

CUL-HOG 867-289-RP414

# nature

Vol 288 No 5786 6 November 1980 £1.25 \$3.00



## Saturn (151) from Voyager 1

(Vol-288)  
(No. 5786-5792)  
(Nov.-Dec.)  
(1-744p)  
(1980)

Seating  
142/81

AUTUMN BOOKS  
SUPPLEMENT





## Ion exchangers from Pharmacia Fine Chemicals

The better choice because ion exchangers from Pharmacia Fine Chemicals have excellent capacities, do not have to be decanted, and require the minimum of preparation.

Better results because ion exchangers from Pharmacia Fine Chemicals are bead formed, making them easy to pack and quick to run. Separations can be repeated many times in the same column.

Better information can be found in the NEW handbook "Ion exchange principles and methods" and the Literature Reference Lists, available free on request from Pharmacia Fine Chemicals.

Pharmacia Fine Chemicals AB  
Box 175  
S-751 04 Uppsala 1  
Sweden

 **Pharmacia  
Fine Chemicals**

Circle No. 24 on Reader Enquiry Card



## nature

Volume 288 No.5786 6 November 1980

## NEWS

|  |   |   |   |
|--|---|---|---|
| <b>What are the research councils for?</b>   | 1 | <b>London University: Medical schools stay</b>  | 6 |
| <b>Ideological trouble ahead for Unesco</b>  | 2 | <b>Séveso scare: Bloat, not poison</b>  | 6 |
| <b>Academics agonize about weapons labs: Livermore and Los Alamos up for grabs</b> | 3 | <b>Bovine tuberculosis: Badgers at risk</b>   | 6 |
| <b>Short commons for Spanish research</b>  | 3 | <b>Swedish Academy: Plugging Nobel gap</b>  | 7 |
| <b>US radioastronomy: Thinking big</b>   | 4 | <b>Franco-Soviet jaunt to Halley?</b>   | 7 |
| <b>Any encounters, any kind</b>  | 4 | <b>Brazilian biology: Humus from wood</b>   | 7 |
| <b>Nuclear protests: Were Croats first?</b>  | 5 | <b>Correspondence: Malaria vaccines? (S. Cohen); Nobel Prize rules (M. Benarie); Fungal food (P. J. Heald); AChE uses (R. A. Davis)</b> | 8 |
| <b>Research councils: Geological setback</b>                                       | 5 |   |   |

## NEWS AND VIEWS

|  |    |   |    |
|--|----|---|----|
| <b>A close look at Saturn: Philip Campbell discusses the forthcoming Voyager 1 encounter</b>                   | 9  | <b>Flat-spectrum radio sources: victim of a conspiracy? Alan Marscher on results of VLBI observations</b> | 12 |
| <b>How much genetic variation? J.S. Jones reviews molecular polymorphism and its evolutionary implications</b> | 10 | <b>Hot foot: Clive Lloyd on focal adhesion plaques</b>  | 13 |

## AUTUMN BOOKS SUPPLEMENT

|  |   |    |                  |  |    |
|--|---|----|------------------|--|----|
| <b>Microprocessors, and the printed word</b> |   | 15 | W.C. McGrew      | <b>The Evolution of Culture in Animals (by John Tyler Bonner)</b>  | 26 |
| Edmund Leach                                 | <b>Gregory Bateson: The Legacy of a Scientist (by David Lipset)</b>   | 16 | Kenneth Mellanby | <b>Hampshire Days (by W.H. Hudson)</b>   | 27 |
| P.B. Medawar                                 | <b>Seeds of Discovery (by W.I.B. Beveridge)</b>   | 17 | Eric Ashby       | <b>The Volta River Project (by David Hart)</b>   | 28 |
| Stuart Sutherland                            | <b>Freud: The Man and Cause (by Ronald W. Clark)</b>  | 18 | Joseph S. Nye    | <b>World Energy Issues and Policies (edited by Robert Mabro)</b>   | 29 |
| D.V. Lindley                                 | <b>The Enterprise of Knowledge: An Essay on Knowledge, Credal Probability, and Chance (by Isaac Levi)</b>           | 20 | Ziauddin Sardar  | <b>Science and Science Policy in the Arab World (by A.B. Zahlan)</b>   | 30 |
| Paul A. Colinvaux                            | <b>The Wooing of Earth (by René Dubos)</b>  | 21 | H.B.G. Casimir   | <b>Landau: A Great Physicist and Teacher (by Anna Livanova)</b>  | 31 |
| Wilma George                                 | <b>A Delicate Arrangement: The Strange Case of Charles Darwin and Alfred Russel Wallace (by Arnold C. Brackman)</b> | 22 | John Stachel     | <b>From X-Rays to Quarks: Modern Physicists and Their Discoveries (by Emilio Segrè)</b>  | 32 |
| John R. Krebs                                | <b>Tooth and Claw: Defensive Strategies in the Animal World (by J.L. Cloudsley-Thompson)</b>                        | 23 | Malcolm C. Scott | <b>Unlocking the Atom: A Hundred Years of Nuclear Energy (by Malcolm Longstaff)</b>  | 33 |
| Bryan Turner                                 | <b>The Complete Encyclopedia of the Animal World (edited by David M. Burn)</b>                                      | 24 | Paul Davies      | <b>Life Beyond Earth: The Intelligent Earthling's Guide to Life in the Universe (by Gerald Feinberg and Robert Shapiro). Earth and Cosmos (by R.S. Kandel)</b> | 34 |
| Alwyne Wheeler                               | <b>The Heyday of Natural History (by Lynn Barber)</b>   | 25 | Joseph Silk      | <b>The State of the Universe (edited by G.T. Bath)</b>   | 34 |

Contents continued overleaf

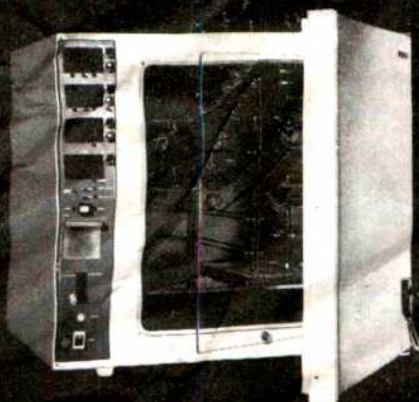
Saturn and Diadne seen by Voyager 1, superimposed on a false-colour image of Saturn's rings. The false colours are designed to enhance intensity contrast in a single-colour image. Voyager 1's mission is discussed on page 9.

M

© 1980 Macmillan Journals Ltd  
 Nature® published weekly ISSN 0028-0836  
 Registered as a newspaper at the British Post Office  
 and the United States Post Office



# Incubator for Tissue Cultures



Heraeus CO<sub>2</sub>-Incubator BL 5060 EK/CO<sub>2</sub>

We build the incubator with appropriate pCO<sub>2</sub>, pH and pO<sub>2</sub> control units.

It is Heraeus that produce incubators incorporating means for control of the pCO<sub>2</sub>, pH, pO<sub>2</sub>, pN<sub>2</sub> and rH, as well as for hot air sterilization.

In the intact living organism, the pCO<sub>2</sub>, pO<sub>2</sub> and pH of the cell environment are in a state of biochemical and physiological equilibrium.

In the Heraeus Incubators for Tissue Cultures, all environmental parameters are ideally matched to the natural environmental conditions of the cells.

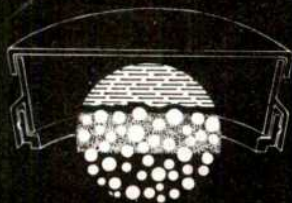
When Petriperm<sup>®</sup> Tissue Culture Dishes are used, gradients of the pCO<sub>2</sub>, pO<sub>2</sub> and pH are avoided in the micro-environment of monolayer cell cultures.

## Petriperm<sup>®</sup>

a novel culture dish with gas permeable membrane as cellular support

Additional advantages of the Petriperm<sup>®</sup> membrane are:

- UV permeable 200 nm
- Suitable for high power light and fluorescence microscopy
- The membrane can be cut for cell cloning, electron microscopy, staining and documentation.
- Chemically resistant to acids, bases and organic solvents.



## Heraeus

W. C. Heraeus GmbH  
Produktbereich  
Elektrowärme  
D-6450 Hanau 1

Agencies all over the world

Circle No. 20 on Reader Enquiry Card.

## Oxford University Press

### Survival in the Wild

Each species of wild animal or plant, beset by a unique series of problems, has evolved its own array of strategies to enable it to survive. The living world, therefore, displays an almost bewildering diversity of these strategies, which this new series aims to describe. The first three books in the series have just been published and they are: *Feeding Strategy* by Jennifer Owen, *Camouflage and Mimicry* by Denis Owen, and *Sexual Strategy* by Tim Halliday. Each book is beautifully illustrated, and includes 32 pages of colour photographs. Illustrated £6.95 each

### Complementary Variational Principles

New edition

A.M. Arthurs

In this book the solution of boundary value problems for linear and nonlinear partial differential equations arising in mathematical physics, chemistry, engineering, and biology is presented for graduate students and for engineers and scientists. There are thirty examples from these fields. This edition is completely revised and enlarged to include many results and new derivations. Second edition £16 Oxford Mathematical Monographs

### The Development of the Vertebrate Limb

An Approach through Experiment, Genetics, and Evolution

J.R. Hinchliffe and D.R. Johnson

Starting with a sketch of the evolutionary history of the pentadactyl limb, the authors describe and analyse the processes of limb development, first at the level of tissue interaction and then at the level of pattern formation. The ectoderm-mesoderm dialogue is approached through the classic grafting experiments on reassembled chick limb buds. Positional-information approaches to pattern formation propose the zone of polarizing activity as a source of an anterior-posterior gradient and a clock-face model to explain amphibian limb regeneration. An account is given of attempts at computer simulation of limb pattern, and the authors conclude with a discussion of the genetic mechanisms controlling limb development. Illustrated £20

*Handwritten:* R513 R41A

### The Mathematical Theory of Quantitative Genetics

M.G. Bulmer

The emphasis in this book is on discussion of the underlying principles illustrated by simple examples. A basic knowledge of statistical methods and theory is assumed and problems for solution are included. £27

Circle No. 16 on Reader Enquiry Card.



## AUTUMN BOOKS SUPPLEMENT

|                 |  |    |
|-----------------|--|----|
| David W. Hughes | <b>Starseekers</b> (by Colin Wilson)   | 35 |
| W.D. Hackmann   | <b>The Construction and Use of a Thermometer</b> (by James Six)  | 36 |
| P.T. Saunders   | <b>Handbook of Applicable Mathematics. Vol. I Algebra</b> (edited by Walter Ledermann and Steven Vajda)                | 37 |
| K.J. Gregory    | <b>Geography: Yesterday and Tomorrow</b> (edited by E.H. Brown)  | 37 |
| Sarah Bunney    | <b>To the Farthest Ends of the Earth: 150 Years of World Exploration</b> (by Ian Cameron)                              | 38 |
| R.J.C. Atkinson | <b>The Enigma of Stonehenge</b> (by John Fowles and Barry Brukoff).<br><b>The Age of Stonehenge</b> (by Colin Burgess) | 39 |

|                  |   |    |
|------------------|---|----|
| J.M. Munn-Rankin | <b>EBLA: An Empire Rediscovered</b> (by Paolo Matthiae)   | 40 |
| Gail Kennedy     | <b>The Cambridge Encyclopedia of Archaeology</b> (edited by Andrew Sherratt)                                    | 41 |
| D.G. Harnden     | <b>The Cancer Syndrome</b> (by Ralph W. Moss)   | 42 |
| J.W.T. Dickerson | <b>Human Nutrition — A Comprehensive Treatise</b> (general editors R.B. Alfin-Slater and D. Kritchevsky)        | 43 |
| John C. Marshall | <b>The Right Brain: A New Understanding of the Unconscious Mind and its Creative Powers</b> (by T.R. Blakeslee) | 44 |

## REVIEW ARTICLE

|   |   |    |
|---|---|----|
| R.C. Newton, J.V. Smith<br>and B.F. Windley | <b>Carbonic metamorphism, granulites and crustal growth</b> | 45 |
|---|---|----|

## ARTICLES

|   |  |    |                                  |  |    |
|---|--|----|----------------------------------|--|----|
| D.A. Adamson, F. Gasse,<br>F.A. Street<br>and M.A.J. Williams | <b>Late Quaternary history of the Nile</b>   | 50 | T.D. Fox<br>and B. Weiss-Brummer | <b>Leaky +1 and -1 frameshift mutations at the same site in a yeast mitochondrial gene</b> | 60 |
| L.R. Harris, C. Blakemore<br>and M. Donaghy                   | <b>Integration of visual and auditory space in the mammalian superior colliculus</b> | 56 |                                  |  |    |

## LETTERS

|   |  |    |   |  |    |
|---|--|----|---|--|----|
| J.G. Davies, B. Anderson<br>and I. Morison                        | <b>The Jodrell Bank radio-linked interferometer network</b>  | 64 | M. Bobrow and J. Heritage   | <b>Nonrandom segregation of nucleolar organizing chromosomes at mitosis?</b>   | 79 |
| C.J. Lonsdale<br>and I. Morison                                   | <b>Rotationally symmetric structure in two extragalactic radio sources</b>   | 66 | G. Janossy, N. Tidman,<br>W.S. Selby, J.A. Thomas,<br>S. Granger, P.C. Kung<br>and G. Goldstein | <b>Human T lymphocytes of inducer and suppressor type occupy different microenvironments</b>   | 81 |
| R.G. Noble and D. Walsh   | <b>MTRLI observations of the double QSO at 408 MHz</b>   | 69 | J.F. Ashmore<br>and D.R. Copenhagen   | <b>Different postsynaptic events in two types of retinal bipolar cell</b>  | 84 |
| S. Halgedahl and M. Fuller  | <b>Magnetic domain observations of nucleation processes in fine particles of intermediate titanomagnetite</b>        | 70 | M. Göthert  | <b>Somatostatin selectively inhibits noradrenaline release from hypothalamic neurones</b>  | 86 |
| R.J. Arculus and J.W. Delano                                      | <b>Implications for the primitive atmosphere of the oxidation state of Earth's upper mantle</b>                      | 72 | J. Rossier, Y. Audigier,<br>N. Ling, J. Cros<br>and S. Udenfriend                               | <b>Met-enkephalin-Arg<sup>6</sup>-Phe<sup>7</sup>, present in high amounts in brain of rat, cattle and man, is an opioid agonist</b> | 88 |
| M.E. Cox, K.E. Cuff<br>and D.M. Thomas                            | <b>Variations of ground radon concentrations with activity of Kilauea Volcano, Hawaii</b>                            | 74 |   |  |    |
| B.J. Cole   | <b>Trophic structure of a grassland insect community</b>   | 76 |   |  |    |
| N.J. Brewin, T.M. DeJong,<br>D.A. Phillips<br>and A.W.B. Johnston | <b>Co-transfer of determinants for hydrogenase activity and nodulation ability in <i>Rhizobium leguminosarum</i></b> | 77 |   |  |    |



# HOW BIG IS YOUR RNA?

The size of the *prokaryotic* and *eucaryotic* Ribosomal RNA Markers produced by P-L Biochemicals is precisely known. These rRNA species remain intact even under denaturing conditions!

**2512 RIBOSOMAL RNA 23S and 16S (*E. coli* MRE-600)**  
**NEW Price:....10 A<sub>260</sub> units....\$52.00\***

**2508 RIBOSOMAL RNA 23S and 16S (*E. coli* R-13)**  
**NEW Price:....10 A<sub>260</sub> units....\$52.00\***

**2510 RIBOSOMAL RNA 28S and 18S**  
**(*Saccharomyces cerevisiae* ATCC 9763)**  
**NEW Price:....10 A<sub>260</sub> units....\$52.00\***

**2506 RIBOSOMAL RNA 28S and 18S (Calf Liver)**  
**NEW Price:....10 A<sub>260</sub> units....\$52.00\***

\*Products must be shipped cold. Insulated container and refrigerant charge—\$10.00. May require air freight.

One unit is that quantity of material which has an absorbance of 1.0 at 260 nm when dissolved in 1 ml water and measured in a 1 cm cuvette.

excellence in biochemistry



**P.L. biochemicals, inc.**

1037 WEST MCKINLEY AVENUE, MILWAUKEE, WIS 53205

® Call 414/347-7442 TWX 910-262-1111

## ANTISERA AGAINST TERMINAL TRANSFERASE

Cross-reacts with human, rat and mouse TdT. Suitable for Rocket immunoelectrophoresis and Immuno inhibition studies. Source of IgG for immunofluorescence.

**New 0102 GOAT ANTI-CALF TdT SERUM**

**Prep:** LIQUID serum with 0.1% sodium azide.

**Price:** 1ml \$65.00 5ml \$275.00

**New 0106 RABBIT ANTI-CALF TdT SERUM**

**Prep:** LIQUID serum with 0.1% sodium azide.

**Price:** 0.4ml \$60.00 2ml \$245.00

excellence in biochemistry



**P.L. biochemicals, inc.**

1037 WEST MCKINLEY AVENUE, MILWAUKEE, WIS 53205

® Call 414/347-7442 TWX 910-262-1111

Circle No. 04 on Reader Enquiry Card.

## Opportunities for small businesses in North Devon

New workshops of 1,000 to 2,000 square feet floor space available shortly in the North Devon village of Bradworthy. They would be very suitable for small firms starting up. New housing is to be built near by. Bradworthy is in a development area.

**For details of these new premises or for further information about activities of the Dartington North Devon Trust, write or phone:**  
**Dr. David Davies,**  
**Bridge Chambers, Barnstaple, North Devon. Phone: Barnstaple (0271) 76365.**

Circle No. 61 on Reader Enquiry Card.

## SYNTHETIC PEPTIDES

**Merseyside Laboratories**  
**at the forefront of peptide chemistry**

Synthetic Peptides  
 Custom synthesis  
 Fmoc, Boc, Z-amino acids  
 Resins for peptide synthesis  
 Unusual amino acids  
 G.I. Hormone antisera

**for information contact:**

**Merseyside Laboratories (Padgate 824856) P.O. Box 62, 21 Aston Court, Kingsland Grange, Warrington WA1 4SL.**

Circle No. 62 on Reader Enquiry Card.



## LETTERS

|   |  |    |
|---|--|----|
| W.D. Hardy Jr,<br>A.J. McClelland,<br>E.E. Zuckerman,<br>H.W. Snyder Jr, E.G. MacEwen,<br>D. Francis and M. Essex | <b>Development of virus non-producer lymphosarcomas in pet cats exposed to FeLV</b>                | 90 |
| R.J. Avery, J.D. Norton,<br>J.S. Jones, D.C. Burke<br>and A.G. Morris   | <b>Interferon inhibits transformation by murine sarcoma viruses before integration of provirus</b> | 93 |

|                            |  |    |
|----------------------------|--|----|
| P.B. Sehgal and A.D. Sagar | <b>Heterogeneity of poly(I).poly(C)-induced human fibroblast interferon mRNA species</b>         | 95 |
| L. Shulman and M. Revel    | <b>Interferon-dependent induction of mRNA activity for (2'-5') oligo-isoadenylate synthetase</b> | 98 |

## MATTERS ARISING

|  |   |     |
|--|---|-----|
| Ch. Hentschel, E. Probst<br>and M.L. Birnstiel | <b>Transcriptional fidelity of histone genes injected into <i>Xenopus</i> oocyte nuclei</b> | 100 |
| J.A. Wolff                                     | <b>Peridotite xenoliths in basalts and mantle dynamics</b>                                  | 103 |
| A.R. Basu                                      | <b>Reply to Wolff</b>   | 103 |

|                              |   |     |
|------------------------------|---|-----|
| E.A. King                    | <b>Late Eocene rings around the Earth?</b>                  | 103 |
| J.A. O'Keefe                 | <b>Reply to King</b>  | 104 |
| W.P. Luckett and L.L. Jacobs | <b>Proposed fossil tree shrew genus <i>Palaeotupaia</i></b> | 104 |

Paleo Ch. City Library  
SCIENCE COLLEGE  
A Upper Circular Road  
DUBLIN 4

## MISCELLANY

|                |        |
|----------------|--------|
| 100 years ago  | 13     |
| Books received | xxxvii |

|                        |       |
|------------------------|-------|
| New on the market      | xxxix |
| Classified advertising | xvi   |

## GUIDE TO AUTHORS

● Review articles should be aimed at a relatively wide readership. Many reviews are invited, but submitted articles may also be accepted; it is advisable to consult us before writing a review article.

● Articles may be up to 3,000 words long with at most six displayed items (figures and tables); they are reports of major research developments.

● Letters are brief reports of original research of unusual and wide interest, not in general longer than 1,000 words; they have at most three or four displayed items.

● 'Matters Arising' permits short discussion (up to 300 words) of papers that have recently appeared in *Nature*.

Articles should be accompanied by an abstract of not more than fifty words. Letters should begin with a paragraph giving the background and main conclusion in terms intelligible to as wide a readership as possible.

**Manuscripts** may be submitted either to London or New York. Three typed copies should be submitted, each including lettered copies of figures. Typing (including references) should be double spaced. The title should be brief and informative. Pages should be numbered. References, tables and figure legends should start on separate pages. Experimental detail vital to the paper yet which would interrupt the narrative is best placed in the figure legends. Units should be identified in the margin on their first appearance. Equations should occupy single lines if possible:  $\exp(a)$  is preferred to  $e^a$  if 'a' is more than one character.

**References** are indicated by superscripts in the text. See any contemporary *Nature* for style, but note:

(i) only one reference number need be used if the reference is to several papers by identical authors.

(ii) first and last pages of references should be cited.

Abbreviations should follow the *World List of Scientific Periodicals*, fourth edn (Butterworth, 1963-65). Symposia are often difficult to refer to and only published or soon-to-be-published volumes should be mentioned in references. Their publisher and place of publication should be clearly indicated 'Personal communication' and 'unpublished' should be incorporated in text.

**Artwork** should be sent with the manuscript and clearly marked with author's name and the figure number. Line drawings should be either photographic prints or in Indian ink on heavy cartridge paper, tracing paper or similar materials. Most figures are reduced to one column width so originals should be about as wide as a page of *Nature*. To enable figures, particularly maps, to be edited in the same style as the text, they should contain only essential material. Ideally, an unlettered original and three lettered copies should be provided; labelling on halftones should, if possible, be avoided entirely. Magnifications quoted should be for the figures as submitted. We are always glad to see artwork for possible use on the cover, but cannot guarantee its return.

In order to save on postal expenses we return only the top copy and artwork of manuscripts that we cannot publish.

*Nature's* publishing policy is outlined in 258, 1 (1975) and 264, v, 11 Nov. (1976).

## New Titles from G+B

### A Perspective of Physics, Vol. 4

Selections from 1979 Comments on  
Modern Physics

Edited by Sir Harrie Massey

The latest volume in the annual serial designed to give an overview of the various fields in modern physics and to keep both the specialist reader and the interested observer abreast of current developments.

December 1980 360 pp 0 677 16190 5 US \$35.50

### Solar Flare Magnetohydrodynamics

Edited by E. R. Priest

Tremendous advances in the observations of solar flares have taken place in recent years, both from high-resolution ground-based instruments and space telescopes such as those on board Skylab and Solar Maximum Mission satellites. This book presents descriptions of previous work together with more recent unpublished calculations.

December 1980 approx 560 pp 0 677 05530 7 In prep.

### Plasma Astrophysics:

Nonthermal Processes in Diffuse Magnetized  
Plasmas

Vol. 1: The Emission, Absorption and Transfer  
of Waves in Plasmas

Vol. 2: Astrophysical Applications

D. B. Melrose

Written primarily for graduate students in plasma astrophysics and for astrophysicists and geophysicists who wish to learn relevant plasma physics. In Volume 1 plasma theory is developed in a systematic way from first principles, and Volume 2 presents the astrophysical applications and source of the more advanced plasma theory.

Volume 1: 290 pp 0 677 02340 5 US \$46.00

Volume 2: 434 pp 0 677 02130 5 US \$64.50

2-vol. set 0 677 03490 3 US \$99.50

July 1980

### A Theoretical Approach to the Preselection of Carcinogens and Chemical Carcinogenesis

Veljo Veljkovic

Presents a simple valence theory of carcinogenesis, using a new approach to quantitative treatment of molecular biology and chemical carcinogenesis problems. A new, quick test for prediction of carcinogenicity of chemical substances is given together with guidance for selection, design and use in therapy of antitumor agents, antibiotics, psychopharmaceuticals and other medical drugs within the framework of valence theory.

November 1980 125 pp 0 677 05490 4 approx US \$25.00

### Physics of the Paranormal

Edited by John Taylor

This book is an attempt to bring the knowledge and critical approach of modern science to bear on supernatural phenomena. Whilst such an approach is not new, this work is almost unique in containing contributions by a group of scientists on their investigations into various paranormal events, and thus the scientific approach is firmly followed in all articles.

October 1980 402 pp 0 677 16170 0 US \$19.50

## G+B

Gordon and Breach Science Publishers  
One Park Avenue, New York, NY10016 USA  
42 William IV Street, London WC2N 4DE England

Circle No. 28 on Reader Enquiry Card.

# Gordon and Breach

# M

© 1980 Macmillan Journals Ltd  
*Nature* is published weekly  
ISSN 0028-0836

Registered as a newspaper at the  
British Post Office

### London

4 Little Essex Street, WC2R 3LF  
Telephone: (01) 836 6633 Telex: 262024  
Telegrams: Phisus London WC2R 3LF

Editor: John Maddox

Deputy Editor: Peter Newmark

### Editorial Staff

Alun Anderson Sara Nash  
Philip Campbell Peta Pickering  
Isobel Collins Judy Redfearn  
Konrad Guettler Miranda Robertson  
Tim Lincoln Robert Walgate  
Mary Lindley Charles Wenz  
Naomi Molson Jonathan Wolfe  
Publishing Director: Christopher Paterson  
Marketing Director: Ray Barker

### New York

15 East 26 Street, New York, NY 10010  
Telephone: (212) 689 5900 Telex: 668497

Robert Ubell (American Publisher)  
and Sheila Kane

### Washington News Bureau

801 National Press Building, DC 20045  
Telephone: (202) 737 2355 Telex: 64280  
David Dickson (Washington News Editor)

### International Advertising Manager:

Richard Webb (London) (01) 836 6633

### USA Advertising Manager

Henry Dale (New York) (212) 689 5900

### Classified Advertising:

4 Little Essex Street, WC2R 3LF  
Telephone: (01) 240 1101

### Classified(USA)

Terence Miller, Suite 832, 50 Rockefeller Plaza,  
New York, NY 10020—(212) 765 5758

### Display and Classified(Canada)

Peter Drake, 32 Front Street West,  
201 Toronto, Ontario M5J 1C5  
(416) 364 1623

### Advertising Representatives in USA

#### Display

Nature New York Office—(212) 689 5900  
Media Group, Inc. (Dallas)—(214) 631 4480  
Didier & Broderick, Inc. (Chicago)—  
(312) 498 4520

Jobson/Jordan/Harrison/Schulz, Inc.  
(San Francisco) (415) 392 6794 (Los Angeles  
& Pasadena) (213) 796 9200  
Daniel Adams Associates, Inc.  
Philadelphia—(215) 353 6191

CEL Associates (Boston)—(617) 383 6136  
Brinker & Brinker (Fort Lauderdale)  
(305) 771 0064

### German Advertising Representative

E. Meckelburg, 6450 Hanau 1, Jahnstrasse 15,  
West Germany Tel:—(49) 61 8115343

### Japanese Advertising Representative

Orient Echo Inc.

11th Fl, Sankyo Bldg. 7-12, Tsukiji 2-Chome,  
Chuo-Ku, Tokyo, Japan, Tel: 541-4923.

### Annual Subscription including Index

|                            |                      |
|----------------------------|----------------------|
| UK & Eire                  | £75                  |
| USA & Canada               | US\$173              |
| Belgium                    | Airspeed only BF5695 |
| West Germany               | Airspeed only DM360  |
| Netherlands                | Airspeed only G390   |
| Switzerland                | Airspeed only SF330  |
| Rest of Europe             | Airspeed only £85    |
| Rest of World              | Surface £85          |
| Rest of World              | Airmail £130         |
| (not USA, Canada & Europe) |                      |

Back numbers (post-paid): UK, £2.00; USA &  
Canada, US\$6.00 (surface), US\$8.50 (air); Rest  
of World, £2.50 (surface), £3.50 (air).

### Orders (with remittance) to:

Macmillan Journals Ltd, Brunel Road,  
Basingstoke, Hants RG21 2XS.  
Telephone: Basingstoke (0256) 29242  
Telex: 858493

*Nature* is published weekly, except the last week  
in December, by Macmillan Journals Ltd.  
Second-class postage paid at New York, NY  
10010 and at additional mailing offices.  
US Postmaster, please send form 3579 to:  
*Nature*, 15 East 26 Street, New York, NY 10010.

Vol. 288 No. 5786 6 November 1980



# nature

Volume 288 No.5787 13 November 1980

Publ. Co. Ltd  
SCIENCE PUBLISHERS  
A Member of the  
SALENTA

## NEWS

|   |     |   |     |
|---|-----|---|-----|
| <b>How to speak out on Sakharov <i>et al.</i>?</b>                                      | 105 | <b>Large space telescope: Delay means money</b>   | 109 |
| <b>Reagan's election cheering for science? Harder line promises more spin-off funds</b> | 107 | <b>Ariane sells three</b>                         | 110 |
| <b>Plusses and minuses, election 1980</b>   | 107 | <b>Biotechnology: Celltech set up</b>             | 110 |
| <b>Polish unions: Science not lost</b>  | 108 | <b>Veal hormones: Total ban proposed</b>          | 111 |
| <b>University of Warsaw changes course</b>  | 108 | <b>Medical research: Born-again basics</b>        | 111 |
| <b>Science council: Mess about money</b>  | 109 | <b>MRC report in brief</b>                        | 111 |
| <b>Hardship everywhere</b>  | 109 | <b>Correspondence: Sakharov (Andrei Sakharov)</b> | 112 |

## NEWS AND VIEWS

|  |     |   |     |
|--|-----|---|-----|
| <b>Why is magnetite not a good conductor?</b>  | 113 | <b>Biosynthesis and processing of cellular and viral polypeptides: Edward Herbert reports a recent conference</b> | 115 |
| <b>Molecular genetics of the mouse: Grahame Bulfield on regulation of gene expression in the mouse</b> | 114 | <b>Lessons from a peptidergic neurone: B.T. Pickering on processing of polypeptide precursors</b>                 | 117 |
| <b>Are QSO absorption lines extrinsic? Derek Wills discusses recent measurements of 3C273</b>          | 114 | <b>The search for the Zvolen fireball: David W. Hughes examines the probability of finding this meteorite</b>     | 118 |

## REVIEW ARTICLE

|                            |                                  |     |
|----------------------------|----------------------------------|-----|
| F. Paresce and P. Jakobsen | <b>The diffuse UV background</b> | 119 |
|----------------------------|----------------------------------|-----|

## ARTICLES

|                                       |  |     |  |   |     |
|---------------------------------------|--|-----|--|---|-----|
| S.H. Zisk and P.J. Mougins-Mark       | <b>Anomalous region on Mars: implications for near-surface liquid water</b>            | 126 | J.R. Bedbrook, M. O'Dell and R.B. Flavell                  | <b>Amplification of rearranged repeated DNA sequences in cereal plants</b>  | 133 |
| S. Neidle, H.M. Berman and H.S. Shieh | <b>Highly structured water network in crystals of a deoxydinucleoside-drug complex</b> | 129 | P. Hobart, R. Crawford, L. Shen, R. Pictet and W.J. Rutter | <b>Cloning and sequence analysis of cDNAs encoding two distinct somatostatin precursors found in the endocrine pancreas of anglerfish</b> | 137 |

## LETTERS

|  |  |     |   |  |     |
|--|--|-----|---|--|-----|
| G.K. Skinner   | <b>Observations of optical flares in the recurrent X-ray transient A0538-66</b>    | 141 | W. Kundt and Gopal-Krishna                  | <b>Extremely relativistic electron-positron twin-jets form extragalactic radio sources</b> | 149 |
| E.M.D. Symbalisty, J. Yang and D.N. Schramm                  | <b>Neutrinos and the age of the Universe</b>                                       | 143 | M. Schüssler                                | <b>Flux tube dynamo approach to the solar cycle</b>  | 150 |
| P. Laques, J.-L. Nieto, J.-L. Vidal, A. Augé and R. Despiaud | <b>Brightening of a hot spot in NCG2903</b>  | 145 | M. Fleischmann, P.J. Hendra and J. Robinson | <b>X-ray diffraction from adsorbed iodine on graphite</b>                                  | 152 |
| C.L. Bhat, M.L. Sapru and C.L. Kaul                          | <b>A nonrandom component in cosmic rays of energy <math>\geq 10^{14}</math> eV</b> | 146 | L.E. Makovsky, S.S. Pollack and F.R. Brown  | <b>TiO<sub>2</sub> on and around a deactivated hydrodesulphurization catalyst</b>          | 154 |

Contents continued overleaf

**Cover:** Kidney epithelial cells treated with a fluorescent monoclonal antibody against a transformation-related protein of the simian virus 40. Why should cells that have not been infected by the virus contain this protein? See page 167.

M

© 1980 Macmillan Journals Ltd  
Nature® published weekly ISSN 0028-0836  
Registered as a newspaper at the British Post Office  
and the United States Post Office

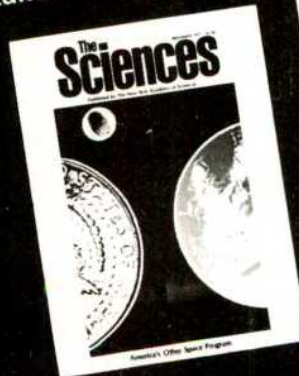
# Spiders

E.O. Wilson: Let me remind you that people everywhere, a large percent of the population, at a very early age have already developed a deep horror at the sight of snakes or spiders with nothing more than gentle nudging from their parents, if that. Yet, in spite of the fact that parents constantly reinforce their children against going near electric sockets, automobiles, knives and the like, phobias against such objects rarely develop.

Marvin Harris: Let's go back again to the possibility that these phobias are genetically programmed — which I'm willing to grant. The overwhelming bulk of the socially conditioned response repertoires of different human societies consists, by your own admission, of culturally determined rather than genetically determined traits. Then it seems to me that when one offers a cogent culturological explanation of these phobias, it has to be considered that this explanation is not offered in isolation.

from a debate between E.O. Wilson and Marvin Harris in sociobiology. In *The Sciences*. From family constellations to galaxies, *The Sciences* takes the critical look. Handsome, original, lively, *The Sciences* represents the best science commentary you'll find anywhere on human behavior, culture, the physical sciences — by Ashley Montagu, Stephen Jay Gould, B.F. Skinner, Napoleon Chagnon, Peter Medawar. ... Subscribe today. It's only \$12.50 a year.

*The Sciences*. More than science.



☐ Here's my check or money order for \$12.50 (\$2.50 off the newsstand price) for the next ten issues of *The Sciences*.  
Foreign individuals add \$5.00  
Foreign institutions add \$10.00  
US institutions add \$5.00

☐ Bill me later.

Name \_\_\_\_\_

Address \_\_\_\_\_

City \_\_\_\_\_

State \_\_\_\_\_

Zip \_\_\_\_\_

**The Sciences**  
2 East 63rd Street  
New York, N.Y. 10021

Published by The New York Academy of Sciences

NAT 6

... instances of human emergence of state-organized societies or the emergence of stratified classes and castes. The enor-



## LETTERS

- |  |  |   |  |
|--|--|---|--|
| A. Lacam, M. Madon<br>and J.P. Poirier       | <b>Olivine glass and spinel formed<br/>in a laser heated, diamond-anvil<br/>high pressure cell</b> 155   | S. Rastan, M.H. Kaufman,<br>A.H. Handyside<br>and M.F. Lyon   | <b>X-chromosome inactivation in<br/>extra-embryonic membranes of<br/>diploid parthenogenetic mouse<br/>embryos demonstrated by<br/>differential staining</b> 172 |
| J.F.R. Gower, K.L. Denman<br>and R.J. Holyer | <b>Phytoplankton patchiness<br/>indicates the fluctuation<br/>spectrum of mesoscale oceanic<br/>structure</b> 157  | M. Perricaudet,<br>J.-M. le Moullec, P. Tiollais<br>and U. Pettersson                                   | <b>Structure of two adenovirus type<br/>12 transforming polypeptides<br/>and their evolutionary<br/>implications</b> 174   |
| K.P. Steel<br>and G.R. Bock                  | <b>The nature of inherited deafness<br/>in deafness mice</b> 159   | T.H. Tötterman, K. Nilsson<br>and C. Sundström  | <b>Phorbol ester-induced<br/>differentiation of chronic<br/>lymphocytic leukaemia cells</b> 176  |
| J.G. Howard, C. Hale<br>and F.Y. Liew        | <b>Genetically determined<br/>susceptibility to <i>Leishmania<br/>tropicalis</i> infection is expressed<br/>by haematopoietic donor cells<br/>in mouse radiation chimaeras</b> 161 | P. De Baetselier, S. Katzav,<br>E. Gorelik, M. Feldman<br>and S. Segal                                  | <b>Differential expression of H-2<br/>gene products in tumour cells is<br/>associated with their<br/>metastatogenic properties</b> 179                           |
| F. Bonhoeffer<br>and J. Huf                  | <b>Recognition of cell types by<br/>axonal growth cones <i>in vitro</i></b> 162  | M. Armstrong-James, J. Millar<br>and Z.L. Kruk  | <b>Quantification of noradrenaline<br/>iontophoresis</b> 181   |
| L.Y. Lu and B.A. Askonas                     | <b>Cross-reactivity for different<br/>type A influenza viruses of a<br/>cloned T-killer cell line</b> 164  | E.J. Goetzl   | <b>Vitamin E modulates the<br/>lipoxygenation of arachidonic<br/>acid in leukocytes</b> 183  |
| D.V. Mohan Das<br>and G. Weeks               | <b>Reversible heat activation of<br/>alkaline phosphatase of<br/><i>Dictyostelium discoideum</i> and<br/>its developmental implication</b> 166                                     | J.G. Lewis<br>and J.A. Swenberg   | <b>Differential repair of<br/>O<sup>6</sup>-methylguanine in DNA of<br/>rat hepatocytes and<br/>nonparenchymal cells</b> 185                                     |
| D.P. Lane<br>and W.K. Hoeffler               | <b>SV40 large T shares an antigenic<br/>determinant with a cellular<br/>protein of molecular weight<br/>68,000</b> 167   | A. Sener<br>and W.J. Malaisse   | <b>L-leucine and a nonmetabolized<br/>analogue activate pancreatic<br/>islet glutamate dehydrogenase</b> 187   |
| G. Ramsay, T. Graf<br>and M.J. Hayman        | <b>Mutants of avian<br/>myelocytomatosis virus with<br/>smaller <i>gag</i> gene-related<br/>proteins have an altered<br/>transforming ability</b> 170                              | M. Knight, P.J. Cayley,<br>R.H. Silverman,<br>D.H. Wreschner, C.S. Gilbert,<br>R.E. Brown and I.M. Kerr | <b>Radioimmune, radiobinding and<br/>HPLC analysis of 2-5A and<br/>related oligonucleotides from<br/>intact cells</b> 189  |

## MATTERS ARISING

- |  |   |              |  |
|--|---|--------------|--|
| R.R. Reisz and M.J. Heaton                 | <b>Origin of mammal-like<br/>reptiles</b> 193                           | K.M. Towe    | <b>Feroxyhyte on Mars?</b> 196                       |
| T.S. Kemp                                  | <b>Reply to Reisz and Heaton</b> 193                                    | R.G. Burns   | <b>Reply to Towe</b> 196                             |
| D.K. Meinke, K. Padian<br>and J. Kappelman | <b>Growth rings in dinosaur<br/>teeth</b> 193                           | S. Chatterji | <b>Anisotropy of Young's modulus<br/>of bone</b> 196 |
| M.S. Boyce                                 |   | J.L. Katz    | <b>Reply to Chatterji</b> 196                        |
| J.R. Bolt and R.E. de Mar                  |   |              |  |
| P.A. Johnston                              | <b>Reply to Meinke <i>et al.</i>, Boyce<br/>and Bolt and de Mar</b> 195 |              |  |

## BOOK REVIEWS

- |                  |  |                   |  |
|------------------|--|-------------------|--|
| Stephen Cotgrove | <b>Environment, Ideology and Policy<br/>(by Francis Sandbach)<br/>The Environment from Surplus<br/>to Scarcity (by Allan<br/>Schnaiberg)</b> 197       | William M. Kaula  | <b>Advanced Physical Geodesy<br/>(by H. Moritz)</b> 199  |
| F.R. Hartley     | <b>Homogeneous Catalysis:<br/>The Applications and Chemistry<br/>of Catalysis by Soluble Transition<br/>Metal Complexes<br/>(by G.W. Parshall)</b> 198 | P.E. Bryant       | <b>Social Interaction and Cognitive<br/>Development in Children<br/>(by A.-N. Perret-Clermont)</b> 199 |
| Donald R. Strong | <b>Evolutionary Biology of Parasites<br/>(by P.W. Price)</b> 198   | Ernst Ungewickell | <b>Coated Vesicles<br/>(edited by C.D. Ockelford and<br/>A. Whyte)</b> 200                             |
|                  |  | T.W. Goodwin      | <b>Lipids in Evolution (by William<br/>R. Nes and W. David Nes)</b> 200                                |

## MISCELLANY

# Compare: Completeness Capability Cost



*Philips Liquid  
Scintillation Counter,  
Mini Vial Model.*



# nature

Volume 288 No.5788 20 November 1980

## NEWS

|   |     |   |     |
|---|-----|---|-----|
| <b>Deciding where to put nuclear plants</b>                                     | 201 | <b>Waste disposal: UK goes French</b>   | 205 |
| <b>Scope for European collaboration?</b>  | 202 | <b>Soviet dissidents: Another taken</b>   | 206 |
| <b>Backlash against DNA ventures? More thoughts at Harvard on business link</b> | 203 | <b>German science: New man arrives</b>  | 206 |
| <b>Science Research Council comes clean</b>                                     | 203 | <b>Indian environment: Ghandi converted</b>   | 207 |
| <b>European science: Foundation stones</b>                                      | 204 | <b>Nuclear fallout: Weapons are worst</b>   | 207 |
| <b>Something ventured, something done</b>                                       | 204 | <b>Correspondence: Museum of errors (L.B. Halstead); Refrigerator brew (Robert T. Green); Frequency tripling (Peter Hammerling)</b> | 208 |
| <b>Fusion research: Livermore looks up</b>                                      | 204 |   |     |
| <b>Radioactive waste: Brussels helps</b>  | 205 |   |     |

## NEWS AND VIEWS

|   |     |  |     |
|---|-----|--|-----|
| <b>What prospects for an X-ray laser?</b>   | 209 | <b>New directions in spectroscopy: Derek Stacey reports a recent conference</b>                                    | 213 |
| <b>Gene regulation: new, old and remote controls: Adrian Minty and Peter Newmark on recent developments</b> | 210 | <b>Precambrian evolution: Thomas D. Brock on the lines of research</b>   | 214 |
| <b>Deep drilling in African lakes: N.J. Shackleton discusses a seismic survey for next year</b>             | 211 | <b>Green light in Heidelberg: Gene organization and expression in green plants</b>                                 | 215 |
| <b>Herpes simplex virus in latent infections: Howard Marsden discusses viral latency</b>                    | 212 | <b>Electrochemistry and the geochemist: H.A. Tourtelot on electrochemical theory for formation of ore deposits</b> | 218 |

## REVIEW ARTICLE

John D. Woods

Do waves limit turbulent diffusion in the ocean? 219

## ARTICLES

|  |   |     |   |   |     |
|--|---|-----|---|---|-----|
| D. Jones                                   | <b>Latitudinal beaming of planetary radio emissions</b>                               | 225 | H. Garoff, A.-M. Frischauf, K. Simons, H. Lehrach and H. Delius | <b>Nucleotide sequence of cDNA coding for Semliki Forest virus membrane glycoproteins</b> | 236 |
| C.U. Hammer, H.B. Clausen and W. Dansgaard | <b>Greenland ice sheet evidence of post-glacial volcanism and its climatic impact</b> | 230 |   |   |     |

## LETTERS

|   |   |     |   |  |     |
|---|---|-----|---|--|-----|
| P.R. Weissman   | <b>Stellar perturbations of the cometary cloud</b>  | 242 | C.J.N. Wilson, N.N. Ambraseys, J. Bradley and G.P.L. Walker | <b>A new date for the Taupo eruption, New Zealand</b>  | 252 |
| A. Bossard and G. Toupance                              | <b>Far UV photolysis of CH<sub>4</sub>-NH<sub>3</sub> mixtures and planetary studies</b>  | 243 | G. Wadge  | <b>Output rate of magma from active central volcanoes</b>  | 253 |
| C.L. Chakrabarti, C.C. Wan, H.A. Hamed and P.C. Bertels | <b>Trace element determination by capacitive discharge atomic absorption spectrometry</b> | 246 | Y. Avnimelech   | <b>Calcium-carbonate-phosphate surface complex in calcareous systems</b>                           | 255 |
| J. Klein  | <b>Forces between mica surfaces bearing layers of adsorbed polystyrene in cyclohexane</b> | 248 | A. Gunatilaka, A. Saleh and A. Al-Temeemi                   | <b>Plant-controlled supratidal anhydrite from Al-Khiran, Kuwait</b>                                | 257 |
| R.C. Morris, M.R. Thornber and W.E. Ewers               | <b>Deep-seated iron ores from banded-iron formation</b>                                   | 250 | E. Suess  | <b>Particulate organic carbon flux in the oceans — surface productivity and oxygen utilization</b> | 260 |

Contents continued overleaf

**Cover:** Contour plot of computer-filtered actin molecules in projection obtained from crystalline *Acanthamoeba* actin sheets. See page 296.

• This issue contains the author index to Vol.287.

M

© 1980 Macmillan Journals Ltd  
 Nature® published weekly ISSN 0028-0836  
 Registered as a newspaper at the British Post Office  
 and the United States Post Office

Raven Press announces a major new journal:

# Journal of Molecular and Applied Genetics

A JOURNAL FOR THE RAPID PUBLICATION OF FULL-LENGTH ARTICLES ON STUDIES UTILIZING MODERN GENETIC TECHNIQUES, ESPECIALLY RECOMBINANT DNA METHODS, TO SOLVE BASIC AND APPLIED PROBLEMS IN GENETICS, BIOCHEMISTRY, MEDICINE, AND AGRICULTURE.

Editor-in-Chief

**Howard M. Goodman, Ph.D.**

*Howard Hughes Medical Institute Laboratory  
Department of Biochemistry and Biophysics  
University of California, San Francisco  
San Francisco, California 94143 U.S.A.*

## Editorial Board

**John Abelson**/La Jolla, Calif., USA  
**Frederick Ausubel**/Cambridge, Mass., USA  
**John R. Bedbrook**/Canberra, Australia  
**Lawrence Bogorad**/Cambridge, Mass., USA  
**Mary-Dell Chilton**/St. Louis, Mo., USA  
**Richard A. Flavell**/London, UK  
**Masayori Inouye**/Stony Brook, N.Y., USA  
**Robert Kamen**/London, UK  
**Yuet W. Kan**/San Francisco, Calif., USA  
**David W. Martin, Jr.**/San Francisco, Calif., USA

**Marc Van Montagu**/Gent, Belgium  
**Richard C. Mulligan**/Cambridge, Mass., USA  
**Alexander Rich**/Cambridge, Mass., USA  
**Jeff Schell**/Cologne, FRG  
**James Shepard**/Manhattan, Kan., USA  
**John Shine**/Canberra, Australia  
**Joan A. Steitz**/New Haven, Conn., USA  
**Robert T. Tjian**/Berkeley, Calif., USA  
**Michael Wigler**/Cold Spring Harbor, N.Y., USA

**CALL FOR PAPERS:** Manuscripts on the synthesis of biologically and medically relevant proteins, genomic organization, chromosomal gene mapping, gene structure, regulation of gene expression, molecular and biochemical studies on genetic diseases, and plant molecular biology are invited for submission. Publication will begin early in 1981. To avoid excessive reduction, the journal will provide generous space for inclusion of figures. The most modern computer typesetting techniques will facilitate rapid publication. The publisher will be Raven Press, New York. Submit manuscripts in triplicate to the Editor-in-Chief at the above address. References should be cited by number in the text and numbered in order of citation; provide complete titles of articles cited, with names of all authors and inclusive pagination. Full instructions to contributors are available from the Editor-in-Chief or from Raven Press.

Circle No. 04 on Reader Enquiry Card.

## SUBSCRIPTION ORDER FORM

TO: **RAVEN PRESS 1140 Avenue of the Americas, New York, N.Y. 10036, U.S.A.** Date \_\_\_\_\_

Please enter my subscription for Volume 1 (1981) of **JOURNAL OF MOLECULAR AND APPLIED GENETICS**.

Published bimonthly. **Personal subscription rates:** U.S. \$80; elsewhere \$90.

**Institutional subscription rates:** U.S. \$135; elsewhere \$145.

Air delivery is *included* for European and Mediterranean countries;  
for air service *elsewhere* add \$15.00.

Name (please print) \_\_\_\_\_

Address \_\_\_\_\_

Country \_\_\_\_\_

Postal Code \_\_\_\_\_

NA112080



## LETTERS

- |  |  |     |   |  |     |
|--|--|-----|---|--|-----|
| H.W. Pearson<br>and R. Howsley   | <b>Concomitant photoautotrophic growth and nitrogenase activity by cyanobacterium <i>Plectonema boryanum</i> in continuous culture</b> | 263 | P. Davies, R. Katzman<br>and R.D. Terry   | <b>Reduced somatostatin-like immunoreactivity in cerebral cortex from cases of Alzheimer disease and Alzheimer senile dementia</b> | 279 |
| A. Roberts and K. Tregonning   | <b>The robustness of natural systems</b>   | 265 | A.A. Patchett, E. Harris,<br>E.W. Tristram, M.J. Wyvratt,<br>M.T. Wu, D. Taub, E.R. Peterson,<br>T.J. Ikeler, J. ten Broeke, L.G. Payne, D.L. Ondeyka,<br>E.D. Thorsett, W.J. Greenlee, N.S. Lohr, R.D. Hoffsommer,<br>H. Joshua, W.V. Ruyle, J.W. Rothrock, S.D. Aster,<br>A.L. Maycock, F.M. Robinson, R. Hirschmann, C.S. Sweet,<br>E.H. Ulm, D.M. Gross, T.C. Vassil and C.A. Stone | <b>A new class of angiotensin-converting enzyme inhibitors</b>   | 280 |
| A.M. Kelly<br>and N.A. Rubinstein  | <b>Why are fetal muscles slow?</b>   | 266 | P. Sokoloff, M.-P. Martres<br>and J.-C. Schwartz  | <b><sup>3</sup>H-apomorphine labels both dopamine postsynaptic receptors and autoreceptors</b>                                     | 283 |
| P.K. Moore and J.R.S. Houlst   | <b>Anti-inflammatory steroids reduce tissue PG synthetase activity and enhance PG breakdown</b>  | 269 | B.P. Roques,<br>M.C. Fournié-Zaluski,<br>E. Soroca, J.M. Lecomte,<br>B. Malfroy, C. Llorens<br>and J.-C. Schwartz   | <b>The enkephalinase inhibitor thiorphan shows antinociceptive activity in mice</b>  | 286 |
| P.K. Moore and J.R.S. Houlst   | <b>Pathophysiological states modify levels in rat plasma of factors which inhibit synthesis and enhance breakdown of PG</b>            | 271 | C.V. Cabrera, C. Wohlenberg,<br>H. Openshaw, M. Rey-Mendez,<br>A. Puga and A.L. Notkins   | <b>Herpes simplex virus DNA sequences in the CNS of latently infected mice</b>   | 288 |
| R.L. Sutherland, L.C. Murphy,<br>M. San Foo, M.D. Green,<br>A.M. Whybourne<br>and Z.S. Krozowski | <b>High-affinity anti-oestrogen binding site distinct from the oestrogen receptor</b>  | 273 | I.D. Walker and A.W. Harris   | <b>Immunoglobulin C<sub>μ</sub> RNA in T lymphoma cells is not translated</b>  | 290 |
| S. Cockcroft, J.P. Bennett<br>and B.D. Gomperts  | <b>Stimulus-secretion coupling in rabbit neutrophils is not mediated by phosphatidylinositol breakdown</b>                             | 275 | B.E.H. Maden  | <b>Methylation map of <i>Xenopus laevis</i> ribosomal RNA</b>  | 293 |
| D.E. Vance<br>and B. de Kruijff  | <b>The possible functional significance of phosphatidylethanolamine methylation</b>  | 277 | U. Aebi, P.R. Smith,<br>G. Isenberg and T.D. Pollard  | <b>Structure of crystalline actin sheets</b>   | 296 |
| J. Axelrod and F. Hirata   | <b>Reply to Vance and de Kruijff</b>   | 278 | G.A. Clegg, R.F.D. Stansfield,<br>P.E. Bourne<br>and P.M. Harrison  | <b>Helix packing and subunit conformation in horse spleen apoferritin</b>  | 298 |

## MATTERS ARISING

- |                             |                                    |     |  |   |     |
|-----------------------------|------------------------------------|-----|--|---|-----|
| L.A. Temerin                | <b>Evolution of the orang-utan</b> | 301 | I.R. Mackay, N.R. Rose<br>and P.R. Carnegie          | <b>Germ-line deletion of genes coding for self-determinants</b> | 302 |
| R.J. Smith and D.R. Pilbeam | <b>Reply to Temerin</b>            | 301 | R. Jemmerson and E. Margoliash                       | <b>Reply to Mackay <i>et al.</i></b>                            | 303 |
| J.C. McGrath                | <b>Noradrenergic transmission</b>  | 301 | S. Lemaire, I. Lemaire,<br>D.M. Dean and G.G. Livett | <b>Opiate receptors and adrenal medullary function</b>          | 303 |
| G.D.S. Hirst and T.O. Neild | <b>Reply to McGrath</b>            | 302 | E. Costa, A. Guidotti<br>and L. Saiani               | <b>Reply to Lemaire <i>et al.</i></b>                           | 304 |

## BOOK REVIEWS

- |                     |   |     |                |  |     |
|---------------------|---|-----|----------------|--|-----|
| George E. Uhlenbeck | <b>The Image of Eternity: Roots of Time in the Physical World (by David Park)</b>                           | 305 | Peter D. Moore | <b>Human Ecology in Savanna Environments (edited by David R. Harris)</b>                               | 307 |
| N.A. Mitchison      | <b>Somatic Selection and Adaptive Evolution: On the Inheritance of Acquired Characters (by E.J. Steele)</b> | 306 | G. Turnock     | <b>Growth and Differentiation in <i>Physarum polycephalum</i> (edited by W.F. Dove and H.P. Rusch)</b> | 307 |
| T.S. West           | <b>Applied Soil Trace Elements (edited by Brian E. Davies)</b>  | 306 | J.L. Gordon    | <b>The Cell Biology of Inflammation. Handbook of Inflammation, Vol. 2. (edited by Gerald Weissman)</b> | 308 |

## MISCELLANY

- |                        |       |
|------------------------|-------|
| 100 years ago          | 218   |
| Index to Vol. 287      | xiii  |
| Classified advertising | xxxiv |

**PRODUCT REVIEW** This week's product review (page xxix) covers general laboratory equipment.

0.00000 g



## NEWS

|  |     |   |     |
|--|-----|---|-----|
| <b>London medical schools stay in limbo</b>  | 309 | <b>Bangladesh: Planning science</b>   | 314 |
| <b>Best not to attend on Mr Moon</b>   | 310 | <b>Soviet fertilizers: Going it alone</b>   | 314 |
| <b>Harvard finally backs off gene venture: Anxiety about conflict of interest wins</b> | 311 | <b>European plutonium: Project denied</b>   | 314 |
| <b>JET fusion experiment seeks growth</b>  | 311 | <b>Project planning: Staged inquiries</b>   | 315 |
| <b>Telecommunications: Monopoly in doubt</b>   | 312 | <b>French museum takes shape</b>  | 315 |
| <b>Malaysian education: Pressures ease</b>   | 312 | <b>Correspondence: Medical education (L.T. Cotton); Risks at NRPB (S.G. Goss); Reagan a plus? (M. Noble <i>et al.</i>); Man's biosphere (J.N.R. Jeffers); Scientific warfare (D. Van Buren)</b> | 316 |
| <b>Antarctic research: Germany joins in</b>  | 313 |   |     |

## NEWS AND VIEWS

|  |     |  |     |
|--|-----|--|-----|
| <b>Sun-climate links: T.M.L. Wigley reports a recent conference</b>                        | 317 | <b>Conversion of solar energy: Sir George Porter looks at the photochemical decomposition of water</b> | 320 |
| <b>Peat — a resource reassessed: J.A. Taylor and R.T. Smith describe new uses for peat</b> | 319 | <b>Far-infrared interstellar carbon: A correspondent reports new spectroscopic measurements</b>        | 321 |
| <b>Cell proliferation: Paul Nurse on genes controlling the cell cycle</b>                  | 319 | <b>Xenobiotic compounds: Phillip R. Lehrbach describes microbial methods of detoxification</b>         | 322 |

## ARTICLES

|  |  |     |  |  |     |
|--|--|-----|--|--|-----|
| <b>W.H.-M. Ku, D.J. Helfand and L.B. Lucy</b>          | <b>X-ray properties of quasars</b>   | 323 | <b>D.R. Burton, J. Boyd, A.D. Brampton, S.B. Easterbrook-Smith, E.J. Emanuel, J. Novotny, T.W. Rademacher, M.R. van Schravendijk, M.J.E. Sternberg and R.A. Dwek</b> | <b>The C1q receptor site on immunoglobulin G</b> | 338 |
| <b>P.J. Coney, D.L. Jones and J.W.H. Monger</b>        | <b>Cordilleran suspect terranes</b>  | 329 |  |  |     |
| <b>R. Blumenthal, R.D. Klausner and J.N. Weinstein</b> | <b>Voltage-dependent translocation of the asialoglycoprotein receptor across lipid membranes</b> | 333 |  |  |     |

## LETTERS

|  |   |     |   |  |     |
|--|---|-----|---|--|-----|
| <b>Gopal-Krishna, E. Preuss and R.T. Schilizzi</b> | <b>Prominent VLBI cores in powerful radio sources with arc second structure</b> | 344 | <b>M. Condomines and C.J. Allegre</b>   | <b>Age and magmatic evolution of Stromboli volcano from <sup>230</sup>Th-<sup>234</sup>U disequilibrium data</b> | 354 |
| <b>W. Bischof, P. Fabian and R. Borchers</b>       | <b>Decrease in CO<sub>2</sub> mixing ratio observed in the stratosphere</b>     | 347 | <b>J.C. Shackleton and T.H. van Andel</b>   | <b>Prehistoric shell assemblages from Franchthi Cave and evolution of the adjacent coastal zone</b>              | 357 |
| <b>R.A. Carrigan Jr</b>                            | <b>Grand unification magnetic monopoles inside the Earth</b>                    | 348 | <b>H.M. Sachs, M. Denking, C.L. Bennett and A.G. Harris</b>                         | <b>Radiometric dating of sediments using fission tracks in conodonts</b>   | 359 |
| <b>M. Del Monte and C. Sabbioni</b>                | <b>Authigenic dolomite on marble surface</b>                                    | 350 | <b>R.E. Molnar and R.A. Thulborn</b>  | <b>First pterosaur from Australia</b>  | 361 |
| <b>H. Okada and A.J. Smith</b>                     | <b>The Welsh 'geosyncline' of the Silurian was a fore-arc basin</b>             | 352 | <b>O. Braddick, J. Atkinson, B. Julesz, W. Kropfl, I. Bodis-Wollner and E. Raab</b> | <b>Cortical binocularity in infants</b>  | 363 |

Contents continued overleaf

**Cover:** Stromboli, part of an active volcano arc in the Mediterranean. The absolute dates for its lavas, reported on page 354, shed new light on the magma evolution of the island.

M

*Nature* (ISSN 0028-0836) is published weekly, except the last week in December, by Macmillan Journals Ltd. Annual subscription for USA and Canada US \$173. Orders (with remittance) and change of address labels to: Macmillan Journals Ltd, Brunel Rd, Basingstoke RG21 2XS, UK. Second class postage paid at New York, NY 10010 and additional mailing offices. US Postmaster send form 3579 to: *Nature*, 15 East 26 Street, New York, NY 10010. © 1980 Macmillan Journals Ltd.

The choice  
is yours



### The Radiochemical Centre Amersham

Full information is available on request.  
The Radiochemical Centre Limited, Amersham,  
England. Telephone: 024-04-4444.

In the U.S.A. and Canada:  
Amersham Corporation, Illinois 60005.  
Telephone: 312-364-7100 and  
800/323-9750 (Tollfree).

In W. Germany:  
Amersham Buchler GmbH & Co KG,  
Braunschweig. Telephone: 05307-4691

Circle No. 06 on Reader Enquiry Card.

## Immunochemicals from Amersham

New, exclusive

**Anti-mouse Fab from rabbit,  $^{125}\text{I}$ -labelled,  $\text{F(ab')}_2$  fragment** IM.113

- ★ For the assay of cell-surface and soluble antigens and hybridoma screening
- ★ Recognizes Fab portion of all classes and subclasses of mouse IgG
- ★ Does not bind to heavy chain Fc fragments
- ★ Specific activity of  $10\text{--}50\mu\text{Ci}/\mu\text{g}$  for optimum binding capacity
- ★ Purified by affinity chromatography and gel filtration
- ★ Biologically tested for binding ability to immobilized mouse IgG

Already available

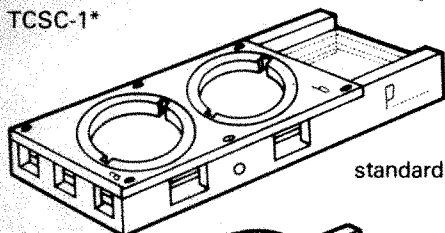
**Protein A,  $^{125}\text{I}$ -labelled with Bolton and Hunter reagent** IM.112

**Protein A, *N*-[propionyl- $^3\text{H}$ ]propionylated** TRK.653

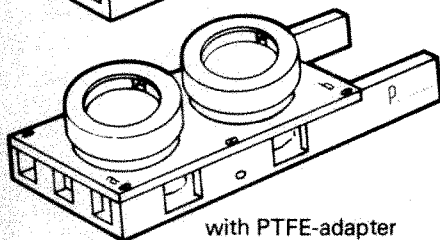
- ★ For the quantitative assay of cell-surface and soluble antigens
- ★ Binds to Fc portions of many classes and subclasses of immunoglobulins
- ★ Biologically tested for binding ability to immobilized mouse IgG

## A new Multipurpose Cell-Test-Chamber-System\* (Pentz-Kammer)

TCSC-1\*



standard



with PTFE-adaptor

### General application

- Cell cultivation in one to ten areas (variable in height and volume) on slides, cover slips or plastic foils.
- Analysis of human, animal and plant tissue and microorganisms.
- Pharmatests, Immunofluorescence, Autoradiography etc.
- Perfusion chamber.
- For still and motion photography.
- The sterilizable chambers ( $+165^\circ\text{C}$ ) enables experiments with infectious bacterial and viral material.

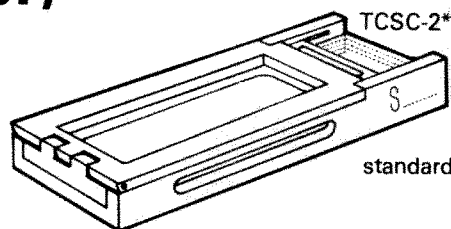
for electrone microscopic investigations

### Additional accessories

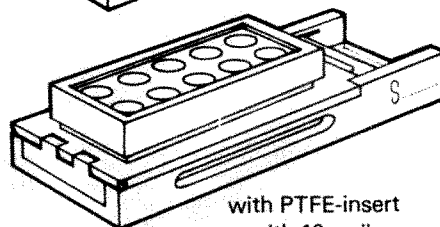
- Different silicone gaskets and PTFE-inserts for numerous inquirments.
- Gas ring ● gas cassette ● heating and gas frame
- heatable work-plate ● temperature control unit

For more information please contact:

**BACHOFER GmbH, P.O. Box 7089,  
D-7410 Reutlingen, FRG (W-Germany), or by  
LEITZ representative (Optical Division).**



standard



with PTFE-insert  
with 10 wells

\* Patents pending

**BACHOFER**

Circle No. 08 on Reader Enquiry Card.



|  |   |            |
|--|---|------------|
| T. Preston, W.D.P. Stewart and C.S. Reynolds               | <b>Bloom-forming cyanobacterium <i>Microcystis aeruginosa</i> overwinters on sediment surface</b>                                   | <b>365</b> |
| M.J. Tucker  | <b>Explanation of sterility in <i>r<sup>h</sup>t<sup>h</sup></i> male mice</b>  | <b>367</b> |
| A.K. Alton, L.M. Silver, K. Artzt and D. Bennett           | <b>Molecular analysis of the genetic relationship of <i>trans</i> interacting factors at the T/t complex</b>                        | <b>368</b> |
| U. di Porzio, M.-C. Daguet, J. Glowinski and A. Prochiantz | <b>Effect of striatal cells on <i>in vitro</i> maturation of mesencephalic dopaminergic neurones grown in serum-free conditions</b> | <b>370</b> |
| R.F. Furchgott and J.V. Zawadzki                           | <b>The obligatory role of endothelial cells in the relaxation of arterial smooth muscle by acetylcholine</b>                        | <b>373</b> |
| M.C. Beinfeld, D.K. Meyer and M.J. Brownstein              | <b>Cholecystokinin octapeptide in the rat hypothalamo-neurohypophyseal system</b>   | <b>376</b> |
| R.K. Goyal, S. Rattan and S.I. Said                        | <b>VIP as a possible neurotransmitter of non-cholinergic non-adrenergic inhibitory neurones</b>                                     | <b>378</b> |
| L.Y. Jan, Y.N. Jan and M.S. Brownfield                     | <b>Peptidergic transmitters in synaptic boutons of sympathetic ganglia</b>  | <b>380</b> |
| A. Reches, A. Eldor, Z. Vogel and Y. Salomon               | <b>Do human platelets have opiate receptors?</b>  | <b>382</b> |
| A. Toniolo, T. Onodera, J.-W. Yoon and A.L. Notkins        | <b>Induction of diabetes by cumulative environmental insults from viruses and chemicals</b>   | <b>383</b> |
| J.M. Teale and N.R. Klinman                                | <b>Tolerance as an active process</b>   | <b>385</b> |
| S.C. Bell and W.D. Billington                              | <b>Major anti-paternal alloantibody induced by murine pregnancy is non-complement-fixing IgG1</b>                                   | <b>387</b> |

|  |   |            |
|--|---|------------|
| A. Ben-Nun, Y. Ron and I.R. Cohen                                  | <b>Spontaneous remission of auto-immune encephalomyelitis is inhibited by splenectomy, thymectomy or ageing</b> | <b>389</b> |
| L. Fainboim, C. Navarrete and H. Festenstein                       | <b>Precursor and effector phenotypes of activated human T lymphocytes</b>                                       | <b>391</b> |
| J.M. Zarleng and P.C. Kung   | <b>Monoclonal antibodies which distinguish between human NK cells and cytotoxic T lymphocytes</b>               | <b>394</b> |
| T. Jørgensen and K. Hannestad                                      | <b>H-2-linked genes control immune response to V-domains of myeloma protein</b>                                 | <b>396</b> |
| A.C. Lopo and V.D. Vacquier  | <b>Sperm-specific surface antigenicity common to seven animal phyla</b>   | <b>397</b> |
| P. Jurdic, J. Huppert, T. Greenland and E. Heller                  | <b>Retroviral antigens on <i>gs<sup>+</sup> chf<sup>+</sup></i> leukocytes</b>                                  | <b>400</b> |
| P.E. Sudbery, A.R. Goodey and B.L.A. Carter                        | <b>Genes which control cell proliferation in the yeast <i>Saccharomyces cerevisiae</i></b>                      | <b>401</b> |
| G. Macino, C. Scazzocchio, R.B. Waring, M.M. Berks and R.W. Davies | <b>Conservation and rearrangement of mitochondrial structural gene sequences</b>                                | <b>404</b> |
| R.R. Schreck and S.A. Latt   | <b>Comparison of benzo (a) pyrene metabolism and sister chromatid exchange induction in mice</b>                | <b>407</b> |
| A.J. Bailey, N.D. Light and E.D.T. Atkins                          | <b>Chemical cross-linking restrictions on models for the molecular organization of the collagen fibre</b>       | <b>408</b> |
| J.M. Squire and A. Freundlich                                      | <b>Direct observation of a transverse periodicity in collagen fibrils</b>                                       | <b>410</b> |
| J. Ramstein and M. Leng  | <b>Salt-dependent dynamic structure of poly(dG-dC).poly(dG-dC)</b>  | <b>413</b> |
| A.A. Kossiakoff and S.A. Spencer                                   | <b>Neutron diffraction identifies His 57 as the catalytic base in trypsin</b>                                   | <b>414</b> |

## BOOK REVIEWS

|                  |  |            |              |  |            |
|------------------|--|------------|--------------|--|------------|
| Gordon R. Willey | <b>Gordon Childe: Revolutions in Archaeology (by Bruce G. Trigger)</b>             | <b>417</b> | V.C. Reddish | <b>Optical and Infrared Telescopes for the 1990s (edited by Adelaide Hewitt)</b> | <b>419</b> |
| J.R.L. Allen     | <b>Continental Red Beds (by P. Turner)</b>   | <b>418</b> | J.M. Thomas  | <b>Intercalated Layered Materials (edited by F.A. Levy)</b>                      | <b>419</b> |
| Timothy D. Heath | <b>Liposomes in Biological Systems (edited by G. Gregoriadis and A.C. Allison)</b> | <b>418</b> | Clive Ellory | <b>Cell Potassium (by Roderick P. Kernan)</b>                                    | <b>420</b> |

## MISCELLANY

|                |            |                        |           |
|----------------|------------|------------------------|-----------|
| 100 years ago  | <b>318</b> | Classified advertising | <b>xv</b> |
| Books Received | <b>421</b> |                        |           |

### Erratum

Due to an error in the *Nature* office, an incompletely revised version of the paper "Anomalous region on Mars: implications for near-surface liquid water" by S. H. Zisk and P. J. Mougins-Mark was published in the issue of 13 November (288, 126-129, 1980). The authors' corrections will appear shortly in an appropriate form.



## Less is more.

Less Work.  
More Dependability.

They're ready-to-use kits with everything you need except your sample. Room temperature set-up, no salting out, no second incubation. We've pre-reacted the first antibody with the second antibody to save you time.

And we've given you NEN quality to assure you of dependable assays — accurate and reproducible. Sensitivity reaches the femtomole range with the acetylating reagents provided. A tritium-labeled marker is included to monitor recovery. The iodinated tracer is exceptionally stable.

These are some of the reasons to choose NEN's Cyclic AMP and GMP [ $^{125}\text{I}$ ] RIA kits, the world's most widely used for their convenience and quality. Send for the whole story in our technical brochure.

Not for use in humans or clinical diagnosis.

**NEN** New England Nuclear

549 Albany Street, Boston, Mass. 02118  
Call toll-free 800-225-1572  
(In Massachusetts and International: 617-482-9595)  
NEN Chemicals GmbH, D-6072 Dreieich, W. Germany  
Postfach 401240 Telephone (06103) 85034 Telex 4-17993 NEN D  
NEN Canada Ltd., 2453 46th Avenue, Lachine, Que H8T 3C9  
Telephone 514-636-4971 Telex 05-821808

Circle No. 01 on Reader Enquiry Card.

# M

©1980 Macmillan Journals Ltd  
Nature® is published weekly  
ISSN 0028-0836  
Registered as a newspaper at the  
British Post Office

London  
4 Little Essex Street, WC2R 3LF  
Telephone: (01) 836 6633 Telex: 262024  
Telegrams: Phusis London WC2R 3LF

Editor: John Maddox  
Deputy Editor: Peter Newmark  
Editorial Staff  
Alun Anderson Sara Nash  
Philip Campbell Peta Pickering  
Isobel Collins Judy Redfearn  
Konrad Guettler Miranda Robertson  
Tim Lincoln Robert Walgate  
Mary Lindley Charles Wenz  
Naomi Molson Jonathan Wolfe  
Publishing Director: Christopher Paterson  
Marketing Director: Ray Barker

New York  
15 East 26 Street, New York, NY 10010  
Telephone: (212) 689 5900 Telex: 668497  
Robert Ubell (American Publisher)  
and Sheila Kane

Washington News Bureau  
801 National Press Building, DC 20045  
Telephone: (202) 737 2355 Telex: 64280  
David Dickson (Washington News Editor)

International Advertising Manager:  
Richard Webb (London) (01) 836 6633

USA Advertising Manager  
Henry Dale (New York) (212) 689 5900

Classified Advertising:  
4 Little Essex Street, WC2R 3LF  
Telephone: (01) 240 1101

Classified(USA)  
Amy Bodiam, Suite 832, 50 Rockefeller Plaza,  
New York, NY 10020—(212) 765 5758

Display and Classified(Canada)  
Peter Drake, 32 Front Street West,  
201 Toronto, Ontario M5J 1C5  
(416) 364 1623

Advertising Representatives in USA

Display  
Nature New York Office—(212) 689 5900  
Media Group, Inc. (Dallas)—(214) 631 4480  
Didier & Broderick, Inc. (Chicago)—  
(312) 498 4520

Jobson/Jordan/Harrison/Schulz, Inc.  
(San Francisco) (415) 392 6794 (Los Angeles  
& Pasadena) (213) 796 9200  
Daniel Adams Associates, Inc.  
Philadelphia—(215) 353 6191

CEL Associates (Boston)—(617) 383 6136  
Brinker & Brinker (Fort Lauderdale)  
(305) 771 0064

German Advertising Representative  
E. Meckelburg, 6450 Hanau 1, Jahnstrasse 15,  
West Germany Tel:—(49) 61 8115343

Japanese Advertising Representative  
Orient Echo Inc.  
11th Fl, Sankyo Bldg. 7-12, Tsukiji 2-Chome,  
Chuo-Ku, Tokyo, Japan, Tel: 541-4923.

Annual Subscription including Index  
UK & Eire £75  
USA & Canada US\$173  
Belgium Airspeed only BF5695  
West Germany Airspeed only DM360  
Netherlands Airspeed only G390  
Switzerland Airspeed only SF330  
Rest of Europe Airspeed only £85  
Rest of World Surface £85  
Rest of World Airmail £130  
(not USA, Canada & Europe)

Back numbers (post-paid); UK, £2.00; USA &  
Canada, US\$6.00 (surface), US\$8.50 (air); Rest  
of World, £2.50 (surface), £3.50 (air).

Orders (with remittance) to:  
Macmillan Journals Ltd, Brunel Road,  
Basingstoke, Hants RG21 2XS.  
Telephone: Basingstoke (0256) 29242  
Telex: 858493

Vol. 288 No. 5789 27 November 1980



# nature

Volume 288 No.5790 4 December 1980

## NEWS

|   |     |  |     |
|---|-----|--|-----|
| <b>Harvard backs off recombinant DNA</b>  | 423 | <b>Cable of protest</b>  | 427 |
| <b>How not to run a public monopoly</b>   | 424 | <b>Brazilian universities: No cash ahead</b>   | 427 |
| <b>Anti-trust waiver for industrial research: Justice blesses inter-company collaboration</b> | 425 | <b>High-energy physics: Machines shut down</b>   | 428 |
| <b>Science foundation all set at last</b>   | 425 | <b>Third World: Consumers arise</b>  | 428 |
| <b>Nuclear power: Border problems</b>   | 425 | <b>Conservation: Bill of rights</b>  | 429 |
| <b>French take Manhattan</b>  | 426 | <b>Fallout from China</b>  | 429 |
| <b>Soviet health: More research</b>   | 426 | <b>Correspondence: Museum pieces (Colin Patterson, M.J. Hughes-Games, Harry Rothman)</b> | 430 |
| <b>Polish science: Advice not taken</b>   | 426 |  |     |

## NEWS AND VIEWS

|  |     |  |     |
|--|-----|--|-----|
| <b>Open debate: M.G. Edmunds on the mass of the Universe</b>                     | 431 | <b>The slow process of succession: Peter D. Moore looks at studies of ecological succession</b>      | 436 |
| <b>Bioenergetics in Europe: Judith Armitage reports a recent conference</b>      | 432 | <b>Actin assembly: Sarah E. Hitchcock-De Gregori on the control of actin filament polymerization</b> | 437 |
| <b>A new view inside cells: Keith Burrige on advances in electron microscopy</b> | 433 | <b>Where do cosmic rays come from: A correspondent reports a recent meeting in Leningrad</b>         | 438 |
| <b>Pathways of endocytosis: Michael Grisow describes routes into the cell</b>    | 434 |  |     |

## ARTICLES

|  |  |     |                                       |   |     |
|--|--|-----|---------------------------------------|---|-----|
| S.A. Collins, A.F. Cook II, J.N. Cuzzi, G.E. Danielson, G.E. Hunt, T.V. Johnson, D. Morrison, T. Owen, J.B. Pollack, B.A. Smith and R.J. Terrile | <b>First Voyager view of the rings of Saturn</b>               | 439 | J.C. Eichelberger                     | <b>Vesiculation of mafic magma during replenishment of silicic magma reservoirs</b>                               | 446 |
| D. McKenzie, A. Watts, B. Parsons and M. Roufosse  | <b>Planform of mantle convection beneath the Pacific Ocean</b> | 442 | M. Shoyab and G.J. Todaro             | <b>Specific high affinity cell membrane receptors for biologically active phorbol and ingenol esters</b>          | 451 |
|  |  |     | G. Isenberg, U. Aebi and T.D. Pollard | <b>An actin-binding protein from <i>Acanthamoeba</i> regulates actin filament polymerization and interactions</b> | 455 |

## LETTERS

|  |  |     |  |  |     |
|--|--|-----|--|--|-----|
| M.H. Ulrich, H. Butcher and D.L. Meier             | <b>B2 1141 + 37: a giant radio galaxy with remarkable radio and optical properties</b> | 459 | A.K. Cheetham                                | <b>Low-temperature preparation of refractory alloys</b>                                      | 469 |
| C. Miller, J.M. Steed, D.L. Filkin and J.P. Jesson | <b>Two-dimensional model calculations of stratospheric HCl and ClO</b>                 | 461 | H. Schouten, J. Karson and H. Dick           | <b>Geometry of transform zones</b>   | 470 |
| E.E. Altshuler                                     | <b>Large rain drops in the bright band</b>   | 464 | S. Mykkeltveit, E.S. Husebye and C. Oftedahl | <b>Subduction of the Iapetus Ocean crust beneath the Møre Gaeiss Region, southern Norway</b> | 473 |
| M. Kunst and J.M. Warman                           | <b>Proton mobility in ice</b>  | 465 | J.S. Kennedy, A.R. Ludlow and C.J. Sanders   | <b>Guidance system used in moth sex attraction</b>   | 475 |
| R.M.J. Cotterill and J.U. Madsen                   | <b>Evidence against a crystal instability in melting</b>                               | 467 | D.E. Kroodsma and R. Pickert                 | <b>Environmentally dependent sensitive periods for avian vocal learning</b>                  | 477 |

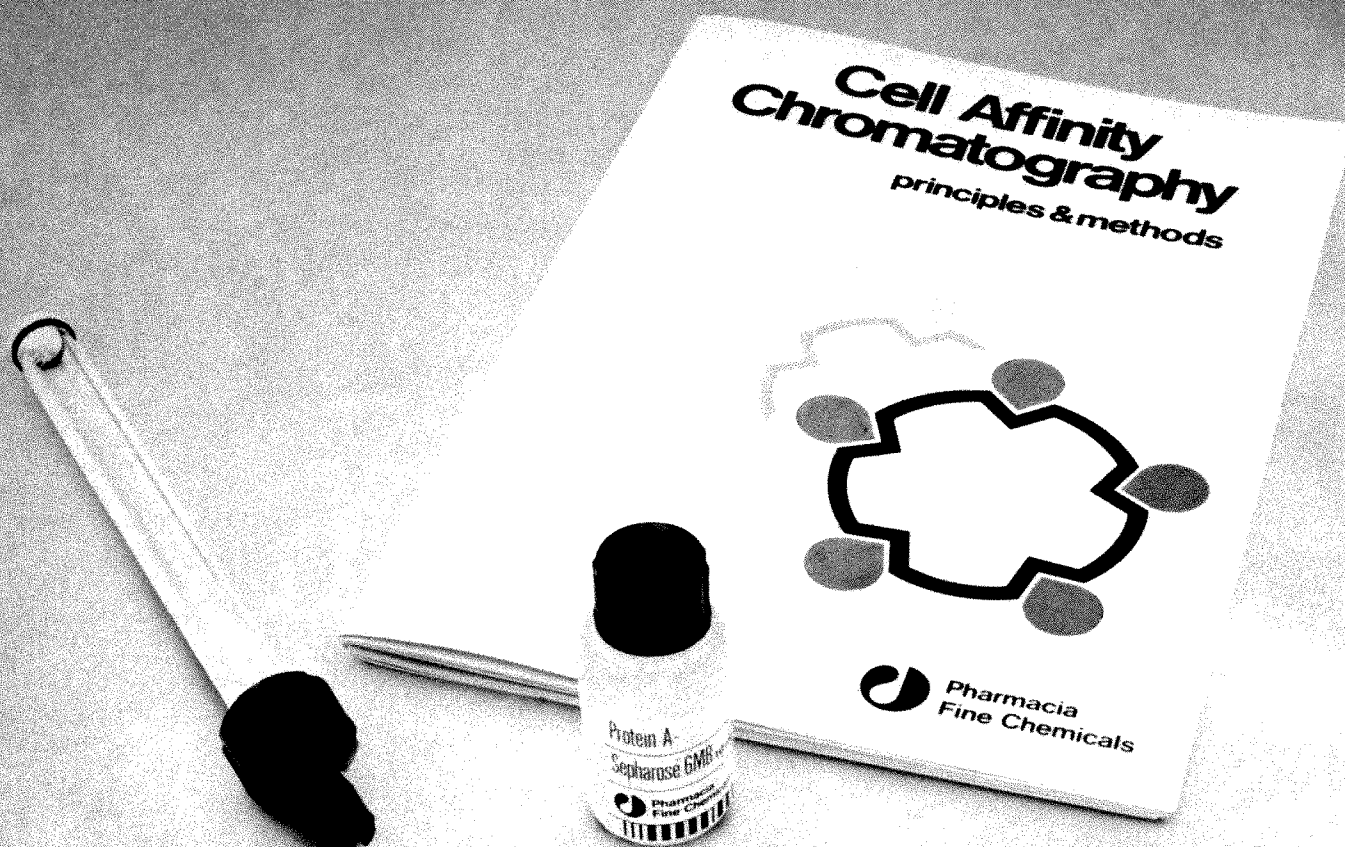
Contents continued overleaf

**Cover:** Arch in the Herodian Winter Palace, Jericho. (Picture by Simon McBride.) Archaeology in the Holy Land is the subject of the lead review in the Christmas Books Supplement which starts on page 503.

# M

*Nature*® (ISSN 0028-0836) is published weekly, except the last week in December, by Macmillan Journals Ltd. Annual subscription for USA and Canada US\$173. Orders (with remittance) and change of address labels to: Macmillan Journals Ltd, Brunel Rd, Basingstoke RG21 2XS, UK. Second class postage paid at New York, NY 10010 and additional mailing offices. US Postmaster send form 3579 to: *Nature*, 15 East 26 Street, New York, NY 10010. ©1980 Macmillan Journals Ltd.

# The Cell Sorters.



## Affinity chromatography is the simplest technique for purifying many macromolecules – now you can use this method for separating cells too!

Affinity chromatography is the simple, rapid technique that separates cell subpopulations according to their unique surface properties. You can separate more than  $10^8$  cells in under 3 hours using only 2–5 ml of affinity adsorbent. The same adsorbent can be used many times, giving you economical and reproducible separations. Choose the adsorbent you need from our range of affinity gels made from Sepharose® 6MB – the gel developed specially for cell separation.

**New!**

**Protein A-Sepharose 6MB**

a versatile new adsorbent for use together with specific antibodies for separating many types of cells

**Helix pomatia Lectin-Sepharose 6MB**

separates T and B cells for immunological studies and tissue typing

**Wheat germ Lectin-Sepharose 6MB**

for subfractionating lymphocytes and other cells

**CNBr-activated Sepharose 6MB**

ready-activated Macrobeads that make it easy to prepare your own adsorbents for cell separation

**Contact us today for your own free copy of our new booklet:  
"Cell affinity chromatography – principles and methods".**

Pharmacia Fine Chemicals  
Division of Pharmacia Inc.  
800 Centennial Avenue  
Piscataway, N.J. 08854

 **Pharmacia  
Fine Chemicals**



## LETTERS

- |   |   |            |   |   |            |
|---|---|------------|---|---|------------|
| C.R. Olson and A.M. Graybiel  | <b>Sensory maps in the claustrum of the cat</b>   | <b>479</b> | J.C. Macartney, S.D. Comis and J.O. Pickles                                       | <b>Is myosin in the cochlea a basis for active motility?</b>  | <b>491</b> |
| N.A. Salibi, N.E. Saadé, N.R. Banna and S.J. Jabbur                       | <b>Dorsal column input into the reticular formation</b>   | <b>481</b> | H.A. Pershadsingh, M.L. McDaniel, M. Landt, C.G. Bry, P.E. Lacy and J.M. McDonald | <b>Ca<sup>2+</sup>-activated ATPase and ATP-dependent calmodulin-stimulated Ca<sup>2+</sup> transport in islet cell plasma membrane</b> | <b>492</b> |
| B.M. Glaser, P.A. D'Amore, H. Seppa, S. Seppa and E. Schiffmann           | <b>Adult tissues contain chemoattractants for vascular endothelial cells</b>                          | <b>483</b> | R. Coronado and C. Miller   | <b>Decamethonium and hexamethonium block K<sup>+</sup> channels of sarcoplasmic reticulum</b>   | <b>495</b> |
| S.-E. Dahlén, P. Hedqvist, S. Hammarström and B. Samuelsson               | <b>Leukotrienes are potent constrictors of human bronchi</b>  | <b>484</b> | J. Traeger, W.G. Wood, J.B. Clegg, D.J. Weatherall and P. Wasi                    | <b>Defective synthesis of HbE is due to reduced levels of <math>\beta^E</math> mRNA</b>   | <b>497</b> |
| M.J. Buchmeier, H.A. Lewicki, O. Tomori and K.M. Johnson                  | <b>Monoclonal antibodies to lymphocytic choriomeningitis virus react with pathogenic arenaviruses</b> | <b>486</b> | W.S. Dallas and S. Falkow   | <b>Amino acid sequence homology between cholera toxin and <i>Escherichia coli</i> heat-labile toxin</b>                                 | <b>499</b> |
| C.M. Croce, A. Linnenbach, W. Hall, Z. Steplewski and H. Koprowski        | <b>Production of human hybridomas secreting antibodies to measles virus</b>                           | <b>488</b> | H. Hori, M. Ikeda-Saito and T. Yonetani   | <b>Freezing induced change in ligand orientation in oxycobalt-myoglobin</b>   | <b>501</b> |
| C.Z. Zielinski, S.D. Waksal, L.D. Tempelis, R.H. Khirya and R.S. Schwartz | <b>Surface phenotypes in T-cell leukaemia are determined by oncogenic retroviruses</b>                | <b>489</b> |   |   |            |

## CHRISTMAS BOOKS SUPPLEMENT

- |                  |   |            |                      |   |            |
|------------------|---|------------|----------------------|---|------------|
| P.J. Parr        | <b>From Dan to Beersheba, and beyond — three recent books on the archaeology and history of the Holy Land</b> | <b>503</b> | John Krebs           | <b>The Mystery of Migration (edited by Robin Baker)</b>                           | <b>510</b> |
| Helmut Gernsheim | <b>Fox Talbot and the Invention of Photography (by Gail Buckland)</b>   | <b>504</b> | Clark T. Rogerson    | <b>Companions for the fungal foray — two guides to mushrooms of North America</b> | <b>511</b> |
| Ashley Montagu   | <b>The Panda's Thumb (by Stephen Jay Gould)</b>   | <b>505</b> | Bernard Wood         | <b>Hands (by John Napier)</b>   | <b>511</b> |
| Richard Mabey    | <b>Contrary natures — natural history books</b>   | <b>505</b> | John C.W. Cope       | <b>The Natural History of Fossils (by C.R.C. Paul)</b>                            | <b>512</b> |
| Arthur Bourne    | <b>The Yachtsman's Naturalist (by Maldwin Drummond and Paul Rodhouse)</b>                                     | <b>506</b> | John Sutton          | <b>Geology of France (by Ch. Pomerol <i>et al.</i>)</b>                           | <b>512</b> |
| Peter D. Moore   | <b>Art in botany . . .</b>  | <b>507</b> | Peter J. Smith       | <b>Earthquakes (by G.A. Eiby)</b>   | <b>513</b> |
| T.R. Halliday    | <b>. . . and art in ornithology</b>   | <b>508</b> | David W. Hughes      | <b>To the planets and beyond — popular astronomy</b>                              | <b>514</b> |
| M.A. Ogilvie     | <b>Edward Lear's Birds (by Susan Hyman)</b>   | <b>508</b> | John Maddox          | <b>Cosmos (by Carl Sagan)</b>   | <b>514</b> |
| G. Pontecorvo    | <b>I Fiori delle Alpi (by F. Rasetti)</b>   | <b>509</b> | Philip Campbell      | <b>Galaxies (by Tim Ferris)</b>   | <b>515</b> |
| H.N. Southern    | <b>The Natural History of Shetland (by R.J. Berry and J.L. Johnston)</b>                                      | <b>509</b> | Silvio A. Bedini     | <b>Antique Scientific Instruments (by Gerard L'E. Turner)</b>                     | <b>516</b> |
| John Lawton      | <b>Evolution for Naturalists (by P.J. Darlington)</b>   | <b>510</b> | Derek de Solla Price | <b>Doing time — two books on time</b>   | <b>516</b> |
|                  |   |            | David Davies         | <b>Science and the Supernatural (by John Taylor)</b>                              | <b>517</b> |
|                  |   |            | John Andrews         | <b>Avian delights — specialist bird books</b>                                     | <b>518</b> |
|                  |   |            | Clayton M. White     | <b>A good year for raptors — books on birds of prey</b>                           | <b>519</b> |
|                  |   |            | C.M. Perrins         | <b>Birds for all seasons — guides for ornithologists</b>                          | <b>520</b> |

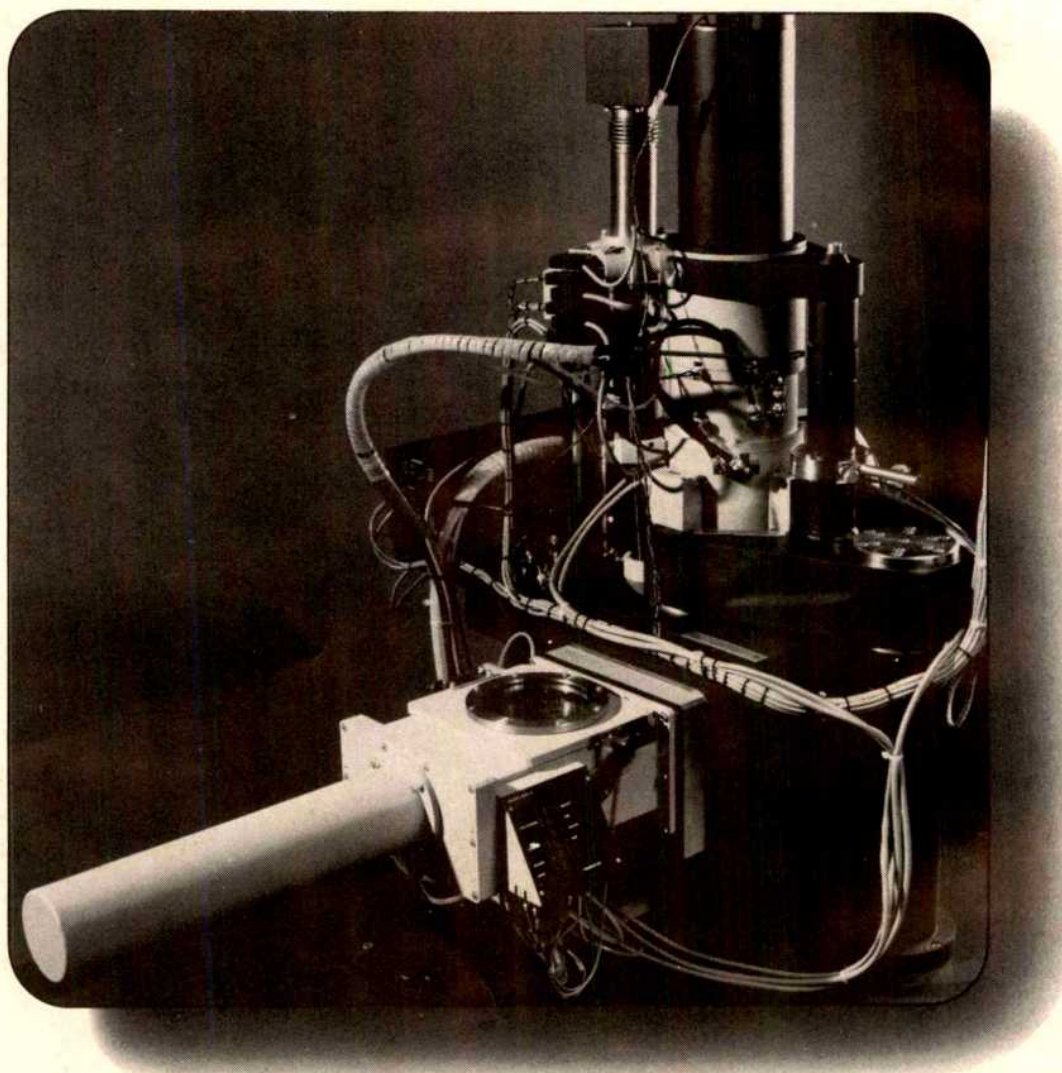
## MISCELLANY

- |                  |     |                        |       |
|------------------|-----|------------------------|-------|
| 100 years ago    | 473 | Announcements          | 524   |
| Books received   | 522 | New on the market      | xxiii |
| Guide to authors | 523 | Classified advertising | xxvii |

# Getting down to the finer details of microelectronics

As a leading manufacturer, and user, of micro-electronic technology, Philips is constantly searching for techniques that will improve the production process, or the product, or – ideally – both. This objective has now been achieved with the development of the 'Beamwriter' vector scan lithography system. In fact, it's the only production-oriented vector scan electron beam writing system available in the world.

Compared to conventional optical lithography techniques, vector scanning produces significant savings in the time taken to produce a set of masks or reticles; hours instead of days. It is also much more efficient than the raster scan E-beam method because the writing beam is directed only to points where exposure is required. The Beamwriter also generates an exposure dosage twenty times greater than other



Circle No. 45 on Reader Enquiry Card.

# PHILIPS



# nature

Volume 288 No.5791 11 December 1980

## NEWS

|   |     |  |     |
|---|-----|--|-----|
| <b>Code of conduct for national academies</b> | 525 | <b>Yugoslavia now: Supek's worry</b>   | 530 |
| <b>Further nonsense on product liability</b>  | 526 | <b>Agricultural research: Ministry at top</b>  | 530 |
| <b>Congress shares out patent licences</b>    | 527 | <b>British dentists: Broader, better</b>   | 531 |
| <b>Stanford and UCLA plasmid patent</b>       | 527 | <b>Israeli science: Crisis at Weizmann</b>   | 531 |
| <b>Genetic engineering: Hormone growth</b>    | 528 | <b>Correspondence: Medical schools (K.E. Webster);<br/>Badgers and TB (Stephen Harris); Court feasibility<br/>(C.R.B. Joyce); Plusses and losses (Editor, <i>Nature</i>)</b> | 532 |
| <b>US Administration: Reagan's men?</b>       | 528 |  |     |
| <b>Soviet plans: Science on tap</b>           | 529 |  |     |
| <b>DNA guidelines: Bowing out</b>             | 529 |  |     |

## NEWS AND VIEWS

|  |     |  |     |
|--|-----|--|-----|
| <b>Conflict and commitment in neural development:</b><br>Miranda Robertson reports a recent conference | 533 | <b>Molecular lines in the red: A correspondent on the<br/>first infra red observations of interstellar clouds</b>                                | 537 |
| <b>Cretaceous ammonites: M.K. Howarth looks at<br/>a new South African study</b>                       | 535 | <b>Drosophila at Kolymbari: M. Ashburner describes<br/>progress in understanding the molecular structure<br/>of the <i>Drosophila</i> genome</b> | 538 |
| <b>Solar oscillations: H.B. von der Raay on ways to<br/>probe the Sun's interior</b>                   | 535 | <b>Comets and the origin of life: N.J. McNaughton and<br/>C.T. Pillinger on a recent chemical evolution conference</b>                           | 540 |
| <b>Coronavirus comes of age: B.W.J. Mahy on the first<br/>international coronavirus meeting</b>        | 536 |  |     |

## ARTICLES

|  |  |     |   |  |     |
|--|--|-----|---|--|-----|
| G. Grec, E. Fossat<br>and M. Pomerantz               | <b>Solar oscillations: full disk<br/>observations from the geographic<br/>South Pole</b> | 541 | L. McIntosh, C. Poulsen<br>and L. Bogorad   | <b>Chloroplast gene sequence for<br/>the large subunit of ribulose<br/>bisphosphatocarboxylase of<br/>maize</b>                  | 556 |
| J. Christensen-Dalsgaard<br>and D.O. Gough           | <b>Is the Sun helium-deficient?</b>  | 544 | A.D.M. van Mansfeld,<br>S.A. Langeveld, P.D. Baas,<br>H.S. Jansz, G.A. van der Marel,<br>G.H. Veeneman<br>and J.H. van Boom | <b>Recognition sequence of<br/>bacteriophage <math>\Phi</math> X174 gene A<br/>protein — an initiator of DNA<br/>replication</b> | 561 |
| J.H. Parkinson, L.V. Morrison<br>and F.R. Stephenson | <b>The constancy of the solar<br/>diameter over the past<br/>250 years</b>               | 548 |   |  |     |
| J. Folkman<br>and C. Haudenschild                    | <b>Angiogenesis <i>in vitro</i></b>  | 551 |   |  |     |

## LETTERS

|                                   |   |     |   |   |     |
|-----------------------------------|---|-----|---|---|-----|
| T. Mullin<br>and T.B. Benjamin    | <b>Transition to oscillatory motion in<br/>the Taylor experiment</b>                    | 567 | I.J. Smalley, C.W. Ross<br>and J.S. Whitton | <b>Clays from New Zealand support<br/>the inactive particle theory of<br/>soil sensitivity</b>                                    | 576 |
| P. Brüggegger and E. Mayer        | <b>Complete vitrification in pure<br/>liquid water and dilute aqueous<br/>solutions</b> | 569 | J.M. Hunt, R.J. Miller<br>and J.K. Whelan   | <b>Formation of C<sub>4</sub>–C<sub>7</sub> hydrocarbons<br/>from bacterial degradation of<br/>naturally occurring terpenoids</b> | 577 |
| P.J. Patchett<br>and M. Tatsumoto | <b>Lu–Hf total-rock isochron for<br/>the eucrite meteorites</b>                         | 571 | D.S. Williams<br>and P. McIntyre            | <b>The principal eyes of a jumping<br/>spider have a telephoto<br/>component</b>  | 578 |
| D. Gapais and C. Le Corre         | <b>Is the Hercynian belt of Brittany<br/>a major shear zone?</b>                        | 574 |   |   |     |

Contents continued overleaf

Cover: A telescope and photospectrometer assembly at the South Pole. Measurements from this observatory of Doppler shifts in solar spectra give the clearest measurements ever of solar oscillations. These results are discussed in two articles on pages 541 and 544.

M

*Nature* (ISSN 0028-0836) is published weekly, except the last week in December, by Macmillan Journals Ltd. Annual subscription for USA and Canada US \$173. Orders (with remittance) and change of address labels to: Macmillan Journals Ltd, Brunel Rd, Basingstoke RG21 2XS, UK. Second class postage paid at New York, NY 10010 and additional mailing offices. US Postmaster send form 3579 to: *Nature*, 15 East 26 Street, New York, NY 10010. ©1980 Macmillan Journals Ltd.

Bethesda Research Laboratories

# Contributions to Cell Science

## FIBRONECTINS




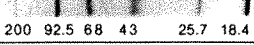
Bethesda Research Laboratories, Inc. is now the source for cell culture growth and regulatory factors. Continuing the tradition of BRL excellence, tissue culture reagents from our Biological Chemistry Laboratory meet the most challenging and rigorous standards of purity and performance. As illustrated below, the electrophoretic homogeneity of BRL Fibronectin (>98%) is far superior to that from other suppliers (Figure 1). Similarly, the murine thymocyte proliferation assay (Figure 2) establishes that our Interleukin-2 (IL-2) is *lectin-free*, the critical factor for selection and long-term maintenance of monospecific T-cell clones.

**Figure 1**

### Electrophoretic and Total Protein Analyses of Fibronectins

To analyze the homogeneity and relative protein content of human plasma fibronectin from BRL and two other commercial sources, 1 milligram vials from each supplier were reconstituted to a volume of 1 milliliter.

Aliquots from each source were then subjected to SDS-polyacrylamide gel electrophoresis and total protein determination.

| SAMPLE                                   | DIRECTION OF MIGRATION  | TOTAL PROTEIN       |               |
|--|---|---------------------|---------------|
|  |   | THEORETICAL (mg/ml) | FOUND (mg/ml) |
| BRL FIBRONECTIN                          |  | 1.0                 | 1.26          |
| SUPPLIER Y FIBRONECTIN                   |  | 1.0                 | 0.24          |
| SUPPLIER Z FIBRONECTIN                   |  | 1.0                 | 1.12          |
| BRL M.W. STANDARDS (x 10 <sup>-3</sup> ) |  | N.A.                | N.A.          |
|  | 200 92.5 68 43 25.7 18.4  |                     |               |

## Ordering Information

| Product                                  | BRL No. | Size  | Quantity | Price    |
|--|---------|-------|----------|----------|
| Human IL-2 Lectin-Free                   | 5372SA  | 500 U | 1-4      | \$80.00  |
|  |         |       | 5 +      | 75.00    |
| Rat IL-2 Lectin-Free                     | 5373SA  | 500 U | 1-4      | \$60.00  |
|  |         |       | 5 +      | 55.00    |
| Mouse IL-2 Lectin-Free                   | 5374SA  | 500 U | 1-4      | \$60.00  |
|  |         |       | 5 +      | 55.00    |
| Human Plasma Fibronectin                 | 6070LA  | 1 mg. | 1-4      | \$55.00  |
| Bulk discount available. Please Inquire. |         |       | 5 +      | 50.00    |
|  | 6070LB  | 5 mg. | 1-4      | \$225.00 |
|  |         |       | 5 +      | 200.00   |

Circle No. 13 on Reader Enquiry Card.

## INTERLEUKIN - 2

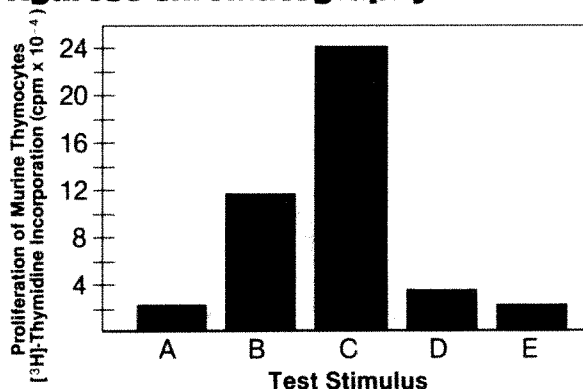
Mouse thymocytes incorporate [<sup>3</sup>H]-thymidine in response to phytohemagglutinin (PHA) and IL-2 stimulation, but will not proliferate (and incorporate [<sup>3</sup>H]-thymidine) following stimulation with IL-2 alone. To assay for PHA-dependent stimulation, 200 µl cultures of murine thymocytes (2 x 10<sup>6</sup> cells/ml) were incubated at 37 °C for 68 hours in the presence of the test medium; pulsed with 0.5 µCi [<sup>3</sup>H]-thymidine for 4 hours, then assayed for incorporation of the radiolabel.

Thyroglobulin-agarose (T-A) chromatography is used to remove lectins from mouse lymphoma-conditioned medium (source of BRL mouse IL-2). Mouse lymphocyte proliferation was measured under each of the following conditions: Stimulus A, Normal culture medium; Stimulus B, Normal culture medium +1% PHA; Stimulus C, Normal culture medium +1% PHA and 312 units IL-2; Stimulus D, Normal culture medium +1% PHA and 326 units IL-2 after one cycle T-A chromatography; Stimulus E, Normal culture medium +1% PHA and 376 units IL-2 after two cycles\* of T-A chromatography.

\*Standard BRL production method

**Figure 2**

### Murine Lymphocyte Proliferation Assay for Lectin Removal from BRL IL-2 Before and After Thyroglobulin-Agarose Chromatography.



## Soon to be available. . .

- Human Cellular and Chick Cellular Fibronectins
- Epidermal Growth Factor

Watch for further data on the unmatched purity and performance of Human plasma fibronectin and Interleukin-2 from the Biological Chemistry Laboratory of BRL.

# BRL

**Bethesda Research Laboratories, Inc.**

P.O. Box 577 • Gaithersburg, MD 20760

Toll Free 800-638-8992 • In Maryland (301) 840-8000

Telex 908750 BRL GARG

Germany Orders: BRL GmbH TELEX 417699 brlni d

## LETTERS

- |   |  |     |   |  |     |
|---|--|-----|---|--|-----|
| S.J. O'Brien, M.H. Gail and D.L. Levin                                    | Correlative genetic variation in natural populations of cats, mice and men   | 580 | L.D. Leserman, J. Barbet, F. Kourilsky and J.N. Weinstein               | Targeting to cells of fluorescent liposomes covalently coupled with monoclonal antibody or protein A   | 602 |
| T.R. Oegema Jr  | Delayed formation of proteoglycan aggregate structures in human articular cartilage disease states                                       | 583 | K. Morimoto and S. Wolff  | Cell cycle kinetics in human lymphocyte cultures   | 604 |
| I.R. Neering and K.G. Morgan  | Use of aequorin to study excitation-contraction coupling in mammalian smooth muscle  | 585 | P. Semm, T. Schneider and L. Vollrath                                   | Effects of an Earth-strength magnetic field on electrical activity of pineal cells   | 607 |
| J.H. Kaplan and R.J. Hollis   | External Na dependence of ouabain-sensitive ATP:ADP exchange initiated by photolysis of intracellular caged-ATP in human red cell ghosts | 587 | S.S. Tenen and J.D. Hirsch  | $\beta$ -Carboline-3-carboxylic acid ethyl ester antagonizes diazepam activity   | 609 |
| W. Lijinsky, M.D. Reuber and W.B. Manning                                 | Potent carcinogenicity of nitrosodethanolamine in rats   | 589 | J. Drouin and H.M. Goodman  | Most of the coding region of rat ACTH- $\beta$ -LPH precursor gene lacks intervening sequences   | 610 |
| D.L. Guernsey, A. Ong and C. Borek  | Thyroid hormone modulation of X-ray-induced <i>in vitro</i> neoplastic transformation  | 591 | D.G. Smyth and S. Zakarian  | Selective processing of $\beta$ -endorphin in regions of porcine pituitary   | 613 |
| D. Mager, T.W. Mak and A. Bernstein                                       | Friend leukaemia virus-transformed cells, unlike normal stem cells, form spleen colonies in <i>Sl/Sl<sup>d</sup></i> mice                | 592 | B.B. Knowles, S. Pan, D. Solter, A. Linnenbach, C. Croce and K. Huebner | Expression of H-2, laminin and SV40 T and TASA on differentiation of transformed murine teratocarcinoma cells                                  | 615 |
| R. Szigeti, M.G. Masucci, G. Masucci, E. Klein, G. Klein and W. Berthold  | Interferon suppresses antigen- and mitogen-induced leukocyte migration inhibition  | 594 | R.K. Craig, I.C. Bathurst and D.G. Herries                              | Post-transcriptional regulation of gene expression in guinea pig tissues   | 618 |
| K.H. Leung and E. Mihich  | Prostaglandin modulation of development of cell-mediated immunity in culture   | 597 | J.P. Langmore and C. Schutt   | The higher order structure of chicken erythrocyte chromosomes <i>in vivo</i>   | 620 |
| S.R. Coughlin, M.A. Moskowitz, B.R. Zetter, H.N. Antoniadis and L. Levine | Platelet-dependent stimulation of prostacyclin synthesis by platelet-derived growth factor   | 600 | R.W. Briehl   | Solid-like behaviour of unsheared sickle haemoglobin gels and the effects of shear   | 622 |
|   |  |     | J.C. Boothroyd, G.A.M. Cross, J.H.J. Hoeijmakers and P. Borst           | A variant surface glycoprotein of <i>Trypanosoma brucei</i> synthesized with a C-terminal hydrophobic 'tail' absent from purified glycoprotein | 624 |

## BOOK REVIEWS

- |                  |   |     |                |   |     |
|------------------|---|-----|----------------|---|-----|
| Nevill Mott      | Experiment, Theory, Practice: Articles and Addresses of P.L. Kapitza                        | 627 | Harvey Lodish  | Cell Membranes and Viral Envelopes (edited by H.A. Blough and J. Tiffany)                                 | 629 |
| Oscar Kempthorne | Theory of Population Genetics and Evolutionary Ecology: An Introduction (by J. Roughgarden) | 628 | Philip England | Atlas of Subsurface Temperatures in the European Community (compiled by R. Haenel)                        | 629 |
| S.P. Spragg      | An Introduction to Physical Properties of Large Molecules in Solution (by E.G. Richards)    | 628 | Sandra Raphael | Herbarium Apulei Platonici and Herbario Volgare (Introductions by Erminio Caprotti and William T. Stearn) | 630 |

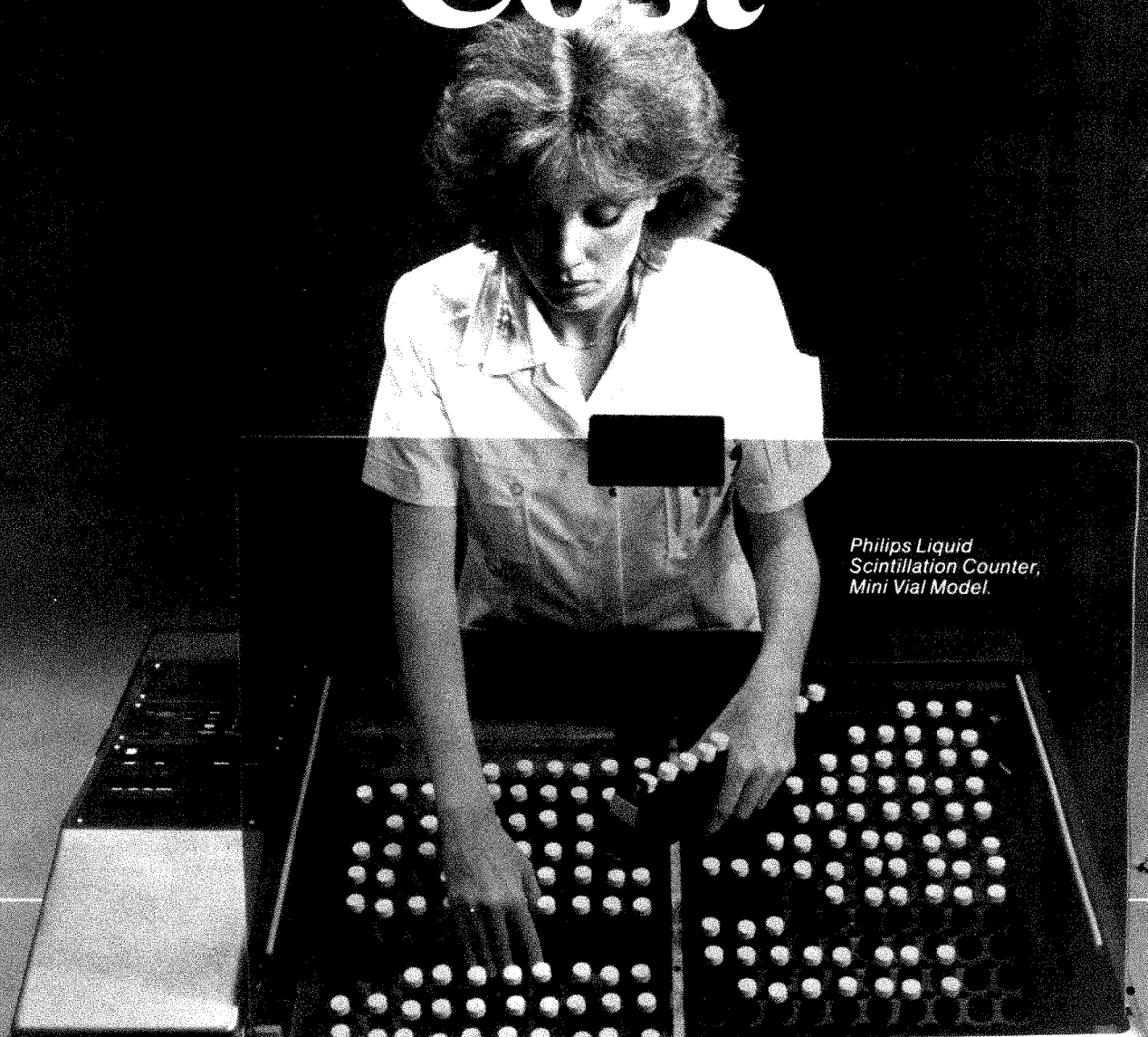
## MISCELLANY

- |                        |      |
|------------------------|------|
| 100 years ago          | 539  |
| Erratum                | 626  |
| New on the market      | xxiv |
| Classified advertising | xxvi |

**PRODUCT REVIEW** This week's product review (page xv) covers laboratory recorders.



# Compare: Completeness Capability Cost



*Philips Liquid  
Scintillation Counter,  
Mini Vial Model.*

# nature

Volume 288 No.5792 18/25 December 1980

|  |            |  |            |
|--|------------|--|------------|
| <b>Britain, France and nuclear weapons</b>   | <b>631</b> | <b>Polish universities: Union snag</b>   | <b>635</b> |
| <b>US research budget now in better shape:</b> Dying Congress restores earlier cut-backs | <b>632</b> | <b>Fissile material: Counting wrong</b>  | <b>635</b> |
| <b>Nuclear safety:</b> European hazards  | <b>633</b> | <b>US research planning:</b> NIH reprieved   | <b>636</b> |
| <b>Fast reactors:</b> Low morale   | <b>633</b> | <b>European environment:</b> Small gains   | <b>636</b> |
| <b>Satellite communications:</b> Free for all ahead?                                     | <b>633</b> | <b>High-energy physics:</b> New man, new style   | <b>636</b> |
| <b>Ariane development:</b> More trouble  | <b>634</b> | <b>Brazilian agriculture:</b> Soya bean feast  | <b>637</b> |
| <b>Halley mission:</b> NASA to go?   | <b>634</b> | <b>Schmitt stars again</b>   | <b>637</b> |
| <b>Beyond Saturn</b>   | <b>634</b> | <b>Correspondence:</b> Nuclear cheap? (P.M.S. Jones); Biospheric works (M. Batisse); More on museums (A. Flew, J. Marks) | <b>638</b> |

## NEWS AND VIEWS

|  |            |  |            |
|--|------------|--|------------|
| <b>Climate and variability in the solar constant:</b> Douglas Gough reports a recent workshop                | <b>639</b> | <b>How heavy is a cold photon?:</b> N. Dombey asks if gauge symmetries may be broken at low temperatures | <b>643</b> |
| <b>Development of spinal sensory systems:</b> T.M. Jessell and M. Yamamoto examine the underlying mechanisms | <b>640</b> | <b>Selfish DNA:</b> reassessments by L.E. Orgel, F.H.C. Crick and C. Sapienza                            | <b>645</b> |
| <b>Human <i>in vitro</i> fertilization:</b> Alex Lopata on the success rate for 'test-tube' babies           | <b>642</b> | Gabriel Dover and W. Ford Doolittle  | <b>646</b> |
|  |            | H.K. Jain  | <b>647</b> |

## REVIEW ARTICLE

|           |                   |            |
|-----------|-------------------|------------|
| H. Georgi | <b>Why unify?</b> | <b>649</b> |
|-----------|-------------------|------------|

## ARTICLES

|   |  |            |  |   |            |
|---|--|------------|--|---|------------|
| F.T. Kyte, Z. Zhou and J.T. Wasson  | <b>Siderophile-enriched sediments from the Cretaceous-Tertiary boundary</b>          | <b>651</b> | D. Moras, M.B. Comarmond, J. Fischer, R. Weiss, J.C. Thierry, J.P. Ebel and R. Giegé | <b>Crystal structure of yeast tRNA<sup>Asp</sup></b>                        | <b>669</b> |
| G.C. Brown, J. Cassidy, E.R. Oxburgh, J. Plant, P.A. Sabine and J.V. Watson | <b>Basement heat flow and metalliferous mineralization in England and Wales</b>      | <b>657</b> | J. Allan, P.G. Hartman, C. Crane-Robinson and F.X. Aviles                            | <b>The structure of histone H1 and its location in chromatin</b>            | <b>675</b> |
| P.J.J. Kamp   | <b>Pacifica and New Zealand: proposed eastern elements in Gondwanaland's history</b> | <b>659</b> | S.H. Zisk and P.J. Mougini-Mark (Erratum)  | <b>Anomalous region on Mars: implications for near-surface liquid water</b> | <b>735</b> |
| E.W. Benz Jr, R.M. Wydro, B. Nadal-Ginard and D. Dina                       | <b>Moloney murine sarcoma proviral DNA is a transcriptional unit</b>                 | <b>665</b> |  |   |            |

## LETTERS

|                                      |  |            |  |  |            |
|--------------------------------------|--|------------|--|--|------------|
| J.R. Primack and M.A. Sher           | <b>Photon mass at low temperature?</b>                                     | <b>680</b> | J.A. Cairns, J.P. Coad, E.W.T. Richards and I.A. Stenhouse | <b>Carbon deposition on metallic surfaces studied by r.f. plasma discharge</b> | <b>686</b> |
| T.H. Hankins and G.A.E. Wright       | <b>A study of PSR1237 + 25 at 430 MHz</b>                                  | <b>681</b> | J.M. Hunt, A.Y. Huc and J.K. Whelan                        | <b>Generation of light hydrocarbons in sedimentary rocks</b>                   | <b>688</b> |
| E. Arijis, D. Nevejans and J. Ingels | <b>Unambiguous mass determination of major stratospheric positive ions</b> | <b>684</b> | G.W. O'Brien and H.H. Veeh                                 | <b>Holocene phosphorite on the East Australian continental margin</b>          | <b>690</b> |
|                                      |  |            | C.P. Wood  | <b>Boninite at a continental margin</b>  | <b>692</b> |

Contents continued overleaf

**Cover:** Scanning electron micrograph of apatite crystallites on the internal surface of foraminiferal test contained in a phosphatic nodule. Holocene apatite formation on the East Australian continental margin is discussed on page 690.

# M

Nature® (ISSN 0028-0836) is published weekly, except the last week in December, by Macmillan Journals Ltd. Annual subscription for USA and Canada US \$173. Orders (with remittance) and change of address labels to: Macmillan Journals Ltd, Brunel Rd, Basingstoke RG21 2XS, UK. Second class postage paid at New York, NY 10010 and additional mailing offices. US Postmaster send form 3579 to: Nature, 15 East 26 Street, New York, NY 10010. ©1980 Macmillan Journals Ltd.

Raven Press announces a major new journal:

# Journal of Molecular and Applied Genetics

A JOURNAL FOR THE RAPID PUBLICATION OF FULL-LENGTH ARTICLES ON STUDIES UTILIZING MODERN GENETIC TECHNIQUES, ESPECIALLY RECOMBINANT DNA METHODS, TO SOLVE BASIC AND APPLIED PROBLEMS IN GENETICS, BIOCHEMISTRY, MEDICINE, AND AGRICULTURE.

Editor-in-Chief

**Howard M. Goodman, Ph.D.**

Howard Hughes Medical Institute Laboratory  
Department of Biochemistry and Biophysics  
University of California, San Francisco  
San Francisco, California 94143 U.S.A.

Pres. Ch. Libr. Bldg.  
SCIENCE COLLEGE  
4 Upper Circular Road  
SINGAPORE

## Editorial Board

John Abelson/La Jolla, Calif., USA  
Frederick Ausubel/Cambridge, Mass., USA  
John R. Bedbrook/Canberra, Australia  
Lawrence Bogorad/Cambridge, Mass., USA  
Mary-Dell Chilton/St. Louis, Mo., USA  
Richard A. Flavell/London, UK  
Masayori Inouye/Stony Brook, N.Y., USA  
Robert Kamen/London, UK  
Yuet W. Kan/San Francisco, Calif., USA  
David W. Martin, Jr./San Francisco, Calif., USA

Marc Van Montagu/Gent, Belgium  
Richard C. Mulligan/Cambridge, Mass., USA  
Alexander Rich/Cambridge, Mass., USA  
Jeff Schell/Cologne, FRG  
James Shepard/Manhattan, Kan., USA  
John Shine/Canberra, Australia  
Joan A. Steitz/New Haven, Conn., USA  
Robert T. Tjian/Berkeley, Calif., USA  
Michael Wigler/Cold Spring Harbor, N.Y., USA

**CALL FOR PAPERS:** Manuscripts on the synthesis of biologically and medically relevant proteins, genomic organization, chromosomal gene mapping, gene structure, regulation of gene expression, molecular and biochemical studies on genetic diseases, and plant molecular biology are invited for submission. Publication will begin early in 1981. To avoid excessive reduction, the journal will provide generous space for inclusion of figures. The most modern computer typesetting techniques will facilitate rapid publication. The publisher will be Raven Press, New York. Submit manuscripts in triplicate to the Editor-in-Chief at the above address. References should be cited by number in the text and numbered in order of citation; provide complete titles of articles cited, with names of all authors and inclusive pagination. Full instructions to contributors are available from the Editor-in-Chief or from Raven Press.

Circle No.29 on Reader Enquiry Card.

## SUBSCRIPTION ORDER FORM

TO: **RAVEN PRESS 1140 Avenue of the Americas, New York, N.Y. 10036, U.S.A.** Date \_\_\_\_\_

Please enter my subscription for Volume 1 (1981) of **JOURNAL OF MOLECULAR AND APPLIED GENETICS**.

Published bimonthly. **Personal subscription rates:** U.S. \$80; elsewhere \$90.

**Institutional subscription rates:** U.S. \$135; elsewhere \$145.

Air delivery is included for European and Mediterranean countries;  
for air service elsewhere add \$15.00.

Name (please print) \_\_\_\_\_

Address \_\_\_\_\_

Country \_\_\_\_\_ Postal Code \_\_\_\_\_

NA121880



## LETTERS

- |  |   |            |  |   |            |
|--|---|------------|--|---|------------|
| R.E. Michod<br>and W.D. Hamilton   | <b>Coefficients of relatedness in sociobiology</b>  | <b>694</b> | E.C. Slater and S. de Vries  | <b>Identification of the BAL-labile factor</b>  | <b>717</b> |
| B.M. Haglund   | <b>Proline and valine — cues which stimulate grasshopper herbivory during drought stress?</b>                                       | <b>697</b> | A.N. Hobden, M. Harding<br>and D.E.M. Lawson   | <b>1,25-Dihydroxycholecalciferol stimulation of a mitochondrial protein in chick intestinal cells</b>                 | <b>718</b> |
| D.A. Jillson   | <b>Insect populations respond to fluctuating environments</b>   | <b>699</b> | G. Parry, J.C. Bartholomew<br>and M.J. Bissell   | <b>Role of <i>src</i> gene in growth regulation of Rous sarcoma virus-infected chicken embryo fibroblasts</b>         | <b>720</b> |
| K. Arikawa, E. Eguchi,<br>A. Yoshida and K. Aoki   | <b>Multiple extraocular photoreceptive areas on genitalia of butterfly <i>Papilio xuthus</i></b>                                    | <b>700</b> | P.T. Mora, K. Chandrasekaran<br>and V.W. McFarland   | <b>An embryo protein induced by SV40 virus transformation of mouse cells</b>  | <b>722</b> |
| B.J. Leckie and N.K. McGhee  | <b>Reversible activation-inactivation of renin in human plasma</b>  | <b>702</b> | R.S. Day III, C.H.J. Ziolkowski,<br>D.A. Scudiero, S.A. Meyer,<br>A.S. Lubiniecki, A.J. Girardi,<br>S.M. Galloway and G.D. Bynum | <b>Defective repair of alkylated DNA by human tumour and SV40-transformed human cell strains</b>                      | <b>724</b> |
| K. Arakawa and H. Maruta   | <b>Ability of kallikrein to generate angiotensin II-like pressor substance and a proposed 'kinin-tensin enzyme system'</b>          | <b>705</b> | L.C. Erickson, G. Laurent,<br>N.A. Sharkey and K.W. Kohn   | <b>DNA cross-linking and monoadduct repair in nitrosourea-treated human tumour cells</b>                              | <b>727</b> |
| S.P. Wilson, R.L. Klein,<br>K.-J. Chang, M.S. Gasparis,<br>O.H. Viveros and W.-H. Yang                   | <b>Are opioid peptides co-transmitters in noradrenergic vesicles of sympathetic nerves?</b>   | <b>707</b> | L. Lindqvist, S. El Mohsni,<br>F. Tfibel and B. Alpert   | <b>Transient haem-globin interactions in photodeligated carboxyhaemoglobin and subunits</b>                           | <b>729</b> |
| T. Michel, B.B. Hoffman<br>and R.J. Lefkowitz  | <b>Differential regulation of the <math>\alpha_2</math>-adrenergic receptor by <math>\text{Na}^+</math> and guanine nucleotides</b> | <b>709</b> | D.L. Bentley<br>and T.H. Rabbitts  | <b>Human immunoglobulin variable region genes — DNA sequences of two <math>V_\kappa</math> genes and a pseudogene</b> | <b>730</b> |
| S.W. de Laat, L.G.J. Tertoolen<br>and C.J.P. Grimmelikhuijzen  | <b>No junctional communication between epithelial cells in hydra</b>  | <b>711</b> | A. Pestronk and D.B. Drachman  | <b>Dimethyl sulphoxide reduces anti-receptor antibody titres in experimental myasthenia gravis</b>                    | <b>733</b> |
| K. Takahashi, M. Tavassoli<br>and D.W. Jacobsen  | <b>Receptor binding and internalization of immobilized transcobalamin II by mouse leukaemia cells</b>                               | <b>713</b> |  |   |            |
| L. Pickart, J.H. Freedman,<br>W.J. Loker, J. Peisach,<br>C.M. Perkins, R.E. Stenkamp<br>and B. Weinstein | <b>Growth-modulating plasma tripeptide may function by facilitating copper uptake into cells</b>                                    | <b>715</b> |  |   |            |

## MATTERS ARISING

- |   |   |            |  |  |            |
|---|---|------------|--|--|------------|
| I. Rosenthal and E. Ben-Hur                     | <b>Superoxide involvement in negative air ion effects</b> | <b>739</b> | R.P. Durbin  | <b>Role of <math>\text{PGE}_2</math> in anion exchange in gastric mucosa</b> | <b>740</b> |
| E.W. Kellogg III, M.G. Yost<br>and A.P. Krueger | <b>Reply to Rosenthal and Ben-Hur</b>                     | <b>739</b> | W. Silen, R. Schiessel,<br>J. Matthews, A. Barzilai<br>and A. Merhav | <b>Reply to Durbin</b>   | <b>740</b> |

## BOOK REVIEWS

- |               |   |            |              |   |            |
|---------------|---|------------|--------------|---|------------|
| Edward Shils  | <b>A Guide to the Culture of Science, Technology and Medicine (edited by Paul T. Durbin)</b>  | <b>741</b> | G.Y. Craig   | <b>Humphry Davy on Geology: The 1805 Lectures for a General Audience (edited by R. Siegfried and R. H. Dott)</b>    | <b>743</b> |
| Tak W. Mak    | <b>Molecular Biology of RNA Tumor Viruses (edited by John R. Stephenson)</b>  | <b>742</b> | John Mowbray | <b>Principles of Metabolic Control in Mammalian Systems (edited by R. H. Herman, R. M. Cohn and P. D. McNamara)</b> | <b>744</b> |
| Adrian Friday | <b>Phylogenetic Patterns and the Evolutionary Process. Method and Theory in Comparative Biology (by Niles Eldredge and Joel Cracraft)</b> | <b>742</b> |              |   |            |

## MISCELLANY

PEARCE LIBRARY  
 SCIENCE COLLEGE  
 3000 GLENVIEW ROAD  
 CHICAGO, ILL. 60637

# THE USE OF CHEMICAL NOMENCLATURE.

**An important symposium.**

**To be held at Church House, Great Smith Street,  
Westminster, London S.W.1., 24th-26th March, 1981.**

**28 internationally known speakers will cover the following subjects:-**

- \* Problems of the day to day use and misuse of chemical nomenclature.
- \* Standardisation.
- \* Industry/Sector problems.
- \* Sources of help.
- \* The use of trivial names, common names, synonyms, trade names and trade marks.
- \* Legal implications.
- \* The use of chemical nomenclature in chemical abstracts.
- \* The problem of translating from English.
- \* Available systems of structure representation.
- \* The problems of using chemical nomenclature to develop an information base.
- \* Problems in the field of biochemical nomenclature.
- \* The need for more effective training.
- \* Symbols and nomenclature as an aid to health and safety.
- \* Harmonisation of nomenclature systems.
- \* Nomenclature - the way ahead.

**Organised by the Laboratory of the Government Chemist in association with the British Crop Protection Council, British Pharmacopoeia Commission, the British Standards Institution, the Chemical Industries Association, the Chemical Notation Association (UK), the Pharmaceutical Society of Great Britain, the United Kingdom Chemical Information Service and the Joint Nomenclature Panel of the Royal Society and Royal Society of Chemistry.**

This three day symposium is designed to help overcome confusion and misunderstandings that exist on the subject of chemical nomenclature.

An internationally known list of speakers will provide a forum in which scientists, educationalists and industrialists can discuss the many problems, as well as learn the latest trends, sources of help and new developments on this subject.

Organised by the Laboratory of the Government Chemist in association with a number of other major organisations, this symposium will create greater understanding of chemical nomenclature in international trade, in the purchase and use of chemicals and in the interpretation of scientific papers.

Inclusive price £69.00. Student reductions and single day rates are available on request.

For full information regarding this symposium, please complete and return the coupon.

To the Symposium Organiser, Laboratory of the Government Chemist, Room 564A, Cornwall House, Stamford Street, London SE1 9NQ.  
Telephone: 01-928 7900, extension 520 or 537.

Please send me full details of the Symposium, 'The Use of Chemical Nomenclature.'

Name: \_\_\_\_\_  
BLOCK LETTERS, PLEASE

Title: \_\_\_\_\_

Organisation: \_\_\_\_\_

Address: \_\_\_\_\_

N2



6 November 1980

# What are the research councils for?

This week will be a testing time for the research councils which are one of the principal means of support for British scientific research. Both the Medical and Science Research Councils are due to publish their annual reports. Hard on the heels of the annual report of the Natural Environment Research Council (see *Nature* 28 October) these documents will between them provide an opportunity for telling where the research councils collectively are heading. Naturally, readers of these annual reports will have to be prepared to read between the lines. Such reports begin with a more or less ritual recitation of honours bestowed on members of the staff and of visits by members of the royal family to council establishments. These days, there usually follows an account of the difficulties of living within a budget which, if not actually shrinking in real terms, is no longer growing. Occasionally, a council may be so moved by some particular consequence of straitened budgets that it will specifically draw attention to the collapse of some special project. This was the spirit in which the Natural Environment Research Council last week let it be known that the Geological Survey of Britain is now jeopardized by the unwillingness of the Department of the Environment to contribute to its continuing cost. Usually, however, the councils tell their tale with as little commotion as they can.

This year things could — or should — be different. No amount of built-in gentility can conceal from the councils themselves the increasing difficulty of sharing out the funds that come their way from the Department of Education and Science in ways that are likely to be both equitable (as between deserving claimants) and effective (in promoting research of high quality and promise). The collapse of the dual-support system is another problem. If the University Grants Committee can no longer ensure that university departments are well-equipped to conduct research, the research councils must either break with their present practice of not financing basic facilities (which means making fewer grants) or must acknowledge that much of what they spend will be used with less than full effectiveness. The trouble is that there is very little that research councils acting individually can do to shape a more rational pattern for academic research. So long as they stick (as they should) to the principle that grants go to the best applicants, they are bound to find themselves spreading their resources more thinly than is reasonable. This recognition is no doubt part of the reason why the Advisory Board for the Research Councils has set up (with the Committee of Vice-Chancellors and Principals, representing the university sector) the Merrison Committee. The hope is that the committee will be able to evolve a framework within which the old goals of concentrating academic research on selected universities (or university departments) can be made acceptable. It remains to be seen whether the University Grants Committee has the stomach for implementing whatever policy may emerge — and whether the universities will allow it to do so.

The research councils will also be perplexed this year by signs of the possible collapse of the Rothschild system with which they have been living since 1971. So they should be. One among them, the Medical Research Council, has been able to claw back from the Department of Health the now inflated funds taken away progressively in the years after 1973 (see *Nature* 23 October).

Others will be tempted to follow suit, and will earn a dusty answer from the government departments concerned. Sir Hermann Bondi, the new chairman of the Natural Environment Research Council, says that he supports the notion that government departments should act as customers for research (see page 5).

Will he be of the same opinion when he discovers how vulnerable his new council is to inconstancy or even downright fickleness on the part of sponsoring ministries?

The trouble with customers is that they are often wrong, but that their actions inevitably create the illusion that they are right. The decision by the Department of the Environment to cut back its contributions to the British Geological Survey can have one of two consequences. Either the survey will be supported by other means (in which case the department will congratulate itself on having saved some money) or it will be stopped; the United Kingdom will not on that account collapse and the department will take pride in having helped bring an apparently worthless activity to an end. Either way, the customer will seem right. Nobody will have made a serious examination of the value of the Geological Survey.

Taken together, these developments are likely to provoke further soul-searching among the research councils and their sponsors. For the Medical Research Council, the most immediate question is whether it can turn from its largely academic ways so as to earn the £12 million a year it will now have to spend on applied medical research. For all of them, the long-term question is how their functions are to be defined and carried out. During the past Rothschild decade, their relative budgets have hardly changed. Each year, one or two of the councils have had an extra one or two per cent in real terms to spend, while the others have fallen back. But is there any reason to suppose that the sums being spent on research in agriculture, medicine and the natural environment in 1970 are still appropriate a decade later? And is it right that the budget of the Science Research Council, exempted from the rigours of Rothschild, should stand in exactly the same relationship with those of what would be called, in the United States, the "mission-oriented" councils? Can it serve either the interests of research or of the public purse that these increasingly elaborate organizations should just grow, like Topsy?

This is why there is emerging an urgent need for yet another review of what the research councils are for. Although it would be convenient that the review should wait until the Merrison inquiry is completed, that is largely a recipe for postponing until tomorrow what should be undertaken right away. The agenda for an inquiry is, after all, easily conceived. Indeed, the final report of such an inquiry should not unduly tax the imagination.

The research councils have two quite different functions, which collectively they must keep. Two of them were set up to sponsor basic research relevant to the practice of agriculture and medicine. A third, the Natural Environment Research Council, is historically an exercise in wish-fulfilment — it was set up in the early 1960s in the hope that it could put flesh on the bones of the then nascent belief that problems of the environment and natural resources would dominate the remainder of the century. The belief has been justified, but the council has turned out to be a manager of a miscellaneous collection of disparate enterprises. (Presumably part of the reason for putting the organization in the hands of Sir Hermann Bondi is that he may be able to weld them into a more coherent whole; but he will have his work cut out.) Almost incidentally, these three research councils help to foster academic research, partly through research grants to academics, partly by links between their research institutes and neighbouring universities. Both kinds of links are valuable, and should be preserved at all costs.

Change is needed elsewhere, and in particular in the definition of the practical functions of the councils with a mission. In medicine, can it make sense that the Medical Research Council



should take back responsibility for the Rothschild money but still stand only on the sidelines in the support of teaching hospitals and the administration of research within the National Health Service? In agriculture, there is also a case for asking that the old boundary between "basic" and "applied" research should be made more flexible. British agriculture has been uncommonly successful in the past few decades. It might have been even more

successful if the customers and the contractors had lived more in each others' pockets. In short, if the Rothschild recipe is now to be eroded, there are the strongest reasons why the balance should be tilted the other way and the research councils given even more practical marching orders than in the recent past. If, at the same time, they can keep their links with the universities, everybody will be the beneficiary.

## Ideological trouble ahead for Unesco

The United Nations Educational, Scientific and Cultural Organization (Unesco) seems bent on cutting its own throat. The General Assembly of the organization just ended in Belgrade has confirmed that Unesco is no longer the high-minded arm of the United Nations concerned with the general enlightenment that recruited the late Sir Julian Huxley as its first director-general. To be sure, last month's proceedings were less sordidly political than those in the past decade when general assemblies were used by the member states as occasions for isolating Israel from Unesco's general activities. The Belgrade assembly was, rather, cynically political. On two important matters, a combination of developing countries (the "group of seventy-seven") and the Eastern bloc was able to force down the throats of the chief contributors to the Unesco budget two thoroughly bad proposals — a controversial resolution about the procedures to be used for the gathering of news throughout the world, and a scheme for the setting up of a "Special Programme" for planning the technical development of developing countries, a kind of hangover from last year's United Nations Conference on Science and Technology at Vienna. Unesco's budget is to be increased by seven per cent (in real terms) to pay for these new ventures. The industrialized Western states who are the chief contributors have to pay up or get out.

The argument about news-gathering is not merely a technical matter of how news agencies operating internationally should be regulated, but an issue of principle going to the root of Unesco's existence. For several years, developing countries have been grumbling about the unpalatable news of their affairs frequently reported by journalists and news agencies from overseas. Unesco responded by mounting a study of the problem by a commission under Mr Sean McBride, a retired Irish diplomat. The McBride report has been a focus of controversy for the past two years, principally because it gave developing countries reason to believe that they are indeed exploited, and even dealt with unfairly, by the international news agencies. So, the argument goes, there must be a "new information order" to match the "new economic order" for which developing countries (with some justice) have been asking for several years. At Belgrade last month, Unesco was given until 1983 to work out the principles on which such a regime should be based.

But why should this be a black mark for Unesco? Surely the gathering of information is properly within the organization's terms of reference? And surely it is right and proper that it should respond to the wishes of the majority of its members? That is the defence of what Unesco is about. These arguments are nevertheless too facile. They entirely overlook the dangers of admitting that governments have a right to expect news of a kind that is welcome, even flattering. The enterprise on which Unesco is embarked also carries explicit approval for the notion that governments should properly be concerned with the management of the means by which news of their own doings is relayed to the wider world. The fear is that governments will use the Unesco resolution as an excuse for telling journalists what they should say.

It is, of course, well known that member governments differ in their estimation of these dangers. Many socialist states take the view, logical enough, that the gathering of information and its dissemination plays such an important role in society that governments must shoulder the responsibility. Most Western governments, with more or less enthusiasm, follow the opposite principle that a free press is a necessary guarantee of personal

freedom and thus of a just society. The governments of developing countries differ among themselves. Some hanker after the Eastern way but lack the facilities. Others — India is perhaps the most creditable example — put up with a free press without too much complaint. Wherever the truth lies (and there is not much doubt of that), the difference is frankly ideological. By backing one side and not the other, Unesco's members have unwisely — some would say foolishly — committed the organization to an ideological position in a way that must surely conflict with its high-minded principles.

Unesco's special programme for redressing the technical balance between the developing and the industrialized countries of the world is similarly born of ideology. Again, there is no complaint that the topic is outside the organization's terms of reference. Nor is it denied that there is an urgent need of more and of more effective technical and financial assistance for the developing countries of the world. There is yet a chance that the message of the Brandt Commission's study will sink in (see *Nature* 21 February). It does not, however, follow that the nostrums that preoccupied the Vienna conference last year would have been effective even if they had been approved (which they were not), that the notion of a "new technological order", ill-defined as it is, makes any sense and that a specially created Unesco secretariat, politicized as it would be, would be competent to define a strategy for the future. It is not, in any case, as if the United Nations system is short of organizations for fostering technical and economic development. Within its special terms of reference, Unesco might have done a useful job by helping to bring about a better understanding of the sharp differences of opinion that abound on the proper relationship between developed and developing countries on science and technology. By plumping for the solution of the new technological order, the majority of Unesco's members have yet again put ideology before good sense.

Unesco is not well placed to take such risks. Over the years, it has won itself an unenviable reputation for unreality, extravagance and maladministration. Some good things have come out of the splendid Corbusier building in the Place de Fontenoy. Unesco helped to focus interest on Abu Simbel and on the hydrology of Venice. Its efforts to encourage innovation in science teaching and the systematization of scientific bibliographies have been well meaning but not sufficiently energetic to make a mark in competition with other free-wheeling agencies. Other projects, the so-called "Biosphere" programme for example, have been chiefly valuable as sources of largely empty generalizations. It is no wonder that people (and member governments) increasingly ask whether it can be worth its cost.

Unesco would be better placed to run ideological risks if it were less open to complaint about the ordinary conduct of its affairs. The chances are that most of the disaffected Western governments will react to the troubles at Belgrade by resolving to pay more attention to Unesco's business in the years immediately ahead. Few of them would wish, at this stage, to incur the opprobrium of taking the initiative to cut it down to size or even to put it to sleep. But things could change — as the United States Congress will change in January. Unesco may yet find itself in the uncomfortable position of the International Labour Organization, which has not yet recovered from the withdrawal of the United States three years ago. It would be unfortunate, but no by any means the end of the world, if Unesco were to find itself in a similar position. The remedy is in its own hands.

# Academics agonize about weapons labs

## Livermore and Los Alamos up for grabs

San Francisco

In what promises to be another stormy round in a long-running debate, the Board of Regents of the University of California is meeting next week to discuss how it should increase its control of research programmes at the two weapons laboratories which the university runs for the Department of Energy (DoE).

The present five-year management contract for the two laboratories — at Livermore and Los Alamos — runs out in 1982, and preliminary moves to negotiate a new contract with the department have restimulated discussion of the implications of the university's responsibility for the research that underpins a major part of the world's nuclear arsenal.

Last year, the Board of Regents, which is responsible to the state for the university's affairs, rejected a proposal from *ex-officio* member Governor Jerry Brown to remove all military research from the Lawrence Livermore Laboratory, and in September voted to open discussions with DoE for a new contract. The focus of debate has therefore shifted from whether the Livermore Laboratory should be carrying out weapons research at all to how the university should exercise its management responsibilities over this research. In particular, opinions differ about the extent to which the Board of Regents — and possibly outside advisers — should be involved in determining research priorities for the laboratory.

Under the present arrangement the university accepts responsibility for the quality of the research but leaves priorities almost entirely to DoE, a situation which many scientists and administrators at the laboratory are reluctant to see changed. "If a car is running well, you don't tamper with the engine", one Livermore official said last week.

Some members of the university faculty are, however, concerned about the lack of control over military research programmes. The autonomy enjoyed by the laboratories under the protection of the university was described in a report as "so delightful as to border on the licentious". More recently, a group of laboratory staff at Livermore, known as the Society of Professional Scientists and Engineers, has suggested that there should be greater outside monitoring of research.

At the same time, the university is keen to keep a contract which brings in \$4 million a year in management fees, and it

points out that several recent reports, including one prepared by the department's Energy Research Advisory Board, have concluded that it is in the best interests of both sides that the basic links with the university be maintained.

At its meeting last month, the Board of Regents received two proposals for modifying the relationship. Professor William Fretter, the university's vice-president, suggested that the regents appoint a new oversight committee to "provide increased accountability to the general public", and that this committee establish three evaluation committees, one of which would be responsible for establishing research priorities.

The second proposal came from Governor Brown and is based on the report of a committee which the university itself set up in 1978. Like Professor Fretter, the governor also proposes a new oversight committee, but this time assisted by an independent advisory board.

The two proposals agree on many points, but also have significant differences. For example, while the evaluation committees proposed by Professor Fretter would essentially be subcommittees of the oversight committee, Governor Brown's advisory committee would have much greater autonomy, being empowered to request that the oversight committee help it evaluate particular programmes or problems.

The composition of the proposed committees would also differ significantly. The evaluation committees proposed by Professor Fretter would chiefly consist of experts from within and outside the university. In contrast, Governor Brown

contemplates an advisory board of scientists, faculty members, students, health experts, theologians and others.

The president's office is now deciding whether the two proposals can be combined. Otherwise, the choice between the two approaches will have to be made by the regents.

Whatever the result, increased control — at least of research not related to weapons, which forms about half of the work of both laboratories — seems inevitable. The university's president, Dr David Saxon, has already proposed setting up a panel of scientists to recommend research priorities in energy research and other unclassified areas at the two laboratories.

More controversial is the extent to which an oversight committee should be involved in policy decisions about weapons research, which is shortly expected to include work on the MX missile system. Here both university and laboratory officials argue that all such policy decisions must be made at the national level in Washington, and that the laboratories should only carry out Washington's requests.

Critics point out, however, that in the past laboratory officials have been far from neutral in policy debates over weapons research and related areas of arms control. For example, pressures from the two weapons laboratories were significant in reducing the scope of the Comprehensive Test-Ban Treaty now being negotiated in Geneva, while other laboratory officials have been active in the debate over whether to ratify the Strategic Arms Limitation Treaty (Salt II).

David Dickson

## Short commons for Spanish research

A ten-month freeze on research grants for scientists in Spanish universities and the Spanish National Research Council ended on 20 October with the distribution of 3,600 million pesetas (£22 million) to groups in the universities and the research council. The average of £24,000 per group must officially last three years — although the period may in practice be longer. Grants were last awarded in 1976.

The distribution has come in for some severe criticism, particularly from members of the group of 200 leading scientists who, just before the grants were announced, had sent a manifesto to the Minister of Universities and Research describing his policies as "derelict" (*Nature* 23 October, p.674). The group now says that the meagre distribution is no surprise. Spain historically has spent only 0.3 per cent of its gross national product (GNP) on research and development compared with about 2 per cent in other Western countries. Passions have,

however, been stirred by the way in which this distribution has been made.

One member of the group says that a key advisory body has been ignored, and that grants have been awarded by subject panels which were not best qualified to make judgements. The result has been a largely random distribution of money, he claims. Some of these discontents were aired at the meeting on European Economic Community (EEC) science policy held two weeks ago in Strasbourg.

The advisory body, the Gabinete de Estudios, was set up four years ago by the now deputy director-general of the United Nations Educational, Scientific and Cultural Organization, Professor Federico Mayor, to provide baseline studies of science in Spain and to advise the Comisión Asesora de Investigación Científica y Técnica (CACT), which distributed last month's grants. But the Gabinete's recommendations of referees for the grant applications were rejected, said the



manifesto spokesman, and CACT took other advice about the composition of the panels of referees.

One curious feature of the grant-making process is that the director of CACT, Professor Marcos Rico, demanded that nobody who was applying for a grant should serve on a review panel. The manifesto group complains that no scientist worth his salt would not be applying after a year without a research grant. The head of one of the panels has since written to one unsuccessful applicant (who with a similar proposal won DM265,000 from the Volkswagen Foundation) to say that a lottery would have been equally fair.

On the other side, the Ministry for Universities and Research claims that the



Seara — handing out

manifesto group is the naive political tool of the far Right, which wants to unseat the minister, Luis Gonzalez Seara, for his attempt to reduce professorial power with a bill now before parliament.

Seara's chief science adviser, sociologist Narciso Pizarro Ponce de la Torre, said at the Strasbourg meeting that his ministry (like Spanish democracy) was new and that the power of the Francoist professors was great, so that change had to be slow. Even so, the ministry is preparing a major policy statement, the 'livre blanc', on science for May 1981, together with a three-year plan that would multiply university research tenfold. But, said the manifesto group spokesman, the same has been said before, by three successive ministers: he will not believe it until it happens.

The seriousness of this conflict cannot easily be gauged. Narciso Pizarro accepts that a 'more scientific' method has to be found for making the next allocation of grants. He is considering the appointment of international referees to some of the review panels for the next grant allocation in 1983. But he argues that the international community can itself be an inequitable power base for those with access to it, and wants to see a 'just' distribution of funds. So does the manifesto group, although its wish that scientific excellence should be rewarded is seen as elitist in a fledgling democracy. The conflict is between the impatient and the gradualists.

Robert Walgate

## US radioastronomy Thinking big

San Francisco

Following the successful completion and inauguration of the Very Large Array (VLA) telescope in New Mexico last month, US radioastronomers are developing an ambitious scheme that would, in effect, turn the country into a single large radio telescope.

The VLA is designed to study relatively close objects whose distance from the Earth is of the order of thousands of light years. But to study the internal structure of quasars and the nuclei of galaxies the necessary resolution can only be achieved by the use of Very Long Baseline Interferometry (VLBI) in which data from several telescopes are combined to form a single image.

To some extent this can be done by linking existing telescopes, and since 1975 seven US radio telescopes have formed such an array. But there are several disadvantages, including the difficulty of coordinating and correlating data from machines designed and built for different purposes.

The new proposal, which has been developed by scientists from the California Institute of Technology (Caltech) and its Jet Propulsion Laboratory (JPL), is for a transcontinental array of ten 25-metre radio dishes, stretching from Massachusetts to Hawaii and controlled by a single central computer.

Such an array should provide an order of magnitude leap in the important parameters that could be measured compared with the data that can be collected from the present *ad hoc* arrangement. It could be used to provide fine detail radio maps of quasars and galaxy nuclei and also for making precise

measurements of the Earth's rotation, even providing information on plate tectonics.

The scientific and the economic feasibility of such a transcontinental array has now been demonstrated in a Caltech study which concludes that for extragalactic astronomy VLBI is the only tool available for detailed study of the energy sources in quasars and galaxies.

One feature of the Caltech proposal is that the array would be two-dimensional, with radio dishes as far north as Alaska. This spread will make it possible to cover almost all of the northern sky, in contrast to a Canadian proposal for a similar array with radio dishes essentially on a linear axis from Europe to British Columbia.

Two particular aspects of the array would improve performance compared with the present system. First, being able to locate the individual dishes in an optimal arrangement would make it possible to increase the dynamic range by an order of magnitude. This would allow detailed studies of the shape, size and evolution with time of the jets which are emitted from quasars and galaxy nuclei, in particular the acceleration and deceleration of so-called 'knots' which occur within the jets.

The second advantage is that the array would be able to make measurements at frequencies of up to 15–20 GHz, considerably higher than some of the telescopes in the present array can achieve. This will make it possible to look much further down the jets to the surface of the objects from which they are emitted.

Radioastronomers in general are enthusiastic about the proposal for a ground-based array, which has been given top priority for funding in the next decade by the Field Committee responsible for overseeing research priorities in all fields of astronomy.

The main problem, inevitably, will be funding. The Caltech group estimates that the array will cost \$38.8 million, considerably less than other astronomical facilities (VLA, for example, cost \$80 million).

But astronomy, like other fields of basic science, is feeling the pinch. Already the National Science Foundation (NSF) has had to postpone plans for the next telescope on its priority list, a 25-metre dish that had originally been requested for funding in the fiscal year 1981 but failed to survive the budget review process.

There are three other schemes vying for funds. The National Aeronautics and Space Administration (NASA) has been working on plans for an advanced X-ray astronomical telescope, a successor to HEAO 2 and HEAO 3. In addition to the ground-based array, the NSF is already considering proposals for a 10–15-metre optical telescope, including designs that have been submitted by the University of California, the University of Arizona and the University of Texas.

Caltech scientists should have detailed plans ready for potential funding by 1982.

## Any encounters, any kind

Voyager 1, now nearing Saturn, is far from innocent of messages to extraterrestrial civilizations (in which respect the article on page 9 is incorrect). Like its partner, Voyager 2, it carries a phonograph disk of copper (for long life) with sound recordings of greetings in 60 languages, a spoken message from Kurt Waldheim, Secretary-General of the United Nations, sounds of the Earth (natural, unnatural and musical) and a list of the members of the pre-election US Congress.

The disk also contains analogue tracks representing 100 photographs of the Earth and a message from President Jimmy Carter referring to 'our progress towards a single global civilization' and 'our wish to become a member of the galactic community'. Voyager 1 was launched before the seizure of the US hostages in Iran.



and on such a schedule their array would be in operation by 1984–85. If the 25-metre dish is approved for funding next year, as hoped, there will be no conflict. However, if it is postponed again, then relations between what could become rival projects would be more delicate.

Experience has taught supporters of the ground-based array that any debate over who should run the facility ought to be resolved before the funding battle begins. Many feel that proposals for a mid-west telescope floundered because of inter-university rivalry for control. "We are determined not to make the same mistake again", says one radioastronomer.

David Dickson

## Nuclear protests

### Were Croats first?

With the Madrid Conference about to commence its review of the Helsinki Accords on Security and Cooperation in Europe and the Campaign for Nuclear Disarmament recently revitalized in the United Kingdom it is interesting to look back at what was almost certainly the first ever anti-nuclear protest — that of Dr Ivan Supek, a Yugoslav physicist, in 1944, more than a year before nuclear bombs were dropped on Hiroshima and Nagasaki.

Before the war, Supek had been a pupil of Heisenberg. In 1941, after a visit to

impossible the final victory of progressive forces — a victory which Marxist theory stated was inevitable. Therefore such weapons could not exist.

Supek, however, remained unconvinced, and a few months later published his papers from the congress in the Croatian popular science journal *Priroda* under the titles "Developments in Modern Physics" and "Science and Society".

Although at that time his main fear was of the perverted use that the Nazi regime could make of science (biology as well as physics), his stand against nuclear weapons has never wavered. He has from the beginning been an active participant in the Pugwash movement, and is extremely wary of proposals for peaceful uses of nuclear energy (including research), lest they be perverted to military ends.

Vera Rich

## Research councils

### Geological setback

The Department of the Environment will slash a third from its spending on geological science over the next three years, raising a question mark over the future of the Geological Survey of Great Britain, officials of the UK Natural Environment Research Council (NERC) said last week.

NERC was launching its first annual report since Sir Hermann Bondi took over a month ago as the new chairman of NERC (see *Nature* 5 June, p. 349). Bondi had no influence over the report and was much less concerned than his colleagues: "This report is not in my style", he said. "As you know, I'm an eternal optimist."

Bondi favours the Rothschild "customer-contractor" principle, which the report described as a threat. In 1973 NERC lost control of a third of its budget to government departments, following Lord Rothschild's recommendations for a shake-up in government science spending. At the time, the council warned that many of its projects — such as the Geological Survey — which were dependent on a group of customer departments would be vulnerable to the whim of any one of its customers. "It is of little comfort that this forecast is proving correct" says the report.

A quarter of NERC's £20 million contract research income depends on multi-customer contracts. The Geological Survey itself costs about £4.5 million a year, of which the Department of the Environment currently contributes £1.5 million. The survey was established in 1835, and produces near-surface and deep geological maps of Britain, improving them area by area as techniques develop. Some 180 scientist-years are spent each year on the survey, which involves 10 field units and a number of palaeontologists and chemists, mostly at the Institute of Geological Sciences (IGS).

The survey, UK geologists argue, is a national resource, drawn on regularly in

major civil engineering works, for example. But if the Department of the Environment takes too short a view, the value of the survey will be diluted and ultimately lost. A thorough survey for a "sheet" covering an area of 12 miles by 18 miles takes around 25 scientist-years and 5 to 7 years. "So you can't turn on a tap when you need a survey" said Dr Brian Kelk, who heads NERC's geosciences division. The survey is not purely an academic exercise. Dr Kelk argues that the survey must be developed on a continuous basis. It is not possible to predict exactly which areas are likely to prove important; for instance, the massive construction work carried out for North Sea oil terminals on the west coast of Scotland and the Shetlands would probably have been slowed without the geological maps which may have seemed of only academic interest when they were made in the 1920s.

Other bodies in the "consortium" which has managed the survey since Rothchild are the Department of Energy (contributing 5 per cent), the Department of Industry (also 5 per cent) and NERC (60 per cent, through the science vote of the Department of Education and Science). But the consortium will now collapse, with the Department of the Environment cutting its share to 20 per cent and offering its money piecemeal for particular areas and purposes. A new management structure must thus be found for the survey — and one is being sought actively by the director of the IGS, Dr G. M. Brown, who will present his proposals to NERC in two weeks' time. Dr Brown will also have to cope with other Department of the Environment cuts at IGS, where the department is reducing its spending from £3 million (at 1979 prices) this year to £2 million in 1982–83, out of a total IGS budget of £16 million. Staff recruitment, for one thing, will be reduced to a trickle.

Nevertheless, NERC's total income of £56.6 million in 1979–80 will hold roughly constant in real terms in 1980–81, largely through a slight increase in funds from the Department of Education and Science; but there is another problem over the replacement of the council's two research ships, *RRS Shackleton* and *RRS Discovery*. The *Shackleton* is older, and will probably be retired around 1983. The *Discovery* should remain effective until about 1987, but a new ship must be found to replace her if Britain is to maintain her place in oceanographic research, says NERC. This would cost £18–20 million at present prices, plus equipment: and to have her ready for the 1988 season, the order must be placed in 1984 at the latest. But there is no sign of the necessary money being made available — except perhaps if the ship were used jointly by the Science Research Council's Marine Technology Directorate and NERC.

It is here, perhaps, that Bondi's contacts and experience in the Advisory Board for the Research Councils — which advises on



Supek (left) and comrade, 1944

Heisenberg in Leipzig, he said that, although his main interest at the time was solid-state physics, he was able to make an "informed guess" that the Germans were working on both fission and fusion bombs.

Supek made his fears known in June 1944, at a congress of Croatian "cultural workers" (a term which included scientists) held in the newly liberated town of Topusko. His views did not go unchallenged. Several Marxist participants were doubtful that such weapons could exist at all. Nuclear weapons in Nazi hands, they argued, would render utterly



the science vote of the Department of Education and Science — may tell. He is reluctant to challenge the Rothschild principle, to which he still adheres firmly — while recognizing the dangers of multi-customer arrangements. He and his staff will redouble their efforts to get new contracts for support for projects in Third World countries.

Robert Walgate

## London university

### Medical schools stay

Two of the medical school of the University of London, whose survival has been in doubt since March this year, were reprieved last Wednesday (29 October) by a resolution of the university Senate. The decision is regarded, within the university, as a sign that the more far-reaching inquiry into the organization of the university as a whole now under way will be less radical than some have feared.

The two medical schools concerned are Westminster Hospital Medical School and King's College Hospital Medical School (which includes a pre-clinical school at King's College proper and a clinical school at King's College Hospital, in south-east London). The disbandment of the two schools was recommended to the university in March by the report on medical teaching in the university prepared by a committee under Lord Flowers, rector of Imperial College.

The politics of last week's narrow Senate decision have a particular interest for the future reorganization of the University of London. The resolution eventually adopted by the Senate was proposed by Dr Bryan Thwaites, principal of Westfield College, one of the smaller institutions of the university. Thwaites and the others supporting the resolution argued that the university should not attempt to coerce constituent academic institutions into courses of action they found unpalatable.

This line of argument has an obvious bearing on the general inquiry into the organization of the university being conducted by a committee under Sir Peter Swinnerton-Dyer and set up by the vice-chancellor, Lord Annan, earlier this year. One possible outcome of that inquiry is a recommendation that the smaller institutions within the university might be merged with larger college or with each other. If however the principle of self-determination has been established, proposals involving loss of independence are less likely to be seriously put forward.

The battle over the independence of the two medical schools is not yet over. Although the decision may in principle be overturned by the Court of the university, this is unlikely without further consideration. A more likely course is that the Academic Planning Board, to which the issue has been referred, will come to a different decision from that of the Senate last week.

## Séveso scare

### Bloat, not poison

A flurry of fear last week that dioxin had reared its head again at Séveso has quickly abated. The local community was alarmed when 150 sheep died after spending a single night on a forbidden field, out of bounds to grazing animals for the past four years. The dead sheep were part of a flock of 250 driven 50 miles from the dry uplands of northern Italy.

First thoughts had blamed dioxin. The field was one of the most exposed when a chemical factory exploded at Séveso in 1976, distributing dioxin over the neighbourhood, and it had not yet been cleared for farming. (The shepherds say they did not see the notices.) But the sheep died too quickly for dioxin poisoning, and the levels in the field are now thought to be quite low. In fact the Séveso special office, headed by Senator Luigi Noé, was planning shortly to open nearby fields for cereal growing, but these plans were halted after the death of the sheep.



Dead sheep, dead landscape

However, the necropsies now show that the sheep died of bloat — severely distended gut, caused by the over rapid fermentation of wet hay, rye and grass in the stomachs of the hungry animals.

The result has been backed up by analysis of the livers of the dead sheep at the Mario Negri pharmacological research institute in Milan, which first detected dioxin in Séveso goats during 1976. According to Dr Luciano Manara, head of

the drug metabolism laboratory at the institute, the sheep had liver dioxin levels below 1 ng per g — compared with 1 µg per g in the most exposed goats in 1976.

Senator Noé has declared himself satisfied with these results, and has restarted the plans to open the Séveso fields.

Robert Walgate

## Bovine tuberculosis

### Badgers at risk

Tuberculous badgers are more of a threat to themselves than to the cattle they infect. This is the nub of Lord Zuckerman's report on the British practice of gassing badgers, suspended a year ago after protests from conservationists (see *Nature* 28 October). Immediately after the publication of his report, *Badgers, cattle and tuberculosis* (HMSO, £5.20), the Secretary of State for Agriculture, Fisheries and Food announced that the practice of gassing infected badger setts is to be resumed as soon as possible and then reviewed after a three-year trial period.

Bovine tuberculosis is most common in south-west England, chiefly in the counties of Avon and Cornwall. The British badger population is to some extent concentrated in southern England, but the agriculture of the eastern counties is more concerned with cultivation than with cattle-rearing.

Evidence in the Zuckerman report for the association between bovine and badger tuberculosis is largely circumstantial. The incidence of bovine tuberculosis is correlated with that of badger tuberculosis and with the density of the badger population. There is also evidence that transmission from one species to the other is feasible. In Britain, the association (long suspected) became the basis for official policy on badger control only in 1971, after experience in New Zealand suggested that opossums were there a feral reservoir for bovine tuberculosis.

The issue has been contentious in Britain for the past decade. The Badger Act of 1973 gave badgers specific protection over and above the provisions of the Protection of Animals Act of 1911, but the Ministry of Agriculture was given power to control badgers (and even to enter farmers' land for that purpose) by later legislation in 1975 and 1976.

The causative organism of bovine tuberculosis, *Mycobacterium bovis*, is the chief cause of tuberculosis in badgers. The most arresting data in the Zuckerman report are those for the incidence of *M. bovis* infection in badgers. The most extensive series of measurements is that carried out by ministry laboratories of badger carcasses submitted for autopsy, usually after being killed on roads. In south-west England, more than 4 per cent of adventitious carcasses yielded *M. bovis*, while elsewhere in Britain isolation of the bacillus from dead badgers was sporadic and not statistically significant. In another



survey of more than 4,000 badgers, 14 per cent were found to be infected.

The rate of badger infection on farms on which outbreaks of bovine tuberculosis have occurred is often much greater, approaching or even exceeding 50 per cent. The report says that the course of the disease among badgers is that of a virulent infection, with pups especially at risk.

In principle, there is no reason why wild animals other than badgers should not be infected with *M. bovis*, which has been found in small numbers of foxes, rats and moles. The Zuckerman report asks for a continuing survey of the occurrence of *M. bovis* and of other related bacilli, including *M. avium*, which has been found in deer, hares and hedgehogs, in particular.

## Swedish Academy

### \* Plugging Nobel gap

A Swedish industrialist, Dr Holger Crafoord, has given £500,000 — with more to come — to the Royal Swedish Academy of Sciences to institute a new series of scientific prizes in fields of science neglected by the Nobel awards — geosciences, biosciences (emphasizing ecology), mathematics with astronomy, and arthritis. The fund, called the Anna-Greta and Holger Crafoord Fund after Dr Crafoord and his wife, will amount to some £1 million by 1984 and the academy estimates it will yield interest of 13 per cent.

Only one third of the interest, perhaps  
★ £45,000 a year, will be spent on prizes. A quarter will go back to capital, and the rest

will go on research grants, to be awarded by international competition. The details of the award system are being worked out by a special commission, which will report to the academy early in 1981 in the hope that the first awards can be made that year. The intention is to avoid the season of the Nobel awards, traditionally made in late September and early October. There will probably be one prize in a single subject each year, rotating on a four-year cycle.

The subjects emphasized in the new award are the result of a few months' consultation between Crafoord and the academy. Dr Crafoord, who is general director of the biomedical firm Gambro AB of Lund, suffers from rheumatoid arthritis — hence the attention given to that disease.

Asked why he made the awards, Crafoord said last week "I had money enough!" Crafoord owns Gambro, which has some 20 per cent of the world market for kidney dialysis units. He felt he wanted to leave money to science, and asked the academy what fields were short of money. The allocation to research grants, as opposed to prizes, was made at his request. "I chose the academy because it was founded in the seventeenth century — it gives some guarantee that the fund will be maintained."

The academy does not see the awards as a chance to improve on the present system for the selection of Nobel prizewinners. "We are very happy with that" said an academy spokesman. "If we could match it for the new prizes we would be well pleased."

Robert Walgate

## Brazilian biology

### Humus from wood

A scheme for turning sawdust into humus, and exporting 600,000 tons of it to the Middle East, is being developed by Nutri-Humus Laboratories of Sao Paulo. This is the latest step in a long-term plan for liberating Brazilian agriculture from dependence on petro-dollars conceived by the bacteriologist Mario Nogueira de Oliveira, who founded Nutri-Humus 20 years ago.

The company began in a small way, supplying a few Brazilian farmers with the fermentation vessels, worms' eggs and organic fertilizers needed for the process. Now that rising oil prices are making the method economically competitive, and there is increased ecological consciousness, there is large-scale acceptance of the new approach.

On the farm, raw vegetable matter (sawdust, rice husks or bagasse from sugar cane) is spread over the fields at 10 to 20 tons per hectare, mixed with two 60-litre bags of pure humus and "earthworms' eggs" as a "primer", plus a third of a ton of natural phosphate obtained as a by-product of mining in the area. Next comes the novel part of the process — the land is sprayed with four types of brew, labelled enigmatically A, B, C and D.

Being something of an empiricist, and not wanting to release too many details of what might be a profitable enterprise, Nogueira does not explain his methods in full. But the additives include *Rhizobium* species bacteria such as *R. japonicum*, nitrogen-fixers and antifungal agents. It is claimed that the process manufactures organic fertilizer in 60 days instead of the usual 4 years at nature's own pace.

Industrially the plan is to use sawdust and wood chips which are the by-products of the timber industry of the Lages area of Santa Catarina state. The wood is hydrolysed with 0.3 per cent sulphuric acid before use and the exportable end-product is the "organic fertilizer", that is, 60-litre plastic bags containing the final humus breakdown products. This is now being made on fields in the Lages area and its market price is one-tenth that of chemical fertilizers in Brazil. It is hoped that a contract will soon be signed with the Libyan and Saudi governments for the sale of 200 shiploads of humus following the successful demonstration of alfalfa production on sandy terrain using Nutri-Humus.

Nogueira's long-term aim is self-reliance for Brazil's agriculture. He proposes a reduced cultivated area for sugar cane to serve as a generator of organic material. Each hectare of cane would fertilize 30 hectares of land in a year. As well as being freely available and high-yielding, sugar cane contains saccharose which facilitates the fermentations on which the Nutri-Humus process is based. Maurice Bazin

## Franco-Soviet jaunt to Halley?

A joint Franco-Soviet mission to visit Halley's comet in 1985 has been announced. This comes as a surprise to many French astrophysicists, including those already involved in the European Space Agency (ESA) mission to the comet which, it seems, the Franco-Soviet experiment will to a large extent replicate. ESA officials confirmed that there is no possibility of France withdrawing from the European effort — participation is mandatory on all members.

France has always had a special relationship with the Soviet space programme. President de Gaulle was the first and so far the only Western leader to visit the Baikonur space centre. French participation in Soviet launches has included a laser experiment aboard the Lunokhod Moon-rover and a joint ionosphere experiment using high-altitude rockets launched from the Arctic and Antarctic ends of the same line of force. And two French cosmonaut candidates are now in training at the Gagarin space centre.

The propaganda value of these trainees, one of whom will become the first Western European to fly aboard a

Soviet spacecraft, has not been overlooked. At the beginning of October, Moscow radio commentator Boris Belitskii, after censuring the British media for neglecting the significance of the joint Soviet-Cuban flight, claimed that the training of the two French cosmonauts was even more "significant in terms of missed opportunity" for Britain. In the Soviet Union, he said, television viewers could watch cosmonauts carried aloft to work on a space programme geared to human needs, whereas in Britain the only rockets to appear on the television screens were American cruise missiles, plus, of course, science fiction epics.

Belitskii's message was clear — a Britain without US military missiles would be eligible for consideration as a future partner for the Soviet Union in space. He made no mention of the financial cost. Judging from the latest Franco-Soviet proposal, this need not be excessive in cosmic terms. The trip to Halley's comet — including the launching of French balloons above Venus — will cost France a mere 150 million francs (£15 million). Vera Rich



# CORRESPONDENCE

## Malaria vaccines?

**SIR** — Considerable effort is being directed towards producing a practical and effective vaccine against the most malignant human malaria, that caused by *Plasmodium falciparum*. The belief that this is feasible was based on the realization that human malaria induces effective specific immune responses which are protective. The best characterized of these are antibody-mediated, directed against stage and species specific antigens of sporozoites and merozoites and seem to act by preventing the entry of these two extracellular forms into their respective target cells, hepatocytes and erythrocytes.

However, the clinical effectiveness of natural immunity in exposed subjects is partially offset by processes generated by living plasmodia which permit evasion of immune effector mechanisms. These include the bewildering degree of antigenic diversity generated by the parasite as it differentiates through successive stages; also its ability to compromise host immunity through induction of immunosuppression and through polyclonal activation of lymphocytes and probably also by production of soluble antigen. Experimental vaccination with, for example, irradiated sporozoites or non-invasive merozoites, induces more effective immunity than does natural infection, indicating that nonviable forms of the parasite can stimulate protective immunity without activating processes favouring parasite survival.

The logical step from these observations is to develop stage-specific vaccines based on sporozoites and merozoites. The difficulty of obtaining these forms in sufficient quantities for even a restricted trial of adequately standardized material has encouraged detailed investigations into the structure of plasmodial antigens in the hope of identifying those involved in inducing protective immunity. This task was beset with technical difficulties, but the prospects have been transformed by the advent of techniques of somatic cell hybridization to generate cell lines which secrete monoclonal antibodies of defined specificity. The very first clone of antibody secreting cells raised against sporozoites led directly to the isolation of a stage-specific, surface-coat component of molecular weight 44,000 with the potential for promoting immunity to this clinically important stage of infection. With these specific probes it is becoming feasible to attempt the *in vitro* production through DNA cloning of plasmodial antigens having putative protective activity.

It is not surprising that such work should attract the attention of commercial interests, not least from those most recently founded and best equipped to exploit its potential. This intervention gives promise of greatly strengthening the malaria vaccine research effort, but some of its consequences may soon retard progress. Work on a malaria vaccine is unusual in requiring access to materials and facilities so diverse as to demand the collaboration of many laboratories. These requirements include a wide range of adequately characterized and geographically remote plasmodial species, their *in vitro* culture, the use of breeding colonies of

appropriate mosquito vectors, access to those few primate species susceptible to human malaria and eventually the organization of adequately controlled and locally acceptable clinical trials in countries which may have only rudimentary public health facilities. Despite these requirements some institutions are contemplating individually beneficial patent rights on segments of the work. This action already threatens to disrupt in part the complex web of collaborative work so central to success.

Malaria menaces over a third of the world's population and is confined almost exclusively to developing countries. There are around 150 million cases per year and over a million African children die annually of the disease. A recent intensive survey has shown that in the vast African savannah no known method of prophylaxis, however thoroughly dispensed, can in practice be effective. Elsewhere, for example in India and Sri-Lanka, it has proved impossible to sustain prophylactic measures and malaria is alarmingly resurgent. The cost of a developed malaria vaccine can never be recouped from the relatively impoverished countries which require it most urgently. Its manufacture and distribution will inevitably require massive subsidy from international governmental and charitable funds. Under these circumstances can any institution justify a claim to benefit individually from a restricted aspect of work, however important, which contributes to the development of a malaria vaccine? Procedural agreement is urgently required in this area of research. Representatives of major organizations involved should meet together forthwith under appropriate international auspices and agree a moratorium on all patent rights relating to the development of a human malaria vaccine. Is it really naïve to believe that this enterprise cannot be sustained solely on the basis of its scientific feasibility and enormous practical potential for the health of mankind?

S. COHEN

Department of Chemical Pathology,  
Guy's Hospital Medical School,  
London SE1, UK

## Nobel Prize rules

**SIR** — Your editorial on changing the Nobel Prize rules (*Nature* 23 October, p.667) is right on all points. However, it does not mention one vital question — the statistics of sampling.

One way that the Nobel Foundation uses to select candidates is to write at random to about 50 universities for proposals. This list is different each year and comprises a sample of the about 900 universities around the globe (*Encyclopaedia Britannica*, *Micropaedia X*, pp.888-1007). As most of these universities are likely to have a chair in nuclear physics, but only about 10% one in spectroscopy, less than 10% in flow phenomena (hydro- and aerodynamics . . .); less than 5% atmospheric physics; less than 2% aerosol physics etc., the odds that a nuclear physicist will get the letter and nominate somebody within his own field, are incomparably greater than for any other branch of physics.

**Proof:** Between 1950 and 1973, 16 Nobel prizes went to some aspect of nuclear physics, 3 were awarded for low-temperature phenomena; 3 for optics; 2 for quantum

electrodynamics and 1 each for magnetism and semiconductors. Probably similar biases exist in chemistry and medicine.

In conclusion: the Nobel Prize goes by preference to the disciplines with the largest number of scientists. In other words, it is biased towards specialities best endowed with funds. This means that governmental budgeting interacts with the award.

It is surprising that such a select scientific body should not be aware of such a basic sampling error. More than a sampling error; this "pseudorandomization" goes against Nobel's will. At the end of the nineteenth century, physics was comprehensive and subdivision in specialities almost unheard of. Since then, electronics, atmospheric physics, rocketry, astrophysics and many, many other branches have become so detached, that scientists working in such areas are almost excluded from being considered for the prize.

M. BENARIE

Institut National de Recherche  
Chimique Appliquée,  
Brétigny, France

## Fungal food

**SIR** — The recent article on fungal foods (*Nature* 4 September, p.6) states that the protein gap that was believed to exist in many developing countries has now been declared a myth. I have discussed a similar problem with Mr J. Todd, Executive Assistant to the Unitarian Service Committee of Canada — a Canadian charitable organization engaged in overseas relief and development in cooperation with governments of the least-developed countries. These countries are specifically chosen on the basis of a per capita income being less than \$200 per year. The agency is working in six such countries.

Mr Todd's description of the protein shortages in the many communities in which he works and the desperate need for protein in a wide variety of forms contrasts sharply with your statement. Although such countries are probably unable to buy protein from overseas, the lack of demand based on such inability can surely not be taken as an absence of need.

P.J. HEALD

Memorial University of Newfoundland,  
St John's, Newfoundland, Canada A1B 3X7

## ACHÉ uses

**SIR** — What, pray, is wrong with the determination of any government to attempt to protect its citizens, be they either soldiers or civilians, against the use of "nerve gas" (organophosphorus) weapons? How can this be thought of as "distortion of technology"? R.G. Elles *et al.* (*Nature* 9 October, p.480) are adopting a stereotyped "holier than thou" attitude more appropriate to the behaviour of our "Praise-the-Lord Barebones" forebears of the post-Civil War period — "smelling-out" evils when they would be better occupied in haranguing protest meetings of a non-scientific nature; such letters are inappropriate for a science-based *Nature*.

R.A. DAVIS

Rodent Research Department,  
Tolworth Laboratory, Tolworth, UK

## NEWS AND VIEWS

## A close look at Saturn

from Philip Campbell

No photograph can do justice to what must surely be one of the most serenely beautiful sights in the solar system — Saturn and its ring system. Just over three years after launching, and having already revolutionized planetary studies with its exploration of Jupiter and its moons, Voyager 1 is about to begin the second exploration by spacecraft of Saturn — planet, rings and moons. The spacecraft's closest encounter will occur at 2345 GMT on 12 November at a distance of 124,200 km; the next two weeks, therefore, should provide a feast for astronomers and, no doubt, a fillip for NASA, troubled by escalating shuttle costs and by repeated budget cuts.

Voyager's encounter is the second of three. The first was by Pioneer 11, just over a year ago. Next August, Voyager 2, carrying similar instrumentation, will carry out a series of investigations complementary to those of Voyager 1. The trajectory of Voyager 1 has been designed to include a study of Titan, Saturn's largest moon, while the path of Voyager 2 is already set for Uranus and, it is hoped, Neptune. For that spacecraft, Saturn is, so to speak, an interesting view on the way. Voyager 1, on the other hand, will eventually pass out of the solar system without further known encounters — and without the hitherto obligatory message to exceedingly intelligent extraterrestrials.

Saturn's rings were first recognized by Huygens in 1656. From the earth, two rings can be seen most easily, rings A and B, separated by a gap known as Cassini's division. Following Pioneer 11, the number of distinct rings now known is five: in order of increasing orbital radius they are labelled C, B, A, F and E. Ring F is very narrow and was discovered by Pioneer 11, while ring E is wide and tenuous, extending from about 2.4 to 5 or 6 Saturn radii ( $R_s \approx 60,000$  km) from the planet. (The existence of ring D, previously suggested by ground-based observations to be inside ring C, was not confirmed by Pioneer 11.) The number-density of particles varies considerably from ring to ring, but ground-based observations and an analysis of Pioneer 11's trajectory both indicate that the rings consist predominantly of low-density particles, covered with or consisting entirely of ices of  $H_2O$  and  $NH_3$ . Moreover, ultraviolet measurements from the International Ultra-Violet Explorer

satellite and from Pioneer 11 have revealed that the rings are surrounded by an envelope of atomic hydrogen, possibly generated by photo-dissociation or the sputtering of the ice molecules.

Saturn's rings pose many problems. How did they form and evolve? Whether the rings originated in the tidal destruction of a moon or are a remnant of the proto-planetary nebula, several questions arise. Thus Cassini's division is known to occur close to the 2:1 orbital resonance of one of Saturn's smaller moons, Mimas. (That resonance is at the radial distance from Saturn at which a particle will orbit twice in the time it takes Mimas to orbit once.) One might expect a gap to appear at such a radius because the repetitive gravitational perturbation of Mimas would act so as to remove the particle from its orbit. But how is it that Mimas, only 350 km in diameter, can clear a division about 10,000 km in extent? And why is the division offset on the outward side of the Mimas resonance? Another question concerns the narrow F ring of Saturn — a question much stimulated by the discovery of other narrow ring systems around Jupiter and Uranus. A ring once formed should flatten and spread as a result of random collisions between the ring particles. Why has this not happened around Jupiter and Uranus? And why does the A ring of Saturn exhibit asymmetric spatial variations in brightness when viewed from the earth?

Whatever the answers to these questions — and several have been suggested over the past few years — they certainly involve interactions between the rings and Saturn's satellites. Two possible clues would be the discovery of moons orbiting within the ring system or the detection of density waves in the rings themselves\*. The fact that spoke-like features have already been detected within the rings by Voyager 1 is a promise of things to come.

Voyager 1 is equipped for several different investigations of the rings. Apart from the two television cameras (which are sensitive enough to detect clumping within the rings but not individual particles), an infrared radiometer will be used to examine the brightness-temperature of particles as sensed in different relative positions of spacecraft, particle and the Sun, and also to monitor the rate at which the particles cool once they have entered the shadow of

Saturn. These measurements should yield particle sizes and compositions. An ultraviolet spectrometer will examine the hydrogen envelope of the rings. Finally, the spacecraft radio telemetry links will be monitored as the spacecraft, after the closest encounter, passes behind the planet and reappears behind the rings. Measurements of refraction and absorption of the radio waves by the rings should reveal details of the larger ring particles together with the overall ring thickness, known to be less than a few kilometres and possible only a few metres.

The body of Saturn itself will be investigated by the same techniques. Analysis of the spacecraft trajectory (monitored by the Doppler shift of the radio telemetry signals) will allow better values of Saturn's mass and gravitational moments to be calculated, enabling a density profile of Saturn's interior to be deduced. The post-Pioneer picture is of an oblate spheroid only 95 times heavier than the earth (although more than 800 times the volume) with one-fifth of the mass concentrated in a rocky core about twice the size of the earth. The core is thought to be surrounded by a layer of metallic hydrogen out to half the radius, beyond which is a gaseous envelope consisting predominantly of hydrogen and helium.

To refine this model, it is hoped that Voyager 1 will provide more details of Saturn's temperature structure and internal rotation. Pioneer 11 shed very little light on the question of rotation. Although the rotation period of the outer atmosphere is known to be about 11 hours, no indication was found of the inner rate. Had Saturn's magnetic field, discovered by Pioneer 11, been inclined to Saturn's axis of rotation, the internal period would have been easily determined. Unlike any other known planetary body, however, the magnetic field and rotation axes are aligned to within  $1^\circ$ . Voyagers 1 and 2 carry plasma and plasma wave detectors, magnetometers and radio receivers to investigate further the magnetic field and its interaction with the Solar Wind. (For a recent detailed discussion of the magnetosphere, see Cowley, *News and Views*, **Nature** **284**, 302; 1980.)

Visual observations of Saturn's atmosphere are greatly hampered by a thick ammonia haze, thought to be formed deep within the atmosphere but spread to considerable heights by convection. Cloud bands have been observed, and Pioneer 11 detected several features found on Jupiter

\*Note added in proof: Two new satellites designated S13 and S14, have been discovered, one on either side of the narrow F ring. This may be consistent with a ring-confinement mechanism suggested by Goldreich and Tremaine (*Nature* **227**, 97; 1979).

to be characteristic of high wind shear. The much more sophisticated imaging cameras of the Voyagers, together with their facilities for detailed infrared and ultraviolet mapping and spectroscopy, should greatly improve understanding of the composition of the atmosphere and of its structural variations over the entire planet. At the time of writing, spot-like features have already been discovered.

The prospect of a close look at Saturn's moons must have the Voyager team salivating in anticipation. Will the outcome be as startling as that of the visit to Jupiter? The moons to be investigated are (in order of decreasing orbital radius) Iapetus, Titan, Rhea, Dione, Tethys, Enceladus

and Mimas. These bodies range in size from 175 km (Mimas) to 800 km (Iapetus), Titan standing out at 2,915 km. They will all be mapped optically and scanned in the infrared and ultraviolet to determine surface temperatures and to detect possible gaseous emissions in molecular, atomic or ionized form. The infrared radiometer will also observe an eclipse of Rhea by Saturn; the cooling should provide some clue to the thermal properties and structure of the satellite's surface.

Titan is, as far as is known, alone among Saturn's moons in possessing a substantial atmosphere. No surface features have yet been detected. Ground-based observations do however suggest that Titan's reflec-

tivity, contrary to what would be expected from a gaseous atmosphere, decreases with increasing frequency, so that Titan appears reddish in colour: this has been interpreted as a manifestation of a high-altitude aerosol layer. On the structure and composition of the atmosphere of Titan, it is agreed that methane, ethylene and ethane are present, and Pioneer 11's ultraviolet instrument detected an extensive atomic hydrogen cloud surrounding Titan and possibly extending around part or all of its orbit. The presence of nitrogen in the atmosphere is a source of controversy. Voyager 1, approaching within 4,000 km of Titan, should certainly resolve these problems. No doubt it will throw up many more. □

## How much genetic variation?

from J.S. Jones

WITHOUT genetic variation, evolution cannot take place. The measurement of the extent of polymorphism is hence a prime task for evolutionary biologists, and a variety of genetic and biochemical techniques have been used to this end. Brown<sup>1</sup> has recently found extensive genetic polymorphism in the mitochondrial DNA of man by using a restriction endonuclease analysis which detects individual differences in the DNA sites susceptible to enzyme degradation. Similar polymorphisms exist in human nuclear DNA<sup>2</sup>. Although the study of polymorphism in the structure of the DNA itself is likely to be a time-consuming affair, improvements in the methods available for the study of proteins have already greatly altered our view of genetic variation at the level of the gene product. This new information has important implications for evolutionary theory.

Gel electrophoresis, which utilizes the migration of proteins in an electric field to detect small differences in their charge and shape, can be used to estimate the proportion of a randomly chosen sample of gene loci which is polymorphic. Simple one-dimensional electrophoresis of a sample of loci coding for soluble enzymes was first carried out about fifteen years ago using *Drosophila pseudoobscura* and many organisms have now been surveyed<sup>3</sup>. In general it seems that about a quarter of the loci tested show genetic variation. Most polymorphic loci have rather few alleles; two or three is the norm although there are occasional loci with up to ten.

The unexpected discovery of widespread genetic variation led to a controversy as to whether protein polymorphism is actively promoted by natural selection, or whether it is largely 'genetic garbage' without much evolutionary relevance. Biochemists and

some theoretical biologists have tended to emphasize the importance of selection, but a number of widely discussed mathematical models incline towards the latter view<sup>4</sup>. In general, theories of the selective maintenance of molecular polymorphism find it difficult to accommodate very large amounts of variation, as such theories depend on, for example, differences in fitness between heterozygotes and homozygotes, or differences in the ability of the various alleles to survive in different ecological niches. As the amount of polymorphism increases, these differences must become vanishingly small. Theories of selective neutrality, however, depend largely on two parameters, one of which (the mutation rate) is very small, while the other (population size) may be very large. Both are difficult to measure, but it is clear that, at least in organisms with large populations (such as *Drosophila*), the neutral theory must predict that while many loci might be invariant, others should have very many alleles. The electrophoretic techniques used until recently, however, have demonstrated a rather limited range of variation over different gene loci and have also shown that the majority of enzyme polymorphisms have rather few alleles. Also, according to a theory of selective neutrality of protein polymorphism, closely related species (which share a common ancestor but which have been unable to exchange genes for many generations) are expected to accumulate a different series of alleles because of the action of a different set of random processes over time. This does not seem to be the case; in *D. pseudoobscura*'s sibling species *D. persimilis*, nearly 90 per cent of the polymorphisms detected by simple electrophoresis show identical patterns of genetic variation, although the last gene interchange between these species occurred several million generations ago<sup>5</sup>.

These observations led many biologists

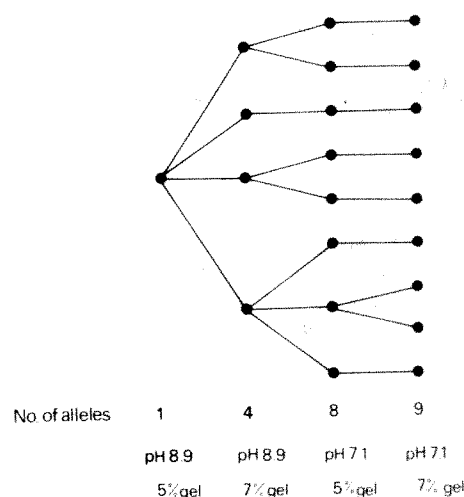
to believe that molecular polymorphism must be actively maintained by natural selection, although the details of the process remained obscure. However, new improvements in the technique of electrophoresis have led to a renewal of support for the theory of selective neutrality. First (as recently discussed by Edwards and Hopkinson<sup>6</sup>) most speculation has been based on data from a very biased sample of gene loci, which ignores structural proteins in favour of genes coding for soluble enzymes. Structural proteins are the most abundant molecules in the cell. Use of the very sensitive new technique of isoelectric focusing in one direction, followed by electrophoresis of the molecules dispersed through the gel at right angles to the focusing path (a method which can detect single charge changes), shows that structural proteins have almost no genetic polymorphism. Estimates of genetic diversity based only on a small sample of enzyme loci are therefore very misleading. In addition, there are serious limitations in the techniques used in enzyme electrophoresis. It has always been accepted that electrophoresis cannot detect all amino acid substitutions. Electrophoretically homogeneous classes of *Drosophila* enzymes are genetically variable in, for example, their resistance to heat treatment and in their ability to form dimers<sup>7,8</sup>. However, only in the last three years has it been realized just how weak the traditional methods of gel electrophoresis may be in detecting enzyme polymorphisms.

Singh, Lewontin and Felton<sup>9</sup> describe some inelegant but practical developments of this technique which they have used to detect new enzyme polymorphisms in *D. pseudoobscura*. They worked first on the xanthine dehydrogenase (*Xdh*) locus. Simple electrophoresis at pH 8.9 on a 5% polyacrylamide gel had revealed only six alleles at this locus. However, sequential analysis of apparently homogeneous

J.S. Jones is in the Department of Genetics and Biometry at University College London, UK.



**Fig. 1** Sequential analysis of an apparently homogeneous xanthine dehydrogenase allele in *Drosophila pseudoobscura*. In all the inbred lines studied, six alleles were revealed in the first set of electrophoretic conditions. After each of the lines were examined on gels of 7% concentration (rather than 5%), 13 variants were discovered. Further examination of these on a 5% gel at pH 7.1 revealed 11 more alleles, and subsequent analysis on a 7% gel at this pH gave 27 genetically different forms. Ten further alleles were distinguished by studying inherited differences in the enzyme's heat stability. Sequential analysis increases the amount of polymorphism detected by six times.



inbred lines on gels of different concentration and pH revealed many previously undetected alleles (Fig. 1). This technique distinguishes 37 alleles, instead of the six previously detected. As only 146 genomes from nature were examined, the total number of alleles at the *Xdh* locus may be even greater.

Sequential electrophoresis does seem to detect most amino acid substitutions. The complete amino acid sequence of many mutant haemoglobins is known; one-step electrophoresis lumps together these different haemoglobins into a series of genetically heterogeneous classes<sup>10</sup>. However, sequential electrophoresis allowed 17 of 20 mutant haemoglobins<sup>11</sup> to be distinguished. This method has now been used on several enzyme systems in *D. pseudoobscura* and *D. melanogaster*<sup>12-15</sup>. Some, but not all, loci have shown a great increase in the extent of their genetic polymorphism. The locus coding for aldehyde oxidase, which was previously thought to have very little genetic variation, is now revealed to possess 16 alleles, while that for esterase-5 increases from 13 to 32. Hexokinase-1 and octanol dehydrogenase show almost no increase in the number of alleles when the new methods are applied. There are no obvious associations between the extent of this newly discovered polymorphism and the enzyme's molecular weight or biochemical function.

These improvements in technique have greatly altered our view of molecular polymorphism. On the one hand there exists a class of structural proteins which are almost invariable, while on the other at least some soluble enzymes show a very high level of genetic variation. This observation accords well with the latest predictions of theoreticians who feel that most molecular polymorphism is not actively favoured by natural selection. The recent models of Kimura<sup>16</sup> and of Ohta<sup>17</sup> incorporate weak natural selection acting against slightly deleterious mutations but

suggest that most mutants have almost no effect on the fitness of their carriers. Structural proteins are highly invariant as they are closely interlocked with each other and have a low tolerance to mutations which change their shape. Any mutants are removed by natural selection. Membrane-bound enzymes are also quite dependent on accurate steric relations with other molecules in the membrane and can thus tolerate only a small amount of polymorphism. Soluble enzymes such as xanthine dehydrogenase, however, are subject to few such constraints; most of the changes in amino acid sequence which result from mutation have no effect on the molecule's function and persist for a period which depends only on the accidents of sampling. Animals which maintain large populations will accumulate very many alleles at such loci, and there is no need to argue that each protein polymorphism is actively maintained because of its biologically useful role.

On previous estimates, *D. pseudoobscura*'s sibling species *D. persimilis* appeared to possess three *Xdh* alleles, two of which were shared with *D. pseudoobscura*<sup>5</sup>. Their close resemblance had been used to suggest that the polymorphism was conserved by natural selection even after speciation. However, when this locus was examined using sequential electrophoresis, 23 alleles were found in a sample of 60 *D. persimilis* genomes<sup>18</sup>. Only three of these are shared with *D. pseudoobscura*, and only one is at all common in both species. The two species, although closely related, have therefore diverged almost completely at this locus since gene exchange was interrupted by speciation. It seems more reasonable to interpret this difference as resulting from a balance between the random origin and extinction of selectively equivalent alleles within each species than to postulate that *pseudoobscura* and *persimilis* (which often occur in the same place) are subject to a completely different set of selective forces.

The existence of the patterns of genetic variation discussed here is not in itself a proof that natural selection is unimportant in maintaining molecular polymorphism. There is experimental evidence for differences in the fitness of electrophoretic alleles at some enzyme loci<sup>19-21</sup> and it is possible that even the dozens of alleles now known to exist may each be found to respond to natural selection, or that new theoretical treatments will show how such extensive polymorphism may be selectively maintained. However, the new data on molecular polymorphism and the cloning a polymorphic enzyme locus in *D. pseudoobscura* into *Escherichia coli*<sup>22</sup> (which may enable large quantities of purified enzyme protein to be produced for further analysis of hidden genetic variation) show that — as so often before in the study of evolution — the experimental cat is among the theoretical pigeons. □

1. Brown, W.M. *Proc. natn. Acad. Sci. U.S.A.* **77**, 3605 (1980).
2. Kan, Y.W., Lee, K.Y., Furbetta, M., Angius, A. & Cao, A. *New Engl. J. Med.* **302**, 185 (1980).
3. Powell, J.R. *Evol. Biol.* **8**, 79 (1975).
4. Kimura, M. & Ohta, T. *Nature* **229**, 467 (1971).
5. Prakash, S. *Proc. natn. Acad. Sci. U.S.A.* **62**, 778 (1969).
6. Edwards, Y. & Hopkinson, D.A. *Nature* **284**, 511 (1980).
7. Singh, R.S., Hubby, J.L. & Throckmorton, L.H. *Genetics* **80**, 637 (1975).
8. Cobbs, G. *Genetics* **82**, 53 (1976).
9. Singh, R.S., Lewontin, R.C. & Felton, A.A. *Genetics* **84**, 609 (1976).
10. Fuerst, P.A. & Farrell, R.E. *Genetics* **94**, 185 (1980).
11. Ramshaw, J.A., Coyne, J.A. & Lewontin, R.C. *Genetics* **93**, 1019 (1979).
12. Singh, R.S. *Genetics* **93**, 997 (1979).
13. Beckenbach, A.T. & Prakash, S. *Genetics* **87**, 743 (1977).
14. Coyne, J.A., Felton, A.A. & Lewontin, R.C. *Proc. natn. Acad. Sci. U.S.A.* **75**, 5090 (1978).
15. Buchanan, B.A. & Johnson, D.E. *Genetics* **94**, 13 (1980).
16. Kimura, M. *Proc. natn. Acad. Sci. U.S.A.* **76**, 3440 (1979).
17. Ohta, T. *Theoret. Pop. Biol.* **10**, 254 (1976).
18. Coyne, J.A. *Genetics* **84**, 593 (1976).
19. Clarke, B. *Genetics* **79**, 101 (1975).
20. Barker, J.S.F. & East, P.D. *Nature* **284**, 166 (1980).
21. De Jong, G. & Scharloo, W. *Genetics* **84**, 77 (1976).
22. Yardley, D.G., Kline, E.L., Chernin, M.I., West, R.W. & Rodriguez, R.L. *Genetics* **94**, 113 (1980).

# Flat-spectrum radio sources: victims of a conspiracy?

from Alan P. Marscher

IN early surveys of the radio sky, taken at wavelengths in the 100-metre range, radio astronomers found that most extragalactic radio sources appear very similar to one another. These objects, identified with radio galaxies and quasars, exhibit spectra which have steep negative slopes, that is the radio flux decreases sharply with increasing frequency. However, later surveys performed at centimetre wavelengths yielded a large number of so-called 'centimetre-excess' objects whose spectral slopes are positive, zero, or undulating. K. I. Kellermann and I. I. K. Pauliny-Toth (*Astrophys. J. Lett.* **155**, L71; 1969) interpreted this to be the result of a superposition of several discrete, compact components, each of which exhibits a turnover in its spectrum at a given wavelength below which the synchrotron emission is self-absorbed. Subsequent observations with very-long-baseline interferometers (VLBI) confirmed that these centimetre-excess sources are indeed very compact, with angular sizes often smaller than 0.001 arc s.

The difficulty with the superposition hypothesis lies in the large number of radio sources whose spectra are both quite flat and rather smooth. A random distribution of several self-absorbed components should yield a much larger percentage of undulating spectra than are observed (D. B. Cook & S. R. Spangler *Astrophys. J.*; in the press). This situation has led several authors to suggest that the flat-spectrum sources are produced by a single component whose magnetic field and relativistic electron density decrease with distance from the centre. In this way, a single, inhomogeneous component mimics the spectrum emitted by an infinite distribution of concentric, uniform components and produces a smooth, flat

spectrum (J. J. Condon & L. L. Dressel *Astrophys. Lett.* **15**, 203; 1973).

One such flat-spectrum radio source, the BL Lacertae object PKS0735 + 178, was suggested by A. P. Marscher (*Astr. J.* **82**, 781; 1977) to be a prime candidate for a study to determine which point of view is correct. Its radio spectrum in 1977 was, to within observational errors, perfectly flat over more than two decades of frequency. It was suggested that multi-wavelength VLBI observations would allow one to differentiate between models involving multiple, uniform components and those invoking a single, tapered component.

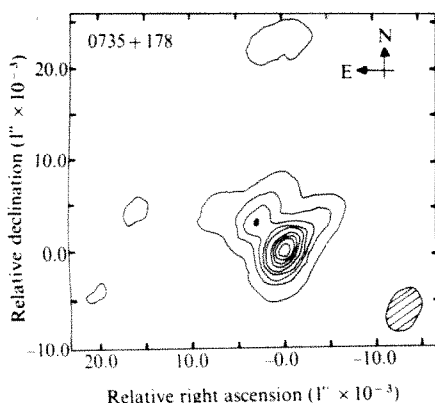
Several groups have performed these critical observations, and the results are now being published. W. D. Cotton *et al.* (*Astrophys. J. Lett.* **238** L123; 1980) have obtained VLBI observations of PKS 0735 + 178 at four wavelengths — 2.8, 3.7, 11–13 and 50 cm. Although their data at any given wavelength are rather limited, they do, in fact, clearly indicate that this radio source is composed of several distinct, compact components, in line with the superposition hypothesis of Kellermann and Pauliny-Toth. Other observers have obtained more detailed data at various frequencies, with a general picture of the source which basically agrees with the Cotton *et al.* interpretation (A. P. Marscher & D. B. Shaffer *Astr. J.* **85**, 668; 1980; L. B. Bååth *et al. Astr. Astrophys.*; in the press). Of particular interest are the detailed 6-cm observations of Bååth *et al.* (see Fig. 1). These authors find that the structure of PKS0735 + 178 is rather complex, consisting of two compact components plus a more diffuse, jet-like feature extending past the weaker hotspot. In addition, there is a weak, even more diffuse, resolved emission region. Thus, as Cotton *et al.* remarked, this flat-spectrum

radio source seems to be the result of a 'cosmic conspiracy' of several compact components which, when superposed, manage to produce a smoothly varying, flat spectrum.

An important clue to the resolution of this conspiracy might lie in the remarkable similarity in appearance of the radio maps of PKS 0735 + 178 and the two well studied objects 3C273 and 3C345 (A. C. S. Readhead *et al. Astrophys. J.* **231**, 299; 1979). All three sources contain a bright, unresolved component, with a jet-like feature emanating to one side of this hotspot, plus one or more 'knots' of enhanced emission embedded in the jet. R. D. Blandford and A. Königl (*Astrophys. J.* **232**, 24; 1979) have interpreted the bright, unresolved component to be the narrow end of a synchrotron-emitting plasma beam, the fluid in which is moving relativistically. The more diffuse jet is then just the fanned-out extension of this beam (which we are viewing nearly end-on, since this configuration enhances the brightness, making such a source more likely to appear in a flux-limited survey of radio sources). The secondary knots are formed through either some instability in the beam or interaction with cooler gas which the beam encounters. If this picture is correct, one would expect all of the components to be physically associated, having been created one way or another by the relativistic beam. The beam itself is smoothly inhomogeneous, with density and magnetic field strength decreasing as the beam widens. Components appearing downstream might then be related by some simple scaling law to those observed upstream. The beam might thus be capable of modulating the physical parameters of the various components in the source such that they 'conspire' to emit a smooth, flat radio spectrum.

Since the beam is smoothly inhomogeneous, the size of the component at its narrow end should appear to increase with wavelength (see A. G. de Bruyn *Astr. Astrophys.* **52**, 439; 1976; A. P. Marscher *Astrophys. J.* **216**, 244; 1977). This should cause the separation between the bright, unresolved hotspot and secondary knots to decrease somewhat with wavelength. Further detailed multi-wavelength VLBI observations should be capable of determining whether this is, in fact, the case, and thereby test the model.

Finally, it is worthwhile noting that the two objects whose radio structures closely resemble PKS0735 + 178, 3C273 and 3C345, both exhibit rapid changes in the separation of their components. If the distances to these quasars are determined through a cosmological interpretation of the optical redshifts, using a standard



**Fig. 1** Radio map at 6 cm of the compact core of PKS0735 + 178. Easily spotted on the map are the bright, unresolved component, the secondary, compact knot to the north-east, and the more diffuse jet, also extending to the north-east. The larger, diffuse component is resolved out on this scale and hence does not appear. From Bååth *et al.* (*Astr. Astrophys.*; in the press).

Alan P. Marscher is a Postgraduate Research Physicist at the Center for Astrophysics and Space Sciences, University of California, San Diego.



Friedmann cosmology, the observed angular velocities of separation correspond to speeds far in excess of the speed of light (see M. H. Cohen *et al.* *Nature* **268**, 405; 1977). The relativistic beam model mentioned above can explain this phenomenon as a consequence of shortened observed arrival intervals of successively emitted wave fronts. This is caused by the motion of the emitting plasma, which approaches

the observer almost as rapidly as do the radio waves (see M. J. Rees *Nature* **211**, 468; 1966). From the above discussion, one can therefore predict that PKS0735 + 178 should also be engaged in such 'superluminal' expansion. Further VLBI monitoring of this source should allow radio astronomers to test this prediction and thereby increase our understanding of compact radio sources. □

## Hot foot

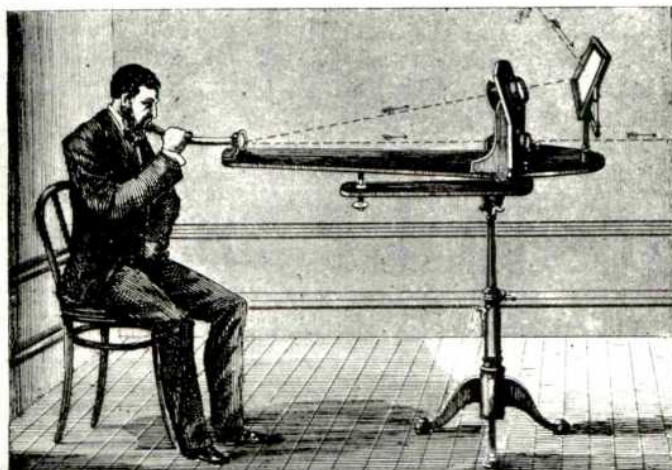
from Clive Lloyd

CONSIDERING its location at the boundary between cell and environment, it is not surprising that the fibroblast's focal adhesion plaque or 'foot' has become a fashionable meeting point for a whole gaggle of animal cell biologists. The reasons for investigating the foot by interference reflection microscopy are diverse — the study of microfilament bundle attachment, cell locomotion,

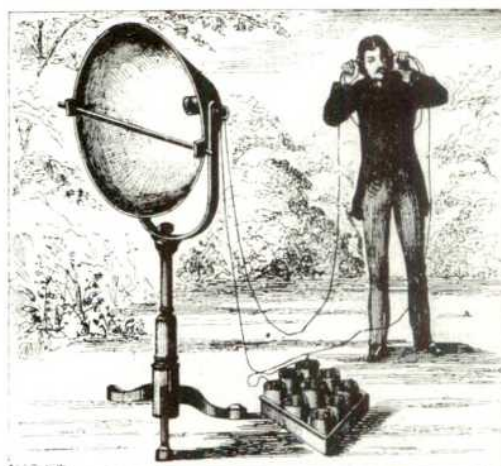
morphology and virus infection — but in coming together at this site, these studies raise universal issues of cell behaviour and growth control.

In a previous article (News & Views *Nature* **279**, 473; 1979), it was reported that extracellular fibronectin and cytoplasmic microfilament bundles had been seen to be co-linear across the membrane suggesting that  $\alpha$ -actinin provided the linkage between

microfilament and membrane in such an assembly. However, research moves so quickly in this field that, already, several refinements are required of this model.  $\alpha$ -actinin does not seem to occur sufficiently close to the dense plaque of epithelial *zonulae adherentes* junctions for it to be the mediator of actin's linkage to the membrane (Geiger *et al.* *Proc. natn. Acad. Sci. U.S.A.* **76**, 2833; 1979). Further work is required to define its location as it is detected within analogous focal adhesion plaques isolated from the cell body (Badley *et al.* *Expl. Cell Res.* **117**, 231; 1978; Rohrschneider & Shriver *Eur. J. Cell Biol.* **22**, 521; 1980). The current view seems to be that  $\alpha$ -actinin collects actin microfilaments laterally to form bundles — a function also tentatively assigned to a new 130 K protein first found as a contaminant in preparations of gizzard  $\alpha$ -actinin. When used to stain cultured chicken cells, antibodies raised against this protein (Geiger *Cell* **18**, 143; 1979) produce a punctate pattern at the ventral surface. These sites turn out to be focal adhesion plaques and Geiger concludes that "the 130 K protein plays a more direct role than either  $\alpha$ -actinin or tropomyosin in the association of actin filaments with the cell membrane". In addition, the protein has been shown to terminate microfilament



The articulating photophone. The transmitter.



The selenium receiver.

## 100 years ago

### BELL'S PHOTOPHONE

By the courtesy of Prof. Graham Bell we are at length able to do somewhat ampler justice to his latest discovery than has hitherto been possible. He has supplied us with certain details not hitherto published, and has also furnished us with drawings of his apparatus and experiments.

Our readers are already aware that the object of the photophone is the transmission of sounds both musical and vocal to a distance by the agency of a beam of light of varying intensity; and that the first successful attempts made by Prof. Bell and his co-labourer, Mr. Sumner Tainter, were based upon the known property of the element selenium, the electric resistance of which varies with the degree of illumination to

which it is exposed. Hence, given a transmitting instrument such as a flexible mirror by which the vibrations of a sound could throw into vibration a beam of light, a receiver consisting of sensitive selenium forming part of an electric circuit with a battery and a telephone should suffice to translate the varying intensities of light into corresponding varying intensities of electric current, and finally into vibrations of the telephone disk audible once more as sound. This fundamental conception dates from 1878, when in lecturing before the Royal Institution Prof. Bell announced the possibility of hearing a shadow fall upon a piece of selenium included in a telephone circuit. The photophone, however, outgrew the particular electrical combination that suggested it; for not the least of the remarkable points in this research is the discovery that audible vibrations are set up in thin disks of almost every kind of material by merely throwing upon them an intermittent

light. Hence in theory, if not in practice, the receiver may be reduced to the divine simplicity of a mere disk of vulcanite or of zinc; on one side of which the listener listens.

We may classify the forms of photophone under two heads, as (1) articulating photophones, and (2) musical photophones; the former being able to transmit speech because they work by beams of light whose intensity can vary in undulatory fluctuations, like those of vocal tones; the latter being able to transmit simple musical tones only, since they work by mere interruptions of a fixed beam of light. The greatest distance to which articulate speech has yet been transmitted by the selenium-cell-photophone is 213 metres, or 233 yards.

Whatever be the future before the photophone, it assuredly deserves to rank in estimation beside the now familiar names of the telephone and the phonograph. From *Nature* **23**, 4 November, 15, 1880.



bundles (in a study which suggests a relationship between the 130 K protein, fibronectin and microfilament bundles, Burridge & Feramisco *Cell* **19**, 587; 1980), and is found at three varieties of tissue junction (Geiger *et al. Proc. natn. Acad. Sci. U.S.A.* **77**, 4127; 1980) and at broad areas of close contact between cultured rat myotubes and glass coverslips (Bloch & Geiger *Cell* **21**, 25; 1980). Its characteristics do not, however, suggest it to be of the integral type which could span the membrane. In fact, it is reported to be virtually nonexistent in isolated HeLa plasma membranes which do contain actin (Burridge & Feramisco *Eur. J. Cell Biol.* **22**, 350; 1980) — properties which hint at a role for the 130 K protein in consolidating microfilaments into bundles rather than linking them to membranes.

This leaves open the question of what actually links actin to the membrane. There are doubts, too, about whether fibronectin is the extracellular limb of the trans-membranous assembly. EM sections had shown that actin microfilaments and fibronectin fibrils are co-linear and come very close to touching across the membrane (Hynes & Destree *Cell* **15**, 875; 1978; Singer *Cell* **15**, 675; 1979). Fibronectin is also found to be concentrated at isolated feet (Badley *et al. Expl Cell Res.* **117**, 231; 1978). Now, by taking double exposures of immunofluorescence (to reveal fibronectin) and interference reflection (to reveal focal adhesion plaques), Birchmeier *et al. (Proc. natn. Acad. Sci. U.S.A.* **77**, 4108; 1980) demonstrate that fibronectin is absent from the foot. Geiger reports a similar conclusion (*Eur. J. Cell Biol.* **22**, 350; 1980). An obvious distinction can be made between the techniques that have localized fibronectin at the foot and those that have not — the former either slice or isolate the target site whereas the latter rely on the ability of antibodies to penetrate stable adhesion plaques borne upon whole cells. Questions of accessibility are bound to be prominent in the coming debate.

In attempting to dissect the molecular anatomy of cell/substratum interactions, there is a natural preoccupation with the foot and its attendant musculature but this is not the only relationship that a cell strikes with the substratum. Fibroblasts which migrate out from pieces of embryonic chick heart are highly motile but this locomotion is based on the formation of the broad, unfocused and transient close contacts which are associated with a diffuse actin meshwork (Couchman & Rees *J. Cell Sci.* **39**, 149; 1979; see also, Abercrombie *et al. Expl Cell Res.* **67**, 359; 1971; Badley *et al. J. Muscle Res. & Cell Motility* **1**, 5; 1980). It is some time later (24–48 h) that the migrating cells become stationary and form the more stable focal adhesion plaques which terminate stress fibres. This conversion from the motile to the sessile condition also coincides with a metamorphosis from polarized to polygonal shapes, a greater abundance of fibronectin and exit

from post-mitotic arrest into the division cycle. Microfilament bundles and feet are therefore not essential for motility and the suggestion is that they set-up cells for anchorage-dependent growth rather than to facilitate movement. This agrees with findings that anchorage-dependent mouse fibroblasts, which had been maintained in suspension, require to re-attach and spread in order to restore DNA synthesis, rRNA synthesis and mRNA production, whereas attachment alone restores only protein synthesis (Ben-Ze'ev *et al. Cell* **21**, 365; 1980).

Observations such as these touch a nerve that runs through much of the fascination with the cytoskeleton: that the way in which it is organized relates to the state of cell growth. It is precisely here that the *src* gene could prove to be an effective probe by disentangling growth control from contact behaviour. This gene of Rous sarcoma virus is responsible for transforming the morphology, motility, metabolism and growth regulation of avian and mammalian cells (Hanafusa in *Comprehensive Virology* **10**, 401, eds Fraenkel-Conrat & Wagner, Plenum, New York; 1977). In order to understand this cluster of responses, it is clearly important to determine the gene product's site of action. That a target for the *src* gene product is the cytoskeleton was suggested by McClain *et al. (Proc. natn. Acad. Sci. U.S.A.* **75**, 2750; 1978) on the basis that dissolution of microfilament bundles occurred within 30 minutes of the microinjection of cytoplasmic extract derived from virus-infected cells. The gene product is now known to be a 60,000 dalton phosphoprotein — a kinase termed pp60<sup>src</sup> which phosphorylates proteins at tyrosine (see Hunter & Sefton *Proc. natn. Acad. Sci. U.S.A.* **77**, 1311; 1980). From its recently determined nucleotide sequence and its association characteristics with plasma membrane preparations (respectively, Czernilofsky *et al. Nature* **287**, 198; 1980; Courtneidge *et al. Proc. natn. Acad.*

*Sci. U.S.A.* **77**, 3783; 1980), it is believed to be embedded in the membrane with its protein kinase activity accessible at the cytoplasmic face. In the light of this, its detection (Rohrschneider *Proc. natn. Acad. Sci. U.S.A.* **77**, 3514; 1980; see Fig. 1) at focal adhesion plaques is highly intriguing since its occurrence there places it at the heart of the adhesion/motility/morphology syndrome. With anti-serum specific to pp60<sup>src</sup>, Rohrschneider detected a speckled pattern of staining on the ventral surface of RSV-transformed rat kidney cells — a pattern which coincided exactly with the distribution of feet (and not with the broader close contacts). The protein kinase was also found in isolated focal adhesion plaques but only from cells infected with the temperature-sensitive mutant when maintained at the permissive temperature; not from cells maintained at the non-permissive temperature at which infected cells appear normal. Since the focal adhesion plaque itself (as distinct from associated microfilament bundles) is formed at both permissive and non-permissive temperatures, it would appear that the protein kinase does not affect foot formation *per se* but perhaps some microfilament-based activity such as their ability to pack into bundles.

A preliminary report provides an interesting postscript to this by suggesting that within adhesion plaques and cell-cell junctions "pp 60<sup>src</sup> was closely associated with actin,  $\alpha$ -actinin and a 130 K protein" (Rohrschneider & Shriver *Eur. J. Cell Biol.* **22**, 521; 1980).

Perhaps further studies on the foot will help nail the persistent idea that cytoskeletal organization and cell growth share something in common. □

Clive Lloyd is in the Biosciences Division, Unilever Research, Bedford, UK.

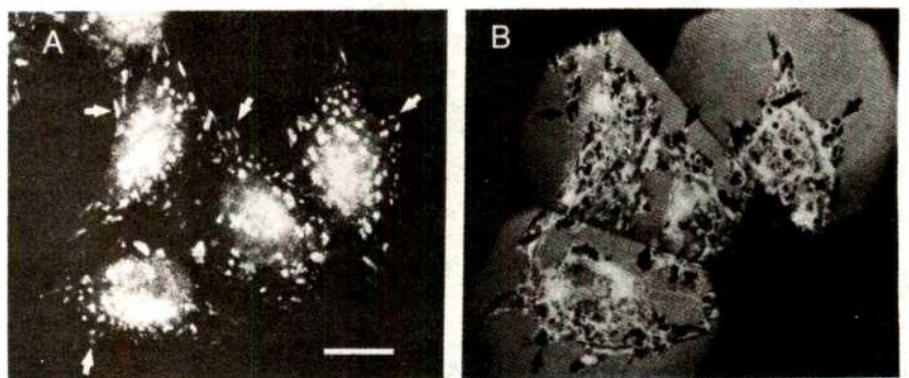


Fig. 1 Comparison of the same NRK cells by immunofluorescence for pp60<sup>src</sup> (A) and interference reflection microscopy (B) demonstrating that the *src* gene product is localized at focal adhesion plaques.



# AUTUMN BOOKS SUPPLEMENT

## Microprocessors and the printed word

There is now a chance that the coming decade will see the flowering of the revolution in communications that the prophets of technology have foretold since the end of the Second World War. Microprocessors, distributed computer facilities and the like offer powerful ways of storing and handling information. Novel kinds of communications channels promise widespread access, flexibility and low cost. Means of turning electronic representations of information into forms that can be read by human eyes and processed by human nervous systems become more versatile as the years go by. The chances that these devices will be welded fruitfully together in the 1980s are greater than in previous decades. It is, of course, far too soon to be certain how the decade will turn out. A severe and probably prolonged economic recession throughout the industrialized West is hardly the best time for launching a major revolution of technology. Lack of capital may yet frustrate the plans being laid for the new communications technology. Yet it is only prudent that people should be asking what will be the consequences of the promised changes. Already there is a vigorous if somewhat shapeless debate about the consequences for employment: will there be more of it, or less? That argument is likely to grumble on, unresolved, for many years to come. What of more specific questions such as the consequences of the new technology for communication in science and technology? In particular, are the days of the conventional journals numbered?

This is one of the questions raised by a study, now published, carried out by the Primary Communications Research Centre at the University of Leicester. (*New technology and developments in the communication of research during the 1980s*, obtainable from the centre at £2.50 within the UK, £3.00 elsewhere.) For what it is worth, the report of the study appears on ordinary paper. The type has been set by pointing cameras at sheets of typewritten paper. Distribution is conventional, by post. Clearly those who pave the way for revolutions must conduct themselves conventionally for a time, as John the Baptist discovered to his cost.

Indeed, the report of the Leicester group, led by Professor Jack Meadows, is largely a sketch of what the future may bring in the communication of information in science and technology. It is a survey of the options that may open up, not a prescription for a preferred course of development. That, too, is seemly. For in the end, the ways in which scientists communicate with each other will be determined by what they want to do.

It is not, however, too soon to think of what the future may be like. The most radical revolution of the scientific literature rejoices in the name of the "electronic journal". The idea is simple. Somewhere there is a computer system capable of storing scientific articles together with the data, in tabular form, as graphs and photographs. People wishing to submit articles for "publication" merely arrange that the text of their contribution is fed into the system. At some stage, human editors must intervene, if only to decide which scientists in which laboratories should be invited to referee which articles, but from that point the process of publication is more or less mechanical. Referees' comments come and go by the same communications system. Authors are invited to amend their manuscripts, and the revised versions are in due course listed in the public file of articles to which all and sundry may have access. Reading a journal will then be simply a process of pressing an appropriate button on a communications terminal to summon up the latest table of contents and then to display whatever articles may be of particular interest.

This version of the future has a number of attractive features. In principle, it is capable of great flexibility. Some readers of some

electronic journals might wish to read the abstracts of all the articles on the file, and could no doubt be satisfied by pressing a few extra buttons – and for an extra charge. The editors of some journals might decide that articles should be available on the network before they have been refereed, so that readers could share with authors the experience of seeing articles take their final form. Some visionaries even dream of schemes in which the whole of some group of interested specialists would be involved in the assessment of each individual's contributions to the literature. The result might be a much greater sense of community, and that the literature of some field of research is truly the collective understanding and the common heritage of those working in it. Such schemes are by no means as fanciful as they sound. Some of the more interesting of the journals in the conventional scientific literature are those in which each article is accompanied by a string of written comments from others with useful things to say about them.

More modest benefits of electronic journals are probably more nearly within grasp. Plainly, there would be great advantages if the same network could provide its users not merely with versions (printed, or electronic) of articles of interest but also with copies of articles cited in the list of references. The utility of such a system will depend critically on the degree to which the literature as a whole accumulates in electronic form. Searches of the electronic literature for relevant contributions not included in the cited references would also be valuable. Electronic versions of the primary journals could be combined in the same network with more advanced versions of the bibliographic files of titles and abstracts that have made a modest contribution to many people's awareness of the scientific literature in the past decade or so. This, however, is yet another benefit that will accrue only when the process of making the literature electronic has absorbed a substantial part of the whole.

The disadvantages of this way of organizing the scientific literature are, unfortunately, less easily identified. Although it is now customary to suppose that computer technology can be adapted to any task whose specification can be defined, experience has shown that computer systems do not always function as smoothly as their designers hope. The development of computer systems which are acceptable to the users of electronic journals, and not just to their designers and editors, will be slow and expensive. The costs of operating and using electronic journals cannot even be guessed at this early stage. The most obvious difficulty is that the initial costs are certain to be very large. Would-be users will have to equip themselves with communications terminals at a cost that far exceeds the annual subscription to even the most high-priced journals.

Even less tangible disadvantages may be more serious impediments to these developments. Even within the scientific community, people are conservative in their habits. Browsing through the scientific literature, not necessarily in a single narrow field, is not merely pleasurable but educative and stimulating. Will the communications terminals of the future lend themselves to such a practice? But people also appear to like carrying their favourite journals around with them, reading them at home or on some journey. Will a sheaf of hard-copy paper produced by a communications terminal serve the same purpose? People are, in short, attached to the printed word in its familiar form. Those who are now planning electronic journals are no doubt aware of the subtlety of the needs they have to satisfy. Defining them, however, will be a formidable undertaking. Experience may yet show that they cannot be met.

# The ecology of mental process: a life of Gregory Bateson

Edmund Leach

*Gregory Bateson: The Legacy of a Scientist.* By David Lipset. Pp. 360. (Prentice-Hall: 1980.) \$16.95, US only.



Gregory Bateson, 1958

MARGARET Mead died in November 1978, Reo Fortune in November 1979, Gregory Bateson in July 1980. The conjunction of these three most unusual anthropologists in New Guinea at the end of 1932 drastically restructured their private lives. Mead, who was then married to Fortune, was later married to Bateson for 14 years. The consequences for scholarship are still difficult to assess. Fortune ceased altogether to be an effective anthropologist; Mead became an international celebrity, mainly by virtue of highly impressionistic, easy to read, accounts of field research which had already been completed when she first met Bateson. Bateson's principal contribution to anthropology, the awkwardly complex but highly original *Naven* (1936), was also based on fieldwork that had been completed by late 1932, and which was written up in Cambridge before his marriage to Mead. But although it is a very different sort of book from anything that

either Mead or Fortune might have written, it would probably never have been written at all without their stimulus.

In 1936 the dominant style in British anthropology was the extreme empirical functionalism adopted by Malinowski and his pupils, Raymond Firth and Audrey Richards. Bateson, while declaring his respect for the work of this school, also argued that the best ethnography has the artistic merits of a great novel. In his opening pages he invoked the names of Jane Austen and Charles Doughty's *Arabia Deserta*.

*Naven* was an attempt to capture what Bateson called the ethos of Iatmul culture rather than simply to describe, in Malinowskian manner, how everything fitted together. The general attitude to ethnographic evidence which Bateson adopted, which was made to seem quite unnecessarily obscure through his mode of presentation, had much more in common with the later work of Evans-Pritchard and of Lévi-Strauss than it had with then current fashions. But although *Naven* was ridiculed at the time by Malinowski, along with Mead's *Sex and Temperament in Three New Guinea Societies* and Benedict's *Patterns of Culture*, it was a book that was read with great interest by Malinowski's younger pupils, as I can vouch from my experience.

Bateson usually described himself as an anthropologist, but he also had polymathic interests in such fields as animal behaviour, cybernetics and the psychology of schizophrenia. His enduring reputation, which may well prove to be very considerable, is likely to derive as much from these other interstitial activities as from his direct contributions to anthropology.

Lipset's biography, which was published a few weeks before Bateson's death, is a brilliant performance. He had the full collaboration of Bateson himself and of all members of his entourage, including access to family papers and letters, but many of the most interesting passages in the book derive from the personal recollections of those who had known Bateson and whose opinions, as expressed in unstructured interviews, were recorded by Lipset on tape. A great variety of people collaborated in this way, including both Mead and Fortune, and the author has shown astonishing skill and tact in deducing, from what must often have

seemed very contradictory and prejudiced evidence, a balanced account of the life and intellectual development of a man whose persistent curiosity about matters which most of us take for granted sometimes came close to genius.

Bateson's family background was academic Cambridge in high degree. His grandfather, W. H. Bateson, was master of St John's College from 1857 to 1882; his father, William Bateson, was the celebrated zoologist whose renown stemmed from his pugnacious vindication of the genetics of Mendel against the statistical biometrics of Weldon and Pearson. William Bateson invented much of the technical language of modern genetics including the word "genetics" itself. Gregory was clearly greatly influenced by his father; indeed his first publication was a joint-authorship contribution to the *Journal of Genetics* "On certain aberrations of the red-legged partridges . . ." (1926), published when Gregory was 22.



William Bateson, July 1907

But Gregory's intellectual heritage was not restricted to biology. It was William Bateson who first introduced Geoffrey Keynes to the art of William Blake, a field in which Sir Geoffrey, at the age of 93, is



now an acknowledged world authority. This was an enthusiasm which Gregory shared and which is somehow reflected in much of his later work. But probably the most important influences on Bateson's thinking came from his close friend C. H. Waddington, the Edinburgh geneticist. Gregory never adopted the Marxist view of science favoured by Waddington, but he did share many of the latter's humanist concerns. What these concerns were is summed up in the titles of Gregory's last two substantial publications, an essay collection, *Steps to an Ecology of Mind* (1972), and *Mind and Nature: A Necessary Unity* (1979), the latter written at a time when Gregory was fully aware that he was suffering from terminal cancer.

Gregory was not a vitalist; he saw very clearly that the scientific explanation of human behaviour must be of essentially the same kind as the scientific explanation of the behaviour of dolphins. But he was too good a cultural anthropologist to be taken in by the kind of reductionism that is favoured by some of the more simple-minded sociobiologists. The human mind cannot be explained away either as a genetically pre-programmed machine or as an illusory side effect of conditioned reflexes.

Gregory's interests always remained biological; but the focus of his attention was not confined to the human being as a biological organism. It was Man in his social interactions and Man as a species adapted to extremely sophisticated forms of interpersonal communication that provoked his most challenging suggestions. But they were suggestions rather than proven facts. His theories about the nature of schizophrenia and about "the double bind" influenced a wide variety of practising psychotherapists, but they were often misunderstood and they were not of a sort which lend themselves to verification.

Academically he was always a loner; he seldom occupied any position which called for formal teaching. He exercised his influence in private informal seminars and conference discussions and it is difficult to pin down just what that influence was. Gregory was a guru. I know that I myself found him one of the most exciting and inspiring "teachers" I have ever met.

Gregory himself would probably have claimed that his main claim to fame was his application of ideas borrowed from cybernetics to an understanding of the feedback which occurs in person to person interactions. But what he had to say on such matters often contained a good deal of blarney; he had a scientific attitude, but he was not an exact scientist and he was not a mathematician.

Lipset recognizes these limitations. Inspired in his youth by the art of Blake and the laws of Mendel, Gregory aspired to make comparable innovations. He did not succeed, but his contributions to our understanding of the position of mind in



From left: Gregory Bateson, Margaret Mead, Lois Bateson and Barkev Kasarjian

the physical world and to the complex relationships which link form and process are far from negligible.

There is much more to Lipset's book than I have been able to summarize here. The account of the intellectual atmosphere

in which Gregory grew up is particularly impressive. The book as a whole makes a most timely and fitting memorial. □

Edmund Leach is a Fellow of King's College, Cambridge.

## Beveridge on discovery

P. B. Medawar

*Seeds of Discovery.* By W.I.B. Beveridge. Pp.130. (Heinemann/W.W. Norton: 1980.) Hardback £6.95, \$12.95; paperback £3.90.

THIS book is a sequel to the author's lively and readable *The Art of Scientific Investigation* (Heinemann, 1957). *Seeds* is readable too — not least because of the wealth of anecdotes and other illustrative material which help the author to make his points; it is a learned man who will learn nothing from Beveridge's pages. Amidst much that is familiar I was very interested to learn that a former Vice President of the National Academy of Sciences had published a demonstration that flight by heavier-than-air machines was not possible.

The present book is not nearly such a success, unfortunately; it is not very original and is in places lamentably trite. Nowhere was I struck, as one always hopes to be, by some felicity of thought or writing. Indeed, I found myself in the disagreeable position of having reason constantly to find fault. As to triteness, consider such a passage as this:

Scientists do not work in isolation. All are members of the world-wide scientific community. It is joined together by

communication through scientific journals and meetings, which are an essential part of science. Formal and informal discussions at scientific meetings, sometimes involving conflict of views and arguments, are a feature of the scientific life.

This is the writing of someone who has nothing very original to say.

The book throughout has a slightly aggrieved and truculent air arising mainly out of the very low opinion Beveridge holds of philosophers of science, whom he accuses of trying to foist on us the notion that scientists operate something that might be called 'the scientific method' — the existence of which, as he rightly says, is a myth. Of the leading philosophers of science, however, it was only Francis Bacon and John Stuart Mill who put before the public an integral body of thought — an organon — that could pass as an exposition of 'the scientific method'. Popper did not, nor did Kuhn. Among Beveridge's many causes of complaint is that philosophers of science have "failed to appreciate the cardinal role that chance and opportunism play in research, and most have dismissed the subject as hardly worthy of their serious consideration".



But what form could such a consideration take? If the story of the remarkable conjunction of events that led to the discovery of penicillin were recounted to a philosopher, what could he say except "Why, gee, what amazing strokes of luck!". If Beveridge himself were a little more philosophical about the matter, he would see that there is an inherent bias in our estimate of the contribution of good fortune to scientific research: we can all recognize when good fortune leads to a discovery or enlarges the understanding, but from the very nature of things we cannot know how often bad luck deprives us of the chance of making a discovery we might otherwise have made.

The most interesting paragraphs in Beveridge's book are those in which he deals with various expedients for promoting the flow of original ideas. Not all are convincing: the more I read and reflect upon the virtues of 'lateral thinking', the more I wonder what all the fuss is about. To be sure, we should all try to be adventurous in our thinking and try to get out of familiar ruts; but this is advice such as Polonius might have given — it cannot come to anyone as a revelation.

Beveridge criticizes Popper, as others have, for failing to throw much light on the process of ideation — the process by which new hypotheses come into being. Popper rebuts this charge perfectly adequately by pointing out that his work is mainly upon the logic of scientific discovery, and that ideation is outside logic and is a logically unscripted process. However Popper is fully aware of the central importance of having ideas as the generative act in scientific enquiry. In spite of Beveridge's criticisms I believe him to be more indebted to Popper than he realizes. In his final chapter, for example, he is clearly feeling his way towards the concept that Popper embodied in the notion of a 'Third World' (Popper's *Third World*; see *Nature* 241, 293; 1973), though Beveridge clothes it in the tiresome terminology of 'hardware' and 'software' — an inappropriate terminology in this context because many ideas and conceptions are embodied in hardware such as machinery, buildings, institutions and so on.

One of the passages in which Beveridge seems to lack philosophic understanding is that in which he deals with frauds. In recounting the Piltown hoax, brought up to date by incorporating Stephen Jay Gould's suggestion that the principal conspirator was none other than Teilhard de Chardin, he says that its main interest is to show "that even the scientific Establishment can be fooled by evidence that in retrospect is seen to be an obvious fake"; but does not Beveridge realize that science, like banking and government and — if that wise man Kenneth Clark is to be believed — civilization itself, rests upon confidence. When we go about our business we do not expect our colleagues and coworkers to be liars; nor do we

scrutinize their statements with wary circumspection, in the manner of men on their guard. If we did so there would be no scientific business to transact. In going on to describe Paul Kammerer's fraud, Beveridge says Kammerer's views on the nature of inheritance were quite incompatible with those of neo-Darwinists "who believed that evolution was due solely to the selection of chance mutations that favour survival". This is a travesty of neo-Darwinism, but it would take too long to explain why.

Accounts of the Summerlin scandal and the fraud implicating Sir Cyril Burt pad out the book readably, but their inclusion may give a rather distorted picture of science to the young scientists who are among those to whom the book is addressed. I surmise — for there can be no proving such a statement — that for every scientist who fiddles his results there are a thousand who do not, and for every scientist who waxes fat on the proceeds of deception a thousand others spend sleepless nights and days of sick anxiety for fear that they have been guilty of a factual misrepresentation — or even, what does not matter nearly so much, of propounding an erroneous hypothesis.

"... most eminent scientists I know do have a lively sense of humour" says Beveridge — a characteristic he chooses to

illustrate by referring to Waddington's witless and disagreeable acronym COWDUNG which stands for 'conventional wisdom of the dominant group'.

Beveridge has some wider views on science in education which I find as difficult to accept as many of those that relate to science itself. He writes that "... it would benefit everybody if the education of scientists included more studies in the humanities ...". I wonder: my own view, as ill-founded as his own, is that the young scientist who has not the initiative and the will to read books or listen to music or visit galleries will be bored out of his mind by lectures of the quality he is likely to receive on subjects such as 'the English novel' or 'the origins of the Romantic movement in Germany'. It would be a different story, of course, if an Ernst Gombrich or Kenneth Clark were to be found on every campus; but what *can* be found on every campus are libraries, radio, television, records and enthusiasts eager to share their enthusiasms — all of which may help to enlarge human sensibilities or human understanding. □

Sir Peter Medawar is Head of the Transplantation Biology Section, Medical Research Council's Clinical Research Centre, Harrow, Middlesex.

## Freudian variations

Stuart Sutherland

*Freud: The Man and the Cause.* By Ronald W. Clark. Pp.652. (Cape/Weidenfeld & Nicolson/Random House: 1980.) £9.95, \$19.95.



Freud was nearly 40 when he began to develop the psychoanalytic ideas for which he is remembered, but even as a youth he was convinced that he would be a famous man. From the age of 21 he periodically tried to destroy all records of his private life in a deliberate attempt to make difficulties for his biographers, each of whom would "be right in his opinion of 'The Development of the Hero'." The latest to take up Freud's challenge is a highly

professional biographer, Ronald Clark, who has already tackled Einstein, J. B. S. Haldane and Bertrand Russell. Fortunately for Clark, Freud's correspondents did not always obey his injunction to destroy his letters and considerable new material has come to light since Ernest Jones wrote the mammoth official biography.

The standard view of Freud's life, as put forward by Jones and other followers, is that he was indeed a hero. They argue that his theories were for long either ignored or derided because of their shocking sexual content, he was denied promotion, he fought with the world in "splendid isolation", and psychoanalysis emerged almost entirely from his own head (or genitals) as a result of his heroic self-analysis. Freud, himself, in his autobiographical writings did everything he could to encourage this view.

In recent years, several scholars have attempted to modify the myth of Freud's heroism. His ideas received considerable support almost from the outset; to the extent to which they were rejected, it was because they were old-fashioned (for example, his attribution of some neuroses to masturbation) or obviously wrong (for example, his belief that many neurotics had been sexually seduced in infancy by an older person). At no time was he isolated from the rest of the scientific community, and many of his ideas were either modifications of existing lines of thought



or were developed in collaboration with others, particularly with Wilhelm Fliess with whom he was in regular correspondence throughout the period when he was developing the basic ideas of psychoanalysis. It is significant that despite their intimacy and the overlap in their work and ideas, Freud does not so much as mention Fliess in his autobiography, and he tried to have his letters to Fliess destroyed. The revisionist view of Freud's career is well summarized by Frank Sulloway in *Freud: Biologist of the Mind* (Deutsch, 1979) which was published too late to be of use to Ronald Clark in writing his own biography.

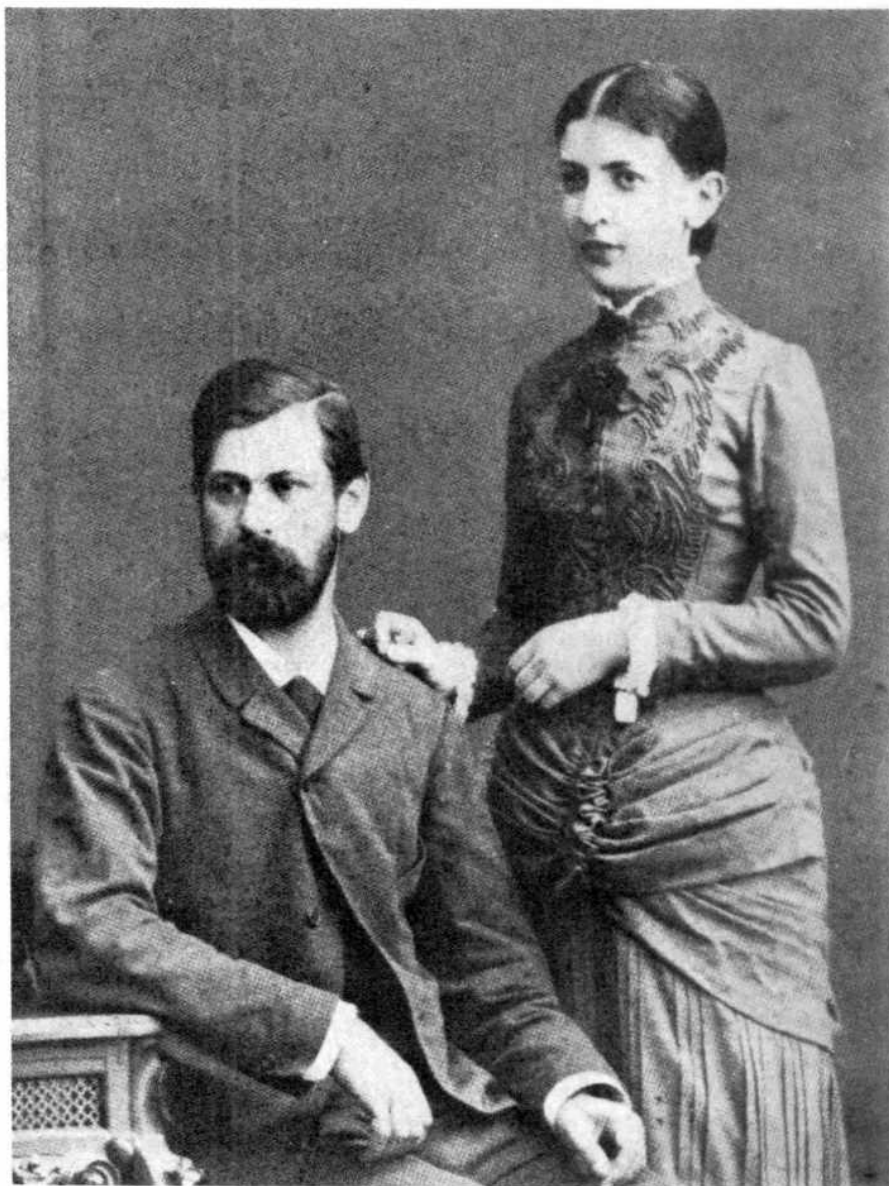
Clark takes a middle-line on these contentious issues. He concentrates on Freud the man rather than on the intellectual content and origins of his work. On Freud's personality there is little new to say. He was often tetchy and intolerant, as when he reproved his wife for talking to strangers in a restaurant. He could be extraordinarily vindictive: although he formed intimate friendships with several men (such as Breuer and Fliess) the friendships did not last and, once they were broken, Freud never forgave. He loudly proclaimed that psychoanalysis was a science, but he treated it as a religion: he was merciless to the many followers who dared to depart from the orthodox doctrine as laid down by himself. On defection, Morton Prince became "an arrogant ass", Magnus Hirschfeld "a flabby, unappealing fellow", and Carl Jung a "megalomaniac" and a "miserable pen-pusher". One wonders how much insight Freud had into his own childishly defensive reactions.

Another of Freud's persistent traits was that he took great delight in annoying others. Of his fiancée's mother, he wrote "I can foresee more than one opportunity of making myself disagreeable to her and I don't intend to avoid them". He stayed away from one neurological congress because "our absence should annoy them and that suits me". It is likely that Freud's failure to achieve rapid academic promotion was caused more by his own prickly personality than by his Jewishness or the unpopularity of his ideas.

His lust for battle and intellectual arrogance polarized opinion on psychoanalysis. He gave those who were not wholly for him no option but to be against. He made matters worse by his reluctance to admit his own mistakes: for example, he did not publicly disavow his infantile seduction theory until many years after he had himself abandoned it.

In contrast to his behaviour with friends, he seems at least in adulthood always to have been generous and kind towards both his immediate family and his more distant relations. But they would appear never to have crossed his wishes and to have treated him as their natural leader.

Perhaps Freud's greatest virtue was courage. In the last 16 years of his life, he had over 30 operations for cancer of the



Freud and Martha Bernays, photographed in Wandsbeck, her home outside Hamburg, in 1885

mouth and had to wear an uncomfortable prosthesis. He bore the pain and danger with the greatest stoicism, continuing both his writing and his clinical work. When it became clear that he was dying, he calmly asked his doctor to put him out of his suffering. In the face of all medical advice, he went on smoking large cigars to the end of his life.

*Freud: The Man and The Cause* records all this and much more, yet at the end of the book most readers will feel that they have not learned what Freud was really like: his own secrecy about himself and his determination to act the part of hero make it difficult to unravel the inner workings of his mind. Moreover Ronald Clark records events, but passes few judgements of his own.

Perhaps wisely, he neither interprets Freud's life in psychoanalytic terms, nor does he derive Freud's psychoanalytic ideas from his life. The clues to the latter problem are tantalizingly few: Freud had a doting mother; as a young man his attitudes towards the opposite sex were

prudish; his friendships with members of his own sex were highly emotional; and he appears to have given up all sexual activity from the age of 41, by which time he was in the midst of his own self-analysis.

Clark describes the elements of Freud's ideas clearly, but at an elementary level: his excellent index contains no reference to such terms as "displacement", "projection", "regression" or "polymorphous perversity". He makes little attempt to evaluate Freud's work and when he does he is often wildly wrong. For example, he attributes recent revisions of psychoanalytic theory to unspecified advances in biochemistry, and quotes with approval Bertrand Russell's silly criticism of Freud's theory of dreams that "we cannot know what a man dreams, but only what he says he dreams": as far as psychoanalytic theory is concerned, it is irrelevant whether the patient has actually dreamt something or merely thinks he dreamt it.

Clark cannot be altogether blamed for his failure to assess the importance of Freud's ideas. Psychologists still know so





Freud (left) with Wilhelm Fliess, his confidant during the early years of psychoanalysis

little about the forces that motivate human action that the ultimate value of Freudian theory cannot be assessed. It is certain only that much of the theory remains vague and that Freud often overgeneralized: his concentration on the libido and the Oedipus complex as the main influences in the development of personality was mistaken. It is doubtful if present-day psychology would be much different had Freud never lived: his main influence has been on the patterns of thought of the layman and hence on much twentieth-century art and culture. Moreover, there are many who feel that Freud sent psychotherapy in a wrong direction, and that it has only recently

begun to recover from the damage done by his ideas. New therapeutic developments are much closer to Adlerian practice than to Freudian.

There are no pyrotechnics in Ronald Clark's new book, but he has made available in one place a mass of previously published material and has added some facts of his own discovery. Although he has not broken the enigma of Freud's personality, he has produced a highly professional biography. □

*Stuart Sutherland is Director of the Centre for Research on Perception and Cognition at the University of Sussex.*

## What is it that we know?

D.V. Lindley

*The Enterprise of Knowledge: An Essay on Knowledge, Credal Probability, and Chance.* By Isaac Levi. Pp.462. (MIT Press: 1980.) \$27.50, £17.

A SUBSTANTIAL part of the knowledge of the world that we have today is the result of the activities of scientists. If knowledge is thought of as a tool by which we may control the world, then scientific thinking is pre-eminent. Artists may help our understanding, but it is scientists who develop the techniques and ideas of control. It is therefore surprising that scientists have paid so little attention to the appreciation of how knowledge is acquired and manipulated. Kuhn has pointed out that most scientific work consists of following through a standard set of techniques, or paradigms, and that the individual is so absorbed in the technicalities of the apparatus, the field, or the mathematics, that he never needs to think about the basis of what he is doing. Other scientists, a small but significant minority, do think more widely but again are

typically not concerned with the nature of knowledge. There are exceptions: for example, Medawar's delightful *The Art of the Soluble* (Methuen, 1967) and, perhaps the most important of all, Harold Jeffreys' *Theory of Probability* (Clarendon, 3rd edn 1961).

There are two groups of people who do think about the knowledge business: statisticians and philosophers of science. The former have developed methods of processing data and reaching conclusions that have gained wide acceptance in some branches of science, so much so that it is scarcely possible to publish a paper without the accepted statistical support. Other scientists pour scorn on statistical methods and regard experiments that require statistical analysis as poor experiments: these are the builders of expensive, laboratory equipment. The philosophers have thought and written a lot about scientific method, and have recently considered the statistical techniques as part of that method.

There is one conclusion that all

statisticians and most philosophers now agree upon: the description of our knowledge, and the way that knowledge is used in control, are essentially probabilistic. There are, however, substantial differences on how probability is to be used and what it means. The accepted paradigm of statistics uses probability only in the sense of frequency, so that we may speak of the probability of the experimental results, which may be repeated, but not of the probability of the hypotheses, which cannot. A minority of statisticians, and perhaps the majority of philosophers, think of probability as a direct descriptor of knowledge, so that probabilities of hypotheses are admitted. Some think of this probability as subjective, some as objective. Here philosophy is providing usable, and — it is to be hoped — useful, results; scientists ought to take note.

In this book, Isaac Levi talks of what he chooses to call credal probability as the way of evaluating hypotheses. Knowledge is thought of, not as a collection of results, but as an input to rational decision-making — "Epistemologists ought to care for the improvement of knowledge rather than its pedigree". The same should be true of scientists. Levi is thus no scholar isolated from practice, but a scholar who is concerned with application as the basis of our thinking. (An appendix discusses the use of his ideas in assessing accident risks in nuclear power plants.)

He therefore disagrees with most statisticians' view of probability as only frequentist — in such situations he talks of "chance" — and devotes a fair portion of the book to a criticism of the methods they have developed, paying special attention to Fisher's concept of fiducial probability, a concept that exerts a fascination out of all proportion to its value. His view is the Bayesian one that probability applies to all uncertainty, not just to repeatable phenomena; so that we can speak of the probability of isolated events, or of hypotheses. What Levi calls a "strict" Bayesian, says this probability is unique and definite, and expresses the totality of our knowledge. In conjunction with utility (which receives little discussion in the book) decisions can be made by maximizing expected utility. Levi does not agree with this uniqueness and admits a set of probabilities. This leads to a difficulty, since the existence of many probabilities leads to many expected utilities, and choice between them has to introduce other considerations. He uses a maximin device in which the worst possible outcome is made as attractive as possible. (It is a pity he does not discuss the objections to maximin that exist, especially as he uses a restricted form of that criterion to which they may not apply.)

Levi writes as a philosopher and the emphasis in his treatment is on the ideas rather than their execution. He discusses at length the related ideas of other



philosophers, especially Kyburg and Hacking who have written on probabilistic ideas and is critical of Popper's appreciation of scientific knowledge. And yet his treatment is often realistic, since it is always set against this decision-making, operational background. Thus he criticizes the adherents of the likelihood view, and Shackle in particular, by saying:

The point is, that calling a mode of appraisal a way of measuring or assessing support is not helpful. A specification of the use or function of the mode of appraisal in inquiry and deliberation is needed, whether the method is probabilistic or not.

This is not an easy book to read. It is very long and parts of it are rather technical. For someone concerned with logical questions, his definitions are not as crisp or as clearly laid out as one might wish. There are many parts where the language is turgid; this is his definition of L-irrelevant:

... the information that a trial is of kind T is L-irrelevant to the issue as to whether an R occurs on that trial relative to information that the trial is of kind S if and only if K contains the information that being of kind T is stochastically irrelevant to yielding an R on a trial of kind S.

A more serious point of style that disturbs me is his failure to help the book's readability by adopting standard notation. For example, experts in the probability calculus use  $p(A|B)$  for the probability of A given B. Why then use  $Q(h;e)$ ? And why use irrelevant instead of independent? Much of the later sections of the book are difficult going because of the apparently unnecessary changes of language and notation.

It is a pity that Levi has so little to say

about works of the "strict" Bayesians, de Finetti, Jeffreys, Savage, Ramsey and others. Is he fully aware of the basic result that a man who is to act sensibly can only do so if he acts in accordance with a *unique* probability and a *unique* utility? And why is there no mention of exchangeability, that brilliant notion expounded by de Finetti in his two-volume treatise *Theory of Probability* (Wiley, 1974/5), that connects chance with belief and embraces the frequentist framework within that of knowledge? Levi says in his discussion of nuclear safety, that "the available evidence fails to warrant a sufficiently definite system of credal probability judgments"; but probability is the only description of the available evidence, as Ramsey and others have shown. We may not like the evidence, but probability should not be the scapegoat.

Where does this book stand as a contribution to the study of knowledge? Its importance lies in its new emphasis on a general, credal probability and in its forward-looking, decision-orientated view of knowledge. It leads us further along the road towards a philosophically satisfying, yet usable, appreciation of scientific method: an appreciation that could do much in a really practical way to assist the development of science and technology. And yet, is that not already with us in the work of the "strict" Bayesians? It is to be hoped that scientists will think about these issues, and read de Finetti and Jeffreys as well as Levi. □

*D.V. Lindley was formerly Professor of Statistics and Head of the Department of Statistics and Computer Science at University College London.*

## Fit for mankind: a vision of Earth

Paul A. Colinvaux

*The Wooing of Earth.* By René Dubos. Pp.183. (Athlone/Scribner's: 1980.) £7.50, \$8.95.

To woo the Earth means to coax our countryside into the human image of what the good Earth should be. And the image is often very good; a land fair and open, contrived to reflect an ancient savanna where our species was moulded by evolution, long, long ago. We have done this everywhere and the carpers among us are wrong to call our doings bad. This is the Dubos message of good cheer.

Europe is beautiful, with its vistas of villages, pastures and trees. The European wilderness of the old times, where immense, dark forest forever hid the view, was a frightening place. Greece is delightful, even though its shimmering hillsides are only kept bare by relentless overgrazing. New Englanders like their patterns of village and farm, and their

legislators are trying to stop land going back to forest as farms are abandoned. Lovely parklands like the Han dynasty Summer Palace or the creations of Capability Brown are not wilderness but nature contrived to fit the human appetite. Hardly any of us want wilderness. Why not admit this — and be optimistic about how we can change the Earth without ruining it.

Dubos points out that the sainted Thoreau had a comfortable time at Walden Pond, close to the safety of tranquil Concord, and that the sight of a real wilderness of trees in Maine shocked him to hasty retreat. We pay lip service to the wilderness, but most still turn away from its frightening possibilities. We urge Africans to save the game herds, but the Africans will destroy them before the year 2000 because farm land is better than wilderness supporting wild beasts. This seems so self-evident that I have long marvelled at the hopes of those who thought the Serengeti would be saved. We

## New books from IRL

### Nucleic Acids Synthesis: Applications to Molecular Biology and Genetic Engineering

Proceedings of the International Symposium on Chemical Synthesis of Nucleic Acids. Held May 1980 in Eggestorf, West Germany. Nucleic Acids Symposium Series No. 7.

In the fields of molecular biology and genetic engineering, synthetic nucleic acids and their constituents have proved to be valuable tools and their uses appear to be infinite. In the present era of 'synthetic biology' it is not surprising that the chemical synthesis of nucleic acids is experiencing a tremendous renaissance.

Thus, it was most opportune that this conference, organized by Hubert Köster, should have been held, and the list of participants reads like a 'Who's Who' in the field, together with representatives from industry. This issue of the Nucleic Acids Symposium Series contains details of the latest methods in oligonucleotide synthesis from practically all the leading laboratories in the world, including those of Eastern Europe, Japan and China and serves as a source not only of their current (and usually unpublished) research, but also of their predictions for the future of the methodology and the use of such oligonucleotides.

396 pp ISBN 0 904147 26 6 (Hard) August 1980 £17.00/US\$40.00

### Obesity: A Bibliography 1974-1979

340 pp ISBN 0904147 17 7 (Hard) £22.50/US\$55.00 October 1980

### Olfaction and Taste VII

Proceedings of the Seventh International Symposium on Olfaction and Taste and Fourth Congress of the European Chemoreception Research Organisation. Held July 1980 in the Netherlands.

500 pp ISBN 0 904147 20 7 (Hard) £22.00/US\$50.00 November 1980

### Immunology of the Eye Workshop 1: Immunogenetics and Transplantation Immunity

Proceedings of a Workshop on Immunogenetics and Transplantation Immunity. Held December 1979 in Chantilly, Virginia. Edited by George M. Steinberg, Igal Gery and Robert B. Nussenblatt

286 pp ISBN 0 904147 25 8 (Soft) £10.00/US\$25.00 November 1980

### Forthcoming Proceedings in the Immunology of the Eye Workshop Series

Autoimmune Phenomena  
Infection, Inflammation  
and Allergy

### Information Retrieval

1 Abbey St., Eynsham,  
Oxford OX8 1JJ, England  
Suite 815, Fisk Building,  
250 West 57th Street, New York,  
NY 10019, U.S.A.



destroyed our wild animals in Europe and North America, and took their land; we even make newspaper headlines of the escape of a lion from the zoo and public peace comes back only when it is known that the animal is shot. Why should we expect poor farmers of Africa to act differently?

Dubos stresses that they will not, that people do not like wilderness, that we may save some areas as places for adventuring or because it seems sense to keep the gene pools of wilderness species as intact as possible, but that we ought to replace most wilderness with something even better.

Dubos is asserting that there is a silent majority of people who want a friendly, humanized Earth to live on — not danger, not wilderness, not even what is productive or the result of good ecological management, but what is familiar or beautiful. Doubtless he is right, and doubtless the silent majority will have its way. I worry, though, at the tyranny of majorities to those few who, people-like, do not always run with the herd. A real wilderness is marvellous in ways that Thoreau could never feel. A desolate mountain top in the Brooks Range is a better place to be than a man-made space above the English Lakes. To stand, thinking yourself into invisibility in the Amazonian forest, alone and as the hours pass, cannot be equalled in a botanic garden or in the landscapes of a potentate. A proper wooing of Earth will see that she keeps bits of her wild temper intact.

Dubos tries to show that what people like is what they were programmed to like in ancient days when our species was fashioned in some forgotten African savanna. These parts of the book make uncomfortable reading. We are the learning species, the animal who learned to live in almost every habitat of the Earth before we discovered, through agriculture, how to transform our habitats. Yet Dubos sees the Peking Summer Palace as an attempt to recreate the supposed savanna of our species' youth. This has a feel of genetic determinism about it which is not quite nice. The essential thesis of wooing the Earth can stand without this.

Nor does the Dubos thesis need bolstering by ecological theory, yet his is a conservation ethic of sorts and all conservation nowadays argues before the "Court of Ecology". Dubos would have done better not to, for his is still the ecology of the environmental movement with the standard errors.

It is not a fact that ecosystem complexity yields stability. This was a hypothesis of the 1960s, built out of inspired speculating by Robert MacArthur (*Ecology* 36, 533-536; 1955) who drew mathematical analogies between junctions in information networks and species in ecosystems. By the mid-1970s, R.M. May (*Stability and Complexity in Model Ecosystems*; Princeton University Press, 1974), D. Goodman (*Q. Rev. Biol.* 50, 237-266; 1975) and others had shown how unrealistic this

was and many of us ecologists felt grave disquiet years before then. Modern conservationists appealing to ecological Courts really must read up the latest Court Decisions before applying their ecological law.

It is dangerous practice to talk about how ecosystems "evolve"; change they do, but to talk of them "evolving" suggests a mechanism of selection, of the stable replacing the unstable, the productive the unproductive. There are indeed ecologists who seek supra-organismal patterns of evolution like these — but they are not all of the profession and they may not be the wave of the future. Far better to remember that most of the energy flux used to drive an ecosystem is degraded in the non-living portions. In temperate forest some 0.7 per cent of incident solar energy enters the biota through photosynthesis and the other 99.3 per cent is degraded by raising temperatures or evaporating water (H. Lieth and R. H. Whittaker, *Primary Productivity of the Biosphere*; Springer-Verlag, 1975).

The biota adapt to this energetic reality much more than they control it. Progress towards a nebulous "climax" is a shuffling in line before the energy soup-kitchen, until everyone has found a place of sorts and there is a quasi peace. Incidentally, this is why our human systems have, in general, worked so well; we have altered the arrangement in the biological energy queue without tampering with the main patterns of energy flux. It is only when we do

something terrible to the landscape, such as promoting soil erosion or building a dam, that major diversions in primary energy flux reflect true system instability.

Dubos has a wise and sane vision — an Earth kept diverse and pleasant for human use, made richer by human invention than wild nature had left it. Leave some wilderness for some of us to spend a few hours in and change the rest, ever so gently, until it is good. Yet he protests how well he understands that all will be vain if our numbers keep on growing and that much will be imperilled if we go to nuclear war. But on the ecological subject of human numbers he has nothing to say. He believes that the remorseless rise of population has something to do with curbs in the death rate made by the medical profession and he savours the hope that our numbers may be levelling off. These are views not tenable in ecological logic. Numbers rise because the human breeding strategy remains that of achieving optimum clutch and the destructions Dubos fears will come about as we seek to find adequate niche-space for the surplus individuals that result (P.A. Colinvaux *Nature* 26, 256-357; 1976. *The Fates of Nations*; Simon and Schuster).

Yet it is good to read honest statements that all things done by mankind to the environment are not bad; indeed that most things done have had satisfactory results.

Paul Colinvaux is a Professor in the Department of Zoology at The Ohio State University.

## Survival of the fittest author

Wilma George

*A Delicate Arrangement: The Strange Case of Charles Darwin and Alfred Russel Wallace.* By Arnold C. Brackman. Pp. 370. (Times Books: 1980.) \$12.50.

THIS is a disappointing book. It promises to uncover a plot but fails to convince and fills up pages with incomplete biography. Many people would agree with the author that Alfred Russel Wallace had less than his fair share of publicity but few would agree with his interpretation that Darwin cheated Wallace and that Lyell and Hooker connived at the plot.

Brackman rests his case on dates: the supposed date that Wallace sent his natural selection paper to Darwin and the supposed date that Darwin received it. Wallace thought he sent it in March 1858 and Darwin thought he received it on 18 June but Wallace's envelope with its postmark has not survived. Brackman claims that because Wallace posted a letter to F. Bates on 9 March which arrived on 3 June he must have posted his article to Darwin on the same date and, therefore, the article must have arrived on 3 June.

This is not evidence. This same "evidence" has been used by H. Lewis McKinney in *Wallace and Natural Selection* (Yale University Press, 1972) to claim that Wallace cheated (to say he was where he was not).

Brackman claims that Darwin cheated by saying he had received Wallace's article on 18 June (and not 3 June) in order to quarry it for data and ideas before writing to Lyell. The "evidence" is supported by the fact that Darwin did not keep letters during the 1850s — and that Wallace was a member of the lower classes.

Brackman implies that Charles Darwin or his son Francis destroyed letters because Wallace was writing to Darwin about his ideas on species. But Darwin did not keep letters systematically until he became famous. Brackman also implies that Darwin was surreptitiously using Wallace's 1855 paper on species when the 1855 paper was in print!

Brackman's narrative style is "surreptitious", to say the least: "A troubled Darwin opened Wallace's letter". In fact, it is downright dishonest: "For Darwin his success in securing Wallace a



Wallace, aged 30 . . .



. . . and at 46.

measure of security for the remainder of his natural life was an act of expiation". It is a dramatic language: "Darwin understandably panicked". And the reader might understandably panic, too: "Both letters exhibit guile, glibness, and guilt mixed with integrity and honor".

Darwin was distressed when Wallace's 1858 article reached him but distress does not prove guilt. There is no evidence that Darwin plundered Wallace's paper for ideas and wrote them into his own manuscript. Darwin had been brooding on his theory for years and had not written his book and I find his outcry about loss of priority entirely natural. Darwin did not seize on Wallace's idea of divergence and make it his own in the supposed two-week interval between receipt and admission of receipt of Wallace's 1858 article. In 1855, Wallace had written in a paper appearing in the *Annals and Magazine of Natural History* (16, 184-196): "But if two or more species have been independently formed

. . . then the series of affinities will be compound and can only be represented by a forked or many branched line". As for the mechanism, Darwin had written to Asa Gray in 1857 (and the letter is not a fake) of: "an unerring power at work in *natural selection* (the title of my book)" and of a principle of divergence "which shows that organic beings seem to branch out into all the places available".

I find no case against Darwin. I think that the explanation for Wallace's partial eclipse from the evolution-by-natural-selection debate is less dramatic. Darwin's fame came not from the appreciation of a new biological theory by a few members of the Linnean Society but from the intelligent reading public. Evolution by natural selection was a revolutionary theory but the public of Victorian England did not read the proceedings of the Linnean Society. It read books. And the readers, shattered by the convincing mechanism for a process which was already a subject of conversation, were troubled by the implications of the theory for the status of man.

Wallace did not write an *Origin* (it was Darwin who provided a detailed account of the process of organic evolution which was accessible to the reading public) and Wallace developed unacceptable ideas about the evolution of man. Finally, Wallace, the younger man by 14 years, insisted that their theory should be called Darwinism, summing up the situation himself when he wrote to Darwin in 1864:

## Animal arms races

John R. Krebs

*Tooth and Claw: Defensive Strategies in the Animal World.* By J. L. Cloudsley-Thompson. Pp.252. (Dent/Biblio: 1980.) £9.95, \$22.50.

THIS is a popular book about the ways in which animals defend themselves against predators and the counter-adaptations of predators to overcome their prey. It covers similar ground to *Defence in Animals* by M. Edmunds (Longmans, 1974) and *The Ethology of Predation* by E. Curio (Springer-Verlag, 1976), but is aimed at a more general audience.

Most of the text consists of examples, many based on the author's own observations of different kinds of anti-predator adaptation and tricks used by predators to catch their prey. Examples of camouflage, mimicry, venoms, defensive spines, armour and so on are described in a charming and entertaining way. Most readers are certain to come away with at least one or two good coffee-time stories. My favourite is about the African water mongoose, which is alleged to catch birds by sticking its rear end in the air and distending its anus to make it look like a

You had worked it out in details I had never thought of, years before I had a ray of light on the subject, and my paper would never have convinced anybody or been noticed as more than an ingenious speculation, whereas your book has revolutionised the study of natural history.

But I am glad to see a book that publicizes Wallace's contribution to the theory of evolution by natural selection, a book that reprints both the 1855 and 1858 species papers — though it is a pity that Darwin's 1858 contributions were not included for the reader to make his own judgement — and a book that has some hilariously scabrous comments in the "Author's Notes". Wallace's name is heard today much more often than it was in the nineteenth century, partly because of the lessened obsession with the evolution of man and the increased interest in other implications of the theory, partly owing to the work of the historians of science and partly because of the return to fashion of evolutionary zoogeography founded by Wallace and stamped indelibly with his "line". But the more Wallace is linked with Darwin as a co-founder of the theory of evolution by natural selection, the more will historical accuracy be served. Thus, even a negative book like this contributes to the subject. □

*Wilma George is a Lecturer in Zoology at the University of Oxford, and the author of Biologist Philosopher: a Study of the Life and Writings of Alfred Russel Wallace (Abelard-Schuman, 1964).*

ripe fruit. Along comes an unsuspecting bird to peck at the fruit and with a smart about turn the wily mongoose snaps it up! Second place goes to the story about frogs' legs and the genitalia of French soldiers in nineteenth century Algeria (without giving too much away, the British are right to stick to pie and chips), and a close third is the account of how large tropical scolopendromorph and scutigermorph centipedes escape from attackers. When attacked or frightened, they shed one of their back legs; the automatized leg leaps around making loud creaking or stridulating sounds to attract the attention of the predator while the nonagintanovipede slips silently away.

Cloudsley-Thompson also tries to extract some general principles about coevolution of predators and prey. He draws a parallel between military arms races and the coevolutionary race between predators and prey. In both military and coevolutionary races, adaptations or innovations by one party call forth counter-adaptations by the other. These counter-adaptations lead in turn to counter-counter-adaptations and so on. One general principle applicable to both kinds of race is the concept of a "trade off" between competing demands. Heavy armour may render a tank less vulnerable



to shell fire, but at the same time it reduces speed and mobility. In the same way animal defences may work well against one kind of attacker but be much less effective against others. The king cobra, for example, is venomous enough to kill an elephant, but is itself killed on occasions by the mongoose with its superior agility.

A closely related idea is that every defensive adaptation has a "cost" which might, for example, be measured in terms of energy that could otherwise be channelled into reproduction. One of the most convincing pieces of evidence for the cost of anti-predator adaptations comes

from the study of chemical defences in plants (and is therefore not discussed by Cloudsley-Thompson). R. G. Cates (*Ecology* 56, 391-400; 1975) has shown that wild ginger plants (*Asarum caudatum*) in places where slugs are common channel more energy into chemical defence (they taste nastier) at the expense of seed production and growth than do plants of the same species where there is little grazing pressure.

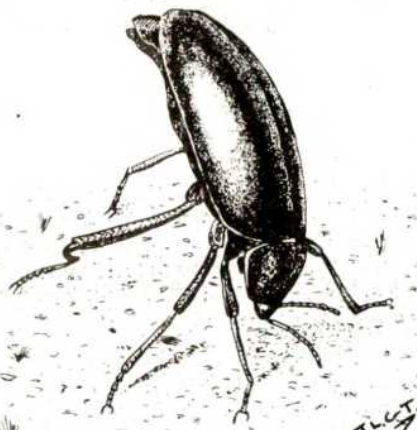
The book touches on some issues without trying to discuss them in their full complexity. For example, in the discussion of Müllerian mimicry (mimicry in which several unpalatable species share the same colour patterns) Cloudsley-Thompson presents the conventional argument that a shared colour pattern reduces the chances that an individual will be killed by a predator in the process of learning to associate colour with distastefulness; the larger the pool of similarly coloured prey

individuals, the smaller the chance that any one of them will be killed. While this argument seems to be correct, it leads one to expect that all unpalatable species living in the same habitat should share the same warning colour patterns. In fact it is known that neotropical butterflies, for example, form several different Müllerian mimicry complexes within the same habitat (C. Papageorgis *Am. Sci.* 73, 522-53; 1975).

The mechanism of evolution of warning coloration is also glossed over, with no mention of R. A. Fisher's suggestion that it might have arisen through kin selection.

However it would be churlish to criticize a popular book for not exploring recondite details. The main aim of Cloudsley-Thompson's book is to entertain and stimulate the reader. In this it succeeds. □

John R. Krebs is a Lecturer in the Edward Grey Institute of Field Ornithology, Department of Zoology, University of Oxford.



Chemical defence: when disturbed, *Eleodes* sprays a secretion at the attacker from its abdomen.

## Animals for the coffee table and student

Bryan Turner

*The Complete Encyclopedia of the Animal World*. Edited by David M. Burn. Pp. 400. (Octopus: 1980.) £12.95, \$17.98.

THE diversity of animals, the sheer numbers of species, and the richness of their differing forms and functions has always fascinated people. It attracts the curious layman and for biologists begs answers to questions of "how?" and "why?". Although this book has been written and designed to adorn the coffee tables of the general public, students of zoology will find much to interest them. The book is of a higher intellectual standard than that customarily associated with this sort of glossy volume, in part due to the impressive list of contributors. Each section has been written by an acknowledged expert in that particular field. Skilful editing has successfully combined the many and varied styles of the contributors in a way that makes section to section differences unobtrusive.

The text is complemented by a beautiful series of colour photographs and novel illustrations. Although most of the illustrations are useful, some are confusing; for instance, in a figure of the distribution of the geological plates of the Earth's crust the key is absent so that the variously coloured boundaries are meaningless. Perhaps somewhat more important than minor irritants of this nature is the discussion on the links between the chordates and the non-chordates (essentially but not precisely equivalent to the vertebrates and invertebrates). Here the widely held ideas of a link involving the hemichordate acorn worms are dismissed and a new but little accepted theory involving the fossil calcichordates is

expounded. In a general text such as this the most widely accepted views of the experts should surely take precedence, and any new and highly controversial ideas take second place.

The main part of the book is a catalogue of the different groups of animals which is sandwiched between chapters on special aspects of animal life. There are introductory chapters on ecology, in which the biologists' "how?" and "why?" questions are briefly considered, and on taxonomy explaining the classificatory process. This latter section is introduced by a full colour photograph of the book's editor in the guise of a lepidopteran taxonomist supposedly illustrating the qualities of "Patience, experience and a good eye" — perhaps a book on brass instruments will be next! Other specialist chapters include such topics as locomotion, migration, senses, associations, endangered species and a useful section on the major zoos and national parks of the world. The foreword, curiously by David Bellamy, the "Botanic Man", is accompanied by a picture of him riding a tortoise. To ensure that we recognize him, the usually sufficient facial characteristics have been supplemented by those other well-aided taxonomic features — the hairy legs!

These asides apart, this book does represent a good, balanced and informative account of the immense variety of animal life. Although unable in 400 pages to live up to its title "Complete", it is none the less a very creditable contribution from the Octopus stables. □

Bryan Turner is a Lecturer in Zoology at King's College, London.



### AMERICAN NUCLEAR SOCIETY'S PUBLICATIONS

*Complete Nuclear  
Publications and  
Services Worldwide.*

Inquire about specific  
interests.

For Free Publications  
and Services Catalog,  
contact:

American Nuclear Society  
555 N. Kensington Avenue  
La Grange Park, IL 60525  
U.S.A.



# The blooming of a hobby: a history of natural history

Alwyne Wheeler

*The Heyday of Natural History.* By Lynn Barber. Pp.320. (Cape/Doubleday: 1980.) £9.50, \$17.95.

THE middle years of the nineteenth century saw a striking flowering of popular interest in natural history in Britain. The economic and social conditions of the time had produced an increase in the number of literate people who had more leisure and were thus able to utilize their time in what was clearly a health-giving, mind-improving hobby — both worthy objectives in the moral climate of the period. In addition, developments in printing, for example stereotyping and electrotyping, permitted a great increase in the number of popular books, often illustrated with colour plates at relatively low prices.

The result was an extraordinary burgeoning of the literature of natural history written for a popular market. The availability of such books stimulated the interest of even more middle-class naturalists, to result in a cycle of demand and supply which saw the nineteenth century out. The consequences of this great increase in popular natural history and its literature have had considerable influence in our time, for it was during the mid-nineteenth century that many local natural history societies were founded (and those that came later were started by people raised during the period). Many such societies started local natural history museums, and even now have their own publications and libraries, and thus still exert a considerable influence on natural history in Britain although, responding to pressures on the environment today, much of the amateur naturalist's efforts go in supporting conservation-orientated societies.

In this view I differ from the conclusion of Lynn Barber that from the 1870s, in the aftermath of the revolution in thought following the acceptance of Darwin's theories, natural history became "dull". The later years of the nineteenth century simply saw a dichotomy between amateur naturalists and professionals, the latter having been few in number before the 1870s. The amateur interest in natural history has continued as strongly as ever, but the professional naturalists have become more specialized in their fields and in their writings, and few have possessed the breadth of knowledge, the ability or the bravery to produce popular writing comparable to that which flourished in the Victorian period.

Lynn Barber's book is a most readable account of the great years of the Victorian naturalists (Victorian being loosely applied). The story is a good one, some



"Scientific Conversazione at Apothecaries' Hall", from the *Illustrated London News*, 1855



"Holiday Time at the Zoo", 1872



The Iguanodon dinner, 1854





## ARCHAEOLOGY

### The Magazine for Past Lovers

Admit it — you've always been secretly fascinated by the mysteries of antiquity... always wondered what life was really like in ancient Egypt, China, Greece, Mexico, Peru. Find out in **ARCHAEOLOGY Magazine!** Six times a year its authoritative clearly-written articles and stunning color photographs bring the ancient world alive. Meet the peoples of the past. Marvel at their achievements, and admire the beauty they left behind. There's nothing else like **ARCHAEOLOGY**. Try it now.

**ARCHAEOLOGY Magazine,**  
Dept. 8603 P.O. Box 385,  
Martinsville, NJ 08836

Please send **ARCHAEOLOGY** to:

Name \_\_\_\_\_

Address \_\_\_\_\_

City \_\_\_\_\_ State \_\_\_\_\_ Zip \_\_\_\_\_

☐ One year \$15 ☐ Payment enclosed

☐ Two years \$27 ☐ Bill me

Add \$3 per year outside U.S.A.

Send gift card signed \_\_\_\_\_

superbly interesting characters appear and the material is handled in a masterly fashion.

The first section recounts the social and historical backgrounds, the second contains accounts of Linnaeus, Cuvier, Audubon, Rafinesque, Swainson and Charles Kingsley. Later sections feature Waterton, Gosse, Ward, Mary Anning, the Bucklands, Owen, Sedgewick, Murchison, Huxley and Darwin. But the treatment is not merely biographical; rather, the work and the influence of these "giants" of the nineteenth century is skilfully woven into an account of the development of British natural history, although biographical details have been included to set them in their background. In working this complicated tapestry into an attractively presented, enjoyable and well-written story Lynn Barber deserves all credit.

No doubt it is because of her background as an experienced journalist and broadcaster that her book is presented with such panache. This background may, however, have led her to include some "human interest" stories which are generally now discredited amongst historians of natural history. Thus, the loss of labels from Cuming's mollusc shell collection due to Mrs Gray's carelessness is now dismissed as a canard. Nor was the unfortunate A.W.E. O'Shaughnessy's appointment in the British Museum to work on insects due solely to the influence of his patron as is inferred here; he was simply transferred from one department within the Museum to another, having passed a test of his knowledge of zoology which the other contender had failed.

One has to say that most of the sources used by Miss Barber are secondary. I doubt whether one can rely overmuch on Kingsley's view of Victorian natural history, or on William Swainson and especially not on Audubon for objective



Frank Buckland, naturalist extraordinary

views of their contemporaries. They were all too involved in the period themselves, and Swainson and Audubon certainly had axes of various kinds to grind. The reliance on secondary sources tends to affect the overall images in the book, and also possibly accounts for some of the more alarming generalizations and particular errors. Surely it is not true that between Cuvier's *Le Règne Animal* of 1817 and Darwin's *Origin of Species* in 1859 "almost no major breakthroughs were made"? Two discoveries alone, that of Schwann (1839) of animal cells, and that of the mammalian ovum by von Baer (1827), would today be given the accolade of "breakthroughs".

For these and other reasons Lynn Barber's book cannot be credited as an original history of natural history, but as a readable and well-produced introduction to the subject it is unsurpassed. □

*Alwyne Wheeler is editor of the Archives of Natural History (formerly the Journal of the Society for the Bibliography of Natural History) and works at the British Museum (Natural History).*

## The "why" of animal culture

W.C. McGrew

*The Evolution of Culture in Animals.* By John Tyler Bonner. Pp.216. (Princeton University Press: 1980.) £8.10, \$14.50.

A DISTINGUISHED cell biologist, J.T. Bonner, has written an ambitious book on the behaviour of animals. In it, he tackles the question of culture as a direct product of the evolutionary processes of natural selection: "[Culture] . . . is as biological as any other function of the organism, for instance, respiration or locomotion". In addressing social scientists, Bonner does not shrink from the implications of this position for human culture and confronts the issues in his opening chapter. From the beginning it is a pleasure to find a book so lucidly written and so free of jargon.

The author's ultimate goal is to explain why we (humans) have culture at all. To

appreciate its adaptive significance requires a step-wise reconstruction of its phylogeny, and it is to this task that much of the book is directed. Bonner starts at the most basic levels of evolutionary mechanisms and advances on a broad front. His definitions are as comprehensive as possible; culture is defined as "... the transfer of information by behavioural means, most particularly by the process of teaching and learning". (Such a definition is not without faults, for instance it gives no inkling of the cumulative nature of the phenomenon). The author compares the genome and the brain as information-processing structures, with genes and "memes", respectively, as the units of information transmission — here, and elsewhere in the book, he calls upon Dawkins's *The Selfish Gene*. The latter



system is speedier and more flexible, but it is ultimately limited by the former. The emergence of large brains in human evolution is credited to neoteny, that is, the retention of juvenile traits whereby the brain goes on growing in size after the growth of the rest of the body has slowed or ceased.

Having laid the structural groundwork, Bonner turns to the most basic behaviours. A long chapter on animal societies (which draws heavily on Wilson's *Sociobiology*) relies on the premise that culture requires communication, which is most developed in social organisms. Here, and throughout the book, Bonner chooses to start with microorganisms and work his way through progressively more complex multicellular forms. An excellent discussion of genetic flexibility is followed by the introduction of the concept of a dichotomy of behavioural flexibility: single-response behaviour versus multiple-choice behaviour; this appears to be "nature versus nurture" re-labelled.

The real problems begin to arise with the author's treatment of learning and teaching. All social learning seems to be classified as imitation, with no distinction being made between types requiring differing degrees of mental ability — mynah birds and human infants may both learn English, but the learning of the bird is merely mindless mimicry. No mention is made of "mixed" forms, for example observational learning by a combination of stimulus enhancement (social) and trial-and-error learning (non-social). Finally, there is no reference to behaviours which involve communication but not (necessarily) learning, social facilitation of pecking in domestic chicks, for example. Crucial to the author's argument is teaching, which he defines as "... the release of sets of signals specifically designed to alter the behaviour of another individual". This presents a rare example of ambiguity: in a general sense such a definition applies to all communication; in a more specific sense, it leaves open the question of whether or not intentionality (or goal-directedness) is involved. The reader is told that a large share of teaching

by higher vertebrates can be considered as parental guidance, and that a parent will shape its offspring's imitative performance with nudges, pokes and slaps. But, apart from a single anecdote, no evidence of this sort of behaviour is presented. Contrary to the author's conclusion, it seems likely that it is just this sort of teaching which is conspicuously absent in non-human animals.

The book builds toward a synthetic final chapter which I found somewhat bewildering. Norton-Griffiths's exemplary work on the intergenerational transmission of feeding techniques in oyster-catchers is given suitable credit, but a number of other, equally significant studies are not mentioned. The "natural experimental" research into cultural innovation and diffusion in Japanese monkeys rates only one paragraph; an admittedly fascinating anecdote of one-trial, avoidance learning by elephants is given preference to the many studies of culture in non-human primates — Menzel's volume on the subject is ignored; fidelity to nesting sites in migratory birds is emphasized, in spite of the fact that no social learning need be posited, just as it is not invoked to explain the homing of Pacific salmon to spawn; even the memorable example of milk-bottle opening by tits merits only three sentences. Finally, the section on human culture cites no specific examples, and some of its general conclusions will cause disquiet amongst the social scientist for whom the book is intended; for example, the author's linking of the rise of culture to the rise of writing seemingly bars extant pre-literate societies from consideration.

Yet, overall, in this book Bonner has produced a clear, compelling and wide-ranging account of the bases for social communication in animals. However, those more interested in the evolutionary mechanisms of transition from non-human to human culture are left wanting. That particular book remains to be written. □

*W. C. McGrew is a Lecturer in Psychology at the University of Stirling and a Visiting Faculty Member at the University of North Carolina at Charlotte.*

## Rural nostalgia

Kenneth Mellanby

*Hampshire Days.* By W.H. Hudson. Pp.250. (Oxford University Press: 1980.) £1.95.

COUNTRY lovers will be grateful to Oxford University Press for reissuing this book in such an attractive paperback edition some 80 years after its first publication. W.H. Hudson was a naturalist who observed the countryside and its wildlife wherever he was, in South America or rural England.

His publishers describe him as "a passionate observer of nature", and this is what emerges from his prose. He gives us accurate and perceptive accounts of the plants, insects, mammals and particularly the birds seen in his garden and in the Hampshire countryside. Some scientists may find his description of his feelings, and his attribution of human emotions to birds and even insects, alien to their tastes, but they will soon be brought back to earth by his unsentimental and accurate accounts of life and death in the countryside.

Hudson's love of rural life was mirrored by his hatred for urban living. He disliked

## SCIENTIFIC BOOKSHOP

H.K. LEWIS can supply works in all branches of Pure and Applied Science. Catalogues on request. Please state interests.

## SCIENTIFIC LENDING LIBRARY

Annual Subscription from £7.50.  
(Available in U.K. only)

Reduced rates for multiple subscriptions.

Prospectus post free on request.

Quarterly List of New Books and new editions added to the Library sent post free to subscribers regularly.

**H.K. LEWIS  
& Co. Ltd.**

136 GOWER STREET,  
LONDON, WC1E 6BS

Telephone: 01-387 4282  
Telegrams: "Publicavit,  
London, WC1E 6BS."

Circle No. 23 on Reader Enquiry Card.

the townsmen, with "their pale civilized faces — they are out of my world — the real world". His passion was for "wildness — the rude heath, the beautiful desolation; furze and ling and bramble and bracken to grow on me, and only wild creatures for visitors and company". He was of course aware that he was observing not the natural face of England, but the result of the interplay of human activities and ecological processes. He describes prehistoric barrows as well as traditional farmhouse and agricultural activities. But at the time he was writing it was possible to imagine that there was a harmony between man and nature which resulted in the beautiful landscape he so vividly describes.

How he would have hated the changes which have taken place in his beloved Hampshire in recent years. Many of the woods and heaths have gone, some of the hedges have been ripped out. Men are even prospecting for oil! Modern farming is very different from that of his day. Yet a great deal remains. We can, if we are lucky, still see most of the sights he so graphically describes. But few of us have his "seeing eye", and in a lifetime of study may not make all the observations his skill and his sympathy made possible in a few brief years at the beginning of this century. □

*Kenneth Mellanby is an editor of Collins' New Naturalist series, which is concerned with wildlife in Britain. His Farming and Wildlife, in this series, will appear in 1981.*



# Retrospective environmental impact assessment

Eric Ashby

*The Volta River Project.* By David Hart. Pp.131. (Edinburgh/Columbia University Press: 1980.) £7.50, \$20.

MEMBER states of the European Community will shortly be asked to adopt a common policy for environmental impact assessment. The individual members already have policies of their own; so the wrangling — and there will be plenty of it — will be about the means for predicting environmental impact rather than whether to do it at all. The ends are clear: to reconcile the inevitable conflict between exploitation of nature for the benefit of Man, and conservation of nature also for the benefit of Man. The wrangling begins when you ask: for whose benefit and at whose cost? And the conflict is confused because we do not know how to predict and we cannot agree about who should participate in assessing predictions.

In Britain the current procedure is to hold ministerial enquiries, commonly under the Town and Country Planning Acts. No one pretends that they are satisfactory (think of the bitterness left after the enquiries at Windscale about fuel reprocessing and at Winchester about the route for a motorway); but even critics of the British procedure prefer it to the bureaucratic hypertrophy of the Environmental Protection Agency in the United States. The trouble is that no one seems to be thinking about the problem in a scholarly way, that is, by examining past experience and trying to draw lessons from it. What we need, before we commit ourselves to European policies for environmental impact assessment, are *retrospective* studies of technology assessment and environmental impact predictions. Academics have done a little work, notably Roy Gregory in his book *The Price of Amenity* (Macmillan, 1971), and a team sponsored by the American Academy of Arts and Sciences in their study *Boundaries of Analysis* (Ballinger, 1976). But much more work needs to be done. That is why this modest study of the Volta River project in Ghana deserves careful reading. We may think we manage environmental affairs better in Westminster than they are managed in Accra, but Ghana has something to teach us, even though it is a cautionary tale.

Among people unfamiliar with West Africa there is still a residual euphoria about the great Volta River project. Isn't it exactly what Third World nations need: to enrich themselves by generating energy, creating industries, raising living standards? The message in David Hart's book is that the Volta River project was not what Ghana needed — at any rate not what the great majority of the people of Ghana needed or ever asked for. It was wished on

Ghana by the West: Britain wanted an assured supply of aluminium from the sterling area; the Kaiser Corporation wanted a large supply of electricity with which to produce cheap aluminium. So under the pure white banner of 'aid' the West descended on Ghana, created a lake which occupies 3.6% of its land-area and dispossessed some 1% of its population. (A rough analogue for England would be to flood the whole of Devonshire and to decant its 460,000 inhabitants into other parts of the country.)

The Volta River project was contemplated as long ago as 1915 by the man who was at that time director of the Gold Coast Geological Survey. The idea was revived about 1948. A special commissioner, Commander Jackson, was appointed in 1953 to report on the whole project and its implications, without prior approval from the legislative assembly in Accra (a sign, as Hart says, "that the real decisions were being made elsewhere"). Even at that stage two influential and distinguished members of the assembly, Danquah and Busia, voiced their doubts. The primary purpose of the Volta River project, they said, was the production of cheap electricity to smelt aluminium; the development of Ghana was only a secondary purpose; the people of Ghana would benefit more from a smaller project to supply electricity to many towns, and to provide irrigation.

And so it has proved to be: aluminium is being smelted, but it has not brought the benefits to Ghana that were promised, and its destiny is in the hands, not of the Ghana government, but of the International Primary Aluminium Institute. As to the benefits to Ghana, Hart's account of the plans which were made to re-settle the 80,000 people occupying 739 villages in the

area to be flooded is a sardonic comment on the incompetence of planners when they have to deal with the human consequences of their decisions. Of course there were plans to compensate the people ejected from their holdings and to give them land elsewhere. In the event the plans were so mismanaged that much of the compensation is not paid, even today, and much of the re-settlement has proved abortive. Polygamous extended families, accustomed to having separate houses, however simple, for their wives and relatives, were given a house suitable only for a nuclear family. In their new locations the pattern of their society, the markets — the familiar locations for buying, selling and making social contracts — vanished; even the styles of agriculture and fishing had to be different. From a world of poverty ameliorated by security they were shovelled into a world of poverty exacerbated by stress. There were tensions among the indigenous occupants of the lands where the re-settlements took place. There were scandalous under-valuations of the property some of them had been obliged to abandon. And, on top of all this, there were alarming increases in the incidence of bilharzia, owing to the opportunities for the snail which transmits the disease to breed in the still waters of the lake; Hart publishes a map of the lake showing places where 70–100% of people sampled were infected.

I said that the experience in Ghana may have lessons for Britain; a remark which will provoke the protest: "It couldn't happen here". Not in the same way, it couldn't. But when we plan airports, motorways, power stations, what proportion of cash, thought and effort is put into the second-order effects of the pro-



The Volta dam — what benefits has it brought to Ghana?



jects? And are the decisions as to what is 'good' for the local populace made locally, or in London? (One perceptive comment on the environmental impact assessment made for the Volta project was that it was made by Westerners for Westerners; what was needed was a team of 'barefoot anthropologists' to live among the people affected by the Volta dam, and then to recommend how they should be handled.) If the people who say "it couldn't happen here" will pause a moment, they may recall the preposterous tragedy of taking people out of down-at-heel terrace houses and hoisting them up into high rise flats; or resettling people from the cohesive and compassionate society of a slum into neat, clean, aseptic villas in a suburb.

Upheavals in our traditional ways of life are inevitable; we are in for a lot more of them; people will have to migrate from the closed steelmills of Corby as surely as they

had to migrate from the waters of the Volta River. The British people are flexible and courageous enough to tolerate these upheavals. What they will not — and should not — tolerate is the pained surprise of planners when some of the remedies proposed from Whitehall are rejected. The way to minimize mistakes — they can't be avoided altogether — is to improve the standard of environmental impact assessment; and the way to do that is to study very carefully case-histories of past assessments, to diagnose where they went wrong and what they left out. David Hart's little book, despite its high price, ought to be on the bookshelves of planners; for he does what he sets out to do: he gives a case-study of politics and technology relevant not only to Ghana but to Britain. □

*Lord Ashby is Chancellor of Queen's University, Belfast, and a Fellow of Clare College, Cambridge.*

## Questions of energy

Joseph S. Nye

*World Energy Issues and Policies.* Edited by Robert Mabro. Pp.367. (Oxford University Press: 1980.) £15, \$44.50.

THIS volume is a collection of papers from the first Oxford Energy Conference, held at St Catherine's College in September 1979, and cosponsored by the Organization of Petroleum Exporting Countries and the Organization of Arab Petroleum Exporting Countries. The Secretaries-General of the two organizations provide two of the 28 papers in the book. Distinguished OPEC contributors also include Kuwait's Minister of Oil and Venezuela's Minister of Energy and Mines. Other essays are contributed by government, industry and academic figures from various oil-consuming and -producing nations. A brief introduction and summary is provided by the editor, Robert Mabro.

As might be expected in a diverse collection of conference papers, there is great unevenness of quality and style. Mabro explains that the essays have "not been heavily edited" in order to avoid lag in publication and to preserve their flavour of authoritative statements. Fair enough, though the disparities on occasion jar somewhat — a brief section, "World Energy Outlook", pairs Wolf Hafele's 23 pages on world regional energy modelling over 50 years with three pages of casual observations by the late C.C. Pocock of Shell Oil.

A more important problem is the gaps in coverage. The resulting tone of the book certainly leans toward the energy establishment. The editor acknowledges some omissions and wishes he had an environmentally orientated paper to balance the

chapter on nuclear energy written by an industry representative. He also regrets the absence of a contribution from a senior official of a major OECD country such as the United States, but explains that official speakers at the seminar were encouraged to speak off the record. A rule that may have been good for the conference, however, is not good for a book. The result is a meagre two chapters, one on the United States by an academic and one on the United Kingdom by a deputy undersecretary of energy, in the section on energy issues and policies of OECD countries. In contrast, there are six papers (including by highly placed OPEC officials) in the section on energy issues and policies of oil-exporting countries. Moreover, the paper on United States' policy entitled "A Critical Overview", hardly purports to be a balanced presentation.

Despite the problems of unevenness and gaps, there are several useful papers in the volume, especially in the opening section on energy supply. Particularly interesting is the paired treatment of natural gas by Nordine Ait-Laoussine of Algeria and James Jensen of the United States. On the other hand, one would have thought coal deserved more than five brief pages. There are descriptive discussions of the Soviet Union and China by Michael Kaser and John Foster, and many of the papers by officials are of interest not because of their analytical insights, but because of their author's positions. If treated as a smorgasbord, the book succeeds in one of the editor's purposes in that it does present some interesting conference fare for a wider audience to sample.

Mabro also has an explicit political objective: "to improve the chances of

success of any future formal dialogue which Governments sooner or later will have to initiate". In his summary, Mabro says that "the urgent need for dialogue was almost unanimously recognized", but there was little agreement on modalities or scope of the agenda.

The idea of a dialogue between OPEC and consumers is currently fashionable in the aftermath of the Brandt Commission Report. A consumer-producer dialogue might help nations shift their focus to the potential long-term joint benefits to be gained. Such a dialogue might seek inter-governmental agreements to stabilize the oil market; for example, OPEC and IEA countries might agree on production targets and consumption limits (at first separately, and then in joint bargaining) which would allow for modest real price rises over the next decade. A band of prices might be established for the duration of the agreement. OPEC countries would agree to maintain sufficient spare capacity to increase production if a shortfall of production from any subgroup of producers threatened to push prices outside the band. They would cut production (or agree to permit consumers to increase demand above the agreed limits) if prices threatened to fall through the bottom of the band. Additional inducements might be needed to assure adequate production levels. For example, consumers might offer indexing of assets and assurances of assistance and market access for the new OPEC industries. Special credit or aid provisions might be agreed for oil-importing developing countries; some such countries could be included in bargaining sessions.

But a number of hard questions must be answered. Could the agenda be focused on energy? If other developing countries participate, will the world replay sterile North-South debates, but with much higher stakes than in the United Nations? Can the "Pandora's Box Effect" be controlled if nations start down the path to serious international collective bargaining?

Is a reasonable bargain likely? At modest prices there are divergent interests between those OPEC surplus producers who lean toward conservation and the high-absorbers interested in maximizing revenues. Large price increases (which maximize revenues and allow painless production cutbacks) tend to reconcile that division. Would OPEC countries be able to agree to a bargain that meant higher production and lower prices than the market would otherwise determine?

Does OPEC have sufficient cohesion to make a bargain stick? Thus far, OPEC countries have been unwilling to limit their separate sovereign control over production decisions concerning the resource that is their major source of power. They compete for power within the oil arena and they reserve the right to use oil as a weapon in wider political games. Given the politics of oil, and the domestic instability of many



OPEC governments, how credible is an OPEC promise to increase production if a shortfall has political ramifications? And if an unintended interruption occurs, how likely is it that OPEC will be able to restrain the high-absorber members from charging what the market will bear? If, as is probable, they cannot, consumers will have paid higher-than-market prices in normal times in return for broken promises.

Would the benefits exceed the costs? Basically, consumers would gain a formal framework for debating production (and price) decisions that are now entirely in OPEC hands. Bilateral diplomacy can have some of the same effect. How much is it worth paying for this framework?

These questions do not mean that conversations with producer states are not useful, or that restoration of an international oil regime is not a worthy long-term goal. Various bilateral and multilateral discussions are essential. But efforts to reconstruct a satisfactory regime are unlikely to be fruitful unless hard questions have been carefully thought through. The volume at hand provides raw material for such thinking, but poses few of those questions and gives disappointingly few of the answers. □

Joseph S. Nye is Professor of Government and Public Policy at Harvard University.

## The state of Arab science

Ziauddin Sardar

*Science and Science Policy in the Arab World.* By A. B. Zahlan. Pp.205. (Croom Helm: 1980.) £13.95.

THE past decade has seen scientific and technological activity in the Middle East really come alive. While much of this activity is little more than simple transfer of equipment, expertise and personnel, there are, nevertheless, a number of projects which aim to make a real contribution to science development in the area and provide it with an indigenous base; to this end a number of technological universities and specialized institutes have been established to meet some of the more demanding needs of manpower and research.

The scale of this transfer of technology and its associated problems are in many respects unique and unparalleled, and demand urgent and detailed scholarly attention. Thus one turns to Antoine Zahlan's book with the hope of seeing these developments charted, analysed and placed in an appropriate scientific, social and political context. Indeed, few would be better qualified for such a job.

With so much to relate and analyse, it is sad to report that Zahlan has missed an excellent opportunity. His book is not just weak in content and rather limp in its

analysis; worse, it is a book apparently based almost entirely on publicity brochures and official handouts. Probably the best part is the introduction where Zahlan allows himself some critical consideration. However, from that point onwards, the book consists of straightforward description, potted history and dubious statistics.

The opening chapter presents a general view of the growth of scientific activity in the Arab World. Zahlan uses three basic sources for his information: UNESCO's *List of Scientific Papers Published in the Middle East (1948-1955)*, the now defunct *Arab Science Abstracts (1973-1975)* and *Who is Publishing in Science*. I would not be able to say anything about Arab science on the basis of these sources. Further I do not believe, as Zahlan does, that "scientific productivity measured in terms of publications of academic institutions is highly correlated with their scientific standing as assessed by leading scientists; it is also related to other outputs such as inventions, patents and the technological performance of the economy". These sorts of criteria for scientific productivity may be applicable to highly developed economies with sophisticated scientific infrastructures, but not to developing economies where scientists have more pressing concerns than

INTERNATIONAL JOURNAL OF

# coal geology

**NOW  
PUBLISHED**

**Editor-in-Chief:**  
**W. SPACKMAN,**  
Pennsylvania State  
University, PA, U.S.A.

**COAL GEOLOGY** is a new international journal committed to treating the basic and applied aspects of the geology and petrology of coal in a scholarly manner. Its scope encompasses -

- the genesis of coal and coal seams, including studies of modern coal-forming processes and environments

- the metamorphosis of coal materials in coal seams and dispersed in other rock types
- the geology of coal measures including stratigraphic, structural, geomorphic, paleogeographic, paleoecologic, hydrogeologic, palynologic, paleozoologic and paleobotanic facets of the subject
- the petrology and petrography of coal and coal seams including coal mineralogy, geochemistry and the chemical and physical constitution of coal.

The journal aims to stimulate the development of the science of coal geology in all parts of the world and to facilitate the dissemination of information on coals from all continents to all those who can benefit from such information.

**Types of contributions to be published are:** papers describing original research results; proceedings of symposia; surveys, reviews, book reviews, overviews, of recent literature, and letters to the editor.

### SUBSCRIPTION INFORMATION

1980-1981: Volume 1 (in 4 issues)  
Price: US \$83.50 / Dfl. 163.00 including postage.

### SUBMISSION OF PAPERS

Authors are invited to submit suitable manuscripts in triplicate to: The Editorial Office, Coal Geology, P.O. Box 1930, Amsterdam, The Netherlands.



**ELSEVIER**

**ELSEVIER**

Send for your sample copy now.



publication. Zahlan himself is aware of the shortcomings of his methodology. However, no one is really any wiser at the end of the exercise.

As Egypt has the most highly developed scientific infrastructure in the Middle East, Zahlan appropriately devotes a whole chapter to the country. It is very much a historical discussion that traces science development in Egypt from 1951. An attempt is made to chart the development of scientific activity by measuring the increases in BSc and PhD degree holders (what is an Egyptian PhD worth, in real scientific terms, anyway?). Most of the statistics are taken from government ministries and technical institutes and no attempt is made to indicate the level of reliability of the figures. After Egypt, scientific activities in "selected countries" are presented: five pages on Kuwait, just over two on Iraq, less than a page on Saudi Arabia — which has one of the most rapidly expanding scientific bases in the Middle East, with astronomical sums being spent on science and technological development — and a half-page on Syria. Is that all that is happening in these countries and in the Middle East as a whole? Is nothing going on in Sudan, Algeria, Tunisia and Jordan?

After a similarly patchy and brief treatment of scientific manpower, we reach the last three chapters on funding, international and regional cooperation, and science policy, where at least an attempt has been made to be more thorough. The chapter on funding does manage to bring out both the channels being developed to fund scientific research and development and the resources available to capital-rich and capital-poor Arab states. The chapter on international and regional cooperation amounts to little more than the minutes of meetings of the Conference of Ministers of Arab States Responsible for the Application of Science and Technology to Development, and relies heavily on national papers submitted by Arab states to the recently held UN Conference on Science and Technology for Development. It is certainly not scholarship, neither is it good journalism, but it works as an account of recent history. This is also true of the chapter on science policy; here the commentary suffers by uncritical reproduction of material from brochures and annual reports such as that of Cairo's National Research Centre.

So, what value can one place on *Science and Science Policy in the Arab World*? The book has little of value to say about science policy, and even less about science, in the Middle East. But the book works, to a certain extent, as a history of science in the Middle East in general, and Egypt in particular, during the 1950s and 1960s. It is surprising that Zahlan has nothing much to say about recent — post-1975 — developments in science and technology. He seems to have overlooked the controversies about "Arabization" of

science, planning and developing technical institutions and universities, scientific bureaucracies and the debate on Islamic science. Perhaps these omissions are deliberate, but some discussion of these issues would have saved him from the accusation that the book is remarkably boring. Perhaps Zahlan feels that he has

said it all elsewhere in one of his many excellent publications. If this is so, then why write such an empty book? □

*Ziauddin Sardar is Middle East Science Consultant to New Scientist and author of Science, Technology and Development in the Muslim World.*

## Landau in retrospect

H.B.G. Casimir

*Landau: A Great Physicist and Teacher.* By Anna Livanova. Pp.217. (Pergamon: 1980.) £10, \$22.50.



Landau in 1936

LEV Davidovich Landau (1908–1968) was a brilliant theoretical physicist, an outstanding teacher and a striking personality, with an influence spreading far beyond the circle of his students and co-workers; his merciless criticism may have antagonized some of its victims, but he was most helpful and encouraging to anyone he considered worth helping. These characteristics are clearly brought out in Anna Livanova's well-written book. Although it is neither an exhaustive biography nor a critical appraisal of the whole of Landau's contributions to physics, the author has succeeded admirably in re-creating the image of this great man and in explaining to a general reader his ways of working and teaching.

The book opens with a brief biography. Landau was born at Baku and entered the university there at the age of 14. In 1924 he moved to Leningrad, graduating in 1927. Livanova gives a short but lively description of his student days. He learnt a little from his professors, quite a bit from discussions with fellow students — but most just by himself.

In 1929 he set out on an extended visit to western Europe and England. He went to see Pauli at Zürich, collaborated there with Peierls and wrote his famous paper on

diamagnetism (the description of which, by Livanova, leaves something to be desired). At Cambridge he met Kapitza, the beginning of a lifelong friendship, but of even greater influence on Landau were his contacts with Niels Bohr at Copenhagen. Livanova reports that Landau later regarded Bohr as his one and only teacher. That may seem surprising; I cannot think of two prominent physicists who differed more widely in their approach to teaching. Livanova calls attention to this difference, but in my opinion she does not sufficiently stress this point. I believe Bohr's influence was so important because his way of looking at physics was complementary to Landau's self-taught virtuosity. Landau had far more in common with Pauli in that they possessed comparable intellectual power and mathematical skills, and both could on occasion be redoubtable critics. Even so, there was a profound difference in their choice of subjects.

In 1932 Landau became head of the theoretical division of the Ukrainian Physicotechnical Institute at Kharkov. There he began teaching in earnest, collaborated with the experimentalists — especially with Shubnikow who had set up a cryogenic laboratory — and published a number of important papers. He left Kharkov in 1937 for Moscow and there he remained as head of the theoretical division of Kapitza's Institute of Physical Problems until his death in 1968; he always refused to become head of an institute of his own.

After a serious motor car accident in 1962, Landau became practically an invalid. One can sympathize with Anna Livanova in not entering into details concerning these later years, but I find it regrettable that, although she hints at difficulties at Kharkov, she does not mention that Shubnikow was arrested and never heard of again, and that Landau spent about one year in prison in 1938 and 1939 and might have perished but for Kapitza's courageous intervention.

For me, the most fascinating chapter is that concerned with "The School of Landau". This shows Landau at the height of his powers and gives a lively picture of his particular style and methods.

About half of the book is devoted to a description of Kapitza's work on the superfluidity of liquid helium and Landau's theoretical work in this field. The author preferred to consider one important and characteristic contribution of Landau's in detail instead of discussing superficially the whole of his work, and in



this she has been most successful in epitomizing the essence of Landau as a scientist. I have only one objection. No mention is made of the analogous and simultaneous experimental work of Allen and Misener at Cambridge, or of the theoretical work of F. London and of Tisza, who predicted second-sound several years ahead of Landau. The work of Landau was hardly influenced by these parallel developments, but the reader should know of them and that Landau's work, important though it was, was neither the only nor the final step towards a theory of superfluidity.

The final chapter, "Dau Away From Physics", recounts some amusing anecdotes but is hardly profound analysis. When I knew Landau at Copenhagen in 1930 and 1931 he was in a state of transition from shyness and reticence to the sociable and self-assured man of later years. He was then already classifying all things. Physicists, people in general and girls in

particular, books, poems, motion pictures, they all received marks from one to five (one the very best, five the worst and three just acceptable). Such grading also entered into his discussion of human relations. A couple where the man was a five, whereas the wife ranked a full three was unsatisfactory and should be broken up. In retrospect such considerations seem to me the immature and not even very witty self-defence of a sensitive and vulnerable man. Livanova takes them more seriously. In those faraway days Landau was not a happy man. Livanova mentions his claim that by his rational approach to human problems he succeeded in teaching himself to be happy. Did he really? I wonder. □

*H.B.G. Casimir studied theoretical physics at Leiden, Copenhagen and Zürich, worked in low temperature physics at Leiden and later joined the Philips Company at Eindhoven. He was for several years President of the European Physical Society.*

## Emilio Segrè on physics and on physicists

John Stachel

*From X-Rays to Quarks: Modern Physicists and Their Discoveries.* By Emilio Segrè. Pp.337. (W.H. Freeman: 1980.) Hardback \$20, £11.80; paperback \$9.95, £5.40.

EMILIO Segrè is one of that group of extraordinarily gifted physicists that gathered around Enrico Fermi in the late 1920s, a

group whose members contributed so much to the development of nuclear and elementary particle physics in the ensuing decades. Like Fermi, Segrè came to the United States in 1938 and worked on the A-bomb project during the Second World War. After the War he returned to Berkeley, where he worked primarily in high-energy physics. An experimentalist,

he shared the 1959 Nobel Prize in physics with Owen Chamberlain for the discovery of the anti-proton.

This book is based on lectures in which, as he says, "I tried to show not only the main discoveries but also the way they were reached, the personalities of the leading physicists and the errors committed before the right path was found". A prospective reader should not be misled by the title: the book is about the development of atomic, nuclear and elementary particle physics and "... does not pretend to be a history of modern physics. It is, rather, an impressionistic view of the events as they appeared to me during my scientific career ...".

Segrè gives fascinating accounts, from his perspective, of the discovery of the electron, X-rays, radioactivity; the old and new quantum theories and special relativity; nuclear structure and nuclear energy; particle accelerators and high-energy physics. The discussion is quite ample until about 1960. More recent developments, and accounts of related areas of physics, are treated in much less detail. For example, quantum electrodynamics, lasers and masers, the Mössbauer effect, superconductivity, astrophysics and biology are crowded into one chapter of 20 pages. In a final chapter, "Conclusions", Segrè points out trends toward greater specialization, industrialization, abstraction, and growing ties with technology in the current development of physics.

While an attempt is made to make the achievements of the major physicists "understandable to the layman", "Some knowledge of physics ... is necessary". Most formulae, however, are relegated to ten appendices ranging from "Stefan's law; Wien's law", to "Quantum Mechanics in a Nutshell".

Most semi-popular survey books of this type seem to be written either by theoretical physicists or non-physicists, and tend to overemphasize theoretical achievements and/or adopt an overawed attitude towards modern experimental techniques. It is therefore valuable to have a book written by such an eminent experimentalist. While he does not neglect the theoretical developments or the theorists, there is a better sense of balance, and of the interplay between experimental achievement and theoretical advance, than in similar books I have read. Since it is an avowedly personal account, Segrè does not hesitate to give his evaluations of the styles of work and personalities of the physicists he is discussing, or to illuminate the text with personal anecdotes and reminiscences. The book is also enlivened by numerous well-chosen illustrations, which really add a great deal of impact to the text. A reader comparing photographs of laboratories and sketches of experimental set-ups in the first few and in the last few chapters, for example, cannot avoid being struck by the growing industrial-



Eight Nobel prize winners at the 1960 Rochester meeting. From left: E. Segrè, C.N. Yang, O. Chamberlain, T.D. Lee, E. McMillan, C.D. Anderson, I.I. Rabi and W. Heisenberg.



ization of experimental research in particle physics, also apparent from the text:

With a pun of dubious taste, I could say that it is no longer sufficient to be a Rutherford, but one must be a Rutherford-Ford, meaning that the physicist must have at least some of the qualities of an industrialist and of a businessman [p.294].

Clearly, Segrè identifies "the physicist" here with the elite of the scientific community. He does not note that if some scientists are to be industrialists and businessmen, this implies that many other scientists and technicians must be workers and wage labourers. To carry his pun a step further, today there is a Reuther-Ford division among scientists (Walter Reuther was the head of the US Auto Workers trades' union).

The comments of a leading physicist such as Segrè on men and events, his views on the development of physics and its place in the scheme of things have an intrinsic interest. But the question naturally arises: how reliable is such an unashamedly personal account? I have the impression that, overall, it is a rather reliable source of information, but have only checked the chapter on Einstein with any care. Judgements of personality will naturally tend to differ. Against Segrè's view of Einstein:

He was not averse to playing the role of the great scientist; clearly, he enjoyed it. Perhaps this explains some of his affectations, his strange manner of dress, and some habits that may have been for show. After all, he was an admirer and friend of Charlie Chaplin [p.97].

one might want to set that of Leo Szilard, who was more closely associated with Einstein:

He is a man as free from vanity as I have ever seen. I have heard him talk to an audience of a thousand in German where he was at his best, and he talked to them as he would talk to a few friends gathered at his fireside . . . If you meet him you are struck with his great modesty and his great simplicity of heart [*Leo Szilard: His Version of the Facts* (MIT Press, 1978) p.12].

As to biographical information, the chapter is fairly accurate, but I must report that there are several errors. For example, Einstein's academic career between 1908 and 1912 is incorrectly given on p.88, which also speaks of Einstein as disturbed by "the anti-Semitic atmosphere" in Prague at that time. The account of Einstein's theories is generally quite good, although Segrè gives more of an operationalist twist to Einstein's development of special relativity than I think is justified. More serious is the statement on p.95 that the experimental effects predicted by general relativity "are small and difficult to observe, so that even now there is no absolute and unequivocal

confirmation of the general theory of relativity". While certainly true, it seems to imply that Segrè believes that some other theories have been absolutely and unequivocally confirmed. This and other statements (for example the first paragraph of p.292) make it clear that philosophical problems of physics are not Segrè's strong point.

No account of the development of nuclear physics can avoid some discussion of the development of nuclear weapons, and the impact of this development on the modern world as well as on the physics community itself. Segrè gives such an account, and makes a number of interesting comments on the personalities and roles of J. Robert Oppenheimer and Ernest O. Lawrence, for example. His stance is that of an enlightened member of the US scientific establishment; one cannot find any searching criticism of either the scientific or political establishments here. His account would have to be supplemented from other sources by anyone seeking a thorough understanding of the origins of our present nuclear predicament. I do not mean to imply by this that Segrè is not well aware of the problem. In the few pages he devotes to "the influence of science on the human condition", as he puts it, he states his views:

. . . science enhances human power. It also permits (at least approximately) anticipation of the consequences of certain courses of action. However, the process of decision at both the individual and the state level is dictated not by science but rather by obscure factors that I understand only dimly. They seem to me to be largely irrational, possibly dictated by behavioural forces, evolutionary drives, or subconscious demons. We thus see courses of action that to an outside observer appear totally irrational and destructive in their consequences. The armament race is an outstanding example. Because science enhances human power, it makes these foolish pursuits more and more dangerous, so much so that they may imperil the survival of the species . . .

While the scientist has the specialized knowledge of his discipline, on other subjects he is pretty much prey to the same dark forces as is anybody else. His training and education may help him to overcome some of his irrational urges, but the idea that the objective, cool scientist is above the crowd is fallacious. This should be recognized by the scientists and by the public at large. Scientists are not priests of a magic religion [pp.288-289].

*John Stachel is a Professor at Boston University, currently working at the Institute for Advanced Study, Princeton, New Jersey.*

## Nuclear technology for the layman

Malcolm C. Scott

*Unlocking the Atom: A Hundred Years of Nuclear Energy.* By Malcolm Longstaff. Pp. 175. (Frederick Muller: London, 1980.) £7.95.

THE story of the development of nuclear energy is striking, both for the intellectual excitement which it has generated as well as for the intense political and moral arguments which have surrounded its use for weapons and for peaceful purposes. Yet, paradoxically, there have been few books which have attempted to cover these developments, particularly the technical aspects, in a way which makes them accessible to the general reader.

Despite the disclaimer in the preface — "... all I have been able to give is a sketchy account of some aspects, and particularly those which interest me most" — the scope of the book is broad. It starts with the discovery of uranium, radioactivity and fission and discusses the work leading to the two atomic bombs dropped on Japan. The post-War development of nuclear reactors for plutonium production is then covered, leading on to the start of the non-weapons orientated reactor programme. The main features of the principal power reactors in use around the world are

outlined, followed by chapters on uranium and its fabrication into fuel (including the use of lasers for enrichment), fuel use and reprocessing, and radioactive waste disposal. There are then separate chapters on safety, on energy and the place of nuclear power, and on other uses of nuclear energy. Finally, in "Looking Ahead", the author touches on some of the current arguments relating to nuclear power (for example, the question of the blackmail value of plutonium and the possible role of thorium in separating the peaceful and non-peaceful uses) and outlines the principles of nuclear fusion. Throughout the book there are well-chosen photographs and numerous other figures.

The author keeps to his intention to give "little chemistry and no mathematics", yet, nevertheless, manages to provide a comprehensive technical coverage of the subject. In doing so he defines the terms which he uses in a non-technical way, so that the lay reader should not find it necessary to read with a technical dictionary at his elbow.

There are a few inconsistencies — for example, the abundance of uranium-235 is given variously as 1 part in 140, 1 part in 139 and 0.3% (1 part in 333: this is certainly a



typographical error). Nevertheless, they are few, and the general tone of the text is one of technical correctness and authority. Yet, despite these undoubted virtues, there is something lacking: it is simply that the author has not succeeded in making the field as enthralling as he found it during his 24 years with the United Kingdom Atomic Energy Authority. Instead, one is left with the uneasy feeling that the book reads like a succession of the carefully worded, technically correct, but bland handouts favoured by public relations officers, particularly in the nuclear industry. The sense of excitement aroused by the initial discovery of fission is missing, as is any sense of the enormous technological achievement in harnessing nuclear power.

After all, the reason why nuclear power bears the brunt of the anti-technologists' onslaught is precisely because it is seen as *the* high technology, an almost unique amalgam of science and engineering. Yet none of this emerges. Everything is under control, doubts are smoothly assuaged and technology rules supreme.

Nevertheless, for the reader who is prepared to accept these limitations, the book provides an accessible and comprehensive survey of the nuclear scene at a level which invites a wide readership. □

*Malcolm C. Scott is Senior Lecturer in the Department of Physics, University of Birmingham, in charge of the MSc course on the physics and technology of nuclear reactors.*

## Life as we know it: does anyone else?

Paul Davies

*Life Beyond Earth: The Intelligent Earthling's Guide to Life in the Universe.* By Gerald Feinberg and Robert Shapiro. Pp.480. (Morrow: 1980.) Hardback \$14.95; paperback \$7.95. *Earth and Cosmos.* By R. S. Kandel. Pp.270. (Pergamon: 1980.) Hardback \$30, £13.50; paperback \$14.90, £6.95.

*Life Beyond Earth*, proclaims the publisher's blurb, "is the result of a three-year collaboration between a theoretical physicist and a biochemist . . .". That sounds like a recipe for disaster, but the end product is remarkably coherent, if a little prolix. It is also somewhat pretentious, because it presents a range of ideas, varying from uncontentious standard biochemistry to the most outrageous and bizarre speculations, in a deceptively uniform and scholarly format.

It is, of course, the outrageous ideas that make this book such fun to read. The authors pin their colours firmly to the mast in Chapter 1: "We believe that most other attempts . . . have not been sufficiently imaginative in examining the possibilities for extraterrestrial life". To remedy this state of affairs, the reader is invited to consider the astonishing prospect of living creatures inhabiting the most unlikely of habitats — wallowing in the molten interior of the Earth, bobbing about inside the Sun, crawling over the surfaces of neutron stars, or floating serenely and nebulously in interstellar space. This is all good sci-fi stuff, but my main misgiving is that while the mere existence of a source of free energy and a mechanism for self-organization are certainly necessary conditions for the appearance of some form of life, can we really believe, as the authors assume, that they are sufficient?

A related problem to the happy prospect of a Universe teeming with exotic life forms is that it is far easier to believe in the evolution of intelligence, once life

has actually gained a foothold, than in the initial appearance of living things. Yet if intelligence abounds in the cosmos, we would expect it to be conspicuous. Where is the alien technology, some of it presumably billions of years more advanced than ours? Unfortunately, Feinberg and Shapiro almost completely ignore the subjects of intelligence and alien communities, so do not attempt to face this central issue.

It would be misleading, however, to over-emphasize the bizarre in this book. The authors provide a valuable service in, for example, drawing attention to the distorted public image of the Viking experiments on Mars, popularly believed to have excluded the possibility of life there. In fact, as the authors' careful analysis shows, the results were ambiguous, and the experiments in any case left a lot to be desired in their underlying assumptions about Martian biology.

One can also be persuaded by their argument that the search for extraterrestrial life contributes hugely to the motivation for the general exploration of space. Public disappointment that space probes have not yet positively encountered even the tiniest form of life has contributed to the widespread disillusionment with these expensive enterprises. Yet the most likely abode for life in the Solar System — Jupiter — has still to be closely explored.

Inevitably, for a book that tackles a subject for which no known subject matter yet exists, *Life Beyond Earth* contains liberal doses of philosophy. Specially singled out for attack are those whom the authors dub as "carbaquists" — biochemical faint-hearts who believe that life based on the chemistry of carbon and water is the only possibility. As a physicist, the carbaquist viewpoint has always seemed to me chauvinistic; biochemists are doubtless more conservative.

Another delicate issue concerns the need for a clear definition of life. Superficial criteria such as the ability to reproduce, response to environment and so on are also displayed by systems that are normally regarded as inanimate, so Feinberg and Shapiro adopt a sort of global definition wherein life is manifested through the activity of a biosphere; that is, one should look to the highly organized and complex structure of interlocking organisms as an unambiguous indicator of life.

At the end of the day we are still left with the depressing fact that the discovery of extraterrestrial biospheres is unlikely to occur in the twentieth century, so all books of this sort really amount to little more than speculation, or at best educated guesses. Nevertheless, there is a real need for us to examine fresh perspectives of mankind and his place in the Universe. With that in mind, I found the book entertaining and generally informative.

In contrast to this ambitious work, *Earth and Cosmos* by Robert Kandel is more modest in aim though wider in scope. The author also provides a cosmic perspective of mankind by discussing in detail a whole range of physical processes that are relevant to the structure of the Earth and its immediate environment. This book is full of fascinating information, ranging from continental drift to the pollution of the atmosphere. There is an extensive discussion of both meteorology and climatology, and a detailed review of the Earth's motion. *Earth and Cosmos* makes good reading for non-specialists who want to know more about the planet we live on. □

*Paul Davies is Professor of Theoretical Physics at the University of Newcastle upon Tyne.*

## Cosmic questions

Joseph Silk

*The State of the Universe.* Edited by G.T. Bath. Pp. 199. (Oxford University Press: 1980.) £8.95, \$24.95.

DESPITE its obscure origin and intemperate past, the Universe has made a good recovery. Conditions have stabilized over the past several eons, and practically all observers now agree that a recession is with us for some time to come. However the long-term outlook remains controversial — some predict that the rate of inflation will eventually drop, heralding the onset of a long era of deflation; other forecasters, perhaps a majority, maintain that the inflation rate will hold steady into the remote future. A vocal minority even persist in finding evidence that the inflation rate is accelerating.

This situation must seem familiar to the student of economics. Likewise, cosmologists also have their differences. It



may seem strange to the layman that experts should disagree on whether the Universe will perpetually continue to cool down, to attain inexorably the ultimate energy crisis, or whether it is destined to overheat and implode into a brilliant fireball, hotter and more intense than anything imaginable by human beings. The uncertainty arises because the currently available indicators are often contradictory; the cosmologist has considerable scope for rejecting evidence that may not fit his model, especially if the evidence is incomplete and tentative. A choice still remains between the "Heat Death" of the Universe and the "Big Squeeze".

Yet our knowledge of the Universe is increasing at an unprecedented rate. The availability of observatories in space has enabled astronomers to study the Universe over much of the electromagnetic spectrum that is inaccessible from ground level, from gamma-rays to infrared radiation. And modern technology has revolutionized ground-based observing. The caricature of the earnest astronomer peering through a telescope in a cold, dark observatory dome is a myth that has long been displaced.

The modern astronomer punches in coordinates on a computer console and views the stars on a video display in a brightly lit room crammed with sophisticated electronic instrumentation. The aim is to probe ever deeper into the mysteries of the Universe, by furthering our understanding of the structures within it, from stars to galaxies, alone and in their great clusters.

Astronomers are now able — albeit barely so — to trace images of ordinary galaxies so distant that their light was emitted before the Earth was formed. In principle, with sufficient information about such systems, one could directly infer their distances and decide whether the rate of expansion of the Universe has changed significantly over this time-scale. The future of the Universe could then be predicted unambiguously. It seems likely that within the next one or two decades, provided that governments continue to make the necessary commitment to science, advances in technology, both ground-based and in space, will enable detailed studies to be made of remote galaxies at the observable edge of the Universe.

*The State of the Universe*, based on the Wolfson College Lectures given at Oxford in the Spring of 1979, provides a fascinating and highly readable account of several of the major developments that have taken place in astronomy and cosmology over the past decade. Eight leading scientists who have played key roles in many of the discoveries cover a diverse array of topics, ranging from G.E. Hunt on the exploration of the planets to D.W. Sciama on the origin of the Universe. Especially memorable is the contribution by R. Penrose on black holes, for its lucid account of space-time singularities. M.J.

Rees writes on galaxies, their nuclei and their origin, and R.J. Tayler describes current views on the origin of the chemical elements. Hunt's beautifully illustrated chapter is one of the highlights of the book, providing a full and timely account of the newly acquired knowledge of the planets from Mercury to Jupiter. Remaining chapters include D.E. Blackwell on the stars as suns, K.A. Pounds on the X-ray Universe and F.G. Smith on new ways of seeing the Universe. Geoffrey Bath is to be commended on having co-ordinated an extraordinary lucid array of timely contributions from a group of the most eminent, and certainly among the busiest, of British astrophysicists.

On reading *The State of the Universe* one cannot fail to be impressed by the immense

vistas that the explosive progress in astronomy has revealed. Much is poorly understood: indeed, a radically new approach to physics may be required if we are to discover the origin of the Universe, for example. But enough has fallen into place for us to be confident that our theories enable us to understand how much of the Universe entered into its present state. Prediction of its future evolution now becomes feasible. We can already do this for stars: it may not be long before enough data is at hand to determine definitively the future of the Universe, no less. □

Joseph Silk is Professor of Astronomy at the University of California, Berkeley, and author of *The Big Bang*, published earlier this year by W.H. Freeman.

## Tuning in to astronomy

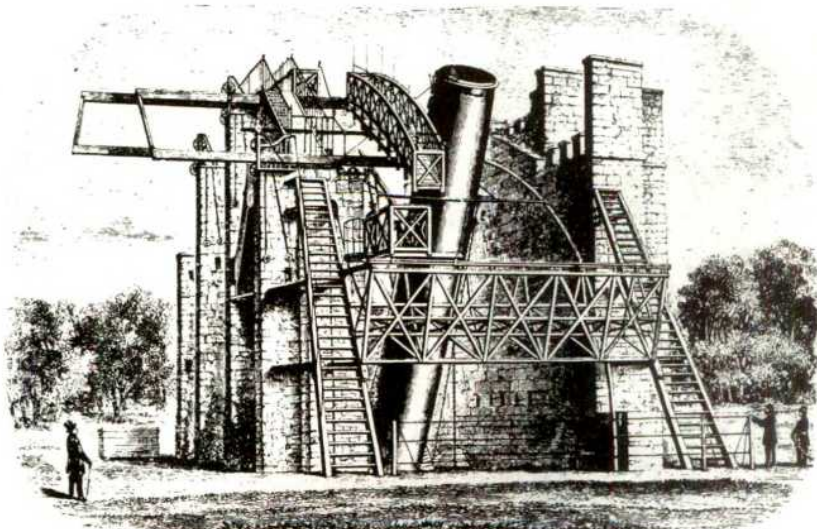
David W. Hughes

*Stargazers*. By Colin Wilson. Pp.271. (Hodder and Stoughton/Doubleday: 1980.) £10.95, \$15.95.

COLIN Wilson, the Colin Wilson who wrote *The Outsider*, *Introduction to the New Existentialism*, *Strange Powers* and a host of other titles, has now turned his attention to astronomy. He has written a fascinating account of how he thinks astronomers tick today, did tick in the past and should tick in the future, if, that is, they ever wish to solve the "fundamental question". What is the question? Bertrand Russell once said that the aim of philosophy is to understand the Universe. Wilson urges us to go a step further. The question is not just "what is the Universe?". It is "what is the *purpose* of the Universe?". Purpose, a word that makes all good scientists shudder. How should we — dry, dusty, intellectual

astronomers, tied to our telescopes, computers and respectable thought processes — delve into the understanding of the purpose of things? Wilson reveals his answer by frequent use of such phrases as "flashes of second sight", "supra-logical processes", "paranormal" and "intuitive insight". We are not told to abandon our scientific principles, we are simply encouraged to recognize that they are incomplete. There is always more than meets the eye.

The book divides into three sections. The first is a review of ancient cosmologies. Why should our ancestors build Stonehenge, what was the real purpose of the pyramids, did the ancient Egyptians know about the precession of the equinoxes? Wilson refers often to bicameralism and has obviously been much affected by Julian Jaynes's book *The Origin of Consciousness in the Breakdown of the*



Lord Rosse's giant six-foot reflector at Birr Castle in Ireland



**Bicameral Mind.** The brain is apparently split into a left half which is the home of rationalist, logical and scientific thought and a right half which houses artistic feelings and intuitive insights. Human development has led to a changeover in the dominant section. Civilization has suppressed the messages from the right brain and allowed the left brain to take over.

The second section of the book deals with the life histories and scientific achievement of some of the great renaissance scientists, Copernicus, Brahe, Kepler, Galileo, Newton and Herschel. The ghosts of Koestler's *The Sleepwalkers* and Dreyer's *A History of Astronomy from Thales to Kepler* haunt these pages.

The third section brings us firmly to the present day and traces the acceleration of

astronomical discovery that has occurred since Einstein's gravitational theory and the advent of quantum mechanics. Planetary exploration, radio astronomy, big bang cosmology, black holes, the origin of life — all are touched upon. Throughout the text echoes the Wilson message that there is more to our astronomical Universe than science can understand. The investigators must try and tune into this ethereal suprahuman influence on our destiny in a manner similar to that used by our ancient ancestors.

I enjoyed reading this book. It was fun. The style is excellent, the production standard and the illustrations are superb. But I continually had an uneasy feeling. It is an axiom that you should not believe all that you read; the reader of this book should not, and Colin Wilson should not

either. He has a regrettable tendency to regard the printed word in the same light as the tablets of Moses. Many eminent authors are quoted — Hoyle, Koestler, Motz, Taylor. When discussing Hoyle's *Lifeclock* and *Ten Faces of the Universe*, Wilson states that "No-one is going to quarrel with what they say". What? Scientists always question what other people say. The scientists such as Galileo, Kepler and Newton who are discussed in Wilson's book thrived on it. So should the readers of *Starseekers*.

But still, I congratulate Colin Wilson. Once you pick the book up it is hard to put it down. Interesting thoughts and problems sparkle from every other page. □

David W. Hughes is a Lecturer in Astronomy and Physics at the University of Sheffield.

## James Six and his thermometer

W. D. Hackmann

*The Construction and Use of a Thermometer.* By James Six. Introduction by Jill Austin and Anita McConnell. Pp.123. (Nimbus: London, 1980.) £15.

THIS small book reproduces the papers of an almost totally forgotten eighteenth century man of science, James Six (1731 – 1793), the descendant of a refugee Walloon family of silk weavers who settled in Canterbury during the reign of Elizabeth I. He was one of a score of amateur scientists who, through their individual small contributions, made scientific progress possible during the eighteenth century.

His tastes were typical of the contemporary intelligensia; painting, astronomy, electrical experiments with the new-fangled frictional electric machines, and meteorological observations. He invented a maximum and minimum self-registering thermometer in 1780; a worthwhile contribution for which he was awarded a Royal Society Fellowship in 1792. His thermometer, in which the extremes of temperature were recorded by sliding indexes, has survived as a popular domestic instrument. With it he observed the night-time inversion of temperature, a phenomenon not explained by meteorologists until the following century.

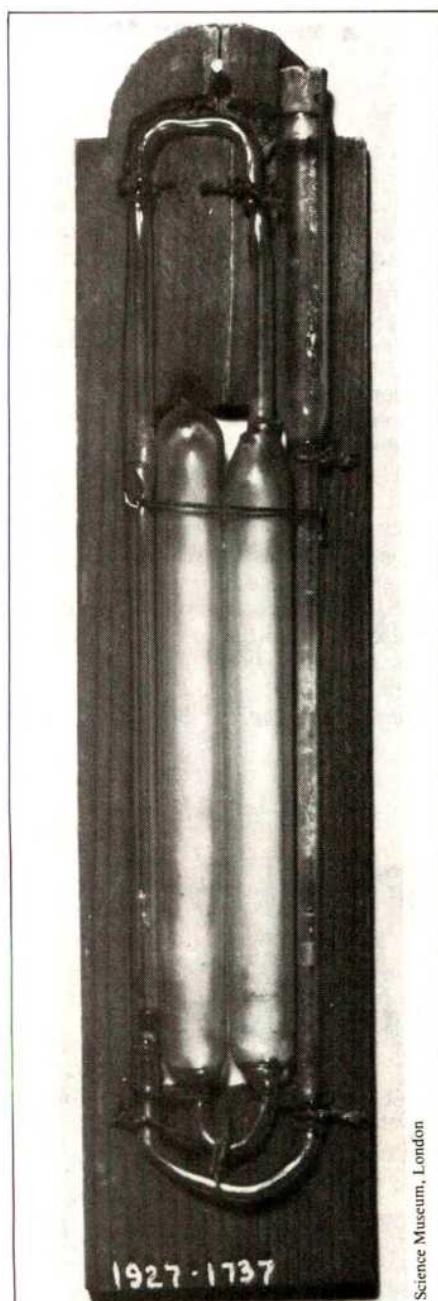
The largest portion of the book is taken up with a reproduction of Six's *Construction and Use of a Thermometer*, published in 1794, and essentially a summary of his three papers on thermometry published in the *Philosophical Transactions* with the addition of a chapter on the deep-sea use of his instrument. Eight pages are devoted to his other scientific communications. The bulk of these are his seven letters to the *Gentleman's Magazine*, a popular organ

for the amateur scientist. In 1770 he described a comet later known as Lexell's Comet. Its orbit was calculated by the American astronomer David Rittenhouse and Six's observations largely agreed with this. In 1771 and 1781 he recorded the appearance of two other comets. Other topics dealt with were the 1784 heat wave, William Herschel's recently discovered "Georgian Star" (Uranus) and a severe frosty spell in 1789. Also reproduced is a letter from the archives of the Cambridge University Library, written in 1785 by Six to a student friend of his son on the use of his thermometer. This series is terminated by a charming obituary of Six, also from the *Gentleman's Magazine*.

The only Six-type thermometer known before the researches of Austin and McConnell was the one in the Museum of the History of Science at Oxford. However, it is not contemporary, having probably been made in the 1820s for Charles Daubeny whose chemistry laboratory was housed in the present basement of this Museum. The authors have identified 26 thermometers made by Six and now part of the King George III Collection at the Science Museum in London, and another specimen of obscure origin at the Copernicus Museum in Rome. These are described in some detail and the subsequent development of the instrument is also given.

All in all, this small, attractively-bound volume not only adds a little to the history of thermometry, it also gives us another glimpse into the world of eighteenth-century men of science. □

W. D. Hackmann is Assistant Curator of the Museum of the History of Science, University of Oxford.



An original maximum and minimum thermometer by James Six, c.1782.

Science Museum, London



# Mathematics for the non-mathematician

P. T. Saunders

*Handbook of Applicable Mathematics.* Chief editor Walter Ledermann. Vol. I *Algebra*. Edited by Walter Ledermann and Steven Vajda. Pp. 532. (Wiley: 1980.) Subscription price for core volumes £27.50, \$75 each, single volumes £32.50, \$85.

UNLIKE their colleagues in physics, workers in the biological and social sciences have generally received very little training in mathematics. Few of them know more than a bit of calculus and some elementary statistics. As a result, they can find themselves totally unable to understand the increasing number of papers in their fields which employ more sophisticated mathematical techniques. Nor is it easy for even the most determined of them to do anything about this. It can be exceedingly difficult for a non-mathematician just to discover where to look up something, and even then he may be not very much further ahead. Mathematics is a cumulative subject; every new idea tends to depend on many that have come before. So he is likely to find that the explanation of the concept he is interested in is in terms of several other concepts which are equally unfamiliar. And as if that were not enough, at least some of these may originate in a different branch of the subject and not even be defined in the book he has consulted.

The *Handbook of Applicable Mathematics* represents an attempt to help "users of mathematics who are not professional mathematicians" when they find themselves in this awkward position. On completion it will consist of 16 volumes. The first six, called "core" volumes — *Algebra, Probability, Numerical Methods, Analysis, Geometry and Combinatorics, and Statistics* — are intended to cover all the mathematics the non-specialist is likely to encounter. There will also be ten "guide books", showing how mathematics is applied to different fields such as chemistry, economics, sociology, management, medicine and so on.

According to the editors, the aim of the *Handbook* is that "professional adults" needing to understand a particular mathematical idea will be able to find in it "just what they want to know". They have therefore tried to make the articles self-contained, to allow the reader to turn directly to the topic in question, rather than start at the beginning of the book. There is an elaborate cross-referencing system throughout the entire *Handbook*, so that any unfamiliar term or result can be located quickly and without searching through other works. They also claim to have "gone to great lengths to ensure that no branch of mathematics is omitted which is useful, and conversely that none is included which is not".

In some respects, the impression given by *Algebra*, the first of the core volumes

and the only one so far available, is encouraging. The general standard of writing and exposition is good, and the authors have kept in mind the desirability of explaining to the reader in plain language what is going on and what some of the definitions "really" mean.

Viewed in the light of the claims made in the introduction, however, some important shortcomings appear. While the explanations are clear and often illustrated by examples, the pace often seems too fast for a newcomer to the topic, and there are no exercises. There are inconsistencies between the chapters with regard to the amount of detail included; this is always a problem in multi-author texts but more could have been done to combat it, especially in such an ambitious work. Further, the selection of topics does not appear to have been made with the care and ruthlessness promised in the introduction; perhaps an analyst might agree that the long account of decimal expansions (without, incidentally, any real mention of other bases) is necessary, but two pages on quaternions seems an avoidable luxury.

The real problem with this book, however, is that in trying to cater for all levels of mathematical competence in one work the editors have set themselves an impossible task. There is a limit to the speed with which mathematics can be assimilated. Most of us can learn a new mathematical idea if it is clearly explained to us in language we can understand. And we may even manage to learn a second new idea based on the first. But before we can grasp a third new idea, and a fourth, we generally need some time and practice to enable us to become familiar with what we have just been taught. Many of the less essential topics which are included in mathematics courses are there for just that purpose. If we try to go on before we have allowed the first ideas to sink in, we are unlikely to understand the later ones, because they will be being explained in terms of ideas which are not yet a secure part of our mathematical vocabulary. So an explanation which is suitable for someone who has a good background in mathematics cannot be made suitable for someone who has not just by referring the novice back through a chain of earlier explanations.

So far as can be judged from the first volume and a proof copy of *Probability*, and without seeing any of the guide books, the *Handbook of Applicable Mathematics* will be of most value to those who already know rather more than the average amount of mathematics. They will find it a useful aid, but if it had been designed specifically for them it would have been a lot better. As it is, it tends to fall between two stools, with too much detail for reference and not enough for real learning, and despite its

virtues many potential users may not feel it worth the considerable outlay. As for someone with only a minimal previous knowledge, he is unlikely to find that the series will open the rich storehouse of mathematics to him, even with the effort the editors warn him will sometimes be required. He would do better to try to acquire a solid foundation from some of the good — and much cheaper — elementary textbooks which are already available. There is, as has been said before, no royal road to geometry. □

P. T. Saunders is a Lecturer in Mathematics at Queen Elizabeth College, University of London.

## Whither geography?

K. J. Gregory

*Geography: Yesterday and Tomorrow.* Edited by E. H. Brown. Pp. 302. (Oxford University Press: 1980.) £10, \$29.95.

THE 150th anniversary of the Royal Geographical Society provides the *raison d'être* for this volume. Founded in 1830, the RGS was third in the world following the establishment of geographical societies in Paris in 1821 and Berlin in 1828; like them its function included the encouragement of exploration and discovery, a tradition which has persisted to the present day.

Although the first professor of geography in Britain was appointed in 1833 at University College, London, the subject took firm root in Oxford and Cambridge, and between 1883 and 1924 the RGS gave grants to these two universities to foster its development. The Geographical Association, concerned with geographical education in schools, was founded in 1893, and in 1933 a group of geographers formed the Institute of British Geographers to provide an outlet for research publications because it was felt that the *Geographical Journal* had insufficient space for both research papers and accounts of exploration and travel.

Today, for the first time, both the President and the two Honorary Secretaries of the RGS are university geographers. Such strong links with university geography have not always featured during the course of the 150 years which are charted by T. W. Freeman in the first third of the book. Freeman concludes that the struggle for recognition of the subject has now been won; the way in which this was done and the subject recognized and established in education is explained in the following contribution by N. J. Graves.

To reveal the yesterday and tomorrow of geography as an academic discipline, the subject is divided into 12 subdisciplines,



each discussed by a different author. Inevitably, perhaps, they do not adopt a consistent approach. Some contributions are stimulating reviews which concentrate on major developments and prospects; W. R. Mead on the essence of the regional ideal, A. G. Wilson on the position of theory in human geography and Emrys Jones on the scope of social geography consider three aspects of the subject that have been prominent and partly sequential in geographical thinking during the past two decades. Other authors give a chronological summary of development in a particular branch of geography — geomorphology, land use survey, leisure and recreation, and medical geography — with passing reference to the role of the RGS. A third type of contribution provides a state-of-the-art summary of the approaches adopted by contemporary research schools; this is very effective in discussions on climate and on biogeography, tends to be somewhat compressed for historical geography, and embraces trends beyond the subject for surveying and mapping and in the chapter "Water as a Geographical Issue". Not all geographers will agree that this range completely portrays the current academic spectrum. In particular, one might have expected a consideration of philosophical approaches to the subject, and of urban geography which has been responsible for a very substantial proportion of the research output in human geography since 1960.

The overall impression of geography given by the book is that it is a subject not as disintegrated as the titles of the chapters might indicate. It is evident that more energy has been devoted to some branches, such as geomorphology, than to others, climatology for example. It is artificial to erect a barrier around a subdiscipline, and it is shown how the development of theory and of surveying and mapping, and of branches such as historical geography and medical geography, have flourished by contact with and exposure to proximal disciplines.

The debate as to whether the physical could, and should, separate from the human part of the subject appears in at least one incisive discussion, but it is apparent from a number of branches that contributions to practical problems associated with earth hazards, and social, recreation and leisure, and medical geography arise because the subject spans the interface between human activity and environment. The geographer thus has to be conversant with some techniques from the pure and applied sciences and others from the humanities and social sciences. This is at once part of the characteristic skill of the geographer. Also clearly emerging as a recurrent theme is the importance of spatial analysis — perhaps geography is really about maps, although the map may today be in the form of an equation, a satellite image or a data bank.

In the final thought-provoking chapter,

W. R. Mead, a former Honorary Secretary of the RGS, epitomizes geography as a synthetic subject in which the regionalists are closer to the heart of the subject than most. Whereas the regional ideal used to be the only crumb of integration that was offered, we now have further applicable links offered by the study of water, biogeography, land use, leisure and recreation, and medical geography. Perhaps geography tomorrow will find its integrity not solely dependent upon the classic regional approach and a book produced for the 200th anniversary could promulgate even closer liaison between the branches of the subject.

The editor introduces the volume as

## To boldly go. . .

Sarah Bunney

*To the Farthest Ends of the Earth: 150 Years of World Exploration.* (The History of the Royal Geographical Society 1830–1980.) By Ian Cameron. Pp.288. (Macdonald/E.P. Dutton: 1980.) £10.95, \$29.95.

I ASSUME it was primarily the shape rather than the subject matter that determined the prominent position of this vignette on a preliminary page of Ian Cameron's book in honour of the Royal Geographical Society, but it was an apt choice nonetheless. The engraving represents two important aspects of Victorian exploration — the appalling hardships endured by the explorers as they strove to satisfy their curiosity, and the disappointments and controversies that accompanied many nineteenth-century expeditions. In particular the picture draws attention to the sadly misguided preference of British Polar

being designed to do many things, among them to explain what is geography, what do geographers do and what use is geography. In answering these questions, particularly the second, the book is a great success. It is enjoyable to read and is extremely stimulating. Students and others should be encouraged to buy this book, but having read it they may find, like me, that an index would have been invaluable because the volume certainly deserves to become a standard work of reference. □

*K. J. Gregory is Professor of Geography and Chairman of Department at the University of Southampton.*

explorers for man-hauling their equipment instead of using dogs. It was this policy, which received the Society's support for some 50 years, that contributed to repeated disappointments on Arctic expeditions and eventually to Captain Scott's defeat in the race for the South Pole in the early 1900s.

Ian Cameron, who had access to the Society's records while writing his book, is scrupulously fair in his treatment of this unhappy story and of the other difficulties that beset many of the expeditions in the Society's first 75 years. Personalities, warts and all, are vividly brought to life. Mr Cameron also gives a balanced account of the Society's more recent — and somewhat insensitive — handling of the choice of leader for the Everest expedition. In the event this expedition was a glorious success and it is, of course, achievement and not failure that this book is mostly about. There is plenty of solid, but never heavy description of the most important expeditions of the past 150 years, accompanied by excerpts from notebooks, dispatches and contemporary accounts in the Society's *Journal*.





All this makes for such fascinating reading that I would have preferred more of the highly readable text and fewer illustrations — even though many of the latter are delightful, particularly the polished sketches by Baines and the early photographs. My one serious complaint concerns the maps. It is ironic that, in this of all books, these are heavily drawn, inadequate and, in at least one case (the Musandam map on p.224), inaccurate. Furthermore the two contemporary maps included are almost illegible, they lack captions and it was only on reading the acknowledgements that I learnt of their source and date.

This book cannot be a comprehensive history of the RGS, and Mr Cameron has wisely concentrated on the expeditions to areas that have long been the favourites of armchair travellers — the Arctic and Antarctic, the Himalayas and Africa. New to me were most of the early explorers of Australia and the brave Pundits who secretly and at great hazard to themselves surveyed on foot almost the whole of the Eastern Himalayas in the 1850s to 1870s. Childhood heroes — Burton, Speke, Livingstone, Stanley, Nansen, Shackleton, Scott, Hunt, Hillary and Tenzing (but only one heroine, Florence Baker) are included. Mr Cameron also gives credit to many other explorers, less well known but equally deserving of fame, who doggedly helped fill in the blanks on the maps. I am only sorry that room could not be found in this catalogue of illustrious names for some



After the summit of achievement: Hillary and Tenzing after the first ascent of Everest, May 1953.

mention of the Arabian travels of Wilfred Thesiger and Freya Stark.

Mr Cameron brings readers up to date with accounts of some of the recent, increasingly scientific, expeditions that the RGS has supported — to the Mato Grosso (1967–1969), the Musandam Peninsula (1971) and the Mulu rain forest in Sarawak

(1977–1978), for example. The book ends with a chapter on the role of the Society today as it continues to advance geographical knowledge. It is a quieter role, without the glamour and heroics of the past, but no less important for that. □

Sarah Bunney is a freelance writer and editor.

## Stonehenge and its times: a layman's and a scholar's view

R.J.C. Atkinson

*The Enigma of Stonehenge.* By John Fowles and Barry Brookoff. Pp.128. (Cape/Summit: 1980.) £6.95, \$19.95. *The Age of Stonehenge.* By Colin Burgess. Pp.402. (Dent/Biblio: 1980.) £12, \$25.

THESE are two very different books, which have in common only the name of Stonehenge in their titles. The first is the result of a most happy collaboration between an English novelist and an American photographer, both of genius, to give a unique picture of Stonehenge itself. The second is a sober and most scholarly interpretation (John Fowles would call it clinical) of the prehistory of the British Isles during the *flourish* of Stonehenge.

Fowles's short account begins with his own first happy visit to Stonehenge as a child, and with his last, less happy because the stones are now closed to the public. His summaries of the archaeological background and of the sequence of building can be faulted in detail by the pedantic specialist; but they are based on a wide and critical reading, and they are written with a delusive ease and with an informed humanity which puts to shame the earnest

but pedestrian locations of most other recent writers about Stonehenge, myself included.

He asks: "What is Stonehenge for?" For me this is an unanswerable question, because I do not think that the mute material evidence of prehistory can tell us, except in a quite trivial sense, what people thought in the remote past, but only, up to a point, what they did. This is not to say, as Fowles hints, "a pox on all speculation"; but speculation and valid inference are two very different things, and must be distinguished, perhaps better than Fowles does.

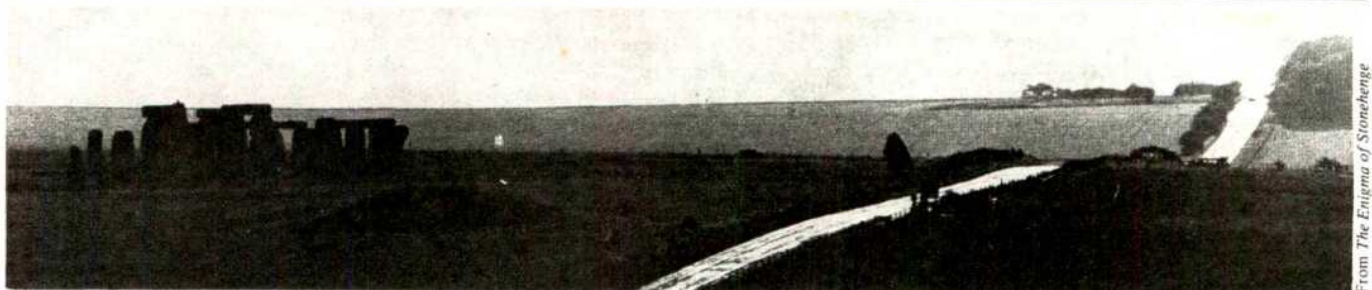
In his longest chapter, "The Moon-Mirror", he perhaps accepts too easily some of the astronomical uses ascribed to Stonehenge by Hawkins, Hoyle, Newham and Thom. Moreover, he confuses the Metonic Cycle with the period of rotation of the lunar nodes, and falsely explains the position of the Heel Stone, as a possible marker for the mid-point of the azimuthal limits of most northerly moonrise, in terms of the latitude of Stonehenge. He also infers, quite incorrectly, that the absence of any discussion of astronomical theories from my own book *Stonehenge* (Hamish

Hamilton, 1956) was intended as a "monumental snub" to Hawkins, Hoyle and Thom. Far from it. My book was written in 1955, before any of these theories were published, and has since been reprinted only with appendices to bring the results of later excavation up to date.

Fowles's luminous text ends with an historical and personal appreciation of Stonehenge-in-the-mind, and not least in the mind of that eerie and disturbing seer, William Blake. He protests throughout against "a quite unnecessary polarity in twentieth-century society between pure science and impure speculation". This echoes what I wrote in *Nature* (265, 11; 1977). The science is far from pure, because much of the basic data are at best uncertain, and at worst corrupt. The speculation is likewise not impure, merely because it is speculation; but it is not inference compelled by the evidence of Stonehenge-on-the-ground.

Barry Brookoff's photographs, unnumbered and uncaptioned, match John Fowles's text in their sensitivity and imagination. No one has better frozen in print an image of Stonehenge. His



From *The Enigma of Stonehenge*

occasional use of a wide-angle lens gives a sense of spaciousness which the monument itself belies, though one which echoes some of William Stukeley's engravings of 1740. Occasionally a Sun or Moon has been added by photomontage for dramatic emphasis at far more than natural size. Not the least haunting of these photographs capture, as none has before, the texture of the surface of some of the sarsen stones, in which each beholder will see his own private vision.

This book, in words and images, will enlarge the consciousness of every visitor to Stonehenge, past and future.

Colin Burgess's book will likewise extend the thinking of every British prehistorian, and of colleagues abroad. It is a major advance in the synthesis of the new evidence which has become available, almost explosively, from excavations and the analysis of museum collections during the past 20 years for the period of 3,000 years from 3,200 BC, which corresponds roughly to the use of Stonehenge.

He divides this into five periods, each identified by a type-site, and each characterized in his view by specific practices or trends, in ritual architecture for worship or burial, and in the design and manufacture of artefacts. This is a convenient chronological device for avoiding the constraints of ill-fitting radiocarbon dates with their present state of uncertainty. He gives also, however, a list of 215 radiocarbon dates in their raw (uncorrected) form. One may ask whether these, when corrected, may not provide a better framework than a series of largely arbitrary periods which, because they are new, may be adopted and maintained long after they have ceased to be significant. He rejects, rightly, the old and now outmoded divisions of the conventional Neolithic and Bronze Age.

Burgess's main thesis is that tribal territories had already been fixed by the end of the fourth millennium BC, and that thereafter cultural change took place by the adoption of innovations across persisting tribal boundaries, with local adaptations increasing in proportion to the distance from the primary source. This is a possible model, though the one which rests on a number of quite unverifiable assumptions, and one which rejects explicitly the "invasion hypothesis" that has long been dominant in explanations of British prehistory.

In his proper desire to emphasize cultural continuity, however, he has

perhaps underestimated the impact of the Beaker people coming from across the North Sea and the Channel in the middle of the third millennium BC. Whether this was an invasion, an incursion or an immigration, or a series of any of these processes, on whatever scale, is largely a semantic question. What is evident is that there was a fairly rapid innovation in material culture, superimposed on native practices which survived by absorption. This cannot be explained except by an incoming from abroad, and a break in the continuity of native traditions. Burgess does admit, quite rightly, that at the end of the "Age of Stonehenge" there may have been an influx of foreigners who established the succeeding "Age of Hill

Forts", though they are far less well represented in the archaeological record than the Beaker people.

This is a book for specialists in British prehistory, and not least for university students. It is well illustrated by photographs of sites and objects. The numerous line-drawings of plans and artefacts have been rather over-inked and thus harshly reproduced, and the inclusion of north-points and scales is a little capricious. Minor defects apart, it is a major contribution to the understanding of a formative period of our prehistoric past. □

R.J.C. Atkinson is Professor of Archaeology at University College, Cardiff.

## The rediscovery of ancient Ebla

J.M. Munn-Rankin

*EBLA: An Empire Rediscovered.* By Paolo Matthiae. Translated by C. Holme. Pp.237. (Hodder and Stoughton/Doubleday: 1980.) £12.95, \$14.95.

THE excavation in 1974 and 1975, at the north Syrian site of Tell Mardikh, ancient Ebla, of a mid-third millennium palace with some 20,000 cuneiform tablets written in a previously unknown Semitic language was an event of outstanding importance for historians of early urban society in the Near East.

Prior to this discovery, archaeological and textual evidence for developments in Syria during the Early Bronze Age (c. 2900–2000 BC) was meagre. As compared with the earliest centres of civilization, Sumer and Egypt, relatively few Syrian excavations had penetrated below second millennium levels and of these most were stratigraphic sondages. At only a few major sites, mainly in the north-east, had more extensive excavation produced significant evidence of urban settlement. Literacy was attested only at Mari on the Euphrates where a Semitic language was written in the cuneiform script of Sumer. Of the population it could be said only that it was probably of mixed ethnic origin and that its social structure ranged from primitive nomadism to complex urbanism. It was, however, apparent that the urban civilization of Sumer, in existence by the second half of the fourth millennium, had

played a major role in the formation and subsequent development of Syrian civilization, the main impetus for the expansion of its influence being the need for the timber, stone and metal in which southern Iraq is deficient. As regards the political geography of Syria, a limited amount of information was provided by the records of Sumer, among the earliest being the campaign reports of Sargon and Naram-Sin of Agade (c. 24th and 23rd centuries BC) which list cities conquered on expeditions to the Mediterranean. Among them is Ebla.

This inadequate picture of the early culture and history of Syria is now being transformed by the excavations of Paolo Matthiae of Rome University at Tell Mardikh. In this report on their progress, he describes and assesses the significance of the finds made between 1964 and 1976. The site was occupied from the latter half of the fourth millennium until the sixteenth century BC, but work has so far been concentrated on the cities of the mid-third and early second millennia. Excavation of the latter has made a major contribution to knowledge of the architecture and art of that period, but of far greater importance are the unique discoveries in the earlier level.

Here was a major urban centre with central acropolis and lower town, perhaps covering some 56 ha, encircled by a defensive wall. Excavation has exposed part of an acropolis palace, including an



administrative block with archive rooms and magazines. The destruction of the building by fire preserved much of its contents: carved furniture, miniature sculpture, seals, decorative stone inlay, pottery and one of the largest collections of cuneiform tablets ever found. The great majority of these tablets are administrative and economic in content but there are also literary compositions, lexical texts, royal edicts and correspondence and treaties. Because of their number and the difficulties posed by the Eblaite language, it will be many years before their publication — entrusted to an international committee — is complete, but preliminary studies provide a foretaste of the rich harvest of information which will eventually be available on the population, economy, institutions, religion, literature and political history of the city.

Any reconstruction of the society and history of Ebla must at this stage be provisional. Matthiae's account, based on the textual evidence available when the 1977 Italian edition went to press, has to a certain extent been amplified and clarified by subsequent research, mainly in the field of linguistics. The population was predominantly but not exclusively Semitic and the closest connections of the Eblaite language are now considered to be with Akkadian, the speech of the Semitic element in the population of Sumer. A considerable amount of information is available on state and municipal administration but there remain many fundamental questions, answers to some of which may not be provided by the type of text found so far. For instance, was kingship hereditary or elective? What proportion of the population was in the service of the state, the temple or large land-owners and under what conditions?

Whether Ebla was the leading state of northern Syria and the centre of an extensive empire, as maintained by Matthiae, requires further investigation, but its conquests included Mari and it was in diplomatic contact with states as far east as the Tigris valley, notably Ashur with which it concluded a commercial treaty. Its far-reaching trading operations are documented by an archive dealing with the state-controlled export of woollen cloth. The destinations of the consignments are distributed over an area extending from Palestine to central Anatolia and from the Mediterranean to Ashur and Kish in northern Sumer. These names of towns and kingdoms provide much new information on political geography but although some are well known, such as Megiddo and Lachish, the majority cannot be located and there are numerous uncertain readings.

The civilization of Early Bronze Age Ebla was formed by the fusion of Syrian and Sumerian cultural traditions. The former are at present most evident in language, religion and architecture; the latter in the use of the cuneiform script, in

literature, art and certain administrative practices. The extent to which political and social institutions were influenced by those of Sumer is not yet clear. Until the lower levels of the site are investigated, the environmental and cultural factors which contributed to the rise of urban life at Ebla must remain a matter of speculation. However, archaic Sumerian elements in the political concepts and art of the palace period suggest that Sumer provided the initial stimulus, probably in the late fourth millennium when it had trading colonies in Syria.

It seems probable that the palace and its archive, which spans the reigns of five kings, was destroyed either by Sargon, founder of the Agade dynasty of Sumer, or by his grandson, Naram-Sin. According to one school of thought, the form of the script employed at Ebla requires the earlier dating. Matthiae prefers the later on the basis of certain artistic features.

The rediscovery of Ebla is of outstanding importance for the early history of civilization in the Near East. The texts and archaeological finds recovered from the palace have revealed the presence in northern Syria in the mid-third millennium of an established urban and literate Semitic society, as advanced as that of contemporary Sumer. The nature of the impact of Sumerian civilization on what was clearly a strong native cultural tradition can already be defined in considerable detail. The texts, when published, will illuminate the history not only of Ebla but also of the numerous states with which it had political and commercial contacts. The significance of the information obtained from Ebla cannot as yet be fully assessed but Matthiae indicates the areas in which it is to be sought. □

*J. M. Munn-Rankin is a Lecturer in Near Eastern History at the University of Cambridge.*



The art of Ebla: wooden figure of a king from Palace G.

## The appeal of archaeology

Gail Kennedy

*The Cambridge Encyclopedia of Archaeology.* Edited by Andrew Sherratt. Pp.495. (Cambridge University Press: 1980.) £18.50, \$35.

THE goal of this handsomely produced volume is to "summarize the present state of knowledge over the whole field of archaeological inquiry". While *The Cambridge Encyclopedia of Archaeology* does not quite achieve that somewhat quixotic goal, it does succeed to an impressive degree.

The overall value of the volume, however, rests as much with its clear presentation of the new directions taken by archaeologists since the 1960s, as with its summarization. In the past most books of this large-format genre have reflected

the earlier emphasis of archaeologists on the exquisitely formed artefact or imaginatively recreated structure; such books have relied more on lavish illustrations and less on informative text. While this volume is indeed well illustrated, the emphasis is on maps and schematic diagrams rather than artefacts, which here are pictured simply and in black and white. The maps — of physical geography, migration patterns, political domains and urban or village street plans — are among the most beautiful and informative in print.

While the maps and diagrams will undoubtedly set a publishing standard for the future, the text is no less attractive and informative. It clearly reflects the trend among archaeologists away from the antiquarian-collector attitudes of the past and



towards data synthesis, broad regional analyses and model building. It demonstrates clearly that archaeology today is problem-orientated rather than artefact-orientated. The problems now under examination by archaeologists often centre on the dynamics of interactions between man, his technology and the environment. Systems theory and feedback models provide valuable ways of examining such interactions, and indeed many of the sections in the *Encyclopedia* are structured either implicitly or explicitly around these conceptual frameworks.

A systems approach becomes a particularly useful tool in archaeology when analysing the emergence of entirely new levels of organization. No longer are such new levels viewed by archaeologists as periods of abrupt revolutionary technological or behavioural change, but instead are seen as periods of adjustment and readjustment to changing configurations of resources and knowledge. The origins of agriculture form one of the more intriguing applications of systems theory. At the end of the last glacial, environmental changes apparently provided both the opportunity and the necessity for the increasingly specialized exploitation of food resources. What is well demonstrated in the chapters on the origins of agriculture in the Near East Africa and the Far East is that this new and unique strategy for human survival occurred, apparently independently, in several areas. Thus, in each of these major regions, and in at least one centre in the New World, human populations responded to the changing post-glacial world in a recurring pattern of increased utilization of a small number of wild foods. It was this emerging dependency on wild foods which led to their ultimate control and domestication. And it was this control over local food resources that paved the way for an increasingly sedentary way of life.

The variety of subjects covered by the book is indeed encyclopaedic. While most of the chapters consist of regional analyses of important phases in human history — the origin and development of agriculture, cities and empires, for example — other relevant topics such as early human evolution and dating techniques have not been neglected. The geographical scope, however, is somewhat uneven. Of a total of 64 chapters, only seven (eight if one includes Oceania) are devoted to the archaeological history of the New World. While it may be conceded that the Old World was long the central focus of human development, surely the entire Western Hemisphere merits more discussion than these few rather perfunctory chapters. Moreover, certain major problems in New World prehistory, such as the probable timing and route of human entry, have not even been mentioned.

In the final analysis, the faults of *The Cambridge Encyclopedia of Archaeology* are few. The short, well-illustrated

chapters are suited for both browsing and more directed reading, while their content will inform all but the specialist. Although price is a drawback, this would be an extremely useful text for broad survey courses in archaeology. The consistent emphasis on method, theory and recent

research, the bibliography and broad geographical and temporal scope all combine to make this a volume with wide appeal. □

Gail Kennedy is at the Department of Anthropology, University of California, Los Angeles.

## Cancer: how much of a business?

D.G. Harnden

*The Cancer Syndrome*. By Ralph W. Moss. Pp.347. (Grove Press: 1980.) \$12.95, US only.

IT is usually assumed that those involved in cancer research are motivated by a desire to rid the world of the disease. While this may be partly true, intellectual curiosity and concern for individual patients are often the most potent driving forces. Ralph Moss, however, tells us something different. Cancer research in the USA is, he says, largely manipulated by big business in the hope of financial gain; manipulated by those who believe that a cancer cure will make a fortune for the holder of the patent and by those who fear that preventive measures will involve cleaning up a profitably polluted environment. The medical profession too, he suggests, are part of this conspiracy, favouring treatments which ensure a handsome profit.

It would be easy to dismiss Moss's book as inaccurate in detail and outrageously biased, but to do so would be to fail to acknowledge that some of the criticisms that he makes seem well aimed and that the issues he raises are of considerable importance. Unfortunately, he does not spell out or consider in any constructive way the main issue that he raises, namely "What is the proper relationship between the fundamental discoveries of biological science and the industry that can make these discoveries available to the general public?"

There are two central allegations around which the book is built. First, that orthodox treatment is unsuccessful and that the cancer establishment in the USA will take any steps to ensure that new developments which are not patentable are stifled at birth or as soon thereafter as possible. Second, that little emphasis has been placed on prevention because it would be more profitable to find a patentable cure and because prevention might involve fundamental and expensive alterations in industrial practices.

Is there any truth in either of them? For the commonest cancers it is true that the results of conventional treatment are not good. In breast cancer the five-year survival rate is approximately 50% (and, as Moss reminds us, five-year survival is not cure), while for lung it is a disastrous 5%. Even worse, neither figure is improving. When we say that improvements have

occurred over the past few years it is essentially in cancers that are uncommon, such as Hodgkin's disease and in the childhood neoplasms such as Wilm's tumour. But many cancer patients are cured and many more are given a greatly improved quality of life, so there is, at least, some over-statement. However, when Moss points to over-optimistic propaganda about cures it is hard to disagree with him — we have a long way to go. He therefore suggests that we turn to unorthodox methods such as laetrile, Coley's toxin, hydrazine sulphate and vitamin C, and says that information that such methods are already successful has been deliberately suppressed. In a vitriolic attack on the Memorial Sloane Kettering Cancer Centre, the American Cancer Society and the National Institutes of Health, he accuses these institutions and specific individuals of blocking grant awards for research in these areas and of granting awards to others for their help in this process.

As a science writer sacked from the Memorial Sloane Kettering for misrepresenting the work of the Institution, Moss can hardly be without bias — but he is well informed. He shows that the governing bodies of the Memorial Sloane Kettering Cancer Centre and the American Cancer Society have a large representation of those whose business connections could lead to a conflict of interest. Obviously there are altruistic reasons why industrialists and financiers would wish to serve on the board of a cancer centre, but there could be less worthy reasons. Although overt attempts to influence scientific policy would obviously be resisted by the scientific staff, the possibility of indirect influences, especially by those who donate very large sums of money to the institutions, must be a matter for concern. Moss also points to the form of contract between the Memorial Sloane Kettering Cancer Centre and the chemical companies which seems to grant all the advantages to the companies. This is not an easy matter, and the link between industry and the scientist often poses a dilemma. Anyone in cancer research who has a connection with industry is liable to be accused of having compromised his scientific integrity. However, Moss is more concerned with undermining the present structure than with suggesting improvements and the important questions are left unasked.

It really does seem hard to believe that successful unorthodox treatments are suppressed because they are not patentable. If they were good then they would have been adopted in countries other than the USA where the allegations of corruption levelled by Moss do not apply. Moreover, Moss mentions, but gives scant attention to the need to protect the public from unscrupulous frauds. There are too many documented cases to ignore the fact that National Institutes of Health, the American Cancer Society and similar bodies have a duty not only to promote research, but also to protect the public from quacks. So the first charge is not entirely proven; nonetheless, Moss's book leaves an uncomfortable feeling that all is not well.

When he turns to cancer prevention (or the lack of it) he is on firmer ground. There is plenty of evidence that in the past, and also at present, some parts of industry have callously ignored the welfare of their workers. Moss revels in the horrors of asbestos and mesothelioma. These facts have been well documented elsewhere, however, and are no longer the main issue. He is quite wrong in saying that research into preventive methods has been ignored;

this only reveals his limited horizons. There is at present a great deal of activity in basic research laboratories and in industrial laboratories to find ways of preventing the widespread use of hazardous chemicals. Again, this needs collaboration between industry and basic research, but the relationship is not always an easy one. Any scientist who helps a company to sort out a problem is likely to be branded a consultant — and therefore suspect — by people such as Moss. This should not be so — the expertise in the universities and research institutes *should* be available to industry. On the other hand, it does cause concern that one distinguished scientist and government adviser should also be found to be a consultant for six large corporations and two manufacturers' associations.

The book is well written and easy to read. In an era in which monoclonal antibodies and the production of specific polypeptides by genetic manipulation are likely to become big business, it raises issues that have to be faced. The manner in which the issues are raised, however, leaves a rather nasty taste in the mouth. □

*D. G. Harnden is Professor of Cancer Studies at the University of Birmingham, UK.*

atherosclerosis may be a paediatric problem is dealt with. Although this is a prudent approach it is emphasized that proof is at present lacking. A brief chapter is devoted to inborn errors — principles and not details. The final chapter discusses the management of chronic diarrhoea in children.

The second volume, concerned with nutrition and growth, draws attention to the diffuse nature of the subject, the value of having different perspectives, and the fact that there are few "absolute" answers to the various problems such as standards for growth and dietary allowances.

The first chapter considers the problem of nutrient needs. In the absence of proper experiment, the tendency is to consider present intake as "ideal requirements". In the next chapter the complex interrelationships between genetic constitution and nutrition are discussed. The influence of non-dietary factors is dealt with, as also is the problem of metabolic anomalies.

Part II is concerned with the ages of man and is introduced by a chapter on maternofoetal nutrition which presents results of the 1969 longitudinal INCAP study. This leads logically to a consideration of the nutrition of the full-term and premature baby. The need for further work on the problems of the latter is emphasized. Four chapters are then devoted to the young child and discuss the normal and failure-to-thrive child, protein-energy malnutrition and obesity respectively. The adolescent, rapidly changing organism and the adult, stabilized situation between development and senescence are then discussed. Part III contains nine contributions which deal with aspects of growth monitoring and nutritional assessment and surveillance, and contains much practical information on different methods and useful tables of reference data.

Volume 3A starts with a discussion of nutrient requirements — what they are and the bases of recommendation — leading on to contributions concerned with energy requirements, the suppliers of energy and their interrelationships, the problem of energy exchange and the partition of food energy. The remaining four chapters deal with nutrients with special functions — proteins and amino acids, essential fatty acids, cholesterol and dietary fibre.

Volume 3B is introduced with a chapter on vitamins, mainly those of the B-group, as co-enzymes. There are five chapters on individual vitamins and one on iron-haemoglobin. The chapter entitled "Trace Elements" starts with a somewhat scant treatment of calcium, phosphorus and magnesium. There are useful discussions of drug-nutrient interrelationships and the effects of oral contraceptives on nutrient requirements. The final chapter on nutrition of the elderly has very much a North American bias.

Volume 4 is concerned with the metabolic and clinical application of nutrition.

## State of the art in nutrition

J.W.T. Dickerson

*Human Nutrition—A Comprehensive Treatise.* General editors R. B. Alfin-Slater and D. Kritchevsky. (Plenum: 1979/1980). Vol. 1. *Nutrition: Pre- and Postnatal Development* (edited by M. Winick), pp.495; £24.89, \$39.50. Vol. 2. *Nutrition and Growth* (edited by D.B. Jelliffe and E.F.P. Jelliffe), pp.450; £23.63, \$37.50. Vol. 3A. *Nutrition and the Adult: Macronutrients*, pp.290; £15.75, \$25. Vol. 3B. *Nutrition and the Adult: Micronutrients*, pp.424; £24.89, \$39.50. (Both edited by R.B. Alfin-Slater and D. Kritchevsky.) Vol. 4. *Nutrition: Metabolic and Clinical Applications* (edited by R.E. Hodges), pp.478; £23.63, \$37.50.

THIS large work has grown out of an idea "to provide the research investigator and the advanced graduate student with an up-to-date report on the state of the art". Originally intended as one volume, the treatise now has four volumes and one (Vol.3) has two parts.

Volume 1 deals with the role of nutrition in pre- and postnatal development, and starts with a discussion of nutrition and the metabolic development of mammals. Metabolic status at various stages of development is closely related to the quality and quantity of the nutrients consumed. The author (Hahn) suggests that the old idea that nutrients act directly on most cells must be discarded and

replaced by a concept that, mostly, nutrients have immediate and long-term effects by acting on selected endocrine cells, which then release their hormone to act on target cells. It is this combined effect which controls the development of enzyme systems, cells and tissues.

The development of the brain is important in controlling the ability of the organism to respond to its environment and malnutrition may, because of the time-scale over which the brain develops, have permanent deleterious effects upon it. The importance of this subject is reflected in several of the following chapters.

Nutrition and pregnancy is largely discussed from the viewpoint of the effects of disturbances in maternal nutrition on the growth and development of the foetus. The effects of nutrient excesses and of interactions of drugs with nutrients are briefly mentioned. This leads logically to a discussion of breast feeding by Jelliffe and Jelliffe who make the point that the matters that need emphasis are the same the world over.

The contribution on the interactions of nutrition and infection includes a discussion of the problem of the septic patient. In the chapter on the relationship of nutrition to dental development and disease the need is emphasized for more studies to explore the mechanisms and consequences of nutrient deficiencies to oral health. The recognition that



The first three chapters discuss the relationship of nutrition to disorders of the haematopoietic, nervous and musculoskeletal systems respectively. These chapters are not exhaustive and are not concerned with therapeutic aspects. The effects of essential nutrients on the gastrointestinal tract and the effects of diseases of the tract on the absorption and utilization of nutrients are dealt with, as also are the nutritional abnormalities occurring in liver disease. Here again there is no discussion of the possible role of nutrition in treatment. This is in contrast to the presentation on cardiac failure which is much concerned with therapeutic aspects and contains a useful table of drug-nutrient interactions of importance in congestive heart failure.

Discussion of the relationship of diet and nutrition to cancer is mainly concerned with their possible involvement in the aetiology of oncological disease, with little mention of the effects of the disease on the nutrition of the patient.

The ageing-nutrition-health triad is discussed by Watkins who points out that education is the prime catalyst for inducing change. The chapter on the endocrine system is concerned with diabetes, vitamin D, and parathyroid and thyroid disorders. Discussion of megavitamins and food fads is largely taken up with doubts about Pauling's well-known views. It is, perhaps, unfortunate that in a text of this sort some consideration is not given to the possibility that larger amounts of vitamins than the currently recommended allowances may have beneficial effects which are difficult to measure and therefore often dismissed as anecdotal.

There is a useful and well-referenced chapter on the effects of ethanol. Nutritional aspects of infectious diseases

are discussed and it is pointed out that nutritional supportive therapy should be employed to prevent or minimize the depletion of body stores during an infection, and to replace lost nutrients as expeditiously as possible during convalescence. Obesity is the most common nutritional disease in Western society. Assessment, risks and treatment of this poorly understood condition are considered. As a consequence of our poor understanding successful treatment is often elusive, and the demand for treatment has led to a multiplication of fad diets, examples of which are given. The final chapter contains a discussion of the interrelationships of nutrition and the kidney. Effects on kidney function and nutritional disturbances in the nephrotic syndrome, hypertension and renal failure are dealt with, as also are the principles of nutritional therapy.

These volumes are a useful addition to the textbooks available on human nutrition. They are not exhaustive, either in respect of subjects covered or the depth to which each subject is discussed, but the material is well presented and well referenced throughout. Moreover, the books have been produced to a high standard and are a pleasure to read. In spite of their inevitably high price, teachers of nutrition at degree level may well consider it worthwhile acquiring one or more of them. They can be said to have achieved their aim and to present in reasonable compass the present state of the art in a dynamic subject. □

*J.W.T. Dickerson is Professor of Human Nutrition at the University of Surrey and Consultant Adviser on Clinical Nutrition to the South West Thames Regional Health Authority.*

subject, of course, to the disabilities consequent upon their pre-operative brain damage.

Here we also had a neurosurgical preparation in which, with appropriate techniques that were lacking in the 1940s, one could investigate the cognitive capacities of the left and right hemispheres isolated from each other except through their brain stem connections. The preparation enabled workers to confirm, extend and fine the deductions that had previously been drawn from the effects of lateralized injury, namely, that the left and right hemispheres (in the majority of the population) are indeed primarily implicated in the exercise of linguistic and visuo-spatial skills, respectively. But because in the commissurotomy patient the left hemisphere has little knowledge of what the right hemisphere is doing (and vice-versa), the enticement of talking about these people as if they had two minds within a single body (brain? person? soul?) proved irresistible (and not only to popularizers). The lure of thinking about the patients in this way is, of course, much more exciting than patiently trying to comprehend the what, how and why of functional localization.

But worse was to come. The disconnected right hemisphere, conspicuously deficient in syntax and verbal reasoning, can yet support dreams, emotions, and a high level of non-verbal memory and intelligence. All that remained was to deify the distinction between the cerebral hemispheres: the left brain became the seat of a cold, calculating, logical and talkative mind, whilst the right brain sustained a warm, intuitive, emotional and artistic mind. In an era in which attitudes towards science are often ambivalent, what could be more attractive than to have science and surgery discover the reality, nay the material substrate even, of intuition, creativity and pure feeling.

Modern times are truly an ideal medium in which to culture the hundreds of articles and books that have attempted to disseminate "the right brain revolution" that Blakeslee describes. Yet there is a sense in which any sociological analysis provides too easy a let-out. Blaming the *Zeitgeist* never takes us very far. The real vacuum that such books attempt to fill arises from the failure of neuroscientists themselves to provide any significant theoretical account of functional localization. The evidence — from anatomy and pathology, and from recordings of the electrical and chemical activity of the normal intact brain — now overwhelmingly supports the notion that distinct cerebral regions are differentially involved in the exercise of higher cognitive functions. How and why this is the case we do not know. It could, however, be an interesting problem for someone to work on. □

*John C. Marshall is in the Neuropsychology Unit, Department of Clinical Neurology, The Radcliffe Infirmary, Oxford.*

## Abdication of reason

John C. Marshall

*The Right Brain: A New Understanding of the Unconscious Mind and its Creative Powers.* By T. R. Blakeslee. Pp.275. (Papermac/Doubleday: 1980.) Hardback £10, \$10.95; paperback £2.95.

THIS is another "popular" book on how to unlock the emotional and creative power of the right cerebral hemisphere. The volume recounts some of the evidence, from both normal and brain-injured people, that has led physicians and clinical psychologists to believe that considerable specialization of function characterizes different areas of the human brain. Blakeslee concentrates on inter- rather than intra-hemispheric localization and leaps somewhat wildly from datum to conclusion. For any reviewer who wants to dip into his repertoire of sarcasm, the volume will provide more than adequate stimulus — why is there no woman Beethoven, the author asks, and answers that the cerebral

hemispheres of women are functionally less differentiated than those of men. It is tempting to regard Blakeslee's offering as beyond satire and plunge immediately into instant sociology. Why do such books exist? What need do they satisfy?

The "right brain revolution" that Blakeslee and so many others have attempted to explain to a lay audience had its genesis in 1962. Two Los Angeles neurosurgeons, Philip Vogel and Joseph Bogen, revived and refined a surgical procedure for the control of pharmacologically intractable epilepsy. The operation involved sectioning the corpus callosum and the anterior and hippocampal commissures — the main fibre tracts that interconnect the two cerebral hemispheres at the cortical level. There can be little doubt that both the original and subsequent series of commissurotomy operations have been a success; patients whose intellectual and social activity had been severely compromised by generalized convulsions have been able to return to an essentially normal life, although still

## REVIEW ARTICLE

# Carbonic metamorphism, granulites and crustal growth

R. C. Newton & J. V. Smith

Department of the Geophysical Sciences, University of Chicago, Chicago, Illinois 60637

B. F. Windley

Department of Geology, University of Leicester, Leicester LE1 7RH, UK

*Stabilization of early crust against melting by high radioactivity and against resorption into the mantle by fast convective overturn requires that water and heat producers were flushed upwards within 50 Myr of accretion. Creation of a refractory base of granulite by metamorphism associated with CO<sub>2</sub> vapour explains CO<sub>2</sub>-rich fluid inclusions in ancient high-grade rocks, minor-element depletions and local phenomena of arrested development of charnockite in Precambrian terrains. The hot-spot and plate-tectonic models of Precambrian crustal evolution lead to different schemes for CO<sub>2</sub> delivery to continental roots. New tectonic concepts may be needed to explain carbonic metamorphism and other features of early crustal evolution.*

THE continental crust consists of a heterogeneous assemblage of rocks whose crystallization ages fall into clusters dating back<sup>1</sup> 3,800 Myr. If earlier crust existed, it was presumably destroyed by resorption into the mantle or by meteorite impacts, by analogy with the Moon<sup>2</sup>. Radiogenic heat production would have halved during the period<sup>3</sup> 4,500 to 3,000 Myr ago, but even by 3,000 Myr the latest estimate of total heat production of the Earth<sup>4</sup> implies an average volcanic activity for the Earth's surface similar to that of Iceland at present<sup>5</sup>. The important problem is thus how the continental crust became stabilized in the Archaean era against melting at its roots, and against resorption into a rapidly convecting mantle.

The well exposed Archaean terrain of south-west Greenland contains areas of tonalitic gneisses with two discrete ages (Amîtsoq, 3,650 to 3,700 Myr; Nûk, 2,800 to 3,000 Myr).<sup>6</sup> Other terrains support the concept of major episodes of crustal accretion from partial melting of mantle, and the similarity of initial isotope ratios to model values for mantle evolution implies little contamination by earlier crust<sup>7</sup>.

Ancient terrains are generally metamorphosed into the amphibolite and granulite grades. The mineral chemistry of the granulites demonstrates reaction over a pressure range<sup>8</sup> ~7–12 kbar (0.7–1.2 GPa), which corresponds to a depth range of ~25–40 km before uplift in response to erosion and tectonic forces<sup>9</sup>. Granulite rocks contain much less H<sub>2</sub>O than lower-grade rocks with similar major-element chemistry: anhydrous pyroxene minerals are prominent in granulites whereas the hydroxylated minerals mica, amphibole and epidote are the mafic equivalents in rocks of amphibolite facies. Charnockite, a pyroxene-bearing rock of granitic composition, is a conspicuous type of granulite which dominates some granulite terrains (for example, southern India). Some charnockites have igneous precursors<sup>10,11</sup>, but some have been attributed to metamorphism of layered sediments<sup>12</sup> and anatexis mobilization of graywackes<sup>13</sup>.

Many granulites have lower contents of large-ion lithophile elements (for example, U, K, Th, Rb) and heavy rare earths than younger crustal rocks with similar major-element chemistry<sup>14,15</sup>. Heat-flow and heat-balance<sup>16</sup> calculations demonstrate that the lower part of the continental crust is strongly depleted in radioactive elements with respect to upper crustal rocks, and show that widespread crustal melting by intrinsic heat produc-

tion would have taken place in the Archaean unless the radioactivity was strongly concentrated in the uppermost part of the crust by some transport mechanism within 50–100 Myr after an accretion episode<sup>3</sup>. Hence granulites are the obvious candidates for deep continental interiors, and granulitization, either by igneous or metamorphic processes, or both, deserves detailed study.

A unique feature of many granulites is CO<sub>2</sub>-rich fluid inclusions in minerals, in contrast to H<sub>2</sub>O-rich inclusions characteristic of lower-grade metamorphic rocks<sup>17,18</sup>. Hence carbonic volatiles may be important in granulite metamorphism and continental stabilization<sup>9,15,19,20</sup>. For carbonic metamorphism to be applicable to entire continental bases, a large, possibly subcrustal, source of CO<sub>2</sub> would be needed. Carbonate-bearing peridotite is stable in the mantle to higher temperature than mica-peridotite<sup>21</sup>, and is a possible source of CO<sub>2</sub>. Interrelations among granulites, crustal growth, carbonic metamorphism and mantle storage of CO<sub>2</sub> are now examined with reference to simple tectonic models currently being discussed for evolution of Precambrian crust.

## Origin of granulites

It has been suggested that granulite terrains in general are the residues of crust depleted in H<sub>2</sub>O and lithophile elements by partial melting (anatexis), with removal of the melt phase to shallow depths<sup>22</sup>. However, there is much evidence against this hypothesis. K-rich granites and higher-level amphibolites are not complementary in either major or minor elements to many granulites<sup>9,15</sup>. Indeed, some granulites, such as the Madras charnockites<sup>23</sup> with granitic chemistry and high Fe/Mg, would themselves qualify as the out-melted fraction. In some migmatite areas, both out-melted and residual fractions are in the granulite facies<sup>24</sup>. Tonalitic gneisses have similar Ba/Sr in both amphibolite and granulite grades; the latter could not be residues from closed-system melting of the former because of greater preference of Ba over Sr for a melt fraction<sup>15</sup>. It has been shown that outmelting did not occur extensively during the 2,700 Myr granulite metamorphism of the Scourian terrain of the Scottish Highlands, the key evidence being preservation of the 2,900 Myr Sm–Nd age<sup>25</sup>. Although granulites cannot in general be anatexis residues, some pyroxene gneisses might be



residual fractions of mantle or deep-crustal melts<sup>26,13</sup>. The pronounced depletion of heavy rare-earth elements of many pyroxene gneisses may require a two-stage formation: original accretion of a basaltic pile and remelting of the basalt to produce tonalite at depths great enough to stabilize garnet in the residue<sup>15</sup>.

Granulite terrains contain a wide variety of bulk compositions matching the metamorphosed igneous and sedimentary components of lower-grade terrains. In Karnataka, India, the metamorphic facies changes southerly from greenschist to granulite<sup>27</sup>. Marbles, basic rocks, pelites, migmatites, Fe-rich quartzites and dominant tonalitic gneisses occur over hundreds of kilometres, and granulite metamorphism, which has affected all of these lithologies, is not obviously associated with partial melting and complementary residues. A similar situation exists in south-west Greenland<sup>9</sup>.

Although many or most granulites have not undergone extensive partial melting, a mineralizing pore fluid is needed to explain the coarse K-feldspar in pegmatoidal charnockites from Enderby Land<sup>28</sup> and Pallavaram, Madras<sup>23</sup>. Kinetic calculations (see ref. 29) show that growth of large garnets at metamorphic temperatures requires a flux. A pervasive fluid would help to transport minor elements<sup>15</sup>. The discovery of dense, CO<sub>2</sub>-rich fluid inclusions in minerals of granulites<sup>18</sup>, and the intimate connection between charnockite and CO<sub>2</sub>-rich inclusions over broad terrains, points strongly to the role of CO<sub>2</sub> in the metamorphism. In the Bamble terrain, southern Norway, fluid inclusions change from aqueous in amphibolite facies to carbonic in granulite<sup>17</sup>. The Kleivan pluton, south-west Norway, grades from normal granite with aqueous inclusions to charnockite with carbonic inclusions<sup>30,31</sup> over 5 km. In the zone of regional transition from amphibolite to granulite in Karnataka, patches of charnockite are locally developed in amphibolitic gneiss<sup>27</sup>. Irregular diffuse stringers of dark-brown charnockite obliterate the pronounced migmatitic banding of gneisses over a scale of 1 cm to 1 m. Amphibole and biotite of amphibolite give way to pyroxenes in patches of charnockite with no textural evidence of melting<sup>20</sup>. Temperatures could not have risen significantly over 1 cm to produce dehydration. Influx of CO<sub>2</sub> along shears was invoked to explain the dehydration. Similar patchy distribution of charnockite occurs in south-west Greenland<sup>9</sup>, south-west Sweden<sup>13</sup> and western Australia<sup>32</sup>. The fluid in cordierite from Finnish granulites has CO<sub>2</sub> mole fractions<sup>33</sup> ranging from 0.35 to 0.85; cordierites from some rocks in the amphibolite facies have much higher H<sub>2</sub>O/CO<sub>2</sub> than cordierites from Norwegian granulites<sup>34</sup>; and cordierites from shallow pegmatites contain no CO<sub>2</sub> in contrast to abundance in cordierites from granulites<sup>35</sup>.

This evidence for abundant CO<sub>2</sub> complements evidence from experimental and theoretical phase-equilibrium studies that granulite-forming fluids must have low  $P_{H_2O}$ . Mineralogical geothermobarometry of granulites consistently yields temperatures of 700–900 °C and pressures<sup>23,36</sup> of 7–12 kbar. However, many rock types yield granitic liquids at 650–700 °C and  $P_{H_2O}$  of a few kbar (ref. 37). In particular, the definitive charnockitic assemblage K-feldspar + orthopyroxene transforms to biotite + quartz or partially melted assemblages at water pressures above 0.7 kbar, regardless of the temperature<sup>38</sup>. To avoid melting, the water fractions of metamorphic fluids must be low, such as the 0.1–0.3 estimated for the amphibolite-to-granulite transition in the Archaean terrain of south-west Greenland<sup>9</sup>.

It must be emphasized that experimental work and geothermobarometry indicate that simple metamorphic dehydration reactions are not sufficient to account for the dryness and minor element depletion of granulites. Some overwhelming pore fluid diluent is called for, and the fluid inclusion evidence implicates CO<sub>2</sub>.

### Amount and source of carbonic fluids

The upper limit of  $P_{H_2O} = 0.3P_{total}$  for granulites from south-west Greenland allows rough estimation of the amount of CO<sub>2</sub> required for conversion of amphibolite to granulite over a

20-km thick layer of crust. A continuous flushing action is needed because H<sub>2</sub>O from the breakdown of hydrous minerals would otherwise dilute the CO<sub>2</sub>. For a conservative estimate of 1 wt% of H<sub>2</sub>O in amphibolitic gneisses and an ideal gas law, about 8 wt% CO<sub>2</sub> is needed ( $44/18 \times 0.7/0.3 \times 1$  wt%), or roughly 0.3 rock volume at average temperature and pressure. This much CO<sub>2</sub> is ultimately necessary to convert an amphibolitic crustal layer to granulite, and the supply may possibly be maintained over the duration of a metamorphic episode, say tens of Myr. The actual amount of CO<sub>2</sub> in the rocks at any instant may be very small, in the form of grain-boundary films.

Thin marbles and calc-silicates occur in greenstone piles and as metamorphic relics in Archaean high-grade terrains<sup>39</sup>. Calc-silicate rocks, possibly representing former limestones, are conspicuous locally in some terrains but are usually subordinate to associated charnockites and other granulites<sup>9</sup>. Although the graphite contained in many Precambrian metasediments<sup>39</sup> might react with H<sub>2</sub>O to produce CO<sub>2</sub> at high temperature and pressure, the mole fraction of CO<sub>2</sub> produced by reaction in a closed system is below 0.7 for a large range of  $T$  and  $P$  (ref. 40). Osmotic escape of H<sub>2</sub>, or fluid immiscibility<sup>41</sup>, might cause CO<sub>2</sub> enrichment.

Some authors have dismissed crustal sources of CO<sub>2</sub> as inadequate to produce the kind and degree of metamorphism observed<sup>9,20</sup>. However, it is very difficult to estimate the original CO<sub>2</sub> content of a highly metamorphosed section. Extensive evaporite sequences rich in carbonate and organic carbon have been recognized recently in the Archaean of Brazil<sup>42</sup>, and stratigraphy of this sort may have been more abundant than generally recognized. We emphasize here mantle outgassing as a more feasible CO<sub>2</sub> source<sup>9,19,43,44</sup>, while recognizing the inherent difficulty of assaying possible crustal contributions.

The present-day mantle contains substantial CO<sub>2</sub> in spite of extensive partial melting. Hawaiian volcanoes emit CO<sub>2</sub>-rich gases<sup>45</sup>. Mid-ocean ridge basalts contain CO<sub>2</sub>-bearing vesicles<sup>46</sup> and xenoliths of mantle peridotites contain fluid inclusions of nearly pure CO<sub>2</sub> (ref. 47). A high CO<sub>2</sub> activity is important for generation of alkali basalts and carbonatites<sup>48–50</sup>. Depending on the  $P$ - $T$  regime, the CO<sub>2</sub>-bearing phase in equilibrium with olivine and pyroxene of the mantle is either a carbonate (dolomite or magnesite), a CO<sub>2</sub>-rich melt, or a free vapour<sup>21,51,52</sup>. To provide 0.3 rock volume of CO<sub>2</sub> for 20 km of crust, 0.04 rock volume would be required from an assumed 150 km of uppermost mantle; this corresponds to ~1–2 wt% of carbonate minerals or interstitial carbonate-rich melt.

Mantle carbon, as represented by diamond and carbonatites, has a smaller amount of <sup>13</sup>C ( $\delta^{13}C \cong -6\%$  relative to the commonly used standard) than limestone, which averages about +20%. Carbon from the CO<sub>2</sub>-rich fluid inclusions of Bamble granulites is near the mantle value, which was used as evidence of a 'primary' carbonic fluid from the upper mantle<sup>53</sup>. However, graphite of biogenic origin is also very light<sup>42</sup>, and it is not clear how much this may have influenced the granulite fluid inclusion carbon. Isotopically light carbon is a necessary, but not sufficient, criterion of a subcrustal source.

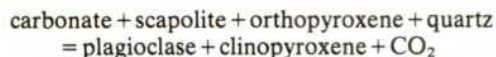
If the whole Earth went through a vapourization stage at the end of accretion<sup>54</sup>, it is not obvious how to explain the presence of CO<sub>2</sub> and other volatiles (for example, <sup>3</sup>He) in the Earth's mantle<sup>55</sup>. Late accretion of cool volatile-rich material on to an Earth that had been cooled by intense volcanic activity during accretion<sup>4</sup> is more plausible. If the primitive mantle was effectively degassed during an early period of high temperature, some form of subduction is needed to carbonate the mantle. Recent experimental data suggest that some pelagic limestone, perhaps inorganically precipitated, might escape dissociation and melting during subduction into the mantle<sup>56</sup>. Carbonate-bearing peridotite is stable to higher temperature and should tend to resist melting better than mica-bearing peridotite above 26 kbar (ref. 21), during convective overturn of the mantle. Although there is no compelling evidence for plate-tectonic subduction in the early Archaean, assimilation of carbonate-bearing sediments into the crust may have occurred during



destruction of crust<sup>4</sup> before 3,900 Myr BP. If the Earth's mantle contained elemental carbon at the end of accretion, oxidation to CO<sub>2</sub> might have occurred during transportation to the surface by convective overturning, or by disproportionation of ferrous iron into ferric iron and iron metal at high pressure<sup>57</sup>.

### Phase-equilibrium constraints on carbonic metamorphism

Some experimental phase-equilibria<sup>58</sup> would allow partial remelting of a basaltic lower crust to yield tonalitic liquid and a garnet-bearing residue. The latter would provide a sink to explain heavy rare-earth depletion in granulite (that is, anhydrous) conditions. A two-pyroxene granulite of basaltic composition begins to melt to garnet + clinopyroxene + liquid at ~1,190 °C for 11 kbar and 1,230 °C for 15 kbar (ref. 58). In the subsolidus region, olivine and orthopyroxene are progressively eliminated with increasing pressure, and garnet becomes stable at ~10 kbar. A late Archaean geotherm<sup>3</sup> would allow dry basalt to melt to a garnet-bearing residue and a tonalitic liquid at ~12.5 kbar and 1,200 °C. The experimental melting relations place an effective limit of ~40 km on the thickness of the Archaean crust with this geotherm, which passes near a *P-T* estimate for Madras granulites<sup>23</sup>. Formation of carbonate-bearing scapolite in basaltic to intermediate compositions places limits on the conditions in which CO<sub>2</sub> may stream through the lower crust. Although calcic CO<sub>2</sub>-scapolite is stable by itself to very high temperatures at elevated pressures, the retention of CO<sub>2</sub> by basalt is limited by the reaction:



The *P-T* location of this reaction is not yet known, but a moderately large geothermal gradient (see, for example, ref. 3) would probably pass through the free-CO<sub>2</sub> field (right-hand side of the above reaction) for about the lower half of the crust. Details depend on the Na/Ca ratio of the plagioclase and the CO<sub>2</sub>/SO<sub>4</sub> ratio of the scapolite, and much further experimentation is needed.

A basaltic liquid rising from the mantle would release CO<sub>2</sub> during ascent, either because of greatly decreased solubility below 20 kbar (ref. 48), or because of crystallization. At 10 kbar, basaltic magma saturated in CO<sub>2</sub> and H<sub>2</sub>O releases a vapour with CO<sub>2</sub> mole fraction<sup>59</sup> near 0.9, and such a vapour would be rich enough in CO<sub>2</sub> to purge overlying crust until it became too diluted in captured H<sub>2</sub>O.

Another possibility is transport of CO<sub>2</sub> during crustal accretion by the dissolved volatile complement of primary tonalitic liquids generated directly by mantle melting<sup>9</sup> leaving a garnet-bearing residue, perhaps in a subduction zone. Evaluation of this and related possibilities requires discussion of tectonic mechanisms of Archaean crustal accretion.

### Tectonics of carbonic metamorphism

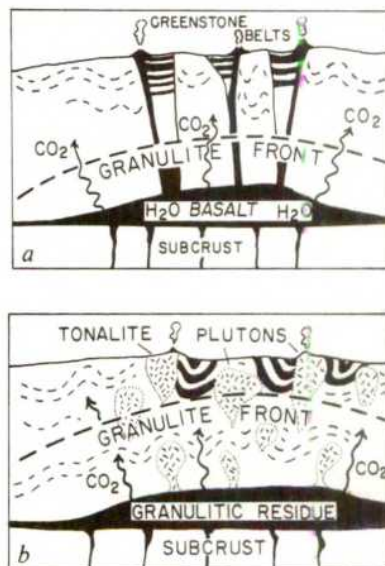
Because many granulites should still be buried and because many must have been destroyed by retrograde metamorphism, there is considerable doubt about the rate of generation of granulites throughout geological time. The simplest tectonic model involves continuous outgassing of CO<sub>2</sub> from the mantle into the lower crust. By analogy with the evidence for generation of crust<sup>1</sup>, the supply of CO<sub>2</sub> would have been episodic. Subduction of carbonate sediments and their assimilation into peridotite might replenish the mantle reservoir, and convective overturning would take newly carbonated peridotite under a continent where CO<sub>2</sub> could be released to cause carbonic metamorphism. However, a comprehensive model should consider the problem of the great concentration of granulites in the age range 3,000–2,500 Myr and show the relationship of these granulites to other components of the Archaean crust.

There is no agreement on the tectonic relationships between low-grade greenstone belts and high-grade regions of the

Archaean era, and simple analogies based on modern plate-tectonic<sup>60,61</sup> and hot-spot<sup>62,63</sup> models may be misleading because of possible change of convective style and melting processes in the mantle as heat flow declined. Hot-spot models are inspired by extrusion of large volumes of basalt at Hawaii and Iceland where generation of proto-continental nuclei may be occurring. Plate-tectonic models draw support from (1) calc-alkaline nature of island-arc volcanic rocks and probable andesitic composition of mean continental crust<sup>64</sup>; and (2) analogies between ancient rocks in granulite-gneiss Archaean belts and deeply eroded Cordilleran batholithic belts<sup>65</sup>. A linear sequence of ridge, trench and subducted slab is probably incompatible with the high heat flow<sup>4</sup> and unstable continental nuclei of early Archaean times. Perhaps numerous plume-like cells with radial rather than lateral spreading<sup>4,63,66</sup> partly coalesced into short ridges as the Earth cooled. It seems certain that a tectonic model for development of granulites in high-grade regions will not prove fully satisfactory until the relationship to greenstone belts is explained. However, the tectonics of ancient carbonic metamorphism will be discussed with reference to the contrasting hot-spot and plate-tectonic models to focus attention on the problems of CO<sub>2</sub> delivery to the lower crust.

### Hot-spot model

Basaltic magma from a rising mantle plume or diapir may escape to form a massive intrusion<sup>63</sup> under existing continental crust (Fig. 1a). Water is retained by amphibole in crystallizing basalt, and CO<sub>2</sub> escapes to flush out water from overlying crustal rocks<sup>18</sup> to produce a granulite front. On cooling, an underplated basaltic pile turns into amphibole-bearing eclogite, garnet granulite, or garnet amphibolite. Underplated crust becomes distended, as perhaps in the present western US, and deep, block-faulted grabens are filled with basic lavas and detritus to become greenstone belts or cratonic supracrustal troughs. Note that the apparent trough-like nature of greenstone belts may actually be due to post-deposition tectonics<sup>67</sup>. As the mantle



**Fig. 1** Hot-spot model of crustal growth and granulite metamorphism. *a*, Basaltic liquid from a mantle diapir (not shown) underplates existing crust, and crystallizing amphibole retains H<sub>2</sub>O. Doming of the crust results in massive grabens filled with volcanic and sedimentary rocks which become metamorphosed into greenstone basins (GB). A granulite front develops from carbonic metamorphism caused by CO<sub>2</sub> released either directly from the mantle or from crystallizing basalt. *b*, Steepening of the geotherm causes remelting of deep-seated rocks to yield a garnet-rich residue and uprising magmas. Resulting tonalite plutons rise through the crust causing isoclinal folding of greenstone basins. Further CO<sub>2</sub> streaming causes rise of a granulite front.



plume continues to rise, geothermal gradients steepen. The basaltic continental roots undergo partial melting to yield magmas of intermediate composition. These rise diapirically as tonalitic plutons which engulf the greenstone belts<sup>68</sup> (Fig. 1b). Escape of tonalitic magma leaves behind a mafic to ultramafic residue. Basaltic magma continues to escape from the mantle bringing further H<sub>2</sub>O and CO<sub>2</sub>. The key to this model is escape of CO<sub>2</sub> as a vapour phase at a pressure near 20 kbar while a secondary amount of H<sub>2</sub>O is either trapped in hornblende in the deep crustal residue or transported upwards in a tonalitic liquid. Whereas H<sub>2</sub>O may be transported to the surface in an undersaturated tonalite melt without significant reaction with crustal rocks, CO<sub>2</sub> vapour may diffuse upwards flushing water in front of it until either the H<sub>2</sub>O/CO<sub>2</sub> ratio of the vapour becomes too high to remove further H<sub>2</sub>O or the stability field of scapolite is reached.

The geochemistry of magma generation in rising mantle diapirs is not fully understood at present, and the possibility of generating intermediate calc-alkaline liquids in the presence of H<sub>2</sub>O and CO<sub>2</sub> components directly by partial melting of the mantle under a hot spot must be retained as an alternative. CO<sub>2</sub> in the mantle might be expelled during partial melting or at least partially dissolved in the tonalitic liquid. Subsequent freezing of this liquid in the crust could release CO<sub>2</sub> for metamorphism.

Factors in favour of a hot-spot model are:

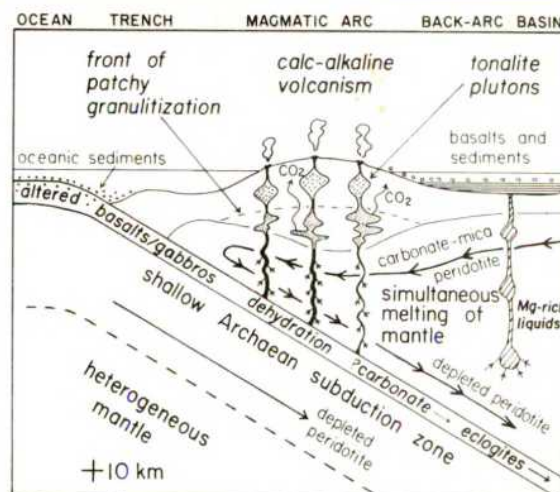
- (1) Field mapping and mineralogical geothermobarometry of post-Archaeon 'hot-spots' in continental settings: Adirondack Highlands<sup>69</sup>, Wilmington Complex, Delaware<sup>70</sup>, Naxos thermal dome<sup>71</sup> and Massif Central, France<sup>72</sup>. Particularly indicative of a mantle origin for CO<sub>2</sub> is the low <sup>13</sup>C of fluid inclusions from Naxos, in spite of abundance of local limestones. <sup>13</sup>C-poor CO<sub>2</sub> of present-day carbonic acid springs in tectonic regions is attributed to a mantle origin<sup>73</sup>.
- (2) Continental underplating provides a heat source for high-grade metamorphism of the lower crust. For Naxos<sup>71</sup>, a heavy CO<sub>2</sub> influx of 0.06–0.8 rock volume was estimated to provide enough heat to raise the regional blueschist terrain to migmatite grade.
- (3) Compelling evidence for escape of CO<sub>2</sub> from the mantle today.

Some problems with the hot-spot model are:

- (1) Although high CO<sub>2</sub> activity in the upper-mantle plume might be expected to produce some alkaline basalts<sup>52</sup>, these are almost unknown in the Archaeon<sup>39</sup>.
- (2) Ancient tonalities are strongly depleted in heavy rare earths<sup>74</sup>. Explanation in terms of residual garnet is not supported by too low seismic velocity in lowermost crust for abundant garnet, and modest amount of garnet in granulite nodules transported by kimberlites through shields. A proposal<sup>19</sup> that heavy rare earths were depleted by complexing and vapour transport is not supported by experimental evidence on rare-earth partitioning between silicate melt and high-pressure CO<sub>2</sub>-rich fluid<sup>75</sup>. Crystallization of very abundant residual amphibole might alleviate this problem.
- (3) In western Greenland, both the 3,700 Myr Amitsoq and 2,900 Myr Nûk tonalites were partly metamorphosed into the granulite facies, and it is not clear how a single mantle reservoir could achieve this: however, continental drift and mantle convection might bring a second reservoir into position.
- (4) No explanation is given for strong horizontal tectonic movements during emplacement of tonalite gneisses (for example, Amitsoq and Nûk gneisses<sup>76</sup>).

## Plate-tectonic model

The margin of an Archaeon proto-continent (Fig. 2) consists of a magmatic arc coupled with a back-arc basin. A batholithic root becomes a high-grade granulitic belt after carbonic metamorphism, and basalts and graywacke detritus of the back-arc basin ultimately collapse into a greenstone belt as the island arc coalesces onto continental foreland<sup>77</sup>. Altered oceanic basalts and sediments rich in H<sub>2</sub>O and CO<sub>2</sub> undergo dehydration and



**Fig. 2** Asymmetric plate-tectonic model for crustal growth and carbonic metamorphism. Subsequent compression converts the back-arc basin into a greenstone belt while the magmatic arc undergoes horizontal deformation to produce a high-grade region. Repeated under-riding of the subducted slab and coalescence of each back-arc basin and magmatic arc produces a complex terrain of greenstone belts and high-grade suites. In the subducted slab, dehydration occurs by loss of either a vapour or a liquid phase which passes into the mantle wedge. Some carbonate may survive with eclogite to become mixed mechanically with depleted peridotite. The volatiles from the descending slab interact with carbonate-mica peridotite in the mantle wedge to basaltic magma which mostly crystallizes in the base of the crust where amphibole retains H<sub>2</sub>O. Carbon dioxide is released into a vapour phase which produces a front of patchy granulitization. Remelting of amphibole-rich rocks produces tonalitic magmas which transport H<sub>2</sub>O in the liquid phase to higher levels, leaving a granulitic residue behind. Earlier igneous rocks underwent later carbonic metamorphism.

decarbonation reactions<sup>21</sup> during shallow subduction to produce a devolatilized residue of eclogite with some surviving carbonate<sup>56</sup>. Either magmas or vapours, or both, rise into the mantle wedge carrying mainly H<sub>2</sub>O but with some CO<sub>2</sub>. Heavy arrows indicate corner flow of the mantle wedge<sup>78</sup>, and small arrows indicate melting simultaneously with devolatilization of the subducted slab and possible partial melting therein. The mantle wedge is assumed to provide more CO<sub>2</sub> than H<sub>2</sub>O. Magmas, generally of quartz tholeiite, differentiate in the lower crust, leaving an amphibole-rich residue which retains water and augments rare-earth fractionation caused by residual garnet in the sinking slab. Magma differentiation produces tonalitic plutons and calc-alkaline volcanism. Release of CO<sub>2</sub>-rich vapour in the lower crust, as for the plume model, produces a granulitic lower crust with a front of patchy granulitization. These processes are envisaged to occur quasi-simultaneously but unevenly over ~50 Myr as subduction varies. Finally, when the island arc coalesces with continental foreland, the supply of volatiles from the subducted slab dies away.

The above scheme is tectonically similar to one<sup>79</sup> for Mesozoic calc-alkaline volcanic-plutonic complexes of the western US in which a postulated basaltic underplate is covered by a 10 km granulite layer succeeded by a lower-grade terrain in which crowding of emplaced plutons caused lateral compression. In western Greenland, rising tonalitic plutons became emplaced along active thrust planes<sup>86</sup>.

Alternative mechanisms for calc-alkaline magma generation are by direct melting of oceanic crust in the subduction zone and by direct melting of the overlying mantle wedge. Given the lack of experimental knowledge of melting in mafic and ultramafic systems with mixed H<sub>2</sub>O and CO<sub>2</sub>, and at relatively low pressures, as in a fast shallow convection system, these possibilities cannot be ruled out.



The relative supply of  $H_2O$  and  $CO_2$  is extremely important for success of the plate-tectonic model. Recent mid-ocean basalts tend to absorb more  $H_2O$  than  $CO_2$ , but the most altered ones can contain roughly equal amounts ( $\sim 2$  wt%)<sup>80,81</sup>. Most  $CO_2$  of a subducted slab probably derives from thin calcareous oozes which permeate brecciated basalts as a matrix in the uppermost part of Layer 2<sup>82</sup>. Amphibolitized gabbros of Layer 3 have very little  $CO_2$ <sup>83</sup>. That ancient oceanic basalts may have absorbed more  $CO_2$  than younger ones because of a higher atmospheric pressure is worth exploration. Nevertheless, it seems difficult to obtain a substantial  $CO_2/H_2O$  ratio for a subducting slab, and it seems necessary to appeal to the mantle wedge for the bulk of the  $CO_2$ . Perhaps some carbonate survives in the subducted slab, and augments the mantle reservoir after mechanical mixing with depleted peridotite.

Attractive features of the plate-tectonic model are:

- (1) The general calc-alkaline composition of ancient gneisses is similar to that of the rocks of modern volcanic and batholithic arcs.
- (2) Young back-arc basins compare fairly well in rock types and overall chemistry with greenstone belts<sup>61</sup>. Although some chemical features differ<sup>84</sup>, temporal evolution of the mantle rather than tectonic mechanism may be the principal cause.
- (3) Structural evidence for horizontal tectonics in ancient terrains suggests plate collision.
- (4) Replenishment of  $CO_2$  under continents is provided by 'conveyor belt' action of the mantle wedge associated with the subducted slab.
- (5) Garnet-rich residues mainly in the mantle, coupled with amphibole precipitation in the lower crust, can explain rare-earth fractionation in the tonalitic gneisses.

As with the hot-spot model, unanswered problems exist in the plate tectonics model:

- (1) How can  $CO_2$  remain stored in the mantle during transport under the back-arc basin into the mantle wedge? Should not the  $CO_2$  have escaped with basaltic magmas into the back-arc basin which is supposed to become a greenstone belt?
- (2) How can complex sequences of greenstone belts and intervening high grade gneisses be developed? For the present model the most obvious mechanism is successive coalescence of volcanic arcs onto continental foreland; however, no lateral age variation in greenstone belt sequences has been found<sup>85</sup>, and andesites, the characteristic rocks of modern island arcs, are apparently rare in some ancient greenstone belts (ref. 39).

## Conclusions

It is important to explain the dryness and  $CO_2$ -rich fluid inclusions of ancient high-grade terrains. Because these features occur in very diverse chemical compositions inherited from igneous and sedimentary parents, a metamorphic process is indicated. Experimental phase-equilibria require removal of  $H_2O$  from hydroxylated minerals in the lower crust ( $\sim 20$ – $40$ -km depth) by a vapour with high  $CO_2/H_2O$ . Consequently carbonic metamorphism deserves detailed consideration. The volume of lower continental crust is so great, and the required ratio of  $CO_2/H_2O$  is so high, that a mantle source of  $CO_2$  may be required. Carbonate-bearing peridotite is stable to higher temperature than mica-bearing peridotite deeper than  $\sim 100$  km, and oxidation of carbon might provide another source of  $CO_2$ . Rising basaltic magma containing both  $CO_2$  and  $H_2O$  in solution should lose  $CO_2$  to the vapour phase as the pressure falls below 20 kbar ( $\sim 75$ -km depth) while water can be retained either in magma or in crystallizing amphibole. It is assumed that rising  $CO_2$  vapour will diffuse through rocks containing hydroxylated minerals and flush out the water to produce a residue of dry granulite until the vapour becomes too diluted in  $H_2O$ , or until  $CO_2$  becomes captured by scapolite. Water trapped in amphibole in deep-crustal basalt may subsequently escape to the surface dissolved in remelted diapirs which undergo little reaction with existing rocks.

Because of the complexity of tectonic processes in the Archaean era before development of large continental masses,

there is unresolved speculation about the origin and development of high-grade regions and greenstone belts. Two simple models based on hot-spot and plate-tectonic features show how the concepts of carbonic metamorphism might be applied. Neither is fully satisfactory, but the models may prove useful for further discussion of Archaean geology.

We thank A. T. Anderson, R. A. Howie and P. J. Wyllie for helpful criticisms, but their endorsement of the present speculative ideas is not implied. The following grants are acknowledged: NSF EAR 78-15939 (R.C.N.), EAR 79-05723 (R.C.N.), and EAR 77-21700 (J.V.S.), NASA 14-001-171 (J.V.S.) and NERC GR3/3198 (B.F.W.). We thank S. Moorbath, P. R. A. Wells, G. N. Hanson and D. H. Eggler for their helpful comments.

1. Moorbath, S. *Chem. Geol.* **20**, 151–187 (1977).
2. Smith, J. V. in *The Early History of the Earth* (ed. Windley, B. F.) 3–31 (Wiley, Chichester, 1976).
3. Lambert, R. St. J. in *The Early History of the Earth* (ed. Windley, B. F.) 363–373 (Wiley, Chichester, 1976).
4. Smith, J. V. *Phil. Trans. R. Soc.* (in the press).
5. Lambert, R. St. J. *Precamb. Res.* **11**, 199–214 (1980).
6. Bridgwater, D., Keto, L. & Myers, J. S. in *The Geology of Greenland* (eds Escher, A. & Watt, W. S.) 18–75 (Geological Survey of Greenland, Copenhagen, 1976).
7. Moorbath, S. in *The Early History of the Earth* (ed. Windley, B. F.) 351–362 (Wiley, Chichester, 1976).
8. Newton, R. C. in *Archaean Geochemistry* (eds Windley, B. F. & Naqvi, S. M.) 221–240 (Elsevier, Amsterdam, 1978).
9. Wells, P. R. A. *J. Petrol.* **20**, 187–226 (1979).
10. Holland, T. H. *Geol. Surv. Ind. Mem.* **28**, pt. 2 (1900).
11. Howie, R. A. *Trans. R. Soc. Edin.* **62**, 725–768 (1955).
12. Cooray, P. G. *Am. J. Sci.* **267**, 969–982 (1969).
13. Hubbard, F. H. *Geol. Förs. Förh.* **100**, 31–38 (1978).
14. Shaw, D. M. *Geochim. cosmochim. Acta* **32**, 573–601 (1968).
15. Tarney, J. & Windley, B. F. *J. geol. Soc.* **134**, 153–172 (1976).
16. Heier, K. S. *Phil. Trans. R. Soc. A* **273**, 429–442 (1973).
17. Tourret, J. *Lithos* **4**, 239–249 (1971).
18. Tourret, J. in *Jubilee P. Michot: Centenaire Soc. Geol. Belg.* 267–287 (1974).
19. Collerson, K. D. & Fryer, B. J. *Contr. Miner. Petrol.* **67**, 151–167 (1978).
20. Janardhan, A. S., Newton, R. C. & Smith, J. V. *Nature* **277**, 511–514 (1979).
21. Wyllie, P. J. *Am. Miner.* **64**, 469–500 (1979).
22. Fyfe, W. S. *Phil. Trans. R. Soc. A* **273**, 457 (1973).
23. Weaver, B. L., Tarney, J., Windley, B. F., Sugavaram, E. B. & Venkata Rao, V. in *Archaean Geochemistry* (eds Windley, B. F. & Naqvi, S. M.) 177–204 (Elsevier, Amsterdam, 1978).
24. Ramaniengar, A. S., Ramakrishnan, M. & Viswanatha, M. M. *J. geol. Soc. Ind.* **19**, 411–419 (1978).
25. Hamilton, P. J., Evensen, N. M. & O'Nions, R. K. *Nature* **277**, 25–28 (1979).
26. Drury, S. A. *Precamb. Res.* **7**, 237–257 (1978).
27. Pichamuthu, C. S. *Ind. Miner.* **6**, 119–126 (1965).
28. Grew, E. S. *Am. Miner.* (in the press).
29. Ahrens, T. J. & Schubert, G. *Rev. Geophys. Space Phys.* **13**, 383–400 (1975).
30. Madsen, J. K. *Am. J. Sci.* **277**, 673–696 (1977).
31. Falkum, T., Wilson, J. R., Petersen, J. S. & Zimmerman, H. D. *Norsk. Geol. Tidsskr.* **59**, 129–140 (1979).
32. Wilson, A. F. in *Archaean Geochemistry* (eds Windley, B. F. & Naqvi, S. M.) 241–267 (Elsevier, Amsterdam, 1978).
33. Hörmann, P. K., Raith, M., Raase, R., Ackermann, D. & Seifert, F. *Bull. Comm. Géol. Finlande* (in the press).
34. Zimmermann, J. L. *Compt. r. heb. Séanc. Acad. Sci., Paris* **275D**, 519–522 (1972).
35. Suknev, V. S., Kitsul, V. I., Lazebnik, Yu. D. & Brovkin, A. A. *Doklady Acad. Sci. USSR, Earth Sci. Sect.* **200**, 156–158 (1971).
36. Hewins, R. H. *Contr. Miner. Petrol.* **50**, 205–209 (1975).
37. Wyllie, P. J. *Tectonophysics* **43**, 41–71 (1977).
38. Luth, W. L. *J. Petrol.* **8**, 372–416 (1967).
39. Windley, B. F. *The Evolving Continents* (Wiley, London, 1977).
40. Eugster, H. P. & Skippen, G. B. in *Researches in Geochemistry* (ed. Abelson, P. H.) 492–520 (Wiley, New York, 1967).
41. Hollister, L. S. & Burrus, R. C. *Geochim. cosmochim. Acta* **40**, 163–175 (1976).
42. Sighinolfi, G. P., Kronberg, B. I., Gorgoni, C. & Fyfe, W. S. *Chem. Geol.* **29**, 323–332 (1980).
43. Drury, S. A. *Chem. Geol.* **11**, 167–188 (1973).
44. Sheraton, J. W., Skinner, A. C. & Tarney, J. in *The Early Precambrian of Scotland and Related Rocks of Greenland* (ed. Park, R. G. & Tarney, J.) 13–20 (University of Keele, 1973).
45. Nordlie, B. L. *Am. J. Sci.* **271**, 417–463 (1971).
46. Moore, J. B., Batchelder, J. N. & Cunningham, C. G. *Geol. Soc. Am. Abstr. Prog.* **9**, 1100–1101 (1977).
47. Roedder, E. *Am. Miner.* **50**, 1746–1782 (1965).
48. Eggler, D. H. *Yb. Carnegie Instn. Wash.* **73**, 215–224 (1974).
49. Wyllie, P. J. & Huang, W. L. *Geology* **3**, 621–624 (1975).
50. Brey, G. & Green, D. H. *Contr. Miner. Petrol.* **61**, 141–162 (1977).
51. Eggler, D. H. *Geology* **6**, 397–400 (1978).
52. Wyllie, P. J. *J. Geol.* **85**, 187–207 (1977).
53. Hoefs, J. & Tourret, J. *Contr. Miner. Petrol.* **52**, 165–174 (1975).
54. Ringwood, A. E. *Composition and Petrology of the Earth's Mantle* (McGraw-Hill, New York, 1975).
55. Smith, J. V. *Miner. Mag.* **43**, 1–89 (1979).
56. Huang, W. L., Wyllie, P. J. & Nehru, C. E. *Am. Miner.* **65**, 285–301 (1980).
57. Mao, H. K. & Bell, P. M. in *Energetics of Geological Processes* (eds Saxena, S. & Bhattacharji, S.) 236–249 (Heidelberg, Springer, 1977).
58. Irving, A. J. *J. Petrol.* **15**, 1–40 (1974).
59. Kadik, A. A. & Lukanin, O. A. *Geokhimiya* **2**, 163–179 (1973).
60. Burke, K., Dewey, J. F. & Kidd, W. S. F. in *The Early History of the Earth* (ed. Windley, B. F.) 113–129 (Wiley, Chichester, 1976).
61. Tarney, J., Dalziel, I. W. D. & DeWit, M. J. in *The Early History of the Earth* (ed. Windley, B. F.) 131–146 (Wiley, Chichester, 1976).



62. Katz, M. B. *Precamb. Res.* **3**, 91–106 (1975).
63. Fyfe, W. S. *Chem. Geol.* **23**, 80–114 (1978).
64. Taylor, S. R. *Tectonophysics* **4**, 17–34 (1967).
65. Windley, B. F. & Smith, J. V. *Nature* **260**, 671–675 (1976).
66. Drury, S. A. in *Archaean Geochemistry* (eds Windley, B. F. & Naqvi, S. M.) 3–23 (Elsevier, Amsterdam, 1978).
67. Platt, J. R. *Tectonophysics* **65**, 127–150 (1980).
68. Barker, F. (ed.) *Trondhjemites, Dacites and Related Rocks* (Elsevier, Amsterdam, 1979).
69. Bohlen, S. R. & Essene, E. J. *Contr. Miner. Petrol.* **62**, 153–169 (1978).
70. Foland, F. K. & Muessig, K. W. *Geology* **6**, 143–146 (1978).
71. Schilling, R. D. & Kreulen, R. *Earth planet. Sci. Lett.* **43**, 298–302 (1979).
72. Froidevaux, C., Brousse, R. & Bellon, H. *Nature* **248**, 749–751 (1973).
73. Irwin, W. P. & Barnes, I. *J. geophys. Res.* **85**, 3115–3121 (1980).
74. O'Nions, R. K. & Pankhurst, R. J. *Earth planet. Sci. Lett.* **38**, 211–236 (1978).
75. Wentlandt, R. F. & Harrison, W. J. *Contr. Miner. Petrol.* **69**, 409–419 (1979).
76. McGregor, V. R. *Phil. Trans. R. Soc. A* **273**, 343–358 (1973).
77. Langford, F. F. & Morin, J. A. *Am. J. Sci.* **276**, 1023–1034 (1976).
78. Andrews, D. & Sleep, N. *Geophys. J. R. astr. Soc.* **38**, 237–251 (1974).
79. Gastil, R. *Geology* **7**, 542–544 (1979).
80. Andrews, A. J. *Can. J. Earth Sci.* **14**, 911–926 (1977).
81. Barragar, W. R. A., Plant, A. G., Pringle, G. J. & Schau, M. *Can. J. Earth Sci.* **14**, 837–874 (1977).
82. Scheidegger, K. F. & Stakes, S. *Earth planet. Sci. Lett.* **36**, 413–422 (1977).
83. Ito, E. thesis, Univ. Chicago (1979).
84. Gill, R. C. O. *Phys. chem. Earth* **11**, 431–447 (1979).
85. Arth, J. G. & Hanson, G. N. *Geochim. cosmochim. Acta* **39**, 325–326 (1975).

## ARTICLES

# Late Quaternary history of the Nile

D. A. Adamson\*, F. Gasse†, F. A. Street‡ & M. A. J. Williams§

\*School of Biological Science and Quaternary Research Unit, and §School of Earth Science and Quaternary Research Unit, Macquarie University, North Ryde, New South Wales 2113, Australia

†Ecole Normale Supérieure, 92260 Fontenay-aux-Roses, France

‡School of Geography, University of Oxford, Mansfield Road, Oxford OX1 3TB, UK

*During the intertropical cold dry phase from ~20,000 to 12,500 yr BP, the aggrading Nile was a braided, highly seasonal river. With a headwaters change to warmer, wetter conditions, it became an incised, sinuous, suspended load river. Overflow from Lake Victoria and severe floods in Egypt heralded the change in Nile regime.*

THE Nile dominates the northeastern quadrant of Africa, flowing 6,700 km from the glaciated highlands and montane forests of Uganda (4° S) through the alluvial plains and desert sands of Sudan and Egypt into the eastern Mediterranean (31° N, Fig. 1). Recently dated river and lake deposits in Sudan<sup>1</sup>, Ethiopia<sup>2</sup> and Uganda<sup>3</sup>, and eastern Mediterranean deep-sea core data<sup>4–6</sup> now allow us to present an integrated history for the entire Nile basin for the past 20,000 yr. It is now possible to reconcile the alluvial history of the main Nile<sup>7,8</sup> with events in the rest of the basin<sup>9</sup>. We focus on the late Pleistocene dry phase (~20,000–12,500 BP) and the terminal Pleistocene to mid-Holocene moister interval (~12,500–5,000 yr BP). As these two intervals contrast strongly in climate, a coherent interpretation of former Nile regime must accommodate both.

## Nile hydrology and headwaters

Key aspects of the present Nile hydrology<sup>10,11</sup> are shown in Table 1. During the dry winter the White Nile provides 83% of main Nile flow and sustains it to the sea when the Blue Nile has fallen 15 m and the Atbara is dry. During the Ethiopian summer floods Blue Nile flow and suspended sediment concentration<sup>12</sup> increase 40-fold. The Blue Nile and Atbara then provide 90% of the flow and 96% of the sediment of the main Nile. Throughout the late Quaternary, the separate contributions of the White Nile and of the Ethiopian tributaries have to be borne in mind.

Of the two major lakes in the upper White Nile basin, Lake Victoria (Fig. 2) was without outlet for at least 2,000 yr before 12,500 yr BP and probably again, briefly, around 10,000 yr BP (ref. 13), but is unlikely to have dried out completely. Closure of Lake Victoria would have reduced White Nile flow and increased its seasonality. Lake Mobutu Sese Seko (Lake Albert) was closed from ~25,000 to 18,000 yr BP and from 14,000 to 12,500 yr BP (ref. 14), during closure of Lake Victoria. Except for these times, it communicated with the White Nile, maintaining winter flow.

Ruwenzori supported the second largest late Pleistocene ice cap in Africa (260 km<sup>2</sup>). Glaciers also developed on Mounts Kenya, Kilimanjaro, Elgon and the Aberdares. Estimates of mean snowline lowering on each mountain range from >480 to 880 m, corresponding to a temperature decrease<sup>15,16</sup> of 3–6 °C if precipitation remained constant. In Lake Mobutu the diatom

flora suggests cooler conditions<sup>17</sup> than today between 28,000 and 25,000 yr BP. If glacial maximum coincided with the minimum level of Lake Mobutu (25,000–18,000 yr BP), and rainfall was decreased by 25%, a temperature lowering of 6–8 °C would be likely<sup>3</sup>.

Pollen spectra from sites in East Africa point to a colder, drier climate than today between ~26,000 and 12,500 yr BP with highland assemblages dominated by small tree, shrub and grass pollen, indicative of widespread suppression of forest trees<sup>3,18</sup>, and a vegetation more open than it is now<sup>19–21</sup>. Cores from Lake Victoria<sup>13</sup> show that lowland forest was either absent or of very limited extent in the White Nile headwaters between 15,000 and 12,000 yr BP. From 12,000 yr BP onwards equatorial and montane forest spread at the expense of grassland and woodland<sup>3,18</sup>, presumably indicating warmer and moister conditions. Lake fluctuations between 26,000 and 12,500 yr BP were apparently more complex in equatorial Africa<sup>22</sup> than in Ethiopia, and the overflow of Lake Mobutu<sup>14</sup> between 18,000 and 14,000 yr BP suggests that glacial aridity here was less prolonged or severe.

The Atbara, Blue Nile and Sobat originate in the Ethiopian highlands (Fig. 1). Although little is known about the history of Lake Tana on the Blue Nile several lake basins in the Ethiopian and Afar Rifts adjacent to the Ethiopian highlands have been studied in detail, including Lake Abhe<sup>3</sup> and the Rift lakes south of Addis Ababa<sup>9</sup> (Fig. 1).

Lake Abhe, the terminal lake of the Awash River, fluctuates in response to hydrological changes on the eastern margin of the Ethiopian plateau as well as in the Afar depression. Lake Abhe was very high several times during the late Pleistocene and also

**Table 1** Nile hydrology<sup>10,11</sup>

|            | Discharge<br>(km <sup>3</sup> ) | Sediment<br>load<br>(mton) | % of<br>maximum<br>monthly<br>flow | % of<br>minimum<br>monthly<br>flow |
|------------|---------------------------------|----------------------------|------------------------------------|------------------------------------|
| White Nile | 27.5                            | 2                          | 10                                 | 83                                 |
| Blue Nile  | 51.0                            | 41                         | 68                                 | 17                                 |
| Atbara     | 12.5                            | 14                         | 22                                 | 0                                  |

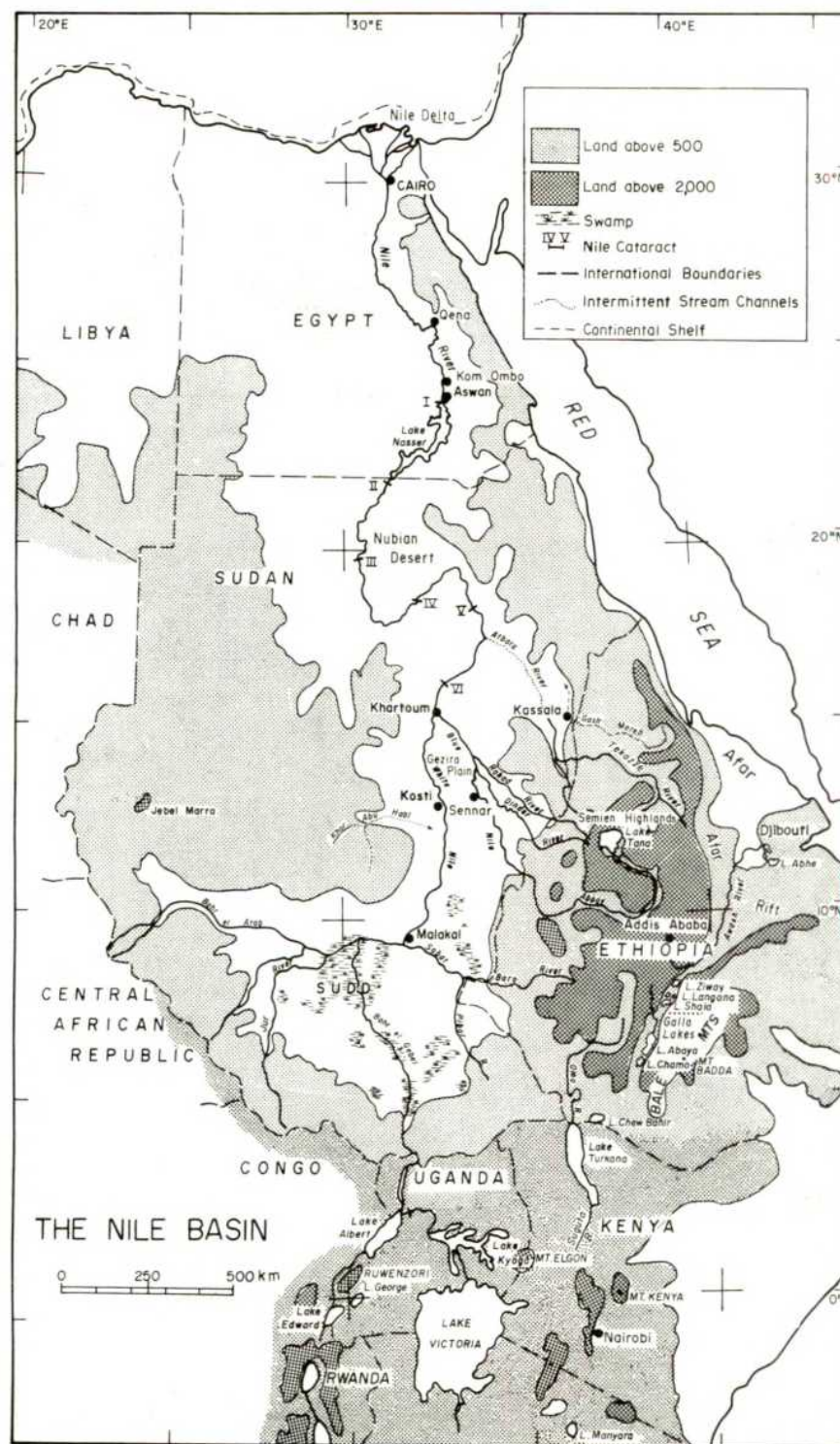


Fig. 1 The Nile basin.

during the early and mid-Holocene but dry from ~17,000 to 10,000 yr BP (Fig. 2). Individual highstands were characterized by quite distinct diatom assemblages and sedimentary facies<sup>9,23,24</sup>, reflecting long-term variations in lake-water chemistry and sediment supply.

The history of the Ziway-Shala basin in the Ethiopian rift (Fig. 1) parallels that of Lake Abhe from at least 30,000 yr BP except that the late Pleistocene lake phases were apparently shorter and less stable<sup>9,25</sup>.

Further south, the Ethiopian plateau drains to the Turkana basin. Since 10,000 yr BP, the fluctuations of Lake Turkana<sup>26-28</sup>

compare closely with those of Lake Ziway-Shala, except for a peak, around  $3,250 \pm 150$  yr BP, which is not evident in the Ethiopian record (Fig. 2). During the early and mid-Holocene, Lake Turkana may have received the overflow from Lakes Chew Bahir<sup>29</sup>, Chalbi (D. Phillipson, personal communication) and, possibly, Suguta<sup>30-32</sup>. It overflowed NNW into the Pibor-Sobat (White Nile) system from ~9,900 to 7,900 yr BP and possibly also between 6,600 and 3,250 yr BP (refs 26-28).

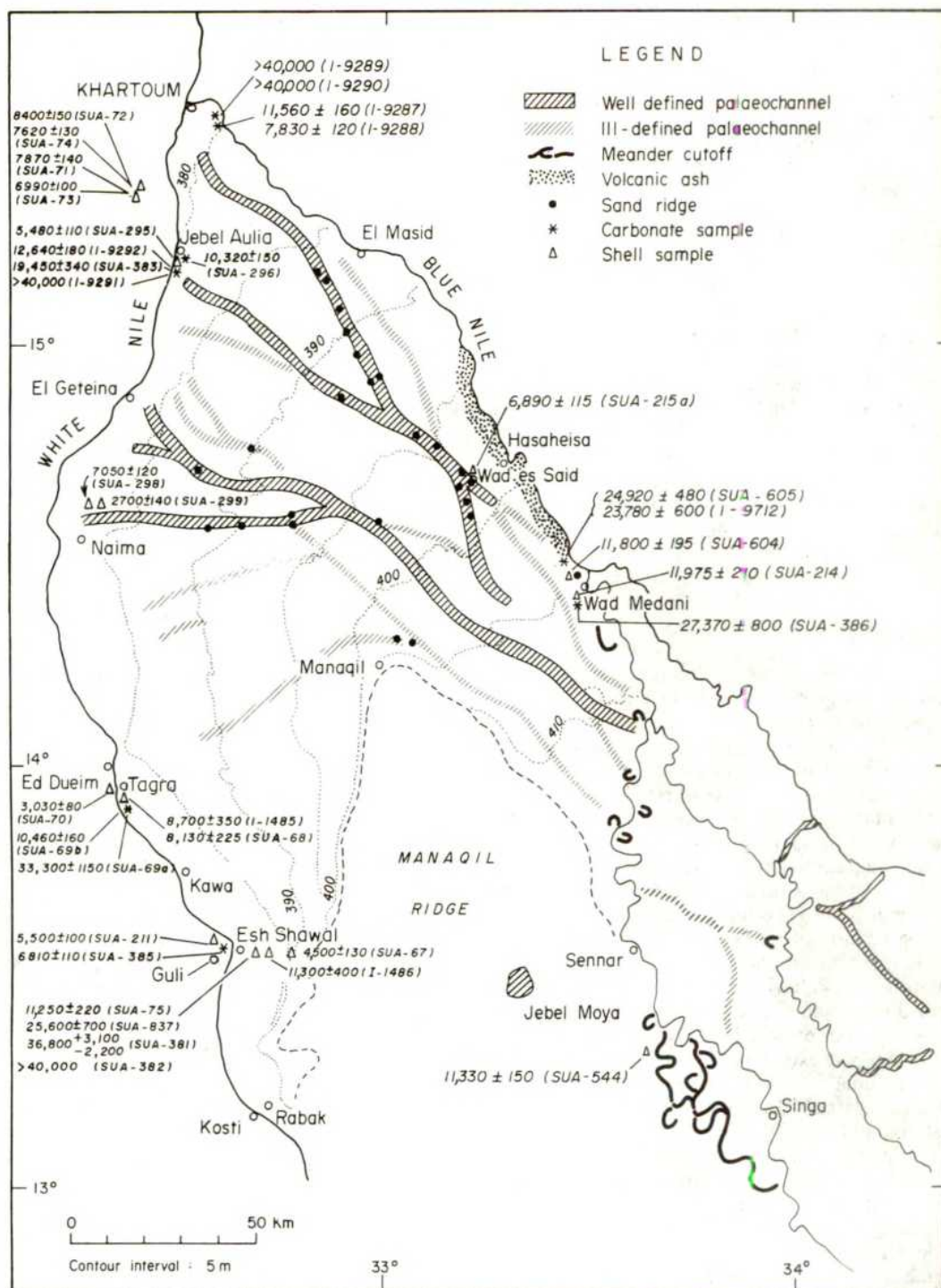
The fluctuations of these lakes stem from variations in water balance resulting from changes in climate. The latter were also reflected in variations in snowlines, vegetation cover, and slope







**Fig. 3** The Blue and White Nile rivers, central Sudan, showing location of dated sites. Field mapping based on over 500 2-m boreholes and trenches.



The extension of closed vegetation types during the early Holocene was reflected in widespread slope stabilization in both highland and lowland areas. Consequently, the rivers transported predominantly fine-grained sediments and the clastic influx into the lakes was reduced by comparison with the preceding period. For example, the Meki River, which enters Lake Ziway from Ethiopian escarpment, began to lay down fine alluvial loams instead of coarse gravels.

We conclude that the phases of highest sediment yield from the Ethiopian highlands and lowlands corresponded to times of maximum aridity, minimum water yield, and highly seasonal runoff during the very cold late Pleistocene interval. These conditions dominated the fluvial regimes of the Blue Nile and Atbara rivers during the late Pleistocene arid period. In contrast, the terminal Pleistocene to mid Holocene was moister, the vegetation cover was more complete, slopes more stable, and sediment yield reduced.

### Alluvial plains of the central Sudan

The alluvial plains of the lower Blue and White Nile rivers in central Sudan provide a depositional legacy of erosional events in their respective catchments<sup>42-44</sup>. A vast low-angle alluvial fan (the Gezira fan), up to 200 m thick and over 200 km in radius<sup>1</sup>, was built up during the past 20 Myr (ref. 45) by ancient Blue Nile distributaries as they emerged from the Ethiopian highlands onto the plains of the Sudan. Our concern here is with the upper 4-5 m of this fan, which contains late Quaternary sediments from the two Niles (Fig. 3).

During a long interval dated<sup>1,46</sup> at  $>40,000$ -25,000 yr BP evaporite deposits of microcrystalline dolomite and calcite accumulated along the White Nile near Esh Shawal. River sands which became progressively more clay-rich were laid down over the evaporites, and were in part reworked by wind to form dunes<sup>1,46</sup> which were later flooded by the White Nile towards 12,000-11,000 yr BP. Radiocarbon ages of unbroken fresh-



water and amphibious mollusca indicate high White Nile flood levels towards 12,500–11,400, 8,400–8,100, 7,000, 5,500, 3,000–2,700, and 2,000–1,500 yr BP (Figs 2, 4). Excavations at Shabona<sup>47,48</sup>, where small groups of elephant, buffalo and hippo hunters camped on low fixed dunes overlooking flooded White Nile swamps from which they collected abundant *Pila* snails dated to 7,000 yr BP confirmed that the White Nile floods were high towards 8,000–7,000 yr BP.

Figure 4 shows that high Blue Nile flood levels tally in detail with those of the White Nile for the intervals 12,000–11,000, 8,000, 7,000 and 5,500 yr BP. There is no evidence of extensive Blue Nile flooding in central Sudan after about 5,500 yr BP when the river entrenched some 10 m into its former floodplain<sup>49–51</sup>. The dated Blue Nile high flood levels coincide with early to mid-Holocene high lake levels and higher water-tables in Ethiopia<sup>2,9,23,52</sup>, with small lakes at En Nahud in Kordofan (6,800 yr BP)<sup>1</sup> and in Wad Mansurab basin 13 km north-west of Jebel Aulia<sup>53</sup> (Fig. 3) (8,400–7,000 yr BP).

Cross-bedded sands and gravels underlie the Blue Nile Holocene clays and occupy channel-fills within them. Borehole data reveal a change from a low-sinuosity bed-load regime to a high-sinuosity mixed- or suspended-load regime towards 12,000–11,000 yr BP (refs 1, 44), coinciding with forest expansion and slope stabilization in the Blue Nile headwaters.

## Main Nile

The intricate response of different parts of the Nile basin to climatic change<sup>7,8,54–56</sup> was first shown by studies of the alluvial stratigraphy of Upper Egypt and Nubia<sup>7</sup>. Here, Nilotic formations of late Quaternary age (Fig. 2) interfinger with local dune, wadi and pond deposits. Phases of aggradation by the main Nile were separated by episodes of rapid downcutting.

The oldest unit, the Korosko Formation<sup>7</sup>, consists of marls, gravelly marls, sandy gravels and Ethiopian silts deposited by a rapidly aggrading, braided Nile which was actively fed by local wadis. A probable minimum age of 27,250 yr BP has come from the upper part of this formation<sup>7,8</sup>.

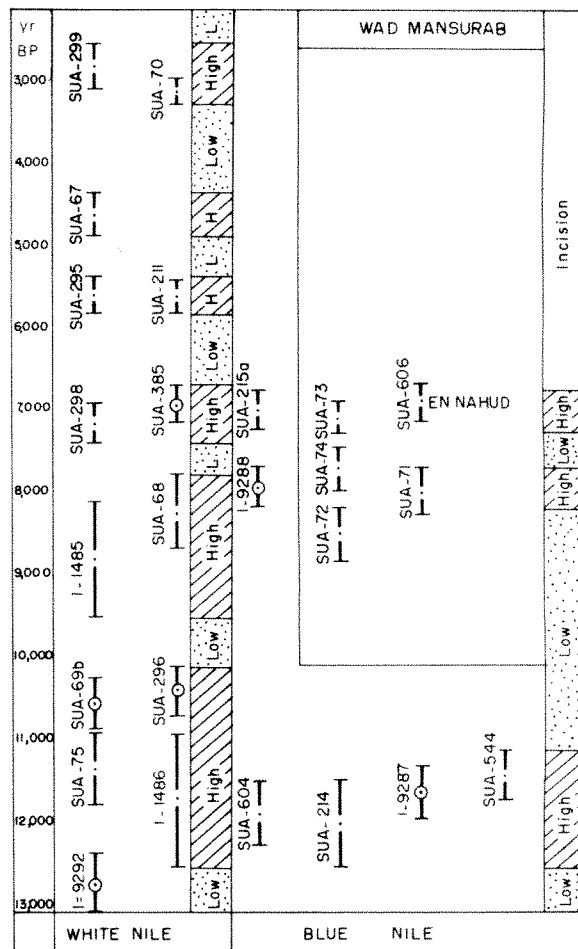
Aggradation of the Masmas Formation<sup>7</sup> began long before 21,000 yr BP, and ended<sup>8</sup> around 18,000 yr BP. The deposits comprise thick, horizontal flood silts of Ethiopian origin with occasional channel sands. They were laid down on a floodplain more than three times broader than today. Frequent crevasse splays suggest extensive seasonal flooding. Contemporary aridity in Nubia<sup>7,8,55,56</sup> is indicated by dunes lining the west bank, which are dated<sup>57,58</sup> at 19,000–17,000 yr BP. Local wadi activity was minimal.

During the Darau substage of the Gebel Silsila Formation<sup>7</sup> (17,000–12,000 yr BP) vigorous braided channels existed on a floodplain twice as wide as today depositing a mixture of sands, gravels and Ethiopian flood silts. Exotic pebbles in the Darau Member as well as further upstream in Blue Nile deposits imply significant fluvial transport from Ethiopia and Sudan. At this time in Nubia and upper Egypt the wadis were intermittently active during the period 17,500–12,000 yr BP<sup>7,8</sup> and pollen and diatom assemblages from permanent ponds indicate a locally cooler and effectively more humid climate than today. The Darau substage ended in a period of exceptionally high floods<sup>8</sup> around 12,000–11,500 yr BP. Recent dates suggest that aggradation of mainly Ethiopian silts took place in the terminal Pleistocene to mid-Holocene intervals 11,200–9,300, 8,000–7,000 and 5,800–5,400 yr BP, with particularly high levels around 7,100 yr BP. Wadi deposits in Nubia indicate several phases of enhanced local runoff between ~11,500 and 5,000 yr BP. From 5,000 yr BP onwards, however, conditions in both Egypt and Nubia became increasingly arid<sup>7,8</sup>.

## Nile cone and eastern Mediterranean

Stratigraphic and isotopic evidence<sup>4–6</sup> from eastern Mediterranean cores now allows partial separation of the effects of changes in river regime and sediment discharge<sup>8,54,59</sup>.

Three recently recognized Nile cone cyclothem<sup>4,5</sup> dated at 58,000–28,000, 28,000–17,000 and 17,000–0 yr BP are broadly coeval with the three alluvial formations in Nubia<sup>8</sup>. Each cyclothem comprises a sapropel unit, muds and turbidites, and a calcareous unit. The three sapropels coincide in time with high lake levels in the Nile basin<sup>9</sup> and Arabia<sup>60</sup>, and with the deposition of Ethiopian silts in central Sudan<sup>1</sup> and Egypt<sup>8,59</sup> (Fig. 2). Sapropel 1 (9,000–7,000 yr BP) also corresponds with the early



**Fig. 4** Dated high Blue and White Nile flood levels in central Sudan. (All ages are corrected for isotopic fractionation; circles are pedogenic carbonates; dots are shells; bars represent 2 standard deviations.)

Holocene expansion of forest in the Nile headwaters<sup>3</sup>. The sapropels reflect stagnation of deep ocean water arising from a major influx of freshwater<sup>6</sup> into the eastern Mediterranean from such sources as the Nile and Black Sea<sup>61,62</sup>. The isotopic change evident towards 9,000–7,000 yr BP in core GA32 is best attributed to both a temperature increase and a freshwater influx<sup>6,61</sup>. The periods of calcareous ooze accumulation<sup>4,5</sup> correspond to times of aridity in the Nile basin. Stable isotope measurements in deep-sea cores from the eastern Mediterranean suggest that at the last glacial maximum, as at present, the eastern Mediterranean had an excess of evaporation over combined precipitation and river input (N. J. Shackleton, personal communication).

Evidence both from the eastern Mediterranean sea floor and from the Nile basin shows that in this region the interval 12,000–5,000 yr BP was generally moister than today and far wetter and warmer than the preceding late Pleistocene phase. Certain inferences may now be drawn about the late Quaternary Nile.

## The 20,000–12,500 yr BP Nile

Cold dry conditions in the headwaters<sup>1–3,36</sup> had profound effects on water and sediment supply to the Nile. Reduced vegetation cover, periglacial processes and summer snow melt gave heavy loads of coarse sediment. Flood peaks were high, annual discharge low. Episodic closure of the headwater lakes<sup>13,14</sup> and consequent reduction in the area of swamps accentuated the seasonality of flow. The White Nile became a seasonal, intermittent river. Annual discharge from the Ethiopian headwaters diminished, so that flow along the main Nile was severely curtailed.

Along the lower White Nile bedload sands were reworked into aeolian dunes during the dry season<sup>46</sup>. Distributaries of the Blue Nile radiated across the Gezira, also furnishing bedload sand for dune formation<sup>63</sup>. The Atbara was even more intermittent than today. Summer floods were substantial, braided distributaries of the Blue Nile and Atbara spread fine gravels (including agate and chalcedony), sands and silts across their alluvial fans. Braided stream channels were characteristic of the main Nile in Egypt and Sudanese Nubia<sup>8</sup>, where mixed sediments similar to those upstream were also deposited. The sharing of flow among braided channels implies that the bedload was moved less efficiently than if flow were concentrated into one or two channels, with minimal frictional loss of stream energy. As flow ceased in the dry season bedload was locally reworked by wind. Channel instability was common during the flood seasons.

## The 12,500–5,000 yr BP Nile

Following overflow from the headwater lakes and rapid expansion of swamps in southern Sudan, Nile flow became permanent and more regular. In the immediate aftermath of overflow from Lake Victoria towards 12,500 yr BP, there was major flooding along the White Nile<sup>1</sup>. Full buffering by the Sudd swamps had not yet developed, so that vast quantities of water were released into the main Nile. The Blue Nile and Atbara also discharged high floods as rainfall increased in Ethiopia at this time. This

helps to explain the few centuries of extremely high floods<sup>8</sup> in Egypt.

Thereafter permanent flow and much reduced seasonal fluctuation allowed the Nile to move its bedload along one or a few dominant channels. Regular Blue Nile floods laid down several metres of clay in the swampy plains of the Sudan Gezira<sup>63,64</sup> and overbank floods deposited the Arminna/Kibdi silts on the narrow Egyptian floodplain<sup>8</sup>.

## Conclusion

The fluvial response of the Nile to late Quaternary climatic changes in the headwaters helps to explain why rivers sometimes aggrade and sometimes degrade their floodplains. Between 20,000 and 12,000 yr BP when timberline in the headwaters was lower and the vegetation cover more open than today, the Nile was a highly seasonal braided river which brought mixed coarse and fine sediments down to Egypt and Sudan. This cold, dry interval had ended by 12,500 yr BP when overflow from Lake Victoria and higher rainfall in Ethiopia sent extraordinary floods down the main Nile, marking a revolutionary change to continuous flow with a superimposed flood peak. The main Nile and its tributaries established more stable channels of higher sinuosity, from which suspended Ethiopian silt and clay was deposited on the floodplains. The Blue Nile began to cut down, thereby depriving the Gezira fan of flood waters. By the mid-Holocene, the modern era of the Nile had begun.

Evidence from earlier periods is consistent with the above interpretation of the relation between Nile behaviour and environmental conditions in the basin (Fig. 2). The thick sequence of evaporite deposits and saline sediments on the lower White Nile also suggest earlier periods of desiccation and intermittent river flow which must have affected the main Nile. Study of the sediments beneath the Sudd and of the little known White Nile evaporites is required for the light they will shed on the earlier history of the basin.

We thank P. Goldberg, J. G. Jones and R. J. Wasson for discussions.

Received 30 June; accepted 27 August 1980.

- Williams, M. A. J. & Adamson, D. A. in *The Sahara and the Nile* (eds Williams, M. A. J. & Faure, H.) 281–304 (Balkema, Rotterdam, 1980).
- Gasse, F., Rognon, P. & Street, F. A. in *The Sahara and the Nile* (eds Williams, M. A. J. & Faure, H.) 361–400 (Balkema, Rotterdam, 1980).
- Livingstone, D. A. in *The Sahara and the Nile* (eds Williams, M. A. J. & Faure, H.) 339–359 (Balkema, Rotterdam, 1980).
- Stanley, D. J. & Maldonado, A. *Nature* **266**, 129–135 (1977).
- Stanley, D. J. & Maldonado, A. *Sediment. Geol.* **23**, 37–75 (1979).
- Luz, B. *Nature* **278**, 847–848 (1979).
- Butzer, K. W. & Hansen, C. L. *Desert and River in Nubia: Geomorphology and Prehistoric Environments at the Aswan Reservoir* (University of Wisconsin Press, Madison, 1968).
- Butzer, K. W. in *The Sahara and the Nile* (eds Williams, M. A. J. & Faure, H.) 253–280 (Balkema, Rotterdam, 1980).
- Gasse, F. & Street, F. A. *Palaeogeogr. Palaeoclimatol. Palaeoecol.* **24**, 279–325 (1978).
- Hurst, H. E. *The Nile: A General Account of the River and the Utilization of its Waters* 2nd edn (Constable, London, 1957).
- Hurst, H. E. & Phillips, P. *The Nile Basin*. Vol. 1 (Physical Department Paper, Government Press, Cairo, 1931).
- Badri, O. E. thesis, Univ. Khartoum (1972).
- Kendall, R. L. *Ecol. Monogr.* **39**, 121–176 (1969).
- Harvey, T. J. thesis, Duke Univ. (1976).
- Osmaston, H. A. thesis, Univ. Oxford (1965).
- Hamilton, A. & Perrott, F. A. *Palaeoecol. Afr.* **11**, 153–161 (1979).
- Gasse, F. *Palaeoecol. Afr.* **12**, 333–350 (1980).
- Hamilton, A. C. in *East African Vegetation* (eds Lind, E. M. & Morrison, M. E. S.) 188–209 (Longman, London, 1974).
- Coetzee, J. A. *Palaeoecol. Afr.* **3**, 1–146 (1967).
- Livingstone, D. A. *Ecol. Monogr.* **37**, 25–52 (1967).
- Hamilton, A. C. *Palaeoecol. Afr.* **7**, 45–149 (1972).
- Holdship, S. A. thesis, Duke Univ. (1976).
- Gasse, F. *Nature* **265**, 42–45 (1977).
- Gasse, F. & Delibrias, G. in *Paleolimnology of Lake Biwa and the Japanese Pleistocene* Vol. 4 (ed. Hori, S.) 529–575 (Kyoto, 1976).
- Gasse, F. & Descourtieux, C. *Palaeoecol. Afr.* **11**, 117–134 (1979).
- Butzer, K. W., Brown, F. H. & Thurber, D. L. *Quaternaria* **11**, 15–30 (1969/70).
- Butzer, K. W., Isaac, G. L., Richardson, R. L. & Washbourn-Kamau, C. *Science* **175**, 1069–1076 (1972).
- Butzer, K. W. in *Earliest Man and Environments in the Lake Rudolf Basin* (eds Coppins, Y., Howell, F. C., Isaac, G. L. & Leakey, R. E. F.) 12–33 (University of Chicago Press, 1976).
- Grove, A. T., Street, F. A. & Goudie, A. S. *Geogr. J.* **141**, 177–202 (1975).
- Bishop, W. W. in *Cambridge Meet. on Desertification* (ed Grove, A. T.) 62 (University of Cambridge, 1975).

- Truckle, P. H. *Nature* **263**, 380–383 (1976).
- Yuretic, R. F. thesis, Princeton Univ. (1976).
- Hastenrath, S. *Erdkunde* **28**, 176–186 (1974).
- Hastenrath, S. *J. Glaciol.* **18**, 309–313 (1977).
- Potter, E. C. *J. Glaciol.* **17**, 148–150 (1976).
- Messerli, B., Winiger, M. & Rognon, P. in *The Sahara and the Nile* (eds Williams, M. A. J. & Faure, H.) 87–132 (Balkema, Rotterdam, 1980).
- Gasse, F. *Rev. Algol.* **NS 13**, 105–149 (1978).
- Williams, M. A. J., Street, F. A. & Dakin, F. M. *Erdkunde* **32**, 40–46 (1978).
- Hamilton, A. C. *Abstr. 10th INQUA Congr.*, 193 (1977).
- Dunne, T. *J. Hydrol.* **42**, 281–300 (1979).
- Rapp, A., Axelsson, V., Berry, L. & Murray-Rust, D. H. *Geogr. Annal.* **54A**, 125–155 (1972).
- Williams, M. A. J. & Williams, F. M. in *The Sahara and the Nile* (eds Williams, M. A. J. & Faure, H.) 207–224 (Balkema, Rotterdam, 1980).
- Williams, M. A. J. & Adamson, D. A. *Economic and Social Research Council Occasional Paper No. 6*, 1–44 (National Council for Research, Khartoum, 1976).
- Williams, M. A. J. & Adamson, D. A. *Geogr. J.* **139**, 498–508 (1973).
- McDougall, I., Morton, W. H. & Williams, M. A. J. *Nature* **254**, 207–209 (1975).
- Williams, M. A. J. & Adamson, D. A. *Nature* **248**, 584–588 (1974).
- Adamson, D., Clark, J. D. & Williams, M. A. J. *Nature* **249**, 120–123 (1974).
- Clark, J. D. *Nyame Akuma* **3**, 56–64 (1973).
- Arkell, A. J. *Early Khartoum* (Oxford University Press, London, 1949).
- Arkell, A. J. *Esh Shaheinab* (Oxford University Press, London, 1953).
- Williams, M. A. J., Clark, J. D., Adamson, D. A. & Gillespie, R. *Bull. ASEQUA (Dakar)* **46**, 75–86 (1975).
- Williams, M. A. J., Bishop, P. M., Dakin, F. M. & Gillespie, R. *Nature* **267**, 690–693 (1977).
- Williams, M. A. J., Medani, A. H., Talent, J. A. & Mawson, R. *Sudan Not. Rec.* **54**, 168–172 (1974).
- Fairbridge, R. W. *Nature* **196**, 108–110 (1962).
- Heinzelin, J. de in *The Prehistory of Nubia* (ed. Wendorf, F.) 19–55 (Southern Methodist University, Dallas, 1968).
- Fairbridge, R. W. *Quat. Res.* **6**, 529–556 (1976).
- Wendorf, F. *et al. Science* **205**, 1341–1347 (1979).
- Wendorf, F., Schild, R., Said, R., Haynes, C. V., Gautier, A. & Kobusiewicz, M. *Science* **193**, 103–144 (1976).
- Hassan, F. A. *Quat. Res.* **6**, 425–444 (1976).
- McClure, H. A. *Nature* **263**, 755–756 (1976).
- Stanley, D. J. *Nature* **274**, 149–152 (1978).
- Thunell, R. C. & Lohmann, G. P. *Nature* **261**, 211–213 (1979).
- Williams, M. A. J. *Nature* **211**, 270–271 (1966).
- Tothill, J. D. *Sudan Not. Rec.* **27**, 153–183 (1946).
- Servant, M. & Servant-Vildary, S. in *The Sahara and the Nile* (eds Williams, M. A. J. & Faure, H.) 133–162 (Balkema, Rotterdam, 1980).
- Roberts, N., Erol, O., de Meester, T. & Uerpman, H.-P. *Nature* **281**, 662–664 (1979).



# Integration of visual and auditory space in the mammalian superior colliculus

Laurence R. Harris\*, Colin Blakemore† & Michael Donaghy‡

The Physiological and Psychological Laboratories, University of Cambridge, Cambridge CB2 3EG, UK

*Recordings of eye movements and single-neurone microelectrode recordings of the superior colliculus in cats show that, for each saccadic movement, their eyes start near to the centre of the orbit so that the coordinates of visual and auditory space are aligned, and complex neural compensation of auditory or visual inputs to the superior colliculus is unnecessary.*

EYES and ears are specialized for detecting events at a distance. Both vision and hearing can be used to localize objects in external space—a function of utmost importance to any animal anxious to avoid its predators or discover its prey. One part of the brain, the midbrain tectum (which in mammals consists of the superior and inferior colliculi), seems especially concerned with the analysis of spatial information derived from both the eyes and the ears. In animals of diverse phylogeny<sup>1–6</sup> there are neurones in the midbrain that have spatially restricted receptive fields in auditory or visual space and which respond when a sound or light stimulus appears (or preferably moves) within the appropriate, limited region of space. These systems of sensory neurones are topographically organized to form neural ‘maps’ of auditory and visual space across the midbrain tectum.

The idea that the roof of the midbrain is devoted to the analysis of positional information in external space is supported by the existence there in some species of other mechanisms for localization. The superior colliculus (SC) of cats<sup>7</sup>, mice<sup>4</sup> and hamsters<sup>8</sup>, as well as having both visual and auditory input, has a topographical representation of the body surface including the whiskers; neurones in the inferior colliculus of the bat<sup>9</sup> may play a part in echo location; and in the SC of the viper there is even a spatial representation of signals from the IR pit organs in the snake’s face<sup>10</sup>.

Damage to the tectum interferes with an animal’s ability to ‘orient’ towards stimuli: indeed, lesions of the hamster’s SC produce a visual defect that renders the animal seemingly blind to novel events in its visual field<sup>11</sup>. In the cat, removal of one SC (which represents primarily the opposite half of space) produces neglect of the contralateral hemifields<sup>12</sup>. Also, lesions of the colliculus in monkeys cause deficits in the timing of eye movements<sup>13</sup>.

Further evidence for the importance of the SC in initiating orienting movements towards sounds or sights comes from the fact that electrical stimulation of this structure in unanaesthetized animals elicits movements of the eyes, head, ears and body towards the opposite side of space<sup>14,15</sup>.

## Correspondence of visual and auditory representations in the superior colliculus

The integrity of the perceptual world clearly demands correlation of positional signals from all sensory systems and especially of messages from the eyes and ears. An animal must know that an object that it both sees and hears is a single thing at one place in space; responses initiated by either auditory or visual cues must be harmonized and coordinated.

The deep layers of the mammalian SC seem ideally equipped for the correlation of spatial cues from the eyes and ears,

for here there are superimposed auditory and visual representations<sup>7,8,16–18</sup>. Neurones in the rostral part of the SC respond to sounds or sights directly in front of the animal, whereas for those further back, visual and auditory receptive fields are shifted into the contralateral hemifield of space. Indeed in cats, many individual cells receive both auditory and visual input<sup>16</sup>: the activity of such neurones could be thought of as providing pure, positional information regardless of the sensory channel mediating it.

In support of this concept, Wickelgren<sup>16</sup>, working on the deep layers of the SC in paralysed cats, found such bimodal cells to have their visual and auditory receptive fields (though large) well matched in their horizontal eccentricity in space. Each neurone responded to either a spot of light or a small sound source presented in one particular region of the field. Could such cells in the cat’s SC be responsible for the functional integration of visual and auditory space, triggering orienting movements towards peripheral objects whether identified by their visual appearance or by the noise they make?

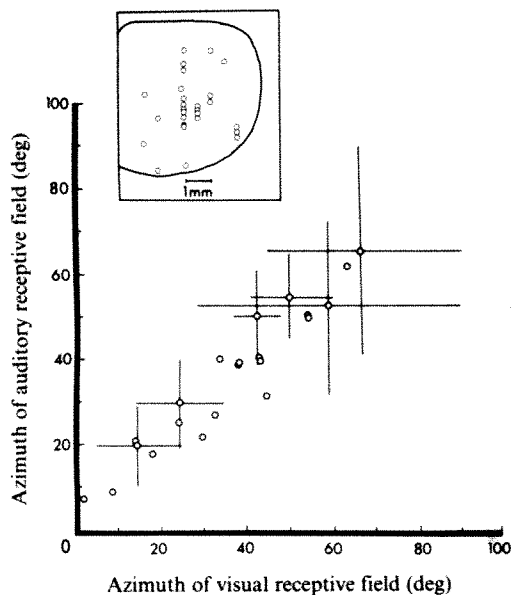
## The effect of eye movements: Pöppel’s paradox

This hypothesis, though attractive in its simplicity, is paradoxical. Cells are able to respond selectively to sounds at a particular position by using the relative timing or intensity of sound at the two ears as the cue to direction: the coordinates of auditory space are defined with respect to the ears and hence the head. The positions of visual receptive fields are, however, defined with respect to the retina. As the eyes can move in their orbits, the coordinates of visual and auditory space used by bimodal neurones should, as Pöppel<sup>19</sup> has pointed out, be torn apart every time an eye movement occurs. Unless some compensatory process occurs, bimodal neurones in the SC should provide ambiguous directional information whenever the eyes are deviated from the straight-ahead position.

There are at least three possible ways in which each bimodal collicular cell might take account of changes in eye position: (1) The cell’s visual receptive field might move with respect to retinal coordinates by an angular distance equal and opposite to each eye movement, thus maintaining spatial correspondence with the auditory receptive field. (2) The cell’s auditory receptive field might move in space by an amount equal to each eye movement and in the same direction, to preserve the correspondence. (3) The auditory or visual input to the cell might simply be switched off whenever the eyes are significantly deviated from the central position, at which the auditory and visual receptive fields are aligned.

The first two possibilities seem implausible because they demand rapid and gross reorganization of the connections between the eyes or the ears and the SC each time the eyes move. The third hypothesis, which was not considered by Pöppel, is perhaps somewhat more likely. We have now examined this perplexing problem in alert cats.

Present addresses: \*Department of Psychology, University of Durham, Durham DH1 3LE, UK; †University Laboratory of Physiology, Parks Road, Oxford OX1 3PT, UK; ‡The National Hospital for Nervous Diseases, Queen Square, London WC1N 3BG, UK.



**Fig. 1** The auditory and visual receptive fields of bimodal cells in the deep layers of the SC are roughly superimposed in space. The inset shows the recording sites (○) of 27 bimodal cells reconstructed with respect to electrolytic lesions and projected on to the horizontal stereotaxic plane within the outline of the right SC. The graph shows the azimuth angle of the centre of the auditory receptive field plotted against that of the visual receptive field for all 22 of the neurones that responded well to the stationary tone used to plot the auditory field. The cat's eyes were centred in the orbits and the head was fixed in the straight-ahead position. For six cells the horizontal extents of the visual and auditory receptive fields are indicated by horizontal (visual) and vertical (auditory) lines.

### Testing the three hypotheses

For three adult female cats we used the techniques of Evarts<sup>20</sup> and Schiller and his collaborators<sup>21</sup> to implant silver-silver chloride electrodes<sup>22</sup> around the eyes (for recording horizontal and vertical eye movements electro-oculographically) and a chamber above the SC (for the introduction of glass-coated tungsten microelectrodes to record from single neurones).

We trained each animal to accept being wrapped in a cloth bag and to lie inside a padded box. Its head protruded through a large aperture and was attached to a superstructure that could be used either to measure horizontal and vertical head movements<sup>23</sup> or to fix the head in one position. With training the cats soon accepted these procedures.

To stimulate cells visually, a spot of light was back-projected on a translucent hemisphere (radius 57 cm) placed directly in front of the cat. Auditory receptive fields were plotted quantitatively by measuring the responses of cells to quiet tone bursts (duration 225 ms, frequency 1.2 Hz) emitted from a small radio earphone suspended from a crane whose centre of rotation was co-axial with the cat's head and whose angular position was varied in 10° steps over 180° in front of the cat and monitored by a potentiometer. The electro-oculogram (EOG) was calibrated<sup>15,24</sup> and the position of the eyes was monitored as a two-dimensional display on a storage oscilloscope. For subsequent computer analysis, horizontal and vertical EOG signals were recorded on tape, together with the neurone's action potentials, the voltage corresponding to the position of the auditory stimulus and pulses to indicate each onset of the sound.

### Precision of correspondence of visual and auditory receptive fields

We studied 27 bimodal cells (giving responses of roughly similar strength to optimal visual and auditory stimulation) in the deep layers of the SC. 50% of the cells recorded in the colliculus

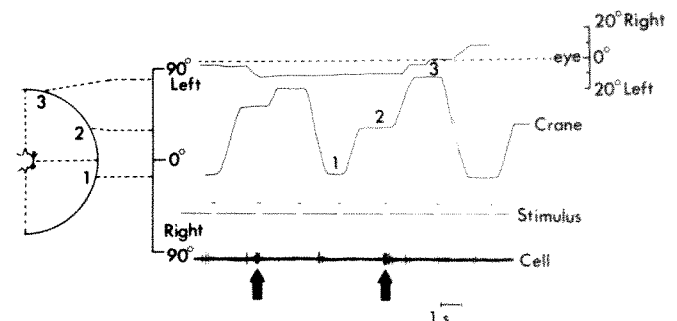
below 1.2 mm from the surface were bimodal. The inset in Fig. 1 shows the position of each recording site at which a bimodal cell was found. With the cat's head held in the straight-ahead position, her attention was constantly attracted to the centre of the hemisphere, and fixation at the centre was constantly checked from the two-dimensional display of eye position. The position of the visual receptive field of the neurone was plotted by monitoring the responses elicited by a small moving spot (~2° in diameter) back-projected on to the hemisphere. Then the hemisphere was removed, all the room lights extinguished and the horizontal extent of the auditory receptive field plotted out by setting the height of the small loudspeaker on the same level as the middle of the visual receptive field, swinging the crane to various positions in front of the cat's head and recording the responses to tone bursts. Only five of the 27 bimodal cells could not be studied in this way because they failed to respond to the pure tone and were excitable only by more complex sounds such as key-jingling or finger-snapping.

Eye position was constantly monitored throughout this procedure. Rapid recalibration of the EOG, by the simple procedure<sup>15</sup> of examining the range of signals produced as the cat made eye movements over the whole oculomotor range, showed little change in the d.c. level or gain of the EOG within the period of darkness in these experiments.

All bimodal cells were spatially selective in their responses to sound and visual stimuli, although in some cases, especially for cells in the more caudal part of the colliculus, representing the more peripheral field, visual and auditory receptive fields were rather large and their borders not sharply defined. However, we were satisfied that our data confirmed Wickelgren's<sup>16</sup> observation that, with the eyes in a straight-ahead position, visual and auditory receptive fields are quite well aligned and usually of about the same horizontal extent. The graph in Fig. 1 plots the horizontal position of the centre of the auditory receptive field against that of the centre of the visual receptive field: total horizontal extents are also indicated for six typical cells.

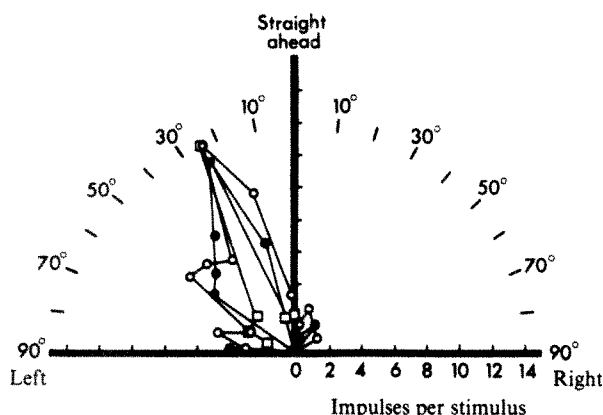
### Is there compensation of the visual receptive field during eye movement?

We did not attempt to measure possible minor variations in the dimensions, sensitivity or retinal positions of the visual receptive fields of bimodal cells during deviation of the eyes. However, for a number of bimodal cells we did informally replot the visual receptive field while attracting the animal's attention to various points on the hemisphere and hence producing deviation of the



**Fig. 2** A sample record from the experiment in which tone-burst stimuli were presented in the dark while the head was held. The position of the tone was randomized and the animal was encouraged to move her eyes. The top trace represents the horizontal eye position (approximate amplitude calibration on the right; interrupted line indicates the centre of the oculomotor range). The second trace shows the position of the crane that carried the loudspeaker (amplitude calibration on the left, with a sketch of the arrangement showing three positions labelled 1, 2 and 3, corresponding to the parts of the trace labelled). The third trace shows the duration of each 1.2 kHz tone burst (duration 225 ms). The bottom trace is an oscillograph recording of action potentials from a bimodal cell. Movements of the crane and noises produced by the experimenter elicited some activity between test stimuli. Clear responses to the tone are indicated by arrows.





**Fig. 3** Quantitative determinations of the spatial location and extent of the auditory receptive field of a bimodal cell. The visual receptive field for this unit was centred  $\sim 25^\circ$  to the left of the vertical meridian of the visual field. Tone stimuli were presented randomly at different positions in front of the cat with the head held in darkness. The animal was encouraged to deviate her eyes. The response (mean number of impulses in the 500-ms period following the onset of the tone averaged over at least five stimulus presentations) is plotted along the radial axis of the polar graph. The average standard deviation is 2.7 impulses per point. The angle of this polar plot represents the angular horizontal position of the loudspeaker. Data are plotted for three conditions of eye fixation: eyes centred (within  $7^\circ$  of straight ahead;  $\circ$ ), eyes deviated more than  $7^\circ$  right ( $\square$ ) or left ( $\bullet$ ). The auditory receptive field seems to be unchanged in spatial position and in sensitivity during deviation of the eyes.

eyes away from the central position. In no case was there any evidence of an obvious change in the retinal position of the receptive field: it always moved with the eyes and, except for possible brief changes in sensitivity associated with saccadic movements themselves<sup>15,25</sup>, no bimodal cells seemed to suffer dramatic reduction in visual sensitivity during deviated gaze. We therefore reject the first hypothesis described above, as well as the possibility of strong attenuation of the visual input during deviated gaze (hypothesis (3)).

### Is there compensation of the auditory receptive field during eye movement?

To test the second hypothesis we performed a detailed quantitative experiment on three bimodal cells (though the result was confirmed informally on many more). For each cell a series of  $\sim 500$  auditory stimuli was delivered in total darkness with the cat's head held straight ahead and with the position of the crane randomly varied from tone to tone. We took care to deliver tones only when the crane was stationary and the room silent. In addition, between tone stimuli, the cat's attention was frequently attracted by tapping or speaking to persuade her to deviate her gaze away from the straight-ahead position. A commentary on the progress of the experiment was made on the voice channel of the tape recorder. Thus we randomized the position of controlled auditory stimuli while the eyes were sometimes straight ahead, sometimes deviated right, sometimes left.

Figure 2 is a typical example of the records obtained, showing eye position, crane position, sound stimuli and the activity of the cell. Note that although the cell was frequently active between the tone stimuli, in response to the relatively loud attention-attracting noises, only two of the tone bursts (marked with arrows) elicited clear responses.

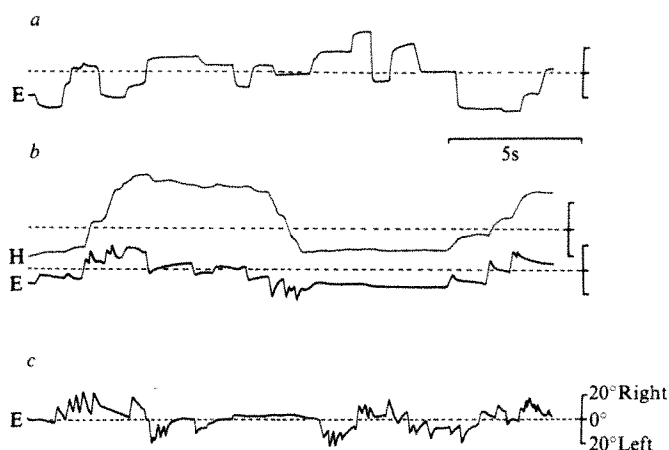
In an off-line computer analysis, the responses of the neurone to tones at each position in auditory space were averaged for three ranges of gaze position: eyes straight ahead (within  $7^\circ$  of the resting position); eyes deviated  $>7^\circ$  right of centre; eyes deviated  $>7^\circ$  left. The data available allowed at least five responses to be averaged for every stimulus condition.

Figure 3 shows the results for one bimodal cell that had its visual receptive field centred about  $25^\circ$  left of the midline. Each point represents the average number of impulses in a 500-ms interval following the onset of the tone. Points are plotted on polar coordinates, the radial axis indicating the magnitude of the response. The data collected within each of the three ranges of gaze position are plotted with different symbols and clearly the maximum response was always of about the same magnitude and always occurred with the loudspeaker placed  $\sim 25^\circ$  to the left of the midline, whatever the position of the eyes. The auditory receptive field did not move with the eyes, neither was the auditory input switched off when gaze was deviated. This result, which was reproduced in two other cells whose receptive fields were centred about  $45^\circ$  and  $70^\circ$  from the midline, seems to eliminate the remaining hypothetical forms of compensation described above.

For some cells the auditory receptive field was replotted with the head fixed not straight ahead but at a  $45^\circ$  angle to the right or left with respect to the body axis. In all cases the auditory receptive field shifted by precisely the same angle as the head. The auditory receptive field seems locked to head-centred coordinates, as one would expect if it depends on timing or intensity differences at the ears for its spatial selectivity. The auditory receptive field is not fixed with respect to the eyes nor with respect to the body axis as it does not move with the eyes when the head is stationary and it does move with the head when the head moves.

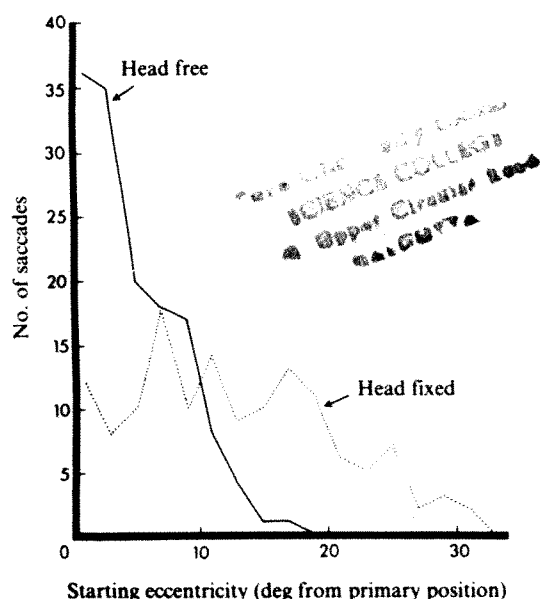
### Recentring of the eyes during gaze shifts

Our results so far indicate that there is no simple mechanism in the cat's SC for compensating for deviations of the eyes. Indeed, we predict that cats might suffer perceptual misalignment of visual and auditory space when the eyes are fixating peripherally. However, further experiments have revealed that a simple motor strategy ensures that this situation very rarely occurs in normal, freely moving cats.



**Fig. 4** Records of natural horizontal eye-in-orbit movements (E) and head movements (H) as a cat looks around a well lit stationary scene, in three conditions. The vertical calibration for each trace shows  $\pm 20^\circ$  deviation from the straight-ahead position, which is indicated by an interrupted line. *a*, Head held stationary. The eyes make a series of characteristic saccades with intervening fixations, lasting up to  $\sim 2$  s, with the eyes deviated up to  $\sim 30^\circ$  from the centre of the orbit. *b*, Head free to move in the head-holder, which transduces head movements but impedes and slows them a little. Now each large eye saccade is accompanied by a head movement in the same direction. The vestibulo-ocular reflex evoked by each head movement results in a compensatory counter-rotation of the eyes, tending to bring them back towards the centre of the orbit. *c*, Head completely unrestrained (hence no trace for head position). Recentring of the eyes after each saccade is now even more efficient, indicating that the head usually executes a movement almost equal in amplitude to that of the eyes. Hence each new change of gaze starts with the eyes near the centre of the orbit.

In these three animals, and in three other cats implanted for EOG recording and head fixation, we used the methods of Blakemore and Donaghy<sup>23,24</sup> to study coordinated movements of the head and eyes during changes of gaze. The superstructure to which the animal's head was fixed could be released to allow relatively free head movement, the horizontal and vertical rotations of which were monitored through potentiometers attached to the axes of rotation. We measured eye movements as the cat simply looked around the room in three conditions: head held still, head free to move in the headholder, and head completely unrestrained (Fig. 4).



**Fig. 5** Histograms showing the frequency of occurrence of eye-in-orbit position during steady fixation in head-fixed (interrupted line) and head-free (solid line) conditions (compare with Fig. 4a, c). The abscissa shows the horizontal position of the eye in the orbit (rightward and leftward deviations pooled) at the start of each saccade. Efficient recentering of the eyes in the head-free condition results in most new saccades starting with the eyes roughly centred in the orbit.

With the head held still the eyes make typical saccadic movements of up to  $\sim 40^\circ$  amplitude with the eyes being held almost stationary for periods of up to 2 s, at deviations in the orbit of up to  $\sim 30^\circ$  from straight ahead (Fig. 4a).

The situation is different when the head is allowed to move (Fig. 4b, c). Gaze changes of more than a few degrees in amplitude are now accomplished by combined movements of the eyes and head, with the eyes' saccade usually starting 25–50 ms before the start of the head movement<sup>23,24</sup>. Large changes in the direction of gaze involve a staircase of saccadic jerks of the eyes superimposed on a large head movement. Whenever the head is in motion, a counter-rotation of the eyes in the orbit, of opposite direction to the head movement and of virtually identical velocity, is superimposed on whatever other

eye movement is occurring. Blakemore and Donaghy<sup>24</sup> and Donaghy<sup>27</sup> have shown that this counter-rotation of the eyes in cats is due to the accurate operation of the vestibulo-ocular reflex. This has the effect of slowing down the saccade if the head begins to move before the eye has reached its target, and of causing a compensatory eye drift in the direction opposite to the saccade as the head movement continues after the end of the saccade (Fig. 4b). As the head rotation is usually of similar angular displacement to the saccadic eye rotation it accompanies, the net effect is to return the eye close to its starting position shortly after each saccade.

The saccadic mechanism can be viewed as a rapid motor system for the fixation of objects of interest, but the complete gaze change in a cat nearly always involves a similar movement of the head that effectively recentres the eyes. Hence, whenever a cat is steadily fixating an object after a whole gaze change is complete, the eyes are nearly always close to the centre of their orbits. This is very clearly shown in records of horizontal eye position when the head is completely unrestrained (Fig. 4c). Nearly all steady fixations occur with the eye close to the orbital centre, and each new change of gaze starts from roughly the straight-ahead position.

Figure 5 plots as a histogram the horizontal starting positions of the eye in the orbit for 70 successive changes of gaze made by each of two cats as they looked around a stationary scene. With the head fixed, the distribution of starting positions has almost constant probability out to  $20^\circ$  deviation and some saccades started with the eyes deviated horizontally by more than  $30^\circ$ . On the other hand, with the head completely unrestrained more than half of all saccades started with the eyes less than  $3^\circ$  from straight ahead in the orbit and very few started with the eyes more than  $10^\circ$  from the primary position.

## Paradox resolved for the cat, but not for primates

Pöppel's paradox<sup>19</sup> turns out not to be a problem for the cat. Complex neural compensation of the auditory or visual inputs to bimodal cells is unnecessary because the motor programme used by the cat to look around ensures that the eyes rapidly return near to the centre of the orbit after each saccade. Every time a new peripheral object attracts the cat's attention its SC can safely assume that the eyes are near the primary position, and hence that the coordinates of visual and auditory space are aligned.

On the other hand, for primates, including humans, the paradox still remains. Quite clearly, monkeys and people do not follow every eye saccade with a head movement of nearly identical amplitude. Occasionally fixation is maintained steadily on a peripheral target with the eyes deviated by  $40^\circ$  or more. We know very little about the neural basis of sensory integration in monkeys (and even less, of course, in man) although bimodal cells have been described in the primate SC<sup>28,29</sup>. The greater independence of the head movements in primates makes Pöppel's paradox a real issue once again.

This work was supported by grants 6973/447B and 6976/346 to C.B. from the MRC. L.R.H. and M.J.D. were MRC Scholars and C.B. held a Locke Fellowship from the RS.

Received 14 July; accepted 9 September 1980.

- Meger, D. L., Schatt, D. & Schaefer, K. P. *Pflügers Arch. ges. Physiol.* **314**, 240–252 (1970).
- Jacobson, M. Q. *J. exp. Physiol.* **47**, 170–178 (1962).
- Frost, B. J. & Di Franco, D. E. *Vision Res.* **16**, 1229–1234 (1976).
- Dräger, U. C. & Hubel, D. H. *Nature* **253**, 203–204 (1975).
- Feldon, S., Feldon, P. & Kruger, L. *Vision Res.* **10**, 135–143 (1970).
- Cynader, M. & Berman, N. *J. Neurophysiol.* **35**, 187–201 (1972).
- Stein, B. E., Magalhães-Castro, B. & Kruger, L. *J. Neurophysiol.* **39**, 401–419 (1976).
- Tiao, Y.-C. & Blakemore, C. *J. comp. Neurol.* **168**, 483–505 (1976).
- Suga, N. *J. Physiol., Lond.* **200**, 555–574 (1969).
- Kaas, L., Loop, M. S. & Hartline, P. H. *J. comp. Neurol.* **182**, 811–820 (1978).
- Schneider, G. E. *Psychol. Forsch.* **31**, 52–62 (1967); *Science* **163**, 895–902 (1969); *Brain Behav. Evol.* **3**, 295–323 (1970).
- Sprague, J. M., Berlucchi, G. & Berardino, A. D. *Brain Behav. Evol.* **3**, 285–294 (1970).
- Wurtz, R. H. & Goldberg, M. F. *J. Neurophysiol.* **35**, 587–596 (1972).

- Hess, W. R., Bürgi, S. & Bucher, V. *Mscr. Psychiat. Neurol.* **112**, 1–52 (1946).
- Harris, L. R. *J. Physiol., Lond.* **300**, 367–391 (1980).
- Wickelgren, B. G. *Science* **173**, 69–72 (1971).
- Gordon, B. G. *J. Neurophysiol.* **36**, 157–178 (1973).
- Dräger, U. C. & Hubel, D. H. *J. Neurophysiol.* **38**, 690–713 (1975).
- Pöppel, E. *Nature* **243**, 231 (1973).
- Evarts, E. *Electroenceph. clin. Neurophysiol.* **24**, 83–86 (1968).
- Schiller, P. H. & Koerner, F. *J. Neurophysiol.* **34**, 920–936 (1971).
- Bond, H. W. & Ho, P. *Electroenceph. clin. Neurophysiol.* **28**, 206–208 (1970).
- Blakemore, C. & Donaghy, M. J. *J. Physiol., Lond.* **242**, 40–41P (1974).
- Blakemore, C. & Donaghy, M. J. *J. Physiol., Lond.* **300**, 317–335 (1980).
- Straschill, M. & Schick, F. *Exp. Brain Res.* **27**, 131–141 (1977).
- Kris, C. *Nature* **182**, 1027–1028 (1958).
- Donaghy, M. J. *J. Physiol., Lond.* **300**, 337–351 (1980).
- Allon, N. & Wollberg, Z. *Brain Res.* **159**, 321–330 (1978).
- Updyke, B. V. *J. Neurophysiol.* **37**, 896–909 (1974).



# Leaky +1 and -1 frameshift mutations at the same site in a yeast mitochondrial gene

Thomas D. Fox & Brigitte Weiss-Brummer\*

Department of Biochemistry, Biocenter, University of Basel, CH-4056 Basel, Switzerland  
\* Genetisches Institut der Universität München, Maria-Ward Strasse 1a, D-8000 München, FRG

Two mutations in a mitochondrial structural gene, which cause leaky premature polypeptide chain termination and leaky growth, are +1 and -1 frameshifts in the same run of five T residues. The partial restoration of reading frame is probably due to ribosomal frameshifting at this site, and may be promoted by the unique structure of the yeast mitochondrial tRNA<sup>Phe</sup> (ref. 1).

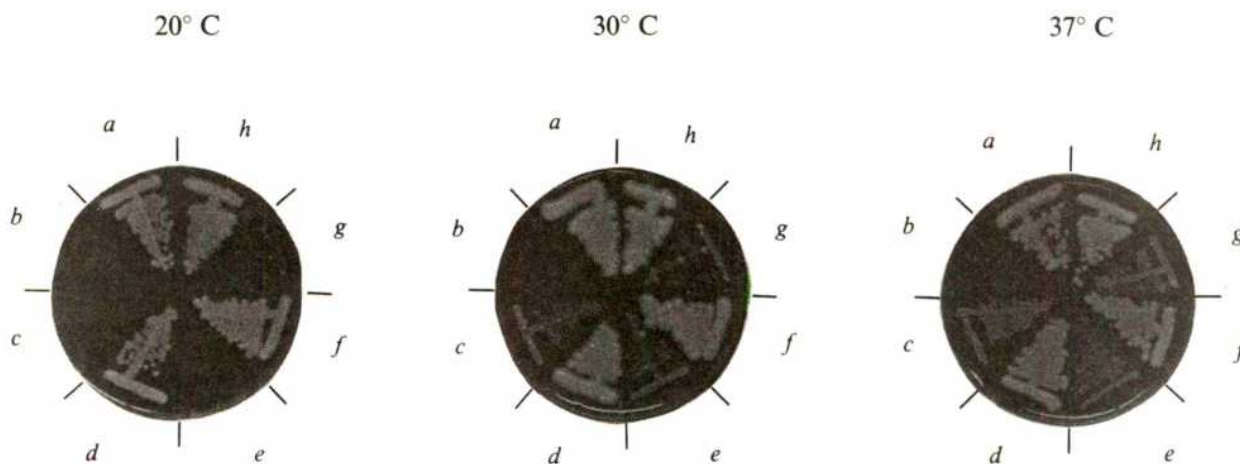
THE mitochondrial genetic system carries out the relatively limited task of making about 10 polypeptides. It has become clear recently that the genetic code specifying these polypeptides is somewhat different from the standard genetic code, and that there are even differences in the code between mitochondria in different species<sup>2-8</sup>. These differences could be due to the ability of mutations that change the code to be tolerated and fixed in a simple genetic system or due to some unknown selection for novelty. They might also reflect some primitive features of the mitochondrial genetic system.

To probe the nature of the mitochondrial genetic system further, we have continued to examine the DNA sequence of mutations in the yeast mitochondrial structural gene termed *oxi-l*, which codes for subunit II of cytochrome *c* oxidase<sup>3,9</sup>. One specific aim of these studies is to investigate the possibility that some codons which do not occur in the wild-type gene might be untranslatable. For this reason we examined several mutations in the *oxi-l* locus that were previously reported<sup>10</sup> to behave like leaky polypeptide chain terminators. Surprisingly, the leaky mutations examined so far have been found to be +1 and -1 frameshift mutations at a particular site in the structural gene. The findings indicate the existence of a mechanism that can promote frequent reading frame errors at specific sites during the expression of yeast mitochondrial genes.

## The leaky phenotype

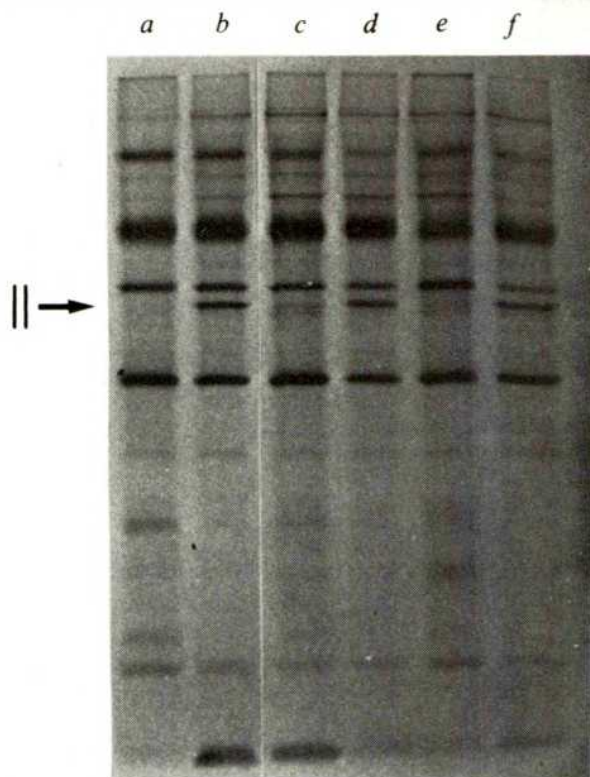
Among a recently described collection of some 90 *oxi-l* mutants<sup>10</sup>, five mutants were reported to have a leaky growth phenotype on medium containing non-fermentable carbon sources, and to synthesize greatly reduced amounts of cytochrome *c* oxidase subunit II. We have re-examined the phenotype of three of these mutants and have confirmed and extended the previous findings. When streaked on plates containing ethanol and glycerol as carbon sources, the three mutants M5661, M5701 and M5631 (Fig. 1c, e, g, respectively) grew significantly at 30 °C and 37 °C but not at 20 °C. In contrast, a non-leaky mutant (M13-249), shown previously by DNA sequence analysis to carry a frameshift, did not grow at any of these temperatures (Fig. 1b). In addition, spontaneous revertants of each of these mutants (Fig. 1d, f, h) grew similarly to wildtype (Fig. 1a). (Subsequent experiments demonstrated that the mutants M5661 and M5701 were independent isolates carrying identical lesions. Therefore, results are presented below only for M5701 and the third strain M5631.)

To examine the products of mitochondrial translation in these strains, yeast cells were treated with cycloheximide to inhibit cytoplasmic protein synthesis, and then labelled by incubation at 30 °C with <sup>35</sup>SO<sub>4</sub>. Crude mitochondrial fractions were prepared



**Fig. 1** Growth of wild-type, *oxi-l* mutant and revertant yeast strains on medium containing non-fermentable carbon sources. Plates containing 1% yeast extract, 2% peptone, 3% ethanol and 3% glycerol were streaked and incubated for 9 days at the temperatures indicated. The yeast strains were: a, wild type; b, M13-249, a non-leaky frameshift mutant<sup>3,26</sup>; c, M5661; d, a spontaneous revertant of M5661; e, M5701; f, a spontaneous revertant of M5701; g, M5631; h, a spontaneous revertant of M5631. The mutants M5661, M5701 and M5631 were isolated from the haploid *pet<sup>-</sup> (rho<sup>0</sup>)* strain 777-3A (ref. 10). To reveal the growth phenotype of these mitochondrial mutations and the wild type, diploids were formed from these strains by crossing them to a *pet<sup>+</sup> (rho<sup>0</sup>)* tester strain. The resulting diploid strains, plated above and used in all experiments described here, are referred to by the original haploid names for simplicity. The spontaneous revertants were isolated from the diploid mutant strains.





**Fig. 2** Mitochondrial translation products of wild type, *oxi-1* mutant and revertant strains. Cells of strains M13-249 (a), wild type (b), M5701 (c), revertant of M5701 (d), M5631 (e) and revertant of M5631 (f) were labelled with  $^{35}\text{S}\text{O}_4^{2-}$  in the presence of cycloheximide in medium containing 2% galactose as described<sup>27</sup>. The mutant cultures contained revertants at frequencies  $<5 \times 10^{-5}$ . Mitochondria were isolated<sup>28</sup> and subjected to electrophoresis in a gel containing 15% polyacrylamide in the presence of SDS. The gel was dried and autoradiographed. The arrow indicates the position of cytochrome oxidase subunit II.

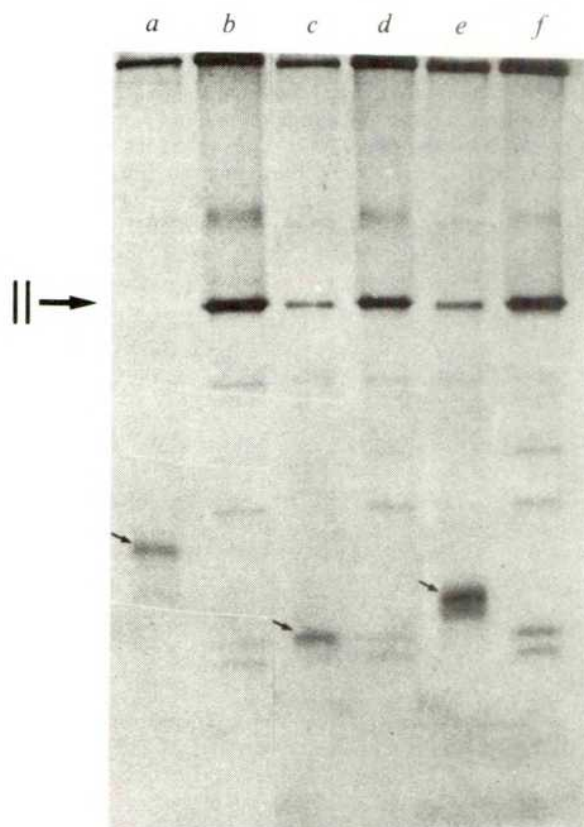
and subjected to SDS-gel electrophoresis. The mitochondrial translation products were visualized by autoradiography. The non-leaky mutant M13-249 failed to synthesize detectable amounts of cytochrome oxidase subunit II (Fig. 2a) as has been previously reported<sup>9</sup>. The leaky mutants M5701 (Fig. 2c) and M5631 (Fig. 2e), on the other hand, both produced small amounts of a polypeptide with the same electrophoretic mobility as wild-type subunit II (Fig. 2b). (A second polypeptide, moving slightly faster than subunit II, is also evident in these mutants and faintly visible in the wild type. As shown below, this protein is apparently not related to subunit II.) By densitometric scanning of autoradiograms, the amount of subunit II labelled in the mutants was estimated to be roughly 5% of that found in wild type at 30 °C. When cells were grown and labelled at 20 °C, the labelling of subunit II in the mutants was further decreased relative to wild type but was still detectable (not shown). Whether this further decrease accounts for the tight negative growth phenotype of the mutants at 20 °C is unknown. Labelling of subunit II was normal in the spontaneous revertants of both mutants (Fig. 2d, f).

To confirm that the faint bands observed in Fig. 2 indeed represented the cytochrome oxidase subunit, the labelled mitochondrial extracts were subjected to antibody precipitation with an anti-subunit II serum. SDS-gel analysis of the precipitates confirmed that the mutants M5701 and M5631 (Fig. 3c, e) had produced small amounts of the full-sized protein (molecular weight (MW) 27,000), whereas the non-leaky mutant (Fig. 3a) had produced none. In addition, a shorter polypeptide fragment

(arrows in Fig. 3). These fragments can also be seen as faint bands in the total mitochondrial translation products<sup>10</sup> (Fig. 2). In the case of the non-leaky frameshift mutant M13-249, the shorter fragment (MW 17,000) is known to result from termination at an out-of-frame nonsense codon downstream from the mutation<sup>3</sup>. As will be shown below, the fragments observed in the mutants M5701 and M5631 (MWs 9,600 and 12,500, respectively) are produced in a similar manner. One might therefore expect the labelling intensity of the mutant fragments to approximate that of subunit II in the wild type, correcting for the lower MW. However, the fragments are much less intense (Figs 2, 3). Possibly they are less stable than the wild type protein. A further caution regarding the quantitative interpretation of these autoradiograms is that the intensity of labelling in the presence of cycloheximide may not accurately reflect the relative level of proteins in growing yeast cells.

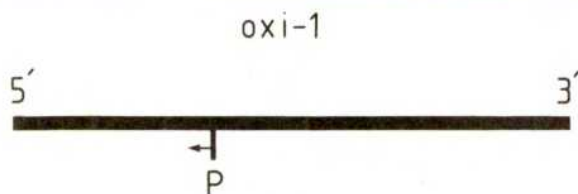
Several minor species are also present in the antibody precipitates of the wild type and revertants. In addition to small amounts of subunits I and III of cytochrome oxidase, at least four lower molecular weight polypeptides can be seen (Fig. 3) which seem to be related to subunit II insofar as they are very strongly reduced in the mutants. The origin of these smaller polypeptides is unknown.

Taken together, the above findings suggest that the leaky growth phenotype of mutants M5701 and M5631 is due to the



**Fig. 3** Antibody precipitation of cytochrome oxidase subunit II and related polypeptides. The radioactively labelled mitochondrial translation products from the experiment of Fig. 2 were solubilized in SDS and subjected to immune precipitation<sup>29</sup> with a rabbit antiserum prepared against purified cytochrome oxidase subunit II (obtained from G. Schatz). The antibody precipitates were dissolved in SDS and electrophoresed on a 15% polyacrylamide gel which was dried and autoradiographed. As in Fig. 2 the labelled proteins were from M13-249 (a), wild type (b), M5701 (c), revertant of M5701 (d), M5631 (e) and revertant of M5631 (f). The position of subunit II in the gel is indicated, and small arrows in the autoradiogram indicate 'fragment' polypeptides specifically precipitated from the mutant extracts.





**Fig. 4** Position of the mutations within the gene sequence. The horizontal line represents the sequence coding for cytochrome oxidase subunit II (753 base pairs), translated from left to right. The *PvuII* site (at position -147 in the sequence of ref. 3) utilized in the experiments of Fig. 5 is indicated by P, and the direction of sequencing by the arrow. The run of T residues affected by the mutations starts five base pairs upstream from the *PvuII* cut.

presence of reduced amounts of a functional form of cytochrome oxidase subunit II, and that this deficiency is caused by frequent premature polypeptide chain termination during translation of the protein.

### Identification of frameshifts in the DNA sequence

To establish the nature of the mutations in strains M5701 and M5631, a 2,400-base pair *HpaII* restriction fragment that carries the entire *oxi-1* locus<sup>3,11</sup> was isolated from the total mitochondrial DNA of each strain for sequence analysis. The positions of the mutations were estimated to be about one-third of the way into the gene based on the apparent MWs of the subunit II fragments observed. A *PvuII* cleavage site lies in this region<sup>3</sup> (Fig. 4) and was utilized for end labelling and sequence determination by chemical degradation<sup>12</sup>. Alterations in the DNA sequence of both mutants were found in a run of five T residues present in the wild type sequence immediately upstream from the *PvuII* site (Fig. 5a). In the mutant M5701, this run is shortened to four T residues by a single base-pair deletion (Fig.

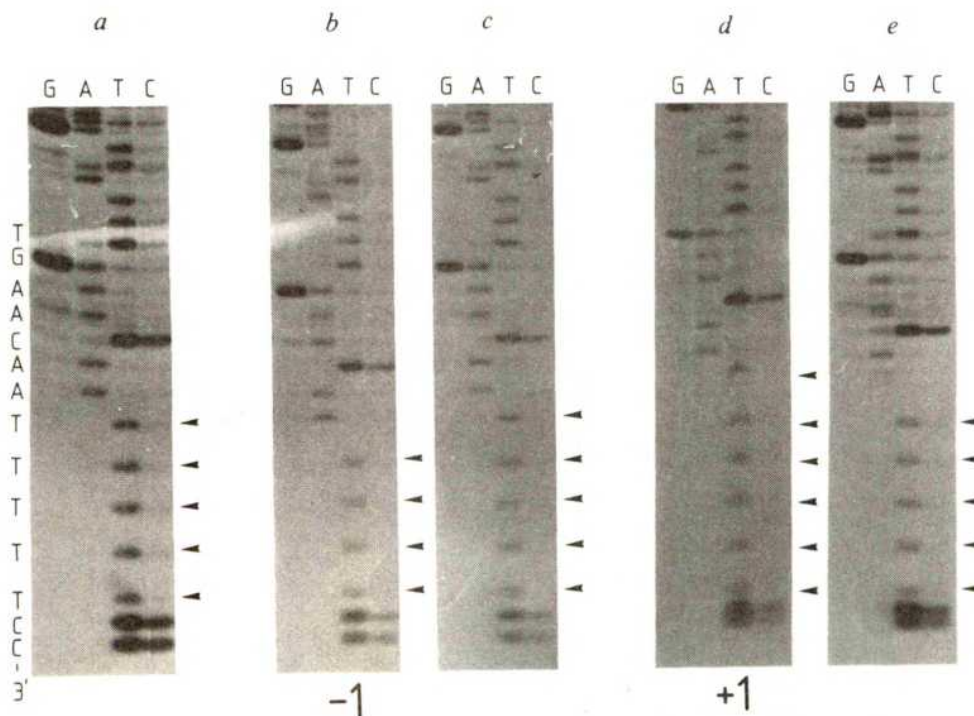
5b) whereas in the mutant M5631 the run is lengthened to six T residues by a single base-pair insertion (Fig. 5d). Spontaneous revertants of each strain (Fig. 5c, e) were restored to wild-type sequence, indicating that no undetected second site mutations are present.

The predicted consequences of the -1 and +1 frameshifts for translation are shown in Fig. 6 based on the known sequence of the wild type gene<sup>3</sup>. Shortening of the T run (underlined) to four bases should lead to a TAA stop codon after the addition of two amino acids out of frame. Lengthening the T run to six should result in the addition of 29 amino acids out of frame, yielding a significantly longer fragment polypeptide. These predictions are in excellent agreement with the apparent MWs of the subunit II fragments detected in the experiment of Fig. 3.

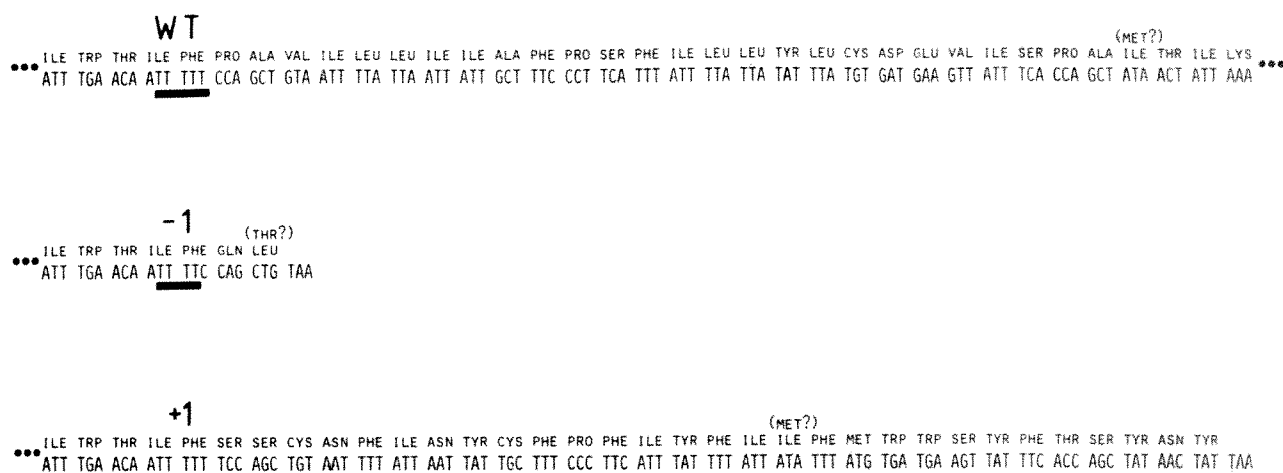
### Restoration of reading frame

The experiments described here show that despite the presence of a +1 or -1 frameshift mutation at a particular site in the yeast mitochondrial gene coding cytochrome oxidase subunit II, a significant amount of the full-sized gene product is formed. Thus, during the expression of these mutant genes, compensating errors must be made at or near the site of the mutations to restore translation to the proper reading frame. Although it is difficult to quantify accurately the frequency of reading frame restoration (see above), it seems to be roughly 5%. Leakiness of frameshift mutations in the  $\beta$ -galactosidase gene of *Escherichia coli* has been previously reported<sup>13</sup>. However, the levels there were 2 to 4 orders of magnitude lower than those described here.

The site affected by these *oxi-1* mutations is a run of five T residues. Whatever the mechanism that restores the reading frame, it is clearly site specific to some extent because at least one other frameshift mutation in this gene (a -1 mutation in a non-monotonous sequence) is not leaky (Figs 1-3 and refs 3, 9). Indeed, it seems likely that the compensating errors are made at the affected T run: eight of the 10 amino acid residues surrounding the site are identical in the yeast and bovine proteins<sup>3,14</sup>, indicating that they have functional significance. If



**Fig. 5** Identification of a single base-pair deletion and a single base-pair insertion in the *oxi-1* locus of the leaky mutants M5701 and M5631, respectively. Mitochondrial DNA fragments labelled on the 3' end<sup>3</sup> at the *PvuII* site indicated in Fig. 4, were isolated from wild type (a), M5701 (b), spontaneous revertant of M5701 (c), M5631 (d) and spontaneous revertant of M5631 (e), and subjected to chemical degradation sequencing reactions<sup>12</sup>. Autoradiograms of the products after separation on 20% polyacrylamide gels are shown. The arrow heads next to the panels point to the T residues in the affected run. As indicated, M5701 is a -1 frameshift and M5631 is a +1 frameshift.



**Fig. 6** Predicted translational consequences of the -1 and +1 frameshifts. A portion of the wild-type sequence (WT) (from ref. 3) including the site of the mutations (underlined) is shown. Out-of-frame translation beyond the mutations is shown up to the first termination codon encountered for the -1 and +1 mutations. Possible alternative codon assignments<sup>2,4</sup> are indicated in parentheses.

compensating errors were made anywhere other than at the site of the mutations, at least some of this conserved amino acid sequence would be garbled.

It seems likely that a single mechanism underlies the reading frame restoration in both the +1 and -1 frameshift mutants. One scheme which immediately suggests itself would suppose that during translation of this monotonous sequence, a slippage of the ribosome and/or peptidyl-tRNA relative to the mRNA can occur in both directions. If, for example during translation in the -1 mutant, the ribosome were to slip back one nucleotide after peptidyl-transfer to the tRNA<sup>Phe</sup>, the next codon exposed to the incoming aminoacyl-tRNA (CCA) would be in the wild type reading frame. Similarly, forward slippage would restore the wild type frame in the +1 mutant. In both cases, the peptidyl-tRNA<sup>Phe</sup> would still be sitting on a Phe codon after the slip. A formally equivalent possibility would be that the ribosome occasionally translocates two or four nucleotides at this site. Similar but less frequent events presumably lead to the observed leakiness of +1 and -1 frameshift mutations in *E. coli*<sup>13,15,16</sup>.

Several lines of evidence indicate that tRNA structures have an important role in maintaining reading frame during translation. First, mutated tRNAs are capable of suppressing +1 frameshift mutations both in bacteria<sup>17-19</sup> and in the nucleocytoplasmic genetic system of yeast<sup>20</sup>. The frameshift-suppressor tRNAs have generally been supposed to 'read' a 4-nucleotide codon, although it now seems that the actual mechanism may involve the induction of ribosomal frameshifting by the altered conformation of these mutant tRNAs<sup>16,21</sup>. Furthermore, some normal tRNAs can also promote ribosomal frameshifting in both directions when added in excess to an *in vitro* translation system<sup>22</sup>. It is therefore very interesting that the wild type yeast mitochondrial tRNA<sup>Phe</sup>, which is involved in translation at the site of the leaky frameshift mutations, has a unique structure:

the TΨC-stem contains an extra nucleotide which cannot be base-paired<sup>1,23</sup>. This extra unpaired nucleotide surely affects the conformation of the tRNA, and it is tempting to speculate that the novel structure may either induce ribosomal frameshifting or promote the slippage of the peptidyl-tRNA<sup>Phe</sup> relative to the mRNA. A precedent for this kind of hypothesis is provided by the case of the *E. coli* tRNA<sup>Trp</sup><sub>UGA</sub> suppressor, in which a sequence alteration in the D-stem confers the ability to read UGA codons on an otherwise normal tRNA<sup>Trp</sup> (ref. 24).

A somewhat different, and perhaps less likely model to explain the frequent frameshifting would suppose that the mitochondrial RNA polymerase occasionally 'slips' while transcribing a run of A residues, thus producing a small amount of wild-type mRNA from a gene carrying a frameshift. This hypothesis can probably now be tested using a heterologous translation system<sup>25</sup> programmed with mitochondrial mRNA from the leaky frameshift mutants.

Whatever the mechanism, it is clear from the results presented here that an extraordinarily high rate of reading frame errors occurs at specific points during the expression of at least some yeast mitochondrial genes. This obviously predicts that small amounts of prematurely terminated (and possibly extended) polypeptides should be synthesized by wild-type mitochondria as a result. Although we have not explicitly tested this prediction, it is not contrary to experience, in that many faint bands can always be detected in cycloheximide labelling experiments like that of Fig. 2 (see also Fig. 3). Such frameshifted proteins might be a burden tolerated by the cell. However, it is also possible that frameshifting at specific sites leads to the synthesis of physiologically important products.

We thank J. Wey and S. Stämpfli for technical assistance and R. Hall for a critical reading of the manuscript. B.W.-B. was supported in part by stipends from EMBO and Euratom. This work was supported by a grant from the Swiss NSF.

Received 1 August; accepted 26 August 1980.

- Martin, R. P. *et al. Nucleic Acids Res.* **5**, 4579-4592 (1978).
- Barrell, B. G., Bankier, A. T. & Drouin, J. *Nature* **282**, 189-194 (1979).
- Fox, T. D. *Proc. natn. Acad. Sci. U.S.A.* **76**, 6534-6538 (1979).
- Li, M. & Tzagoloff, A. *Cell* **18**, 47-53 (1979).
- Macino, G., Coruzzi, G., Nobrega, F. G., Li, M. & Tzagoloff, A. *Proc. natn. Acad. Sci. U.S.A.* **76**, 3784-3785 (1979).
- Heckman, J. E., Sarnoff, J., Alzner-De Weerd, B., Yin, S. & RajBhandary, U. L. *Proc. natn. Acad. Sci. U.S.A.* **77**, 3159-3163 (1980).
- Barrell, B. G. *et al. Proc. natn. Acad. Sci. U.S.A.* **77**, 3164-3166 (1980).
- Bonitz, S. G. *et al. Proc. natn. Acad. Sci. U.S.A.* **77**, 3167-3170 (1980).
- Cabral, F. *et al. J. biol. Chem.* **253**, 297-304 (1978).
- Weiss-Brummer, B., Guba, R., Haid, A. & Schweyen, R. J. *Curr. Genet.* **1**, 75-83 (1979).
- Fox, T. D. *J. molec. Biol.* **130**, 63-82 (1979).
- Maxam, A. M. & Gilbert, W. *Proc. natn. Acad. Sci. U.S.A.* **74**, 560-564 (1977).
- Atkins, J. F., Elseviers, D. & Gorini, L. *Proc. natn. Acad. Sci. U.S.A.* **69**, 1192-1195 (1972).
- Steffens, G. J. & Buse, G. *Hoppe-Seyler's Z. physiol. Chem.* **360**, 613-619 (1979).

- Yarus, M. *Prog. Nucleic Acid Res. molec. Biol.* **23**, 195-225 (1979).
- Kurland, C. G. in *Nonsense Mutations and tRNA Suppressors* (eds Celis, J. E. & Smith, J. D.) 97-108 (Academic, New York, 1979).
- Roth, J. R. *A. Rev. Genet.* **8**, 319-346 (1974).
- Riddle, D. & Carbon, J. *Nature new Biol.* **242**, 230-234 (1973).
- Kohn, T. & Roth, J. R. *J. molec. Biol.* **126**, 37-52 (1978).
- Culbertson, M. R., Charnas, L., Johnson, M. T. & Fink, G. R. *Genetics* **86**, 745-764 (1977).
- Bossi, L. & Roth, J. R. *Nature* **286**, 123-127 (1980).
- Atkins, J. F., Gesteland, R. F., Reid, B. R. & Anderson, C. W. *Cell* **18**, 1119-1131 (1979).
- Martin, N. C. *et al. in Extrachromosomal DNA* (eds Cummings, D. J., Borst, P., Dawid, I. B., Weissman, S. M. & Fox, C. F.) 357-375 (Academic, New York, 1979).
- Hirsch, D. *J. molec. Biol.* **58**, 439-458 (1971).
- De Ronde, A., Van Loon, A. P. G. M., Grivell, L. A. & Kohli, J. *Nature* **287**, 361-363 (1980).
- Slonimski, P. P. & Tzagoloff, A. *Eur. J. Biochem.* **61**, 27-41 (1976).
- Douglas, M. & Butow, R. A. *Proc. natn. Acad. Sci. U.S.A.* **73**, 1083-1086 (1976).
- Needleman, R. B. & Tzagoloff, A. *Analyt. Biochem.* **64**, 545-549 (1975).
- Maccacchini, M.-L., Rudin, Y., Blobel, G. & Schatz, G. *Proc. natn. Acad. Sci. U.S.A.* **76**, 343-347 (1979).



# LETTERS

## The Jodrell Bank radio-linked interferometer network

J. G. Davies, B. Anderson & I. Morison

University of Manchester Nuffield Radio Astronomy Laboratories,  
Jodrell Bank, Macclesfield, Cheshire SK11 9DL, UK

The Multi Telescope Radio Linked Interferometer (MTRLI) has just been brought into operation at Jodrell Bank and here we introduce the instrument, describe its capabilities, and present some of the first maps to be made with it. MTRLI produces high quality maps of radio sources with resolutions varying from  $\sim 1$  arcs to  $\sim 0.02$  arcs depending on the frequency of operation. The obvious astronomical use of the instrument is for the mapping of powerful extragalactic radio sources to investigate the physical processes within them, but it will also have the capability to map galactic line as well as galactic continuum sources. The maps presented here were made at 408 MHz and are all of extragalactic sources. They illustrate the ability of MTRLI to map at low frequencies the steep spectrum emission which tends to be overlooked with existing synthesis instruments which have to work at much higher frequencies to obtain the same resolution.

The MTRLI which has been under construction since 1975 and is an extension of the long baseline interferometers first operated at Jodrell Bank<sup>1</sup> in 1954 over a baseline of 0.91 km (480 wavelengths). Subsequently the baselines were suc-

cessively increased by using radio links<sup>2</sup> to 127 km (2 million wavelengths) by 1967 (ref. 3). The present MTRLI concept was proposed in 1974 by Palmer as a further improvement and extension of these two telescope interferometer systems. The MTRLI uses one of the two large telescopes at Jodrell Bank, (the MK IA 76-m telescope or the MK II 25 $\times$ 37-m telescope) and the existing outstations at Defford and Wardle, together with three new 25-m telescopes sited at Knockin Darnhall and Tabley which are of the E-Systems design as used in the VLA. The first phase of the instrument using four telescopes is now working; the second phase in which the Darnhall and Tabley telescopes are added to the array will be complete by the end of 1980. When all telescopes are in use, data can be obtained from 15 baselines simultaneously ranging from 133 to 6 km in length. The system will be operated at a variety of wavelengths ranging from 73 to 1.35 cm, although at the higher frequencies not all telescopes are usable. Figure 1 indicates the position of the telescopes and the orientation of the baselines. The three new telescopes were sited to provide reasonably uniform coverage of the spatial frequency components of the sky brightness distribution. This is shown in Fig. 2 for declinations 10° and 50° north for the 15 baselines of the array. Because of the large N-S component in many of the baselines the resolution in the N-S direction remains comparable to that in the E-W direction even at low declinations.

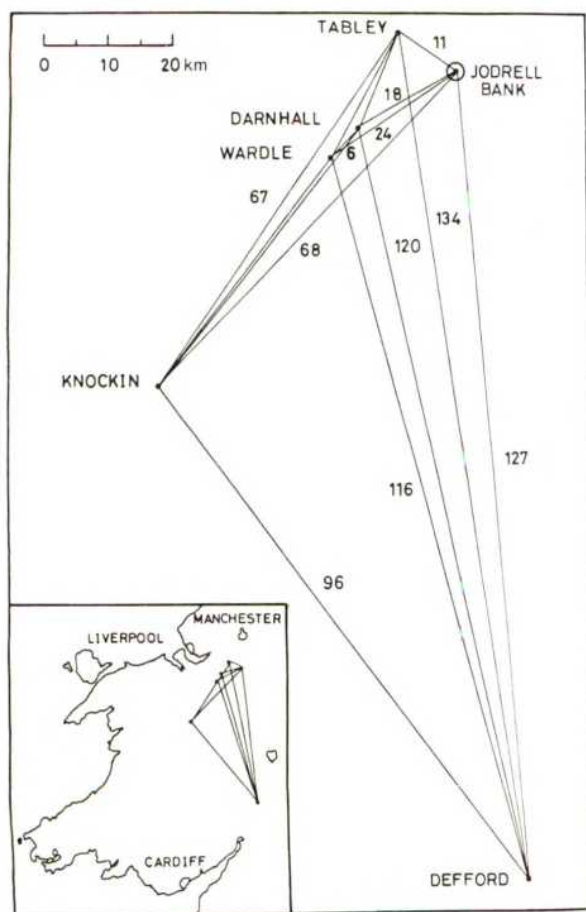


Fig. 1 The relative positions of the MTRLI telescopes with the baseline lengths given in kilometres.

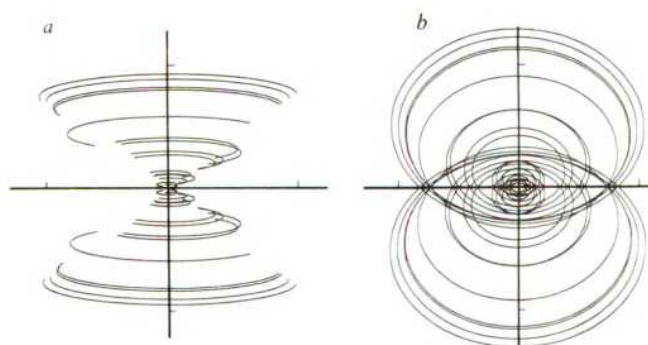
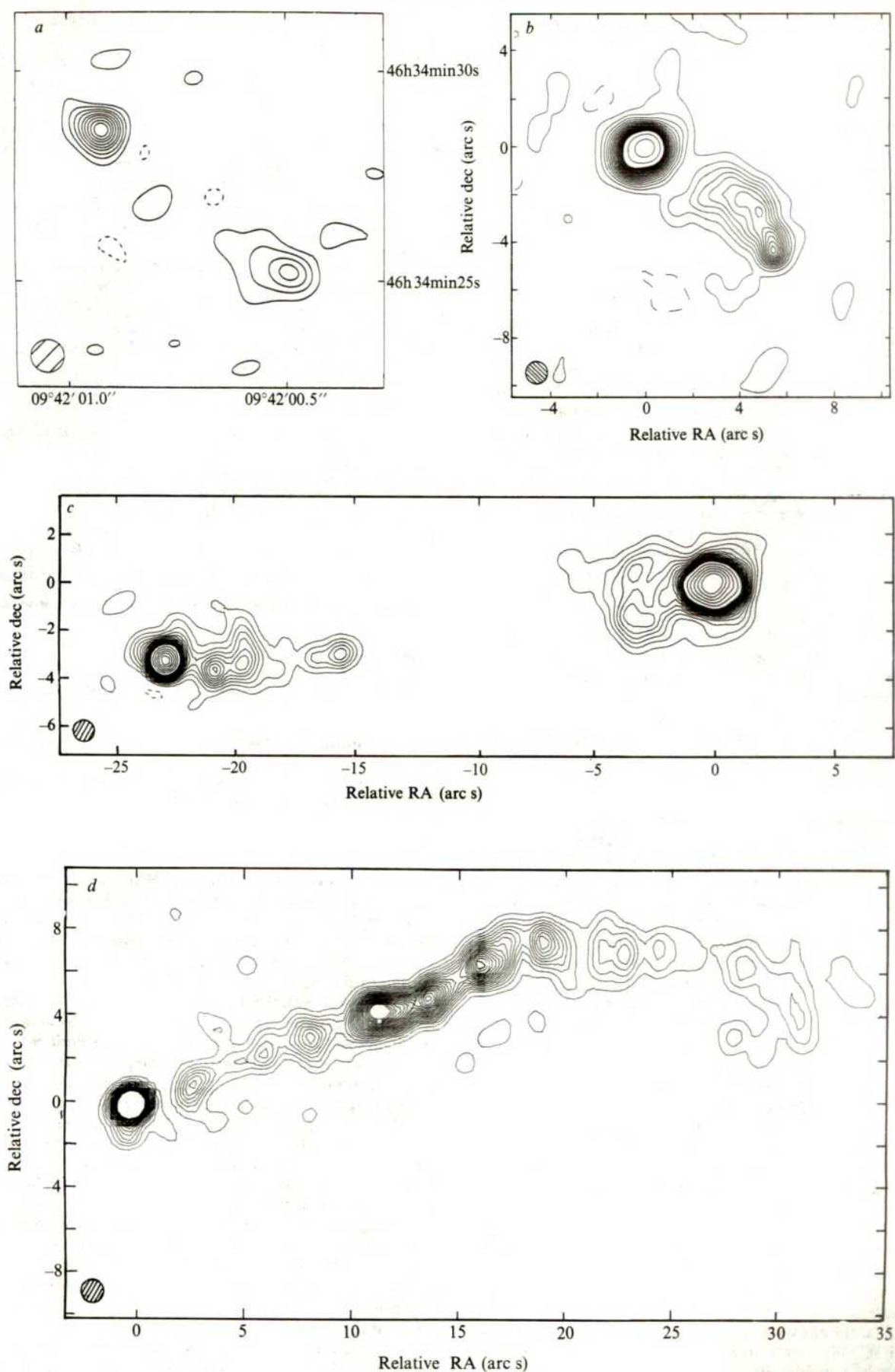


Fig. 2 The projected spacings of the MTRLI baselines for sources of declination: a, 10°; b, 50°. One division represents 100 km.

Each outstation telescope has an on-line computer to provide local control of the telescope and receiver or allow remote operation by land line from Jodrell Bank. Standard microwave links with a bandwidth of 10 MHz carry the radio signals from the outstations to Jodrell Bank, using two repeater stations in the case of Defford and Knockin, and direct for the nearer telescopes. Local oscillators at all sites are phase locked using a single frequency near 1,500 MHz. Pulses at this frequency are transmitted from Jodrell Bank to the outstations over the same paths as are used for the microwave links, locking high quality crystal oscillators at each repeater site and telescope. Pulses are then returned over the same paths and the received phase compared with that transmitted. In this way changes in the electrical path lengths are continuously measured with an accuracy of about 1 mm in 150 km, and corrections made to the phase of the received signals.

At Jodrell Bank the signals from each telescope are passed through phase rotators to remove the effects of the Earth's rotation, an analogue delay continuously variable between 0 and 75 ns and a digital delay of up to 1 ms in 50-ns steps to compensate for the varying geometry of the telescope baselines. The signals are then taken in pairs and correlated in a set of



**Fig. 3** The MTRLI maps. *a*, 5C5.168 at 408 MHz; the contour interval is 2 mJy per beam area. *b*, 3C153 at 408 MHz; the contour levels are 1, 3, 5...33, 35, 50, 75% of peak brightness; *c*, 3C249.1 at 408 MHz; the contour levels are 2, 4, 6, 8...28, 30, 40, 50, 60, 70, 80% of peak brightness. *d*, Virgo A at 408 MHz; the contour levels are 2, 4, 6, 8...38, 40% of peak brightness. The half-power beamwidth of the circular gaussian restoring beam is shown in each case in the lower left-hand corner.



one-bit correlators. These are normally connected as 16 complex correlators each with 32 channels of delay. If two or more sources are to be observed simultaneously in one telescope beam, the differential delay for the longer baselines may exceed the  $32 \times 50$  ns available from one of these correlators. In this event the correlators can be connected together to provide fewer independent correlators with a larger number of delays. Integration over 1 s is performed within the correlators, and the data are then passed to a purpose designed computer where further integration, processing and storage takes place.

Sources are typically observed at all hour angles where the elevation remains above  $5^\circ$  and maps of the brightness distribution are produced by the CLEAN<sup>4</sup> technique to remove unwanted sidelobe responses of  $\sim 5\%$  caused by the incomplete spatial frequency coverage of the array.

The inherent phase stability of the interferometers and hence the map making capability of the system is fundamentally limited by the atmosphere above each telescope, with tropospheric effects being most important at high frequencies and ionospheric effects at low frequencies. These limitations may be overcome by determining the phase of the source being mapped relative to that of a nearby reference source. At low frequencies the source and a suitable reference can often be observed simultaneously within the telescope beam<sup>4</sup>, but at high frequencies it will be necessary to alternate between the source and reference on a time scale short compared with that of the fluctuations. Alternatively, with the sacrifice of positional information, one can produce maps which use the closure phase relationships<sup>6</sup> between different combinations of telescopes. Cornwell and Wilkinson<sup>7</sup> developed a mapping algorithm which corrects amplitude and phase errors arising at the separate telescopes in the array. This is exactly equivalent to using the closure amplitudes and phases as in the approach adopted by the standard 'hybrid' mapping algorithms of Readhead and Wilkinson<sup>8</sup> and Readhead *et al.*<sup>9</sup>. The new algorithm is rather more general than these earlier ones and extensive tests on simulated data have shown that maps of complex sources made from typical MTRLI data are reliable down to  $\sim 1\%$  of the peak brightness.

Observations of about 30 extragalactic sources were made during January and February 1980 at 408 MHz with a four-telescope array comprising the MK IA and the Wardle, Knockin and Defford telescopes. The observations provide an extreme test of the mapping ability of the system in that there were only six baselines available and the data were obtained in severe ionospheric conditions near the time of maximum solar activity. A full astronomical discussion of most of the results will be given elsewhere but we present in Fig. 3 a few of the maps produced from the observations to illustrate the capabilities of the system. The map of 5C5.168 was produced by reference to a source elsewhere in the beam, the remaining maps were produced using the new hybrid mapping technique.

5C5.168 (Fig. 3a) is one of four 5C sources mapped simultaneously using 5C5.175 as a reference source. This is a double source of 6 arc s separation with a total flux of 70 mJy. The contour interval is limited by noise at 2 mJy per beam area. Because an accurate position measurement for the reference source is available, the positions of the components of 5C5.168 are determined to  $\sim 0.2$  arc s, but even with such accuracy the source remains unidentified on the Palomar Sky Survey down to 20th magnitude. The ability of MTRLI to map such weak sources means that we can investigate how the morphologies of radio sources depend on luminosity. This in turn is a prerequisite for the investigation of angular size evolution.

Figure 3b, and c shows maps of two high luminosity sources 3C153 and 3C249.1 respectively. The large dynamic range of the maps enables the details of the point features between the main peaks of emission to be seen clearly. Note that in both sources there is emission stretching from near the optical object out to just one of the lobes; in each case the second lobe appears completely isolated. Perhaps the emission is from the beam which is thought to transport energy from the nucleus to the

outer lobes, and then the asymmetry could be explained by relativistic beaming.

The map of Virgo A is included to illustrate how well MTRLI can map complicated sources with just four telescopes. That the details of the map are substantially correct is demonstrated by the coincidence of the radio and optical knots and by the good agreement found between the main features in the present map and that made with the VLA at 5 GHz (ref. 10).

MTRLI observations at 1,666 MHz of all the present sources are planned and detailed astrophysical discussion of the combined 408- and 1,666-MHz observations will be given elsewhere.

The construction of the MTRLI has involved major effort by many members of staff at Jodrell Bank, but we particularly thank J. A. Battilana, M. Bentley, A. Brown, D. C. Brown, R. D. Davies, R. J. Davis, M. Doggett, J. S. Haggis, J. Hopkins, R. G. Noble, H. P. Palmer, L. Pointon, R. S. Pritchard, D. Stannard and P. Thomasson.

Received 14 July; accepted 18 September 1980.

1. Hanbury Brown, R., Palmer, H. P. & Thompson, A. R. *Phil. Mag.* **46**, 857 (1955).
2. Morris, D., Palmer, H. P. & Thompson, A. R. *The Observatory* **77**, 103, (1957).
3. Palmer, H. P. *et al. Nature* **213**, 789 (1967).
4. Hogbom, J. A. *Astr. Astrophys. Suppl.* **15**, 417-426 (1974).
5. Peckham, R. J. *Mon. Not. R. astr. Soc.* **165**, 25-38 (1973).
6. Jennison, R. C. *Mon. Not. R. astr. Soc.* **188**, 276-284 (1958).
7. Cornwell, T. J. & Wilkinson, P. N. (in preparation).
8. Readhead, A. C. S. & Wilkinson, P. N. *Astrophys. J.* **223**, 25-36 (1978).
9. Readhead, A. C. S., Walker, R. C., Pearson, T. J. & Cohen, M. H. *Nature* **285**, 137-140 (1980).
10. Owen, F. N., Hardee, P. E. & Bignell, R. C. *Astrophys. J. Lett.* **239**, L11-15 (1980).

## Rotationally symmetric structure in two extragalactic radio sources

C. J. Lonsdale & I. Morison

University of Manchester, Nuffield Radio Astronomy Laboratories, Jodrell Bank, Macclesfield, Cheshire SK11 9DL, UK

Many extragalactic radio sources exhibit radio structures with some degree of rotational symmetry<sup>1,2</sup>, which in extreme cases (for example, 3C315 (ref. 3) and NGC326 (ref. 4)) suggests precession of the source axis, such as might result if a relativistic beam of particles<sup>5,6</sup> or stream of plasmoids<sup>7</sup> were to change its orientation during the source lifetime<sup>1</sup>. In such circumstances we might expect radiative and other energy losses to steepen the spectrum of the older regions of emission<sup>8</sup> away from the current sites of activity, and so make them more prominent on low-frequency maps of the source structure. The new multi-telescope radio-linked interferometer (MTRLI)<sup>9</sup> at Jodrell Bank was used during January and February 1980 at a frequency of 408 MHz to map the extragalactic radio sources 3C196 and 3C305 with a resolution of  $\sim 1$  arc s. We show here that both the markedly symmetric structures observed and the spectral index distributions inferred from comparison with previously published 5-GHz maps<sup>10</sup> provide evidence for the source axes having rotated during the lifetime of the emitting regions.

The sources were observed using four telescopes of the MTRLI, with projected interferometer spacings ranging between  $\sim 15$  and 127 km. Over such distances the effects of ionospheric disturbances at the low observing frequency are large and the absolute phase information was not recoverable. Consequently, the closure-phase hybrid mapping technique described by Readhead and Wilkinson<sup>11</sup> was used, though with a significantly improved algorithm<sup>12</sup>. The absolute positions of the components on these maps, lost in the hybrid mapping technique, were inferred from a comparison with the Cambridge 5-GHz maps. The main characteristics of the two sources are given in Table 1.



**Table 1** Some relevant characteristics of 3C196 and 3C305

| Source                             | 3C196   | 3C305   |
|------------------------------------|---|---|
| Optical identification             | 18 m OVV quasar   | 13.5 mag Sa pec galaxy <sup>14</sup>                              |
| Redshift                           | 0.871   | 0.0416  |
| Radio structure at 5 GHz (ref. 10) | 2 main components. Third weaker component at 90° to source axis from N main component | 2 main components surrounded by an extended low-brightness region |
| Separation of 2 main components    | 5 arc s   | 3.4 arc s   |
| Projected linear size              | 43 kpc  | 3.8 kpc   |
| Overall radio spectrum             | Power law $\alpha = -0.81$  | Power law $\alpha = -0.86$  |
| Integrated radio luminosity        | $4.2 \times 10^{45}$ erg s <sup>-1</sup>  | $1.8 \times 10^{42}$ erg s <sup>-1</sup>                          |

\* Assuming  $H_0 = 50 \text{ km s}^{-1} \text{ Mpc}^{-1}$  and  $q_0 = \frac{1}{2}$ .

The MTRLI map of the high luminosity radio source 3C196, a quasar, is based on 16-h observation and is shown in Fig. 1. The projected linear size of the source is  $\sim 50$  kpc. Components A and B are assumed to correspond to the main components on the Cambridge 5-GHz map. Component B' is identified as the third component on the Cambridge map, and is revealed to be an extended region of emission with a steep spectrum. Component A', which was not detected at 5 GHz and therefore has a steep spectrum, is a much weaker extended region, with a slight plateau at some distance from component A. A line drawn from this plateau to the peak of component B' passes through the position of the optical object. The physical properties of the components are listed in Table 2. Note that component A is significantly more extended than component B. The spectral indices of the components have been obtained by comparison with other published<sup>10,13</sup> data. Note that in addition to the spectral differences between the compact components A and B in 3C196, the extended components A' and B' display markedly different morphologies and luminosities which may indicate time-dependent asymmetry in the power supply mechanism. Planned observations with higher resolution should enable this aspect of the source properties to be investigated.

The source 3C305, which is highly unusual for a 3C source in being identified with a 13.5 mag Sa peculiar galaxy<sup>14</sup> of dimensions  $\sim 20 \times 30$  kpc, is a relatively low-luminosity radio source, and the two compact components are separated by a projected linear distance of only 3.8 kpc. A strong absorption lane crosses the body of the galaxy at an oblique angle, and there is a region of O II [ $\lambda 3,727$ ] emission centred in a position 3 arc s to the NE of the nucleus<sup>14</sup>. The MTRLI map of 3C305, based on 24-h data, is shown in Fig. 2. The rotational symmetry displayed on this map is striking. The extent of the low brightness regions A' and B' may be somewhat greater than is shown because only 85% of the total flux has been accounted for in the map. The spectral indices of the two main components and extended regions are given in Table 2. The apparent symmetry in this source is greater than in 3C196 because the intensity ratios A:A' and B:B' are similar. Component C is a possible candidate for a compact source associated with the optical nucleus of the galaxy. If this is the case, the region of O II [ $\lambda 3,727$ ] emission lies close to the strong component B, but the uncertainty in the optical position prevents positive association.

In both 3C196 and 3C305, the rotational symmetry and the steep spectral indices (normally associated with the ageing of synchrotron electrons) of the extended components suggest that the axes of the radio sources have changed their orientation relative to the medium in which the sources are embedded. Hitherto, examples of such symmetry have been confined to

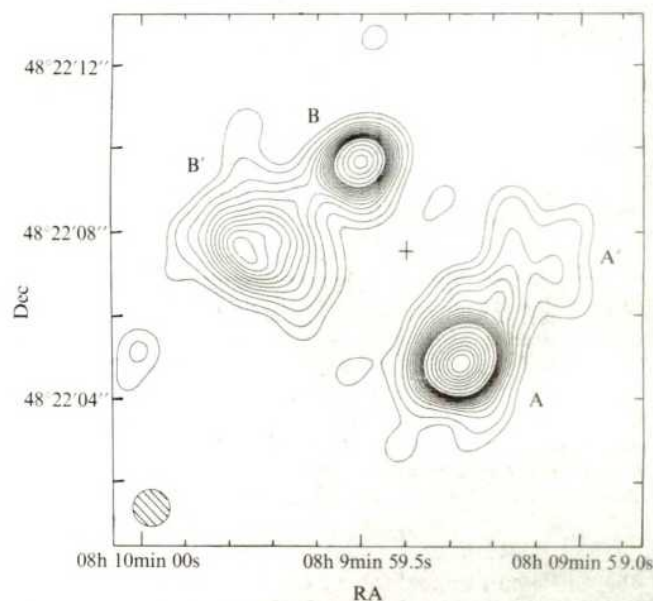
sources of large linear extent and relatively low luminosity. Thus these sources are very unusual not only for the degree of symmetry displayed, but also because they are small in linear size, and because 3C196 is an exceptionally powerful source.

Clearly, it is important to know the time scale on which such a rotation of the axis occurs. However, the determination of such a time scale is hampered by our ignorance of the physical conditions prevailing in and around the radio source components, and our lack of understanding of the mechanisms governing source evolution.

For component B' in 3C196 the spectral information in Table 2 allows us to make a rough estimate of the cut-off frequency  $\nu_c$ , above which we expect the spectrum to steepen markedly due to the energy losses of the radiating electrons<sup>8</sup>. If we assume that these energy losses are purely radiative, we can deduce how long the component has been radiating without any fresh input of high-energy electrons. This time is  $\sim 2 \times 10^5$  yr, which is thus the corresponding time scale  $t$  for the rotation of the source axis. The accuracy of this estimate depends critically on the validity of neglecting both adiabatic expansion losses and particle reacceleration gains.

If we accept that in 3C196 the energy supply from the quasar was once directed at component B' and is now directed at component B, it is reasonable to assume that in the past, component B' was a similar distance from the QSO as component B is now. Because component B' is now only slightly more distant from the QSO than component B, it cannot have moved by more than  $\sim 10$  kpc in the time taken for the source axis to swing through 65°. By assuming (1) that component B' is confined by ram pressure and (2) that the average internal energy density of the component during this period was no lower than it is now, we can deduce the minimum velocity of the component through the intergalactic medium which is required to confine it. Assuming an upper limit for the density of the intergalactic medium<sup>15</sup> of  $\sim 10^{-27} \text{ g cm}^{-3}$ , we find that a velocity of  $\geq 0.03c$  is required to confine the component by ram pressure, and so the time scale  $t$  for the source axis rotation is  $t \leq 10^6$  yr.

The rate of advance of a component through the surrounding medium deduced from the internal energy density of that component may enable us to set a lower limit on the time scale for the source axis rotation at present. From the appearance of component B' in 3C305 and the apparent gap between



**Fig. 1** The MTRLI map of 3C196 at 408 MHz. The contour levels are 1, 2, 4, 6... 24, 30, 40... 90% of peak brightness. The HPBW of the circular gaussian beam is shown in the bottom left corner. +, The position of the 18-mag quasar.



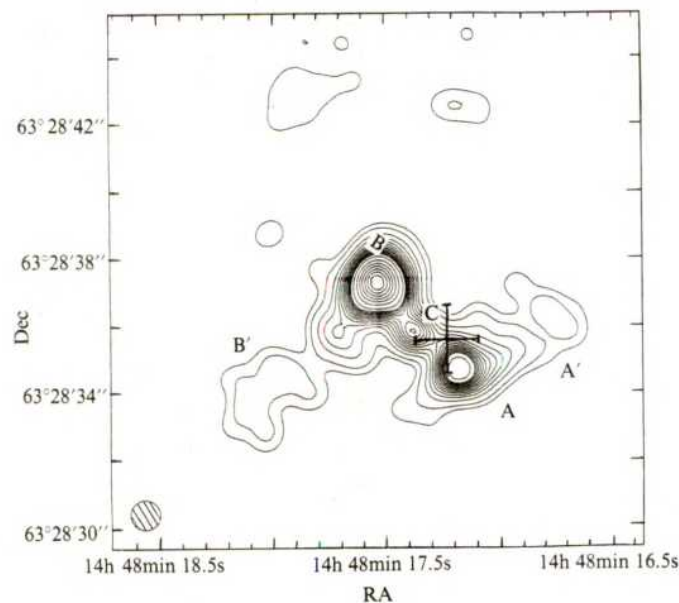
**Table 2** Physical parameters of components in 3C196 and 3C305

| Component | $\alpha_{408}^{5000}$ | $\pm$ | $\alpha_{5000}^{15000}$ | $\pm$ | Size (kpc)              | $E_{\min}^{\text{tot}}$ (erg) | $B_{\text{eq}}$ (G)   | $T_{\text{sp}}$ (yr) |
|-----------|-----------------------|-------|-------------------------|-------|-------------------------|-------------------------------|-----------------------|----------------------|
| 3C196     |                       |       |                         |       |                         |                               |                       |                      |
| A'        | <-1.0                 | —     | —                       | —     | $12 \times 10$          | —                             | —                     | —                    |
| A         | -0.72                 | 0.05  | -1.05                   | 0.06  | $6 \times 4$            | $3.0 \times 10^{58}$          | $3.7 \times 10^{-4}$  | $4.6 \times 10^4$    |
| B         | -0.60                 | 0.09  | -0.69                   | 0.06  | $<2 \times 4$           | $<8.1 \times 10^{57}$         | $>4.7 \times 10^{-4}$ | $<1.8 \times 10^4$   |
| B'        | -1.21                 | 0.15  | <-1.5                   | —     | $16 \times 13$          | $1.6 \times 10^{59}$          | $1.7 \times 10^{-4}$  | $2 \times 10^5$      |
| 3C305     |                       |       |                         |       |                         |                               |                       |                      |
| A'        | $\sim -1$             | —     | —                       | —     | $\sim 2.8 \times 1.1^*$ | —                             | —                     | —                    |
| A         | -0.62                 | 0.09  | -1.35                   | 0.23  | $0.9 \times 0.9$        | $2.6 \times 10^{55}$          | $1.2 \times 10^{-4}$  | $4.4 \times 10^5$    |
| C         | —                     | —     | —                       | —     | $<0.5 \times <0.5$      | —                             | —                     | —                    |
| B         | -0.72                 | 0.06  | -1.15                   | 0.09  | $0.75 \times 0.75$      | $3.6 \times 10^{55}$          | $2.0 \times 10^{-4}$  | $2.0 \times 10^5$    |
| B'        | $\sim -1$             | —     | —                       | —     | $\sim 4.8 \times 1.1^*$ | —                             | —                     | —                    |

\* Approximate values only, see text.

The spectral indices are defined in the sense  $S \propto \nu^\alpha$ . The sizes given are the dimensions of an equivalent gaussian. The minimum energy was calculated assuming that there are no relativistic protons, and assuming cylindrical component geometry. Equipartition of energy between relativistic particles and magnetic field was also assumed. The spectral age  $T_{\text{sp}}$  was calculated by assuming that spectral steepening is caused only by radiative energy losses, and by estimating the cut off frequency  $\nu_c$  from the spectral data. Assuming  $H_0 = 50 \text{ km s}^{-1} \text{ Mpc}^{-1}$  and  $q_0 = \frac{1}{2}$ .

components B' and B in 3C196, it is reasonable to suppose that the beam may have been switching on and off. If the source axis rotated through a significant angle whilst the beam was switched off, it would then have to re-excavate a channel through the surrounding medium, and this would take place at the above mentioned rate. Clearly, during the time taken for this excavation, the axis cannot rotate by more than the angle subtended between two discrete emitting regions. Assuming for 3C196 a typical intracluster medium density of  $\sim 5 \times 10^{-28} \text{ g cm}^{-3}$ , and for 3C305 (because it is embedded in the galaxy) a typical interstellar medium density of  $\sim 10^{-25} \text{ g cm}^{-3}$ , we find that the present rotation time scale for 3C196 is  $t \geq 10^6 \text{ yr}$  and for 3C305 is  $t \geq 5 \times 10^6 \text{ yr}$ . If the assumptions inherent in these values are valid, this may indicate that the rotation rate in 3C196 has slowed down.



**Fig. 2** The MTRLI map of 3C305 at 408 MHz. The contour levels are 1, 2, 4, 6, ..., 24, 30, 40, 50, 60, 70, 80, 90% of peak brightness. The HPBW of the circular gaussian beam is shown in the bottom left corner. +, The position of the nucleus of the galaxy.

The time scales we find for the rotation in these sources are very much shorter than those typically deduced for the larger sources. For example, Ekers *et al.*<sup>4</sup> arrive at a value of  $\sim 2 \times 10^8 \text{ yr}$  for NGC326, and this difference may indicate that the size of a source such as 3C196 is limited by the rapid rotation. Alternatively, we may be seeing the results of two completely

different mechanisms for producing the rotational symmetry. Ekers *et al.*<sup>4</sup> mention that the precession of gaseous disk in the galaxy would probably lead to a long time scale. We will briefly consider an alternative mechanism that seems capable of producing a more rapid rotation.

Rees<sup>16</sup> has discussed the possibility that the Bardeen-Peterson<sup>17</sup> effect couples the radio axis to the rotation axis of a massive black hole at the centre of a galaxy, thereby stabilizing the beam against 'jitter' resulting from uneven accretion. If the accreted mass had an angular momentum direction different to that of the black hole, the radio source axis would swing appreciably on a time scale equal to the time it would take for the black hole to double its mass. If the postulated black hole in 3C196 is radiating at its Eddington luminosity, (see, for example, ref. 18) it must have a mass of at least  $5 \times 10^7 M_\odot$  deduced from the radio power alone, and so to produce a rotation of the source axis on a time scale of  $\sim 10^6 \text{ yr}$ , the accretion rate would have to be at least  $50 M_\odot \text{ yr}^{-1}$ . The implied efficiency of conversion of accreted rest mass into relativistic particle energy leading to radio emission is  $\sim 0.2\%$ . The corresponding efficiency for 3C305 is  $\sim 1\%$  assuming a rotation time scale of  $5 \times 10^6 \text{ yr}$ . If the efficiency of conversion of accreted rest mass into energy was as much as  $\sim 30\%$ <sup>19</sup>, the rotation time scale would be at least  $\sim 10^8 \text{ yr}$ , and the low efficiencies deduced here might create difficulties if 3C196, in particular, was found to be a strong X-ray or IR source.

In the case of 3C305, an alternative origin of the rotational symmetry is possible. The radio source is embedded in the galaxy, and if the axis of this source is not aligned with the rotation axis of the galaxy, then we might expect the galactic rotation to sweep energetic particles away from the compact hotspots in a rotationally symmetric fashion, thus producing the observed morphology. Sandage<sup>14</sup> deduces a rotation period of  $6.8 \times 10^7 \text{ yr}$  for the galaxy corresponding to a time scale of  $\sim 2 \times 10^7 \text{ yr}$  for the degree of rotation observed here, and thus does not conflict with the lower limit of  $\sim 5 \times 10^6 \text{ yr}$  deduced earlier.

The present observations strongly suggest that, in 3C196 and 3C305, the orientation of the source axis has rotated through a large angle over the source lifetime. Not only does the fact of source rotation place constraints on the source mechanism itself but its result is to separate spatially the radio emission generated at different stages in the source evolution. Future observations of such sources may thus provide valuable insights into the nature of radio sources in general.

We thank Drs D. Stannard and I.W.A. Browne for helpful discussions and comments. C.J.L. acknowledges an SRC research studentship.

Received 15 July; accepted 16 September 1980.

1. Miley, G. K. *The Physics of Non Thermal Radio sources* (ed. Setti, G.) (Reidel, Dordrecht, 1976).
2. Willis, A. G. *Phys. Scr.* **17**, 243–255 (1978).
3. Northover, K. J. E. *Mon. Not. R. astr. Soc.* **177**, 307–317 (1976).



4. Ekers, R. D., Fanti, R., Lari, C. & Parma, P. *Nature* **276**, 588–590 (1978).
5. Rees, M. J. *Nature* **229**, 312–317 (1971).
6. Blandford, R. D. & Rees, M. J. *Mon. Not. R. astr. Soc.* **169**, 395–415 (1974).
7. Christiansen, W. A., Pacholczyk, A. G. & Scott, J. S. *Nature* **266**, 593–596 (1977).
8. Laan, H. van der & Perola, G. C. *Astr. Astrophys.* **3**, 468–476 (1969).
9. Davies, J. G., Anderson, B. & Morison, I. *Nature* **288**, 66–68 (1980).
10. Pooley, G. G. & Henbest, S. N. *Mon. Not. R. astr. Soc.* **169**, 477–526 (1974).
11. Readhead, A. C. S. & Wilkinson, P. N. *Astrophys. J.* **223**, 25–36 (1978).
12. Cornwell, T. J. & Wilkinson, P. N. (in preparation).
13. Laing, R. A. Preprint (Cambridge University, 1980).
14. Sandage, A. *Astrophys. J.* **145**, 1–5 (1966).
15. Stocke, J. *Astrophys. J.* **230**, 40–48 (1979).
16. Rees, M. J. *Nature* **275**, 516–517 (1978).
17. Bardeen, J. M. & Petterson, J. A. *Astrophys. J. Lett.* **195**, L65–L67 (1975).
18. Rees, M. J. *Phys. Scr.* **17**, 193–200 (1978).
19. Lynden-Bell, D. *Phys. Scr.* **17**, 185–191 (1978).

## MTRLI observations of the double QSO at 408 MHz

R. G. Noble & D. Walsh

University of Manchester, Nuffield Radio Astronomy Laboratories, Jodrell Bank, Macclesfield, Cheshire SK11 9DL, UK

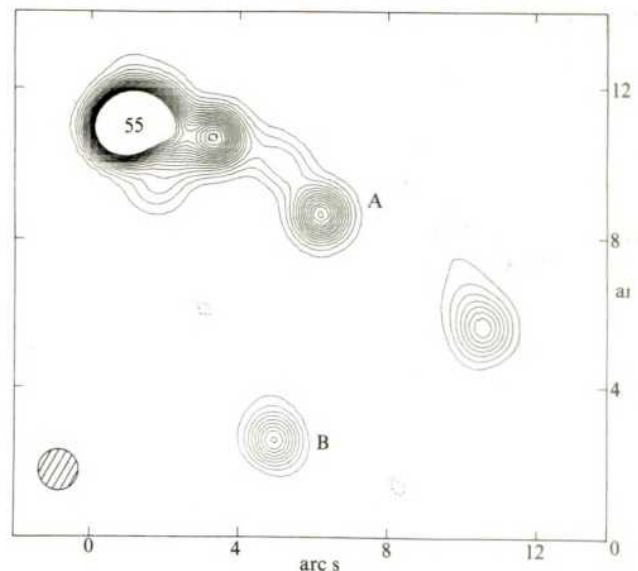
The suggestion<sup>1</sup> that the twin QSOs 0957 + 561 A, B, which are separated by  $\sim 6$  arc s and have emission redshifts 1.41, are images of a single QSO formed by a gravitational lens now seems to be generally accepted. This is a result of a wide range of data including optical spectroscopy<sup>2,3</sup> and, more particularly, direct imaging by CCD camera<sup>4</sup> and image-intensified photography (A. Stockton, personal communication) which reveal a galaxy, G1, with  $m_r \sim 18.5$  within 1 arc s of the QSO B. G1 can account for the splitting of the images<sup>4</sup>. It is the brightest member of a cluster<sup>4</sup>, has a redshift  $0.375 \pm 0.005$  (ref. 3) and IR observations confirm that it is a giant elliptical<sup>5,6</sup>. The flux density ratio of the two QSO components is nearly constant,  $B/A \approx 0.75$ , from  $\sim 3,000$  Å (ref. 7) to decimetre wavelengths<sup>8,9</sup>, as expected for gravitational imaging. The first radio maps<sup>10,11</sup> showed a complex structure and their initial interpretation was ambiguous, but there now seems to be agreement on the overall interpretation<sup>4,11,12</sup> in terms of gravitational imaging. Early observations at 408 MHz (ref. 10) suggested the flux density ratio of the two QSO components may differ significantly from that at shorter wavelengths, which would cast doubt on the gravitational lens interpretation. Recent observations at 5 GHz (ref. 13) indicate a point source 1 arc s from QSO B, coinciding closely with the position of G1. We present here a 408-MHz map which provides spectral information on all components of the radio source, removes the doubt raised by the earlier 408 MHz observations and sheds light on the nature of the source coincident with G1.

0957+561 was observed at 408 MHz for 24 h on 8–9 January 1980 with the Jodrell Bank multi-telescope radio-linked interferometer (MTRLI)<sup>14</sup> using four stations with six simultaneous independent baselines up to 127 km. Data were reduced by a CLEAN technique using closure phase and amplitude relations<sup>15</sup>, and restored with a synthesized beam of circular-gaussian shape with FWHM of 1.1 arc s. Using phase-closure relations means a loss of absolute positional information. Amplitude-closure relations were used to adjust gains of individual telescopes by amounts which in practice never exceeded 5%, and the resulting uncertainty contributed to the final flux scale is  $\leq 2\%$ . The flux scale was derived by reference to the compact source 3C119 which was assumed to have flux density 16 Jy. The peak of the resulting hybrid map (Fig. 1) is  $\sim 200$  times the r.m.s. noise.

The 408-MHz map shows the general features of the map made with higher resolution ( $0.66 \times 0.41$  arc s FWHM) at 5 GHz (ref. 13). In Fig. 1 the component associated with QSO A is unresolved. Component B shows extension in a direction roughly that of G1, presumably due to the point source detected

at 5 GHz. The emission north-following A shows similar structure to that at 5 GHz; it has a steeper spectrum than A and accounts for more than two-thirds of the flux of the whole source. The emission south-preceding A is extended in a similar direction to that seen at 5 GHz and has a spectrum similar to that of the north-following emission.

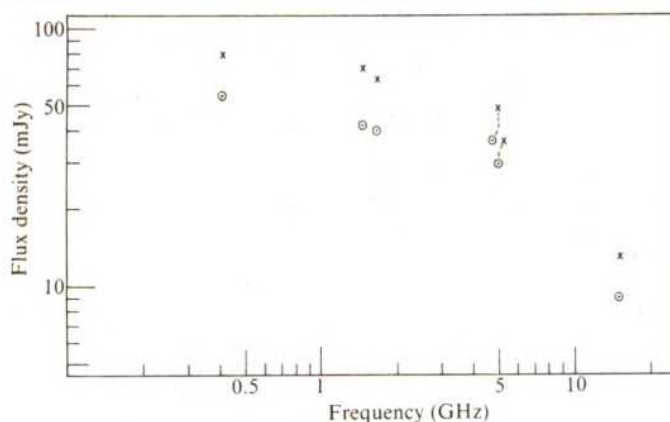
The structure of the emission in the neighbourhood of component B was investigated as follows. Profiles through the peak of B were examined in the direction of G1 and the perpendicular direction; lower-level contours than shown in Fig. 1, extending down to the noise limit, were used for this. (The best estimate of the position of G1, 0.99 arc s N and 0.19 arc s E of QSO B, comes from the photograph by Stockton (personal communication) in seeing of half arc s.) The sections in the E–W direction and southwards from the peak showed no deviation from the point-source response down to the noise level, whereas the northern skirt showed a systematic broadening. Accordingly we assume that the contribution of QSO B is that of a point source at the position of the peak on the map. (This is supported by the fact that the peaks of A and B on the map are separated by  $6.170 \pm 0.005$  arc s, in close agreement with the value of 6.175 arc s determined by VLBI<sup>8</sup>.) The flux density of B is 55 mJy. Subtraction of this point source leaves residual emission which is well represented by a point source of  $3.3 \pm 1.3$  mJy at a distance  $1.2 \pm 0.2$  arc s from B. This separation agrees well with the optical value quoted above for G1 and the 5 GHz value of 1.07 arc s (ref. 13).



**Fig. 1** Map of 0957 + 561 at 408 MHz. The zeros on both axes are arbitrary. The contour interval corresponds to a point source of 6 mJy; the zero contour is omitted, and negative contours are broken. The lowest contour is  $\sim 4\sigma$ . The half-power beam is indicated in the lower left corner.

The flux density of component A is 79 mJy. The ratio of flux densities,  $B/A$  is  $0.70 \pm 0.03$ , where the standard deviation quoted is derived from the estimated noise on the map. This value is within the range of published flux density ratios at shorter wavelengths from radio to UV. It extends by a factor of more than three the longest wavelength at which the ratio is accurately determined and replaces the anomalous value obtained previously<sup>10</sup> using single baselines of the present interferometer. There is evidence for variability of flux density at optical<sup>16</sup> and radio<sup>13</sup> wavelengths. Because sources generally vary less at 408 MHz than at higher frequencies, the new 408-MHz flux density ratio may be the most accurate value





**Fig. 2** Spectra of the compact components A (x) and B (o). 0.408 GHz, epoch January 1980 (this paper); 1.5 GHz, October 1980 (ref. 9); 1.67 GHz, February 1980 (ref. 17); 5.0 GHz (higher values), May 1979 (ref. 10); 5.0 GHz (lower values), February 1980 (ref. 13); 15 GHz, October 1979 (ref. 9).

available for the ratio inherent in the gravitational imaging process.

The radio spectra of A and B have now been determined over the range 0.408–15 GHz and are shown in Fig. 2, where the epochs of measurement are indicated. The values at 1,666 MHz are from VLBI observations using the European Network<sup>17</sup> and supersede those published previously<sup>8</sup>. The disagreement between the two values at 5 GHz is unlikely to be due to variation as the values determined in May 1979 with the Cambridge 5-km telescope<sup>10</sup> are considerably higher than the values determined with the VLA at three epochs<sup>11–13</sup> June and October 1979 and February 1980; one or both measurements are likely to have systematic errors. The spectra show marked curvature with a high-frequency fall-off, although the extent of this is strongly dependent on the 15-GHz values<sup>9</sup> which are only preliminary.

The weak component coincident with G1 may be emission from G1 itself or, more intriguingly, a third image of the QSO (or a combination of the two). Attention was drawn to the possibility of multiple imaging in the first published maps<sup>10</sup> and more thorough calculations<sup>4</sup> show a wide range of imaging geometries is possible, including ones giving rise to a third image close to the centre of G1. If the radio component is in fact a third image, its spectrum should be similar to that of A and B. We find the flux density ratio of B to this component is  $16 \pm 7$  at 408 MHz whereas the value at 5 GHz (ref. 13) is  $12.7 \pm 1.1$ . Thus it is possible that a third QSO image has been detected.

We thank our many colleagues at Jodrell Bank for the construction and operation of the MTRLI, and the development of data reduction techniques. We thank Dr Alan Stockton and Professor Bernard Burke for results before publication.

## Magnetic domain observations of nucleation processes in fine particles of intermediate titanomagnetite

S. Halgedahl & M. Fuller

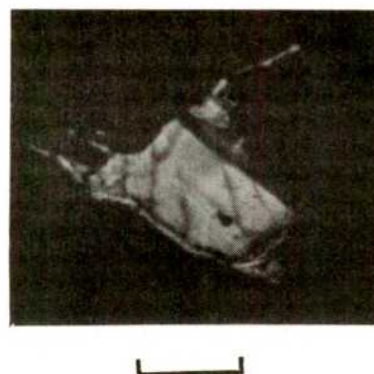
Department of Geological Sciences, University of California, Santa Barbara, Santa Barbara, California 93106

The stable carriers of the palaeomagnetic record in rocks are commonly fine grains of magnetite or titanomagnetite ( $\text{Fe}_{3-x}\text{Ti}_x\text{O}_4$ ) between 1 and 15  $\mu\text{m}$  in diameter. The magnetic properties of these particles are therefore of interest to palaeomagnetists who must rely on them to preserve the Earth's magnetic field record over geological time. We report here domain observations of titanomagnetites in samples from Leg 49 of the Deep Sea Drilling Project. The results indicate that a major contributor to 'pseudosingle-domain' (PSD) saturation remanence is single domain remanence of particles larger than the classical single-domain threshold size which fail to nucleate domain walls in this magnetization state.

In contrast to larger, typically multidomain particles, the magnetic properties of titanomagnetites  $\leq 15 \mu\text{m}$  are strongly grain-size dependent. Within this range, the coercivity  $H_c$ , the ratio  $J_{rs}/J_s$  of saturation remanence to saturation magnetization, and the low-field ( $< 1 \text{ Oe}$ ) thermoremanent magnetization (TRM) acquired per unit volume of material increase roughly as  $1/L$  ( $L$  is grain size)<sup>1,2</sup> from nearly size-independent, multidomain values to their maxima at the single-domain boundary. The rapid rise of stability and remanence with decreasing grain size in particles still large enough to accommodate domain walls has led to their being referred to as 'pseudosingle-domain'<sup>3</sup>.

Stacey originally proposed that Barkhausen discreteness of domain wall position resulted in an intrinsic, undemagnetizable PSD moment<sup>3</sup>. It was later suggested<sup>4</sup> that PSD moments arise within surface closure domains, or within a fine structure in domain walls which terminate at the surface. Domain wall moments have also been considered as a source of PSD remanence in sub-micrometre size magnetite by Dunlop<sup>5</sup>, who referred to such moments as 'psarks'.

These PSD models are based on the assumption that particles larger than the classical single-domain threshold size contain domain walls, regardless of their magnetization state. The role of nucleation—the process by which domain walls are initially formed—has not been considered in PSD models. Yet Becker<sup>6,7</sup> has shown that the high coercivity of fine  $\text{Co}_5\text{Sm}$  particles is nucleation-controlled, and Banerjee<sup>8</sup> noted that nucleation sites



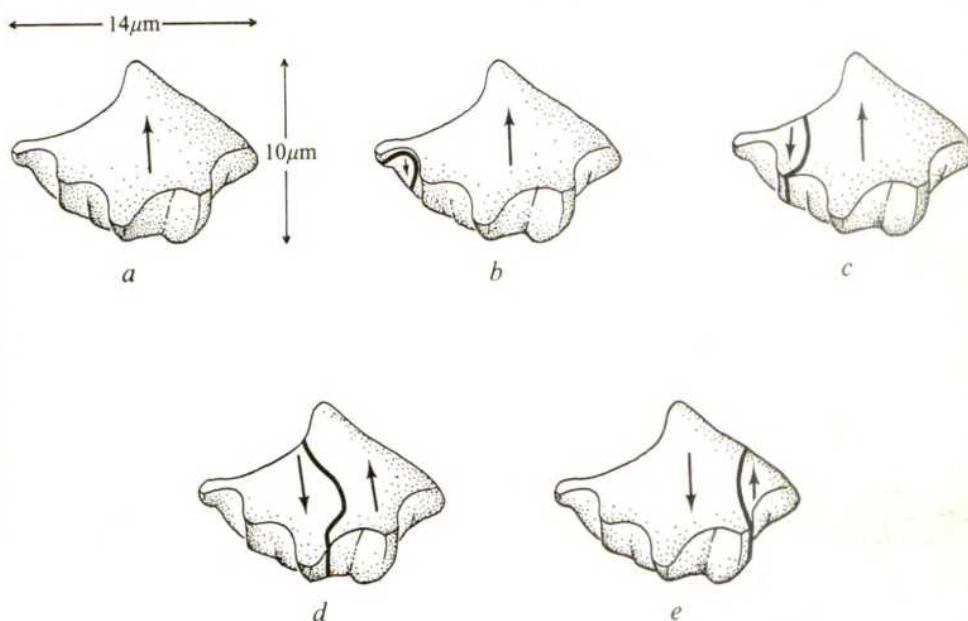
**Fig. 1** Domain pattern on an ionically polished titanomagnetite particle, using the Bitter technique. Scale bar, 20  $\mu\text{m}$ .

Received 1 August; accepted 12 September 1980.

- Walsh, D., Carswell, R. F. & Weymann, R. J. *Nature* **279**, 381 (1979).
- Weymann, R. J. *et al. Astrophys. J. Lett.* **233**, L43 (1979).
- Wills, B. J. & Wills, D. *Astrophys. J.* **238**, 1 (1980).
- Young, P. *et al. Astrophys. J.* (in the press).
- Soifer, B. T. *et al. Nature* **285**, 91 (1980).
- Lebofsky, M. J. *et al. Nature* **285**, 395 (1980).
- Gondhalekar, P. M. & Wilson, R. *Nature* **285**, 461 (1980).
- Porcas, R. W. *et al. Nature* **282**, 385 (1979).
- Burke, B. F., Greenfield, P. E. & Roberts, D. H. *Bull. Am. astr. Soc.* **11**, 620 (1980).
- Pooley, G. G. *et al. Nature* **280**, 461 (1979).
- Roberts, D. H., Greenfield, P. E. & Burke, B. F. *Science* **205**, 894 (1979).
- Greenfield, P. E., Roberts, D. H. & Burke, B. F. *Science* **208**, 495 (1980).
- Greenfield, P. E., Burke, B. F. & Roberts, D. H. *Nature* **286**, 865 (1980).
- Davies, J. G., Anderson, B. & Morison, I. *Nature* **288**, 66–68 (1980).
- Cornwell, T. J. & Wilkinson, P. N. *Mon. Not. R. astr. Soc.* (submitted).
- Keel, W. *IAU Circ. No.* 3481 (1980).
- Porcas, R. W. *et al. Nature* (submitted).



**Fig. 2** Small titanomagnetite particle undergoing hysteresis in an applied field parallel to the magnetization: *a*, state of saturation remanence after reducing saturating field of 1,500 Oe to zero. Arrow indicates sense of domain magnetization, which is parallel to grain surface. *b*, Nucleation of small reverse domain in a reverse field of -12 Oe. Domain wall is indicated by heavy black line. *c*,  $H = -30$  Oe. Note that this grain displays three-dimensional relief, and that the surface domain structure penetrates the grain volume. *d*,  $H = -40$  Oe, *e*,  $H = -48$  Oe.



may be the origin of high coercivity in fine-grained magnetite. The present domain observations strongly suggest that the nucleation process is important in determining the PSD properties of fine-grained titanomagnetite. These observations will be incorporated in a simple model which accounts for much of the grain-size dependence of  $J_{rs}/J_s$  in the PSD range.

Selected samples of oceanic basalt collected on Leg 49 of the DSDP were used for domain observations; their rock magnetic properties have been reported elsewhere<sup>9</sup>. The rocks chosen contain fresh titanomagnetite particles of composition  $x = 0.6$ . Specimens were first mechanically polished, and then ionically polished using the method of Soffel and Petersen<sup>10</sup> to obtain the strain-free surfaces necessary for domain observation. The walls were observed with the Bitter technique (Fig. 1).

A small ( $\approx 12 \mu\text{m}$ ) titanomagnetite particle undergoing hysteresis is shown in Fig. 2. The particle is initially saturated in a 1,500-Oe field. When the applied field is reduced to zero, the grain remains in the saturated state. On applying a 12-Oe reverse field, a small, reversely magnetized domain is nucleated. Further increase of the reverse field drives the wall towards the grain's interior, and magnetization reversal takes place by wall motion. The second half-cycle of hysteresis is identical to the first, except that the magnetization and field polarities are reversed.

Nucleation always occurs at the same location during each half-cycle, indicating that this grain utilizes only one nucleation site. As the polarity of the freshly nucleated reverse domain is always opposite to that of the saturating field, the grain has been truly saturated.

Similar behaviour has been observed in many particles of this size or smaller. In a population of 60 particles whose grain sizes are uniformly distributed between 5 and  $15 \mu\text{m}$ , 40% are observed to remain as single domains in saturation remanence, although one or more walls are subsequently nucleated in reverse fields. Another 40% of the grains contain two domains in saturation remanence, while the remainder contain three domains or more. It is also observed that grain size alone does not uniquely determine the saturation-remnant domain state, because particles of the same grain size exhibit a range of domain multiplicities.

These observations are consistent with the calculations of Brown<sup>11</sup>. For a wall to nucleate, the spins must initially overcome an energy barrier originating in the various anisotropy energies. Brown's nucleation condition requires that  $H_{ap} + H_d \geq 2K/J_s$ , where  $H_{ap}$  is the applied field,  $H_d$  is the demagnetizing field,  $2K/J_s$  is the anisotropy field, and where it is understood

that the sense of  $H_{ap} + H_d$  is opposite to that of  $J_s$ . Particles of certain materials will, therefore, theoretically never develop domain structure in saturation remanence ('Brown's paradox')<sup>12</sup>. However, there is considerable experimental evidence that nucleation occurs at surface imperfections at which there is either a strong, local demagnetizing field or an anomalously low anisotropy field<sup>6,13</sup>. When a particle contains no nucleation sites which satisfy the above condition, it will remain as a single domain in saturation remanence, and will require a reverse field which aids  $H_d$  before domain walls appear. Such 'back-field' nucleation has been directly observed in iron whiskers<sup>13</sup>, in individual  $\text{Co}_2\text{Sm}$  particles<sup>6</sup> and in the titanomagnetites described here.

If a sizeable percentage of grains fail to nucleate in saturation remanence, then these same particles will contribute significantly to the remanence of the assemblage. Moreover, the 'single-domain-like' fraction of a sized assemblage will increase as the mean grain size of the assemblage decreases, as the average number of nucleation sites per particle will decrease as the grain's surface area diminishes. The exact relationship between the number of sites and the number of walls is not understood, because the number of sites which actually succeed in nucleating will depend on the sites available as well as the number of domains which an individual particle can contain. However, we can still propose a simple model for the contribution to  $J_{rs}/J_s$  from particles which fail to nucleate in saturation remanence.

On the basis of the domain observations, it is first reasonable to assume that the nucleation sites are randomly distributed throughout a population of particles. Thus, the number of walls per particle in grains of a given size will vary probabilistically. Second, because nucleation sites vary in 'strength' according to whether or not the condition  $H_d \geq 2K/J_s$  is fulfilled, it is likely that the fraction of sites which nucleate in  $J_{rs}$  is small ( $\ll 1$ ). If nucleation can thus be defined to be a 'rare' event, then the number of walls per particle present in  $J_{rs}$  can be most simply described by a Poisson distribution.

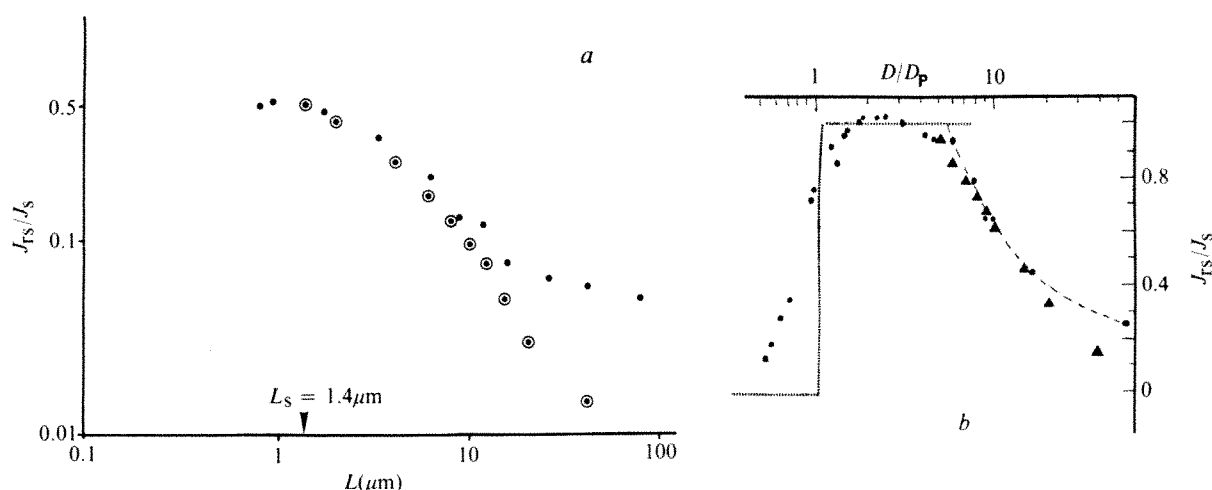
Let  $w$  be the number of walls present in a grain of size  $L$  in  $J_{rs}$ , and let  $\lambda$  be the average number of walls, per particle, in  $J_{rs}$ . In general,  $\lambda$  will be a function of the grain size  $L$ . Therefore, the probability of there being  $w$  walls is

$$P(w) = \lambda^w e^{-\lambda} / w!$$

The contribution to  $J_{rs}/J_s$  from particles which do not nucleate in  $J_{rs}$  will be

$$J_{rs}(w=0)/J_{s,\text{total}} = e^{-\lambda} (J_{rs}/J_s)_{\text{SD}}$$





**Fig. 3** *a*,  $J_{rs}/J_s$  versus grain size in randomly oriented  $x = 0.6$  titanomagnetite. ●, Experimental data<sup>1</sup>; ○,  $P(w=0) (j_{rs}/j_s)_{SD}$ . *b*,  $J_{rs}/J_s$  versus grain size in randomly oriented Co-Fe alloy at 76 K (ref. 16). Grain size is normalized to superparamagnetic size  $D_p = 64 \text{ \AA}$ ; and  $D_{SD} = 286 \text{ \AA}$  (after ref. 16). ●, Experimental data; ▲,  $P(w=0) (j_{rs}/j_s)_{SD}$ .

where  $(j_{rs}/j_s)_{SD}$  is the ratio of saturation remanence to saturation magnetization for single-domain particles of the material under consideration.

Once  $\lambda$  is known, then the single-domain-like contribution to  $J_{rs}$  may be calculated as a function of grain size. Ultimately,  $\lambda$  must be experimentally determined, but it is possible to set an upper limit for  $\lambda$  as follows.

Kittel<sup>14</sup> predicted that the number of domains,  $n$ , contained by a cubic particle of length  $L$  should be

$$n = J_s(1.705L/\gamma)^{1/2}$$

where  $J_s$  is the spontaneous magnetization (G);  $\gamma$ , the specific wall energy (erg cm<sup>-2</sup>); and  $L$  the grain size (cm). This relationship has been verified for  $x = 0.55$  titanomagnetite<sup>15</sup>. Because this calculation minimizes the sum of wall and demagnetizing energy without considering the magnetization state or nucleation difficulties, we will set  $\lambda_{\max} = J_s(1.705L/\gamma)^{1/2} - 1$ .

The single-domain size  $L_{SD} = \gamma/(1.705J_s^2)$  by the Kittel calculation, so that

$$J_{rs}(w=0)_{\min}/J_{s,\text{total}} = \exp[-(L/L_{SD})^{1/2} + 1](j_{rs}/j_s)_{SD}$$

This model therefore gives the minimum contribution to  $J_{rs}/J_s$  from the particles which fail to nucleate in an assemblage of identical particles with grain size  $L$ .

This model has been compared to  $J_{rs}/J_s$  in randomly oriented grains of  $x = 0.6$  titanomagnetite, measured by Day<sup>1</sup>. The single-domain size is estimated to be  $1.4 \mu\text{m}$ , at which the experimental value of  $J_{rs}/J_s = 0.5$ . This estimate is consistent with that of Soffel for  $x = 0.55$  titanomagnetite<sup>15</sup>. Figure 3a shows that there is good agreement between the model and the data in the PSD range. The model ceases to be important above  $20 \mu\text{m}$  where the grains are truly multidomain.

In Fig. 3b the model has been compared to  $J_{rs}/J_s$  in randomly oriented Co-Fe alloy particles at 76 K, after Kneller and Luborsky<sup>16</sup>.  $J_{rs}/J_s$  is normalized with respect to the single-domain value of 0.46. Again, the model accounts for nearly all of  $J_{rs}/J_s$  in the PSD region which, for this material at 76 K, lies approximately between 300 and 1,300 Å.

The present domain observations indicate that, at least in  $x = 0.6$  titanomagnetite, a major contribution to PSD saturation remanence is due to the single-domain remanence of particles which fail to nucleate domain walls in this magnetization state. The present model agrees well with the grain-size dependence of  $J_{rs}/J_s$  in two very different magnetic materials, thereby indicating that nearly all of the saturation remanence in the PSD range may be due to particles that do not nucleate walls in this state. The observations and the model suggest that the remanence stored by domain wall displacement is of minor importance in the PSD range, and is significant only when the particles are truly

multidomain. However, additional domain observations are in progress to test the validity and generality of the model, as well as its applicability to other aspects of PSD behaviour such as the size-dependence of coercivity and weak-field TRM.

We thank Professor Dr H. Soffel for details of his ionic polishing technique.

Received 14 April; accepted 12 September 1980.

1. Day, R. thesis, Univ. Pittsburgh (1973).
2. Hamano, Y. *Rock Magn. Paleogeophys.* **6**, 137–142 (1979).
3. Stacy, F. D. *Adv. Phys.* **12**, 45–133 (1963).
4. Stacey, F. D. & Banerjee, S. K. *The Physical Principles of Rock Magnetism* (Elsevier, New York, 1974).
5. Dunlop, D. J. *J. Geomagn. Geoelect.* **29**, 293–318 (1977).
6. Becker, J. J. *IEEE Trans. MAG-5*, 211–244 (1969).
7. Becker, J. J. *IEEE Trans. MAG-12*, 965–967 (1976).
8. Banerjee, S. K. *J. Geomagn. Geoelect.* **29**, 319–329 (1977).
9. Day, R., et al. *Init. Rep. DSDP Leg 49*, 781–791 (1978).
10. Soffel, H. & Petersen, N. *Earth planet. Sci. Lett.* **11**, 312–316 (1971).
11. Brown, W. F. *Micromagnetics* (Wiley, New York, 1963).
12. Shtrikman, S. & Treves, D. *J. appl. Phys.* **31**, 72–73S (1960).
13. De Blois, R. W. & Bean, C. P. *J. appl. Phys.* **30**, 225–226S (1959).
14. Kittel, C. *Rev. Mod. Phys.* **21**, 541–583 (1949).
15. Soffel, H. Z. *Geophys.* **37**, 451–470 (1971).
16. Kneller, E. F. & Luborsky, F. E. *J. appl. Phys.* **34**, 656–658 (1963).

## Implications for the primitive atmosphere of the oxidation state of Earth's upper mantle

R. J. Arculus & J. W. Delano

Research School of Earth Sciences, Australian National University, PO Box 4, Canberra, ACT 2600, Australia

Knowledge of the oxidation state of the Earth's mantle is critical for understanding the processes of magma genesis and the composition of deep-seated volatiles. Measurements reported here of the intrinsic oxygen fugacities ( $f_{O_2}$ ) of mantle-derived spinels from peridotite and megacryst assemblages show that the Earth's upper mantle is close to the synthetic iron-wüstite (IW) buffer curve in  $f_{O_2}$  versus  $T$  space. It seems likely that most erupted volcanics are oxidized after their formation, perhaps by diffusive  $H_2$  loss<sup>1</sup>. There is a strong possibility that the mantle was in equilibrium with a core-forming metal phase, and that subsequent oxidation of the upper mantle resulted from an interaction between the present oxidizing atmosphere-hydrosphere and the mantle by subduction processes. Evidence in support of this mechanism has been supplied by rare-gas analyses of deep-seated nodules from kimberlites<sup>2</sup>.

The gas species composing the early terrestrial atmosphere that formed through the degassing of the mantle having an oxygen state close to IW would have been profoundly different from those gases emitted from present-day volcanoes. The early primitive atmosphere would have been dominated by  $H_2$ ,  $CH_4$ ,  $CO$  and  $H_2S$  (that is reduced) rather than by the present-day, oxidized assemblage of  $H_2O$ ,  $CO_2$  and  $SO_2$ .

It has generally been assumed that the abundance ratios of gases emitted by recent volcanic activity reflect equilibrium with the sources of erupted magmas<sup>3</sup>, and that these relative abundances have remained essentially unchanged through geological time<sup>4-6</sup>. These assumptions have led to the supposition that the oxidation state of the Earth's upper mantle is, and always has been, close to the  $f_{O_2}$  defined by the quartz-fayalite-magnetite (QFM) buffer at any given temperature<sup>7,8</sup>.

Oxygen ion-specific properties of stabilized, solid  $ZrO_2$  electrodes<sup>1,9</sup> can be used to measure the oxidation state of mantle-derived materials directly. By modifying the published techniques<sup>9</sup> we have improved the precision, accuracy and reversibility of  $ZrO_2$  cell signals obtained<sup>10,11</sup>. Our approach involves isolating the e.m.f. signal generated by the sample from that unavoidably imposed by the residual atmosphere inside the sample-bearing cell. By varying the  $f_{O_2}$  of the residual atmosphere inside the cell, it is possible to determine a 'plateau' value of constant  $f_{O_2}$  relative to an external furnace atmosphere which represents a reversed, intrinsic  $f_{O_2}$  measurement for the sample alone. The extent of the plateau reflects the innate  $O_2$ -buffering capacity of the sample relative to the residual atmosphere. All previous measurements of intrinsic  $f_{O_2}$ s of geological samples have failed to achieve true reversals of the cell signals, and the published data<sup>1,9,12-14</sup> must represent upper, oxidized limits to the true values.

Our techniques have been used to measure the intrinsic  $f_{O_2}$  of spinels from peridotite and megacryst assemblages from Victoria (Australia), Arizona (US) and West Germany. These peridotite samples are considered to be representative of portions of the upper mantle in the pressure range  $\approx 20$ –25 kbar, whereas the spinel megacrysts are believed to be high-pressure ( $\geq 10$  kbar) equilibrium cumulates from basaltic magmas<sup>15,16</sup>. The major element compositions of the peridotites are similar to samples from the same region of Victoria and Dreiser Weiher described by Frey *et al.*<sup>17</sup> and Jagoutz *et al.*<sup>18</sup> as somewhat depleted in basaltic components.

The intrinsic oxidation states relative to the IW buffer range from  $\approx 0.25 \log_{10} f_{O_2}$  units more oxidized to 1  $\log_{10} f_{O_2}$  unit more reduced (Fig. 1). The overall reduced nature of the spinels, as well as the considerable range of  $f_{O_2}$ s obtained, are striking features of the data. We note that recent electrochemical cell data obtained by Ulmer *et al.*<sup>12</sup> on upper mantle-derived olivines plot close to the IW buffer, but the true values must be more reduced than that in view of the experimental technique. Figure 1 also shows  $f_{O_2}$  plotted against  $T$  for common basic eruptive rocks determined from analysis of coexisting Fe-Ti oxide minerals<sup>19</sup>. The difference of  $\sim 4 \log_{10} f_{O_2}$  units between the oxidation states of peridotites and igneous rocks may be due to late-stage oxidation of the latter, perhaps by  $H_2$  loss<sup>1</sup>. Alternatively the generation of magma in the upper mantle might involve a precursor, metasomatizing event<sup>20,21</sup> that causes localized oxidation and lowering of solidus temperatures relative to the bulk of the mantle. Limited data on the intrinsic  $f_{O_2}$  of kimberlite<sup>22</sup> suggest that some mantle-derived magmas may be as oxidized as values of  $f_{O_2}$  equivalent to QFM. In general, however, the proposed mechanism of  $H_2$  loss by magmas at shallow depths within the Earth is the favoured explanation for the contrast in oxidation states of erupted and deep-seated rocks due to the highly reduced nature of the spinel megacrysts from Arizona, and a deep-sea Hawaiian basalt<sup>1</sup> (Fig. 1).

We have noted<sup>10,11</sup> that the intrinsic  $f_{O_2}$  of a spinel peridotite sample from Australia is only  $\approx 2 \log_{10} f_{O_2}$  units more oxidized than that required for saturation with a potential core-forming Fe-Ni alloy. If oxygen is the main contributor towards lowering of the mean atomic weight of the Earth's core<sup>23</sup>, rather than S

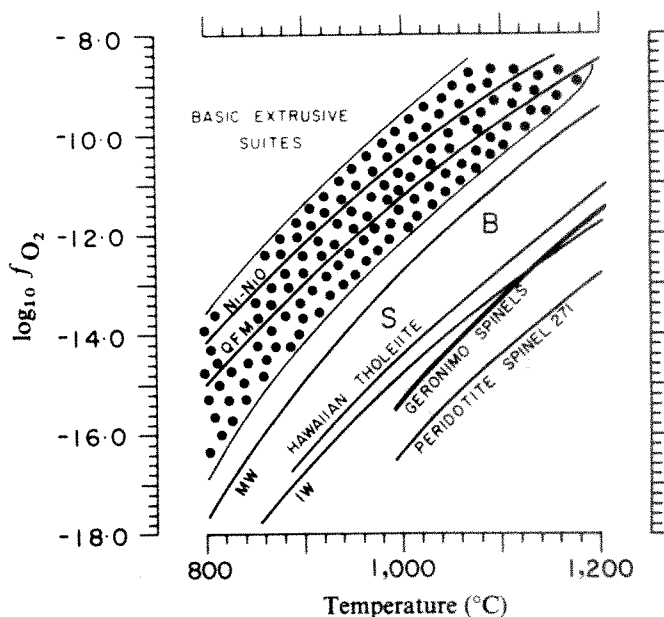
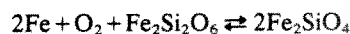


Fig. 1  $f_{O_2}$  versus  $T$  data for common basic eruptive rocks compared with electrochemical cell determinations of intrinsic  $f_{O_2}$ s for plutonic and one volcanic rock. The dots outline the area of  $T$  versus  $f_{O_2}$  space in which  $>95\%$  of the available data for basic volcanic rocks fall<sup>7</sup>. S and B represent the intrinsic  $f_{O_2}$ s and  $T$ s recorded for specific horizons in the Stillwater<sup>9</sup> and Bushveld<sup>13</sup> intrusions. The line for the Hawaiian tholeiite is data obtained by Sato<sup>9</sup> for a submarine basalt on the flanks of Kilauea. Given the experimental techniques used for S, B and the Hawaiian tholeiite, these earlier data must represent the upper (oxidized) limits of the true intrinsic  $f_{O_2}$ s of the samples. Our data for one spinel peridotite from West Germany fall very close to the curve for Hawaiian tholeiite. Geronimo spinels are megacryst samples from Arizona while spinel 271 is from Victoria, Australia. Buffers: MW, magnetite-wüstite; Ni-NiO, nickel-nickel oxide; IW, iron-wüstite; QFM, quartz-fayalite-magnetite.

(ref. 24) or Si (ref. 25), then the values of intrinsic  $f_{O_2}$  reported here for portions of the Earth's upper mantle must be even closer to those required for equilibrium with the core. During the separation of a core-forming metal phase from the proto-mantle, an equilibrium of the sort described by



would buffer the  $f_{O_2}$  of the system, at least at low pressures ( $<100$  kbar). At higher pressures, phases other than orthopyroxene and olivine would be involved and the disproportionation of  $Fe^{2+}$  to  $Fe^{3+}$  and Fe metal would be a significant redox control<sup>26</sup>.

The variation in  $f_{O_2}$ s for mantle-derived samples collected from widely separated locations on the Earth could be due either to (1) the persistence of primary accretional heterogeneities in the Earth that have lasted for 4,600 Myr or (2) localized oxidation of the mantle following the onset of plate-tectonics.

The development of subduction as a major terrestrial tectonic feature raises the possibility that volatiles (for example, seawater bound in hydrous minerals,  $CO_2$  in carbonates) and oxidized oceanic crust can be transported into the upper mantle causing a progressive and irreversible oxidation of the Earth's upper mantle, especially at shallow levels. While no consensus has emerged in the petrological debate over the involvement of the subducted slab as a source of volatiles and magmas at island arcs and collisional continental margins<sup>27-29</sup>, there is no doubt that devolatilization of the subducted slab must occur especially at pressures  $<25$  kbar (refs 30, 31). Because the upper layers of the subducted lithosphere reflect prolonged interaction with the atmosphere-biosphere-hydrosphere system, which is dramatically oxidized relative to the  $f_{O_2}$ s prevailing in the upper



mantle, contamination of the mantle by a subducted component is a plausible oxidation mechanism over geological time.

Since the studies of Rubey<sup>32</sup> and Holland<sup>33</sup> on the evolution of the atmosphere and hydrosphere, it has been assumed<sup>3</sup> that the present-day volcano-associated gas abundances constrain the oxidation state of the upper mantle to that equivalent to the QFM buffer. This assumption, together with the supposed overabundance of siderophile elements in the upper mantle<sup>3</sup>, have led to conclusions that the mantle was never in equilibrium with a core-forming metallic phase. We have proposed<sup>34</sup> that the relatively high abundances of siderophile elements in the mantle (for example, Ni, Co, Pt group metals, W, Mo, Sn, Ag, Sb, Cu) can be explained by a combination of early equilibrium between a metal-silicate-sulphide system, and incomplete separation of sulphide into the core-forming metal, followed by meteoritic contamination<sup>35</sup> after core separation ( $\approx 4,500$  Myr). As at low  $f_{O_2}$ s and relatively high  $f_{S_2}$ , a significant proportion of the siderophile elements are partitioned into the sulphide phase, the supposed overabundance of siderophile elements in the mantle does not negate the possibility of core-mantle equilibrium.

Assuming a mantle close to the IW buffer in terms of oxidation state, it is possible to compute the nature of the gas species in the system C-O-H-S that would be in equilibrium with Fe-Mg silicates and oxides<sup>36-38</sup>. If the Earth's interior was an effectively closed system with respect to gaseous constituents during the earliest stages of planetary differentiation, then the volatile species residing in the mantle after core formation would have been in chemical equilibrium with the core-mantle system. In these conditions, gas-species computations show that CH<sub>4</sub>, H<sub>2</sub>, H<sub>2</sub>S and CO become volumetrically significant with respect to H<sub>2</sub>O, CO<sub>2</sub> and SO<sub>2</sub> (refs 36-38). Although the latter species may remain collectively the most abundant, it is important to note that condensation and low-temperature, selective reaction of the primitive crust with H<sub>2</sub>O, CO<sub>2</sub> and SO<sub>2</sub> could have resulted in a strongly reducing primitive atmosphere composed of CH<sub>4</sub>, NH<sub>3</sub>, H<sub>2</sub>, CO and H<sub>2</sub>S with lesser amounts of H<sub>2</sub>O vapour and CO<sub>2</sub>. Diffusive loss of H<sub>2</sub> from the atmosphere<sup>39</sup>, together with the evolution of life that was initially promoted in this reducing environment<sup>40</sup>, has ultimately resulted in a progressive oxidation and alteration of the primitive atmosphere<sup>6</sup>.

We propose that during partial melting of the upper mantle to produce basaltic magmas, the intrinsic  $f_{O_2}$  prevailing in the melt-residue system is close to the IW buffer. However, as these magmas rise towards the Earth's surface, their systems become open by H<sub>2</sub>-loss and interaction with the oxidized crust-hydrosphere-atmosphere resulting in oxidation levels in the vicinity of QFM. This is generally supported by the observation that magmatic systems are dominated by low-pressure equilibria<sup>41</sup>. While the oxidation state of the Earth's upper mantle is presently not in equilibrium with a metallic phase (the core), probably due to its contamination by oxidized, subducted components, it is significantly more reduced than the erupted magmas. Finally, our results on the intrinsic  $f_{O_2}$  of the Earth's upper mantle support the view that the early terrestrial atmosphere, which is known to have been formed by degassing of the Earth's interior, was strongly reducing relative to the present atmosphere and volcanic gases.

Received 16 June; accepted 28 August 1980.

1. Sato, M. *Geophys. Res. Lett.* **5**, 447-449 (1978).
2. Kaneoka, I., Takaoka, N. & Aoki, K.-I. *Earth planet. Sci. Lett.* **36**, 181-186 (1978).
3. Ringwood, A. E. *The Origin of the Earth and Moon* (Springer, New York, 1979).
4. Johnson, F. S. *Space Sci. Rev.* **9**, 303-324 (1969).
5. Levine, J. S. in *Comparative Planetology* (ed. Ponnampetuma, C.) 165-182 (Academic, New York, 1978).
6. Walker, J. C. G. *Evolution of the Atmosphere* (Macmillan, New York, 1977).
7. Haggerty, S. E. *Geophys. Res. Lett.* **5**, 443-446 (1978).
8. Bence, A. E., Grove, T. L. & Papke, J. J. *Precamb. Res.* **10**, 249-279 (1980).
9. Sato, M. *Geol. Soc. Am. Mem.* **135**, 289-307 (1972).
10. Arculus, R. J. & Delano, J. W. *Lunar planet. Sci.* **11**, 28-30 (1980).
11. Arculus, R. J. & Delano, J. W. *Geochim. cosmochim. Acta* (in the press).
12. Ulmer, G. C., Rosenhauer, M. & Woermann, E. *Trans. Am. Geophys. Un.* **61**, 413 (1980).
13. Flynn, R. T., Ulmer, G. C. & Sutphen, C. F. *J. Petrol.* **19**, 136-152 (1978).
14. Snethlage, R. & Klemm, D. D. *Contr. Miner. Petrol.* **67**, 127-138 (1978).
15. Binns, R. A., Duggan, M. B. & Wilkinson, J. F. G. *Am. J. Sci.* **269**, 132-168 (1970).
16. Evans, S. H. Jr & Nash, W. P. *Am. Miner.* **64**, 249-267 (1979).

17. Frey, F. A., Green, D. H. & Roy, S. D. *J. Petrol.* **19**, 463-513 (1978).
18. Jagoutz, E. et al. *Proc. 10th Lunar planet. Sci. Conf.* 2031-2050 (1979).
19. Haggerty, S. E. *Miner. Soc. Am. Short Course* **3**, Hg 101-277 (1976).
20. Boettcher, A. L. & O'Neil, J. R. *Am. J. Sci.* (in the press).
21. Menzies, M. & Murthy, V. R. *Earth planet. Sci. Lett.* **46**, 323-334 (1980).
22. Ulmer, G. C. et al. *Am. Miner.* **61**, 653-660 (1976).
23. Ringwood, A. E. *Geochim. J.* **11**, 111-135 (1977).
24. Murthy, R. V. & Hall, H. *Phys. Earth planet. Inter.* **2**, 276-282.
25. Ringwood, A. E. *Geochim. cosmochim. Acta* **15**, 195-212 (1958).
26. Mao, H.-K. *Yb. Carnegie Instn Wash.* **73**, 510-518 (1974).
27. DePaolo, D. J. & Wasserburg, G. J. *Geophys. Res. Lett.* **4**, 465-468 (1977).
28. Taylor, S. R., Johnson, R. W., Arculus, R. J. & Perfit, M. R. *Basaltic Volcanism*, Ch. 1 (NASA, in the press).
29. Arculus, R. J. *Tectonophysics* (in the press).
30. Wyllie, P. J. *Tectonophysics* **17**, 189-209 (1971).
31. Wyllie, P. J. in *Energetics of Geological Processes* (eds Saxena, S. K. & Bhattacharji, S.) 389-433 (Springer, New York, 1977).
32. Rubey, W. W. *Bull. geol. Soc. Am.* **62**, 1111-1147 (1951).
33. Holland, H. D. in *Petrologic Studies: A Volume in Honor of A. F. Buddington* (eds Engle, A. E. J., James, H. L. & Leonard, B. F.) 447-477 (Geological Society of America, New York, 1962).
34. Arculus, R. J. & Delano, J. W. *Geochim. cosmochim. Acta* (submitted).
35. Chou, C.-L. *Proc. 9th Lunar planet. Sci. Conf.* 219-230 (1978).
36. French, B. M. *Rev. Geophys.* **4**, 223-253 (1966).
37. Heald, E. F. *Am. J. Sci.* **266**, 389-401 (1968).
38. Karzhavin, V. K. & Vendillo, V. P. *Geochim. Int.* **7**, 797-803 (1970).
39. Hunten, D. M. *J. Atmos. Sci.* **30**, 1481-1494 (1973).
40. Miller, S. L. & Urey, H. C. *Science* **130**, 245-251 (1959).
41. O'Hara, M. J. *Scott. J. Geol.* **1**, 19-40 (1965).

## Variations of ground radon concentrations with activity of Kilauea Volcano, Hawaii

Malcolm E. Cox, Kevin E. Cuff & Donald M. Thomas

Hawaii Institute of Geophysics, University of Hawaii, Honolulu, Hawaii 96822

Measurements of the concentration of the radioactive gas radon, in particular relative areal variations in Rn outgassing (mainly isotopes <sup>222</sup>Rn,  $t_{1/2} = 3.82$  days and <sup>220</sup>Rn,  $t_{1/2} = 54.5$  s), at shallow ground depths (30 cm) are being used extensively in Hawaii in the exploration for geothermal resources<sup>1,2</sup>. Zones showing a greater than usual degree of Rn ground gas outgassing have delineated areas of anomalous subsurface heat and increased permeability. The patterns of outgassing suggest that thermally induced ground gas convection systems have developed<sup>1</sup>. Nine measurement stations have been established on the upper east rift of Kilauea volcano along the Chain of Craters Road (Fig. 1) to observe: (1) temporal variations in Rn outgassing; (2) relationship between Rn outgassing and variations in seismicity; and (3) whether this technique can assist in understanding the 'plumbing' of Kilauea and whether monitoring of a larger number of stations could assist in indicating pre-eruptive activity. These nine stations, initially included in a summit-wide survey (August-September 1978), were re-established in October 1979 because of the increased seismic activity within the upper east rift. Fortunately, a small eruption of Pauahi Crater occurred on 16-17 November 1979 at the end of the first one-month period of measurement. The present results indicate that the Rn concentration increases before and during seismic events, then decreases before returning to a 'normal' value.

Variations of Rn concentration associated with changes in the activity of volcanoes and volcanically-induced earthquakes are most commonly reported from measurements of hot spring waters and fumarolic or spring gases<sup>3-6</sup>. These Rn values often have large fluctuations that cannot always be correlated with variations in volcanic or seismic activity. Rn measured in groundwaters on Karymsky volcano has, however, shown such correlation<sup>7</sup> and in Hawaii, widely spaced measurements on Kilauea's summit and east rift indicated increased ground Rn outgassing during periods of increased seismic activity associated with the September 1977 eruption of Kilauea<sup>8</sup>.

In the current survey, the concentrations of Rn in ground gas were measured by using  $\alpha$  particle-sensitive films (Kodak, LR 115, II) that were field exposed for periods of three to four

weeks<sup>1,9,10</sup>. To distinguish between the Rn contribution from soil immediately below the measuring device and Rn derived from a greater depth and transported by convection, the Rn emanation was measured in the laboratory by using one sample of soil from each station, and then was subtracted from the total measurement<sup>1,11</sup>. The Rn concentration units are  $\alpha$  tracks ( $T$ )  $\times 10^{-2} \text{ cm}^{-2} \text{ h}^{-1}$  (1 unit  $\approx 1.03 \times 10^{-4} \text{ nCi l}^{-1}$ ). The Rn emanation from the soil samples (all derived from tholeiitic basalt lavas) ranged from 0.5 to  $2.15 T \times 10^{-2} \text{ cm}^{-2} \text{ h}^{-1}$ . Duplicate laboratory measurements of Rn emanation from five different soil samples had a mean precision of  $\pm 3.5\%$ . Quadruplicate measurements in the field at one location gave a mean observed variation in corrected values of 10%. When these corrected field-measured concentrations at a station were lower than the Rn emanation from the soil at that location, the Rn concentrations are reported as negative values. Negative or very low positive values suggest that the flow of ground gas at that site is downward or, in some cases, static.

Areal variations in concentration measured during the summit-wide survey of Kilauea suggest that the long-term pattern on the summit is of strong outgassing within the caldera and associated major fractures, with a net downflow of ground gas in the peripheral area and on the upper flanks of Kilauea. This net downflow is, however, variable and responds to localized events such as described here, as well as being affected by the existence and location of faults and fractures that enable strong upflows to occur. The development of similar, but linear and areally restricted convection systems has also been observed over rift zones in Hawaii<sup>1</sup>.

The data for August 1978 were collected during a period of slow inflation in the Kilauea summit region<sup>12</sup>. This buildup of activity followed a flank eruption in the central east rift in September 1977. The Pauahi eruption of 16–17 November 1979 was a minor eruption that lasted  $\sim 22$  h and produced only a small volume of tholeiitic lava ( $\approx 700,000 \text{ m}^3$ ) at relatively low temperatures<sup>12</sup> ( $1,040$ – $1,080^\circ \text{C}$ ). Radon outgassing at the nine stations during August–September 1978 produced low positive values (Fig. 2). For the month up to and including the November 1979 eruption, values of Rn outgassing increased from 0.5 to 20.5 times the August–September 1978 measurements at seven of the nine stations (Fig. 2). The highest concentration was

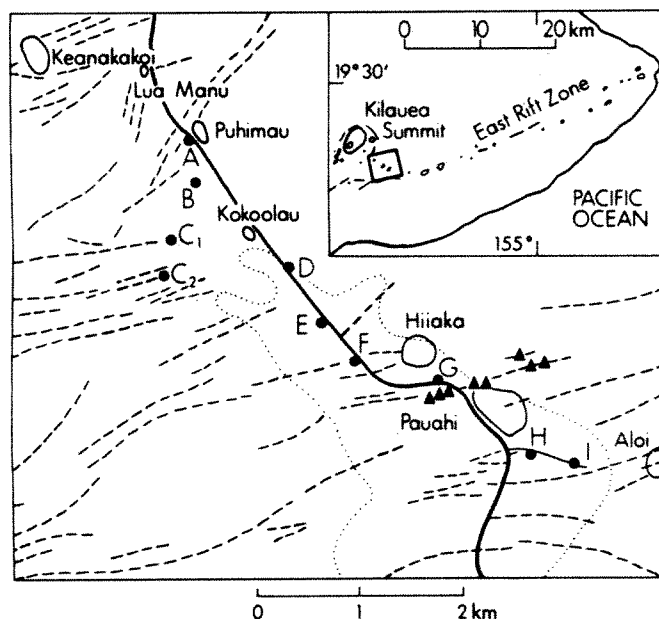


Fig. 1 Survey area. The inset shows the location of the survey area on the island of Hawaii, and solid lines show the craters and the Chain of Craters Road; ●, measurement locations; ▲, vents of November 1979 Pauahi eruption; broken lines show faults and major fractures; small dots show the outline of the area of concentration of shallow epicentres (1–5 km) preceding the eruption<sup>12</sup>.

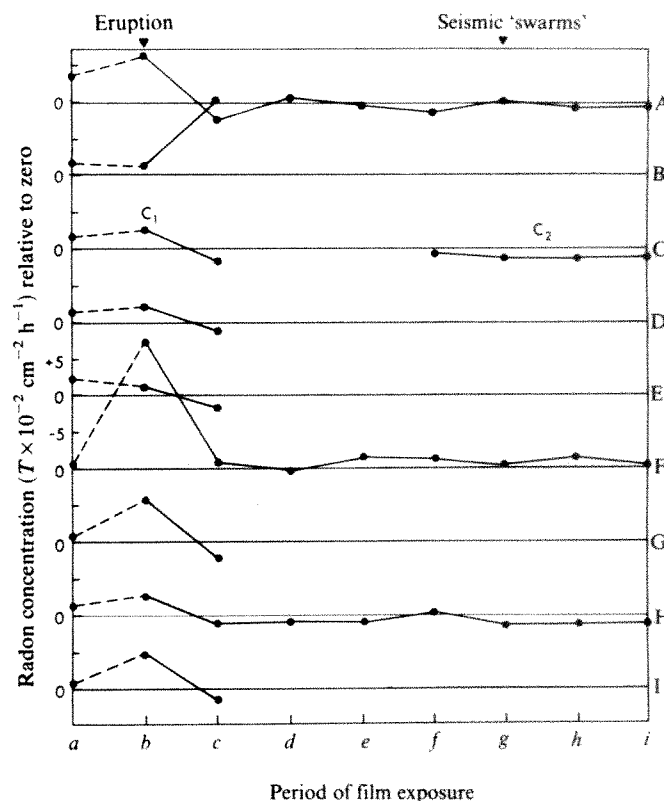


Fig. 2 Plot of Rn concentration at each station; each point is the value measured over an approximately four-week period and normalized to exposure time and surface area of film. The mean precision of the measurements was determined by field experiments to be  $\pm 5\%$ . a, 4 August–3 September 1978; b, 27 October–17 November 1979; c, 17 November–19 December 1979; d, 19 December 1979–15 January 1980; e, 15 January–6 February 1980; f, 6 February–27 February 1980; g, 27 February–20 March 1980; h, 20 March–10 April 1980; i, 10 April–3 May 1980.

recorded at Station F, next to an eruptive fissure that was active during the eruption of Hiiaka Crater in 1973. Rn outgassing was also high from a fracture associated with Puhimau Crater. This fracture extends to an area of steaming ground (between B and C), related to an intrusive event that occurred in 1938. At Stations B and E, Rn concentration before and during the eruption was 0.11 and 0.41 lower, respectively, than in August–September 1978. In the month following the Pauahi eruption, Rn concentration decreased significantly, mostly to negative values, at eight stations, and increased only at B. Stations A, F and H were monitored over the subsequent six months, and Station C was relocated and monitored over three months. During this latter period two episodes of seismic 'swarms' were significant. The first (2 March 1980) was located near Pauahi Crater, and the second (a week later) began in the same area and migrated  $\sim 6$  km eastwards (D. M. Moore, personal communication); these seismic events were probably caused by intrusive activity. At this time the summit was experiencing its fourth week of deflation.

Smaller changes in Rn concentration occurred in association with the seismic swarms. At Station H, the closest to the activity, the Rn concentration increased during the month before the events and decreased after them. (Note that this seismic activity occurred in the first part of the measurement period 27 February–20 March 1980). At Station F, the Rn concentration gradually decreased before and during these events, behaviour which was inverse to that at H and which is considered to be a result of localized convective ground gas flow related to the activity below Pauahi Crater. At Station C<sub>2</sub>, Rn concentrations remained much the same, but at A, concentrations increased to positive values during and immediately after these events, and then returned to negative values. This change is not fully



understood but could demonstrate some delay effect from the activity below Pauahi or possibly localized activity in the vicinity of Station A. Overall, Rn outgassing at three of the four stations underwent changes during the period of these seismic events, and subsequently returned to values apparently characteristic for each station.

We attribute the increases in outgassing associated with the eruption and the seismic events to various causes related to the movement of magma towards the surface and the associated deformation of the country rock. The rise of magma causes local temperature increases within the volcano and increases the fracture permeability. These conditions seem to permit Rn directly volatilized from the magma at high temperature to migrate towards the surface, transported by the escaping steam<sup>6,13,14</sup>. This steam and the overall thermally stimulated, increased outgassing act as a transport medium for other available Rn encountered during migration towards the surface<sup>1,7</sup>. The major sources of this additional Rn are the groundwater through which the vapour phases pass (Rn is more soluble in the vapour) and Rn within pore spaces and fractures in lava above the water table. A further source may be the decay of Ra within secondary mineralization (largely CaSO<sub>4</sub>) deposited on fracture surfaces in zones where hydrothermal activity has occurred<sup>1,15</sup>. Availability of minor quantities of Rn is possibly also enhanced by stress buildup and deformation, causing a greater diffusion of Rn by destruction of crystalline lattices of minerals and a greater pore space-transporting fluid area in contact at depth.

The common decrease in Rn concentration following the eruption and seismic swarms seems to be caused by depletion of Rn available in rock fractures and pores from 'flushing' by increased outgassing before and during these events. The Rn regenerates by decay of Ra and by diffusion into rock fractures over a period of several weeks, allowing an overall return to levels characteristic of periods of normal seismicity (no specific events). Similar post-eruptive Rn depletion was observed in thermal springs on Karymsky volcano<sup>4</sup> and has been proposed as creating <sup>226</sup>Ra-<sup>222</sup>Rn disequilibrium in pumice ejected during eruptions of Japanese volcanoes<sup>16</sup>. In both cases, a subsequent period of buildup was observed. In the case of ground Rn outgassing associated with an eruption, the post-eruptive reduction of near-surface heat and stresses at depth, partially decrease fracture permeability and allow the re-establishment of groundwater flow and consequent dissolution of much of the Rn being generated below the normal water table. After equilibrium conditions are again established, the greatest source of Rn to the surface is probably from the lava pile above the water table. The most important change, however, seems to be a reduction of thermally induced ground gas outgassing, which allows re-establishment of ground gas flow patterns. The greatest changes in outgassing were measured at stations close to fractures or faults below which there was magma migration, or other phenomena that produced increased seismic activity. Where Rn values at a station are atypical relative to adjacent stations (for example, B), they are apparently a consequence of localized ground gas convection systems developed around or between fractures. The flow of ground gas (whether upflow or downflow) in these systems is increased during these events, and in some cases, reversals in ground gas flow can occur usually within specific zones of fracturing.

Due to the apparent success of this study 25 stations (including the above) are now being monitored on the summit and along the east rift of Kilauea. The results from these stations reinforce the above findings, specifically, that the Rn concentration increases before and during seismic events (caused by either extrusive, intrusive, or earthquake activity) and decreases over several weeks after the event, then tends to return to a normal or characteristic value for each station. Atypical variations at some stations are indicated to result from location of fractures relative to each other and to the location of the event. Continuous monitoring of the larger number of stations will aid understanding of the fracture systems and the ground gas flow

patterns on the volcano, and may assist in indicating pre-eruptive activity.

We thank J. J. Naughton and D. B. Jackson for reviews and the staff of the Hawaii Volcano Observatory for cooperation. The study was carried out under US Department of Energy Contract no. EW-78-S-07-0713.

Received 29 April; accepted 19 August 1980.

1. Cox, M. E. *Geophys. Res. Lett.* **7**, 4, 283-286 (1980).
2. Cox, M. E. & Cuff, K. E. *Trans. Geotherm. Resour. Coun.* **4**, 451-454 (1980).
3. Chirkov, A. M. *Bull. volcan.* **39**, 126-131 (1976).
4. Iwasaki, I., Katsura, T., Shimojima, H. & Kamada, M. *Bull. volcan.* **18**, 103-123 (1956).
5. Iwasaki, I. *Bull. volcan.* **39**, 82-90 (1976).
6. Lambert, G., Bristeau, P. & Polian, G. *Geophys. Res. Lett.* **3**, 12, 724-726 (1976).
7. Gasparini, P. & Mantovani, M. S. M. *J. Volcan. Geotherm. Res.* **3**, 325-341 (1978).
8. King, C.-Y. *Pap. 3rd Conf. Nat. Radiat. Envir. Houston* (1978).
9. Fleischer, R. L., Alter, H. W., Furman, S. C., Price, P. B. & Walker, R. M. *Science* **178**, 255-262 (1972).
10. Gingrich, J. E. *Trans. Soc. Min. Engrs.* **258**, 61-64 (1975).
11. Fleischer, R. L. & Mogro-Campero, A. *J. geophys. Res.* **83**, 3539-3549 (1978).
12. HVO Staff Sci. *Event Alert Network Bull.* **4**, 11-17 (1979).
13. Björnsson, S. *Geochim. cosmochim. Acta* **32**, 815-821 (1968).
14. Polian, G. & Lambert, G. *J. Volcan. Geotherm. Res.* **6**, 126-137 (1979).
15. Kruger, P., Stoker, A. & Umana, A. *Geothermics* **5**, 13-19 (1977).
16. Sato, K. & Sato, J. *Nature* **266**, 439-440 (1977).

## Trophic structure of a grassland insect community

Blaine J. Cole

Museum of Comparative Zoology, Harvard University, Cambridge, Massachusetts 02138

The idea that there is some underlying trophic structure to ecological communities has long been attractive<sup>1-3</sup>. Energy, biomass or nutrients are undeniably transferred from one trophic level to another. However, does the number of species at one trophic level place constraints on the number of species at another trophic level? Cohen<sup>4</sup> has shown that, in a sample of 14 community food webs, the ratio of prey species to predator species remains virtually constant. In an analysis of a grassland insect community, Evans and Murdoch<sup>5</sup> have shown that the ratio of herbivorous insects to entomophagous insects remains fairly constant throughout the growing season. They speculated that this reflects an underlying trophic pattern that persists in the face of a continuing turnover of species. I have now found that a close examination of this pattern shows that an appearance of constancy can be generated by replicate samples taken from the pool of all available species.

The number of species of herbivorous and entomophagous insects in each sample interval may be envisioned as a random draw of species from the total pool of available species. In this case the number of herbivorous species would be a function of the total number of species drawn from the pool and the proportion of herbivorous species present in the species pool. The number of herbivorous species will have a hypergeometric distribution

$$P(k) = \frac{\binom{n}{n_1} \binom{n-n_1}{r-k}}{\binom{n}{r}} \quad (1)$$

Equation (1) gives the probability that exactly  $k$  herbivorous species will be found in a sample of  $r$  species taken from a total pool of  $n$  species of which  $n_1$  are herbivorous species. The expected number of herbivorous species in a sample of size  $r$  is given by

$$E(H) = r \left( \frac{n_1}{n} \right) \quad (2)$$

The variance of this expectation is given by

$$\text{Var}(H) = r \left( \frac{n_1}{n} \right) \left( 1 - \frac{n_1}{n} \right) \left( 1 - \frac{r-1}{n-1} \right) \quad (3)$$

**Table 1** The observed and expected numbers of herbivores in a grassland insect community

| Fortnightly interval | No. of species | Observed no. of herbivores | Expected no. of herbivores | Expected variance in herbivore no. |
|----------------------|----------------|----------------------------|----------------------------|------------------------------------|
| 1                    | 20             | 12                         | 12.4                       | 4.4                                |
| 2                    | 32             | 22                         | 19.9                       | 6.6                                |
| 3                    | 64             | 40                         | 39.7                       | 10.8                               |
| 4                    | 92             | 62                         | 57.1                       | 12.6                               |
| 5                    | 116            | 77                         | 72.0                       | 12.7                               |
| 6                    | 137            | 88                         | 85.1                       | 11.7                               |
| 7                    | 147            | 98                         | 91.3                       | 10.8                               |
| 8                    | 150            | 95                         | 93.2                       | 10.5                               |
| 9                    | 133            | 79                         | 82.6                       | 12.0                               |
| 10                   | 144            | 91                         | 89.4                       | 11.1                               |
| 11                   | 127            | 78                         | 78.9                       | 12.3                               |
| 12                   | 98             | 64                         | 60.9                       | 12.8                               |
| 13                   | 52             | 29                         | 32.3                       | 9.5                                |
| 14                   | 22             | 18                         | 13.7                       | 4.8                                |

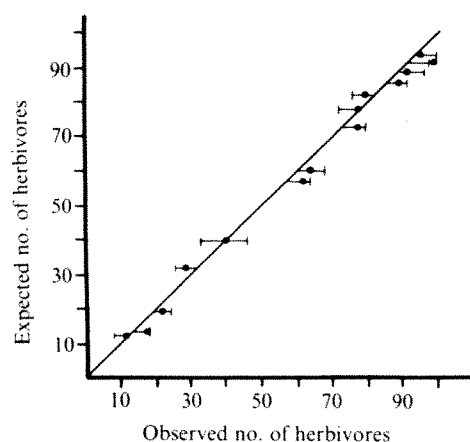
The data from the 14 sample intervals of Evans and Murdoch specify all quantities of equations (2) and (3). The number of species is the quantity  $r$ . Other quantities are given in the text. The fit of observed values to theoretical expectations is tested by a  $\chi^2 = 3.45$ , d.f. = 13,  $P > 0.995$ .

The data from the 14 fortnightly intervals given by Evans and Murdoch are shown in Table 1. The total number of herbivorous and entomophagous species in this grassland community is given as 131 and 80, respectively. This represents values of  $n = 211$  and  $n_1 = 131$ . All values of equations (2) and (3) are known and thus the expected number of herbivores and the expected variance can be calculated.

Figure 1 shows the observed number of herbivores and the expected number of herbivores. Points fall on the line if the expected number of herbivores equals the observed number. The bars through the points are 2 s.d. from the expected values. All but one of the points (fortnightly interval 7) lie within 2 s.d. of the expected value.

There seems to be no systematic tendency in the samples to lie either above or below the line. Four samples are found to have more herbivores than expected, 10 have fewer than expected. The two-tailed binomial probability for this, or a more deviant event, is  $P = 0.284$ .

There does not seem to be any trend in deviation from the expected as one considers various numbers of species. Two of the four values greater than expectations are above the median of total species, two of the values are below the median. When there are few species, at either the beginning or end of the



**Fig. 1** The expected number of herbivores is plotted against the observed number of herbivores. The bars represent 2 s.d. from the expected number of herbivores.

season, there does not seem to be any less trophic structure. Nor does there seem to be more trophic structure during the period of greatest species diversity.

In conclusion, there does not seem to be any evidence that the ratio of herbivores to predators in this grassland insect community is maintained at a constant level by any other force than a statistical one. Analysis at another, deeper, level, well beyond the scope of this report, might ask why the ratio of herbivorous insects to their predators is 1.64. Given that it is, however, no further evidence for trophic structuring exists.

Received 2 June; accepted 10 September 1980.

1. Ricklefs, R. E. *Ecology* (Chiron, Portland, Oregon, 1973).
2. Emlen, J. M. *Ecology: An Evolutionary Approach* (Addison-Wesley, London, 1973).
3. May, R. M. *Theoretical Ecology* (Saunders, Philadelphia, 1976).
4. Cohen, J. *Nature* **270**, 165-167 (1977).
5. Evans, F. C. & Murdoch, W. W. *J. Anim. Ecol.* **37**, 259-273 (1968).

## Co-transfer of determinants for hydrogenase activity and nodulation ability in *Rhizobium leguminosarum*

N. J. Brewin\*, T. M. DeJong†, D. A. Phillips† & A. W. B. Johnston\*

\*John Innes Institute, Colney Lane, Norwich NR4 7UH, UK

†Department of Agronomy and Range Science, University of California, Davis, California 95616

In all organisms that fix atmospheric nitrogen a by-product of the nitrogenase reaction is hydrogen gas<sup>1</sup> which may dissipate up to one-third of the energy flux through nitrogenase<sup>2</sup>. Some nitrogen-fixing bacteria, including certain strains of the root nodule bacterium *Rhizobium*, possess an active hydrogen uptake (Hup) system permitting hydrogen to be re-cycled<sup>3,4</sup>. For this reason Hup<sup>+</sup> *Rhizobium* strains are thought to be more energy-efficient symbionts than their Hup<sup>-</sup> counterparts<sup>5-8</sup>. We report here that determinants for hydrogenase activity (*hup*) in a particular strain of *R. leguminosarum* (128C53) are genetically linked to determinants for nodulation ability (*nod*), and are probably carried on a plasmid, pRL6JI, of molecular weight (MW) ~19 × 10<sup>7</sup>. Although pRL6JI was not self-transmissible, the determinants for nodulation ability and hydrogenase activity (*hup*) could be transferred to other strains of *R. leguminosarum* after recombination with a derivative of a transmissible *R. leguminosarum* plasmid.

Nodulation ability is plasmid-determined in *R. leguminosarum*<sup>9-12</sup> and several determinants for nodule formation and function may be carried on a single plasmid<sup>11-15</sup>. We therefore attempted to transfer determinants for nodulation ability from strain 128C53, a Hup<sup>+</sup> field isolate of *R. leguminosarum*<sup>8,16</sup>, into a non-nodulating (Nod<sup>-</sup>) mutant of the Hup<sup>-</sup> field-isolate *R. leguminosarum* strain 300 in the hope that determinants for Nod<sup>+</sup> and Hup<sup>+</sup> were genetically linked and might consequently be co-transferred. The recipient strain was 16015, a derivative of strain 300, which contains *str-37* and *spc-54* markers and a plasmid deletion in a region determining nodule formation (Nod<sup>+</sup>) and nodule function (Fix<sup>+</sup>)<sup>11-13</sup>.

Strain 128C53 contains two large plasmids (MW ~19 and 23 × 10<sup>7</sup>) but no evidence for self-transmissible plasmids was obtained using methods which had identified such plasmids in other *Rhizobium* strains<sup>9,14,17</sup>. Therefore two self-transmissible plasmids, which did not themselves suppress the Nod<sup>-</sup> phenotype of strain 16015 but which were known to mobilize nodulation plasmids from other strains<sup>13</sup>, were introduced into strain 128C53. The transmissible plasmids used were pVW3JI and pVW5JI, kanamycin-resistant derivatives of pRL3JI and pRL4JI respectively<sup>13</sup>.



**Table 1** Co-transfer of Nod<sup>+</sup> and Hup<sup>+</sup> determinants from derivatives of strain 128C53 to strain 16015 following recombination with transmissible plasmids determining kanamycin resistance

| Donor strain | Plasmid from which <i>kan</i> marker was derived | Recipient strain | Frequency of transfer of <i>kan</i> per recipient | No. of Kan <sup>r</sup> transconjugant clones tested on plants |                  |                  |                  |
|--------------|--|------------------|---|--|------------------|------------------|------------------|
|              |  |                  |   | Total  | Nod <sup>+</sup> | Fix <sup>+</sup> | Hup <sup>+</sup> |
| <i>a</i>     |  |                  |   |  |                  |                  |                  |
| 2515         | pVW3JI   | 128C53           | 2 × 10 <sup>-4</sup>                              | 5  | 5                | 5                | 5                |
| 2517         | pVW5JI   | 128C53           | 1 × 10 <sup>-4</sup>                              | 5  | 5                | 5                | 5                |
| <i>b</i>     |  |                  |   |  |                  |                  |                  |
| 3856         | pVW3JI   | 16015            | 5 × 10 <sup>-7</sup>                              | 15   | 11               | 11               | 11               |
| 3957         | pVW5JI   | 16015            | 5 × 10 <sup>-7</sup>                              | 15   | 10               | 10               | 10               |
| <i>c</i>     |  |                  |   |  |                  |                  |                  |
| 2515         | pVW3JI   | 16015            | 3 × 10 <sup>-2</sup>                              | 10   | 0                | —                | —                |
| 2517         | pVW5JI   | 16015            | 5 × 10 <sup>-2</sup>                              | 10   | 0                | —                | —                |

*a*, Introduction of transmissible plasmids into 128C53 derivatives; *b*, transfer of plasmid-linked determinants from 128C53 derivatives to the non-nodulating strain 16015; *c*, control crosses: direct transfer of plasmids from 300 derivatives to strain 16015. Two derivatives of strain 300, each carrying a different transmissible plasmid conferring kanamycin resistance, were mated with strain 3854, a spontaneous *rif* mutant of strain 128C53 (itself a Hup<sup>+</sup> field isolate of *R. leguminosarum*). The genotypes of the donor strains were as follows:— 2515:300 *phe-1 ade-27 rif-45* pVW3JI; 2517:300 *phe-1 ade-27 rif-45* pVW5JI. Kanamycin-resistant derivatives of 3854 (128C53 *rif-397*) were obtained by introducing pVW3JI or pVW5JI into this strain and these derivatives were termed 3856, 3957 respectively (*a*). These two strains, together with the corresponding strain 300 donors were used in crosses to the Nod<sup>−</sup> strain 16015 (*b* and *c*). Kan<sup>r</sup> derivatives of 16015 were repurified and scored for nodulation ability on duplicate peas, var. Wisconsin Perfection. Roots of nodulated plants were tested for acetylene reduction (Fix<sup>+</sup>) and for the incorporation of tritiated hydrogen gas (Hup<sup>+</sup>) into the aqueous phase as described in Table 2.

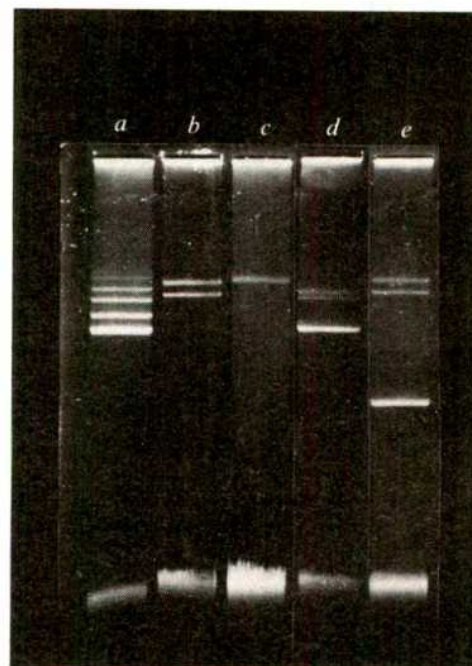
When the 128C53 derivatives into which pVW3JI or pVW5JI had been introduced were used as donors to strain 16015, transfer of *kan* occurred at low frequency ( $10^{-6}$  to  $10^{-7}$  per recipient). However, more than half of the 16015 transconjugant clones were now able to nodulate peas (Table 1). In all cases the nodules formed had hydrogenase activity comparable to that for strain 128C53 and the rate of hydrogen evolution was correspondingly diminished compared with a Hup<sup>−</sup> strain (Table 2).

Because strain 300 itself is Hup<sup>−</sup> and neither Nod<sup>+</sup> nor Hup<sup>+</sup> phenotypes are conferred by pVW3JI or pVW5JI (data not shown), both Nod<sup>+</sup> and Hup<sup>+</sup> determinants must have been derived from strain 128C53 and must therefore be genetically linked in that strain. This was confirmed in further crosses between the 16015 Kan<sup>r</sup> Nod<sup>+</sup> Hup<sup>+</sup> transconjugants and strain 6015 (which carries the same *nod-6007* deletion as strain 16015<sup>9</sup>; in these crosses *kan* was transferred at high frequency ( $5 \times 10^{-3}$  per recipient) and most (22/25) of the Kan<sup>r</sup> 6015 transconjugants were also Nod<sup>+</sup>. In all cases Nod<sup>+</sup> transconjugants were Hup<sup>+</sup>. The very high-frequency co-transfer of *nod* and *hup* with *kan* suggests that there has been genetic recombination between these markers, and the high-frequency transfer of *kan* suggests the involvement of a plasmid, at least at this stage.

The transfer frequency of *kan* from the 128C53 derivatives to strain 16015 was inexplicably low but was at least 10-fold higher than for transfer of chromosomal alleles (data not shown). When similar crosses were performed using the P1 group R plasmid pJB3JI (which confers tetracycline resistance<sup>14</sup>), the Tet<sup>r</sup> determinant was transferred into and out of strain 128C53 at normal frequencies ( $10^{-2}$ – $10^{-3}$ ), but no co-transfer of Nod<sup>+</sup> to strain 16015 was observed (data not shown).

Because the Nod<sup>+</sup> determinants of strain 128C53 were probably plasmid-borne, the plasmids from many of the strains described here were examined after electrophoresis on agarose gels (Fig. 1). In strain 2515, a 300 derivative, the plasmid pVW3JI was visible as the second-fastest migrating band, MW  $13 \times 10^7$  (Fig. 1 track *a*, and see ref. 12). However, in all three Kan<sup>r</sup> derivatives of 128C53 examined after transfer of pVW3JI into this strain, no band corresponding to pVW3JI was visible (Fig. 1 track *c*): furthermore, the smaller of the two plasmids (MW  $19 \times 10^7$ ) visible in strain 128C53 (Fig. 1 track *b*) had also disappeared. An identical plasmid pattern was observed in Kan<sup>r</sup> derivatives of 128C53 obtained after the transfer of pVW5JI (MW  $16 \times 10^7$ ) into this strain. However, when the P1-group plasmid pJB3JI was transferred into strain 128C53 (Fig. 1, track *e*) the two resident plasmids of strain 128C53 remained visible and in addition there was a band corresponding in mobility to that of pJB3JI.

The simplest interpretation that is consistent with both the genetical and physical observations described is that the smaller plasmid of strain 128C53 is the likely carrier of the linked Nod<sup>+</sup> and Hup<sup>+</sup> determinants. We term this plasmid pRL6JI, and we propose that pRL6JI recombined (or co-integrated) with the introduced plasmid to form a transmissible plasmid carrying determinants for Nod<sup>+</sup> and Hup<sup>+</sup> from pRL6JI, Kan<sup>r</sup> from



**Fig. 1** Physical interaction between pVW3JI and a plasmid from strain 128C53. See Tables 1 and 2 for a description of the relevant strains. Lysates were prepared and analysed by electrophoresis on agarose gels following the method of Hirsch *et al.*<sup>12</sup>. In each track the fastest migrating band represents sheared (chromosomal) DNA. *a*, Strain 2515. The plasmid band corresponding to pVW3JI is the second-fastest migrating plasmid band. The two high molecular weight plasmids of strain 300 are just visible on this gel (see ref. 12). *b*, Strain 3854 = 128C53 *rif-397*. *c*, Strain 3856 = 3854 carrying *kan* determinant from pVW3JI. *d*, Strain 3892 = kan<sup>r</sup> Nod<sup>+</sup> Fix<sup>+</sup> Hup<sup>+</sup> transconjugant from the cross 3856 × 16015. *e*, Strain 3955 = 3854 pJB3JI. Two tracks have been removed from this gel corresponding to lysates from 3957 (pVW5JI derivative, identical to track *c*) and 16015 (identical to track *d*).

pVW3JI (or pVW5JI) and *Fix*<sup>+</sup> determinants from either or both moieties. The failure to detect the recombinant plasmid as a band on agarose gels might be due to the fact that its very large size ( $MW > 30 \times 10^7$ ) would make it too susceptible to breakage to be recovered intact in our plasmid preparations. Inter-plasmid recombination might have occurred if pRL6JI shared homologous sequences with pVW3JI and pVW5JI.

There are at least two explanations for the fact that the introduced plasmid was never observed in Kan<sup>r</sup> derivatives of strain 128C53. Either the introduced plasmids are incompatible with pRL6JI which itself might carry genes essential for the growth of this strain or, alternatively, pVW3JI or pVW5JI might be incapable of autonomous replication within this host. Both possibilities are consistent with the relatively low initial transfer frequency ( $10^{-4}$ ) of the transmissible plasmids into strain 128C53 and with the observed disappearance of the band corresponding to pRL6JI from Kan<sup>r</sup> transconjugants.

**Table 2.** Quantitative measurements of pea root nodule activity following inoculation with Hup<sup>+</sup> and Hup<sup>-</sup> strains of *R. leguminosarum*

| Inoculant  | Acetylene reduction<br>( $\mu\text{mole C}_2\text{H}_4$<br>per plant per h) | Hydrogen evolution<br>( $\mu\text{mole H}_2$<br>per plant per h) | Tritium incorporation<br>( $\mu\text{mole H-T}$ per<br>g-nodule fresh<br>wt per h) |
|------------|---|--|--|
| 300        | 5.11 ( $\pm 0.32$ )   | 3.16 ( $\pm 0.23$ )  | 0.002 ( $\pm 0.001$ )  |
| 300 pRL3JI | 8.81 ( $\pm 0.77$ )   | 4.57 ( $\pm 0.69$ )  | 0.001 ( $\pm 0.001$ )  |
| 3740       | 8.46 ( $\pm 0.24$ )   | 5.01 ( $\pm 0.30$ )  | 0.001 ( $\pm 0.001$ )  |
| 128C53     | 7.97 ( $\pm 0.99$ )   | 0.57 ( $\pm 0.20$ )  | 0.738 ( $\pm 0.063$ )  |
| 3892       | 6.84 ( $\pm 0.48$ )   | 0.32 ( $\pm 0.04$ )  | 1.013 ( $\pm 0.112$ )  |
| 3894       | 9.43 ( $\pm 1.09$ )   | 0.37 ( $\pm 0.04$ )  | 0.844 ( $\pm 0.074$ )  |

'Alaska' peas grown in modified Leonard-jar assemblies were assayed 25 days after inoculation as previously described<sup>8</sup>. Tritium incorporation by nodulated roots was measured in 25-ml incubation vessels containing tritiated hydrogen gas (2.4%, v/v,  $2.4 \text{ mCi mmol}^{-1}$ ) in the presence of acetylene (10%, v/v) to inhibit hydrogen production by nitrogenase<sup>8</sup>. Incubation was for 30 min and means ( $\pm$  s.e.) were computed for six replicates. Bacteria recovered from surface-sterilized nodules were tested for the appropriate drug-resistance markers and plasmid patterns. Strains 3740, 3892 and 3894 were all Nod<sup>+</sup> Kan<sup>r</sup> derivatives of strain 16015. In strain 3740, which was Hup<sup>-</sup>, *kan* was derived from pVW5JI and *nod* from strain 300 (see ref. 13 for the construction of this strain). In strains 3892 and 3894, *kan* was derived from pVW3JI and pVW5JI respectively, *nod* and *hup* determinants were derived from 128C53 (see Table 1).

The plasmids of the 300 Nod<sup>-</sup> strain 16015 have already been described<sup>12,14</sup>. In the Kan<sup>r</sup> derivatives that were Nod<sup>+</sup> Hup<sup>+</sup>, no new plasmid bands could be seen (Fig. 1 track d). This implies either that any co-transferred plasmid co-migrated on gels with a resident plasmid from strain 16015 or that the co-transferred plasmid was too large to be visualized on gels (as was suggested for the donor strain itself). However, Kan<sup>r</sup> 16015 derivatives that were Nod<sup>-</sup> (Table 1b) contained a new plasmid band present in neither strain 16015 nor in the donor strain, but corresponding in size to the original plasmid band of pVW3JI as seen in lysates of normal strain 300 derivatives (Fig. 1 track a). In these cases it seems that the original pVW3JI plasmid may have been regenerated by a reversal of the original recombination event that caused its disappearance from derivatives of 128C53.

We have demonstrated that two apparently unrelated symbiotic phenotypes, nodulation ability for peas and the presence of hydrogenase activity, are genetically linked in strain 128C53. It is possible that a large proportion of the genes concerned specifically with the nitrogen-fixing symbiosis, the so-called symbiotic genes, will be found to be clustered and located on one or a few plasmids. Such an arrangement would certainly make it easier to develop genetically improved strains of *Rhizobium*.

This work was supported in part by NATO grant 1533 and by US NSF grant PFR77-07301. We thank Dr M. G. Yates and Professor J. R. Postgate for help and advice on the measurement of tritium incorporation by root nodules, Miss E. A. Wood for technical assistance, and Professor D. A. Hopwood for criticism of the manuscript.

**Note added in proof:** A. H. Christensen and K. R. Schubert (personal communication) have informed us that their culture of 128C53 (obtained from Dr J. C. Burton) has a different plasmid profile from that described here for our culture of this strain. It is not clear whether our Hup<sup>+</sup> strain has undergone plasmid rearrangements during its history or whether two different strains exist bearing the designation 128C53.

Received 25 July, accepted 17 September 1980

- Orme-Johnson, W. H. in *Genetic Engineering for Nitrogen Fixation* (ed. Hollander, A.) 317-332 (Plenum, New York, 1977).
- Shanmugam, K. T., O'Gara, F., Anderson, K. & Valentine, R. C. A. *Rev. Pl. Physiol.* 29, 263-276 (1978).
- Evans, H. J., Ruiz-Argüeso, T., Jennings, H. & Harris, J. J. in *Genetic Engineering for Nitrogen Fixation* (ed. Hollander, A.) 333-335 (Plenum, New York, 1977).
- Ruiz-Argüeso, T., Emerich, D. W. & Evans, H. J. *Biochem. biophys. Res. Commun.* 86, 259-264 (1979).
- Schubert, K. R. & Evans, H. J. *Proc. natn. Acad. Sci. U.S.A.* 73, 1207-1211 (1976).
- Moser, R. J., Postgate, J. R. & Evans, H. J. *Nature* 276, 494-495 (1978).
- Albrecht, S. L. *et al. Science* 203, 1255-1257 (1979).
- Bethlenfalvy, G. J. & Phillips, D. A. *Pl. Physiol.* 63, 816-820 (1979).
- Johnston, A. W. B. *et al. Nature* 276, 635-636 (1978).
- Cano, F., Boncher, C., Julhot, J. S., Michel, M. & Décarlé, J. J. *gen. Microbiol.* 113, 229-242 (1979).
- Buchanan-Wollaston, A. V., Berlinger, J. E., Brown, N. J., Hirsch, P. R. & Johnston, A. W. B. *Molec. gen. Genet.* 178, 185-190 (1980).
- Hirsch, P. R., van Montagu, M., Johnston, A. W. B., Brown, N. J. & Schell, J. J. *gen. Microbiol.* 120, 403-412 (1980).
- Brown, N. J., Berlinger, J. E., Buchanan-Wollaston, A. V., Johnston, A. W. B. & Hirsch, P. R. *J. gen. Microbiol.* 116, 261-270 (1980).
- Brown, N. J., Berlinger, J. E. & Johnston, A. W. B. *J. gen. Microbiol.* 120, 413-420 (1980).
- Beynon, J. L., Berlinger, J. E. & Johnston, A. W. B. *J. gen. Microbiol.* 120, 421-429 (1980).
- Ruiz-Argüeso, T., Harris, J. & Evans, H. J. *Arch. Microbiol.* 116, 113-118 (1978).
- Berlinger, J. E., Beynon, J. L., Buchanan-Wollaston, A. V. & Johnston, A. W. B. *Nature* 276, 633-634 (1978).
- Hirsch, P. R. *J. gen. Microbiol.* 113, 219-228 (1979).

## Nonrandom segregation of nucleolar organizing chromosomes at mitosis?

Martin Bobrow & Jane Heritage

Department of Medical Genetics, Old Road, Headington, Oxford OX3 7LE, UK  
Genetics Laboratory, Oxford University, South Parks Road, Oxford OX1 3BD, UK

The random assortment of non-homologous chromosomes at meiosis is one of the fundamental tenets of genetics, to which few exceptions have been documented<sup>1</sup>. The segregation of mitotic chromatids is believed to be similarly random. We report here that we seem to have discovered a new exception to this rule, in that nucleolar organizing chromosomes remain associated with one another, held in the same lateral orientation, for several mitotic cycles.

Five pairs of human chromosomes (nos 13, 14, 15, 21 and 22) carry rDNA sequences in specific chromosome segments, known as nucleolar organizing regions (NORs). The chromosomes are all acrocentrics, and the NORs are on their short arms. More than one chromosome may participate in the formation of a single nucleolus, DNA from their NORs uncoiling and extending deep into the substance of the nucleolus<sup>2</sup>. During mitosis, the nucleoli disappear, but the chromosomes may be seen at metaphase grouped together with their short arms in close proximity. These configurations are called 'satellite associations' (ref. 3). A very close association of nucleoprotein complexes between associated chromosomes has been demonstrated autoradiographically<sup>4</sup>.



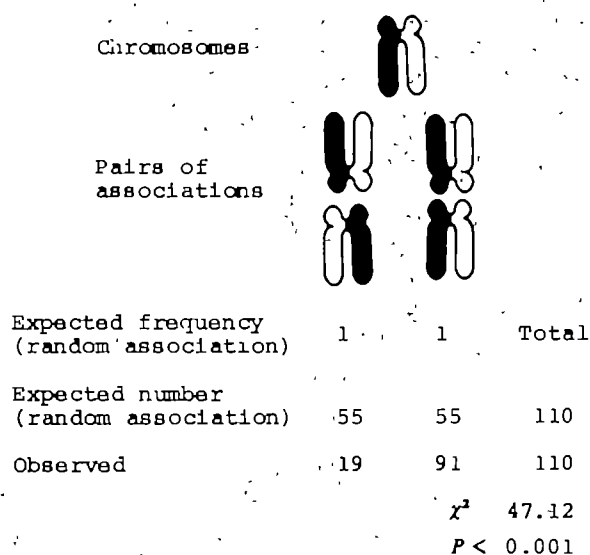


Fig. 1 Expected and observed satellite-association pairs in second-generation BUdR-substituted cells.

Methods have recently been developed which differentially stain the two chromatids of each chromosome. Cells grown in the presence of bromodeoxyuridine (BUdR) incorporate this base into their DNA in place of thymidine, and such BUdR-substituted chromatids stain less intensely with the dye 33258-Hoechst<sup>5</sup>, or with a combination of 33258 and Giemsa<sup>6</sup>. By growing cells in BUdR-containing medium for two cell cycles, chromosomes are produced with one-chromatid half-substituted and one fully substituted with BUdR. The 'old' and 'new' chromatids can be differentially stained. After a third round of

DNA replication in the presence of BUdR, one-quarter of the chromatids will still be thymidine containing and darkly stained; half of the chromosomes will therefore have differentially stained chromatids, and the other half will consist of two bifilarly substituted, poorly stained chromatids.

We have examined satellite-associated chromosomes in both second- and third-generation BUdR cells, using standard peripheral blood chromosome cultures from five normal people. (Similar observations were made on a culture from an orangutan, although these cells are not included in the totals scored.) To minimize subjective scoring bias, we selected satellite associations consisting of only two chromosomes, where the chromosomes were closely paired (less than about 1 chromatid width apart), directly end-on to one another, and reasonably straight. All such configurations were scored. In second-generation cells, either a dark-to-dark or dark-to-light chromatid alignment may be seen, and assuming random segregation of chromatids at mitosis, these should be equally common. Our observations on 110 associations are set out in Fig. 1. It is clear that there is a highly significant tendency for old, thymidine-containing, darkly staining chromatids to be aligned with one another. There is about a 17% frequency of discordant (dark-to-light) associations. This may be an underestimate of stability, as many of the 17% exceptional associations seemed to be minimally twisted, but these were, nevertheless, scored as 'discordant' to avoid any possibility of artificially inflating the rate of concordant segregation.

In the absence of sister chromatid exchanges near the centromere, metacentric chromosomes generally show the dark-staining strand to go straight, rather than diagonally, across the centromere. In a purely descriptive sense, pairs of associated acrocentric chromosomes are behaving like single metacentric chromosomes with a centromere breakage rate of ~17% per cell cycle.

It is similarly simple to define the expected frequencies of various configurations in third-division cells, on the assumption either of random assortment or of a given dissociation rate per

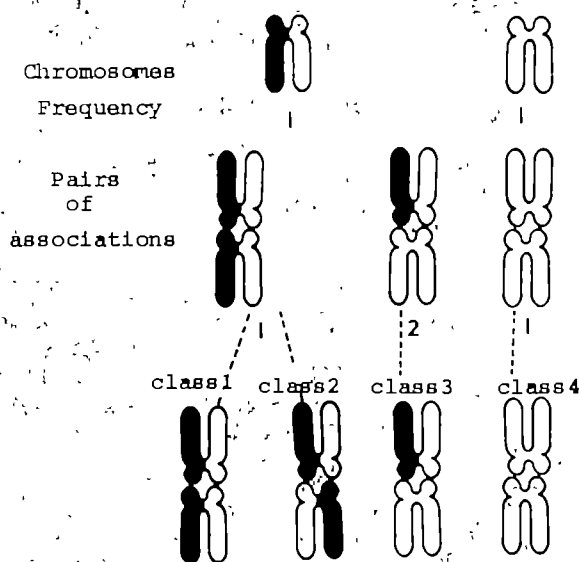


Fig. 2 Expected and observed satellite-association pairs in third-generation BUdR-substituted cells. If association pairs dissociate at the rate 'p' per cell cycle, and single chromosomes reassociate at random, the frequencies of the four classes of association after three cell cycles can be calculated as:

$$\text{Class 1} = \frac{1}{8}(4 - 7p + 6p^2 - 2p^3)$$

$$\text{Class 2} = \frac{p}{8}$$

$$\text{Class 3} = \frac{1}{8}(3p - 3p^2 + p^3)$$

$$\text{Class 4} = \frac{1}{8}(2 - 3p + 3p^2 - p^3)$$

The 'expected' values in the last line of the figure are derived by substituting  $p = 0.2$  in these formulae. NS, not significant.

|   |      |      |      |      |       |
|---|------|------|------|------|-------|
| Expected frequency (random association) | 1    | 1    | 2    | 1    | Total |
| Expected number (random association)    | 6.25 | 6.25 | 25   | 12.5 | 50    |
| Expected number (20% dissociation)      | 17.6 | 1.3  | 12.2 | 18.9 | 50    |
| Observed                                | 15   | 4    | 15   | 16   | 50    |

$\chi^2$  18.04  
 $P < 0.001$

$\chi^2$  7.08  
NS

cell cycle with random rejoining of dissociated chromosomes. These expectations, and our observations on 50 relevant associations, are set out in Fig. 2. The data clearly fit well with the observations on second-division cells.

The staining of a chromatid in this system depends on the presence of either thymidine or BUdR in a single DNA strand. Similar staining of opposed chromatids therefore implies that they are being held in alignment during mitosis by forces operating at the level of the single DNA strand.

There are several possible explanations for this phenomenon. (1) Chromatids of associated chromosomes may be held oriented relative to one another by the establishment of physical connectives within the nucleolar substance. The existence of ribonucleoprotein connections has been demonstrated<sup>4</sup>. Inter-chromosomal DNA connections have also been reported, and have led to suggestions of the same DNA strand continuing through more than one chromosome<sup>7</sup>, although there is now a strong suspicion that these interchromosomal fibres are artefacts<sup>8</sup>. Our observations require that single DNA strands are held together for several cell cycles, and it is easier to envisage such a rigid orientation from a nucleic acid connection than from mere enmeshment in a common nucleoprotein matrix. (2) One cannot exclude the possibility that chromatids do segregate randomly at mitosis, but that their involvement in new satellite associations is nonrandom, thymidine-containing chromatids selectively aligning opposite one another. Even this implies a pairing phenomenon at the level of the single DNA strand. The restrictions on joining imposed by DNA strand polarity would not adequately explain our observations, as the number of active nucleolus-organizing chromosomes per cell is such that there would almost always be both thymidine- and BUdR-containing strands of each polarity available. (3) Presumably, not all nucleolus-associated chromosome groups survive into metaphase as visible satellite associations, but there seems to be no reason that 'concordant' pairs should be more likely to survive than 'discordant' pairs.

Any attempt to choose between these possibilities, or to consider the basic mechanism of this phenomenon, would be purely speculative. However, the most economic hypothesis seems to be that a physical continuity, at the DNA single-strand level, is actually established between non-homologous chromosomes, and can persist through several cell cycles.

The most common form of chromosome rearrangement in man is the Robertsonian fusion, in which acrocentric chromosomes become permanently joined by their short arms, the translocation chromosomes sometimes remaining demonstrably dicentric. Such translocations may segregate to produce aneuploid offspring, particularly Down's syndrome. If the NOR-bearing chromosomes regularly establish physical connections with one another, this may be related to the generation of such translocations.

There are conflicting data on the randomness with which particular chromosomes are involved in satellite associations<sup>9</sup>, and on whether such associations are causally related to the production of trisomic children<sup>10-12</sup>. If such a relationship does exist, it may also be concerned with the phenomenon of intimate chromosome association described here.

We thank H. J. Evans for useful comments. This work was supported by a programme grant from the MRC.

Received 2 June; accepted 4 September 1980.

1. Sybenga, J. *General Cytogenetics*, 310-314 (North-Holland, Amsterdam, 1972).
2. Busch, H. & Smetana, K. *The Nucleolus* (Academic, New York, 1970).
3. Ferguson-Smith, M. A. & Handmaker, S. D. *Lancet* i, 638 (1961).
4. Henderson, A. S., Warburton, D. & Atwood, K. C. *Nature* **245**, 95 (1973).
5. Latt, S. A. *Proc. natn. Acad. Sci. U.S.A.* **70**, 3395 (1973).
6. Perry, P. & Wolff, S. *Nature* **251**, 156 (1974).
7. du Praw, E. J. *DNA and Chromosomes* (Holt, Rinehart & Winston, New York, 1970).
8. White, M. J. D. *The Chromosomes*, 14-15 (Chapman & Hall, London, 1973).
9. Sele, B. *et al. Hum. Genet.* **39**, 39 (1977).
10. Hansson, A. *Hereditas* **90**, 59 (1979).
11. Taysi, K. *Clin. Genet.* **8**, 319 (1975).
12. Cooke, P. & Curtis, D. J. *Hum. Genet.* **23**, 279 (1974).

## Human T lymphocytes of inducer and suppressor type occupy different microenvironments

George Janossy, Nicholas Tidman, Warwick S. Selby, J. Alero Thomas & Sylvia Granger

Department of Immunology, Royal Free Hospital School of Medicine, London NW3 2QG, UK

Patrick C. Kung & Gideon Goldstein

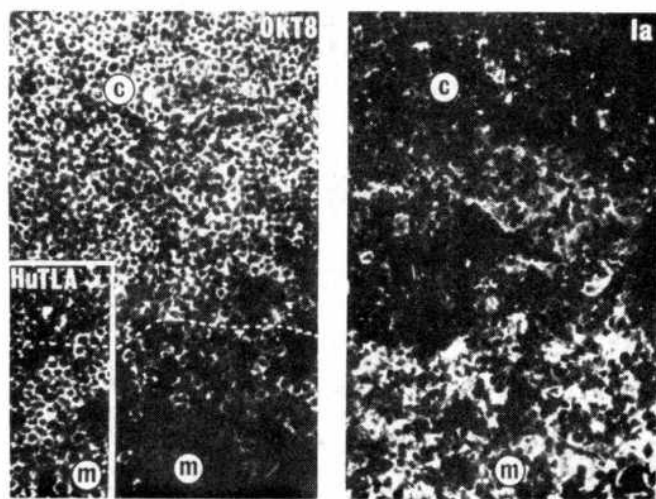
Ortho Pharmaceutical Corporation, Division of Immunobiology, Raritan, New Jersey 08869

Distinct subsets of human peripheral T-cell populations have recently been characterized using mouse monoclonal antibodies and conventional hetero-antisera in functional tests *in vitro*<sup>1-6</sup>. 'Inducer' or 'helper' T cells have been shown to react with a monoclonal antibody termed OKT4. These OKT4<sup>+</sup> cells respond to soluble antigens<sup>3</sup>, help B-lymphocyte differentiation into plasma cells in pokeweed mitogen stimulated cultures<sup>4</sup> and assist the development of cytotoxic T cells in mixed lymphocyte cultures (MLC)<sup>5</sup>. In contrast, the 'suppressor-cytotoxic' T-cell subset is recognized by the monoclonal antibodies OKT5<sup>5</sup> and OKT8<sup>6</sup>. The same subset can also be labelled with a conventional horse antiserum which (after extensive absorption) recognizes TH<sub>2</sub> antigen<sup>5,7</sup>. These OKT8<sup>+</sup>, TH<sub>2</sub><sup>+</sup> cells fail to respond optimally to soluble antigen<sup>3</sup> but contain the concanavalin-A induced suppressor cell population<sup>5,7</sup> and the cells which develop cytotoxic activity in mixed lymphocyte reaction (MLR)-induced cell-mediated lympholysis<sup>3</sup>. The physiological role, tissue distribution and recirculation patterns of 'inducer' and 'suppressor' T cells are unknown, although changes in the proportion and activity of blood-borne T-cell subsets have been observed in various immunoregulatory disorders<sup>8,9</sup>. We have therefore now analysed the distribution of these T-cell subsets in the lymphohaematopoietic organs and the gut. OKT4<sup>+</sup>, OKT8<sup>+</sup> cells of inducer type predominate in the thymic medulla, blood and T-cell traffic areas such as tonsillar paracortex and intestinal lamina propria. OKT4<sup>+</sup>, OKT8<sup>+</sup> cells of suppressor-cytotoxic type, on the other hand, constitute the larger part of T-cell population in normal human bone marrow and gut epithelium. Furthermore, a close micro-anatomical relation can be seen between the OKT4<sup>+</sup>, OKT8<sup>+</sup> T cells and non-lymphoid cells expressing large amounts of Ia-like (p 28, 33) antigens, for example, interdigitating (ID) cells and Ia<sup>+</sup> macrophages, suggesting that Ia-like antigens may play a part in the local regulation of inducer T cell activity. Thus the T-cell subsets which have been shown to have different functions *in vitro* seem also to have different patterns of tissue distribution, implying different immunological functions *in vivo*.

The principle of the study was to apply well characterized antibodies from different species in various combinations using second layer antibodies coupled with different fluorochromes (fluorescein-isothiocyanate FITC: green and tetramethylrhodamine isothiocyanate TRITC: red) in order to determine whether the antibodies detect identical, overlapping or distinct populations. Table 1 shows the distribution of OKT4<sup>+</sup> and OKT8<sup>+</sup>, TH<sub>2</sub><sup>+</sup> T lymphoid cells analysed in cell suspensions. Preliminary experiments showed that all three reagents (OKT4, OKT8 and anti-TH<sub>2</sub>) reacted exclusively with T-lymphoid cells which were identified with a rabbit antiserum reacting to human T-lymphocyte antigen (HuTLA<sup>+</sup>; Table 1). These findings confirmed that the antibodies were T-lineage markers<sup>1-6,10</sup>. Furthermore, the OKT8 and anti-TH<sub>2</sub> antibodies labelled the same populations (>98% double-labelled cells). Thus these two reagents were used interchangeably in this study.

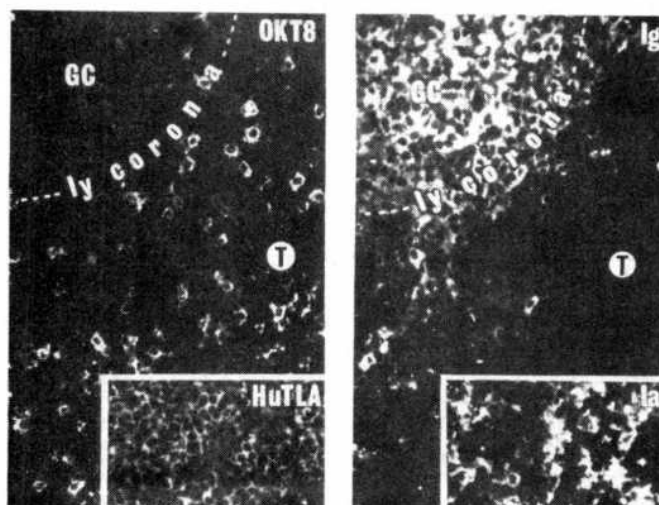


In the human thymus 78% of all cells were OKT4<sup>+</sup>, TH<sub>2</sub><sup>+</sup> (see also refs 1–6). The majority (80%) of these double-labelled cells expressed nuclear terminal deoxynucleotidyl transferase (TdT), a marker of cortical thymocytes<sup>11</sup>. 20% of the OKT4<sup>+</sup>, TH<sub>2</sub><sup>+</sup> population was TdT<sup>+</sup>.



**Fig. 1** Cells in the human thymic cortex (c) and medulla (m) reacting with antisera to OKT8 (OKT8, a mouse monoclonal antibody), to human thymocyte/T-cell antigen (HuTLA; a rabbit antiserum) and to Ia-like p 28, 33 antigen (Ia; a chicken antiserum detecting core determinants of p 28, 33)<sup>11,12</sup>. Sections of frozen tissue biopsies from infant thymus were fixed for 10 min in ethanol and washed in saline<sup>11</sup>. OKT8 (1:100 dilution) and chicken anti-Ia-like antiserum (1:40) were added, incubated for 30 min at room temperature and washed for 30 min. Goat anti-mouse Ig-FITC (affinity purified antibody; 0.5 mg ml<sup>-1</sup>) and sheep anti-chicken Ig-TRITC (1:20 dilution) were added for 30 min and washed again. The same areas were photographed with filters for FITC (OKT8) and TRITC (Ia). The broken line indicates the cortico-medullary boundary. Insert shows the same area photographed in an adjacent section. This had been incubated with anti-HuTLA (1:20 dilution), washed and stained with goat anti-rabbit Ig-FITC (1:40 dilution). OKT8 reacts with virtually all cortical thymocytes and 20% of medullary thymocytes. Anti-HuTLA detects all thymocytes. Anti-Ia stains cortical epithelial cells strongly and large medullary cells corresponding to interdigitating cells (ID) very strongly.  $\times 200$ .

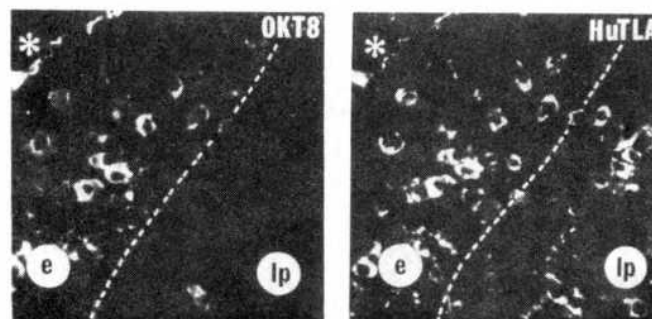
Within the population of thymic cells with only a single label (putative thymic medullary lymphocytes; see below), the OKT4<sup>+</sup>, TH<sub>2</sub><sup>+</sup> cells were more frequent (76%) than the OKT4<sup>+</sup>, TH<sub>1</sub><sup>+</sup> cells (24%). Previous studies<sup>1–6</sup> suggested that the majority of T cells in peripheral human blood are either OKT4<sup>+</sup>, TH<sub>2</sub><sup>+</sup> or OKT4<sup>+</sup>, TH<sub>1</sub><sup>+</sup>, although the existence of a few double-labelled cells has not been formally excluded. Our study has extended these previous findings (Table 1). The calculated proportions of OKT4<sup>+</sup>, TH<sub>2</sub><sup>+</sup> cells (inducer phenotype) within the HuTLA<sup>+</sup> T-lymphoid population were 66% in blood, 64% in tonsil and 13% in bone marrow from children. In contrast, the proportions of OKT4<sup>+</sup>, TH<sub>1</sub><sup>+</sup> cells (suppressor-cytotoxic phenotype) were 27% in blood, 20% in tonsil and 82% in bone marrow. A small number of double-labelled OKT4<sup>+</sup>, TH<sub>2</sub><sup>+</sup> lymphocytes were found in the periphery—2.6% of blood T cells and 6.5% of tonsil T cells. (These cells could have been immature T cells but they failed to express cortical thymocyte markers such as TdT and reactivity with monoclonal antibody to cortical thymocyte antigen, HTA-1<sup>11,12</sup>.) Thus the definition of 'inducer' and 'suppressor-cytotoxic' T subsets with the available reagents in man seems to be more convenient and distinct than the definition of corresponding cell types in the mouse where large proportions (20–50%) of peripheral T cells simultaneously express 'inducer' (Ly-1) and 'suppressor' (Ly-2,3) markers<sup>14,15</sup>.



**Fig. 2** Cells in the human tonsil reacting with antisera to OKT8 (OKT8), to immunoglobulin (Ig), to human T-cell/thymocyte antigen (HuTLA) and to Ia-like p 28, 33 antigen (Ia). GC, germinal centre, containing lacy deposits of immunoglobulin; ly corona, lymphocyte corona containing Ig<sup>+</sup> B lymphocytes; T, paracortical area with T cells which are HuTLA<sup>+</sup> (see insert); only 20% of these T cells react with OKT8. In this area large ID cells stain brightly for Ia (see insert). The reagent combinations were OKT8 (FITC) together with goat anti-human IgM (TRITC; a purified antibody used at 0.5  $\mu$ g ml<sup>-1</sup>), and HuTLA (FITC) with Ia (TRITC). The same areas were photographed with selective filters.  $\times 200$ .

An immunohistological analysis of T-cell subsets was performed using OKT8 antibody with an affinity purified goat anti-mouse Ig-FITC. Bright membrane staining was obtained on a subset of lymphoid cells in sections of frozen biopsies. The OKT8 antibody could also be used in double-marker combinations with rabbit anti-HuTLA antiserum and other reagents (Figs 1–3). Since the OKT4 antibody showed only weak staining in tissue sections of peripheral lymphoid organs, T-cell subsets of 'inducer' and 'suppressor-cytotoxic' type were defined as HuTLA<sup>+</sup>, OKT8<sup>+</sup> and HuTLA<sup>+</sup>, OKT8<sup>+</sup>, respectively.

In the thymic medulla, 60–75% of HuTLA<sup>+</sup> cells were OKT8<sup>+</sup> (Fig. 1). This is consistent with the cell suspension analysis discussed earlier (Table 1), indicating that the majority of mature thymic medullary lymphocytes express the 'inducer' phenotype. Note that some of the medullary OKT8<sup>+</sup> cells may be recent arrivals from the cortex which express TdT and cortical thymocyte antigen HTA-1<sup>11</sup>. These cells, which represent 6–15% of the medullary cell population, may not have



**Fig. 3** Cells in the human jejunum reacting with antisera to OKT8 (OKT8) and to human T-cell/thymocyte antigen (HuTLA). e, Epithelium; lp, lamina propria. (\*) intestinal lumen. Most intra-epithelial lymphocytes are double-stained for HuTLA and OKT8 ('suppressor-cytotoxic' phenotype). In the lamina propria many T cells are HuTLA<sup>+</sup>, OKT8<sup>+</sup> ('inducer' phenotype).  $\times 220$ .



**Table 1** Distribution of T lymphoid cells expressing the inducer (OKT4<sup>+</sup>, TH<sub>2</sub><sup>+</sup>, OKT8<sup>-</sup>) and 'suppressor-cytotoxic' (OKT4<sup>-</sup>, TH<sub>2</sub><sup>-</sup>, OKT8<sup>+</sup>) phenotypes

|                   | No. of cases | % Labelled with rabbit anti-HuTLA* | % Of cells labelled with mouse OKT4 and horse anti-TH <sub>2</sub> (SUP) antibodies |                        |                                   |   | % Labelled with mouse OKT8† |
|-------------------|--------------|------------------------------------|---|------------------------|-----------------------------------|---|-----------------------------|
|                   |              |                                    | All cells labelled‡   | OKT4 <sup>+</sup> only | TH <sub>2</sub> <sup>+</sup> only | OKT4 <sup>+</sup> , TH <sub>2</sub> <sup>+</sup> double |                             |
| Thymus            | 5            | 96 ± 2.1                           | 89 ± 0.8  | 8.5 ± 0.9              | 2.7 ± 0.5                         | 78 ± 3.7  | 80                          |
| Peripheral blood¶ | 7            | 75 ± 3.3                           | 72 ± 3.1  | 50 ± 1.9               | 20 ± 1.5                          | 2.0 ± 0.4   | 23                          |
| Tonsil*           | 4            | 60 ± 5.6                           | 55 ± 5.1  | 39 ± 1.8               | 12 ± 2.3                          | 3.9 ± 1.3   | 17                          |
| Bone marrow**     | 6            | 4.5 ± 0.9                          | 4.4 ± 0.2   | 0.6                    | 3.7 ± 0.2                         | 0.1   | 5                           |

10<sup>6</sup> cells in 50 µl buffered saline were incubated with conventional antisera (1:20 dilution) and monoclonal antibodies (peritoneal exudate; 1:200 to 1:500 dilution), washed twice and reincubated with goat anti-mouse-Ig-TRITC and goat anti-rabbit or horse Ig-FITC (1:20 dilution), followed by washing and counting the labelled cells under a fluorescence microscope.

\* A rabbit antiserum reacting with human thymocytes/T cells was made against monkey thymocytes and extensively absorbed (with human red cells, liver powder, chronic lymphoid leukaemia and lymphoid cell lines of B type and acute myeloid leukaemia; ref. 12). The second layer used (goat anti-rabbit-Ig) was conjugated to FITC. The horse anti-HuTLA prepared from an anti-human thymocyte globulin (ATGAM; Upjohn, Lot 17.923) with similar absorptions gave identical results. Values are mean ± s.e.m.

† These percentages are consistently lower than the proportion of HuTLA<sup>+</sup> cells in the same sample. The HuTLA<sup>+</sup>, OKT4<sup>+</sup>, TH<sub>2</sub><sup>+</sup> cells appear to be larger blasts in the thymus (prothymocytes? see refs 6, 11, 13) and small lymphocytes of unknown function in the blood and tonsils.

‡ Horse anti-TH<sub>2</sub> serum was prepared from horse anti-HuTLA serum at the Royal Free Hospital by further absorption with OKT4<sup>+</sup> leukaemic lymphocytes obtained from a patient with chronic lymphocytic leukaemia of T-cell type. This reagent gave identical results to the control horse anti-TH<sub>2</sub> reagent (see ref. 7).

§ Similar double-labelling experiments using anti-TH<sub>2</sub> and OKT8 showed that these two reagents reacted with an identical population of cells; >98% of labelled cells in thymus, blood and tonsil were reactive with both antisera.

|| Infant thymus cell suspensions from patients undergoing elective cardiac surgery.

¶ Normal donors of 30–42 years of age.

\* The donors (10–15 yr) had tonsillitis in the past. The tonsillectomy was performed after antibiotic treatment.

\*\* From children (5–15 yr). No haematological abnormality.

yet matured into OKT8<sup>-</sup> lymphocytes. There was an abundance in the medulla of non-lymphoid cells which strongly expressed Ia-like (p 28, 33) antigens. Some of these could be Ia<sup>+</sup> epithelial cells which were also present in the cortex. Nevertheless the most brightly stained population appeared to be a group of interdigitating (ID) cells with prominent veils and processes<sup>11,16</sup>. These Ia<sup>+</sup> cells could also be detected in the interlobular septae and may have been migrating cells (Fig. 4 and refs 11, 17).

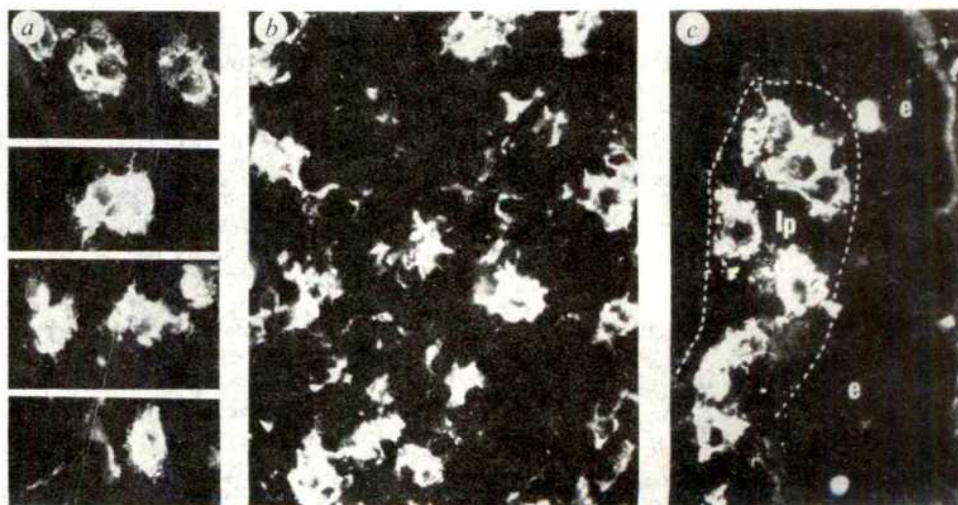
In serial sections of tonsil the germinal centres (which contained lacy deposits of immunoglobulin complexes surrounded by a B-lymphocyte corona) and paracortical T-cell areas were identified (Fig. 2). In the B-lymphocyte corona less than 5% of cells were HuTLA<sup>+</sup>. This small T-lymphocyte population contained both OKT8<sup>+</sup> and OKT8<sup>-</sup> cells. In the paracortical areas 70–80% of HuTLA<sup>+</sup> cells were OKT8<sup>-</sup> and 20–30% were OKT8<sup>+</sup>. In these areas large ID cells expressed Ia-like antigens very strongly (Figs 2 and 4; see also refs 18–20). It appeared that the Ia<sup>+</sup> ID cells were preferentially surrounded by OKT8<sup>-</sup> T lymphocytes and tended to be apart from the OKT8<sup>+</sup> cells. Further studies will be needed to determine

whether isolated ID cells form rosettes with T lymphocytes of the 'inducer' or 'suppressor' phenotype.

Finally, histologically normal jejunal biopsies were studied from patients undergoing investigation of diarrhoea. In the lamina propria the HuTLA<sup>+</sup> population contained more OKT8<sup>-</sup> cells than OKT8<sup>+</sup> cells (65–75% OKT8<sup>-</sup> T cells in the three samples studied; Fig. 3). When adjacent sections were stained for Ia-like antigens, the abundant macrophages in the lamina propria stained very strongly for Ia-like antigens (Fig. 4) and resembled the light microscopic appearance of Ia<sup>+</sup> ID cells observed in tonsils or in the thymic medulla and septae. Furthermore, the intra-epithelial lymphocytes in human gut have recently been shown to be almost exclusively HuTLA<sup>+</sup> T lymphocytes<sup>21</sup>. In contrast to the T cells in the lamina propria, this intra-epithelial T-cell population consisted mainly of OKT8<sup>+</sup> cells (70–90% OKT8<sup>+</sup> cells within the HuTLA<sup>+</sup> population in the three samples analysed).

The observations outlined above are compatible with the view that subsets of peripheral T lymphocytes develop from immature OKT4<sup>+</sup>, OKT8<sup>+</sup> thymocytes through a series of

**Fig. 4** Interdigitating (ID) cells and macrophages in the human thymus (a), tonsil (b) and gut (c). All three preparations are sections from frozen biopsies stained for human Ia-like (p28, 33) antigen with chicken-anti-Ia-like serum (1:40) followed by sheep anti-chicken Ig-TRITC (1:20). a, Areas of interlobular septae contain ID cells (migrating cells?) which resemble circulating lymph-borne veiled cells<sup>28</sup>. The cells exhibit characteristic strongly Ia<sup>+</sup> 'veils' and 'whiskers'. Similar cells are seen around the cortico-medullary junction within the thymus (see Fig. 1). b, A paracortical area from tonsil. The Ia<sup>+</sup> ID cells again show extensive processes which surround the T lymphocytes (not stained, but see insert in Fig. 2). c, A jejunal villus with epithelium (e) very weakly stained for Ia-like antigen and lamina propria (lp) containing large macrophages with abundant Ia-like antigens. The staining patterns suggest that the expression of Ia-like antigens might be cytoplasmic in many of these cells. ×315.





differentiation steps<sup>6,13</sup>. The preponderance of OKT8<sup>+</sup> T cells in the bone marrow suggests that T cells are normal inhabitants of this tissue with a definite physiological role (suppression of immunoglobulin synthesis?) rather than representing contaminating blood-borne T cells.

Intriguingly, while the OKT8<sup>+</sup> subset shows 'affinity' to the gut epithelium which expresses Ia-like antigens poorly, the lymphoid microenvironments (thymic medulla, paracortex, lamina propria) which contain high proportions of 'inducer' T cells exhibit large numbers of Ia<sup>+</sup> non-lymphoid cells. These stain more brightly for Ia-like antigens than B lymphocytes, dendritic cells in the germinal centres or sinus histiocytes<sup>20</sup>. In the literature these cells are variably referred to as ID cells<sup>15-19,22,23</sup>, cells of the cortico-medullary junction<sup>24</sup> or macrophages of the lamina propria<sup>21,25</sup>. Further immuno-electron microscope studies are needed to determine the ultrastructural characteristics, lineage derivation (from marrow precursors? see ref. 26) and cytoplasmic Ia-content (secretion or shedding of Ia?) of this apparently migratory Ia<sup>+</sup> population. It is already known that at least a proportion of ID cells contain Birbeck granules and are related to skin Langerhans cells<sup>23,27</sup> and circulating 'veiled' cells in the lymph<sup>27,28</sup>. These cells all express large amounts of Ia-like antigens<sup>28-30</sup>. The full characterization of this strongly Ia<sup>+</sup> ancillary system for 'inducer' T lymphocytes throughout the body is important since Langerhans cells have already been shown to play a part in transporting foreign antigens from skin to the regional lymph nodes and to 'present' these antigens to T cells<sup>28,29,31</sup>. A similar role could be postulated for the lamina propria macrophages, the 'Cinderella' cells of the gastrointestinal system<sup>25</sup>.

It is also known that 'inducer' T cells see foreign antigens in the context of Ia antigen (in the mouse)<sup>32</sup> or Ia-like HLA-DR antigens (in man)<sup>33</sup> according to the previous thymic education of these cells<sup>32</sup>. In both species, thymic cortical epithelial cells as well as medullary ID cells express large quantities of Ia or Ia-like antigens<sup>11,34</sup>. The close anatomical relation of 'inducer' T cells and Ia<sup>+</sup> cells in the tonsil and gut further suggests that this physiological control of T-cell recognition is maintained in the peripheral lymphoid tissues.

The use of well characterized monoclonal antibodies to T-cell subsets in studies of both cell suspensions and tissue sections of biopsies taken from patients with viral infections, immunoregulatory ('autoimmune') disorders and graft-versus-host disease may well contribute to the understanding of virus control and disease development<sup>7,8,35</sup>.

We thank Dr F. J. Bollum for anti-TdT antibody and Professor S. F. Schlossman for a sample of anti-TH<sub>2</sub> antiserum. Human thymus and bone marrow samples were provided by Mrs L. Layward and Dr N. Rapson of the Institute of Child Health and Dr H. G. Prentice of the Royal Free Hospital, London. Gut biopsies were obtained in collaboration with Dr D. Jewell, Royal Free Hospital, London. W.S.S. was supported by the Coppleson Postgraduate Medical Foundation.

Received 20 June; accepted 16 September 1980.

- Kung, P. C., Goldstein, G., Reinherz, E. L. & Schlossman, S. F. *Science* **206**, 347-349 (1979).
- Reinherz, E. L., Strelkaskas, A. J., O'Brien, C. & Schlossman, S. F. *J. Immun.* **123**, 83-86 (1979).
- Reinherz, E. L., Kung, P. C., Goldstein, G. & Schlossman, S. F. *Proc. natn. Acad. Sci. U.S.A.* **76**, 4061-4065 (1979).
- Reinherz, E. L., Kung, P. C., Goldstein, G. & Schlossman, S. F. *J. Immun.* **123**, 2894-2896 (1979).
- Reinherz, E. L., Kung, P. C., Goldstein, G. & Schlossman, S. F. *J. Immun.* **124**, 1301-1307 (1980).
- Reinherz, E. L. *et al. Proc. natn. Acad. Sci. U.S.A.* **77**, 1588-1592 (1980).
- Reinherz, E. L. & Schlossman, S. F. *J. Immun.* **122**, 1335-1341 (1979).
- Reinherz, E. L. *et al. New Engl. J. Med.* **300**, 1061-1068 (1979).
- Reinherz, E. L. *et al. New Engl. J. Med.* **301**, 1018-1022 (1979).
- Tidman, N. *et al.* (in preparation).
- Janosy, G. *et al. J. Immun.* **125**, 202-212 (1980).
- Janosy, G. *et al. J. Immun.* **123**, 1525-1529 (1979).
- Bradstock, K. F. *et al. J. natn. Cancer Inst.* **65**, 33-42 (1980).
- Cantor, H. & Boyce, E. *Contemp. Topics Immunobiol.* **7**, 47-62 (1977).
- Simon, M. M. & Abenhardt, B. *Eur. J. Immun.* **10**, 334-341 (1980).
- Kaiserling, E., Stein, H. & Muller-Hermelink, H. K. *Cell. Tissue Res.* **155**, 47-55 (1974).
- Gaudecker, B. von & Muller-Hermelink, H. K. *Adv. exp. med. Biol.* **114**, 19-22 (1979).
- Heusermann, U., Stutte, H. J. & Muller-Hermelink, H. K. *Cell Tissue Res.* **153**, 415-417 (1974).

- Kaiserling, E. & Lennert, K. *Virchows Arch. Cell Path.* **16**, 51-61 (1974).
- Lampert, I. A., Pizzolo, G., Thomas, J. A. & Janosy, G. *J. Path.* **131**, 145-156 (1980).
- Selby, W., Janosy, G. & Jewell, D. *Gut* (in the press).
- Veerman, A. J. P. *Cell Tissue Res.* **148**, 247-251 (1974).
- Hoefmit, Ch. M. *et al. in Structure and Morphology of the Reticuloendothelial System* (ed. Curr, E.) 417-468 (Plenum, New York, 1980).
- Olah, I., Röhlick, P. & Törö, I. *Ultrastructure of Lymphoid Organs* (Lippincott, Philadelphia, 1975).
- LeFevre, M. E., Hammer, R. & Joel, D. D. *J. reticuloend. Soc.* **26**, 553 (1979).
- Katz, S. I., Tamaki, K. & Sachs, D. H. *Nature*, **282**, 324-326 (1979).
- Kelly, R. H., Balfour, B. M., Armstrong, J. A. & Griffiths, S. *Anat. Rec.* **190**, 5-22 (1978).
- Spry, C. J. F., Pflug, J., Janosy, G. & Humphrey, J. H. *Clin. exp. Immun.* **39**, 750-754 (1980).
- Stingl, G. *et al. J. invest. Derm.* **71**, 59-64 (1978).
- Rowden, G., Lewis, M. G. & Sullivan, A. K. *Nature* **268**, 247-248 (1977).
- Silberberg Sinakin, I. *et al. Cell. Immun.* **25**, 137-151 (1976).
- Zinkernagel, R. M. *et al. J. exp. Med.* **147**, 882-896 (1978).
- Thorsby, E. *et al. Transplant Proc.* **9**, 393-399 (1977).
- Rouse, R. V., van Ewijk, W., Jones, P. P. & Weissman, I. L. *J. Immun.* **122**, 2508-2515 (1979).
- Janosy, G. *et al. Br. J. Cancer* **42**, 1-20 (1980).

## Different postsynaptic events in two types of retinal bipolar cell

Jonathan F. Ashmore & David R. Copenhagen

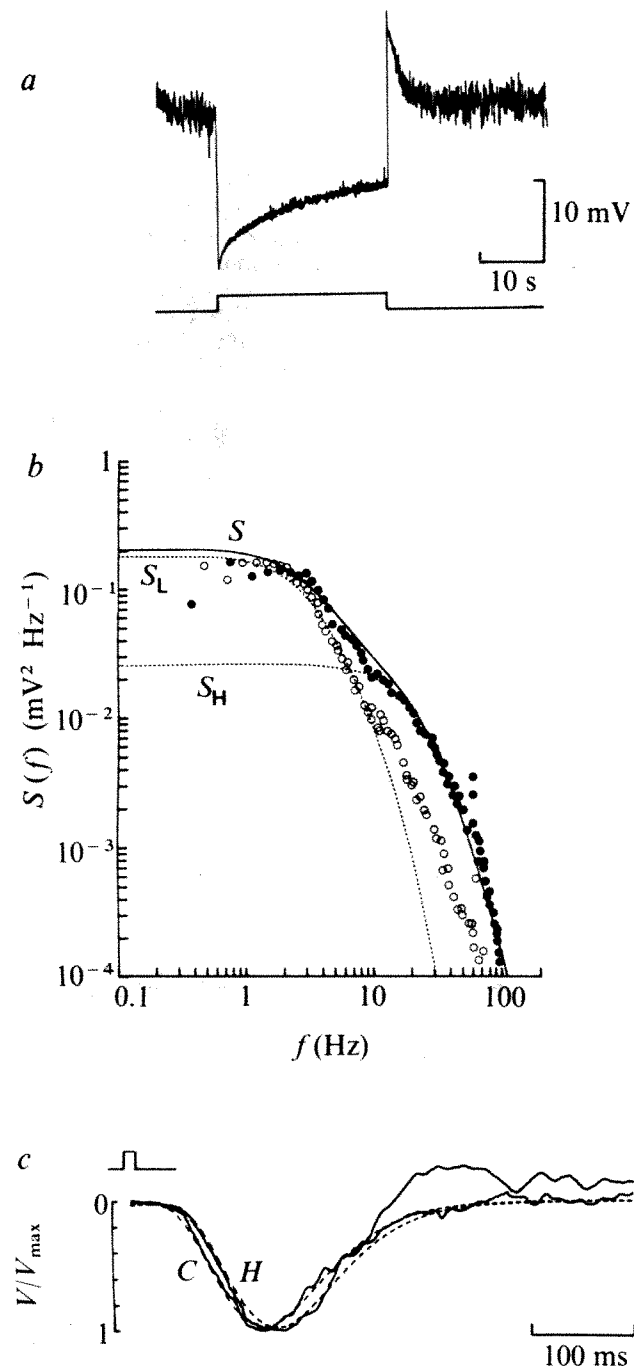
Departments of Ophthalmology and Physiology, University of California, San Francisco, California 94143

The first synapse in the vertebrate visual system is made between the photoreceptors and the bipolar cells. Bipolar cells fall into two distinct classes according to whether the cell hyperpolarizes or depolarizes to small centred spots of light. Most evidence indicates that the light-induced hyperpolarization of the photoreceptors suppresses transmitter release from the synaptic terminals<sup>1-3</sup>, and it is probable that the differences between the two bipolar cell classes results from the different actions of the photoreceptor transmitter<sup>4</sup>. In analysing the membrane potential fluctuations in both types of bipolar cell we find that the voltage noise spectra differ. It is to be expected that postsynaptic noise would be composed of the sum of noise generated in and transmitted from the cones<sup>5,6</sup> and the noise arising from the statistical nature of synaptic transmission. We report here evidence for two such components in the voltage noise spectra recorded from each type of bipolar cell. The differences in the frequency distribution of the presumed transmitter-related components indicates that the transmitter generates events of longer duration in the depolarizing bipolar cells.

Eyecup preparations from the snapping turtle (*Chelydra serpentina*) were mounted in a chamber through which moist oxygen flowed and such that small spots of light could be focused on the impaled cell<sup>7</sup>. Bipolar cells were recorded at depths of 120-180  $\mu$ m distal to the vitreal surface of the retina. A sample of studied cells were stained with either Procion yellow or Lucifer<sup>8</sup> and all positively identified as bipolar cells. Although a rod input may be demonstrated in certain cells, we have investigated the red cone input only<sup>9</sup>. The stimulus was a 100  $\mu$ m spot of 650 nm light centred on the impaled cell.

In hyperpolarizing bipolar cells, steps of light reduced potential fluctuations<sup>10</sup> (Fig. 1a). The total noise variance decreased 27-fold for this cell, from 1.1 mV<sup>2</sup> in the dark to 0.04 mV<sup>2</sup> in bright light. This reduction appears to reflect primarily the cutoff of the cone transmitter and cannot be attributed to a potential-dependent membrane resistance decrease since we find that the hyperpolarization is associated with an increase in cell input resistance. In addition, we find that hyperpolarization of the cell to the light evoked levels by extrinsic current does not suppress the noise in the dark.

The potential fluctuations were Fourier analysed to obtain a difference spectrum between the spectra in the dark and in the light. The difference spectra were found to have the same form at all light levels, the effects of illumination being to rescale their amplitude. A difference spectrum between dark and bright light



**Fig. 1** Voltage noise in hyperpolarizing bipolar cells. *a*, Response of a cell to a 100- $\mu\text{m}$  spot of 650-nm light with an intensity of  $9.85 \times 10^4$  photons  $\mu\text{m}^{-2} \text{s}^{-1}$ . Maximum response to flashes; 21 mV. *b*, Difference spectrum (dark – bright) of the voltage noise for the hyperpolarizing bipolar cell (●) and a cone (○). The cone spectrum has been multiplied by a factor of 26 for normalization. The records were filtered at 100 Hz, and sampled at 400 Hz (bipolar cells) or 500 Hz (cones) for processing using a 1,024-point FFT program. The spectrum is frequency smoothed. The extracellular electrode noise variance was less than 0.01  $\text{mV}^2$ . The continuous curve *S*, is the sum of the two functions shown as dotted curves<sup>10</sup>. *S<sub>H</sub>* is proportional to the modulus squared of the Fourier transform of equation (1) with  $T = 5.9$  ms; *S<sub>L</sub>* is the product of *S<sub>H</sub>* and two lorentzian functions with time constants 54.9, 9.2 ms required to fit the cone spectrum<sup>6</sup>. The ratio of the variances associated with the components *S<sub>L</sub>*:*S<sub>H</sub>* is, by numerical computation, 1.57:1. *c*, Signal-averaged and normalized responses of a cone and hyperpolarizing bipolar cell, both cells within their linear ranges. The dotted lines are *C*, seven-stage low-pass filter model with time constant per stage = 20 ms (ref. 5), and *H*, the function after passing through a filter given by equation (1) with  $T = 5.9$  ms. The difference in times to peak is 13 ms.

is shown in Fig. 1*b* and falls off asymptotically as  $1/f^4$  with more power at high frequencies than found in cones<sup>6</sup>. In some cells there was a very pronounced inflection at around 10 Hz and, unlike the voltage noise spectrum recorded in cones, the spectrum could not be fitted by the simple product of lorentzian functions<sup>6</sup>. Instead, the following model leads to a fit of the noise difference spectrum as a sum of two components, *S<sub>L</sub>* and *S<sub>H</sub>*. The release of transmitter from the cones and its postsynaptic action may be considered to be a shot process, and will result post-synaptically in a noise spectrum *S<sub>H</sub>*(*f*) (ref. 11). If the rate of transmitter release were a linear function of the presynaptic cone membrane potential, with fluctuations described by a spectrum *S<sub>C</sub>*(*f*) (ref. 6), it can be shown that there will be an additional term *S<sub>L</sub>*(*f*) = constant  $\times S_C(f) \times S_H(f)$  present in the spectrum of the postsynaptic fluctuations (compare ref. 11, equation 2.6–11). The term *S<sub>L</sub>*(*f*) will have power restricted to lower frequencies than *S<sub>H</sub>*(*f*) and arises because the synapse acts to filter the noise transmitted from the cones.

The simplest unitary event sufficient to describe the component *S<sub>H</sub>* has the form  $\alpha(t)$  given by

$$\alpha(t) = (\alpha/T) \exp(-t/T + 1) \quad (1)$$

where  $\alpha$  is the amplitude, *T* the time to peak, is 5.9 ms and the event halfwidth is 14.5 ms. The spectrum associated with the event given by equation (1) is then

$$S_H(f) = \frac{S_H(0)}{(1 + 4\pi^2 T^2 f^2)^2} \quad (2)$$

$\alpha(t)$  is formally equivalent to the impulse response of a two-stage low pass filter<sup>12</sup>, where both stages have the time constant *T*. One stage of this filter most probably represents the membrane time constant,  $\tau$ . In a sample of nine cells we found  $\tau = 9.2 \pm 5.0$  ms (mean  $\pm$  s.d.). Hence, the likely duration of transmitter action corresponding to the second filter stage, would be no greater than 6 ms.

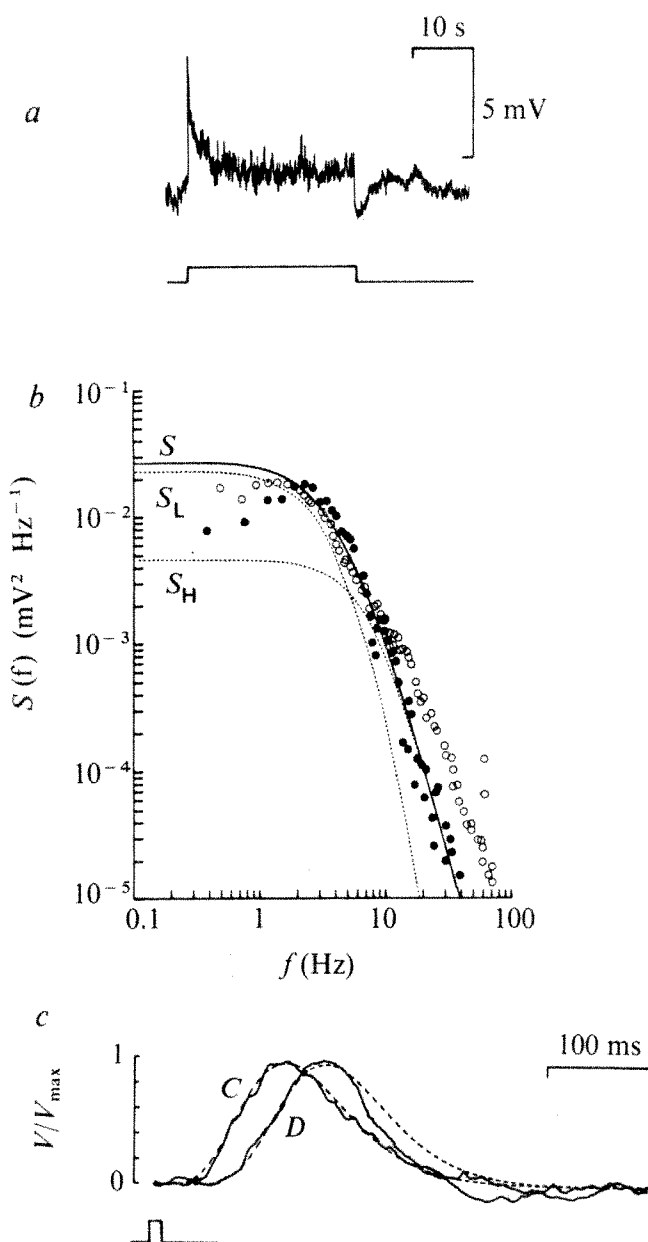
Equation (1) also describes the effective filter representing the cone–bipolar synapse. Figure 1*c* shows that the response in the hyperpolarizing bipolar cell can be predicted by simply passing the cone response through this filter. The early phase of the bipolar response is predicted well, corresponding to frequencies in the spectrum above 1 Hz. The overshoot in the repolarization of the bipolar cell response can be ascribed to an additional differentiation occurring for frequencies below about 1 Hz, which is not included in this model. Such a differentiating stage has also been postulated in the retinal signal pathway from the photoreceptors to account for some of the properties of ganglion cell firing patterns in the turtle retina<sup>13</sup>.

A similar analysis of the fluctuations may be made for depolarizing bipolar cells. Dim lights usually, but not always, produced an increase in intracellularly recorded voltage noise. In the cell shown in Fig. 2, the noise variance increased from 0.055  $\text{mV}^2$  to 0.154  $\text{mV}^2$  for a 1.5-mV depolarization, with an accompanying cell input resistance decrease<sup>1</sup>. Further increase in the light intensity produced a noise suppression to a level close to that in the dark. The initial increase in noise might be expected if the postsynaptic action of transmitter were to block ionic channels<sup>1,4</sup> and if a majority of the channels were blocked in the dark<sup>10</sup>.

Figure 2*b* illustrates the difference spectrum of voltage noise between dim light and the dark. Although, in contrast to the hyperpolarizing bipolar cells, there was no clearly indicated inflection point in the noise spectra, it was found that the noise had a narrower bandwidth than for hyperpolarizing bipolar cells or cones. A decomposition of the voltage noise spectrum was obtained by considering the synaptic filtering required to produce the delay in the flash response (Fig. 2*c*). The observed delay can be obtained using equation (1) with  $T = 21$  ms as the synaptic filter, in which case the associated unitary voltage event would have a half duration of 49 ms. For the input time constant



of depolarizing bipolar cells, it was found that  $\tau = 7.2 \pm 3.5$  ms ( $n = 5$ ). The membrane time constant,  $S_H(f)$ , in the spectral decomposition (Fig. 2b) can be consistently interpreted as accounting for one stage of the filter if the duration of transmitter-activated conductance change is not less than 21 ms, corresponding to the other stage of the synaptic filter. Conversely, an upper bound for the duration of the event in the depolarizing bipolar cell can be obtained if the spectrum is fitted



**Fig. 2** Voltage noise in depolarizing bipolar cells. *a*, Response of a cell to a 100  $\mu\text{m}$  spot with an intensity of 1,380 photons  $\mu\text{m}^{-2} \text{s}^{-1}$ . Maximum response to flashes, 11 mV. *b*, Difference spectrum (dim - dark) of the voltage noise for the bipolar cell (●). Cone spectrum (○) as before, multiplied by 4.8 for normalization. The dotted curve  $S_H$  is obtained from equation (2) with  $T = 21$  ms.  $S_L$  is constructed as in the text. The ratio of the variances associated with the components  $S_L : S_H$  is computed to be 2.66 : 1 to provide the best fit to the data. *c*, Normalized linear range responses to a flash of light in a cone (inverted) and the bipolar cell with computed cone *C* and bipolar cell *D* responses. The difference in time to peak between the responses is 41 ms. The hyperpolarization during recovery of the bipolar cell indicates differentiation at this stage of synaptic processing.

by a single component of the form of equation (2), which would lead to an event with a half duration of 82 ms. Thus it appears by either analysis that the transmitter event in the hyperpolarizing bipolar cell may be much shorter than in the depolarizing bipolar cell.

The differences in the temporal properties of the synapses between the two cell types may indicate that each is specialized for a different role. By recording ganglion cell spikes elicited by current injection into cones differences in the latency between the on- and off-pathways to the ganglion cells have been described<sup>13</sup>. It is possible that this functional difference may be established at the level of the outer plexiform layer. The wider passband of the cone-hyperpolarizing bipolar cell synapse may be appropriate for signals in the photopic range when the response of the photoreceptors themselves speed up<sup>12</sup>.

However the narrower range of frequencies passed by the depolarizing bipolar cell synapse is matched closely to the temporal characteristics of the cell's response to a flash of light. Such an arrangement would be advantageous in the detection of light in the mesopic range.

We thank Drs Juan Korenbrot and Julie Schnapf for helpful comments on the manuscript. This work was supported by NIH grant EY-01869.

Received 7 April; accepted 20 August 1980.

1. Toyoda, J. *Vision Res.* **13**, 283-294 (1973).
2. Dowling, J. E. & Ripps, H. *Nature* **242**, 101-103 (1973).
3. Schachter, S., Holtzman, E. & Hood, D. J. *Cell Biol.* **70**, 178-192 (1976).
4. Ashmore, J. F. & Falk, G. *J. Physiol., Lond.* **300**, 115-150 (1980).
5. Ashmore, J. F. & Falk, G. *Nature* **270**, 69-71 (1977).
6. Lamb, T. D. & Simon, E. J. *J. Physiol., Lond.* **272**, 425-468 (1977).
7. Copenhagen, D. R. & Owen, W. G. *J. Physiol., Lond.* **259**, 251-282 (1976).
8. Stewart, W. *Cell* **14**, 741-759 (1978).
9. Richter, A. & Simon, E. J. *J. Physiol., Lond.* **248**, 317-334 (1975).
10. Simon, E. J., Lamb, T. D. & Hodgkin, A. L. *Nature* **256**, 661-662 (1975).
11. Rice, S. O. *Bell Syst. Tech. J.* **23**, 282-332 (1944).
12. Baylor, D. A. & Hodgkin, A. L. *J. Physiol., Lond.* **242**, 729-758 (1974).
13. Baylor, D. A. & Fettiplace, R. *J. Physiol., Lond.* **271**, 425-448 (1977).

## Somatostatin selectively inhibits noradrenaline release from hypothalamic neurones

M. Göthert

Institute of Pharmacology, University of Essen, Hufelandstr. 55, D-4300 Essen 1, FRG

Somatostatin is a hypothalamic peptide hormone which inhibits growth hormone release from the anterior pituitary<sup>1</sup>. However, biochemical and morphological investigations have revealed that somatostatin is located not only in the hypothalamus but also in other brain areas (for example the cerebral cortex) where it occurs and in nerve cell bodies and fibres<sup>2-5</sup> from which it can be released in a  $\text{Ca}^{2+}$ -dependent manner<sup>6</sup>. It has therefore been suggested that the neuropeptide may have functions in the central nervous system other than its effect on growth hormone release<sup>7</sup>; one possible action is that of a neuromodulator<sup>4,6</sup>. Therefore, hypothalamic and cerebral cortical slices of the rat were used to examine whether somatostatin modifies the electrically or  $\text{CaCl}_2$ -evoked release of tritiated monoamines from monoaminergic neurones. It is reported here that somatostatin inhibits  $^3\text{H}$ -noradrenaline release from the hypothalamus (but not from the cerebral cortex) but does not affect the release of  $^3\text{H}$ -dopamine and  $^3\text{H}$ -serotonin.

Slices of hypothalamus or occipital cortex (0.3 mm thick, diameters 2.0 and 3.0 mm, respectively) from male Wistar rats (200-300 g) were incubated for 60 min in physiological salt solution (of composition described in Fig. 1 legend) containing one of the following tritiated monoamines at a concentration of

0.1  $\mu\text{M}$ :  $^3\text{H}$ -(-)noradrenaline (21.3–25.4 Ci  $\text{mmol}^{-1}$ ),  $^3\text{H}$ -dopamine (32.6 Ci  $\text{mmol}^{-1}$ ) or  $^3\text{H}$ -serotonin (25 Ci  $\text{mmol}^{-1}$ ). In these conditions the tritiated monoamines are selectively taken up into noradrenergic, dopaminergic and serotonergic neurones of the slices, respectively.<sup>8–10</sup>

After incubation, the slices were superfused with either physiological salt solution or  $\text{Ca}^{2+}$ -free solution containing 25 mM  $\text{K}^+$  (isomolar replacement of  $\text{NaCl}$  by  $\text{KCl}$ ). Each slice was stimulated 40 and 90 min after the onset of superfusion ( $S_1$ ,  $S_2$ , duration 2 or 6 min; Fig. 1). Slices superfused with physiological salt solution were stimulated by an electrical field (13 mA; rectangular pulses) generated between two platinum ring electrodes, and slices superfused with  $\text{Ca}^{2+}$ -free,  $\text{K}^+$ -rich solution were stimulated by introduction of 0.65 mM  $\text{CaCl}_2$ . In the experiments with somatostatin, the peptide was present from 25 min before  $S_2$  until the end of the experiments. The radioactivity in the superfusates and slices was determined by liquid scintillation counting. All details of the methods used and the calculation of stimulated  $^3\text{H}$  overflow above basal efflux have been described previously.<sup>11,12</sup> The electrically or  $\text{CaCl}_2$ -evoked  $^3\text{H}$  overflow (for absolute values, see Table 1) from slices preincubated with a  $^3\text{H}$ -labelled monoamine mainly consists of the respective, nonmetabolized  $^3\text{H}$ -monoamine<sup>11–14</sup> which is released from the corresponding neurones.

Somatostatin at up to 1  $\mu\text{M}$  did not affect the basal efflux of  $^3\text{H}$ -noradrenaline,  $^3\text{H}$ -dopamine or  $^3\text{H}$ -serotonin. However, at

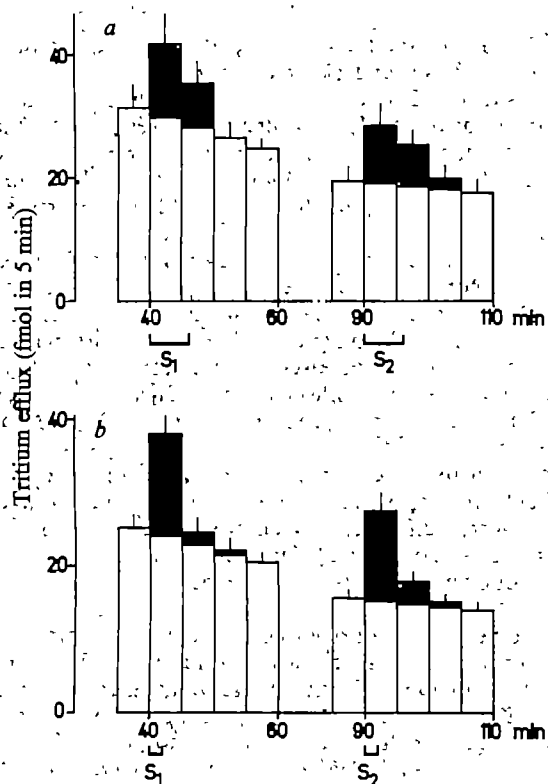
**Table 1** Stimulation-evoked tritium overflow above basal efflux from superfused rat brain slices preincubated with tritiated monoamines

| Slices preincubated with $^3\text{H}$ -noradrenaline |                  |                      |
|--|------------------|----------------------|
| Tissue<br>(mode of stimulation*)                     | Tritium overflow |                      |
|  | fmol             | % Of tissue tritium† |
| Hypothalamus (1 Hz)                                  | 17.9 $\pm$ 2.3   | 1.16 $\pm$ 0.16      |
| Hypothalamus (3 Hz)                                  | 15.9 $\pm$ 1.9   | 1.38 $\pm$ 0.24      |
| Hypothalamus ( $\text{CaCl}_2$ )                     | 8.6 $\pm$ 1.5    | 0.40 $\pm$ 0.03      |
| Cortex (3 Hz)  | 61.6 $\pm$ 10.1  | 4.35 $\pm$ 1.00      |
| Hypothalamic slices stimulated electrically (3 Hz)*  |                  |                      |
| Preincubation<br>with                                | Tritium overflow |                      |
|  | fmol             | % Of tissue tritium† |
| $^3\text{H}$ -dopamine                               | 15.7 $\pm$ 2.8   | 1.09 $\pm$ 0.18      |
| $^3\text{H}$ -serotonin                              | 32.6 $\pm$ 6.8   | 2.22 $\pm$ 0.44      |

All values represent tritium overflow evoked by the second period of stimulation ( $S_2$ ; 90 min after onset of superfusion; control experiments; means  $\pm$  s.e.m.;  $n = 5-7$ ).

\* Slices were stimulated either electrically (1 or 3 Hz, 360 pulses, 13 mA; superfusion with physiological salt solution) or by introduction of 0.65 mM  $\text{CaCl}_2$  for 6 min after superfusion with  $\text{Ca}^{2+}$ -free,  $\text{K}^+$ -rich solution containing 1  $\mu\text{M}$  tetrodotoxin.

† % of tissue tritium at the onset of the respective stimulation period.



**Fig. 1** Tritium efflux from rat hypothalamic slices preincubated with  $^3\text{H}$ -noradrenaline (means  $\pm$  s.e.m.). The slices were superfused with physiological salt solution of the following composition (mM):  $\text{NaCl}$  118,  $\text{KCl}$  4.8,  $\text{CaCl}_2$  1.3,  $\text{KH}_2\text{PO}_4$  1.2,  $\text{MgSO}_4$  1.2,  $\text{NaHCO}_3$  25, ascorbic acid 0.06, disodium-EDTA 0.03, glucose 10 (aeration with 95%  $\text{O}_2$  and 5%  $\text{CO}_2$ ; 37  $^{\circ}\text{C}$ ). The superfusate was collected in 5-min samples, and the radioactivity was measured by liquid scintillation counting. The slices were stimulated electrically with 360 pulses at frequencies of either 1 Hz (a;  $n = 7$ ) or 3 Hz (b;  $n = 7$ ). Two periods of stimulation were applied, 40 ( $S_1$ ) and 90 min ( $S_2$ ) after the onset of superfusion (duration of stimulation indicated by the horizontal bars). The stimulation-evoked  $^3\text{H}$  overflow above basal efflux is indicated by the shaded areas of the columns.

concentrations of 0.32 and 1.0  $\mu\text{M}$  the peptide inhibited electrically (3 Hz, 2 min) induced  $^3\text{H}$ -noradrenaline overflow from hypothalamic slices (Table 2). This inhibition was of a similar magnitude when the slices were stimulated at a frequency of 1 Hz for 6 min. Thus, in seven controls the ratio of  $^3\text{H}$  overflow evoked by  $S_2$  to that evoked by  $S_1$  ( $S_2/S_1$ ) was  $1.14 \pm 0.12$  (means  $\pm$  s.e.m.), whereas it was  $0.84 \pm 0.04$  ( $P < 0.05$ , Student's  $t$ -test;  $n = 7$ ) when 0.32  $\mu\text{M}$  somatostatin was present from 25 min before  $S_2$ . In contrast, the electrically (3 Hz) induced overflow of  $^3\text{H}$ -dopamine or  $^3\text{H}$ -serotonin from hypothalamic slices was not altered by somatostatin at up to 1  $\mu\text{M}$  (Table 2). Interestingly, the impulse-evoked  $^3\text{H}$ -noradrenaline overflow from cortical slices was also not inhibited by the peptide, although the experimental conditions were identical to those used in hypothalamic slices (see Fig. 1 legend; frequency of stimulation 3 Hz). Thus the ratio  $S_2/S_1$  was  $1.04 \pm 0.04$  ( $n = 5$ ) in control conditions, and  $0.96 \pm 0.06$  (no significant difference) in six experiments with 0.32  $\mu\text{M}$  somatostatin.

Because electrically evoked  $^3\text{H}$ -noradrenaline release from brain slices is  $\text{Ca}^{2+}$  dependent<sup>12</sup>, the inhibitory effect of somatostatin on impulse-evoked release from hypothalamic slices may be due to a decrease in the availability of  $\text{Ca}^{2+}$  ions for stimulus-release coupling. This hypothesis was tested by investigating the effect of somatostatin on  $^3\text{H}$ -noradrenaline

**Table 2** Effect of somatostatin on electrically evoked tritium overflow from superfused slices of rat hypothalamus preincubated with  $^3\text{H}$ -monoamines

| Somatostatin<br>( $\mu\text{M}$ ) | Tritium overflow ( $S_2/S_1$ )<br>after preincubation with |                        |                         |
|-----------------------------------|--|------------------------|-------------------------|
|                                   | $^3\text{H}$ -noradrenaline                                | $^3\text{H}$ -dopamine | $^3\text{H}$ -serotonin |
| 0                                 | 1.12 $\pm$ 0.07  | 1.05 $\pm$ 0.09        | 1.00 $\pm$ 0.04         |
| 0.1                               | 0.96 $\pm$ 0.03  | —                      | —                       |
| 0.32                              | 0.77 $\pm$ 0.03*   | 0.97 $\pm$ 0.05        | —                       |
| 1.0                               | 0.73 $\pm$ 0.08*   | 1.08 $\pm$ 0.13        | 0.99 $\pm$ 0.05         |

The slices were superfused with physiological salt solution. Tritium overflow was stimulated twice, after 40 ( $S_1$ ) and 90 min ( $S_2$ ) of superfusion (3 Hz, 2 min), and the ratio of the overflow (above basal  $^3\text{H}$  efflux; expressed as % of tissue tritium at the onset of stimulation) evoked by  $S_2$  and that evoked by  $S_1$  was determined ( $S_2/S_1$ ; means  $\pm$  s.e.m.;  $n = 5-7$ ). Somatostatin was present from 25 min before  $S_2$  until the end of the experiments.

\*  $P < 0.005$  (compared with the experiments without somatostatin).



release from hypothalamic slices evoked by the introduction of  $0.65 \text{ mM Ca}^{2+}$  after superfusion with  $\text{Ca}^{2+}$ -free solution containing  $25 \text{ mM K}^+$  and  $1 \mu\text{M}$  tetrodotoxin throughout the experiments. This  $\text{Ca}^{2+}$ -induced  $^3\text{H}$  overflow is due to  $\text{Ca}^{2+}$  influx into the noradrenergic fibres via the potential-sensitive permeability channel of the cell membrane<sup>11</sup>. In five control experiments, the ratio  $S_2/S_1$  was  $1.18 \pm 0.18$ , decreasing to  $0.63 \pm 0.14$  ( $n = 5$ ;  $P < 0.05$ ) when  $0.32 \mu\text{M}$  somatostatin was present from 25 min before  $S_2$  until the end of the experiments.

In conclusion, the present investigation revealed that somatostatin selectively inhibits the stimulated release of  $^3\text{H}$ -noradrenaline from noradrenergic nerve fibres of the hypothalamus, leaving that from cerebral cortex and also the release of  $^3\text{H}$ -dopamine and  $^3\text{H}$ -serotonin from hypothalamus unaffected. The terminal fibres of central noradrenergic neurones are known to possess various presynaptic

receptors<sup>12,15,16</sup> which modulate release by modifying  $\text{Ca}^{2+}$  influx via the potential-sensitive permeability channel<sup>17</sup>. Therefore, it is possible that presynaptic somatostatin receptors exist on the noradrenergic fibres of the hypothalamus. The presynaptic site of action seems likely, because the effect of somatostatin was also observed in the presence of tetrodotoxin (which inhibits the propagation of action potentials by decreasing the  $\text{Na}^+$  permeability of the cell membrane), thus excluding the possibility that interneurons are involved in this effect. Our experiments in which  $\text{Ca}^{2+}$  ions were used for stimulation revealed that the inhibition is probably due to a decrease in  $\text{Ca}^{2+}$  influx into the terminal noradrenergic fibres.

I thank Miss B. Giesen and Miss G. Werthmann for technical assistance and Serono for the gift of cyclic somatostatin. This study was supported by the Deutsche Forschungsgemeinschaft.

Received 14 July; accepted 18 August 1980.

1. Brazeau, P. *et al.* *Science* **179**, 77–79 (1973).
2. Brownstein, M., Arimura, A., Sato, H., Schally, A. V. & Kizer, J. S. *Endocrinology* **96**, 1456–1461 (1975).
3. Koyabashi, R. M., Brown, M. & Vale, W. *Brain Res.* **126**, 584–588 (1977).
4. Bennett-Clarke, C., Romagnano, M. A. & Joseph, S. A. *Brain Res.* **188**, 473–486 (1980).
5. Hökfelt, T., Johansson, O., Ljungdahl, Å., Lundberg, J. M. & Schultzberg, M. *Nature* **284**, 515–521 (1980).
6. Iversen, L. L. *et al.* *Nature* **273**, 161–163 (1978).
7. Olpe, H. R., Balcar, V. J., Bittiger, H., Rink, H. & Sieber, P. *Eur. J. Pharmac.* **63**, 127–133 (1980).

8. Farnebo, L. -O. *Z. Zellforsch.* **122**, 503–519 (1971).
9. Kuhar, M. J. *Life Sci.* **13**, 1623–1634 (1973).
10. Lidbrink, P. & Jonsson, G. *J. Neurochem.* **22**, 617–626 (1974).
11. Göthert, M. *Naunyn-Schmiedeberg's Archs Pharmac.* **307**, 29–37 (1979).
12. Taube, H. D., Starke, K. & Borowski, E. *Naunyn-Schmiedeberg's Archs Pharmac.* **299**, 123–141 (1977).
13. Perkins, N. A. & Westfall, T. C. *Neuroscience* **3**, 59–63 (1978).
14. Chase, T. N., Katz, R. I. & Kopin, I. J. *J. Neurochem.* **16**, 607–615 (1969).
15. Starke, K. *Rev. physiol. biochem. Pharmac.* **77**, 1–124 (1977).
16. Langer, S. Z. in *Catecholamines: Basic and Clinical Frontiers* Vol. 1 (eds Usdin, E., Kopin, I. J. & Barchas, J.) 387–398 (Pergamon, Oxford, 1979).
17. Göthert, M., Pohl, I. -M. & Wehking, E. *Naunyn-Schmiedeberg's Archs Pharmac.* **307**, 21–27 (1979).

## Met-enkephalin-Arg<sup>6</sup>-Phe<sup>7</sup>, present in high amounts in brain of rat, cattle and man, is an opioid agonist

Jean Rossier\*, Yves Audigier†, Nicholas Ling‡, Jean Cros† & Sidney Udenfriend§

\* Physiologie Nerveuse, CNRS, 91190 Gif-sur-Yvette, France

† Pharmacologie et Toxicologie, CNRS, Toulouse, France

‡ The Salk Institute, La Jolla, California 92138

§ The Roche Institute, Nutley, New Jersey

**The enkephalins Met-enkephalin and Leu-enkephalin were first isolated from porcine brain by Hughes and co-workers<sup>1</sup>. We have recently isolated from bovine adrenals another enkephalin with the structure Tyr-Gly-Gly-Phe-Met-Arg-Phe, or Met-enkephalin-Arg<sup>6</sup>-Phe<sup>7</sup> (ref. 2). We report here that this new heptapeptide is found in human, rat and bovine striatum in concentrations comparable with or greater than that of Leu-enkephalin. This molecule should not be considered as a mere precursor of Met-enkephalin. A pharmacological study indicates that this naturally occurring enkephalin has similar properties to the two enkephalins characterized earlier.**

To demonstrate the presence of this molecule in brain extracts, we used an HPLC system coupled with a new radioimmunoassay (RIA) which used an antiserum whose specificity is directed against the N-terminus (Tyr<sup>1</sup>-) of the enkephalins. This antiserum reacts as well with Leu-enkephalin as it does with Met-enkephalin. Molecules with a C-terminus deletion (des-Met, Met-enkephalin) or a C-terminus addition (Met-enkephalin-Arg<sup>6</sup>, Met-enkephalin-Lys<sup>6</sup> and Met-enkephalin-Arg<sup>6</sup>-Phe<sup>7</sup>) also react strongly with this serum (Fig. 1).

HPLC enables all the known enkephalin congeners to be separated in a single run. The system described in Table 1 uses an Ultrasphere octyl column eluted by a gradient of propanol. To detect minute amounts of enkephalins in the eluate we used the RIA described above, which has a sensitivity of 20 pg per tube. The broad specificity of this antiserum is an advantage in that all the characterized enkephalins can be quantified by the same assay.

Table 1 shows that in the striatum and in isolated chromaffin cells Met-enkephalin and Leu-enkephalin were not the only compounds detected by our RIA. We found compounds corresponding to oxidized Met-enkephalin, Met-enkephalin-Arg<sup>6</sup> and Met-enkephalin-Arg<sup>6</sup>-Phe<sup>7</sup>. Trace amounts of Leu-enkephalin-Arg<sup>6</sup> (retention time 24 min) and of oxidized Met-enkephalin-Arg<sup>6</sup>-Phe<sup>7</sup> (retention time 72 min) were also detected.

In all the species examined, Met-enkephalin was always the predominant compound. This contrasts with a report from Simantov and Snyder, who have claimed that in cattle, Leu-enkephalin is the predominant peptide<sup>3</sup>. To ensure that our relatively lower values for Leu-enkephalin were not due to our RIA procedure, we have confirmed these values with two other assays, a RIA specific for the C-terminus of Leu-enkephalin and a radioreceptor assay<sup>4,5</sup>.

Compared with values for Met-enkephalin, the amount of Met-enkephalin-Arg<sup>6</sup> was important in man and rat but not in cattle, a species difference which we cannot explain. This compound has also been isolated from porcine hypothalamus by another group who have called the molecule a pro-Met-enkephalin<sup>6</sup>.

The relative amount of oxidized Met-enkephalin was quite high in human and bovine extracts but not in the rat extracts. The possibility that the oxidation of Met-enkephalin had occurred after death or before or during the preparation of the extracts with 10% trichloroacetic acid, cannot be ruled out.

Met-enkephalin-Arg<sup>6</sup>-Phe<sup>7</sup> was found in high amounts in the three species examined. In rat and human striatal extracts the concentration was higher than that of Leu-enkephalin. This is seen particularly in the human extract, which contained four times more Met-enkephalin-Arg<sup>6</sup>-Phe<sup>7</sup> than Leu-enkephalin. This very high ratio of Met-enkephalin-Arg<sup>6</sup>-Phe<sup>7</sup> to Leu-enkephalin was also found in chromaffin cells isolated from the bovine adrenal medulla.

The presence of this compound in high amounts in all species examined raises some questions about its role in the brain. We have recently reported that this molecule has analgesic activity when administered intraventricularly to mice. On a molar basis, Met-enkephalin-Arg<sup>6</sup>-Phe<sup>7</sup>, with an ED<sub>50</sub> of 38.5 nmol per mouse, was 8 times more potent than Met-enkephalin in the tail flick test but 63 times less potent than morphine<sup>7</sup>. However, it

**Table 1** Enkephalin congeners in striatum of rat, cattle and man and in isolated chromaffin cells

| Retention time on HPLC (min) | Compound  | Striatum |                   |       | Isolated bovine chromaffin cells (ng per 10 <sup>6</sup> cells) |
|------------------------------|---|----------|-------------------|-------|---|
|                              |   | Rat      | Cattle (ng per g) | Human |   |
| 5                            | Oxidized Met-enkephalin                           | 2.0      | 26.0              | 9.3   | 0.88  |
| 13                           | Met-enkephalin-Arg <sup>6</sup>                   | 83.0     | 5.0               | 8.6   | 0.63  |
| 19                           | Met-enkephalin                                    | 220.0    | 450.0             | 28.0  | 2.22  |
| 45                           | Leu-enkephalin                                    | 30.0     | 38.0              | 1.6   | 0.78  |
| 75                           | Met-enkephalin-Arg <sup>6</sup> -Phe <sup>7</sup> | 50.0     | 25.0              | 7.5   | 2.50  |

Striata from 10 rats (Sprague-Dawley, 200 g) were dissected out and frozen immediately after decapitation. Striata from three bovine brains were obtained in the 3 h following death. The human tissue was obtained at autopsy, 8 h after death, from a 68-yr old woman who died from a pulmonary embolism. In this case only the two putamens were used. Isolated bovine chromaffin cells were prepared as described by Livett *et al.*<sup>10</sup>. In all cases the pooled tissues were incubated for 10 min at 95 °C in 10 vol of 1 M acetic acid before homogenization as described in ref. 11. The supernatant (3,000g × 30 min) was precipitated with 10% final trichloroacetic acid, the precipitate was discarded and the solution extracted three times with an equal volume of diethyl ether. The solution was adjusted to pH 4 with pyridine and applied to an Ultrasphere octyl column (5 µm, 4.6 × 250 mm). The column was eluted by a linear gradient of 1-propanol (from 7 to 14% in 100 min) in 0.5 M formic acid/0.4 M pyridine as described elsewhere<sup>12</sup>. Flow rate was 30 ml h<sup>-1</sup>. Fractions of 0.75 ml were collected. After evaporation, the residue was resuspended in the RIA buffer and assayed as described in Fig. 1 legend. Positive fractions were reassayed at two or three appropriate dilutions.

**Table 2** Inhibition of binding to rat brain membranes

| Peptide   | <sup>3</sup> H-etorphine IC <sub>50</sub> (nM) | <sup>3</sup> H-(D-Ala <sup>2</sup> )-Leu-enkephalinamide IC <sub>50</sub> (nM) |
|---|--|--|
| Met-enkephalin                                    | 25 ± 6 (3)                                     | 17 ± 2 (3)   |
| Met-enkephalin-Arg <sup>6</sup> -Phe <sup>7</sup> | 35 ± 2 (3)                                     | 36 ± 8 (3)   |
| Leu-enkephalin                                    | 51 ± 10 (3)                                    | 35 ± 3 (3)   |

Rat brain minus the cerebellum was homogenized with a Teflon-glass homogenizer (1,500 r.p.m., 5 strokes) in 10 ml of 0.05 M Tris-HCl buffer pH 7.4, centrifuged at 49,000g for 10 min, the pellet rehomogenized in 10 ml of Tris buffer and re-centrifuged. The pellet was resuspended in Tris buffer to obtain a final concentration of 1 mg per ml. The suspension (0.8 ml) was incubated for 150 min at 0 °C in the presence of either <sup>3</sup>H-etorphine (1 nM) or <sup>3</sup>H-(D-Ala<sup>2</sup>)-Leu-enkephalinamide (3.5 nM) and unlabelled peptides. Nonspecific binding was determined with 1 µM levorphanol for <sup>3</sup>H-etorphine and 1 µM (D-Ala<sup>2</sup>)-Leu-enkephalinamide for <sup>3</sup>H-(D-Ala<sup>2</sup>)-Leu-enkephalinamide as described in ref. 13. The values are the means ± s.e.m.; the number of observations is given in parentheses.

**Table 3** Inhibition of contraction of guinea pig ileum (g.p.i.) and mouse vas deferens (m.v.d.)

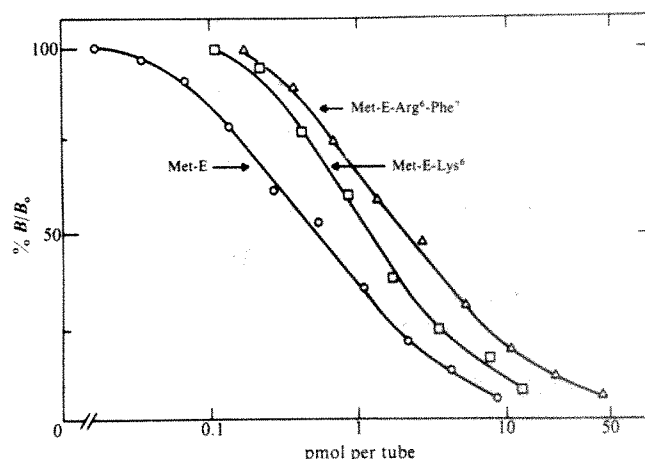
| Compound  | Guinea pig ileum IC <sub>50</sub> (nM) | Mouse vas deferens IC <sub>50</sub> (nM) | Ratio IC <sub>50</sub> g.p.i./m.v.d. |
|---|--|--|--------------------------------------|
| Morphine  | 80 ± 12 (4)                            | 417 ± 75 (4)                             | 0.19                                 |
| Met-enkephalin                                    | 219 ± 29 (3)                           | 68 ± 6 (3)                               | 3.22                                 |
| Met-enkephalin-Arg <sup>6</sup> -Phe <sup>7</sup> | 322 ± 52 (3)                           | 67 ± 14 (3)                              | 4.81                                 |
| Leu-enkephalin                                    | 601 ± 18 (3)                           | 42 ± 4 (3)                               | 14.3                                 |

Assays were performed as described in ref. 13. The values are means ± s.e.m.; the number of observations is given in parentheses.

was possible that the analgesic effect of the heptapeptide was due to its biotransformation. Indeed, *in vitro* Met-enkephalin-Arg<sup>6</sup>-Phe<sup>7</sup> can be converted to Met-enkephalin by a sequential digestion with trypsin and carboxypeptidase B. To eliminate this possibility we have characterized the new compound in conditions where biotransformation should not occur.

To minimize any enzymatic transformation in our radioligand displacement assay, we have used washed rat brain membranes and incubated them at 0 °C. As Table 2 shows, Met-enkephalin-Arg<sup>6</sup>-Phe<sup>7</sup> was as potent as Leu-enkephalin in displacing <sup>3</sup>H-etorphine or <sup>3</sup>H-(D-Ala<sup>2</sup>)-Leu-enkephalinamide from the purified rat brain membranes. The heptapeptide was slightly less active than Met-enkephalin.

We further characterized the new compound on two classical preparations for opiates, the guinea pig ileum and the mouse vas deferens<sup>8</sup>. On the guinea pig ileum, Met-enkephalin-Arg<sup>6</sup>-Phe<sup>7</sup> inhibited the electrically induced twitch with an IC<sub>50</sub> of 322 nM.



**Fig. 1** Cross-reactivities of the N-terminus Met-enkephalin (E) antiserum. A rabbit was injected intradermally at multiple sites with 2 mg of the immunogen emulsified in Freund's complete adjuvant. A month after the first injection it was boosted and serum collected 10 days later. The immunogen was prepared as follows: 40 mg of crystalline bovine serum albumin and 76 mg of 1-ethyl-3-(3-dimethyl-aminopropyl)-carbodiimide HCl were dissolved in 2 ml water. The pH was adjusted to 3. After 4 min in an ice bath, 57 mg of Boc-Met-enkephalin-NH-(CH<sub>2</sub>)<sub>2</sub>-NH<sub>2</sub> pre-dissolved in 4 ml was added. After 1 h the resulting milky solution was dialysed and lyophilized. The powder was treated with trifluoroacetic acid for 15 min. The trifluoroacetic acid was pumped off under high vacuum, and the resulting brown gelatinous precipitate resuspended in 30% acetic acid/water and dialysed against water. The RIAs were carried out at a final serum dilution of 1/600. The maximum binding was 21%. Serum, trace and standard were incubated for 48 h at 4 °C in a final volume of 300 µl of a 10 mM sodium phosphate buffer pH 7.5, 145 mM NaCl, supplemented with thimerosal 0.01%, gelatine 0.1% and crystalline bovine serum albumin 0.01%. Trace was monoiodo-(<sup>125</sup>I)-Leu-enkephalin prepared as described in ref. 4 and purified by HPLC. Similar results were obtained with monoiodo-(<sup>125</sup>I)-Met-enkephalin. γ-Globulins were precipitated with 0.5 ml of a preparation of formalin-treated *Staphylococcus aureus* after an incubation of 10 min at room temperature. This preparation (Ig Sorb, Enzyme Center, Boston) was diluted 20 times with phosphated-buffered saline before use. After centrifugation (2,000g × 10 min) the supernatant was discarded and the pellet counted. Results are in % of B/B<sub>0</sub>. Expressed in molar ratio, the cross-reactivities relative to Met-enkephalin were 100% with sulphoxide Met-enkephalin and Leu-enkephalin, 42% with Met-enkephalin-Lys<sup>6</sup>, 30% with Tyr-Gly-Gly-Phe, 23% with Met-enkephalin-Arg<sup>6</sup>-Phe<sup>7</sup>, 19% with Met-enkephalin-Arg<sup>6</sup>, 1.5% with γ-endorphin, 0.75% with α-endorphin, 0.25% with β-endorphin and 0.20% with δ-endorphin. Parallelism was found for all these compounds except for Met-enkephalin-Lys<sup>6</sup>. No cross-reactivity was found with morphine, tyrosine, des-Tyr<sup>1</sup>-β-endorphin or β-lipotropin tested at concentration up to 1 µg per tube.



On this preparation Met-enkephalin was slightly more active and Leu-enkephalin 50% less active. These effects were almost completely antagonized by naloxone ( $5 \times 10^{-7}$  M).

Kosterlitz and co-workers have demonstrated the existence of at least two types of opiate receptor— $\mu$  and  $\delta$  in the guinea pig ileum and mouse vas deferens, respectively<sup>8,9</sup>. Leu-enkephalin was considered to be a  $\delta$  agonist, being much more potent on the vas deferens than on the guinea pig ileum. On the other hand, morphine was considered to be a  $\mu$  agonist, being much more potent on the guinea pig ileum than in the vas deferens. In our preparations the ratios of the activity on the guinea pig ileum to that on the mouse vas deferens were 0.19 for morphine and 14.3 for Leu-enkephalin (Table 3). Met-enkephalin-Arg<sup>6</sup>-Phe<sup>7</sup> had a ratio of 4.81 against 3.22 for Met-enkephalin. Kosterlitz *et al.*<sup>9</sup> recently showed that compounds with high ratios interacted mainly with  $\delta$  receptors. Thus, it seems reasonable to consider that the new heptapeptide binds preferentially to the  $\delta$  receptor rather than to the  $\mu$  receptor.

Received 28 July, accepted 10 September 1980

- 1 Hughes, J. *et al.* *Nature* **258**, 577–579 (1975)
- 2 Stern, A. S. *et al.* *Proc. natn. Acad. Sci. USA* **76**, 6680–6683 (1979).
- 3 Semantov, R. & Snyder, S. H. *Proc. natn. Acad. Sci. USA* **73**, 2515–2519 (1976)
- 4 Rosner, J., Vargo, T., Minick, S., Ling, N., Bloom, F. E. & Guillemin, R. *Proc. natn. Acad. Sci. USA* **74**, 5162–5165 (1977).
- 5 Gerber, L. D., Stern, S., Rubenstein, M., Wideman, J. & Udenfriend, S. *Brain Res* **151**, 117–126 (1978)
- 6 Huang, W. Y., Chang, R. C., Kastin, A. J., Coy, D. H. & Schally, A. V. *Proc. natn. Acad. Sci. USA* **76**, 6177–6180 (1979)

Met-, Leu-enkephalin and  $\beta$ -endorphin have previously been considered as the main endogenous opioid ligands in the brain. Our report shows that Met-enkephalin-Arg<sup>6</sup>-Phe<sup>7</sup> is another important endogenous opioid peptide. The crucial problem now is to determine by immunocytochemistry whether or not this compound is present in neurones containing Met- or Leu-enkephalin.

We thank Drs J. Pablo Huidobro-Toro, Sadao Kimura, Randolph Lewis, Stanley Stein, Alvin Stern and Jean-Jacques Vanderhaeghen for their help. J.R. is Chargé de Recherche INSERM (France).

**Note added in proof:** The analgesic properties of the heptapeptide were markedly enhanced by preparing an analogue more resistant to degradation by peptidases. This compound (D-Ala<sup>2</sup>)-Met-enkephalin-Arg<sup>6</sup>-Phe<sup>7</sup>-NH<sub>2</sub> was, on a molar basis, 130 times more potent than the natural compound and twice as potent than morphine when administered intraventricularly to mice.

- 7 Inturris, C. E. *et al.* *Proc. natn. Acad. Sci. USA* **77** (in the press)
- 8 Lord, J. A., Waterfield, A. A., Hughes, J. & Kosterlitz, H. W. *Nature* **267**, 495–499 (1977)
- 9 Kosterlitz, H. W., Lord, J. A. H., Paterson, S. J. & Waterfield, A. A. *Br. J. Pharmac.* **68**, 333–342 (1980).
- 10 Livett, B. G., Koprowski, V., Mizobe, F. & Dean, D. M. *Nature* **278**, 256–257 (1979)
- 11 Rosner, J., Bayon, A., Vargo, T., Ling, N., Guillemin, R. & Bloom, F. *Life Sci* **21**, 847–852 (1977)
- 12 Kimura, S., Lewis, R. V., Stern, A. S., Rosner, J., Stein, S. & Udenfriend, S. *Proc. natn. Acad. Sci. USA* **77**, 1681–1685 (1980)
- 13 Audigier, Y., Mazarguil, H., Gout, R. & Cros, J. *Eur. J. Pharmac.* **63**, 35–46 (1980).

## Development of virus non-producer lymphosarcomas in pet cats exposed to FeLV

W. D. Hardy Jr\*, A. J. McClelland\*, E. E. Zuckerman\*, H. W. Snyder Jr\*, E. G. MacEwen†, D. Francis‡ & M. Essex‡

\* Laboratories of Veterinary and Viral Oncology, Memorial Sloan-Kettering Cancer Center, New York, New York 10021

† Donaldson Atwood Cancer Clinic, Animal Medical Center, New York, New York 10021

‡ Department of Microbiology, Harvard School of Public Health, Boston, Massachusetts 02115

Naturally occurring oncoviruses of several species<sup>1–6</sup> are transmitted contagiously and cause lymphosarcoma (LSA) or leukaemia in their hosts<sup>7</sup>. All naturally occurring oncoviruses replicate *in vivo* in the tumours they induce or, as with bovine leukaemia virus, can be isolated from tumour cells grown in short-term cell culture<sup>7,8</sup>. However, we have shown that feline leukaemia virus (FeLV) is not present in a significant minority of pet cats that develop LSA<sup>9–11</sup>. Unlike experimentally induced virus-negative leukaemias and sarcomas of other species, LSA cells from FeLV-negative LSA cats lack any FeLV proteins, including p15 or p12, and complete functional copies of FeLV provirus and thus do not produce FeLV when grown in cell culture<sup>9–11</sup>. Thus, except for FeLV, the naturally occurring animal leukaemogenic oncoviruses seem to induce only virus-producing lymphoid tumours. Our earlier findings prompted a study to determine the frequency of occurrence of FeLV non-producer (NP) LSA in pet cats and whether NP LSAs develop in cats exposed to FeLV. We report here epidemiological data which indicate that development of NP LSAs in pet cats is associated with exposure to FeLV and suggest that FeLV may be the aetiological agent for FeLV NP feline LSAs. Thus, feline NP LSAs may be suitable for studying the potential viral aetiology and mechanism of leukaemogenesis of human lymphoid tumours in which no oncoviruses have, as yet, been proved to cause the disease.

The FeLV status of most cats with LSA was determined by the immunofluorescent antibody (IFA) test for FeLV performed on

peripheral blood leukocytes using a multivalent rabbit anti-FeLV serum which detects FeLV gp70, p30, p15, and p12 (ref. 17); but an immunodiffusion test<sup>2</sup>, tissue culture isolation<sup>9</sup>, and radioimmunoassays (RIAs)<sup>18</sup> were also done to determine the FeLV status of some cats. The presence of RD114 viral proteins was determined by RIAs of LSA cell lysates<sup>19</sup>. In general, the results of the IFA test for FeLV correlated well with all other immunological tests and with tissue culture isolation (Table 1 and refs 9, 11, 13, 17, 19 and 20). We compared the results of the IFA test from 274 cats with our ability to recover infectious FeLV in tissue culture from these cats. We could isolate FeLV from only three of the 153 IFA test-negative cats, a 98% concordance between the two methods of FeLV detection. Conversely, FeLV was isolated from 118 of 121 IFA test-positive cats, a 97.5% concordance. Similar results were obtained when we studied cats with LSA. Of the 57 IFA test-positive LSA cats, 56 (98.3% concordance) were found to have FeLV by tissue culture isolation and of the 33 IFA test-negative LSA cats 31 (93.9% concordance) had no FeLV. These results indicate that detection of FeLV antigens by the IFA test is equivalent to the detection of infectious FeLV. Furthermore, the IFA test can detect even the partial FeLV expression that occurs in FeSV-transformed NP mink cells which do not replicate FeLV or FeSV but which express only FeLV p15 and p12 (ref. 21).

We tested 507 LSA cats for the presence of FeLV and 14 LSA cats for the presence of RD114 viral proteins. We found that 360 of the 507 cats tested (71.0%) had FeLV-positive LSAs and 147 (29.0%) had NP LSAs (Table 2). NP LSAs occurred most frequently in cats with the alimentary form of LSA (Table 2). As reported previously, we found that cats with NP LSA were markedly older than cats which developed FeLV-positive LSAs<sup>14</sup>. The mean age of cats with NP LSAs was 6.7 yr; and the median age was 7 yr. In contrast, the mean age of the cats with FeLV-positive LSA was 2.9 yr; and their median age was only 2 yr. Nine FeLV-positive LSAs were tested by RIA and were found to contain large quantities of FeLV structural proteins (Table 1), whereas nine NP LSAs were found to have no detectable FeLV gp70, p30, p15, or p12. However, as reported previously<sup>14</sup>, both the FeLV-positive and NP LSAs had low levels of RD114 gp70 (21–22 ng per mg protein) and p15 (34–36 ng per mg protein) whereas FeLV-positive and -negative normal lymphoid tissues had no detectable RD114 antigens (Table 1).

**Table 1** Expression of feline leukaemia and RD114 viral antigens and the feline oncornavirus-associated cell membrane antigen (FOCMA) in normal and lymphosarcoma tissues of pet cats

| Diagnosis                          | No. of cats tested | FeLV* status | FOCMA† status | RIA competition assay‡: average viral antigen expression (ng competitor per mg total protein) |      |     |     |                          |     |
|------------------------------------|--------------------|--------------|---------------|---|------|-----|-----|--------------------------|-----|
|                                    |                    |              |               | FeLV antigen expression   |      |     |     | RD114 antigen expression |     |
|                                    |                    |              |               | gp70  | p30  | p15 | p12 | gp70                     | p15 |
| Normal lymphoid cells              | 4                  | —            | —             | <10   | <5   | <5  | <5  | <10                      | <5  |
| Normal lymphoid cells              | 2                  | +            | —             | ND  | 1084 | 259 | 321 | <10                      | <5  |
| Lymphosarcoma (FeLV non-producers) | 9                  | —            | +             | <10   | <5   | <5  | <5  | 21                       | 34  |
| Lymphosarcoma (FeLV producers)     | 9                  | +            | +             | 483   | 859  | 304 | 463 | 22                       | 36  |

\* Determined by the fixed-cell IFA test<sup>17</sup>.† Determined by the viable cell membrane IFA test<sup>13,19</sup>.‡ RIA competition assays were performed as described in ref. 30 with 5 ng of <sup>125</sup>I-labelled purified viral protein and a limiting amount of specific antibody diluted to the point of ~50% precipitation of the labelled protein. Competition with protein from detergent-lysed cells was quantified by comparison with a standard competition curve with known amounts of purified unlabelled viral protein corresponding to the <sup>125</sup>I-labelled protein and expressed as the amount required to give 50% reduction in labelled protein precipitation<sup>30</sup>.**Table 2** Occurrence of feline leukaemia virus in naturally occurring lymphosarcomas of pet cats

| Gross form of lymphosarcoma | No. of cats tested | Per cent of cases | No. FeLV positive | Per cent FeLV-positive LSA | No. FeLV-negative | Per cent FeLV non-producer LSA |
|-----------------------------|--------------------|-------------------|-------------------|----------------------------|-------------------|--------------------------------|
| Multicentric                | 198                | 39.1              | 159               | 80.3                       | 39                | 19.7                           |
| Thymic                      | 174                | 34.3              | 134               | 77.0                       | 40                | 23.0                           |
| Alimentary                  | 69                 | 13.6              | 16                | 23.2                       | 53                | 76.8                           |
| Unclassified                | 13                 | 2.6               | 5                 | 38.5                       | 8                 | 61.5                           |
| Form unknown                | 53                 | 10.4              | 46                | 86.8                       | 7                 | 13.2                           |
| Total                       | 507*               | 100               | 360               | 71.0                       | 147               | 29.0                           |

\* All pet cats with lymphosarcoma were histologically confirmed clinical cases and were examined by W.D.H. or E.G.M. at the Henry Bergh Memorial Hospital of the ASPCA or the Animal Medical Center in New York City.

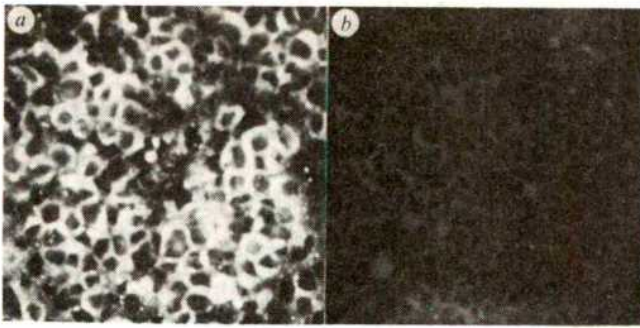
**Table 3** Occurrence of lymphosarcoma in FeLV-exposed and unexposed pet cats

| Cat exposure history | Observation years based on: | No. of cats | FeLV status  | Observation years |                 | Observed cases of lymphosarcoma |       | No. of LSAs developing per cat observation year |
|----------------------|-----------------------------|-------------|--------------|-------------------|-----------------|---------------------------------|-------|---|
|                      |                             |             |              | Total             | Average per cat | FeLV+                           | FeLV— |   |
| Never exposed        | Ages of cats                | 1,074       | 1,074—       | 3,235             | 3.1             | 0                               | 0†    | 0   |
| Exposed              | From time of FeLV exposure* | 538         | 149+<br>389— | 2,334             | 4.3             | 30                              | 11†   | 0.018   |
| Total cats           |                             | 1,612       |              |                   |                 |                                 |       |   |

\* The observation periods for both FeLV-unexposed control cats and FeLV-infected and -uninfected exposed cats were determined in the following ways. For the unexposed FeLV-uninfected control cats the observation period was the age of the cat on the date of its last FeLV test. The observation periods for the exposed cats was the period between the date of the first positive FeLV test of any cat in the household and the termination of this study. The total number of cat observation years for the unexposed and exposed cats was calculated by adding the individual observation periods of all cats in each group. The observation periods for the exposed and unexposed groups of cats were not the same as the exposed cats because the exposed cats had not been exposed for their entire life. To ensure that the difference in the observation periods did not bias our results, we also calculated the observation period for exposed cats in the same way as we did for the unexposed cats—according to their age. In this analysis there was a total of 558 cats, the additional 20 cats were cats that died before our study began and had not been tested for FeLV. The 558 cats were observed for their entire lives for a total observation period of 3,199 yr (an average of 5.7 yr—range 1–24 yr). We found 56 cases of LSA among these 558 exposed cats (30 FeLV-positive, 11 NPLSA and 15 whose status was unknown). The development of LSA per cat observation year was found to be the same (0.018 case) when the observation period was calculated from either (1) the time of FeLV exposure (41 cases of LSA per 2,334 cat observation years = 0.018), or (2) the ages of the cats (56 cases of LSA per 3,199 cat observation years = 0.017). Thus, the difference between the two methods of determining the observation period of the unexposed and exposed tested cats did not alter the conclusion of this study.

• †  $P < 0.001$ .





**Fig. 1** Examination of feline lymphosarcoma cells for FeLV antigens by the fixed-cell indirect IFA test. The test was done with a multivalent rabbit antiserum against disrupted FeLV that had known reactivity to FeLV gp70, p30, p15 and p12 antigens. *a*, Strong cytoplasmic fluorescence indicates presence of FeLV, but *b*, no such fluorescence is seen in NP LSA cells. Thus the NP LSA cells are devoid of replicating FeLV and FeLV gp70, p30, p15 and p12 expression.

A total of 1,612 FeLV-exposed and unexposed pet cats from all regions of the US were observed for the development of LSA (Table 3). A cat was classified as unexposed if the cat was FeLV-negative and if, according to the owner, the cat had not lived with any FeLV test-positive cat or with any cat which had an FeLV disease. The FeLV status of all cats was determined by the IFA test for FeLV antigens<sup>17</sup>. Of the 1,612 cats, 1,074 living in 96 households had never been exposed to FeLV and were uninfected with FeLV. These cats served as controls and were observed for a total of 3,235 cat observation years (an average of 3.1 yr per cat). None of the unexposed control cats developed LSA during this study. In contrast, the remaining 538 pet cats living in 23 households had been exposed to an FeLV-infected cat (Table 3). All of these exposed cats were tested for FeLV and 389 were found to be uninfected whereas 149 were infected. These cats were observed for a total of 2,334 cat observation years (an average of 4.3 yr per cat with a range of 1 to 6 yr) and 41 of these cats developed LSA; 30 of these LSAs were FeLV-positive and 11 were NP LSAs. The difference in the occurrence of NP LSA between the unexposed control cats and the exposed cats is highly significant by the  $\chi^2$  test,  $P < 0.001$ . In one household where there were four unrelated cats, one cat was infected with FeLV and died of FeLV-induced anaemia. What made the household unique was that all three uninfected cats died of NP alimentary LSA.

As infectious FeLV particles, FeLV antigens, and complete copies of FeLV provirus cannot be detected in feline NP LSAs by electron microscopy<sup>9</sup>, tissue culture isolation<sup>4,9,17</sup>, immunofluorescence (Fig. 1)<sup>4,17</sup>, RIA<sup>10,14,19</sup>, or by nucleic acid hybridization<sup>14,15,16</sup>, the aetiological role of FeLV in these tumours has been uncertain. In contrast to FeLV NP LSA cells, virtually all other oncovirus-transformed cells including FeSV- and MSV-transformed NP fibroblasts, Abelson MuLV and the acute avian leukaemia virus-transformed fibroblasts or leukaemia cells and bovine leukaemia cells are positive for at least the N-terminal viral gag protein by RIA even though they are negative for replicating virus<sup>22</sup>. We have recently reported that the FeLV-associated tumour-specific antigen, the feline oncornavirus-associated cell membrane antigen (FOCMA), is present on the surface of all FeLV- and FeSV-transformed, virus-producing cat cells, but not on non-transformed virus-producing cat cells. We found that FOCMA is also present on FeLV NP LSA cells suggesting that FeLV may play a role in the transformation of normal lymphocytes into NP LSA cells<sup>13,22,23</sup>. Our finding that there is a comparable epidemiological association between FeLV exposure and the development of both NP- and FeLV-positive LSAs (Koch's postulates have been fulfilled for the FeLV-positive LSAs)<sup>24</sup> supports the hypothesis

that FeLV may be the aetiological agent for most feline LSAs regardless of whether or not they express FeLV.

At least three possible hypotheses explain the mechanism by which a replicating oncovirus such as FeLV causes NP feline LSAs<sup>25</sup>. First, FeLV may be involved in the generation of a recombinant replication-defective leukaemogenic virus from cat cellular genes and FeLV provirus, similar to the Abelson MuLV, AK-T8 mink cell focus-inducing virus and several avian oncoviruses, although in these NP tumours some viral gag gene expression is present<sup>26-28</sup>. Second, only a fragment of the FeLV genome may be present as provirus in leukaemic cell chromosomes. If such a fragment was present, it would presumably be unable to code for the production of any detectable viral structural proteins, but may be able to initiate transformation<sup>29</sup>. Third, a 'hit and run' phenomenon might occur in which FeLV alters, but does not stably integrate into the chromosomes of the leukaemic cell.

Feline NP LSA is the only known example of a naturally occurring lymphoid tumour which develops after exposure to a leukaemogenic virus but in which no evidence of that leukaemogenic virus remains. NP LSAs may thus be valuable for the study of the basic mechanism by which viruses, chemicals or radiation induce transformation.

We thank R. Markovich, T. Paino and H. Perry for technical assistance, and Ms S. Passe for statistical analysis. We thank numerous practicing veterinarians and cat owners, especially Mrs S. Bernard, for assistance, and the National Veterinary Laboratory of Franklin Lakes, New Jersey for performing tests for FeLV and helping to obtain cats with FeLV non-producer lymphosarcomas. We also thank Drs Robert Gallo, Nancy Gutensohn and Peter Besmer for helpful discussions. This work was supported in part by grants and contracts from the NCI, The Cancer Research Institute, and the American Cancer Society. During this study W. D. H. was a Scholar and H. W. S. is a Special Fellow of the Leukemia Society of America.

Received 12 May; accepted 29 August 1980.

- Papas, T. S., Dahlberg, J. E. & Sonstegard, R. A. *Nature* **261**, 506-508 (1976).
- Burmeister, B. R. & Gentry, R. F. *Cancer Res.* **14**, 34-42 (1954).
- Aoki, T., Boyse, E. A. & Old, L. J. *J. natn. Cancer Inst.* **41**, 103-110 (1968).
- Hardy, W. D. Jr, Old, L. J., Hess, P. W., Essex, M. & Cotter, S. *Nature* **244**, 266-269 (1973).
- Miller, J. M., Miller, L. D., Olson, C. & Gillette, K. G. *J. natn. Cancer Inst.* **43**, 1297-1305 (1969).
- Kawakami, T. G., Buckley, P. M., McDowell, T. S. & DePaoli, A. *Nature* **246**, 105-107 (1973).
- Hardy, W. D. Jr in *The Immunopathology of Lymphoreticular Neoplasms* (eds Twomey, J. J. & Good, R. A.) 129-180 (Plenum, New York, 1978).
- Ferrer, J. F., Stock, N. D. & Lin, P. S. *J. natn. Cancer Inst.* **27**, 613-621 (1971).
- Hardy, W. D. Jr *et al. Science* **166**, 1019-1021 (1969).
- Hardy, W. D. Jr *et al. in Viruses in Naturally Occurring Cancer* (eds Essex, M., Todaro, G. J. & zur Hausen, H.) (Cold Spring Harbor Laboratory, New York, in the press).
- Francis, D. P., Cotter, S. M., Hardy, W. D. Jr & Essex, M. *Cancer Res.* **39**, 3866-3870 (1979).
- Stephenson, J. R., Kahn, A. S., Sliski, A. H. & Essex, M. *Proc. natn. Acad. Sci. U.S.A.* **74**, 5608-5612 (1977).
- Hardy, W. D. Jr, Zuckerman, E. E., MacEwen, E. G., Hayes, A. A. & Essex, M. *Nature* **270**, 249-251 (1977).
- Niman, H. L., Stephenson, J. R., Gardner, M. B. & Roy-Burman, P. *Nature* **266**, 357-360 (1977).
- Levin, R., Ruscetti, S. K., Parks, W. P. & Scolnick, E. M. *Int. J. Cancer* **18**, 661-671 (1976).
- Koshy, R., Wong-Stall, F., Gallo, R. C., Hardy, W. D. Jr & Essex, M. *Virology* **99**, 135-144 (1979).
- Hardy, W. D. Jr, Hirshaut, Y. & Hess, P. in *Unifying Concepts of Leukemia* (eds Dutcher, R. M. & Chieco-Bianchi, L.) 778-799 (Karger, Basel, 1973).
- Snyder, H. W. Jr, Hardy, W. D. Jr, Zuckerman, E. E. & Fleissner, E. *Nature* **275**, 656-658 (1978).
- Snyder, H. W. Jr *et al. in Cold Spring Harb. Symp. quant. Biol.* **44**, 787-799 (1980).
- Stephenson, J. R., Essex, M., Hino, S., Hardy, W. D. Jr & Aaronson, S. A. *Proc. natn. Acad. Sci. U.S.A.* **74**, 1219-1223 (1977).
- Khan, A. S. & Stephenson, J. R. *J. Virol.* **23**, 599-607 (1977).
- Stephenson, J. R., Khan, A. S., van de Ven, W. J. M. & Reynolds, F. H. Jr *J. natn. Cancer Inst.* **63**, 1111-1119 (1979).
- Essex, M., Cotter, S. M., Stephenson, J. R., Aaronson, S. A. & Hardy, W. D. Jr in *Origins of Human Cancer* (eds Hiatt, H. H., Watson, J. D. & Winsten, J. A.) 502-510 (Cold Spring Harbor Laboratory, New York, 1977).
- Jarrett, W. F. H., Martin, W. B., Crighton, G. W., Dalton, R. G. & Stewart, M. F. *Nature* **202**, 566-567 (1964).
- Gallo, R. C. *et al. in Origins of Human Cancer* (eds Hiatt, H. H., Watson, J. D. & Winsten, J. A.) 1253-1286 (Cold Spring Harbor Laboratory, New York, 1977).
- Rosenberg, N. & Baltimore, D. *J. exp. Med.* **147**, 1126-1141 (1978).
- Sacks, T. L., Reynolds, F. H. Jr, Deobagkar, D. N. & Stephenson, J. R. *J. Virol.* **27**, 809-814 (1978).
- Graf, T. & Beug, H. *Biochim. biophys. Acta* **516**, 269-299 (1978).
- Tsichlis, P. N. & Coffin, J. M. *J. Virol.* **33**, 238-249 (1980).
- Strand, M. & August, J. T. *J. Virol.* **14**, 1584-1596 (1974).



## Interferon inhibits transformation by murine sarcoma viruses before integration of provirus

R. J. Avery, J. D. Norton, J. S. Jones,  
D. C. Burke & A. G. Morris

Department of Biological Sciences, University of Warwick,  
Coventry CV4 7AL, UK

Neoplastic transformation by C-type retroviruses requires synthesis of a DNA copy (the provirus) of the RNA genome and its integration into the host cell DNA. We have previously shown that interferon (IFN) can stably prevent transformation of murine fibroblasts by the Kirsten strain of murine sarcoma virus (KIMSV)<sup>1,2</sup>, a murine leukaemia virus (MLV). A series of cell clones (IFN clones), isolated in the presence of IFN ( $10^4$  U ml<sup>-1</sup>) from cultures of NIH-3T3 cells which had been treated with IFN, and then infected with KIMSV (KiMLV) in conditions where every cell was infected, were shown to be phenotypically untransformed. These untransformed cells did not produce virus or contain rescuable KIMSV. However, cells isolated using an identical procedure, but in the absence of IFN, were uniformly transformed and all produced KIMSV (KiMLV) or contained rescuable KIMSV<sup>2,3</sup>. It was concluded that IFN either prevents synthesis or integration of the provirus, or else that in the presence of IFN the provirus is integrated such that it is not expressed. We now show that five representative clones contain no detectable KIMSV proviral DNA, and also that the initial stages of infection by KIMSV (KiMLV) are inhibited by IFN treatment. IFN seems to act before integration, preventing either the synthesis or the integration of proviral DNA.

We initially sought to establish whether the IFN clones contained integrated KIMSV provirus in their cellular genomes, by hybridizing cell DNA with a representative <sup>3</sup>H-cDNA probe synthesized from purified KIMSV (KiMLV) RNA. As normal uninfected mouse DNA contains multiple copies of endogenous retrovirus sequences closely related to MLV genomes<sup>4</sup>, it was necessary to reduce the proportion of KiMLV cDNA sequences in the probe by annealing with KiMLV RNA. After this procedure the cDNA hybridized to a maximum level of about 16% with KiMLV RNA and 78% with KIMSV (KiMLV) RNA. It was then used as a cDNA probe for hybridization with various cell DNAs. The results (Table 1) show that there was some annealing of the cDNA probe with the DNA from uninfected NIH-3T3 cells, reflecting the inefficiency of the selection procedure, and that a much higher level of hybridization (~58%) occurred between the cDNA probe and the DNA from a non-producer, transformed cell line, CCl, which is known to contain a rescuable KIMSV genome.<sup>3</sup> The level of hybridization with DNA from the IFN clones was no higher than that seen with DNA from uninfected cells, strongly suggesting that the IFN clone DNAs do not contain integrated KIMSV proviral DNA.

The cell DNAs were further investigated for the presence of integrated provirus by restriction enzyme analysis using the Southern blotting procedure. Figure 1A shows the restriction map of unintegrated linear KIMSV DNA using endonuclease *Pst*I (details of the restriction mapping will be presented elsewhere). *Pst*I analysis of a number of KIMSV-transformed non-producer cell DNAs has shown each to contain the two large internal fragments *P*<sub>1</sub> (molecular weight  $2.6 \times 10^6$ ) and *P*<sub>2</sub> (molecular weight  $1.05 \times 10^6$ ) (Fig. 1A). These two internal *Pst*I fragments (representing 80% of the KIMSV genome) therefore provided a means of detecting integrated provirus. *Pst*I-digested cell DNAs were electrophoresed on an agarose gel and the fragments transferred to a filter which was then annealed with KIMSV (KiMLV) <sup>32</sup>P-cDNA to give the result shown in Fig. 1B.

Lane a shows the hybridization of the cDNA with the MLV-related sequences of uninfected cell DNA. In lane b, which contains a digest of CCl DNA, the two internal *Pst*I fragments (arrowed) are clearly visible against the background of hybridization. However, these fragments are absent from the IFN clone DNAs (c-g) showing that intact integrated provirus was not present. The use of other restriction enzymes, which cleave once or twice within the provirus, confirmed that no KIMSV-specific fragments were detectable in the IFN clone DNAs (data not shown).

Thus, we conclude that cells infected in the presence of IFN do not contain complete integrated proviral genomes and are unlikely to contain truncated forms of proviral DNA. IFN must therefore prevent transformation by KIMSV at a stage before integration.

The possibility that IFN was acting by inhibiting adsorption or penetration of the virus was investigated by determining the effect on KIMSV (KiMLV) transformation of IFN added after infection. Transformation was assayed by focus formation on monolayer cultures of C3H10T $\frac{1}{2}$  cells; the virus stock used contained an excess of KIMSV and focus formation using this stock at high dilution follows one-hit kinetics, that is, a focus is initiated by infection of a cell by KIMSV alone and enlargement of the focus is due to outgrowth from this cell alone rather than by virus spread or recruitment<sup>1</sup>. In such conditions, any effects of

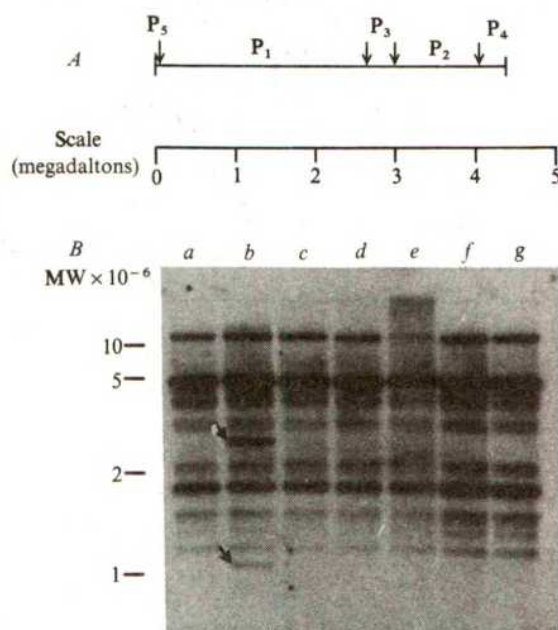
Table 1 Hybridization of KIMSV cDNA with cellular DNAs

| Source of DNA | % Hybridization |            |
|---------------|-----------------|------------|
|               | Cell DNA        | cDNA probe |
| NIH 3T3       | 82              | 19         |
|               | 78              | 16         |
| CCl           | 82              | 58         |
|               | 86              | 57         |
| IFN 49        | 89              | 19         |
|               | 83              | 16         |
| IFN 81        | 77              | 14         |
|               | 76              | 15         |
| IFN 85        | 71              | 14         |
|               | 82              | 10         |
| IFN 61        | 76              | 16         |
|               | 73              | 14         |
| IFN 91        | 86              | 16         |
|               | 76              | 15         |

NIH-3T3 cells and a KIMSV-transformed non-producer line, CCl, were grown as described previously<sup>3</sup>. Details of the isolation of the IFN clones (IFN 49, 61, 81, 85 and 91) are given by Morris and Burke<sup>2</sup>. Cell DNAs were prepared by deproteinization with phenol/chloroform (1:1, v/v), spooling under ethanol (EtOH), RNase A digestion (50 µg ml<sup>-1</sup> for 1 h at 37 °C), further deproteinization, ether extraction and spooling under EtOH. The high molecular weight DNA was dissolved in 10<sup>-3</sup> M EDTA and sheared by sonication. Virion RNA (35S) was prepared from a purified KiMLV preparation containing excess KIMSV and used as a template for the *in vitro* synthesis of <sup>3</sup>H-cDNA by AMV reverse transcriptase essentially as described by Taylor *et al.*<sup>5</sup>. The reaction mixture contained 50 mM Tris pH 8.3, 40 mM KCl, 8 mM MgCl<sub>2</sub>, 5 µg calf thymus DNA primer, 100 µCi <sup>3</sup>H-TTP (42 Ci mmol<sup>-1</sup>), 0.2 mM dATP, dGTP, dCTP, 0.5 mM dithiothreitol, 4 mM Na pyrophosphate, 0.5 µg RNA and 7.5 units of AMV reverse transcriptase in a volume of 50 µl. Incubation was for 1 h at 37 °C. cDNA was purified by phenol/chloroform extraction, EtOH precipitation, alkali hydrolysis, a second EtOH precipitation; Sephadex G-100 chromatography and further EtOH precipitation. The cDNA was then selected by self-annealing and annealing with poly(rA) to remove anticomplementary (+ strand) sequences and oligo(dT) polymers, and annealed with KIMSV (KiMLV) RNA (at a ratio of 1:5 RNA:cDNA) to produce a representative cDNA probe. At this ratio 90% of the RNA hybridized to DNA. Finally the cDNA was hybridized with a 100-fold excess of KiMLV RNA to reduce the proportion of KiMLV cDNA sequences which can anneal with mouse DNA. Hybridizations were carried out in 2.4 M phosphate buffer (PB) (1.2 M Na<sub>2</sub>HPO<sub>4</sub>, 1.2 M NaH<sub>2</sub>PO<sub>4</sub>, pH 7.0) at 76 °C. These conditions, devised by D. E. Kohne (La Jolla Cancer Research Foundation), give a reproducible stimulation of the rate of hybridization (D. E. Kohne, personal communication). The cDNA was annealed with cell DNA, with the latter in at least 5 × 10<sup>6</sup>-fold excess, ensuring that a single integrated provirus would be in at least fivefold excess over the cDNA. The extent of hybridization with cDNA and reassociation of cell DNA (demonstrating the validity of each hybridization experiment) were determined by retention on hydroxypatite in 0.14 M PB at 61 °C.



IFN are due to an influence on the initial transformation event or on growth of transformed cells, rather than to effects on virus spread<sup>1</sup>. Murine C-type viruses penetrate and uncoat rapidly (within 80 min in NIH-3T3 cells at 37 °C)<sup>11</sup>, whereas at least 3 h are required for the antiviral effect of IFN to develop (ref. 12 and A.G.M., unpublished data). Thus, the addition of IFN to cells after their infection would be expected to have very little effect on transformation if its effects were exerted at this early stage. However, it was found that IFN added as much as 4 h after infection was virtually as effective at blocking transformation as pretreatment with IFN (Table 2). Even when added as late as 24 h post infection, IFN still inhibited focus formation to some extent (Tables 2 and 3) indicating that, in some infected cells, the IFN-sensitive stage was not complete. However, in reconstruction experiments treatment with IFN for 24 h had no effect on focus formation by cells stably transformed by KiMSV (KiMLV) and producing KiMSV (KiMLV) (data not shown),



**Fig. 1** A, Restriction endonuclease cleavage map of unintegrated linear KiMSV DNA. B, Hybridization of KiMSV (KiMLV) cDNA with endonuclease *Pst*I fragments of cell DNAs. High molecular weight DNA was prepared as described in Table 1 legend and 10- $\mu$ g samples were cleaved with an excess of endonuclease *Pst*I (Boehringer) and then run on a 1.0% agarose horizontal slab gel. DNA fragments were denatured *in situ* and transferred to a nitrocellulose filter (BA 85, Schleicher and Schuell) by the method of Southern<sup>6</sup>. For hybridization, a <sup>32</sup>P-labelled cDNA was synthesized as for the <sup>3</sup>H-cDNA probe (Table 1) except that pyrophosphate was omitted and actinomycin D (100  $\mu$ g ml<sup>-1</sup>) was included in the reaction mixture to suppress (+) strand cDNA synthesis<sup>7</sup> and <sup>3</sup>H-TTP was replaced by unlabelled TTP and dCTP by 125  $\mu$ Ci [ $\alpha$ -<sup>32</sup>P]dCTP (350 Ci mmol<sup>-1</sup>). The <sup>32</sup>P-cDNA was purified as described for the <sup>3</sup>H-cDNA (Table 1) and used without further selection. The filter was annealed with 2.5  $\times$  10<sup>6</sup> c.p.m. of <sup>32</sup>P-cDNA in a volume of 2.0 ml in a sealed polythene bag for 60 h using hybridization conditions described by Shank *et al.*<sup>8</sup>. Unlabelled KiMLV RNA (5.0  $\mu$ g ml<sup>-1</sup>) was included in the hybridization medium to suppress the level of background hybridization of cDNA with KiMLV-related sequences present in mouse DNA. After annealing, the filter was washed<sup>8</sup> and treated with RNase A (10  $\mu$ g ml<sup>-1</sup>) in 15 mM NaCl, 1.5 mM Na<sub>3</sub> citrate at 37 °C for 20 min. The filter was exposed to X-ray film (Fuji RX) at -70 °C for 1 week using a Dupont Cronex 'Lightning Plus' intensifying screen. a, Uninfected NIH-3T3 DNA; b, CCI DNA; c-g, DNA from IFN clones<sup>2</sup>, IFN 49, 61, 81, 85 and 91 respectively. Molecular weights of restriction fragments were determined using *Eco*RI<sup>9</sup> and *Hind*III<sup>10</sup> fragments of bacteriophage  $\lambda$  DNA as size markers.

**Table 2** Effect of IFN treatment before and after infection with KiMSV (KiMLV)

| Time of IFN addition (h) | Mean no. of foci per plate |
|--------------------------|----------------------------|
| -24                      | 0.5                        |
| +1                       | 0                          |
| +2                       | 1.0                        |
| +4                       | 0                          |
| +6                       | 2.5                        |
| +24                      | 10.5                       |
| None                     | 13.25                      |

IFN (10<sup>4</sup> U ml<sup>-1</sup> and 2  $\times$  10<sup>8</sup> U mg<sup>-1</sup>) was added to cultures of C3H10T $\frac{1}{2}$  cells at the times indicated and removed 24 h later. All cultures were infected with 30 FFU of KiMSV (KiMLV) at 0 h. Transformed foci were scored 10 days later.

**Table 3** Effect of IFN treatment on KiMSV (KiMLV) infection of serum-deprived cells

| Period of serum deprivation (h) | Period of IFN treatment (h) | Mean no. of foci per culture |
|---------------------------------|-----------------------------|------------------------------|
| None                            | None                        | 27                           |
| -24 to 264                      | None                        | 0                            |
| None                            | -24 to 0                    | 0                            |
| None                            | 24 to 48                    | 10.5                         |
| -24 to 72                       | None                        | 12                           |
| -24 to 72                       | 24 to 48                    | 0                            |

Cultures of C3H10T $\frac{1}{2}$  cells<sup>13</sup>, otherwise maintained in medium containing 5% serum, were shifted into medium containing 0.25% serum (serum deprivation) and treated with IFN (10<sup>4</sup> U ml<sup>-1</sup>) for periods as indicated. All cultures were infected at 0 h with KiMSV (KiMLV) at 30 FFU per culture. Transformed foci were scored 10 days later.

showing that the effect was not due to an inhibition of growth of transformed cells. These data indicated that IFN probably does not act by inhibiting adsorption, penetration or uncoating of the virus.

An extension of this experimental approach suggested that IFN acts at or after provirus synthesis. In cells arrested in G<sub>0</sub> by serum deprivation, C-type virus replication is blocked<sup>14,15</sup>. It seems that in such conditions synthesis of proviral DNA begins but is not completed and integration does not occur. Cultures of normal mouse fibroblasts (C3H10T $\frac{1}{2}$ ) were blocked in G<sub>0</sub> by prolonged serum deprivation and then infected with KiMSV (MLV) (30 FFU (focus-forming units) per culture). Addition of serum 48 h later allowed transformation (again scored by focus formation), showing the block to be reversible. However, when IFN was added 24 h post infection, so that it is present for the 24-h period before serum addition, transformation was essentially completely prevented (Table 3). A similar IFN treatment of cells which had not been serum deprived was much less effective in preventing transformation. This suggests that IFN acts at, or later than the stage blocked by serum deprivation.

It therefore seems that IFN can block infection by C-type viruses at a stage after uncoating but before integration of the provirus. This is not due to the cell growth inhibitory effect of IFN as in these and other experiments IFN had no significant effect on the growth of the cells used; nor is it likely to be an effect of IFN on translation of viral mRNA, as translation of input genomic RNA is probably not significant in the virus life cycle<sup>16-18</sup>.

This effect of IFN is at least superficially similar to the Fv-1 restriction phenomenon<sup>19-21</sup> in which the Fv-1 gene product appears to prevent integration of proviral DNA; it may be that here IFN is acting in a way that is analogous to the effect of the Fv-1 gene product.

This work was supported by grants from the Cancer Research Campaign.

Received 28 July; accepted 17 September 1980.

- Morris, A. G. & Clegg, C. *Virology* **88**, 400-402 (1978).
- Morris, A. G. & Burke, D. C. *J. gen. Virol.* **43**, 173-181 (1979).
- Morris, A., Clegg, C., Jones, J., Rodgers, B. & Avery, R. J. *J. gen. Virol.* **49**, 105-113 (1980).
- Steffen, D. & Weinberg, R. A. *Cell* **15**, 1003-1010 (1978).
- Taylor, J. M., Illmensee, R. & Summers, J. *Biochim. biophys. Acta* **442**, 324-330 (1976).
- Southern, E. M. *J. molec. Biol.* **98**, 503-517 (1975).
- Ruprecht, R. M., Goodman, N. C. & Spiegelman, S. *Biochim. biophys. Acta* **294**, 192-203 (1973).
- Shank, P. R. *et al. Cell* **15**, 1383-1395 (1978).
- Thomas, M. & Davis, R. W. *J. molec. Biol.* **91**, 315-328 (1975).
- Wellauer, P. K. *et al. Proc. natn. Acad. Sci. U.S.A.* **71**, 2823-2827 (1974).
- Aboud, M., Shoor, R. & Salzberg, S. J. *J. Virol.* **30**, 32-37 (1979).
- Sonnabend, J. A. & Friedman, R. M. in *Interferons and Interferon Inducers* (ed. Finter, N. B.) 201-239 (North-Holland, Amsterdam, 1973).
- Reznikoff, C. A., Brankow, D. W. & Heidelberger, C. *Cancer Res.* **33**, 3231-3238 (1973).
- Fritsch, E. F. & Temin, H. M. *J. Virol.* **24**, 461-469 (1977).
- Varmus, H. E., Padgett, T., Heasley, S., Simon, G. & Bishop, J. M. *Cell* **11**, 307-319 (1977).
- Parsons, J. T., Coffin, J. M., Haroz, R. K., Bromley, P. A. & Weissmann, C. *J. Virol.* **11**, 761-774 (1973).
- Sveda, M. M., Fields, B. N. & Soeiro, R. *J. Virol.* **18**, 85-91 (1976).
- Takano, T. & Hatanaka, M. *Proc. natn. Acad. Sci. U.S.A.* **72**, 343-347 (1975).
- Krontiris, T. G., Soeiro, R. & Fields, B. N. *Proc. natn. Acad. Sci. U.S.A.* **70**, 2549-2553 (1973).
- Jolicœur, P. & Baltimore, D. *Proc. natn. Acad. Sci. U.S.A.* **73**, 2236-2240 (1973).
- Sveda, M. & Soeiro, R. *Proc. natn. Acad. Sci. U.S.A.* **73**, 2356-2360 (1976).

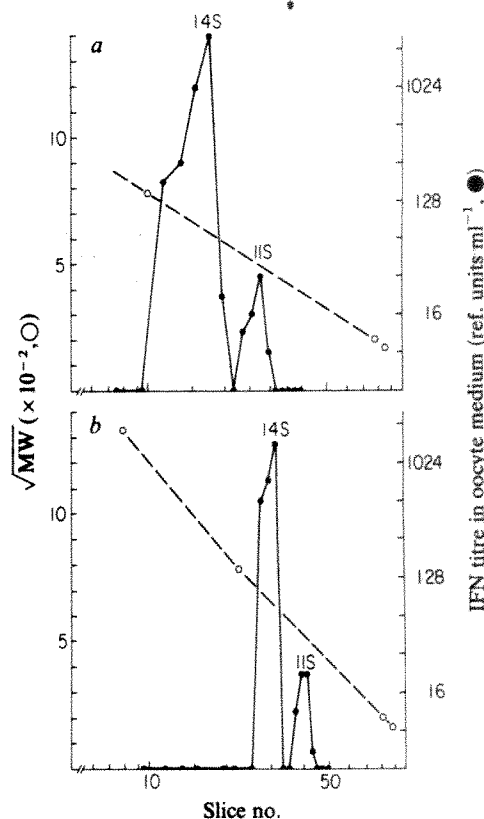
## Heterogeneity of poly(I).poly(C)-induced human fibroblast interferon mRNA species

Pravinkumar B. Sehgal & Anurag D. Sagar

The Rockefeller University, New York, New York 10021

Three classes of human interferons (IFNs) have been defined on the basis of their immunological properties: the 'Le' or ' $\alpha$ ' IFN, mainly derived from leukocyte or lymphoblastoid cells; the 'F' or ' $\beta$ ' IFN, mainly derived from fibroblast cultures; and the 'T', 'immune' or ' $\gamma$ ' IFN, mainly derived from mitogen- or antigen-stimulated lymphoid cells<sup>1</sup>. Whereas several individual species of Le IFN have been purified to homogeneity<sup>2-4</sup>, it is generally considered that F IFN represents a single protein<sup>5,6</sup>. Thus current efforts to clone human fibroblast IFN mRNA sequences are based on the observation that F IFN mRNA sediments in sucrose gradients as a single RNA species of size corresponding to 12-14 S (refs 7-10). We show here, using gel electrophoresis of mRNA, that two populations of translationally active human fibroblast IFN mRNA molecules exist—an abundant '14 S' species and a scarce '11 S' species. Microinjection of either species of mRNA into *Xenopus* oocytes leads to the synthesis of biologically active F-type human IFN. These data agree with and complement recent RNA hybridization studies of Weissenbach *et al.*<sup>10</sup>.

Polyadenylated IFN mRNA was prepared from diploid human fibroblast cultures (FS-4 strain) exposed to poly(I).poly(C) and cycloheximide for 4 h as described earlier<sup>7,11</sup>. In some experiments the induced cells were fractionated using hypotonic swelling and Dounce homogenization<sup>7,11</sup> and cytoplasmic polyadenylated RNA was prepared. Appropriate amounts of IFN mRNA preparations were mixed with <sup>32</sup>P-labelled HeLa cytoplasmic RNA, the samples made 6 M in urea, heated at 95 °C for 2 min, cooled rapidly in an ice bath and electrophoresed through a cylindrical agarose-6 M urea gel<sup>12,13</sup>. Adjacent slices in the appropriate region of the gel were pooled, the RNA eluted and assayed for IFN mRNA activity by microinjection in oocytes of *Xenopus laevis*. Figure 1a shows the electrophoretic profile of translationally active IFN mRNA in preparations of cellular polyadenylated RNA from induced FS-4 cells. Figure 1b shows a similar profile of IFN mRNA in preparations of cytoplasmic polyadenylated RNA. At least two populations of IFN mRNA are clearly resolved in each



**Fig. 1** Electrophoresis of human fibroblast IFN mRNA preparations through agarose-6 M urea gels. Polyadenylated RNA preparations obtained from FS-4 cultures induced with poly(I).poly(C) (30  $\mu$ g ml<sup>-1</sup>, P.-L. Biochemicals) and cycloheximide (50  $\mu$ g ml<sup>-1</sup>, Calbiochem) for 4 h were mixed with an appropriate amount of <sup>32</sup>P-labelled HeLa cell cytoplasmic RNA in 50  $\mu$ l distilled water. The samples were made 6 M in urea (Eastman or Schwarz-Mann) and 50 mM in NaCl, and 5  $\mu$ l glycerol saturated with bromophenol blue was added. The samples were then heated at 95 °C for 2 min, cooled rapidly in an ice bath and electrophoresed through a 2.5% (a) or 2% (b) agarose (Biorad)-6 M urea cylindrical gel (0.6  $\times$  11 cm) in half-strength Loening's buffer (Tris-HCl 0.02 M, sodium acetate 0.01 M, EDTA 0.001 M, pH 7.8) at 4 °C and 5-6 mA per tube ( $\sim$ 8 V cm<sup>-1</sup>) using the modified<sup>13</sup> procedure of Locker<sup>12</sup>. After electrophoresis, the gels were sliced manually into 1-mm slices and the <sup>32</sup>P content of each slice monitored by Cerenkov counting to locate the positions of 28 S, 18 S, 5 S and 4 S marker RNA species (O). The MWs for marker RNA species were taken to be 1.75  $\times$  10<sup>6</sup>, 0.605  $\times$  10<sup>6</sup>, 3.9  $\times$  10<sup>4</sup> and 2.6  $\times$  10<sup>4</sup> for 28 S, 18 S, 5 S and 4 S RNA species, respectively<sup>29</sup>. Adjacent slices in the appropriate regions of the gel were pooled (2 slices per pool) and the RNA eluted as described elsewhere<sup>13</sup>. The RNA recovery was in the 50-80% range as estimated by the recovery of <sup>32</sup>P-labelled RNA present in each slice. Each RNA pellet was washed with 2 M LiCl and then with ethanol, dried and dissolved either in 2  $\mu$ l (a) or in 5  $\mu$ l (b) sterile distilled water. A 2- $\mu$ l aliquot of each RNA sample was microinjected into 15-20 oocytes of *X. laevis* and the oocytes incubated in 0.2 ml Barth's medium for  $\sim$ 40 h<sup>11,30</sup>. The IFN content (●) of the oocyte incubation medium (ref. 31; P.B.S., in preparation) was estimated by a semi-microassay on GM258, GM2767 or FS-4 cells with VSV as the challenge virus<sup>32,33</sup>. All IFN titres are expressed in terms of the 69/19 reference standard for human IFN. a, Cellular polyadenylated RNA (37  $\mu$ g) electrophoresed through a 2.5% agarose-6 M urea gel. b, Cytoplasmic polyadenylated RNA (30  $\mu$ g) electrophoresed through a 2% agarose-6 M urea gel.

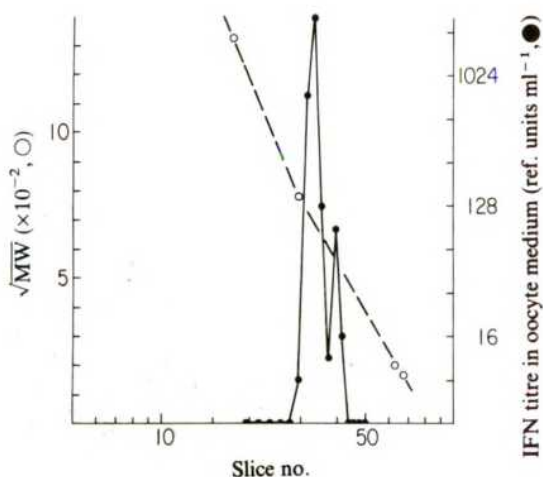


case: an abundant species of length 1,100–1,200 residues (corresponding to a sedimentation value of 14 S using the relationship  $MW/330 = \text{number of residues} = 4.7 S^{2.1}$ ) and a less abundant species of length 700–800 residues (corresponding to a sedimentation value of 11 S). For convenience we refer to these two species of mRNA as the '14 S' and '11 S' IFN mRNAs.

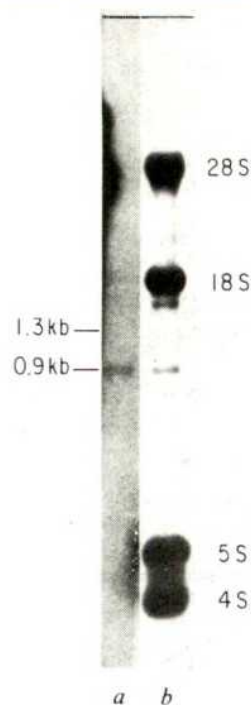
In the experiment illustrated in Fig. 1b only 40% of each RNA sample eluted from gel slices was assayed in oocytes. The remaining 60% of RNA corresponding to the individual 14 S and 11 S species was denatured once more and electrophoresed individually through another agarose-urea gel. The second set of gels was then sliced and appropriate gel slices assayed for IFN mRNA activity. Both the 14 S and 11 S species re-electrophoresed as RNA corresponding to 14 S and 11 S respectively (data not shown).

We have electrophoresed a sample of IFN mRNA through an agarose- $\text{CH}_3\text{HgOH}$  gel<sup>14–17</sup> in fully denaturing conditions (10 mM  $\text{CH}_3\text{HgOH}$ ). Figure 2 indicates that the two populations of IFN mRNA can also be resolved when RNA electrophoresis is carried out in stringent denaturing conditions. Whereas a 1.75% agarose gel was used in the experiment illustrated in Fig. 2, we now routinely use a 2% agarose gel. In these conditions the abundant species is of length 1.3 kilobases (six determinations,  $\pm 40$  residues, s.e. of mean), whereas the less abundant species is of length 0.9 kilobases (six determinations,  $\pm 40$  residues).

The translation product of the 14 S and 11 S mRNA species has been characterized as the human F-type IFN (Table 1). The antiviral activity synthesized by *Xenopus* oocytes in response to



**Fig. 2** Electrophoresis of a human fibroblast IFN mRNA preparation through an agarose- $\text{CH}_3\text{HgOH}$  gel. Cellular polyadenylated RNA (45  $\mu\text{g}$ ) obtained from induced FS-4 cells was mixed with  $^{32}\text{P}$ -labelled marker RNA and was made 10 mM in  $\text{CH}_3\text{HgOH}$  (stock 1.27 M, Alfa Division, Ventron) in half-strength borate buffer (full strength corresponds to: 0.1 M boric acid, 6 mM sodium borate, 1 mM EDTA, 10 mM sodium sulphate, pH 8.2) in a total volume of 50  $\mu\text{l}$  and was allowed to stand for 5 min at room temperature. 5  $\mu\text{l}$  of glycerol saturated with bromophenol blue was then added and the RNA electrophoresed through a 1.75% agarose-10 mM  $\text{CH}_3\text{HgOH}$  cylindrical gel (0.6  $\times$  11 cm) in borate buffer at room temperature (4 mA per tube; 3.5  $\text{V cm}^{-1}$ ) until the dye was close to the bottom of the tube gel (5 h; ref. 17). After electrophoresis the gel was placed in 100 ml of a solution containing 100 mM  $\beta$ -mercaptoethanol and 0.01 M Tris-HCl, pH 7.4, for 40 min on a rotary shaker at room temperature. The gel was then sliced manually, the locations of marker RNA (O) monitored by Cerenkov counting, RNA in appropriate regions of the gel eluted (the elution buffer contained 1 mM dithiothreitol<sup>13</sup>), dissolved in 2  $\mu\text{l}$  distilled water and assayed for IFN mRNA activity (●) as indicated in Fig. 1 legend.



**Fig. 3** Hybridization analysis of human fibroblast IFN mRNA species using  $^{32}\text{P}$ -labelled *Pst*I/*Bgl*II fragment of the IFN cDNA insert in clone TpIF319-13. Cellular polyadenylated RNA (12  $\mu\text{g}$ ) obtained from induced FS-4 cells was glyoxylated in 50% dimethylsulphoxide at 50  $^{\circ}\text{C}$  for 45 min, electrophoresed through a 1.5% agarose slab gel in 10 mM sodium phosphate buffer (pH 6.5) until the bromophenol blue dye had moved  $\sim 15$  cm from the origin.  $^{32}\text{P}$ -labelled HeLa cytoplasmic RNA was also glyoxylated and electrophoresed in an adjacent slot in the gel. After electrophoresis the RNA was transferred to APT-paper and hybridized as described by Alwine *et al.*<sup>34</sup>  $^{32}\text{P}$ -labelled *Pst*I/*Bgl*II DNA fragment of clone TpIF319-13 ( $1.7 \times 10^5$  Cerenkov c.p.m.) was heat-denatured (65  $^{\circ}\text{C}$  for 10 min in 50% formamide) and hybridized to the RNA-containing paper in 1 ml of hybridization buffer (50% formamide, 0.75 M NaCl, 0.075 M sodium citrate, 1X Denhardt's solution, 20 mM sodium phosphate buffer, pH 6.5, and 0.2% sodium dodecyl sulphate) for 72 h at 37  $^{\circ}\text{C}$ . The hybridized DNA was detected by autoradiography. The presence of the 0.9- and 1.3-kilobase translatable IFN mRNA species in the mRNA preparation used in this experiment was verified using the procedure in Fig. 2 legend. Lane a, IFN mRNA preparation; lane b,  $^{32}\text{P}$ -labelled HeLa cytoplasmic RNA. kb, Kilobases.

microinjection with individual 14 S and 11 S mRNA species is completely neutralized by anti-F IFN antiserum but is largely unaffected by anti-Le IFN antiserum.

The results presented here are directly relevant to the interpretation of recent data obtained using cloned human fibroblast IFN mRNA sequences<sup>8–10,18</sup>. Weissenbach *et al.*<sup>10</sup> have described plasmids containing cDNA inserts (in pBR322) derived from polyadenylated RNA extracted from poly(I).poly(C)-induced human diploid fibroblasts (FS-11 strain). DNA from one of these clones (clone A341), which has been identified as an 'interferon' clone, hybridizes to two populations of polyadenylated RNA from induced cells: an RNA of length 1,100–1,200 residues hybridizes strongly to this DNA probe whereas another species of length  $\sim 750$  residues hybridizes weakly. Their data do not allow one to determine whether the two populations of RNA function as translationally active IFN mRNA species as sucrose gradient sedimentation analysis by these investigators reveals a single peak of biologically active IFN mRNA sedimenting at 12–14 S (corresponding to a length of 1,100–1,200 residues). The enhanced resolution of gel electrophoretic analyses of IFN mRNA described here clearly

**Table 1** Neutralization of IFNs synthesized by *Xenopus* oocytes in response to microinjection with separated 14 S and 11 S mRNA species

| Expt               | mRNA | Residual IFN titre (ref. units ml <sup>-1</sup> ) after mixing with anti-IFN antiserum |        |                    |         |
|--------------------|------|--|--------|--------------------|---------|
|                    |      | No antiserum   | Anti-F | Anti-F and anti-Le | Anti-Le |
| 1                  | 11 S | 256  | <8     | Not done           | 128     |
|                    | 14 S | 192  | <8     | Not done           | 128     |
| 2                  | 11 S | 1,280  | <10    | <10                | 640     |
|                    | 14 S | 160  | <10    | <10                | 80      |
| 3                  | 14 S | 120  | <10    | <10                | 120     |
| Antiserum controls |      |  |        |                    |         |
| Fibroblast IFN     |      | 512  | <2     | <2                 | 256     |
| Leukocyte IFN      |      | 2,408  | 1,024  | <16                | <16     |

RNA recovered from gel slices corresponding to the peaks of 14 S and 11 S IFN mRNA as described in Fig. 1a was injected into groups of oocytes (20–30 per group), which were then incubated in 0.2 ml Barth's medium for 30–40 h at room temperature. The clarified oocyte homogenate was used to set up neutralization assays<sup>28</sup>. Briefly, 100- $\mu$ l aliquots of a 1:4 or 1:5 dilution of the oocyte homogenate in cell culture medium (Eagle's minimal essential medium containing heat-inactivated fetal bovine serum, 10% v/v) was mixed with 2  $\mu$ l (expts 2, 3 and control IFN preparations or 10  $\mu$ l (expt 1) anti-F IFN antiserum (batch 2 + 282) or 10  $\mu$ l of a 1:10 dilution of anti-Le IFN antiserum (batch 903) or both. Controls free of antiserum were mixed with an appropriate volume of culture medium. The samples were incubated for 60–90 min at 37 °C and serial twofold dilutions (50- or 100- $\mu$ l aliquots) of each sample were added to confluent, 1-day-old monolayers of human GM258 cells in multiwell microtitre dishes. The cultures were incubated for 20–24 h at 37 °C, the IFN- and antiserum-containing medium was removed and replaced with fresh culture medium containing vesicular stomatitis virus (VSV). The residual IFN titre represents the reciprocal of the highest dilution of the original oocyte homogenate that protected GM258 cell monolayers and is expressed in terms of the 69/19 reference standard for human IFN. Fibroblast IFN used to test the specificity of the antisera was prepared by superinduction of FS-4 cell cultures with poly(I):poly(C), cycloheximide and actinomycin D<sup>33</sup>, whereas the leukocyte IFN used was prepared by induction of human peripheral blood buffy coat preparations with Sendai virus.

demonstrates that both populations of RNA represent translationally active mRNA species for human F-type IFN.

Human fibroblast IFN mRNA sequences have also been cloned by a group of Japanese investigators<sup>8,9,18</sup>. The DNA restriction map and nucleotide sequence obtained by Taniguchi *et al.* (clone TpIF319-13, ref. 18) is different from that for clone A341 (M. Revel and M. Zeevi, personal communication). Therefore it seemed likely that clone A341 would correspond to the 1.3-kilobase IFN mRNA and that clone TpIF319-13 would correspond to the 0.9-kilobase mRNA species. Figure 3 presents a test of this hypothesis. Polyadenylated RNA obtained from induced FS-4 cells was denatured by glyoxylation, electrophoresed in a 1.5% agarose slab gel, transferred to APT-paper and hybridized to <sup>32</sup>P-labelled, nick-translated, 359-base pair, *Pst*I/*Bgl*II DNA fragment of the cDNA insert in clone TpIF319-13. This DNA fragment corresponds to the middle and carboxy-terminal portions of the human fibroblast IFN coding sequence. It can be seen from Fig. 3 that this probe hybridized exclusively to an RNA species of approximate length 0.9 kilobase. Thus the 1.3-kilobase fibroblast IFN mRNA has a sequence which is substantially different from that of clone TpIF319-13.

Although we have resolved two size classes of human F IFN mRNA by electrophoresis in agarose gels, we cannot exclude further sequence heterogeneity within each size class.

Data on the effect of glycosylation inhibitors on the physical properties of fibroblast IFN synthesized in their presence (ref. 19; Y. K. Yip and J. Vilček, personal communication) as well as recent protein fractionation studies (refs 20, 21; E. Knight Jr,

personal communication) suggest the existence of more than one human F-type IFN protein. This heterogeneity may reflect the existence of distinct chromosomal genes for fibroblast IFN such as on human chromosome 2 or 5 or 9 (refs 22, 23). Alternatively, the heterogeneity may arise from the existence of alternative pathways for processing the primary transcript of IFN gene(s) in the cell nucleus.

The existence of multiple species of human leukocyte (Le)-type human IFNs as well as of murine IFNs has been clearly demonstrated<sup>2-4,24,25</sup>. Furthermore, recent nucleic acid cloning experiments demonstrate the existence of at least two distinct sequences for human Le IFN<sup>26,27</sup>. Gel electrophoretic analyses of IFN mRNA species from these sources may be highly instructive. It is likely that IFN genes constitute a large multi-genic family of inducible genes which code for cellular proteins with antiviral, anticellular and immunomodulatory effects in eukaryotic cells.

This investigation was partly stimulated by a seminar given by Dr Michel Revel at The Rockefeller University on 18 February 1980. We thank Dr T. Taniguchi for the <sup>32</sup>P-labelled *Pst*I/*Bgl*II DNA fragment of clone TpIF319-13 and Mr Benjamin Neel for assistance in carrying out the blot-hybridization experiment. We also thank Drs I. Tamm, J. Vilček, E. A. Havell, E. Knight and M. Zeevi for helpful discussions, Drs J. Vilček and E. A. Havell for the anti-IFN antisera, Dr W. E. Stewart II for a sample of human Le IFN and Drs T. Taniguchi, M. Revel and K. Cantell for preprints. We thank Mr Ira Augenzucker for technical assistance. This investigation was supported by NIAID, DHEW grant AI-16262. P.B.S. is the recipient of a Junior Faculty Research Award from the American Cancer Society.

**Note added in proof:** In accordance with current guidelines for interferon nomenclature [*Nature* **286**, 110 (1980)], we suggest that the translation product of the 0.9-kilobase IFN mRNA (Fig. 2) be designated human interferon- $\beta_1$  and that of the 1.3-kilobase IFN mRNA be designated human interferon- $\beta_2$ .

Received 9 April; accepted 26 August 1980.

- Stewart, W. E. II *The Interferon System* (Springer, Berlin, 1979).
- Rubinstein, M. *et al. Proc. natn. Acad. Sci. U.S.A.* **76**, 640–644 (1979).
- Zoon, K. C., Smith, M. E., Bridgen, P. J., Zur Nedden, D. & Anfinson, C. B. *Proc. natn. Acad. Sci. U.S.A.* **76**, 5601–5605 (1979).
- Zoon, K. C. *et al. Science* **207**, 527–528 (1980).
- Tan, Y. H., Barakat, F., Berthold, W., Smith-Johannsen, H. & Tan, C. J. *biol. Chem.* **254**, 8067–8073 (1979).
- Knight, E. Jr, Hunkapiller, M. W., Korant, B. D., Hardy, R. W. F. & Hood, L. E. *Science* **207**, 525–526 (1980).
- Sehgal, P. B., Lyles, D. S. & Tamm, I. *Virology* **89**, 186–198 (1978).
- Taniguchi, T. *et al. Proc. Jap. Acad.* **55**, Ser. B, 464–469 (1979).
- Taniguchi, T., Fujii-Kuriyama, Y. & Muramatsu, M. *Proc. natn. Acad. Sci. U.S.A.* **77**, 4003–4006 (1980).
- Weissenbach, J. *et al. Proc. natn. Acad. Sci. U.S.A.* (in the press).
- Sehgal, P. B., Dobberstein, B. & Tamm, I. *Proc. natn. Acad. Sci. U.S.A.* **74**, 3409–3413 (1977).
- Locker, J. *Analyt. Biochem.* **98**, 358–367 (1979).
- Sehgal, P. B. *Meth. Enzym.* (Academic, New York, in the press).
- Bailey, J. M. & Davidson, N. *Analyt. Biochem.* **70**, 75–85 (1976).
- Bryan, R. N., Cutler, G. A. & Hayashi, M. *Nature* **272**, 81–83 (1978).
- Dunn, A. R., Mathews, M. B., Chow, L. T., Sambrook, J. & Keller, W. *Cell* **15**, 511–526 (1978).
- Maxwell, I. H., Maxwell, F. & Hahn, W. E. *Analyt. Biochem.* **99**, 146–160 (1979).
- Taniguchi, T., Ohno, S., Fujii-Kuriyama, Y. & Muramatsu, M. *Gene* **10**, 11–15 (1980).
- Havell, E. A., Yamazaki, S. & Vilček, J. *J. biol. Chem.* **252**, 4425–4427 (1977).
- Davey, M. W., Sulikowski, E. & Carter, W. A. *Biochemistry* **15**, 704–713 (1976).
- Senussi, O. A., Cartwright, T. & Thompson, P. *Arch. Virol.* **62**, 323–331 (1979).
- Slate, D. L. & Ruddle, F. H. *Cell* **16**, 171–180 (1979).
- Meager, A., Graves, H., Burke, D. C. & Swallow, D. M. *Nature* **280**, 493–495 (1979).
- DeMaeyer-Guignard, J., Tovey, M. G., Gresser, I. & De Maeyer, E. *Nature* **271**, 622–625 (1978).
- Taira, H. *et al. Science* **207**, 528–530 (1980).
- Nagata, S. *et al. Nature* **284**, 316–320 (1980).
- Mantei, N. *et al. Gene* **10**, 1–10 (1980).
- Havell, E. A. *et al. Proc. natn. Acad. Sci. U.S.A.* **72**, 2185–2187 (1975).
- Spohr, G., Mirault, M.-E., Imaizumi, T. & Scherrer, K. *Eur. J. Biochem.* **62**, 313–322 (1976).
- Reynolds, F. H. Jr, Premkumar, E. & Pitha, P. *Proc. natn. Acad. Sci. U.S.A.* **72**, 4881–4885 (1975).
- Colman, A. & Morser, J. *Cell* **17**, 517–526 (1979).
- Armstrong, J. A. *Appl. Microbiol.* **21**, 723–725 (1971).
- Havell, E. A. & Vilček, J. *Antimicrob. Ag. Chemother.* **2**, 476–484 (1972).
- Alwine, J. C., Kemp, D. J. & Stark, G. R. *Proc. natn. Acad. Sci. U.S.A.* **74**, 5350–5354 (1977).



## Interferon-dependent induction of mRNA activity for (2'-5')oligo-isoadenylate synthetase

Lester Shulman & Michel Revel

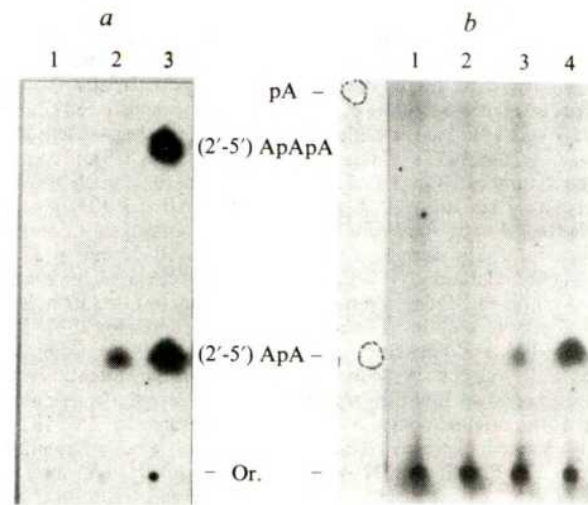
Department of Virology, Weizmann Institute of Science, Rehovot, Israel

At least three different enzymes involved in the regulation of protein synthesis are induced in a variety of cells by interferon (IFN)<sup>1-5</sup>. Sensitive assays for these enzymes have been developed and used to establish the specificity, dose dependence and time course of their induction by IFN<sup>5-8</sup>. One of these enzymes, the oligo-isoadenylate synthetase E, whose product (2'-5')pppApApA<sup>9</sup> activates the latent ribonuclease F<sup>10-11</sup>, is increased over 50-fold after IFN treatment. We describe here the assay for an mRNA from IFN-treated mouse L cells, that produces oligo-isoadenylate synthetase activity when injected into *Xenopus* oocytes. This mRNA is found in the cells only after exposure to IFN. The mRNA increases in mouse L cells with the same time course as the enzyme activity itself. In particular, there is a 3-h lag period between IFN addition and the onset of enzyme and mRNA accumulation. Using anti-IFN antibodies, we show that during this lag period the continued interaction of IFN with the cells is necessary for the full induction of the oligo-isoadenylate synthetase.

Poly(A)-containing RNAs<sup>12</sup> were prepared from cytoplasmic extracts of L929 monolayer cultures which had been exposed for different times to 200 U ml<sup>-1</sup> mouse IFN<sup>5</sup>. The RNAs were injected into *Xenopus laevis* oocytes<sup>13</sup>, extracts from these oocytes were added to poly(rI)·(rC)-agarose beads, which were then incubated with [ $\alpha$ -<sup>32</sup>P]ATP to measure the synthesis of (2'-5')oligo-isoadenylate as previously described<sup>5</sup>. In parallel, the cellular level of the oligo-isoadenylate synthetase was measured in the NP40 cytoplasmic extracts from the same cultures (Fig. 1a). Formation of the phosphatase-resistant (2'-5')(Ap)<sub>n</sub>A oligonucleotides is only seen with extracts from IFN-treated cells. Figure 1b (lane 1) shows that extracts of *Xenopus* oocytes do not normally form any (2'-5')ApA by themselves (see also ref. 6), but (2'-5')ApA synthesis appeared clearly in extracts of oocytes injected with poly(A)<sup>+</sup>-mRNA from IFN-treated cells (lane 4). Identification of this activity in injected oocytes, with the IFN-induced oligo-isoadenylate synthetase, is based on the following arguments: (1) Formation of the (2'-5')ApA results from an enzymatic activity which binds to the poly(rI)·(rC)-agarose beads, no significant activity being detected without this purification step. (2) The activity appears only if mRNA from IFN-treated cells is injected into the oocytes (compare lanes 2 and 4 in Fig. 1). (3) The phosphatase-treated products, labelled with [ $\alpha$ -<sup>32</sup>P]ATP, co-migrated in several thin-layer chromatography and electrophoresis systems<sup>9,10</sup>, with chemically synthesized (2'-5')ApA markers. The predominance of dimers in the oocyte products is due to the low level of enzyme used; the same is found when a limited reaction is carried out with purified synthetase<sup>10</sup>. (4) Finally, the products of a large-scale reaction (with 1 ml oocyte extract instead of the 0.02 ml routinely used) inhibited Mengo RNA translation in L-cell extracts (Table 1) proving that biologically active (2'-5')oligo(A) is formed. In these conditions (2'-5')oligo trimers were seen by electrophoresis of the phosphatase-treated products (not shown). No translational inhibition was found with the products of mRNA from cells not treated with IFN.

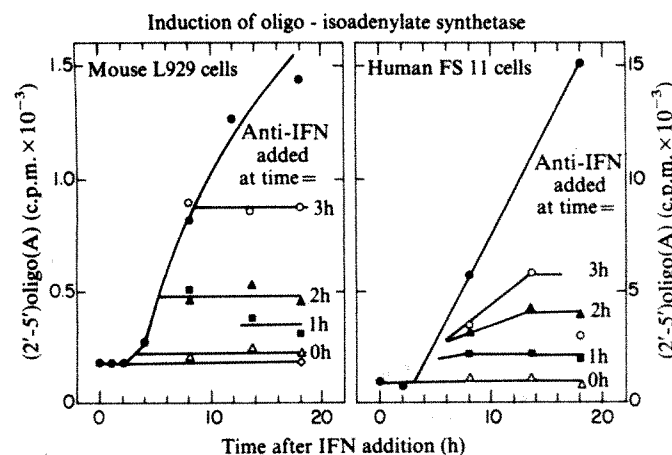
In conditions where (2'-5')oligo(A) synthesis is proportional to the amount of extract used, we compared the oligo-iso-

adenylate synthetase activity in L cells and in mRNA-injected oocytes (Table 1, right). The enzyme activity produced in oocytes by injection of mRNA from L cells treated for 8 h with IFN represents ~1% of the enzyme activity present in the same volume of cell extract from which the mRNA was prepared. We verified that untreated-cell mRNA, which does not yield synthetase activity, is not inhibitory in our assay: 33,400 c.p.m. (2'-5')ApA were formed with extracts of oocytes injected with 1  $\mu$ g of 8h-mRNA, against 3,600 c.p.m. for 0h-mRNA, and 45,100 c.p.m. for the mixture of 0h- and 8h-mRNA. The accumulation of oligo-isoadenylate synthetase in L cells exposed to IFN is, therefore, accompanied by a proportional increase in an mRNA yielding this enzymatic activity in the oocyte assay. In similar experiments, we have found that exposure of human lymphoblastoid Namalva cells to leukocyte



**Fig. 1** Formation of active oligo-isoadenylate synthetase by translation of IFN-induced mRNA in *Xenopus* oocytes. L929 monolayer cultures in minimal Eagle's medium with 8% calf serum were exposed for 0, 3 or 8 h at 37°C to 200 U ml<sup>-1</sup> mouse IFN (induced in L cells by Newcastle disease virus and purified at 10<sup>7</sup> U per mg protein<sup>5</sup>). Cells from seven plates were washed with 35 mM Tris-HCl pH 7.5, 140 mM KCl, 3 mM Mg acetate and lysed with 0.5% Nonidet P40 (NP40) in 5 mM Tris-HCl pH 7.8, 100 mM NaCl, 3 mM Mg acetate (2 ml per plate). After 30 min, nuclei were removed by centrifugation at 2,000g for 10 min. **a**, Enzyme activity in cell extracts. 20  $\mu$ l cytoplasmic extract was mixed with 50  $\mu$ l poly(rI)·(rC)-agarose beads (P.L. Biochemicals). After 10 min at 30°C, unbound proteins were removed by washing the beads twice in 20 mM HEPES buffer pH 7.5, 120 mM KCl, 5 mM MgCl<sub>2</sub>, 1 mM dithiothreitol, 10% glycerol (Buffer B). Beads were incubated in 10  $\mu$ l of 2.5 mM [ $\alpha$ -<sup>32</sup>P]ATP (0.24 Ci mmol<sup>-1</sup>) and 2.5 mM dithiothreitol for 20 h at 30°C. Beads were centrifuged down, washed with 10  $\mu$ l water and the two supernatants combined. 6  $\mu$ l were treated with bacterial alkaline phosphatase and subjected to paper electrophoresis at pH 3.5 (4 kV, 3 h) and autoradiography as previously described<sup>3</sup>. Positions of (2'-5')ApA and ApApA were indicated by synthetic markers. Extracts of cells treated 0 h (lane 1), 3 h (lane 2) and 8 h (lane 3) with IFN are shown. **b**, Enzyme synthesized in oocytes. To the cytoplasmic extracts, 3 mM EDTA and 0.5% dodecyl sulphate were added and RNA was extracted three times by 1 vol phenol-chloroform-isoamylalcohol (50:50:1), precipitated with 2 vol ethanol and the poly(A)<sup>+</sup> sequences was purified on oligo(dT)-cellulose<sup>12</sup>. Groups of 10 *Xenopus* oocytes were injected with 50 ng RNA (in 50 nl) per oocyte as described by Gurdon *et al.*<sup>13</sup>. The oocytes were kept in 0.15 ml Barth's medium for 20 h and then homogenized with 0.5 ml Buffer B. Aliquots (20  $\mu$ l) of homogenate were used to assay (2'-5')oligo(A) synthesis as above. Lane 1, water-injected oocytes; lanes 2, 3 and 4, oocytes injected with mRNA from L cells, treated 0, 3 and 8 h with IFN, respectively. UV spots of markers are shown. All radioactive spots were cut out and counted by Cerenkoff radiation in a scintillation counter. Results are given in Table 1.





**Fig. 2** Delayed effect of anti-IFN antibodies on oligo-isoadenylate synthetase E induction by IFN. Monolayer cultures of mouse L929 or human foreskin FS11 cells (about  $3 \times 10^4$  cells per well of a 96-well microplate) received  $50 \text{ U ml}^{-1}$  mouse L-cell IFN or  $15 \text{ U ml}^{-1}$  human fibroblast IFN<sup>19</sup>, respectively. The level of enzyme E was measured as before<sup>5</sup>, at the time indicated on the abscissa. Antibodies to mouse L-cell IFN or antiserum to human fibroblast IFN obtained in rabbits<sup>19</sup> were added (at dilutions of 1/100 and 1/20, respectively, see Table 2) at the indicated times after IFN addition. The lower activity of the L cells reflects use of less radioactive ATP in this assay.

IFN also induces mRNA yielding oligo-isoadenylate synthetase activity in the oocyte assay (not shown).

In cell cultures exposed to IFN, induction of the oligo-isoadenylate synthetase does not start immediately on addition of IFN but is preceded by a 2–3-h lag period (ref. 5 and Fig. 2). This lag is characteristic of IFN action and does not depend on the amount of IFN used. With the oocyte assay we compared the level of mRNA activity for the oligo-isoadenylate synthetase, at 3 and 8 h after IFN addition. Although some mRNA activity can be detected at 3 h (Fig. 1b, lane 3), over 90% of the mRNA present at 8 h is formed during the 3–8-h period, whereas less than 10% is made from 0–3 h after IFN addition (Table 1). A more than 10-fold increase in mRNA activity from 3 to 8 h could also be calculated from the translation inhibition experiment shown in Table 1: 50% inhibition was seen at a 1:1,000 dilution for the 3-h mRNA products and at 1:20,000 for the 8-h mRNA products. Like enzyme synthesis, induction of the mRNA seems, therefore, to be a slow process.

This delayed response to IFN prompted us to examine how long IFN has to interact with the cells to trigger oligo-isoadenylate synthetase induction. Antibodies against mouse IFN were added to L-cell cultures to interrupt the action of IFN at different times after its addition. When added together with IFN, the antibodies blocked completely induction of oligo-isoadenylate synthetase, whereas replication of vesicular stomatitis virus (VSV) was able to proceed normally as in the absence of IFN (Table 2). Antibodies, therefore, block the cell response to IFN but do not impair other cell functions such as viral replication. The effect is specific as anti-mouse IFN did not inhibit oligo-isoadenylate synthetase induction by human IFN in human cells and, conversely, anti-human fibroblast IFN did not inhibit the effect of mouse IFN on L cells (Table 2). Figure 2 shows that, in mouse and human cells, the delayed addition of antibodies, at 1, 2 or 3 h after IFN addition, can still interrupt the already initiated process of enzyme induction. Enzyme accumulation starts but stops at a certain level. The enzyme level reached increases with the time between IFN and anti-IFN additions. Thus, when anti-mouse IFN is added to L cells 3 h after IFN, the induction proceeds for 8 h but then stops. Thus, to complete the induction process, IFN has to act for more than 3 h,

that is, beyond the lag period. In human foreskin cells, the kinetics of synthetase induction are somewhat slower than in mouse L cells<sup>5</sup>, and as shown in Fig. 2, the inhibition by delayed addition of antibodies is even more pronounced than in L cells. The antiviral effect of IFN against VSV replication in these cells was also inhibited by antibodies against human IFN, 3 h after IFN addition (not shown).

Antibodies do not penetrate inside living cells<sup>14</sup>. The inhibitory effects of anti-IFN added 2 or 3 h after IFN probably results, therefore, from neutralization of IFN molecules still present outside the cell. Although IFN binds rapidly to cells<sup>15</sup>, it does not seem to enter the cell rapidly, as already suggested by experiments with antibodies to the chromosome 21-coded human IFN receptor<sup>16,17</sup>. The lag period in the oligo-isoadenylate synthetase induction could then be explained by a prolonged action of IFN outside the cell, the resistance to neutralization by antibodies developing only just before the enzyme and its mRNA activity measured in the oocyte assay start to accumulate in the cytoplasm of the cells. The parallel increase in translatable mRNA and in enzyme observed in our

**Table 1** Induction by interferon of mRNA for oligo-isoadenylate synthetase

| Time after IFN addition (h) | Oligo-isoadenylate synthetase activity      |       |  |               |
|-----------------------------|---|-------|--|---------------|
|                             | % Translation inhibition with               |       | <sup>32</sup> P-(2'-5')oligo(A) synthesis† |               |
|                             | products of mRNA-injected oocytes* Dilution | 1:250 | 1:25,000                                   |               |
| 0                           | 2   | 0     | 45 (1)                                     | 13,660 (4)    |
| 3                           | 87  | 6     | 275 (8)                                    | 54,170 (17)   |
| 8                           | 95  | 44    | 3,410 (100)                                | 316,670 (100) |

Figures in parentheses are per cent of the 8-h enzyme level.

\* Measured by Mengo virus RNA translation in L-cell extracts as in ref. 3. <sup>35</sup>S-methionine incorporation without oligonucleotides was 94,500 c.p.m. A background without mRNA of 3,000 c.p.m. was subtracted. The oligonucleotide products from 1 ml oocyte extract were diluted as indicated in the 0.25 ml translation reaction mixture.

† Measured by [ $\alpha$ -<sup>32</sup>P]ATP incorporation into (2'-5')ApA + ApApA cores with 0.02 ml oocyte extract as in Fig. 1 legend; calculated for 1  $\mu$ g poly(A)<sup>+</sup> mRNA and for the 0.25 ml cytoplasmic extract from which this RNA originates.

**Table 2** Use of anti-interferon antibodies to inhibit oligo-isoadenylate synthetase induction

| IFN       | Antibodies to IFN | Oligo-isoadenylate synthetase <sup>32</sup> P-(2'-5')oligo(A) (c.p.m.) |             | VSV growth (PFU ml <sup>-1</sup> ) |
|-----------|-------------------|--|-------------|------------------------------------|
|           |                   | Mouse cells  | Human cells | Mouse cells                        |
| None      | None              | 1,750  | 725         | $4.4 \times 10^{10}$               |
| Mouse IFN | None              | 20,500   | —           | $2 \times 10^8$                    |
| Mouse IFN | Anti-mouse IFN    | 2,120  | —           | $4.3 \times 10^{10}$               |
| Human IFN | None              | —  | 5,175       | —                                  |
| Human IFN | Anti-mouse IFN    | —  | 5,270       | —                                  |
| None      | None              | 4,610  | 2,500       | —                                  |
| Mouse IFN | None              | 32,830   | —           | —                                  |
| Mouse IFN | Anti-human IFN    | 32,055   | —           | —                                  |
| Human IFN | None              | —  | 16,100      | —                                  |
| Human IFN | Anti-human IFN    | —  | 2,600       | —                                  |

IFN and anti-IFN antibodies were added together to the cells, in the conditions described in Fig. 2 legend. The enzyme assay was carried out after 8 h for mouse L929 cells and after 14 h for human foreskin FS11 cells. Where indicated, mouse cells were infected at 8 h with 4 PFU per cell VSV and the virus growth was measured 24 h later. PFU, plaque-forming units.



experiments suggests that the main control of enzyme accumulation is formation of new mRNA. This is consistent with the inhibition of induction by actinomycin D, and by cycloheximide, which also indicates that there is no activation of a preformed enzyme in the cells<sup>5</sup>. We had previously reported<sup>3</sup> that actinomycin D added 2 h after IFN does not block any more oligo-isoadenylate synthetase induction in L cells: this seems to contradict the more than 10-fold increase in mRNA measured by the oocyte assay from 3 to 8 h after IFN addition. On the other hand, the results obtained by delayed antibody addition are in line with the kinetics of mRNA accumulation. Actinomycin D causes a phenomenon of superinduction<sup>5</sup>, and the normal level of enzyme found when actinomycin D is added at 2 h may reflect a more efficient expression of a smaller amount of mRNA. Actinomycin D cannot, therefore, be easily used to analyse the induction process.

The mRNA assay described here should facilitate the study of the mechanism by which IFN induces oligo-isoadenylate

synthetase, a process tightly correlated with its biological activity<sup>5,7,8</sup>. An important question still to be solved is whether the mRNA product is the enzyme itself, a regulatory factor or a combination of polypeptides. This question cannot be answered until the polypeptide structure of the enzyme is determined. Farrell *et al.*<sup>18</sup> have described the synthesis of some proteins by translation of IFN-induced mRNAs in reticulocyte lysates, but could not identify any enzymatic activity. The oocyte assay demonstrates for the first time that IFN induces in the cells an mRNA involved in the synthesis of oligo-isoadenylate synthetase.

We acknowledge helpful suggestions from Dr H. Sorek and D. Givon and the technical assistance of Ms Sara Tzur. Synthetic markers for the assay were given by Dr S. Rapoport and Y. Lapidot, and antibodies to mouse L-cell IFN by Dr G. Galasso. This work was supported by GSF (Israel) and NCRD (München).

Received 28 February; accepted 2 September 1980.

1. Roberts, W. K., Hovanessian, A., Brown, R. E., Clemens, M. J. & Kerr, I. M. *Nature* **264**, 477–480 (1976).
2. Revel, M. *et al. Proc. 11th FEBS Meet.* **43**, 47–58 (1977).
3. Zilberstein, A., Kimchi, A., Schmidt, A. & Revel, M. *Proc. natn. Acad. Sci. U.S.A.* **75**, 4734–4738 (1978).
4. Farrell, P. J. *et al. Proc. natn. Acad. Sci. U.S.A.* **75**, 5893–5897 (1978).
5. Kimchi, A. *et al. Proc. natn. Acad. Sci. U.S.A.* **76**, 3208–3212 (1979).
6. Stark, G. R., Dower, W. J., Schimke, R. T., Brown, R. E. & Kerr, I. M. *Nature* **278**, 471–473 (1979).
7. Ball, L. A. *Virology* **94**, 282–296 (1979).

8. Baglioni, C., Maroney, P. A. & West, D. K. *Biochemistry* **18**, 1765–1768 (1979).
9. Kerr, I. M. & Brown, R. E. *Proc. natn. Acad. Sci. U.S.A.* **75**, 256–260 (1978).
10. Schmidt, A. *et al. FEBS Lett.* **25**, 257–264 (1978).
11. Slattery, E., Ghosh, N., Samanta, H. & Lengyel, P. *Proc. natn. Acad. Sci. U.S.A.* **76**, 4778–4782 (1979).
12. Aviv, H. & Leder, P. *Proc. natn. Acad. Sci. U.S.A.* **69**, 1408–1412 (1972).
13. Gurdon, J. B., Lane, C. D., Woodland, H. R. & Marbaix, G. *Nature* **233**, 177–182 (1971).
14. Nicolson, G. L. in *Membrane Research* (ed. Fox, C. P.) 53–70 (Academic, New York, 1972).
15. Bermann, B. & Vilcek, J. *Virology* **57**, 378–386 (1974).
16. Revel, M., Basch, D. & Ruddle, F. H. *Nature* **260**, 139–141 (1976).
17. Revel, M. in *Interferon 1979* (ed. Gresser, I.) 154–156 (Academic, New York, 1979).
18. Farrell, P., Broeze, R. J. & Lengyel, P. *Nature* **279**, 523–525 (1979).
19. Weissenbach, J., Zeevi, M., Landau, T. & Revel, M. *Eur. J. Biochem.* **98**, 1–8 (1979).

## Transcriptional fidelity of histone genes injected into *Xenopus* oocyte nuclei

Ch. Hentschel, E. Probst & M. L. Birnstiel

Institut für Molekularbiologie II der Universität Zürich, Hönggerberg, 8093 Zürich, Switzerland

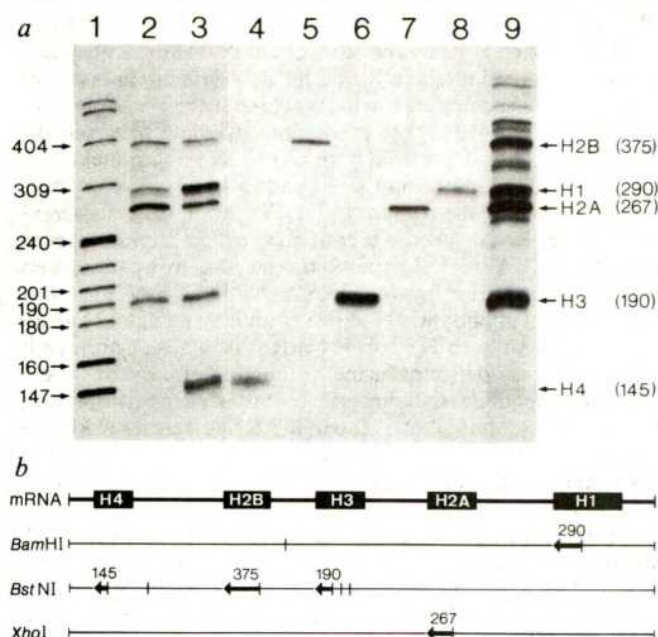
Previous work has indicated that at least some of the genetic information required for the expression of sea urchin histone genes is recognized following injection of the gene repeat (h22) into *Xenopus* oocyte nuclei<sup>1,2</sup>. The ability to elicit the expression of cloned genes and their sequence-manipulated counterparts is proving invaluable in analysing the molecular details of gene expression<sup>2,3</sup>. Direct injection of such genes into *Xenopus* oocyte nuclei remains one of the simplest methods for obtaining such expression and a remarkable degree of transcriptional fidelity has been demonstrated using this system with RNA polymerase III genes<sup>4–9</sup>, and to a lesser extent with rDNAs transcribed by RNA polymerase I<sup>10,11</sup>. In the case of polymerase II genes there is ample evidence for coupled transcription-translation<sup>12–14</sup>, but the degree of transcriptional fidelity involved may, as has recently been shown for the ovalbumin gene<sup>15</sup>, be minimal. However, clearly if the oocyte is to be used to investigate transcriptional regulation of such genes, transcriptional fidelity defined as the production of correct RNA termini, rather than the production of 'functional mRNAs' (ref. 15), must pertain<sup>16</sup>. Here we demonstrate such fidelity in the expression of all five *Psammechinus miliaris* histone genes comprising a repeat unit. However, we find large quantitative variations in the levels of synthesis of the individual correct termini and hence of the mRNAs. In addition to the mRNAs, species with no detectable counterparts in the sea urchin are generated off the coding strand, as are heterogeneous noncoding species.

We have previously shown that RNA electrophoretically indistinguishable from authentic H2A and H2B mRNAs is synthesized by polymerase II-transcribing supercoiled micro-

injected histone gene repeats<sup>1</sup>. Moreover, the histone DNA must be free of vector DNA<sup>1</sup> because its presence (both in *trans* and in *cis*) is strongly inhibitory. We have also argued that these mRNAs are essentially primary transcripts<sup>17</sup>, and thus reflect faithful transcription in the oocyte<sup>1,2</sup>. Consequently, the lack of high levels of the other mRNAs (H3, H4, H1) implied some transcriptional deficiency such as a lack of fully functional promoters for these genes with respect to the *Xenopus* enzymes. This explanation seemed most probable for the H1 and H4 genes, as they (in contrast to the H3 as well as the H2A and the H2B genes) lack clear versions of the TATAAATA and cap sequence upstream of the structural genes<sup>17</sup>.

To test this idea we needed to assay levels of correct promotion (production of 5' termini) independent of termination. We therefore cut the h22 repeat with a combination of restriction enzymes which produced fragments five of which gave suitable overlaps to all the h22 5'-mRNA termini from within the coding sequence (Fig. 1b). As the 5' termini of the mRNAs have been mapped previously<sup>17</sup>, the lengths of the overlaps could be predicted and the relative levels of the correct 5' termini in RNA samples visualized by a multi-probe 5' S<sub>1</sub> mapping technique (see Fig. 1 legend). When authentic sea urchin RNA is used with this probe, there are, as predicted, strong bands protected by the 5'-terminal sequences of the five histone mRNAs and with the anticipated sizes (Fig. 1, lane 3). Positive identification of the correspondence of bands to given mRNAs was achieved by mapping partially purified mRNAs with the multiple probe (lanes 4–8, H4, H2B, H3, H2A, H1 mRNAs, respectively). The faint high-molecular-weight bands are due to renatured DNA probe fragments whose labelled ends were not removed by S<sub>1</sub> nuclease because they co-migrate with the input DNA and are observed independently of the RNA (not shown).

These results with authentic sea urchin mRNAs may be compared with the strikingly similar pattern of protected bands observed when h22-injected oocyte RNA is used as the RNA component of the reaction (Fig. 1, lane 2). Bands corresponding to all the correct mRNA 5'-terminal sequences are present, indicating a qualitatively correct promotion of these genes but with relative intensities significantly different from those present in the sea urchin RNA. This is most evident for the H4 5' band which, although relatively very faint, is nevertheless clearly

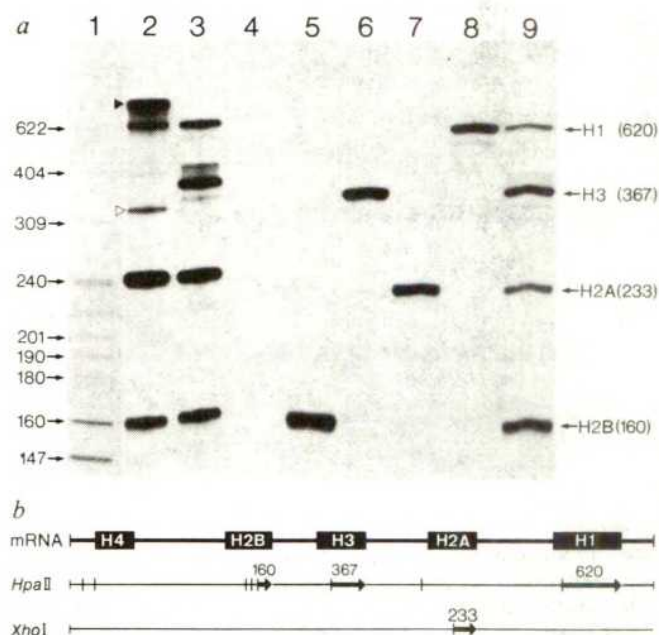


**Fig. 1** Multiple-probe  $S_1$  mapping of h22 5' mRNA terminal sequences present in sea urchin-derived RNA or in h22-injected *Xenopus* oocyte RNA.  $S_1$  mapping was carried out essentially as described previously for individual 5' mRNA termini<sup>17</sup>, but scaled down to 10  $\mu$ l and with a 5'  $^{32}$ P-labelled, triple restriction digest (*Bam*II, *Bst*NI and *Xho*I) of the h22 repeat DNA as probe. The cognate DNA protected by the histone mRNA 5'-terminal sequences is shown in panel b. The indicated lengths of DNA protection by the individual mRNAs are calculated from previous mapping of the 5' termini and the DNA sequence<sup>17</sup>. Note that labelled 5' ends outside the mRNA map cannot be protected from  $S_1$  within a mRNA/DNA hybrid and are even susceptible in DNA duplex because they overhang the 3' termini. a, Lane 1,  $^{32}$ P-labelled DNA size marker<sup>19</sup>; lane 2, 5–14S sucrose gradient-purified h22-injected oocyte RNA from approximately two oocytes each injected with 4 ng of h22 circles and incubated overnight at 18 °C (ref. 20); lane 3, 5  $\mu$ g of total RNA from *P. miliaris* embryos at the 128-cell stage of development; lanes 4–8, partially purified *P. miliaris* histone mRNAs<sup>21</sup>, in order H4, H2B, H3, H2A and H1; lane 9, longer exposure of lane 2. Experiments in lanes 2 and 3 and 4–8 were carried out in parallel. Faint high-molecular-weight bands are due to renatured probe (see text). Numbers in parentheses indicate the size in bases.

present with longer exposure (lane 9). The H1 band is also relatively less intense than the H2B, H2A and, surprisingly, the H3 band. We interpret these differences in abundance of 5'-terminal sequences as reflecting differential promotion of the mRNA transcripts<sup>1,2,17</sup>. The alternative explanation of differential stabilities can be ruled out by our observation that the *de novo* synthesized histone mRNAs are essentially stable in the oocyte (ref. 1 and unpublished data), in apparent contrast to histone mRNAs directly injected into the oocyte cytoplasm<sup>18</sup>.

Thus, we also conclude from this experiment that differential transcription of correct histone mRNA 5'-terminal sequences in h22-injected oocyte RNA reflects the differential pattern of expression of the complete mRNAs except in the case of H3 gene, where the high levels of correct H3 5'-terminal sequences are not matched by an equal abundance of the mRNA<sup>1</sup>. A deficiency in the production of the correct 3' terminus for this mRNA, presumably as a result of poor termination, could account for this discrepancy. To test this idea and to demonstrate the fidelity in the production of 3' termini by the oocyte, we performed a multiple-probe  $S_1$  mapping similar in concept to that used for the 5' termini but with 3'-end-labelled *Xho*I/*Hpa*II fragments capable of mapping all but the H4 histone mRNA 3'

termini (Fig. 2b). The results using the sea urchin RNA or partially purified individual mRNA are shown in Fig. 2, lanes 3–9. When the h22-injected oocyte RNA is used with this probe (Fig. 2, lane 2), presumptive correct termination is indicated by strong bands corresponding to correct H1, H2A and H2B 3'-terminal sequences, but, as anticipated, only a faint band at the H3 position is observed. In fact, the H3 mRNA 3' terminus seems to be the only mRNA 3' terminus whose production is quantitatively deficient, because in a separate experiment (not shown) we detected H4 mRNA 3'-terminal sequences in an abundance which matched transcripts originating from correct H4 mRNA 5' termini. In contrast, the large imbalance of correct H3 mRNA 5' over 3' termini must be compensated by H3 RNA species with incorrect 3' termini. Further examination of Fig. 2, lane 2 suggests synthesis in the oocyte of RNA species comprising the correct H3 5'-terminal sequences but with long 3' extensions compared with the mRNA. Thus, the input *Hpa*II fragment used to probe the H3 3' region (indicated by a closed arrowhead) is protected from the  $S_1$  to a much greater extent than other input fragments, as is the next fragment transcriptionally downstream (*Hpa*II/*Xho*I; open arrowhead) which

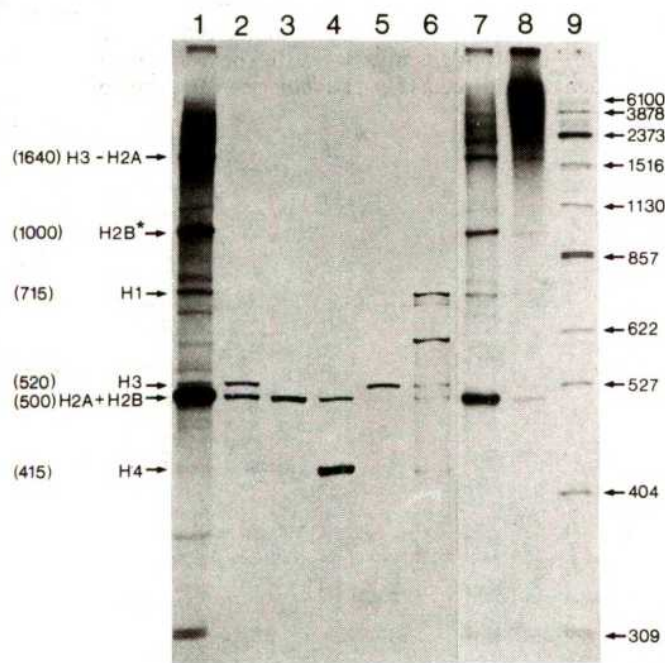


**Fig. 2** Multiple-probe  $S_1$  mapping of the h22 3'-terminal sequences of the H2B, H3, H2A and H1 mRNAs present in sea urchin- or h22-injected oocyte RNA.  $S_1$  mapping was as in Fig. 1 legend except that the probe comprised 3'  $^{32}$ P-end-labelled *Hpa*II/*Xho*I restriction fragments of h22 as shown in panel b. The 3'-end labelling was achieved by filling in recessed 3' ends with highly purified DNA polymerase I<sup>22</sup> (from NEN nick-translation system) in the presence of [ $\alpha$ - $^{32}$ P]dCTP and using the nick-translation protocol of the supplier but without DNase addition and with a reduced incubation period (15 min at 12 °C). A low level of internal labelling nevertheless occurred, causing the background of faint, spurious band with this probe. The indicated lengths of expected DNA protection by the H2B, H3, H2A and H1 mRNA 3'-terminal sequences are calculated from previous mapping of the 3' terminal and from the DNA sequence<sup>17</sup>. a, Lane 1,  $^{32}$ P-labelled DNA size marker<sup>19</sup>; lane 2, 5–14S sucrose gradient-purified h22-injected oocyte RNA from approximately two oocytes<sup>20</sup>; lanes 3 and 9, 5  $\mu$ g of total RNA from *P. miliaris* embryos at the 128-cell stage of development; lanes 4–6, partially purified *P. miliaris* histone mRNAs in order H4, H2B, H3, H2A and H1<sup>21</sup>. Note that the H4 3'-terminal sequence is not mapped by this probe because the *Hpa*II site lies just upstream of the mRNA<sup>17</sup>. Arrowheads indicating non-mRNA-derived band in lane 2 (oocyte RNA) co-migrate with two specific input DNA fragments and are discussed in the text.



starts in the H3-H2A spacer and ends in the middle of the H2A coding region. Protection of these fragments is not apparent when sea urchin RNA is used (compare lanes 2 and 3). The exact end(s) of the H3 3' extensions cannot be unambiguously deduced from these data but the fact that one can follow specifically protected DNA fragments into the H2A coding region suggests that a significant proportion of the species starting with the correct H3 5' sequence read through to the correct H2A 3' terminus and are thus 'di-cistronic' H3/H2A mRNAs (see below). Evidence of a minor level wholly incorrect termination is revealed by the presence of discrete oocyte RNA-derived bands not present when sea urchin RNA is used (compare lanes 2 and 3).

Taken together, the  $S_1$  mapping data discussed above predict the synthesis in the injected oocyte of all five correct histone



**Fig. 3** Strand-selected transcripts of h22 in microinjected oocytes. Lane 1, overexposure of  $^{32}\text{P}$ -GTP-labelled coding strand-selected RNA transcripts of h22-injected oocytes. Lane 7 shows normal exposure. h22 strands were separated on alkaline CsCl gradients (density at  $4^\circ\text{C}$  1.700, 0.1 M NaOH, 6 mM EDTA, 30,000 r.p.m. for 3.5 days in a VT:50 rotor). Recovered single strands were judged to be about 95% pure and were bound to diazobenzylloxymethyl (DBM) paper<sup>23</sup>. Complementary injected oocyte RNA was purified by hybridization in 60% formamide, 0.15 M NaCl, 25 mM phosphate buffer, pH 7.1, and 0.2% SDS at  $45^\circ\text{C}$  for 2–12 h and elution with 90% formamide at  $60^\circ\text{C}$ . RNA was analysed on a 6% acrylamide 8 M urea gel containing 10 mM TBE buffer and 0.2% SDS, and with continuous buffer recirculation. Gels were treated with diphenylloxazole and dried before exposure. Lanes 2–6,  $^3\text{H}$ -labelled *P. miliaris* histone mRNAs<sup>21</sup> further purified with DBM filters loaded with restriction fragments comprising H2B and H3 sequences, H2A sequences, H2A and H4 sequences, H3 sequences and H1 sequences, respectively. Lane 8, noncoding strand-selected h22 transcripts obtained as for coding transcripts (lanes 1 and 7) but by hybridization to noncoding-strand on DBM paper. Note that there are several discrete 'coding' RNA species visible in this lane and similarly some polydisperse RNA is visible in the overexposed coding-strand RNA (lane 1) consistent with cross-contamination of the strands on the DBM filters accentuated by the conditions of local DNA excess in the hybridizations<sup>23</sup>. Lane 9,  $^{32}\text{P}$ -DNA size marker. The band labelled H2B\* is an example of a coding-strand RNA species whose length precludes it comprising both normal 5' and 3' termini (see text). In the hybridization conditions used for strand-selected RNA, essentially no endogenous *Xenopus* transcripts were recovered in control experiments (not shown).

mRNAs, albeit with large quantitative variations, as well as species with correct starts and stops but with readthrough at one or more termination signal (such as an H3/H2A di-cistronic transcript) and species arising from erroneous initiation and/or termination. To verify these predictions, we have analysed the h22-coded oocyte RNA from both coding and noncoding DNA strands on fully denaturing gels as shown in Fig. 3. The RNA species selected by the coding strand (Fig. 3, lane 7) are discrete and include RNA species identifiable by co-migration with authentic mRNAs (Fig. 3, lanes 2–6) as well as by hybridization (not shown) as correct histone mRNAs, with the H2A and H2B mRNAs being abundant, H1 showing an intermediary concentration and with both H3 and H4 mRNAs, whose synthesis is respectively very deficient in the production of correct 3'- and 5'-terminal sequences, being scarce but clearly visible with overexposure (lane 1). An abundant RNA species with the expected length of an H3-H2A di-cistronic mRNA (about 1,640 bases) is present, as are other species in the size range ( $\geq 1,700$  bases) expected for di- or even tri-cistronic mRNAs. The presence of an abundant di-cistronic H3-H2A mRNA explains our recent finding (ref. 1 and E.P., unpublished) that, despite the very low levels of correct H3 mRNAs, the H3 protein is synthesized in the oocyte at levels comparable to the H2A and H2B proteins. These large RNA species are not mRNA precursors because they are stable in the oocyte and exit like the mRNAs into the cytoplasm (ref. 1 and unpublished data). In addition, a minor proportion of discrete RNA species are synthesized whose length precludes the possibility that they comprise both normal 5' and 3' mRNA termini. An example is the species H2B\* which hybridizes to the H2B region of the repeat. The RNA selected by the noncoding strand (lane 8) is, in contrast, of high molecular weight and polydisperse. Although contributing a significant amount to the total mass of RNA transcripts<sup>1</sup>, it presumably arises from relatively infrequent, erroneous promotion and/or termination.

In conclusion, our results show definitely that all five genes of the sea urchin histone repeat are capable of being faithfully transcribed within an amphibian nucleus but with strikingly different efficiencies, generally reflecting the differential rates of promotion but in the case of the H3 gene reflecting defective termination. It will be interesting to know whether analogous experiments with *Strongylocentrotus purpuratus* histone genes<sup>14</sup>, or with chicken histone genes (J. Wells, personal communication) yield comparable results.

We thank Mrs S. Oberholzer and Mr F. Ochsenbein for assistance in preparing the manuscript, and K. Gross for providing partially purified mRNAs. This work was supported by a grant from the State of Zürich, by Swiss National Research Foundation grant 3.257.077 and by an EMBO fellowship for C.H.

Received 25 July; accepted 22 September 1980.

1. Probst, E., Kressmann, A. & Birnstiel, M. L. *J. molec. Biol.* **135**, 709 (1979).
2. Grosschedl, R. & Birnstiel, M. L. *Proc. natn. Acad. Sci. U.S.A.* **77**, 1432 (1980).
3. Birnstiel, M. L. & Chipchase, M. *Trends biochem. Sci.* **2**, 149 (1977).
4. Brown, D. D. & Gurdon, J. B. *Proc. natn. Acad. Sci. U.S.A.* **74**, 2064 (1977).
5. Kressmann, A., Clarkson, S. G., Pirrotta, V. & Birnstiel, M. L. *Proc. natn. Acad. Sci. U.S.A.* **75**, 1176 (1978).
6. Telford, J. L. *et al. Proc. natn. Acad. Sci. U.S.A.* **76**, 2590 (1979).
7. Kressmann, A., Hofstetter, H., Di Capua, E., Grosschedl, R. & Birnstiel, M. L. *Nucleic Acids Res.* **7**, 1749 (1979).
8. Cortese, R., Melton, D., Tranquilla, T. & Smith, J. D. *Nucleic Acids Res.* **5**, 4593 (1978).
9. De Robertis, E. M. & Olson, M. V. *Nature* **268**, 137 (1979).
10. Trendelenburg, M. F., Zentgraf, H., Franke, W. W. & Gurdon, J. B. *Proc. natn. Acad. Sci. U.S.A.* **75**, 3791 (1978).
11. Trendelenburg, M. F. & Gurdon, J. B. *Nature* **276**, 292 (1978).
12. De Robertis, E. D. & Mertz, J. E. *Cell* **12**, 175 (1977).
13. Rungger, D. & Türlér, H. *Proc. natn. Acad. Sci. U.S.A.* **75**, 6073 (1978).
14. Etkin, L. D. & Maxam, R. E. *Dev. Biol.* **75**, 13 (1980).
15. Wickens, M. P., Woo, S., O'Malley, B. W. & Gurdon, J. B. *Nature* **285**, 628 (1980).
16. Kressmann, A., Clarkson, S. G., Telford, J. L. & Birnstiel, M. L. *Cold Spring Harb. Symp. quant. Biol.* **42**, 1077 (1977).
17. Hentschel, C., Irmlinger, J. C., Bucher, P. & Birnstiel, M. L. *Nature* **285**, 147 (1980).
18. Woodland, H. R. & Wilt, F. H. *Dev. Biol.* **75**, 199 (1980).
19. Sutcliffe, J. G. *Nucleic Acids Res.* **5**, 2727 (1978).
20. Kressmann, A. & Birnstiel, M. L. *NATO Advanced Study Institutes Ser. A31* (1980).
21. Gross, K., Probst, E., Schaffner, W. & Birnstiel, M. L. *Cell* **8**, 455 (1976).
22. Wu, R. J. *J. molec. Biol.* **51**, 501 (1970).
23. Stark, G. R. & Williams, J. G. *Nucleic Acids Res.* **6**, 195 (1979).



## MATTERS ARISING

## Peridotite xenoliths in basalts and mantle dynamics

BASU<sup>1</sup> has described jointed and angular xenoliths of mantle peridotite in alkali basalts from California. He considers their morphology to be due to brittle fracture at the site where the xenoliths were incorporated into the rising magma, and thus to be representative of dynamic conditions in the upper mantle. I believe this conclusion to be unwarranted, for the following reasons.

Mitchell *et al.*<sup>2</sup> have modelled the thermal response of xenoliths to enclosing magma, and have demonstrated that blocks of the size described by Basu are heated to the temperature of their surroundings in a matter of hours. Exceptionally high magma ascent rates are, therefore, required if xenoliths are to be brought from the mantle to the surface unaffected by incorporation into basalt.

Basu assumed a newtonian rheology for alkali basalt magma when calculating nodule settling rates. This assumption is invalid as magmas commonly possess a yield strength at subliquidus temperatures. Sparks *et al.*<sup>3</sup> have considered the effect of non-newtonian rheology on the transport of xenoliths by magmas. They conclude that blocks of the sizes observed have zero settling velocity in the majority of magmas. Thus, Basu's calculation of magma ascent rate cannot be justified.

In xenolith suites where a range of rock types is represented, fragment angularity is highly variable and unrelated to mineralogy or depth of origin.

Non-newtonian magma rheology favours xenolith transport by slow, rather than rapid, ascent of magma<sup>3</sup>. Thus xenoliths are likely to have been in a state of internal chemical and mechanical disequilibrium for a considerable time before their arrival at the surface. Brittle failure occurs as a response to changing conditions after incorporation of a xenolith into rising magma. Angular ultrabasic blocks from La Palma, Canary Islands, show such clear evidence of disequilibrium as partial melting induced by heating by the host magma (my unpublished data). Ultrabasic xenoliths in basalts should be regarded as unreliable guides to dynamic conditions in the mantle.

J. A. WOLFF

Geology Department,  
Imperial College,  
London SW7 2BP, UK

BASU REPLIES—Central to Wolff's criticism is the conclusion by Sparks *et al.*<sup>1</sup> that the abundance of ultramafic xenoliths in alkalic basalts is due to the slow rates of ascent of such magmas from mantle depths. Using thermal diffusivity arguments based on such measurements in olivines, Wolff also suggests that blocks of ultramafic xenoliths will attain thermal equilibrium with their enclosing basalts in a matter of hours.

The xenoliths under discussion and other associated xenoliths in the same lava flow in San Quintin volcanic field show evidence of strong plastic deformation. My conclusion that these xenoliths could not have spent longer than a few hours in the ascending magmas is also compatible with conclusions based on recovery kinetics in deformed olivines<sup>2,3</sup>. The deformed porphyroclasts of olivine in these xenoliths are expected to be completely recrystallized in a few hours due to the relatively fast kinetics of grain growth in conditions of high temperature thermal equilibration with the host lava. The survival of the plastically deformed porphyroclasts of olivine attests to their very short-lived association with the host basalt. Thus, Wolff's contention that "brittle failure occurs as a response to (slowly) changing conditions after incorporation of a xenolith into rising magma" is untenable.

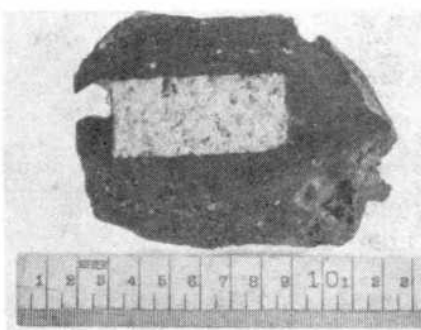


Fig. 1 Perfectly rectangular block of ultramafic xenolith in alkaalic lava from the Mt Schank volcano in SE Victoria, Australia. (Photograph courtesy of Dr Alan Moore, University of Cape Town, South Africa.)

Wolff favours a non-newtonian basalt rheology for slow xenolith transport and suggests that the "xenoliths are likely to have been in a state of internal chemical and mechanical disequilibrium for a considerable time before their arrival at the surface." Figure 1 shows an almost perfect rectangular slab of an ultramafic xenolith surrounded on all sides by the alkaalic vesicular lava from the Mt Schank volcano in SE Victoria, Australia. Could the orthogonal joint planes in Fig. 1 have

formed by brittle failure as a response to changing conditions after incorporation of this xenolith by the host magma? Or did these joint planes form before the xenolith was included in the magma? The xenolith in Fig. 1 shows typical porphyroclastic texture and evidence of plastic deformation. This evidence alone, because of the nature of the recovery kinetics as discussed above, refutes Wolff's central thesis that the joint planes formed after incorporation of the xenolith by the magma.

A. R. BASU

Department of Geological Sciences,  
University of Rochester,  
Rochester, New York 14627

1. Sparks, R. S. J., Pinkerton, H. & MacDonald, R. *Earth planet. Sci. Lett.* **35**, 234–238 (1977).
2. Goetze, C. & Kohlstedt, D. L. *J. geophys. Res.* **78**, 5961–5971 (1973).
3. Radcliffe, S. V. & Green, H. W. *Trans. Am. geophys. Un.* **54**, 453 (1973).

## Late Eocene rings around the Earth?

THE suggestion by O'Keefe<sup>1</sup> that the "terminal Eocene event" was caused by rings of tektite material encircling the Earth deserves criticism. O'Keefe assumes tektites to be of cosmic origin and cites his book<sup>2</sup> in which it is suggested that tektites originate from lunar volcanoes. This assumption is unwarranted and contrary to the numerous existing data<sup>3–6</sup>. Four specific difficulties are obvious. First, there are no known lunar rocks that are chemically suitable parent materials for tektites or which even appear possibly related to objects of this composition<sup>3–7</sup>. Second, there are no known lunar rocks of the correct age to satisfy O'Keefe's hypothesis. This is not trivial, as the most recent lunar rocks that have been dated are two orders of magnitude older than those required by O'Keefe. Third, we do not find that the North American tektites fell or were initially deposited throughout a sedimentary rock column of a few million years. Fourth, we have not found even a single tektite with a measurable cosmic ray exposure age, and the detection limits are well below the lifetime of the rings as deduced by O'Keefe.

What then caused the "terminal Eocene event?" I do not propose to answer that question. However, I do suggest that those who are interested in this problem consider the great volume of volcanic ash, air-fall tuff and bentonite (altered volcanic ash and tuff) that occurs in the late Eocene

1. Basu, A. R. *Nature* **284**, 612–613 (1980).

2. Mitchell, R. H., Carswell, D. A. & Clarke, D. B. *Contr. Miner. Petrol.* **72**, 205–217 (1980).

3. Sparks, R. S. J., Pinkerton, H. & MacDonald, R. *Earth planet. Sci. Lett.* **35**, 234–238 (1977).



sedimentary rocks of the Gulf Coastal Plain from Texas to Georgia<sup>8-10</sup>. Some of these tuffs and tuffaceous sedimentary rocks are similar in composition to the North American tektites<sup>9</sup> and are the probable target rocks from which the North American tektites were derived by a terrestrial impact. Thus, the terrestrial impact mechanism proposed by Urey<sup>11</sup> and others for faunal extinctions and major breaks in the geological record also should be considered, particularly in view of the recent work by Alvarez *et al.*<sup>12</sup> which supports this possibility.

If there ever were rings around the Earth, it is certain that the North American tektites (or any of the other presently known tektites) were never a cosmically derived fraction of those rings.

ELBERT A. KING

Lunar and Planetary Institute,  
3303 NASA Road 1,  
Houston, Texas 77058

1. O'Keefe, J. A. *Nature* **285**, 309-311 (1980).
2. O'Keefe, J. A. *Tektites and their Origin* 180-187 (Elsevier, New York, 1976).
3. King, E. A. *Space Geology: An Introduction* 69-80 (Wiley, New York, 1976).
4. Taylor, S. R. *Earth Sci. Rev.* **9**, 101-123 (1973).
5. King, E. A. *Am. Scient.* **65**, 212-218 (1977).
6. Haskin, L. A. *et al. Lunar planet. Sci.* **11**, 410-412 (1980).
7. King, E. A., Martin, R. & Nance, W. *Science* **170**, 199-200 (1970).
8. King, E. A. *Nature* **196**, 569-570 (1962).
9. King, E. A. & Rodda, P. U. *Trans. Gulf Coast Ass. Geol. Soc.* **12**, 265-270 (1962).
10. King, E. A. *Geochim. cosmochim. Acta* **28**, 915-919 (1964).
11. Urey, H. C. *Nature* **242**, 32-33 (1973).
12. Alvarez, L. W., Alvarez, W., Asaro, F. & Michel, H. V. *Science* **208**, 1095-1108 (1980).

**O'KEEFE REPLIES**—The present issue is whether tektites are cosmic or terrestrial in origin. The main point<sup>1,2</sup> is that the terrestrial hypothesis is found to conflict with the laws of physics, and these arguments have not been answered. Two examples are given below.

First, tektites are good glasses; that is, even in decimetre-sized pieces they are homogeneous and non-porous, unlike impact glasses. The production by meteorite impact (and immediate distribution over distances of thousands of kilometres) of good glass having very low water content, starting from ordinary rocks or soil, is not possible. The diffusion coefficients are too small to permit rapid homogenization<sup>3</sup>, and the bubbles will not escape in free flight because they have no buoyancy.

Second, many tektites were obviously shaped by surface tension. Certain hollow tektites, when liquid, were so delicate that a breath (literally) would have destroyed them<sup>4</sup>. But the terrestrial origin idea demands non-isotropic launch pressures of over half a million atmospheres (50 GPa), followed by entrainment in air behind a shock wave capable, as a minimum, of blowing out the top of the atmosphere<sup>4</sup>.

As regards King's first difficulty, lunar quartz monzonites and rhyodacites having tektitic major-element composition have been reported<sup>5-7</sup>.

On his second difficulty, note that terrestrial obsidians are also largely confined to the Cenozoic<sup>8</sup>, and further that although most lunar basalts are more than 3,000 Myr in age, others<sup>9</sup> are distributed over younger ages.

The remaining two difficulties and the conclusion are invalidated by the fact, which I had mentioned, that the (dominant) solar Poynting-Robertson effect seems to move the particles outward.

I have discussed elsewhere<sup>2,10</sup> the detailed chemical arguments in King's references, and my discussion of them has not been answered. Those arguments are, in any case, merely appeals to plausibility, which should not persuade us to accept violations of physical law.

JOHN A. O'KEEFE

Code 681, Laboratory for Astronomy  
and Solar Physics,  
NASA Goddard Space Flight Center,  
Greenbelt, Maryland 20771

1. Chapman, D. R. & Larson, H. K. *J. geophys. Res.* **68**, 4305-4358 (1963).
2. O'Keefe, J. A. *Tektites and their Origin* 179-194 (Elsevier, New York, 1976).
3. Varshneya, A. K. & Cooper, A. R. *J. geophys. Res.* **74**, 6845-6851 (1969).
4. Lin, S. C. *J. geophys. Res.* **71**, 2427-2437 (1966).
5. Chapman, D. R. *J. geophys. Res.* **76**, 6309-6338 (1971).
6. Ryder, G. *Earth planet. Sci. Lett.* **29**, 255-268 (1976).
7. Glass, B. P. *Lunar Sci.* **7**, 296, 297 (1976).
8. Ewing, R. C. & Haaker, R. F. *Pacific Northwest Laboratory Report PNL-2776/UC-70* (Richland, Washington, 1979).
9. Maurer, P. *et al. Geochim. cosmochim. Acta* **42**, 1687-1720 (1978).
10. O'Keefe, J. A. *Scient. Am.* **239**(2), 116-125 (1978).

## Proposed fossil tree shrew genus *Palaeotupaia*

CHOPRA and Vasishat<sup>1</sup> described a skull fragment with partial dentition of a fossil tree shrew (family Tupaiidae) from Miocene Siwalik deposits in India. Together with a maxillary fragment and an isolated lower molar from the same locality<sup>2</sup>, and some incomplete craniodental remains from the Miocene Siwaliks of Pakistan<sup>3</sup>, these specimens provide the first documentation of the fossil history of tree shrews. No generic or specific allocation was attempted for the Pakistani fossils or for the maxillary and isolated dental remains from India.

In contrast, Chopra and Vasishat<sup>1</sup> assigned their skull fragment to the new genus and species *Palaeotupaia sivalicus*. Although acknowledging that *Palaeotupaia* closely resembles *Tupaia*, they asserted that generic distinction was warranted because of "morphological differences and the large age gap between

our specimens and the living genus". However, their only discussion of differences between the two genera was limited to enumerating several cranial and dental traits that distinguish between *Palaeotupaia* and *Tupaia minor*. All the supposed differences of *Palaeotupaia* (proportionately longer face, less posterior incisive foramina, distinct protocone on P<sup>3</sup>, more transverse P<sup>4</sup>, and divided mesostyles on upper molars) occur in some species of *Tupaia*<sup>4-6</sup>. No assessment was presented of the possible primitive or derived nature of resemblances among Siwalik fossils and extant tupaiids. Few, if any, dental traits of *Tupaia* are uniquely derived within the subfamily Tupaiinae. Although at least two derived cranial features (posterior palatal vacuities and enlarged zygomatic foramen) distinguish *Tupaia* and *Lyomgale* from other tupaiines<sup>6,7</sup>, these regions are unfortunately missing from both the Indian and Pakistani fossil skull fragments. Finally, the geological age of the Indian skull fragment is not a biological attribute and is irrelevant in evaluating its possible generic affinities. There are several extant eutherian genera whose geological history extends back to the Miocene or earlier, including the chiropteran genera *Rhinolophus*, *Hipposideros*, *Megaderma*, and *Myotis*<sup>8</sup>.

Because no essential differences in craniodental morphology which might serve to distinguish between *Tupaia* and *Palaeotupaia* were identified, it is premature to propose generic distinction for the Indian Siwalik skull fragment. Instead, the evolutionary relationship of this fossil can be expressed best by either including it questionably in the genus *Tupaia*, or, perhaps more appropriately, by stressing its essentially modern aspect while withholding generic allocation until more complete specimens are recovered, or the holotype of *Palaeotupaia* is studied more thoroughly.

W. P. LUCKETT

Department of Anatomy,  
Creighton University,  
Omaha, Nebraska 68178

L. L. JACOBS

Museum of Northern Arizona,  
Flagstaff,  
Arizona 86001

1. Chopra, S. R. K. & Vasishat, R. N. *Nature* **281**, 214-215 (1979).
2. Chopra, S. R. K., Kaul, S. & Vasishat, R. N. *Nature* **281**, 213-214 (1979).
3. Jacobs, L. L. in *Comparative Biology and Evolutionary Relationships of Tree Shrews* (ed. Luckett, W. P.) 205-216 (Plenum, New York, 1980).
4. Lyon, M. W. Jr. *Proc. U.S. natn. Mus.* **45**, 1-188 (1913).
5. Steele, D. G. *Symp. fourth int. Cong. Primatol.* **3**, 154-179 (1973).
6. Butler, P. M. in *Comparative Biology and Evolutionary Relationships of Tree Shrews* (ed. Luckett, W. P.) 171-204 (Plenum, New York, 1980).
7. Luckett, W. P. in *Comparative Biology and Evolutionary Relationships of Tree Shrews* (ed. Luckett, W. P.) 3-31 (Plenum, New York, 1980).
8. Sigé, B. *Palaeovertebrata* **1**, 65-133 (1968).

## nature

13 November 1980

How to speak out on Sakharov *et al.*?

Gor'kii, where Andrei Sakharov is under house arrest, is well to the east of Moscow. Those who live there, willingly or otherwise, cannot at this time of the year forget that the long winter has begun. The sun will not shine strongly again until the best part of half a year has passed. The central isolation from which the inhabitants of Gor'kii suffer even at the best times of the year will for a long time to come be indistinguishable from desolation. Andrei Sakharov's letter (see page 112) is thus a reminder of the plight of others than himself. In some respects it may be as bad to have to live in Gor'kii because nothing else suggests itself, as to happen to live in Gor'kii because one has been taken there by force. If imprisonment is the lack of freedom, and if the sense of freedom is the sense of having chosen to live in a chosen way, many of Sakharov's fellow residents may be as deprived of liberty as he without question is. Sakharov should not blame himself if his letter prompts those who read it to remember that his problem is part of a larger problem, one that will still be with us in the spring. How could it be otherwise, in the week that the first review conference on the Helsinki accords begins in Madrid?

Sakharov makes several points, some of them particular. Plainly he is dismayed that the conference at the Hague at the beginning of September should have been based on assumptions that are incorrect. The KGB may have tried to prevent him publishing his three recent papers in English in the West, but it had no influence with the editors of *Zhurnal éksperimental'noi i teoreticheskoi fiziki*. There is no scientific library across the street, only "mud and piles of rubbish". (No doubt the snow has by now made them less unsightly.) The reason that he cannot talk to scientific colleagues is not that the others who work in Gor'kii work on classified projects but that he is prevented from going out, and from receiving visitors. (The personalized radio jamming equipment is a refinement.) There is no telephone.

Sakharov also raises more general questions. Why, he asks, is it supposed that his treatment is mild simply because he has not been sent to a labour camp? Is loss of liberty now measured on a discontinuous spectrum, with hardly anything between full citizenship and endangered life? If so, he implies, any loss of liberty is absolute. To know that the KGB can break into your flat when it chooses may be as intolerable as to know that you may be worked to death on somebody else's whim. Naturally he is sorry for his friends and fellow-scientists — Orlov, Shcharanskii, Velikanova, Nekipelov, Lavut, Ternovskii, Osipova and the rest. The severity of their plight does not make his own supportable.

**Imprisonment without trial**

Then, he asks, what happens when a person's loss of liberty comes about because a government has assumed the right to break its own laws? The constitution of the Soviet Union resembles that of other modern states in its assurance that people will not be deprived of liberty without due process, usually a trial by a court. So, Sakharov asks, how has the word got about that it can be in his interest not to make too much fuss outside the Soviet Union in the hope that the authorities will then quietly relent and let their illicitly imprisoned prisoner return to Moscow? What Sakharov wants, he says, is due process — a formal charge, a fair trial and either a fair sentence or a discharge.

Sakharov appears not to appreciate the enormity of his demand. The Russians (which is not necessarily a synonym for "the Soviets") have had a flair in the past few centuries for mingling tyranny with essays at rebellion. The one, of course, provokes the other. Tolstói might have been as complacent as his fellow-landowners if the feudal state of the nineteenth century

had been less repressive. Dostoevskii might have consented to entertain the middle classes with popular romances if only there had been more romance to brood about. Sakharov is one of the many who, in the past few years, have dug in their heels and insisted on the rule of law and the validity of international agreements such as the Helsinki accords. By doing so, he runs great risks for himself and his family. Forced emigration would solve nothing, but would be the ultimate humiliation. Sakharov's plight is haunting.

What, if anything, can be done to help? Sakharov's letter provides some clues. He is concerned about his relatives and about his son's fiancée. Experience in the past few years has shown that it may sometimes help if the names of those threatened with trouble of some kind are well known outside the Soviet Union. But publicity is not a certain remedy, as the cases of the Orlovs of that world demonstrate. Perhaps the best that can be offered is the occasional message of good cheer, perhaps even a reprint of a scientific paper that might interest him. It is sad that there is so little else to offer, with the winter setting in at Gor'kii.

But is this not an issue on which the interests of the scientific community as a whole should be engaged? The question is unfortunately more complicated than it seems. Sakharov may be a member of the scientific community, but he is also a citizen of the Soviet Union, and his disagreement with his government is about civil liberties, not scientific issues. To what extent, in these circumstances, is the scientific community entitled to be engaged?

**Constraints on protest**

To a first approximation the answer is that the international scientific community has no special duty to protest at what is happening to Sakharov and those of his fellow scientists who are formally imprisoned. The Soviet Union has a constitution which guarantees due process, but also a criminal code which arranges that people are brought to trial for reasons that are elsewhere unacceptable. The trouble is that the scientific community as such has no special competence in persuading national governments to follow seemingly legal practices. And even where Soviet citizens such as Sakharov have been harmed outside the law, by being deprived of jobs or deprived of liberty without even an unfair trial, to a first approximation the issue is not one for the scientific community. Others than scientists are dealt with in such ways. Injustice, it appears, is impartial. This is why, in the past several years, the problems of those such as Sakharov have been such a rich source of frustration for their colleagues elsewhere.

The second approximation, fortunately, offers a little more hope, and for two reasons. Scientists are fond of saying that science is international and that the scientific community is inherently more interdependent than other communities of scholarly or professional people. Too much is often made of these propositions, which, nevertheless, contain a germ of truth. We are all the losers if people like Sakharov cannot work as effectively as they might, and talk as freely as they would wish about what they have done. Ironically, the past few decades have demonstrated the eagerness of even the Soviet government to make formal arrangements for the movement of Soviet scientists in and out of the Soviet Union.

The second chink of hope is that the Helsinki accords exist. They are not a formal international convention, but a declaration of intent. The declared intention is liberal, if only vaguely so. People are to be free to move from one country to another if they wish, free to correspond with colleagues elsewhere, free to do a variety of things now often denied. The objective of the



conference opening this week in Madrid is to assess progress and to decide what should next be done. The outcome will not carry the Helsinki accords much further. The most immediate danger is that such hard things will be said that the process of relaxation will be set back. Yet the accords provide a licence for scientists outside the Soviet Union to speak their minds from time to time.

This is the spirit in which more than 270 distinguished scientists bought advertisement space in the London *Times* last week asking for the release of fellow scientists now locked up. Lord Todd, the President of the Royal Society, followed this on Friday with a letter in *The Times* asking that the British government should make an issue with the Soviets about Sakharov, Orlov, Shcharanskii and the rest. These developments are creditable. The US National Academy of Sciences declared itself to the same effect more than a year ago. But it is important that the scientific community in the West should clearly appreciate what it is about with such declarations. Because of its connections, because science is indeed international, it happens to have learned of some appalling injustice. But classicists, farmers and lorry drivers are similarly deprived of liberty without good cause. The scientific community must appreciate that by asking that Western governments should do what they can to persuade the Soviet government to change its ways, it is asking a political and not a scientific favour. The scientific community is entirely within its rights to do so. Science will continue to be diminished if the Soviet contribution is inhibited by illiberality. The knowledge that protest is bound to be understood as political protest has no doubt helped to keep the scientific community silent all these years. To urge governments to take up cudgels is the proper course.

### No boycott

Talk of boycotting relations with Soviet scientists is, however, mistaken. In the past few weeks, Sir Brian Pippard and others have been drumming up support for a temporary boycott. Scientists in the West, they say, should not receive Soviet scientists in their laboratories and should not attend conferences in the Soviet Union until the diplomatic conference in Madrid is over. The argument would make sense if there were reasons to suppose that a boycott would succeed in influencing what happens at Madrid. The chances of that are small.

Although there will be many in the West who will now follow their individual inclinations and boycott Soviet science, it will be best if those not that way inclined can try to strengthen relationships with their Soviet colleagues, at the same time leaving them in no doubt of how the illiberality of the Soviet state offends the consciences of others and impedes the advancement of science as well. Soviet colleagues should be welcomed, if anything more warmly than in the past, but also spoken to more openly than has been the custom. The genteel convention that one does not embarrass a visitor by talking politics is now outmoded. For the best but cruel hope for Sakharov and his like is that there should be more of them.

In following such a line stridency must be avoided. A sense of perspective is essential. It is thus relevant that what the Soviet government has done to Sakharov *et al.* does not hold a candle to, say, what Pol Pot did in Cambodia between 1976 and 1978. Moreover, the West cannot be too smug in its complaints against the Soviet way of dealing with people such as Sakharov — it is after all only a quarter of a century since Senator Joseph McCarthy was riding high in the United States administering injustice in an arbitrary way. Russian illiberality is, however, a special challenge because the Russian state is within an ace of being decent. Personal freedom is guaranteed by the constitution. The Soviet educational system, much admired elsewhere, creates expectations of freedom. The industrial development of the past half century depends on the involvement of trained people in a variety of occupations, technical and managerial, that are efficiently carried out only when people are free to move about within the system and free to contribute to industrial development in ways that best suit individual talents. Is it too much to hope that some future Soviet government will recognize that economic and industrial stagnation is too high a price to pay for the right to lock

people up on flimsy charges?

The revolution, ostensibly directed at Tsarist feudalism, seems not have touched what is the essence of feudalism — the notion that people's lives belong in their entirety to the state. This is the basis on which it is supposed that ordinary unrebelling people in the Soviet Union should have less freedom than is habitual elsewhere to choose what they work at and where they live. The institution of the collective farm is not very different from that of the mediaeval *desmesne*, while the recent understanding that members of the collectives should be allowed to work some land on their own account is the Soviet analogue of the mediaeval practice of granting the right to work strips of land in a common field to the dutiful dependants of a manor.

Experience of the Dark Ages in Western Europe shows clearly enough that in such a feudal system the lack of freedom is not absolute and the condition of society not entirely static. Just as, in mediaeval society, bright young people escaped from the villages in which they were brought up by joining some influential religious order and moving on a wider stage, so in the Soviet Union there is a constant and substantial flux of young bright people through the special schools and through the universities into the professions, the scientific professions among them. For other people, it also helps that the modern equivalents of the lords of the manor — the local party bosses — are susceptible to influence: a person may reasonably expect to improve the lot of himself and his family and never get into trouble provided he is willing never to ask for what may be forbidden. For every Sakharov, there may be 100,000 content to live within the system. The course of events will be determined not by the number of open rebels but by the unknown influence of those with similar inclinations still undeclared.

So does it follow that Sakharov and his fellows in adversity have no choice but to wait for a counter-revolution? That gloomy logic is fortunately unsound. Although the feudal practices of the Soviet government have the obvious advantage of keeping the government of the day in power, there is no reason to suppose that they are essential to the survival of socialism, communism, Marxism or whatever blend of those ingredients may be fashionable. To be sure, it is a depressing truth about the past half century that most communist governments have kept their ideology intact by restricting liberty, if only at the margin. The fate of Mr Michael Manley's government in last month's elections in Jamaica will no doubt reinforce them in their prejudices. Yet is it not ironical that many of those who find themselves in Sakharov's plight are as concerned with the survival of the Marxist state as are their governments? Liberty need not spell the end of the Revolution even though each year that passes makes the conflict between them sharper.

### No choice

So what is to be done? The wisest assumption is that nothing much will change: that Madrid will be a disappointment but that the Helsinki accords will remain in being; that Mr Reagan's government in the new year will reopen discussions about arms limitation but will not embrace detente with much enthusiasm; that Soviet troops will stay indefinitely in Afghanistan but will not take day t day charge in Poland; and that Soviet scientists will not be free to travel overseas. Western governments at Madrid will no doubt make the best they can of what the scientific community has been asking of them in the past few months, but are likely afterwards to be preoccupied with other things. The scientific community will then be left to its own devices, which are primitive yet potentially effective. The objective must be to strengthen, and not let lapse, the recent pathetic trickle of intercourse with Soviet scientists on scientific matters in the hope that there will be a growing company of Soviet scientists prepared to acknowledge the value of liberty. It sounds an insubstantial remedy, yet the scientific enterprise is more robustly international in character than other branches of scholarship. The scientific community is now challenged to show that its faith in this principle can be upheld. And that is the best hope that Sakharov will not still be living against his will in Gor'kii for many winters to come.

# Reagan's election cheering for science?

## Harder line promises more spin-off funds

### Washington

A big step for US politics, but a relatively small step for US science seems to be the main verdict on last week's presidential and congressional elections, with scientists unlikely to suffer as much from a swing to the right as other recipients of government spending.

President-elect Ronald Reagan has already said that he wants a 2 per cent across-the-board cut in the budgets of all federal agencies next year. But he is on record as supporting increased funds for research and development, a larger defence budget (with its spill-over into basic research) and the retention of both the Office of Science and Technology Policy (OSTP) and the post of President's Science Advisor.

The Republican takeover in the Senate has been as significant as Reagan's victory. The defeat of a significant handful of liberal Democrats will mean a major shift in the content of legislation. Again, however, the science budget may escape serious cuts, partly because key committee positions are likely to be filled by liberal Republicans, such as Senator Charles Mathias of Maryland, who have long been supporters of increased research funding.

Although little was said about science during the presidential election campaign, Mr Reagan has made it known in the past few weeks that he favours increased spending on science, particularly in areas related to defence needs. His main publicly-stated reservations were about the organization of OSTP, whose new staff would, he said, gather information in an informal way "rather than relying on 'blue ribbon panels' which are often partisan and work in secret".

The key question is who will fill the major science and technology positions in the new Reagan administration. Many of these choices are unlikely to be made until the new year. But preliminary discussions were held last weekend by a task force whose members indicate the likely directions of a Reagan science policy.

The task force was brought together by Dr Simon Ramo, co-founder of the advanced engineering firm TRW Inc., an adviser to Mr Reagan during the election campaign and former chairman of a congressionally-established federal science and technology committee under President Ford.

Co-chairman of the task force is Dr Arthur Bueche, vice-president of research and development for the General Electric

Company, a strong supporter of nuclear power and a possible Science Advisor.

Other members of the task force include Dr Harold Agnew, past director of the Los Alamos Scientific Laboratory; Dr Ed David, president of Exxon Research and, for a time, President Nixon's Science Advisor; Dr Frederick Seitz; Dr Guy Stever, ex-director of the National Science Foundation (NSF) and President Ford's Science Advisor; Dr Bill Baker, past president of Bell Laboratories; and Dr Edward Teller, a close adviser to Mr Reagan when he was governor of California.

Also included are several senior administrators from the defence and aerospace industries, including Dr Albert D. Whelan, vice-president of the Hughes

Aircraft Corporation and a strong supporter of the commercialization through private industry of communications and Earth monitoring satellites.

One immediate task for the committee is to select a new administrator for the National Aeronautics and Space Administration (NASA) to succeed Dr Robert Frosch, who has already announced his intention to take up the position of president of the new National Association of Engineering Societies in January.

Less certain is whether an immediate successor will be sought for Donald Dr Fredrickson, director of the National Institutes of Health. Dr Fredrickson was

## Plusses and minuses, election 1980

### Plus

**Fast breeder research.** One of Mr Reagan's first actions as President is likely to be to lift the embargo on the construction of the Liquid Metal Fast Breeder Reactor at Clinch River in Tennessee. Most of the major components have been built, but the test reactor's completion was held up by President Carter because of proliferation dangers and also a belief that fast breeder reactors are unlikely to be needed in the United States until well into the next century. Utility companies, however, which have provided a substantial amount of the funds, are keen to see the project completed, and are now likely to get their way.

**Chemical weapons.** President-elect Mr Reagan is also likely to give the go-ahead to a new facility for producing binary chemical weapons, favoured in Congress but, following President Nixon's earlier ban on their production, requiring a presidential declaration that such weapons are needed. In a campaign statement, Mr Reagan said that since binary weapons are much safer to stockpile and transport than existing stockpiles of poison gas, "we should proceed with preparation to convert to binary weapons".

**Science court.** In another statement, Reagan also said that he would explore the feasibility of a "science court" to help arrange public discussions of controversial scientific issues, a proposal that generated considerable publicity four years ago, but has since lapsed into relative obscurity.

**House of Representatives.** The House has lost one of its three scientist members, Mr Mike McCormack (see below), but has gained another, Mr Jim Coyne, an energy analyst and president of the Coyne Chemical Corporation. With Mr Coyne's election, all three scientists in the House are now Republican.

### Minus

**Mr Mike McCormack,** previously chairman of the House Science and Technology Committee's powerful energy research subcommittee, a strong advocate of nuclear power and a leading architect of recent nuclear fusion research legislation. Mr McCormack lost a tight race in Washington, where his district included the Department of Energy's Hanford Reservation.

**Mr Jerome A. Ambro.** A Democrat from Long Island, Mr Ambro was chairman of the Science and Technology Committee's subcommittee on natural resources and environment. He played a significant role in generating congressional approval for the 400-GeV particle accelerator, ISABELLE, at the Brookhaven National Laboratory.

**Environmental regulation.** The loss of liberals such as Senators Frank Church (Idaho), John Culver (Iowa) and Gaylord Nelson (Wisconsin) and Representatives Bob Eckardt (Texas) and Andrew Maguire (New Jersey) will be a major blow to supporters of tough environmental regulation. Their only consolation is the re-election of another liberal, Congressman Morris Udall, chairman of the House Interior Committee. Mr Reagan has promised to repeal environmental and health legislation that is considered unnecessarily burdensome to industry.

**Alfred Carnesale.** The change in administration makes it unlikely that, as proposed by Mr Carter, Dr Alfred Carnesale, professor of public policy at Harvard's Kennedy School of Management, will now become chairman of the Nuclear Regulatory Commission. Although respected as a negotiator, Dr Carnesale is closely identified with a Ford-Mitre study that strongly influenced President Carter's stand against fast breeders.

**David Dickson**



initially appointed by President Ford and was retained by President Carter; he had previously indicated that, even if Carter won, he would probably leave some time next year.

At NSF, although the Senate has approved the nomination of Dr John Slaughter as the new director, he has yet to be sworn in by the President and it is possible that Mr Reagan will wish to propose another candidate for what is supposed to be a relatively non-partisan appointment.

In the Senate, much will depend on how the chairmanships of the various committees are allocated. One of the most prominent election casualties was Senator Warren Magnusen, long-time representative of the state of Washington, who as chairman of both the Senate Appropriations Committee and its health subcommittee had presided over a period of substantially increased funds for biomedical research.

If the Democrats had retained control, the subcommittee chairmanship could have passed to Mr William Proxmire, the scourge of NSF. As ranking Republican, however, the position could now be taken by Senator Mathias — unless he prefers to take over Mr Proxmire's committee, which is responsible for the budgets of both NSF and NASA.

NASA's hopes for a relatively sympathetic hearing in the Senate have also been raised by the likelihood that the chairmanship of the Commerce Committee's science, technology and space committee will pass to Republican Senator and former astronaut Jack Schmitt, a keen supporter of the space programme and of increased funds for space science.

In the House of Representatives, which remains in the hands of the Democrats, the main changes will result from a possible reorganization of the Science and Technology Committee, where three subcommittee chairmen — Mr Mike McCormack, Mr Jerome Ambro and Mr John Lloyd — all lost their seats.

David Dickson

## Polish unions

## Science not lost

### Gdańsk

In spite of the legal wrangles over registration and the need to prepare contingency plans for a possible nationwide protest strike, Poland's new independent self-governing trade union, *Solidarność*, has already started work. Among other things, it established, at the end of last month, its All-Poland Coordinating Commission for Science.

This at first glance is somewhat surprising, because the present policy of *Solidarność*, as the very name implies, is to build a strong union organization without subdivisions by trade or profession. Profession-based branches were originally

planned for a later stage. Such a policy meets with the aspirations of the many briefly established new unions which, after the creation of *Solidarność* in mid-September, were quick to amalgamate with it. As Dr Zdzisław Bibrowski, erstwhile chairman of the Independent Trade Union of Scientific, Technical and Educational Workers (founded 8 September — see *Nature* 18 September — merged with *Solidarność* 13 October) explained, the members felt that in the present fluid situation they needed greater bargaining power and protection than a single small union could afford.

The *Solidarność* commission for science is not intended to be a separate interest group but rather a working party to elaborate the union's practical suggestions on the strengthening and renewal of the role of science in Poland.

Such a renewal is widely accepted as a major factor in getting the Polish economy out of its present crisis. It was the theme of last month's extraordinary General Assembly of the Polish Academy of Sciences and of a number of statements by academic and scientific bodies throughout the country. Lech Walesa, the leader of

*Solidarność*, told me last week "Speeches and declarations are not the point. We need concrete activity."

Such activity will be the role of the *Solidarność* commission. As Dr Wojciech Gruszecki, a chemistry lecturer at the Gdańsk Technical University and the *Solidarność* spokesman on science and technology explained, the commission, which has already met several times in Poland's leading academic centres (Krakow, Warsaw, Gdańsk, Wrocław) hopes to work out some concrete proposals and submit them to the government; so too during the next few months will the Academy of Sciences and the country's various learned bodies. New legislation on science in Poland is now being drafted and will shortly be presented to the Sejm (parliament). In the current atmosphere of greater "openness" a lively public debate is expected.

On many points, including the need for greater autonomy in academic life and the lifting of censorship restrictions, the scientific and academic community is unanimous. *Solidarność*, however, would go further. As Dr Gruszecki explained, the union urges that science be treated as a non-

## University of Warsaw changes course

### Warsaw

The expected liberalization of Polish academic life is not entirely a consequence of the Gdańsk accords, according to a spokesman for the Polish Ministry of Higher Education and Science. Rather, he said, it is the culmination of a continuing process. Thus the promise of a greater degree of self-government for the universities was already foreseen in guidelines drawn up several months ago.

The ministry, it appears, wishes to seem well abreast of developments. This has been especially the case since the surprise resignation at the end of September of the rector of Warsaw University. With widespread talk of academic autonomy, the ministry found it prudent to offer a compromise solution for the appointment of his successor. It proposed a list of three candidates, from whom the university senate made its final selection.

The senate is now committed to the principle of academic autonomy. The pro-rector, Dr Kazimierz Dobrowolski, stresses that the university should be able to draw up its own syllabuses and courses. Even under the present system, he says, some latitude is possible. In his own subject, biology, the university has been able to initiate courses in such new fields as environmental biology and molecular genetics. The result, he says, is that no student can graduate with simply a nineteenth century knowledge of biology.

The academic staff at the university is

nevertheless concerned with falling standards among candidates for entry. The educational reform, introduced three years ago, which replaced the traditional eight years of primary schooling and four years lyceum by a comprehensive ten-year schooling, alarmed both parents and university staff. Although three years is strictly too short a time in which to assess the new system, the Ministry of Education has been quick to read the signs. Although no official announcement has yet been made, a recent article in the weekly *Perspektywy* suggests that the new Minister of Education, Krzysztof Kruszewski, intends to revert to the former system, with certain changes in syllabus incorporated from the ill-fated ten-year system.

A recent development at Warsaw University has been the inauguration of a course of Friday evening lectures by members of the Society for Academic Courses (the "Flying University") whose aim is to fill the gaps left by the state system of instruction. The lectures, held in the Adam Mickiewicz Hall (the largest lecture room in the university) are not, however, formally sponsored by the Society for Academic Courses. The hall is leased to the new Independent Students' Union, which invited the speakers. But, as one of the student organizers said, the correspondence between the list of lecturers in the Mickiewicz Hall and the members of the Society for Academic Courses is hardly coincidental.

Vera Rich

commercial activity and financed by a budget which would ensure the total autonomy and freedom of scientific research. Research, he said, should not be "cramped" by government plans. Industrial research should be carried out in the research institutes of the ministries concerned (a network of such institutes does exist), or contracted out to academic institutes; but the overall direction of research by the government should cease.

In effect, Solidarność is seeking a major change in Poland's science policy. Since the early 1970s, research has been organized and funded on the basis of a complex hierarchy of "problems" (governmental, key, interdepartmental, departmental and branch problems) geared to the needs of the national economy. Research on a given problem will generally be carried out at many institutes simultaneously, and problems of coordination and control, including the interface between the academic and governmental sides, have led to a proliferation of bureaucracy. The establishment view, however, as represented by Dr Ignacy Malecki, director of the Institute of Fundamental Problems of Technology of the Polish Academy of Sciences, is that the problem structure is not in itself a bad thing. Dr Malecki, a member of a special commission looking into the management of the "problem" system, said that the consensus was that the system should stay, although trimmed of its bureaucracy. He added that in his opinion there was room for improvement in financing. **Vera Rich**

## Science council

### Mess about money

The UK Science Research Council is in a financial mess. But nobody can say how serious the trouble is, because figures and tables released in the 1979-80 annual report last week are wrong. The SRC now confirms the misuse of a computer program, as a result of which some research grants which have ceased have been displayed as current. A claim in the report that grant payments had increased by 72 per cent since the previous year took SRC officials four working days to disown once the inconsistencies had been pointed out to them.

Behind this is a more serious problem — what chairman Sir Geoffrey Allen last week called a "hiccup" in the council's cash flow. He and his officials are being coy about the size of this financial spasm. Some say that the council must find at least £10 million from within its current budget to pay for excesses last year in grant-giving by the Science Board, responsible for small science and neutron and synchrotron radiation physics, thus shedding doubt on claims earlier this year that the Science Board was turning away "alpha quality" grant applications for lack of cash.

The anomaly dates back to a success:

### Hardship everywhere

The Science Research Council's report for 1979-80 (HMSO, £7.10) is liberally spattered with references to the consequences of financial stringency, within a budget totalling £176 million. The budget last decreased 1 per cent in real terms in 1980-81, and will show a modest increase after that — but, says the report, new initiatives will be impossible without producing stagnation in favoured areas of the council's programme, or markedly reducing other programmes.

**Nuclear physics** is the most vulnerable of the big spenders — although contributions to CERN fell from £27.7 million in 1978-79 to £25.3 million in 1979-80 largely because of the stronger pound. The nuclear physics budget is not one of the "favoured areas" of the SRC's programme, and it has fallen a factor of two in real terms since 1975-76. It will fall again by 18 per cent this year, and another 9 per cent the year after, says the report, to £2 million below a "minimum programme"; but despite this the board sees LEP, the large electron positron ring that CERN plan, as its accelerator for the late 1980s, as its highest priority. It is "seeking council support" on this project. Meanwhile, equipment for the 30 MV Van de Graaff Nuclear Structure Facility under construction at Daresbury is to be further delayed.

**X-rays and neutrons** provided by the synchrotron radiation source at Daresbury, opened last week, and the Spallation Neutron Source under construction at the Rutherford Laboratory are threatened by lack of money to exploit them; and existing neutron sources will be run down. The high proportion of the Science Board's funds devoted to neutron scattering will fall after 1981-82, when the modernization programme at the Institut Laue-Langevin high flux reactor at Grenoble, in which the UK is a partner, is completed.

**Computers.** The SRC needs to find £8 million capital "over the next few years" to replace its central computers, and more if allowance is to be made for an increasing demand.

**Research students** supported by the SRC will continue to be a falling proportion of good graduates in science or engineering. In 1972, 46 per cent of such graduates, applying for SRC grants, were awarded them. In 1979-80 the proportion was 36 per cent, and now the number of grants must be held constant against an increase — for the next few years — of about 4 per cent a year in university output. But there should be a few more cooperative awards in science and education (CASE awards), designed to link students with industry as well as university. Even so, this council hopes to fund more in-service training.

**Robert Walgate**

that of Mrs Shirley Williams, Secretary of State for Education and Science in the last government, in convincing her Cabinet colleagues that Britain should spend more on science. Uniquely, she brought in research council heads to convince other ministers that basic science was important — and in late 1978 won another £47 million for the councils, of which SRC would have received £33 million, payable from 1979-80 to 1982-83. Then came the new government; spending cuts, announced in the budget of June 1979, lopped off most of Mrs Williams's gift.

But well before the election she had privately warned the council chairmen to beware of Tory zeal. In case the government changed, she hinted, it would be wise to spend the money soon. In April 1979, SRC sent out a circular requesting applications for grants to buy equipment. £37 million of applications flooded in; SRC panels thought £20 million of them were deserving, and committed themselves to £7.5 million. In the event, the council received only £5 million of the Williams money.

The flood of applications, however, continued, and not just for equipment. The universities had seen the tap turned on after years of drought. It was against this background that "alpha quality" applications had to be turned down. Even so, the boards over-committed themselves and now all are being asked to cut back by delaying grant renewals.

Other factors worsen the SRC's current financial picture. Universities are putting in their bills earlier than usual, because they too have cash flow problems; and the largest price of SRC construction work — the spallation neutron source at the Rutherford laboratory — is going ahead on time (the council had allowed for slippage).

The only light comes from the strong pound, which reduced the council's subscriptions — totalling £42 million a year — to international bodies such as the European centre for subnuclear physics (CERN) and the European Space Agency by about £7 million; and from the volcanic rock underneath the new Isaac Newton telescope house at La Palma in the Canaries. Engineers had overestimated the strength of the rock, and the foundations must be rebuilt, causing a six-month delay and pushing a £500,000 bill into next year.

**Robert Walgate**

## Large space telescope

### Delay means money

*Washington*

US astronomers have successfully persuaded the National Aeronautics and Space Administration (NASA) to request additional funds in next year's budget to ensure the successful development of scientific instruments due to fly on the space telescope.

Previously, scientists had complained



that significant cost and schedule overruns with the 2.4-metre telescope, whose planned 1984 launch from the space shuttle will probably have to be postponed for up to a year, were leading the agency to cut corners in developing and testing the instrumentation thus prejudicing some of the scientific experiments.

For example, no reserve funds to meet unexpected difficulties had been included in the budget of the Goddard Space Flight Center, which is responsible for the development of the scientific instruments which will be located at the telescope's focal plane.

Partly as a result of this delay, caused chiefly by greater than expected technical difficulties in various parts of the project, cost overruns could amount to \$50–\$100 million, compared with an initial estimate of \$435–\$470 million.

The space telescope is only one of a growing list of NASA projects in the same trouble. In some cases, such as the Galileo mission to Jupiter, and the solar polar mission — delayed two years — these have been the direct result of problems with the space shuttle itself.

## Ariane sells three

*Washington*

Intelsat — the international telecommunications satellite organization — has given a major boost to European space efforts with its decision to launch three of its nine satellite global communication systems from the French-built Ariane rocket.

Intelsat had originally hoped to launch the satellites from the National Aeronautics and Space Administration (NASA)'s space shuttle. Delays in the shuttle development programme, however, have caused concern about whether the launcher will be available in time. (Even after the first launch next year, it is uncertain whether NASA will be able to keep up its promised schedule of launches.)

Ariane is also experiencing problems, and following the failure of a test flight earlier this year there is no guarantee that it will be available for the Intelsat launches, which would be the sixth, seventh and eighth in the nine-satellite, \$300 million system. In this case, Intelsat would use Atlas Centaur rockets, which because of the shuttle delays are already being used for the first five satellite launches, with the first launch due to take place next month.

The launch vehicle for the final satellite in the series has not yet been decided, because Centaur launches are likely to be considerably more expensive than the shuttle. When all satellites are in orbit, the system will double the number of international telephone calls and television transmissions that can be handled simultaneously.

**David Dickson**

But in the case of the space telescope, there have been separate problems with each of the three parts of the project: the scientific instrumentation, the optical telescope assembly and the support system module.

In the case of the scientific instrumentation there have been what one scientist describes as a not unusual set of technical problems, extra costs caused by delays and a few "minor screw-ups" in all instruments except the high-speed photometer.

It is a similar story with Perkin-Elmer, which was awarded a \$58.5 million contract for the optical telescope assembly and which has also had difficulty in keeping work on schedule, finding that it lacked sufficient manpower for design needs and that a computer-controlled method for grinding one of the two optical mirrors was not as successful as had been hoped.

More recently, the other main contractor, Lockheed, awarded a \$73 million contract for the support systems module, reported that revised cost estimates were substantially larger than those originally submitted.

Both NASA officials and staff members of the relevant congressional oversight committees are looking closely for the reasons behind the delays. In particular, Congress wants to know whether tight limits on personnel have reduced the agency's ability to review contracts awarded to private companies.

In Europe, where several companies are working on apparatus to be included on the telescope, a delayed launch will relieve pressure on schedules that were said to be getting tight.

The delay seems unlikely, however, to have a significant impact on plans for a space telescope institute, which will be responsible for analysing the data received from the telescope.

NASA is expected to announce within the next few weeks the site that it has selected for the institute. Of the original four proposals submitted earlier this year, two remain in the running. One is from the Association of Universities for Research in Astronomy (AURA), which proposes building the institute at Johns Hopkins University in Baltimore; the other is a proposal from Associated Universities Inc. to locate the institute at Princeton University.

Although both proposals are accepted by astronomers as having strong merits, the balance may have been swung in favour of Princeton by a recent federal indictment against Computer Sciences Corporation (CSC). This company, which AURA intended to use to help develop the software for handling telescope data, is being indicted on charge of fraud and racketeering arising from a 1972 time-sharing contract.

AURA officials pointed out last week, however, that the section of CSC which has

been indicted is completely separate from that which would help operate their proposed space telescope institute, and hope that this will insulate them from any action which the federal government might take against the company. The General Services Administration (GSA), against which the frauds are said to have been carried out, has suspended the company from acquiring new business from the agency until a trial which is expected to open in January. The action by the GSA could affect 200 federal users of CSC's Infonet time-sharing system.

**David Dickson**

## Biotechnology

### Celltech set up

The formation of Celltech Limited, the first British company predominantly concerned with the exploitation of biotechnology, was completed on 6 November, according to an announcement earlier this week from the National Enterprise Board (NEB), the public corporation supported with public funds. The board will be the largest shareholder in the company, with 44 per cent of the shares. The remainder of the equity will be divided equally between the four remaining shareholders, the Prudential Assurance Company, the Midland Bank, British and Commonwealth Shipping and TDC (a venture capital investment trust, itself an offshoot of Finance for Industry, a joint venture between the clearing banks and the British government).

The shareholders have already subscribed the first tranche of the £12 million that will serve as the initial capital base of the company. The board of the company will chiefly be representative of the principal shareholders, with Mr G. Jackson of Philips Electronics Limited nominated by the National Enterprise Board (NEB), but will also include Dr J. L. Gowans, the secretary of the Medical Research Council, and Sir Michael Stoker, until recently director of the Imperial Cancer Research Fund Laboratories and foreign secretary of the Royal Society. Sir Michael will also be the chairman of the company's advisory board, to be known as the Science Council.

The council will also have as a member Dr Sydney Brenner, director of the MRC Laboratory for Molecular Biology at Cambridge, who has been involved with the planning of Celltech from the beginning. Other members of the council are to be announced in the near future.

Apart from the managing director of the company, Mr S. Fairtlough, the director of research and development will be Dr N. Carey, at present director of research at G. D. Searle Limited. Dr Caroline Vaughn, like Mr Fairtlough at present on the staff of the board, will be director of marketing. Other members of the staff of the company have yet to be appointed. The chairman of the company will be Mr Wynn Denman, a

director of British and Commonwealth Shipping.

The announcement of the setting up of the new company said that Celltech has reached an agreement with the Medical Research Council (MRC) that provides a "framework" within which the company will have access to research carried out in the council's laboratories. It has also come to an arrangement with the National Research Development Corporation, the public corporation which is the principal repository of patent rights arising from research carried out in university and public laboratories in the United Kingdom. Plainly the negotiation of these agreements, no details of which have been made public, has taken up some of the time that has elapsed since the Celltech project was first announced nearly four months ago (see *Nature* 24 July).

### Veal hormones

## Total ban proposed

### Brussels

The Commission of the European Economic (EEC) has lost no time in taking steps to ban the use of all natural and artificial hormones in livestock — a draft regulation is due to come into effect on 1 January 1981. At the Council of EEC Agricultural Ministers on 30 September the Commission promised to respond speedily to a request to draw up proposals on the use of hormones and anabolic steroids. This week's Agricultural Council meeting on 10 and 11 November was to be given an account of the Commission's proposals, but will hardly have had a chance to digest them.

Although the ministers have committed themselves to speedy action there are several hurdles ahead of them. The proposals are far reaching — covering all meats intended for human consumption (veal, pork, beef and fowl). The only exception is for the use of natural hormones in therapeutic treatment, which must be carried out under strict supervision. Furthermore, the marketing of animals or carcasses containing residues above a certain level (yet to be specified) will also be prohibited.

None of this will be easy to enforce. The commission still has to devise a foolproof way of controlling the supply of hormones to vets, ways of monitoring animals from the farm to the abattoir, and ways of checking meat on retail sale. These controls are bound to involve a system of identification so that the animal's origin can be traced if the regulations are broken.

The commission's proposals will be particularly welcome in Italy, where in September a magistrate imposed a nationwide ban on veal sales and the sale of twenty-two brands of baby foods containing veal was suspended. The British position is one of traditional restraint, partly due to unwillingness to yield too

much power to Brussels and partly due to scepticism over the implementation of EEC regulations. This scepticism is shared in Germany, where laws on the import of meats have already been tightened.

Jasper Becker

### Medical research

## Born-again basics

The UK Medical Research Council (MRC) and the departments of health in London and Edinburgh are making a valiant effort to defend the transfer of Rothschild contract research monies back to the control of the MRC (*Nature* 23 October, p.669). Last week, on the publication of the MRC annual report for 1979-80, MRC secretary Dr J.L. Gowans said that his council is expected to double its commitment to "health services research" in the next five years. And Professor Arthur Buller, Chief Scientist at the Department of Health and Social Security, said that his department had pressed the MRC into the deal, rather than the other way about.

The doubling of health services research is said to be the MRC price for gaining control of the £13.85 million per annum of Rothschild cash. Since 1972 and the adoption of the Rothschild customer-contractor principle, these funds have been controlled by the health departments but spent by MRC. Under a concordat reached in 1973 between the departments and the MRC they were spent exclusively on biomedical research. Each year the departments defined their interests in a voluminous report under headings such as "blood", "mental illness", "cancer and infections" and so on; and MRC responded, detailing exactly how its biomedical research was relevant. Each year, the health departments passed the Rothschild allocation to MRC, duly increased for inflation.

Health services research, which involves social and economic as well as medical matters (for example, does amniocentesis yield a net benefit?) was, strangely, not covered by the 1973 concordat — so that the £2 million or so a year of health services research at present undertaken by the MRC was in fact funded with money outside the Rothschild principle.

The health departments themselves have thus pressed MRC into the new arrangement under which MRC must spend an extra £2 million on health services research by 1985. Professor Buller, no fan of the 1973 arrangement, considers this a net gain for health services researchers, who might expect, for example, two or three new MRC units in the area by 1985.

Both Professor Buller and Dr Gowans, however, insist that the definition of health services research must be broad, and that the creation of new units will depend on the availability of good people to head them. The agreement is to be reviewed in five years, when the health departments could

## MRC report in brief

The 1979-80 report makes the following specific points:

**Neutron therapy.** Another £1½ million is needed by the end of this year to buy and set up a new cyclotron for neutron therapy research at Clatterbridge Hospital, Liverpool — which would thus overtake the Hammersmith Hospital, London, in this work. The cyclotron would be outside the MRC budget, and would be funded largely by the Imperial Cancer Research Fund, the Mersey Regional Hospitals Authority, and a Liverpool cancer research fund. But quotations for the equipment expire in December, when inflation would probably put the cyclotron out of reach.

**Tropical medicine.** The Tropical Medicine Research Board of MRC met last Friday for the first time since 1979, having cancelled two meetings for lack of money for research grants since cutbacks in Overseas Development Administration spending in 1979. No new projects could be funded — and overseas cooperation is threatened by the new round of government spending cuts. Recruitment into the field has halted.

**Budgets.** Total expenditure by MRC in 1979-80 was £74 million, including £57 million from the Department of Education and Science and £12.7 million of Rothschild money. The council notes with approval the stability promised in the most recent public expenditure plans, but is apprehensive about the effects of cash limits in inflationary times. Anxious to increase its room for manoeuvre, the council says it has deliberately reduced its commitments to long-term research programmes. During the year, it opened two new research units and closed seven.

**Private practice.** The council has confirmed its longstanding policy that members of the MRC research staff should not be allowed to engage in private medical practice. The review was made necessary by the decision that physicians working for the National Health Service might take on private patients. The MRC council says that private practice would be incompatible with full-time research appointments, promises to secure adequate salaries for those members of its staff concerned and hopes that British universities will follow a similar policy.

Robert Walgate

claw back the money if MRC has not performed according to plan. MRC should undertake "brick upon brick" health services research, says Buller, without the constraint of contracts tied to particular policy objectives. The subject is just at the point of requiring such academic treatment, he believes, and it is best handled under the dual support system. The departments' own £20 million of research money will continue to be spent on pragmatic matters.

Robert Walgate



## CORRESPONDENCE

## Sakharov

SIR—Your journal of 11 September contained a short article by Vera Rich about a conference in the Hague devoted to the "Sakharov affair". On the basis of this article (and I have no grounds for doubting its accuracy, so my grievances are not directed at the author and editors) I was left with the impression that the participants of the conference had received distorted information. This information then reached the pages of your journal. Factual inaccuracies in the description of my situation at the conference and other significant facts and a kind of general demobilizing trend of these inaccuracies aroused perplexity and anxiety, causing me to send this letter to your journal.

I suppose that the participants of the conference and its organizers sincerely wished to help me and others who are suffering from repression, but excessive haste and other errors in its organization have almost cancelled its usefulness.

In my time I have taken part in defending the organizer of the conference, Dr Shtern, but I have never made his acquaintance. I have had no communication with him during the preparation for the conference or at any other time. I am also not acquainted with Dr Lozansky and did not meet him at the Jewish seminar of "refusnik" scientists in Moscow. Shortly before the start of the conference Dr Shtern contacted my representative abroad, Efrem Yankielevich, with a request for him to participate in the work of the conference. Yankielevich declined, expressing some apprehension concerning his unpreparedness, though he submitted some concrete advice about desirable witnesses (which, as far as I know, was not used). Yankielevich also commented on the excessively pretentious (in his, and my, opinion) title of the conference.

The article, however, does not refer to Efrem Yankielevich but to his wife, my adopted daughter Tanya Yankielevich (erroneously called Tamara), who it seems objected to "garish" actions, as if they might interfere with the plans of the Soviet authorities to return me to Moscow. This is not simply an inaccuracy, but something outrageous. A stance that is completely alien to us is ascribed to a person close to me, and thereby, indirectly, to myself also.

I, and persons of a kindred spirit, regard openness as the only weapon in the fight for justice. The plans of the authorities are known to no-one. Our actions and statements must be based on fundamental considerations as we perceive them, without accommodating ourselves to these plans, which are unknown to us, or to anyone's ambitions or other considerations of the political situation. This applies both to my defence, and to the defence of other victims of repression, and to general questions such as disarmament and international security, human rights, environmental protection and nuclear power.

Now to some concrete inaccuracies. In Moscow, publication of preprints of my articles in English was forbidden, and the manuscripts were removed by the KGB from the office of the Institute, evidently to preclude any possibility of acquaintance with my work in the West. The preprints were published at Stanford University, and I am deeply grateful to my colleagues there. I am also very grateful to my colleagues in the USA and in other countries who send me their preprints. The Russian texts of my articles are published in *Zh. éksp. teor.*

*Fiz.* in June, August and September, according to normal schedules. I am confident that the Politbureau has had nothing to do with these publications, and, on the whole, references to the Politbureau without stating the sources of information seem unfounded.

My isolation in Gor'kii is of an entirely different nature than appears from the conference. There is no scientific library opposite my home, to which I might have access. Opposite there is only mud and piles of rubbish. I have no contact with scientists in Gor'kii, not because there are only secret institutes here, but because I am in a state of almost total isolation, deprived of the possibility of meeting anybody at all apart from my wife and two people from Gor'kii, who obtained permission for this from the KGB, and one visit from my university colleague, also by permission of the KGB. Any others are kept away by a militiaman, on duty round the clock, one metre from the door.

I don't even get to know about the majority of visitors, and they have great trouble. After some time I merely learn of people who are close to me. Our friend and doctor, who travelled from Leningrad, was not admitted, nor was our 82-year old aunt from Moscow. They do not even admit my son's fiancée, who has lived with us nearly three years — Liza Alekseeva. The authorities will not allow her out of the country to join the person she loves, she is subjected to persecution, threats of physical and legal reprisals. Fear for her, for her life compels my wife to divide her time between Gor'kii and Moscow. Liza Alekseeva has become a hostage of my public activity, and now her defence is, perhaps, the most realistic form of supporting me.

To describe my situation, I might add that I have no telephone and it is not possible to make a call from a post office; I am deprived of the medical aid of those doctors who used to treat me; my correspondence is carefully inspected by the KGB and only a fraction of correspondence reaches me; in the house where I live there is a personal radio jamming device, which was even in operation before jamming of radio transmissions was resumed in the USSR.

In July my wife found two KGB agents in the flat, who had entered through a window and, without the knowledge of the militiaman on duty, rummaged through my papers, and erased tape recordings. Illegal entry like this, the purposes of which may be even more dangerous, has happened before. I have not received a reply to a single one of my letters or telegrams to officials. Two months ago I sent a letter to the vice president of the Academy of Sciences of the USSR, E. P. Velikhov, and would like to hope for a reply.

The Soviet press, Soviet representatives abroad and some of my Soviet colleagues during foreign missions, in contacts with people in the West who are concerned about my fate, in an attempt to disorganize my defence, assert that I am against détente, have spoken out against SALT, and have even permitted the divulgence of state secrets; they also emphasize the mildness of the measures taken against me. My attitude and open way of life and actions are well known and show how absurd these accusations are.

I have never infringed state secrecy, and any talk of this is slander. I regard thermonuclear war as the main danger threatening mankind, and consider that the problem of preventing it takes priority over other international problems; I am in favour of disarmament and a strategic balance, I support the SALT-II agreement as a necessary stage in disarmament

negotiations. I am against any expansion, against Soviet intervention in Afghanistan, but in favour of aid to refugees and the starving throughout the world. I regard as very important an international agreement on refusal to be the first to use nuclear weapons, concluded on the basis of a strategic balance in the field of conventional weapons. I am convinced of the interrelatedness of international security and defence of human rights, and am in favour of freedom of convictions and exchange of information, freedom to choose one's country of domicile and place of domicile within that country, and freedom of religion. I am deeply anxious about the fate of political prisoners in the USSR, unjust courts, illegal repression. The most important aim for me is the release of prisoners of conscience throughout the world, including the USSR, the countries of Eastern Europe, and China.

I do not make it my task to give special support to the viewpoint of Western governments, or anyone else, but express precisely my own viewpoint on matters causing me anxiety. As for the mildness of the measures taken against me, they are not as severe as the terms of imprisonment lasting many years for my friends and scientists—prisoners of conscience Sergei Kovalev, Yurii Orlov, Toli Shcharanskii (Anatoli Shcharansky), Tanya Velikanova, Viktor Nekipelov, nor as the fate of those awaiting trial — Aleksandr Lavut, Leonard Ternovskii, Tanya Osipova and many others.

But my banishment, without trial in infringement of all constitutional guarantees, the isolation measures applied, interference of the KGB in my life, are completely illegal and inadmissible as an infringement of my personal rights, and as a dangerous precedent of the actions of the authorities, who are casting aside even that pitiful imitation of legality in the persecution of dissidents that they displayed in recent years. Only a court has the right to establish that a law has been infringed and to define the manner of punishment. Any deliberations about culpability and mercy without a trial are inadmissible and against a person's rights.

Therefore I insist on a public trial, and attach fundamental importance to this. It is this that should have been heard at the conference in my defence, and not the greater or lesser mildness of the measures taken against me. Unfortunately, albeit unwittingly, the conference adopted the formulation of the problem that is most advantageous to the Soviet authorities, but even then there were the factual inaccuracies stated above.

I do not know how the fate of others was described (this is not mentioned in the article), but the report concerning the only other person apart from myself mentioned in the article — Dr Gol'fand — is incorrect. He was not dismissed from his work in connection with an application to leave for Israel, but long before he decided to emigrate. Those colleagues of his in the West who are helping him in his struggle for the right to emigrate will, I fear, be misinformed and will cease their efforts after reading such a cheerful paragraph about his reinstatement.

In conclusion I should like to draw attention to the possibility of obtaining accurate information on my situation and attitude directly from my statements and from the reports originating from my wife and from my representative abroad, Efrem Yankielevich.

ANDREI SAKHAROV

6 October 1980,  
Gor'kii 137, Gagarina 214 kv.3, USSR

© 1980 Macmillan Journals Ltd

## NEWS AND VIEWS

## Why is magnetite not a good conductor?

MAGNETITE is a remarkable material, as the first users of lodestones were well aware. When reasonably pure, it looks and feels like a metal. Lumps of magnetite such as can be picked up in some iron mines even sound metallic when struck or thrown to the ground. It is therefore worth recalling that there are some grounds for thinking that magnetite should also conduct electricity as if it were a conventional material. The argument, which of course is false, goes something like this. The crystal structure of magnetite is technically that of the inverse spinel structure. Iron cations turn up on two different kinds of sites within the lattice, conventionally known as A and B sites. The A sites are occupied by  $\text{Fe}^{3+}$  cations and are tetrahedrally related to surrounding oxygen anions. The B sites, on the other hand, have octahedral symmetry and are occupied by equal numbers of  $\text{Fe}^{2+}$  and  $\text{Fe}^{3+}$  ions. This is entirely consistent with the old school textbook notion that magnetite,  $\text{Fe}_3\text{O}_4$ , is a molecular compound of the divalent and trivalent oxides of iron,  $\text{FeO}$  and  $\text{Fe}_2\text{O}_3$ . Considered in isolation, however, the lattice of B sites is potentially a candidate for conduction as if it were a metal. It is possible to think of it as a lattice of  $\text{Fe}^{3+}$  cations with one conduction electron for each pair of cations. How good a conductor of electricity magnetite should be at, say, ordinary temperatures would nevertheless be a matter for detailed calculation and even speculation but one thing would seem to stand out — at some sufficiently low temperature, and certainly near the absolute zero, magnetite should conduct electricity. The fact is that it does not.

If anything, the truth is the opposite. At low temperatures, magnetite has the electrical conductivity of an insulator, but at about 110K there is a first-order transition (recognizable as a specific heat anomaly, for example) and the electrical conductivity of magnetite increases by a factor of about 100 to  $100\ \Omega^{-1}\text{cm}^{-1}$ . With further increase of temperature, the conductivity increases by a further order of magnitude until, as with all conductors, the disruptive effects of lattice vibrations eventually take over and the conductivity decreases with increasing temperature. The conductivity of magnetite above 110K is thus more or less what would be expected. The puzzle is to know why the material does not conduct at lower temperatures. The explanation is by no means novel, although it retains something of the flavour of a surprise. It appears that at low temperatures magnetite is not a conductor because, below the transition temperature, the electrons from the cations at B sites arrange themselves in such a way that there is some form of long-range ordering of the  $\text{Fe}^{2+}$  and  $\text{Fe}^{3+}$  ions. So much was guessed at in the 1940s by E. J. W. Verwey, after whom are now named transitions from states in which ionic charges are ordered to states in which they are not. It is salutary, therefore, to be reminded that people are still unsure what happens to magnetite below 110K. So much at least is clear from the issue of the *Philosophical Magazine* (Series B, Volume 42) for September 1980.

Magnetite is by no means the only material now known to exhibit transitions of this kind. The oxide of titanium with the composition  $\text{Ti}_4\text{O}_7$  is another. The low-temperature state in which electrical conduction is inhibited consists of an ordered arrangement of  $\text{Ti}^{3+}$  and  $\text{Ti}^{4+}$  cations. But there are also materials typified by the samarium sulphide  $\text{Sm}_3\text{S}_4$  in which cations of different charge (in this case  $\text{Sm}^{2+}$  and  $\text{Sm}^{3+}$ ) sit on the same lattice and appear not to form a highly ordered (and thus a markedly non-conducting) state at low temperatures. Why should there be these differences? And why, in any case, is it turning out to be so difficult to come to grips with properties of

what might at first sight seem to be among the simplest of phase transitions? The special issue of *Philosophical Magazine* consisting of papers stimulated by a symposium on the Verwey transition a year ago at the Cavendish Laboratory, and obviously fostered by Sir Nevill Mott, for long the editor of the journal and who contributes an introductory paper, is a splendid way of finding out.

The first surprise is that, until very recently, the actual arrangement of the cations in magnetite at low temperatures was in doubt. That this should have been the case is no surprise if the ordered structure now described by S. Iida (*Phil. Mag. B* 42, 239; 1980) is anything like correct. Especially in the past few years, data bearing on the structure of magnetite at low temperatures have been derived from a variety of sources — Mossbauer spectroscopy, nuclear magnetic resonance measurements and neutron diffraction. The underlying difficulty is that any state in which there is long-range order of cations of different electrical charges on the B sites of the lattice is bound to entail substantial distortion of the shape of the lattice. (Some lattice distances are indeed changed by more than two per cent.) Iida's solution to what is plainly a problem of great complexity involves the description of a superlattice in which eight unit cells in the inverse spinel structure become a single unit cell in a lattice with a larger repeating unit. In the ordered state, below the first-order transition at 110K,  $\text{Fe}^{2+}$  and  $\text{Fe}^{3+}$  cations turn up as pairs or as groups of three similar cations in a row. Although the outcome of the tortuous chain of inference leading to this conclusion is outwardly simple, it is easy enough to see why it could not have been predicted, and why even now its calculation would be a formidable undertaking.

The complications are indeed even more serious than might be thought. Magnetite is not a simple conductor (above the Verwey transition) or a simple insulator (below). The interaction between the relatively large magnetic moments of the cations on the A and B sites makes magnetite a ferromagnetic material below the relatively high Curie temperature of 850K or thereabouts. (The large influence of small quantities of impurities makes the temperature uncertain.) The result is still greater strain of the lattice structure. But magnetite is also a ferroelectric at low temperatures, making for even more lattice distortion. Against this background, the recognition in recent years of further low-temperature transitions (recognizable as specific heat anomalies) is to be expected. The experimental difficulty is that the transition temperatures are sensitive not merely to the stoichiometric purity of the magnetite but to its physical condition. Iida's paper points to an explanation of the transition at 12 K, but there remains room for further argument.

The properties of  $\text{Ti}_4\text{O}_7$  are similarly complex, although C. Schlenker and M. Marezio from the CNRS in Grenoble have a somewhat simpler tale to tell (*Phil. Mag. B* 42, 453; 1980). Two distinct first-order transitions are recognized and, at the lowest temperatures, pairs of titanium cations of different charge are frozen into the lattice. Between the two transition temperatures, pairs can migrate by a process described as 'hopping' and then, at high temperatures, long-range order disappears and the conduction becomes possible. The explicit calculations of what may be happening purport to be little more than crude approximations. Plainly, the experimentalists will make the running for some time to come. Indeed, the study of this curious and still somewhat unexpected transition is likely to serve chiefly as a pointer to fresh problems in lattice structure. □



# Molecular genetics of the mouse

from Grahame Bulfield

WORKERS from two rather different areas came together at a recent conference\* in an attempt to relate structure to function in the regulation of mammalian gene expression. One group of workers has been studying the large number of structural and regulatory gene loci controlling enzyme levels that have been discovered in the mouse. A second group, exploiting recent advances in molecular biology, has been looking at the arrangement and sequence of some mammalian structural genes.

The system most completely characterized by genetic analysis in the mouse is that of  $\beta$ -glucuronidase (K. Paigen, Buffalo; see also *A. Rev. Genet.* **13**, 417; 1980) and by molecular techniques is the globin system (H. Dahl, National Institute of Medical Research, London). However, the only gene family where both approaches have already converged is the amylase one. Genetic analysis shows that the genes for pancreatic and salivary amylase isoenzymes are tightly linked. The different pancreatic isoenzymes are coded for by up to 20 tandemly repeated structural genes (T. Nielsen, Aarhus) but the sole salivary isoenzyme is the product of a single locus (J.P. Hjorth, Aarhus). These workers have identified over 20 different haplotypes of the complex in wild-caught mice and backcrossed them into the C3H inbred strain. Some of the genetically distinct pancreatic isoenzymes have been characterized by peptide analysis and partial amino acid sequencing (M. Meisler, Ann. Arbor). The A/J inbred strain has one salivary and one pancreatic isoenzyme and a single mRNA species is present in each tissue. The active salivary and pancreatic genes are respectively about 28 and 13 kilobases long and contain at least ten exons. Overall there is a family of about eight amylase-like genes, including one salivary gene, but six of the genes are not expressed in the A/J strain (R. Young, Lausanne) demonstrating a remarkable fit with the genetic evidence. The rat amylase gene has also been cloned as part of an analysis of the structure of the pancreas-specific genes and 12 amylase-like genes have been found (W. Rutter, University of California, San Francisco). The complimentary approaches of the geneticists (in providing a large number of congenic haplotypes) and of the molecular biologists (in providing methods for analysing gene structure) should produce a much better understanding of the regulation of expression of the amylase system.

The workshop provided many reports of new variation available to geneticists, the

characterization of some of the systems and their use in analysing both the regulation of gene activity and of development. Expression of  $\beta$ -glucuronidase is affected by several regulatory loci which map at or near the structural gene and control systemic levels of the enzyme, androgen inducibility and developmental profile (K. Paigen; K. Pfister, Zürich). The different haplotypes of this gene complex should provide valuable analytical material once the gene has been cloned.

Genetic variation in regulatory or tissue-specific mechanisms was reported for many enzyme systems including: alcohol-metabolizing enzymes (R. Holmes, Brisbane), H-2 and related systems (M. Boubelik, Prague; K. Fisher Lindahl, Basel), glycerophosphate dehydrogenase (L. Kozak, Bar Harbor), histidine decarboxylase (S.A.M. Martin, Leicester University), metallothioneins (D.M. Hunt, Queen Mary's College, London), neuraminidase (J. Peters, Harwell) and pyruvate kinase (K.J. Moore, Leicester University). Novel methods of investigating genetic regulation were introduced for teratocarcinomas (W.F. Dove, Madison), by the use of spontaneously occurring trisomics (A. Gropp, Lübeck; R. Fündele, München) and by the flow sorting of mammalian chromatin (L. Bolund, Aarhus). Many of the variants in the enzyme systems listed above have unusual features suggesting that the complexities of genetic regulation will be various and may be difficult to unravel. Further extensive genetic variation, so far little used, was shown to be available in different species (interfertile with laboratory mice) and sub-species of feral mice throughout Eurasia (L. Thaler,

Montpelier; E. Capanna and A. Gropp, Rome/Lübeck; K. Moriwaki, Mishima).

The use of biochemical variants to analyse the nature of one developmental problem — X-chromosome inactivation — was discussed in depth. An electrophoretic variant of G6PDH found in *Mus caroli* has been used to show that, in the germ cells of heterozygous fetuses, one X chromosome is active at the 10th day *post coitum*, whereas both are active between days 11 and 14 *post coitum* during the leptotene to pachytene stage of meiosis (V. Chapman, Buffalo). A 'Catherine-wheel' model has been proposed to incorporate the X-chromosome activation-inactivation cycle in the germ cells with the progressive X-inactivation of extraembryonic and embryonic tissues during fetal development (as demonstrated by gene dosage of X-linked enzymes and X-linked electrophoretic alloenzymes (M. Monk, M. Harper and A. McMahon, University College London). That X-inactivation may itself be under genetic control was shown by three alleles of the *Xce* locus which modify the extent of inactivation on the X chromosome they inhabit (B. Cattaneach, Harwell).

Most of the discussions that took place during the conference were concerned with the validity of the genetical and molecular approaches and how they might compliment one other. Two important points were made: first, the need to concentrate on a few systems and analyse them in detail and second, the need to overcome the geneticists' inability to obtain recombinants between structural and regulatory loci within a tightly linked gene complex. Such recombinants will be essential to relate different DNA sequences to changes in phenotype. □

Grahame Bulfield is a Lecturer in Genetics at the University of Leicester Medical School.

## Are QSO absorption lines extrinsic?

from Derek Wills

THE observation of quasi-stellar objects (QSOs) in the ultraviolet (UV), made possible by rocket and satellite developments in the past few years, promises to help decide between alternative explanations of some properties of these still puzzling objects. One of the latest developments is that improved measurements of 3C273 in the UV lend support to the hypothesis that the absorption lines in the spectra of this and other QSOs are due to intervening galaxies (or other material) and that they are not intrinsic to the QSOs themselves.

Derek Wills is associate professor of astronomy at the University of Texas, Austin.

The first QSO whose redshift was determined is the radio source 3C273, which was observed spectroscopically by M. Schmidt (*Nature* **197**, 1040; 1963). Although more than 1,500 QSO redshifts are now known, 3C273 is still the brightest (magnitude 13) and has almost the smallest redshift (0.16). Observations of 3C273 in the UV region are of particular interest because, at this relatively small redshift, it is possible to examine a spectral region that is seen from the ground only in QSOs at much larger redshifts. The result is a direct comparison of physical conditions in objects at quite different cosmological distances and, thus, at different cosmological epochs. Study of the UV

\*Workshop on the Molecular Genetics of the Mouse II held at Sandbjerg Slot, Sønderborg, Denmark, on 11-16 August, organised by J. Peter Hjorth of the Institute of Ecology and Genetics, University of Aarhus and supported by the Danish Natural Science Research Council and Gl. Bomholtgaard Ltd. The abstracts will be published in *Hereditas*.

absorption-line spectrum also makes it possible to probe the medium between 3C273 and the Earth.

The first UV observations of 3C273 were made from a rocket (A. Davidsen *et al.* *Nature* **269**, 203; 1977) and were soon followed by broad-band UV measurements from the ANS satellite (C.-C. Wu *Astrophys. J. Lett.* **217**, L117; 1977). Not surprisingly, 3C273 was one of the small number of extragalactic objects observed during the commissioning phase of the International Ultraviolet Explorer (IUE) satellite by a team of twenty-six astronomers (A. Boksenberg *et al.* *Nature* **275**, 404; 1978), and two separate groups then obtained more detailed spectra of the QSO. One team published their results last year (A. Boggess *et al.* *Astrophys. J. Lett.* **230**, L131; 1979) and the latest contribution, by M.-H. Ulrich *et al.* (*Mon. Not. R. astr. Soc.* **192**, 561; 1980), is a collaborative effort by twenty astronomers at twelve institutions in five European countries. These spectra represent a total of about 16 hours of observing time with the 45-cm diameter telescope on board IUE, and their quality is comparable with those of spectra obtained by ground-based telescopes observing much fainter QSOs at larger redshifts.

It was clear from the first rocket spectra of 3C273 that its emission-line spectrum is indistinguishable from those of typical QSOs at large redshifts, and the details now reported reinforce this conclusion. The similarity is perhaps not as surprising as the fact that the emission-line spectra of QSOs at even the earliest cosmological epochs can be satisfactorily reproduced by simple models involving photo-ionization of a gas with chemical element abundances similar to those in the Sun. The underlying continuum of 3C273 can be represented fairly well by a power law over a large frequency range, except for a considerable excess of radiation in the UV-optical region. It was suggested by G.A. Shields (*Nature* **272**, 706; 1978) that this excess is attributable to thermal radiation from the vicinity of the black hole that is supposed to supply the enormous energy emitted by QSOs, and the observations of Ulrich *et al.* lend support to this interpretation of the UV-optical excess, in part by excluding some other suggested mechanisms.

The absorption-line spectrum of 3C273 is of particular interest. Virtually all large-redshift QSOs contain one or more sets of narrow absorption lines, usually at smaller redshifts than the corresponding emission lines. The strongest absorption lines are due to Lyman- $\alpha$  of hydrogen and other transitions in the UV, so that they are detectable from the ground only when the redshifts are large.

There is long-standing argument about the origin of these absorption lines. One interpretation is that they are caused by clouds of material ejected at high speeds (up to 0.1–0.5 of the speed of light), perhaps by the radiation pressure of the

QSO; another is that they arise in normal galaxies or intergalactic clouds that happen to intersect the very long path between us and the QSO. The two explanations are not mutually exclusive, although the minority of astronomers who still doubt the cosmological interpretation of QSO redshifts (see the recent review by G.R. Burbidge in *Nature* **282**, 451; 1979) cannot accept the second.

An obvious prediction from the ejection hypothesis is that absorption systems should be seen in nearby QSOs just as frequently as in the distant ones; even if, as in the early rocket observations, the wavelength resolution is not quite sufficient to detect individual, narrow absorption lines, the blending of lines below the wavelength of the Lyman- $\alpha$  emission should produce a noticeable drop in the continuum level in that part of the observed spectrum. On the other hand, if the 'intervening galaxy' hypothesis is valid, a relatively nearby object such as 3C273 would be unlikely to show displaced absorption lines or a drop in the continuum level below the Lyman- $\alpha$ .

No such change in the continuum level has been unambiguously seen in any of the UV spectra of 3C273, and the improved data from Ulrich *et al.* still show no evidence for individual absorption lines like those seen in high-redshift QSOs. Adherents of the ejection hypothesis will probably reply that observations of more than one low-redshift QSO are needed before their model can be ruled out, and that large ejection velocities (greater than about one-fifth that of light) would place the strong Lyman- $\alpha$  absorption below the IUE low-wavelength limit.

The latest data on the absorption lines in 3C273 also improve on the earlier evidence for absorption lines at zero redshift, arising in our galaxy. In particular, Ulrich *et al.* confirm the earlier IUE evidence (Savage and de Boer *Astrophys. J. Lett.* **230**, L77;

1979) for absorption due to CIV at 1,549 Å. This line indicates the presence of a highly ionized region at a temperature of  $\approx 10^5$  K, and confirms the prediction (L. Spitzer *Astrophys. J.* **124**, 20; 1956) that our galaxy possesses a hot, gaseous corona, perhaps as a result of accretion of hot, intergalactic gas (D. Sciama *Nature* **240**, 456; 1972) or supernova explosions in the disk.

The presence of the CIV line in some of the absorption systems seen in high-redshift QSOs was formerly used as an argument against the 'intervening galaxy' model, on the grounds that there was no convincing evidence for such high temperatures and metal abundances in the haloes of normal galaxies. The detection of this spectral line in our own galaxy at roughly the intensity seen in the absorption spectra of high-redshift QSOs clearly removes this objection. Thus the presence of absorption lines at zero redshift and their absence at other redshifts must both be counted in favour of the idea that intervening galaxies similar to our own are responsible for many of the QSO absorption-line systems.

Undoubtedly, 3C273 will be among the first objects observed when the Large Space Telescope is launched in a few years. That eagerly awaited development will greatly increase the number of low-redshift QSOs whose UV spectra can be examined, perhaps leading to final agreement on the origin of QSO absorption lines and to a more detailed comparison of conditions in objects believed to have been formed at quite different cosmological epochs. In the meantime, the latest observations confirm that we can now use UV observations of QSOs as probes of the hot, outer regions of our galaxy — for even if there is still some lack of unanimity about QSO distances, there is at least agreement that they are outside our own galaxy. □

## Biosynthesis and processing of cellular and viral polyproteins

from Edward Herbert

THAT active forms of polypeptides can be generated from inactive forms by proteolytic cleavages is an idea dating back to the discovery of precursor forms of gastrointestinal proteases (zymogens) in the early thirties. This type of activation is now known to occur with polypeptide hormones, proteases, blood coagulation factors and viral proteins. The activation process can be either an intracellular or extracellular event and is usually accomplished by trypsin-like enzymes.

Edward Herbert is Professor of Chemistry at the University of Oregon.

The discovery of viral and cellular proteins that serve as precursors to more than one biologically active entity has added a new level of complexity to the subject of protein processing.

At a recent conference\*, scientists working on cellular and viral polyproteins were brought together to discuss similarities and differences in processing of these two classes of proteins.

Among the cellular proteins, pro-opiomelanocortin and proneurophysins

\*Held in Hamburg, FRG in May 1980.



have attracted the most interest. Pro-opiomelanocortin, which contains 260 amino acids, is the precursor to adrenocorticotropin (ACTH),  $\alpha$ - and  $\beta$ -melanocyte-stimulating hormones (MSHs),  $\beta$ -lipotropin ( $\beta$ -LPH) and  $\beta$ -endorphin [ $\beta$  (61–91)LPH]. The amino acid sequence of the precursor was worked out in 1979 by Nakanishi *et al.* (*Nature* **278**, 423, 1979) using recombinant DNA technology. This revealed that each biologically active domain in the precursor is preceded by a tryptic cleavage site (Lys-Lys or Lys-Arg). At the Hamburg meeting, A.C.Y. Chang (Stanford University) presented a partial sequence of the human pro-opiomelanocortin gene. One intron was found at a position 93 amino acids from the amino terminus of the protein but no other interruptions of the coding sequence were detected showing that genetic information for ACTH and  $\beta$ -LPH is contiguous. M. Chrétien (Montreal) presented the amino acid sequence of a 103-amino acid N-terminal fragment of the precursor isolated from the human pituitary. Sequencing work revealed two N-terminal amino acids (Trp and Arg) suggesting that there may be two pro-opiomelanocortin genes in humans.

Pro-opiomelanocortin is present in both anterior and intermediate lobes of mouse and rat pituitary (E. Herbert, University of Oregon). However, the precursor is processed to different end products in the two lobes. The major end products in the anterior lobe are glycosylated and unglycosylated forms of ACTH,  $\beta$ -LPH and N-terminal fragments of the precursor. In the intermediate lobe ACTH is processed further to  $\alpha$ -MSH and  $\beta$ -LPH is processed to  $\beta$ -endorphin. The initial core glycosylation of the precursor and the first proteolytic cleavage appear to be the same in the two lobes, suggesting that processing differences in the two tissues arise at later stages. In the intermediate lobe of rat pituitary,  $\beta$ -endorphin [ $\beta$  (61–91)LPH] is rapidly converted to an N-acetyl derivative and a derivative missing four C-terminal amino acids (Zakarian, National Institute of Medical Research, London). These derivatives, which account for most of the endorphin in the intermediate lobe, have no opioid activity. In contrast to this situation, the major form of endorphin in the hypothalamus is  $\beta$ -endorphin.

Processing of pro-opiomelanocortin occurs quite early in the secretory pathway as subcellular fractions from rat pituitary enriched in endoplasmic reticulum and Golgi vesicles have a precursor/product ratio of 10. This ratio reaches a value greater than 100 in subcellular fractions enriched in secretory vesicles (Glembotski, University of Colorado). Loh (National Institutes of Health) showed that processing of pro-opiomelanocortin in the intermediate lobe of toad pituitary is similar to that in rat pituitary, and that inhibition of

glycosylation by tunicamycin leads to enhanced intracellular degradation of pro-opiomelanocortin to atypical peptides.

Considerable progress has been made in the past year in the study of the synthesis of neurophysins I and II. Three groups reported the synthesis of pre-pro-forms of neurophysins I and II in cell-free protein-synthesizing systems operating under the direction of hypothalamic mRNA (Chaiken, National Institutes of Health; Richeter, University of Hamburg; McKelvy, University of Pittsburgh). Pre-pro-neurophysin I has a molecular weight of 17,000–19,000 and contains an antigenic determinant for oxytocin. Pre-pro-neurophysin II has a molecular weight of 23,000–25,000 and contains an antigenic determinant for vasopressin (Richter). Peptide mapping studies confirm the presence of the neurophysin sequences in pre-pro-neurophysins I and II but sequences of vasopressin and oxytocin could not be detected (Chaiken). The possibility that still higher-molecular-weight forms of neurophysins exist was raised by P. Cohen (University of Paris) who fractionated hypothalamic proteins by gel filtration in denaturing solvents. A protein moiety of molecular weight greater than 50,000 was reported to contain antigenic determinants of neurophysins I and II and oxytocin and vasopressin.

Do these findings about polyprotein precursors of hormones and other biologically active entities have any relevance to what has been found for viral polyproteins? Host cell proteases are most likely involved in very early steps (initial translation of a polyprotein) or in very late steps (transport through membranes or at maturation) of viral replication. In addition, proteolytic enzymes are synthesized by many viruses that are responsible for very specific steps in protein processing. Finally, interesting modifications of viral proteins take place as prerequisite for or as the result of function.

For example, the initial cleavage of the polyprotein of picornaviruses (molecular weight 220,000) is likely to occur by a host cell protease. Such function could reside in the 80S ribosome (Korant, University of Wilmington). One of the initial cleavage products of the polyprotein of encephalomyocarditis virus (a picornavirus), on the other hand, is capable of autocatalytic cleavage yielding a virus-specific protease, p24, which in turn processes other viral proteins (Rueckert, University of Cleveland). In contrast, the precursor protein Pr76<sup>gag</sup> of avian retroviruses is incapable of autocatalytic cleavage, although its C-terminal portion (p15) is a virus-specific protease. p15 must be generated first by a host function before it can proceed to process the rest of the viral precursor protein (Eisenmann, University of Washington; Dittmar, University of Berlin). Both p24 of encephalomyocarditis virus and p15 of retrovirus have a narrow

range of specificity but a definition of their action must await further studies on the structure of viral proteins.

Late reactions in viral maturation taking place as the virus buds from the cell in the completed viral particle were also discussed. Evidence was presented for the involvement of several proteases with unique specificities in cleavage of murine leukaemia virus proteins during viral morphogenesis (Luftig, University of Ohio). One activity exhibited characteristics of serine proteases, another hydrolysed two X-Pro bonds (with X being either tyrosine or phenylalanine). The haemagglutinin of influenza virus also has to be hydrolysed at a critical site to expose a new amino-terminal region which is crucial for infectivity (H.-D. Klenk, Giessen). This cleavage requires a trypsin-like enzyme which must be supplied by the host. Other proteases may cleave adjacent peptide bonds but this does not yield infectious viral particles. A similar example has been described in the maturation of Semliki Forest virus — in cells infected with this virus, a 26S mRNA is produced which codes for a polyprotein cleaved into capsid protein and two transmembrane proteins. The nucleotide sequence of the 26S mRNA has recently been completed (H. Garoff, Heidelberg) and it was found to contain an uninterrupted reading frame which can code for more than 1,200 amino acids. In conjunction with data on the termini of mature virus proteins, the cleavage sites, membrane-spanning segments and putative signal sequences can be discerned. Interestingly, the last cleavage of this polyprotein, the extracellular processing of the transmembrane protein p62 to yield proteins E2 and E3, again involves a trypsin-like specificity.

Viral glycoproteins undergo cleavage by host cellular signal peptidase while being transported to the cell surface. The value of viral proteins as probes to study modification and transport of polypeptides was documented by Lodish (University of Cambridge), who also discussed the interesting phenomenon of fatty acid acylation of certain cellular and viral glycoproteins. Another novel modification of polypeptides is the polyadenylation diphosphate ribosylation of some reovirus capsid proteins (Carter, State University of New York), a phenomenon that may play a role in regulating events in reovirus morphogenesis. Finally, all newly synthesized viral RNA of poliovirus is covalently linked to a small protein, VPg, at the 5' end via a  $O^4$ -(5'-uridylyl)-tyrosine bond (Wimmer, State University of New York). VPg maps in the precursor (NCVP1b) for the viral RNA polymerase as well as viral protease (Rueckert; Wimmer). Since no free VPg can be detected in the infected cell, initiation of RNA synthesis may be linked to a step of proteolytic cleavage of the precursor for the viral RNA polymerase, a situation unique among animal RNA viruses. ■



# Lessons from a peptidergic neurone

from B. T. Pickering

SECRETED polypeptides are known to begin their lives as parts of larger precursors but for many biosynthetic pathways the question persists of 'how large is larger'. This question has recently been asked for the precursors of vasopressin by Paul Cohen and his associates in Paris (*Proc. natn. Acad. Sci. U.S.A.* 77, 2587; 1980). They have found evidence, primarily based on Sephadex chromatography in the presence and absence of urea, of a large ( $\approx 140,000K$ ) precursor molecule in beef posterior pituitaries which showed immunoreactivity with both antivasopressin and antineurophysin sera.

The posterior pituitary hormones were the first recognized members of the neuropeptides, a group which has been growing in both size and importance. Although the hormones oxytocin and vasopressin are released from the posterior pituitary, the gland consists essentially of a collection of the ends of nerve fibres whose neuronal cell bodies are located in the supraoptic and paraventricular nuclei of the hypothalamus. Protein synthesis occurs only in the cell body but the synthetic product is packaged into granules and transported along the nerve fibres for storage in, and release from, the posterior pituitary gland. Along with the non-peptide hormones, the gland contains a family of polypeptides with molecular weights around 10,000 — the neurophysins. These molecules form strong ionic complexes with the hormones with a *pH* optimum of 5.5, close to that inside the secretory granule. It is not surprising, therefore, that neurophysins have been regarded as carrier proteins necessary to keep the hormones inside the granules during their intra-axonal journey.

The hypothesis that vasopressin and its neurophysin share a common precursor was first put forward by Howard Sachs in the mid-sixties. Sachs and Takabatake

(*Endocrinology* 75, 943; 1964) presented the first real evidence for post-translational processing of a polypeptide hormone precursor and the group went on to include neurophysin in the precursor, summarizing their views at the same Laurentian conference that received Steiner's evidence for the existence of proinsulin (*Recent Prog. Horm. Res.* 25; 1969). The hypothesis became much more plausible when it was realised that almost all species elaborate at least two neurophysins — one which is biosynthetically related to vasopressin and another related to oxytocin. Other minor neurophysins seem to be metabolic products of these two (see *Ann. N. Y. Acad. Sci.* 248; 1975).

Undoubtedly the major breakthrough in this field, which provided some hard data to back up the circumstantial evidence, came from Hal Gainer and his group at the US National Institutes of Health (*J. Cell Biol.* 73, 366; 1977; *Science* 207, 373; 1980). In brief, the Gainer group has used pulse-chase studies to show that the two major neurophysins of the rat are formed from two precursors ( $\approx 20,000K$ ) and that processing continues within the secretory granule while it is travelling along the axon. Although the NIH group has not been able to demonstrate conclusively that the precursors do contain hormone as well as neurophysin sequences within their molecules, they have shown that the putative vasopressin precursor is absent from animals unable to make vasopressin (Brattleboro rats). Also, after limited tryptic digestion, the precursor produces molecules with characteristics similar to vasopressin as well as to neurophysin.

The recent paper of Cohen *et al.* (*op. cit.*) reports evidence for a similar ( $\approx 25,000K$ ) precursor in beef pituitaries and this did have immunological determinants for both neurophysin and vasopressin, as did the larger ( $\approx 140,000K$ ) component.

Moreover, protease activity generated molecules with the characteristics of the fully processed secretory products. Similar 20,000–25,000K neurophysin precursors have been synthesized in cell-free systems using mRNA extracted from the supraoptic nuclei of cattle by Guidice and Chaiken (*Proc. natn. Acad. Sci. U.S.A.* 76, 3800; 1979) and of mice by McKelvy and colleagues (*Biochem. biophys. Res. Commun.* 89, 943; 1979). The neurophysin (10,000) and hormone (1,000) sequences would account for about 11,000 of the precursor molecular weight, leaving some 10,000 to be accounted for, and Gainer's group has evidence that in the putative vasopressin precursor this is represented by a 10,000K glycopeptide.

Thus the 20,000–25,000K precursor can be readily accounted for in terms of processed products and has an extractable mRNA to direct its synthesis. What constitutes the residual 110,000 in the larger molecule? Does it form part of the biosynthetic pathway? Certainly there seem to be comparable amounts of 140,000 and 25,000K forms remaining in the granules when they reach the posterior pituitary gland where processing is all but complete (96%). If the 140,000K form is an early stage of the usual pathway, the products of the residual 110,000 should be present in the secretory granule in amounts equimolar with neurophysins and hormones. If not, it must follow that the 140,000K form is a polymer of the 25,000K precursor, perhaps coming from the translation of a polycistronic message; such a possibility is allowed by the Paris workers. The solution to this problem, along with the exclusion of aggregation arising from disulphide interchanges, must await a re-examination of pulse-chase studies in the hypothalamus where precursor/product ratios are more favourable than in the posterior pituitary.

Quite apart from the size of the primary translation product, in my view (*Essays in Biochemistry* 14, 45; 1978) the great attraction of the hypothalamo-neurohypophyseal system is that it provides a good model system for studying polypeptide secretion. Its constituent neurones show all the properties of secretory cells but there is a division of labour (see Fig. 1) such that synthesis and packaging take place in the perikaryon, transport of granules occurs along the axon, and storage and release of the product is restricted to the nerve terminal. This permits the constituent phases of secretion to be studied in some degree of isolation one from another, leading, for example, to the evidence that processing continues while the granule is in

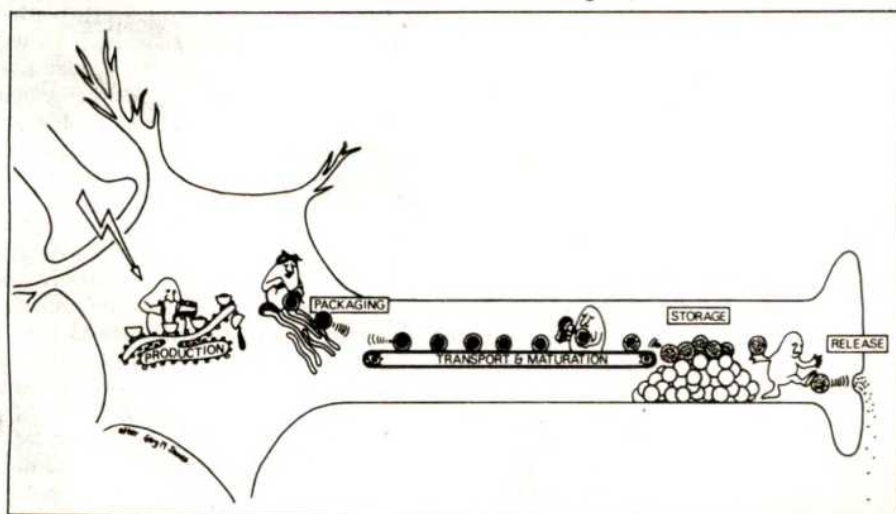


Fig. 1 The division of labour in a peptide-secreting neurone. (After an idea by N. McC. Mortensen.)

B. T. Pickering is a Professor of Anatomy at Bristol University, UK.



transit. The peptidergic neurone as a model system was the dominating theme of the recent 8th International Symposium on Neurosecretion\*. Also at this meeting, H.-D. Dellman (Iowa) showed that, in the developing neurone, secretory material appears within the cisternae of the endoplasmic reticulum before the appearance of Golgi complexes or secretory granules. It is tempting to relate this observation to the almost simultaneous report of A. G. Robinson (Pittsburgh), at another meeting†, that while immunoreactive neurophysin appeared in the brains of fetal

\*Held at Friday Harbor, Washington on 4–10 September 1980

rats on day 13 of gestation, peaked on day 14 and fell slowly towards term, the hormones were undetectable on day 13 but their content in the brain increased towards term. If, as Robinson suggests, these results reflect a high relative concentration of precursor forms in the third fetal week, then, taken together with Dellman's findings, they suggest that the developing hypothalamo-neurohypophysial system presents a tool for the study of the role of the Golgi complex in precursor processing. □

†'Neuropeptides, development and ageing'; held at Rochester, New York on 3–5 September 1980.

## The search for the Zvolen fireball

from David W. Hughes

FIVE all-sky camera stations of the European Fireball Network recorded a bright fireball which penetrated low into the atmosphere on 27 May 1979 at 20h 39min. The fireball terminated close to Zvolen in central Slovakia and may have produced several meteorites.

Geometric, dynamic, photometric and orbital data have been calculated by Z. Cepelach, J. Boček and M. Ježková of the Astronomical Institute of the Czechoslovak Academy of Sciences, Ondřejov, V. Porubčan of the Astronomical Institute of the Slovak Academy of Sciences, Bratislava and G. Polnitzky of the University Observatory, Vienna. Their results have been published in a recent edition of the *Bulletin of the Astronomical Institutes of Czechoslovakia*

31, 176; 1980.

The photometric and positional data on all the available photographic records were measured using a Zeiss Ascocord device. Computational analysis gave the light curve shown in Fig. 1. It is interesting to note that the magnitude remained reasonably constant during a considerable portion of the trajectory. The luminous power is approximately proportional to the kinetic energy lost per unit time by the incident body and it can be seen that mass loss dominates the constant luminosity phase. The maximum deceleration occurs well inside the luminous trajectory and this is typical for meteorite-dropping fireballs. The end height, coupled with the initial mass, velocity and trajectory, indicates that the meteorite was an ordinary

chondrite (a 'strong' stone). The low initial velocity is responsible for the maximum luminosity occurring between heights of 60 and 30 km. Two of the photographs showed the separation of three fragments from the main trail. Fragmentation occurred at heights of 28, 33 and 40 km.

The computational analysis also gave the orbit of the incident meteorite. This had a perihelion distance of 0.89 AU (just inside the Earth's orbit), an aphelion distance of 2.84 AU (right in the asteroid belt) and an inclination to the ecliptic of only 2.3°.

The mass of the final falling meteorite and fragments was estimated to be a kilogram or so. The statistics of meteoritic events from fireball camera networks in the American and Canadian Prairies, demonstrate that one observable meteorite fall per year should occur within a network area of about  $1.4 \times 10^6 \text{ km}^2$ . As the cameras can only register fireballs efficiently when the sky is completely dark, the influx rate of meteorites will be about three times higher than this figure. This is equivalent to about 1,100 meteorite falls per year over the whole surface of the Earth and about 300 over the land masses. In the regions where the networks are active it has been found that the searches that follow the observed falls only have, on average, a 10 per cent chance of recovering the meteorite. Under these assumptions, the Slovakian part of the European network should observe a meteorite fall every 30 years and recover one every 300 years.

The search area for the Zvolen meteorite was estimated to be about  $10 \text{ km}^2$ . This is larger than usual. The photographic station which predicts the fall site most accurately is the one closest to the terminal point of the luminous trail. The camera at Močiar was only 15 km from the predicted position but the gremlins that haunt all scientific endeavour were at work. The Močiar camera was opened on that evening two minutes after the apparition of the fireball. The central part of the search area lies in the eastern part of the town of Zvolen, a region containing many urban dwellings, two large factories, a railway depot with piles of coal and a small river that is swampy in parts. The other regions of the predicted fall area are hilly and covered with woods, fields and meadows. The possibilities of finding a strange, 1-kg rock, about 10-cm across, do not seem too great.

Great publicity was given to the event in the hope of obtaining eye-witness reports of the fireball flight near the impact point. It was surprising that only seven reports were forthcoming in a region of such dense population and only two reports helped to reconstruct the whole path of the flight.

Well over a year has passed, including an early spring when vegetation is much thinner than usual. Nothing has yet been found. □

David W. Hughes is in the Department of Physics, University of Sheffield.

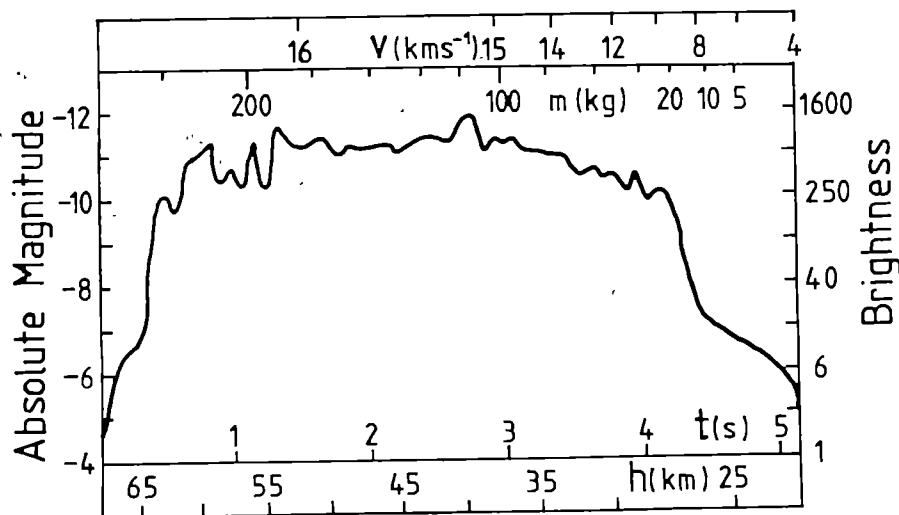


Fig. 1 The light curve of the Zvolen Fireball over the brightest part of its trajectory. The left ordinate gives the absolute photometric magnitude, which is the magnitude the fireball would have if it was at a standard position 100 km from the observer at the zenith. The right-hand ordinate gives the brightness, standardized so that a brightness of 1 arbitrary unit is equivalent to an absolute magnitude of -4. The main abscissa is time, measured in seconds. Secondary abscissae show the decrease in the height of the causative meteorite and also its mass loss and deceleration. At  $t = 0$ , the meteorite had a calculated mass of 223 kg and a velocity of  $16.12 \text{ km s}^{-1}$ .

## REVIEW ARTICLE

## The diffuse UV background

Francesco Paresce &amp; Peter Jakobsen\*

Space Sciences Laboratory, University of California, Berkeley, California 94720

*The diffuse radiation field in the UV (900–3,000 Å) affects the structure of galactic molecular clouds and conveys important information concerning the physical characteristics and spatial distribution of gas and dust in the Universe. Continuum emission in this range is probably dominated by interstellar dust scattering in our Galaxy. For view directions and angular resolutions allowing observations in the rifts between galactic dust clouds, the background due to the integrated light of spiral galaxies may be detected, providing important information on their structure and evolution. The redshifted emission from an intergalactic medium may be observable in the regions between nearby bright galaxies. Present observations provide weak constraints on the radiation field required to ionize the intergalactic medium at the level required by the Gunn–Peterson test.*

THE recent enhanced capabilities of UV instrumentation and observing platforms, a better understanding of basic emission processes coupled with rapid progress in associated fields (especially dust grain characteristics and distribution and galactic luminosity functions) have contributed to a rapid growth of diffuse UV astronomy. UV spectra of galaxies from the OAO, IUE and ANS satellites have enabled their contribution to a diffuse background in the UV to be assessed. New optical observations of hot objects and of high latitude reflection nebulae have become useful for probing the origin of the observed UV radiation field and assessing the likelihood of reaching extragalactic sources.

These factors make the present situation more complex than that envisaged by Davidsen *et al.*<sup>1</sup>, but there are still conflicting observations indicative of the fundamental difficulty of observation. We attempt here, using these latest findings, to determine as accurately as possible the characteristics of the most likely sources of the diffuse UV background. We have placed special emphasis on assessing the probability that information of cosmological significance can be gleaned from this work. Galactic dust and external galaxies are likely to have an important role. These sources must be well understood before the intergalactic medium contribution, if any, can be properly quantified especially if it is emitting by recombination radiation rather than collisional excitation as has been assumed in the past.

### Local sources

The most serious difficulty in analysing diffuse cosmic background data from UV instruments is to account for the large number of sources that may contaminate the observations. The inherent instrument background is not as easily removable for diffuse emission spectrophotometry as it is for point sources. Shutters that can exclude the outside world periodically are the only reliable method, but complex moving parts in spacecraft instrumentation are not always considered ideal. Pointing the instrument at some dark object is a common alternative but the actual darkness of the object is questionable. Dark Earth may not be so dark at certain altitudes and latitudes. In fact, it may be brighter than the sky due to various electromagnetic or particle induced emissions in the UV.

This atmospheric emission—another source of diffuse radiation—must be fully understood when observing from an Earth orbiting platform. There are at least 20 known or suspected UV line and band emission features in the Earth's airglow and aurora. Particle induced emissions are probably the most

treacherous of these sources because of their intensity and uncertain spatial and temporal variation over the Earth's surface. This source is not restricted to the auroral zones, but may appear almost anywhere at any time, including the equatorial regions due to ring current precipitation<sup>2,3</sup>. It is essential to exclude at least the most intense emission lines from the instrument's bandpass. However, this may not be a sufficient precaution as weak band emissions throughout the far UV may contribute to a broad band observation<sup>4</sup>.

A more drastic solution would be to escape the Earth's atmosphere and observe from a platform in the interplanetary medium. However, even this medium is a source of diffuse UV radiation. In this case, scattering of solar light by zodiacal dust grains and by atomic and singly ionized interstellar gas atoms must be considered. The former source of emission is probably not important below about 2,000 Å (refs 5, 6) but becomes troublesome just above this wavelength. At an elongation of 30° on the ecliptic plane, the zodiacal light intensity at 2,000 Å may reach  $\approx 500$  photons  $\text{cm}^{-2} \text{s}^{-1} \text{sr}^{-1} \text{Å}^{-1}$ , a value uncomfortably close to the observed cosmic background intensities plotted in Fig. 1. Any correction for this effect should include systematic exploration of the ecliptic plane at many elongations and observations as far removed from this plane as possible.

Backscattered UV line radiation at the resonance transitions of interstellar hydrogen and helium flowing into the interplanetary medium because of the large relative motion of the Solar System with respect to the interstellar medium is also of considerable importance<sup>7</sup>. Observed emissions include the H I 1,216 Å and 1,026 Å and the He I, 584 Å resonance lines with suspected weaker contributions from He II 304 Å, He I 537 Å, N II 1,085 Å, O I 1,304 Å, and C II 1,336 Å that have the necessary corresponding exciting lines in the solar spectrum. These emission lines influence UV observations by their strength (especially Ly $\alpha$  at  $\approx 3 \times 10^8$  photons  $\text{cm}^{-2} \text{s}^{-1} \text{sr}^{-1}$ ) and seasonal variability.

### Point sources

Progress in understanding point sources of UV emission critically influences the results of the UV background observations because some of these sources will be in the field of view of an instrument attempting to measure the diffuse background. The best way of correcting for stellar contamination is to use the TD1 catalogue of stellar UV fluxes<sup>8</sup> covering the range 1,500–2,500 Å down to  $m_v \approx 8-9$ , supplemented, where possible, by the corresponding spectrophotometric catalogue<sup>9,10</sup>. For this technique to be accurate enough, the instrument response and

\* Permanent address: Copenhagen University Observatory.



the field of view must be well known, preferably by means of careful in-flight calibrations.

For fainter stars or for  $\lambda < 1,500 \text{ \AA}$  we have to use theoretical models for the stellar emission and luminosity functions for hot stars obtained in the optical band; large errors are, therefore, to be expected.

Henry<sup>11</sup> has described a technique to overcome some of these problems in which stars in the SAO catalogue are integrated in conjunction with a UV stellar calibration<sup>12</sup>. Although simple, this method may overestimate the stellar contribution due to errors in the listed spectral types and the lack of a suitable correction for differential interstellar dust extinction.

A simpler method, in principle, is to reduce the instrument field of view to a size such that the number of stars having a certain limiting magnitude becomes very small. This limiting magnitude has been estimated for observations at  $1,500 \text{ \AA}$  to be near  $m_v = 9.5-10$  (ref. 11). This is effective provided the collecting area of the telescope rises simultaneously as the square root of the decrease in the field of view to maintain the same signal-to-noise ratio: this may become impractical or too expensive. As a rule, with recent technology, a 1-m diameter telescope is necessary to achieve a sensitivity slightly below that needed to detect the lowest observed UV intensity ( $\approx 300 \text{ photons cm}^{-2} \text{ s}^{-1} \text{ sr}^{-1} \text{ \AA}^{-1}$  at  $1,500 \text{ \AA}$ ) with a 15–20 arc min field of view.

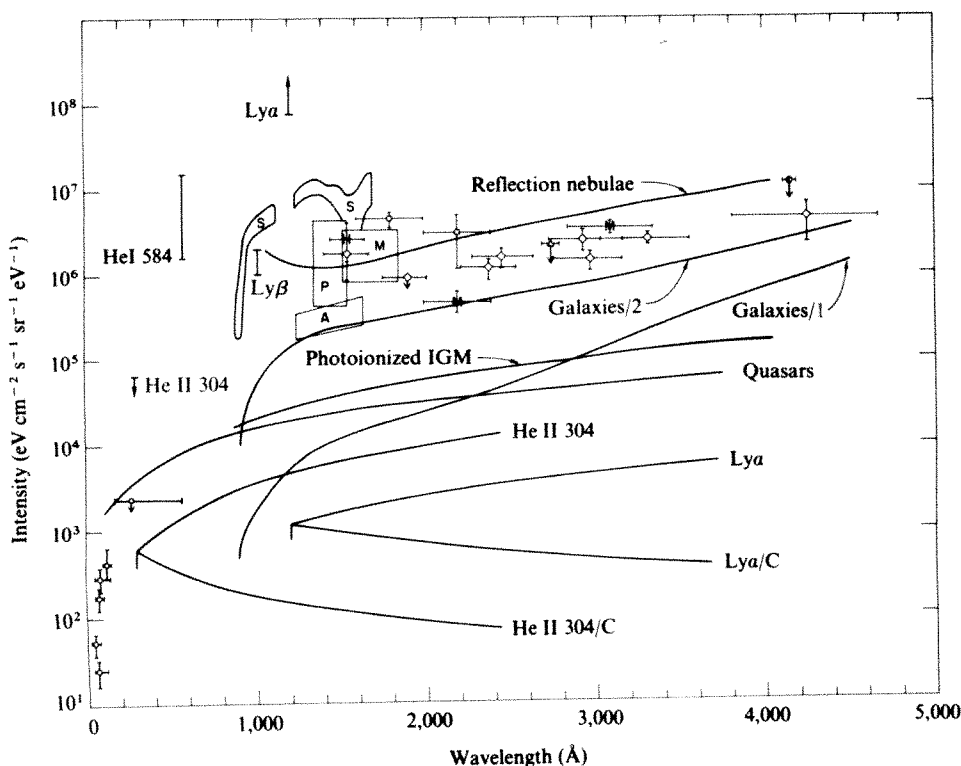
An added advantage can be envisaged by restricting one's background observations to high galactic latitudes where hot stars are few and far between. This works well for O and B stars, is dubious for A stars and of no use for F and later stars. Because A stars (especially A0 stars) contribute substantially to the background above  $1,500 \text{ \AA}$  (ref. 11), this technique is best suited to observations in the range  $\approx 1,000-2,000 \text{ \AA}$ .

After these precautions, there remains the important question of the residual faint ( $m_v > 10$ ) star distribution and the possible magnitude of its contribution to the observed UV background. We have estimated this contribution using standard main sequence colours, absolute visual magnitudes, scale heights and luminosity functions. Conversion to the UV is accomplished by using observed mean  $(m_v - m_\lambda)_0$  versus  $(B - V)_0$  relations<sup>12,13</sup>, with the result that the contribution due to the sum of all main sequence stars of  $m_v > 10$  in the Galaxy at  $1,500 \text{ \AA}$  in the direction of the galactic poles cannot exceed  $30 \text{ photons cm}^{-2} \text{ s}^{-1} \text{ sr}^{-1} \text{ \AA}^{-1}$ .

Not all hot stars, however, can be assumed to be on the main sequence. Green<sup>14</sup> has shown that hot white dwarfs comprise  $\approx 64\%$  of the known faint blue star population down to a  $B$  mag of  $\approx 16$ . Using his derived luminosity function and scale height for these objects and assuming that all the hot white dwarfs in his sample are as hot as HZ43, one of the hottest white dwarfs known<sup>15</sup> we can calculate a strict upper limit to their effect on an UV background measurement. We find that their contribution at the poles and at  $1,500 \text{ \AA}$  cannot exceed  $\approx 20 \text{ photons cm}^{-2} \text{ s}^{-1} \text{ sr}^{-1} \text{ \AA}^{-1}$ . Other possible sources of stellar UV radiation such as subdwarf OB stars and blue horizontal branch stars are probably too scarce in space to give a substantial contribution<sup>16</sup>. Thus with the accuracy allowed by the input astronomical data, unresolved faint stars will contribute  $< 50 \text{ photons cm}^{-2} \text{ s}^{-1} \text{ sr}^{-1} \text{ \AA}^{-1}$  at  $1,500 \text{ \AA}$  in the direction of the galactic poles.

## Observations

All observers have to deal with at least some of the above problems to claim a measurement of a truly cosmic (galactic or extragalactic) background. Henry *et al.*<sup>17</sup>, using a rocket-borne  $10^\circ \times 10^\circ$  Geiger counter sensitive to the  $1,425-1,640 \text{ \AA}$  range, mapped the entire sky observable in March from White Sands, New Mexico. After in flight calibrations and subtraction of the average count rate observed when the detector was pointed  $25^\circ$  or more below the horizon were performed, the residual signal was compared with the signal expected from the integration of the stars in the SAO catalogue. The data for  $b < 45^\circ$  are reasonably well accounted for by the predictions but a large observational excess is evident in the range  $b > 45^\circ$ . At high galactic latitudes Henry *et al.* find the intensity of the UV background corrected for stellar contributions to be in the range  $1,000-1,900 \text{ photons cm}^{-2} \text{ s}^{-1} \text{ sr}^{-1} \text{ \AA}^{-1}$ . The high galactic latitude measurement is displayed in Fig. 1 where we have plotted the observed background intensity in units of  $\text{eV cm}^{-2} \text{ s}^{-1} \text{ sr}^{-1} \text{ eV}^{-1}$  as a function of wavelength in  $\text{\AA}$  for each measurement discussed here. According to Henry *et al.*, the reported excess is due to airglow in the  $1,425-1,640 \text{ \AA}$  band and one may hypothesize the presence of weak emissions of  $\text{N}_2$  in the Lyman-Birge-Hopfield bands<sup>4</sup> as a possible source of this contamination.



**Fig. 1** Observations and theoretical estimates of the diffuse UV background at high galactic latitudes as a function of wavelength (delete  $\text{eV}^{-1}$  for the interplanetary lines). Sources of the observations: A, ref. 22; H, ref. 17;  $\diamond$ , ref. 18; M, refs 24, 28;  $\triangle$ , ref. 29; P, refs 25, 26;  $\circ$ , ref. 34;  $\square$ , ref. 23; S, ref. 31;  $\odot$ , ref. 35.

Lillie and Witt<sup>18</sup> used the Wisconsin Experiment Package  $10 \times 10$  arc min broadband photometers on OAO 2 to study the intensity, spectrum and spatial distribution of the UV background between 1,550 and 4,250 Å. Their results are summarized in Fig. 1 which displays their average intensities in the  $40^\circ < b < 90^\circ$  range. Their  $S_{10}$  units are converted to our physical units using the TD1 spectrum of  $\alpha$  Lyr<sup>9</sup>. These results supersede the earlier published observations from OAO 2 (ref. 19) because of their superior accuracy, spatial coverage and signal-to-noise ratio.

The OAO 2 measurements plotted in Fig. 1 are corrected for instrumental background using mechanically actuated shutters, for zodiacal light by means of an empirical correction formula incorporating several observational results and for light of stars of  $m_v > 11.5$  by optical photoelectric drift scanning of the observational fields. For the reasons outlined above we would expect the most accurate numbers in this case to be those corresponding to the shortest wavelengths and to the highest galactic latitude range observed. In this case, however, the weakness of the signals in the very small OAO field of view at high galactic latitudes introduces a substantial observational error that may approach 100% of the observed signal in some cases. The fact that the adopted zodiacal light spectrum below 2,000 Å (ref. 20) may be too high<sup>6</sup> probably has very little influence on the results because of the vanishing solar flux at 1,500 Å.

With a  $12^\circ \times 12^\circ$  scanning spectrometer sensitive to the 1,180–1,680 Å range, Henry *et al.*<sup>21</sup> observed the sky near the south and north galactic poles from Apollo 17 on trans-Earth coast, free from the effects of the terrestrial atmosphere. The resulting UV background spectrum consisted of a wide emission feature centred at 1,450 Å, of maximum intensity  $\approx 250$  photons  $\text{cm}^{-2} \text{s}^{-1} \text{sr}^{-1} \text{Å}^{-1}$  and with little or no emission at 1,250 and 1,650 Å. Unfortunately, a large and complex correction for instrumental background, starlight and Ly $\alpha$  scattering in the instrument amounting to  $\approx 85\%$  of the signal significantly reduces the confidence level of the result.

In a repeat experiment performed from a rocket by Anderson *et al.*<sup>22</sup>, the 1,450 Å 'feature' at the galactic pole disappears and is replaced by a featureless constant background of  $\approx 285$  photons  $\text{cm}^{-2} \text{s}^{-1} \text{sr}^{-1} \text{Å}^{-1}$  between 1,250 and 1,650 Å. A suggestion of a ledge or discontinuity at  $\approx 1,650$  Å is found in this experiment which, because of its smaller field of view ( $1.4^\circ \times 5.8^\circ$ ) is less susceptible to large starlight subtraction errors. The outer envelope of the spectrometer results from this experiment is plotted in Fig. 1 rather than the results from Apollo 17 as the latter are far more uncertain and highly discrepant with the rocket results at 1,250 and 1,650 Å. The former should be considered essentially free of the problems encountered by the Apollo 17 experiment because the instrumental background was low, a crystal filter shielded the Instrument from Ly $\alpha$  radiation and the stellar correction for two of the three targets observed was quite small. From the results on these three targets, Anderson *et al.* suggest that the UV background is spatially uniform at this intensity.

A three channel UV polychromator with a  $2^\circ$  circular field of view flown on a rocket by Pitz *et al.*<sup>23</sup> measured the UV sky brightness at 1,800, 2,200 and 2,600 Å. After the data were purged of instrumental effects and corrected for airglow and zodiacal light and starlight contaminations, the intensities for  $b = 60^\circ$  displayed in Fig. 1 were reported. The quasi twilight observing configuration (solar zenith angle  $\sim 110^\circ$ ) makes correction for airglow risky. Pitz *et al.*<sup>23</sup> claim that the brightness distribution with view direction is uniform but it is not clear at what level of accuracy. Only a few observations at different latitudes are reported—the result of an extensive averaging procedure that might easily mask a more pronounced spatial variation.

A similar difficulty of interpretation is encountered with data of Maucherat-Joubert *et al.*<sup>24</sup> obtained from the ELZ photometer on board the D2B satellite. This experiment consisted of a  $1.3^\circ \times 1^\circ$  objective grating-photomultiplier detector

combination sensitive to the 1,525–1,855 Å range surveying the entire sky from a 600-km altitude orbit. The outer envelope of the validity range of their results for  $b > 40^\circ$  is shown in Fig. 1. Because of the altitude of the satellite, the wavelength band, the small field of view and the observing configurations, airglow, zodiacal light and starlight probably form a small part of the observed signals after elimination of the bright star fields ( $m_v > 8$ ). Because the instrumental background was high and difficult to assess properly, the data was averaged over relatively large spatial zones, thereby losing possible spatial information. As the observed range of intensities was much wider than expected from counting statistics alone, an additional source of emission was invoked. Faint stars with the true UV background consequently uniform were suggested in accordance with the results of Anderson *et al.* and Pitz *et al.* Another possibility is that the spread is due to an actual spatial variation of the UV background itself.

The latter conclusion would be more compatible with the results of the survey carried out with the  $2.5^\circ$  field of view telescope on board the Apollo-Soyuz Test Project (ASTP). A patchy spatial distribution of the UV background is reported<sup>25,26</sup> with intensities ranging from a sharp minimum of 300 to  $\approx 4,000$  photons  $\text{cm}^{-2} \text{s}^{-1} \text{sr}^{-1} \text{Å}^{-1}$  after correction for stars of  $m_v \leq 9-10$ , instrument background and airglow. The latter corrections were made using a moveable shutter and observation of the Earth from the 225 km altitude of the spacecraft. The range of intensities observed for  $b > 40^\circ$  is also shown in Fig. 1 at the appropriate wavelength band.

There are two obvious explanations for the radiation pattern observed: (1) diffuse radiation scattered by galactic dust or (2) random airglow contamination not accounted for by the Earth pointed observations and not satisfying the standard rules to airglow phenomenology<sup>27</sup>. The latter explanation of the discrepancy between the Paresce *et al.* results and those of Anderson *et al.* is the simplest because, for at least two of the Anderson *et al.* targets, there corresponds an ASTP observation made in essentially identical conditions and yielding a factor of  $\approx 3$  difference in intensities. However, the clear correlation found<sup>26</sup> between the ASTP UV background intensity and galactic N (H I) column density as determined by 21-cm radio observations suggests a galactic origin of a good part of the observed signal.

This result has been confirmed by Maucherat-Joubert *et al.*<sup>28</sup> after a reanalysis of the D2B data. They constructed histograms of individual count rates corresponding to areas in the sky of 24–40 square degrees, regions much smaller than those considered in the original analysis. After removal of resolved stars, subtraction of dark current and zodiacal light, a reasonably good correlation between observed 1,690 Å intensity and N (H I) is found for all view directions corresponding to  $b > 40^\circ$ . The large scatter in the correlation may be partly due to variations in galactic plane brightness and dust-to-gas ratio from point to point in the sky<sup>26</sup>.

Further analysis<sup>28</sup> of the UV background with the ELZ instrument at 2,200 and 3,100 Å is reproduced in Fig. 1. The similarity in shape of the UV background spectrum towards the poles and towards the Coal Sack nebula has been used to favour the scattered galactic light hypothesis.

Morgan *et al.*<sup>29,30</sup> have reported TD-1 measurements of the UV background. Unfortunately, because of substantial airglow contamination (especially Ly $\alpha$ ) of uncertain magnitude, only the variation of the signal with galactic latitude could be ascertained with any accuracy. Thus these results have limited value except to confirm that the albedo of interstellar grains is  $\sim 0.5$  in the 1,550–2,740 Å range and to set an upper limit to the UV background at 2,740 Å which is shown in Fig. 1.

The UV spectrometer on the Voyager spacecraft<sup>31</sup> has the capability of measuring the UV background in the 500–1,700 Å region with  $\approx 10$  Å wavelength and  $0.9^\circ \times 0.1^\circ$  spatial resolution with high sensitivity due to the long observing times available and the absence of terrestrial airglow contamination. Large instrumental backgrounds, uncertain corrections for Ly $\alpha$



interplanetary emission and uncertainties in instrument calibration still hamper attainment of the ultimate instrument sensitivity to weak diffuse fluxes.

These problems necessitate subtracting a background spectrum obtained in one view direction and used as a 'scattering background spectrum' from a spectrum obtained in another direction as was done in the Voyager results analysis. Hence spatial variations conveying basic physical facts concerning the radiation field may be obliterated. The outer envelope of the results of this experiment are shown in Fig. 1. The generally higher values may, in part, be due to the generally lower galactic latitudes ( $b < 40^\circ$ ) of the Voyager view directions than for the other measurements displayed in Fig. 1 which generally pertain to the  $b > 40^\circ$  region.

The spectral feature at  $\approx 1,450 \text{ \AA}$ , first detected by Henry *et al.*<sup>21</sup> and not confirmed by Anderson *et al.*<sup>22</sup>, is also reported by Hua *et al.*<sup>32</sup> but of varying intensity in the two places in the sky observed. This experiment consisted of a  $53 \text{ \AA}$  resolution,  $6^\circ \times 6^\circ$  field of view scanning spectrometer sensitive to the  $1,100\text{--}1,900 \text{ \AA}$  region flown on the Prognost-6 satellite. Because calibration of the instrument is uncertain it is premature to give it the same weight as the other measurements shown in Fig. 1.

The UV background is almost certainly made up of components displaying widely different physical characteristics in the emitted radiation field including different intensities, spatial variations and polarization at different wavelengths. Attempts to unify these properties into a diagram similar to Fig. 1 will probably turn out to be an oversimplification. Because of our limited knowledge, however, it is useful for gaining a general perspective on the problem that would be difficult if we were restricted to a small subset of the UV spectrum. It also ensures that any postulated source of UV radiation does not violate observational limits in the adjacent spectral regions. For these reasons we have expanded the scale of Fig. 1 to include the EUV on one end, the visible on the other, and have included results pertaining to different phenomena that must be present whenever a measurement of the UV background is attempted. It also vividly displays the variety of physical emission mechanisms operating in the UV and the information one can obtain concerning the structure of the interstellar gas and dust components.

Figure 1 thus includes observations of the EUV background in the  $50\text{--}600 \text{ \AA}$  wavelength region<sup>33,34</sup>, the range of observed intensities of the diffuse interplanetary emission lines at  $304$ ,  $584$ ,  $1,026$  and  $1,216 \text{ \AA}$  and the limit on the night sky background at  $4,150 \text{ \AA}$  (ref. 35). Although the scatter, individually and collectively, of the data is large, there seems to be remarkable agreement over a wide range of wavelengths from the visible to the beginning of the EUV that the UV background is relatively constant between  $10^6$  and  $10^7 \text{ eV cm}^{-2} \text{ s}^{-1} \text{ sr}^{-1} \text{ eV}^{-1}$  at high galactic latitudes. The largest deviations occur in the far UV ( $1,000\text{--}2,000 \text{ \AA}$ ) where most observations are concentrated. It is not yet possible to decide whether the large scatter at these wavelengths reflects reality or is due to the observational problems discussed above. If the scatter is real and due to variations in observing direction and wavelengths, for example, the relative lack of such scatter at wavelengths longer than  $2,000 \text{ \AA}$  may simply be fortuitous and due to the much smaller number of observations available. The most difficult region of observation is at  $\lambda > 2,000 \text{ \AA}$  where the effects of zodiacal light and starlight contamination become severe.

Below  $1,000 \text{ \AA}$  observations become extremely difficult both because of the insensitivity of presently available EUV instrumentation<sup>36</sup> and the large interstellar H I absorption cross-section below  $912 \text{ \AA}$  (ref. 37). A large gap in our knowledge of the UV background between  $300$  and  $1,000 \text{ \AA}$  is due to these difficulties and more local interplanetary line emission phenomena dominate the EUV at present. After a drop of  $\sim 3$  orders of magnitude, the background due to hot ( $T > 10^5 \text{ K}$ ) gas in the galaxy as attenuated by intervening H I, perhaps the same gas responsible for the O VI absorption feature in hot stars<sup>38</sup>, is probably the dominant diffuse emission mechanism in the EUV.

## Diffuse galactic light

Interstellar dust particles may scatter starlight that was initially travelling out of the Galaxy back to an observer in the plane. The intensity of this reflected radiation at a specific wavelength  $\lambda$  will depend on the albedo,  $a(\lambda)$ , the phase function asymmetry factor,  $g(\lambda)$ , the optical depth of the dust and the galactic disk, and the source function of starlight. Davidsen *et al.*, using then standard dust models, estimated the brightness of this source at the poles to be  $\approx 250 \text{ photons cm}^{-2} \text{ s}^{-1} \text{ sr}^{-1} \text{ \AA}^{-1}$  at  $1,400 \text{ \AA}$ , quite a large amount if the expected extragalactic contribution is much fainter. A convenient solution to this problem was suggested by Sandage's observations of  $E(B - V) = 0$  for  $b > 50^\circ$  (ref. 39). There is now considerable doubt about the validity of this result. Sandage<sup>40</sup> was, in fact, the first to discover faint filamentary structured reflection nebulae in the visible at latitudes as high as  $|b| \approx 50^\circ$ . The brightest of these filaments have an optical extinction as high as  $A_v \sim 0.3 \text{ mag}$  and are clearly visible on the Sky Survey Palomar prints where they can be traced to regions not covered by Sandage's work. These clouds possibly cover a large part of the sky around the galactic poles. Recent measurements of polarization and reddening of high-latitude stars<sup>41-43</sup> give further evidence of the existence of dust near the galactic poles.

An H I column density of at least  $2 \times 10^{20} \text{ cm}^{-2}$  at the poles<sup>44</sup>, and the canonical dust-to-gas ratio<sup>45-47</sup>, recently extended to the poles by Knude<sup>43</sup> ensure that  $E(B - V) > 0.03$ , and it seems safe to claim that  $0.03 < E(B - V) < 0.3$  for  $|b| > 50^\circ$ . This result implies that dust could be a source of diffuse galactic radiation, but its presence alone is not a sufficient condition for this effect to be noticeable as the scattered intensity is also very sensitive to the values of  $a(\lambda)$  and  $g(\lambda)$ . As far as the albedo of the dust is concerned, there seems to be general acceptance of values near  $a \approx 0.5$  for  $\lambda > 1,400 \text{ \AA}$ , which is consistent with a recent model of the interstellar grains<sup>48,49</sup>. The value of the parameter  $g$ , is, however, a subject of some controversy. Henry *et al.*<sup>50</sup> argued for values of  $g$  higher than  $0.9$ , implying that the interstellar dust is strongly forward scattering, whereas others<sup>51-53</sup> argued for much lower values, that is,  $g \approx 0.2$ , or much more isotropically scattering dust grains. The above dust model predicts an intermediate value of  $g \approx 0.6$  at UV wavelengths which agrees well with previously<sup>26</sup> derived value on the basis of a comparison with Jura's predictions<sup>53</sup> and with recent TD-1 observations of UV radiation around  $\lambda \text{ Ori}$  (ref. 54).

The patchiness of the background radiation at  $1,450 \text{ \AA}$  and the reported correlation<sup>26,28</sup> with hydrogen column density does indeed suggest that backscattered galactic disk starlight is an important contributor to the diffuse background at UV wavelengths. The question then arises of whether the general level of the measured background is compatible with this view. This problem has been discussed by Jura<sup>53,55</sup>.

An uncertainty in calculating the amount of backscattered starlight lies in estimating the intensity of the radiation incident on the high latitude dust. As the reflecting material is essentially seeing the Milky Way from well above the galactic plane, this problem is connected with the general question of the amount of UV radiation emerging from spiral galaxies. The curve 'Reflection nebulae' in Fig. 1 gives the predicted UV surface brightness of the densest of Sandage's filaments placed at  $b \sim 90^\circ$  as a function of wavelength, calculated in terms of Jura's reflection nebula model<sup>55</sup> and assuming the White<sup>49</sup> model for interstellar dust. The incident radiation was determined by using a value of  $A_v \sim 0.3 \text{ mag}$  for the optical depth of the galactic disk and by assuming that the Milky Way as seen from outside the galactic plane has the same UV spectrum as the spiral galaxies observed with the OAO 2 satellite<sup>56</sup>. The magnitude of the UV radiation field was determined by normalizing to the total local radiation density at  $1,450 \text{ \AA}$  observed onboard Apollo-Soyuz<sup>26</sup>.

In spite of all the uncertainties, the general level of the theoretically expected backscattered light is in rough accord with the observed background level throughout the far UV into the visible. Note that the calculation refers to the very brightest filaments observed, and that Sandage reported filamentary

structure on scales from arc minutes to several degrees. Because most measurements are performed with instruments having fields of view larger than this, the observed smeared out background could be lower in those cases. However, the order of magnitude agreement between predictions and observations supports the claim that backscattered starlight is an important source of background light and an obstacle that must be overcome before the true extragalactic component of the UV background can be determined.

The possibility of large amounts of reflecting material existing at high galactic latitudes could limit the performance of the Space Telescope at short wavelengths but the patchiness of the filaments as indicated by Sandage and the Apollo-Soyuz data, suggests we may find rifts in the interstellar cloud cover through which it may be possible to catch unobstructed glimpses of extragalactic sources in the UV.

## Extragalactic sources

The background light due to distant galaxies and quasars arises as the emission from all objects along a given line of sight looking out into the Universe. But because of redshift and lookback-time effects, more distant sources contribute to the background at a given wavelength today with light emitted at earlier epochs at shorter wavelengths. In a Friedman Universe with Hubble constant  $H_0$  and density parameter  $\Omega$ , the background intensity  $I_{\lambda_0}$  at wavelength  $\lambda_0$  due to a class of objects with luminosity density  $\epsilon_{\lambda_0}$  can be written<sup>57</sup>

$$I_{\lambda_0} = \left( \frac{c}{H_0} \right) \frac{\epsilon_{\lambda_0}}{4\pi} A_{\lambda_0}$$

with  $A_{\lambda_0}$ , 'the accumulation factor' given by

$$A_{\lambda_0} = \int_0^\infty \chi_\lambda(z, \lambda_0/(1+z)) \phi(z) (1+z)^{-4} (1+\Omega z)^{-1/2} dz$$

$\chi_\lambda(z, \lambda)$  describes the mean spectra and  $\phi(z)$  the comoving density evolution of the objects under consideration, both normalized to  $\chi_\lambda(0, \lambda_0) = 1$  and  $\phi(0) = 1$ .

To estimate the expected UV background due to galaxies and QSOs, detailed information on the UV spectra and evolution of these objects is required. Conversely, measurements of the background radiation field can, in principle, constrain different galaxy and quasar evolution hypotheses.

Despite recent advances in space borne instrumentation, surprisingly little is known about the UV spectra of galaxies. This is mainly because the instruments that have been launched up until now have been of moderate size and optimized for stellar work. For example, IUE galaxy observations have been restricted to spectra of the central regions of elliptical galaxies and bulge components of spirals, that is of portions of objects with large surface brightness. The spectra of these regions fall off rapidly shortwards of the *B*-band at  $\sim 4,400 \text{ \AA}$  down to  $\sim 2,000 \text{ \AA}$  after which a relatively flat residual remains at a level of  $f_\lambda \sim 0.05 f_\lambda(B)$  (refs 58, 59). The origin of the far UV galactic radiation is controversial but if this behaviour is assumed typical of all galaxies, the expected galaxy background contribution, neglecting evolution and calculated for  $\Omega = 0$ , is plotted as the curve 'Galaxies/1' in Fig. 1. Note that there is an overall uncertainty in all calculations of this type of a factor  $\sim 2$  due to the uncertainty in the total *B*-luminosity density in galaxies alone, but that the calculations are otherwise insensitive to the cosmological model.

In the other extreme case one can, following Anderson *et al.*<sup>22</sup>, adopt as the typical galaxy spectrum the mean Scd galaxy spectrum<sup>56</sup> observed with OAO 2, extrapolated to the Lyman limit. The expected background contribution in this case, neglecting evolution, is shown as the curve 'Galaxies/2' in Fig. 1.

Thus if all galaxies have as energetic short wavelength spectra as the Scd galaxies observed by the OAO 2, and our extrapolation to the Lyman limit is valid, the integrated light from distant galaxies could be a substantial contributor to the UV background light.

Because all galaxies are not spirals, the true galaxy background is probably between the two cases shown in Fig. 1. Recent estimates of the colour distribution of galaxies<sup>60,61</sup>, suggest that only about 5–10% of the total *B*-light from galaxies is emitted by ellipticals, implying that the latter estimate is perhaps the most realistic. Tinsley<sup>62</sup> showed that the accumulated galaxy radiation at visible wavelengths is very sensitive to the effects of galaxy evolution, but the situation in the far UV may be less complicated<sup>63</sup>. This is because the short wavelength light emitted by spiral galaxies originates almost entirely from the young, short-lived *O* and *B* star population continuously forming in the spiral arms. Aside from the disturbing effects of dust absorption, the intensity and slope of the far UV spectrum of a spiral galaxy at a given epoch directly mirror the rate of formation and the initial mass function of the young hot star population. If, for example, the initial mass function is independent of epoch and the rate of star formation decreases exponentially with the galaxy age, this will give rise to an exponential increase in the overall far-UV luminosity of spiral galaxies with look back time<sup>64</sup>. In this way, the background measurements shortward of  $2,000 \text{ \AA}$  together with the adopted OAO 2 spiral spectrum set a rough lower limit on the e-folding time for stellar formation of about a quarter of the Hubble time or  $\approx 5,000 \text{ Myr}$ . Taking such evolution effects into account will raise our background estimate  $\sim 50\%$  shortwards of  $2,000 \text{ \AA}$ , making galaxies even more important contributors to the UV background.

Results from the HEAO 2 satellite concerning the contribution to the X-ray background from quasars<sup>65</sup>, suggest that these objects might be expected to also play an important part in generating the background at UV wavelengths. Adopting the estimated QSO-luminosity function<sup>66</sup> and  $\phi(z) = e^{10z/(1+z)}$  density evolution<sup>67</sup> together with a  $\chi_\lambda \propto \lambda^{-1}$  powerlaw spectrum extending unattenuated beyond the Lyman limit, the expected background is shown as the curve 'Quasars' in Fig. 1. A quasar turn on epoch of  $z \sim 3$  was assumed, but with the adopted density evolution, the result is not very sensitive to the exact redshift at which QSOs first appear. Although the predicted background falls far below the UV measurements, it is interesting that the integrated light from quasars does exceed the EUV background in Fig. 1. Because this radiation is reasonably well accounted for by hot interstellar gas emission<sup>34</sup>, this suggests that QSOs are less bright at soft X-ray energies than expected from an extrapolation of the  $\chi_\lambda \propto \lambda^{-1}$  continuum observed in the optical, either because of intrinsic shielding or because of a true steepening of the continuum<sup>68</sup>.

Although the integrated light from quasars seems unimportant in connection with the UV background, a large fraction of the QSO radiation is emitted at wavelengths shortwards of the Lyman limit at distant epochs and may play an important part in photoionizing the mythical intergalactic medium.

Although most cosmological information suggests that the Universe is open by a large margin<sup>69,70</sup> and that the major fraction of matter in the Universe is in the form of galaxies, many attempts have been made to detect a dense intergalactic medium (IGM).

Whereas the observed X-ray background could arise as emission from a very hot ( $T \approx 10^8 \text{ K}$ ) IGM<sup>71,72</sup>, the intensity of the background at UV wavelengths is relevant in the case of a "lukewarm" or photoionized IGM with a temperature between  $\approx 10^3 \text{ K}$  and  $\approx 10^5 \text{ K}$ . Several IGM models which predict temperatures in this range, at least at some epoch, have been proposed<sup>73–77</sup>. This case has been discussed recently in terms of the resulting background radiation<sup>26,57</sup>.

At temperatures  $10^3 < T < 10^5 \text{ K}$  a mixture of hydrogen and 10% helium radiates strongly in the two resonance lines of H I at  $1,216 \text{ \AA}$  and He II at  $304 \text{ \AA}$ . This line emission, smeared by the redshift, should turn up as background radiation in the UV. The two more or less complementary mechanisms for generating such line radiation are (1) collisional excitation which dominates in an IGM heated by dissipative processes; and (2) recombination which dominates in a highly photoionized medium.



Although the emissivity in the collisional excitation case is in general much larger than in the recombination case, very specific conditions, that is a combination of incomplete ionization and high electron temperatures, are necessary to maintain this large emissivity and corresponding high level of background radiation.

Very strict upper limits on the possible amounts of dense, well-distributed intergalactic neutral hydrogen are set by the lack of strong absorption troughs between emitted and observer frame Ly $\alpha$  in the spectrum of high redshift quasars<sup>78</sup>. It follows that if a dense IGM does exist, the intergalactic hydrogen must be highly ionized, typically to a level of 1 p.p.m. This severely constrains all IGM models and reduces the chances of detecting the IGM in emission by excluding the case for a  $T \approx 2 \times 10^4$  K IGM radiating strongly in Ly $\alpha$  by collisional excitation.

The curve 'Ly $\alpha$ ' in Fig. 1 shows the expected background contribution due to redshifted recombination Ly $\alpha$  from a dense, fully ionized IGM of temperature  $10^4$  K, having a closure density appropriate for a Hubble constant of  $50 \text{ km s}^{-1} \text{ Mpc}^{-1}$ . The expected background intensity increases at longer wavelengths corresponding to emission from earlier, more dense, epochs as the recombination emissivity is proportional to density squared. This estimate scales with cosmological parameters as  $\Omega_b^2 h_{50}^3$ , where  $\Omega_b$  denotes the IGM density in units of the critical density and  $h_{50}$  the Hubble constant in units of  $50 \text{ km s}^{-1} \text{ Mpc}^{-1}$ .

Regarding redshifted He II 304 Å line radiation, there is no direct information on the ionization of intergalactic helium, but the Space Telescope will make it possible to carry out the He I 584 Å and He II 304 Å equivalents of the Gunn-Peterson test<sup>68</sup>, and set upper limits on the concentrations of neutral and once ionized intergalactic helium. Until then it cannot be completely excluded that the IGM at some epoch has gone through a phase of intense collisional excitation generated He II 304 Å emission as predicted by some IGM-reheating models<sup>74,76</sup>. Although the reported 1,450 Å background feature<sup>21,32</sup> is suggestive of such radiation, its existence is in doubt. In any case, at 1,450 Å the observations<sup>22,25,26</sup> can be used to set a rigorous upper limit to an extragalactic component of  $300 \text{ photons cm}^{-2} \text{ s}^{-1} \text{ sr}^{-1} \text{ Å}^{-1}$ .

The curve 'He II 304' in Fig. 1 shows the expected background due to redshifted He II 304 Å recombination radiation from a fully ionized IGM calculated for a temperature of  $10^4$  K and the combination  $\Omega_b^2 h_{50}^3 = 1$ . The He II 304 Å emissivity in the collisional excitation case with these parameters is, at most, a factor  $\approx 5$  higher than that of the recombination case, still giving a background well below the measurements.

The measured intensities of the UV background do not set very interesting limits on the density of a photoionized intergalactic medium in terms of redshifted IGM recombination emission ( $\Omega_b^2 h_{50}^3 \leq 280$  from Ly $\alpha$  and  $\Omega_b^2 h_{50}^3 \leq 70$  from He II 304 Å). A more interesting constraint is that, as any existing IGM must be highly transparent according to the Gunn-Peterson test, the ionizing flux that maintains the implied high level of ionization must turn up as background radiation at the appropriate wavelengths. The curve 'Photoionized IGM' in Fig. 1 shows the background level produced by the redshifted Lyman continuum radiation necessary to photoionize a dense intergalactic medium to the required level. This curve also scales with cosmological parameters as  $\Omega_b^2 h_{50}^3$ , so even assuming that the lowest background measurement at 1,450 Å of  $300 \text{ photons cm}^{-2} \text{ s}^{-1} \text{ sr}^{-1} \text{ Å}^{-1}$  consists of the sum of contributions from redshifted recombination Ly $\alpha$  from  $z = 0.2$ , redshifted Lyman continuum radiation from  $z = 0.6$  and redshifted recombination He II 304 Å radiation from  $z = 3.8$  leads to the inequality  $\Omega_b^2 h_{50}^3 \leq 10$ , leaving a wide margin for a closed universe in the dense photoionized IGM picture. We cannot rigorously exclude that a major portion of the UV background radiation is redshifted Lyman continuum radiation, but this interpretation seems unlikely because no known sources, quasars included, seem capable of producing such a large ionizing flux.

The discussion above refers to a dense well-distributed intergalactic medium. On the other hand a very plausible interpretation of the numerous absorption lines seen shortwards of

emitted Ly $\alpha$  in the spectra of high redshift quasars is that at least some of these lines arise as Ly $\alpha$  absorption in intervening intergalactic clouds<sup>79-81</sup>.

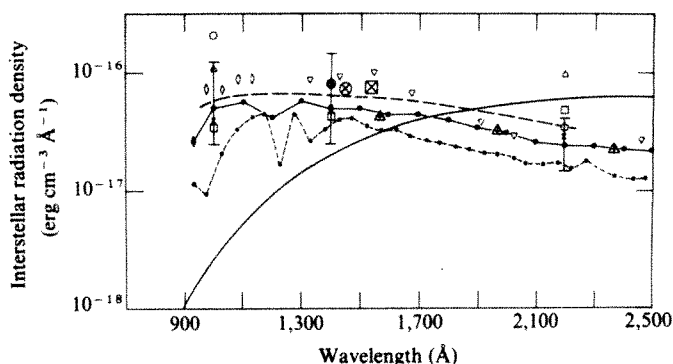
Taking clumping into account increases the IGM emissivity by the 'clumping factor',  $C(z) = \langle n^2 \rangle / \langle n \rangle^2$ , but the redshifted line radiation decreases in intensity towards longer wavelengths because the clumping is expected to increase with time at least as  $C(z) \propto (1+z)^{-3} \propto \lambda^{-3}$ , corresponding to comoving clouds of fixed dimensions<sup>26</sup>. As an example, curves 'Ly $\alpha$ /C' and 'He II 304/C' show the expected redshifted Ly $\alpha$  and He II 304 Å background from unevolving photoionized intergalactic clouds, for simplicity calculated for  $\Omega_b^2 h_{50}^3 C(0) = 1$ . Sargent *et al.*<sup>81</sup> presented a homogeneous sample of QSO Ly $\alpha$  absorption lines observed in high resolution spectra of six quasars. Unfortunately, the interpretation of these spectra in terms of the physical parameters of the absorbing matter is not unique. However, Sargent *et al.*<sup>81</sup> proposed a low density IGM photoionized by quasars consisting of clouds of density  $\sim 10^{-4} \text{ cm}^{-3}$  and temperature  $T \sim 3 \times 10^4$  K embedded in a medium with a density  $\sim 10^{-5} \text{ cm}^{-3}$  and temperature  $\sim 3 \times 10^5$  K (at redshift  $z \sim 2.5$ ). If so, the expected background due to IGM emission is very low, as these parameters translate to  $\Omega_b^2 h_{50}^3 C(0) \approx 10^{-1}$  for the intergalactic clouds giving rise to the QSO absorption lines and  $\Omega_b^2 h_{50}^3 \approx 10^{-2}$  for the surrounding medium. As far as the background radiation is concerned, the above is mainly interesting in that the true integrated light from quasars must be similar to that given in Fig. 1 for these objects to supply sufficient Lyman continuum radiation to photoionize the intergalactic clouds to the required level.

The expected level of IGM emission under reasonable assumptions is far below the measured UV background intensity. The present measurements do not rule out a dense photoionized IGM, but future observations with higher sensitivity together with a better understanding of the other background contributions should place interesting limits on this possibility.

## The interstellar radiation density

UV photons have sufficient energy to ionize, dissociate and heat the interstellar medium<sup>82-84</sup>. The heating effect of UV photons on diffuse clouds and the periphery of larger clouds is quite important. For example, the proposed heating mechanisms of diffuse interstellar clouds require UV photons to photoeject electrons from grains<sup>85,86</sup> or to excite H<sub>2</sub> to vibrationally bound levels<sup>87</sup>. Absorption of UV radiation by H<sub>2</sub> controls the abundance of this and other molecules in cool clouds<sup>88</sup>.

Most of the UV radiation in the solar neighbourhood probably originates in O and B stars<sup>88-90</sup> and hot white dwarfs<sup>14</sup> within 1 kpc of the Sun. Just below the H I ionization threshold at 912 Å, the mean free path of UV photons is small<sup>37</sup> and the radiation field is characteristic of a smaller region around the



**Fig. 2** Observations and theoretical estimates of the interstellar radiation density as a function of wavelength. Sources of the observations:  $\square$ , ref. 17;  $\otimes$ , ref. 26;  $\triangle$ , ref. 97. Sources of the calculations:  $\square$ , ref. 98;  $\bullet$ — $\bullet$ , ref. 99; —, ref. 89;  $\boxtimes$ , ref. 96; —, ref. 11;  $\diamond$ , ref. 88;  $\circ$ , ref. 100;  $\nabla$ , ref. 101;  $\triangle$ , ref. 102;  $\bullet$ — $\bullet$ , ref. 97.

Sun out to  $\approx 10$  pc or so. The field in this case will be dominated by the combined effects of the  $\approx 10$  early type B stars to be found at these distances from the Sun<sup>91</sup> and hot white dwarfs, subdwarfs, novae, and other possible EUV sources<sup>92-94</sup>. Enough radiation below 912 Å will seriously affect the He I/H I ratio in the ISM and observations of the interstellar/interplanetary wind<sup>89,95</sup>.

Several theoretical or empirical determinations of the expected energy density in the UV have been attempted. For heating, ionization and dissociation of ISM atoms and molecules, the important parameter is clearly the mean intensity of the UV radiation field or the equivalent energy density  $U_\lambda$ . The results of the calculations of  $U_\lambda$  in  $\text{erg cm}^{-3} \text{Å}^{-1}$  as a function of wavelength are plotted in Fig. 2.

The computations shown in Fig. 2 are hampered by many of the uncertainties encountered when establishing the total luminosity of the galaxy because they depend on an integration of all the possible galactic sources of UV radiation. Specifically, the uncertainties reflect our incomplete knowledge of the flux and space density of hot stars, especially below 1,200 Å, and of the distribution and scattering characteristics of dust grains. The calculations are, in principle, very sensitive to the exact location in space but as long as the chosen spot is well removed from the vicinity of very hot stars and associations, this effect is not very important in practice<sup>96</sup>.

Only three direct observations of the interstellar radiation density exist: Henry *et al.*'s rocket observation<sup>17</sup>, the ASTP results<sup>26</sup>, and the TD-1 sky survey<sup>97</sup> indicated in Fig. 2. The measurements are compatible with Witt and Johnson's, Henry's and an extrapolation of Jura's results but are higher than the Gondhalekar and Wilson, Grewing and Dunham estimates. Grewing's curve can be made compatible with the observations if  $n_e \approx 0.2-0.4 \text{ cm}^{-3}$ , a value much higher than the canonical value of  $0.03 \text{ cm}^{-3}$  from pulsar dispersion measures, but not to be excluded *a priori*.

## Conclusions

The scatter of the data and of the theoretical expectations in Figs 1 and 2 are due, probably in roughly equal measure, to the natural variation of the physical parameters and to observational and theoretical difficulties. This is not unexpected if the present observations are dominated by the dust scattering mechanism described above. Thus future work should explore systematically the magnitude and extent of the galactic dust source by an all-sky survey at high sensitivity (a  $3\sigma$  detection of  $\approx 100 \text{ photons cm}^{-2} \text{s}^{-1} \text{sr}^{-1} \text{Å}^{-1}$ ) and moderate angular ( $0.1-0.5^\circ$ ) and spectral resolution ( $10-100 \text{ Å}$ ). A direct comparison with optical and far IR deep surveys as described by Sandage<sup>40</sup>, King *et al.*<sup>103</sup> and Drapatz<sup>104</sup> would be very useful in this context. Such surveys in the UV are being planned for some large ( $\approx 1\text{-m}$  diameter) space borne telescopes and by the wide field far UV camera on Spacelab I<sup>105</sup>.

The background spectrum at moderate spectral resolutions ( $\sim 10 \text{ Å}$ ) can provide valuable information on the emission mechanism. Measurement of the polarization of the radiation field would be valuable. Jura<sup>55</sup> has shown that one can expect a linear polarization of the backscattered light by dust grains up to 11% at  $b = 60^\circ$ , an amount easily detectable by a simple UV polarimeter mounted at the focus of presently available or planned UV telescopes. Such a measurement would be an important test of hypotheses on the origin of the observed diffuse UV background. However, extragalactic radiation might also be polarized due to transmission through aligned dust grains.

A better understanding of or a bigger effort at minimizing or avoiding contaminating sources of diffuse emissions is clearly required. Spacecraft orbits should be high enough to avoid most of the terrestrial molecular band emission in the UV that is at least above  $\approx 500 \text{ km}$  but not in the radiation belts where particle induced background can be severe. Zones subject to auroral precipitation should be avoided completely. A completely opaque shutter periodically occulting the outside

world and precise calibrations of overall throughput and field of view are a must for accurate absolute measurements of UV intensities. Techniques by which Ly $\alpha$  is rejected by at least a factor of  $10^6$  must be perfected for the region 1,050-1216 Å where no crystal filter or grating on its own can do the job.

As long as the field of view is small and/or the observations are made near the galactic poles, point sources can be avoided or corrected for fairly accurately at least in the 1,200-2,000 Å range especially if deep Schmidt plates of the UV targets are available. Below 1,200 Å more information on the space density and the luminosity of UV emitters is badly needed. A complete survey of the sky in the 100-1200 Å band of the spectrum down to limiting sensitivities of  $M_v \approx 15-20$  is also critical. A UV survey of this type is being planned by NASA for an Explorer mission.

Present observations summarized in Fig. 1 set very weak constraints on extragalactic sources of UV emissions. The question remains about the general validity over the sky of the observational lower limit of  $\approx 300 \text{ photons cm}^{-2} \text{s}^{-1} \text{sr}^{-1} \text{Å}$  at 1,450 Å that presently pertains only to the limited region surveyed so far. We also need to establish whether the observed minimum is due to a veil of backscattering dust or to an extragalactic source observed through a rift in the galactic dust cloud. This will be a difficult point to resolve and polarization measurements and additional studies of dust to gas correlations may be required.

Additional sources of diffuse UV emissions might be envisioned. For example, recent observations from IUE<sup>106</sup> have been interpreted as evidence for the existence of a hot gaseous halo around our galaxy. This hot gas cools by emitting lines in the UV which could turn up in or influence moderate to high spectral resolution observations of the far UV background.

Clearly a better understanding of all contributions to the UV background is necessary before any information of cosmological significance can be distilled from the observations. First, integrated galaxy and QSO spectra extending to very short wavelengths are required to assess the background contributions and the output of ionizing radiation from these sources. With the Space Telescope it should become possible to subtract the bulk of the galaxy and QSO background light in specific fields in much the same way as star subtraction is now performed, leaving a residual presumably due to IGM emission. The intensity of this residual radiation together with information on the physical state of intergalactic Helium obtained from the He I 584 Å and He II 304 Å equivalents of the Gunn-Peterson test should set interesting constraints on or establish the amount of intergalactic matter present in the Universe.

We thank Drs Stuart Bowyer, Chris McKee, Michael Jura, Richard Henry, Jean Michel Deharveng, Gustavo Bruzual, and Adolf Witt for valuable discussions. This research is supported in part by NASA grant NGR 05-003-450 and a grant from the Danish Space Board.

*Note added in proof:* Very recently, various particle experiments have indicated that neutrinos may possess mass. Because large numbers of light leptons are produced in the big bang, the implications of this for cosmology are far reaching<sup>107</sup>. One possibility is that such massive neutrinos are unstable to radiative decay. An extragalactic component of the UV background could conceivably be due to the redshift-smeared emission from such a cosmological sea of decaying neutrinos<sup>108</sup>.

1. Davidsen, A., Bowyer, S. & Lampton, M. *Nature* **247**, 513 (1974).
2. Paresce, F. *J. geophys. Res.* **84**, 4409 (1979).
3. Tinsley, B. A. *J. geophys. Res.* **84**, 1855 (1979).
4. Huffman, R. E., LeBlanc, F. J., Larrabee, J. C. & Paulsen, D. E. *J. geophys. Res.* (in the press).
5. Röser, S. & Staude, H. *J. Astr. Astrophys.* **67**, 381 (1978).
6. Maucherat-Joubert, M., Cruvellier, P. & Deharveng, J. M. *Astr. Astrophys.* **74**, 218 (1979).
7. Thomas, G. E. *A. Rev. Earth planet. Sci.* **6**, 173 (1978).
8. Thompson, G. I. *et al. Catalogue of Stellar Ultraviolet Fluxes* (Science Research Council, 1978).
9. Jamar, C. *et al. ESA SR-27* (1976).
10. Macau-Hercot, D. *et al. ESA SR-28* (1978).
11. Henry, R. C. *Astronomical J. Suppl.* **33**, 451 (1977).
12. Henry, R. C., Weinstein, A., Feldman, P. D., Fastie, W. G. & Moos, H. W. *Astrophys. J.* **201**, 613 (1975).



13. Crawford, R., Margon, B., Paresce, F., Lampton, M. & Bowyer, S. *Astr. Astrophys. Suppl.* **36**, 371 (1979).
14. Green, R. F. *Astrophys. J.* **238**, 685 (1980).
15. Margon, B. *et al.* *Astrophys. J.* **209**, 525 (1976).
16. Laget, M. *Astr. Astrophys.* **81**, 37 (1980).
17. Henry, R. C., Swandic, J. R., Shulman, S. D. & Fritz, G. *Astrophys. J.* **212**, 707 (1977).
18. Lillie, C. F. & Witt, A. N. *Astrophys. J.* **208**, 64 (1976).
19. Witt, A. N. & Lillie, C. F. *Astr. Astrophys.* **25**, 397 (1973).
20. Lillie, C. F. in *The Scientific Results from the Orbiting Astronomical Observatory* (NASA SP-310, 1972).
21. Henry, R. C., Feldman, P. D., Fastie, W. G. & Weinstein, A. *Astrophys. J.* **223**, 437 (1978).
22. Anderson, R. C., Brune, W. H., Henry, R. C., Feldman, P. D. & Fastie, W. G. *Astrophys. J. Lett.* **233**, L39 (1979).
23. Pitz, E., Leinert, C., Schultz, A. & Link, H. *Astr. Astrophys.* **72**, 92 (1979).
24. Maucherat-Joubert, M., Cruvellier, P. & Deharveng, J. M. *Astr. Astrophys.* **70**, 467 (1979).
25. Paresce, F., Margon, B., Bowyer, S. & Lampton, M. *Astrophys. J.* **230**, 304 (1979).
26. Paresce, F., McKee, C. & Bowyer, S. *Astrophys. J.* (in the press).
27. Chamberlain, J. W. *Physics of the Aurora and Airglow* (Academic, New York, 1961).
28. Maucherat-Joubert, M., Deharveng, J. M. & Cruvellier, P. *Astr. Astrophys.* **88**, 323 (1980).
29. Morgan, D. H., Nandy, K. & Thompson, G. I. *Mon. Not. R. astr. Soc.* **117**, 531 (1976).
30. Morgan, D. H., Nandy, K. & Thompson, G. I. *Mon. Not. R. astr. Soc.* **185**, 371 (1978).
31. Sandel, B. R., Shemansky, D. E. & Broadfoot, A. L. *Astrophys. J.* **277**, 808 (1979).
32. Hua, C. T. in *(COSPAR) X-ray Astronomy* (eds Baity, W. A. & Peterson, L. E.) 551 (Pergamon, New York, 1978).
33. Stern, R. & Bowyer, S. *Astrophys. J.* **230**, 755 (1979).
34. Paresce, F. & Stern, R. *Astrophys. J.* (in the press).
35. Spinrad, H. & Stone, R. P. S. *Astrophys. J.* **226**, 609 (1979).
36. Paresce, F., Bowyer, S., Cash, W., Lampton, M. & Malina, R. in *(COSPAR) New Instrumentation for Space Astronomy*, Vol. 1, 77 (Pergamon, Oxford, 1977).
37. Cruddace, R., Paresce, F., Bowyer, S. & Lampton, M. *Astrophys. J.* **187**, 497 (1974).
38. Jenkins, E. B. & Shaya, E. J. *Astrophys. J.* **231**, 55 (1979).
39. Sandage, A. *Astrophys. J.* **183**, 711 (1973).
40. Sandage, A. *Astr. J.* **81**, 954 (1976).
41. Appenzeller, I. *Astr. Astrophys.* **38**, 313 (1975).
42. Markkanen, T. *Astr. Astrophys.* **74**, 201 (1979).
43. Knude, J. in *Astronomical Papers Dedicated to Bengt Strömberg* (eds Reiz, A. & Andersen, T.) 273 (Copenhagen University Observatory, 1978).
44. Heiles, C. *Astrophys. J.* **204**, 379 (1976).
45. Burstein, D. & Heiles, C. *Astrophys. J.* **225**, 40 (1978).
46. Bohlin, R. C., Savage, B. D. & Drake, J. F. *Astrophys. J.* **224**, 132 (1978).
47. Knapp, G. R. & Kerr, F. J. *Astr. Astrophys.* **35**, 361 (1974).
48. Mathis, J. S., Rimpl, W. & Nordstreck, K. H. *Astrophys. J.* **217**, 425 (1977).
49. White, R. L. *Astrophys. J.* **229**, 954 (1979).
50. Henry, R. C., Anderson, R., Feldman, P. D. & Fastie, W. G. *Astrophys. J.* **222**, 902 (1978).
51. Witt, A. N. *Publ. Astr. Soc. Pacif.* **89**, 750 (1977).
52. Andriess, C. D., Piersma, Th. R. & Witt, A. N. *Astr. Astrophys.* **54**, 841 (1977).
53. Jura, M. *Astrophys. J.* **231**, 732 (1979).
54. Morgan, D. H. *Mon. Not. R. astr. Soc.* **190**, 825 (1980).
55. Jura, M. *Astrophys. J.* **227**, 798 (1979).
56. Code, A. D. & Welch, G. A. *Astrophys. J.* **228**, 95 (1979).
57. Jakobsen, P. *Astr. Astrophys.* **81**, 66 (1980).
58. Bruzual, A., G. & Spinrad, H. in *The Universe at Ultraviolet Wavelengths. The First Two Years of IUE* (NASA, 1980).
59. Norgaard-Nielsen, H. U. & Kjaergaard, P. *Astr. Astrophys.* (in the press).
60. Tinsley, B. M. *Astrophys. J.* **220**, 816 (1978).
61. Bruzual, A., G. & Kron, R. G. *Astrophys. J.* (in the press).
62. Tinsley, B. M. *Astrophys. J.* **211**, 621 (1978).
63. Bruzual, A., G. thesis, Univ. California, Berkeley (1980).
64. Tinsley, B. M. in *The Scientific Results from the Orbiting Astronomical Observatory* (NASA SP-310, 1972).
65. Tananbaum, H. *et al.*, *Astrophys. J. Lett.* **234**, L9 (1979).
66. Schmidt, M. *Phys. Scr.* **17**, 135 (1978).
67. Schmidt, M. *Phys. Scr.* **17**, 329 (1978).
68. Green, R. F., Pier, J. R. & Schmidt, M. *Astrophys. J.* **239**, 483 (1980).
69. Gott, J. R., Gunn, J. E., Schramm, D. N. & Tinsley, B. M. *Astrophys. J.* **194**, 543 (1974).
70. Penzias, A. A. *Astrophys. J.* **228**, 430 (1979).
71. Field, G. B. & Perrenod, S. C. *Astrophys. J.* **215**, 717 (1977).
72. Marshall, F. E. *et al.* *Astrophys. J.* **235**, 4 (1980).
73. Kurt, V. G. & Sunyaev, R. A. *Cosmic Res.* **5**, 496 (1967).
74. Weymann, R. *Astrophys. J.* **147**, 887 (1967).
75. Arons, J. & Wingert, D. W. *Astrophys. J.* **177**, 1 (1967).
76. Sherman, R. D. & Silk, J. *Astrophys. J. Lett.* **231**, L61 (1979).
77. Sherman, R. D. *Astrophys. J.* **238**, 794 (1980).
78. Gunn, J. E. & Peterson, B. A. *Astrophys. J.* **142**, 1633 (1965).
79. Ellis, R. S. *Mon. Not. R. astr. Soc.* **185**, 613 (1978).
80. Young, P. J., Sargent, W. L. W., Boksenberg, A. & Carswell, R. F. & Whelan, J. A. J. *Astrophys. J.* **229**, 891 (1979).
81. Sargent, W. L. W., Young, P. J., Boksenberg, A. & Tytler, D. *Astrophys. J. Suppl.* **42**, 41 (1980).
82. Dalgarno, A. & McCray, R. A. A. *Rev. Astr. Astrophys.* **10**, 375 (1972).
83. Spitzer, L. *Physical Processes in the Interstellar Medium* (Wiley, New York, 1978).
84. McCray, R. & Snow, T. P. A. *Rev. Astr. Astrophys.* **17**, 213 (1979).
85. Watson, W. D. *Astrophys. J.* **208**, 64 (1972).
86. de Jong, T. *Astr. Astrophys.* **55**, 137 (1977).
87. Stecher, T. P. & Williams, D. A. *Mon. Not. R. astr. Soc.* **161**, 305 (1973).
88. Jura, M. *Astrophys. J.* **191**, 375 (1974).
89. Grewing, M. *Astr. Astrophys.* **38**, 391 (1975).
90. Torres-Peimbert, S., Lazcano-Araujo, A. & Peimbert, M. *Astrophys. J.* **191**, 401 (1974).
91. Allen, C. W. *Astrophysical Quantities* (Athlone, London, 1973).
92. Hill, J. K. & Silk, J. *Astrophys. J.* **198**, 299 (1975).
93. Paresce, F. *Earth Extrater. Sci.* **3**, 55 (1977).
94. Bowyer, S. *IAU Colloq. No. 53* (1979).
95. Blum, P. W. & Fahr, H. J. *Astrophys. Space Sci.* **39**, 321 (1976).
96. Habing, H. J. *Bull. astr. Inst. Netherlands* **19**, 421 (1968).
97. Gondhalekar, P. M., Phillips, A. P. & Wilson, R. *Astr. Astrophys.* **85**, 272 (1980).
98. Dunham, T. *Proc. Am. phil. Soc.* **81**, 277 (1939).
99. Gondhalekar, P. M. & Wilson, R. *Astr. Astrophys.* **38**, 329 (1975).
100. Lambrecht, H. & Zimmerman, H. *Mitt. Univ. Sternw. Jena* **13** (1956).
101. Witt, A. N. & Johnson, M. W. *Astrophys. J.* **181**, 363 (1973).
102. Zimmerman, H. *Astr. Nachr.* **228**, 95 (1965).
103. King, D. J., Taylor, K. N. R. & Tritton, K. P. *Mon. Not. R. astr. Soc.* **188**, 719 (1979).
104. Drapatz, S. *Astr. Astrophys.* **75**, 26 (1979).
105. Riviere, G. & Deharveng, J. M. in *(COSPAR) New Instrumentation for Space Astronomy* Vol. 1, 13 (Pergamon, Oxford, 1977).
106. Savage, B. D. & de Boer, K. S. *Astrophys. J. Lett.* **230**, L77 (1979).
107. De Rújula, A. & Glashow, S. L. *Nature* **286**, 755 (1980).
108. Kimble, R., Bowyer, S. & Jakobsen, P. *Phys. Rev. Lett.* (submitted).

## ARTICLES

# Anomalous region on Mars: implications for near-surface liquid water

S. H. Zisk

NEROC Haystack Observatory, Westford, Massachusetts 01886

P. J. Mouginis-Mark

Department of Geological Sciences, Brown University, Providence, Rhode Island 02912

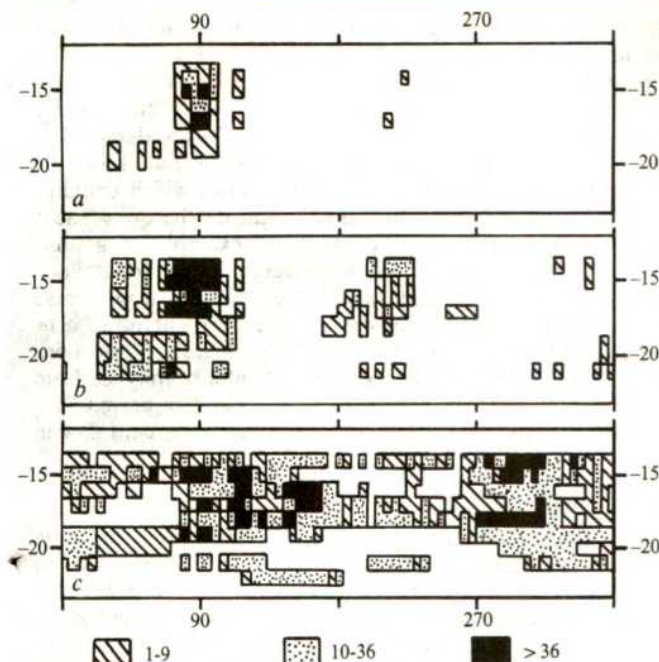
*An anomalous region has been identified on Mars from the 1971 and 1973 Earth-based Goldstone radar data. This region is characterized by coincident very high radar reflectivities and unusual smoothness. Very few realistic surface morphologies can generate such return-signals. Liquid water within ~50–100 cm of the surface is one possibility, an interpretation strengthened by an apparent seasonal variation in surface reflectivity for the same locality.*

ANALYSIS of radar measurements of the martian surface provides the possibility of interpreting textural/compositional differences of materials on a scale unobtainable from orbital images<sup>1–3</sup>. Estimations of the dielectric constant (from radar reflectivity) and small-scale slope statistics (see, for example, the C-factor analysis developed by Hagfors<sup>4</sup>) can be used to help characterize surface units<sup>5</sup> or to delineate areas with unusual material properties. Radar can provide additional evidence regarding the existence of near-equatorial regions of H<sub>2</sub>O outgassing ('oases') as proposed by Huguenin *et al.*<sup>6,7</sup>. Liquid water should produce an obvious effect on the radar characteristics of the surface (if the overburden is relatively transparent to the

radar energy), because of the very high dielectric constant of liquid water (~10 times that of solid rock and 20 times that of water ice).

### Data base

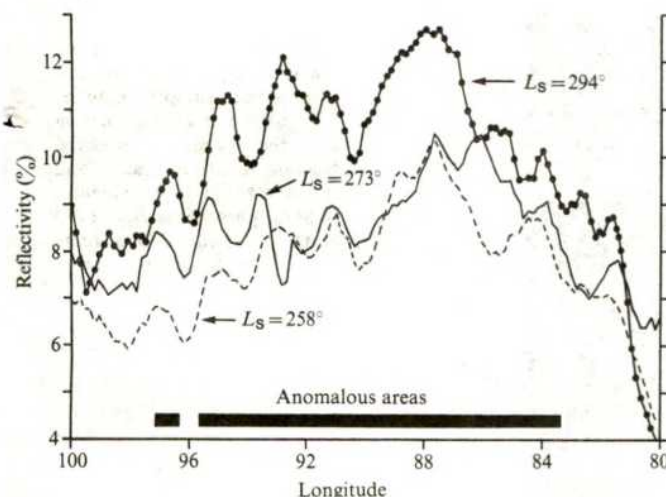
Earth-based radar measurements of the martian surface were carried out at the Jet Propulsion Laboratory's Goldstone Facility by Downs and others<sup>2</sup> in 1971 and 1973. The combined set of observations gave almost complete coverage between latitudes 14 and 22° S. Where possible, the measurements were reduced to obtain inherent reflectivity and smoothness (C-factor) of the surface material, as well as topography and other data not



**Fig. 1** Number density of radar sample points with given characteristics per 1° lat., 5° long. sample bins. *a*, Reflectivity > 9% and *C*-factor > 3,200 coincidentally; *b*, *C*-factor > 3,200; *c*, reflectivity > 9%. Note that although data points with high reflectivity or *C*-factor occur over a wide area of Mars, coincident high values in both parameters are found exclusively at the "oasis" areas proposed by Huguenin *et al.*<sup>6,7</sup> (Solis Lacus, at 20–30° S, 80–90° W; and Noachis–Hellas, at 15–25° S, 305–315° W).

considered here. In some cases the *C*-factor and hence the reflectivity could not be obtained, usually because of low signal strength resulting from rough and low-dielectric constant surfaces. In any case, a very low smoothness (*C*-factor) measurement would be suspect because of the limited Doppler bandwidth of the radar, usually resulting in an overestimate of the smoothness and a consequent underestimate of the reflectivity.

Hence the most productive type of search seemed to be for a uniform layer of liquid or of damp soil, where both reflectivity and *C*-factor were expected to be high.

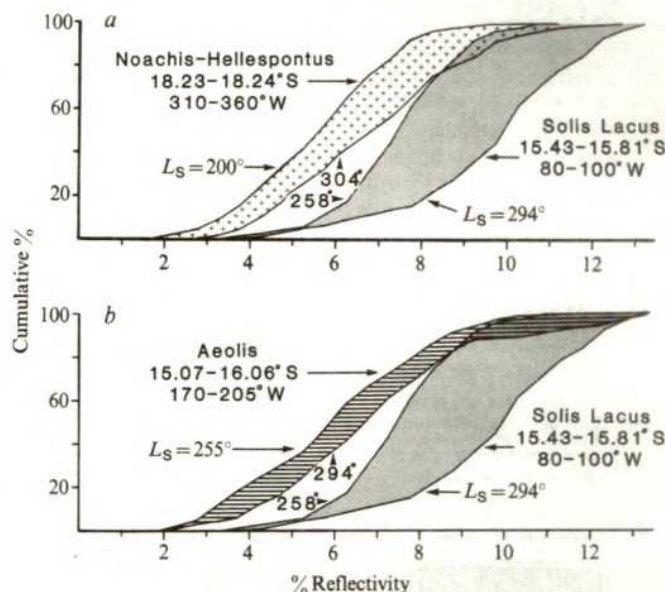


**Fig. 2** Temporal variations in radar reflectivity for an area of Solis Lacus at 15.43–15.81° S. Curves represent a running five-point average at 0.16 long. intervals. Radar data was taken during 1971 ( $L_s = 258^\circ$ ) and 1973 ( $L_s = 273^\circ$  and  $294^\circ$ ) Mars oppositions at latitudes 15.44, 15.43 and 15.81° S respectively. The 'anomalous areas' refer to parts of the ground track at  $L_s = 294^\circ$  where reflectivity is > 9% and *C*-factor > 3,200. See also Fig. 4a.

## Analysis

The data were scanned for regions with a coincident high reflectivity and smoothness. Limits of 9% reflectivity and 3,200 *C*-factor (r.m.s. slopes < 1°) were chosen somewhat arbitrarily. Variations from 9 to 11% and from 2,400 to 3,200 respectively had only a slight effect on the shape of the anomalous area and on the number of observation points. For these measurement values, the formal errors (standard deviations) were ~10% of the data value.

Figure 1a illustrates the areocentric position and number densities of these high-reflectivity, high-smoothness measurements. Only two regions on the planet share this combined radar characteristic. The most prominent is a region centred at 16° S 90° W. There is also a pair of smaller areas to the north-west of Hellas. These two regions are remarkably close to the Solis Lacus (25° S, 85° W) and Noachis–Hellas (20° S, 310° W) oases proposed by Huguenin *et al.*<sup>6,7</sup>.



**Fig. 3** The seasonal variations in radar reflectivity are compared here for three regions of Mars. The horizontal axis is reflectivity and the vertical axis is the percentage of data points having less than the indicated reflectivity. *a*, Compares the strongly anomalous Solis Lacus area with the weakly anomalous Noachis–Hellas region. *b*, Compares Solis Lacus with an area in Aeolis, which is taken to be representative of Mars as a whole and shows no anomaly. Note that all three areas display an increase in percentage reflectivity with increasing martian season, but that Solis Lacus has a much more pronounced seasonal change, in addition to its higher absolute radar reflectivity.

For comparison, Fig. 1b, c indicates the areas having only their reflectivity or *C*-factor above the defined limits. Note that areas of high reflectivity are abundant, indicating a profusion of well-compacted or rocky soils on the martian surface. Areas of high smoothness are clearly less common, although they are not only restricted to the anomalies described here.

As an argument for the reality of the anomalous areas, note that the map of Fig. 1a includes radar measurements from both the 1971 and 1973 conjunctions. Almost no anomalous data points occur elsewhere on the planet, despite the near-global coverage of the data set between 14 and 22° S. In the 300 × 300 km anomaly itself, on the other hand, there are several hundred points.

## Seasonal variability

Additional characteristics of Solis Lacus can be determined by comparing radar data derived for nearly coincident ground tracks at different times of the martian year. Note that practical limitations of Earth-based radar systems dictate that radar



observations of the sub-Earth-region must be made near opposition, and hence near local martian summer. Winter measurements would at best be extremely difficult to make using Earth-based radar.

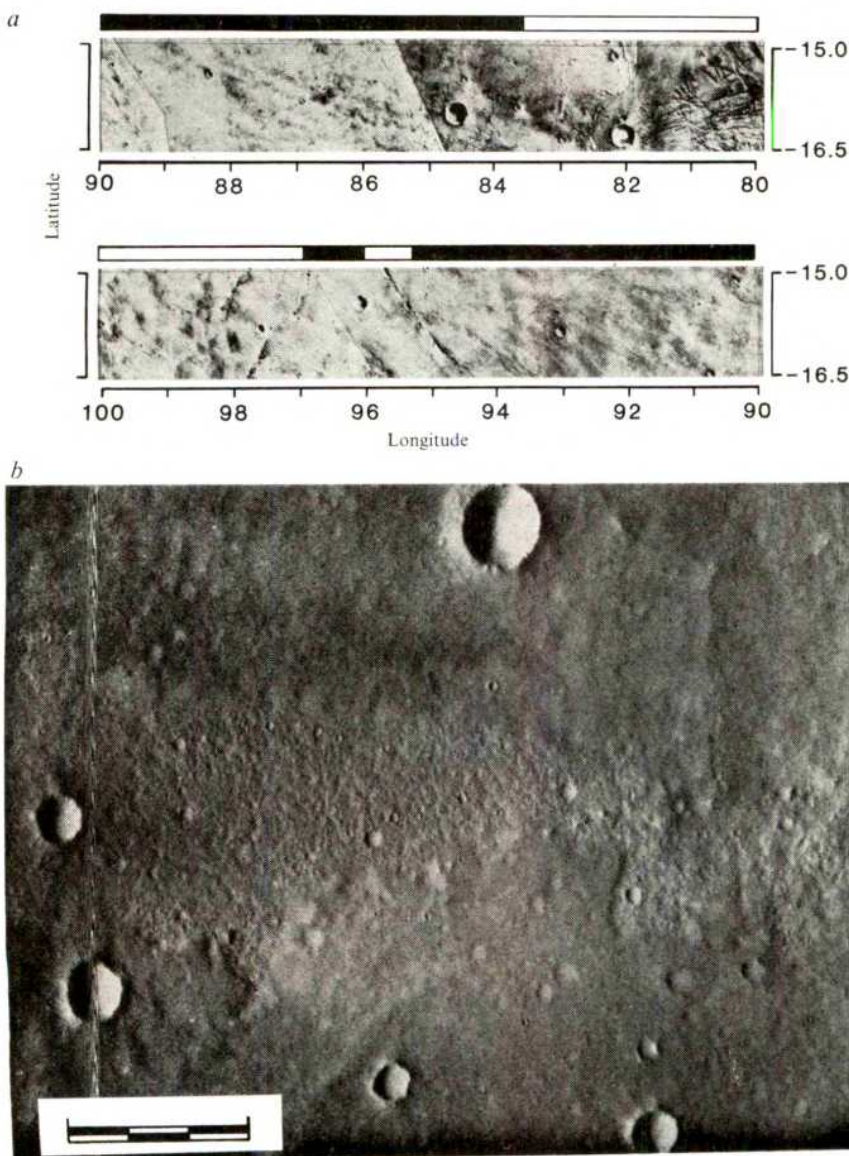
A combination of data from the 1971 and 1973 oppositions provides one example of overlapping radar swaths: Latitudes  $15.45^\circ$  S,  $15.43^\circ$  S, and  $15.81^\circ$  S were sampled between  $80$  and  $100^\circ$  W during the seasonal range from early to middle local martian summer ( $L_s = 258^\circ$ ,  $273^\circ$  and  $294^\circ$  respectively). Note that, as  $L_s$  represents the longitude of the Sun as seen from Mars, the difference between  $L_s = 258^\circ$  and  $294^\circ$  is roughly equivalent to the shift from early June to mid-July on Earth (Northern Hemisphere). Because of the nearly identical locations of these radar profiles (the north-south extent of the radar resolution cell is  $1.3^\circ$ , giving an overlap of at least 70% between swaths), the reflectivity curves for identical surfaces should be very similar. However, Fig. 2 indicates that there is a discrepancy in the reflectivity between  $L_s = 258^\circ$  and  $273^\circ$ . The  $273^\circ$  profile indicates an increase of 1.0–1.5% in the reflectivity compared with the same longitude at  $L_s = 258^\circ$ , while the  $294^\circ$  profile shows a further enhancement of 2.5–3.5%. For large parts of the region between  $82$  and  $100^\circ$  W, there is a systematically higher reflectivity with advancing  $L_s$ , that is, with season. Such a phenomenon seems to be real, as some parts of the data (for example, between  $83$ – $84^\circ$  W and  $88$ – $92^\circ$  W for  $L_s = 258^\circ$  and  $273^\circ$ ) show no difference in reflectivity despite their respective acquisition dates in 1971 and 1973. This is strong evidence for the adequacy of the calibration of the original radar data, and

also for the lack of any temporal variation in the data from instrumental causes.

In another test for possible systematic effects, we are searching the radar data at areas other than the observed anomaly for quasi-seasonal variability. Some of the results are depicted in Fig. 3. Figure 3a shows a plot of the range of variability of the reflectivity with  $L_s$  for Noachis–Hellas, which contains the only cluster of anomalous points outside the Solis Lacus region. Figure 3b shows Aeolis as an example of a non-anomalous region. Figure 3 demonstrates the 'seasonal' variability in much of the observed area, in the same sense (increased reflectivity with advancing summer), but Solis Lacus exhibits the greatest range by more than a factor of 2 of those areas so far examined. The general variability may indicate scattered expressions of near-surface water and/or permafrost, or possibly a low-level, systematic and time-dependent flaw in the calibration.

## Discussion

Measurements showing a high radar reflectivity (high dielectric constant) would be expected not only for water surfaces, but also for large areas of smooth rock within 1 m of the surface. In these conditions, anorthositic rock, with a dielectric constant  $K$  of  $\sim 5$ , would have a reflectivity of about 15% (basalt, with  $K = 9$ , is  $> 25\%$ ; water, with  $K = 81$ , is  $> 65\%$ ) if it covered the entire surface area of the radar cell ( $\sim 750 \text{ km}^2$ ). Figure 4 presents Viking Orbiter images of the same area as Fig. 2. Although few craters larger than  $\sim 10 \text{ km}$  diameter are within the radar



**Fig. 4** Viking Orbiter Images of the anomalous radar areas. *a*, Ground track shown in Fig. 2. *b*, High resolution for an area in Solis Lacus at  $18.7^\circ$  S,  $91.4^\circ$  W;  $C$ -factor, 3,186;  $L_s = 250$ ; reflection, 10.77%. Note that the images do not support a hypothetical smooth, mantle-free surface as an explanation of the radar anomaly. Numerous 10-km craters and lava flow fronts are in evidence. (USGS photomosaics I-1183 and I-1190; and Viking frame 773A10.) Scale bar, 3 km.

ground track, many moderately well preserved lava flow fronts can be easily identified. Morphologically comparable lava flows elsewhere on Mars either have radar reflectivities of 2–6% or *C*-factors <2,000 (refs 5, 8, 9). Unless the small-scale surface texture of the Solis Lacus region is unrelated to its large-scale appearance in Fig. 3, the hypothesis of an extensive rock pediment is untenable as an explanation for the high values of radar reflectivity and *C*-factor.

Moreover, to explain a seasonal variability in the reflectivity of a solid rock surface, one must hypothesize, for example, an absorptive overburden which is regularly scoured away as the summer progresses. The thickness of overburden required for the observed changes in dielectric constant have been calculated on the basis of published dielectric constants and absorption lengths for basaltic rock and loosely-compacted rock powder<sup>10</sup>. Although resonant effects of thin highly-planar soil and rock layers might be observed in laboratory conditions, such conditions do not exist on a planetary surface. Consequently, the reflectivity was calculated for a random-thickness soil layer masking a solid rock surface. Assuming dielectric constants of 2.0 for soil and 8.0 for rock, the net reflection coefficient for bare rock is 23%; for a soil layer at least 14 cm (one wavelength) thick, is 11.1%; and drops to 6% for a soil depth of 1.4 m. For lunar rock chemistry rather than terrestrial rock chemistry, the 6% reflectivity would require >10 m of rock-free soil. The problem is complicated by other factors such as variation in soil porosity with depth, but the conclusion, nevertheless, is that for rock and soil surface to exhibit a measured reflectivity of more than 11%, the soil thickness must be in the range 10–20 cm over the entire area; and that an additional deposit of the order of 1 m of soil would be required to reduce further the dielectric constant to 8%. Although there is undoubtedly a seasonal redistribution of martian dust, photographs at the Viking Lander sites<sup>11</sup> do not show the buildup of the tens of centimetres of dust that would be needed to effect a change from 11 to 8% in

the average radar reflectivity. Alternative explanations, such as seasonal changes in the bulk chemistry of the near-surface rocks, also seem to be unlikely.

Conversely, a transition from frozen water (reflectivity >7%) to liquid water (reflectivity >64%) would produce just such a striking difference in the observed radar reflectivity. Surface temperatures in the range 230–250 K have been observed, for example, at the Viking Lander sites<sup>12</sup>. While this is well below the freezing temperature for pure water, salt solutions may well exist, and have been shown<sup>13</sup> to be stable at temperatures as low as 210 K.

We conclude, therefore, that only surface materials containing liquid water are consistent with: (1) the coincident very high radar reflectivities and *C*-factor values; (2) the photographically observed surface morphology; and (3) the increase in reflectivity values from spring to summer. Some inferences can also be made about the regional extent of the near-surface expression of the liquid water at Solis Lacus. An extensive liquid water surface would have a much higher reflectivity than the observed maximum value of ~16%. More likely is a reduction in the reflectivity by an overlying layer of soil, as outlined above for the rock-soil combination, or, alternatively (or additionally), the liquid water might be observable only through random patches of the surface because of variations in the thickness or density of the overburden. In the latter case, the observed reflection values would be from a mixture of high and low reflectivity surface elements. In this case, the *C*-factor measurements would depend mainly on the highly reflecting regions (the oases) rather than the dry intervening areas. In either case, we are convinced by the radar data that liquid water does indeed exist near the surface of Solis Lacus during southern hemisphere summer.

We thank George Downs for the radar data discussed here, and Richard Simpson and Gordon Pettengill for helpful comments. This work was funded in part under NASA grant NSG 7197.

Received 7 April; accepted 13 October 1980.

- Pettengill, G. H., Shapiro, I. I. & Rogers A. E. E. *Icarus* **18**, 22–28 (1973).
- Downs, G. S., Reichley, P. E. & Green, R. R. *Icarus* **26**, 273–312 (1975).
- Simpson, R. A., Tyler, G. L. & Lipa, B. J. *Icarus* **32**, 147–167 (1977).
- Hagfors, T. *J. geophys. Res.* **69**, 3779–3784 (1964).
- Mouginis-Mark, P. J. & Zisk, S. H. *Lunar planet. Sci.* **11**, 771–773 (1980).
- Huguenin, R. L., Clifford, S. M., Sullivan, C. A. & Miller, K. J. *NASA Tech. Mem.* 80339, 208–214 (1979).

- Huguenin, R. L. & Clifford, S. M. *Bull. Am. astr. Soc.* **11**, 580 (1979).
- Mouginis-Mark, P. J. & Zisk, S. H. *Lunar planet. Sci.* **11**, 768–770 (1980).
- Mouginis-Mark, P. J., Cintala, M. J. & Whitford-Stark, J. L. *Lunar planet. Sci.* **11**, 762–764 (1980).
- Campbell, M. J. & Ulrichs, J. J. *geophys. Res.* **74**, 5867–5880 (1969).
- Arvidson, R., Guinness, E. & Lee, S. *Nature* **278**, 533–535 (1979).
- Hess, S. L., Leoxy, C. B., Ryan, J. A. & Tillman, J. E. *J. geophys. Res.* **82**, 4559–4574 (1977).
- Brass, G. W. *Icarus* **42**, 20–28 (1980).

# Highly structured water network in crystals of a deoxydinucleoside–drug complex

Stephen Neidle

Department of Biophysics, University of London King's College, London WC2B 5RL, UK

Helen M. Berman & H. S. Shieh

Institute for Cancer Research, Fox Chase Cancer Center, Philadelphia, Pennsylvania 19111

*X-ray diffraction analysis of crystals of the intercalative complex between the deoxyribonucleoside phosphate d(CpG) and the mutagen proflavine shows a highly structured arrangement of water molecules linked together by networks of hydrogen bonds to form four edge-linked pentagons per asymmetric unit. These pentagons have a general role in maximizing hydrogen bonding at 3.4-Å intervals. The conformation of the deoxyribose sugar ring at the 3' end of one strand can depend on its local aqueous environment.*

THE role of water in stabilizing and mediating the structure and conformation of nucleic acids has long been the subject of study and speculation (see, for example, refs 1–3). The conformational transitions of DNA are dependent on the level of humidity; it has been established<sup>4–6</sup> that in A-DNA each nucleotide is associated with about 8–10 water molecules whereas B-DNA has a rather greater number. As the primary hydration shell of a nucleotide can maximally accommodate fewer water molecules

than even this lower limit, it has been suggested<sup>2,7,8</sup> that 'bulk' water molecules are involved in addition to those actually hydrogen-bonded to the bases and backbone.

Features of the environment involving these latter water molecules have been investigated in several ways; the crystal structures of both ribodinucleoside phosphates GpC<sup>9</sup> and ApU<sup>10</sup> have all potential nucleobase hydrogen-bond donors and acceptors utilizing their maximum possible water interactions;



**Table 1** Characteristics of two crystals of the 2:2 complex of d(CpG)-proflavine

|                        | Crystal 1   | Crystal 2   |
|------------------------|---|---|
| Final unit cell        | $a = 32.871 \text{ \AA}$<br>$b = 22.187 \text{ \AA}$<br>$c = 13.506 \text{ \AA}$<br>Volume = 9,850 $\text{\AA}^3$<br>Space group $P2_12_12$ | $a = 32.991 \text{ \AA}$<br>$b = 21.995 \text{ \AA}$<br>$c = 13.509 \text{ \AA}$<br>Volume = 9,802 $\text{\AA}^3$ |
| Resolution limit       | 1.00 $\text{\AA}$   | 0.83 $\text{\AA}$   |
| No. of water molecules | 27.5  | 26  |

this finding has been used to investigate sequence-specific nucleic acid recognition<sup>11</sup> using water molecules as a probe of a variable group. The hydration of base pairs has been examined by quantum-mechanical methods<sup>12</sup>. Recently the solvent-accessible surfaces of tRNA<sup>8,13</sup> as well as of double-stranded DNA and RNA have been investigated, the overall important conclusion being that conformationally different forms of double-helical polynucleotides exhibit differing degrees of exposure to the proings of clustered water molecules.

It remains true that there are no simple descriptions for the water structures in oligonucleotides<sup>14,15</sup> which can be extrapolated to generalized descriptions for the hydration of nucleic acids.

We report here on the details of the arrangements of water molecules in crystals of the deoxydinucleoside phosphate d(CpG) intercalative complex with the mutagenic agent proflavine<sup>16</sup>. This structure reveals hitherto unsuspected highly ordered and structured networks of water molecules. These arrangements may provide insight into the structure of aqueous environments around nucleic acids in general, and also demonstrate the importance of water molecules in maintaining oligonucleotide and nucleic acid structure.

### Crystallographic details

X-ray diffraction data were collected on two different crystals of the d(CpG):proflavine complex. Table 1 details some data for these crystals. The superior quality of crystal 2, coupled with more observed data compared with crystal 1, enabled the structure to be successfully and fully refined by standard full-matrix least-squares techniques. Aspects of the refinement and the conformational features of this structure have already been

discussed elsewhere<sup>16</sup>. Crystal 1 proved less amenable to conventional techniques of refinement, which initially resulted in unacceptable and abnormal bond distances and angles. Successful refinement of the structure obtained from data on crystal 1 was contingent on (1) a careful procedure of constrained restrained refinement, and (2) the realization that the 3' deoxy-ribose sugar in one strand (of clear C3'-endo conformation in crystal 2) was disordered between ~50% populations of C2'-endo and C3'-endo conformers. We shall show that this disorder phenomenon is related to the water environment. Except where otherwise stated, the following descriptions are of the crystal 2 structure.

To determine the water structure, difference Fourier maps were calculated. A peak was considered to be a water molecule only if it formed reasonable hydrogen-bonding contacts with the duplex or with another water molecule candidate. The positions and temperature factors were refined; a peak was accepted to be a water molecule if there was convergence and the temperature factors remained below  $B = 30 \text{ \AA}^2$ . After the refinement, detailed analysis of distances and angles involving water molecules revealed the networks to be described. Thus, no bias towards any particular arrangement was introduced during structure solution and refinement. Water-contact distances in the structure average 2.8  $\text{\AA}$ , with a few deviating from this norm (Table 2). The maximum distance found was 3.2  $\text{\AA}$ , which, although near the limit of an acceptable hydrogen-bonding distance, did fulfill the other requirements for hydrogen-bonding geometry. The average mean-square amplitude of vibration for the first-shell water molecules is 0.18  $\text{\AA}^2$ , and for the bulk waters is 0.26  $\text{\AA}^2$ ; these relatively high degrees of thermal motion and the large estimated standard deviations of the positional parameters necessarily lead to some ambiguities in geometry which cannot be resolved by X-ray data alone. Unfortunately, the small crystal size does not make neutron analysis possible at this time.

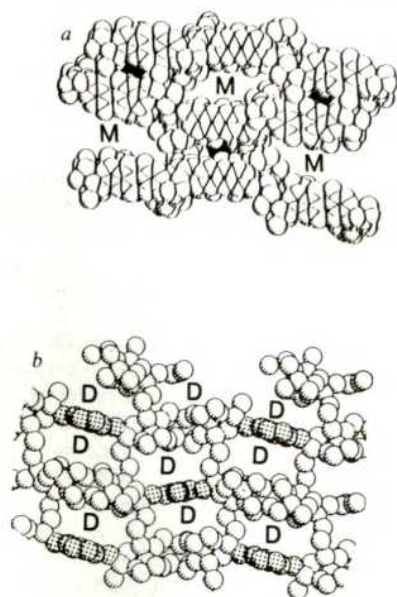
### Overall view of the crystal structure

The asymmetric unit of the crystal contains a 2:2 complex of d(CpG) and proflavine. These pack as infinite columns of symmetry-related stacked molecules. Figure 1 shows that these columns have a stacking sequence of base pair, proflavine, base pair, proflavine, base pair, and so on. The ring nitrogen atoms and the exocyclic amino groups of the proflavine cations face the major groove. The duplex columns are grouped such that diad-

**Table 2** Hydrogen bonds involved in pentagon water network in the crystal structure of d(CpG)-proflavine

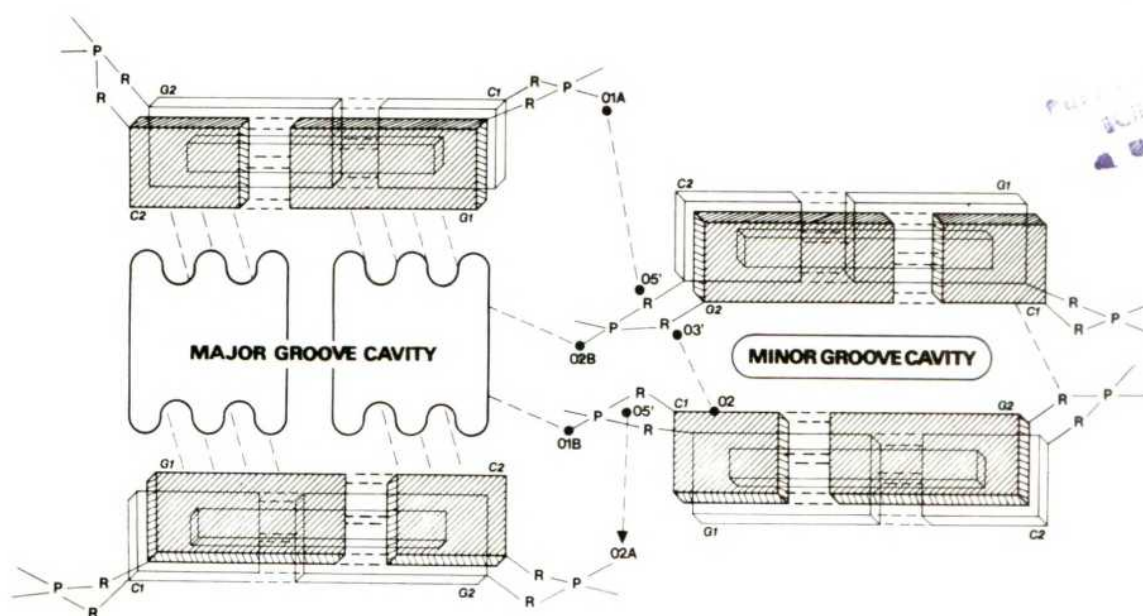
| Pentagons |        |          |                           | Branches from pentagons |        |          |                           |
|-----------|--------|----------|---------------------------|-------------------------|--------|----------|---------------------------|
| Atom i    | Atom j | Pentagon | $D_{ij}$ ( $\text{\AA}$ ) | Atom i                  | Atom j | Pentagon | $D_{ij}$ ( $\text{\AA}$ ) |
| W3        | W20    | I        | 2.91                      | W3                      | N7G1   | I        | 2.77                      |
| W20       | W13    | I        | 3.25                      | W20                     | O6G1   | I        | 2.88                      |
| W13       | W23    | I        | 2.87                      | W9                      | W12    | I        | 3.02                      |
| W23       | W15    | I,II     | 2.41                      | W13                     | N10PF1 | I,II     | 2.85                      |
| W15       | W3     | I        | 2.90                      | W16                     | W10    | II       | 2.78                      |
|           |        |          |                           | W16                     | W21    | II       | 2.68                      |
| W23       | W9     | II       | 2.96                      | W14                     | N4C1   | III,IV   | 2.91                      |
| W9        | W22    | II,III   | 2.96                      | W6                      | W24    | IV       | 3.23                      |
| W22       | W16    | II       | 2.75                      | W6                      | N7G2   | IV       | 2.87                      |
| W16       | W15    | II       | 3.06                      | W24                     | O6G2   | IV       | 2.90                      |
| W17       | W9     | III      | 3.22                      |                         |        |          |                           |
| W17       | W14    | III,IV   | 2.85                      | W18                     | N15PF2 | IV       | 2.97                      |
| W14       | W2     | III,V    | 2.74                      | W18                     | O1B    | IV       | 2.66                      |
| W2        | W22    | III      | 2.76                      | W25                     | O1B    | IV,V     | 2.92                      |
| W17       | W6     | IV       | 2.62                      | W25                     | W11    | IV,V     | 2.77                      |
| W6        | W18    | IV       | 3.15                      | W11                     | N10PF2 |          | 2.76                      |
| W18       | W25    | IV       | 3.23                      | W8                      | N16PF2 | V        | 2.97                      |
| W25       | W14    | IV,V     | 2.87                      |                         |        |          |                           |
| W25       | W8     | V        | 2.78                      |                         |        |          |                           |
| W8        | O2B    | V        | 2.89                      |                         |        |          |                           |
| W2        | O2B    | V        | 2.73                      |                         |        |          |                           |

$D_{ij}$ , distance between atoms i and j.



**Fig. 1** *a*, Packing of the intercalated duplexes as viewed along the *c* axis. *m*, The major groove cavities; minor groove cavities are shaded. *b*, Water contents of the major and minor groove cavities, also viewed along the *c* axis. The minor groove polygon atoms are shaded; *D* indicates the positions of the intercalated duplexes (shown in *a*).

related pairs, which have their minor grooves facing one another, form minor groove cavities. These alternate with pairs which have their major grooves facing one another forming major groove cavities (Fig. 2). The minor-groove dimers are held together by two hydrogen bonds, and are related to the symmetry-related major groove ones by two (other) hydrogen bonds (see Fig. 2 for details). The minor groove gaps are relatively small and are filled by two-dimensional disk-like assemblies of water molecules, in contrast to the water-filled major groove cavities which are large in two dimensions and extend in infinite channels along the third (Figs 1*b*, 2).



**Fig. 2** A schematic illustration of the crystal structure viewed along the *c* axis. R, ribose; P, phosphate; C1, cytidine in strand 1; C2, cytidine in strand 2; G1, guanine in strand 1; G2, guanine in strand 2. Shaded areas indicate the base pairs on top. The dashed lines represent hydrogen bonds. The major and minor groove cavities are shown filled with water.

## Structure of the water assemblies

One might suppose that the water molecules in the major groove channels would be disordered, especially as seven of the eight waters per asymmetric unit that do not directly coordinate to the duplexes are located in these channels. However, this is not so. As Fig. 3 shows, the water molecules are linked together in a regular framework, forming edge-linked hydrogen-bonded pentagons. There are four such pentagons per asymmetric unit, each set being joined to the next via water molecule W8. A fifth pentagon is formed by two water molecules (2 and 8) which branch off two pentagons and bridge to a phosphate oxygen of a dinucleoside strand. The major groove channels are thus filled with two diad-related chains of water pentagons, with each chain coordinated to four dinucleoside strands as shown in Fig. 4. The pentagons are constructed to maximize the number of hydrogen-bonding contacts at 3.4-Å intervals along the *c* direction. The water molecules hydrogen bond with the nucleobase atoms in the major groove, as well as with the ring nitrogen atoms and the exocyclic amino groups of the proflavine cations. These hydrogen bonds are all of the 'in-plane variety'<sup>17</sup>; that is, the water molecules are in the same plane as the bases and drugs. The arrangement of the pentagons resembles that of the crystal structure of piperazine hexahydrate<sup>18</sup>, which has a 'partial pentagonal dodecahedral motif'<sup>19</sup> and is a close relative of the clathrate hydrates<sup>19</sup>.

The water arrangements in the small minor groove cavities are precisely one water molecule thick; in each one we see a planar hydrogen-bonded polygon disk of water molecules which in turn hydrogen bond to the atoms in the minor grooves of the bases. Figure 4 shows how, in contrast to the major groove structure, these interactions are 'out of plane'.

Note that in this structure, as in r(CpG)-proflavine<sup>20</sup>, some of the ribose oxygen atoms are hydrated (O1'C1 and O1'G2). Thus, this type of hydration may in fact be the rule rather than the exception as had been believed previously. Another feature of this structure is that not all the possible shell-water coordination has been observed; for example, N4C2 only forms one hydrogen bond and is not hydrated. A similar feature occurs in r(CpG)-proflavine but not in the uncomplexed dinucleoside phosphates<sup>9,10</sup>. It is not yet clear whether incomplete hydration of bases is characteristic of drug-nucleic acid complexes.



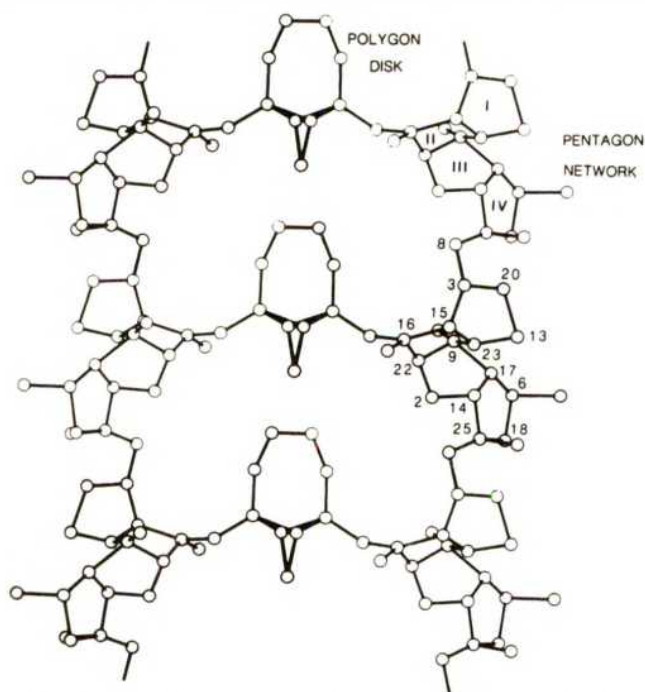


Fig. 3 The water structure alone viewed along the *b* axis. The pentagon network and polygon disk are labelled.

### Relationship between water structure and molecular conformation

Comparison of the structures of the more highly hydrated crystal 1 with the less hydrated crystal 2 shows that environmental factors may affect the conformation of a particularly flexible part of a molecule. Crystal 2 is the more highly ordered of the two, both with respect to the conformation of the molecule and the structure of the water network. In this crystal, strand 1 has C3'-endo(3', 5')C3'-endo deoxyribose conformations. Water 7 bridges O3'G1 and a phosphate oxygen, possibly stabilizing the

C3'-endo conformation at the 3' end. Strand 2 has C3'-endo(3'5')C2'-endo deoxyribose conformation (the 'mixed sugar pucker'<sup>21</sup>). In crystal 1, strand 2 has the same conformation as in crystal 2. However, on strand 1 the 3' deoxyribose sugar is disordered, albeit in a specific manner. The significant populations of this disorder are C3'-endo and C2'-endo (each ~50%). In crystal 1, water 7 is not hydrogen-bonded to either of the two disordered O3' hydroxyl positions.

These findings on sugar pucker elucidate further the contentious issue of the role ascribed to sugar conformations in intercalated dinucleosides. Our earlier analysis of a ribo(CpG)-proflavine complex structure<sup>20</sup> showed C3'-endo ribose pucker at both ends of the two dinucleoside strands. Even though this structure, by its very existence, showed that intercalation did not necessarily require (or produce) 'mixed sugar' pucker, it has been suggested that proflavine is a special intercalator<sup>21</sup>, presumably on account of the hydrogen bonding of a proflavine cation to the exterior of a duplex via the 3' sugar. Our observation<sup>22</sup> that dinucleoside intercalation is concomitant with an increase in the glycosidic torsion angle at the 3' end to a relatively high value suggested that C2'-endo sugar pucker at this end might be slightly favoured in view of the correlation between C2'-endo pucker and high  $\chi$  values. This deoxy(CpG)-proflavine complex, on the other hand, clearly shows no major preference for either pucker at the 3' end. We conclude that this pucker is unimportant and plays no real part in defining the intercalation geometry. The precise nature of the pucker is dependent on the environment around the sugar and may be considered as an end effect. We would expect the situation in solution to parallel that found in these crystals, with states flipping between the major C2'/C3'-endo puckers to be present.

### Discussion

Such highly structured water has never been observed in crystal structures of nucleic acids, their constituents or other biological molecules although circular networks of hydrogen bonds (involving hydroxyl as well as water atoms) have been reported in the structure of  $\alpha$  cyclodextrin<sup>23</sup>. Although the structures of the nucleic acid fragments, GpC and ApU, are highly hydrated, the waters are evenly distributed in a first hydration shell.

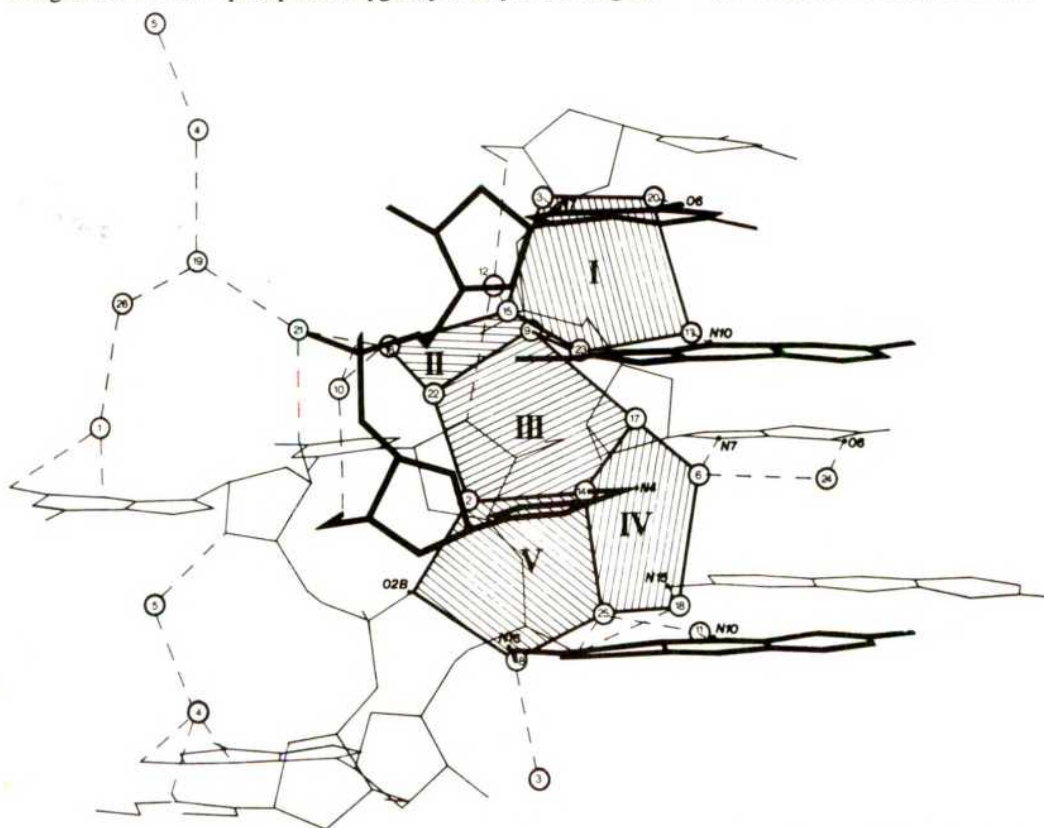


Fig. 4 The hydrogen bonding of the water molecules to the four dinucleoside phosphate strands. The five pentagons are labelled and shaded. The numbering of each water molecule is shown. The view is similar to Fig. 3. Waters 3 and 20 of pentagon I form a square-planar hydrogen-bonding arrangement with N7G and O6G of strand 1, and water 14 hydrogen bonds to N4 of that same strand. Waters 6 and 24, which branch off pentagon IV, form a similar pattern with N7G and O6G of strand 2 of the diad-related duplex. Water 13 of pentagon I hydrogen bonds to N10 of the intercalated proflavine, and water 11, which branches off pentagon IV, hydrogen bonds to N10 of the stacked proflavine. The exocyclic amino groups N15 and N16 of the diad-related stacked proflavine molecules hydrogen bond to waters 18 and 8 respectively.

Two questions arise: (1) Why does this orderly framework appear in this crystal? and (2) is the pentagon network of any wider significance? Although neither question is fully answerable some observations may be made.

The characteristics of the water framework are partially due to the crystal packing. This structure exhibits very few duplex-duplex interactions (Fig. 2), possibly because it contains deoxyribose sugars. It therefore lacks the hydrogen bonding of the O2' hydroxyl which in the most extreme example helped mediate the proflavine-duplex cross-linking observed in proflavine-CpG. Instead, the crystal contains two water-filled cavities. Probably the water disks in the minor groove cavities merely accommodate themselves to the relatively small space allowed by the hydrogen-bonded dimers. The major groove cavities are considerably more hydrophilic with two positively charged nitrogen atoms facing one another. As there are no anions such as  $\text{SO}_4^{2-}$  mediating these charges, the cavity is necessarily quite large. Solvent-solvent interactions, therefore, become as important as solvent-solute interactions in maintaining the crystal order. In this structure the solvent-solvent interactions take the form of a pentagon network of waters, which can be

likened to a trellis to which the major groove heteroatoms hydrogen bond.

Presumably the pentagon network is not the only plausible arrangement of water molecules—a network of hydrogen-bonded hexagons can also be envisaged. However, aside from the frequent observation of pentagonal water networks in clathrate crystals<sup>19</sup>, the geometry observed is such that it clearly forms an optimum number of attachments to drug and dinucleoside atoms. Indeed, the pentagon geometry is well suited to link 3.4-Å-separated heterocycles. Furthermore, the evident propensity of the pentagons to readily associate together and the inherent flexibility of the individual pentagon strongly suggest that nucleic acids of size greater than the dinucleoside level could readily accommodate related pentagonal clusters.

We thank Drs S. H. Kim and J. L. Finney for discussions of this manuscript. The support of NIH grants GM 21589, CA 22780, CA 06927 and RR 055390, NATO, the Cancer Research Campaign and an appropriation from the Commonwealth of Pennsylvania are gratefully acknowledged. S.N. is a Career Development Awardee of the Cancer Research Campaign.

Received 29 July; accepted 3 October 1980.

1. Texter, J. *Prog. Biophys. molec. Biol.* **33**, 83–97 (1978).
2. Lewin, S. *J. theor. Biol.* **17**, 181–212 (1967).
3. Clementi, E. & Corongiu, G. *Biopolymers* **18**, 2431–2450 (1979).
4. Bloomfield, V. A., Crothers, D. M. & Tinoco, I. in *Physical Chemistry of Nucleic Acids* (Harper & Row, New York, 1974).
5. Tunis, M. J. B. & Hearst, J. E. *Biopolymers* **6**, 1345–1353 (1968).
6. Wolf, B. & Hanlon, S. *Biochemistry* **14**, 1661–1670 (1975).
7. Falk, M., Hartman, K. A. Jr & Lord, R. C. *J. Am. chem. Soc.* **85**, 387–391 (1963).
8. Alden, C. J. & Kim, S. H. *J. molec. Biol.* **132**, 411–434 (1979).
9. Rosenberg, J. M., Seeman, N. C., Day, D. O. & Rich, A. *J. molec. Biol.* **104**, 145–167 (1976).
10. Seeman, N. C., Rosenberg, J. M., Suddath, F. L., Kim, J. J. P. & Rich, A. *J. molec. Biol.* **104**, 109–144 (1976).
11. Seeman, N. C., Rosenberg, J. M. & Rich, A. *Proc. natn. Acad. Sci. U.S.A.* **73**, 804–808 (1976).

12. Goldblum, A., Perahia, D. & Pullman, A. *FEBS Lett.* **91**, 213–215 (1978).
13. Thiagarajan, P. & Ponnuswamy, P. K. *Biopolymers* **18**, 2233–2247 (1979).
14. Viswamitra, M. A. *et al. Nature* **273**, 687–688 (1978).
15. Wang, A. H.-J. *et al. Nature* **282**, 680–686 (1979).
16. Shieh, H.-S., Berman, H. M., Dabrow, M. & Neidle, S. *Nucleic Acids Res.* **8**, 85–97 (1980).
17. Pullman, A. in *Structure and Conformation of Nucleic Acids and Protein-Nucleic Interactions* (eds Sundaralingam, M. & Rao, S. T.) 457–484 (University Park Press, Baltimore, 1975).
18. Schwartenbach, D. *J. chem. Phys.* **48**, 4134–4140 (1968).
19. Jeffrey, G. A. *Acct. Chem. Res.* **2**, 344–352 (1969).
20. Berman, H. M. *et al. Biopolymers* **18**, 2405–2429 (1979).
21. Sobell, H. M. in *Nucleic Acid Geometry and Dynamics* (ed. Sarma, R. H.) 83–108 (Pergamon, New York, 1980).
22. Berman, H. M., Neidle, S. & Stodola, R. K. *Proc. natn. Acad. Sci. U.S.A.* **75**, 828–832 (1978).
23. Saenger, W. *Nature* **279**, 343–344 (1979).

## Amplification of rearranged repeated DNA sequences in cereal plants

J. R. Bedbrook\*, M. O'Dell & R. B. Flavell

Cytogenetics Department, Plant Breeding Institute, Trumpington, Cambridge CB2 2LQ, UK

*A simple repeating unit of the rye genome, previously known in tandem arrays, has now been shown to occur also in more complex repeating units. One such unit has been cloned and found to contain some sequences unrelated to the simple repeat. It is proposed that tandem arrays of complex repeats are often produced by amplification of DNA segments formed by recombination of different repeats and possibly unique sequences. Some complex variants of repeats are not in high copy number on all rye chromosomes.*

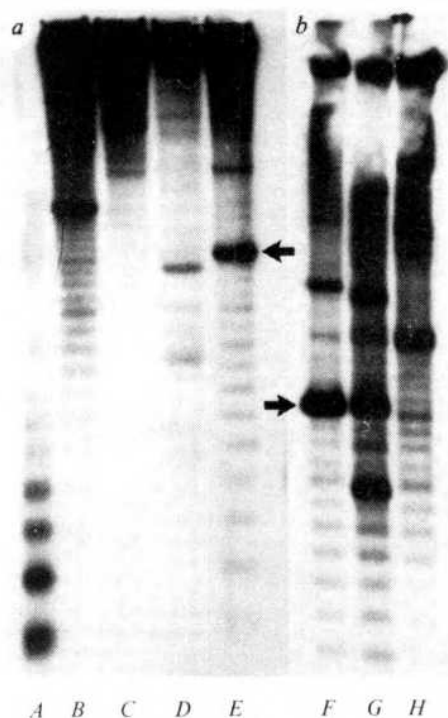
REPEATED sequences constitute much of the chromosomal DNA of higher eukaryotes. Many higher plant species have more than 70% of their DNA in the form of repeated sequences<sup>1</sup>. Consequently, studies of the formation and organization of families of repeated sequences may contribute substantially to our understanding of plant chromosome structure. Formation of families of repeated sequences must occur often during evolution to account for the differing spectra of repeated DNA sequences in the chromosomes of closely related species<sup>2</sup>. Repeated sequences are frequently reamplified during evolution<sup>2</sup>. This was concluded from comparative studies on repeated sequences common to the genomes of the related gramineae species—wheat, rye, barley and oats<sup>2</sup>. About 20% of the rye genome consists of short, species-specific, repeated sequences interspersed with short repeated sequences also found in wheat and other related cereals<sup>3,4</sup>. These results suggested that the repeated sequences which are reamplified are often in new combinations which must have been generated by

sequence rearrangement. Studies of the structure of specific repeated sequences of rye heterochromatin have also suggested sequence rearrangement before amplification because each has a simple sub-repeat interspersed with an unrelated non-subrepeating unit<sup>5</sup>. If closely related sequences are amplified in different combinations then different repeating units should have sub-repeats in common.

To investigate this prediction we have probed the wheat and rye genomes with a simple 120-base pair repeating unit that is predominantly organized in tandem arrays<sup>5</sup> to search for more complex units which are likely to have been created by recombination of the 120-base pair sequence with other sequences before amplification. We describe here the identification, structure and chromosome distribution of such complex forms of this repeat. One of the many complex reamplified forms has been purified by cloning in a bacterial plasmid. Its repeating unit is 2.2 kilobases long and consists of a few of the simple repeat units interspersed with unrelated sequences. The 2.2-kilobase repeat is present on all seven rye chromosomes but other repeats containing sequences related to those in the 2.2-kilobase repeat seem to be present only on some rye chromosomes.

\* Present address: CSIRO Division of Plant Industry, Canberra, ACT Australia.





**Fig. 1** Hybridization of a cloned repeated sequence to rye DNA digested with various restriction endonucleases. Rye DNA (15 µg) prepared from purified nuclei<sup>5</sup> was digested to completion *a*, with *Hae*III (A), *Bam*HI (B), *Bgl*II (C), *Hind*III (D), *Eco*RI (E) and *b*, with *Eco*RI (F), *Eco*RI + *Bam*HI (G) and *Bam*HI (H), and fractionated by agarose gel electrophoresis. The agarose concentration in the gel was 1.5%. Electrophoresis conditions were as described previously<sup>5</sup>. Electrophoresis was from top to bottom of the panel. The DNA was transferred from the gel to a sheet of nitrocellulose filter as described by Southern<sup>19</sup>. The filter was hybridized using a <sup>32</sup>P-labelled cRNA probe prepared *in vitro* by *E. coli* RNA polymerase using a cloned example of a 120-base pair highly repeated DNA sequence as the template (see text for details of repeat). 5 × 10<sup>5</sup> c.p.m. were used in the hybridization. Hybridization was in 2 × SSC containing 100 µg tRNA at 62 °C for 18 h. (SSC is 0.15 M sodium chloride + 0.015 M sodium citrate). Unhybridized probe was removed from the filters by extensive washing with 1 × SSC at 60 °C. Stable hybridization was revealed by autoradiography. The major 2.2-kilobase repeats in the *Eco*RI digests are arrowed.

### Complex forms of a simple tandem repeat

The family of rye repeats we have analysed for more complex reamplified forms comprises ~2% of the genome<sup>5</sup>. It consists principally of 120-base pair repeating units arranged in tandem arrays. This was determined by digesting rye DNA with *Hae*III restriction endonuclease, fractionating the resulting fragments by agarose gel electrophoresis, transferring the fragments to a nitrocellulose filter and hybridizing them with <sup>32</sup>P-labelled cRNA prepared from a cloned 120-base pair repeat. (The cloning of this repeat unit in the bacterial plasmid pBR322 is described elsewhere<sup>5</sup>.) *Hae*III digestion (Fig. 1, track A) revealed a progression of fragments at intervals of 120 base pairs. This pattern would be expected from a family of tandemly arranged repeats in which each unit repeat sequence contains a *Hae*III site but occasionally loses it by random mutation so that some dimers, trimers and higher multimers remain after *Hae*III digestion. Figure 1 also shows that the restriction enzymes *Bam*HI (track B), *Bgl*II (track C), *Hind*III (track D) and *Eco*RI (track E) cut sequences complementary to the 120-base pair repeat probe DNA infrequently. *Bam*HI and *Eco*RI produce an integral series of fragments with a periodicity of 120 base pairs. Such fragments presumably arise from the creation of restriction sites by mutation. *Bgl*II and *Hind*III do not generate such an integral series of fragment lengths. Therefore there is probably no sequence closely related to the *Bgl*II and *Hind*III recognition sites within the basic repeating unit. That *Bam*HI and *Eco*RI sites occur randomly in the 120-base pair family is supported by double-enzyme digestion. Digestion with both *Eco*RI and *Bam*HI (Fig. 1, track G) produces a higher proportion of the family in lower molecular weight fragments than does

digestion with either *Eco*RI (Fig. 1, track F) or *Bam*HI (Fig. 1, track H) alone.

The results in Fig. 1 (tracks B–E) also show that the clone of the 120-base pair unit hybridizes to specific restriction fragments which are in relatively much higher copy number than the integral progression of 120-base pair fragments. All hexanucleotide restriction enzymes used produce such fragments. These fragments could have arisen in the genome by (1) amplification of specific arrays of 120-base pair units, one member containing a particular hexanucleotide recognition site, or (2) the amplification of more complex pieces of DNA that include 120-base pair units. That at least some of these major variant forms contain sequences other than 120-base pair units is suggested by their being present in *Hind*III and *Bgl*II digests, even though these enzymes do not produce an integral series of 120-base pair fragments. We have shown that the major variant revealed in the *Eco*RI digests (arrowed in Fig. 1) does contain a complex piece of DNA besides 120-base pair units. This was achieved by characterizing cloned examples of the major variant.

### Major *Eco*RI variant is not a simple tandem array of 120-base pair units

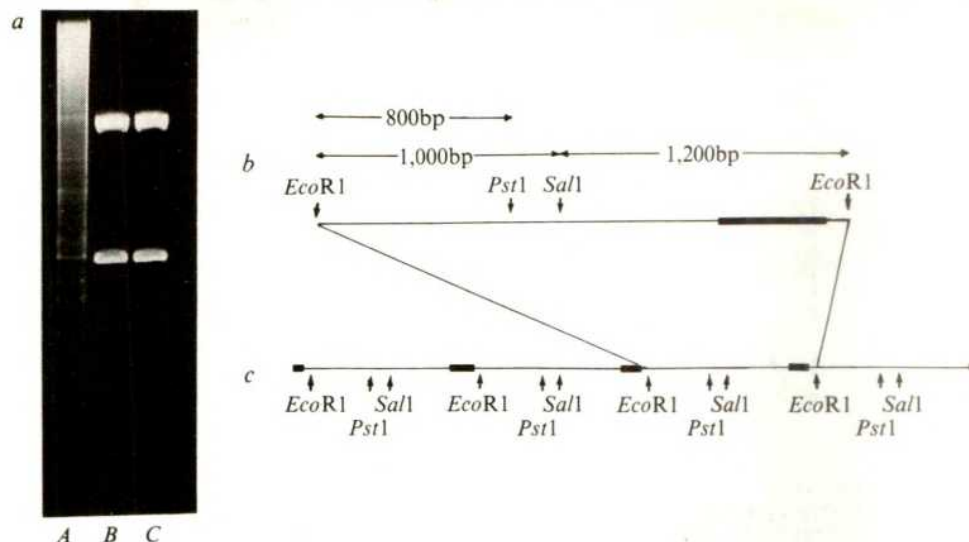
The major high copy number variant in *Eco*RI digests is 2.2 kilobases long and migrated with a DNA band of strong fluorescence in *Eco*RI digests of total rye DNA (Fig. 2a). This band was recovered from an agarose gel and cloned in the vector plasmid pACYC184. The resulting clones were screened with the 120-base pair sequence by the method of Grunstein and Hogness<sup>6</sup>. Two clones that hybridized with the 120-base pair repeat sequence and co-migrated with the major band in *Eco*RI digests of *Secale cereale* DNA were obtained (Fig. 2a). A physical map of one of the cloned 2.2-kilobase rye DNA fragments is shown in Fig. 2b. The sequence contains sites for endonucleases *Pst*I and *Sal*I. The 120-base pair repeat unit hybridizes only to the 1,200-base pair *Sal*I-*Eco*RI fragment and the 1,400 base pair *Pst*I-*Eco*RI fragment and not to the 1,000-base pair *Sal*I-*Eco*RI fragment or the 800-base pair *Pst*I-*Eco*RI fragment (results not shown). The 120-base pair repeat unit hybridizes to only three *Hae*III fragments of 220, 200 and 120 base pairs which map within the 1,200-base pair *Sal*I-*Eco*RI fragment. Thus it was deduced that the 120-base pair repeat unit in the high copy *Eco*RI variant is interspersed with unrelated sequences, all the sequences together forming a unit repeat defined by *Eco*RI, *Pst*I or *Sal*I. For ease of discussion we shall refer to the DNA unrelated to the 120-base pair unit as 'spacer' DNA. The 2.2-kilobase repeat units are clustered in rye chromosomes because dimer and trimer forms can be seen in partial *Eco*RI digests of rye DNA. Fig. 2c illustrates the deduced arrangement of the 2.2-kilobase repeat in the genome.

### The 2.2-kilobase repeat unit family may have been formed later than the 120-base pair repeat unit family

Two lines of evidence suggest that the 2.2-kilobase repeat unit family may have been formed in the rye genome more recently than the 120-base pair repeat unit family. First, in complete digests of rye DNA >80% of the 2.2-kilobase repeat DNA is in the monomer form after digestion with *Eco*RI, whereas <40% of the 120-base pair repeat DNA is in the monomer form after complete digestion with *Hae*III (Fig. 1). Assuming that dimer, trimer and such forms result from the random loss of restriction sites with time, and that each base has an equal probability of being altered, then more of the six-base pair *Eco*RI sites would be expected to have been lost than four-base pair *Hae*III sites if the families were of equal age. Second, the 2.2-kilobase repeat family is not highly repeated in wheat (see below; Fig. 5) whereas the 120-base pair family is<sup>5</sup>. This suggests that the 120-base pair family was amplified before wheat and rye diverged from their common ancestor<sup>2</sup>, and the 2.2-kilobase repeat family was amplified after the rye and wheat ancestors diverged,



**Fig. 2** The structure of a cloned example of a complex form of the 120-base pair repeat. Rye DNA (100 µg) was digested to completion with *EcoRI* and fractionated on a 1.5% low melting point agarose (LMP Seakem) gel. The major repeat band in this digest (see a, lane A) was excised and heated at 65 °C together with 2 vol (w/v) 50 mM Tris-HCl, pH 8.0, 0.5 mM EDTA for 3 min. The solution was cooled to 37 °C and an equal volume of water-saturated phenol (at 37 °C) was added. The mixture was homogenized, allowed to equilibrate to room temperature and the phases separated by centrifugation at room temperature. The phenol phase was removed and the aqueous phase re-extracted with phenol. The final aqueous phase was precipitated with 2.5 vol ethanol. The precipitated DNA was washed twice with 70% ethanol, dried and dissolved in 20 µl H<sub>2</sub>O. The DNA was ligated to 0.1 µg *EcoRI*-linearized pAC184 DNA<sup>5</sup>. The ligated DNA was used to transform the *E. coli* strain HB101. Transformants were selected on media containing tetracycline at 5 µg ml<sup>-1</sup>. Transforming plasmids containing inserted fragments were screened by testing for chloramphenicol sensitivity. These transformants were then screened for sequences complementary to the 120-base pair repeat using the assay described by Grunstein and Hogness<sup>6</sup>. Plasmid DNA from such transformants was prepared<sup>20</sup>, digested with *EcoRI* and fractionated by agarose gel electrophoresis together with rye DNA. a, Track A shows rye DNA, tracks B and C show two plasmids. b, A physical map of one such plasmid. The double thickness line shows the region complementary to the 120-base pair repeat. This was determined by hybridizing cRNA prepared from a cloned example of the 120-base pair repeat to the plasmid illustrated in 2a (track B), digested with *EcoRI* + *SalI*, *EcoRI* + *PstI*, and *EcoRI* + *HaeIII*, fractionated by gel electrophoresis and transferred to nitrocellulose paper. We have assumed that the three *HaeIII* fragments (see text) which hybridize to the clone of the 120-base pair repeat are adjacent. The region has been positioned as illustrated because the 200-base pair fragment carries the *EcoRI* site. c, The deduced structure of the complex cloned repeat (the 2.2-kilobase repeat, see text) in the genome. The double thickness line represents that portion of the repeat assumed to include sequences complementary to the 120-base pair repeat. bp, Base pairs.



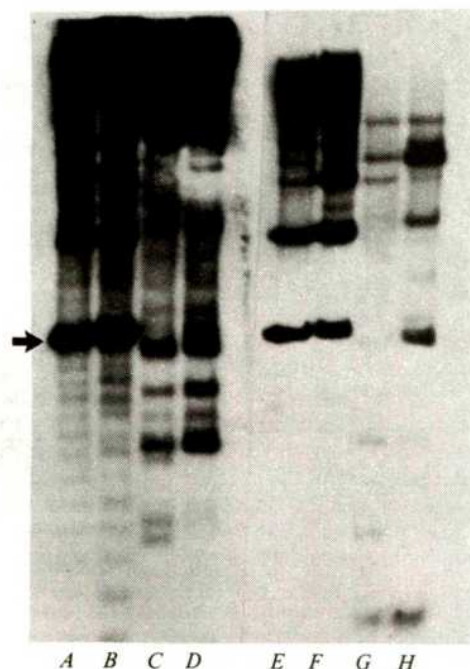
although we cannot rule out the possibility that the 2.2-kilobase repeat has been deleted from wheat.

### Origin of the 2.2-kilobase repeat family

To investigate the arrangement of the spacer DNA sequences in *Secale* genomes, a probe prepared from DNA fragments within the 2.2-kilobase spacer DNA (the 800-base pair *EcoRI*-*PstI* fragment) was hybridized to size-fractionated *Secale cereale* (rye) and *Secale silvestre* DNAs digested with *EcoRI* and *HindIII* endonucleases. Figure 3 (tracks E-H) shows that the spacer DNA hybridizes to many repeated sequence DNA bands in DNAs digested with *EcoRI* or *HindIII*. The pattern of hybridization produced when the 120-base pair repeat DNA was used as probe is shown as a control (Fig. 3 A-D). The spacer DNA probe hybridized to DNA fragments containing from >20

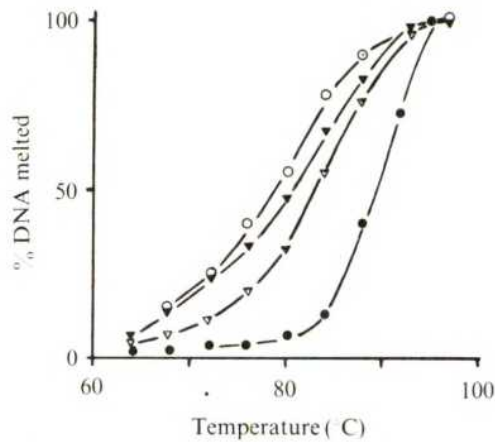
kilobases to >0.5 kilobases. This hybridization pattern suggests that sequences related to those in the 2.2-kilobase spacer DNA exist in many diverse arrangements in the genome. This diversity and the origin of the 2.2-kilobase repeat can be explained by proposing that short pieces of DNA frequently undergo re-arrangement by recombination during genome evolution to form many permutations of linear order. Specific permutations of these sequences are then amplified to create repeat families, such as the 2.2-kilobase repeat family, definable by their unique length and linear permutation of rearranged sequences.

The 2.2-kilobase repeat contains two components that we have distinguished—the 120-base pair sequences and what we have called 'spacer sequences'. Two pieces of evidence suggest that these subcomponents have existed as repeats in cereal genomes for long evolutionary time periods. First, much of the 2.2-kilobase spacer DNA is present in rye, wheat and barley genomes because most (but not all) of the 800-base pair *EcoRI*-*PstI* fragment of the 2.2-kilobase repeat (see Fig. 2b) renatures with repeated sequence kinetics when sheared and renatured with a large excess of sheared wheat and barley DNAs<sup>7</sup>. This suggests that these sequences were first amplified before wheat, rye and barley diverged<sup>2</sup>. The presence of the 120-base pair sequence in wheat is shown in Fig. 5 and has also been demonstrated by *in situ* hybridization to wheat chromosomes<sup>5</sup>. Second, sequences in the rye genome related to the subcomponents of the 2.2-kilobase repeat are very heterogeneous. This was determined by forming hybrid duplexes *in vitro* between rye DNA fragments and a cloned example of 120-base pair repeats or the 800-base pair *EcoRI*-*PstI* fragment from the 2.2-kilobase repeat. The thermal stabilities of these duplexes were



**Fig. 3** Organization of spacer DNA from the 2.2-kilobase repeat in *Secale* species DNA. The 800-base pair *EcoRI*-*PstI* fragment (see Fig. 2b) was prepared from preparative *EcoRI* + *PstI* double digests of the cloned 2.2-kilobase repeat fractionated on agarose gels as described in Fig. 2 legend. <sup>32</sup>P-labelled cRNA prepared from this fragment was hybridized to *S. cereale* (rye) DNA digested with *EcoRI* (E) or *HindIII* (G) and *S. silvestre* DNA digested with *EcoRI* (F) and *HindIII* (H). As a control, <sup>32</sup>P-labelled cRNA prepared from the 120-base pair repeat was hybridized to *S. cereale* digested with *EcoRI* (A) or *HindIII* (C) and to *S. silvestre* DNA digested with *EcoRI* (B) or *HindIII* (D). The DNA was fractionated by electrophoresis on 1.0% agarose gels (from top to bottom) and transferred to nitrocellulose filters before hybridization. Hybridization and washing conditions were as in Fig. 1 legend. Hybridization was assayed by autoradiography. The major 2.2-kilobase repeats are arrowed.





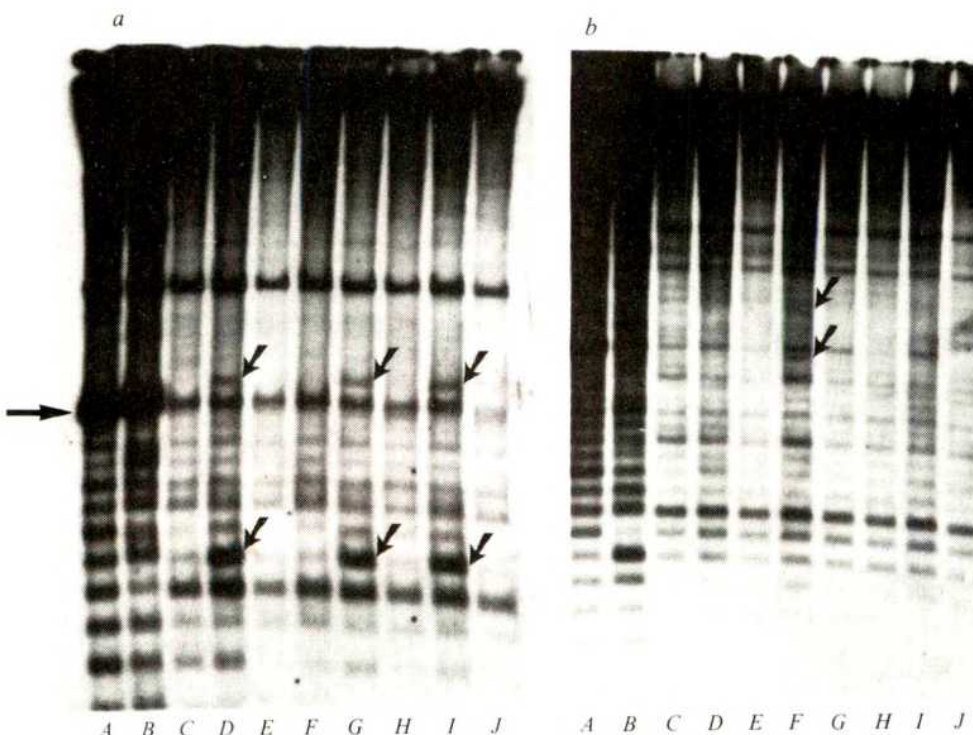
**Fig. 4** Thermal stability of duplexes formed *in vitro* between rye DNA and the 120-base pair or 2.2-kilobase spacer DNA. DNA from a clone of the 120-base pair repeat or the 800-base pair *EcoRI-PstI* fragment from 2.2-kilobase spacer, radiolabelled with  $^{32}\text{P}$  by nick translation ( $10^5$  c.p.m. of specific activity,  $10^8$  c.p.m.  $\mu\text{g}^{-1}$ ) and was mixed with 200  $\mu\text{g}$  rye DNA sheared to 300–400 nucleotide lengths. After denaturation the DNA was incubated to  $C_0t$  0.3 in 0.12 M phosphate buffer at 60°C. The renatured DNA was adsorbed on to hydroxyapatite at 60°C in 0.12 M phosphate buffer, then melted off by raising the temperature in defined steps. Denaturation of total rye repeated DNA was determined by measuring the elution of  $A_{260}$ . Denaturation of the labelled DNA duplexes was determined by precipitating the eluted DNA with 5% TCA in the cold, collecting it on GF/B filters and scintillation counting. Sheared native rye DNA was similarly eluted as a control.  $\circ$ , 2.2-kilobase spacer duplexes;  $\blacktriangledown$ , 120-base pair DNA duplexes;  $\nabla$ , total renatured repeated rye DNA;  $\bullet$ , native rye DNA. Results plotted are means from two experiments.

determined by binding them to hydroxyapatite and melting them off by raising the temperature in defined steps. Both sets of duplexes show a very broad melting curve with a  $\Delta T_m$  of  $\sim 11^\circ\text{C}$  with respect to native DNA (Fig. 4). A broad melting curve is expected of hybrids with a large range of mispaired bases. These melting curves therefore indicate considerable heterogeneity amongst sequences related to the 120-base pair and spacer DNA. Assuming that repeated sequence divergence is related to the age of the repeated sequence family, sequences related to the 120-base pair and to spacer DNA have existed as repeats for a long and similar time period. The sequence heterogeneity of

these families contrasts with the relative homogeneity of a family described elsewhere which is specific to *S. cereale* and absent from *S. silvestre* and which was amplified presumably relatively recently<sup>5</sup>.

The hybridization experiments of Fig. 3 provide evidence that both subcomponents of the 2.2-kilobase repeat have been involved in rearrangements. Probes prepared from both the 120-base pair sequence and the spacer sequence hybridize to a smear of DNA fragments ranging in size from  $>20$  to 0.5 kilobases suggesting that sequences complementary to these DNAs are interfaced with many different sequences in the chromosomes. Figure 3 also shows that many permutations of the ancestral sequences are reamplified. The two subcomponents of the 2.2-kilobase repeat hybridize to many bands other than the integral size progression of the 120-base pair tandem repeat. Furthermore, several of the bands (other than the 2.2-kilobase repeat itself) which hybridize to the two subcomponents of the 2.2-kilobase repeat have the same length. This suggests that sequences related to the 120-base pair and spacer DNA sequences have been amplified together to form repeat families differing from the 2.2-kilobase repeat family. DNA sequences homologous with 2.2-kilobase spacer DNA have been involved in amplification (and possibly rearrangement) events since the separation of *S. cereale* and *S. silvestre* because repeated DNA bands visible in hybridizations to *S. cereale* (Fig. 3, tracks E and G) are absent from the hybridizations to *S. silvestre* (Fig. 3, tracks F and H) and vice versa.

The heterogeneity of the sequences in the genome related to the subcomponents of the 2.2-kilobase family makes it unlikely that these sequences have been rearranged or translocated to new sites in the genome as 'intact, mobile' elements such as a bacterial insertion sequence<sup>8</sup> or the copia, 412 or 279 elements in *Drosophila*<sup>9</sup>. If spacer DNA always inserted itself intact, all the *HindIII* restriction fragments from the genome which hybridize to spacer DNA would be expected to be larger than the spacer itself because spacer DNA in the 2.2-kilobase repeat does not contain a *HindIII* recognition sequence. The results in Fig. 3 (tracks G and H) show three repeat families in *S. cereale* and two in *S. silvestre* which hybridize to 2.2-kilobase spacer DNA but which are shorter than the calculated size of the 2.2-kilobase repeat spacer. Thus spacer DNA must at least undergo deletion or be the target of insertion itself by a DNA sequence containing a *HindIII* recognition sequence.



**Fig. 5** The presence of complex forms of the 120-base pair repeat in individual chromosomes of rye. DNAs from rye (variety King II), *S. silvestre* and *Triticum aestivum* (variety Holdfast) and the complete set of alien addition lines of the *S. cereale* variety King II in the *T. aestivum* variety Holdfast were digested with *EcoRI* (a) and *BamHI* (b) and fractionated by electrophoresis on 1.5% agarose gels. The fractionated DNA was transferred to nitrocellulose filters and hybridized with  $^{32}\text{P}$ -labelled cRNA prepared using a cloned example of the 120-base pair repeat. Hybridization was assayed by autoradiography. Track A, rye DNA; track B, *S. silvestre* DNA; track C, *S. cereale* chromosome 5R in a *T. aestivum* background DNA; track D, chromosome 6R; track E, chromosome 2R; track F, chromosome 4R; track G, chromosome 1R; track H, chromosome 3R; track I, chromosome 7R; track J, *T. aestivum* DNA. The major 2.2-kilobase repeats revealed by *EcoRI* digestion are indicated by the arrow at the extreme left. The other arrows mark bands which vary in different addition line tracks.

## Chromosomal distribution of reamplified variants of the 120-base pair repeat

Wheat-rye addition lines have enabled us to investigate quantitative variation of specific reamplified variants of the 120-base pair repeat between the chromosomes of the rye variety King II. Each wheat-rye addition line has a full complement of wheat chromosomes and a single pair of rye chromosomes<sup>10</sup>. DNA isolated from each of the addition lines, from King II rye, from *S. silvestre* and from wheat (variety Holdfast) were digested with *Eco*RI (Fig. 5a) or *Bam*HI (Fig. 5b) restriction endonucleases, fractionated by gel electrophoresis, transferred to nitrocellulose paper and hybridized with a probe prepared from the 120-base pair repeat. The results in Fig. 5 show that *S. cereale* (rye) (track A) and *S. silvestre* (track B) have essentially the same set of amplified variants of the 120-base pair repeat. Wheat DNA (track J), however, lacks a high concentration of the major variant in the *Eco*RI digest. It is therefore possible to use the addition lines to investigate the chromosomal distribution of the rye 2.2-kilobase repeats. Figure 5a shows that the 2.2-kilobase family is present in each of the seven rye chromosomes examined as is the major family in *Bam*HI digests (Fig. 5b). However, two variants in *Eco*RI digests are present in high copy number only in chromosomes 1R, 6R and 7R (Fig. 5a, arrowed in tracks D, G and I) and one or two relatively minor variants in *Bam*HI digests (Fig. 5b, arrowed in track F) may be present in high copy number only in chromosome 4R.

That some amplified variant forms of the 120-base pair repeat may be chromosome specific or on only some chromosomes suggests that specific amplified sequences may occur initially at a specific location in the genome and are only subsequently distributed to other chromosomes by recombination.

## Discussion

High copy number variants within families of repeated sequences have been found in a few other species by methods similar to ours—in satellite DNAs of mouse<sup>11</sup>, *Drosophila*<sup>12</sup> and man<sup>13-15</sup>. Only for *Drosophila*<sup>12,16,17</sup> and man<sup>13-15</sup>, as far as we

are aware, have results been previously reported which illustrate chromosome-specific variants of repeated sequences. An intriguing question is whether chromosome-specific variation is maintained for functional reasons or merely reflects the site of reamplification before dispersal<sup>14</sup>.

The hypothesis described here to account for the origin of the complex 2.2-kilobase family of repeated sequences is relevant to the structure and evolution of a large proportion of plant chromosome DNA because complex permutations of short repeated and single-copy sequences are common in plant chromosomes<sup>18</sup>. Furthermore, in cereal species, a large fraction of the DNA consists of short repeated sequences common to many species, interspersed with repeated sequences which are species-specific or found only in very closely related species<sup>3,4</sup>. DNA with this sequence arrangement has probably evolved by sequence rearrangement and amplification like the 2.2-kilobase repeat family described here.

We thank Dr D. Lonsdale for criticisms of an earlier version of this paper.

Received 19 March; accepted 26 August 1980.

1. Flavell, R. B., Bennett, M. D., Smith, J. B. & Smith, D. B. *Biochem. Genet.* **12**, 257-269 (1974).
2. Flavell, R. B., Rimpau, J. & Smith, D. B. *Chromosoma* **63**, 205-222 (1977).
3. Rimpau, J., Smith, D. B. & Flavell, R. B. *J. molec. Biol.* **123**, 327-359 (1978).
4. Rimpau, J., Smith, D. B. & Flavell, R. B. *Heredity* **44**, 131-149 (1980).
5. Bedbrook, J. R., Jones, J., O'Dell, M., Thompson, R. & Flavell, R. B. *Cell* **19**, 545-560 (1980).
6. Grunstein, M. & Hogness, D. S. *Proc. natn. Acad. Sci. U.S.A.* **72**, 3961-3965 (1975).
7. Flavell, R. B. *4th John Innes Symposium* 15-30 (John Innes Institute, Norwich, 1979).
8. Bukhari, A.I., Shapiro, J. A. & Adhya, S. L. (Cold Spring Harbor Laboratory, New York, 1977).
9. Cameron, J. R., Loh, E. Y. & Davis, R. W. *Cell* **16**, 739-751 (1979).
10. Riley, R. & Chapman, V. C. *Heredity* **12**, 301-305 (1958).
11. Horz, W. & Zachau, J. G. *Eur. J. Biochem.* **73**, 383-392 (1977).
12. Peacock, W. J. et al. *Cold Spring Harb. Symp. quant. Biol.* **42**, 1121-1135 (1977).
13. Cooke, H. J. & McKay, R. D. G. *Cell* **13**, 453-460 (1978).
14. Beauchamp, R. S., Mitchell, A. R., Buckland, R. A. & Bastock, C. J. *Chromosoma* **71**, 153-166 (1979).
15. Cooke, H. J. & Hindley, J. *Nucleic Acids Res.* **6**, 3177-3197 (1979).
16. Brutlag, D. & Peacock, W. J. *J. molec. Biol.* **135**, 565-580 (1979).
17. Fry, K. & Brutlag, D. *J. molec. Biol.* **135**, 581-593 (1979).
18. Flavell, R. B. *A. Rev. pl. Physiol.* **31**, 569-596 (1980).
19. Southern, E. M. *J. molec. Biol.* **98**, 503-517 (1975).
20. Clewell, D. B. & Helinski, D. R. *Proc. natn. Acad. Sci. U.S.A.* **62**, 1159-1166 (1969).

# Cloning and sequence analysis of cDNAs encoding two distinct somatostatin precursors found in the endocrine pancreas of anglerfish

Peter Hobart, Robert Crawford, LuPing Shen, Raymond Pictet & William J. Rutter

Department of Biochemistry & Biophysics, University of California, San Francisco, California 94143

Complementary DNAs for two distinct anglerfish somatostatin peptides (termed I and II) have been cloned in bacterial plasmids and sequenced. The nucleotide sequence for somatostatin I encodes a large precursor peptide (molecular weight 13,300) in which the somatostatin hormone is at the carboxyl terminus. The predicted 14-amino acid sequence for anglerfish somatostatin I is the same as mammalian somatostatin. Somatostatin II is also synthesized as part of a larger precursor (molecular weight 14,100) with the presumptive somatostatin hormone also at the carboxyl terminus. The 14-amino acid sequence of somatostatin II differs from somatostatin I at two internal residues (Tyr in place of Phe 7 and Gly in place of Thr 10). The two different somatostatins may have distinct biological activities. Homologies in the amino acid sequences of the two peptides outside the somatostatin moiety suggest other regions of the molecules have biological functions.

SOMATOSTATIN is a 14-amino acid peptide which modulates the secretion of several peptide hormones and may also have a role in neurotransmission. Somatostatin was originally isolated from the hypothalamus as an inhibitor of pituitary growth hormone secretion<sup>1</sup>, but it has more recently been localized in

the D cells of the endocrine pancreas<sup>2,3</sup> and shown to be an inhibitor of both insulin and glucagon secretion<sup>4</sup>. In addition, it has been detected in discrete epithelial cells lining the gut<sup>5</sup> and can inhibit the secretion of several gastrointestinal hormones including secretin<sup>6</sup>, gastrin<sup>7</sup> and cholecystokinin<sup>8</sup>. However,



somatostatin is not universally involved in regulating peptide hormone secretions because it does not affect the secretion of several other hormones including follicle-stimulating hormone and luteinizing hormone<sup>9</sup>. Studies on the localization of somatostatin in neuronal tissue reveal its presence in several other regions of the brain<sup>10,11</sup> as well as the spinal cord<sup>12</sup> and the sympathetic nerve fibres<sup>13</sup>. Injection of somatostatin into the cranium results in loss of motor activity, suggesting that it is a potent depressant of certain parts of the central nervous system<sup>14</sup>. These properties have led to the postulate that somatostatin is a neurotransmitter. That a single hormone exhibits this spectrum of biological activities is a regulatory paradox.

These observations have engendered considerable interest in the regulation of somatostatin synthesis and secretion by the various dispersed somatostatin-producing cells. In common with several other peptide hormones, somatostatin is synthesized as part of a larger precursor peptide that is subsequently processed<sup>15,16</sup>. Peptides up to 10 times the size of somatostatin have been found which react with somatostatin antibodies<sup>17,18</sup> and there is evidence that this larger peptide is also able to inhibit growth hormone secretion by the pituitary<sup>19</sup>. Furthermore, a 28-residue peptide containing somatostatin has recently been isolated from porcine intestinal tissue<sup>20</sup>.

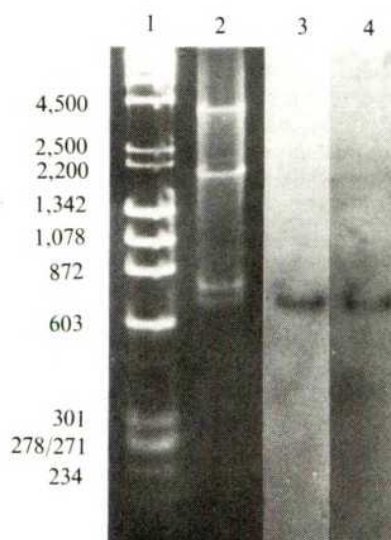
A direct approach to characterizing the complete somatostatin precursor, as well as the somatostatin mRNA and gene, involves construction of bacterial plasmids containing the somatostatin mRNA sequence, using nucleic acid technology. This approach is facilitated by the availability of a tissue which is highly enriched in somatostatin mRNA. In most vertebrates, there is no tissue with a sufficiently high proportion of somatostatin-producing cells to undertake such experiments. However, in some fish, and in particular the anglerfish (*Lophius americanus*), the endocrine pancreas (termed Brockmann body) is easily separated from exocrine tissue and, furthermore, in comparison with mammals, is highly enriched in D (somatostatin-producing) relative to B (insulin-producing) cell types<sup>21</sup>. Therefore, we have used the anglerfish Brockmann body as a source of somatostatin mRNA.

We present here the results of cloning in bacteria and subsequent sequence analysis of a cDNA molecule which predicts the complete preprosomatostatin peptide sequence (somatostatin I) synthesized by the fish endocrine pancreas. In addition, we present the sequence of another cDNA molecule, also present in the fish endocrine pancreas, encoding a second preprosomatostatin precursor (somatostatin II) which differs by two amino acids in the 14-residue hormone sequence. The finding that two distinct precursor peptides are synthesized in the fish pancreas leads us to suggest that more than one gene may be involved in the hormonal activities now attributed to somatostatin.

## Synthesis and cloning of fish cDNA

Poly(A)<sup>+</sup> mRNA from Brockmann body tissue was isolated as described in Fig. 1 legend. This fraction contains two major classes of mRNA: 700 ± 25 and 840 ± 25 bases. This is consistent with a previous report that *in vitro* translation of the mRNA from anglerfish Brockmann bodies results in only a few predominant protein products<sup>22</sup>. Double-stranded cDNA was synthesized from poly(A)<sup>+</sup> mRNA, tailed with deoxycytidine residues and cloned in the *Pst*I site of the plasmid pBR322 which had been previously tailed with deoxyguanosine (described in Fig. 1 legend). Approximately 3,000 tetracycline-resistant transformants were obtained from 75 ng of tailed cDNA.

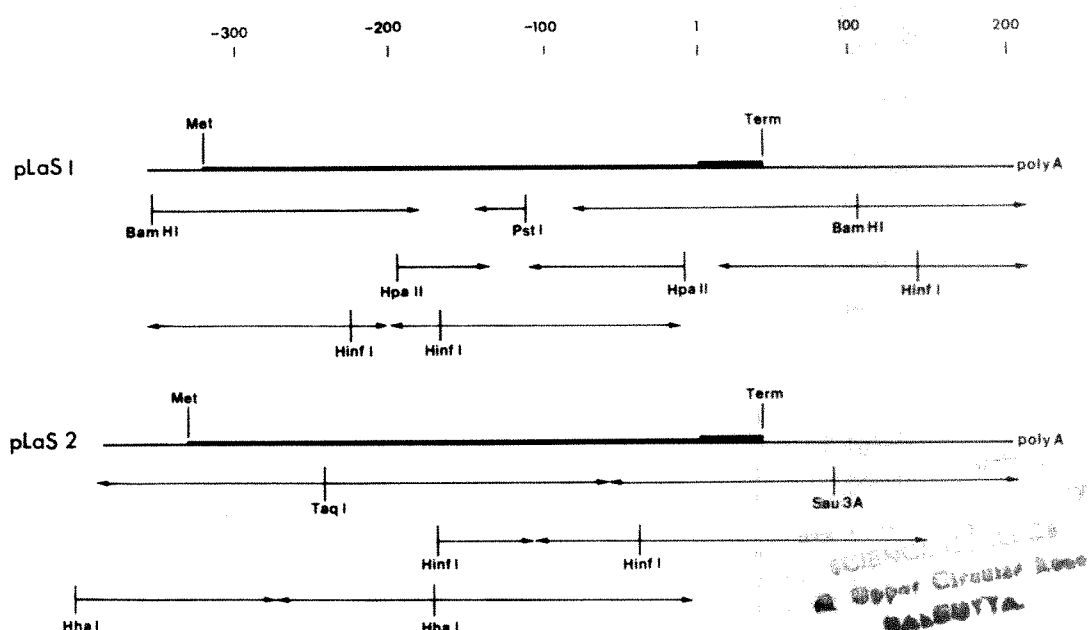
To screen the transformants, the most frequent cDNA inserts were selected by hybridization to a single-stranded cDNA probe synthesized from Brockmann body poly(A)<sup>+</sup> RNA. A few plasmids containing large inserts were prepared from the cDNA-positive colonies. Purified inserts from these plasmids were labelled by 'nick translation' and tested for their ability to cross-hybridize with each other. The most frequent cDNA insert among the colonies selected by this method has been subsequently sequenced and found to be fish preproinsulin<sup>23</sup>.



**Fig. 1** RNA was extracted from anglerfish Brockmann bodies (Biological Associates) by the guanidine thiocyanate method<sup>23</sup>. One gramme of Brockmann body tissue yields approximately 6.5 mg of total RNA. Polyadenylated RNA was purified using oligo(dT)-cellulose affinity chromatography. 1.35 µg of single-stranded cDNA was made from 10 µg polyadenylated RNA using AMV reverse transcriptase (J. Beard, lot no. 1577) in the following reaction mix; 40 mM Tris-HCl, pH 8.3, 10 mM MgCl<sub>2</sub>, 56 mM β-mercaptoethanol, 0.5 mM dATP, dGTP, dTTP, 0.15 mM <sup>3</sup>H-dCTP (specific activity 5.2 mCi µmol<sup>-1</sup>), 25 µg ml<sup>-1</sup> oligo(dT) (P-L Biochemicals), 40 µg ml<sup>-1</sup> poly(A)<sup>+</sup> RNA, 15 units reverse transcriptase per µg RNA. Incubation was at 42 °C for 30 min and then at 68 °C for 2 min. The reaction was stopped by the addition of NaEDTA (pH 8.0) to 20 mM, chromatographed over Sephadex G-75 and precipitated with ethanol. RNA was removed by alkali treatment (0.2 M NaOH, 23 min at 68 °C) and the second strand cDNA synthesis was carried out in the following reaction mixture using DNA polymerase I; 100 mM Na HEPES pH 6.9, 75 mM KCl, 10 mM MgCl<sub>2</sub>, 10 mM dithiothreitol (DTT), 100 mM dNTPs, 0.8 µg ml<sup>-1</sup> single-stranded cDNA (boiled for 3 min just before addition), and 75 units per µg *Escherichia coli* DNA polymerase I (Biolabs). Incubation was at 14 °C for 2 h. The reaction volume was made 20 mM NaEDTA, extracted once with phenol/chloroform/isoamyl alcohol (50:48:2) and passed over a Sephadex G-75 column. In preparation for dC tailing, the hairpin loops of the double-stranded DNA (ds-cDNA) were clipped and made blunt ended using S<sub>1</sub> micrococcal nuclease (Miles) in a 30-min reaction at 37 °C (175 units per µg ds-cDNA). After organic extraction and Sephadex G-75 chromatography to remove small DNA fragments, 300 ng of trimmed double-stranded (ds)-cDNA was tailed using calf thymus terminal transferase in a 30-min reaction at 37 °C containing 140 mM K cacodylate, 30 mM Tris base (pH 7.8), 1 mM CoCl<sub>2</sub>, 0.1 mM DTT, 25 µM dCTP ([α-<sup>32</sup>P]dCTP, 8.36 µCi nmol<sup>-1</sup>), and 150 units terminal transferase per µg ds-cDNA<sup>24</sup>. Preliminary experiments indicated approximately 30 bases are added to the 3' end in these conditions. The dC-tailed ds-cDNA was then annealed to an equimolar amount of dG-tailed pBR322 at a concentration of 1 µg ml<sup>-1</sup> using sequential 2 h incubations at 42, 30 and 14 °C (ref. 35). The hybrid plasmid DNA was precipitated with ethanol and used to transform *E. coli* λ1776 in P2/HV2 containment conditions in compliance with NIH Recombinant DNA Guidelines<sup>36</sup> and selected for tetracycline resistance. To screen with various labelled probes, recombinant colonies were grown on Whatman 541 cellulose paper, lysed *in situ* and prepared for hybridization according to the Grunstein and Hogness procedure<sup>37</sup>. The filters were hybridized to a <sup>32</sup>P-labelled cDNA probe synthesized from anglerfish Brockmann body RNA and plasmid DNA was isolated from those colonies giving a strong autoradiographic signal using a cleared lysate procedure<sup>38</sup>. Two plasmids (pLaS1 and pLaS2) were selected on the basis of their size and their cDNA inserts purified on preparative acrylamide gel electrophoresis. Purified insert cDNA from these plasmids was labelled by 'nick translation'<sup>39</sup> and hybridized to anglerfish poly(A)<sup>+</sup> RNA which had been previously chromatographed on a 2% agarose methyl mercury gel<sup>40</sup> and transferred to diazotized cellulose paper<sup>24</sup>. Hybridization was for 48 h at 42 °C. Hybridized filters were autoradiographed after washing three times (100 ml volume, 10 min each) in 0.3 M NaCl, 0.03 M Na citrate, 0.1% (w/v) SDS at 20 °C and then in the same manner using 15 mM NaCl, 1.5 mM Na citrate, 0.1% SDS at 50 °C. Lane 1, *Hind*III-digested λ DNA and *Hae*III-digested ΦX174 DNA MW standards. Lane 2, ethidium bromide staining of anglerfish Brockmann body (1 µg poly(A)<sup>+</sup>-enriched RNA); lane 3, hybridization of transferred anglerfish poly(A)<sup>+</sup> RNA to pLaS1 <sup>32</sup>P insert DNA; lane 4, hybridization of transferred anglerfish poly(A)<sup>+</sup> RNA to pLaS2 <sup>32</sup>P insert



**Fig. 2** Sequencing strategy for pLaS1 and pLaS2 cDNA inserts. Both cDNAs are oriented 5' to 3' according to the mRNA sequence and are numbered so that the first base coding for the hormone somatostatin I or somatostatin II is no. 1, and with all bases in the 5' direction given negative numbers. Thickened areas of the line for each cDNA indicate the predicted translated region of the mRNA sequence and the double thickness at the 3' end of the translated sequence indicates the region coding for the hormone. Not included are the poly(dG)-poly(dC) tails at the ends of the cDNA inserts which were between 12 and 25 base pairs long. Below each sequence are arrowed lines indicating the restriction sites used for kinasing the DNA and the direction and extent of DNA sequence determined using that labelled fragment. To prepare purified fragments for each labelling or sequencing reaction, DNA fragments were cut by the indicated restriction endonuclease, separated by polyacrylamide slab gel electrophoresis and electroeluted. All acrylamide gel electrophoreses were carried out in 100 mM Tris-borate pH 8.1, 2.5 mM NaEDTA using 5–7% polyacrylamide (20:1, acrylamide/bisacrylamide). To end-label, the DNA fragments were treated for 30 min at 65 °C with 8–20 units of bacterial alkaline phosphatase (Worthington) in 0.1 M Tris-HCl pH 7.4, 0.1 M NaCl, phenol extracted (2×), and then treated with 4–8 units of T4 polynucleotide kinase (BioLabs) at 37 °C for 30 min in a reaction mixture containing 50 mM Tris pH 7.6, 10 mM MgCl<sub>2</sub>, 5 mM DTT, 200  $\mu$ Ci (3,000–4,000 Ci mmol<sup>-1</sup>) [ $\gamma$ -<sup>32</sup>P]ATP. The 5' end-labelled DNA fragment was subsequently cut by an intervening restriction endonuclease, separated by gel electrophoresis, eluted, concentrated and ethanol precipitated as described above. Sequence reactions were carried out according to Maxam and Gilbert<sup>41</sup>.



Two additional non-cross-hybridizing non-insulin cDNA inserts (later termed pLaS1 and pLaS2) were selected. The size of the mRNAs specific to both pLaS1 and pLaS2 were determined by 'Northern' gel transfer<sup>24</sup> analysis to be approximately 700 bases (see Fig. 1, lanes 3, 4). By a similar analysis, the other major poly(A)<sup>+</sup> mRNA of 840 bases corresponds to preproinsulin (data not shown). The two non-insulin cDNA inserts were sequenced according to the strategy presented in Fig. 2. The nucleotide sequence of pLaS1 (563 base pairs) predicts the entire peptide sequence of preprosomatostatin I whereas pLaS2 (594 base pairs) predicts the sequence of preprosomatostatin II. The 14-amino acid sequence of the hormone in fish preprosomatostatin I is identical to mammalian somatostatin. This corroborates an earlier sequence analysis of fish somatostatin<sup>25</sup>.

As expected from the lack of cross-hybridization and its restriction map (Fig. 2), the nucleotide sequence of pLaS1 insert DNA differs substantially from that of pLaS2; nevertheless, the molecules are clearly related. As shown in Fig. 3, the nucleic acid sequences were aligned based on the recognized homologies present in the regions coding for the hormone and the signal peptides. Additional homologies in the translated and in the untranslated regions were revealed by computer analysis. A molecule of approximately 45% overall homology can be constructed by the insertion of gaps in the nucleotide sequence. Beginning with the first AUG codon at the 5' end of the sense strand, translation of pLaS1 predicts the sequence of a 121-amino acid peptide which contains the somatostatin hormone at its carboxyl terminus (Fig. 3). This leaves 37 bases of untranslated sequence at the 5' end of the cDNA and 158 bases 3' to the stop codon and before the poly(A) tail. If translation is initiated at the first AUG codon (amino acid position -107), the predicted preprosomatostatin I peptide has a molecular weight of 13,328. This is approximately the size of somatostatin precursors which have been detected in both mammalian and fish tissue<sup>17,18,42</sup>. The region of the peptide following this AUG comprises a sequence of hydrophobic amino acids characteristic of the signal peptide described for other precursors of secretory proteins<sup>26</sup>. The sequence Leu-Leu-Val-Leu-Leu in position

-96 to -92 of this region is found in the signal peptide of fish preproinsulin and is located at approximately the same distance from the initiating methionine in both precursor molecules<sup>22,23</sup>.

Translation from the first AUG codon in pLaS2 predicts a 125-amino acid peptide (MW 14,100) which also contains a characteristic signal peptide at its amino terminus and a 14-residue somatostatin-like peptide at its carboxyl terminus. This somatostatin II peptide differs from somatostatin I by two internal amino acids at position 7 (Tyr instead of Phe) and position 10 (Gly instead of Thr). The hormone sequences are flanked at their amino terminus by the residues Arg-Lys. Such contiguous basic residues are frequent sites for post-translational processing of hormone precursors<sup>27,28</sup> and suggest that both somatostatins are cleaved from their precursors by a trypsin-like enzyme activity. There is additional homology extending to amino acid -18. This region of the anglerfish precursors is in turn homologous with a 28-amino acid somatostatin-containing peptide isolated from porcine gut<sup>20</sup> (see Fig. 4). The anglerfish somatostatins have arginine residues at position -15 and thus can both be cleaved by a trypsin-like activity to give similar 28-amino acid peptides. These conserved features of the molecules suggest that this 28-amino acid sequence may have biological activity. The additional 2-amino acid homology evident in the two fish precursors may indicate a recognition sequence for a processing enzyme. This same Leu-Glu-Arg sequence is found at a second position (-66/-64) in preprosomatostatin II.

Apart from the characteristic hydrophobic amino acid composition, there is little homology in the signal peptide region of the two preprosomatostatins.

The untranslated regions of pLaS1 and pLaS2 have some areas of sequence homology when aligned as shown in Fig. 3. However, it is not clear that these common sequences have a functional role. The homologies (>55%) in the cloned portion of the 5'-untranslated region are largely due to the repeated sequence XCAGAX. In the 3'-untranslated region, as in many other eukaryotic mRNA sequences, pLaS1 has a AAUAAA sequence beginning 20 bases from the polyadenylation site<sup>28-31</sup>. This same sequence is present in pLaS2 but at a position 40



GAUCCGACAGCCGCGCCAGACGUACAGACAUACGUG  
 \* \* \* \* \*  
 CAGAGACAAACCCAGCAGAACAGUAGAACCAGCAGAAGACACAGACAGCAGACAGU:::  
 -107 -100  
 met lys met val ser ser ser arg leu arg cys leu leu val leu leu  
 AUG AAG AUG GUC UCC UCC UCG CGC CUC CGC UGC CUC CUC GUG CUC CUG  
 \*\*\* \*\* \* \* \* \* \*  
 AUG CAG UGU AUC CGU UGU CCC GCC AUC UUG GCU CUC CUG GCG UGU GUU  
 met gln cys ile arg cys pro ala ile leu ala leu leu ala leu val  
 -111 -110 -100  
 -90 -80  
 leu ser leu thr ala ser ile ser cys ser phe ala gly gln arg asp  
 CUG UCC CUG ACC GCC UCC AUC AGC UGC UUC GCC GGA CAG AGA GAC  
 \*\*\* \*\* \* \* \* \* \*  
 CUG UGC GGC CCA AGU GUU UCC UCC CAG CUC GAC AGA GAG CAG AGC GAC  
 leu cys gly pro ser val ser ser gln leu asp arg glu gln ser asp  
 -90 -80  
 -70  
 ser lys leu arg leu leu leu his arg tyr pro leu gln gly ser  
 UCC AAA ::: CUC CGC CUG CUG CUG CAC CGG UAC CCG CUG CAG GGC UCC  
 \* \* \* \* \*  
 AAC CAG GAC CUG GAC CUG GAG CUG CGU CAG CAC UGG CUG CUG GAG AGA  
 asn gln asp leu asp leu glu leu arg gln his trp leu leu glu arg  
 -70  
 -60  
 lys  
 AAA ::: ::: ::: ::: ::: ::: gln asp met thr arg ser ala leu  
 CAG GAC AUG ACU CGC UCC GCC UUG  
 \*\*\* \*\* \* \* \*  
 GCC CGG AGC GCC GGA CUC CUG UCC CAG GAG UGG AGU AAA CGG GCG GUG  
 ala arg ser ala gly leu leu ser gln glu trp ser lys arg ala val  
 -60 -50  
 -50 -40  
 ala glu leu leu leu ser asp leu leu gln gly glu asn glu ala leu  
 GCC GAG CUG CUC CUG UCG GAC CUC CUG CAG GGG GAG AAC GAG GCU CUG  
 \* \* \* \* \*  
 GAG GAG CUG CUG GCU CAG AUG UCU CUG CCA GAG GCC ACG UUC CAG CGG  
 glu glu leu leu ala gln met ser leu pro glu ala thr phe gln arg  
 -40  
 -30 -20  
 glu glu glu asn phe pro leu ala glu gly gly pro glu asp ala his  
 GAG GAG GAG AAC UUC CCU CUG GCC GAA GGA GGA CCC GAG GAC GCC CAC  
 \*\*\* \*\* \* \* \* \* \*  
 GAG GCG GAG GAC GCG UCC AUG GCA ACA GAA GGA CGG :: :: :: ::  
 glu ala glu asp ala ser met ala thr glu gly arg  
 -30 -20  
 -10  
 ala asp leu glu arg ala ala ser gly gly pro leu leu ala pro arg  
 GCC GAC CUA GAG CGG GCC GCC AGC GGG GGG CCU CUG CUC GCC CCC CGG  
 \*\*\* \*\* \* \* \* \* \*  
 AUG AAC CUA GAG CGG UCC GUG GAC UCU ACC AAC AAC CUA CCC CCU CGU  
 met asn leu glu arg ser val asp ser thr asn asn leu pro pro arg  
 -10  
 Somatostatin I  
 1 10  
 glu arg lys ala gly cys lys asn phe phe trp lys thr phe thr ser  
 GAG AGA AAG GCC GGC UGC AAG AAC UUC UUC UGG AAA ACC UUC ACC UCC  
 \*\*\* \* \*\* \* \* \* \* \*  
 GAG CGU AAA GCU GGC UGU AAG AAC UUC UAU UGG AAG GGC UUC ACU UCC  
 glu arg lys ala gly cys lys asn phe tyr trp lys gly phe thr ser  
 1 10  
 Somatostatin II  
 14  
 cys OP  
 UGC UGA GCCGCUCCUCAUCCUGCGCGCUCCUCCGUCUCCAAACGGACGUUUU:::ACAG  
 \* \* \* \* \*  
 UGU UAA ::AGCUCCGCCAGCCAAAGCUACACCGUACACCGACCAACCAAUCCAGAUACG  
 cys OC  
 14  
 ACGCUGAAUGGAUCCCGGUUUGCAGCUCUCCUUUUGUGGGCGGAGUCUGAAUGUAAACUUGA  
 \* \* \* \* \*  
 ACCCUGAAAUUACCCUGAAGAACUGGACCGACCAAUACAGCAGCUC::UCCGGAUGGAUUGUACC  
 UGAAACUAUUUUUAAUGGUUGUUGAAUAAUAAUACUGUUUGAGAC Poly A  
 \* \* \* \* \*  
 UGAAUAAA:::UAAUACUGUUAUGAAUUAAGCAUAAUCCGUC Poly A

**Fig. 3** The mRNA nucleotide sequence and single-frame translation of pLaS1 and pLaS2. For comparative purposes, the two nucleic acid sequences are aligned (by the use of gaps) to show regions with a significant amount of base homology. The translated amino acid sequences are numbered by designating the first residue (Ala) of the somatostatin I and somatostatin II peptides as no. 1. The amino acids towards the amino terminus of the precursors are numbered negatively and those towards the carboxy terminus of the hormones are numbered positively. The asterisks indicate homologous bases along the pLaS1 and pLaS2 nucleotide sequence. We have, in addition, sequenced two other cDNA fragments which cross-hybridized with pLaS1 and two which cross-hybridized with pLaS2. In all three cases the sequences were identical to those presented here, eliminating the possibility of any significant errors resulting from the reactions involved in cDNA synthesis.

bases from the poly(A) site whereas a slightly different sequence, AAUUA AAA, is found at the corresponding position closer to the 3' end of the mRNA.

## Characteristics of somatostatin I and II precursors

Our results show that, in common with many other hormones, somatostatin is synthesized as part of a larger precursor peptide. This precursor contains a signal peptide which may be released during the transit into the endoplasmic reticulum; the resultant prosomatostatin would be approximately 97 residues for somatostatin I and 101 residues for somatostatin II (with MWs 10,600 and 11,600 respectively). The function of this form of the precursor, which is more than five times the size of somatostatin, is interesting. It may be cleaved in one step to yield somatostatin alone and thus have no function other than to act as a connecting peptide between the somatostatin hormone and the signal peptide. Alternatively, prosomatostatin, or a smaller, intermediate-sized precursor containing the somatostatin sequence, may be biologically active because 'big somatostatin' exhibits somatostatin activity<sup>19</sup>. Finally, there may be a related or separate biologically active peptide encoded in the precursor in analogy with the adrenocorticotropin (ACTH) precursor<sup>28</sup>. However, a computer analysis of both preprosomatostatin I and II detected no distinct homologies with any known protein sequence (search completed by the National Biomedical Research Foundation, Georgetown University).

## Two somatostatin activities?

The finding of two distinct mRNAs which generate different somatostatin molecules raises questions concerning possible functions of multiple somatostatins and the nature of somatostatin hormone activity measured in animal tissues by immunological procedures. The somatostatin I and II hormones are sufficiently closely related structurally for it to be likely that they cross-react to some degree in biological activity and/or radioimmunoassays. However, it is unclear whether they exhibit the same range of biological activities. Previous studies using chemically synthesized somatostatin analogues have shown selective inhibition of secretion of insulin or glucagon by the pancreas and/or growth hormone by the pituitary<sup>32</sup>. These studies indicate significant functional differences in somatostatin receptors of the different target cells. Therefore, it is possible that there are several somatostatins with common immunological determinants but with selective activities on different target cells. A test of the biological activity of somatostatin II as well as prosomatostatins I and II may help to resolve these questions.

We thank Dr John McCosker of the Steinhardt Aquarium for help in obtaining fish specimens, Leslie Spector for assistance in

ANGLERFISH SOM. I LEU GLU ARG ALA ALA SER GLY GLY PRO LEU LEU ALA PRO ARG GLU ARG LYS ALA GLY CYS LYS ASN PHE PHE TRP LYS THR PHE THR SER CYS  
 ANGLERFISH SOM. II LEU GLU ARG SER VAL ASP SER THR ASN ASN LEU PRO PRO ARG GLU ARG LYS ALA GLY CYS LYS ASN PHE TYR TRP LYS GLY PHE THR SER CYS  
 PORCINE SOM-28 SER ALA ASN SER ASN PRO ALA MET ALA PRO ARG GLU ARG LYS ALA GLY CYS LYS ASN PHE PHE TRP LYS THR PHE THR SER CYS

**Fig. 4** Alignment of porcine somatostatin-28 (ref. 20) to the corresponding peptide region of preprosomatostatin I and II. Boxed residues show homologies present in the precursor peptides; residues underlined within the hormone sequence indicate those that are unique to anglerfish somatostatin II.

preparing the manuscript, and Dr Hugo Martinez and Sonja Bock for assistance in computer analyses. This work was supported by NIH grant AM 21344. P.H. is the recipient of an American Cancer Society Postdoctoral Fellowship. R.C. is the holder of a National Health and Medical Research Council (Aust.) C. J. Martin Fellowship. L.P.S. is funded in part by the Academia Sinica, the People's Republic of China.

**Note added in proof:** It was recently reported that an

Received 24 March; accepted 10 September 1980.

- Vale, W. *et al.* *C. R. hebdomadaire Séances Acad. Sci., Paris* **275**, 2913 (1972).
- Luft, R., Efendic, S., Hokfelt, T., Johansson, O. & Arimura, A. *Med. Biol.* **52**, 428–430 (1974).
- Dubois, M. *Proc. natn. Acad. Sci. U.S.A.* **72**, 1340–1343 (1975).
- Koerker, D. *et al.* *Science* **184**, 482–484 (1974).
- Polak, J., Pearce, A., Grimelius, L., Bloom, S. & Arimura, A. *Lancet* **ii**, 1220–1222 (1975).
- Boden, G., Sivitz, M. & Owen, D. *Science* **190**, 163–164 (1975).
- Bloom, S. *et al.* *Lancet* **ii**, 1106–1109 (1974).
- Konturek, S., Tasler, J., Obtulowicz, W., Coy, D. & Schally, A. *J. clin. Invest.* **58**, 1 (1976).
- Guillemin, R. & Gerich, J. A. *Rev. Med.* **27**, 379–388 (1976).
- Vale, W., Rivier, C., Palkovits, M., Saavedra, J. & Brownstein, M. *Endocrinology* **94**, 14–78 (1974).
- Brownstein, M., Arimura, A., Sato, H., Schally, A. & Kizer, J. *Endocrinology* **96**, 1456–1461 (1975).
- Vale, W. *et al.* *Recent Prog. Horm. Res.* **31**, 365–397 (1975).
- Hokfelt, T., Elde, R., Johansson, O., Luft, R., Nilsson, G. & Arimura, A. *Neuroscience* **1**, 131–136 (1976).
- Cohn, M. L. & Cohn, M. *Brain Res.* **96**, 138–141 (1975).
- Lauber, M., Camier, M. & Cohen, P. *Proc. natn. Acad. Sci. U.S.A.* **76**, 6004–6008 (1979).
- Noe, B., Fletcher, D. & Spiess, J. *Diabetes* **28**, 724–730 (1979).
- Conlon, J., Zyznar, E., Vale, W. & Unger, R. *FEBS Lett.* **94**, 327–330 (1978).
- Noe, B., Fletcher, D., Bauer, G., Weir, G. & Patel, Y. *Endocrinology* **102**, 1675–1685 (1978).
- Spiess, J. & Vale, W. *Metabolism* **27**, Suppl. 1, 1175–1178 (1978).
- Pradagroi, L., Jörnvall, H., Mutt, V. & Ribet, A. *FEBS Lett.* **109**, 55–58 (1980).
- Johnson, A., Torrence, J., Elde, R., Bauer, G., Noe, B. & Fletcher, D. *Am. J. Anat.* **147**, 119–122 (1976).

18,000 MW peptide synthesized *in vitro* by translation of anglerfish Brockmann body mRNA is immunoprecipitable using somatostatin specific antibody<sup>43</sup>. A second report using the same method of analysis indicated that two peptides (16,000 and 14,000 MW) synthesized by anglerfish Brockmann body mRNA *in vitro* are immunoprecipitable using somatostatin specific antibody<sup>44</sup>. The exact relationship between the peptides in these reports and the predicted peptides reported here is unclear.

- Shields, D. & Blobel, G. *Proc. natn. Acad. Sci. U.S.A.* **74**, 2059–2063 (1977).
- Hobart, P., Shen, L. P., Crawford, R., Pictet, R. & Rutter, W. *Science* (in the press).
- Alwine, J. C., Kemp, D. J. & Stark, G. R. *Proc. natn. Acad. Sci. U.S.A.* **74**, 5350–5354 (1977).
- Noe, B., Spiess, J., Rivier, J. & Vale, W. *Endocrinology* **105**, 1410–1415 (1979).
- Devillers-Thiery, A., Kindt, T., Scheele, G. & Blobel, G. *Proc. natn. Acad. Sci. U.S.A.* **72**, 5016–5020 (1975).
- Steiner, D., Kemmler, W., Tager, H. & Peterson, J. *Fedn Proc.* **33**, 2105–2115 (1974).
- Nakanishi, S. *et al.* *Nature* **278**, 423–427 (1979).
- Kafatos, F., Efstratiadis, A., Forget, B. & Weissman, S. *Proc. natn. Acad. Sci. U.S.A.* **74**, 5618–5622 (1977).
- Ullrich, A. *et al.* *Science* **196**, 1313–1319 (1977).
- Bell, G. *et al.* *Nature* **282**, 525–527 (1979).
- Brown, M., Rivier, J. & Vale, W. *Science* **196**, 1467–1468 (1977).
- Chirgwin, J., Przybyla, A., MacDonald, R. J. & Rutter, W. J. *Biochemistry* **24**, 5294–5299 (1979).
- Roychoudhury, R., Jay, E. & Wu, R. *Nucleic Acids Res.* **3**, 101–116 (1976).
- Villa-Komaroff, L. *et al.* *Proc. natn. Acad. Sci. U.S.A.* **75**, 3727–3731 (1978).
- Federal Register* **43**, 60080–60105 (1978).
- Grunstein, M. & Hogness, D. *Proc. natn. Acad. Sci. U.S.A.* **72**, 3961–3965 (1975).
- Staudenbauer, W. L. *Molec. gen. Genet.* **145**, 273–280 (1976).
- Rigby, P., Dieckmann, M., Rhodes, C. & Berg, P. *J. molec. Biol.* **113**, 237–251 (1977).
- Bailey, J. & Davidson, N. *Analyt. Biochem.* **70**, 75–85 (1976).
- Maxam, A. & Gilbert, W. *Meth. Enzym.* **65**, 499 (1980).
- Patzelt, C., Tager, H., Carroll, R. & Steiner, D. *Proc. natn. Acad. Sci. U.S.A.* **77**, 2410–2414 (1980).
- Shields, D. *Proc. natn. Acad. Sci. U.S.A.* **77**, 4074–4078 (1980).
- Goodman, R. *et al.* *J. biol. Chem.* **255**, 6549–6552 (1980).

## LETTERS

### Observations of optical flares in the recurrent X-ray transient A0538–66

G. K. Skinner

Department of Space Research, University of Birmingham, Edgbaston, Birmingham B15 2TT, UK

The recurrent transient X-ray source A0538–66 probably lies at the distance of the Large Magellanic Cloud (LMC) and is consequently among the most luminous stellar sources known ( $L_x \sim 8 \times 10^{38} \text{ erg s}^{-1}$ , 2–17 keV) (refs 1–4). It has a unique combination of properties. The X-ray outbursts which have been observed were separated by multiples of a 16.6-day period. Some were relatively long, for example the  $n=3$  and  $n=4$  events (using the nomenclature of Johnston *et al.*<sup>2</sup>) lasted ~14 days and ~1 day respectively, but others lasted only a few hours. Observation of the  $n=3$ , 4, 11 outbursts<sup>3</sup> recently led to an improved error box and the proposal of a  $B \sim 15$  optical counterpart<sup>4</sup> (star 'Q' in Fig. 1 of ref. 4) shown on archival plates to be variable. The star was found to have an absorption spectrum characteristic of a  $B$  star. I report here an examination of 85 plates taken with the UK Schmidt telescope at Siding Spring, between 1974 and 1979 including some taken at the time of the X-ray observations. Dramatic flares observed on three of the plates, separated by intervals of 16 days and synchronized with the X-ray outbursts, confirm the proposed identification.

The region of sky containing A0538–66 has been included in numerous plates taken with the UK Schmidt telescope, both in its survey role and as part of non-survey programmes. The plates have been taken in various colours but in particular a series of 35  $B$  plates overlapping the Ariel 5 and HEAO 1 X-ray observations have been measured with an iris photometer. The plates were taken largely on nights when conditions were not sufficiently good for survey work and are of rather variable quality. The plate-to-plate consistency obtained for a series of

comparison stars was 0.15 mag r.m.s. Excluding two plates, the r.m.s. scatter of the observations of the proposed candidate, star 'Q', about their mean was only slightly greater (0.20 mag) and this difference may be attributable to the influence of a  $B \sim 17$  star 4 arc s away which is resolvable from Q on some, but not all, plates and which complicates the photometry. On each of the two remaining  $B$  plates Q was brighter by  $\Delta B = 1.8$ . Of these two plates one was taken during the 1-day long  $n=4$  X-ray outburst (17.1 UT on 4 September 1977) (Fig. 1a) and the other close to the time that the  $n=5$  X-ray outburst was expected (at 18.4 UT on 20 September 1977)<sup>3</sup>. Scans through the region made by the Large Area Sky Survey (LASS) instrument on HEAO 1 1.7 h before the latter optical observation and 4.7 h after it did not detect any X-ray activity (Fig. 1b).

The candidate star lies within the boundary of the stellar association NGC2034 and the surrounding region of the plates contains several stars of similar magnitude with which visual comparisons are easily made. This enabled a simple search to be made for optical flares on 50 further original plates and copies. The plates were of various colours but at least three of each type were compared (3U, 3B, 7V, 3R, 12I, 11J, 4H $\alpha$ , 7 non-standard). In most cases photographic enlargements of the region were used in the comparison. Changes of 0.5–1 mag would have been detectable, depending on the plate quality and colour. The flares of  $\Delta B = 1.8$  are immediately apparent in this way.

The search led to the discovery of a third flare, on a plate taken using 098 emulsion and only a polaroid filter and therefore sensitive to a wide range of wavelengths from ~4,000 to 7,000 Å. The plate was taken during the  $n=6$  X-ray outburst, at 17.1 UT on 7 October 1977 (Fig. 1c). No detailed measurements have been made as the original plate is still in Australia, but comparison with copies of other plates taken with the same filter/emulsion combination suggests that the increase above the quiescent level is about the same as the 1.8 mag increase during the flares seen on  $B$  plates.

On eight plates taken between those on which the flares are seen the star was apparently in its normal state. These include two plates taken 23 and 24 h before that showing the third flare.



As there is no certainty that the optical luminosity was the same at the time of the 7 October plate as it was for the two *B* plates showing flares, there is no firm information on the colour in the flare state. The similarity of the three events suggests that the colour may not be very different from that in the quiescent state. Colour measurements based on the measurements of UK Schmidt plates are given in Table 1. Compared with the results of Johnston *et al.*<sup>4</sup> these figures suggest the star is brighter (by 0.8 mag) and suggest a UV excess not apparent from their spectrum. Their results are based on plates taken in 1941–45, when the mean level may have been different, and on a spectrum obtained with the Anglo-Australian Telescope in July 1979, when the zenith distance was large, perhaps making the figures unreliable at shorter wavelengths (M. J. Ward, personal com-

**Table 1** Photometry of the counterpart of A0538–66

|                 | <i>B</i> | <i>U</i> – <i>B</i> | <i>B</i> – <i>V</i> | <i>V</i> – <i>R</i> | Broad band |
|-----------------|----------|---------------------|---------------------|---------------------|------------|
| Quiescent state | 15.0     | –1.5                | 0.1                 | 0.6                 |            |
| During flares   | 13.2     |                     |                     |                     |            |
| Difference      | 1.8      |                     |                     |                     | ~1.8       |

UVR measurements are from plates taken on the same night (10–11 h UT on 19 March 1979) presumably in the quiescent state. Colours are calculated assuming the mean *B* magnitude from 33 plates taken between November 1976 and January 1978 (not including those showing flares). Standards from refs 6–8 were used for calibration but none is close to star Q both in brightness and position and in addition to the effects of the internal scatter discussed in the text each measurement is subject to a calibration uncertainty of the order of 0.25 mag. Thus errors in colours could be as large as 0.4 mag.

munication). In addition the calibration uncertainties are large, as indicated in Table 1.

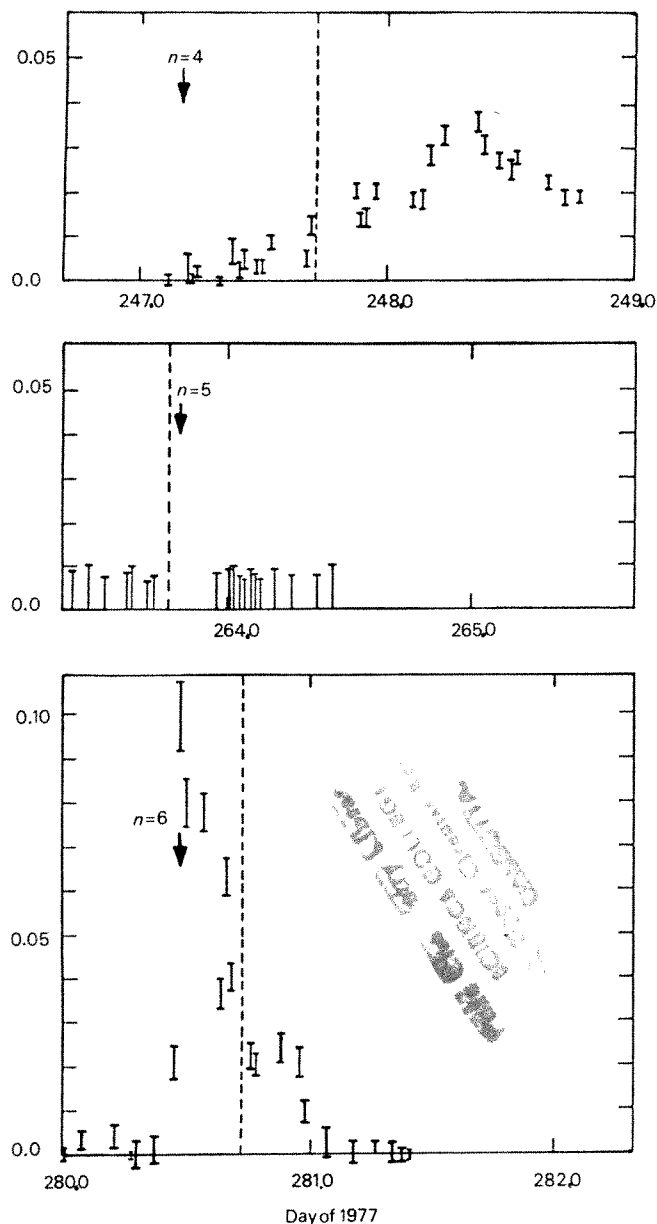
To estimate the optical luminosity we assume that the flares had the same spectrum as a *B*2.5 main sequence star, consistent with the quiescent-state spectrum discussed above. Then, assuming a distance modulus of 18.6 corresponding to the LMC and allowing for an extinction of 0.2, the *B* = 13.2 flare state corresponds to  $M_{\text{bol}} = -7.6$  or an optical luminosity of  $3 \times 10^{38} \text{ erg s}^{-1}$ . This is ~3 times higher than the X-ray flux measured at very nearly the same time as the *n* = 3 optical observation. If the spectrum is not that of a *B* star but is similar to the emission spectrum expected from an accretion disk<sup>5</sup> then the optical luminosity would be higher still. Thermal bremsstrahlung from an optically thin plasma at 6.6 keV (ref. 1) capable of producing the observed X-ray flux would produce a *B* band flux ~250 times below that observed.

The star was observed by Johnston *et al.* in what can now be recognized as its flare state (although not as bright as those reported here) on a plate taken on 12 November 1945. Combining this with all other optical and X-ray observations (except the anomalously long and late *n* = 3, 4 events) and assuming a constant period plus a random phase jitter, best fits are obtained for periods of  $16.668 \pm 0.002$  or  $16.645 \pm 0.002$  days depending on whether the 1945 event is attributed to *n* = –693 or *n* = –594. The r.m.s. deviation is 1.5 h in either case. Other periods differing by steps of 0.023 days from these are possible but imply a jitter at least twice as large.

The three UK Schmidt telescope plates showing flares were among 26 obtained between September 1977 and March 1978 which have been examined. They occurred on consecutive cycles of the 16.6-day period. The fact that none of the 59 plates from other times during the period 1974–79 which have been examined shows any sign of flares suggests that the source may not always be active, although the X-ray activity lasted at least from June to December 1977 and there was previous optical activity in 1945. Plates taken near the times when outbursts would have been predicted on the basis of each of the above possible periods are among the 59 from other years which have been examined without detecting further activity. However, because of the uncertainty in the duration of the flares and of the existence of phase jitter, this evidence is inconclusive. The observation of the optical flare at *n* = 5 shows that either the X-ray outburst was very short or an optical flare occurred without a corresponding X-ray outburst.

Measurements of the plates to determine the position of the centroid of the emission in the flare state place it within 0.1 arc s of that in the quiescent state, effectively excluding the possibility of another, normally invisible star being the source of the events. Thus these results place beyond doubt the association of star Q with A0538–66, as proposed by Johnston *et al.*<sup>4</sup>

The discovery of the flaring optical counterpart considerably improves the chances of establishing whether there is a true constant period, perhaps a binary orbital period, controlling the activity of the system or whether a roughly constant characteristic time between outbursts produces a pseudo-periodic



**Fig. 1** The times of the three observations of optical flares (dotted lines) compared with the HEAO 1 LASS X-ray data. Plate exposures and X-ray measurement times are short compared with the ordinate scale (10–20 min; 5 s). The graphs are aligned and labelled according to the ephemeris given in ref. 4. In each case the ordinate shows X-ray intensities in units of the intensity of the Crab Nebula. The *n* = 4 X-ray event (a) is one of two anomalously long and late ones; the *n* = 6 event (c) is more typical. The points plotted in b are all  $2\sigma$  upper limits. Not all available upper limits are shown but there were no observations during the gap around the time of the optical observation as the satellite was being used in pointed mode.

behaviour. The surprising absence of emission lines in the spectrum of the counterpart suggests that away from outburst the star is comparatively normal and the prospects of spectroscopic studies helping to unravel the nature of this unique system are consequently also good.

Regarding A0538-66 as an X-ray transient, its X-ray spectrum and the properties of the optical counterpart suggest that it should be classed with systems such as A0535+26, 4U0115+63 and A1118-61, which tend to have hard spectra and high mass counterparts, rather than the soft, low mass transients such as A0620-00, A1524-617 and 1H1705-250. Optical flares coincident with X-ray outbursts are common in the latter class (see review in ref. 9), but in these cases the optical flux is only a minor contribution to the overall luminosity during outburst. For example, although during the X-ray transient outburst of A0620-00 the optical counterpart increased in brightness by 3 mag, the optical luminosity was still less than the X-ray luminosity by a factor of 85. Much of the increase in optical flux in such cases is probably due to reprocessing of X rays in the atmosphere of a star whose quiescent state luminosity is low or in an accretion disk.

Similarly, optical bursts have been detected in coincidence with X-ray bursts from MXB1735-44 (refs 10, 11) and 4U1837+04 (ref. 12) but again the X-ray luminosity greatly exceeds the optical luminosity (by factors of  $5 \times 10^4$  and  $3 \times 10^5$  respectively) and the optical flux can be attributed to reprocessing.

Optical luminosities comparable with, or in excess of, the X-ray luminosity are known to occur in bright, high mass systems. Optical variability has been reported in several cases, but the changes have shown no correlation with X-ray outbursts. Nor have they been as large as those described here. Even if the distance of A0538-66 is regarded as uncertain, the relative increase in optical flux compared with the X-ray flux is unique. If the source is indeed at the distance of the LMC, then the absolute value of the increase is even more remarkable.

Many existing plates must contain records of the behaviour of A0538-66 and I would be pleased to liaise between astronomers having such material. A position and finding chart are given in ref. 4.

I thank P. Murdin for pointing out the existence of the plate material and for valuable discussions, S. Shulman for assistance with HEAO 1 data and the following for making plates and copies available: R. Davies, J. Meaburn, W. Garner and C. Butler. I particularly thank Miss M. Sims and other members of the UK Schmidt Telescope Unit both at Edinburgh and Siding Spring for their help.

**Note added in proof:** Since completing the above work I have identified a further flare on a blue plate from the Harvard plate stack. The plate was taken at Bloemfontein, South Africa, on 8-9 October 1932. The plate quality does not permit good measurements to be made but the increase seems to be similar to that on the UK Schmidt plate events. A plate taken 24 h earlier shows possible signs of some brightening but on others from the same year star Q seems to be similar to the 1974-79 quiescent state. Measurements of other plates from the collection confirm that the star was generally  $\sim 0.5$  mag less bright in 1941-46. The 1932 event is consistent with a period of 16.667 days if a rather large jitter is assumed, but excludes the possibility of a 16.645-day period.

Received 4 August, accepted 3 October 1980.

- Whita, N. E. & Carpenter, G. F. *Mem. Nat. R. astr. Soc.* **183**, 11-15P (1978)
- Johnston, M. D. *et al. Astrophys. J. Lett.* **230**, L11-14 (1979)
- Stimmer, G. K. *et al. Astrophys. J.* **240**, 619-627 (1980)
- Johnston, M. D., Griffiths, R. E. & Ward, M. J. *Nature* **288**, 26-27 (1980)
- Hartar, T., Lacasse, M. G., Wesemael, F. & Wingot, D. B. *Astrophys. J. Suppl.* **39**, 513-535 (1979)
- Dachs, J. *Astr. Astrophys.* **18**, 271-286 (1972)
- Eggen, O. J. & Sandage, A. R. *Mem. Nat. R. astr. Soc.* **120**, 79-88 (1960).
- Bodler, C. J. *Durham Observatory Publ.* **1**, No. 6 (1972)
- Bradt, N. V., Donnelly, R. E. & Jernigan, J. G. *Astr. Space Explor.* **3**, 3-66 (1979)
- Gratlay, J. E., *et al. Nature* **274**, 567-568 (1978).
- McClintock, J. E. *et al. Nature* **279**, 47-48 (1979)
- Hackwell, J. A. *et al. Astrophys. J. Lett.* **233**, L115-199 (1979).
- Stor, M. & Liller, W. *Astrophys. J.* **206**, 257-259 (1976)

## Neutrinos and the age of the Universe

E. M. D. Symballsty, J. Yang & D. N. Schramm

Astronomy and Astrophysics Center, Enrico Fermi Institute, The University of Chicago, 5640 South Ellis Ave, Chicago, Illinois 60637

The age of the Universe should be calculable by independent methods with similar results. Previous calculations<sup>1,2</sup> using nucleochronometers, globular clusters and dynamical measurements coupled with Friedmann models and nucleosynthesis constraints have given different values of the age. We report here a consistent age,  $T_U$ , whose implications for the constituent mass density are very interesting and are affected by the existence of a third neutrino flavour,  $\tau$ , and by allowing the possibility that neutrinos may have a non-zero rest mass.

Nucleocosmochronology places a lower limit on  $T_U$  of  $\geq 8.7$  Gyr essentially model independently<sup>3</sup> as this value represents the mean age of the  $r$ -process elements. A model dependent  $T_U$  can be determined from a chemical evolution model of the Galaxy. The major uncertainty entailed is relating the mean age of the elements to the duration of nucleosynthesis. Such an analysis leads to a model dependent upper limit<sup>4</sup> on  $T_U$  of  $\sim 20$  Gyr. However, there are non-standard galactic evolution models which cannot be eliminated and which give ages greater than this.

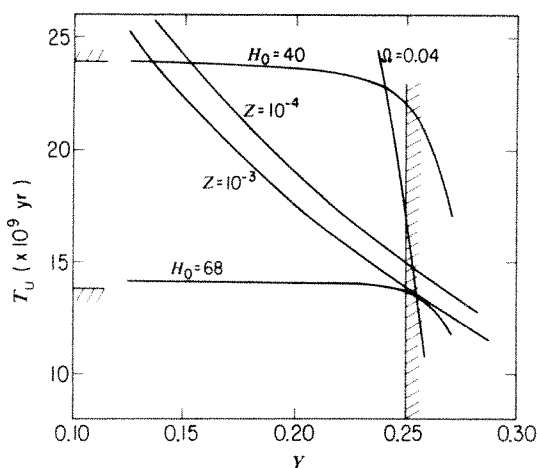
Big-bang nucleosynthesis began with Gamow<sup>5</sup> who recognized that an early hot universe would allow nuclear reactions to occur to build heavier elements. With the microwave radiation confirming the hot early universe it is obvious that the primordial abundances of the light elements— $^2\text{H}$ ,  $^3\text{He}$ ,  $^4\text{He}$  and  $^7\text{Li}$ —become useful probes<sup>6</sup>. For example, the observed primordial  $^4\text{He}$ ,  $Y$ , leads to constraints on the number of light ( $M_e \leq 1\text{ MeV}$ ) neutrino types<sup>7,8</sup>. Detailed big-bang nucleosynthesis calculations relates  $Y$  to the present baryon density,  $\rho_B$ , which is at the very least a lower limit to the universe density,  $\rho$ . The exact relationship between  $Y$  and  $\rho_B$  is weakly dependent on the neutron half life and we have used  $\tau_n$  of 10.61 min (ref. 9). The deuterium density decreases with increasing baryon density thereby setting a  $\rho_B$  upper bound from D/H lower bound. In addition,  $Y$  increases with increasing  $\rho_B$ , and the observational limit,  $Y \leq 0.25$  and the fact that at least three neutrino flavours exist also sets an upper limit<sup>7,8</sup> on  $\rho_B$ . The fact that both D and  $Y$  measurements argue against large  $\rho_B$  coupled with the fact that these arguments are rather insensitive to baryon density fluctuations<sup>10,11</sup> further supports the big-bang model. Kazanas *et al.*<sup>2</sup> and Gott *et al.*<sup>1</sup> achieved their restrictive limits on  $T_U$  by equating the nucleosynthesis constrained  $\rho_B$  with the  $\rho$  implied by galactic dynamics. Here by allowing for non-zero mass neutrinos  $\rho > \rho_B$  is possible. The resulting age constraints are somewhat relieved but are still significant.

Globular cluster ages,  $T_{GC}$ , independently determine  $T_U$  and it has been found that  $T_{GC}$  may be written in terms of the primordial stellar helium abundance and their metal abundances,  $Z$ . The result from stellar evolution models is<sup>12</sup>:

$$\log_{10} T_{GC} \approx 0.035 + 2.085(0.3 - Y) - 0.034(\log_{10} Z + 3) \quad (1)$$

where  $10^{-3} \leq Z \leq 10^{-4}$  and  $T_{GC}$  is in 10 Gyr units. The range for  $Z$ , following Iben<sup>12</sup>, encompasses metal poor clusters ( $Z \sim 10^{-4}$ ) to clusters where turnoff ages indicating young stars are observed ( $Z \geq 10^{-3}$ ). The  $Y$  uncertainty will be discussed elsewhere. Carney<sup>13</sup> has recently calculated globular cluster ages by comparing effective temperatures of main sequence turnoff points with model isochron results and he has compared his results with the evolutionary isochrons of other workers. When these results are normalized to the proper  $Y$  and  $Z$  values they are in good agreement with equation (1). We assume a negligible time interval between the big bang and cluster formation.





**Fig. 1** The age of the Universe,  $T_U$  plotted against the primordial helium abundance,  $Y$ . The vertical line representing  $Y = 0.25$  corresponds to the  $Y$  upper limit. The globular cluster ages are bracketed by their metal abundance,  $10^{-4} \leq Z \leq 10^{-3}$ . The constant density line,  $\Omega = 0.04$ , represents a lower limit to the total Universe density and  $H_0 = 40$  ( $\text{km s}^{-1} \text{Mpc}^{-1}$ ) represents the lower limit on the Hubble constant. The maximum allowed Hubble constant is found to be  $68$  ( $\text{km s}^{-1} \text{Mpc}^{-1}$ ).

The third independent calculation of  $T_U$  involves a Friedmann model using zero cosmological constant ( $\Lambda = 0$ ) representing a homogeneous isotropic universe presently matter dominated with negligible pressure. One can write:

$$T_U = F(\Omega)H_0^{-1} \quad (2)$$

where  $H_0$  is the Hubble constant and  $F(\Omega)$  is a monotonically decreasing function of  $\Omega$ , where  $\Omega = \rho/\rho_c = 8\pi\rho GH_0^{-2}/3$  (an exact description of  $F(\Omega)$  is given in ref. 1). The density parameter,  $\Omega$ , determines whether the Universe is open ( $\Omega \leq 1$ ) or closed ( $\Omega > 1$ ).

As pointed out by Kazanas *et al.*<sup>2</sup> precise values for the quantities necessary for  $T_U$  through the three methods—production and element abundance ratios for nucleocosmochronology,  $Y$  and  $Z$  for globular clusters, and  $H_0$  and  $\rho$  (or  $\Omega$ ) for Friedmann calculations—would enable exact independent  $T_U$  determinations which could then be compared for consistency. Unfortunately none of the sets of quantities is known precisely and hence it is more useful to explore the range of the parameters that intersect  $T_U$  domains for a consistent age. A non-zero intersection will restrict  $T_U$  whereas a null intersection suggests a model flaw and forces one to question some of our basic astrophysical theories.

The calculation is most easily shown by plotting  $T_U$  against  $Y$  (Fig. 1). We expect a firm upper limit of  $Y$  to be 0.25 and a possible lower limit of 0.20. This range follows from Yang *et al.*<sup>7,8</sup> who pointed that a  $Y$  value between 0.20 and 0.25 seems to be emerging from various experimental and theoretical determinations based on quite different input physics and assumptions. Recent measurements of population II subdwarfs indicating<sup>14</sup>  $Y \sim 0.19 \pm 0.04$  falls into this range within its uncertainty. However, it does cause concern in that the lower limit of 0.20 may be too restrictive.

From galaxy dynamics<sup>15</sup> the probable limits for the total density parameter are  $0.04 \leq \Omega \leq 0.4$  whereas the baryon lower bound is  $\Omega_B \geq 0.001$  obtained from the local stellar neighbourhood<sup>16</sup> or from the extremes of the mass implied for central regions of galaxies.

The previous calculation of Kazanas *et al.*<sup>2</sup> assumed a two neutrino standard big-bang model, that is the electron and muon neutrinos contributed to the radiation dominated early Universe density. The standard model now assumes three massless neutrinos because of the discovery of the  $\tau$  lepton<sup>17</sup>. Even though the current experimental upper limit<sup>18</sup> of the  $\nu_\tau$  mass is 250 MeV, which does not qualify as low mass for big-bang

nucleosynthesis calculations, the  $\nu_\tau$  is expected to be of low mass. Astrophysical constraints require it to be either very low mass and long lived or to have a mass  $\geq 10$  MeV and a lifetime  $\leq 10^3$  s (refs 19, 20).

Figure 1 shows  $T_U$  plotted against  $Y$  for the standard  $3\nu$  model. If  $\Omega = 0.04$  is an accurate lower limit and if it represents a baryon density then no concordant age is found. Even if 1 Gyr was allowed between the big bang and cluster formation no consistent age would be found. Thus if  $\nu_\tau$  is a low mass or massless neutrino then  $\Omega_B$  must be less than the lower limit on  $\Omega$ . This means that the bulk of the mass of the Universe would not be in the form of 'normal' baryonic matter. The most obvious alternative form is lepton matter. The recent reports of neutrino masses reported by Reines<sup>21</sup> and the scales of neutrino clustering with galaxies are consistent with this<sup>22</sup>. In fact one could argue that this discrepancy almost requires that neutrinos have mass or that some other form of nonbaryonic matter exist.

It is also interesting that the maximum allowed Hubble constant is  $68 \text{ km s}^{-1} \text{Mpc}^{-1}$ . This conclusion is independent of the neutrino/baryonic mass ratio and derives only from the upper limit on  $Y$  and the globular cluster age consistency. This is true even in a lepton dominated universe as equation (2) requires  $\Omega (\geq \Omega_B) \leq 1$  and as a result for a given  $T_U$ ,  $H_0$  may only be lower than  $H_0$  calculated for a baryon dominated universe because  $F(\Omega) \leq F(\Omega_B)$ . This  $H_0$  upper limit conflicts with claims<sup>23</sup> of  $H_0 \sim 100 \text{ km s}^{-1} \text{Mpc}^{-1}$ . If  $H_0$  were unequivocally shown to be large then the standard globular cluster age calculations and the assumption that the cosmological constant is zero would be questioned. However, the difficulties in direct measurements at  $H_0$  suggest that there is no need to question such assumptions at present. It is probable that observationally  $H_0 \geq 40 \text{ km s}^{-1} \text{Mpc}^{-1}$ . This limit crosses the globular cluster ages at  $\rho_B \sim 1.7 \times 10^{-32} \text{ g cm}^{-3}$  and  $\Omega_B \sim 0.0053$  implying that  $Y \geq 0.135$  and  $T_U \leq 24$  Gyr. The aforementioned baryon density bound,  $\Omega_B \geq 0.001$ , is not very restrictive as such a constant density line would not intersect globular cluster ages until well above 25 Gyr. Likewise, the  $\Omega < 0.4$  bound is not restrictive as  $T \leq 0.25$  already requires  $\Omega_B \leq 0.1$  (ref. 22). Likewise any  $\Omega$  upper bound greater than 0.4 which may arise from lepton density considerations would not be restrictive.

The existence of a massive neutrino allows for a large lepton contribution to the Universe density and hence a lower baryon density (and lower  $Y$ ) is possible. In fact, should neutrinos dominate the Universe density, which would be the case for a neutrino mass of a few electron volts<sup>22</sup>, then the  $T_U/Y$  relationship is broken as we have assumed  $\Omega_B$  to be the dominant fraction of  $\Omega$  in relating  $T_U$  to  $Y$ . Then, the aforementioned  $T_U \leq 24$  Gyr would be the upper limit. We recognize that nucleocosmochronology coupled with a galactic evolution model set an upper bound of 20 Gyr and is more restrictive than this but we hesitate to use the 20 Gyr bound because of the uncertainties in the galactic evolution models. Significantly the 20 Gyr limit straddles the allowed range for  $Y$  and its credibility is also strengthened by the fact that the mean age of the elements normalized by the duration of nucleosynthesis has been found to be approximately constant for several galactic models<sup>4</sup>.

If the  $\tau$  neutrino should be discovered to be massive ( $\geq 1$  MeV) then the standard big-bang model should include only two neutrinos contributing to the early Universe density. The electron and muon neutrino model allows for a consistent age of 13.8–15.8 Gyr assuming  $\Omega_B = \Omega \geq 0.04$ . This restricts  $0.237 \leq Y \leq 0.250$  and constrains the maximum Hubble constant to  $64 \text{ km s}^{-1} \text{Mpc}^{-1}$ . There would be no consistent age should  $Y < 0.237$  or  $\Omega_B > 0.18$ . If we allow for a lepton dominated universe in this case as well and extend the lower bound to  $Y > 0.13$  then one again finds  $T_U \leq 24$  Gyr.

We have shown that there is no consistent age in the standard cosmological model if the  $\tau$  neutrino has a mass  $< 1$  MeV unless the density of the universe is significantly greater than the baryon density. Such a result argues for an earlier suggestion<sup>22</sup> that neutrinos having masses of the order of tens of electron volts. Regardless of the mass of  $\nu_\tau$  and the mass of neutrinos in

general we re-emphasize that no consistent solution exists between standard globular cluster models and high values of the Hubble constant. If  $H_0$  were shown observationally to be  $\geq 70 \text{ km s}^{-1} \text{ Mpc}^{-1}$ , then either standard globular cluster calculations must be seriously in error or else there must be a cosmological constant so that  $H_0^{-1}$  is no longer an upper limit for  $T_U$ .

Allowing for  $\rho$  to be  $\gg \rho_B$  we find that the consistent age is

$$13.8 \text{ Gyr} \leq T_U \leq 24 \text{ Gyr}$$

If  $\rho_B = \rho$  then consistent solutions are only possible if  $M(\omega_\tau) > 1 \text{ MeV}$  which from ref. 18 would require  $M(\nu_\tau) > 10 \text{ MeV}$  and  $\tau(\nu_\tau) \leq 10^3 \text{ s}$ . If these constraints are satisfied then the consistent age is similar to that of Kazanas *et al.*<sup>2</sup> and is,

$$13.8 \text{ Gyr} \leq T_U \leq 15.8 \text{ Gyr}$$

If neutrinos are shown to have electron volt masses then we are forced to conclude  $\rho > \rho_B$  and the less restrictive age limits result.

We thank Keith Olive, Jim Fry, and Gary Steigman for useful discussions. This work was supported by NASA grant NSG 7212.

Received 27 May; accepted 28 August 1980.

- Gott, J. R., Gunn, J. E., Schramm, D. N. & Tinsley, B. M. *Astrophys. J.* **194**, 543–553 (1974).
- Kazanas, D., Schramm, D. N. & Hainebach, K. *Nature* **274**, 672–674 (1978).
- Schramm, D. N. & Symbalisty, E. M. D. *Rep. Prog. Phys.* (in the press).
- Hainebach, K. & Schramm, D. N. *Astrophys. J.* **212**, 347–359 (1977).
- Alpher, R. A., Bethe, H. & Gamow, G. *Phys. Rev.* **73**, 803 (1948).
- Schramm, D. N. & Wagoner, R. A. *Rev. Nucl. Sci.* **27**, 37–74 (1977).
- Yang, J., Schramm, D. N., Steigman, G., & Rood, R. T. *Astrophys. J.* **227**, 697–704 (1979).
- Shvartsman, V. F. *JEPT Lett.* **9**, 184–186 (1969).
- Christensen, C. J., Nielsen, A., Bahnsen, A., Brown, W. K. & Rustad, B. M. *Phys. Rev. D*, **5**, 1628–1640 (1972).
- Harrison, E. R. *Astr. J.* **73**, 533–534 (1968).
- Epstein, R. I. & Petrosian, V. *Astrophys. J.* **197**, 281–284 (1977).
- Iben, I. A. *Rev. Astr. Astrophys.* **12**, 215 (1974).
- Carney, B. W. *Astrophys. J. Suppl.* **42**, 481–500 (1980).
- Carney, B. W. *Astrophys. J.* **223**, 877–887 (1979).
- Faber, S. M. & Gallagher, J. S. A. *Rev. Astr. Astrophys.* **17**, 135–188 (1979).
- Peebles, P. J. E. *Lecture Notes for the 1979 Les Houches Summer School* (Reidel, Dordrecht, in the press).
- Perl, M. L. *et al. Phys. Lett.* **63B**, 466 (1976).
- Wolf, G. *Selected Topics on  $e^+e^-$  Physics* 38 (DESY Rep. 80/13, 1980).
- Gunn, J. E., Lee, B. W., Lerche, I., Schramm, D. N. & Steigman, G. *Astrophys. J.* **223**, 1015–1031 (1978).
- Falk, S. & Schramm, D. N. *Phys. Lett.* **79B**, 511–513 (1978).
- Reines, F. *et al. Phys. Rev. Lett.* (in the press).
- Schramm, D. N. & Steigman, G. Preprint No. 80–20 (Enrico Fermi Institute, 1980).
- de Vaucouleurs, G. & Bollinger, B. *Astrophys. J.* **233**, 433–452 (1979).

## Brightening of a hot spot in NCG2903

P. Laques, J.-L. Nieto, J.-L. Vidal, A. Augé & R. Despiaud

Observatoires du Pic du Midi et de Toulouse (Laboratoire Associé au CNRS n° 285), 65200 Bagnères de Bigorre, France

The nuclear region of the Sc galaxy NGC2903 exhibits a very chaotic structure with eight knots, described by Sandage<sup>2</sup> as “giant H II regions”. Others<sup>3,4</sup> called these knots ‘hot spots’. This nuclear region has a very strong blue and UV emission<sup>5–7</sup> and is a 1,420-MHz radio source<sup>8</sup>. Oka *et al.*<sup>1</sup> made photographic and spectroscopic observations of the central region, giving magnitudes and colour indices for the knots which they designated a–g. Physical conditions and stellar content of the 3-arc s central region were investigated by Alloin<sup>10</sup> whereas Turnrose<sup>11</sup> analysed the stellar population in the knot c. The nucleus was identified on near IR photographs<sup>9</sup>. During high resolution—broad band and narrow band—photometric studies of the central region of NGC2903, we have observed and report here that one of the knots (a, according to Oka *et al.*<sup>1</sup>) appears 1.3 mag brighter on plates taken in February 1980 than on a plate taken in January 1978, which agrees with other observations taken<sup>1</sup> in 1966–68.

Our observational material is described in Table 1. The 1978 plate was taken with the Griboval electrographic camera on the 30-inch reflector at the McDonald Observatory. Two other plates (167 P5 and 167 P6) were taken at Pic du Midi Observatory with the 20-mm Lallemand camera attached to the 106-cm reflector on 13 February 1980 as well as a test plate (167 P8) to correct for the S 20 photocathode inhomogeneities. On plates 167 P5 and 167 P6 the knot appeared brighter than on the McDonald plate by between 1 and 1.5 mag. On 18 March, knot a was observed visually with the camera eyepiece to be roughly as bright as the others, whereas in February the object was visually much brighter. The nuclear region as it appeared in January 1978 (McDonald plate with no filter) and in February 1980 (Pic du Midi plate 167 P6 with a V filter) is shown in Fig. 1. de Vaucouleurs has estimated from an electrographic B plate taken on 28 March, 1979 with the 76-cm McDonald reflector that the brightness of spot a was then about the same as in 1978.

The four plates mentioned above were scanned with the PDS microdensitometer at Nice Observatory. The field of the McDonald plate (15 arc min) allowed a reduction procedure following the numerical mapping technique<sup>12</sup> adapted to the interactive CDCA system<sup>13</sup>. The small field of the Lallemand plates (2.5 × 4 arc min) compared with the size of the galaxy did not allow such a procedure and only correction for the inhomogeneities of the photocathode was possible. Thus, the sky density was assumed to be constant and determined in one of the galaxy-density-free corner of the plates. Linearity between plate densities and light intensities were assumed on all plates after checking that densities were in the commonly adopted linear part of the characteristic curves of electrographic plates ( $d < 3$ ). The zero point for the magnitudes was obtained from the integrated V magnitudes measured in various apertures by

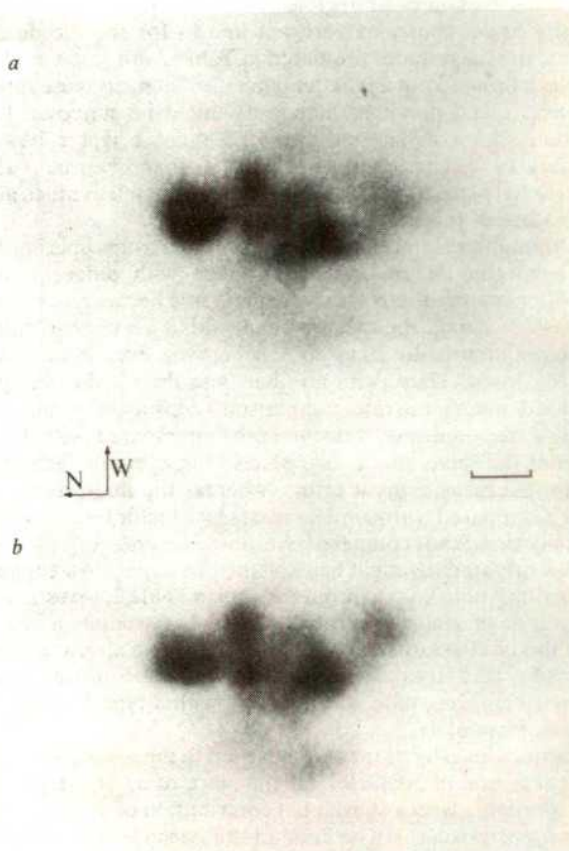


Fig. 1 Nuclear region of NGC2903. a, Pic du Midi plate taken with the Lallemand electrographic camera on 13 February 1980, with a V filter. b, McDonald plate taken with the Griboval electrographic camera on 31 January 1978 with no filter, a is the northernmost knot. Scale bar, 5 arc s.



Table 1 Observational material

| Plate  | Date             | Camera    | Telescope aperture (cm) | Emulsion           | Filter   | Exposure time (min) |
|--------|------------------|-----------|-------------------------|--------------------|----------|---------------------|
| GC1218 | 31 January 1978  | Griboval  | McDonald 76             | Electro Image Film | No       | 30                  |
| 167 P5 | 13 February 1980 | Lallemand | Pic du Midi 106         | Ilford G5          | [O III]* | 30                  |
| 167 P6 | 13 February 1980 | Lallemand | Pic du Midi 106         | Ilford G5          | V        | 10                  |

\* Centred on 5,000 Å with FWHM of 100 Å.

Table 2 Magnitudes and intensity ratios of the brightest knots

| Knot | Okayama plates (1966–68) |                 | Griboval plates (31 January 1978) |                 | Pic du Midi V plate (13 February 1980) |                 | Pic du Midi [O III] plate (13 February 1980) |                 |
|------|--------------------------|-----------------|-----------------------------------|-----------------|--|-----------------|--|-----------------|
|      | Magnitudes V             | Intensity ratio | Magnitudes                        | Intensity ratio | Magnitudes V                           | Intensity ratio | Magnitudes                                   | Intensity ratio |
| a    | 14.2                     | 1               | 14.0                              | 1               | 12.7                                   | 1               | —  | 1               |
| c    | 14.3                     | ~0.9            | 14.2                              | 0.83            | 13.9                                   | 0.33            | —  | 0.33            |
| d    | 14.8                     | ~0.6            | 15.0                              | 0.40            | 14.6                                   | 0.18            | —  | 0.18            |

photoelectric photometry, for plate 167 P6, taken with a V filter, as well as for the McDonald plate, taken with no filter. For the latter, this procedure does not lead to a strong error as most of the central intensity of the galaxy comes from the knots which have very similar colour indices ( $B-V \sim 0.4-0.5$ ) (see ref. 1). Unfortunately for the [O III] plate, no absolute calibration can be derived. The derived V magnitudes may have errors of 0.1–0.2 mag. Note that Oka *et al.*'s V measurements for knots a and c correspond respectively to  $5 \times 6$  arc s and  $4 \times 5$  arc s elliptical regions whereas ours correspond respectively to  $5 \times 5$  arc s and  $4 \times 4$  arc s circular regions. As the variations of the sky density under the galaxy are not known for the Pic du Midi plates, the magnitudes presented in Table 2 are just a guide, so the variation of knot a is better perceived intensity-wise relative to knots c and d, whose luminosity might be supposed to be constant: knot a has become ~2.3 times brighter between January 1978 (possibly even March 1979) and February 1980. The [O III] plate corroborates this but cannot tell us much about the nature of this luminosity variation.

Although the knots have an emission spectrum superimposed on a continuum, measurements made with different detector/filter combinations are still comparable because, in one case at least (V band), the spectral bandwidth is very broad and the same as that used by Oka *et al.*<sup>1</sup> Moreover, even in the case of the McDonald plate (with no filter) and the Pic du Midi plate (with a V filter), the intercomparison keeps its full significance because the intensity ratio of knot c compared with knot d remains the same for the two plates (and even for Oka *et al.*), within the measurement errors, whereas the intensity ratio of knot a compared with c or d increases by a factor (~2.3) which is actually significant compared with these errors.

This brightening might be explained by supernova explosion occurring within knot a. From the data in Table 2, we estimate V magnitude of such a supernova at ~13.1. Assuming a distance modulus of 29.43 (distance 7.7 Mpc)<sup>14</sup> gives an absolute magnitude of -16.5 after correction for absorption in our Galaxy ( $A_v = 0.17$ ). This value is compatible with a type II supernova near maximum<sup>15</sup>.

Previous investigations<sup>1,10,11</sup> have led to the description of the nuclear region of NGC2903 as the place of an active phase of star formation with a substantial contribution of young massive stars ionizing the gas. The knot a itself because of its off-centre position was missed in all relevant observations, but we may assume that these considerations are also valid for knot a as well as for hot spot nuclei in general<sup>9-11,16-20</sup>. Therefore, the explosion of a supernova would not be surprising in such a region. Only a few examples are known of supernova phenomena in central regions of galaxies (for example, SN1885 in M31, SN1968 in M83 (ref. 21)). This might be due to

observational bias because an exploding object is harder to detect in a high-surface brightness region, but is probably more frequent than believed. We therefore suggest routine observations of such hot spots to investigate whether such brightenings are the result of supernova outbursts or hot spots are intrinsically variable objects. We hope that other observations of the nuclear region of NGC2903 in 1979–80 will be found to reconstruct the history of this event.

J.-L. N. thanks P. Griboval for the use of the electronographic camera on the McDonald 76-cm telescope. We also thank G. de Vaucouleurs for information on the McDonald electronographic plate taken in March 1979.

Received 26 August; accepted 26 September 1980.

- Oka, S., Wakamatsu, K., Sakka, K., Nishida, M. & Jugaku, J. *Publ. astr. Soc. Jap.* **26**, 289–298 (1974).
- Sandage, A. R., *The Hubble Atlas of Galaxies* (Carnegie Institution of Washington, Washington DC, 1961).
- Sérsic, J.-L. & Pastoriza, M. *Publ. astr. Soc. Pacif.* **79**, 152–155 (1967).
- Sérsic, J.-L. *Publ. astr. Soc. Pacif.* **85**, 103–104 (1973).
- Tift, W. G. *Astr. J.* **66**, 390–404 (1961).
- Tift, W. G. *Astr. J.* **74**, 354–365 (1979).
- de Vaucouleurs, G. *Astrophys. J. Suppl.* **5**, 233–289 (1961).
- Lequeux, J. *Astr. Astrophys.* **15**, 30–41 (1971).
- Prabhu, T. P. *Astrophys. Space Sci.* **68**, 519–523 (1980).
- Alloin, D. *Astr. Astrophys.* **27**, 433–448 (1973).
- Turnrose, B. E. *Astrophys. J.* **210**, 33–57 (1976).
- Jones, W. B., Obbits, D. L., Gallet, R. M. & de Vaucouleurs G. *Publ. astr. Dept Univ. Tex., Austin, Ser II, Vol. 1* (1967).
- Davoust, E., Nieto, J.-L. & Paturel, G. *Colloq. Photométrie Bidimensionnelle*, Toulouse (in the press).
- de Vaucouleurs, G. *Astrophys. J.* **227**, 729–755 (1979).
- Barbon, R., Ciatti, F. & Rosino, L. *Astr. Astrophys.* **72**, 287–292 (1979).
- Tift, W. G. *Astr. J.* **68**, 302–318 (1963).
- Alloin, D. *Astr. Astrophys.* **33**, 337–342 (1974).
- Alloin, D. & Sareyan, J.-P. *Astr. Astrophys.* **33**, 331–336 (1974).
- Alloin, D. & Kunth, D. *Astr. Astrophys.* **71**, 335–343 (1979).
- Osmer, P. S., Smith, M. G. & Weedman, D. W. *Astrophys. J.* **192**, 279–291 (1974).
- Wood, R. & Andrews, P. J. *Mon. Not. R. astr. Soc.* **167**, 13–29 (1974).

## A nonrandom component in cosmic rays of energy $\geq 10^{14}$ eV

C. L. Bhat, M. L. Sapru & C. L. Kaul

Nuclear Research Laboratory, Bhabha Atomic Research Centre, Srinagar, India

We have been studying<sup>1</sup> the distribution of the arrival times of atmospheric Cerenkov light pulses, initiated by cosmic rays of energy  $\geq 10^{14}$  eV. We have now detected a nonrandom component for time separations  $< 40$  s, and here we discuss the possibility that it has a point-source origin.

The light pulses were detected at Gulmarg (altitude 2,743 m), India, on clear moonless nights, by two, coincidentally operating wide-angle photomultipliers (EMI 9545 B; viewing angle with respect to zenith,  $50^\circ$ ). Each Cerenkov light pulse, identified by its characteristic shape, was recorded with its occurrence time by a logic system with a dead-time of  $\leq 100$  ms. The amplitude discrimination levels of both the detector channels were held constant above the shot-noise fluctuations in the night-sky background light. The detection system was regularly checked with a standard light-pulsar to ensure that the photomultiplier and amplifier gains remained unaltered. Between June 1976 and June 1978 observations were possible for 180 h and 9,879 events were recorded, corresponding to an average rate of  $\sim 55$  events per h. The observed hourly rates show a fairly symmetrical scatter around this value.

Using all the data, we have plotted the arrival-time distribution of the events, that is, the distribution of time-separation  $t$  between consecutive events on a 10-s bin size (Fig. 1). The smooth curve shows the expected exponential distribution of the arrival times assuming that the time of occurrence of the events is completely random; the inset to Fig. 1 represents standard deviations of the frequencies of the events with respect to the fitted curve. Deviations at  $\geq 5\sigma$  are apparent for  $t \leq 40$  s, the implied overabundance constituting  $\sim 12\%$  of the total number of events.

The possibility that this overabundance was of instrumental origin was examined by subjecting the detection system to a random time-series simulation, in which the system photomultipliers were simultaneously exposed to light pulses from a pair

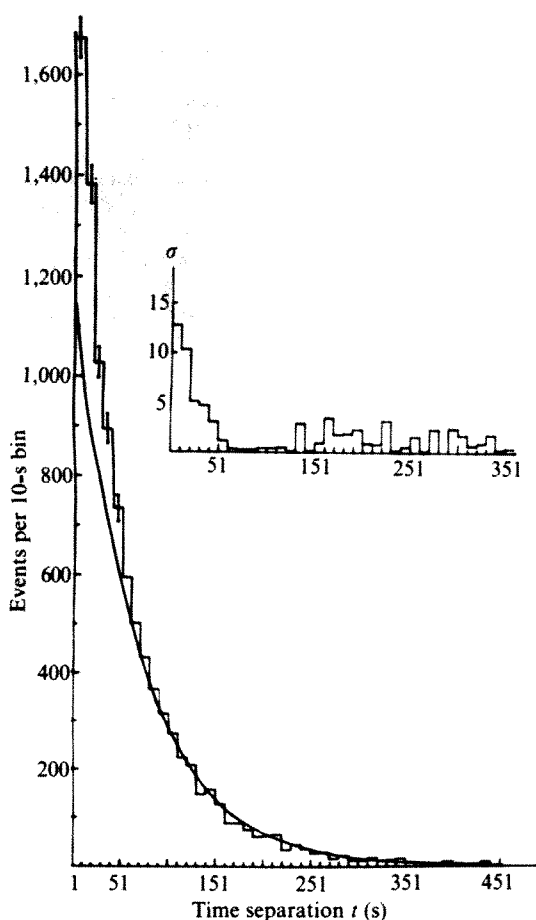


Fig. 1 The histogram shows the observed distribution of time separations,  $t$ , between consecutive events on a 10-s bin-size. Error bars up to  $t = 50$  s are also shown. The smooth curve is the exponential fit to this histogram. Standard deviations,  $\sigma$ , of the event frequencies with respect to the fitted curve are shown in the inset.

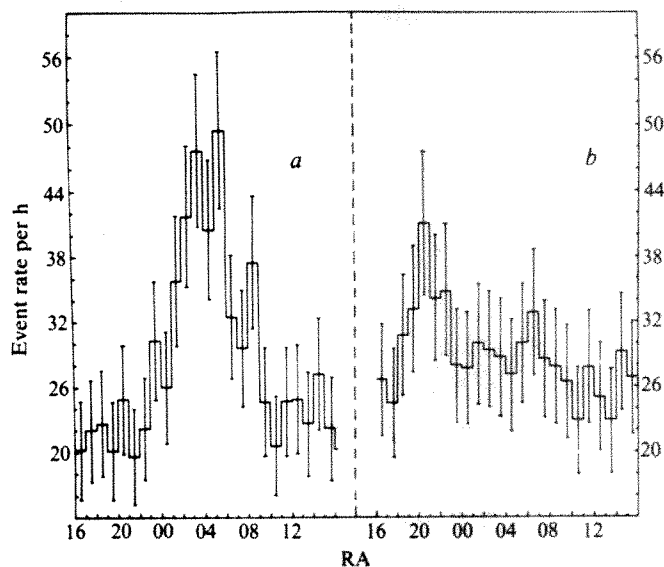


Fig. 2 *a* Shows the rate per h of events as a function of the RA values. Events with  $t \leq 40$  s only are included, *b*, Same as *a* except that events with time separations of 41–450 s alone are included in the distribution.

of LED lamps. The flashing rate of the lamps was so controlled by a random pulse generator that pulses with time separations of 1–500 s were possible. The output from the detection system in this case was found to reproduce quite accurately the expected exponential variation in time. Likewise, solar-terrestrial origin of the overabundance also seems improbable because the event rates did not exhibit systematic solar time variations and also because the arrival-time distributions for days of high and low values of the geomagnetic disturbance index  $A_p$ , when considered separately, reproduced the excess contribution for  $t \leq 40$  s to the same extent. Clearly, also, at these energies the effect cannot be understood in terms of the interplanetary magnetic field fluctuations. Furthermore, Baadino *et al.*<sup>2</sup>, following our earlier work<sup>1</sup>, have also observed a significant extra contribution for  $t \leq 37.5$  s in muons produced by cosmic-ray primaries of energy  $\sim 5 \times 10^{13}$  eV. Therefore, the observed excess is not peculiar to the optical method of detecting high-energy cosmic rays.

To find whether the observed excess has a sidereal association, the rates of two subsamples with  $t \leq 40$  s and  $40 < t \leq 450$  s, constituting 5,033 and 4,846 events, respectively, were plotted (Fig. 2) as a function of right ascension (RA), the RA value of an event being derived from its absolute occurrence time. It is clear that, whereas events with  $t > 40$  s do not show a directional preference (Fig. 2*b*), those with  $t \leq 40$  s, constituting the excess region, exhibit a statistically significant peak at  $RA = 05 \pm 03$  h (Fig. 2*a*). To investigate this association further, events with  $t \leq 40$  s were divided into two 1-year subsamples, and the directional enhancement at  $RA = 05 \pm 03$  h was observed in each of them separately. The large width of the peak in Fig. 2*a* is compatible with the response function of our wide-angle detection system for Cerenkov light from EAS<sup>3</sup>. The large angular response of the detection system was also responsible for our observation of a significant excess of events for  $t \leq 40$  s even for the period December 1978–January 1979, when, during a search for optical bursts from primordial black-hole explosions<sup>1,4</sup>, a similar experiment was carried out simultaneously at Gulmarg and 30 km away at Srinagar (altitude 1,524 m). Figure 3 shows the sidereal distribution of the event rates for  $t \leq 40$  s for the two data samples obtained from this experiment. It is apparent that the rates in both the samples show a clear rising trend beyond 22 h RA, which, if data beyond January 1979 were available, would probably reproduce the peak observed in Fig. 2*a* and so provide additional confirmation



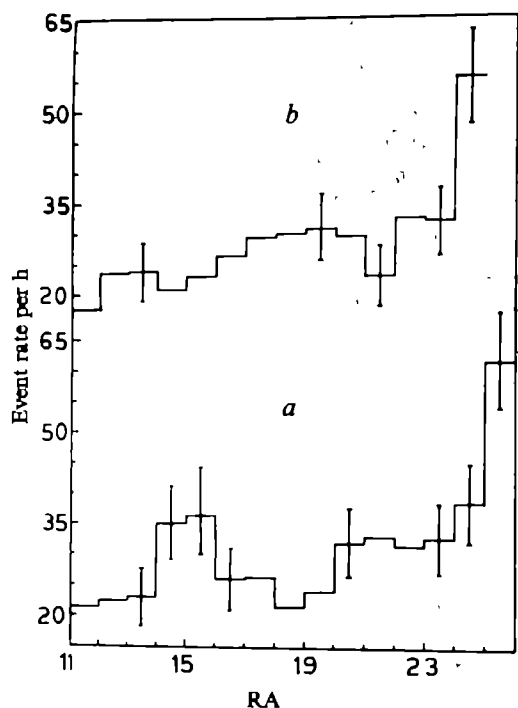


Fig. 3 Hourly rates of events with  $t < 40$  s as a function of RA for December 1978–January 1979. Data recorded at Gulmarg (a) and Srirangar (b).

regarding the sidereal association of the excess. In view of this, it is useful to determine whether this excess contribution is due to a high flux of  $>10^{14}$  eV charged particles or to  $\gamma$ -rays coming presumably from a cosmic source with  $RA \approx 05 \pm 03$  h.

For a cosmic-ray proton of energy  $>10^{14}$  eV, the gyro-radius in the galactic magnetic field is  $>0.03$  pc, which is quite small relative to the typical scale-lengths of the interstellar magnetic field irregularities, generally believed to be  $\sim 1$ – $100$  pc (ref. 5). According to the compound diffusion model<sup>6</sup>, a cosmic-ray proton follows the field lines for distances less than  $1$ – $100$  pc and is then transferred to other field lines in a random manner. Accordingly, charged particles coming from a galactic source, a

few kpc away, suffer scattering in the interstellar space and are not, therefore, expected to retain original source direction. On the contrary, one may, following Barrowes<sup>7</sup>, hypothesize that there are very few small-scale irregularities in the interstellar magnetic field in the direction of the source, so that charged primaries, gyrating around a quite well ordered magnetic field, reach us without undergoing sufficient randomization. The observed directional enhancement is, however, more easily understood if one assumes that the source is emitting  $\gamma$ -ray photons of energy  $>10^{14}$  eV, which the present detection system cannot distinguish from charged primaries. Several instances of discrete source anisotropies have been reported<sup>8,9</sup> including the point sources at  $RA = 6$  h, dec.  $\delta = 6^\circ \pm 1^\circ$  and at  $RA = 5$  h,  $\delta = 0.5^\circ$ .

If this view of the point-source origin of the excess contribution is valid, its time-structure will probably provide further information on the nature of the source. Accordingly, we plotted (Fig. 4a) the arrival-time distribution of events with RA values between 22 and 9 h only, which correspond to the abscissa limits of the peak in Fig. 2a. The distribution of the arrival times of the excess events, plotted in Fig. 4b, shows a significant peak at  $\sim 4$  s, suggesting that there is a departure from time-randomness and that in the case of source events,  $t \sim 4$  s is more probable than smaller arrival times, conceivably a manifestation of some kind of modulation due to the source. Extensive theoretical work by Ostriker and Gunn<sup>10</sup> and others shows that indeed a rotating neutron star is capable of producing cosmic rays of energy  $>10^{14}$  eV. In view of this and the fact that the excess contribution peaks at  $\sim 4$  s, it is tempting to infer that the source may be the pulsar PSR 0525+21, which has a period of 3.7 s and lies at a distance of 1.6 kpc (ref. 11). If so, it may be argued that high-energy particles, probably  $\gamma$  rays, are emitted randomly in time from a restricted region on or near this pulsar. The effect of the pulsar rotation period of 3.7 s would be seen by an Earth-bound observer as an enhanced frequency for  $t$  near 3.7 s and its harmonics relative to the other arrival times, which would be reduced in frequencies depending on the angle of the emission cone. Obviously, the event rate from the source cannot depend on the pulsar rotation period alone but also depends on distance, intrinsic flux and other emission characteristics of the source.

One may surmise, alternatively, that intense particle bursts are emitted towards the Earth with the pulsar period of 3.7 s. As the observed average interval between consecutive events is  $\sim 1$  min, that is, nearly 16 pulsar periods, one would rule this out

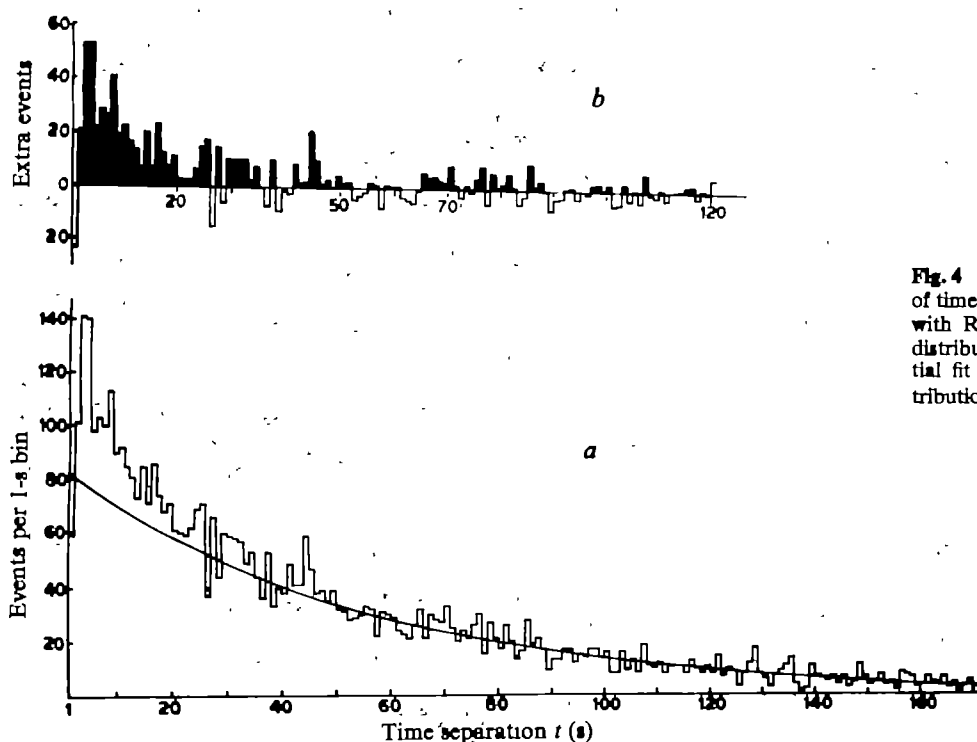


Fig. 4 a, The histogram shows the distribution of time separations,  $t$ , on a 1-s bin size. Events with RA values 22–9 h are included in this distribution. The smooth curve is the exponential fit to this distribution. b Shows the distribution of extra events obtained from a as a function of  $t$ .

unless an additional restriction is imposed that the bursting activity lasts only for a fraction of the total observing time. Further experiments in the Northern Hemisphere by air shower arrays and optical detection systems, designed with improved angular resolution and a bias towards photon-initiated showers, would be helpful in this connection.

Received 28 April; accepted 28 August 1980.

1. Bhat, C. L., Sarma, P. R., Sapru, M. L. & Kaul, C. L. *Proc. 16th Int. Cosmic Ray Conf.* **8**, 57 (1979).
2. Baadino, G., Galeotti, P., Periale, L. & Saavedra, O. Preprint (Laboratories di Cosmogeofisica del CNR, Torino, Italy, 1980).
3. White, J., Porter, N. A. & Long, C. D. *J. atmos. terr. Phys.* **20**, 40 (1961).
4. Bhat, C. L., Razdan, H. & Sapru, M. L. *Astrophys. Space Sci.* (in the press).
5. Allen, C. W. *Astrophysical Quantities*, 262 (Athlone, London, 1976).
6. Lingelfelter, R. E., Ramaty, R. & Fisk, L. A. *Astrophys. Lett.* **8**, 93 (1971).
7. Barrowes, S. C. *Proc. 12th Int. Cosmic Ray Conf.* **1**, 423 (1971).
8. Jokisch, H. & Carstensen, K. *Proc. 14th Int. Cosmic Ray Conf.* **2**, 575 (1975).
9. Sekido, Y., Yoshida, S. & Kamiya, Y. *Phys. Rev.* **113**, 1108 (1975).
10. Ostriker, J. P. & Gunn, J. E. *Astrophys. J.* **157**, 1395 (1969).
11. Groth, J. E. *Neutron Stars, Black-Holes and Binary X-Ray Sources* (eds Gursky, H. & Ruffini, R.) 119 (Reidel, Dordrecht, 1975).

## Extremely relativistic electron-positron twin-jets form extragalactic radio sources

W. Kundt

Institut für Astrophysik und Extraterrestrische Forschung der Universität Bonn, Auf dem Hügel 71, D-5300 Bonn, FRG

Gopal-Krishna\*

Max-Planck-Institut für Radioastronomie, Auf dem Hügel 69, D-5300 Bonn, FRG

The extended extragalactic double radio sources—quasars, BL Lac-type-objects (blazars), and radio galaxies—are commonly interpreted as synchrotron sources in which extremely relativistic electrons gyrate in enhanced magnetic fields. The detection of narrow emission bridges between hot spots inside these sources and the centre of an intermediate galaxy has strongly favoured the existence of a continuous power-line feeding the extended source<sup>1,3,5</sup>. Such beams may be a universal phenomenon occurring in many—if not all—massive galaxies, including our own<sup>4</sup>. But whereas early interpretations involved low-frequency electromagnetic waves and/or relativistic particle beams, more recent work favoured non-relativistic ( $\beta < 10^{-1}$ ) (refs 3, 6–8), or mildly relativistic ( $\gamma < 10$ ) (refs 9–11) bulk velocities for the power supply. In particular, non-relativistic bulk velocities  $c\beta$  have been derived from estimates of the involved kinetic energy densities  $u$  and mass densities  $\rho$  in the form  $\beta \approx (2u/\rho)^{1/2}$ . This can lead to large underestimates of  $\beta$  when  $\rho$  is derived from Faraday rotation and depolarization data, because the observed jets are likely to have a two-fluid structure, with light relativistic plasma streaming inside of heavy ‘walls’ of thermal matter, or traversing ‘swarms’ of heavy quasistatic filaments<sup>12</sup>. We suggest here that these beams consist of extremely relativistic electrons and positrons, of typical Lorentz factor  $\gamma \geq 10^2$ .

The power streaming in the jets must be liberated inside the galactic nucleus, from matter spiralling into the central powerhouse. This power  $\dot{E}_{\text{lobes}}$  should be a small fraction  $\eta$  ( $\ll 1$ ) of the total liberated power  $\dot{E}_{\text{tot}}$  because of its comparatively low entropy. The power  $\dot{E}_{\text{tot}}$  in turn is a small fraction  $\epsilon$  ( $< 1$ ) of the accreted mass-energy rate  $\dot{M}_{\text{in}}c^2$ , where  $\epsilon \leq 0.1$  is suggested by black-hole models whereas hydrogen burning<sup>13</sup> (of  $\leq 20\%$  of the fuel) amounts to  $\epsilon \leq 2 \times 10^{-3}$ . The rest mass rate  $\dot{M}_{\text{lobes}} = \dot{E}_{\text{lobes}}/(\gamma - 1)c^2$  injected into the lobes cannot exceed the fuel-

ling rate  $\dot{M}_{\text{in}}$ , hence

$$1 < \dot{M}_{\text{in}}/\dot{M}_{\text{lobes}} = (\gamma - 1)/\epsilon\eta \quad (1)$$

or  $\gamma > 1 + \epsilon\eta$ ; which would imply, for non-relativistic values of  $\beta = (1 - \gamma^{-2})^{-1/2}$ :

$$\beta > (2\epsilon\eta)^{1/2} = 1.4 \times 10^{-2}(\epsilon\eta/10^{-4})^{1/2} \quad (2)$$

that is slow bulk speeds  $c\beta$  of the beam material imply a small ‘beaming efficiency’  $\eta$ . But  $\eta$  is likely to be above  $10^{-2}$ . To see this, note that  $\dot{E}_{\text{lobes}}$  can exceed the luminosity  $L_{\text{lobes}}$  of the lobes when most of the beam energy is stored in relativistic gyrations, and that a substantial fraction of  $L_{\text{lobes}}$  can be emitted near optical frequencies<sup>14</sup>, whereas the compact nuclear source is expected to emit its excess energy instantaneously as high surface-brightness electromagnetic radiation, mainly between IR and  $\gamma$ -ray energies. We thus have

$$\eta = \dot{E}_{\text{lobes}}/\dot{E}_{\text{tot}} \geq L_{\text{lobes}}/L_{\text{core}} = 10^{-2 \pm 2} \quad (3)$$

the latter for well-studied sources like 3C273, Cen A, Cyg A, and from source statistics. Equation (2) then implies beam particle velocities in excess of  $10^9 \text{ cm s}^{-1}$ .

A second estimate of  $\beta$  derives from the speed at which the lobes of double sources separate. This speed has been estimated from the core-hot spot separations<sup>15,16</sup> to be of the order of  $v_r = 10^{-1 \pm 0.3}c$ . Similar values for  $v_r$  can be obtained from force balance calculations<sup>12</sup>. The flow inside the jets must reach the outer ends of the radio lobes, hence its velocity must exceed  $v_r$ .

The flow inside the (almost free) jets is expected to be supersonic, although it must go subsonic at its termination point. Consequently,  $v_r$  is even a lower limit on the sound speed of the hot-spot material, whose temperature  $T_+$  must therefore exceed  $m v_r^2/3k \geq 10^{10} \text{ K}(m/10^{-24} \text{ g})$ . Were the jets subsonic,  $T_+$  would at the same time be a lower limit to the jet temperature. For a supersonic jet, on the other hand, there must be an inner shock surface towards the ambient medium where the flow passes from supersonic to subsonic. One can then relate the post-shock temperature  $T_+$  to the pre-shock temperature  $T_-$  and get a more severe lower limit to the jet velocity.

If we assume that the jet velocity were sub-relativistic, its pre-shock sound speed  $v_{s,-}$  would be related to its post-shock sound speed  $v_{s,+}$  by<sup>17</sup>

$$v_{s,-}/v_{s,+} \approx [(\Gamma + 1)/(\Gamma - 1)]^{1/2}(p^-/p^+)^{1/2} \quad (4)$$

where  $p^\pm$  are the pressures before and behind the shock respectively, and  $\Gamma$  is the adiabatic index. The pressure ratio  $p^+/p^-$  is unlikely to exceed 30; it can be estimated from the brightness ratio at different parts of the hot spot: In a few cases, a scintillating component has been found inside the hot spot whose inferred pressure is about 10 times higher than that of its surroundings<sup>18,19</sup>. For  $\Gamma \leq 5/3$ , equation (4) therefore yields  $v_{s,-}/v_{s,+} \geq 0.6$ . But  $v_{s,+}$  must exceed the post-shock flow velocity  $v^+$  which is larger than the lobe velocity  $v_r$ , hence  $v_{s,-} \geq 0.6 v_r \geq 0.06 c$ , corresponding again to a pre-shock temperature  $T_- \geq 10^{10} \text{ K}(m/10^{-24} \text{ g})$ . This lower limit conflicts with independent temperature estimates<sup>3</sup> ( $T_- \leq 10^7 \text{ K}$ ) of the jet material, that is excludes non-relativistic jet velocities. Also, adiabatic cooling in the jet would imply extremely relativistic temperatures near the origin.

Relativistic bulk velocities of the beam material are also suggested by the following independent observations whose details are discussed elsewhere<sup>12</sup>:

(1) Roughly half of the strongest compact extragalactic radio sources show intermittent superluminal expansion, on scales between 10 and  $10^2$  light yr, with apparent expansion speeds ranging up to  $40 c$  (for 3C454.3)<sup>20,21</sup>. These speeds must, of course, be phase velocities, but all reasonable models involve relativistic bulk velocities<sup>22</sup> of the beam material.

(2) In most cases, the observed jets are one-sided, both in radio, optical, and X rays. Even in sources with a large inclination angle of their axis, like Cyg A, the VLBI structure is one-sided<sup>21</sup>. Relativistic beaming is the only convincing explanation<sup>12</sup>.

\* Permanent address: Tata Institute of Fundamental Research, PO Box 8, Ootacamund-643001, India.



(3) The largest extragalactic radio sources<sup>23</sup> have unprojected tails of length  $r \geq 3 \times 10^7$  light yr, and their central engines are still active. A non-relativistic power supply would make the central engine very old, and its fuel demand very high.

(4) When a beam of magnetized plasma is blown into some ambient plasma, its hot-spot develops at the far end of the resulting jet only if its mass density is much lower than that of the surroundings. In the opposite case, the hot-spot develops at the near end. But a lower mass density implies a higher sound speed (than some  $10^8$  cm s<sup>-1</sup>), and an even higher (supersonic) bulk velocity.

(5) The beams of most sources are bent, in particular those of the head-tail galaxies. The standard explanation of bent beams uses ram pressure confinement<sup>5,7</sup>, in which case the bending angle is proportional to the bulk velocity of the power supply (for a given power). Non-relativistic supply velocities would in some cases ask for implausibly high ram pressures of the intergalactic medium.

(6) For non-relativistic power supply velocities, all the relativistic electrons in the jets and lobes would have to be accelerated *in situ*. According to the second law of thermodynamics, this is only possible for a small fraction of the total power.

(7) The observed stability of the (often curved!) jets, on length scales exceeding  $10^5$  light yr, poses problems for non-relativistic bulk velocities<sup>12</sup>.

We shall now suggest that the beams consist of electrons and positrons, with ions being energetically insignificant. Consider if there were no positrons, and  $n_e$  was the particle number density of the electrons,  $n_i$  the corresponding density of the (positive) ions. Charge neutrality in the beam implies  $n_e = n_i$ . The ratio  $\xi$  of energy densities in ions and electrons then reads

$$\xi = n_i \gamma_i m_i c^2 / n_e \gamma_e m_e c^2 \geq 1,836 \gamma_i / \gamma_e \quad (5)$$

where  $\gamma_i$ ,  $\gamma_e$  are the average Lorentz factors of ions and electrons respectively.  $\xi$  should not exceed unity by much because the power stored in ions is invisible, and the lobe power  $\dot{E}_{\text{lobes}}$  inferred from the synchrotron radiation of the electrons ought to stay significantly below the core power  $\dot{E}_{\text{core}}$  not to violate the second law of thermodynamics, see equation (3). But then equation (5) implies large Lorentz factors for the electrons:  $\gamma_e \geq 2 \times 10^3 \gamma_i$ , larger than inferred from equipartition estimates for the energetic peak of the electron distribution. In other words, if the charge of the electrons were neutralized by the charge of ions, the necessary inequality  $1 \gg \eta = \dot{E}_{\text{lobes}} / \dot{E}_{\text{core}}$  would be violated, either by a power excess in the ions, or by a significant deviation from equipartition (between magnetic and electron kinetic energy).

This argument can be strengthened by interpreting the frequent and pronounced one-sidedness of the jets as being due to extreme bulk velocities ( $\gamma_{\text{bulk}} \geq 10^2$ ) of the electrons radiating when their path is obstructed<sup>12</sup>, rather than as being due to mildly relativistic motion at a small beam inclination angle: The bulk velocities of oppositely charged particles cannot differ by more than  $10^{-11} c$  ( $\dot{E}_{\text{lobes}} / 10^{44} \text{ erg s}^{-1}$ )<sup>1/2</sup> because their relative motion would otherwise generate higher than equipartition magnetic fields. Consequently, the bulk Lorentz factor of the electrons must equal  $\gamma_i$ , and the condition  $\gamma_e \geq 2 \times 10^3 \gamma_i$  would imply  $\gamma_e \geq 2 \times 10^5$ , that is extreme deviation from equipartition.

There are other indications of the near-absence of ions in the beams<sup>12</sup>; briefly they are:

(1) The direct supply of extremely relativistic electrons to the lobes avoids the difficulty of upgrading thermal energy of a mildly relativistic plasma to much higher energies of most of the electrons.

(2) No booster of two relativistic electron-ion plasma beams is known; the situation is different for an electron-positron plasma wave-riding a strong spherical wave, and focused by a magnetic pinch<sup>13</sup>.

(3) The smallness of observed Faraday rotation in compact sources rules out the presence of a significant fraction of low-

energy electrons, but does not rule out a neutral electron-positron plasma<sup>27</sup>.

(4) It has been suggested that the relativistic wind of the Crab pulsar consists of an extremely relativistic electron-positron plasma<sup>24,25</sup>. Galactic centre sources are likely to follow a similar working scheme<sup>13</sup>.

(5) The observed positron annihilation radiation from our galactic centre<sup>26</sup> is reported to exceed that likely to be injected by young pulsars by roughly two orders of magnitude. An active past of our galactic centre would yield a plausible interpretation.

Received 10 January; accepted 21 August 1980.

- Butcher, H. R., Van Breugel, W. & Miley, G. K. *Astrophys. J.* **235**, 749 (1980).
- Dufour, R. J. & Van den Bergh, S. *Astrophys. J.* **226**, L73 (1978).
- Schreier, E. J. *et al. Astrophys. J.* **234**, L39 (1979).
- Burton, W. B. & Liszt, H. S. *Astrophys. J.* **225**, 815; **226**, 790 (1978).
- Rees, M. J. *Nature* **275**, 516 (1978).
- Blandford, R. D. & Icke, V. *Mon. Not. R. astr. Soc.* **185**, 527 (1978).
- Begelman, M. C., Rees, M. J. & Blandford, R. D. *Nature* **279**, 770 (1979).
- Perley, R. A., Willis, A. G. & Scott, J. S. *Nature* **281**, 437 (1979).
- Scheuer, P. A. G. & Readhead, A. C. S. *Nature* **277**, 182 (1979).
- Blandford, R. D. & Königl, A. *Astrophys. J.* **232**, 34 (1979).
- Blandford, R. D. & Königl, A. *Astrophys. J.* **232**, 34 (1979).
- Kundt, W. & Gopal-Krishna *Astrophys. Space Sci.* (submitted).
- Kundt, W. *Astrophys. Space Sci.* **62**, 335 (1979).
- Bridle, A. H. & Fomalont, E. B. *Astr. J.* **84**, 1679 (1979).
- Longair, M. S. & Riley, J. M. *Mon. Not. R. astr. Soc.* **188**, 625 (1979).
- Banhatti, D. G. *Astr. Astrophys.* **84**, 112 (1980).
- Landau, L. D. & Lifshitz, E. M. VI (1966).
- Gopal-Krishna & Swarup, G. *Mon. Not. R. astr. Soc.* **178**, 265 (1977).
- Simkin, S. M. *Astrophys. J. Lett.* **222**, L55 (1978).
- Cotton, W. D. *et al. Astrophys. J. Lett.* **229**, L115 (1979).
- Pauliny-Toth, I. *5th European Regional IAU Meet., Liège* (1980).
- Blandford, R. D., McKee, C. F. & Rees, M. J. *Nature* **267**, 211 (1977).
- Reich, W., Stute, U., Reif, K., Kalberla, P. M. W. & Kronberg, P. P. *Astrophys. J. Lett.* **236**, L61 (1980).
- Kundt, W. & Krotscheck, E. *Astr. Astrophys.* **83**, 1 (1980).
- Kundt, W. *Am. N.Y. Acad. Sci.* **336**, 429 (1980).
- Leventhal, M., Mac Callum, C. J. & Stang, P. D. *Astrophys. J.* **225**, L11 (1978).
- Noerdlinger, P. D. *Phys. Rev. Lett.* **41**, 135 (1978).

## Flux tube dynamo approach to the solar cycle

Manfred Schüssler

Universitäts-Sternwarte, Geismarlandstraße 11,  
D-3400 Göttingen, FRG

In the past two decades dynamo models of solar activity and the physical foundations of the solar cycle have become acceptable. However, recent observations revealing the concentrated form of photospheric magnetic flux<sup>1</sup>, the distribution and cyclic appearance of X-ray bright points<sup>2,3</sup> and ephemeral active regions<sup>4</sup>, as well as the discovery of sunspot brightness variations during the solar cycle<sup>5,6</sup>, have raised some questions about the dynamo theory of solar activity<sup>7</sup>. Both observation and theory<sup>8</sup> suggest that most of the magnetic flux in the solar convection zone is in the form of concentrated isolated magnetic flux tubes. The turbulent dynamo theory<sup>9,10</sup> has, therefore, to be modified and attempts have been made to include concentrated fields<sup>11</sup>. Nevertheless, the dynamo problem for a convective medium pervaded by concentrated flux tubes, the 'flux tube dynamo', has not yet been solved. The problem is to regenerate the poloidal magnetic field out of which toroidal field is produced by differential rotation. Here the consequences and the structure of the resulting cycle are considered if a field regeneration process operating on flux tubes is assumed. A calculation similar to Leighton's magneto-kinematic model<sup>12</sup> shows that a flux tube dynamo model can operate and reproduce the essential features of the solar cycle. It can also explain the cyclic variation of sunspot brightness and ephemeral active regions.

I conjecture that the variation of sunspot brightness and appearance of ephemeral active regions (EAR) or X-ray bright points (XBP) is caused by different age of the basic flux tubes. If EAR are interpreted as products of 'shredding' of big flux tubes by violent convective motions, older flux tubes will suffer longer

from this influence than younger tubes. Consequently, they yield more EAR and some may be totally disrupted before they reach the photosphere. The effect of age on sunspot brightness is not as obvious because of the lack of a detailed theory of the deep structure and cooling of sunspots. As sunspots are already cool when they appear in the photosphere, the cooling 'machine' must work beneath it. A plausible mechanism is the formation of loops with subsequent adiabatic downflow within the solar convection zone through a convective instability. If this happens at the beginning of the tube's existence it will subsequently be heated by radiation (and possibly convection of reduced efficiency because of the magnetic field). The older a flux tube, the longer the time available for heat exchange: emerged older tubes will appear brighter than younger ones. If the convective instability happens in the upper (more superadiabatic) layers of the convection zone, the initial conditions depend on flux tube age: older tubes are more severely distorted and 'shredded' by convective motions and possibly the instability will not be as efficient in cooling as for younger tubes. Finally, distorted old tubes might produce more umbral dots after emerging as sunspots, leading to a brighter appearance of the umbra when observed with normal resolution.

As long as the subphotospheric cooling of magnetic flux is not well understood the above arguments are speculative. Nevertheless, convection causes old flux tubes to be physically different from young tubes and the above considerations suggest that they are less coherent and not as cool as younger tubes.

Age differences between flux tubes can arise as follows. Consider a shear region of strong differential rotation where toroidal flux is produced out of a poloidal magnetic field. The flux tubes built by this process leave the shear region due to their magnetic buoyancy depending on the magnetic field strength: stronger fields are more buoyant and rise faster. The stronger the poloidal field, the faster the toroidal field increases and the faster (and younger) the flux tube leaves the shear region<sup>13</sup>. If the poloidal field strength varies during the cycle, the age of the flux tubes which appear in the photosphere also shows a cyclic variation.

To study the value of the age hypothesis and to get some insight into the behaviour of a flux tube dynamo I have investigated a simple one-dimensional model.

Consider a sphere with a thin shear region due to differential rotation  $\partial\Omega/\partial r$ , idealized by a shell at  $r = r_1$ . In the axisymmetric case, the magnetic field in the shell only depends on the colatitude  $0 \leq x \leq \pi$  and time  $t$ .

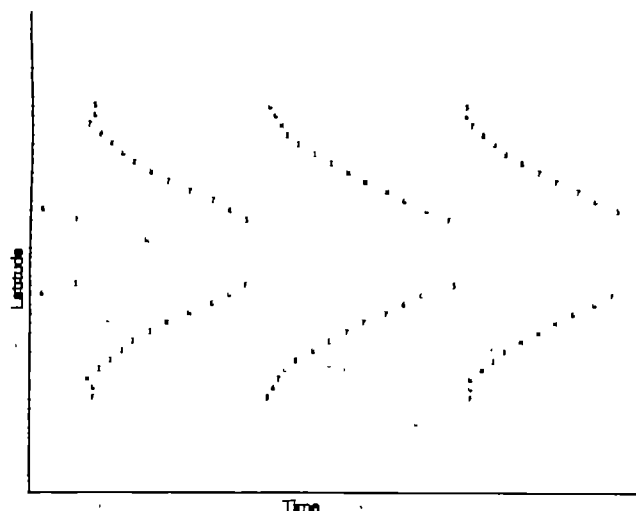


Fig. 1 A synthetic butterfly diagram. The latitude of appearance of flux tubes is plotted against time. Their activity lasts for months and leads to the broad wings of observed butterfly diagrams. Tubes appearing in high latitudes are weak and old: they are probably disrupted totally and do not build big active regions with spots.

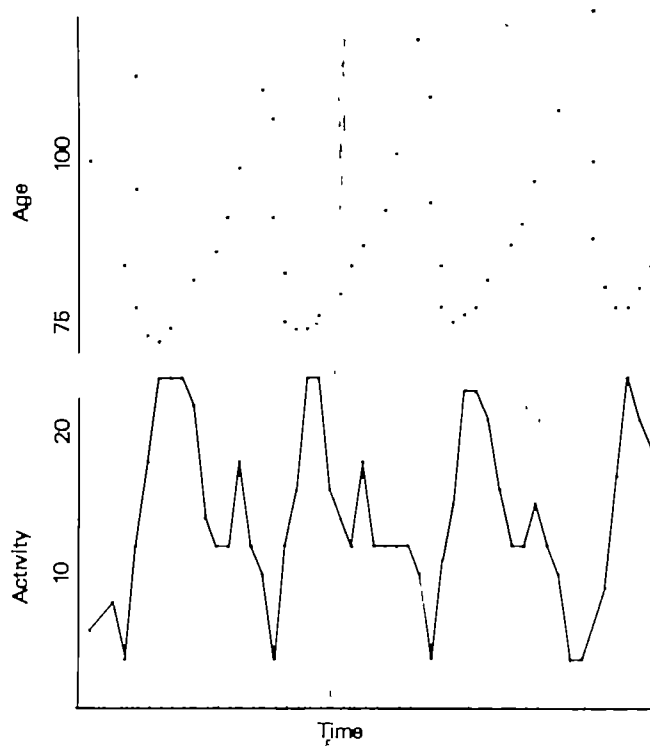


Fig. 2 Activity index and flux tube age: oldest flux tubes appear during activity minimum and vice versa. The age as a function of time shows a striking similarity to the variation of sunspot brightness and the number of XBP in time<sup>5,6</sup>.

The toroidal field is determined by the  $\phi$ -component of the induction equation at  $r = r_1$ :

$$\frac{\partial B_\phi}{\partial t} = B_r \cdot \sin(x) \cdot r_1 \cdot \left( \frac{\partial \Omega}{\partial r} \right)_{r=r_1} \quad (1)$$

We define a critical field strength,  $B_c$ , comparable with the equipartition with the convective kinetic energy. For  $B_\phi \gg B_c$  convection is suppressed within the flux tube, the tube has an 'identity' and we start to count the age,  $A$ . The tube tends to leave the shear region because of its buoyancy with a probability assumed to depend on the product of field strength and age,  $B_\phi \cdot A$ . We allow for a random component in the cycle by defining the eruption probability  $P$  in the following way, using constants  $C_1, C_2$ :

$$\begin{aligned} 0 &\leq B_\phi \cdot A < C_1: P = 0 \\ C_1 &\leq B_\phi \cdot A < C_2: P = \frac{B_\phi A - C_1}{C_2 - C_1} \\ C_2 &\leq B_\phi \cdot A: P = 1 \end{aligned} \quad (2)$$

Whether the tube leaves the shear region or not is determined by a random number generator, according to the above defined probabilities. The relevant poloidal field component,  $B_r$ , is regenerated by an unspecified dynamo process yielding a current parallel (Northern Hemisphere) or antiparallel (Southern Hemisphere) to the toroidal field  $B_\phi$ . The radial component of the field produced by this current for a flux tube situated at  $x = x_0$  is assumed to have the triangular profile  $R(x - x_0) = R(\bar{x})$ , for simplicity.

$$R(\bar{x}) = \begin{cases} \frac{\bar{x}}{x_m} & \text{for } |\bar{x}| \leq x_m \\ \frac{\bar{x} - \text{sgn } \bar{x} \cdot D}{x_m - D} & \text{for } x_m \leq |\bar{x}| \leq D \\ 0 & \text{for } D \leq |\bar{x}| \end{cases} \quad (3)$$



The parameters  $x_m$  and  $D$  define the location of the maximum and the total extension of the poloidal field produced by one flux tube, respectively. Therefore,  $D$  is a measure for the efficiency of (turbulent) diffusion in dispersing the weak poloidal fields spatially. The regeneration term for the poloidal field coming from one flux tube at  $x = x_0$  is hence:

$$r(x, x_0) = \alpha(x_0) B_\phi(x_0, t) R(x - x_0) \quad (4)$$

where  $\alpha(x)$  measures the strength of the regeneration process. As the role of rotation and Coriolis forces seem essential for any relevant mechanism we take  $\alpha = \alpha_0 \cos x$ . Now consider a distribution of  $N$  flux tubes at  $x = x_1, \dots, x_N$ . The poloidal field at the location  $x_i$  of one flux tube which is necessary for the amplification of  $B_\phi(x_i)$  throughout equation (1) is given by

$$\frac{\partial B_r(x_i)}{\partial t} = -\gamma B_r(x_i) + \sum_{j=1}^N r(x_i, x_j) \quad (5)$$

The contributions of all flux tubes to the poloidal field are summed and  $-\gamma B_r$  is a simple dissipation term. (A dissipation term for the toroidal field has not been included in equation (1) because turbulence is assumed to be suppressed within the flux tubes and the molecular diffusivity is neglected. This is not possible for the much weaker poloidal field.)

Equations (1) and (5) have been integrated forward in time, paying attention to flux eruption determined by equation (2) through random numbers. In spite of the considerable number of free parameters, the results sensitively depend only on a few of these. The quotient  $\alpha/\gamma$  determines whether the dynamo is excited or not: a critical value has to be exceeded. The other sensitive parameter is  $D$ , the half width of the regenerated poloidal field due to one flux tube. To get a butterfly diagram comparable with the observations  $D \geq 0.1 \pi$ , otherwise the butterfly wings overlap severely or the large-scale structure changes totally to irregular fluctuations. Therefore, even a flux tube dynamo depends on strong turbulent diffusion allowing for effective superposition of the poloidal field contributions of the individual flux tubes.

The results for a model with  $D = 0.125 \pi$ ,  $x_m = 0.025 \pi$  are shown in Figs 1 and 2. Figure 1 shows a 'synthetic' butterfly diagram in which the latitude of erupted flux tubes is drawn against eruption time. Numbers indicate positive field strength (in arbitrary units), letters negative field strength ( $A \triangleq -1$ ,  $B \triangleq -2 \dots$ ). Although only the time of the first appearance of a flux tube is shown, activity caused by it can last for months. This must be remembered when Fig. 1 is compared with observed butterfly diagrams showing broad wings. We can also define an activity index by monitoring the number and field strength of erupting flux tubes per time interval. This index is given in Fig. 2 together with the age of erupted flux tubes as a function of time. Looking first on the activity index, we observe a fast rise of the cycle, followed by a slower descent towards the minimum in accordance with the typical behaviour of the sunspot cycle (the secondary maximum is possibly accidental).

The cyclic variation of flux tube age seems to be very significant. The youngest tubes appear at activity maximum, flux tube age increases gradually during the decline of activity and reaches a maximum at activity minimum, followed by a sharp falling-off during the rise to the activity maximum. This variation is almost identical to the behaviour of sunspot brightness in time<sup>5,6</sup> and supports our hypothesis. Moreover, the anticyclic variation of XBP and EAR can be interpreted as an effect of age, too: older and therefore more severely 'shredded' tubes appear about activity minimum. It is quite plausible that the oldest of them are disrupted totally and only appear as XBP and EAR in high latitudes as the first messengers of the new cycle<sup>4</sup>. This would also decrease the latitude at which the first spots of a new cycle appear and thus remove the excess extension of the butterfly wings in Fig. 1 (XBP and EAR are not included in the classical activity measures, sunspot numbers and butterfly diagram). The problem of activity appearing in high latitudes was encountered by most dynamo models and was usually dealt with by ad hoc arguments.

Results from this crude and simplified model are thus very encouraging: the variations of sunspot brightness and of the appearance of XBP and EAR can be interpreted as an effect of age of the basic flux tubes. In considering the 'solar clock' proposed by Dicke<sup>14</sup> and the Maunder minimum, the present calculations, Leighton's and many other dynamo models show that non-linear dynamo action has a self-stabilization of phase, even if random fluctuations are allowed for.

Phase fluctuations in certain activity measures as sunspot number or the D/H indicator can easily be interpreted as fluctuations in the ratio of magnetic flux appearing in EAR to the flux appearing in big active regions with spots and flares, that is fluctuations of the amplitude of dynamo action (poloidal field), not phase. As the dynamo operates deep down in the convection zone with constant phase, then phase fluctuations of surface activity do not lead to a random walk of phase: the dynamo itself is the solar chronometer. The low sunspot numbers during the Maunder minimum may not be interpreted by a total stop of the 'machine', but can be understood as a period of weaker poloidal field causing the production of older flux tubes which have been disrupted by convection and only appeared as EAR, not sunspots. The dynamo has operated all the time and no phase problems arise at the end of this period.

Received 4 July; accepted 12 September 1980.

1. Harvey, J. W. *Highlights of Astronomy* Vol. 4, II (ed. Müller, E. A.) 223-239 (Reidel, Dordrecht, 1977).
2. Davis, J. M., Golub, L. & Krieger, A. S. *Astrophys. J. Lett.* **214**, L141-144 (1977).
3. Golub, L., Davis, J. M. & Krieger, A. S. *Astrophys. J. Lett.* **229**, L145-150 (1979).
4. Martin, S. F. & Harvey, K. L. *Sol. Phys.* **64**, 93-108 (1979).
5. Albrechtsen, F. & Maltby, P. *Nature* **274**, 41-42 (1978).
6. Maltby, P. & Albrechtsen, F. *Astrophys. J.* **234**, L147-149 (1979).
7. Jensen, E., Nordø, J. & Ringnes, T. S. *Astrophys. Norv.* **5**, 167-205 (1955).
8. Galloway, D. J., Proctor, M. R. E. & Weiss, N. O. *J. Fluid Mech.* **87**, 243-261 (1978).
9. Parker, E. N. *Cosmical Magnetic Fields* (Clarendon, Oxford, 1979).
10. Moffat, H. K. *Magnetic Field Generation in Electrically Conducting Fluids* (Cambridge University Press, 1978).
11. Childress, S. *Pap. Conf. on Origins of Planetary Magnetism*, Houston (1978).
12. Leighton, R. B. *Astrophys. J.* **156**, 1-26 (1969).
13. Schüssler, M. *Astr. Astrophys.* **71**, 79-91 (1979).
14. Dicke, R. H. *Nature* **276**, 676-680 (1978).

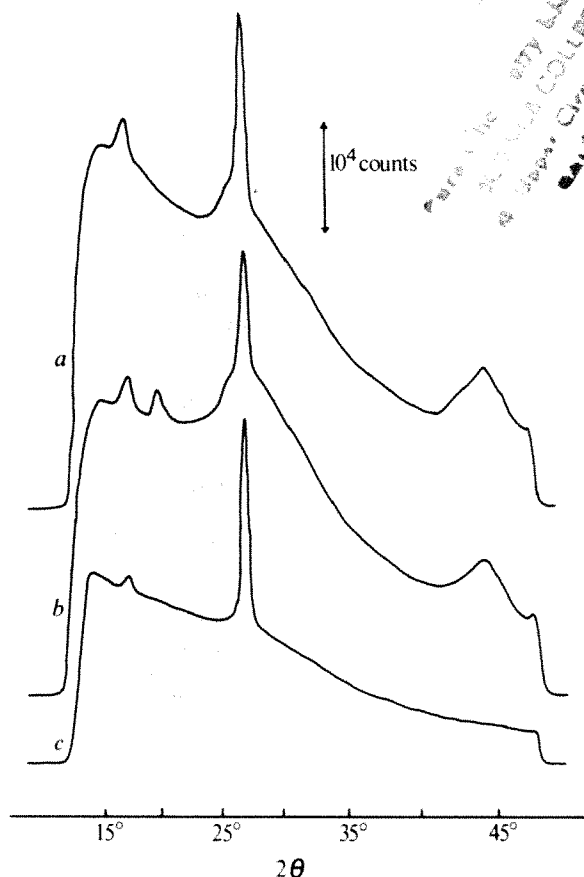
## X-ray diffraction from adsorbed iodine on graphite

M. Fleischmann, P. J. Hendra & J. Robinson

Department of Chemistry, The University, Southampton SO9 5NH, UK

Our knowledge of surface structure at the solid-vacuum interface has been acquired largely through high-vacuum analytical techniques. Unfortunately these may not be applied *in situ* to solid-liquid or solid-high-pressure gas interfaces which are of greater practical importance. *Ex situ* investigations have been made but the transfers involved probably result in surface restructuring. It is therefore apparent that *in situ* techniques are required. Raman spectroscopy<sup>1</sup> is applicable but lacks versatility, whilst neutron diffraction<sup>2</sup> and SEXAFS<sup>3</sup> are promising but depend on a reactor and synchrotron respectively. X-ray diffraction, on the other hand, is routinely performed and the theory is well developed though it has been assumed to be insensitive to surfaces. We report here the first observation of X-ray diffraction from a two-dimensional adsorbate formed at the solid-liquid interface,  $I_2$  on carbon, using position-sensitive detection to enhance sensitivity.

The adsorption of  $I_2$  from aqueous  $KI_3$  solution, on carbon was chosen as a test system as it has been widely studied and also because it is particularly suited to X-ray investigation in view of the large scattering cross-section of  $I_2$  with respect to carbon. The adsorbent chosen was Papyex; a graphitic material (in the form of 0.15-mm thick sheets) in which approximately half the graphite basal planes lie within a few degrees of parallel to the surface. This material has recently found wide use in neutron



**Fig. 1** Diffraction patterns of Papyex in: *a*, 0.1M KI, in-plane geometry; *b*, 0.02M I<sub>2</sub> in 0.1M KI, in-plane geometry; *c*, 0.02M I<sub>2</sub> in 0.1M KI, out-of-plane geometry. The sample thickness for *a* and *b* was 0.3 mm and for *c* 0.8 mm. The count time was 4,000 s.

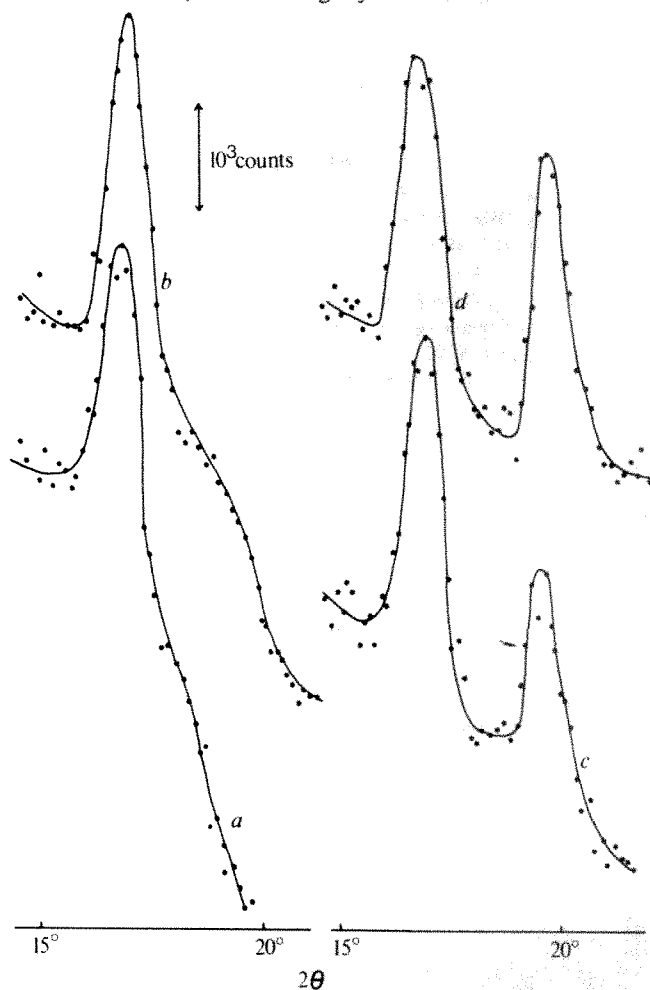
diffraction studies of gas-phase adsorption<sup>4</sup> and has a surface area of  $\sim 20 \text{ m}^2 \text{ g}^{-1}$ . Whilst higher surface area graphites are available, the preferred orientation of the graphite flakes in Papyex make it particularly useful; one can perform diffraction experiments either in the in-plane geometry (X-ray beam normal to the surface) probing primarily correlations in the plane of the surface or (by turning the sample through 90°) in the out-of-plane geometry, probing correlations perpendicular to this plane.

In the experiments reported here, Papyex sheets were equilibrated for 48 h with aqueous solutions of I<sub>2</sub> in KI before transfer to a cell fitted with Mylar windows for the entrance and exit of the X-ray beam. A stack of two Papyex sheets was used and the cell was designed to minimize the thickness of solution through which the beam passed.

The scattering from an adsorbate is obviously very small compared with the total observed (the substrate and H<sub>2</sub>O molecules contribute the major portion). A high photon count is therefore necessary to obtain adequate signal-to-noise ratios. This precludes the use of conventional counting techniques because of the prohibitive times involved. However, the past few years has seen the introduction of X-ray position-sensitive proportional counters (PSPC) which have proved very useful in biological applications where low exposure times are desirable<sup>5</sup>. A PSPC similar to that described by Borkowski and Kopp<sup>6</sup> was used in this study. Briefly, the anode is a high-resistance wire, parallel to the entrance window, which behaves as a distributed delay line. The position on the wire of the charge pulse caused by the X-ray photon is determined by the risetime of the pulse at each end of the wire and the output of the signal-processing electronics is a pulse, the height of which is related to the position of the X-ray event. These pulses are then sorted by a multichannel analyser which displays the intensity-position spectrum of the diffracted X-rays. The detector used had a

20-cm active length, a window height of 1 cm and a depth of 1 cm. A copper anode X-ray tube operating at 40 kV, 20 mA was the source.

Typical diffractograms are shown in Fig. 1 for Papyex in I<sub>2</sub>-free KI solutions and with a monolayer coverage of I<sub>2</sub>, both for in-plane geometry, and for monolayer coverage in the out-of-plane geometry. The peak at  $2\theta = 26.6^\circ$  on all the diffractograms is the (002) diffraction of graphite, whilst the broad peak at  $2\theta = 44.2^\circ$  is that for the (100) and (101) planes. The peak at  $2\theta = 16.3^\circ$  is due to the Mylar windows as is the shoulder on the low-angle side of the (002) diffraction. The peak in Fig. 1*b* at  $2\theta = 19.6^\circ$  is assigned to the (10) diffraction of a two-dimensional layer of hexagonally close-packed adsorbed I<sub>2</sub> molecules. Figure 2*a-d* shows this region of the diffractogram in more detail for increasing values of I<sub>2</sub> coverage (as determined by titration techniques which indicated a Langmuir-type isotherm with a maximum coverage of  $3.9 \times 10^{-2} \text{ g I}_2 \text{ per gC}$ ). Whilst the position of the (10) diffraction is independent of coverage, the intensity is proportional to it. This indicates that the forces between the adsorbed I<sub>2</sub> molecules are attractive and that the adsorbate is present as islands. From the half width of the (10) peak the size of these islands may be estimated<sup>7</sup>; for the coverage range 0.1–1.0 this was found to be constant at  $110 \pm 20 \text{ \AA}$ ; a value identical to the crystallite size for adsorbed Kr on Papyex as determined by neutron diffraction<sup>4</sup>. This dimension has been attributed to the size of the graphite flakes. It is, therefore, better to regard the iodine adsorption process as a higher-order phase transition. The position of the (10) peak, in the Warren formalism<sup>7</sup> for diffraction from a two-dimensional structure corresponds to a layer spacing of 4.6 Å, which in the hexagonally close-packed structure gives a nearest-neighbour distance of 5.3 Å, which is slightly less than the value at the



**Fig. 2** Details of diffractograms of Papyex, equilibrated with I<sub>2</sub> solutions in KI, between  $2\theta = 15^\circ$  and  $20^\circ$ . The coverages were: *a*, 0; *b*, 0.05; *c*, 0.7; *d*, 1.0.



minimum of the Lennard-Jones potential, 5.6 Å. The calculated nearest-neighbour distance, in conjunction with the value of the maximum coverage, gives the surface area of Papyex as 22 m<sup>2</sup> g<sup>-1</sup>, in close agreement with values obtained by other methods.

While these results were obtained for a favourable system, they indicate that X-ray diffraction can be successfully applied to adsorption studies in condensed media. It is inherent in these studies that there will always be a large background signal arising from scattering by the solution, therefore, accurate background subtraction techniques are required. These subtractions are difficult because of the large X-ray absorption cross-sections of potential adsorbates. This is overcome in diffraction studies of gas phase adsorption by recording the background at a temperature where the adsorbate is present as a 'liquid' and not an ordered array, but such a technique is not possible with condensed phases. In electrochemistry, however, it is possible to modulate the electrode potential and therefore accurate background subtraction should be possible. Experiments of this type are now in progress.

We thank the US Office of Naval Research for support of this work under contract no. N00014-77-G-0006.

Received 28 July; accepted 30 September 1980.

1. Fleischmann, M. & Hendra, P. J. in *Topics in Surface Chemistry* (eds Kay, E. & Bagus, P. S.) 373-402 (Plenum, New York, 1978).
2. Bomchil, G. & Rekel, C. J. *electroanal. Chem.* **101**, 133-5 (1979).
3. Stern, E. A. *J. vac. Sci. Technol.* **14**, 461-465 (1977).
4. Marti, C. & Thorel, P. *J. Phys.* **38**, C4, 26-30 (1977).
5. Faruqi, A. R. *IEEE Trans. Nucl. Sci.* **NS22**, 2066-2073 (1975).
6. Borkowski, C. J. & Kopp, M. K. *Rev. Scient. Instrum.* **39**, 1515-1522 (1968).
7. Warren B. E. *Phys. Rev.* **59**, 693-698 (1941).

## TiO<sub>2</sub> on and around a deactivated hydrodesulphurization catalyst

L. E. Makovsky, S. S. Pollack\* & F. R. Brown

US Department of Energy, Pittsburgh Energy Technology Center, PO Box 10940, Pittsburgh, Pennsylvania 15236

Deactivation of catalysts used to promote the liquefaction and desulphurization of coal is usually attributed to structural changes in the catalyst and the buildup of carbonaceous materials, minerals, iron and titanium. We discuss here the nature of the titanium which, though it is one of the major metals to deposit on and around catalysts, has never been characterized. The titanium deposited around a used catalyst removed from a fixed-bed reactor is very similar to one of the TiO<sub>2</sub> polymorphs (anatase) except that the *c* axis is 0.054 Å shorter. Two possible explanations for the origin of the anatase-like material are (1) that the titanium was originally organically bound in the coal, but it became oxidized during coal liquefaction, or (2) that small crystallites of the oxide existed in the coal and were simply concerned on and around the catalyst during liquefaction.

The need for clean fuel sources has led to the development of new processes for the liquefaction of coal. Some, such as the solvent refined coal (SRC) processes, do not use a catalyst, apart from the effects produced by the mineral matter in the feed coal. Others, such as the H-coal process, use an added catalyst, typically Mo promoted with Co or Ni supported on high surface area aluminas. Present usage requires ~1 lb of catalyst with 10% Mo as metal to hydrodesulphurize 1 ton of coal and produce three barrels of liquid fuels; thus it would take ~10 × 10<sup>6</sup> lb of Mo per year to produce one million barrels of liquid per day. (A production of approximately this amount would be required for a catalytic process to influence significantly the generation of liquid fuels in the US.) Because US production of Mo was estimated at 65 × 10<sup>6</sup> lb in 1978 and world production was 194 × 10<sup>6</sup> lb the need for lifetime maximization for Mo-based catalysts is obvious<sup>1</sup>.

Catalyst deactivation has been extensively studied for both petroleum and coal hydrodesulphurization catalysts<sup>2-4</sup>, but the nature of the titanium in the latter was not determined.

Much work at the Pittsburgh Energy Technology Center (PETC) has been devoted to a study of deactivated catalysts (supported Co-Mo on alumina) removed from the SYNTHOIL (fixed-bed) reactor. After 300 h of operation at 450 °C, 4,000 p.s.i., and exposure to 1.3 tons of Homestead, Kentucky coal, the 11 lb of Mo catalyst had become deactivated, as shown by the increase in sulphur content of the liquid product from 0.25 to 0.75%, the latter value equivalent to that found in non-catalytic operations<sup>5</sup>. The studies at PETC have shown that part of the catalyst deactivation may be due to the growth of the MoS<sub>2</sub> crystallites from single layers into three-dimensional stacks containing nine layers<sup>6</sup>. The work reported here is limited to the nature of the titanium deposits found on and around the spent catalyst.

The titanium found in the catalyst is concentrated in the outer 150 μm of the 1/8-inch catalyst pellets and is difficult to separate from the rest of the catalyst. However, surrounding the pellets in the reactor is a greyish deposit similar in composition to the spent catalyst except for lower Al, Mo, and Co contents. (The unused catalyst contains 3% CoO, 15% MoO<sub>3</sub> and 5% SiO<sub>2</sub> on eta Al<sub>2</sub>O<sub>3</sub>.) An X-ray diffraction pattern of this deposit, which contains ~20% Ti, is shown in Fig. 1 *b*. The anatase form of TiO<sub>2</sub>, with lines slightly shifted, is the major crystalline compound in the sample. Calcite, gypsum and quartz which occur in the original coal and pyrrhotite which forms during liquefaction are also present. The strongest line of anatase at 3.52 Å can easily be seen on diffraction patterns of the whole unground pellets, but long counting times are needed to reveal the second-strongest line at 1.89 Å.

The composition of the reactor deposit (shown in Fig. 1) is listed in Table 1. For comparison the analysis of used catalyst from the same portion of the reactor, the outlet side, is also shown.

After treatment with HCl and HF, all but ~15% of the reactor deposit dissolves. (Although Vorres and Donohue<sup>7</sup> showed in 1955 that TiO<sub>2</sub> reacts with HF to form TiOF<sub>2</sub>, this information does not yet seem widely disseminated.) The acid-insoluble residue contains a coke-like material, MoS<sub>2</sub>, and an unidentified magnetite-type spinel (see Fig. 1*a*). From X-ray diffraction linewidth measurements, corrected for instrumental broadening, the crystallite size of the anatase-like material in the reactor deposit was estimated<sup>8</sup> to be in the range 190-260 Å. The positions of the peaks, except the (200), are shifted to

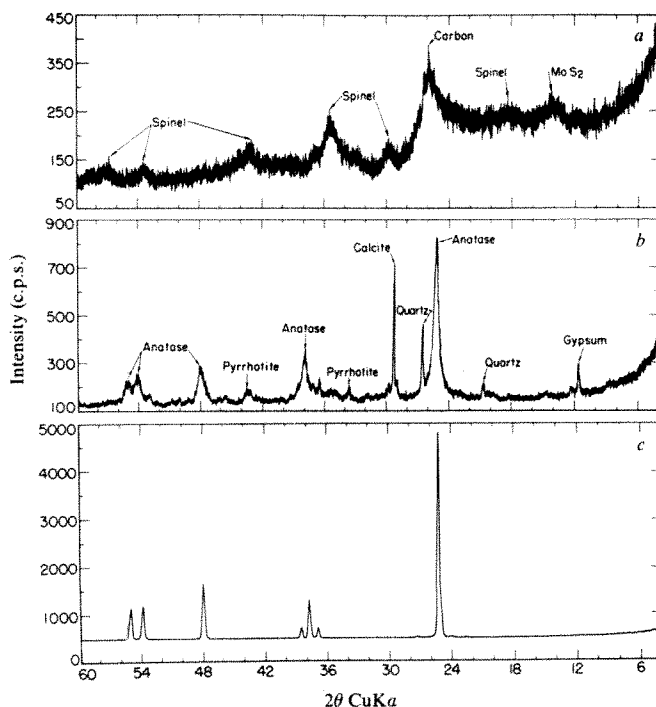


Fig. 1 Diffraction patterns of: *a*, Reactor deposit that has been treated with HCl and HF; *b*, reactor deposit; *c*, pure anatase.

\* To whom correspondence should be addressed.

**Table 1** Selected metals, *C* and *H* content of reactor deposit and used catalyst pellets from outlet section of SYNTHOIL reactor

| Element | Reactor deposit % | Used catalyst pellets % |
|---------|-------------------|-------------------------|
| Ti      | 24.5              | 2.9                     |
| Fe      | 7.82              | 0.5                     |
| Al      | 7.81              | 30.1                    |
| Ca      | 1.74              | 0.3                     |
| Mo      | 1.92              | 7.8                     |
| Co      | 0.55              | 1.2                     |
| C       | 15.3              | 9.8                     |
| H       | 1.3               | 0.9                     |

slightly higher angles, and from measurement of six peaks, a *c* axis of 9.460 Å with a standard deviation of 0.006 Å has been calculated using Appleman's<sup>9</sup> least-squares program. This indicates a decrease of 0.054 Å from that measured by Swanson *et al.*<sup>10</sup> for pure anatase. No change in the *a* axis was detected. The reason for the slightly shorter *c* axis of the anatase-like material in the reactor deposit is not known. This material also contains ~1% boron, but when treated with HCl, the boron is found in the soluble fraction, whereas the titanium-rich material is insoluble. Scanning transmission electron microscopy (STEM) studies showed no element other than Ti in the anatase-like crystallites from the reactor deposit. Attempts have been made to study by STEM the TiO<sub>2</sub> on and in the pellets but the preparation of TiO<sub>2</sub> crystallites thin enough to produce electron diffraction patterns has not been achieved.

A sample of the raw coal (Homestead, Kentucky) was treated to concentrate any TiO<sub>2</sub> minerals present. The coal was first ashed at low temperature and then fractionated using bromoform. HCl and HNO<sub>3</sub> were then used to remove calcite and pyrite from the residue. No titanium minerals were detected in the residue even though the coal contains ~0.1% titanium. Quantitative estimates of the inorganic titanium in the Homestead coal have not been made, but Finkelman<sup>11</sup>, using a novel procedure based on SEM and energy-dispersive X-ray fluorescence, has attempted to do this for a Waynesburg coal. He found that approximately half the titanium is in minerals >2 µm in diameter, and the remainder of the titanium is either organically bound or in smaller crystals. The presence of 200-Å anatase crystallites in the Homestead coal is possible because Lin *et al.*<sup>12</sup> have found mineral crystallites 40–1,000 Å in an Illinois no. 6 coal, although they did not specifically find anatase.

Recent work here at PETC has shown that titanium bound as the cresylate, nonylate, or tetraphenyl porphine, when mixed with catalyst, penetrated several hundred micrometres into the pellets. After treatment in an autoclave at 450° and 2,000 p.s.i. hydrogen for 30 min, the titanium in between the pellets had been converted to 600–800-Å anatase crystallites with normal *a* and *c* axes, and the structure of the titanium inside the pellets is under investigation. This work shows that organically bound titanium will form anatase in liquefaction conditions. However, until more conclusive studies rule out the presence of small crystallites of TiO<sub>2</sub> in the original coal, the inorganic origin remains a possibility. Scanning transmission electron microscopy studies and additional differential solubility experiments to concentrate any inorganic TiO<sub>2</sub> present in the raw Homestead coal are in progress. Hopefully, this information will permit resolution of the origin of titanium deposits on at least one coal hydrodesulphurization catalyst.

We thank George Noles at Sandia laboratories for the scanning transmission electron microscopy of the TiO<sub>2</sub> crystallites from the reactor deposit.

Received 23 June; accepted 12 September 1980.

- Goth, J. W. *Engng Min. J.* **180**, 122 & 129 (1979).
- Mosby, J. F., Hoekstra, G. B., Kleinhenz, T. A. & Sroka, J. M. *Hydrocarbon Proc.* **52**, 93–97 (1973).
- Holloway, P. H., Granoff, B., Nowak, F. J., Mellendore, A. W. & Lieberman, M. L. *1st A. Rep. Chem. Studies on SYNTHOIL Process* (Sandia Laboratories, Albuquerque, New Mexico, 1976).
- Stanulonis, J. J., Gates, B. C. & Olson, J. H. *A.I.Ch.E.J.* **22**, 576–581 (1976).

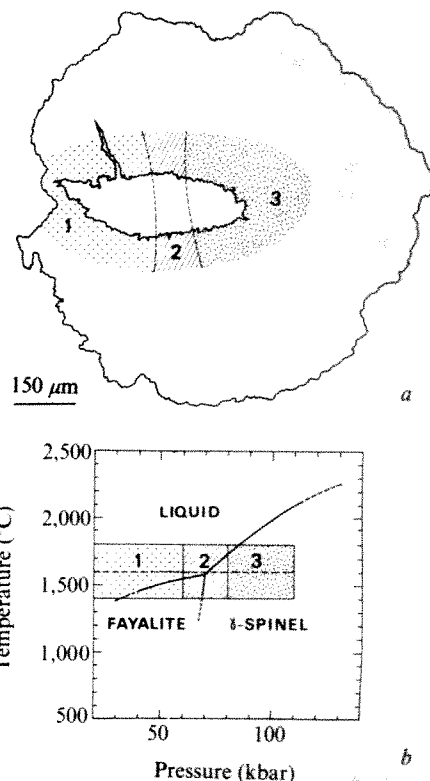
- Internal Quarterly Technical Progress Rep.*, July–September 1977 (Pittsburgh Energy Technology Center, Pennsylvania, 1977).
- Pollack, S. S., Makovsky, L. E. & Brown, F. R. *J. Catal.* **15**, 452–459 (1979).
- Vorres, K. & Donohue, J. *Acta Crystallogr.* **8**, 25–26 (1955).
- Klug, H. P. & Alexander, L. E. *X-Ray Diffraction Procedures for Polycrystalline and Amorphous Materials* 2nd edn 698 (Wiley, New York, 1974).
- Appleman, D. E. & Evans, H. T. *Job 9214: Indexing and Least Squares Refinement of Powder Diffraction Data* (National Technical Information Service, Springfield, PB 216 188, 1973).
- Swanson, H. E., McMurdie, H. F., Morris, M. C. & Evans, E. H. *Standard X-Ray Diffraction Patterns* (National Bureau of Standards Monogr. 25, Section 7, 82, 1969).
- Finkelman, R. B. *Scanning Electr. Microsc.* **1**, 143–148 (1978).
- Lin, S. J., Hendricks, R. W., Harris, L. A. & Yust, C. S. *J. appl. Crystallogr.* **11**, 620–625 (1979).

## Olivine glass and spinel formed in a laser heated, diamond-anvil high pressure cell

A. Lacam, M. Madon & J. P. Poirier

Institut de Physique du Globe, Université Paris VI, 4 Place Jussieu, 75230 Paris Cedex 05, France

Laser-heated, diamond anvil cells have produced a major breakthrough in the understanding of the physics of the Earth's interior, by making it possible to synthesize mineral phases that are stable at very high pressure. The synthesized phases are usually identified by X-ray powder diffraction techniques. We report here the results of the first local examination by transmission electron microscopy of a sample prepared by heating fayalite in a diamond-anvil cell. We have identified three phases produced, in the pressure gradient from the edge to the centre of the cell: olivine glass (to our knowledge, the first case to be reported); phases corresponding to a transition zone between olivine and spinel; and spinel. The phases are similar to those found in shocked chondritic meteorites.



**Fig. 1** *a*, Scheme of a sample recovered from the diamond-anvil cell and ion-beam thinned. The edges of the hole are transparent to the electrons. *b*, Location of the different zones of the sample in the phase diagram after Ohtani. Zone 1, glass quenched from the melt at lower pressure near the rim. Zone 2, transition zone. Zone 3, γ-spinel at higher pressures near the centre.



Fayalite  $\text{Fe}_2\text{SiO}_4$  is the iron end member of the ferro-magnesian olivine series, which constitute most of the Earth's upper mantle, and whose transition to spinel structure under high pressure has important geodynamic consequences. Pure, single crystalline, synthetic fayalite prepared by zone-melting<sup>3</sup>, was ground in an agate mortar; the powder, consisting mostly of grains  $\sim 3 \mu\text{m}$  in size with a few larger ones ( $\approx 30 \mu\text{m}$ ), was loaded between the diamonds, without a gasket, as a disk 0.8 mm in diameter. Pressure was applied for 2 days before heating. The maximum pressure, measured by the shift of ruby fluorescence lines, was  $109 \pm 10$  kbar in the centre of the specimen and was found to be the same when measured before and after heating. The distribution of pressure across the cell was not measured but the absence of a gasket meant that the pressure at the edge would be close to atmospheric pressure. The beam of a 60-W YAG laser was focused on the sample and scanned across it. The powder density was of the order of  $1 \text{ MW cm}^{-2}$  and the luminance temperature was estimated to be  $1,450^\circ\text{C} \pm 50^\circ\text{C}$  by optical pyrometry. The sample was then recovered and ion-beam thinned until a hole appeared. The elongate hole extended from the centre of the sample to the edge of the transformed zone (Fig. 1). Its edges were thin enough to be examined by transmission electron microscopy in a 100-keV Philips EM300 microscope. From the rim to the centre three structurally different zones were distinguished and could be interpreted in the light of Ohtani's recent phase diagram for melting of  $\text{Fe}_2\text{SiO}_4$  under pressure<sup>4</sup> (Fig. 2). These results were reproduced in two experiments with nominally the same conditions. (In one experiment the recovered sample broke but fragments could be thinned and examined, they yielded the same results).

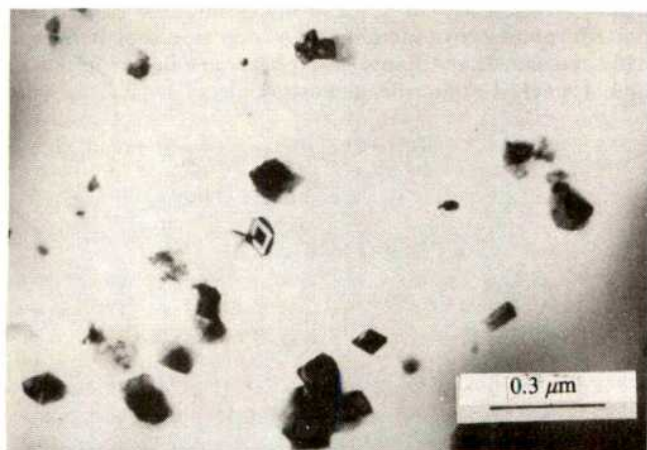


Fig. 2 Fayalite glass with small fayalite crystals in zone 1.

Zone 1, close to the rim, consists mostly of a material which was totally nondiffracting, melted easily when heated in the beam by removing the condenser apertures of the microscope (this prevented X-ray microanalysis), and contained a few idiomorphic micro crystals of a size much too small ( $< 1,000 \text{ \AA}$ ) to allow characterization by electron diffraction. These three features together with the fact that the pressure at the rim is low enough for fayalite to melt under the impact of the laser beam lead us to believe that we have observed olivine glass quenched from the melt. We believe that this is the first report of an olivine glass quenched from the melt, the only glass previously reported having been produced in the solid state during shock experiments<sup>5</sup>. The highly conducting diamonds can evacuate heat from the very thin layer of melt, fast enough to obtain very high quenching rates comparable with rates ( $\approx 10^6^\circ\text{C s}^{-1}$ ) obtained in the preparation of metallic glasses<sup>6</sup>. We can get an idea of the quenching rate by a rough calculation assuming that a quantity of heat  $Q = 2\lambda\rho cT_0$  per unit area is released instantaneously at

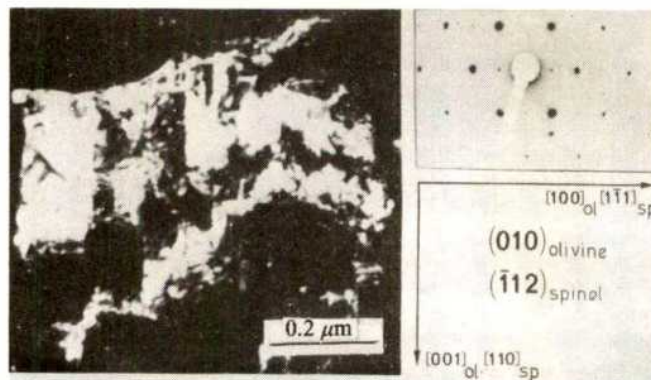


Fig. 3  $\gamma$ -spinel and olivine intergrowths in the transition zone 2. The plane of the foil can be indexed as (010) in olivine or (112) in spinel, the boundaries between the areas in and out of contrast are (100) planes in olivine or ( $\bar{1}\bar{1}\bar{1}$ ) planes in spinel.

time  $t = 0$  in a thin layer of thickness  $2\lambda$  at  $x = 0$  (the sample) and evacuated on both sides by conduction in semi-infinite diamond anvils along the  $x$  axis. If we assume that  $\rho c$  (density  $\times$  heat capacity) is not very different in the thin sample and in the diamonds; the temperature  $T$  at time  $t$  and  $x = 0$  (the temperature of the sample) is given<sup>7</sup> by:  $T = T_0\lambda/(\pi\kappa t)^{1/2}$  where  $\lambda \approx 10^{-3} \text{ cm}$  and  $\kappa$  is the thermal diffusivity of diamond,  $\kappa \approx 1 \text{ cm}^2 \text{ s}^{-1}$ ,  $T_0$  is the temperature of the liquid  $T_0 \approx 1,500^\circ\text{C}$  (the temperature of the diamonds at  $t = 0$  is taken as  $0^\circ\text{C}$ ). We see that for  $t = 10^{-6} \text{ s}$ ,  $T$  falls to  $\sim 850^\circ\text{C}$ , well below the freezing point: the quenching rate is probably higher than  $10^6^\circ\text{C s}^{-1}$ .

Zone 2, inwards of zone 1, probably corresponds to the vicinity of the triple point liquid-fayalite- $\gamma$ -spinel, in the solid state region. It seems to be a transition zone between the olivine and spinel structure, where the electron diffraction patterns can be indexed both as (010) plane in olivine and (112) plane in spinel (Fig. 4). If various spots are used to form the image, different tabular regions of the grains are seen in contrast, the boundaries between these regions lie on (100) plane in olivine or (111) plane in spinel. This structure could be interpreted as corresponding to conditions close to the olivine-spinel boundary in the phase diagram, and is compatible with a model recently proposed<sup>8</sup>, of a martensitic olivine-spinel transition effected by the motion of dissociated [001] dislocations on the (100) close packed planes of olivine, with accompanying synchroshear of the cations.

Zone 3, close to the central region, consists only of  $\gamma$ -spinel. Further from the centre the grains are quite small,  $1 \mu\text{m}$  in diameter, with a polygonal shape; they contain planar defects (stacking faults or antiphase boundaries) (Fig. 4) on (110) planes

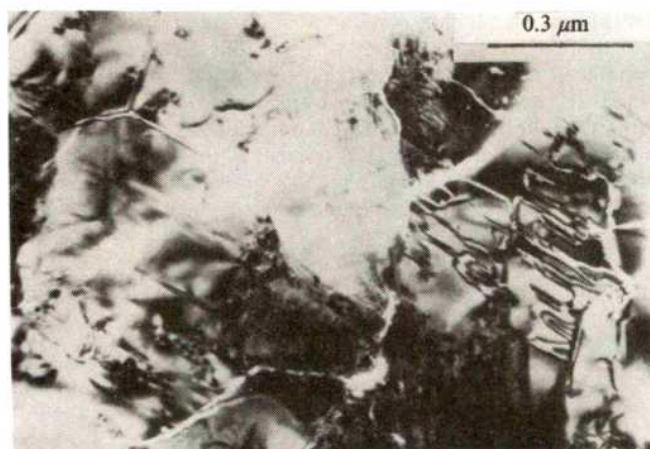


Fig. 4  $\gamma$ -spinel with antiphase boundaries in zone 3.



with displacement vector  $1/4[110]$ , identical to the defects previously identified in the ringwoodite of the meteorite Tenham<sup>9-11</sup>. Closer to the centre, the grains become larger (several micrometres), planar defects are no longer visible but numerous straight dislocations aligned along  $\langle 110 \rangle$  directions are present.

In conclusion, transmission electron microscopy has shown that processes taking place in fayalite inside a laser-heated diamond-anvil cell are rather complex and range from melting and olivine glass formation during rapid quench to solid state transition to spinel. Note that the observed phases: glass with small idiomorphic crystals and mosaic spinel polycrystal with antiphase boundaries are very similar to those found in shocked hypersthene chondrites.

We thank Dr H. Takei for the fayalite and C. Guillemin for help with the electron microscopy. This work was supported by INAG (ATP Geodynamique 1979). Contribution IPG NS 417.

Received 14 July; accepted 23 September 1980.

1. Bassett, W. A. *Rev. Earth planet. Sci.* **7**, 357-384 (1979).
2. Bell, P. M. *Rev. Geophys. Space Phys.* **17**, 788-791 (1979).
3. Takei, H. *J. Cryst. Growth* **43**, 463-468 (1978).
4. Ohtani, E. *J. Phys. Earth* **27**, 189-208 (1979).
5. Jeanloz, R. *et al. Science* **197**, 457-459 (1979).
6. Gilman, J. J. *Phys. Today* 46-53 (1979).
7. Jaeger, J. C. & Starfield, A. M. *An Introduction to Applied Mathematics*, 435 (Oxford University Press, 1974).
8. Poirier, J. P. *Anelastic Properties and Related Processes in the Earth's Mantle* (AGU Monograph, in the press).
9. Poirier, J. P. & Madon, M. *EOS* **60**, 370 (1979).
10. Madon, M. & Poirier, J. P. *Science* **207**, 66-68 (1980).
11. Putnis, A. & Price, G. D. *Nature* **280**, 217-218 (1979).

## Phytoplankton patchiness indicates the fluctuation spectrum of mesoscale oceanic structure

J. F. R. Gower\*, K. L. Denman\* & R. J. Holyer†

\* Institute of Ocean Sciences, PO Box 6000, Sidney, British Columbia, Canada V8L 4B2

† Oceanography Division, Naval Ocean Research and Development Activity, NSTL Station, Mississippi 39529

Satellite imagery and large-scale oceanic experiments have replaced traditional concepts of broad sluggish currents moving throughout the ocean by the concept of a continuous distribution of more energetic eddies, the dominant eddies having space scales<sup>1,2</sup> of the order of 100 km. Near the ocean boundaries in such areas as the Gulf Stream and the California Current, these eddies exhibit strong thermal contrast, of the order of 2-6°C, and their structure and distribution can be mapped using satellite thermal IR imagery<sup>3,4</sup>. Over most of the ocean, however, the thermal contrasts are much lower, of the order of 0.1-0.5°C, and tend to be masked from satellite observation by small-scale atmospheric variations. To map the structure associated with mesoscale horizontal water motions in these areas, another indicator must be used for observation from space. We present here the first results of spectral analysis of satellite imagery of what we believe is phytoplankton patchiness controlled by mesoscale (10-100 km) water motions.

The surface layer of the ocean is inhabited by organisms ranging in scale from plankton (~1 µm) to whales (~10 m). Whereas whales often migrate over hemispheric distances, phytoplankton, the microscopic plants in the ocean, have the least mobility, limited to vertical migration over a few metres per day<sup>5</sup> accomplished by buoyancy changes. The phytoplankton may, therefore, be considered as a passive scalar being advected about by the variable ocean currents. Phytoplankton do, however, grow and reproduce; a healthy population can double its biomass in a time period of the order of 1 day<sup>6</sup>. Several

models have been developed to describe growing phytoplankton patches being redistributed and diffused horizontally by a partially turbulent ocean<sup>7-9</sup>. These models have tried to describe the observed spatial variations of biomass in terms of wavenumber spectra. It has recently been concluded<sup>7,8,10</sup> that shipborne sampling cannot achieve sufficient spatial coverage in times short enough to be considered synoptic and that airborne or satellite sampling is required.

The biomass of phytoplankton is usually quantified by determining the amount of chlorophyll *a* pigment present. Remote measurement of chlorophyll concentration uses the colour changes caused by the combination of absorption or fluorescence of chlorophyll pigments and backscattering by associated suspended matter<sup>11-15</sup>. Variations in phytoplankton concentration cause measurable changes in the intensity and spectral distribution of visible light backscattered from the ocean, especially in the blue and green bands where water transmission is a maximum. Normal, low plankton concentrations cause colour changes which can be detected from space only by using specialized processing on selected wavelength bands to remove atmospheric effects. The Coastal Zone Colour Scanner on Nimbus 7 is now available as a sensor designed for this purpose. Areas of high chlorophyll concentration, however, can give large changes in water reflectivity detectable by less sophisticated systems.

Figure 1 shows an area of the ocean 180×250 km in size, south of Iceland, as imaged by the LANDSAT multispectral scanner on 19 June 1976. The image shown is a mosaic of spectral band 4 from frames 2514-12015 and 2514-12021. Band 4 is the shortest wavelength band on the instrument, covering 500-600 nm, corresponding roughly to green light. The south-west coast of Iceland is visible at the top of the image, and the 400-m depth contour crosses the middle of the scene. The land is partly cloud covered and some bands of cloud are visible at the lower right. The island of Westmannaeyjar can be seen just off the coast with the volcanic island, Surtsey, to its south-west. The swirls and eddies in the remaining area of the water show a structure characteristic of mesoscale turbulence as observed in satellite thermal imagery. This structure is much less visible in the red band, while the longest wavelength band 7 (800-1,100 nm) shows only the clouds above featureless dark water. Because this band-spectral signature is typical of suspended matter in the ocean, we interpret the eddy patterns in Fig. 1 as representing the distribution of phytoplankton biomass or of detritus derived from phytoplankton.

A phytoplankton survey tow was made in the area as part of a programme of the Institute for Marine Environmental Research, UK, on the day this image was taken. The ship travelled westwards parallel to the coast ~20-km offshore passing between Westmannaeyjar and Surtsey. The concentration of phytoplankton observed was well below average for the time of year confirming, at least, that the darker area near the top of the image corresponds to a low concentration of phytoplankton. Measurements made along the same line six weeks earlier, however, showed the strongest phytoplankton bloom observed in this area during May for five years. Repeated measurements made on a section to the west of Westmannaeyjar by staff of the Marine Research Institute of Reykjavik<sup>16</sup> showed that the main peak of growth in this area also occurred about a month earlier. Their data for 1976-78 show that the blooms tend to occur earlier in the shallower water on the continental shelf than in the deeper water offshore where the bloom in Fig. 1 is observed. These data also showed that an exceptionally high productivity of phytoplankton occurred in the spring of 1976. The available data, then, confirm strong productivity near this place and time and do not invalidate our interpretation of Fig. 1 as showing the effects of a phytoplankton bloom. The area of the bloom covers at least 180×180 km, the area of a single frame of LANDSAT imagery. The increase in reflectance caused by the bloom is high, but not unreasonable for plankton of the appropriate species<sup>11</sup> or in the appropriate stage of development<sup>17</sup>. No other LANDSAT scenes were collected over the area near this time



except for an image overlapping the area of Fig. 1 but farther east, largely cloud covered, recorded on 30 May. This image shows no discernible bloom. Scarcity of satellite data is largely due to there having been no satellite receiving station capable of receiving directly image data of Iceland.

The characteristic spatial scales of the eddies and ocean turbulence structure can best be determined from a two-dimensional spectral analysis<sup>18</sup> of the image in which we assume that the increase in pixel value over the level for clear water is proportional to phytoplankton concentration. The resulting power spectrum can then be averaged over all directions to get a spectrum as a function of a nondirectional wave number<sup>19</sup>.



**Fig. 1** Enhanced image formed from two LANDSAT Multispectral Scanner band 4 frames showing increased reflectance in the Atlantic Ocean south of Iceland on 19 June 1976. The patterns are interpreted as due to a plankton bloom in water advected by ocean mesoscale turbulence.

Before beginning this analysis, the effects of cloud were reduced by subtracting the band 7 image, suitably scaled, from the band 4 image. As water looks very dark in band 7 (near IR), the subtraction is equivalent to removing the light backscattered by aerosol particles in thin clouds and haze above the water. This scaling allows for the different instrument gain and solar irradiance between bands 4 and 7 and also, in effect, selects different values of mean Angstrom coefficient for the spectral dependence of aerosol scattering in the scene<sup>20</sup>. The scaling constant was adjusted to reduce the visibility of cloud features in the band 4 image. In ~10% of the area of Fig. 1 analysed, thin cloud contributed an additional 15–30% to the radiance enhancement in band 4 that is due to light scatterers in the water. The subtraction reduced this cloud contribution to ~5%. Less correction is possible in areas with thicker cloud, but these were largely avoided in the analysis.

Picture elements in the raw image are spaced on a grid with element spacing  $57 \times 79$  m. The pixel values were averaged over groups of  $8 \times 6$  pixels to reduce instrument noise and to give a roughly square grid of about 474-m spacing for further processing. Three overlapping areas of  $256 \times 256$  averaged pixels each about 120 km square were then selected for Fourier transforming. The mean pixel value for each was subtracted from each pixel in the area, and the areas were Hanned (weighted with a cosine taper in both dimensions) to reduce edge effects.

Although the three areas overlapped by ~55%, the Hanning reduced the correlation of the coefficients of the resulting transforms to ~25%, low enough for reasonable statistical independence. The Fourier transforms of the pixel arrays were then converted to power or signal-variance spectra, and circular ring areas in the transform plane were summed and normalized by their areas to give non-directional estimates of the variance as a function of wavelength. Wedge-shaped areas were similarly summed to give estimates of the directional effects in the water or introduced by residual cloud signals. These were found to be <10% except at the shortest wavelengths (<3 km) where a larger value (up to 20%) appears in the direction range appropriate to the cloud streaks in Fig. 1.

The logarithms of the spectral components of signal variance, averaged over all directions, are plotted in Fig. 2 against the logarithm of the inverse wavelength,  $K$ . If the spectral components are dependent on  $K$  in a power law manner, proportional to  $K^n$ , then such a plot should yield a straight line with slope  $n$ . The spectral components computed for the three areas are plotted separately and all yield a similar relation for the wavelength range 2–60 km ( $K = 0.015$  to  $0.5$ ); the relations can be well fitted by straight lines. The regression line slopes are  $-3.11$ ,  $-2.83$  and  $-2.82$  for the three areas giving an average value of  $-2.92$ . The average regression line is plotted as the dashed line in Fig. 2. At long wavelengths, the points lie below this line, but some roll off is expected for components having wavelengths comparable to the dimensions of the sample area. The point for a wavelength of 1 km lies above the line indicating reduction in slope at the short wavelength. This value may be increased by components of scene radiance due to residual cloud reflections. Variance due to small streaks of cloud such as can be seen in Fig. 1 would be expected to have more energy at the higher frequencies.

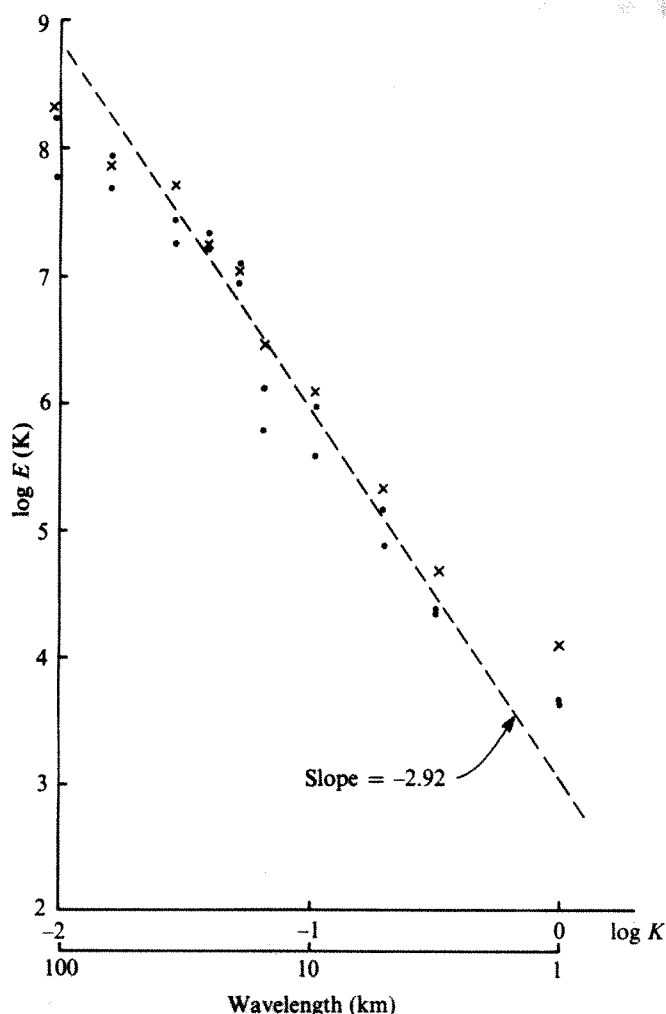
For wavelengths between 2 and 60 km the distribution of signal variance is related to inverse wavelength to the power  $-2.9$ . If the observed pixel values are interpreted as proportional to particulate backscatter from phytoplankton, then this power law also applies to the phytoplankton density and the above result can be compared with other measurements of the power law index in ocean mesoscale turbulence.

Spectra of sea-surface temperatures derived from airborne radiometer measurements have varied between  $-2$  and  $-3$  (refs 18, 19). Shipboard estimates of phytoplankton patchiness have varied widely, but a similar range is most typical<sup>10,21–23</sup>. Theoretical estimates<sup>7–9</sup> of the index for turbulence-controlled phytoplankton patchiness tend to be between  $-2$  and  $-3$ . The  $-3$  slope is consistent with the concept of two-dimensional geostrophical turbulence<sup>24,25</sup>, where the growth rate of the phytoplankton has a negligible effect on the horizontal distribution of biomass. The signal discontinuities resulting from the small (~10) number of discrete pixel values or grey scale levels in the original image would shift the slope towards  $-2$  (ref. 26), but this effect is reduced to a negligible amount by averaging over 48 pixels.

The relationship between phytoplankton concentration and the amount of radiance upwelling from beneath the sea surface is not in general linear. The absorption by chlorophyllous pigment increases along with the increased backscatter from the suspended planktonic matter<sup>12,13</sup>. In the range 500–600 nm, this leads to saturation in the reflectance values after an initial increase. Over a limited range of chlorophyll concentrations, however, the relationship can be approximated by a linear function so that the above discussion holds. The reflectance values in the areas analysed range over ~3–7% reflectance. The expected linearity of the reflectance-to-chlorophyll relation depends on the properties of the plankton actually present. The relatively high reflectivity of the water implies a high backscatter to absorption ratio, a condition which improves the linearity of the relationship.

We interpret patterns on a LANDSAT band 4 multispectral scanner image as being due to phytoplankton and show that the fluctuation spectrum is consistent with the phytoplankton dis-





**Fig. 2** Power spectra computed from three overlapping areas of Fig. 1 as described in the text. A slope of  $-3$  in a log-log plot is characteristic of turbulent motion, and indicates that growth rate of the plankton itself is having a relatively small effect. The distribution of enhanced water reflectance in Fig. 1 should, therefore, be a useful tracer of the eddy motions.

tribution being controlled by advection in variable ocean currents, while being unaffected by their reproduction rate.

The phytoplankton are, therefore, behaving as a passive scalar and the distribution of enhanced water reflectance in Fig. 1 can be used as a tracer of eddy motion. The spatial distribution of areas showing increased reflectance can certainly be mapped more precisely from a satellite than by any other means available, and this may be why the resulting slope of the power spectrum agrees so well with theory. The problem of relating this reflectance increase to exact measures of chlorophyll concentration remains, but this should soon be possible using the improved data from NASA's Coastal Zone Colour Scanner.

In comparing satellite IR and colour mapping of ocean eddy structure both have their limitations, and the two methods will to some extent be complementary. Both methods are blocked by clouds, and both are affected by atmospheric absorption and scattering. Both measure only surface phenomena, though wind mixing, particularly at high latitudes, will tend to average properties over a surface mixed layer, often of the order of 50 m deep. Thermal measurements are more susceptible to skin effects related to the very small penetration depth ( $\leq 0.1$  mm) of thermal radiation. Both measurements are of ocean properties interesting and important in themselves. Taken together they can show how solar heating, water mixing and stratification, and plankton growth lead to the productivity variations that are of such importance to the world's fisheries.

Received 28 May; accepted 2 September 1980.

- Bernstein, R. L. & White, W. B. *J. phys. Oceanogr.* **4**, 613 (1974).
- Gould, J., Schmitz, W. J. & Wunsch, C. *Deep-Sea Res.* **21**, 911 (1974).
- Legeckis, R. V. *J. phys. Oceanogr.* **9**, 483 (1979).
- Bernstein, R. L., Breaker, L. & Whritner, R. *Science* **195**, 353 (1977).
- Smayda, T. J. *Oceanogr. mar. Biol. A. Rev.* **8**, 353 (1970).
- Eppler, R. W. *Fish Bull. U.S.* **70**, 1063 (1972).
- Denman, K. L. & Platt, T. *J. mar. Res.* **34**, 593 (1976).
- Denman, K. L., Okubo, A. & Platt, T. *Limnol. Oceanogr.* **22**, 1033 (1977).
- Fasham, M. J. *Oceanogr. mar. Biol. A. Rev.* **16**, 43 (1978).
- Horwood, J. W. *J. mar. Biol. Ass. U.K.* **58**, 487 (1978).
- Yentsch, C. S. *Deep-Sea Res.* **7**, 1 (1960).
- Clarke, G. L., Ewing, G. C. & Lorenzen, C. J. *Science* **167**, 1119 (1970).
- Morel, A. & Prieur, L. *Limnol. Oceanogr.* **22**, 709 (1977).
- Gower, J. F. R. *Boundary Layer Met.* **18**, 235 (1980).
- Smith, R. C. & Baker, K. S. *Limnol. Oceanogr.* **23**, 247 (1978).
- Frueger, E., Einarrson, S., Olafsson, J. & Thordarson, T. *International Council for the Exploration of the Sea, Early Life History of Fish Symp.* (Woods Hole, 1979).
- Kiefer, D. A., Olson, R. J. & Wilson, W. H. *Limnol. Oceanogr.* **24**, 664 (1979).
- Saunders, P. M. *Deep-Sea Res.* **19**, 467 (1972).
- Holladay, C. G. & O'Brien, J. J. *J. phys. Oceanogr.* **5**, 761 (1975).
- Gordon, H. R. & Clark, D. K. *Boundary Layer Met.* **18**, 299 (1980).
- Denman, K. L. & Platt, T. *Mem. Soc. r. Sci. Liège* **7**, 19 (1975).
- Denman, K. L. *Deep-Sea Res.* **23**, 539 (1976).
- Fasham, M. J. & Pugh, P. R. *Deep-Sea Res.* **23**, 527 (1976).
- Kraichnan, R. H. *Phys. Fluids* **10**, 1417 (1976).
- Charney, J. G. *J. atmos. Sci.* **28**, 1087 (1971).
- Phillips, O. M. *J. phys. Oceanogr.* **1**, 1 (1971).

## The nature of inherited deafness in deafness mice

Karen P. Steel & Gregory R. Bock

MRC Institute of Hearing Research, University of Nottingham, Nottingham NG7 2RD, UK

Many mouse mutants have an apparent deficiency in their responsiveness to sound<sup>1</sup>. Most of these mutants have other abnormalities in addition to their hearing deficit, and the only two which have been subjected to a detailed anatomical and physiological study, *shaker-1* and *Ames waltzer*, also have motor abnormalities<sup>2,3</sup>. The existence of such motor abnormalities throws some doubt on the usefulness of these two mutants as possible models for hereditary deafness in man, which is most frequently uncomplicated<sup>4</sup>. Deol and Kocher have described the *deafness* mutation in which mice homozygous for the recessive *deafness* gene (*dn/dn*) were unresponsive to sound and had no significant behavioural abnormality<sup>5</sup>. Cochlear hair cells in *deafness* mice develop normally and then degenerate, and the adult animals are completely deaf<sup>6</sup>. We have now studied *deafness* mice in order to determine the nature of their inherited deafness. Our data indicate that stimulus-related cochlear potentials do not develop even though hair cells are present in the young animal. The endocochlear potential is present in the scala media, but behaves abnormally during anoxia.

*Deafness* mice were bred in our laboratory from stock obtained from M.S. Deol, University College, London. Heterozygotes (*+dn*) were used as controls, and were distinguished from their homozygous (*dn/dn*) littermates by the failure of the latter to exhibit a Preyer reflex in response to a metallic click. Gross VIIIth nerve action potential thresholds for control animals are presented in Fig. 1. No action potentials could be detected in *deafness* mice in any age group at any frequency, even when 5,000 stimulus repetitions were included in the average.

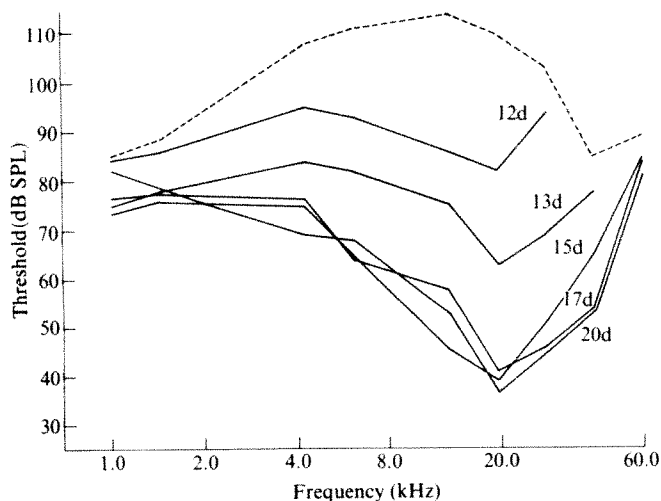
Cochlear microphonics in response to discrete continuous tones between 1 kHz and 60 kHz were recorded from the same electrode and measured with a computer-controlled lock-in amplifier. No cochlear microphonic could be recorded at any age in the mutant mice, although normal microphonics with maximum amplitudes of about 100  $\mu$ V were found in control animals. Resting noise levels for these measurements were below 0.1  $\mu$ V.



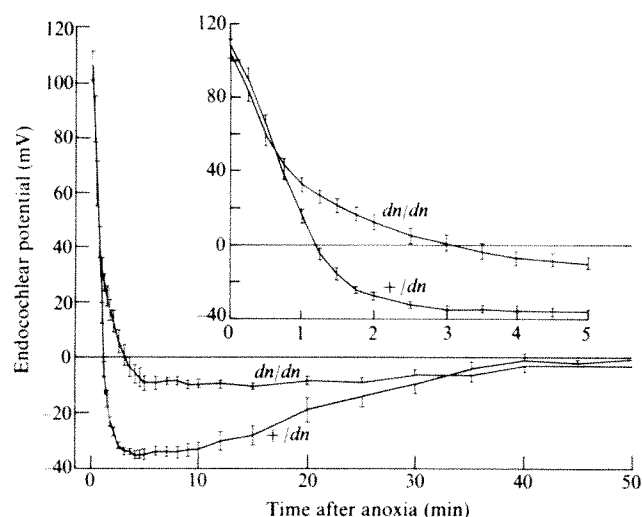
After the electrophysiological experiments, the cochleas were removed and fixed in a buffered paraformaldehyde/glutaraldehyde fixative and embedded in Spurr low-viscosity resin. In surface preparations, most of the cochlear hair cells are present and apparently intact in young (13 to 17 day) *dn/dn* mice, but there is a progressive degeneration so that fewer than 15% of the hair cells remain at 40 days. However, 2- $\mu$ m thick sections from young *deafness* mice revealed structural abnormalities in the organ of Corti even at the time when hair cells are still present. In particular, the fluid spaces around the outer hair cells and in the tunnel of Corti do not develop normally. There were no gross abnormalities in the stria vascularis.

Endocochlear potential (the positive d.c. resting potential in the scala media) was examined in mice aged 26–30 days. Potentials were measured and anoxia was induced by sealing the tracheal cannula. The data presented in Fig. 2 show that the resting potentials are identical in control and *deafness* animals, but that *deafness* animals do not show the large negative anoxia potential usually observed in scala media during anoxia<sup>7</sup>.

The present study shows a normal pattern of development in control animals<sup>8</sup>, and suggests that *deafness* mice are profoundly deaf during all stages of cochlear development, including the early stages when most hair cells are intact. There are two possible explanations for the absence of microphonics in *deafness* mice: (1) mechanical stimulation of the hair cells is absent, or (2) the mechanism of generating the microphonic from mechanical stimulation is not functioning. The first possibility seems unlikely because we can detect no external or middle ear abnormalities in the mutants. It is generally assumed that the positive endocochlear potential provides a driving force for potassium ions to cross the apical surfaces of hair cells, and that mechanical stimulation controls the opening of ion channels in the hair cell membrane, thus giving rise to the cochlear microphonic<sup>9,10</sup>. Since the positive endocochlear potential is present in *deafness*, the most likely explanation for the absence of microphonics is that the ion channels are not opening normally. It is not yet clear whether this failure constitutes the primary action of the *deafness* gene, or whether it follows as a consequence of some other genetically determined abnormality.



**Fig. 1** Mean gross VIIIth nerve action potential thresholds (as sound pressure level in dB SPL) recorded from control mice aged 12, 13, 15, 17, and 20 days after birth. Animals were anaesthetized with urethane (1.5 mg per g intraperitoneally), a tracheal cannula was inserted and the gross VIIIth nerve action potentials were recorded from a silver wire electrode on the round window. Action potentials were amplified, digitized, and averaged on a microcomputer. Responses to tone bursts (40-ms duration, 2-ms rise/fall time) delivered through a closed sound system were recorded, and threshold at a given frequency was taken to be 2.5 dB SPL below the lowest intensity producing a detectable response in an average of 50 stimulus repetitions. Six animals were studied in each age group. The broken line shows the peak output of the sound system at various frequencies.



**Fig. 2** Animals were prepared as described for Fig. 1 and a glass microelectrode filled with 3 M potassium acetate was inserted into the scala media through a fenestra over the stria vascularis of the basal turn. The potential was recorded as a function of time after the onset of anoxia induced by sealing the tracheal cannula. Each curve shows mean potentials from six animals, and the vertical bars indicate s.e.m. The insert shows the first 5 min of anoxia on an expanded scale. Mean resting potentials were 109 mV (s.e.m. = 2.6 mV) in control animals (+/dn) and 104 mV (s.e.m. = 3.1 mV) in *deafness* animals (*dn/dn*). Mean minimum anoxia potentials were -35 mV (s.e.m. = 1.4 mV) and -9 mV (s.e.m. = 2.7 mV) respectively. Analysis of variance indicated a significant ( $F = 48$ , d.f. = 1,  $P < 0.001$ ) interaction between genetic constitution and recording condition (resting potential versus anoxia potential).

Recent work on acoustic trauma and ototoxic drug-induced cochlear damage has indicated that an increase in the electrical resistance of the boundaries of the scala media as a result of this damage leads to a decrease in the negativity of the anoxia potential.<sup>11,12</sup> This is consistent with our suggestion that the ion channels across the apical surfaces of the hair cells are not opening correctly, which would lead to an increase in the electrical resistance, and a reduction in the negativity of the anoxia potential, as observed. However, our endocochlear potential data are difficult to reconcile with the generally accepted mechanism of endocochlear potential generation. It is widely assumed that the resting endocochlear potential is the sum of an active positive electrogenic component and a passive negative diffusion potential, the latter being the only component present during anoxia<sup>7,13</sup>. The absence of a large negative diffusion potential in *deafness* mice might be expected to lead to the occurrence of a significantly larger positive resting potential compared with the resting potential in control mice. This is clearly not the case in our data. We are currently measuring potassium concentration in scala media of *deafness* mice in an attempt to resolve this problem.

Finally, we suggest that the *deafness* mutant offers a promising animal model of profound hereditary deafness in man. The mutant can be used to study both the primary action of a mutation giving an uncomplicated form of deafness, and the central consequences of the total absence of auditory input during development.

We thank Dr M. S. Deol for providing mice from the *deafness* stock, Mr A. C. Davis for statistical advice and Drs M. P. Haggard and G. K. Yates for critical comments on the manuscript. This research was carried out within the framework of the European Economic Communities' Concerted Action programme for auditory research.

Received 17 July; accepted 10 September 1980.

1. Deol, M. S. *J. med. Genet.* **5**, 137–158 (1968).
2. Mikaelian, D. O. & Ruben R. J. *Arch. Otolaryngol.* **80**, 418–430 (1964).
3. Osako, S. & Hilding, D. A. *Acta oto-lar.* **71**, 365–376 (1971).

4. Fraser, G. R. *The Causes of profound Deafness in Childhood* (Johns Hopkins University Press, Baltimore, 1976)
5. Deol, M. S. & Kocher, W. *Heredity* **12**, 463-466 (1958)
6. Niauxat, M.-M., Chevance, L.-G. & Adrian, M. *C.r. Séanc. Soc. Biol.* **171**, 991-1002 (1977)
7. Bosher, S. K. *J. Physiol., Lond.* **293**, 329-345 (1979)
8. Mikaelian D. & Ruben, R. J. *Acta oto-lar.* **59**, 451-461 (1965).
9. Russell, I. J. & Sellick, P. M. *J. Physiol., Lond.* **257**, 245-255 (1976).
10. Dallos, P. *The Auditory Periphery* (Academic, New York, 1973).
11. Konishi, T. *Acta oto-lar.* **87**, 506-516 (1979).
12. Konishi, T., Salt, A. N. & Hamrick, P. E. *Hearing Res.* **1**, 325-342 (1979).
13. Johnstone, B. M. & Sellick, P. M. *Q. Rev. Biophys.* **5**, 1-57 (1972)

## Genetically determined susceptibility to *Leishmania tropica* infection is expressed by haematopoietic donor cells in mouse radiation chimaeras

J. G. Howard\*, Christine Hale\* & F. Y. Liew†

\* Division of Experimental Biology and † Department of Experimental Immunobiology, The Wellcome Research Laboratories, Beckenham, Kent BR3 3BS, UK

Models of the different disease patterns of cutaneous leishmaniasis can be established by infecting various inbred strains of mice with *Leishmania tropica*. The BALB/c strain is exceptionally susceptible in that the infection is dosage independent and inexorably progressive, terminating in cutaneous and fatal visceral metastasis<sup>1-3</sup>. This is largely determined by a single autosomal non-H-2-linked gene<sup>3</sup>, seemingly not identical to the well-characterized *Lsh* gene which determines innate susceptibility to systemic *Leishmania donovani* infection<sup>4,5</sup>. Although H-2-linked genetic influences are also detectable in the immune stage of both leishmanial infections<sup>3,6</sup>, they are relatively minor in the case of *L. tropica*. Thus, although progression of disease induced by lower infecting doses is slower in congenic BALB/K (H-2<sup>b</sup>) than in BALB/c or BALB/B (H-2<sup>b</sup>) mice, the eventual outcome is similar in all three<sup>3</sup>. This inability to control *L. tropica* infection seems to involve profound impairment of potentially curative cell-mediated immunity by the generation of a specific suppressor T-cell population<sup>7</sup>. With two other pathogens which infect mononuclear phagocytes, *Listeria monocytogenes* and *Mycobacterium lepraemurium*, differences in mouse strain susceptibility have been attributed to extrinsic factors regulating macrophage activity rather than to intrinsic gene expression within the cells themselves<sup>8,9</sup>. The relative strain susceptibility of mice to myxoviruses (determined by the dominant allele *Mx*) is also a genetic characteristic of their macrophages *in vitro*<sup>10</sup>. Nevertheless, radiation chimaeras exhibit the myxovirus resistance profile of the host despite near-total haematopoietic cell replacement, including donor macrophages which can still express their original susceptibility *in vitro*<sup>11</sup>. In contrast, the experiments described here indicate unequivocally that susceptibility to *L. tropica* in radiation chimaeras compatible at the major histocompatibility (H-2) locus is determined by the descendants of donor haematopoietic cells and not by host environmental factors.

Lethally irradiated mice injected with allogeneic bone marrow cells develop not only haematopoietic and lymphoid cells but also macrophages which are predominantly of donor type<sup>12,13</sup>. When an H-2 incompatibility is involved, mature T lymphocytes must be excluded from the donor cells to avoid the development of fatal graft-versus-host disease<sup>14</sup>. This complication is very rare when untreated marrow is transferred across a non-H-2 incompatibility and the chimaeras survive with extensive replacement of lympho-haematopoietic tissues by donor cells<sup>15</sup>. We have adapted this situation to establish reciprocal chimaerism between two H-2-compatible pairs of strains which differ widely in their susceptibility to *L. tropica*<sup>3</sup>: (1) BALB/B and C57BL/6, respectively highly susceptible and resistant,

both H-2<sup>b</sup>; (2) BALB/c and B10.D2, respectively highly and intermediately susceptible, both H-2<sup>d</sup>.

BALB/B and BALB/c mice were given 800 rads whole body irradiation, C57BL/6 and B10.D2 900 rads at a rate of 50 rads min<sup>-1</sup> from a <sup>137</sup>Cs source. They were injected the same day with  $5 \times 10^6$  bone marrow cells either syngeneic or from the H-2-compatible paired strain. Twelve weeks later they were injected over the shaved rump with  $2 \times 10^7$  viable *L. tropica* promastigotes and the ensuing lesions were observed and measured for 80-100 days as previously described<sup>3</sup> (Figs 1, 2). Syngeneically reconstituted chimaeras behaved indistinguishably from intact untreated members of the same strain. With strain pair (1), lesions in BALB/B grew progressively to fatal termination by 80-110 days, whereas in C57BL/6 they remained small and arrested by 20-30 days, with gradual healing. The same two diverging patterns were presented by the allogeneic chimaeras according to the behaviour of the donor: BALB/B → C57BL/6 highly susceptible, C57BL/6 → BALB/B relatively resistant. Complementary findings were obtained with strain pair (2), although here the differences were smaller, reflecting the lesser resistance of B10.D2 than C57BL/6. In this instance, BALB/c → B10.D2 or BALB/c chimaeras were equally susceptible, whereas B10.D2 → BALB/c or B10.D2 showed a similar intermediate profile.

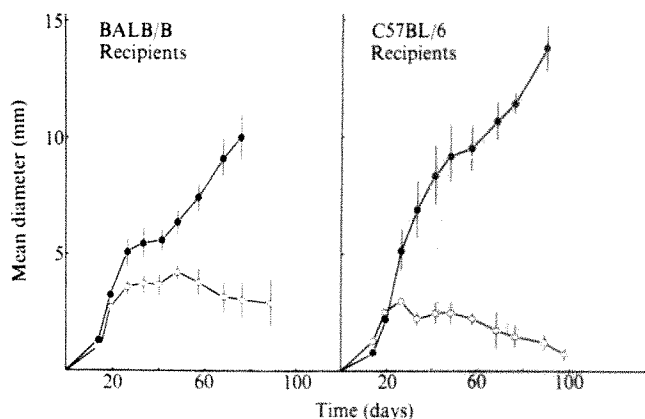
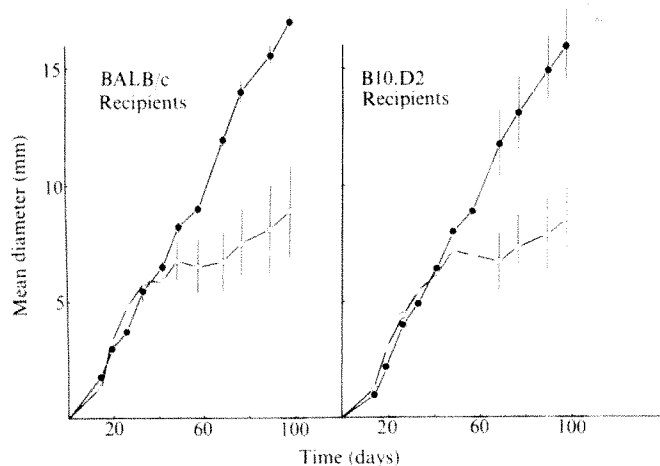


Fig. 1 The course of *L. tropica* infection in H-2<sup>b</sup>-compatible radiation chimaeras. BALB/B and C57BL/6 male mice were injected subcutaneously over the rump with  $2 \times 10^7$  promastigotes 12 weeks after lethal irradiation and reconstitution at age 8-10 weeks with  $5 \times 10^6$  bone marrow cells from BALB/B (●) or C57BL/6 (○) donors. The mean lesion size  $\pm$  s.e. is represented ( $n=5$ ). (Recipients of BALB/B cells died from disseminated leishmaniasis within 80-110 days.) The susceptibility profiles in both recipient strains are those characteristic of the donor.

These results clearly indicate that the susceptibility to *L. tropica* infection of all four recipient strains studied assumed that of the donor used to establish chimaerism, whether it be more or less resistant. Hence, the exceptional susceptibility of BALB/c and its H-2-congenic derivative lines is expressed intrinsically in some population(s) of haematopoietically derived cells, as this property is transferable by them to a resistant strain. The converse effect implies equally that BALB/c susceptibility is not an environmental influence, in striking contrast with *L. monocytogenes* infection, where reciprocal B10.A and A strain chimaeras have consistently retained resistance characteristic of the host<sup>8</sup>. Similar extrinsic regulation of macrophage activity underlying strain differences in susceptibility to *M. lepraemurium* infection is implicit in recent *in vitro* studies<sup>9</sup>, but this has not been evaluated in chimaeric animals. The fact that radiation chimaeras between strains resistant or susceptible to myxoviruses retain the





**Fig. 2** The course of *L. tropica* infection in H-2<sup>d</sup>-compatible radiation chimaeras. BALB/c and B10.D2 mice were irradiated and reconstituted with BALB/c (●) and B10.D2 (○) bone marrow cells, infected and their lesions followed as in Fig. 1 ( $n = 7$ ). (Recipients of BALB/c cells died from disseminated leishmaniasis within 90–110 days.) As in Fig. 1, the susceptibility profiles again correspond with those of the donor.

characteristic of the recipient, despite replacement of their macrophages by cells displaying donor phenotype *in vitro*<sup>11</sup>, suggests a wider distribution of cell targets for this infection. In the case of avian leukosis virus, however, where the target is the B lymphocyte alone, transference of genetic resistance and susceptibility has been achieved in chickens by post-hatching exchange of semi-allogeneic bursal cells<sup>16</sup>. The conversion of resistance to *Salmonella typhimurium* into donor-type susceptibility has been achieved by establishing bone marrow chimaerism with the C57BL/10→(C57BL/10×A/J)F<sub>1</sub> combination<sup>17</sup>, although the shift from susceptibility to resistance using the converse was detectable only in the early stage of infection and did not persist. The fact that *L. tropica* is an obligate macrophage parasite clearly contributes to the successful conversion of susceptibility into that of the haematopoietic cell donor in the present study. Although our data do not formally establish that the major gene expression is in macrophages rather than suppressor T-cell lineage, this does seem the more likely possibility by analogy with *L. donovani*, towards which isolated Kupffer cells behave *in vitro* as predicted by their strain of origin (J. Blackwell and D. J. Bradley, personal communication).

In conclusion, we report an example in which genetically determined susceptibility to a parasite infection is restricted to haematopoietic cell lineage, such that its replacement by radiation-induced chimaerism is accompanied by acquisition of the resistance/susceptibility phenotype of the donor.

Received 7 July; accepted 17 September 1980.

- Kellina, O. I. *Med. Parasit.* **42**, 279–285 (1973).
- Handman, E., Ceredig, R. & Mitchell, G. F. *Aust. J. exp. Biol. med. Sci.* **57**, 9–29 (1979).
- Howard, J. G., Hale, C. & Chan-Liew, W. L. *Parasite Immunology* (in the press).
- Bradley, D. J. *Clin. exp. Immun.* **30**, 130–140 (1977).
- Bradley, D. J., Taylor, B. A., Blackwell, J., Evans, E. P. & Freeman, J. *Clin. exp. Immun.* **37**, 7–14 (1979).
- Blackwell, J., Freeman, J. & Bradley, D. *Nature* **283**, 72–74 (1980).
- Howard, J. G., Hale, C. & Liew, F. Y. *J. exp. Med.* **152**, 594–607 (1980).
- Kongshavn, P. A. L., Sadarangani, C. & Skamene, E. *Cell. Immun.* **53**, 341–349 (1980).
- Preston, P. M. *Trans. R. Soc. trop. Med. Hyg.* **73**, 212–215 (1979).
- Lindenmann, J., Deuel, E., Fanconi, S. & Haller, O. *J. exp. Med.* **147**, 531–540 (1978).
- Haller, O., Arnheiter, H. & Lindenmann, J. *J. exp. Med.* **150**, 117–126 (1979).
- Balner, H. *Transplantation* **1**, 217–223 (1963).
- Virolainen, M. *J. exp. Med.* **127**, 943–952 (1968).
- Onoé, K., Fernandes, G. & Good, R. A. *J. exp. Med.* **151**, 115–132 (1980).
- Korngold, R. & Sprent, J. *J. exp. Med.* **148**, 1687–1698 (1978).
- Purchase, H. G., Gilmour, D. G., Romero, C. H. & Okazaki, W. *Nature* **270**, 61–62 (1977).
- Hormaeche, C. E. *Immunology* **37**, 329–332 (1979).

## Recognition of cell types by axonal growth cones *in vitro*

Friedrich Bonhoeffer & Julita Huf

Max-Planck-Institut für Virusforschung, Abteilung Physikalische Biologie, Tübingen, FRG

One of the most intriguing problems in neuroembryology is that of how growing axons find the correct way to their proper target cells. Several pathfinding mechanisms have been envisaged, including mechanical guidance through channels, guidance by diffusible substances and guidance by non-diffusible chemical cues expressed on cell surfaces and sensed by axonal growth cones. Here we describe experiments in which axons growing out from retinal explants are given the choice between two cell monolayers consisting of either retinal or tectal cells and we find that they grow preferentially over the surface covered with tectal cells. This preferential adhesion between retinal growth cones and cells originating from the *in vivo* target seems to be a property specific to the growth cone. In contrast, sorting experiments indicate that the perikarya of retinal cells adhere preferentially to retinal rather than tectal cells. It is likely that this adhesive property is due to recognition of cues expressed on the cell surfaces.

The experimental design is shown in Fig. 1. Axons originating from explants of chick retina grow through a zone where they are simultaneously exposed to two different cell types (retinal and tectal cells) and where they may 'choose' the more attractive one. A retinal explant is spread on a black membrane filter with the layer containing the ganglion cells facing up. The explant is stained with a fluorescent dye and placed upside down on the cell monolayer I. In growth medium, fluorescent axons grow from the explant towards a glass rod coated with monolayer II. Axons reaching the second monolayer have the choice between two cell types: either they decide to grow along monolayer I (Fig. 1, axon a) or along monolayer II (Fig. 1, axon b). This decision reveals their preference for a certain cell type. The ratio of fibres growing upwards along monolayer II and therefore out of the focal plane of monolayer I to that of the fibres which stay in that focal plane reflects the preference of the growth cones for the cell type of monolayer II.

To follow living axons growing in tissue or on a monolayer of cells, we have developed a technique using rhodamine-isothiocyanate (RITC) as a vital stain. Retinal explants stained with RITC and subsequently washed produce axons which remain well stained over 2 days. Figure 2 shows outgrowing fibres on an unstained monolayer of retinal cells. Outgrowing axons tend to keep their original direction over a long distance. The original direction of the fibres leaving the explant corresponds closely with the orientation of axonal growth within the retina *in vivo* where the axons are growing towards the optic fissure.

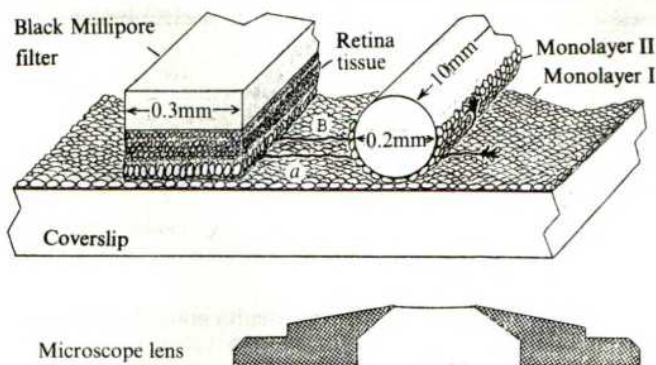
In control experiments both monolayers I and II consist of the same cell type. Our expectation is that half the axons reaching monolayer II on the glass rod should grow along monolayer I and the other half along monolayer II. However, as demonstrated in Table 1, only about 30% grow along monolayer II.

**Table 1** Fraction of fibres growing along monolayer II

| Monolayer I derived from | Monolayer II derived from |                 |                     |
|--------------------------|---------------------------|-----------------|---------------------|
|                          | Retinal cells             | Tectal cells    | Telencephalic cells |
| Retinal cells            | 0.31 (158/352)            | 0.72 (1075/417) | 0.39 (79/124)       |
| Tectal cells             | 0.036 (63/1687)           | 0.34 (289/565)  | 0.16 (94/480)       |
| Telencephalic cells      | 0.35 (46/86)              | 0.75 (130/43)   | —                   |

The total number of axons counted is shown in parentheses. The first number refers to axons growing along monolayer II, the second number refers to those which grow along monolayer I.





**Fig. 1** Principle of experimental arrangement. The retina of a 6-day-old chick embryo was surgically isolated. A black membrane filter (Sartorius, SM 13006,  $0.45\ \mu\text{m}$  pores) was soaked in Ca-Mg-free Hank's solution containing Con A ( $0.1\ \text{mg ml}^{-1}$ ) for 1 h and subsequently washed with the same buffer. The retina was spread on the membrane filter in Ca-Mg-free Hank's solution. The membrane filter containing the retina preparation was placed briefly on a dry filter paper; thus, the retina becomes firmly attached to the membrane filter. This was then placed into a staining solution, prepared as follows: 1 mg of RITC is dissolved in  $20\ \mu\text{l}$  dimethyl sulphoxide; this solution is diluted 1:5,000 with vigorous shaking into Ca-Mg-free Hank's solution. After 15 min of incubation in staining solution at room temperature, the retina and the supporting membrane filter were washed three times with Hank's solution and then incubated in culture medium (Eagle's medium containing 10% calf serum and 2% chicken serum) for 1 h at  $37^\circ\text{C}$ . Then the supporting filter with the retina was again briefly placed on a filter paper to remove the liquid and chopped into strips  $0.3\ \text{mm}$  wide. These strips were placed on the monolayer as indicated in the figure. The layer of ganglion cells touches the monolayer. The strips were held in position by small stainless steel weights at the ends of the strips where they were not covered by retina. The monolayers were prepared as follows: retina, tectum or telencephalon of chick embryos was prepared and incubated for 10 min at room temperature and for another 10 min at  $37^\circ\text{C}$  in Hank's solution containing  $1\text{--}2\ \text{mg ml}^{-1}$  trypsin. The tissue was then thoroughly washed, taken up in culture medium containing  $25\ \mu\text{g ml}^{-1}$  DNase I at a concentration corresponding to  $2\text{--}5 \times 10^6$  cells per ml, incubated for 5 min at  $37^\circ\text{C}$  and carefully dispersed by forcing the tissue twice through a capillary (10 cm long,  $0.4\ \text{mm}$  in diameter). This cell suspension was diluted with an equal volume of Ca-Mg-free Hank's solution and centrifuged for 10 min at 600 r.p.m. and  $4^\circ\text{C}$ . The sediment was taken up in Hank's solution at a concentration of  $3 \times 10^7$  cells per ml. About  $0.25\ \text{ml}$  of the cell suspension was placed on top of a pretreated coverslip ( $20\ \text{mm}$  in diameter) and the cells were allowed to settle at room temperature. After 15 min the coverslip was carefully rinsed with culture medium and kept in culture medium at  $37^\circ\text{C}$  until used for the experiment. The monolayers on the glass rods were prepared correspondingly. Pretreatment of coverslips and glass rods was necessary to achieve good cell adhesion. The silan treatment was done according to a method described by Gottlieb<sup>6</sup>. Before being used for production of monolayers, the derivatized glass was cleaned by wiping with cotton, then incubated in a Con A solution ( $1\ \text{mg ml}^{-1}$  Con A in Hank's solution) at room temperature for 1 h and finally rinsed in Hank's solution. Microscopic observation was done at  $\sim 24\ \text{h}$  after explantation, as described in Fig. 2 legend. Whether an axon is rising or staying on monolayer I was determined for each axon by changing the focal plane of observation.

It should be mentioned that the monolayers are contiguous, that the axons grow exclusively on cell monolayers and that they are completely unable to use pretreated glass covered with concanavalin A (Con A) as a substratum. At the interface of monolayer I and II, neither branching nor growing back on monolayer II has been observed.

It would be interesting to know whether axons arising from a certain position within the retina show a preference for tectal cells from a corresponding tectal area in this *in vitro* system. Experiments on antero-posterior positional effects are in progress.

Our experiments show that the growth cones of retinal axons have a clear preference for tectal cells. Is this preference a general surface property of retinal cells or is it specific to their outgrowing axons? This question can be answered by sorting experiments of the kind extensively used by Moscona<sup>1</sup>. Single-cell suspensions of retinal and tectal cells are mixed and allowed to form aggregates. If these aggregates are incubated for 24 h the cells sort out in such a way that the core preferentially



**Fig. 2** Fluorescent retinal axons growing on a monolayer of retinal cells. The edge of the stained explant is at the left. Staining of explant and preparation of monolayer are described in Fig. 1 legend. The microscopic observation is done with epifluorescence at a wavelength  $>590\ \text{nm}$  in an inverted Zeiss microscope with an image-intensifying TV camera (Siemens). The incident light range is  $510\text{--}560\ \text{nm}$ . With this technique the axons can easily be detected on a monolayer of cells.

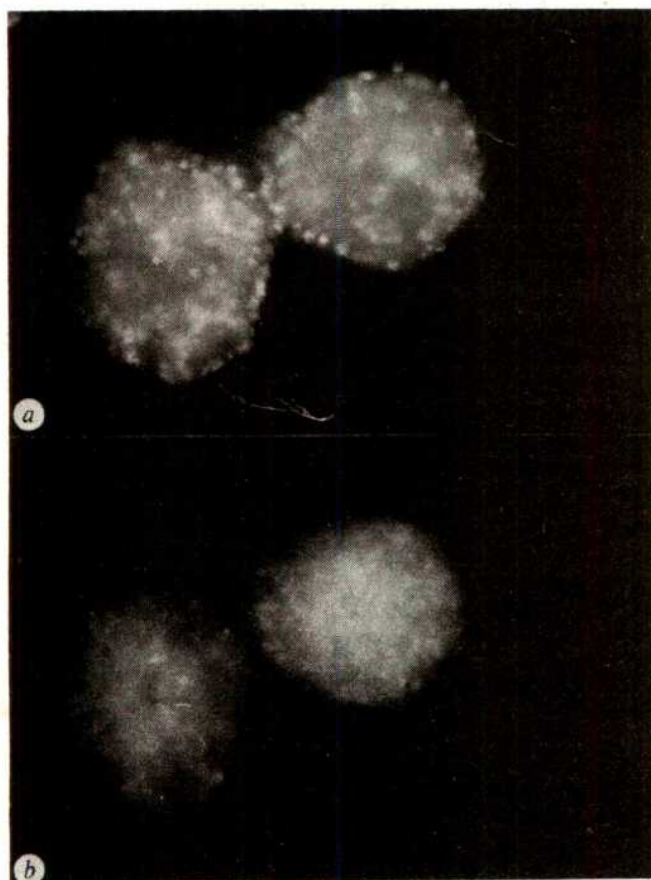
The tendency of axons to remain on the coverslip monolayer may reflect a tendency to grow in straight rather than curved paths, or incomplete contact between the monolayers.

In test experiments, one of the monolayers was prepared from retinal cells, the other from tectal cells. In all experiments retinal axons show a strong preference for cells derived from the tectum, their *in vivo* target. The preference is more pronounced if monolayer I contains tectal cells (Table 1). In 15 separate experiments, 72% of a total of 1,492 fibres preferred tectal cells on the glass rod to retinal cells on the coverslip, whereas only 4% of 1,416 fibres grew to the glass rod when it was covered with retinal cells and the coverslip contained the tectal cells. There are slight variations between experiments but in all 15 in which the glass rod carried the tectal cells, appreciably more than 50% of the axons grew along the glass rod; in none of the experiments with tectal cells on the coverslip did more than 10% of the axons grow along the glass rod carrying retinal cells. Telencephalon monolayers are no more attractive for retinal axons than retinal monolayers, and much less attractive than tectal monolayers (Table 1).

contains retinal cells, whereas the periphery consists preferentially of cells derived from the tectum. This sorting out can be observed in a fluorescence microscope if, for example, the retinal and tectal cells have been stained before mixing with RITC and fluorescein isothiocyanate (FITC), respectively. Pictures of two typical aggregates after sorting are shown in Fig. 3. The fluorescence of tectal cells is seen in Fig. 3a, that of retinal cells in Fig. 3b. Black-and-white pictures of the whole aggregates taken in one plane of focus inadequately demonstrate the clear sorting out of the two cell types, whereas direct observation of the stained cells in various focal planes show sorting out very clearly. In experiments with tectal and retinal cells derived from embryos of various ages (6, 7, 9 days), retinal cells are always in the centre of the aggregates and tectal cells always in the outer shell. According to Steinberg<sup>2</sup>, sorting experiments of this kind reveal a hierarchy of cell adhesiveness; those cells in the middle adhere more tightly to each other than to the cells of the outer shell. This indicates that for cell perikarya retina-retina adhesion is stronger than retina-tectum adhesion, in contrast to the adhesion of the retinal growth cones which, in spite of their retinal origin, adhere preferentially to tectal cells.

The combination of axon choice and cell-sorting experiments suggests that growth cones have adhesive properties which differ from the adhesive properties of the perikarya from which they





**Fig. 3** Sorting out of tectal and retinal cells. Tectal and retinal cells were labelled with RITC and FITC, respectively, as described by Burt and Gierer<sup>5</sup>, and taken up in Eagle's medium containing 20% calf serum, mixed at a concentration of about  $10^7$  cells  $\text{ml}^{-1}$  for each cell type. They were incubated on a gyratory shaker in an Erlenmeyer flask (25 ml) with 60 r.p.m. at 37 °C for 18–30 h. *a*, Fluorescence of tectal cells was observed at wavelengths  $>590$  nm with an illumination at 546 nm. *b*, Fluorescence of retinal cells was observed at wavelengths of 520–560 nm with an illumination of 450–490 nm.

originate. However, remember that sorting experiments are concerned with a mixture of all types of retinal and tectal cells and not with a pure population of retinal ganglion cells—probably the only origin of all fibres observed—and tectal target cells.

It has long been known that axonal growth is very dependent on the material offered as substratum (see, for example, ref. 3). Our experiments show that the growth cones of retinal cells can discriminate *in vitro* between various neural cell types and this capability may be used for *in vitro* axonal guidance. It remains to be shown that the guidance of axons *in vitro* corresponds with the axonal guidance in a developing brain. We believe that the present experiments strongly support the idea that growth of axons along specific pathways *in vivo* may be mediated by characteristic affinities of growth cones for specific cell surfaces. The system we describe lends itself to biochemical analysis of the specific recognition of cell types by growth cones.

We thank Dr Alfred Gierer and Michael Claviez for stimulating discussions, and Alfred Schöffski for help with the sorting experiments.

Received 9 June; accepted 12 September 1980.

1. Moscona, A. A. in *Cells and Tissues in Culture* Vol. 1 (ed. Willmer, E. N.) 689–729 (Academic, New York, 1965).
2. Steinberg, M. S. in *Cell-Cell Recognition* (ed. Curtis, A. S. G.) 25–49 (Cambridge University Press, 1978).
3. Letourneau, P. C. *Dev Biol.* **44**, 92–101 (1975).
4. Gottlieb, D. J. & Glaser, L. *Biochem. biophys. Res. Commun.* **63**, 815–821 (1975).
5. Burt, R. & Gierer, A. *Wilhelm Roux Arch. EntwMech. Org.* **187**, 367–373 (1979).

## Cross-reactivity for different type A influenza viruses of a cloned T-killer cell line

Lin Yun Lu & Brigitte A. Askonas\*

National Institute for Medical Research, The Ridgeway, Mill Hill, London NW7 1AA, UK

Spleen cytotoxic T cells killing influenza virus-infected target cells are cross-reactive for the different type A influenza viruses, in contrast to the circulating antibodies, which show fine specificity for each A virus subtype variant<sup>1,2</sup>. This finding has raised the question of whether a single T cell can recognize cells infected with all the type A viruses. T-killer cell lines with specificity for alloantigens and the male Y antigen can be selected by means of growth factors present in the supernatant of T cells stimulated with concanavalin A (refs 3–7). We report here that we have been able to establish clones of mouse T cells killing target cells infected with influenza virus. Our cell line maintains the same specificity as the heterogeneous spleen cell population from infected mice, in as far as the T-killer cells are specific for A influenza virus, but do not discriminate between the different type A viruses. The cell line maintains H-2 restriction and does not kill cells infected with B influenza virus. The cells grow in the presence of T-cell growth factor and do not require antigen for growth although they maintain their receptors for type A virus. They can also be stimulated by irradiated T-helper cells from mice primed by type A influenza infection in the presence of type A virus-infected cells.

The type A influenza specific killer cells were selected by methods similar to those described for allogeneic killer cell lines<sup>3–8</sup>. Briefly, BALB/c donor mice were primed by infection with A/X-31 (H3N2, WHO nomenclature<sup>9</sup>) influenza virus and cytotoxic T cells (CTLs) were generated by culture of the primed spleen cells with A/X-31-infected lymphoblasts<sup>1</sup>. The cells were restimulated in the same way every 10–12 days ( $7.8 \times 10^5$  cells stimulated with  $1.5 \times 10^5$  ml irradiated infected lymphoblasts) and after 2 months the cells grew well in the absence of antigen in RPMI 1640 medium containing 10% fetal calf serum and 30% rat cell supernatant (RS). RS supernatant supporting the growth of the T cells was prepared by stimulating  $3 \times 10^6$  rat spleen cells per ml with  $3 \mu\text{g ml}^{-1}$  concanavalin A for 48 h (refs 3–8). The presence of T-killer cells were ascertained by assaying lysis of <sup>51</sup>Cr-labelled P815 (H-2<sup>d</sup>) mastocytoma cells infected with type A influenza virus, or non-histocompatible infected target cells. After 4 weeks the cells could be cloned on layers of syngeneic mouse peritoneal macrophages (irradiated with 1,600 rad) using two to five cells per well in 0.1 ml in a Linbro microplate. One of the clones (L4) was highly cytotoxic for influenza-infected cells at low killer/target cell ratios. On recloning the L4 killer cells, all the subclones lysed A/X-31-infected target cells (Table 1). The clones with the highest activity were grown and tested for their specificity. Clone L4 was found to show the same specificity as the mixed population of T-killer cells generated *in vitro* by culture of primed spleen cells with infected stimulators (Table 2). The L4 killer cells do not discriminate between the different subtypes and variants of influenza virus A. Target cells infected with any of the type A viruses are lysed equally well (USSR/70) (H1N1), Jap 305 (H2N2) or X-31 (H3N2), whereas cells infected with B/HK influenza virus, or H-2<sup>k</sup>-infected target cells are not attacked. Thus, H-2 restriction is preserved.

\* To whom correspondence should be addressed.

**Table 1** Cytotoxicity of clone L4 and its subclones

|       | K/T | % Target cell lysis |      |      |
|-------|-----|---------------------|------|------|
|       |     | 5/1                 | 4/1  | 3/1  |
| L4    |     |                     |      | 26.5 |
| L4/1  |     |                     | 62.9 |      |
| L4/2  |     |                     | 40.1 |      |
| L4/5  |     |                     | 44.2 |      |
| L4/9  |     | 33.9                |      |      |
| L4/11 |     |                     |      | 31.0 |
| L4/13 |     |                     |      | 35.9 |
| L4/14 |     |                     | 29.2 |      |

<sup>51</sup>Cr-labelled P815 target cells (H-2<sup>d</sup>) were infected with A/X-31 virus for 1 h. Following the addition of killer cells, lysis of  $2 \times 10^4$  target cells was assayed after 6 h by estimating the amount of <sup>51</sup>Cr released by the killer cells<sup>17</sup>. Control spontaneous release was 18%. Target cell lysis was expressed as %<sup>51</sup>Cr released = c.p.m. (experimental) - c.p.m. (spontaneous release)/c.p.m. (total) - c.p.m. (spontaneous release). K/T, killer/target cell ratio.

With time of culture, cytotoxicity and the rate of growth of L4 clones seem to decline. However, we have been able to grow the cells from frozen stock and to reclone on irradiated macrophages and have maintained highly cytotoxic clones for 8 months.

Although the established L4 cell line does not require antigen for its growth, because growth is supported by nonspecific and non-H-2- or strain-restricted growth factors produced by activated T cells, the cells clearly preserve their receptors for antigen recognition. First, L4 cells retain their killer specificity for type A influenza viruses, and second, 20% of the continuously growing T cells form clusters with P815 cells infected with type A virus but not with cells infected with influenza B virus (experiments with W. A. Taylor, using the method of Berke *et al.*<sup>10</sup>).

Growth and killer activity of L4 clones can also be induced in the presence of macrophages by stimulation with infected stimulator cells (irradiated spleen) and irradiated T-helper cells<sup>11</sup> from mice primed by infection with type A virus (Table 3). The L4 killer cells die in the absence of T-cell growth factor (RS) or irradiated T-helper cells plus antigen. The requirement for T-cell growth factor on its own distinguishes the T-cell clones from memory precursors of cytotoxic T cells in mice primed by infection. We find that the memory cells require antigen and T-cell growth factors for the generation of cytotoxic cells (B.A.A., unpublished results). This indicates that the continuously growing cells are at the last stage of differentiation. Fluorescent staining with monoclonal rat antibodies showed

**Table 2** Specificity of L4 killer cells, H-2 restriction and cross-reactivity between different type A influenza viruses

| H-2 | Target cells<br>Influenza<br>infection | K/T | % <sup>51</sup> Cr release |      |      |      |
|-----|--|-----|----------------------------|------|------|------|
|     |  |     | 10                         | 5    | 2.5  | 1.2  |
| d   | A/X-31 (H3N2)*                         |     | 60.4                       | 54.7 | 39.8 | 27.7 |
| d   | A/Jap (H2N2)                           |     | 71.6                       | 62.9 | 49.1 | 41.2 |
| d   | A/USSR (H1N1)                          |     | 79.6                       | 65.8 | 59.9 | 54.9 |
| d   | B/HK                                   |     | 6.5                        | 4.7  | 1.9  | 1.6  |
| d   | Uninfected                             |     | 4.7                        | 2.1  | 1.1  | 1.3  |
| k   | A/X-31 (H3N2)                          |     | 7.5                        | 7.7  | 4.5  | 0    |

The L4 cells were derived from mice primed with A/X-31 virus and induced *in vitro* with the same virus. Target cells were labelled with <sup>51</sup>Cr and infected with influenza virus<sup>17</sup>. H-2<sup>k</sup> target cells were CBA lymphoblasts induced with lipopolysaccharide and infected with A/X-31 virus. Such target cells are lysed by CBA T-killer cells. H-2<sup>d</sup> target cells were similarly infected P815 mastocytoma cells. <sup>51</sup>Cr-release assay was as in Table 1.

\* H = viral haemagglutinin, WHO nomenclature<sup>9</sup>; N = viral neuraminidase.

**Table 3** Cloned T-killer cells respond to virus-stimulated T-helper cells

| Clone L4/2<br>(cells $\times 10^{-4}$<br>per well) | 10 <sup>5</sup><br>Stimulator<br>cells | 4 $\times 10^4$<br>Macrophages | 1.5 $\times 10^5$<br>T-helper<br>cells + | % Target<br>cell lysis |
|--|--|--------------------------------|--|------------------------|
| 2.5  | +                                      | +                              | +  | 10.4 ( $\pm 1.1$ )     |
| 5  | +                                      | +                              | +  | 19 ( $\pm 0.6$ )       |
| 5  | -                                      | +                              | -  | 0                      |
| 5  | -                                      | +                              | +  | 0                      |
| -  | +                                      | +                              | +  | 0                      |
| 2.5  | -                                      | +                              | -  | 0                      |
| 5  | -                                      | +                              | -  | 0                      |
| 5  | +                                      | +                              | -  | 0                      |

Stimulator cells are normal spleen cells irradiated (1,200 rad) and infected with A/X-31 influenza virus. Peritoneal exudate macrophages were seeded into microwells and irradiated at 1,600 rad before addition of the T-killer clone. +T-helper cells were spleen cells irradiated at 600 rad (ref. 11) and derived from mice primed intranasally by infection with A/X-31 virus 2 months previously. Target cell lysis on day 4 was assayed on  $10^4$  A/X-31 infected P815 mastocytoma cells, labelled with <sup>51</sup>Cr and added to the microwells after centrifuging the plate and removing the culture medium. Values for mean lysis by 6-12 culture wells are given ( $\pm$ s.e.).

that the L4 killer cells bear the Lyt 2 marker, but are Lyt 1 negative.

We have not been able to convert the L4 cytotoxic cells into memory cells by transferring them into syngeneic mice and challenging with influenza virus. However, we have been able to protect mice from death following lethal infection with A/X-31 virus. BALB/c mice were irradiated at 450 rad (Co source) and infected with A/X-31 influenza intranasally (25-50 haemagglutinin units in 100  $\mu$ l of 1/100 allantoic fluid). One day later, the mice received normal spleen cells, or our continuously growing cytotoxic T cells. Mice receiving no cells, or  $3 \times 10^6$  normal spleen cells intravenously died by day 17 or earlier, whereas the mice which had received  $3 \times 10^6$  L4 cytotoxic cells survived for more than 4 weeks. The cloned cells therefore show protective activity *in vivo* as do primed normal T cells restricted at the K and D end of H-2 (ref. 12).

It is not certain which viral protein is being recognized by A influenza-specific T-killer cells, but our killer cell line should help resolve this question. The internal matrix protein shared between the different type A viruses was previously thought to be recognized by cross-reactive T cells<sup>13,14</sup>; however, recent data indicate that killer T cells recognize a region of the haemagglutinin molecule homologous in all type A influenza viruses<sup>15-17</sup>.

L.Y.L. is a British Council-Chinese Exchange Scholar, Shanghai First Medical College. Monoclonal rat antibodies were provided by Dr L. Herzenberg.

Received 30 July; accepted 22 September 1980.

- Zweerink, H. J., Courtneidge, S. A., Skehel, J. J., Crumpton, M. J. & Askanas, B. A. *Nature* **267**, 354-356 (1977).
- Effros, R. B., Doherty, P. C., Gerhard, W. & Bennink, J. J. *exp. Med.* **145**, 557-568 (1977).
- Von Boehmer, H. *et al. Eur. J. Immun.* **9**, 592-597 (1979).
- Gillis, S., Baker, P. E., Ruscetti, F. W. & Smith, K. A. *J. exp. Med.* **148**, 1093-1098 (1978).
- Gillis, S. & Smith, K. A. *Nature* **268**, 154-156 (1977).
- Dennert, G. *Nature* **277**, 476-478 (1979).
- Glasebrook, A. L. & Fitch, F. W. *J. exp. Med.* **151**, 876-895 (1980).
- Nabholz, M., Engers, H. D., Collavo, P. & North, M. in *Current Topics in Microbiology and Immunology* (eds Melchers, F., Potter, M. & Warner, N.) 81-176 (Springer, New York, 1978).
- Bull. Wild Hlth Org.* **45**, 119 (1971).
- Berke, G., Sullivan, K. A. & Amos, D. B. *J. exp. Med.* **135**, 1335-1350 (1972).
- Ashman, R. B. & Müllbacher, A. *J. exp. Med.* **150**, 1277-1282 (1979).
- Yap, K. L., Ada, G. L. & McKenzie, F. C. *Nature* **273**, 238-239 (1978).
- Biddison, W. E., Doherty, P. C. & Webster, R. G. *J. exp. Med.* **146**, 690-697 (1977).
- Braciale, T. J., Ada, G. L. & Yap, K. L. *Contemporary Topics molec. Immun.* **7**, 319-364 (1978).
- Koszinowski, U. H., Allen, H., Gething, M. J., Waterfield, M. D. & Klenk, H. D. *J. exp. Med.* **151**, 945-958 (1980).
- Hackett, C. J., Askanas, B. A., Webster, R. G. & van Wyke, K. J. *J. exp. Med.* **151**, 1014-1025 (1980).
- Askanas, B. A. & Webster, R. G. *Eur. J. Immun.* **10**, 151-156 (1980).



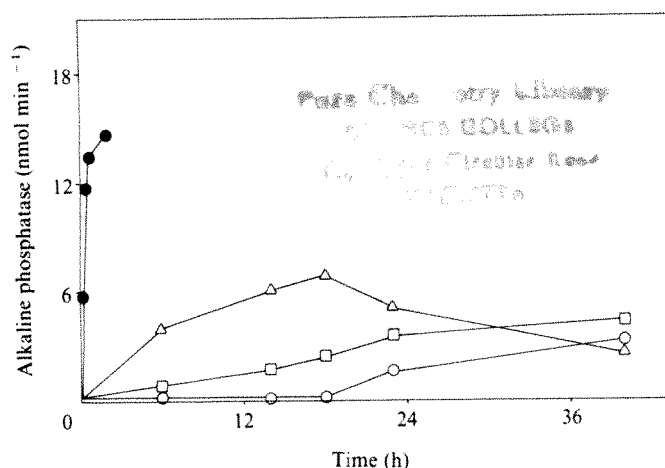
# Reversible heat activation of alkaline phosphatase of *Dictyostelium discoideum* and its developmental implication

D. V. Mohan Das & Gerald Weeks

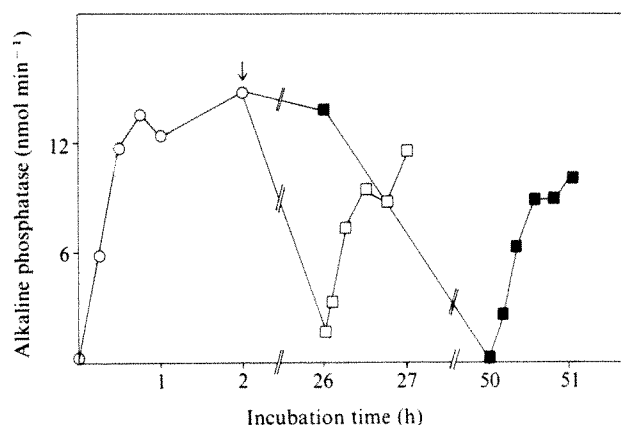
Department of Microbiology, University of British Columbia, Vancouver, Canada V6T 1W5

The activities of some enzymes increase during the development of the cellular slime mould, *Dictyostelium discoideum*. Because optimal specific activity is attained by each enzyme at a specific developmental stage<sup>1</sup>, development can be followed as a function of enzyme activity. The activity of one of these enzymes, alkaline phosphatase, increases markedly during the late stages of development, making it a potentially useful marker for terminal differentiation<sup>2,3</sup>. It has been suggested that this increase in activity is due to *de novo* enzyme synthesis because the increase in activity does not occur in the presence of inhibitors of RNA and protein synthesis<sup>2</sup>. However, we present evidence here of reversible heat activation of membrane-bound alkaline phosphatase which suggests that the increase in alkaline phosphatase activity may be due to an unmasking of pre-existing enzyme by a novel membrane regulatory mechanism.

Alkaline phosphatase is firmly membrane bound, and evidence suggests that it is located on both the plasma membrane<sup>3-5</sup> and the internal contractile vacuole membrane<sup>6</sup>. We found that there was a considerable decrease in alkaline phosphatase activity if a crude membrane preparation from vegetative-phase cells was stored at 4 °C. Activity was restored, however, if the membrane preparation was incubated at room temperature, and a dramatic increase in activity was observed if the enzyme was incubated at elevated temperatures. With increasing temperature the rate and amount of the enzyme activation increased (Fig. 1), reaching a maximum at 50 °C. Although not shown in



**Fig. 1** The effect of preincubation temperature on the activity of membrane-bound alkaline phosphatase. Crude membranes of vegetative cells of *D. discoideum*, strain Ax-2, were prepared as described previously<sup>8</sup>, resuspended in 5 mM Tris-Cl, pH 7.4, at 4 mg ml<sup>-1</sup> and incubated at 13.5 °C (○), 21 °C (□), 33.5 °C (△) or 50 °C (●). After the indicated periods of incubation, 0.1-ml aliquots of the membrane were assayed for alkaline phosphatase activity at 30 °C in a total assay volume of 1.0 ml as described previously<sup>3</sup>, with the addition of 30 mM NaF to inhibit acid phosphatase.



**Fig. 2** The reversible heat activation of alkaline phosphatase. Crude membrane preparations of vegetative cells were incubated at 50 °C and aliquots were removed at the indicated time points (○) and assayed for alkaline phosphatase activity at 30 °C. After 2 h of incubation at 50 °C (at the arrow) the preparation was divided into two and one portion (□) was incubated for 24 h at 0 °C followed by 1 h at 50 °C. At the indicated time points (□), aliquots were removed and assayed for alkaline phosphatase at 30 °C. The second sample (■) was rapidly cooled to -70 °C, maintained at -70 °C for 24 h and then incubated at 0 °C for 24 h, followed by 1 h at 50 °C. At the indicated time points (■), aliquots were assayed for alkaline phosphatase activity at 30 °C.

this experiment, activity at 50 °C is stable for up to 6 h. Incubation at 60 °C led to variable results (data not shown), whereas incubation at 70 °C resulted in a total inactivation of the enzyme.

This heat activation is totally reversible. A membrane preparation was heated at 50 °C for 2 h, and alkaline phosphatase activity increased markedly (Fig. 2). The preparation was then divided and one portion stored at 0 °C for 24 h, whereas the other was rapidly frozen in acetone/dry ice and stored at -70 °C for 24 h. The membrane fraction stored at 0 °C lost considerable alkaline phosphatase activity, but when reheated at 50 °C, activity was rapidly restored (Fig. 2). This heat activation-cold inactivation cycle could be repeated three times (data not shown) indicating that the phenomenon was totally reversible. The sample stored at -70 °C retained the elevated heat-activated level (Fig. 2), but when transferred to 0 °C, the activity declined markedly over a 24-h period. The enzyme could be reactivated by incubating at 50 °C.

Thus, membrane-bound alkaline phosphatase activity is markedly dependent on the temperature of storage. The mechanism of the reversible temperature-dependent activation is not known, but the factor(s) involved in the phenomenon are tightly membrane bound, as even after recentrifugation at 100,000g and resuspension in fresh buffer, both heat-activated and cold-inactivated membranes retained their capacity for the reversible activation or inactivation of the enzyme.

**Table 1** Comparison of the effects of preincubation at 50 °C and 0 °C on the alkaline phosphatase activity of intact membrane and butanol-extracted preparations

| Preparation   | No treatment | Preincubated at 50 °C for 60 min | Preincubated at 0 °C for 24 h |
|---|--------------|----------------------------------|-------------------------------|
| Specific activity of alkaline phosphatase (nmol min <sup>-1</sup> per mg protein) |              |                                  |                               |
| Intact membrane   | 9.2          | 74.0                             | 3.1                           |
| Butanol extract*  | 105.0        | 56.0                             | 96.0                          |

\* The butanol-extracted preparation was prepared by briefly vortexing a mixture of 0.4 ml butanol and 1.0 ml of a suspension of crude membranes in 5 mM Tris-Cl, pH 7.4 (10 mg protein ml<sup>-1</sup>). The aqueous phase was removed carefully, dialysed for 24 h against 0.01 M Tris-Cl, pH 7.4, and assayed for alkaline phosphatase activity at 30 °C after the indicated preincubation conditions. Over 70% of the activated membrane-bound alkaline phosphatase is solubilized by this procedure.

To investigate this phenomenon further, alkaline phosphatase activity was solubilized from the membrane by butanol treatment. Following butanol extraction the alkaline phosphatase activity of the aqueous phase was elevated to a level slightly higher than that observed following heat treatment (Table 1). When this solubilized enzyme was incubated at 0 °C for 24 h there was no loss in activity, whereas incubation at 50 °C for 60 min caused a reduction in activity, characteristics quite different from those of the enzyme of the intact membrane (Table 1). Thus, maintenance of membrane integrity seems to be essential for the expression of the reversible heat activation-cold inactivation of the enzyme.

The alkaline phosphatase activity of freshly prepared membranes from cells at later stages of development is considerably higher than that of vegetative cells, reaching peak levels at the culminating stages of development (Table 2). The activity of culminating cell membranes is not markedly responsive to heat activation or cold inactivation; there is no decrease in activity on storage at 0 °C for 24 h, and only a slight elevation on incubation at 50 °C for 1 h (Table 2). Alkaline phosphatase from pseudoplasmodial-stage cells is partially responsive to the heat activation phenomenon (Table 2). There is a slight cold-activation effect in pseudoplasmodial membranes but at present this phenomenon is not understood. As the peak activities of alkaline phosphatase in culminating membranes is of the same order of magnitude as the maximum activated levels of vegetative membranes, clearly vegetative-phase cells express only a small proportion of their potential alkaline phosphatase activity, whereas the culminating-phase cells express most of theirs. There is a twofold increase in the heat-treated levels of activity in culminating cells compared with vegetative cells (Table 2). This may indicate that heat treatment does not fully unmask the vegetative activity. Alternatively, as the amount of protein per cell decreases during differentiation<sup>7</sup>, the amount of membrane protein per cell probably decreases concomitantly, and the twofold increase in the specific activity of a membrane-bound enzyme would reflect no change in the amount of enzyme per cell. We have not investigated this possibility further due to the difficulty of determining accurately the yields of differentiating cells.

**Table 2** Comparison of the effects of preincubation of 0 °C and 50 °C on the alkaline phosphatase activity of membranes prepared from Ax-2 cells at various stages of development

| Developmental stage   | Developmental time (h) | Freshly prepared membranes | Preincubated at 0 °C for 24 h | Preincubated at 50 °C for 1 h |
|---|------------------------|----------------------------|-------------------------------|-------------------------------|
| Alkaline phosphatase specific activity (nmol min <sup>-1</sup> mg <sup>-1</sup> ) |                        |                            |                               |                               |
| Vegetative  | 0                      | 9.2                        | 3.1                           | 74.0                          |
| Pseudoplasmodium  | 22                     | 43.0                       | 71.0                          | 105.0                         |
| Preculmination  | 30                     | 108.0                      | 105.0                         | 139.0                         |
| Late culmination  | 34                     | 105.0                      | 92.5                          | 133.0                         |

It should be emphasized that the alkaline phosphatase activity of vegetative cells is the same, whether the membranes are prepared at 4 °C or 22 °C (data not shown), indicating that the low activity of freshly prepared vegetative membranes is not due to the low temperature of the preparative procedure<sup>8</sup>. We believe, therefore, that the apparent increase in alkaline phosphatase activity is due to unmasking of existing enzyme rather than to an increase in amount of enzyme. McCleod and Loomis<sup>9</sup> have recently presented evidence that the vegetative and developmentally determined enzymes are products of the same gene, a finding not inconsistent with the above suggestion.

This lack of correlation between the observed level of the enzyme and the amount of enzyme protein has also been reported during *D. discoideum* development (for example, see ref. 10). However, this is the first instance of an apparent unmasking of a presumptive developmentally regulated enzyme by heat treatment.

Although there is probably no direct physiological significance to the reversible heat activation of the membrane-bound alkaline phosphatase, this phenomenon apparently simulates the effect of a plasma membrane modification that occurs during development. This could involve the removal of a low-molecular-weight effector molecule or the dissociation of inactive protein aggregates within the plane of the membrane. We are investigating these possibilities.

We thank Dr G. Webb for helpful discussions and the National Science and Engineering Research Council of Canada for financial support.

Received 12 June; accepted 2 September 1980.

1. Loomis, W. F. Jr *Dictyostelium discoideum: A Developmental System* (Academic, New York, 1975).
2. Loomis, W. F. Jr *J. Bacteriol.* **100**, 417 (1969).
3. Lee, A., Chance, K., Weeks, C. & Weeks, G. *Archs Biochem. Biophys.* **171**, 407 (1975).
4. Green, A. A. & Newell, P. C. *Biochem. J.* **140**, 313 (1974).
5. Parish, R. W. & Pelli, C. *FEBS Lett.* **48**, 293 (1974).
6. Quiviger, B., De Chastellier, C. & Rytter, A. J. *Ultrastruct. Res.* **62**, 228 (1978).
7. White, G. L. & Sussman, M. *Biochim. biophys. Acta* **53**, 285 (1961).
8. Gilkes, N. R. & Weeks, G. *Biochim. biophys. Acta* **464**, 142 (1977).
9. McCleod, C. L. & Loomis, W. F. *Dev. Genet.* **1**, 109 (1979).
10. Kessin, R. H., Orlov, S. J., Shapiro, R. I. & Franke, J. *Proc. natn. Acad. Sci. U.S.A.* **76**, 5450 (1979).

## SV40 large T shares an antigenic determinant with a cellular protein of molecular weight 68,000

D. P. Lane\* & W. K. Hoeffler

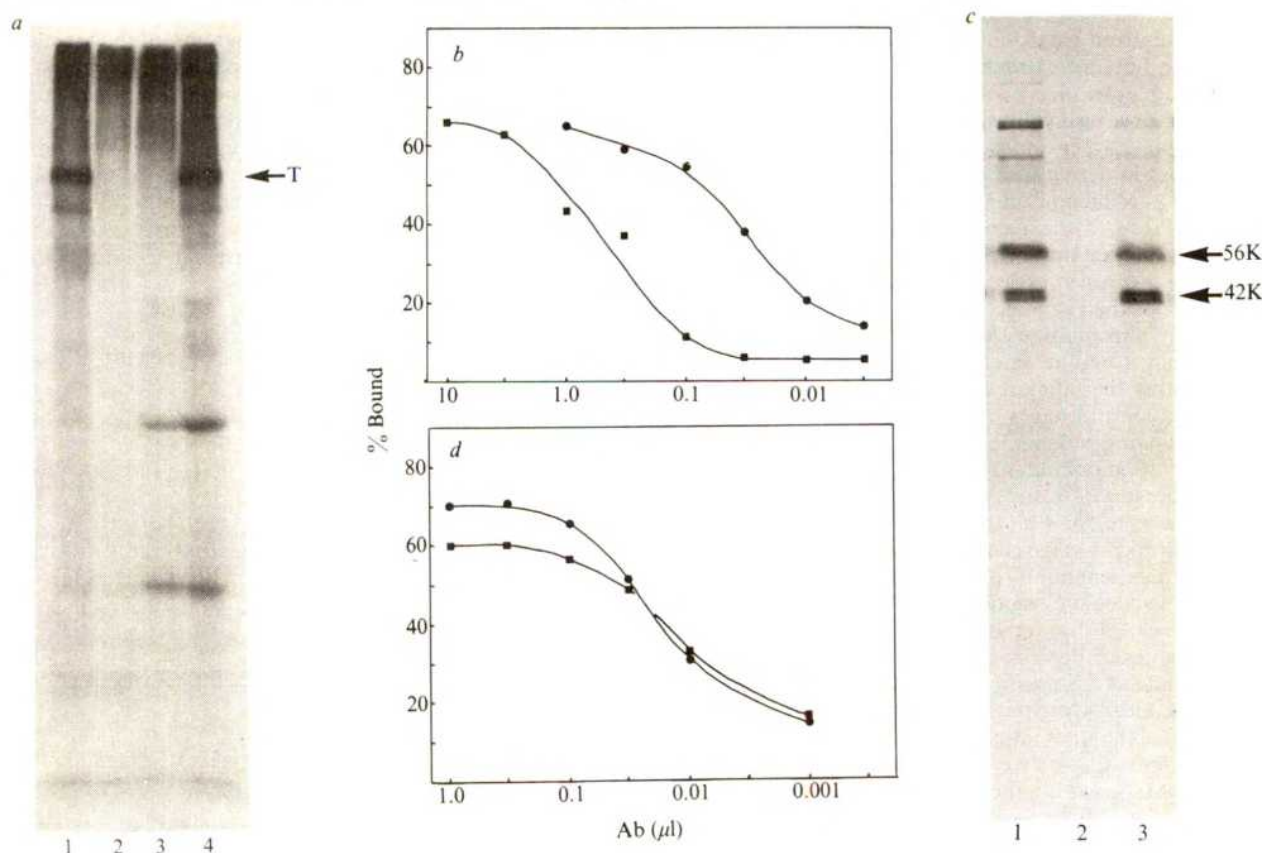
Cold Spring Harbor Laboratory, Cold Spring Harbor, New York 11724

The large T protein coded by the early region of simian virus 40 (SV40) is involved in the induction and maintenance of cell transformation<sup>1</sup>. It is not clear which properties of T are important in causing the transformation, since the protein is multifunctional<sup>2-9</sup>. To clarify the action of T proteins in transformation, we have prepared several monoclonal antibodies directed against different regions of the T molecule. One of these antibodies, DL 3C4, recognizes an antigenic determinant on T that is also present on a host cell protein of molecular weight 68,000. This cross-reactive 68K protein is located within the nucleus of all mammalian cell types examined and has a characteristic granular distribution as shown by immunofluorescence. The antigenic determinant recognized by DL 3C4 is resistant to denaturation. Studies on Adeno-SV40 hybrid viruses show that the antigenic site on T is coded for by sequences located between 0.44 and 0.29 on the SV40 map.

The cell line producing the monoclonal antibody DL 3C4 was derived from a fusion between the HAT (hypoxanthine, aminopterin and thymidine)-sensitive myeloma cell line Sp2/O-Ag14 (refs 10-12) and spleen cells from a BALB/c mouse which had been hyperimmunized with the T antigen-related protein purified from Ad2<sup>+</sup> D2-infected HeLa cells<sup>5</sup>. Ten days after fusion cell culture supernatants were screened, using an indirect immunofluorescence test, for antibodies capable of staining the nuclei of SV40-transformed cells (SV80). The supernatants from 11 out of 96 wells were positive by this test and the cells from these wells were cloned using a soft-agarose method. (A detailed description of the methods will be published elsewhere, D. L., in preparation.)

\* Present address: Department of Zoology and Cancer Research Campaign Eukaryotic Molecular Genetics Research Group, Imperial College, London SW7 2AZ, UK.





**Fig. 1** Monoclonal antibody 3C4 binds to a specific region of SV40 large T antigen. *a*, SV80 cells, in a 60-mm Petri dish, were labelled for 1 h in phosphate minus E4 medium with 1 mCi of  $^{32}\text{P}$  and the labelled proteins extracted in 1 ml of 1% NP40, 120 mM NaCl, 50 mM Tris, pH 8.0. 100  $\mu\text{l}$  of the extract were incubated with (1) 10  $\mu\text{l}$  hamster anti-tumour serum, (2) 10  $\mu\text{l}$  normal hamster serum, (3) 50  $\mu\text{l}$  E4 medium and (4) 50  $\mu\text{l}$  supernatant E4 medium from a culture of 3C4 cells. After 1 h at room temperature 20  $\mu\text{l}$  of rabbit anti-mouse immunoglobulin serum (Rb $\alpha$  Mlg) were added to tubes (3) and (4) as 3C4 does not bind to protein A directly and then 1 h later 40  $\mu\text{l}$  of a 10% suspension of fixed *Staphylococcus aureus* Cowan 1 (ref. 21) were added. The bacteria were collected by centrifugation, washed four times in NET buffer<sup>21</sup> and the adsorbed immune complexes eluted by boiling in 50  $\mu\text{l}$  of SDS-gel sample buffer. The eluted proteins were analysed on a 15% polyacrylamide slab gel<sup>20</sup> and the labelled proteins detected by autoradiography of the stained fixed and dried gel. (The minor band below large T is a 73K breakdown product of T). *b*, Purified  $^{35}\text{S}$ -labelled large T antigen was isolated by immunoprecipitation and preparative SDS-gel electrophoresis from lysates of  $^{35}\text{S}$ -labelled SV40-infected CV1 cells as before<sup>13</sup>. It was then used to titrate the relative T-binding capacity of a rabbit antibody to large T (■) and of the monoclonal antibody 3C4 (●). The monoclonal antibody was used as the ascites fluid from a BALB/c mouse which had been injected intraperitoneally 10 days earlier with  $10^7$  3C4 cells. The radioimmunoassay was as described previously except in the case of the monoclonal antibody 20  $\mu\text{l}$  of Rb $\alpha$  Mlg were added, 1 h before the addition of 50  $\mu\text{l}$  SAC. Input was 1,000 c.p.m. of T. *c*, A 60-mm Petri dish contained HeLa cells, labelled with 500  $\mu\text{Ci}$  of  $^{35}\text{S}$ -methionine in met E4 medium 30 h after infection with Ad2<sup>+</sup>ND2 virus. After labelling for 1 h the labelled proteins were extracted as described in *a* and immunoprecipitated with (1) 10  $\mu\text{l}$  rabbit anti-T serum, (2) 20  $\mu\text{l}$  Rb $\alpha$  Mlg, and (3) 0.1  $\mu\text{l}$  3C4 ascites fluid + 20  $\mu\text{l}$  Rb $\alpha$  Mlg. The antibody-bound proteins were collected and analysed as in *a* except that a 10% SDS-polyacrylamide gel was used. *d*, Purified  $^{35}\text{S}$ -labelled 56K and 42K T-related proteins were isolated from extracts of  $^{35}\text{S}$ -labelled Ad2<sup>+</sup>ND2-infected HeLa cells as described for large T in *b*. The isolated proteins were then individually used in the radioimmunoassay to titrate the 3C4 ascites fluid binding to (■), the 56K protein (input 2,070 c.p.m.) and to (●), the 42K protein (input 2,360 c.p.m.).

The hybridoma cell line DL 3C4 has been cloned four times and grows well in culture. When injected into pristane-primed mice it induces an ascites tumour and the ascites fluid contains extremely high titres of the antibody ( $>1/10^4$  in the immunofluorescence test). The antibody synthesized by 3C4 specifically immunoprecipitates T antigen from lysates of  $^{32}\text{P}$ -labelled SV80 cells (Fig. 1*a*) and confirmation of its specificity for large T was obtained by radioimmunoassay<sup>13</sup>. The ascites fluid and supernatant tissue culture media of 3C4 cells were able to bind specifically pure  $^{35}\text{S}$ -labelled T antigen. (Isolated from  $^{35}\text{S}$ -methionine-labelled SV40-infected monkey cells by immunoprecipitation with a defined anti-T serum<sup>13</sup> followed by SDS-gel electrophoresis.) Figure 1*b* shows the titration 3C4 ascites fluid in such a radioimmunoassay. The monoclonal antibody could also immunoprecipitate the T-related proteins of molecular weights 56,000 and 42,000 present in extracts of Ad2<sup>+</sup>ND2-infected HeLa cells (Fig. 1*c*). Furthermore the antibody bound specifically to both polypeptides after they had been isolated by immunoprecipitation and elution from SDS gels (Fig. 1*d*). These experiments show that the 3C4 antibody

recognizes a determinant on T which is coded by the SV40 DNA present in the Ad2<sup>+</sup>ND2 virus (0.44–0.11 map units)<sup>14</sup> and which is resistant to the denaturing effects of SDS-gel electrophoresis. The 3C4 antibody did not immunoprecipitate or bind to the 30,000-molecular weight T-related protein synthesized in Ad2<sup>+</sup>ND1-infected cells (data not shown) and it is reasonable to assume that the determinant is therefore not coded by the SV40 DNA in this virus (0.29–0.11 map units)<sup>15</sup>. This approximately localizes the region coding for the determinant to sequences between 0.44 and 0.29 on the SV40 map. The determinant must be present on the majority of T-antigen molecules as the monoclonal antibody can bind the same proportion of the isolated  $^{35}\text{S}$ -labelled T antigens as a variety of other anti-T sera (Fig. 1).

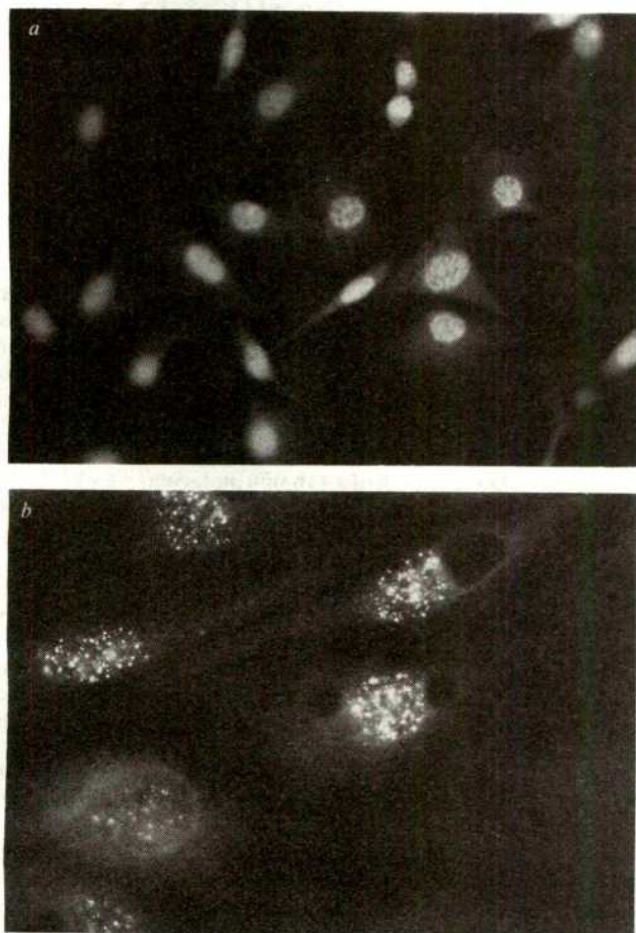
Having observed the specificity of 3C4 for a particular region of T antigen, it was surprising to discover that the antibody gave a positive specific nuclear fluorescent staining pattern on a wide variety of different cell types that do not contain SV40 DNA or the SV40 T antigen. Figure 2 shows examples of this staining pattern on two different mammalian cell lines: KA31 cells are RNA-virus transformed murine fibroblast cells and PtK1 cells



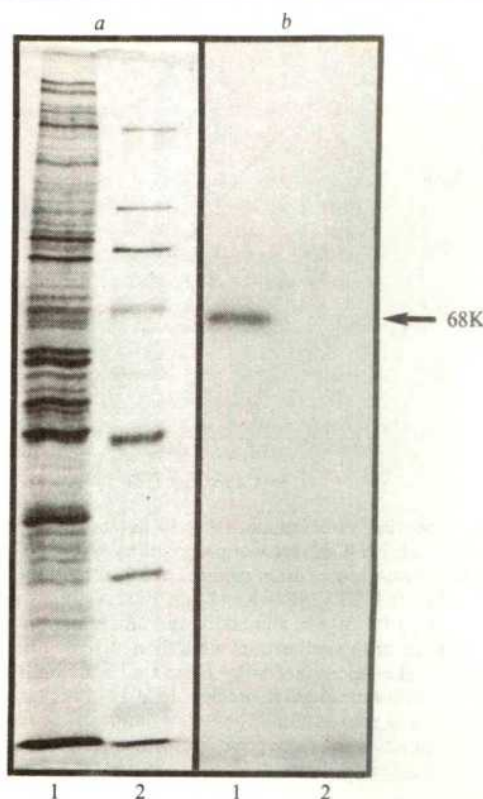
are untransformed kidney epithelium cells from the marsupial *Potorous tridactylis*<sup>16</sup>. In both lines, especially PtK1 cells, the staining pattern is clearly nuclear and strikingly granular. Various cell lines, including cells of human, monkey and rat origin, all show the positive nuclear staining pattern, so the determinant being recognized is clearly highly conserved in the mammals. None of the other anti-T monoclonal antibodies examined, nor a variety of conventional anti-T sera, show such positive reactions on these cells, so the effect seems to be restricted to the DL 3C4 monoclonal antibody.

The species recognized by 3C4 in one of these SV40 T antigen-negative cell lines was identified using the immunautoradiography technique described by Burrige<sup>17</sup>. A single protein of molecular weight 68,000 is detected in extracts of mouse L cells (Fig. 3). Attempts to identify this protein by immunoprecipitation of conventional NP40 lysates of these cells were only partially effective. The protein is present in low concentration and poorly solubilized by buffers that effectively extract the viral T antigen from SV40-infected or -transformed cells, most of the antigen remaining in the insoluble pellet.

One hypothesis to explain the apparent dual specificity of 3C4 for the virally coded SV40 T antigen and the 68K host cell protein is that these two proteins share a common structural



**Fig. 2** Detection of a T-related protein in the nuclei of cells that do not contain SV40 DNA. Cells for immunofluorescence were grown on glass coverslips, washed in PBS, fixed in a 1:1 mixture of acetone and methanol at room temperature for 2 min, then overlaid with a 1/50 dilution of 3C4 ascites fluid. After 20 min of incubation the coverslips were washed in phosphate-buffered saline (PBS) and then overlaid with a 1/30 dilution of rhodamine-conjugated rabbit antibody to mouse immunoglobulin (Cappel). After a 20-min incubation the coverslips were washed in PBS and then with distilled water before mounting in gelvatol (Monsanto Chemicals) on clean glass slides. The coverslips were examined under a fluorescence microscope. *a*, Staining of KA31 cells. *b*, Staining pattern of PtK-1 cells.

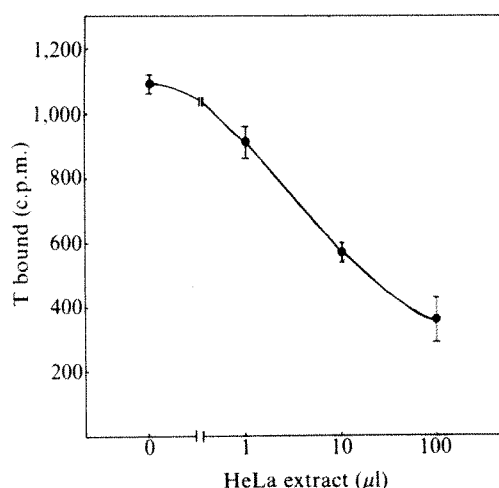


**Fig. 3** Immunautoradiographic detection of the protein bound by 3C4 in cells that do not contain T-antigen. A complete nuclease-treated extract of mouse L cells, solubilized in sample buffer, was electrophoresed on a 10% SDS-polyacrylamide gel. Track 1, 40  $\mu$ l L cell extract ( $2 \times 10^5$  cells). Track 2, Marker proteins: 200K, 130K, 94K, 45K, 30K, 21K. *a*, Shows the gel stained with Coomassie blue. In *b*, the same gel strip was fixed lightly, equilibrated, and then overlaid first with monoclonal antibody DL 3C4 (as tissue culture supernatant) for 4 h and then after extensive washing in Tris-buffered saline it was overlaid with  $^{125}$ I-labelled rabbit anti-mouse immunoglobulin antibody for 3 h. After further extensive washing, the gel strip was stained dried and autoradiographed. *b*, Shows the result of a 46-h exposure to Kodak XR-1 film with a lightening-plus intensification screen at  $-70^\circ\text{C}$ . The method used is precisely that of Burrige<sup>17</sup>.

element that forms the antigenic site recognized by 3C4 antibody. That extracts of cells that did not contain T could, nevertheless, inhibit the binding of 3C4 to purified  $^{35}\text{S}$ -labelled T antigen (Fig. 4) supports this hypothesis. This result forms the basis of a radioimmunoassay for the host cell protein and eliminates a trivial explanation for the pattern of 3C4 reactivity—that the cell line produces two different antibodies, one specific for T and one specific for the 68K protein. Possibly some conventional anti-T sera have arisen that recognize this cross-reactive 68K protein. Indeed Renart *et al.*<sup>18</sup>, using a novel gel-transfer technique, detected a 68K protein in T-negative cells. However, in these cases it would be difficult to define the basis of the reaction as the natural assumption would be that it represented a contaminating independent antibody activity rather than a cross-reaction.

The detection of a host cell protein sharing a common structure with a virally coded transforming gene product has already been described for the RNA tumour viruses and led to the hypothesis that the RNA virus has 'stolen' a host gene<sup>19</sup>. The present finding should not be interpreted in the same way, because, although the monoclonal antibody discussed here does recognize a structure common to a DNA virus oncogene and a normal host protein, the common structure may be very limited in extent. For example, most of the anti-T sera and the other anti-T monoclonal antibodies we have isolated do not recognize the 68K species and the T protein therefore has several unique antigenic determinants.





**Fig. 4** Competition radioimmunoassay to detect the T-related protein. The HeLa cell extract was prepared by lysing  $10^9$  uninfected cells (grown in suspension culture) in 15 ml buffer (0.01 M phosphate, pH 7.0, 0.25% NP40 and 1 mM EDTA) on ice, centrifuging at 10,000g for 30 min and taking the supernatant fraction. Varying amounts of this cell extract were then mixed with a fixed amount of  $^{35}$ S-labelled purified large T (isolated as in Fig. 1b) and sufficient 3C4 antibody added to precipitate 50% of the large T in the absence of any competition. The radioimmunoassay was then carried out as described<sup>13</sup>. Each point shows the mean and  $\pm$ s.d. of a triplicate determination.

The extreme evolutionary conservation of the determinant recognized by 3C4 and the unusual nuclear localization of the host protein make it unlikely that the cross-reactivity is fortuitous, rather we would propose that the 68K protein and T share some common function. This function would involve an interaction with another host cell component and be highly conserved in evolution. In this model the interaction would be mediated through the region of T or of the 68K protein that form the 3C4 binding site; the SV40 T antigen thus mimics a structure on the host cell protein to usurp its function and thereby modify an aspect of the cells behaviour to suit the virus. Initial studies on the monoclonal antibody and the 68K protein support this: (1) 3C4 antibody is a potent inhibitor of the ATPase activity of the T-related protein made in Ad2<sup>+</sup>D2-infected Hela cells (R. Tjian, personal communication). (2) The intensity of nuclear fluorescence seen with the antibody varies with the growth state of the cell, so that nuclei of quiescent rat embryo fibroblasts are barely positive whereas the same cells growing exponentially stain brightly. The 68K protein may be involved in the initiation of host DNA synthesis in much the same way as the T protein acts in the initiation of viral DNA synthesis. The two proteins would then share a common need to interact with the host cell DNA replication machine. Clearly the determination of the function of the 68K protein may aid our understanding of the role of T antigen both in lytic infection and in transformation.

We thank Dr P. Beverley, Dr Clive Slaughter and Dr R. Kennett for advice and help with the hybridization technique, Dr E. B. Lane for help with the immunautoradiography, and all our colleagues at Cold Spring Harbor for supporting the project. Dr R. Kennett provided myeloma cell line Sp2/O-Ag14, Dr M. Wigler the L cells, Dr E. B. Lane the PtK-1 cells, and the pure D2 protein was a gift from R. Tjian and A. Robbins. This study was financed by the Cancer Center Grant to Cold Spring Harbor; D.P.L. was supported by a Post-doctoral Fellowship from the Cancer Research Institute Inc. and thanks the Department of Zoology, Imperial College, London, UK for granting him leave of absence.

Received 4 June; accepted 2 September 1980.

1. Tooze, J. (ed.) *The Molecular Biology of Tumor Viruses* 2nd Edn, Vol. 2 (Cold Spring Harbor Laboratory, New York, 1980).
2. Tjian, R., Fey, G. & Graessmann, A. *Proc. natn. Acad. Sci. U.S.A.* **75**, 1279–1282 (1978).
3. Tegtmeyer, P. *J. Virol.* **10**, 591–598 (1972).
4. Carroll, R., Hager, L. & Dulbecco, R. *Proc. natn. Acad. Sci. U.S.A.* **72**, 3754–3757 (1974).

5. Tjian, R. *Cell* **13**, 165–180 (1978).
6. Chang, C., Luborsky, S. W. & Mora, P. T. *Nature* **269**, 438–440 (1977).
7. Tjian, R. & Robbins, A. *Proc. natn. Acad. Sci. U.S.A.* **76**, 610–614 (1979).
8. Griffen, J. D., Spangler, G. & Livingstone, D. M. *Proc. natn. Acad. Sci. U.S.A.* **76**, 2610–2614 (1979).
9. Lane, D. P. & Crawford, L. V. *Nature* **278**, 261–263 (1979).
10. Kohler, G. & Milstein, C. *Nature* **256**, 495–497 (1975).
11. Shulman, M., Wilde, C. D. & Kohler, G. *Nature* **276**, 269–270 (1978).
12. Kennett, R. H., Denis, K. A., Tung, A. S. & Klinman, N. R. *Curr. Topics Microbiol. Immun.* **81**, 77–91.
13. Lane, D. P. & Robbins, A. K. *Virology* **86**, 182–193 (1978).
14. Lebowitz, P., Kelly, T. J., Nathans, D., Lee, T. H. & Lewis, A. M. *Proc. natn. Acad. Sci. U.S.A.* **71**, 441–445 (1974).
15. Kelly, T. J. & Lewis, A. M. Jr *J. Virol.* **12**, 653–658 (1973).
16. Walen, K. H. & Brown, S. W. *Nature* **194**, 406 (1962).
17. Burridge, K. *Proc. natn. Acad. Sci. U.S.A.* **73**, 4457–4461 (1976).
18. Renart, J., Reiser, J. & Stark, G. R. *Proc. natn. Acad. Sci. U.S.A.* **76**, 3116–3120 (1979).
19. Collett, M. S., Erikson, E., Purchio, A. F., Brugge, J. S. & Erikson, R. L. *Proc. natn. Acad. Sci. U.S.A.* **76**, 3159–3163 (1979).
20. Laemmli, U. K. *Nature* **227**, 680–685 (1970).
21. Kessler, S. W. *J. Immun.* **115**, 1617–1624 (1975).

## Mutants of avian myelocytomatosis virus with smaller gag gene-related proteins have an altered transforming ability

Gary Ramsay\*, Thomas Graf† & Michael J. Hayman\*

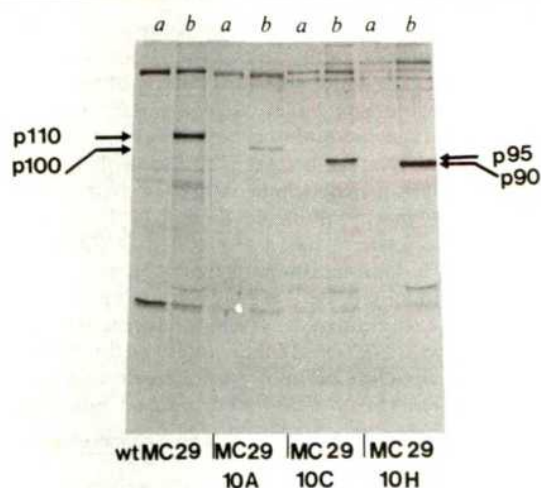
\* Tumour Virology Laboratory, Imperial Cancer Research Fund, Lincoln's Inn Fields, London WC2A 3PX, UK

† Institut Für Virusforschung, Deutsches Krebsforschungszentrum, Im Neuenheimer Feld 280, 6900 Heidelberg, FRG

Avian myelocytomatosis virus strain MC29 is a replication-defective<sup>1</sup> avian oncovirus which in newborn chickens causes myelocytomatosis and liver and kidney tumours<sup>2,3</sup>. *In vitro* infection of bone marrow cells gives rise to colonies of transformed macrophage-like cells<sup>4</sup>, and cloned virus is also capable of transforming fibroblasts<sup>5</sup>. The genome of MC29 contains cellular sequences<sup>6–8</sup> which are closely related to those in other defective leukaemia viruses with similar transforming spectra. Consequently, these cellular sequences have been postulated to represent a new oncogene which has been designated *mac*, for macrophage transformation<sup>4,9</sup>. MC29-transformed cells contain a gag gene-related protein of a 110,000 molecular weight (MW) (p110)<sup>10</sup>, which by tryptic peptide analysis has been shown to be a fusion product comprised of gag gene-derived sequences and sequences which are presumed to be coded by the adjacent *mac* gene<sup>11,12</sup>. These findings suggest that this protein may be implicated in transformation by MC29. We now describe three mutants of MC29 that synthesize smaller gag gene-related proteins. These mutants have an altered ability to transform bone marrow cells but not fibroblasts. This demonstrates for the first time a direct involvement of the p110 protein of MC29 in transformation.

The starting point of our studies was the observation that the Q10 cell line, a MC29-transformed quail fibroblast line producing MC29 plus MC29 associated helper virus (MCAV)<sup>10</sup>, on prolonged periods in culture synthesized smaller gag gene-related proteins in addition to p110. To determine whether we could isolate from this cell line virus mutants that would direct the synthesis of these smaller proteins, we infected fresh quail fibroblasts at a low multiplicity of infection and analysed single transformed clones for the synthesis of the gag-related proteins. Of 12 clones analysed, 6 produced a protein smaller than p110. Figure 1 shows an analysis by immune precipitation of non-producer clones transformed by three of the mutants (non-producer cells being cells transformed by MC29 but unable to release infectious virus due to the absence of helper virus). Cells transformed by MC29 virus clones 10A, 10C and 10H contained proteins of respective approximate MWs 100,000, 95,000 and 90,000. These proteins were shown to be related to the MC29 p110 protein by tryptic peptide analysis which revealed that they contained gag- and *mac*-specific peptides (data to be published elsewhere).





**Fig. 1** Altered gag gene-related proteins synthesized in three clones of quail fibroblasts infected with MC29 virus derived from the MC29 Q10 line. Virus was collected from the supernatant fluids of the MC29 (MCAV) infected quail fibroblast line Q10 developed by Bister *et al.*<sup>10</sup>, and used to infect fresh quail embryo cells at various dilutions of the virus. Foci of transformed cells were isolated 10 days later from dishes (50 mm) containing less than 10 foci and grown up to approximately  $2 \times 10^7$  cells. Clones were screened for p110-related proteins by radioimmunoprecipitation analysis. For this,  $5 \times 10^6$  cells were labelled with  $^{35}\text{S}$ -methionine for 60 min and gag-related proteins immunoprecipitated by anti-virus serum and analysed by SDS-polyacrylamide gel electrophoresis as detailed elsewhere<sup>10</sup>. Immunoprecipitates were made using either normal rabbit serum (a) or rabbit anti-RSV serum (b).

The mutant MC29 genomes were rescued from the non-producer cells by superinfection with the helper virus *td* B77 and the rescued viruses tested for their ability to transform fibroblasts and bone marrow cells in comparison with wild-type virus. Table 1 shows that although the three mutant viruses still transform fibroblasts with titres similar to wild-type virus they transform haematopoietic cells at an approximately 100-fold reduced efficiency. Wild-type MC29 transforms both cell types with roughly equal efficiency. In addition, the colonies of bone marrow cells transformed by the mutant viruses were smaller than the wild-type colonies and proved difficult to grow. This difference in efficiency of transformation of bone marrow cells can also be shown directly on transformation of chick embryo

**Table 1** Transforming ability of the MC29 mutants assayed on chick embryo cells and chick bone marrow cells

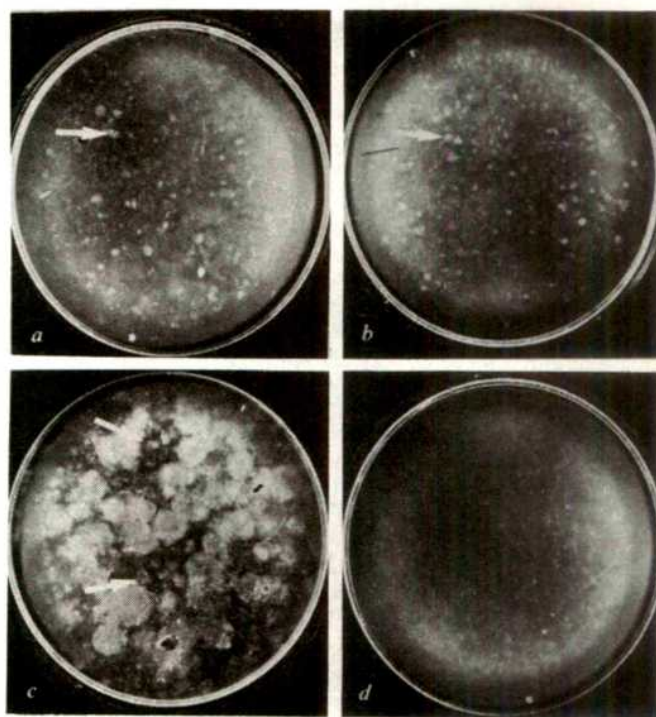
| Virus                     | Transforming activity                    |   |   |       |
|---------------------------|--|---|---|-------|
|                           | Chicken embryo cells                     |   | Chicken bone marrow cells                   |       |
|                           | Fibroblasts foci (FFU ml <sup>-1</sup> ) | Macrophage foci (FFU ml <sup>-1</sup> ) | Macrophage colonies (CFU ml <sup>-1</sup> ) | Ratio |
| wt MC29 ( <i>td</i> B77)* | $2.3 \times 10^3$                        | $1.9 \times 10^3$                       | $2 \times 10^3$                             | 0.9   |
| wt MC29 (RAV-2)           | $1.3 \times 10^6$                        | $7.0 \times 10^5$                       | NT  | 0.5   |
| MC29-10A ( <i>td</i> B77) | $5 \times 10^4$                          | $3.2 \times 10^2$                       | $6 \times 10^2$                             | 0.009 |
| MC29-10C ( <i>td</i> B77) | $1 \times 10^6$                          | NT                                      | $6 \times 10^3$                             | 0.006 |
| MC29-10H ( <i>td</i> B77) | $1 \times 10^4$                          | $2 \times 10^2$                         | $5 \times 10^1$                             | 0.01  |

Non-producer clones of quail fibroblasts were superinfected with the avian leukosis virus *td* B77, passaged once and virus collected from the supernatant fluids 5–7 days later. FFU, focus-forming units. Titres were obtained following serial 10-fold dilutions of the virus stocks as described<sup>5</sup>. CFU, colony-forming units. The ratio was calculated by dividing the macrophage transforming titre, from CEC and bone marrow, by the fibroblast transforming titre. NT, not tested.

\* The wild-type virus used was derived either from the Q8 fibroblast line<sup>10</sup> superinfected with *td*B77 or from a MC29 (RAV-2)-producing macrophage cell line (H. Beug *et al.*, in preparation).

cells (CEC) that contain a mixture of cell types, including fibroblasts and macrophage-like cells (Table 1). Wild-type MC29 can transform both these cell types giving rise to small tight colonies of fibroblasts and large diffuse colonies of macrophage-like cells<sup>5</sup>. Figure 2 shows that CEC infected by two of these mutants, 10A and 10H, give rise exclusively to small tight fibroblast foci (Fig. 2a, b), whereas, as expected, wt MC29 gave rise to both types of focus (Fig. 2c). Cells newly infected with the mutant pseudotypes synthesized gag-related proteins corresponding in MW to those detected in the original isolates (unpublished observations).

The finding that a deletion in the p110 protein of MC29 leads to a large reduction in the macrophage transforming ability of the virus without affecting its fibroblast transforming potential could be taken to indicate that there are two separate gene products responsible for the transformation of different host cells. The fact that no messenger RNA other than that which codes for the MC29 p110 protein has been found in transformed cells (D. Stehelin *et al.*, personal communication) argues against this possibility. Another possibility is that there are domains in the molecule which are required for macrophage but not for fibroblast transformation. A third, not necessarily mutually exclusive alternative is that more transforming activity is required to transform bone marrow cells than is required to transform fibroblasts. The deletion observed in our mutants could have reduced the biological activity of the gag-related protein to a level which is insufficient to transform macrophages efficiently. The isolation of further DLV mutants altered in their ability to transform fibroblasts but still able to transform bone marrow cells would be useful in resolving this question. Interestingly, a mutant of avian erythroblastosis virus has been isolated which has also lost the ability to transform bone marrow cells but is still able to transform fibroblasts<sup>13</sup>. This mutant also has a deletion in the gag gene-related protein (p75) of this particular virus<sup>14</sup>.



**Fig. 2** Foci of chick embryo cells infected with mutants of MC29. The focus assay was prepared as described earlier<sup>5</sup> and pictures taken 10 days after infection. a, Foci induced by *td* 10A; b, by *td* 10H; and c, by wt MC29. All dishes were inoculated with 0.2 ml of virus containing approximately 200 FFU. d, Uninfected control. The foci in a and b as well as the small foci in c (indicated by the arrows) represent fibroblast foci. The large plaque-like foci seen only in c represent foci derived from transformed macrophages.



Studies are under way to locate the alterations in the proteins of the MC29 mutants by tryptic peptide mapping techniques and oligonucleotide mapping. Preliminary results indicate that the mutant proteins have lost several *mac*-specific peptides and have gained a *gag*-specific peptide and this can be correlated with a deletion(s) in the *mac* sequences in the genomic RNA (G.R., K. Bister, P. H. Duesberg and M.J.H., preliminary observations). This could indicate that our MC29 mutants arose by crossing-over between helper leukemia virus and the MC29 genome.

We thank Eva Korzeniewska and Gay Kitchener for technical assistance, Dr H. Beug for helpful discussions, Drs G. Peters and J. Wyke for their advice on preparing the manuscript and Joyce Newton for typing the manuscript.

Received 11 July; accepted 12 September 1980.

1. Ishizaki, R., Langlois, A. J., Chabot, J. & Beard, J. W. *J. Virol.* **8**, 821-827 (1977).
2. Ivanov, X., Mladenov, Z., Nedyalkov, S., Todorov, T. G. & Yakimov, B. *Bull. Inst. Path. comp. Anim. Acad. Bulg. Sci.* **10**, 5-38 (1964).
3. Mladenov, Z., Heine, U., Beard, D. & Beard, J. W. *J. nat. Cancer Inst.* **38**, 251-285 (1967).
4. Langlois, A. J. *et al. Cancer Res.* **29**, 2056-2074 (1969).
5. Graf, T. *Virology* **54**, 398-413 (1973).
6. Roussel, M. *et al. Nature* **281**, 452-455 (1979).
7. Stehelin, D., Saule, S., Roussel, M., Lagrou, C. & Rommens, C. *Cold Spring Harb. Symp. quant. Biol.* **44**, (1980).
8. Sheiness, D., Fanshier, L. & Bishop, J. M. *J. Virol.* **28**, 600-610 (1978).
9. Graf, T., Beug, H., Kirchbach, A. V. & Hayman, M. J. *Cold Spring Harb. Symp. quant. Biol.* **44**, (1980).
10. Bister, K., Hayman, M. J. & Vogt, P. K. *Virology* **82**, 431-448 (1977).
11. Kitchener, G. & Hayman, M. J. *Proc. natn. Acad. Sci. U.S.A.* **77**, 1637-1641 (1980).
12. Mellon, P., Pawson, A., Bister, K., Martin, G. S. & Duesberg, P. H. *Proc. natn. Acad. Sci. U.S.A.* **75**, 5874-5878 (1978).
13. Royer-Pokora, B., Grieser, S., Beug, H. & Graf, T. *Nature* **282**, 750-752 (1979).
14. Beug, H., Kitchener, G., Döderlein, G., Graf, T. & Hayman, M. J. *Proc. natn. Acad. Sci. U.S.A.* (in the press).

## X-chromosome inactivation in extra-embryonic membranes of diploid parthenogenetic mouse embryos demonstrated by differential staining

S. Rastan\*, M. H. Kaufman†, A. H. Handyside† & M. F. Lyon\*

\*MRC Radiobiology Unit, Harwell, Didcot, Oxon OX11 0RD, UK

†Department of Anatomy, University of Cambridge, Cambridge CB2 3DY, UK

In somatic cells of female mammals one of the two X chromosomes is genetically inactive and heterochromatic, resulting in dosage compensation for X-linked genes<sup>1-3</sup>. In marsupials the paternally derived X chromosome is preferentially inactivated. In eutherian mammals, although either X chromosome can be inactivated at random in somatic cells, preferential inactivation of the paternally derived X chromosome has been demonstrated cytologically in mouse and rat yolk sac<sup>4,6</sup> and mouse chorion<sup>5</sup> and biochemically in mouse yolk sac<sup>7</sup>, chorionic ectoderm<sup>8</sup> and trophoblast. In mouse yolk sac the non-random element has been shown both biochemically<sup>7</sup> and cytologically<sup>9</sup> to be confined to the endoderm layer in which there is almost total paternal X-chromosome inactivation. We have therefore looked at X-chromosome activity in the separated yolk sac layers of diploid parthenogenetic mouse embryos in which both X chromosomes are maternally derived. Kaufman *et al.*<sup>10</sup> have demonstrated X inactivation in somatic cells of diploid parthenogenetic embryos, and we have used a modification of Kanda's method<sup>11</sup>, which renders the presumptive inactive X dark staining, to reveal an inactive X chromosome in both endoderm and mesoderm layers of separated yolk sacs from parthenogenones. Thus even in tissues in which there is normally total non-random paternal X inactivation, in the absence of a paternally derived X chromosome a maternally derived X can be inactivated.

Kanda identified the inactive X chromosome at metaphase in female mice<sup>11</sup> and other rodents<sup>12</sup> by treating bone marrow cells with hot hypotonic potassium chloride solution before fixation. The inactive X chromosome then stained much more darkly with Giemsa dyes than the other chromosomes in the cell. The modification of the Kanda method for use with embryonic material involved placing the whole embryo and/or embryonic membranes for 90 min in culture medium 199 (Flow Laboratories) to which colchicine had been added ( $4 \mu\text{g ml}^{-1}$  final concentration) to accumulate metaphases. The embryos were then placed individually in Petri dishes containing 0.5% (w/v) potassium chloride solution at room temperature and incubated in a water bath at 50°C for 15 min, followed by fixation in freshly made 3:1 absolute ethanol/glacial acetic acid solution. After fixation the embryos were isolated, touched lightly to filter paper to remove excess fixative and disaggregated in 0.5 ml of 60% acetic acid for 5 min. Chromosome spreads were made by allowing small drops of the acetic acid mixture to evaporate on slides placed on a 40°C hot plate. The preparations were stained in 2% Giemsa buffered at pH 6.8 for 20 min.

A dark-staining X chromosome was seen in more than 80% of metaphase cells from female embryos at 5½, 6½, 7½ and 13½ days post-coitum (p.c.) (Table 1 and Fig. 1a, b). Strong evidence that the dark staining chromosome is the inactive X chromosome is that it is seen in such a high proportion of XX female cells, but not in XO female cells nor XY male cells. A dark staining X chromosome was also present in more than 75% of cells from a bone marrow preparation of an adult XX male mouse carrying *Sxr*, the autosomal gene for sex reversal<sup>13</sup>.

Five experimental diploid parthenogenetic embryos were produced by the method of Kaufman *et al.*<sup>14</sup> by suppression of second polar body formation, and dissected out of their decidua at a stage equivalent to 9½-10½-day gestation (10-25 somites present). Their yolk sacs were removed, washed in medium 199 and placed in medium 199 with colchicine ( $4 \mu\text{g ml}^{-1}$  final concentration) for 3 h at room temperature to accumulate metaphases. The yolk sacs were then separated into their endodermal and mesodermal components by partial digestion for 3 h in a mixture of 2.5% pancreatin and 0.5% trypsin (w/v) made up in  $\text{Ca}^{2+}$  and  $\text{Mg}^{2+}$ -free Tyrode solution at 4°C<sup>15</sup>, followed by dissection with watchmaker's forceps. The cleanly separated cell layers were then individually treated by the modified Kanda method, as described above. Chromosome spreads from the two separated yolk sac components from normal fertilized zygotes at the same developmental stage were also obtained. The slides were all stained in 2% Giemsa at pH 6.8 for 20 min, randomized and coded, and cells at metaphase were scored for the presence or absence of a dark staining X chromosome (Table 2). A dark staining X

Table 1 Staining of metaphase cells from female embryos

| Age of embryos (days p.c.) | No. of female embryos | Total metaphases | Metaphases with a dark X chromosome | Per cent with a dark X chromosome |
|----------------------------|-----------------------|------------------|-------------------------------------|-----------------------------------|
| 5½                         | 8                     | 221              | 192                                 | 86.88                             |
| 6½                         | 13                    | 1,188            | 1,019                               | 85.77                             |
| 7½                         | 6                     | 545              | 455                                 | 83.49                             |
| 13½                        | 8                     | 598              | 495                                 | 82.78                             |

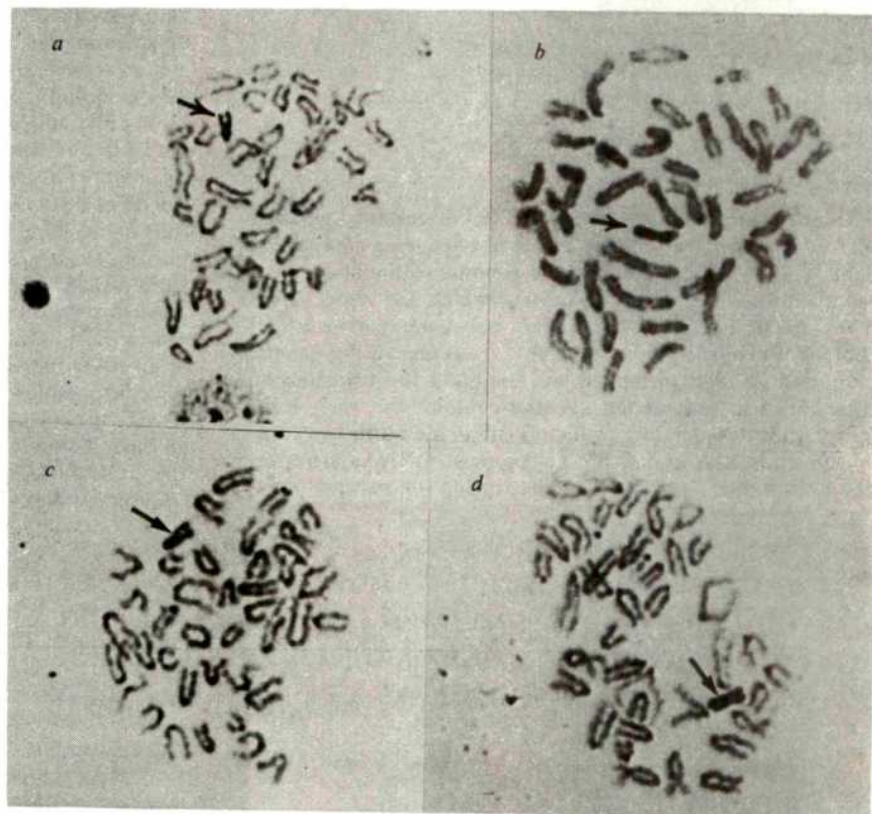
Virgin female mice of the 3H1 strain ( $F_1$  hybrids between two inbred strains, C3H/HeH and 101/H) were injected with 5 IU pregnant mare's serum gonadotropin (PMS) followed 44 h later by an injection of 5 IU human chorionic gonadotropin (HCG) to synchronize ovulation, and were mated to 3H1 males. Females were checked for vaginal plugs early the next morning, and the day of the plug was designated day ½. Pregnant females were killed by cervical dislocation at various stages of pregnancy, and the embryo was dissected out under a dissecting microscope. Whenever possible Reichert's membrane was removed to ensure that there was no contamination by maternal cells. The 13½-day embryos were sexed by dissecting out the gonad, which has visibly differentiated by this stage, and the earlier embryos were sexed cytologically.

**Table 2** Staining of metaphases from yolk sacs

| Tissue            | No. embryos     |          | No. metaphases scored |          | No. metaphases with a dark X chromosome |              |
|-------------------|-----------------|----------|-----------------------|----------|---|--------------|
|                   | Parthenogenones | Controls | Parthenogenones       | Controls | Parthenogenones (%)                     | Controls (%) |
| Yolk sac endoderm | 5               | 14       | 94                    | 914      | 76(80.85)                               | 742(81.18)   |
| Yolk sac mesoderm | 5               | 14       | 328                   | 675      | 255(77.74)                              | 558(82.67)   |

This table shows the number of cells at metaphase from parthenogenetic separated yolk sac endoderm and mesoderm exhibiting a dark-staining X chromosome after treatment with the modified Kanda method, compared with controls of fertilized material which have received the same treatment.

**Fig. 1** Metaphase cells showing an inactive dark-staining X chromosome after hypotonic treatment at 50 °C. *a*, Metaphase from a normal 5½-day p.c. embryo; *b*, metaphase from a normal 7½-day p.c. embryo; *c*, metaphase from the endoderm layer of diploid parthenogenetic yolk sac; and *d*, metaphase from the mesoderm layer of diploid parthenogenetic yolk sac.



chromosome was seen in 76 out of 94 metaphases in parthenogenetic yolk sac endoderm (Fig. 1c) and in 255 out of 328 metaphases scored from parthenogenetic yolk sac mesoderm (Fig. 1d). We therefore conclude that X-chromosome inactivation has taken place in both endodermally and mesodermally-derived layers of yolk sac from diploid parthenogenones.

Cooper<sup>16</sup> has suggested that passage of the X chromosome through male gametogenesis or fertilization led to imprinting of the paternal X chromosome and was an important factor in paternal X inactivation in marsupials. It has been further suggested that imprinting also occurs in eutherian mammals<sup>17</sup> and results in paternal X inactivation in those tissues of the embryo that differentiate early, such as yolk sac endoderm which is derived from the primitive endoderm<sup>18</sup>, but that cells of the embryo proper escape from imprinting before the time of X-chromosome differentiation so that in them X inactivation is random<sup>19,20</sup>. Our results show that even in a tissue such as yolk sac endoderm in which primary non-random inactivation of the paternal X is thought to occur, a maternal X chromosome can be inactivated in the absence of a paternal one. In our parthenogenetic material neither X chromosome could have been imprinted, either by passage through male gametogenesis, fertilization or re-entry of the polar body, and so we conclude that imprinting cannot be essential to the mechanism of X inactivation in the tissues in which non-random paternal X inactivation normally occurs. One cannot, however, assume that absence of an imprinted X chromosome has not affected X inactivation in any way; for example, is the onset of X inactivation

in these tissues delayed? Homozygous diploid uniparental mice, produced by the removal of one or other pronucleus after fertilization, followed by diploidization in cytochalasin B, are viable<sup>21</sup>, which suggests that X inactivation in all tissues has occurred normally. However, as no live-born mammalian parthenogenones have been produced so far, one cannot rule out the possibility that some abnormality of X inactivation is involved in their premature death.

We thank Mrs A. Burling for technical assistance.

Received 7 July; accepted 17 September 1980.

1. Lyon, M. F. *A. Rev. Genet.* **2**, 31–52 (1968); *Biol. Rev.* **47**, 1–35 (1972); *Proc. R. Soc. B* **187**, 243–268 (1974).
2. Eichler, E. M. *Adv. Genet.* **15**, 175–259 (1970).
3. Gartler, S. M. & Andina, R. J. *Adv. hum. Genet.* **7**, 99–140 (1976).
4. Cooper, D. W. *et al.* in *Isozymes III: Developmental Biology* (ed. Market, L. C.) 559 (Academic, New York, 1975).
5. Takagi, N. & Sasaki, M. *Nature* **256**, 640–642 (1975).
6. Wake, N. *et al.* *Nature* **262**, 580–581 (1976).
7. West, J. D. *et al.*, *Cell* **12**, 873–882 (1977).
8. Freis *et al.* *Dev. Genet.* **123**–132 (1979).
9. Rastan, S. (in preparation).
10. Kaufman, M. H. *et al.* *Nature* **271**, 547–549 (1978).
11. Kanda, N. *Expl. Cell Res.* **80**, 463–467 (1973).
12. Kanda, N. & Yosida, T. H. *Cytogenet. Cell Genet.* **23**, 12–22 (1979).
13. Cattaneach, B. M. *Cytogenetics* **10**, 318–337 (1971).
14. Kaufman, M. H., Barton, S. C. & Surani, M. A. H. *Nature* **265**, 53–55 (1977).
15. Levak-Svajger, B., Svajger, A. & Skreb, N. *Experientia* **25**, 1311–1312 (1969).
16. Cooper, D. W. *Nature* **230**, 292–294 (1971).
17. Brown, S. W. & Chandra, H. S. *Proc. natn. Acad. Sci. U.S.A.* **70**, 195–199 (1973).
18. Gardner, R. L. & Papaioannou, V. in *The Early Development of Mammals* 107–132 (Cambridge University Press, London, 1975).
19. Lyon, M. F. in *Reproduction and Evolution*, Proc. 4th Symp. comp. Biol. Reprod. (Australian Academy of Science, 1977).
20. Takagi, N., Wake, N. & Sasaki, M. *Cytogenet. Cell Genet.* **20**, 240–248 (1978).
21. Hoppe, P. C. & Illmensee, K. *Proc. natn. Acad. Sci. U.S.A.* **74**, 5657–5661 (1977).



## Structure of two adenovirus type 12 transforming polypeptides and their evolutionary implications

Michel Perricaudet, Jean-Michel le Moullec & Pierre Tiollais

Unité de Recombinaison et Expression Génétique, Institut Pasteur, 28 rue du Docteur Roux, 75724 Paris Cedex 15, France

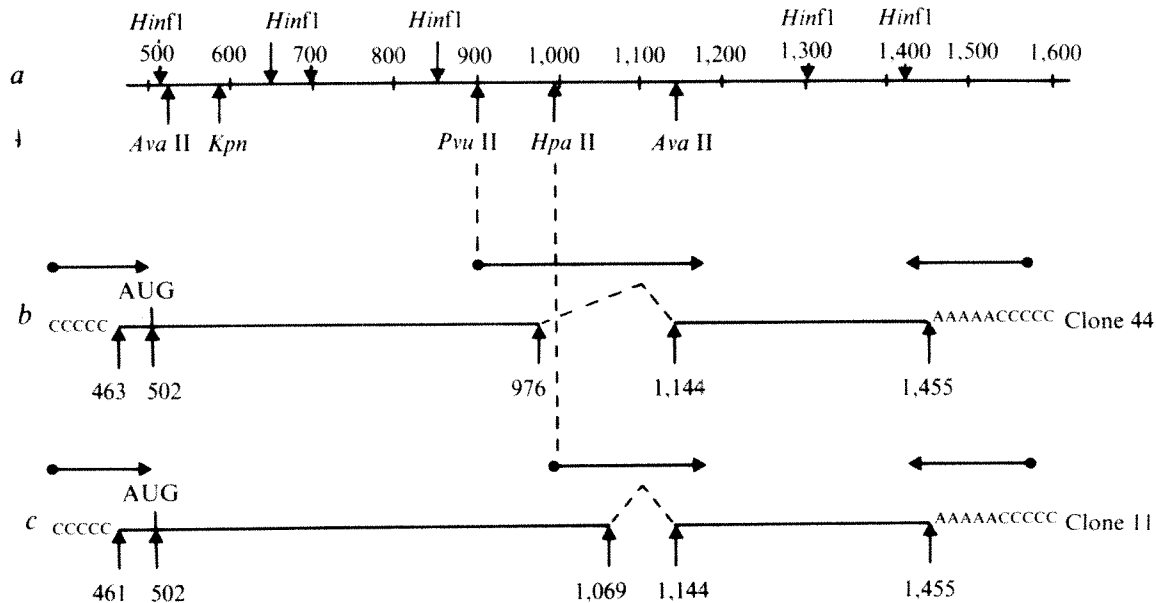
Ulf Pettersson

Department of Microbiology, The Biomedical Center, Box 581, S-751 23 Uppsala, Sweden

The human adenoviruses are classified according to their nucleotide sequence homology and their oncogenic potential in rodents<sup>1,2</sup>. The left-hand end of the genome of the adenovirus types 5 (ad5), 7 (ad7) and 12 (ad12), which are respectively, non-oncogenic (subgroup C), weakly oncogenic (subgroup B) and highly oncogenic (subgroup A)<sup>3-5</sup>, contains all the genetic information needed to induce and maintain the transformed phenotype. This part of the genome contains the early transcription unit designated E<sub>1</sub>, which is subdivided into two transcription units E<sub>1</sub>A and E<sub>1</sub>B<sup>6</sup>. Two spliced mRNAs are transcribed from the E<sub>1</sub>A region which codes for several phos-

phorylated polypeptides. These polypeptides play a key role by controlling the expression of the other early transcription units<sup>7,8</sup>. The major role of region E<sub>1</sub>A in adenovirus cell transformation might be to activate the true transforming genes of the region E<sub>1</sub>B. An additional role probably consists of the activation of some cellular genes as a restriction fragment containing this region can immortalize rodent cells *in vitro*. An important question is why some adenoviruses are oncogenic and others are not. We report here differences in the structures of the E<sub>1</sub>A polypeptides from ad7 and ad12, compared to ad5, which may partially account for their differing oncogenicity.

To answer this question, we have cloned in *Escherichia coli* double-stranded complementary DNA (cDNA) copies of the transforming mRNAs from region E<sub>1</sub>A of ad12 and compared their structures and their translation products with those of the corresponding mRNAs of ad5 (ref. 9) and ad7 (ref. 10). The cloning procedure and the determination of the physical structure of the cDNA were as described in Fig. 1. The two clones designated 11 and 44 contain the longest inserts and describe two different spliced mRNAs of the region E<sub>1</sub>A. Structural study of the cloned cDNAs at the nucleotide level shows that the splicing events of the mRNAs result in the deletion of a markedly AT-rich region, between nucleotides 1,069 and 1,144, which contains many stop codons<sup>11</sup> (Fig. 2). In clone 44 position 976 (donor site D<sub>1</sub>) is spliced to position 1,144 (acceptor site A), and in clone 11 position 1,069 (donor site D<sub>2</sub>) is spliced to position 1,144 (Fig. 1). The sequence of the donor site D1 (UU ↓ GUAAGU) is unexpected as a pyrimidine precedes the dinucleotide GU. The sequence of the other donor site D2 (CA ↓ GUAAGU) is very similar to the prototype sequence for a donor site described by Seif *et al.*<sup>12</sup>.



**Fig. 1** Structure of the two mRNAs of the E<sub>1</sub>A region from ad12 genome. cDNA copies of RNA from ad12-infected KB cells, 8-h post-infection and grown in the presence of cycloheximide were synthesized as described elsewhere<sup>14</sup> except that RNA was not poly(A) selected. cDNA was inserted into the *Pst*I restriction site of plasmid pBR322 after dG-dC tailing with the terminal transferase<sup>9</sup>. The recombinant plasmids were propagated in the *E. coli* DP 50 bacterial strain. Bacterial clones containing ad12-specific sequences of the transforming region were identified by *in situ* hybridization using the *Eco*RI-C restriction fragment (0–16%) as a probe; 30 clones gave a positive hybridization signal. Subsequent hybridization using <sup>32</sup>P-labelled poly(dT) as a probe was then performed to detect clones containing a poly(A) tract. Six clones gave a positive signal. Plasmid was extracted from the 30 clones and analysed by restriction endonuclease digestion. The size of the insert was determined by sizing of the *Pst*I restriction fragment and the plasmids containing the longest cDNAs as well as a poly(A) tail were selected for further analysis. Plasmid, <sup>32</sup>P-labelled *in vitro* by nick translation, hybridized only to the *Hind*III-G restriction fragment (0–6.8% of the genome) and therefore must contain cDNA sequences corresponding to mRNA of region E<sub>1</sub>A. *a* Represents the physical map of a part of the left-hand end of the ad12 genome. *b* Represents the cDNA structure from clone 44. It is 900 base pairs long and possesses the *Ava*II restriction site at nucleotide 525, but not the *Ava*II restriction site at position 1,143 suggesting it is located in the intron. The five *Hinf*I restriction sites are present and the *Hinf*I DNA fragment located between positions 853 and 1,307 is about 150 base pairs shorter than the corresponding genomic DNA fragment suggesting that this fragment contains the splice junction. *c* Represents the cDNA structure from clone 11. It is 1,000 base pairs long and possesses the same restriction sites as clone 44. However, the *Hinf*I DNA fragment located between positions 853 and 1,307 is 75 base pairs shorter than the homologous genomic restriction fragment, suggesting that this fragment contains different splice junctions. The 5' end, the polyadenylation site and the splice points were located by the nucleotide sequence determination of the appropriate region. Sequence analysis was carried out according to the Maxam and Gilbert procedure<sup>15</sup>. The horizontal arrows show the strategy adopted for our sequencing approach. Due to the presence of tandem repeats at the splice points (GU in both mRNAs) it is not possible to pinpoint precisely the positions where splicing has taken place. However, by following the GU/AG rule, tentative location for the splice points can be established and are indicated by vertical arrows. Following this assumption, nucleotide 976 is connected to nucleotide 1,144 in the mRNA corresponding to the clone 44 (*b*) and nucleotide 1,069 is connected to nucleotide 1,144 in the mRNA corresponding to clone 11 (*c*).

GAG TTT TCT CTG CCA GCT CAT TTT CAC GGC GGC <sup>502</sup> ATG AGA ACT GAA ATG ACT CCC TTG  
Met Arg Thr Glu Met Thr Pro Leu

GTC CTG TCG TAT CAG GAA GCT GAC GAC ATA TTG GAG CAT TTG CTG GAC AAC TTT TTT AAC  
Val Leu Ser Tyr Gln Glu Ala Asp Asp Ile Leu Glu His Leu Val Asp Asn Phe Phe Asn

GAG GTA CCC AGT GAT GAT GAT CTT TAT GTT CCG TCT CTT TAC GAA CTG TAT GAT CTT GAT  
Glu Val Pro Ser Asp Asp Asp Leu Tyr Val Pro Ser Leu Tyr Glu Leu Tyr Asp Leu Asp

GTC GAG TCT GCC GGT GAA GAT AAT AAT GAA CAG GCG GTG AAT GAG TTT TTT CCC GAA TCG  
Val Glu Ser Ala Gly Glu Asp Asn Asn Glu Gln Ala Val Asn Glu Phe Phe Pro Glu Ser

CTT ATT TTA GCT GCC AGT GAG GGG TTG TTT TTA CCG GAG CCT CTT GTA CTT TCT CTT GTC  
Leu Ile Leu Ala Ala Ser Glu Gly Leu Phe Leu Pro Glu Pro Pro Val Leu Ser Pro Val

TGT GAG CCT ATT GGG GGC GAA TGT ATG CCA CAA CTG CAC CTT GAA GAT ATG GAT TTA TTG  
Cys Glu Pro Ile Gly Gly Glu Cys Met Pro Gln Leu His Pro Glu Asp Met Asp Leu Leu

TGC TAC GAG ATG GGC TTT CCC TGT AGC GAT TCG GAA GAC GAG CAA GAC GAG AAC GGA ATG  
Cys Tyr Glu Met Gly Phe Pro Cys Ser Asp Ser Glu Asp Glu Gln Asp Glu Asn Gly Met

GCG CAT GTT TCT GCA TCC GCA GCT GCT GCT GCC CTT GAT AGG GAA CTT GAG GAG TTT CAG  
Ala His Val Ser Ala Ser Ala Ala Ala Ala Ala Asp Arg Glu Arg Glu Glu Phe Gln

TTA GAC CAT CCA GAG TTG CCC GGA CAC ATT TGT AAG TCC TGT GAG CAC CAC CGG AAT AGT  
Leu Asp His Pro Glu Leu Pro Gly His Asn Cys Lys Ser Cys Glu His His Arg Asn Ser

ACT GGA AAT ACT GAC TTA ATG TGC TCT TTG TGC TAT CTG CGA GCC TAC AAC ATG TTC ATT  
Thr Gly Asn Thr Asp Leu Met Cys Ser Leu Cys Tyr Leu Arg Ala Tyr Asn Met Phe Ile

TAC A GTAAGTGTGCTATGGGAGTGGGAGGTGATTTTCTTAAAGCAGTAAAAAATAATTTTGTGTGTTTATG  
Tyr Ser

CT CCT GTT TCC GAT AAT GAG CCT GAA CCT AAT AGC ACT TTG GAT GCC GAT GAG CGA CCC  
Pro Val Ser Asp Asn Glu Pro Glu Pro Asn Ser Thr Leu Asp Gly Asp Glu Arg Pro

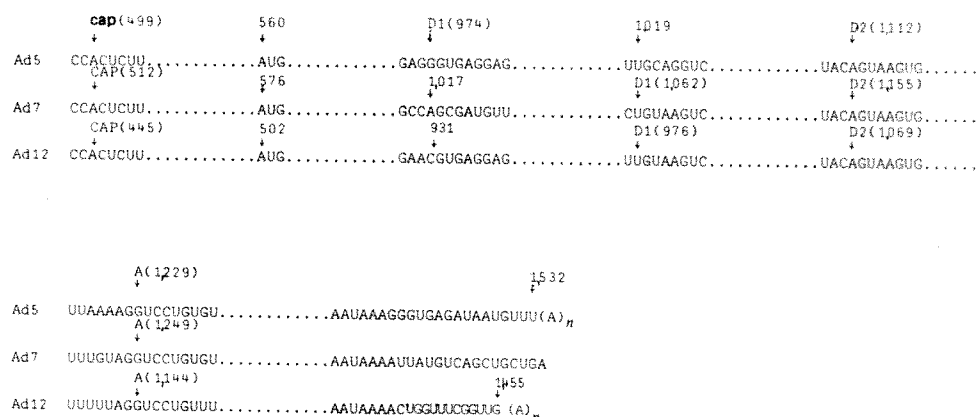
TCA CCC CCG AAA CTA GGA AGT GCG GTT CCA GAA GGA GTA ATA AAA CCT GTG CCT CAG CGG  
Ser Pro Pro Lys Leu Gly Ser Ala Val Pro Glu Gly Val Ile Lys Pro Val Pro Gln Arg

GTG ACT GGG AGG COT AGA TGT GCT GTG GAA AGC ATT TTG GAT TTG ATT CAA GAG GAA GAA  
Val Thr Gly Arg Arg Arg Cys Ala Val Glu Ser Ile Leu Asp Leu Ile Gln Glu Glu Glu

AGA GAA CAA ACA GTG CTT GTT GAT CTG TCA GTG AAA CCG CTT AGA TGT AAT TAA TGG ACT  
Arg Glu Gln Thr Val Pro Val Asp Leu Ser Val Lys Arg Pro Arg Cys Asn

TTG AGC ACC TGG GCA ATA AAA TAG GGG TAA TGT GGT TTT TGT GAG TCA TGT ATA ATA  
CTG GTT TCG GTT GAA GTG TCT TGT TAA TGT TTG TTT

**Fig. 2** The proposed primary structure for the two mRNAs and for the corresponding polypeptides of the ad12 E<sub>1</sub>A region. These structures are deduced from our analysis of the cDNA clones together with the nucleotide sequence for the left-hand end of ad12 DNA. The sequence which is absent in the shortest mRNA is underlined. The hexanucleotide AATAAA present close to the poly(A) junction of eukaryotic mRNA<sup>16</sup> is indicated by a box. Nucleotides which become connected after splicing are shown in boxes (see also Fig. 3). The nucleotide sequence is indexed according to the nomenclature of Sugisaki *et al.*<sup>17</sup>.



**Fig. 3** Comparison of the homologous regions for donor and acceptor sites of the mRNAs from the E<sub>1</sub>A early region of ad5, ad7 and ad12. The nucleotide sequences of the ad5 capping site are from ref. 18. The nucleotide sequences of the ad5 splicing and poly(A) sites are from ref. 9. The nucleotide sequences of the ad7 capping and splicing sites are deduced from comparing the homologous nucleotide sequences of ad5 (ref. 13), ad7 (ref. 10) and ad12 (ref. 11) genomes. The nucleotide A, position 1,017 of ad7 from the region homologous to the ad5 D<sub>1</sub> site, cannot be used as a splice donor site as it is followed by the dinucleotide GC. On the contrary the sequence UGUAAGU of the ad12 D<sub>1</sub> site (U: donor nucleotide) is found around the ad7 nucleotide U, position 1,062. The donor site D<sub>2</sub> and the acceptor site A of ad7 have been localized respectively at positions 1,155 and 1,249 by a similar method.

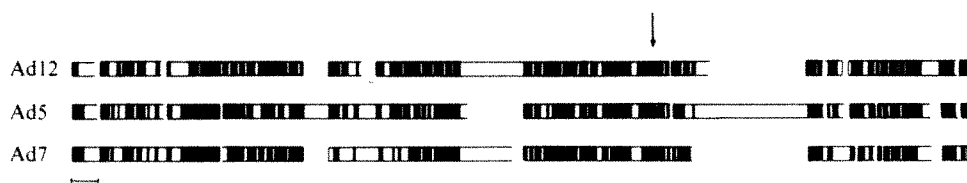
Sequence analysis from the *Pst*I cleavage sites of both clones 11 and 44 allowed us to describe the boundaries of the mRNAs. Sequencing gels revealed the same poly(A) addition sites for both mRNAs. However, it was not possible to predict exactly where the poly(A) addition had occurred because two As follow the G residue at position 1,455 in the DNA sequence<sup>11</sup> (Fig. 2) as is frequently the case for eukaryotic mRNAs. The poly(A) addition site is located 14–16 nucleotides after the typical hexanucleotide sequence AAUAAA. Note that two other hexanucleotide sequences AAUAAA are encountered at positions 1,397 and 1,241. However, no poly(A) addition seems to occur downstream of these positions, thus indicating that the hexanucleotide sequence alone may not be a sufficient signal for polyadenylation. Sequence analysis performed at the 5' ends of both cDNAs located the 5' boundaries at nucleotides 461 and 463, respectively, for clones 11 and 44, that is about 40 nucleotides upstream from the AUG presumed to be the initiation codon (Fig. 1). However, these positions probably do not represent the true 5' ends of the mRNAs because a few nucleotides are usually lost at the extremities during mRNA cloning. The cap site is probably located at position 445 as the sequence at this position is identical to the sequence at the cap site in region E<sub>1</sub>A of ad5 (Fig. 3).

A comparison of the sequences for donor and acceptor sites of ad5, ad7 and ad12 is very informative (Fig. 3). The results from our cloning experiments show that the donor sites D<sub>2</sub> and the acceptor sites A are located in homologous sequences in both serotypes 5 and 12 whereas the donor sites D<sub>1</sub> are not. Thus donor site D<sub>1</sub> is displaced 45 nucleotides further along the serotype 12 sequence as compared to the homologous sequence of serotype 5. Although the splices for the E<sub>1</sub>A mRNAs from ad7 have not yet been established by cloning experiments, they can be predicted by comparing the DNA sequences of the three serotypes 7, 12 and 5 (refs 10, 11 and 13, respectively) around the presumed splice points. Thus, the only alternatives are the positions 1,062 and 1,155 for donor sites D<sub>1</sub> and D<sub>2</sub> and nucleotide 1,249 for the acceptor site. The donor site D<sub>1</sub> would be located in homologous sequences in both serotypes 7 and 12 and the dinucleotide GU would in both cases be preceded by a U residue. The donor site D<sub>2</sub> and the acceptor site A would be located in homologous sequences in the three serotypes.

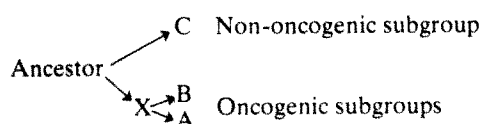
The established DNA sequence together with the positions of splice points allow us to predict the primary sequences of the polypeptides which are encoded by each of the ad12 E<sub>1</sub>A spliced mRNAs (Fig. 2)<sup>11</sup> and to compare them with those of the two other serotypes 5 (refs 13, 9) and 7 (ref. 10) to find common features (Fig. 4). In the three serotypes both mRNAs are translated before and after the splice. Thus for each serotype the two E<sub>1</sub>A polypeptides have identical amino- and carboxy-



**Fig. 4** Diagram showing the homologous amino acids occurring in the longest E<sub>1</sub>A polypeptides among the three adenovirus types 5, 7 and 12. Black areas (■) represent homologies and colourless areas non-homologies. Ile, Leu and Val, Ser and Thr, Asn and Gln, Asp and Glu, were respectively considered as similar amino acids. Gaps are left whenever necessary to maximize homology. The vertical arrow indicates the position where the intron is found in the genome. The black areas show the good conservation of the amino acid sequences of the three polypeptides. However, a deletion corresponding to about 40 amino acids and an insertion corresponding to about 20 amino acids are present in both ad7 and ad12 compared to ad5. The left part of the figure corresponds to the N-terminal end of the polypeptides. Scale bar denotes a peptide 10 amino acids long.



terminal ends, their only difference being an internal deletion due to different positions of the donor sites for splicing. A comparison of the amino acid sequences shows an important deletion located in the C-terminal part of the polypeptides, and an insertion and another deletion in homologous regions of ad7 and ad12 compared to ad5. However, several identical amino acid stretches are encountered along the three polypeptide sequences showing the existence of highly conserved regions. This suggests a common ancestor for these adenoviruses. The different locations of the splice sites and the differences observed in the primary structures of the polypeptides also suggest that subgroups A and B had some evolutionary steps in common. A scheme for the evolutionary path might be:



The different primary structures observed for the ad7 and ad12 E<sub>1</sub>A polypeptides compared to ad5 might explain in part the oncogenic properties of these serotypes. Nevertheless, a similar comparison of primary structures of ad12 E<sub>1</sub>B polypeptides with those of ad7 and ad5 is necessary. Among the 10,000 clones so far analysed, not one was found to contain sequences from region E<sub>1</sub>B. A hybridization experiment between single-stranded <sup>32</sup>P-DNA copies of ad12 mRNA and

ad12 HindIII restriction fragments, showed no signal for the HindIII-I restriction fragment (6.8–10.9% of the genome). This result suggests that the region E<sub>1</sub>B is not transcribed early during the lytic cycle. Therefore there may be a fundamental difference in the expression of region E<sub>1</sub>B in adenovirus subgroups A and C. Further studies of the protein products from the E<sub>1</sub>B region are clearly required to resolve this issue and we are currently extending our analysis to the region E<sub>1</sub>B.

This work was supported by grants from the Swedish Cancer Society, the Swedish MRC, the Délégation Générale à la Recherche Scientifique et Technique, the CNRS and INSERM. We thank Dr Beard for reverse transcriptase.

Received 24 June; accepted 2 September 1980.

1. Mackey, J., Wold, W., Rigden, P. & Green, M. J. *Virology* **29**, 1056–1064 (1979).
2. Van der Eb, A. J. *et al. Cold Spring Harb. Symp. quant. Biol.* **44**, (1979).
3. Graham, F. L. *et al. Cold Spring Harb. Symp. quant. Biol.* **39**, 637–650 (1974).
4. Sekikawa, K., Shiroki, K., Shimojo, H., Ojima, S. & Fujinaga, K. *Virology* **88**, 1–7 (1978).
5. Shiroki, K. *et al. Virology* **82**, 462–471 (1977).
6. Wilson, M. C., Fraser, M. W. & Darnell, J. E. *Virology* **94**, 175–184 (1979).
7. Jones, N. & Shenk, T. *Proc. natn. Acad. Sci. U.S.A.* **76**, 3665–3669 (1979).
8. Berk, A. J., Lai, F., Harrison, T., Williams, J. & Sharp, P. A. *Cell* **17**, 935–944 (1979).
9. Perriacaudet, M., Akusjarvi, G., Virtanen, A. & Pettersson, U. *Nature* **281**, 694–696 (1979).
10. Dijkema, R., Dekker, B. M. M. & Van Ormondt, H. *Gene* **9**, 141–156 (1980).
11. Fujinaga, K. *et al. Cold Spring Harb. Symp. quant. Biol.* **44**, (1979).
12. Seif, I., Khoury, G. & Dhar, R. *Nucleic Acids Res.* **6**, 3387–3398 (1979).
13. Van Ormondt, H., Maat, J., De Waard, A. & Van der Eb, A. J. *Gene* **4**, 309–328 (1978).
14. Persson, H., Pettersson, U. & Mathews, M. G. *Virology* **90**, 60–79 (1978).
15. Maxam, A. & Gilbert, W. *Proc. natn. Acad. Sci. U.S.A.* **74**, 560–564 (1977).
16. Proodfoot, N. J. & Brownlee, G. G. *Nature* **263**, 211–214 (1976).
17. Sugisaki, H. *et al. Cell* **20**, 777–786 (1980).
18. Baker, C. & Ziff, E. *Cold Spring Harb. Symp. quant. Biol.* **44**, 1980.

## Phorbol ester-induced differentiation of chronic lymphocytic leukaemia cells

Thomas H. Tötterman, Kenneth Nilsson & Christer Sundström

The Wallenberg Laboratory and the Departments of Internal Medicine and Pathology, University of Uppsala, Uppsala, Sweden

The croton oil-derived tumour-promoting agent 12-*O*-tetradecanoyl-phorbol-13-acetate (TPA) exerts pleiotropic effects on the differentiation and proliferation of both normal and malignant animal and human cells *in vitro*. TPA is mitogenic in nanomolar concentrations to chicken embryo fibroblasts<sup>1</sup> and human T lymphocytes<sup>2</sup> and inhibits the terminal differentiation of various committed embryonic cells<sup>3,4</sup> and mouse Friend erythroleukaemia<sup>5</sup> or myeloid leukaemia<sup>6</sup> cells. TPA induces a terminal cell differentiation in some murine<sup>7</sup> and human<sup>7–11</sup> myeloid leukaemia and histiocytic lymphoma cells<sup>12</sup>. We report here the effect of TPA on chronic lymphocytic leukaemia (CLL) biopsy cells *in vitro*. In four out of five CLL patients studied, TPA induced the appearance of 90–100% lymphoblastoid and plasmacytoid cells after 4 days of culture. Under the influence of TPA, 86–97% of the cells expressed with time increasing amounts of intracytoplasmic immunoglobulin (C-Ig) of the same phenotype as that detected on the surface (S-Ig) of fresh, non-induced CLL cells. A parallel decrease in both monoclonal S-Ig density and DNA synthesis of the CLL cells was observed. Electron microscopic studies showed a maturation towards plasma cells. We therefore conclude that TPA is capable of inducing differentiation of CLL cells *in vitro*.

Three patients with CLL (AK, EJ and MW) and one patient (EB) with prolymphocytic leukaemia (a clinical variant of CLL<sup>13</sup>) were selected for this study on the basis of high blood levels ( $>10^5 \text{ mm}^{-3}$ ) of monoclonal B lymphocytes. Blood mononuclear cells were separated by density-gradient centrifugation<sup>14</sup> and analysed for relative numbers of E rosetting<sup>15</sup> (on average 8%) and S-Ig-positive cells (on average 91% stained cells using polyvalent fluorescein isothiocyanate (FITC)-conjugated rabbit anti-human Ig F(ab')<sub>2</sub> fragment, Kallestad). The S-Ig isotypes of the cells were determined using fluorescent F(ab')<sub>2</sub> antisera specific for human heavy ( $\mu$ ,  $\delta$ ,  $\gamma$ ,  $\alpha$ ,  $\epsilon$ ) and light ( $\kappa$ ,  $\lambda$ ) chains (Kallestad; anti- $\epsilon$  serum produced by Behring).

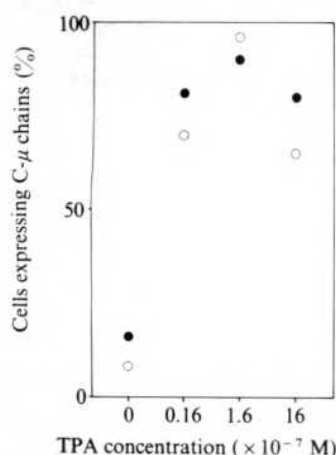
In preliminary experiments, the cells were plated and cultured with different concentrations of TPA. Figure 1 shows that the maximal frequency of C-Ig-positive cells ( $>90\%$  at day 3) was found with a TPA concentration of  $1.6 \times 10^{-7} \text{ M}$ . This concentration was used in later experiments.

Figures 2, 3 and 4 demonstrate the morphological features of CLL cells exposed to TPA. Within 4–12 h after plating, most of the cells became larger and acquired variable shapes. About 70% formed free-floating or surface-adherent clusters which increased in size with time (Fig. 3b). MGG-stained cytocentrifuge preparations at day 1–2 revealed a rapid enlargement of the cytoplasm together with an increasing basophilia and the appearance of a prominent nucleolus (lymphoblastoid cells). At day 3–4, cells with a large basophilic and frequently vacuolized cytoplasm and an eccentrically located nucleus (plasmacytoid cells) dominated the cultures together with the lymphoblastoid cells; only ~5% small lymphocytes were observed (Figs 2, 3c). Morphologically mature plasma cells were, however, only rarely seen. The viability remained  $>90\%$  in both the TPA-treated and control cultures as judged by Trypan blue exclusion. The

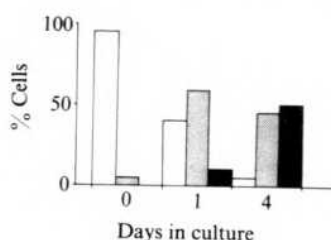
**Table 1** Effect of TPA on the expression and density of monoclonal surface and cytoplasmic immunoglobulin (S- and C-Ig) in CLL cells

| Day of culture | Treatment of cells | Patient                   |    |      |    |                               |    |      |    |                           |    |      |    |                               |    |      |    |
|----------------|--------------------|---------------------------|----|------|----|-------------------------------|----|------|----|---------------------------|----|------|----|-------------------------------|----|------|----|
|                |                    | EB ( $\mu, \lambda$ )     |    |      |    | AK ( $\mu, \delta, \lambda$ ) |    |      |    | EJ ( $\mu, \lambda$ )     |    |      |    | MW ( $\mu, \delta, \lambda$ ) |    |      |    |
|                |                    | Staining for $\mu$ chains |    | S-Ig |    | Staining for $\mu$ chains     |    | S-Ig |    | Staining for $\mu$ chains |    | S-Ig |    | Staining for $\mu$ chains     |    | S-Ig |    |
|                |                    | %                         | I  | %    | I  | %                             | I  | %    | I  | %                         | I  | %    | I  | %                             | I  | %    | I  |
| 0              | —                  | 93                        | 13 | 5    | 5  | 95                            | 10 | 7    | 7  | 96                        | 18 | 9    | 10 | 77                            | 12 | 1    | 3  |
| 1              | Control            | 82                        | 13 | 6    | 6  | 73                            | 6  | 4    | 7  | 85                        | 16 | 4    | 6  | ND                            | ND | ND   | ND |
|                | TPA                | 20                        | 7  | 28   | 8  | 10                            | 7  | 62   | 8  | 61                        | 11 | 58   | 16 | ND                            | ND | ND   | ND |
| 2              | Control            | 47                        | 6  | 2    | 2  | 75                            | 6  | 6    | 9  | 67                        | 9  | 24   | 7  | ND                            | ND | ND   | ND |
|                | TPA                | 10                        | 6  | 72   | 16 | 8                             | 7  | 78   | 19 | 17                        | 4  | 87   | 18 | ND                            | ND | ND   | ND |
| 3              | Control            | 52                        | 6  | 14   | 7  | ND                            | ND | 8    | 7  | 71                        | 7  | 16   | 11 | 83                            | 10 | 4    | 4  |
|                | TPA                | 11                        | 6  | 80   | 46 | ND                            | ND | 96   | 30 | 8                         | 4  | 90   | 15 | 19                            | 4  | 96   | 13 |
| 4              | Control            | 42                        | 6  | 8    | 8  | 74                            | 8  | 11   | 8  | 58                        | 5  | 11   | 4  | ND                            | ND | ND   | ND |
|                | TPA                | 4                         | 6  | 86   | 32 | 4                             | 6  | 97   | 38 | 10                        | 3  | 88   | 18 | ND                            | ND | ND   | ND |

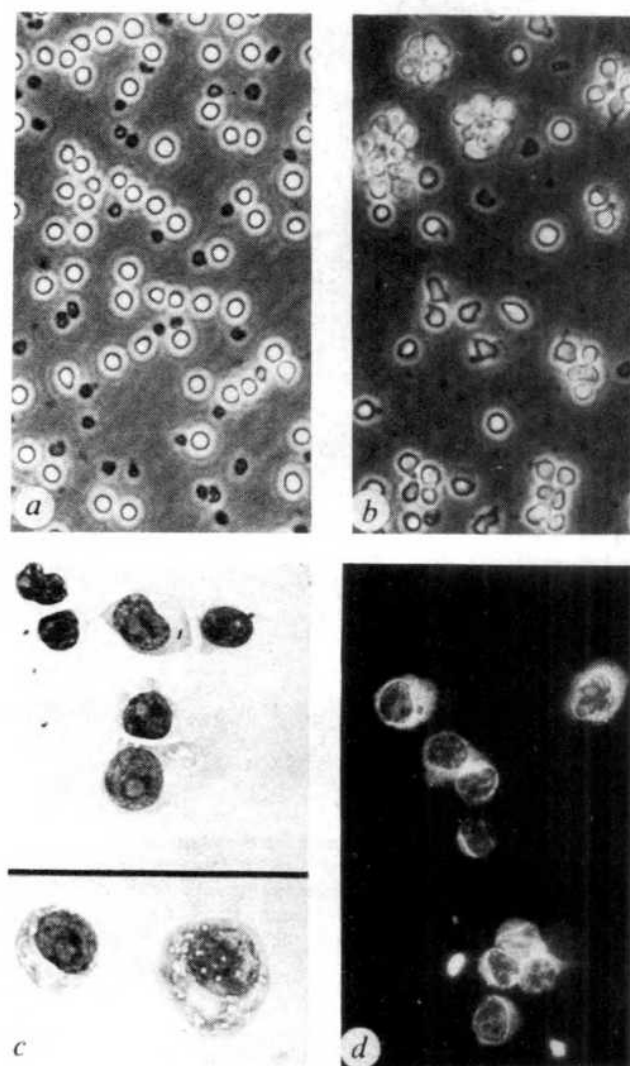
The S-Ig isotype of the CLL cells is given in brackets for each of the four patients (EB, AK, EJ, MW). Fresh biopsy cells (day 0) or cells cultured (day 1–4) in the absence (control) or presence of TPA ( $1.6 \times 10^{-7}$  M) were stained for surface and cytoplasmic  $\mu$  chains using FITC-coupled goat anti-human  $\mu$  serum (F(ab')<sub>2</sub> fragment, Kallestad at dilutions 1:3 and 1:10, respectively). The proportion of stained cells (%) and mean intensity ( $I$ , relative units; 20–30 cells measured per sample) of cellular fluorescence were measured using a Zeiss surface fluorescence cytophotometer (UV light source HBO 100 W, excitation filter BG12, barrier filter 50; objectives Neofluar Ph2 40 $\times$  and Ph3 100 $\times$  for C-Ig and S-Ig, respectively). ND, not determined.



**Fig. 1** Effect of different concentrations of TPA on the relative number of CLL cells expressing monoclonal cytoplasmic immunoglobulin. ○, Patient AK (S-Ig isotype  $\mu, \delta, \lambda$ ); ●, patient EJ ( $\mu, \lambda$ ). CLL cells ( $10^6 \text{ ml}^{-1}$ ) were cultured on plastic Petri dishes in Ham's F-10 medium supplemented with 10% fetal calf serum, antibiotics and TPA (Sigma, stock solution  $1 \text{ mg ml}^{-1}$  dissolved in 100% ethanol) at indicated final dilutions. Cultures were collected on day 3. The cells were washed, cytocentrifuged on to microscope slides, fixed in ice-cold methanol:acetone (1:1) and stained for intracytoplasmic  $\mu$  (C- $\mu$ ) chains using specific 1:10 diluted FITC-conjugated rabbit anti-human  $\mu$  serum (F(ab')<sub>2</sub> fragment, Kallestad). Fluorescent cells were quantified using the microscope equipment described in Table 1 legend.



**Fig. 2** TPA-induced morphological differentiation of CLL cells. Relative distribution (means for four CLL patients) of small lymphocytes (open bars), lymphoblastoid cells (shaded bars) and plasmacytoid cells (closed bars) at different times of culture. Cells were cultured in the continuous presence of  $1.6 \times 10^{-7}$  M TPA, collected on days 1 and 4, cytocentrifuged on to microscope slides and stained with May-Grünwald-Giemsa (MGG). Differential counts were calculated from 250 scored cells. Day 0 = untreated biopsy cells.



**Fig. 3** Morphology of CLL cells (patient AK) cultured for three days in the presence of  $1.6 \times 10^{-7}$  M TPA. *a* and *b*, Cultures of living untreated and TPA-treated cells, respectively ( $\times 220$ ). *c*, TPA-treated cells stained with MGG ( $\times 660$ ). *d*, Immunofluorescence of TPA-treated cells stained for cytoplasmic  $\mu$  chains ( $\times 450$ ).



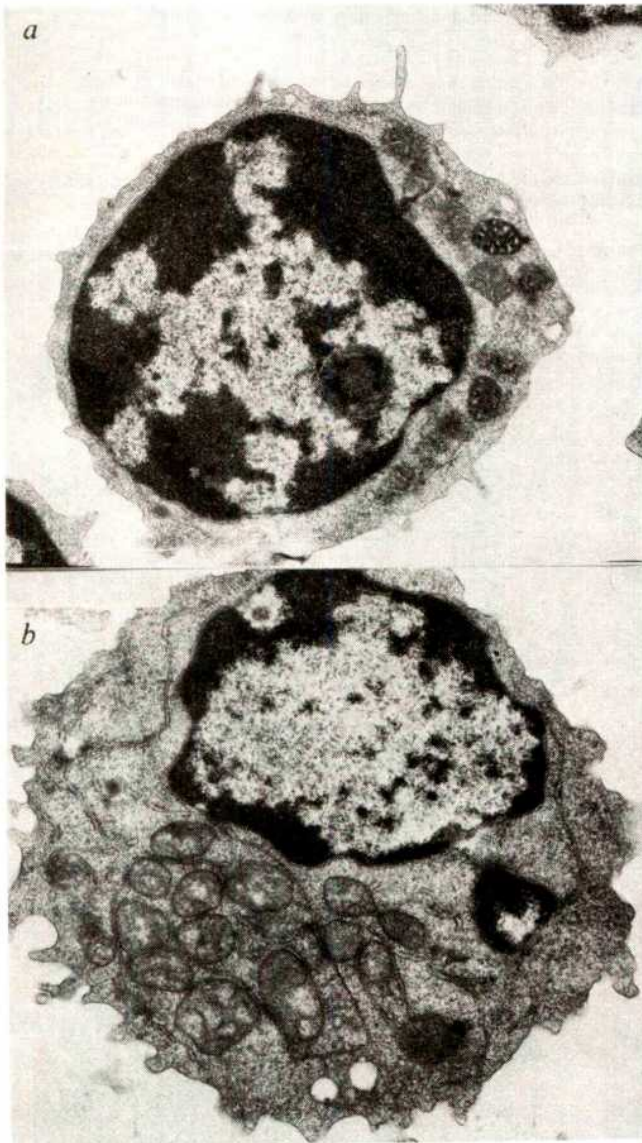
lymphoblastoid and plasmacytoid cells, but not the small fraction of small lymphocytes, stained strongly for C-Ig (Fig. 3d and Table 1). In control experiments, TPA-induced CLL cells (day 3–4) from the four patients were stained for C-Ig using monospecific antisera against the immunoglobulin heavy chains  $\mu$ ,  $\delta$ ,  $\gamma$ ,  $\alpha$  and  $\epsilon$  as well as  $\kappa$  and  $\lambda$  light chains. The C-Ig was always of the same isotype as the S-Ig detected on the corresponding freshly separated blood cells, whereas irrelevant

CLL cells, as reflected by heavy-chain ( $\mu$ ) variations. On average 5.5% of the fresh CLL cells contained cytophotometrically detectable amounts of C-Ig, and the proportion of such cells increased only slightly in the control cultures during 4 days. However, in cultures containing TPA there was a rapid increase in the percentage of C-Ig-positive lymphoid cells from (on average) 49% after 1 day to 92% after 3–4 days of culture. The relative amount of  $\mu$  chains increased two- to ninefold in TPA-treated CLL cells as compared with untreated cells. Under the influence of TPA, the S-Ig of CLL cells behaved reciprocally, as the proportion of S- $\mu$  chain-positive cells decreased from (on average) 90 to 9% together with a decrease in fluorescence intensity. However, a slight to moderate reduction in the percentage of S- $\mu$  chain-positive cells was also seen in untreated control cultures (Table 1).

The poor *in vitro* proliferative response of CLL cells to various mitogens<sup>16–18</sup> has previously led to the conclusion that CLL represents a clonal expansion of malignant B-lymphoid cells arrested at the stage of differentiation roughly corresponding to that of small resting lymphocytes. However, Fu and colleagues<sup>19</sup> recently studied two CLL patients expressing monoclonal serum Ig components idiotypically identical with the S-Ig of the CLL cells. When assisted by allogeneic helper T cells or Epstein-Barr virus (EBV), a fraction of the CLL cells matured into monoclonal, Ig-secreting plasma cells. A variable *in vitro* differentiation can also be induced in some ordinary CLL tumour populations using polyclonal B/T lymphocyte activators or EBV<sup>20</sup>.

The present study demonstrated that TPA, which has been previously found to be effective in inducing differentiation of mouse<sup>7</sup> and human<sup>7–11</sup> myeloid and monocytic<sup>12</sup> malignant cells, also effects CLL cells. The sequence of changes in the immunoglobulin expression and the ultrastructure of TPA-treated CLL cells is similar to that observed during differentiation of normal B cells. It is, therefore, possible that TPA-induced differentiation of CLL cells may be a useful model for human B-cell differentiation *in vitro*. In contrast to the EBV- or mitogen-induced differentiation, TPA seems to affect the whole tumour cell population, as more than 90% of the CLL cells changed both morphologically and with respect to C- and S-Ig expression. A second difference between EBV/mitogen and TPA as differentiation inducers in CLL cells seems to be that differentiation with TPA is associated with concomitant inhibition of DNA synthesis, as suggested by preliminary thymidine incorporation studies. Biosynthetic studies with TPA-induced CLL cells using a plaque assay and immunoprecipitation<sup>21</sup> indicate a cytoplasmic accumulation but only a minimal secretion of monoclonal immunoglobulin. Possibly the B cells do not reach the degree of maturation necessary for substantial immunoglobulin secretion. Alternatively, TPA may block secretion perhaps as a result of the inhibition of DNA synthesis.

Received 14 April; accepted 22 September 1980.



**Fig. 4** TPA-induced ultrastructural maturation of CLL cells. Lymphocytes cultured for three days in the absence (a) and presence (b) of TPA ( $\times 18,500$ ). Note the increase in the number of mitochondria, the amount of endoplasmic reticulum and the higher cytoplasmic:nuclear ratio in the TPA-treated cells.

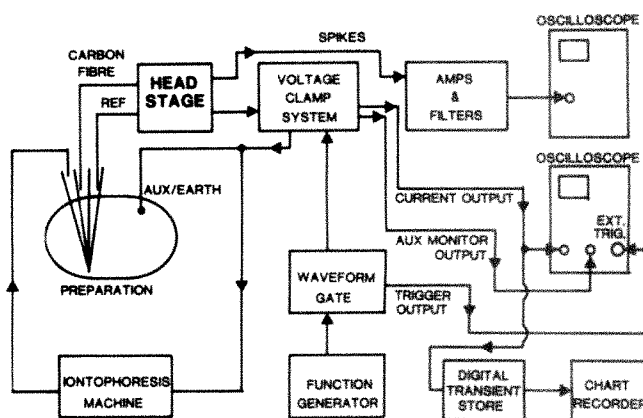
antisera stained only 0–1% of the cells weakly (data not shown). Therefore, TPA clearly induced the tumour cell population and not merely contaminating normal cells in these experiments. The TPA-induced ultrastructural changes in CLL cells (Fig. 4) consisted of an increased cytoplasmic:nuclear ratio together with increased amounts of mitochondria, endoplasmic reticulum and Golgi structures.

Table 1 shows the time-dependent TPA-induced changes in the expression and amounts of monoclonal C-Ig and S-Ig of

1. Driedger, P. E. & Blumberg, P. M. *Cancer Res.* **37**, 3257–3265 (1977).
2. Touraine, J.-L. *et al. J. exp. Med.* **143**, 460–465 (1977).
3. Cohen, R., Pacifici, M., Rubinstein, N., Biehl, J. & Holtzer, H. *Nature* **266**, 538–540 (1977).
4. Diamond, L., O'Brien, T. G. & Rovera, G. *Nature* **269**, 247–248 (1977).
5. Rovera, G., O'Brien, T. & Diamond, L. *Proc. natn. Acad. Sci. U.S.A.* **74**, 2894–2898 (1977).
6. Kasukabe, T., Honma, Y. & Hozumi, M. *Gann* **70**, 119–123 (1979).
7. Lotem, J. & Sachs, L. *Proc. natn. Acad. Sci. U.S.A.* **76**, 5158–5162 (1979).
8. Huberman, E. & Callahan, M. F. *Proc. natn. Acad. Sci. U.S.A.* **76**, 1293–1297 (1979).
9. Rovera, G., Santoli, D. & Damsky, C. *Proc. natn. Acad. Sci. U.S.A.* **76**, 2779–2783 (1979).
10. Rovera, G., O'Brien, T. & Diamond, L. *Science* **204**, 868–870 (1979).
11. Vorbrodt, A., Meo, P. & Rovera, G. *J. Cell Biol.* **83**, 300–307 (1979).
12. Nilsson, K., Andersson, L. C., Gahrberg, C. G. & Forsbeck, K. in *New Trends in Human Immunology and Cancer Immunotherapy* (eds Serrou, B. & Rosenfeld, C.) (Holt-Saunders & Doin, in the press).
13. Galton, D. A. G. *et al. Br. J. Haemat.* **27**, 7–23 (1974).
14. Böyum, A. *Scand. J. clin. Lab. Invest.* **21**, suppl. 97 (1968).
15. Pellegrino, M. A., Ferrone, S., Dierich, M. P. & Reisfeld, R. A. *Clin. Immun. Immunopath.* **3**, 324–333 (1975).
16. Smith, J. L., Cowling, D. C. & Barker, C. R. *Lancet* **i**, 229–233 (1972).
17. Wybran, J., Chantler, S. & Fudenberg, H. *Lancet* **i**, 126–129 (1973).
18. Han, T. & Dadey, B. *Cancer* **43**, 109–118 (1979).
19. Fu, S. M., Chiorazzi, N. & Kunkel, H. G. *Immun. Rev.* **48**, 23–44 (1979).
20. Robèrt, K.-H. *Immun. Rev.* **48**, 123–143 (1979).
21. Tötterman, T. H. *et al. Human Lymphocyte Differentiation* (submitted).



4. Fidler, I. J. & Kripke, M. L. *Science* **197**, 893-895 (1977).
5. Liotta, L. A., Kleinerman, J., Catanzaro, P. & Rynbrandt, D. *J. natn. Cancer Inst.* **58**, 1427-1431 (1977).
6. Apffel, C. A. *Cancer Res.* **36**, 1527-1537 (1976).
7. Gorelik, E., Fogel, M., Feldman, M. & Segal, S. *J. natn. Cancer Inst.* **63**, 1397-1403 (1979).
8. Gasic, G. J., Gasic, T. B., Galanti, N., Johanson, R. & Murphy, S. *Int. J. Cancer* **11**, 704-718 (1973).
9. Poste, G. & Fidler, I. J. *Nature* **283**, 139-145 (1980).
10. Yogeewaran, G., Stein, B. S. & Sebastian, H. *Cancer Res.* **38**, 1336-1344 (1978).
11. Tao, T. W. & Burger, M. M. *Nature* **270**, 437-438 (1977).
12. Sugarbaker, E. & Cohen, A. *Surgery* **72**, 155-158 (1972).
13. Fogel, M., Gorelik, E., Segal, S. & Feldman, M. *J. natn. Cancer Inst.* **62**, 585-588 (1979).
14. Shearer, G. M., Rehn, T. G. & Carbarino, C. A. *J. exp. Med.* **141**, 1348-1364 (1975).
15. Zinkernagel, R. M. & Doherty, P. C. *J. exp. Med.* **141**, 1427-1436 (1975).
16. Permiani, G. *et al. Immunogenetics* **9**, 1-24 (1979).
17. Schmidt, W., Atfield, G. & Festenstein, H. *Immunogenetics* **8**, 311-321 (1979).
18. Brodt, P. & Gordon, J. *J. Immun.* **121**, 359-365 (1978).
19. Kerbel, R. S., Twiddy, R. R. & Robertson, D. M. *Int. J. Cancer* **22**, 583-594 (1974).
20. Pluznik, D. H. & Sachs, L. *J. cell. comp. Physiol.* **66**, 319-324 (1965).



**Fig. 1** A block diagram of the apparatus used for spike recording and high-speed polarography. Switches are incorporated in the headstage and voltage-clamp systems. For extracellular single-unit (spike) recording, the signal from the carbon fibre-containing microelectrode barrel (CARBON FIBRE) is switched into a low-noise voltage follower in the headstage and then amplified and filtered in a conventional way. The auxiliary electrode (AUX/EARTH) is switched to ground. For polarography, a triangular waveform (see Fig. 2a) is obtained from a function generator and a waveform gate. This is fed into the preparation using the auxiliary electrode. The voltage at the tip of the microelectrode is monitored by the reference barrel (REF) and via a voltage-clamp system makes the voltage at the tip exactly follow the applied waveform. The current flow to ground through the carbon fibre caused by this voltage pattern is displayed on an oscilloscope, and may be output to a chart recorder through a digital transient store. A second channel of the oscilloscope monitors the voltage appearing at the auxiliary electrode.

## Quantification of noradrenaline iontophoresis

M. Armstrong-James & J. Millar

Department of Physiology, The London Hospital Medical College, Turner Street, London E1 2AD, UK

Z. L. Kruk

Department of Pharmacology and Therapeutics, The London Hospital Medical College, Turner Street, London E1 2AD, UK

Several problems are encountered when iontophoresis<sup>1,2</sup> is used to study the effects of putative neurotransmitters. The most significant is that it is not usually practical to estimate the concentration of drug obtained at the tip of the microelectrode by a current of a given strength. The usual methods, albeit rarely used, include measurement of transport numbers<sup>3,4</sup>, the use of ion-sensitive microelectrodes<sup>5,6</sup> and quantitative fluorescent microscopy<sup>7</sup>. With the exception of the ion-sensitive microelectrodes developed for acetylcholine<sup>5</sup>, these techniques are elaborate and time consuming, and cannot be routinely applied to every electrode used. Furthermore, conventional multibarrel microelectrodes have high-impedance recording barrels and thus often display low signal-to-noise ratios when recording single-cell activity, the noise being increased during iontophoresis. We describe here a technique which largely overcomes the problem of low spike signal-to-noise ratio in conventional multibarrel electrodes, and which, unlike the latter, also allows precise determination of the concentration of noradrenaline in the environment of the cell, which affects its excitability. The recording and iontophoretic properties of these electrodes have been described previously<sup>8</sup>. The use of these electrodes to quantify precisely iontophored noradrenaline by adapting polarographic techniques is described.

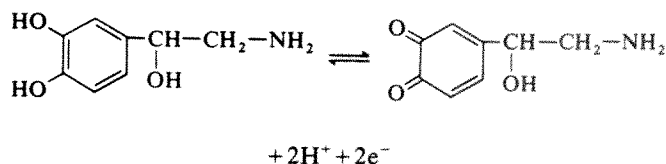
The high-speed polarographic technique was developed from systems being used for evaluating catecholamine levels in the central nervous system<sup>9,10</sup>. Our system differs principally in that it is some hundreds of times faster, is carried out at the single-cell, rather than macrocellular, level, and combines iontophoresis and single-cell recording. Full details of the methodology will be presented elsewhere; however, the principal features and a block diagram of the system (Fig. 1) are described here.

Three barrel microelectrodes were constructed in which one barrel contained a carbon fibre (outer diameter 7-8  $\mu\text{m}$ ), protruding 15  $\mu\text{m}$  from the glass, and etched to a 1- $\mu\text{m}$  point<sup>11,12</sup>. The other two (fluid-filled) barrels had outside diameters of 2-3  $\mu\text{m}$ . The carbon fibre electrode was connected via saline solution in the stem of the pipette to a current-to-voltage 'virtual-ground' field effect transistor (FET) operational amplifier. One other (reference) barrel was filled with 2 M NaCl, and connected to a voltage-follower FET. The third barrel was

filled with 0.1 M noradrenaline (NA) in dilute HCl ( $\text{pH} \sim 2$ ) for iontophoresis.

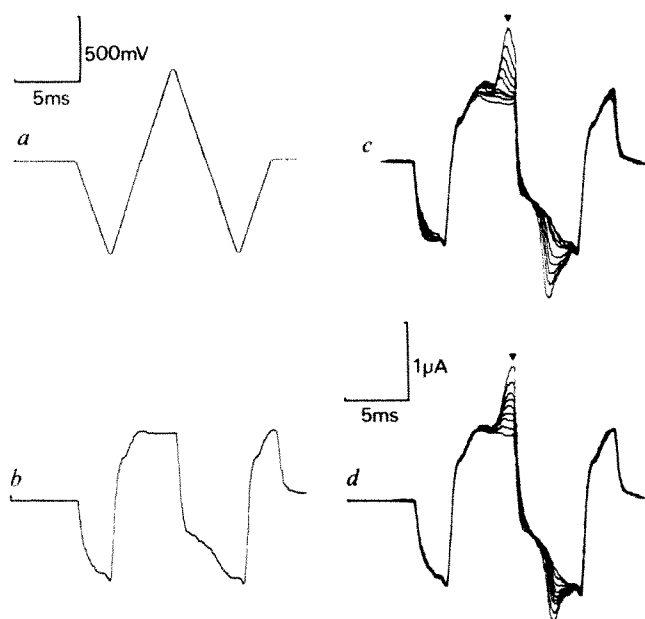
For *in vitro* calibration, the electrode tip was lowered into a beaker of 0.9% NaCl. Also dipping into the saline was a chlorided silver wire (the auxiliary electrode). The reference electrode was connected in a negative feedback loop with the auxiliary electrode, such that the auxiliary electrode would supply current to force the potential at the tip of the carbon microelectrode (monitored by the reference electrode) to follow any desired input voltage pattern. The current flow through the carbon fibre caused by these voltage changes was measured and displayed on an oscilloscope and printed out on a chart recorder via a digital transient store. A triphasic triangular waveform was used as the input voltage pattern. It was obtained by gating the output of a function generator. This waveform had a peak voltage of  $\pm 0.7$  V, a duration of 15 ms and was repeated twice per second (Fig. 2a). The precise current flow in the carbon electrode caused by this voltage pattern was determined by the impedance of the electrode-saline system<sup>11</sup>, and varied slightly from electrode to electrode, but was always similar to that shown in Fig. 2b.

When NA was added to the saline in the beaker, electro-oxidation of the amine occurred during the part of the cycle when the carbon fibre was anodic, according to the formula



It is generally accepted that the electrons liberated are taken into the working electrode (carbon fibre) and cause an increase in anodic current, and that subsequent reversal of potential causes a reduction of the quinone product back to NA, producing a corresponding increase in cathodic current<sup>9</sup>. Figure 2c





**Fig. 2** Polarographic currents recorded with carbon fibre microelectrodes. *a*, The voltage pattern applied to the carbon fibre tip of the microelectrode; *b*, shows the resultant current flow through the carbon fibre produced by this voltage pattern, when the microelectrode tip was immersed in 0.9% saline in a beaker; *c* shows a set of nine such polarographic current sweeps from a microelectrode in saline and eight different concentrations of NA in saline. The concentrations were  $2.8 \times 10^{-4}$  M for the largest trace, and then  $1.4 \times 10^{-4}$  M, 7, 5, 3, 2 and  $1 \times 10^{-5}$  M, and finally  $5 \times 10^{-6}$  M, for the second-smallest trace. The 'peak incremental current' for each concentration was measured at the time marked by the filled triangle. This was the extra current over the saline current caused by the oxidation of NA. *d* shows a set of current sweeps obtained with the microelectrode in saline using nine different levels of iontophoretic eject (tip positive) current through the NA-containing barrel of the microelectrode. They were 0, 10, 20, 40, 60, 80 and 120 nA. Scale in *a* applies only to *a*; scale in *d* applies to *b*, *c* and *d*.

The similarity between Fig. 2c and d is apparent. From the data in Fig. 2c, a calibration curve was constructed relating peak incremental current (measured at the points indicated by filled triangles) to the molar concentration of NA. From this curve and the data in Fig. 2d, a second curve relating iontophoretic eject current to tip concentration of NA in steady-state conditions could be produced. This curve is shown in Fig. 3.

For *in vivo* studies, the electrode was inserted into the primary somato-sensory cortex of urethane-anaesthetized rats. The auxiliary electrode was pushed into the retracted neck muscle. Figure 4 illustrates *in vitro* and *in vivo* data taken from another microelectrode. Figure 4a shows a set of current sweeps taken in different concentrations of NA in saline, ranging from  $10^{-5}$  to  $2 \times 10^{-3}$  M NA. Figure 4b shows current sweeps during iontophoresis in saline at different currents ranging from 20-nA retain to 100-nA eject. Figure 4c shows two sweeps with 20-nA retain, one in saline and the other *in vivo* (1,000- $\mu$ m down in the rat cortex). Apart from a slight increase in cathodic current *in vivo*, the sweeps are identical. Finally, Fig. 4d shows a set of current sweeps *in vivo* using the same iontophoretic eject currents as in Fig. 4b, taken after 60 s of iontophoretic eject current for each sweep. The catecholamine signals can be seen to be bigger *in vivo* than *in vitro*, presumably due to restricted diffusion of NA *in vivo*. In other cases, *in vivo* NA levels were less than *in vitro* ones, or fluctuated from second to second despite steady iontophoretic ejection, possibly reflecting variations in active noradrenergic uptake. Anyway, the signal shows the moment-to-moment variation in catecholamine levels at the investigated cell.

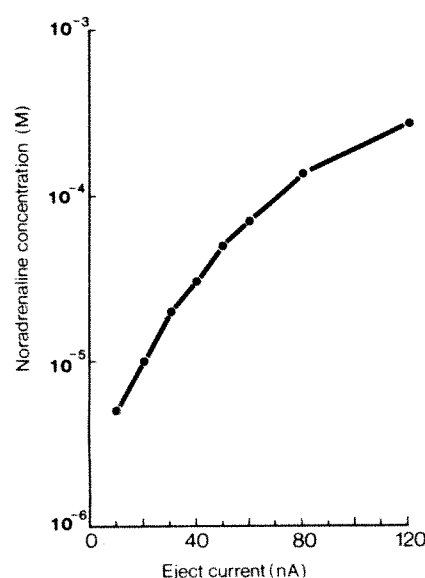
By switching the auxiliary electrode connection to ground and the carbon fibre electrodes into a low-noise voltage follower, extracellular voltage spikes were recorded from the investigated cortical neurone. The response of such neurones to iontophoretic NA was complex and will be reported elsewhere. Used as recording microelectrodes, carbon fibres had significantly lower noise than micropipettes and could distinguish axon and soma-dendrite spikes by waveshape<sup>8,13,14</sup>.

The technique of high-speed polarography using carbon fibre microelectrodes should have wide application in the study of the neurobiology of electroactive neurotransmitters. The method combines three techniques at the single-cell level—iontophoresis, recording of unit activity changes elicited by the

shows polarographic current sweeps in a series of different NA concentrations. Increasing concentrations of NA produced progressively increasing increments on the sweep at the peaks of oxidation and reduction. The reason for using a fast-gated triangular waveform was that this voltage pattern minimized build-up of reaction product and consequent poisoning of the electrode.

These experiments were done with a 'retain' (tip negative) iontophoretic current on the NA barrel. By reducing the retain current to zero, it was found that most of the NA-containing iontophoresis barrels showed appreciable 'leak' or passive diffusion of NA. By applying polarographic current sweeps at 2–10 Hz during iontophoretic eject currents of various levels, one could measure the concentrations of NA at the electrode tip. To establish adequate retain current, retain current was increased during polarographic pulses at 2 Hz. When the catecholamine signal disappeared, and further increase in retain current gave no change in signal, the retain current was considered adequate. For establishing steady levels of iontophoretically ejected catecholamine, we waited until the level of catecholamine signal maximally stabilized at a constant iontophoretic current. This 'lag time' varied in different electrodes and will be reported elsewhere. Signals from successive sweeps in these conditions invariably showed no detectable variations in amplitude, even when iontophoresis was continued for up to 30 min. Longer periods were not investigated.

Figure 2d shows a set of current sweeps made during NA iontophoresis using several different levels of ejection current.



**Fig. 3** Calibration curve relating the concentration of NA present at the tip of a multibarrel microelectrode immersed in saline to the level of steady iontophoretic ejection current through a NA-containing barrel. (The curve is constructed from data shown in Fig. 2c, d).

## Differential expression of H-2 gene products in tumour cells is associated with their metastatogenic properties

Patrick De Baetselier, Shulamit Katzav, Eliezer Gorelik, Michael Feldman & Shraga Segal

Department of Cell Biology, The Weizmann Institute of Science, Rehovot, Israel

Many neoplasms seem to be heterogeneous in nature<sup>1,2</sup>, producing metastases by pre-existing variant cells<sup>3,4</sup> with inherent biochemical and biological properties. The survival and proliferation of metastatic cells depend on various biological properties, such as enzymes which degrade basement membranes<sup>5</sup>, resistance to various host defence systems<sup>6,7</sup>, association with host cellular components<sup>8</sup>, adhesiveness<sup>9</sup> and expression of certain membrane glycoproteins<sup>10,11</sup>. Recent studies have indicated that metastatic cells may differ from the local tumour cells in the expression of immune recognizable membrane-associated antigens<sup>12,13</sup>. Such antigenic differences may result from an immunoselection of cells with distinct antigenic properties due to a specific immune response evoked against the local tumour. In view of the role of the major histocompatibility complex (MHC) system in controlling and restricting the function of immune effector cells against modified self-components<sup>14,15</sup>, one could assume that the modulation of the expression of MHC-encoded antigens on the membrane of tumour cells influenced the interclonal relationship within a local heterogeneous tumour cell population and the subsequent generation of metastasis. The modulation of the expression of H-2 antigens on several murine tumours is well documented<sup>16,17</sup>; however, practically no attempts were made to relate H-2 modulation with invasiveness. We now describe principal differences in the expression of H-2 parental haplotypes between a local F<sub>1</sub> methylcholanthrene-induced tumour and its descendant pulmonary metastases. These results suggest that both the expression and the immunogenicity of MHC products strongly influence the immune relationship between the tumour and the host's immune system, thus determining the generation and dissemination of metastases.

Mouse (T10) methylcholanthrene-induced sarcoma cells were serially transferred in syngeneic (C3HeB×C57BL/6)F<sub>1</sub> mice (H-2<sup>b</sup>×H-2<sup>k</sup>). Animals carrying subcutaneous solid T10 tumours regularly show the appearance of metastatic nodules in the lungs<sup>18</sup>. Because we intended to probe quantitative and qualitative differences in the membrane expression of murine MHC-encoded antigens on the local tumour and its metastatic descendants, local T10 (L-T10) and metastatic T10 (M-T10) cells were analysed for the membrane expression of both parental H-2<sup>b</sup> and H-2<sup>k</sup> haplotypes. The membrane expression of H-2 antigens was analysed using fluorescence serology carried out with the fluorescence-activated cell sorter (FACS-II). The use of the FACS allowed us to screen only for cells expressing high density of the relevant H-2 antigen. Such cells will be referred to as brightly stained cells. Solid tumours originating from subcutaneous transplants of L-T10 or M-T10 cells in (C3HeB×C57BL/6)F<sub>1</sub> mice were trypsinized and single-cell suspensions analysed for the relative number of cells stained either with anti-H-2<sup>k</sup> or with anti-H-2<sup>b</sup> antisera. From the comparison of the relative number of tumour cells expressing H-2<sup>b</sup> and H-2<sup>k</sup> antigens (data outlined in Table 1) and of the fluorescence distribution of M-T10 and L-T10 cells stained with either anti-H-2<sup>b</sup> or anti-H-2<sup>k</sup> antisera (Fig. 1), a clearcut difference was observed in the membrane expression of the parental H-2 haplotype on L-T10 compared with M-T10 cells. The data suggest that L-T10 cells express mainly or exclusively the H-2<sup>b</sup> parental haplotype whereas M-T10 cells express both the H-2<sup>b</sup> haplotype (although at a lower level than L-T10 cells)

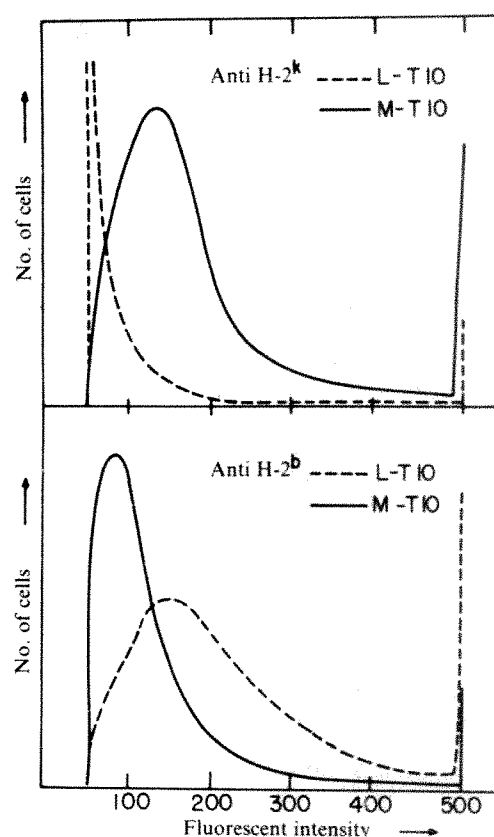


Fig. 1 Fluorescence distribution of L-T10 and M-T10 cells stained with anti-H-2<sup>k</sup> or anti-H-2<sup>b</sup> antisera. The same staining conditions were used as described in Table 1 legend.

and the H-2<sup>k</sup> haplotype. These differential characteristics in H-2 expression were stable despite several serial transfers. In addition, different M-T10 clones (obtained from single metastatic nodules) showed identical staining patterns, implying the homogeneous nature of this variant. The H-2<sup>k</sup>-encoded molecules expressed on the M-T10 cells consisted of the serological determinants encoded by the different subregions, as the M-T10 cells were stainable with anti-H-2<sup>k</sup> antisera directed against both the H-2D and H-2K end products of the H-2<sup>k</sup> haplotype (Table 1). Again, L-T10 tumour cells were found to be serologically negative when analysed with these specific antisera. To test whether the M-T10 cells were pre-existing variants in the local tumour population, the L-T10 tumour cells were cloned in semi-solid agar, and individual clones which were passaged in F<sub>1</sub> recipients were analysed for the presence of H-2<sup>k</sup> or H-2<sup>b</sup>

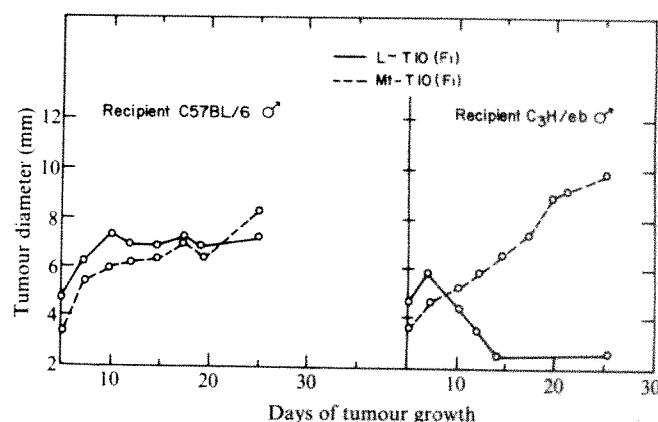


Fig. 2 The capacity of L-T10 and M-T10 tumour cells to grow in parental hosts. 10<sup>6</sup> L-T10 or M-T10 cells were inoculated into the hind footpad of normal C57BL/6 or C3H/eb mice. At the indicated time intervals, the mean tumour diameter was recorded. Each group consisted of 10 mice.



membrane antigens. As shown in Table 2, the fluorescence analyses of 10 randomly chosen T10 clones revealed the presence of two clones (that is, IE7 and IB9) expressing both the H-2<sup>k</sup> and the H-2<sup>b</sup> parental haplotypes. The remaining clones were found to be H-2<sup>k</sup> negative but H-2<sup>b</sup> positive.

These last findings suggest that the original local T10 tumour consisted of a mixture of H-2<sup>k</sup>-positive and H-2<sup>k</sup>-negative cells, with a predominance of H-2<sup>k</sup>-negative cells. To approach the question of whether the H-2<sup>k</sup>-positive T10 tumour cells were identical in nature to the M-T10 cells, the capacity of the different L-T10 clones to produce lung metastases was tested by injecting 10<sup>6</sup> viable tumour cells intravenously (i.v.) and 2 weeks later examining the organs for the appearance of tumour nodules. The data outlined in Table 2 clearly indicate that the H-2<sup>k</sup>-positive clones are potentially able to survive in the peripheral blood stream and to develop subsequently in one organ, the lungs. No such features were observed with the H-2<sup>k</sup>-negative clones. These two concomitant characteristics—membrane expression of the H-2<sup>k</sup> parental haplotype and homing to the lung tissue—were stable, remaining unchanged even after 10 serial passages in syngeneic F<sub>1</sub> mice.

Additional evidence for the ability of H-2<sup>k</sup>-positive T10 tumour cells to circumvent the host's resistance mechanisms was obtained by analysing the growth capacities of L-T10 and M-T10 cells in parental recipients. When 10<sup>6</sup> viable L-T10 cells or M-T10 cells were grafted intra footpad to C57BL/6 (H-2<sup>b</sup>) mice or C3H/eb (H-2<sup>k</sup>) mice, differential growth patterns were observed, depending on the origin of the T10 tumour cells (Fig. 2). M-T10 cells were found to grow both in an H-2<sup>b</sup> and in an H-2<sup>k</sup> environment, whereas L-T10 cells grew only in H-2<sup>b</sup> mice

**Table 1** Parental H-2 haplotype expression on L-T10 and M-T10 tumour cells

| Expt no. | Tumour cells (origin) | Relative no. of cells stained with: |                   |                    |                    |
|----------|-----------------------|-------------------------------------|-------------------|--------------------|--------------------|
|          |                       | aH-2 <sup>b</sup>                   | aH-2 <sup>k</sup> | aH-2D <sup>k</sup> | aH-2K <sup>k</sup> |
| 1        | L-T10                 | 85                                  | 0                 | 0                  | 0                  |
|          | M-T10 <sub>1</sub>    | 44                                  | 71                | 74                 | 42                 |
|          | M-T10 <sub>2</sub>    | 45                                  | 78                | 80                 | 38                 |
|          | M-T10 <sub>3</sub>    | 40                                  | 71                | 60                 | 45                 |
| 2        | L-T10                 | 93                                  | 24                | 8                  | 7                  |
|          | M-T10                 | 55                                  | 85                | 86                 | 50                 |
|          | M-T10 <sub>1</sub>    | 61                                  | 86                | 87                 | 42                 |
|          | M-T10 <sub>3</sub>    | 40                                  | 82                | 73                 | 53                 |
| 3        | L-T10                 | 84                                  | 16                | —                  | —                  |
|          | M-T10 <sub>1</sub>    | 47                                  | 90                | —                  | —                  |
|          | M-T10 <sub>2</sub>    | 37                                  | 75                | —                  | —                  |

The T10 sarcoma tumours from the original local tumour (L-T10) or from different metastatic pulmonary nodules (M-T10<sub>1,2,3</sub>) were maintained by subcutaneous transfers of 1 × 10<sup>6</sup> viable cells in (C3HeB × C57BL/6)F<sub>1</sub> mice. Single cell suspensions from solid tumours were prepared by treatment of minced tumour tissue with a solution of 0.3% trypsin (hog pancreas; Nutritional Biochemicals). The fluorescence stainings of the L-T10 and M-T10 tumour cells were performed using the following experimental protocol: 0.1 ml cells (3 × 10<sup>7</sup> cells ml<sup>-1</sup>) in Dulbecco's balanced salt solution with 0.02% NaN<sub>3</sub> (DBSS) were incubated with 0.01 ml antiserum (optimal concentration) at 4 °C during 30 min followed by two washings with DBSS. After resuspension in 0.1 ml DBSS, 0.010 ml of an optimal dilution of fluorescein-labelled rabbit anti-mouse Ig (Nordic Immunological Laboratory) was added and the cells were incubated for 20 min at 4 °C. After two washings with DBSS, the cells were analysed on the FACS-II (Becton-Dickinson). A scatter window was set to eliminate dead cells and cell debris. The frequency and fluorescence profile of the stained cells were determined using a laser output of 400 mW, photomultiplier at 450 V and fluorescent gain 4. The anti-H-2 antisera were obtained using the following immunization protocol: C3H.SW (H-2<sup>b</sup>) or C3H.DiSn (H-2<sup>k</sup>) were immunized intraperitoneally with 10<sup>8</sup> spleen cells of either C3H.DiSn or C3H.SW, respectively, weekly, for 4 weeks. Five days after the last injection the mice were bled and the obtained antisera checked for specificity using spleen cells and hydrocortisone-resistant thymocytes of different H-2<sup>k</sup> or H-2<sup>b</sup> congenic strains. The staining experiments outlined here were repeated on three successive serial transfers of L-T10 and M-T10 tumour cells (expts 1–3).

**Table 2** Parental H-2 haplotype expression and metastatic potential of T10 clones

| Expt no. | Tumour cells (origin) | Relative no. of cells stained with |                       | Presence of nodules in lung | Experimental metastases after i.v. inoculation |
|----------|-----------------------|------------------------------------|-----------------------|-----------------------------|--|
|          |                       | Anti-H-2 <sup>b</sup>              | Anti-H-2 <sup>k</sup> |                             |  |
| 1        | L-T10                 | 84                                 | 23                    | ±                           | 300  |
|          | T10 clone IC9         | 66                                 | 14                    | —                           | 212  |
|          | IG2                   | 67                                 | 16                    | —                           | 214  |
|          | IIF3                  | 73                                 | 8                     | —                           | 241  |
|          | IG3                   | 81                                 | 11                    | —                           | 232  |
|          | IB9                   | 93                                 | 65                    | +++                         | 655  |
|          | IE7                   | 97                                 | 73                    | +++                         | 759  |
|          | IF7                   | 94                                 | 17                    | ND                          | ND   |
|          | IID6                  | 77                                 | 14                    | ND                          | ND   |
|          | IID9                  | 82                                 | 15                    | ND                          | ND   |
|          | IB7                   | 85                                 | 14                    | ND                          | ND   |
| 2        | L-T10                 | 87                                 | 12                    | ±                           | 241  |
|          | T10 clone IE7         | 91                                 | 93                    | +++                         | 765  |
|          | IID6                  | 77                                 | 10                    | —                           | 214  |
|          | IB9                   | 73                                 | 74                    | +++                         | 704  |
|          | IC9                   | 71                                 | 7.8                   | —                           | 205  |
| 3        | L-T10                 | 82                                 | 13                    | ±                           | 256  |
|          | T10 clone IE7         | 80                                 | 77.4                  | +++                         | 960  |
|          | IB9                   | 89                                 | 94                    | +++                         | 803  |

T-10 cells were cloned in soft agar as previously described<sup>20</sup>. Briefly, tumour cells were seeded in soft agar medium (0.3%) on a harder agar (0.5%) medium supplemented with 15% FCS. After 10–14 days of incubation colonies were picked, expanded in liquid medium and transplanted subcutaneously into syngeneic F<sub>1</sub> mice. Single cell suspensions obtained after trypsin treatment of the different T10 tumours were analysed for the expression of H-2 antigens and for the capacity to form experimental metastases. The fluorescent stainings with anti-H-2<sup>b</sup> and anti-H-2<sup>k</sup> antisera on L-T10 tumour cells and different T10 clones were performed as described in Table 1 legend. The metastatic potential of different T10 clones was assessed by injecting 10<sup>6</sup> cells i.v. and 2–3 weeks later mice were killed and examined macroscopically for evidence of metastases to the lungs (—, no metastases; ±, <10 nodules, +, +, +, extensive involvement by tumour, numerous metastases). The level of infiltration was estimated by weighing the lungs (weight of normal lung = ±200 mg). The membrane expression of the parental H-2 haplotypes and the metastatic potential were repeated on some of the T10 clones obtained after different serial transfers (expt 1 = first transfer, expt 2 = 5th transfer; expt 3 = 10th transfer). ND, not done.

and were completely rejected in H-2<sup>k</sup> mice. This result suggests that the presence of H-2<sup>k</sup> antigens on the surface of T10 tumour cells somehow impairs semialloantigenic recognition.

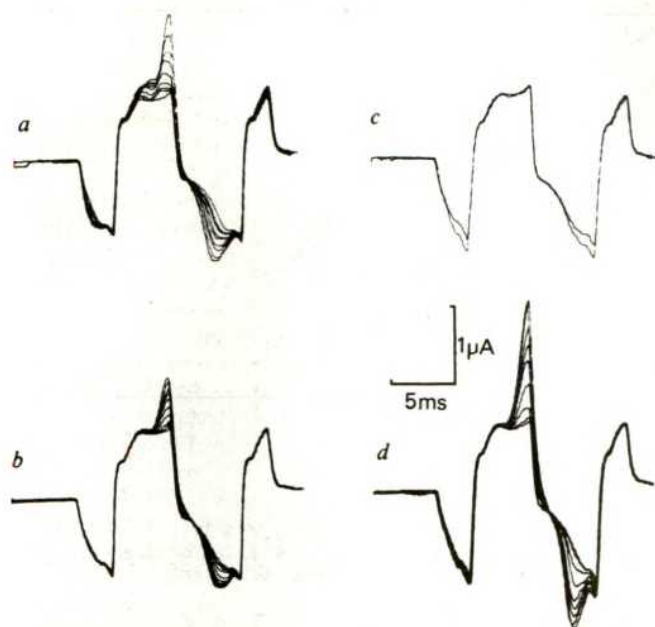
Using a methylcholanthrene-induced tumour in (DBA/2 × A)/F<sub>1</sub> mice (MDAY), Kerbel *et al.*<sup>19</sup> recently reported that serial transfers of MDAY tumour cells through the parental DBA/2 mice led to the selection or formation of a putative H-2K<sup>k</sup> loss variant, with highly metastatic characteristics. This finding and our present results may suggest that the modulation in the expression of MHC products generates in certain instances neoplastic cells with higher ability to resist immune destruction, resulting in increased survival in the peripheral blood, before seeding in distant anatomical locations.

We thank Dr R. N. Apte for his help and expertise in isolating the T10-derived clones, Dr D. Meruelo for anti-H-2 antisera, and Mr Ezra Vaday and Ms Ziona Frenkel for technical assistance. The work was supported by the NCI under contract no. CB-74185. P.D.B. is a EURATOM and EMBO postdoctoral fellow.

Received 30 June; accepted 12 September 1980.

1. Prehn, R. T. *J. natn. Cancer Inst.* **45**, 1039–1045 (1970).
2. Olsson, L. & Ebbesen, P. *J. natn. Cancer Inst.* **62**, 623–627 (1979).
3. Fidler, I. J. *Cancer Res.* **38**, 2651–2660 (1978).





**Fig. 4** Polarographic current sweeps *in vitro* and *in vivo*. *a*, A series of current sweeps for microelectrode in different concentrations of NA in saline, from  $10^{-5}$  to  $2 \times 10^{-3}$  M. *b*, The same microelectrode in saline using a series of different NA iontophoretic ejection currents. Current levels were, from smallest to largest, 20 nA tip negative, 0 mA (passive leak), 20, 40, 60, 80, 100, 120, 160 nA tip positive. *c*, Control current sweeps (20-nA retain) in saline and in the cerebral cortex of an anaesthetized rat. The current *in vivo* is slightly larger on the cathodal (reducing) part of the cycle. *d*, A set of sweeps in the cerebral cortex using the same series of steady iontophoretic NA ejection currents as in *b*. In *b* and *d* the sweeps were made 1 min after the start of iontophoresis.

iontophored substance and accurate measurement of the concentration of the iontophored substance. The sensitivity of the technique allows concentrations of  $5 \times 10^{-8}$  M NA and dopamine to be distinguished from background signal<sup>15</sup>. In comparison, other polarographic techniques<sup>10,16,17</sup> do not have the facility for iontophoresis, unit activity recording or electrode calibration *in vitro* before use *in vivo*. Finally, the time course of this polarographic recording technique (15 ms) approaches the time courses encountered during changes in neuronal activity in the nervous system. By using suitable high-speed switching between recordings of unit spike activity and polarographic measurement of catecholamine concentration, studies of the time course of responses in relation to known concentrations of drug in the central nervous system, which has previously been impossible, should now become feasible.

Received 9 May; accepted 26 September 1980.

- Kelly, J. S. in *Handbook of Psychopharmacology* Vol. 2 (eds Iversen, L. L., Iversen, S. H. & Snyder, S. D.) 29-67 (Plenum, New York, 1975).
- Bradshaw, C. M. & Szabadi, E. *Neuropharmacology* **13**, 407-415 (1974).
- Hoffer, B. J., Neff, N. & Siggins, G. R. *J. Neuropharmacol.* **10**, 175-180 (1971).
- Clarke, G., Hill, R. G. & Simmonds, M. A. *Br. J. Pharmacol.* **48**, 156-161 (1973).
- Dionne, V. E. *Biophys. J.* **16**, 705-717 (1976).
- Morris, M. E. & Krnjevic, K. in *Ion-selective Microelectrodes* (eds Berman, H. J. & Herbert, N. C.) 145-156 (Plenum, New York, 1974).
- Purves, R. D. *J. Neurosci. Meth.* **1**, 165-178 (1979).
- Armstrong-James, M. & Millar, J. *J. Neurosci. Meth.* **1**, 279-287 (1970).
- Adams, R. N. *J. pharmac. Sci.* **58**, 1171-1183 (1969).
- McCreery, R. L., Dreiling, R. & Adams, R. N. *Brain Res.* **73**, 23-33 (1974).
- Armstrong-James, M., Fox, K. & Millar, J. *J. Neurosci. Meth.* (in the press).
- Fox, K., Armstrong-James, M. & Millar, J. *J. Neurosci. Meth.* (in the press).
- Armstrong-James, M. & Millar, J. *J. Physiol., Lond.* (in the press).
- Armstrong-James, M. & Millar, J. *J. Physiol., Lond.* (in the press).
- Armstrong-James, M., Kruk, Z. L. & Millar, J. *J. Physiol., Lond.* (in the press).
- Marsden, C. A., Conti, J., Strobe, E., Curzon, G. & Adams, R. N. *Brain Res.* **171**, 85-99 (1979).
- Ponchon, J. L., Cespuglio, R., Gonon, F., Juvet, M. & Pujol, J. F. *Analyt. Chem.* **51**, 1483-1486 (1979).

## Vitamin E modulates the lipoxygenation of arachidonic acid in leukocytes

Edward J. Goetzl

Howard Hughes Medical Institute Laboratory at Harvard Medical School, and the Departments of Medicine, Harvard Medical School and the Brigham and Women's Hospital, Boston, Massachusetts 02115

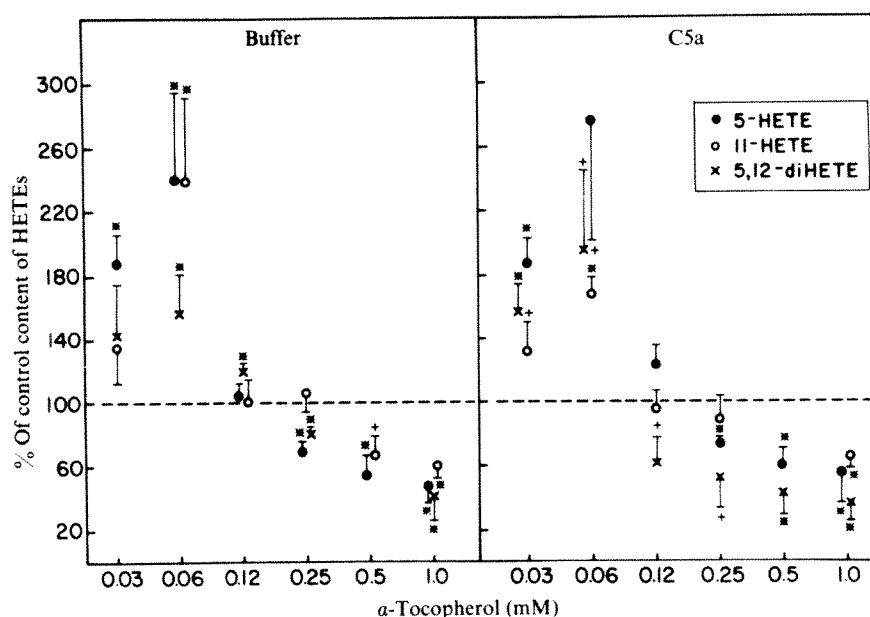
The arachidonic acid released from cellular phospholipids of specifically stimulated platelets and leukocytes is oxygenated enzymatically by two major pathways<sup>1-5</sup>. A complex cyclo-oxygenase converts some of the free arachidonic acid to labile endoperoxides that are transformed to prostaglandins, thromboxanes and prostacyclin (PGI<sub>2</sub>). Lipoxygenases convert part of the arachidonic acid to unstable hydroperoxy-eicosatetraenoic acids (OOHETEs) that are transformed to monohydroxy-eicosatetraenoic acids (HETEs), oligohydroxy-eicosatetraenoic or -eicosatrienoic acids such as di-HETEs and tri-HETEs, and, in some instances, more complex humoral mediators, including slow-reacting substances<sup>5-9</sup>. Both the nature of the HETEs and the ratio of the HETEs to the cyclo-oxygenase products are specific characteristics of each type of cell<sup>12,5</sup>. In human neutrophils, the sum of the lipoxygenase products 5-HETE, 11-HETE and 5,12-di-HETE substantially exceeds the total amount of PGE<sub>2</sub> and other cyclo-oxygenase metabolites that are generated concurrently<sup>3,4</sup>, and the endogenous lipoxygenase products regulate neutrophil function. The present data indicate that vitamin E ( $\alpha$ -tocopherol) bidirectionally modulates the activity of the lipoxygenase pathway of human neutrophils *in vitro*. Normal plasma concentrations of  $\alpha$ -tocopherol enhance the lipoxygenation of arachidonic acid, whereas higher concentrations of  $\alpha$ -tocopherol exert a suppressive effect that is consistent with its role as a hydroperoxide scavenger.

As extracellular mediators, the HETEs stimulate polymorphonuclear leukocyte random and chemotactic migration<sup>10-12</sup>, enhance the expression of C3b receptors<sup>12</sup> and increase the intra-leukocyte concentration of cyclic GMP (ref. 13). As the bulk of HETEs generated by human neutrophils and eosinophils is retained in the cellular membranes, whereas the PGE<sub>2</sub> produced is secreted, it has been suggested that the HETEs are functionally critical intracellular constituents<sup>14,15</sup>. In support of this, preincubation of neutrophils or eosinophils for 30-60 min with specific lipoxygenase inhibitors (for example, nordihydroguaiaric acid (5  $\mu$ M)) was observed to result in both significant depletion of cellular HETEs and suppression of random and chemotactic migration. The suppression of migration was reversed by the addition of purified exogenous HETEs to neutrophils and eosinophils deficient in endogenous HETEs as a result of pretreatment with lipoxygenase inhibitors<sup>14,15</sup>.

The levels of endogenous HETEs in neutrophils not stimulated by a chemotactic factor were enhanced a mean of two- to threefold by preincubation for 20 min at 37°C with 0.03-0.12 mM  $\alpha$ -tocopherol and were suppressed substantially by 0.5-1 mM  $\alpha$ -tocopherol ( $n = 3$ ). Neutrophils incubated with a chemotactic concentration of C5a exhibited mean increases of 2-, 1.5- and 2.5-fold, respectively, in the intracellular content of 5-HETE, 11-HETE and 5,12-di-HETE ( $n = 4$ ), and  $\alpha$ -tocopherol similarly modulated the enhanced level of HETEs in a concentration-dependent manner. In each instance, the increases and decreases were greatest for 5-HETE, whereas those of 5,12-di-HETE proved to be most resistant to suppression by 0.5-1 mM  $\alpha$ -tocopherol. The quantities of HETEs in the extracellular fluid were consistently less than 20% of those in the neutrophils, but the alterations elicited by  $\alpha$ -tocopherol paralleled those in the corresponding neutrophil pellets. To establish that the mechanism of action of  $\alpha$ -tocopherol was not a function of changes in the rate of mobilization of arachidonic acid from



**Fig. 1** Effects of  $\alpha$ -tocopherol on the lipoxygenation of exogenous arachidonic acid by human neutrophils. Portions of  $1 \times 10^8$  purified neutrophils were preincubated in 6 ml of Hanks' solution/0.1% ovalbumin (w/v), without or with various concentrations of highly purified  $\alpha$ -tocopherol (Supelco) for 20 min at 37 °C. Neutrophils were then washed twice, resuspended in 6 ml of the corresponding buffer without or with the same concentration of  $\alpha$ -tocopherol and incubated for 15 min at 37 °C with 160  $\mu$ g of arachidonic acid and 100  $\mu$ l of buffer (left-hand frame) or 100  $\mu$ l of the purified 15,000-molecular weight chemotactic fragment of the fifth component of complement, designated C5a (right-hand frame)<sup>12-15</sup>. The neutrophils were sedimented at 100g and the supernatant and neutrophil pellet, which had been resuspended in 6 ml of Hanks' solution and sonicated, were acidified to pH 4 with 2 M citric acid. After the addition of 40,000 c.p.m. of  $^3$ H-12-L-HETE<sup>14,15</sup> to each sample, the HETEs were extracted from each supernatant and sonicated with two 6-ml portions of chloroform/methanol (2:1, v:v) and two 3-ml portions of ether. The HETEs in the pooled extracts were separated from  $\alpha$ -tocopherol, resolved and purified by sequential silicic acid chromatography and reversed-phase HPLC<sup>14,15</sup> and quantified by optical density at 235 nm (mono-HETEs) or 280 nm (5,12-di-HETE) with a correction for recovery according to the yield of  $^3$ H-12-L-HETE. The range of intracellular content of 5-HETE, 11-HETE and 5,12-di-HETE in control neutrophils (100%) was 3,711–5,841, 1,833–3,271 and 594–1,071 ng per  $10^8$  neutrophils, respectively, in buffer alone and 6,914–11,046, 3,774–5,650 and 1,468–2,348 ng per  $10^8$  neutrophils with C5a. Each data point and bar are the mean  $\pm$  s.d. for four experiments. The level of statistical significance of the difference between each value and the corresponding control value were determined by a standard two-sample *t*-test and are depicted by \*  $P < 0.01$  and †  $P < 0.05$ .



phospholipids, the studies were repeated using 160  $\mu$ g of exogenous arachidonic acid per  $10^8$  neutrophils, of which over 90% was taken up by the neutrophils to provide a quantity that exceeded by approximately twofold the total amount in the native cellular pool<sup>14,15</sup>. Although the introduction of exogenous arachidonic acid augmented the content of intracellular HETEs by nearly 10-fold, the bidirectional effects of  $\alpha$ -tocopherol (Fig. 1) were similar in magnitude to those elicited in the absence of exogenous arachidonic acid. The optimal increase in the content of each of the HETEs was evoked by 0.06 mM  $\alpha$ -tocopherol and maximal suppression was achieved by 1 mM  $\alpha$ -tocopherol.

As  $\alpha$ -tocopherol reacts specifically with OOH-groups, it was also anticipated that the generation by neutrophils of 5-OOHETE and other OOHETEs would be influenced by alterations in the cellular level of  $\alpha$ -tocopherol (Table 1). The ratio of the quantities of 5-OOHETE to 5-HETE was increased more than twofold by 0.03 mM  $\alpha$ -tocopherol and was suppressed to ~30% of control values by 0.5 mM  $\alpha$ -tocopherol in the absence of a specific agonist. Despite the 5.1-fold higher mean levels of 5-HETE in neutrophils exposed to the calcium ionophore A23187, the same concentrations of  $\alpha$ -tocopherol exerted effects on the ratio of 5-OOHETE to 5-HETE that were of similar magnitude to those observed for neutrophils in buffer (Table 1). Alterations by  $\alpha$ -tocopherol in the ratio of OOHETE to HETE secreted by neutrophils would influence the net

activity of any concentration of the lipid factors as extracellular mediators. 12-OOHETE and 5-OOHETE elicit maximal neutrophil chemotactic responses at 4  $\mu$ g ml<sup>-1</sup> and 0.4  $\mu$ g ml<sup>-1</sup>, respectively, that exceed by over 50% the maximal chemotactic responses to 10–20  $\mu$ g ml<sup>-1</sup> of 12-HETE and 1–2  $\mu$ g ml<sup>-1</sup> of 5-HETE<sup>10-13</sup>. Similarly, both OOHETEs are more active than the respective HETEs in evoking an optimal neutrophil chemokinetic response. Not only are the OOHETEs 10-fold more potent than the HETEs in augmenting the intra-neutrophil concentration of cyclic GMP, but also the elevation achieved lasts for 30 min or longer, compared with between 10 and 20 min for that achieved by the HETEs.

$\alpha$ -tocopherol modulates human neutrophil migration *in vitro* at concentrations that affect the lipoxygenase pathway. The preincubation of neutrophils with 0.06 mM  $\alpha$ -tocopherol for 20 min enhanced neutrophil random migration by 18–54% and chemotaxis to C5a by 29–106% ( $n = 3$ ), whereas 1 mM  $\alpha$ -tocopherol inhibited neutrophil random migration by 53–70% and chemotaxis by 32–56%, as assessed by a modified Boyden micropore filter assay<sup>12-15</sup>. The addition of nanogramme amounts of exogenous 5-HETE to  $2 \times 10^6$  neutrophils depleted of endogenous 5-HETE and 11-HETE by prior treatment with lipoxygenase inhibitors, such as nordihydroguaiaretic acid, completely reverses the defect in neutrophil migration that is characteristic of the HETE-depleted neutrophils<sup>14,15</sup>. Thus, it would be expected that the addition of 5-HETE to neutrophils preincubated in 1 mM  $\alpha$ -tocopherol would reverse the inhibition of migration, if the sole abnormality were a depletion of endogenous HETEs. Preincubation of neutrophils with 1 mM  $\alpha$ -tocopherol depleted the intracellular content of 5-HETE by a mean of 71% ( $n = 3$ ), suppressed the ratio of 5-OOHETE to 5-HETE from a mean of 0.18 to 0.10 and concurrently inhibited random migration by 64% and chemotaxis to C5a by 52%. In contrast to the results with lipoxygenase inhibitor-treated neutrophils, however, the addition of 0.2–2.5 ng 5-HETE without or with 10–200 ng 11-HETE to  $2 \times 10^6$   $\alpha$ -tocopherol-treated neutrophils failed to reverse the migration defects. The effects of  $\alpha$ -tocopherol on human neutrophil function thus are not solely attributable to alterations in the cellular content of endogenous HETEs, and may also reflect changes in the concentrations of OOHETEs or non-lipoxygenase-related actions of  $\alpha$ -tocopherol.

$\alpha$ -tocopherol serves an important role as 'biological antioxidant' by preventing the peroxidation of polyunsaturated fatty acid constituents of cellular membranes, including arachidonic

**Table 1** Modification of the ratio of 5-OOHETE to 5-HETE in human neutrophils by  $\alpha$ -tocopherol

| Concentration of $\alpha$ -tocopherol (mM) | Buffer           | A23187          |
|--|------------------|-----------------|
| 0  | 0.16 $\pm$ 0.04* | 0.17 $\pm$ 0.07 |
| 0.03                                       | 0.36 $\pm$ 0.12  | 0.32 $\pm$ 0.15 |
| 0.12                                       | 0.10 $\pm$ 0.06  | 0.12 $\pm$ 0.09 |
| 0.50                                       | 0.05 $\pm$ 0.01  | 0.08 $\pm$ 0.02 |

Portions of  $3 \times 10^8$  purified neutrophils were preincubated in buffer without or with  $\alpha$ -tocopherol, washed and resuspended in buffer of the same composition as described in Fig. 1 legend, with 160  $\mu$ g arachidonic acid per  $10^8$  neutrophils, and calcium ionophore A23187 at a final concentration of 5  $\mu$ M. After 10 min at 37 °C, the neutrophils were sedimented and the 5-OOHETE and 5-HETE extracted and purified as described in Fig. 1 legend. The ratio of 5-OOHETE to 5-HETE was determined by assessing the concentration of OOH-groups in the mixtures of the two compounds based on the conversion of triphenylphosphine to triphenylphosphine oxide and measurement of the quantity of triphenylphosphine oxide by gas-liquid chromatography<sup>27</sup>.

\* Each value is the mean  $\pm$  s.d. of the results from three separate experiments.

acid<sup>16-19</sup>. A deficiency of  $\alpha$ -tocopherol in rat or human neutrophils results in greater than normal release of hydrogen peroxide, augmented peroxidation of membrane lipids and impairment of chemotaxis and phagocytosis that are corrected rapidly by either the addition of  $\alpha$ -tocopherol *in vitro* or the prior administration of several doses of  $\alpha$ -tocopherol to the neutrophil donors<sup>20</sup>. Although the optimal cyclooxygenation of arachidonic acid to prostaglandins in rabbit tissues requires physiological concentrations of  $\alpha$ -tocopherol<sup>21,22</sup>, the mechanism of this apparent facilitation of oxidation by  $\alpha$ -tocopherol is unknown. The present data document for the first time the bidirectional modulation by  $\alpha$ -tocopherol of the lipoxygenation of arachidonic acid to products which serve as both specific extracellular mediators and functionally critical intracellular constituents. The generation of endogenous neutrophil 5-HETE, 11-HETE and 5,12-di-HETE was significantly enhanced *in vitro* by 0.03 mM and 0.06 mM  $\alpha$ -tocopherol, which approximate the normal human serum concentration of 0.01–0.05 mM (refs 23, 24). The neutrophil lipoxygenase pathway was inhibited significantly by levels of 0.25–1 mM  $\alpha$ -tocopherol, which increase the content of  $\alpha$ -tocopherol in platelets and leukocytes by up to 5–17-fold within 5 min of incubation *in vitro* and are obtainable *in vivo* by the ingestion of pharmacological doses of  $\alpha$ -tocopherol<sup>23,24</sup>. The mechanism of the enhancement of lipoxygenation of arachidonic acid in neutrophils by physiological levels of  $\alpha$ -tocopherol is not related simply to alterations either in the formation of lipid hydroperoxides or in the liberation of endogenous arachidonic acid from phospholipids. The demonstration that the function of some acetylcholine receptors in phospholipid liposomes is

optimal only when  $\alpha$ -tocopherol represents a substantial fraction of the total lipid content<sup>25</sup> and that  $\alpha$ -tocopherol is required for the incorporation of excitability-inducing material into black lipid membranes<sup>26</sup>, suggests that a normal content of  $\alpha$ -tocopherol in neutrophil membranes also may be required for maximal expression of lipoxygenase activity.

Received 17 July, accepted 3 September 1980

- Samuelsson, B., Granstrom, E., Green, K., Hamberg, M. & Hammarstrom, S. *A Rev Biochem* 44, 669–695 (1975)
- Nugteren, D. H. *Biochim biophys Acta* 380, 299–307 (1975)
- Goldstein, I. M. *et al J exp Med* 148, 787–792 (1978)
- Stenson, W. F. & Parker, C. W. *J clin Invest* 64, 1457–1465 (1979)
- Borgeat, P., Hamberg, M. & Samuelsson, B. *J Biol Chem* 251, 7816–7820 (1976)
- Borgeat, P. & Samuelsson, B. *Proc natn Acad Sci USA* 76, 3213–3217 (1979)
- Jones, R. L., Korry, P. J., Poyser, N. L., Walker, I. C. & Wilson, N. H. *Prostaglandins* 16, 583–589 (1978)
- Murphy, R. C., Hammarstrom, S. & Samuelsson, B. *Proc natn Acad Sci USA* 76, 4275–4280 (1979)
- Morris, H. R., Taylor, G. W., Piper, P. J., Sanboun, M. W. & Tippins, J. R. *Prostaglandins* 19, 185–201 (1980)
- Goetzl, E. J., Woods, J. M. & Gorman, R. R. *J clin Invest* 59, 179–183 (1977)
- Goetzl, E. J. & Sun, F. F. *J exp Med* 150, 406–411 (1979)
- Goetzl, E. J., Brash, A. R., Tauber, A. I., Oates, J. A. & Hubbard, W. C. *Immunology* 39, 141–151 (1980)
- Goetzl, E. J., Hill, H. R. & Gorman, R. R. *Prostaglandins* 19, 71–85 (1980)
- Goetzl, E. J., Weller, P. F. & Sun, F. F. *J Immunol* 124, 926–933 (1980)
- Goetzl, E. J. *Immunology* 48, 709–726 (1980)
- Tappel, A. L. *Vitam Horm* 28, 493–510 (1962)
- Tappel, A. L. *Ann NY Acad Sci* 283, 12–28 (1972)
- Hoeftstra, W. G. *Fedin Proc* 34, 2083–2089 (1975)
- Combs, G. F. Jr., Noguchi, T. & Scott, M. L. *Fedin Proc* 34, 2090–2095 (1975)
- Harris, R. E., Boxer, L. A. & Boelmer, R. L. *Blood* 55, 338–343 (1980)
- Chan, A. C., Hegarty, P. V. J. & Allen, C. E. *J Nutr* 110, 74–81 (1980)
- Chan, A. C., Allen, C. E. & Hegarty, P. V. J. *J Nutr* 110, 66–73 (1980)
- Stamer, M. & Anastasi, J. *J clin Invest* 57, 732–737 (1976)
- Hatam, L. J. & Kayder, H. J. *J Lipid Res* 20, 639–645 (1979)
- Kiban, P. L. *et al Biochim biophys Res Commun* 93, 409–414 (1980)
- Mueller, P. & Rodan, D. O. *J Amer Biol* 18, 222–258 (1968)
- Boymans, J. M., Oates, J. A. & Hubbard, W. C. *Prostaglandins* 19, 87–91 (1980)

## Differential repair of $O^6$ -methylguanine in DNA of rat hepatocytes and nonparenchymal cells

J. G. Lewis

Department of Pathology, Duke University Medical Center, Durham, North Carolina 27710

J. A. Swenberg\*

Department of Pathology, Chemical Industry Institute of Toxicology, Research Triangle Park, Durham, North Carolina 27709

Chronic administration of several chemical carcinogens to laboratory animals induces a variety of tumours which arise from specific cell populations within the liver. In the rat, diethylnitrosamine induces hepatocellular carcinomas<sup>1</sup>, dimethylnitrosamine induces both angiosarcomas<sup>2</sup> and hepatocellular carcinomas<sup>3</sup>, vinyl chloride primarily induces angiosarcomas<sup>4</sup>, and 1,2-dimethylhydrazine induces malignant haemangioendotheliomas<sup>5,6</sup>. One of the principal mechanisms thought to be involved in initiating carcinogenesis is the alkylation of specific sites on DNA, such as the  $O^6$  position of guanine<sup>7</sup>. Previous investigations of alkylation and repair have, however, analysed DNA prepared from whole liver. This approach does not localize alkylation or repair capacity in the different cell types which give rise to neoplasia. Furthermore, although hepatocytes account for more than 90% of the liver's mass, they only comprise 60–70% of its cells<sup>8</sup>. The nonparenchymal cell (NPC) population, which consists almost entirely of endothelial and Kupffer cells, accounts for the remaining 30–40% and contains 10–20% of the DNA. Therefore, we decided to investigate the alkylation and repair of  $O^6$ - and 7-methylguanine in the target and non-target cells following oral administration of 1,2-dimethylhydrazine. We report here that although initial alkylation was slightly less in NPCs, removal of  $O^6$ -methylguanine was significantly slower. This led to a preferential accumulation of  $O^6$ -methylguanine in NPC 24 h after administering a second daily dose. In contrast, 7-

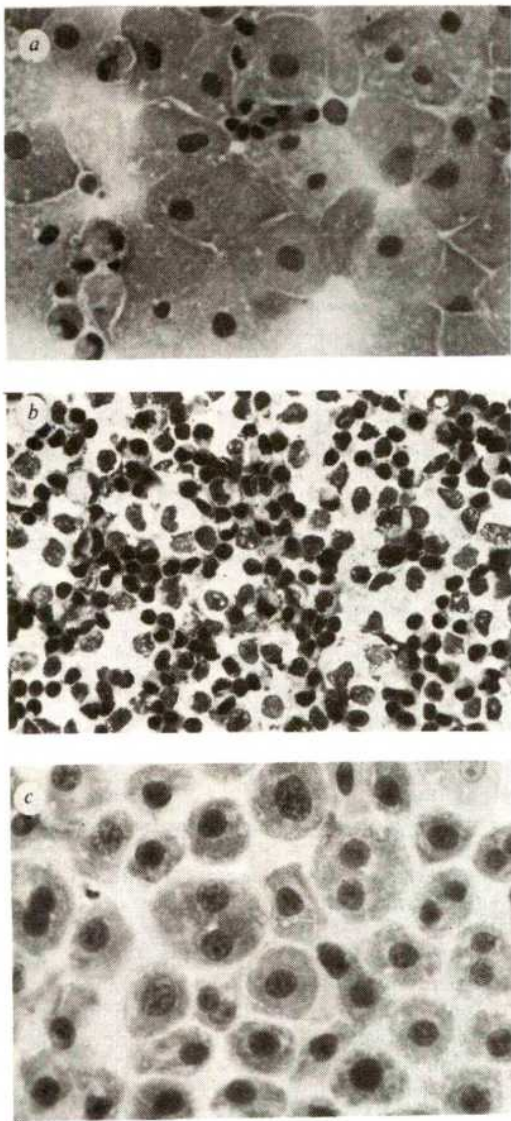
methylguanine decreased at similar rates, resulting in a 28-fold greater  $O^6$ -methylguanine/7-methylguanine ratio in the target cell population.

Administration of 1,2-dimethylhydrazine (DMH) at a dose of 3 mg per kg per day in the drinking water induces a high incidence of tumours arising from the vascular lining cells of the liver in BDIX rats. Investigations of DMH-induced alkylation and repair in whole liver have demonstrated that maximal DNA alkylation occurs within 12 h for doses ranging from 4 to 20 mg per kg (refs 9, 10).  $O^6$ -Methylguanine is rapidly removed from DNA by an enzymatic process, whereas 7-methylguanine is lost at a slower rate by chemical depurination, leading to a decreasing  $O^6$ -/7-methylguanine ratio<sup>11</sup>. This pattern is similar to that observed after the administration of dimethyl- or diethylnitrosamine<sup>12</sup>. Nothing is known of the localization of methylated purines within the two major liver cell populations or the capacities of the different cells to repair  $O^6$ -methylguanine.

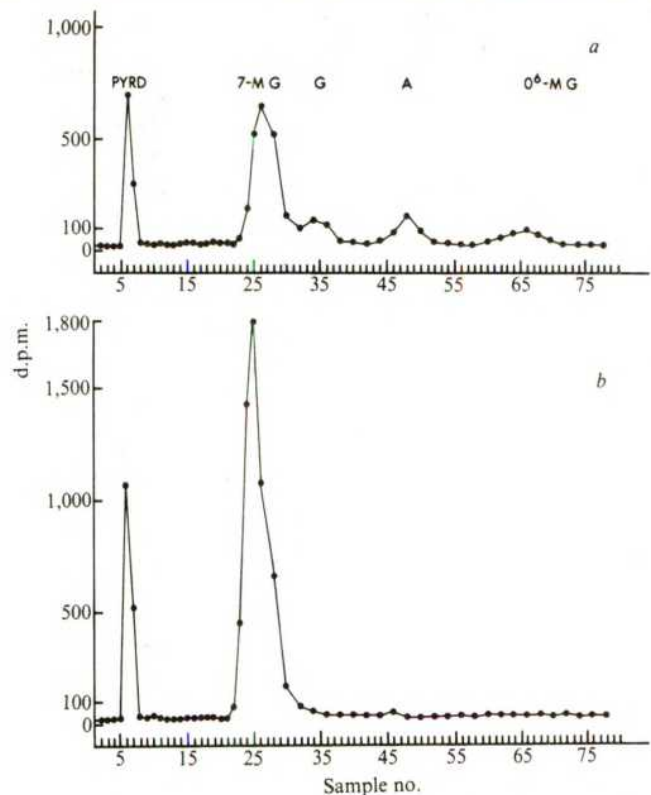
Previous attempts to separate NPCs from hepatocytes have used density gradient centrifugation<sup>13</sup> or the selective destruction of hepatocytes by pronase digestion<sup>14</sup>. Both these methods have serious limitations for use in a comparative study of alkylation and repair. When density gradient centrifugation is used, yields are inversely proportional to purity and many of the media used are hyperosmotic or mildly toxic. With pronase digestion, high yields of relatively pure NPCs can be obtained; however, destruction of the hepatocytes negates the possibility of studying two populations of cells from the same liver. In addition, the massive destruction of hepatocytes in the presence of the NPCs results in phagocytosis of hepatocellular debris by Kupffer cells<sup>8</sup>, possibly contaminating them with hepatocellular DNA. Elutriation centrifugation<sup>15</sup>, which separates mainly on the basis of cell volume, exploits the enormous difference between the volume of the hepatocyte and NPC<sup>8</sup>. This technique can be used to separate a mixed liver cell suspension derived from collagenase perfusion<sup>16</sup> into populations of NPCs and hepatocytes with a purity of 95% or greater. The NPC population consists almost entirely of Kupffer and endothelial cells<sup>17</sup>. Bile duct cells remain in the filter leavings during the preparation of the mixed liver cell suspension. Purity of the populations can easily be monitored by light microscopy due to

\* To whom correspondence should be addressed





**Fig. 1** Separation of a mixed liver cell suspension (MLCS) (a) into hepatocytes (b) and NPCs (c) by elutriation centrifugation (haematoxylin and eosin stain for hepatocytes, Wrights stain for NPCs  $\times 400$ ). A MLCS was prepared as previously described<sup>16</sup> by *in situ* perfusion of the liver with collagenase through the portal vein. The resultant MLCS was washed three times in HBSS without  $\text{Ca}^{2+}$  and  $\text{Mg}^{2+}$  at  $4^\circ\text{C}$ . After washing, the cells were resuspended in 20 ml of HBSS without  $\text{Ca}^{2+}$  and  $\text{Mg}^{2+}$  and slowly injected into the large mixing chamber (70 ml) of the Beckman JE-6 elutriation rotor containing a Sanderson separation chamber in a Beckman J2-21 refrigerated centrifuge equipped with a fine speed control. The rotor speed was held constant at 1,500 r.p.m., and the media flow rate varied. The MLCS was washed into the rotor at a flow rate of  $18\text{ ml min}^{-1}$  until the separation chamber became approximately 50% full of retained hepatocytes. The flow of media was then diverted around the mixing chamber directly through the separation chamber and the retained hepatocytes washed until 200 ml of media containing the NPCs had been collected. The hepatocytes were then flushed from the rotor at a flow rate of  $100\text{ ml min}^{-1}$ . After the separation chamber was emptied the flow rate was returned to  $18\text{ ml min}^{-1}$  and the flow again routed through the mixing chamber washing in a second portion of the MLCS. This procedure was repeated four or five times until all the cells that could be washed from the mixing chamber had been separated. Yields varied from  $2\text{--}5 \times 10^6$  NPCs and  $6\text{--}11 \times 10^6$  hepatocytes per liver and were  $\geq 95\%$  pure as determined by counting on a haemocytometer. The absence of bile duct epithelium in the NPC and hepatocyte fractions was confirmed using  $\gamma$ -glutamyl transpeptidase enzyme histochemistry.



**Fig. 2** Representative radiochromatograms of hydrolysed DNA from NPCs (a) and hepatocytes (b) of a rat killed 24 h after two daily doses of  $^{14}\text{C}$ -DMH. DNA was extracted from the cell pellets by hydroxyapatite chromatography as previously described<sup>18</sup> and the purines liberated by mild acid hydrolysis ( $0.1\text{ M HCl}$  at  $80^\circ\text{C}$  for 30 min). After hydrolysis the solution was made  $0.01\text{ M NaPO}_4$ , the pH adjusted with  $1\text{ M NaOH}$  to 5.5, filtered and applied to a  $45 \times 0.9\text{-cm}$  glass column containing 20 g (dry weight) of ultra fine Sephasorb HP (Pharmacia). The column was eluted with  $0.01\text{ M NaPO}_4$  buffer pH 5.5 at a flow rate of  $1\text{ ml min}^{-1}$  (100 p.s.i.) using a Laboratory Data control HPLC pump. The concentrations of guanine and adenine were determined by integrating the area under the curve for their absorbance at 254 nm using a Shimadzu C-EIA integrator and a Uvicord S monitor. Samples of 3 ml were collected until the beginning of the guanine peak, after which 6-ml samples were collected. Two volumes of ACS scintillation fluid were added to each sample and they were counted for 10 min at a counting efficiency of 79% in a Searle mark III scintillation counter using channel 3. The concentrations of 7- and  $\text{O}^6$ -methylguanine were expressed as a fraction of guanine and were calculated assuming that the specific activity of the alkylation products was one-half that of the carcinogen because only one labelled methyl group is available for alkylation<sup>19</sup>.

the large difference in size and morphology (Fig. 1). An additional advantage of elutriation centrifugation is that it can be performed at  $4^\circ\text{C}$ .

To quantify differences in alkylation and repair and to test for possible accumulation of alkylation products, nine male BDIX rats weighing 150–200 g were given an oral dose of  $^{14}\text{C}$ -DMH (3 mg per kg, specific activity  $7.5\text{--}8.0\text{ }\mu\text{Ci mmol}^{-1}$ ). Three animals were killed at 2 and 24 h, their livers perfused and the cells separated and frozen. The remaining three animals received a second dose of  $^{14}\text{C}$ -DMH 24 h after the first dose, and were killed and their liver cells separated 24 h later. DNA from the different cell populations was purified by hydroxyapatite chromatography<sup>18</sup>, hydrolysed in  $0.1\text{ M HCl}$  at  $80^\circ\text{C}$  for 30 min and the purines separated by gel filtration chromatography (Fig. 2).

The extent of the initial alkylation was slightly less in NPCs than in hepatocytes 2 h after carcinogen administration (Table 1). In contrast, after 24 h only 10% ( $8.9 \pm 4.4\text{ pmol}$  of  $\text{O}^6$ -methylguanine per  $\mu\text{mol}$  of guanine) of the initial amount of  $\text{O}^6$ -methylguanine persisted in the hepatocytes, whereas 53%

**Table 1** Alkylation of hepatocyte and nonparenchymal cell DNA following oral exposure of rats to  $^{14}\text{C}$ -1,2-dimethylhydrazine

| Cell type  | No. of doses | Survival time (h) | Alkylation of DNA per $10^6$ guanine |                |                          | Metabolic incorporation of $^{14}\text{C}$ |                                     |
|------------|--------------|-------------------|--------------------------------------|----------------|--------------------------|--|-------------------------------------|
|            |              |                   | $\text{O}^6\text{MG}$                | 7-MG           | $\text{O}^6/7\text{-MG}$ | Guanine (d.p.m. per $\mu\text{M}$ )        | Adenine (d.p.m. per $\mu\text{M}$ ) |
| Hepatocyte | 1            | 2                 | $89.0 \pm 7.5^*$                     | $1,032 \pm 70$ | 0.086                    | ND†  | ND                                  |
| NPC        | 1            | 2                 | $65.4 \pm 8.4$                       | $783 \pm 78$   | 0.083                    | ND   | ND                                  |
| Hepatocyte | 1            | 24                | $8.9 \pm 2.5$                        | $753 \pm 80$   | 0.011                    | $7.6 \pm 7.7$                              | $18.3 \pm 10.4$                     |
| NPC        | 1            | 24                | $34.6 \pm 0.7$                       | $525 \pm 60$   | 0.067                    | $79.4 \pm 46.8$                            | $78.7 \pm 15.3$                     |
| Hepatocyte | 2‡           | 48                | $4.6 \pm 3.6$                        | $1,362 \pm 54$ | 0.003                    | $8.1 \pm 8.1$                              | $21.5 \pm 13.6$                     |
| NPC        | 2            | 48                | $56.3 \pm 4.3$                       | $689 \pm 90$   | 0.085                    | $375.6 \pm 35.9$                           | $369.3 \pm 53.8$                    |

\* Mean  $\pm$  s.e. of three rats.

† Not detectable.

‡ Second dose administered 24 h after the first dose.

( $34.6 \pm 1.1$  pmol of  $\text{O}^6$ -methylguanine per  $\mu\text{mol}$  of guanine) remained in the NPCs ( $P < 0.01$ , 1-tailed  $t$ -test). 7-Methylguanine decreased at a similar rate in the NPC (27%) and hepatocyte (30%) populations during the 24 h following oral administration of  $^{14}\text{C}$ -DMH.

With 53% of the initial  $\text{O}^6$ -methylguanine remaining in the NPCs, and assuming that previous and newly formed  $\text{O}^6$ -methylguanine are repaired at the same rate, the amount of  $\text{O}^6$ -methylguanine accumulating in the NPCs 24 h after a second dose of  $^{14}\text{C}$ -DMH was estimated to be 53 pmol of  $\text{O}^6$ -methylguanine per  $\mu\text{mol}$  of guanine. The observed value was  $56.3 \pm 4.3$  pmol  $\text{O}^6$ -methylguanine per  $\mu\text{mol}$  guanine. No accumulation of  $\text{O}^6$ -methylguanine was detected in the corresponding hepatocytes whereas, in contrast, 7-methylguanine accumulated in both populations (Table 1). An additional indication of the marked differences in the two cell populations' capacity for repair of  $\text{O}^6$ -methylguanine is demonstrated by comparing the  $\text{O}^6/7$ -methylguanine ratios. These ratios were similar at 2 h, 6 times higher in the NPCs at 24 h and 28 times higher in the NPCs 24 h after administration of the second dose of  $^{14}\text{C}$ -DMH (Table 1). As the 7-methylguanine was removed at a similar rate for both cell populations, the change in ratio clearly demonstrates that the hepatocytes were more efficient than the NPCs at removing  $\text{O}^6$ -methylguanine from their DNA.

An additional difference observed between the two cell populations was the incorporation of  $^{14}\text{C}$  from  $^{14}\text{C}$ -DMH into normal purine bases via the C-1 pool. Incorporation of  $^{14}\text{C}$  was much higher in the NPCs than the hepatocytes 24 h after the second dose of  $^{14}\text{C}$ -DMH (Table 1). The slower rate of DNA repair and increased amount of metabolic incorporation suggest that non-repair-related DNA synthesis, that is, cell replication, is occurring in the NPCs. This may be due to selective cytotoxicity for the NPCs leading to repopulation.

This present study demonstrates that different cell populations in the intact rat liver possess different capacities for DNA repair. It further shows that in DMH-induced carcinogenesis the target cell population (NPCs) accumulates the promutagenic alkylation product,  $\text{O}^6$ -methylguanine, whereas the non-target cell (hepatocyte) does not. It also suggests that the rate of cell division may be higher in the target cells. These data are consistent with the hypothesis that the extent of promutagenic DNA damage, the capacity to repair such damage, as well as the degree of cell replication represent critical events which correlate with carcinogenesis. Previous investigations of organ-specific carcinogenesis<sup>7,11</sup> have supported this conclusion; however, this is the first demonstration of cell specificity within the target organ.

We thank Ms Kathryn Caton Billings for technical assistance and Ms Mary Bedell and Dr Gerhard Doerjer for their thoughtful advice.

Received 23 June; accepted 12 September 1980.

1. Weisburger, J. H., Madison, R. M., Warel, J. M., Vigueva, C. & Weisburger, E. K. *J. natl. Cancer Inst.* **54**, 1185-1188 (1975).
2. Abanobi, S. E., Farber, E. & Sarma, D. S. R. *Cancer Res.* **39**, 1592-1596 (1979).
3. Magee, P. N. & Barnes, J. M. *Br. J. Cancer* **10**, 114-122 (1956).
4. Lee, C. C. *et al. J. Tox. envir. Hlth* **4**, 15-30 (1978).

5. Druckrey, H. in *Topics in Chemical Carcinogenesis* (eds Nakahara, W., Takayama, S., Sugimura, T. & Odashima, S.) 73-101 (University Park Press, Tokyo, 1972).
6. Druckrey, H. in *Carcinoma of the Colon and Antecedent Epithelium* (ed. Brudette, W. J.) 267-279 (Thomas, Springfield, 1970).
7. Pegg, A. E. *Adv. Cancer Res.* **25**, 195-269 (1977).
8. Wisse, E. & Knook, D. L. in *Progress in Liver Disease* Vol. 6 (eds Popper, H. & Schaffner, F.) 153-171 (Grune & Stratton, New York, 1979).
9. Rogers, K. J. & Pegg, A. E. *Cancer Res.* **37**, 4082-4087 (1977).
10. Swenberg, J. A., Cooper, H. K., Bücheler, J. & Kleihues, P. *Cancer Res.* **39**, 465-467 (1979).
11. Kleihues, P. *et al. Archs Tox. Suppl.* **2**, 253-261 (1979).
12. Pegg, A. E. & Nicol, J. W. in *Screening Tests in Chemical Carcinogenesis* (eds Montesano, R., Bartsch, H. & Tomatis, L.) 571-590 (IRC Scientific Publ. 12, IARC, Lyon, 1976).
13. Munthe-Kaas, A. C. & Segler, P. O. *FEBS Lett.* **43**, 252-257 (1974).
14. Mills, D. M. & Zucker-Franklin, D. *Am. J. Path.* **54**, 147-155 (1969).
15. Sanderson, R. J. & Bird, K. E. *Meth. Cell Biol.* **15**, 1-14 (1977).
16. Berry, M. N. & Friend, D. S. *J. Cell Biol.* **43**, 506-520 (1969).
17. Knook, D. L. & Sleyster, E. Ch. *Expl Cell Res.* **99**, 444-449 (1976).
18. Beland, F. A., Dooley, K. L. & Casciano, D. A. *J. Chromat.* **174**, 177-186 (1979).
19. Fiala, E. S. *Cancer* **40**, 2436-2445 (1977).

## L-leucine and a nonmetabolized analogue activate pancreatic islet glutamate dehydrogenase

Abdullah Sener & Willy J. Malaisse

Laboratory of Experimental Medicine, Brussels University, Brussels, Belgium B-1000

The release of insulin evoked by nutrients in the pancreatic  $\beta$ -cell is attributed to either the activation of a stereospecific receptor by the nutrient molecule itself or the generation of one or more signal(s) through the intracellular metabolism of the nutrient secretagogue<sup>1</sup>. The first of these hypotheses is apparently supported by the fact that nonmetabolized amino acids, especially the L-leucine analogue b(-)-2-amino-bicyclo[2, 2, 1]heptane-2-carboxylic acid (BCH), stimulate insulin release<sup>2</sup>. However, we now report evidence in support of the second hypothesis. We present data consistent with the idea that BCH induces insulin release through the allosteric activation of glutamate dehydrogenase. This is compatible with the fuel hypothesis, which states that the secretory response to nutrient secretagogues depends always on an increase of catabolic fluxes in the islet cells<sup>3,4</sup>.

The activity of glutamate dehydrogenase in islet homogenates was measured at pH 8.0 and 25 °C in the presence of  $\text{NH}_4^+$  50.0 mM,  $\alpha$ -ketoglutarate 7.0 mM and NADH 0.1 mM, as described elsewhere<sup>5</sup>. L-leucine and b(-)-BCH were equally potent in causing allosteric activation of the enzyme (Fig. 1). D-leucine had no effect on enzyme activity (data not shown). The velocity of the reaction catalysed by glutamate dehydrogenase was considerably increased by ADP (0.5 mM). Even in the presence of ADP, L-leucine and b( $\pm$ )BCH still caused a significant increase in reaction velocity (Fig. 1). L-norvaline and L-isoleucine also caused activation of glutamate dehydrogenase, although to a lesser extent than L-leucine (Table 1). Glycine,



**Table 1** Effect of amino acids on glutamate dehydrogenase and insulin release

| Amino acid (mM)       | Glutamate dehydrogenase (nmol per islet per 60 min) | Insulin release ( $\mu$ U per islet per 90 min) |                        |
|-----------------------|---|---|------------------------|
|                       |   | No glutamine                                    | L-glutamine (10.0 mM)  |
| Nil                   | 2.5 $\pm$ 0.5 (7)                                   | 15.4 $\pm$ 1.8 (56)                             | 13.6 $\pm$ 2.2 (40)    |
| L-leucine (10)        | 9.3 $\pm$ 1.0 (7)*                                  | 51.7 $\pm$ 3.0 (54)*                            | 206.7 $\pm$ 18.0 (19)* |
| b( $\pm$ )BCH (10–20) | 8.9 $\pm$ 1.7 (3)†                                  | 24.5 $\pm$ 3.0 (20)‡                            | 185.1 $\pm$ 4.0 (20)*  |
| L-norvaline (20)      | 6.2 $\pm$ 0.6 (3)†                                  | 38.6 $\pm$ 3.0 (29)*                            | 93.1 $\pm$ 8.1 (19)*   |
| L-isoleucine (20)     | 5.0 $\pm$ 0.9 (5)§                                  | 15.7 $\pm$ 1.4 (18)                             | 50.2 $\pm$ 5.5 (28)*   |
| Glycine (10)          | 3.0 (1)   | 18.0 $\pm$ 2.7 (19)                             | 25.1 $\pm$ 2.2 (9)     |
| L-serine (10)         | 3.1 (1)   | 20.2 $\pm$ 2.5 (10)                             | 19.7 $\pm$ 2.1 (10)    |
| L-valine (20)         | 2.6 $\pm$ 1.2 (2)                                   | 14.8 $\pm$ 2.1 (20)                             | 21.8 $\pm$ 3.9 (20)    |
| L-norleucine (10–20)  | 2.1 $\pm$ 0.2 (2)                                   | 12.7 $\pm$ 1.6 (9)                              | 14.6 $\pm$ 2.2 (17)    |
| L-lysine (20)         | 2.9 (1)   | 44.7 $\pm$ 5.0 (30)*                            | 40.3 $\pm$ 7.9 (10)    |

The activity of glutamate dehydrogenase was measured in islet homogenates. Insulin release was measured in islets incubated in the absence or presence of L-glutamine. Mean values ( $\pm$  s.e.m.) are shown together with the number of individual determinations (in parentheses).

\* $P < 0.001$ ; † $P < 0.005$ ; ‡ $P < 0.02$ ; § $P < 0.05$ . The statistical indices refer either to the differences between basal (first line) and experimental values (first and second columns) or to the glutamine-induced increment in insulin output (third column).

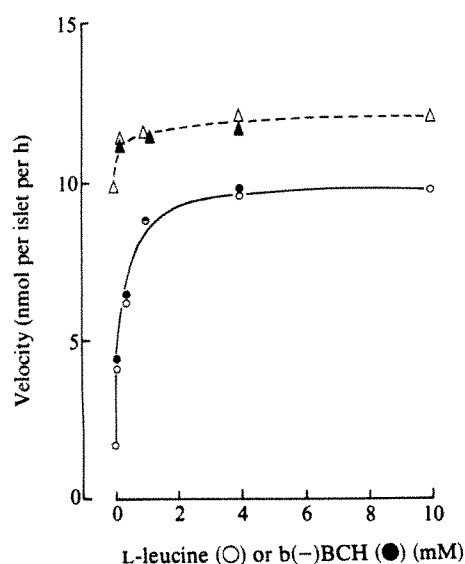
L-serine, L-valine, L-norleucine and L-lysine failed to activate glutamate dehydrogenase. These results are virtually identical to those found in isolated rat liver mitochondria or with purified glutamate dehydrogenase extracted from bovine liver<sup>6–8</sup>.

The possible relevance of changes in enzyme activity to the secretory behaviour of the  $\beta$ -cell was investigated by examining the influence of L-glutamine (10 mM) on insulin release in islets exposed to various amino acids. This approach was motivated by the following considerations. First, in the islets, L-glutamine is extensively converted to glutamate and, hence, provides much larger amounts of substrate for glutamate dehydrogenase than exogenous glutamate, which is poorly transported into the islet cells<sup>9</sup>. Second, L-glutamine itself fails to affect insulin release by the islets, whether in the absence or presence of D-glucose<sup>9</sup>. Insulin release was measured in groups of eight islets each incubated for 90 min at 37 °C in a bicarbonate-buffered medium<sup>10</sup>.

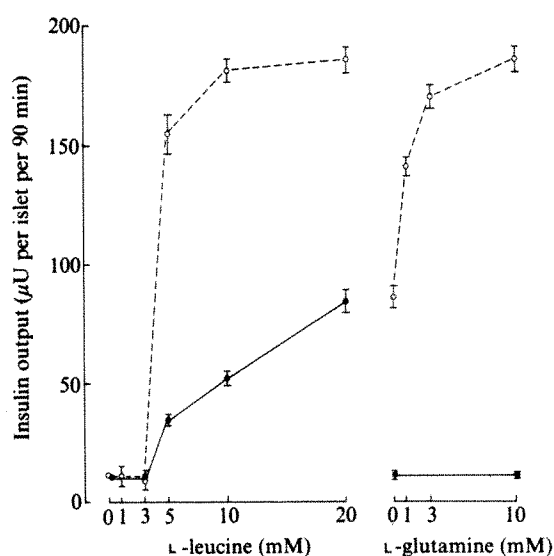
As shown in Table 1, L-glutamine markedly enhanced insulin release provoked by L-leucine or b( $\pm$ )BCH, augmented

secretion to a lesser extent in the presence of L-norvaline or L-isoleucine, and failed significantly to increase insulin output in the presence of glycine, L-serine, L-valine, L-norleucine or L-lysine. There was a highly significant correlation ( $r = 0.9786$ ;  $P < 0.001$ ) between the magnitude of the glutamine-induced increment in insulin output in the presence of different amino acids and their capacity to activate glutamate dehydrogenase in islet homogenates. In contrast, the magnitude of the glutamine-induced increment in insulin output was not closely related to the capacity of a given amino acid to stimulate secretion in the absence of L-glutamine.

The dose-response relationship for the effect of L-leucine and L-glutamine on insulin release, as illustrated in Fig. 2, indicated that a dramatic augmentation of L-leucine-induced insulin release occurred in the presence of 1.0 mM L-glutamine, at a concentration close to physiological value. The threshold value for L-leucine-induced release (3.0–5.0 mM) was the same in the absence or presence of L-glutamine. However, at higher concentrations of L-leucine, the dose-response relationship was



**Fig. 1** Effect of L-leucine (open symbols) and b(-)BCH (assumed to represent half of the b( $\pm$ )BCH concentration effectively used; closed symbols) on the activity of glutamate dehydrogenase measured in islet homogenates in the presence (triangles) or absence (circles) of ADP (0.5 mM). Each value was measured in triplicate.



**Fig. 2** Mean values ( $\pm$  s.e.m.) for insulin release from pancreatic islets refer to 7–136 individual observations. Left panel: effect of increasing concentrations of L-leucine in the absence (solid line) or presence (dotted line) of L-glutamine (10.0 mM). Right panel: effect of increasing concentrations of L-glutamine in the absence (solid line) or presence (dotted line) of L-leucine (20.0 mM).

different in the presence and absence of L-glutamine, respectively. In the presence of L-glutamine, the secretory rate virtually reached a maximal value at a 10 mM concentration of L-leucine. In the absence of L-glutamine, even 20 mM L-leucine was not sufficient to evoke a maximal secretory response, the output of insulin being further increased when the concentration of L-leucine was raised to 40 mM (ref. 11). This difference in dose-response relationship may be explained as follows. In the presence of L-glutamine, the secretory response is largely dependent on the rate of glutamate metabolism, the catabolism of L-leucine itself being severely impaired (data not shown). Hence, a maximal secretory rate will be reached whenever the mitochondrial concentration of L-leucine (or  $b(\pm)$ BCH) is sufficient to cause full activation of glutamate dehydrogenase. In the absence of L-glutamine, however, the secretory response is largely dependent on the rate of L-leucine catabolism<sup>11</sup> and, hence, may require higher concentrations of this amino acid to reach its maximal value. This is not to deny that, in the absence of exogenous L-glutamine, the secretory response to L-leucine depends in part on the rate of endogenous glutamate metabolism, as activated by the branched-chain amino acid. In fact, the extent to which L-leucine, independently of its own catabolism, stimulates insulin release by facilitating the metabolism of glutamate derived from endogenous precursors can be judged from the effect of  $b(\pm)$ BCH on insulin release in the absence of exogenous L-glutamine (Table 1 and ref. 12).

Several findings suggest the existence of a causal link between activation of glutamate dehydrogenase and stimulation of insulin release. Thus, in addition to the above-mentioned correlation between enzyme activation by different amino acids and the magnitude of the glutamine-induced increment in insulin output, both the enzyme activation and secretory response<sup>12</sup> are stereospecific for the L-form of leucine. Moreover, detailed biochemical and functional studies performed in intact islets exposed to the combination of L-leucine and L-glutamine indicated that the secretory response to these amino acids is indeed linked to activation of the NAD(P)H-dependent enzyme glutamate dehydrogenase, and is associated with a more reduced state of cytosolic redox couples, abolished by menadione, and triggered by the cellular accumulation of calcium and subsequent activation of the  $\beta$ -cell microtubular-microfilamentous effector system (data not shown). These findings emphasize the essential role of reducing equivalents in the coupling between metabolic and cationic events in the process of nutrient-induced insulin release<sup>3</sup>.

In conclusion, the present data indicate that the capacity of a nonmetabolized amino acid to augment  $O_2$  consumption by the islets<sup>13</sup>, to increase their content in NAD(P)H (ref. 14), to provoke a phosphate flush<sup>15</sup> and to stimulate insulin release<sup>2</sup> is compatible with the fuel hypothesis for insulin release<sup>3</sup>.

We thank J. Schoonheydt and M. Urbain for technical help. This work was supported in part by grants of the Belgian Foundation for Scientific Medical Research.

Received 30 June; accepted 2 September 1980.

1. Randle, P. J., Ashcroft, S. J. H. & Gill, J. R. in *Carbohydrate Metabolism and its Disorders* (eds Dickens, F., Randle, P. J. & Whelan, W. J.) 427-447 (Academic, London, 1968).
2. Christensen, H. N. et al. *Biochim. biophys. Acta* **241**, 341-348 (1971).
3. Malaisse, W. J., Sener, A., Herchuelz, A. & Hutton, J. C. *Metabolism* **28**, 373-386 (1979).
4. Ashcroft, S. J. H. *Diabetologia* **18**, 5-15 (1980).
5. Hutton, J. C., Sener, A. & Malaisse, W. J. *Biochem. J.* **184**, 291-301 (1979).
6. Gylfe, E. *Acta diabet. lat.* **13**, 20-24 (1976).
7. McGivan, J. C., Bradford, N. M., Crompton, M. & Chappell, J. B. *Biochem. J.* **134**, 209-215 (1973).
8. Chapelle, S. *Archs int. Physiol. Biochim.* **80**, 25-33 (1972).
9. Malaisse, W. J. et al. *Molec. cell. Endocr.* (in press).
10. Malaisse, W. J., Brisson, G. & Malaisse-Lagae, F. *J. Lab. clin. Med.* **76**, 895-902 (1970).
11. Malaisse, W. J., Hutton, J. C., Carpinelli, A. R., Herchuelz, A. & Sener, A. *Diabetes* **29**, 431-437 (1980).
12. Sener, A. & Malaisse, W. J. *C. r. hebdom. Séanc. Acad. Sci., Paris* **290**, 1135-1137 (1980).
13. Hellerström, C., Anderson, A. & Welsh, M. *Horm. Metab. Res.* (in press).
14. Joost, H. U., Panten, U., Ishida, H., Poser, W. & Hasselblatt, A. *Life Sci.* **16**, 247-254 (1975).
15. Freinkel, N., Younsi, C. E. & Dawson, R. M. C. *Proc. natn. Acad. Sci. U.S.A.* **73**, 3403-3407 (1976).

## Radioimmune, radiobinding and HPLC analysis of 2-5A and related oligonucleotides from intact cells

M. Knight\*, P. J. Cayley\*, R. H. Silverman\*,  
D. H. Wreschner†, C. S. Gilbert\*,  
R. E. Brown\* & I. M. Kerr\*

National Institute for Medical Research, Mill Hill,  
London NW7 1AA, UK

The enzyme (2-5A synthetase) which synthesizes  $ppp(A_2'p)_nA$  where  $n = 2$  to 4 (collectively referred to as 2-5A)<sup>1</sup> is widely distributed in a variety of cells and tissues in amounts which increase in response to interferon<sup>2-5</sup> and vary with growth and hormone status<sup>6</sup>. 2-5A activates a nuclease which inhibits protein synthesis<sup>7-10</sup>. The non-phosphorylated 'core' of 2-5A ( $(A_2'p)_nA$ ,  $n = 2$  to 4) can inhibit DNA synthesis and cell growth<sup>11,12</sup>. Here we describe convenient and sensitive radioimmune (RI) and radiobinding (RB) assays for core and 2-5A. In combination with more satisfactory high performance liquid chromatography (HPLC) methods using reverse-phase C18 columns, these assays have been used to detect core and 2-5A in crude extracts from interferon-treated cells. The novel 2-5A synthetase products  $NAD_2'p_5'A_2'p_5'A$  and  $A_5'p_5'A_2'p_5'A_2'p_5'A$  (ref. 13), which can also be detected using the RB assay, were not found in significant amounts. The natural occurrence of core has not been described previously.

The RI and RB assays are based on the high affinities of core for antibody and of 2-5A for the 2-5A-dependent nuclease<sup>9,10</sup> respectively. In both cases the amount of <sup>32</sup>P-labelled core or 2-5A bound to antibody or nuclease is determined by its retention on nitrocellulose filters. The concentration of unknown samples is measured by the ability of suitable dilutions to

Present addresses: \*ICRF Laboratories, Lincoln's Inn Fields, London WC2A 3PX, UK;  
† Department of Microbiology, Tel Aviv University, Ramat Aviv, Israel.

**Table 1** Specificity of the radioimmune and radiobinding assays

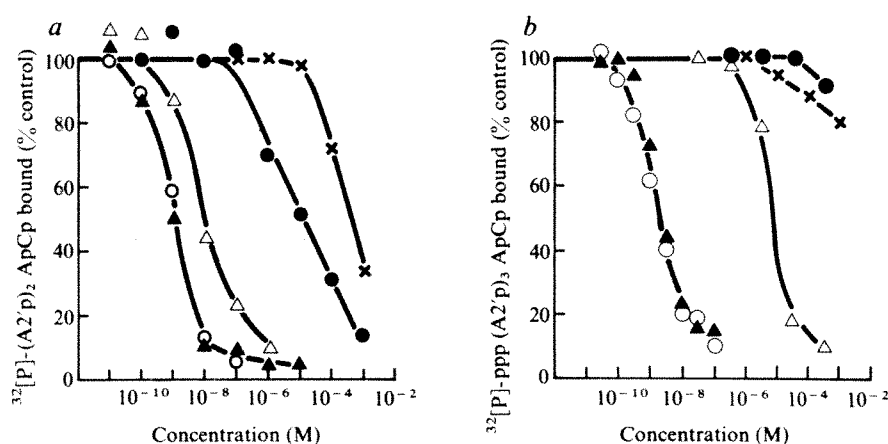
| Compound                          | Concentration for 50% displacement of probe* |
|-----------------------------------|--|
| <b>a, Radioimmune assay</b>       |  |
| $(A_2'p)_2A$ and $(A_2'p)_3A$     | 1 nM   |
| $p(A_2'p)_2A$                     | 5 nM   |
| $pp(A_2'p)_2A$                    | 100 nM                                       |
| $ppp(A_2'p)_2A$                   | 500 nM                                       |
| 2'- and 3'-AMP                    | 5 $\mu$ M                                    |
| 5'-AMP                            | 10 $\mu$ M                                   |
| $(A_3'p)_2A$ and $(A_3'p)_3A$     | 10 $\mu$ M                                   |
| $A_3'p_5'A$                       | 50 $\mu$ M                                   |
| Adenosine                         | 500 $\mu$ M                                  |
| ATP, CTP, pCp, 2'-, 3'- and 5'-   | >1 mM  |
| <b>CMP</b>                        |  |
| <b>b, Radiobinding assay</b>      |  |
| $ppp(A_2'p)_nA$ , ( $n = 2$ to 4) | 1 nM   |
| $pp(A_2'p)_2A$                    | 1 nM   |
| $p(A_2'p)_2A$                     | 7 nM   |
| $(A_2'p)_2A$                      | 300 nM                                       |
| $(A_3'p)_2A$ and $(A_3'p)_3A$     | >0.3 mM                                      |
| 2'-, 3'-, and 5'-AMP, ADP, ATP    | >1 mM  |
| 2'-, 3'- and 5'-CMP, pCp          | >1 mM  |

The assays were carried out as for Fig. 1. Concentration curves were constructed for each of the compounds tested for which the 50% displacement values given were obtained. Essentially identical results to those shown in Fig. 1a and Table 1b were obtained using the RI assay with <sup>3</sup>H-(A<sub>2</sub>'p)<sub>2</sub>A as probe except that the assay was approximately 20-fold less sensitive, reflecting the lower specific activity of this material.

\* In the RI and RB assays the radioactive probes were  $(A_2'p)_2A$ -[<sup>32</sup>P]pCp and  $ppp(A_2'p)_3A$ -[<sup>32</sup>P]pCp respectively.



**Fig. 1** Radioimmune (RI) and radiobinding (RB) assays for A2'p5'A2'p5'A, pppA2'p5'A2'p5'A and related oligonucleotides. *a*, The RI assay. Inhibition of the binding of (A2'p)<sub>2</sub>A-[<sup>32</sup>P]pCp to (A2'p)<sub>2</sub>A antiserum by different concentrations (abscissa) of unlabelled (A2'p)<sub>2</sub>A, (○); (A2'p)<sub>3</sub>A, (▲); A2'p5'A, (△); (A3'p)<sub>2</sub>A, (●) and adenosine (×). *b*, The RB assay. Inhibition of the binding of ppp(A2'p)<sub>3</sub>A-[<sup>32</sup>P]pCp to the 2-5A-dependent nuclease by different concentrations (abscissa) of unlabelled ppp(A2'p)<sub>2</sub>A, (○); ppp(A2'p)<sub>3</sub>A, (▲); pppA2'p5'A, (△); (A3'p)<sub>2</sub>A, (●) and adenosine, (×). The RI assay (55 μl) contained 3,000 c.p.m. of (A2'p)<sub>2</sub>A-[<sup>32</sup>P]pCp ( $1-3 \times 10^6$  Ci mol<sup>-1</sup>), 15 μl of the sample being tested and 25 μl of a 1:2,000 dilution of antiserum. All dilutions were in Tris-HCl-buffered saline pH 7.6 (TBS); 0.1% gelatin. Incubation was for 1 h at 30 °C. Samples (40 μl) were applied to nitrocellulose filter discs (2.5 cm diameter, 0.45 μm pore size; Sartorius) which were washed in three changes of TBS, dried and counted in a toluene-based scintillant. The RB assays (20 μl) contained 3,000 c.p.m. of ppp(A2'p)<sub>3</sub>A-[<sup>32</sup>P]pCp ( $1-3 \times 10^6$  Ci mol<sup>-1</sup>), 2 μl of competitor, 10 μl of a post-mitochondrial supernatant fraction<sup>19</sup> from Ehrlich ascites tumour cells as the source of the 2-5A-dependent nuclease and 8 μl of 20 mM Tris-HCl pH 7.6, 8.5 mM magnesium acetate, 1 mM ATP and 5% glycerol (v/v). Incubation was for 60 min at 0 °C. Samples (19 μl) were applied to pre-wet nitrocellulose filters as above which were washed in TBS, dried and counted. In both assays the conditions were chosen to give 30 to 50% binding of the radioactive probe in the absence of competitor. This corresponds to the 100% point of the ordinate. The (A2'p)<sub>2</sub>A antiserum was prepared in rabbits with (A2'p)<sub>2</sub>A bound to bovine serum albumin as antigen<sup>20-22</sup>. The 5'-[<sup>32</sup>P]pCp labelled derivatives were synthesized with T<sub>4</sub> RNA ligase and purified by HPLC (R.H.S., unpublished results and ref. 22).



displace 50% of the bound <sup>32</sup>P-labelled derivative in comparison with the concentration of pure core or 2-5A required to produce a similar displacement. (A similar nitrocellulose filter procedure, but for the detection of the nuclease, was used by Slattery *et al.*<sup>10</sup>.)

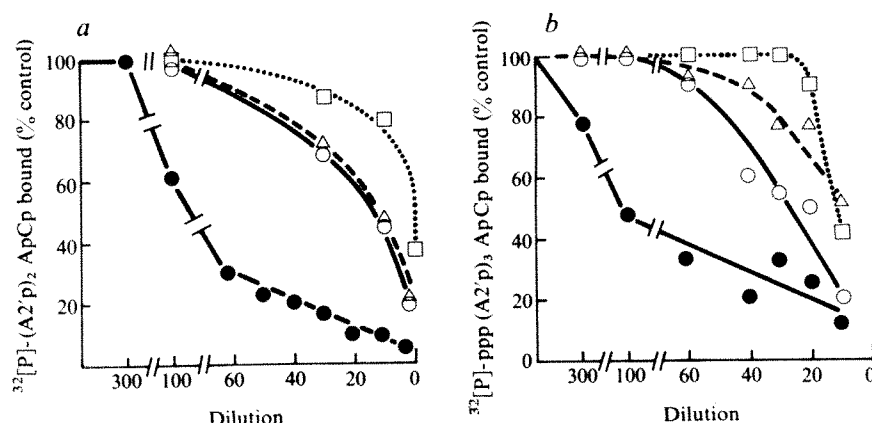
The difficulty in developing suitable assays has been in the production of 2-5A of sufficiently high specific activity (to detect  $\leq 10$  μl of nanomolar 2-5A). In our experience, very poor yields of 2-5A are obtained with the 2-5A synthetase when substrate (ATP) concentrations of  $\leq 100$  μM are used, making the production of 2-5A of specific activity  $\geq 10,000$  Ci per mole of nucleotide costly and impractical. Accordingly, here we have utilized T<sub>4</sub> RNA ligase<sup>14,15</sup> to label preformed (A2'p)<sub>2</sub>A or ppp(A2'p)<sub>n</sub>A ( $n = 2$  or  $3$ ) with [5'-<sup>32</sup>P]pCp to specific activities of  $2-3 \times 10^6$  Ci per mole of oligonucleotide.

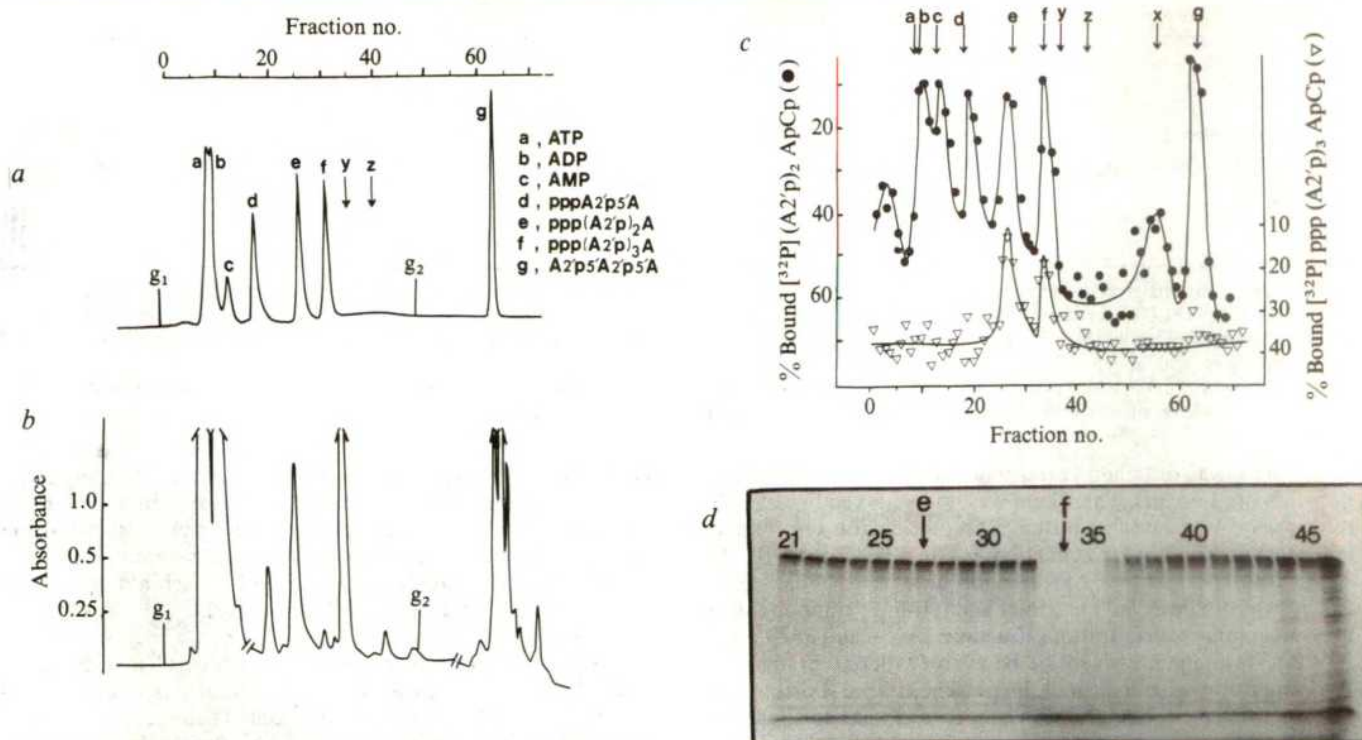
The RI assay shows high but incomplete specificity for the 2'-5' linkage (Fig. 1a, Table 1a). Fifty per cent displacement of the radioactive probe is observed with nM (A2'p)<sub>2</sub>A or (A2'p)<sub>3</sub>A (○, ▲, Fig. 1a) and 10 nM A2'p5'A (△, Fig. 1a). The concen-

tration at which other potentially cross-reacting materials displace 50% of the probe are given in Table 1a. The RI assay provides a sensitive method for the detection of core but without prior fractionation it cannot be used to measure core in the presence of higher concentrations of 2-5A (Table 1a). In addition, problems will arise in the assay of crude material of low titre if it contains sufficient AMP, ADP and ATP to yield  $\geq 500$  μM adenosine on dilution into the assay after digestion with bacterial alkaline phosphatase (BAP), or  $\geq 10$  μM 3'-5' (Ap)<sub>n</sub>A ( $n = 2$  or  $3$ ) (Table 1a). It is possible that other 3'-5'-linked oligonucleotides may also cross-react.

The RB assay shows even greater specificity for 2-5A (Fig. 1b and Table 1b). The 5' triphosphorylated (○, Fig. 1b) and diphosphorylated (Table 1b) trimer, the tetramer (▲, Fig. 1b) and pentamer (Table 1b), all displace 50% of the bound probe at nanomolar concentrations. In fact it shows almost as great a specificity as the 'biological' assays for 2-5A. It falls short of this in detecting relatively low concentrations of the trimer 5'-monophosphate and higher concentrations of core (Table 1b),

**Fig. 2** Radioimmune (a) and radiobinding (b) assays for the natural occurrence of 2-5A in extracts from interferon-treated, EMC virus-infected (●); interferon-treated (○); EMC virus-infected (△) and control (□) mouse L-cells. The assays were carried out as described in Fig. 1 legend. The 100% values correspond to 1,300 c.p.m. representing the 30 to 50% of the radioactive probes bound in the absence of competitor. Mouse L-cells ( $0.75 \times 10^6$  cells) were treated for 17 h at 37 °C with 400 reference (20 effective) units per ml of partially purified ( $5 \times 10^7$  reference units per mg of protein) mouse interferon, infected with 20 plaque-forming units (PFU) per cell of EMC virus and incubated for 4 h at 37 °C. Interferon-treated cells and control cells with or without EMC infection were incubated in parallel. Cells were collected, washed and the packed cells (2.5 ml) lysed into an equal volume of 0.5% NP40 in 10 mM HEPES buffer pH 7.5; 90 mM KCl; 1.5 mM magnesium acetate at 0 °C. Trichloroacetic acid (50%) was added immediately to 5% and the mixture centrifuged at 2,000g for 20 min. The supernatant solutions were extracted 10 times with water-saturated ether, lyophilized and resuspended in 500 μl of 10 mM HEPES buffer pH 7.5 (the pH was adjusted to 7 with NH<sub>4</sub>OH). These extracts were assayed with (radioimmune) or without (radiobinding) prior BAP digestion (40 units of enzyme (Sigma) per ml overnight at 30 °C). Control experiments in which radioactive 2-5A or core (200 nM) were added at the time of cell lysis showed recovery through the remainder of the procedures to be  $\geq 50\%$ .





**Fig. 3** HPLC analysis of 2-5A from interferon-treated EMC virus-infected L-cells. *a*, A mixture of standards containing ATP, ADP, AMP and the dimer trimer, tetramer and core of 2-5A (a-g). The positions y and z at which A5'p45'A2'p5'A2'p5'A and NAD2'p5'A2'p5'A, respectively, eluted in parallel runs are also indicated on the figure. *b-d*, Cell extract (150  $\mu$ l) from 0.75 ml of packed cells. *b*, Absorbance profile: absorbance was measured at 256 nm and at fraction 17 and fraction 57 the full-scale deflection (2.56) was reduced twofold (to 1.28) and 32-fold (to 0.08). *c*, RB assay: column fractions (5  $\mu$ l) were assayed for their ability to displace ppp(A2'p)3A- $^{32}$ P]pCp and RI assay: column fractions (15  $\mu$ l) were assayed after BAP digestion (as in Fig. 2) for their ability to displace (A2'p)2Ap- $^{32}$ P]pCp. The amounts of trimer, tetramer and core detected in the RI assay were unaffected by prior digestion of the fractions with ribonuclease T<sub>2</sub>. This excludes any possibility that the titres obtained reflect the presence of as yet unidentified cross-reacting 3'-5'-linked material. *d*, Nuclease assay<sup>17</sup>: fractions (25-46 and 58-70) (1  $\mu$ l) were analysed for their ability to activate a nuclease and degrade  $^{32}$ P-RNA in a reticulocyte lysate system<sup>17</sup>. Activation of the nuclease by: C, no additions; S1-6, 0.02, 0.06, 0.2, 0.6, 2.0 and 6.0 nM 2-5A tetramer standard; D1-5, dilutions, 1,250-, 375-, 125-, 37.5- and 12.5-fold of the interferon-treated, EMC virus-infected L-cell extract. The interferon treatment and EMC infection of the L-cells and preparation of the trichloroacetic acid extracts were as described in Fig. 2 legend. The HPLC analysis was on a  $\mu$ Bondapak C18 column (Waters Associates) run in 50 mM ammonium phosphate, pH 7.0 at 1 ml min<sup>-1</sup> with a 25-min linear gradient of 50:50 methanol:water applied at g<sub>1</sub> to reach a final of 20% of the total flow by g<sub>2</sub> where the methanol:water was increased to 50% in a 5-min gradient. This second gradient does not separate the 2'-5'-linked oligomers. Good separation of these can be achieved if a shallower gradient is applied at g<sub>2</sub>. The individual 2'-5' and 3'-5'-linked core from the corresponding 3'-5'-linked core components can be resolved in a gradient of methanol in 4 mM potassium phosphate pH 6.5. (It is advisable in the routine analysis of cell extracts that a dry packed pre-column should be inserted to protect the main column.)

both of which are without effect in the activation of the 2-5A-dependent nuclease or on cell-free protein synthesis. All of the other potentially cross-reacting materials tested were essentially without effect (Fig. 1*b*, Table 1*b*).

The specificity is sufficient for the RB assays to be performed with crude cell extracts as the source of the 2-5A-dependent nuclease as binding protein. The results presented here were obtained with post-mitochondrial supernatant fractions from Ehrlich ascites tumour (EAT) cells and very similar results have been obtained with rabbit reticulocyte lysates. It is possible that crude extracts of this type contain other proteins which contribute to the specific binding of 2-5A. However, the results obtained after partial purification of the nuclease and in experiments involving the analysis of radioactive 2-5A covalently bound to protein in such extracts favour the nuclease as the major component involved (D.H.W., C.S.G., R.H.S. and I.M.K., unpublished results). Less extensive studies with similar extracts from HeLa and L-cells suggest that they (and probably any extract containing significant amounts of the 2-5A-depen-

dent nuclease) can also be used in this type of assay. Care should, however, be taken to monitor for significant degradation of 2-5A by such extracts in the development of suitable assays<sup>9,16</sup>.

Despite the relatively high specificity of the RI and RB assays, the exclusion of cross-reacting material is potentially a problem in the assay of crude extracts. Nevertheless, in agreement with our previous results using 'biological' assays<sup>17</sup>, both the RI (after BAP) and RB assays (Fig. 2*a* and *b*, respectively) indicated relatively high concentrations (~100 nM in trimer equivalents) of 2-5A±core in a trichloroacetic acid-soluble extract from interferon-treated, EMC virus-infected mouse L-cells (●) and only much lower concentrations in corresponding extracts from interferon-treated (○), or EMC-infected (Δ), or control (□) cells. That the majority of the material registering in these assays was indeed 2-5A or core was confirmed by HPLC.

The results presented in Fig. 3*b-d* are of an HPLC analysis of an acid-soluble extract from interferon-treated, EMC virus-infected mouse L-cells. The eluates were first assayed by their ability to activate a nuclease in reticulocyte lysates (Fig. 3*d*)<sup>17</sup>. A



**Table 2** Levels of 2-5A and related oligonucleotides in interferon-treated and control mouse L-cells with or without EMC virus infection

| Pretreatment of cells        | Concentration in the intact cell (nM) |          |       |                 |                 |
|------------------------------|---------------------------------------|----------|-------|-----------------|-----------------|
|                              | 2-5A                                  |          | Core  | NAD2'p5'A2'p5'A | ApA2'p5'A2'p5'A |
|                              | Trimer                                | Tetramer |       |                 |                 |
| Interferon and EMC infection | 100                                   | 100      | 150   | <5              | <5              |
| Interferon                   | 30                                    | 30       | 20    | <5              | <5              |
| EMC infection                | 10                                    | 10       | <2.5* | <5              | <5              |
| Control                      | <2.5                                  | <2.5     | <2.5  | <5              | <5              |

The concentrations given are based on the packed cell volumes from which the extracts were made. They are calculated from the concentrations recovered after HPLC analysis carried out as for Fig. 3. No allowance has been made for losses during the extraction and processing of the samples. Control experiments in which 2-5A and the related oligonucleotides (50 nM) were added at the time of cell lysis indicated that the recovery of each component was  $\geq 50\%$ .

\* In one experiment in which two- to fourfold higher concentrations of 2-5A were found in the interferon-treated cell extracts (with or without EMC infection) a low level of core ( $\leq 8$  nM) was detected in the extract from EMC-infected cells.

single peak was obtained corresponding to the tetramer (fractions 33–36, Fig. 3d). The trimer was not observed because the reticulocyte nuclease is unusual in requiring the tetramer or higher oligomers for its activation<sup>17</sup>. The RB ( $\nabla$ ) and RI ( $\bullet$ ) assays (the latter after BAP digestion of the individual HPLC fractions) both detected the trimer and tetramer components of 2-5A at similar concentrations (fractions 25–30 and 33–35, Fig. 3c). Interestingly, however, the RI assay (with or without prior BAP digestion) also indicated the presence of pre-existing core ( $\bullet$ , fractions 62–64, Fig. 3c) in amounts similar to those observed for the phosphorylated components. Further HPLC analysis of this material using a gradient of methanol in 4 mM potassium phosphate pH 6.5 showed it to consist largely of the trimer core ((A2'p)<sub>2</sub>A). There was no evidence for significant breakdown of 2-5A to core in control experiments in which low concentrations (<100 nM) of 2-5A were added at the time of cell lysis. This, together with the results of experiments in which the time taken to wash and disrupt the cells was deliberately varied, suggests that the core is not an artefact.

The RI assay also detected dimer ( $\bullet$ , fractions 19–21, Fig. 3c) and cross-reacting material in fractions 1–15 which is probably adenosine produced by the BAP digestion of ATP, ADP and AMP. The concentration of this material is high compared with that in the corresponding control extract (not shown). This emphasizes the necessity for HPLC or alternative additional analysis of material detected by the RI assay in crude extracts in order to establish its identity.

The nature of peak X (Fig. 3c) is not known. It does not seem to be 2-5A joined to NAD<sup>13</sup>. The latter has been synthesized *in vitro* from NAD and ATP with the 2-5A synthetase bound to poly(I)-poly(C)-paper in conditions similar to those used for 2-5A<sup>2,6,13</sup>. The products NAD2'p5'A and NAD2'p5'A2'A were purified by chromatography (on DEAE-cellulose) and the structure of the latter was confirmed by proton NMR spectroscopy. On HPLC analysis the product NAD2'p5'A2'p5'A (Z, Fig. 3a) eluted after NAD. It can be detected at nanomolar concentrations using the RB assay. With the extract from interferon-treated, EMC-infected cells, only very low levels of material (equivalent to  $\leq 5$  nM of putative NAD2'p5'A2'p5'A) were detected in this region of the gradient (Fig. 3c). Control experiments in which NAD2'p5'A2'p5'A at 50 nM was added at the time of cell lysis have shown 75% recoveries. Similar results have been obtained in a less extensive investigation into the possible presence of A5'p<sub>4</sub>A2'p5'A2'p5'A (Y, Fig. 3a, c). It is unlikely, therefore, that either NAD or A5'p<sub>4</sub>A (ref. 18) modified by the addition of 2-5A occurs naturally in these cells at concentrations greater than 5 nM.

Similar HPLC analysis of extracts from interferon-treated L-cells and from EMC virus-infected L-cells, have shown that they contain 2-5A and (in the case of the interferon-treated cells at least) core at lower concentrations (Table 2). It is not yet clear whether very low levels (3 nM in the intact cell) of core and 2-5A are also present in control extracts (Fig. 2 and Table 2).

The results presented establish the validity of the RI and RB assays to detect core and 2-5A. They are now the methods of

choice for the assay of preformed core and 2-5A being much more convenient than the 'biological' assays. In addition the assays are suitable for the routine screening of cells and tissues for 2-5A. The identity of any putative 2-5A components or 2-5A-related oligonucleotides detected in such material must, however, be confirmed by further HPLC (or alternative) analysis.

The natural occurrence of 2-5A and 'core' in interferon-treated cells, although at lower concentrations than in interferon-treated EMC virus-infected cells (Table 2), emphasizes the possible involvement of the 2-5A system in the cell growth inhibitory activity of interferon. The presence of low levels of 2-5A in virus-infected cells may reflect the low levels of synthetase known to be present in the absence of interferon treatment and its activation by viral double-stranded RNA<sup>6</sup>.

The natural occurrence of substantial amounts of core (Table 2) is of considerable interest and emphasizes that in the analysis of the 2-5A system it is not adequate to measure only 2-5A. The amount of core seems to be independent of the concentration of 2-5A and it may, therefore, play a separate role in the inhibition of DNA synthesis and cell growth.

We thank B. F. Erlanger and S. Zakarian for advice in setting up the radioimmune assays, B. F. Erlanger for antisera to 3'-5'-linked ApApA used in preliminary studies, and S. Jones and C. B. Reese for chemically synthesized 2-5A trimer, 5'-mono-, di- and triphosphates. M.K. was the recipient of a grant from the government of Ghana and D.H.W. of an EMBO fellowship.

Received 11 June; accepted 16 September 1980.

- Kerr, I. M. & Brown, R. E. *Proc. natn. Acad. Sci. U.S.A.* **75**, 256–260 (1978).
- Hovanessian, A. G., Brown, R. E. & Kerr, I. M. *Nature* **265**, 537–540 (1977).
- Ball, L. A. *Virology* **94**, 282–294 (1979).
- Kimchi, A. *et al. Proc. natn. Acad. Sci. U.S.A.* **76**, 3208–3219 (1979).
- Minks, M. A., Benven, S., Maroney, P. A. & Baglioni, C. *J. biol. Chem.* **254**, 5058–5064 (1979).
- Stark, G. R., Dower, W. J., Schimke, R. T., Brown, R. E. & Kerr, I. M. *Nature* **278**, 471–473 (1979).
- Clemens, M. J. & Williams, B. R. G. *Cell* **13**, 565–572 (1978).
- Baglioni, C., Minks, M. A. & Maroney, P. A. *Nature* **273**, 684–687 (1978).
- Williams, B. R. G., Kerr, I. M., Gilbert, C. S., White, C. N. & Ball, L. A. *Eur. J. Biochem.* **92**, 445–462 (1978).
- Slattery, E., Ghosh, N., Samanta, H. & Lengyel, P. *Proc. natn. Acad. Sci. U.S.A.* **76**, 4778–4782 (1979).
- Reisinger, D. M. & Martin, E. M. *Proceedings of the Sloan Kettering International Workshop on Interferons* (in the press).
- Kimchi, A., Shure, H. & Revel, M. *Nature* **282**, 849–851 (1979).
- Ball, L. A. & White, C. N. in *Regulation of Macromolecular Synthesis by Low Molecular Weight Mediators* (eds Koch, G. & Richter, D.) 303–317 (Academic, New York, 1980).
- Silber, R., Malathi, V. G. & Hurwitz, J. *Proc. natn. Acad. Sci. U.S.A.* **66**, 3009–3014 (1972).
- England, T. E. & Uhlenbeck, O. C. *Nature* **275**, 560–561 (1978).
- Minks, M. A., Benven, S., Maroney, P. A. & Baglioni, C. *Nucleic Acids Res.* **6**, 769–780 (1979).
- Williams, B. R. G., Golgher, R. R., Brown, R. E., Gilbert, C. S. & Kerr, I. M. *Nature* **282**, 582–586 (1979).
- Rapaport, E. & Zamecnik, P. *Proc. natn. Acad. Sci. U.S.A.* **73**, 3984–3988 (1976).
- Kerr, I. M., Oleshevsky, U., Lodish, H. F. & Baltimore, D. *J. Virol.* **18**, 627–635 (1976).
- Erlanger, B. F. & Beiser, S. M. *Proc. natn. Acad. Sci. U.S.A.* **52**, 68–74 (1964).
- D'Alisa, R. M. & Erlanger, B. F. *Biochemistry* **13**, 3575–3579 (1974).
- Knight, M., Wreschner, D. H., Silverman, R. H. & Kerr, I. M. *Meth. Enzym.* (in the press).

# MATTERS ARISING

## Origin of mammal-like reptiles

KEMP<sup>1</sup> has recently hypothesized that "the synapsid [mammal-like reptile] skull evolved from a limnoscelid-like skull rather than from that of a romeriid, and that the temporal fenestra of the mammal-like reptiles evolved directly from the remnant of the crossopterygian hinge line". This disagrees with the widely accepted theory that the Protorothyrididae (Romeriidae), a group of small reptiles with unfenestrated skull roofs, include the ancestors or near-ancestors of the Pelycosauria, the earliest synapsid or mammal-like reptiles<sup>2-4</sup>. Both Kemp<sup>1</sup> and Reisz<sup>5,6</sup> have recognized that the protorothyridid skull is advanced in some cranial features compared with pelycosaurids and, hence, could not be ancestral to the primitive pattern of early synapsids. Kemp's hypothesis replacing a protorothyridid ancestor with a "limnoscelid-like" ancestor also seems invalid.

Kemp uses the common occurrence of a large supratemporal that contacts the postorbital, and a large tabular that contacts the paraoccipital process of the opisthotic, as the basis of his hypothesis. These, however, are primitive tetrapod characters present in virtually all primitive amphibians and reptiles. Thus they have no phylogenetic significance in the context of synapsid origins. The proper methodology for developing a theory of phylogenetic relationships of any group of organisms is to study the distribution pattern of morphological characters among a whole range of generally similar organisms so that a determination of whether a particular character is primitive or derived may be made (only derived characters are of any significance when trying to deduce phylogenetic relationships). Because Kemp has failed to do this, he has been badly misled by phylogenetically insignificant primitive characters.

The thesis that the synapsid temporal fenestrae evolved directly from a remnant of the crossopterygian hinge-line between the skull roof and cheek is untenable. There is no evidence that any true cotylosaur, including seymouriamorphs or diadectomorphs (limnoscelids belong to the latter group<sup>7</sup>) or primitive reptiles, ever had a cardinal line of weakness (or hinge) between the skull roof and cheek in the living animals. The presence of such a feature in the above animals is an old misconception based on the fact that post-depositional crushing tends to concentrate forces along the sharp angle between the skull roof and cheek leading to breakage of the bone or suture. The only known skull of *Limnoscelis* is compressed dorsolaterally so that the bone has broken in this region to give the impression of a

hinge, or line of weakness. As Heaton<sup>8</sup> has noted, this often happened in captorhinomorphs as well, where there was a solid wide suture between the skull roof and cheek. The only known specimen of *Romeriscus*, a possible limnoscelid on which Kemp placed much emphasis, is so poorly and incompletely preserved that it cannot be used as the basis of a major hypothesis.<sup>9</sup>

Hypotheses on the origin of the Synapsida based on the development of the temporal fenestrae<sup>10</sup> are inappropriate because these are not restricted to them (lateral temporal fenestrae are present in mesosaurs, bolosaurs, diapsids and some millerosaurs) and because fenestration is only one aspect of the development of the synapsid skull. Any hypothesis of the origin of the synapsid reptiles should be linked to the structural innovations seen in the braincase, occiput, adductor chamber, mandibles and dentition as a whole, because these changes gave rise to a morphological complex that is unique among higher vertebrates.

R. R. REISZ  
M. J. HEATON

Erindale College,  
University of Toronto,  
Mississauga, Ontario,  
Canada L5L 1C6

1. Kemp, T. S. *Nature* **283**, 378-380 (1980).
2. Carroll, R. L., *J. Paleont.* **43**, 151-170 (1969).
3. Clark, J. & Carroll, R. L. *Bull. Mus. comp. Zool. Harv.* **144**, 353-407 (1973).
4. Carroll, R. L. *Forma et Functio*, **3**, 165-178 (1970).
5. Reisz, R. R. *Univ. Kansas Paleont. Contrib., Vertebrata* (in the press).
6. Reisz, R. R. in *The Terrestrial Environment and the Origin of Land Vertebrates* (ed. Panchen, A. L.) (Academic, London, in the press).
7. Heaton, M. J. in *The Terrestrial Environment and the Origin of Land Vertebrates* (ed. Panchen, A. L.) (Academic, London, in the press).
8. Heaton, M. J. *Bull. Okla. geol. Surv.* **127**, 1-84 (1979).
9. Baird, D. & Carroll, R. L. *Science* **157**, 56-59 (1967).
10. Reisz, R. R. *Bull. Mus. comp. Zool. Harv.* **143**, 27-62 (1972).

KEMP REPLIES—Reisz and Heaton's criticism of the use of primitive characters to demonstrate phylogenetic relationships ignores my specific disclaimer that I was proposing any particular relationship between limnoscelids and synapsids. My object was simply to suggest that the character-state of the temporal region of the skull of the direct ancestor of synapsids resembled that retained in the limnoscelids, for example, and not that of romeriid or protorothyridid reptiles. Of course any hypothesis about the phylogenetic relationships of synapsids to particular tetrapod groups would require a comprehensive study of the distribution of derived characters of the whole skeleton. It was for this reason that I

carefully avoided any taxonomic implications at all, and indeed the possibility of a primary sister-group relationship between romeriids and synapsids is nowhere excluded.

The exact nature of the connection between the skull table and cheek of *Limnoscelis* is difficult to determine from a single, damaged skull. Even if the 'hinge-line' is merely the consequence of distortion, as Reisz and Heaton now claim, the similar manner of breakage of the two sides of the skull, between the table and the cheek, suggests nevertheless that this line was weak. So also does the fact that the suture between the post-orbital and squamosal is continued posteriorly in a straight line by the suture between the supratemporal and squamosal to the hind margin of the skull. My contention that the synapsid temporal fenestra appeared within this suture line remains unaffected, even if the contact between the respective bones was rather firmer than supposed. There would still have been a thin layer of connective tissue between the bones, as in the case of any suture, which could have expanded, eventually forming the temporal aponeurosis.

T. S. KEMP

The Zoological Collections,  
University Museum,  
Parks Road,  
Oxford OX1 3PW, UK

## Growth rings in dinosaur teeth

THERE are several difficulties with Johnston's interpretation of the growth rings he has observed in dinosaur teeth<sup>1</sup>. The first problem is whether the rings are annual. Such growth rings are found in living and fossil ectothermic vertebrates, but in the bones, not the teeth, which are replaced frequently in most non-mammalian vertebrates<sup>2</sup>. The teeth of crocodiles are replaced at intervals of 8-16 months<sup>3</sup>, making it impossible for more than two annual rings to occur within any given tooth. There is no evidence that replacement ceases during adult life, nor that the rate was substantially different in fossil crocodilians. Data on the manner and rate of tooth replacement for dinosaurs are limited, although evidence suggests multiple replacement and rapid turnover<sup>2</sup>.

Dinosaurs and crocodiles would be expected to share some similarities in hard-tissue deposition and to differ from mammals, for the ancestors of archosaurs and mammals were separated perhaps as



far back as latest Carboniferous<sup>4</sup>. Johnston ignores conclusions based on extensive studies of fossil reptile bones<sup>5</sup> which show that dinosaur bone resembles more that of large living endotherms than ectotherms. He argues that, because crocodiles are ectothermic and their teeth are similar to those of dinosaurs, then dinosaurs also must have been ectothermic. But similar teeth are also found in Cretaceous birds<sup>6,7</sup>, implying either that they were ectothermic or that dental growth rings are not a sufficient indicator of overall physiology.

The precise connection between growth rings and thermal physiology is unknown, and it is likely that a complex set of phenomena is involved. Mammalian growth rings appear in constant as well as seasonal environments<sup>8</sup>; neither temperature nor moisture are proven causal factors. Endo/ectothermy is not a sharp dichotomy, but a continuous spectrum, as is homeo/poikilothermy<sup>9</sup>. Calcium stress may be due to seasonal, dietary, reproductive, structural, phylogenetic or other poorly understood influences; the pitfall of 'one-factor' ecology is that no one factor, internal or external, is likely to explain all observed metabolic responses. Mammals and birds have used various strategies to solve problems in energetics; the diversity of dinosaurs suggests that many physiological solutions may also have been available to them<sup>10</sup>. It seems imprudent to rule out other factors contributing to the growth of hard tissues merely because they cannot be accounted for.

DEBORAH K. MEINKE  
KEVIN PADIAN  
JOHN KAPPELMAN

Peabody Museum of Natural History,  
Yale University,  
New Haven, Connecticut 06520

1. Johnston, P. A. *Nature* **278**, 635-636 (1979).
2. Edmund, A. G. *Contr. Life Sci. R. Ont. Mus.* **52**, 1-190 (1960).
3. Edmund, A. G. *Contr. Life Sci. R. Ont. Mus.* **56**, 1-42 (1962).
4. Romer, A. S. *Vertebrate Paleontology* 3rd edn (University of Chicago, 1966).
5. Ricqlès, A. de *Evol. Theory* **1**, 51-80 (1974); in *Morphology and Biology of Reptiles* No. 3 (eds Bellairs, A. d'A. & Cox, C. B.) 123-150 (Linnean Society, London, 1976).
6. Ostrom, J. H. *A. Rev. Earth planet. Sci.* **3**, 55-75 (1975).
7. Marsh, O. C. *Prof. Paper Engineer. Dept. US Army* **18**, 1-201 (1880).
8. Gaskin, D. E. & Blair, B. A. *Can. J. Zool.* **55**, 18-30 (1977).
9. Cowles, R. B. *Science* **135**, 670 (1962).
10. Dodson, P. *Evolution* **28**, 494-497 (1974).

CONTRARY to Johnston's interpretation, the skeletal annuli he observed in dinosaur teeth<sup>1</sup> need not imply any seasonal temperature fluctuation but may simply be a result of seasonal variation in food resources created by seasonal rainfall patterns. Spinage<sup>2</sup> has shown that two distinct annual cementum lines are

formed in the teeth of African buffalo (*Syncerus caffer*) from regions with bimodal precipitation whereas one exceptionally distinct annulation forms each year in buffalo from southern Tanzania where rainfall patterns are unimodally seasonal. Also, desert bighorn sheep (*Ovis canadensis*) possess annuli in both cementum and dentine resulting from a cessation of growth during dry summer months<sup>3</sup>. These observations of seasonal dental annuli formation in endotherms counter Johnston's arguments for ectothermy in dinosaurs.

MARK S. BOYCE

Department of Zoology and Physiology,  
University of Wyoming,  
Laramie, Wyoming 82071

1. Johnston, P. A. *Nature* **278**, 635-636 (1979).
2. Spinage, C. A. *J. Zool.* **178**, 117-131 (1976).
3. Turner, J. C. *J. Wildlife Management* **41**, 211-217 (1977).

JOHNSTON<sup>1</sup> claims that 'growth zones' observable in dinosaur teeth give tooth age in years, and suggest that dinosaurs were crocodile-like ectotherms. Individual ages in many mammalian species can be determined by counting various types of growth rings, including those in dentine. But if the results are not checked against individuals of known age<sup>2-4</sup>, serious errors can be made. One possibility is that annual growth lines are confused with the contour lines of Owen. Johnston says that there are "two main types of rings" in dinosaur teeth, with the implication that annual rings are easily distinguished. Studies on mammalian teeth suggest that true annual rings are apparently formed in the same way as, and are morphologically similar to, contour lines of Owen<sup>2</sup>.

In the absence of studies on a living relative or other acceptable analogue, it is easy in growth ring studies for hypothesis to bias observations. We suspect that Peabody's paper<sup>5</sup> cited by Johnston gives an example of this. Peabody recognized as many as four annual growth zones in some teeth of the small Lower Permian reptile *Captorhinus*. Although he did not discuss tooth replacement, a common opinion among vertebrate palaeontologists at the time was that the teeth of *Captorhinus* were not replaced. It would have been reasonable to expect individual teeth to persist for 4 yr. However, it is now known that all the teeth of *Captorhinus* were being actively replaced<sup>7</sup>. It is unlikely that a single tooth in such a small animal would persist for 4 or more years; Peabody's 'annual growth zones' probably reflect a less than annual periodicity if they had a regular periodicity at all.

Because dinosaurs are extinct Johnston's 'annual growth zones' cannot be verified, and his counts can at best be established only as more or less reason-

able by study of living animals. The crocodilians are the closest living toothed relatives of dinosaurs, but there is no substantial evidence as to how long their teeth last or whether they can be aged by counting growth zones. Although Edmund<sup>8</sup> found a life span of slightly more than 2 yr in *Alligator* teeth, his specimens were very small and do not provide a good parallel with dinosaurs. Neill<sup>9</sup> states that old alligators cease replacement and may become nearly toothless. Even if this is confirmed, it tells us nothing about the age of the remaining teeth or the number of growth zones they may contain. In any case Johnston's counts of eight annual rings in each of two tyrannosaur teeth seems rather high (though not impossible) in view of the fact that tyrannosaurs, as well as the other dinosaurs he cites, show active tooth replacement<sup>6,10</sup> which seems to have continued throughout life as we know of no evidence to the contrary.

Johnston notes that de Ricqlès' histological surveys<sup>11,12</sup> did not reveal seasonal growth rings in dinosaur bone. However, histology did not simply produce negative evidence. de Ricqlès argued cogently, on the basis of long-bone histology, that dinosaurs were probably relatively endothermic. Absence of cyclical growth lines in dinosaur periosteal bone was attributed to the rapid growth characteristic of endotherms. The growth zones observed in dinosaur teeth thus should not be considered in isolation; their interpretation must be consistent with a total histological picture that includes the rest of the skeleton.

Johnston's suggestion of crocodile-like endothermy in dinosaurs at first appears to contradict de Ricqlès, but the latter noted that animals may be neither fully endothermic nor fully ectothermic and that, although dinosaurs were relatively endothermic, they probably had their own peculiarities in thermal physiology. It is impossible to correlate environmental and/or endogenous factors with the formation of growth zones in dinosaur teeth. But even if Johnston is right in calling these growth rings seasonal, their existence simply suggests that de Ricqlès was right in supposing that dinosaurs were not completely comparable to large mammals in thermal physiology. It does not imply, in view of the total histological evidence that dinosaurs were crocodile-like ectotherms.

JOHN R. BOLT

Department of Geology,  
Field Museum of Natural History,  
Chicago, Illinois 60605

ROBERT E. DE MAR

Department of Geology,  
University of Illinois,  
Chicago, Illinois 60680

1. Johnston, P. A. *Nature* **278**, 635-636 (1979).
2. Kleveland, G. A. & Klemberg, S. E. *Age Determination of Mammals from Annual Layers in Teeth and Bones* (in Russian) (translation by Israel Program for Scientific Translations, Jerusalem, 1969).
3. Morris, P. *Mamm. Res.* **2**, 69-104 (1972).
4. Morris, P. in *Development, Function and Evolution of Teeth* (eds Butler, P. M. & Joysey, K. A.) 483-494 (Academic, London, 1978).
5. Peabody, F. E. *J. Morph.* **108**, 11-62 (1961).
6. Edmund, A. G. *Contr. Life Sci. Div. R. Ont. Mus.* **82**, 1-190 (1960).
7. Bolt, J. R. & DeMar, R. E. *J. Paleont.* **49**, 814-832 (1975).
8. Edmund, A. G. *Contr. Life Sci. Div. R. Ont. Mus.* **96**, 1-42 (1962).
9. Noddi, W. T. *The Last of the Ruling Reptiles* (Columbia University Press, New York, 1971).
10. Edmund, A. G. in *Biology of the Reptiles* 1, Morph. A (ed. Gans, C.) 117-200 (Academic, London and New York, 1969).
11. Rucicla, A. de *Biol. Theory* **1**, 51-60 (1974).
12. Rucicla, A. de in *Morphology and Biology of Reptiles* (eds Bellairs, A. & Coss, C. B.) 123-150 (Linnæan Society, London, 1976).

JOHNSTON REPLIES—Meinke *et al.* acknowledge that annual layers occur in bone of fossil (and living) ectotherms but deny that the similar rings which occur in the dentine of those animals are annual or even extrinsically induced by the change in seasons. Irrespective of anything else, however, this view is illogical: dentine is itself simply acellular bone. Furthermore, in Recent temperate and arctic terrestrial mammals<sup>1,2</sup> (marine mammals, cited by Meinke *et al.*, are ecologically inappropriate as analogues of terrestrial crocodiles and dinosaurs): (1) the most conspicuous dentine bands form simultaneously with annual layers in periosteal bone, and (2) dentine has been shown to be a sensitive indicator of annual, seasonally induced disruptions of growth. Meinke *et al.* give no evidence that the dentine in ectotherms (living or extinct) behaves differently.

Boyce, noting that severe seasonal contrasts can produce rings in the dentine of certain terrestrial mammals, overlooks my citation of the same phenomenon<sup>3</sup>; and Boyce provides no evidence that Alberta dinosaurs lived in seasonally xeric conditions comparable to those of desert bighorn sheep. Instead, palaeontological evidence<sup>4,5</sup> indicates that the western interior of North America was a humid, warm temperate to subtropical environment without extreme seasonal fluctuation of precipitation and temperature during Late Cretaceous time.

Bolt and DeMar cite possible uncertainty in distinguishing the boundaries of annual layers in dentine (and bone) owing to the production of accessory bands (accentuated contour lines of Owen); however, these difficulties no more detract from the reality of seasonal disruptions in dentine deposition than does the occurrence of false annuli negate the phenomenon of true annuli in fish scales. Furthermore, annual layers in the calcified tissues of Recent terrestrial mammals (and by extrapolation, crocodiles and dinosaurs) can usually be distinguished: they are more pronounced and regularly spaced than are accessory bands<sup>1,2</sup>.

Meinke *et al.* err in claiming the impossibility of finding more than two annual rings within a crocodile tooth: the number of annual layers in crocodile dentine gives the age of the tooth (minimum age if the pulp cavity is occluded), not just its functional age. In one 100-yr-old crocodile<sup>6</sup>, each tooth probably has been replaced about 50 times—an average of about once every 2 yr. In the Nile crocodile, two or three replacing teeth can be lodged beneath a functional one, and as many as six replacing teeth have been recorded at a single locus<sup>6</sup>. Thus, in a mature individual, a tooth could easily reside in the jaw for 4 yr, two before eruption and two after (longer if more than one successional tooth occurs below a given functional tooth), resulting in the accumulation of four annual layers in the dentine.

The number of major bands in dinosaur teeth is consistent with probable replacement rates: a maxilla of *Antrodemus* sp. (Princeton University Museum No. 16554-9), for example, exhibits three generations of teeth<sup>7</sup>, and if the average tooth replacement interval in mature *Antrodemus* was 2 yr (not unreasonable by analogy with Recent crocodiles), each tooth must have been held for 6 yr (4 yr before eruption and two while functional), yielding six annual layers in the dentine. If the replacement interval ranged from 1 to 3 yr during the life of an individual, the total life of a given tooth could be from 3 to 9 yr depending on the age of the individual. Although absolute replacement rates are not known for dinosaurs, relative rates can sometimes be inferred: hadrosaur and ceratopsian teeth, which are stacked for evident rapid replacement in a specialized grinding mill, generally have fewer rings than do carnosaur teeth, the function of which is not dependent on occlusal wearing of crowns.

Bolt and DeMar's model<sup>8</sup> of tooth replacement in *Captorhinus* describes the pattern of replacement but says nothing of rate. Small size alone is not necessarily indicative of rapid replacement: *Sphenodon* (Rhynchocephalia) and certain acrodont lizards are *Captorhinus*-sized or smaller, yet the lateral teeth wear heavily with age and are probably not replaced at all in mature individuals<sup>9</sup>. There is no histological evidence to support Bolt and DeMar's model of rapid replacement (in fact, heavy wear on many specimens of *Captorhinus*<sup>8,10</sup> suggests relatively slow replacement) nor can the model account for the occurrence of the tallest teeth at or near the centre of the rows of teeth, a definitive feature of *Captorhinus* multiple-rowed dentitions<sup>11</sup> (R. C. Fox, personal communication). Consequently, Peabody's interpretation<sup>12</sup> of growth zones in *Captorhinus* teeth remains a reasonable one.

Mesozoic toothed birds do not show dinosaur or crocodile-like zones in their

teeth (*contra* Meinke *et al.*) (see Yale Peabody Museum specimens 1206, 1474, uncatalogued thin-sections, all teeth of *Hesperornis*, YPM 1728, teeth of *Ichthyornis*); possibly Meinke *et al.* observed ringed teeth in small mosasaur (*Lepidosauria*) jaws (having lacertilian rows of nutritive foramina), for dentigerous fragments of two such jaws are in the Yale toothed-bird collections (R. C. Fox, personal communication).

Meinke *et al.* attribute the undeniably close resemblance of dentinal rings in dinosaurs and crocodiles to phylogenetic propinquity. *Champsosaurus*, a Late Cretaceous-Eocene eosuchian (and undoubted ectotherm), displays dentinal rings like those in Upper Cretaceous dinosaurs and crocodiles. Would Meinke *et al.* explain this in terms of "phylogenetic propinquity" of archosaurs and eosuchians, groups whose last common ancestry is no younger than Permian and perhaps Carboniferous<sup>13</sup> (almost as remote as for archosaurs and mammals)?

Phylogenetic 'explanations' only describe results of process, not process itself (at least for those who believe natural selection is the source of adaptive resemblance between organisms), and it is clearly self-contradictory that resemblances purported to stem from phylogenetic relationship would have completely different physiologic origins, as Meinke *et al.* would have us believe.

Finally, Meinke *et al.* argue that, owing to their diversity, dinosaurs might be expected to show a range of physiological thermoregulation. Perhaps, but if so diversity by itself will not carry the argument: after all, Recent reptiles are far more diverse taxonomically than are dinosaurs, yet all are ectothermic.

I thank J. Osborn, D. Wigglesworth, R. C. Fox and R. Barwick for helpful comments.

PAUL A. JOHNSTON

Department of Geology,  
The University of Alberta,  
Edmonton, Alberta,  
Canada T6G 2E9

1. Kleveland, G. A. & Klemberg, S. E. *Age Determination of Mammals from Annual Layers in Teeth and Bones* (in Russian) (translation by Israel Program for Scientific Translations, Jerusalem, 1969).
2. Morris, P. *Mamm. Res.* **2**, 69 (1972).
3. Johnston, P. A. *Nature* **278**, 635-636 (1979).
4. Dodson, P. *Paleogeogr. Paleoclimatol. Paleogeol.* **18**, 10 (1971).
5. Estes, R. *Univ. Calif. Publ. Geol. Sci.* **49**, 1 (1964).
6. Poole, D. F. G. *Proc. zool. Soc. Lond.*, 136 (1961).
7. Edmund, A. G. *Contr. Life Sci. Div. R. Ont. Mus.* **82** (1960).
8. Bolt, J. & DeMar, R. E. *J. Paleont.* **49**, 814 (1975).
9. Edmund, G. in *Biology of the Reptiles* (eds Gans, C., Bellairs, A. & Parsons, T.) **1**, 117 (Academic, London, 1969).
10. Clark, J. & Carroll, R. *Bull. Mus. comp. Zool. Harv.* **144**, 353 (1973).
11. Fox, R. C. and Bowman, M. C. *Paleont. Contr. Univ. Kans.* **11** (1966).
12. Peabody, F. E. *J. Morph.* **108**, 11 (1961).
13. Osborn, J. & Carroll, R. in *The Encyclopedia of Paleontology* (eds Peabody, R. & Jablonski, D.) 705 (Dowden, Hutchinson and Ross, Stroudsburg, 1979).



## Feroxyhyte on Mars?

BURNS discussion<sup>1</sup> on the possibility of the mineral feroxyhyte occurring on the surface of Mars is potentially misleading. In the original description of this mineral Chukhrov *et al.*<sup>2</sup>, following Feitknecht<sup>3</sup>, distinguished between a strongly magnetic phase,  $\delta$ -FeOOH, and a "practically nonmagnetic" phase  $\delta'$ -FeOOH. It was the weakly or nonmagnetic  $\delta'$  phase to which the mineral name feroxyhyte was applied. Burns seems to have equated the two phases and uses data in support of his hypothesis most of which are derived from the synthetic  $\delta$ -FeOOH. The difference may be of more than semantic significance because the ferromagnetic, deep brownish  $\delta$ -FeOOH is formed by the vigorous, rapid oxidation and topotactic replacement of Fe(OH)<sub>2</sub>. As this is a process unlikely to occur in natural conditions at the Earth's surface,  $\delta$ -FeOOH has yet to be reported as a mineral. On the other hand,  $\delta'$ -FeOOH (feroxyhyte), while also requiring the topotactic replacement of precipitated Fe(OH)<sub>2</sub>, is obtained by a slower oxidation and is a yellow-brown ochreous material when dried<sup>2</sup>. This is the mineral reported from marine sediments and gley soils<sup>2</sup>. The yellow-brown colour is almost identical to the description of the soils at the Viking Lander sites<sup>4</sup>. However, if feroxyhyte is nonmagnetic then its major presence on the weak magnets attached to the Viking Lander backhoes<sup>5</sup> is improbable. Chukhrov *et al.* noted that some of the  $\delta'$ -FeOOH samples they studied contained admixed maghaemite ( $\gamma$ -Fe<sub>2</sub>O<sub>3</sub>) which they felt contributed to the weak magnetism of these individual samples. Thus, on the basis of colour, feroxyhyte ( $\delta'$ -FeOOH) might indeed be a constituent of the surface of Mars and the magnetic experiments may have picked up admixed maghaemite<sup>5</sup>, but the possibility of  $\delta$ -FeOOH on Mars seems remote.

KENNETH M. TOWE

Department of Paleobiology,  
Smithsonian Institution,  
Washington DC 20560

1. Burns, R. G. *Nature* **285**, 647 (1980).
2. Chukhrov, F. V. *et al.* *Int. Geol. Rev.* **19**, 873-890 (1977).
3. Feitknecht, W. Z. *Elektrochem.* **63**, 34-43 (1959).
4. Huck, F. O. *et al.* *J. geophys. Res.* **82**, 4401-4411 (1977).
5. Hargraves, R. B., Collinson, D. W., Arvidson, R. E. & Spitzer, C. R. *J. geophys. Res.* **82**, 4547-4558 (1977).

BURNS REPLIES—When it was suggested that feroxyhyte might occur on the surface of Mars<sup>1</sup>, I was well aware<sup>2,3</sup> of the claimed distinction between the ferromagnetic phase  $\delta$ -FeOOH and the terrestrial mineral feroxyhyte ( $\delta'$ -FeOOH). Towe points out that in their original descriptions of feroxyhyte, Chukhrov *et al.* thought the weak magnetism in some  $\delta'$ -FeOOH samples was due to maghaemite ( $\gamma$ -Fe<sub>2</sub>O<sub>3</sub>) impurities<sup>4,5</sup>. Note, however, that synthetic  $\delta$ -FeOOH phases display variable saturation

magnetization<sup>6-13,17</sup> as a result of particle size variations, implying the coexistence of  $\delta$ -FeOOH and  $\delta'$ -FeOOH in most synthesis products. Maghaemite, too, shows similar tendencies towards superparamagnetism<sup>14-16</sup>. Towe has focused his attention on the magnetic properties of  $\delta$ -FeOOH- $\delta'$ -FeOOH assemblages without commenting on other favourable properties of them relevant to martian geochemistry. I contend that feroxyhyte  $\delta'$ -FeOOH- $\delta$ -FeOOH admixtures must be reckoned as a prime candidate for the colour, chemisorption, spectral, redox, paragenesis and magnetic properties of the surface of Mars.

ROGER G. BURNS

Department of Earth and  
Planetary Sciences,  
Massachusetts Institute of  
Technology,  
Cambridge, Massachusetts 02139

1. Burns, R. G. *Nature* **285**, 647 (1980).
2. Burns, R. G. (ed.) *Marine Minerals*, Ch. 2 (Mineralogical Society of America Monograph 6, 1979).
3. Burns, R. G. & Burns, V. M. in *The Sea* Vol. 7 (ed. Emiliani, C.) (Wiley-Interscience, New York, in the press).
4. Chukhrov, F. V. *et al.* *Izv. Akad. Nauk SSR, Ser. geol. no.* **5**, 5 (1976); *Int. geol. Rev.* **19**, 873 (1977).
5. Chukhrov, F. V., Zvyagin, B. B., Yermilova, L. P. & Gorshkov, A. I. *Miner. Depos.* **11**, 24 (1976).
6. Okamoto, S. J. *Am. ceram. Soc.* **51**, 594 (1968).
7. Kulgawczuk, D. S., Obuszko, A. & Szytula, A. *Phys. Status Solidi* **26**, K83 (1968).
8. Dezi, I., Keszthelyi, L., Kulgawczuk, D., Moinar, B. Eissa, N. A. *Phys. Status Solidi* **22**, 617 (1967).
9. Feitknecht, W., Haeni, H. & Dvorak, V. *Proc. 6th Int. Symp. on Reactivity in Solids*, 237 (Wiley-Interscience, New York, 1969).
10. Sara, J. *Chem. Listy* **63**, 112 (1969).
11. Vlasov, A. Ya., Loseva, G. V. & Murashko, N. V. *Izv. Vyssh. ucheb. Zaved., Fiz.* **13**, 129 (1970).
12. Loseva, G. V., Murashko, N. V. *Izv. Akad. Nauk. SSSR, Neorg. Mater.* **7**, 1467 (1971).
13. Kukoz, F. I., Emets, A. A. *Trudy novozerk. politekh. Inst.* No. 269, 61 (1972).
14. Coey, J. M. D. *Phys. Rev. Lett.* **27**, 1140 (1971).
15. Coey, J. M. D. & Khalafala, D. *Phys. Status Solidi* **11**, 229 (1972).
16. Shipin'kov, N. I., Olefirenko, P. P. *Soviet Phys. Solid State* **20**, 222 (1978).
17. Muller, O., Wilson, R. & Krakow, W. *J. Mater. Sci.* **14**, 2929 (1979).

## Anisotropy of Young's modulus of bone

The Hashin-Rosen model was recently applied by Katz<sup>1</sup> to bone to explain the variation of Young's modulus,  $E$ , for bovine femoral specimen with respect to the orientation of specimen axes cut at the angle  $\phi$  to the long axis of the bone. From Fig. 4 of Katz's report it can be seen that (1) in the case of dry bones  $E$  fell from 20 GN m<sup>-2</sup> at 0° to 13 at 10°. At 20°, 50°, 60° and 70°  $E$  was 13. Only at 30° and 40° was it 14; (2) in the case of wet bone  $E$  was 17 GN m<sup>-2</sup> at 0° then fell steadily to 10 at 50°.  $E$  then increased to 14 at 60°, remained steady at 14 up to 70° and thereafter gradually declined to about 11 GN m<sup>-2</sup>.

If values of  $E$  for the dry and wet bone specimens are considered to be significantly different, water must have an important role in determining the mechanical properties of bone. The Hashin-Rosen model does not take this role into account.

If, on the other hand, values of  $E$  for the dry and wet bone specimens are not considered to be significantly different,  $E$  values between 10° to 80° lie between 13 and 14 GN m<sup>-2</sup>, that is,  $E$  does not seem to be affected by  $\phi$ . This result is contrary to the Hashin-Rosen model. Accordingly, I wonder whether the Hashin-Rosen model can be profitably applied to bone.

S. CHATTERJI

Research and Development,  
1A, Lundtoftevej,  
DK-2800 Lyngby,  
Denmark

1. Katz, *Nature* **283**, 106 (1980).

KATZ REPLIES—Further explanation seems necessary for the role of the Hashin-Rosen calculation in modelling the elastic properties of bone. This is the structural composite phase of the hierarchical modelling. It cannot *per se* account for the effects of wet compared with dry bone. This entails considering the material composite nature of the system during the hierarchical modelling.

First, as I stated<sup>1</sup>, dry bone is stiffer and more rigid than the same specimen when wet. This is attributed to changes in the elastic properties of the organic matrix of bone. Second, the Young's modulus,  $E$ , of bone does vary with angle  $\phi$  as shown by many experimenters for haversian bone, for so-called plexiform bone and for mixed specimens. The bovine bone specimens used by Bonfield and Grynepas<sup>2</sup> probably included all three kinds; unfortunately, they reported no structural observations. Indeed, this might explain why some wet specimens were stiffer than some dry ones (plexiform bone is stiffer than haversian bone).

These facts can be incorporated in the Hashin-Rosen calculation; values of  $E_{GS}$ ,  $\nu_{GS}$ ,  $E_{Ost}$  and  $\nu_{Ost}$  can be adjusted. Thus,  $E(\phi)$  in Fig. 3 of my report is approximately 30% greater than the equivalent  $E(\phi)$  on Fig. 4. Also,  $E(\phi)$  at any angle  $\phi$  can vary as much as 80% (see Fig. 4 of ref. 1) simply by altering the percentage of longitudinal osteonic collagen fibres. Thus, curve *a* of Fig. 4 simulates dry bone, and curves *b*, *c* and *d* in effect simulate wet bone behaviour. In reality, this calculation accounts for the effects of sample variation described above, that is, more longitudinal fibres, and thus stiffer lamellae, so simulating plexiform bone.

Unfortunately, my original report<sup>1</sup> could not be expanded to discuss all this; a longer, more complete paper is being prepared. Finally, a hierarchical model wherein a structural composite is superimposed on a material composite does simulate the elastic properties of bone.

J. LAWRENCE KATZ

Rensselaer Polytechnic Institute,  
Troy, New York 12181

1. Katz, J. L. *Nature* **283**, 106-107 (1980).
2. Bonfield, W. & Grynepas, M. D. *Nature* **270**, 453-454 (1977).

## BOOK REVIEWS

SCIENCE COLLEGE  
Upper Circular Road  
DUBLIN 4

# Environmental issues: how much science, how much politics?

Stephen Cotgrove

THE 1970s could well be remembered as the decade of the environment, a decade that was ushered in by warnings of impending disaster. But it was also a time of controversy. Opinions differed widely both on the nature of the threat to the environment and on its causes and cures. During the decade, the focus of attention shifted from pollution to a growing concern over the exhaustion of fossil fuels and resources. The period also saw the emergence of a more radical environmentalist movement, impatient with mere cosmetic meliorist strategies, arguing that the roots of the environmental crisis lie deep in the structure and values of contemporary society, and that no mere technical fix can solve the problem. Now, in the 1980s, nuclear power looks set fair to become the focus for continuing radical protest.

The controversies spawned a vast literature. Any attempt to master the thousands of articles and books and to achieve some kind of diagnosis and stock-taking is a daunting prospect. These two books, however, are both impressive efforts to generate an interpretative framework. Together with Tim O'Riordan's earlier study (*Environmentalism*; Pion, 1976), they constitute a guide through the massive literature and complexities of the issues.

One conclusion is inescapable. Environmental controversies go far beyond scientific and technical debate about reserves of non-renewable resources, methods for safe disposal of radioactive waste and the "risks" of various methods of generating energy. Pollution, for example, is not a scientific term: it conflates a value judgement. In the words of Mary Douglas, pollution is dirt in the wrong place. Similarly, "safe" systems always entail a judgement about an acceptable level of hazard. Behind controversies about low-level radiation, the routing of a motorway or optimum levels for the control of pollution, there is a hidden agenda involving the increasing powerlessness of individuals to influence decisions affecting their lives and the question of the extent to which economic growth should be at the expense of other values.

There are, of course, other blatant and obvious interests underlying the protest of those who do not want a motorway through their own back gardens or a hydro-electric scheme that might spoil their

*Environment, Ideology and Policy.* By Francis Sandbach. Pp.254. (Basil Blackwell/Allanheld, Osmun: 1980.) Hardback £12.50, \$26.50; paperback £4.95. *The Environment from Surplus to Scarcity.* By Allan Schnaiberg. Pp.464. (Oxford University Press: 1980.) Hardback \$14.95; paperback \$9.95, £6.75.

fishing. But beyond this, environmental policies are essentially political in the sense that the interests of some are safeguarded, while those of others are threatened. The central thesis of Sandbach's book is that it is political ideologies that mould both policy and action.

This point is not easily taken by many who see the debate over nuclear risk, for example, as essentially factual. For them it is a question of an objective analysis of degrees of risk for various sources of energy as the basis for a rational decision to choose those methods which the calculus shows to be least risky. From this perspective the rejection of nuclear power is at best ill-informed, and at worst emotional and irrational. But there is a hidden agenda on both sides of the debate. Both are essentially rooted in the alternative ideologies which Stephen Del Sesto has discussed (*Public Policy* 28 (1); 1980); both come to conclusions which are perfectly sensible and reasonable within their respective frameworks of meaning. The problem is to unpack the debate in such a way that the hidden beliefs and values of both sides are made explicit. Even this will not go far enough. Each side is convinced of the self-evident logic of its own position. In short, the debate is embedded in competing doctrines about the nature of society, and above all, about what are the overriding values that policy should seek to maximize.

Despite the central role which the notion of ideology plays in Sandbach's analysis, nowhere does he unpack the concept. It is necessary to distinguish at least two senses in which the term is used. First, there is the argument that ideology refers to knowledge which is distorted by the interests of different groups. In order to substantiate this usage, it would be necessary to demonstrate ways in which scientific knowledge — of the effects of low-level radiation, for example — is

actually related to interests. Of course, it is easy to show that a substantial proportion of the total scientific effort is related to production and defence. The other side of the coin is to demonstrate that much research does not get done because it is not in the interests of dominant interest groups. Schnaiberg's analysis has essentially the same message: that it is the distribution of economic and political power which shapes the kind of research which does get done. So, argues Schnaiberg, there has been a major emphasis on production research to the relative neglect of research on environmental impacts. But he is more convincing than Sandbach in presenting supporting evidence. Equally important, he provides evidence of the subtle (and not so subtle) pressure in the USA against the communication of evidence contrary to powerful interests. Consequently, he argues, society simply lacks the necessary scientific intelligence for realistic environmental policies.

There is a second sense in which it is possible to distinguish between science and ideology. Whenever knowledge and beliefs are used to justify and legitimize policies and courses of action, science is being put to ideological uses to support particular interests. This does not necessarily mean that the knowledge is distorted by interests. It simply draws attention to the distinction between knowledge and its uses. So when scientists give evidence at public inquiries, they are, willingly or not, caught up in political debate. This may help to explain the lack of confidence and trust in science among environmentalists. The achievements of science in modern industrial societies underlie the generally high respect for science and scientists. To appeal to expert opinion is a powerful weapon in political debate. But to sustain respect, science must be seen to be impartial and objective; it is this that many environmentalists doubt. Interestingly, the appearance of scientists at inquiries has contributed to the erosion of confidence. It has increased awareness of the extent of disagreement: on almost all major issues, expert opinion can be ranged on both sides of debate.

The two books are especially critical of the claims of such techniques as cost-benefit analysis, technology assessment and environmental impact analysis to be objective and scientific. The great



weakness, say both Sandbach and Schnaiberg, is that such approaches fail to investigate the original basis for technological choice. Much of the debate over nuclear power, for example, has focused on its social and environmental consequences without asking what, for Sandbach, is the fundamental question: what are the interests which promote this form of energy? Only by uncovering the hidden agenda can there be a debate about nuclear power which comes to grips with the fundamental issues.

Both books challenge the notion of technological determinism — technology as some independent and impartial force, there being no escape from its imperatives — and explore the ways in which technology is shaped by the economic and political system. Sandbach gives a particularly interesting and thought-provoking account of technology and the environment in China. Chinese economic policy would not be judged efficient in market economy terms precisely because it has sought to incorporate non-economic political goals, such as rural self-sufficiency, worker management of factories, and protection of the natural environment and resources. And it has deliberately sought to develop technologies which are appropriate to the achievement of such goals. This has not, incidentally, been without its environmental problems, notably that of organic pollution in the rural areas.

Sandbach and Schnaiberg, then, make a powerful case for the view that environmental policy goes far beyond technical issues. The way a society treats its environment is rooted in the fundamental structure and values of that society. Science and technology, too, are functions of social systems.

While both books attempt to explore the implications of different political positions for the environment, both are more optimistic about the ability of the left to find benign solutions avoiding the more extreme forms of centralized state control which scarcity may generate. While Schnaiberg manages to avoid obvious partiality, Sandbach is not so successful. He is less than convincing, for example, about the possibility of an "objective" Marxist science, free from political and ideological distortions.

Both books are scholarly and well researched. Both carry the same essential message — that science and technology function within a political context. Few scientists and even fewer technologists will like this. By education and inclination, many would prefer a de-politicized world in which policy is determined by "facts" and expertise. Environmental controversies, however, supply convincing evidence to the contrary. □

Stephen Cotgrove is Professor of Sociology and Director of the Science Studies Centre at the University of Bath.

## At the core of chemical catalysis

F. R. Hartley

*Homogeneous Catalysis: The Applications and Chemistry of Catalysis by Soluble Transition Metal Complexes.* By George W. Parshall. Pp.240. (Wiley-Interscience: 1980.) £14.90, \$35.

THIS book by Dr G. W. Parshall, Director of Chemical Science at du Pont, aims to provide a balanced description of homogeneous catalytic reactions. In this it succeeds admirably. There are few people better qualified to write such a book and everyone involved in the field, student or research worker in an academic or industrial laboratory, will be grateful to Dr Parshall for wading through the enormous literature of homogeneous catalysis to expose the real core of the subject to close scrutiny.

After two brief, but valuable, introductory chapters there follow nine chapters on homogeneously catalysed chemical reactions. All the major industrial processes that use homogeneous catalysis are covered, as well as the more useful laboratory syntheses. Clearly, some selection has been necessary here, but in my judgement it has been well done. The final chapter looks to the future, considering the known as well as likely developments in feedstocks as well as possible future developments in catalysis, including supported metal complex catalysts.

The strengths of this book are many. Foremost amongst them is the air of industrial reality that pervades the whole book. This is beautifully illustrated by the comment that the intensive study of homogeneous olefin hydrogenation catalysts seems anomalous because soluble catalysts are rarely used either in industrial or laboratory hydrogenations. Many of the chapters end with a number of important general references to guide the reader into the wider literature. Key references in the text have been chosen with great care.

This book is one that everyone working in the field of homogeneous catalysis will want to have close to hand, and lecturers will want several copies available in the library for their students. The book summarizes what is known and where the applications of the subject lie; it emphasizes areas in which more research is needed to increase our understanding of the mechanisms of homogeneously catalysed reactions; it provides pointers to the future. I recommend it unreservedly to anyone starting or established in the fields of synthetic, industrial and catalytic chemistry. □

F. R. Hartley is a Professor in the Department of Chemistry and Metallurgy at the Royal Military College of Science, Shrivenham, Wiltshire.

## New ideas about parasites

Donald R. Strong

*Evolutionary Biology of Parasites.* By Peter W. Price. Pp.237. (Princeton University Press: 1980.) Hardback \$22, £9.70; paperback \$8.75, £3.80.

PRICE's thoughtful and ambitious little book is an ecumenical overview which considers phytophages, parasitoids and hemiparasitic green plants, as well as the subjects of classical parasitology, as functional analogues. Such general perspectives have not been of great interest to parasitologists, who are more concerned with details of the taxonomy, life-cycles and pathology of the myriad pests of animals and plants. Price, in contrast, is an ecologist and evolutionist, and as such works in an alternative tradition of broad generalization and synthesis. I hope that this does not deter mainstream parasitologists. Ecologists will read the book; the author's reputation and that of the *Princeton Monographs in Population Biology* ensure this. But biologists who

work on specific parasitic groups have much to contribute to an eco-evolutionary synthesis in parasitology; and much to gain from the book. Ultimate success for Price's efforts towards a synthesis will come only from a rapprochement of these two camps.

After an introduction, chapters on general concepts, non-equilibrium ecology and evolution, genetics, radiation and host-specificity, niches and orthodox community theory, and parasite influences on host evolution follow. Finally there is a coda of ideas for further study.

The most interesting chapter to me is that on communities. Here, Price represents the new academic ecology well, in questioning the basic assumptions of the old, ideal Hutchinsonian school. The most important assumption of the idealists is, of course, that communities are primarily a product of the competitive interactions among their component species. Price meets this head-on with Table 6.1, which shows that the literature indicates non-

Put in the Library  
BIOLOGY COLLECTION  
at the Royal College of Science  
SHRIVENHAM

interactive coexistence to be quite common among species of gut parasite. In summary he says: "There is little evidence to suggest that competition has been an organizing force [for many parasites]". K. Rohde's important overview of species interaction among fish gill parasites was published after this book went to press (*Am. Nat.* 114, 648; 1979), but his earlier work is reviewed. For gill parasites, Rohde comes to a conclusion similar to Price's; so do John Lawton and myself for the phytophagous insects, in a paper now in press (*Am. Nat.*).

Clearly, exceptions to this generalization exist in both zoophagous and phytophagous groups; interspecies competition does sometimes affect coexistence. But the great preponderance of cases involve loose organization (if any) among parasitic species at similar trophic levels, with no substantial shift from fundamental to realized niche in the presence of another species.

I like Price's book so much that I feel entitled to make two suggestions as to how it might be improved. First it is unfortunate that "community interaction" is treated only in the purblind Hutchinsonian sense, which studies competition to the virtual exclusion of all else. Interactions can occur horizontally in food webs — as competition or mutualism among species at very similar trophic levels — and they can occur vertically as predation and parasitism from above, or through factors such as the noxious and nutritious aspects of hosts as food from lower in the web. Perhaps this omission was made from modesty; Price has published much about community influences of natural enemies on phytophagous insects.

My second reservation concerns "coevolution", a term which here has as many references in the subject index as any other process. Price deals critically with most conceptual flabbiness in ecology and evolution, but he is soft on coevolution. For example, specialization of parasites is discussed as if it were necessarily a coevolutionary process — need it be? In another example, the inverse relationship between host breadth of agronomid flies and the diversity of their hosts' phytochemicals is treated as if it were a necessarily coevolutionary phenomenon. Again, need it be? Coevolution implies more than just the evolution of two species that live together. It implies reciprocity of influence. Evolutionary influence of host upon parasite can occur without any influence being returned, especially with benign parasites living in a non-equilibrium world.

But this is niggling. Price's book is exciting, imaginative and its influence might even be enduring, if parasitologists and eco-evolutionists find common interests as its result. □

Donald R. Strong is Associate Professor of Biology at Florida State University, Tallahassee.

## Developments in geodetic theory

William M. Kaula

*Advanced Physical Geodesy.* By H. Moritz. Pp.500. (Abacus: Tunbridge Wells, UK/International Scholarly Book Services: Oregon, 1980.) £26, \$57.

THIS treatise concerns developments in the theory of "classical" physical geodesy that have taken place since the publication of *Physical Geodesy* by W. A. Heiskanen and H. Moritz (W. H. Freeman, 1967). The implication of "classical" is that the figure and gravitational field of the Earth are considered as constant in time. The book is intended for research workers and graduate students in geodesy and gravity, and opens with a thorough introductory exposition on the background to the subject. About half the book is devoted to advanced least-squares collocation theory and one-third to the geodetic boundary-value problem. A topic not treated is the differential geometry of the gravitational field; for this *Mathematical Geodesy* by M. Hotine (US Dept of Commerce, 1969) is still the best book available.

The strengths of the book lie in the soundness of its mathematical foundations, the clarity of the writing and the authoritative tone of its discussion of modern developments in geodetic theory. Despite the rigour of the mathematics the text has an easy style, understandable to engineers and physical scientists. The authoritative tone arises naturally from Helmut Moritz being a leading contributor to the field, but work by others, such as Molodenskiy, Krarup, Bjerhammar and Sanso, has been well integrated.

To me the weaknesses of the book all appear to be in the area of least-squares collocation: firstly, an excessive simplification of gravity field properties, leading to an under-estimation of some difficulties; and secondly, a failure to take advantage of concepts and techniques developed outside geodesy.

The principal simplification is that gravity is taken to be homogeneous and isolated: a global covariance curve is taken as given, and no cross-covariance with other variables, such as topography, is considered (although accounting for topography by isostatic reduction is mentioned). However, it is in these areas that the greatest difficulties occur in applying collocation: the appropriate data selection to determine the covariance curve, and how to take into account topography as an influence on the distribution of data, as well as a correlate, and hence predictor, of gravity. Although Moritz recognizes that complete representation of a continuum like gravity requires an unlimited number of parameters, he does not present tools like singular value analysis or the resolution

matrix to select the limited parameter set which can be determined from a finite data base. The discussion of "improperly posed problems" does not bring out the idea of "trade-offs" between accuracy and resolution, and the heuristic opportunity of comparing similar inference problems in different fields is not taken.

Moritz's treatise is essential for any researcher specializing in physical geodesy. However, for the non-geodesist wishing to obtain some insight about the nature of the gravity field and the methods applied to it the 1967 text by Heiskanen and Moritz seems preferable. □

William M. Kaula is a Professor of Geophysics at the University of California, Los Angeles.

## Causal dilemmas

P.E. Bryant

*Social Interaction and Cognitive Development in Children.* By Anne-Nelly Perret-Clermont. Pp.206. (Academic: 1980.) £14.80, \$34.

NO subject is going to solve its problems until it realizes how difficult those problems are. A poignant example can be found in child psychology, which is faced with the major difficulty which it does not recognize and is certainly nowhere near to solving.

The problem is one of causes. Children's behaviour changes as they grow older, and it is easy enough to say what these changes are. But what makes them happen? What are the causes of, for example, intellectual development? Child psychologists have typically relied on quite inadequate techniques for answering this kind of question. An obvious example is their use of correlation. To find, as someone did, that the more a father talks to his children at breakfast the brighter they are, is, in child psychology, to conclude that parental chatter determines intelligence. But what about the possibility, *mutatis mutandis*, that brighter children provoke the tired parent into talking while dim children do not?

Psychologists have one other major technique for tracking the causes of development, and that is the training experiment, which also has weaknesses. These weaknesses are to be found in the work described in Perret-Clermont's book which attempts to demonstrate that social interactions in the form of discussions and arguments between children are an



important factor in causing intellectual changes.

The rationale behind the training experiment is simple. You think that social interaction is important, so you give a child a pre-test on some important cognitive skill like Piaget's conservation test, then give them a training period, and then a post-test exactly like the pre-test. If they are better on the post-test than a control group, you conclude that social interaction normally causes the development in question.

There are two difficulties, neither solved by Perret-Clermont. The first is that these positive results might be quite artificial. Many other people have done successful conservation training experiments using quite different methods. There must be at least a dozen successful ways, most of which do not involve social interaction between children. There is no way of knowing which has isolated the real cause.

Secondly, it's peculiarly difficult to get the controls right. For example we cannot say from Perret-Clermont's data whether it is social interaction with anyone or social interaction with children that is important. She does not take her effects apart. Nevertheless her work is simple and ingenious, and she presents an attractive causal hypothesis. But how are we ever to test it properly? □

*P.E. Bryant is Watts Professor of Psychology at the University of Oxford.*

## Vesicle in a basket

Ernst Ungewickell

*Coated Vesicles.* Edited by C.D. Ockleford and A. Whyte. Pp.344. (Cambridge University Press: 1980.) £40, \$90.

FOR more than 10 years, up to about 1975, the study of coated vesicles was almost exclusively the province of morphologists who early on had recognized the importance of these organelles in exo- and endocytotic processes. This state of affairs changed dramatically when B. Pearse succeeded in isolating pure vesicles in quantity, and thus made them available to biochemists. It is this latter group who will profit most from this monograph.

The volume contains contributions by representatives of a number of specialized fields, most of whom offer stimulating discussions and speculations on what are often rather fragmentary data. The 12 chapters fall into three groups: an introductory survey of the field; exploration of specific functions of the vesicles; and discussions of models aimed at describing endocytotic events at a molecular level.

The book opens with a classification of

endocytotic processes, and an evaluation of the role of coated vesicles in micropinocytosis and their comparison structurally and functionally with smooth-walled micropinocytotic vesicles. This is followed by a summary of the occurrence of coated vesicles in different species and cell types, and a discussion of the different pathways of intracellular transport.

The logical sequence of the contributions proceeds with a consideration of the coated vesicle in plant cells. Subsequent chapters describe in detail the involvement of coated vesicles in IgG transmission, their role in membrane retrieval in neurosecretory cells, and their function in vitellogenesis and secretory processes. All of these reviews are supplemented with high-quality electron micrographs showing the characteristic appearance of coated vesicles from different sources in both median and tangential sections.

Molecular aspects of receptor-mediated transport are discussed next, and models proposed by various researchers are compared. The authors of this contribution

conclude that specific protein transport is too complex a process to be described by any one of the proposed models. It is my impression that the same might be said of the models which try to explain how membranes invaginate to assume the configuration of coated vesicles, a topic which is also discussed. In the penultimate chapter, structural aspects of coated vesicles are reviewed; this reveals that surprisingly little work has been done on the structure of the major coat protein, clathrin. The book concludes with a cautious discussion of the importance of coated vesicles in medical science.

In summary, the book provides comprehensive coverage of the knowledge of coated vesicles up to the end of 1978 (a list of more recent publications appears in an appendix) and clearly indicates directions for future research. I recommend it to anyone who is new to the field or who is considering working with coated vesicles.

*Ernst Ungewickell is at the Biological Laboratories, Harvard University.*

## Much to ponder in lipid evolution

T.W. Goodwin

*Lipids in Evolution.* By William R. Nes and W. David Nes. Pp.195. (Plenum: 1980.) \$29.50, £18.59.

THE authors of this book, *père et fils*, are clearly fascinated by the problem of relating biochemical parameters to the classical ideas on evolution. Concentrating on lipids, they have sifted through a great amount of information and bravely attempted to discern clear evolutionary patterns. A perusal of their final chapter indicates how difficult this data analysis was and how few new correlations have emerged. In almost every aspect studied, facts crop up which invalidate an emerging generalization. Indeed the authors' occasional frustrations are revealed by such comments as "The situation is made worse by the phylum Mollusca". This follows the view that as arthropods cannot synthesize sterols it would be reasonable to assume that molluscs, which from fossil records pre-date arthropods, would also not synthesize sterols; alas, "biosynthesis of sterols is a common property of molluscs".

The first four main chapters deal succinctly with dating and chronology, the palaeontological record, the origin of oxygen, and the temperature and pH problem. It is clear from the chapter on oxygen that anaerobic organisms can make some unsaturated fatty acids and isoprenoids anaerobically from acetyl-CoA. A discussion of how anaerobic

organisms make acetyl-CoA would have been most welcome, as would some comment on the quantitative aspects of acetyl-CoA, lipid and isoprenoid production in the presence and absence of oxygen in organisms such as yeast.

"Phylogenetics and Occurrence", the next chapter, is a straightforward and thorough account of lipid and sterol distribution in nature. The main conclusion is that no lipid distribution is unique to prokaryotes or to eukaryotes, and this is emphasized by the observation that the fatty acid pattern in blue-green bacteria (algae) is much closer to that of the eukaryote algae than to that of the photosynthetic bacteria.

The authors next turn to a consideration of phylogenetics and biosynthesis, paying particular attention to the important bifurcation in sterol synthesis at the point of cyclization of squalene 2,3-oxide. This clearly separates non-photosynthetic from photosynthetic organisms. In the former, the first cyclization product is lanosterol, whereas in the latter it is cycloartenol. The reason for this bifurcation is still obscure.

This is a book packed with interesting information and spiced with enjoyable speculation. It will help to broaden the outlook of conventional natural-product chemists and will give biologists much to ponder over. □

*T.W. Goodwin is Johnston Professor of Biochemistry at the University of Liverpool.* ●

20 November 1980

# Deciding where to put nuclear plants

Even the most embittered opponents of nuclear power must be surprised at the good luck that has come their way in the past few months. First, there was the accident at Three Mile Island in March 1979, the chief casualty of which was the reputation of the US Nuclear Regulatory Agency. In the wake of the report of the Presidential Commission of Inquiry, it was inevitable that the regulatory commission would have to be reorganized and that its chairman, Dr Joseph M. Hendrie, would eventually be required to practise his talents elsewhere. In due course, President Carter nominated a new chairman (Professor Al Carnesale), but so soon before the election that his appointment to the job was legitimately blocked by the Republicans in Congress and will now, presumably, fall by the wayside. In the interregnum, the commission has been behaving with accustomed but quite alarming timorousness. The second reactor at Three Mile Island, entirely undamaged and now more fully understood than ever, is still out of service. The granting of operating licences for plants already built has proceeded at a snail's pace. Then, almost as if to ensure that no utility will be so rash as to order a nuclear plant for some time to come, the commission embarked at the end of July on a series of inquiries aimed at defining the criteria to be met by the sites proposed for nuclear plants. The outcome of this inquiry, known technically as a rulemaking procedure and thus designed to yield rules applicable throughout the United States, is naturally unforeseeable. Several years, perhaps five, may pass before putative builders of nuclear plants know where they stand. If they are wise, they will in the meantime put their capital into growing trees. That way, they will at least have something to burn.

Elsewhere than in the United States, stasis is less complete but of longer standing. In Britain, for example, it now seems likely that the Central Electricity Generating Board will be allowed to order one new nuclear plant in each of the next two years, but that 1982 will be largely given over to a public inquiry about the proposal to build a single pressurized water reactor of Westinghouse design. (The Three Mile Island reactors use pressurized water, but were built by Babcock.) As yet, the terms of reference of the inquiry (promised by Mr Tony Benn, previously Mr Anthony Wedgwood Benn, when a minister in the previous government) have not been decided. It remains to be seen whether the inquiry will be organized around a site-specific proposal or, alternatively, drawn in such a way that pressurized water reactors as such will be pronounced usable or otherwise. But only after that inquiry is complete will the same group of people embark on the more contentious job of preparing for an inquiry into the safety of full-sized fast reactors, now on the calendar for 1984.

Both the opponents of the nuclear construction industry and those who think it prudent to build more of them must surely agree that these are not ways in which decisions should be made about the future development of nuclear power. Whatever the rights and wrongs of the safety argument, procrastination cannot substitute for rational decision, although it may be responsible for decision by default. Since the problem of winning public acceptance, or at least of creating a sense that justice has been done, applies to other kinds of technological enterprises than the construction of nuclear power stations, it is obviously important that better mechanisms should be devised.

The regulation of nuclear power plants in the United States has been a controversial issue for the best part of twenty years. To begin with, the Atomic Energy Commission was both the sponsor of nuclear power and the licensing authority. Understandably,

and rightly, the two functions were separated a decade ago. Again rightly, the Nuclear Regulatory Commission is an independent body whose members are appointed by the president of the day for fixed terms, and who are collectively responsible to Congress and not the Administration for the proper regulation of nuclear safety. Like other regulatory agencies, the Federal Communications Commission for example, the Nuclear Regulatory Commission enjoys a kind of delegated authority to make rules which elsewhere would have the status of laws. It is empowered to make generic rules applying, say, to all reactors of a specific type, and also particular rules, as on the licensing for operation of a particular reactor. Other government agencies are powerless to influence decisions by the commissions, but those who dissent can appeal to the courts. Such appeals have been one of the most frequent means of impeding the construction of nuclear plants in the United States.

The British system is at the other end of the regulatory spectrum. Broadly speaking, all new industrial developments are subject to planning legislation. Applications for planning consent are first submitted to the lowest planning authority in the hierarchy, a county council for example. Necessarily, they are site-specific. One applicant may want to build an abattoir at the end of some village high street, another (invariably a nationalized industry) a nuclear power station on an estuary. The planning legislation provides that the Secretary of State at the Department of the Environment may order a public inquiry if either the proposers or the opponents of some innovation are aggrieved, or if he and his officials consider that the issue has wider importance. The planning legislation also allows for the appointment of commissions of inquiry to determine generic questions — are motorways, or nuclear power stations, or fast reactors, really necessary, for example? But this procedure has not so far been used, no doubt for fear of creating precedents.

Both the British and the American systems are intended to serve similar ends — to allow objectors, especially disappointed objectors, a proper sense that their objections have been fully heard, but also to give the public at large a sense that important questions have been properly examined. That, at least, is the theory. The reality is usually less than satisfying. Private objectors are usually less well equipped, at least financially, to put their case to government inspectors. In the United States, the Internal Revenue Service allows charitable foundations to contribute to the cost of putting objections to a public hearing. In Britain, where this is not permitted, the government might think it worthwhile making some funds available for objectors to important schemes. (Inspectors at present have a right to penalize frivolous objectors with an order to pay costs, but that is hardly the same thing.) A more serious difficulty under British planning law is that objectors to a novel scheme have only restricted rights to argue that the objective of a new plant might be better achieved by siting it somewhere else.

These, however, are relatively minor difficulties. The most serious objection to both the British and the American systems for deciding whether and, if so, where nuclear power stations should be built is that both of them are inevitably subject to political forces in the broadest sense, and are thus far from being objective. In Britain, the more fuss that can be made about a proposal to build a nuclear power station, the greater the chance that there will be a public inquiry. All nuclear plants so far built have been brought into the world with ceremonies of this kind. No minister with an eye to re-election would think otherwise. In the United



States, similar pressures affect the Nuclear Regulatory Commission, whose reputation would quickly sink still further if it were often defeated in the courts on the grounds of not having been scrupulous about due process. And at inquiries of both kinds, there is nothing to prevent the most local objectors from raising the biggest questions that come to mind. Does the country need nuclear power anyway? Is this kind of reactor safe? Why should Blanksville or Dashby be the first prisoner of the plutonium economy, as it is called? In the United States, these pressures have led to a quite absurd proliferation of the subjects on which the Nuclear Regulatory Commission is holding public hearings. The inevitable result is more prevarication, more delay.

As things are, the only seemly escape from the dilemma is to devise a means of limiting the scope of public hearings without limiting the right of objectors to object. On the construction of

nuclear plants, it is pointless that public hearings should rehash questions of whether nuclear power as such is necessary, or economic, or likely to be overtaken by solar power. Both Britain and the United States have elected governments which reckon to include such questions in the fields of their competence. Similarly, there are questions about the relative (not absolute) safety of different reactor types which are generic in character, and which could (and should) be argued out once and for all. Questions of siting, on the other hand, are essentially local or regional matters (which is not to imply that they should not be disputed nationally). But it should be open to objectors to argue that some other site would be more suitable. The British log-jam of nuclear inquiries will not be broken until 1984. Is there a chance that Mr Reagan will be able to move more quickly in the United States when January has come?

## Scope for European collaboration?

The famous conjuring trick in which the Cheshire Cat was made to disappear but to leave its smile behind is no doubt the envy of the professionals who still work the music-halls. The European Science Foundation, which held its annual assembly last week in Strasbourg (see page 204), is trying to do much the same. Its members are research councils and learned academies from most Western European nations, all of them supported financially by their national governments. Their membership of the foundation is voluntary, as are their contributions to the special research projects which are from time to time devised. It is just as if they belonged to a club for organizations like themselves and, like the members of other respectable clubs, they spend some time each year considering what the fees for membership should be. The trick, which has worked well in the past six years, lies in the foundation's insistence that it is strictly a non-governmental organization, free (if its members agree) to criticize developments at which its members' paymaster-governments may have connived. This is the spirit in which the European Space Agency has been taken to task in the past two years for the inadequacy of its plans for launching scientific satellites. On other occasions, the foundation assumes the freedom to put pressure on the same governments to act in some specific way — to build a synchrotron radiation source, for example. The hapless governments see the smile (or the grimace) but appear not to recognize the body.

That, fortunately, has been the foundation's experience so far. Part of the explanation is that it has been run on a kind of shoestring. The members' contributions to the foundation are such modest proportions of the national public funds they receive that even the most hyper-touchy governments would feel foolish if they reacted against the foundation's members' modest show of independence. But will it be the same if the foundation grows, becoming less inconspicuous in the process? That, inevitably, must be one of the concerns of those who now think that the time has come for modest growth. The time has come to ask what the foundation is for, and what it might be for. For the past few months, a domestic think-tank has been brooding on the same two questions.

The bread and butter of the foundation's business is easily justified. Plainly it is useful that there should be an umbrella under which organizations with a responsibility for the support of research and scholarships can meet from time to time, even if they talk only about administrative matters such as how to adjust research grants for inflation. In principle, it is also plainly beneficial that there should be some mechanism for tackling research problems of common European concern. European taxonomy is an obvious candidate. So too was the project to mount a coordinated study of the problems of preserving mediaeval stained glass, but that fell foul of the chauvinistic quarrelsomeness of the experts in the field. Unexpectedly, but not surprisingly, most enthusiasm seems to have been generated by the common interest of European scholars in external problems — the literature of China and Byzantine history, for example.

Collaborative research programmes within Europe itself seem more easily arranged in the social than the hard sciences — partly because of the costs involved but also because international comparisons come more naturally to mind in the social sciences; in the hard sciences, inevitably, everything is everywhere the same. Yet there is obviously plenty of scope for further collaborative research. The geophysicists have for example an ambition to mount a seismic traverse of Europe from north to south, reaching into North Africa, that could probably be mounted within the necessarily limited time-scale of *ad hoc* voluntary contributions by the member organizations. The plan to build a source of synchrotron radiation would, by contrast, require a continuing commitment of funds, and thus endanger the loyalty of some members or the compliance of their governments. The strategy the foundation has pursued — to interest governments in the idea — is thus the only practicable way of seeing such a machine built.

So where does the foundation go from here? For the time being, there are grounds for being cautious. Inevitably, in only six years, the foundation has comparatively little to show for the trouble it has been taking. Ultimately — and there should not be long to wait — it will be judged by the quality of its collaborative research. If the outcome is worthwhile, the result should be a rash of other projects crying out for supplementary contributions. In the meantime, however, there are other tasks on which the foundation could busy itself. The recent study on the mobility of academic scientists within the European Community (see *Nature* 23 October) made much of the lack of movement between European countries (as distinct from the now common journeys across the Atlantic). As things are, several of the foundation's committees organize research workshops, symposia and the like in their narrow fields, but the scale of such activities within Europe is nothing like enough, in spite of the efforts of the European Molecular Biology Organization and the federations of specialist scientific societies that have sprung up. More ambitiously, there is a case for asking the foundation to share in the administration of the European exchange fellowship scheme, so far in the hands of national academies but much in need of escaping from the strictly bilateral basis on which it was set up eight years ago. (With a little luck, an international organization might even be able to tap supranational sources of funds, the European Community for example.) Finally, there are some crucial housekeeping tasks not at present being done (or done well) for European science. There is, for example, a crying need for a directory showing who does what in European research, some means of knowing who is where and a systematic way of telling which national organizations spend how much. Coherently compiled statistics of the working (and output) of European university systems would be a great boon. If one immediate objective is to ensure that the smile remains visible and the rest of the animal inconspicuous, this must surely be the best way forward.

# Backlash against DNA ventures?

## More thoughts at Harvard on business link

### Washington

Harvard University's announcement that it is considering setting up a company to exploit the results of its recombinant DNA research (*Nature* 30 October, p.769) has provoked a backlash on university campuses that may lead Harvard to drop the idea. The company is seen by some as a threat to academic freedom.

University administrators have, in general, welcomed the Harvard proposal, particularly since many of them are already discussing similar ideas of their own but have not yet made them public.

Yet at the same universities both scientific and non-scientific faculty members have warned of the dangers of steering basic research towards commercial objectives, suggesting that there are elements in the Harvard proposal which make it qualitatively different from more conventional arrangements for linking university research and its industrial applications.

One group which has taken up the issue is the academic freedom committee of the American Civil Liberties Union (ACLU). The committee has set up a subcommittee to draft a possible policy statement for ACLU to consider on guidelines to cover relationships between universities and industry.

"I do not think that you can divorce the universities from industry, but the contribution that we can make is to set guidelines down for the future, for which we feel both faculty and administrators would be appreciative, as they have been in the past on issues such as military research", Dr Bernard Belush, chairman of the academic freedom committee, said last week.

Other universities considering new ways to profit from their research are going through similar debates to that at Harvard, where more than half the faculty members were reported by the *Wall Street Journal* to have told Harvard president Derek Bok that they were opposed to the idea.

At Yale University in New Haven, for example, the faculty has asked for a revision of proposals which have been put to it for encouraging greater links with industry, and has expanded the committee looking at these proposals — which might, as at Harvard, include the idea of setting up a research development company — to include more non-scientists, who had been among the critics of the original proposal.

• A similar debate is expected at the

University of Michigan at Ann Arbor, where there is a proposal to link up with a local pharmaceutical company, Warner Lambert, to provide training facilities for the company's research personnel.

Dr Charles Overberger, vice-president for research at Ann Arbor, said last week that although there were no firm plans to set up a separate company, talks had been held with a venture capitalist, Mr Herbert Doan, an ex-chairman of the Dow Chemical Company.

At Stanford University in California, where much of the original recombinant DNA research was carried out, the debate is already at an advanced stage. A proposal similar to Harvard's was made several years ago that the university should become more directly involved as an investor in exploiting its research results, rather than merely offering patent rights.

The proposal was, however, shelved after strong opposition from several faculty members, including Professor Paul Berg of the university medical school's biochemistry department.

Rather than getting directly involved, the department is now setting up an industrial affiliates programme under which companies which sign up will be able to send representatives to one seminar a year on the department's work, to receive one visit a year from a faculty member to discuss the company's research and to send a representative to Stanford to discuss this research with faculty members.

In return, the company will give \$12,000

annually to the university, which the department hopes will be used to support junior research posts. Fifteen companies — including Cetus, Genentech and several major pharmaceutical firms — have already signed up, and the department has a growing waiting list.

Dr Donald Kennedy, who took over as Stanford's president earlier this year after spending four years as head of the Food and Drug Administration in Washington, admits that the new commercial pressures on biological research have thrown up a variety of problems which biomedical researchers have never previously had to face. "Quite possibly it is time for some leadership to be sought or to well up in universities on this point as it has done on other points in the discussion of the social responsibilities of scientists", says Dr Kennedy. "Perhaps it is time for another Asilomar, but it ought to come from the people who are doing the science."

At Harvard, university officials insist that they have gone to considerable lengths to prevent any potential conflict of interests between the academic goals of the institution and its investment policies. For example, no university administrators would be directly involved in investment decisions taken by the new company, which would be completely separate from the university. Although the university would be a minority shareholder, it would not be investing any of its endowment, since the shares would be provided in return for access to research results.

## Science Research Council comes clean

The UK Science Research Council (SRC), which could not say (*see Nature* 13 October) how many research grants were outstanding at the end of the last financial year because of a computer oversight, has now produced reliable figures. According to the revised account, 3,933 grants were current on 31 March 1980, of a total value of £120.5 million. This is an increase in number of 15 per cent and in value of 34 per cent over the previous year.

The increase is still substantial and unplanned. Indeed, it is the first major increase of grant allocations for many years. It is only partly accounted for by the "equipment round", a £7.5 million handout for major items of equipment in universities which took place in the summer of 1979.

Last week the Department of Education and Science (DES) came to SRC's aid, allowing the council to transfer £5.7 million of its savings on foreign subscriptions, due to the strong pound, to other accounts. SRC can thus pay for some of this year's increased expenditure on grants. Even so, the council was due this week to seek another £2 million of savings on current spending, on top of £4 million

worth of cuts already made.

SRC will therefore scrape through the current financial year without requiring extra finance from DES — but the year to follow (April 1981 to March 1982) looks increasingly bleak. The pound seems unlikely to rise further against the European currencies in which foreign subscriptions are mostly paid, and indeed it may fall if interest rates in London money markets are reduced. Thus the £5.7 million found on exchange rates this year may vanish or even become negative next year, while the grant commitment will remain obstinately high.

Next year, accordingly, the council will have to seek an increase in its funding above the £175.3 million included in the provisional 1980 five-year forward look, to pay for its support for the universities last year. There is no reason to suppose that the other dependants of the Advisory Board for the Research Councils will be sympathetic. The council's finances are, however, unlikely to be seriously affected if it is required to refund the price of its annual report (HMSO, £7.50) to purchasers complaining that the figures it contains are wrong.

Robert Walgate



Whether this will be sufficient to answer the critics remains uncertain. While scientists were voicing their fears about academic freedom, several investment houses were saying in public last week that they thought it was a bad thing for a university to get involved in commercial operations. Dr Bok's announcement about whether the university intends to go ahead with plans to set up the new company is therefore awaited with great interest.

David Dickson

## European science

### Foundation stones

#### Strasbourg

The European Science Foundation ended its annual general assembly here last week (13 November) in a vaguely hesitant frame of mind. Unlike previous assemblies, this was less a general amplification of the enthusiasm for international collaboration of member organizations (now 47 research councils and learned academies from 18 countries) than a reluctant recognition that the next six years may be more difficult than the past — and first — six.

Part of the hesitancy stems from changes of personnel. Lord Flowers, rector of Imperial College, London, and president of the foundation for the past six years, handed over at this year's assembly to Professor H. Curien, director of the CNRS (Centre National d'Etudes Spatiales) in Paris, while Dr. John Goormaghtigh succeeded Dr Friedrich Schneider as secretary-general only a year ago. But the member organizations seem also to be preoccupied with domestic funding problems and thus less able to think expansively than in recent years.

Several of the foundation's recent initiatives appear also to be at critical, even

anxious, stages. Thus the development of a plan for what is called the European Synchrotron Radiation Facility, on which a foundation study group has been working for the past three years, is in the air. At the general assembly in 1979, the retiring secretary-general, Dr Schneider, was asked to spend a year sounding out European governments on their willingness to contribute towards the cost of the machine, estimated at something of the order of \$100 million.

Dr Schneider appears to have found this a disappointing year. Potential contributors to the cost of the machine have taken the view that haste might jeopardize eventual construction. Some governments also appear to be suspicious that the foundation is usurping their role of making treaties among themselves for multinational projects. The study group (under Professor Y. Farge of Orsay) will, nevertheless, remain in being during 1981, concentrating on the further refinement of its proposals.

The foundation is also despondent about the prospects for space research in Europe. A year ago, one of the foundation's published reports took the European Space Agency to task for the degree to which its then programme was biased to the development of the Ariane launching system, to the detriment of plans for launching scientific satellites. At this assembly, delegates were told that there has been no substantial improvement. Plans for launching European scientific satellites are so sparse that scientists who are members of space research groups in Europe may have to wait about five to seven years between successive experiments. Professor Curien told the assembly that this might be inevitable in studies of "the reproduction of the elephant, or of silviculture", but that it was

an entirely artificial circumstance in space research.

The foundation is not, however, entirely frustrated. Its programme on polymer structure is going well (see box), while the assembly agreed to launch a number of new projects in the social sciences while continuing most of its past successes, the programme of training in "brain and behavioural research", for example.

On more general questions, the foundation has decided to keep in being the Liaison Committee on Recombinant DNA Research even though, according to a statement from the committee, the need for attempts to coordinate containment guidelines has melted away. The focus of anxiety has moved to what are called "second generation" issues, including the pace and the manner in which recombinant DNA techniques are being commercialized with the possible consequential risks to academic research. Dr Philip Handler, president of the US National Academy of Sciences, said in his invited address to the assembly that academics forming commercial links with DNA companies were "creating a great deal of difficulty for the others working in this field".

The foundation has also issued a statement asking that national governments planning new legislation on the confidentiality of computerized data banks should also bear in mind the value of such data, suitably shorn of identification, for the research community.

The assembly approved the foundation's budget for 1981, which exceeds FF5 million for the first time, and which does not include the cost of the special research projects (called "additional activities") to which member organizations contribute on a voluntary basis.

Lord Flowers estimated, in his final address to the assembly, that the total expenditure on the foundation's activities amounted to less than 0.1 per cent of the budgets of member organizations, and hoped that the next six years would see a tenfold increase in this proportion in the next six years, as well as a further extension of the foundation's sphere of interest. The academy of Finland was admitted as a full member of the foundation with effect from 1981.

## Fusion research

### Livermore looks up

#### Washington

After a period of considerable uncertainty, scientists in the two main fusion energy programmes at the US Department of Energy's Lawrence Livermore Laboratory in California are confident that recent technical advances are given a significant boost to the chances of being able to exploit nuclear fusion as a commercial source of power.

In the magnetic confinement programme, successful tests with so-called tandem mirrors, which could be used to

## Something ventured, something done

Both the new research projects approved by the 1980 assembly are in the social sciences. One, under the rubric of "comparative law", and to which ten countries have agreed to contribute, includes an attempt to define and compare the medical responsibility within Europe. The study will include the responsibilities of physicians and drug firms towards patients and the influence of medical insurance on the behaviour of physicians. There is also to be a European study of procedures for summary jurisdiction in civil and other courts.

The social scientists are preoccupied with migration and language, and have won approval for two other research projects — the problems of language acquisition by adult migrants within Europe (of whom there are estimated to be 11 million) and a series of research workshops on the human and cultural aspects of migration within Europe.

There is also to be a one-year study of

problems of technical innovation and social change, chiefly so as to identify fields in which coordination by the foundation might be beneficial.

Continuing projects that appear to be flourishing, or nearing fruition, include:

- *Chinese studies.* A handbook of Chinese literature in the period 1900-49 is nearing completion, while a descriptive catalogue of the body of fifteenth century Chinese literature known as the *Tao-Tsang* is well under way.

- *Brain and behaviour research.* The foundation plans to spend in 1981 a total of FF1.3 million on this programme of training awards and travel grants.

- *Taxonomy.* The *ad hoc* group on European taxonomy is to be disbanded, and its final report published in March next year. The draft report claims to have made substantial progress towards understanding the difficulties of coordinating European taxonomic nomenclature.

"plug" the ends of a solenoid containing plasma, have led to the decision to include the mirror devices in the Mirror Fusion Test Facility (MFTF) at present under construction. Work is already under way on plans for a new, larger machine, tentatively referred to as the Tandem Mirror Next Step (TMNS), which could become a serious rival to the tokamak design.

The programme based on inertial confinement techniques is also looking well. Recent experimental data indicate that solid state lasers made from vanadium-doped magnesium fluoride crystals have characteristics, high energy efficiency chief among them, which may overcome the difficulties experienced with the use of more conventional solid state lasers to ignite a deuterium-tritium pellet.

The tandem mirror is a device first proposed in 1976, when experimenters were experiencing considerable difficulty in preventing plasma from escaping its containing magnets along field lines which are open rather than closed (as they are in a tokamak). Its ancient ancestor is the machine called DCX, developed at the Oak Ridge National Laboratory in the 1950s.

Proposed simultaneously by Ken Fowler and Grant Morgan at the Livermore Laboratory, and Soviet scientists at Novosibirsk, the mirror acts by using two magnets to contain a plasma in an electrostatic potential well, the plasma being positively charged because electrons are able to escape faster than protons.

Small-scale experiments were carried out by research workers at the University of Tsukuba in Japan last year, demonstrating that, in principle, a tandem mirror designed to contain a plasma in this way does create the predicted potential well.

Subsequently, Livermore scientists have concluded a series of experiments on the tandem magnet experiment (TMX) in which they have been able to demonstrate that a solenoid with such plugs at each end can contain a heated plasma at a mean energy of 0.2 keV per atom, as compared with 13 keV within the end mirrors.

The attraction of a commercial fusion reactor based on this design would not only be the easier design tasks presented by a straight solenoid rather than a toroidal tokamak, but also that, once the end plugs have been produced to the tandem mirror design, the length of the solenoid between them can be adjusted at will to provide the power characteristics required.

The US Congress has already been sufficiently impressed to approve substantially increased funding for the MFTF now being built.

Its success or otherwise will determine whether the department should proceed to the next logical step, the TMNS. Livermore scientists feel that magnetic mirror designs could catch up with tokamak technology, the most likely design for a Fusion Energy Device (FED), and which the department hopes to build over five to ten years.

• Meanwhile, those working on the

inertial confinement techniques are hoping that the promise of vanadium-doped magnesium fluoride lasers may overcome doubts about the ultimate potential of solid state lasers as fusion drivers.

Most of the research so far has been done on glass lasers, initially with red light and more recently, following the development of techniques for doubling the wavelength, with green and blue light which has a greater ability to focus energy on a small deuterium-tritium pellet.

Preliminary evidence suggests that, in contrast with the conventional krypton fluoride laser, which only has an efficiency of between 5 and 7 per cent, a V:MgF<sub>2</sub> solid state laser would have an efficiency of between 5 and 10 per cent. With other advantages, this would help to reduce the cost of electricity from an estimated \$300 million to \$100 million per megajoule.

Livermore scientists are now carrying out further experiments to determine whether crystals with such characteristics can in fact be grown for use in lasers. If so, solid state lasers will remain a serious contender in the fusion stakes.

David Dickson

## Radioactive waste

# Brussels helps

The parallel research programmes of the European Economic Community (EEC) and Canada on the storage of radioactive waste are to be linked. A five-year agreement was signed in Brussels on 3 November between the European Atomic Energy Community (Euratom) and Atomic Energy of Canada Ltd. It follows on from the original Euratom/Canada agreement of 1959.

The new agreement relates particularly to the evaluation of the environmental impact of the storage of wastes in hard rocks, and to collecting data on the development of safe waste storage systems. There has already been considerable cooperation between scientists in these fields, so the agreement puts this on a more formal basis and opens the way for even closer cooperation.

Initially the agreement will lead to exchanges of technical information, organization of joint scientific meetings, and exchange visits of scientists between Canadian and European laboratories.

The agreement is the first in this field between the community and an outside country. It is likely to be a pointer to a trend towards more international cooperation, and the United States is already showing interest in closer cooperation with the EEC.

The community's own research programme was unveiled with a great fanfare in Luxembourg in May this year. The community's contribution, US\$130 million, is planned to extend over four years. Of the total, \$100 million will be contributed on a fifty-fifty basis to national research programmes, while \$30 million will be spent at the joint research

centre at Ispra.

Research on the disposal of high-level wastes is well advanced in France, West Germany and the United Kingdom. In each case, the objective is to embody high-level radioactive wastes in some solid form — France and the United Kingdom are chiefly interested in vitreous solids, while West German studies have also taken account of bitumen-like materials.

In several member states, investigations are also under way to identify disposal sites for solidified radioactive waste. France and the United Kingdom are exploring granite formations, West Germany salt formations while Belgium and Italy are concentrating on siliceous (clay) formations.

Jasper Becker

## Waste disposal

# UK goes French

British Nuclear Fuels Ltd (BNFL) whispered last week its intention to use the French AVM process for vitrifying highly active nuclear waste emerging from the Windscale reprocessing plant, thus bypassing the British "Harvest" vitrification research programme which has been under way at Harwell. There was no official announcement by BNFL: rather, the news emerged during a routine meeting of the Windscale local liaison committee, a group convened to keep the local community aware of developments at the plant. The leak was intentional, and confirmed rumours that BNFL had chosen AVM some time before.

A full commercial agreement between BNFL and Cogema, the French company which developed AVM, has not yet been reached, and if Cogema's price is too high the deal may still fail through. As presently envisaged, it would entail constructing an AVM (*atelier de vitrification à Marcoule*) plant at Windscale in the late 1980s, under licence from Cogema.

BNFL will not say at this stage why it has chosen AVM, though the reasons are not far to seek. Both the French and the British began work on vitrification in the late 1950s but work halted in Britain in 1966 when the principle had been demonstrated. (It was felt at the time that it would be possible to store liquid high active waste indefinitely in tanks.) Political pressure led to the setting up of the Harvest programme (Harwell vitrification engineering study) in 1973, but by then Cogema had established a seven-year technological lead.

While the Harvest team at Harwell is even now using only simulated nuclear waste, a plant called PIVER was built at Marcoule eleven years ago to handle the real stuff in commercial quantities. PIVER ran from 1969 to 1973, and produced 12 tonnes of vitrified waste containing 5 million curies of activity — roughly speaking the arisings of a 1 GW nuclear power plant working over the same period.

PIVER was a batch process, like





Product of Harvest

Harwell's Harvest; its successor AVM, incorporated in a plant at Marcoule which began operation two years ago, is continuous, allowing — it is claimed — a roughly twofold saving in capital equipment costs for the same waste throughput. The AVM plant is remotely controlled, and is constructed from units none larger than 500 kg for ease of handling and replacement. The French process is thus many years ahead of its British — or any — rival.

Nevertheless there is still a question mark over BNFL's haste to conclude an agreement with Cogema. The decision to abandon Harvest is as much a political as a commercial one. At present, about 1,000 m<sup>3</sup> of high active waste is stored in liquid form in tanks at Windscale, and BNFL still considers that it could remain in these tanks, or new ones, for some decades. Further tanks could be built for the oncoming nuclear power programme, but it is felt that public opposition to the programme — which will be expressed in the promised PWR enquiry — may be less if vitrification work is seen to be progressing apace. The argument, however, turns a

blind eye to local opposition to drilling tests, to find sites for future long-term disposal of the glass.

At Harwell, Dr Ron Flowers, who heads the chemical technology division that developed Harvest, says that he expects to close work on the project by next March, once experiments are completed and final publications prepared. Loss of the Harvest contract — which was paid for by BNFL, the Central Electricity Generating Board, and the Department of the Environment — will not be a serious blow to the division, he says.

Robert Walgate

### Soviet dissidents

## Another taken

Viktor Brailovskii, the Moscow Jewish mathematician who regularly hosts the Sunday seminars for *refusnik* scientists, was arrested last week, reportedly under Article 109/1 of the Criminal Code which deals with slander of the Soviet Union and the socialist system and the circulation of "publications known to be false".

News of the arrest, coming shortly after the opening of the Madrid review conference on implementation of the Helsinki Final Act, has caused consternation among his colleagues and friends abroad, who see it not only as a threat to Brailovskii himself, but also an adverse omen for Soviet intentions regarding "Basket 3" of the Final Act, which deals with human rights.

Brailovskii, who is a specialist in cybernetics and computer programming, first applied to emigrate to Israel in 1972. His application was refused, and he was then dismissed from his academic post. Since then, he has had no chance of obtaining any job in science.

It was to help such "*refusnik*" scientists keep up their academic interests that the Sunday seminars were founded in 1973 by Aleksandr Voronel'. When Voronel' and then his successor as seminar leader Mark Azbel' finally managed to emigrate, Brailovskii and his wife Irina (also a mathematician) became hosts to the seminar.

A recent Western visitor reports that in spite of a total lack of access to scientific facilities, including journals, the standard of discussion remains high, and there is considerable participation by young Jewish scientists who are attempting to carry out some kind of postgraduate study on their own.

A frequent visitor to the seminar, the traveller said, is Evgenii Chudnovskii of Khar'kov — a city where the refusal rate has always been particularly high — who is now trying to organize what he calls a "Jewish university" for young *refusniks*.

According to Mrs Brailovskaya, the seminars will continue in spite of her husband's arrest. The citation of Article 109/1 presumably refers to the *samizdat* journal *Jews in the USSR*, of which

Brailovskii was for a time editor. However, this journal ceased publication in summer 1979, and the long delay before an accusation on this charge seems unreasonable.

### German science

## New man arrives

Germany has a new Minister for Science and Technology: 43-year-old Andreas von Bülow, who since 1976 has been Parliamentary Undersecretary of State for Defence. The Bundesministerium für Forschung und Technologie BMFT is Dr von Bülow's first ministerial appointment — as it was for his predecessor, Dr Volker Hauff. Dr Hauff now moves on to the Ministry of Transport, which is considered to be a more senior political appointment.

Dr von Bülow has had no time yet to form his policies for the BMFT, but he is expected to lean more to the right of his party, the SPD, than Dr Hauff, who attempted to use the ministry as an



instrument of economic policy (through its involvement in technology). But Dr Hauff — after seven years in some capacity at the BMFT — was said to be becoming impatient at the inertia of the research community, and particularly the big science institutions like the Karlsruhe nuclear research centre and others which had grouped themselves into a powerful lobby, the Arbeitsgemeinschaft der Grossforschungseinrichtungen (AGF). It remains to be seen what Dr von Bülow will do with that. His ministry plays a coordinating role in German science, akin to that of the Delegation Générale à Recherche Scientifique et Technique in France; but it controls a much larger budget — around DM 6 billion (£1.25 billion). This is the bulk of the federal finance applied to R&D Germany, another DM 3 billion or so being under the direct control of other ministries. (A further DM 6 billion is spent by the state governments, mostly to support universities, and DM 16 billion by industry.) The BMFT, along with the state governments, supports the institutions of the AGF, the Max Planck Gesellschaft (which runs the Max Planck institutes), the Deutsches

### The differences

High active waste emerges as a liquid from the reprocessing of spent fuel: it is a solution in concentrated nitric acid of the nitrates of actinides and fission products. The object of vitrification is to immobilize the radioactive elements. In the Harvest process, which is only at the pilot stage, a simulated waste is mixed with the components of a borosilicate glass, poured into a tube, evaporated and glassified in one step in a furnace. The tube becomes the primary container for the glass. The process is a batch process. In the AVM technique, a high active liquid stream is evaporated and calcined (converted to oxides) in a rotary calciner. Each hour, the calciner accepts 40 litres of liquid waste and converts it to brown granules, which leave the furnace continuously. The granules are mixed with borosilicates and melted in a stainless steel container. Every eight hours, the container pours out 140 kg of glassified waste into storage drums. The drums are moved out, lids are welded on, and the drums moved to storage caves — all automatically.



Forschungs-gemeinschaft (which funds research projects in the universities), the Fraunhofer Gesellschaft (the equivalent of Max Planck, but for applied science), and other science promotion bodies. The ministry also promotes research and innovation in industry through a number of mechanisms.

Robert Walgate

## Indian environment

### Shandi inverted

#### Bangalore

Mrs Gandhi's new government seems to have taken the environment to heart, to judge from the spate of decisions since the election at the beginning of the year and the appearance of the environment in the newly published Sixth Development Plan.

In recent years, environmental abuse in India has increased alarmingly. Urbanization, industrialization and river pollution have all conspired to make a mockery of the United Nation's slogan of "development without destruction" in a country renowned for its religious regard for the variety and greatness of nature. The repercussions of this indiscriminate assault on the ecological system are telling:



Barren hill

landslides and flash floods in the Himalayan foothills have caused heavy loss of human lives and property, top-soil erosion and growing aridity in the Ganges plains have had severe consequences for agriculture.

Successive Indian governments during the past 30 years have shown little awareness of the cardinal importance of environmental planning in developmental activities. It was only after Mrs Gandhi's return to power in early 1980 that the environment assumed significance.

Since then, work on the controversial Silent Valley hydroelectric project in the tropical rain forests of southern India has been suspended and the rate of deforestation in the Himalayan foothills has been

greatly reduced.

It is a measure of the growing public ecological awareness that the last session of the Indian parliament witnessed perhaps one of the liveliest debates on the environment. Intervening in the debate, Mrs Gandhi made it clear that the nation must not repeat its earlier mistake of allowing industrial projects, despite their economic importance, to damage the delicate environmental web.

During the debate, a ruling party member, Dr Karan Singh, expressed shock over the "ruthless denudation of Himalayan vegetation by corrupt politicians, corrupt officials and corrupt contractors". He further lamented that even the Ganges had now been contaminated.

Another member, Mr Digvijaya Narain Singh, said that, as a result of top-soil erosion, 90 million hectares — equal to 28 per cent of the total land area — had now become practically barren. He urged that there should be a separate department concerned with land use, forestry, wild life, pollution control, marine ecosystems and the promotion of environmental protection.

This suggestion seems likely to be incorporated into the government's long-term environmental strategy, which will be based on the recommendations of a 14-member committee set up to suggest legislative measures and administrative machinery for environmental protection. The committee, headed by Mr Narayan Dutt Tiwari, deputy chairman of the Planning Commission, has come out strongly in favour of immediate coordinated action at both central and state levels to give environmental protection a crucial place in the country's programmes and policies.

The Indian government is also contemplating introducing a bill on the prevention of air pollution in which would be based on proposals put forward by an expert committee appointed in 1978 to study air and water pollution in the urban areas of India. Air pollution has become a major health hazard in cities such as Bombay, where the content of carbon dioxide in the atmosphere has been increasing by 4.2 per cent a year due to the 65 tonnes of dust ejected into the air each day by industry and vehicles.

B. Radhakrishna Rao

## Nuclear fallout

### Weapons are worst

States with substantial nuclear industries should do everything they can to avoid strategic nuclear attacks. That is one of the inevitably ironical conclusions of a study of catastrophic nuclear radiation releases by Steve Fetter and Kosta Tsipis of the Program in Science and Technology for International Security at Massachusetts Institute of Technology.

The chief objective of the study has been to compare the long-term consequences of nuclear weapons exploded in the air and on the ground, catastrophic releases of radioactivity in reactor accidents and the explosion of nuclear weapons on or near nuclear reactors or reprocessing plants. Although it is recognized that the immediate effects of weapons explosions as distinct from reactor accidents will consist largely of the death of people and the destruction of property, the calculations are aimed at estimating the area of surrounding land that will be unfit for human habitation after an explosion or some other catastrophe.

For the purposes of the calculation, the authors assume that half the energy released in a one-megaton thermonuclear explosion is provided by fusion reactions and the remainder by the fission induced in a surrounding blanket of uranium-238. For weapons burst in the atmosphere, radioactivity from the fission of uranium-238 will be the sole source of long-term contamination, and much of its debris will be distributed by stratospheric processes.

The areas rendered uninhabitable after a nuclear explosion are sensitively dependent on the criteria used for deciding what doses of radioactivity are acceptable. For a ground burst weapon whose debris is spread in the lower atmosphere by a 15-mile per hour wind, the authors calculate that 5,700 square miles of land would be uninhabitable for a year if doses greater than 2 rem per year were considered unacceptable, but that fewer than 50 square miles would be uninhabitable a year after the explosion if 100 rem per year were taken as the cut-off dose.

Inevitably the consequences of the explosion of a nuclear weapon on or near a reactor are more startling. Using the somewhat stringent criterion of a limiting dose of 2 rem per year, the authors conclude that 50,000 square miles of land would be uninhabitable for a year. The destruction of a waste storage facility would have still more horrendous consequences, putting 64,000 square miles out of action for a year. By comparison, the report concludes, the consequences of a reactor melt-down and a subsequent release of radioactivity would be comparatively small, sterilizing only 900 square miles for a period of one year.

The obvious but impractical import of these calculations, Fetter and Tsipis say, is that countries seeking to avoid devastating damage from distributed radioactivity in a nuclear war should either dispense with a nuclear industry or build reactors and reprocessing plants underground. They also point out that because the permanent damage done by a single nuclear weapon detonated on the ground is so much greater than that in the "worst conceivable nuclear reactor accident", it is hard to understand the greater anxiety of the general public about the risks of civil nuclear accidents than with the consequences of nuclear war.



## CORRESPONDENCE

## Museum of errors

SIR — Two years ago (*Nature* 275, 683; 1978), I questioned the wisdom of what is happening at the Natural History Museum in South Kensington. If a national museum is concerned with aspects of social engineering, by promoting concepts that happen to be current in the present climate of opinion, are there not sinister implications? I was especially alarmed by the museum's new exhibition scheme, and asked that sufficient pressure should be brought to bear to "curb the activities of the Public Services Department and to ensure the survival of the museum's reputation for scholarship in its public galleries".

Since then, time has passed. It is no longer a question of raising the alarm but simply of reporting what has already happened.

Two areas of the museum's work have already succumbed: dinosaurs in 1979 and fossil man in 1980. Both the new exhibits are simply vehicles for the promotion of a system of working out relationships known as cladistics. The accompanying booklets *Dinosaurs and their living relatives* (1979) and *Man's place in evolution* (1980) explain with startling clarity the essence of cladistics. In both books the fundamental assumptions are spelt out unequivocally. "First we assume that new species arise when one species splits into two. This assumption allows us to test the relationship we suggest, because it means that every species must have a closest relative. Second we assume that none of the species we are considering is the ancestor of any of the others." It is axiomatic, therefore, that no species in the fossil record can be considered ancestral to any other nor can one species evolve directly into another.

With regard to both dinosaurs and fossil man, it is evident that the application of cladistics is quite inappropriate. The well attested sequence of human fossils representing samples of succeeding populations has, until the Natural History Museum's latest exercise, been taken as a classic example of the gradual evolution of a single gene pool. Certainly there is not any serious doubt about *Homo erectus* being directly ancestral to *Homo sapiens*.

Yet the concept of one species being directly ancestral to another is contrary to the rules of cladistics. So we read in the section on *Homo erectus* (under the heading "Not our direct ancestors"), that "The *Homo erectus* people were not quite like us. . . the *Homo erectus* skull has several characteristics that the modern skull does not share. Because of these special characteristics, we think that the *Homo erectus* people were not our direct ancestors".

But then on the opposite page is a photograph of the Petralona skull, from Greece, which the author considers an example of *Homo sapiens* or *Homo erectus* because of its mixture of features. This particular skull makes nonsense of the entire methodology being promoted in the books and exhibition. According to the stated assumptions of cladistics none of the fossil species can be ancestral by definition. This presents the public for the first time with the notion that there are no actual fossils directly antecedent to man. What the creationists have insisted on

for years is now being openly advertised by the Natural History Museum.

The scientists on the museum staff, be they experts on dinosaurs or on fossil man, have had their scientific judgement over-ridden by the Department of Public Services. What exactly is the cladistic framework to which the Public Services Department is so fervently dedicated? Why is there such a fanatical insistence that data should be presented within such a framework?

And why should there be a deliberate policy that involves the removal from the public gaze of important and scholarly exhibits in the museum such as the Insect Gallery and the Fossil Mammal Gallery? Is it because they provide too dramatic a contrast with the propaganda of the new-style exhibits?

The questions that should arise in everyone's mind are: what is this all about, what actually is going on and what is behind it all? The answers can be found by reading the literature of cladistics. The tenor of this is seen in its abuse of E. Mayr and G.G. Simpson, and indeed of Charles Darwin himself, because of their firm adherence to the concept of gradualism and to the idea that the processes that can be observed at the present day, when extrapolated into the past, are sufficient to explain changes observed in the fossil record. The synthesis of population genetics and palaeontology presented by Simpson in his two seminal works *Tempo and mode in evolution* (1944) and *The major features of evolution* (1953) is anathema to cladists.

The next question is why should the notion of gradualism arouse passions of such intensity? The answer to this is to be found in the political arena. There are basically two contrasting views with regard to human society and the process of change through time: one is the gradualist, reformist and the other is the revolutionary approach. The key tenet of dialectical materialism, the world outlook of the Marxist-Leninist party according to J.V. Stalin, is in the recognition of "a development in which the qualitative changes occur not gradually but rapidly and abruptly, taking the form of a leap from one state to another" (Engels). This is the recipe for revolution. If this is the observed rule in the history of life, when translated into human history and political action it would serve as the scientific justification for accentuating the inherent contradictions in society, so that the situation can be hurried towards its appropriate "nodal point" and a qualitative leap supervenes.

With regard to evolution and the fossil record, neither Engels nor Lenin, both of whom discussed the subject at length — to their great credit — insisted upon a pattern of such qualitative leaps, they were merely content to see in evolution and the fossil record evidence of change, albeit gradual.

This has always been a matter of some disquiet for Marxist theorists. If it could be established that the pattern of evolution was a saltatory one after all, then at long last the Marxists would indeed be able to claim that the theoretical basis of their approach was supported by scientific evidence. Just as there are "scientific" creationists seeking to falsify the concept of gradual change through time in favour of catastrophism, so too there are the Marxists who for different motives are equally

concerned to discredit gradualism.

What is going on at the Natural History Museum needs to be seen in this overall context. If the cladistic approach becomes established as the received wisdom, then a fundamentally Marxist view of the history of life will have been incorporated into a key element of the educational system of this country. Marxism will be able to call upon the scientific laws of history in its support, with a confidence that it has previously enjoyed.

This is the course of action to which the authorities of the Natural History Museum seem to have committed themselves either unwittingly or willingly.

L.B. HALSTEAD

Department of Zoology and Geology,  
University of Reading, UK.

## Refrigerator brew

SIR — One of the problems associated with Legionnaires' disease lies in the tracking down of the source of infection. Air conditioning systems seem to be prime suspects. So far as I am aware, nobody has thought of looking behind refrigerators. Having had occasion to do this recently, I was taken aback to discover that a self-defrosting refrigerator may provide the ideal breeding ground for a wide range of microorganisms.

At the back of a self-defrosting refrigerator there is a reservoir to collect the water as it is discharged. This water remains stagnant, gradually evaporating until it is replenished by the next automatic defrosting. With some designs the cooling coil passes through this reservoir to hasten evaporation. The result is a warm broth ideally suited to the proliferation of microorganisms. After a year or two stood around in a hospital environment such reservoirs might well harbour some very interesting cultures indeed. Even the ordinary household must pick up some pretty virulent infectious agents from time to time.

I have now taken the precaution of adding a dash of disinfectant to the brew. Hospital authorities might care to adopt the same simple measure.

ROBERT T. GREEN

15 Clifton Gardens,  
London NW11, UK

## Frequency tripling

SIR — Your correspondent's comments on the US inertial-confinement fusion (ICF) programme contains a minor inaccuracy (*Nature* 16 October p.573). University of Rochester scientists have, in fact, frequency-tripled the output of their glass laser thus converting the 1.054  $\mu\text{m}$  light to 0.3513  $\mu\text{m}$  radiation at high efficiency. Experiments using frequency-doubled light, at 0.53  $\mu\text{m}$  have been done or are underway at many laboratories, notably the Science Research Council Rutherford Laboratory, the Centre d'Etudes de Limeil (France), GRECO-Interaction Laser Matiere, Ecole Polytechnique (Palaiseau, France), KMS Fusion Inc., and the Lawrence Livermore National Laboratory. The Ecole Polytechnique group recently has reported on experiments using 0.26  $\mu\text{m}$  radiation, the 4th harmonic of 1.06  $\mu\text{m}$  light.

La Jolla Institute,  
La Jolla, California

PETER HAMMERLING

## NEWS AND VIEWS

## What prospects for an X-ray laser?

WHAT are the chances that one day there will be machines capable of producing short but intense pulses of virtually monochromatic X rays, for all the world like lasers that function at the short-wavelength end of the spectrum? And if such machines can be built, what purposes will they serve? The notion that a machine with such a specification might be the basis of yet another military weapon will no doubt quickly capture the imagination of newspaper-headline writers. In reality, of course, the Earth's atmosphere is as opaque, more or less gram for gram, as are other materials. For those who brood about "death rays" for the benefit of science fiction literature, what matters (or should matter) is not the wavelength of the radiation but the amount of energy that can be delivered by a radiation beam and the efficiency with which it is absorbed by the target. Reflection will also show that the present attempts to develop X-ray lasers, centred as they are on machines that differ very little from high-energy particle accelerators, suggest that X-ray lasers — if they can be built — will hardly be the kinds of portable devices of which generals and their staffs are fond. In other roles, however, and especially in strictly scientific applications, devices of this kind, however cumbersome, would be of great benefit. So what are the chances that they will eventually be constructed?

This question has obviously perplexed those within the European Science Foundation who have been concerned with the project to plan a European facility for synchrotron radiation. At the general assembly of the foundation last week in Strasbourg, those responsible for this project, which is essentially a scheme for building an electron storage ring operating at 3 GeV and designed to produce copious amounts of synchrotron radiation, let it be known that they are undeterred by the chance that an X-ray laser may eventually make their own project unnecessary. In this phlegmatic view, the planning group is surely on safe ground. The chances that it will be possible to construct machines operating as lasers in the X-ray range within the lifetime of the proposed European synchrotron machine are small. Further ahead, however, there is a reasonable chance that something may be possible.

The starting point for this speculation is the wave of excitement generated in the past few years by the concept of the "free-electron laser", an innovation largely due to Dr J. Madey at Stanford University in 1976 (Elias, L.R. *et al. Phys. Rev. Lett.* **36**, 717; 1976). The working principle of these devices is a curious amalgam of old-fashioned 1940s technology and the more recent sophistication of the particle-beam technologists (see J.N. Elgin *Nature News and Views*, 1 May 1980, and references therein). Suppose a beam of electrons travelling along a tube is subjected to a sequence of transverse magnetic fields, alternately in one direction and the opposite. At each step, the electrons (accelerated as they will be along the third cartesian axis) will radiate electromagnetic energy. As Maxwell's equations have it, a beam of electrons processed in this way should be a source of a radiation beam directed along the axis of the system. Moreover, the wavelength of the radiation should be determined to a first approximation only by the energy of the electrons and the geometrical periodicity of the magnetic field. The more frequent the alternation of the direction of the magnetic field along the axis of the beam, the shorter the wavelength of the radiation, which is (or should be) related inversely to the square of the energy of the electrons. The planning of the proposed European synchrotron radiation facility is based almost entirely on the notion that a circulating beam of stored electrons should be subjected to a sequence of such corrugated magnetic fields, called "wigglers" in the trade.

The novel development at Stanford University was the recognition that a beam of electrons travelling through a corrugated magnetic field should also behave as if it were the working material of a laser. In other words, if an electron beam traversing a wiggling magnetic field is also exposed to radiation of the frequency characteristic of the geometry and the electron energy, radiation at that same frequency will be stimulated and, if there is a pair of mirrors somewhere, energy from the mechanical motion of the electrons will be converted into a beam of radiation of wavelength determined in advance only by geometry and electronic energy (with the actual strength of the magnetic field as a second approximation correction). So, would-be designers of X-ray lasers will say, why not go the whole hog, pushing the electron energy as high as possible but reducing the geometrical wavelength of the alternation of the wiggling magnetic fields until the predicted wavelength is in the X-ray region?

There seems little doubt that lasers working on this principle will be designed and built in the years ahead. For the time being, however, the wavelengths at which free-electron lasers are being designed or played with are modestly long. The first experiments at Stanford University demonstrated laser action at 10.6  $\mu\text{m}$ , well into the infrared. Although there are more conventional types of lasers which function in this region of the spectrum, the prospect that the wavelength of radiation from a free-electron laser may be adjusted simply by changing the energy of the electron beam suggests that devices built on such a principle should be more 'tuneable' than more conventional infrared lasers. The immediate prize in the sights of those now developing this new technology is, however, that of being able to construct lasers that operate in the ultraviolet. The potential benefits of such devices are self-evident. For the first time, it would, for example, be possible to make precise studies of several photochemical processes at present inaccessible to observation. The snags are unfortunately also clear. Free-electron lasers are likely to be less efficient at increasing energies (although much depends on the geometry) while technical problems of arranging for a geometrically rapid corrugation of a magnetic field entail the complications of handling superconducting magnets. This part of the game, nevertheless, may be well worth the candle because of the potential usefulness of ultraviolet lasers in the separation of uranium isotopes or the stimulation of thermonuclear fusion.

The potential of free-electron lasers seems to have been clearly recognized in the United States, where much technical development is under way. The best known plan is that of the Brookhaven National Laboratory on Long Island, where a 700-MeV storage ring will be commissioned next year with the intention of producing laser radiation in the optical and near-ultraviolet in 1982. Most other projects, in which industrial companies such as TRW Incorporated and Bell Telephone Laboratories have taken an interest, appear to be aimed at exploring still inaccessible parts of the infrared spectrum. Given the present limitations of even superconducting magnet design, it is inevitable that people should be forced to use beams of electrons with energies approaching 1 or more GeV. But these, of course, are early days. With any luck, free-electron lasers should be operating in the ultraviolet within the next few years. There after, it should be relatively easy to decide how the technology might be pushed still further. By the end of the decade, soft X-ray laser sources, however inefficient, should be in operation. The hard X-ray source that will make possible direct measurement of atomic and molecular energy levels will be further ahead, but not out of reach.



# Gene regulation: new, old and remote controls

from Adrian Minty and Peter Newmark

A few months ago in these columns, due warning was given that the 5' ends of every gene under the sun were "in for a beating with mutagens and nucleases in the quest for the eukaryotic promoter" (*Nature* 285, 356; 1980). Two European meetings\* with many presentations in common have since demonstrated the validity of that prediction, whilst illustrating that introns and regions far removed from the 5' ends of genes (see Fig. 1) are also coming under close scrutiny as possible sites of gene regulation.

## The Hogness/Goldberg/TATA box

It has been recognized for some time that most of the eukaryotic genes which are transcribed by RNA polymerase II have a very similar, short nucleotide sequence about 30 nucleotides upstream from the place where transcription begins. The sequence is invariably AT rich and is most commonly known as the TATA (tar-tar) box but at other times as the Hogness box, since it was first recognized in the Stanford laboratory of D. Hogness. Purists, however, note that the only formal citation for the discovery at present is to the 1979 Stanford University thesis of M. Goldberg and hence refer to the Goldberg-Hogness box.

Is the TATA box essential for the initiation of transcription? An answer of sorts is emerging from a comparison of the *in vitro* and *in vivo* transcription of intact, cloned genes with cloned genes that have mutated, deleted and/or replaced TATA boxes.

For *in vitro* transcription there is, at first sight, a good deal of evidence that the TATA box is essential. Most strikingly, mutation of the chicken conalbumin gene box from TATA to TAGA reduces

transcription by more than 95 per cent (P. Chambon *s*, Strasbourg). In cruder tests, the elimination of TATA box regions of the chicken ovalbumin gene (M. J. Tsai *a*, Houston), the  $\beta$  globin gene (R. Flavell *a*, National Institute for Medical Research, London) or the adenovirus late region (P. Sharp *s*, MIT) reduced or halted the initiation of transcription.

Unfortunately, matters are more complicated than that. For example, several viral genes do not have TATA boxes. Furthermore, both R. Kamen (*s*, ICRF), working with the polyoma virus early region, and P. Chambon, working with the SV40 early region, reported that deletion of the TATA box regions did not prevent transcription but did shift the position(s) at which it started. From TATA box deletions and a series of other deletions, Chambon is of the view that the efficiency of transcription is controlled both by the TATA box and by regions lying downstream from it, close to the site of initiation of transcription, while the TATA box alone is responsible for fixing the site of initiation. Not everyone's data seem to fit even that fairly unspecific view and that is the way matters are likely to stay until a good deal of progress has been made in defining the ideal conditions for *in vitro* transcription.

Meanwhile, a complementary approach is to look at *in vivo* transcription. Here there is general agreement that deletion of the TATA box affects the site far more than the efficiency of initiation. This is so for the SV40 early region in monkey cells (Chambon *s*), sea urchin H2A histone genes in *Xenopus* oocytes (M. Birnstein *a*, Zurich), yeast iso1-cytochrome *c* genes in yeast (G. Faye *s*, Seattle and Orsay) and mouse  $\beta$  globin genes in monkey cells (D. Hamer *s*, NIH).

## Upstream controlling region

Much the most interesting and broadly consistent result to come, in recent months,

from a spectrum of *in vivo* studies, is that there are regions further upstream than the TATA box which can modulate RNA polymerase II-dependent transcription. What is more, whereas deletion of these upstream controlling regions can drastically reduce *in vivo* transcription, it can be without effect on *in vitro* systems.

For example, P. Dierks (Institute of Molecular Biology, Zurich) reported that deletion of the CAAT box, found 80 nucleotides upstream from the cap site of a number of globin genes, markedly reduced their transcription in mouse L-cells, although he agreed with Flavell that this deletion was ineffective *in vitro*. In the case of the SV40 early region, Chambon reported that the crucial upstream region lay within a GC-rich region of a 72-base pair repeated sequence that, at its closest, is some 100 base pairs upstream from the TATA box.

Another interesting example is the histone H2A gene (C. Hentschels, Zurich). Deletion of a segment of DNA positioned from 184 to about 520 base pairs upstream of the initiation site reduced transcription by 15–20-fold. Mysteriously, the inversion of this region, which is characterized by its AT-richness and some largish palindromes, led to a fivefold increase in transcription.

As a final example of remote control of gene activity, there are the wild-type strains of *Drosophila* which do not show the normal 'puffing' of band 3C11-12 on the X chromosome in response to ecdysone. D. Hogness (*s*, Stanford) reported that the relevant gene in each of four such strains had a 50–150-base pair deletion approximately 200 base pairs upstream from the 5' end.

How does the remote control of transcription work? There are at least three possibilities. The first is that the upstream region binds a protein which affects transcription. The second is that it binds

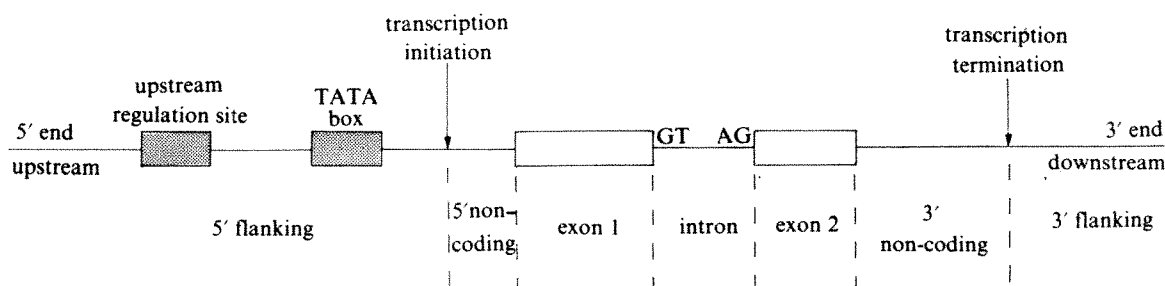


Fig. 1 Consensus polymerase II gene structure. Not to scale.

\*Fourth Arolla Workshop, Arolla, Switzerland, 18–22 August 1980 and INSERM conference on 'Structure and Expression of Eukaryotic Genomes', Domaine de Seillac, 21–25 September 1980. Speakers at the former are identified by an *a* before their affiliation and those at the latter by an *s*.

RNA polymerase II, secondary structure being invoked to explain how the enzyme also binds to sites near to the point of initiation. And the third, and most fashionable, explanation is that the upstream sites phase (determine the spacing of) the nucleosomes in relation to the DNA sequence, the phasing determining whether or not a downstream gene is transcribed.

That chromatin structure plays a part is suggested by the hypersensitivity to DNase I of the 5' ends of the heat-shock genes (S. Elgin *a*, Harvard; see also Wu, C. *Nature* **285**, 854; 1980) and histone genes (A. Worcel *a*, Princeton) of *Drosophila*. Results that fit that trend are also beginning to emerge from a study of the DNase I hypersensitivity of SV40 in infective or integrated form (C. Cremisi *s*, Fred Hutchinson Cancer Center, Seattle). Furthermore, electron microscopy shows there to be a break in the regular dispersal of nucleosomes around the SV40 minichromosome close to the presumed promoter site (Y. Aloni *a*, Weizmann Institute and *Nature* **285**, 263; 1980; M. Yaniv *s*, Pasteur Institute and *Cell* **20**, 65; 1980). Polyoma virus, which has a similar nucleosome-free region, does not normally grow on undifferentiated teratocarcinoma cells. Yaniv, however, described a mutant which could grow on those cells and which had an altered DNA sequence in the presumed promoter region and a displaced nucleosome-free region, reinforcing the view that there is a relationship between the sequence of DNA, its organization into nucleosomes and the control of transcription.

#### Introns

As more introns are sequenced, new features of interest emerge. These include the recognition of repetitive sequences within the introns of the ovalbumin-related 'X' gene (J.-P. Mandel *s*, Strasbourg) and the vitellogenin gene (G. Ryffel *a*, University of Bern).

It is customary to believe that introns are spliced out whole, from the GT at the 5' end to the AG at the 3' end (the junction or boundary sequences). But E. Avvedimento (*s*, NIH; see *Cell* **21**, 689; 1980) has identified three possible internal splice sites in an intron of the chick  $\alpha$ 2-collagen (type 1) gene. He proposed that a first step in the removal of this intron could be the splicing of the 3' end to any one of the three internal sites and backed up that proposal with evidence of the presence of the predicted RNA species in the nucleus of chick fibroblasts. A two-step splicing out of one of the introns of a mouse  $\alpha$ -amylase gene is similarly indicated (O. Hagenbuehle and U. Schibler *a* and *s*, ISREC, Lausanne).

A more interesting feature of the  $\alpha$ -amylase system is that it may provide the first example in eukaryotes higher than viruses of the production of mRNAs with alternative 5' ends from the same DNA sequence. That at least is the explanation favoured by the Lausanne group for the

fact that the major species of  $\alpha$ -amylase mRNA in the mouse liver is identical to that in the salivary gland except that its 5' non-coding sequence is extended by about 100 nucleotides. Analysis of genomic clones from the two tissues supports the view that the alternative mRNAs are derived by tissue-specific transcription and splicing of an identical DNA sequence. Why and how this happens is uncertain.

It has been postulated that splicing is initiated by the base-pairing of one of the small nuclear (Sn) RNAs, called U1, to the intron-exon boundary sequences in gene transcripts. M. Jacob (*a*, Strasbourg) presented a list of 60 intron-exon boundary sequences in eukaryotic pre-mRNAs and concluded that, in the majority of cases, the homology between these and U1 was probably not, in itself, sufficient to ensure a stable hybrid. Approximately 40 per cent of SnRNAs in the cell are associated with heterogeneous nuclear RNA at a ratio of 1 or 2 molecules of SnRNA per 2,500 nucleotides, indicating that they are not structural components of heterogeneous nuclear ribonucleoproteins (Jacob). T. Pederson (*a*, Worcester Foundation) reported from cross-linking studies *in vivo*, that U1 is actually bound to heterogeneous nuclear RNA in the cell. This appears not to be the case for another 'processing RNA' candidate, the adenovirus VA RNA, which is not found in adenovirus nuclear ribonucleoproteins (Jacob *a*; J.M. Blanchard, Montpellier).

A different mediator of splicing was proposed by P. Slonimski (*a,s*, Gif) for the transcript of the yeast mitochondrial gene for cytochrome *b*. He proposes that certain introns are spliced out with the help of proteins ('maturases') encoded in the introns themselves.

Several facts favour that interpretation. They include the recent discovery that the second intron of the cytochrome *b* gene contains an open reading frame of considerable length while mutants containing stop codons within that intron accumulate unspliced transcripts of the gene, a defect that can be corrected by *in vivo* complementation. Furthermore,

those mutants contain proteins of the right size to be the 'maturase' truncated in accordance with the position of the stop codon. Neat though this system is, particularly in terms of autoregulation, there is very little evidence for its generality.

#### Post-transcriptional regulation

That gene expression can be regulated after, as well as at, transcription was made clear by several contributors. M. Rosbash (*a*, Rosenstiel Center, Waltham) described a temperature-sensitive mutant of yeast (RNA 2) in which the synthesis of ribosomal protein is inhibited despite normal transcription of the ribosomal protein gene. Since the unspliced transcript accumulates in the nucleus, it seems probable that the primary defect lies in the processing of the transcript to mRNA. A similar situation exists for globin mRNA in erythroblasts transformed by avian erythroblastosis virus (A. Therwath *a*, IRBM). J. Nevins (*a*, Rockefeller, New York) showed evidence that a part of the adenovirus genome expressed late in infection is also efficiently transcribed early in infection but that few cytoplasmic mRNA molecules are formed from the transcripts; again this reflects a defect in processing since polyadenylated precursor molecules accumulate in the nucleus. However, the effects of inhibitors of protein synthesis on adenovirus expression led L. Phillipson (*a*, University of Uppsala) to propose that a viral gene product encoded in the early region controls, either directly or indirectly, translation of early adenovirus mRNA *in vivo*.

Finally, Hereford (*a*, Rosenstiel Center) reported that duplicating the yeast histone genes by genetic manipulation resulted in a doubling of transcription whilst the overall level of histone mRNA remained constant due to a halving of the mRNA half-life. Further elucidation, at a molecular level, of the control of eukaryotic mRNA production remains a major task for the 1980s. □

*Adrian Minty is a research fellow at the Pasteur Institute. Peter Newmark is Deputy Editor of Nature.*

## Deep drilling in African lakes

*from N.J. Shackleton*

THE climatic environmental history of Africa is a major unknown on a time scale from thousands to millions of years. So far as the Pleistocene is concerned, we are building up a fairly complete picture of the characteristics of climatic change, both on the northern continents and over the oceans. Moreover, we have sufficient information to relate reliably the time sequences from the oceans with those of

glaciated areas. To a first approximation, climate changed more or less synchronously in North America, Europe and over much of the sea surface; however, the picture of climatic change in Africa has been surprisingly different.

In the past, the dry areas of Africa have experienced episodes of much greater wetness, which gave rise to increased lake areas, bigger rivers and more extensive



vegetation. At first it was assumed that these 'pluvial episodes' occurred at times of glaciation in the north. However, the most recent 'pluvial' is reliably dated over large areas of Africa to about between 12,000 and 5,000 years ago. Unfortunately, our records from Africa are too young to allow investigation of the previous occurrence of similar pluvial episodes. Thus we cannot usefully integrate the history of tropical rainfall with older records of other climatic variables. Indeed, we have no idea of the frequency of pluvials during the Pleistocene.

Between 21 and 27 August, an international working group, convened by Dr Dan Livingstone (Duke University, North Carolina) and Dr Neil Opdyke (Lamont Doherty Geological Observatory), met at the offices of the National Science Foundation (NSF) in Washington to plan a major drilling project to tackle this and related problems. Funds for the meeting came from the Anthropology Division of the NSF, but the disciplines represented were numerous, including palynology, magnetostratigraphy, organic and inorganic geochemistry, and the study of diatoms, stable isotopes and evolutionary biology as well as African prehistory. As well as conventional dry-land drilling expertise, we had a representative of the

Deep-Sea Drilling Project whose presence was appreciated partly because of the potential value of their drilling experience (especially with the new Hydraulic Piston Corer) and partly because of their unique experience in managing a major sediment-sampling programme for the benefit of a very large scientific community.

The NSF has already funded a seismic survey which will be conducted during the next year and which will hopefully cover three lakes. A great deal of the meeting was devoted to a discussion of the relative scientific and logistical merits of over a dozen tropical lakes in Africa (we resisted the temptation to spend much time on lakes which seem logistically impossible at present). The lake most suitable for a first sampling is Lake Bosumtwi in Ghana. This occupies a crater that is thought to have been formed by meteoric impact about a million years ago. Preliminary study of short cores covering the past 30,000 years or so shows that it preserves a good vegetational history and, so far as the million years recorded is concerned, is the most attractive of the lakes we discussed. Drilling of this lake should recover very valuable material for studying the early diagenesis of organic-rich sediments. The hypothetical origin of the Ivory Coast tectite-strewn field will be tested at source.

Most important, we will have a datable and continuous record of the climate of the past million years in the tropics where rain, rather than temperature, is the most important climatic variable. The extent to which this record can be explained in terms of current hypotheses will be an important test of our present understanding of the causes of climatic change.

With regard to the potential for a record spanning many million years, Lakes Malawi, Tanganyika and Turkana seem to offer the greatest number of advantages and should be covered in the seismic survey effort.

It was clear to the meeting delegates that the environmental history of any of the East African lakes must, over the long term, be intimately connected with its tectonic evolution, and conversely, that any deep drilling in one of these will arouse considerable interest from a wider section of the geological community. The consensus of the meeting was that a project to drill in the major African lakes, although expensive, will certainly be worthwhile in terms of the interest the results will hold for many different disciplines. □

*N.J. Shackleton is at the Sub-department of Quaternary Research, University of Cambridge, UK.*

## Herpes simplex virus in latent infection

*from Howard Marsden*

FOLLOWING initial infection of humans, herpes simplex virus (HSV) appears to be maintained in a latent state either for the lifetime of the individual<sup>1</sup> or in some individuals is periodically reactivated to produce overt lesions. Important questions arise, such as: in what tissue(s) is the virus latent, and what is the molecular basis of latency?

Goodpasture's suggestion<sup>2</sup> that HSV is latent in neuronal tissue has been substantiated in the mouse<sup>3</sup> where, after experimental infection in the footpad, two phases could be distinguished. First is an acute phase of one or two weeks during which virus can be recovered from cell-free homogenates of lumbrosacral ganglia. This is followed by a latent phase during which infectious virus is no longer detectable but in some animals virus can be recovered by co-cultivating explanted ganglia with sensitive cell monolayers on which the virus can form plaques. In this way, HSV-1 could be recovered not only from the peripheral but also, less frequently, from the central nervous system, though not from any non-neural tissue<sup>4</sup>. This observation suggested that in

the mouse, HSV latency is restricted to tissues of neural origin. However, Scriba subsequently demonstrated<sup>5</sup> that HSV-2 was recovered preferentially, and HSV-1 exclusively, from the footpad (the site of primary inoculation) of latently infected guinea pigs. More recently, Hill, Harbor and Blythe similarly recovered HSV-1 from the skin of latently infected mice<sup>6</sup>, although earlier attempts by other investigators had been unsuccessful. Are these really conflicting observations or do they reflect differences in the efficiency with which virus can be detected?

Latency involves three separate but related processes — not only establishment and maintenance but also reactivation. The virus assay method by nucleic acid hybridization used by Cabrera *et al.* (*Nature* this issue, p.288) does not necessitate formation of infectious virus particles and thus allows discrimination between the establishment and maintenance steps and the reactivation step. During the acute stage following corneal inoculation of HSV, infectious virus could be detected both in brain tissue (90 per cent of mice positive) and

trigeminal ganglia (100 per cent of mice positive); 8 weeks after inoculation, during the latent phase, virus could be reactivated by explantation and co-cultivation from 95 per cent of the trigeminal ganglia but from only 5 per cent of the brain tissue explants — yet by DNA reassociation techniques, HSV DNA sequences were detected in 30 per cent of brains of mice harbouring latent HSV in their trigeminal ganglia. The authors conclude that virus is not eliminated from the brain tissue but is maintained in a state which cannot be reactivated by the explantation techniques used.

What is this state and are all sequences of the HSV genome present? Inability to reactivate in the absence of complete genomic sequences would hardly be surprising. However, the presence and expression of an incomplete genome could have considerable consequences for the organism. Perhaps nucleic acid hybridization studies using cloned fragments of the genome will provide some insight.

Another approach to detect HSV genetic material in explant organ cultures is to superinfect explanted human ganglion

tissue with temperature-sensitive (*ts*) mutants of HSV-1 (ref. 7). Using this method, Brown *et al.* recovered wild-type virus from explant cultures which had been negative by co-cultivation for 45 days, and inferred that the *ts* mutant must have been complemented or rescued by genetic information in the ganglia. The authors suggest use of restriction enzymes to try to detect in the putative rescued virus DNA sequences which are not present in the *ts* mutant.

An important question is whether any of the viral genome is expressed during the latent state. Puga *et al.*<sup>8</sup> could find no HSV mRNA using reassociation techniques capable of detecting one genome equivalent of mRNA in 2,000 cells. On the other hand, using *in situ* hybridization, Galloway *et al.*<sup>9</sup> reported HSV mRNA in 0.4–8 per cent of human ganglia. HSV-specific thymidine kinase (TK) activity was observed in the sensory ganglia of mice up to 60 days after infection<sup>10</sup> but not in the skin or ganglia of quinea pigs, even with an assay which could detect the activity of one lytically infected cell in 3,000 uninfected cells<sup>11</sup>. We do not yet know whether any of the observed expressions are necessary for maintenance of the latent state or whether they reflect the spontaneous reactivation of cells which may subsequently be eliminated from the animal.

A different approach with potential for recognition of the viral functions necessary for latency is the use of HSV mutants. Tenser and colleagues<sup>12,13</sup> found that TK-negative mutants of HSV established latent infections in the trigeminal ganglia of both guinea pigs and mice with a lower frequency than that of TK-positive virus, suggesting that expression of this enzyme is necessary for latency. A collaborative study between Stevens' group (University of California, Los Angeles) and Subak-Sharpe's (Glasgow, UK) identified six temperature-sensitive mutants of HSV-1 which produce latent infections in mice with reduced frequency. One of these mutants (*tsK*) has a lesion in the immediate-early polypeptide  $V_{mw}$  175 (ref. 14) and appears to be blocked at or near the immediate-early stage of infection. The combined results of Preston<sup>14</sup> and those of the mutant latency study suggest that expression of at least one immediate-early function and one or more later virus functions is necessary for latency<sup>15</sup>.

The techniques hitherto employed in the isolation of *ts* mutants generate mutations in genes essential for growth in tissue culture. Genetic manipulation techniques will also allow isolation of mutants lacking sequences not essential for growth in tissue culture but which might be essential for latency. Screening of such deletion mutants for latency should be informative. □

Howard Marsden is at the MRC Virology Unit, Glasgow, UK.

1. Barringer, J.R. & Swoveland, P. *New Engl. J. Med.* **288**, 648 (1973).
2. Goodpasture, E.W. *Medicine* **8**, 233 (1929).
3. Stevens, J.G. & Cook, M.L. *Science* **173**, 843 (1971).
4. Cook, M.L. & Stevens, J.G. *J. gen. Virol.* **31**, 75 (1976).
5. Scriba, M. *Nature* **267**, 529 (1977).
6. Hill, T.J., Harbourn, D.A. & Blyth, W.A. *J. gen. Virol.* **47**, 205 (1980).
7. Brown, S.M., Subak-Sharpe, J.H., Warren, K.G., Wroblewska, Z. & Koprowski, H. *Proc. natn. Acad. Sci. U.S.A.* **76**, 2364 (1979).
8. Puga, A., Rosenthal, J.D., Openshaw, H. & Notkins, A.L. *Virology* **89**, 102 (1978).
9. Galloway, D.A., Benoglio, C., Shevchuk, M. & McDougall, J.K. *Virology* **95**, 265 (1979).
10. Yamanoto, J., Walz, M.A. & Notkins, A.L. *Virology* **76**, 866 (1977).
11. Fong, B.S. & Scriba, M. *J. Virol.* **34**, 644 (1980).
12. Tenser, R.B. & Dunstan, M.E. *Virology* **99**, 417 (1979).
13. Tenser, R.B., Miller, R.L. & Rapp, F. *Science* **205**, 915 (1979).
14. Preston, C.M. *J. Virol.* **32**, 357 (1979).
15. Watson, K., Stevens, J.G., Cook, M.L. & Subak-Sharpe, J.H. *J. gen. Virol.* **49**, 149 (1980).

## New directions in spectroscopy

from Derek Stacey

ATOMIC SPECTROSCOPY has a long and distinguished tradition. Its history is closely linked with that of quantum mechanics; atomic structure and the interaction of atoms with radiation provided both the inspiration and the testing ground for many of the theoretical advances which took place in the first half of this century, from the early quantum theory of Bohr to quantum electrodynamics (QED). Now that the emphasis has been passed on to elementary-particle physics, what remains to be done in atomic spectroscopy? A recent conference\* showed how spectroscopists have responded to this challenge.

First, there are some areas in which fundamental questions can still be studied. One paper, given by a team from CERN and the University of Pisa, described progress in an experiment to measure the birefringence of empty space (E. Iacopini and E. Zavattini *Phys. Lett.* **85B**, 151; 1979). According to QED, ordinary plane-polarized light becomes slightly elliptically polarized when travelling through an evacuated region in which a magnetic field exists. As there is nothing else present, it follows that the photon-photon interaction itself is responsible for the birefringence. Measurement of the induced ellipticity would give a direct test of this interaction at very low energies; this would be interesting because the birefringence is a genuine vacuum-polarization effect, arising only as a result of virtual pair creation. Apart from the interest in testing QED, the effect could have implications for astrophysics when one is dealing with the propagation of light through regions which may be subject to strong magnetic fields.

The problem with the experiment is the smallness of the effect. The idea is to shine a linearly polarized beam from an argon-ion laser into an evacuated region where there is a magnetic field of 8 teslas, provided by superconducting magnets; the effect is proportional to the fourth power of the field, so it is important to make this as large as possible. A mirror system causes the beam to cross this region many times, so that the effective path length through

the field is several kilometres. Even so, the ellipticity predicted for the emerging beam is only around  $10^{-12}$ . The measurement is carried out using familiar methods of analysing polarized light, the object being to detect changes which occur synchronously with the switching of the magnetic field.

The project brings to mind the experiments which use rather similar optical techniques to measure the rotation of the plane of polarization of light when it passes through an atomic vapour; the rotation gives a measure of parity non-conserving effects in the atomic system and hence demonstrates the presence of weak, neutral currents in atoms. These experiments are of fundamental interest and considerable effort has been put into them, but they have still taken several years to measure effects at the  $10^{-7}$  level. Thus the prospects for the new test of QED seem discouraging at first sight, but this could be a misleading comparison. Much of the difficulty of the parity experiments arises because one has to search for an effect which is sensitively dependent on wavelength. This problem does not arise in the QED test, in which the switching of the magnetic field provides the only necessary discriminating factor. Nevertheless, success in this experiment would be a major technical achievement.

Although comparatively few groups are working on such fundamental problems, the contributed papers showed that the field of atomic spectroscopy, far from declining, is showing a remarkable resurgence. This is largely due to the profound influence that the tuneable dye laser has had on atomic physics. During its early days, powerful spectroscopic techniques based on the device were developed but were usually applied to systems already well understood. Only now is the full potential of dye-laser methods becoming apparent; they have transformed established fields of study and opened entirely new areas for investigation — Rydberg states, collisional redistribution of radiation, super-radiance and so on. The attraction of this type of work is easy to see; in many branches of physics, anyone wishing to take advantage of advances in technology must join a team working at a major central faculty. The tuneable laser is a comparatively cheap

\*Annual conference of the European Group for Atomic Spectroscopy, held in Pisa, 2–5 September 1980.



device which permits a whole range of new experiments to be carried out in an ordinary laboratory.

Several papers described improvements in dye-laser techniques, but the most significant development in this area has been the emergence of the new generation of dye lasers based on the ring geometry. Ring lasers are inherently much more powerful and stable than the earlier standing-wave devices, and one reason for their importance is that they allow tuneable-laser methods to be applied in the ultra-violet. Most atoms have hitherto been inaccessible to the simpler dye-laser techniques because the tuning range of available dyes does not extend to short enough wavelengths. A ring laser operates with the same dyes but gives sufficient power to allow frequency doubling, or frequency generation, by mixing with the output of fixed-frequency lasers.

Another reason for the present interest in atomic spectroscopy is that the various techniques developed over the years primarily as spectroscopic tools are finding wider application. An invited paper presented at the conference by F. Laloë (Saclay Nuclear Research Centre, Paris) dealt with the properties of polarized  $^3\text{He}$  (that is, nuclear spins all parallel) (C. Lhuillier and F. Laloë *J. Phys.* **40**, 239;

1979). The connection with atomic spectroscopy is that the most promising of the methods proposed to prepare a sample of this material is based on the standard spectroscopic technique of optical pumping. (In particular, a newly explored colour centre in NaF seems well suited for pumping the  $2^3\text{--}2^3\text{P}$  transition, an important step in the preparation process [L.F. Mollenauer *Opt. Lett.* **5**, 188; 1980].) The talk reviewed the remarkable properties predicted for this fluid; they derive from the indistinguishability of the particles and can give rise to 'quantum effects' even when the system is in the form of a low-density gas. This is because the transport properties depend on the collision cross-section, and the Pauli Principle prevents the atoms from hitting each other. Other intriguing predictions include changes in the liquid-vapour and liquid-solid equilibrium pressures (C. Lhuillier and F. Laloë, *op. cit.*). It may be some time before any of these effects are demonstrated practically. However, the project is a good example of the way in which atomic spectroscopy continues to influence the development of other areas of physics. □

Derek Stacey is at the Clarendon Laboratory, University of Oxford, UK.

the rock record for minerals or chemical constituents that require oxygen for their formation. Unfortunately, although they exist, the time of their formation in the geological record fails to provide unequivocal evidence for an oxygenic atmosphere, and one major point to come out of the conference was that no single piece of evidence, in itself, would be sufficient to establish the existence of an oxic atmosphere. Rather, a whole sequence of analyses must be done on the same rocks in order for valid interpretations to be possible. Analyses have so far been too fragmentary to provide firm conclusions, although the weight of opinion, based primarily on the microfossil record and on iron and uranium mineralogy, is that oxygen probably first arose in significant quantities around 2 to 2.6 billion years BP. However, the interpretation of microfossil evidence is fraught with difficulty, as there are no microbial structures that can be unequivocally associated with oxygen evolution.

One of the four groups evaluated the evidence concerning Precambrian banded-iron formation. These formations are extremely important because they provide over 90 per cent of the minable iron deposits of the world. There was a major period in Earth history between 2 and 2.6 billion years BP when iron was precipitated in vast amounts, and after this time only very small deposits of this type of iron have deposited. The main Precambrian iron formation is rich in silica (chert) and has extensive characteristic banding (macro-, meso- and micro-bands), thus prompting the name banded-iron formations (BIF). These deposits probably formed as a result of sedimentation of oxidized iron on to ocean shelves, and because of the known chemistry of iron, it is clear that the Precambrian oceans could only have held in solution the vast amounts of iron necessary for BIF if the ocean waters were much less oxygenated than they are today.

The favoured model involves a circulating Precambrian ocean with an upper oxygenated layer and a lower anaerobic zone, the latter of which held a vast amount of ferrous iron. Movement of reduced iron into the surface waters, perhaps as a result of oceanic upwelling (analogous to the movements which bring up deep, cold, nutrient-rich waters on to shallow shelves in the present oceans), brought soluble iron to surface waters from where it was probably carried into closed basins for precipitation and sedimentation. The upwelling analogy involving marginal basins is strengthened by the facts that iron formations are enriched in phosphorus,

## Precambrian evolution

from Thomas D. Brock

THE PRECAMBRIAN constitutes the longest but least understood period of Earth history. In terms of biology, it is the period during which life arose and underwent extensive biochemical diversification. In terms of geology, it is when the continents and oceans became segregated and defined. Although today life plays a crucial role in geochemical processes at the surface of the Earth, geochemical events during at least part of the early Precambrian probably occurred in the absence of biological catalysis.

A number of ancient sedimentary deposits, some with important ore-bearing rocks, are accessible for study and analysis, the oldest of which is the Isua Supracrustal Group in Greenland (around  $3.8 \times 10^9$  years before the present [BP]). The only real clues to evolutionary processes in the Precambrian are found in the chemical and biological constituents present in these ancient rocks, and the aim of students of the Precambrian is to try to make sense out of the fragmentary records available. Although this is interdisciplinary research at its highest level, chemists, geologists and biologists rarely have the opportunity of meeting and working with one another. It was therefore particularly appropriate that a conference\* on Precambrian evolution was arranged that involved both geochemists and bioscientists.

Four separate topics were considered, each by a separate group containing chemists, geologists and biologists: (1) banded-iron formations; (2) stratified sulphide deposits; (3) organic geochemistry and palaeomicrobiology of ancient sediments; and (4) biogeochemical evolution of the ocean/atmosphere system. Although these topics were considered by separate groups, they so greatly overlapped that it was necessary for individuals to move from one group to another from time to time, a process encouraged by the format of the Dahlem Conferences.

Of over-riding importance for an understanding of Earth history is the estimation of the sequence of events leading to the formation of an oxygen-containing atmosphere. Oxygen arises today almost exclusively through plant photosynthesis, and the single most important feature in the evolution of higher-life forms was the appearance of this process. This must have occurred early in Earth history, but we do not know precisely when. Data from studies on chemical evolution suggest that life probably arose in an initially anoxic environment, and micropalaeontological evidence is strong that, by the Cambrian, the Earth's atmosphere contained nearly as much oxygen as it does today.

The geochemist looks carefully through

\*The Dahlem Conference on Mineral Deposits and the Evolution of the Biosphere, held during the first week of September 1980. A workshop report is also available: H.D. Holland and M. Schidlowski (eds) *Mineral Deposits and the Evolution of the Biosphere*, Dahlem Konferenzen (Verlag Chemie, Weinheim, FRG, in the press).

and by the purity of these deposits (absence of heavy metals). It is thought that the world-wide appearance of BIF between 2 and 2.6 billion years BP may be largely due to the development, for the first time, of wide continental shelves and enclosed basins adjacent to the deeper, oceanic areas. The cyclicity which led to banding was probably the result of seasonal climatic changes, perhaps controlling phytoplankton oxygen production.

During the discussion, it became clear that considerably more information is needed on iron oxidation states in Precambrian iron formations, as an indication of the oxidation states of the Precambrian oceanic waters. Since the presence of iron in Precambrian rocks provides some of the best evidence for the oxygen status of the atmosphere, it is essential that the oxidation state of iron during primary precipitation be established with certainty. Does the massive development of iron formation at 2 to 2.6 billion years BP represent the initial rise in oxygen in the atmosphere, or is it more related to the initial development of continental shelves, providing an appropriate habitat for iron deposition?

Stratified sulphide deposits display a host of features indicating that they formed at or near the sediment-water interface. Although it had been considered previously that some of these deposits were biogenic, the conclusion of the Dahlem workshop was that they had to have an external (possibly exhalative) source of metal and that the sulphur may represent a mixing of multiple sources (biogenic and hydrothermal).

An important biogeochemical tool, sulphur isotope fractionation, was carefully re-examined in the light of the evidence. Two components are needed for the formation of a sulphide deposit — a source of sulphide and a source of iron (to tie up the sulphide). Sulphide can come from either abiotic sources (hydrothermal or volcanogenic) or biotic sources (sulphate-reducing bacteria). Because bacterial sulphate reduction leads to the discrimination of  $^{34}\text{S}$  against  $^{32}\text{S}$ , it has been conventional to use isotope ratios of sulphur in sulphide deposits to infer biogenicity. However, more recent work on the isotope ratio distributions in sedimentary and hydrothermal deposits shows that a clear-cut conclusion on biogenicity is not possible. Most ancient sulphide deposits have a high iron content, and it was shown that such a high iron content is unlikely to develop in a typical modern sedimentary setting where biogenic sulphide is depositing. Modern analogues for the ancient stratified sulphide deposits are the Red Sea brine pools and the 'black smokers' at 21°N on the East Pacific Rise. If the Precambrian sulphide deposits are indeed largely abiotic, then it is impossible to determine

from an examination of these deposits the time of onset of biological sulphate reduction. It was concluded that extensive new data will be needed to elucidate the onset of this important step in biochemical evolution.

Many Precambrian deposits have extensive amounts of reduced carbon, analysis of which may provide clues to biological evolution. However, interpretation of such analyses requires careful application of concepts developed during studies on modern ecosystems. There is now available a wide variety of techniques that could be used in the study of Precambrian organic matter, including ion microprobe, pyrolysis-gas chromatography, high-resolution mass spectrometry (MS), photoacoustic spectroscopy, laser pyrolysis, high-pressure liquid chromatography (HPLC), HPLC-MS, high-resolution capillary gas chromatography,  $^{13}\text{C}$  nuclear magnetic resonance and X-ray diffraction. It is clear that a vast amount of information can be obtained, but it is vital that the analyses be carried out on carefully collected specimens, and that, as far as possible, combinations of methods be used, to permit cross-checking and a more precise interpretation.

Organic matter in ancient rocks can be divided into two major fractions, extractable organic matter (EOM) and kerogen (nonextractable). Because of the ease of analysis, EOM has been studied more extensively, but it is essential that the EOM studied be syngenetic with the rock and not a post-depositional replacement or contamination arising during processing.

The interpretation of the chemistry of both EOM and kerogen requires a knowledge of the organic chemistry of modern ecosystems and of how organic matter changes during diagenesis and catagenesis. Micropalaeontological studies are also vital as they provide clear evidence that life was involved in organic matter deposition or modification. Studies on carbon isotopes in ancient organic matter may provide evidence for biogenicity, provided the data can be interpreted properly in relation to modern processes (although the example for sulphur isotopes discussed above shows the dangers involved).

During the conference, it was frequently the case that biologists were turning to chemists for appropriate chemical evidence that would aid their studies, and that geologists were seeking biological evidence to confirm or expand their conclusions. One of the main conclusions of this conference was that no one science alone would provide an answer, and that progress can be made only when all proceed together. Much discussion during the conference centred on the problems of communication between biologists and geologists, and the need for more formal mechanisms of interchange. Although 'biogeochemistry' has been used as a term since the mid-1930s, it is only now emerging as a discipline in its own right. Another result of the Dahlem workshop was strong consideration for the formation of a new society to be called the 'BioGeo-Chemistry Society' that would bring together workers from a variety of fields for a concerted attack on some of the most fundamental problems of our times. □

## Green light in Heidelberg

*from a correspondent*

THE 200 or so molecular biologists who attended the sixth EMBO symposium\* in Heidelberg spent 3½ days discussing gene organization and expression in green plants. The surprisingly large size of the audience might suggest that the organizers had found a patch of fertile ground and that the topic was scientifically ripe. In the event, however, there turned out to be few converts to the green revolution. For the most part, the audience consisted of those already in the field, together with a sprinkling of volunteers from other disciplines and a few weeds from the recombinant DNA companies whose presence seemed to presage a new meaning for the term 'seed-money'.

### Nuclear genes

Much of the meeting was devoted to the presentation of the results of molecular cloning experiments. cDNA and genomic libraries of the genomes of several species of plants have been constructed and several genes, particularly those expressed at high levels, have been analysed in some detail. Most attention has been paid to the genes coding for the storage proteins of cereals and legumes, which are silent in vegetative tissues but extremely active at specific stages of seed development. For example, the set of genes coding for the ten or so superabundant proteins of soybeans is turned on immediately after flowering; the concentration of their mRNAs in the cotyledons increases steadily for the next 75 days, by which time 50 per cent of the total mRNA is composed of only these few species (Goldberg, University of California, Los Angeles). None or very

\*Thomas D Brock is at the University of Wisconsin.

\*'Molecular Biologists look at Green Plants', European Molecular Biology Laboratory, Heidelberg, 29 September — 2 October 1980.



little of this RNA is ever detected in axis or leaf cells.

DNA copies of seven superabundant mRNAs have been made and cloned in prokaryotic vectors. By hybridization selection, *in vitro* translation and immunoprecipitation, four of them have been shown to code for polypeptides of the 7 and 11S storage proteins as well as the Kunitz trypsin inhibitor. Although these proteins appear to be coordinately synthesized, their genes are not closely clustered. Hybridization experiments between cDNAs and representative clones from a genomic library show that the genes for superabundant mRNAs occur at most a few times within the soybean genome and do not map within 20 kilobases of one another.

A major problem, therefore, is that of how small, dispersed families of apparently unrelated genes such as these are controlled and simultaneously activated. Reassociation kinetic experiments rule out the possibility that the genes are differentially amplified during embryogenesis. Furthermore, no common feature has appeared from an analysis of the gross structure of the genes that would explain their behaviour. In fact, their organization appears to be quite dissimilar — for example, the gene for Kunitz trypsin inhibitor contains an 9.7-kilobase intervening sequence, while that for 11S storage protein is apparently colinear with its mRNA. Because no nuclear transcripts of these genes can be detected in cells which do not contain storage proteins (leaf cells, for example), it seems likely that their expression is regulated primarily at the level of transcription.

The storage proteins of barley (hordein) and maize (zein) are encoded by gene families which appear to contain at least ten to twenty highly homologous members. Interestingly, the expression of the entire family is drastically influenced by the activity of other genes (Larkins, Purdue University; Feix, University of Freiburg; Brandt, Carlsberg Laboratory, Copenhagen). Thus, mutations at the *lys 3A* locus of barley and the *opaque 2* locus of maize effectively abolish expression of the respective gene families. Again, this effect seems to be mediated at the transcriptional level. Clearly it will be interesting to compare the DNA sequences which lie upstream from the structural genes coding for these various storage proteins.

#### Chromosomal rearrangements

Several genes coding for abundant proteins (for example, the 11S storage protein and the Kunitz trypsin inhibitor of soybeans) appear to be located in the immediate vicinity of middle-repetitive DNA (Goldberg, University of California, Los Angeles). The evolution of analogous sequences in the genome of cereals was discussed at Heidelberg by R. Flavell (Plant Breeding Institute, Cambridge). By using cloned segments of repetitive DNA as

probes in *in situ* hybridization experiments, he has shown that the greatest concentration of several species of repetitive DNA maps at the ends of cereal chromosomes.

The detailed organization of these sequences, however, varies from species to species and even from chromosome to chromosome within a single species. Thus certain repetitive sequences are present more than  $10^6$  times in one secale species but fewer than 50 times in another; and several examples are known where different chromosomes of a single plant species carry different repetitive sequences at their ends. All of these observations are consistent with a model in which most of the non-coding DNA of cereal chromosomes 'turns over' relatively rapidly during evolution by a process of amplification and deletion, and new sets of repetitive sequences are created by the translocation of small pieces of DNA into new sites. Why repetitive sequences in plant genomes should be sequestered to the ends of chromosomes is not known.

Chromosomal rearrangements in plants are, of course, not limited to non-coding sequences. Burr (Brookhaven) has analysed mutations at the *shrunk* locus of maize caused by the transposable element *DS* (McClintock *Yb. Carnegie Instn Wash.* 51, 212–219; 1952) which causes chromosome breaks in the endosperm leading to dicentric chromosome formation. The *shrunk* locus codes for the enzyme sucrose synthetase, a partial cDNA copy of whose mRNA has been cloned. Using this as a probe in Southern hybridizations, Burr has been able to show alterations in the structure of the *shrunk* locus as a result of *DS* action, but because of the small size of the probe the extent of these alterations is not known. At least one of them involves deletion of part of the gene while others appear to result from insertion of sizeable tracts of DNA, perhaps multiple copies of *DS* itself.

#### Splicing

By contrast with this plasticity, sequences coding for some plant proteins have not changed appreciably over large spans of evolutionary time: for example, the leghaemoglobins of soybeans which, judged by their amino acid sequences, appear to be related to the ancestral haemoglobin of higher animals. The leghaemoglobins are encoded by a set of six separate genes, four of which are closely linked in a single 30-kilobase DNA fragment (Marcker, University of Aarhus). This arrangement is reminiscent of those found in the haemoglobin genes of mouse and man. The leghaemoglobin *c* gene contains two intervening sequences (between nucleotides coding for amino acids 34/35 and 103/104) which map at positions almost identical with those occupied by intervening sequences in mammalian haemoglobins. A third intervening sequence, not yet recognized in

any other haemoglobin, has been detected in leghaemoglobin *c* gene and has been mapped between sequences coding for amino acids 67 and 68. Whether this is a general feature of all six leghaemoglobin genes or is specific to the one copy which by chance has been cloned and sequenced is not known.

The DNA sequences at intron–exon boundaries have also now been determined for the phaseolin gene of beans (Hall, University of Wisconsin) — it contains three intervening sequences — and for the 23S ribosomal RNA gene of *Chlamydomonas* chloroplasts, which contains one (Rochaix, University of Geneva). All of these have the dinucleotides GT and AG at their 5' and 3' ends and correspond in many other respects to the common sequence across splice junctions in heterogeneous nuclear RNA of mammalian cells. Presumably, therefore, the mechanism by which transcripts of plant genes are spliced into mature functional RNAs is fundamentally similar to that in animal cells. There are indications that small 'adaptor' RNAs may be involved in splicing of mammalian RNAs (Lerner and Steitz *Proc. natn. Acad. Sci. U.S.A.* 76, 5495; 1979). A similar set of RNAs has now been discovered in green plants. Working with *Chlamydomonas*, Rochaix has shown that the 5.85S nuclear RNAs, and the 3S and 7S RNAs encoded by the chloroplast, are partially complementary to the sequences flanking the intron within the chloroplast gene coding for 23S ribosomal RNA. By pairing with the coding sequences in the precursor RNA, these small RNAs could cause the intervening sequence to loop out, making it more accessible to the enzymatic machinery involved in splicing.

#### Chloroplast genes

That chloroplasts carry genes essential for plant growth and survival has been known since the early years of this century. However, it is only during the past few years that chloroplast chromosomes have been physically dissected. Restriction endonuclease mapping and electron microscopy have shown that chloroplast genomes are always circular and large in size, varying from 135–210 kilobases in different plant species. A commonly occurring feature is the presence of two large, inverted and repeated segments, which in the case of maize are 22.5 kilobases in length. Within these repeats are arranged the genes for the chloroplast ribosomal RNAs in the order 16S–spacer–23S–5S. Spacers are a constant feature of all plant chloroplast genomes so far examined but vary in size from species to species. Within the genus *Oenothera*, insertions and deletions are found to occur within them. Because such alterations always occur in both copies of the spacers simultaneously, it seems likely that a mechanism exists which corrects one copy of the spacer against the other. Why this correction process occurs is not known.

The spacer regions are neither silent nor empty, containing genes for tRNAs and, in the case of *Chlamydomonas*, for 3S and 7S RNAs as well (Rochaix). Genes for additional species of tRNA (perhaps 30 in all) are scattered throughout the repeated and unique regions of the chloroplast genome. At least some of these are split by intervening sequences, which in *Chlamydomonas*, as in yeast, are located 1–2 bases distal of the anticodon loop (Kossel, University of Freiburg).

The sequences of the 16S, 23S and 5S genes of the chloroplast of several plant species are remarkably homologous with the corresponding sequences of *Escherichia coli* (Delius, Embl; Kossel; Rochaix). These highly conserved sequences include those near the 3' end of 16S rDNA as well as those immediately flanking the intervening sequences in *Chlamydomonas* 23S RNA. It therefore appears that part of the genome of present-day chloroplasts is derived from prokaryotic precursors.

Although chloroplast and nuclear genes are carried on separate pieces of DNA, at least two lines of evidence indicate that they are not evolving independently of one another. First, within the genus *Oenothera*, where five different types of chloroplast genome can be recognized by restriction-enzyme digestion, interspecific crossing can result in combinations of nuclear and chloroplast genomes not normally found in nature (Herrmann, Botanisches Institute, Dusseldorf). Often these hybrids are extremely unhealthy, displaying a bleached phenotype. Apparently, there is a mutual dependence between the two genomes such that chloroplasts are adapted to express in only one or a few nuclear backgrounds.

Secondly, the chloroplast genome is now known to code for more than 100 polypeptides. Some of the proteins found in the chloroplast, however, are not coded by the genome of the organelle but by the nucleus of the cell. Among these polypeptides are subunits of the thylakoid-located ATP synthetase of photosystems I and II, of cytochrome *f* and of the large subunit of ribulosebiphosphate carboxylase. These examples of cooperation between the chloroplast and nucleus argue strongly that the two genomes evolve as a binary pair.

The most detailed analysis of this phenomenon has come from studies of ribulosebiphosphate carboxylase — an enzyme built from two non-identical subunits. The larger of these subunits (LS) is coded by the unique region of the chloroplast genome, the smaller (SSU) by a nuclear gene. Both genes have now been cloned (the former from maize and the latter from pea) and sequenced. The mRNA for the small subunit is 760 nucleotides in length and is derived by splicing from a nuclear precursor some 200 nucleotides longer. It codes for a protein which contains at its N-terminal end at least 13 hydrophobic amino acids which are not

found in the mature subunit. Presumably they form a signal sequence which is cleaved off as the small subunit is transported into the chloroplast.

The LS subunit of ribulosebiphosphate carboxylase occupies a special place in the history of plant molecular biology in that its gene was the first to be mapped on the chloroplast genome. The entire gene, together with its flanking sequences, has been cloned and sequenced. The coding sequence is 1.6 kilobases in length and is colinear with the polypeptide. Located on the opposite DNA strand, some 300 nucleotides away, is the *his* gene. Despite their close proximity, the two genes are expressed in entirely different ways: that for *his* is expressed constitutively in both mesophyll and the neighbouring bundle-sheath cells of maize, while that for the large subunit is expressed efficiently only in mesophyll cells. It seems quite possible that this differential control is achieved at the level of transcription, since efficient and accurate transcription of the cloned LS gene *in vitro* by DNA-dependent RNA polymerase requires a 26K polypeptide isolated specifically from chloroplasts.

#### Plant vectors

The relative merits were discussed of two vectors which, potentially, can replicate both in plant and bacterial cells and also allow the expression of foreign genes in plants. Both have highly unusual properties. The double-stranded DNA of cauliflower mosaic virus has recently been sequenced and has been shown to contain single-strand discontinuities at unique sites — two in one strand and one in the other (Frank *et al.* Cell 21, 285; 1980). The viral DNA propagated in bacterial plasmids and therefore without discontinuities, retains its infectivity. However, the viral genomes arising from such infections and encapsidated into progeny virus particles reacquire single-strand breaks and the tangled topology typical of the viral DNA. Thus, neither the discontinuities nor the knotted topology are necessary for establishing infection but are formed in DNA which has been replicated in plants (Howell, University of California, San Diego; Hull, John Innes Institute, Norwich).

Only the DNA strand with the single discontinuity is transcribed during infection: at early times, a single species of RNA is detected with a molecular weight equivalent to that of one entire strand of the viral genome. Later, at least four other transcripts are found, the most prominent of which is about 2,200 nucleotides in length and codes for the inclusion body protein of molecular weight 65,000. Despite intensive searching, no sites have been detected in the genome which can accept foreign sequences without affecting the viability of the virus. Until such sites are found or until a system is established in which defective viruses can be complemented, cauliflower mosaic virus cannot be used as a vector.

The second potential vector is the Ti plasmid of the Gram-negative soil bacterium *Agrobacterium tumefaciens*, which induces crown gall tumours on most dicotyledonous plants. The Ti plasmid causes the neoplastic transformation of plant cells and the resulting transformed cells contain a segment of the Ti plasmid (T-DNA) which is 12–24 kilobases long and which is integrated and transcribed (Schell, Cologne; Chilton, Saint Louis). The boundaries of the integrated T-DNA have now been cloned from a line of transformed tobacco cells and analysed by DNA sequencing and hybridization. One of the clones examined contains the right and left borders of the T-DNA linked together; another contains the right end of the T-DNA linked to repetitive plant DNA (Zambryski, University of California, San Francisco).

These data suggest that the integrated T-DNA is arranged as a tandemly repeated element within repetitive plant sequences. However, they do not shed light on the mechanism by which the integration event occurs, nor do they prove that the T-DNA can become a stable part of the plant chromosome that can be transmitted through meiosis. It is the latter property which will determine whether T-DNA can fulfill its promise of serving as vector to carry foreign genes into dicotyledonous plants.

#### Viroids

Of all infectious agents so far discovered, viroids must rank among the most bizarre. The best characterized — potato spindle tuber viroid — is a single-stranded circular RNA molecule 359 nucleotides in length, with so much base-pairing that it is thermodynamically equivalent to double-stranded DNA. Several strains of potato spindle tuber viroid are known which differ greatly in their capacity to cause disease. Surprisingly, these strains differ from each other in only three nucleotides (Sanger, Giessen). How such seemingly insignificant changes can result in vast alterations in biological properties is unknown.

The mechanism by which viroids replicate has long been puzzling. Too small to code for an elaborate replication machinery, it had been assumed that, like retroviruses, they may integrate into the host genome and then be transcribed into new progeny viroids. This view has been challenged by two exciting findings. First, viroids are efficient *in vitro* templates for RNA polymerase II isolated from tomato callus or leaf cells. The product is equivalent in size to full-length viroid RNA (Sanger). Secondly, viroid replication in cells is inhibited by amanitin (Sanger; Diener, Beltsville). These results open the possibility that viroids replicate by an entirely novel mechanism in which the infecting RNA molecules are copied by the host enzyme which is normally responsible for synthesis of nuclear precursors to mRNA. □



# Electrochemistry and the geochemist

from H.A. Tourtelot

ELECTROCHEMISTRY deals with the relation of electron flow to chemical transformations that either create electricity or are caused by the flow of electric current. Geochemistry generally deals with Earth materials that are poorly conductive so that electrochemical transformations take place only within very short distances. In contrast, the term 'electrochemistry' seems to be used by geochemists to describe transformations involving highly conductive materials, such as sulphide minerals, and some others through which electrons travel easily. Transformations separated by considerable distances thus also are coupled by electron flow. Morris *et al.* describe in this issue of *Nature* (ref.1, p.250) such an electrochemical model for the formation of deep-seated iron ores.

Electrical phenomena around ore deposits were recognized long ago and provide the basis for the self-potential method of geophysical prospecting<sup>2,3</sup>. The electrochemical mechanism for self-potentials associated with sulphide ore bodies was examined by Sato and Mooney<sup>4</sup> based on the theoretical work of Pourbaix<sup>5</sup> and Latimer<sup>6</sup>. The paper by Sato and Mooney seems to be the chief introduction to geochemists of electrochemical theory applied to ore deposits. An ore body of conducting minerals connects oxygenated ground water near the surface of the Earth with ground water at a depth deficient in oxygen. This redox gradient is 'short-circuited' by upward electron flow in the conductive ore minerals<sup>7</sup>. Reduced compounds at depth thus are oxidized (electrons lost) and oxidized compounds near the surface are reduced (electrons gained). The circuit is closed by ionic conduction in the pore fluids around the

ore body. Cations move upwards towards the surface and anions move downwards. The diagram shown by Morris *et al.* (*Nature* this issue, p.251, Fig.1a) illustrates the general character of electrochemical systems as well as the specific system involved in iron ores where magnetite is the conductor of electrons, ferrous iron is oxidized to ferric at depth and oxygen is reduced to OH<sup>-</sup> at or near the surface.

Most economic iron ores consist of ferric oxide minerals that have formed largely by the oxidation of pre-existing ferrous minerals, such as magnetite, siderite, and iron silicates originally deposited in the Precambrian in an association known as banded-iron formation<sup>8</sup>. At some deposits, such as those in Brazil, formation of supergene ferric oxides that make up the ore is related to present and relatively recent weathering conditions<sup>9</sup>. As Morris *et al.* point out, some ferric-oxide ore deposits, such as those at Krivoy Rog, Russia and in the Hamersley Ranges, Western Australia, now exist at such great depths that their origin cannot be explained by the action of oxygenated ground waters, either now or at any time in the geological past. At Krivoy Rog, for example, oxide ores are found at depths as great as 2,400 m and in the Hamersley Ranges at depths greater than 400 m.

Explanation of the origin of the deep-seated iron oxide ores in the Hamersley Ranges by processes other than electrochemical are not offered by Morris *et al.* They suggest that electrochemical processes based on the conductivity of magnetite can be called upon to explain the origin of deep-seated oxidized banded-iron formation for ore deposits where the action of 'normal' oxidation processes cannot be comfortably accepted. Differing opinions, no doubt, will be expressed.

An earlier application of electrochemical theory to the genesis of ore deposits is that of Constantinou and Govett<sup>10,11</sup>. They considered the idea that electric potential differences within a sulphide body could cause movement of metals and could affect the distribution of elements in rocks overlying ore of the Cypress sulphide deposits. Experiments by Govett and Whitehead<sup>12</sup> showed that sulphides of different metals develop zoning patterns that are consistent with electrochemical theory and that are similar to the arrangement of minerals in some stratiform sulphide bodies such as Rammelsberg.

Another application of electrochemical theory is in exploration geochemistry. The electrochemical model for the formation of the Hamersley deep-seated iron deposits is

H.A. Tourtelot is a geologist with the US Geological Survey, Denver, Colorado.

based on work by Thornber, one of the co-authors with Morris *et al.*, on the supergene alteration of massive nickel sulphide deposits at Kambella, Western Australia<sup>13</sup>. Thornber's main effort was to explain supergene alteration of sulphides, according to electrochemical principles with a view to recognizing parameters useful in geochemical prospecting. He concluded that, under favourable conditions, *Eh* and *pH* patterns could indicate the presence of an oxidizing ore body.

Govett, taking a different approach to exploration geochemistry, suggested that metal contents in soils above some mineral deposits resulted largely from the upward flow of metal cations around a conducting sulphide ore body<sup>11</sup>. Later, he emphasized the importance of soil-slurry conductivities that give patterns at least as good as those from trace metals, that arise from the same electrochemical processes, and that are easier to determine in the field<sup>14</sup>. Patterns of conductivity are clarified if the measurements are corrected for H<sup>+</sup> concentrations that can be derived from *pH* measurements on the soil slurry. H<sup>+</sup> concentrations in soil slurries show typical anomalies in profiles across some ore deposits even though the deposits are covered by as much as 10 metres of glacial deposits<sup>15,16</sup>. Lithium gives a similar anomaly around an ore deposit in Norway probably, according to Bölviken and Logn<sup>17</sup>, because Li<sup>+</sup>, like H<sup>+</sup>, has high ionic equivalent conductance and should be one of the principal current carriers in an electrochemical system.

Many other processes besides electrochemical ones influence the formation of ore deposits as well as the zoning of metals around them, but an understanding of electrochemical effects may explain the origin of some ore deposits and provide a means for exploring for them. The work reviewed here has been done mostly by scientists in government and university research organizations, with extensive cooperation from mining companies to which the subject is of great interest and potential value.



100 years ago

The Jablochhoff light has been introduced by M. Hervé-Mangon into the Conservatoire. It will be fed by a Gramme machine, which the establishment has purchased for its constant use. The light will be placed in the amphitheatre, where M. Hervé-Mangon delivers, twice a week, his own lectures.

The lighting of the Victoria Station of the District Railway by means of the Jablochhoff electric light has been so successful that it has been also applied to the Charing Cross Station, and will shortly be introduced at Earl's Court.

From *Nature* 23, 18 November, 64, 1880.

1. Morris, R.C., Thornber, M.R. & Ewers, W.E. *Nature* **288**, 250-252 (1980).
2. Dobrin, M.B. *Introduction to Geophysical Prospecting* (McGraw-Hill, New York, 1960).
3. Jakosky, J.J. *Exploration Geophysics* (Tijja, Los Angeles, 1950).
4. Sato, M. & Mooney, H.M. *Geophysics* **25**, 226 (1960).
5. Pourbaix, M. *Thermodynamics of Dilute Aqueous Solutions* (Arnold, London, 1949).
6. Latimer, W.M. *The Oxidation States of Elements and their Potentials in Aqueous Solutions*, 2nd edn (Prentice-Hall, New York, 1952).
7. Rose, A.W., Hawkes, H.E. & Webb, J.S. *Geochemistry in Mineral Exploration* (Academic, New York, 1979).
8. James, H.L. & Sims, P.K. (eds) *Econ. Geol.* **68**, 913 (1973).
9. Dorr, J. van N. II *Econ. Geol.* **59**, 1203 (1964).
10. Constantinou, G. & Govett, G.J.S. *Trans. Instn Min. Metall.* **81**, B34 (1972).
11. Govett, G.J.S. *J. Geochem. Explor.* **1972** (Instn Min. Metall., London, 1973).
12. Govett, G.J.S. & Whitehead, R.E.S. *Econ. Geol.* **69**, 551 (1974).
13. Thornber, M.R. *Chem. Geol.* **15**, 1, 117 (1975).
14. Govett, G.J.S. *J. Geochem. Explor.* **1974** (Elsevier, Amsterdam, 1975).
15. Govett, G.J.S. *J. Geochem. Explor.* **6**, 359 (1976).
16. Govett, G.J.S. & Chork, C.Y. *Prospecting in Glaciated Terrain* (Instn Min. Metall., London, 1977).
17. Bölviken, B. & Logn, O. *J. Geochem. Explor.* **1974** (Elsevier, Amsterdam, 1975).



## REVIEW ARTICLE

## Do waves limit turbulent diffusion in the ocean?

John D. Woods

Institute für Meereskunde an der Universität Kiel, Düsternbrooker Weg 20, D2300 Kiel 1, FRG

*Recent theoretical and observational studies of fluctuating motions in the stable interior of the ocean suggest that the rate of turbulent diffusion of scalars may be sensitive to the influence of waves on the energy balance of eddies and fronts. A new flow diagram is used to describe the turbulent cascades of energy and enstrophy in the ocean.*

REYNOLDS introduced the idea of separating motion into two parts, steady and fluctuating. In the ocean the gyre circulations can be thought of as the steady part and all the other motions as the fluctuating part. This division is clear in the climatological mean spectrum of oceanic kinetic energy (Fig. 1). The fluctuating part is normally divided into two categories.

(1) Wave-like motions that radiate energy and momentum through the ocean. Their propagation through the ocean can be described kinematically in terms of linear theory, plus resonant wave-wave interaction and dynamical interaction with the environment through which they pass.

(2) Advective-like motions that can only transport momentum and energy by advection of water particles from one place to another. The fluctuating motions in this category are often sufficiently energetic to require nonlinear description of their development with time. They can be further subdivided into (i) those motions that do not overturn isentropic surfaces (notably quasi-geostrophic eddies, and fronts); (ii) those that do overturn isentropic surfaces (billows, Langmuir cells, and the motion within patches of three-dimensional turbulence).

Many fluid dynamicists prefer to restrict the term 'turbulence' to the category (2ii). In this limited definition oceanic turbulence occurs only at the boundary layers, in deep-convection and in thin, transient blini in the interior. Oceanographers, however, talk about lateral diffusion in the interior of the ocean, occurring at rates ( $\sim 1,000 \text{ m}^2 \text{ s}^{-1}$ ) that cannot possibly be explained by the restricted picture of the fluid dynamicist. Oceanographers accept that the fluctuating motions in category (2i), those that do not overturn isentropic surfaces, demand statistical treatment in the spirit of turbulence theory. They too must be included in any description of 'turbulence in the ocean'. Recently, there has been increasing discussion about the need to include wave-like as well as advective-like fluctuations in any complete model of turbulence in the ocean designed to predict the rates of scalar diffusion. The basis for this is that the rate of turbulent diffusion depends on the kinetic energy density of the advective-like fluctuations which is limited by leakage of energy to waves that radiate the surplus energy away and dissipate it.

This article summarizes the main features of the conceptual model of ocean turbulence that emerges if waves play a significant part. The problem can be simplified by ignoring the well documented regional variation of turbulent kinetic energy. The method, a common one in turbulence theory, considers the statistics of fluid-dynamically important properties such as momentum and vertical component of vorticity, and in particular describes how their variances (kinetic energy and enstrophy, respectively) are transferred from one place to another and from one scale to another. The transfer from one place to another is achieved by advection (by mean circulation) and by radiation (of energy but not enstrophy) by waves. The transfer from one scale to another is called a cascade, which is a transfer

from one position to another in the wavenumber spectrum. We can also think of it as a flux of variance (energy, enstrophy, and so on) from one place to another in Fourier space. An integrated picture of turbulence in the ocean is developed by considering the budgets of kinetic energy and enstrophy, taking account of their fluxes through both physical and Fourier space by advection, radiation and cascading. To achieve this conservation laws are used which are like the laws of thermodynamics, but concerned with kinetic energy and enstrophy of the fluctuations of oceanic motion. There are important relations between the conservation laws of thermodynamics and turbulence theory. The most important law of ocean turbulence is that potential vorticity is conserved in adiabatic motion, that is, those that do not involve overturning and subsequent mixing of isentropic surfaces. Oceanographers have long relied on this law in developing theories of the gyre scale mean circulation; it is the basis of the Sverdrup balance. The law is also valid for fluctuating motions with scales ranging down to the order of 1 m in the interior of the ocean. This is because the vertical density gradient in the ocean interior is so large that the rate of kinetic energy input (of the order of  $\text{mW m}^{-2}$ ) is only sufficient to sustain intermittent overturning of isentropic surfaces on scales of 1 m or less. Between these rare and short-lived overturning events there is no three-dimensional turbulence; so, at any instant the interior of the ocean is in laminar flow almost everywhere. The law of potential vorticity conservation can be applied across the spectrum from the scale of the ocean basin down to the scale of overturning (of the order of 1 m). The climatological spectrum in Fig. 1 shows that this covers almost the whole of the range now under discussion. Conservation of potential vorticity is an approximation but the largest source of error—intermittent overturning and mixing of isentropic surfaces in the interior—is negligible for the present discussion. There is a striking similarity between this law and the law of conservation of relative vorticity in a strictly two-dimensional flow and many of the results of two-dimensional turbulence theory can be applied to oceanic turbulence. In discussing the statistics of the fluctuating oceanic flow we shall therefore use 'enstrophy' to describe 'variance of potential vorticity'.

### The gyres

In this article the main features of the new conceptual model of oceanic cascade physics are summarized using a new flow diagram presented in Fig. 2. On the left lies the largest scale of motion, the gyres of the upper ocean (A), driven by the wind through the agency of Ekman pumping (a). The gyres exhibit seasonal variation in response to the wind, but we can think of their streamlines as being steady compared with the fluctuating motions associated with the smaller-scale eddies, fronts, waves, and so on. The gyre circulation represents the mean flow, in

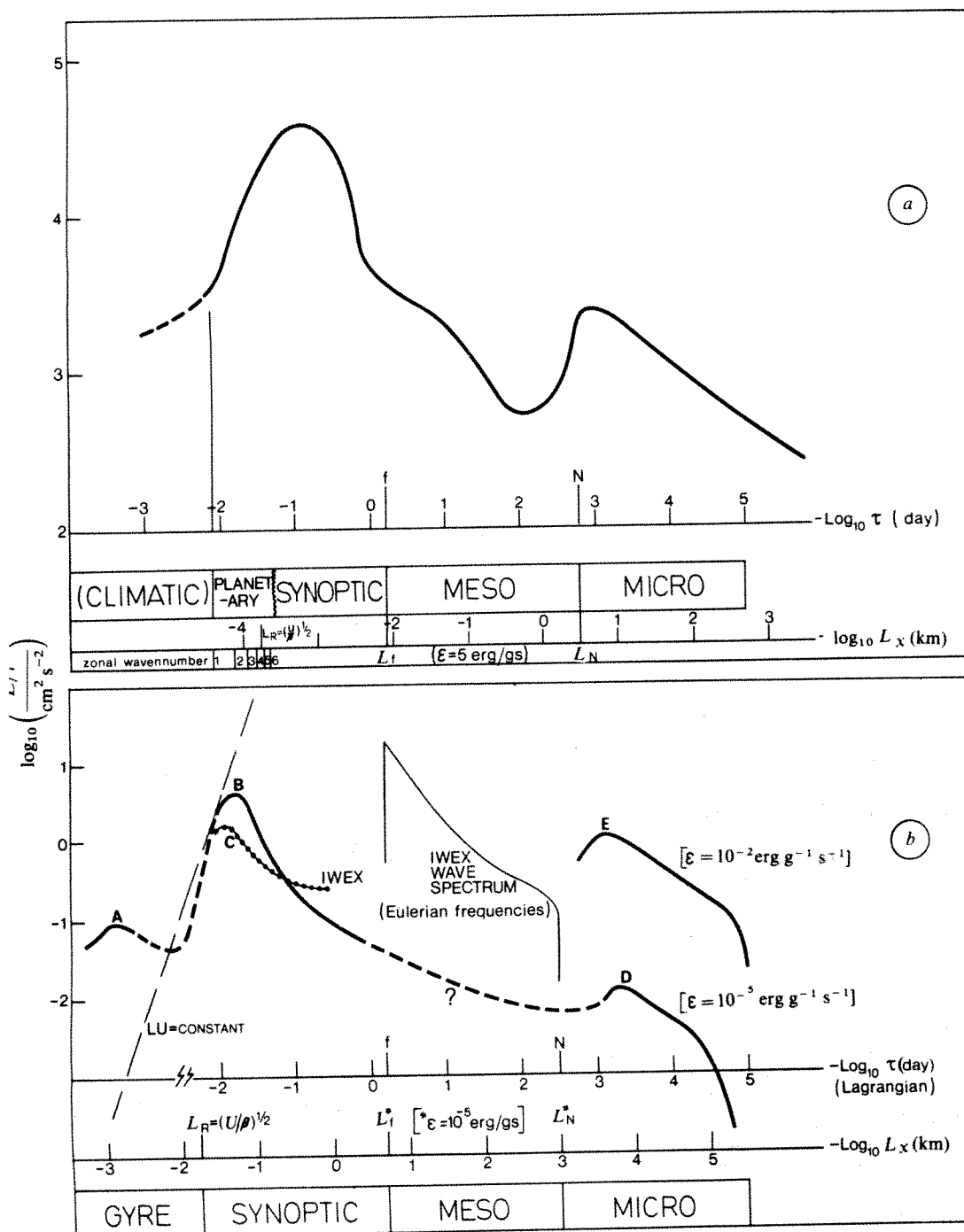


terms of Reynolds's division of a turbulent flow. Between adjacent gyres there are relatively sharp permanent fronts, characterized by maxima in both thermoclinicity and baroclinicity. The gyre streamlines pack closer in these frontal jets and in western boundary currents (for example, the Gulf Stream). Water particles take a decade or so to circulate around an upper ocean gyre. The size, location and number of gyres remains controversial<sup>2</sup>, so we are discussing the physics of the fluctuations without knowing the mean flow. This difficulty arises largely from uncertainty over the influence of the fluctuations on the mean motion; a first-order problem in both diagnostic and prognostic models of oceanic circulation.

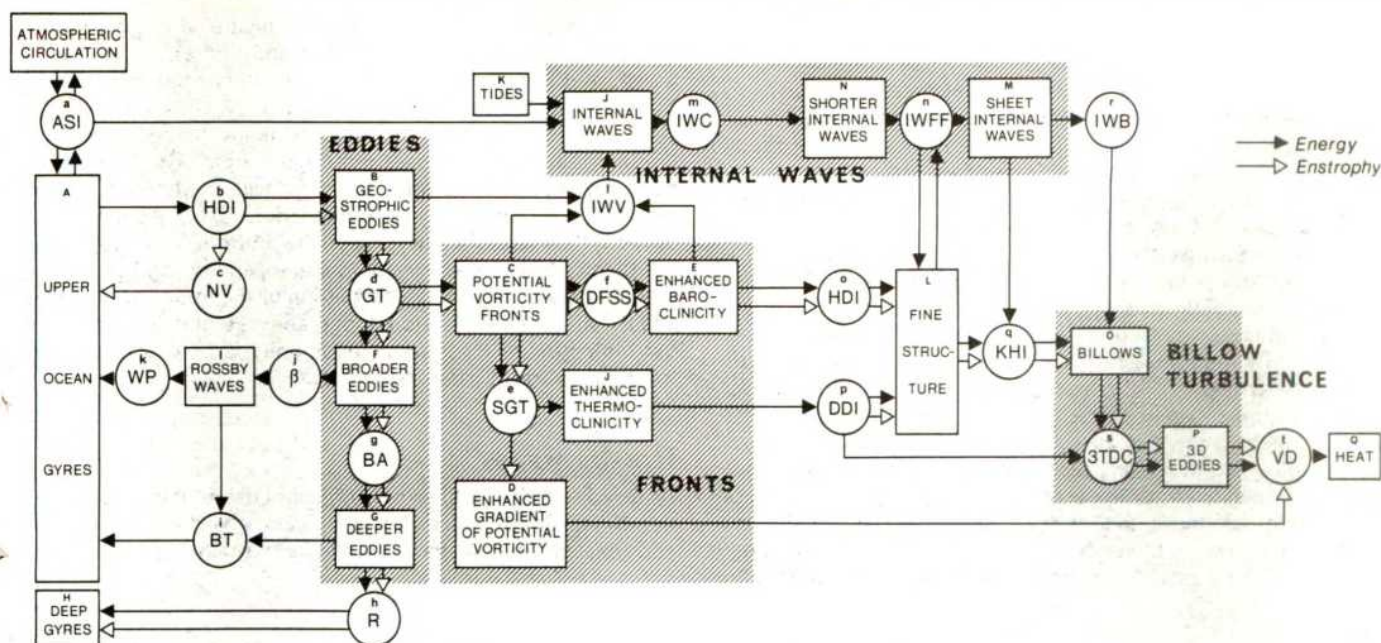
## The eddies

Hydrodynamic instability (b) of the gyres<sup>3,4</sup> and unsteady external forcing effects (wind, surface heat and moisture transfer) generate eddies (B) whose horizontal dimensions are of the order of 100 km and circulation speed of the order of 10 km

day<sup>-1</sup>. These eddies have a Rossby number ( $R_0 = U/Lf$ ) of the order of 0.01 and are, therefore, quasi-geostrophic. Field observations<sup>5</sup> during the 1970s have shown that such eddies occur widely (believed throughout the ocean) albeit with considerable regional variation (being strongest around the baroclinicity maxima of permanent fronts and western boundary currents). They are readily detected in oceanographic sections by the order of 100 m vertical displacement of isopycnals (and isotherms). The energy density in the spectral peak associated with the eddies (Fig. 1) exceeds that of the gyres by a factor of nearly 100; they are the energy-containing eddies of oceanic turbulence<sup>6</sup>. As detached eddies form from meanders, they interact with the gyre scale circulation in the upper ocean, influencing the pattern of mean streamlines<sup>7</sup>. There is some evidence<sup>8</sup> that, like their atmospheric counterparts<sup>9</sup>, eddy stress profoundly influences (c) the general circulation as though by negative viscosity. On the other hand, the eddies spread passive scalar anomalies along density surfaces at a rate equivalent to a (positive) diffusivity of  $\sim 70 \text{ km}^2 \text{ day}^{-1}$  (refs 6, 10).



**Fig. 1** A comparison of the climatological spectra for: a, turbulent kinetic energy in the atmosphere; b, turbulent kinetic energy and internal wave energy in the ocean based on recent observations. The space and time scales are in both cases approximate, being based on a mixture of eulerian and lagrangian estimates. (Figure reproduced from ref. 38.)



**Fig. 2** The new flow diagram for cascades of energy and enstrophy in the ocean. Letters on each box are indexed in the text. The following abbreviations have been used in labelling the circled processes: (a) ASI, air-sea interaction; (b) HDI, hydrodynamic instability (baroclinic and barotropic); (c) NV, negative viscosity, associated with baroclinic instability; (d) GT, geostrophic turbulence, which initiates the process of kinematic frontogenesis; (e) SGT, semi-geostrophic turbulence; (f) DFSS, dynamic frontogenesis at the (baroclinic) sea surface; (g) BA, baroclinic adjustment; (h) R, rectification of deep eddy enstrophy to give deep gyres; (i) BT, interaction with bottom topography; (j)  $\beta$ , interaction between eddies and Rossby waves; (k) WP, westward propagation of Rossby wave energy; (l) IWC, internal wave cascade of energy to higher wavenumbers; (m) IWCFF, interaction between internal waves and fine structure—internal wave strain produces fine structure, and fine structure permits very short trapped 'sheet' waves; (n) HDI, hydrodynamic instability of mesoscale fronts; (o) DDI, double-diffusive instability, leading to convection; (p) KHI, Kelvin-Helmholtz instability; (q) IWB, internal wave breaking (other than KHI); (r) 3DTC, three-dimensional turbulence cascade; (t) VD, dissipation of turbulent kinetic energy and enstrophy by molecular viscosity.

## Eddy decay

Observations of the streamline patterns associated with the eddies show a slow evolution with a lagrangian correlation time scale of  $\sim 50$  days (ref. 6); so, although they are the oceanic equivalent of the synoptic scale storms of the atmosphere, the eddies decay very much more slowly. (Rings, as distinct from eddies, decay an order of magnitude more slowly). One of the principal challenges in the study of oceanic turbulence is to develop a theory for this observed rate of decay. To decay, the eddies must lose both energy and enstrophy. The observed lifetimes indicate that this must occur at rates given, to order of magnitude, by the following example:

Eddy width

$$L = 100 \text{ km}$$

Rotation speed

$$U = 10 \text{ km day}^{-1}$$

Energy density

$$E = \frac{U^2}{2} = 50 \text{ km}^2 \text{ day}^{-2} \text{ per unit mass}$$

Enstrophy density

$$\Omega' = \frac{U^2}{2L^2} = 5 \times 10^{-3} \text{ day}^{-2} \text{ per unit mass}$$

Observed lifetime

$$T = 100 \text{ days}$$

Deduced dissipation rates:

$$(1) \text{ Energy } \quad \epsilon = 0.5 \text{ km}^2 \text{ day}^{-3}$$

$$(2) \text{ Enstrophy } \quad \eta = 5 \times 10^{-5} \text{ day}^{-3}$$

Ultimately the energy and enstrophy are dissipated by molecular viscosity ( $\nu = 10^{-2} \text{ cm}^2 \text{ s}^{-1}$  for seawater). Neglecting, for the moment, the complex processes shown in Fig. 2, we can estimate dissipation scales for the above example.

Dissipation scales:

$$(1) \text{ Energy } \quad l_e = (\nu^3 \epsilon^{-1})^{1/4} = 1 \text{ cm}$$

$$(2) \text{ Enstrophy } \quad l_n = (\nu^{1/2} \eta^{-1/6}) = 1 \text{ m}$$

In this primitive model, the eddy energy and enstrophy have to cascade through seven and five decades respectively of Fourier space before molecular viscosity can dissipate them, a requirement not significantly changed by the new model.

## The enstrophy cascade

The basic mechanism of the enstrophy cascade has been recognized for well over a decade, being closely related to the theoretical idealization of inviscid two-dimensional turbulence, in which particles retain their relative vorticity because there is no vortex stretching. Although the eddy motion in the interior of the ocean is not strictly two-dimensional it is—to a much better approximation—adiabatic, with the result that particles effectively retain their potential vorticity as they are swept around the complicated, fluctuating eddy streamline patterns. Below the wind-mixed layer and below the top few metres of the ocean, where the Sun warms the water diabatically, the most serious cause of error in the assumption of potential vorticity conservation arises from diabatic mixing by motion that overturns isentropic surfaces. Identifying this with billow turbulence we can estimate the magnitude of the error. The time scale for potential vorticity change due to diabatic mixing at rate  $K$ , in a region where the curvature of the vertical profile of  $N$  has a scale depth  $L_N$ , is given by  $T \approx L_N^2/K$ . Taking  $L_N = 0.1 \text{ km}$  for the oceanic thermocline, and estimating  $K$  from the above example

$$K = \epsilon N^{-2} = 5 \times 10^{-7} \text{ km}^2 \text{ day}^{-1}$$

where  $N = 1,000 \text{ day}^{-1}$ , we calculate that  $T \sim 2 \times 10^5$  days, which is so much longer than the eddy lifetime that we can neglect the effect of diabatic mixing. (The same calculation also justifies the assumption of potential vorticity conservation in gyre dynamics, for which the circulation time is of the order of 10 yr.)



## Fronts

The enstrophy cascade is, therefore, assumed to be adiabatic, and to proceed by lateral redistribution of potential vorticity<sup>12</sup>. As Batchelor<sup>11</sup> showed in the simpler case of two-dimensional turbulence, this leads to kinematic frontogenesis (d). A multiplicity of ever-extending, ever-thinning fronts (C) develop in the eddy contours of constant potential vorticity. This advective redistribution of eddy enstrophy has important consequences. First, the stretching of contours of constant potential vorticity into long, thin fronts introduces a local anisotropy involving sharp gradient of vorticity (D) and correspondingly large Rossby number in the cross-front direction. The resulting flow field is described by the semi-geostrophic equations used in studies of mesoscale fronts<sup>13,14</sup>. We therefore call this motion occupying the waveband 10 km to 1 m 'semi-geostrophic turbulence'. Most of the kinetic energy in each front is in its horizontal, quasi-geostrophic jet; however, the weak ageostrophic cross-front motion associated with the continuous thinning of the front is not horizontal, but rather it runs up and down the density surfaces inclined by the eddy baroclinicity. (Roughly speaking, the axes of the fronts lie tangentially to the adjacent eddies, like the bands of a spiral nebula.) At the sea surface, where density surfaces outcrop, this ageostrophic motion redistributes the strong near-surface thermoclinicity (due to solar heating) to give the characteristic modulation of sea surface temperature seen in



**Fig. 3** An IR image of the central Mediterranean Sea from NOAA 5 showing eddies sharply outlined by sea-surface temperature gradients at mesoscale fronts. (Photograph reproduced by permission of Dr P. Baylis, University of Dundee.)

satellite IR images (Fig. 3). At the same time, the kinematic frontogenesis (d, e) forced by the eddy motion interacts with the upper boundary (f) causing the frontal baroclinicity to peak strongly in the top few decametres, but to flatten below<sup>14</sup> (E), so that the kinetic energy of the semi-geostrophic turbulence becomes concentrated near the sea surface.

## Eddy expansion

As the eddy vorticity becomes teased out into fronts that extend beyond the original dimensions of the eddy, the mean eddy circulation also expands (F), carrying with it a small portion of the original eddy vorticity<sup>12</sup>. This lateral expansion is the oceanic realization of the reverse energy cascade in two-dimen-

sional turbulence theory. The broadening introduces baroclinic adjustment (g) with the result that eddy potential energy is transferred to eddy kinetic energy; the eddy rotates faster. At the same time, due to potential vorticity conservation, the vertical distribution of eddy energy tends to become more uniform; the eddy becomes more barotropic (G). This drives eddy enstrophy down into the deep ocean, where it can be rectified (h) to force deep gyre circulations<sup>15</sup> (H). As the eddies deepen they also begin to feel the bottom topography (i) producing the observed spatial inhomogeneity<sup>5</sup> and providing the link between the mean circulation of the upper ocean gyres and the much deeper bottom topography. Hence the steering of the Gulf Stream by bottom topography is a consequence of frontogenesis in the Gulf Stream eddies.

## Rossby waves

As an eddy broadens it soon approaches the limit beyond which the North-South difference in planetary vorticity across the eddy exceeds the mean eddy (relative) vorticity

$$\beta L > U/L$$

For the eddy in our example, this occurs when  $L > 200$  km. At this scale the eddy motion becomes influenced by the rotating Earth's sphericity (j) and energy begins to radiate as Rossby waves<sup>16</sup> (I), which propagate westwards. Streamline patterns derived from the MODE data exhibit this characteristic westward phase drift<sup>5</sup>. Compared with the full spectrum from millimetres to megametres, the eddies expand very little before Rossby wave radiation takes hold. The proximity of the scales at which the eddies first receive energy from the gyres and subsequently are converted to Rossby waves explains the narrowness of the observed spectral valley (not quite a 'gap') between the spectral peaks of the eddies and the gyres (Fig. 2). The Rossby waves powered by eddy expansion radiate energy to the distant ocean (possibly after scattering by bottom topography (i)), allowing mean circulation to be driven from a distance. The effect may be intensified at a western boundary, where energy tends to be trapped (k), accelerating the western boundary current and so contributing to the associated gyre circulation<sup>15,16</sup>.

## Internal waves

In classical inviscid, two-dimensional turbulence theory<sup>17,18</sup> all eddy energy is transferred to larger scale and eventually to the gyres, but in the ocean much of the energy cascades to smaller scale to be dissipated locally by molecular viscosity. The mechanism for this energy cascade cannot be turbulent frontogenesis for, although it efficiently cascades enstrophy to small scale, the associated energy cascade rate,  $\epsilon_t$ , is reduced in proportion to the square of the dissipation scale,

$$\epsilon_t = \eta_t l^2$$

For our example ( $\eta_t = 5 \times 10^{-5} \text{ day}^{-3}$ ,  $\epsilon = 0.5 \text{ km}^2 \text{ day}^{-1}$ ,  $l_e = 10^{-5} \text{ km}$ )

$$\epsilon_t = 5 \times 10^{-15} \text{ km}^2 \text{ day}^{-1} = 10^{-10} \epsilon$$

Thus, frontogenesis cannot dissipate much of the eddy energy. On the other hand, observations of ocean microstructure<sup>20,21</sup> are broadly consistent with the mean energy dissipation rate of our example ( $\epsilon = 0.5 \text{ km}^2 \text{ day}^{-1}$ ). How then does energy cascade from the eddies to small scale? One solution is that internal waves (J) extract energy from the eddies (and from the fronts) through the Reynolds stress they exert on the shear in the eddy/front flow<sup>22</sup>. The magnitude of the corresponding 'internal wave viscosity' (I) has recently caused controversy<sup>23,24</sup>, earlier estimates of  $0.1 \text{ km}^2 \text{ day}^{-1}$  being later revised downwards by a



factor of 10–100. The higher values were estimated on the basis of dynamical theory; the lower values are based on field observations. Nevertheless, the concept of internal wave viscosity is generally accepted, only the magnitude is in doubt. Taking an intermediate value of  $K_w = 0.005 \text{ km}^2 \text{ day}^{-1}$ , we estimate the rate of energy extraction from eddies with a mean vertical shear of  $10 \text{ day}^{-1}$  to be

$$\varepsilon_w = K_w (dU/dz)^2 = 0.5 \text{ km}^2 \text{ day}^{-3}$$

This is precisely the value of  $\varepsilon$  in our example, so we tentatively conclude that internal wave viscosity provides an important mechanism for extracting energy from the eddies.

Once the energy enters the internal wave spectrum it is believed to cascade efficiently by wave–wave interaction to the smallest scales of wave motion. This concept of an internal wave energy cascade is based on a combination of dynamical theory and empirical knowledge acquired during the past decade. In particular, observations have revealed a remarkable homogeneity of spectral form and level in the interior of the ocean<sup>25</sup>, with significant modifications in the upper ocean<sup>24</sup>. This is interpreted in terms of the universal saturation of the internal wave field<sup>23</sup>. Whenever additional energy is added at any scale (for example, by interaction with an eddy) the surplus is rapidly cascaded through the spectrum by wave–wave interaction (m) until it reaches the smallest scales, where the waves break, transferring the energy to three-dimensional turbulence<sup>24</sup>. Orlanski<sup>26</sup> has suggested that the shedding of surplus energy may occur even more efficiently by the enhanced large-scale wave strain causing small waves to break directly without a cascade through the whole wave spectrum. Either way, the large (1–10 km) internal waves that extract energy from the eddies/fronts pass it to small scales (~5 m) so efficiently that the energy is not propagated far from the point of injection before it is lost to breaking<sup>27</sup>. Energy removed from eddies by internal wave viscosity is dissipated locally, probably within some tens of kilometres. Note that the internal wave spectrum is not kept saturated by the energy loss from the eddies; there are other important sources, including air–sea interaction (a) and tides (K). Nor need the energy extraction from eddies come exclusively from internal wave viscosity: a significant part may come from the interaction of the eddies with bottom topography (not shown in Fig. 2). Finally the local character of energy dissipation by internal waves suggests that observed spatial inhomogeneity in the internal wave field, especially in the upper ocean, may reflect recent interactions with eddies and, especially in the upper ocean, with fronts<sup>28</sup> (E).

## Fine structure

Turning back to Fig. 1, we now arrive at the fine structure box (L). We have no theory for ocean fine structure just observations interpreted speculatively on the basis of analogy with laboratory experiments or otherwise. Some of the observed fine structure in density stratification can be explained by the transient straining (n) of the mean density field by internal waves<sup>29</sup>. The thermohaline characteristics of the fine structure suggests that water masses of different characteristics have intruded into one another in layers with vertical scales in the range 1–100 m and horizontal scales of up to several tens of kilometres<sup>24</sup>. Such structure is particularly sharply defined, with thin sheets (vertical scale ~10 cm) separating the layers, near fronts where the mean cross-front thermoclinicity is enhanced by kinematic frontogenesis<sup>28</sup> (J). A correlation between intrusions and meanders on fronts has suggested that the dynamical instability (o) of mesoscale fronts may provide an important mechanism for fine structure generation<sup>30</sup>. Theoretical studies of frontal instability showing complex vertical structure in the growing waves support this conjecture (M. K. MacVean, personal communication). An alternative proposal is that intrusions are driven by double diffusive convection (p), which is also most

effective in the enhanced thermoclinicity at fronts<sup>31</sup>. Most observations of fine structure comprise single profiles or sections, which do not provide the information needed to discriminate between these three main mechanisms: (1) internal wave straining (n<sub>1</sub>); (2) dynamical intrusion associated with frontal baroclinicity (o); (3) convective intrusion driven by the double diffusive release of latent static instability associated with frontal thermoclinicity (p). New techniques yielding time series of three-dimensional surveys of fine structure may help to overcome these limitations<sup>32</sup>.

The net influence of fine structure on the overall cascades of energy and enstrophy in the ocean remains uncertain, but its presence significantly modifies the details of the important transition from the cascades of frontogenesis and wave–wave interaction, in which isentropic surfaces are not overturned, to

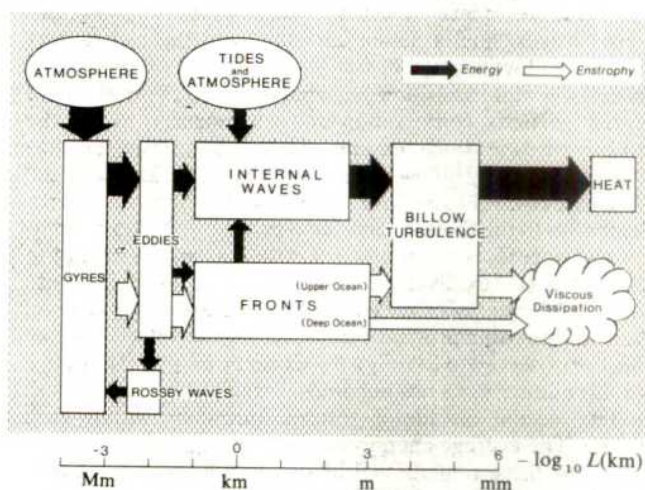


Fig. 4 A simplified cascade diagram showing the principal paths by which oceanic eddy energy and enstrophy flow through the spectrum. The scale provides an indication of the approximate positions of the various classes of motion in the overall spectrum megametres to millimetres. The breadths of the cascade arrows are intended to suggest a possible distribution between competing paths.

the cascade of three-dimensional quasi-isotropic turbulence, in which they are. I envisage fine structure as the bridge between these two classes of cascade; not a single-span bridge—more like a complicated tropical bamboo construction. We may be able to develop theories for the statistical properties of ocean fine structure on the basis of some thermodynamic-like principle of optimum energy and enstrophy transfer between the three cascades. But for the present we must merely note elements of the fine structure mechanism. First, the internal wave community has drawn attention to the importance of fine structure in determining the high wavenumber cutoff of the internal wave spectrum<sup>33</sup>. Flow visualization observations have shown that the shortest internal waves—'sheet waves' (M)—are trapped on the thin sheets of enhanced static stability. It is not clear how they are generated; presumably by interaction (n<sub>2</sub>) between the fine structure and the shortest free internal waves. The trapped sheet waves are important because they and not the free waves are observed to break<sup>34</sup>. Breaking has been observed to result from Kelvin–Helmholtz instability (q), which occurs when the local Richardson number is <0.25.

$$Ri = \left| N / \frac{\partial U}{\partial z} \right|^2, \quad \left( \text{where } \frac{\partial U}{\partial z} \text{ is the shear} \right)$$

Kelvin–Helmholtz instability occurs infrequently when a sheet wave provides additional fluctuating shear (due to the orbital motion of the water particles) to supplement the more steady



shear of the fine structure currents<sup>34</sup>. Wave breaking may also occur independently of shear instability ( $r$ )<sup>35</sup>, but this has not been observed in the ocean.

## Billow turbulence

Kelvin-Helmholtz instability causes density (and isentropic) surfaces to overturn giving billows (O). Observations show that billows occur in rows on a sheet making blini several metres across in otherwise laminar flow<sup>36</sup> (defined here as being flow devoid of motion that overturns density surfaces). Empirical estimates of the instantaneous volume fraction occupied by billows in the upper ocean range from a few ( $\sim 5$ ) per cent in calm weather to an order of magnitude greater in stormy weather<sup>37</sup>. There is also considerable regional variability, with the highest concentrations found at intense currents and near fronts<sup>20,21,38</sup>. This intermittency must be allowed for as we follow the cascade of energy from the non-overturning motions (internal waves, fine structure currents) into the overturning motions of billow turbulence.

In making this transition we abandon the assumption of potential vorticity conservation and no longer consider the enstrophy cascade which becomes lost in the explosive generation of enstrophy by billow turbulence. The dual cascade of the mesoscale becomes fused into one as we pass into the microscale, thanks to the three-dimensional process of vortex stretching, which increases enstrophy at a rate that allows energy to cascade with no flux divergence until it becomes scattered into heat by molecular viscosity. The billows, the energy-containing eddies of three-dimensional turbulence in the interior of the ocean, are observed to be only a few decimetres high. They have Reynolds numbers of a few hundreds, barely sufficient to permit a modest inertial cascade of isotropic turbulence inside each billow ( $r$ ). The average energy cascade rate,  $\bar{\epsilon}_B$ , inside such tiny cylinders of three-dimensional billow turbulence is related to the mean energy flux  $\bar{\epsilon}_w$  through the internal wave cascade (neglecting contributions from sources other than the eddies) by the mean billow intermittency factor  $\bar{I}$ : that is

$$\bar{I}\bar{\epsilon}_B \equiv \bar{\epsilon}_w$$

For  $\bar{I} = 0.05$  and  $\bar{\epsilon}_w = 0.5 \text{ km}^2 \text{ day}^{-3}$ ,  $\bar{\epsilon}_B = 10 \text{ km}^2 \text{ day}^{-3}$ , which is typical of direct estimates from velocity microstructure measurements<sup>20,21</sup>. For this value of the billow turbulence energy cascade rate, the Kolmogorov microscale of molecule dissipation is

$$l_e = (\nu^3 \bar{\epsilon}_B^{-1})^{1/4} = 3 \text{ mm}$$

And the Ozmidov scale of largest overturning (taking  $N = 1,000 \text{ day}^{-1}$ ) is

$$l_N = (\epsilon_B / N^3)^{1/2} = 10 \text{ cm}$$

in good agreement with direct observation.

## Conclusion

The conversion of turbulent kinetic energy to heat ( $Q$ ) and the associated molecular dissipation of enstrophy ( $t$ ) complete the cascades begun with the creation of geostrophic eddies by instability of the mean gyre circulation. The cascades span 10 decades of Fourier space, a waveband one hundred million times broader than that of the most advanced prognostic model of ocean circulation. I have discussed the physics of processes that influence the mean circulation but which can never be resolved in such models. These unresolved processes must be treated statistically in the model equations—their effect on the large-scale circulation and distributions must be parameterized. Current practice relies on eddy transport coefficients invented by Boussinesq in the nineteenth century. Systematic investigation of the physics of ocean turbulence began in the 1960s and has progressed rapidly during the 1970s, with major advances in our understanding of eddies, waves, fronts, fine structure and billows. The new cascade flow diagram is not claimed to be correct, but it seems to offer the simplest conceptual model consistent with contemporary theoretical ideas and with the admittedly still primitive estimates of cascade rates. I anticipate and invite modifications. For example, the role of the ocean surface in modifying the cascade physics has scarcely been mentioned and the role of the seasonal change not at all. The interior of the ocean has been emphasized rather than the boundary layers, although these are likely to be important. Finally, according to the model, energy is extracted from the eddies by both internal waves and Rossby waves, but the latter only after the eddies have expanded by a factor of about two. If the internal wave viscosity is higher in some regions, a larger proportion of eddy energy will cascade to billow turbulence leaving less to feed Rossby waves, and vice versa. Does this imply less eddy expansion in regions of greater wave viscosity? If so, then there will also be less eddy deepening in these regions, and therefore weaker interaction with bottom topography and more feeble powering of deep gyres. But the wave viscosity depends on the internal wave saturation level and therefore on the mean static stability (and perhaps on the fine structure intensity). This suggests that the cascade physics described by the proposed new flow diagram should be inherently stable when applied to oceanic circulation models.

This article is based on a lecture presented at the IAPSO General Assembly, Canberra, December 1979 and uses material presented at the Second International Symposium on Turbulence in the Ocean (Liège, May 1979) co-sponsored by IAPSO and SCOR with support from UNESCO, IOC and IDOE. (Contributed papers are reported in ref. 39 and invited papers in ref. 40.) I thank Konstantin Fedorov, Terry Joyce, Sergei Kitaigorodskii, Dirk Olbers, Peter Rhines and Stewart Turner for helpful comments on an earlier version of the article.

1. IOC Workshop Rep. No. 21 (UNESCO, 1979).
2. Worthington, V. *On the North Atlantic Circulation* (Johns Hopkins, Baltimore, 1976).
3. Gill, A. E., Green, J. S. A. & Simmons, A. *Deep-Sea Res.* **21**, 499–528 (1974).
4. Rhines, P. B. in *The Sea* Vol. 6, 189–318 (Wiley-Interscience, London, 1979).
5. The MODE group *Deep-Sea Res.* **25**, 859–910 (1978).
6. Freeland, H. J., Rhines, P. B. & Rossby, H. T. *J. mar. Res.* **33**, 383–404 (1975).
7. Holland, W. R. in *The Sea* Vol. 6, 3–46 (Wiley-Interscience, London, 1979).
8. Webster, F. *Deep-Sea Res. Suppl.* **16**, 357–368 (1969).
9. Green, J. S. A. *Q. J. R. met. Soc.* **96**, 157–185 (1970).
10. Veronis, G. in *The Sea* Vol. 6, 169–188 (Wiley-Interscience, London, 1979).
11. Batchelor, G. K. *Phys. Fluids Suppl.* **II** **12**, 233–238 (1969).
12. Rhines, P. B. A. *Rev. Fluid Mech.* **11**, 401–441 (1979).
13. Hoskins, B. & Bretherton, F. P. *J. atmos. Sci.* **29**, 11–37 (1972).
14. MacVean, M. K. & Woods, J. D. *Q. J. R. met. Soc.* **106**, 293–311 (1980).
15. Holland, W. & Rhines, P. B. *J. phys. Oceanogr.* (submitted); *Dyn. Atmos. Oceans* **3**, 289–325 (1979).
16. Rhines, P. B. *J. Fluid Mech.* **69**, 417–443 (1975).
17. Taylor, G. I. *Phil. Trans. R. Soc. A* **A240**, 1–26 (1915).
18. Fjortoft, A. *Tellus* **5**, 225–230 (1953).
19. Lilly, D. in *Dynamic Meteorology* (Reidel, Dordrecht, 1974).
20. Gibson, C., Vega, L. A. & Williams, R. B. in *Advances in Geophysics* **18A**, 353–370 (Academic, London, 1974).
21. Monin, A. S. & Ozmidov, R. V. in *Physics of the Ocean* **1** (Woods, Moscow, 1978).

22. Müller, P. & Olbers, D. *J. geophys. Res.* **80**, 3848–3860 (1975).
23. Garrett, C. J. & Munk, W. H. A. *Rev. Fluid Mech.* **11**, 339–69 (1979).
24. Gregg, M. & Briscoe, M. G. *Rev. Geophys. Space Phys.* **17**, 1524–1528 (1979).
25. Müller, P., Olbers, D. & Willebrand, J. *J. geophys. Res.* **83**, 479–500 (1978).
26. Orlandi, I. in *Marine Turbulence* 65–100 (Elsevier, Amsterdam, 1980).
27. Olbers, D. in *Turbulence in the Ocean* (Springer, Berlin, in the press).
28. Woods, J. D. in *Physics of Fronts in the Ocean* (in preparation).
29. de Saubies, Y. *Proc. 14th Liège Ocean Hydrodynamics Colloq.* (Elsevier, Amsterdam, 1980).
30. Woods, J. D., Wiley, R. L. & Briscoe, M. G. in *A Voyage of Discovery*, 253–275 (Pergamon, Oxford, 1978).
31. Turner, J. S. in *Turbulence in the Ocean* (Springer, Berlin, in the press).
32. Woods, J. D. & Minnett, P. J. *Deep-Sea Res.* **26A**, 85–96 (1979).
33. Garrett, C. J. R. *Dyn. Atmos. Oceans* **3**, 239–266 (1979).
34. Woods, J. D. *J. Fluid Mech.* **32**, 791–800 (1968).
35. Thorpe, S. A. *J. geophys. Res.* **80**, 328–338 (1975).
36. Woods, J. D. in *Turbulence in the Ocean* (Springer, Berlin, in the press).
37. Nasmyth, P. *ICES Symp. Rep. No. 6* (ICES, 1969).
38. Proc. JOC-SCOR Study Conf. on Models of Oceanic Circulation and Climate (WMO, Geneva, 1977).
39. Nihoul, J. C. J. (ed.) *Marine Turbulence* (Elsevier, Amsterdam, 1980).
40. Woods, J. D. (ed.) *Turbulence in the Ocean* (Springer, Berlin, in the press).

## ARTICLES

# Latitudinal beaming of planetary radio emissions

Dyfrig Jones\*

Space Science Department, ESA, Estec, Noordwijk, The Netherlands

*The Voyager missions have revealed that jovian kilometric radiation (emanating from Jupiter's magnetosphere) is beamed away from the zenomagnetic equator. Results from GEOS 1 show that terrestrial non-thermal continuum or myriametric radiation is similarly beamed away from the geomagnetic equator. A mode-coupling mechanism is proposed such that measurements of the direction of propagation of the escaping O-mode radiations may allow the construction of the first high-resolution maps of the shapes of the equatorial plasmopause and Io torus.*

THE two Voyager spacecraft, which flew by Jupiter in March and July 1979, have shown that Jupiter's magnetosphere has many similarities to the Earth's as far as radio-wave observations are concerned<sup>1-4</sup>. Close parallels had already been drawn between jovian decametric emission, which has been observed from Earth for over two decades, and terrestrial kilometric radiation which has only recently been seen by Earth-orbiting spacecraft<sup>5</sup>. (Decametric and kilometric refer to the free-space wavelengths at which the radiations are predominantly observed.)

One wave component observed by the Voyager spacecraft—jovian kilometric radiation (JKR)—had seemed to have no counterpart within the Earth's magnetosphere. It is suggested here, however, that JKR is the analogue of the Earth's non-thermal continuum radiation<sup>6,7</sup>, the latter being termed terrestrial myriametric radiation (TMR). Both radiations seem to have their source in the intense electrostatic waves observed to be closely confined to the magnetic equators of both planets<sup>8,9</sup> in regions of large plasma density gradients—the Earth's plasmopause and the outer edge of the Io plasma torus.

## Terrestrial myriametric radiation

A particularly clear example of TMR was obtained for ~80 min on 4 March (day 63) 1978 by the GEOS 1 S-300 wave experiment which incorporates high resolution on-board correlators<sup>10,11</sup> and sweep frequency analysers<sup>12</sup> (SFAs). The spectrogram shown in Fig. 1 depicts signals from the 40 m tip-to-tip electric dipole as analysed by the SFAs. The start time is 02.50 UT and the end time is ~04.00 UT. During these observations, the satellite moved from ~5.4  $R_E$  to ~4.2  $R_E$ , where  $R_E$  is an Earth radius (6,370 km) and from a magnetic latitude of ~16°N to ~8°N. TMR is the striated emission seen in two frequency bands. Other natural emissions occur in the vicinity of the electron plasma frequency ( $f_{pe} = 9 \cdot 10^{-3} N_e^{1/2}$  kHz;  $N_e$  is the electron density per  $m^3$ ) and at the  $f_q$  'resonance' respectively. The increase in plasma frequency occurs because the spacecraft is moving towards the Earth and encountering increasing plasma density as the plasmopause is approached. Weak noise at lower frequencies is probably at  $3f_{ce}/2$  (ref. 8), where  $f_{ce}$  is the electron gyrofrequency ( $f_{ce} = 1.8 \cdot 10^3 B_0$  kHz,  $B_0$  is the magnetic field strength) which must also increase as GEOS 1 moves inwards. Clearly the low-frequency cut-off of TMR cannot be depended on to yield unambiguously the local plasma density, as has been suggested previously<sup>7</sup>.

The TMR increases in strength as the spacecraft approaches the plasmopause where intense radiation occurs in the vicinity of  $f_{pe}$  (where  $f_{pe}$  is the electron plasma frequency). The striations in the TMR are due to a beat between the satellite spin frequency ~0.2 Hz and the frequency ~0.04 Hz with which the SFAs are sweeping through the frequency range 0–75 kHz. The nulls in

the pattern occur when the dipole antenna used for receiving is aligned parallel to the direction of the emission's propagation, the antenna spin plane being approximately parallel to the equatorial plane. The fact that the pattern is so well-defined for so long is an indication that the radiation is arriving from preferred directions as GEOS 1 moves in towards the plasmopause. Such patterns have been used for direction-finding to locate the sources of TMR (ref. 7, and P. J. Christiansen, M. P. Gough and J. Etcheto, personal communication), and the sources were found to lie on the dayside plasmopause and on the morning magnetosheath<sup>7</sup>. It was also established that the radiation is significantly, if not predominantly, propagating in the left-hand ordinary (L–O) magnetoionic mode.

The hypothesis for the production of TMR considered here<sup>13,14</sup> is that electrostatic waves close to the upper-hybrid-resonance (UHR) frequency  $f_{UHR} = (f_{pe}^2 + f_{ce}^2)^{1/2}$  are the source of TMR. These intense UHR waves, which exist in a warm plasma, are tightly confined to within a few degrees of the magnetic equator at, and beyond, the Earth's plasmopause<sup>8</sup>. They are probably produced by a warm loss-cone component of the energetic electron distribution as outlined by Ronnmark *et al.*<sup>15</sup>. By virtue of their propagation into a slowly varying plasma density, it is suggested that their wave numbers decrease such that they access directly the cold-plasma Z-mode branch<sup>16</sup> of the dispersion relation, which is a natural extension of the warm-plasma branch. Ray-tracing of Z-mode waves show how subsequent access can be gained by these waves to magnetoionic window points<sup>17,18</sup>; these allow the direct coupling of energy to L–O mode waves which then propagate to lower density regions. These L–O waves are found to be beamed away from the geomagnetic equator by the presence of the local magnetic field.

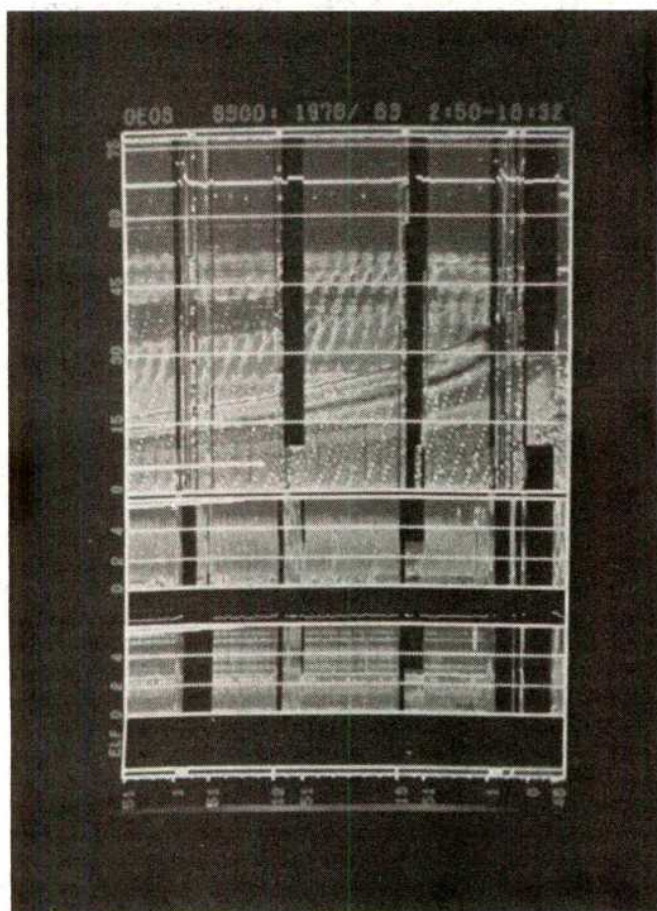
## Jovian kilometric radiation

The Voyager spacecraft observed radio emissions in the frequency range 10 kHz–1 MHz, emanating from Jupiter's inner magnetosphere<sup>1-4</sup>. The emissions seem to suffer a distinct latitudinal beaming such that beyond the orbit of Io, a shadow zone exists with virtually no radiation seen within  $\pm 10^\circ$  of the zenomagnetic equator<sup>19</sup>. Furthermore, the latitudinal extent of the shadow zone increases with increasing wave frequency, so that the higher frequencies are beamed to higher magnetic latitudes. Polarization measurements<sup>4</sup> have shown that radiation seen north of the shadow zone, that is when the jovian magnetic north pole is tilted towards the spacecraft, is left-hand polarized, whereas that observed in the southern magnetic hemisphere is right-hand polarized; polarization is defined with respect to the direction of the wave-normal at the observer.

Two distinct and separate locations have been suggested as being possible source regions of JKR. The first source is assumed to lie along auroral magnetic field lines linked to the Io torus<sup>20</sup>. The torus is a region of enhanced plasma density believed to extend around Jupiter, threaded by the orbit of Io, and therefore

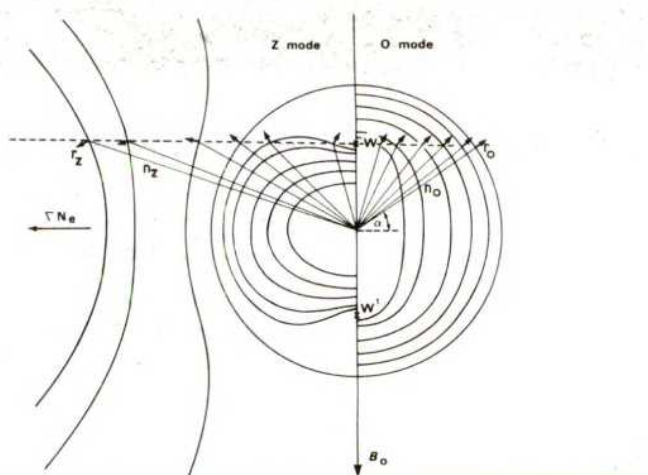
\*Present address: British Antarctic Survey, NERC, Madingley Road, Cambridge CB3 0ET, UK.





**Fig. 1** Diagrammatical representation of wave spectrogram obtained on GEOS 1 on 4 March 1978. Terrestrial myriametric radiation appears as inclined striations due to the preferential direction of arrival of the waves. Intense upper hybrid waves occur at  $\sim 30$  kHz after 04.00 UT.

lies close to the centrifugal and zenomagnetic equatorial planes. The auroral emission has been assumed to occur at  $2f_{pe}$  in the L-O mode<sup>20</sup>, and different frequencies would come from different altitudes above Jupiter, the higher frequencies being emitted from regions of higher densities closer to the planet. In this first theory, the Io torus acts merely as a passive obstacle to wave propagation, and ray-tracing in a model magnetosphere



**Fig. 2** Refractive index curves for the Z and O modes assuming that the gradient of electron density  $\nabla N_e$  is perpendicular to the magnetic field  $B_0$  as at the magnetic equator. A Z wave with initial wave normal  $n_z$  and corresponding ray  $r_z$  passes through the coupling point W to become an O wave finally having wave normal  $n_0$  and ray  $r_0$ , which make angle  $\alpha$  with the magnetic equator.

has shown that the equatorial shadow effect observed can be reasonably accounted for by this model, although the detailed extent of the shadow zone must depend on the assumed plasma density along auroral field lines. No specific mechanism has been suggested for wave emission at  $2f_{pe}$ , and as far as we know no unambiguous identification of  $2f_{pe}$  emissions has as yet been made within the terrestrial and jovian magnetospheres.

The other possible source is the Io torus itself<sup>2</sup>. To produce a shadow zone beyond the torus requires some sort of beaming mechanism, possibly inherent to the source. Another difficulty is an observation by Voyager 1, whose periapsis was at  $5 R_J$  which allowed it to traverse the torus centred at  $\sim 5.8 R_J$ . Peak densities within the torus were found to correspond to  $f_{pe} \sim 600$  kHz, whereas JKR extending up to  $\sim 1$  MHz has been detected. These results suggest that the Io torus may be unable to support emission at  $f_{pe} \sim 1$  MHz, the plasma frequency having been a possible candidate for the source emission. However, Voyager 1 probably did not pass through the region of peak density and Voyager 2, whose periapsis was at  $10 R_J$ , did encounter higher densities outside the torus than did Voyager 1 (ref. 4). Therefore plasma frequencies in the torus could exceed 1 MHz.

It is proposed here that JKR is created at, and beyond, the Io torus in a manner similar to that suggested for TMR. Within  $\sim 23 R_J$  of Jupiter, the Voyager spacecraft observed durable, intense UHR waves which, as was found at Earth, were very tightly confined to within  $\pm 2^\circ$  or less of the zenomagnetic equator<sup>9</sup>. However, much less is known about the Io torus than about the Earth's plasmopause and JKR may yield a significant insight into the characteristics of the torus at the magnetic equator.

## Theory

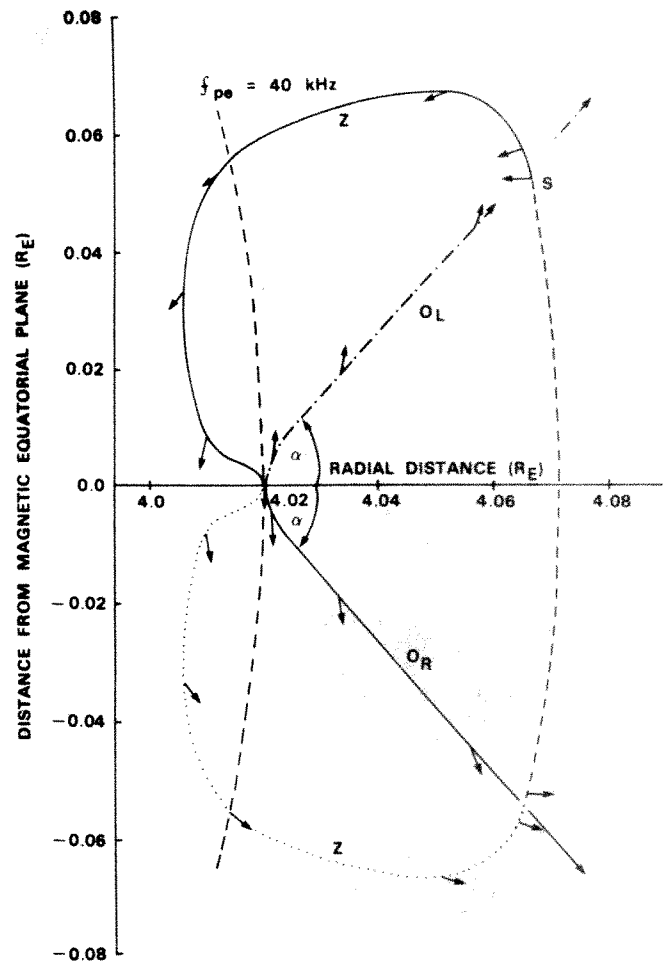
If a region of large density gradients<sup>13,14</sup> is located at the magnetic equator as at the plasmopause, then mode-coupling of Z-mode to O-waves could occur, and its consequences on the radiation can be illustrated by the refractive index surfaces in Fig. 2. The magnetic field  $B_0$  is shown with the electron-density gradient,  $\nabla N_e$ , assumed perpendicular to it as expected at the equatorial plasmopause. Z-mode refractive index surfaces have rotational symmetry about the magnetic field, but only one half is shown. The O-mode refractive index surfaces are also shown. The surfaces are for various plasma densities assuming the magnetic field to be constant; density in this refractive index domain increases towards the centre. The points W and W' are the window points through which Z waves can escape as O waves<sup>12,18</sup>. Snell's law requires that, during propagation,  $n \cos \theta$  remains constant,  $n$  being the modulus of the refractive index

vector in the direction of the wave normal, and  $\theta$  its angle with respect to the magnetic field. Therefore, a line parallel to the density gradient through point W represents the locus of the tips of the vectors from  $n_Z$  to  $n_O$  for the wave which couples from Z to O mode. The wave frequency, which is greater than the electron gyrofrequency, is assumed constant, the wave encountering the window when  $f = f_{pe}$ . Clearly, as the Z-O waves propagate through the coupling point to lower densities, the ray direction swings from  $r_Z$  to  $r_O$  and tends towards an angle  $\alpha$  with the equator, where  $\alpha$  is arcs in  $(f_{ce}/f_{ce} + f)^{1/2}$  (see ref. 17) and  $f_{ce}$  is the gyrofrequency at the window point, where  $f = f_{pe}$ . A similar ray will exist for window point  $W^1$ , and if mode coupling is the mechanism for TMR and JKR emission then the radiation would be beamed away from the magnetic equator at an angle  $\alpha$ . Figure 3 shows how  $\alpha$  depends on  $f_{pe}/f_{ce}$ , and for typical plasmaspheric densities, this ratio is in the region of 10 yielding an  $\alpha$  of  $\sim 17^\circ$ , although if the plasmapause moves to smaller radial distances such that  $f_{ce}$  increases, then  $\alpha$  may be much larger. Clearly if there is a large density gradient such that  $f_{pe}$  is increasing more rapidly than  $f_{ce}$ , then the higher frequencies from that region will be beamed to lower latitudes, and if the gradients are small so that  $f_{ce}$  increases more rapidly than  $f_{pe}$ , then the converse is true. If the plasma density gradient is radial, the beams will lie in the magnetic meridian plane; if it is not radial, the beams will lie in the plane containing the density gradient and magnetic field vectors.

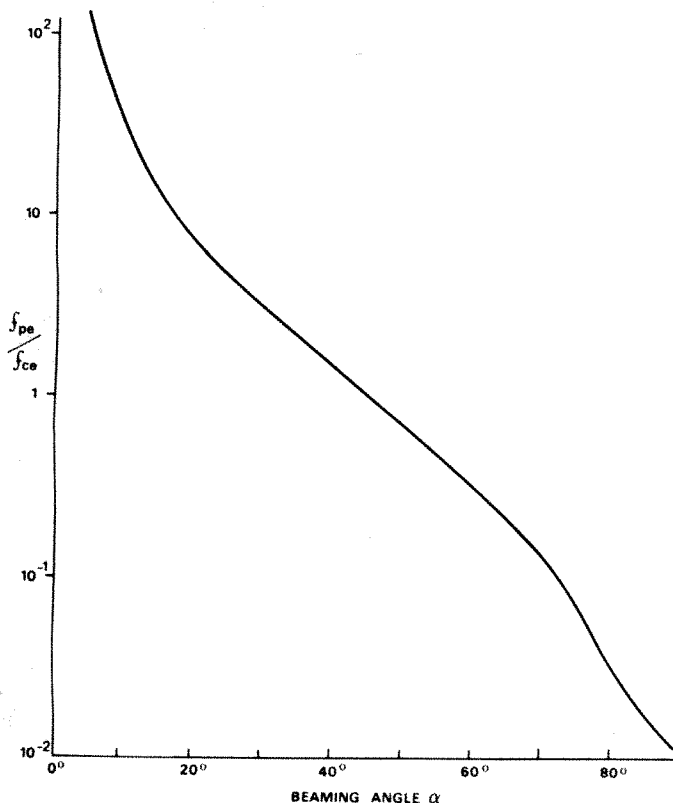
### TMR ray paths

The terrestrial magnetospheric model used for the ray tracing has been described elsewhere<sup>21</sup>, although the plasmasphere model has been updated using information from GEOS 1.

Figure 4 shows the ray path in the magnetic meridian plane at  $4R_E$  of the Z-mode wave which couples to the O-mode, and which was in fact traced back from the coupling point. The arrows on the ray path indicate the directions of the wave normal. At S the wave normal is approximately parallel to the density gradient and perpendicular to the magnetic field. (The computations were stopped at S because the wave moves very slowly and the computation time becomes excessive.) The wave



**Fig. 4** The ray path in the magnetic meridian plane of a 40-kHz wave which starts at S with its wave normal, depicted by the small arrow, approximately perpendicular to the magnetic field and parallel to the density gradient. Mode-coupling occurs at the magnetic equator and the escaping  $O_R$  wave (solid line) propagates to free space at angle  $\alpha$  to the magnetic equator; the contour  $f_{pe} = 40$  kHz is shown. Reversing the wave-normal of the Z wave in the southern hemisphere allows coupling to occur at the other window to produce the  $O_L$  ray as shown in Fig. 2.

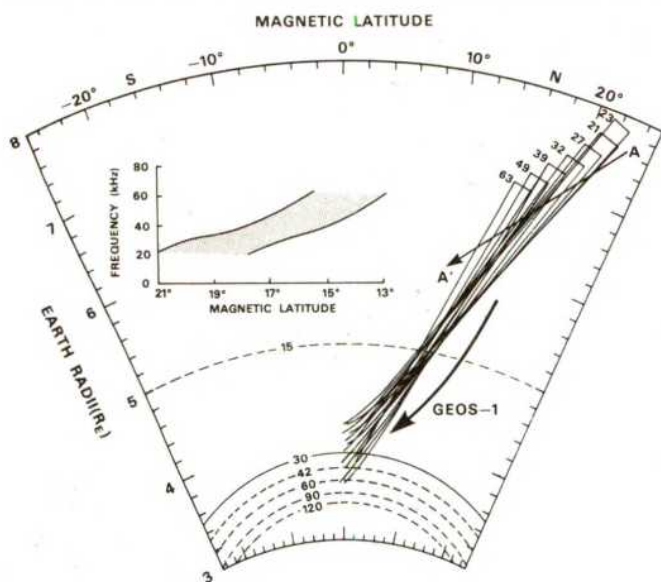


**Fig. 3** The variation of the beaming angle  $\alpha$  as a function of the ratio of electron plasma frequency to gyrofrequency,  $f_{pe}/f_{ce}$ .

normal in this direction is very important because electrostatic UHR waves can propagate<sup>15</sup> without damping only with their wave normals close to perpendicular to the magnetic field. Therefore if the warm-plasma electrostatic waves propagate to link on to the cold-plasma Z-mode, it might be expected that at that point (S) the Z wave-normal will be as shown. The possible significance of such Z wave-normals, parallel to the density gradient, had been pointed out previously<sup>22</sup>. The Z ray eventually reaches the coupling point with its wave normal parallel to the magnetic field, and the O ray which couples from it moves to lower plasma densities at an angle  $\alpha$  to the geomagnetic equator. This ray,  $O_R$ , will be observed to be right-hand polarized by a satellite; the ray  $O_L$  from the other window point will be observed to be left-hand polarized. Unfortunately, no polarization measurements of TMR have yet been performed.

It is significant that had the initial Z wave normal at S been such that the window had been just missed, the Z ray would propagate symmetrically about the equator, becoming electrostatic again, with its wave normal reversed, and possibly yielding its energy back to the charged particles on passing once more into the equatorial interaction region. Note that the latitudinal excursion of the Z ray which couples out is only  $\sim \pm 1^\circ$  from the magnetic equator, which was found to be approximately the extent of the intense UHR waves seen on GEOS and other spacecraft.





**Fig. 5** Beams of O radiation for different frequencies assuming each has coupled out at the levels corresponding to  $f = f_{pe}$ . The plasma frequency contours are labelled 15–120 kHz. The GEOS 1 track is shown and the inset shows the type of spectrogram observed by a satellite moving along track AA'.

If one assumes that the window points are distributed  $\pm 0.5^\circ$  about the Equator, then the resulting beams of TMR in the Northern Hemisphere are as shown in Fig. 5; identical beams exist in the Southern Hemisphere. The beams for a whole range of frequencies  $f$  are illustrated, each being assumed to have penetrated the window at the relevant level where  $f = f_{pe}$ . The track of GEOS 1 corresponding to the event on 4 March 1978 is also shown. The plasmopause in the model used in the ray-tracing needs to be moved inwards to slightly smaller radial distances. For a given frequency the latitudinal beam angle  $\alpha$  will then increase because  $f_{ce}$  increases, and  $f_{pe}/f_{ce}$  decreases. That the TMR above 45 kHz in the GEOS-1 spectrogram remains virtually unchanged throughout the time of observation indicates that the satellite was moving within and parallel to the beam at those frequencies. A satellite moving along track AA' in Fig. 5 would record a spectrogram similar to that shown in the inset. However, much more complicated spectrograms can be envisaged depending on the satellite track chosen. (An example of a TMR spectrogram in which the frequency decreases as the satellite moves inwards towards the plasmopause may be seen in Fig. 7 of ref. 23.) The frequency bandwidth of the TMR received at a given satellite position is indicative of the width of the beam, and the assumed  $\pm 0.5^\circ$  latitudinal extent of the source seems to be approximately that required to explain the GEOS 1 spectrogram.

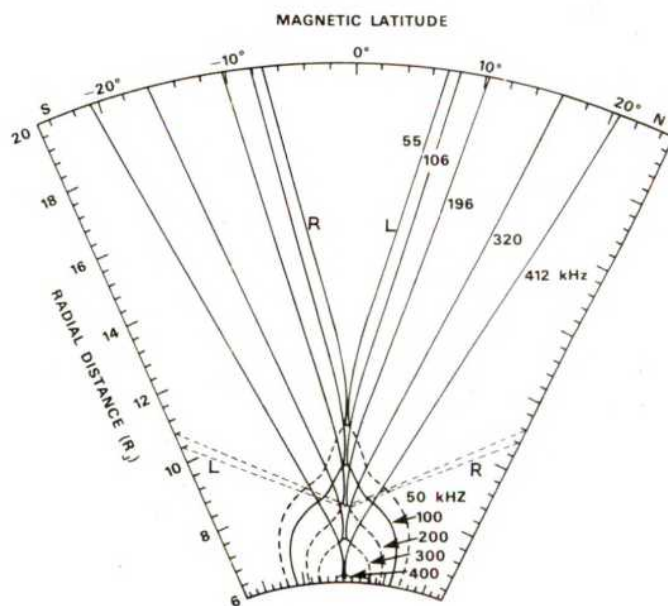
### JKR ray paths

Ray-tracing has also been performed in a model jovian magnetosphere assuming that UHR waves at the Io torus and beyond are responsible for JKR. The model magnetosphere, detailed elsewhere<sup>24</sup>, is largely similar to that of the Earth's taking into account the opposite polarity of the magnetic dipole, the different magnetic field strength and the existence of the Io plasma torus. If the Io torus has a low-curvature rounded outer edge at the equator, the O waves, which come from the proposed coupling process, will be beamed in a similar manner to those from the Earth's plasmopause. Because Jupiter's magnetic dipole is inverted compared with that of the Earth's, the beam which would be observed in the northern magnetic hemisphere would be left-hand polarized as seen by a spacecraft. This is opposite to what was observed by the Voyager spacecraft, and to

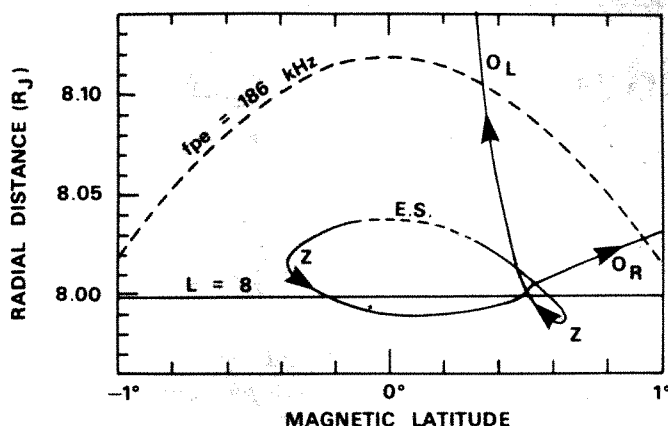
adjust the model to account for this, a distended torus is necessary, as shown in Fig. 6. The contours of constant plasma density are labelled with their corresponding plasma frequencies and the ray paths are shown for different wave frequencies, assuming that mode-coupling has occurred at  $\pm 0.5^\circ$  latitude. Provided the torus distension tilts with the tilting magnetic field, a spacecraft located at a given centrifugal latitude will observe tapered emissions of the type seen by the Voyager spacecraft; as the magnetic latitude of the spacecraft increases, higher frequencies are observed, and a shadow zone exists within  $\sim \pm 10^\circ$  of the magnetic equator.

This beaming of JKR depends on the shape of the torus, distension at the equator and hence a detailed analysis of JKR could yield valuable information on those torus regions not visited by the Voyager spacecraft. The rocking of the torus by the magnetic field is to be expected as the Io torus is believed to contain anisotropic charged particle distributions favouring large pitch angles, and any gradual tilting of the magnetic field would cause the particles to be moved bodily with it.

Also, if there were propagation through the other window point, then in Fig. 6 the result would appear as very narrow beams (dashed lines) going to high latitude as shown for a source at  $8 R_J$ . Whether these exist probably depends on the ray-paths of the corresponding Z-mode waves. Figure 7 shows the ray paths of Z waves which would couple through the two windows. The coupling is assumed to occur at  $8 R_J$  at latitude  $0.5^\circ$ ; also shown are the resulting O-mode rays,  $O_L$  going to a low latitude and  $O_R$  to a high latitude. Data from the Voyager Planetary Radio Astronomy experiment should confirm whether the high-latitude beams exist. As Voyager 2 moved inwards towards the torus the plasma wave experiment observed that at about  $46.5 R_J$  the Northern source split into two<sup>3</sup>, and this effect may be produced by a single narrow beam which is cut twice by the spacecraft—once as its magnetic latitude increases and once as it decreases. On Voyager 2 the strong JKR at  $\sim 17$ –56 kHz disappeared at  $\sim 33 R_J$ , indicating that the source region for these frequencies had been passed, and clearly there was a fairly large density gradient at  $\sim 33 R_J$ , such that the plasma frequency



**Fig. 6** The low-latitude limits of the 'main' beams of jovian kilometric radiation showing the latitudinal dependence on frequency. The plasma density contours representing the distended Io torus are labelled according to plasma frequency (50–400 kHz). The narrow beams to high latitudes are from propagation through the second coupling point (see text), the L and R depicting left-hand and right-hand polarization respectively as observed by a spacecraft.



**Fig. 7** Details of ray paths close to the coupling region. ES shows where the upper hybrid waves are electrostatic. One Z ray propagates to  $-0.4^\circ$  magnetic latitude before it reaches the coupling point at  $+0.5^\circ$  latitude, subsequently propagating as the  $O_R$  ray going to high latitude. The other Z ray turns at  $+0.65^\circ$  latitude and becomes the  $O_L$  ray. For reference the  $L = 8$  magnetic field line is shown as is the plasma frequency contour corresponding to 186 kHz. The wave frequencies are all 196 kHz.

increased rapidly from 17 kHz to above 56 kHz in a relatively short distance. Perhaps narrow-band JKR sometimes observed as a stronger emission within wide-band JKR has its source in such large density gradients, which increase the window width, thereby allowing the escape of more Z-mode energy<sup>18</sup>. There has been some controversy as to the identification of the UHR frequency on Voyager 2 (refs 3, 4) and, on the basis of the theory proposed here, the 56 kHz UHR frequency was at  $\sim 30 R_J$  and the UHR frequency at  $\sim 10 R_J$  was probably  $\sim 193$  kHz. However, in a highly distended torus latitudinal variations are an important factor when interpreting the *in situ* density estimates made by the Voyager experiments.

## Discussion

The theory that intense electrostatic UHR waves coupling to L-O waves through the Z-mode are the source of JKR and TMR can account for many characteristics of the radiations. Detailed ray tracing of the electrostatic UHR waves in a realistic magnetospheric model and calculations of the width of the coupling windows are underway to confirm some features of the hypothesis, and to calculate the efficiency of the processes. The powers of TMR and JKR previously estimated on the basis of isotropic emission will have to be correspondingly reduced. Limiting the symmetrical Z-mode ray paths to  $\pm 1^\circ$  of the magnetic equator is believed to be significant and may be a crucial factor in the instability and in the energy exchange between waves and particles at the equator. That the UHR waves can access the Z-mode branch may indicate where exactly on the warm dispersion branch the UHR waves are produced<sup>25</sup>.

Note also that the confinement of UHR waves and associated particle distributions<sup>8,26</sup> may allow the first determination of the actual position of the magnetic equator, which would be very important within the context of other types of equatorially produced emissions, such as whistler-mode 'chorus'<sup>27</sup>.

A more detailed analysis of Voyager wave data should yield much new information on the Io torus. For example, the theory proposed here would predict that lower-frequency long-lived features of JKR should exhibit less co-rotation than higher frequencies because the former have their source at larger radial distances.

An important consequence of the theory, because the propagation windows are only a few degrees wide in practice<sup>18</sup>, is that JKR and TMR will be beamed away from the source region such that the rays lie very close to the plane containing the magnetic field and the density gradient vectors. This provides a powerful diagnostic technique allowing one to map the shapes of the plasmopause and Io torus in their respective equatorial planes by performing direction-finding measurements on the radiation. JKR shows long-lasting co-rotating features which reappear at approximately the same longitude for many jovian rotations. The Earth's plasmopause may co-rotate without large changes in its shape provided that one is not in regions affected temporally by large substorm electric fields<sup>28,29</sup>. High-resolution direction finding (DF) measurements are being performed using GEOS and ISEE data and the results will be reported later.

These comments on the plasmopause source are equally valid for the other source of TMR—the morning magnetosheath. Gurnett *et al.*<sup>30</sup> have reported ISEE observations of narrow band emissions near the electron plasma/upper hybrid frequencies in this region of the magnetosheath and I suggest that the energy in these waves also escapes as L-O mode radiation in a manner similar to that proposed for the plasmopause source. The magnetosheath magnetic field and plasma flow velocities are continuously changing depending on the direction of the interplanetary magnetic field and solar wind velocity and it is more difficult to determine the shape of the magnetosheath on the basis of the DF measurements. However, in stable conditions and with high time-resolution DF data it may be possible to map the magnetosheath and to see the propagation of irregularities and large-scale waves within it.

Finally, I re-emphasize that the determination by spacecraft of the local plasma density from the sharp low-frequency cut-off of TMR should be treated with caution. Clearly the cut-off is often due to beaming effects and bears no relation to the local plasma frequency at the satellite except in that it provides an upper limit to it. This may be equally valid for the low frequency jovian emissions tentatively identified as non-thermal continuum, which were detected by Voyagers 1 and 2 on their outbound passes<sup>1,3</sup>, and which were observed also to have a shadow zone at the magnetic equator.

I thank K. G. Budden, P. Christiansen, J. Etcheto, C. Goertz, P. Gough, R. Grard, D. Gurnett, R. Helliwell, R. Herring and M. J. Rycroft for stimulating discussions, R. M. Laws for support, and E. Gershuny, M. Trischberger and C. Boucher for computing assistance.

Received 24 July; accepted 12 September 1980.

1. Scarf, F. L., Gurnett, D. A. & Kurth, W. S. *Science* **204**, 991-995 (1979).
2. Warwick, J. W. *et al. Science* **204**, 995-998 (1979).
3. Gurnett, D. A., Kurth, W. S. & Scarf, F. L. *Science* **206**, 987-991 (1979).
4. Warwick, J. W. *et al. Science* **206**, 991-995 (1979).
5. Gurnett, D. A. *J. geophys. Res.* **80**, 2751-2763 (1975).
6. Brown, L. W. *Astrophys. J.* **180**, 359-370 (1973).
7. Shaw, R. R. & Gurnett, D. A. *J. geophys. Res.* **78**, 8136-8149 (1973).
8. Gough, M. P., Christiansen, P. J., Martelli, G. & Gershuny, E. J. *Nature* **279**, 515-517 (1979).
9. Kurth, W. S., Barbosa, D. D., Gurnett, D. A. & Scarf, F. L. *Geophys. Res. Lett.* **7**, 57-70 (1980).
10. Jones, D. *IEEE Trans. Geosci. Electron.* **GE-12**, 9-18 (1974).
11. Jones, D. *Annls. Télécommun.* **35**, 187-195 (1979).
12. Jones, D. *Space Sci. Rev.* **22**, 327-332 (1978).
13. Jones, D. *Nature* **260**, 686-689 (1976).
14. Jones, D. *The Scientific Satellite Programme During the International Magnetospheric Study*, 281-291 (Reidel, Dordrecht, 1976).

15. Ronnmark, K., Borg, H., Christiansen, P., Gough, P. & Jones, D. *Space Sci. Rev.* **22**, 401-417 (1978).
16. Oya, H. *Planet. Space Sci.* **22**, 687-708 (1974).
17. Budden, K. G. *Radio Waves in the Ionosphere* (Cambridge University Press, 1966).
18. Budden, K. G. *J. Atmos. Terr. Phys.* **42**, 287-298 (1980).
19. Gurnett, D. A., Kurth, W. S. & Scarf, F. L. *Science* **206**, 987-990 (1979).
20. Green, J. L. & Gurnett, D. A. *Geophys. Res. Lett.* **7**, 65-68 (1980).
21. Jones, D. & Grard, R. J. L. *The Scientific Satellite Programme During The International Magnetospheric Study* 293-302 (Reidel, Dordrecht, 1976).
22. Jones, D. *J. Geomagn. Geoelectr.* **30**, 291-293 (1978).
23. Gurnett, D. A., Anderson, R. R., Scarf, F. L., Fredericks, R. W. & Smith, E. J. *Space Sci. Rev.* **23**, 103-122 (1979).
24. Jones, D. *Proc. COSPAR Symp. on Planetary Magnetospheres*, Helsinki (in the press).
25. Barbosa, D. D. *J. Geophys. Res.* **85**, 2341-2345 (1980).
26. Wrenn, G. L., Johnson, J. F. & Sojka, J. J. *Nature* **279**, 512-514 (1979).
27. Helliwell, R. A. & Crystal, T. L. *J. geophys. Res.* **78**, 7357-7371 (1973).
28. Carpenter, D. L. *J. geophys. Res.* **71**, 693-709 (1966).
29. Carpenter, D. L., Park, C. G. & Miller, T. R. *J. geophys. Res.* **84**, 6559-6563 (1979).
30. Gurnett, D. A. *et al. J. geophys. Res.* **84**, 7043-7058 (1979).



# Greenland ice sheet evidence of post-glacial volcanism and its climatic impact

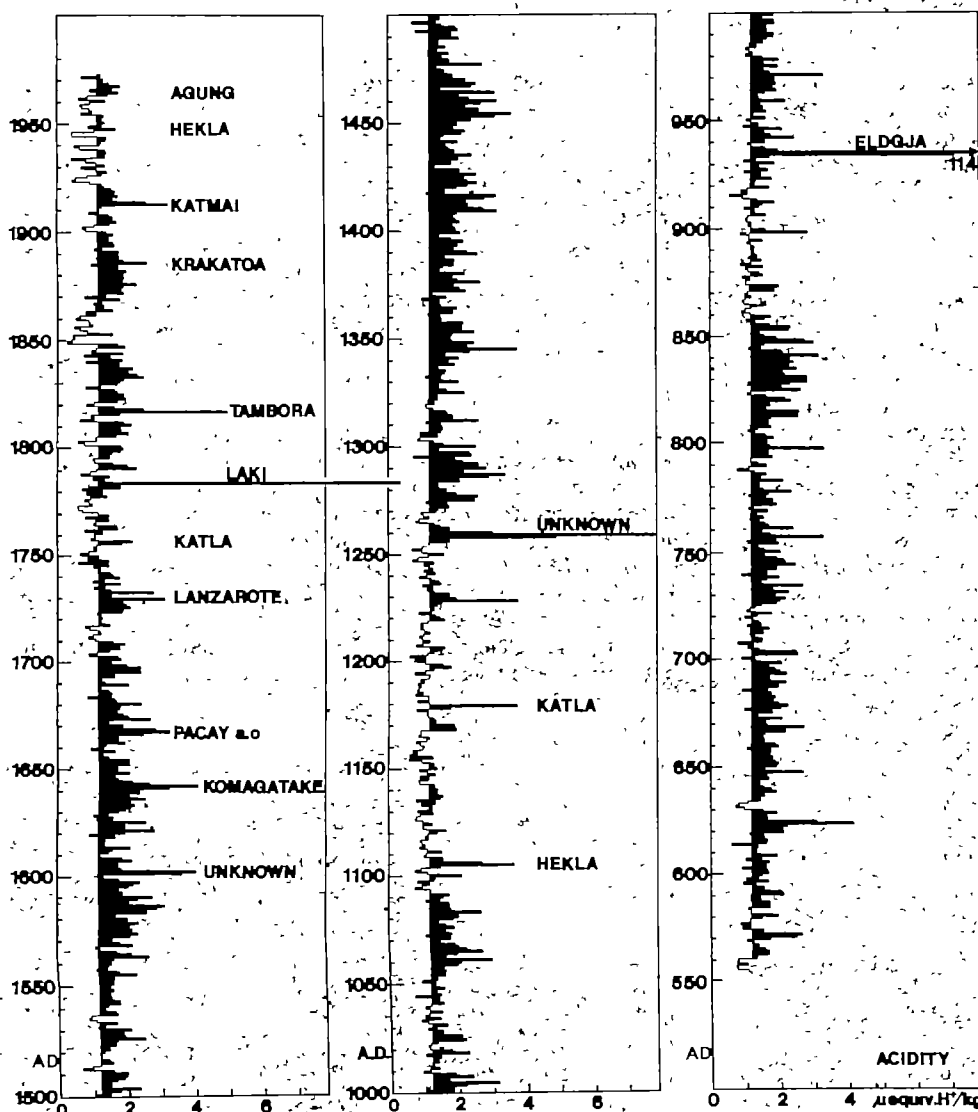
C. U. Hammer, H. B. Clausen & W. Dansgaard

Geophysical Isotope Laboratory, University of Copenhagen, Haraldsgade 6, DK 2200 Copenhagen N, Denmark

*Acidity profiles along well dated Greenland ice cores reveal large volcanic eruptions in the Northern Hemisphere during the past 10,000 yr. Comparison with a temperature index shows that clustered eruptions have a considerable cooling effect on climate, which further complicates climatic predictions.*

HISTORICALLY, man has often been directly influenced by volcanic eruptions: for example Mont Pélée (Caribbean, 1902), Krakatoa (Indonesia, 1883), Tambora (Indonesia, 1815), Laki (Iceland, 1783), Vesuvius (Italy, AD 79), and Thera (Santorini, ?). Other great eruptions have been observed only by the associated optical phenomena in the atmosphere caused by volcanic aerosols, for example AD 1601–02 (ref. 1) and 44 BC (ref. 2). But, before AD 1600 most volcanism was not recorded, and not even noticed outside the regional areas that suffered from the direct impact of the eruptions.

However, indirect impacts may be expected, because great volcanic eruptions inject huge amounts of silicate micro-particles and acid gases into the stratosphere. The main effect of the silicates is probably to heat up the stratosphere by absorption of solar radiation<sup>3,4</sup>, but they disappear by settling during the first few months<sup>5,6</sup>. At the same time a sulphate aerosol, mainly sulphuric acid, is building up from SO<sub>2</sub> to become the dominant aerosol<sup>6,7</sup>, the main effect of which seems to be cooling the lower troposphere by back scattering of solar radiation<sup>3,4</sup>. Most of this information has been obtained by directly monitor-



**Fig. 1** Mean acidity of annual layers from AD 1972 to 553 in the ice core from Crête, Central Greenland. Acidities above the background,  $1.2 \pm 0.1$   $\mu\text{equiv. H}^+$  per kg ice, are due to fallout of volcanic acids, mainly H<sub>2</sub>SO<sub>4</sub>, from eruptions north of 20°S. The ice core is dated with an uncertainty of  $\pm 1$  yr in the past 900 yr, increasing to  $\pm 3$  yr at AD 553 (ref. 10), which makes possible the identification of several large eruptions known from historical sources, and the accurate dating of the Icelandic Eldgjá eruption shortly after the settlement that was completed AD 930.

**Table 1** Magnitudes (in terms of global acid fallout) of some volcanic eruptions north of 20°S, roughly estimated from the acidity of annual layers in ice cores from Greenland

| Volcano               | Location    | Year of eruption<br>AD | Volcanic acid<br>fallout in<br>Greenland<br>(H <sub>2</sub> SO <sub>4</sub> + HX)<br>kg km <sup>-2</sup> | Latitude<br>correction<br>factor* (1/F) | Global acid<br>fallout<br>(H <sub>2</sub> SO <sub>4</sub> + HX)<br>(× 10 <sup>6</sup> tons) |
|-----------------------|-------------|------------------------|--|---|---|
| <b>Crête</b>          |             |                        |  |   |   |
| Agung                 | Indonesia   | 1963                   | 9  | 3                                       | 20  |
| Hekla                 | Iceland     | 1947                   | 6  | 1                                       | 5   |
| Katmai                | Alaska      | 1912                   | 37   | 1                                       | 30  |
| Krakatoa              | Indonesia   | 1883                   | 21   | 3                                       | 55  |
| Tambora               | Indonesia   | 1815                   | 58   | 3                                       | 150   |
| Laki                  | Iceland     | 1783                   | 116  | 1                                       | 100   |
| Lanzarote             | Canary Isl. | 1730-36                | 36   | 2                                       | 60  |
| Krafla (Myvatn fires) | Iceland     | 1724-30                | 63   | 1                                       | 55  |
| Unknown               | ?           | 1666?                  | 60   | ?                                       | (100)   |
| Pacaya                | Guatemala   | 1664                   |  | 3                                       |   |
| Awu                   | Indonesia   | 1641                   |  | 3                                       |   |
| Adiksa                | Indonesia   | 1641                   | 81   | 3                                       | (190)   |
| Komagatake            | Japan       | 1640                   |  | 2                                       |   |
| Unknown               | ?           | 1600/01                | 61   | 1?                                      | (50)  |
| Raudubjallar          | Iceland     | 1554                   | 23   | 1                                       | 20  |
| Unknown               | ?           | 1257/58                | 128  | 1?                                      | (110)   |
| Hekla 1               | Iceland     | 1104                   | 51   | 1                                       | 45  |
| Eldgjá                | Iceland     | 934                    | 189  | 1                                       | 165   |
| Unknown               | ?           | 622/23                 | 52   | 1?                                      | (45)  |
| <b>Camp Century</b>   |             |                        |  |   |   |
| Unknown               | ?           | 50 ± 30                | 192  | 1?                                      | (120)   |
| Unknown               | ?           | 210 ± 30               | 72   | 1?                                      | (45)  |
| Unknown               | ?           | 260 ± 30               | 54   | 1?                                      | (35)  |
| Hekla 3               | Iceland     | 1120 ± 50              | 99   | 1                                       | 60  |
| Thera                 | Greece      | 1390 ± 50              | 98   | 2                                       | 125   |
| Hekla 4               | Iceland     | 2690 ± 80              | 96   | 1                                       | 60  |
| Unknown               | ?           | 3150 ± 90              | 255  | 1?                                      | (160)   |
| Mt Mazama             | Oregon, USA | 4400 ± 110             | 156  | 2                                       | 200   |
| Hekla 5/Thjórsá flow  | Iceland     | 5470 ± 130             | 90   | 1                                       | 60  |
| Unknown               | ?           | 6060 ± 140             | 119  | 1?                                      | (75)  |
| —                     | ?           | 6230 ± 140             | 102  | 1?                                      | (65)  |
| —                     | ?           | 7090 ± 160             | 79   | 1?                                      | (50)  |
| —                     | ?           | 7240 ± 160             | 124  | 1?                                      | (80)  |
| —                     | ?           | 7500 ± 160             | 51   | 1?                                      | (35)  |
| —                     | ?           | 7640 ± 170             | (412)  | 1?                                      | (260)   |
| —                     | ?           | 7710 ± 170             | 69   | 1?                                      | (45)  |
| —                     | ?           | 7810 ± 170             | 73   | 1?                                      | (45)  |
| —                     | ?           | 7910 ± 170             | 95   | 1?                                      | (60)  |

\* See ref. 8.

ing the atmosphere in the years after the few great eruptions that have occurred in the past 20 yr, but this period of observation is obviously too short to allow any conclusion as to a possible persistent climatic effect of volcanic activity.

In the Northern Hemisphere (north of 20° S), the Greenland ice sheet is a rich source of information on past volcanism. This is not due to deposition of volcanic micro-particles<sup>8</sup>, as these are apparently too large and/or too few to reach the high-altitude regions of the Greenland ice sheet in amounts that significantly raise the (continental) dust concentration background. However, volcanic acids in snow layers deposited shortly after a large volcanic eruption can be detected—as elevated specific conductivities measured on melted ice samples<sup>8</sup>, or as elevated acidities revealed by an electric current through the solid ice, when pulling a simple pair of electrodes (voltage difference ~1,250 V) along a clean cut surface of an ice core<sup>9</sup>. We used the latter method because it is fast, non-destructive and more selective, the current being almost entirely determined by the protons from the strong acids.

### The Crête acidity record

A 404-m long ice core from Crête, Central Greenland (71° N, 37° W), was recovered in 1974 by US Cold Regions Research Engineering Laboratory under the American-

Danish-Swiss Greenland Ice Sheet Program (GISP). It has been dated to an accuracy of ±1 yr through the past 900 yr and to ±3 yr at the oldest annual layer deposited AD 553 (ref. 10).

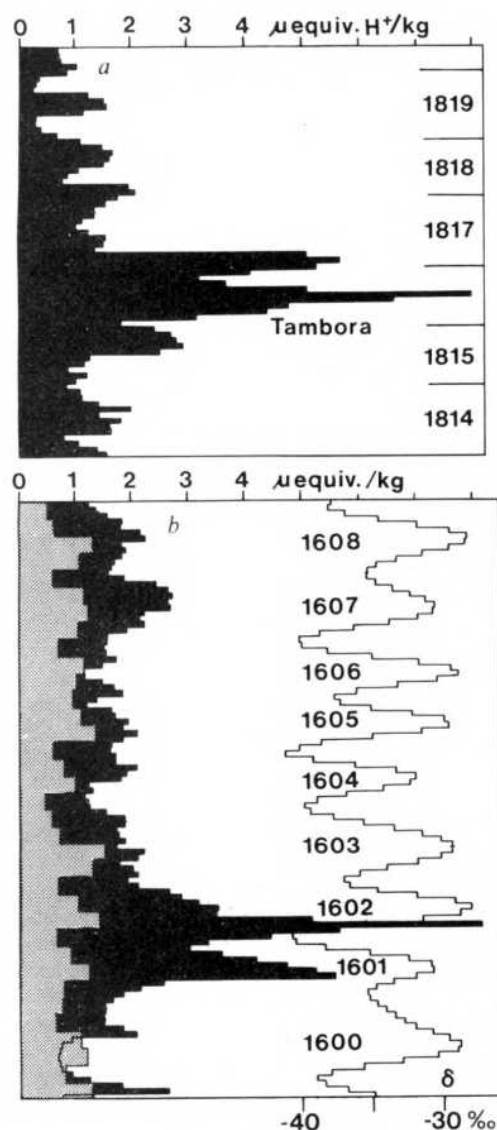
Electrical measurements on the solid ice provide the acidity record shown in Fig. 1, except for the upper porous part of the core (back to AD 1840), where the acidity values are based mainly on pH measurements on melted samples. Some of the very low values recorded since AD 1840 may be due to the difficulty of making a proper correction for CO<sub>2</sub>-induced H<sup>+</sup> in water of low acidity. The same reason may have caused a few small signals to be omitted in the uppermost part of the record.

Low-latitude eruptions generally show up with a time lag of ~1 yr due to the long travel time of the aerosols before deposition in Greenland. Some of the easily identified eruptions are denoted in Fig. 1. The layers of highest acidity coincide with internal reflection horizons in radio-echo sounding<sup>8,11</sup> and are thus recognizable all over Greenland.

The increase of the acid concentration in ice layers containing debris from a high northern latitude eruption can be used to estimate the global H<sup>+</sup> fallout by applying the same latitudinal distribution pattern observed for <sup>90</sup>Sr fallout from high northern latitude bomb tests. In 1962, the global fallout of <sup>90</sup>Sr (mainly from the Soviet tests in 1961) was 1.2 MCi which was 8.6 × 10<sup>8</sup> and 6.4 × 10<sup>8</sup> times the fallout per km<sup>2</sup> at Crête and Camp Century, respectively. Applying this factor to the time-



integrated fallout of volcanic acids per  $\text{km}^2$  from a given eruption gives the magnitude of the eruption in terms of acid-gas injection into the stratosphere. The fallout from mid-latitude ( $20^\circ\text{--}50^\circ\text{N}$ ) or low-latitude ( $20^\circ\text{S--}20^\circ\text{N}$ ) eruptions should be multiplied by factors of 2 or 3, respectively, to account for the spread of the eruption cloud during the travel to high northern latitudes, judged from fallout data (more extensive than in ref. 8) on debris from bomb tests outside the polar region. Magnitude estimates on several eruptions listed in Table 1 could easily be wrong by a factor of 2 for several reasons. For example, they may be underestimated, because some acid may have been neutralized before deposition, and in the case of Tambora, a higher fraction of the acid gases than during the explosive Krakatoa eruption may have remained in the troposphere where they were washed out at low latitudes. On the other hand, a high tropospheric wind pattern, favourable for deposition of volcanic acids in Greenland, may lead to an overestimation, particularly in the Icelandic eruptions.



**Fig. 2** The acid fallout (black curves; scale on top) from two long volcanic eruptions, found in annual layers at Crête. *a*, The Tambora eruption in Indonesia began AD 1815, and the fallout in Greenland peaked in 1816, "the year without a summer" (ref. 12). *b*, The  $\delta(^{18}\text{O})$  curve to the right shows that the fallout from an eruption in AD 1600 or early 1601 at an unknown locality lasted to the end of 1602. The  $\text{NO}_3^-$  concentration (shaded curve to the left) varies seasonally, but it was not above normal shortly after the supernova 1604 (see ref. 16).

Most of the eruptions recorded in the Crête core (Fig. 1) and listed in the upper part of Table 1 will now be considered individually.

Krakatoa (1883,  $6^\circ\text{S}$ ) and Tambora (1815,  $8^\circ\text{S}$ ) are revealed by relatively low signals due to the long distance to Greenland. Figure 2*a* shows that the acid fallout from the Tambora eruption peaked in mid 1816, "the year without a summer"<sup>12</sup>.

Laki (1783) and Eldgjá (tenth century) are the two highest signals in the record; revealing the two greatest eruptions in Iceland since the landnam (settlement) of 875–930, perhaps since the last glaciation. The fallout from Laki (1783) has been detailed elsewhere<sup>8</sup>. The exact year of the Eldgjá eruption does not appear in Icelandic annals, but according to Thorarinnsson (personal communication, and ref. 13) the eruption took place some time during or shortly after the landnam, although not later than AD 950. The eruption is identified (at AD  $934 \pm 2$ ) in the Crête record with high certainty, because (1) the eruption was of the same magnitude as Laki (1783), at least  $10 \text{ km}^3$  of lava, which is more than any other lava extrusion on Earth in historical time, and (2) there is no other signal comparable to that of Laki (1893) in the said period.

Hekla (1104) is the greatest Hekla eruption (H1) in Icelandic historical time, that is, in the past thousand years. The annals generally date it at 1104, and "the winter of sand-rain" 1104–05 is discussed which suggests that the eruption began late in 1104. In a detailed acidity record<sup>9</sup> the acidity increases upward from the top of the annual layer previously dated at 1104 by the  $\delta$  method, and Fig. 1 shows an acidity peak in 1105, which is strong evidence that the time scale is correct at around AD 1100.

Most signals, particularly before AD 1600, are due to unknown eruptions somewhere in the Northern Hemisphere. The three strongest such signals are those in AD 1601–02, 1258–59 and 623–24 (see Fig. 1). The eruption corresponding to the first signal caused "a constant haze over southern Scandinavia in 1601. . . The Sun and Moon appeared 'reddish, faint and lacked brilliance' in central Europe all through the year 1601 and up to the end of July 1602" (ref. 1). Figure 2*b* spans the period 1599–1608, according to the dating based on counting seasonal  $\delta$ -variations downward from top of the core. The  $\delta$ -curve is first order corrected for smoothing by diffusion<sup>14</sup>. The acidity curve in the middle shows that the acid fallout lasted from the beginning of 1601 to the end of 1602. The location of the 1601–02 eruption cannot be deduced from these measurements, but the high peak of the signal suggests mid- or high latitudes (Alaska, Kamchatka?) because otherwise a low-latitude eruption causing this amount of fallout in Greenland would have to be of the Tambora class and could hardly have escaped the attention of the early colonialists. The  $\text{NO}_3^-$  concentration curve in Fig. 3 measured on melted samples<sup>15</sup> shows that  $\text{HNO}_3$  did not contribute to the elevated acidity signals in 1601 and 1602. Nor did the  $\text{NO}_3^-$  concentration increase above normal in 1604 and 1605 (the  $\text{NO}_2^-$  concentration was close to zero), which heavily influences the hypothesis of elevated nitrate production in the atmosphere during the supernova observed in 1604 (ref. 16), as will be discussed elsewhere<sup>17</sup>. Note that the  $\text{NO}_3^-$  concentration exhibits persistent seasonal variations (compare with the  $\delta$  curve, which usually peaks in late summer), suitable for stratigraphic dating independent of volcanic eruptions. The  $\text{NO}_3^-$  summer peak may be due to the nitrate production in the atmosphere being determined by the intensity of the solar radiation, but the explanation is probably more complicated.

The third highest signal in the record spans three years and peaked in 1259. It cannot be ascribed to any Icelandic eruption, because the closest one in time (1262, probably a minor eruption of Katla; Thorarinnsson, personal communication) is not within our uncertainty limits of about one year. The eruption must also have been large, because the integrated fallout is at least of the same order as that of Laki (1783).

Before AD 900 the volcanism revealed in the Crête record cannot be ascribed to any known eruptions. The highest signal on an annual basis is that of 623, and the absolute maximum acidity ( $\sim 10 \text{ } \mu\text{equiv. H}^+ \text{ kg}^{-1}$ ) on a more detailed record occur.

red in 757. We doubt whether any of these signals were caused by the great eruption in the Yukon basin of Alaska some 1,400 yr ago, because an Alaskan eruption, estimated at 50% of Tambora (1815) in terms of ash production<sup>18</sup>, would be expected to cause considerably higher acid fallout in Greenland than indicated in Fig. 1. It is more likely that the Yukon eruption will show up if the acidity record is extended beyond AD 553—the year of deposition of the oldest layer in the 404-m long Crête core.

### The Camp Century acidity record

The Camp Century, north-west Greenland (77° N, 61° W), ice core is the only one reaching from the surface to the bedrock in Greenland. The core is 1,390 m long, corresponding to 1,367 m of ice equivalent, and the deepest part of it is >100,000 yr old<sup>19</sup>. Unfortunately, there is a gap of ~510-yr between the oldest layer in the Crête ice core and the youngest part of the Camp Century core that is in sufficiently good physical condition for continuous acidity analyses (only a few outstanding events since AD 43 have been safely identified, for example, 1259 and Laki 1783, the fallout from which has approximately the same acidity as at Crête).

The dating of the Camp Century core cannot compare with that of the Crête core, although it has been dated by the  $\delta$  method to better than  $\pm 2\%$  through the interval<sup>10</sup> 2,000–10,000 yr BP. Further improvement of the time scale over the past 4,000 yr has been obtained by using the AD 1259 and 1783 reference horizons as fixed points and also using all presently available data on the annual layer thickness  $\lambda$ , which decreases from 19 cm in 2,000-yr-old ice to 2 cm in 10,000-yr-old ice due to plastic thinning of the annual layers as they sink towards greater depths<sup>10</sup>.

A continuous acidity profile (one acidity mean value for each 10-cm increment) has been measured along the Camp Century

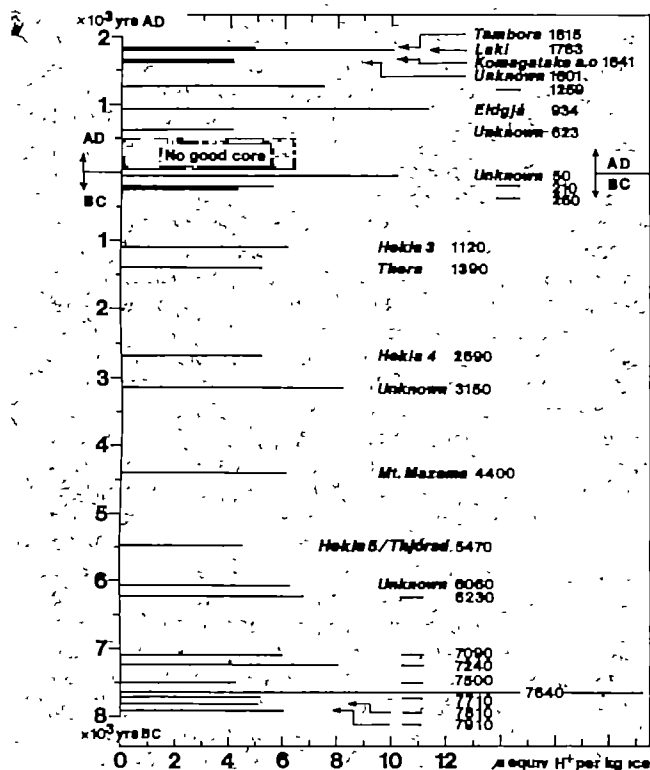


Fig. 3 Acidity signals exceeding  $4 \mu\text{equiv. H}^+$  per kg ice in the past 10,000 yr, but for AD 44–552. Large eruptions have occurred most frequently in the earliest and in the latest millenium of the period (compare with ref. 30). Up to AD 43 the analyses were performed on the Camp Century ice core; since AD 553 on the Crête ice core.

ice core from a depth of 558 m of ice, corresponding to AD 43, to the bedrock. Very high acidity spikes were analysed back to 8,000 BC with a resolution higher than  $\lambda$  at the particular depths. For clarity Fig. 3 shows only the mean acidity of the most acid annual layer within each one of those signals that can be ascribed to a single violent eruption. This procedure probably reveals all the large, violent eruptions, whereas all the eruptions up to medium magnitude, as well as large long-lasting but less violent eruptions are deleted. For comparison, the Crête record in Fig. 1 has been treated in the same way and added to the top of Fig. 3. The approximate magnitudes of some of the eruptions in terms of acid-gas production are listed in Table 1, estimated by the same procedure as used on the Crête core.

The frequency of violent eruptions is clearly relatively low from 1500 to 7000 BC, in particular from 3500 to 5500 BC. Some of the most outstanding events are now discussed.

**50  $\pm$  30 BC:** The acid fallout lasted ~3 yr (compare with Fig. 4a) and must be due to one of the largest eruptions in the Northern Hemisphere since the last glaciation. There is no evidence of any great eruption in Iceland at this time. If Etna really had an eruption in the year of Caesar's death<sup>20</sup>, 44 BC, it could explain Virgil's statement<sup>21</sup> that "when Caesar died, the Sun felt pity for Rome, as it covered its beaming face by darkness, and the impious generation feared an eternal night". But, if the heavy fallout in Greenland were to be ascribed to Etna, the magnitude of the eruption and its impact on the Roman society would have been so great that there would undoubtedly be geological and historical evidence. A century later the Elder Plinius mentioned<sup>2</sup> the "feebleness of the Sun through nearly a year, when the dictator Caesar was killed", which suggests there was a widespread aerosol from an unusually large eruption somewhere else.

**210  $\pm$  30 or 260  $\pm$  30 BC:** Might reveal the Younger Laxar-lava (Iceland; Thorarinnsson, personal communication).

**1100  $\pm$  50 BC:** The greatest post-glacial eruption of Hekla (H3) has been radiocarbon dated at  $950 \pm 130$  BC (ref. 22), that is not significantly different from  $1100 \pm 50$  BC. The estimated total volume of freshly fallen tephra was  $12 \text{ km}^3$  (ref. 23), corresponding to some 30% of the material extruded by Laki (1783).

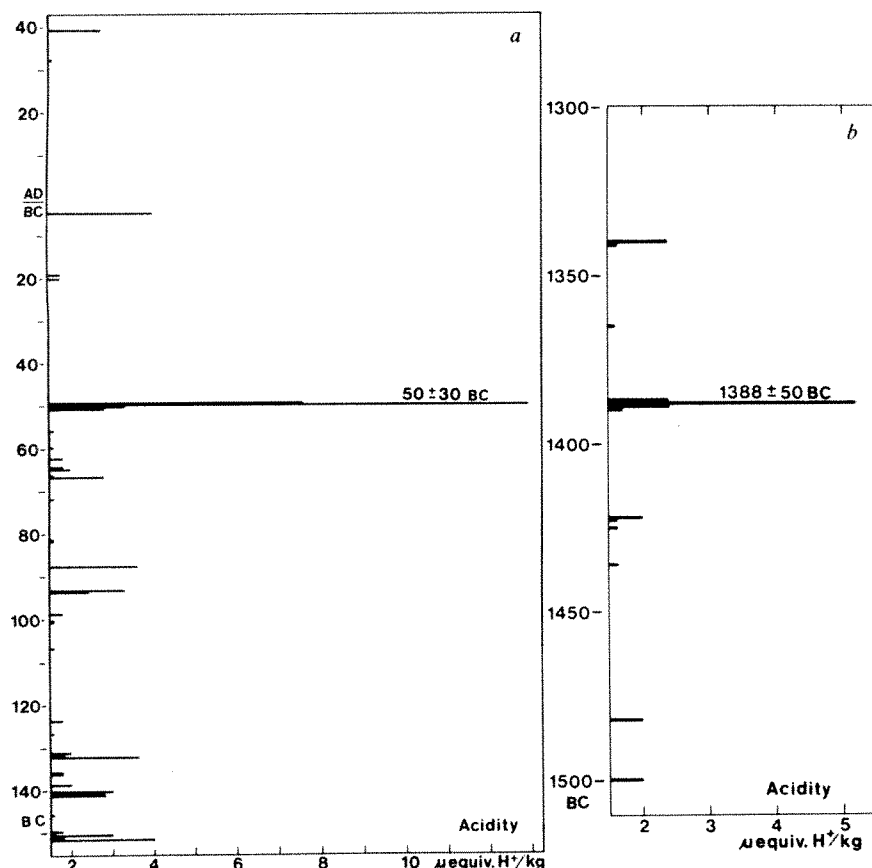
**1390  $\pm$  50 BC:** (Compare details in Fig. 4b). This is the only signal exceeding  $2.6 \mu\text{equiv. H}^+$   $\text{kg}^{-1}$  between 1100 and 2700 BC, and we therefore interpret it as being due to the large eruption of Thera (Santorini) in the Aegean Sea, which is generally agreed to have been of the same magnitude as that of Tambora (1815). The tephra production has recently been estimated at more than  $28 \text{ km}^3$  ( $13 \text{ km}^3$  of dense rock equivalent)<sup>24</sup>. This unusually large eruption has been radiocarbon dated at  $1720 \pm 50$  BC on the calibrated radiocarbon scale (ref. 25, and H. Tauber, personal communication). However, archaeological evidence from the excavation of the Minoan settlement near Akrotiri on Santorini strongly suggests<sup>26</sup> that the island was inhabited at least up to 1500 BC judging by Egyptian pottery style chronology; it was apparently abandoned shortly before the eruption, and in good order because no valuables have been found nor people killed by the heavy ash fall (10–40 m). The discrepancy between the datings may be partly explained if the organic material used for the radiocarbon dating were partly built up by radioactively dead  $\text{CO}_2$  exhausted from the volcano before the eruption (an effect which has been observed recently<sup>27</sup>). Our dating around 1400 BC supports Marinatos' theory<sup>28</sup> of a causal connection between the Thera eruption and the decline of the Minoan civilization centred on the island of Crete. The dating can be further improved to  $\pm 10$  yr, if and when a deep Central Greenland ice core becomes available.

**2700  $\pm$  70 BC:** Agrees with the radiocarbon dating  $2550 \pm 120$  BC of the Hekla eruption H4, which is estimated to have been almost as great as H3 (ref. 23).

**3250  $\pm$  80 BC:** This signal is difficult to reconcile with any known giant eruption, but the one at

**4400  $\pm$  100 BC:** Agrees with Mt Mazama, Oregon, the radio-





**Fig. 4** Unambiguous volcanic signals in Camp Century ice core increments spanning the AD 43–140 BC, and the 1300–1500 BC time intervals. *a*, The unusually large event at  $50 \pm 30$  BC may be the one that caused the optical phenomena in the atmosphere described at Julius Caesar's death 44 BC. *b*, The only high signal in the entire period (in fact between 1120 and 2690 BC) occurred at  $1388 \pm 50$  BC. With the only reservation that another high signal might be lost in the few per cent of missing core, the observed event can be identified with the large Thera eruption in the Aegean Sea that deeply influenced the ancient Minoan society.

carbon datings of which range from 4200 to 4600 BC<sup>29</sup>. The amount of freshly fallen ash is estimated at 30 km<sup>3</sup>.

**5400 ± 120 BC:** Agrees with the Hekla eruption H5, radio-carbon dated at  $5450 \pm 190$  BC<sup>22</sup>, and with the largest Thjórsá lava flow, dated by Thorarinsson at ~5500 BC.

None of the high signals before 6000 BC can be safely ascribed to any eruption known by us. Not less than seven great eruptions seem to have occurred between 7000 and 8000 BC. According to Thorarinsson (personal communication), at least some of these must be Icelandic shield volcanoes, such as Skjaldbreidur (15 km<sup>3</sup>; ~10,000 yr ago).

No unambiguous evidence of volcanic fallout has been found in the deep ice, which was deposited during the last glaciation, judging from very low  $\delta$  values in the complete  $\delta$  profile<sup>19</sup>. As the volcanic activity was hardly negligible in this period<sup>30</sup>, our measuring technique, at least in the present form, obviously cannot be applied to the Camp Century core before 8000 BC. One reason is the limited resolution power of the electrodes, but the main reason is that, disregarding the interstadials revealed by intermediate  $\delta$  values, the ice from the last glaciation is slightly alcalic, which makes the current between the electrodes nearly zero. In alcalic ice the chemical element content measured so far<sup>31</sup> is higher than in post-glacial time by factors of, for example, 1.5–3 for Na and SO<sub>4</sub><sup>2-</sup>; 2.5–11 for K, Mg, Si and Al; and 10–30 for Ca. The elevated sulphate values are probably just part of the generally increased impurity background, and measuring the volcanic contribution calls for very detailed sulphate analyses. The extremely high calcium values probably originate from CaCO<sub>3</sub> dust from the exposed continental shelves<sup>31</sup>, indicating an alcalic aerosol able to neutralize an acid aerosol that would otherwise cause acidities of up to 8 μequiv H<sup>+</sup> per kg ice.

In preglaciation ice, characterized by high  $\delta$  values, the chemical impurity concentrations and the acidity background come close to post-glacial values. There is some indication of periods of intense volcanism, but the resolution is too poor for further details.

## The climatic impact of volcanism

Volcanic aerosols influence the radiation balance in the atmosphere. The optical thickness  $\tau$  of an atmospheric aerosol is an index of the loss of radiation by scattering and absorption (the optical thickness of a layer is  $\tau$ , if the fraction  $\exp(-\tau)$  of radiation impinging perpendicularly on the layer is transmitted).  $\tau$  is an important parameter in radiation balance models for calculating the temperature effect of volcanic aerosols in the stratosphere. The optical properties of an assumed sulphuric acid aerosol have been estimated<sup>3</sup> using the measured global 'average' optical depths since 1882. It was thereby possible to calculate temperature changes ( $\Delta T$ ) close to those observed in the atmosphere after volcanic eruptions, including the Agung eruption 1963 that caused up to several degrees warming of the low latitude stratosphere<sup>32</sup> and a 0.4 °C cooling of the low-latitude troposphere<sup>33</sup>. However, an important drawback in these calculations is "that the sign and magnitude of  $\Delta T$  depends critically on the real and imaginary parts of the refractive indices of the added particles, their size distribution, and the surface albedo"<sup>3</sup>, which, of course, stresses the need for a direct comparison between volcanic activity and climatic changes before the instrumental epoch.

The Crête excess-acidity data given in Fig. 1 must be expected to be proportional to the volcanic contribution  $\Delta\tau$  to the optical depth in the high northern latitude atmosphere. As a first approximation we further assume that this  $\Delta\tau$  is just as relevant for comparison with climatic temperature changes as is the global averaged  $\Delta\tau$ . This is often implicitly assumed in model calculations, where the latitude-dependent back scattering has been averaged.

Figure 5e shows the Crête acidity profile in 50-yr averaged values. Note that periods of low volcanic activity have been marked in black. The maximum deviation from the overall mean is  $< 0.5 \mu\text{equiv H}^+ \text{ kg}^{-1}$  (measured on solid ice<sup>9</sup>), corresponding to only 0.03 and 0.05 deviation of pH measured on melted samples, assuming saturation with CO<sub>2</sub> in ambient air at 0° and

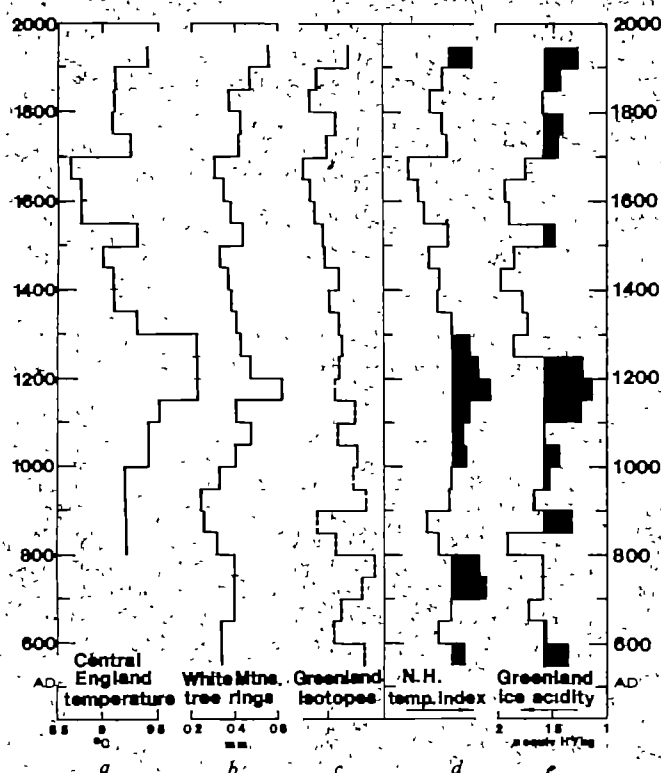


Fig. 5 Correlation between climatic temperature variations (curve *d*, composed of the three indirectly determined records *a* through *c*; warm periods are set out in black) and volcanic activity (curve *e*, showing an acidity profile along the Crête ice core; lower than normal volcanism corresponds to low acidities set out in black).

25 °C, respectively. This might be why 'remarkably stable' 50-yr mean pH values in meltwater from most of the Devon Island ice core<sup>34</sup> were interpreted to indicate that 'volcanic activity has not altered significantly' during the period 50–5300 yr BP.

To examine the possible influence of volcanic activity on climate we compare below the Crête acidity record with some absolute-dated climatic records of proxy data reaching far beyond the period of direct temperature observations. As the ice acidity data are more or less representative of aerosol conditions in the Northern Hemisphere in general, they ought to be compared with temperatures of similar general validity, rather than data representative of regional climatic conditions, for example, central England temperature estimates (Fig. 5a; ref. 35); or white Mountains, California, tree ring widths (Fig. 5b; ref. 36); or the long-term  $\delta$ -variation in Greenland ice sheet precipitation (Fig. 5c; combination of four normalized  $\delta$ -profiles back to AD 1250; two back to AD 550; ref. 37). But, if

these three climatic curves are combined after normalization, the resulting record (Fig. 5d) may be a first approximation to the Northern Hemisphere temperature index needed for making a useful comparison with past volcanic activity. Unfortunately, most other long-term climatic records do not meet the strict requirement to the dating accuracy needed in this context.

The Northern Hemisphere temperature index in Fig. 5d does not have a temperature scale, of course. Most of its trends are recognized, more or less, in each of its components—the warm first half of the twentieth century; the cooler nineteenth century; the relatively warm eighteenth century; the 'Little Ice Age' AD 1350–1700 with a minor 'interstadial' AD 1500–1550 (or AD 1350–1900 with 'interstadials' 1500–1550 and 1700–1800), and the mediaeval warmth AD 1000–1300, although the latter seems to have occurred earlier in Greenland.

Many of the above-mentioned features can be recognized in the Crête acidity curve (Fig. 5e), warmth generally occurring in periods of lower than average volcanic activity. The correlation coefficient between curves 5d and 5e is  $R = -0.52$  ( $P > 95\%$  for 12 d.f.). The curves exhibit a few clear discrepancies, particularly between the data in the AD 850–900 interval. Such occasional discrepancies are not surprising in view of the increasing uncertainty of the temperature index backward in time (for example Lamb gives only one mean temperature estimate for the entire period AD 800–1000). Furthermore, curve *e* is hardly the best obtainable representative of volcanic activity. It could, for example, be improved by replacing the simple acidity measurements by a more differentiated chemical investigation.

The significant correlation between curves *d* and *e* (Fig. 5) indicates that persistent volcanic activity north of 20° S is probably an important, but not necessarily the only, cause of climatic fluctuations of up to several hundred years duration at mid- and high-latitudes. If true, a solution of the extremely important and difficult problem of predicting climatic changes by atmospheric model calculations implies a scarcely easier prediction of volcanic activity.

*A priori*, the acid aerosol load at low latitudes cannot be expected to vary in parallel with curve *e* (Fig. 5) nor, therefore, with the Northern Hemisphere temperature index (curve *d* Fig. 5). This suggests that future climate models should account for the latitudinal variation of the optical depth of volcanic aerosols, rather than using a global average.

A similar treatment of the Camp Century data has been attempted with some success and will be reported elsewhere.

We thank Professor Chester C. Langway, for permission to analyse the Camp Century ice core, and Dr S. Thorarinsson for valuable help. The Danish Commission for Scientific Investigations in Greenland funded the study.

*Note added in proof:* In a new ice core from South Greenland, a strong acidity signal was found and preliminarily dated at AD 540 ± 10. This might be the Yukon eruption mentioned above. If so, the global acid fall out was of the order of 70 million tons.

Received 4 June; accepted 26 August 1980.

- Lamb, H. H. *Met. Trans. R. Soc. A* **226**, 425–533 (1970).
- Pinus the Elder *Historia Naturalis* II, 98 (~AD 70).
- Baldwin, B., Stumens, A., Toon, O. B., Segen, C. & Van Camp, W. *Nature* **263**, 551–555 (1976).
- Hansen, J. B., Wang, W.-C. & Latta, A. A. *Science* **199**, 1065–1068 (1978).
- Moscow, S. C. *Nature* **263**, 824–827 (1964).
- Pollack, J. B. *et al. J. geophys. Res.* **81**, 1071–1083 (1976).
- Castleson, A. W., Munkelwitz, H. R. & Manowitz, T. *Science* **206**, 222–234 (1974).
- Hannar, C. U. *Nature* **278**, 482–486 (1977).
- Hannar, C. U. *J. Glaciol.* **93** (in the press).
- Hannar, C. U. *et al. J. Glaciol.* **20**, 3–26 (1978).
- Gudmundsson, P. & Overgaard, S. *Rep. P. 312* (Electromagnetic Institute, Lyngby, 1978).
- Stommel, H. & Stommel, E. *Science* **140**(6), 134–140 (1979).
- Larsen, G. *Nordfjella glaciol. (Rykjavik)*, **49**, 1–26 (1979).
- Johnsen, S. J. *Proc. I.U.G.G. Symp. Isotopes and Impurities in Snow and Ice*, Grenoble, 210–219 (1975).
- Greenhoff, K. *Methods of Sea Water Analysis* 137–145 (Chepka, Wormsheim, 1976).
- Rood, R. T., Sarason, C. L., Zoller, E. J. & Parker, B. C. *Nature* **282**, 701 (1979).
- Riebo, T., Olsson, H. B. & Lund-Rasmussen, K. (in preparation).
- Macdonald, G. A. *Volcanoes* (Prentice-Hall, New Jersey, 1972).
- Johnsen, S. J., Dingsgaard, W., Olsson, H. B. & Langway, C. C. *Nature* **238**, 429–434 (1972).
- Seppert, K. *Katalog der geologischen Vulkanvorkommen* (Schriften, Straßburg, 27. Heft, 1917).
- Virgil *Georgicon* I, 466 (37–31 BC).
- Tambor, H. *Am. J. Sci., Radiocarbon Suppl.* **2**, 5–11 (1960).
- Larsen, G. & Thorarinsson, S. *Jökull* **27**, 28 (1977).
- Watkins, N. D. *et al. Nature* **271**, 122–126 (1980).
- Olsson, I. A. & Broecker, W. S. *Am. J. Sci. Radiocarbon Suppl.* **1**, 1 (1959).
- Popham, M. *Atmospheric* **83**, 57–59 (1979).
- Brown, M., Levin, I., Mifflin, K. O. & Hubberton, H. H. *Proc. 10th Int. Radiocarbon Conf., Bern, Radiocarbon* (in the press).
- Marshall, S. *Atmospheric* **13**, 425–439 (1959).
- Ruben, M. & Alexander, C. *Am. J. Sci. Radiocarbon Suppl.* **2**, 129–185 (1960).
- Bryson, R. A. & Goodson, B. M. *Science* **207**, 1041–1044 (1980).
- Cragin, J. H., Horton, M. M., Langway, C. C. & Klondike, G. *SCOR/SCAR Polar Ocean Conf., Montreal* (1974).
- Newell, R. E. *J. Atmos. Sci.* **27**, 977–978 (1970).
- Newell, R. E. & Weare, B. C. *Science* **194**, 1413–1414 (1976).
- Fabry, D. A. & Koerner, R. M. *Geostrophics* (in the press).
- Lamb, H. H. *The Changing Climate* 186 (Methuen, London, 1968).
- Labeyrie, V. C. *Jr. Science* **183**, 1043–1048 (1974).
- Hannar, C. U., Olsson, H. B. & Dingsgaard, W. *Proc. I.U.G.G. Symp. on Volcanism and Climate*, Canberra (in the press).



# Nucleotide sequence of cDNA coding for Semliki Forest virus membrane glycoproteins

Henrik Garoff, Anne-Marie Frischauf, Kai Simons, Hans Lehrach & Hajo Delius

European Molecular Biology Laboratory, Postfach 102209, 6900 Heidelberg, FRG

*The genes coding for the three membrane polypeptides of Semliki Forest virus have been sequenced and the primary structures of the proteins deduced. The amino acid sequence gives further insight into how the transmembrane structure of the three-chain virus membrane glycoprotein is generated in the infected cell.*

MANY enveloped animal viruses acquire their membranes at the host cell surface<sup>1</sup>. The virus membranes are highly differentiated plasma membranes which can be studied as models for plasma membrane assembly<sup>2-7</sup>. Semliki Forest virus (SFV) consists of a nucleocapsid surrounded by a lipid envelope. The virus membrane is studded with glycoprotein spikes which are essential for virus attachment and penetration into host cells<sup>8</sup>. Each spike glycoprotein contains three different glycopolypeptides: E1 (molecular weight ( $M_r$ ) 49,000), E2 ( $M_r$  52,000) and E3 ( $M_r$  10,000)<sup>9,10</sup>. E3 is external to the lipid bilayer whereas E1 and E2 are attached by short hydrophobic polypeptide segments to the membrane. E2 spans the membrane, having about 30 amino acid residues of its carboxy terminus internal to the bilayer<sup>11</sup>. In infected cells, two species of virus mRNA are found—the 42S RNA, the virus genome and the 26S RNA<sup>12</sup>. The latter RNA molecule is homologous to the 3' end of the 42S RNA<sup>13</sup> and serves as mRNA not only for the E1, E2 and E3 polypeptides but also for the capsid protein of the virus nucleocapsid. All four polypeptides are translated from the 26S RNA using a single initiation site in the order: capsid, p62 and E1<sup>14,15</sup>. The p62 polypeptide is the precursor of E3 and E2<sup>9</sup>. The capsid protein is cleaved from the nascent chain immediately after it is completed and is left in the cytoplasm<sup>16</sup>. The amino-terminal end of p62 then directs the polysomes to the endoplasmic reticulum where the synthesis of the glycoproteins continues concomitantly with membrane translocation and glycosylation<sup>16</sup>. The newly synthesized p62 and E1 glycopolypeptides form a complex which migrates through the intracellular membrane system to the plasma membrane, where the p62 protein is cleaved to form E2 and E3<sup>17</sup>.

We now report the nucleotide sequence of the cloned cDNA made from the 26S RNA, which codes for the SFV membrane proteins. The amino acid sequence suggests how the glycoproteins are attached to the membrane and provides further insight into how one mRNA directs the synthesis of four polypeptides destined for two different locations of the cell.

## Cloning of membrane protein genes

The viral genome (42S RNA) obtained from virus particles and 26S RNA isolated from infected cells were used as templates for cDNA synthesis from the 3' end of the RNA molecules<sup>18</sup>. The first strand was made with reverse transcriptase and the second with DNA polymerase<sup>19</sup>. The double-stranded cDNA was inserted into the vector pBR322 at the *Pst*I site using the oligo(dG-dC) tailing procedure described by Röwekamp and Firtel<sup>20</sup>. The hybrid plasmid was then used to transform *Escherichia coli*  $\chi$ 1776 (ref. 21). Tetracycline-resistant colonies, which hybridized strongly to <sup>32</sup>P-labelled cDNA made from 42S RNA<sup>22</sup>, were screened to determine the length of the insert molecule<sup>23</sup>.

Several clones containing hybrid plasmids with inserts larger than 1 kilobase were found. Electron microscopic analysis of hybrids<sup>18,24,25</sup> formed between the 42S RNA and DNA inserts showed that three hybrid plasmid clones—pBR SFV 1, 2 and

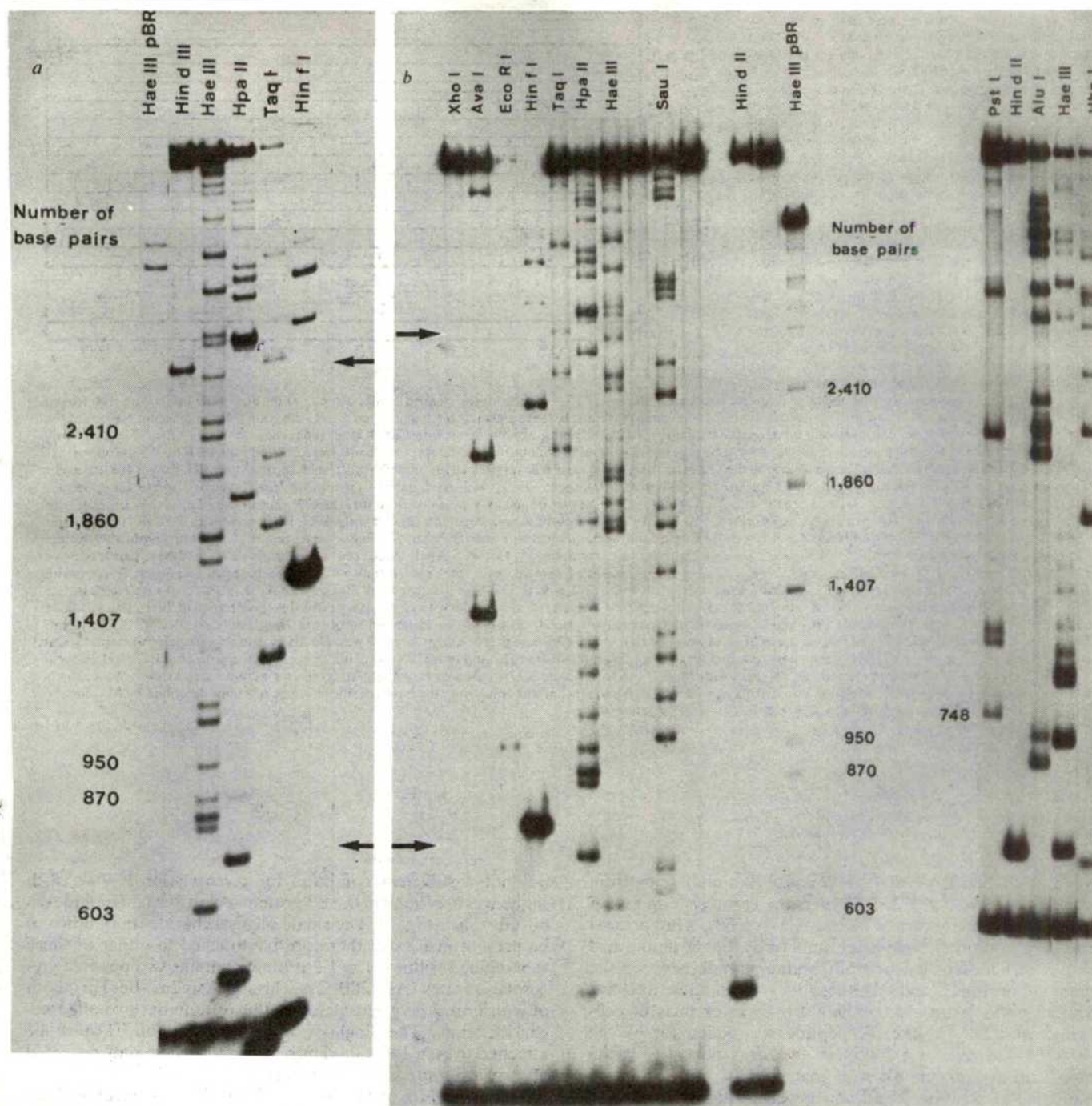
3—covered the entire 26S RNA region with the exception of about 150 bases from the 3' end. The insert molecule in pBR SFV 1 contained about 2.0 kilobases from the 3' end of the 26S RNA. pBR SFV 2 contained some 2.25 kilobases from the middle region of the 26S RNA. It overlapped by about 1.35 kilobases with the insert of pBR SFV 1. The insert of pBR SFV 3, made from the 42S RNA, contained 1.6 kilobases and was some 250 bases longer than the 5' end of the 26S RNA. It had an overlap of 300 bases with the pBR SFV 2 insert. All inserts were mapped with restriction endonucleases using the technique described by Smith and Birnstiel<sup>26</sup>. Figure 1 shows agarose gel analyses of the partial digestion products of pBR SFV 1 and pBR SFV 2. The restriction endonuclease mapping of pBR SFV 3, which covers the entire gene of the capsid protein, is presented elsewhere<sup>18</sup>. Figure 2 shows the restriction map of the region coding for the membrane proteins. The capsid protein gene ends some 100 bases away from the *Xho*I site in the direction towards the 5' end<sup>18</sup>.

## Nucleotide sequencing

DNA fragments for sequencing were prepared using two different approaches. The first one was based on the restriction map (Fig. 2). The DNA was cleaved using a suitable restriction endonuclease. After labelling either the 3' or the 5' ends of the DNA fragments, these were cleaved a second time to produce pieces of DNA that had only one labelled end<sup>27</sup>. The various fragments were isolated and sequenced as described in Fig. 2 legend. In the second procedure we deleted *in vitro* the DNA region of the vector between the *Eco*RI site and the *Pst*I site (748 base pairs)? together with different-sized portions of the insert molecule (see Fig. 2 legend). When these molecules were recloned, it was possible to sequence directly from the *Eco*RI site of the subcloned plasmid into the insert region (see Fig. 2 legend). This sequencing procedure will be presented in detail elsewhere (A.-M. F., H.G. and H.L., in preparation). The sequenced stretches of DNA are indicated by the arrows in Fig. 2. The sequences were overlapped using a computer program (H. L., unpublished). Figure 3 shows the nucleotide sequence of the region coding for the membrane proteins. The C at the 3' end of the sequence corresponds to the nucleotide before the poly(A) tail in the 26S RNA<sup>30</sup>. We have included the nucleotide sequence on the 5' side of the *Xho*I site that codes for the carboxy terminus of the capsid protein<sup>18</sup>. The complete sequence of the capsid protein will be published elsewhere<sup>18</sup>.

## Amino acid sequence

Translation of the nucleotide sequence into amino acids using the same reading frame that was earlier used to deduce the primary structure of the capsid protein resulted in a continuous sequence of amino acids (Fig. 3). Reading in the two other frames was interrupted by 40 and 45 nonsense codons, respectively. The coding region of the 26S RNA thus starts with the amino terminus of the capsid protein and terminates 3,759.



**Fig. 1** Analyses of partial digestion products of end-labelled pBR SFV 1 (a) and pBR SFV 2 (b) by electrophoresis on 1.4% agarose gels (20 cm × 40 cm, 1.5-mm thick). pBR SFV 1 (10 µg) was linearized with *EcoRI* and the same amount of pBR SFV 2 was cleaved with *Clal*. The 5' ends were dephosphorylated and labelled using polynucleotide kinase and  $^{32}\text{P}$ -ATP (ref. 27). After a second cleavage with *Bam*HI, both DNA samples were subjected to partial digestions with the restriction endonucleases indicated at the top of the figure. The exact incubation conditions as well as the electrophoresis procedure, the drying of the gel and the autoradiography are described elsewhere<sup>18</sup>. Fragments generated by cleavages within the insert of pBR SFV 1 are distributed between the two arrows in a. Cleavage sites in the insert molecule of pBR SFV 2 are shown by the bands between the arrows in b. Some of the digestions of pBR SFV 2 were either too complete or incomplete. These are repeated in a second experiment (right part of b). Here the smallest (748 base pairs) and the largest *Pst*I fragments indicate the limits of the fragments derived from the insert. The partial digestion products of pBR322 that were end labelled in the *EcoRI* site were used as standards<sup>28</sup>.

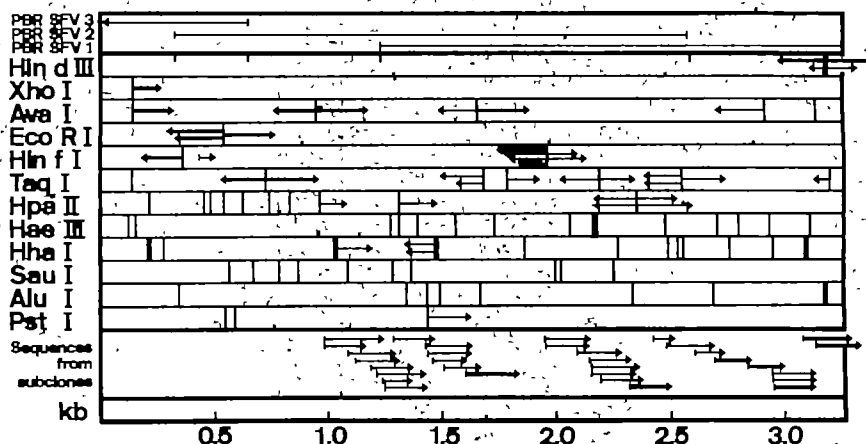
nucleotides later when the first stop codon (TAA in Fig. 3) is reached. The regions coding for the E3, E2 and E1 polypeptides were localized in this sequence using data available from amino-terminal amino acid sequencing (refs 31, 32 and H. Garoff, H. Riedel and H. Lehrach, in preparation) and carboxypeptidase digestions of the isolated polypeptides<sup>33</sup>.

The amino terminus of the isolated E3 polypeptide contains a methionine residue in position 8 and leucine residues in positions 4 and 11 (W. Welch and B. Sefton, personal communication). This amino acid sequence is found immediately after the region coding for the capsid protein (Fig. 3). Bonatti

and Blobel have reported a highly homologous sequence at the amino terminus of the precursor for the E3 and E2 polypeptides from the closely related Sindbis virus<sup>32</sup>. The carboxy-terminal sequence His-Arg, determined from the isolated E3 polypeptide<sup>33</sup>, is found 64 amino acid residues from the carboxy terminus of the capsid protein preceding the known amino terminus of E2 (Ser-Val-Ser-Gln-His-Phe-)<sup>31</sup>. As there are two arginine residues before the amino terminus of E2, the last one might be excised by a host protease during cleavage of the p62 polypeptide to E3 and E2 (see below). The amino-terminal sequence determined from the isolated E1 polypeptide



**Fig. 2** Restriction endonuclease map of the SFV membrane protein region in pBR-SFV 1-3. Thick arrows indicate stretches of DNA where both strands have been sequenced. Thin arrows indicate either 3' end or 5' end sequences. There are no sequence data that overlap the *Xho*I site. However, the corresponding region in the E3 protein is covered with partial amino acid sequence data from a cyanogen bromide peptide (H. Garoff, H. Riedel and H. Lehrach, in preparation). The arrows inside the restriction map represent sequences obtained from isolated DNA fragments and those below the map represent sequences obtained using the subcloning approach. The preparation of subcloned plasmids for sequencing from pBR-SFV 1 and 2 will be described elsewhere (A.M.F., H.G. and H.L., in preparation). The steps were as follows: (1) Random linearization of the hybrid plasmid with DNase I. (2) Ligation of *Eco*RI linkers to the ends. (3) Cleavage of the linkers and the vector with *Eco*RI. (4) Separation of DNA molecules by electrophoresis in agarose gels and elution of such molecules which were expected to have deletions extending from the *Eco*RI site of the vector to different positions in the insert. (5) Ligation of the cleaved *Eco*RI octamer at the end of the insert with the cleaved *Eco*RI site of the vector. (6) Transformation and isolation of subcloned plasmids. In these plasmids the regenerated *Eco*RI site is adjacent to different regions of the original insert. The subcloned plasmids were prepared for sequencing using the simple approach: cut with *Eco*RI, label and recut with *Cl*AI. As *Cl*AI cleaves only 20 bases from the *Eco*RI site, the plasmid preparation could be sequenced without further purification steps. Fragments were isolated from pBR-SFV 3 as follows: (1) Cut with *Xho*I, label, recut with *Cl*AI which cleaves in the vector, isolate 4,106-base pair fragment. (2) Cut with *Ava*I, label, recut with *Eco*RI, isolate 408-base pair fragment. (3) Cut with *Eco*RI, label, recut with *Xho*I, isolate 408-base pair fragment. (4) Cut with *Hind*III, label, (i) recut with *Hae*III (vector), isolate 422-base pair fragment, (ii) isolate 697-base pair fragment, recut with *Xho*I, isolate 224-base pair fragment. Fragments from pBR-SFV 2: (1) Cut with *Taq*I, label, (i) recut with *Hind*III (vector), isolate 701-base pair fragment; (ii) recut with *Hae*III, isolate 546-base pair fragment. (2) Cut with *Ava*I, label, recut with *Pst*I, isolate 620- and 488-base pair fragments. (3) Cut with *Hpa*II, label, isolate 345-base pair fragment, recut with *Hae*III, isolate 307-base pair fragment. (4) Cut with *Hae*III, label, isolate 437-base pair fragment, recut with *Hpa*II, isolate 277- and 160-base pair fragments. (5) Cut with *Ava*I, label, recut with *Pst*I, isolate 1,612-base pair fragment. Fragments from pBR-SFV 1: (1) Cut with *Hpa*II, label, (i) isolate 1,036-base pair fragment, recut with *Hind*III, isolate 648- and 388-base pair fragments, (ii) recut with *Hind*III, isolate 830-base pair fragment. (2) Cut with *Pst*I, label, recut with *Hind*III, isolate 521-base pair fragment. (3) Cut with *Ava*I, label, recut with *Hae*III, isolate 1,789- and 950-base pair fragments. (4) Cut with *Taq*I, label, (i) isolate 865-base pair fragment, recut with *Hpa*II, isolate 369-base pair fragment, (ii) isolate 405-base pair fragment, recut with *Hind*III, isolate 176- and 229-base pair fragments, (iii) isolate 354-base pair fragment, recut with *Hpa*II, isolate 159- and 195-base pair fragments, (iv) isolate 1,768-base pair fragment, either recut with *Hind*III, isolate 635-base pair fragment, or recut with *Hae*III, isolate 86-base pair fragment. (5) Cut with *Hind*III, label, (i) recut with *Hpa*II, isolate 648-base pair fragment, (ii) recut with *Hind*III, isolate 1,218-base pair fragment. (6) Cut with *Hind*III, label, (i) recut with *Eco*RI, isolate 2,708-base pair fragment, (ii) recut with *Bam*HI (vector), isolate 3,320-base pair fragment. All fragments were isolated by electrophoresis in agarose gels and subsequent electroelution into hydroxyapatite<sup>28</sup>. DNA sequencing was done using the base-specific cleavage reactions described by Maxam and Gilbert<sup>27</sup>. We used five reactions: G, G+A, C+T, C, C+A. kb, Kilobases.



(Tyr-Glu-His-Ser-Thr-Val)<sup>31</sup> is found 482 amino acids from the amino terminus of E2. However, the carboxy terminus of E2, which has been shown to be His-Ala (ref. 33), is not present immediately before the amino terminus of E1, but 60 amino acid residues earlier. This leaves a 60-residue peptide between the regions coding for E2 and E1. Recently, Welch and Sefton have found a peptide with a  $M_r$  of 6,000 (6K) in extracts of cells infected with SFV<sup>34</sup>. The 6K peptide was coded for by the 26S RNA, but was not found in the virus particle. Partial amino acid sequencing showed that the 6K peptide has a methionine at position 7 and leucines at positions 10 and 17. (W. J. Welch and B. M. Sefton, personal communication), in agreement with the sequence of the 60-amino acid residue segment beginning after the carboxy terminus of E2. The E1 polypeptide terminates at the TAA-438 amino acids after its amino terminus. Carboxypeptidase experiments have shown that the E1 polypeptide terminates with an arginine residue<sup>35</sup>, in agreement with the sequence shown in Fig. 3.

The deduced amino acid sequences of the polypeptides have been fully confirmed by partial amino-terminal amino acid sequencing of fragments obtained by cyanogen bromide cleavage of the isolated E1, E2 and E3 polypeptides (H. Garoff, H. Riedel and H. Lehrach, in preparation). The calculated amino acid compositions of the E3, E2 and E1 polypeptides are in good agreement with those obtained experimentally<sup>9</sup>.

### Sites of glycosylation

All three membrane polypeptides contain carbohydrate units linked to asparagines<sup>35,36</sup>. Carbohydrate units in glycoproteins are known to appear either in Asn-X-Ser or in Asn-X-Thr sequences, the presence of these sequences being a necessary

but not a sufficient condition for glycosylation<sup>37</sup>. Two such sequences are found in the E3 protein (Asn 13-Ala-Thr and Asn 60-Gly-Thr) (Fig. 3). The single oligosaccharide unit known to be present in E3 can therefore be attached to either of these asparagine residues. The E2 protein contains two possible glycosylation sites (Asn 200-Cys-Thr and Asn 262-Ile-Thr), both of which must be glycosylated as this protein has two oligosaccharide units. The single carbohydrate unit of E1 must be attached to Asn 141-Gln-Thr because this is the only potential glycosylation site in the E1 protein.

When the  $M_s$  of the protein (from the sequence) and the carbohydrate parts (from previous gel filtration data) are summed for E1 (47,386+3,400), E2 (46,755+5,100) and E3<sup>35</sup> (7,369+4,000), there is good agreement with the apparent  $M_s$  determined for the proteins by SDS gel electrophoresis<sup>9</sup>.

### Location of the transmembrane segments

We used the criteria devised by Segrest and Feldman<sup>38</sup> to search for hydrophobic sequences in the SFV proteins. Peptides longer than 10 amino acids and lacking charged residues (lysine, arginine, glutamic acid and aspartic acid) were identified and plotted according to their hydrophobicity per unit length. Most of the sequences that were found fall within the triangular area where apolar peptides of globular proteins map. Four peptides mapped in the region to the right of the triangle where the transmembrane domain of glycoprotein<sup>39</sup> and the hydrophobic domains of the haemagglutinins of Influenza virus<sup>40,41</sup> are located (Fig. 4). Three of these peptides were in the SFV membrane proteins, the fourth was in the non-structural 6K peptide. Peptide 24 from E1 (Fig. 4) and peptide 10 from E2 are

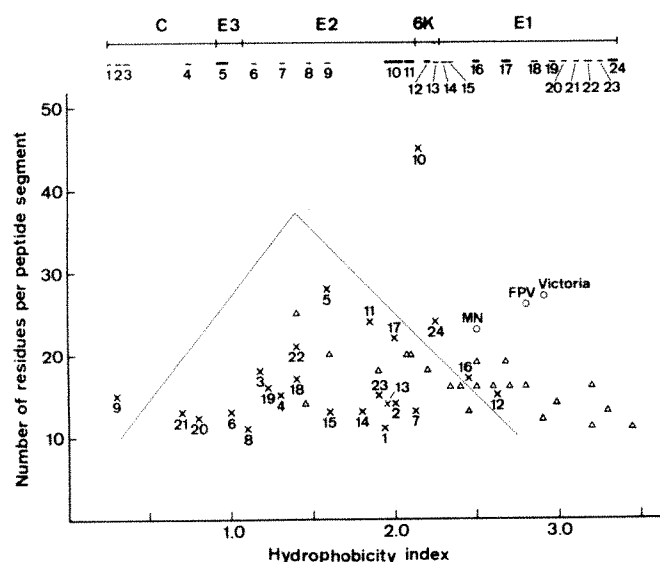
[illegible]

**Fig. 3** The nucleotide sequence of the membrane protein genes. The deduced amino acid sequences of the membrane proteins are shown below. The amino acid residues are numbered from the amino terminus of each polypeptide. The positions are shown in the parentheses to the right. Membrane-spanning segments are underlined and potential glycosylation sites are marked (●).



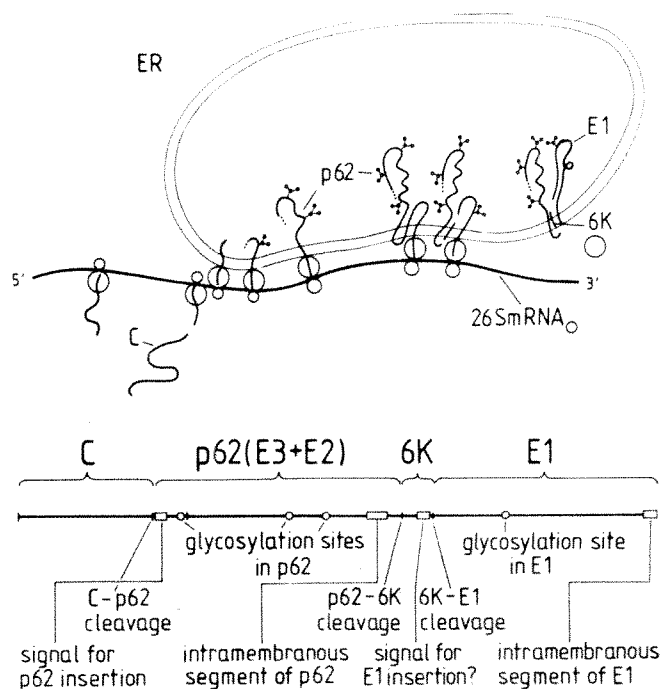
long enough to span the lipid bilayer in the form of an  $\alpha$ -helix<sup>38</sup>. These peptides are located in the carboxy-terminal regions of E1 and E2, respectively, where the hydrophobic domains of E1 and E2 have previously been mapped<sup>11</sup>. The presumptive transmembrane domain of E2 is located between Lys 346 and Arg 392, 31 amino acids away from the carboxy terminus, in complete agreement with our previous biochemical data<sup>11</sup>. The transmembrane domain of E2 is rather long, as defined in the diagram shown in Fig. 4. However, scrutiny of the amino acid sequence shows that it contains two histidines at positions 348 and 352 and two glutamines at positions 353 and 356. These may be located in the external domain outside the bilayer because these amino acids have not been found in the other known transmembrane domains. Furthermore, if we assume an  $\alpha$ -helix for the membrane-spanning segment, the proline residue at position 363 would also be excluded from the bilayer, leaving 28 residues in the transmembrane domain. However, we cannot exclude the possibility that more of the segment is in the bilayer.

The hydrophobic domain of E1 is 24 residues long, only two amino acid residues away from the carboxy terminus. There is no evidence from previous studies that this domain spans the membrane, but the methods we previously used to demonstrate spanning would not have detected the very short segment of two arginine residues<sup>11,42</sup>. Examination of the known and presumptive transmembrane domains of cell surface<sup>39,43,44</sup> and virus glycoproteins<sup>40,41</sup> (including E2) show that they are all characterized by hydrophobic segments at least 23 amino acid residues long (lacking Lys, Arg, Asp, Glu, Gln, Asn, His and Pro residues) followed by one or several closely spaced basic amino acids on their carboxy-terminal side marking the start of the cytoplasmic domain. The hydrophobic domain of the E1 polypeptide fulfills these criteria. Its cytoplasmic domain would thus be only two arginine residues long.



**Fig. 4** Hydrophobicity diagram of apolar sequences in SFV proteins. The hydrophobicity of apolar peptides containing 10 or more amino acids was calculated as described by Segrest and Feldman<sup>38</sup> and these values were plotted against the lengths of the peptides. The upper part of the figure shows the location of the apolar sequences on the polypeptides translated from the 26S RNA. Symbols:  $\times$ , apolar peptides from SFV proteins; these are numbered according to their location.  $\circ$ , Membrane-spanning peptides from glycoporin (marked MN)<sup>39</sup>, the haemagglutinin protein from fowl plague virus (FPV)<sup>40</sup> and influenza virus A strain Victoria<sup>41</sup>.  $\Delta$ , Apolar segments of amino-terminal extensions (signal peptides) of various secreted proteins (see ref. 60).

The third hydrophobic peptide mapping to the right of the triangle in Fig. 4 is located between Lys 79 and Asp 97 in the external hydrophilic domain of E1. This region is amino terminal to the presumptive attachment site for the oligosaccharide side chain. It is 16 amino acids long and is interrupted by a proline residue, much in the same way as the hydrophobic domain of cytochrome  $b_5$  (ref. 45). This region could be involved in the membrane fusion activity displayed by the SFV spike glycoprotein during virus entry into the host cell through the lysosomes<sup>46</sup>. At  $\leq$  pH 6, the membrane of SFV fuses with cholesterol-containing phospholipid bilayers<sup>47</sup>. One could envisage that the low pH induces a conformational change in the E1 polypeptide, exposing this hydrophobic peptide which could then insert into a neighbouring lipid bilayer to initiate fusion of the apposed membranes. The amino-terminal region of the Sendai virus fusion protein, thought to be involved in membrane fusion, is also relatively hydrophobic<sup>48</sup>.



**Fig. 5** Scheme for the assembly of SFV membrane glycoprotein into the membrane of the endoplasmic reticulum. C is the capsid protein which remains in the cytoplasm.

## Proteolytic cleavages involved in synthesis of SFV proteins

The nucleotide sequence of the DNA, copied from the 26S RNA, has confirmed the order determined previously for the genes coding for the SFV proteins<sup>11,14</sup>. The coding regions are contiguous except between E2 and E1, where an additional gene segment was found coding for 60 amino acids, the 6K peptide described by Welch and Sefton<sup>34</sup>. This would imply that at least four proteolytic cleavages are needed to generate the four structural polypeptides of the virus. Previous studies have shown that the capsid protein is cleaved from the nascent chain as soon as translation of the protein is completed<sup>16</sup>. This cleavage is mediated either by the capsid protein itself<sup>49</sup> or by a ribosomal protease<sup>50</sup>, as it has been observed *in vitro* in all eukaryotic protein-translation systems tested. The excision of the 6K peptide also occurs on the nascent chain and may involve host proteases. The fourth cleavage which generates the E3 and E2 polypeptides from the p62 protein occurs about 30 min after synthesis<sup>17</sup>. The cleavage is blocked by antibodies against the SFV spike glycoproteins added to the infected cells, and prob-

ably occurs at the plasma membrane<sup>17,51</sup>. The cleavage site is next to an arginine pair located before the amino terminus of E1. Many prohormones and proproteins are processed to their final forms through specific cleavages at sites bearing pairs of basic amino acid residues (lysine and arginine). This is the case for proinsulin<sup>52</sup>, progastrin<sup>53</sup>, proglucagon<sup>54</sup>, proalbumin<sup>55</sup>, parathyroid hormone<sup>56</sup> and the common precursor for melanotropins, corticotropin, lipotropin and endorphins<sup>57</sup>. These cleavages which probably involve a combined trypsin-like and carboxypeptidase B-like specificity occur late in secretion, shortly before extracellular release. The haemagglutinin of fowl plague virus is also split late during intracellular transport or at the plasma membrane by a host protease into two polypeptide chains by two cleavages involving the excision of a -Lys-Arg-Glu-Lys-Arg- connecting peptide<sup>40</sup>. It is tempting to speculate that the secreted proproteins and the virus membrane glycoproteins are processed by the same family of host proteases, part of the post-Golgi pathway to the cell surface. This would mean that the cleavage of the p62 polypeptides begins before their appearance on the cell surface.

### Assembly of SFV membrane proteins

Previous studies indicate that the p62 and the E1 polypeptides are transferred across the membrane of the endoplasmic reticulum as they are being synthesized<sup>16,32</sup>. Both polypeptide chains seem to have their own independent signal peptides for membrane insertion<sup>16,58,59</sup>. Membrane insertion and transfer of the p62 polypeptide occur *in vitro* only if microsomal vesicles are present in the translation assay before about 100 amino acids from the amino terminus of the p62 polypeptide have been made<sup>16</sup>. This region must therefore contain a functional signal peptide. There seems to be no significant homology in the primary structures of the different signal sequences so far known<sup>16,60</sup>. The only common feature is a central core of at least nine predominantly hydrophobic amino acids uninterrupted by charged amino acids<sup>61</sup>. This criterion is fulfilled by the amino-terminal region of the p62 protein (Fig. 3). The hydrophobicity of this peptide (no. 5 in Fig. 4) is low but not lower than that of other signal peptides (Fig. 4). An unusual observation is that the signal peptide of the p62 polypeptide is not removed during translation (ref. 32 and W. Welch and B. Sefton, personal communication). It is completely translocated through the membrane with the rest of the external p62 domain of the protein.

The evidence suggesting that the E1 polypeptide has its own independent signal peptide is based on observations using a temperature-sensitive mutant of SFV. Kääriäinen and co-workers have found a mutant of SFV in which the cleavage between the capsid and the p62 polypeptides is blocked at the nonpermissive temperature<sup>39</sup>. Although the p62 polypeptide is not inserted into the membrane of the endoplasmic reticulum in these conditions, the E1 polypeptide seems to be correctly translocated. Judging from the *M<sub>s</sub>* of the E1 polypeptide and the uncleaved capsid-p62 polypeptide, the 6K peptide seems also to be normally excised. It is not possible to define the exact location of the signal peptide for E1 from the amino acid sequence of this region (Figs 3, 4), but one possibility is that it is in the 6K peptide preceding the amino terminus of E1. In this case, polypeptide E1 would be released from the 6K peptide, presumably by a signal peptidase cleavage.

A scheme for the assembly of the SFV spike glycoprotein into the membrane of the endoplasmic reticulum is depicted in Fig. 5. The signal peptide of the p62 polypeptide mediates insertion into the membrane soon after capsid protein cleavage. Translocation of the growing chain continues until the carboxy-terminal transmembrane domain stops transfer of the polypeptide. The ribosome would either be detached from the membrane at this stage or remain bound to the membrane. When the signal peptide for E1 emerges from the ribosome, renewed membrane insertion and transfer would take place. We do not know exactly when and on what side of the membrane the cleavage releasing the 6K peptide occurs during translation. It would be helpful to know the location of the 6K peptide with respect to the membrane after excision. Translocation of the E1 polypeptide is not complete when the nonsense codon in the 26S RNA terminates translation but the transmembrane domain of E1 must be pulled into the membrane either by the spontaneous folding of the external glycosylated domain in the lumen of the endoplasmic reticulum or by the postulated translocation machinery in the membrane<sup>7</sup>. The cluster of basic amino residues on the carboxy-terminal side of the membrane-spanning segments may be needed to fix the polypeptides into the membrane.

We thank Evelyn Kiko and Hilkka Virta for technical assistance, Annie Biais for typing the manuscript, N. Kalkkinen, L. Kääriäinen, B. Sefton, J. Strauss for permission to use unpublished data, and A. Helenius, K. Matlin and G. Warren for helpful criticism. This work has been done in accordance with the German guidelines for recombinant DNA research.

Received 7 July, accepted 22 September 1980

- Samons, K. & Garoff, H. *J. gen. Virol.* (in the press)
- Rothman, J. E. & Lodish, H. F. *Nature* **269**, 775-780 (1977)
- Langguth, V. R., Katz, F. N., Lodish, H. F. & Blobel, G. *J. Biol. Chem.* **253**, 8667-8670 (1978)
- Dobbertstein, B., Garoff, H. & Warren, G. *Cell* **17**, 759-769 (1979)
- Ploegh, H. L., Cammer, L. E. & Strominger, J. L. *Proc. natn. Acad. Sci. USA* **76**, 2273-2277 (1979)
- Jokinen, M., Gehlberg, C. G. & Anderson, L. C. *Nature* **279**, 604-607 (1979)
- Blobel, G. *et al. Proc. Nat. Acad. Sci. USA* **76**, 9-16 (1979)
- Uhrmann, G. & Samons, K. *J. molec. Biol.* **88**, 569-587 (1974)
- Garoff, H., Samons, K. & Ronkainen, O. *Virology* **61**, 493-504 (1974)
- Zasmeck, A. & Garoff, H. *J. molec. Biol.* **122**, 259-269 (1978)
- Garoff, H. & Soderlund, H. *J. molec. Biol.* **124**, 535-549 (1978)
- Samons, D. T. & Strauss, J. H. *J. molec. Biol.* **71**, 599-613 (1972)
- Kennedy, S. I. T. *J. molec. Biol.* **108**, 491-511 (1976)
- Clegg, J. C. S. *Nature new Biol.* **284**, 454-455 (1975)
- Glanville, N., Rankin, M., Morner, J., Kaaramen, L. & Smith, A. E. *Proc. natn. Acad. Sci. USA* **73**, 3059-3063 (1976)
- Garoff, H., Samons, K. & Dobbertstein, B. *J. molec. Biol.* **124**, 587-600 (1978)
- Zasmeck, A., Garoff, H. & Samons, K. *J. gen. Virol.* (in the press)
- Garoff, H., Frisch, A.-M., Samons, K., Lohr, H. & Delmas, H. *Proc. natn. Acad. Sci. USA* (in the press)
- Lehrach, H. *et al. Biochemistry* **18**, 3146-3152 (1979)
- Rowekamp, W. & Pritzel, R. *Dev. Biol.* (in the press)
- Vila-Komaroff, L. *et al. Proc. natn. Acad. Sci. USA* **75**, 3727-3731 (1978)
- Grunstein, M. & Hogness, D. S. *Proc. natn. Acad. Sci. USA* **72**, 3961-3965 (1975)
- Barnes, W. M. *Science* **198**, 393-394 (1977)
- Chow, L. T., Roberts, J. M., Lewis, J. B. & Broker, T. R. *Cell* **11**, 819-836 (1977)
- Prins, H., Koller, B., Hess, B. & Delmas, H. *Molec. gen. Genes* **178**, 27-34 (1980)
- Smith, H. O. & Birnstiel, M. L. *Nucleic Acids Res.* **3**, 2387-2398 (1976)
- Maxam, A. M. & Gilbert, W. *Meth. Enzym.* **65**, 499-560 (1980)
- Satchell, J. G. *Nucleic Acids Res.* **5**, 2721 (1978)
- Tabak, H. F. & Flavell, R. A. *Nucleic Acids Res.* **5**, 2321-2332 (1978)
- Ou, J.-H., Strauss, E. G. & Strauss, J. H. *Virology* (in the press)
- Kalkkinen, N., Jörnwall, H., Soderlund, H. & Kaaramen, L. *Eur. J. Biochem.* **100**, 31-37 (1980)
- Boemth, S. & Blobel, G. *J. Biol. Chem.* **254**, 12261-12264 (1979)
- Kalkkinen, N. *FEBS Lett.* **115**, 163-166 (1980)
- Welch, W. J. & Sefton, B. M. *J. Virol.* **33**, 230-237 (1980)
- Mattila, K., Lunkkainen, A. & Ronkainen, O. *Biochim. biophys. Acta* **419**, 435-444 (1976)
- Pesonen, M. & Ronkainen, O. *Biochim. biophys. Acta* **485**, 510-525 (1976)
- Neuberger, A., Gottschalk, A., Marshall, R. D. & Sporo, R. G. In *The Glycoproteins: their Composition, Structure and Function* (ed. Gottschalk, A.) 450-490 (Elsevier, Amsterdam, 1972)
- Sagrest, J. P. & Feldman, R. J. *J. molec. Biol.* **87**, 853-858 (1974)
- Toimila, H. & Marchon, V. T. *Proc. natn. Acad. Sci. USA* **72**, 2964-2968 (1975)
- Porter, H. G. *et al. Nature* **282**, 471-477 (1979)
- Min Jou, W. *et al. Cell* **19**, 683-696 (1980)
- Garoff, H. & Samons, K. *Proc. natn. Acad. Sci. USA* **71**, 3988-3992 (1974)
- Robb, R. J., Terborst, L. & Strominger, J. L. *J. Biol. Chem.* **253**, 5319-5324 (1978)
- Rogovin, J. *et al. Cell* **20**, 303-312 (1980)
- Ozols, J. & Gerard, C. *Proc. natn. Acad. Sci. USA* **74**, 3725-3729 (1977)
- Helenius, A., Kartenbeck, J., Samons, K. & Prins, E. *J. Cell Biol.* **84**, 404-420 (1980)
- White, J. & Helenius, A. *Proc. natn. Acad. Sci. USA* **77**, 3273-3277 (1980)
- Gething, M. J., White, J. & Waterfield, M. D. *Proc. natn. Acad. Sci. USA* **76**, 2737-2740 (1978)
- Alpert, G. & Schlesinger, M. *J. Virology* **90**, 366-369 (1978)
- Langner, J., Wiedersheim, S., Ansoerg, P., Bohley, P. & Krachko, H. *Acta biol. med. germ.* **38**, 1527-1538 (1979)
- Jones, K. J., Witte, M. R. F. & Bose, H. R. *J. Virol.* **13**, 809-810 (1974)
- Kemmer, W., Steiner, D. F. & Borg, J. *J. Biol. Chem.* **248**, 4544-4551 (1973)
- Gregory, R. A. & Tracy, H. J. *Lancet* **ii**, 797 (1972)
- Tager, H. S. & Steiner, D. F. *Proc. natn. Acad. Sci. USA* **70**, 2321-2325 (1973)
- Russell, J. H. & Geller, D. M. *J. Biol. Chem.* **250**, 3409-3413 (1975)
- Habener, J. F., Chang, H. T. & Potts, J. T. Jr. *Biochemistry* **16**, 3910-3917 (1977)
- Nakamitsu, S. *et al. Nature* **278**, 423-427 (1979)
- Wirth, D. F., Katz, F., Smith, B. & Lodish, H. F. *Cell* **10**, 253-263 (1977)
- Hashimoto, K., Erdei, S., Keranen, S., Saraste, J. & Kaaramen, L. *J. Virol.* (in the press)
- Anstötz, B. M. *FEBS Lett.* **103**, 308-313 (1979)
- Emr, S. D., Hedgpeth, J., Clement, J. M., Silhavy, T. J. & Hoffnung, M. *Nature* **286**, 82-85 (1980)



# LETTERS

## Stellar perturbations of the cometary cloud

Paul R. Weissman

Jet Propulsion Laboratory, Earth and Space Sciences Division,  
Pasadena, California 91103

The existence of a cloud of  $\sim 2 \times 10^{11}$  comets surrounding the Solar System and extending out to interstellar distances has been suggested by Oort<sup>1</sup> based on the observed distribution of inverse semi-major axes of the long-period comets. Simple statistical arguments can be used to update the current understanding of how stellar perturbations act on the Oort cloud, and to infer some of the cloud properties. Using such an approach it is shown here that the cloud radius is  $\sim 10^5$  AU, the mean 'thermal' velocity in the cloud is  $\sim 110$  m s<sup>-1</sup>, and the resulting perihelion distribution in the planetary region is uniform with  $q$ . Stars passing through the Oort cloud over the history of the Solar System have ejected at least 9% of the initial population, and have randomized the orbits of the remaining comets so as to leave little record of their initial state.

Dynamical studies using analytical<sup>2</sup>, statistical<sup>3</sup>, and Monte Carlo<sup>4</sup> techniques have shown that the cometary cloud hypothesis can explain the observed distribution of cometary orbits. While these studies have tended to emphasize the orbital evolution of the long-period comets once they enter the planetary region from the cloud, relatively little attention has been given to the dynamics of comets in the cloud, controlled principally by perturbations from passing stars. Previous studies of the stellar perturbation problem<sup>1,5-9</sup> have demonstrated that no simple, complete solution exists.

The general method of treating the problem is to assume the comet is stationary in space relative to the Sun and that stars move by at high velocity along straight line paths. This is a good approximation because comets in the Oort cloud are moving at speeds of the order of 1–100 m s<sup>-1</sup> while the entire Solar System is moving through the local group of stars at a velocity of 20 km s<sup>-1</sup>. The Sun's gravity perturbs the passing star but the deflection from a straight line is negligible: 0.12 degrees for a star passing 0.01 pc (2,063 AU) away at a velocity of 20 km s<sup>-1</sup>. The velocity change imparted to the comet by the passing star is

$$\Delta V = 2GM_s/RV_s \quad (1)$$

where  $G$  is the gravitational constant,  $M_s$  the mass of the star,  $R$  the impact parameter, and  $V_s$  the velocity of the passing star. The velocity impulse is directed towards the point at which the star makes its closest approach to the comet. For a typical  $1 M_\odot$  star passing at a distance of 1 pc and a velocity of 20 km s<sup>-1</sup> the velocity impulse  $\Delta V = 43$  cm s<sup>-1</sup>.

The Sun receives a similar impulse from the passing star though typically different in magnitude and direction. It is the net difference between the velocity impulse on the comet and the impulse on the Sun that determines the perturbation of the comet's orbit relative to the Sun. Previous studies have pointed out the importance of close stellar encounters where the comet-star distance is comparable with or less than the comet-Sun distance. The velocity changes from distant encounters are small in magnitude and tend to impart nearly the same impulse to the Sun and the comet, yielding little net effect. Close encounters, however, show much greater variation in both magnitude and direction of the velocity impulse on the comet relative to the Sun, and thus are dominant in determining the total perturbation on the comets, even though they are less frequent than the distant encounters.

The frequency of encounters between the Solar System and passing stars can be found by considering the volume of space swept out by the Solar System in a time  $T$

$$N = \pi R^2 VT \rho_s \quad (2)$$

where  $N$  is the number of encounters,  $V$  is the velocity of the Sun relative to the local group of stars,  $\rho_s$  is the local density of stars, and  $R$  is the radius of the Solar System cross-section to be considered. Taking  $V = 20$  km s<sup>-1</sup> and  $\rho_s = 0.08$  pc<sup>-3</sup> (from ref. 10) then

$$N = 5.1 \times 10^{-6} R^2 T \quad (3)$$

where  $R$  is in parsecs and  $T$  in years. For  $R = 1$  pc there is on the average one stellar encounter every  $2.0 \times 10^5$  yr or 5.1 encounters per Myr. If these parameters have been constant over the history of the Solar System then the cometary cloud has experienced  $2.3 \times 10^4$  stellar encounters at a distance of 1 pc or less in that time.

The mean energy perturbation caused by the passing stars can be found by integrating over concentric shells around the comet in space, with the number of stars passing at any distance  $R$  proportional to the volume of the shell at that distance.

$$\overline{\Delta V^2} = \int_{R_1}^{R_2} (\Delta V)^2 4\pi R^2 dR / \int_{R_1}^{R_2} 4\pi R^2 dR \quad (4)$$

Substituting for  $\Delta V$  in equation (1) and performing the integration gives

$$\overline{\Delta V^2} = 12 (GM/V)^2 (R_2 - R_1) / (R_2^3 - R_1^3) \quad (5)$$

The lower limit of the integration can be taken to be that distance at which a single encounter will eject a comet from the cloud. At  $5 \times 10^4$  AU from the Sun the escape velocity,  $V_e = 188$  m s<sup>-1</sup> and the impact parameter  $R_1 = 472$  AU for a  $1 M_\odot$  star passing at 20 km s<sup>-1</sup>; for  $10^5$  AU from the Sun  $V_e = 133$  m s<sup>-1</sup> and  $R_1 = 667$  AU. For the upper limit it has already been stated that  $R_2$  must be of the order of the dimensions of the cometary cloud or larger:  $\geq 10^5$  AU. Thus  $R_2 \gg R_1$  and the expression above can be simplified to

$$\overline{\Delta V^2} \approx 12 (GM/VR)^2 \quad (6)$$

where  $R$  is now equal to  $R_2$ , the upper limit of the Solar System radius of cross-section being considered. Again taking  $V = 20$  km s<sup>-1</sup> and assuming a  $1 M_\odot$  stars gives

$$\overline{\Delta V^2} = 0.55/R^2 \quad (\text{m s}^{-1})^2 \quad (7)$$

where  $R$  is in parsecs.

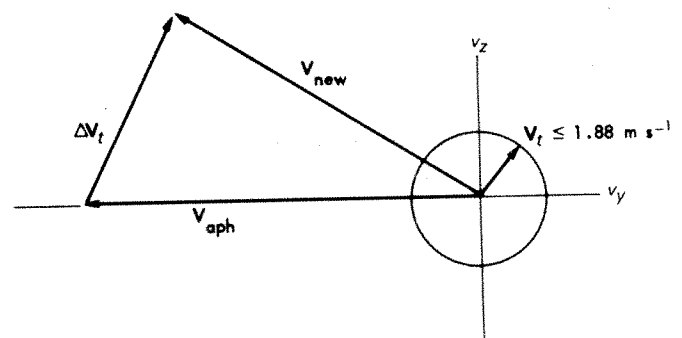


Fig. 1 Velocity phase space normal to a comet's radius vector showing relationship between initial aphelion velocity  $V_{\text{aph}}$ , tangential perturbation  $\Delta V_t$ , and new velocity  $V_{\text{new}}$ . Comets falling within the  $1.88$  m s<sup>-1</sup> circle around the origin will have perihelia  $\leq 5$  AU. An aphelion distance of  $5 \times 10^4$  AU is assumed.

The total r.m.s. velocity perturbation in any period of time is then given by the square root of the number of stellar passages within distance  $R$  times the mean energy perturbation

$$\Delta V_{r.m.s.} = (N \cdot \overline{\Delta V^2})^{1/2} = 1.7 \times 10^{-3} T^{1/2} \text{ m s}^{-1} \quad (8)$$

where  $T$  is the time in yr. This could result in a significant perturbation on comets far from the Sun. The aphelion velocity of an Oort cloud comet with perihelion distance of 1 AU is  $\sim 0.84 \text{ m s}^{-1}$  while its period is  $4 \times 10^6$  yr, most of which is spent near aphelion. During that time the mean stellar perturbation from the above equation would be  $3.4 \text{ m s}^{-1}$ , capable of raising the comet's perihelion distance to over 25 AU (assuming the velocity perturbation is parallel to the aphelion velocity), outside the observable region. The angular orbit elements would also be expected to change radically. But the maximum possible change in semi-major axis for the same typical perturbation is only 0.05%. Thus comets which leave the planetary region on orbits with large aphelion distances may again be subject to significant changes in angular momentum by passing stars, but not in orbital energy. This could be an important factor in following the evolution of such comets during their lifetimes. The fraction of comets for which this occurs, however, is not large. For comets originating in the cloud and with perihelia inside the orbit of Jupiter, only  $\sim 9\%$  will be returned to orbits with aphelion distances between  $10^4$  and  $10^5$  AU.

It is worthwhile to consider the total velocity perturbation on comets in the cloud over the history of the Solar System. From equation (8)  $\Delta V_{r.m.s.} = 113 \text{ m s}^{-1}$ , which agrees well with previous results<sup>1,7</sup>. This is equal to the circular orbital velocity at  $6.9 \times 10^4$  AU from the Sun or the escape velocity at twice that distance. Thus one would expect the present dynamical limits on the cloud to be of the order of  $10^5$  AU or less. Note that the dimensions of the cloud will shrink with time as the stellar perturbations continue to strip away the outermost shells. The mean aphelion distance of observed new comets entering the planetary region from the cloud has been shown<sup>11</sup> to be  $4.32 \pm 0.12 \times 10^4$  AU. The dynamical limit<sup>12</sup> on the Sun's sphere of influence due to perturbations by the galactic nucleus is of the order of  $2 \times 10^5$  AU.

The perihelion distribution of comets entering the planetary region from the Oort cloud can be obtained by considering the velocity phase space in the plane perpendicular to each comet's heliocentric radius vector, shown in Fig. 1. The component of the comet's aphelion velocity in this plane determines the perihelion distance. Comets are randomly scattered on this plane by stellar perturbations whose r.m.s. magnitude is  $(2/3)^{1/2}$  that given by equation (8). If a comet's initial tangential velocity is given by  $V_{\text{orb}}$  then after a stellar perturbation of  $\Delta V$ , it will have some velocity  $V_{\text{new}}$ . Those comets whose new velocity vectors fall within a relatively small circle around zero transverse velocity ( $1.88 \text{ m s}^{-1}$  for a perihelion of 5 AU and aphelion of  $5 \times 10^4$  AU) will enter the planetary region and possibly be observed. The typical value for  $\Delta V$  is of the order of  $2.8 \text{ m s}^{-1}$  so comets can be expected to be randomly scattered over the near-zero velocity region in phase space. Thus the number in the circle is proportional to the area of the circle, or to its radius squared, that is  $\propto V_t^2$ . But  $V_t \propto q^{1/2}$  so the cumulative number of comets between zero and any value  $q$  is proportional to  $q$ , or  $dN/dq$  is constant. This result has also been demonstrated by Monte Carlo simulations of the problem<sup>13</sup>.

Another implication drawn from the magnitude of the total r.m.s. perturbation is that the orbits of the comets in the cloud have been 'randomized' over the history of the Solar System. Thus it is unlikely that orbital data could be used to discriminate between various theories of cometary origin, that is, formation among the outer planets with subsequent ejection to the cloud, versus formation in satellite fragments of the primordial solar nebula.

Finally, one can also consider the number of comets ejected from the cloud due to single passes of stars through it. Using the estimated population of  $2 \times 10^{11}$  comets and assuming a radius of  $10^5$  AU yields a number density of  $\rho_c = 4.8 \times 10^{-5} \text{ AU}^{-3}$ . Each

star will eject from the cloud comets for which the velocity perturbation is greater than the escape velocity:

$$2GM_*/DV_* > (2GM_\odot/R)^{1/2} \quad (9)$$

where  $D$  is the minimum comet-star distance and  $R$  is the comet-Sun distance. Solving for  $D$  gives

$$D = (2GR/M_\odot)^{1/2} M_*/V_* \quad (10)$$

Assuming a  $1 M_\odot$  star and a relative velocity of  $20 \text{ km s}^{-1}$  one finds  $D = 2.1 R^{1/2}$  where  $R$  is in AU.

From equation (3) there would be  $N_* = 5.4 \times 10^3$  stellar encounters within  $10^5$  AU over the history of the Solar System. Approximating the volume swept out by each star by a cylinder with radius equal to  $D$  at  $R = 5 \times 10^4$  AU and with length equal to the mean chord length through the cloud of  $10^5$  AU gives

$$N_{\text{ejected}} = N_* \pi D^2 10^5 \rho_c = 1.8 \times 10^{10} \quad (11)$$

This is 9% of the estimated cloud population, a small but significant fraction. Note that this is the fraction ejected by single stellar encounters only, and that the cumulative effect of many encounters will eject additional comets.

I thank colleagues at JPL for review of an earlier draft of this paper. This paper presents one phase of work performed at the Jet Propulsion Laboratory/California Institute of Technology under NASA contract NAS 7-100.

Received 30 June, accepted 26 September 1980

1. Oort, J. H. *Bull. astr. Inst. Nech* 11, 91 (1950)
2. Whipple, F. L. *Astr. J.* 67, 1 (1962)
3. Kendall, D. G. 4th Berkeley Symp. on Mathematical Statistics and Probability 3, 99 (1961)
4. Westman, P. R. *IAU Symp.* No. 81, 277-282 (1979)
5. Opik, E. J., *Proc. Am. Acad. Arts Sci.* 67, 169 (1932)
6. Sekanina, Z. *Bull. Astr. Inst. Czech* 19, 223 (1968) and 19, 291 (1968)
7. Puntich, M. B. thesis, Univ. Illinois (1971)
8. Ruckman, H. *Bull. astr. Inst. Czech* 27, 92 (1976)
9. Yabushita, S. *Astr. Astrophys.* 16, 395 (1972)
10. Allen, C. W. in *Astrophysical Observations* (Athlone, London, 1963)
11. Marston, B. G., Sekanina, Z. & Everhart, E. *Astr. J.* 83, 64 (1978)
12. Chabotzov, G. A. *Soviet Astr. J.* 8, 787 (1965), 10, 341 (1966)
13. Westman, P. R., *Comets, Asteroids, Meteoroids: Interrelations, Evolution, and Origins* (ed. Dolosenc, A. H.) 87-91 (University of Toledo Press, 1977)

## Far UV photolysis of $\text{CH}_4$ - $\text{NH}_3$ mixtures and planetary studies

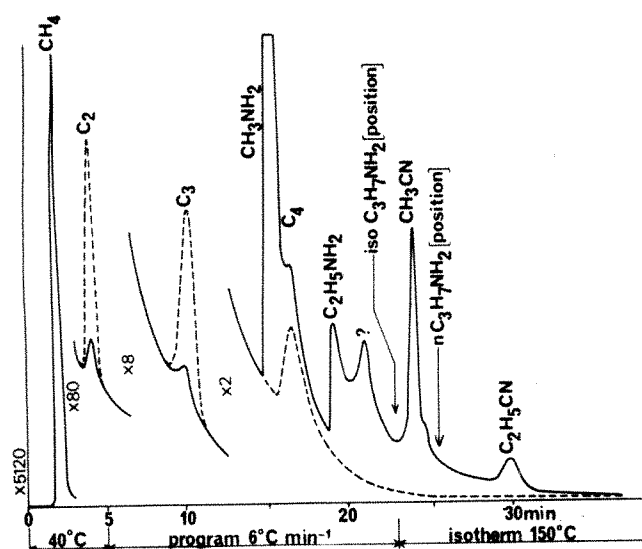
Alain Boesard & Gérard Toupance

Laboratoire de Physico-Chimie de l'Environnement,  
Université Paris Val de Marne, Avenue du Général de Gaulle,  
94010, Créteil Cedex, France

The far UV photochemistry of  $\text{CH}_4$  and of  $\text{NH}_3$  has been widely studied<sup>1,2</sup> and the primary processes are relatively well known. In contrast no experimental study of far UV photochemistry of  $\text{CH}_4$ - $\text{NH}_3$  mixtures had been published before our preliminary report<sup>3</sup>. We report here new photochemical data on the effect of the mole fraction of  $\text{NH}_3$  on the production of N-containing organics. Photolysis of  $\text{CH}_4$ - $\text{NH}_3$  mixtures at 147 nm leads to the formation of nitriles when the mole fraction of  $\text{NH}_3$  is low and to the formation of amines when the mole fraction of  $\text{NH}_3$  is high. Study of mixtures in which the  $\text{NH}_3$  mole fraction is very low has been particularly emphasized. The main conclusions are that (1) important quantities of nitriles may have been photo-produced on the primitive Earth if a low partial pressure of  $\text{NH}_3$  remained and (2) nitriles are the main N-containing organics that may be photoproduced in the atmosphere of the giant planets.

The far UV photolysis of various  $\text{CH}_4$ - $\text{NH}_3$  mixtures was carried out under a total pressure of 13 mbar into a cylindrical all-pyrex reactor ( $l = 35 \text{ cm}$ ; i.d. =  $4 \text{ cm}$ ) with a low-pressure Xe-lamp attached (window,  $\text{MgF}_2$ ;  $\lambda = 147 \text{ nm}$ , monochromatic; flux emitted =  $8 \times 10^{15} \text{ photon s}^{-1}$ ). The apparatus has been described elsewhere<sup>4</sup>. The reactor was evacuated to a





**Fig. 1** Chromatogram obtained after irradiation of an equimolar  $\text{CH}_4$ - $\text{NH}_3$  mixture during 30 min with a xenon lamp emitting  $8 \times 10^{15}$  photons per second. Solid line,  $\text{CH}_4$  (6.5 mbar)- $\text{NH}_3$  (6.5 mbar); dashed line,  $\text{CH}_4$  (13 mbar). Chromatograms were obtained with a Varian apparatus model 1520 using FID. Chromatographic conditions, glass column (6 mm i.d.  $\times$  3 m) packed with Chromosorb 103 (100–120 mesh). Carrier gas,  $\text{N}_2$  (40 ml  $\text{min}^{-1}$ ).

pressure  $< 10^{-5}$  mbar before each experiment; care was taken to ensure that there were no mercury-containing devices in any part of the apparatus. Samples were analysed mostly by gas chromatography (FID detector).

Two series of experiments were performed. In the first the irradiation time was 30 min and the mole fraction of  $\text{NH}_3$  in the mixture ranged from 0.1 to 1; in the second the respective values were 7 min, and 0.01 to 0.1. The irradiation times were chosen to ensure a significant synthesis of products and a negligible decomposition of the initial compounds,  $\text{NH}_3$  being the most critical, during the experiment.

The solid curve (Fig. 1) applies to an equimolar  $\text{CH}_4$ - $\text{NH}_3$  mixture irradiated for 30 min: amines, nitriles and hydrocarbons are synthesized. Gas chromatography on a Porapak Q package shows that the hydrocarbons are mainly saturated,  $\text{C}_2\text{H}_6$  and  $\text{C}_3\text{H}_8$  representing respectively more than 99% of the  $\text{C}_2$  and  $\text{C}_3$  hydrocarbons. The dashed curve applies to  $\text{CH}_4$  irradiated for 30 min at the same total pressure. Figure 1 shows that  $\text{NH}_3$  in the mixture strongly inhibits the synthesis of hydrocarbons. A gas chromatography on a Porapak Q package has shown that this inhibitory effect of  $\text{NH}_3$  is much more important for unsaturated hydrocarbons than for saturated ones.

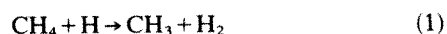
$\text{CH}_3\text{NH}_2$ ,  $\text{C}_2\text{H}_5\text{NH}_2$ ,  $\text{HCN}$ ,  $\text{CH}_3\text{CN}$ ,  $\text{C}_2\text{H}_5\text{CN}$  and many aliphatic hydrocarbons have been definitively identified as products of the photolysis. As quantitative gas chromatographic analysis of  $\text{HCN}$  is not possible in the presence of  $\text{NH}_3$ , a colorimetric titration<sup>5</sup> has been achieved for this compound. For a  $\text{CH}_4$ - $\text{NH}_3$  mixture where the mole fraction of  $\text{NH}_3$  is 0.1, the amount of  $\text{HCN}$  synthesized has been found to be approximately equal to the amount of  $\text{CH}_3\text{CN}$  synthesized during the same experiment. There has not been a search for hydrazine.

Figure 2 shows how the mole fraction of  $\text{NH}_3$  affects the synthesis of  $\text{CH}_3\text{CN}$  and  $\text{CH}_3\text{NH}_2$ . An opposite effect is evident: increasing the mole fraction of  $\text{NH}_3$  strongly increases the synthesis of  $\text{CH}_3\text{NH}_2$  but strongly decreases the synthesis of  $\text{CH}_3\text{CN}$ . In fact, for mole fractions of  $\text{NH}_3 \leq 0.2$ , no  $\text{CH}_3\text{NH}_2$  has been detected by gas chromatography. To have a better limit of detectability, a spectrophotofluorimetric analysis of  $\text{CH}_3\text{NH}_2$  using the fluorecamine<sup>6</sup> technique has been performed. For a mixture containing a mole fraction of  $\text{NH}_3$  equal to 0.1, we have

found that the quantity of  $\text{CH}_3\text{NH}_2$  synthesized was at best 20 nmol, that is 7% of that of  $\text{CH}_3\text{CN}$ .

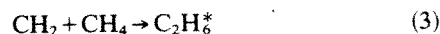
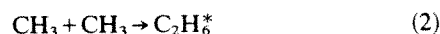
The second series of experiments, using mole fractions of  $\text{NH}_3$  in the range 0.01–0.1, has been performed to determine more precisely the portion of the curve plotted with a dashed line on Fig. 2. The results are shown in Fig. 3. Synthesis of  $\text{CH}_3\text{CN}$  is efficient even when the mole fraction of  $\text{NH}_3$  is very low. There was no search for amines.

The photochemistry involved in these experiments, especially for the synthesis of nitriles, is not yet clear. At 147 nm both  $\text{CH}_3$  and  $\text{CH}_2$  may be photoproducts from  $\text{CH}_4$  (ref. 7) (the relative amount of the two species is not known) while both  $\text{NH}_2$  and  $\text{NH}$  may be photoproducts from  $\text{NH}_3$  (ref. 8). However, as molar absorption coefficients<sup>9</sup> at 147 nm, are respectively  $0.2 \text{ cm}^{-1} \text{ atm}^{-1}$  for  $\text{CH}_4$  and  $80 \text{ cm}^{-1} \text{ atm}^{-1}$  for  $\text{NH}_3$ , in every considered mixture  $\text{CH}_4$  absorbs only a minor part of the incident light (that is 2% or less when the  $\text{NH}_3$  mole fraction is 0.1 or above). Consequently, the predominant radicals in the system are:  $\text{NH}_2$  and  $\text{NH}$  photoproducts from  $\text{NH}_3$ , and  $\text{CH}_3$  mainly produced through reaction of  $\text{CH}_4$  with energetic H atoms resulting from the photodissociation of  $\text{NH}_3$ :



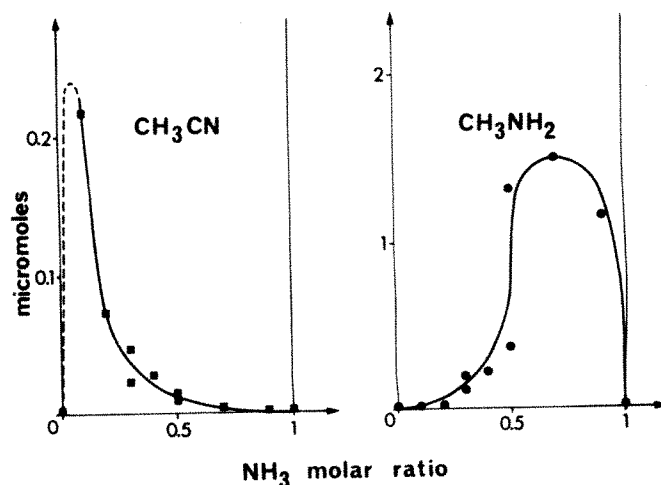
$\text{CH}_2$  which can be produced only from the photodissociation of  $\text{CH}_4$  is present at a lower concentration.

The key step for the synthesis of hydrocarbons is the formation of  $\text{C}_2\text{H}_6^*$  through:

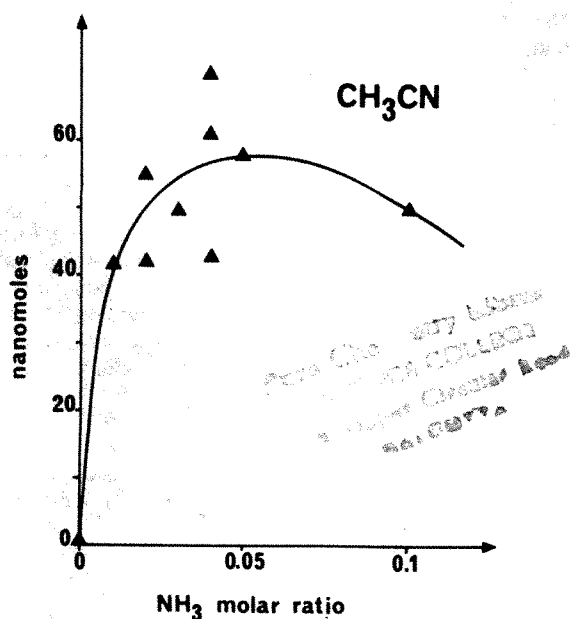


It seems likely that the reaction pathway for  $\text{CH}_3\text{NH}_2$  synthesis combines  $\text{CH}_3$  and  $\text{NH}_2$ . The production of nitriles is more difficult to explain. A reaction pathway in steps must be invoked but unfortunately there is very little knowledge of the reactions of the  $\text{NH}$  radical nor of the chemistry of intermediate species which should be considered, such as  $\text{CH}_2\text{NH}$ ,  $\text{CH}_3\text{NH}$  or  $\text{CH}_3\text{CHNH}$ . In fact, although the production of  $\text{HCN}$  has been reported in similar experiments<sup>10</sup>, no reaction pathway has been proposed.

Nevertheless, it seems likely that the photodissociation of  $\text{CH}_4$  is not necessary for the production of nitriles because first,  $\text{HCN}$  is synthesized in experiments performed at 185 nm where photodissociation of  $\text{CH}_4$  cannot occur<sup>10</sup>; and second, because of the calculated quantum yield of synthesis of  $\text{CH}_3\text{CN}$ , relative to the photons absorbed by  $\text{CH}_4$ , obtained in our experiments.



**Fig. 2** Influence of the mole fraction of  $\text{NH}_3$  on the synthesized quantities of acetonitrile and methylamine. In all these experiments, there is total absorption of the incident UV light.



**Fig. 3** Influence of the mole fraction of  $\text{NH}_3$  on the synthesis of acetonitrile. Analysis has been performed by GC on Porapak Q support. The chromatogram obtained and analytical conditions have been previously reported<sup>4</sup>. Absorption of the incident UV light is not total, except when the mole fraction of  $\text{NH}_3$  is 0.1.

Let us assume, as an extreme situation, that the photodissociation of  $\text{CH}_4$  at 147 nm gives only  $\text{CH}_2$ . As long as  $\text{CH}_4$  and  $\text{NH}_3$  remain the most concentrated species, the most frequent reactions of  $\text{CH}_2$  are (3) and:



The kinetic parameters of reactions (3) and (4) are not known; however, as reaction (3) is very exothermic ( $\Delta G^\circ = -84.4 \text{ kcal mol}^{-1}$ ) its probability is  $\sim 1$  when a collision occurs. Consequently, in a  $\text{CH}_4\text{-NH}_3$  mixture where the mole fraction of  $\text{NH}_3$  is 0.1, <10% of the  $\text{CH}_2$  produced from photodissociation of  $\text{CH}_4$  may react through reaction (4). If we assume that some of the products formed in reaction (4) are involved in the synthesis of  $\text{CH}_3\text{CN}$ , we can conclude that the quantum yield of synthesis of  $\text{CH}_3\text{CN}$  through reaction (4), calculated with respect to the photons absorbed by  $\text{CH}_4$ , should be, at best, 0.1. It is probably very much less. As we have found that the experimental quantum yield of synthesis of  $\text{CH}_3\text{CN}$ , calculated in respect of the photons absorbed by  $\text{CH}_4$ , is 0.4, we conclude that reaction (4) is not important for the synthesis of  $\text{CH}_3\text{CN}$ . As the second important reaction of  $\text{CH}_2$ , reaction (3), leads to the same product as reaction (2), we also conclude that production of  $\text{CH}_2$  is not needed to explain the bulk of the results we have obtained. Finally, as  $\text{CH}_3$  may also be produced from reaction (1) (that is from photodissociation of  $\text{NH}_3$ ) as well as from photodissociation of  $\text{CH}_4$ , it may be assumed that photolysis of  $\text{CH}_4$  does not introduce any significant specificity in the system.

Figure 4 represents the quantum yield of synthesis of  $\text{CH}_3\text{CN}$  and of  $\text{CH}_3\text{NH}_2$  calculated from the data reported in Figs 2 and 3, and with respect to the photons absorbed by  $\text{NH}_3$  during each experiment. The quantum yield of synthesis of  $\text{CH}_3\text{CN}$  is shown to increase continuously when the mole fraction of  $\text{NH}_3$  decreases, whereas a drastically opposite effect is observed for  $\text{CH}_3\text{NH}_2$ . Experimental constraints limited our study to mixtures in which the mole fraction of  $\text{NH}_3$  was  $\geq 0.01$ . Nevertheless, we conclude that the quantum yield of synthesis of  $\text{CH}_3\text{CN}$  continues to increase slowly when the mole fraction of  $\text{NH}_3$  is decreased to  $<0.01$ . A limit value of  $3 \times 10^{-2}$  can be accepted for very low mole fractions of  $\text{NH}_3$ . We have also reported that

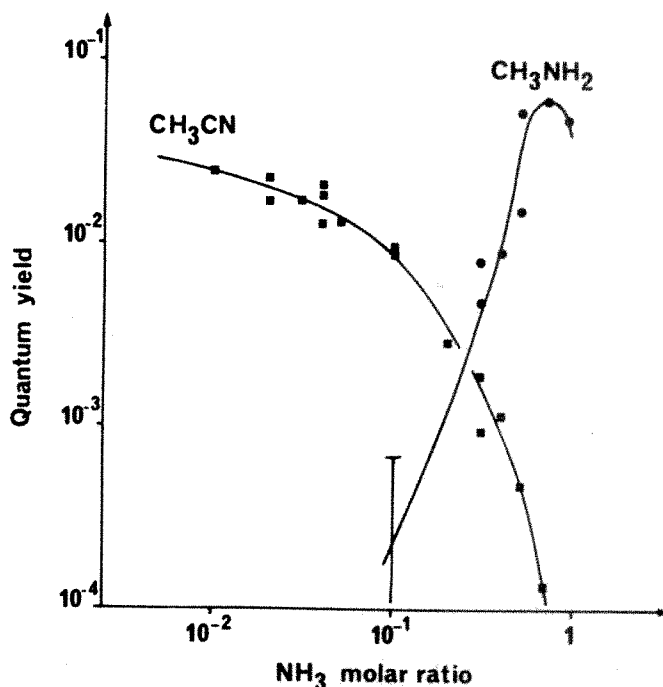
$\text{HCN}$  is synthesized with the same efficiency as  $\text{CH}_3\text{CN}$  when the mole fraction of  $\text{NH}_3$  is 0.1. If we assume that the same results apply at lower mole fractions of  $\text{NH}_3$ , the limit value for the total quantum yield of synthesis of nitriles at very low mole fractions of  $\text{NH}_3$  is probably  $\sim 5 \times 10^{-2}$ .

The new photochemical data on the qualitative and quantitative production of N-containing organics in  $\text{CH}_4\text{-NH}_3$  mixtures may be applied to the jovian troposphere and to the atmosphere of the primitive Earth.

The photochemistry of the atmosphere of Jupiter is generally approached by computer modelling based on photochemical data from  $\text{CH}_4$  and  $\text{NH}_3$ . Many difficulties occur in the building up of a convenient photochemical model mainly due to the lack of numerous kinetic data and even the lack of reaction pathways that would be considered. Amines are the only N-containing organics which are considered in such calculations<sup>11-13</sup>. The present experimental results show that, to a large extent this assumption is wrong.

In fact at altitudes where UV light may be absorbed by  $\text{NH}_3$  (that is middle troposphere), the  $\text{NH}_3$  mixing ratio calculated by respect to  $\text{CH}_4$  is  $\sim 10^{-4}$ . The shape of the curves in Fig. 4 suggests that the UV photosynthesis of nitriles is far more efficient than the UV photosynthesis of amines. However, this assumption must be discussed with respect to the wavelength of the UV light and to the  $\text{H}_2$  content of the mixture.

In our experiments both  $\text{NH}$  and  $\text{NH}_2$  are produced by photolysis of  $\text{NH}_3$ . This is possible only for wavelengths shorter than 160 nm. At longer wavelengths only  $\text{NH}_2$  is produced. We have previously reported<sup>4</sup> the effect of important quantities of  $\text{H}_2$  on the photochemical synthesis (147 nm) of nitriles from  $\text{H}_2\text{-CH}_4\text{-NH}_3$  mixtures where the  $\text{NH}_3$  mole fraction relative to  $\text{CH}_4$  was 0.5. The increase of the amount of  $\text{H}_2$  decreases the synthesis of the nitriles. We do not have similar data for amines; however, the same effect can be expected if we assume that most of the synthesis of N-containing organics is initiated by  $\text{NH}$  and  $\text{NH}_2$  photoproducted from  $\text{NH}_3$ . In the presence of  $\text{H}_2$  these species are neutralized into  $\text{NH}_3$  which should probably decrease the yield of synthesis of the different N-containing organics in similar proportions.



**Fig. 4** Influence of the mole fraction of  $\text{NH}_3$  on the quantum yield of formation of acetonitrile and of methylamine. These curves have been built from the experimental results shown in Figs 2 and 3. The quantum yields are calculated with respect to the photons absorbed by  $\text{NH}_3$ .



The present data may contribute to the study of the evolution of the atmosphere of the primitive Earth in the limits of the reducing atmosphere hypothesis. They show that the presence of large amounts of  $\text{NH}_3$  were not necessary for the photochemical synthesis of nitriles. If a low molar mixing ratio of  $\text{NH}_3$  had remained for a significant time, an efficient production of these nitriles may have occurred.  $10^{12}$  mol of nitriles per year would be produced only with photons of wavelengths ranging from 150 to 160 nm (quantum yield of production of nitriles =  $5 \times 10^{-2}$ ; present solar flux). As a cyano group cannot be easily destroyed<sup>14</sup> by the UV light which reaches the altitude where it is produced, most of the synthesized nitriles would have reached the oceans. The presence of other gases such as  $\text{N}_2$  or  $\text{H}_2\text{O}$  in the atmosphere should be tested.  $\text{CH}_4\text{-NH}_3$  and  $\text{CH}_4\text{-NH}_3\text{-H}_2\text{O}$  gaseous mixtures have been irradiated (147 nm) in the same experimental conditions: the rate of production of HCN is about the same in both cases.

This study has been supported by the French Space Agency, CNES. We thank Dr J. P. Ferris for helpful comments.

Received 1 May; accepted 3 October 1980.

1. Calvert, J. G. & Pitts, J. N. Jr in *Photochemistry*, 203–204, 498 (Wiley, New York, 1966).
2. Okabe, H. in *Photochemistry of Small Molecules*, 269–272, 298–299 (Wiley, New York, 1978).
3. Toupance, G., Bossard, A. & Raulin, F. *Origins of Life* **8**, 259–266 (1977).
4. Raulin, F., Bossard, A., Toupance, G. & Ponnamperna, C. *Icarus* **38**, 358–366 (1979).
5. Bark, L. S. & Higson, H. G. *Talanta* **11**, 471–479; 621–631 (1964).
6. Stein, S., Bohlén, P., Stone, J., Dairman, W. & Udenfriend, S. *Archs. Biochem. Biophys.* **155**, 202–212 (1973).
7. Hellner, L., Masanet, J. & Vermeil, C. *J. chem. Phys.* **55**, 1022–1028 (1971).
8. Masanet, J., Fournier, J. & Vermeil, C. *Can. J. Chem.* **51**, 2946–2951 (1973).
9. Watanabe, K., Zelikoff, M. & Inn, E. C. Y. *Geophys. Res. Pap. No. 21* (1953).
10. Ferris, J. P. & Chen, C. T. *Nature* **258**, 587–588 (1975); Ferris, J. P., Nakagawa, C. & Chen, C. T. *Commun. 29th COSPAR Meet.* Philadelphia (1976).
11. McNesby, J. R. *J. atmos. Sci.* **26**, 594–599 (1969).
12. Kuhn, W. R. & Atreya, S. K. *Geophys. Res. Lett.* **4**, 203–206 (1977).
13. Atreya, S. K. & Donahue, T. M. *Rev. Geophys. Space Sci.* **17**, 388–396 (1979).
14. Mizutani, H., Mikuni, H., Takahashi, M. & Noda, H. *Origins of Life* **6**, 513–526 (1975).

## Trace element determination by capacitive discharge atomic absorption spectrometry

C. L. Chakrabarti, C. C. Wan, H. A. Hamed & P. C. Bertels

Department of Chemistry, Carleton University, Ottawa, Ontario, Canada K1S 5B6

Conventional instrumental analytical techniques require careful calibration of the instrument with chemically analysed standards or synthetic standards of known composition. When analyses of miscellaneous materials are required, providing the required range of standards becomes impossible. As a way to an absolute method of atomic absorption analysis, L'vov<sup>1</sup> suggested using a capacitive bank as a source of electrothermal energy for heating graphite atomizers. We describe here a new analytical technique which uses a capacitor bank for electrothermal heating of an anisotropic pyrolytic tube atomizer in atomic absorption spectrometry producing very fast rates of heating and an isothermal condition, both in space and in time<sup>1,2</sup>, and uses a direct relationship: peak absorbance = constant  $\times$  mass of analyte, thereby dispensing with analytical calibration curves. Sensitivity is almost independent of the matrix and matrix interferences are greatly reduced. Background correction is not required.

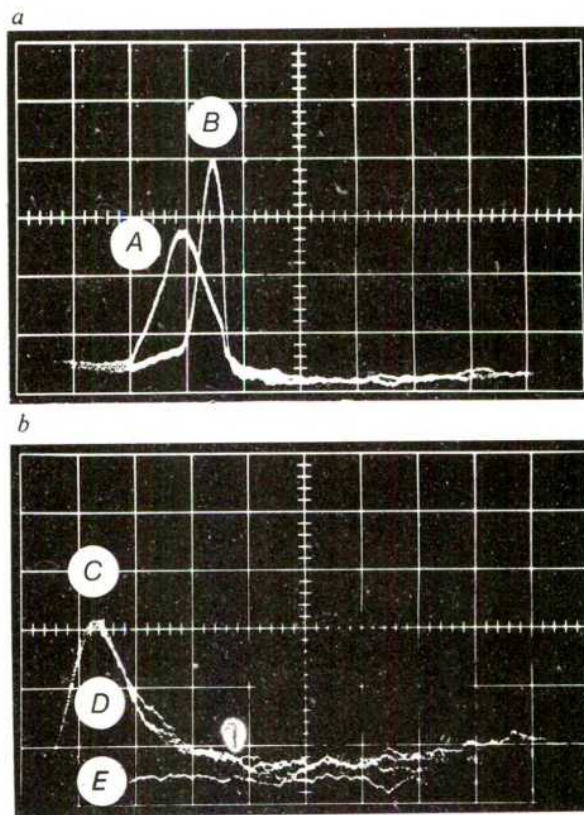
Equation (1) is a modified version of that given by L'vov<sup>3</sup>.

$$A_{\text{peak}} = \alpha(T^{0.7}/SP)M = \beta M \quad (1)$$

where  $A_{\text{peak}}$  is the peak absorbance,  $\alpha$  a coefficient determined by atomic and spectroscopic constants and by experimental conditions,  $T$  the absolute temperature,  $S$  the cross-sectional

area,  $P$  the pressure inside the graphite tube,  $M$  is the mass of the analyte and  $\beta$  the proportionality constant. The apparatus and its operation have been described elsewhere<sup>1</sup>.

Absorption pulses are recorded with a model 549 storage oscilloscope (Techtronix) fitted with a type 1A7A high-gain differential plug-in. The signal trace is photographed with a Polaroid camera (Tektronix). Three standard solutions of the analyte of different concentrations were analysed, three times each, and the arithmetic mean of these determinations was averaged to provide the value for  $\beta$ . The concentrations of the unknown samples were determined from their absorbance values obtained using the above conditions and suitable mass of solid samples or  $5.0 \times 10^{-6}$  dm<sup>3</sup> volume of the dissolved samples as appropriate and solving equation (1) for the unknown mass of the analyte element.



**Fig. 1** a, Oscilloscopic traces for  $5.0 \times 10^{-13}$  kg of Pb (as nitrate) atomized at a heating rate of  $1.3 \text{ K ms}^{-1}$  and temperature of 2200 K. Curve A, Pb (as nitrate) in 0.5% (wt/v) NaCl aqueous solution. Curve B, Pb (as nitrate) in an aqueous solution. Vertical scale, 0.1 absorbance per scale division. Horizontal scale, 500 ms per scale division. Pb  $\lambda$  283.3 nm. b, Oscilloscopic traces for  $2.5 \times 10^{-13}$  kg of Pb (as nitrate) in an aqueous solution with (curve C) and without 0.5% (wt/v) NaCl aqueous solution (curve D), atomized at a heating rate of  $40 \text{ K ms}^{-1}$  and temperature of 2,200 K. Curve E, the blank made of an aqueous solution of 0.5% (wt/v) NaCl. Vertical scale, 0.1 absorbance/scale division. Horizontal scale, 100 ms per scale division. Pb  $\lambda$  283.3 nm.

Table 1 shows the experimental conditions used, and also, the precision of the proportionality constant for equation (1). From Table 1, within-the-day precision of the mean is seen to have varied from 2.5 to 7.6% r.s.d. These relatively low values of the % r.s.d. are a measure of the validity of the proportionality expressed by equation (1). The large variations in the proportionality constants between the days were mainly due to change in the resistance of the atomizer circuit caused by change in the contact resistance between graphite electrodes and graphite tubes—the change was considerable with new tubes inserted at the beginning of each day. Substitution of automatic electronic

**Table 1** Experimental conditions and the precision of the proportionality constant ( $\beta$ ) for equation (1)

| Day no. | Element | Analysis line (nm) | Atomization temperature (K) | $\beta$ of equation (1) | % r.s.d.* |
|---------|---------|--------------------|-----------------------------|-------------------------|-----------|
| 1       | Pb      | 283.3              | 2,670                       | $5.85 \times 10^{11}$   | 4.3       |
| 2       | Pb      | 283.3              | 2,670                       | $7.43 \times 10^{11}$   | 6.6       |
| 1       | Mn      | 279.5              | 2,820                       | $7.90 \times 10^{12}$   | 7.6       |
| 2       | Mn      | 403.1              | 2,820                       | $8.89 \times 10^{10}$   | 4.0       |
| 3       | Mn      | 403.1              | 2,820                       | $1.21 \times 10^{11}$   | 2.5       |
| 1       | Cd      | 228.8              | 2,300                       | $2.30 \times 10^{13}$   | 3.5       |
| 2       | Cd      | 228.8              | 2,300                       | $9.90 \times 10^{13}$   | 7.6       |

\* Three different concentrations, each concentration was determined three times, making nine determinations. The value represents % relative standard deviation of the mean of three determinations.

control of resistance for the present manual control will improve both the between-day reproducibility and the within-the-day precision—the latter is largely determined by change in resistance due to change in contact tension and in the porosity of graphite with firings.

Table 2 presents the results of analysis. Table 2b shows a comparison of the results obtained by the technique with those obtained by the conventional graphite furnace atomic absorption spectrometry (GFAAS) using the Perkin-Elmer Heated Graphite Atomizer (HGA) 76B and optimized experimental conditions. Table 2b shows that results of the conventional GFAAS suffer from extremely severe depression by the matrix, whereas the matrix interferences have been almost completely eliminated by this technique. Another problem with commercial graphite furnaces is that they are non-isothermal, both spatially and temporally<sup>4</sup>.

The sensitivity of the technique is almost independent of matrix. This is important because analysis by GFAAS suffers from severe matrix interferences. There is also another significant difference—background correction is not required with this technique. Because analysis of complex materials by the conventional GFAAS usually requires removal of interfering matrices (including those that give extremely intense background absorption) from samples before the determination of the analytes, background correction represents a serious limiting factor in the speed and accuracy of analysis by the conventional GFAAS. Even removal of the bulk of the interfering matrices in the charring (pyrolysis) stage of the heating cycles of the conventional GFAAS by using the time-resolved selective volatilization and atomization technique<sup>5,6</sup> requires precise determination of the heating programme to remove the bulk of the matrix without any loss of the analytes, and correction for the residual background absorption by the background correction technique. The solid-sampling technique<sup>6</sup>, applied with this technique eliminates the large dilution factor involved in the solution-sampling technique, and thereby enhances greatly the relative sensitivity. This is in addition to the large enhancements in the absolute sensitivity of this technique, for example, for Cu, Ni and Al, the enhancements are 27-fold, 24-fold and 20-fold, respectively<sup>2</sup>.

The effect of high heating rates and isothermal atomization is seen from Fig. 1a, which shows oscilloscopic traces of  $5 \times 10^{-13}$  kg of Pb atomized at a heating rate of  $1.3 \text{ K ms}^{-1}$  and an atomization temperature of 2,200 K, using the conventional GFAAS but with an anisotropic pyrolytic graphite tube. In the chloride matrix the lead signal appears earlier in time and, hence, the lead appearance temperature is lower; also the pulse amplitude is lower than that of the aqueous solution of lead nitrate without the matrix. Figure 1b shows oscilloscopic traces for the above systems using the capacitive discharge technique, a heating rate of  $40 \text{ K ms}^{-1}$ , and isothermal atomization at a

**Table 2** Recoveries: a, solid sampling; b, solution sampling capacitive discharge technique

## a, Solid sample. National Bureau of Standards oyster tissue, SRM 1566

| Element | Analysis line (nm) | Certified value (kg per kg)      | Recovered value (kg per kg)*     | Recoveries (%)† |
|---------|--------------------|----------------------------------|----------------------------------|-----------------|
| Pb      | 283.3              | $(4.8 \pm 0.3) \times 10^{-7}$   | $(4.7 \pm 0.10) \times 10^{-7}$  | 98.5            |
| Cd      | 326.1              | $(3.2 \pm 0.4) \times 10^{-6}$   | $(3.4 \pm 0.22) \times 10^{-6}$  | 105             |
| Mn      | 403.1              | $(1.75 \pm 0.06) \times 10^{-5}$ | $(1.72 \pm 0.06) \times 10^{-5}$ | 98.3            |

\* The  $\pm$  values represent one standard deviation of five successive replicate determinations.

† Arithmetic means of five successive replicate determinations.

## b, Synthetic aqueous samples

| Element | Analysis line<br>(nm) | Mass of analyte          | Matrix in excess<br>over the analyte | Recoveries (% of the amount<br>of analyte taken) |                   |     |
|---------|-----------------------|--------------------------|--------------------------------------|--|-------------------|-----|
|         |                       |                          |                                      | Conventional<br>technique<br>using HGA 76B*      | New<br>technique† |     |
| Cd      | 228.8                 | $1.0 \times 10^{-14}$ kg | NaCl                                 | 700,000 fold                                     | 37                | 100 |
|         |                       |                          | +MgCl <sub>2</sub>                   | 84,000 fold                                      |                   |     |
|         |                       |                          | +CaCl <sub>2</sub>                   | 28,000 fold                                      |                   |     |
| Pb      | 217.0                 | $5.0 \times 10^{-13}$ kg | NaCl                                 | 30,000 fold                                      | 12                | 100 |
|         |                       |                          | +MgCl <sub>2</sub>                   | 3,600 fold                                       |                   |     |
|         |                       |                          | +CaCl <sub>2</sub>                   | 1,200 fold                                       |                   |     |
| Mn      | 279.5                 | $2.0 \times 10^{-13}$ kg | NaCl                                 | 25,000 fold                                      | 75                | 100 |
|         |                       |                          | +MgCl <sub>2</sub>                   | 3,000 fold                                       |                   |     |
|         |                       |                          | +CaCl <sub>2</sub>                   | 1,000 fold                                       |                   |     |

\* HGA 76B is Heated Graphite Atomizer 76B used with an atomic absorption spectrophotometer, model 603 (Perkin-Elmer). The relative standard deviation of the mean of five replicate determinations by the conventional graphite furnace atomic absorption spectrometry using HGA 76B = 8%.

† The relative standard deviation of the mean of five replicate determinations by the capacitive discharge technique = 12%.



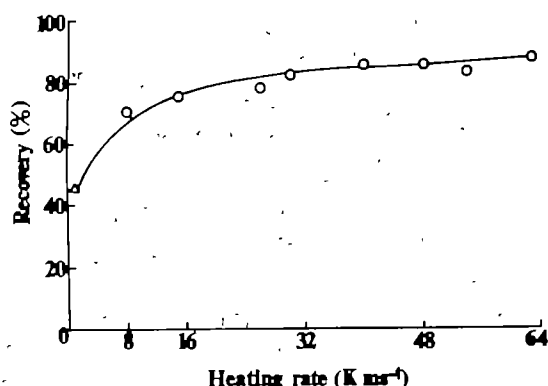


Fig. 2 Recoveries of Cd as a function of heating rate from an aqueous solution containing NaCl  $1.0 \times 10^{-8}$  kg + MgCl<sub>2</sub>  $1.2 \times 10^{-9}$  kg + CaCl<sub>2</sub>  $4.0 \times 10^{-10}$  kg as a function of the heating rate. Cd  $\lambda$  228.8 nm. Cd =  $4.0 \times 10^{-14}$  kg. Atomization temperature, 1,900 K.

temperature of 2,200 K (same as that of Fig. 1a); curve E is for the blank containing an aqueous solution of 0.5% (wt/v) NaCl, and shows that the background absorption due to the NaCl matrix is completely absent, which is highly significant. Figure 1b shows that the two absorption pulses are identical in both amplitudes and areas, and the matrix effects have been completely eliminated. In Fig. 1b the lead signal appears much later in time (compared with Fig. 1a), and hence, the appearance temperature for lead is considerably higher than that in Fig. 1a. In Fig. 1b the considerably higher appearance temperature for Pb and atomization in constant temperature are crucial for eliminating chloride matrix interferences. In Fig. 1a, atomization of lead occurred in non-isothermal conditions at a temperature which was considerably lower than that in Fig. 1b and at a time when the temperature of the atomizer increased at a very rapid rate from 600 to 2,200 K; hence, the pressure inside the graphite tube changed from 1 to 3.7 atm, which resulted in partial expulsion of the lead chlorides vapour; also the extent of dissociation of lead chlorides to lead atoms was less at the lower temperature. It is concluded that the elimination of the matrix effect in Fig. 1b is due to atomization at a constant temperature and at a much faster rate of heating with the technique.

Figure 2 shows the recoveries of Cd from an aqueous solution of NaCl + MgCl<sub>2</sub> + CaCl<sub>2</sub> matrices as a function of heating rates at the isothermal atomization temperature of 1,900 K. Even at the highest heating rate used (63 K ms<sup>-1</sup>), the recovery curve is seen to rise slightly, indicating a need for still higher heating rates for greater recoveries.

We conclude that even with the present laboratory-made instrumentation, the technique gives fairly accurate and precise results, which should improve with better instrumentation.

The technique with its simplified and shortened analytical procedure should save considerable time and cost per analysis. The limitation of this technique is that in the solid-sampling technique, the small sample (mg) requirement may present a sampling problem if the solid sample is inhomogeneous.

H.A.H. thanks the Government of Iraq for a postgraduate scholarship. This work was supported by grants from the Natural Sciences and Engineering Research Council of Canada.

Received 14 April, accepted 30 September 1980

## Forces between mica surfaces bearing layers of adsorbed polystyrene in cyclohexane

Jacob Klein

Polymer Department, Weizmann Institute of Science, Rehovot, Israel

Direct measurements of the forces acting between polymer surface phases adsorbed at interfaces have only recently been reported<sup>1-3</sup>. These were carried out in good solvents and showed that repulsive forces were acting between the adsorbed layers; these forces increased monotonically as the surfaces approached each other. In certain conditions, however, for example, those leading to the flocculation of sterically stabilized colloidal systems, one expects the surfaces bearing the adsorbed phases to attract before repelling each other<sup>4,5</sup>. I have measured the forces acting between two curved mica surfaces immersed in cyclohexane at 24 °C (a worse than  $\theta$  solvent at this temperature), each bearing a surface layer of adsorbed polystyrene ( $M_w = 6 \times 10^5$ ). No forces are observed at surface separations larger than about three radii of gyration of the polymer; on closer approach a strong attraction develops between the surfaces, changing to an ultimate repulsion as the surfaces approach closer than about one radius of gyration. Between times of a few minutes and several hours the forces are stable, well behaved and reproducible.

The experimental technique (Fig. 1) is an extension of that developed by Tabor *et al.*<sup>6,7</sup>, and recently modified by Israelachvili and Adams<sup>8</sup>, to measure (1) the forces  $F(D)$  acting between two curved mica surfaces a distance  $D$  apart; (2) the mean refractive index  $n(D)$  of the medium separating the surfaces.

$F(D)$  was first determined between the mica surfaces in pure cyclohexane; polystyrene solution was then added to the cell, to a final concentration of  $7 \pm 2 \times 10^{-6}$  g ml<sup>-1</sup>. After 10 h incubation in the polymer solution,  $F(D)$  was measured both in compression and decompression; measurements were repeated in the solution over a period of some hours, following which the polymer solution was entirely removed (save for ~1 ml between the mica surfaces) and replaced by pure cyclohexane. The surface-surface forces were then measured at intervals of between 5 min and several hours, and at compression/decompression rates of between 20–60 min per cycle, over a period of 48 h. The temperature of all experiments was  $24 \pm 0.5$  °C.

The results are shown in Fig. 2. No forces are observed as the surfaces approach from  $D \approx 300$  nm down to  $D \approx 60$  nm; on closer approach an attractive force arises between the surfaces, and on further decreasing  $D$  they jump from A (Fig. 2b) to a new stable position at B (such jumps are expected<sup>6</sup> whenever  $dF/dD > K$ , the force constant of the spring supporting the lower mica surface—see Fig. 1). Further approach results in a strong repulsion. On separation (decompression) the surfaces jump from C to a new stable position at E. The region AC is a region of instability ( $dF/dD > K$ ), where  $F(D)$  and  $n(D)$  cannot be determined<sup>8</sup>. The 'jumps' (A  $\rightarrow$  B, C  $\rightarrow$  E) are not instantaneous, and up to 300 s are required for new stable positions to be established; this is interpreted as the time taken by the opposing adsorbed layers to interdiffuse (on compression) or disentangle (on decompression). The forces are stable, and within the estimated errors, reversible and reproducible over the several compression/decompression cycles. In particular, the surfaces could be held in a strongly repulsive region around  $D \approx 14$  nm under a fixed force for up to 3 h with no resulting change in the separation.

1 L'vov, B. V. *Spectrochim. Acta* **33B**, 153–193 (1978).

2 Chakrabarti, C. L. *et al. Anal. Chem.* **52**, 167–176 (1980).

3 L'vov, B. V. *Atomic Absorption Spectrochemical Analysis*, 221 (Hilger, London, 1970).

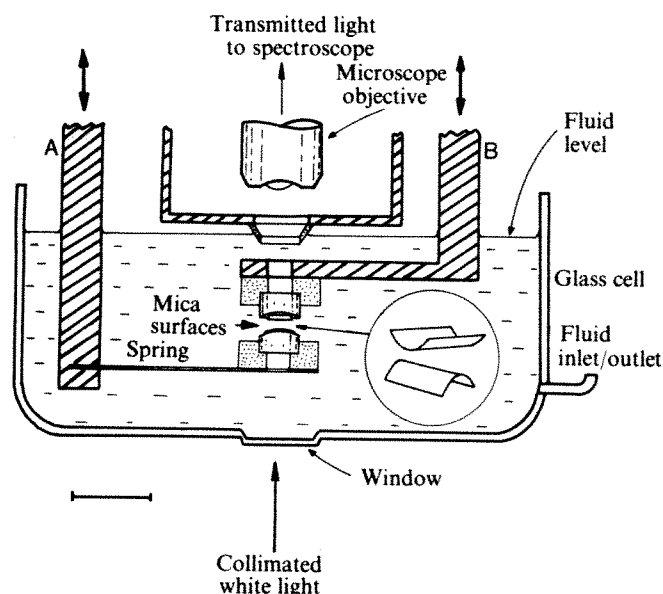
4 Sturgeon, R. E. & Chakrabarti, C. L. *Prog. Analyt. Atom. Spectrosc.* **1**, 1–199 (1978).

5 Nakahara, T. & Chakrabarti, C. L. *Anal. Chem. Acta* **104**, 99–111 (1979).

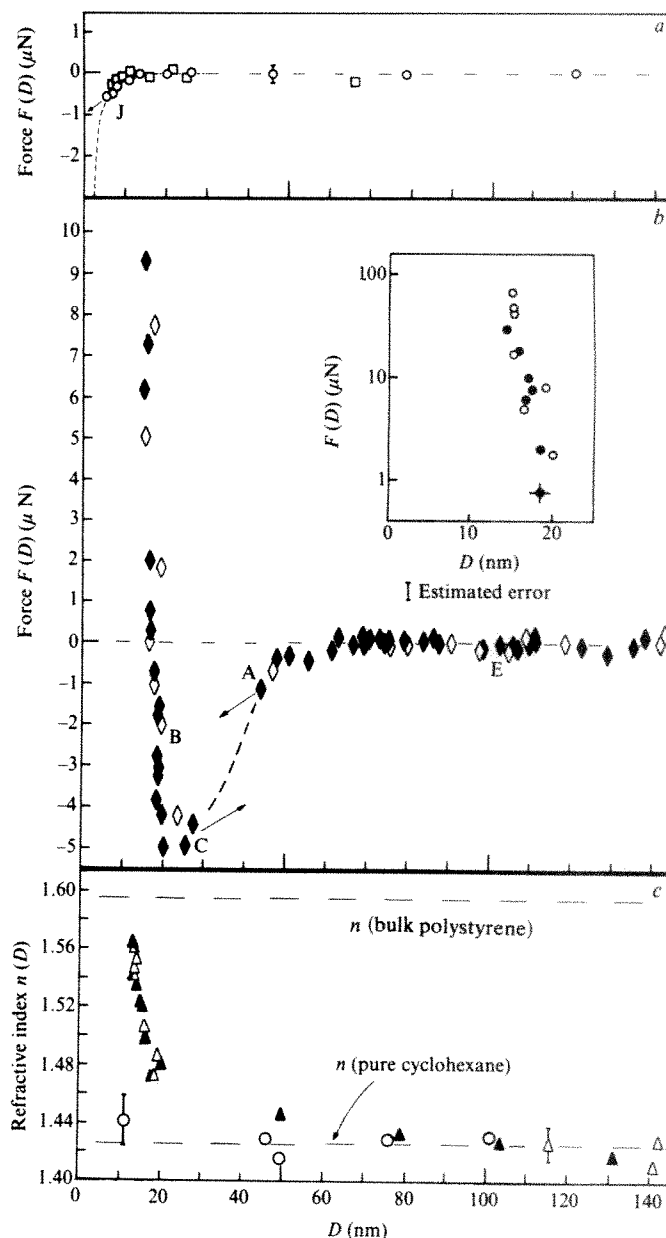
6 Chakrabarti, C. L., Wen, C. C. & Li, W. C. *Spectrochim. Acta* **36B**, 93–105 (1980).

The refractive index  $n(D)$  of the medium separating the mica surfaces varied between  $n = 1.56 \pm 0.02$  at  $D = 14$  nm and  $n = 1.43 \pm 0.012$  for  $D \geq 80$  nm (Fig. 2c). The values of  $n$  were determined, following incubation, in the polymer solution, and were unchanged on replacing the solution by pure solvent, and up to 48 h later. From the bulk refractive indices of cyclohexane (1.426) and polystyrene (1.595) the value of  $n$  ( $D = 14$  nm) corresponds to an adsorbance on each mica surface of around  $6 \text{ mg m}^{-2}$  of polymer. This compares with equilibrium adsorbances of  $3\text{--}8 \text{ mg m}^{-2}$  for polystyrene adsorbed onto various substrates from cyclohexane at the  $\theta$  temperature<sup>9</sup>.

In the conditions of only moderately high polymer molecular weight and extremely low bulk concentration of polymer used in the present study, the polymer solution, though considerably below the Flory  $\theta$ -temperature for this system ( $35^\circ\text{C}$ ), is above its cloud-point temperature<sup>5,10</sup>. Thus no phase-separation occurs<sup>10</sup> (other than adsorption); polymer dimensions are expected to be somewhat smaller than their unperturbed value<sup>5,11</sup>. Because very long times may be required before an adsorbed layer reaches equilibrium, we cannot be sure that, given much longer times, the system may not undergo further change. The fact that replacing the polymer solution by essentially pure solvent does not significantly change the adsorbed layer suggests that the adsorption may behave irreversibly. The onset of interaction between the surfaces at  $D \approx 60$  nm indicates that significant overlap between the opposing polymer layers begins at this value of  $D$ , corresponding to adsorbed layers extending some 30 nm from each mica surface. This compares with an unperturbed radius of gyration  $R_g = 21$  nm for this polymer<sup>13</sup>, and with ellipsometrically<sup>9</sup> and viscometrically<sup>12</sup> measured equilibrium layer thicknesses of 40 nm for poly-



**Fig. 1** Section of the apparatus used to measure forces between mica surfaces in a liquid medium. The surfaces are mounted in a crossed-cylinder configuration (inset) on cylindrical quartz lenses, within a glass cell (volume  $\sim 150$  ml); their separation  $D$  is controlled (to 0.2 nm) by the rigid arms A, B, using a three-stage mechanism (two micrometers and a piezoelectric crystal) similar to that previously described<sup>8</sup>. The method is based on an optical technique utilizing white-light multiple-beam interferometry, which can measure both  $D$  (to 0.3 nm) and the refractive index  $n(D)$  of the medium separating the surfaces, as well as their radii of curvature<sup>6,7</sup>. The top mica surface is directly mounted on the rigid arm B, while the bottom surface is mounted on A through a leaf spring of force constant  $K$  ( $75 \text{ N m}^{-1}$ ). By measuring the change in  $D$  in response to known, applied relative displacements of the rigid arms A and B,  $F(D)$  may be determined<sup>8</sup>. The glass cell is mounted within an airtight stainless steel box, which is in turn placed on a mechanically insulated platform within a thermally insulated chamber. Scale bar, 2 cm.



**Fig. 2** Forces  $F(D)$  and refractive index  $n(D)$  between curved mica surfaces in cyclohexane (Fluka, spectroscopic grade) at  $24.0 \pm 0.5^\circ\text{C}$ . **a**, Forces between bare mica surfaces in pure cyclohexane. At  $J(7 \pm 1 \text{ nm})$  the surfaces jump into contact within  $\pm 0.3$  nm of their air contact position. Mica surfaces (where  $R$  is the mean radius of curvature of mica):  $\square$ ,  $R = 0.35 \times 10^{-2} \text{ m}$ ;  $\circ$ ,  $R = 0.66 \times 10^{-2} \text{ m}$ . The broken line is the theoretical Van der Waals force  $F(D) = -AR/6D^2$ , with  $R = 0.66 \times 10^{-2} \text{ m}$  and a Hamaker constant  $A = 1.4 \times 10^{-20} \text{ J}$ , estimated from optical data for mica in cyclohexane. **b**, Forces between the curved mica surfaces of **a** ( $R = 0.66 \times 10^{-2} \text{ m}$ ) following 10 h incubation in a polystyrene cyclohexane solution. Solutions were prepared by overnight stirring of the polystyrene (Pressure Chemicals,  $M_w = 5.99 \times 10^5$ ,  $M_w/M_n \leq 1.06$ ) in cyclohexane, followed by 1-h ultracentrifugation at  $160,000g$  before use. The inset extends the range of  $F(D)$  on a semi-log plot.  $\diamond$ ,  $\circ$ , Forces measured in the polymer solution;  $\blacklozenge$ ,  $\bullet$ , forces following replacement of solution by pure solvent. At A, C the surfaces jump to new stable positions B, E (see text); AC (broken curve) is a region for which  $\partial F/\partial D > K$  and  $F(D)$  cannot be measured<sup>8</sup>. **c**, Refractive index  $n(D)$ , of the medium separating the mica surfaces.  $\circ$ , in pure cyclohexane.  $\Delta$ , in solution, following 10-h incubation.  $\blacktriangle$ , 20–44 h after replacing the polymer solution by pure solvent.



styrene (of similar molecular weight) adsorbed from cyclohexane onto various surfaces in  $\theta$  conditions.

The initially attractive nature of the interactions, however, is to be expected: it arises because the polymer molecules adsorbed on each mica surface have a much greater affinity for those adsorbed on the opposing surface, than they do for the solvent molecules. As Flory has shown<sup>5</sup>, bringing two polymer-segment distributions into overlap in worse than  $\theta$  conditions (a negative second virial coefficient) results in a negative free energy change. Thus, on initial overlap, an attractive force arises between the surfaces; as they approach to much closer than a radius of gyration, the compression of the adsorbed layers by the mica surfaces leads to extensive configurational constraints on the polymer molecules<sup>4</sup>, resulting in the ultimate strong repulsion observed at  $D \leq 18$  nm.

Over the range of times and experimental parameters described, the present results indicate that: (1) in certain conditions the steric repulsion observed when two adsorbed polymer layers are mutually compressed is preceded by an attractive region; (2) the onset of steric interaction between the adsorbed layers may take place at surface separations comparable with the polymer dimensions and with layer thicknesses measured by other means; and (3) the polymer adsorption may be an irreversible process.

I thank Professor A. Silberberg for encouragement, interest and helpful discussions; also the design and workshop staff of the Weizmann Institute for technical assistance, and Dr J. N. Israelachvili for useful suggestions. This work was partly supported by the Basic Research Division of the Israel Academy of Sciences.

Received 17 June; accepted 12 September 1980.

1. Lyklema, H. & Van Vliet, T. *Faraday Discuss.* **65**, 25 (1978).
2. Cain, F. W., Ottewill, R. H. & Smitham, J. B. *Faraday Discuss.* **65**, 33 (1978).
3. Israelachvili, J. N., Tandon, R. K. & White, L. R. *Nature* **277**, 120 (1979); *J. Coll. Interface Sci.* (in the press).
4. Vincent, B. *Adv. Coll. Sci.* **4**, 193 (1974).
5. Flory, P. J. *Principles of Polymer Chemistry* (Cornell University Press, Ithaca, 1953).
6. Tabor, D. & Winterton, R. H. S. *Proc. R. Soc. A* **312**, 435 (1969).
7. Israelachvili, J. N. & Tabor, D. *Proc. R. Soc. A* **331**, 19 (1972).
8. Israelachvili, J. N. & Adams, G. E. *JCS Faraday I* **74**, 975 (1978); *Nature* **262**, 774 (1976).
9. Stromberg, R. R., Tutas, D. J. & Passaglia, E. *J. phys. Chem.* **69**, 3955 (1965).
10. Schultz, A. R. & Flory, P. J. *J. Am. chem. Soc.* **74**, 4760 (1952).
11. Outer, P., Carr, C. I. & Zimm, B. H. *J. chem. Phys.* **18**, 830 (1950).
12. Rowland, F., Bulas, R., Rothstein, E. & Eirich, F. *Ind. Eng. Chem.* **57**, 49 (1965).
13. Brandrup, J. & Immergut, E. H. (eds) *Polymer Handbook* 2nd edn (Wiley, New York, 1975).

## Deep-seated iron ores from banded-iron formation

R. C. Morris, M. R. Thornber & W. E. Ewers

Division of Mineralogy, Institute of Earth Resources, CSIRO, Wembley, Western Australia 6014, Australia

Very large iron ore deposits have formed in many parts of the world, evidently by the supergene alteration of Precambrian banded-iron formation (BIF). Some of these deposits extend to great depths, ranging to 2,400 m at Krivoyrog<sup>1</sup>, beyond the likely reach of oxygenated water. We propose here, on the basis of studies in the Hamersley Ranges, Western Australia, a mechanism for deep-seated ore formation in which electronic conduction through the magnetite layers in BIF connects a cathodic region near the surface, where oxygen is reduced, to an anode at depth, where iron (II) from magnetite, carbonates and silicates is oxidized and precipitated as iron (III) hydroxides. The electrical circuit is completed by ionic conduction through groundwaters. The model is based broadly on a mechanism suggested by Sato and Mooney<sup>2</sup> to explain self-potentials associated with sulphide ore bodies. It is based more specifically on a model demonstrated by Thornber<sup>3</sup> for the

weathering of massive nickel-iron sulphide deposits at Kambalda, Western Australia, but with substantial differences in the physical situation and the reactions at depth.

The iron ore reserves of the Hamersley Iron Province exceed  $33 \times 10^9$  tonnes, much of it contained in huge ore bodies, some of them exceeding 5 km along strike and extending below the present water table to as much as 400 m down dip. They conform to the bedding of the host BIF and, in common with many ore bodies of this kind throughout the world, grade from >60% Fe in ore to <30% Fe in BIF over distances that are always negligible in relation to the size of the ore body and sometimes much less than a metre.

BIF in the Hamersleys is characterized by compositional layering of the centimetre scale in mesobands, some of them magnetite-rich, alternating with others containing chert, haematite, magnetite, silicates and carbonates in varied proportions. Many of these mesobands can be traced individually for hundreds of kilometres<sup>4</sup>.

Morris<sup>5</sup> has provided petrographical evidence that the Hamersley orebodies, in general, have formed from BIF by a combination of residual enrichment of the original iron oxides (magnetite, now martite, and primary haematite) by removal in solution of silica and other gangue, together with replacement of part of this gangue by hydrous iron oxide.

A key factor in the formation of ore at depth by such a process is the electrical conductivity of the magnetite-rich layers in BIF, and this may explain Dorr's<sup>6</sup> observation that ores "form best from the oxide facies iron-formation in most places of the world".

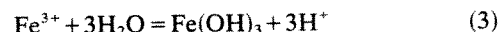
Table 1 lists some field and laboratory resistivity measurements which indicate that BIF is highly conductive along the layers of magnetite. This conductivity is retained even where the magnetite has been partially altered by weathering. Thus the BIF can be considered as an adequate conductor to allow higher oxidation potentials to penetrate to considerable depths as shown in Fig. 1a. The cathode, with a potentially vast area exposed along strike, comprises magnetite in contact with waters oxygenated by the atmosphere. Here electrons drawn from below would be consumed by the reduction of oxygen, summarized by the reaction:



The reaction that can take place at anodic surfaces of magnetite at depth, remote from sources of atmospheric oxygen, is:



The supply of  $\text{Fe}^{2+}$  to the anode, mainly from the dissolution of iron (II) minerals, all of the carbonates and silicates, and some of the magnetite, is facilitated by the release of acid in the hydrolysis reaction which will occur close to the anode surface:



The chief apparent difficulty with this model is that galvanic processes would normally favour near-surface oxidation, that is, with the anode and cathode close together; for example, where an iron bar immersed in damp soil corrodes through near the soil-air interface. However, our experimental data, as well as field and mineragraphic observations, indicate that the

Table 1 Some resistivity measurements on banded-iron formation

| Measured on                          | Resistivity ( $\Omega\text{m}$ ) |                     | Anisotropy coefficient $\lambda((\rho_t/\rho_e)^{1/2})$ |
|--------------------------------------|----------------------------------|---------------------|---|
|                                      | Longitudinal $\rho_e$            | Transverse $\rho_t$ |   |
| Cliff face at Dales Gorge            |                                  |                     |   |
| Mostly BIF                           | 2.7                              | 7,574               | 53  |
| BIF + shale                          | 4.5                              | 7,800               | 42  |
| Isolated slab $2 \times 0.9$ m thick | 0.87                             | $5.5 \times 10^5$   | 795   |
| Rods 1-cm <sup>2</sup> cross-section |                                  |                     |   |
| Magnetite band                       | 0.4                              | —                   | —   |
| Chert-magnetite                      | 740                              | $8.6 \times 10^5$   | 34.2  |

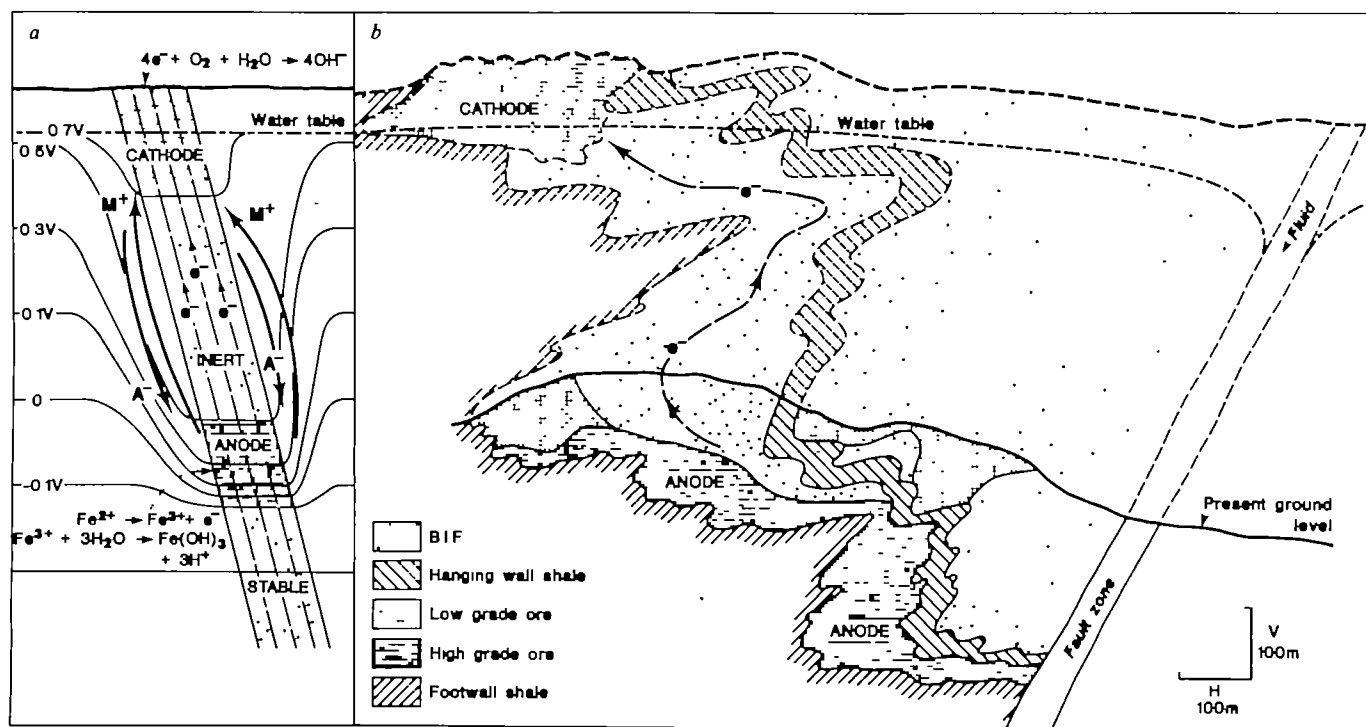


Fig. 1 a, Cross-section illustrating the proposed electrochemical model for the formation of iron ore at depth. Magnetite layers in the BIF provide electron paths between cathode and a deep-seated, initially porous, anodic zone. Cations ( $M^+$ ) and anions ( $A^-$ ) in groundwaters move through internal and external fluid pathways to complete the cell circuit. b, Cross-section from the Whaleback Mine at Newman, Western Australia, with a hypothetical reconstruction of the now eroded extension of the structure, illustrating the proposed electrochemical model at an advanced stage of deep iron ore formation during the Proterozoic. Fluid pathways at depth are provided initially by the fault zone, later extending laterally and vertically, by leaching of BIF.

magnetite usually weathers more slowly than other susceptible components in BIF.

Polarization tests, at pH values 4–9, on electrodes of magnetite indicate that it is an essentially inert electrode. Addition of ferrous ion to the solution produced oxidation reactions in the region of +0.3 V (SHE). With BIF electrodes the response was the same when ferrous ion was added. In the absence of added ferrous ion, however, there was still a slight indication of reaction at +0.3 V (SHE) which led us to investigate this phenomenon in a different cell.

The cell used was designed to allow current and voltage levels to be varied while surface reactions could be observed under the microscope; its design will be reported in detail elsewhere. We have shown that reactions are controlled not only by the level of conductivity of the specimens, and by the potentials to which they are subjected, but also by the proximity of reactive non-conductive minerals to the conducting bands of magnetite.

A build-up of iridescent coatings of iron oxide on magnetite surfaces is controlled by conduction, as electrically isolated grains of magnetite within the generally conductive zones are relatively unaffected, although build-up of iron oxide eventually becomes general. Silicates and carbonates in close proximity to conductive magnetites are rapidly attacked, and stilpnomelane in particular tends to swell, often to the extent that flakes of the mineral are released into the cell solution. At the same time other parts of the exposed surface become pitted as carbonate grains are dissolved; in some cases corrosion extends beyond the area of the specimen initially exposed in the cell, as solution penetrates along susceptible bands below plastic masking.

Comparable features have been observed in outcrop samples where, for example, certain bands of magnetite, carbonates and silicates may be extensively oxidized or corroded while adjacent bands are relatively fresh.

Supergene alteration of BIF does not necessarily involve oxidation of magnetite. Deep drilling in the vicinity of ore bodies at various sites in the Province has intersected severely altered and friable BIF in which chert has been strongly leached, but in

which magnetite is still fresh. In some cases this altered but unoxidized BIF grades downward into strongly goethitized zones. In the Paraburdoo 4E deposit<sup>7</sup> a high-grade haematite ore lens occurs 200 m down dip below surface ore. The intervening BIF is still fresh in places despite the precambrian age<sup>4</sup> of this ore.

Thus the evidence suggests that the electronic paths will be left relatively intact during deep ore formation, although leaching of other minerals takes place.

Oxidation potentials favourable for reaction (2) will exist along much of the conducting paths, but an essential requirement for deep-seated ore formation in our model is a zone at depth with greater initial porosity and better fluid access than in almost impermeable zones closer to the surface. The 'corrosion cell' is completed by electrolytic conduction through the general groundwater system, connecting the permeable anode with the cathode at the surface. These conditions would be favoured by faulting (Tom Price<sup>8</sup>, Whaleback<sup>9</sup>, Paraburdoo<sup>6</sup>), and by some structural situations involving damming by intrusives (Paraburdoo<sup>6</sup>) or cross-folding<sup>10</sup>. A hypothetical situation based on Whaleback is shown in Fig. 1b.

The geometry of the systems makes it difficult to test realistically the feasibility of the model in terms of rates of ore formation. A simple approach is to assume the anode and cathode to be of the same area and to regard the BIF conductor as a column of cross-section 1 m<sup>2</sup> and an appropriate length, say 400 m. Such a column will contain ~400 tonnes Fe, about one-third of it as iron (II). If a similar amount of iron (II) is introduced during ore formation, the total amount to be oxidized from iron (II) to iron (III) is about 265 tonnes. Using 4.5 Ωm as the resistivity, 0.7 V as the potential difference, and assuming the conducting path constant at 400 m, the current will be  $0.39 \times 10^{-3}$  A and the time to oxidize all of the iron (II)  $3.7 \times 10^7$  yr. In the actual situation, we envisage that the current from a very large exposed cathode (that is the BIF outcrop), will be concentrated on a much smaller permeable zone at depth, thus increasing the current density and therefore the oxidation



rate at the anode. Even so, the calculated current density, though smaller by at least an order of magnitude than that observed in the slow corrosion of resistant alloys, such as stainless steel<sup>11</sup>, is sufficient to form an ore body in reasonable geological time.

The natural BIF corrosion cell contrasts strongly, in terms of the extent of the cathode and the size of the conductor, with the situation described for Kambalda nickel ores<sup>3</sup>, in which relatively small bodies of conducting sulphides are surrounded by non-conducting country rock. A second major difference is that, whereas the conducting nickel-iron sulphides are oxidized at the anode, in the BIF it is primarily ferrous iron from the interlayered non-conducting carbonates and silicates that is oxidized as a result of the anodic reaction. This was demonstrated in the corrosion cell experiments described above.

Although the iron (II) content of the magnetite is included above in the calculation of the required current density the oxidation of magnetite, *per se*, is not considered to be essential to the first stage of ore-forming process, and will indeed inhibit it unless the oxidation forms conducting maghaemite, for which there is some evidence<sup>5</sup>. Ultimately much of the magnetite will be converted to haematite by a slow solid-state process, or to goethite by hydration<sup>5</sup>. Initial permeability to groundwater is essential, and this will be extended to an enlarged porous zone as attack on carbonates and silicates proceeds. Reactions (1), (2) and (3) will persist as long as there is magnetite and a conducting path to the surface, and diffusion along gradients of  $a_{Fe}^{2+}$  and pH will extend the effective anodic zone. Chert is a major component of these rocks and its removal, an essential part of the ore-forming process, will be facilitated by increased permeability. This leaching is governed by silica activity in ground waters, which is independent of *Eh* and, within normal levels, of pH.

The evidence that some iron has been added to the ore from external sources<sup>5</sup> requires that the deep groundwater which transported it was anoxic. If an electrochemical mechanism were not responsible for precipitating this iron, one would need to invoke a confluence with oxygenated water from the surface which, at the depth of 2,400 m at Krivoyrog or >400 m in the Hamersley Province, would call for remarkable hydrological regimes. James *et al.*<sup>11</sup> invoked oxygenated deep artesian water during extremely arid conditions, but they pointed out that the best ore development seemed to occur in the zones most likely to remain stagnant in their model, suggesting that some other process was operating.

Finally, we stress that the electrochemical model we have proposed is an attempt to explain the more deep-seated ore bodies, and we do not doubt that many ore bodies have resulted from the penetration by oxygen-bearing surface water and, with seasonally fluctuating water tables, from processes akin to lateritization<sup>6,13</sup>. These processes are to some extent electrochemical. Many such ore bodies in the Hamersley Iron Province are closely related to the Tertiary erosion surface, and some indeed form a capping<sup>7-9</sup> on the deeper ore bodies. This capping probably represents the final stage in which downward progression of surface enrichment and erosion meets the upward extension of the deep-seated processes.

Received 16 April; accepted 24 September 1980.

- Belevtsev, Y. N. in *Proc. Kiev. Symp. Genesis of Precambrian Iron and Manganese Deposits*, 167-180 (Unesco, Paris, 1973).
- Sato, M. & Mooney, H. M. *Geophysics* **25**, 226-249 (1960).
- Thornber, M. R. *Chem. Geol.* **15**, 1-14 (1975).
- Trendall, A. F. & Blockley, J. G. *Bull. 119. Geol. Surv. West. Australia* (1970).
- Morris, R. C. *Econ. Geol.* **75**, 184-209 (1980).
- Dorr, J. van N. II *Econ. Geol.* **59**, 1203-1240 (1964).
- Bourn, R. & Jackson, D. G. *Proc. West Australia Conf. 1979*, 187-201 (Australasian Institute of Mining and Metallurgy, 1979).
- Gilhome, W. R. *Economic Geology of Australia and Papua New Guinea*, 892-898 (Australasian Institute of Mining and Metallurgy, 1975).
- Kneeshaw, M. *Economic Geology of Australia and Papua New Guinea*, 910-916 (Australasian Institute of Mining and Metallurgy, 1975).
- Berge, J. W., Johansson, K. & Jack, J. *Econ. Geol.* **72**, 582-607 (1977).
- Jones, D. A. *Ind. Engng Chem. Prod. Res. Devel.* **11**, 12-23 (1972).
- James, H. L., Dutton, C. E., Pettijohn, F. J. & Wier, K. L. *U.S. Geol. Survey. Prof. Pap.* 570 (1968).
- Berge, J. W. *Econ. Geol.* **66**, 947-960 (1971).

## A new date for the Taupo eruption, New Zealand

C. J. N. Wilson\*, N. N. Ambraseys†, J. Bradley‡ & G. P. L. Walker§

\* Geology Department and †Civil Engineering Department, Imperial College, London SW7 2BP, UK

‡ East Asian History of Science Library, 16 Brooklands Avenue, Cambridge CB2 2BB, UK

§ Geology Department, University of Auckland, Private Bag, Auckland, New Zealand

**The Taupo eruption was a complex volcanic event that represents the most recent activity at the Taupo Volcanic Centre<sup>1</sup> in the North Island of New Zealand. The average<sup>2</sup> of many radiocarbon ages dates the eruption at ~AD 130. The records of ancient China and Rome refer to events in ~AD 186 of the type which follow a major volcanic eruption, and we present here reasons for considering that these events were due to the Taupo eruption, and that the true date of the eruption is ~AD 186.**

The products of the Taupo eruption are rhyolitic and are dispersed over a large part of the North Island<sup>2</sup>. They consist of an initial plinian pumice-fall deposit (the Hatepe Pumice)<sup>2</sup>, two phreatoplinian<sup>3</sup> ashes (the Putty Ash and Rotongaio Ash)<sup>4</sup> which are separated by an erosion break, the 'ultraplinian' Taupo pumice-fall deposit<sup>5</sup> and finally the non-welded Taupo ignimbrite<sup>6-8</sup>.

Preliminary calculations indicate an erupted volume of >60 km<sup>3</sup> (20-25 km<sup>3</sup> dense-rock equivalent), of which 24 km<sup>3</sup> and >30 km<sup>3</sup> are represented by the Taupo ultraplinian pumice-fall deposit and Taupo ignimbrite respectively. This eruption was thus comparable in magnitude to the ~1500 BC eruption of Santorini<sup>9</sup>.

Recent studies on the Taupo ultraplinian pumice-fall deposit<sup>5</sup> and Taupo ignimbrite<sup>6-8</sup> show that they were the most violent eruptions of their type yet documented. The eruption column which produced the ultraplinian pumice-fall deposit was of great power and height. Inserting the estimated dense-rock equivalent eruption rate<sup>5</sup> of 10<sup>6</sup> m<sup>3</sup> s<sup>-1</sup> in published eruption-column models<sup>10,11</sup> yields estimates of the eruption column height of not less than 50 km. Estimates of the initial grain-size population for the ultraplinian eruption column indicate the presence of an unusually large proportion of fine-grained material (ref. 5; and G.P.L.W. and C.J.N.W., unpublished data). It is evident that large quantities of fine ash must have been injected into the stratosphere and incorporated into the upper-atmosphere circulation.

Numerous <sup>14</sup>C ages were determined before 1962<sup>12</sup> on carbonized vegetation enclosed in the eruption products, and 22 selected values were averaged by Healy<sup>2</sup> to yield the eruption-date estimate of 1,819 ± 17 yr BP, or AD 131. Note, however, that the individual <sup>14</sup>C ages used to compile this average have much larger standard deviations (usually at least ±50 yr) than the average date itself.

A search within the ancient Chinese and Roman histories revealed the occurrence of phenomena similar to those that followed the 1883 eruption of Krakatoa<sup>13</sup>.

In the Chinese literature, it is recorded that:

"During the reign of (the emperor) Ling Ti (AD 168-189) several times the Sun rose in the east red as blood and lacking light, only when it had risen to an elevation of more than two *zhàng* was there any brightness. When it set in the west, at two *zhàng* above the horizon it was similarly red. . . . Also during this period, several times when the Moon rose and set and was two to three *zhàng* above the horizon, all was red as blood."<sup>14</sup>

‡ Present address: 18 Juniper Lane, Amherst, Massachusetts 01002.

A *zhàng* is approximately equal to 12° (ref. 15).

In the Roman literature, two sources refer to unusual appearances of the sky in, or just before, AD 186.

"Before the war of the deserter (autumn 186), the heavens were ablaze."<sup>16</sup>

"Stars were seen all the day long and that some did stretch in length hanging as it were in the midst of the ayre which was a token of a cloud not kindled but drouen together for it seemed kindled in the night, in the day when it was far off it vanished away."<sup>17</sup>

These descriptions are reminiscent of the effects observed to follow the 1883 Krakatoa eruption and particularly the characteristics of the Krakatoa dust haze (ref. 13, pp. 223–225) in higher latitudes. The appearance and description of the haze as being too thin to produce blue or green-coloured suns, as having a rippled or striated appearance and only being visible around dawn and dusk (recall "... in the day when it was far off it vanished away") and the accompanying glow effects, seem to correspond closely with the above descriptions.

These records of phenomena resulting from a major eruption in or just before AD 186 and the absence of records of similar effects between then and the Vesuvius eruption of AD 79, suggest that the records do indeed refer to the Taupo eruption and therefore that the true date of this eruption is ~AD 186.

Two problems arise. First, what chance is there of material erupted at Taupo (38° 50' S) being able to spread across the tropics and into the Northern Hemisphere in quantities sufficient to cause noticeable effects? Although Northern Hemisphere temperature records<sup>18,19</sup> show a minor change at the time of the 1886 Tarawera (New Zealand) eruption<sup>20</sup>, this is not considered as significant enough to indicate that material can cross the tropics. Lamb<sup>21,22</sup> has stated (for example, ref. 22, p. 416) that: "... volcanic dust originating in high latitudes hardly spreads in significant quantities beyond about latitude 30° in the hemisphere of origin; though small quantities may reach any part of the Earth, it effectively covers only latitudes 30°–90° in the hemisphere of origin...". Note that Lamb was referring to the dispersal of volcanic ash in the lower stratosphere, from the tropopause up to ~25–27 km. On the other hand, data quoted earlier indicate that the Taupo ultraplinian eruption-column penetrated the upper stratosphere and reached the mesosphere. Fine ash injected at such levels would take times of the order of months to years to fall to lower levels<sup>21</sup> and in the meantime be subject to the high level (>30 km) drift which crosses the equatorial regions between the hemispheres (see ref. 21, p. 455). Thus the finest ash, injected at the greatest heights, could spread from New Zealand to the Northern Hemisphere with little difficulty.

This is in accord with the above descriptions; the absence of blue or green suns or moons suggests that the causative particles were <5 µm across<sup>13,22</sup>. Also, the nature of the Chinese description implies that the glow effects appeared gradually and lasted for some time; other reports of sunset-glow effects found by one of us (J.B.) in the Chinese literature (almost certainly caused by middle or northern-latitude eruptions) are generally closely dated (often to the nearest month) as to when they first appear.

The second problem is that an AD 186 eruption date lies just outside three standard deviations of the average of the <sup>14</sup>C dates (1,819 ± 17 yr BP). However, since the dates were published, much work has been done on the corrections required to convert <sup>14</sup>C ages to true ages derived by dendrochronology. Michael and Ralph<sup>23</sup> have obtained <sup>14</sup>C dates of AD 118 and AD 148 on samples with true dates of AD 150 and AD 197 respectively, while Suess<sup>24</sup> has obtained a <sup>14</sup>C date of AD 119 on material of true date AD 185. (All these <sup>14</sup>C dates were calculated using the 5,568-yr half life, for valid comparison with the New Zealand dates; reported standard deviations are ±40, 44 and 45 yr respectively.) The difference between the proposed AD 186 true and AD 131 <sup>14</sup>C eruption dates is, therefore, very close to that between true and <sup>14</sup>C dates obtained on samples from the same true-age period.

One slight possibility is that these atmospheric phenomena resulted from the eruption which produced the north lobe of the White River Tephra in Alaska<sup>25</sup>, <sup>14</sup>C dated at about 1,890 yr BP (average of 11 determinations<sup>25</sup>). Applying the true date to <sup>14</sup>C date corrections as above<sup>23,24</sup> suggests that in this case, the <sup>14</sup>C date of ~AD 60 is close to the true age, and that the White River eruption did not produce the effects seen in or just before AD 186 here ascribed to the Taupo eruption.

We conclude that the Taupo eruption, previously dated by <sup>14</sup>C methods at AD 131, actually occurred in ~AD 186. The scale of the eruption, its violence, and the wide dispersal of the resulting air-fall deposits suggest that enough fine dust escaped into the upper-atmospheric circulation to reach the Northern Hemisphere and produce the optical effects observed in China and Europe.

Whilst this new date is only a proposal, we hope that we have demonstrated the potential of using historical records in dating and characterizing the distant effects of large volcanic eruptions.

Confirmation of this new date for the Taupo eruption might be sought in Antarctic or Arctic ice cores. Alternatively, a New Zealand dendrochronology time scale could be constructed and correlated with the timber enclosed abundantly in the Taupo ignimbrite.

We thank Dr J. Needham for assistance and Drs J. Westgate and L. Wilson for helpful comments. C.J.N.W. is an NERC research student and G.P.L.W. a Captain James Cook Research Fellow of the Royal Society of New Zealand. J.B. thanks the East Asian History of Science Library for facilities.

Received 9 July, accepted 8 October 1980

1. Hooley, J. *Bull volcan* 26, 141–151 (1963)
2. Hooley, J., Vucetich, C. G. & Poller, W. A. *Bull NZ geol Surv* no. 73 (1964)
3. Self, S. & Sparks, R. S. J. *Bull volcan* 41, 1–17 (1978)
4. Walker, G. P. L. *J volcan geotherm Res* (in the press)
5. Walker, G. P. L. *J volcan geotherm Res* 8, 69–94 (1980)
6. Walker, G. P. L., Hemming, R. F. & Wilson, C. J. N. *Nature* 283, 286–287 (1980)
7. Walker, G. P. L., Wilson, C. J. N. & Froggatt, P. C. *Geology* 8, 245–249 (1980)
8. Walker, G. P. L., Wilson, C. J. N. & Froggatt, P. C. *J volcan geotherm Res* (in the press)
9. Watkins, N. D. *et al Nature* 271, 122–126 (1978)
10. Sottile, M. J. *J volcan geotherm Res* 3, 309–324 (1978)
11. Wilson, L., Sparks, R. S. J., Huang, T. C. & Watkins, N. D. *J geophys Res* 83, 1829–1836 (1978)
12. Grant-Taylor, T. L. & Rafter, T. A. *Radiocarbon* 8, 118–162 (1963)
13. Symons, G. J. (ed.) *The Eruption of Krakatoa and Subsequent Phenomena* (Report of the Krakatoa Committee of the Royal Society, London, 1888)
14. *Hou Han Shu* Vol. 11, 3373, lines 2–3 Peking (punctuated) edn (1965).
15. Kung, T. *Mem R astr Soc* 76, 27–66 (1972)
16. *Scriptores Historiae Augustae Cosmographia Antonina* xvi, 2 (Loeb, 1967)
17. Herodotus, *Metis Maritima vixitatis hystoria* 1, 10 (ed. K. Stronach, 1922)
18. Humphreys, W. J. *The Physics of the Air* (McGraw Hill, New York, 1940)
19. Rampino, M. R., Self, S. & Fairbridge, R. W. *Science* 206, 826–829 (1979)
20. Cole, J. W. N. Z. *J Geol. Geophys* 13, 879–902 (1970)
21. Lamb, H. H. *Phil Trans R Soc A266*, 425–533 (1970)
22. Lamb, H. H. *Climate Present, Past and Future* Vol. 1 (Methuen, London, 1972)
23. Michael, H. N. & Ralph, E. K. *Radiocarbon* 16, 198–218 (1974)
24. Suess, H. E. *Radiocarbon* 20, 1–18 (1978)
25. Lerbekmo, J. F., Westgate, J. A., Smith, D. G. W. & Denton, G. H. *Quaternary Studies* (eds Saggate, R. P. & Crosswell, M. M.) 203–209 (Royal Society of New Zealand, Wellington, 1975)

## Output rate of magma from active central volcanoes

G. Wadge

Lunar and Planetary Institute, 3303 NASA Road One, Houston, Texas 77058

For part of their historic records, nine of the most active volcanoes on Earth have each erupted magma at a nearly constant rate. These output rates are very similar and range from 0.69 to 0.26 m<sup>3</sup> s<sup>-1</sup>. The volcanoes discussed here—Kilauea, Mauna Loa, Fuego, Santiaquito, Nyamuragira, Hekla, Piton de la Fournaise, Vesuvius and Etna—represent almost the whole spectrum of plate tectonic settings of volcanism. A common mechanism of buoyantly rising magma-filled cracks in the upper crust may contribute to the observed restricted range of the rates of output.



**Table 1** Historic output rates of magma from selected volcanoes

| Volcano               | Plate tectonic setting | Product                             | Period    | Volume ( $\times 10^6 \text{ m}^3$ ) | No. of eruptions | Output rate ( $\text{m}^3 \text{ s}^{-1}$ ) | Refs   |
|-----------------------|------------------------|-------------------------------------|-----------|--------------------------------------|------------------|---|--------|
| Kilauea               | Intraoceanic           | Tholeiitic basalt                   | 1823–1975 | 3,323                                | 54               | 0.69  | 1–3    |
| Mauna Loa             | Intraoceanic           | Tholeiitic basalt                   | 1823–1975 | 3,158                                | 37               | 0.66  | 1, 4   |
| Fuego                 | Subduction             | High $\text{Al}_2\text{O}_3$ basalt | 1932–1979 | 700                                  | 28               | 0.5   | 5      |
| Santiaguito           | Subduction             | Dacite                              | 1922–1972 | 658                                  | 14               | 0.42  | 6      |
| Piton de la Fournaise | Intraoceanic           | Hawaiite                            | 1931–1974 | 529                                  | 21               | 0.39  | 7      |
| Nyamuragira           | Intracontinental       | Leucite basanite                    | 1901–1971 | 838                                  | 12               | 0.38  | 8      |
| Hekla                 | Spreading ridge        | Basaltic andesite<br>Dacite         | 1693–1970 | 2,731                                | 4                | 0.31  | 9      |
| Vesuvius              | Intracontinental?      | Leucite basanite                    | 1760–1944 | 1,660                                | 20               | 0.29  | 10, 11 |
| Etna                  | Subduction             | Hawaiite                            | 1759–1974 | 1,746                                | 31               | 0.26  | 12     |

The volumes of lava and tephra have been corrected to magmatic volumes at liquidus temperatures. The bulk densities of the lava flows are not accurately known, but the corrections are small. A factor of 0.85 was applied to the lavas of Kilauea<sup>14</sup> and also to Mauna Loa and Hekla. A factor of 0.94 based on my unpublished data for lavas of Etna, was applied to the lavas of Etna, Nyamuragira and Santiaguito. For the dacitic tephra of Hekla a correction factor of 0.20 was used<sup>33</sup>, and one of 0.45 was used for the basaltic tephra of Etna and Nyamuragira. The number of eruptions is a general guide, and in the cases of Etna and Vesuvius refers only to the major lava-forming eruptions. For Hekla with its long repose periods, the time used to calculate the output rates starts after the 1693 eruption and ends after the 1970 eruption. The output rate for Piton de la Fournaise as originally published<sup>7</sup> was too great by a factor of 10.

The rates at which magmas have been erupted at these nine volcanoes have been calculated from estimates of the volumes of their historic products<sup>1–12</sup> (Table 1). These volcanoes were chosen because of the availability of data of similar quality. Each is a major central volcano of considerable age ( $>10,000$  yr) which has been active for much of the recent historic past. Using volumetric data to calculate output rates can only be justified for those volcanoes whose cumulative volume curves are approximately linear (Fig. 1). The volcanoes of Table 1 not shown in Fig. 1 also satisfy this criterion. It has been suggested that the combined output rate for Mauna Loa and Kilauea is constant<sup>13</sup>. Because of the uncertainties in the data for the summit, caldera-filling lavas for both these volcanoes, complete cumulative volume curves are not shown in Fig. 1. However, judged solely on the historic flank eruptions of Mauna Loa which account for ~80% of the total for this volcano, the curve is linear. Hence the output rate is considered valid for Mauna Loa and probably also for Kilauea.

The nine volcanoes of Table 1 show a very restricted range of output rates which cannot be considered an artefact of a single observer's bias despite the levels of uncertainty (several tens of per cent) in the volume estimates. This small sample cannot be considered representative of volcanism in general in that these volcanoes have been unusually active and unusually well studied. Nevertheless, there is no ready explanation for such a common output rate and its significance may extend beyond the individual volcanoes reported here. Departures from linearity in the cumulative volume curves of Vesuvius and Etna are apparent in Fig. 1 and have been previously discussed in terms of the evolution of intravolcanic magma chambers and magma supply<sup>11,12</sup>. An episodic character to the recurrence of activity at Fuego, represented here in its most recent history has been detected<sup>5</sup>. Thus a constant output rate may represent a state of equilibrium that can only be maintained for a limited period of time.

Not all magmas that rise beneath volcanoes reach the surface. Some may freeze in intrusions<sup>14</sup>, or become involved in crystal fractionation and host rock digestion<sup>15</sup>. Kilauea is the only volcano for which there is geological and geophysical evidence that magma is supplied at a constant rate which is greater than the subaerial output rate<sup>14</sup>. This supply rate of  $3.6 \text{ m}^3 \text{ s}^{-1}$  is about five times the observed historic output rate, the balance being taken up mainly by submarine effusion and dyke intrusion. This has been applicable for the past 30 yr (refs 14, 16, 17). Supply rates for magma entering the other volcanoes can only be guessed at. The evidence from Kilauea suggests that constant output rates at each of the nine volcanoes represent a partitioning of ascending magma into a fraction which is erupted and a fraction which remains below the surface. Thus it is conceivable that each volcano has a constant supply rate that is larger than its

output rate but falling within a similarly restricted range of values.

Buoyant rise of magma in cracks is a mechanism which may explain a constant supply rate to these volcanoes. A magma-filled crack experiences a net force of  $(\rho - \rho')gV$ , where  $\rho$  is the density of the rock,  $\rho'$  is the density of the magma,  $g$  is the value of gravity and  $V$  is the volume of the crack<sup>18</sup>. The densities of the magmas considered here range from  $\sim 2,600 \text{ kg m}^{-3}$  (olivine tholeiite) to  $2,300 \text{ kg m}^{-3}$  (dacite) at liquidus temperatures and atmospheric pressure. Up to 5 kbar pressure the increase in densities is small ( $<100 \text{ kg m}^{-3}$ )<sup>19,20</sup>. The density contrast for basalts will be smaller than for andesites and dacites, and for an average crustal density of  $2,670 \text{ kg m}^{-3}$  a factor of five covers the range of density contrasts  $(\rho - \rho')$ , though this is sensitive to the local rock density.  $V$  is restricted by the lithospheric stress field; the greater stress at the base closes the crack as its tip migrates upwards. A free crack has a stable vertical length,  $L$ , given by

$$L \leq 2 \left[ \frac{K_c}{\sqrt{\pi} g (\rho - \rho')} \right]^{2/3}$$

where  $K_c$  is the fracture toughness of the rock<sup>21</sup>. For a density contrast of  $100 \text{ kg m}^{-3}$  in rocks of fracture toughness of  $100 \text{ MN m}^{-2/3}$   $L$  is  $\sim 3,000 \text{ m}$ . The width of the crack is variable but an average width of 10 m is geologically realistic and this would give a typical volume for a disk-shaped crack of about  $70 \times 10^6 \text{ m}^3$  and a net buoyancy of 70 GN.

This crack volume is of the same order of magnitude as the individual eruption volumes for most of the volcanoes in Table 1. Such cracks would need to arrive at the volcano every 6–7 yr to account for the observed output rates, more frequently if there is subsurface loss of magma. Magma-filled cracks, therefore, are of appropriate size and the ascending magma has a buoyancy controlled by parameters which may vary within sufficiently narrow limits to produce the observed similarity of output rates of volcanoes from very different tectonic settings.

If the magma is to remain liquid during conduction of heat to the cold walls it must have a minimum average ascent velocity. The calculations of Marsh for andesite-filled cracks<sup>22</sup> give a velocity of  $10^{-3} \text{ m s}^{-1}$ . A recent quantitative model of magma ascent at Kilauea<sup>23</sup> involves magma rising along cracks at velocities between  $10^{-2}$  and  $10^{-1} \text{ m s}^{-1}$ . The petrology and geochemistry of the products of the October 1974 eruption of Fuego have been interpreted<sup>24</sup> in terms of a magma-filled crack of volume  $100 \times 10^6 \text{ m}^3$  rising at an average velocity of  $10^{-3} \text{ m s}^{-1}$  for the last 8 km to the surface. These figures indicate the minimum average velocities though the real motion will be incremental<sup>25</sup>. In addition, the viscosity of the liquid has an important limiting effect on crack velocity<sup>26</sup>. The limiting effect will be much stronger for highly viscous siliceous magmas than for that for less viscous basaltic magmas. Although this problem

cannot be considered here it has an important bearing on volcanic magma supply.

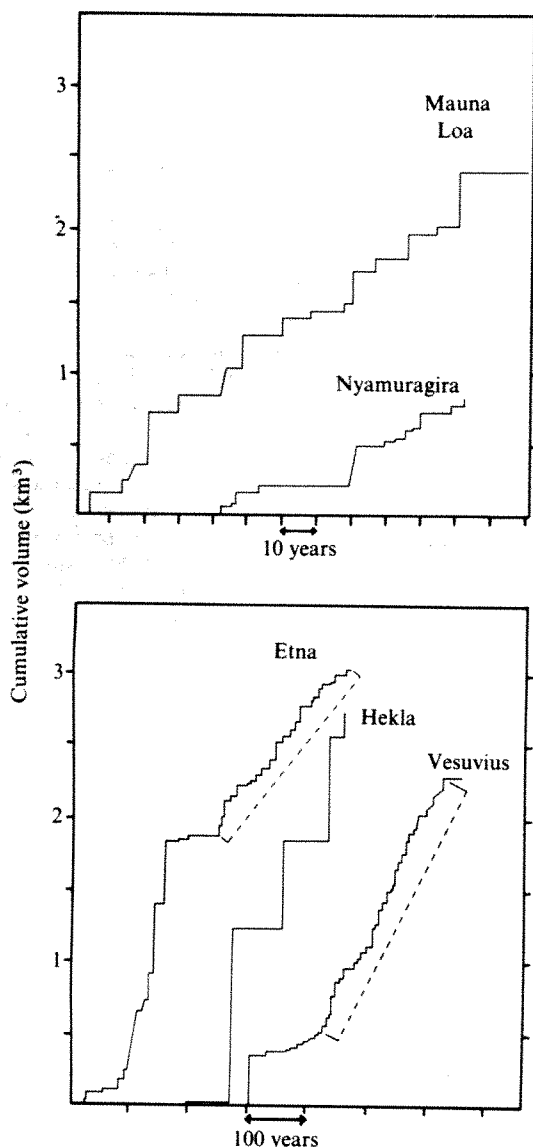
Most of the world's mature, subaerial central volcanoes have been considerably less active in historical times than those discussed here. Many have erupted no magma for hundreds of years. This may mean that magma is not being supplied to these volcanoes because it is being intercepted by a large crustal reservoir or because magma is not entering the crust at all. In a review of ash flow eruptions of all sizes, Smith<sup>27</sup> proposes a tentative correlation between ejecta volume and the time taken to produce this material. This rate is  $0.03 \text{ m}^3 \text{ s}^{-1}$  ( $10^{-3} \text{ km}^3 \text{ yr}^{-1}$ ), which is about 1/10th of the output rates presented here. There have been several published estimates of the volumetric productivity of large sections of several volcanic arcs situated above subduction zones. These estimates are usually expressed in  $\text{km}^3 \text{ Myr}^{-1} \text{ km}^{-1}$  of arc, and range from 5 to  $30 \text{ km}^3 \text{ Myr}^{-1} \text{ km}^{-1}$  (refs 28–32) for various periods of the Quaternary. If an average of 50 km of arc is allocated to each volcanic centre, each volcano produces  $\sim 250\text{--}1,500 \text{ km}^3 \text{ Myr}^{-1}$  or  $0.008\text{--}0.05 \text{ m}^3 \text{ s}^{-1}$ . This is between 2 and 10% of the historic

output rates shown by the Table 1 volcanoes near subduction zones. These two comparisons suggest that if the output rates reported here are more generally applicable to arc volcanoes when they are in an active state, then their corresponding periods of inactivity must last about 10–50 times longer.

I thank W. I. Rose Jr, S. Self and C. A. Wood for reviews of an earlier manuscript. Part of this work was done while I was a visiting scientist at the Lunar and Planetary Institute which is operated by the Universities Space Research Association under Contract NSR-09-051-001 with NASA.

Received 23 July; accepted 29 September 1980.

- MacDonald, G. A. *Catalogue Active Volcanoes of the World* Vol. III (1956).
- MacDonald, G. A. & Abbott, A. T. *Volcanoes in the Sea* (University of Hawaii Press, 1970).
- Tilling, R. I., Holcomb, R. T., Lockwood, J. P. & Peterson, D. W. *Int. Colloq. Planet. Geol.*, Rome, 149–152 (1975).
- Lockwood, J. P., Koyanagi, R. Y., Tilling, R. I., Holcomb, R. T. & Peterson, D. W. *Geotimes* 21, 12–15 (1976).
- Martin, D. P. *EOS* 61, 70 (1980).
- Rose, W. I. Jr *Bull. volcan.* 37, 73–94 (1973).
- Ludden, J. N. *J. Volcan. geotherm. Res.* 2, 385–395 (1977).
- Poulet, A. *Bull. volcan.* 29, 1–13 (1975).
- Thorarinsson, S. *The Eruption of Hekla 1947–48 I* (1–170 Visindafelg Islendinga 1967).
- Imbo, G. *Annali. Oss. vesuv.* 5, 185–379 (1951).
- Yokoyama, I. in *Volcanoes and Tectonosphere* (eds Aoki, H. & Iizuka, S.) 93–101 (Tokai University Press, 1976).
- Wadge, G., Walker, G. P. L. & Guest, J. E. *Nature* 255, 385–387 (1975).
- Moore, J. G. *Bull. volcan.* 34, 562–576 (1970).
- Swanson, D. A. *Science* 175, 169–170 (1972).
- O'Hara, M. J. *Nature* 266, 503–507 (1977).
- Dzurisin, D. *EOS* 61, 70 (1980).
- Swanson, D. A., Duffield, W. A., Jackson, D. B. & Peterson, D. W. *U.S. Geol. Surv. Prof. Pap.* 1056 (1979).
- Weertman, J. *J. geophys. Res.* 76, 1171–1183 (1971).
- Fujii, T. & Kushi, I. *Yb. Carnegie Instn Wash.* 76, 419–424 (1977).
- Kushi, I. *Yb. Carnegie Instn Wash.* 77, 675–677 (1978).
- Muller, O. H. & Muller, M. R. *Abstr. 11th lunar planet. Sci. Conf.*, Houston, 774–776 (1980).
- Marsh, B. D. *Phil. Trans. R. Soc. A288*, 611–625 (1978).
- Wright, T. L., Shaw, H. R., Tilling, R. I. & Fiske, R. S. *Abstr. Hawaii Symp. Intraplate Volcanism and Submarine Volcanism*, Hilo, 108 (1979).
- Rose, W. I. Jr, Anderson, A. T. Jr, Woodruff, G. & Bonis, S. B. *J. Volcan. geotherm. Res.* 4, 3–53 (1978).
- Weertman, J. *J. geophys. Res.* 76, 8544–8553 (1971).
- Anderson, O. L. *Bull. volcan.* 41, 341–353 (1978).
- Smith, R. L. *Geol. Soc. Am. Spec. Pap.* 180, 5–27 (1979).
- Sapper, K. *Vulkankunde* (Engelhorn, Stuttgart, 1927).
- Nakamura, K. in *The Utilization of Volcano Energy* (ed. Colp, J. L.) 273–285 (Sandia Laboratories, Albuquerque 1976).
- McBirney, A. R. *Can. Miner.* 14, 245–254 (1976).
- Marsh, B. D. *Am. Sci.* 67, 161–172 (1979).
- Sigurdsson, H., Sparks, R. S. J., Carey, S. & Huang, T. C. *J. Geol.* (in the press).
- Thorarinsson, S. *Geol. Rdsch.* 57, 705–719 (1967).



**Fig. 1** Cumulative volume curves compiled from the historic records of five volcanoes. The curve for Mauna Loa is for flank eruptions during 1843–1978. The curves for Nyamuragira and Hekla are for the periods used in Table 1, whilst the linear portions of the curves for Etna and Vesuvius used in Table 1 are bracketed by the dashed lines. The solid curves for Etna<sup>12</sup> are for 1535–1974, and for Vesuvius<sup>10,11</sup>, 1630–1979. Note that the abscissa scale for Mauna Loa and Nyamuragira is different from that for the other three volcanoes.

## Calcium-carbonate-phosphate surface complex in calcareous systems

Yoram Avnimelech\*

Faculty of Agricultural Engineering, Technion,  
Israel Institute of Technology, Haifa, Israel

The interactions between soluble orthophosphates and lime ( $\text{CaCO}_3$ ) have been extensively studied because of the frequent occurrence of soil systems rich in  $\text{CaCO}_3$  and the dominant effect of calcium carbonate on phosphate solubility. Several investigators have suggested that in these systems chemically defined calcium phosphate species are precipitated. Cole and Olsen<sup>1</sup> found that the solubility of phosphate in calcareous soils seems to be controlled by a di-calcium phosphate (DCP) solid phase, although the solubility product inferred ( $2.89 \times 10^{-9}$ ) is significantly less than that measured<sup>2</sup> for DCP ( $2 \times 10^{-7}$ ). Similar results have been reported for the interaction between fish-pond sediments and the aqueous phase<sup>3</sup>. On the other hand, Stum and Leckie<sup>4</sup> have suggested that the solubility of phosphate in calcareous systems may be controlled by the chemisorption of phosphate on  $\text{CaCO}_3$  particles, with the formation of amorphous calcium phosphates<sup>5</sup> or of surface complexes.<sup>4</sup> We now describe experiments which argue for the formation of a surface complex of calcium-carbonate-phosphate with well defined chemical composition.

\* Present address: The USDA-SEA Water Quality Management Laboratory, Durant, Oklahoma 74701.



The experiments consisted of adding phosphate to suspensions of analytical grade  $\text{CaCO}_3$ . In the first series,  $\text{K}_2\text{HPO}_4$  solutions, buffered with KOH to pH 8.4, were added drop by drop. Later, phosphate-enriched anion exchange resin (Dowex 2) contained in a fine nylon cloth was used to maintain a slow supply of phosphorus. The suspensions were shaken for periods of 3–25 days. Systems planned to provide data on material balance were tightly sealed to avoid gains or losses of  $\text{CO}_2$ . The samples were filtered and measurements made of: pH with a glass electrode, calcium with atomic adsorption using nitrous oxide flame, phosphate colorimetrically<sup>6</sup> and carbonates by titration<sup>7</sup>. Ionic distribution in the solution was computed using constants for the dissociation of the orthophosphoric and carbonic acids and stability constants for the ionic pairs  $\text{CaHPO}_4$ ,  $\text{CaH}_2\text{PO}_4^+$  (ref. 2),  $\text{CaCO}_3^\circ$ ,  $\text{CaHCO}_3^-$  (ref. 8) and  $\text{CaOH}^+$  (ref. 9).

The material balance of components in the solution during the reaction of potassium phosphate with calcium carbonate in a sealed system over 25 days is given in Table 1. A transfer of a component from the solution to the solid is defined as a negative change whereas dissolution, or desorption, is defined as a positive change. The balance for hydrogen is made on its free ionic species,  $\text{H}_3\text{O}^+$ , as well as on other species containing protons, such as  $\text{HCO}_3^-$  and  $\text{HPO}_4^{2-}$ .

Calcium is lost from the solution after the addition of phosphorus, but the losses become smaller with the increased phosphorus concentration and are not related to the changes in phosphorus concentration. The changes in total carbonate concentration follows the same pattern, but in the range of high phosphorus losses (above  $\sim 3 \times 10^{-4} \text{ mol P l}^{-1}$ ), carbonate is released from the solid into the solution. The transfer of hydrogen from the solution to the solid is linearly related to that of phosphorous. The linear regression is:

$$\Delta\text{H} = 0.59 + 2.11 \Delta\text{P}, \quad r = 0.965 \quad (1)$$

and the best estimate of  $\Delta\text{H}$  as a function  $\Delta\text{P}$  is

$$\Delta\text{H} = 2.625 \Delta\text{P} \quad (2)$$

If the reaction occurring in the system tested here was the precipitation of any known calcium phosphate, the ratio of precipitated calcium to that of phosphorus should be constant and in the range between 1.67 to 1.0, the stoichiometric Ca/P ratios in hydroxyapatite and DCP, respectively, that is

$$\frac{\text{Ca precipitated}}{\text{P precipitated}} = \text{constant}; \quad 1.0 \leq \text{constant} \leq 1.67 \quad (3)$$

The precipitated calcium includes that disappearing from the original solution, as well as calcium that is possibly added into the solution, by a dissolution of  $\text{CaCO}_3$ . Any gain of soluble calcium is associated with an identical gain in carbonate. Thus, calcium precipitated with phosphate is given by

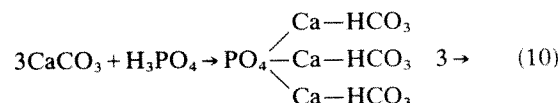
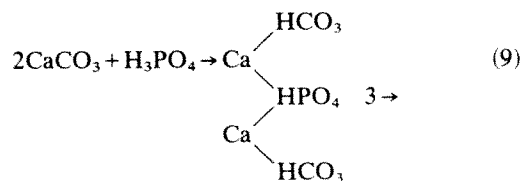
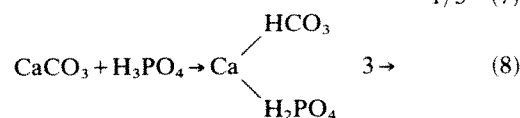
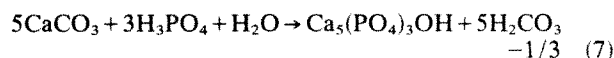
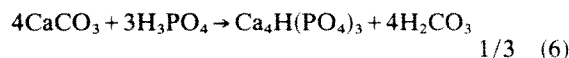
$$\text{Ca (P-p.p.t.d.)} = -(\Delta\text{Ca} + \Delta\text{CO}_3) \quad (4)$$

where  $\Delta\text{Ca}$  and  $\Delta\text{CO}_3$  are the changes in total calcium and carbonate respectively, from the time of phosphorus addition until the end of the experiment.

The ratio of precipitated Ca to precipitated P, averaged for

the data presented in Table 1, is 0.620. This ratio is not within that defined by equation (3) and thus is not consistent with the hypothesis that a known calcium phosphate shall have precipitated.

Equations (5)–(10) describe six possible reactions between  $\text{CaCO}_3$  and phosphoric acid, together with the resultant  $\Delta\text{H}/\Delta\text{P}$  ratios.



Reactions (5)–(7), leading to the formation of distinct calcium phosphates (DCP, octa-calcium phosphate or hydroxyapatite) do not lead to an appreciable binding of hydrogen to the solid phase. Reactions (8)–(10), describing the formation of calcium-carbonate-phosphates, lead to an equivalent binding of phosphate and hydrogen ions to the solid phase. The necessary  $\Delta\text{H}/\Delta\text{P}$  ratio is 3.

The linear relation found between the transfer of hydrogen and phosphorus from the solution to the solid (equation (2)), yields a  $\Delta\text{H}/\Delta\text{P}$  ratio of 2.6. This ratio tends to decrease, however, with the increase in phosphate concentration. This trend, and the fact that the experimental  $\Delta\text{H}/\Delta\text{P}$  ratio is lower than that demanded by equations (8)–(10), is probably because some fraction of the phosphate had reacted with calcium according to reactions (5)–(7).

These considerations and results suggest that the reaction between  $\text{CaCO}_3$  and orthophosphate can be formulated as



According to equation (11), and the potential diagram suggested by MacGregor and Brown<sup>10</sup>, the chemical potentials of the components participating in reactions (8)–(10) can be related through equation (12).

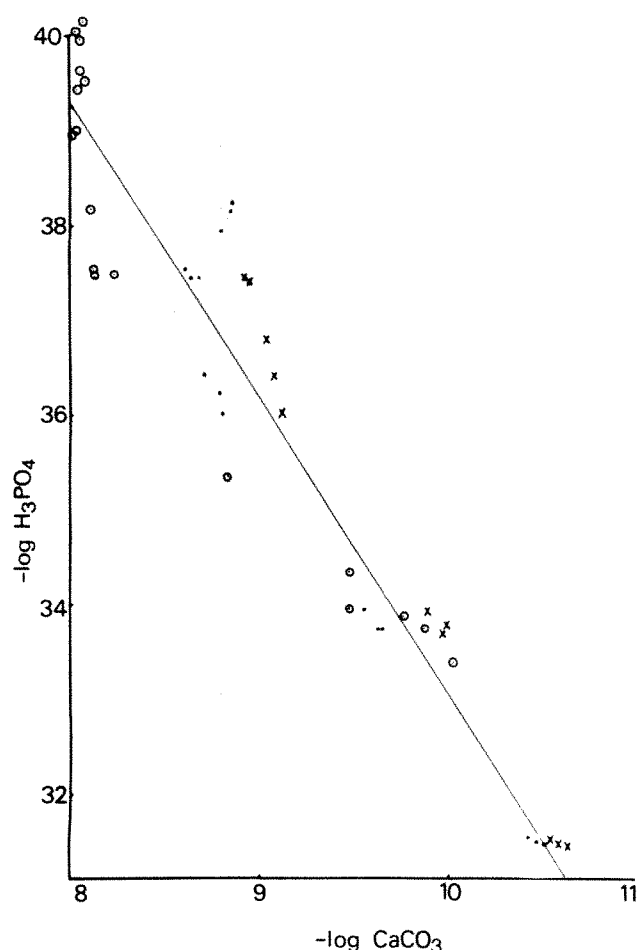
$$n\mu\text{CaCO}_3 + \mu\text{H}_3\text{PO}_4 = F^\circ \text{ solid} \quad (12)$$

or

$$n \ln(\text{CaCO}_3) + \ln(\text{H}_3\text{PO}_4) = \text{constant} \quad (13)$$

**Table 1** Material balance in  $\text{CaCO}_3$  suspensions enriched with phosphate

| Changes in solution composition ( $\text{mol l}^{-1}$ ) |                                    |                                   |                                   |                                   |
|---|------------------------------------|-----------------------------------|-----------------------------------|-----------------------------------|
| Initial phosphorus                                      | $\Delta\text{P}$                   | $\Delta\text{H}$                  | $\Delta\text{Ca}$                 | $\Delta\text{CO}_3$               |
| $2 \cdot 10^{-5}$                                       | $-(3.94 \pm 0.11) \times 10^{-6}$  | $-(2.95 \pm 0.23) \times 10^{-5}$ | $-(2.32 \pm 0.31) \times 10^{-5}$ | $-(2.31 \pm 0.26) \times 10^{-5}$ |
| $4 \cdot 10^{-5}$                                       | $-(7.89 \pm 0.22) \times 10^{-6}$  | $-(3.43 \pm 0.28) \times 10^{-5}$ | $-(2.49 \pm 0.13) \times 10^{-5}$ | $-(1.97 \pm 0.28) \times 10^{-5}$ |
| $8 \cdot 10^{-5}$                                       | $-(1.59 \pm 0.01) \times 10^{-5}$  | $-(4.63 \pm 0.26) \times 10^{-5}$ | $-(2.38 \pm 0.2) \times 10^{-5}$  | $-(1.56 \pm 0.25) \times 10^{-5}$ |
| $1.6 \cdot 10^{-4}$                                     | $-(3.02 \pm 0.04) \times 10^{-5}$  | $-(6.17 \pm 0.33) \times 10^{-5}$ | $-(1.97 \pm 0.17) \times 10^{-5}$ | $-(2.71 \pm 2.02) \times 10^{-6}$ |
| $1.2 \cdot 10^{-4}$                                     | $-(2.37 \pm 0.004) \times 10^{-5}$ | $-(3.93 \pm 0.52) \times 10^{-5}$ | $-(2.7 \pm 1.95) \times 10^{-6}$  | $(4.7 \pm 5.1) \times 10^{-6}$    |
| $2.4 \cdot 10^{-4}$                                     | $-(4.36 \pm 0.03) \times 10^{-5}$  | $-(7.65 \pm 0.39) \times 10^{-5}$ | $-(5.46 \pm 0.46) \times 10^{-6}$ | $(1.18 \pm 0.38) \times 10^{-5}$  |
| $4.8 \cdot 10^{-4}$                                     | $-(7.64 \pm 0.13) \times 10^{-5}$  | $-(1.29 \pm 0.03) \times 10^{-4}$ | $-(5.81 \pm 0.77) \times 10^{-6}$ | $(4.11 \pm 0.34) \times 10^{-5}$  |
| $9.6 \cdot 10^{-4}$                                     | $-(1.15 \pm 0.1) \times 10^{-4}$   | $-(2.78 \pm 0.04) \times 10^{-4}$ | $-(5.89 \pm 1.19) \times 10^{-6}$ | $(2.55 \pm 1.01) \times 10^{-5}$  |



**Fig. 1**  $\text{H}_3\text{PO}_4$  potential as a function of  $\text{CaCO}_3$  potential in  $\text{CaCO}_3$  suspensions equilibrated with phosphorus adsorbed on anion exchange resin. ●, Experiment (1), 5 g  $\text{CaCO}_3$  per 200 ml; ×, experiment (2), 5 g  $\text{CaCO}_3$  per 200 ml; ○, experiment (3), 1 g  $\text{CaCO}_3$  per 200 ml.

where the values in parentheses represent the activity of the given components.

According to equation (13), the logarithm of  $\text{CaCO}_3$  activity plotted against that of  $\text{H}_3\text{PO}_4$  should yield a straight line, the slope of which is equal to  $n$ , the stoichiometric ratio of  $\text{CaCO}_3$  to  $\text{H}_3\text{PO}_4$ .

Calcium carbonate suspensions were equilibrated during three days with phosphated anion exchange resin. The experimentally derived data are presented, in a potential diagram form, in Fig. 1. The points follow a straight line defined by

$$\log (\text{H}_3\text{PO}_4) = 64.23 - 3.11 \log (\text{CaCO}_3); \quad r = -0.951 \quad (14)$$

This line is in accordance with equation (13), and the slope suggests that the reaction occurring and controlling the system is that described by equation (10).

The formation of a surface compound  $\text{Ca}_3(\text{HCO}_3)_3\text{PO}_4$  agrees with the crystal structure of calcite or aragonite. In both crystals, three calcium ions are located on the surface for each unit cell<sup>11</sup>.

The linear relation between the  $\text{CaCO}_3$  and  $\text{H}_3\text{PO}_4$  potentials seems to disagree with the reported relationship between the chemical potentials of  $\text{Ca}(\text{OH})_2$  and  $\text{H}_3\text{PO}_4$  (refs 1, 3), but the present experimental data also yield a straight line when  $\log \text{H}_3\text{PO}_4$  is plotted against  $\log \text{Ca}(\text{OH})_2$ . This ambiguity stems from the fact that in any system at which  $\text{H}_2\text{CO}_3$  potential is constant (systems in equilibrium with the atmosphere),  $\text{Ca}(\text{OH})_2$  potential is related to  $\text{CaCO}_3$  potential. Thus, in any system controlled by equation (14), and maintaining a constant  $p\text{CO}_2$ ,

the phosphoric acid potential will show an apparent dependence on  $\text{Ca}(\text{OH})_2$  potential.

The existence of the surface compound,  $\text{Ca}_3(\text{HCO}_3)_3\text{PO}_4$ , also has an effect on the solubility of  $\text{CaCO}_3$ . The activity of  $\text{CaCO}_3$  in the solution is equivalent to the ionic product  $(\text{Ca}) \cdot (\text{CO}_3)$ . The data in Fig. 1 clearly indicate that this product is a function of the phosphoric acid potential and not a constant value. When the phosphoric acid potential is high, the ionic product drops significantly below the solubility product of calcite ( $pK = 8.31$  (ref. 8)).

This work has been supported by a research grant from the Lake Kinneret Authority.

Received 9 May; accepted 24 September 1980.

1. Cole, C. V. & Olsen, S. R. *Proc. Soil Sci. Soc. Am.* **23**, 116–118 (1959).
2. Gregory, T. M., Moreno, E. C. & Brown, W. E. *J. Res. natn. Bur. Standards* **74A**, 461–475 (1970).
3. Avnimelech, Y. *Verh. int. Verein. Limnol.* **19**, 2305–2308 (1975).
4. Stumm, W. & Leckie, J. O. *Proc. 5th int. Conf. on Advances in Water Pollution Research* (Pergamon, Oxford, 1971).
5. Rootare, H. M., Deitz, V. R. & Carpenter, F. G. *J. Colloid Sci.* **17**, 179–206 (1962).
6. Olsen, S. R. & Watanabe, J. S. *Proc. Soil Sci. Soc. Am.* **21**, 144–149 (1975).
7. Rand, M. C., Greenberg, A. E. & Taras, M. T. (eds) *Standard Methods for the Examination of Water and Wastewater* 14th edn (American Public Health Association, Washington DC, 1976).
8. Nakayama, F. S. *Soil Sci.* **106**, 429–434 (1968).
9. Gimblett, F. G. R. & Mohk, C. B. *Trans. Faraday Soc.* **50**, 965–972 (1959).
10. MacGregor, J. & Brown, W. E. *Nature* **205**, 359–361 (1965).
11. Grimshaw, R. W. *The Chemistry and Physics of Clays and Other Ceramic Materials* (Benn, London, 1971).
12. Avnimelech, Y., Moreno, E. C. & Brown, W. E. *J. Res. natn. Bur. Standards* **77A**, 149–155 (1973).

## Plant-controlled supratidal anhydrite from Al-Khiran, Kuwait

A. Gunatilaka, A. Saleh & A. Al-Temeemi

Department of Geology, Kuwait University, Kuwait

We report here that in the supratidal zone of the Al-Khiran sabkha, diagenetic anhydrite occurs exclusively in association with the living halophyte *Halocnemum strobilaceum* (Pallas) M.B. This anhydrite has a hair cream-like consistency and the bulk of it has formed as pseudomorphs after gypsum crystals. On the death of the plant at the end of its life cycle, the anhydrite is hydrated back to gypsum. This two-way transformation results in a series of characteristic textures, whose preservation could be due to the comparative 'youth' of the sabkha, which is in the very earliest stages of evaporite diagenesis.

A Recent carbonate–algal stromatolite–evaporite cycle <2-m thick and covering an area >60 km<sup>2</sup> occurs in the Al-Khiran area of Kuwait. The depositional area is in contact with the open waters of the Arabian Gulf by means of two large tidal channels (khors) which provide the main hydraulic energy input into the system. The physiography and sedimentary pattern of the region is shown in Fig. 1.

The supratidal zone proper or sabkha is marked by the occurrence of the halophyte *Halocnemum strobilaceum* (Pall.) M.B., which covers an area 1–3 km wide and extends continuously for ~15 km. Here the groundwater table is no more than 50–70 cm from the surface. Tidal flooding of this zone has not been observed, but probably occurs when strong winds and high tides coincide. The summer temperatures on the sabkha surface can vary between 42 and 55 °C (April to October) and winter temperatures from 20 to 35 °C (November to March). Evaporation rates are very high and rainfall (1979–80) can be up to 12 cm yr<sup>-1</sup>. Relative humidity values are generally <50%. The tidal range in the khors is >2 m at the mouth and <30 cm at the extremities. In all cases, the evaporite minerals present were confirmed by X-ray diffraction studies.



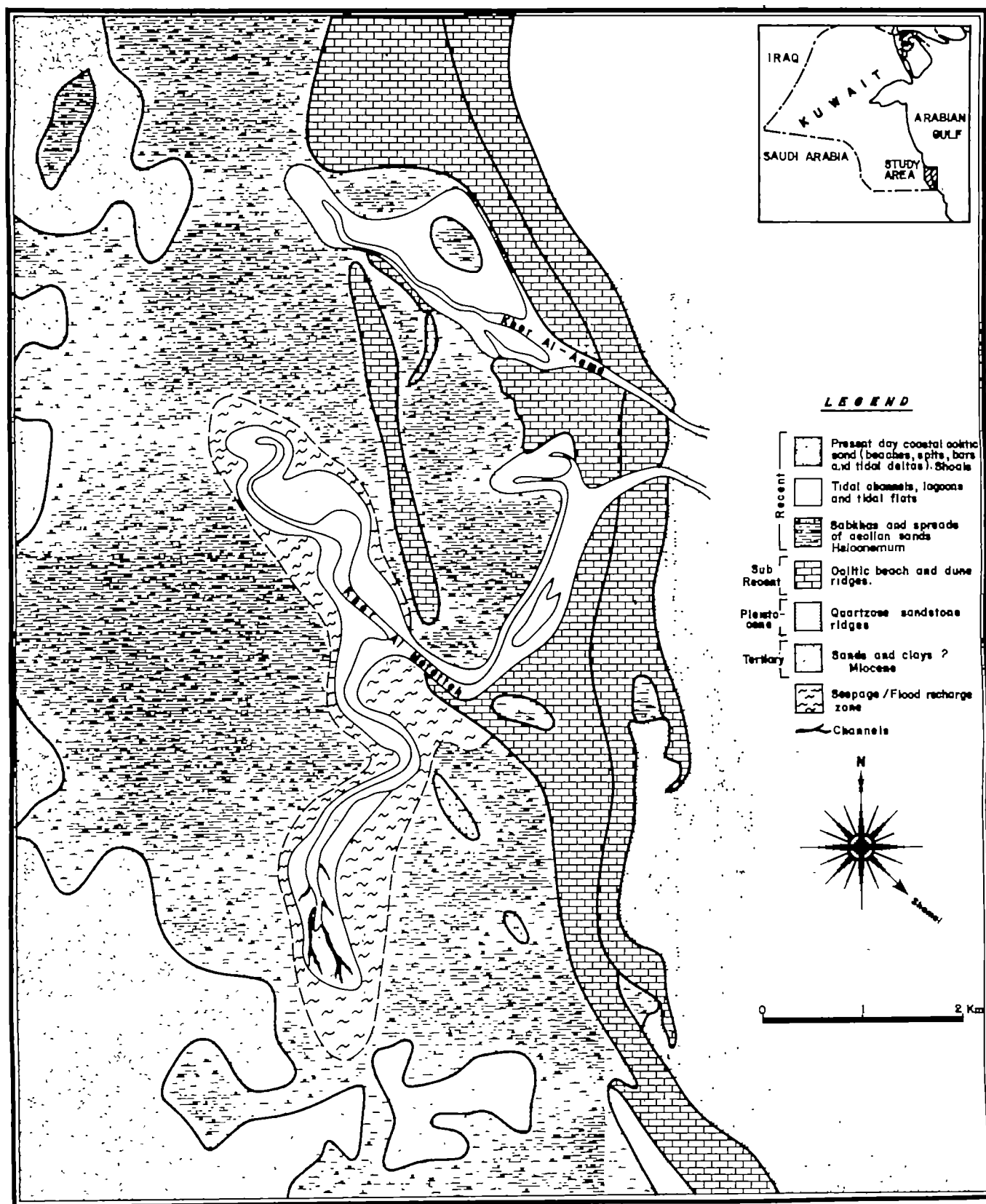


Fig. 1 Physiography and sedimentary pattern of the Al-Khiran area.

The first occurrence of anhydrite in the supratidal zone coincides with the appearance of the *Halocnemum* plant. It occurs as white patches exclusively around the plants, forming small elevated humps above the general surface (Fig. 2). It was also observed that the anhydrite is formed only around the mature, fully grown plants, in layers 3–12-cm thick with the characteristic consistency of hair cream (not the 'cottage cheese'

consistency as in Abu Dhabi). The stratigraphic relationships in a 30-cm core taken through the plant has the features shown in Table 1.

The anhydrite first begins to form as single nodules in the gypsum mush, a few centimetres below the sabkha surface, around the roots. Several of these nodules eventually coalesce to form irregular laminae, which in turn form the anhydrite layers



**Table 1** Stratigraphic features of a *Halocnemum* plant taken from the Al-Khiran area of Kuwait

| Depth (cm) | Dominant minerals   |
|------------|---|
| 0–1        | Wind-blown material, aragonite, gypsum, anhydrite, dolomite, halite |
| 1–7        | Anhydrite nodules or layers, some gypsum + trace dolomite           |
| 7–9        | Cemented gypsum crust   |
| 9–10       | Gypsum + some anhydrite   |
| 10–19      | Gypsum mush + minor aragonite + dolomite                            |
| 19–25      | Aragonite + gypsum + some dolomite                                  |
| >25        | Aragonite mud   |

around the plant. The continued growth of the gypsum below this zone contorts the layering, eventually resulting in structures resembling enterolithic veins. In section, the anhydrite layer looks like a 'diapir' with a *Halocnemum* bush in the middle. In fact, the surface expression of the anhydrite is directly related to the extent of the root network at depth. The diameter of these patches vary from 20 to 70 cm.

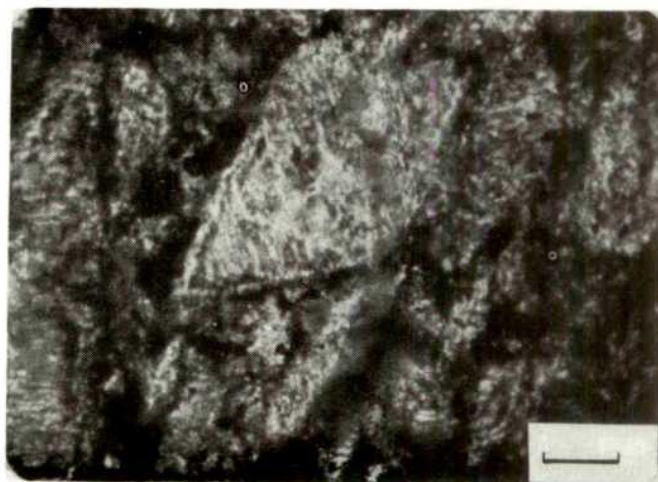
In thin section, the anhydrite occurs as perfect pseudomorphs after diskoid gypsum crystals of variable size (Fig. 3). The pseudomorphs are not formed by the infilling of diskoid voids left by the dissolution of gypsum crystals as suggested by Butler<sup>1</sup>. The gypsum–anhydrite transformation is a direct dehydration *in situ*, and the bulk of the nodules in the sabkha formed originally as pseudomorphs after gypsum within the host sediment. The evaporite minerals developing in the sabkha include aragonite, gypsum, bassanite, anhydrite, halite, protodolomite, celestite and magnesite. Detailed microscopic and X-ray diffraction studies indicate that the anhydrite and protodolomite are formed through replacement reactions between gypsum and aragonite and coexisting sabkha brines within the sediment. Note that in all the textures studied, the anhydrite had a gypsum precursor. There is no evidence for any orthochemical precipitation of anhydrite as a primary mineral in this sabkha<sup>2,3</sup>.

We believe that a brine concentration of 7–8 × SSW (standard seawater of chlorinity 19.377‰) necessary to form the anhydrite, is achieved by combining the effects of evapotranspiration activity of the *Halocnemum*, the osmotic activity of the roots and the cemented gypsum layer below, which regulates the capillary flow of the water. The mass dehydration around the plant results in a series of evaporitic textures caused mainly by the creation of new voids. The gypsum–anhydrite transformation results in a volume reduction<sup>4</sup> of ~36%.

Many dead plants occur within the supratidal zone. When associated with such plants, the anhydrite changes to a dirty grey or buff colour and the area around the plant becomes hum-

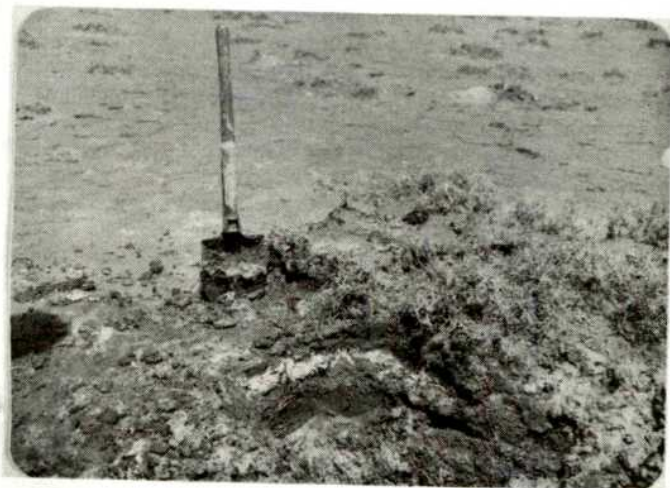
mocky. Vuggy features tend to develop and the entire surface starts breaking up, by which time the thixotropic consistency of the anhydrite has changed to one resembling moist and hardened flour. Microscopically this change is reflected in the rehydration of the anhydrite back to gypsum. The original pseudomorphs are destroyed and are replaced by a new series of hydration textures which are quite unlike that of any reported before from sabkhas. Around the dead plants optimal physico-chemical conditions probably do not prevail to concentrate the brines sufficiently (7–8 × SSW) and keep the system within the metastable field of anhydrite.

In thin section, the first change observed is the splaying open of the anhydrite pseudomorphs, brought about by the increase in volume due to rehydration (a 66% volume increase)<sup>4</sup>. Most pseudomorphs are flattened along their *c*-axes and the best developed cleavages are normal to the long axis of a crystal. The crystal is split along the latter cleavages, resulting in small, discrete sub-crystals or cleavage laths of anhydrite having rectangular cross-sections. These are very soon hydrated to gypsum laths pseudomorphic after the anhydrite cleavage laths. This is alabastrine secondary gypsum because of its microcrystalline–cryptocrystalline nature. Clumps or aggregates of these laths always show undulating extinction shadows when the microscope stage is rotated. The range of new textures developed vary from collapsing nodules of anhydrite/secondary gypsum laths (both of which originated in diskoid anhydrite

**Fig. 3** Photomicrograph of anhydrite pseudomorph after gypsum from the supratidal *Halocnemum* zone. Scale bar, 0.1 mm.

pseudomorphs) to 'granoblastic and preferred orientation textures'<sup>5</sup>. Perhaps the most interesting intermediate stage is the generation of a nested or 'augen'-like texture, where a nodule of anhydrite pseudomorphs or a single anhydrite grain is surrounded by gypsum laths showing a distinct lineation and indicating some flowage (Fig. 4). Compaction settling and pore water pressures causing liquefaction in poorly draining sediments are believed to cause lineation fabrics in anhydrite laminites<sup>6</sup>. If so, the inter- and intra-nodular permeability characteristics within the sediments could play a crucial part in their genesis. The compact and hardened nature of the alabastrine gypsum is probably due to the decrease in the void space between the laths, caused by the volume increase during hydration.

The hydration mechanism is thought to be dominantly one of dissolution of anhydrite followed by reprecipitation as gypsum<sup>7</sup>. However, there is no evidence that this occurs in Al-Khiran. Finally, when camel herds trek across the *Halocnemum* zone, their footprints soon convert the alabastrine gypsum pseudomorphic laths back into anhydrite, but with an aphanitic, felted texture<sup>5</sup>. Although the latter is probably a result of sustained compaction, followed by slippage or gliding of the breaking microcrystalline laths, the exact mechanisms involved are

**Fig. 2** Occurrence of hair-cream anhydrite (white patches) around the *Halocnemum* plants.



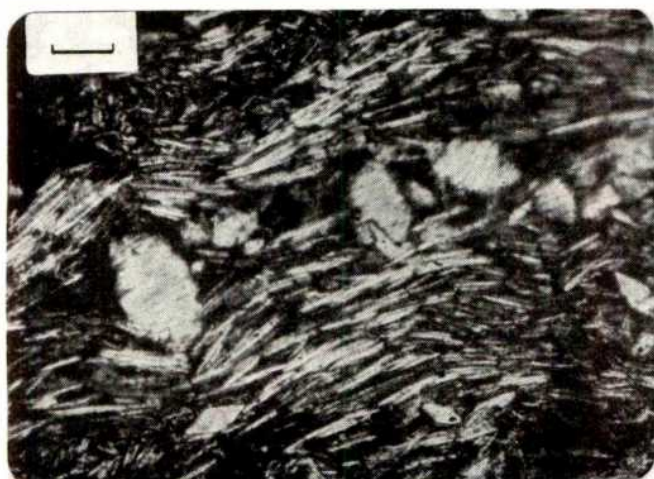


Fig. 4 Photomicrograph showing aligned fabric of gypsum laths. Note the nested anhydrite crystals. Scale bar, 500  $\mu\text{m}$ .

obscure. The main changes observed are:

Diskoid primary gypsum  $\rightarrow$   
 anhydrite pseudomorphs  $\rightarrow$   
 anhydrite cleavage laths  $\rightarrow$   
 alabastrine secondary gypsum pseudomorphic laths  $\rightarrow$   
 felted-aphanitic anhydrite.

Supratidal anhydrite associated with plants is of interest and there is experimental evidence regarding anhydrite precipitation in the presence of organic matter<sup>8</sup>. The occurrence of anhydrite in Al-Khiran is obviously controlled by the physiological requirements of the halophyte. Whether this difference with the widespread Trucial Coast anhydrite is due to the different climatic regimes (less rainfall and no vegetative cover in Abu Dhabi) is not clear. The absence of anhydrite in the North African sabkhas is probably due to the large influx of continental groundwaters and the semi-arid climatic regime<sup>9,10</sup>. We have also observed incipient anhydrite formation in a very restricted intertidal channel area, where a reducing organic-rich (algal/bacterial) laminated sediment is forming. Isolated gypsum grains altering to anhydrite were observed 4–5 cm below the intertidal surface in scattered locations. Though quantitatively insignificant, this, albeit rare, occurrence indicates that Perthuisot's oxidizing environment theory for the Arabian Gulf anhydrites needs to be treated with caution<sup>11</sup>. The Al-Khiran chemical data are yet incomplete to assess the general applicability of this idea.

The present conclusions made regarding the genesis of this unique occurrence of anhydrite in an Arabian Gulf sabkha are tentative because studies are continuing to relate the evaporite mineral assemblages to the chemistry of the coexisting brines within each zone. Many of the features reported here are either absent or not well represented in the classic Trucial Coast sabkhas. The comparatively youthful Al-Khiran sabkhas are still in the 'early' stages of a first cycle of carbonate sedimentation. Here, the intertidal algal mat does not extend inland below the present sabkha surface, and typical chicken-wire anhydrite is absent.

We thank Dr Graham Evans for visiting the study area and making critical comments on many aspects of this study.

Received 6 June; accepted 18 September 1980.

- Butler, G. P. *Ohio geol. Soc. J.* 120–152 (1970).
- Kinsman, D. J. J. *Am. Petrol. Inst. Prog. Rep.* (1969).
- Shearman, D. J. *Inst. Min. Metall. Trans. B* 75, 208–215 (1969).
- Mossop, G. D. & Shearman, D. J. *Inst. Min. Metall. Trans. B*, 147–154 (1973).
- Holliday, D. W. *Inst. Min. Metall. Trans. B*, 81–84 (1973).
- Shearman, D. J. & Fuller, J. G. *Bull. Can. petrol. Geol.* 17, 496–525 (1969).
- Ostroff, A. G. *Geochim. cosmochim. Acta* 28, 1363–1372 (1964).
- Cody, R. D. & Hull, A. B. *Geology* (in the press).
- Rouse, J. E. & Sherif, N. *Nature* 285, 470–472 (1980).
- West, I. M., Ali, Y. A. & Hilmy, M. E. *Geology* 7, 354–358 (1979).
- Perthuisot, J. P. *Bull. geol. Soc. Fr.* 19, 1145–1149 (1977).

## Particulate organic carbon flux in the oceans—surface productivity and oxygen utilization

Erwin Suess

School of Oceanography, Oregon State University, Corvallis, Oregon 97331

Organic detritus passing from the sea surface through the water column to the sea floor controls nutrient regeneration, fuels benthic life and affects burial of organic carbon in the sediment record<sup>1–3</sup>. Particle trap systems have enabled the first quantification of this important process. The results suggest that the dominant mechanism of vertical transport is by rapid settling of rare large particles, most likely of faecal pellets or marine snow of the order of  $>200 \mu\text{m}$  in diameter, whereas the more frequent small particles have an insignificant role in vertical mass flux<sup>4–6</sup>. The ultimate source of organic detritus is biological production in surface waters of the oceans. I determine here an empirical relationship that predicts organic carbon flux at any depth in the oceans below the base of the euphotic zone as a function of the mean net primary production rate at the surface and depth-dependent consumption. Such a relationship aids in estimating rates of decay of organic matter in the water column, benthic and water column respiration of oxygen in the deep sea and burial of organic carbon in the sediment record.

The relationship is based on flux data compiled from particle traps installed throughout the world's oceans<sup>7–19</sup> by many investigators and from annual mean organic carbon production rates of the respective surface waters<sup>20–29</sup> (Table 1). In a few cases biological production rates were determined at the time of installing the sediment trap<sup>12,16</sup>, the remaining data were compiled from other sources, often using annual mean rates from the general area of investigation. The predicted flux may overestimate the proportion of surface production intercepted at any given depth, when traps were installed during times of peak productivity (which was mostly the case) but then were normalized to lower mean annual production rates. Accordingly, equation (1) gives an upper limit of the net vertical carbon flux, if the production is known:

$$C_{\text{flux}(z)} = \frac{C_{\text{prod}}}{0.0238z + 0.212};$$

$$n = 33, \quad r^2 = 0.79, \quad z \geq 50 \quad (1)$$

$C_{\text{prod}}$  is the primary production rate of carbon at the surface,  $C_{\text{flux}}$  is the organic carbon flux at depth measured by the sediment traps, both in units of  $(\text{g m}^{-2} \text{ yr}^{-1})$ ,  $z$  ( $\geq 50$ ) is the water depth (m) at which the traps were moored,  $n$  is the number of observations, and  $r^2$  the coefficient of correlation. Only flux data from below the euphotic zone ( $>50 \text{ m}$ ) are used in defining equation (1). This limitation also causes the non-zero intercept for  $b = 0.212$ . Moreover carbon fluxes in shallow waters, as in the western Baltic Sea<sup>12,13</sup> and along cross-shelf transects of the Peru coastal upwelling regime<sup>16–18</sup>, are consistently less than predicted by extrapolating equation (1) to such depths (Fig. 1). These low yields are probably due to non-vertical motions of particles caused by advection, horizontal currents and locomotion of live plankton, thus exporting particulate matter from the site of sediment trap deployments.

Effects of  $\pm 15\%$  uncertainty in primary production estimates are also shown in Fig. 1. This uncertainty is of the same magnitude as the variations and ranges of repeated flux measurements obtained using several traps at the same location. For example, particle flux measurements below the California Current<sup>10</sup> were repeated within the same season whereas the data from the Peru coastal upwelling system<sup>17,18</sup> are averaged.

over several seasons, as indicated in Table 1. The collection and closure efficiency of certain trap designs, the problems of *in situ* decay of non-poisoned collectors, horizontal and resuspended flux probably contribute even more significantly to the scatter of the data<sup>30,31</sup>.

However large the present uncertainties may be for the relationship of vertical fluxes of particulate carbon in the oceans, they have interesting implications. First, if depth can be adequately transformed into time, the slope of equation (1) implies some sort of rate constant. Actual measurements of large particle size spectra with depth are not available. For small particles ( $d < 100 \mu\text{m}$ ) many theoretical models and empirical distribution patterns have been presented which suggested that particle populations get smaller in diameter with increasing depth<sup>4,32</sup>. The decrease in particle diameter with depth is thought to be a function of various chemical dissolution or oxidation processes<sup>33-35</sup>. Thus one would expect a gradual decrease in particle settling rates with depth. However, recent investigations suggest that biological repacking by successive feeding actually produces larger particles at the expense of smaller ones and that settling rates are extremely rapid<sup>36</sup>. A relationship of carbon-flux to surface-production from which minimum sinking rates can be inferred was recently also observed by Deuser and Ross<sup>14</sup> who showed that seasonality in surface production is reflected in like changes of the carbon flux in the deep Sargasso Sea. The coupling between production at the surface and deep flux—here at a depth of 3,200 m—within a period of a month or less, requires sinking rates of particles in excess of  $100 \text{ m day}^{-1}$ . Also Shanks and Trent<sup>6</sup> measured sinking rates of  $\sim 50\text{--}100 \text{ m day}^{-1}$  for other large aggregates (marine snow) primarily involved in vertical mass transfer.

As a first approximation, then, depth and residence time may be linearly related and for simplicity a settling velocity of  $w_s = 100 \text{ m day}^{-1}$  may be assumed in transforming depth ( $z$ ) of equation (1) into time. This then enables the definition of an

Table 1 Organic carbon fluxes in the water column and mean primary production rates

| Latitude         | Longitude   | Water depth (m) | Carbon flux ( $\text{g m}^{-2} \text{ yr}^{-1}$ ) | Production ( $\text{g m}^{-2} \text{ yr}^{-1}$ ) | Refs.      |
|------------------|-------------|-----------------|---|--|------------|
| 31°32.5' N       | 55°55.4' W  | 976             | 0.89  | 40   | 8, 29      |
|                  |             | 3,694           | 0.32  |  |            |
|                  |             | 5,206           | 0.026(?)  |  |            |
| 31°32.0' N       | 55°00.8' W  | 5,367           | 0.45  | 45   | 8, 29      |
| 13°30.2' N       | 54°00.1' W  | 389             | 2.46  | 50   | 8, 26      |
|                  |             | 988             | 1.44  |  |            |
|                  |             | 3,755           | 0.63  |  |            |
|                  |             | 5,068           | 0.62  |  |            |
| 15°21.1' N       | 151°28.5' W | 378             | 1.30  | 40   | 8, 26      |
|                  |             | 978             | 0.20(?)   |  |            |
|                  |             | 2,778           | 0.40  |  |            |
|                  |             | 4,280           | 0.32  |  |            |
|                  |             | 5,582           | 0.24  |  |            |
| 25 nm SE Bermuda |             | 3,200           | 0.77  | 40   | 14, 23     |
| 0°36' N          | 86°6' W     | 2,570           | 2.0   | 100  | 15, 22     |
| 27°42' N         | 78°54' W    | 660             | 5.3   | 100  | 9, 24, 26  |
| 33°30' N         | 76°15' W    | 1,350           | 10.9  | 200  |            |
| 38°23' N         | 69°45' W    | 3,520           | 5.6   | 250  |            |
| 24°51' N         | 77°39' W    | 2,100           | $2.0 \pm 0.3$                                     | 100  | 7          |
| 36°42' N         | 122°13' W   | 50              | $158 \pm 5$                                       | 500  | 10, 20, 21 |
|                  |             | 250             | $92 \pm 5$  |  |            |
|                  |             | 700             | $42 \pm 2$  |  |            |
| 36°42' N         | 122°13' W   | 50              | $33 \pm 7$  | 150  |            |
|                  |             | 250             | $19 \pm 2$  |  |            |
|                  |             | 700             | $17 \pm 2$  |  |            |
| 32°47' N         | 144°26' W   | 75              | $25 \pm 10$                                       | 100  |            |
|                  |             | 575             | $5.3 \pm 1$                                       |  |            |
|                  |             | 1,050           | $4.4 \pm 2$                                       |  |            |
| 38°50' N         | 72°31' W    | 2,160           | $6.4 \pm 0.2$                                     | 200  | 11, 26, 28 |
| 38°28.5' N       | 72°02.3' W  | 2,800           | $3.5 \pm 0.7$                                     | 200  |            |
| 38°19' N         | 69°37' W    | 3,500           | $5.4 \pm 1.0$                                     | 250  |            |
| 55°38.6' N       | 15°22.9' E  | 55              | 65  | 460±, 150  | 12         |
| 7°39.5' S        | 79°31.9' W  | 22              | 378†  | 650  | 17, 25     |
| 10°04.2' S       | 78°11.2' W  | 19              | 370†  | 450  |            |
| 11°58.5' S       | 77°11.0' W  | 20              | 253†  | 300  |            |
| 13°40.4' S       | 76°17.3' W  | 13              | 167†  | 350  |            |
| 15°04.5' S       | 75°26.6' W  | $50 \pm 10$     | $240 \pm 100$ ‡                                   | $1,200 \pm 600$                                  | 16, 17, 25 |
| 15°05.4' S       | 75°28.1' W  | 70              | $130 \pm 20$ †                                    | 600  | 17, 25     |
| 15°06.3' S       | 75°29.7' W  | $100 \pm 10$    | $110 \pm 30$ ‡                                    | 600  |            |
| 53°30' N         | 10°02' E    | <20             | $30 \pm 10$                                       | 150  | 13, 19, 27 |

\* Plotted as one datum point.

† Flux measured during one season only.

‡ Flux measured during two or more seasons.

§ Productivity determined during the same season when sediment traps deployed.

apparent rate constant for organic carbon decomposition from equation (2):

$$\frac{1}{C_{\text{flux}(z)}} - 0.212 = 2.38t \quad (2)$$

$$\frac{C_{\text{prod}}}{C_{\text{prod}}}$$

where  $C_{\text{prod}}$  = production at  $t = 0$ , and the constant  $k = 2.38$ , (that is  $z(0.0238)$ ), has the dimension  $\text{day}^{-1}$  and the properties of a second-order rate constant. This is inferred because equation (2) is analogous to the expression for second-order rates in chemical kinetics:  $1/C_t - 1/C_0 = kt$ . In testing experimental data to ascertain second-order rate kinetics,  $1/C_t$  plotted against  $t$  should yield a straight line relationship whose slope is equal to the rate constant  $k$  and the intercept equal to  $1/C_0$ . Accordingly, a fit for the carbon flux data in relation to depth ( $z$ ), to settling velocity ( $w_s$ ) and to primary production  $C_{\text{prod}}$  defines the equation above.

As a second implication, the extrapolation of the predicted carbon flux from equation (1) to the interception with the sea floor at any site yields the net carbon sedimentation before burial. This is independent of the actual rate laws and mechanisms that control organic matter consumption at depth or the variation in sinking rates of particulate matter. Net carbon sedimentation is an important parameter because it gives the upper limits of organic carbon accumulation in the sediment column. The preserved rate of burial can only be smaller than this flux. The magnitude of continued consumption of organic matter from the time it arrives at the sediment surface to the

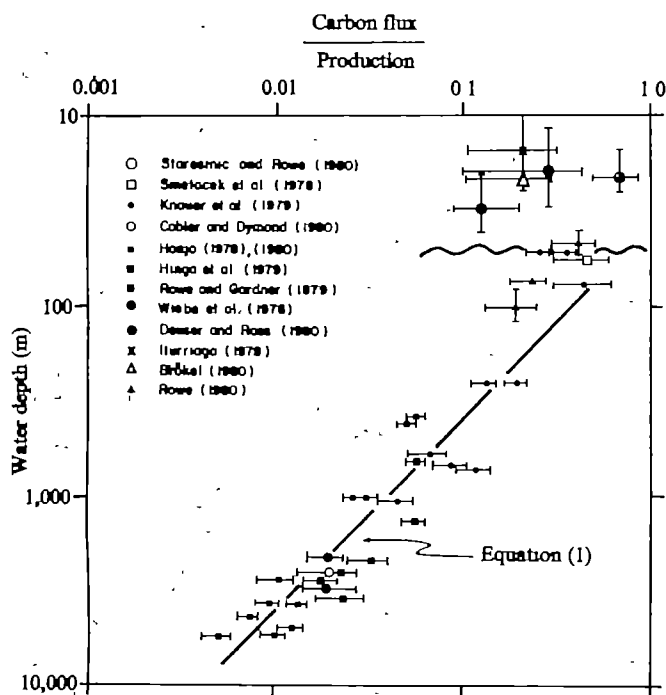


Fig. 1 Organic carbon fluxes with depth in the water column normalized to mean annual primary production rates at the sites of sediment trap deployment. The undulating line indicates the base of the euphotic zone; the horizontal error bars reflect variations in mean annual productivity as well as in replicate flux measurements during the same season or over several seasons; vertical error bars are depth ranges of several sediment trap deployments and uncertainties in the exact depth location. The data points by Rowe (1980) represent selected averages of 2–5 single sites at  $\sim 10 \text{ m}$  above the bottom, where resuspension was assumed to be minimal.



**Table 2** Organic carbon utilization by benthic processes at two sites of the coastal upwelling regime off Peru

|  | Station 7706-39                                      | Station 7706-36 |
|--|--|-----------------|
| Latitude   | 11°15.1' S   | 13°37.3' S      |
| Longitude  | 77°57.4' W   | 76°50.5' W      |
| Water depth (m)  | 186  | 370             |
|  | C-org (g m <sup>-2</sup> yr <sup>-1</sup> )          |                 |
| Production annual mean                                 | 500  | 400             |
| Flux to seafloor using equation (1)                    | 108  | 44              |
| Burial rate from sediment accumulation <sup>37</sup>   | 40   | 17              |
| Benthic utilization as carbon difference <sup>37</sup> | 68   | 38*-142†        |
|  | O <sub>2</sub> (l m <sup>-2</sup> yr <sup>-1</sup> ) |                 |
| Oxygen demand  | 160  | 93-345†         |

\* Equivalent oxygen consumption rates are based on 2.43 ml O<sub>2</sub> consumed = 1.0 mg C utilized<sup>41</sup>.

† Ref. 38.

time it is effectively removed from decomposition through burial is related to benthic respiration. In many cases the burial rate of organic carbon can be independently determined from linear bulk sedimentation rates, sediment densities, porosities and organic carbon contents. Consequently, the benthic respiration is the difference between the net vertical flux as predicted by equation (1) and the burial rate. The burial rate of organic matter, in turn, seems to be primarily controlled by the linear rate of sedimentation, as discussed elsewhere<sup>37</sup>. Results in Table 2 at two stations from the coastal upwelling regime off Peru illustrate how to estimate benthic respiration from vertical carbon flux minus carbon burial rate. The carbon utilization rates and the inferred bottom oxygen demand are well within the ranges reported from other coastal upwelling areas. Based on benthic production and faunal analyses, Christensen and

Packard<sup>38</sup> estimated benthic oxygen utilization rates at water depths ranging from 20 to 200 m for coastal upwelling areas off north-west Africa and Baja California to be between 93 and 345 (l m<sup>-2</sup> yr<sup>-1</sup>). Also, oxygen utilization rates of 60-550 (l m<sup>-2</sup> yr<sup>-1</sup>), with strong seasonal fluctuations, are reported from the first direct measurements of O<sub>2</sub>-distribution profiles *in situ* and from incubation experiments of near-shore anoxic sediments from the western Baltic Sea<sup>39,40</sup>.

The most far-reaching, yet tentative implication, is coupling oxygen consumption in the water column to the observed changes in vertical flux of particulate organic carbon. If for every 106 mol organic carbon consumed, 138 mol oxygen are utilized<sup>41</sup> and if the residence time of the particles within a parcel of seawater can be ascertained, rates of oxygen utilization at any depth can be predicted. Again for simplicity, assuming a mean sinking rate for particles  $w_s = 100 \text{ m day}^{-1}$  yields the distribution of the total cumulative oxygen utilization with depth as:

$$\Delta O_2 = C_{\text{prod}}(6.66 \times 10^{-5}) \left[ 1 - \frac{1}{0.0238(z) + 0.212} \right] \quad (3)$$

where the constant  $6.66 \times 10^{-5}$  converts carbon consumption to oxygen utilization in units of (ml l<sup>-1</sup> day<sup>-1</sup>); that is  $\frac{1}{365} \text{ g C-org}$

m<sup>-2</sup> day<sup>-1</sup> utilizes  $2.43 \times \frac{1}{100} \text{ m}^3$  when assuming settling velocity

of particles  $w_s = 100 \text{ m day}^{-1}$ ; therefore,  $\frac{2.43}{365} \times 10^{-5} \times 10^3 =$

$6.66 \times 10^{-5} \text{ ml l}^{-1} \text{ day}^{-1}$ . The proportion of organic carbon

consumed is given by the expression  $1 - \frac{1}{0.0238(z) + 0.212}$  and

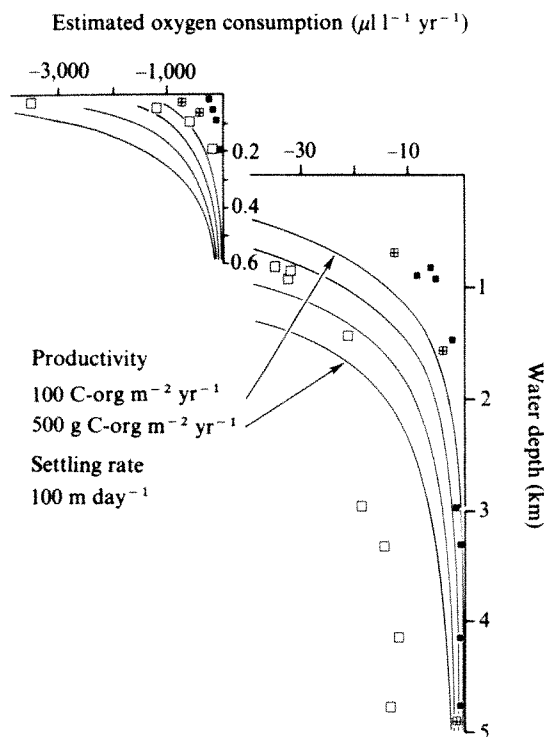
again,  $z$  is limited to depths  $\geq 50 \text{ m}$ . To illustrate the usefulness of equation (3), vertical distribution profiles of oxygen consumption rates are generated for a water-column profile where the input of oxidizable particulate organic matter from the euphotic zone is between 100 and 500 g C m<sup>-2</sup> yr<sup>-1</sup> and the vertical mass transfer is assumed to be primarily through large particles at sinking rates of  $100 \text{ m day}^{-1}$ . Comparable oxygen consumption rates in water-column profiles deduced from electron transport activities, bacterial utilization rates and respirometer measurements are in general agreement with these predicted values, although ETS O<sub>2</sub>-consumption rates appear higher by an order of magnitude at greater water depths (Fig. 2)<sup>42-45</sup>. Equation (3) also assumes O<sub>2</sub>-consumption to be only by the utilization of particulate organic matter, whereas actually, dissolved organic carbon is also utilized<sup>46</sup>.

The oxygen distribution resulting from the predicted consumption rates of equation (3) largely follows that of the classical circulation model by Wyrki<sup>47</sup>, the basic difference being that his model utilizes an exponential oxygen consumption term with depth following first-order rate kinetics, that is  $C_t = C_0 e^{-kz}$ , whereas the carbon flux measurements presented here are better approximated by a second-order fit. The only way that the carbon flux data would follow a first-order rate expression is in the case of accelerated settling of particles; that is, if sinking rates were actually to increase with depth in the water column.

These early results from particle traps apparently tie together successfully processes of organic carbon cycling in the oceans that previously have been treated separately by marine biologists, chemists and sedimentologists. Sizes and shapes of particles involved in vertical mass flux and seasonally adjusted surface productivity and deep carbon fluxes hold the key to understanding fully organic carbon cycling in the ocean and related oxygen and nutrient distributions.

This work was supported by the NSF and the Office of Naval Research through grants OCE-77-20376 and N00014-79-C-0004, Project NRO83-1026 to Oregon State University. I thank J. Dymond, P. D. Komar and R. Pytkowicz for helpful discussions.

I dedicate this work to Richard Cobler, an inspiring student of oceanography and a friend.



**Fig. 2** Vertical distribution of oxygen consumption rates in the ocean derived from changes of particulate carbon fluxes. The profiles are generated from equation (3) for mean primary productivities of between 100 and 500 g C-org m<sup>-2</sup> yr<sup>-1</sup>, respectively. Vertical transfer of particles is at constant sinking rate of  $100 \text{ m day}^{-1}$ . Maximum potential oxygen consumption rates are shown for comparison from electron transport activities (□) and the corresponding estimated actual oxygen utilization (■). □, Oxygen consumption from bacterial utilization rates. The data points represent a composite profile from the eastern Pacific Ocean<sup>42-45</sup>; note scale changes.

Received 18 June, accepted 10 September 1980

1. Redfield, A. C., Ketchum, B. H. & Richards, F. A. in *The Sea*, Vol. 2 (ed. Hill, M. N.) 26-77 (Wiley, New York, 1963).
2. Smith, K. L. *Mar. Biol.* **47**, 337-347 (1978).
3. Müller, P. J. & Soosa, E. *Deep-Sea Res.* **26**, 1347-1362 (1979).
4. McCave, I. N. *Deep-Sea Res.* **22**, 491-502 (1975).
5. Schrader, H. J. *Science* **174**, 55-57 (1971).
6. Shanks, A. L. & Trent, D. *Deep-Sea Res.* **27**, 137-143 (1980).
7. Woabe, P. H., Boyd, S. H. & Winget, C. J. *Mar. Res.* **34**, 341-354 (1976).
8. Honjo, S. J. *Mar. Res.* **36**, 469-492 (1978), **38**, 53-97 (1980).
9. Hinga, K. R., Seabarth, J. & Heath, G. R. J. *Mar. Res.* **37**, 557-579 (1979).
10. Kinner, G. A., Martin, J. H. & Bruland, K. W. *Deep-Sea Res.* **26**, 97-108 (1979).
11. Rowe, G. T. & Gardner, W. D. J. *Mar. Res.* **37**, 581-600 (1979).
12. Smetacek, V., von Brökel, K. & Zentchel, Zank, W. *Mar. Biol.* **47**, 211-226 (1978).
13. Iturza, R. *Mar. Biol.* **55**, 157-169 (1979).
14. Donner, W. G. & Ross, E. H. *Nature* **283**, 364-365 (1980).
15. Cobler, R. & Dymond, J. *Science* **209**, 801-802 (1980).
16. von Brökel, K. *Abstr. IDOE int. Symp. on Coastal Upwelling*, Los Angeles (1980).
17. Rowe, G. T. *Symp. on Bio-productivity of Upwelling Ecosystems*, Moscow (1979).
18. Starosom, N. & Rowe, G. T. *Abstr. IDOE int. Symp. on Coastal Upwelling*, Los Angeles (1980).
19. Zentchel, B. *Koeler Meeresforsch.* **21**, 55-80 (1965).
20. Owen, R. W. *California Cooperative Oceanic Fisheries Investigations*, Atlas No. 20, 98-109 (State of California, Marine Research Commission, 1974).
21. Ryther, J. H. *Science* **166**, 72-76 (1969).
22. Love, C. M. & Allen, R. M. (eds) *Estuarine Atlas 10* (US Government Printing Office, Carc 330, 1975).
23. Menzel, D. W. & Ryther, J. H. *Deep-Sea Res.* **6**, 351-367 (1960).
24. Ryther, J. H. in *The Sea*, Vol. 2 (ed. Hill, M. N.) 347-380 (Wiley, New York, 1963).
25. Guilleen, O., de Mendonça, B. R. & de Rondon, R. I. *Oceanography of the South Pacific* (New Zealand National Committee for UNESCO, Publ. 405-418, 1973).
26. Koblenz-Mishka, O. J., Volkovskiy, V. V. & Kabanova, J. G. *Scientific Exploration of the South Pacific*, (ed. Wooster, W.) 183-193 (National Academy of Sciences, Washington, 1970).
27. von Bodungen, B. *ibidem*, *Umw. Kael* (1975).
28. Ryther, J. H. & Yentsch, C. S. *Limnol. Oceanogr.* **3**, 327-335 (1958).
29. Ryther, J. H. & Menzel, D. W. *Deep-Sea Res.* **6**, 235-238 (1960).
30. Dymond, J. *et al. Earth planet. Sci. Lett.* (in the press).
31. Kinner, W. B. *Limnol. Oceanogr.* **28**, 657-660 (1975).
32. Brun-Cottan, J. C. J. *geophys. Res.* **81**, 1601-1606 (1976).
33. Lal, D. & Lerman, A. J. *geophys. Res.* **80**, 423-430 (1975).
34. Wollett, R. *The Sea*, Vol. 5 (ed. Goldberg, E. D.) 369-392 (Wiley, New York, 1974).
35. Lal, D. *Science* **190**, 997-1008 (1977).
36. Honjo, S. & Roman, M. R. J. *Mar. Res.* **36**, 45-75 (1978).
37. Müller, P. J. & Soosa, E. *Deep-Sea Res.* **26**, 1347-1362 (1979), *Colloq. int. du C.N.R.S.* No. 293, 17-26 (1980).
38. Christensen, J. P. & Packard, T. T. *Deep-Sea Res.* **24**, 331-343 (1977).
39. Ravnsbock, N. P., Jørgensen, B. B. & Blackburn, T. H. *Science* **207**, 1355-1356 (1980).
40. Ravnsbock, N. P., Jørgensen, J., Blackburn, T. H. & Lombolt, J. P. *Limnol. Oceanogr.* **28**, 403-411 (1980).
41. Richards, F. A. *Chem. Oceanogr.* **1**, 611-645 (1965).
42. Packard, T. T., Hooley, M. L. & Richards, F. A. *Limnol. Oceanogr.* **16**, 67-70 (1971).
43. Kroopnick, P. *Deep-Sea Res.* **21**, 211-227 (1974).
44. Craig, H. J. *geophys. Res.* **76**, 5078-5086 (1971).
45. Carlucci, A. F. & Wilbur, P. M. *Naturwissenschaften* **65**, 541-542 (1978).
46. Williams, P. M. & Carlucci, A. F. *Nature* **262**, 810-811 (1976).
47. Wyrtki, K. *Deep-Sea Res.* **9**, 11-23 (1962).

## Concomitant photoautotrophic growth and nitrogenase activity by cyanobacterium *Plectonema boryanum* in continuous culture

H. W. Pearson &amp; R. Howley

Department of Botany, University of Liverpool, PO Box 147, Liverpool L69 3BX, UK

Since the discovery that nitrogenase activity will develop in cultures of *Plectonema boryanum* in microaerobic conditions<sup>1</sup>, this phenomenon has been demonstrated in numerous other non-heterocystous cyanobacteria<sup>2-4</sup>. However, there is controversy as to whether such organisms are capable of sustained concomitant nitrogenase activity and photoautotrophic growth<sup>2,4,5</sup>. An exogenous carbohydrate source (fructose) and strongly reducing conditions (produced by bubbling liquid cultures with a N<sub>2</sub>/CO<sub>2</sub>/H<sub>2</sub>S gas mixture) have been deemed necessary for continuous logarithmic green growth and nitrogenase activity by batch cultures of *Plectonema boryanum* in the light. We report here sustained exponential growth and nitrogenase activity by *P. boryanum* in continuous culture gassed with nitrogen in the absence of further chemical reducing agents and exogenous carbohydrate sources.

An aerobic continuous culture of *P. boryanum* was established in a chemostat with nitrate (1 mM) in the medium as the combined-nitrogen source and light intensity the factor controlling the rate of growth. General conditions for culture were as described in Fig. 1 legend, except that the fermenter was gassed with air (instead of nitrogen) and the rate of dilution was faster ( $D = 0.072 \text{ h}^{-1}$  rather than  $0.048 \text{ h}^{-1}$ ). With the population in steady state in these carbon-limited growth conditions, the ratio of phycobiliprotein to chlorophyll *a* (an indication of the nitrogen status of the cells<sup>1,5</sup>) was 1.030, the cell density 0.115 absorbance units and the cell doubling time 9.6 h. After 10 d of steady-state growth, nitrogen starvation was imposed by omitting nitrate from the inflowing medium. The culture turned yellow within ~36 h, growth virtually stopped (as evidenced by a rapid rate of washout) and the ratio of phycobiliprotein to chlorophyll *a* dropped from 1.030 to 0.903. Thus the higher ratio was obtained when nitrogen was not limiting growth, whereas the lower ratio occurred in conditions of nitrogen starvation.

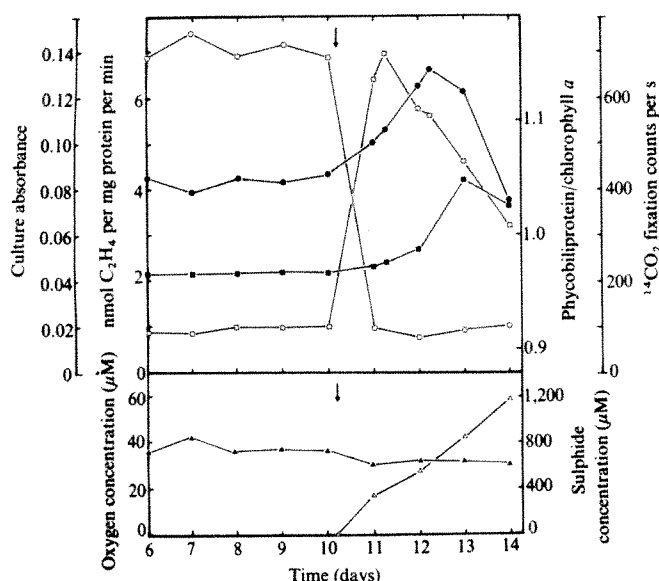
We used the basic conditions established for aerobic photoautotrophic growth of *P. boryanum* in continuous culture; cells previously grown with nitrate were inoculated into combined-nitrogen-free medium under an atmosphere of nitrogen and grown in the fermenter for 3-4 d in batch culture. During this period nitrogenase activity commenced and cell density increased. The fermenter was then switched to the continuous mode by pumping combined-nitrogen-free medium through the culture while bubbling it with oxygen-free nitrogen gas (inorganic carbon was supplied as bicarbonate in the inflowing medium). The culture stabilized to give a steady-state cell density after approximately 48 h. Figure 1 shows that simultaneous photosynthesis, nitrogenase activity and photoautotrophic exponential growth were sustained by *P. boryanum* in this microaerobic continuous culture. The filaments showed no visible signs of yellowing in spite of a ratio of phycobiliprotein to chlorophyll *a* of 51.56% of the value recorded for the aerobic cultures grown with nitrate.

Our nitrogenase activity (1.00 nmol C<sub>2</sub>H<sub>4</sub> per mg protein per min) for *P. boryanum* in continuous culture was substantially less than that quoted for batch cultures grown in a sulphide-stat amended with fructose<sup>5</sup>. Nevertheless it provided sufficient fixed nitrogen to support a higher specific growth rate ( $\mu = 0.048 \text{ h}^{-1}$ ), equivalent to a cell doubling time of 14.4 h compared to ~24 h reported by Rogerson<sup>5</sup>. The growth pattern described here could be maintained almost indefinitely.

We next investigated the effect of adding sulphide at levels known to suppress oxygenic photosynthesis. To establish the range of inhibitory concentrations, we incubated samples of the culture with various concentrations of sulphide: photosynthesis was severely inhibited above 300  $\mu\text{M}$ . We therefore incorporated sulphide into the inflowing medium and it reached a concentration of 300  $\mu\text{M}$  in the fermenter after 20 h, at which time the photosynthetic rate of *P. boryanum* had dropped to 14% of its initial steady-state value. In spite of this severe reduction in carbon fixation, nitrogenase activity was stimulated sevenfold and the specific growth rate of the culture steadily increased for 48 h before falling again in response to carbon starvation. Thus, while previously maintaining a high rate of growth in nitrogen-fixing photoautotrophic conditions, *P. boryanum* accumulated sufficient photosynthetically derived carbon to support a prolonged period of increased growth in the light, in conditions favouring nitrogen fixation but inhibiting photosynthesis. The stimulation of nitrogenase by the added sulphide was reflected in the increased production of phycobiliprotein relative to chlorophyll *a* to a value higher than during growth with nitrate.

Although sulphide reduced the dissolved oxygen concentration in the medium to  $31.7 \pm 1.7 \mu\text{M}$ , the studies of Stewart and Lex<sup>1</sup> suggest that this alone could not account for all the increase in nitrogenase activity. In microaerobic conditions the controlling factor seems to be intracellular accumulation of photosynthetically produced oxygen, rather than the diffusion of





**Fig. 1** Nitrogen-fixing photoautotrophic growth of *Plectonema boryanum* (UTEX 594) in chemostat continuous culture. The growth medium was a modified ASM recipe<sup>11</sup>, free of combined-nitrogen but with  $\text{NaHCO}_3$  (12 mM final concentration) added as the source of carbon dioxide. The culture (1,000-cm<sup>3</sup> volume) had a dilution rate of 48 cm<sup>3</sup> h<sup>-1</sup> and was gassed with oxygen-free nitrogen (100 cm<sup>3</sup> min<sup>-1</sup>) and stirred continuously. The pH of the medium in the fermenter was adjusted to 8.9. When required, sulphide was pumped into the fermenter (the arrow denotes the start of this procedure) from a separate reservoir of  $\text{Na}_2\text{S}$  solution maintained in anoxic conditions. The dilution rate of the culture was kept constant. Illumination by 125-W white fluorescent tubes provided a light intensity at the fermenter surface of 97.5  $\mu\text{E m}^{-2} \text{s}^{-1}$  photosynthetically active radiation (6,000 lux) and the temperature was maintained at  $29 \pm 1^\circ\text{C}$ . Dissolved oxygen ( $\blacktriangle$ ) was determined using a Clark-type oxygen electrode housed in a small chamber remote from the main fermenter body into which a sample of the culture could be diverted when measurements were to be made. This prevented poisoning of the electrode by prolonged contact with the medium when it contained sulphide. The optical density of the culture ( $\bullet$ ) was estimated spectrophotometrically at 540 nm (1 cm pathlength) and the phycobiliprotein to chlorophyll *a* ratio ( $\blacksquare$ ) calculated from measurements at 625 and 678 nm respectively. Nitrogenase activity ( $\square$ ) was estimated by the acetylene reduction technique in a gas phase of 10%  $\text{C}_2\text{H}_2$  balance nitrogen, as described previously<sup>11</sup> but by means of a Perkin Elmer FII gas chromatograph. Sulphide concentration ( $\triangle$ ) was determined by the methylene blue photometric method<sup>12</sup>. Rates of carbon fixation ( $\circ$ ) were measured as before<sup>7</sup> except that  $\text{NaH}^{14}\text{CO}_3$  was added directly to samples from the fermenter.

oxygen into the cells from the culture medium. Sulphide thus allowed increased expression of nitrogenase activity by penetrating the cells<sup>7</sup> and reducing the intracellular oxygen tension by two possible mechanisms: (1) the chemical reduction of photosynthetically produced oxygen, as was likely in Rogerson's work<sup>5</sup>, because 5–8  $\mu\text{M}$  sulphide at pH 7.8 does not appreciably inhibit oxygenic photosynthesis in *Plectonema* (Fig. 2), and (2) the direct suppression of photosynthetic oxygen production as in our experiments (Fig. 1).

Nagatani and Haselkorn<sup>8</sup> have suggested that the shortage of reductant is the major factor limiting induced nitrogenase activity in microaerobic cultures of *Plectonema*. If so the increased rate of nitrogenase activity in the presence of sulphide might be due not just to the elimination of molecular oxygen *in vivo* but also to the supply of reductant directly to the nitrogenase system by sulphide. This could explain the high rates of acetylene reduction we observed with sulphide present, even

when the specific growth rate had started to decline rapidly after day 12 (Fig. 1) due to carbon starvation. In such conditions supplies of reductant and ATP from respiration are likely to be severely restricted. But because sulphide, at the concentrations used, inhibits photosynthetic electron transport through photosystem II while photosystem I is unaffected, cyclic photophosphorylation could provide the ATP in the light and sulphide could donate the bulk of the electrons directly to the nitrogenase system.

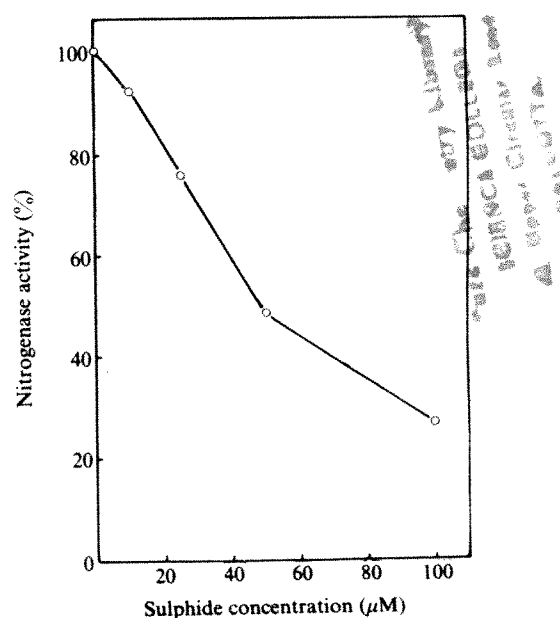
Because nitrogenase activity due to stimulation by sulphide leads to the apparent 'luxury' production of phycobiliprotein, as a nitrogenous reserve compound, it seems unwise to draw conclusions about the functioning of photosystem II based solely on a high phycobiliprotein to chlorophyll *a* ratio especially as sulphide inhibited virtually all photosynthetic activity in our culture. Nevertheless, our results point to the potential for renewed photosystem II activity should inhibitory sulphide concentrations prove transitory, as in many natural environments such as temperate salt marshes, mud flats and sand dune slacks.

Our data show that in microaerobic continuous culture *P. boryanum* can sustain a high rate of exponential growth based solely on its own photosynthetic and nitrogen-fixing capacities. The simultaneous and stable rates of photosynthesis and nitrogenase activity do not support the idea of temporal separation of these processes as a mechanism for protecting the nitrogenase from inactivation by oxygen<sup>9</sup>.

Sulphide probably stimulates nitrogenase activity by eliminating intracellular photosynthetically produced oxygen, but sulphide ions may also provide reductant to the nitrogenase system. Oxygenic photosynthesis was markedly more sensitive to sulphide poisoning than was nitrogenase activity but *P. boryanum* can exploit this situation by using stored photosynthate as shown here, or by switching to photoheterotrophic growth if suitable exogenous substrates are available<sup>10</sup>.

Given the apparent absence of a special cellular mechanism to permit microaerobic nitrogen-fixing photoautotrophic growth by *P. boryanum*, it is likely that other non-heterocystous cyanobacteria with oxygen-sensitive nitrogenase systems *in vivo* could grow similarly.

R.H. was supported by a NERC studentship.



**Fig. 2** Carbon fixation by *P. boryanum* at different sulphide concentrations (pH 7.8). Values are expressed as a percentage of the sulphide-free controls and are the means of triplicate samples. Experimental procedure was similar to that described previously<sup>7</sup>.

Received 1 August, accepted September 19, 1980

1. Stewart, W. D. P. & Lee, M. *Arch Microbiol* 73, 250–260 (1970)
2. Ruppia, R. & Waterbury, J. B. *FEMS Microbiol Lett* 2, 83–86 (1977)
3. Kopyov, C. N., Ruppia, R. & Stamer, R. Y. *Arch Microbiol* 83, 216–236 (1972)
4. Pearson, H. W. & Tomlinson, D. L. in *Proc. Second Int. Symp. Photosynthetic Prokaryotes* (eds Codd, G. A. & Stewart, W. D. P.) 161–163 (University of Dundee, 1976)
5. Rogers, A. C. *Nature* 284, 563–564 (1980)
6. Fay, P. & Kuleshova, S. A. *Br. J. Appl. Phys.* 24, 51–57 (1973)
7. Howley, R. & Pearson, H. W. *FEMS Microbiol Lett* 6, 287–292 (1979)
8. Nagatani, H. N. & Hasekura, R. *J. Bact* 134, 597–605 (1978)
9. Womers, N. M. & Benemann, J. R. *J. Bact* 119, 258–265 (1974)
10. Khoja, T. M. & Whittow, B. A. *Br. J. Appl. Phys.* 18, 139–148 (1975)
11. Stewart, W. D. P. & Pearson, H. W. *Proc. R. Soc., Lond.* B178, 293–311 (1970)
12. Truper, H. G. & Schögel, H. G. *Auton. o. Lebensw.* 30, 225–238 (1964)

## The robustness of natural systems

Alan Roberts\* & Ken Tregonning†

\*Physics Department, Monash University, Clayton, Victoria 3168, Australia

†Research Branch, Forests Commission, 1 MacArthur Place, Melbourne, Victoria 3000, Australia

Although the relation between complexity and stability in natural systems has been widely investigated<sup>1</sup>, a number of other basic questions remain largely unstudied. For example: can we find fundamental properties which identify a persistent natural system? Are these properties due to the process by which such a system emerges? Is this process—natural selection—also responsible for that robustness which is so generally superior to that of an artificial system? This peculiar robustness of a natural system can show itself in a wide variety of ways; the resistance to shock and efficient nutrient conservation of a climax community<sup>2</sup>, for example, or the physical stability of proteinoid microparticles<sup>3</sup>. Can we find other system properties which help to explain this robustness—properties which transcend the particular type of system under consideration? Such a 'universal' set of requirements is indeed suggested by the results reported here. In the model studied, the survivor systems turn out to be composed, at every subsystem level, of subsystems each of which is independently viable. These viable subsystems are nested, overlapping, strongly connected and extraordinarily numerous, implying a 'defence in depth' for the main system against major collapse. Some important conclusions can be made about these model systems: first, an artificial system comparable in its size and complexity could hardly have this robust structure built into it; second, if grossly damaged, a natural system will usually be reduced to one of its viable subsystems. The components eliminated could, of course, include ones vital to human interests. Full restoration of the damage would not generally be practicable.

We have not followed the procedure usually applied to examining related questions, which has focused on the system's stability. This mathematical concept assumes that an attainable equilibrium is already present, and examines how the system reacts to subsequent departures from it, but clearly one should first look for factors which determine whether an equilibrium will be attained at all. (This is obviously true when local equilibrium about an equilibrium point is studied, but also applies to more complicated cases such as limit cycle behaviour, where a stable cycle loop cannot exist unless an attainable equilibrium point lies within it.) This is all the more advisable because, in a whole range of important cases, the existence of an attainable equilibrium effectively guarantees stability anyway<sup>4</sup>.

Here, then, we look for properties which distinguish a system with an attainable equilibrium. More specifically, we consider interacting variables  $N_1, N_2, \dots$ , varying with time, which can take only positive values. (Examples may include the 'populations' of animal, plant or chemical species, measured in numbers of individuals or (bio)mass.) Thus a set of mathematically possible equilibrium values  $N_1^*, N_2^*, \dots$  can be attained

only if they are 'feasible'—that is, all  $N_i^* > 0$  (ref. 5). Terms used here are 'species', 'populations' and 'feasible' equilibria.

This approach has a further substantial advantage: the model examined can be a very general one, so that any findings are widely applicable and far less dependent on the minutiae of a particular model specification. We write

$$dN_i/dt = f_i(N_i) [r_i + A_i(N_1, N_2, \dots, N_M)], \quad i = 1 \text{ to } M \quad (1)$$

Here the functions  $A_i$  describe the interactions between and within species; we will see that their form can be left almost completely open. The functions  $f_i$  are likewise left unspecified; they describe the species' reproductive (or decay) behaviour, as do the constants  $r_i$ . We require, however, that  $f_i(0) = 0$ , to exclude spontaneous creation.

In many types of system there are mechanisms by which the species can 'adapt' to each other, so that, over a long enough period of coexistence, the interactions take on a systematic character. However, because it is precisely the conditions for this initial coexistence which interest us, we exclude this possibility by requiring the species to interact randomly. We also exclude any species which, if left in isolation, would increase without limit, by requiring all species to be self-regulated.

The randomness of interaction will generally result in the disintegration of the assemblage as time goes on, with one or more species dying out. When  $M$  is large, only a small fraction of the solutions will survive intact, corresponding to rare configurations of the  $A_i$ . The nature of this survival can be mathematically various (local stability about  $N^*$ , limit cycle, strange attractor—see ref. 1, Ch. 2), and can generally be unravelled only if the  $A_i$  are fully known. However, for its survival to be possible, a system must first have a feasible equilibrium point. Thus, by studying the assemblages described by feasible solutions of equation (1), we are studying all possible candidates for survival as a persistent system.

Because we use numerical methods, definite probability distributions must be chosen. We first rewrite equation (1) formally as

$$dN_i/dt = f_i(N_i) \left[ r_i + \sum_{j=1}^M A_{ij}^* N_j \right] \quad (2)$$

Here the  $A_{ij}^*$  are partial derivatives, and only mild restrictions need be imposed on the interactions  $A_i$  to justify rewriting in this form. (All first partial derivatives must be continuous; the first mean value theorem then gives equation (2), the derivatives being evaluated at a point which depends on the specific form of  $A_i$  but not on  $j$ .)

We now express the randomness of interaction by choosing

$$A_{ij}^* = \pm g (i \neq j), \quad r_i = \pm 1 \quad (3)$$

Here  $g$  is a constant measuring interaction strength; all variates are independent and + or – with equal probability. For self-regulation, we use  $A_{ii}^* = -1$ , all  $i$ .

In our computer studies, we started with a feasible solution for  $M = 25$  variables, generated by the method of 'natural-selective elimination' (ref. 6). We then examined the structure of this solution, proceeding as follows: we selected  $q$  different species at random and eliminated them from the system; the resulting subsystem of  $m = 25 - q$  species was then tested for feasibility. For a given value of  $m$ , 20 such subsystems were sampled (with replacement). This procedure was repeated for all subsystem orders from  $m = 24$  to  $m = 1$ . In all, 100 systems of 25 species each were treated in this way, so that 2,000 subsystems of each order were examined. The value of  $g$  chosen was 0.16, corresponding to a May parameter<sup>7</sup>  $\gamma = (M-1)^{1/2}g = 0.8$  in the 25-species system under study. The number of species with  $r_i < 0$  was 2–11, with a mean of 5.33.

The results are summarized in Table 1. Line *a* shows the mean percentage of  $m$ -species subsystems found to be feasible, for  $m = 1$ –24. (The s.e.m., as estimated from the sample variance, did not exceed 2%.) To appreciate how significantly large these percentages are, they should be compared with those in line *b*. These were derived from a control group of 100 initially



**Table 1** Analysis of the feasibility structure of feasible and unfeasible solutions to equations (2) and (3)

| Subsystem order<br>(no. of species) | 24 | 23 | 22 | 21 | 20 | 19 | 18 | 17 | 16 | 15 | 14 | 13 | 12  | 11 | 10 | 9   | 8   | 7  | 6  | 5  | 4  | 3  | 2  | 1  |
|-------------------------------------|----|----|----|----|----|----|----|----|----|----|----|----|-----|----|----|-----|-----|----|----|----|----|----|----|----|
| Mean % feasible:                    |    |    |    |    |    |    |    |    |    |    |    |    |     |    |    |     |     |    |    |    |    |    |    |    |
| a, In initially feasible system     | 51 | 31 | 21 | 15 | 11 | 9  | 8  | 8  | 6  | 7  | 7  | 7  | 9   | 9  | 9  | 12  | 15  | 19 | 22 | 29 | 39 | 46 | 61 | 80 |
| b, In initially unfeasible system   | 0  | 0  | 0  | 0  | 0  | 0  | 0  | 0  | 0  | 0  | 0  | 0  | 0.1 | 0  | 0  | 0.2 | 0.4 | 1  | 2  | 4  | 6  | 13 | 26 | 51 |

a Analyses the feasibility structure of 100 feasible solutions and b that of unfeasible solutions to equations (2) and (3), with scaled interaction strength  $\gamma = 0.8$  ( $g = 0.16$ ). A zero entry means that no feasible subsystem was found among the 2,000 tested.

unfeasible solutions ('non-survivors'), processed in exactly the same way. Even for  $m = 16$ , where the percentage feasible is least (6%), of the 2,000 subsystems examined, 122 were feasible, compared with the control group figure of zero.

To consider what these results mean, we should relate them to existing concepts of complex-system structure. Here, looking at the quantitative features of a definite model, we can confirm and significantly develop some of these mainly qualitative ideas. The concept is familiar, for example, of a persistent system built up from subsystem components which are themselves persistent. Thus the above results may be viewed as a concrete realization of, for example, Simon's 'Chinese box' picture<sup>8</sup>; but in further and important respects, it differs strikingly from all the previous realizations known to us.

The 'nesting' of subsystems is usually seen as achieved by linking them 'externally' to each other, so that  $k$  subsystems, each of order  $m$ , form a system of order  $km$ . Such an arrangement relates well to the needs of control theory, where an externally imposed negative feedback can stabilize each subsystem, and the links between subsystems can be made deliberately weak to preserve overall stability (see for example ref. 9, Ch. 1, 2). This concept seems particularly well adapted to subsystems which are 'mechanical', both in the everyday sense as well as Bertalanffy's more general one<sup>10</sup>.

However, the subsystems in the model above cannot be seen as just 'externally' linked in this way. On the contrary, the feasible subsystems of a given order overlap each other to an extraordinary degree. If we look once again at the least feasible case ( $m = 16$ ), we easily calculate that each 25-species system contains, on average, over 120,000 feasible subsystems of order 16; a pair of these subsystems have, on average, over 10 species in common. Another striking comparison is provided by the feasible 5-species subsystems: the most economical Chinese box packing would need just five of these—the average above is over 15,000.

This overlapping suggests what might be termed a 'third level' on which to characterize a complex system. On the first level, we specify the single-species properties (intrinsic increase rate, and self-regulation parameter ( $s$ )) and on the second level, the pair interactions. The third level concerns the details of 'persistence structure', that is, the nesting and degree of overlap of component subsystems which are themselves viable. Such a characterization would be possible, and perhaps of some use, even when first- and second-level knowledge was deficient or altogether absent (as in catastrophe theory).

A further novelty in this model should be stressed—the strength of interaction involved. When the links between subsystems are external, stability is easiest to assure by keeping the interaction strength down to values within the 'weakly interacting' region. In our case, this corresponds to  $\gamma < [M - 1]^{-1} = 0.04$ . (The system is then biased towards stability by the Gersgorin criterion<sup>11</sup>.)

The value used above is 20 times greater ( $\gamma = 0.8$ ), therefore we are well into the 'significant' region. It is only here (Ashby's 'richly joined' case<sup>12</sup>) that system properties are primarily determined by the interactions; in the weaker regime, the behaviour of the isolated components is only weakly modified by the interactions.

These considerations suggest, then, that the nested, overlapping structure found in the model may be generally required if a truly autonomous ('natural') system is to persist in time, when

the interactions are numerous and strong enough to produce fully developed system behaviour. The robustness of such a structure, and the formidable difficulties in trying to reproduce it artificially (whether *ab initio* or after damage) when no control level is present, are apparent.

Received 23 April; accepted 7 October 1980.

1. May, R. M. *Stability and Complexity in Model Ecosystems* (Princeton University Press, 1973).
2. Odum, E. P. *Fundamentals of Ecology* (Saunders, Philadelphia, 1971).
3. Fox, S. W., & Dose, K. *Molecular Evolution and the Origin of Life* (Freeman, San Francisco, 1972).
4. Tregonning, K. thesis, Monash Univ. (1979).
5. Roberts, A. *Nature* **251**, 607 (1974).
6. Tregonning, K. & Roberts, A. *Nature* **281**, 563–564 (1979).
7. May, R. M. *Nature* **238**, 413–414 (1972).
8. Simon, H. A. in *Hierarchy Theory* (Braziller, New York, 1973).
9. Siljak, D. D. *Large-scale Dynamic Systems* (North-Holland, New York, 1978).
10. von Bertalanffy, L. *General System Theory* (Braziller, New York, 1969).
11. Marcus, M. & Minc, H. *A Survey of Matrix Theory and Matrix Inequalities* (Allyn & Bacon, Boston, 1964).
12. Ashby, W. R. *Design for a Brain* (Wiley, New York, 1960).

## Why are fetal muscles slow?

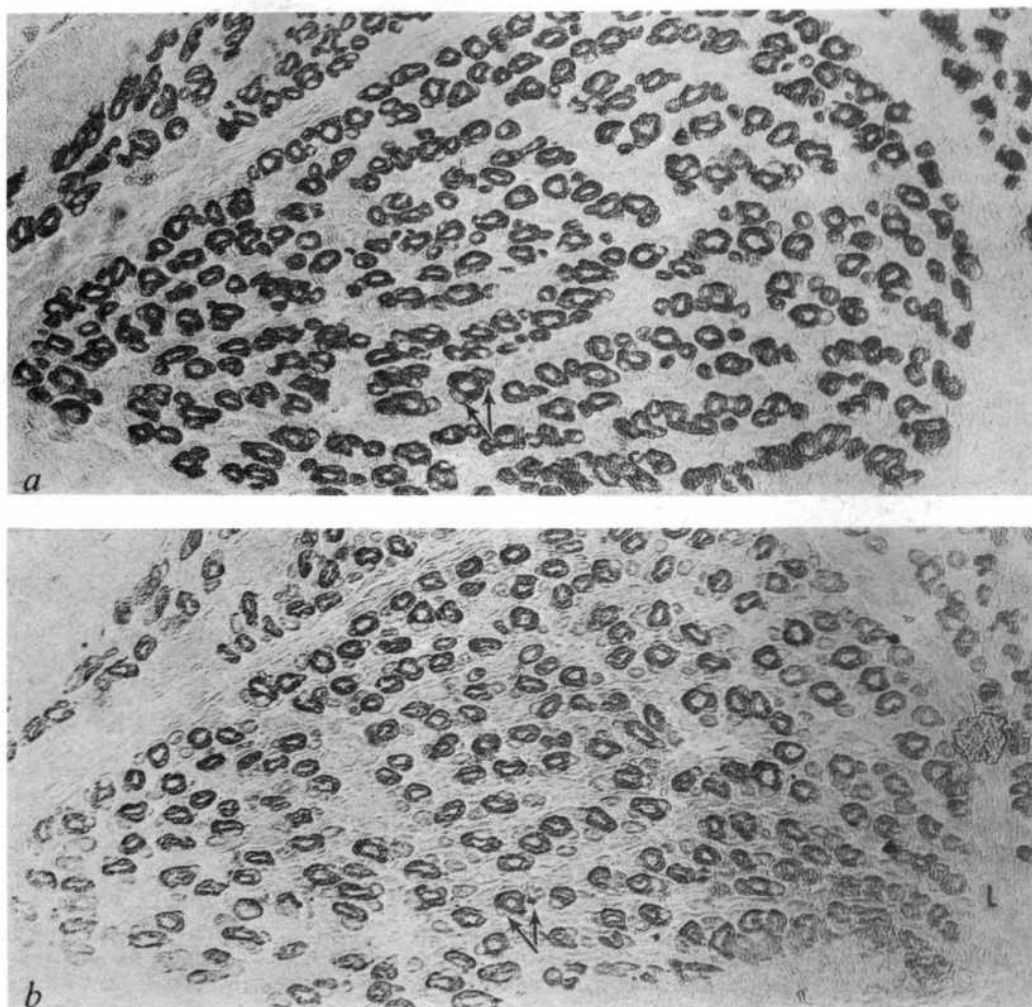
A. M. Kelly & N. A. Rubinstein

Departments of Pathobiology, School of Veterinary Medicine and of Anatomy, School of Medicine, University of Pennsylvania, Philadelphia, Pennsylvania 19174

**Differentiating fast and slow mammalian muscles contract slowly at birth and increase their speed during the first few weeks of life<sup>1,2</sup>. However, only small proportions of slow myosin light chains are found in early developing muscles and the fast type of light chains predominate<sup>3–7</sup>. In addition, differentiating muscle contains unique, embryonic forms of myosin which may partially determine the early slow responses<sup>8–15</sup>. The present study suggests additional reasons for these slow twitch times. Most skeletal muscles are initially formed from a small population of primary generation cells<sup>16,17</sup> which are innervated by pioneering axons early in myogenesis<sup>18</sup>. Subsequently, numerous secondary generation cells develop along the walls of primary myotubes, then separate and become independent units of contraction. Using affinity-purified antibodies to fast and slow myosin<sup>5</sup>, it was found that most primary myotubes react with anti-slow myosin and are destined to become slow, Type I fibres. By contrast, secondary generation cells stain exclusively with anti-fast myosin and develop into Type II, fast fibres. We propose that primary myotubes constitute the fundamental motor units of the developing neuromuscular system and are responsible for early slow movements. Secondary generation cells become organized into large, fast motor units later in development, eclipsing the original slow response.**

Serial, frozen sections were prepared from the extensor digitorum longus (EDL) and soleus muscle of fetal, neonatal and adult rats. At 16 days gestation primordia of the EDL and soleus stain with anti-fast myosin and the reaction with anti-slow is equivocal. Specification into fibre types in the EDL occurs between 17 and 18 days<sup>19,20</sup>. This muscle is then composed of

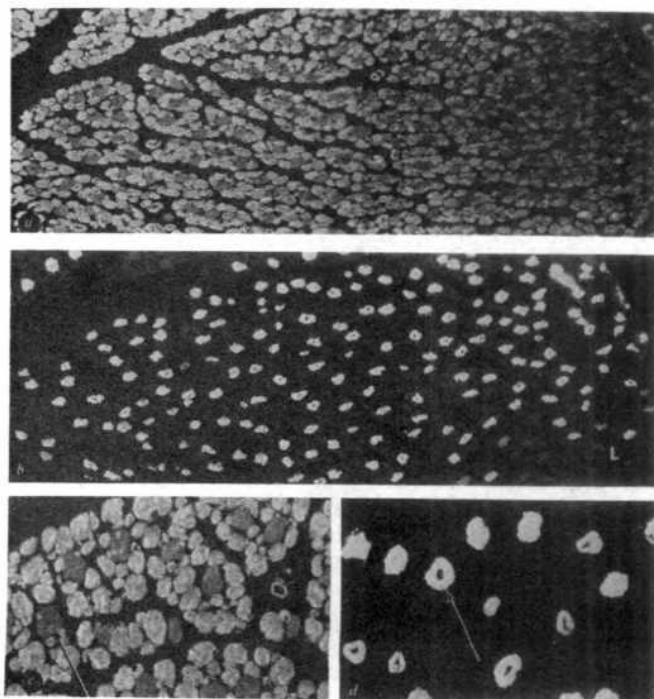
**Fig. 1** Serial sections of the EDL from an 18-day fetus stained by the indirect peroxidase anti-peroxidase method<sup>20</sup> with anti-fast myosin (*a*) and anti-slow myosin (*b*). The muscle primordium is mainly composed of large primary myotubes most of which stain with both anti-fast and anti-slow myosin. There are a few secondary generation cells attached to the walls of primary myotubes. All of these react strongly with anti-fast and weakly, if at all, with anti-slow myosin (arrows). The large myotubes containing anti-slow myosin are least numerous on the lateral side of the muscle (L). They are interpreted as components of fundamental motor units in the evolving neuromuscular system.  $\times 210$ .



150 to 200 large, primary myotubes most of which stain intensely with both anti-fast and anti-slow myosin (Fig. 1). There are numerous, less differentiated, secondary generation cells clustered around the walls of the primary myotubes, which stain intensely with anti-fast and weakly, if at all, with anti-slow myosin.

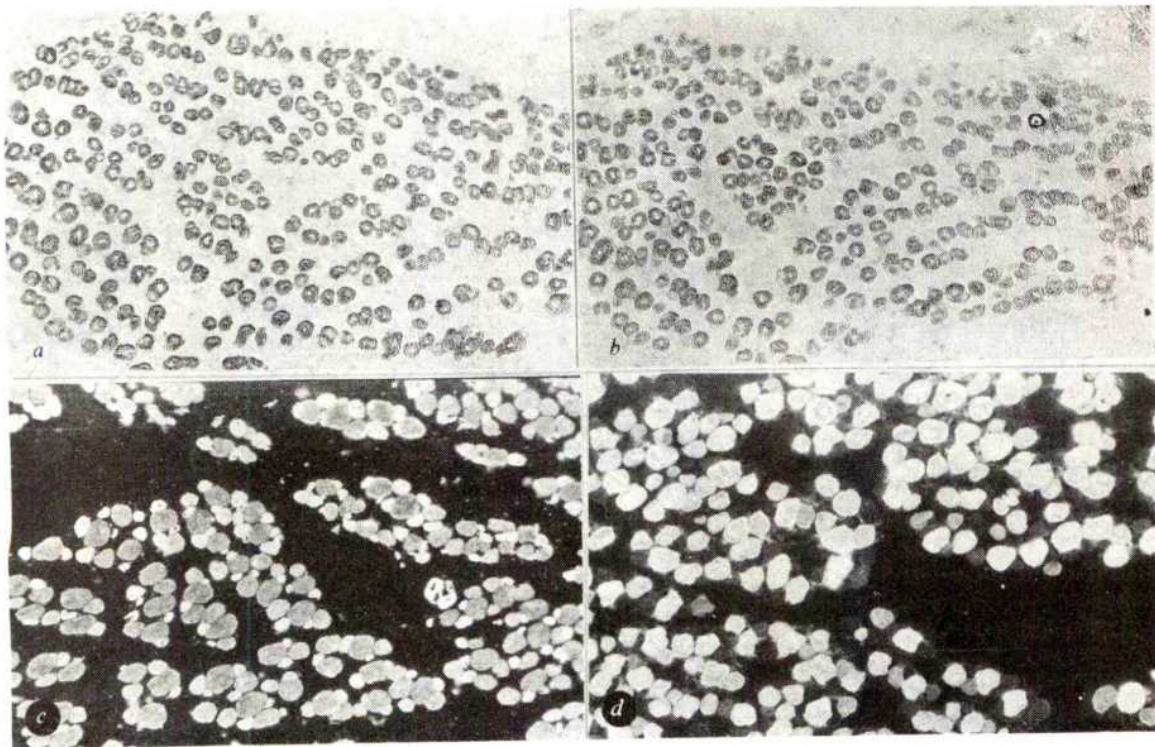
At 2 days post partum, comparable numbers of large fibres in the EDL stain with both anti-myosins (Fig. 2), but they are now widely separated by intervening fibres which stain only with anti-fast myosin. We interpret fibres staining with both anti-myosins as the primary generation cells, within which reactivity to anti-slow myosin is intense whereas the response with anti-fast is weak. This suggests that slow myosin is starting to dominate these cells and they are differentiating into Type I fibres (Fig. 2*b, c*). Studies of the adult EDL stained with anti-myosins and myofibrillar ATPase support this—there are approximately 200 Type I fibres amongst a total population of about 4,000 (ref. 21). Other fibres, which number at least 2,000 by 2 days, stain with anti-fast and not with anti-slow myosin. These correspond to the secondary generation cells which have now separated from primary cells and become independent

units of contraction. We interpret them as the precursors of Type II fibres. This pattern of assembly results in primary and secondary generation cells which are intermingled in a mosaic reminiscent of the checkerboard distribution of histochemically distinct fibres in adult muscle<sup>22,23</sup>.



**Fig. 2** Serial sections of the EDL at 2 days post partum stained by direct fluorescence with anti-fast myosin (*a, c*) and anti-slow myosin (*b, d*). Almost all fibres stain intensely with anti-fast myosin. There are a few, widely distributed fibres which stain weakly with anti-fast myosin (arrows, *c*). This selected population stains intensely with anti-slow myosin (arrows, *d*). These fibres are least numerous on the lateral side of the muscle (L) and correspond in distribution to the primary myotubes of the fetal EDL. They are interpreted as developing Type I fibres. Fibres staining only with anti-fast myosin are interpreted as secondary generation differentiating into Type II fibres. *a, b*  $\times 75$ ; *c, d*  $\times 140$ .





**Fig. 3** Serial sections of the 18-day fetal soleus stained by the indirect peroxidase, anti-peroxidase method with anti-fast myosin (a) and anti-slow myosin (b). All fibres stain with both antibodies. There are very few secondary generation cells. At 2 days post partum (c, d, direct fluorescence) the intensity of staining with anti-fast myosin of large primary fibres has decreased but is intense with anti-slow myosin (d). In addition, there are now secondary generation cells developing along the walls of primary fibres all of which stain with anti-fast and not with anti-slow myosin. a, b  $\times 170$ , c, d  $\times 190$ .

Previous studies imply a close dependence of slow myosin synthesis on stimulation by the nervous system<sup>6,24,25</sup>. In the 18-day EDL, primary myotubes are innervated and contain differentiating endplates<sup>20</sup>. The appearance of slow myosin within these cells thus correlates with the development of neuromuscular relations. In addition, reflex hind limb movements develop in the fetus at approximately the same stage of gestation<sup>26-28</sup>, implying that motor unit activity is evolving. Hence we interpret the development of slow myosin within most primary myotubes as the reflection of a fundamental neuromuscular organization. In view of the muscle architecture, movements of the EDL at 18 days must be predominantly generated by primary myotubes containing significant proportions of slow myosin, which may be one reason why early contractions of the EDL are slow.

Secondary generation cells seem not to be separately innervated when in contact with primary myotubes<sup>6,29,30</sup>. Many do not extend the entire length of the muscle<sup>16,31</sup> but are attached to the primary cells by various forms of membrane junction. It is therefore doubtful that they can contract and relax independently. As the muscle matures, they gain independence<sup>16,31</sup> and a separate nerve supply<sup>32</sup>. We propose that they are then added as developing fast motor units to the contractile machinery and as this occurs, they prevail over the early slow response and the muscle increases its speed of contraction.

Differentiation of the soleus follows the same pattern but the temporal sequence and ratio of primary to secondary fibres is different. Using our antibodies the 18-day fetal soleus is the only primordium amongst leg muscles in which almost all fibres stain uniformly with both anti-fast and anti-slow myosins (Fig. 3). In this muscle the results are consistent with those of Gauthier *et al.*<sup>33</sup>. One reason for the uniformity of staining is that this primitive soleus is composed of myotubes which are small and have little variation in size. We interpret these as the primary myotubes of the soleus and there is little evidence of secondary orders of cells as in the EDL at this stage. Thus the soleus seems less developed than the EDL at 18 days.

Development of secondary generation fibres is evident in the soleus at 2 days post partum where their strong reactivity with anti-fast myosin contrasts with the less intense response of the larger primary generation fibres (Fig. 3c, d). As in the EDL, these secondary generation cells do not stain with anti-slow myosin whereas staining of primary fibres is intense. Slow myosin thus is the dominant species in the primary generation cells, which seem to be progressing towards Type I differentiation. Secondary generation cells are progressing towards Type II differentiation. They are as numerous as primary cells in the soleus at 2 days. Significantly, using myofibrillar ATPase stains, there are equal numbers of Types I and II fibres at 15 days post partum<sup>6</sup>.

These findings suggest that initial movements of the soleus, as in the EDL, result from contraction of primary fibres. They contain abundant slow myosin and slow rates of contraction may be anticipated. After birth, secondary generation, fast fibres appear and, once independent, these cells become separately innervated and are added as fast motor units to the original slow response. This may explain why the twitch time course of the soleus is initially slow and then becomes faster in the first few weeks of life. The work of Kugelberg<sup>34</sup> showing the transitions of whole motor units from fast to slow in the maturing animal accounts for the final slowing of the muscle.

This study was supported by NIH grants HL 15835 to the Pennsylvania Muscle Institute, NS 14332, BRSG 5 207, RR5464 and by a grant from the Muscular Dystrophy Association of America. We thank Dr Gerta Vrbova for first suggesting the interpretation of our fluorescence micrographs in terms of developing motor units.

Received 2 July; accepted 18 September 1980.

1. Buller, A. J., Eccles, J. & Eccles, R. J. *Physiol., Lond.* **150**, 399-416 (1960).
2. Close, R. J. *Physiol., Lond.* **173**, 74-95 (1964).
3. Sréter, F., Holtzer, S., Gergely, J. & Holtzer, H. *J. Cell Biol.* **55**, 586-594 (1972).
4. Pelloni-Mueller, G., Ermini, M. & Jenny, E. *FEBS Lett.* **67**, 68-74 (1976).
5. Rubinstein, N., Pepe, F. & Holtzer, H. *Proc. natn. Acad. Sci. U.S.A.* **74**, 4524-4527 (1977).
6. Rubinstein, N. & Kelly, A. *Dev. Biol.* **62**, 473-485 (1978).
7. Sirovy, J. & Gutmann, E. *Pflügers Arch. ges. Physiol.* **369**, 85-89 (1977).
8. Trayer, I. P., Harris, C. I. & Perry, S. V. *Nature* **217**, 452-453 (1968).
9. Huszar, G. *Nature new Biol.* **240**, 260-264 (1972).



10. Sréter, F., Balint, M. & Gergely, J. *Dev Biol.* **46**, 317–325 (1975).
11. Whalen, R., Butler-Browne, G. & Gros, F. *J. molec. Biol.* **126**, 415–431 (1978).
12. Whalen, R., Butler-Browne, G., Sell, S. & Gros, F. *Biochemie* **61**, 625–632 (1979).
13. Whalen, R., Schwartz, K., Bouveret, P., Sell, S. & Gros, F. *Proc. natn. Acad. Sci. U.S.A.* **76**, 5197–5201 (1979).
14. Hoh, J. & Yeoh, A. P. S. *Nature* **280**, 321–323 (1979).
15. Rushbrook, J. & Stracher, A. *Proc. natn. Acad. Sci. U.S.A.* **76**, 4331–4334 (1979).
16. Kelly, A. & Zacks, S. *J. Cell Biol.* **42**, 135–153 (1969).
17. Church, J. J. *Anat.* **105**, 419–438 (1969).
18. Bennett, M. & Pettigrew, A. J. *Physiol., Lond.* **241**, 515–545 (1974).
19. Rowleron, A. J. *Physiol., Lond.* **301**, 19 (1980).
20. Rubinstein, N. & Kelly, A. *J. Cell Biol.* (in the press).
21. Carlson, B. & Gutmann, E. *Expl Neurol.* **58**, 82–93 (1976).
22. Ashmore, C., Robinson, D., Rattray, P. & Doerr, L. *Expl Neurol.* **37**, 241–255 (1972).
23. Kelly, A. & Schotland, D. in *Muscle Development and the Muscle Spindle* (ed. Banker) (Excerpta Medica, Amsterdam, 1972).
24. Salmons, S. & Sréter, F. *Nature* **263**, 30–34 (1976).
25. Salmons, S. & Vrbova, G. *J. Physiol., Lond.* **210**, 535–549 (1969).
26. East, E. *Anat. Rec.* **50**, 201–212 (1931).
27. Strauss, S. & Weddell, G. *J. Neurophysiol.* **3**, 358–369 (1940).
28. Windle, W., Minear, W., Austin, M. & Orr, D. *Physiol. Zool.* **8**, 156–185 (1935).
29. Kelly, A. & Zacks, S. *J. Cell Biol.* **42**, 154–169 (1969).
30. Kikuchi, T. & Ashmore, C. *Cell Tissue Res.* **171**, 233–251 (1977).
31. Ontell, M. *Anat. Rec.* **189**, 669–690 (1977).
32. Betz, W., Caldwell, J. & Ribchester, R. *J. Physiol., Lond.* **297**, 463–478 (1979).
33. Gauthier, G., Lowey, S. & Hobbs, A. *Nature* **274**, 125–129 (1978).
34. Kugelberg, E. *J. Neurol. Sci.* **27**, 269–289 (1976).

## Anti-inflammatory steroids reduce tissue PG synthetase activity and enhance PG breakdown

P. K. Moore\* & J. R. S. Hoult

Department of Pharmacology, King's College, Strand, London WC2R 2LS, UK

Anti-inflammatory steroids reduce prostaglandin (PG) synthesis in intact cells and isolated organs<sup>1–9</sup> by interfering indirectly with the phospholipase(s) which release the polyunsaturated fatty acid precursors for both cyclooxygenase and lipoxygenase pathways. This action requires nucleic acid transcription and synthesis of new protein,<sup>10–12</sup> and a soluble factor capable of inhibiting PG generation has been identified<sup>11,13</sup>. However, it is not known whether these steroids affect either the actions or content of the enzymes of the PG system after administration *in vivo*, nor is it known if they affect PG-metabolizing enzymes. We show here that treatment of rats with anti-inflammatory steroids causes rapid changes in tissue activities of enzymes which synthesize and inactivate PGs, with apparent levels reduced and increased respectively.

Tissue activities of enzymes which synthesize and break down PGs were assayed by preparing homogenates of organs taken from animals pretreated with anti-inflammatory steroids or with vehicle alone. PG synthetase activity was generally measured by assaying the conversion of arachidonic acid to bioassayable PG-like material in freshly prepared 100,000g microsomal preparations<sup>14,15</sup>, whereas that of the PG-metabolizing enzymes (here called 'prostaglandinases') was assayed by a radiochemical method using the 100,000g cytosolic supernatants and radiolabelled PGF<sub>2α</sub> as substrate<sup>14,15</sup>.

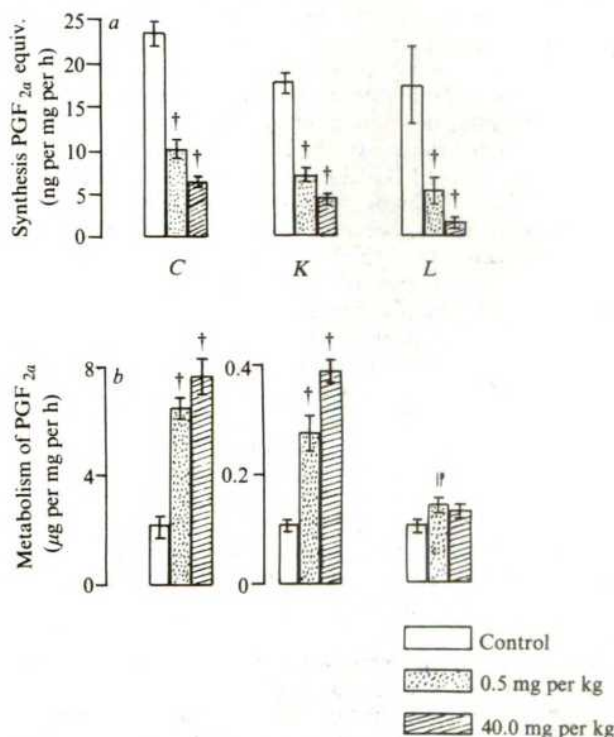
Treatment of rats with prednisolone, 0.5 and 40.0 mg per kg, for 10 days produced a dose-related decrease in activity of microsomal PG synthetase in caecum, kidney and lung; by contrast, the activities of prostaglandinase in these organs were increased (Fig. 1). An experiment investigating the time course of these reciprocal changes in the PG system showed that they occurred within 48 h, that is, after two subcutaneous injections of prednisolone, in caecum and kidney (Table 1) as well as in stomach (not shown).

Further experiments using prednisolone at 0.5, 5.0 and 40.0 mg per kg (given for 2 days only) also elicited dose-related decreases in apparent PG synthetase levels and increased prostaglandinase activity in stomach, caecum and kidney. The lowest

dose is similar to that recommended for a variety of clinical applications in man (10–100 mg per day)<sup>16</sup>. Several other anti-inflammatory steroids were tested at doses selected to reflect their established clinical potencies. As expected, these treatments caused a reduction in apparent microsomal PG synthetase activity, and in most cases also increased the prostaglandinase activity (Table 1). Correlations between anti-inflammatory potency and the anti-phospholipase actions of these steroids have been noted previously<sup>6,9</sup>.

Taken together, the results suggest that these pharmacological effects of the glucocorticoids on the enzymes of the PG system might be related to their anti-inflammatory properties. To test this idea we treated rats with cortisone, 17 $\alpha$ -methyltestosterone and tetrahydrocortisone (all at 20 mg per kg for 2 days), but they did not produce typical steroid-like reciprocal changes (Table 1). These therapeutically inactive compounds are closely related to hydrocortisone and may bind to glucocorticoid receptors, but are not agonists<sup>17</sup>. In most cases the treatments caused small changes in enzyme activities in the opposite direction (and represented in Table 1 as negative values), although in most cases the changes were not significant.

The simplest explanation for our findings is that the anti-inflammatory steroids modify cellular protein synthesis such that the amounts or levels of PG synthetase are decreased and those of PG-metabolizing enzymes increased. However,



**Fig. 1** Treatment of rats with prednisolone at 0.5 and 40.0 mg per kg for 10 days decreases activity (apparent level) in caecum (C), kidney (K) and lung (L) of microsomal PG synthetase (a), and increases activity of prostaglandin-metabolizing enzymes (b). Male Sprague-Dawley rats (five or six per group, 200 g) were injected with prednisolone sodium succinate or 0.2 ml vehicle (0.9% saline containing 0.5% CM-cellulose, 0.4% Tween 80 and 0.9% ethyl alcohol). Low-dose prednisolone animals appeared normal, but the growth and spleen size of rats treated with prednisolone 40 mg per kg were much reduced. However, histological examination of sections of stomach, lung and kidney did not reveal any differences between tissues from the three treatment groups. Organs were worked up individually as previously described<sup>14,15</sup> and assayed for PG metabolism (100,000 g supernatants incubated at 37 °C pH 7.5, with 5 mM NAD<sup>+</sup>, 0.05 μCi [<sup>3</sup>H]-PGF<sub>2α</sub> and 10 μg ml<sup>-1</sup> PGF<sub>2α</sub> and extracted for radio-TLC caecum 5 min, kidney 60 min and lung 90 min incubation), or PG synthesis (100,000g microsomes pooled and resuspended for 60 min incubation at 37 °C pH 7.5, with 10 μg ml<sup>-1</sup> arachidonic acid, 3 mM reduced glutathione and extracted for bioassay using PGF<sub>2α</sub> as reference standard). Results show means  $\pm$  s.e.m. for 6–12 determinations and are expressed in terms of protein content (not different between experimental groups for any single organ) using bovine serum albumin as standard. The significance of differences was evaluated using Student's *t*-test, and the key symbols are the same as those used in Table 1.

\* Present address: Department of Pharmacology, Chelsea College, Manresa Road, London SW3 3TW, UK.



**Table 1** Reciprocal changes in activity of enzymes of the prostaglandin system are induced *in vivo* within 2 days by anti-inflammatory steroids but not by their inactive analogues

| Steroid                         | Dose<br>(mg per kg) | Potency* | Duration of<br>treatment<br>(days) | % Reduction in tissue PG synthesis |              | % Enhancement of tissue prostaglandinase<br>activity |               |
|---------------------------------|---------------------|----------|------------------------------------|------------------------------------|--------------|--|---------------|
|                                 |                     |          |                                    | Caecum                             | Kidney       | Caecum   | Kidney        |
| Corticosterone                  | 20                  | 0.35     | 2                                  | 57.6 ± 6.8¶                        | 5.0 ± 13.7#  | 124.4 ± 33.3†  | -14.7 ± 19.8# |
| Triamcinolone                   | 5                   | 5        | 2                                  | 66.5 ± 5.4¶                        | 49.8 ± 10.6§ | 95.3 ± 38.1¶   | 67.3 ± 4.2†   |
| Dexamethasone                   | 1                   | 25       | 2                                  | 65.3 ± 4.3¶                        | 54.1 ± 9.3†  | 226.2 ± 19.2†  | -6.4 ± 24.8#  |
| Prednisolone                    | 5                   | 4        | 2                                  | 40.1 ± 4.6†                        | 46.0 ± 5.2†  | 292.9 ± 20.6†  | 222.1 ± 42.1† |
| Hydrocortisone                  | 20                  | 1        | 2                                  | 58.6 ± 2.4†                        | 57.5 ± 7.1†  | 228.4 ± 35.3†  | 185.7 ± 43.9‡ |
| Fludrocortisone                 | 1.25                | 10       | 2                                  | 67.9 ± 1.3‡                        | 67.9 ± 2.3‡  | 303.6 ± 55.8‡  | 170.3 ± 39.3‡ |
| Tetrahydrocortisone             | 20                  | 0        | 2                                  | -64.9 ± 45.5#                      | 42.2 ± 3.5‡  | -47.6 ± 4.7‡   | -22.7 ± 9.4#  |
| Cortexolone                     | 20                  | 0        | 2                                  | -49.1 ± 7.9‡                       | 23.2 ± 9.3#  | -13.7 ± 6.0#   | -19.8 ± 8.4#  |
| 17 $\alpha$ -Methyltestosterone | 20                  | ?        | 2                                  | -7.7 ± 20.3#                       | -6.6 ± 9.4#  | -26.8 ± 11.0¶  | -16.9 ± 8.6#  |
| Prednisolone                    | 40                  | 4        | 2                                  | 67.2 ± 4.2†                        | 51.4 ± 5.8†  | 89.0 ± 7.2†  | 49.9 ± 5.6†   |
| Prednisolone                    | 40                  | 4        | 4                                  | 66.6 ± 7.5†                        | 45.5 ± 14.9  | 39.6 ± 21.1#   | 52.4 ± 16.4   |
| Prednisolone                    | 40                  | 4        | 8                                  | 62.9 ± 5.2†                        | 41.2 ± 10.2§ | 32.9 ± 9.3§  | 88.5 ± 49.3#  |

Groups of three or four rats were injected daily for 2–8 days with steroids as indicated. Doses refer to base: the steroids (all Sigma) were in the form corticosterone 21-acetate, triamcinolone acetate, dexamethasone acetate, prednisolone sodium succinate, hydrocortisone 21-acetate, fludrocortisone acetate, tetrahydrocortisone, cortexolone (=11-deoxycortisol) and 17 $\alpha$ -methyltestosterone. Enzyme activities are expressed as per cent change relative to vehicle-injected control rats. Results show mean  $\pm$  s.e.m. for 4–10 determinations. Each block of results represents experiments with different batches of Sprague–Dawley rats.

\* Relative anti-inflammatory potency, hydrocortisone = 1 (from ref. 16).

†  $P < 0.001$ ; ‡  $P < 0.002$ ; §  $P < 0.01$ ; ||  $P < 0.02$ ; ¶  $P < 0.05$ ; # not significant relative to control treated rats, using Student's *t*-test.

alternative explanations are possible, and for this reason we refer to the changes in terms of 'activities' rather than 'levels'. It is recognized that many of the varied metabolic effects of glucocorticoids (and other steroid hormones) occur as a result of changes in the rates of synthesis of specific proteins<sup>18,19</sup>.

It is unlikely that the PG synthetase results can be accounted for by a redirection of PG endoperoxide breakdown away from PGE<sub>2</sub> and PGF<sub>2 $\alpha$</sub>  formation towards other non-spasmogenic prostanoid derivatives, because the reaction conditions (high substrate concentration, presence of reduced glutathione) favour the formation of the classical PGs (refs 20, 21). Furthermore, we obtained direct evidence from radiochemical experiments that the conversion of arachidonic acid to the various prostanoid products was reduced in freshly prepared homogenates of kidney, spleen and stomach prepared from rats treated for 2 days with prednisolone at 40 mg per kg. The overall percentage utilization of 0.5  $\mu$ g ml<sup>-1</sup> arachidonic acid (labelled with 0.4  $\mu$ Ci [1-<sup>14</sup>C]-arachidonic acid, Radiochemical Centre, specific activity 56.4 Ci mol<sup>-1</sup>, no cofactor added) in 10-min incubations decreased from 41.0  $\pm$  5.9 to 20.0  $\pm$  4.9 in kidney, from 56.9  $\pm$  5.3 to 10.9  $\pm$  0.4 in spleen and from 26.7  $\pm$  1.5 to 7.1  $\pm$  2.6 in stomach, results obtained using six control and three steroid-treated animals.

We have shown that the activity of PG-metabolizing enzymes is increased in steroid-treated rats and believe that this may reflect increased tissue levels of prostaglandin 15-hydroxy-dehydrogenase (PGDH, the first enzyme in the PG degradative pathway<sup>22</sup>). However, we cannot exclude the possibility that these changes can be partly explained by the presence in the supernatants of factor(s) which enhance PGDH activity (see accompanying paper<sup>23</sup>) rather than by increases in PGDH levels. Nevertheless, this factor cannot be the steroid itself: in the range 1  $\mu$ M to 1 mM, prednisolone (four tests each at four concentrations) did not affect PGF<sub>2 $\alpha$</sub>  breakdown in 60-min incubations of rat kidney 100,000g supernatant.

To confirm these findings, prostaglandinase activities in supernatants were also measured by bioassay of the rate of disappearance of 10  $\mu$ g ml<sup>-1</sup> PGE<sub>2</sub> and PGF<sub>2 $\alpha$</sub>  from incubations of kidney and caecum. PGE<sub>2</sub> metabolism was more rapid than that of PGF<sub>2 $\alpha$</sub> , consistent with the known affinities of these PGs for PGDH<sup>22</sup>. A plot of disappearance of PGF<sub>2 $\alpha$</sub>  activity against time in 100,000g supernatants of kidney prepared from rats pretreated for 2 days with prednisolone 40 mg per kg showed it to be accelerated (*t*<sub>1/2</sub> ~ 10 min compared with ~ 32 min in control kidney). Both PGE<sub>2</sub> and PGF<sub>2 $\alpha$</sub>  inactivation in caecum and kidney were enhanced in the steroid-treated rats.

Our results show that in the rat, pharmacological doses of anti-inflammatory steroids administered *in vivo* have a more pervasive 'anti-prostaglandin' effect than has previously been realised: they cause bidirectional enzymatic changes which may lead to reduced tissue PG synthesis and enhanced breakdown. We believe that the effects relate directly to their anti-inflammatory actions because PGs and related substances have predominantly pro-inflammatory properties<sup>24,25</sup>; however, this effect is likely to be only one among many which contribute to the powerful anti-inflammatory spectrum of these compounds (see refs 16, 26). Although we do not understand how the changes in enzyme activities are brought about, it is probable that they reflect altered tissue levels of the enzymes concerned; this in turn suggests dependence on changes in cellular protein synthesis in the manner described for the steroid-induced release of anti-phospholipase factor<sup>11,13</sup>.

We thank Dr J. E. Pike (Upjohn) for gifts of prostaglandins, the MRC and May & Baker Ltd for financial support and Dr J. G. Hoult and P. D. Brinck for assistance with histological studies.

Received 11 July; accepted 18 September 1980.

- Gryglewski, R. J., Panczenko, B., Korbut, R., Grodzinska, L. & Ocetkiewicz, A. *Prostaglandins* **10**, 343–355 (1975).
- Lewis, G. P. & Piper, P. J. *Nature* **254**, 308–311 (1975).
- Kantrowitz, F., Robinson, D. R., McGuire, M. B. & Levine, L. *Nature* **258**, 737–739 (1975).
- Tashjian, A. H., Voelkel, E. F., McDonough, J. & Levine, L. *Nature* **258**, 739–741 (1975).
- Floman, Y. & Zor, U. *Prostaglandins* **12**, 403–413 (1976).
- Nijkamp, F. P., Flower, R. J., Moncada, S. & Vane, J. R. *Nature* **263**, 479–482 (1976).
- Hong, S.-C. L. & Levine, L. *Proc. natn. Acad. Sci. U.S.A.* **73**, 1730–1734 (1976).
- Blackwell, G. J., Flower, R. J., Nijkamp, F. P. & Vane, J. R. *Br. J. Pharmac.* **62**, 79–89 (1978).
- Tam, S., Hong, S.-C. L. & Levine, L. *J. Pharmac. exp. Ther.* **203**, 162–168 (1977).
- Danon, A. & Assouline, G. *Nature* **273**, 552–554 (1978).
- Flower, R. J. & Blackwell, G. J. *Nature* **278**, 456–459 (1979).
- di Rosa, M. & Persico, P. *Br. J. Pharmac.* **66**, 161–163 (1979).
- Carnuccio, R., di Rosa, M. & Persico, P. *Br. J. Pharmac.* **68**, 14–16 (1980).
- Hoult, J. R. S. & Moore, P. K. *Br. J. Pharmac.* **68**, 719–730 (1980).
- Hoult, J. R. S. & Moore, P. K. *Clin. Sci.* **59**, 63–66 (1980).
- Haynes, R. C. Jr & Lerner, J. in *The Pharmacological Basis of Therapeutics* 5th edn (eds Goodman, L. S. & Gilman, A.) 1472–1506 (Macmillan, New York, 1975).
- Samuels, H. H. & Tomkins, G. M. *J. molec. Biol.* **52**, 57–74 (1970).
- Baxter, J. D. & Forsham, P. A. *Am. J. Med.* **53**, 573–589 (1972).
- Thompson, E. B. & Lippmann, M. E. *Metabolism* **23**, 159–202 (1974).
- Chan, J. A., Nagasawa, M., Takeguchi, C. & Sih, C. J. *Biochemistry* **14**, 2987–2991 (1975).
- Cottee, F., Flower, R. J., Moncada, S., Salmon, J. A. & Vane, J. R. *Prostaglandins* **14**, 413–423 (1977).
- Hansen, H. S. *Prostaglandins* **12**, 647–679 (1976).
- Moore, P. K. & Hoult, J. R. S. *Nature* **288**, 271–273 (1980).
- Ferreira, S. H. & Vane, J. R. A. *Rev. Pharmac.* **14**, 57–73 (1974).
- Bonta, I. L. & Parnham, M. J. *Biochem. Pharmac.* **27**, 1611–1623 (1978).
- Parrillo, J. E. & Fauci, A. S. A. *Rev. Pharmac. Tox.* **19**, 179–201 (1979).

## Pathophysiological states modify levels in rat plasma of factors which inhibit synthesis and enhance breakdown of PG

P. K. Moore\* & J. R. S. Hoult

Department of Pharmacology, King's College, Strand, London WC2R 2LS, UK

We have shown recently that adaptive changes in the apparent amount of enzymes which synthesize and inactivate prostaglandins (PGs) occur in a reciprocal manner (see accompanying paper<sup>1</sup> and refs 2–4). For example, PG synthetase activity in several rat organs is reduced but that of PG-metabolizing enzymes ('prostaglandinases') is increased after treatment with anti-inflammatory steroids<sup>1</sup>. In view of recent reports that the synthesis of PG-like substances may be influenced by plasma factors<sup>5–7</sup>, we wondered whether our findings may be explained in whole or in part by the presence in varying amounts of substances which affect PG synthesis and inactivation in opposite directions. We show here that rat plasma contains a protein factor(s) which inhibits the synthesis of PGs and enhances their enzymatic breakdown *in vitro* and which we provisionally call prostaglandin 'reciprocal coupling factor' (RCF). Furthermore, RCF is rapidly released in response to anti-inflammatory steroids and its levels are altered in the two model pathophysiological states so far investigated.

The effects of plasma from male rats were tested in standardized assays of PG synthesis (in seminal vesicle microsomal preparations) and inactivation (using rat caecum 100,000g supernatants) as described in Fig. 1 legend. In both assays plasma was generally tested at final concentrations (v/v) of 0.5, 5.0 and 10.0%.

Low concentrations of rat plasma caused dose-related inhibition of PG synthesis in bovine seminal vesicle microsomes (Fig. 1a) and enhanced the enzymatic inactivation of PGF<sub>2α</sub> in rat caecum supernatants (Fig. 1b). We suggest the provisional term prostaglandin 'reciprocal coupling factor' to designate the

plasma component(s) responsible for these effects. The dose-response curves obtained at the three concentrations tested were usually not linear (with characteristic upward inflections in 25 out of 34 synthesis-inhibition curves and in 29 of 30 metabolism-activation curves), suggesting that the observed effects might be caused by more than one plasma component.

Rat plasma at 5% (v/v) also inhibited the synthesis of bioassayable PG-like material in microsomal systems from four other species (see Fig. 1 legend). That the synthesis inhibition is not due to redirection of endoperoxide breakdown towards other products which cannot be detected by the bioassay (for example, the stable metabolites of prostacyclin or thromboxane A<sub>2</sub>) was shown by incubating bovine seminal vesicle microsomes with radio-labelled arachidonic acid. In the presence of 0.5–10% plasma there was a progressive reduction in the utilization of arachidonic acid and in the amounts of each of the prostanoate products formed. The experiments did not distinguish whether inhibition of synthesis is due to depletion of substrate by binding (perhaps to albumin, as demonstrated previously<sup>8–10</sup>), or to a specific inhibitory effect on the cyclooxygenase component of prostaglandin synthetase.

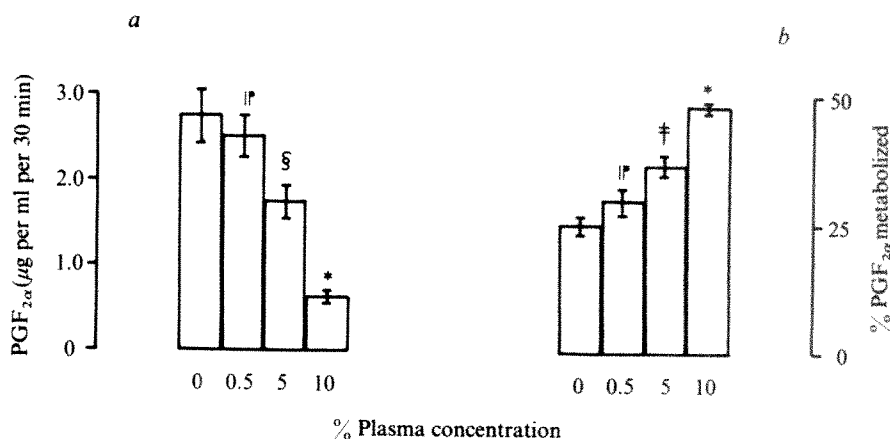
Enhancement of PGF<sub>2α</sub> inactivation by rat plasma was shown in several other 100,000g supernatants using the radiochemical assay (Fig. 1 legend). To check these results, the time courses of breakdown of prostaglandins E<sub>2</sub> and F<sub>2α</sub> in rat caecum supernatants were also measured by bioassay: as expected, PGE<sub>2</sub> was the better substrate (*t*<sub>1/2</sub> ~ 1.6 min compared with ~ 5.6 min for PGF<sub>2α</sub>), and the rate of disappearance of both PGs was enhanced in the presence of 5% plasma (*t*<sub>1/2</sub> reduced to ~ 0.8 and ~ 2.9 min, respectively).

We wondered whether alterations in the amounts of RCF might contribute to the adaptive changes in apparent levels of PG-synthesizing and metabolizing enzymes which were observed previously in certain animal models of pathophysiological states<sup>1–4</sup>.

Rats were injected subcutaneously (s.c.) for 2 days with prednisolone (5 mg per kg) or vehicle. As expected<sup>1</sup>, apparent levels of PG synthetase and prostaglandinase in kidney, lung, stomach and caecum were reduced and increased, respectively (Fig. 2 legend). Blood samples were collected by cardiac puncture and the plasmas assayed for RCF activity. The dose-response curves in Fig. 2a and b show that the steroid-treated plasmas contained considerably larger amounts of synthesis-inhibiting and inactivation-enhancing activity than those from the control group. The results in Fig. 2a confirm those of Saeed

\* Present address: Department of Pharmacology, Chelsea College, Manresa Road, London SW3 3TW, UK.

**Fig. 1** Demonstration of prostaglandin 'reciprocal coupling factor' (RCF) in rat plasma by assays on PG synthesis (a) and breakdown (b). Synthesis assays: Bovine seminal vesicle microsomes (5 mg ml<sup>-1</sup> lyophilized powder, Miles) were incubated for 30 min at 37 °C in pH 8.0 100 mM Tris-HCl buffer with 10 μg ml<sup>-1</sup> arachidonic acid (Sigma) and 3 mM reduced glutathione to favour conversion to classical PGs, and the amounts of PG-like material assayed after extraction on the isolated rat fundus strip preparation in terms of PGF<sub>2α</sub> equivalents. Bars show mean values ± s.e.m., *n* = 12–16. Breakdown experiments: Freshly prepared 100,000g supernatants of rat caecum homogenized in pH 7.4 50 mM phosphate buffer (final protein concentration 8.6 ± 0.2 mg ml<sup>-1</sup>, *n* = 67) were incubated at 37 °C for 4–10 min as appropriate with 5 mM NAD<sup>+</sup> and 10 μg ml<sup>-1</sup> PGF<sub>2α</sub> containing 0.02–0.05 μCi [9β-<sup>3</sup>H]-PGF<sub>2α</sub> (Radiochemical Centre, specific activity 15 Ci mmol<sup>-1</sup>), and the extent of PGF<sub>2α</sub> breakdown estimated by radiochromatography<sup>19</sup>. Results show mean values ± s.e.m., *n* = 4–8. RCF was found in both plasma and serum, was unaffected by the presence of heparin or if urethane or ether were given to anaesthetize the rats. Both synthesis-inhibiting and breakdown-enhancing properties exhibited similar characteristics: they were completely destroyed after 30 s boiling or pronase digestion (250 U ml<sup>-1</sup>, 16 h at 4 °C), but unchanged by incubation for 5 min at 37 °C or 18 h at 4 °C, by dialysis or by storage at -20 °C and repeated thawing. Most activity was recovered after precipitation by ammonium sulphate and 5 min heating at 60 °C. In Figs 1 and 2 the significance of differences was evaluated by Student's *t*-test, and the following key is used: \* *P* < 0.001, † *P* < 0.002, ‡ *P* < 0.01, § *P* < 0.02, ¶ *P* < 0.05, ¶ not significant. With regard to others systems: 5% (v/v) rat plasma inhibits microsomal PG synthesis in frog skin by 60.8 ± 8.8% (*P* < 0.001), rat kidney 37.3 ± 6.8% (*P* < 0.01), rabbit kidney 59.7 ± 1.5% (*P* < 0.001) and guinea pig kidney 49.3 ± 2.1% (*P* < 0.001) (*n* = 10) and enhances PGF<sub>2α</sub> inactivation in 100,000g supernatants of rat kidney by 54.4 ± 12.9% (*P* < 0.02), rat stomach 18.4 ± 2.2% (*P* < 0.01), rat lung 130.6 ± 22.5% (*P* < 0.01), guinea pig stomach 60.3 ± 15.8% (*P* < 0.001), guinea pig kidney 69.8 ± 11.9% (*P* < 0.01) and guinea pig colon 74.1 ± 6.5% (*P* < 0.001) (*n* = 5).





*et al.*<sup>5</sup> showing that glucocorticoid treatment increases the ability of plasma to inhibit microsomal PG synthesis, but they did not examine organ enzyme levels or test the effects of plasma on PG degradation. A further experiment (not shown) revealed that RCF is released within 30 min of the intra-arterial injection of prednisolone (2.5 mg per kg) as determined by both synthesis-inhibition and metabolism-enhancement assays.

Furthermore, we confirmed (Fig. 2 legend) a previous report that the apparent PG synthetase content in kidneys of rats made diabetic with alloxan is decreased whereas prostaglandinase

activity is elevated<sup>3</sup>. Plasmas collected from alloxan-diabetic rats contained considerably more RCF than those from control animals (Fig. 2c, d).

We anticipated that it might be possible to induce adaptive changes in the opposite direction (increased PG synthesis and decreased breakdown) by treatment of rats with thyroxine. Earlier experiments showed that this reduces prostaglandinase activity in lung and kidney<sup>11</sup>. Lungs, caeca, kidneys and blood samples were taken from rats injected s.c. for 2 days with 200 µg thyroxine. In all organs tested there was a decrease in prostaglandinase and increase in PG synthetase activity (Fig. 2 legend). The plasmas from the thyroxine-treated animals contained markedly less RCF activity than the control plasmas, according to both the microsomal synthetase and the caecum supernatant assays (Fig. 2e, f).

These data show that pathophysiological adaptations in apparent levels of enzymes of the PG system are indeed accompanied by 'appropriate' changes in the amounts of RCF, at least in the three examples studied. To what extent might the plasma factor be responsible for the changes in apparent enzyme activities? At present we cannot exclude the possibility that altered tissue prostaglandinase activities in the cell-free 100,000g supernatants may simply reflect the presence of different amounts of RCF taken up by the tissue or present in the blood entrapped in it, rather than differences in absolute enzyme levels. (Indeed, several authors<sup>12-15</sup> have noted that cytosolic high-speed supernatants are inhibitory to microsomal PG synthesis, perhaps because they contain RCF). It is unlikely that the changes in apparent PG synthetase levels can be explained in terms of altered amounts of RCF because these assays are performed using resuspended microsomes separated from the cytosol, and in some pathophysiological models (such as diabetes, Fig. 2) changes were found in some organs but not in others. Additional experiments (not shown) verified that RCF does not significantly bind to microsomes, thus making it unlikely that the large differences in apparent levels of PG synthetase can be simply due to differences in amounts of adsorbed RCF.

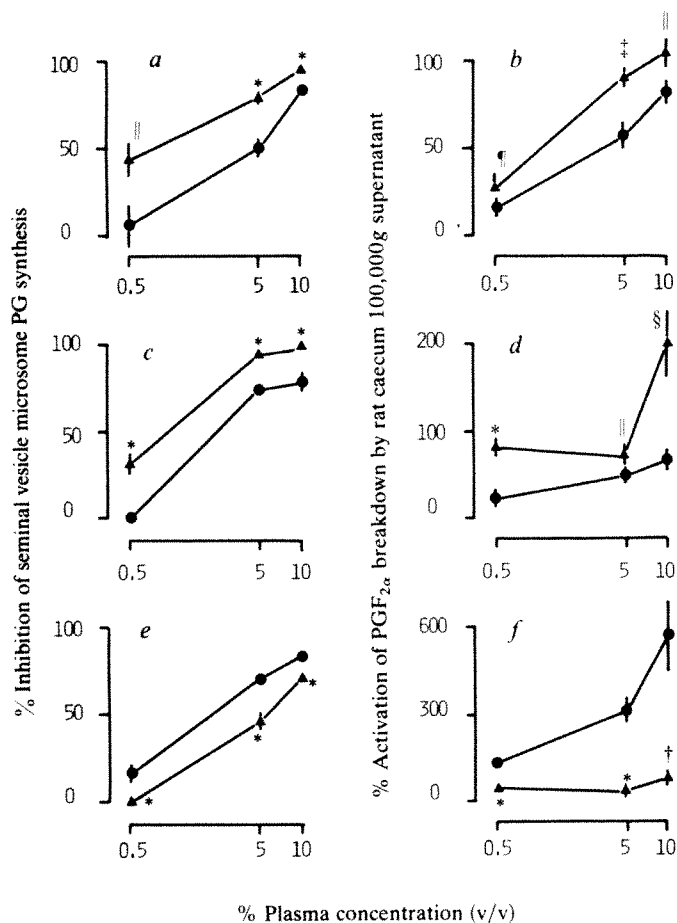
These studies suggest that the activities of the enzymes of the PG system are under sensitive metabolic control and may be susceptible to regulation by rapidly releasable blood-borne factors. Saeed, Collier and co-workers<sup>5,15</sup> have also identified a factor(s) capable of inhibiting microsomal PG synthesis *in vitro* (calling it 'endogenous inhibitor of prostaglandin synthesis'), and others have subsequently shown that serum or plasma may influence the amount or direction of arachidonate metabolism in both intact and broken cell preparations<sup>6,7,16-18</sup>. However, ours is the first demonstration of alterations in plasma factors in model pathophysiological states and shows for the first time that the enzymatic destruction of PGs may also be influenced by blood-borne factors. These results reinforce our view that the functional control and adaptive versatility of the PG system are likely to depend on modulation of breakdown as well as regulation of synthesis.

Finally, it should be noted that the consequences of RCF action, if functionally effective *in vivo*, would be 'anti-homeostatic': thus, high levels would cause or enhance a PG deficiency whereas its absence would favour a PG excess. Either way, this may lead to pathological changes. It is therefore important to discover the identity and mechanism of action of RCF and to find out how and why it is released in the intact animal.

We thank the MRC, Pharmacia AB, May & Baker Ltd and the Central Research Fund of the University of London for financial support, and Drs J. E. Pike, R. L. Jones, H. O. J. Collier and K. Crowshaw for gifts of prostaglandins and seminal vesicles. E. Ramcharan provided technical help.

Received 11 July; accepted 22 September 1980.

1. Moore, P. K. & Hoult, J. R. S. *Nature* **288**, 269-270 (1980).
2. Hoult, J. R. S. & Moore, P. K. *Br. J. Pharmac.* **69**, 272-273 (1980).
3. Hoult, J. R. S. & Moore, P. K. *Clin. Sci.* **59**, 63-66 (1980).
4. Hoult, J. R. S., Moore, P. K., Marcus, A. J. & Watt, J. *Ag. Actions Suppl.* **4**, 232-244 (1979).
5. Saeed, S. A. *et al. Nature* **270**, 32-36 (1977).



**Fig. 2** Alterations in rat plasma RCF activity accompany the reciprocal changes in tissue enzyme activities of the PG system in three model pathophysiological states (prednisolone treatment, panels a and b; experimental diabetes, panels c and d; thyroxine administration, panels e and f). Panels a, c and e show inhibition of sheep seminal vesicle microsomal PG synthesis by RCF in rat plasma; panels b, d and f show activation of PGF<sub>2α</sub> breakdown in rat caecum 100,000g supernatants by RCF in rat plasma. ● Denotes plasma from control and ▲ that from treated animals. Points show mean values  $\pm$  s.e.m. (unless smaller than symbol) for 16-20 (synthesis) and 8-10 determinations (breakdown). See Fig. 1 legend for key to statistical evaluation and details of experimental methods. Reciprocal changes in tissue activities of enzymes which synthesize and inactivate PGs were seen after each of the three treatments as shown below. Prednisolone treatment (five Sprague-Dawley rats per group injected s.c. with prednisolone 5 mg per kg or vehicle for 2 days): PG synthetase activity in kidney, caecum, stomach and lung reduced by 45.0  $\pm$  5.0% ( $P < 0.02$ ), 38.0  $\pm$  7.6% ( $P < 0.05$ ), 29.5  $\pm$  12.2% (not significant) and 46.0  $\pm$  5.9% ( $P < 0.05$ ) compared with activity in organs from vehicle-injected animals; prostaglandinase activity increased by 102  $\pm$  9.8% ( $P < 0.001$ ), 122.5  $\pm$  17.0% ( $P < 0.001$ ), 70.3  $\pm$  4.6% ( $P < 0.001$ ) and 57.8  $\pm$  12.9% ( $P < 0.01$ ) compared with control (see also ref. 1). Diabetic rats (five Wistar rats per group injected intravenously with alloxan 50 mg per kg or saline 3 days before death, blood sugar levels  $> 3.5$  mg per ml in diabetic animals): kidney PG synthetase activity reduced by 48.9  $\pm$  5.7% ( $P < 0.002$ ) and prostaglandinase activity increased by 188.8  $\pm$  41.9% ( $P < 0.001$ ), lung activities not changed (see also ref. 3). Thyroxine administration (five Sprague-Dawley rats per group injected s.c. for 2 days with L-thyroxine 200 µg per kg): PG synthetase activity in kidney, caecum and lung enhanced by 169.5  $\pm$  13.2% ( $P < 0.001$ ), 30.4  $\pm$  7.1% ( $P < 0.05$ ), and 304.3  $\pm$  65.4% ( $P < 0.001$ ) compared with activity in control organs, prostaglandinase activity reduced by 48.3  $\pm$  5.1% ( $P < 0.01$ ), 29.9  $\pm$  2.6% ( $P < 0.01$ ) and 40.2  $\pm$  3.2% ( $P < 0.001$ ).

- 6 Herman, E. A., Yamamoto, M. & Rapoport, B. *J. cell. Physiol.* 100, 401-406 (1979).
- 7 MacIatyre, D. E., Pearson, J. D. & Gordon, J. L. *Nature* 271, 549-551 (1978).
- 8 Putnam, F. W. in *The Proteins* Vol. 3, 2nd edn (ed. Neurath, H.) 153-267 (Academic, London, 1965).
- 9 Ball, T. K., Smith, J. B. & Silver, M. *J. Biochem. biophys. Acta* 424, 303-314 (1976).
- 10 Jackson, P. C., Ratz, A., Denny, S. E., Wyche, A. & Noddeman, P. *Prostaglandins* 14, 853-871 (1977).
- 11 Moore, P. K. & Hout, J. R. S. *Prostaglandins* 16, 335-350 (1978).
- 12 Takaguchi, C., Kohno, E. & Shi, C. *Biochemistry* 10, 2372-2376 (1971).
- 13 Rose, A. J. & Collins, A. J. *Prostaglandins* 8, 271-283 (1974).
- 14 Wlodawer, P., Kindahl, H. & Hamberg, M. *Biochem. biophys. Acta* 431, 603-614 (1976).
- 15 Collier, H. O. J., Deeming-Kendall, P. A., McDonald-Gibson, W. J. & Saeed, S. A. in *Hormones, Prostaglandins and Renal Disease* (eds Remuzzi, G., Mocca, G. & de Zeeuw, D.) (Raven, New York, in the press).
- 16 Hong, S. L. & Levine, L. *J. Biol. Chem.* 251, 5814-5816 (1976).
- 17 Remuzzi, G. et al. *Thromb. Res.* 13, 1007-1015 (1978).
- 18 di Rosa, M., Capasso, F. & Mascolo, N. in *Advances in Diarrhoeal Research* Vol. 1 (eds Weinstein, G., Samelson, B. & Proietti, R.) 493-498 (Raven, New York, 1979).
- 19 Hout, J. R. S. & Moore, P. K. *Br. J. Pharmac.* 61, 615-626 (1977).

## High-affinity anti-oestrogen binding site distinct from the oestrogen receptor

Robert L. Sutherland\*, Leigh C. Murphy,  
Ming San Foo, Michael D. Green  
& Anne M. Whybourne

Ludwig Institute for Cancer Research, University of Sydney, Sydney,  
New South Wales 2006, Australia

Zygmunt S. Krozowski

Department of Biochemistry, Royal Prince Alfred Hospital,  
Camperdown, New South Wales 2050, Australia

Non-steroidal anti-oestrogens such as tamoxifen, CI 628, nafoxidine and clomiphene, are structurally related synthetic compounds that antagonize the effects of oestrogen on its target tissues<sup>1,2</sup>, and this activity has led to the use of tamoxifen to treat advanced breast cancer<sup>3</sup>. All these compounds inhibit the binding of tritiated oestradiol to cytosol from oestrogen target tissues<sup>2,4-7</sup>, suggesting that anti-oestrogens bind to the oestrogen receptor. This is supported by reports that in the rat uterus<sup>7-10</sup> and dimethyl-benz ( $\alpha$ )-anthracene (DMBA)-induced rat mammary carcinoma<sup>9</sup>, oestradiol and anti-oestrogens bind directly to the same number of saturable binding sites. Furthermore, oestrogens and anti-oestrogens are mutually competitive for binding to these sites<sup>8,10</sup>. It has thus been generally accepted that the anti-oestrogens exert most of their effects through the specific oestrogen receptor. We now report a further high-affinity, anti-oestrogen binding site which may have a role in regulating the effects of non-steroidal anti-oestrogens.

Our evidence comes from comparison of the concentrations of high-affinity, saturable binding sites for oestradiol and anti-oestrogens in the same cytosol preparations, and from competition experiments with tritiated anti-oestrogens. Typical results of saturation analysis experiments with anti-oestrogens are shown in Fig. 1. The binding curves for the four oestrogen target-tissue cytosols were curvilinear (Fig. 1a) but could readily be resolved into a high-affinity, saturable binding site and non-specific binding<sup>11,12</sup> (Fig. 1b). The straight-line Scatchard plot<sup>13</sup> obtained by correction for non-specific binding (Fig. 1b) indicated a single high-affinity site or several saturable sites with similar affinities. No high-affinity sites were detected in the muscle cytosol (Fig. 1a).

Table 1 summarizes the apparent equilibrium dissociation constants ( $K_d$ ) and concentrations ( $C$ ) of high-affinity sites for oestradiol and tamoxifen in cytosol from eight oestrogen target tissues. With the exception of immature rat uterus, all these cytosols contained significantly more anti-oestrogen binding

sites than could be accounted for by oestrogen receptors alone. We have subsequently shown that the anti-oestrogen binding site is also present in immature rat uterus but was masked in the study reported here by a high concentration of oestrogen receptor<sup>14</sup>.

To test the ability of oestradiol to inhibit the binding of tritiated anti-oestrogen to its saturable binding sites, cytosol was

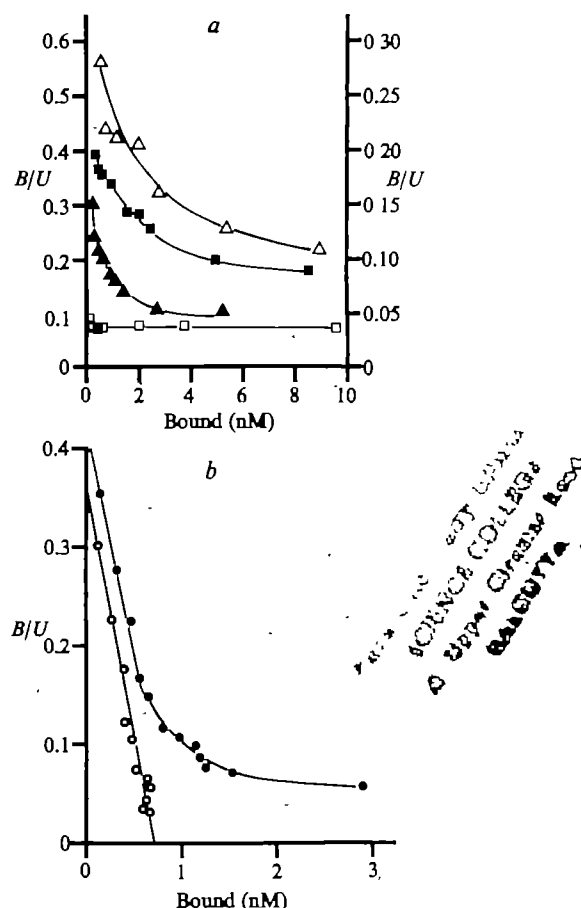


Fig. 1 Scatchard plots of anti-oestrogen binding to human endometrium, rat liver, chick oviduct, rat uterus and chick muscle cytosol. All tissues were homogenized with a Polytron and/or Teflon-glass tissue grinder, in 5-25 volumes (w/v) of 10 mM Tris-HCl buffer, pH 7.4, containing 1.5 mM EDTA and 0.5 mM dithiothreitol. A high-speed cytosol was prepared. Saturation analysis was performed at 4 °C by incubating 100  $\mu$ l of cytosol with a fixed concentration of tritiated tamoxifen (ICI, specific activity 19.5 Ci mmol<sup>-1</sup>) or CI 628 (1.25 nM, Radiochemical Centre, Amersham, specific activity 8-25 Ci mmol<sup>-1</sup>) and increasing concentrations of unlabelled ligand in the range of 1.25 nM-2  $\mu$ M. After 16 h of incubation, protein-bound and unbound ligand were separated by charcoal adsorption (0.5% charcoal for 30 min at 4 °C) and concentrations of bound and unbound ligand were calculated. The apparent equilibrium dissociation constant ( $K_d$ ) and binding site concentration ( $C$ ) of the saturable anti-oestrogen binding sites were calculated from measured bound and unbound ligand concentrations by a non-linear regression analysis technique<sup>11</sup> or by a graphical linearization technique<sup>12</sup>. The former technique was preferred but in the only tissue (chick oviduct) where the techniques were compared on several samples both gave similar results. a, Binding of CI 628 to human endometrium cytosol ( $\Delta$ ) and rat liver cytosol ( $\blacksquare$ ), and binding of tamoxifen to mature rat uterine cytosol ( $\blacktriangle$ ) and chick skeletal muscle cytosol ( $\square$ ). The scale of the left-hand ordinate applies to human endometrium only. b, Binding of CI 628 to chick oviduct cytosol before ( $\bullet$ ) and after ( $\circ$ ) correction for nonspecific binding. Tritiated CI 628 was greater than 97% pure at dispatch but was a 40:60 mixture of the *cis* and *trans* isomers. Tritiated tamoxifen was 88-90% pure on dispatch and was pure *trans* isomer. Purity was monitored continually by thin-layer chromatography and did not differ significantly from that at dispatch during the course of the experiments.

\*To whom correspondence should be addressed.



**Table 1** Binding parameters for interactions between oestradiol, tamoxifen and cytosol from eight oestrogen target tissues

| Tissue                   | Mean cytosol protein conc. (mg ml <sup>-1</sup> ) | No. of observations | Oestradiol                |                     | Tamoxifen                 |                     | Tamoxifen/oestradiol      |               |
|--------------------------|---|---------------------|---------------------------|---------------------|---------------------------|---------------------|---------------------------|---------------|
|                          |   |                     | <i>K<sub>d</sub></i> (nM) | <i>C</i> (nM)       | <i>K<sub>d</sub></i> (nM) | <i>C</i> (nM)       | <i>K<sub>d</sub></i> (nM) | <i>C</i> (nM) |
| Rat uterus (immature)    | 1.85  | 10                  | 0.17 ± 0.02               | 0.99 ± 0.07         | 2.54 ± 0.37               | 1.08 ± 0.08         | 14.9                      | 1.09          |
| Rat uterus (mature)      | 0.88  | 2                   | 0.24<br>(0.23–0.25)       | 0.13<br>(0.12–0.14) | 3.20<br>(2.28–4.11)       | 0.56<br>(0.55–0.56) | 13.3                      | 4.31          |
| Rat liver                | 29.5  | 2                   | 0.31<br>(0.16–0.46)       | 0.21<br>(0.14–0.28) | 3.52<br>(2.97–4.06)       | 1.70<br>(1.66–1.74) | 11.4                      | 7.98          |
| Rat kidney               | 18.9  | 2                   | 0.14<br>(0.13–0.14)       | 0.12<br>(0.12–0.12) | 5.60<br>(3.25–7.94)       | 0.80<br>(0.76–0.83) | 40.0                      | 6.67          |
| Chick oviduct            | 3.4   | 6                   | 0.07 ± 0.02<br>0.93       | 0.19 ± 0.01<br>0.11 | 9.82 ± 1.96<br>3.62       | 0.66 ± 0.24<br>0.50 | 140.3                     | 3.47          |
| Chick liver              | 20.3  | 2                   | (0.90–0.96)               | (0.09–0.13)         | (2.93–4.31)               | (0.49–0.51)         | 3.9                       | 4.55          |
| Human endometrium        | 3.0   | 1                   | 0.52                      | 0.21                | 3.43                      | 0.74                | 6.7                       | 3.45          |
| Human mammary carcinoma* | 3.6   | 5                   | 0.18 ± 0.07               | 0.17 ± 0.05         | 6.04 ± 1.60               | 1.47 ± 0.50         | 33.6                      | 8.65          |

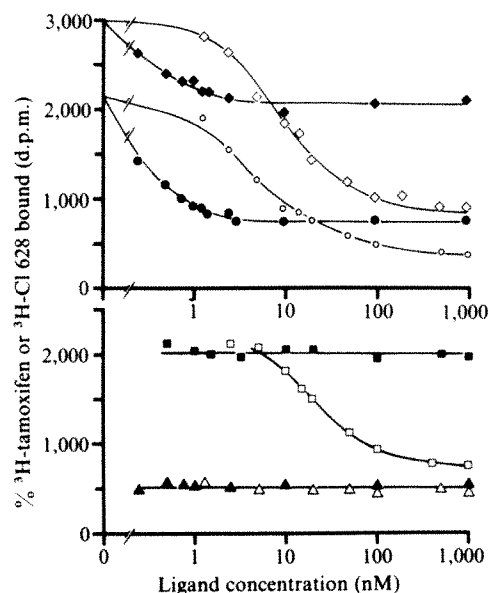
Experimental procedures are described in Fig. 1 legend. Binding-site concentration (*C*) is expressed as nmol of oestradiol or tamoxifen specifically bound per litre of reaction mixture, which was a twofold dilution of the cytosol. Data are presented as the mean ± s.e.m. or the mean plus range in parentheses.

\* With oestrogen receptors.

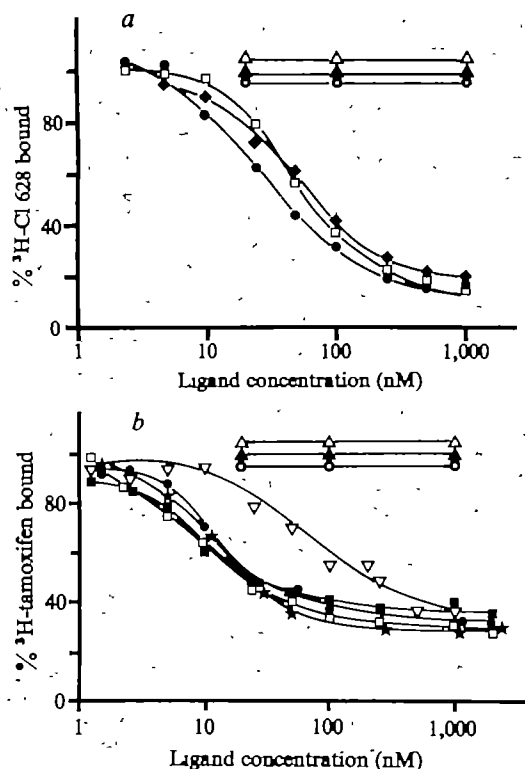
incubated with tritiated CI 628 or tamoxifen and increasingly higher concentrations of oestradiol or anti-oestrogen. Figure 2 shows that the degree of inhibition by oestradiol varied with the tissue. With immature rat uterine cytosol, inhibition was complete<sup>7–10</sup>, whereas in mature rat uterus and chick oviduct it was partial (Fig. 2). In human mammary carcinoma that had oestrogen receptors, oestradiol did not inhibit anti-oestrogen binding, whereas only non-specific binding occurred in chick muscle (Fig. 2). This can probably be explained by the relative affinities and concentrations of oestrogen and anti-oestrogen binding sites in cytosols, because those factors govern the amount of tritiated anti-oestrogen bound to the oestrogen receptor and thus the proportion of label displaced by oestradiol. For example, using data presented in Table 1 and elsewhere<sup>15</sup>, we calculated that only 5–7% of tritiated tamoxifen was bound to the oestrogen receptor in the mammary carcinoma cytosol, so that oestradiol could not displace significant amounts of label.

To assess the ligand specificity of the anti-oestrogen binding site we used cytosol from MCF 7 cells grown in 10% fetal calf serum because the relative concentration of saturable anti-oestrogen binding sites and oestrogen binding sites is greater than 50:1 (L.C.M. and R.L.S., unpublished data). As a result, essentially no tritiated anti-oestrogen was bound to the oestrogen receptor and competition curves represent the inhibition of binding of tritiated anti-oestrogen to anti-oestrogen binding site alone. Tamoxifen, CI 628 and nafoxidine all inhibited the binding of tritiated CI 628 to its saturable binding site (Fig. 3a), whereas natural and synthetic oestrogens, androgens, and progestins did not (Fig. 3a), indicating that the high-affinity anti-oestrogen binding site was not a sex steroid hormone receptor. To show that these results were not due to a contaminant of tritiated CI 628, similar experiments were performed with tritiated tamoxifen (Fig. 3b). Again anti-oestrogens (tamoxifen, CI 628, ICI 47,699, enclomiphene and *N*-desmethyltamoxifen) inhibited binding whereas the same steroids were ineffective.

The structural requirements for binding to the anti-oestrogen binding site are different from those for the binding of these anti-oestrogens to the oestrogen receptor. The *cis* isomers of tamoxifen and clomiphene (ICI 47,699 and zuclophene) have only 5–10% of the affinity of the *trans* isomers for the oestrogen receptor<sup>16</sup> but both *cis* and *trans* tamoxifen have similar affinities for the anti-oestrogen binding site (Fig. 3b). Studies with 4-hydroxytamoxifen, a metabolite with 5–10 times the affinity of tamoxifen for the oestrogen receptor<sup>17,18</sup>, showed that aromatic monohydroxylation had no effect on the affinity of tamoxifen for the anti-oestrogen binding site (A.M.W. and R.L.S., unpublished data). In contrast, demethylation in the



**Fig. 2** Competition of oestradiol and anti-oestrogens (CI 628 or tamoxifen) for anti-oestrogen binding sites in chick oviduct, rat uterus, human mammary carcinoma with oestrogen receptors and chick muscle cytosol. Aliquots of cytosol were incubated for 16 h at 4 °C with 1.25 nM tritiated CI 628 or tamoxifen and increasingly high concentrations of unlabelled oestradiol or anti-oestrogen (tamoxifen or CI 628). Protein-bound radioactivity was separated by charcoal adsorption and the data were plotted as d.p.m. tritiated anti-oestrogen bound against log of the added ligand concentration. Results for chick oviduct (diamonds), mature rat uterus (circles), oestrogen receptor-positive human mammary carcinoma (squares) and chick skeletal muscle cytosols (triangles) are illustrated. Binding of tritiated anti-oestrogen in the presence of increasingly high concentrations of unlabelled oestradiol or anti-oestrogen are represented by solid and open symbols, respectively. Tamoxifen was the anti-oestrogen in the experiment with mammary carcinoma cytosol whereas in the other three experiments CI 628 was the anti-oestrogenic ligand. The protein concentrations of the cytosols are listed in Table 1 and the oestrogen receptor concentrations in fmol per mg protein were: chick oviduct, 112; mature rat uterus, 297; human mammary carcinoma, 119; and chick muscle, 0. For clarity the ordinate for the chick oviduct data has been expanded twofold, that is  $B_0$  for chick oviduct = 1,500 d.p.m.



**Fig. 3** Specificity of the saturable anti-oestrogen binding site in MCF 7 human mammary carcinoma cell cytosol. Tritiated CI 628 (a) or tamoxifen (b), cytosol and increasingly high concentrations of: tamoxifen (●), CI 628 (□), nafoxidine (◆), enclomiphene (★), ICI 47,699 (■), *N*-desmethyltamoxifen (▽); androgens: testosterone, 5 $\alpha$ -dihydrotestosterone, R1881 (○), oestrogens: oestradiol, oestrone, diethylstilboestrol (▲), and progestins: progesterone, R5020 (△), were incubated for 16 h at 4°C and the protein-bound radioactivity was measured after adsorption on charcoal. Data are presented as the amount of tritiated anti-oestrogen bound in the presence of added ligand, expressed as a percentage of tritiated anti-oestrogen bound in the absence of added ligand against log of the concentration of added ligand.

alkylaminoethoxy side chain had little effect on receptor binding<sup>19</sup> but markedly reduced the affinity for the anti-oestrogen binding site (compare tamoxifen with *N*-desmethyltamoxifen in Fig. 3b).

These data (Figs 1–3, Table 1), demonstrating an excess of high-affinity, saturable anti-oestrogen binding sites over oestrogen receptor sites and the inability of oestradiol to compete for all these sites, are evidence for an anti-oestrogen binding site. The site has a high affinity ( $K_d = 3$ –10 nM) for CI 628 and tamoxifen and is saturable at nanomolar concentrations of the drugs. It shows a surprising degree of specificity, binding a series of structurally related synthetic non-steroidal anti-oestrogens but not several steroid hormones (Fig. 3). There is also an indication of tissue specificity in that the site was present in all oestrogen target tissues studied but not in human mammary carcinoma that lacked oestrogen receptors<sup>15</sup> nor in rat plasma and skeletal muscle. In addition we have shown that it is a protein, for binding activity can be destroyed by trypsin but not by lipase, RNase or DNase. The observation that its concentration changes during the oestrous cycle in rats<sup>20</sup> suggests that this intracellular binding protein is under hormonal control.

Our data are consistent with anti-oestrogen binding to the cytoplasmic oestrogen receptor as well as to the anti-oestrogen binding site. Indeed the competition curves illustrated in Fig. 2 and elsewhere<sup>7</sup> demonstrate partial or complete inhibition of anti-oestrogen binding by oestradiol. We believe that anti-oestrogens bind to two saturable binding components *in vivo* which often cannot be resolved *in vitro* because of their relative

concentrations and affinities and the range of ligand concentrations used. However, experiments with human mammary carcinoma containing high titres of oestrogen receptor generated curves which could be resolved<sup>11</sup> into two saturable binding components (oestrogen receptor and anti-oestrogen binding site) in addition to non-specific binding<sup>21</sup>.

We have no evidence that this binding site mediates the effects of anti-oestrogen on target tissues. The possibility that it has a natural ligand and mediates the antagonistic effects of the drugs whereas agonist effects are mediated through the oestrogen receptor warrants investigation. In any case, the affinity and concentration of the anti-oestrogen binding site are such that it must bind a significant proportion of the drugs *in vivo* and so may regulate the amounts of anti-oestrogen available for binding to the oestrogen receptor.

We thank ICI, Warner Lambert/Parke-Davis, Merrell and Upjohn for anti-oestrogens, and Professor M. H. N. Tattersall for interest, encouragement and critical comment.

Received 14 March, accepted 25 September 1980

- 1 Katzenellenbogen, B. S. *et al.* *Rec. Prog. Horm. Res.* **35**, 259–300 (1979)
- 2 Jordan, V. C., Dix, D. J., Naylor, K. E., Prestwich, G. & Rowley, L. *J. Toxicol. Clin. Toxicol.* **4**, 363–390 (1978)
- 3 Mourad, H., Palahol, T., Patterson, J. & Battersby, L. *Cancer Treat. Res.* **5**, 131–141 (1978)
- 4 Horwitz, K. B. & McGuire, W. L. *J. Biol. Chem.* **253**, 8185–8191 (1978)
- 5 Lippman, M., Bolan, G. & Huff, K. *Cancer Res.* **36**, 4595–4601 (1976)
- 6 Stodmore, J., Walpole, A. L. & Woodburn, J. *J. Endocrinol.* **52**, 289–298 (1972)
- 7 Sutherland, R. L. & Foo, M. S. *Biochem. Biophys. Res. Commun.* **91**, 183–191 (1979)
- 8 Katzenellenbogen, B. S., Katzenellenbogen, J. A., Ferguson, E. R. & Krauthammer, N. *J. Biol. Chem.* **253**, 697–707 (1978)
- 9 Nicholson, R. L., Syne, J. S., Daniel, C. P. & Griffiths, K. *Eur. J. Cancer* **15**, 317–329 (1979)
- 10 Capony, F. & Rochefort, H. *Mol. Cell. Endocrinol.* **11**, 181–198 (1978)
- 11 Sutherland, R. L. & Simpson-Morgan, M. W. *J. Endocrinol.* **63**, 319–332 (1975)
- 12 Chamness, G. C. & McGuire, W. L. *Steroids* **26**, 538–542 (1976)
- 13 Scatchard, G. *Ann. N.Y. Acad. Sci.* **51**, 660–672 (1949)
- 14 Murphy, L. C. & Sutherland, R. L. *J. Endocrinol.* (in the press)
- 15 Sutherland, R. L. & Murphy, L. C. *Eur. J. Cancer* (in the press)
- 16 Sutherland, R. L. & Foo, M. S. in *Non-Steroidal Anti-Oestrogens* (eds Sutherland, R. L. & Jordan, V. C.) (Academic, Sydney, in the press)
- 17 Jordan, V. C., Collins, M. M., Rowley, L. & Prestwich, G. *J. Endocrinol.* **75**, 305–316 (1977)
- 18 Benart, N. *et al.* *Biochem. Biophys. Res. Commun.* **91**, 812–818 (1979)
- 19 Wakeling, A. E. & Slater, S. R. *Cancer Treat. Rep.* **63**, 1150 (1979)
- 20 Paye, J. C., Lamerre, B. & Bayard, F. *Biochem. Biophys. Res. Commun.* **93**, 1225–1231 (1980)
- 21 Murphy, L. C. *et al.* in *Non-Steroidal Anti-Oestrogens* (eds Sutherland, R. L. & Jordan, V. C.) (Academic, Sydney, in the press)

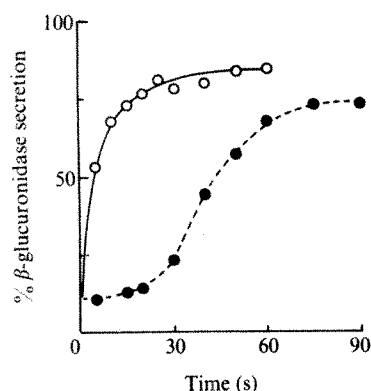
## Stimulus–secretion coupling in rabbit neutrophils is not mediated by phosphatidylinositol breakdown

S. Cockcroft, J. P. Bennett & B. D. Gomperts

Department of Experimental Pathology,  
School of Medicine, University College London, University Street,  
London WC1E 6JJ, UK

In common with other cells which use intracellular  $Ca^{2+}$  to mediate specific cell function, when rabbit neutrophils are stimulated with specific agonists the rate of metabolism of phosphatidylinositol (PI) increases<sup>1–3</sup>. This is normally measured as the incorporation of radioactive phosphate or inositol into PI, but these reactions are presumed to be secondary processes following the initial breakdown of pre-existing PI to diacylglycerol<sup>4</sup>. The radioactive labels are incorporated during the stepwise resynthesis of PI via phosphatidic acid (PA). It has been suggested that in the sequence of biochemical events, starting with the binding of the ligand to a receptor, and finally resulting in the expression of cellular activity, the breakdown of PI is an early event immediately directed by activation of the receptor<sup>1,4</sup>. This could then control the increase in cytoplasmic  $Ca^{2+}$  and other processes dependent on this. Here we report an analysis of the temporal relationship between these phospholipid changes and cell stimulation. Our evidence suggests that in neutrophils, PI breakdown and PA labelling are both consequences and not causes of a rise in intracellular  $Ca^{2+}$ .





**Fig. 1** Time course of  $\beta$ -glucuronidase secretion from rabbit neutrophils stimulated with  $10^{-8}$  M fMet-Leu-Phe (○) and  $5 \times 10^{-6}$  M ionomycin (●). Neutrophils were obtained from the rabbit peritoneal cavity 4–6 h after infusion of 250 ml 0.1% glycogen in saline<sup>3</sup>. They were suspended at  $4 \times 10^7$  cells  $\text{ml}^{-1}$  in a buffered salt solution, pH 7.5, comprising 137 mM NaCl, 2.7 mM KCl, 1 mM  $\text{MgCl}_2$ , 1.8 mM  $\text{CaCl}_2$ , 20 mM HEPES, 5.6 mM glucose and 1 mg  $\text{ml}^{-1}$  bovine serum albumin. The cells were incubated at 37 °C for 45 min. After addition of cytochalasin B ( $5 \mu\text{g ml}^{-1}$ ), the cells were immediately added to fMet-Leu-Phe or ionomycin contained in small volumes of buffer. Samples containing  $\sim 4 \times 10^7$  cells were quenched into ice-cold saline at the times indicated. The secreted  $\beta$ -glucuronidase released into the extracellular fluid was measured as previously described<sup>3</sup>. There was no detectable increase in the released  $\beta$ -glucuronidase in the absence of added ligands.

As agonists for neutrophil activation, we have used the synthetic tripeptide formylmethionyl-leucyl-phenylalanine (fMet-Leu-Phe) and ionomycin, which is a  $\text{Ca}^{2+}$ -carrying ionophore<sup>5</sup>. Activation of neutrophils normally results in an increase in cell motility, but in the presence of cytochalasin B ( $5 \mu\text{g ml}^{-1}$ ), the cells secrete lysosomal enzymes (we measure  $\beta$ -glucuronidase) and the motile functions are suppressed<sup>6</sup>. Chemotaxis and secretion are known to be different expressions of the same cell-surface receptors<sup>7</sup>, and we have previously demonstrated that cytochalasin B does not significantly affect the binding of fMet-Leu-Phe to its receptor and the induced  $\text{Ca}^{2+}$  fluxes; nor does it alter the extent of PI labelling<sup>3</sup>.

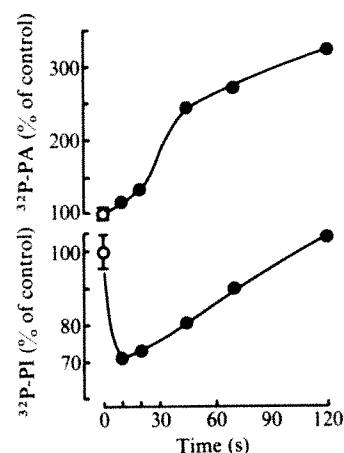
Figure 1 shows the time course of  $\beta$ -glucuronidase secretion from cytochalasin B-treated neutrophils due to fMet-Leu-Phe ( $10^{-8}$  M) and ionomycin ( $5 \times 10^{-6}$  M). The secretion due to the receptor-directed tripeptide is 90% complete within 10 s of adding the ligand, and so any early events which could dictate or modulate the course of the secretory process must be expressed within this time. Secretion due to the ionophore is characterized by a delay of about 20 s and is complete within about 60 s.

Figure 2 shows the changes in the radioactivity of PA and PI during 120 s following the addition of fMet-Leu-Phe to neutrophils which had been preincubated for 45 min in the presence of  $^{32}\text{P}$ -phosphate to label phospholipids and the ATP pool. The radioactivity in these cells was quenched by direct addition to a mixture of chloroform/methanol (1:2), and the lipids were extracted and separated by TLC. Within 10 s of the addition of the ligand, the radioactivity of PI had declined by 30% whereas that of PA had increased slightly. Thereafter, the radioactivity in both lipids increased due to the incorporation of  $^{32}\text{P}$  from ATP into the intermediates for PI resynthesis. In other experiments (data not shown), in which cells prelabelled with  $^3\text{H}$ -glycerol were used, the radioactivity of PI declined to a similar extent within 10 s. In this case, the ensuing increase in radioactivity was not observed, because  $^3\text{H}$ -glycerol can only enter PI as a consequence of *de novo* synthesis and, unlike  $^{32}\text{P}$ -phosphate, is not incorporated during the resynthesis cycle<sup>1</sup>.

Although the time dependence of PI breakdown certainly justifies its designation as an early event, our previous work showed that PI resynthesis (labelling) is unrelated to  $\text{Ca}^{2+}$  movements and the stimulation of secretion<sup>2</sup>. Secretion due to fMet-Leu-Phe will occur in the absence of extracellular  $\text{Ca}^{2+}$  due to mobilization of  $\text{Ca}^{2+}$  from intracellular sources<sup>8</sup>, but in these circumstances we found that PI labelling does not occur<sup>2</sup>. Table 1 shows that this is also true of PI breakdown. In addition, we show that when  $\text{Ca}^{2+}$  is introduced into the cell using ionomycin, secretion is accompanied by PI breakdown, and we have found that both responses are  $\text{Ca}^{2+}$  dependent. In this case, PI breakdown follows a slower time course similar to that of the ionomycin-stimulated secretion illustrated in Fig. 1 (results not shown).

We conclude that, in neutrophils, breakdown of PI is not essential for  $\text{Ca}^{2+}$  mobilization and secretion. Ionomycin and the receptor-directed agonist were equally effective in causing PI breakdown. Although the breakdown of PI is rapid, it is apparently a consequence and not a cause of the elevation of  $\text{Ca}^{2+}$  in the cytosol. Implicit in the results presented (Table 1) is the possibility that the concentration of intracellular  $\text{Ca}^{2+}$  required to induce PI breakdown might be higher than that needed for secretion. These results also exclude the recently suggested<sup>9,10</sup> possibility that PA generated during resynthesis of PI could be the intrinsic ionophore which permits  $\text{Ca}^{2+}$  movement into agonist-stimulated cells. In neutrophils the appearance of PA is a late event and furthermore (unlike secretion), is dependent on extracellular  $\text{Ca}^{2+}$  (see Table 1).

There is a close correlation between cell activation processes mediated by an elevation of cytosol  $\text{Ca}^{2+}$  and the stimulation of PI metabolism<sup>1,4,11</sup>. The possibility that PI breakdown could precede and thus regulate the fluxes of  $\text{Ca}^{2+}$  which lead to



**Fig. 2** Time course of the changes in radioactivity of PI and PA after addition of fMet-Leu-Phe to neutrophils. Neutrophils ( $4 \times 10^7$  cells  $\text{ml}^{-1}$ ) were incubated at 37 °C for 45 min with  $50 \mu\text{Ci ml}^{-1}$   $^{32}\text{P}$ -P<sub>i</sub>. Four samples (1 ml) were then quenched directly into 3.75 ml of chloroform/methanol (1:2) (zero time control) and the remainder of the cells were immediately added to fMet-Leu-Phe (final concentration  $10^{-8}$  M) contained in a small volume. Samples were taken and quenched at the times indicated. The lipids were extracted<sup>13</sup> and separated by TLC as previously described<sup>14</sup>. The lipids were identified by staining with iodine vapour and by autoradiography. The spots containing PI and PA were scraped into vials and the radioactivity measured by liquid scintillation counting. Open symbols indicate zero time control, mean  $\pm$  s.e.m.,  $n = 4$ ; PA =  $1,890 \pm 110$  c.p.m.; PI =  $2,470 \pm 100$  c.p.m. There was no detectable increase in the radioactivity of these two lipids in control samples during the 2-min period of incubation. A similar kinetic pattern of phospholipid changes was obtained when cytochalasin B-treated neutrophils were used, and the cells quenched with ice-cold saline. In 12 independent experiments, using fMet-Leu-Phe at  $10^{-8}$  M, we found that at 10 s breakdown of labelled PI was  $26 \pm 2\%$  and the increment in PA labelling was  $32 \pm 5\%$ .

**Table 1** Effects of  $\text{Ca}^{2+}$  on agonist-induced secretion and changes in radioactivity of  $^{32}\text{P}$ -labelled phosphatidylinositol and phosphatidic acid

|                                 | c.p.m. in PI<br>(% of control) | c.p.m. in PA<br>(% of control) | $\beta$ -glucuronidase<br>secretion<br>(% of total) |
|---------------------------------|--------------------------------|--------------------------------|---|
| a Control                       | 100 $\pm$ 1                    | 100 $\pm$ 1                    | 3 $\pm$ 1   |
| fMet-Leu-Phe                    | 107 $\pm$ 3                    | 102 $\pm$ 7                    | 15 $\pm$ 1  |
| Control + $\text{Ca}^{2+}$      | 100 $\pm$ 1                    | 100 $\pm$ 3                    | 4 $\pm$ 1   |
| fMet-Leu-Phe + $\text{Ca}^{2+}$ | 69 $\pm$ 5                     | 153 $\pm$ 4                    | 60 $\pm$ 1  |
| b Control + $\text{Ca}^{2+}$    | 100 $\pm$ 2                    | 100 $\pm$ 3                    | 4 $\pm$ 1   |
| Ionomycin + $\text{Ca}^{2+}$    | 78 $\pm$ 2                     | 137 $\pm$ 3                    | 50 $\pm$ 3  |

a, Effect of  $\text{Ca}^{2+}$  on secretion and changes in radioactivity of PI and PA after 10-s exposure of cytochalasin B-treated neutrophils to fMet-Leu-Phe. b, Secretion and changes in the radioactivity of PI and PA after 45-s exposure of cytochalasin B-treated neutrophils to ionomycin +  $\text{Ca}^{2+}$ . Neutrophils ( $4 \times 10^7$  cell  $\text{ml}^{-1}$ ) were incubated for 45 min in a  $\text{Ca}^{2+}$ -free buffer (EGTA 10  $\mu\text{M}$ ) containing  $^{32}\text{P}$ . After the addition of cytochalasin B (5  $\mu\text{g ml}^{-1}$ ), three pairs of samples (1 ml) were transferred in succession to tubes containing agonist (fMet-Leu-Phe  $10^{-8}$  M or ionomycin  $5 \times 10^{-6}$  M) and buffer, with or without  $\text{Ca}^{2+}$  (1.8 mM); these were quenched after 10 s (fMet-Leu-Phe) or 45 s (ionomycin) by addition of 5 ml of ice-cold saline. The whole operation was complete within 2 min. After centrifugation at 4  $^{\circ}\text{C}$ , the supernatant was sampled for estimation of  $\beta$ -glucuronidase and the cell lipids were extracted and analysed as described in Fig. 2 legend.  $\text{Ca}^{2+}$  had no effect on secretion and phospholipid changes in the absence of fMet-Leu-Phe. Results are expressed as mean  $\pm$  s.e.m.,  $n=3$ . Concentration of  $\text{Ca}^{2+}$  in  $\text{Ca}^{2+}$ -free buffer (measured with a  $\text{Ca}^{2+}$  electrode) was less than 5  $\mu\text{M}$ .

activation has been a popular concept because in many of the earlier systems studied, PI responses seemed to be independent of extracellular  $\text{Ca}^{2+}$  (ref. 2). If breakdown of PI has a universal role in cell activation processes, our results with neutrophils, and those of others with platelets<sup>12</sup>, indicate that this is not in the regulation of  $\text{Ca}^{2+}$  fluxes.

This investigation was supported by grants from the Wellcome Trust and the MRC.

Received 21 April; accepted 30 September 1980.

1. Mitchell, R. H. *Biochem Biophys Acta* **418**, 81–147 (1975).
2. Cockcroft, S., Bennett, J. P. & Gomperts, B. D. *FEBS Lett* **118**, 115–118 (1980).
3. Bennett, J. P., Cockcroft, S. & Gomperts, B. D. *Biochem Biophys Acta* **601**, 584–591 (1980).
4. Mitchell, R. H., Jaffer, S. S. & Jones, L. M. *Adv exp Med Biol* **83**, 447–465 (1977).
5. Bennett, J. P., Cockcroft, S. & Gomperts, B. D. *Nature* **282**, 851–853 (1979).
6. O'Flaherty, J. P. & Ward, P. A. *Semin Hematol* **16**, 163–174 (1979).
7. Showell, H. J. *et al J exp Med* **143**, 1154–1169 (1976).
8. Naccache, P. H., Volpe, M., Showell, H. J., Becker, E. L. & Shaul, R. I. *Science* **203**, 461–463 (1979).
9. Salmon, D. M. & Honeyman, T. W. *Nature* **284**, 344–345 (1980).
10. Putney, J. W., Weiss, S. J., van de Walle, C. M. & Hadden, R. A. *Nature* **284**, 345–347 (1980).
11. Gomperts, B. D., Cockcroft, S., Bennett, J. P. & Pettrell, C. M. *J Physiol, Paris* **76**, 383–393 (1980).
12. Bell, R. L. & Majerus, P. W. *J Mol Chem* **288**, 1790–1792 (1980).
13. Mitchell, R. H. & Jones, L. M. *Biochem J* **136**, 47–52 (1974).
14. Skipski, V. P., Peterson, R. F. & Barclay, M. *Biochem J* **96**, 374–378 (1964).

## The possible functional significance of phosphatidylethanolamine methylation

Dennis E. Vance & Ben de Kruijff\*

Department of Biochemistry, University of British Columbia, Vancouver, British Columbia, Canada V6T 1W5

The conversion of phosphatidylethanolamine to phosphatidylcholine was first reported in rat liver microsomes by Bremer and Greenberg<sup>1</sup>. The reaction requires three successive methylations of the ethanolamine moiety by *S*-adenosylmethionine. The highest activity for this enzyme has been found in liver microsomes and the enzyme from rat liver was recently solubilized and partially purified<sup>2</sup>. Although the activity is highest in liver, it is the minor pathway in this tissue for the synthesis of phosphatidylcholine<sup>3</sup>. The enzyme has recently been identified in bovine adrenal medulla<sup>4</sup> and reports exist on the activity of phosphatidylethanolamine methyltransferase in erythrocyte ghosts<sup>5</sup>, reticulocyte ghosts<sup>6,7</sup> and mammary gland membranes<sup>8</sup>. In view of the relatively minor importance of the

methylation pathway in phosphatidylcholine biosynthesis in liver, we were intrigued by the reports of significant physiological changes attributed to phospholipid methylation<sup>9–11</sup>. Calculations reported here show that this enzymatic activity in reticulocytes, erythrocytes and mammary gland membranes is 0.1% of that observed in liver microsomes. Furthermore, in conditions where marked changes in microviscosity of the erythrocyte membrane were observed, only extremely small amounts of phosphatidylethanolamine were methylated<sup>9</sup>. For these and other reasons, there is considerable doubt that methylation of phosphatidylethanolamine could account for the many physiological responses attributed to this activity.

Table 1 compares the activity for *N*-methylation of phosphatidylethanolamine in rat liver microsomes with the highest activity reported for several other membrane preparations. The activity in the microsomes from adrenal medulla is 100-fold lower than in liver microsomes and 1,000-fold lower in the three other membrane preparations. In the presence of exogenously added phosphatidyl-*N*-monomethylethanolamine, the activity in liver microsomes and in erythrocyte ghosts was 0.58 (ref. 2) and 0.0003 nmol (Fig. 1 of ref. 5)  $^3\text{H}$ -methyl transferred per min per mg protein, respectively. In view of the very low enzymatic activities of the last three membrane preparations listed in Table 1, we question whether or not the activity is associated with these membranes. Perhaps the activity is due to cellular impurities in the preparation.

Because such low methylation activity was observed with the erythrocyte membrane, we decided to calculate the number of molecules of phosphatidylethanolamine methylated during these incubations. In one reported experiment, erythrocyte ghosts were incubated for 1 h at 37  $^{\circ}\text{C}$  with 100  $\mu\text{M}$  *S*-adenosylmethionine<sup>9</sup>. During this incubation 4.4 pmol of phosphatidylethanolamine were methylated per mg of membrane protein. The ratio of protein to lipid in rat erythrocytes is 1.1 (ref. 10). Thus, there would be 0.91 mg lipid per mg protein, and on a molar ratio half of this lipid (0.62 mg) is polar lipid<sup>10</sup>. Most, if not all, of the polar lipid is phospholipid. The phospholipids of the rat erythrocyte include 47.5% phosphatidylcholine and 21.5% phosphatidylethanolamine<sup>11</sup>. From these data and the assumption of 750 and 800 as the respective molecular weights of phosphatidylethanolamine and phosphatidylcholine, we can calculate that rat erythrocyte membranes contain 173,000 pmol of phosphatidylethanolamine and 362,000 pmol of phosphatidylcholine per mg protein. During the incubation described above, 2.0 pmol of phosphatidyl-*N*-monomethylethanolamine, 1.2 pmol of phosphatidyl-*N,N*-dimethylethanolamine and 1.2 pmol of phosphatidylcholine were apparently formed<sup>9</sup>. Thus, 0.0012% of the phosphatidylethanolamine was converted to the monomethyl derivative. Of the phosphatidylcholine molecules present, only 0.00033% were formed via methylation of phosphatidylethanolamine in the 1-h incubation. Despite these extremely small amounts of lipids converted or formed, a relatively large change in microviscosity from 1.62 to 1.09 P was observed in the same experiment. Therefore, it seems highly unlikely that the changes in membrane microviscosity could have been caused by methylation of phosphatidylethanolamine. Some other explanation must be sought for the observed changes in microviscosity. This conclusion is supported by the studies of Schroeder *et al.*<sup>12</sup> with LM cells. There was no change in the fluidity of the membranes or membrane lipid (as measured by several different probes) when the polar head group of the phospholipid in the cell or subcellular membranes was altered by more than 50%.

Another area of concern in the reports on methylation of phosphatidylethanolamine is the extremely small amounts of  $^3\text{H}$  incorporated into the lipids. There is a serious possibility that the  $^3\text{H}$  radioactivity originates from contaminating compounds in the *S*-adenosyl-L-[Me- $^3\text{H}$ ]methionine. For instance, in the

\* Permanent address: Department of Molecular Biology, Padualaan 8, de Uithof, Utrecht, The Netherlands.



**Table 1** Comparison of various enzymatic activities for methylation of phosphatidylethanolamine

| Source of enzyme   | Enzyme activity<br>(nmol <sup>3</sup> H-methyl<br>transferred per<br>min per mg protein) |
|--|--|
| Rat liver microsomes (ref. 2)                            | 0.45   |
| Bovine adrenal medulla microsomes<br>(Table 1 of ref. 4) | 0.0040   |
| Rat erythrocyte ghosts (Table 2 of ref. 5)               | 0.0005   |
| Rat reticulocyte ghosts (Fig. 3 of ref. 6)               | 0.0001   |
| Mammary gland membranes (Table 3 of<br>ref. 8)           | 0.0003   |

Information in parentheses indicates the source of the data.

experiment reported in Table 1 of ref. 5, only 0.05% of the radioactivity is incorporated into phosphatidyl-*N*-monomethyl-ethanolamine. The radiopurity of the *S*-adenosyl-*L*-[Me-<sup>3</sup>H]methionine as supplied by New England Nuclear is approximately 99% by the time this compound is used. Thus, the amount of contaminating <sup>3</sup>H-labelled compounds is many times higher than the actual amount of <sup>3</sup>H incorporated. Therefore, it is essential that for each system quantitative data are provided which show that the only radioactivity incorporated in the membrane is that of <sup>3</sup>H-methyl in the polar head group of the methylated phospholipid. In the reports<sup>6-8,13-17</sup> that suggest a link between physiological effects and phospholipid methylation, such studies are lacking. In addition, these experiments are subject to the same criticisms as detailed above. Hence, we are not convinced that methylation of phosphatidylethanolamine is related to any physiological response or change in membrane fluidity.

We thank the MRC, the Canadian Heart Foundation and the BC Health Care Research Foundation for the support of B.K. while in Canada. This work was supported by grants from the MRC, BC Heart Foundation and NIH.

Received 18 March, accepted 18 September 1980

1. Brauner, J. & Greenberg, D. M. *Biochim Biophys Acta* **46**, 205-216 (1961)
2. Schneider, W. J. & Vance, D. E. *J. Biol. Chem.* **254**, 3886-3891 (1979).
3. Sundler, R. & Akesson, B. *J. Biol. Chem.* **250**, 3359-3367 (1975)
4. Hirata, F., Vivieros, O. H., Diliberto, E. J. & Axelrod, J. *Proc. natn. Acad. Sci. USA* **75**, 1718-1721 (1978)
5. Hirata, F. & Axelrod, J. *Proc. natn. Acad. Sci. USA* **75**, 2348-2352 (1978).
6. Strittmatter, W. J., Hirata, F. & Axelrod, J. *Science* **204**, 1205-1207 (1979)
7. Hirata, F., Strittmatter, W. J. & Axelrod, J. *Proc. natn. Acad. Sci. USA* **76**, 368-372 (1979).
8. Bhattacharya, A. & Vanderbeek, B. K. *Proc. natn. Acad. Sci. USA* **76**, 4489-4492 (1979)
9. Hirata, F. & Axelrod, J. *Nature* **275**, 219-220 (1978)
10. Quinn, P. J. *The Molecular Biology of Cell Membranes*, 31 (Macmillan, London, 1976)
11. van Deenen, L. L. M. & de Gier, J. in *The Red Blood Cell* Vol. 1 (ed. Sargent, D. M.) 147-211 (Academic, London, 1974)
12. Schroeder, F., Holland, J. F. & Vagelos, P. R. *J. Biol. Chem.* **251**, 6747-6756 (1976)
13. Pike, M. C., Krodach, W. M. & Strydoman, R. *Proc. natn. Acad. Sci. USA* **76**, 2922-2926 (1979).
14. Hirata, F., Axelrod, J. & Crews, F. T. *Proc. natn. Acad. Sci. USA* **76**, 4813-4816 (1979)
15. Mato, J. M. & Martin-Cao, D. *Proc. natn. Acad. Sci. USA* **76**, 6106-6109 (1979)
16. Strittmatter, W. J. *et al. Nature* **282**, 857-859 (1979)
17. Hirata, F., Corcoran, B. A., Venkatesubramanian, K., Schiffman, E. & Axelrod, J. *Proc. natn. Acad. Sci. USA* **76**, 2640-2643 (1979)

## Reply from J. Axelrod and F. Hirata

Section on Pharmacology, Laboratory of Clinical Science,  
National Institute of Mental Health, Bethesda, Maryland 20205

From papers published in our own and other laboratories, Vance and de Kruijff make calculations showing that phospholipid methylation activities observed in a variety of tissues and cells are very low. They then argue that because of these low enzyme activities, all the reported findings on the association between phospholipid methylation and biological responses are due to an impurity in *S*-adenosyl-Me-[Me-<sup>3</sup>H]methionine.

Vance and de Kruijff have not provided any experimental evidence for this assumption.

The reports on the methylation of membrane lipids satisfy the biochemical criteria of enzymatic reactions<sup>1-4</sup>: (1) no significant activity in a heated preparation, (2) saturated substrate concentration-velocity curves, (3) pH dependency, (4) subcellular localization, (5) sensitivity to proteolytic enzymes, (6) stimulation by exogenous phospholipid substrates and cofactors and (7) competitive inhibition by *S*-adenosylhomocysteine. All the methylated lipids arising from *S*-adenosyl-[Me-<sup>3</sup>H]methionine were identified by TLC with several solvent systems, chemical and enzymatic degradation and column chromatography with ion-exchange resin of products from chemical degradation<sup>1,2,4-6</sup>. These observations exclude the possibility of measuring the impurities as phospholipid methylation. The alternative explanation is that an impurity of <sup>3</sup>H-*S*-adenosylmethionine has the capacity to transmethyrate an acceptor lipid and an exceedingly high affinity ( $K_m$  in  $10^{-9}$  M range) for the reaction. In experiments using intact cells (mast cells<sup>5,7</sup>, basophils<sup>8</sup>, neutrophils<sup>9</sup>, astrocytoma cells<sup>10</sup> and lymphocytes<sup>11</sup>), [Me-<sup>3</sup>H]methionine, a precursor of *S*-adenosylmethionine, was used for the assay of phospholipid methylation. Therefore, the impurity should also be formed in intact cells from methionine and the transfer of the methyl group should be blocked by methyltransferase inhibitors such as *S*-adenosylhomocysteine and its analogues<sup>7-11</sup>. It would be extremely unlikely that an as yet unidentified artefact would have all of the above properties.

Vance and de Kruijff make the sweeping claim (without providing any evidence) that "... we are not convinced that methylation of phosphatidylethanolamine is related to any physiological response or change in membrane fluidity". Experiments have shown a dose-dependent increase of phospholipid methylation, with the methyl donor, *S*-adenosylmethionine, which is associated with a decrease in membrane viscosity of red blood cells<sup>12</sup>. When the methyltransferase inhibitor, *S*-adenosylhomocysteine is added with *S*-adenosylmethionine, changes in membrane viscosity are abolished with a concomitant inhibition of phospholipid methylation. It has been previously shown that extremely low concentrations of prostaglandins (a few molecules per cell) cause changes in membrane viscosity<sup>13</sup>. Therefore, the fact that small amounts of phospholipid are methylated is no indication that phospholipid methylation is not involved. The amounts of phospholipids methylated after the stimulation of  $\beta$ -adrenergic receptors in reticulocytes<sup>14</sup> and C<sub>6</sub> astrocytoma<sup>10</sup> are calculated to be 30 molecules per receptor molecule, a value which is almost equivalent to that of the annulus lipids around Ca<sup>2+</sup>-ATPase, a typical transmembrane protein<sup>15</sup>. Such changes in lipid composition may be sufficient to change the fluidity and to enhance the coupling of receptor to adenylate cyclase. As 1,6-diphenyl-1,3,5-hexatriene, a fluorescence probe we used for measuring membrane fluidity, is preferentially embedded in the boundary of lipid domains<sup>16</sup>, local and bulk changes of membrane fluidity cannot be separated by measuring its anisotropy. The order of potency for several agonists to increase methylation is similar to their ability to generate cyclic AMP<sup>10,14</sup>. Increased methylation could be blocked by  $\beta$ -adrenergic antagonists. These observations are consistent with the previous reports that increasing membrane fluidity with vaccenic acid facilitates coupling of receptor to adenylate cyclase<sup>17</sup> and that decreasing fluidity with cholesterol reduces the coupling<sup>18</sup>. Almost all the changes in phospholipid methylation reported were shown to be receptor mediated ( $\beta$ -adrenergic<sup>10,14</sup>, concanavalin A<sup>5,11</sup>, chemotactic peptide<sup>9</sup>, benzodiazepine<sup>10</sup> and IgE receptors<sup>7,10</sup>). Because receptors occupy only a tiny fraction of the cell surface, it would require only small amounts of methylating enzymes clustered near the receptor to produce changes in phospholipid composition. Note that phosphatidylcholine formed by transmethylation contains the major portion of arachidonic acid although transmethylation is only a minor pathway for the phosphatidylcholine synthesis compared with the CDP-choline pathway<sup>19,20</sup>. Arachidonic acid

(a fatty acid of great importance for cell function) is liberated by receptor stimulation<sup>8,9,11</sup>, suggesting a close coupling of receptor, methyltransferases and phospholipases and a rapid turnover of methylated phospholipids.

When cells are labelled with [ $^3\text{H}$ ]methionine, the methyl group is mainly incorporated into the phospholipid fraction via *S*-adenosylmethionine after receptor stimulation<sup>7</sup>. The subsequent physiological responses such as lymphocyte mitogenesis<sup>11</sup>, histamine release from mast cells<sup>5,7</sup> and basophils<sup>8</sup>

and leukocyte chemotaxis<sup>9</sup> can be inhibited by treatment with 3-deazaadenosine and its analogues, which are intracellularly transformed to *S*-adenosylhomocysteine analogues, inhibitors of transmethylation reactions<sup>21</sup>. By treating cells with 3-deazaadenosine and its analogues, phospholipid methylation but not the transmethylation of nucleotides and proteins is inhibited, in the conditions used by us. All these experiments show the close association between receptor-mediated phospholipid methylation and physiological responses.

- Hirata, F., Vivarona, O. H., Diliberto, E. Jr & Axelrod, J. *Proc. natn. Acad. Sci. U.S.A.* **75**, 1718-1720 (1978).
- Bloomquist, J. K., Zisapel, S. H. & Wortman, R. J. *Brain Res.* **179**, 319-327 (1979).
- Hirata, F. & Axelrod, J. *Proc. natn. Acad. Sci. U.S.A.* **75**, 2348-2352 (1978).
- Crews, F. T., Hirata, F. & Axelrod, J. *J. Neurochem.* **34**, 1491-1498 (1980).
- Hirata, F., Axelrod, J. & Crews, F. T. *Proc. natn. Acad. Sci. U.S.A.* **76**, 4813-4816 (1979).
- Crews, F. T., Hirata, F. & Axelrod, J. *Neurochem. Res.* (in the press).
- Ishizuka, T., Hirata, F., Ishizuka, K. & Axelrod, J. *Proc. natn. Acad. Sci. U.S.A.* **77**, 1903-1906 (1980).
- Crews, F. T., Morita, Y., Hirata, F., Axelrod, J. & Stragman, R. P. *Biochem. biophys. Res. Commun.* **93**, 42-49 (1980).
- Hirata, F., Corcoran, B. A., Venkatasubramanian, K., Schiffmann, E. & Axelrod, J. *Proc. natn. Acad. Sci. U.S.A.* **76**, 2640-2643 (1979).
- Strittmatter, W. J. *et al. Nature* **282**, 857-859 (1979).
- Hirata, F., Toyoshima, S., Axelrod, J. & Wexler, M. J. *Proc. natn. Acad. Sci. U.S.A.* **77**, 862-865 (1980).

- Hirata, F. & Axelrod, J. *Nature* **278**, 219-220 (1978).
- Kury, P. G., Ruzewicz, P. W. & McCormell, H. M. *Biochem. biophys. Res. Commun.* **86**, 178-185 (1974).
- Hirata, F., Strittmatter, W. J. & Axelrod, J. *Proc. natn. Acad. Sci. U.S.A.* **76**, 368-372 (1979).
- Bonnett, J. P., McChil, K. A. & Warren, G. B. *Nature* **274**, 823-825 (1978).
- Klemm, R. D., Klemm, A. M., Hoover, R. L. & Karnovsky, M. J. *J. Biol. Chem.* **255**, 1286-1295 (1980).
- Rimon, G., Hanaki, E., Brann, S. & Levitzki, A. *Nature* **276**, 394-396 (1978).
- Klein, L., Moore, L. & Pastan, I. *Biochem. biophys. Res. Commun.* **80**, 42-53 (1978).
- Ketyl, S. L. & Lombardi, B. *Lipids* **11**, 513-516 (1976).
- Trowbridge, M. A. & Collins, F. D. *Biochem. biophys. Res. Commun.* **296**, 51-61 (1973).
- Carroll, G. L., Richards, H. H. & Chang, P. K. in *Transmethylation* (eds Uchida, E., Borchard, R. T. & Creveling, G. R.) 155-165 (Elsevier, Amsterdam, 1979).

## Reduced somatostatin-like immunoreactivity in cerebral cortex from cases of Alzheimer disease and Alzheimer senile dementia

Peter Davies\*, Robert Katzman† & Robert D. Terry\*

Departments of \*Pathology and of Neuroscience, and of †Neurology and of Neuroscience, Albert Einstein College of Medicine, 1300 Morris Park Avenue, The Bronx, New York 10461

Both Alzheimer's disease and senile dementia of the Alzheimer type (AD/SDAT) are progressive dementias characterized neuropathologically by the presence in the cerebral cortex of numerous neurofibrillary tangles and neuritic plaques<sup>1</sup>. We use the abbreviation AD/SDAT to denote all such cases, irrespective of age of onset<sup>2</sup>. Studies of neurotransmitter-related parameters in autopsied brain tissues from patients with AD/SDAT have, to date, been confined to five putative transmitter systems. Acetylcholine-releasing neurones seem to be most markedly and consistently affected, as judged by the extensive reductions in choline acetyltransferase (ChAT) and acetylcholinesterase activities that have been reported<sup>3-6</sup>. Despite numerous studies, there is no consistent evidence for the involvement of neurones releasing dopamine, noradrenaline, serotonin, or  $\gamma$ -aminobutyric acid in AD/SDAT<sup>4</sup>, nor for loss of muscarinic cholinergic receptors<sup>7</sup>. Thus, the involvement of cholinergic neurones in AD/SDAT seems to be specific. However, the possible involvement of neurones using other chemicals as transmitters has yet to be explored. The recent recognition of the existence of so-called 'peptidergic neurones' in the mammalian brain (for review see ref. 8) and the availability of radioimmunoassay (RIA) techniques for studying these peptides, have led us to begin a systematic investigation of neuropeptides in autopsied brain tissue from cases of AD/SDAT, and from neurologically normal individuals. We report here results obtained with a RIA for somatostatin, showing that somatostatin-like immunoreactivity in the cerebral cortex is reduced in tissue from AD/SDAT patients.

Synthetic somatostatin (Peninsula) was coupled to bovine serum albumin as described by Arimura *et al.*<sup>9</sup>, and an antiserum was raised in rabbits. The serum was used in RIA at a final dilution of 1:48,000 with <sup>125</sup>I-labelled tyr<sup>1</sup>-somatostatin as tracer (NEN; 2,200 mCi mmol<sup>-1</sup>). The presence of 1  $\mu\text{g}$  per

tube of substance P, insulin, proinsulin, glucagon, Met-enkephalin, thyrotropin releasing hormone, gastrin, cholecystokinin octapeptide or neurotensin did not interfere with the assay. The limit of sensitivity of the assay was about 5 pg of synthetic somatostatin, the intra-assay variability was  $\pm 7\%$  and inter-assay variation  $\pm 12\%$ .

Samples of right cerebral cortex were obtained at autopsy from 12 neurologically normal individuals (mean age 74 yr, range 40-101 yr) within 24 h of death (mean delay death to autopsy 11 h, range 3-24 h). The areas studied were mid-frontal gyrus, superior temporal gyrus, inferior parietal cortex and hippocampus. Neuropathological examination of left cerebral hemispheres revealed no gross or microscopic abnormalities. Similar samples were obtained from 12 cases of AD/SDAT (mean age 74 yr, range 49-92 yr; mean delay 10 h, range 2-16 h). Neuropathologically, all 12 AD/SDAT cases showed many neurofibrillary tangles and neuritic plaques in sections of frontal and parietal cortex, and in hippocampus, with no evidence of cerebrovascular disease, Parkinson's disease or other abnormality.

Extracts of brain tissues were made by boiling in 2 M acetic acid, homogenization and centrifugation at 10,000g for 30 min. Aliquots of supernatants were freeze-dried and residues were re-dissolved in phosphate-buffered saline, pH 8.2, containing 0.1% bovine serum albumin. The efficiency of extraction of <sup>125</sup>I-labelled somatostatin added to frozen tissue samples was 89%. The slopes of displacement curves produced by the addition of serial dilutions of extracts of brain regions were not significantly different from those produced by addition of various amounts of synthetic somatostatin. Although this indicates immunochemical similarity between material in brain extracts and synthetic somatostatin, it does not prove identity. Our preliminary studies with gel filtration have so far failed to

Table 1 Choline acetyltransferase activity in cerebral cortex samples from normal and AD/SDAT cases

|                         | Normal            |    |         | AD/SDAT           |    |        |
|-------------------------|-------------------|----|---------|-------------------|----|--------|
|                         | Mean $\pm$ s.e.m. | n  | Range   | Mean $\pm$ s.e.m. | n  | Range  |
| Hippocampus             | 575 $\pm$ 77      | 11 | 203-960 | 168 $\pm$ 31      | 10 | 58-367 |
| Frontal cortex          | 394 $\pm$ 59      | 12 | 91-751  | 48 $\pm$ 9        | 11 | 7-112  |
| Parietal cortex         | 305 $\pm$ 49      | 12 | 112-681 | 35 $\pm$ 8        | 12 | 7-77   |
| Superior temporal gyrus | 428 $\pm$ 69      | 12 | 97-673  | 49 $\pm$ 16       | 12 | 9-164  |

Choline acetyltransferase activity is expressed as nmol acetylcholine produced per h per 100 mg protein. Values for all regions of AD/SDAT cases are significantly lower than those of normals ( $P < 0.01$ ).



**Table 2** Somatostatin-like immunoreactivity in cerebral cortex samples from normal and AD/SDAT cases

|                         | Normal     |    |           | AD/SDAT    |    |           |
|-------------------------|------------|----|-----------|------------|----|-----------|
|                         | Means.e.m. | n  | Range     | Means.e.m. | n  | Range     |
| Hippocampus             | 3.56±0.40  | 10 | 0.84–5.35 | 0.95±0.04  | 8  | 0.77–1.10 |
| Frontal cortex          | 2.99±0.39  | 12 | 1.11–5.79 | 0.72±0.15  | 12 | 0.17–1.45 |
| Parietal cortex         | 3.28±0.70  | 12 | 1.27–8.89 | 1.47±0.40  | 12 | 0.07–3.83 |
| Superior temporal gyrus | 3.05±0.39  | 12 | 0.75–5.04 | 0.97±0.30  | 12 | 0.00–2.86 |

Somatostatin-like immunoreactivity is expressed as ng per mg protein. Values for hippocampus, frontal cortex and superior temporal gyrus are significantly lower in AD/SDAT than in normal tissue ( $P < 0.01$ ), as are those in parietal cortex ( $P < 0.05$ ).

reveal evidence for the presence of high molecular weight (>3,000) putative precursors of somatostatin in acetic acid extracts of human cerebral cortex. We therefore refer to immunoreactive material in human brain as somatostatin-like immunoreactivity. Choline acetyltransferase activities from these cases were determined on separate samples of the same brain regions by methods previously described<sup>3</sup>.

In agreement with our own and other published data, all four regions of AD/SDAT brains investigated showed marked, statistically significant reductions in the activity of ChAT (see Table 1). The reductions in ChAT reported here, and by one of us previously, are larger than those reported by others. One reason for this may be the ages of the patients chosen as controls, as we have discussed elsewhere<sup>3</sup>. A second factor may be our selection of only severe cases of AD/SDAT; that is, of only those cases with many plaques and tangles in both the cerebral cortex and hippocampus. The amounts of somatostatin-like immunoreactivity in all four regions of AD/SDAT brains were also significantly below those found in brains from normal individuals (Table 2). In the hippocampus, both ChAT activity and somatostatin-like immunoreactivity were reduced by about the same extent, 70.8% and 73.3%, respectively. It is possible that these two parameters are within the same neuronal structure: co-existence of peptide and amine transmitters in a single neurone has been demonstrated in other systems<sup>8</sup>. However, there is no other evidence for the presence of somatostatin in cholinergic terminals in the hippocampus. In the cortical regions studied, there is a greater loss of ChAT activity than of somatostatin-like immunoreactivity. The greatest loss of somatostatin-like immunoreactivity seems to occur in frontal cortex (75.9%), and the least in parietal cortex (55.2%). In both these regions the ChAT activity is reduced by almost 90%.

We have considered the possibility that the reduced somatostatin-like immunoreactivity found in the AD/SDAT cases might result from factors other than the disease. However, we have been unable to find any evidence of correlation between the amount of somatostatin-like immunoreactivity and the age of the patient, either in the control or AD/SDAT groups. Similarly, there was no correlation between the somatostatin-like immunoreactivity concentration and the delay period between death and autopsy. Because of the large number of different drug treatments administered to both the controls and the AD/SDAT cases before death, we have been unable to determine whether any one such treatment might be of particular significance.

Thus, our data seem to indicate the involvement of a second putative neurotransmitter system in AD/SDAT, and provide the first evidence for loss of a neuronal peptide in AD/SDAT cases. Efforts must now be directed towards characterizing the immunoreactive material in both normal and AD/SDAT brain. We do not yet know whether or not the loss of somatostatin-like immunoreactivity has functional significance to the patient with AD/SDAT. Further clinical and biochemical work is needed before this most important point can be clarified.

Our thanks to Aurora Thompson for technical assistance. This work was supported in part by NIH grants AG-01066, NS-03356 and NS-02255, and by a gift from A. and B. Condiolti.

Received 16 May; accepted 15 October 1980.

1. Wisniewski, H. M. & Terry, R. D. in *Neurobiology of Aging* (eds Terry, R. D. & Gershon, S.) 265–280 (Raven, New York, 1976).
2. Katzman, R. *Archs Neurol., Chicago* **33**, 217 (1976).
3. Davies, P. *Brain Res.* **171**, 319 (1979).
4. White, P. *et al. Lancet* **i**, 668 (1977).
5. Perry, E. K., Perry, R. H., Blessed, G. & Tomlinson, B. E. *Lancet* **i**, 189 (1977).
6. Terry, R. D. & Davies, P. *A. Rev. Neurosci.* **3**, 77 (1980).
7. Davies, P. & Verth, A. H. *Brain Res.* **138**, 385 (1977).
8. Hokfelt, T., Johansson, O., Ljungdahl, A., Lundberg, J. M. & Schultzberg, M. *Nature* **284**, 515 (1980).
9. Arimura, A., Sato, H., Coy, D. H. & Schally, A. V. *Proc. Soc. exp. Biol. Med.* **148**, 784 (1975).

## A new class of angiotensin-converting enzyme inhibitors

A. A. Patchett, E. Harris, E. W. Tristram, M. J. Wyvratt, M. T. Wu, D. Taub, E. R. Peterson, T. J. Ikeler, J. ten Broeke, L. G. Payne, D. L. Ondeyka, E. D. Thorsett, W. J. Greenlee, N. S. Lohr, R. D. Hoffsommer, H. Joshua, W. V. Ruyle, J. W. Rothrock, S. D. Aster, A. L. Maycock, F. M. Robinson & R. Hirschmann

New Lead Discovery Department, Basic Research, Merck Sharp and Dohme Research Laboratories, Division of Merck and Co. Inc., Rahway, New Jersey 07065

C. S. Sweet, E. H. Ulm, D. M. Gross, T. C. Vassil & C. A. Stone

Merck Institute for Therapeutic Research, West Point, Pennsylvania 19486

**Much current attention focuses on the renin-angiotensin system in relation to mechanisms controlling blood pressure and renal function. Recent demonstrations (ref 1, ref. 2 and refs therein) that angiotensin-converting enzyme inhibitors show promising clinical antihypertensive properties have been of particular interest. We now report on the design of a novel series of substituted N-carboxymethyl-dipeptides which are active in inhibiting angiotensin-converting enzyme at nanomolar levels. We suggest that these compounds are transition-state inhibitors and that extensions of this design to other metalloendopeptidases merit further study.**

The biological profile of three of these inhibitors was assessed in rats and dogs by the antagonism of the pressor response to angiotensin I. High converting-enzyme inhibitory activities (at doses as low as 2.3 µg per kg) were demonstrated after intravenous (i.v.) administration. Given orally (p.o.) in dogs these three compounds showed good activities with a duration of action of at least 6 h at doses of 0.3 mg per kg. This particularly long duration of action and their apparent specificity may make these compounds useful in the treatment of hypertension.

Angiotensin-converting enzyme (peptidyl dipeptide hydrolase, EC 3.4.15.1) generates the powerful vasoconstrictor substance angiotensin II by removing the C-terminal dipeptide from the precursor decapeptide angiotensin I (ref. 3). The enzyme also inactivates the vasodilating substance bradykinin<sup>4</sup>. That angiotensin-converting enzyme inhibitors might display useful antihypertensive properties has been demonstrated clinically by the nonapeptide SQ 20,881 (ref. 1) and more recently by many studies<sup>2</sup> on the orally active angiotensin-converting enzyme inhibitor captopril (SQ 14,225)<sup>5</sup>. The latter structure, D-3-mercapto-2-methylpropanoyl-L-proline (resulting from work by the Squibb group) inhibits the enzyme with a reported IC<sub>50</sub> of  $2.3 \times 10^{-8}$  M (ref. 6).

**Table 1** *In vitro* converting-enzyme inhibitory activities of *N*-carboxymethyl-L-alanyl-L-proline, derivatives and analogues\*

| <div><math display="block">\begin{array}{c} R_1 \\   \\ CH-Ala-Pro \\   \\ CO_2H \end{array}</math></div> |   |                          |   |                |                          |
|---|---|--------------------------|---|----------------|--------------------------|
| No.   | R <sub>1</sub>                                      | IC <sub>50</sub>         | No.                                     | R <sub>1</sub> | IC <sub>50</sub>         |
| 1   | H—†   | 2.4 × 10 <sup>-6</sup> M | Related analogues                       |                |                          |
| 2   | CH <sub>3</sub> —                                   | 9 × 10 <sup>-8</sup> M   | 9                                       |                | 5.8 × 10 <sup>-6</sup> M |
| 3   | CH <sub>3</sub> CH <sub>2</sub> —                   | 1.7 × 10 <sup>-8</sup> M |   |                |                          |
| 4   |   | 2.6 × 10 <sup>-9</sup> M | 10                                      |                | 1.2 × 10 <sup>-6</sup> M |
| 5   |   | 3.9 × 10 <sup>-8</sup> M |   |                |                          |
| 6   |   | 3.8 × 10 <sup>-9</sup> M | Maleate salt<br>(S, S, S configuration) |                |                          |
| 6a  | <br>(S configuration)                               | 1.2 × 10 <sup>-9</sup> M | 11                                      |                | 1.3 × 10 <sup>-6</sup> M |
| 6b  | <br>(R configuration)                               | 8.2 × 10 <sup>-7</sup> M |   |                |                          |
| 7   | NH <sub>2</sub> —(CH <sub>2</sub> ) <sub>4</sub> —§ | 2.2 × 10 <sup>-9</sup> M | 12                                      |                | 4.8 × 10 <sup>-6</sup> M |
| 8   | NH <sub>2</sub> —(CH <sub>2</sub> ) <sub>5</sub> —  | 5.2 × 10 <sup>-9</sup> M |   |                |                          |

Converting enzyme was prepared from fresh citrated hog plasma by the method of Dorer *et al.*<sup>17</sup> up to fraction 'B', followed by chromatography on Sephadex G-200 and collection of the fractions of highest specific activity. This enzyme was chloride-dependent, 90% inhibited by EDTA at  $1 \times 10^{-4}$  M and yielded His-Leu from angiotensin I as determined by TLC. Assays adapted from the method of Piquilloud *et al.*<sup>18</sup> were conducted in the following manner. Test compounds were dissolved at  $5 \times 10^{-3}$  M in 0.05 M borate-phosphate buffer, pH 8.0, 0.17 M in NaCl. Further dilutions were made with this buffer. To 100  $\mu$ l of each test-compound solution was added 100  $\mu$ l each of  $3.7 \times 10^{-4}$  M substrate solution Cbz-Phe-His-[<sup>14</sup>C-Leu]-OH, 5,500 c.p.m. per tube and converting-enzyme solution diluted from stock so as to give approximately 1,200 c.p.m. in the control supernatant after incubation. The final concentration of substrate was  $1.23 \times 10^{-4}$  M.  $K_m$  in this assay system was between 1 and  $2 \times 10^{-4}$  M. The reaction was incubated 1 h at 30 °C, then terminated by the addition of 1 ml of a 40% (settled solids) suspension in 0.05 M borate buffer of benzoylated DEAE (BD) cellulose (Schwarz-Mann 100–200 mesh, defined), pH 11 or 20% BD Sephadex (Biorad) in 0.05 M borate buffer, pH 7.7. Unreacted substrate was bound to the BD adsorbant and separated from supernatant by filtration through a cotton-plugged Sarpette (size 102/2, Walter Sarstedt). The entire supernatant plus a 0.5-ml buffer wash of the BD residue was collected in a scintillation vial. Counting was done in 10 ml PCS (Amersham Searle) for 10 min. Minus-enzyme blanks were run through the assay and subtracted from each control and test count. IC<sub>50</sub> values (concentration for 50% inhibition) were determined by linear regression of logit against log concentration over a 20–80% inhibition range.

\* Except where indicated, compounds were synthesized by the reductive condensation of  $\alpha$ -ketoacids or esters with dipeptides and were assayed without the separation of diastereomers. All compounds were characterized by satisfactory mass spectra and NMR data and by TLC on silica-gel plates.

† This compound was prepared by the alkylation of L-alanyl-L-proline in aqueous solution at 85 °C by the portion-wise addition of chloroacetic acid over 1 h with maintenance of pH 8–9.

‡ Diastereomers were separated by chromatography on 200–400 mesh XAD-2 polystyrene resin (Rohm and Haas) using 95:5 (v/v) 0.1 M aqueous NH<sub>4</sub>OH-methanol and were crystallized from water. Compound 6a (eluted first) [ $\alpha$ ]<sub>D</sub><sup>25</sup> =  $-67.0^\circ$  C (0.1 M HCl); compound 6b (eluted second) [ $\alpha$ ]<sub>D</sub><sup>25</sup> =  $-101.6^\circ$  C (0.1 M HCl). Compound 6a: Analyses calculated for C<sub>18</sub>H<sub>24</sub>N<sub>2</sub>O<sub>5</sub>·1/2H<sub>2</sub>O: C, 60.40; H, 7.05; N, 7.84. Found: C, 60.60; H, 7.01; N, 7.79.

§ Compound 7 was prepared from  $\epsilon$ -benzyloxycarbonyl-L-lysine ethyl ester and *N*-pyruvoyl-L-proline in dry tetrahydrofuran. Sodium cyanoborohydride was added to this mixture after it had been stirred at room temperature for 4 h with powdered no. 4A molecular sieves. Protecting groups were removed by saponification of the ethyl ester with 0.1 M NaOH overnight followed by hydrogenolysis of the benzyloxycarbonyl group in 1:1 ethanol-water over 10% Pd/C catalyst at 40 p.s.i. Diastereomers were not separated.

|| Hydrocinnamaldehyde was reductively condensed with L-alanyl-L-proline using sodium cyanoborohydride in aqueous ethanol.

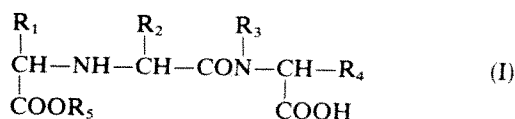
¶ This salt was precipitated from an acetonitrile solution of *N*-(1-ethoxycarbonyl-3-phenylpropyl)-L-alanyl-L-proline (mixed diastereomers) using a half-molar equivalent of maleic acid. Repeated recrystallization from acetonitrile afforded pure compound 10 [ $\alpha$ ]<sub>D</sub><sup>25</sup> =  $-42^\circ$  (CH<sub>3</sub>OH). Analyse calculated for C<sub>24</sub>H<sub>22</sub>N<sub>2</sub>: C, 58.53; H, 6.55; N, 5.69. Found: C, 58.49; H, 6.53; N, 5.61. As even traces of 6a in this sample would give significant inhibition, the IC<sub>50</sub> may overestimate its potency.

# Compound 10 is also designated MK-421.

\*\* Compound 11 was prepared from *N*-pyruvoyl-L-proline and L-proline benzyl ester using sodium cyanoborohydride in methanol. The benzyl group was subsequently removed by hydrogenolysis using 10% Pd/C in aqueous ethanol at 40 p.s.i. Diastereomers were not separated.

†† Compound 12 was prepared from d1-2,4-dimethylglutaric acid<sup>19</sup> which as its anhydride was reacted with L-proline benzyl ester in CH<sub>2</sub>Cl<sub>2</sub>. The benzyl group was removed by hydrogenolysis and the diastereomers separated by successive chromatography over LH-20 using CH<sub>3</sub>OH followed by HPLC on a Whatman Partisil-10 ODS-2 preparative column using H<sub>2</sub>O:CH<sub>3</sub>CN:HOAc (75:25:1).

The most common side effects accompanying the clinical use of captopril are rashes and loss of taste both of which usually clear on withdrawal or reduction of dose<sup>2</sup>. As similar side effects are observed with penicillamine<sup>7</sup>, we looked for potent specific inhibitors of angiotensin-converting enzyme lacking a mercapto function and characterized by weak chelating properties. We report here the design of such compounds illustrated by generic formula (I).



These substituted *N*-carboxymethyl-dipeptides are conveniently prepared by the reductive coupling of  $\alpha$ -ketoacids or esters to the amino terminus of suitably protected dipeptides utilizing sodium cyanoborohydride or hydrogenation with palladium-on-carbon or Raney nickel. Typically, 1.42 g of 2-oxo-4-phenylbutyric acid was dissolved in 5 ml of water by adjusting the pH to 6.8 with 50% NaOH. L-Alanyl-L-proline (0.27 g) was then added and the solution treated with 0.28 g of sodium cyanoborohydride in 5 ml of water. After stirring at room temperature overnight, 35 ml of Dowex 50 X-2, 50–100 mesh on the acid cycle, was added to absorb the product and destroy any residual sodium cyanoborohydride. The slurry was then added to a column containing 20 ml of Dowex 50 and



**Table 2** *In vitro* converting-enzyme inhibitory activities of *N*-(1-carboxy-3-phenylpropyl)-dipeptides

| $\text{C}_6\text{H}_5-\text{CH}_2\text{CH}_2-\underset{\text{CO}_2\text{H}}{\text{CH}}-\text{A}_1-\text{A}_2$ |                            |                    |                        |
|---|----------------------------|--------------------|------------------------|
| No.   | A <sub>1</sub>             | A <sub>2</sub>     | IC <sub>50</sub>       |
| 13  | L-alanine                  | L-4-thiaproline    | $7.6 \times 10^{-9}$ M |
| 14*   | L-alanine                  | L-4-hydroxyproline | $1.2 \times 10^{-9}$ M |
| 15  | L-alanine                  | L-pipecolic acid   | $2.2 \times 10^{-9}$ M |
| 16  | L-alanine                  | L-lysine           | $1.9 \times 10^{-8}$ M |
| 17  | glycine                    | L-proline          | $2.3 \times 10^{-7}$ M |
| 18  | D-alanine                  | L-proline          | $2.5 \times 10^{-6}$ M |
| 19  | <i>N</i> -methyl-L-alanine | L-proline          | $1.0 \times 10^{-7}$ M |
| 20  | L-fluoroalanine            | L-proline          | $3.6 \times 10^{-9}$ M |
| 21  | L-lysine                   | L-proline          | $6.8 \times 10^{-9}$ M |
| 21a†  | L-lysine                   | L-proline          | $1.2 \times 10^{-9}$ M |
| 22  | L-arginine                 | L-proline          | $6.4 \times 10^{-9}$ M |

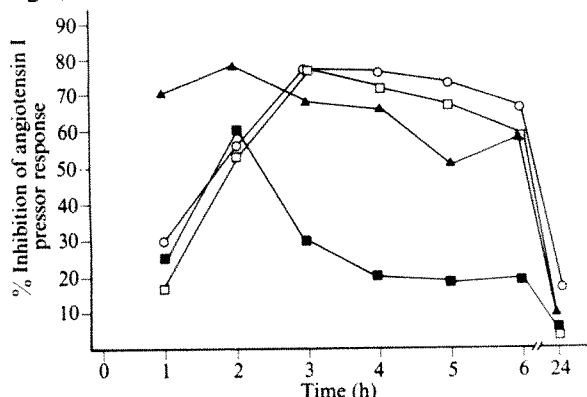
See Table 1 legend for methods.

\* The data reported are for the more active diastereomer which was separated from the mixture of isomers by chromatography on a 200–325 mesh XAD-2 polystyrene resin column using 0.1 M NH<sub>4</sub>OH as the eluant.

† Compound 21a was isolated from the mixture of diastereomers (compound 21) by initial LH-20 chromatography using methanol followed by chromatography on a jacketed 200–400 mesh XAD-2 polystyrene resin column at 50°C utilizing 3% acetonitrile in 0.1 M NH<sub>4</sub>OH as the eluant. The more active diastereomer 21a eluted first and was crystallized from methanol/ethyl acetate;  $[\alpha]_D^{25} = -23.3^\circ$  (CH<sub>3</sub>OH). Analyses calculated for C<sub>21</sub>H<sub>31</sub>N<sub>3</sub>O<sub>5</sub>·H<sub>2</sub>O: C, 59.56; H, 7.85; N, 9.92. Found: C, 59.56; H, 7.88; N, 9.77.

neutrals eluted with methanol and water. The product was eluted with 8 × 50 ml of 2% pyridine in water, and the product-rich cuts were lyophilized to yield 0.43 g of *N*-(1-carboxy-3-phenylpropyl)-L-alanyl-L-proline as a mixture of two diastereomers. Alternatively some compounds have been synthesized as indicated in Tables 1 and 2 legends by reductive coupling of amino acids to pyruvoyl-L-proline or via dipeptide alkylation using the appropriate α-haloacid.

A new asymmetric centre is created when ketoacids or esters are reductively coupled to dipeptides to yield structures of formula (I). These diastereomers can be separated by chromatography. For example, compound 6 after chromatography on milled XAD-2 polystyrene resin with 0.1 M NH<sub>4</sub>OH in 95:5 (v/v) water/methanol yielded diastereomers 6a and 6b differing in their *in vitro* potencies by roughly 700-fold. The more active diastereomer 6a was determined by X-ray diffraction to have the *S, S, S* configuration (the structure was determined by Dr J. P. Springer).



**Fig. 1** The p.o. converting-enzyme inhibitory activity of captopril (■), inhibitors 6a (▲), 10 (□) and 21a (○) at 0.3 mg per kg p.o. in unanaesthetized dogs. Dogs were fasted overnight. The per cent inhibition of the pressor response to angiotensin I, 150 ng per kg i.v. over 6 h is shown. Each compound was evaluated in at least three dogs. The animals were not challenged with angiotensin I between 1 and 2 h. Thus the possibility exists that captopril's peak effect could have occurred between 1 and 2 h.

We synthesized over 200 variants of structure (I) to explore requirements for tight inhibitor binding. Representative structures are shown in Tables 1 and 2. In apparent parallel with studies on captopril analogues<sup>5,6,8</sup>, we found that cyclic imino acids such as proline confer particularly high activity at the dipeptide's carboxyl terminus. Consistent with the enzyme's specificity<sup>9–11</sup> imino acids in the position penultimate to the carboxyl terminus were not compatible with high inhibitory activities (for example, compounds 11 and 19). Note that both hydrophobic and basic substituents could be incorporated at R<sub>1</sub> and R<sub>2</sub> in highly active analogues. Inhibitory specificity was demonstrated by the inactivity of compounds 6a and 10 when tested at  $3.3 \times 10^{-5}$  M against renin, plasmin, trypsin, chymotrypsin and carboxypeptidases A and B (E.H.U. and T.C.V., details to be reported elsewhere). Note also that the amino acid analogue *N*-(1-carboxy-3-phenylpropyl)-L-alanine inhibited carboxypeptidase A and angiotensin-converting enzyme by less than 10% at  $1 \times 10^{-5}$  M.

Studies on the mechanism of action of these inhibitors are in progress. Inhibition by a chelating effect to remove Zn<sup>2+</sup> from the active site of the enzyme can be ruled out because the *in vitro* enzyme inhibitory activity of these compounds is unaffected by added Zn<sup>2+</sup>. Indeed, their chelating ability for Zn<sup>2+</sup> is only comparable to that of α-amino acids<sup>12</sup>. For example, log K<sub>1</sub> for compound 6a is 4.9. The kinetics of inhibition by compounds 6a and 21a are consistent with a competitive mechanism (H. Bull, E. H. Cordes and N. Thornberry, to be reported elsewhere). Furthermore, the importance of the NH in structure (I) for inhibitory potency is suggested by the marked reduction in activity resulting from the replacement of the NH in compound 2 by a CH<sub>2</sub> group (compound 12). This finding is consistent with the enzyme's well-documented<sup>9,11</sup> requirement for an —NH at the corresponding position in peptide substrates. We suggest that our inhibitors should be broadly classified as transition-state inhibitors (ref. 13 and refs therein). In this interpretation

**Table 3** *In vivo* comparisons of selected converting-enzyme inhibitors including captopril

| Compound  | IC <sub>50</sub> *<br><i>In vitro</i> | ID <sub>50</sub> (rat)<br>i.v. (μg per kg) | ID <sub>50</sub> (dog)<br>i.v. (μg per kg) |
|-----------|---------------------------------------|--|--|
| Captopril | $2 \times 10^{-8}$ M                  | 60.5<br>(51.3–71.6)                        | 80<br>(67–97)                              |
| 6a        | $1.2 \times 10^{-9}$ M                | 8.2<br>(6.6–10.6)                          | 6.4<br>(4.7–8.0)                           |
| 10        | $1.2 \times 10^{-6}$ M                | 14<br>(12.2–16.2)                          | 278<br>(240–324)                           |
| 21a       | $1.2 \times 10^{-9}$ M                | 2.3<br>(1.7–3.0)                           | 6.5<br>(5.6–7.6)                           |

The ability of the compounds to inhibit the pressor response to angiotensin I (see text for doses) was determined in mecamylamine (1.0 mg per kg i.v.)-pretreated anaesthetized (Dial-urethane, 0.8 mg per kg intraperitoneally) rats and in anaesthetized (vinbarbital sodium, 60 mg per kg) normotensive dogs. These doses of angiotensin I in rats and dogs caused an approximately equivalent pressor response (50–60 mm Hg). The ID<sub>50</sub> (dose of inhibitor which produced a 50% inhibition of angiotensin I) was computed in both rats and dogs by increasing the doses of the antagonist in logarithmic intervals and in a cumulative manner. In rats and dogs the ID<sub>50</sub> varied with the dose of angiotensin I. Rubin *et al.*<sup>20</sup> found considerably lower values for captopril's ID<sub>50</sub>, for example, 15 (13–18) μg per kg i.v. in anaesthetized rats. The reason for the higher ID<sub>50</sub> in the present experiments may reflect differences in anaesthetic, presence of ganglionic blockade and interval between doses. Our *in vitro* results with captopril are consistent with those reported by Ondetti *et al.*<sup>5</sup> regarding the inhibition of converting enzyme (see above) and the potentiation of bradykinin in which we determined an AC<sub>50</sub> of 2.4 nM in the guinea pig ileum. The ID<sub>50</sub> values in rats and dogs were also computed in a nmol per kg basis. In rats for captopril, compounds 6a, 10 and 21a, the following values were computed: 253.1, 23.5, 37.2 and 5.7 nmol per kg, respectively. In the dog, the corresponding ID<sub>50</sub> values in nmol per kg were as follows: captopril, 334.7; compound 6a, 18.4; compound 10, 738.6; and compound 21a, 16.0. The values in parentheses are the 95% confidence intervals.

\* See Tables 1 and 2. The IC<sub>50</sub> for captopril varied from  $3.4 \times 10^{-8}$  M to  $2.9 \times 10^{-9}$  M with the most of the determinations at  $2 \times 10^{-8}$  M.

transition state-like geometry is attained at the scissile CONH locus via the  $\text{CHCO}_2\text{H}$  and  $\text{NH}$  groups. Cumulative binding contributions are provided by the  $\text{CO}_2\text{H}$ ,  $\text{NH}$  and  $\text{R}_1$  groups as indicated in the analogue studies. It remains to be determined if the  $\text{NH}$  is protonated while bound to the enzyme, thus contributing a potential electrostatic interaction.

These compounds were evaluated for their ability to antagonize the pressor effect of angiotensin I administered i.v. to rats and dogs. Doses of angiotensin I were selected which represented the midpoint of their respective dose-response curves. In anaesthetized rats this was 100 ng per kg i.v., and it was 600 ng per kg i.v. in anaesthetized dogs. In conscious dogs, angiotensin I was administered at 150 ng per kg i.v. Data for three of our inhibitors are summarized in Table 3 and compared with captopril. Clearly compounds 6a, 10 and 21a were highly active by the i.v. route in rats. The same was true in dogs except for compound 10 whose ester functionality was found to be hydrolysed by dog liver homogenates but poorly so by dog plasma. Hydrolysis of compound 10 in rat plasma was rapid. (Hydrolysis of  $^{14}\text{C}$ -(Proline UL) compound 10 to compound 6a was estimated by incubation of  $10^{-5}\text{ M}$  compound 10 with undiluted plasma or a 1:5 homogenate of liver in  $5\text{ mM}$   $\text{NaHCO}_3$ . The reaction was stopped at various times by acidification with  $\text{HCl}$  and after isolation using XAD-4 resin the proportion of compounds 6a to 10 was determined by TLC (Quantum LQDF developed with  $n\text{-BuOH}:\text{HOAc}:\text{H}_2\text{O}$ , 4:1:1) and by the degree of inhibition of angiotensin-converting enzyme.)

All three compounds were orally active in rats and dogs. Comparative p.o. converting-enzyme inhibitory activities in dog are shown in Fig. 1. Compounds 6a, 10 and 21a displayed high potency in inhibiting the blood pressure response to angiotensin I and all had a long duration of action. Detailed pharmacological studies further demonstrating the p.o. and i.v. activities of some of these compounds and their antihypertensive properties will be reported elsewhere<sup>14,15</sup>.

Clinical studies now in progress<sup>16</sup> with compound 10 (MK-421) should help to determine if converting-enzyme inhibitors lacking a mercapto function have advantages in respect to side effects. More importantly, we believe that our angiotensin-converting enzyme inhibitors have important design implications for the synthesis of inhibitors of other metallopeptidyl carboxypeptidases and possibly of metalloendopeptidases more generally. In our design a  $\text{CO}_2\text{H}$ , an  $\text{NH}$  and an  $\text{R}$  group are arranged in tetrahedral geometry at the locus of the scissile amide group. Their binding energies in concert replace the  $\text{Zn}^{2+}$ /sulphydryl interaction which is a required feature of captopril<sup>3,6,8</sup>.

We thank Drs C. Hoffman, S. Michelson and H. Schwam for isolations of angiotensin-converting enzyme, and Dr J. A. McCauley for determination of the zinc metal stability constant.

Received 14 May, accepted 18 September 1980

- Ovras, H. *et al* *New Engl. J. Med.* **291**, 817-821 (1974)
- Atkinson, A. B. & Robertson, J. I. S. *Lancet* **ii**, 836-839 (1979)
- Skoggs, L. T., Marsh, W. H., Kahn, J. R. & Shumway, N. P. *J. exp. Med.* **99**, 275-282 (1954)
- Yang, H. Y. T., Erdos, E. G. & Levin, Y. *Biochem. Biophys. Acta* **214**, 374-376 (1970)
- Ondetti, M. A., Ruben, B. & Cushman, D. W. *Science* **196**, 441-444 (1977)
- Cushman, D. W., Cheung, H. S., Sabo, E. F. & Ondetti, M. A. *Biochemistry* **16**, 5484-5491 (1977)
- Lovine, W. G. in *The Pharmacological Basis of Therapeutics* 5th edn (eds Goodman, L. S. & Gilman, A.) 919-920 (Macmillan, New York, 1975)
- Cushman, D. W., Cheung, H. S., Sabo, E. F. & Ondetti, M. A. *Fed. Proc.* **33**, 2778-2782 (1979)
- Soffer, R. L. *A. Rev. Biochem.* **45**, 73-94 (1976)
- Cheung, H. S., Wang, F. L., Ondetti, M. A., Sabo, E. F. & Cushman, D. W. *J. Biol. Chem.* **255**, 401-407 (1980)
- Bockner, C. F. & Caprioli, R. M. *Biochem. Biophys. Res. Commun.* **93**, 1290-1296 (1980)
- Stability Constants of Metal Ion Complexes* 520 (Spec. Publ. no. 17, The Chemical Society, London, 1964)
- Wolfenden, R. *A. Rev. Biophys. Bioeng.* **8**, 271-306 (1976)
- Sweet, C. S. *et al* *J. Pharmac. exp. Ther.* (submitted)
- Gross, D. M. *et al* *J. Pharmac. exp. Ther.* (submitted)
- Bodlitz, J. *et al* *Clin. Pharmac. Ther.* (submitted)
- Dorje, F. E., Kahn, J. R., Lantz, K. E., Lovine, M. & Skoggs, L. T. *Circulation Res.* **34**, 824-827 (1974)
- Pearlman, Y., Romberg, A. & Roth, M. *Biochem. Biophys. Acta* **206**, 136-142 (1970)
- Allinger, N. L. *J. Am. chem. Soc.* **81**, 232 (1959)
- Ruben, B. *et al* *J. Pharmac. exp. Ther.* **204**, 271 (1978).

## <sup>3</sup>H-apomorphine labels both dopamine postsynaptic receptors and autoreceptors

Pierre Sokoloff, Marie-Pascale Martres & Jean-Charles Schwartz

Unité 109 de Neurobiologie, Centre Paul Broca de l'INSERM, 2ter, rue d'Alésia, 75014 Paris, France

Evidence points to the existence of multiple classes of dopamine (DA) receptor in mammalian brain which can be distinguished by their pharmacological specificities and localizations, and by the actions they mediate<sup>1</sup>. Among them, dopaminergic autoreceptors are regulatory receptors presumed to be present in the membrane of the DA neurones themselves, and believed to mediate an inhibition of these neurones' activity, either at nerve endings or on cell bodies<sup>2-4</sup>. However, the pharmacology of autoreceptors remains to be established because attempts to characterize autoreceptors by <sup>3</sup>H-ligand binding techniques have produced controversial data. Thus Seeman and co-workers stated that <sup>3</sup>H-apomorphine selectively labels autoreceptors<sup>5,7</sup>, whereas Creese *et al.* concluded that this ligand selectively labels postsynaptic DA receptors<sup>8,9</sup>. In addition, large differences in the capacity and drug specificity of <sup>3</sup>H-apomorphine receptor sites in rat striatum have been reported<sup>10-13</sup>. We demonstrate here that <sup>3</sup>H-apomorphine labels two classes of DA receptor, distinguishable using domperidone, a selective DA antagonist<sup>14-17</sup>. Lesion studies indicate that they correspond to a certain class of postsynaptic receptor and to autoreceptors, respectively. Each of these classes displays a clearly distinct pharmacological specificity for antipsychotics and DA agonists.

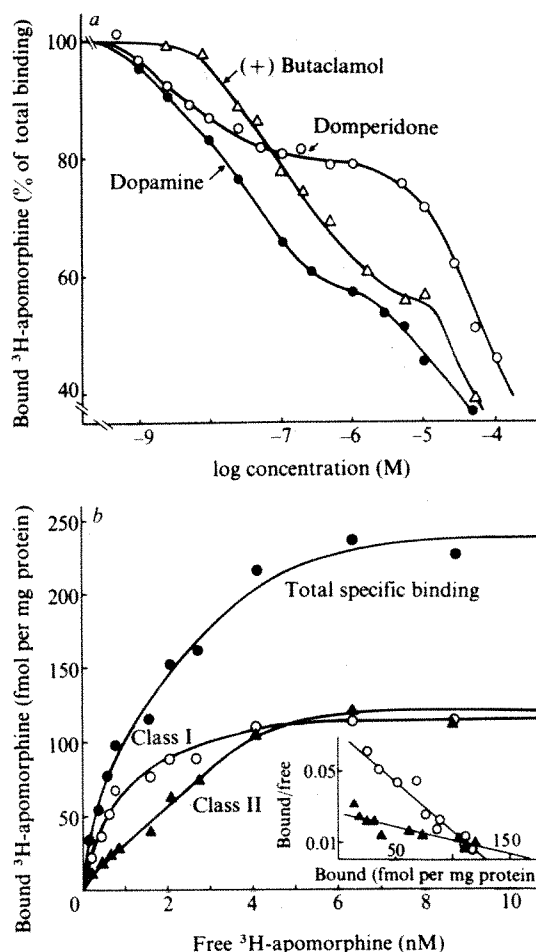
Total binding of <sup>3</sup>H-apomorphine was studied at 6 nM in the presence of increasing concentrations of DA, (+)butaclamol (an antipsychotic drug) or domperidone. As shown in Fig. 1a, DA and (+)butaclamol displayed monophasic inhibition curves up to concentrations of 1 and 10  $\mu\text{M}$  respectively. At these concentrations, a small but reproducible plateau was observed allowing definition of the specific binding (45% of total binding) in conditions similar to those used by others<sup>6,8,10,18</sup>. In contrast, domperidone inhibited this specific binding in a clearly biphasic manner, and a wide plateau appeared between approximately 50 nM and 2  $\mu\text{M}$ . This allowed definition of two pharmacologically distinct classes of <sup>3</sup>H-apomorphine binding site: class I, comprising sites recognized by low concentrations of domperidone ( $\text{IC}_{50} = 5\text{ nM}$ ), and class II, composed of sites poorly recognized by domperidone ( $\text{IC}_{50} \sim 10\text{ }\mu\text{M}$ ).

Saturation of these two classes of binding site by <sup>3</sup>H-apomorphine in increasing concentrations was studied separately—class I sites by determining the fraction of binding inhibited by 200 nM domperidone, and class II sites by determining the binding which occurred in the presence of 200 nM domperidone and was inhibited by 1  $\mu\text{M}$  dopamine (Fig. 1b). Both classes of binding site distinguished by domperidone are characterized by high affinities for <sup>3</sup>H-apomorphine ( $K_d$  0.9 and 2.6 nM), and the capacity of each one amounts to about 120 fmol per mg protein (7 pmol per g tissue).

Lesion data show that these two classes of site are located on different populations of striatal neurones (Table 1). Class I sites seem to be mostly, if not exclusively, present on intrinsic neurones, as the drop in their binding capacity after kainate lesion (-57%) is the same as the reduction occurring in the activity of glutamate decarboxylase, a marker of striatal  $\gamma$ -aminobutyric acid neurones. In addition, the number of class I sites is significantly enhanced after 6-hydroxydopamine (6-OHDA)-induced degeneration of afferent DA



**Fig. 1**  $^3\text{H}$ -Apomorphine binding to rat striatal particulate fraction. The dissected tissues (40–50 mg) from Sprague-Dawley rats (C. River, 200–250 g) were gently sonicated (Ultrasons-Annemasse; sonotrode  $d = 4.5$  mm) at  $4^\circ\text{C}$  in 2 ml 50 mM Tris-HCl buffer pH 7.4 (in 15 ml borosilicated glass tubes). After a three-fold dilution, the homogenate was centrifuged (5,000 g min) and the supernatant diluted two-fold and centrifuged (200,000 g min) in 12 ml cellulose nitrate test tubes. The pellet was resuspended in 2 ml Tris-HCl buffer using a glass-glass homogenizer (Dounce, clearance 70–120  $\mu\text{m}$ ) and incubated for 12 min at  $37^\circ\text{C}$  in a metabolic shaker (140  $\text{cm}^{-1}$ ). After fivefold dilution and centrifugation (200,000 g min), the particulate fraction was resuspended with the Dounce homogenizer in 2 ml freshly prepared 50 mM Tris-HCl buffer pH 7.4 containing 120 mM NaCl, 5 mM KCl, 1 mM  $\text{CaCl}_2$ , 1 mM  $\text{MgCl}_2$ , 0.1% ascorbic acid and 10  $\mu\text{M}$  pargyline ('Tris-ions buffer'). The suspension was briefly sonicated (4 s) before use. In preliminary experiments, we checked that this procedure for tissue preparation led to an almost complete elimination of  $^3\text{H}$ -DA added before homogenization. In the binding assay, 200  $\mu\text{l}$  freshly prepared tissue suspension were preincubated for 20 min at  $30^\circ\text{C}$  in polystyrene test tubes. Incubations were initiated by addition of 200  $\mu\text{l}$  Tris-ions buffer containing  $[8, 9\text{-}^3\text{H}]\text{apomorphine}$  (30.6 Ci  $\text{mmol}^{-1}$ , NEN) and various drugs, and were carried on for 30 min at  $30^\circ\text{C}$ . Drugs were dissolved in either Tris-ions buffer or 0.01–0.05% lactic acid and diluted into glass tubes with Tris-ions buffer. Lactic acid at the final concentration used did not interfere with the binding. Incubations were stopped by dilution with 3 ml ice-cold Tris-ions buffer followed by rapid filtration under vacuum (0.2–0.4 bar) through Whatman GF/B filters. Tubes were rinsed with 3 ml ice-cold Tris-ions buffer and the filters were washed with  $2 \times 5$  ml of the same slowly delivered buffer. After drying the filters, the radioactivity was counted by liquid scintillation spectrometry in 12 ml toluene-Triton X-100-PP-POP (21-11-16.5 g-0.45 g) at an efficiency of 45%. Binding on filters represented less than 0.5% of the total radioactivity. *a*, Inhibition by three dopaminergic agents. Striatal particulate fractions were incubated in the presence of 6 nM  $^3\text{H}$ -apomorphine and dopamine (●), (+) butaclamol ( $\Delta$ ) or domperidone ( $\circ$ ) in increasing concentrations. Values are expressed in per cent of total binding ( $523 \pm 73$  fmol per mg protein) and represent the mean of 6–8 determinations performed in two separate experiments. s.e.m. of these values (not shown) were less than 3% of total binding. *b*, Saturability and Scatchard analysis (inset). Total specific binding (●) was that inhibited by 1  $\mu\text{M}$  dopamine. Binding to class I sites ( $\circ$ ) was that inhibited by 200 nM domperidone. Binding to class II sites ( $\Delta$ ) was that occurring in the presence of 200 nM domperidone minus that in the presence of 1  $\mu\text{M}$  dopamine. At 6 nM  $^3\text{H}$ -apomorphine, radioactivity bound to the tissue was about 3,500 c.p.m. without inhibiting drug, 2,700 c.p.m. in the presence of 200 nM domperidone and 1,900 c.p.m. in the presence of 1  $\mu\text{M}$  dopamine. Total specific binding as well as binding to class I or II sites increased linearly with protein level between 0.1 and 0.3 mg per incubation. Values are the means of 3–10 determinations performed in three independent experiments. Analysis of these data by an iterative computing method based on the least squares<sup>32</sup> gave the following parameters:  $(B_{\text{max}})_I = 131 \pm 12$  fmol per mg protein,  $(K_d)_I = 0.92 \pm 0.24$  nM,  $(nH)_I$  (Hill constant) =  $0.95 \pm 0.17$  for the first class and  $(B_{\text{max}})_{II} = 151 \pm 32$  fmol per mg protein,  $(K_d)_{II} = 2.64 \pm 1.18$  nM,  $(nH)_{II} = 1.17 \pm 0.30$  for the second; values are in good agreement with those obtained by Scatchard plot analysis.



neurones. On the other hand, the number of class II sites is not affected by kainate lesions but is significantly reduced after two kinds of selective lesion of DA neurones (Table 1). The changes observed after degeneration of DA neurones consist of a reduction in the number of class II sites and a rise in the number of class I sites, with no change in the affinity of domperidone for either class of site. Thus, when  $^3\text{H}$ -apomorphine binding in striata of 6-OHDA-lesioned animals (eight rats in two separate experiments) was displaced by domperidone in increasing concentrations, a curve (not shown) similar to that in Fig. 1a was obtained. It also exhibited a large plateau whose height on the ordinate was reduced compared to the control.

The highly heterogeneous but more or less parallel distribution of the two classes of site among the various regions of rat brain reflects DA terminal distribution and thus supports the idea that DA receptors are labelled in both cases<sup>19</sup>.

The drug specificity of sites I and II was established in conditions allowing selective labelling of each class (Table 2). For class I sites, which displayed the highest affinity for  $^3\text{H}$ -apomorphine, a low ligand concentration was used (0.8 nM). For class II sites, inhibitory potencies were established in the presence of 6 nM  $^3\text{H}$ -apomorphine plus 200 nM domperidone to prevent labelling of class I sites. In both cases it was checked that 'nonspecific' binding (binding in the presence of 200 nM domperidone and of 1  $\mu\text{M}$  DA for class I and II sites, respectively) was not significantly inhibited by the various drugs at their  $\text{IC}_{50}$ .  $^3\text{H}$ -Apomorphine binding to both classes of site was stereospecific and exhibited distinct pharmacological specificity, as shown by the relative affinities of several DA agonists and antagonists, which contrasted with the lack of potency of a variety of non-dopaminergic agents (Table 2). The low potency

of benztropine, an inhibitor of DA uptake, rules out the possibility that class II sites might be linked to this transport system.

Hence the two classes of site have clearly different localizations and pharmacological specificities. Class I sites consist of postsynaptic DA receptors, present on intrastriatal neurones. The increase in their number after ablation of DA neurones probably reflects denervation hypersensitivity<sup>8,20,21</sup>. They are characterized by the high affinity of DA and both DA agonists and DA antagonists ( $K_i$  in nanomolar range), and thus resemble the  $^3\text{H}$ -apomorphine binding sites described by others<sup>13</sup>. Their capacity is about one-third that of DA receptors labelled with  $^3\text{H}$ -butyrophenones<sup>22–24</sup> or  $^3\text{H}$ -domperidone<sup>16</sup>. However, class I sites correspond to a subpopulation of sites constituting ~30% of the total<sup>25</sup> that have a much higher affinity for DA ( $K_i = 7$  nM) than most of the  $^3\text{H}$ -domperidone binding sites ( $K_i = 2$   $\mu\text{M}$ )<sup>26</sup>. Class I sites cannot be  $D_1$  receptors, that is DA receptors linked to adenylate cyclase<sup>1</sup>, because the affinities of domperidone and sulpiride for these sites ( $K_i$  0.5 nM and 100 nM, respectively) are several orders of magnitude higher than for the DA-sensitive cyclase of rat striatum ( $K_i > 10$   $\mu\text{M}$  in both cases)<sup>16,17,27</sup>. They may be postsynaptic DA receptors mediating certain behavioural effects of low doses of DA agonists which are prevented by neuroleptics in moderate dosage and which have often been ascribed to the stimulation of autoreceptors<sup>28,29</sup>. In accordance with the nomenclature of Keabian and Calne<sup>1</sup> we suggest calling these sites  $D_2$  receptors.

On the other hand, class II sites correspond, at least in part, to DA autoreceptors, as shown by the effects of the two neurotoxins 6-OHDA and kainate (Table 1). However, the partial decrease of class II sites, in contrast to the nearly complete loss of tyrosine hydroxylase activity after 6-OHDA, does not

exclude the possibility that ~50% of these sites may be localized on cells other than DA neurones. Autoreceptors, like class I sites, but unlike the major fraction of post-synaptic receptors labelled by  $^3\text{H}$ -butyrophenones and  $^3\text{H}$ -domperidone, are characterized by their high affinity ( $K_i$  in nanomolar range) for most DA agonists. This agrees with electrophysiological, behavioural, and biochemical observations suggesting that autoreceptors are stimulated by DA agonists at low dosage<sup>2,4,28,29</sup>. An interesting exception is bromocriptine, which is approximately 60 times less potent on autoreceptors than on postsynaptic receptors labelled either with  $^3\text{H}$ -apomorphine (class I sites) or  $^3\text{H}$ -butyrophenones<sup>23</sup>. Antipsychotic agents belonging to various chemical groups are recognized by autoreceptors but note that their potency is always lower than on postsynaptic receptors, that is class I sites (Table 2) or  $^3\text{H}$ -butyrophenones and  $^3\text{H}$ -domperidone binding sites<sup>16,23-24</sup>. The number of class II sites found here is approximately five times higher than reported earlier<sup>6</sup> but only slightly higher than that of the  $^3\text{H}$ -apomorphine sites recently described by Titeler *et al.* under the name of  $D_3$  receptors. These  $D_3$  receptors display a drug specificity similar to that of class II sites but were not localized by lesion studies<sup>12</sup>. Thus, class II sites could be termed  $D_3$  receptors.

The discrepancies between various studies concerning drug specificity and localization of sites labelled by  $^3\text{H}$ -apomorphine might be attributable to their heterogeneity with preferential labelling of either class I or class II sites in a given laboratory according to small differences in experimental conditions.

Finally, note that the differential drug specificity of autoreceptors might have therapeutic implications. Because 'on-off' reactions in the treatment of Parkinson's disease (paradoxically inhibitory effects produced by DA agonists when their plasma levels are low) are attributed to selective stimulation of autoreceptors, the low frequency of such reactions in patients treated with bromocriptine<sup>30</sup> might be explained by the low potency of this compound on autoreceptors. In addition, it is unlikely that the antipsychotic activity of antagonists is related to the block-

**Table 2** Inhibition by various agents of the  $^3\text{H}$ -apomorphine binding on the two classes of striatal sites

| Agent                   | $K_i$ values (nM) |          | $(K_i)_{II}/(K_i)_I$ |
|-------------------------|-------------------|----------|----------------------|
|                         | Class I           | Class II |                      |
| <b>DA antagonists</b>   |                   |          |                      |
| Spiperone               | 0.20              | 522      | 2,610                |
| Domperidone             | 0.52              | 3,150    | 6,050                |
| (+)-Butaclamol          | 1.7               | 13.5     | 8                    |
| $\alpha$ -Flupentixol   | 6.8               | 167      | 25                   |
| Haloperidol             | 7.2               | 332      | 46                   |
| Sulpiride               | 97.3              | 100,600  | 1,030                |
| (-)-Butaclamol          | 1,121             | 1,090    | 1                    |
| <b>DA agonists</b>      |                   |          |                      |
| N-Propyl-norapomorphine | 0.40              | 3.5      | 9                    |
| Apomorphine             | 0.65              | 2.9      | 4                    |
| ADTN                    | 1.1               | 4.5      | 4                    |
| Bromocriptine           | 7.2               | 420      | 58                   |
| Dopamine                | 9.9               | 6.1      | 0.6                  |
| <b>Miscellaneous</b>    |                   |          |                      |
| Noradrenaline           | -                 | 65       | -                    |
| Phentolamine            | -                 | 6,100    | -                    |
| Clonidine               | -                 | >30,000  | -                    |
| Serotonin               | -                 | 5,780    | -                    |
| Morphine                | -                 | >150,000 | -                    |
| Benzotripine            | -                 | 4,900    | -                    |

Binding on sites of class I was measured in the presence of 0.8 nM  $^3\text{H}$ -apomorphine and defined as the excess over blank values obtained in the presence of 200 nM domperidone. Values in a typical experiment were: 650 c.p.m. (total binding), 350 c.p.m. (in the presence of 200 nM domperidone) and 250 c.p.m. (in the presence of 1  $\mu\text{M}$  dopamine). Binding on sites of class II was measured in the presence of 6 nM  $^3\text{H}$ -apomorphine and 200 nM domperidone and defined as the excess over blank values obtained in the presence of 1  $\mu\text{M}$  dopamine (see Fig. 1b legend). The effect of each agent was determined at 4-6 concentrations (triplicate determinations) and  $\text{IC}_{50}$  calculated by log-probit analysis of pooled data from 2-4 separate experiments.  $K_i$  values were derived from  $\text{IC}_{50}$  according to the relationship  $K_i = \text{IC}_{50}/(1 + S/K_d)$ .  $(K_d)_I = 0.92$  nM and  $(K_d)_{II} = 2.64$  nM.

ade of autoreceptors as indicated, for instance, by the extremely low potency of sulpiride and by the low potency of spiperone. Furthermore, autoreceptors are probably not blocked during clinical treatment with most antipsychotics at a moderate dosage. In the treatment of psychotics it would therefore seem rational to combine DA agonists with high potency for autoreceptors, and DA antagonists with high relative affinity for postsynaptic receptors. Note that such an apparently paradoxical combination of apomorphine and antipsychotics was recently reported to improve psychotic symptoms significantly, whereas bromocriptine did not show the same activity as apomorphine<sup>31</sup>.

This work was supported by a grant from the CNRS (Pharmacologie des récepteurs des neuromédiateurs).

**Table 1** Effect of various lesions on the capacity of the two classes of  $^3\text{H}$ -apomorphine binding site in rat striatum

| Type of lesion                              |               | $^3\text{H}$ -Apomorphine binding (fmol per mg protein) |              |              |
|---|---------------|---|--------------|--------------|
|   |               | Total specific  | Class I      | Class II     |
| Kainate into the striatum (7)               | Contralateral | 203 $\pm$ 15  | 120 $\pm$ 10 | 83 $\pm$ 14  |
|   | Ipsilateral   | 133 $\pm$ 14  | 50 $\pm$ 11  | 83 $\pm$ 10  |
|   | Difference    | -33 $\pm$ 8%  | -57 $\pm$ 9% | +3 $\pm$ 13% |
| 6-OHDA into the medial forebrain bundle (5) | Control       | 249 $\pm$ 31  | 120 $\pm$ 16 | 129 $\pm$ 12 |
|   | Lesioned      | 219 $\pm$ 28  | 155 $\pm$ 24 | 64 $\pm$ 12  |
|   | Difference    | -12%  | +28%         | -50%         |
| 6-OHDA into the substantia nigra (14)       | Contralateral | 235 $\pm$ 7   | 126 $\pm$ 8  | 109 $\pm$ 5  |
|   | Ipsilateral   | 220 $\pm$ 10  | 153 $\pm$ 9  | 68 $\pm$ 8   |
|   | Difference    | -5 $\pm$ 4%   | +24 $\pm$ 7% | -37 $\pm$ 8% |

Lesions were performed in chloral-anaesthetized rats positioned in a David Kopf stereotaxic apparatus. Kainic acid (2.5  $\mu\text{g}$  in 1  $\mu\text{l}$  of solution titrated at pH 7.4) was unilaterally injected (2.5 min infusion) into the striatum at coordinates<sup>32</sup> A = 7.5 mm, L = 2.8 mm and H = 5.1 mm and animals were killed 10-15 days later. Striatal glutamate decarboxylase<sup>33</sup> was decreased by 57  $\pm$  5% in the lesioned compared to contralateral sides (94.2  $\pm$  2.2 nmol per h per mg protein of  $^{14}\text{CO}_2$  formed). In contrast, DOPA decarboxylase activity<sup>33</sup> was not significantly affected (46.2  $\pm$  0.9 compared to 46.3  $\pm$  2.1 nmol per h per mg protein of  $^{14}\text{CO}_2$  formed). 6-OHDA (8  $\mu\text{g}$  in 4  $\mu\text{l}$  of saline containing 0.1% Na ascorbate) was bilaterally injected (5-min infusion) into the medial forebrain bundle at coordinates<sup>34</sup> A = 3.2 mm, L = 1.4 mm, H = -3.0 mm and animals were killed 6-9 days later. Striatal tyrosine hydroxylase activity<sup>37</sup> was significantly decreased by 79% (0.64  $\pm$  0.19 compared to 3.09  $\pm$  0.21 nmol per h per mg protein of  $^3\text{H}_2\text{O}$  formed). In the third group of animals, 6-OHDA (8  $\mu\text{g}$ ) was unilaterally injected into the substantia nigra as described<sup>38</sup> and animals killed 4-5 weeks later. Striatal tyrosine hydroxylase activity was decreased by 89  $\pm$  3% in the lesioned compared to contralateral sides. Binding was measured in the presence of 6 nM  $^3\text{H}$ -apomorphine in the conditions described in Fig. 1b legend. Triplicate determinations on tissues from single animals, the number of which is indicated in parentheses. Binding on the contralateral side of animals lesioned unilaterally with either kainate or 6-OHDA did not significantly differ from that on unlesioned animals (not shown).

NS, not significant. \*  $P < 0.01$ , †  $P < 0.005$ , ‡  $P < 0.001$ ; two-tailed *t*-test. §  $P < 0.05$ ; one-tailed *t*-test.

Received 24 March, accepted 17 September 1980

- Kobben, J. W. & Calne, D. B. *Nature* **277**, 93-96 (1979)
- Carlsson, A. in *Pre- and Post-synaptic Receptors*, Annual ACNP Meet., Puerto-Rico (eds Ueda, E. & Bunney W. B.) (Dekker, New York, 1975)
- Roth, R. H. *Commun. Psychopharmacol.* **3**, 429-443 (1979)
- Aghajanian, G. K. & Bunney, B. S. *Neuromy-Schmiedberg's Arch. Pharmacol.* **297**, 1-7 (1977)
- Glowinski, J. & Cheramy, A. in *Catecholamines: Basic and Clinical Frontiers* Vol 1 (eds Ueda, E., Kopan, I. J. & Bardes, J.) 231-239 (Pergamon, New York, 1978)
- Nagy, J. I., Lee, T., Seeman, P. & Fildes, H. C. *Nature* **274**, 278-281 (1978)
- Wonnacott, P., Lee, T. & Seeman, P. *Soc. Neurosci. Abstr.* **4**, 1687 (1978).
- Croese, I. & Snyder, S. H. *Eur. J. Pharmacol.* **56**, 277-281 (1979)
- Croese, I., Ueda, T. & Snyder, S. H. *Nature* **278**, 577-578 (1979)
- Croese, I., Proulx, T. & Snyder, S. H. *Life Sci.* **23**, 495-500 (1978)
- Croese, I., Stewart, K. & Snyder, S. H. *Eur. J. Pharmacol.* **68**, 55-66 (1979)
- Titeler, M., Lee, T. & Seeman, P. *Commun. Psychopharmacol.* **3**, 411-420 (1979)
- Layson, J. E. *Commun. Psychopharmacol.* **3**, 397-410 (1979)
- Nicomogers, C. J. F. & Janssen, P. A. J. *Proc. 7th Int. Congr. Pharmacol.* Paris, Abstr. no. 68 (1978).
- Martres, M. P., Baudry, M. & Schwartz, J. C. *Life Sci.* **23**, 1781-1784 (1978)
- Baudry, M., Martres, M. P. & Schwartz, J. C. *Neuromy-Schmiedberg's Arch. Pharmacol.* **308**, 231-237 (1979).
- Wadding, K. J., Dowling, J. E. & Iversen, L. L. *Nature* **281**, 578-580 (1979)
- Thal, L., Croese, I. & Snyder, S. H. *Eur. J. Pharmacol.* **49**, 295-299 (1978).
- Sokoloff, P., Martres, M. P. & Schwartz, J. C. *Neuromy-Schmiedberg's Arch. Pharmacol.* (in press).
- Croese, I., Burt, D. R. & Snyder, S. H. *Science* **197**, 596-598 (1977).
- Schwartz, J. C., Costentin, J., Martres, M. P., Protas, P. & Baudry, M. *Neuropharmacology* **17**, 665-685 (1978)
- Seeman, P., Chau-Wong, M., Todaro, J. & Wong, K. *Proc. natn. Acad. Sci. U.S.A.* **72**, 1376-1380 (1975)



23. Burt, D. R., Creese, I. & Snyder, S. H. *Molec. Pharmac.* **12**, 800–812 (1976).
24. Leysen, J. E., Gommeren, W. & Laduron, P. M. *Biochem. Pharmac.* **27**, 307–316 (1978).
25. Baudry, M., Martres, M. P. & Schwartz, J. C. in *Catecholamines: Basic and Clinical Frontiers* Vol. 1 (eds Usdin, E., Kopin, I. J. & Barchas, J.) 565–567 (Pergamon, New York, 1978).
26. Martres, M. P., Sokoloff, P. & Schwartz, J. C. in *The Psychopharmacology and Biochemistry of Neurotransmitter Receptors* (eds Olsen, R. N. & Yamamura, H. I.) (Elsevier, Amsterdam, in the press).
27. Trabucchi, M., Longoni, R., Fresia, P. & Spano, P. F. *Life Sci.* **17**, 1551–1556 (1975).
28. Martres, M. P. *et al.* *Brain Res.* **136**, 319–337 (1977).
29. Di Chiara, G., Porceddu, M. L., Fratta, W. & Gessa, G. L. *Nature* **267**, 270–272 (1977).
30. Lieberman, A. N. *et al.* *Adv. Neurol.* **24**, 461–473 (1979).
31. Tamminga, C. A., Schaffer, M. H., Smith, R. C. & Davis, J. M. in *Catecholamines: Basic and Clinical Frontiers* Vol. 2 (eds Usdin, E., Kopin, I. J. & Barchas, J.) 1836–1838 (Pergamon, New York, 1978).
32. Parker, R. B. & Waud, D. R. *J. Pharmac. exp. Ther.* **177**, 1–12 (1971).
33. Albe-Fessard, D., Stutinsky, F. & Libouban, S. *Éditions du CNRS*, Paris (1971).
34. Moskal, J. R. & Basu, S. *Analyt. Biochem.* **65**, 449–457 (1975).
35. Aures, D., Håkanson, R. & Schauer, A. *Eur. J. Pharmac.* **3**, 217–234 (1968).
36. König, F. R. & Klippel, R. A. *The Rat Brain* (Krieger, Huntington, New York, 1970).
37. Buda, M., Roussel, B., Renaud, B. & Pujol, J. F. *Brain Res.* **93**, 564–569 (1975).
38. Llorens-Cortes, C., Pollard, H. & Schwartz, J. C. *Neurosci. Lett.* **12**, 165–170 (1979).

## The enkephalinase inhibitor thiorphan shows antinociceptive activity in mice

B. P. Roques\*, M. C. Fournié-Zaluski\*, E. Soroça\*, J. M. Lecomte†, B. Malfroy‡, C. Llorens‡ & J.-C. Schwartz‡

\* Département de Chimie Organique, Université René Descartes, 4, avenue de l'Observatoire, 75006 Paris, France

† Centre de Recherche Janssen-Lebrun, 93 Aubervilliers, France

‡ Unité de Neurobiologie, Centre Paul Broca de l'INSERM, 2ter, rue d'Alésia, 75014 Paris, France

There is both theoretical and therapeutic interest in establishing whether the signals conveyed by the enkephalins are turned off under the action of a specific peptidase which might, in this case, represent a target for a new class of psychoactive agents. Enkephalinase, a dipeptidyl carboxypeptidase cleaving the Gly<sup>3</sup>-Phe<sup>4</sup> bond of enkephalins<sup>1,2</sup> and distinct from angiotensin converting enzyme (ACE)<sup>3–6</sup>, might be selectively involved in enkephalineric transmission. It is a membrane-bound enzyme<sup>1,7,8</sup> whose localization in the vicinity of opiate receptors in the central nervous system is suggested by parallel regional<sup>1,7,9</sup> and subcellular<sup>10</sup> distributions as well as by the effects of lesions<sup>9</sup>. Such a role is further supported by the ontogenetic development of enkephalinase<sup>11,12</sup>, its substrate specificity accounting for the increased biological activity of several enkephalin analogues<sup>13</sup> and its adaptive increase following chronic treatment with morphine<sup>1,14</sup>. To investigate the functional role of this enzyme further, we have designed a potent and specific enkephalinase inhibitor. We report here that this compound, thiorphan [(DL-3-mercapto-2-benzylpropanoyl)-glycine; patent no. 8008601] protects the enkephalins from the action of enkephalinase *in vitro* in nanomolar concentration and *in vivo* after either intracerebroventricular or systemic administration. In addition, thiorphan itself displays antinociceptive activity which is blocked by naloxone, an antagonist of opiate receptors.

Thiorphan was designed to interact with critical residues of the active site of enkephalinase, as postulated on a hypothetical model (Fig. 1). The model was developed on the assumption that binding of enkephalins to this active site occurs in a manner analogous to that established at the molecular level for carboxypeptidase A (ref. 15). In thiorphan, most of the putative interactions of enkephalins are retained and the binding with the zinc atom at the catalytic site is strongly increased by the introduction of a thiol group in the proper position<sup>16,17</sup>.

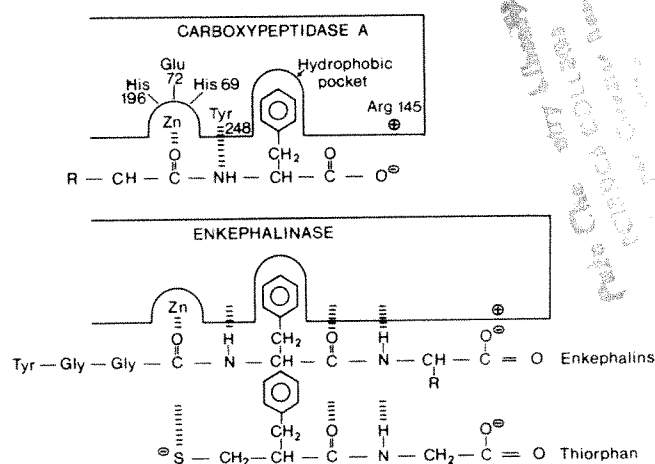
Evidence for the validity of the hypothetical model of the enkephalinase active site was suggested by the high inhibitory potency of thiorphan (Fig. 2). The inhibition of enkephalinase activity from striatal membranes is of a competitive type and the mean  $K_i$  value obtained in various experiments similar to those described in Fig. 2 was  $4.7 \pm 1.2$  nM.

Furthermore, thiorphan displays a good selectivity towards enkephalinase among the various enkephalin-hydrolysing

activities already described in brain tissues. Regarding ACE activity in mouse striatum<sup>18</sup> which is also able to cleave the Gly<sup>3</sup>-Phe<sup>4</sup> peptide bond of enkephalins<sup>19</sup>, the  $K_i$  of thiorphan was  $150 \pm 30$  nM (not shown) which corresponds to a 30-fold lower potency than towards enkephalinase. It is interesting that captopril (SQ 14,225), an inhibitor of ACE, displays an inverse specificity pattern, being much more potent on this enzyme ( $K_i = 7$  nM) than on enkephalinase ( $K_i = 10$   $\mu$ M)<sup>4,16</sup>. These observations further demonstrate that enkephalinase and ACE, in spite of their analogies<sup>3</sup>, are different enzymes<sup>4,14</sup>. In addition, the formation of either <sup>3</sup>H-Tyr or <sup>3</sup>H-Tyr-Gly, as detected by TLC, following incubation of striatal membranes in the presence of 20 nM <sup>3</sup>H-Leu<sup>5</sup>-enkephalin and in the absence of puromycin (which inhibits the formation of both compounds) was not affected by thiorphan in concentrations as high as 10  $\mu$ M. This indicates that thiorphan does not significantly inhibit the aminopeptidase<sup>20–26</sup> or the putative endopeptidase<sup>6</sup> activities responsible for *in vitro* cleavage of the enkephalin molecules at peptide bonds other than Gly<sup>3</sup>-Phe<sup>4</sup>.

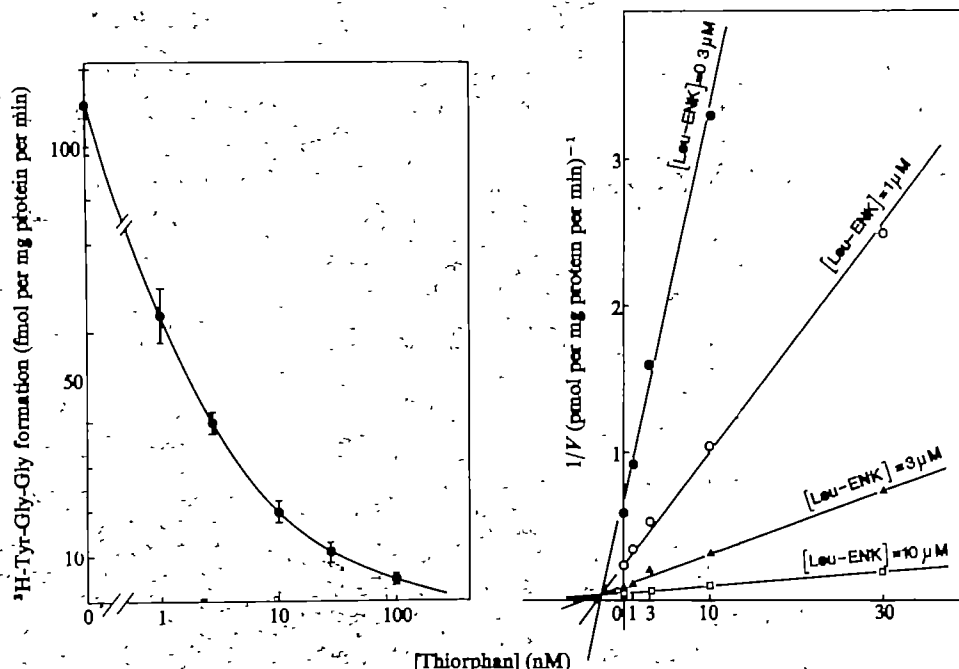
The ability of thiorphan to inhibit enkephalinase activity *in vivo* was evaluated by determining the effect of the drug on the analgesia elicited by (D-Ala<sup>2</sup>-Met<sup>5</sup>)-enkephalin administered intracerebroventricularly (i.c.v.) in low dosage. The D-Ala<sup>2</sup> substitution in this compound preserves opiate receptor affinity and bestows resistance to aminopeptidases<sup>27</sup>, but does not markedly impair recognition by enkephalinase as long as the carboxyl of Met<sup>5</sup> is not amidified<sup>13</sup>.

A short-lasting, nonsignificant analgesia was recorded on the tail-withdrawal test<sup>28</sup> when (D-Ala<sup>2</sup>-Met<sup>5</sup>)-enkephalin was administered (20  $\mu$ g, i.c.v.) alone (Fig. 3 and Table 1). Co-administration of thiorphan, either i.c.v. or systemically, resulted in a strong potentiation of the analgesic effect of the opioid pentapeptide which was nearly maximal in all animals over ~90 min and still significant ~2 h after intravenous (i.v.) administration and 4 h after i.c.v. administration. In contrast, the effect elicited by (D-Ala<sup>2</sup>-Met<sup>5</sup>)-enkephalinamide, an analogue poorly recognized by enkephalinase<sup>13</sup>, was not significantly modified by thiorphan. Interestingly, neither thiorphan alone (30  $\mu$ g or 60  $\mu$ g, i.c.v.) nor the opiate receptor antagonist naloxone (1 mg per kg, subcutaneously (s.c.))



**Fig. 1** Hypothetical model of the active site of enkephalinase and of the binding of enkephalins and thiorphan. The model was developed by analogy with the active site of carboxypeptidase A (upper part) as proposed by Quiocho and Lipscomb<sup>15</sup>. Enkephalinase is likely to contain a zinc atom<sup>3</sup> that, as in carboxypeptidase A, would bind the carbonyl group of the peptide bond to be cleaved. Evidence for the presence of a 'dead-end hydrophobic pocket' analogous to that of carboxypeptidase A<sup>15</sup> but which seems absent in ACE<sup>16</sup> is given by the recognition of di- and tripeptides only when containing an aromatic amino acid<sup>37</sup>. Interaction of the two C-terminal peptide bonds of enkephalins with the active site is suggested by the diminished recognition of analogues in which they are modified<sup>37</sup>. The free carboxyl would interact with a positively charged residue (corresponding to Arg 145 in carboxypeptidase A) as shown by the diminished recognition of enkephalin analogues in which it is replaced by an alcohol group, amidified, esterified or localized in a proline ring<sup>13,14</sup>.

**Fig. 2** Inhibition of enkephalinase activity from mouse striatum by thiorphan. A washed particulate fraction from mouse striatum was prepared according to Malfroy *et al.*<sup>1</sup>. Protein concentration in the assay mixture was 40 µg per 100 µl but similar results were obtained for concentrations varying over 1–200 µg per 100 µl. After a 15-min preincubation at 25 °C, incubations were started by addition of a mixture containing 20 nM (<sup>3</sup>H-Leu<sup>5</sup>)-enkephalin previously purified by Porapak column chromatography<sup>24</sup>, 0.1 mM puromycin, an aminopeptidase inhibitor<sup>25</sup>, 1 µM captopril, an ACE inhibitor<sup>16</sup>, 0.1 mM 2-mercaptoethanol and unlabelled (Leu<sup>5</sup>)-enkephalin in the indicated concentrations (all final concentrations in 50 mM Tris-HCl buffer, pH 7.4). Incubations (15 min at 25 °C) were stopped by addition of HCl (0.07 M, final molarity). Blanks were obtained by adding HCl before the beginning of incubation and represented ~20% of the uninhibited enzyme activity. <sup>3</sup>H-Labelled metabolites plus unlabelled carriers were separated by TLC on silica gel plastic sheets (Merck, Darmstadt) using the following system: BuOH, AcOH, AcOEt, H<sub>2</sub>O (1:1:2:1). Spots, localized after a ninhydrin spray, had the following *R<sub>f</sub>* values: Tyr 0.55, Tyr-Gly 0.47, Tyr-Gly-Gly 0.39, (Leu<sup>5</sup>)-enkephalin 0.81. The Tyr-Gly-Gly spots were cut out and their radioactivity estimated by liquid scintillation counting. Left: Effect of thiorphan in increasing concentrations on the hydrolysis of (<sup>3</sup>H-Leu<sup>5</sup>)-enkephalin (20 nM) by mouse striatal enkephalinase. Means ± s.e.m. of triplicate determinations in the same experiment. This experiment was repeated 12 times leading to an IC<sub>50</sub> value of 4.7 ± 1.2 nM. Right: Dixon plots of enkephalinase inhibition by thiorphan. Each point represents the mean of duplicate determinations. *K<sub>i</sub>* value obtained in this experiment was 3 nM and was confirmed in another similar experiment.



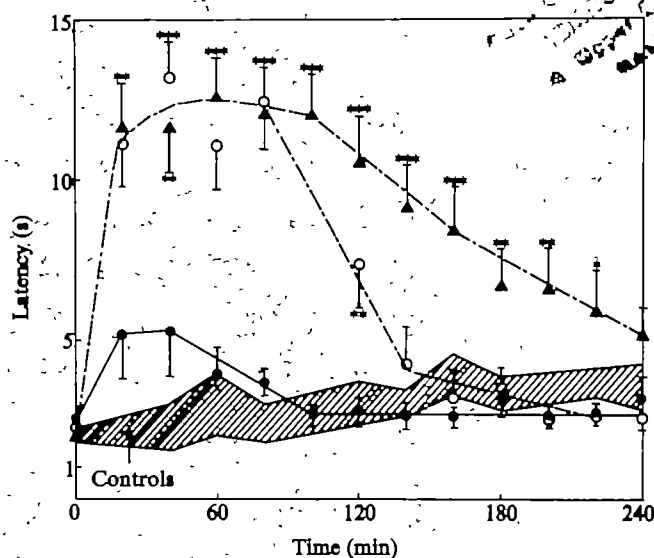
**Table 1** Activity of thiorphan on responses to nociceptive stimuli in mice

| Tests                   | Treatments   | Latency (s)    | P       |
|-------------------------|--|----------------|---------|
| Tail withdrawal (48 °C) | Controls   | 3.1 ± 0.4 (15) |         |
|                         | Thiorphan (30 µg, i.c.v.)  | 4.2 ± 1.1 (6)  |         |
|                         | Thiorphan (60 µg, i.c.v.)  | 2.7 ± 0.4 (9)  |         |
|                         | Naloxone (1 mg per kg, i.v.)   | 3.2 ± 0.3 (9)  |         |
|                         | (D-Ala <sup>2</sup> -Met <sup>5</sup> )-enkephalin (20 µg, i.c.v.)                                   | 3.4 ± 0.2 (14) |         |
|                         | (D-Ala <sup>2</sup> -Met <sup>5</sup> )-enkephalin (20 µg, i.c.v.) + thiorphan (30 µg, i.c.v.)       | 9.6 ± 0.9 (14) | <0.001  |
|                         | (D-Ala <sup>2</sup> -Met <sup>5</sup> )-enkephalin (20 µg, i.c.v.) + thiorphan (100 mg per kg, i.v.) | 7.6 ± 0.8 (14) | <0.001  |
|                         | (D-Ala <sup>2</sup> -Met <sup>5</sup> )-enkephalinamide (2.5 µg, i.c.v.)                             | 3.2 ± 0.4 (6)  |         |
|                         | (D-Ala <sup>2</sup> -Met <sup>5</sup> )-enkephalinamide (2.5 µg, i.c.v.) + thiorphan (30 µg, i.c.v.) | 3.3 ± 0.6 (6)  |         |
|                         | (D-Ala <sup>2</sup> -Met <sup>5</sup> )-enkephalinamide (15 µg, i.c.v.)                              | 12.5 ± 1.1 (6) | <0.001  |
|                         | (D-Ala <sup>2</sup> -Met <sup>5</sup> )-enkephalinamide (15 µg, i.c.v.) + thiorphan (30 µg, i.c.v.)  | 13.8 ± 1.2 (6) | <0.001* |
| Hotplate jump (55 °C)   | Controls (solvent, i.c.v.)   | 70 ± 6 (14)    |         |
|                         | Thiorphan (30 µg, i.c.v.)  | 121 ± 8 (10)   | <0.001  |
|                         | Thiorphan (60 µg, i.c.v.)  | 134 ± 17 (14)  | <0.01   |
|                         | Controls (solvent, i.v.)   | 63 ± 11 (20)   |         |
|                         | Thiorphan (100 mg per kg, i.v.)  | 129 ± 22 (10)  | <0.02   |
|                         | Thiorphan (100 mg per kg, i.v.) + naloxone (1 mg per kg, s.c.)                                       | 68 ± 16 (10)   | <0.05†  |
| Hotplate jump (50 °C)   | Naloxone (1 mg per kg, s.c.)   | 43 ± 8 (10)    | <0.05   |
|                         | Controls   | 186 ± 11 (20)  |         |
|                         | Thiorphan (60 µg, i.c.v.)  | 245 ± 14 (20)  | <0.05   |
|                         | Thiorphan (60 µg, i.c.v.)  | 129 ± 13 (20)  | <0.05   |
|                         | + naloxone (1 mg per kg, s.c.)   | 129 ± 13 (20)  | <0.001† |

The tail withdrawal test was performed as described in Fig. 3 legend. The latency values obtained for each animal during the 240-min experimental period (13 determinations) were averaged. The hotplate test<sup>24,26</sup> was carried out at either 55 °C or 50 °C and the jump latency recorded 15 min after drug administration, without 'cutoff time'. Naloxone was administered at the same time as thiorphan. Results are the means ± s.e.m. of the number of experiments indicated in parentheses.

\* Non-significant compared with (D-Ala<sup>2</sup>-Met<sup>5</sup>)-enkephalin alone.

† Compared with thiorphan alone.



**Fig. 3** Effects of thiorphan on the analgesic activity of (D-Ala<sup>2</sup>-Met<sup>5</sup>)-enkephalin in the mouse tail withdrawal test. Swiss mice (20–22 g, Charles River) were tested at 20-min intervals over 4 h. The time (in seconds) between tail immersion into a water bath maintained at 48 °C and withdrawal was recorded as the response latency<sup>26</sup>. The 'cutoff time' was 15 s and the value at zero time represents the average of three determinations carried out before drug injection. (D-Ala<sup>2</sup>-Met<sup>5</sup>)-enkephalin (20 µg) was administered i.c.v. under a volume of 5 µl (3% ethanolic solution) either alone or together with thiorphan (30 µg). In the third group of animals thiorphan was administered i.v. (100 mg per kg) 15 min before (D-Ala<sup>2</sup>-Met<sup>5</sup>)-enkephalin (20 µg, i.c.v.). Controls received an i.c.v. administration of solvent alone. Each point represents the mean ± s.e.m. of data from 14 or 15 experiments. The shaded area corresponds to means ± s.e.m. of controls. Δ, (D-Ala<sup>2</sup>-Met<sup>5</sup>)-enkephalin + thiorphan (i.c.v.); ○, (D-Ala<sup>2</sup>-Met<sup>5</sup>)-enkephalin + thiorphan (i.v.); □, (D-Ala<sup>2</sup>-Met<sup>5</sup>)-enkephalin alone. \* *P* < 0.05; \*\* *P* < 0.01; \*\*\* *P* < 0.001.



modified the responsiveness of mice in the tail-withdrawal test, at any time after administration (Table 1).

Because the involvement of endogenous opioid peptides in the response to various nociceptive stimuli, as revealed by the hyperalgesic effect of naloxone, seems to vary according to the type of nociceptive stimulus used<sup>29-33</sup>, we have determined the effect of thiorphan in the hotplate jump test<sup>34,35</sup>. On this test, performed at either 55 °C or 50 °C, thiorphan administered either i.c.v. or i.v. displayed a clear antinociceptive activity which was probably mediated by opiate receptors as it was completely prevented by administration of naloxone in moderate dosage (Table 1). This opiate antagonist, when administered alone, significantly decreased the latency of the jump response as previously shown<sup>29,32</sup>.

The effect of thiorphan cannot be mediated by inhibition of aminopeptidase and is unlikely to involve ACE inhibition because its antinociceptive activity was observed at dosages approximately 30 times lower than those required for captopril<sup>36</sup>, whereas the latter compound is approximately 20 times more potent than thiorphan as an ACE inhibitor. Hence, the present observations strongly support the hypothesis that enkephalinase is selectively responsible for the metabolism of endogenous enkephalins. The reasons for which thiorphan elicits analgesia (and naloxone hyperalgesia) in one test but not in others are unclear but might be that different noxious stimuli elicit release of endogenous opioid peptides to a variable extent. Thus, thiorphan might constitute a useful tool for investigating the involvement of enkephalins in a variety of behavioural situations and might also represent the prototype of a new class of pharmacological agent.

We thank J. L. Coignet, M. Schwob and M. De Munck for technical assistance. This work was supported by grants from the Délégation Générale à la Recherche Scientifique et Technique, the Centre National de la Recherche Scientifique (PIRMED), the Institut National de la Santé et de la Recherche Médicale, and the Fondation pour la Recherche Médicale.

Received 6 June, accepted 17 September 1980.

- 1 Malfroy, B., Swerts, J. P., Guyon, A., Roques, B. P. & Schwartz, J.-C. *Nature* **276**, 523-526 (1978)
- 2 Guyon, A. *et al.* *Life Sci* **25**, 1605-1612 (1979)
- 3 Swerts, J. P., Perdrinat, R., Malfroy, B. & Schwartz, J.-C. *Eur. J. Pharmacol.* **53**, 209-210 (1979)
- 4 Swerts, J. P., Perdrinat, R., Patay, G., De La Baume, S. & Schwartz, J.-C. *Eur. J. Pharmacol.* **87**, 279-281 (1979)
- 5 Sullivan, S., Akil, H., Blacker, D. & Barchas, J. D. in *Endogenous and Exogenous Opiate Agonists and Antagonists* (ed. Way, E. L.) 357-360 (Pergamon, New York, 1980)
- 6 Goronstein, C. & Snyder, S. H. *Life Sci* **25**, 2065-2070 (1979)
- 7 Sullivan, S., Akil, H. & Barchas, J. D. *Commun. Psychopharmacol.* **2**, 525-531 (1979)
- 8 Vogel, Z. & Alston, M. in *Endogenous and Exogenous Opiate Agonists and Antagonists* (ed. Way, E. L.) 353-356 (Pergamon, New York, 1980)
- 9 Malfroy, B., Swerts, J. P., Llorens, C. & Schwartz, J.-C. *Neurosci. Lett.* **11**, 329-334 (1979)
- 10 De La Baume, S., Patay, G. & Schwartz, J.-C. *Neurosci. Lett.* (in the press)
- 11 De La Baume, S., Patay, G., Gros, C. & Schwartz, J.-C. in *Endogenous and Exogenous Opiate Agonists and Antagonists* (ed. Way, E. L.) 179-182 (Pergamon, New York, 1980)
- 12 Patay, G., De La Baume, S., Gros, C. & Schwartz, J.-C. *Life Sci* **27**, 245-252 (1980)
- 13 Fournie-Zalinski, M. C. *et al.* *Biochem. Biophys. Res. Commun.* **91**, 130-135 (1979)
- 14 Schwartz, J.-C. *et al.* *Auto. Biochem. Psychopharmacol.* **22**, 219-235 (1980)
- 15 Quischo, F. A. & Lapecomb, W. N. *Adv. Protein Chem.* **15**, 1-48 (1971)
- 16 Ondetti, M. A., Rubin, B. & Coulman, D. W. *Science* **196**, 441-444 (1977)
- 17 Ondetti, M. A. *et al.* *Biochemistry* **18**, 1427-1430 (1979)
- 18 Yang, H. Y. T. & Neff, N. H. *J. Neurochem.* **19**, 2443-2450 (1972)
- 19 Erdos, E. G., Johnson, A. R. & Boyden, N. T. *Biochem. Pharmacol.* **27**, 843-848 (1978)
- 20 Hambrook, J. M., Morgan, B. A., Rance, M. J. & Smith, C. F. *Nature* **262**, 782-783 (1976)
- 21 Lane, A. C., Rance, M. J. & Walter, D. S. *Nature* **269**, 75-76 (1977)
- 22 Marika, N., Grybaum, A. & Noolde, A. *Biochem. Biophys. Res. Commun.* **74**, 1552-1559 (1977)
- 23 Mook, J. L., Yang, H. Y. T. & Costa, E. *Neuropharmacology* **16**, 151-154 (1977)
- 24 Vogel, Z. & Alston, M. *FEBS Lett.* **88**, 332-336 (1977)
- 25 Knight, M. & Klose, W. A. *J. Biol. Chem.* **253**, 3843-3847 (1978)
- 26 Guyon, A. *et al.* *Biochem. Biophys. Res. Commun.* **88**, 919-926 (1979)
- 27 Port, C. B., Port, A., Chang, J. K. & Fong, B. T. W. *Science* **194**, 331-332 (1976)
- 28 Bon-Bassat, J., Perez, E. & Salpán, P. G. *Arch. int. Pharmacodyn. Ther.* **122**, 434-477 (1959)
- 29 Jacob, J., Tremblay, E. C. & Colombl, M. C. *Psychopharmacology* **37**, 217-223 (1974)
- 30 Goldstein, A., Pryor, G. T., Ott, L. S. & Linnon, F. *Life Sci* **18**, 599-604 (1976)
- 31 Sowell, R. D. E. & Spencer, P. S. *J. Neuropharmacol.* **13**, 683-688 (1976)
- 32 Fredrickson, R. C. A., Bergers, V. & Edwards, J. D. *Science* **198**, 756-757 (1977)
- 33 Wood, C. J. *Brain Res.* **198**, 578-583 (1980)
- 34 Eddy, N. B., May, E. L. & Moentag, E. J. *org. Chem.* **17**, 321-326 (1952)
- 35 Jacob, J. & Blazynski, M. *Arch. int. Pharmacodyn. Ther.* **133**, 296-309 (1961)
- 36 Sims, S. M., Yang, H. Y. T. & Costa, E. *Brain Res.* **188**, 295-299 (1980)
- 37 Llorens, C. *et al.* *Biochem. Biophys. Res. Commun.* (in the press)

## Herpes simplex virus DNA sequences in the CNS of latently infected mice

Carlos V. Cabrera\*, Charles Wohlenberg, Harry Openshaw†, Manuel Rey-Mendez‡, Alvaro Puga & Abner Louis Notkins

Laboratory of Oral Medicine, National Institute of Dental Research, National Institutes of Health, Bethesda, Maryland 20205

It has been amply documented that herpes simplex virus (HSV) persists in sensory ganglia of the peripheral nervous system (PNS)<sup>1-4</sup>. In contrast, HSV latency in the central nervous system (CNS) has not been well characterized. Corneal inoculation of virus results in a productive viral infection in the CNS during the first week after inoculation<sup>5</sup>, indicating that the virus can progress from the PNS to the CNS. During latency, HSV has been found by co-cultivation of CNS tissue in only a very small fraction of inoculated mice<sup>7,8</sup>. We have used here molecular hybridization techniques to analyse the fate of viruses that reach the CNS by anatomical pathways. We show that 6 days after corneal inoculation of HSV-1 a productive viral infection was present in brain tissue as well as in peripheral ganglia in at least 90% of the inoculated mice. The mortality during this acute phase was only 2%. In the survivors, latent HSV could be recovered by explantation from 95% of the trigeminal ganglia, but only 5% of the brain tissue explants of the same mice yielded infectious virus. However, HSV DNA sequences were detected in the brains of 30% of mice which harboured latent HSV in their trigeminal ganglia. These results suggest that viruses that progress from the PNS into the CNS are not eliminated, but are capable of establishing a latent infection in the CNS that cannot be reactivated by explantation techniques.

Six- to eight-week-old female BALB/cJ mice were inoculated by corneal scarification with approximately  $5 \times 10^6$  plaque-forming units (PFU) of the F strain of type 1 HSV (American Type Culture Collection). The virus was grown in primary rabbit kidney cells and concentrated by ultracentrifugation (stock pool of  $10^6$  PFU ml<sup>-1</sup>). For infectivity assays, homogenates or minced explants of individual organs were monitored for ability to induce cytopathic effects in monolayers of primary rabbit kidney cells<sup>3-5</sup>. For hybridization experiments, DNA was extracted from individual brain stems and hemispheres. Hybridization was to a <sup>32</sup>P-labelled HSV DNA probe prepared by nick translation<sup>9</sup>, purified in alkaline Sephadex G-200 (ref. 10) and free of fold-back DNA<sup>4</sup>. The conditions for the DNA-DNA hybridization reactions were as described previously<sup>4,11,12</sup>.

Table 1 shows that infectious HSV could be detected in homogenates of trigeminal ganglia from all of the mice killed 6 days after corneal inoculation of HSV (acute stage). At this time, infectious HSV was also detected in the brain stems of 18 out of 20 mice, and in the brain hemispheres of 6 out of 20 mice. DNA-DNA hybridization confirmed and extended these findings. Figure 1a shows the hybridization kinetics of a trace of <sup>32</sup>P-HSV DNA with DNA from individual brain stems and hemispheres taken from mice 6 days after inoculation. All 10 DNA preparations increased the rate of reassociation of the tracer over the self-reassociation rate in the presence of uninfected mouse brain DNA. However, the extent of the rate increase was not the same for the different preparations tested. The slopes of the curves show that the brain stems from acutely infected mice contained more viral DNA than the hemispheres from the same mice. The range of viral equivalents per 100 cells was 1-5 for the brain hemispheres and 22-178 for the brain stems (Table 2). In each animal the brain stem had more viral

Present addresses: \*Division of Biology, California Institute of Technology, Pasadena, California 91125; †Dept of Neurology, UC Davis Medical Center, Sacramento, California 95817; ‡Depto de Bioquímica, Facultad de Ciencias Biológicas, Universidad de Santiago, Santiago, Spain

**Table 1** Infectivity assay of mouse ganglia and brains

| Time after inoculation | Trigeminal ganglia | Brain stem | Brain hemispheres |
|------------------------|--------------------|------------|-------------------|
| <b>6 days</b>          |                    |            |                   |
| Homogenates*           | 20/20              | 18/20      | 6/20              |
| <b>8 weeks</b>         |                    |            |                   |
| Homogenates*           | 0/20               | 0/20       | 0/20              |
| Explant†               | 38/40              | 0/20       | 1/20              |

Results are expressed as the ratio of positive isolates from individual mice to the total number of mice tested.

\* The appropriate tissue was homogenized in glass Ten-Broek tissue grinders. After freezing and thawing to disrupt viable cells, the cell debris was pelleted by low-speed centrifugation and the supernatant fluid was cultured on primary rabbit kidney cells. Cultures were followed for viral-induced cytopathology (CPE) for 5 days.

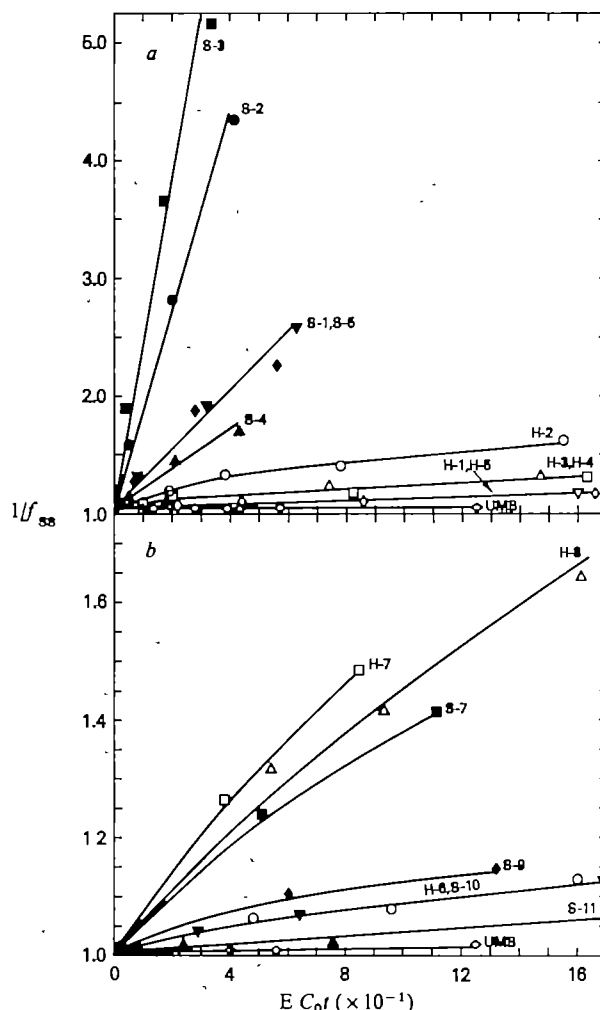
† Ganglia were explanted on monolayers of primary rabbit kidney cells in Eagle's minimal essential media supplemented with 3% fetal bovine serum (MEM). CPE appeared in the cell monolayer by 8 days in over 95% of the explant cultures that yielded HSV. For CNS explants, the appropriate tissues were minced and placed in MEM without a cell monolayer. The media was changed on alternate days and cultured for HSV. After 6–8 days, the explant tissue was homogenized and assayed for infectious virus\*. As shown previously, this technique can detect *in vitro* reactivation in 100% of latently infected ganglia after only 48 h of culture<sup>5</sup>. In contrast, CPE does not usually appear on the indicator cell monolayer before 5 days in the standard explantation and co-cultivation technique<sup>3</sup>.

sequences than the brain hemispheres, ranging from 8-fold for animal no. 4 to 60-fold for animal no. 3.

Mortality in the inoculated animals was only 2%, despite the productive viral infection in the CNS. Furthermore, 8 weeks after inoculation, trigeminal ganglionic homogenates were negative, but 38 of 40 ganglionic explants yielded infectious HSV by *in vitro* reactivation. Although these conditions essentially define the latent stage of the ganglionic infection, they did not apply to the CNS tissue, as HSV could be recovered by explantation in only 1 of 20 mice (Table 1). This low recovery rate from CNS explants could be explained in two ways: either the virus is eliminated from the CNS during the acute infection or the viral genome is present in the CNS in a form that cannot be readily reactivated by explantation techniques. To investigate these alternatives, a total of 20 mice in three separate inoculation schedules were killed 8 weeks after inoculation with HSV. DNA was extracted from the brain stems and hemispheres and each individual preparation was hybridized to a <sup>32</sup>P-HSV DNA probe.

The highest possible mass ratios of brain DNA to probe were used to maximize the detection level. However, due to the limited amount of DNA available from single organs, the sensitivity level was never higher than 1 viral equivalent per 1,500 cells, and usually it was in the range of 1 viral equivalent per 300–800 cells. Notwithstanding, DNA from 3 out of 20 hemispheres and 4 out of 20 stems increased significantly the reassociation rate of the probe over the control (Fig. 1*b*). An average number of copies per cell was calculated for the seven positive organs using the rates determined experimentally and the known parameters of each hybridization reaction. The three positive hemispheres had 0.4–9 copies per 100 cells; the four positive stems had 0.5–6 copies per 100 cells. Unlike the acute stage, latently infected brain stems and hemispheres had comparable amounts of viral DNA, although the number of sequences in either tissue varied over a 10–20-fold range (Table 2; only positive cases shown). These calculations are based on the assumption that the entire viral genome is present, although the maximum extent of hybridization never exceeded 40% (H-8) and more often was 12–20% (S-9; S-11). This assumption is only valid to determine an average number of copies for the DNA sequences that hybridize. Only one animal (no. 7) contained viral sequences in both brain stem and hemispheres; all other positive animals had viral DNA in either tissue, but not both.

Latent HSV has previously been detected by co-cultivation in 9% of mouse brains following experimentally induced viraemia<sup>7</sup> and in 9% of mouse spinal cords after rear-footpad inoculation<sup>8</sup>. In those reports mortality was high, unlike the present study. However, in our experiments, 5% of the brain hemispheres were shown to contain virus, a number not very different from those reported previously. Clearly, explantation results in a large underestimation of the actual number of animals that harbour viral DNA sequences in the CNS. As shown, a total of 6 out of 20 mice (30%) have HSV DNA in the brain stem and/or hemispheres, a fraction six times higher than that found by explantation. Inoculation of a viral dose sufficiently large to increase the mortality rate may increase the fraction of surviving animals with detectable viral DNA sequences in the CNS.



**Fig. 1** Hybridization kinetics of <sup>32</sup>P-HSV DNA ( $1.2 \times 10^8$  c.p.m. per  $\mu$ g) in the presence of DNA from brain stems (S) or brain hemispheres (H) of HSV-infected mice. Brain tissues were homogenized in 2.2M sodium trichloroacetate (NaTCA), pH 7.4, 10 mM EDTA, followed by phenol-chloroform extraction and ethanol precipitation. NaTCA inhibits DNase activity present in large quantities in nervous tissue. DNA preparations were treated with RNase, proteinase K, re-extracted and sonicated to an average piece size of 7S in alkaline sucrose. DNA yield was  $300 \pm 50 \mu$ g for brain hemispheres and  $40 \pm 15 \mu$ g for brain stems. *a*, 6 days post-inoculation; the reaction mixtures contained 0.8–1.0 ng ml<sup>-1</sup> <sup>32</sup>P tracer and 11–12 mg ml<sup>-1</sup> brain hemisphere DNA or 5–6 mg ml<sup>-1</sup> brain stem DNA. *b*, 8 weeks post-inoculation; the reaction mixtures contained 1 ng ml<sup>-1</sup> <sup>32</sup>P tracer and 15 mg ml<sup>-1</sup> hemisphere DNA or 13–20 mg ml<sup>-1</sup> stem DNA. A control was run in the presence of uninfected mouse brain DNA (UMB). Mixtures were adjusted to 0.48 or 1.0 M phosphate buffer, pH 6.8, and incubated in siliconized glass capillaries at 70–72 °C. The inverse of the fraction of <sup>32</sup>P-DNA remaining as single strands ( $1/f_{\infty}$ ) is plotted as a function of the equivalent  $C_0 t$  ( $E C_0 t$ ), corrected to 0.18 M Na<sup>+</sup> (ref. 12).



The detection level of the hybridization reactions is limited by the scarcity of DNA from single CNS tissues and by the uncertainty as to which areas of the brain are most likely to be positive for viral sequences. The hybridization rates used to calculate the number of viral copies have been obtained from a least-squares regression fit of three experimental points to a straight line, but in many cases a fit to a two-component curve may also be possible (as shown in Fig. 1). A fit to a straight line provides only valid information for comparisons to be drawn between the various tissues. Thus, the results would not warrant the conclusion that all of the viral genome is present in the CNS during the latent stage. In fact, the sequences detected may correspond to an unbalanced representation of portions of the genome, such as is found in defective particles. The presence of defective particles may explain the absence of significant reactivation by explantation.

HSV reaches sensory ganglia in the PNS by intra-axonal retrograde transport<sup>13-15</sup>. The same anatomical pathway is the most likely route for virus to reach the CNS, as the bipolar axon of trigeminal neurones continues past the ganglion and synapses into the brain stem. A productive viral infection in the brain stem and hemispheres can then occur concomitantly with the acute stage of the ganglionic infection, setting the stage for subsequent latency in the CNS.

The finding of latent viral DNA in the brains of experimental animals suggests a possible role for HSV in neurological disorders of unknown aetiology. If the viral genome or portions of it were shown to be present in human brains, in the absence of complete viral reactivation certain genes could be expressed

under the influence of various stimuli. The resulting viral proteins might interfere with nerve cell function by altering cell membranes, setting up abnormal storage material or provoking a local immune response.

We thank Dr Edouard Cantin for helpful discussions, Drs Patrick McClintock and Martin Haspel for criticisms, Mrs Jeannette Murphy and Edith Rian for secretarial help, and Dr D. E. Kohne for communicating methodology before its publication.

Received 3 July; accepted 17 September 1980.

1. Stevens, J. G. & Cook, M. L. *Science* **173**, 843 (1971).
2. Price, R. W., Katz, B. J. & Notkins, A. L. *Nature* **257**, 686 (1975).
3. Walz, M. A., Price, R. W. & Notkins, A. L. *Science* **184**, 1185 (1974).
4. Puga, A., Rosenthal, J. D., Openshaw, H. & Notkins, A. L. *Virology* **89**, 102 (1978).
5. Openshaw, H., Asher, L. S. V., Wohlberg, C., Sekizawa, T. & Notkins, A. L. *J. gen. Virol.* **44**, 205 (1979).
6. Baringer, J. R. & Griffith, J. F. *J. Neuropath. exp. Neurol.* **29**, 89 (1970).
7. Knotts, E. P., Cook, M. L. & Stevens, J. G. *J. exp. Med.* **138**, 740 (1973).
8. Cook, M. L. & Stevens, J. G. *J. gen. Virol.* **31**, 75 (1976).
9. Maniatis, T., Jeffrey, A. & Kleid, D. G. *Proc. natn. Acad. Sci. U.S.A.* **72**, 1184 (1975).
10. Britten, R. J., Graham, D. E. & Neufeld, B. B. *Meth. Enzym.* **29**, 363 (1974).
11. Kohne, D. E. *Biophys. J.* **8**, 1104 (1968).
12. Britten, R. J. & Smith, J. *Yb. Carnegie Instn Wash.* **68**, 378 (1970).
13. Hill, T. J., Field, H. J. & Roome, A. P. C. *J. gen. Virol.* **15**, 253 (1972).
14. Cook, M. L. & Stevens, J. G. *Infect. Immun.* **7**, 272 (1973).
15. Baringer, J. R. & Swoveland, P. *Lab. Invest.* **30**, 230 (1974).

## Immunoglobulin C<sub>μ</sub> RNA in T lymphoma cells is not translated

Ian D. Walker & Alan W. Harris

The Walter and Eliza Hall Institute of Medical Research,  
Post Office, Royal Melbourne Hospital, Victoria 3050, Australia

**Table 2** Viral DNA sequences in brain stems and hemispheres of HSV-infected mice

| Time after inoculation | CNS tissue and animal no. | Rate increase | DNA copies per 100 cells |
|------------------------|---------------------------|---------------|--------------------------|
| 6 days                 | Brain hemispheres         |               |                          |
|                        | 1                         | 5 ± 1         | 1 ± 0.3                  |
|                        | 2                         | 19 ± 2        | 5 ± 0.6                  |
|                        | 3                         | 9 ± 1         | 3 ± 0.4                  |
|                        | 4                         | 9 ± 1         | 3 ± 0.5                  |
|                        | 5                         | 5 ± 2         | 1 ± 0.5                  |
|                        | Brain stem                |               |                          |
|                        | 1                         | 61 ± 5        | 38 ± 3                   |
|                        | 2                         | 138 ± 11      | 120 ± 10                 |
|                        | 3                         | 154 ± 21      | 178 ± 24                 |
|                        | 4                         | 27 ± 3        | 22 ± 3                   |
|                        | 5                         | 42 ± 9        | 28 ± 6                   |
| 8 weeks                | Brain hemispheres         |               |                          |
|                        | 6                         | 2 ± 0.3       | 0.4 ± 0.2                |
|                        | 7                         | 55 ± 7        | 9 ± 1                    |
|                        | 8                         | 4 ± 0.5       | 3 ± 0.4                  |
|                        | Brain stem                |               |                          |
|                        | 7                         | 38 ± 6        | 6 ± 1                    |
|                        | 9                         | 29 ± 9        | 2 ± 0.5                  |
|                        | 10                        | 8 ± 1         | 1 ± 0.2                  |
|                        | 11                        | 5 ± 1         | 0.5 ± 0.1                |
|                        | R-15                      | 15 ± 2        | —                        |
|                        | R-24                      | 24 ± 7        | —                        |

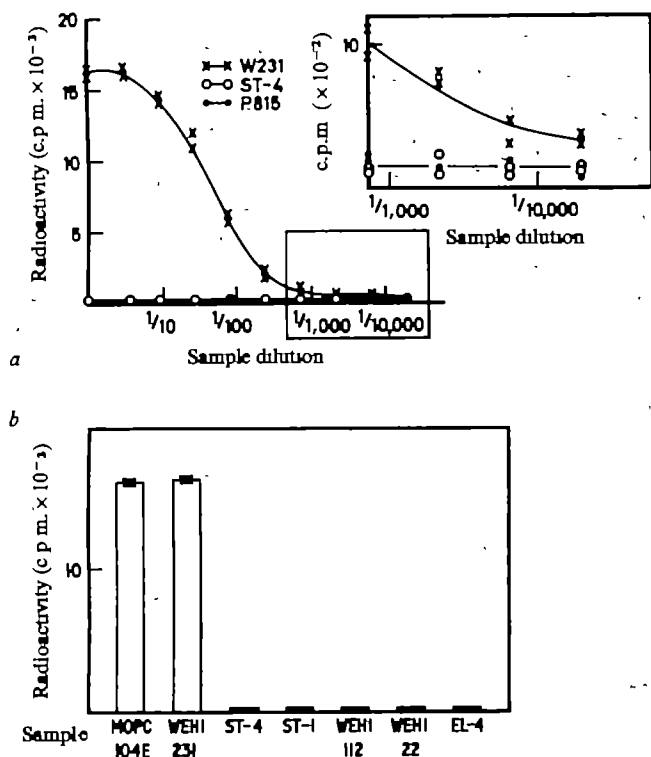
Rate increase factors and copies per cell were determined as described<sup>4</sup>, using  $2.46 \pm 0.171 \text{ mol}^{-1} \text{ s}^{-1}$  as the rate constant for the reassociation of nick-translated HSV DNA in the presence of uninfected mouse brain DNA (an average of five experiments). The rate constants of the hybridization reactions were determined from the least-squares fit of the curves in Fig. 1. A total of 20 brain stems and their corresponding hemispheres were tested at 8 weeks post-inoculation; only organs that gave rate increase  $\geq 2$  were considered positive and are reported here. The mass ratios of brain DNA to <sup>32</sup>P-HSV DNA ranged from  $5 \times 10^6 : 1$  to  $1 \times 10^8 : 1$ . Results are indicated  $\pm$ s.e. R-15 and R-24 are reconstitution experiments containing 15-fold and 24-fold excess of unlabelled HSV DNA over <sup>32</sup>P tracer, respectively; the rate increases in these two reactions agree with those expected from the reconstitution conditions.

It is widely believed that immunoglobulin genes might encode at least part of the receptor for antigen on the T lymphocyte. Evidence supporting this comes from the effects of anti-immunoglobulin idiotype antibodies on cellular immune networks<sup>1-4</sup> and from the presence of idiotypes on immunologically active factors from T cells<sup>5-7</sup>. Detailed molecular characterization of the receptor, however, has been seriously hampered by the lack of a suitable cellular source from which it might be isolated. The recent demonstration by Kemp *et al.*<sup>8,9</sup> that thymocytes and certain cultured lines of mouse T lymphoma cells contain polyadenylated RNA molecules encoded by the immunoglobulin C<sub>μ</sub> gene (C<sub>μ</sub> RNA) prompted us to identify the corresponding protein molecules in those cells. As the haploid mouse genome contains a single C<sub>μ</sub> gene<sup>10</sup>, any polypeptide encoded by this gene should react with at least some of the antibodies present in rabbit anti-mouse IgM antiserum. In this letter we report that a number of T lymphoma lines, regardless of whether they contain C<sub>μ</sub> RNA, synthesize no detectable  $\mu$  polypeptides.

The cloned T lymphoma lines chosen for study were STRij-4-2.2 (ST4), STRij-1.3 (ST1), WEHI-22.1 (W22), EL-4.1 (EL4) (described in ref. 8) and WEHI-112.1 (W112): they contained 33, <1.5, 3, <1.5 and 30–50 molecules of C<sub>μ</sub> RNA per cell, respectively. In addition, two B lymphoma cell lines, WEHI-231 (W231) ( $\mu$ ,  $\kappa$ ) and WEHI-279 (W279) ( $\mu$ ,  $\kappa$ ), a mastocytoma line P815 (respectively, 95, 195 and <0.3 C<sub>μ</sub> RNA molecules per cell<sup>8</sup>) and an Abelson pre-B lymphoma cell line 18–81 (ref. 11) were used as positive or negative controls in the search for  $\mu$  polypeptide chains.

The presence of C<sub>μ</sub> RNA molecules in ST4 and W112 was repeatedly confirmed during experiments described here, indicating that C<sub>μ</sub> gene transcription occurs continuously in these cell lines.

A 'sandwich' radioimmunoassay (RIA) technique using <sup>125</sup>I-labelled antibodies was used to test cell extracts for  $\mu$  polypeptide content and Fig. 1a shows the results of an experiment in which extracts of W231, P815 and ST4 were examined. No binding whatever was apparent with ST4 or P815, whereas in



**Fig. 1** Detection of  $\mu$  polypeptides in detergent lysates of lymphoma cells. Cells ( $10^6 \text{ ml}^{-1}$ ) were solubilized in Triton X-100 buffer (0.01 M Tris-HCl, 0.15 M NaCl, 0.5% Triton X-100, pH 7.5) containing 1% (w/v) bovine serum albumin (BSA), by incubation at  $0^\circ\text{C}$  for 20 min. Nuclei were removed by centrifugation at 10,000 r.p.m. for 30 min. Supernatants were tested by solid-phase RIA<sup>16</sup>. Anti- $\mu$  antiserum, obtained from rabbits immunized with purified myeloma HPC-76 IgM ( $\mu, \kappa$ ), was affinity-purified on myeloma MOPC 104E IgM ( $\mu, \lambda$ )-Sepharose adsorbent. Microtitre plates were coated with purified anti- $\mu$  Ig ( $20 \mu\text{g ml}^{-1}$ ) and then incubated with dilutions of cell extracts or of purified 104E IgM. After washing, anti- $\mu$   $^{125}\text{I}$ -Ig was added ( $10 \mu\text{Ci } \mu\text{g}^{-1}$ , 20,000 c.p.m. per well), and incubation carried out overnight. Plates were washed and individual wells counted in a Packard  $\gamma$  counter. *a*, Titration curves for extracts of W231, P815 and ST4; *b*, binding data for detergent extracts of various cell lines, each tested at a concentration of  $10^6 \text{ cells ml}^{-1}$  compared to MOPC 104E at  $10 \mu\text{g ml}^{-1}$ .

W231, activity (IgM) could be detected even after a 10,000-fold dilution. Using purified myeloma MOPC 104E IgM as a reference standard, the amount of IgM in W231 was estimated at  $3 \times 10^5$  molecules per cell. Thus the number of  $\mu$  molecules in P815 or ST4 cannot exceed 30 per cell. Other  $C_\mu$  RNA-containing T lymphoma lines (W112 and W22) were tested by sandwich RIA and again no  $\mu$  polypeptides were detected (Fig. 1*b*).

We considered the following possibilities to account for our failure to detect  $\mu$  polypeptides in cells producing  $C_\mu$  RNA: (1) The anti- $\mu$  antibodies bind only to carbohydrate determinants present on IgM but not on T lymphoma cell  $\mu$  polypeptides.

(2) A specific protease in T lymphoma cells degrades  $\mu$  polypeptides.

(3) The anti- $\mu$  antibodies cannot bind  $\mu$  chains that are not associated with light chains.

(4)  $\mu$  polypeptides in T lymphoma cells are associated with other proteins which render antigens, which would otherwise bind anti- $\mu$  antibodies, inaccessible.

(5) A fragment of  $\mu$  chain containing only one or a few antigenic sites is synthesized by T lymphoma cells.

Possibility (1) was eliminated by demonstrating that oxidation of HPC-76 myeloma IgM with  $\text{NaIO}_4$ , in conditions known to degrade serologically detectable carbohydrate<sup>12</sup>, did not affect

its reactivity towards anti- $\mu$  antibodies as determined by RIA.

Possibility (2) was ruled out by an experiment in which equal numbers of ST4 and W231 cells were mixed before lysis and the mixed extract titrated for IgM activity after overnight incubation at room temperature. No reduction in IgM titre compared to an extract of W231 alone was found. To test the further possibility that cellular proteases could act on T-cell  $\mu$  polypeptides but not on IgM, we pulse-labelled cells with  $^{35}\text{S}$ -methionine and searched for labelled proteins after immunoprecipitation of cell extracts with anti- $\mu$  antibodies (Fig. 2). Only with the two B lymphoma lines, W231 and W279, was specifically precipitated labelled protein apparent. As little as 1% of the material present in W231 would have been detected as a specific band, but none was found in the T lymphoma cell lysates. As W231 cells contain on average  $3 \times 10^5$  IgM molecules per cell and have a doubling time in culture of 12–14 h, they must synthesize at least 6,000 molecules per cell during a 15-min labelling period. ST4 cells contain 33  $C_\mu$  RNA molecules per cell compared with 95 in W231 and would be expected to synthesize 2,000 molecules in the same time period. Thus, if fewer than 60 out of 2,000 newly synthesized  $\mu$  molecules remain in ST4 cells after 15 min, their half life would have to be less than 1 min, a considerably shorter time than that required for complete translation of a  $\mu$  polypeptide chain.

Possibility (3), that anti- $\mu$  antibodies bind only to antigens formed by H chain-L chain association was ruled out by demonstrating that  $\mu$  polypeptides, even after SDS-gel electrophoresis, could specifically bind the antibodies. Figure 3 shows the results of a filter affinity transfer experiment<sup>13,14</sup> in which purified IgM (MOPC 104E) was electrophoresed in SDS and transferred to chemically activated paper to which anti- $\mu$  antibodies had been attached. Subsequent incubation with anti- $\mu$   $^{125}\text{I}$ -antibodies revealed the presence of a radioactive protein zone corresponding in size to  $\mu$  chain in the purified IgM channel. Thus, at least a fraction of the antibody molecules can recognize  $\mu$  chains not associated with L chains.

This conclusion was confirmed in RIA of extracts of an Abelson lymphoma cell line, 18-81, which synthesizes  $\mu$  chains but no L chains<sup>11</sup>. In these experiments (not shown), neither the shape of the titration curve nor the maximum counts per min bound with 18-81 was different from the corresponding parameters for W231, implying that L chains contributed few, if any, antigens reactive with the present antiserum.

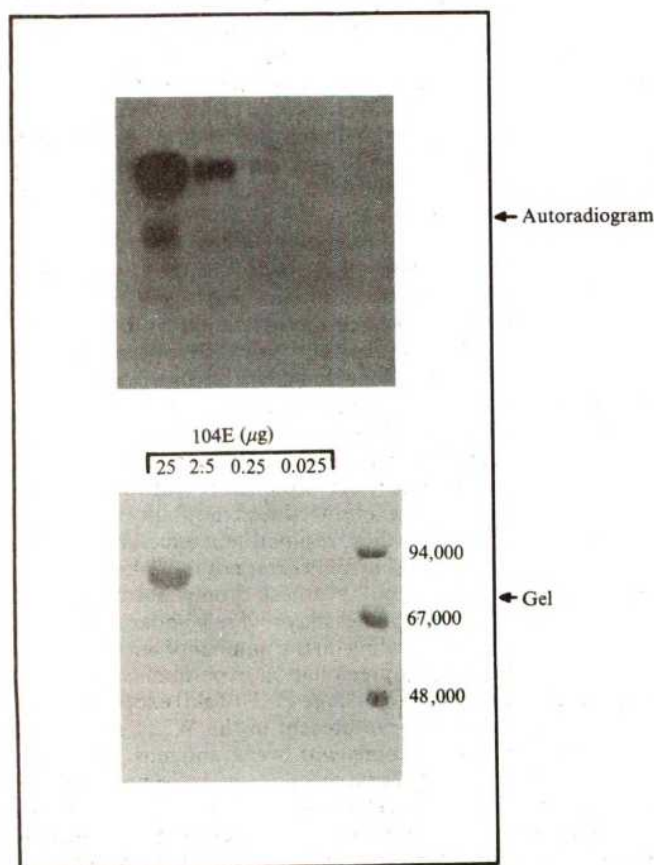
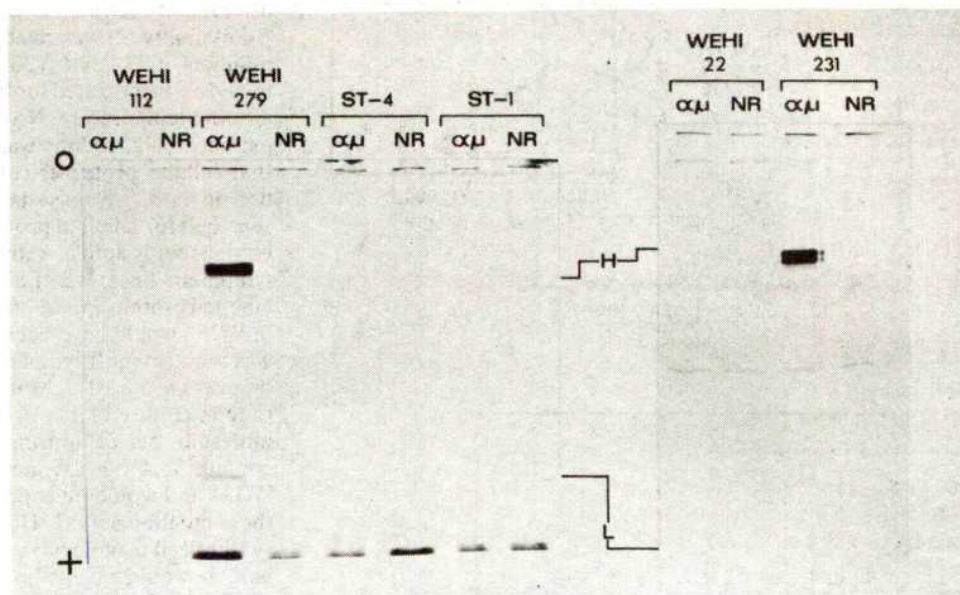
Possibility (4) was tested by performing RIA on extracts of W231 and ST4 cells which had been subjected to SDS treatment before assay so as to dissociate protein-protein interactions. Although SDS treatment severely reduced the ability of W231  $\mu$  chain to fix anti- $\mu$  antibodies, residual antigenic activity was nonetheless clearly present in W231 but not in ST4.

Should T lymphoma cells synthesize only a fragment of normal  $\mu$  chain, RIA techniques may severely underestimate or even fail to detect it, depending on the number of antigenic sites contained. In the immunoprecipitation experiments of Fig. 2, anti- $\mu$  antibodies were used in large ( $> 10$ -fold) excess over the amount of IgM known to be present in the W231 extract, to facilitate antibody interactions with weak antigens. However, only in the two B lymphoma cell lines were  $\mu$  polypeptides detected: in the T lymphoma lines, neither intact  $\mu$  polypeptides nor polypeptides of altered size were detected. A single  $\mu$  antigenic determinant per molecule would have resulted in specific precipitation in this test.

At face value, the data herein do not support the inference, from the existence of  $C_\mu$  RNA in T lymphoma and thymus cells, that the  $C_\mu$  gene may specify part of the T-cell antigen receptor<sup>8,9</sup>. If  $C_\mu$  RNA concentration was the sole determinant of  $\mu$  polypeptide production, ST4 cells should contain about  $10^5$   $\mu$  molecules per cell, which would have been readily detected. Furthermore, the  $C_\mu$  RNA molecules in ST4 cells contain nucleotide sequences corresponding to all four  $C_\mu$  domains<sup>15</sup> and, if translated, their protein products would be expected to express the antigenic determinants required for serological detection. Therefore, neither the qualitative characteristics (as



**Fig. 2** Immunoprecipitation of detergent extracts of biosynthetically labelled lymphoma cells.  $2 \times 10^7$  cells were labelled for 15 min at  $37^\circ\text{C}$  in 10 ml culture medium containing 10% fetal calf serum and  $50 \mu\text{Ci ml}^{-1}$   $^{35}\text{S}$ -methionine (specific activity  $\sim 1,000 \text{ Ci mmol}^{-1}$ ). Incubations were terminated by the addition of 1 ml  $10\times$  concentrated Triton X-100 buffer and supernatants were prepared as in Fig. 1 legend. Samples of each supernatant containing equal amounts of radioactivity were reacted with  $10 \mu\text{g}$  anti- $\mu$  ( $\alpha\mu$ ) Ig, or with  $10 \mu\text{g}$  normal rabbit IgG (NR) by overnight incubation at  $4^\circ\text{C}$ .  $10 \mu\text{l}$  of packed, formalin-fixed *Staphylococcus A* organisms were added to each sample, incubated for 1 h at  $4^\circ\text{C}$  and then washed twice in Triton X-100 buffer containing 1% (w/v) BSA, pH 8.5 (HCl), and once in Triton X-100 buffer lacking BSA. Samples were subject to SDS electrophoresis on 12% polyacrylamide gels<sup>17</sup>, stained to visualize molecular weight marker proteins and then fluorographed<sup>18</sup>. H, L, positions of IgM heavy chain and light chain, respectively.



**Fig. 3**  $\mu$  polypeptides do not require associated L chains to react with anti- $\mu$  antibodies. The indicated amounts of purified MOPC 104E IgM and a molecular weight marker mixture of proteins containing phosphorylase *b* (94,000), BSA (68,000) and ovalbumin (48,000) were separated by SDS-gel electrophoresis. The gel was then soaked in phosphate-buffered saline (PBS) containing 1% Triton X-100 to leach out SDS. Proteins were transferred from the gel to a strip of Whatman 540 paper to which anti- $\mu$  Ig had previously been attached. After transfer, the gel was stained with Coomassie blue 250R and the paper was reacted by overnight incubation with  $20 \text{ ml}$  anti- $\mu$ - $^{125}\text{I}$ -Ig ( $2 \times 10^6 \text{ c.p.m. ml}^{-1}$ , specific activity  $10 \mu\text{Ci } \mu\text{g}^{-1}$ ) dissolved in PBS containing 0.05% Tween 20, 1% (w/v) BSA. Filter paper was chemically activated<sup>14</sup> and antibodies were attached as described<sup>13</sup>. After 'radioactive staining', the paper was washed six times with 1 l of PBS, dried and autoradiographed at  $-70^\circ\text{C}$  using preflashed X-ray film (Kodak XRP-5) and a fast tungstate intensifying screen (Ilford). The autoradiogram (a) was obtained after a 4-h exposure and is aligned with the stained gel (b). The lower molecular-weight radioactive material beneath the  $\mu$  chain band in the leftmost channel is a degradation product of 104E IgM.

presently known) nor the relative amounts of T lymphoma  $\mu$  RNA compared to its B cell (e.g. W231) counterpart provide an explanation for the absence of  $\mu$  polypeptides.

It therefore seems that post-transcriptional control of  $\mu$  polypeptide synthesis may operate in T lymphoma cells. Further evidence for the occurrence of untranslated  $C_\mu$  RNA comes from some of our recent observations with Abelson virus-transformed pre-B cell lines. Four lines contain  $C_\mu$  RNA but only one of them, 18-81, produces  $\mu$  chains (I.D.W., A.W.H. and D. J. Kemp, unpublished observations). Thus, in the B lineage, the ability to translate  $\mu$  RNA molecules may be

acquired during later states of differentiation. If the same programme were to apply to the T-cell lineage, then  $\mu$  polypeptide synthesis could be expected at a later stage of development than that represented by the T lymphoma lines of this study.

We thank Dr D. J. Kemp for making data available to us before publication and for critically reading this manuscript, and Drs K. Shortman and E. Siden for providing rabbit anti-IgM antiserum and the 18-81 cell line respectively. Sue Gherashe and Angela Apa gave excellent technical assistance.

Received 12 August; accepted 1 October 1980.

1. Eichmann, K. *Eur. J. Immun.* **4**, 296-302 (1974).
2. Cosenza, H., Julius, M. & Augustin, A. *Immun. Rev.* **34**, 3-33 (1977).
3. Eichmann, K. & Rajewsky, K. *Eur. J. Immun.* **5**, 661-666 (1975).
4. Nisonoff, A., Ju, S. T. & Owen, F. *Immun. Rev.* **34**, 89-118 (1977).
5. Bach, B. A., Sherman, L., Benacerraf, B. & Greene, M. I. *J. Immun.* **121**, 1460-1468 (1978).
6. Hirai, Y. & Nisonoff, A. *J. exp. Med.* **151**, 1213-1231 (1980).
7. Sy, M. S., Dietz, M. H., Germain, R. N., Benacerraf, B. & Greene, M. I. *J. exp. Med.* **151**, 1183-1195 (1980).
8. Kemp, D. J., Harris, A. W., Cory, S. & Adams, J. M. *Proc. natn. Acad. Sci. U.S.A.* **77**, 2876-2880 (1980).
9. Kemp, D. J., Wilson, A., Harris, A. W. & Shortman, K. *Nature* **286**, 168-170 (1980).
10. Cory, S. & Adams, J. M. *Cell* **19**, 37-51 (1980).
11. Siden, E. J., Baltimore, D., Clark, D. & Rosenberg, N. E. *Cell* **16**, 389-396 (1979).
12. Mattes, M. J. & Steiner, L. A. *Nature* **273**, 761-763 (1978).

- 13 Ehrlich, H. A., Levmore, J. R., Cohen, S. N. & McDavitt, H. O. *J. Biol. Chem.* **10**, 12240-12247 (1979)  
 14 Alwine, J., Kemp, D. J. & Stark, G. R. *Proc. natn. Acad. Sci. U.S.A.* **74**, 5350-5354 (1977)  
 15 Kemp, D. J., Harris, A. W. & Adams, J. M. *Proc. natn. Acad. Sci. U.S.A.* (in the press)  
 16 Kinnison, N. R. et al. *Arab. J. Bot.* **127**, 489-495 (1976)  
 17 Lamm, U. K. *Nature* **227**, 680-685 (1970)  
 18 Leakey, R. A. & Mills, A. D. *Eur. J. Biochem.* **86**, 335-341 (1975)

## Methylation map of *Xenopus laevis* ribosomal RNA

B. E. H. Maden

Department of Biochemistry, University of Glasgow,  
Glasgow G12 8QQ, UK

One of the most enigmatic features of eukaryotic ribosomal RNA is the presence of many methylated nucleotides. The numbers of RNA methyl groups range from approximately 70 per ribosome in yeast<sup>1</sup> to over 100 in vertebrates<sup>2,3</sup>. Here it is shown that the methylated nucleotides in *Xenopus laevis* rRNA are broadly but non-uniformly distributed. In 18S rRNA 2'-O-methylations are partly concentrated in the 5' region and base methylations near the 3' end. In 28S rRNA methyl groups are infrequent in the 5' region, moderately frequent in the central region and abundant in an 1,100-nucleotide tract near the 3' end.

To map the methylated nucleotides rRNA was radioactively labelled in *X. laevis* cultured kidney cells. 18S or 28S rRNA was then hybridized to cloned restriction fragments of rDNA (Fig. 1) or to smaller, purified restriction fragments derived from the clones (see Fig. 3, below). As only part of the rRNA was complementary to each restriction fragment, the noncomplementary RNA could be eliminated by digestion with T<sub>1</sub> ribonuclease. The complementary rRNA was then eluted, examined by fingerprinting, and the methylated oligonucleotides in each region identified. (Limited, partial mapping data were previously obtained by this general method<sup>4,5</sup>.)

Figure 2 shows some representative fingerprints. Numerous further fingerprints were obtained covering all the regions and subregions in Fig. 3. As most methylated T<sub>1</sub> products occur once per molecule of 18S or 28S rRNA<sup>2,3</sup>, the presence or absence of particular products in different fingerprints was usually clearly recognizable, especially when autoradiographs of fingerprints which had been run simultaneously were superimposed. Additional criteria for sequence identification were alkaline hydrolysis followed by electrophoretic analysis of methylated components<sup>2,3</sup>, and use of the combined T<sub>1</sub> plus pancreatic ribonuclease fingerprinting system<sup>6,7</sup>. This system resolves, in the form of well separated digestion products, several methylated components that occur within high-numbered T<sub>1</sub> products that are not well resolved in Fig. 2.

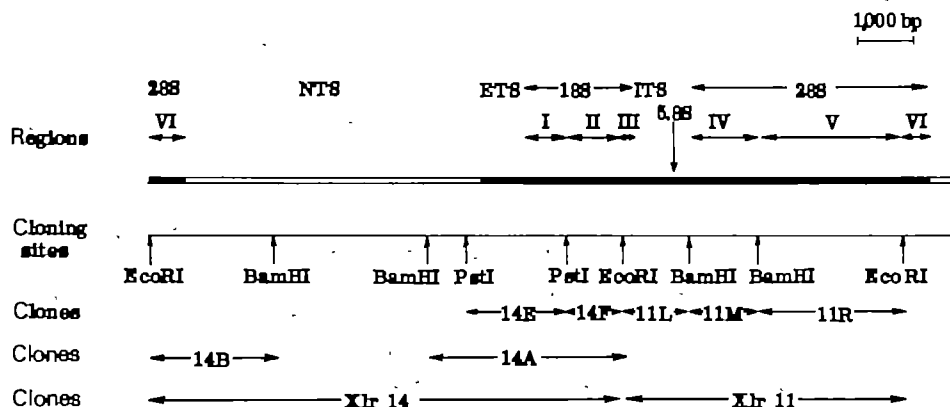
Nearly all unimolar products mapped uniquely within a single rRNA region or subregion, and in general the relative molar recoveries were in good agreement with the yields previously determined for whole 18S or 28S rRNA. A few products hybridized to two adjacent rDNA fragments (see Table 1). In each case the most likely explanation is that the RNA methylated oligonucleotide is encoded across or very close to the respective restriction site in rDNA. There were no instances of methylated sequences cross-hybridizing to widely separated regions in rDNA. Of the few methylated oligonucleotides that occur more than once per 18S or 28S rRNA, approximately correct aggregate recoveries were obtained from the sub-region(s) in which the spots mapped.

The findings are summarized in Fig. 3 and Table 1. In 18S rRNA methyl groups occur in all subregions, but their distribution is strikingly non-uniform, especially when 2'-O-ribose methylation and base methylation are scored separately. This distinction is biologically important because during eukaryotic ribosome formation 2'-O-methyl groups are added very rapidly to ribosomal precursor RNA in the nucleolus<sup>2,8</sup> probably to nascent chains<sup>9</sup>, whereas the few base methyl groups in 18S rRNA are added later during ribosome maturation<sup>2,10</sup>. 2'-O-methyl groups are relatively much more abundant in the 5' part of the molecule than in the central or 3' parts. 60% of the 2'-O-methyl groups are in the 5' 40% of the molecule. In contrast, the dimethyl A sequence (product 30) is close to the 3' end<sup>4,11</sup> and the m<sup>6</sup>A sequence (product 34) is also in region III. The m<sup>7</sup>G sequence (product 49) is on the boundary between regions II and III, and the sequence containing the hypermodified base, am<sup>ψ</sup>, (product 37)<sup>10</sup> is within the rather large subregion IIb.

In 28S rRNA the distribution of methyl groups is quite different from that found in 18S rRNA. At the 5' end there is a long tract of about 900 nucleotides containing only one methylated component, Am-G. There is then a small cluster of methyl groups in region IVb and the first part of Va, followed by a 'trough' in the second part of Va. Near the middle of the molecule a group of 16 methyl groups occupies the first two parts of region Vb. There follows another, distinct trough between the first of two PvuII sites and the second PvuII site or possibly the adjacent HincII site. The next 1,100 nucleotides (regions Vc and VIa) contain by far the highest abundance and concentration of methyl groups in 28S rRNA—36 2'-O-methyl groups and four of the five base methyl groups, or 60% of the total 28S methyl groups in little over 25% of the molecule. Finally, the 200 nucleotides at the 3' end contain only one methyl group. These 28S findings confirm and much extend in detail those of Brand and Gerbi<sup>5</sup>.

28S rRNA possesses several sequences in which two or more methyl groups occur within a single T<sub>1</sub> ribonuclease oligonucleotide<sup>3</sup>. These multiply methylated sequences are distributed between the three larger-scale clusters. One such oligonucleotide occurs in region IVb (product 14, containing the

**Fig. 1** Slightly more than one repeat of *X. laevis* rDNA, showing cloning sites, cloned fragments and rRNA regions. Cloned fragments Xlr14 and Xlr11 have been described elsewhere<sup>4,5,11,22</sup> (Xlr)14B and 14A were subcloned from Xlr14 into pBR322 (ref. 23). Remaining fragments were subcloned into pBR322 in this work. Cloning sites in rDNA permit division of rRNA into following principal regions: I, 18S 5' end→PstI (628); II, 18S PstI→EcoRI (~950); III, 18S EcoRI→3' end (227); IV, 28S 5' end→BamHI (~1,100); V, 28S BamHI→EcoRI (~2,500); VI, 28S EcoRI→3' end (500). Numbers in parentheses are numbers of RNA nucleotides, determined from sequencing, hybridization and restriction data (refs 13, 23-25 and unpublished work of M. Salm, L. Hall and B.E.H.M.). NTS, ETS, ITS denote nontranscribed, external-transcribed and internal-transcribed spacers, respectively. NTS contains additional BamHI (ref. 22) and PstI sites not shown by Base notes.

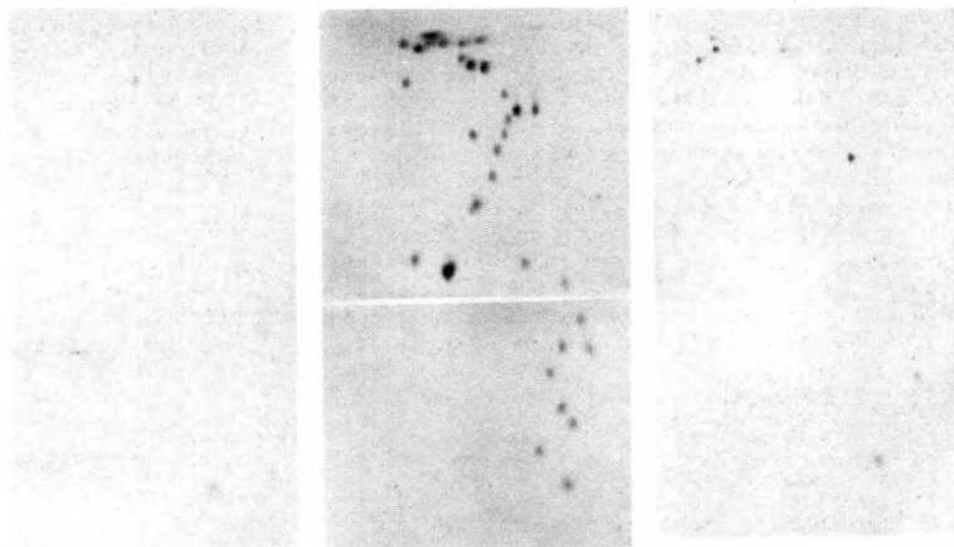
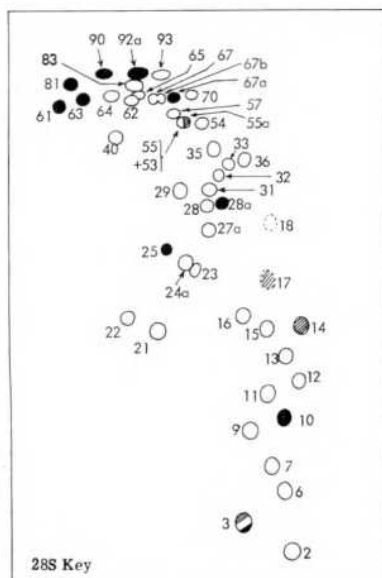
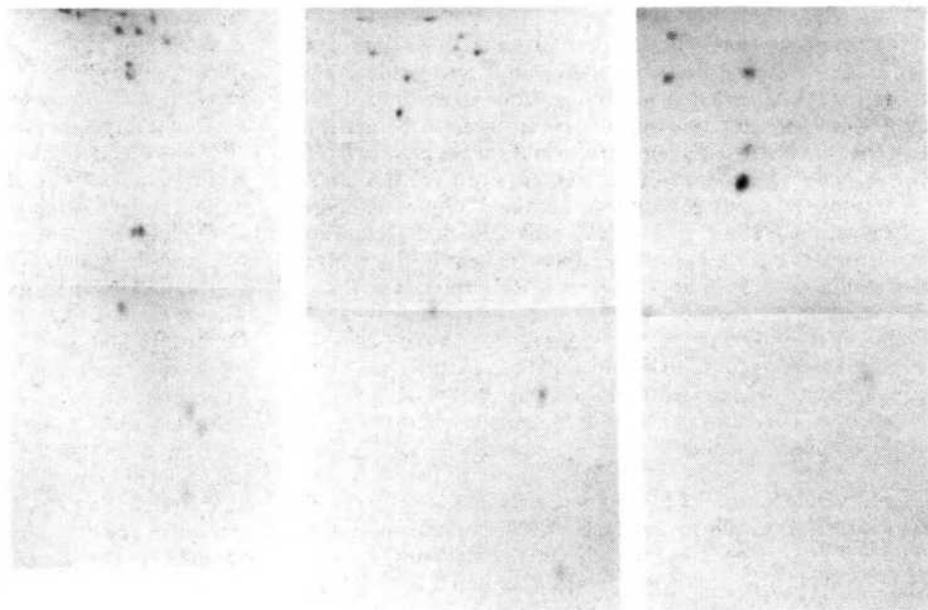
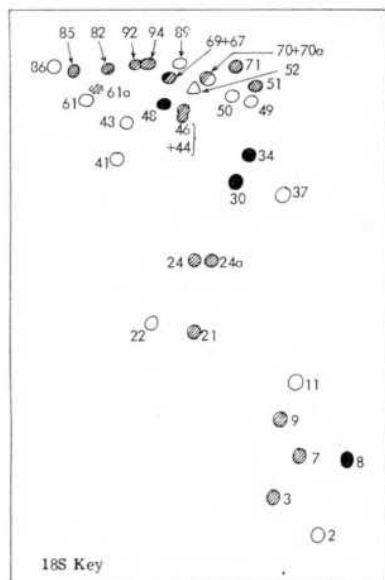




unusual, base-modified m<sup>1</sup>A), another in the adjacent part of region Va, two more in the first part of region Vb and three in regions Vc plus VIa. The central location of the triply methylated sequence, Am-Gm-Cm-A in region Vb, is of particular interest, as an identical component was once assigned to the 5' end of mammalian 28S rRNA<sup>12</sup>, although results from our laboratory did not support this assignment<sup>6</sup>.

The most striking feature of the methyl group distribution is its large-scale nonuniformity, both in 28S rRNA and to a lesser extent in 18S rRNA. Methylation requires recognition by methylases of specific sites in ribosomal precursor RNA or (for the few late methylations) in mature 18S rRNA. The recognition sites are evidently much more abundant in some regions of rRNA than in others. It seems likely that the frequencies of methylation sites in different parts of rRNA are somehow

related to other aspects of ribosome structure and function. Some indications of a possible link between rRNA methylation and biological function may be gained from the following. (1) The resolution of the methylation map is sufficient in many regions to permit accurate pinpointing of methyl groups in relation to sequence data obtained from rDNA<sup>13</sup>. This analysis is currently being extended for 18S rRNA with a view to definitive characterization of the methylation sites in this rRNA. (2) The rRNAs of several vertebrates yield similar fingerprints of methylated oligonucleotides to *X. laevis*, with a few distinguishing features<sup>3</sup>. It is therefore likely that the methylated sequences are similarly distributed along the primary structure of rRNAs in other vertebrates. (3) Gerbi and co-authors<sup>5,14</sup> have pointed out that much of the highly methylated region near the 3' end of *Xenopus* 28S rRNA is highly conserved between

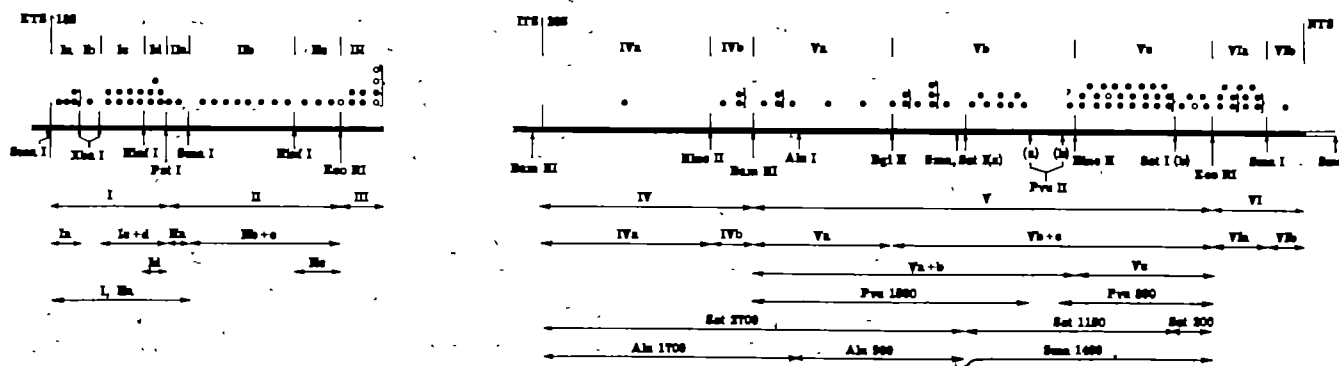


**Fig. 2** T<sub>1</sub> ribonuclease fingerprints of regions of *X. laevis* methyl-labelled rRNA. *X. laevis* cultured kidney cells were labelled with sufficient [<sup>14</sup>C]-methionine (Amersham, ~50 mCi mmol<sup>-1</sup>) to permit growth for 3–4 generations, and 18S and 28S rRNA were prepared as described elsewhere<sup>6</sup>. A slight molar excess of the appropriate rRNA was hybridized to ~100 µg of linearized recombinant plasmid DNA containing fragment 14E for region I, 14F for region II and so on (see Fig. 1). Details of hybridization, trimming of hybrids with T<sub>1</sub> ribonuclease and recovery of T<sub>1</sub>-resistant, hybridized RNA are given in ref. 13. Fingerprinting was as described<sup>26</sup>. First panel on upper line shows diagram of whole 18S rRNA; fingerprint has been published<sup>3</sup>. Shaded spots (3, 7, 9...) are in region I (fingerprint in second panel), open spots (2, 11...) are in region II (third panel), filled spots (8, 30...) are in region III (last panel). Spots 44 and 46 usually co-migrate<sup>3</sup>, but have separated in (I). 61a is a faint component (0.3 M) which is not included in Table 1. First panel on lower line shows diagram of whole 28S rRNA; fingerprint has been published<sup>3</sup>. Shaded spots are in region IV (second panel), open spots in region V (third panel), filled spots in region VI (last panel). Spot 3 occurs in each of the three regions. Spot 17 (region IV) is almost certainly a derivative of spot 14 resulting from isomerization of m<sup>1</sup>A to m<sup>6</sup>A during hybridization at elevated temperature and subsequent elution<sup>7,27</sup>; individually the yields of the two spots varied but collectively they always amounted to two methyl groups (mA plus Am-C; Table 1). Spot 18 is recovered in low yield and is not included in Table 1. 83 in the key is a mixture of 83, 83a and 83b (Table 1); 93 in the key is a mixture of 93, 93a and probably another component, 93b, in Table 1. Products 85 upwards in 18S and 28S rRNA showed variable mobilities or streaking in T<sub>1</sub> fingerprints but were definitively mapped by additional criteria outlined in text.

Table 1 Methylated sequences in *X. laevis* rRNA

| 18S subregion    | Methylated sequences   | Methyl 2'-O, base | Length  | Methyl 2'-O, base | Length | 2'-O-methyl per 100N |
|------------------|--|-------------------|---------|-------------------|--------|----------------------|
| Ia               | 46... Am-U-G; 87... Am-U...; 85, U-Um-C-C-U-U-Um-G   | 4 (-)             | 160     | 13 (-)            | 502    | 2.59                 |
| Ib               | 3, Am-G  | 1 (-)             | 102     |                   |        |                      |
| Ic               | 7, A-Cm-G; 9, Am-A-G; 24, U-Am-G; 24a, A-Gm-G(x2); 44... Um-C...; 51... Cm-C...; 71... Am-A-A-U...   | 8 (-)             | 240     |                   |        |                      |
| Id               | 21, Gm-G; 67... Um-A-A-U...; 70... A-Gm-C...; 82... Am-U...; 92... A-A-Am-U  | 5 (-)             | 126     | 7 (-)             | 246    | 2.85                 |
| IIa              | 52... Am-A...; 61, U-U-Gm-G  | 2 (-)             | 120     |                   |        |                      |
| IIb              | 2, Cm-G; 11, A-Am-C-G(x2); 22, Um-G; 37... am $\Psi$ ...; 41, Gm-U-G; 43, A-Um-U-G; 86, Um-U...  | 7 (1)             | ~550    | 7 (1)             | ~550   | 1.27                 |
| IIc              | 50, A-Gm-G; 70a... Cm-C...; 89... Um-C...; 49, m <sup>7</sup> G-A-A-U...   | 3 (1)             | ~250    | 6 (6)             | ~480   | 1.25                 |
| III              | 48... Am-A-G; 8, Cm-C-C-G; 69... Um-G; 34... (m <sup>6</sup> A, A)C...; 30, m <sup>2</sup> A-m <sup>2</sup> A-C  | 3 (5)             | 227     |                   |        |                      |
|                  |  | Total             | 33 (7)  | ~1,800            | 1.83   |                      |
| 28S subregion    |  |                   |         |                   |        |                      |
| IVa              | 3, Am-G  | 1 (-)             | ~900    | 1 (-)             | ~900   | 0.1                  |
| IVb              | 14, (m <sup>1</sup> A, A)C, AmC...; 55a... Cm-U...   | 2 (1)             | ~230    | 6 (1)             | ~480   | 1.25                 |
| Va Bam-Alu       | 21, Gm-G; 36... Gm-A-Am-A-G; 57, A-Am-C...   | 4 (-)             | ~250    |                   |        |                      |
| Va Alu-Bgl       | 6, C-Am-G; 23, Cm-U-G(x0.5)  | 2 (-)             | ~500    | 2 (-)             | ~500   | 0.4                  |
| Vb Bgl-Ssr(a)    | 3, Am-G; 22, Um-G; 62, Cm-A-Gm-U...; 64, A-U-Cm-U...; 93... Am-Gm-Cm-A...  | 8 (-)             | ~400    | 16 (-)            | ~750   | 2.13                 |
| Vb Ssr(a)-Pvu(a) | 15... C-Am-G; 21, Gm-G; 27a, U-Cm-A-G; 35, A-A-Um-G; 54... CmC, UmC...; 70... Am-U...; 83a... Gm-G...  | 8 (-)             | ~350    |                   |        |                      |
| Vb Pvu(a)-Hinc   | 21, Gm-G(x0 or 1)  | 0-1 (-)           | ~250    | 0-1 (-)           | ~250   | <0.5                 |
| Vc Hinc-Ssr(b)   | 2, Cm-G; 7, A-Cm-G; 9, A-Am-G; 11, A-Am-C-G; 12... Cm-A-G; 13, Cm-C...; 16, C-C-Gm-G   | 21-22 (2)         | ~580    | ~35 (4)           | ~1,100 | 3.18                 |
| Vc Ssr(b)-EcoRI  | 21, Gm-G(x2 or 3); 28... (m <sup>6</sup> A, A)C...; 29, A-A- $\Psi$ m-G; 31, A(A, Gm-A)G; 32... A-Am-A-G; 33, mC, A-A-Am-U   |                   |         |                   |        |                      |
| Vla              | 53, Gm-U...; 55... Um-C...; 65... A-Am-C...; 67b... Am-U...; 83... Um-Gm-U...; 93a... A-Cm-U...; 93b... Cm-C... (?)  | 4 (1)             | ~200    | 10 (1)            | 300    | 0.5                  |
| Vlb              | 21, Gm-G; 24a, A-Gm-G; 40, Um-A-U-G; 67... mC...; 83b... A-Gm-C  | 10 (1)            | 300     |                   |        |                      |
| Vlb              | 3, Am-G; 10, A-Cm-C-G; 25, Am-U-G(x0.5); 61, U-U-Gm-G; 63, m <sup>2</sup> U-U...; 67a... A-Am-U... (0.5); 81... Gm-U-G; 90... Um-C, (A, Gm-A)C; 92a... Um-Gm- $\Psi$ | 1 (-)             | 200     | 1 (-)             | 200    |                      |
|                  |  | Total             | ~62 (5) | ~4,150            | 1.49   |                      |

The methylated sequences shown here are as reported in ref. 3, although the two low-yield products, 61a (18S) and 18 (28S), are not shown as they have not been precisely mapped. Most sequences longer than tetranucleotides are given only in part. Further details, where available, are in refs 3 and 13. The nomenclature (revised) is as follows: The former 18S spot 70 (ref. 3) has two components, now called 70 (region Id) and 70a (region IIc). Spot 89 is correct identification for a spot previously designated 87. Former 28S spot 67 has two components now called 67 and 67b (both in region Vc). Identification and mapping of product 93b are tentative. In regions Ia, IIa and III, products are listed in the order in which they appear in the sequence. In other regions they are listed in arbitrary order. In the last columns data are grouped to highlight main features of methyl group distribution, firstly by subregions, then by larger rRNA segments with differing methylation densities. Further details on experimental methods are given in Fig. 3 legend.



**Fig. 3** The general features of methyl group distribution and restriction fragments used. Restriction map is to scale and methyl groups were reliably assigned to each subregion, but precise locations within each subregion are so far known in only a few instances<sup>11,13</sup>. Closed circles denote 2'-O-ribose methyl groups, open circles denote base methyl groups, brackets denote multiply methylated oligonucleotides. Preparative hybridization required rDNA fragments at least a few hundred nucleotides long; shorter fragments did not adhere to nitrocellulose filters. There was no upper limit to useful fragment length, and presence of vector DNA (which adjoined many of the fragments in Fig. 3) did not cause spurious hybridization. As large quantities of restriction fragments were required (equivalent to ~100 µg of whole plasmid per  $M_{16}$ - $^{14}$ C) fingerprint separations were usually on sucrose gradients (10–25%, in 1 M NaCl, 0.001 M EDTA, 0.025 M Tris-HCl, pH 8); restriction enzymes which cut infrequently were chosen where possible, and several subregions were mapped by 'overlaps' (lower part of figure). Restriction digests were planned from published maps of rDNA<sup>24,25</sup>, unpublished data (below), map of pBR322 (ref. 28) and known orientation of rDNA insert. In the 18S gene, sites shown for PstI, SmaI and EcoRI are only sites for those enzymes. There are several HincII sites, those shown are next left of PstI and EcoRI sites respectively<sup>25</sup>. HincII digestion of appropriate plasmids yielded these short rDNA regions attached to an easily separated fragment of pBR322 DNA. In the 28S gene, sites shown for HincII, BamHI, BglII, SsrI, PvuII and EcoRI are only sites for those enzymes. There are several SmaI sites<sup>24,25</sup>; those shown are the last two in the gene. There are also several AluI sites<sup>24,25</sup>, the one shown is first in 28S gene. The SsrI and PvuII sites are subsets of AluI sites and were mapped in this work. They are the second and sixth or seventh AluI sites (SsrI) and the third and fourth AluI sites (PvuII). Left-hand sites defining SsrI, 700 and AluI, 700 are in ITS and 5.8S gene respectively in Xlr11. See ref. 24 for AluI map. After purification of rRNA fragments by preparation hybridization, most products were recovered in ~100 µg yield in T<sub>1</sub> ribonuclease fingerprints. Those marked (x2) or (x0.5) in Table 1 occur in approximately these frequencies. (0.5 M spots were treated as unimolar in the quantitative summary) Spot 37 and some of highest-numbered spots showed variable mobilities and yields in T<sub>1</sub> fingerprints. Smaller 'derivative' products occurred in good yields in combined T<sub>1</sub> plus pancreatic ribonuclease fingerprints. See ref. 7 for correlation between the two fingerprinting systems. A few products hybridized weakly to two adjacent fragments. In each case the probable explanation is that the methylated sequence occurs close to a restriction site. Spot 52 hybridized with region IIa and weakly with region Id. Sequence data (M. Salm and B.E.H.M., unpublished) place this sequence as next product to right of PstI site. Spot 49 hybridized with regions IIc and III. Data on RNA oligonucleotide are consistent with DNA sequence encompassing EcoRI site (M. Salm, L. Hall and B.E.H.M., unpublished). Spot 64 in 28S RNA hybridizes with region Vb and weakly with Va. Sequence G-A-U-Cm-U-U-G probably overlaps BglII site, (A)-G-A-T-C-T... One of the Gm-G residues in 28S RNA is probably close to second HincII site (demarcating regions Vb and Vc), it is not yet known on which side.



*Xenopus* and yeast, whereas the almost unmethylated region near the 5' end shows little sequence conservation between these distantly related eukaryotes. It will be extremely useful to determine at the level of nucleotide-sequence analysis the precise relationship between sequence conservation and secondary modification sites during eukaryotic rRNA evolution. (4) The only region of clear sequence homology so far identified between *Xenopus* 18S rRNA and *Escherichia coli* 16S rRNA is a short region at the 3' end<sup>11,14</sup>. This short, homologous region contains the dimethyl A sequence. The 5' one-third of *E. coli* 16S rRNA is completely unmethylated<sup>15,16</sup> in contrast to the highly 2'-O-methylated 5' one-third of *Xenopus* 18S rRNA.

Received 14 July, accepted 18 September 1980

- 1 Klotzwyk, J. & Planta, R. J. *Eur J Biochem* **39**, 325-333 (1973).
- 2 Maden, B. E. H. & Salim, M. J. *molec. Biol.* **88**, 133-164 (1974).
- 3 Khan, M. S. N., Salim, M. & Maden, B. E. H. *Biochem J* **169**, 531-542 (1978).
- 4 Maden, B. E. H. & Reeder, R. H. *Nucleic Acids Res* **6**, 817-830 (1979).
- 5 Brand, R. C. & Gerbs, S. A. *Nucleic Acids Res* **7**, 1497-1511 (1979).
- 6 Khan, M. S. N. & Maden, B. E. H. *J molec Biol* **101**, 235-254 (1976).
- 7 Maden, B. E. H. & Khan, M. S. N. *Biochem J* **167**, 211-221 (1977).
- 8 Brand, R. C., Klotzwyk, J., Van Steenberg, T. J. M., De Kok, A. J. & Planta, R. J. *Eur J Biochem* **78**, 311-318 (1977).
- 9 Groenbergh, M. & Pouman, S. J. *molec. Biol* **21**, 527-535 (1966).
- 10 Brand, R. C., Klotzwyk, J., Planta, R. J. & Maden, B. E. H. *Biochem J* **169**, 71-77 (1978).
- 11 Hagenbüchle, O., Sauter, M., Stott, J. A. & Maas, R. J. *Cell* **13**, 551-563 (1978).
- 12 Choi, Y. C. & Branch, H. *Biochem biophys Res Commun* **88**, 674-682 (1974).
- 13 Salim, M. & Maden, B. E. H. *Nucleic Acids Res* **8**, 2871-2884 (1980).
- 14 Gourme, R. L. & Gerbs, S. A. *J molec Biol* **140**, 321-339 (1980).
- 15 Carbon, P., Ehresmann, C., Ehresmann, B. & Ebel, J. P. *FEBS Lett* **94**, 152-156 (1978).

This region of *E. coli* 16S rRNA plays a crucial role in ribosome assembly through interaction with ribosomal protein S4 (refs 17-20). As yet the function of the 5' one-third of eukaryotic 18S rRNA is unknown.

I started this work at the Carnegie Institution of Washington, Department of Embryology, Baltimore: I thank D. D. Brown, S. McKnight, R. Peterson, R. Reeder and Barbara Sollner-Webb for discussion, advice on cloning and gifts of restriction enzymes. I also thank J. Forbes and Mary Robertson for technical assistance in Glasgow, and J. Sheddon for discovery of the SsrI sites. The work was supported by the MRC.

- 16 Brown, J., Palmer, M. L., Pondexter, J. K. & Noller, H. F. *Proc natn Acad Sci USA* **78**, 4801-4805 (1978).
- 17 Minto, A., Ehresmann, C., Fellner, P. & Zimmermann, R. A. *J molec Biol* **86**, 411-432 (1976).
- 18 Cole, M. D., Bear, M., Koller, Th., Strycharz, W. A. & Nomura, M. *Proc natn Acad Sci USA* **75**, 270-274 (1978).
- 19 Newberry, V., Yaguchi, M. & Garrett, R. A. *Eur J Biochem* **76**, 51-61 (1977).
- 20 Ehresmann, C., Stogler, P., Carbon, P., Ungewickell, E. & Garrett, R. A. *Eur J Biochem* **183**, 439-446 (1980).
- 21 Dawid, I. B. & Wolfner, P. K. *Cell* **8**, 443-448 (1976).
- 22 Botchan, P., Reeder, R. H. & Dawid, I. B. *Cell* **11**, 599-607 (1977).
- 23 Sollner-Webb, B. & Reeder, R. H. *Cell* **18**, 485-499 (1979).
- 24 Bosley, P. G., Tuys, A. & Bernstein, M. L. *Nucleic Acids Res* **5**, 1121-1137 (1978).
- 25 Bosley, P. G., Moss, M., Mächler, M., Portmann, R. & Bernstein, M. L. *Cell* **17**, 19-31 (1979).
- 26 Brownlee, G. G. *Determination of Sequences in RNA* (North Holland, Amsterdam, 1972).
- 27 Macon, J. B. & Wolfenden, R. *Biochemistry* **7**, 3453-3458 (1968).
- 28 Sutcliffe, J. G. *Nucleic Acids Res* **5**, 2721-2728 (1978).

## Structure of crystalline actin sheets

Ueli Aepli, Phillip Ross Smith\*, Gerhard Isenberg & Thomas D. Pollard

Department of Cell Biology and Anatomy, The Johns Hopkins University School of Medicine, Baltimore, Maryland 21205

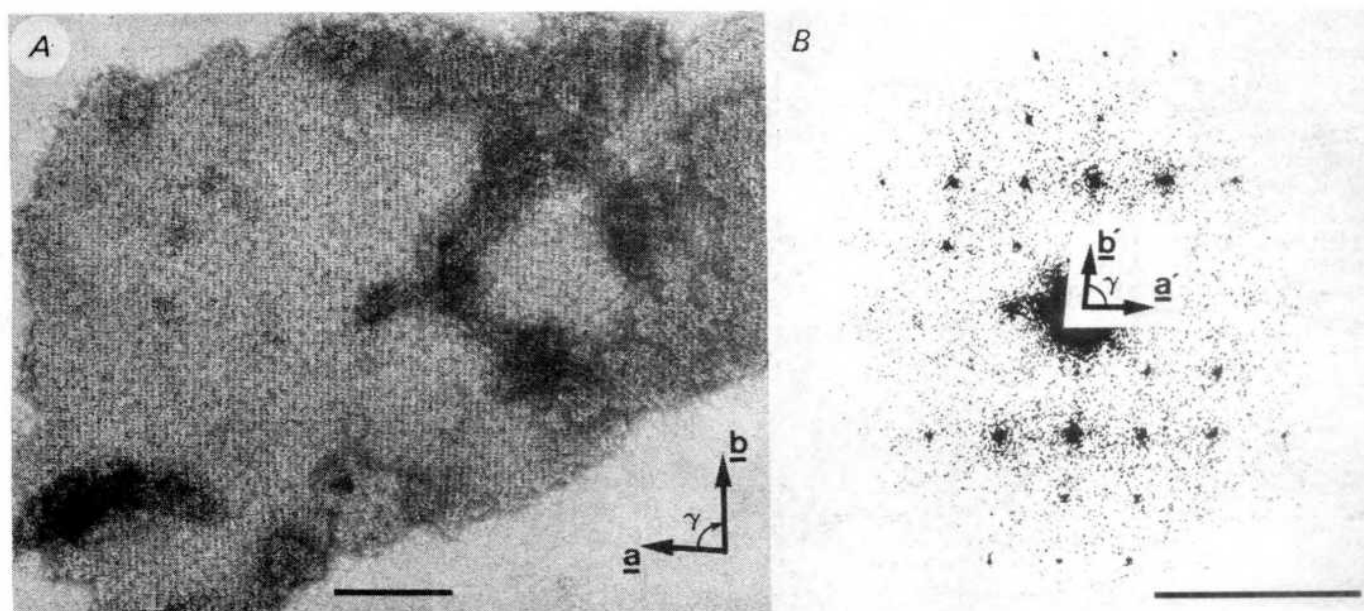
\* Department of Cell Biology, New York University Medical Center, New York, New York 10016

Although actin is one of the most abundant proteins found in nature, little detailed information about its molecular structure is available beyond the amino acid sequence<sup>1,2</sup>. Electron microscopy of negatively stained filaments combined with three-dimensional image reconstruction techniques have revealed the overall size and shape of the actin monomer at 25 Å resolution<sup>3-5</sup>. Higher resolution structural data can be expected from electron microscopy of two-dimensional crystalline arrays<sup>6,7</sup> and X-ray diffraction analysis of three-dimensional crystals<sup>8-11</sup>, but only very preliminary results have been reported so far. The original finding by Dos Remedios and Dickens<sup>4</sup> was that skeletal muscle actin forms microcrystals and tubes in the presence of the trivalent lanthanide gadolinium (Gd<sup>3+</sup>). We have modified and refined their conditions to obtain large crystalline sheets of *Acanthamoeba* actin and present here a model of the actin monomer in projection to 15 Å resolution. We have found that, depending on the ionic strength used, these sheets occur in three different forms: 'cylinders', 'square type' sheets and 'rectangular type' sheets. These different polymorphic forms are built from the same fundamental two-dimensional crystalline actin lattice, which we call the 'basic sheet'. The present concerns the structural analysis of these basic sheets; the crystal polymorphism will be discussed in detail elsewhere (U.A. *et al.*, in preparation). Furthermore, in addition to demonstrating that actin is an elongated globular molecule with a pronounced asymmetric shape in and perpendicular to the plane of the sheet, our results indicate that these crystalline actin sheets might be suitable for three-dimensional structure determination by low-dose electron microscopy of unstained specimens<sup>12,13</sup> to at least 10 Å resolution.

An electron micrograph of a negatively stained basic sheet from an opened-up cylinder (Fig. 1A) reveals that these sheets

are made of a near-rectangular lattice with average lattice parameters  $a = 56.5$  Å,  $b = 65.5$  Å and  $\gamma = 85.5^\circ$  (average of 60 sheets). Figure 1B displays an optical diffraction pattern recorded from a circular area of the micrograph including about 1,000  $56.5 \times 65.5$  Å unit cells. The fact that strong  $(33 \text{ Å})^{-1}$  second order reflections are visible along  $b'$ , with the  $(65.5 \text{ Å})^{-1}$  first order reflections being almost completely absent, is consistent with the observation of a pronounced 33 Å pseudo-repeat along  $b$  in the images (see Fig. 1A), indicating that there might be two molecules per unit cell, related to one another by a two-fold axis of symmetry. Optical diffraction analysis of basic sheets indicates that the long-range order can extend to 5,000 Å in both directions within the plane of the sheet, with sharp diffraction spots extending out to  $(15 \text{ Å})^{-1}$  (see Fig. 1B for example  $(\pm 1, \pm 4)$  reflections). We have found right- and left-handed basic sheet lattices with about equal frequencies with negatively stained specimens. However, the sheets appearing left-handed on the grid (see Fig. 1A) invariably showed better structural preservation and higher resolution detail. As is illustrated in Fig. 2, the handedness of the basic sheet observed on the grid depends on which of the two sheet surfaces is in contact with the carbon support film on adsorption.

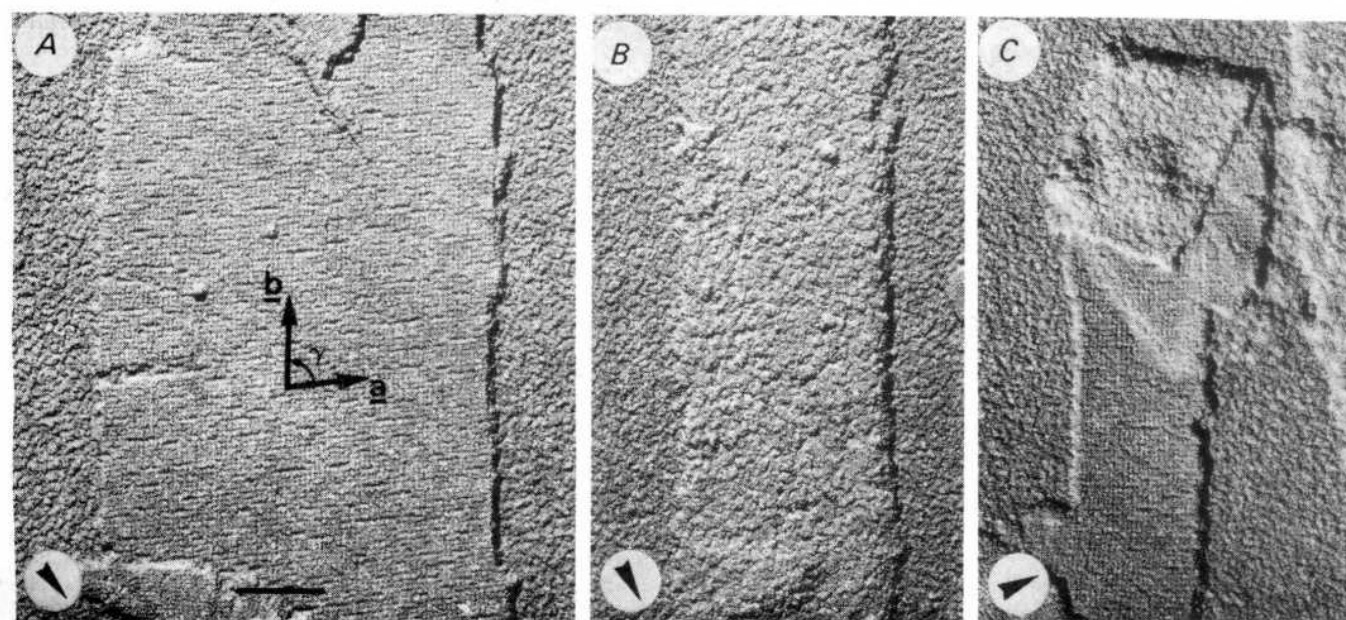
Basic sheets prepared for electron microscopy by adsorption freeze-drying and shadowing<sup>14,15</sup> showed two surface topographies. One surface was smooth and regular, with a near-rectangular right-handed lattice texture (Fig. 2A) and average lattice parameters  $a = 55$  Å,  $b = 63.5$  Å and  $\gamma = 86.5^\circ$  (average of 40 regular-looking sheets). The other surface appeared coarse and irregular, with no indication of a lattice texture, and showed a granularity similar to that found in the background (Fig. 2B). Occasionally, basic sheets folded over, allowing the two distinct surface topographies to be seen simultaneously (Fig. 2C). Optical diffraction patterns recorded from the regular surface of shadowed basic sheets yielded the  $(55 \text{ Å})^{-1}$  and  $(63.5 \text{ Å})^{-1}$  first order reflections along  $a'$  and  $b'$ , respectively, with no indication of the  $(32 \text{ Å})^{-1}$  second order reflections along  $b'$  observed with negatively stained sheets (Fig. 1B). This must be due to the inability to resolve the two molecules in the unit cell by our freeze-drying and shadowing technique. In contrast, basic sheets with the irregular surface topography did not produce any reciprocal lattice reflections on optical diffraction. From the lengths of the shadows cast at the edges of the sheets we calculated their average thickness to be 45 Å (average of



**Fig. 1** A, Electron micrograph of a negatively stained actin basic sheet arising from an opened-up cylinder. Basic sheets were prepared as follows: *Acanthamoeba* G-actin, purified by a modification of the methods described<sup>16,17</sup>, was diluted to  $1.5 \text{ mg ml}^{-1}$  and subsequently dialysed against  $2.5 \text{ mM}$  imidazole,  $\text{pH } 7.25$  ( $4^\circ\text{C}$ ),  $0.25 \text{ mM}$  dithiothreitol (DTT) and  $0.005\%$   $\text{NaN}_3$  for  $5 \text{ h}$  at  $4^\circ\text{C}$ . The sample was then spun in a Beckman Airfuge for  $15 \text{ min}$  at  $130,000\text{g}$  to remove aggregated material and the supernatant dialysed against  $2.5 \text{ mM}$  PIPES,  $\text{pH } 7.00$  ( $4^\circ\text{C}$ ),  $150 \text{ mM}$  KCl,  $0.25 \text{ mM}$  DTT,  $0.005\%$   $\text{NaN}_3$  and  $\text{GdCl}_3$  (molar ratio  $\text{Gd}^{3+}$ : actin  $\geq 6:1$ ) for  $15 \text{ h}$  at  $4^\circ\text{C}$ . At this stage the sample consisted of a mixture of filaments ( $30\text{--}50\%$  of aggregated material), rectangular and square type sheets, and cylinders (U. A. *et al.*, in preparation). A low-speed pellet ( $5,000\text{g}$  for  $5 \text{ min}$ ) of this material was resuspended in one-third volume assembly buffer (see above) and immediately dialysed against  $2.5 \text{ mM}$  PIPES,  $\text{pH } 7.00$ , and  $0.005\%$   $\text{NaN}_3$  for at least  $12 \text{ h}$  at  $4^\circ\text{C}$ . The sample was then spun for  $10 \text{ min}$  at  $5,000\text{g}$  and the pellet resuspended in the same volume  $2.5 \text{ mM}$  PIPES,  $\text{pH } 7.00$  ( $4^\circ\text{C}$ ), and  $0.005\%$   $\text{NaN}_3$ . On dilution of this material to  $\leq 0.75 \text{ mg ml}^{-1}$  with the same buffer, basic sheets started peeling off the rectangular and square type sheets, and the cylinders opened up into basic sheets when diluted material was left for a few hours at  $4^\circ\text{C}$ . For electron microscopy,  $2\text{-}\mu\text{l}$  drops were adsorbed for  $60 \text{ s}$  to carbon-coated  $400\text{-mesh}$  per inch copper grids which were rendered hydrophilic by glow discharge in a reduced atmosphere of air. The grids were then washed for  $30 \text{ s}$  on several drops of distilled water and stained for  $30 \text{ s}$  on several drops of  $0.75\%$  uranyl formate,  $\text{pH } 4.25$ . Electron micrographs of these specimens were recorded on Kodak 4463 Electron Image Film in a Zeiss EM 10A electron microscope at  $\times 50,000$  nominal magnification and developed for  $4 \text{ min}$  in  $1:2$  times diluted Kodak D-19 developer. To minimize the accumulated electron dose on the areas to be photographed, a beam rocking technique<sup>18</sup> was used. The example shows a basic sheet with its regular surface in contact with the carbon support (see text and Fig. 3), and therefore its near-rectangular lattice appears left-handed (indicated by the lattice vectors **a** and **b**). Scale bar,  $1,000 \text{ \AA}$ . B, Optical diffraction pattern recorded from a circular area of the electron micrograph shown in A including about  $1,000$  unit cells. The reciprocal lattice vectors corresponding to the  $56.5 \times 65.5 \text{ \AA}$  near-rectangular lattice have been drawn to scale in the central inset. Scale bar,  $(20 \text{ \AA})^{-1}$ .

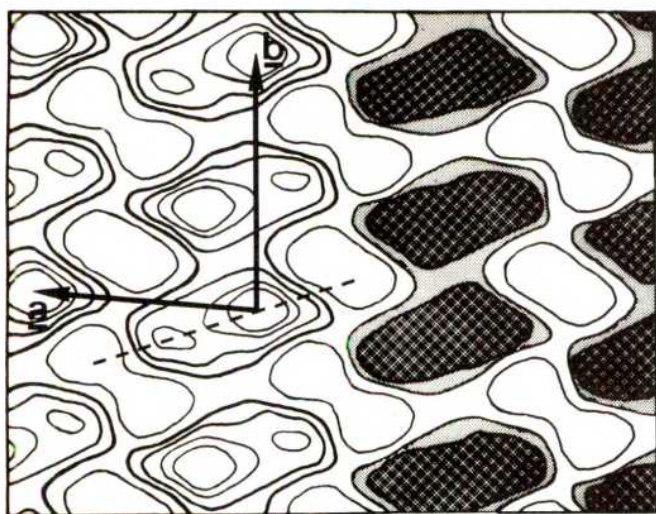
24 sheets), suggesting that the basic sheets are spanned by one actin molecule. The two distinct surface topographies of the basic sheets reflect two things: (1) the actin monomer must have a very asymmetric shape in the direction perpendicular to the plane of the sheet, and (2) all actin molecules are packed with the same polarity perpendicular to the plane of the sheet.

We have computer-filtered several micrograph areas containing well preserved negatively stained basic sheets, and have obtained the quaternary structure of the actin molecule within the sheet, and its overall size and shape in projection to  $15 \text{ \AA}$  resolution. The average unit cell morphology obtained from five different  $12 \times 10 \text{ } 56.5 \times 65.5 \text{ \AA}$  unit cell areas chosen



**Fig. 2** Electron micrographs of freeze-dried and shadowed basic sheets exhibiting the two different surface topographies. Samples of unfixed material were prepared for electron microscopy by the adsorption freeze-drying technique described elsewhere<sup>14,15</sup>. Unidirectional shadowing of the specimens was done with platinum from an electron gun at an elevation angle of about  $30^\circ$ . A, Example of a sheet displaying a regular, right-handed near-rectangular lattice surface (as indicated by the lattice vectors). B, Example of a sheet showing an irregular surface with no indication of a periodic lattice. C, Example of a folded-over sheet simultaneously exposing its two surfaces. The arrows in A, B and C indicate the direction of metal shadowing. Scale bar,  $1,000 \text{ \AA}$  (for A, B and C).





**Fig. 3** A contour plot showing the average two-fold symmetrized unit cell morphology obtained from five different electron micrograph areas of computer-filtered negatively stained actin basic sheets. All five sheets selected for filtering were left-handed (see text and Figs 1, 2). The electron micrographs were digitized with an Optronics P-1000 microdensitometer using a 50- $\mu\text{m}$  square raster, from photographic enlargements onto Kodak 4147 Plus-X pan film to give an effective sampling rate of 3.25 Å. Computer filtering was performed essentially as described previously<sup>19,20</sup> using  $12 \times 10$   $56.5 \times 65.5$  Å near-rectangular unit cell sheet areas. The filtered unit cells were two-fold symmetrized after searching for the best symmetry centre<sup>19,21</sup>: the power loss on two-fold symmetrization averaged to 2.1% over the five samples. The filtered and two-fold symmetrized unit cells from the five samples were then aligned with respect to their two-fold centres of symmetry and summed to give the average unit cell morphology shown. The near-rectangular unit cell (as indicated by the lattice vectors **a** and **b**) contains two actin molecules related to one another by P2 symmetry. Actin dimers and monomers are indicated by the light and dark shaded regions, respectively, in the right-hand side of the figure. The broken line marks the longer axis of the actin monomer, and is defined through the major and minor peak of the subunit in projection. Scale bar, 50 Å.

from four different micrographs is shown in Fig. 3. The following reproducible features were observed. (1) The  $56.5 \times 65.5$  Å near rectangular unit cell contains two actin molecules which are related to each other by a two-fold axis of symmetry perpendicular to the plane of the sheet (space group P2). (2) The actin monomer is elongated and measures about  $56 \times 33$  Å in projection, with its longer axis (indicated by a broken line) being tilted by about  $23^\circ$  with respect to the lattice vector **a**. (3) The projected mass density of the actin subunit possesses a pronounced asymmetry with a major and a minor peak along its longer axis. (4) The negative stain accumulates as a distinctive 2-and-1 pattern between columns of actin dimers.

The unit cell parameters of the basic sheets are in agreement with those determined previously by optical diffraction of negatively stained skeletal muscle actin tubes<sup>7</sup>. The overall dimensions of the actin monomer are similar to those obtained from three-dimensional reconstructions of average actin filaments computed by deconvolution from filament paracrystals<sup>3</sup>. Moreover, the distinct asymmetric shape of the subunit within and perpendicular to the plane of the basic sheet is consistent with the polarity of the actin monomer found by three-dimensional reconstruction of individual actin filaments<sup>5</sup>. A more quantitative comparison with the actin filament structure must await completion of a three-dimensional map of the molecule computed from tilted views of the crystalline sheets. However, the quaternary structure of the actin molecules in the basic sheet differs substantially from their packing in the filament. Although it is possible that the head-to-tail bonds between actin molecules are similar in the sheets (for example along **a**) and the filaments (for example along a single strand), the lateral associations cannot be the same in the two cases. In the sheets, adjacent rows

of subunits have opposite polarity, whereas in filaments the two strands have the same polarity with respect to the filament axis. Consequently, the assembly of the basic sheets cannot be explained as an 'unwinding' of the double-helical filaments into linear double strands, followed by a side-by-side association of these linear double strands.

From the size and long-range order of the crystalline actin sheets described here, we are confident that a three-dimensional model of the actin molecule can be determined to at least 10 Å resolution by low-dose electron microscopy and three-dimensional reconstruction of tilted views of unstained specimens<sup>12,13</sup>. Finally, it might be possible to decorate basic sheets stoichiometrically with actin-interacting proteins such as myosin S-1, troponin, gelation factors, profilin, DNase I and 5'-nucleotidase, and thus to map the binding sites for these molecules on the three-dimensional model of actin.

We thank Dr V. G. Allfrey for allowing us to use his Optronics P-1000 microdensitometer. This work was supported by National Institute of General Medical Sciences grants GM 27765 to U.A., GM26723 to P.R.S. and GM26338 to T.D.P. G.I. is supported by a Heisenberg Fellowship from the Deutsche Forschungsgemeinschaft.

Received 11 August; accepted 30 September 1980.

- Collins, J. H. & Elzinga, M. *J. biol. Chem.* **250**, 5915–5920 (1975).
- Vandekerckhove, J. & Weber, K. *Nature* **276**, 720–721 (1978).
- Moore, P. B., Huxley, H. E. & DeRosier, D. J. *J. molec. Biol.* **50**, 279–295 (1970).
- Spudich, J. A., Huxley, H. E. & Finch, J. T. *J. molec. Biol.* **72**, 619–632 (1972).
- Wakabayashi, T., Huxley, H. E., Amos, L. A. & Klug, A. *J. molec. Biol.* **93**, 477–497 (1975).
- Dos Remedios, C. G. & Dickens, M. J. *Nature* **276**, 731–733 (1978).
- Dickens, M. J. *Proc. R. microsc. Soc.* **13**, 80–81 (1978).
- Carlsson, L. *et al. J. molec. Biol.* **105**, 353–366 (1976).
- Mannherz, H. G., Kabsch, W. & Leberman, R. *FEBS Lett.* **73**, 141–143 (1977).
- Oriol, C., Dubord, C. & Landon, F. *FEBS Lett.* **73**, 89–91 (1977).
- Sugino, H. *et al. J. Biochem.* **86**, 257–260 (1979).
- Unwin, P. N. T. & Henderson, R. *J. molec. Biol.* **74**, 425–440 (1975).
- Henderson, R. & Unwin, P. N. T. *Nature* **257**, 28–32 (1975).
- Kistler, J., Aebi, U. & Kellenberger, E. *J. ultrastruct. Res.* **59**, 76–86 (1977).
- Smith, P. R. *J. ultrastruct. Res.* **72**, 380–384 (1980).
- Pollard, T. D., Stafford, W. F. & Porter, M. E. *J. biol. Chem.* **253**, 4798–4808 (1978).
- Gordon, D. J., Eisenberg, E. & Korn, E. D. *J. biol. Chem.* **251**, 4778–4786 (1976).
- Williams, R. C. & Fisher, H. W. *J. molec. Biol.* **52**, 121–123 (1970).
- Aebi, U., Smith, P. R., Dubochet, J., Henry, C. & Kellenberger, E. *J. supramolec. Struct.* **1**, 498–522 (1973).
- Smith, P. R. *Ultramicroscopy* **3**, 153–160 (1978).
- Aebi, U. *et al. J. molec. Biol.* **130**, 255–272 (1979).

## Helix packing and subunit conformation in horse spleen apoferritin

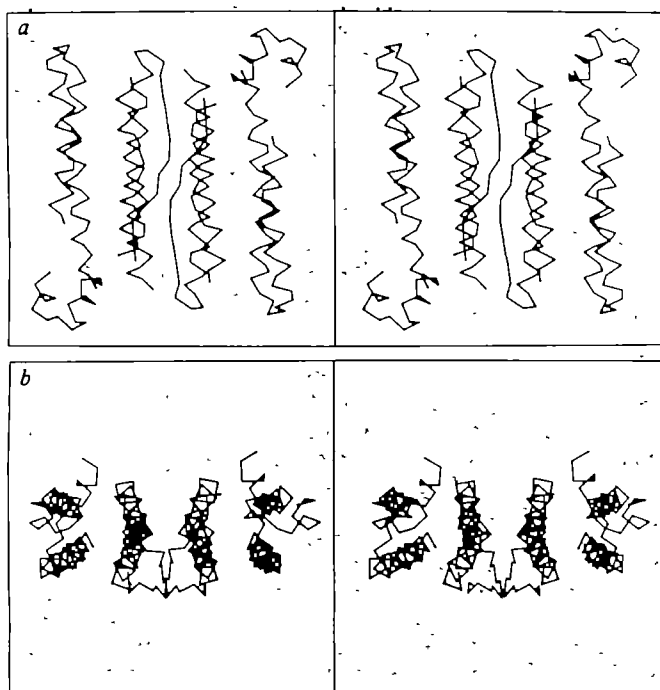
George A. Clegg, Robert F. D. Stansfield, Philip E. Bourne & Pauline M. Harrison

Department of Biochemistry, The University, Sheffield S10 2TN, UK

An electron density map of horse spleen apoferritin at 0.28-nm (2.8 Å) resolution and its preliminary interpretation have been described previously<sup>1</sup>. Rigorous examination of this and newer maps at the same nominal resolution but calculated from more extensive data sets, including model building in a Richards' comparator<sup>2</sup>, now allows us to report on structural features in more detail. We list inter-helical angles within and between neighbouring subunits, and describe a new short region of inter-subunit anti-parallel pleated sheet. A short section of electron density not properly accounted for in the first model has also been found. We also report on two alternative ways of connecting helical regions which account almost equally well for the observed electron density, and we assess these two alternative conformations and compare them with the conformations of other known proteins.

The iron storage molecule ferritin consists of a protein shell comprising 24 subunits in 432 symmetry surrounding an inorganic 'core' of hydrated ferric oxide-phosphate. Horse





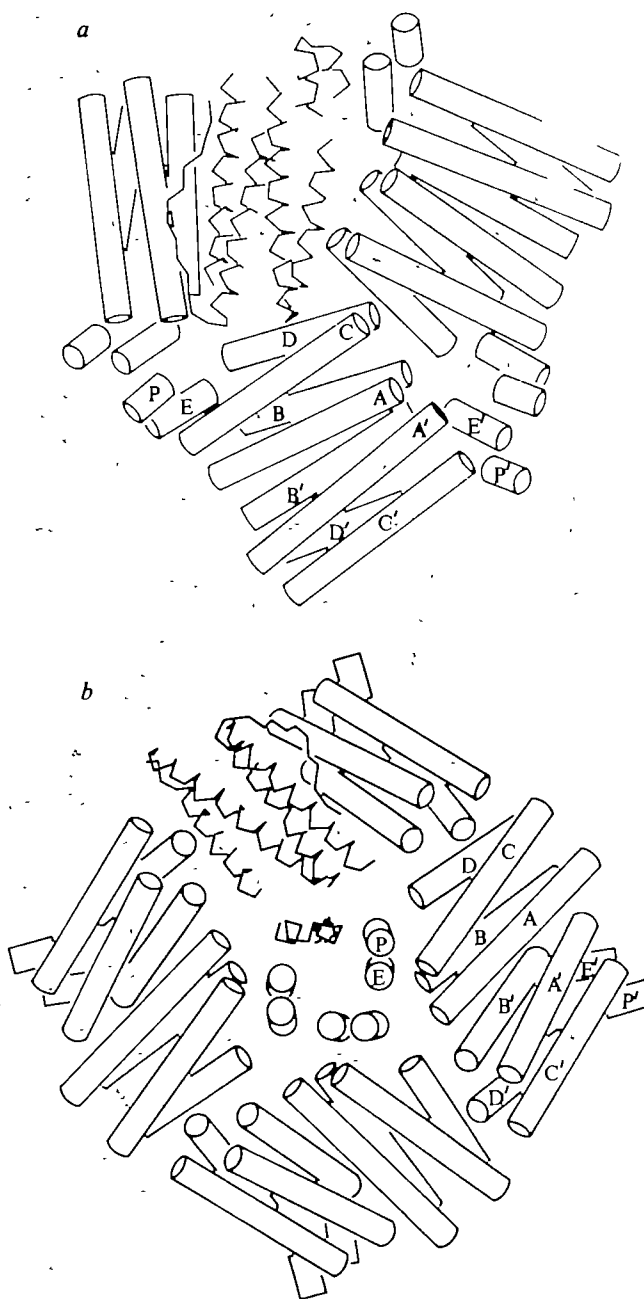
**Fig. 1** Stereoscopic views of connected  $\alpha$ -carbon coordinates for well established regions in an apoferritin dimer. *a*, The view down a molecular diad from outside the molecule. The four major helices A, B, C, D in the leftmost subunit occur: above right, below right, above left and below left, respectively. *b*, 'End-on' view perpendicular to the diad and parallel to a molecular triad. The four major helices A, B, C, D in the leftmost subunit occur: below right, above right, below left and above left, respectively. The atomic positions used here and in Fig. 2 have regular geometry and are faithful to the electron density map, but may not be correct in every detail.

spleen apoferritin (subunit molecular weight 19,000) crystallizes from  $\text{CdSO}_4$  solution in space group  $F432$  with  $a = 18.40$  nm (184.0 Å). The asymmetric unit contains a single subunit. Electron density maps show clearly that each subunit consists of a bundle of four long helices lying parallel or anti-parallel to one another; together with two much shorter helices and stretches of irregular conformation. It is in the inter-helical connecting regions that the electron density is weakest and where difficulties are experienced in tracing the course of the polypeptide chain unambiguously. Preliminary sets of  $\alpha$ -carbon and carbonyl oxygen atomic coordinates have been measured in the Richards' comparator and used to derive regularized sets of coordinates for main chain and  $\beta$ -carbon atoms.

We will first describe the regions which we consider to be reasonably well established. These are the long helices A, B, C and D, containing approximately 27, 25, 28 and 20 amino acid residues respectively, and two short helices, P, 7 residues (formerly described as a helical turn), and E, comprising about 10 residues. The total number of helical residues (117) accounts for about 68% of the main chain density. Helix B uniquely seems to contain an irregularity near the middle of its length, and N-terminal regions of helices C and D seem to be fitted best by one to two turns of  $3.0_{10}$  helix. There is also good density for the sharp turn connecting C and D, for the long loop L and (less so) for the connecting regions between D-P to E. The directions of the helices are confirmed to be those previously assigned, and angles between pairs of helices are given in Table 1. Among the four major helices of one subunit, adjacent anti-parallel pairs lie within the range  $166 \pm 5^\circ$  to one another, and diagonally opposite parallel pairs are inclined at  $\sim 17^\circ$ . The four helices are thus related by 222 pseudo-symmetry with pseudo-diads passing between helical pairs A, C and B, D and between C, D and A, B and a third lying nearly parallel to the long axes of the helices (and this is the long axis of the subunit). In the apoferritin 432 quaternary structure, pairs of subunits related by molecular

diads lie with their long axes anti-parallel. Angles relating all pairs of helices within this 'dimer' are given in Table 1. Interestingly, angles relating neighbouring anti-parallel helices A, A' and B, B' related by the molecular two-fold axis are similar to those within the subunit, and the same is true of the diagonally related pairs A, B' and B, A'. Thus, a complete system of eight helices is formed comprising two layers, each of which contains four anti-parallel helices, and this system itself has pseudo-222 symmetry.

In Fig. 1 stereo views of the helices and other well established regions within the dimer are shown as connected  $\alpha$ -carbon diagrams down the diad (Fig. 1*a*) and approximately end-on to the major helices, perpendicular to the diad and parallel to a molecular three-fold axis (Fig. 1*b*). It can be seen in Fig. 1*b* that the four major helices within a single subunit together show a left-handed twist when viewed down their lengths, whereas the two pairs of A and B helices near the diad are arranged so that diagonally related pairs A, B' and B, A' converge at opposite



**Fig. 2** Illustration of the subunit packing around a molecular triad, showing three dimers (*a*) and around a molecular tetrad, showing four dimers (*b*).



ends of the arrangement. The dimer has a rather flat, lozenge shape, and the overall arrangement within the molecule is such that each dimer lies roughly on the face of a rhombic dodecahedron with subunit axes nearly parallel to one pair of edges of the rhomb. A better molecular envelope is a rhombic dodecahedron truncated to give a polyhedron inscribable within a sphere. Figure 2 shows the packing of three dimers around a three-fold axis (a) and four dimers around a four-fold axis (b), with  $\alpha$ -carbon coordinates used for one subunit only.

Another feature of the structure which has become apparent as a result of model building is a short stretch of anti-parallel  $\beta$ -pleated sheet which joins the loops (L) from neighbouring diad-related subunits over a region around the two-fold axis. Four hydrogen bonds are formed, involving a total of five residues in each subunit, and the  $\beta$ -strands exhibit a characteristic right-handed twist when viewed along their length<sup>3</sup>. This pleated sheet structure lies on the outside surface of the molecule (see Fig. 1) at a region of intermolecular contact.

The two alternative ways of joining the defined segments which best fit the electron density are as follows. Each of these starts with the same extended N-terminal sequence of about 12 residues preceding the A helix. Only four residues were previously described and a section of electron density, relatively isolated but tenuously connected to these residues, was missed in our first interpretation. The C-terminal end of A may be connected through a short turn to the N-terminus of either B (as in our original interpretation) or C. The peptide segments are joined subsequently in order A  $\rightarrow$  B  $\rightarrow$  L  $\rightarrow$  C  $\rightarrow$  D  $\rightarrow$  P  $\rightarrow$  E (Fig. 3a) or A  $\rightarrow$  C  $\rightarrow$  D  $\rightarrow$  P  $\rightarrow$  E  $\rightarrow$  B  $\rightarrow$  L (Fig. 3b). Note that all the interhelix connections in both alternative conformations, except for the long loop joining B and C in Fig. 3a, exhibit the usual right-handed character<sup>4</sup> (viewed parallel to the helix-pair contact vector). The alternative subunit conformations are shown schematically in Fig. 3a and b, respectively, and in c and d using the mode of representation of Levitt and Chothia<sup>5</sup>. The differences between these connectivities depend on whether density beyond A is attributed to side-chain or main-chain density, and whether the short tail at the C-terminus of E is free, leaving the C-terminus of the molecule inside the shell, or whether it is joined to B. Overall, the chain length seems to be a few residues longer than in our earlier description.

The packing of the four long helices in the apoferritin subunit resembles that of several other proteins, including myo-

**Table 1** Angles between the helices within an apoferritin dimer

|   | A   | A'  | B'  | C'  | D'  | P'  | E'  |
|---|-----|-----|-----|-----|-----|-----|-----|
| A |     | 154 | 29  | 17  | 156 | 142 | 41  |
| B | 171 |     | 151 | 159 | 20  | 33  | 145 |
| C | 170 | 16  |     | 174 | 20  | 48  | 129 |
| D | 18  | 168 | 161 |     | 171 | 138 | 42  |
| P | 62  | 119 | 126 | 51  |     | 88  | 90  |
| E | 116 | 62  | 57  | 130 | 172 |     | 94  |

A, A' and so on are related by the symmetry ( $z, -y, x$ ). Intra-subunit angles, in degrees, are found in the leftmost (lower) triangle and inter-subunit angles on the (upper) right.

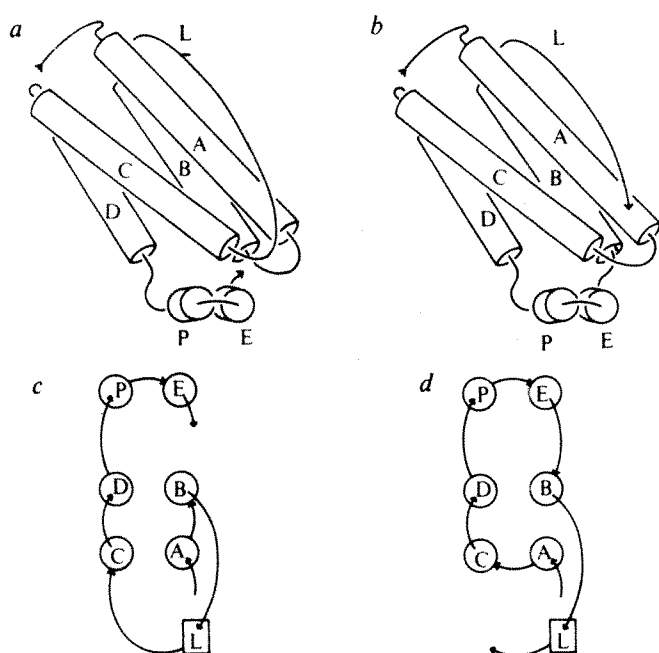
haemerythrin<sup>6,7</sup>, haemerythrin<sup>8,9</sup>, tobacco mosaic virus<sup>10</sup>, cytochrome *b*<sub>562</sub> (ref. 11) and cytochrome *c'* (P. Weber, personal communication). Moreover, angles between helices shown in Table 1 closely resemble those in myohaemerythrin<sup>6</sup>, and the bundle of four helices in all these structures apparently has a left-handed twist. It does seem that this mode of helical packing may indeed be considered as a stable 'super-secondary structure' as suggested earlier<sup>12</sup>. Furthermore, the subunit relationship in the apoferritin shell dimer closely resembles that in cytochrome *c'* (P. Weber, personal communication). An attractive feature of the alternative conformation shown in Fig. 3b is that the connectivity closely resembles that in the other proteins. However, a feature of the connectivity of Fig. 3a, which is attractive from another point of view, is that this subunit structure seems to be constructed from two approximately equal parts (A to L inclusive and C to E inclusive, comprising sequences of approximately equal length) which could conceivably have arisen from gene duplication. Some support, however slight, for this suggestion is the structural similarity of the A, B and C, D helical pairs and the finding of mercury sites (and therefore presumably cysteine) near the N-terminal ends of helices B and D. An unequivocal assignment of the apoferritin subunit conformation awaits the completion of the amino acid sequence by Crichton and colleagues, and the extension to higher resolution and refinement of the structure. Although it has been reported earlier that the C-terminus is available to carboxypeptidase action, this has not been confirmed in recent work on human liver ferritin (J. M. Sowerby and J. E. Fitton, unpublished preliminary observation). This latter result would favour Fig. 3a rather than b. Partial proteolysis gives rise to two fragments of molecular weights approximately 7,500 and 11,000, the smaller of which is thought to include the N-terminus<sup>13,14</sup>. Such fragments could arise in either connectivity by splitting at the BL connection in Fig. 3a or at the CD turn in b.

We thank the SRC, MRC, the Royal Society and the Blood Research Fund for support, and Mr Graeme Dolderson for technical assistance.

**Note added in proof:** Details of the cytochrome *c'* structure have now been published<sup>15</sup>, and a more detailed comparison of the 4- $\alpha$ -helical proteins has been made<sup>16</sup>. Completion of the amino acid sequence of horse spleen apoferritin has also recently been reported<sup>17</sup>.

Received 6 June; accepted 26 September 1980.

- Banyard, S. H., Stammers, D. K. & Harrison, P. M. *Nature* **271**, 282-284 (1978).
- Richards, F. M. *J. molec. Biol.* **37**, 225-230 (1968).
- Chothia, C. *J. molec. Biol.* **75**, 295-302 (1973).
- Sternberg, M. J. E. & Thornton, J. M. *J. molec. Biol.* **105**, 367-382 (1976).
- Levitt, M. & Chothia, C. *Nature* **261**, 552-558 (1976).
- Hendrickson, W. A., Klippenstein, G. L. & Ward, K. B. *Proc. natn. Acad. Sci. U.S.A.* **72**, 2160-2164 (1975).
- Hendrickson, W. A. & Ward, K. B. *J. biol. Chem.* **252**, 3012-3018 (1977).
- Ward, K. B., Hendrickson, W. A. & Klippenstein, G. L. *Nature* **257**, 818-821 (1975).
- Stenkamp, R. E., Sieker, L. C., Jensen, L. H. & Loehr, J. S. *J. molec. Biol.* **100**, 23-24 (1976).
- Bloomer, A. C., Champness, J. N., Bricogne, G., Staden, R. & Klug, A. *Nature* **276**, 362-368 (1978).
- Mathews, F. S., Bethge, P. H. & Czerwinski, E. W. *J. biol. Chem.* **254**, 1699-1706 (1979).
- Argos, P., Rossmann, M. G. & Johnson, J. E. *Biochem. biophys. Res. Commun.* **75**, 83-86 (1977).
- Collet-Cassart, D. & Crichton, R. R. in *Proteins of Iron Storage and Transport in Biochemistry and Medicine* (ed. Crichton, R. R.) 185-192 (North-Holland, Amsterdam, 1975).
- Ishitani, K., Niitsu, Y. & Listowsky, I. *J. biol. Chem.* **250**, 3142-3148 (1975).
- Weber, P. C. *et al. Nature* **286**, 302-304 (1980).
- Weber, P. C. & Salemme, F. R. *Nature* **287**, 82-84 (1980).
- Heusterspreute, M., Mathijs, J. M., Wustefeld, C. & Crichton, R. R. *16th Congr. Int. Soc. Hematology*, Montreal (1980).



**Fig. 3** Two alternative conformations of the apoferritin subunit—A-B-L-C-D-P-E (a) and A-C-D-P-E-B-L (b)—together with their Levitt-Chothia<sup>5</sup> representations, c and d, respectively.

# MATTERS ARISING

## Evolution of the orang-utan

SMITH AND PILBEAM<sup>1</sup> have argued that "the available evidence... justifies the concept of a Pliocene orang-utan ancestor at least as terrestrial as the modern chimpanzee". It is, however, questionable whether they have established their thesis as equally, or more, plausible than the one they wish to replace (that the ancestral lineage of orang-utans was arboreal).

The authors have used both palaeontological and neontological records, but their arguments are unconvincing. First, there are no unequivocal data on the body sizes of Pleistocene orang-utans so that inferences on arboreality or terrestriality are tenuous. Although Smith and Pilbeam acknowledge the difficulty of drawing conclusions about body size from tooth size alone when considering subfossil orang-utan populations, they conclude that mid-Pleistocene mainland forms were larger-bodied and hence less arboreal than the extant form. The basis for such a conclusion is not evident. Second, plausibility alone does not constitute empirical (or theoretical) support for a thesis. Smith and Pilbeam suggest that it is plausible to view the large body size and marked sexual dimorphism of living orang-utans as remnants of a more terrestrial pattern. This is a possibility but they offer no direct support. Thus there is no reason to consider this alternative of greater importance than any other (sexual selection, niche separation, and such) that may have an influence on whether or not animals are terrestrial. Third, Kay<sup>2</sup> has shown that (1) there is no relationship between tooth enamel thickness and arboreality or terrestriality, and (2) thick enamel, as found in *Pongo*, seems to be associated with the consumption of hard fruits, nuts and seeds. This weakens arguments by Smith and Pilbeam that ancestral orang-utans may not have been arboreal frugivores.

If there are data that do not support a particular hypothesis, then the inconsistency should be explained. The postcranial anatomy of living orang-utans is the least equivocal source of data on possible "remnants... of a more terrestrial pattern". Morphological studies of orang-utan cheiridia<sup>3</sup>, wrist<sup>4</sup>, and hip and thigh<sup>5</sup> have all revealed marked specializations consistent with arboreal progression in a large-bodied primate. No features suggesting adaptations for terrestrial locomotion, present or past, have been reported. Smith and Pilbeam have not accorded these data the attention they deserve, nor explained why extant orang-utans should not display evidence of terrestriality in an ancestral form. It is unclear, for example, whether the authors postulate a stage of terrestriality so brief

that terrestrial adaptations had not time to evolve, or, if arguing for a longer period of terrestriality, whether the return to arboreal progression was to have been accompanied by an exact reversal of evolutionary changes.

Despite the available fossil evidence suggesting that "typical Neogene hominoids (including our hypothetical Pliocene orang-utan) were probably... woodland creatures", one cannot yet eliminate the possibility that this is a simple artefact of the still very limited fossil record. Similarly, there is no reason to expect that all fossils displaying an affinity to extant forms represent populations directly ancestral to living species. It may be worthwhile to consider the possibility, for example, that the mid-Pleistocene orang-utans represented by fossil teeth were a related, but not ancestral, species. Until the competing hypotheses of arboreality or terrestriality can be tested by unequivocal data from the fossil record, they must be considered viable alternatives.

I thank H. McHenry, P. Rodman and L. Scott for reading an earlier version of this manuscript.

L. ALIS TEMERIN

Department of Anthropology,  
University of California,  
Davis, California 95616

1. Smith, R. J. & Pilbeam, D. R. *Nature* **284**, 447-448 (1980).
2. Kay, R. *Am. J. phys. Anthropol.* **62**, 243 (1980).
3. Tuttle, R. H. *J. Morph.* **128**, 309-364 (1969); *The Chimpanzee* **2**, 167-253 (1970); *Gibbon* **1**, 136-206 (1972).
4. Lewis, O. J. *Am. J. phys. Anthropol.* **30**, 251-268 (1969); in *Primate Locomotion* (ed Jackson, F. A.) 143-169 (Academic, New York, 1974).
5. Sigmon, B. A. *J. Hum. Evol.* **3**, 161-185 (1974).

SMITH AND PILBEAM REPLY—We do not know whether Miocene ancestors of the orang-utan were arboreal or terrestrial, and evidence marshalled in favour of either hypothesis is tenuous at best. Nevertheless, it seems to us that hypotheses for hominoid evolution generally have assumed with confidence that the orang lineage has always been arboreal. In offering evidence for the possibility of a terrestrial ancestor, our purpose was also to lead others to re-evaluate the supposed evidence for arboreality. We completely agree with Temerin's conclusion that arboreality and terrestriality "must be considered viable alternatives".

RICHARD J. SMITH

Department of Orthodontics,  
Dental School,  
University of Maryland,  
Baltimore, Maryland 21201

DAVID R. PILBEAM

Department of Anthropology,  
Yale University,  
New Haven, Connecticut 06520

## Noradrenergic transmission

I WISH to raise two points concerning the discussion and conclusion in a recent report by Hirst and Nield<sup>1</sup>.

First, evidence quoted to illustrate that a portion of sympathetic postganglionic transmission is resistant to adrenoreceptor antagonists was derived from work on rodent vasa deferentia: the authors had concluded that in these tissues a component of the motor transmission was 'non-adrenergic' (refs. 2-5). From the reported results<sup>1</sup>, however, noradrenergic transmission resistant to  $\alpha$ -adrenoreceptor antagonists is postulated. This conclusion may be justified in the case of the arteriolar preparation under study and, if so, constitutes an important observation. However, if this is offered as an explanation for the 'non-adrenergic' component of transmission in vas deferens, it should be noted that all previous reports quoted as having supported this latter concept, did so not only on the evidence of resistance to antagonists but also because the response persisted after depletion of noradrenaline by reserpine, for example, to less than 1% of control levels<sup>6</sup>. Furthermore, responses persisted even after chemical sympathectomy when virtually all adrenergic nerve terminals had been removed<sup>7</sup>. In contrast, the 'conventional', adrenergic,  $\alpha$ -blocker-susceptible component was completely absent following reserpine or chemical sympathectomy<sup>7</sup>. If allowance for this adrenergic component in the control is made, the 'non-adrenergic' response is not reduced at all following the latter treatments<sup>2,8</sup>. There is, therefore, no evidence to connect this response in vas deferens with noradrenaline or noradrenergic nerves. To associate this with a discussion of the postulated mechanism in arteriolar muscle can only attract irrelevant criticism of the latter. It is also possible that the intracellular excitatory junctional potential and the 'non-adrenergic' contraction of the muscle layers reflect different cellular processes.

Secondly, the conclusion that there are 'two populations of excitatory receptors for noradrenaline in arteriolar smooth muscle' could be confused with the other recent evidence for two distinct types of excitatory  $\alpha$ -adrenoreceptor on vascular and non-vascular smooth muscle<sup>9,10</sup>; in this case, each response was blocked by the appropriate antagonist<sup>9-11</sup>. Furthermore, in contrast to the newly reported observation on arteriolar muscle<sup>1</sup>, the pressor response to sympathetic nerve stimulation was even more sensitive to blockade by the  $\alpha_1$ -adrenoreceptor antagonist, prazosin, than was the response to exogenous noradrenaline<sup>11,13</sup>. The 'phentolamine-resistant' effect of



noradrenaline<sup>1</sup> may thus point to a 'third' excitatory mechanism for noradrenaline. This may be supported by the observation that a small, residual, pressor response to catecholamines remains even after combined  $\alpha$ - and  $\beta$ -adrenoreceptor blockade<sup>12</sup>.

J. C. MCGRATH

*Institute of Physiology,  
The University,  
Glasgow G12 8QQ, UK*

1. Hirst, G. D. S. & Neild, T. O. *Nature* **283**, 767-768 (1980).
2. McGrath, J. C. *J. Physiol., Lond.* **283**, 23-39 (1978).
3. Ambache, N. & Zar, M. A. *J. Physiol., Lond.* **216**, 359-389 (1971).
4. Ambache, N., Dunk, P., Verney, J. & Zar, M. A. *J. Physiol., Lond.* **227**, 433-456 (1972).
5. Euler, U. S. von & Hedqvist, P. *Acta physiol. scand.* **93**, 572-573 (1975).
6. Gillespie, J. S. & McGrath, J. C. *Br. J. Pharmac.* **52**, 585-590 (1974).
7. Booth, F. J., Connell, G. J., Docherty, J. R. & McGrath, J. C. *J. Physiol., Lond.* **280**, 19-20P (1978).
8. Docherty, J. R. & McGrath, J. C. *J. Physiol., Lond.* **307**, 18-19 (1980).
9. Drew, G. M. & Whiting, S. B. *Br. J. Pharmac.* **67**, 207-215 (1979).
10. Docherty, J. R., MacDonald, A. & McGrath, J. C. *Br. J. Pharmac.* **67**, 421P-422P (1979).
11. Docherty, J. R. & McGrath, J. C. *Naunyn-Schmiedeberg's Archs Pharmac.* **312**, 107-116 (1980).
12. Flavanhan, N. A. & McGrath, J. C. *Br. J. Pharmac.* **69**, 355-357 (1980).
13. Docherty, J. R. & McGrath, J. C. *Naunyn-Schmiedeberg's Archs Pharmac.* **313**, 101-111 (1980).

**HIRST AND NEILD REPLY**—We take the view that there are many similarities between the mechanisms of excitatory transmission in arterioles and vasa deferentia of guinea pigs. Both are innervated by catecholamine-containing nerves which when stimulated cause an excitatory junction potential (e.j.p.) in the underlying smooth muscle. The e.j.ps recorded from both tissues are to all intents and purposes identical<sup>1,2</sup>; e.j.ps from both tissues are rapidly reduced in amplitude by guanethidine and persist in high concentrations of adrenergic blocking agents. We consider that the failure of  $\alpha$ -blockade in arterioles arises because the neuronally released transmitter activates receptors which are unlike  $\alpha$ -receptors. In our preparation we are able to mimic the action of the neurotransmitter only when noradrenaline is applied to specific regions of the muscle; until similar experiments have been conducted on vas deferentia it seems unnecessary to reject the hypothesis that noradrenaline is the primary transmitter substance<sup>3-6</sup>.

McGrath rightly points out that some of the authors who take the view that a second unknown transmitter is released in addition to noradrenaline, base their opinion on further experiments in which tissue noradrenaline was in some way reduced<sup>3,6</sup>. A common method is by prior treatment with reserpine, which dramatically reduces but does not eliminate tissue noradrenaline<sup>7</sup>. However, it is by no means clear that a dramatic reduction in tissue noradrenaline leads to an equally dramatic reduction in the actual amount of noradrenaline released per nerve impulse<sup>8</sup>.

Concerning McGrath's second point, we did not mean to imply that arteriolar smooth muscle contained two distinct populations of  $\alpha$ -receptors, although this may well be the case. We stressed that the 'junctional' receptors that we were able to activate by noradrenaline were completely different from  $\alpha$ -receptors. To avoid the possibility of confusion it might perhaps be more appropriate to call the 'junctional' receptors  $\gamma$  gamma-receptors.

G. D. S. HIRST  
T. O. NEILD

*Department of Physiology,  
Monash University,  
Clayton, Victoria,  
Australia 3168*

1. Hirst, G. D. S. & Neild, T. O. *J. Physiol. Lond.* **280**, 87-104 (1978).
2. Byewater, R. A. R. & Taylor, G. S. *J. Physiol., Lond.* **300**, 303-316 (1980).
3. Ambache, N. & Zar, M. A. *J. Physiol., Lond.* **216**, 359-389 (1971).
4. Ambache, N., Dunk, P., Verney, J. & Zar, M. A. *J. Physiol., Lond.* **227**, 433-456 (1972).
5. Euler, U. S. von & Hedqvist, P. *Acta physiol. scand.* **93**, 572-573 (1975).
6. Booth, F. J., Connell, G. J., Docherty, J. R. & McGrath, J. C. *J. Physiol., Lond.* **280**, 19P-20P (1978).
7. Rand, M. J. & Jurevics, H. *Handbk Expl Pharmac.* **39**, 77-159 (1977).
8. Enero, M. A. & Langer, S. Z. *Br. J. Pharmac.* **49**, 214-225 (1973).

## Germ-line deletion of genes coding for self-determinants

JEMMERSON AND MARGOLIASH's article<sup>1</sup> raises provocative questions about immunological unresponsiveness to self-antigens. They found that the autoantigenic sites on rabbit cytochrome *c* correspond to those regions in the molecule where other mammalian cytochromes *c* differ, and suggested that archaic genes coding for V-region specificities of immunoglobulin recognizing shared portions of the cytochrome *c* molecule were eliminated by evolutionary pressures. This would result in immunologically silent peptide sequences, there remaining mainly V genes for the more recently evolved species-specific determinants. Thus, one mechanism of self-tolerance would be evolutionary germ-line deletion of V genes coding for specificities against self-molecule determinants.

Previous studies by one of us (N.R.R.) were directed to the antigenic properties of thyroglobulin in rabbits<sup>2</sup>. Two sorts of autoantibodies in rabbits were compared, those induced by immunization with rabbit thyroglobulin and those induced by immunization with foreign thyroglobulins, such as those of hog or beef. The first kind of autoantiserum resembled the rabbit antisera to rabbit cytochrome *c* described by Jemmerson and Margoliash. Tested for reaction with rabbit thyroglobulin, the rabbit thyroglobulin readily absorbed all reaction, whereas the hog (or beef) antigen removed only a small part of the antibody content. We concluded that

the rabbit preferred to form antibodies to the non-shared antigenic determinants of thyroglobulin.

In contrast, rabbits immunized with hog thyroglobulin showed relatively weak reactions with rabbit thyroglobulin, and these reactions could be absorbed equally well with hog, beef and rabbit thyroglobulins. Thus, autoantibodies induced by foreign thyroglobulin are directed mainly to the shared antigenic determinants of thyroglobulin.

On the basis of absorption behaviour, then, we could distinguish two types of autoantibodies. Those elicited by thyroglobulin of the same species were directed primarily to species-specific determinants, whereas the autoantibodies evoked by foreign thyroglobulins reacted mainly with the shared antigenic determinants. Of further interest, rabbits immunized with rabbit thyroglobulin showed severe lesions of thyroiditis. Only after repeated injections were even mild lesions seen in rabbits given foreign thyroglobulin.

The basic protein of myelin (BPM), a linear-folded protein without a tertiary structure, is another well characterized autoantigen. There are some 170 amino acid residues, and the sequences for the molecule of several mammalian species reveal a number of substitution sites. Because immunization with BPM induces experimental autoimmune encephalomyelitis (EAE) in all species studied, attention has focused on the capacity of BPM, and various peptides derived from it, to induce disease. The review by Bergstrand<sup>3</sup> indicates that different portions of the BPM molecule have greatly differing potency in terms of induction of (1) EAE, (2) cell-mediated immunity and (3) humoral antibody.

In the induction of EAE, which requires the participation of a T-cell response, detailed studies have defined the different amino acid sequences in the homologous proteins which induce EAE in different species. Minor sequence substitutions have an enhancing effect, for example, the encephalitogenic Ser-Thr substitution at residue 79 for the rat<sup>4</sup>, with other changes abrogating activity<sup>5</sup>.

With heterologous BPM injected into rabbits, one of the main determinants of humoral antibody was identified in the region 90-116 (ref. 6), and this does not vary between mammalian species. Unfortunately, relatively little information is available on the amino acid sequence(s) involved in the homologous response. Studies by microcomplement fixation assays in the rabbit<sup>7</sup> could be interpreted as showing a pattern of cross-reactivity between homologous and heterologous BPM equivalent to that described above for thyroglobulin. In particular, when rabbits were immunized with rabbit BPM, the antibody was predominantly reactive with rabbit BPM but with extensive cross-reaction with BPM of other species. It is assumed, although not

directly tested, that rabbit antibody to BPM is directed to the invariant 92–116 sequence.

Thus for thyroglobulin and BPM, genes specifying reactions to shared determinants do not seem to be eliminated by evolutionary pressures. However, examination of autoantigens in the light of the concept of Jemmerson and Margoliash would be interesting with respect to association of autoimmunity with disease.

IAN R. MACKAY

NOEL R. ROSE

*Clinical Research Unit,  
The Walter and Eliza Hall  
Institute of Medical Research,  
Post Office, Royal Melbourne  
Hospital,  
Victoria 3050, Australia*

PATRICK R. CARNEGIE

*School of Agriculture,  
La Trobe University, Bundoora,  
Victoria 3083, Australia*

1. Jemmerson, R. & Margoliash, E. *Nature* **282**, 468–471 (1979).
2. Rose, N. R. in *Textbook of Immunopathology* 2 edn Vol. 1 (eds Miescher, P. & Muller-Eberhard, H.) 215–229 (Grune & Stratton, New York, 1977).
3. Bergstrand, H. *Immunochim. Proteins* **1**, 315–370 (1977).
4. Kibler, R. F. *et al. J. exp. Med.* **146**, 1323–1331 (1977).
5. Hashim, G. A. *Immun. Rev.* **39**, 60–107 (1978).
6. Driscoll, B. F., Kramer, A. J. & Kies, M. W. *Science* **184**, 73–75 (1974).
7. Whitaker, J. N. *Comp. Biochem. Physiol.* **59B**, 299–306 (1978).

**JEMMERSON AND MARGOLIASH REPLY**—A serious problem with the comparative study of protein antigens of unknown amino acid sequence and spatial structure is that one tends to invoke qualitative all-or-none differences, based on the particular antibody-binding test used, when in fact the differences may be merely quantitative. Thus, in the experiments on thyroglobulin cited by Mackay, Rose and Carnegie, it is possible that rabbit thyroglobulin injected into rabbits does not elicit antibodies which bind to hog or beef thyroglobulin because determinant sites on the rabbit protein, which would elicit such cross-reactive antibodies, bind too weakly to the rabbit immune system to effect the needed cell stimulation. In contrast, once antibody production to these same sites has been stimulated by the higher-affinity hog thyroglobulin determinants, the antibodies will bind to the cross-reactive sites on the rabbit protein.

So-called 'shared' determinants can be merely cross-reactive and certainly do not need to be identical. One might be able to distinguish between these categories if the antibodies are tested in assays where binding affinities are measurable (not in immunoabsorption where very low antibody affinities allow binding); in such conditions the appropriate differences in binding have been observed with several

families of protein antigens<sup>1–4</sup>, as well as with cytochrome *c*. With this last protein family, the data are clearly contrary to any generalization that antibodies reactive with self, elicited by foreign thyroglobulins, react mainly with shared antigenic determinants. Indeed, only one of 13 distinct, site-specific antibody populations isolated from sera of rabbits immunized against foreign cytochromes *c* was shown to bind to a region of the molecule where the host and immunizing proteins were identical<sup>5</sup>. This seems to be the result of a special cross-reaction situation.

With proteins having poorly defined or plastic conformations, a further problem is that amino acid sequence variations distant from a site where amino acid sequences are conserved may possibly change the conformation of that region from the protein of one species to that of another, thus making it antigenic. This is not the case with cytochrome *c* where it has been shown with several different antibody populations that amino acid sequence variations outside the antigenic determinant have no effect on the conformation of that determinant<sup>6–7</sup>. Moreover, the purification procedure in the case of thyroglobulin seems to change the molecular conformation to some degree<sup>8</sup>, and regions which should be antigenically silent on the basis of amino acid sequence could become immunogenic.

Furthermore, and perhaps most importantly, although our evidence<sup>9</sup> supports the thesis that evolutionary germ-line deletion of V genes coding for anti-self protein specificities can occur, one need not assume that all selective pressures affecting anti-self antibodies would be negative. Indeed, certain anti-self antibody specificities may be preserved if the antibody itself is important biologically, such as in regulation. Recent observations supporting this idea are that normal animals possess low levels of antibodies having specificities ranging from cellular antigens of the surface<sup>10</sup>, cytoplasm<sup>11</sup> and organelles (R. J., N. Klinman and E. M., unpublished results) to intermediates in metabolism<sup>12</sup>. Anti-idiotypic antibodies which are specific for self-immunoglobulin determinants seem to be involved in regulation of the immune system itself<sup>13</sup>. Certain anti-self antibodies could serve as a clearance mechanism for cell debris resulting from killing of, for example, virus-infected cells, or ageing and death in the normal cell cycle<sup>14</sup>. Depending on the nature of the self-antigen (structural lability, physiological location and biological role), the regulatory role of antibodies could vary. Therefore, not all self-antigens would be expected to express only the determinants in evolutionarily variable regions, as was observed with cytochrome *c*. However, immunization with cytochrome *c* has never led to any autoimmune pathology, in sharp contrast to what occurs with thy-

roglobulin and basic myelin protein. Thus, it would be surprising if the V genes corresponding to self-antigenic determinants in the latter two proteins were not as vigorously selected against as those for the former, unless there exists a biological mechanism of which we are unaware.

Finally, even if the V genes corresponding to the antigen studied were treated by the evolutionary process as seems to be the case for cytochrome *c*, one must take into account the appearance of the proteins on the evolutionary time scale relative to the appearance of the antibodies and their average rates of evolutionary change. More recently evolved self-antigens may not show complete antibody deletion of conserved region specificities as not enough time would have been allowed for selective pressures to take effect.

RONALD JEMMERSON

*Department of Cellular  
and Developmental  
Immunology, Scripps Clinic  
and Research Foundation,  
La Jolla, California 92037*

EMANUEL MARGOLIASH

*Department of Biochemistry  
and Molecular Biology,  
Northwestern University,  
Evanston, Illinois 60201*

1. Atassi, M. Z. in *Immunochemistry of Proteins* Vol 2 (ed. Atassi, M. Z.) 77–176 (Plenum, New York, 1977).
2. Garver, F. A. & Talmage, D. W. *Biochem. Genet.* **13**, 743–755 (1975).
3. Prager, E. M. & Wilson, A. C. *J. biol. Chem.* **246**, 5978–5989 (1971).
4. Welling, G. W., Groen, G., Beintema, J. J., Emmens, M. & Schroder, F. P. *Immunochimistry* **13**, 653–658 (1976).
5. Urbanski, G. J. & Margoliash, E. *J. Immun.* **118**, 1170–1180 (1977).
6. Eng, J. & Reichlin, M. *Molec. Immun.* **16**, 225 (1979).
7. Jemmerson, R. & Margoliash, E. *J. biol. Chem.* **254**, 12706 (1979).
8. Rose, N. R. & Witebsky, E. in *Textbook of Immunopathology* Vol. 1 (eds Miescher, P. & Muller-Eberhard, H.) 150–163 (Grune & Stratton, New York, 1968).
9. Jemmerson, R. & Margoliash, E. *Nature* **282**, 468–471 (1979).
10. Eisenberg, R. A. *et al. J. Immun.* **122**, 2272–2278 (1979).
11. Steele, E. J. & Cunningham, A. J. *Nature* **274**, 483–484 (1978).
12. Bartos, D., Bartos, F., Campbell, R. A., Grettie, D. P. & Smejtek, P. *Science* **208**, 1178–1181 (1980).
13. Jerne, N. K. *Annls. Immun. Inst. Pasteur, Paris* **125c**, 373–389 (1974).
14. Kay, M. M. B. *Proc. natn. Acad. Sci. U.S.A.* **72**, 3521–3525 (1975).

## Opiate receptors and adrenal medullary function

THERE is much interest in the role of enkephalins and opiates as transmitters or modulators of neuronal function. Costa and colleagues recently demonstrated<sup>1</sup> that high-affinity opiate receptors are present in the plasma membranes of adrenal chromaffin cells and proposed that "the activation of these receptors causes a non-competitive inhibition of catecholamine release elicited by the stimulation of nicotinic receptors." From



the data presented in their Table 1, it is apparent that morphine and several endogenous opioid peptides inhibit the nicotinic release of catecholamines from isolated chromaffin cells (approximate  $ID_{50}$ s: morphine,  $>10^{-4}$  M;  $\beta$ -endorphin,  $10^{-6}$  M; Met-enkephalin,  $>10^{-4}$  M).

We have performed similar experiments both on freshly isolated bovine chromaffin cells<sup>2</sup> and on the cells maintained as primary monolayer cultures<sup>3,4</sup> for up to 16 days. We agree with their findings on inhibition of catecholamine release by morphine ( $ID_{50}$   $1.6 \times 10^{-4}$  M),  $\beta$ -endorphin ( $5 \times 10^{-5}$  M), Met-enkephalin ( $5 \times 10^{-4}$  M) and Leu-enkephalin ( $>5 \times 10^{-4}$  M). Like Costa *et al.*, we found that the nicotine-evoked release but not the  $K^+$ -evoked release of catecholamines was inhibited by these compounds<sup>5</sup>. We also agree that the inhibition by these opiate compounds is noncompetitive with nicotinic agonists; however, we are not convinced by the specificity of the inhibitory effects of opioid compounds for the opiate receptor. In our hands, the two opiate antagonists naloxone ( $10^{-8}$ – $10^{-4}$  M) and naltrexone ( $10^{-8}$ – $10^{-4}$  M) did not reverse the inhibition produced by morphine, but rather they acted like morphine to inhibit the release of catecholamines (naloxone  $ID_{50}$ ,  $10^{-5}$  M; naltrexone,  $>10^{-4}$  M). Further, the effect of naloxone ( $10^{-6}$ – $10^{-4}$  M) and naltrexone ( $10^{-6}$ – $10^{-4}$  M) was additive to that of  $\beta$ -endorphin ( $5 \times 10^{-5}$  M) and morphine ( $10^{-4}$  M).

We were rather concerned that the levels of morphine and the endogenous opiates required to inhibit catecholamine secretion ( $10^{-3}$ – $10^{-5}$  M) were far in excess of the concentrations of these compounds required for effective receptor occupancy ( $10^{-8}$ – $10^{-9}$  M)<sup>1,6</sup>. In our search for compounds with higher potency, we found that levorphanol inhibited catecholamine release with an  $ID_{50}$  of  $4 \times 10^{-6}$  M. However, dextrorphan, the inactive enantiomer of levorphanol, was equipotent ( $ID_{50}$   $4 \times 10^{-6}$  M) in inhibiting the release of catecholamine from the chromaffin cells.

It is therefore unlikely that the receptor that is involved in these inhibitory actions of morphine and the endogenous opiates on catecholamine release is the same as that described in membrane preparations from the cells<sup>1</sup> and adrenal medullary homogenates<sup>6</sup> that is stereospecific and has high-affinity binding for Met-enkephalinamide ( $K_d$   $0.9 \times 10^{-9}$  M), naloxone ( $3.2 \times 10^{-9}$  M) and naltrexone ( $+Na^+$   $1.3 \times 10^{-9}$  M;  $-Na^+$   $3.93 \times 10^{-9}$  M).

Before any physiological role for opiates in the adrenal gland is considered it is necessary to demonstrate stereospecificity and reversal by antagonists. Although it is possible that slight differences in the way the cells are isolated and maintained in culture could account for the differences we observe, the basic question we raise here of the lack of stereospecificity and the

discrepancy between the levels required for receptor occupancy ( $10^{-9}$  M) and the biological effects ( $10^{-5}$ – $10^{-4}$  M) are still relevant and raise serious doubts about the proposed functional role of high-affinity opiate receptors in the modulation of catecholamine release from chromaffin cells.

SIMON LEMAIRE  
IRMA LEMAIRE

Department of Pharmacology,  
Centre Hospitalier Universitaire,  
Sherbrooke, Quebec,  
Canada J1H 5N4

DEANNE M. DEAN  
BRUCE G. LIVETT

Division of Neurology,  
The Montreal General Hospital and  
McGill University,  
Montreal, Quebec,  
Canada H3G 1A4

1. Kumakura, K., Karoum, F., Guidotti, A. & Costa, E. *Nature* **283**, 489–492 (1980).
2. Schneider, A. S., Herz, R. & Rosenheck, K. *Proc. natn. Acad. Sci. U.S.A.* **74**, 5036–5040 (1977).
3. Livett, B. G., Kozousek, V., Mizobe, F. & Dean, D. M. *Nature* **278**, 256–257 (1979).
4. Mizobe, F., Kozousek, V., Dean, D. M. & Livett, B. G. *Brain Res.* **178**, 555–566 (1979).
5. Mizobe, F., Dean, D. M. & Livett, B. G. *Soc. Neurosci. Abstr.* **5**, 534 (1979).
6. Chavkin, C., Cox, B. M. & Goldstein, A. *Molec. Pharmac.* **15**, 751–753 (1979).

COSTA ET AL. REPLY—Lemaire *et al.* have confirmed our report that opioids, when added to primary cultures of chromaffin cells, inhibit the release of catecholamines elicited by nicotinic receptor agonists. They pointed out that this inhibitory effect is nonspecific because the required dose of morphine is too high and the phenomenon lacks stereospecificity. Moreover, as the doses of naloxone required to reverse the action of morphine are also high, at these doses naltrexone acts as a partial agonist. Lemaire *et al.* failed to give significance to our finding that lower concentrations of naloxone are required to antagonize the inhibition of catecholamine release caused by  $\beta$ -endorphin. This peptide seems to have a greater affinity and a greater intrinsic activity with the opiate receptor of chromaffin cells which are operative in regulating the action of nicotinic receptor agonists on chromaffin cell stores of catecholamines. In conclusion, the data obtained by us and confirmed by Lemaire *et al.* show that this opiate receptor has peculiar properties (a low sensitivity to morphine, high sensitivity to  $\beta$ -endorphin). Moreover, as expected, the dose of naloxone required to antagonize the inhibition of catecholamine release elicited by opioids depends on the specificity of the agonist used.

These considerations are in line with current thinking suggesting that there are multiple forms of opiate receptors. Hence, it is not surprising that those located on

the membrane of the chromaffin cells have peculiar properties which must be studied before concluding that these receptors do not have a physiological role.

We studied the binding characteristics of the opiate recognition sites of chromaffin cell membranes and compared them with the recognition sites located in synaptic membranes prepared from frontal cortex of bovine brain. The opiate recognition sites of adrenal medulla have a high affinity, and a large capacity to bind etorphine and its structurally related antagonist, diprenorphine. This prompted us to study the action of both compounds on the nicotine-induced release of catecholamines. Diprenorphine, in concentrations of  $10^{-8}$ – $10^{-6}$  M, is devoid of any action, whereas etorphine prevents the action of nicotine with an  $IC_{50}$  of  $2 \times 10^{-7}$  M. The  $IC_{50}$  of diprenorphine to inhibit the action of an  $IC_{50}$  dose of etorphine is about  $3 \times 10^{-7}$  M. These results show a specific ability of etorphine to antagonize nicotine, and a great specificity of diprenorphine to antagonize etorphine.

We believe that the opiate peptides stored in the splanchnic nerve act on specific receptors located on the chromaffin cell membrane. When these peptides are released from the splanchnic nerve they may function as co-transmitters and modulate the number of receptors for acetylcholine that are available in the chromaffin cell membrane. According to this view, the receptor for the co-transmitter, when occupied by a specific agonist, can influence the number of acetylcholine recognition sites and the extent of the response to acetylcholine.

This type of synaptic regulation could be of interest in the development of new neuropharmacological agents that may modify synaptic transmission by acting on co-transmitter receptors. Theoretically, these potential drugs could minimize or maximize the response to primary transmitters without altering the frequency of neuronal activity, because they will not act on the receptor for the primary transmitter and obliterate the transmitter action. Probably, such drugs would not trigger as many side effects as those that block the primary transmitter receptor. The benzodiazepines are a good example of drugs that act on the co-transmitter regulation. By knowing the nature of various co-transmitters operative in different synapses, we might develop specific drugs that, similarly to the benzodiazepines, will modulate synaptic activity and be relatively devoid of untoward side effects.

E. COSTA  
A. GUIDOTTI  
L. SAIANI

Laboratory of Preclinical  
Pharmacology,  
National Institute of Mental Health,  
Saint Elizabeths Hospital,  
Washington, DC 20032

## BOOK REVIEWS

## Time for thought

George E. Uhlenbeck

THIS book is a kind of essay about the age-old problem of the nature of time and especially about the question whether time "flows" or whether there is an arrow in time. Since these questions affect every human being, David Park has tried to reach both the general "time amateur" and the scientific expert — a considerable task. I think he has not quite succeeded, but as a result the style of the book is charmingly unpretentious and the author really does try to be clear.

The main line of the book is an attempt to elucidate the development of thought on the two kinds of time, physical time and time of human consciousness, which nowadays seem quite familiar, although they are still full of riddles. In ten short chapters the author traces the development from prehistoric times via the Greek philosophers and the Newtonian and post-Newtonian era to the most recent cosmological theories.

I liked especially the two early chapters entitled "The Greek Questions" and "The Newtonian Answer". The foreshadowing of the two times by Parmenides and Heraclitus, the speculations of Plato about these ideas and the discussion of the atomic theory introduced by Leucippus (perhaps to understand the causal direction in time) I found quite illuminating. The Newtonian chapter starts with a nice evocation of the wonders of the motions in the sky and then the author gives a concise but clear discussion of Newton's laws of dynamics and the law of gravitation. He scrutinizes especially the notion of absolute time, and tries to make clear that in Newtonian dynamics it is *not* necessary to think of a flow of time but that in fact the laws are time-reversible, as we would say nowadays. Here, he also touches on the special theory of relativity, the Einstein-Minkowski space-time concept, the Mach principle and the general theory of relativity. In the appendices he gives more details about these difficult subjects. I am afraid that for the general reader these appendices will be too technical, but they are a good reminder for the physicist, although Appendix 3 on the Mach principle is perhaps rather too speculative.

Now that Newton has clarified the

*The Image of Eternity: Roots of Time in the Physical World.* By David Park. Pp. 149. (University of Massachusetts Press: 1980.) \$14.50.

universal physical time, the question arises how to measure this time. This is of course done by a clock, but the author asks: What is a clock, and, especially, what is a good clock? He argues that a clock is a device whose law of motion is known, and the better this law is known, the better the clock is. Particularly he discusses the use of the rotation of the Earth from this point of view. This is all quite interesting, but I do have some qualms. Following Ernst Mach, I think that the question of what is a good clock is quite similar to the question of what is a good thermometer. In both cases the answer is essentially determined by convention. From the strictly operational point of view there is in my opinion no "true" time just as there is no "true" temperature.

Park devotes most of the rest of his book to the basic problem of the origin of the idea of the direction or "arrow" in time. If one accepts the Greek concept of the world as a huge collection of moving and interacting atoms, and if one believes that the Newtonian laws of dynamics describe these motions, how can one then reconcile the time-reversibility of these laws with the overwhelming common experience of the natural phenomena? We all know that we grow older and that we have to die. Further, a fundamental law of physics, the second law of thermodynamics, states that a closed system (as the world is supposed to be) tends to a state of equilibrium (or of maximum entropy) in which nothing further happens, the so-called *Wärme Tod*.

Early in this latter part of the book the author gives a short summary of the statistical interpretation of the second law. He illustrates it by a nice discussion of the so-called Maxwell Demon and of the little-known paper by Leo Szilard, which shows why the Demon is not able to violate the second law (in Appendix 1 a simplified but clear summary of Szilard's proof is presented.) Park also emphasizes the enormous length of the so-called Poincaré recurrence time for non-equilibrium states of macroscopic systems, and later argues that as a result these systems can be described causally in time producing our sense of past and future. Hence the arrow

of time on the macroscopic scale is guaranteed by the second law. Although this is certainly the generally accepted view, I feel qualms that the author's presentation now has its faults. I miss, for instance, a deeper discussion of the probabilistic aspects of the second law. No mention is made of the fluctuations around the macroscopic states which produce so many striking phenomena (such as the blue colour of the sky) and which limit the strict causality of the macroscopic laws of motion. But my main reservation is that the author does not make any distinction between living and non-living matter. He says (p. 54) that there is no doubt that our mortality is decreed in some way by the second law. He also does not mention the enormous amount of evidence for the existence of a biological evolution, which seems in such an apparent conflict with the second law. I think this is a serious omission.

The book goes on to tackle the cosmological time problem. After an instructive historical introduction about models of the Universe, the author discusses the modern cosmological "myth", the so-called canonical big bang theory. In my opinion this is the weakest part of the book. It is very speculative and I found it sometimes difficult to follow. The development of the Universe starting from the big bang clearly defines an arrow in time, and I think the author tries to reconcile this with the arrow of time of the second law of thermodynamics. Apparently his arguments have not yet been published in detail. They depend on the notion of microscopic order, which quite escapes me. He touches on the question of a possible end of time for oscillating models of the Universe, and also discusses the possible cosmological significance of the large dimensionless numbers occurring in the present theories.

The last chapter has the charmingly modest title: "Can We Finally Say Anything Sensible?". It is a summary of the basic theme of the book, the existence of two kinds of time, the physical time as measured by clocks and the time of human consciousness which is marked by events. Is there a relation between the two? The author notes that this profound question, which goes back to Plato, is clearly related to the great dilemma between the apparent causality of all natural phenomena and our obvious sense of free will. He makes the



interesting suggestion that perhaps the two times are a pair of concepts which are — like the pair of concepts, free will and determinism — complementary in the sense of Bohr. They are two aspects of human knowledge which are both required for our understanding of the world but which exclude each other. Park hopes that this view will lead to a unification of the two times on a higher abstract level. I am

sceptical, mainly because of my qualm about the neglect of the life sciences. To understand time 2 one surely should know what life is!

In all, I think that this is a stimulating book and I gladly recommend it. Each reader will undoubtedly have several objections as I had, but there is also no doubt that the book will make him think again about the roots of time. □

## Inheritance: the immunological challenge

N.A. Mitchison

*Somatic Selection and Adaptive Evolution: On the Inheritance of Acquired Characters.* By E. J. Steele. Pp.92. (Williams and Wallace: Toronto/Croom Helm: London, 1980.) \$14.95, £8.95.

THIS rather thin little book advocates the inheritance of acquired characteristics. Its interest lies in the opportunity it offers of observing how a competent young cellular immunologist came to hold such a view, and in the papers published earlier this year by the author, jointly with R. Gerczynski of Toronto, claiming to establish the validity of such inheritance in respect of immunological reactivity. Whether this idea need be considered seriously is a matter of opinion. R. B. Taylor (*Nature* 286, 837; 1980) does so. I do not, on the grounds that such an implausible claim need not be taken seriously to start with except by extreme specialists, in the sense of those willing and able to attempt to repeat the work. Otherwise, let time be the test: if Steele and Gerczynski can make something of their story — pursuing its implications and mechanisms — then let them do so. The rest of us can afford to wait and see. Fortunately, Steele shares the view that their work will stand or fall by what he can accomplish in a follow-up. For example, can heightened as well as diminished reactivity be transmitted by males to their offspring? Can genetically tolerant (heterozygous at H-2) as well as experimentally tolerant males transmit?

The idea is that retroviruses transmit genes from one cell to another by picking up messenger RNA, an old speculation of Temin's. To this is added the thought that the hypothetical flow of genes will favour those genes expressed in clonally expanded cells. As ideas there is nothing wrong with these, except that they are a little old hat now that DNA transfection has become an established technique — which can be used, as M. J. Cline has shown, to transmit methotrexate resistance genes from one mouse to another. The question is whether gene transfer between cells occurs naturally on any appreciable scale. The stability of Mendelian segregation ratios argues that it

does not, particularly when account is taken of segregation from a parent carrying a non-functional allele and from females with X-chromosome inactivation. Steele does not try to rebut or even evaluate this evidence. Instead he quotes a handful of apparent exceptions. Of course, apparent exceptions will turn up if one looks hard enough, but as exceptions they surely deserve critical examination. This they do not receive here.

For instance, Steele cites the apparent transmission of "individual-specific" antibody idiomorph from immunized rabbits to their offspring. But interpreting these data is tricky, because the assignment of idiotypes to the "individual-specific" as distinct from the "germline-encoded" category is doubtful. Furthermore, when a female is immunized before giving birth, as was the case for the data showing apparent transmission, there is a possibility that passively transmitted antibody may have favoured production of the idiomorph in the offspring. Or to take another instance, Steele cites the apparent production of sickle-cell haemoglobin trait offspring from normal parents as evidence of gene transfer. What is critical here is whether the parents were correctly typed, and to the extent that the typing is more rigorous (that is detects smaller amounts of HbS-type haemoglobin) the argument for gene transfer is weakened. These are technical points, but they indicate the incomplete nature of Steele's argument.

Much the same applies to the musings on the history and future of Lamarckian ideas. A scholarly discussion of these topics would require a coverage of nineteenth-century intellectual history and twentieth-century population genetics which is not the aim here. It is particularly disappointing to find no mention of the problem of conserving genetic variation under any scheme such as that proposed.

If Steele's work can be repeated, and if his interpretation stands, here is one colleague who will most humbly eat his words. □

N.A. Mitchison is Professor of Zoology at University College London.

## B, Cu, Co, Fe, Mn, Mo, Zn . . .

T.S. West

*Applied Soil Trace Elements.* Edited by Brian E. Davies. Pp.482. (Wiley: 1980.) £22.50, \$67.50.

PROBLEMS associated with contamination of the environment by traces of heavy metals are of considerable concern to many scientists and laymen. Somewhat strangely, relatively little interest is shown in the equally important problems associated with deficiencies of the trace elements that are essential to all forms of life. Elements such as boron, copper, cobalt, iron, manganese, molybdenum and zinc act as essential catalytic components in most enzyme systems in plants and, boron excepted, in animals where many other elements are vital to the considerably more complex biochemical processes involved.

All trace elements in biological systems are derived from the Earth's crustal rocks originally, but come mainly via weathering of the primary minerals of the parent rocks in soils through plants and, to a lesser extent, through the water supply. This somewhat curiously titled book is a synthesis of most of our knowledge of the trace elements that are known, at the present time, to be "biosignificant". Written by agronomists, chemists and geologists, it is an excellent account which can be recommended to all who are directly concerned with these matters, to others who work in associated areas in the medical sciences and indeed to all who are scientifically aware. It is well written and in many places quite fascinating.

I would have preferred to have seen a fuller account of the chemistry, particularly chemical speciation, of these elements in the soil, and a more systematic consideration of the demands made by plants on the soil. This could have been done at the expense of the rather over-detailed account given of analytical procedures, although one of course does recognize that virtually all present trace-element work in soils is heavily dependent on advances in the analytical sciences.

However, there is no doubt that this book is a major contribution to the subject and in my opinion it is one of the most important to have been published. It is well written and illustrated, and handsomely produced. One hopes that the editor will keep the team together to produce a second edition, when many of the exciting developments that are now taking place — particularly in speciation and synergism between elements — could be given as well as an account of the "new" elements.

This book deserves to be widely read and it probably will. □

T.S. West is Director of the Macaulay Institute for Soil Research, Craigiebuckler, Aberdeen.



# Anthropology and ecology of the world's savannas

Peter D. Moore

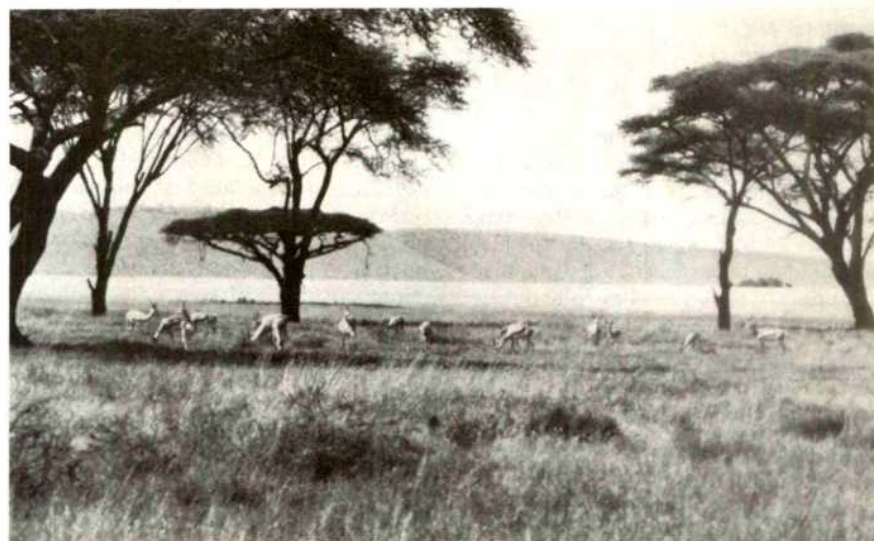
*Human Ecology in Savanna Environments*. Edited by David R. Harris. Pp.522. (Academic: 1980.) £21.50, \$49.50.

THERE is a romantic appeal about certain of the world's biomes which defies scientific explanation. What is there about desert, rain forest and tundra which excites the imagination, and why does the savanna lack the same magic? It was a similar concern which led David Harris to co-ordinate the Wenner-Gren Foundation conference in 1976 which formed the basis for this book. The general lack of public, and perhaps even scientific, interest in the savanna regions is all the more surprising when one considers the close association of early Man with these tropical grasslands, together with the modern problems of pastoral societies in these regions and the growing conflict with wildlife conservation.

The book is divided into three parts. The first deals with the occupation and exploitation of savanna environments since early prehistoric times. J. Desmond Clark attempts a synthesis of the pollen and vegetation data of Van Zinderen Bakker with the rapidly accumulating information concerning prehistoric communities in Africa. Man, he claims, remained restricted to the open savanna environments until about one million years ago, when *Homo erectus* first invaded the Ethiopian highlands. Hammond provides a similar synthesis for Central and South America, although the palaeoecological data is very much thinner. Within this section of the book also fall a number of anthropological studies of tropical Australia, Africa, India and South-east Asia. To an ecologist, some of the uses of ecological terms in an anthropological context may seem a little misplaced; is it reasonable, for example, to say that pastoral behaviour in East Africa shows the elements of an r-strategy? The statement is largely based upon the process of local resource exhaustion, followed by a moving on to new grazing land. The MacArthur and Wilson model is becoming unrecognizable.

Overall, one is left with the impression, from this first part of the book, that anthropologists have now gathered much field data from their respective study sites and are searching avidly for generalized models.

In the second part of the book, the emphasis moves from savanna history and exploitation systems, to present ecology and management. Here some authors use the ecosystem approach and one is supplied with data concerning production rates and nutrient distributions, particularly in relation to human land use. Among these papers that of P. A. Jewell, concerning the management of game and domestic livestock in African savanna, is outstanding,



East African savanna: Grant's gazelle grazing in the Serengeti.

both in the clarity of its presentation and in the wealth of carefully chosen data it contains. Beside it, the paucity of information from other areas is apparent.

The final part of the book concerns the human biology of savanna peoples. This contains largely physiological, nutritional and epidemiological information concerning the savanna populations, which is vital for an understanding of the ecology of Man in these areas.

One can always think of other subjects which could have been included to make any book more comprehensive in its coverage. High on my list here would be a

contribution by a palaeoecologist, who could put into perspective the limitations of the pollen data, to which so many of the authors refer. Also, a chapter concerning the ecology and importance of fire in savanna would have been helpful. But one must draw the line somewhere, and this book contains more than enough to whet one's appetite and enthusiasm for that neglected biome where Man himself has his roots. □

Peter D. Moore is Senior Lecturer in the Department of Plant Sciences, King's College, London.

## Slime mould jubilee

G. Turnock

*Growth and Differentiation in Physarum polycephalum*. Edited by W. F. Dove and H. P. Rusch. Pp.250. (Princeton University Press: 1980.) £13.70, \$25.

THE true slime mould, *Physarum polycephalum*, has a respected position in the catalogue of lower eukaryotes used for studies of cell biology in general and of differentiation in particular. Two features of its complex life cycle are of especial interest: first, the high degree of synchrony that is characteristic of nuclear division in the coenocytic plasmodium, and, second, the dramatic degree of differentiation involved in the transition from amoebae, which grow and divide as single cells, to plasmodia, which grow without any further cell division. Thus the amoebal-plasmodial transition is a link between two vegetative growth phases; it provides a refreshing contrast for the study of differentiation by comparison with

formation of spores or resting stages — not that *Physarum* cannot supply these as well.

One person, H. P. Rusch, played a particularly important role in stimulating biochemical studies of *Physarum*, and this book celebrates the silver jubilee of the work begun by his group at the McArdle Laboratory at the University of Wisconsin. Cancer research is the remit of the McArdle Laboratory and Rusch chose *Physarum* as a model organism for the basic analysis of growth and differentiation, although he admits in the Introduction that his work on carcinogens was becoming hampered by

James Six

*The Construction and Use of a Thermometer* by James Six, reviewed in the Autumn Books Supplement of *Nature* (288, 36; 1980), is available from Nimbus Books, 84 Sydney Road, London N10 2RN, price £15 + 60p post and packing.



the development of an allergy to rodents.

With Rusch as one of the co-editors, several of his former collaborators and others have contributed a series of essays describing the progress achieved in the study of *Physarum*. The collection will be of value to all who work with the organism and to others who wish to learn about its peculiarities for the first time.

The potential of genetic studies is emphasized in several of the articles, and the defined strains now available make possible, for example, the biochemical analysis of mutants defective in their ability to undergo the amoebal-plasmodial transition. Heat-sensitive mutants have

been isolated in several laboratories and there is optimism that this class will contribute to our understanding of the control of the synchronous nuclear division cycle in the plasmodial phase. Here, the major challenge, as Holt points out in the first article, is to relate the coordinated replication of the genome to the control of nuclear division.

It is a tribute to the interest that Rusch was able to stimulate that most areas of research on *Physarum* can be covered by his former associates. Transcription, the nuclear replication cycle, genetics and details of the different developmental phases are amongst the topics described.

Throughout there is a discussion of possible areas of progress, although some of the suggestions have a slightly frenetic ring, more appropriate to a grant application than to a collection of critical essays. Another minor criticism is the overlap in details provided in the different chapters. This could have been avoided by stringent editorial control; on the other hand, the argument for repetition is that it does enable each essay to be read individually, and the book as a whole can certainly be recommended. □

G. Turnock is a Senior Lecturer in Biochemistry at the University of Leicester.

## All you wanted to know about inflammation

J. L. Gordon

*The Cell Biology of Inflammation. Handbook of Inflammation, Vol. 2.* Edited by Gerald Weissman. Pp.714. (Elsevier/North-Holland Biomedical: 1980.) Dfl. 230, \$112.25.

THE topics embraced by the title *Cell Biology of Inflammation* cover a fair proportion of many lecture courses in pre-clinical pathology and also touch on several aspects of fundamental research into cell biology — including cell maturation, adhesion, locomotion, phagocytosis, secretion and intercellular interactions —

as well as tissue catabolism, remodelling and repair. Any editor attempting to assemble a book under this catch-all title is faced with a daunting task.

The first point to make, therefore, is that this book succeeds unusually well — better than any other single volume I have read. Several of the authors are acknowledged leaders in their field, and the overall quality is high, with some of the chapters being quite outstanding. I particularly liked Dee Bainton's general view of "The Cells of Inflammation", and there are two excellent contributions on mononuclear

phagocytes from Edelson and from Egal and Davies.

It is impossible to do justice to all the book's 18 chapters in a brief review; the topics cover an astonishingly wide range, from "template activity of isolated lymphocyte nuclei in priming exogenous bacterial RNA polymerase" through "eosinopoiesis and mast cell desensitisation" to "the ultrastructure of pre-lymphatics and tissue channels that constitute the sol phase of interstitial tissue". However, although the coverage is eclectic, this book is not a collection of esoterica — the balance is good and the tone is authoritative, inasmuch as it can be with a subject such as this where so much still remains to be learned.

There are, of course, some disappointments: for example, the reviews of the fast-moving areas of research are already dated, because most of the literature surveys seem to have stopped at the beginning of 1978, and some even earlier. Also, there is inevitable overlap with some parts of Vol. 1 in this series (*Chemical Messengers of the Inflammatory Process*), but this is a much better book than its predecessor — so much so that one wonders what remains for future volumes in this series. The standard of production is high and the copy is clean — Graham Lewis's criticism of the proof-reading of Vol. 1 (*Nature* 286, 89; 1980) perhaps had a salutary effect.

In summary, this is a substantial and important volume, and it deserves to be widely read; it left me with the impression that it could have been subtitled "all you wanted to know about inflammation but were afraid to look for in the original literature". It provides a valuable source of information and reference for those already working on some aspect of the cell biology of inflammation, and it may also stimulate those working on other topics to enter this fascinating field. □

J. L. Gordon is a Principal Scientific Officer in the Department of Cell Biology, ARC Institute of Animal Physiology, Cambridge.

## Until winning isn't everything, the public is damned.

Nuclear waste v. cheap energy; the DC-10 disaster v. air travel; genetic engineering v. reducing birth defects. Complex socio-scientific issues like these cannot be adequately addressed by our "either/or" system of dispute resolution, asserts legal scholar Milton R. Wessel. How to truly serve the public interest—by replacing winner-take-all adversary law with "the rule of reason"—is spelled out in *SCIENCE AND CONSCIENCE*, a work that every concerned citizen should read.

**SCIENCE  
and  
CONSCIENCE**  
Milton R. Wessel

\$20.70

**COLUMBIA UNIVERSITY PRESS**  
15A Epsom Road, Guildford, Surrey GU1 3JT



27 November 1980

# London medical schools stay in limbo

The University of London is making heavy weather of its attempts to reorganize its pattern of medical education. For most of the past year, the university but especially the medical schools which are constituent parts of it have been engaged in a fierce and frequently public argument about the proposals for rationalization put forward in February by a committee under Lord Flowers. Normally staid academics and, even more surprising, college principals with their origins in the civil service, have been writing to the newspapers, making public speeches and behaving as if this or that recommendation could be implemented only over their dead bodies. In one respect, at least, the volume (and the manner) of the protest has been effective. For the time being, nothing will be done. At its last meeting, the court of the university decided to postpone a decision until its next meeting, in February. This was a consequence of the decision of the senate of the university on 29 October (see *Nature*, 6 November) that no part of the proposed reorganization should be implemented without the consent of the medical schools concerned. So the hapless planning committees of the university are once more in session, seeking a formula that will win the consent of legally autonomous and temperamentally unruly medical schools to a measure of central government which is at once unpalatable and unfamiliar. If the issue is again postponed in February, the university will be running true to form. In the process, the foundations of its medical education will be further eroded.

Delay is of course a familiar response of academic institutions to the need for decision. The University of London has been grappling with problems of medical education since 1966, when the report of the Royal Commission on Medical Education, recognizing that the university is the chief source of qualified physicians in the United Kingdom, made specific proposals for reorganization. Since then, nothing much has happened, although the need that something should have become more urgent. The continuing decline of the population of London has reduced the numbers of patients to whom medical students in London have access; the National Health Service has embarked on a policy of redistributing hospitals and other medical services in accordance with these demographic trends and is now faced with a more permanent decision about the provision of hospital beds in London (brought about by the need either to replace old hospitals or to close them down). Although five among the twelve medical schools have been rehoused during this long period, resources available for teaching have steadily declined. Since 1973, the university has been trying to follow the advice of the University Grants Committee that more funds should be channelled to the medical schools. Its admission of failure provoked the Flowers inquiry. Things can only get worse while the university broods about its response. Given the importance of the university's medical schools in the pattern of medical education in the United Kingdom as a whole, the consequences of delay are not merely parochial. All medical schools will be affected.

The essential ingredient of the reorganizations proposed by the Royal Commission in 1966 and the Flowers committee in 1980 is the shotgun marriage. The Royal Commission had the twelve medical schools marrying off in pairs. In the event, one of these marriages was partly consummated in the relationship which has grown up between the London Hospital and St Bartholomew's Hospital (or, more accurately, the corresponding medical colleges). The other prescribed partners have fallen back jealously on their habitual celibacy, to which they have a legal right which they can surrender only voluntarily. The Flowers recommen-

dations took a similar form, but were inevitably more specific. Some marriages were to be arranged, two pre-clinical schools (at King's College and Westminster Hospital) were to be abandoned and the twelve postgraduate institutes within the university were either to be merged with teaching hospitals or to be relocated (in premises vacated by Middlesex Hospital). The Joint Planning Committee set up by the university senate and court acknowledges that the putative partners are within their rights when they insist that they would prefer to remain as they are. The university could nevertheless force change upon them by robbing them of funds — or by telling the National Health Service what future it sees for them. The effect of the senate's decision is that the pre-clinical schools at King's College and Westminster Hospital should be closed (and the clinical school at the latter merged with that at Charing Cross).

The university's dilemma is thus familiar to all those who work in universities in the process of change. Should a university administration force reorganization on unwilling academics? Should it, by failing to decide on a course of action, at the same time connive at a further deterioration in the quality of education? Or should it go all out for a decision in February, and if so which of the several canvassed options should it be? The greatest danger now is that the university will find itself plumping for one and sticking with it, come what may.

In reality, none of the schemes that have been advocated is ideal, although many of them contain common elements of agreed good sense. The shotgun marriages which have been proposed would often result in widely scattered groups of buildings united only by the new (and synthetic) names on their letterheads. What the university now needs is not a once and for all solution but a less ambitious and more persuasive programme of immediate action and a framework of management within which a more economical pattern of medical education can evolve, and be made to evolve, in the course of, say, a decade.

In the short run, there are administrative steps that should be taken — the rump of the Royal Free Hospital School of Medicine should, for example, be decanted from its old building, allowing the site to be sold. Similarly, the weaker among the postgraduate medical institutes — at a guess, six out of the twelve — should be looked at critically and perhaps even deprived of their academic pretensions. (Many of them would still have a useful service role within the National Health Service.) For the longer term, however, the university should be prepared to settle for a mechanism, not a prescription. And if the National Health Service demands some simple plan, it must be told that if the London medical schools are such an important part of British medical education, it is folly that their quality should be jeopardized by too hasty a solution.

In any case, the collective brooding about the future of the London medical schools has surprisingly left entirely out of account the paramount consideration — the character of the medical education the schools at present provide. The Flowers committee had some telling points to make about the way in which several of the existing schools are so short of resources that they cannot employ the full range of the academic staffs they need, but otherwise raised only the arid issue of whether it is better, within the peculiar pattern of British medical education, that intending physicians should be taken straight from secondary school and plunged into a hospital environment ('vertical integration') or, alternatively, allowed to spend their three pre-clinical years in a more normal type of college (the 'multi-faculty' approach).



Nobody has seriously considered whether some quite different pattern, perhaps the American pattern, might be preferable, at least in some of the London medical schools. No serious consideration has been given by the university (as distinct from individual medical teachers or schools) to the pattern of the medical curriculum. The relationship between postgraduate education and postgraduate research is almost entirely unexplored. So is it not high time that the university that happens to be the most prolific source of physicians in the United Kingdom should ask for a stay of execution while these difficult but important issues are hammered out?

The obvious difficulty is that, as on many previous occasions, the medical schools and even the university would use delay as an opportunity for doing nothing. What can make them change their ways? One good sign is that the troubles of the past few months have given all concerned a nasty shock, which they will not quickly forget. But there are also obvious combinations of stick and carrot that could persuade the medical schools that it is in their common interest to find out what changed pattern would best suit the long-term needs of medical education. One present absurdity is that the twelve medical schools, nominally constituent parts of the same university, appear to be even more concerned with their independence than with the education of their students. The university has a committee to scrutinize

developments by the separate schools, but the joint planning board says it would be impossible for that body to arbitrate between the existing medical schools on questions such as which should do what.

Why ever not? Membership of even the loose federation called the University of London surely entails some sacrifice in a common cause. They should be willing, and if not should be compelled, to sacrifice some of their autonomy. The only basis on which they can continue to resist recurrent proposals of shotgun marriage is that they should be willing to join in a still more ambitious venture, one intended to weld the London medical schools into a single coherent complex of institutions concerned with the training of doctors. Whatever the separate schools now pretend, many of them are too weak to stand indefinitely on their own feet. Too many academic departments are too small to be viable. What the schools need is a system in which the university as a whole provides certain common academic services which are beyond their separate resources. Then they might have the best of both worlds — diversity of style but effectiveness (and efficiency) in their teaching. As things are, they invite only the further erosion of their resources, the continued impairment of the quality of their teaching and the loss of such sympathy as they retain from those who share the schools' own distrust of coercion in the administration of universities.

## Best not to attend on Mr Moon

Next to Pope John Paul II and, possibly, the Reverend Ian Paisley, the internationally best-known religious leader is probably the Korean Sun Myung Moon, the founder of the organization called the Unification Church. In the past few years, the church has been constantly in hot water throughout the world, defending itself against complaints that in recruiting members to its ranks it frequently exerts undue influence on people who are temperamentally far from robust. The Unification Church is less well known (through its subsidiary organization, the International Cultural Foundation) as a sponsor of scientific conferences. The ninth "International Conference on the Unity of the Sciences" is now under way in Miami Beach (27–30 November), with the theme "Absolute values and the search for the peace of mankind". The chairman is the distinguished scholar Morton A. Kaplan from the University of Chicago. The vice-chairmen include Dr Frederick Seitz, most recently president of the Rockefeller University, and Dr J. S. von Euler, professor of medicine at the Karolinska Institute in Stockholm. This conference is as well blessed with distinction at the top as anybody can ask. The same, for what it is worth, is true of earlier conferences in the series — last time, for example, the chairman was Professor Eugene Wigner of Princeton. With such credentials, why should the question repeatedly be asked why people keep turning up?

The question is a controversial one. Those who participate in these conferences are usually at pains to emphasize that they have found them valuable, even stimulating. The same people are usually willing to keep on going back. The case for doing so was well put by Professor Nicholas Kurti two years ago, on the eve of the seventh conference held in Boston (see *Nature* 276, 206; 1978). The broadness of the themes of the conferences (in 1978 the subject was "the re-evaluation of existing values and the search for absolute values") does not always lead to the confusion that might be expected. Professor Kurti has said (and others have echoed him) that he has on the contrary found it useful to be required to think and talk about subjects that do not ordinarily come his way. Professor Kurti in his article made no secret of his view of the Unification Church ("many distasteful aspects") and of what he thinks of Mr Moon (not much), but he stoutly affirmed that the Unification Church could have derived no substantial propaganda value from the proceedings of the conferences, and that in any case no continuing obligation to the Unification Church would be incurred by accepting Mr Moon's hospitality (which is generous, to say the least). There is no reason to dispute

those opinions. It does not, unfortunately, follow that attendance is without consequence.

Quite apart from the source of their sponsorship, the conferences have some curiously shabby attributes. Perhaps the most serious complaint against them is that they are not so much sponsored as made possible by patronage. A part of the price paid by the assembly is that Mr Moon himself may choose to deliver an address of such vacuity that its thesis would not survive for ten minutes in an undergraduate seminar. By all accounts, however, Mr Moon's ideas survive more or less unscathed the gathering of Nobel prizewinners and other distinguished people who are required to listen to them. It is unseemly that scholars, but especially distinguished scholars, should behave in such a way. It is also unseemly that people should participate in conferences in which the participants, however individually distinguished, cannot collectively boast that they are the group ideally suited for the discussion of the broad themes with which they are faced. (To judge from the Miami Beach programme, some of the committee meetings, on the other hand, should be rewarding.)

Above all, it is unseemly that serious people should turn up at meetings where every other session title includes the word "values", where the title of the conference as a whole includes the phrase "absolute values" and where there is no means of knowing what these terms mean. It is true that participants are not required to assent to the "chairmen's affirmations" (read by Sir John Eccles to the fifth conference in 1976) that "scholars and scientists throughout the world should endeavour to search for absolute values and harmony among the sciences". Mr Moon might, however, get better value for his money if he required participants in advance to write a brief note of what they understand by these high-sounding words. As things are, participants are allowed to write on a subject of their own choice, receiving \$200 if the manuscript is sent in before 1 September and a further \$300 when what they write is "approved" for publication.

The case against these conferences, then, is self-contained. Professor Kurti may have been right two years ago to assert that participation does not necessarily give comfort (or much comfort) to the Unification Church, but the conferences themselves appear not to be as distinguished as those who participate in them, and should therefore be encouraged to wither away. For it is bad for the reputation of scholarship, dedicated as it is to the pursuit of excellence, that it should be seen to lend its name to extraneous causes. It matters less that they are those of the Unification Church than that they are second-rate.

# Harvard finally backs off gene venture

## Anxiety about conflict of interest wins

Harvard University's flirtation with the commercial exploitation of recombinant DNA research came to an end last week. After a period of agonizing and second thoughts by the faculty and administration (see *Nature* 20 November), the president of the university, Dr Derek Bok, put out a statement that the university would not after all participate in a company to exploit the work of Professor Mark Ptashne's laboratory.

What seems to have persuaded the university not to go ahead were the arguments of faculty members that a direct commercial interest by Harvard in the exploitation of ideas generated by one of its professors would create intolerable conflicts of interest. One argument was that the university would have found itself favouring the academics working for the commercial company in routine academic matters such as the appointment of staff, the allocation of laboratory space and even the provision of research funds.

It seems that the university administration has accepted these arguments only reluctantly. Mr Daniel Steiner, the university's Chief Counsel, said earlier this week that the university had approached Professor Ptashne as long ago as last February, suggesting the formation of a commercial company to exploit some of the research on which he was then engaged. It seems that until the faculty meeting in October, the university administration had not anticipated the strength of the reaction by some academics.

Other members of the faculty complain that the university administration was naive in its expectations of the commercial exploitation of recombinant DNA research. Under the proposed arrangements, the new company to be set up would have been financed by venture capital from commercial sources, would have had its own premises and its own managers and would not have been connected with Harvard by name. The university would have been given between 10 and 15 per cent of the equity without direct investment and there was also to have been a royalty on sales at a level not fixed.

In return, the university would have licensed the new company to use such patents as emerged only from Professor Ptashne's laboratory. Critics point out that the university would nevertheless have been a serious shareholder in the new company and that it could not have avoided committing resources of its own if,

for example, the new company ran into trouble.

Whether a commercial company based on Professor Ptashne's work will now be set up (without a shareholding by the university) remains to be seen. Professor Ptashne is thought to have been working since February this year, with the help of Professor T. Kanaguchi, on a novel method of making fibroblast interferon by cloning the gene at a more efficient expressing site in a plasmid in *Escherichia coli*. It is thought that the university has already committed some funds to this research.

Harvard's interest in the exploitation of patents arising from academic research dates back to 1975, when the university took advantage of a change in rules on patent law promulgated by the National Institutes of Health, and set up an office to encourage the patenting of inventions and the assignment of rights to the university.

Within the Harvard faculty, opinions remain divided. Some erstwhile supporters of the proposal regret the collapse of the administration's plan and hope that, in the

months ahead, less formal and perhaps more profitable ways of making progress may be possible.

Opponents, however, include some who argue that conflicts of interest are unavoidable if the university is to have a commercial interest in the exploitation of one professor's academic research. One irony that has emerged is that the university has indirectly acquired an interest in the recombinant DNA company Biogen, of which one of its professors, Dr W. A. Gilbert, is a prominent member. This interest has arisen independently, through a commercial investment in a venture capital company and in the normal process of university investment.

Among the critics, there are some who would use the events of the past few months as an occasion for a more general inquiry into the propriety of external entrepreneurial activities by any members of the faculty. One such critic said, earlier in the week, that Harvard was nevertheless comparatively "clean" — "You ought to look into what happens at MIT, down the river".

## JET fusion experiment seeks growth

The case for making Europe's big fusion experiment, the joint European torus (JET), bigger and better — and twice as expensive — is now being argued by physicists connected with the project. They are arguing that the machine, now being built at Culham in Britain, should be equipped to allow full thermonuclear experiments using deuterium-tritium mixtures.

This proposal for "extended performance" is being discussed by the JET Council, the governing body for the project. It could be presented to energy ministers of the European Community in mid-1981, when the community's five-year fusion research programme is due for reappraisal.

"Extended performance" to reach ignition conditions was envisaged in the original JET design (completed in 1975) but was thought at the time to be financially too risky, for theorists had predicted that new high-temperature instabilities might set in before the plasma ignited. Since then, experiments in existing devices have led to much greater optimism. In particular, an experiment in the Princeton tokamak is taken to indicate that the feared instabilities do not exist.

This development makes the basic JET now look rather tame, and suggests that it should be possible to aim quite quickly at deuterium-tritium experiments. But this requires a greater power supply to increase the toroidal field power by 50 per cent and the heating power by 150 per cent, new diagnostic devices, remote handling

equipment and a degree of radiation protection (from neutrons emitted by the ignited plasma). There will also have to be facilities for storing and handling tritium (itself an expensive commodity).

The latest estimate for the cost of basic JET is 263 million European Units of Account (EUA) (£147 million), a figure largely explained by inflation since the original amount fixed in 1977 (185 million EUA). The cost of the extensions now proposed is not yet fixed, but is likely to double that amount.

Meanwhile, JET construction is going well, though building delays have made the mid-1983 physics target look tight. Twenty of the 36 toroidal coils have been delivered and tested successfully; and buildings are now either complete and occupied or well under way. The vacuum vessel is a little late — the first octant was due in October but is not now expected until January — but it is hoped to make up the time lost. Staffing is up to target: 300 out of 320 appointed.

Contracts have now been placed for almost all the major items for the basic machine but it will be necessary to place contracts soon for the sophisticated equipment needed for the extended version if the momentum is to be maintained. Under this programme, JET will be commissioned early in 1983, and will begin physics proper in the summer of that year. There would be two years of experiments with hydrogen, investigating scale effects, a year with deuterium, and then, if everything went smoothly, work with a deuterium-tritium mixture in late 1986. It



is not known how long JET could work with a radioactive plasma, until its materials become too active to handle efficiently.

The Princeton tokamak fusion test reactor (TFTR), which is of similar scale to JET, is already being installed in its buildings. According to JET officials, the TFTR will be running some six months before JET itself.

Robert Walgate

## Telecommunications

### Monopoly in doubt

Sir Keith Joseph, allegedly the British Cabinet's hard man on monetarism and other issues of grand policy, last week published a soft, even muddled, bill for the reorganization of the nationalized British telecommunications industry. The bill, which the government hopes will be law before the end of this session of parliament, would split the nationalized British Post Office into two parts, one (called the Post Office) concerned with mail and the other (British Telecommunications) with the development and operation of the telecommunications network.

The bill confirms British Telecommunications in its monopoly of the telecommunications services in Britain including — a minor surprise — the right to maintain all equipment connected to the network. But the bill provides for "approved" equipment to be attached to the network, for private organizations to use the network for selling what are called "value-added services" and even for letting the Secretary of State license private telecommunications networks if he thinks fit.

Although these developments were foreshadowed in Sir Keith Joseph's policy statement last July, the extent to which the bill leaves final decisions about the shading of the monopoly in the hands of the Department of Industry is surprising. Instead of attempting to define what technical criteria should be satisfied by privately supplied terminal equipment, for example, the bill gives the Secretary of State power to arrange for an approval procedure. Questions of when outsiders would be allowed to lease the telecommunications network (and at what cost) are being looked into by Professor Michael Beesley, but again it will be the Secretary of State who will decide what should be permitted.

British Telecommunications (which will not formally exist until the bill is law) is plainly unhappy with the extent to which the bill would give the Department of Industry a crucial and perhaps arbitrary say in its future business. Sir Keith's dilemma seems to be that, having shrunk from going the whole hog and defining British Telecommunications as a common carrier, he has had to fall back on ministerial direction as a way of nudging the corporation in his preferred direction.

The bill may thus be a recipe for constant wrangling between the communications network and the civil service (which, paradoxically, has been much involved with the affairs of all nationalized industries since the election of May 1979).

The new regime at British Telecommunications also promises continued uncertainty about the financing of the telecommunications network. The new corporation will be encouraged by the bill to set up new subsidiaries to compete with private manufacturers of terminal equipment, but will be required to finance these developments within the tight restrictions at present applied — and which, in effect, imply that most of the capital cost of renewing the British telecommunications network is paid for by current users of the network.

Last week, Sir Keith Joseph offered no escape from this corset except to the extent that British Telecommunications may be able to set up joint ventures with private industry which are financed privately and not under the corporation's financial control. Delphically, he declined last week to say what sorts of ventures he was thinking of, thus lending credence to the view at British Telecommunications that the proposed device will offer very little escape from the present squeeze.

Despite reports to the contrary, there appears to be no threat of interference with the programme of telecommunications research and development, based at the laboratories at Martlesham Heath in Suffolk. The government intends this bill to be law within a year. Its plan to sell off Cable and Wireless is the most likely snag.

## Malaysian education

### Pressures ease

#### Kuala Lumpur

Faced with internal racial pressures and a growing concern about academic quality, educational authorities in Malaya seem to be easing up slightly on the harshness of previous measures to reform the country's education system.

Two aspects of this policy have come under particular criticism. The first, known as restructuring, is the preference that has been given to Malay students and staff over those from Malaya's other two major ethnic groups, the Chinese and the Indians. The second, nationalization, has been the requirement that all school and university courses should eventually be taught in Malay rather than in English, both initially used as official languages after the country's independence from colonial rule in 1957.

Both goals are part of a new economic policy introduced by the Malay government in 1971. This followed widespread racial riots sparked off by Malay fears that their post-colonial political dominance was about to be challenged by the economically more powerful Chinese, who had voted

strongly for the main opposition party in the 1969 elections.

One result of the subsequent "reforms" is that, from 1985, all university courses will have to be taught in Malay, the culmination of a process which started in 1976 with the requirement that Malay be the language taught in primary schools, and which has been climbing the educational ladder one year at a time ever since.

The policy has been effective in increasing an awareness and use of Malay, now the official language in which all communications with civil servants, for example, must be carried out. But many university teachers now argue that an excessive concentration on Malay is already placing students at a disadvantage, particularly in science subjects where most textbooks and almost all scientific journals are written in English, and many scientific concepts have no Malay counterpart.

Partly in response to this criticism, the government is now boosting the teaching of English as a second language in Malaysian schools, arguing, for example, that English is necessary for graduates entering technical employment or intending to pursue postgraduate studies abroad.

A recent decline in the standard of English teaching in secondary schools was "alarming", said one education official last week, arguing that if it continued unchecked it would be a serious setback to the government's plans to increase the number of scientists and technologists on whom the country depended for its future.

A concern for educational standards has also prompted the government to relax slightly the constraints placed on foreign university staff — exceptions are now frequently made to the ruling that a non-Malaysian can only be given two consecutive three-year teaching appointments — as well as the strong preference given to Malays in awarding university places over Chinese and Indian students with equal academic achievement.

The latter relaxation has proved to be controversial, particularly as many Malays see positive discrimination in their favour as necessary to eliminate the dominance of the Chinese in many professional fields, including scientific research.

For example, opening a conference on the role of universities in the developing countries last week, the vice-chancellor of the University Kebangsaan Malaysia, Professor Datuk Awang Had Salleh, said that solutions based on groups rather than individuals remained an appropriate strategy for university entrance.

## Erratum

The title of the article on the Indian environment, which appeared on page 207 of the 20 November issue of *Nature* should have been "Indian environment: Gandhi converted".



However, Malaya's Education Minister, Datuk Musa Hitam, is currently tightening up on the ease with which Malay students can at present enter university. In particular, he is reducing the proportion of Malay to Chinese and Indian students by 2 per cent a year until a final figure of 55 per cent *bumiputra* — literally "sons of the soil" — and 45 per cent non-*bumiputra* is achieved in the country's five universities. This is roughly equivalent to the racial balance in the country, but between 1970 and 1975, for example, the preference given to Malays increased their size as a proportion of student intake from 50 to 65 per cent.

Speaking at the opening of an educational building in Kuala Lumpur, Mr Datuk Musa was quoted as saying that this development should be taken as a "warning signal" to both *bumiputra* students and their parents that entrance to universities would in future depend less on their racial status and more on their academic achievement.

There is less political pressure to change the impact of present policies on the make-up of university staff. Part of the restructuring policy has been to increase considerably the number of Malay teachers and administrators in both schools and universities, again with the intention of redressing previous imbalances.

Chinese and Indian teachers accept both the logic of this policy and the political needs on which it is based. But in private, many express unhappiness that appointments, even at relatively senior administrative levels, are sometimes made with little respect for academic merit, and that in the process their own promotion prospects have been significantly reduced.

University staff in Malaya, however, are forbidden as government employees from taking part in any attempt to change policy. Lacking significant political power, their only options are frequently either to accept their reduced prospects or to seek teaching or research appointments abroad.

David Dickson

## Antarctic research

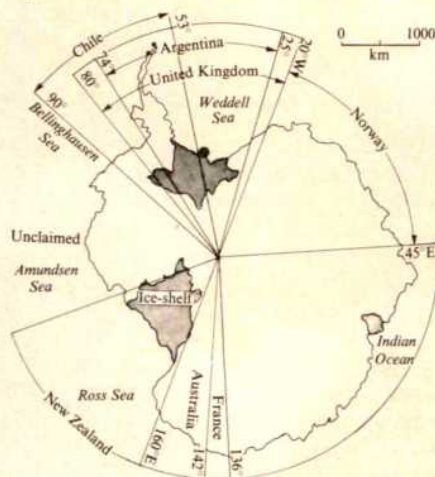
### Germany joins in

A bid for a voice in the future development of the Antarctic may be behind West Germany's massive new research programme in the area. Details published recently\* show that West Germany will become second only to the United States in the size of its investment in Antarctic research.

Although West Germany acceded to the Antarctic Treaty in 1979, it is still not admitted to the inner consultative group of countries which discuss matters beyond research, such as the exploitation of krill,

\*Antarktisforschungsprogramm der Bundesrepublik Deutschland, Bundesministerium für Forschung und Technologie, Bonn. An English summary is available.

one of the last great untapped food resources of the sea, and the development of possible offshore oil supplies. In the wording of the treaty, admission to the consultative group is reserved for the original 12 signatories (which did not include West Germany) and for any later signatory demonstrating its interest in Antarctica either by conducting substantial scientific research activity there — such as the establishment of a scientific station — or by the despatch of a scientific expedition.



Germany for blob in Weddell Sea

West Germany is doing both. It is creating a new 20-man research and training institute at Bremerhaven to direct its Antarctic programme, building a supply and research ship and purchasing one or two Lockheed C130 transport aircraft (the largest planes on skis). Its commitment will cost DM 385 million (£85 million) to the end of 1983, with a large fraction going on capital equipment and buildings.

The Bremerhaven centre will be called the "Alfred Wegener Institut für Polarforschung" after the originator of the concept of continental drift, who died on an expedition to Greenland in 1930. The institute will open in January 1981 under the directorship of Dr Gotthilf Hempel, a marine biologist now at the University of Kiel, while the research ship, which has been placed on order at a German shipyard, will be launched in 1982.

Officials at the federal research ministry were at pains last week to demonstrate West Germany's long research interest in Antarctica. Germans were among the first explorers of the polar continent, with expeditions in 1873, 1901, 1911 and 1938. The last expedition, according to some commentators, was not research but an effort by Hitler to establish a territorial claim and was overtaken by the events of the Second World War. The region explored at that time (called New Schwabenland and Queen Maud Land) is now claimed by Norway. After the war, West Germany was too preoccupied with economic reconstruction to bother with the Antarctic. Interest revived in 1975 when a research ship was sent to investigate krill.

## Antarctic politics

Antarctic politics are tortuous, a product of random historical and geographical factors and the current interest in food and oil resources. The Antarctic Treaty was set up after the International Geophysical Year of 1957–58, and ratified in 1961 by twelve nations: Argentina, Australia, Belgium, Chile, France, Japan, New Zealand, Norway, South Africa, the United Kingdom, the United States and USSR. Since then Bulgaria, Brazil, Czechoslovakia, Denmark, East Germany, West Germany, the Netherlands, Poland and Romania have acceded to the treaty, but of these only Poland has so far joined the all-important "consultative group" (which otherwise consists of the first 12 signatories). West Germany has applied to do so and is awaiting admittance.

The treaty forbids new territorial claims on Antarctica, but has no effect on previously asserted rights or claims. Before the treaty, Argentina, Australia, Chile, France, New Zealand, Norway and the United Kingdom had claimed sectors of the continent centred on the South Pole. These states recognize each other's claims, except Chile, Argentina and the United Kingdom, which have largely overlapping claims. The claims do not affect the placing of research stations: West Germany's proposed station will be on the edge of the Ronne ice shelf, near Berkener Island in the krill-rich Weddell Sea, on territory disputed between Argentina and the United Kingdom. The Antarctic Treaty confirms free access to all areas of Antarctica to all signatories. The legal status of the territorial claims, relevant only to resource development, is untested.

Surveys for an Antarctic research station began in 1979. The chosen site near Berkener Island is on the edge of the Ronne ice shelf, an extension of the Antarctic ice sheet over the shallows of the Weddell Sea. The station is now under construction and by late 1981 it will begin to serve as a scientific observatory for 45 scientists and technicians and a supply base for expeditions within a 1,000 km radius, wide enough to include the geologically interesting Palmer, Ellsworth, Pensacola and Shackleton mountain ranges.

Two other nations are also increasing their efforts in Antarctica — Australia and Argentina. Australia announced recently that it would completely re-equip its existing stations in Antarctica, at a cost of £20 million. Argentina is planning to construct the first all-weather, hard-surface landing strip as a potential refuelling base for commercial transpolar flights. Argentina is also constructing a new icebreaker for Antarctic work.

Robert Walgate



## Bangladesh

### Planning science

#### Dacca

Better use of the existing facilities and manpower for scientific research and development are given special attention in the Bangladesh government's Second Five-Year Plan, now published. In research and development, priority is given to agriculture, light and heavy industry, energy provision including nuclear power, housing and sanitation and transport.

The contribution of science and technology to the socio-economic development of the country has so far been relatively insignificant. Although Bangladesh boasts about 30,000 scientists and technologists with postgraduate qualifications, some 7,000 engineering graduates and more than 100,000 lower-level scientists, university research has often been "too academic" and in the government establishments research has often duplicated work done elsewhere. In nationalized industries there has been little initiative for innovative research, and in the private sector there has been virtually no research and development work.

#### Allocation for science and technology in the Bangladesh Second Five-Year Plan

|                                      | Estimated budget<br>(in millions of taka*) |
|--------------------------------------|--|
| Agriculture                          | 2,400                                      |
| Industry                             | 1,570                                      |
| Flood control and water<br>resources | 750  |
| Transport and<br>communication       | 210  |
| Health                               | 390  |
| Education                            | 50   |
| Natural resources                    | 260  |
| Nuclear power                        | 1,000                                      |
| Science, technology and<br>research  | 1,550                                      |
| Others                               | 200  |
| <b>Total:</b>                        | <b>8,380</b>                               |

\*US\$1 = 15.30 taka.

Main spending areas in the new plan (see table) are agriculture, industry, flood control and water resources, nuclear power plants and science and technology research. Of the allocation to science and technology research, nearly half of the 1,550 million takas budget goes to the Bangladesh Atomic Energy Commission. The bulk of the rest goes to the Bangladesh Council of Scientific and Industrial Research, the Space Research and Remote Sensing Organization and the Museum of Science and Technology.

The nuclear power programme includes a plan for the country's first research reactor for the production of radio-isotopes, a new 125-MW nuclear power plant in the western zone of the country and a study of the feasibility of extracting nuclear minerals from beach sand.

The space research organization is to concentrate on the completion of Bangladesh's advanced multipurpose

satellite ground station. The station's equipment is to be developed so that it can receive data from the various satellites including CMS (Japan), TROS-N and NOAT (United States) and METEOR (USSR). Important aspects of the satellite-based work for a developing country such as Bangladesh are a natural resources survey and a disaster-warning network. The five-year plan includes policy recommendations aimed at improving links between research centres and industry, improving primary and secondary education and giving further education a more practical bias. **M. Kabir**

### Soviet fertilizers

### Going it alone

Fertilizer production has been hived off from the Soviet Ministry of the Chemical Industry and now merits a ministry of its own, under Minister Aleksei Petrishchev, previously deputy chairman of the State Committee for Material and Technical Supply. At the same time, a new Minister of the Chemical Industry, Vladimir Listov, has been appointed. He was formerly deputy minister and has been working in the Party Central Committee since 1977.

These changes provide an indication of the direction of Soviet planning in the next five years, coming as they do in the closing weeks of the five-year plan. "Chemicization", as it is called, was launched by Khrushchev in 1958 and was continued by his successors. But Krushchev himself was less fond of chemical fertilizers than of the "virgin lands" — horizon-to-horizon grainfields in the erstwhile uncultivated steppelands of Asia. In 1965, his successors introduced a new agricultural strategy based on increased investment in agriculture, land improvement (drainage and irrigation) and an emphasis on intensive methods of cultivation, increasing the yield per hectare by the use of fertilizers rather than by expanding the total area cultivated.

The expansion of the chemical fertilizer industry was initially heavily dependent on Western technology, particularly the Pullman-Kellogg ammonia system and urea plants. Indeed, much of the capacity of these plants is still being used to pay off the cost of the equipment under compensation agreements.

Recently, however, the Soviet Union has been stressing its independence in all matters of chemical production. To some extent, this may be a reaction to world events. The main raw materials of the Soviet chemical industry are oil and natural gas, and the Gulf war has produced a spate of assurances that there is no oil shortage in the Soviet Union.

Poland is the Soviet Union's main supplier of another raw material vital to the fertilizer industry — sulphur. Political changes there may force Soviet planners to look more seriously at plans to utilize their

own relatively inaccessible sulphur beds.

Irrespective of politics, however, the Soviet fertilizer industry does seem to have reached a stage of relative technological independence. The new Chirchik ammonia plant, for example, is based on Russian technology and Russian contracting.

In spite of official emphasis on increasing the yield of food crops, Soviet agriculture's capacity for fertilizer remains far from satisfied. In 1976 only 50 per cent of the total grain cultivated area received any fertilizer at all.

The setting up of the new Ministry for the Production of Chemical Fertilizers strongly suggests that all branches of the fertilizer industry are to receive a boost in research and development. It also suggests that the forthcoming five-year plan will maintain the current emphasis on the "non-black-earth" regions in the west of the USSR, where the relatively poor soil demands considerable use of fertilizers.

If, as seems likely, the new ministry plans to build more fertilizer plants, the siting of these plants will be a major policy decision. At present, most plants lie in the non-black-earth zone, handy for the market, but far from Siberia, the main source of raw materials. Plants could, of course, be set up in Siberia, but the Siberian economy is in a bad way. **Vera Rich**

### European plutonium

### Project denied

#### Brussels

The future of the European Commission's support of research and development on plutonium cycling is in doubt. Last month, after a year-long search for a compromise, the Committee of Permanent Representatives (COREPER) rejected Euratom's second four-year plan even though this had been approved by the European Parliament last May. Officials now seem at a loss to know how an acceptable proposal can be devised.

The first programme ended in 1979 with what the commission described as "highly significant results" and encouraged it to draw up the more ambitious plan for 1980-84 now rejected. A total of 30 million European Units of Account (1 EUA = £0.56) was for research on the environmental effects of using plutonium (including the reprocessing of plutonium fuel), the transport of plutonium, the fabrication of mixed plutonium oxide and uranium oxide fuels and the recycling of used mixed-oxide fuels from light-water reactors.

France and the United Kingdom have led the opposition to the programme while Germany and Belgium have shown the greatest enthusiasm. The French and British are anxious to have cheap plutonium with which to fuel fast-breeder reactors and would rather buy plutonium from fellow member states than use recycled plutonium from their own reactors — the theory being that this would



increase the supply of plutonium and keep prices down.

Commercial rivalry is also said to have contributed to the rejection of the plan. The United Kingdom has already developed a process for fabricating mixed-oxide fuels and fears that a new research programme may compromise its capacity to collect royalties from the licensing of the process.

The desire to cut back on the commission's budget also probably contributed to the rejection of the programme, and thoughts are therefore now turning towards a "supplementary programme". Unlike a joint programme, this would be financed only by the interested countries.

Germany is committed to the plutonium-cycle programme because it wants to keep all options open, and public pressure at home makes any movement towards improving nuclear safety particularly attractive. Belgium, which generates 20 per cent of its electricity from nuclear power stations, feels that the programme would help towards securing steady fuel supplies. Italy and Holland seem prepared to go along with the programme but Ireland and Denmark are less sure — Ireland because it would draw little benefit in the foreseeable future and Denmark because it is interested only in the safety aspects of the plutonium cycle and would prefer the budget to be halved.

Jasper Becker

## Project planning

### Staged inquiries

The proposal that major planning issues of national importance, such as the fast-breeder reactor, should be decided in two stages, with a "project inquiry" followed by a local planning inquiry, was debated at a seminar on "The future of the big public inquiry" held at the Royal Institution, London on Monday 24 November.

The proposal has its origins in the work of a working party of the Council for Science and Society which issued a report in July 1979 recommending that project inquiries should investigate major proposals in depth, paying attention to the need for the project and considering all possible alternatives. One objective was to avoid lengthy and sterile wrangles at statutory local planning inquiries and even disruption by frustrated environmentalists.

There has recently been growing dissatisfaction with inquiries on national issues such as the building of major airports and motorways and nuclear installations. The siting of motorways seems to have been a particularly contentious subject and inquiries on such subjects have often been disrupted by highly regarded citizens.

The working party of the Council for Science and Society relied on the assistance

of Justice (the British section of the International Commission of Jurists) and the Outer Circle Policy Unit. The chairman was the barrister Paul Sieghart, vice-chairman of Justice, and the members were drawn from public administration, industry and planning.

At this week's meeting, Lord Kearton (with an extensive background of manufacturing industry) welcomed the proposal for preliminary project inquiries. He said few "big" inquiries were likely to arise in the near future and these would consist of proposals by the government for new motorways or for nuclear installations or refineries from bodies concerned with energy.

Sir Wilfred Burns, chief planner at the Department of the Environment, however, attacked the notion of the project inquiry. He argued that such a process would bring into question decisions reached democratically by parliament, the ultimate arbiter in matters of general policy.

The audience, consisting of officials, planners, consultants and members of pressure groups, seemed on the whole to have been in favour of the concept of a project inquiry. John Tyme, the veteran motorway protester, summed up the need for change by saying that many developers were "biased and ignorant, and many so-called experts on traffic or energy needs had been shown to be wrong".

Kenneth Mellanby

## French science museum takes shape

### Paris

The new French Museum of Science and Industry is at last beginning to take shape, even if at present only in the form of an architect's model. Two years after the commissioning of a report on the possibility of a new museum, and a year after that report was handed in, the final architectural plan has been selected. This pace, extraordinarily slow even for France, is a result of the problems attendant on a prestige project of this kind in a country in which "prestige" often equals "personal politics".

As originally conceived by the President of France, Valéry Giscard d'Estaing, the museum was to be the scientific equivalent, in grandeur and prestige, of the immensely successful Centre for the Arts created by his predecessor Georges Pompidou. To be erected on the 52-hectare site of La Villette in the north of Paris, the project was to be the largest, most modern science museum in the world. The original report, prepared by Maurice Lévy of the University of Paris, envisaged the conversion of an existing building on the site to a 100,000 square metre showplace of scientific and technical advance (*Nature*, 3 January).

Since then, however, a number of problems have surfaced which threaten to delay the project or to change it a great deal. There have been problems of money; the floor space available to the museum has

had to be reduced by more than half, to 40,000 m<sup>2</sup>; even so, the whole project is expected to cost 800 million francs — at a time of growing austerity in France. There have been clashes of personality; early in the year Lévy resigned as head of project, to be replaced after a three month interregnum by André Lebeau of the Conservatory of Arts and Crafts, an older, very traditional Paris museum.

Nor has the departure of Lévy ended all the differences of emphasis on policy questions among the museum staff. For example, the director of exhibitions, Goery Delacote, speaks of using the history of science and technology to "show the failures as well as the successes" so as to avoid a "triumphalist" conception of

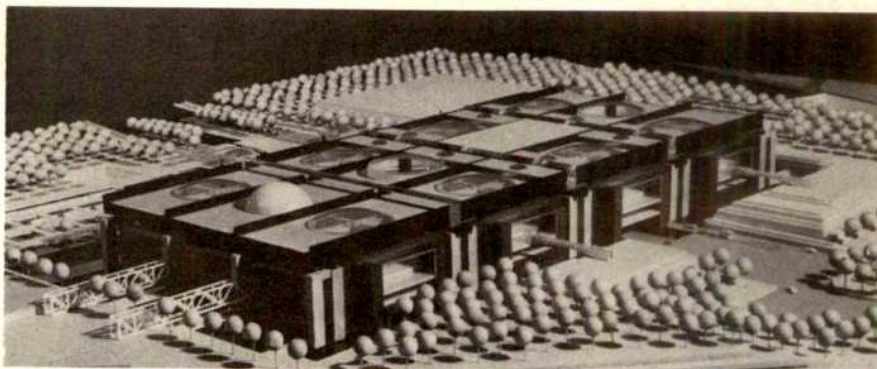
science, while general director Lebeau maintains that "the historical dimension should be present more to enlighten the comprehension of contemporary science than to tell the story of past science".

Added to all this is the fact that President Giscard d'Estaing retains a final say over all aspects of the museum's planning. Nor is this merely a formality. It was the president who chose the design of the winning architect Adrien Fainsilber from among the seven preselected by an international committee.

Thus the problems of a multiplicity of power centres, ambiguities in conception and increasingly tight financial resources suggest that the new museum is in for a prolonged and difficult gestation period which may last beyond 1984, the proposed date of completion.

Jim Ritter

*Will Giscard, like Pompidou, have a centre . . . . . ?*





# CORRESPONDENCE

## Medical education

SIR — In the article "Medical schools stay" (*Nature* 6 November, p.6) you say that King's College Hospital Medical School is rerieved. The Flowers Report did not in fact envisage the closure of King's College Hospital Medical School but suggested a fusion with Guy's Hospital, the product to be called the Lister Hospital. This idea has been replaced by a proposal that King's, Guy's and St Thomas's Medical Schools should form a consortium of equal partners under a common management body.

The debate in the University is now centred on the possible closure of the Medical Faculty of King's College London, from which the majority of our pre-clinical students come. The University has set up a subcommittee of its Joint Planning Committee called the Medical Costing Committee which is urgently to review pre-clinical education in London and to report its findings by January 1981. From its report the Senate and Court of London University will be able to make a decision on where medical students will derive their basic scientific training in London.

L. T. COTTON

King's College Hospital  
Medical School,  
London SE5, UK

## Risks at NRPB

SIR — Confidence in nuclear energy (*Nature* 19 June p.521) is not helped when individuals interested in the risks associated with it are inhibited either from expressing their opinions or from performing their work. The uninitiated who read the section on "Quality and integrity of the advisory and control authorities" in the Parker Report of the Windscale Enquiry would probably conclude that the record of the National Radiological Protection Board (NRPB) was clear in this respect, and moreover that although its late Director of Research, Dr G.W. Dolphin, in his generally censured paper on the Windscale workers, had underestimated radiation risks through a "mistake in methodology", the affair only showed that Dolphin was not infallible.

I have written (*New Scientist* letter, 13 January 1977) about the conditions at NRPB where my paper on radiation risks in the Japanese A-bomb survivors was held up by Dolphin for a year. One reason was his ignorance of statistics but he also objected strongly to risk estimates which were larger than he expected. The increases were not extraordinary but Dolphin's loyalties apparently remained with the Atomic Energy Authority (AEA) for he cautioned against making risk estimates which could be used against the fast breeder reactor. In contrast to the openly expressed bias supporting nuclear energy, there were no discussions about the possible risks from its development.

Before the merger forming the NRPB, the director of the Medical Research Council Radiological Protection Service publicly

warned staff, in the presence of the NRPB chairman and director elect, that the new management could not be trusted. Similarly, many of the AEA staff that joined the NRPB strongly distrusted the management who, they said, had abused their power in the AEA and exercised control over staff by, for example, making false reports on their work. However, they took care not to express any criticism in public and warned that it was futile to resist management decisions.

These management practices continued in the NRPB. Members of the staff found that it did not pay to disagree with the management who, in contrast, were apparently free to do as they pleased. When I objected to the management's duplicity and views on risks, the director of research warned that it would do me no good and became intent on making the conditions intolerable even at the expense of the work.

In 1977, soon after the Flowers Report made its criticisms of the NRPB, I wrote to Sir Edward Pochin, a member of the NRPB and an assessor at the Windscale Enquiry, concerning the working conditions at the Board but, although he promised to investigate, I received no reply. Recently my MP made enquiries and in the Board's answer it is claimed that Dolphin was the real author of the NRPB paper, published in my name, on risks in the A-bomb survivors, a statement which is clearly false from Dolphin's Windscale paper.

Evidently the regard shown to NRPB staff employed on similar projects depends primarily on who they are and not on the quality of their results. However, such anomalies do show the standard of the NRPB.

S.G. GOSS

Sutton, Surrey, UK

## Reagan a plus?

SIR — It is with a mixture of incomprehension, dismay and disgust that we read David Dickson's assessment of the "plusses and minuses" of the 1980 United States elections (*Nature* 13 November, p.107), where Mr Dickson notes completion of the Clinch River Fast Breeder Reactor and resumed production and stockpiling of chemical warfare agents as expected plusses of the Reagan election. Since when is the development of a questionable technology with very likely adverse ramifications for the environment and for attempts to limit nuclear proliferation a positive direction in which to proceed? Since when is the development of new tools of murder and mayhem a plus for anyone, or does *Nature* — or at least its Washington editor — hold the view that science prospers when humanity is threatened?

MARK NOBLE  
MICHAEL KLIMKOWSKY  
TOM VOLLIAMY  
JACK PRICE

Department of Zoology,  
University College London,  
London, UK

## Man's biosphere

SIR — I was sorry to see, in the unsigned editorial on Unesco (*Nature* 6 November, p.2), the passing reference to the Unesco "Man and the Biosphere Programme" as "chiefly valuable as sources of largely empty generalizations". Whoever wrote this editorial must have done so from a position of almost total ignorance of the MAB Programme. A research programme which has been endorsed by 79 countries, with more than 960 field projects, and involving more than 5,000 scientists is no empty generalization.

It is, of course, true that government departments and agencies in this country have shown relatively little interest once they have discovered that there is no "pot of gold" which can be readily tapped, as in the International Biological Programme. Nevertheless, scientists in research council institutes and in British universities have made, and are continuing to make, valuable contributions to the research of Third World countries in Asia, Africa and South America. They and their colleagues in these countries will be surprised, if not angry, at the glib dismissal of one of the most exciting and ambitious environmental research programmes as insignificant.

J.N.R. JEFFERS

Institute of Terrestrial Ecology,  
Merlewood Research Station,  
Grange-over-Sands,  
Cumbria, UK

## Scientific warfare

SIR — R.A. Davis (*Nature* 6 November, p.8) has failed to notice that science and scientists do not exist in a social vacuum. Applications of technology generally raise questions concerning its impact on society and it is irresponsible for scientists to ignore these questions, especially when the technology concerned is to be applied to warfare.

One cannot help but be concerned when the US Army is interested in research directly related to chemical weapons, particularly since the recent go-ahead for the construction of a binary nerve gas plant. The United States is a signatory to several international agreements which specifically prohibit the use of these weapons — weapons which are indiscriminate in their effects upon noncombatants. To suggest that the development of an antidote will render these weapons useless is akin to suggesting that building fallout shelters makes the world safer from nuclear war.

It is incumbent on the participants of a democratic society to call attention to, and question policies which they do not believe serve the common good. When these participants are scientists and the policy concerns science then the pages of *Nature* are indeed the appropriate place to raise the issue.

DAVE VAN BUREN

Astronomy Department,  
University of California,  
Berkeley, California

## NEWS AND VIEWS

## Sun-climate links

from T. M. L. Wigley

DOES the Sun vary in ways which could affect our climate and, if so, are these variations sufficiently large to have noticeable effects? The question of the Sun's influence on climate was examined in detail at a recent conference\* where new data and recent advances in solar physics and Sun-climate links were presented.

If the Sun is to affect the Earth's climate, then some part of the Sun's output must vary. So far, the only variations observed seem unlikely to have a direct impact on climate. The solar 'constant' (that is the radiation output in the visible region, 300–400 nm, which accounts for 99 per cent of the Sun's energy flux) may not be a constant but evidence for its variability on annual and greater time scales is inconclusive. P. Foukal (Atmospheric and Environmental Research) reviewed this evidence and pointed out that changes have been observed directly only on shorter time scales; for example, those associated with the 27-day solar rotation period. The magnitude of these changes is extremely small, less than 0.1 per cent.

Longer-period and much larger-magnitude changes are well documented at shorter ultra-violet (UV) wavelengths. The magnitude of these fluctuations becomes larger as wavelength decreases, at least down to around 120 nm (Ly $\alpha$ ). D. Heath (NASA, Goddard Space Flight Centre) presented intriguing evidence that the direction of change over the past ten years has been different above and below 190–210 nm, with indications that these changes are associated with either the 11-year sunspot cycle, or the 22-year magnetic cycle.

Particle fluxes associated with the solar wind and recorded by their effect on the

Earth's magnetic field also follow the solar cycle. P. Simon and J. P. Legrand (Observatoire de Meudon and Laboratoire de Geophysique, EXTERNE-CNRS, Saint-Maure respectively) argued on physical and statistical grounds that the solar wind has two distinct components. The frequency of high-energy (10–100 MeV) proton events from solar flares and heliomagnetic disturbances, although the disturbances themselves are only short-lived (up to 100 min), varies approximately in phase with the sunspot cycle, while the lower-energy (around 1 MeV) particles emanating continuously from (mainly polar) coronal-hole regions show an out-of-phase relationship, the two combining to give a complex pattern of cyclic variations which is mirrored by variations in the Earth's magnetic field. These geomagnetic cycles have already been studied by Crooker *et al.* (*J. geophys. Res.* **82**, 1933, 1977) and by Feynmann and Crooker (*Nature* **275**, 626; 1978).

Just how UV and particle flux changes might affect climate is uncertain as direct effects, resulting from photochemical processes, are only observed in the stratosphere or above. We do not yet know how (or whether) these effects can be translated to the troposphere. Various mechanisms have been proposed (summarized by J. J. Berthelier, Laboratoire de Geophysique, EXTERNE-CNRS, Saint-Maure, and by A. P. Mitra, National Physical Laboratory, New Delhi) involving stratospheric aerosols, dynamic coupling between troposphere and stratosphere, changes in the Earth's electric field and/or direct radiative effects. These mechanisms are still speculative and require more detailed theoretical study and empirical testing; although the latter is hampered by the quality of currently available data. For example, although there is clear evidence that the solar proton event of 4 August 1972 affected stratospheric ozone, changes in ozone on longer (year-to-year) time scales have not yet been convincingly linked to solar activity (see Pittock *Rev.*

*Geophys. & Space Phys.* **16**, 400; 1968; Dutsch *J. atmos. Terr. Phys.* **41**, 771; 1979).

Statistical evidence of tropospheric changes associated with day-to-day solar variations was presented by J. M. Wilcox (Stanford University). Wilcox and his colleagues (see *J. atmos. Sci.* **33**, 1113; 1976) have found a relationship between the vorticity area index and the passage of solar magnetic sector boundaries, but the reality of this as a stable phenomenon has been questioned (Williams & Gerety *Nature* **275**, 200; 1978; Shapiro *J. atmos. Sci.* **36**, 1105; 1979). Russian work of a similar nature, reported by E. R. Mustel and co-workers (Astronomy Council of the Academy of Sciences of the USSR), apparently shows significant changes in surface pressure patterns 2 to 4 days after intense geomagnetic storms. Both of these phenomena are most evident in regions of large baroclinicity and in winter. It was suggested that this might imply some conditionally unstable initial condition in the atmosphere which is triggered in some way by a solar event, although recent modelling work by B. G. Hunt (*J. geophys. Res.* in the press) does not support this hypothesis. Further work is required before the reality of these short-term Sun-weather links is firmly established.

On the decadal time scale, tropospheric effects associated with the 11- or 22-year solar cycle remain controversial (see Pittock *Rev. Geophys. & Space Phys.* **16**, 400; 1978; *Nature* **283**, 605; 1980) and lack causal links. Interesting statistical relationships shown by R. G. Vines (CSIRO Division of Chemical Technology) and by C. J. E. Schuurmans (Royal Netherlands Meteorological Institute) (see also Schuurmans *Climatic Change* **1**, 231; 1978) point to a solar influence on the general circulation and may relate to the

T. M. L. Wigley is in the Climatic Research Unit, University of East Anglia, UK.

\*'Sun and Climate', Toulouse, France, 30 September – 3 October was sponsored by the Centre National d'Etudes Spatiales, Centre National de la Recherche Scientifique and the Délégation Générale à la Recherche Scientifique et Technique. The proceedings of this conference will be published by the Centre National d'Etudes Spatiales as a companion volume to *Evolution of Planetary Atmospheres and Climatology of the Earth* (the proceedings of a conference in Nice in 1978; *Nature* **276**, 213; 1978).



recent solar-jet stream link found by Nastrom and Belmont (*J. geophys. Res.* **85**, 443; 1980).

On the century time scale, it was suggested long ago (de Vries *Koninkl. Ned. Akad. Wetenschap. Proc. B* **61**, 98; 1958) that changes in atmospheric  $^{14}\text{C}$  levels might reflect changes in solar activity and climatic change. This idea was cautiously revived by Eddy (*Climatic Change* **1**, 173; 1977), and recent work by Stuiver and Quay (*Science* **207**, 11; 1980) has quite firmly linked changes in atmospheric  $^{14}\text{C}$  to solar wind changes. Atmospheric  $^{14}\text{C}$  changes also run roughly parallel to the envelope of solar activity as measured by the mean number of sunspots over a sunspot cycle. The Maunder minimum (1645 to 1715), a period of reduced solar activity, was a time of high atmospheric  $^{14}\text{C}$ .  $^{14}\text{C}$  fluctuations like that seen during the Maunder minimum have occurred frequently in the past and further observations were presented by H. E. Suess (University of California, San Diego, see also *Endeavour* **4**, 113; 1980). We can thus be fairly certain that the Sun does vary on the 100-year time scale. Conclusive proof could come from measuring the minute concentrations of cosmogenic  $^{10}\text{Be}$  found in ice cores, using accelerator spectrometry (G. M. Raisbeck and F. Yiou, Laboratoire Renais Bernes du Centre de Spectrométrie, Nucleaire). Although these isotopic ( $^{14}\text{C}$  and  $^{10}\text{Be}$ ) variations do not in themselves indicate changes in solar output in the visible part of the spectrum, there is some indirect evidence of such changes. Changes in the Sun's radius should be accompanied by changes in luminosity (Sofia *et al. Science* **204**, 1306; 1979) and

radius changes can be calculated from eclipse data. Using material from the eclipse of 3 May 1715 collected originally by Sir Edmund Halley, NASA scientist, S. Sofia (Goddard Space Flight Centre), suggested that the Sun was about half an arc second bigger (and thus brighter) in 1715 than today. However, Parkinson (*New Scientist* 24 April, p203, *Nature* in the press;) has also examined eighteenth century eclipse data and deduces no changes in solar radius.

The link between atmospheric  $^{14}\text{C}$  activity and the Sun is through the solar wind, and does not yet encompass changes in the solar constant. A statistically significant link between  $^{14}\text{C}$  and climate had not yet been established either, in spite of the rough coincidence in timing between the Maunder minimum and the Little Ice Age. Thus, as for shorter time scale solar fluctuations, the Sun-climate link on the century time scale is still not proven. Recent work by Stuiver (*Nature* **286**, 868, 1980) has revealed only a few, barely significant correlations between reconstructed variations in solar activity (based on atmospheric  $^{14}\text{C}$  variations) and climate data over the past 1,000 years. Results presented by L. D. Williams (University of East Anglia), T. M. L. Wigley and P. M. Kelly extend the analysis to the past 4,000 years and to a wider range of proxy climate variables, but still fail to find any statistically significant relationships. The main problem now is with the climate data base. On the 100-year time scale, our knowledge of the details of climatic change over the past millennia is very sketchy. As more palaeoclimatic information becomes available, the picture of past climates

becomes more and more complex. Although many significant fluctuations, similar qualitatively if not in magnitude to the Little Ice Age, have clearly occurred in the past, it is also evident that the response to solar forcing would involve circulation changes which might lead to considerable differences in trend and timing of, for example, temperature changes from place to place.

Changes in the Sun and in the Earth's climate on time scales significantly greater than 100 years, while of less immediate importance to mankind, are nevertheless fundamental to the understanding of the workings of the Sun and the climate system. Since the first solar model of J. Homer Lane in 1869, and especially in the last decade, solar physics has progressed enormously (reviewed by I. W. Roxburgh, Queen Mary College, London). The faintness of the youthful Sun (with luminosity only about 70 per cent of today's), predicted by stellar evolution theories is now quite firmly established and has led to a greater understanding of the importance of changes in atmospheric composition in determining changes in climate on the  $10^9$ -year time scale (Owen *et al. Nature* **277**, 640; 1979). But, as pointed out by M. B. McElroy (Harvard University), this factor is equally important today because of the large anthropogenic input of  $\text{CO}_2$  resulting from fossil-fuel burning.

On intermediate time scales, between the century time scale variations implied by  $^{14}\text{C}$  data and the long-term stellar evolution trend in solar luminosity, the possibility of fluctuations in the Sun's output is speculative yet still important. J.-C. Duplessy and A. Berger (CNRS, Gif-sur-Yvette) reviewed respectively the observational and astronomical evidence for the Milankovitch theory, which relates the periodic glaciations of the past few million years to changes in Earth orbital parameters. Although the evidence for this theory is very strong, it is still difficult to explain how the small total changes in incoming radiation, which result from orbital changes, can produce such major climatic effects. The key lies in the nature of orbit-related changes in radiation input, which occur not in total input, but in the seasonal and latitudinal distribution of incoming radiation. Although the global average change in radiation is only 0.1% or less, local variations of more than 10% can occur and the effects of even small changes can be amplified by ice-albedo and other feedbacks.

A more significant problem with the Milankovitch theory is that the observational data available for the past 400,000 years shows the strongest periodicity of radiation at 100,000 years with lesser peaks at around 40,000 and 20,000 years (Hays *et al. Science* **194**, 1121; 1976), while the astronomical data implies that the 100,000-year peak should be relatively less prominent. Hays *et al.*



## 100 years ago

Herr V. Bergso, in a recent work, "Fra Mark og Skov," has given some interesting data in regard to the habits of the Tarentula, *Lycosa tarentula*, Latr., whose nests he has traced and examined on the Roman Campagna. He found that the nest, which was well rounded and smooth, was approached by a tunnel which, after running about a foot straight down below the surface of the ground, made a sudden short turn before it finally descended for about another foot into the spider's abode. The superstitious error of assuming that the bite of the animal induces an irresistible desire of dancing is due to the fact, that dancing having been originally employed as a remedy against the poison, which is believed to be eliminated by profuse perspiration, the action of the poison was confounded with the means of its eradication.

"We the undersigned, captain, officers, and crew of the barque *Pauline* (of London) of Liverpool, in the county of Lancaster, in the United Kingdom of Great Britain and Ireland, do solemnly and sincerely declare that on July 8,

1875, in lat.  $5^{\circ}3'$  S., long.  $35^{\circ}$  W., we observed three large sperm-whales, and one of them was gripped round the body with two turns of what appeared to have a length beyond the coils of about 30 feet, and its girth 8 or 9 feet. The serpent whirled its victim round and round for about fifteen minutes, and then suddenly dragged the whale to the bottom head first.

"GEORGE DREVAR, MASTER  
"HORATIO THOMPSON  
"JOHN HENDERSON LANDELLS  
"OWEN BAKER  
"WILLIAM LEWARN

"Again, on July 13, a similar serpent was seen about 200 yards off, shooting itself along the surface, head and neck being out of the water several feet. This was seen only by the captains and one ordinary seaman, whose signatures are affixed.

"A few moments after it was seen elevated some sixty feet perpendicularly in the air by the chief officer and the following able seamen, whose signatures are also affixed —

"HORATIO THOMPSON  
"WILLIAM LEWARN

"And we make this solemn declaration, &c.  
"Severally declared and subscribed at Liverpool aforesaid the 10th day of January, 1877, before

"T. S. RAFFLES, J.P. for Liverpool."  
From *Nature* **23**, 25 November, 84, 1880.



suggested that this may be related to a non-linear response. Two different explanations were presented here. C. Nicolis (Institut d'Aeronomic Spatiale, Belgium) presented a very simple model which showed how internal feedbacks could amplify an otherwise weak 11- or 22-year sunspot-related signal. A very different model developed by J. Oerlemans and J. M. Bienfiet (Royal Netherlands Meteorological Institute; see also *Nature* 287, 430; 1980) also produces a 100,000-year periodicity in the climate record, but in this case resulting entirely from internal factors related to isostatic rebound. This interesting result may, paradoxically, support the

Milankovitch theory. The strength of the 100,000-year periodicity is not constant and almost vanishes about  $10^6$  years BP. This would be hard to understand if the cause were purely internal, but less so if climatic changes were the result of orbital forcing. The lack of a 100,000-year periodicity in the early climate record may be related to the fact that perennial sea-ice cover in the Arctic only began around 700,000 years ago (Margolis and Herman *Nature* 286, 145; 1980). However, it may well be that around  $10^6$  years BP, the orbital parameters themselves, if more accurately known, have no 100,000-year signal.

deep in northern latitudes) or thinner blankets in persistent oceanic, montane or tundra conditions. In the tropics peat is normally located in badly drained, riverine and coastal flats but can also occur in wet, cool climates at high altitudes. Tropical peats are usually deeper (up to 20m or more have been recorded) and contain many more macro-remains of vegetation plus mineral matter than their temperate counterparts.

The value of peat as an alternative energy source has perhaps been under-assessed and a broad spectrum of work is now being undertaken to harness its potential more effectively. Canadian authorities estimate that there is more energy potential in their peat deposits than in their forests or their reserves of natural gas. The National Energy Board calculates Canadian peat reserves at 89 billion tons which is equivalent to 500 trillion cubic feet of natural gas. The peat reserves of the US are put at 13 billion tons and the US Department of Energy has recently allocated \$2.2 billion for the development of alternative fuels, including peat as a major component. In the USSR peat fuels no less than 76 large electric generating plants. The Republic of Ireland generates one-third of its electricity and one-fifth of its total energy requirement from peat. Finland is in a stage of rapidly advancing technology in this field and it is estimated by 1990 that up to 8 per cent of the national energy requirement will be met from peat. Peat consumption in Europe has reached a point where regional producers cannot meet the demand. In the United Kingdom,

## Peat — a resource reassessed

from J. A. Taylor and R. T. Smith

REPORTS at the Sixth International Peat Conference\* suggest a need for a fundamental reassessment of the world's peat resources in industrial, agricultural and environmental terms. The total area of the world's peatlands is now estimated to be about 500m ha, equivalent to an area over half that of the United States. Canada (150m ha, 36%) and the USSR (170m ha,

40%) together monopolize over three quarters of the world's peatlands but there are also extensive tropical peatlands in the lowlands of S. America, Central Africa and parts of SE Asia.

Peat is organic matter derived from the slow decay of plant remains by the action of bacteria and fungi. Decay is finally arrested in the absence of free oxygen and sunlight, normally under conditions of ground or soil waterlogging which may be aided by an accompanying wet and cool climate. Peat may thus accumulate in badly drained basins forming mires (up to 10-m

J. A. Taylor is University Reader in Geography, University College of Wales, Aberystwyth and R. T. Smith is a Lecturer in Geography, University of Leeds.

## Genes controlling cell proliferation

from Paul Nurse

AN attractive hypothesis for the control of eukaryotic cell proliferation is that it is regulated at a particular point during the  $G_1$  period before the initiation of DNA replication. This  $G_1$  control has been called the 'restriction point' in mammalian cells (Pardee, A. B. *Proc. natn. Acad. Sci. U.S.A.* 71, 1286; 1974) and 'start' in the budding yeast *Saccharomyces cerevisiae* (Hartwell, L. H. *Bact. Revs.* 38, 164; 1974; *J. Cell Biol.* 77, 627; 1978). Cells made quiescent in a variety of ways become blocked at this  $G_1$  control point, and cells shifted to conditions favouring proliferation have to pass this point before they become committed to the mitotic cell cycle. The control has been investigated genetically in *S. cerevisiae* by Hartwell and his colleagues, who have identified a gene *cdc 28* whose function is required before 'start' can be traversed. These workers

have suggested that before a cell traverses 'start', it monitors various conditions such as cell size, nutrient level, and the presence of conditions promoting conjugation and sporulation. If these conditions are satisfactory for cell proliferation, the cell begins a new mitotic cell cycle, but if they are not, the cell either becomes quiescent and enters stationary phase, or differentiates and undergoes conjugation or sporulation.

A recent study that has extended this genetic analysis in *S. cerevisiae* is described by Sudbery, Goodey and Carter in the current issue of *Nature* (p 401). They have isolated a novel series of mutants defining two *whi* genes, which undergo bud emergence and cell division at a reduced cell size compared with wild type. The *whi 1* mutants show a reduced cell size both during exponential growth and in stationary phase, whilst the *whi 2* mutation has a major effect only in stationary phase. When these mutants are made quiescent by deprivation of nutrients, they do not enter

stationary phase by becoming blocked at 'start'. They stop increasing in mass but they continue to initiate new cell cycles and to undergo division. When they eventually do stop proliferating, they are of a reduced cell size and have a reduced cell viability compared with wild type, and are also blocked in later stages of the cell cycle than the normal block point 'start'. These mutants are clearly defective in the gene functions required for an orderly transition of cells from the proliferating state to the quiescent state.

It has been suggested that mammalian cells may become malignant if they lose their 'restriction point' control (Pardee op. cit.), and as a consequence cells fail to accumulate at the proper point in  $G_1$  when shifted to conditions favouring quiescence. If this is the case, then the *whi* mutants may be analogous to some types of malignant cell lines. Therefore, the further study of the *whi* and *cdc* 'start' mutants may also have implications for the problem of malignancy in mammalian cells.

Paul Nurse is in the School of Biological Sciences, University of Sussex.



the peat cover is quite extensive but to date has been regarded as too thin, too variable, too remote (that is, in the uplands) and not economically harvestable — a situation that may change with the introduction of new technology.

The most costly and time consuming aspect of peat exploitation is the treatment of the peatland before harvesting and the initial winning and drying of the peat. The technology for these purposes already exists, thanks to forest industries which have already solved many of the problems of mire drainage. In northern lands the short harvesting season has led to much effort being put into mechanization and into improving techniques to remove the water from either sods or milled peat. In Sweden, a centrifugation and belt press process has been developed which can process 6 cubic metres of peat slurry per hour down to 50 percent dry substance (that is, water content reduced to 50 per cent by weight). From Finland comes a method of de-watering peat — the wet carbonization process — which produces dry pellets of partly carbonized peat, perhaps the most marketable product of the peat industry. Milled peat production is becoming more adaptable to mechanization, and subsequent processing is far and away more prevalent than traditional sod peat cutting. However, Finnish experience suggests that on the local scale at modest production, sod peat enterprises are likely to remain the more cost-effective. Peat is a most inconvenient source of energy compared to gas or oil but various gasification and liquefaction schemes are currently being tried out and may lead to major improvements. In these schemes processing plants will be located on the peat lands themselves as they are usually at great distances from centres of energy consumption. Peat-burning power stations, operated mainly by briquette peats, are commercially successful in the Soviet Union, Finland and Ireland but because of the variable consistency and calorific value of the peat, such stations are at least 5 percent less efficient than coal-fired ones.

As well as its value as an energy source, there appear to be many potential uses of peat as a raw material. Successful attempts have been made to use peatland for sewage disposal, on account of its great absorption capacity and its effectiveness in sequestering metallic cations. Other uses of peat include its role in activated carbon manufacture as a catalyst when treated with heavy metals, as a source of pharmaceutical and curative preparations, as a possible starting point for fertilizer manufacture, as a soil conditioner and even as a food additive.

The revaluation of the commercial potential of peat raises the question of the

possible harmful effects of its exploitation. The vast areas of peat function as stores of carbon, Bramryd (University of Lund) estimating that the annual average global rate of peat accumulation is 0.7mm — equivalent to about  $0.21 \times 10^{15}$  gC. Clearly, large-scale exploitation of peat and, in northern latitudes, interference in the fragile tundra ecosystem could help to trigger changes in the CO<sub>2</sub> balance. Only 10 per cent of the world's middle-latitude mires, mostly in Europe, USSR, USA and Canada, remain untouched. Accessibility for peat extraction and agricultural and

forestry development has been their demise.

New surveying techniques of peatlands are involving remote sensing, satellite imagery and georadar, notably in Sweden (Ultiksen, Lund Institute of Technology) the US (Hagen & Meyer, Minnesota Department of Natural Resources) and Scotland (Robertson, Macaulay Institute of Soil Research, Aberdeen). Automated monitoring of peatlands will boost not only scientific research into mires but also, ironically, their commercial exploitation in 'non-renewable' fashion.

## Photochemical conversion and storage of solar energy

from Professor Sir George Porter, FRS

PHOTOCHEMICAL decomposition of water into its elements is potentially of great importance. It is theoretically possible in sunlight with efficiencies exceeding 10 per cent, and there are several routes to success which seems tantalizingly close. Yet so far, no satisfactory and efficient system has been discovered. This is the stuff that photochemists' dreams are made of and it is not surprising that many of them are now as excited as the molecules which characterize their craft.

The Third International Conference on 'Photochemical Conversion and Storage of Solar Energy' brought together most of the active research workers in this field under the Colorado sun and appropriately close to the new Solar Energy Research Institute which sponsored the very successful and well organized conference on photochemical conversions held in September. One hundred and fifty papers were presented, either as plenary lectures or as posters, all of which were on view and open for discussion throughout the week — a most satisfactory arrangement.

It was clear from the beginning that the principal interest of the participants would be in the rapidly developing subject of the conversion of light into chemical potential by methods which, although inspired by the mechanisms used in natural photosynthesis, are entirely abiological or artificial or, if you must, 'biomimetic'. Dr Mary Archer's (University of Cambridge) review of photogalvanic cells for electrical-power generation was decidedly pessimistic and there have been no significant advances in the use of photochemical reactions for the storage and release of

thermal energy. On the other hand, liquid-junction photovoltaic cells are developing rapidly and appear quite promising.

The photochemical reaction which attracts most attention at present is the production of hydrogen and oxygen, by the visible-light photolysis of water. The methods by which this desirable objective might be achieved range from biological ones, which retain some part of the *in vivo* system, for example isolated chloroplasts, through completely homogeneous photochemical reactions in solution to photoelectrochemical cells with one or two semiconductor electrodes, of the type originally used by Fujishima and Honda.

The apparently large gap between the last two is now, however, bridged, first by the use of colloidal metals and semiconductor suspensions in solution and, second, by the use of 'photochemical diodes' which consist of 'wireless' particles in which the two electrodes, usually a metal and a semiconductor, are in direct contact in a single entity which may be microscopically small. There is now an almost continuous transition between these different approaches and much success is being achieved with photochemical electron-transfer reactions in solutions which contain suspensions of such catalytic particles.

One of the principal difficulties in bringing about the liberation of gaseous hydrogen and oxygen in electron-transfer reactions in solution has always been that hydrogen requires the accumulation of two electrons while oxygen requires the accumulation of four. In an electrochemical cell these processes occur

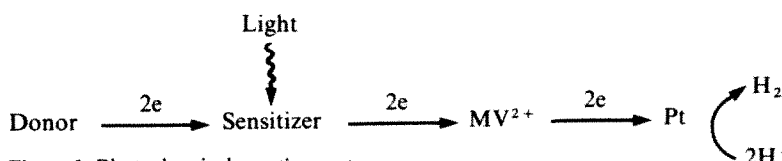


Figure 1: Photochemical reaction system

\*The Sixth International Peat Congress was held in Duluth, Minnesota from August 17th to 23rd, 1980. Over 600 delegates from 25 countries attended, including, for the first time, scientists from China, Japan, New Zealand and Burundi.

at the electrodes and, if the overpotential is to be made as small as possible, platinum is usually preferred for hydrogen liberation at the cathode and ruthenium dioxide for oxygen liberation at the anode. The most important advance of the last few years has been the discovery that suspensions of these two substances will catalyse the evolution of hydrogen and oxygen in homogenous solution. Recent progress was reviewed by two of the principal contributors to this progress, Jean Marie Lehn (Strasbourg) and Michael Gratzel (Lausanne).

The natural photosynthetic system carries out the oxidation and reduction in separate steps, with a redox couple of quinone/hydroquinone between them, and most research has been concerned with one or other of these processes, using a sacrificial donor for the hydrogen elimination and a sacrificial acceptor for the oxygen liberation half-reactions. The water reduction reaction has been studied in many laboratories, nearly all of which use the system shown in Fig. 1.

$MV^{2+}$  is methyl viologen (paraquat), which acts as electron carrier, and the sacrificial donor is usually EDTA, although many other substances which are irreversibly oxidized are equally satisfactory. As sensitizer, ruthenium

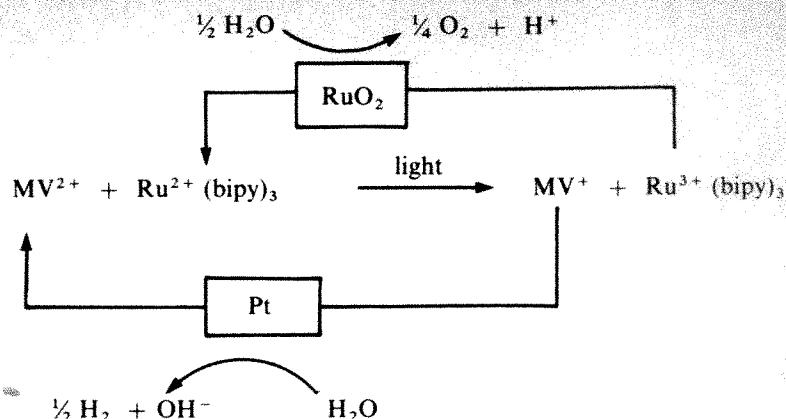


Figure 2: A four component system for the photochemical decomposition of water

trisbipyridyl has been most popular but water-soluble porphyrins have been used more recently and have many advantages; quantum yields of hydrogen production as high as 60 percent in green light were reported with zinc tetramethylpyridyl porphyrin as sensitizer.

The oxidation half-reaction, liberating oxygen, is in a less satisfactory state and, although ruthenium dioxide does act as a catalyst and liberates oxygen in the presence of an electron acceptor of sufficiently high redox potential, overall yields are low. Most surprisingly however, Gratzel and Kalyanasundaram reported oxidation and reduction with the simultaneous evolution of hydrogen and oxygen in a single system without sacrificial

electron donors or acceptors. The system was of four-components containing both catalysts, with methyl viologen as carrier and ruthenium trisbipyridyl as sensitizer (see Figure 2).

Of course, the liberation of hydrogen and oxygen together is not altogether desirable. Yields are low and the mechanism is not clearly understood; if confirmed it must obviously involve some specific kinetic selectivity of the redox components for the two catalysts.

In a highly competitive and developing field of research, preliminary reports which await confirmation are not uncommon. But this was a stimulating symposium in which everybody shared the excitement of a rapidly developing science.

Professor Sir George Porter, FRS, is Director of The Royal Institution

## Far-infrared interstellar carbon

from a Correspondent

IN interstellar clouds, carbon is taken up partly in dust grains and partly in the gas phase, where it is distributed between ionized carbon  $C^+$ , neutral carbon  $C$  and various molecules, mostly carbon monoxide with lesser amounts of other compounds such as  $HCN$ ,  $H_2CO$ ,  $HCO^+$ ,  $CH$  and  $CH_2$ . Because  $CO$  is widely taken as a measure of the densities of clouds in which  $H_2$  is the major constituent, the fraction of  $C$  existing as  $CO$  is a critical parameter in the determination of the cloud masses.

Observations of  $CO$  also provide information on the galactic isotopic ratio of  $^{12}C$  and  $^{13}C$  but, because of chemical exchange reactions, the relationship between  $^{12}C$  and  $^{13}C$  and the parent  $CO$  molecules depends, through a complicated chemical reaction scheme, on the density, temperature and age of the clouds. Information on the abundances of  $C$  and  $C^+$  would thus help to make more certain the estimation of cloud masses.

Most of the radiant energy emitted by the gaseous component of interstellar clouds is contained in fine-structure transitions of  $C$  and  $C^+$  and rotational transitions of  $CO$ . Emissions in the 1-0 and 2-1 rotational transitions of  $CO$  have been

measured at 1.3 and 2.6 millimeters, but it is the higher-lying transitions in the sub-millimeter region which contribute most of the cooling.

Recently the  $^3P_1$ - $^3P_0$  fine-structure transition of neutral carbon, the  $^2P_{3/2}$ - $^2P_{1/2}$  fine-structure transition of ionized carbon and the 6-5 rotational transition of  $CO$  have been detected from interstellar space. Laboratory measurements at the National Bureau of Standards using far-infrared laser magnetic resonance (R.J. Saykally and K.M. Evenson *Ap. J. Lett.* **238**, L107; 1980) established that the  $^3P_1$ - $^3P_0$  transition of  $^{12}C$  has a frequency of 492.1623(7) GHz (and that the  $^3P_2$ - $^3P_1$  transition has a frequency of 809.3446(29) GHz). These accurate measurements made possible a search for and led to the discovery of the  $^3P_1$ - $^3P_0$  emission from several molecular clouds in the interstellar gas (T.G. Phillips, P.J. Huggins, T.B.H. Kuiper and R.E. Miller *Ap. J. Lett.* **238**, L103, 1980). The detection system used an InSb heterodyne bolometer receiver. The bandwidth is only 1 MHz and several observations were necessary to record a single Doppler-broadened spectral line.

A heterodyne system has also been used,

but with a GaAs mixer diode, to observe the 6-5 rotational transition of  $CO$  at 692.9495 GHz (P.F. Goldsmith, N.R. Erickson, H.R. Felterman, B.J. Clifton, D.D. Pack, P.E. Tannenwald, G.A. Koept, D. Bull and N. McAvoys, *Ap. J. Lett.* in the press) in emission from the Kleinman-Low plateau source in the Orion molecular cloud.

The  $^2P_{3/2}$ - $^2P_{1/2}$  transition of  $C^+$  has a frequency of 1910 GHz and it has been detected towards the interstellar regions NGC 2024 and M42 (R.W. Russell, G. Melnick, G.E. Gull and M. Harwit *Ap. J. Lett.* in the press). The Cornell group used as a detector a stressed Ge:Ga photoconductor, cooled to 2K by pumping with liquid helium coolant, and a grating spectrometer (J.R. Houck and D. Ward, *Pub. A.S.P.* **91**, 140, 1979).

These papers demonstrate that a new region of the electromagnetic spectrum is accessible to observation. Sub-millimeter astronomy permits the direct observation of the major energy losses from the gaseous components of many regions of the interstellar gas and will provide powerful diagnostic probes of the physical environment in interstellar clouds where star formation is in progress.



# Microbial degradation of xenobiotic compounds

from Philip R. Lehrbach

MOST organic compounds released into the environment are rapidly broken down by the activities of fungi and bacteria. However, certain man-made compounds (xenobiotics) are not quickly degraded. Public concern over the persistence of such compounds stems from their accumulation in food chains and their toxicity to living organisms. Xenobiotics in the form of pesticides, dye stuffs, surfactants and the waste products of industrial processes require detoxification before they are allowed to enter the environment and new techniques are needed to bring this about.

At a recent meeting\* convened to discuss the capabilities of microbes and microbial communities to degrade exotic compounds, several strategies were considered from the viewpoints of industrial chemists, microbiologists and molecular biologists. H. Bretscher (Ciba-Geigy, Basel) discussed various methods for the total chemical and physical destruction of many xenobiotic compounds. Thermal degradation at incineration temperatures of 1,100°C, and the less developed but lower energy-consuming wet air oxidation (300°C) process were mentioned. But these processes have the disadvantages of high-energy expenditure and the total destruction of a potentially useful resource. In the future, economic constraints may dictate the use of biotechnical methods for the treatment of effluent. Such methods would be aimed at eliminating the environmental dangers while providing the basis for recovery of useful organic compounds used in the production of chemicals or microbial proteins.

Procedures are available (batch or continuous culture) for the isolation of bacteria or fungi able to grow on a particular organic compound. However, it is difficult to adapt these isolates so that they perform the same degradative function in the complex mixture of organic chemicals and salts present in industrial effluent. Reviewing the topic, W. Harder (Rijksuniversiteit Groningen, Haren) said that failure to isolate a pure culture able to utilize a particular compound may indicate that metabolism involves a community of bacteria and/or fungi. Important parameters such as culture conditions, interfaces, salt or acid gradients may have been overlooked. One example among many which illustrates the complexity of degradative processes is dichlorodiphenyltrichloroethane (DDT) metabolism. DDT is slowly broken down anaerobically to *o*-dichlorophenylmethane by

*Aerobacter aerogenes*. This compound is then co-metabolised by *Hydrogenomonas* to other less-toxic, chlorinated compounds.

One approach to the problem of waste disposal (D. Munnecke, University of Oklahoma), which applies a detailed knowledge of enzyme technology but eliminates the frailty of the living organism, is to supply the appropriate inactivating enzyme to a contaminated area. Such an approach has been taken to detoxify contaminating amounts of the insecticide parathion from liquid waste effluent and industrial or domestic containers. In this case parathion is detoxified to *p*-nitrophenol in the presence of the enzyme hydroxylase. This enzyme can be used successfully in soluble (whole cell or partially purified) or immobilized (glass matrix) form. This example serves as a useful model for the development of other enzyme systems. However, several limitations are placed on this method of waste disposal. The enzymes used must be readily obtainable at relatively low cost, simple in their application particularly for domestic uses, stable, and not require an expensive cofactor to function. To justify this approach the chemicals to be inactivated must be of considerable environmental and public hazard (as was the case with parathion). The quantity and dispersal of the compound must be sufficient to require a concerted effort for its eradication.

U. Gasche (Cellulose Attishelz, Luterbach) and H. Kern (Institut für Botanik und Microbiologie, Jülich) focused on the complex problems of dealing with effluents from cellulose manufacturers. To achieve high yields of cellulose fibres, mechanical and chemical treatment of wood is necessary to convert lignin into physically and chemically altered derivatives which become a predominant by-product in the effluents. Lignosulphonates are lignin products formed in the acidic sulphite pulping process and are more resistant to microbial degradation than lignin itself. H. Kern discussed the possibility of enzymatic removal of the sulphonate acid groups and the subsequent bio-oxidation of the desulphonated products. He quoted data of Ban *et al.* (*Biotechnol. Bioengng* 21 1917; 1979) on mixed cultures containing yeasts and bacteria as an approach to economically feasible processing systems.

An understanding of the numerous biochemical pathways necessary for the bacterial degradation of various organic compounds is well advanced. Several participants suggested that this knowledge

could be used to develop bacteria with new metabolic capabilities. The reasoning is that bacteria able to degrade organic compounds that are structurally related to xenobiotics may be 'modified' to metabolize these new compounds. Modification using established mutation/-selection procedures or the specific genetic manipulation of appropriate genes determining catabolic enzymes to form new biochemical pathways were suggested. Such an approach has already been taken in the construction of haloaromatic-utilizing bacteria (H.-J. Knackmuss, Institut für Mikrobiologie, Göttingen, see *Nature* 277, 385; 1979). A similar approach was suggested from an appreciation of the metabolic diversity of methane-utilizing bacteria (methanotrophs) (I. J. Higgins, D. J. Best and R. C. Hammond *Nature* 286, 561; 1980).

Several important recent developments in molecular biology make this approach attractive to biotechnologists and may aid in the industrial exploitation of these organisms. First, the discovery that many catabolic pathways, including the degradation of substituted aromatic compounds (toluene, xylenes, naphthalene and styrene), are determined by the presence of transmissible plasmids. This makes possible the transfer of metabolic capabilities between various Gram-negative bacteria. Second, powerful new *in vivo* and *in vitro* techniques for the analysis and manipulation of genetic material permit rapid characterization of the structure and regulation of important degradative pathways, precise manipulation of the expression and the construction of multipathway organisms. The recent development of suitable vector systems in *Escherichia coli* and *Pseudomonas* (M. Bagdasarion and K. Timmis, Max-Planck Institut für Molekulare Genetik, Berlin) make this approach feasible.

The molecular analysis of the plasmid involved in the degradation of toluene and xylenes (the TOL plasmid) is probably the most advanced. F. H. C. Franklin and K. Timmis (Max-Planck Institut für Molekulare Genetik, Berlin) presented a functional map of the catabolic enzymes of the TOL plasmid based on the phenotypic properties of Tn5 (kanamycin resistance) insertion mutants. In this manner three genes, including the *xylE* gene encoding 2, 3-oxygenase, were located. A subsequently cloned *XhoI* restriction fragment (*XhoI*-I) verified these data and showed expression of catechol 2, 3-oxygenase activity in the *Pseudomonas* host strain. These and similar studies on various catabolic plasmids will provide important information for the future construction of organisms capable of the specific degradation of xenobiotic compounds. □

\*The 12th FEMS symposium on 'Microbial Degradation of Xenobiotic and Recalcitrant Compounds' held at Zürich, 15-19 September 1980. The proceedings will be published by Academic Press.

Phillip R. Lehrbach is in the Department of Molecular Biology, University of Edinburgh.

## ARTICLES

## X-ray properties of quasars

William H.-M. Ku, David J. Helfand &amp; L. B. Lucy

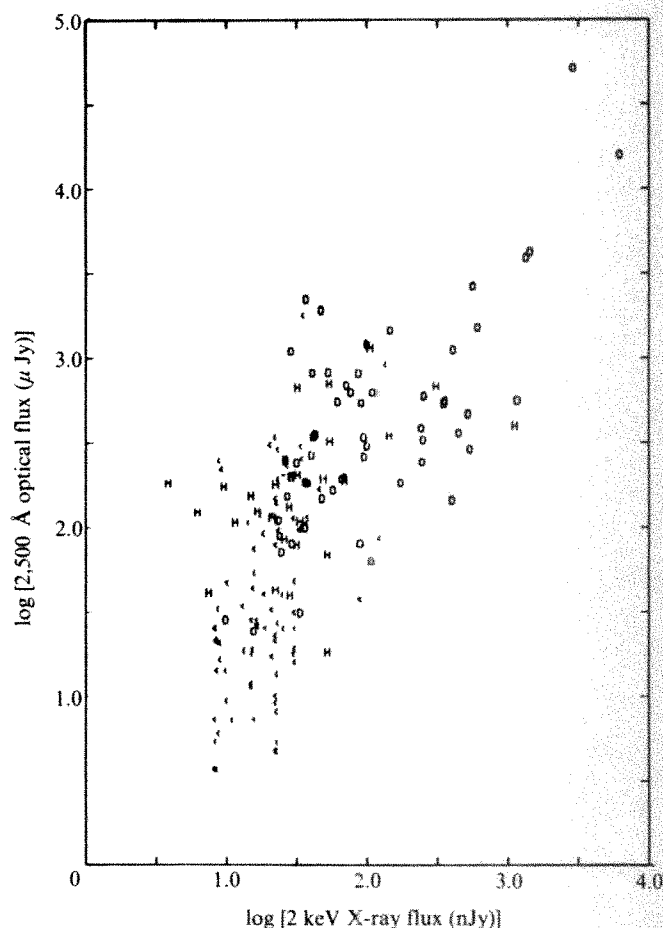
Columbia Astrophysics Laboratory, Departments of Astronomy and Physics, Columbia University, 538 West 120th Street, New York, New York 10027

*The X-ray properties of 111 catalogued quasars have been examined with the imaging proportional counter on board the Einstein Observatory. Thirty-five of the objects, of redshift between 0.064 and 3.53, were detected as X-ray sources. The 0.5–4.5-keV X-ray properties of these quasars are correlated with their optical and radio continuum properties and with their redshifts and variability characteristics. The X-ray luminosity of quasars tends to be highest for those objects which are bright in both the optical and radio regimes and which exhibit optically violent variability. These observations suggest that quasars should be divided into two classes on the basis of radio luminosities, spectra, evolution and underlying morphology and, thus, that quasars can make up a significant portion of the diffuse soft X-ray background only if the slope of the optical quasar log  $N$ –log  $S$  relation is steeper than 2 to  $m_B \approx 21.5$ .*

AS the most distant and luminous objects in the Universe, quasars have commanded considerable interest since their discovery nearly two decades ago. In the past few years, they have been surveyed by IR, UV, X-ray and  $\gamma$ -ray observers as well as optical and radio astronomers. X-ray emission from 3C273 was first recorded with a rocket-borne detector a decade ago<sup>1</sup>, but before the launch of HEAO 2 on 13 November 1978, only four other quasars had been detected: MR2251-178 (ref. 2), 4U0241+622 (ref. 3), NRAO 140 (ref. 4) and NRAO 530 (ref. 4).

The first results of an Einstein Observatory quasar survey<sup>5</sup>, however, make it clear that a significant new window, the soft X-ray band, has been opened for the study of these objects. Thirty-two of the 40 sources in that survey were detected in the 0.5–4.5-keV range, with luminosities from  $10^{43}$  to  $10^{47}$  erg s<sup>-1</sup>. These observations suggested that the summed contribution from the number of predicted optical quasars at faint magnitudes would exceed the diffuse soft X-ray background unless the optical quasar log  $N$ –log  $S$  relation is flattened significantly above  $m_B = 20$ , disagreeing with some optical measurements<sup>6</sup>. This surprising conclusion followed from the assumptions that: (1) the effect of the sample selection bias in favour of 'radio-bright' quasars was small, and (2) the effect of optical variability on the calculation of the X-ray-to-optical luminosity ratio could be ignored—simultaneous data at optical wavelengths were unavailable.

A second survey of quasars being carried out with the Einstein Observatory is reported here. Our sample consists of two components: a pointed survey in which 31 fields (one square degree each) containing 41 catalogued quasars were observed for an average of  $\sim 2 \times 10^3$  s, and a serendipitous survey in which each of our other  $\sim 500$  fields were examined for the presence of known quasars. The pointed survey sources were chosen to have a roughly uniform redshift distribution and to include many of the objects well studied in the radio and optical regimes. The 70 quasars in the other fields form a random collection of largely optically selected objects. Of this combined total of 111 quasars, 35 were detected as soft X-ray sources. For all of our observations, we have tried to obtain simultaneous optical measurements whenever possible but otherwise have tried to assess separately the contribution of the optically violent variables (OVVs) and to establish their optical-to-X-ray properties on the basis of nearly simultaneous measurements in the optical by A. Smith (personal communication). The initial results of this



**Fig. 1** Log of the flux at 2,500 Å (at the source) plotted against log of the flux at 2 keV (at the source). O, Objects with redshifts < 1; H, redshifts > 1; <, 3 $\sigma$  upper limits for objects. A clear positive correlation can be seen.

survey are reported, and their implications for quasar continuum emission mechanisms are considered. The significance of the revised values of X-ray brightness for the contribution of quasars to the diffuse soft X-ray background is also examined.



## Observations

All of the quasar measurements discussed in this article were obtained with the imaging proportional counter (IPC) on board the Einstein Observatory<sup>7</sup>. Thirty-five quasars met the detection criteria of a counting rate  $\geq 3\sigma$  above the background and coincidence within 80 arc s of the optical position (that is, within the 90% confidence X-ray error circle). For the stronger sources ( $>5\sigma$ ), the positional coincidences were all better than 50 arc s. The common names of the 111 quasars examined, their positional designations, their redshifts  $z$  and the times of the observations are given in Table 1.

The IPC has sufficient time resolution to permit searches for flux variations down to time scales of milliseconds. Searches for flaring activity have been conducted for the 10 sources with counting rates  $>0.05$  counts  $s^{-1}$ . No statistically significant variations ( $>3\sigma$ ) were found on time scales of 10–1,000 s. However, several of the sources have been observed more than once several months apart. In some of these cases, large ( $>100\%$ ) changes in the flux were recorded. These variability studies will be discussed elsewhere in conjunction with simultaneous observations obtained in other spectral regimes by ground-based observers.

As well as recording the arrival time and position of each photon, the IPC also provides crude spectral information. Although residual systematic uncertainties in the calibration of the IPC have so far prevented detailed analysis of the X-ray spectra, we believe that the fluxes calculated, following the

procedure suggested by Tananbaum *et al.*<sup>5</sup>, are correct to within 30%. The  $(0.5-4.5)/(1+z)$ -keV flux incident on the Galaxy,  $S_x$ , is used to calculate the 0.5–4.5-keV X-ray luminosity  $L_x$  (ref. 8):

$$L_x = S_x D \frac{4\pi c^2}{H_0^2} [z(1+0.5z)]^2 \quad (1)$$

where a Friedmann cosmology with  $H_0 = 50$  km (s Mpc) $^{-1}$  and  $q_0 = 0$  has been assumed. The logarithms of  $L_x$  and, where appropriate, the  $3\sigma$  upper limits are given in column 5 of Table 1. We compare  $S_x$  and  $L_x$  to the optical  $S_0$  and  $L_0$ , calculated for the 3,000–6,000-Å band (at the source and corrected for galactic reddening<sup>9</sup>) using *UBV* magnitudes and a common energy index of 0.7, and to the radio  $S_r$  and  $L_r$ , calculated for the 3.1–8.1-GHz band (at the source) from published 1.4-GHz fluxes and spectral indices following the prescription given by Schmidt<sup>10</sup>. Where no radio flux has been measured, upper limits corresponding to the best available limiting fluxes are used. The spectral indices  $\alpha_{ro}$ , from 5 GHz to 2,500 Å, and  $\alpha_{ox}$ , from 2,500 Å to 2 keV, can then be found from

$$\alpha_{ro} = \frac{\log [L_r/L_0]}{5.380} + 0.595 \quad (2)$$

$$\alpha_{ox} = \frac{\log [L_0/L_x]}{2.605} + 1.200 \quad (3)$$

assuming power-law behaviour within each bandpass (see Table 1).

**Table 1** Properties of 111 quasars examined with the imaging proportional counter on board the Einstein Observatory

| Name*    | Coordinates<br>(1950.0) | Redshift<br>$z$ | Epoch<br>(JD-2443000) | $\log [L_x(0.5-4.5 \text{ keV})]$<br>(erg s $^{-1}$ )† | $\alpha_{ro}$ | $\alpha_{ox}$ |
|----------|-------------------------|-----------------|-----------------------|--|---------------|---------------|
| UMT301‡  | 0100+0205               | 1.8             | 1075.7                | 45.54  | <0.56         | 1.32          |
| PHL957   | 0100+1300               | 2.690           | 1052.3                | <46.54   | <-0.02        | >1.62         |
| PKS      | 0106+0119               | 2.170           | 1512.5                | 46.66  | 0.75          | 1.19          |
| PKS      | 0109+1737               | 2.157           | 1077.0                | <46.19   | 0.60          | >1.44         |
| PKS      | 0237-2322               | 2.263           | 897.7                 | 47.16  | 0.70          | 1.29          |
| NGC1073‡ | 0241+0109               | 0.599           | 1076.9                | <44.41   | <0.51         | >1.43         |
| NGC1073‡ | 0241+0108               | 1.945           | 1076.9                | <45.75   | <0.53         | >1.31         |
| NGC1073‡ | 0241+0107               | 1.411           | 1076.9                | <45.35   | 0.60          | >1.27         |
| PKSO420  | 0420-0127               | 0.915           | 1099.8                | 46.12  | 0.70          | 1.16          |
| NRAO190  | 0440-0023               | 0.844           | 1125.4                | 45.82  | 0.81          | 1.06          |
| PKS      | 0736+0143               | 0.191           | 1167.0                | 44.44  | 0.58          | 1.53          |
| 4C05.34  | 0805+0441               | 2.877           | 1166.9                | 46.65  | 0.60          | 1.43          |
| KP2‡     | 0805+0445               | 2.060           | 991.4                 | <46.23   | <0.44         | >1.19         |
| MC5      | 0830+1115               | 0.589           | 1169.2                | 44.90  | 0.39          | 1.49          |
| MC5      | 0830+1133               | 2.974           | 1169.2                | <46.91   | 0.36          | >1.35         |
| KP‡      | 0847+1530               | 2.190           | 1169.9                | <46.31   | <0.37         | >1.08         |
| KP4‡     | 0847+1540               | 2.660           | 1169.9                | <46.54   | <0.22         | >1.24         |
| KP5‡     | 0847+1539               | 2.200           | 1169.9                | <46.32   | <0.37         | >0.93         |
| LB8755   | 0848+1533               | 2.010           | 1169.9                | 46.02  | 0.56          | 1.54          |
| LB8796   | 0849+1530               | 1.320           | 1169.9                | <45.67   | <0.25         | >1.43         |
| OT1      | 0854+1910               | 0.331           | 1168.8                | <44.23   | <0.53         | >1.53         |
| LB8956   | 0854+1907               | 1.891           | 1168.8                | <46.11   | <0.36         | >1.48         |
| LB8991   | 0855+1846               | 1.013           | 1168.8                | <45.36   | <0.24         | >1.52         |
| LB9010   | 0856+1837               | 1.711           | 1168.8                | <45.98   | <0.32         | >1.38         |
| LB9029   | 0856+1855               | 1.286           | 1168.8                | <45.63   | <0.32         | >1.47         |
| 0906+015 | 0906+0133               | 1.018           | 1013.1                | 45.85  | 0.68          | 1.31          |
| NGC2859‡ | 0921+3444               | 2.250           | 1172.4                | <46.17   | <0.72         | >1.20         |
| NGC2859‡ | 0921+3444               | 1.460           | 1172.4                | <45.61   | <0.78         | >1.13         |
| NGC2859‡ | 0921+3444               | 0.230           | 1172.4                | <43.72   | <0.73         | >1.30         |
| TON 490  | 1011+2504               | 1.633           | 1017.2                | 46.60  | 0.39          | 1.55          |
| NGC3384  | 1045+1253               | 1.111           | 1216.4                | <45.59   | <0.73         | >1.14         |
| NGC3384  | 1045+1253               | 1.107           | 1216.4                | <45.59   | <0.77         | >1.06         |
| NGC3384  | 1045+1253               | 1.131           | 1216.4                | <45.61   | <0.75         | >1.09         |
| NGC3384  | 1045+1253               | 1.134           | 1216.4                | <45.62   | <0.68         | >1.24         |
| NGC3384  | 1045+1253               | 1.192           | 1214.4                | <45.67   | <0.71         | >1.17         |
| NGC3384  | 1045+1253               | 1.280           | 1216.4                | <45.75   | <0.75         | >1.08         |
| NGC3384  | 1045+1253               | 0.520           | 1216.4                | <44.80   | <0.82         | >0.98         |
| NGC3384  | 1045+1253               | 0.497           | 1216.4                | <44.75   | <0.83         | >0.96         |
| WE1058W1 | 1058+7241               | 0.375           | 1152.3                | 44.61  | 0.68          | 1.34          |
| 3C273    | 1226+0220               | 0.158           | 1045.5                | 45.89  | 0.62          | 1.30          |
| 1246-057 | 1246-0542               | 2.212           | 1052.0                | <45.93   | <0.50         | >1.70         |
| 3C277.1  | 1250+5650               | 0.321           | 1040.2                | 44.35  | 0.70          | 1.41          |
| 5C04.105 | 1258+2846               | 0.650           | 1064.7                | 45.06  | 0.57          | 1.42          |
| 5C04.127 | 1258+2837               | 1.373           | 1064.7                | 45.71  | 0.56          | 1.26          |

Table 1 contd.

| Name*      | Coordinates<br>(1950.0) | Redshift<br><i>z</i> | Epoch<br>(JD-2443000) | $\log [L_X(0.5-4.5 \text{ keV})]$<br>( $\text{erg s}^{-1}$ )† | $\alpha_{r0}$ | $\alpha_{0x}$ |
|------------|-------------------------|----------------------|-----------------------|---|---------------|---------------|
| W61972     | 1258+2839               | 1.922                | 1064.7                | <46.26  | <0.32         | >1.39         |
| B201       | 1257+3439               | 1.375                | 1221.7                | <45.73  | 0.23          | >1.59         |
| B246       | 1258+3404               | 0.690                | 1221.7                | <44.91  | <0.15         | >1.62         |
| B471       | 1258+3422               | 0.774                | 1221.7                | <45.06  | <0.22         | >1.40         |
| KP31‡      | 1258+3432               | 2.010                | 1221.7                | <46.21  | <0.50         | >1.19         |
| KP32‡      | 1258+3417               | 1.800                | 1221.7                | <46.05  | <0.56         | >1.03         |
| KP33‡      | 1258+3416               | 1.930                | 1221.7                | <46.11  | 0.51          | >1.14         |
| KP34‡      | 1258+3442               | 2.080                | 1221.7                | <46.24  | <0.34         | >1.00         |
| KP35‡      | 1258+3425               | 2.820                | 1221.7                | <46.69  | <0.38         | >1.25         |
| BSO6       | 1259+3427               | 1.956                | 1221.7                | <46.13  | <0.22         | >1.46         |
| KP36‡      | 1300+3433               | 2.880                | 1221.7                | <46.73  | <0.41         | >1.17         |
| KP37‡      | 1300+3427               | 1.700                | 1221.7                | <45.97  | <0.43         | >1.16         |
| KP38‡      | 1300+3421               | 1.800                | 1221.7                | <46.05  | <0.52         | >1.02         |
| W22722     | 1303+3050               | 1.770                | 1064.8                | <46.25  | <0.25         | >1.34         |
| W21541     | 1303+3123               | 2.047                | 1064.8                | <46.44  | <0.25         | >1.35         |
| 1435+248   | 1435+2452               | 1.010                | 1065.3                | 45.45   | 0.69          | 1.20          |
| OQ172      | 1442+1011               | 3.530                | 1077.2                | 47.06   | 0.68          | 1.41          |
| NGC5866‡   | 1505+5557               | 0.706                | 879.7                 | <45.10  | <0.56         | >1.35         |
| PKS        | 1510-0854               | 0.361                | 1089.0                | 45.30   | 0.67          | 1.29          |
| KP57‡      | 1544+2112               | 2.050                | 1099.4                | <46.22  | <0.46         | >0.91         |
| KP58‡      | 1545+2054               | 1.850                | 1099.4                | <46.08  | <0.52         | >0.91         |
| KP59‡      | 1545+2100               | 1.890                | 1099.4                | <46.11  | <0.68         | >1.17         |
| 3C323.1    | 1545+2101               | 0.264                | 1116.0                | 45.30   | 0.61          | 1.13          |
| A2151*     | 1601+1747               | 1.430                | 1100.7                | <45.61  | <0.40         | >1.43         |
| A2151*     | 1601+1825               | 1.940                | 1100.7                | <46.01  | <0.47         | >1.26         |
| A2151*     | 1602+1753               | 3.020                | 1100.7                | <46.61  | <0.45         | >1.24         |
| A2151*     | 1603+1818               | 1.610                | 1100.7                | <45.68  | <0.51         | >1.22         |
| A2151*     | 1603+1755               | 1.770                | 1100.7                | <45.87  | 0.69          | >1.04         |
| A2151*     | 1603+1806               | 2.060                | 1100.7                | <46.05  | <0.50         | >1.20         |
| A2151*     | 1604+1810               | 1.870                | 1100.7                | <45.92  | <0.54         | >1.12         |
| A2151*     | 1604+1739               | 2.010                | 1100.7                | <46.02  | <0.46         | >1.27         |
| A2151*     | 1604+1743               | 2.300                | 1100.7                | <46.21  | <0.42         | >1.34         |
| A2151*     | 1604+1756               | 2.740                | 1100.7                | <46.47  | <0.45         | >1.25         |
| A2151*     | 1605+1758               | 0.890                | 1100.7                | <45.05  | <0.45         | >1.37         |
| KP63       | 1604+2903               | 1.950                | 1258.0                | <45.72  | 0.36          | >1.36         |
| KP64       | 1605+2851               | 1.800                | 1258.0                | <45.61  | <0.08         | >1.04         |
| KP65       | 1606+2910               | 0.060                | 1258.0                | <42.25  | <0.03         | >1.10         |
| KP66       | 1605+2902               | 2.000                | 1258.0                | <45.75  | <-0.07        | >1.35         |
| KP67       | 1606+2859               | 2.560                | 1258.0                | <46.11  | <-0.04        | >1.11         |
| KP68       | 1607+2849               | 2.300                | 1258.0                | <45.95  | <-0.03        | >1.25         |
| KP69       | 1607+2903               | 0.350                | 1258.0                | <43.85  | <-0.02        | >1.23         |
| 4C28.40    | 1606+2857               | 1.989                | 1258.0                | 45.70   | 0.69          | 1.43          |
| TON 256    | 1612+2612               | 0.131                | 903.1                 | 44.53   | 0.25          | 1.31          |
| NAB1612    | 1612+2640               | 0.395                | 903.1                 | 44.40   | <0.24         | 1.52          |
| KP70       | 1622+2648               | 2.100                | 1263.9                | <45.82  | <0.46         | >1.10         |
| KP71       | 1622+2656               | 3.160                | 1263.9                | <46.45  | <0.42         | >1.16         |
| KP72       | 1623+2709               | 2.400                | 1263.9                | <46.01  | <0.50         | >1.32         |
| KP73       | 1623+2700               | 2.300                | 1263.9                | <45.95  | <0.48         | >1.03         |
| KP74       | 1623+2654               | 1.900                | 1263.9                | <45.68  | <0.62         | >1.15         |
| 4C26.48    | 1623+2657               | 0.779                | 1263.9                | 45.16   | 0.61          | 1.47          |
| KP76       | 1623+2651               | 2.400                | 1263.9                | <46.01  | <0.33         | >1.39         |
| KP77       | 1623+2653               | 2.460                | 1263.9                | 45.91   | <0.25         | 1.64          |
| KP78       | 1623+2651               | 2.600                | 1263.9                | <46.13  | <0.13         | >1.72         |
| KP79       | 1624+2657               | 2.180                | 1263.9                | <45.87  | <0.36         | >1.33         |
| 4C39.46    | 1632+3906               | 1.082                | 1101.0                | <45.61  | 0.65          | >1.34         |
| 4C38.41    | 1633+3814               | 1.814                | 1101.0                | 46.23   | 0.71          | 1.35          |
| 3C345      | 1641+3954               | 0.595                | 1112.6                | 45.96   | 0.73          | 1.22          |
| KP90‡      | 1703+6051               | 1.980                | 1080.0                | 46.17   | <0.55         | 1.49          |
| 3C351      | 1704+6048               | 0.371                | 879.5                 | 44.92   | 0.55          | 1.56          |
| PKS        | 1725+0429               | 0.293                | 1114.6                | 44.12   | 0.67          | 1.44          |
| 1729+501** | 1729+5009               | 1.111                | 959.9                 | <45.77  | 0.64          | >1.38         |
| 3C418      | 2037+5108               | 1.686                | 1019.4                | 46.12   | 0.81          | 1.30          |
| OX 036     | 2121+0522               | 1.878                | 1190.8                | 46.45   | 0.63          | 1.38          |
| PKS        | 2216-0350               | 0.901                | 1017.7                | 45.80   | 0.53          | 1.52          |
| MR††       | 2251-1750               | 0.068                | 1017.2                | 44.49   | -0.07         | 1.33          |
| PKS        | 2251+1121               | 0.323                | 1406.4                | <44.91  | 0.52          | >1.49         |
| PKS        | 2345-1647               | 0.600                | 1212.8                | 45.24   | 0.71          | 1.33          |

\* Unless otherwise specified, data are from ref. 28.

† Systematic errors of  $\pm 30\%$  ( $\pm 0.12$  in logarithm) dominate all errors.‡ Quasar from Michigan-Tololo survey<sup>29</sup>.

§ Redshift uncertain.

¶ Quasars near NGC galaxies<sup>30</sup>.‡ Quasar candidates suggested by Sramek and Weedman<sup>31,32</sup>.

¶ Quasars near Abell cluster 2151 discussed by A. A. Hoag (personal communication).

\*\* QSO candidate from Jodrell Bank 966-MHz survey<sup>33</sup>.

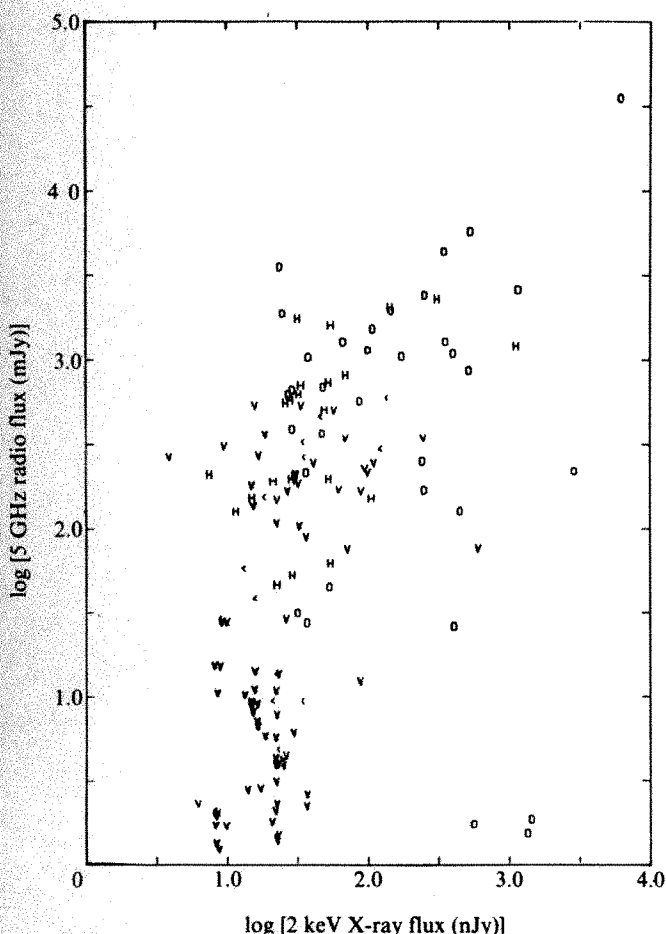
†† X-ray-selected quasar.



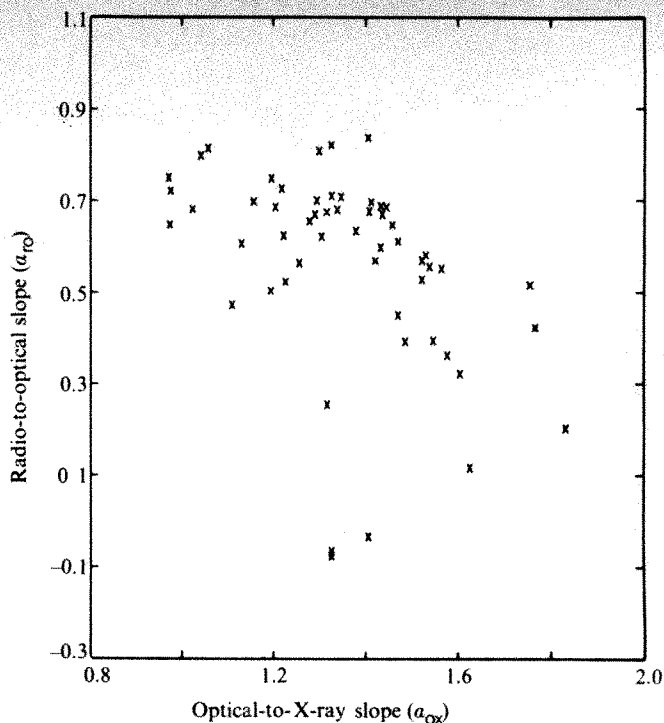
## Data analysis

The data in Table 1 have been combined with data for 39 quasars previously discussed by Tananbaum *et al.*<sup>5</sup> (excluding their data for 3C273, MR2251-178 and 3C351, which are included in our sample), two quasars claimed by Marscher *et al.*<sup>4</sup> and 19 quasars discovered by Chanan *et al.*<sup>11</sup>. The data were then analysed for possible correlations between X-ray behaviour and quasar continuum properties in other regions of the electromagnetic spectrum. The combined sample thus comprises 171 quasars of which 87 are positive detections. Twenty-six of these quasars were first discovered through X-ray observations. Sixty-five of the combined sample have a measured 1.4-GHz flux greater than 10 mJy. Of these 'radio-bright' quasars, 11 are classified as OVV's, 9 of which are known to be active<sup>12</sup>.

A positive correlation was found between  $S_X$  and  $S_0$  for the detected quasars. Although considerable scatter is evident in the correlation diagram (see Fig. 1), the correlation coefficient of 0.67 is significant at the  $6.9\sigma$  level (using the Fisher  $z$ -statistic). Positive correlations also result from comparisons between  $S_X$  and the flux in the IR and at radio frequencies down to 15 GHz. Formally, however, there is no correlation between  $S_r$  and  $S_X$  for the sample of 65 quasars detected in both bands—the correlation coefficient is 0.04. This lack of correlation is largely attributable to three quasars: MKn205, PG0026+129 and MR2251-178. Nevertheless, Fig. 2, which is a plot of the detections and upper limits for all sources, shows a clear association between 'radio-quiet' quasars and a lack of X-ray emission. The fact that the X-ray and radio emissions are related can



**Fig. 2** Log of the flux at 5 GHz (at the source) plotted against log of the flux at 2 keV (at the source). Symbols as in Fig. 1. V, appropriate survey limiting fluxes for objects not detected in the radio. While the plot of detections forms a scatter diagram, the preponderance of X-ray upper limits corresponds to 'radio-quiet' objects in the lower left-hand corner of the diagram.



**Fig. 3** A 'colour-colour' diagram of quasars. The radio-to-optical slopes for detected quasars are plotted against the optical-to-X-ray slopes. The radio-bright objects cluster near the upper left of the diagram; the radio-quiet objects cluster near the lower right of the diagram.

be seen from a comparison of  $\alpha_{r0}$  and  $\alpha_{0x}$ . A correlation coefficient of  $-0.41$  (significant at the  $3.1\sigma$  level) was found, implying that higher radio emission leads to higher X-ray emission when both are normalized to the optical output (see Fig. 3).

Differences in the X-ray behaviour of radio quasars and optical quasars can be seen more clearly in a plot of the number of sources versus  $\alpha_{0x}$ . Figure 4 presents histograms for the 87 detected quasars segregated into: *a*, nearby radio quasars ( $z > 1$ ;  $L_r > 10^{41}$  erg s<sup>-1</sup>); *b*, distant radio quasars; *c*, nearby optical quasars ( $L_r < 10^{41}$  erg s<sup>-1</sup>, or undetected); and *d*, distant optical quasars. The total number of objects sampled in each  $\alpha_{0x}$  interval, including upper limits, are plotted as dotted histograms in the same figures. The total detected fractions along with  $\langle \alpha_{0x} \rangle$ , the mean values of  $\alpha_{0x}$ , and the standard errors of these means for the detected quasars in each of the subsamples are indicated in the figures. Clearly when the optical quasars are detected in X rays, they are detected with larger values of  $\alpha_{0x}$ . For a more quantitative analysis, a simple comparison of the measured means and their standard errors is inadequate because it does not take the upper-limit information into account. A maximum likelihood (ML) technique has therefore been applied to calculate  $\langle \alpha_{0x} \rangle$  for the total sample and for each of the subsamples.

We assume that the spectral index  $\alpha_{0x}$  is a random variate with distribution function  $f(\alpha)$  which is postulated to be independent of other quasar characteristics. Best-fit parameters are determined from the principle of maximum likelihood using standard techniques for treating censored samples and truncated distributions (see, for example, refs 13, 14). Specifically, the likelihood function to be maximized in our case is

$$L = \prod_i f(\alpha_i) \prod_j F(\beta_j) \prod_k f(\alpha_k)/F(\gamma_k) \quad (4)$$

where  $F(\beta) = \int_{\beta}^{\infty} f(\alpha) d\alpha$ . The first two factors take account of the optically selected quasars, both X-ray detected (*i*) and nondetected (*j*), and the third factor takes account of the quasars (*k*) first discovered as X-ray sources. The quantity  $\beta_j$  is the threshold on the index  $\alpha_{0x}$  of the *j*th quasar below which it would have been detected as an X-ray source. Similarly,  $\gamma_k$  is the



threshold on the index of the  $k$ th quasar below which quasar-confirming spectroscopic observations would not yet have been made. Where the optical thresholds are known (see, for example, ref. 11), we have used them. Otherwise we have adopted an arbitrary threshold one magnitude fainter than the measured quasar magnitude. For the actual data samples, changing these thresholds by  $\pm 1/2$  magnitude changes  $\langle\alpha_{0x}\rangle$  by  $<0.01$ .

A nonparametric approach following Avni *et al.*<sup>14</sup> may be used to estimate  $f(\alpha)$ . However, strict adherence to such a procedure results in  $f(\alpha)$  being identically zero outside the range of the measured values for  $\alpha$ . If, as is most likely, the present quasar samples do not span the entire range of  $\alpha$ , this unphysical cutoff will introduce a slight bias in the calculated values of  $\alpha_{\text{eff}}$ . To avoid this source of bias, we take  $f(\alpha)$  to be the normal distribution, consistent with the distribution measured for all detected quasars. The sample mean  $\langle\alpha_{0x}\rangle$  and the variance  $\sigma^2$  are then obtained by maximizing  $L$  numerically, and the standard errors of these parameters are determined in the usual way from the co-variance matrix. Monte-Carlo simulations have shown that these ML estimators are unbiased.

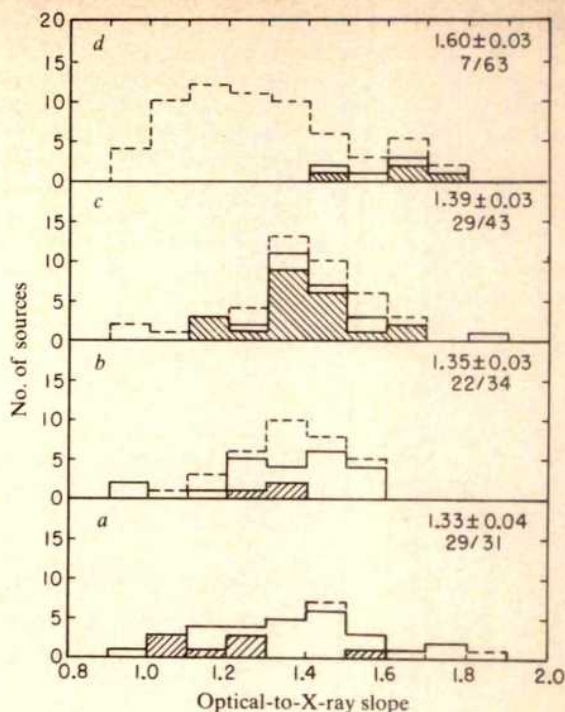
Using the above procedure, we find for the total sample of 171 quasars a value  $\langle\alpha_{0x}\rangle = 1.46 \pm 0.02$ . The 26 X-ray-selected quasars with  $\langle\alpha_{0x}\rangle = 1.41 \pm 0.03$  are indistinguishable from the remainder of the sample; they also do not differ significantly from other nearby optically selected, radio-quiet quasars (see Fig. 4c). Dividing the sample into radio quasars and optical quasars, we find values of  $1.38 \pm 0.03$  and  $1.52 \pm 0.03$ , respectively. Dividing the two classes into low- and high-redshift groups renders the distinction even more striking. Although there is no difference between the low- and high-redshift radio quasars ( $\langle\alpha_{0x}\rangle = 1.36 \pm 0.04$  and  $1.40 \pm 0.03$ , respectively), the optical quasars do show evidence of evolution with  $\langle\alpha_{0x}\rangle = 1.44 \pm 0.03$  and  $1.65 \pm 0.04$ , respectively.

Most of the difference in the values of  $\langle\alpha_{0x}\rangle$  for the two classes arises from a difference in X-ray luminosity. The luminosity distribution histograms shown in Fig. 5 suggest that, in general, optical quasars have lower X-ray luminosities than radio quasars. The mean log X-ray luminosities are  $44.61 \pm 0.16$  and  $45.64 \pm 0.13$ , respectively, for detected quasars.

We note that a subset of the radio quasars, the flat-spectrum radio sources in general and the OVV's in particular, plays a large part in establishing the distinction between radio quasars and optical quasars. The OVV's are shown as crosshatched objects in Fig. 4. For the 11 OVV's,  $\langle\alpha_{0x}\rangle = 1.25 \pm 0.05$ , compared with  $1.41 \pm 0.04$  for radio quasars without the OVV's. Discounting the OVV's, the mere absence or presence of radio emission does not strongly correlate with the level of X-ray emission from nearby objects. However, the separation at high redshifts seen in Fig. 4 remains significant.

## Discussion

The present data suggest that an instructive segregation of quasars into two types can be made: those with  $L_r < 10^{41}$  erg s<sup>-1</sup> (Type I) and those with  $L_r > 10^{41}$  erg s<sup>-1</sup> (Type II). Type I quasars make up  $\sim 90\%$  of the total population. For these objects, the typical luminosity in the 3,000–6,000-Å band



**Fig. 4** Optical-to-X-ray slope distributions for: *a*, nearby ( $z < 1$ ) radio-bright ( $L_r > 10^{41}$  erg s<sup>-1</sup>); *b*, distant radio-bright; *c*, nearby radio-quiet or undetected; and *d* distant radio-quiet or undetected quasars. The dashed histograms represent the total number of objects with a detection or a  $3\sigma$  upper limit in the appropriate  $\alpha_{0x}$  bin. The solid histogram represents only those objects which were detected in the X-ray. The hatched histograms in *a* and *b* represent the OVV's in our sample. The hatched histograms in *c* and *d* represent X-ray-discovered quasars. The total detected fraction and the mean and standard deviations for the detected quasars in each subsample are given.

ranges from  $10^{43}$  to  $10^{47}$  erg s<sup>-1</sup>. In the 0.5–4.5-keV soft X-ray regime, their output ranges from  $10^{43}$  to  $10^{46}$  erg s<sup>-1</sup> with  $\langle\alpha_{0x}\rangle \sim 1.5$  and  $\alpha_{r0} < 0.2$ . In contrast, Type II quasars are much more luminous, most notably in the radio and X-ray regimes, with  $\langle\alpha_{0x}\rangle \sim 1.35$  and  $\alpha_{r0} > 0.2$ . (If one considers the total energy radiated by several typical Type I and Type II quasars, it is clear that, though substantial overlap exists from one class to the other, Type I quasars are typically 1–2 orders of magnitude less luminous than Type II objects in the range  $10^8$ – $10^{18}$  Hz.) Our results, along with previous studies by Schmidt<sup>10</sup> and most recently by Turner<sup>15</sup>, indicate that these two types of quasars evolve quite differently: the radio-bright, flat-spectrum type II quasars are consistent with no evolution, whereas radio-quiet Type I objects exhibit a strong luminosity and/or density enhancement at earlier epochs. The parameters of the two classes are summarized in Table 2.

Data from our larger sample of active galactic nuclei provide an important clue to the underlying cause of this class distinction. N-galaxies and BL Lac objects, which are generally bright radio sources, are found to be luminous soft X-ray emitters; we find values of  $\langle\alpha_{0x}\rangle = 1.30 \pm 0.07$  and  $1.31 \pm 0.05$  for 15 and 16 observed sources, respectively. These values are consistent with  $\alpha_{0x}$  calculated for the few previously discovered BL Lacs<sup>16</sup> and N-galaxies<sup>17</sup>. A large number of these active nuclei are associated with underlying elliptical galaxies<sup>18</sup>. On the other hand, Seyfert galaxies, which are typically weak radio sources, are also found to have lower X-ray luminosities<sup>19,20</sup> and a larger  $\langle\alpha_{0x}\rangle$  when compared with nearby radio-bright active galaxies. More than 90% of Seyferts are identified with spiral or barred spiral galaxies<sup>21</sup>. This distinction in the morphology of the galaxies underlying Type I and Type II objects may signal differences in the nature of the compact nuclear source and/or its immediate environment.

**Table 2** Properties of the two quasar classes

|  | Type I                | Type II                |
|--|-----------------------|------------------------|
| % Of total population                        | 90%                   | 10%                    |
| $L_r$ (3.1–8.1 GHz) (erg s <sup>-1</sup> )   | $<10^{41}$            | $>10^{41}$             |
| $L_0$ (3,000–6,000 Å) (erg s <sup>-1</sup> ) | $10^{43}$ – $10^{47}$ | $10^{43}$ – $10^{47}$  |
| $L_x$ (0.5–4.5 keV) (erg s <sup>-1</sup> )   | $10^{43}$ – $10^{46}$ | $10^{44}$ – $10^{47}$  |
| $\langle\alpha_{0x}\rangle$                  | 1.5                   | 1.35                   |
| $\alpha_{r0}$                                | $<0.2$                | $>0.2$                 |
| Evolution                                    | Strong                | Weak                   |
| Related AGNs                                 | Seyferts              | BL Lacs,<br>N galaxies |
| Related Hubble type                          | Spirals               | Ellipticals            |
| Time variability                             | ...                   | $\times 10$ (OVV's)    |



Our observation that the X-ray flux correlates with other quasar continuum measurements from the UV region to the millimetre region, along with the observation that the mean value of the IR-optical slope of 1.3–1.4 (ref. 22) is similar to  $\langle\alpha_{\text{ox}}\rangle$ , supports the view that synchrotron radiation from a single power-law distribution of electrons is responsible for most of the  $10^{13}$ – $10^{18}$ -Hz emission in quasars. The lack of correlation between the emission at X-ray and radio frequencies may be partly due to low-frequency radio emission generally coming from a halo or extended lobe components and thus not measuring the power of the central nuclear source which is presumably responsible for all of the X-ray emission. Furthermore, the compact component may become opaque at frequencies below a few gigahertz due either to synchrotron self-absorption or to free-free absorption by intervening clouds. Absorption by such clouds can also decrease the level of measured soft X-ray emission, although very large column densities ( $n_{\text{H}} \geq 10^{23} \text{ cm}^{-2}$  at  $z = 3$ ) would be required to explain the low X-ray outputs of the high-redshift Type I objects.

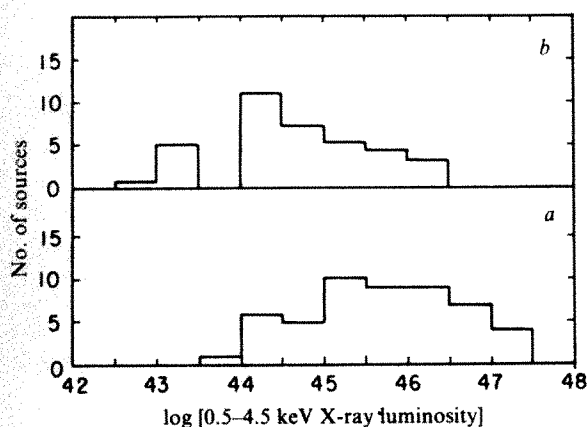


Fig. 5 Histograms of the number of sources plotted against log [0.5–4.5-keV X-ray luminosity ( $\text{erg s}^{-1}$ )] for a, radio-bright objects and b, radio-quiet objects.

Although at soft X-ray energies direct synchrotron radiation seems to be dominant for nearly all quasars, a second mechanism could explain the enhanced X-ray emission from Type II objects in general and OVV in particular. Compton scattering of flat-spectrum centrimetric radio photons off relativistic electrons with a Lorenz factor of  $\sim 10^3$  can add significantly to the total X-ray emission above a few kiloelectron volts<sup>23</sup>. For the OVVs, the problem has been that the incoherent synchrotron self-Compton (SSC) process predicts high X-ray fluxes that are inconsistent with the upper limits derived from the early 2–10-keV all-sky surveys<sup>24</sup>. However, the level of X-ray emission we now observe from these sources can be made consistent with the SSC model if the emitting plasma is moving at relativistic velocities with an energy density in the electrons

comparable to that in the magnetic fields<sup>4</sup>. For the non-OVVs, the observation that there is little difference in the X-ray behaviour between the two classes for nearby quasars suggests that the Compton contribution is relatively unimportant below a few kiloelectron volts. Above a few kiloelectron volts, however, a change in spectral slope from  $\sim 1.5$  to a value  $\leq 0.5$  is expected as the dominant emission mechanism changes from synchrotron to SSC. Recent observations of the X-ray spectra of BL Lac objects<sup>25,26</sup> support the idea of spectral flattening in the 1–10-keV region. In this picture, the effective power-law index in the spectral band sampled by the IPC is  $\sim 1$  for Type II objects. As there is no  $K$  correction for a power law of index one, the lack of any distinction between  $\langle\alpha_{\text{ox}}\rangle$  at low and high redshifts for Type II objects follows directly. For Type I objects, only the synchrotron power law with  $\alpha_{\text{ox}} \sim 1.5$  is present, explaining the greater difficulty we have in detecting high-redshift Type I objects.

One important consequence of the separation of quasars into two distinct classes is that preliminary conclusions reached by Tananbaum *et al.*<sup>5</sup> concerning the contribution of quasars to the diffuse X-ray background need to be modified. Because neither the samples of quasars studied by Tananbaum *et al.*<sup>5</sup> nor by us are statistically complete, we cannot derive an X-ray luminosity function directly but must rely instead on optical quasar counts and  $L_{\text{x}}/L_0$  values for different quasars. As the surface density of quasars at faint magnitudes is generally derived from objective prism surveys sensitive to  $z > 1.7$  and as most of these sources are not strong radio sources, the proper value of  $\alpha_{\text{ox}}$  to apply to the optical quasar count is that associated with distant optical quasars. The effective  $\alpha_{\text{ox}}$ ,  $\alpha_{\text{eff}}$  (see ref. 5), inferred from the mean  $L_{\text{x}}/L_0$  ratio for all distant optical quasars, is  $1.63 \pm 0.04$ . This value means that, on average, optical quasars contribute a factor of 8 less to the diffuse X-ray background than the value of  $\alpha_{\text{eff}} = 1.27$  used by Tananbaum *et al.*<sup>5</sup>. If Type II objects comprise 10% of all quasars, their value of  $\alpha_{\text{eff}} = 1.26 \pm 0.03$  implies that they contribute  $\sim 70\%$  of the amount from all optical quasars. Treating the OVVs separately may alter the estimate, but the net result is to reduce the contribution from all quasars by a factor of  $\geq 4$  from the value given by Tananbaum *et al.*<sup>5</sup>. To explain the entire diffuse soft X-ray background as resulting from quasars, then, one must integrate the optical log  $N$ –log  $S$  relation to  $m_{\text{B}} = 21.5$  and assume that the slope of the log  $N$ –log  $S$  curve remains steeper than 2. Similar results have been reported by Zamorani *et al.*<sup>27</sup>.

We believe that the data presented here support a picture incorporating the differing importance of synchro-Compton radiation in Type I and Type II quasars, possibly enhanced to some degree by an excess of absorbing material in the radio-quiet objects. While simultaneous spectral and time variability studies over as wide a frequency range as possible are essential for further progress in this field, it is clear that X-ray observations will play a major part in our future understanding of the evolution of quasars, their connection to other active galaxies, and their precise contribution to the diffuse X-ray background.

This work was supported by NASA under contract NAS8-30753.

Received 10 April; accepted 16 October 1980.

1. Bowyer, C. S., Lampton, M. Mack, J. & de Mendonca, F. *Astrophys. J. Lett.* **161**, L1–7 (1970).
2. Ricker, G. R. *et al.* *Nature* **271**, 35–36 (1978).
3. Apparo, K. M. V. *et al.* *Nature* **273**, 450–453 (1978).
4. Marscher, A. P. *et al.* *Astrophys. J.* **223**, 498–503 (1979).
5. Tananbaum, H. *et al.* *Astrophys. J. Lett.* **234**, L9–13 (1979).
6. Wills, D. *Phys. Scr.* **17**, 333 (1978).
7. Giacconi, R. *et al.* *Astrophys. J.* **230**, 540–550 (1979).
8. Sandage, A. *Astrophys. J.* **133**, 353–391 (1961).
9. Sandage, A. *Astrophys. J.* **178**, 1–24 (1972).
10. Schmidt, M. *Astrophys. J.* **151**, 393–409 (1968).
11. Chanan, G. A., Margon, B. & Downs, R. Preprint (Columbia University, 1980).
12. Pollock, J. T. *et al.* *Astr. J.* **84**, 1658–1675 (1979).
13. Kendall, M. G. & Stuart, A. *The Advanced Theory of Statistics* Vol. 2 (Charles Griffin, London, 1961).
14. Avni, Y., Soltan, A., Tananbaum, H. & Zamorani, G. *Astrophys. J.* **238**, 800 (1980).
15. Turner, E. L. *Astrophys. J. Lett.* **228**, L51–54 (1979).
16. Schwartz, D. A., Doxsey, R. E., Griffiths, R. E., Johnston, M. D. & Schwartz, J. *Astrophys. J. Lett.* **229**, L53–57 (1979).

17. Marshall, F. E. *et al.* *Nature* **275**, 624–625 (1978).
18. Stein, W. A., O'Dell, S. L. & Strittmatter, P. A. *Rev. Astr. Astrophys.* **14**, 173–195 (1976).
19. Elvis, M. *et al.* *Mon. Not. R. astr. Soc.* **183**, 129–157 (1978).
20. Tananbaum, H., Peters, G., Forman, W., Giacconi, R., Jones, C. & Avni, Y. *Astrophys. J.* **223**, 74–81 (1978).
21. Adams, T. F. *Astrophys. J. Suppl.* **33**, 19–34 (1977).
22. Neugebauer, G., Oke, J. B., Becklin, E. E. & Mathews, K. *Astrophys. J.* **230**, 79–94 (1979).
23. Jones, T. W., O'Dell, S. L. & Stein, W. A. *Astrophys. J.* **188**, 353–368 (1974).
24. Burbidge, G. R., Jones, T. W. & O'Dell, S. L. *Astrophys. J.* **193**, 43–54 (1974).
25. Agrawal, P. C. & Riegler, G. R. *Astrophys. J. Lett.* **231**, L25–29 (1979).
26. Mushotzky, R. F. *et al.* *Astrophys. J. Lett.* **226**, L65–67 (1978).
27. Zamorani, G. *et al.* *Bull. Am. astr. Soc.* **11**, 776 (1979).
28. Burbidge, G. R., Crowne, A. H. & Smith, H. E. *Astrophys. J. Suppl.* **33**, 113–188 (1977).
29. Lewis, D. W., MacAlpine, G. M. & Weedman, D. W. *Astrophys. J.* **233**, 787–795 (1979).
30. Burbidge, G. *Nature* **282**, 451–455 (1979).
31. Sramek, R. A. & Weedman, D. W. *Astrophys. J.* **221**, 468–480 (1978).
32. Sramek, R. A. & Weedman, D. W. Preprint (1980).
33. Walsh, D., Wills, B. J. & Wills, D. *Mon. Not. R. astr. Soc.* **189**, 667–670 (1979).

# Cordilleran suspect terranes

Peter J. Coney

Department of Geosciences, University of Arizona, Tucson, Arizona 85717

David L. Jones

US Geological Survey, Menlo Park, California 94025

James W. H. Monger

Canadian Geological Survey, Vancouver, British Columbia, Canada

*Over 70% of the North American Cordillera is made up of 'suspect terranes'. Many of these geological provinces are certainly allochthonous to the North American continent and seem to have been swept from far reaches of the Pacific Ocean before collision and accretion into the Cordilleran margin mostly in Mesozoic to early Cenozoic time.*

RECENT tectonic studies and a new geological and geophysical data base support earlier theories<sup>1-3</sup> that much of the North American Cordillera is a vast mosaic or collage<sup>4,5</sup> of what are here termed 'suspect terranes'<sup>6</sup>. The terranes are suspect because we cannot be certain of their palaeogeographical setting with respect to North America through much of Phanerozoic time. Most are truly allochthonous and seem to have collided and accreted to the North American cratonic margin mostly during Mesozoic and early Cenozoic time<sup>7</sup>. Large-scale concurrent and post-accretionary horizontal translations of hundreds of kilometres<sup>8</sup> and significant rotations around vertical axes<sup>9,10</sup> are also indicated, both of which are continuing to the present.

## Distribution and character of terranes

The distribution of the major Cordilleran suspect terranes is shown in Fig. 1. More than 50 terranes are recognized some of which are here grouped for simplicity and designated composite terranes. Some terranes are too small to show at the scale of this map.

Once the Palaeozoic miogeocline is identified in the geology of western North America all geological terranes outside it are inherently suspect in that their palaeogeographical distribution or their palaeotectonic setting with respect to North America is uncertain. The reason is based on a simple plate tectonic concept. During most of latest Precambrian through early Palaeozoic time the western margin of North America was a passive continental margin across which was draped a growing miogeoclinal terrace<sup>11</sup> as some proto-Pacific Ocean opened. Brief periods of convergence and collision are inferred during mid-Palaeozoic time<sup>12</sup>, but the progressive out-building of the terrace was almost uninterrupted for at least 700 Myr. This regimen changed in latest Triassic to middle Jurassic time<sup>13</sup> and since then the margins of the Pacific Ocean have been convergent or transform. Subduction related to convergence consumed all of the vast Palaeozoic Pacific Ocean<sup>12</sup> and it follows that all Palaeozoic terranes now found outside the edge of the original Palaeozoic passive continental margin must have somehow accreted against that margin during Mesozoic-Cenozoic time. It also follows that all younger geological terranes outside that margin (many of which sit on older Palaeozoic rocks) are also suspect, until proved otherwise, and may have been accreted against that margin.

The terranes shown in Fig. 1 are characterized by internal homogeneity and continuity of stratigraphy, tectonic style and history. The boundaries between terranes are fundamental discontinuities in stratigraphy that cannot be explained easily by conventional facies changes or unconformity. Most boundaries separate totally distinct temporal or physical rock

sequences<sup>15,19</sup>, and many juxtapose different faunas<sup>16</sup>. Some terranes carry palaeomagnetic records that differ strongly from those of cratonic North America<sup>9,10</sup>. These data suggest large displacements and/or rotations between the terranes themselves and between the terranes and stable North America.

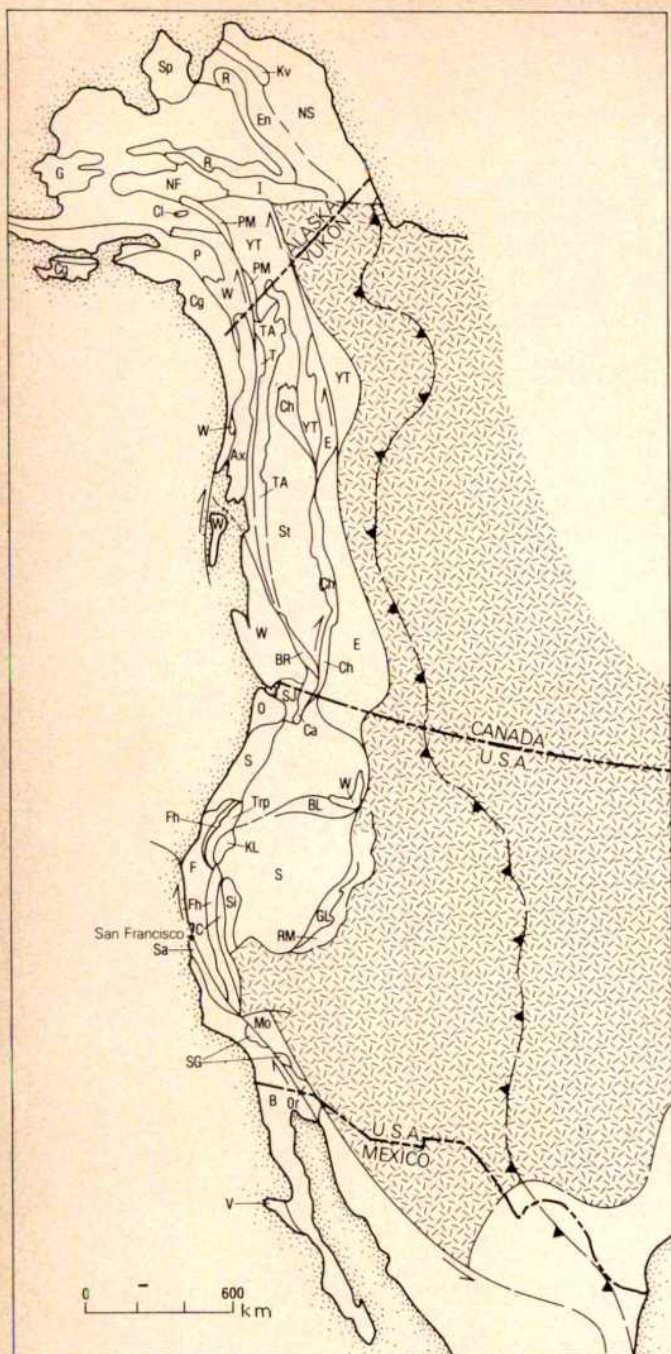
Note that identification of a terrane is based primarily on its stratigraphy<sup>14</sup> and need not carry any genetic or even plate tectonic implication. At the start of investigations, the identified terranes are simply considered as domains in the descriptive sense. Their identification and description has provided great insight into Cordilleran geological and tectonic history.

In support of the concept of terranes and their suspect character it is important that most of them display sedimentary and volcanic rock sequences that are of oceanic affinity rather than continental. It is also significant that rocks proved to be older than middle Palaeozoic are not common in the larger suspect terranes<sup>15</sup>. Most contain only upper Palaeozoic and/or Mesozoic sequences and most seem to have formed far removed from any continental influence, or at best at the most distal reaches of continental influence.

Most of the boundaries between terranes are known or suspected faults that usually display complex structural history (for example, see ref. 19). Many of the boundaries are certainly sutures, now largely cryptic, and most have been reactivated by concurrent and post-collisional large-scale, right-lateral strike-slip movements. High-pressure mineral assemblages of the blueschist facies from some of these boundaries have yielded Mesozoic radiometric ages<sup>5</sup>. Also, several boundaries are marked by thick and highly deformed Mesozoic sequences of turbidite flysch<sup>7</sup>.

The allochthonous terranes are of several types. A few are, or contain, pieces of oceanic crust (Ch, Cl, Br, SJ, BL, Trp, C) and represent last vestiges of large late Palaeozoic-early Mesozoic oceans now trapped well within the Cordillera far from the present Pacific margin<sup>15</sup>. The Permian Tethyan faunas characteristic mainly of the Cache Creek terrane are totally distinct from coeval faunas found on both sides<sup>16</sup>. Other terranes contain fragments of oceanic arcs subsequently swept against the Cordilleran margin (R, I, G, YT, W, P, St, E, Ca, BL, KL, S, Si). A significant proportion of these arcs are late Palaeozoic in age, many are late Triassic to Jurassic in age, but at least one (the Gravena-Nutzotin belt)<sup>17</sup> is as young as early Cretaceous. The major Palaeozoic and Mesozoic arcs (St, P, W) have no known basement other than presumed oceanic crust. Some of the arcs, although submarine in character, rode passenger on older basement terranes. Other terranes seem to be fragments or slices off distal parts of unknown continental edges (E, NF, PM, YT, Ax, Sa, RM) and they possess what might be termed a





**Fig. 1** Generalized map of Cordilleran Suspect Terranes. Dashed pattern, North American autochthonous cratonic basement. Barbed line, eastern limit of Cordilleran Mesozoic-Cenozoic deformation. Barbed arrows, direction of major strike-slip movements. Terranes are described below.

#### Alaska

(for further information on the distribution and character of terranes in Alaska, see refs 14, 17–20, 53)

- Sp, Seward Peninsula—structurally complex assemblage of Precambrian metamorphic and sedimentary rocks, and Palaeozoic carbonate rocks.
- NS, North Slope—Precambrian, Palaeozoic, and Mesozoic clastic and carbonate sequence—part of North America, but may have moved from original position.
- Kv, Kavik—Thin sequence of radiolarian chert, argillite, shale, and minor volcanics, Mississippian to Triassic in age.
- En, Endicott—metamorphosed Lower to Upper Palaeozoic clastic and carbonate rocks intruded by Palaeozoic granitic rocks.
- R, Ruby—composite terrane comprising at least three separate units, including Precambrian metamorphic rocks, mid to Upper Palaeozoic volcanic and sedimentary rocks, and thick piles of Lower Mesozoic basalt and chert.
- I, Innoko—structurally deformed sequence of Upper Palaeozoic to early Mesozoic chert, argillite, graywacke, and basic to intermediate volcanics.
- NF, Nixon Fork—Precambrian metamorphic rocks overlain by Palaeozoic and Mesozoic carbonate, clastic, and cherty rocks.

- G, Goodness (composite)—includes three terranes: (1) a complex assemblage of deformed Upper Palaeozoic volcanics, chert, and graywacke with blocks of older limestone; (2) Precambrian gneisses and schist; and (3) Mesozoic arc-derived volcanic flows, tuff, and graywacke, with interbedded chert.
- Cl, Chulitna (composite)—includes three terranes: (1) Devonian ophiolite overlain by Palaeozoic chert, volcanic conglomerate, limestone, and flysch, and Mesozoic limestone, redbeds, flysch, and chert; (2) Mesozoic chert, argillite, crystal tuff, and conglomeratic sandstone; (3) Upper Palaeozoic tuff, and chert, volcanic graywacke, with blocks of Lower Palaeozoic limestone.
- PM, Pingston & McKinley (composite)—includes three terranes: (1) Upper Palaeozoic phyllite and Triassic thin-bedded limestone and sooty black shale; (2) Upper Palaeozoic chert, Triassic pillow basalt, and Upper Mesozoic flysch and conglomerate; (3) Lower Palaeozoic limestone, tuff and flysch of unknown ages.
- YT, Yukon-Tanana (composite)—includes regionally metamorphosed schist and gneiss of Precambrian(?) age, Devonian limestone, Upper Palaeozoic silicic metavolcanic rocks, Permian ophiolite, and foliated granitic rocks of unknown age.
- W, Wrangellia—Upper Palaeozoic arc complex composed of flows, breccias, and volcanoclastic rocks overlain by limestone, clastics, and chert, and Mesozoic pillowed and subaerial basalt flows succeeded by limestone, cherty limestone, and clastic rocks.
- P, Peninsular—rare Palaeozoic limestone, Triassic basalt, argillite, and limestone, Lower Jurassic volcanic and volcanoclastic rocks, younger clastics.
- Cg, Chugach (composite)—includes (1) deformed Upper Mesozoic flysch and melange units, and (2) deformed Lower Cenozoic flysch and volcanic rocks.
- Ax, Alexander—complex terrane of Precambrian(?) and Palaeozoic volcanic rocks, clastics, and limestone, and Mesozoic volcanics, limestone, and clastic rocks.
- T, Taku—structurally complex assemblage of Upper Palaeozoic volcanoclastics, limestone, flysch(?), and Lower Mesozoic basalt, limestone, and flysch.
- TA, Tracy Arm—structurally complex assemblage of marble, pelitic gneisses, and schist of unknown ages.

#### Canada

(for further information on distribution and character of terranes in Canada, see refs 2, 5, 8, 15, 16, 19, 25, 33)

- Ch, Cache Creek terrane—Mississippian to Middle (Upper?) Triassic, highly disrupted radiolarian chert, argillite, basalt, alpine-type ultramafics, large shallow-water carbonates, and local blueschist metamorphism.
- BR, Bridge River terrane—Middle Triassic to Lower Middle Jurassic, highly disrupted radiolarian chert, argillite, basalt, alpine-type ultramafics and minor carbonate.
- St, Stikine terrane—Mississippian and Permian volcanoclastics, basic to acidic volcanics and carbonates, locally deformed and intruded in middle to late Triassic time, overlain by Upper Triassic to Middle Jurassic volcanogenic strata.
- E, Eastern assemblage (composite)—includes possible late Precambrian-early Palaeozoic metamorphic terranes, of possible continental affinity, together with Mississippian to Triassic basalt, ultramafics and chert and volcanoclastics and carbonates, overlain unconformably by Middle Triassic to Lower Jurassic volcanogenic strata.

#### Washington and Oregon

- SJ, San Juan (composite)—includes highly deformed Mesozoic chert, argillite, graywacke, and volcanic rocks, partly in melanges, with blocks of lower Palaeozoic plutonic rocks, Palaeozoic chert, carbonates, and volcanic rocks. Permian limestone blocks contain Tethyan fusulinids (see ref. 54).
- Ca, Northern Cascades (composite)—includes crystalline and pelitic gneisses, and thrust sheets composed of (1) Upper Palaeozoic andesitic volcanics and associated sedimentary rocks; (2) green schist and blue schist; and (3) Jurassic ophiolite (see ref. 55).
- O, Olympic—Lower Cenozoic volcanic rocks and associated deep and shallow water sedimentary rocks. Basement unknown, but presumed to be oceanic (see ref. 56).
- S, Lower Cenozoic volcanic and sedimentary rocks lying west of the Cascade Range. Palaeomagnetic data imply post-Eocene clockwise rotation of 70° (see refs 35, 36).
- BL, Blue Mountains (composite)—includes melange with blocks of Palaeozoic ophiolite, limestone, and chert, and Mesozoic chert and sandstone, structurally overlain by Triassic and Jurassic volcanic sandstone, conglomerate, and argillite (see refs 57, 58).

#### California

- Fh, Foothills—Upper Jurassic andesitic volcanic and volcanoclastic rocks associated with phyllite, slate, and graywacke, and Upper Jurassic ophiolite (see refs 59, 60).
- Trp, Triassic and Palaeozoic of Klamath Mountains (composite)—includes a structurally complex assemblage of Lower Mesozoic ophiolite, chert, basalt, Jurassic andesitic rocks, and associated sedimentary rocks (see refs 61, 62).
- KL, Eastern Klamath Mountains—Middle to Upper Palaeozoic clastic, volcanic, and carbonate rocks, overlain by Triassic and Jurassic volcanics and minor limestone (see refs 63, 64).



- Si, Northern Sierra—Lower Palaeozoic clastic sedimentary rocks, Upper Palaeozoic and Lower Mesozoic volcanic and associated sedimentary rocks (see ref. 65).
- C, Calaveras (composite)—including a western belt of melange with ophiolite and Mesozoic chert, and an eastern belt of quartzose clastic rocks, argillite, and minor Permian limestone (see ref. 66).
- F, Franciscan (composite)—includes Upper Mesozoic Great Valley sequence with ophiolite at base, and structurally underlying disrupted and partially metamorphosed rocks of the Franciscan Complex (see ref. 67).
- Sa, Salinia—includes metamorphosed pelitic rocks, marble, and graywacke of unknown ages, intruded by Cretaceous granite plutons (see ref. 68).
- SG, San Gabriel (composite)—two structurally complex and juxtaposed Precambrian crystalline terranes intruded by Mesozoic plutons (see ref. 69).
- OR, Orocopia—metagraywacke and mudstone and minor chert and basic volcanic rocks, age unknown. No known basement (see ref. 70).
- Mo, Mohave (composite)—juxtaposed and disrupted Palaeozoic sedimentary sequences, Lower Mesozoic sedimentary and volcanic rocks intruded by Mesozoic plutons (see ref. 71).

#### Mexico

- B, Baja—includes scattered localities of Upper Palaeozoic limestone and Lower Mesozoic clastic rocks, overlain by a thick pile of Upper Mesozoic volcanic and volcanoclastic rocks, capped by latest Cretaceous quartzofeldspathic sandstone (see ref. 72).
- V, Vizcaino (composite)—includes Triassic basalt, chert, and limestone, Upper Jurassic arc-derived volcanic and volcanoclastic rocks, Upper Jurassic and Cretaceous clastic rocks, ophiolite, and structurally underlying Upper Mesozoic blue schist and disrupted rocks similar to the Franciscan Complex (see ref. 73).

#### Nevada

- S, Sonoma (composite)—includes Upper Palaeozoic volcanics in the south, and Lower Mesozoic volcanics in the north. Si and KL terranes originally included in Sonoma (see ref. 74).
- GL, Golconda—structurally deformed assemblage of chert, argillite, minor limestone, and volcanics of Mississippian to Permian age (see ref. 75).
- RM, Roberts Mountains—structurally complex assemblage of chert, argillite, sandstone, basalt, and minor limestone of Cambrian to latest Devonian or early Mississippian ages (see ref. 76).

'quasi-continental' character. A few terranes are of uncertain origin. A significant number of the terranes have basalt or gabbroic rocks, particularly of late Triassic age (I, PM, W and so on) suggesting they are fragments from rifting events, intraplate volcanism, or oceanic plateaus of unknown origin or setting<sup>18</sup>.

In a few cases it can be shown by stratigraphical and structural controls that disparate terranes amalgamated before final accretion against the North American margin<sup>18,19</sup>. One of the largest and best documented cases is the amalgamation of Wrangellia<sup>20</sup> with the Alexander terrane. Wrangellia everywhere comprises a late Palaeozoic submarine arc assemblage, with no known basement, overlain by a distinctive and very thick (up to 6,000 m) partly submarine, partly subaerial Upper Triassic basalt, overlain in turn by sedimentary rocks which extend into the early Jurassic. Palaeomagnetic data from identical Upper Triassic basalt sequences in eastern Oregon (J. Hillhouse, personal communication), Vancouver Island in western Canada<sup>21</sup>, and from southern Alaska<sup>22</sup> all record the same low Triassic palaeolatitudes with respect to Triassic North America. The Alexander terrane is a complex assemblage of volcanosedimentary rocks of Palaeozoic age<sup>17</sup>. Somewhere on route from its equatorial origins, Wrangellia amalgamated with the Alexander terrane<sup>3,19</sup>, as demonstrated by the overlapping Upper Jurassic and Cretaceous strata of the Gravina-Nutzotin belt, and with the Lower Jurassic arc of the Peninsular terrane<sup>18</sup>. Once amalgamated the resulting super-terranes was the site of variably distributed Jurassic to Lower Cretaceous Gravina-Nutzotin<sup>17</sup> arc activity before its final consolidation into the Cordilleran orogen. Since accretion Wrangellia has been fragmented by major horizontal translations and rotations so that its pieces are now scattered over almost 2,000 km of the Cordilleran margin from Oregon to Alaska<sup>20</sup>.

Some terranes are very small (most are not shown on Fig. 1) and have no known counterparts in the Cordillera. A remarkable example is in the Chulitna terrane<sup>23</sup> in southern Alaska. It lies with other small, but totally distinct, terranes embedded in a mass of late Jurassic to early Cretaceous flysch north of the Wrangellia terrane in the Central Alaska Range. Only several

tens of kilometres long, the terrane is a nappe-like structure exposing in continuous sequence late Devonian ophiolite, Mississippian chert, Permian volcanic conglomerate and breccia, flysch, chert and limestone, Lower Triassic limestone, Upper Triassic red beds and basaltic to silicic volcanics, Jurassic sandstone and chert, and Cretaceous argillite, chert, sandstone and coquinooid limestone. No other stratigraphic section such as this is known anywhere in the Cordillera. Lower Triassic ammonites from this terrane are of equatorial affinity<sup>24</sup> and indicate a southern origin.

Not shown in Fig. 1 are some overlap assemblages termed superjacent terranes. These terranes are sedimentary and volcanic sequences deposited on the basement terranes shown in Fig. 1 and tie together previously disjunct terranes. The Gravina-Nutzotin belt<sup>17</sup> is an example. Analyses utilizing basement and superjacent stratigraphy, biostratigraphy and palaeomagnetic data combined with consideration of belts of dated cross-cutting plutonic rocks provide critical data for unraveling the pre-, syn-, and post-accretionary history of these complex structural units.

### Accretionary history

A full understanding of the history of accretion and post-accretionary consolidation of Cordilleran suspect terranes into the North American Cordillera is incomplete. Although we review here what is known or suspected for the assembly as a whole, much of what we say is preliminary as additional complexities continue to unfold.

Southern Alaska is made up of several large terranes with numerous smaller ones scattered along the margins and between the larger ones<sup>18,23</sup>. The Yukon-Tanana terrane is largely made up of heterogeneous gneiss and schist, scattered deformed plutons, and high-level sheets of chert, basalt and ultramafic rock. The terrane is probably composite with nappes of upper Palaeozoic oceanic assemblages thrust across a quartzofeldspathic and silicic volcanic-rich protolith of probable Precambrian to known Palaeozoic age and of unknown continental affinity. The time of final emplacement of the composite terrane against North America is not known, but may have been as recent as Cretaceous time with earlier amalgamation in the Triassic<sup>25</sup>. Subsequently, in post-Early Cretaceous time Wrangellia, already amalgamated with the Lower Jurassic Peninsular arc terrane and Alexander terrane, collided with the Yukon-Tanana terrane entrapping many smaller terranes of unknown origin (including Chulitna terrane) within a flysch-filled suture zone<sup>18,26</sup>. The successive accretions must have caused subduction systems to step southward and from late Cretaceous to early Tertiary time, the Chugach and younger accretionary flysch prisms were emplaced against the newly formed North American margin<sup>27</sup>. Concurrent and post-accretionary convergence has caused translation and intra-plate deformation with reactivation of old sutures. This has resulted in northwestward strike-slip displacements of hundreds of kilometres along the Tintina, Denali and other faults in Alaska and adjacent Canada<sup>25,28-30</sup>.

The largest allochthonous terrane in Canada is the Stikine terrane<sup>15</sup>. It has a basement of upper Palaeozoic submarine arc rocks overlain by Upper Triassic to Middle Jurassic submarine and subaerial volcanic and sedimentary rocks (Takla-Hazleton assemblage)<sup>15</sup> and intruded by coeval granitic plutons. This major block seems to have accreted between early Triassic and mid-Jurassic time<sup>25,31</sup> entrapping between itself and the North American margin Tethyan ocean floor (Ch) and a collage of Palaeozoic 'oceanic' arcs and possible distal fragments of the Cordilleran continental terrace (E). The late Jurassic and Cretaceous Bowser Basin<sup>32</sup> overlap assemblage is deposited on Stikine terrane and records the first clear sediment source to the east, of both continental and oceanic (Ch) character. Final stages of the accretionary process were emplacements of nappes eastwards and westwards from the suture zone and on to the former continental margin. This eastern accretion was followed by the arrival of Wrangellia<sup>7</sup>, which, from Vancouver Island north,



seems to have been in middle Cretaceous time. In eastern Oregon, its arrival time may be earlier. The northern part of Wrangellia had already amalgamated with the Alexander terrane, as explained above, and arrived bearing a Jurassic arc and the Gravina–Nutzotin late Jurassic to early Cretaceous submarine arc terrane on it. Subsequent thrusting and northward translation on intra-plate strike-slip faults<sup>8,33</sup> largely during late Cretaceous to early Tertiary time, have disrupted the original relationships, but left a detached fragment of Wrangellia isolated in eastern Oregon. Once again, subduction zones must have stepped outboard through successive accretions, for by late Cretaceous–early Tertiary time the trench was on or near the present Pacific margin<sup>8</sup>.

Much of the central western part of the Cordillera in the US is underlain by several terranes (S, BL, KL, Si, Trp, C) whose very poorly exposed relationships to one another are still imperfectly understood<sup>34</sup>. Certainly the Permian Tethyan fauna-bearing terranes of Oregon and California are important and which move to positions much closer to the Pacific margin as they are tracked southward from their more internal position in Canada. No Tethyan fauna-bearing terranes are known south of central California. The Roberts Mountain allochthon of west-central Nevada is probably a distal continental terrace or marginal oceanic assemblage emplaced across the Cordilleran miogeocline in middle Palaeozoic time<sup>12</sup>. This is the oldest known example of accretion in western North America. Most of the remaining suspect terranes in the northern Sierra Nevada, Klamath Mountains and western Nevada are Palaeozoic to Mesozoic volcanic and sedimentary sequences of oceanic and arc-trench affinity which were swept against the Cordilleran margin in late Palaeozoic to middle Mesozoic time<sup>7</sup>. By mid-Cretaceous time the Franciscan accretionary assemblage was forming on the outboard margin of North America. Siletzia, a submarine basalt province of early Tertiary age in western Oregon certainly rotated clockwise over 70° since Eocene time<sup>35,36</sup> and was only finally emplaced in mid-Tertiary time.

In southwestern North American Precambrian basement extends nearly to the present coastline in southern California and northwestern Mexico. This precludes major large accretionary masses there, but several smaller displaced terranes (Sa, SG, Or) of both oceanic and quasi-continental character are known along this margin. Another important relationship is that some Jurassic magmatic arc terranes were intruded into, or deposited on, North American cratonic basement in northwestern Mexico and the southwestern US. This is in direct contrast to arcs of similar age north of central California which are ubiquitously found outside confirmed North American basement and intruded into or deposited on the suspect terranes themselves. As stated earlier, this makes the northern Mesozoic arc terranes as suspect as the terranes they sit on until it is proved otherwise. How all these Upper Triassic to Jurassic arcs relate to one another along strike and which way they faced are problems currently under much discussion and investigation. Note that major low-angle thrusting in southern California and southwestern Arizona is emerging from recent work and large-scale emplacement of allochthons in this region is not precluded<sup>37,38</sup>.

The major displaced terrane in southwestern North America so far proposed is of totally different character from those described northwards in the Cordillera. This terrane is that part of the North American craton which is supposed to have moved up to 800 km southeastwards relative to stable North America along the Mojave–Sonora megashear<sup>39</sup> or transform fault. This movement is said to have taken place in late Jurassic time and was kinematically linked to the opening of the Atlantic Ocean and the Gulf of Mexico as Africa–South America separated from North America.

## Conclusions

The collisions and accretions in western North America discussed above have profound implications for Cordilleran tecto-

genesis<sup>25,40</sup>. The mechanical process of these accretions and their effect on the accreted masses themselves and on the Cordilleran margin are poorly understood. Certainly thrust faulting has played a dominant part and if the thrust faulting within the accreted terranes is linked to the thrust belts<sup>41,42</sup> along the eastern Cordilleran margin as has been suggested<sup>25</sup>, the resulting telescoping is unprecedented in Cordilleran tectonic thought. Concurrent and post-accretionary telescoping, and consolidation apparently took place by major intra-plate thrusting and strike-slip translations<sup>25</sup>. The entire process seems to have endured over a period of at least 120 Myr or from mid-Jurassic well into early Tertiary time. Much northward translation and clockwise rotation occurred which suggest oblique convergence from a general northward Pacific 'mega-drift'<sup>7</sup>, as implied by palaeomagnetic data.

The analogy with the Himalayan orogen and the internal disruption of Asia<sup>43</sup> is striking, but there are major differences. Unlike India, a large continental mass which remains coupled to the Indian Ocean plate as the subcontinent indents Asia, the comparatively smaller accreted terranes in western North America became uncoupled from Pacific Ocean plates by formation of subduction zones near the present Pacific margin in late Mesozoic time. Much of the telescoping and translation continued inside the marginal subduction zones well into Tertiary time. During the late Cretaceous to early Tertiary period of Laramide deformation<sup>6</sup> possible elevated convergence rates between North America and the Farallon and Kula plates combined with variably dipping subducting slabs<sup>44</sup> may have produced deep-seated Laramide tectonism and complex shifting magmatic patterns across the Cordilleran foreland as a final stage to consolidation of the Cordilleran mosaic and its cratonic foreland. Also North America's generally northwestward and westward motion over the mantle against the generally northward-moving accretions may have been dynamically important<sup>41,42,45</sup>. It is not accidental that Cordilleran telescoping on the foreland only began after the Middle Jurassic initiation of opening of the Central Atlantic Ocean which sent the North American plate northwestward then westward over the Pacific Ocean<sup>41,8</sup>. Post-middle Tertiary successive overriding of Pacific spreading centres by North America has produced the complex transform regimen which has affected North America's western edge down to the present<sup>46</sup>.

The numerous upper Palaeozoic and lower to middle Mesozoic arcs that so characterize the allochthonous terranes are of special interest. None of these can be confirmed to have stood on the North American cratonic margin. They may have stood offshore in the manner of the present western Pacific Ocean arcs, but if they did we still do not know which way they faced. In any event they would have to have eventually collapsed against the North American margin by subduction of various sorts of small ocean basins caught behind them. This view is attractive because of the example of the western Pacific Ocean, but it does present some difficulties. The principal difficulties are the scraps of Tethyan ocean floor caught inside these arcs and preliminary palaeomagnetic evidence<sup>9,10,47,48</sup> which suggest large northwards translations of some of these arcs before final accretion. All this presents the possibility that the arcs may indeed be far travelled and totally unrelated to North America and thus exotic fragments from far reaches of the Pacific Ocean<sup>7</sup>. It is not until Cretaceous time that a semi-continuous magmatic arc along the Cordilleran margin can be substantiated by plutonic, volcanic and stratigraphical data<sup>6,52</sup>.

Either of these models is consistent with possible plate palaeogeographies of the time. During late Palaeozoic and early Mesozoic time two-thirds of our planet's surface was paved with a single enormous ocean<sup>49</sup>. The other third was Pangea. Assuming that lengths and spacings of spreading centres were similar then to that now, a single large ocean would statistically favour more percentage area of old ocean crust lying around ready to be subducted than at any other time before or since the Phanerozoic. If offshore and/or intra-oceanic arcs correlate with subduction of cold and dense old oceanic crust, as has been

suggested<sup>50</sup>, large parts of the late Palaeozoic-early Mesozoic palaeo-Pacific Ocean could have been festooned with magmatic arcs<sup>51</sup>. As Pangea began to break up and North America began to advance over that Ocean, the arcs could have been swept northwards against large sectors of North America's margin to

produce much of the Cordilleran mosaic which has been considered here. During this process, the Pacific was cleared of older arcs, oceanic plateaus and continental fragments, leading thus to the creation of the simple plate configuration that characterizes the present eastern Pacific.

Received 19 May; accepted 25 September 1980.

1. Wilson, J. T. *Proc. Am. phil. Soc.* **112**, 309-320 (1968).
2. Monger, J. W. H., Souther, J. G. & Gabrielse, H. *Am. J. Sci.* **272**, 577-602 (1972).
3. Jones, D. L., Irwin, W. P. & Owenshine, A. T. *U.S. Geol. Surv. Prof. Pap.* 800-B, B211-B217 (1972).
4. Helwig, J. *Soc. Econ. Paleontologists and Mineralogists Spec. Publ.* **19**, 359-376 (1974).
5. Davis, G. A., Monger, J. W. H. & Burchfiel, B. C. in *Mesozoic Paleogeography of the Western United States* (eds Howell, D. G. & McDougall, K. A.) 1-32 (Pacific Coast Paleogeography Symp. No. 2, 1978).
6. Coney, P. J. *Geol. Soc. Am. Mem.* 152, 000-000 (1978).
7. Jones, D. L., Silberling, N. J. & Hillhouse, H. W. in *Mesozoic Paleogeography of the Western United States* (eds Howell, D. G. & McDougall, K. A.) 71-74 (Pacific Coast Paleogeography Symp. No. 2, 1978).
8. Monger, J. W. H. & Price, R. A. *Can. J. Earth Sci.* **16**, 770-791 (1979).
9. Beck, M. E. Jr *Am. J. Sci.* **276**, 694-712 (1976).
10. Irving, E. *Can. J. Earth Sci.* **16**, 669-694 (1979).
11. Stewart, J. H. & Poole, F. G. in *Tectonics and sedimentation* (ed. Dickinson, W. R.) 57 (Society of Economists Paleontologists and Mineralogists Spec. Publ. 22, 1974).
12. Dickinson, W. R. in *Paleozoic Paleogeography of the Western United States* (eds Stewart, J. H., Stevens, C. H. & Fritsche, A. E.) (Pacific Coast Paleogeography Symp. No. 1, 1977).
13. Burchfiel, B. C. & Davis, G. A. *Am. J. Sci.* **275A**, 363-396.
14. Churkin, M. & Eberlein, G. D. *Bull. geol. Soc. Am.* **88**, 769-786 (1977).
15. Monger, J. W. H. *Can. J. Earth Sci.* **14**, 1832-1859 (1977).
16. Monger, J. W. H. & Ross, C. A. *Can. J. Earth Sci.* **8**, 259-278 (1971).
17. Berg, H. C., Jones, D. L. & Richter, D. H. *U.S. Geol. Surv. Prof. Pap.* 800-D, D1-D24 (1972).
18. Jones, D. L. & Silberling, N. J. *U.S. Geol. Survey Open-File Rep.* 79-1200 (1979).
19. Berg, H. C., Jones, D. L. & Coney, P. J. *U.S. Geol. Survey Open-File Rep.* 78-1085 (1978).
20. Jones, D. L., Silberling, N. J. & Hillhouse, J. *Can. J. Earth Sci.* **14**, 2565-2577 (1977).
21. Irving, E. & Yole, R. W. *Earth Phys. Branch Publ. Ottawa* **42**, 87-95 (1972).
22. Hillhouse, J. W. *Can. J. Earth Sci.* **14**, 2578-2592 (1977).
23. Jones, D. L., Silberling, N. J., Csejty, B. Jr, Nelson, W. H. & Blome, C. D. *U.S. Geol. Surv. Prof. Pap.* **1121A** (1980).
24. Nichols, K. M. & Silberling, N. J. *U.S. Geol. Surv. Prof. Pap.* 1121B (1979).
25. Tempelman-Kluit, D. J. *Geol. Surv. Can. Pap.* 79-14, 1-27 (1979).
26. Coney, P. J., Silberling, N. J., Jones, D. L. & Richter, D. H. *U.S. Geol. Surv. Circ.* (in the press).
27. Plafker, G., Jones, D. L. & Pessagno, E. A. Jr *U.S. Geol. Surv. Circ.* **751B**, 41-43 (1977).
28. Grantz, A. *U.S. Geol. Survey Open-File Rep.* 267 (1966).
29. Roddick, J. A. *J. Geol.* **75**, 2333 (1964).
30. Owenshine, A. T. & Brew, D. A. *Int. 24th Geol. Congr., Montreal, Sec. 3*, 245-254 (1972).
31. Tempelman-Kluit, D. J. *Geol. Surv. Can. Pap.* 73-41 (1974).
32. Eisbacher, G. H. *Soc. Econ. Paleontol. Miner. Spec. Publ.* **19**, 274-291 (1974).
33. Monger, J. W. H., Richards, T. A. & Peterson, I. A. *Can. J. Earth Sci.* **15**, 823-830 (1978).
34. Speed, R. C. *J. Geol.* **87**, 279-292 (1979).
35. Cox, A. V. *Nature* **179**, 685-686 (1957).
36. Simpson, R. W. & Cox, A. *Geology* **5**, 585-589 (1977).
37. Haxel, G., Wright, J. E., May, D. J. & Tosdel, R. M. *Arizona Geol. Soc. Digest* **12** (1980).
38. Reynolds, S. J., Keith, S. B. & Coney, P. J. *Arizona Geol. Soc. Digest* **12** (1980).
39. Silver, L. T. & Anderson, T. H. *Geol. Soc. Am. Abstr. Prog.* **6**, 955-956 (1974).
40. Nur, A. & Ben-Avraham, Z. *J. Phys. Earth* **26**, 5-21 (1978).
41. Coney, P. J. *Nature* **233**, 462-465 (1971).
42. Coney, P. J. *Am. J. Sci.* **272**, 603-628 (1972).
43. Molnar, P. & Tapponnier, P. *Science* **189**, 419-426 (1975).
44. Coney, P. J. & Reynolds, S. J. *Nature* **270**, 403-406 (1977).
45. Wilson, J. T. & Burke, K. *Nature* **239**, 448-449 (1972).
46. Atwater, T. *Bull. geol. Soc. Am.* **81**, 3513-3526 (1970).
47. Packer, D. R. & Stone, D. B. *Can. J. Earth Sci.* **11**, 976-997 (1974).
48. Stone, D. B. & Packer, D. R. *Tectonophysics* **37**, 183-201 (1977).
49. Irving, E. *Nature* **270**, 304-309 (1977).
50. Molnar, P. & Atwater, T. *Earth planet. Sci. Lett.* **41**, 330-340 (1978).
51. King, L. C. Q. *Jl geol. Soc. Lond.* **114**, 47-77 (1958).
52. Hamilton, W. in *Mesozoic Paleogeography of the Western United States* (eds Howell, D. G. & McDougall, K. A.) 33-70 (Pacific Coast Paleogeography Symp. No. 2, 1978).
53. Jones, D. L., Silberling, N. J., Berg, H. C. & Plafker, G. *U.S. Geol. Surv. Open-File Rep.* (in the press).
54. Whetten, J. T., Jones, D. L., Cowan, D. S. & Zartman, R. E. in *Mesozoic Paleogeography of the Western United States* (eds Howell, D. G. & McDougall, K. A.) 117-132 (Pacific Coast Paleogeography Symp. No. 2, 1978).
55. Misch, P. *Can. Instn. Min. Metall. Spec. B*, 101-148 (1966).
56. Tabor, R. W. & Cady, W. M. *U.S. Geol. Surv. Prof. Pap.* 1033 (1978).
57. Brooks, H. C. & Vallier, T. L. in *Mesozoic Paleogeography of the Western United States* (eds Howell, D. G. & McDougall, K. A.) 133-145 (Pacific Coast Paleogeography Symp. No. 2, 1978).
58. Dickinson, W. R. & Thayer, T. P. in *Mesozoic Paleogeography of the Western United States* (eds Howell, D. G. & McDougall, K. A.) 147-161 (Pacific Coast Paleogeography Symp. No. 2, 1978).
59. Irwin, W. P. *Calif. Div. Min. Geol. Bull.* **190**, 19-37 (1966).
60. Behrman, P. G. & Parkinson, G. A. in *Mesozoic Paleogeography of the Western United States* (eds Howell, D. G. & McDougall, K. A.) 349-360 (Pacific Coast Paleogeography Symp. No. 2, 1978).
61. Irwin, W. P. *U.S. Geol. Surv. Prof. Pap.* 800C, C103-C111 (1972).
62. Irwin, W. P., Jones, D. L. & Pessagno, E. A. Jr *Geology* **5**, 557-562 (1977).
63. Irwin, W. P. *Geol. Soc. America Map Char. Ser.* MC-33, Sheet 1 (1979).
64. Potter, A. W., Hotz, P. E. & Rohr, D. M. in *Paleozoic Paleogeography of the Western United States* (eds Stewart, J. H., Stevens, C. H. & Fritsche, A. E.) 421-440 (Pacific Coast Paleogeography Symp. No. 1, 1977).
65. D'Aillura, J. A., Moores, E. M. & Robinson, L. in *Paleozoic Paleogeography of the Western United States* (eds Stewart, J. H., Stevens, C. H. & Fritsche, A. E.) 395-408 (Pacific Coast Paleogeography Symp. No. 1, 1977).
66. Schweickert, R. A., Saleeby, J. B., Tobisch, O. T. & Wright, W. H. III in *Paleozoic Paleogeography of the Western United States* (eds Stewart, J. H., Stevens, C. H. & Fritsche, A. E.) 381-394 (Pacific Coast Paleogeography Symp. No. 1, 1977).
67. Blake, M. C. Jr & Jones, D. L. in *Mesozoic Paleogeography of the Western United States* (eds Howell, D. G. & McDougall, K. A.) 397-400 (Pacific Coast Paleogeography Symp. No. 2, 1978).
68. Ross, D. C. in *Mesozoic Paleogeography of the Western United States* (eds Howell, D. G. & McDougall, K. A.) 509-522 (Pacific Coast Paleogeography Symp. No. 2, 1978).
69. Powell, R. E. & Silver, L. T. *Geol. Soc. Am. Abstr. Prog.* **11**, 498 (1979).
70. Haxel, G. & Dillon, J. in *Mesozoic Paleogeography of the Western United States* (eds Howell, D. G. & McDougall, K. A.) 453-470 (Pacific Coast Paleogeography Symp. No. 2, 1978).
71. Miller, E. L. & Carr, M. D. in *Mesozoic Paleogeography of the Western United States* (eds Howell, D. G. & McDougall, K. A.) 283-290 (Pacific Coast Paleogeography Symp. No. 2, 1978).
72. Gastil, G., Morgan, G. J. & Krummenacher, D. in *Mesozoic Paleogeography of the Western United States* (eds Howell, D. G. & McDougall, K. A.) 107-116 (Pacific Coast Paleogeography Symp. No. 2, 1978).
73. Rangan, C. in *Mesozoic Paleogeography of the Western United States* (eds Howell, D. G. & McDougall, K. A.) 85-106 (Pacific Coast Paleogeography Symp. No. 2, 1978).
74. Speed, R. C. *J. Geology* **87**, 179-192 (1979).
75. Silberling, N. J. & Roberts, R. J. *Geol. Soc. Am. Spec. Pap.* 72 (1962).
76. Poole, F. G., Sanberg, C. A. & Boucot, A. J. in *Paleozoic Paleogeography of the Western United States* (eds Stewart, J. H., Stevens, C. H. & Fritsche, A. E.) 39-66 (Pacific Coast Paleogeography Symp. No. 1, 1977).

# Voltage-dependent translocation of the asialoglycoprotein receptor across lipid membranes

Robert Blumenthal, Richard D. Klausner & John N. Weinstein

Section on Membrane Structure and Function, LTB, DCBD, National Cancer Institute, National Institutes of Health, Bethesda, Maryland 20205

*A membrane receptor protein for asialoglycoproteins induces voltage-dependent increases in ion conductance across a lipid bilayer, probably reflecting penetration of the protein into the bilayer towards an electrically positive pole. In the presence of specific ligand for the receptor, this penetration leads to a 'translocation' of the receptor from one side of the bilayer to the other. These observations suggest a mechanism by which biological membranes might regulate the disposition of their proteins, and a way in which membrane receptors involved in endocytosis might be spared lysosomal destruction in order to be recycled to the plasma membrane.*

BOTH the lipid and the protein components of biological membranes seem to be asymmetrically distributed<sup>1</sup>. A key question is whether the biosynthetic process determines once

and for all the orientation of a given membrane component, or whether later processes can affect the component's disposition. At least some membrane lipids do seem to redistribute between



the inner and outer leaflets of the bilayer in a relatively rapid process whose nature is at present not clear<sup>2</sup>. We show here that a membrane receptor protein for asialoglycoproteins induces voltage-dependent increases in ion conductance across a lipid bilayer, probably reflecting penetration of the protein into the bilayer towards an electrically positive pole. In the presence of specific ligand for the receptor, this penetration leads to a 'translocation' of the receptor from one side of the bilayer to the other. These observations suggest that the membrane potential might have a role in regulation of the disposition and function of membrane proteins.

To investigate the assembly and disposition of proteins in membranes we have studied the interaction with lipid bilayers of a membrane receptor purified from rabbit hepatocytes. This hepatic binding protein (HBP) has been studied extensively<sup>3</sup>. When serum glycoproteins are desialylated to expose penultimate galactose moieties, they are removed from circulation by binding to this receptor, with subsequent endocytosis.

A general outline of receptor-mediated endocytosis is the following. After the ligand has bound to the receptor it is rapidly endocytosed and delivered to a lysosome, where it is degraded. The process has a half life of 15–60 min. The receptor, on the other hand, has a half life of ~88 h (ref. 4). This raises a topological problem: the receptor's binding sites face outwards from the plasma membrane. After ligand binding and endocytosis, they would be expected to face the inside of the lysosome and to be destroyed. However, evidence<sup>4</sup> suggests that the receptor in fact faces the outer, cytosolic surface of vesicles in the lysosome-enriched fraction. Thus the receptor may cross the membrane at some point during endocytosis, and we present here a possible mechanism for such a translocation.

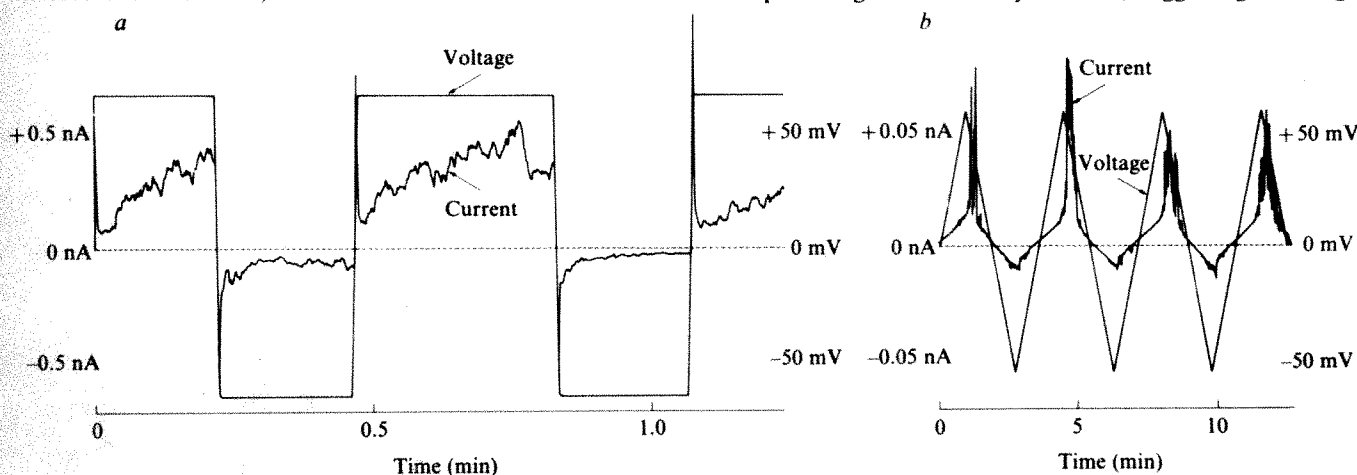
Rabbit HBP can be purified to homogeneity and, as shown by SDS polyacrylamide gel electrophoresis, has two subunits, of molecular weights 40,000 and 48,000 (ref. 5). By precipitation with ethanol it can be obtained in water-soluble form, free of detergent and of bilayer lipid. Our previous studies<sup>6</sup> showed that this protein forms a stable association with phosphatidylcholine vesicles merely by mixing of the protein with vesicles. Here we report the interaction of HBP with black lipid membranes (BLMs). Advantages of the BLM were the accessibility of both sides of the membrane for addition of reagents and the ease with which the membrane potential could be controlled. Partial insertion of a protein into a BLM can perturb the membrane's structure and increase the permeation of ions across it (that is, increase its conductance)<sup>7</sup>.

## The nature of HBP-induced BLM conductance

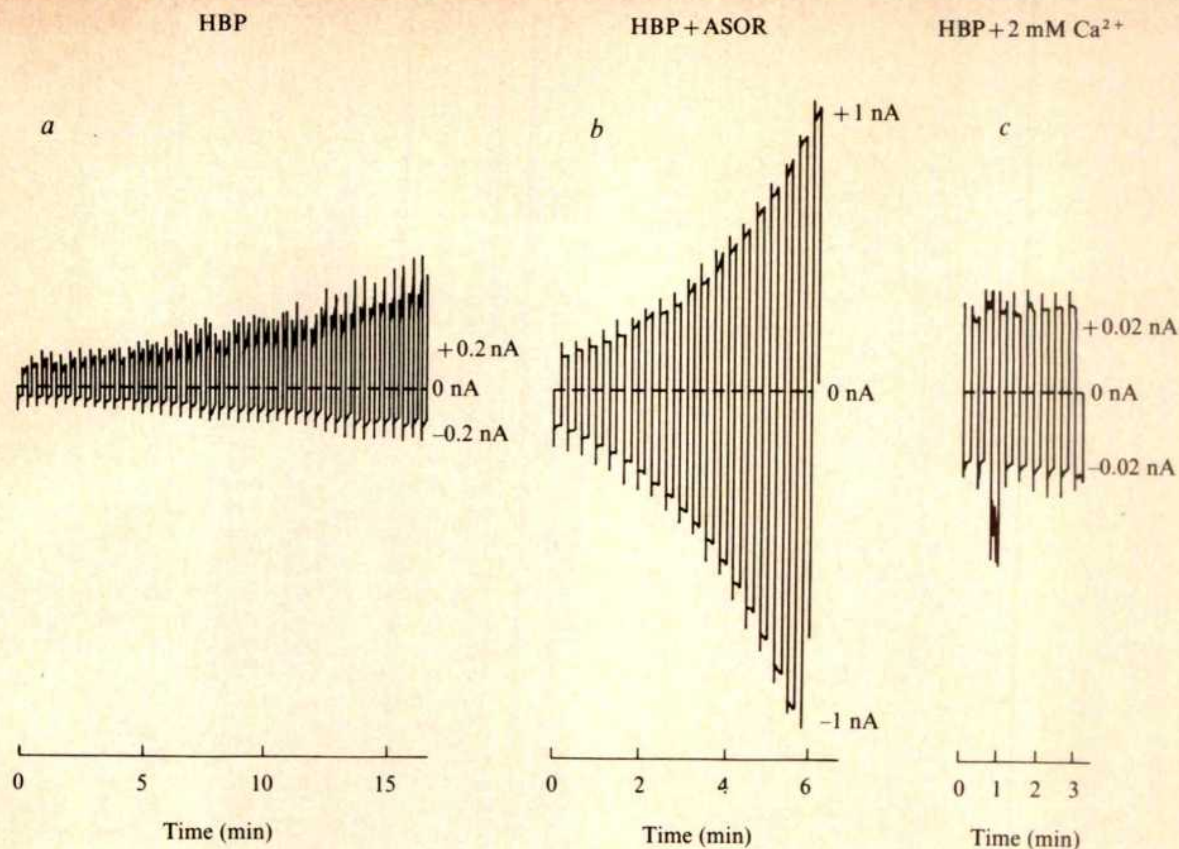
Figure 1 shows an asymmetrical conductance increase seen when HBP was added to one side (*cis*) of a BLM. When the potential was negative on the *trans* side, the conductance was that of an unmodified BLM. When the potential was positive on the *trans* side, HBP induced a conductance increase to about 10 times that of the unmodified BLM. In most such experiments the conductance changed to 10–100-fold the unmodified BLM level (see below). Conductance changed in the form of rapid fluctuations rather than in the discrete, uniform steps characteristic of channels or the fast, smooth rise characteristic of carriers<sup>8</sup>. This form suggests that the conductance was induced by a perturbation of membrane structure<sup>7</sup> rather than by an ionophore associated with HBP. Figure 1 shows the asymmetrical time dependence and voltage dependence of the conductance increase. In Fig. 1a the voltage was switched at time intervals of about 30 s between +60 and –60 mV. During *trans*-positive intervals the conductance increased, and during *trans*-negative periods it decreased. The time required for conductance increase was much longer than that for the decrease. When the voltage was imposed in the form of a triangular wave (Fig. 1b), the result suggested a threshold effect; that is, the conductance started to rise steeply as the voltage increased and then decreased sharply as the voltage fell below 20–30 mV *trans*-positive. With a *trans*-positive voltage above threshold the conductance increased with time (Fig. 2). If the voltage was held below threshold a low conductance could be maintained for hours.

The diffusion potential of an HBP-modified BLM, measured as a function of potassium nitrate concentration ratio, showed a slope of about 10 mV per decade of concentration ratio  $[K^+]_{cis}/[K^+]_{trans}$ , indicating a slight selectivity for cations over anions.

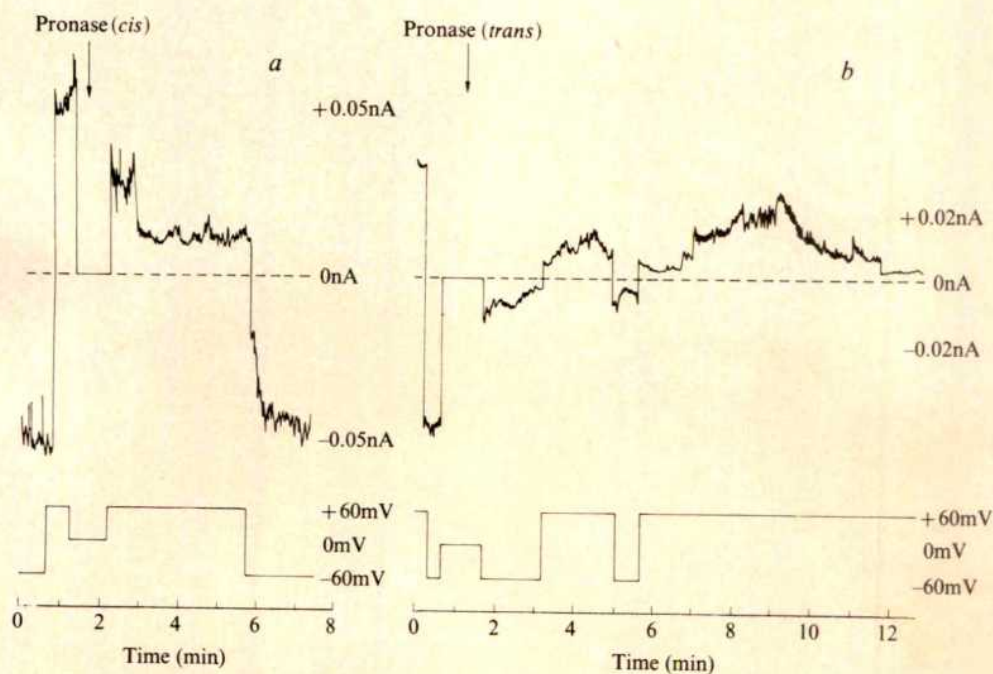
The suggestion from the BLM experiment (Fig. 1) that HBP moves towards a *trans*-positive potential was supported by studies of HBP inserted into phospholipid vesicles by methods described elsewhere<sup>6</sup>. We determined the exposure of the protein's tryptophan groups to aqueous quenchers, iodide and acrylamide. The fluorescence intensity of the tryptophan residues in vesicle-associated HBP decreased with increasing concentration of quencher. When we imposed a *trans*-positive voltage gradient across the vesicles by adding the  $K^+$ -selective ionophore valinomycin in the presence of a  $K^+$  gradient, the quenching was markedly reduced, suggesting a voltage-



**Fig. 1** Asymmetric conductances in a HBP-modified BLM. The BLM was formed from a solution of oxidized cholesterol (2% in *n*-decane) applied across an aperture (1-mm diameter) in a Teflon partition separating two 3-ml chambers, according to the procedure developed by Mueller and Rudin<sup>24</sup>. Each chamber contained an aqueous solution of KCl (6 mM), NaCl (139 mM), and HEPES (10 mM) at pH 7.4. The solution contained about 50  $\mu$ M  $Ca^{2+}$ . HBP (final concentration 10  $\mu$ g ml<sup>-1</sup>) was added to one compartment (*cis*) and the solution was stirred by means of Teflon-covered magnets turned by a d.c. motor fixed below the bilayer chamber. The records were taken immediately after adding the HBP. The initial conductance was 0.1 nS. The area of the BLM was  $8 \times 10^{-3}$  cm<sup>2</sup>. The voltage was applied from a d.c. battery switched at arbitrary times by hand (a) or in the form of a triangular wave at a frequency of 0.003 Hz using a function generator (Hewlett-Packard 3310B) (b). Current was passed through the BLM by means of Ag/AgCl electrodes and fed into a current transducer that converted membrane current (I) into a voltage signal. The output of the voltage source and of the current transducer were fed into two channels of a d.c. recorder (Leeds and Northrup 624). The voltage is defined as  $\psi_{trans} - \psi_{cis}$ . Note that in Fig. 2b there is a small capacitive current.



**Fig. 2** Symmetrization of conductance on addition of specific ligand or  $\text{Ca}^{2+}$  to an HBP-modified BLM. The conditions were as described in the legend to Fig. 1. Voltage (not shown) was applied in a rectangular wave form alternating between +50 and -50 mV, at a frequency of 0.04 Hz. *a*, The same buffer as in Fig. 1; *b*,  $10 \mu\text{g ml}^{-1}$  ASOR added to the *cis* side; *c*, 2 mM  $\text{Ca}^{2+}$  present on both sides.



**Fig. 3** The effect of pronase on the current through an HBP-ASOR-modified BLM. HBP and ASOR were added to the *cis* side. The conditions were as described in Fig. 2b legend.  $100 \mu\text{g ml}^{-1}$  *Staphylococcus aureus* (Sigma) protease (equivalent to pronase) was added to the *cis* chamber (*a*) or to the *trans* chamber (*b*).



dependent penetration of the HBP into the vesicle bilayer. Valinomycin, in the presence of  $K^+$  but without a  $K^+$  gradient, had no effect on quenching.

### The effects of ligand and $Ca^{2+}$

Figure 2 shows the pattern of conductance change induced in the BLM by HBP in the presence of the ligand asialo-orosomucoid (ASOR) and in the presence of  $Ca^{2+}$ . In each case the reagents were added to the *cis* side only. ASOR alone did not affect BLM conductance. With HBP alone (Fig. 2a), the conductance remained asymmetric, but it became symmetrical and increased rapidly when ASOR was added (Fig. 2b). To test the specificity of this effect, the terminal galactose residues of ASOR were removed by enzymatic hydrolysis with  $\beta$ -galactosidase. In accordance with the known specificity of the binding protein, the resulting product, agalacto-orosomucoid, failed to increase or symmetrize the conductance of an HBP-modified BLM.

In the presence of 2 mM  $Ca^{2+}$  (Fig. 2c) the conductance symmetrized, but the rate of conductance increase was relatively slow.  $Mg^{2+}$  had no effect. When ASOR (see Fig. 4) or  $Ca^{2+}$  (not shown) was added to the *trans* side of an asymmetrically conducting HBP-modified BLM, there was no effect on conductance and no symmetrization. As expected, addition of HBP alone to both sides of the BLM induced a symmetrical conductance (not shown). The simplest interpretation of the symmetrization seen with HBP and either ASOR or  $Ca^{2+}$  (Fig. 2) is movement of (part of) the HBP to the opposite side of the membrane.

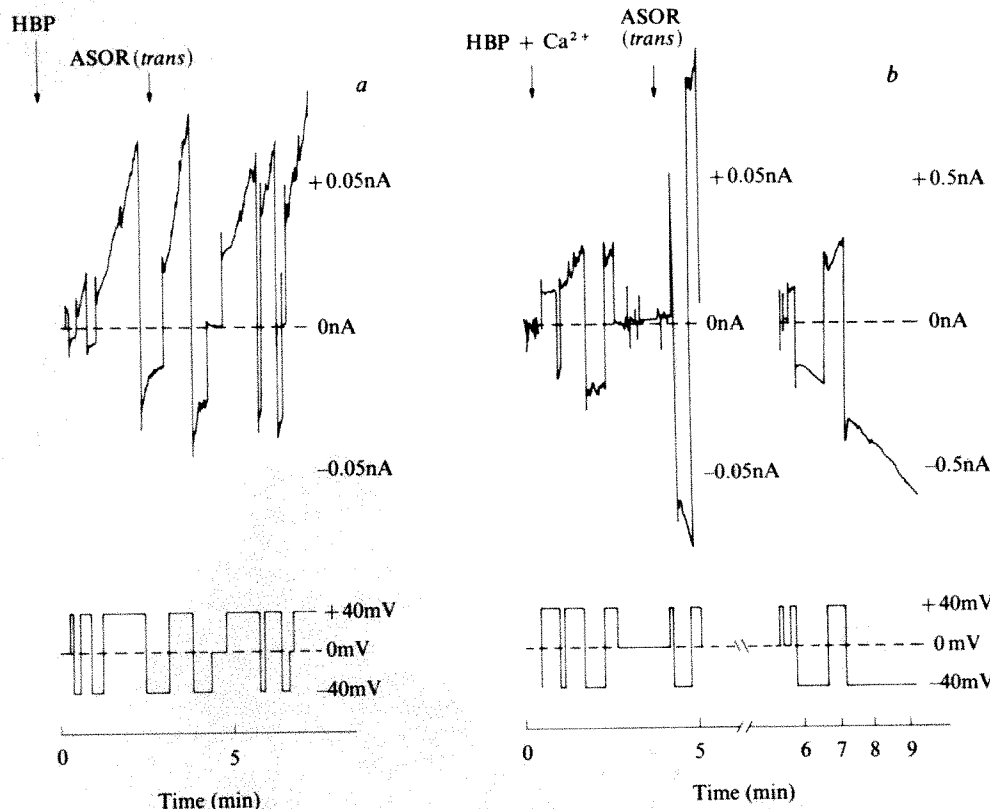
### Evidence for translocation of HBP across the membrane

We tested this notion of membrane crossing or 'translocation' by adding pronase to the *cis* side of an asymmetrically conducting BLM. This abolished the conductance increase, indicating degradation of HBP on that side; pronase had no effect when

added to the *trans* side. However, after conductance had been symmetrized by addition of HBP and ligand to a BLM, addition of pronase to the *cis* side resulted in an asymmetric conductance of the polarity corresponding to addition of HBP to the *trans* side of the membrane only (Fig. 3a). Thus with a *trans*-positive potential the conductance decreased. With a *trans*-negative potential the conductance initially increased, indicating that the HBP had entered a conducting state on the *trans* side. With prolonged exposure to *trans*-negative potential, all conductance eventually disappeared (not shown). This finding is consistent with a gradual potential-induced translocation of HBP back to the *cis* side, where it could be degraded by pronase. On the other hand, when the potential was maintained *trans*-positive, the protein was not degraded, and the new asymmetry could be maintained (not shown), indicating that pronase had not crossed the BLM.

When pronase was added to the *trans* side of a symmetrically conducting BLM (Fig. 3b), the pattern of conductance change was complicated but consistent with translocation of the conducting moiety of HBP. When the potential was made *trans*-negative, there was a decrease in conductance consistent with transition of HBP to a non-conducting state on the *trans* side and an inability to recruit conducting moieties from the *trans* side because those had been degraded by pronase. When the voltage was switched to *trans*-positive there was a transient increase in conductance due to transition of HBP into a conducting state, followed by a conductance decrease due to exposure of HBP which had apparently crossed over towards the pronase on the *trans* side. The conductance eventually disappeared when the potential was held *trans*-positive for longer times. Adding new HBP and ASOR to the *cis* side resulted in a repetition of the pattern.

Figure 4 suggests that a binding moiety of HBP is translocated. With HBP on the *cis* side, ligand had no effect when added to the *trans* side (Fig. 4a); when added to the *cis* side it increased and symmetrized the conductance (Fig. 2b). However,



**Fig. 4** Effect of adding ligand to the '*cis* and *trans*' sides. The conditions were as described in Fig. 1 legend. *a*,  $10 \mu\text{g ml}^{-1}$  ASOR added to the *trans* side at about 2 min; *b*, 2 mM  $Ca^{2+}$  present on both sides and  $10 \mu\text{g ml}^{-1}$  ASOR added to the *cis* side at ~3 min.

when a symmetrical conductance was induced in the presence of 2 mM  $\text{Ca}^{2+}$ , the conductance further increased markedly and symmetrically when ligand was added to the *trans* side (Fig. 4b). Again this was specific for the ligand; agalacto-orosomucoid had no effect on the conductance.

Figure 5 shows the absolute dependence of a conductance increase and subsequent symmetrization on the *trans*-positive potential. In the presence of HBP and ASOR a *trans*-negative voltage of 50 mV was applied across the BLM for 60 min giving no conductance change. When the voltage was then switched to a *trans*-positive polarity, the conductance started to increase and became symmetrical.

## Discussion

Figure 6 shows a hypothetical view of the interaction between HBP and lipid bilayers. The protein first associates with the bilayer without requiring a membrane potential (a). Our previous studies<sup>6</sup> have shown this to be hydrophobic interaction involving perturbation of the lipid bilayer and a conformational change in the HBP. Under the influence of a *trans*-positive membrane potential the protein can be promoted reversibly into a conducting state (b) in which it seems to perturb the bilayer sufficiently to permit passage of ions, that is, to increase the conductance of the membrane. The polarity of this effect makes sense, as HBP is negatively charged (isoelectric point at pH 4.7). The increase in conductance does not have the characteristics of a well defined channel or carrier. It does correlate, however, with the finding in lipid vesicles that HBP tryptophans become markedly less accessible to fluorescence quenchers in the aqueous phase when valinomycin and a  $\text{K}^+$  gradient are used to generate a *trans*-positive potential. The conductance increase and the tryptophan sequestration suggest a further penetration by the protein, perhaps sufficient to perturb the second leaflet of the bilayer. However, these observations could also be accounted for by an aggregation, or by a combination of penetration and aggregation such as that in Fig. 6b. Analogously, Shinitzky has considered that vertical displacement of membrane proteins could be mediated by changes in lipid packing<sup>9</sup>.

The next stage (Fig. 6b, c) is a translocation of the protein from the *cis* to the *trans* side of the membrane under the influence of a *trans*-positive electric field in the presence of a galactose-terminal ligand or  $\text{Ca}^{2+}$ . Observations supporting translocation are (1) that the membrane conductance becomes symmetrical, (2) that part of the HBP becomes exposed on the *trans* side and is destroyed by pronase there, and (3) that ligand

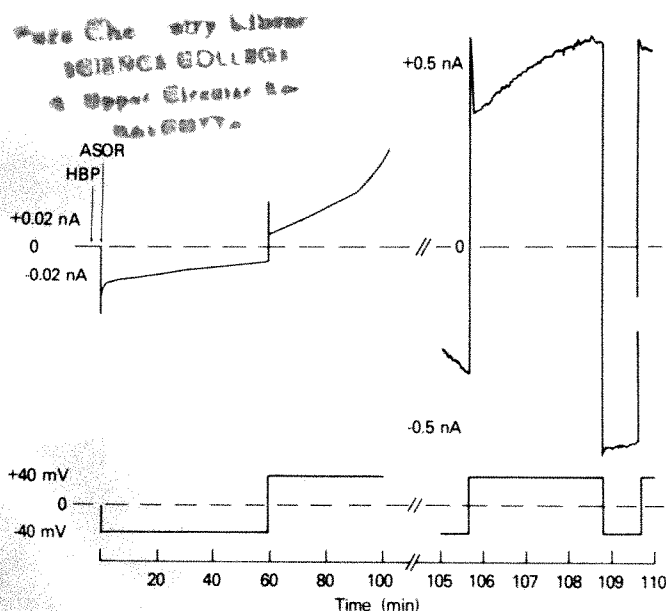


Fig. 5 Requirement of *trans*-positive potential for translocation of HBP across a BLM. The conditions were as described in Fig. 2b legend.

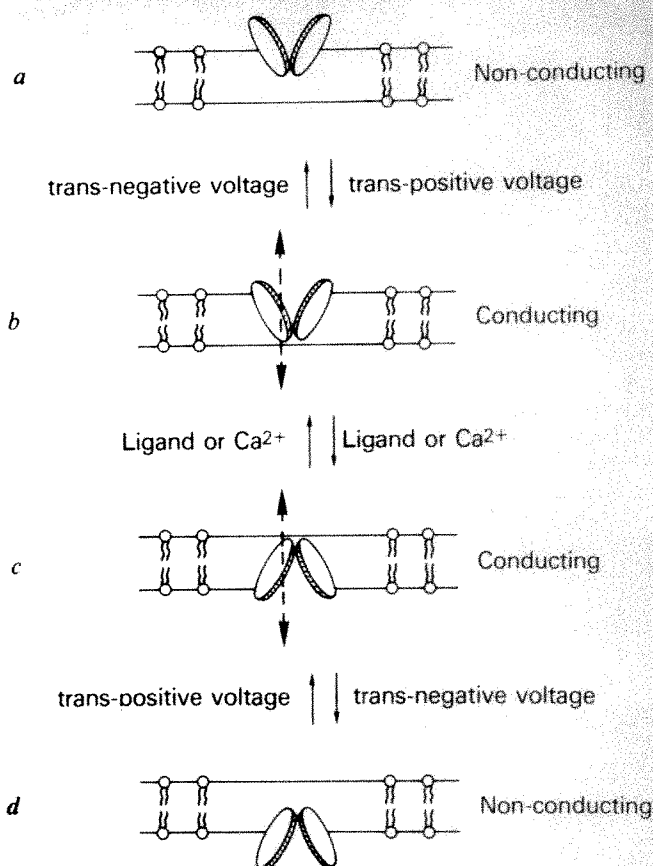


Fig. 6 Model for the translocation of the receptor protein (see text for explanation). The schematic rendering of two protein molecules is meant to suggest possible protein-protein interaction, not necessarily dimeric.

binding sites also become exposed on the *trans* side, where they are available for binding and cause a further increase in conductance. We do not know whether a given binding site exposed on the *cis* side becomes exposed on the *trans* side or whether an initially buried site is simply pushed through to the other side. Furthermore, we cannot say whether the protein actually flips over.

Two protein molecules are shown in Fig. 6 to indicate the possibility that protein-protein interaction is important in the translocation. It would provide an alternative to the energetically improbable movement of hydrophilic and charged residues directly through the low dielectric bilayer interior. Thus, charge delocalization and neutralization, by apposition of charged residues (either within a molecule of HBP or by aggregation as shown), could drastically lower the barrier. A possible role for  $\text{Ca}^{2+}$  in charge neutralization is suggested by the symmetrization seen in Fig. 2c.

Despite the topological problem outlined earlier, biochemical data suggest that the binding sites of HBP are on the cytosolic surface in the lysosomal fraction, and that they survive, presumably to be recycled to the plasma membrane. Although one must be cautious about the correspondence<sup>10</sup> between biological membranes and a model system such as the BLM, our observations do provide a conceptual basis for the translocation that may be required. The hepatic cells are inside-negative<sup>11</sup>, and the receptor is directed outward; measurements of ion distribution suggest that lysosomes are also inside-negative<sup>12,13</sup>, and the receptor's binding sites are on the cytosolic, electrically positive surface.

There is considerable precedent for potential-dependent behaviour of peptides and proteins in membranes. Electrical conductance can be modulated asymmetrically by antibiotic ionophores<sup>14</sup>, toxins<sup>15,16</sup>, transport molecules isolated from



biological systems<sup>17,18</sup>, immune cytotoxic factors<sup>19,20</sup>, and by 'gating' components of the sodium and potassium channels of nerve<sup>21,22</sup>. However, none of the physiologically interesting examples of these processes is understood in much detail. Wickner and co-workers<sup>23</sup> have speculated that an electrical gradient might drive newly synthesized M13 coliphage coat

proteins across the host membrane. This work on HBP provides the first direct evidence for the voltage-dependent translocation of a membrane protein across a membrane.

We thank K. Bridges and H. Tsunoo for purified HBP and ASOR, and G. Ashwell for stimulating discussions and encouragement.

Received 4 May; accepted 26 September 1980.

1. Rothman, J. E. & Lenard, J. *Science* **195**, 743-753 (1977).
2. Op den Kamp, J. A. F. *Rev. Biochem.* **48**, 47-71 (1979).
3. Ashwell, G. & Morell, A. G. *Adv. Enzym.* **41**, 99-128 (1974).
4. Tanabe, T., Pricer, W. E. Jr & Ashwell, G. *J. biol. Chem.* **254**, 1038-1043 (1979).
5. Kawasaki, T. & Ashwell, G. *J. biol. Chem.* **251**, 1296-1302 (1976).
6. Klausner, R. D. *et al. Proc. natn. Acad. Sci. U.S.A.* **77**, 5087-5091 (1980).
7. Blumenthal, R. & Shamoo, A. E. in *The Receptors* Vol. 1 (ed. O'Brien, R. D.) 215-245 (Plenum, New York, 1979).
8. Haydon, D. A. & Hladky, S. B. *Q. Rev. Biophys.* **5**, 187-282 (1972).
9. Shinitzky, M. in *Physical-Chemical Aspects of Cell Surface Events in Cellular Regulation* (eds DeLisi, C. & Blumenthal, R.) 173-181 (Elsevier, New York, 1979).
10. Tien, H. *Bilayer Lipid Membranes (BLM) Theory and Practice* (Dekker, New York, 1974).
11. Somlyo, A. P., Somlyo, A. V. & Friedmann, N. *Ann. N.Y. Acad. Sci.* **185**, 108-114 (1971).

12. Goldman, R. & Rottenberg, H. *FEBS Lett.* **33**, 233-238 (1973).
13. Henning, R. *Biochim. biophys. Acta* **401**, 307-316 (1975).
14. Ehrenstein, G. & Lecar, H. *Q. Rev. Biophys.* **10**, 1-344 (1977).
15. Finkelstein, A., Rubin, L. L. & Tzeng, M. *Science* **193**, 1009-1011 (1976).
16. Schein, S. J., Kagan, B. L. & Finkelstein, A. *Nature* **276**, 159-163 (1978).
17. Blumenthal, R. & Shamoo, A. E. *J. Membrane Biol.* **19**, 141-162 (1974).
18. Schein, S. J., Colombini, M. & Finkelstein, A. *J. Membrane Biol.* **30**, 99-120 (1976).
19. Michaels, D. W., Abramovitz, A. S., Hammer, C. H. & Mayer, M. M. *Proc. natn. Acad. Sci. U.S.A.* **73**, 2652-2856 (1976).
20. Henkart, P. & Blumenthal, R. *Proc. natn. Acad. Sci. U.S.A.* **72**, 2789-2793 (1975).
21. Hodgkin, A. L. & Huxley, A. F. *J. Physiol., Lond.* **117**, 500-544 (1952).
22. Miller, C. & Rosenberg, R. L. *J. gen. Physiol.* **74**, 457-478 (1979).
23. Date, T., Zwizinsky, C., Ludmerer, S. & Wickner, W. *Proc. natn. Acad. Sci. U.S.A.* **77**, 825-831 (1980).
24. Mueller, P., Rudin, D. O., Tien, H. T. & Wescott, W. C. *Nature* **194**, 979-981 (1962).

# The C1q receptor site on immunoglobulin G

D. R. Burton, J. Boyd, A. D. Brampton, S. B. Easterbrook-Smith, E. J. Emanuel, J. Novotny, T. W. Rademacher, M. R. van Schravendijk, M. J. E. Sternberg & R. A. Dwek

Department of Biochemistry and Laboratory of Molecular Biophysics, South Parks Road, Oxford OX1 3QU, UK

*We propose that the binding site for the complement subcomponent C1q on immunoglobulin G involves the last two (C-terminal)  $\beta$ -strands of the C<sub>2</sub> domain. This region contains a large number of accessible and highly conserved charged residues and charge is postulated as an important component of the C1q-IgG interaction. The conclusions are reached on the basis of accessibility and sequence conservation analyses of C<sub>2</sub> amino acid residues, the use of specific inhibitors and chemical modification studies.*

ANTIBODIES are the basis of the body's defence against infection. This central role is expressed in the functional versatility of the antibody molecule and realized through its unique structure. Thus, the organization of the antibody molecule into domains (Fig. 1a) allows recognition of a virtually unlimited range of antigens by the variable part of the structure, while the constant part mediates a small number of effector systems related to antigen elimination and/or immobilization. The best characterized of these effector systems is the classical pathway of complement.

Complement is a cascade process<sup>1</sup> generating a repertoire of biological activities with consequences<sup>2</sup> that are both local (for example, cytolysis and increased vascular permeability) and systemic (such as induced peripheral leukocytosis). Although the complement system presumably evolved as a beneficial antimicrobial mechanism, its inappropriate activation may lead to a variety of harmful consequences such as tissue damage secondary to complement-induced leucoembolization<sup>3</sup>, as occurs in adult respiratory distress syndrome, or complement-mediated cytolysis *in situ* such as occurs in autoimmune disorders<sup>2</sup>.

The triggering event in the classical pathway is the binding of the first component C1 to the Fc region of aggregated immunoglobulin. C1 is a macromolecular complex of three subcomponents—C1q, C1r and C1s—of total molecular weight (MW) approximately 700,000. The binding site for the Fc region of Ig is found on the C1q subcomponent (MW ~400,000). The structure of C1q has been proposed by Reid and Porter<sup>4</sup> as having the appearance of a 'bunch of tulips' (Fig. 1b). Eighteen chains, each some 200 amino acid residues long, are linked in threes in the base and stalk regions to form collagen-like triple helices. Each of the six fibres terminates in a globular head region which is thought to contain the Fc binding site(s).

The crystallographic structure of human Fc from pooled IgG

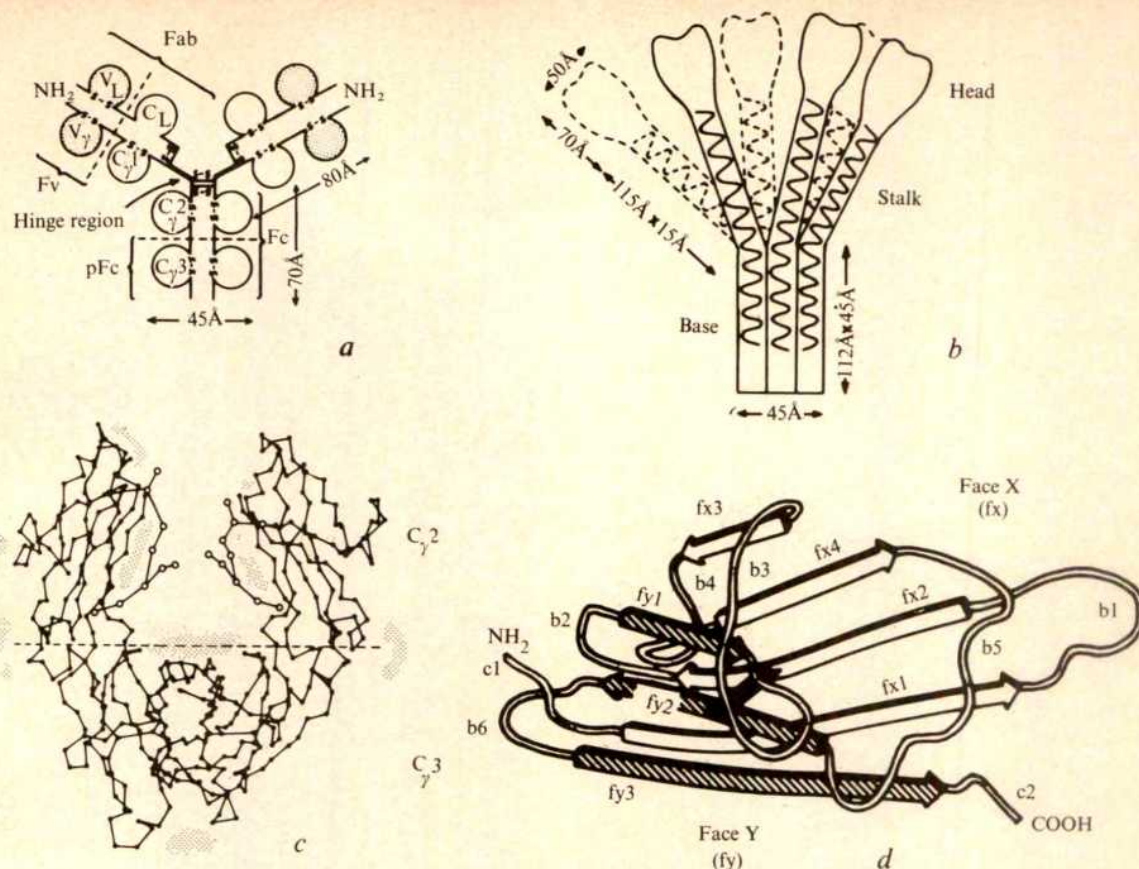
has been determined to 3.5 Å by Huber and colleagues<sup>5</sup>. The overall structure has been described as a 'Mickey Mouse', with the C<sub>2</sub> domains forming the ears and the C<sub>3</sub> domains the head (Fig. 1c). The tertiary structure of both these domains corresponds to the 'immunoglobulin fold'. However, whereas the pair of C<sub>3</sub> domains are in close interaction (Fab 'C-like' pairing<sup>6</sup>), the C<sub>2</sub> domains show no interaction with one another. The carbohydrate chains attached to Asn 297 are in between the C<sub>2</sub> domains. Although it is generally accepted that recognition of IgG by C1q occurs via a site on the C<sub>2</sub> domains<sup>6,7</sup>, the precise location of the amino acid residues constituting this site has not been described.

We now propose an identification of the C1q binding site based on a novel approach containing three lines of investigation. These are: (1) amino acid residue accessibility and sequence conservation analyses which are used to locate potential binding regions on Fc; (2) specific inhibitors of the protein-protein interaction (IgG-C1q) which are investigated to give information on the nature of the groups involved in the interaction; (3) specific chemical modifications of residues on Fc and C1q which are studied to implicate particular types of residues in the protein-protein interaction.

The C1q binding site we propose is rather novel in that it consists mainly of charged side chains (glutamate and lysine) on the last two (C-terminal end)  $\beta$ -strands of the C<sub>2</sub> domain. The approach used may prove to be generally useful in studying protein-protein interactions, in particular, where a detailed structure is known for one of the proteins but little structural information is available for the second protein or the complex formed between the two.

The residues in the C<sub>2</sub> domain involved in interaction with C1q should fulfil two criteria. First, they should be accessible for C1q binding, that is, not buried in the interior of the domain. This can be quantified by the surface area of the residue which





**Fig. 1** *a*, The domain structure of IgG. The different domains are shown by circled regions where V signifies variable domain, C constant domain,  $\gamma$  the heavy chain and L the light chain. Various proteolytic fragments Fc, pFc, Fab and Fv are also indicated. The IgG molecules of different classes and species differ most noticeably at the hinge region. Human IgG1 is represented here. *b*, Molecular structure of C1q proposed by Reid and Porter<sup>4</sup> (after whom the figure is taken) to account for the effects of collagenase and pepsin digestion and the dimensions and shape of the images seen in the electron microscope. Analysis and sequencing of the three types of polypeptide chain present show clear similarities between them, notably the repeating collagen-like triplets of residues which occupy some 85 positions starting near the N-terminal end. The characteristic Gly-X-Y pattern, where the residue Y is often either hydroxyproline or hydroxylysine, is broken at position 39 of the A chain and 36 of the C chain, allowing the bend of the triple helices forming each stalk away from those in the base region. *c*, The structure of the Fc fragment from pooled human IgG after Huber *et al.*<sup>5</sup>. ●,  $\alpha$ -C carbon positions; ○, approximate centres of carbohydrate hexose units. The very approximate locations of the main hydrophobic patches of the molecule (see Table 1 and text) are represented as shaded areas. *d*, Peptide chain folding of a constant domain<sup>6</sup>. The segments fx1-4 (unshaded) and fy1-3 form two roughly parallel faces of anti-parallel  $\beta$ -pleated sheet linked by an intra-chain disulphide bridge (filled rectangle, Cys 261 to Cys 321 in C $\gamma$ 2). Between the  $\beta$ -pleated segments are other segments (b1-6) forming helices, bends and other structures. Segments fx3, fx4, fy1 and b4 are foreshortened in this three-dimensional representation. A generalized view of constant domain folding is represented here—the C $\gamma$ 2 domain shows some deviations from this description, chiefly in b3 and fx3 (ref. 5).

can be in contact with the solvent. Second, they should be highly conserved in IgG molecules that bind C1q. This follows from the observation of the cross-species reactivity of C1q and IgG<sup>8,9</sup>. These two criteria are now considered separately.

### Accessibility analysis

In exploring those residues accessible for C1q binding, an analysis would ideally be carried out on the C $\gamma$ 2 domain of IgG in an immune complex. However, the only structure available at sufficient resolution is that of the isolated Fc fragment determined by crystallography to 3.5 Å (ref. 5). In using this structure in the accessibility analysis, the assumption is thus made that Fc has essentially the same structure in the isolated fragment and in intact IgG. Further, it is assumed that antigen binding does not significantly perturb the Fc structure in IgG, in line with evidence from this and other laboratories<sup>10</sup>.

Starting with the crystallographic structure of the Fc fragment for which the positions of most of the atoms are known, those residues of the C $\gamma$ 2 domain in contact with solvent can be identified using a computer program<sup>11</sup>. This program calculates the solvent contact area by constructing the van der Waals surface of the protein and 'rolling' a sphere (in our case of 1.4 Å radius to represent a water molecule) over the surface. It is found that of the 104 residues of the C $\gamma$ 2 domain, about 72 are accessible to water (contact area  $>5 \text{ Å}^2$ ).

As the energy which drives protein-protein interactions often comes from shielding protein hydrophobic surfaces<sup>12</sup> (the area

buried being proportional to the free energy of the interaction,  $1 \text{ Å}^2 \text{ contact area} \approx 80 \text{ cal mol}^{-1}$ )<sup>13</sup>, first interest centres on accessible residues which are predominantly nonpolar. Groupings of residues to form exposed hydrophobic patches are of particular interest and the principal features of those located in the C $\gamma$ 2 domain are summarized in Table 1 (see also Fig. 1c, d).

Table 1 shows that 35 residues have their nonpolar atoms (main chain  $\alpha$ -C, side chain C excepting those attached to O or N and side chain S) accessible to solvent with a contact area  $>5 \text{ Å}^2$ . Of these, 27 are clustered into four large patches ( $>100 \text{ Å}^2$ ) (shown in Fig. 1) and the remaining residues are found in two smaller patches and as isolated residues.

The location of patches 1-3 makes it unlikely that they are involved in C1q binding (Table 1, Comments). Use of our second criterion that a potential C1q binding site should be conserved between species then helps to eliminate the remaining patches (Table 1, Conservation).

In the absence of suitable accessible hydrophobic residues the next stage is to examine hydrophilic residues. Most of these are, of course, solvent accessible and prime interest now centres on the conservation between species of these hydrophilic residues.

### Sequence comparison analysis

Nine C $\gamma$ 2 primary structures are available<sup>14-16</sup>: three human myeloma proteins [ $\gamma$ 1 (Eu),  $\gamma$ 3 (Zuc),  $\gamma$ 4 (Vin)], rabbit chain, guinea pig  $\gamma$ 1 and  $\gamma$ 2 chains, two mouse myeloma proteins [ $\gamma$ 1 (MOPC 21),  $\gamma$ 2a (MOPC 173)] and mouse  $\gamma$ 2b chain. Human



**Table 1** The exposed hydrophobic patches of the C<sub>γ</sub>2 domain of Fc from human IgG1

| Patch  | Approximate area (Å <sup>2</sup> ) | Residues  | Conservation   | Comments  |
|--|------------------------------------|---|--|---|
| Concave surface of the 4-strand β-sheet layer (x face) | 150                                | Phe 241, Phe 243, Pro 244<br>Lys-Pro-Lys 246-248<br>Val-Val-Val 262-264 | Very highly conserved. All residues, except Pro 247, identical in nine C <sub>γ</sub> 2 primary structures | Mostly covered by Fc carbohydrate*. Lys-Pro-Lys is very close to C <sub>γ</sub> 3 and probably inaccessible to C1q  |
| N-proximal bend (b6)                                   | 130                                | Lys-Ala-Leu-Pro-Ala-Pro-Ile 326-332                                     | Not highly conserved. Only Pro 329 and Ile 332 identical in nine C <sub>γ</sub> 2 primary structures       | Hinge nearby could increase hydrophobic area. In the case of antibody recognition of cell-surface determinants, C1q binding to this patch would be under severe, if not prohibitive, steric restrictions from the cell  |
| C-proximal bulge (b1, b5)                              | 100                                | Met-Ile 252-253<br>Val-Leu 308-309                                      | Not highly conserved. Only Ile 253 identical in all nine C <sub>γ</sub> 2 sequences                        | C1q binding to this patch would necessarily involve contact with C <sub>γ</sub> 3 residues (compare with protein A <sup>22</sup> ). The ability of the Fabc fragment (IgG with the C <sub>γ</sub> 3 domains removed) to bind C1 and activate complement by the classical pathway <sup>7</sup> argues against the involvement of this patch in C1q binding |
| Outside edge between β-sheet layers (fx3, fx4)         | 100                                | Val 279<br>Ala-Lys 287-288<br>Lys-Pro 290-291<br>Val 303<br>Leu 306     | Not highly conserved. Only Ala 287 and Leu 306 identical in nine C <sub>γ</sub> 2 primary structures       |   |
| C <sub>γ</sub> 2/C <sub>γ</sub> 3 switch region        | 40                                 | Ala-Lys 339-340   | Ala 339 found in only four of nine C <sub>γ</sub> 2 sequences  | Relatively small area   |
| b3 bend  | 40                                 | Val 282, Val 284  | Val 282 (most of nonpolar area) is identical in six of nine C <sub>γ</sub> 2 sequences                     | Relatively small area   |
| Isolated residues                                      | Total area 60 Å <sup>2</sup>       | Pro 271, Lys 274, Tyr 296, Ile 336                                      | Ile 336 highly conserved, others not   |   |

\* The crystallographic coordinates used in this analysis did not include those for the carbohydrate.

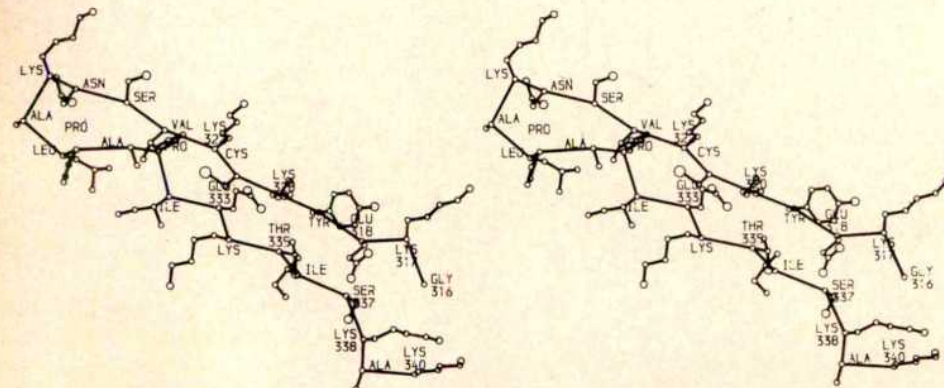
IgG1, IgG2 and IgG3, and rabbit and mouse IgG2a and IgG2b proteins are known to activate complement. Two mouse IgG1 subclasses—one activating complement, one not—have recently been proposed<sup>17</sup>. The C1q binding properties of MOPC 21 are not known. Guinea pig IgG1<sup>16</sup> and human IgG4 proteins are known not to bind C1, although the Fc fragment of IgG4 does<sup>18</sup>. This latter observation has led to the suggestion that the C1q binding site may be present in the primary structures of all IgGs but unavailable in some cases because of, for example, obstruction by the Fab arms<sup>18</sup>. Furthermore, comparison of the C<sub>γ</sub>2 sequences reveals no obvious correlation between primary structure and complement-fixing ability. Hence, all nine C<sub>γ</sub>2 primary structures are considered in the detailed sequence comparison here.

The analysis reveals that of the 104 positions in the nine C<sub>γ</sub>2 domains, 39 are identical throughout, and a further 36 may be considered conservative replacements (defined as any having a chemical relatedness index >0 according to McLachlan<sup>19</sup>; in the case of uncertainties, homology was maximized). Nineteen positions are particularly variable in that they show more than

one non-conservative substitution. As expected, these are almost exclusively surface residues and include two distinct regions: Gly-Val-Gln 281-283 and His 285 on bend b3 and Lys 288, Lys-Pro-Arg-Glu 290-294 on the fx3 sheet (nomenclature according to Fig. 1c). Interestingly, this latter region has been proposed as a C1q binding site by Brunhouse and Cebra<sup>16</sup>.

If we now consider the 39 invariant residue positions, some can be readily eliminated from being involved in C1q binding: 10 are buried, 5 are covered by carbohydrate and 2 (Asn 297, Thr 299) are related to sugar attachment. It then becomes necessary to establish positions for which invariance can be understood on structural grounds without invoking functional significance.

A comparison of the alignments of the primary structures of 23 constant domains<sup>20</sup> (including λ, κ, C<sub>H</sub>1, C<sub>H</sub>2, C<sub>H</sub>3 and the 'extra' domains of various species) is now used to reveal whether any of the remaining 22 invariant positions are involved in general immunoglobulin domain architecture. The percentage of domains having the same amino acid residue as C<sub>γ</sub>2 at the same position (the identity index) is computed. A high index



**Fig. 2** A stereoview of the region of the C<sub>γ</sub>2 domain containing the proposed C1q binding site. Residues 316 and 317 are part of a bend structure; residues 318-322 form a β-strand (fy2); residues 323-331 are on a bend as shown; residues 332-337 form a β-strand (fy3) antiparallel to fy2 and residues 338-340 continue into the C<sub>γ</sub>3 domains.



indicates that the residue is important for the constant domain fold in general, a low index indicates it is unusual for constant domains and possibly associated with the unique function of the C<sub>γ</sub>2. Table 2 shows identity indices for the 22 key invariant positions; Leu 306 and Trp 313 seem to be general features of constant domains.

At this stage, however, the most striking observation is the emergence of the contiguous residues on the  $\gamma$  face, Gly-Lys-Glu 316–318, Lys 320 (b5, fy2), Thr 335, Ser 337 and Lys 338 (fy3) (underlined, Table 2), as a potential binding region (Fig. 2). The charged residues have noticeably low identity indices. Further examination of other exposed residues in this region reveals that Lys 322 (fy2) is conserved as Lys in eight of nine C<sub>γ</sub>2 domains, being replaced by Arg in guinea pig IgG2 and having an identity index of 13%. Pro 331 (b6) (replaced by Thr in guinea pig IgG1), Glu 333 (fy3) (Thr in guinea pig IgG1) and Lys 340 (e2) (Arg in rabbit), with identity indices of 35, 26 and 9%, are similarly conserved. The entire region (Fig. 2) is then one of exposed, highly conserved, mostly charged (five Lys, two Glu) residues.

Of the remaining residues of Table 2, Thr 260 and Arg 301 could be involved in interaction with the carbohydrate; Ser 239, Asp 265 and Ser 267 may be involved in hinge or Fab arm conformation; Lys 248 (possibly interacting with Glu 380) and His 310 are at the C<sub>γ</sub>2/C<sub>γ</sub>3 interface; Pro 329 is involved in bend architecture and Gly 341 in the C<sub>γ</sub>2/C<sub>γ</sub>3 switch region. Reasons for conservation of the remaining residues, Ala 287, Ile 253, Ile 332 and Ile 336, are unclear.

Note, finally, that the carbohydrate forms an exposed, probably conserved, continuous region and therefore must also be considered as a potential or part of a potential C1q binding site.

## Inhibitor studies

In the light of the charged potential binding region on Fc discussed above, we have compared the ability of several salts, in a variety of experimental conditions, to inhibit C1q binding to anti-ovalbumin-ovalbumin aggregates. Table 3 compares the  $K_{50}$  values for a number of inhibitors.

Figure 3a illustrates the well known dependence of C1q binding to antibody aggregates on NaCl concentration<sup>21,22</sup> and further reveals a marked anion dependence of inhibitory ability,  $I^- > Cl^- > F^-$ . Appropriate controls show that salt is not dissociating the aggregates over the concentration range used<sup>23</sup>. Figure 3 also shows that the C1q-antibody aggregate reaction is reversible and therefore, at a given NaCl concentration, can be

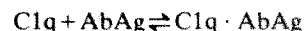
**Table 3** Comparison of the ability of a number of molecules to inhibit the C1q-antibody aggregate reaction

| Molecule                                 | $K_{50}$ (mM) | Molecule             | $K_{50}$ (mM) |
|--|---------------|----------------------|---------------|
| <b>Inorganic salts</b>                   |               | <b>Polyions</b>      |               |
| NaSCN                                    | 170           | DNA*                 | 0.0005        |
| NaI                                      | 200           | Polylysine           | <0.1          |
| NaCl                                     | 260           | Suramin              | 3.5           |
| Na <sub>2</sub> SO <sub>4</sub>          | 450           | Heparin              | 1             |
| NaF                                      | >450          |                      |               |
| NaI                                      | 150           | <b>Carbohydrates</b> |               |
| KI                                       | 175           | Mannan               | 60            |
| RbI                                      | 200           | N-acetyl glucosamine | 450           |
| MgCl <sub>2</sub>                        | 145           | Raffinose            | 575           |
| CaCl <sub>2</sub>                        | 165           | Xylose               | 575           |
| CsCl                                     | 300           | Glucose              | >600          |
|  |               | Mannose              | 700           |
|  |               | Glucose-6-phosphate  | >19           |
| <b>Organic ions</b>                      |               | Lactose              | >18           |
| N-(p-nitrophenyl)-2-aminoethyl phosphate | 2             | Inulin               | >225          |
| N-(DNP)-2-aminoethyl phosphate           | 2.5           |                      |               |
| DNP-lysine                               | 2.5           |                      |               |
| DNP-glycine                              | 12.5          |                      |               |
| DNP-leucine                              | >22.5         |                      |               |
| DNP-OH                                   | >10.5         |                      |               |
| 2,4-dinitronaphthol-7-sulphonate         | 2             |                      |               |
| ATP                                      | 10            |                      |               |
| ADP                                      | 9             |                      |               |
| MnATP                                    | 11            |                      |               |
| AMP                                      | 13            |                      |               |
| Adenosine                                | >12           |                      |               |
| Diaminobutane                            | 55            |                      |               |
| Spermine                                 | 25            |                      |               |
| Glycine                                  | >50           |                      |               |

$K_{50}$  indicates the concentration of inhibitor at which C1q binding to antibody aggregates assayed as described in Fig. 3 legend is reduced by 50% from the maximum value (compare with Fig. 3a). For the inorganic ions, NaCl was present in concentrations such as to maintain a constant ionic strength of 170 mM. For the polyions and carbohydrates, the NaCl concentration was constant at 170 mM. > Indicates a full inhibition curve was not obtained and the value quoted is an extrapolation. >> Indicates that no inhibitory effect was observed up to the quoted concentration. For polylysine an upper limit is described because of uncertainties in the molecular weight of this polymer.

\* NaCl = 120 mM.

described as an equilibrium process:



where AbAg represents antibody aggregate, measured in units of antibody concentration, and C1q · AbAg the complex, measured as the amount of C1q bound to the aggregates. Binding studies at variable C1q and NaCl concentration (Fig. 3b) can then be used to estimate a phenomenological dissociation constant,  $K_{obs}$ , at each NaCl concentration for this equilibrium. The plot of  $\log K_{obs}$  against  $a_{\pm}$  ( $a_{\pm}$  defined as  $a_{NaCl}^{1/2}$ ) in Fig. 3c reveals that  $K_{obs}$  increases with increasing NaCl concentration. This increase, together with a fall in C1q binding capacity, is responsible for the inhibitory effect of NaCl seen in Fig. 3a. The gradient of a  $\log K_{obs}$  against  $\log a_{\pm}$  plot can be interpreted in terms of a general equation for the effect of an electrolyte on a macroion equilibrium<sup>24</sup>. Although a detailed analysis is probably not justified by the limited scope of our data, the clearly positive gradient of the  $\log K_{obs}$ - $\log a_{\pm}$  plot indicates that ions participate directly in the association of C1q and antibody aggregate. The most straightforward interpretation of the slope is that a net total of  $12 \pm 2$  ions are released when 1 molecule of C1q binds to antibody aggregates. A similar plot for CaCl<sub>2</sub> between 22 and 50 mM gives a slope of  $15 \pm 2$ . Although both cations and anions could be involved, some indication of the importance of anions is provided by the dependence of inhibitory ability on the lyotropic series (Fig. 3a, Table 3),  $SCN^- > I^- > Cl^- > F^- > SO_4^{2-}$  and the relative potency of organic

**Table 2** The identity indices of selected C<sub>γ</sub>2 residues

|                | Identity index (%) | Total accessibility (Å <sup>2</sup> ) |
|----------------|--------------------|---------------------------------------|
| Ser 239        | 30                 | 16                                    |
| Lys 248        | 13                 | 28                                    |
| Ile 253        | 10                 | 38                                    |
| Thr 260        | 30                 | 11                                    |
| Asp 265        | 35                 | 22                                    |
| Ser 267        | 22                 | 11                                    |
| Ala 287        | 4                  | 21                                    |
| Arg 301        | 4                  | 30                                    |
| Leu 306        | 87                 | 26                                    |
| His 310        | 4                  | 34                                    |
| Trp 313        | 65                 | 7                                     |
| Gly 316        | 35                 | 11                                    |
| <u>Lys 317</u> | 22                 | 23                                    |
| <u>Glu 318</u> | 17                 | 24                                    |
| Lys 320        | 4                  | 15                                    |
| Pro 329        | 17                 | 40                                    |
| Ile 332        | 15                 | 13                                    |
| Thr 335        | 35                 | 21                                    |
| Ile 336        | 13                 | 10                                    |
| Ser 337        | 30                 | 12                                    |
| Lys 338        | 13                 | 6                                     |
| Gly 341        | 38                 | 13                                    |

Underlined residues are those on the  $\gamma$  face, forming a potential binding region (see text).



anions such as dinitrophenyl (DNP) ethyl phosphate and ATP as inhibitors (Table 3). It is interesting that the  $K_{50}$  values observed for NaCl (~250 mM) and ATP (~10 mM) are comparable with the binding constants to the organic phosphate site of oxyhaemoglobin of ~50 mM (NaCl) and ~2.5 mM (ATP), respectively<sup>24</sup>. The inhibitory ability of organic ions listed in Table 3 may explain the widespread observation of various polypeptides (all containing negative charges) as inhibitors of the C1q-IgG interaction<sup>25,26</sup>.

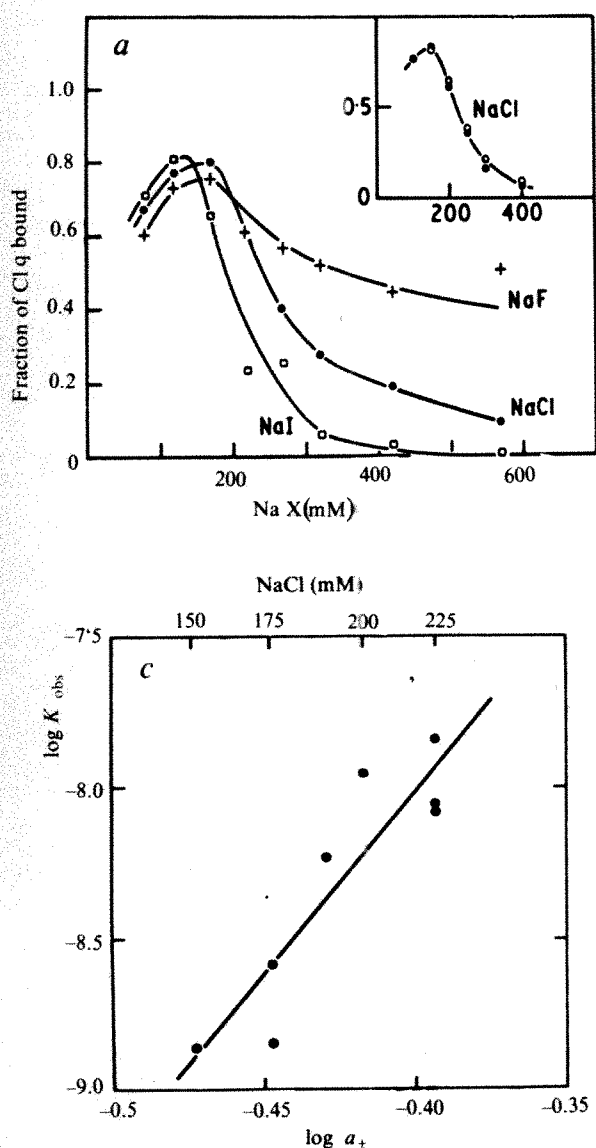
That the interaction between C1q and antibody-antigen aggregates involves ions does not, of itself, rule out the possibility that other interactions are important. In particular, the Fc carbohydrate could be involved because it fulfils the criteria of accessibility and conservation. However, neither monosaccharides (Table 3) nor the carbohydrate isolated from transferrin (similar to the human Fc carbohydrate) had any significant inhibitory ability<sup>27</sup>. The inhibition by heparin is probably due to its polyionic nature.

### Chemical modification studies

The effect of chemical modification of a number of groups on both C1q and rabbit IgG on the interaction between the two has been studied. Table 4 shows that modification of  $19 \pm 1$  (30%) of the lysines on IgG by methyl acetimidate, a mild reagent leaving the positive charge on lysine intact, produces no decrease in the binding capacity of IgG aggregates for C1q, with a significant increase in the dissociation constant. A qualitatively similar

result is obtained for the modification of 4 or 10 lysines using acetic anhydride. A decrease in binding capacity and an increase in  $K_d$  are observed for modification of  $12 \pm 2$  carboxyl groups on IgG by glycine methyl (or ethyl) ester (Table 4). (A recent report describes a similar observation of the effect of carboxyl modification on the C1q-human Fc interaction<sup>28</sup>.) Control experiments in these and other modification experiments involved showing that: (1) circular dichroism (CD) spectra and (2) precipitin curves of modified and unmodified IgG were the same. A further control for methyl acetimidate modification of lysines and cyclohexanedione modification of arginines (see below) was that similar effects were observed whether the modification was carried out before or after antigen aggregation.

In contrast to the above, cyclohexanedione modification of  $10 \pm 1$  arginines in IgG, of which 7 or 8 were estimated to be in the C<sub>γ</sub>2 domains, has little effect on C1q binding, as shown in Table 4. The number of residues modified in the C<sub>γ</sub>2 domains was determined from pepsin digestion of modified IgG as the difference between the number modified in intact IgG and the number modified in the F(ab')<sub>2</sub> and pFc' fragments<sup>29</sup>. Six of the seven C<sub>γ</sub>2 arginine residues in rabbit IgG are found in the general region between x and y faces. As the modification described involves complexing a very bulky cyclohexanedione-borate group to each arginine, our results provide evidence against the involvement of this region in C1q binding, which includes the region proposed by Brunhouse and Cebra as a C1q binding site<sup>16</sup>. This conclusion is also substantiated by the absence in rabbit from this region of the C<sub>γ</sub>2 domain of lysine



**Fig. 3** The involvement of ions in the C1q-antibody aggregate reaction. *a*, The binding of C1q to antibody aggregates as a function of sodium halide concentration. Human C1q (ref. 38) and <sup>125</sup>I-labelled human C1q (ref. 39) were prepared as described elsewhere. Rabbit antisera were prepared by the injection of ovalbumin, emulsified in Freund's complete adjuvant 1:1, into each hind footpad and shoulder muscle. The anamnestic response was elicited by intraperitoneal injection of alum-precipitated ovalbumin. Purification to yield IgG was according to ref. 40. The C1q binding assay involved incubating <sup>125</sup>I-labelled C1q (typically 1–30 μg ml<sup>-1</sup>) with antibody aggregates (typically 25 μg ml<sup>-1</sup>) in a 12 mM Tris, 0.15% gelatin, pH 7.2, solution of the appropriate salt concentration at 37 °C for 45 min. Bound and free <sup>125</sup>I-labelled C1q were determined after centrifugation. The inset data points were obtained as normal (●) or (○) by incubating as above for 30 min at 400 mM NaCl, performing the appropriate dilution to the specified NaCl concentration, reincubating and assaying in the normal manner. *b*, Representative binding curves for the reaction of C1q and antibody aggregates at varying NaCl concentration. Binding was measured as in *a*. The curves were fitted to a hyperbola using a nonlinear least squares program. The program yielded a value for  $K_{obs}$ , the phenomenological dissociation constant for the reaction, at each NaCl concentration. It was found that 10–20% (depending on the C1q preparation) of the C1q was not available for binding to antibody aggregates (possibly through denaturation). The binding curves shown have been appropriately corrected. *c*, log  $K_{obs}$  as a function of the log of the ion activity parameter,  $a_{\pm}$ , for the C1q-antibody aggregate reaction in the presence of NaCl.  $a_{\pm}$  is defined as the square root of the NaCl activity ( $a_{NaCl}^{1/2}$ ). The plot makes use of the type of data seen in *b*. The slope of the plot is  $12 \pm 2$ .

**Table 4** The effect of various chemical modifications of groups on IgG and C1q on the interaction between C1q and antibody aggregates

| Modification                          | Extent of modification (per IgG or C1q molecule) | $K_d$ modified<br>$K_d$ unmodified | Capacity modified<br>Capacity unmodified |
|---------------------------------------|--|------------------------------------|--|
| <b>Modifications to IgG</b>           |  |                                    |  |
| Lysine                                |  |                                    |  |
| Methyl acetimidate                    | 19 ± 1 (30%)<br>40 ± 5 (60%)                     | 3–4                                | 1  |
| Acetic anhydride                      | 4 ± 1 (6%)<br>10 ± 2 (15%)                       | 2<br>4–5                           | 1<br>1                                   |
| Arginine                              |  |                                    |  |
| Cyclohexanedione                      | 10 ± 1 (30%)                                     | 1                                  | 0.8                                      |
| Carboxylate                           |  |                                    |  |
| Glycine methyl ester/<br>carbodiimide | 4 ± 1 (3%)<br>12 ± 2 (10%)                       | 1<br>2                             | 1<br>0.5                                 |
| Glycine ethyl ester/<br>carbodiimide  | 12 ± 2 (10%)                                     | 3–4                                | 0.7                                      |
| Tryptophan                            |  |                                    |  |
| Hydroxynitrobenzyl<br>bromide         | 1.5–2  | 1                                  | 1  |
| <b>Modifications to C1q</b>           |  |                                    |  |
| Lysine                                |  |                                    |  |
| Methyl acetimidate                    | 95 ± 15 (75%)                                    | 1                                  | 1  |
| Arginine                              |  |                                    |  |
| Cyclohexanedione                      | 18 ± 1 (10%)                                     | —                                  | 0  |

For each modification a C1q binding curve is obtained (compare with Fig. 3b) and compared with unmodified reactants. The  $K_d$  and capacity of IgG for C1q in each case were determined from the binding curves as described in Fig. 3b legend. Methyl acetimidate modification<sup>33</sup> of lysines on IgG (10 mg ml<sup>-1</sup>) was carried out at pH 8.06 and 4 or 25 °C in 0.1 M triethanolamine using 0.1 M methyl acetimidate for 3 min (30% modification) or 10 min (60%). The reaction was stopped by lowering the pH to below 8.0. Similar conditions were used for modification of C1q with 7 min modification time and the inclusion of 150 mM NaCl in all buffers. Acetic anhydride modification<sup>34</sup> of lysines was carried out at pH 5.1, 0 °C in 1 M sodium acetate using 0.5% (v/v) acetic anhydride for 5 min. The reaction was stopped by adding a large excess of lysine. The extent of lysine modification for both modifying reagents was determined using trinitrobenzene sulphonate as described elsewhere<sup>35</sup>. Arginine modification<sup>29,36</sup> was carried out using 1 M cyclohexanedione in 0.2 M sodium borate at pH 9 and 25 °C for 1 h. The reaction was stopped by lowering the pH to 4 and the extent of modification estimated from amino acid analysis. Similar conditions were used for modification of C1q with 45 min modification, a lowering of the pH to 6 to stop the reaction and the inclusion of 150 mM NaCl in all buffers. Carboxylate modification<sup>35</sup> of IgG made use of a 30–50-fold (over IgG) molar excess of carbodiimide in 1 M glycine methyl (or ethyl) ester at pH 4.75 and 25 °C for appropriate times. Excess sodium acetate was added to stop the reaction and the extent of modification estimated from amino acid analysis. Tryptophan modification<sup>37</sup> of IgG was carried out using a 300-fold (over IgG) excess of hydroxynitrobenzyl bromide in 0.1 M sodium acetate at pH 4.5. The extent of modification was estimated spectrophotometrically. Modifications were carried out on IgG in the range 10–70 µM.

residues which are shown here to be important in the interaction with C1q.

In sharp contrast to IgG, cyclohexanedione modification of 18 arginines on C1q (equivalent to 3 residues modified per C1q monomer unit) abolishes binding to IgG aggregates whereas methyl acetimidate modification of 75 ± 15% of the lysines on C1q has little or no effect.

## Conclusions

The accessibility and conservation analyses described strongly suggest that a charged region on the last two (C-terminal end)  $\beta$ -strands of the C<sub>2</sub> domain of IgG has functional importance. Specific inhibitor and chemical modification studies are consistent with this function being the binding of the complement subcomponent, C1q, and we therefore propose that this charged region (Fig. 2) contains residues which are directly involved in the C1q binding site on IgG.

At the other end of the antibody molecule, recognition of antigen generally involves binding of the antigen in a cleft or groove in the antibody structure. On the basis of our hypothesis, recognition of C1q would involve quite different principles. Thus, the Fc site proposed by us consists of a virtually planar array of (mostly charged) residues which is unlikely to act as or bind into a cleft or groove. It is far more probable that recognition involves some form of surface 'matching' of charged

residues on Fc and C1q. This kind of protein-protein interaction involving charge has been described in the extended salt-bridge system between subunits in tobacco mosaic virus (TMV)<sup>30</sup>. Whereas TMV uses residues on helices, our Fc site consists mainly of residues on two  $\beta$ -strands. A surface complementary to this would be provided by suitably arranged charged residues on two  $\beta$ -strands of C1q.

The type of approach we have adopted here is limited by the fact that it is not possible to describe the size of the proposed C1q binding site precisely. However, examination of Fig. 2 shows that Glu 318, Lys 320, Lys 322, Pro 331, Glu 333, Thr 335 and Ser 337 are fairly close in space and Gly 316, Lys 317, Lys 338 and Lys 340 (the residues not in the  $\beta$ -strands) are more distant. The former residues form a roughly planar area of approximately 150 Å<sup>2</sup>. The location of this area in the C<sub>2</sub> domain is such that a bulky molecule such as a C1q head could be denied access for certain orientations of the Fab arms. In addition, our data do not definitively rule out the possible involvement of the contiguous carbohydrate moieties (compare with ref. 31).

Clearly, a crystallographic structure of Fc and C1q heads would provide a definitive identification of the C1q binding site. Progress in this formidable task could be made with the availability of a crystal structure for C1q heads. For instance, matching of this structure with that of Fc could be considered. In the short term, however, exhaustive testing of chemical modifications of Fc may allow selective labelling of particular residues in the site which can be identified by the usual protein chemical methods. Alternatively, crystallographic studies of Fc in the presence of an inhibitor could be useful. Such chemical modification and crystallographic studies are now in progress.

Finally, it is interesting that preliminary results on IgM (in collaboration with A. Feinstein) again indicate the importance of charged groups in the recognition of C1q. It remains to be shown whether the same site on C1q is recognized for both IgG and IgM.

We thank Professors R. R. Porter and D. C. Phillips for their continued interest and encouragement, Professor R. J. P. Williams, Drs K. Reid, A. Feinstein, F. E. Cohen and I. O. Walker for useful discussion, Professor R. Huber for supplying the coordinates of the Fc crystal structure and Dr S. R. Martin for CD measurements. This work was supported by the MRC and is a contribution from the Oxford Enzyme Group. D.R.B. is an MRC Training Fellow, S.B.E. is a Junior Beit Fellow, E.J.E. is an F. J. Moore Fellow, T.W.R. is a Fellow of the Institute for Medicine and Mathematics and M.J.E.S. is a Stothert Fellow of the Royal Society. J.N. held a Royal Society Fellowship during this study.

Received 4 July; accepted 17 September 1980.

- Porter, R. R. & Reid, K. B. M. *Adv. Protein Chem.* **33**, 1–71 (1980).
- Fearon, D. T. & Austen, K. F. *Essays med. Biochem.* **2**, 1–35 (1976).
- Jacob, H. S., Craddock, P. R., Hammerschmidt, D. E. & Moldow, C. F. *New Engl. J. Med.* **302**, 789–794 (1980).
- Reid, K. B. M. & Porter, R. R. *Biochem. J.* **155**, 19–23 (1976).
- Huber, R., Deisenhofer, J., Colman, P. M., Matsushima, M. & Palm, W. *Nature* **264**, 415–420 (1976).
- Beale, D. & Feinstein, A. *Q. Rev. Biophys.* **9**, 135–180 (1976).
- Colomb, M. & Porter, R. R. *Biochem. J.* **145**, 177–183 (1975).
- Alexander, R. J. & Steiner, L. A. *J. Immun.* **124**, 1418–1425 (1980).
- Höfken, K., McLaughlin, P. J., Price, M. R., Preston, V. E. & Baldwin, R. W. *Immunochimistry* **15**, 409–412 (1978).
- Fewtrell, C. et al. *Molec. Immun.* **16**, 741–754 (1979).
- Richmond, T. J. & Richards, F. M. *J. molec. Biol.* **119**, 537–555 (1978).
- Richards, F. M. *A. Rev. Biophys. Bioengng* **6**, 151–156 (1977).
- Chothia, C. H. *Nature* **248**, 338–339 (1974).
- Dayhoff, M. O. *Atlas of Protein Sequence and Structure* **5**, Suppl. 3, 202 (1978).
- Yamawaki-Kakao, Y., Kataoka, T., Takahashi, N., Obata, M. & Tasuku, H. *Nature* **283**, 786–789 (1980).
- Brunhouse, R. & Cebra, J. J. *Molec. Immun.* **16**, 907–917 (1979).
- Ey, P. L., Prowse, S. J. & Jenkin, C. R. *Nature* **281**, 492–493 (1979).
- Iseman, D. E., Dorrington, K. J. & Painter, R. H. *J. Immun.* **114**, 1726–1729 (1975).
- McLachlan, A. D. *J. molec. Biol.* **64**, 417–437 (1972).
- Dayhoff, M. O. *Atlas of Protein Sequence and Structure* **5**, Suppl. 3, 168–169 (1978).
- Lin, T. Y. & Fletcher, D. S. *Immunochimistry* **15**, 107–117 (1978).
- Hughes-Jones, N. C. & Gardner, B. *Immunology* **34**, 459–463 (1978).
- Rademacher, T. W. & Dwek, R. A. (in preparation).
- Record, M. T., Anderson, C. F. & Lohman, T. M. *Q. Rev. Biophys.* **11**, 103–178 (1978).
- Johnson, B. J. & Thames, K. E. *J. Immun.* **117**, 1491–1494 (1976).



26. Boackle, R. J., Johnson, B. J. & Caughman, G. B. *Nature* **282**, 742–743 (1979).
27. Barclay, N. *et al.* (in preparation).
28. Vivanco-Martinez, F., Bragado, R., Albar, J. P., Juarez, C. & Ortiz-Maslorems, F. *Molec. Immun.* **17**, 327–336 (1980).
29. Zavodsky, P. *et al.* (in preparation).
30. Bloomer, A. C., Champness, J. N., Bricogne, G., Staden, R. & Klug, A. *Nature* **276**, 362–367 (1978).
31. Winkelhake, J. L., Kunicki, T. J., Elcombe, B. M. & Aster, R. H. *J. biol. Chem.* **255**, 2822–2828 (1980).
32. Deisenhofer, J., Jones, T. A., Huber, R., Sjödh, J. & Sjöquist, J. *Hoppe-Seyler's Z. physiol. Chem.* **359**, 975–985 (1978).
33. di Marchi, R. D., Garner, W. H., Wang, C. C., Hanania, G. I. H. & Gurd, F. R. N. *Biochemistry* **17**, 2822–2829 (1978).
34. Oppenheimer, H. L., Labouesse, B. & Hess, G. P. *J. biol. Chem.* **241**, 2720–2730 (1966).
35. Means, G. E. & Feeney, R. E. *Chemical Modification of Proteins* (Holden-Day, San Francisco, 1971).
36. Pattay, L. & Smith, E. L. *J. biol. Chem.* **250**, 557–564, 565–569 (1975).
37. Allan, R. & Isliker, H. *Immunochimistry* **11**, 175–180 (1974).
38. Reid, K. B. M. *Biochem. J.* **141**, 189–203 (1974).
39. Heusser, C., Boesman, M., Nardin, J. H. & Isliker, H. *J. Immun.* **110**, 820–828 (1973).
40. Fanger, M. W. & Smyth, D. G. *Biochem. J.* **127**, 757–765 (1972).

## LETTERS

### Prominent VLBI cores in powerful radio sources with arc second structure

Gopal-Krishna\* & E. Preuss

Max-Planck-Institut für Radioastronomie, Bonn, FRG

R. T. Schilizzi

Netherlands Foundation for Radio Astronomy, Dwingeloo, The Netherlands

VLBI and aperture-synthesis techniques have produced better understanding of the structural details of extragalactic radio sources of both compact ( $<1$  arcs) and extended ( $>10$  arcs) types. Much less is known about the radio morphologies of sources with an overall size of just a few arc seconds, though such information is essential for understanding the evolutionary link between compact and extended sources. It has been predicted that the radio nucleus of a double source should appear Doppler brightened due to relativistic beaming, if the source axis is oriented close to the line of sight<sup>1–3</sup>. To investigate this, we examined two samples of double radio sources whose axes are expected to be inclined respectively at large and small angles from the line of sight. The statistics of the 'core fraction'—fraction of the total flux of the source which is contributed by its nuclear core at some reasonably high frequency, say 5 GHz, can then be obtained. Sources with large inclination angles would probably dominate the samples of extended, well-resolved double sources and hence their core-fraction can be readily estimated from published aperture synthesis surveys. Double sources oriented close to the line of sight are expected to be more common in samples containing only those sources whose angular sizes are a couple of times smaller than the median size for that flux density range. A large, unbiased sample of this type can be constructed using the nine Ooty lunar occultation lists (see ref. 4). We have selected all sources lying north of declination  $-25^\circ$  for which a flux density  $\geq 1$  Jy and an overall size between 1 and 4 arc s have been estimated at 327 MHz in the occultation observations. These 30 'few-arc second' sources are expected<sup>5</sup> to be distant objects ( $z > 0.3$ ) and hence intrinsically powerful radio emitters radiating  $>10^{33}$  erg s<sup>-1</sup> Hz<sup>-1</sup> at 327 MHz ( $H_0 = 50$  Km s<sup>-1</sup> Mpc<sup>-1</sup>,  $q_0 = 0.5$ ). Sources of such high radio power have a classical double morphology<sup>6</sup> and there exists evidence for double structure in 8 of these 30 few-arc second sources. We report here a search for compact cores among these sources by VLBI at 5 GHz using the large antennas at Effelsberg and Westerbork which provide a minimum fringe spacing of 0.045 arc s at this frequency. Radio cores were found to be much more prominent in this representative sample of 30 few arc-second sources, as compared with the cores found typically in extended double sources.

The nine Ooty occultation lists provide high resolution data for an unbiased sample of 711 radio sources in the Moon's path, down to a flux level of  $S_{327} \sim 0.25$  Jy. Due to the low frequency of this survey (327 MHz), it is believed that the sources have been selected without bias in orientation. Parts of these data have been used to study the angular size properties of weak

extragalactic radio sources<sup>5,7,8</sup>. By excluding all sources with  $S_{327} < 1$  Jy or  $\delta < -25^\circ$ , we first formed a sample A of 266 occultation sources, which should have properties very similar to the 4C complete sample (defined by  $S_{178} > 2$  Jy). The median angular size<sup>9</sup> of sources in sample A is  $\sim 12$  arc s and three-quarters of them have been resolved in the occultation observations at 327 MHz (these low-frequency observations are suitable for measuring the overall size because the outer radio structure usually has a steep spectrum). The optical identification work for sample A has been carried out using PSS plates and using mostly a combined 'radio+optical' position accuracy of better than a few arc seconds, aided by the knowledge of radio structure. It was found that  $\sim 39\%$  of the sources have optical counterparts brighter than the PSS plate limit<sup>4</sup>.

Our sample of 30 few-arc second sources was formed by selecting from the sample A all those sources for which occultation scans along position angles at least  $20^\circ$  apart had been observed and the derived maximum angular size at 327 MHz fell in the range 1–4 arc s. Note that a comparable number of similarly extended sources may have failed to be selected because, either the coverage in position angle during occultations was not wide enough or the angular resolution attained was insufficient to resolve them (the achieved resolution for the same source can vary by up to a factor of  $\sim 2$  depending on the observational circumstances such as the speed of the Moon's limb relative to the source<sup>9</sup>).

The VLBI observations of the 30 few arc-second sources were made on 11 and 12 January 1980 for 26 h, using the 100-m Effelsberg telescope and 11 of the 14 telescopes of the Westerbork array in total power mode. The latter provides at the zenith a beamwidth of 7 arc s (EW)  $\times$  10 arc min (NS) and is equivalent to an 83-m dish in collecting area. A central frequency of 4,996 MHz and right circular polarization were used.

For each source, up to three short observations each lasting 10–15 min were made, interspersed with calibration observations. The minimum fringe spacing was 0.045 arc s, increasing by up to a factor of 3 for the southern sources. We also measured, on the first day, the integrated flux densities of all these sources at Effelsberg by taking cross scans at the source positions (known to an accuracy of  $\sim 1$  arc s).

The VLBI data recording was done using the standard MKIIc system with a bandwidth of 2 MHz. A hydrogen maser oscillator at Effelsberg and a rubidium oscillator at Westerbork provided the time and frequency standards. The cross correlation and further reduction of the data were carried out at the Max-Planck-Institut für Radioastronomie, Bonn.

The values of integrated flux densities  $S_T$ , calibrated on 3C161 and 3C286, are given on the scale of Baars *et al.*<sup>10</sup>. These have an r.m.s. uncertainty of  $\Delta S_T(\text{mJy}) = [(5)^2 + (0.05 S_T)^2]^{1/2}$ . The correlated flux density scale was calibrated using the sources 0J287, 2134+004 and 3C454.3 whose flux densities measured at Effelsberg during the observations were 2.7, 9.8 and 8.3 Jy at 5 GHz, respectively. The calibration factor for all three sources has an r.m.s. scatter of 7%. Using the observations of these strong calibration sources and of a few weaker sources belonging to our observed sample (Table 1), the loss of correlated amplitude due to phase drifts in oscillators was determined as a function of the coherent integration time. Accordingly, a correction of 20% to the correlated amplitude was applied for a

\* Permanent address: Tata Institute of Fundamental Research, Ootacamund, India.

Table 1 Observed parameters of the 30 'few-arc sec' sources\*

| IAU name | Optical field† | Structure‡ and size at 327 MHz (arc s) | $S_{327}$ (mJy) | $S_{4,996}$ (mJy) | $\alpha_{327}^{4,996}$ | VLBI parameters at 4,996 MHz |            |             |       |          |
|----------|----------------|--|-----------------|-------------------|------------------------|------------------------------|------------|-------------|-------|----------|
|          |                |  |                 |                   |                        | PA (deg.)                    | FS (arc s) | $S_c$ (mJy) | $C_5$ | Class    |
| 0011+054 | EF             | D (3.5)                                | 4,200           | 360               | 0.90                   | -47                          | 0.049      | <30         | —     | —        |
| 0057+105 | EF             | S (1.7)                                | 1,000           | 168               | 0.65                   | -26                          | 0.057      | <30         | —     | —        |
|          |                |  |                 |                   |                        | 39                           | 0.051      | <30         |       |          |
| 0352+210 | 18 mag NSO     | S (2.7)                                | 3,300           | 328               | 0.85                   | -24                          | 0.051      | 94          | 0.31  | <i>a</i> |
|          |                |  |                 |                   |                        | 45                           | 0.047      | 107         |       |          |
| 0405+258 | EF             | S (2.0)                                | 1,000           | 107               | 0.82                   | -25                          | 0.049      | <30         | —     | —        |
|          |                |  |                 |                   |                        | 44                           | 0.046      | <30         |       |          |
| 0410+266 | EF             | D (3.0)                                | 2,100           | 98                | 1.12                   | -26                          | 0.049      | 29          | 0.30  | <i>b</i> |
|          |                |  |                 |                   |                        | 42                           | 0.046      | 30          |       |          |
| 0500+270 | Crowded        | S (3.5)                                | 1,200           | 164               | 0.73                   | -19                          | 0.049      | 31          | 0.20  | <i>b</i> |
|          |                |  |                 |                   |                        | 43                           | 0.046      | 36          |       |          |
| 0632+189 | EF             | PD (1.5)                               | 3,000           | 124               | 1.17                   | -04                          | 0.055      | 34          | 0.26  | <i>b</i> |
|          |                |  |                 |                   |                        | 32                           | 0.050      | 32          |       |          |
|          |                |  |                 |                   |                        | 44                           | 0.047      | 30          |       |          |
| 0646+184 | EF             | S (3.0)                                | 1,400           | 107               | 0.94                   | -04                          | 0.055      | 31          | 0.29  | <i>b</i> |
|          |                |  |                 |                   |                        | 46                           | 0.046      | 30          |       |          |
| 0656+213 | 19 mag G       | S (1.5)                                | 2,400           | 123               | 1.09                   | -05                          | 0.053      | 47          | 0.39  | <i>a</i> |
|          |                |  |                 |                   |                        | 45                           | 0.047      | 50          |       |          |
| 0706+261 | 20 mag RO      | D (3.5)                                | 2,500           | 454               | 0.63                   | -09                          | 0.051      | <30         | —     | —        |
|          |                |  |                 |                   |                        | 44                           | 0.046      | <30         |       |          |
| 0710+241 | 18.5 mag NSO   | S (3.6)                                | 1,200           | 74                | 1.02                   | -16                          | 0.051      | <30         | —     | —        |
|          |                |  |                 |                   |                        | 39                           | 0.047      | <30         |       |          |
| 0736+167 | EF             | D (4.0)                                | 1,800           | 82                | 1.13                   | -14                          | 0.055      | <30         | —     | —        |
|          |                |  |                 |                   |                        | 30                           | 0.052      | <30         |       |          |
| 0746+162 | EF             | PD (3.4)                               | 1,400           | 135               | 0.86                   | -14                          | 0.056      | 85          | 0.47  | <i>a</i> |
|          |                |  |                 |                   |                        | 28                           | 0.052      | 50          |       |          |
|          |                |  |                 |                   |                        | 37                           | 0.049      | 56          |       |          |
| 1055+018 | 18 mag QSO     | D (1.5)                                | 4,000           | 2,985             | 0.11                   | 38                           | 0.058      | 3266        | 0.97  | <i>a</i> |
|          |                |  |                 |                   |                        | 48                           | 0.049      | 2546        |       |          |
| 1123+012 | 20 mag G       | PD (3.5)                               | 1,200           | 190               | 0.68                   | -50                          | 0.047      | 36          | 0.18  | <i>b</i> |
|          |                |  |                 |                   |                        | 29                           | 0.064      | 32          |       |          |
| 1159-060 | EF             | S (1.6)                                | 1,900           | 175               | 0.87                   | -48                          | 0.054      | 87          | 0.50  | <i>a</i> |
| 1304-101 | EF             | S (4.0)                                | 1,400           | 105               | 0.95                   | -51                          | 0.054      | 27          | 0.34  | <i>b</i> |
|          |                |  |                 |                   |                        | -39                          | 0.073      | 44          |       |          |
| 1348-129 | EF             | EXT                                    | 3,500           | 280               | 0.93                   | -52                          | 0.059      | 69          | 0.26  | <i>a</i> |
|          |                |  |                 |                   |                        | -47                          | 0.067      | 76          |       |          |
| 1350-154 | EF             | S (3.0)                                | 1,000           | 45                | 1.14                   | -43                          | 0.082      | 36          | 0.80  | <i>b</i> |
| 1456-165 | 20 mag BO      | S (3.0)                                | 1,500           | 189               | 0.76                   | 7                            | 0.125      | 66          | 0.35  | <i>a</i> |
| 1632-199 | EF             | S (3.5)                                | 1,000           | 67                | 0.99                   | -45                          | 0.097      | 47          | 0.72  | <i>a</i> |
|          |                |  |                 |                   |                        | 37                           | 0.113      | 50          |       |          |
| 1924-193 | Crowded        | D (2.8)                                | 1,100           | 80                | 0.96                   | -45                          | 0.093      | <30         | —     | —        |
| 2019-202 | EF             | S (2.0)                                | 1,200           | 320               | 0.48                   | -47                          | 0.092      | 280         | 0.88  | <i>a</i> |
|          |                |  |                 |                   |                        | 43                           | 0.104      | 283         |       |          |
| 2023-142 | EF/20 mag G    | S (2.7)                                | 1,000           | 32                | 1.26                   | -46                          | 0.074      | <30         | —     | —        |
|          |                |  |                 |                   |                        | 41                           | 0.082      | <30         |       |          |
| 2050-188 | EF             | D (2.6)                                | 2,100           | 140               | 0.99                   | -49                          | 0.084      | <30         | —     | —        |
|          |                |  |                 |                   |                        | 43                           | 0.095      | <30         |       |          |
| 2058-179 | 19.5 mag BSO   | S (3.3)                                | 3,500           | 325               | 0.87                   | -11                          | 0.079      | 33          | 0.10  | <i>b</i> |
|          |                |  |                 |                   |                        | 41                           | 0.095      | 30          |       |          |
| 2243-032 | 19 mag BO      | EXT                                    | 3,500           | 503               | 0.71                   | -40                          | 0.060      | 144         | 0.29  | <i>a</i> |
|          |                |  |                 |                   |                        | 40                           | 0.061      | 147         |       |          |
| 2245-022 | EF             | D (3.5)                                | 1,250           | 264               | 0.57                   | -46                          | 0.053      | 50          | 0.20  | <i>a</i> |
|          |                |  |                 |                   |                        | -42                          | 0.058      | 57          |       |          |
|          |                |  |                 |                   |                        | 38                           | 0.062      | 48          |       |          |
| 2257-048 | EF             | S (2.2)                                | 1,500           | 193               | 0.75                   | -44                          | 0.058      | 33          | 0.17  | <i>b</i> |
| 2335+031 | 18 mag BL Lac  | S (2.0)                                | 4,300           | 603               | 0.72                   | -46                          | 0.051      | 108         | 0.17  | <i>a</i> |
|          |                |  |                 |                   |                        | -31                          | 0.059      | 95          |       |          |

\* The optical and the radio (327 MHz) data are taken from Joshi and Singal<sup>4</sup> and the references therein.

† NSO, neutral stellar object; QSO, quasi-stellar object; BSO, blue stellar object; RO, red object; BO, blue object; EF, empty field; G, galaxy.

‡ D, double; S, single; PD, possible double; EXT, bright core with a faint extension of a few arc s.

typical observation of 9 min. The r.m.s. noise for a coherent integration over such a period is  $\sim 8$  mJy. The formal error of the correlated amplitude  $S_c$  is the quadratic sum of this noise and  $0.05S_c$ .

The results for the 30 few-arc second sources are summarized in Table 1, together with their parameters at 327 MHz, derived from the occultation observations, and their optical identifications. The VLBI results include the fringe spacing FS, position angle PA of the projected baseline and the correlated flux density  $S_c$  at 5 GHz for each observation. The 'core fraction' at 5 GHz ( $C_5$ ) gives the ratio of the mean correlated flux density of a source to its integrated flux density. The last column gives the fringe detection class: *a* indicates all detections above 5 r.m.s. (12 sources) and *b* the detections between 3.5 and 5 r.m.s. in at least one observation (9 sources). We consider the above 21 sources to be clearly detected because in each case, the maximum correlated amplitude: (1) lies well above the noise and

in the correct frequency side band; (2) it lies within the same range of three delay channels in which the calibration sources were also detected; and (3) its residual fringe rate falls in a narrow range from  $-58$  to  $-74$  mHz which is similar to the value  $-68 \pm 4$  mHz observed for the calibration sources.

Further, such consistent behaviour in at least two observations was a prerequisite for calling a fringe detection positive in all those class *b* sources where the maximum correlated amplitude was only between 3.5 and 4 r.m.s. It can be shown<sup>11</sup> using random noise statistics together with the above checks that at most 1 of the claimed 21 detections can be spurious. As a further check, we again correlated the data after artificially introducing an extra time delay of  $2.5 \mu\text{s}$ , which is equivalent to looking at 'empty sky' because the delay is  $\sim 5$  times the coherence time defined by the system bandwidth of 2 MHz. Of the available 70 sets of observations, in only one case was a peak found on the correlated output which could satisfy all our detection criteria



specified above. Again, this empirical result on 'empty sky' suggests that all the 21 detections in our sample are most probably real.

For most sources, the position angle of the projected baseline changed appreciably between the observations. However, the fringe spacing remained around 0.05 arc s for sources at positive declinations but varied between 0.05 and 0.125 arc s for the southern sources. Two noticeable trends from Table 1 are: the correlated amplitude of a source changed little with position angle and showed no definite tendency to increase with fringe spacing, and the core fractions of the southern sources are not higher than those of the northern sources, though the former were observed at considerably larger fringe spacings. These two points together strongly suggest that all the detected compact components are essentially unresolved even at the smallest fringe spacing used and hence they are smaller than  $\sim 0.02$  arc s in size. We expect these compact components to be associated with the optical nuclei of the sources, as there is not enough evidence that such compact and prominent structures occur in the outer lobes of radio sources. For instance, Broderick and Condon<sup>12</sup> made a sensitive VLBI search at 430 MHz for components smaller than  $\sim 0.03$  arc s in a large sample of 100 extragalactic sources, which also includes some few-arc second sources. They found such compact components, contributing a significant fraction ( $>3\%$ ) of the total flux density, exclusively in those sources which either have a flat radio spectrum or a quasar identification and therefore probably also possess a prominent nuclear radio core. A similar absence of compact hot spots ( $\leq 0.02$  arc s) in the outer lobes has been reported for some few-arc second sources, such as 3C225B and 3C309.1, for which sufficiently detailed observations are now available<sup>13-16</sup>. Note that in recent VLBI work<sup>17</sup> on 35 3CR sources with a fringe spacing of 0.16 arc s at 1.4 GHz, compact components have been detected in the outer lobes of many double sources. However, whenever they were found to be sufficiently strong (emitting  $>5\%$  of the total flux density), these components showed evidence of resolution by the 0.16 arc s beam. In contrast, the compact components found in the present observations at 5 GHz seem to be considerably smaller and their contribution to the total emission is generally much higher than 5% (see Table 1). It therefore seems more appropriate to suppose that our detected compact components in the few-arc second sources are associated with their nuclear regions.

Each of the 30 few-arc second sources in our sample is probably a distant object located at a redshift  $z > 0.3$  (and hence a powerful radio source radiating  $\geq 10^{33}$  erg s<sup>-1</sup> Hz<sup>-1</sup> at 327 MHz). This follows from the analysis of radio source properties by Swarup and Subrahmanya<sup>5</sup> and is also indicated by the optical identifications of these 30 sources (Table 1). Excluding two that lie in crowded fields, seven are identified with blue-stellar objects and hence are probably distant quasars; 18 lie in empty fields and are likely to be galaxies at  $z \geq 0.4$  (refs 18-21). The remaining three sources have galaxy-like counterparts but even the brightest (and probably the nearest) of them is an object of  $m_R \sim 19$  which translates to  $z \sim 0.3$ . These relatively high redshifts of the few-arc second sources should not, however, be systematically any different from the redshifts of the remaining 236 sources (mostly of larger angular size) in the parent sample A. This is because the optical identification rate of 37% among the 30 few-arc second sources is nearly identical to the identification rate of 39% mentioned above for the entire sample A. Consequently, the emission wavelengths of the observed radiation should not be systematically different for the two sets of sources. Among the few-arc second sources, there seems to be no obvious correlation between the presence of an optical identification and of a bright radio nucleus (Table 1). We notice a similar trend in the published VLBI observations of a complete sample of 100 extragalactic radio sources selected from the BDFL catalogue<sup>12</sup>.

Table 1 shows that in 15 of the total 30 few-arc second sources, the radio nucleus accounts for more than a quarter of the total flux density at 5 GHz (in fact, similarly dominant radio

nuclei may exist in a few more of the 30 sources but these would have escaped detection because the sources are so weak that their total flux densities lie well below 100 mJy at 5 GHz). The above result on the fraction of sources with a core fraction  $C_s > 1/4$  can be parametrized by  $F_s(>1/4) \geq 15/30 = 0.5$  and below we compare it with the corresponding values found for four fairly large and well-studied representative samples of extended radio sources again derived from metre wavelength catalogues.

(1) Sample 1 (galaxies): at NRAO, Bridle and Fomalont<sup>22</sup> have mapped a large sample of 4C sources identified with galaxies brighter than 18 mag (double or triple morphology was commonly observed). Considering only those 150 sources with size  $>20$  arc s and lying at  $\delta > 15^\circ$ , we estimate that a sub-arc s component with a core fraction  $C_s > 1/4$  at 5 GHz occurs in only 12 sources. This gives  $F_s(>1/4) = 0.08$ .

(2) Sample 2 (galaxies and quasars): in the 3CR complete sample, 66 sources show a classical double morphology with an established optical counterpart<sup>23</sup>. In only two of them, is a core fraction  $C_s > 1/4$  seen<sup>24</sup>. Thus,  $F_s(>1/4) \sim 0.03$ .

(3) Sample 3 (quasars): at Westerbork, Miley and Hartsuijker<sup>25</sup> have mapped at 5 GHz a sample of 114 4C quasars. Of them, 43 are classified as double with a size  $>20$  arc s and possibly having a compact radio core which is clearly distinguishable from the straddling outer lobes. Of these 43, only seven have  $C_s > 1/4$ . Thus,  $F_s(>1/4) = 0.16$ .

(4) Sample 4 (quasars): at NRAO, Potash and Wardle<sup>26</sup> have mapped a sample of 52 4C quasars at 2.7 and 8.1 GHz, of which 16 are larger than 20 arc s and show a double morphology with a possible central radio core. From these data, we estimate that three of the 16 quasars have  $C_s > 1/4$ . Thus,  $F_s(>1/4) = 0.19$ .

The above comparison shows that in double sources of large angular size, whose axes are mostly expected at large angles from the line of sight, the radio nuclei are much less prominent as compared with those detected in the few-arc second sources by the present VLBI observations. In reality, the contrast is even more striking if one takes into account that the few-arc second sources were selected from a metre wavelength survey and hence  $\sim 80\%$  are likely to be associated with galaxies (see above and refs 4, 18-21, 27), and that the radio nuclei in galaxies are an order of magnitude weaker than those in quasars of the same total luminosity (see ref. 28).

To understand fully the meaning of the very different levels of nuclear radio emission observed in the few-arc second sources and in sources of larger angular extent, one needs to assess the importance of projection in the former case. Generally, few-arc second sources can arise in two ways and depending on the relative strength of these two types among our 30, the present VLBI results can be taken as evidence for either or both of the following, each of which represents an extreme situation:

(1) If all the few-arc second sources are intrinsically normal sized doubles reduced to small angular size because of projection, the observed high core-fraction in them would be consistent with the hypothesis of beaming of the nuclear radio emission along the source axis<sup>1-3</sup>. The implication of such beaming on the large scale structure of double sources has been discussed elsewhere<sup>24</sup>. Note also that the occurrence of beaming in the nuclei of extended radio sources need not conflict with the opposite claim made recently for optically selected quasars<sup>29</sup>, because the entire radio source in these quasars is visualized<sup>29</sup> as being so compact that the relativistic particles have yet to break out of the nuclear cloud of thermal plasma.

(2) Alternatively, the small angular size of few-arc second sources could be due to their being intrinsically small. If so, their physical sizes would only be  $\sim 10$ -50 kpc but they would probably have a double morphology, as is typical for powerful radio sources<sup>6</sup> (high radio luminosities for them were inferred above from their estimated large redshifts  $z \geq 0.3$ ). Such an interpretation would assign to them properties radically different from what is known about powerful radio sources in nearby space, hinting that very strong cosmological effects would have to be present. For instance, at  $z < 0.1$ , intrinsic sizes<sup>30</sup> of

powerful double sources ( $P_{1400} > 10^{32} \text{ erg s}^{-1} \text{ Hz}^{-1}$  for  $H_0 = 50 \text{ km s}^{-1} \text{ Mpc}^{-1}$ ) are very rarely, if ever,  $< 200 \text{ kpc}$ . However, if the few-arc second sources are intrinsically small, the detection of very prominent nuclear radio cores in them would mean that the time scale over which the nuclear ratio emission in powerful sources declines markedly, relative to the lobe emission, is comparable with the time needed by the lobes to emerge out of the main body of the parent galaxy.

To distinguish between the above two possibilities the extent to which projection determines their angular sizes needs to be assessed. Some insight into this question can be gained by mapping their arc second structures. Were the projection important, the two lobes might still be distinguishable but they would probably not appear elongated parallel to the line joining them. Note that such a morphology has been observed in the quasar 3C309.1 (a few-arc second source) mapped recently with a sub-arc second beam<sup>16</sup>, but is in contrast to the elongation of the lobes parallel to the source axis, as seen in extended double sources for which projection effects are expected to be minimal.

We thank H. Blaschke, U. Stursberg and W. Alef for help with data processing and R. Porcas for useful discussions. G.K. acknowledges support received from the Alexander-von-Humboldt Foundation.

Received 3 September; accepted 3 October 1980.

- Blandford, R. D., McKee, C. F. & Rees, M. J. *Nature* **267**, 211–216 (1977).
- Blandford, R. D. & Königl, A. *Astrophys. J.* **232**, 34–48 (1979).
- Scheuer, P. A. G. & Readhead, A. C. S. *Nature* **277**, 182–185 (1979).
- Joshi, M. N. & Singal, A. K. *Mem. astr. Soc. India* **1**, 49–72 (1980).
- Swarup, G. & Subrahmanya, C. R. *IAU Symp. No. 74*, 125–132 (1977).
- Fanaroff, B. L. & Riley, J. M. *Mon. Not. R. astr. Soc.* **167**, 31–35 (1974).
- Swarup, G. *Mon. Not. R. astr. Soc.* **172**, 501–512 (1975).
- Kapahi, V. K. *Mon. Not. R. astr. Soc.* **172**, 513–533 (1975).
- Swarup, G. *et al. Nature phys. Sci.* **230**, 185–188 (1971).
- Baars, J. W. M., Genzel, R., Pauliny-Toth, I. I. K. & Witzel, A. *Astr. Astrophys.* **61**, 99–106 (1977).
- Moran, J. M. in *Methods of Experimental Physics* (Part C) (Academic, London, 1976).
- Broderick, J. J. & Condon, J. J. *Astrophys. J.* **202**, 596–602 (1975).
- Bentley, M., Haves, P., Spencer, R. E. & Stannard, D. *Mon. Not. R. astr. Soc.* **173**, 93–97P (1975).
- Jenkins, C. J., Pooley, G. G. & Riley, J. M. *Mem. R. astr. Soc.* **84**, 61–99 (1977).
- Kapahi, V. K., Joshi, M. N. & Gopal-Krishna *Astrophys. Lett.* **11**, 155–158 (1972).
- Kus, A. J., Wilkinson, P. N. & Booth, R. S. *Mon. Not. R. astr. Soc.* (in the press).
- Kapahi, V. K. & Schilizzi, R. T. *Astr. Astrophys. Suppl.* **38**, 11–13 (1979).
- Bolton, J. G. *IAU Symp. No. 74*, 85–97 (1977).
- Grueff, G. & Vigotti, M. *Astr. Astrophys. Suppl.* **20**, 57–82 (1975).
- Laing, R. A., Longair, M. S., Riley, J. M., Kibblewhite, E. J. & Gunn, J. E. *Mon. Not. R. astr. Soc.* **183**, 547–548 (1978).
- Wills, B. J. *Astr. J.* **81**, 1031–1052 (1976).
- Bridle, A. H. & Fomalont, E. B. *Astr. J.* **83**, 704–724 (1978).
- Longair, M. S. & Riley, J. M. *Mon. Not. R. astr. Soc.* **188**, 625–635 (1979).
- Gopal-Krishna *Astr. Astrophys.* **86**, L1–L2 (1980).
- Miley, G. K. & Hartsuiker, A. P. *Astr. Astrophys. Suppl.* **34**, 129–163 (1978).
- Potash, R. I. & Wardle, J. F. C. *Astr. J.* **84**, 707–717 (1979).
- Venkatakrishna, K. L. & Swarup, G. *Mem. astr. Soc. India* **1**, 25–47 (1979).
- Miley, G. K. *A. Rev. Astr. Astrophys.* (in the press).
- Strittmatter, P. A., Hill, P., Pauliny-Toth, I. I. K., Steppe, H. & Witzel, A. *Astr. Astrophys.* **88**, L12–L15 (1980).
- Gavazzi, G. & Perola, G. C. *Astr. Astrophys.* **66**, 407–416 (1978).

## Decrease in CO<sub>2</sub> mixing ratio observed in the stratosphere

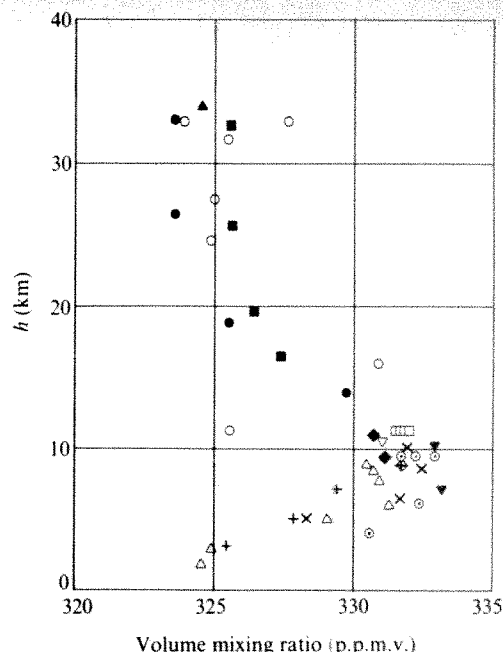
W. Bischof

Department of Meteorology, University of Stockholm,  
S-10691 Stockholm, Sweden

P. Fabian & R. Borchers

Max-Planck-Institut für Aeronomie, D-3411 Lindau, FRG

**Air samples, collected cryogenically at different heights of the stratosphere, were analysed for carbon dioxide with an IR absorption technique. Supplementary tropospheric air samples were taken aboard commercial airliners. The results reported here show that the CO<sub>2</sub> mixing ratio is not constant with altitude but rather decreases in the stratosphere, by about 7 p.p.m.v., between the tropopause and 33 km. One conclusion is that recently increased concentrations of CO<sub>2</sub> in the troposphere have not propagated far into the stratosphere.**



**Fig. 1** Balloon and aircraft samples taken from 1977 to 1979. Balloon samples: ▲, September 1977; ●, June 1978; ■, 28 June 1979; ○, 9 November 1979. Aircraft samples 27 June 1979: ○, Stockholm; +, Copenhagen descent; ×, Copenhagen ascent; □, Zürich–Copenhagen; △, Zürich. Aircraft samples November 1979: ◆, Copenhagen, 12 November; ▼, Copenhagen, 15 November.

The balloon-borne cryogenic sampler is described elsewhere<sup>1</sup>, together with mid-latitude, vertical profiles of H<sub>2</sub>, CH<sub>4</sub>, CO, N<sub>2</sub>O, CFCl<sub>3</sub> and CF<sub>2</sub>Cl<sub>2</sub> obtained from gas-chromatographic analysis of the samples. CO<sub>2</sub> can also be analysed by gas chromatography, but the total error is of the order of  $\pm 1\%$ , corresponding to  $\sim \pm 3 \text{ p.p.m.v.}$  With the IR absorption technique, however, flask samples can be analysed with a total error of less than  $\pm 0.2 \text{ p.p.m.v.}$ , a figure which already includes the error from the absolute calibration<sup>2</sup>.

For the first set of samples, taken during balloon flights in 1977 and 1978, which had been stored for more than one year, we found that some drifted considerably. In Fig. 1 we plot only the data from those samples which appeared to be stable—those that varied by less than 0.5 p.p.m.v. over a 3-month period. These clearly show that the stratospheric CO<sub>2</sub> mixing ratio is not constant with height but rather decreases with increasing height. This was confirmed by the results from samples collected on 28 June 1979. The CO<sub>2</sub> IR gas analysis was carried out 4 months after the flight. Although two samples whose CO<sub>2</sub> concentration drifted considerably were discarded, an apparently similar vertical profile was obtained from the stable samples. To demonstrate the vertical CO<sub>2</sub> distribution in the troposphere at the same time, supplementary air samples were collected on 27 June aboard commercial airliners, at different mid-latitude locations and different heights, and also analysed for CO<sub>2</sub>. The results, also shown in Fig. 1, demonstrate that the highest CO<sub>2</sub> mixing ratios are observed at the tropopause level, which was at  $\sim 10 \text{ km}$ . The three stratospheric samples taken at 10.6-km altitude, during a Zürich–Copenhagen flight, suggest that the decrease in the CO<sub>2</sub> mixing ratio starts immediately at the tropopause. The decreasing CO<sub>2</sub> content from the tropopause level down, which is also noticeable in Fig. 1, is a result of CO<sub>2</sub> uptake by the vegetation at this time of the year.

The CO<sub>2</sub> mixing ratios analysed from seven stratospheric samples collected during a balloon flight on 9 November 1979, supplemented by five tropospheric samples from 12 and 15 November, fit fairly well with the vertical distribution of carbon dioxide, although some scatter is noticeable. Because no repeated analysis checks could be made for this last set of air



samples, we cannot decide whether or not this scatter is real or due to concentration drifts in some sample containers.

Our results show that the stratospheric  $\text{CO}_2$  mixing ratio decreases from 332 p.p.m.v. at the tropopause to  $\sim 325$  p.p.m.v. at a height of 25 km. These values are related to the Scripps 1959 manometric scale (see ref. 2). Our data do not give any indication of a vertical gradient higher up. This decrease of 7 p.p.m.v. disagrees with results obtained by Volz *et al.*<sup>3</sup>. They found, through gas-chromatographic analysis of stratospheric air samples, a constant  $\text{CO}_2$  mixing ratio of  $\sim 320$  p.p.m.v. for the whole height range discussed here.

Because the presently known photochemical reactions cannot account for the stratospheric  $\text{CO}_2$  decrease we found, this is likely to be the result of long-range transport and exchange between the troposphere and stratosphere. In fact, due to the burning of fossil fuel, the tropospheric  $\text{CO}_2$  mixing ratio increases by  $\sim 1\text{--}1.5$  p.p.m.v. every year<sup>2</sup> and had an annual average for 1979 of 332 p.p.m.v. This man-made increase in tropospheric  $\text{CO}_2$  is gradually propagating upwards with a delay that increases with increasing altitude. The vertical gradient shown in the diagram, which is a result of this slow vertical mixing, suggests a delay of 5–6 yr between the tropopause and an altitude of 25 km.

The stratospheric balloon sampling project was sponsored by the German Federal Ministry of Research and Technology, grant no. FKW-03. The  $\text{CO}_2$  project at Stockholm University is supported by the Swedish SRC.

Received 18 July; accepted 25 September 1980.

1. Fabian, P. *et al.* *J. geophys. Res.* **84**, 3149–3154 (1979).
2. Bischof, W. *Tellus* **29**, 435–444 (1977).
3. Volz, A. *et al.* *WMO Technical Conf. on Regional and Global Observation of Atmospheric Pollution Relative to Climate*, Boulder, 171–179 (WMO-no. 549, 1979).

## Grand unification magnetic monopoles inside the Earth

R. A. Carrigan Jr

Fermi National Accelerator Laboratory, Batavia, Illinois 60510

**Elementary particle grand unification theories admit the possibility of very massive magnetic monopoles, but standard cosmology gives too many poles. Massive monopoles are affected both by gravity and magnetism, requiring reassessment of existing monopole searches. Monopoles inside the Earth would be able to annihilate with each field reversal, thereby giving rise to additional internal heat. This perspective is used to estimate an upper limit for the monopole-to-baryon ratio at accretion of  $10^{-28}$ .**

Grand unification particle theories such as  $\text{SU}(5)$  allow the existence of massive magnetic monopoles<sup>1</sup>. Polyakov and 't Hooft<sup>2,3</sup> observed that theories such as  $\text{SU}(5)$  with an imbedded  $\text{U}(1)$  symmetry could contain a magnetic monopole solution<sup>4,5</sup>. Goddard and Olive<sup>6</sup> noted that this approach can reproduce Dirac charge quantization<sup>7</sup> by using a massive vector boson. Bogomol'nyi<sup>8</sup> has found a lower limit on the monopole mass of  $M > 4M_v/g^2$  where  $M_v$  is the mass of the boson and  $g^2$  is a dimensionless coupling constant. If  $M_v$  is the vector boson of weak interactions,  $g^2$  is equal to  $\alpha$ , and the Bogomol'nyi limit is of the order of  $10^4$  GeV.

Many grand unification theories are characterized by the presence of super heavy bosons with a mass<sup>9,10</sup> of the order of  $M_x = 10^{14}$  GeV. The mass of a grand unification magnetic monopole (GUMM) is set by the Bogomol'nyi limit with the related coupling constant of the order of  $1/50$  (ref. 11), so that GUMMs are expected to have masses of the order of  $10^{16}$  GeV or  $0.02 \mu\text{g}$ .

Such massive particles might have been produced in the big bang in the early Universe. It has been shown<sup>12–14</sup> that for standard cosmology and plausible grand unification models that the number of GUMMs would be close to the number of baryons even now. The evidence is against this in our corner of the Universe. Several ways of circumventing Preskill's paradox have been suggested. These include first-order phase transitions<sup>15</sup>, electric charge non-conservation<sup>16,17</sup>, unusual group structures<sup>18</sup> and cosmological statistical non-equilibrium<sup>19</sup>. The grand unification–standard cosmology system is then faced with a paradox that can be moderated or even turned off but with difficulty. Grand unification remains to be established as a fundamental relevant theory and standard cosmology seems to leave some room for adjustments. However, this paradoxical situation means we need to understand better the limits on the existence of massive magnetic monopoles.

A massive magnetic monopole could be produced either in the big bang or in a cosmic-ray interaction. Bludman and Ruderman<sup>20</sup> have shown that it is not feasible to produce particles with the masses of GUMMs in cosmic ray collisions. A GUMM born in the primordial fireball that survives annihilation can be accelerated to  $10^{11}$  GeV by galactic fields<sup>21,22</sup> of the order of  $3 \times 10^{-6}$  G acting over distances of  $10^{21}$  cm (ref. 23). As these are non-relativistic energies, previous conventional wisdom on energy loss of relativistic monopoles and on transit times must be used with discretion.

No magnetic monopoles have been found<sup>24</sup>. In a typical search, magnetic charges are expected to produce heavy ionization in matter, but for non-relativistic energies the energy loss is smaller<sup>25</sup>. Where timed counters are used, care must be taken. Typically<sup>26</sup> a pole accelerated for 50 cm in an 80-kg field and detected with counters spaced 25-cm apart and a timing window of 20 ns, would give a minimum  $\beta$  of 0.04 and an upper limit for mass that could be detected of  $10^5$  GeV.

A monopole passing through a coil should produce an induced voltage<sup>27</sup>. This technique has been exploited to show that the monopole-to-baryon ratio is  $< 3 \times 10^{-28}$  near the surface of the Moon<sup>28</sup>. As with all other searches this limit is affected by the circumstances of the monopole trapping.

Parker has shown that monopoles would have a profound effect in dissipating and neutralizing large-scale magnetic fields. For relativistic Dirac poles this sets a limit on the monopole-to-baryon ratio for the galactic system of  $2 \times 10^{-26}$ , while for non-relativistic poles it would be around  $10^{-24}$ . Solar and terrestrial field limits are less stringent and the galactic limit is less stringent than the lunar search.

A primordial magnetic monopole is subjected to forces from cosmological magnetic fields, gravitational forces, other magnetic monopoles, and interactions with ordinary electronic matter through processes such as ionization. Many analyses of pole behaviour only consider the magnetic effects. For GUMMs, the force of gravity will approach the effect of cosmic magnetic fields. The gravitational energy acquired by a typical GUMM falling into a galactic disk is  $10^{10}$  GeV while the energy gained in passing through a galactic magnetic field fluxuation (300 light yr) is  $2 \times 10^{10}$  GeV. A GUMM with this energy could go deep into the Earth. The magnetic force at the galaxy is 500 times the gravitational force but the gravitational force acts over a much larger distance. The gravitational energy from solar or terrestrial sources exceeds the energy acquired from the corresponding magnetic field. For a magnetic dipole Earth acting in a repulsive sense (not a realistic approximation here) the magnetic and gravitational forces are in equilibrium at  $R = 0.18 R_e$ . This is well inside the radius of the core ( $R_c = 0.55 R_e$ ).

In a dense material a GUMM will be thermalized and move to an equilibrium position of the magnetic, gravitational, and other forces. In a dipole Earth this would be on a line with the opposite terrestrial magnetic pole and the gravitational centre. The same is true for magnetic fields generated by currents. If the pole is in a fluid it will be able to move freely. In a solid it may have to move by lattice jumps<sup>29</sup>.

Because gravitation forces and magnetic forces are intermingled, one must be cautious about where one looks for GUMMs. A heavy pole that accretes in equilibrium with the material of the Earth will move preferentially closer to the Earth's centre because of the presence of a terrestrial magnetic field. Thus, the Earth's surface is a poor place to look for GUMMs.

The Earth's magnetic field reverses irregularly<sup>23,30</sup> with epochs lasting typically a million years interspersed with occasional events of shorter duration. The reversal takes of the order of 1,000 yr and is turbulent. The Earth's magnetic field is due to a convective dynamo in the fluid core. The dipole field lines flow into the core and then spiral around the Earth's axis of rotation, resulting in larger axial (100 G) than poloidal fluxes (5 G). Further complexity is introduced by convective cells within the dynamo.

When the field reverses, GUMMs of one polarity would move to positions previously held by the opposite polarity. Some of them would pass close enough to opposite sign poles to attract, bind and annihilate, resulting in the release of an extraordinary amount of energy. What, then, would be the contribution of such an energy source to the terrestrial heat inventory?

The heat generation inside the Earth is not completely understood<sup>31</sup>. Heat comes from both gravitational forces and radioactivity. Differentiation processes concentrate radioactive materials selectively in the silicates which form the Earth's crust so that much of the radioactivity is near the surface. Estimates of average heat flow per unit area over the surface area have been revised upwards in the past decade by 20–40%. Uncertainties include the amount of radioactivity, thermal properties of the high-pressure core material, and the contributions of the ocean basins. Clearly, then, understanding the relevant contributions to this heat flow is no easy matter. The average heat flow at the surface is of the order of  $1.5 \times 10^{-6}$  cal cm<sup>-2</sup> s<sup>-1</sup>. The total heat output is  $3 \times 10^{20}$  erg s<sup>-1</sup> ( $2 \times 10^{23}$  GeV s<sup>-1</sup>).

To estimate an upper limit on monopole annihilation as a heat source, we assume that of the order of 25% of the Earth's heat generation could easily come from this source. This corresponds to a heat source of  $5 \times 10^{22}$  GeV s<sup>-1</sup>. For a field reversal every 500,000 yr each reversal must supply  $8 \times 10^{35}$  GeV. If the annihilation energy is perfectly coupled to terrestrial material this requires the annihilation of  $10^{20}$  GUMMs. If the annihilation region is confined to the Earth's core the annihilation event density is  $n_a = 4 \times 10^{-7}$  cm<sup>-3</sup>.

One model to get a monopole density for one polarity,  $n$ , is to assume that the core is uniformly filled with north and south poles. Poles are moving with some relative velocity  $v_D$  as they wander through the liquid core. When they approach within  $r_a$  where the pole-antipole force is sufficiently strong to overcome external forces, they will annihilate, provided the angular momentum between the poles is small enough. The annihilation event density is

$$n_a = \pi r_a^2 v_D t n^2 \quad (1)$$

where  $t$  is the time during which annihilation can occur in the reversal. Initial inhomogeneities would have to be present because the monopoles with opposite polarity would be separated. But, as the reversal proceeds, the equilibrium condition could exist over different smaller regions of the core. The model would still be satisfactory provided  $t$  represented the average time for some region to pass through equilibrium.

For a monopole in equilibrium with the liquid core at a temperature of 4,000 K, the thermal velocity is of the order of  $10^{-2}$  cm s<sup>-1</sup>, as is the average mass drift velocity. But for an axial field of 100 G, the characteristic monopole velocity might be  $10^5$  cm s<sup>-1</sup> based on extrapolating the Ahlen energy loss formula<sup>25</sup> to low  $\beta$  values. With the complex field geometry fully on, monopoles would move to equilibrium positions probably near the surface of the solid core or the inner surface of the mantle in  $\sim 1$  yr. If the reversal is turbulent, though, monopoles might slow substantially for some period even as they moved to regions where field lines had moved in again. At a velocity of

$10^{-2}$  cm s<sup>-1</sup> the time to produce a homogeneous condition is of the order of  $10^{10}$  s.

The capture distance,  $r_a$ , is sensitive to gravity, the terrestrial magnetic field and relative pole velocity. For characteristic forces that would be present ( $10^{-5}$  dyne), a plausible capture distance would be  $10^{-5}$  cm.

For these conditions, the monopole density in the core to produce one-quarter of the Earth's heat is  $n = 1.5 \times 10^{-3}$  cm<sup>-3</sup>. This is equivalent to an upper limit on the monopole-to-baryon ratio at accretion of  $2 \times 10^{-28}$ . The baryon number is taken for the entire Earth rather than the core alone as it is presumed that monopoles were differentially attracted to the core. The pole density could not be too much larger because the poles would cancel the Earth's field. Field dissipation due to magnetic currents is less of a constraint.

This limit depends on the pole mass. Turbulence and inhomogeneities could also change the limit. It is difficult to attach any estimate of accuracy to a limit based on such a speculative mechanism. Nevertheless, the picture suggests that the upper limit on the monopole-to-baryon ratio in the Earth is extremely small and consistent with the upper limit on the ratio observed at the surface of the Moon. This strengthens the Preskill paradox and indicates that the grand unification-standard cosmology-GUMM collection picture must break down at some point.

A GUMM density near this limit would be sufficient to supply energy for of the order of  $10^4$  field reversals (the age of the Earth). Such a density would degrade the Earth's field by 10% with the details depending on the equilibrium configuration. For a constant dynamo strength over the life of the Earth the average net field would rise with time as the monopoles annihilated.

There has been little consideration of the details of annihilation of GUMM pairs but they would probably annihilate rapidly into many particles with energies of  $10^{14}$  GeV, some of which would decay quickly into muons and neutrinos. Muons at these energies lose nearly all of their energy by radiation rather than ionization<sup>33</sup> so that the energy is dissipated within 20 km of the annihilation point. The neutrino cross-section<sup>34</sup> is expected to be of the order of  $\sigma_\nu = 10^{-34}$  cm<sup>2</sup>, so that a substantial fraction of the neutrinos would interact in the Earth. During a field reversal much of the GUMM mass would be converted to heat in the core. Heat transfer times from the core are of the order of the age of the Earth so that the individual field reversals would be averaged out. Some portion of the neutrino energy deposited in a layer close to the surface (roughly 10 km) would appear as an effective heat pulse during a field reversal. This is only 0.1% of the neutrino energy and substantially less of the total but appears in 1/500 the time so that it might constitute a thermal spike of the order of 0.01–0.1 of the average heat flow. This spike seems to be insufficient to have an effect on the polar ice caps<sup>35</sup>.

The Moon has no dipole-like field<sup>36</sup>, but a field of 0.05–1 G would have been necessary to produce the magnetization<sup>37</sup>. It is difficult to model a lunar dynamo that would have produced the field<sup>23</sup>. If the Moon accreted from a mix with a GUMM-to-baryon ratio five times larger than the upper limit earlier suggested for the Earth and the GUMMs differentiated out into opposite poles during the process their presence could explain a slowly decaying relic field of the order of 0.1 G. Some mechanism such as an external field from the Earth or the solar wind would have been needed to establish the north-south separation.

Thus even small admixtures of GUMMs would produce noticeable changes in planetary conditions. On the other hand the search for massive primordial monopoles should continue. Possibilities might include meteors from the cores of large asteroid bodies. Perhaps some reconsideration should be given to tracks in emulsion purported to come from one-third of Dirac charge monopoles in experiments on meteorites<sup>38</sup>. These could have been due to massive, slowly moving monopoles with concomitantly smaller energy loss. A later experiment was more sensitive but not to GUMM masses.



Received 30 June; accepted 15 September 1980.

1. Scott, D. M. Preprint 78-79/32 Imperial College (1979).
2. 't Hooft, G. *Nucl. Phys.* **B79**, 276 (1974).
3. Polyakov, A. *Soviet. Phys. JETP Lett.* **20**, 194 (1974).
4. Carrigan, R. A. Jr *Fermilab* **77**, 42 (1977).
5. Stevens, D. M. *VPI-EPP-73-5* (1973).
6. Goddard, P. & Olive, D. I. *Rep. Prog. Phys.* **41**, 1360 (1978).
7. Dirac, P. A. M. *Proc. R. Soc. A* **133**, 60 (1931).
8. Bogomol'nyi, E. *Soviet. J. nucl. Phys.* **24**, 449 (1976).
9. Buras, A. J., Ellis, J., Gaillard, M. K. & Nanopoulos, D. V. *Nucl. Phys.* **B135**, 66 (1978).
10. Goldman, T. J. & Ross, D. A. *Phys. Lett.* **84B**, 208 (1979).
11. Scott, D. M. *Cambridge DAMTP* 80/2 (1980).
12. Preskill, J. P. *Phys. Rev. Lett.* **43**, 1365 (1979).
13. Einhorn, M. B., Stein, D. L. & Toussaint, D. *Michigan UM HE* 80-1 (1980).
14. Zeldovich, Ya. B. & Khlopov, M. Yu. *Phys. Lett.* **79B**, 239 (1978).
15. Guth, A. H. & Tye, S.-H. *SLAC-Publ.* 2448 (1979).
16. Langacker, P. & Pi, S.-Y. *SLAC-Publ.* 2496 (1980).
17. Langacker, P. *1st Workshop on Grand Unification* (1980).
18. Lazarides, G. & Shafi, Q. *Phys. Lett.* **94B**, 149 (1980).
19. Fry, J. N. & Schramm, D. N. *Phys. Rev. Lett.* **44**, 1361 (1980).
20. Bludman, S. A. & Ruderman, M. A. *Phys. Rev. Lett.* **36**, 840 (1976).
21. Porter, N. A. *Nuovo Cim.* **16**, 958 (1960).
22. Goto, E. *Prog. theor. Phys.* **30**, 700 (1963).
23. Parker, E. N. *Cosmical Magnetic Fields* (Clarendon Oxford, 1979).
24. Price, P. B., Shirk, E. K., Osborne, W. Z. & Pinsky, L. S. *Phys. Rev. Lett.* **35**, 487 (1975).
25. Ahlen, S. P. *Rev. Mod. Phys.* **52**, 121 (1980).
26. Carrigan, R. A. Jr, Nezzick, F. A. & Strauss, B. P. *Phys. Rev.* **D10**, 3867 (1974).
27. Tassie, L. J. *Nuovo Cim.* **38**, 1935 (1965).
28. Vant-Hull, L. L. *Phys. Rev.* **173**, 1412 (1968).
29. Ross, R. R., Eberhard, P. H., Alvarez, L. W. & Watt, R. D. *Phys. Rev.* **D8**, 698 (1973).
30. Amaldi, E. *et al.* *CERN* 63-13 (1963).
31. Cox, A., Dalrymple, G. B. & Doell, R. R. *Scient. Am.* **216**, 44 (1967).
32. Oxburgh, E. R. & Turcotte, D. L. *Rep. Prog. Phys.* **41**, 1249 (1978).
33. Schubert, G. A. *Rev. Earth planet. Sci.* **7**, 289 (1979).
34. Wilson, R. R. *Fermilab Summer Study*, 465 (1969).
35. Halprin, A. 1978 *DUMAND Summer Workshop* Vol. 2, 27 (Fermilab 1978).
36. Andrews, J. T. & Barry, R. G. A. *Rev. Earth planet. Sci.* **6**, 205 (1978).
37. Ness, N. F. A. *Rev. Earth planet. Sci.* **7**, 249 (1979).
38. Dyal, P., Parkin, C. & Daly, W. *Rev. Geophys. Space Phys.* **12**, 56 (1974).
39. Kolm, H. H., Villa, F. & Odian, A. *Phys. Rev.* **D4**, 1285 (1971).

## Authigenic dolomite on marble surface

M. Del Monte

Istituto di Geologia, Università di Bologna, 40126 Bologna, Italy

C. Sabbioni

Laboratorio FISBAT-CNR, 40126 Bologna, Italy

The formation of dolomite remains controversial. Various hypotheses have been proposed, including primary precipitation from seawater, authigenesis or penecontemporaneous alteration of  $\text{CaCO}_3$  by seawater, and postdiagenetic secondary replacement of  $\text{CaCO}_3$  by groundwater, connate water, or other solutions. Although the existence of authigenic dolomite in recent sediments has been confirmed<sup>1-3</sup>, all attempts to synthesize ordered dolomite at temperatures of sedimentary environments have failed<sup>4</sup>. It has been suggested that organic material<sup>5,6</sup> and clay minerals<sup>7,8</sup> may be important in the formation mechanism of dolomite. Here we present evidence that authigenic dolomite is formed on marble surfaces exposed to urban atmospheres. This discovery suggests that a relatively short period of time (of the order of a century) is actually required for dolomite formation in the natural system described here.

We have studied for many years the effects of the atmosphere on the deterioration of building stones. Samples from San Petronio (fourteenth century) and other more recent buildings in Bologna (Northern Italy) have been examined. Analyses on many altered layers found on limestone and marble surfaces have shown the following parageneses:

- (1) authigenic dolomite and calcite, quartz, K-feldspar;
- (2) authigenic calcite, quartz, K-feldspar;
- (3) authigenic gypsum and calcite, K-feldspar, Na-feldspar, graphite;

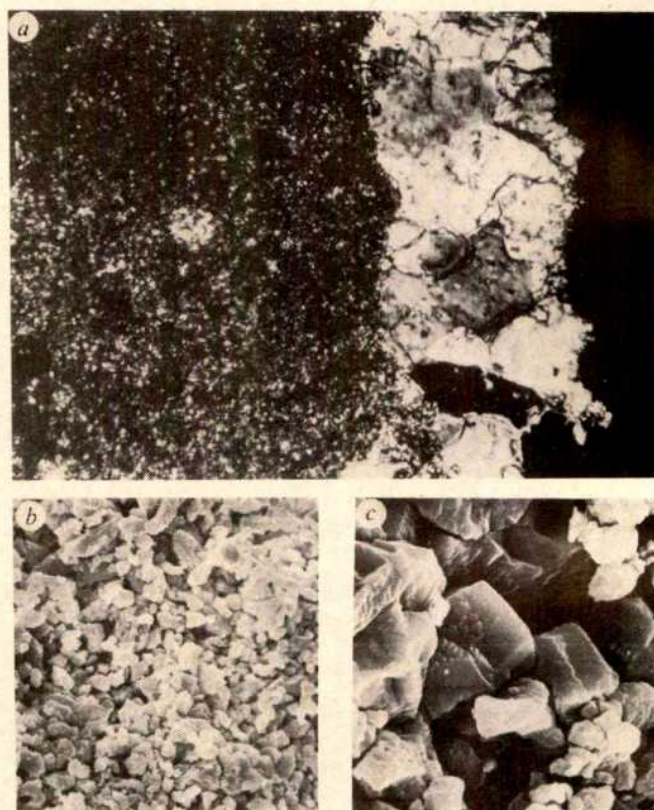
- (4) authigenic gypsum, quartz, K-feldspar, graphite.

The thickness of the altered layer varies between <1 mm to several mm (Fig. 1).

The variation in the mineralogical parageneses of the altered layer is outlined in Fig. 2. The dolomite clearly prevails in the external layer (A) and decreases progressively from the outside towards the inside until it disappears on contact with the unaltered rock. In the samples where it is only present in traces it is exclusively observed in the superficial layer.

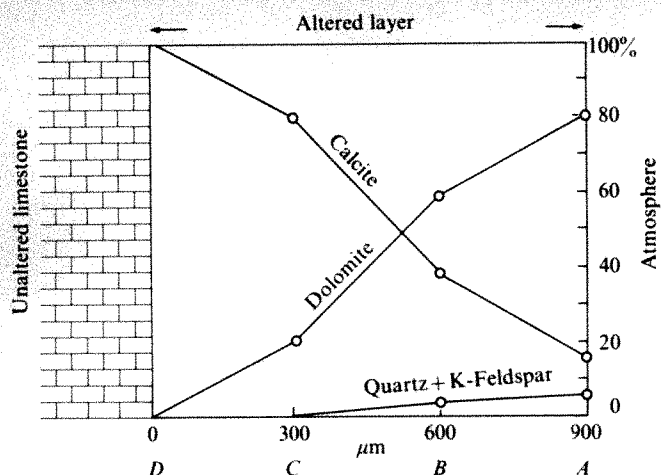
Representative X-ray diffraction analyses (XRD) of samples of calcite and dolomite are shown in Fig. 3. Our results indicate that: (1) in layers A, B, C and D the dolomite presents a slight excess of calcium<sup>12</sup> ( $\text{Ca}_{53}\text{Mg}_{47}$ ) and the calcite shows a  $\text{MgCO}_3$  mole content of 2%; (2) the calcite in the original marble has also a 2 mole %  $\text{MgCO}_3$ ; (3) in the layer where only the calcite precipitates, that is in the sample of the second paragenesis, a high-Mg calcite ( $\text{Ca}_{90}\text{Mg}_{10}$ ) is present. The error in the determination is <1 mole.

The XRD analyses of marble samples dissolved in a 2% solution of acetic acid show that dolomite is not present in the unaltered rock. Sedimentation of dolomite on the surfaces observed as wind-blown dust seems unlikely as then dolomite should also be found in the other parageneses as occurs for quartz and K-feldspar, which seem to be derived from soil erosion. This observation together with optical analyses which show euhedral or subhedral forms and intergrowth texture (Fig. 1) excludes this origin. Nearly stoichiometric calcite was observed alongside dolomite. This phenomenon together with the absence of magnesian calcites means that a metasomatic origin can be excluded. These observations lead us to think that the



**Fig. 1** The altered layer consists of rhombohedral crystals of dolomite and calcite, often twins, with greater dimensions (5–10  $\mu\text{m}$ ) than the crystals of calcite in the unaltered marble. The porosity of the altered layer is high. It is impossible to discriminate calcite from dolomite by optical analysis, but X-ray analyses show that dolomite prevails in the outer layer. *a*, Thin section, Nicols  $\times$ ,  $\times 100$ ; *b*, scanning electron microscopy (SEM),  $\times 1,000$ ; *c*, SEM,  $\times 3,000$ .





**Fig. 2** Schematic diagram of the mineralogical concentrations of the altered layer. The altered layer is of an average thickness of 1 mm. For each area the samples were taken successively A, B, C, D and each were 200–300  $\mu\text{m}$  thick. Quartz and K-feldspar percentages were determined after dissolution of the samples in acetic acid.

dolomite is formed by direct crystallization from aqueous solution. The unaltered rock contains between 0.25 and 0.30% Mg. We think that the Mg in our system does not derive exclusively from the dissolution of the underlying rock, but also from the washing away of the surrounding area. Besides, there is evidence<sup>9</sup> (even though our thermodynamic and chemical conditions differ) of a mobilization of the Mg ion in the solid state, which could affect a limited thickness of the underlying rock in a way which is difficult to evaluate. Quantitative analyses by atomic absorption spectrometry (AAS) of bulk samples of the altered layer have been performed. The presence of elements such as Zn ( $320 \pm 15$  p.p.m.), Cu ( $156 \pm 8$  p.p.m.), V ( $25 \pm 1$  p.p.m.) and Pb ( $20 \pm 2$  p.p.m.), which are absent in the original rock was detected. These elements are evidence of the contribution made by atmospheric particulate. Mg is associated mainly with inorganic salts in coal fly-ash (1,000–10,000 p.p.m.), industrial dust (100–1,000 p.p.m.) and sea spray (3.7%)<sup>10</sup>. Particulate transport phenomena and deposition effects cause serious difficulties in determining an average Mg concentration in our system.

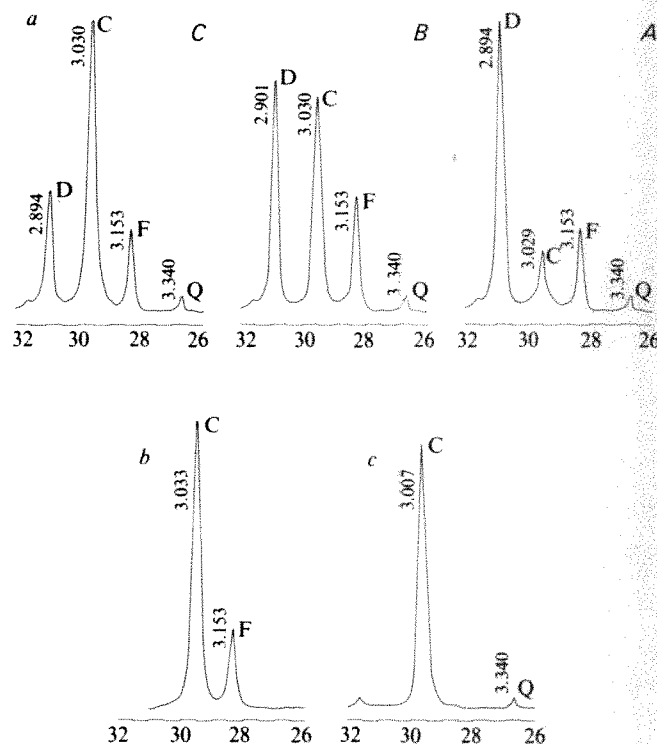
It has been thought<sup>4,11</sup> that a high ratio of Mg/Ca favours the precipitation of dolomite, but this does not seem to be true in our case. However, the circulating solution is being analysed. Moreover the part played by pH, clay minerals and algae in the origin of dolomite must be considered. In none of the samples that we analysed, were dolomite and gypsum present at the same time. Because the hydration of  $\text{SO}_2$  and its oxidation in sulphuric acid produces a lowering of pH in solution, we agree that the formation<sup>5</sup> of dolomite is favoured by a high pH level.

The insoluble residues of some dolomite samples dissolved in 2% acetic acid show either no or only minor quantities of clay minerals. Thus no relationship between clay minerals and dolomite was detected which accords with the results obtained by Lumsden<sup>8</sup>. The presence of algae (*Gleocapsa* sp. and lichen *soredium*) and Basidiomycetes and Ascomycetes spores were observed.

Microclimatic conditions (temperature and humidity) led us to consider the possibility of the local reproduction of these microorganisms with consequent chemical alteration of the medium.

We have shown that authigenic dolomite is present in a different environment from those reported previously, at low (0–50°C) temperatures at one atmosphere with a low Mg/Ca ratio and no clay minerals present. Furthermore the period of formation is fairly short. The upper limit is 500 yr and is even

lower if the effects of restoration carried out subsequently and the presence in the altered layer of elements like Pb, Zn, V, Cu, resulting from industrial development over the past few decades are considered. Dolomite crystals show dimensions up to 10  $\mu\text{m}$ , which together with a low time period of formation suggests a high growth rate. A model for the formation of the altered layer could be: water vapour condenses on the surface and penetrates the porous altered layer. The less porous unaltered rock forming a discontinuity in the system favours an accumulation of water at the interface of the altered and unaltered rock. Here the transformation of the carbonates by the various elements dissolved in



**Fig. 3** X-ray Cu-K $\alpha$  diffraction patterns of: a, altered layer dolomite-calcite; b, unaltered marble; c, altered layer with only precipitation of calcite. The composition of dolomite (D) and calcite (C) was determined by the position of the  $d$  (104). Fluorite (F:  $d_{111}$ ) and quartz (Q:  $d_{101}$ ) were used as internal standards as their peaks fall reasonably close to the main calcite peak.

the water takes place. The growth of crust occurs in an inward direction so that the altered layers of more recent formation are in contact with the unaltered rock. As this phenomenon proceeds the formation of a protecting coating on the surface which reduce the chemical activity of the rock, or the detachment of the altered layer occurs.

We thank O. Vittori and E. Bonatti for helpful discussions, E. MacLoren for creating interest in the aspect of the dolomite formation, and P. Mandrioli for biological analyses. This work was supported, by a grant of Piano Finalizzato Promozione della qualità dell'ambiente CNR.

Received 13 May; accepted 3 October 1980.

1. Von Der Borch, C. *Geochim. cosmochim. Acta* **29**, 781–799 (1965).
2. Clayton, R. N., Jones, B. F. & Berner, R. A. *Geochim. cosmochim. Acta* **32**, 415–432 (1968).
3. Clayton, R. N., Skinner, M. C. W., Berner, R. A. & Robinson, M. *Geochim. cosmochim. Acta* **32**, 983–988 (1968).
4. Glover, E. D. & Sippel, R. F. *Geochim. cosmochim. Acta* **31**, 603–613 (1967).
5. Gebelein, C. D. & Hoffman, P. J. *Sedim. Petrol.* **43**, 603–613 (1973).
6. Davies, P. J., Ferguson, J. & Bubela, B. *Nature* **255**, 472–474 (1975).
7. Kahle, C. F. *J. Sedim. Petrol.* **35**, 448–453 (1965).
8. Lumsden, D. N. *J. Sedim. Petrol.* **44**, 450–455 (1974).
9. Gomborg, D. N. & Bonatti, E. *Science* **168**, 1451–1453 (1970).
10. Lee, R. E. & von Lehmden, D. J. *J. Air Pollut. Control Ass.* **23**, 853–857 (1973).
11. Folk, R. L. *J. Sedim. Petrol.* **44**, 40–53 (1974).
12. Goldsmith, J. R., Graf, D. L. & Heard, H. C. *Am. Miner.* **46**, 453–457 (1961).



## The Welsh 'geosyncline' of the Silurian was a fore-arc basin

H. Okada

Department of Geosciences, Shizuoka University, Shizuoka, Japan

A. J. Smith

Department of Geology, Bedford College, University of London, London NW1 4NS, UK

The Welsh 'geosyncline'<sup>1</sup>, an example of the classic geosyncline, has often been viewed in terms of plate tectonics as a Japan Sea-type marginal sea<sup>2-15</sup>. It is generally agreed that in the Welsh area during Cambrian and Ordovician times, Anglesey, with its north-east and south-west extensions, was an island arc complex with a trench to the north-west, the trench being accompanied by a south-east dipping subduction zone which caused the Ordovician volcanism of Wales<sup>2,5,10-14</sup>. Some authors believe that the Welsh region was the site of a back-arc tensional basin at the time of Ordovician volcanism. We believe that in Silurian times the subduction zone migrated landwards, that is southeastwards, due to tectonic erosion<sup>16</sup>, a process which has been implied for the modern Japan Trench<sup>17</sup>. Here, we compare the Welsh Silurian Basin with the modern Japan Sea and the sedimentary basins of the Pacific offshore of Japan, and conclude that a different interpretation is possible, that the Silurian Basin could have been a fore-arc basin.

In south-west Japan, between 132°E and 136°E in the vicinity of the Nankai Trough, the present subduction started at the earliest some 5 Myr ago<sup>18</sup> and the subducting slab is thought to have now reached a depth of only about 50 km (ref. 19). Because the subduction is still young, there has been no Quaternary volcanism in this segment of the Japanese islands. We believe a similar situation existed in the Welsh region in the Silurian. In middle to late Llandovery times, the renewed subduction following a landward migration of the subduction

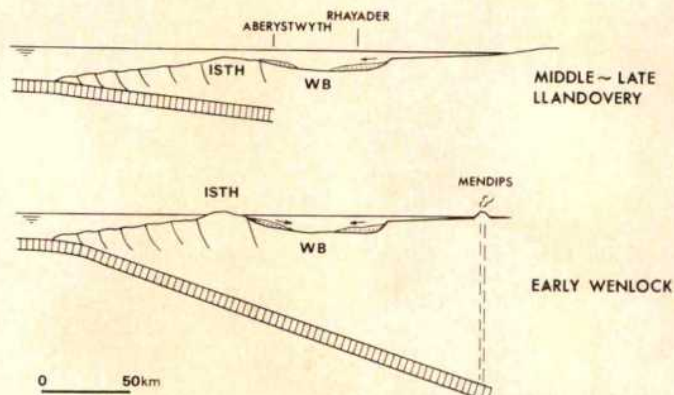


Fig. 1 Geotectonic profiles of the Welsh Basin in the Silurian. Arrows indicate derivation of clastics. WB, Welsh Basin; ISTH, Irish Sea Tectonic High.

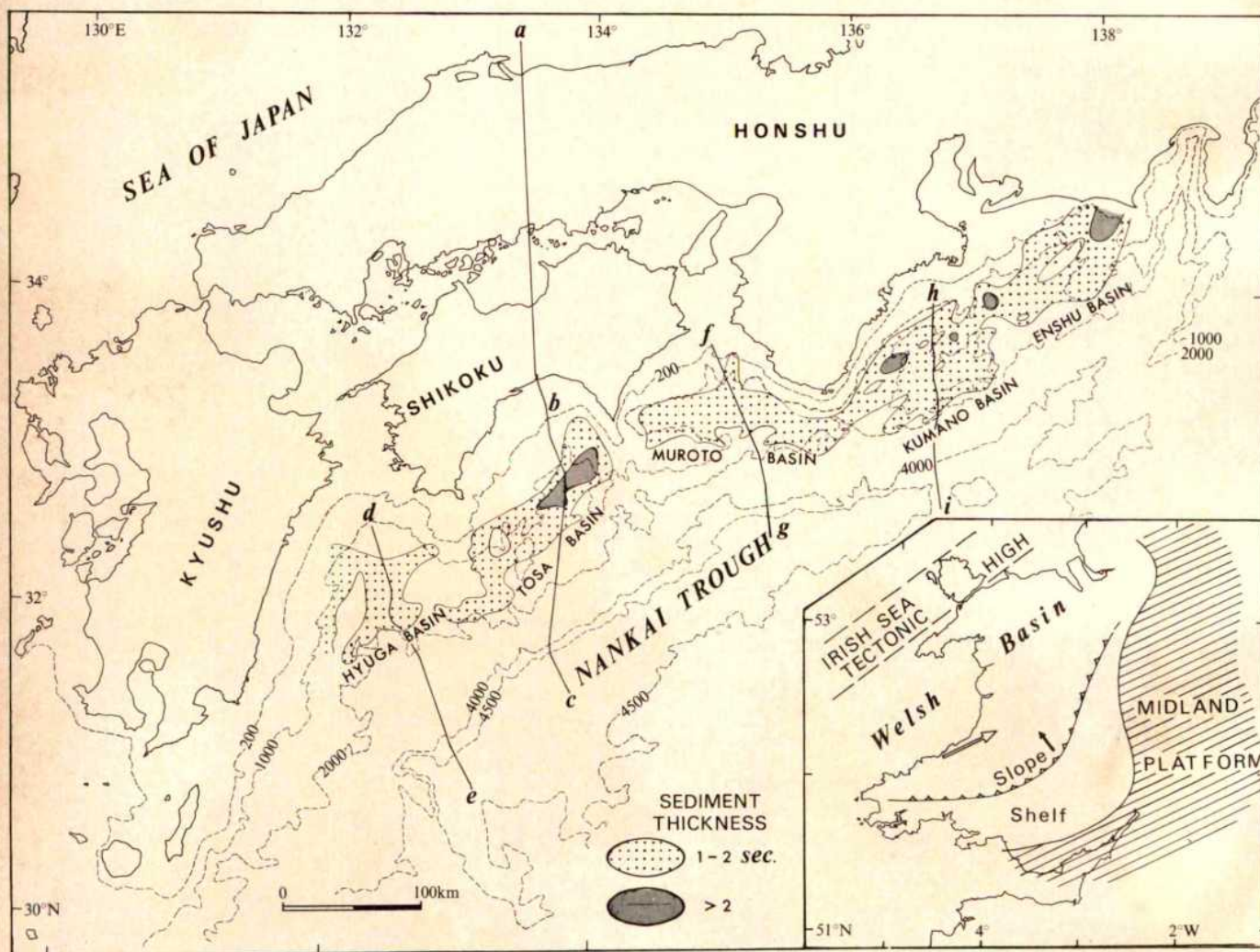
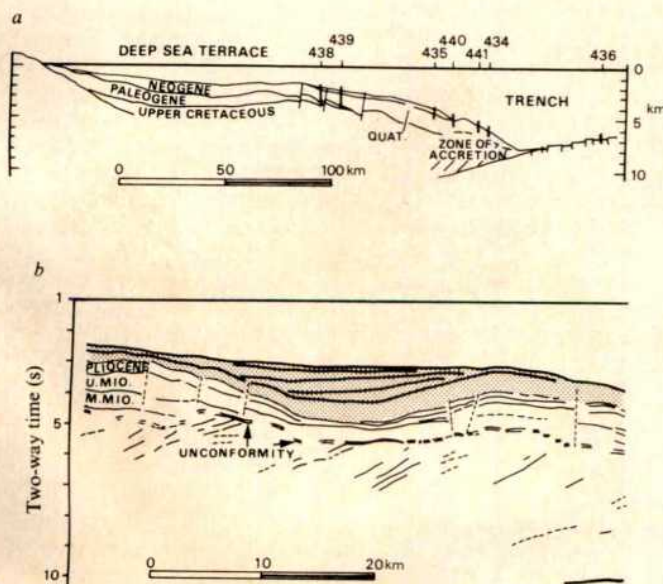
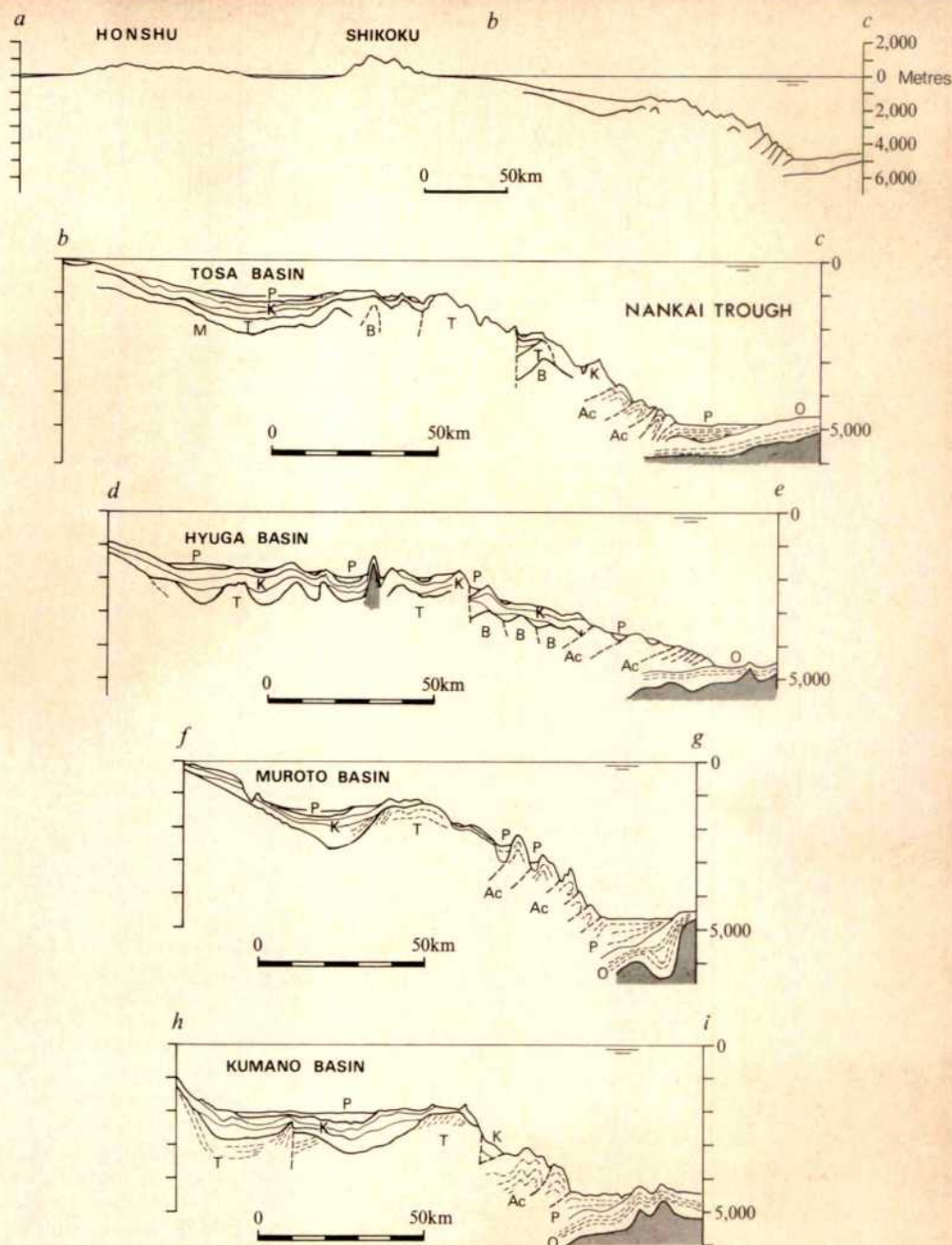


Fig. 2 Comparisons in dimensions between the Welsh Basin of Llandoveryan time (inset on same scale as main map) and the modern fore-arc basins behind the Nankai Trough off south-west Japan (modified from Okada *et al.*<sup>22</sup>). White arrow in the Welsh Basin shows axial turbidity currents; black arrow shows lateral currents. a-i In the Nankai Trough area correspond to the profiles in Fig. 3.



**Fig. 3** Geological profiles of the fore-arc basins behind the Nankai Trough off south-west Japan (modified from Okuda<sup>25</sup>). M, B, acoustic basement; T, early-middle Miocene; K, late Miocene-late Pliocene; P, Pleistocene-Recent; Ac, accreted Pliocene to Recent; O, oceanic sediments. Shading indicates igneous rocks. *a-i* Correspond to areas shown in Fig. 2.



zone caused compressional uplift of North Wales and the adjacent Irish Sea Tectonic High. Such uplifts can be compared with the Oyashio ancient landmass postulated at the trench-slope break of the modern Japan Trench (Fig. 1)<sup>20</sup>. At this stage the angle of the newly subducting slab was too small and the subducting edge of the slab too shallow to allow arc volcanism. Only by Wenlock times was volcanism again possible in Wales and adjacent areas (Fig. 1).

If the Welsh Basin of the Silurian could be represented as the Japan Sea-type marginal basin, then it should be characterized somewhere by tholeiitic ocean-floor basement and by ridge and trough features formed by rifting. No such characteristic features have yet been discovered. Conversely, the major faults found in Wales and the Welsh Borderland such as the Bala and Church Stretton Faults, are not dissimilar from those found in

**Fig. 4** Seismic profiles of the Japan Trench transect at 40°N *a*, General structural profile, redrawn from ref. 20. Numbers along the top of *a* refer to DSDP sites of Leg 56/57; indicated depth in km. *b*, Detailed seismic section of the fore-arc basin in *a* showing landward migration of depocentres<sup>17</sup>. U. Mio, Upper Miocene; M. Mio, Middle Miocene.



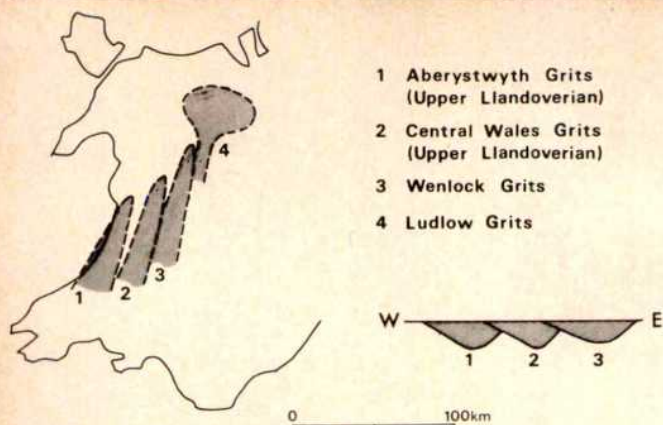


Fig. 5 Schematic diagrams showing landward migrations of depocentres of major Silurian turbidite sequences in Wales.

fore-arc basins—see, for example, those of the Sumatran continental margin<sup>21</sup>.

It seems possible to compare closely the Silurian Welsh Basin with modern arc-trench gap basins or fore-arc basins in several ways: tectonic position, volcanicity or its absence, the scale, size and shape of the basin and sedimentation types, styles and patterns. To emphasize this, we consider some fore-arc basins behind, that is landward, of the Nankai Trough (Figs 2, 3)<sup>22</sup> and the Japan Trench. The Tosa Basin, for example, is about 80 km across and 200 km long and accommodates late Miocene to Quaternary sediments to more than 1 km in thickness. These sediments are characteristically terrigenous turbidites and moreover they exhibit the tendency of depocentres to migrate inwards or landwards with time as the trench-slope break tectonic high is uplifted (see Fig. 4, which illustrates the Japan Trench situation). A similar trend of migration of depocentres is seen in the succeeding stages of the Silurian in the Welsh geosyncline (Fig. 5).

Changes in the subduction angles inferred for the Welsh geosyncline can be explained by Kanamori's<sup>23</sup> cyclic evolutionary model of oceanic plate subduction. According to Niitsuma's estimates<sup>24</sup>, the time length of unit cycles of plate subduction in the Japanese Neogene sequences is 10–20 Myr. Such an interval fits well with those of the Welsh Basin.

Such a multiplicity of coincidences between the fore-arc situation as has existed from early Neogene times on the Pacific side of Japan and the evidence from the Silurian rocks of Wales at least demands serious consideration of the conclusion that the Silurian Basin of Wales could have been a fore-arc basin.

Received 29 July; accepted 16 October 1980.

1. Jones, O. T. Q. *J. geol. Soc. Lond.* **94**, 60 (1938).
2. Fitton, J. G. & Hughes, D. J. *Earth planet. Sci. Lett.* **8**, 223 (1970).
3. Bird, J. M., Dewey, J. F. & Kidd, W. S. F. *Nature phys. Sci.* **231**, 28 (1971).
4. Mitchell, A. H. G. & Reading, H. G. *J. Geol.* **79**, 253 (1971).
5. Gass, I. G. *et al. Historical Geology* (Open University Press, London, 1972).
6. McKerrow, W. S. & Ziegler, A. M. *24th int. geol. Congr.*, sect. 6, 4 (1972).
7. Baker, J. W. *Geol. Mag.* **110**, 447 (1973).
8. Jeans, P. J. F. *Nature phys. Sci.* **245**, 120 (1973).
9. Owen, T. R. *The Geological Evolution of the British Isles* (Pergamon, Oxford, 1976).
10. Phillip, W. E. A., Stillman, C. J. & Murphy, T. J. *geol. Soc. Lond.* **132**, 579 (1976).
11. Wright, A. E. *Nature* **264**, 156 (1976).
12. Windley, B. F. *The Evolving Continents* (Wiley, New York, 1977).
13. Holland, C. H., Kelling, G. & Walton, E. K. in *The Caledonides of the British Isles—Reviewed* (eds Harris, A. L., Holland, C. H. & Leake, B. E.) (Geological Society of London, 1979).
14. Anderton, R., Bridges, P. H., Leeder, M. R. & Sellwood, B. W. *A Dynamic Stratigraphy of the British Isles* (Allen & Unwin, London, 1979).
15. Dunkley, P. N. in *Caledonides of the British Isles—Reviewed* (eds Harris, A. L., Holland, C. H. & Leake, B. E.) (Geological Society of London, 1979).
16. Murauchi, S. *Mar. Sci. Mon.* **11**, 799 (1979).
17. von Huene, R., Langseth, M., Nasu, N. & Okada, H. *Init. Rep. DSDP*, 56–57 (in the press).
18. Ingle, J. C. Jr *et al. Init. Rep. DSDP*, 31 (1975).
19. Kanamori, H. *Kagaku* **42**, 203 (1972).
20. von Huene, R. *et al. Geotimes* **23**, 16 (1978).
21. Karig, D. E., Lawrence, M. B., Moore, G. F. & Curran, J. R. *J. geol. Soc. Lond.* **137**, 77 (1980).
22. Okuda, Y., Kumagai, M. & Tamaki, K. *J. Jap. Ass. Petrol. Technol.* **44**, 279 (1979).
23. Kanamori, H. *Tectonophysics* **12**, 187 (1971).
24. Niitsuma, N. *J. Phys. Earth* **26**, Suppl. 367 (1978).
25. Okuda, Y. *Mar. Geology Map Ser.* **8** (Geol. Surv. Japan, 1977).

## Age and magmatic evolution of Stromboli volcano from $^{230}\text{Th}$ – $^{238}\text{U}$ disequilibrium data

Michel Condomines & C. J. Allegre

Laboratoire de Géochimie et Cosmochimie, Département des Sciences de la Terre, 4, Place Jussieu, 75230 Paris Cedex 05, France

The Eolian archipelago is one of the two active volcanic arcs in the Mediterranean. Of its seven islands, only Vulcano and Stromboli have erupted recently. Stromboli is well known for its continuous explosive activity. Whereas the relative ages of volcanism are fairly well known from stratigraphical methods<sup>1,2</sup> there has been little absolute dating. Precise age determinations for the different islands are, however, necessary to study the evolution of the whole Eolian arc volcanism, notably the transition from calc-alkaline series to shoshonitic series<sup>3,4</sup>. We report here the age determination of lavas on Stromboli using a method based on the radioactive disequilibrium  $^{230}\text{Th}/^{238}\text{U}$  applied to volcanic rocks<sup>5–7</sup>. The analytical techniques have been described elsewhere<sup>8</sup>. The activity ratio ( $^{230}\text{Th}/^{232}\text{Th}$ ) is determined through  $\alpha$  spectrometry and the U/Th ratio through isotopic dilution and mass spectrometry.

Stromboli Island can be divided into two parts, an older one to the east and a western, younger part to which the active craters of Stromboli belong (Fig. 1). The oldest part comprises three main formations<sup>9</sup>: (1) a basal pyroclastic complex with interstratified lava flows outcropping at the bottom of canyons and on the east coast (La Petrazza); (2) an intermediate complex made up of scoria and lava flows lying unconformably on the previous complex in the north-east; and (3) an upper complex or Vancori complex (lava flows and sills, tuffs in its uppermost part) which still forms the actual top of the volcano. The lavas of these old complexes belong to the calc-alkaline series and most are either K-rich andesites or Al-rich basalts<sup>4,8</sup>. However, some rare shoshonites have also been observed<sup>9</sup>.

The younger, western part comprises several formations made of lava flows and scoria. The 'Sciara del Fuoco' consists of superimposed historical flows running all the way from the uppermost, active craters down to the sea. The lava from this young area are shoshonitic with a  $\text{SiO}_2$  content usually in the range 50–53%, a variable but high  $\text{K}_2\text{O}$  content (up to 4% or more) and a  $\text{K}_2\text{O}/\text{Na}_2\text{O}$  ratio of  $\sim 1$  (refs 4, 10).

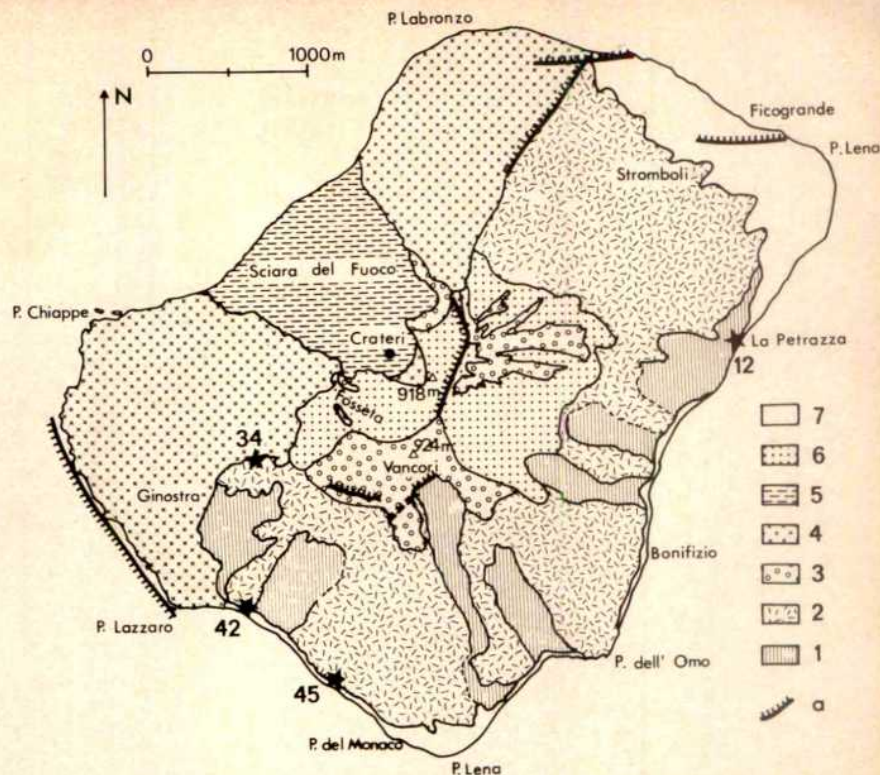
The samples analysed all come from the older eastern region of the island (Fig. 1). Specimen number 12 is from the oldest part of the basal complex around La Petrazza; the other specimens are from the intermediate complex on the south-west coast of the island (Stb 42, 45), and from the slope of the volcano itself (Stb 34; 400-m altitude). Samples Stb 12, 34 and 45 are K-rich andesites whereas Stb 42 is a Si-poor andesite according to Taylor's terminology<sup>11</sup> (F. Barberi, personal communication).

Analytical data and petrographical descriptions are given in Table 1: U and Th contents (Th from  $\sim 10$  to  $\sim 20$  p.p.m.) agree with other Th and U data<sup>12,13</sup> on volcanics from the Stromboli calc-alkaline series. Our data confirm that these series have a higher content of hygromagmatophile elements than do the classic calc-alkaline series. On the ( $^{230}\text{Th}/^{232}\text{Th}$ ), ( $^{238}\text{U}/^{232}\text{Th}$ ) activity-ratio diagram (Fig. 2a) representative whole-rock values fall to the left of the equiline (first bisectrice) which indicates a ( $^{230}\text{Th}/^{238}\text{U}$ ) disequilibrium ratio of  $>1$ .

In an activity-ratio diagram, representative data for minerals from a volcanic rock must fit an isochron of slope  $(1 - e^{-\lambda t})$  thereby giving the age  $t$  of the rock. The intersection between the isochron and the equiline gives the initial ratio ( $^{230}\text{Th}/^{232}\text{Th}$ )<sub>0</sub>.



**Fig. 1** Geological map of Stromboli (after ref. 8): 1, oldest complex (calc-alkaline series); 2, intermediate complex (calc-alkaline series); 3, Vancori complex (calc-alkaline series); 4, young shoshonitic volcanics; 5, Sciara del Fuoco; 6, present cinder cover; 7, alluvions and reworked volcanics; a, faults or ancient caldera edges.



The results of internal isochrone dating on samples Stb 12, 42 and 34 are plotted in Fig. 2. The most important mineral for this type of dating is titanomagnetite because of its higher Th/U fractionation relative to the whole rock (as we pointed out in our studies on lavas from Costa Rica and Etna<sup>5,6</sup>). Nevertheless, for

**Table 1** Analytical data and petrographical descriptions of samples from Stromboli volcano

| Sample                              | U<br>(p.p.m.) | Th<br>(p.p.m.) | Th/U | $(^{238}\text{U}/^{232}\text{Th})\%$ | $(^{230}\text{Th}/^{232}\text{Th})\%$ |
|-------------------------------------|---------------|----------------|------|--------------------------------------|---------------------------------------|
| Stb 12*                             |               |                |      |                                      |                                       |
| Whole rock                          | 3.81          | 15.7           | 4.12 | 0.728                                | $0.834 \pm 0.016$                     |
| Magnetite M1<br>80–20 $\mu\text{m}$ | 0.525         | 2.20           | 4.19 | 0.72                                 |                                       |
| Magnetite M2<br>20–8 $\mu\text{m}$  | 1.59          | 8.74           | 5.50 | 0.546                                | $0.690 \pm 0.012$                     |
| Plagioclase Pl                      | 0.377         | 1.41           | 3.73 | 0.802                                | $0.883 \pm 0.018$                     |
| Clinopyroxene Cpx                   | 0.316         | 1.49           | 4.73 | 0.634                                | $0.767 \pm 0.016$                     |
| Stb 42†                             |               |                |      |                                      |                                       |
| Whole rock                          | 2.57          | 9.77           | 3.80 | 0.790                                | $0.841 \pm 0.008$                     |
| Magnetite M1<br>80–20 $\mu\text{m}$ | 0.683         | 3.25           | 4.76 | 0.63                                 |                                       |
| Magnetite M2<br>20–8 $\mu\text{m}$  | 1.51          | 9.91           | 6.57 | 0.457                                | $0.697 \pm 0.007$                     |
| Stb 34‡                             |               |                |      |                                      |                                       |
| Whole rock                          | 4.61          | 17.2           | 3.72 | 0.810                                | $1.007 \pm 0.017$                     |
| Magnetite M1<br>80–20 $\mu\text{m}$ | 1.01          | 2.47           | 2.45 | 1.23                                 | $1.12 \pm 0.02$                       |
| Magnetite M2<br>20–8 $\mu\text{m}$  | 1.85          | 5.15           | 2.79 | 1.08                                 | $1.09 \pm 0.02$                       |
| Stb 45                              |               |                |      |                                      |                                       |
| Whole rock                          | 5.18          | 21.5           | 4.15 | 0.720                                | $0.85 \pm 0.01$                       |

\* Stb 12: K-rich andesite with zoned plagioclase phenocrysts rich in glass inclusions, clinopyroxene, orthopyroxene and magnetite. The groundmass is made of plagioclase, pyroxene and magnetite microliths. Apatite is also present as needles in plagioclase.

† Stb 42: Si-poor, K-rich andesite with olivine, clinopyroxene and plagioclase (rich in glass and pyroxene inclusions) phenocrysts and magnetite microphenocrysts. The groundmass consists primarily of plagioclase and pyroxene microliths.

‡ Stb 34: K-rich andesite with zoned plagioclase phenocrysts rich in inclusions, clinopyroxene, orthopyroxene, biotite and magnetite in a groundmass of brown glass with tiny plagioclase and pyroxene microliths. Apatite is abundant as inclusions in plagioclase and pyroxenes.

§ Activity ratios: standard error on  $(^{238}\text{U}/^{232}\text{Th})$  is estimated at 1%. The error on  $(^{230}\text{Th}/^{232}\text{Th})$  is the  $\alpha$ -counting error ( $1\sigma$ ).

samples Stb 12 and 42, this fractionation occurs in the opposite direction, that is Th/U for magnetite is greater than for the total rock. For Stb 34 fractionation is 'normal'.

The age of Petrazza lava (Stb 12) from the eastern basal complex is  $\sim 156,000$  yr ( $^{+45,000}_{-32,000}$ ) and its initial ratio close to 1.16. The lack of precision on dating this lava is due to its great age and also, and mostly, to moderate Th/U fractionation between the different minerals and the whole rock. The age of sample Stb 42 from the intermediate complex on the southwestern coast is  $61,500$  yr ( $\pm 6,500$ ) and its initial ratio  $(^{230}\text{Th}/^{232}\text{Th})_0$  0.880 ( $\pm 0.015$ ). The age of sample Stb 34 from the upper part of the intermediate complex is  $35,000$  yr ( $\pm 9,000$ ) and its initial ratio  $1.084$  ( $\pm 0.005$ ).

These ages agree with the relative stratigraphical position of the different lava flows and can be used to infer a general pattern for the chronology of Stromboli volcanism: the oldest-emerged part of the island is at least  $160,000$  yr old, the formation of the intermediate complex probably started at least  $60,000$  yr ago and lasted until  $\sim 30,000$  yr ago. The Vancori complex was then formed, followed by the younger western part of the island.

The transition to shoshonitic volcanism thus occurred  $< 35,000$  yr ago. Barberi *et al.*<sup>4</sup> and Keller<sup>3</sup> consider that this significant transition corresponds to an important change in the subduction process underneath the Eolian arc.  $\text{K}_2\text{O}$ -rich shoshonitic lava could result from fast subduction of the lithosphere<sup>4</sup> or from the presence of an isolated fragment of lithosphere sinking into the mantle<sup>3</sup>. The transition to shoshonitic volcanism must, then, be synchronous along to the strike of the subducting lithosphere. Seismic data show a  $50$ – $60^\circ$  dip towards WNW (refs 14, 15), and Vulcano and Stromboli should thus be in a similar position relative to the subduction zone. Unfortunately, the age of early shoshonitic volcanism for Vulcano has not yet been exactly determined (though it is probably  $< 100,000$  yr (ref. 3)). Our data put limitations on this model and will eventually allow age correlations with neighbouring islands of the Eolian archipelago.

There are too few petrographical and chemical data for older lava from Stromboli to allow a detailed study of magmatic evolution of this island; however, the  $^{230}\text{Th}$ – $^{238}\text{U}$  disequilibrium method can be used to determine the main steps. Indeed, the study of the variation throughout time of the initial ratio  $(^{230}\text{Th}/^{232}\text{Th})_0$  for lavas gives valuable information<sup>5</sup>.



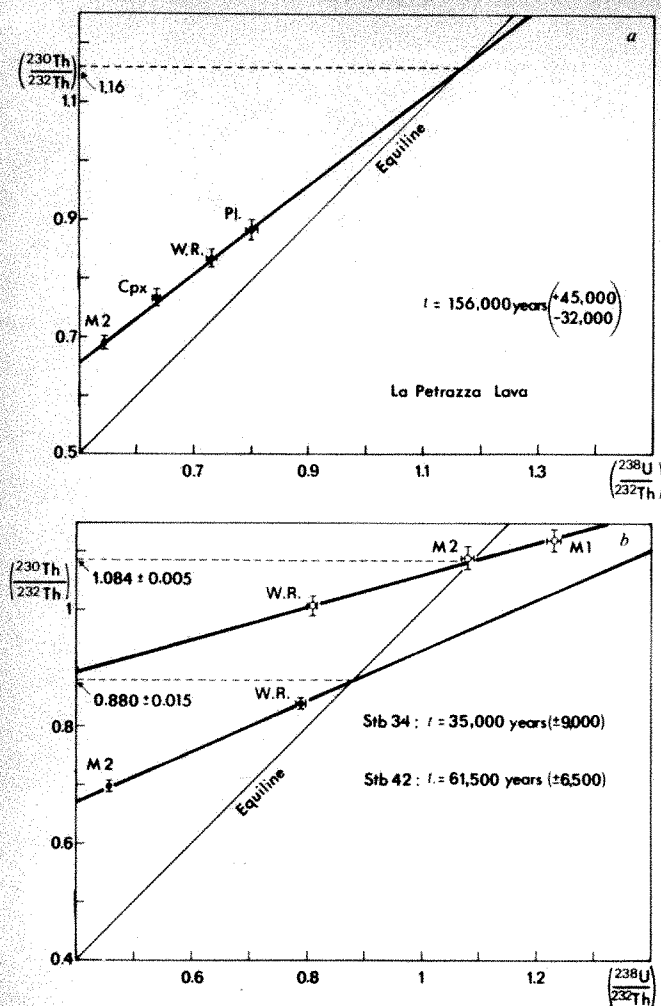


Fig. 2 Isochron diagram for: a, sample Stb 12; b, samples Stb 42 (●) and 34 (○).

When lavas derive from deep magma through evolution in a chemically closed system since a certain time  $T$  (the age of magma isolation), their initial ratios obey the following equation<sup>5</sup>:

$$\left(\frac{^{230}\text{Th}}{^{232}\text{Th}}\right)_0 = \left[\left(\frac{^{230}\text{Th}}{^{232}\text{Th}}\right)_{M_0} - \left(\frac{^{238}\text{U}}{^{232}\text{Th}}\right)_M e^{-\lambda T} + \left(\frac{^{238}\text{U}}{^{232}\text{Th}}\right)_M\right]$$

where  $t$  is the age of lava and  $(^{238}\text{U}/^{232}\text{Th})_M$  and  $(^{230}\text{Th}/^{232}\text{Th})_{M_0}$  the initial ratios of the deep magma. This relation is valid as long as the  $(^{238}\text{U}/^{232}\text{Th})_M$  ratio remains the same throughout fractional crystallization; which is probably the case for such hygromagmatophile elements except, perhaps, for the products resulting from late differentiation.

Indeed, Th/U ratios for calc-alkaline series seem to remain constant. Figure 3 shows Th and U values plotted for our samples as well as those of Guillard<sup>13</sup> for calc-alkaline and shoshonitic series and those determined by Capaldi *et al.*<sup>16,17</sup> for recent Stromboli lavas. On such a diagram, the two series can be readily differentiated on the basis of their Th/U ratios, ~4 for the calc-alkaline series and ~6.5 for the shoshonitic series, which indicates that the primary magma for the two series seems to be different.

Considering the hypothesis that the  $(^{238}\text{U}/^{232}\text{Th})_M$  ratio of the deep primary magma has not been affected during fractional crystallization, one can use the above equation to study the evolution of initial ratios in a  $(^{230}\text{Th}/^{232}\text{Th})_0 - e^{-\lambda T}$  diagram. Representative data for lavas derived from the same deep magma evolving in a chemically closed system must fit a straight line of slope  $[(^{230}\text{Th}/^{232}\text{Th})_{M_0} - (^{238}\text{U}/^{232}\text{Th})_M]e^{-\lambda T}$ , and knowing the position of a lava on such a diagram and the  $(^{238}\text{U}/^{232}\text{Th})_M$  ratio of the deep magma, we can then determine the evolution line for the initial ratios and find out whether other dated lavas belong to the same series—whether they derive from the same deep magma. This method has been used in Fig. 4: samples Stb 12 (156,000 yr) and 42 (61,500 yr) may belong to the same series whereas Stb 34 (35,000 yr) and present lavas from Stromboli seem to have a different origin. Thus, we have to distinguish at least three series:

- (1) A calc-alkaline series starting at least 160,000 yr BP and lasting until about 60,000 yr BP.
- (2) Another younger calc-alkaline series from 60,000 yr BP to <35,000 yr BP. The primary magma of this series seems to be identical with the previous series, the  $(^{230}\text{Th}/^{232}\text{Th})_{M_0}$  ratios being very close.
- (3) The present shoshonitic series for which Th/U ratio is different from that of older shoshonites and would even be

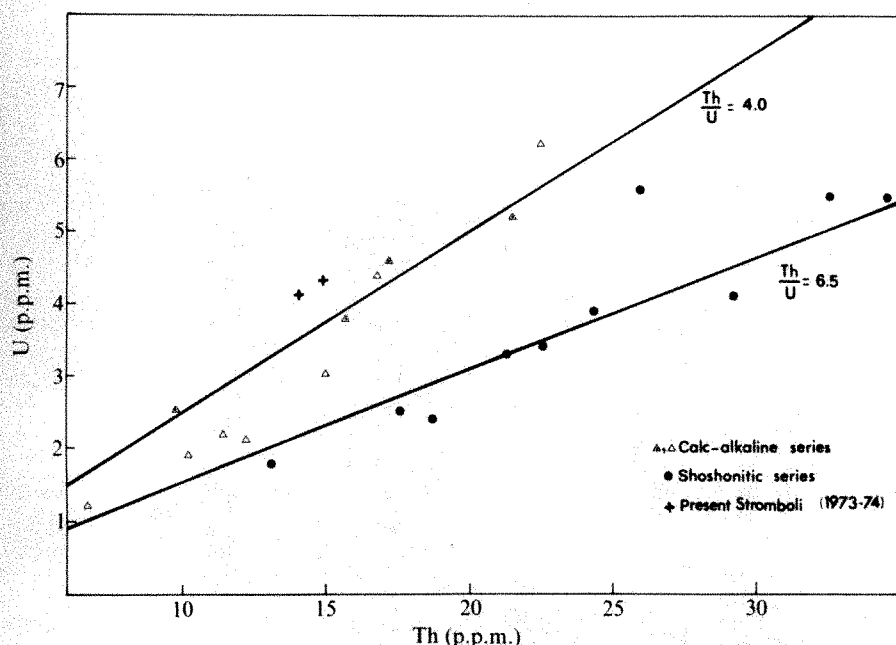


Fig. 3 Th/U diagram for Stromboli lavas: ▲, △, our data; ●, Guillard's data<sup>13</sup>; ✦, Capaldi *et al.*'s data<sup>16,17</sup>.

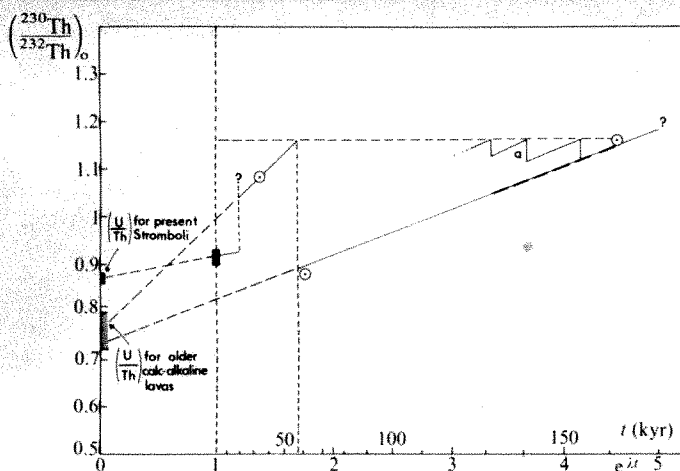


Fig. 4  $(^{230}\text{Th}/^{232}\text{Th})_0$ - $e^{\lambda t}$  diagram (see text for explanation).

closer to that of calc-alkaline series (Fig. 3). This series would obviously be derived from an initial magma different from that of the calc-alkaline series as their  $(^{230}\text{Th}/^{232}\text{Th})_0$  ratio is much lower (Fig. 4). Besides, the older shoshonites with high Th/U ratios could belong to an intermediate series not shown on Fig. 4.

Samples Stb 12 and 42 and sample Stb 34 which belong to two different series also have opposite Th/U fractionation trends for magnetite compared with the whole rock. This could be due to different crystallization conditions where oxygen fugacity could have an important role (in preparation). This parameter may explain differences between fractional crystallization of the calc-alkaline series and of the shoshonitic series<sup>4,18</sup>.

The series defined above are based on the hypothesis of evolution in a chemically closed system of a deep magma successively feeding the dated eruptions. This deep magma can be isolated in a zone where it generated through partial melting, for example, at the top of the subducting lithospheric plate, or at an intermediate level.

The magma has probably not evolved in a superficial closed-system magma chamber for several tens of thousand years. If it had, then the initial ratio evolution for a given series would be correlated with the differentiation degree of lava, whereas there seem to be several cycles of differentiation, for calc-alkaline series, for example, slightly differentiated lavas alternating with more evolved ones<sup>5</sup>. Therefore, there may have been several reinjections of primary magma into the chamber but the basic magma added could not have the same  $(^{230}\text{Th}/^{232}\text{Th})_0$  ratio because the reduction of  $(^{230}\text{Th}/^{232}\text{Th})_0$  initial ratios would thus be much lower than that actually calculated for the oldest calc-alkaline series, for example. The evolution curve of  $(^{230}\text{Th}/^{232}\text{Th})_0$  would be above the line corresponding to the evolution in a closed system (Fig. 4a). If  $(^{230}\text{Th}/^{232}\text{Th})_0$  ratios variations actually correspond to the evolution line for a closed system, it implies a really deep magma evolving as a chemically closed system with a  $(^{230}\text{Th}/^{232}\text{Th})_0$  ratio decreasing with time and imposing the general variation of the  $(^{230}\text{Th}/^{232}\text{Th})_0$  ratios. The successive reinjection-differentiation cycles would thus be represented by straight segments on the evolution line representing the deep magma evolution (Fig. 4).

The proposed model would thus be: a deep permanent magma evolving as a closed system and feeding through successive reinjections one or several superficial magma chambers, where the main differentiation would take place through fractional crystallization. If this model were verified, there would be important geodynamic implications for the subduction beneath the Eolian arc and for the size of the deep magma reservoirs relative to subduction rates. The problem of calc-alkaline to shoshonitic volcanism transition cannot be solved here because of the lack of data especially on the older shoshonites. We have

shown that shoshonitic series seem to generate from an initial magma different from the calc-alkaline series primary magma which has a higher  $(^{230}\text{Th}/^{232}\text{Th})_0$  ratio. Two hypotheses can be proposed for the origin of this magma: either it comes from a source region different from that of the calc-alkaline primary magma, with a different Th/U ratio, or it results from a modification of the calc-alkaline series primary magma through a more or less complex contamination process. A contamination by relatively high Th/U and low  $(^{230}\text{Th}/^{232}\text{Th})_0$  crust could explain the transition to ancient shoshonites. But there is no evidence for continental type crust underneath the Stromboli volcano, whereas such evidence does exist for other islands in the Eolian arc<sup>1</sup>. Dupuy *et al.*<sup>19</sup> use a fluid-transfer mechanism to explain the important enrichment of shoshonitic magma in hygromagmatophile elements such as K, U and Th. Detailed studies on ancient shoshonites might help solve the problem of their origin. In this respect Th/U ratio measurements and determination of initial  $(^{230}\text{Th}/^{232}\text{Th})_0$  ratios would then be of great interest.

We thank F. Barberi and M. Rosi for samples, and Claude Mercier for the English translation of the manuscript.

Received 1 August; accepted 29 September 1980.

1. Pichler, H. *Geol. Rdsch.* **57**, 102-126 (1967).
2. Keller, J. *Ber. naturf. Ges. Freiburg* **57**, 33-67 (1967).
3. Keller, J. *Contr. Miner. Petrol.* **46**, 29-47 (1974).
4. Barberi, F., Innocenti, F., Ferrara, G., Keller, J. & Villari, L. *Earth planet. Sci. Lett.* **21**, 269-276 (1974).
5. Allegre, C. J. & Condomines, M. *Earth planet. Sci. Lett.* **28**, 395-406 (1976).
6. Condomines, M. & Tanguy, J. C. *r. hebdomadaire Séanc. Acad. Sci., Paris D282*, 1661-1664 (1976).
7. Condomines, M. *Nature* **276**, 257-258 (1978).
8. Rosi, M. *Carta Geologica dell'isola di Stromboli* (1975).
9. Girod, M. *Pétrologie* **1**, 3, 189-196 (1975).
10. Ninkovich, D. & Hays, J. D. *Earth planet. Sci. Lett.* **16**, 331-345 (1972).
11. Taylor, S. R. *Bull. Oregon Dept. Geol. Miner. Ind.* **65**, 43-63 (1969).
12. Civetta, L., Gasparini, P. *Scritti in onore del Prof. G. IMBO* (1973).
13. Guillard, M. A. thesis, Univ. Paris VII (1976).
14. Caputo, M., Panza, G. F. & Postpischl, D. *Tectonophysics* **15**, 219-231 (1972).
15. Barberi, F., Gasparini, P., Innocenti, F. & Villari, L. *J. geophys. Res.* **78**, 5221-5232 (1973).
16. Capaldi, G., Cortini, M., Gasparini, P. & Pece, R. *J. J. geophys. Res.* **81**, 350-358 (1976).
17. Capaldi, G. *et al. Bull. volcan.* **41**, 259-285 (1978).
18. Girod, M. & Magonthier, M. C. *4ème R. Ann. Sci. Terre*, Paris (1976).
19. Dupuy, C., Dostal, J., Girod, M. & Liotard, M. (in the press).

## Prehistoric shell assemblages from Franchthi Cave and evolution of the adjacent coastal zone

Judith C. Shackleton

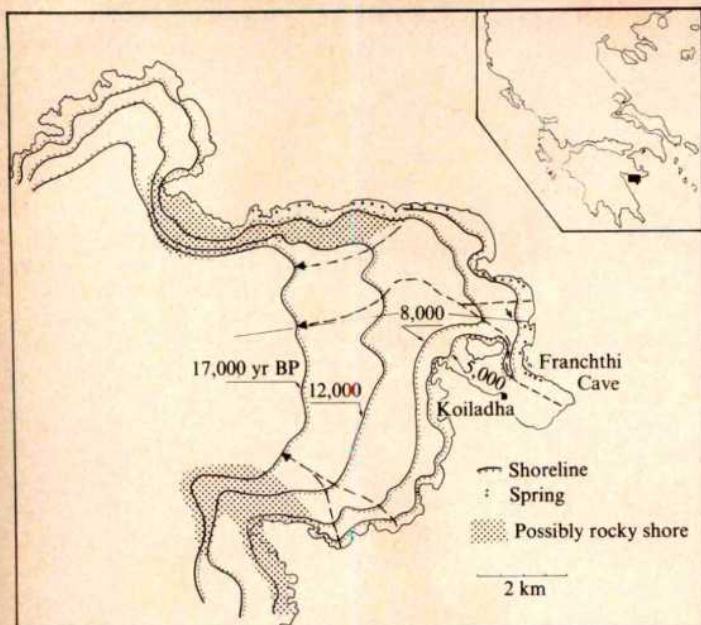
Clare Hall, University of Cambridge, Cambridge CB3 9AL, UK

Tjeerd H. van Andel

Geology Department, Stanford University, Stanford, California 94305

Franchthi Cave, Greece, virtually continuously occupied from the late Palaeolithic to the Final Neolithic<sup>1</sup>, is situated at the entrance to Koiláda Bay on the Gulf of Argos, where the sea meets a steep rocky shore just outside the cave entrance (Fig. 1). The deposits of the cave reveal much evidence of man's use of marine resources. For much of the occupational history of the cave, however, the shore was actually quite far away due to the glacial lowering of sea level, for example, 6-7 km during the latest Palaeolithic. Perhaps this is why the earliest deposits examined contain little shell material. A second phase has a mixed shell assemblage of short duration (Fig. 2) but a third one from the late Mesolithic has abundant shell remains dominated by a single species. We show here that these shell assemblages reflect environmental changes resulting from the rising post-glacial sea level.



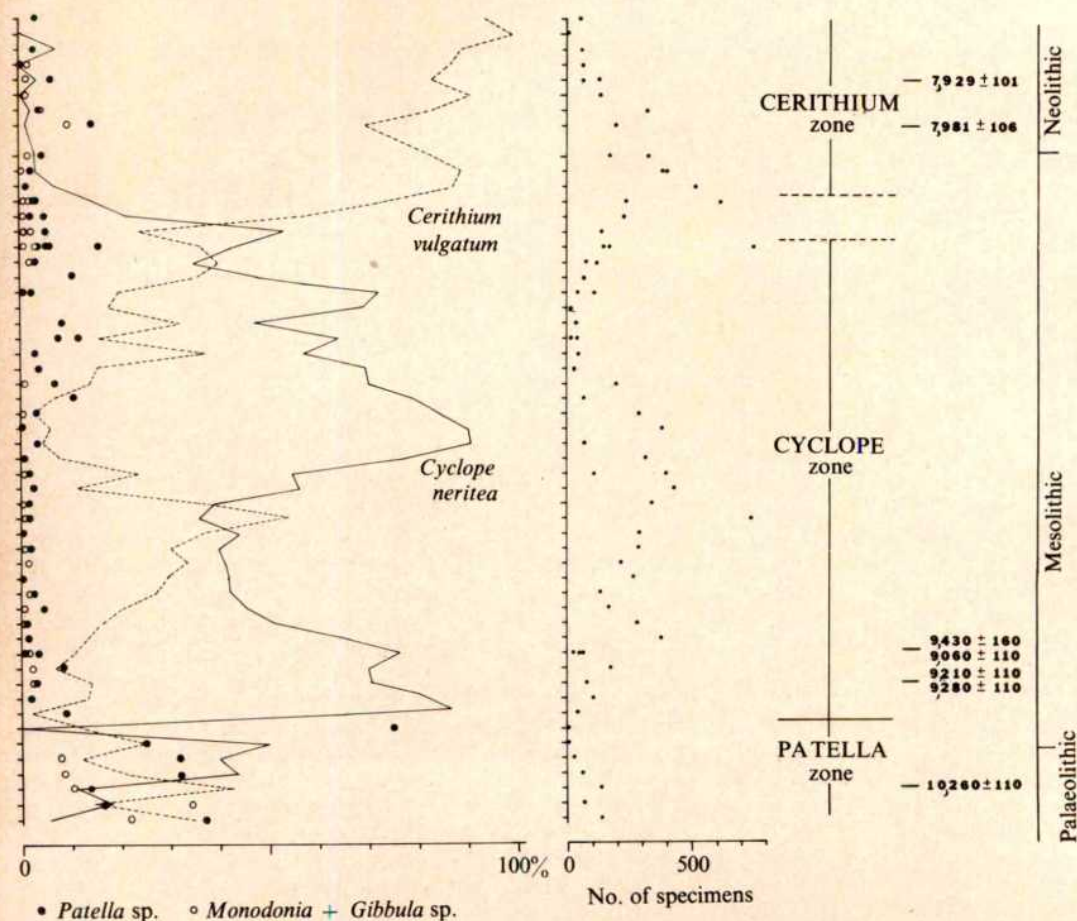


**Fig. 1** Shoreline positions (yr BP) for the Franchthi area during the late Pleistocene and early Holocene. Based on contours prepared from British Admiralty chart 1518/1954. Data point spacing gives a contour position uncertainty of about  $\pm 200$  m. Sea-level rise curve uncertainty produces a shoreline position uncertainty of 200–500 m. Dashed arrows are streams. Solid lines are seismic reflection traverses and arrow indicates a submerged bar after ref. 6.

From ~9,000 to 8,000 yr BP the inhabitants collected mainly *Cyclope neritea*<sup>2</sup>, a small (~15 mm) species which lives in the littoral zone near the mud surface and also flourishes in brackish water. It is gregarious and a carnivore. Although small it is easy to catch because it occurs in large numbers in very shallow water<sup>3</sup> and can be attracted with bait (M. Bishop, personal communication). It might be eaten raw or as a soup. At about 8,000 yr BP this assemblage is abruptly replaced by another, dominated by *Cerithium vulgatum*<sup>2</sup>, a rock-dweller.

Although the ethnographical evidence provides instances of hunter-gatherers choosing to go long distances to collect delicacies<sup>4</sup>, this behaviour is the exception. Whatever the reason for the change in shell assemblages, we have adopted the view that a group will normally harvest a resource because it is accessible. We also assume that a change in economic or social behaviour may be triggered by environmental factors<sup>5</sup>. Obviously, both changes in shell composition could have been caused by various factors but here we discuss them in terms of an environmental/economic approach. Our interpretation rests on the fact that the post-glacial sea-level rise beginning 17,000 yr ago created a succession of coastal environments which must have influenced the lives of the inhabitants of Franchthi Cave.

There are two explanations for the dominance of *Cyclope* and its sudden replacement around 8,000 yr BP by the *Cerithium* assemblage (Fig. 2). First, *Cyclope* might have flourished on extensive, very shallow and sheltered nearshore flats near the cave. Such an environment might have existed temporarily during the early Holocene. Further migration of the shore into the bay and establishment of present conditions could have eliminated the species. Simultaneously, the advance of the sea produced rocky shores north of the cave, 2–3 km away, where *Cerithium* could be collected instead. Alternatively, the mouth of the river then flowing seaward between Franchthi and the island opposite<sup>6</sup> might have been converted into a perhaps brackish estuary with quiet, shallow, sandy shores where *Cyclope* could be collected. Further rise of the sea destroyed this environment.



**Fig. 2** Stratigraphy of late Palaeolithic through early Neolithic marine shell assemblages from a trench (F/AS) in Franchthi Cave. Sampled units are shown vertical to no scale. Left, percentages of most important species; centre, total number of specimens in each sampled unit; right, shell zones and radiocarbon dates (yr BP).



Figure 1 shows a series of past shorelines using the shelf bathymetry and sea-level positions determined from a post-glacial sea-level rise curve. The present best value for the maximum lowering is 90–95 m and the shape of the following rise curve is still uncertain<sup>7–10</sup> and complicated by isostatic responses to ice removal and water addition<sup>11,12</sup>. Comparison of various proposed curves shows vertical uncertainties of 5–15 m for each of the chosen intervals which, for the shelf topography in our area, translate into horizontal uncertainties of a few hundred metres. For our purpose the shorelines so determined are adequate. Little modern sediment is present on the shelf<sup>6</sup> and the present water depths are a sufficient guide. In Koiládha Bay, where sediments are thicker, we have used coastal outlines from a more detailed study<sup>6</sup>.

It has been argued that the Holocene sea-level rise around the Peloponnese was accompanied by vertical crustal movements<sup>13–16</sup>, including a subsidence of 1–2 m kyr<sup>-1</sup> for the southern Argolid. If true this would shift all shoreline positions seaward by 0.51 km. The evidence for the southern Argolid is weak<sup>13–17</sup>, but if true it lengthens the walking distance to the sea before 8,000 yr BP by at least 1 km.

Three aspects of the reconstructed early Holocene shores are of interest; the rocky or sandy/muddy nature, the distance to the cave, and the presence of sheltered shoals or brackish lagoons or estuaries. The present coast is mainly rocky with offshore rocky flats and occasional pocket beaches. Large sand or gravel beaches exist only in Koiládha Bay and the bay north of Franchthi. During the early Holocene the situation was quite different. The smooth offshore topography with a slope of less than 0.6° implies an alluvial coastal plain, confirmed by seismic reflection data<sup>6</sup>. Only along the extreme north and south coasts a rough bottom suggests a possible rocky shore before 8,000 yr BP. Thus only 30–45% of the coast was rocky as contrasted to >75% today.

During the late Palaeolithic and much of the Mesolithic the coast was from 3.5 to 6.5 km away depending on whether one assumes subsidence. It is thus not surprising that whatever the shore may have yielded in seafood did not find its way into the cave deposits in quantity. The gradual approach of the sea to 4 km is, however, reflected in the appearance of some shells around 11,000 yr BP.

Shortly before 9,000 yr BP shells increase in number (Fig. 2). At this time the simple, straight shoreline had begun to develop embayments and capes ~2 km away, but remained sedimentary. Of the several streams the largest, the Koiládha river, was much larger than its modern successor<sup>6</sup> and flowed semi-permanently until ~7,000 yr BP. On the open coastal plain its valley was wide and had little effect on the shoreline, but as the sea approached Franchthi a bay was formed around 9,000 yr BP in the here much steeper and narrower valley. By 8,000 yr BP a narrow estuary existed just west of the present cave entrance which may have been closed by a bar at the outer shore; a sediment ridge occurs at the appropriate spot and depth (25 m) on seismic profiles<sup>6</sup>. Given the larger and more permanent river flow and the presence of copious freshwater springs at the foot of the Franchthi cliffs<sup>18</sup> it is possible that the estuary was brackish or had a variable salinity rather than the high salinity typical for lagoons in the Argolid today. Such an estuary, with sheltered and shallow shores, would provide an ideal habitat for *Cyclope* within a few hundred metres of the cave.

Thus the environments postulated earlier are probable at the right time and in the right place to explain extensive utilization of *Cyclope* on an open shore or in a sheltered and perhaps brackish bay<sup>19</sup>. Later, between 8,000 and 7,000 yr BP, further advance of the sea eliminated the bar<sup>9</sup> and opened the estuary. Simultaneously, however, the limestone cliffs north of Franchthi became part of the littoral zone and their rocky shores provided a good habitat for *Cerithium* within a few kilometres from the cave.

Bones of large tunny appear at the base of the *Cyclope* zone, a species hitherto not used<sup>18</sup>. N. J. Shackleton (personal communication) has postulated an increase in biological productivity

in the Aegean at this time which might explain this use of a new species. We also suggest that the development of an embayed coast around 9,000 yr BP may have facilitated the capture from shore of this open sea fish. The same productivity increase would also have enlarged the shellfish available.

During the next few years much evidence from Franchthi will become available to test and amplify ideas such as those we have presented. We hope that this paper will stimulate the integration of archaeological and environmental information.

In the summer of 1980, we found abundant live *Cyclope neritea* near the beach at the head of the Gulf of Argos between Nauplion and Nea Kios, and also in small numbers in the Bay of Astakos in Acharnania. In both cases *Cyclope* lived at the surface of fine silty-muddy sand in very shallow depths of 5–15 cm, on quiet and extensive shallow flats off the beach, an environment that corresponded exactly to the first of the two postulated here.

J.C.S. acknowledges support from the University of Indiana Foundation and the NSF through grants to T. W. Jacobsen. We thank T. W. Jacobsen and S. Payne for stimulating discussion, and M. Bishop and S. Whybrow for their assistance with identifications of Mollusca.

Received 9 June; accepted 27 September 1980.

- Jacobsen T. W. *Scient. Am.* **234**, 76–87 (1976).
- D'Angelo, G. & Gargiullo, S. *Guida alle Conchiglie Mediterranee* (Fabbi, Milan, 1978).
- Morton, J. E. *Proc. malac. Soc. Lond.* **34**, 96–105 (1960).
- Maddox, D. M. in *Maritime Adaptations in the Pacific* (eds Casteel, R. W. & Quimby, G. I.) 210 (Mouton, The Hague, 1975).
- Struever, S. in *Anthropological Archaeology in the Americas* (ed. Meggers, B.) 131–135 (1968).
- Van Andel, T. J. H., Jacobsen, T. W., Jolly, J. & Lianos, N. *Field Archaeol.* (in the press).
- Dillon, W. P. & Oldale, R. N. *Geology* **6**, 56–60 (1978).
- Oldale, W. P., O'Hara, C. J. *Geology* **8**, 102–106 (1980).
- Kraft, J. C., Rapp, G. Jr & Aschenbrenner, S. E. *Bull. geol. Soc. Am.* **86**, 1191–1208 (1975).
- Kraft, J. C., Aschenbrenner, S. E., & Rapp, G. Jr. *Science* **195**, 941–947 (1977).
- Clark, J. A., Farrell, W. E., & Peltier, W. R. *Quat. Res.* **9**, 265–287 (1978).
- Clark, J. A. & Lingle, C. S. *Quat. Res.* **11**, 279–298 (1979).
- Flemming, N. C. *Nature* **217**, 1031–1032 (1968).
- Dufaure, J. *Quaterni* **15**, 179–185 (1971).
- Kelletat, D., Kowalczyk, G., Schroeder, B. & Winter, K. P. *Z. dt. geol. Ges.* **127**, 447–465 (1976).
- Schroeder, B. & Kelletat, D. *Neues Jb. Geol. Paläont. Mh.* 174–186 (1976).
- Bintliff, J. L. *Br. Archaeol. Rep. Suppl. Ser.* **28**, 13–29 (1977).
- Jacobsen, T. W. *Hesperia* **42**, 45–86 (1973).
- Williams, D. F. & Thunnell, R. C. *Sedim. Geol.* **23**, 81–93 (1979).

## Radiometric dating of sediments using fission tracks in conodonts

H. M. Sachs\*, M. Denkinger\*, C. L. Bennett† & A. G. Harris‡

\* Geological and Geophysical Sciences and †Physics Departments, Princeton University, Princeton, New Jersey 08544

‡ US Geological Survey, US National Museum, Washington, DC 20560

Conodonts are microfossils which are commonly found in marine rocks of Cambrian to Triassic age. Although their biological affinities are difficult to assess, conodonts are valuable stratigraphical indices for much of their geological range<sup>1</sup>. Recent work has also established that conodont colour alteration indices (CAI) are useful guides to diagenetic temperatures and hence burial depth<sup>2</sup>. Fission tracks<sup>3</sup> in conodonts allow measurement of uranium concentrations and estimates of 'age' to be made using isotopic methods<sup>4</sup>. We report here that fission tracks counted in irradiated, thermally unaltered (as indicated by CAI) middle Palaeozoic conodonts indicate typical uranium concentrations of ~1 part in 10<sup>9</sup>, with some samples higher. A single specimen of *Siphonodella* from the Lower Mississippian yielded an age estimate of 380 ± 140 Myr consistent with conventional interpolations. This method may also allow the unroofing of deeply buried sediments to be dated.



Table 1 Summary of data

| Sample code | Mineral | Spontaneous            |         | Induced                 |         | Fluence ( $\Phi t$ ) neutrons $\text{cm}^{-2}$ | $T$ (Myr) | $\pm 1\sigma$ (Myr) | No. of grains or fields | p.p.b. |
|-------------|---------|------------------------|---------|-------------------------|---------|--|-----------|---------------------|-------------------------|--------|
|             |         | Track $\text{cm}^{-2}$ | Tracks† | Tracks $\text{cm}^{-2}$ | Tracks† |  |           |                     |                         |        |
| C-2-22*     | Apatite | —                      | —       | $2.0 \times 10^3$       | 5       | $3.0 \times 10^{15}$                           | —         | —                   | 8                       | 1.9    |
| C-2-22*     | Apatite | —                      | —       | $2.6 \times 10^3$       | 4       | $3.0 \times 10^{15}$                           | —         | —                   | 6                       | 2.4    |
| C-2-32      | Apatite | —                      | —       | $8.1 \times 10^4$       | 101     | $1.62 \times 10^{17}$                          | —         | —                   | 6                       | 1.4    |
| C-2-33      | Apatite | —                      | —       | $2.4 \times 10^4$       | 52      | $1.62 \times 10^{17}$                          | —         | —                   | 7                       | 0.4    |
| CDR-2       | Apatite | —                      | 12      | —                       | —       | $2.0 \times 10^{16}$                           | —         | —                   | —                       | —      |
| CDR-4       | Apatite | —                      | 10      | —                       | 35      | $2.0 \times 10^{16}$                           | 380       | $\pm 140$           | —                       | —      |

\* Slide contains two conodonts.

† No. of tracks actually counted to determine the reported track density.

Conodonts consist of carbonate apatite and trace amounts of organic material<sup>5</sup> and their structure consists of concentric lamellae, usually around a single growth centre. Lamellae of many conodonts average 2–3  $\mu\text{m}$  thickness, with some interlamellar spaces of 0.5–1.0  $\mu\text{m}$  thickness<sup>6</sup>. Individual crystallites are generally smaller than 0.01  $\mu\text{m}$  and optically unresolvable (R. Phillips, cited in ref. 7). The crystallites are predominantly co-parallel, with optic  $c$ -axes parallel to the direction of growth (perpendicular to lamellae) in most cases<sup>8,9</sup>.

The heavy nuclear particles released from spontaneous fission of  $^{238}\text{U}$  leave narrow damage tracks in most dielectric solids, generally 8–20  $\mu\text{m}$  long (track lengths vary among mineral species). In crystals, the trajectory is marked by vacant lattice sites and/or interstitial atoms. These features are permanent unless the solid is heated to its annealing temperature, at which point the tracks begin to disappear<sup>3</sup>. In general, fission tracks are exposed by chemically etching random polished surfaces of solids, and examining the specimen optically at high magnification. Etch kinetic arguments, based on the expectation of high dissolution rates along crystallite boundaries, have discouraged earlier efforts to find fission tracks in conodonts.

Assuming reasonable etch efficiency, the feasibility of fission track work depends on the weight concentration of uranium ( $c$ ) and the age ( $A$ ) of the sample. Fleisher and Price<sup>3</sup> suggested a minimum track density of 100  $\text{cm}^{-2}$  for routine searches, corresponding to  $cA \geq 0.3$ . This requires  $\sim 2$  h in favourable conditions. For middle Palaeozoic conodonts (300 Myr), this corresponds to  $[U] \geq 1$  part in  $10^9$ . Because conodonts are small ( $\sim 1$  mm),  $cA = 0.3$  will substantially underestimate the time required to count many grains instead of a single homogeneous surface.

For dating, only the relative densities of spontaneous and induced tracks in the same specimen are needed. In contrast, using fission tracks to measure uranium concentration requires determining the specimen size, the number of spontaneous (fossil) tracks (or, alternatively, annealing the sample to remove pre-existing tracks), and counting the tracks from fission events caused by irradiation with a known dose of thermal neutrons. In this context, the first step is to establish methods which allow the tracks to be seen and which allow the conodonts to be handled for irradiation.

Surface preparation requires mounting and fine polishing. Each set of conodonts was randomly mounted in epoxy wafers and one surface ground until all specimens were exposed. The mount was then reversed, ground face to glass, and cemented to standard petrographical slides. Samples were ground to  $\sim 0.05$  mm and the surface finally polished with 0.25  $\mu\text{m}$  diamond grit—the minimum surface roughness acceptable for high magnification optical searches. Parallel-ground specimen surfaces seem crucial for reliable optical examination. After many trials, we chose as standard etch 0.25% nitric acid for 60 s (ref. 4).

Following a thorough search (using transmitted light differential interference contrast microscopy at  $\times 1,250$ ) to determine the number of spontaneous tracks, the wafer was cleaned and removed from the glass slide for irradiation (both glass and Lexan became unacceptably radioactive when irradiated).

Each sample was wrapped in aluminium foil, as was the NBS calibration glass<sup>10</sup>, when used.

A thermal neutron dose of  $2.0 \times 10^{16}$  neutrons  $\text{cm}^{-2}$  yielded usable results (Brookhaven National Laboratory, HFBR facility, V-II Port, D. Rohrer, personal communication). Epoxy-embedded, foil-wrapped samples were 'cool' enough for shipment almost immediately, and handling required only modest precautions. No special facilities were required.

Irradiated wafers were remounted on petrographical slides (for ease of handling), reground and etched again for optical examination and track counting. Grinding to a new surface maintained a 'solid' counting geometry—the expectation of finding track fragments from the solid volume instead of a half-space.

We obtained the following results: (1) Middle Ordovician simple conodonts and conodonts with 'white-matter'<sup>11</sup> which we tested darkened and become opaque during irradiation; we were unable to count tracks. (2) Although the track densities were very low, the distribution of induced tracks in platform conodonts appeared uniform, with no apparent concentration near edges, interlamellar spaces or other obvious features. We inferred that the uranium was disseminated in the apatite structure. Altschuler *et al.*<sup>11</sup> have suggested that uranium in conodonts would replace calcium. This is reasonable because the ionic radii of divalent Ca (0.99 Å) and tetravalent U (0.97 Å) are so similar<sup>12</sup>. (3) Our best results were obtained with platform conodonts which showed no visible colour alteration (CAI = 1). Induced track densities of  $2.0$ – $2.6 \times 10^3$  tracks  $\text{cm}^{-2}$  and  $2.4$ – $8.1 \times 10^4$  tracks  $\text{cm}^{-2}$  for  $3 \times 10^{15}$  and  $1.6 \times 10^{17}$  thermal neutrons  $\text{cm}^{-2}$ , respectively, yielded concentrations of 1.9–2.4 and 0.4–1.4 parts per  $10^9$  (p.p.b.) (Table 1), comparable with estimates by Naeser (personal communication). In eight nonirradiated specimens searched for fossil tracks, we found no tracks in five specimens, one each in two, and two tracks in one specimen. These track densities are expected for Palaeozoic samples with  $\sim 1$  p.p.b. [U]. (4) Two specimens tested 'blind' (CDR-2 and CDR-4) yielded 12 and 10 well defined fossil tracks respectively, indicating order-of-magnitude higher [U] than other samples studied. CDR-2 was ground off inadvertently while repolishing after irradiation, but CDR-4 yielded 35 tracks from which we compute an age of  $380 \pm 140$  Myr, from  $A = 6.45 \ln [1 + 0.76 \Phi t (N_s/N_i)]$ , where age is  $10^9$  yr,  $\Phi t$  is the thermal neutron dose in  $10^{17}$  neutrons  $\text{cm}^{-2}$  and  $N_s(N_i)$  is the density of spontaneous (induced) fission tracks in the solid. In addition to the 10 (spontaneous) and 35 (induced) unambiguous tracks (see ref. 3), there were respectively 6 and 12 'track-like' markings rejected during counting by M.D. In addition to the criteria of ref. 3, we compared the observed distribution of track lengths and orientations with that expected for randomly oriented tracks. The two specimens counted were large platform conodonts of the genus *Siphonodella* from the lower Chappel Limestone, Llano region, Texas, locality C-25 of ref. 13. The age of this interval is given as 340 Myr (ref. 14).

Thus, it is possible to count fission tracks in conodonts and to compute reasonable age estimates from these data. Many improvements in procedures could be made. Our preparation routines work well but are tedious: for example, methods which



allow irradiation of specimens with their mounts would save time and eliminate the risks inherent in handling unsupported epoxy wafers. Fossil track counting statistics would be greatly improved by examining more than one surface on each specimen: multiple grind-etch-count cycles will greatly increase the number of tracks per conodont without affecting the induced track densities. We have limited information on the distribution of uranium concentrations in conodonts, but over 90% of the conodonts we have tested have had very low [U] (~1 p.p.b.). The precision of age estimates improves with the square root of the number of tracks counted. A reasonable target would be 100 spontaneous (fossil) tracks/age determination, which implies 10–100 conodonts examined for each accurate age determination.

Fission track dating of conodonts at stratotype boundaries and elsewhere may challenge conventional indirect age estimates based on correlation and interpolation from igneous rocks<sup>15</sup>. However, the scarcity of fission tracks in our conodonts suggests that much effort will be required to rival the precision of good radiometric determinations published for igneous rocks.

Nonetheless, the general dichotomy between (isotopically) datable but fossil-free igneous rocks and fossiliferous sedimentary rocks (which are the basis of the relative geological time scale) has complicated stratigraphical codes<sup>16</sup>. Except for <sup>14</sup>C dating of uppermost Pleistocene fossils, direct dating of fossils has been virtually impossible, but by eliminating the need to correlate datable rocks with those whose position in the stratigraphic column is secure errors may be reduced. The benefits of directly dating mid-Palaeozoic rocks justify studying fission tracks in conodonts.

The greatest value of dating conodonts directly probably lies in studying the thermal history of sedimentary basins<sup>17</sup>. Because the annealing temperature of apatite is ~90–100 °C, corresponding to burial of 3–5 km (ref. 18), the fission track 'clock' only begins to run as deeply buried sediments are uplifted and unroofed. If we can count tracks in thermally altered conodonts, we can date the time at which the overburden thinned (structurally or by erosion) to 3–5 km. (If one tests conodonts from various burial depths in the same section, the fission track 'ages' (unroofing times) will decrease with increasing depth (depositional age) in the rock column, as seen in igneous and metamorphic rocks in an Alaskan drill hole<sup>19</sup>.)

This work was begun with a question by S. T. Crough. We thank Z. S. Altschuler and A. G. Fischer for reviewing the manuscript, C. W. Naeser for advice and assistance, and R. Milwicz for monitoring radiation safety protocols. This work was supported by Princeton University Department of Geological and Geophysical Sciences and in part by NSF grant PHY 78-01473.

Received 30 July; accepted 7 October 1980.

1. Lindstrom, M. *Conodonts* (Elsevier, Amsterdam, 1964).
2. Epstein, A. G., Epstein, J. B. & Harris, L. D. *U.S. Geol. Surv. Prof. Pap.* 995 (1977).
3. Fleischer, R. L. & Price, R. B. *Geochim. cosmochim. Acta* **28**, 1705–1714 (1964).
4. Fleischer, R. L., Price, R. B. & Walker, R. M. *Nuclear Tracks in Solids—Principles and Applications* (University of California Press, Berkeley, 1975).
5. Pietzner, H., Vahl, J., Werner, H. & Ziegler, W. *Palaeontographica* **128**, 115–152 (1968).
6. Barnes, C. R., Sass, D. B. & Monroe, E. A. in *Conodont Paleozoology* (ed. Rhodes, F. H. T.) 1–30 (Geological Society of America, 1973).
7. Rhodes, F. H. T. *Biol. Rev. Camb. Phil. Soc.* **29**, 419–452 (1954).
8. Lindstrom, M. *Conodonts*, 30 (Elsevier, Amsterdam, 1964).
9. Mueller, K. J. & Nogami, Y. *Mem. Fac. Sci. Kyoto Univ. Ser. Geol. Miner.* **38**, 1–87 (1971).
10. Carpenter, B. S. & Reimer, G. M. *NBS Spec. Publ.* 260–49 (National Bureau of Standards, Washington, DC, 1974).
11. Altschuler, Z. S., Clarke, R. S. & Young, E. J. *U.S. Geol. Survey Prof. Pap.* 314-D, 45–90 (1958).
12. McConnell, D. *Econ. Geol.* **48**, 147–148 (1953).
13. Hass, W. H. *U.S. Geol. Surv. Prof. Pap.* 249-J, 365–399 (1959).
14. *Upper Kinderhookian, Lower Mississippian*. (U.S. Geological Survey, in the press).
15. Hedberg, H. D. et al. (eds) *Contributions to the Geological Time Scale* (American Association of Petroleum Geologists Studies in Geology, Tulsa, 1978).
16. Hedberg, H. D. (ed.) *International Stratigraphic Guide* (Wiley, New York, 1976).
17. Naeser, C. W. in *Aspects of Diagenesis*, 109–112 (eds Scholle, P. A. & Schlager, P. R.) (Society Economic Paleontologists Mineralogists Spec. Publ. 26, 1979).
18. Naeser, C. W. in *Lectures in Isotope Geology*, 154–169 (Springer, Berlin, 1979).
19. Naeser, C. W. & Forbes, R. B. *EOS* **57**, 353 (1976).

## First pterosaur from Australia

R. E. Molnar

Queensland Museum, Gregory Terrace, Fortitude Valley, Queensland 4006, Australia

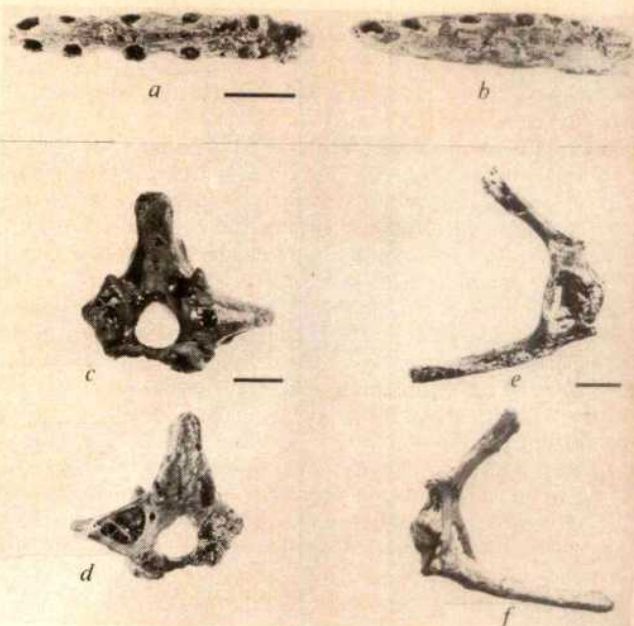
R. A. Thulborn

Department of Zoology, University of Queensland, St Lucia, Queensland 4067, Australia

**We report here the first evidence of pterosaurs from Australia. Our report is based on fragmentary material from marine Lower Cretaceous sediments, of the Eromanga Basin, western Queensland. These fragments represent at least one pterosaur allied to the well-known *Pteranodon*<sup>1,2</sup>, and establish a new southern limit of distribution for Cretaceous flying reptiles.**

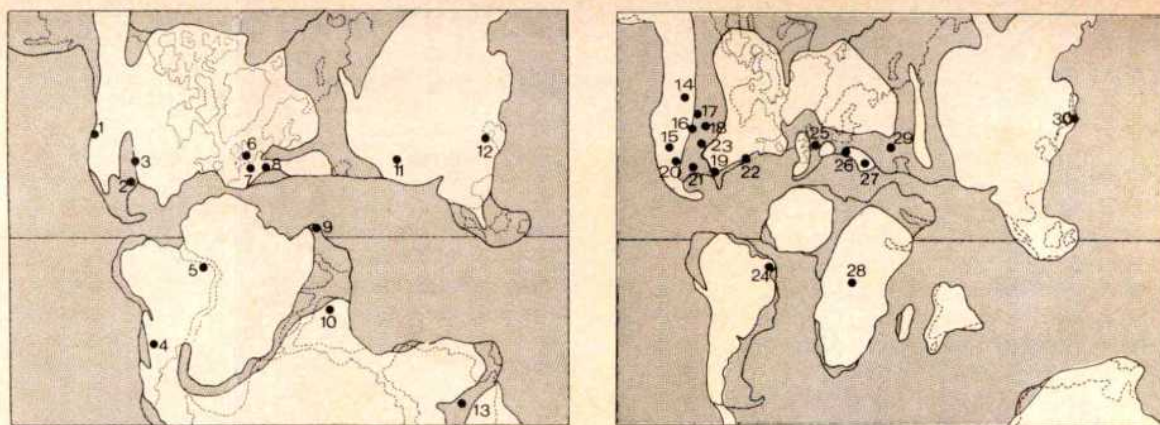
The material (Fig. 1) comprises three uncrushed specimens—the front of the fused mandibles (QM F10613), a single vertebra (QM F10614) and an isolated left scapulocoracoid (QM F10612). These were collected from flaggy limestones of the Toolebuc Formation at an unnamed locality 13 km south of Hamilton Hotel and about 70 km east of Boulia, west Queensland. The skull fragment and vertebra came from a single slab, and the scapulocoracoid was found about 500 m away. The Toolebuc Formation consists of crystalline and, in places, concretionary limestones with minor bands of shale; it has been dated as Lower Cretaceous (Albian)<sup>3,4</sup> on the basis of its rich and varied marine fauna (including lamellibranchs, gastropods, belemnites, ammonites, fishes and marine reptiles).

The skull fragment (Fig. 1a, b) comprises the slender extremities of both mandibles, showing several characteristic pterosaur features: (1) the long fused symphysis; (2) the interior



**Fig. 1** a, Anterior region of mandibles of pteranodontid (Queensland Museum (QM) F10613) from Toolebuc Formation of Queensland, in palatal view. Note replacement crown in fourth left alveolus. Scale bar, 2 cm. b, The same in lateral view. c, Vertebra of pterosaur (QM F10614) from the same locality, in anterior view. Scale bar, 1 cm. d, The same in posterior view; note large aperture into hollow transverse process. e, Pteranodontid scapulocoracoid (QM F10612) in anterior view. Scale bar, 2 cm. f, The same in posterior view.





**Fig. 2** Distribution of Cretaceous pterosaurs. Lower Cretaceous occurrences (left): 1, Oregon, *Pteranodon*?; 2, east Texas, unidentified; 3, Kansas, *Apatomerus*; 4, San Luis, *Pterodaustro* and *Puntanipiterus*; 5, Ceara, *Araripidactylus* and *Araripesaurus*; 6, southern England, *Criorhynchus*, *Ornithocheirus* and *Ornithodesmus*; 7, France, *Ornithocheirus*; 8, Germany, 'Ornithocheirus'; 9, Jordan, *Titanopteryx*; 10, Rajasthan, unidentified; 11, Dzungaria, *Dsungaripterus* and *Noriopterus*; 12, Shandong, unidentified; 13, Queensland, aff. *Ornithocheirus*. Upper Cretaceous occurrences (right): 14, Alberta, 15, Arizona, 16, Wyoming, 17, Montana, 18, South Dakota and 19, Alabama, unidentified; 20, west Texas, *Quetzalcoatlus*; 21, east Texas and 22, Delaware, *Pteranodon*; 23, Kansas, *Nyctosaurus* and *Pteranodon*; 24, Paraíba, *Nyctosaurus*; 25, southern England, *Criorhynchus*, *Ornithocheirus* and *Ornithostoma*; 26, Austria-Bohemia, 'Ornithocheirus'; 27, Transylvania, unidentified; 28, Zaire, cf. *Ornithocheirus*; 29, Petrovsk, *Ornithostoma*; 30, Hokkaido, *Pteranodon*.

of the jaws, exposed through breaks, was coarsely cancellous, or perhaps hollow; (3) the flat lateral surface of each ramus slopes down and inwards, giving a triangular cross-section (slightly deeper than wide); (4) the oral surface is transversely convex with a narrow median groove marking the line of the symphysis; (5) a distinctive arrangement of the teeth.

On each side are five deep and widely spaced alveoli, whose thin outer walls form distinct bulges in the jaw margins. Each alveolus is elliptical (with long axis longitudinal), and opens upwards and slightly laterally. The first alveolus on each side evidently carried a near-procumbent tooth; the second is more steeply inclined, whereas the following alveoli are almost vertical. Structure and size of the alveoli indicate a thecodont, near-isodont dentition at the front of the lower jaw. The fourth left alveolus contains a damaged replacement tooth; its crown is latero-medially compressed, and seems to have been tall and sharply pointed. In all respects the specimen is very similar to jaw fragments attributed to *Ornithocheirus*<sup>5,6</sup> from the Cambridge Greensand (Cenomanian<sup>7,8</sup>) of England.

The single vertebra (Fig. 1c, d) is incomplete, but shows most of the neural arch and the anterior part of the centrum. The centrum is relatively small and has a deeply concave anterior face, kidney-shaped in outline (concave above) and much broader than high. The walls and processes of the arch are virtually hollow, containing large cavities traversed by fine struts of bone. This system of cavities opens to the exterior in three places (seen on the well-preserved right side of the specimen): through a large triangular opening in the rear surface of the stout transverse process, and through smaller openings beneath the transverse process and below the base of the prezygapophysis. The robust neural spine is almost square in profile; its anterior margin is thick and flat, whereas its rear margin is narrower and carries a shallow vertical groove. The stout prezygapophyses have large articular facets inclined at about 30° from vertical; the postzygapophyses are smaller and sharper, each supported by a low ridge extending up and back from the base of the transverse process.

This pneumatic vertebra, with its depressed and probably procoelous centrum, is clearly from the presacral region of a pterosaur<sup>6,9</sup>. The postzygapophysial facets are much smaller than the prezygapophysial, which may indicate that the vertebra was transitional between the flexible cervical series and the rigid notarium<sup>6,9</sup>. The grooved rear margin of the neural spine suggests an articulation with the front of the notarium. Detailed comparisons are difficult because the vertebrae of other pterosaurs are usually crushed flat. Presacral vertebrae of *Pteranodon*

have similar oblique ridges supporting the postzygapophyses, but have relatively thin neural spines and seem to lack pneumatic openings<sup>1</sup>. The rather thick neural spine is matched in *Ornithodesmus latidens*<sup>10</sup>, from the Wealden of England, and in the notarium of *Dsungaripterus weii*<sup>11</sup>, from the Lower Cretaceous of China.

The scapulocoracoid (Fig. 1e, f) lacks only its uppermost tip and parts of the antero-medial margin. In postero-lateral view the specimen is roughly V-shaped (open posteriorly), with scapular and coracoidal wings enclosing an angle of about 75°. It shows a combination of features unknown in vertebrates other than pterosaurs<sup>6,9,12</sup>: (1) A cancellous interior overlain by a smooth cortex less than 1-mm thick, revealed at the damaged areas. (2) Scapula and coracoid are basically rod shaped with oval cross-sections, expanding considerably where they meet to form the glenoid; the intervening suture has been obliterated by fusion, but probably ran horizontally through the central and deepest part of the glenoid. (3) On the medial side the glenoid region is strengthened by a vertical buttress enclosing a narrow slit-like fenestra. (4) The large glenoid opens laterally, and slightly to the front, with margins developed into thick 'lips' of bone. It is essentially an open groove, aligned antero-posteriorly, with flattened upper and lower walls meeting at slightly more than a right angle. In outline it resembles three-quarters of a square: its upper (scapular) wall is about twice as long as its lower (coracoidal) wall, and forms a distinct overhang posteriorly. (5) The scapula is nearly straight, and extends medially as well as up and backwards from the glenoid; this oblique, and partly transverse, orientation suggests that the scapula may have articulated with a notarium<sup>9,12,13</sup>.

Just above the postero-dorsal corner of the glenoid the rear margin bears a prominent triceps tubercle<sup>12</sup>. The coracoid is slightly curved (convex downwards), and about halfway along its dorsal surface bears a low longitudinal crest probably marking the coracobrachialis attachment<sup>2</sup>. The tip of the coracoid is damaged, but enough remains to show a rounded surface for articulation with the sternum.

In general appearance the specimen is very similar to scapulocoracoids of the Upper Cretaceous pterosaurs *Nyctosaurus*<sup>14</sup> and *Pteranodon*<sup>1</sup>, the most obvious difference being the less strongly developed triceps tubercle in these latter forms. The specimen seems to be virtually identical to an incomplete scapulocoracoid attributed to *Ornithocheirus sedgwickii*<sup>5,6</sup>, from the Cambridge Greensand of England.

Evidently, the Toolebuc material represents one or more pterosaurs of the suborder Pterodactyloidea. The specimens are



most closely matched in pterodactyloids such as *Ornithocheirus* and *Pteranodon*, and the medial buttress of the scapulocoracoid occurs only in certain pterodactyloids<sup>12</sup>. In addition, there is indirect evidence of a notarium, a structure unknown outside the Pterodactyloidea. It is difficult to assign the Toolebuc material to a family because the two most similar forms, *Ornithocheirus* and *Pteranodon*, are at present in different families<sup>12</sup>. The Toolebuc scapulocoracoid is nearly identical to that attributed to *O. sedgwickii*<sup>6,9</sup>, but this species is known only from dissociated fragments and the referred scapulocoracoid might belong to another Cambridge Greensand pterosaur, *Ornithostoma seeleyi*<sup>15</sup>. *Ornithostoma* may, in turn, be identical with *Pteranodon*<sup>2,6,15</sup>. The jaw fragment is clearly from a pterosaur unlike the toothless *Pteranodon*, and is most closely matched in *Ornithocheirus*. Adherence to the pterosaur classification given by Wellnhofer<sup>12</sup> would require assignment of the Toolebuc jaw fragment to one family (Ornithocheiridae) and of the scapulocoracoid to another (Pteranodontidae). Distinctions between Ornithocheiridae and Pteranodontidae are, perhaps, of doubtful validity, largely because material attributed in the past to *Ornithocheirus* is fragmentary and of uncertain status. The problem is exacerbated by a possibility that the Toolebuc material represents more than one animal. In view of these difficulties, we recommend that the Toolebuc material be provisionally assigned to the family Pteranodontidae *sensu lato* (including Ornithocheiridae *sensu stricto*), following the usage of Romer<sup>6,16</sup>. The Toolebuc pterosaur material may be identified as aff. *Ornithocheirus*.

The best-known members of the Pteranodontidae *s.l.*, *Nyctosaurus* and *Pteranodon*, are of Upper Cretaceous age, whereas the earliest representatives come from about the boundary between Lower and Upper Cretaceous: from the Cambridge Greensand (Cenomanian<sup>7,8</sup>) of England<sup>6,12,15</sup> and the Hudspeeth Formation (Albian, possibly Cenomanian<sup>17</sup>) of Oregon<sup>12</sup>. The Toolebuc pterosaur is certainly Albian in age<sup>5,4</sup> and, hence, one of the earliest pteranodontids yet discovered.

*Pteranodon* and its allies were probably soaring maritime creatures<sup>2</sup>, similar in their habits to oceanic birds of today, and it is not surprising that they should have been widely distributed. Even so, few pteranodontids have been discovered in the Southern Hemisphere (Fig. 2), and the material described here establishes a new southern limit for their occurrence (indeed, for the occurrence of any Cretaceous pterosaur).

In *Pteranodon*, which attained a wing-span of about 7 m, the maximum dorso-ventral height of the scapulocoracoid is equivalent to some 5% of the total wing-span (calculated from data in ref. 2). The Toolebuc scapulocoracoid is only slightly damaged and probably had a maximum height of about 10.7 cm when complete. We estimate, by comparison with *Pteranodon*, that this scapulocoracoid was derived from a pterosaur with a wing span of about 2 m.

We thank Mr S. Van Dyck for his assistance in the field, and also Drs J. H. Ostrom and P. Wellnhofer. This work was supported by a grant from the Australian Research Grants Committee.

Received 7 July; accepted 30 September 1980.

1. Eaton, G. F. *Mem. Conn. Acad. Arts Sci.* **2**, 1–38 (1910).
2. Bramwell, C. D. & Whitfield, G. R. *Phil. Trans. R. Soc. B* **267**, 503–581 (1974).
3. Vine, R. R. & Day, R. W. *Qd Govt Mining J.* **68**, 416–421 (1965).
4. Senior, B. R., Mond, A. & Harrison, P. L. *Bull. Bur. Miner. Resour. Geol. Geophys. Aust.* **167**, 1–102 (1978).
5. Owen, R. *A History of British Fossil Reptiles* (Cassell, London, 1884).
6. Seeley, H. G. *Dragons of the Air* (Appleton, London, 1901).
7. Hart, M. B. *Proc. geol. Ass.* **84**, 65–82 (1973).
8. Carter, D. J. & Hart, M. B. *Bull. Br. Mus. nat. Hist. (Geol.)* **29**, 1–135 (1977).
9. Romer, A. S. *Osteology of the Reptiles* (Chicago University Press, 1956).
10. Hooley, R. W. *Q. J. geol. Soc. Lond.* **69**, 372–422 (1913).
11. Young, C. C. *Mem. Inst. vertebr. Paleont. Paleanthrop. Acad. Sinica* **11**, 18–35 (1973).
12. Wellnhofer, P. *Handb. Paläoherp. 19*, 1–82 (1978).
13. Seeley, H. G. *Ann. Mag. nat. Hist. Ser. 6*, **7**, 438–445 (1891).
14. Williston, S. W. *Publs Field Mus. nat. Hist., geol. Ser. 2*, 123–163 (1901).
15. Hooley, R. W. *Ann. Mag. nat. Hist. Ser. 8*, **13**, 529–557 (1914).
16. Romer, A. S. *Vertebrate Paleontology*, 3rd edn (Chicago University Press, 1966).
17. Wilkinson, W. D. & Oles, K. F. *Bull. Am. Ass. Petrol. Geol.* **52**, 129–161 (1968).

## Cortical binocularity in infants

Oliver Braddick\* & Janette Atkinson

Kenneth Craik Laboratory, University of Cambridge, Cambridge CB2 3EB, UK

Bela Julesz & Walter Kropff

Bell Laboratories, Murray Hill, New Jersey 07974

Ivan Bodis-Wollner & Edward Raab

Mount Sinai School of Medicine, New York 10029

The primate visual cortex, including that of man, receives separate input from each eye and these interact in binocular cortical neurones. This organization is known to be vulnerable to disruption in early life<sup>1</sup>. To understand the development of human visual cortex, and to detect and assess disorders of binocular function at the earliest possible age, a robust method is needed for detecting binocular interactions in the infant's visual system. We have done this by recording cortical visual evoked responses (VERs) to the onset and offset of binocular correlation in a large-screen dynamic random dot display. We report here that, in general, the human infant has a functional binocular visual cortex by 3 months of age, with some individuals showing cortical binocularity at an earlier age.

We used a stimulus display which has been found to yield prominent VERs in adult subjects with normal binocular vision<sup>2,3</sup> and in an alert macaque monkey<sup>4</sup>, and which does not produce VERs in patients whose binocular function has been impaired by monocular retrobulbar neuritis<sup>5</sup>. It consists of a random dot pattern generated on red and green channels of a projection video monitor (Advent 1000 A), producing a large-screen back-projected display (157 × 130 cm), with each dot 8 × 5 mm; at the infant's viewing distance of 40 cm this gave dots 1.1 × 0.7 degrees in a display 126 × 117 degrees. The stimulus alternates between a correlated phase, in which the dot patterns are identical in the red and green channels, and an anti-correlated phase in which a dark dot in the green channel corresponds to every bright dot in the red and vice versa. Because a fresh random dot pattern is generated for each TV frame (that is, at 30 Hz), the alternation between these phases is not detectable in either channel viewed alone. When the channels are displayed to the two eyes separately, by means of red and green Wratten filters over the projection lenses and corresponding filters in lightweight goggles worn by the infant, the stimulus alternation can only be detected by binocular interaction, that is, it is 'strongly cyclopean' (ref. 6). The use of correlation/anti-correlation has the merit for infant testing that the binocular relationship is not affected by head tilt. At slow rates of alternation, the correlated phase appears to an adult as dynamic noise on a well-defined flat surface, whereas the anti-correlated phase appears rivalrous and incoherent in depth. In preliminary experiments we found that an alternation rate of 1.9 Hz was optimal for VER recording. At this rate it was difficult to differentiate the two alternating percepts, but a clear pulsation of the display at the alternation frequency was visible with binocular viewing.

Bipolar VERs were recorded from a pair of Grass gold electrodes 1 cm above the inion and at the vertex, with an indifferent electrode on the forehead. Interelectrode resistances between 5 and 20 kΩ were generally attained. Potentials were amplified with a passband of 0.25–15 Hz and cumulated in a signal averager with a 1.024 s sweep, each sweep containing two

\*Present address: Department of Experimental Psychology, University of Cambridge, Downing St, Cambridge CB2 3EB, UK.



**Table 1** Proportion of infants showing significant VERs with cyclopean stimulus, compared with control conditions

| Age range*       | No. of infants in group | Number of infants showing cyclopean VER |
|------------------|-------------------------|---|
| 4 weeks–2 months | 9                       | 4                                       |
| 3–5 months       | 9                       | 9                                       |
| 5–8 months       | 8                       | 6                                       |

\* There were no infants in the age range 10–13 weeks inclusive in the sample.

cycles of the stimulus alternation. The averager automatically rejected sweeps containing high-amplitude artefacts, and averaging was manually interrupted when the infant was drowsy, agitated, making gross movements, or looking away from the display. (The success of the experimenter holding the infant in minimizing these states is critical to the success of the procedure.) The cumulated evoked response was plotted after 25, 50, 75, and 100 sweeps, and the waveforms were digitized for analysis.

Subjects were healthy infants attending the paediatric clinic at Mount Sinai Hospital, and relatives of ophthalmological patients, and ages ranged between 4 and 36 weeks. They were tested when calm and alert, as far as possible, although it was more difficult to sustain this state through preparation and testing in the younger infants, especially following a long clinic attendance.

Five stimulus conditions were used for VER recording: (1) 'Contrast': when viewed without goggles, the display appears to alternate between a yellow-black (correlated) and a red-green (anti-correlated) dot pattern. This served to check that we could record VERs from a particular subject. (2) 'Red-green': viewed with goggles so that any VER recorded was due to activation of binocular cortical neurones. (3) 'Red-red' control: with goggles so that each eye saw the same channel. Any VER recorded here must be due to crosstalk between the channels, visibility of contrast changes round the edge of the goggles, or electrical artefact. (4) 'Misaligned control': correlation and anti-correlation were both destroyed by misaligning the patterns vertically by 10 degrees; again any VER is an indicator of crosstalk or artefact. (5) 'Looking away control' in which the infant was directed away from the display—this served principally as a control for the contrast condition. It was not possible to run all conditions on all infants, but in all the 27 infants whose data are reported, recordings were obtained in contrast, red-green, and one or more of the control conditions. In only five cases was it necessary to compare the red-green with the weakest, 'looking-away' control.

Figure 1 shows VERs recorded successively from a 2-month infant. In (a) a VER waveform at twice the frequency of the correlated/anti-correlated alternation clearly emerges in the course of 100 sweeps, (b) the patterns displayed to the two eyes are misaligned vertically and the VER is completely absent. In (c) the patterns are realigned and the VER reappears, (d) a single channel is displayed to both eyes and the VER is again absent. This infant therefore showed VERs which can only be a cortical response to binocular correlation.

In many infants the VER records were not so noise-free as in Fig. 1 (although amplitudes were generally greater—of the order of 10  $\mu$ V). We therefore adopted a statistical procedure for confirming the presence of a VER that cumulated over sweeps in the 'red-green' condition and was absent in controls.<sup>7</sup> The amplitude of a constant VER signal increases linearly with the number of sweeps which are cumulated, whereas noise amplitude, present in both test and control runs, increases as the square root of the number of sweeps. For each run we obtained a record of the cumulated signal after 25, 50, 75 and 100 sweeps. Each of these records was digitized, and its products computed with sine and cosine functions at the stimulus alternation frequency and its second harmonic, to give the amplitude and

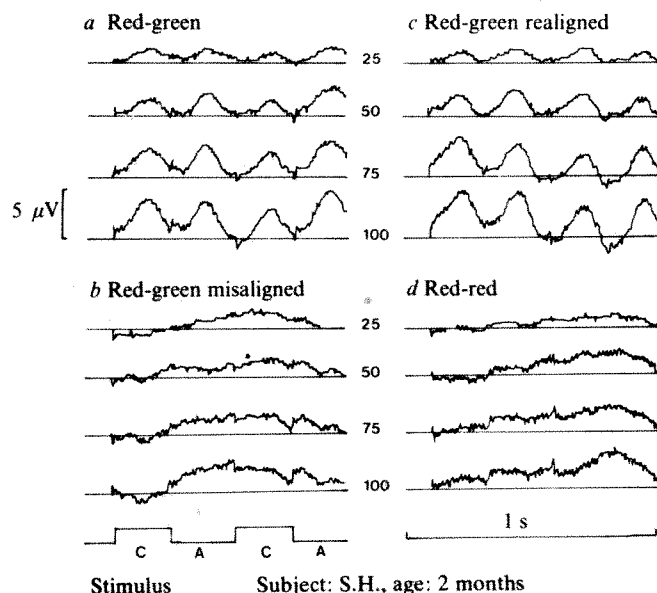
phase of components at these frequencies in the waveform. Regression lines were computed for the amplitude of each component as a function of number of sweeps for the records from a single run. It was taken as positive evidence for a binocular VER if the slope of the regression line for either component for a 'red-green' run was statistically significantly greater (at the  $P < 0.05$  level) than the slope for a control run.

The group of infants tested were divided by age into three groups. Table 1 shows the number of infants in each group from whom positive evidence of binocular VERs was obtained. All the infants who gave negative results showed satisfactory VERs in the contrast condition.

The VERs found could be either at the first or the second harmonic of the stimulus frequency. Generally, but not invariably, the VER obtained in the 'red-green' binocular condition was the same harmonic as that obtained with the same individual in the contrast condition.

In addition to the 27 infants included in Table 1, one 17-week infant with congenital esotropic strabismus was tested both before and the day after corrective surgery, and on both occasions this child showed a VER in the contrast condition but not in 'red-green' binocular viewing. It is too soon to know whether subsequent development of binocularity will be possible in this case, or whether the lack of binocularity was congenital and permanent.

We conclude that, at least by the age of 12 weeks, the normally developing human visual cortex contains neurones which are activated by binocularly correlated stimuli. Such neurones are clearly present in some younger infants. We do not know whether the failure to elicit VERs in half the infants under two months indicates a true absence of functional binocularity, or simply the more labile attentional state of these younger infants. It is possible, but in our view unlikely, that the apparent lack of binocularity in some younger infants could have been due to errors of convergence<sup>8</sup>. We believe that the failure to



**Fig. 1** Visual evoked responses (VERs) recorded from a 2-month infant using a 'cyclopean' stimulus: (a) the infant wore 'red-green' goggles so that the two eyes saw different pattern components. The stimulus trace (bottom left) shows the alternation between binocular correlation (C) and anti-correlation (A): a VER synchronized with the stimulus changes is clearly present; (b) when a vertical misalignment of the two eyes' patterns was introduced the VER disappeared; (c) the alignment of the patterns was restored and the VER reappeared; (d) when both eyes see the same pattern component (through 'red-red' goggles) no VER is present. The four traces for each condition represent the cumulated signal after 25, 50, 75 and 100 sweeps within a single run. Any true VER will appear with progressively increasing amplitude in such a series.



demonstrate binocular VERs in two infants of the oldest group can be ascribed to the very noisy signals obtained from these more active individuals.

Other behavioural investigations have tested whether infants can discriminate areas of stereoscopic disparity within a static or dynamic random dot stereogram<sup>9,10</sup>. The most extensive of these<sup>9</sup> found evidence for stereoscopic discriminations in 3½-month but not in younger infants. It is possible that an infant could have cortical neurones which responded to binocular correlation in our experiment, but which did not respond differentially to binocularly correlated patterns with varying disparities. Binocular cells without any fine degree of disparity tuning have been reported in the immature visual cortex of the cat<sup>11</sup>. Further behavioural and evoked potential studies, which compare the random dot correlograms used here with random dot stereograms, are required to test whether the binocularity found in at least some infants under 3 months is of this nature. In

adults, both dynamic random dot correlograms (the stimulus used in this study) and stereograms yield large VERs, but of different shapes<sup>2</sup>.

Animal<sup>1,12</sup> and human<sup>13</sup> studies have shown that binocular organization is vulnerable to environmental modification, implying that early correction of binocular disorders such as strabismus may be critical. Our demonstration of cortical binocularity in normal 3-month-old infants opens the possibility that this robust VER method could be used to diagnose and assess early abnormalities of binocular development and effects of treatment.

This work was supported by a grant from the Ophthalmology Department, Mount Sinai School for Medicine, and by the Medical Research Council of Great Britain.

We thank Lesley Ayling for assistance in data analysis, Hilda Rivera for help with infant subjects, and Lee Mylin and John Camisa for technical assistance.

Received 11 June; accepted 29 September 1980.

- Hubel, D. H. & Wiesel, T. N. *J. Neurophysiol.* **28**, 1041–1059 (1965).
- Julesz, B., Kropff, W. & Petrig, B. *J. opt. Soc. Am.* **68**, 1420 (1978); *Proc. natn. Acad. Sci. U.S.A.* (in the press).
- Lehmann, D., Skrandies, W. & Lindenmaier, C. *Neurosci. Lett.* **10**, 129–134 (1978).
- Miezin, F., Myerson, J., Julesz, B. & Allman, J. *Vision Res.* (in the press).
- Bodis-Wollner, I., Julesz, B. & Kropff, W. *Pap. 28th int. Congr. on Physiological Science*, Budapest (1980).

- Julesz, B. *Foundations of Cyclopean Perception* (University of Chicago Press, 1971).
- Atkinson, J., Braddick, O. & French, J. *Invest. ophthalmol. & Vis. Sci.* **18**, 210–213 (1979).
- Aslin, R. N. *J. exp. Child Psychol.* **23**, 133–150 (1977).
- Fox, R., Aslin, R. N., Shea, S. L. & Dumais, S. T. *Science* **207**, 323–324 (1980).
- Atkinson, J. & Braddick, O. *Perception* **5**, 29–38 (1976).
- Pettigrew, J. D. *J. Physiol.* **237**, 49–74 (1974).
- Vital-Durand, F., Garey, L. J. & Blakemore, C. *Arch. ital. Biol.* **116**, 444–448 (1978).
- Banks, M. S., Aslin, R. N. & Letson, R. D. *Science* **190**, 675–677 (1975).

## Bloom-forming cyanobacterium *Microcystis aeruginosa* overwinters on sediment surface

T. Preston & W. D. P. Stewart

Department of Biological Sciences, University of Dundee, Dundee DD1 4HN, UK

C. S. Reynolds

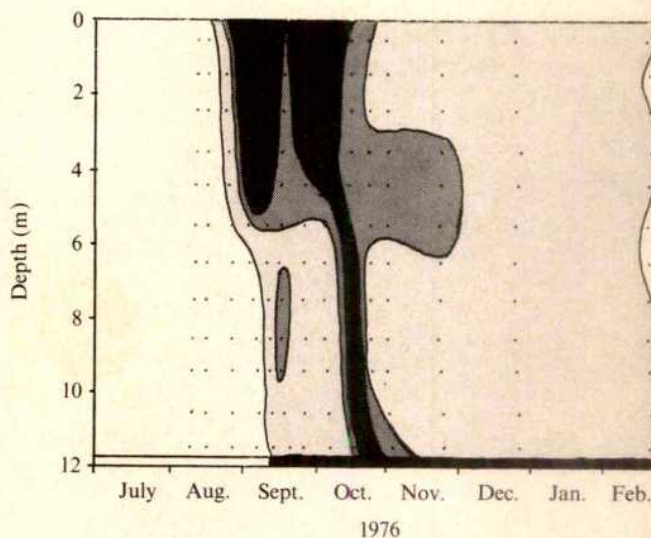
Freshwater Biological Association, Ambleside, Cumbria LA22 0LP, UK

Cyanobacteria (blue-green algae) commonly occur in the phytoplankton of lakes and reservoirs and sometimes develop as blooms which can cause deoxygenation, toxin production and nuisance odours<sup>1</sup>. The factors which govern the occurrence and seasonal development of such blooms in surface waters are imprecisely understood and little is known about the origins of the bloom-forming populations within particular water bodies (see, however, refs 2, 3). Using <sup>15</sup>N as tracer, we show here that the appearance of *Microcystis* in the phytoplankton of an experimental enclosure in the summer of 1977 correlated directly with the presence of particulate <sup>15</sup>N which could only have been sediment-derived and which originated mainly from *Microcystis* cells deposited on the sediment surface the previous year. The most plausible explanation is that *Microcystis* overwinters on the sediment surface and by so doing provides an inoculum of colonies from which the epilimnetic population develops the following summer<sup>4–8</sup>. Possible mechanisms which allow the mass recruitment of *Microcystis* to the plankton are considered elsewhere<sup>2,3</sup>.

On 19 August 1976, 11 kg NaNO<sub>3</sub> (enriched with 9.63 atom% excess <sup>15</sup>N) and 789 g KH<sub>2</sub>PO<sub>4</sub> (N:P atomic ratio, 10:1) were dissolved and sprayed onto the surface waters of an 18,500 m<sup>3</sup> experimental enclosure (45.7 m diameter, 12 m deep)<sup>9</sup> in Blelham Tarn in the English Lake District when the waters were thermally stratified<sup>10</sup>.

When the fertilizer was added, algal biomass in the water column was low (<5 µg chlorophyll *a* per l) but within 14 days an extensive bloom dominated by the cyanobacterium *Microcystis aeruginosa* developed in the epilimnion. In October,

stratification broke down and the particulate <sup>15</sup>N in the water column (7.2 kg N enriched with 1.31 atom% excess <sup>15</sup>N) sedimented out (Fig. 1). Light microscopy showed the sedimenting material to be almost entirely (>90% by volume) *Microcystis* colonies. This was deposited on the sediment surface as a layer approximately 1.0 cm thick and clearly visible in sediment core samples. On 19 February 1977 the layer of *Microcystis* still dominated the sediment surface and the cells then had a <sup>15</sup>N enrichment of 1.33 atom% excess <sup>15</sup>N; only 7.5% (9 g <sup>15</sup>N) of



**Fig. 1** The distribution of particulate <sup>15</sup>N (total particulate N × atom% excess <sup>15</sup>N enrichment) in the water column and sediment of a Lund enclosure (enclosure A) in Blelham Tarn, English Lake District from July 1976 to February 1977. ■, >8; ▒, 5–8; □, 1–5; □, 0–1 (all µg per l). Water samples were collected using a 5 l Friedinger bottle; sediment core samples were obtained using a Jenkins surface sediment corer<sup>12</sup>, particulate material was separated by filtration onto precombusted Whatman GF-C disks; organic C and total N were measured using a Hewlett Packard 185B elemental analyser or by Kjeldahl digestion. Isotope analyses were carried out on Kjeldahl distillates after conversion of the NH<sub>4</sub><sup>+</sup> to N<sub>2</sub> using LiOBr (ref. 13). Isotope ratios were determined using a VG Micromass MM601 mass spectrometer.



the total isotope present in the sediment had been mineralized. The experiment therefore provided a labelled sediment population whose subsequent fate could be followed.

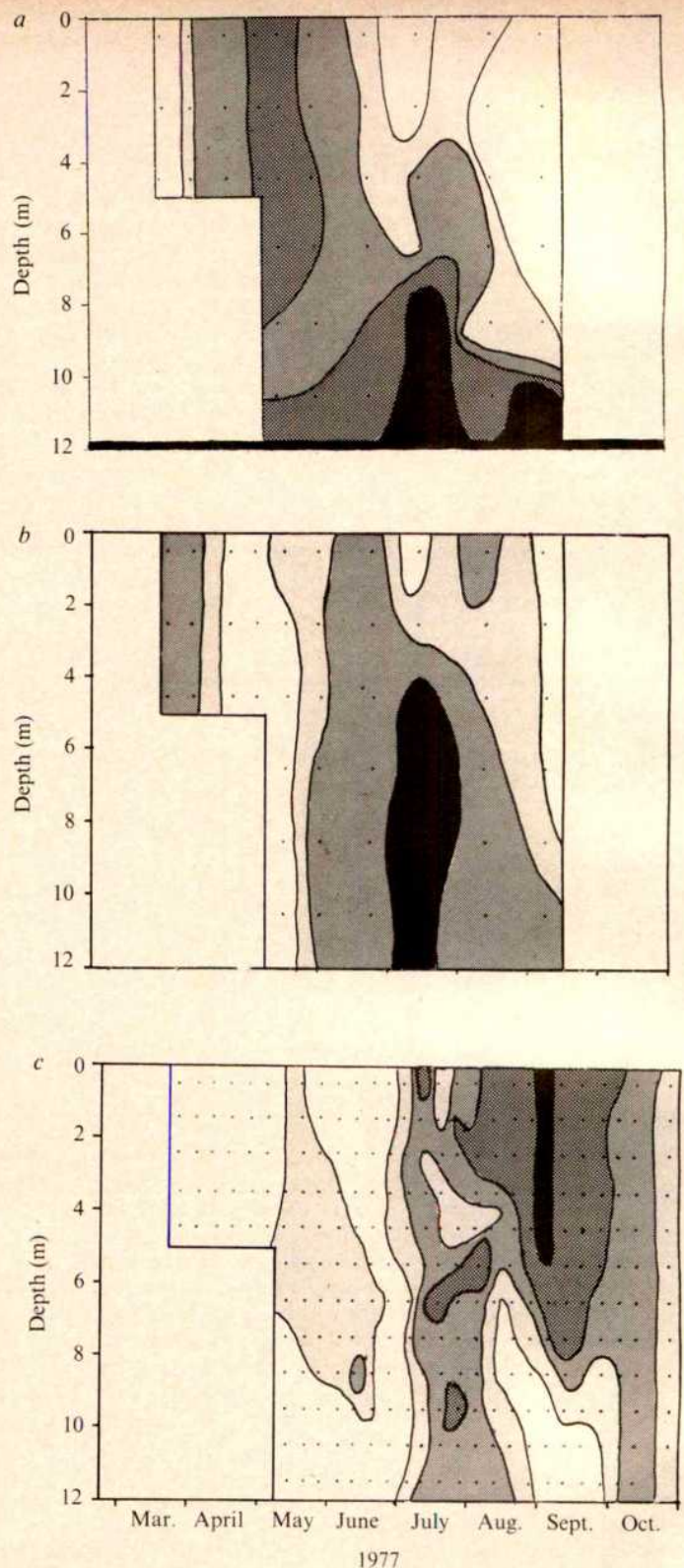
The walls of the enclosure were lowered on 20 February 1977 to equilibrate the isothermal waters with those of the Tarn and thus remove  $^{15}\text{N}$  from the water column. After 30 days the walls were raised and the  $^{15}\text{N}$  content of the particulate and soluble material in the water column was subsequently monitored.

Figure 2a presents data on the particulate  $^{15}\text{N}$  found in the water column from the time of isolation of the enclosure (22 March 1977) until late September 1977. It is seen that very little particulate  $^{15}\text{N}$  was present in the water column immediately after isolation (10–100-fold lower than that present before opening the enclosure; see Figs 1 and 2a), indicative of the success of the flushing procedure. Particulate  $^{15}\text{N}$  concentrations in the surface waters then increased to a maximum in May. As soluble  $^{15}\text{N}$  was undetectable in the water column until August when  $^{15}\text{NH}_4^+$  was first released from the sediment into the anoxic hypolimnion, the particulate  $^{15}\text{N}$  increase must have been sediment-derived. This particulate  $^{15}\text{N}$  increase in May corresponded with the first appearance of *M. aeruginosa* in the water column (see Fig. 2c). An epilimnetic decline in particulate  $^{15}\text{N}$  then occurred with the onset of stratification in June.

In mid-July a very pronounced input of  $^{15}\text{N}$  was noted below 7.5 m. Over the period 21 June–12 July this input was 230 mg  $^{15}\text{N}$  and the net increase in the whole enclosure was 84 mg  $^{15}\text{N}$ . That is, there was significant movement of sediment-derived  $^{15}\text{N}$  particulate material into the hypolimnion. The integrated water column  $^{15}\text{N}$  concentration in mid-July was 940 mg  $^{15}\text{N}$  (1% of that present on the sediment surface). On analysing the subsequent changes in particulate  $^{15}\text{N}$  over the period 12 July–11 August, a net decrease in particulate  $^{15}\text{N}$  occurred, due presumably to some material sedimenting. However, of more importance, there was an input of 122 mg  $^{15}\text{N}$  to the epilimnion. That is, the particulate  $^{15}\text{N}$  which originated in quantity from the sediment in mid-July had reached the surface waters. In late September the particulate  $^{15}\text{N}$  sedimented.

Figure 2b, c provides information on the nature of the particulate material in the water column. The carbon-to-nitrogen (C:N) ratio data (Fig. 2b) show that immediately after isolating the enclosure in March the particulate material had a C:N ratio of 10.4:1. This ratio then increased to a maximum of 12.2:1 in early May indicating that the particulate material had a large detrital component. A particulate  $^{15}\text{N}$  maximum also occurred then (see Fig. 2a). In mid-July the C:N ratio changed sharply at depth to <9 indicative of the presence of phytoplankton (the C:N ratios of healthy *Microcystis* the previous year were 7–8:1) with minimum C:N values (8:1) being found where the particulate  $^{15}\text{N}$  concentration was also highest (8.5 m; see Fig. 2a). In August the C:N ratios in the surface waters decreased to a minimum.

The abundance of *Microcystis* (Fig. 2c) was then examined and correlated with changes in particulate  $^{15}\text{N}$  (Fig. 2a) and in C:N ratios (Fig. 2b). *Microcystis* was first detected in very low numbers in the surface waters during May 1977. These colonies failed to develop and *Microcystis* colonies present in May could not have been solely responsible for the total particulate  $^{15}\text{N}$  noted. This May 1977 *Microcystis* (based on cell volume estimates and a  $^{15}\text{N}$  enrichment of 1.33 atom % excess  $^{15}\text{N}$ ) accounted for <25% of the observed water column  $^{15}\text{N}$  concentration. Together with the high C:N ratio this suggested that the labelled material was largely cell debris derived from the sediment surface. Also, at that time the colonial chrysophyte *Uroglenopsis americana*<sup>11</sup> developed. This alga, which was absent from the phytoplankton the previous year, may exist, like other chrysophytes, as cysts on the sediment surface until germination, possibly obtaining some  $^{15}\text{N}$  from sediment pore water and then moving into the water column. In late July *Microcystis* became clearly detectable in the water column and was concentrated at 8.5 m, the site of highest  $^{15}\text{N}$  concentration. In August, *Microcystis* developed in the surface waters and its presence there correlated with the presence of particulate  $^{15}\text{N}$



**Fig. 2** a, The distribution of particulate  $^{15}\text{N}$  in the water column and sediment of a Lund enclosure in Blelham Tarn from March 1977 to September 1977. ■, >80; ▨, 50–80; ▩, 35–50; □, 25–35; □, 0–25 (all ng per l). b, The distribution of particulate organic carbon-to-nitrogen ratio of water column material of a Lund enclosure in Blelham Tarn from March 1977 to September 1977. □, >12:1; □, 12:1–11:1; ▨, 11:1–9:1; ▩, <9:1. c, The distribution of *M. aeruginosa* colonies in the water column of a Blelham Tarn enclosure from March 1977 to October 1977. ■, >7; ▨, >3; ▩, 1–3; □, 0.1–1; □, <0.1 (per ml). The colonies were counted by sedimentation and microscopy<sup>14</sup>.



(the *Microcystis* biomass then could easily account for the total particulate  $^{15}\text{N}$  in the epilimnion) although, because of its undoubted assimilation of unlabelled nitrogen during growth, the  $^{15}\text{N}$  enrichment of *Microcystis* decreased. In late September *Microcystis*, like the particulate  $^{15}\text{N}$ , sedimented.

The above data collectively provide evidence that *Microcystis* overwinters on the sediment surface and serves as an inoculum for the following year's epilimnetic growth.

We thank the ARC and NERC for support and Dr J.W.G. Lund for helpful advice and encouragement.

Received 19 May; accepted 22 September 1980.

1. Fogg, G. E., Stewart, W. D. P., Fay, P. & Walsby, A. E. *The Blue-Green Algae* (Academic, London, 1973).
2. Reynolds, C. S. & Walsby, A. E. *Biol. Rev.* **50**, 437–481 (1975).
3. Reynolds, C. S. *Proc. R. Soc. B* **154**, 24–50 (1973).
4. Topachevskiy, A. V., Bradinskiy, L. P. & Sirenko, L. A. *Hydrobiol. J.* **5**, 1–10 (1969).
5. Sirenko, L. A. *BLL Translation* RTS8132.
6. Kappers, F. E. *Hydrobiol. Bull.* **10**, 164–171 (1976).
7. Reynolds, C. S. & Rogers, D. A. *Hydrobiologia* **48**, 17–23 (1976).
8. Tow, M. J. *Limnol. Soc. Sth Afr.* **5**, 9–10 (1979).
9. Lack, T. J. & Lund, J. W. G. *Freshwater Biol.* **4**, 399–415 (1974).
10. Christofi, N., Preston, T. & Stewart, W. D. P. *Water Res.* (in the press).
11. Reynolds, C. S. & Butterwick, C. *Algalological Studies* **23**, *Arch. Hydrobiol., Suppl.* **56**, 166–183 (1979).
12. Mortimer, C. H. *J. Ecol.* **30**, 147–200 (1942).
13. Ross, P. J. & Martin, A. E. *Analyst* **95**, 817–822 (1970).
14. Lund, J. W. G., Kipling, C. & LeCren, E. D. *Hydrobiologia* **11**, 143–170 (1958).

## Explanation of sterility in $t^x t^y$ male mice

Michael J. Tucker

Department of Zoology and Comparative Physiology,  
University of Birmingham, PO Box 363, Birmingham B15 2TT, UK

The lethal ' $t$  alleles' of the T complex on mouse chromosome 17 (refs 1, 2) have been assigned to six complementation groups (the definitive classes being  $t^0$ ,  $t^9$ ,  $t^{12}$ ,  $t^{w1}$ ,  $t^{w5}$  and  $t^{w73}$ ), each causing embryonic death at a particular stage. Intercomplementation heterozygotes ( $t^x t^y$ ) show 'partial' complementation, so that only some  $t^x t^y$  offspring survive<sup>3,4</sup>. These survivors appear morphologically normal; indeed the females, being fertile, seem entirely normal. The  $t^x t^y$  males, however, are sterile. Among the reasons given for this sterility in some  $t^x t^y$  males are low motility of the  $t^x t^y$  spermatozoa<sup>5</sup>, and an inability to effect fertilization either *in vitro* or *in vivo* even when already present at the site of fertilization<sup>6,7</sup>. Spermatozoa from sterile  $t^x t^y$  males were reported to be apparently present in 'normal' numbers in the uterus, although actual ejaculate numbers have not been quoted for these, or indeed for normal fertile males<sup>5–8</sup>. In the human, typical ejaculate counts of less than  $20 \times 10^6$  spermatozoa, where the normal ejaculate contains  $100\text{--}250 \times 10^6$ , are judged to indicate clinical sterility<sup>9</sup>. The comparison of numbers of spermatozoa<sup>10</sup> ejaculated into the female tract by sterile  $t^6 t^{w5}$ ,  $t^6 t^{w32}$  and  $t^{w5} t^{w32}$  (all 'strong' mutations<sup>2</sup>) and control mice clearly shows an even greater oligozoospermia (about 100 times less than controls) occurring in the  $t^x t^y$  males.

Balanced lethal stocks of  $Tt^6$ ,  $Tt^{w5}$  and  $Tt^{w32}$  mice are maintained in the Department of Zoology at the University of Birmingham;  $t^x t^y$  tailed males were produced from crosses between these tail-less stocks ( $Tt^x \times Tt^y$ ). I investigated the numbers of spermatozoa ejaculated by sterile  $t^x t^y$  and control males by mating them with females at times ranging from 2 h before until 4 h after ovulation. Ovulating  $++$ (C3H),  $T+$ ,  $++$  and  $Tt$  females aged 2–10 months were used. (No differences were observed between results from induced or naturally ovulating females of differing ages or genotypes.) Females were killed as soon as a vaginal plug was seen (30 min observations). Control females were artificially inseminated with known

numbers of spermatozoa. The uterus and 'plugged' vagina were removed complete, after the ovarian end of the uterine horns had been ligatured, into a small (50 mm) Petri dish with as little blood as possible, and flushed with phosphate-buffered saline (PBS, Oxoid Dulbecco A) from a syringe and 21-gauge needle. The uterus was cut open, washed and scraped gently to transfer all spermatozoa to the wash-medium. All medium was taken up into 10 ml PBS and this was centrifuged at 250g for 15 min. The pellet was resuspended by gentle agitation into a further 10 ml PBS; 0.02-ml drops of this suspension were spotted out and air-dried on clean, marked slides. The dried spots were stained for 1 min in Wells and Awa stain<sup>11</sup>, air-dried and mounted in DPX (Hopkins and Williams Chemicals). All spermatozoa in each spot were counted in order to calculate the number in the 10 ml PBS, which was assumed to be the number ejaculated. When a visual estimate suggested a count greater than 1,000 per drop, the spermatozoa in 10 random  $\times 40$  objective fields (area  $0.16 \text{ mm}^2$ ) were counted and used to calculate total numbers in the dried drop of known size. The area of the spot was measured either by taking two diameter measurements at  $90^\circ$  where the spot was circular, or by making a trace on fine graph paper to calculate the area where the spot was misshapen. This was done to ensure standard treatment of all samples. I checked the multi-field count method by further diluting sperm suspensions and counting every sperm in each spot (diluted to contain 100–1,000 spermatozoa per drop). That gave numbers in agreement with the counts from the spots of lesser dilution ( $<10\%$  error). Table 1 shows the recovery of artificially inseminated spermatozoa, and makes possible estimation of the efficacy of the flushing technique; Table 2 shows the recovery of spermatozoa from females mated to control and  $t^x t^y$  males.

**Table 1** Assessment of efficacy of the flushing technique

|            | Spermatozoa artificially<br>inseminated log $\pm$ s.d.<br>of counts<br>(linear value $\times 10^6$ ) |     | Spermatozoa recovered<br>log $\pm$ s.d. of counts<br>(linear value $\times 10^6$ ) |
|------------|--|-----|--|
| Male       |  |     |  |
| $+t^6$     | $6.78 \pm 0.12$ ( $6.28 \pm 2.0$ )   | (1) | $6.50 \pm 0.11$ ( $3.23 \pm 0.8$ )   |
|            |  | (2) | $6.80 \pm 0.03$ ( $6.30 \pm 0.4$ )   |
|            |  | (3) | $6.66 \pm 0.18$ ( $4.83 \pm 2.0$ )   |
| $Tt^{w5}$  | $6.36 \pm 0.10$ ( $2.34 \pm 0.6$ )   | (1) | $6.33 \pm 0.14$ ( $2.21 \pm 0.7$ )   |
|            |  | (2) | $6.38 \pm 0.12$ ( $2.50 \pm 0.7$ )   |
| $+t^{w32}$ | $6.34 \pm 0.09$ ( $2.23 \pm 0.5$ )   | (1) | $6.09 \pm 0.25$ ( $1.39 \pm 0.9$ )   |
|            |  | (2) | $6.49 \pm 0.08$ ( $3.09 \pm 0.6$ )   |
|            |  | (3) | $5.98 \pm 0.16$ ( $1.00 \pm 0.3$ )   |

Spermatozoa from these control males were stripped from vasa deferentia and epididymides into warm ( $37^\circ\text{C}$ ) PBS. 0.05–0.10-ml sperm suspension was carefully injected per cervix as soon as possible (5–8 min) into etherized, oestrous females, and samples were diluted for counting to estimate the number of spermatozoa injected per female. Females were killed within 10 min of insemination, by cervical dislocation, and the uteri were exposed. Cervices were clamped and the uteri flushed as described in the text. Sperm numbers are given as log means  $\pm$  s.d. as recommended by Cohen<sup>10,12</sup>, and the linear values are also presented.

Recovery of spermatozoa from artificially inseminated females was relatively successful considering the difficulty of attempting to deposit known numbers of spermatozoa into the uterus. On the worst interpretation of the figures, recovery was usually 85% (the very worst was 43%). So the estimates of numbers of ejaculates from control and  $t^x t^y$  mice can be assumed to be at least as representative. The numbers assessed for C57BL males are close to previous estimations<sup>12</sup>, but are higher than those obtained by electroejaculation<sup>14</sup>. The figures for the  $t^x t^y$  mice of all three types are very variable between males, and even, to some extent, between copulations by one



**Table 2** Recovery of spermatozoa from females mated with  $t^x t^y$  and control males

| $t^x t^y$ sterile males |                |   | Control males |                |  |
|-------------------------|----------------|---|---------------|----------------|--|
| Male                    | No. of matings | Sperm count<br>log mean $\pm$ s.d.*<br>(linear value) | Male          | No. of matings | Sperm count<br>log mean $\pm$ s.d.*<br>(linear value $\times 10^6$ ) |
| $t^6 t^{w5}$            | 4              | $4.30 \pm 0.25$ (22,500 $\pm$ 12,000)                 | $Tt^{w32\pm}$ | 1              | $6.96 \pm 0.04$ (9.13 $\pm$ 0.9)                                     |
| $t^6 t^{w5}$            | 4              | $5.10 \pm 0.53$ (209,000 $\pm$ 244,000)               | $Tt^{w32\pm}$ | 1              | $6.77 \pm 0.09$ (5.95 $\pm$ 1.1)                                     |
| $t^6 t^{w5}$            | 3              | <3.00 (<1,000) <sup>†</sup>                           | $Tt^{w5\pm}$  | 2              | $6.85 \pm 0.35$ (8.35 $\pm$ 6.0)                                     |
| $t^6 t^{w5}$            | 4              | <3.00 (<1,000) <sup>†</sup>                           | $Tt^{w5\pm}$  | 2              | $7.11 \pm 0.08$ (13.00 $\pm$ 2.5)                                    |
| $t^6 t^{w5}$            | 2              | <3.00 (<1,000) <sup>†</sup>                           | $T+$          | 1              | $7.30 \pm 0.05$ (19.82 $\pm$ 1.9)                                    |
| $t^6 t^{w32}$           | 5              | $4.99 \pm 0.30$ (113,000 $\pm$ 54,000)                | $T+$          | 1              | $6.44 \pm 0.13$ (2.82 $\pm$ 0.8)                                     |
| $t^6 t^{w32}$           | 1              | 3.79 (7,000) <sup>†</sup>                             | $+ + C57BL$   | 1              | $7.14 \pm 0.06$ (13.87 $\pm$ 1.8)                                    |
| $t^{w5} t^{w32}$        | 2              | $4.88 \pm 0.51$ (100,000 $\pm$ 98,000)                | $+ + C57BL$   | 2              | $6.86 \pm 0.04$ (7.17 $\pm$ 0.6)                                     |
|                         |                |   | $+ t^{w5}$    | 1              | $7.23 \pm 0.06$ (16.77 $\pm$ 2.5)                                    |

Female mice were either induced to ovulate (5 IU follicle stimulating hormone followed 48 h later by 5IU human chorionic gonadotropin; ovulation assumed to occur 13 h later<sup>13</sup>), or used when naturally ovulating as assessed by vaginal smear test.  $T+$  and  $+t$  mice were obtained as  $F_1$  from  $C57BL \times +t$  crosses. The  $t^x t^y$  males were considered sterile if they were run with five known-fertile females for 4 weeks or more without pregnancies (five 'mating units'<sup>4</sup>).

\* Standard deviations of pooled counts per mating where the s.d. of each count <20% of mean; except where only one count is given, then the s.d. of that count is shown.

<sup>†</sup> These counts were based on very few (<20) spermatozoa per spot.

<sup>‡</sup> Known fertile control males.

male. However, they are at least two orders of magnitude lower than the figures from the control males. In the human just one order of magnitude difference seems to confer a state of clinical sterility, so this hundredfold difference would adequately explain the sterility of these  $t^x t^y$  males.

In addition to the other suggested causes of the sterility<sup>5-7</sup>, the extreme  $t^x t^y$  oligozoospermia reported here presents a convincing explanation; it is tempting to consider this as the chief cause, with reduced motility and lack of fertilizability being secondary phenotypic expressions arising from the infertile state<sup>15</sup>. In this simple solution to the  $t^x t^y$  sterility it is not necessary to invoke altered sperm surface antigens interacting within the female<sup>16</sup>; the answers appear to lie in the course of spermatogenesis, which is in accordance with and extends the suggestion<sup>17</sup> that events before mating affect  $t^x t^y$  fertility. Preliminary studies so far indicate fewer spermatozoa present in the epididymides and vasa deferentia of  $t^x t^y$  males compared with controls<sup>18</sup>. It is to be hoped that further work will elucidate the actual processes resulting in this severe oligozoospermia found in these heterozygous  $t^x t^y$  male mice.

I thank Dr Jack Cohen for helpful criticism. This research was supported by a studentship from the SRC.

Received 1 August; accepted 19 September, 1980.

- Bennett, D. *Cell* **6**, 441-454 (1975).
- Sherman, M. I. & Wudl, L. R. in *Concepts in Mammalian Embryogenesis* (ed. Sherman, M. I.) 136-234 (MIT Press, Cambridge, 1977).
- Silagi, S. *Dev Biol.* **5**, 35-67 (1962).
- Bennett, D. *Science* **144**, 263-267 (1964).
- Bennett, D. & Dunn, L. C. *J. reprod. Fert.* **13**, 421-428 (1967).
- Mcgrath, J. & Hillman, N. *J. Cell Biol.* **75**, Abstr. G689 (1977).
- Olds, P. J. *J. exp. Zool.* **177**, 417-434 (1971).
- Olds, P. J. *Biol. Reprod.* **2**, 91-97 (1970).
- Freund, M. & Peterson, R. N. in *Human Semen and Fertility Regulation in Men* (ed. Hafez, E. S. E.) 344-354 (Mosby, St Louis, 1976).
- Cohen, J. *Adv. comp. Physiol. Biochem.* **4**, 267-380 (1971).
- Wells, M. E. & Awa, O. A. *J. Dairy Sci.* **53**, 227-232 (1970).
- Cohen, J. *Nature* **215**, 862-863 (1967).
- Gates, A. H. in *Methods in Mammalian Embryology* (ed. Daniel, J. C.) 64-75 (Freeman, San Francisco, 1971).
- Snyder, R. L. *Anat. Rec.* **155**, 11-14 (1966).
- Singer, R. *et al. Experimentia* **36**, 578-579 (1980).
- Yanagisawa, K. *et al. Immunogenetics* **1**, 57-67 (1974).
- Archer, J. R. *et al. Genet. Res., Camb.* **32**, 79-84 (1978).
- Bryson, V. *J. Morphol.* **74**, 131-179 (1944).

## Molecular analysis of the genetic relationship of *trans* interacting factors at the T/t complex

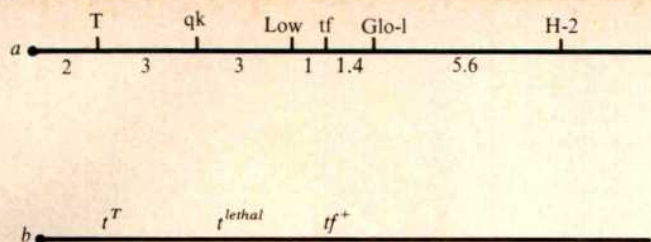
Althea K. Alton, Lee M. Silver, Karen Artzt & Dorothea Bennett

Laboratory of Developmental Genetics, Sloan-Kettering Institute, 1275 York Avenue, New York, New York 10021

The T/t complex is an extensive genetic region proximal to the H-2 complex on mouse chromosome 17, with multiple effects on embryonic development, spermatogenesis and recombination<sup>1-3</sup>. Recently, two-dimensional gel analysis of testicular cell proteins identified a gene within the T/t complex that codes for a major cell surface-associated protein, p63/6.9 (ref. 4). The wild-type gene, *Tcp-1*<sup>b</sup>, codes for a 63,000-molecular weight protein (p63/6.9b), whereas a mutant allele, *Tcp-1*<sup>a</sup>, which occurs in all intact *t* haplotypes, codes for a more acidic form of the protein (p63/6.9a). Analysis of partial *t* haplotypes obtained from rare recombination events showed that *Tcp-1*<sup>a</sup> correlated completely with the tail interaction factor *t*<sup>T</sup>, which is thought to be a genetic allele of *T*, thus raising the possibility that the locus of *T* codes for the p63/6.9 protein. We report here that the p63/6.9 proteins produced by seven chromosomes carrying independently derived dominant mutations at the locus of *T* are all indistinguishable from the wild-type form; thus, the cumulative data indicate that the *Tcp-1* gene is most probably not at the locus of *T*.

The T/t complex was originally defined by the dominant mutation *Brachyury* (*T*), which shortens the tails of heterozygotes and is lethal at 10.5 days of gestation when homozygous. Recessive lethal *t* haplotypes are found at high frequency in wild mice and are identified by their interaction with *T* to produce a tailless phenotype. Recombination data demonstrate that naturally occurring *t* haplotypes are separable into at least two well defined genetic factors (see Fig. 1): a proximal factor, *t*<sup>T</sup>, is allelic to and interacts in *trans* with *T* to produce taillessness; a distal factor, *t*<sup>lethal</sup>, results in embryonic death when it is homozygous. Other data indicate that the *t* haplotype may be





**Fig. 1** *a*, Mouse chromosome 17 and relevant markers. Genetic distance between markers is given in centimorgans. *b*, *t* Haplotype showing the separation of *t* factors.

separated into several other factors including those factors responsible for male sterility and distorted segregation ratios<sup>5</sup>.

Partial *t* haplotypes, recovered from recombination events, were used to map the *Tcp-1* gene: *Tcp-1*<sup>a</sup> was not associated with the one available partial haplotype (*t*<sup>h17</sup>) carrying only the *t*<sup>lethal</sup> factor, but correlated completely with the presence of the tail interaction factor, *t*<sup>T</sup>, in a variety of partial haplotypes examined. As *t*<sup>T</sup> and *T* behave as genetic alleles, the simplest explanation for the data was that the p63/6.9 protein was the direct gene product of the locus of *T*. However, the form of p63/6.9 produced by the one *T* mutation examined (*Brachyury*) was indistinguishable by two-dimensional gel analysis from wild type.<sup>4</sup> Nevertheless, as two-dimensional gel analysis is capable of defining only about one-third of all point mutations, the possibility remained that the locus of *T* codes for the p63/6.9 protein.

Seven independently derived dominant tail mutations at the locus of *T* have been analysed here (Table 1). These include two radiation-induced mutations and five spontaneous mutations which occurred in laboratory stocks. Of the five spontaneous mutations at *T*, two seem to be deletions of a portion of chromosome 17 including the *T* locus and another locus, *quaking* (*qk*). All *T*-locus mutations meet the following criteria: (1)

they are dominant mutations mapped to the *T/t*-complex region of chromosome 17, and are lethal when homozygous; (2) they interact with *t* to produce a tailless phenotype in *T/t* individuals; (3) they fail to complement one another and hence *T*<sup>x</sup>/*T*<sup>y</sup> individuals die during embryonic development.

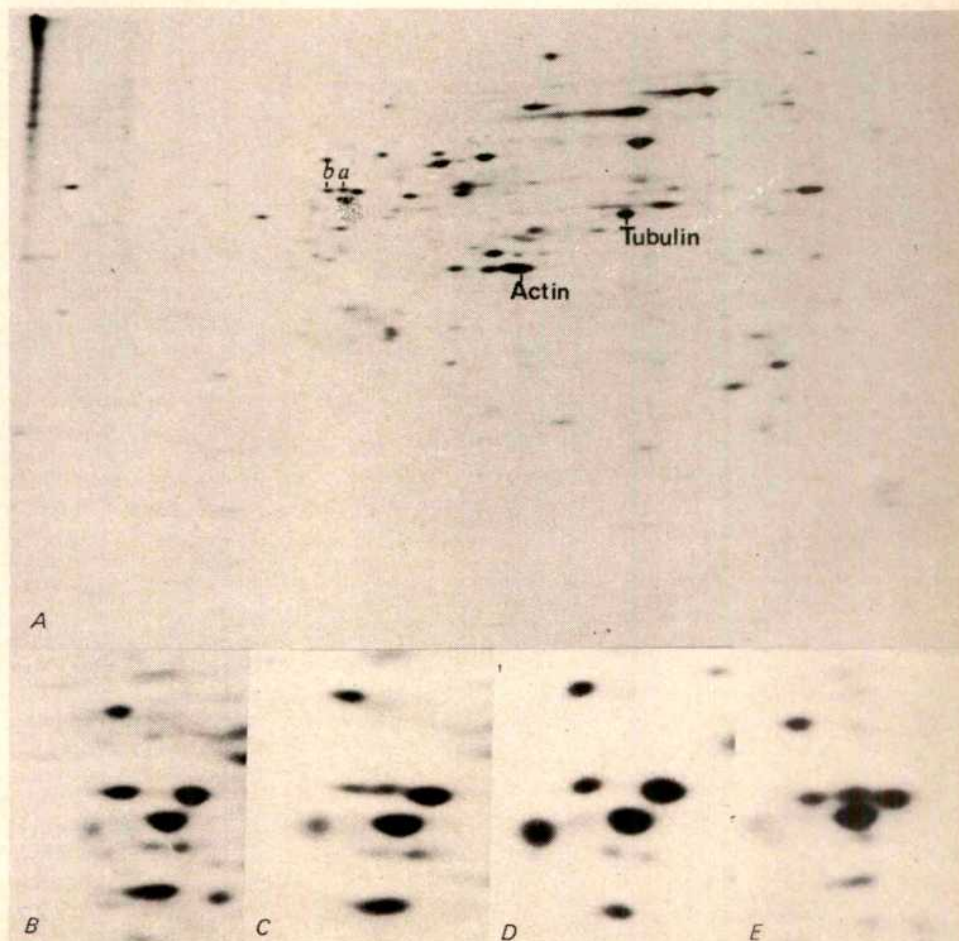
The expression of the p63/6.9 protein in heterozygotes for seven independent *T*-locus mutations was analysed by two-dimensional gel electrophoresis of radio-labelled testicular cell proteins (Fig. 2, Table 2). Animals which carried *T*, *T*<sup>hp</sup>, *T*<sup>Wis</sup>, *T*<sup>J</sup>, *T*<sup>c</sup> and *T*<sup>OR4</sup> opposite a chromosome with a wild-type *Tcp-1*<sup>b</sup> allele expressed a distinct p63/6.9b protein spot, but showed no additional spots (relative to known *Tcp-1*<sup>b</sup> homozygotes) in the p63/6.9 region of two-dimensional gels. In each case, this result indicates that the chromosome opposite *Tcp-1*<sup>b</sup> either expresses p63/6.9b or does not express any form of the p63/6.9 protein.

To distinguish between these two possibilities, we analysed the protein patterns of mice carrying each of these mutations opposite a chromosome carrying a *Tcp-1*<sup>a</sup> allele. Animals which carried *T*, *T*<sup>Wis</sup>, *T*<sup>J</sup>, *T*<sup>c</sup> and *T*<sup>OR4</sup> and a *Tcp-1*<sup>a</sup> allele all expressed both p63/6.9b and p63/6.9a. Therefore, each of these *T*-locus mutations expresses the wild-type form of the p63/6.9 protein. As described previously, mice with a *T*<sup>hp</sup>/*Tcp-1*<sup>a</sup> genotype express only p63/6.9a (ref. 4). Therefore, chromosomes with the *T*<sup>hp</sup> deletion do not have a functional *Tcp-1*<sup>a</sup> gene.

The apparent deletion *T*<sup>Orl</sup> was analysed for *Tcp-1* gene expression. *T*<sup>Orl</sup>/*Tcp-1*<sup>a</sup> mice express both p63/6.9b and p63/6.9a. This indicates that the *T*<sup>Orl</sup> deletion does not cover the *Tcp-1* gene. However, *T*<sup>Orl</sup>/*Tcp-1*<sup>b</sup> mice also express both p63/6.9b and p63/6.9a. These data imply that the *T*<sup>Orl</sup> chromosome, far from containing a deletion of *Tcp-1*, actually possesses both the *Tcp-1*<sup>b</sup> and *Tcp-1*<sup>a</sup> alleles. Further analysis of this chromosome is in progress.

The *Tcp-1* gene codes for a major cell surface-associated protein, p63/6.9. Two structural alleles of this gene have been

**Fig. 2** *A*, Complete two-dimensional fluorograph of Nonidet P40-soluble proteins from *T*<sup>c</sup>/*t*<sup>w73</sup> testicular cells. *b*, p63/6.9b; *a*, p63/6.9a. The basic side of the gel is on the left. *B-E*, The p63/6.9 regions of fluorographs are shown for the following genotypes: *B*, *T*<sup>Wis</sup>/+; *C*, *T*<sup>Wis</sup>/*t*<sup>w73</sup>; *D*, *T*<sup>OR4</sup>/+; *E*, *T*<sup>OR4</sup>/*t*<sup>w18</sup>. Testicular cells were isolated essentially as described by Romrell *et al.*<sup>12</sup> as modified by Silver *et al.*<sup>4</sup>. Cells were labelled in medium containing 200–250  $\mu$ Ci ml<sup>-1</sup> <sup>35</sup>S-methionine, for 4–5 h at 34 °C. Cells were washed and lysed at a concentration of 10<sup>7</sup> cells ml<sup>-1</sup> with phosphate-buffered saline containing 1% Nonidet P40, 2 mM methionine and 1 mM phenylmethylsulphonyl-fluoride. Nonidet P40-soluble proteins were obtained after centrifugation at 15,000g at 4 °C for 60 min and were stored at -80 °C. Proteins were separated according to the procedure described by O'Farrell and O'Farrell<sup>13</sup> as modified by Silver *et al.*<sup>4</sup>.





**Table 1** Origin of the various *T* mutations

| <i>T</i> Mutation                                    | Origin                               | Ref.                             |
|--|--------------------------------------|----------------------------------|
| <i>T</i> <i>Brachyury</i>                            | Spontaneous in laboratory stock      | 7                                |
| <i>T<sup>hp</sup></i> <i>T<sup>hairpin</sup></i>     | Spontaneous in an AKR mouse          | 8                                |
| <i>T<sup>Orl</sup></i> <i>T<sup>Orleans</sup></i>    | Spontaneous in a Swiss/Orleans mouse | 9                                |
| <i>T<sup>Wis</sup></i> <i>T<sup>Wisconsin</sup></i>  | Spontaneous in laboratory stock      | Moutier (personal communication) |
| <i>T<sup>J</sup></i> <i>T<sup>Jackson</sup></i>      | Spontaneous in a BALB/CHU mouse      | D.B. (unpublished data)          |
| <i>T<sup>c</sup></i> <i>T<sup>curtailed</sup></i>    | Radiation induced                    | Hummel (personal communication)  |
| <i>T<sup>OR4</sup></i> <i>T<sup>Oak Ridge4</sup></i> | Radiation induced                    | 10                               |
|  |                                      | 11                               |

identified. All wild-type chromosomes carry *Tcp-1<sup>b</sup>* whereas all naturally occurring *t* haplotypes carry *Tcp-1<sup>a</sup>*. As *Tcp-1<sup>a</sup>* and the *t<sup>T</sup>* allele of the *T* locus seemed to be completely correlated<sup>4</sup>, we sought to determine whether the *Tcp-1* gene and the locus of *T* were identical. Of seven independently derived *T*-locus mutations examined, six allowed expression of a form of p63/6.9 which seems to be identical to the wild-type p63/6.9. The seventh, *T<sup>hp</sup>*, acted as a null allele of *Tcp-1* (*Tcp-1<sup>a</sup>*).

At least 33% of all single base pair substitutions will result in an alteration in protein charge that can be readily detected by standard isoelectric focusing techniques<sup>6</sup>. If we take a conservative estimate, 66% of all single base pair substitutions go undetected (that is, those resulting in a neutral-to-neutral amino acid change). If we assume that the *Tcp-1* gene is at the locus of *T*, the probability that in six independent mutational events at *T* such a shift has occurred and that it remains undetected is (0.66)<sup>6</sup>. The probability of detecting at least one such shift is 1 - (0.66)<sup>6</sup> or 92%. Because, in fact, no shifts were detected, we can say with 92% probability that the *Tcp-1* gene is separate from the locus of *T*. This view is compatible with other genetic evidence. *T<sup>hp</sup>* is known to be a deletion covering at least the 3-centimorgan region between and inclusive of *T* and *qk* as well as the locus of *Tcp-1*. *T<sup>Orl</sup>* seems to be a deletion covering at least the same 3-centimorgan region, but *Tcp-1* is not within the deletion. Thus, the *Tcp-1* gene must be localized to the region of the *T<sup>hp</sup>* deletion either proximal to *T* or distal to *qk* and, therefore, cannot be equivalent to *T*. Previous results have demonstrated that the *Tcp-1* gene is separate from the loci of *qk*, *low*, *tf* and *t<sup>lethal</sup>* (see Fig. 1 and ref. 4).

We have demonstrated that the *Tcp-1* gene is separate from the locus of *T*; however, as *Tcp-1<sup>a</sup>* is completely correlated with the presence of *t<sup>T</sup>*, the possibility still exists that p63/6.9a is a product of *t<sup>T</sup>*. If this proves to be the case, then *T* and *t<sup>T</sup>* cannot, as previously assumed, be alleles at the same locus. Although *T* and *t<sup>T</sup>* are not separable by recombination, one must remember

that one of the effects of *t* haplotypes is the suppression of recombination along chromosome 17. *T* and *t<sup>T</sup>* interact in *trans* to produce taillessness, but it is possible that *trans* interactions can occur even between two interacting factors at separate loci. Until the precise relationship between *t<sup>T</sup>* and *Tcp-1* can be determined, one cannot comment on the validity of the assumption that *T* and *t<sup>T</sup>* are alleles at the same locus.

Although it is possible that the p63/6.9 protein may be associated with some other property of the *T/t* complex, such as segregation distortion or sterility, for which others had suggested factors existed<sup>5</sup>, our data do not fit the distribution of any known *T/t*-complex factor other than *t<sup>T</sup>*.

This work was supported in part by NCI core grant CA-08748, grants CA 21651 and HD 10668, and research contract EV04159. A.K.A. is a pre-doctoral fellow at the Sloan-Kettering Division of the Cornell Graduate School of Medical Sciences and received support from the American Cancer Society institutional grant IN-114. We thank Dr T. Alton for his help with the figures, and Drs H. Axelrod, P. McCormick and T. Alton for their critical reading of the manuscript.

Received 19 June; accepted 25 September 1980.

- Bennett, D. *Cell* **6**, 441-454 (1975).
- Klein, J. & Hammerberg, C. *Immun. Rev.* **33**, 70-104 (1977).
- Sherman, M. I. & Wudl, L. R. in *Concepts in Mammalian Embryogenesis* (ed. Sherman, M. I.) 136-234 (MIT Press, Massachusetts, 1977).
- Silver, L. M., Artzt, K. & Bennett, D. *Cell* **17**, 275-284 (1979).
- Lyon, M. F., Evan, E. P., Jarvis, S. E. & Sayers, I. *Nature* **279**, 38-42 (1979).
- Edwards, Y. & Swallow, D. *Nature* **272**, 309-310 (1978).
- Dobrovolskaia-Zavadskaja, N. C. *r. Séanc. Soc. Biol.* **97**, 114-116 (1927).
- Johnson, D. R. *Genetics* **76**, 795-805 (1974).
- Erickson, R. P., Lewis, S. E. & Slusser, K. S. *Nature* **274**, 163 (1978).
- Searle, A. G. *Genet. Res.* **7**, 86-95 (1966).
- Bennett, D. *et al. Genet. Res.* **26**, 95-108 (1975).
- Romrell, L. G., Bellve, A. R. & Fawcett, D. J. *Dev. Biol.* **49**, 119-131 (1976).
- O'Farrell, P. H. & O'Farrell, P. Z. *Meth. Cell Biol.* **16**, 407-420 (1977).

## Effect of striatal cells on *in vitro* maturation of mesencephalic dopaminergic neurones grown in serum-free conditions

Umberto di Porzio, Marie-Christine Daguet, Jacques Glowinski & Alain Prochiantz

INSERM U.114, Collège de France, 11 place Marcelin Berthelot, 75231 Paris Cedex 05, France

It is well documented that target cells can regulate the morphological and biochemical development of peripheral afferent neurones<sup>1,2</sup>, but little is known about the existence of such regulatory mechanisms in the central nervous system. We therefore investigated previously the influence of striatal target cells on the maturation *in vitro* of nigrostriatal dopaminergic neurones, which survive in culture for more than 5 weeks, develop dense arborizations and both take up <sup>3</sup>H-dopamine (DA) by a high-affinity specific process and synthesize <sup>3</sup>H-DA from <sup>3</sup>H-tyrosine<sup>3</sup>. Furthermore, depolarization by potassium or veratridine stimulates the release of DA through a calcium-dependent mechanism and tetrodotoxin prevents the veratridine-evoked release of the transmitter<sup>4</sup>. Both the number of <sup>3</sup>H-DA uptake sites and the capacity for <sup>3</sup>H-DA synthesis were at least doubled when the neurones were cultured with target cells from the striatum<sup>3</sup>. To determine whether glial cells which proliferate in serum-complemented medium are partly responsible for the maturation of dopaminergic neurones and/or for the effect of striatal cells, we have now repeated the experiment using serum-free medium in which virtually pure neuronal populations can be obtained<sup>5-7</sup>. The reduction in the number of glia did not affect either the maturation of dopaminergic cells alone, or the effect of striatal cells. Autoradiographic analysis of the number of dopaminergic cells strongly suggests that the stimulatory effect is related to increased capacities of <sup>3</sup>H-DA uptake and synthesis per dopaminergic neurone.

**Table 2** Summary of the p63/6.9 pattern of expression for the various *T<sup>s</sup>*

| Genotype                 | p63/6.9b | p63/6.9a |
|--------------------------|----------|----------|
| <i>T/+</i>               | +        | -        |
| <i>T/t</i>               | +        | +        |
| <i>T<sup>hp</sup>/+</i>  | +        | -        |
| <i>T<sup>hp</sup>/t</i>  | -        | +        |
| <i>T<sup>Wis</sup>/+</i> | +        | -        |
| <i>T<sup>Wis</sup>/t</i> | +        | +        |
| <i>T<sup>J</sup>/+</i>   | +        | -        |
| <i>T<sup>J</sup>/t</i>   | +        | +        |
| <i>T<sup>c</sup>/+</i>   | +        | -        |
| <i>T<sup>c</sup>/t</i>   | +        | +        |
| <i>T<sup>OR4</sup>/+</i> | +        | -        |
| <i>T<sup>OR4</sup>/t</i> | +        | +        |
| <i>T<sup>Orl</sup>/+</i> | +        | +        |
| <i>T<sup>Orl</sup>/t</i> | +        | +        |



**Table 1** Composition of various serum-free media and their effects on dopaminergic cell survival

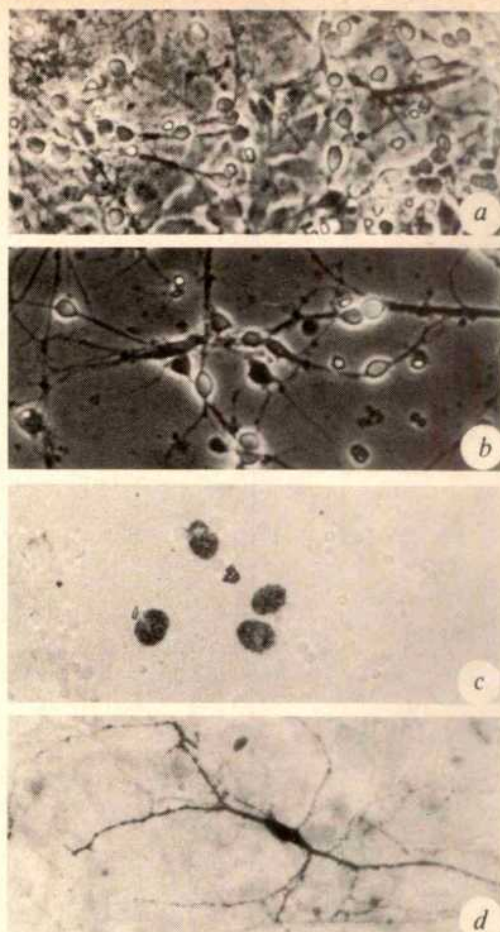
|                          | Medium 1 | Medium 2 | Medium 3 |
|--------------------------|----------|----------|----------|
| Basal medium             | —        | +        | —        |
| Proteins, hormones, salt | +        | +        | +        |
| Conditioned medium       | +        | —        | +        |
| Survival time            | ≥14 days | ≤10 days | ≥14 days |

In all cases, cells were grown on non-irradiated collagen plus polyornithine as substrate. Basal medium was as described in Fig. 1a legend; proteins, hormones, salt refer to transferrin, insulin, progesterone, putrescine, selenium salt (see text for concentrations); conditioned medium 1 was basal medium incubated for 48 h with cells (fibroblasts or total brain cells) previously grown with a serum-complemented medium for 1–4 weeks; conditioned medium 3 was medium obtained after 8 days from total brain cells directly plated and grown with medium 2.

Preliminary experiments indicated that the use of non-irradiated collagen markedly reduced the overall population of glial cells when mesencephalic cells of 13-day-old mouse embryos were cultured with serum. Furthermore, autoradiography of the cultures (Fig. 1c) after a 48-h pulse of  $^3\text{H}$ -thymidine (during days 3–5) revealed that the number of labelled cells with large nuclei (presumptive astrocytes<sup>8</sup>) was only 2.3% ( $742 \pm 109$ ,  $n = 3$ ) of that found in cultures grown on UV-irradiated collagen plus polyornithine ( $31,600 \pm 1,500$ ,  $n = 3$ ). To eliminate glial elements further, mesencephalic cells were dissociated in a serum-free medium and then plated on non-irradiated collagen plus polyornithine in a conditioned medium obtained by 48-h incubation of the serum-free medium with monolayers of primary cultures of embryonic cells from whole mouse brain or of fibroblasts previously grown with serum. Thereafter, this conditioned medium was supplemented with  $100 \mu\text{g ml}^{-1}$  transferrin (Sigma),  $25 \mu\text{g ml}^{-1}$  insulin (Sigma),  $2 \times 10^{-8}$  M progesterone (Sigma),  $6 \times 10^{-5}$  M putrescine (Sigma) and  $3 \times 10^{-8}$  M selenium salt (Merck), and filtered (Millex; Millipore). In this medium (medium 1), the number of labelled glial cells (estimated as above) was only 0.06% ( $20 \pm 14$ ,  $n = 3$ ) of that found with serum using UV-irradiated collagen plus polyornithine (Fig. 1a, b). In medium 1, despite the virtual absence of glial cells, the overall neuronal population survived for 2–4 weeks according to the experiments (Table 1). The incubation of mesencephalic cells with exogenous  $^3\text{H}$ -DA allowed the autoradiographic visualization of dopaminergic neurones, which exhibit numerous varicose fibres (Fig. 1d). As illustrated by Table 2, the capacities of  $^3\text{H}$ -DA uptake and of  $^3\text{H}$ -DA synthesis from  $^3\text{H}$ -tyrosine increased with time in culture (up to 15 days at least). Medium 1 is thus preferable to the serum-complemented medium used in our previous study because in the latter case  $^3\text{H}$ -DA uptake and synthesis did not increase between days 8 and 15 in mesencephalic cultures. However, as in the presence of serum<sup>3</sup>, the extent of  $^3\text{H}$ -DA uptake or synthesis in mesencephalic cultures grown with medium 1 varied between experiments; this did not seem to be related to the cell type used to condition the medium.

When mesencephalic cells were cultured in medium 1 in the presence of striatal target cells from 15-day-old embryos (co-cultures), the glial cell population was still negligible ( $26.5 \pm 2$ ,  $n = 3$ ). Nevertheless, as revealed by the enhanced capacities of  $^3\text{H}$ -DA uptake and synthesis in co-cultures, the striatal cells stimulated the maturation of the mesencephalic dopaminergic neurones (Table 2). These stimulatory effects varied (1.5–3 times) between experiments but were always significant, at both 8 and 15 days. These effects cannot be attributed to the higher cell concentration used in co-cultures ( $2.5 \times 10^6$  cells per dish) because  $^3\text{H}$ -DA uptake in mesencephalic cultures alone is directly proportional to the number of cells plated (between  $1 \times 10^6$  and  $3.5 \times 10^6$  cells, results not shown).

Complementary experiments were carried out to determine whether the development of the dopaminergic neurones and their enhanced maturation in the presence of striatal cells were dependent on the occurrence in medium 1 (Table 1) of



**Fig. 1** a, Thirteen-day-old mouse embryonic mesencephalic cells were dissociated in a mixture of minimum essential medium and nutrient mixture F-L2 (both Gibco, 1:1) complemented with  $3.3 \times 10^{-2}$  M glucose,  $2 \times 10^{-3}$  M glutamine and  $0.3 \times 10^{-2}$  M sodium bicarbonate without serum (basal medium). Cells ( $1.5 \times 10^6$  per dish) were then plated on UV-irradiated collagen plus polyornithine and grown in basal medium plus 7.5% fetal calf serum (Irvine Scientific) as previously described<sup>1</sup>. Arabinosylcytosine ( $10^{-5}$  M, Sigma) was added at day 5, the medium (2 ml) was replaced at day 7 and thereafter weekly. The extensive development of both neurones and glial cells at day 5 can be seen.  $\times 187$ . b, Mesencephalic cells were dissociated as above, plated on non-irradiated collagen plus polyornithine and grown in 1 ml of medium 1 (a serum-free, conditioned medium prepared as described in the text); cells were not exposed to arabinosylcytosine and the medium was not renewed. In these conditions, in contrast to that observed in a, the development of glial cells was impaired. The development of neurones in the virtual absence of glial cells at day 5 is seen.  $\times 187$ . c, Visualization by autoradiography at day 5 of glial cell nuclei labelled by incubating mesencephalic cells for 48 h between days 3 and 5 with  $9 \times 10^{-7}$  M  $^3\text{H}$ -thymidine ( $28 \text{ Ci mmol}^{-1}$ , CEA) added to the culture medium.  $\times 180$ . After three washes with cold phosphate-buffered saline (PBS), the cells were fixed for 1 h at  $4^\circ\text{C}$  with 2.5% glutaraldehyde (Taab Laboratories) in PBS, rinsed four times with cold PBS, air dried and covered with Ilford K5 emulsion. Autoradiograms were developed 1 week later using Kodak Dektol. d, Visualization of labelled dopaminergic neurones at day 8 by autoradiography.  $\times 183$ . Cells were incubated at  $37^\circ\text{C}$  for 1 h with  $5 \times 10^{-7}$  M  $^3\text{H}$ -DA ( $9.9 \text{ Ci mmol}^{-1}$ , NEN) in 1 ml PBS complemented with  $10^{-3}$  M magnesium,  $10^{-3}$  M calcium and  $3.3 \times 10^{-2}$  M glucose. Cells were then washed and processed for autoradiography as described in c. No labelling was seen when the incubation was carried out at  $0^\circ\text{C}$ . Incubation at  $37^\circ\text{C}$  in the presence of  $5 \times 10^{-6}$  M desmethyl-imipramine (Geigy) or  $10^{-6}$  M fluoxetine (Lilly), drugs known to inhibit  $^3\text{H}$ -DA uptake into noradrenergic and serotonergic neurones respectively, did not modify the number of labelled cell bodies. This number was reduced to 5% of control values when the incubation was performed in the presence of  $5 \times 10^{-6}$  M benztropine (Merck), a potent inhibitor of  $^3\text{H}$ -DA uptake into dopaminergic nerve cells.



substances of cellular origin or of contaminating serum components released into the medium during the 48-h conditioning period. Mesencephalic cell cultures or co-cultures with striatal cells were thus directly plated in medium 2, which consisted of a non-conditioned serum-free basal medium supplemented with hormones, proteins and salts as above (Table 1). In this medium, the development of glial cells was equally impaired ( $8.5 \pm 3.5$ ,  $15 \pm 4.2$ ,  $n = 3$ ,  $^3\text{H}$ -thymidine-labelled cells in cultures and co-cultures, respectively). The dopaminergic neurones could be characterized as in medium 1 by autoradiography and by the estimated capacities for  $^3\text{H}$ -DA uptake and synthesis. However,  $^3\text{H}$ -DA uptake was lower than that observed with medium 1 and the survival of the mesencephalic neurones never exceeded 10 days. Nevertheless, the stimulatory effect of the striatal target cells on  $^3\text{H}$ -DA uptake and synthesis was present at 8 days, as observed with medium 1 (Table 2). From these results we conclude that the use of a conditioned medium containing traces of serum components is not required for the influence of target striatal cells on dopaminergic neurones, although it favours their overall development.

A possible role of serum contaminants in the improved survival of cultures and co-cultures in medium 1 over that in medium 2 was excluded by studies with a third type of conditioned medium. Dissociated cells from the whole brain of 15-day-old mouse embryos were directly plated in the serum-free medium 2 and grown for 8 days. The medium was then removed, filtered, further complemented with proteins, hormones and salts (as described for media 1 and 2) and used as conditioned medium (medium 3, Table 1). Results comparable with those reported for experiments performed with medium 1 were obtained: absence of glial cells, satisfactory development of the neuronal populations including the dopaminergic neurones, which survived for 2 weeks at least, and facilitated maturation of the dopaminergic neurones in the presence of striatal cells, as revealed by measurement of  $^3\text{H}$ -DA uptake at 8

and 15 days (Table 2). Thus, substances of cellular origin are apparently responsible for the longer survival of neurones in medium 1. Furthermore, these substances could originate from neurones because medium 3 was prepared in conditions impairing the development of glial cells.

**Table 3** Mean value of  $^3\text{H}$ -dopamine uptake per dopaminergic cell at 8 days in medium 1

|                 | -STR            | +STR              |
|-----------------|-----------------|-------------------|
| Expt 1          |                 |                   |
| Uptake          | $6,143 \pm 924$ | $9,555 \pm 661^*$ |
| Cell number     | $1,556 \pm 574$ | $1,495 \pm 276$   |
| Uptake per cell | 3.9             | 6.4               |
| Expt 2          |                 |                   |
| Uptake          | $6,207 \pm 523$ | $9,134 \pm 561^*$ |
| Cell number     | $1,880 \pm 416$ | $1,207 \pm 118$   |
| Uptake per cell | 3.3             | 7.7               |

$^3\text{H}$ -dopamine uptake in cultures (-STR) and co-cultures (+STR) was estimated as described in Table 2 legend (mean of four determinations). Sister cultures and co-cultures were used to count the number of labelled dopaminergic cell bodies after autoradiography as described in Fig. 1d legend. Results are the mean  $\pm$  s.e.m. of triplicates.  $^3\text{H}$ -DA uptake per cell is expressed as c.p.m. per cell.

\* Difference between values obtained with cultures and co-cultures is significant ( $P < 0.05$ ).

Due to the marked reduction of the glial cell population in the various experimental conditions used, it is unlikely that glial cells contribute to the stimulatory effect of striatal cells on the development of mesencephalic dopaminergic neurones. However, it is just possible that a minor population of striatal glial cells distinct from those evaluated by  $^3\text{H}$ -thymidine incorporation is still present and thus involved in the phenomenon observed.

To determine whether the stimulatory effect of striatal neurones on  $^3\text{H}$ -DA uptake and synthesis is related to a better survival or to an increased maturation of individual dopaminergic cells, the numbers of neurones labelled with  $^3\text{H}$ -DA in cultures and co-cultures were estimated on autoradiograms. The effects of various inhibitors of amine uptake in aminergic neurones on the number of labelled cells indicated that the neurones labelled in these conditions corresponded to dopaminergic cells (Fig. 1d legend). By counting all labelled dopaminergic cell bodies, analysis of several experiments carried out with medium 1 indicated that after 8 days in culture, the total number of dopaminergic cells was not modified by the presence of striatal cells (Table 3). Similar observations were made with media 2 and 3 (data not shown). These results suggest an increased development of individual dopaminergic neurones in co-cultures and confirm previous estimations made after histochemical visualization of dopaminergic neurones grown in serum-complemented medium<sup>3</sup>.

Autoradiograms also revealed that some dopaminergic neurones were more intensely labelled than others. This may be related to the presence in the cultures of subpopulations of dopaminergic cells involved in the formation of the various ascending dopaminergic pathways. It is not known whether these subpopulations of mesencephalic dopaminergic cells respond in a similar way to the influence of striatal neurones.

We draw three main conclusions from our study: (1) the mesencephalic dopaminergic neurones could develop when cultured in serum-free medium (conditioned or not), which markedly impaired the proliferation of glial cells; (2) the dopaminergic neurones survived for a longer time when the synthetic medium was conditioned in the presence of different cell types, indicating that diffusible cellular products are required for long-term survival; (3) in the virtual absence of glial elements the striatal cells exerted a stimulatory effect on the

**Table 2** Influence of striatal cells on  $^3\text{H}$ -DA uptake or synthesis in mesencephalic cells grown in various serum-free media

|                                      | 8 Days            |                      | 15 Days           |                      |
|--------------------------------------|-------------------|----------------------|-------------------|----------------------|
|                                      | -STR              | +STR                 | -STR              | +STR                 |
| Medium 1: $^3\text{H}$ -DA uptake    |                   |                      |                   |                      |
| Expt 1:                              | $5,882 \pm 204$   | $8,234 \pm 980^*$    | $8,100 \pm 904$   | $17,820 \pm 1,390^*$ |
| 2:                                   | $6,207 \pm 523$   | $9,134 \pm 561^*$    | $9,194 \pm 1,935$ | $22,112 \pm 2,002^*$ |
| 3:                                   | $4,449 \pm 1,021$ | $13,436 \pm 2,231^*$ | ND                | ND                   |
| Medium 2: $^3\text{H}$ -DA uptake    |                   |                      |                   |                      |
| Expt 1:                              | $2,147 \pm 641$   | $5,920 \pm 135^*$    | —                 | —                    |
| 2:                                   | $1,422 \pm 144$   | $2,573 \pm 368^*$    | —                 | —                    |
| Medium 3: $^3\text{H}$ -DA uptake    |                   |                      |                   |                      |
| Expt 1:                              | ND                | ND                   | $3,119 \pm 941$   | $8,206 \pm 646^*$    |
| 2:                                   | $2,286 \pm 192$   | $3,372 \pm 104^*$    | $1,666 \pm 484$   | $3,620 \pm 421^*$    |
| Medium 1: $^3\text{H}$ -DA synthesis |                   |                      |                   |                      |
| Expt 1:                              | $375 \pm 72$      | $621 \pm 55^*$       | $1,359 \pm 58$    | $2,605 \pm 288^*$    |
| 2:                                   | $1,673 \pm 210$   | $2,773 \pm 313^*$    | $3,198 \pm 730$   | $6,235 \pm 413^*$    |
| 3:                                   | $497 \pm 163$     | $1,467 \pm 103^*$    | ND                | ND                   |
| Medium 2: $^3\text{H}$ -DA synthesis |                   |                      |                   |                      |
| Expt 1:                              | $510 \pm 55$      | $846 \pm 98^*$       | —                 | —                    |

Mesencephalic (13-day-old) and striatal (15-day-old) mouse embryonic cells were dissociated in basal medium as described in Fig. 1a legend, plated on non-irradiated collagen plus polyornithine and grown in 1 ml of medium 1, 2 or 3 (see Table 1 and text). Cultures (-STR) were obtained by plating  $1.5 \times 10^6$  mesencephalic cells per dish;  $1.5 \times 10^6$  mesencephalic cells and  $1 \times 10^6$  striatal cells per dish were used in co-cultures (+STR). In several experiments  $^3\text{H}$ -DA uptake or synthesis was estimated in 8- and/or 15-day-old cultures and co-cultures. Cells were incubated with  $5 \times 10^{-8}$  M  $^3\text{H}$ -DA ( $9.9 \text{ Ci mmol}^{-1}$ ) for 15 min or with  $1.5 \times 10^{-6}$  M  $^3\text{H}$ -tyrosine ( $52.5 \text{ Ci mmol}^{-1}$ , NEN) for 1 h at  $37^\circ\text{C}$  and then treated as described previously<sup>3</sup> to measure their  $^3\text{H}$ -DA content. Results expressed in c.p.m. are the mean  $\pm$  s.e.m. of four determinations, the yield of the counter for tritium being 40%. ND, not determined.

\* The difference between values obtained with cultures and co-cultures is significant using the Student's *t*-test ( $P < 0.05$ ).

maturation of individual dopaminergic neurones whatever the serum-free medium used (conditioned or not). Therefore, serum-free media should facilitate the characterization of the molecules and of the neuronal interactions that intervene in the survival of mesencephalic dopaminergic neurones and in their enhanced maturation in the presence of striatal target cells.

This study was supported by INSERM grant ATP 81.79.113.

Received 26 June; accepted 26 September 1980.

1. Black, I. B. A. *Rev. Neurosci.* **1**, 183–214 (1978).
2. Patterson, P. H. A. *Rev. Neurosci.* **1**, 1–17 (1978).
3. Prochiantz, A., di Porzio, U., Kato, A., Berger, B. & Glowinski, J. *Proc. natn. Acad. Sci. U.S.A.* **76**, 5387–5391 (1979).
4. Daguet, M. C., di Porzio, U., Prochiantz, A., Kato, A. & Glowinski, J. *Brain Res.* **191**, 564–568 (1980).
5. Barnes, D. & Sato, G. *Analyt. Biochem.* **102**, 255–302 (1980).
6. Bottenstein, J. E., Skaper, S. D., Varon, S. S. & Sato, G. H. *Expl Cell Res.* **125**, 183–190 (1980).
7. Faivre-Bauman, A., Rosenbaum, E., Puymirat, J., Grouselle, D. & Tixier-Vidal, A. *Dev. Neurosci.* (in the press).
8. Labourette, G., Roussel, G., Ghandour, N. S. & Nussbaum, J. L. *Brain Res.* **179**, 199–203 (1979).

## The obligatory role of endothelial cells in the relaxation of arterial smooth muscle by acetylcholine

Robert F. Furchgott & John V. Zawadzki

Department of Pharmacology, State University of New York  
Downstate Medical Center, Brooklyn, New York 11203

Despite its very potent vasodilating action *in vivo*, acetylcholine (ACh) does not always produce relaxation of isolated preparations of blood vessels *in vitro*. For example, in the helical strip of the rabbit descending thoracic aorta, the only reported response to ACh has been graded contractions, occurring at concentrations above 0.1  $\mu$ M and mediated by muscarinic receptors<sup>1,2</sup>. Recently, we observed that in a ring preparation from the rabbit thoracic aorta, ACh produced marked relaxation at concentrations lower than those required to produce contraction<sup>3,4</sup> (confirming an earlier report by Jelliffe<sup>5</sup>). In investigating this apparent discrepancy, we discovered that the loss of relaxation by ACh in the case of the strip was the result of unintentional rubbing of its intimal surface against foreign surfaces during its preparation. If care was taken to avoid rubbing of the intimal surface during preparation, the tissue, whether ring, transverse strip or helical strip, always exhibited relaxation to ACh, and the possibility was considered that rubbing of the intimal surface had removed endothelial cells<sup>4</sup>. We demonstrate here that relaxation of isolated preparations of rabbit thoracic aorta and other blood vessels by ACh requires the presence of endothelial cells, and that ACh, acting on muscarinic receptors of these cells, stimulates release of a substance(s) that causes relaxation of the vascular smooth muscle. We propose that this may be one of the principal mechanisms for ACh-induced vasodilation *in vivo*. Preliminary reports on some aspects of the work have been reported elsewhere<sup>4,6</sup>.

Descending thoracic aortas were excised from white, male, New Zealand rabbits (2–3 kg), and trimmed free of adhering fat and connective tissue as previously described<sup>2</sup>. Transverse rings of 2.5-mm width were cut with scissors or with a special cutting device containing five parallel razor blades. A transverse strip was made by cutting across a ring. Strips and rings were mounted for isometric recording of tension in oxygenated Krebs–bicarbonate solution. Throughout the preparation and mounting of rings and transverse strips, the tissue was kept wet with Krebs solution, and special care was taken to avoid unintentional rubbing of the intimal surface against a foreign surface or itself.

Figure 1a, b shows typical records illustrating both the concentration-dependent relaxation by ACh of a ring and a transverse strip of aorta precontracted with noradrenaline (NA), and the loss of the relaxing response after rubbing of the intimal surface of each preparation. If care was taken not to over-stretch the preparation during the rubbing and to allow sufficient re-equilibration time (30–60 min) after the rubbing, the procedure did not lead to any loss of sensitivity to contracting agents; indeed, apparent sensitivity to ACh as a contracting agent is increased. Rubbing also had no effect on the sensitivity of aortic preparations to a variety of nonmuscarinic relaxing agents, including glyceryl trinitrate, sodium nitrite, sodium azide, adenosine, adenylic acid and isoprenaline, or to photorelaxation<sup>7</sup>.

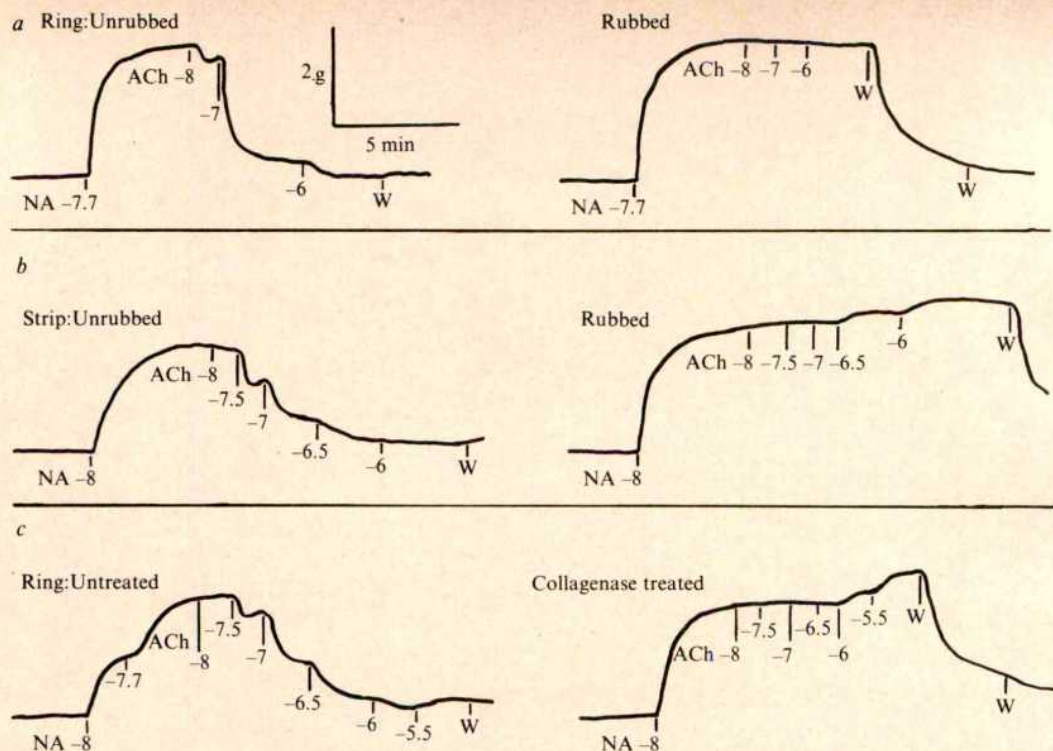
The relaxation at lower concentrations of ACh, like the contraction at higher concentrations<sup>1,2</sup>, was highly sensitive to blockade by atropine. From the ratio of ACh concentrations giving equal relaxation with and without atropine (10  $\mu$ M, 30 min), the dissociation constant ( $K_B$ ) of the atropine–receptor complex was estimated to be  $0.35 \pm 0.04$  nM ( $n = 14$ ). This  $K_B$  value and the relative potencies of ACh, methacholine and carbachol (about 1, 0.3 and 0.1, respectively) in eliciting relaxation indicate that the receptor involved is of the muscarinic type. Physostigmine (0.3  $\mu$ M) did not significantly increase the sensitivity to ACh.

The range of concentration over which ACh produced graded relaxation in aortic preparations precontracted with NA was usually 0.01–1  $\mu$ M (Fig. 1). Occasionally, in preparations with higher than usual sensitivity to the contracting action of ACh, contraction would begin to supercede relaxation at 1  $\mu$ M. Half-maximal relaxation usually occurred between 0.03 and 0.10  $\mu$ M. Prolonged exposure to a fixed concentration of ACh usually resulted in some 'fade' of its relaxing effect. The degree of relaxation elicited by addition of a fixed concentration of ACh tended to decrease as the level of initial tonic contraction (tone) was increased.

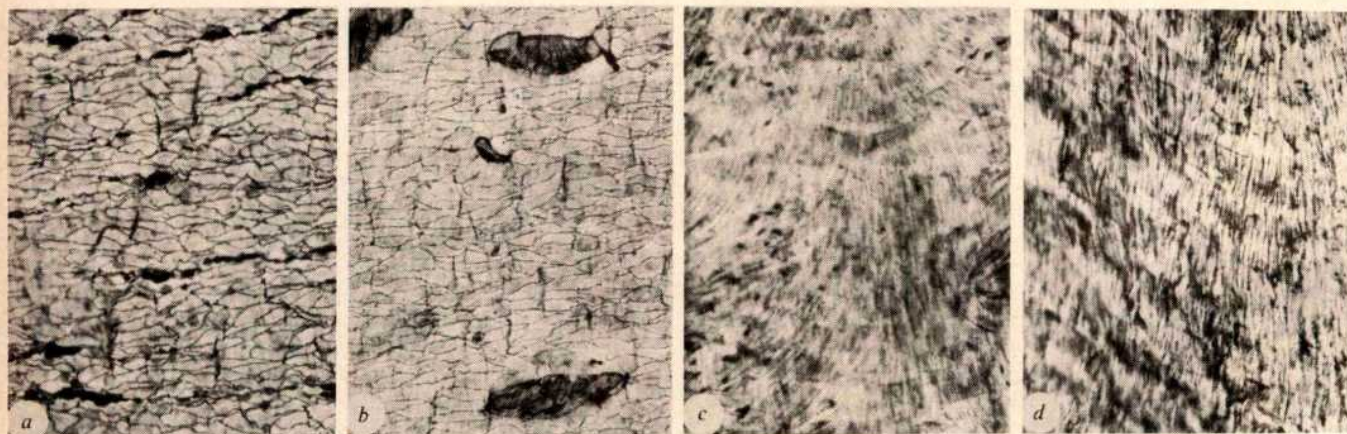
ACh was about equally effective in relaxing contractions of the same magnitude produced by NA, histamine, serotonin, angiotensin or prostaglandin  $F_{2\alpha}$ . However, moderate to high contractions produced by increasing  $K^+$  in the Krebs solution (by adding 12–18 mM KCl) were less sensitive to ACh, showing maximal relaxation 10–50% of that of comparable NA-induced contractions. In two experiments in which the Krebs solution bathing the aortic rings was replaced by a ' $K_2SO_4$ –Krebs solution' (NaCl and  $NaHCO_3$  of the regular solution substituted for by equimolar concentrations of  $K_2SO_4$  and  $KHCO_3$ , respectively), the contractions obtained, which were ~75% of maximal NA-contractions, were relaxed about 20% by 1  $\mu$ M ACh. As the  $K_2SO_4$ –Krebs solution should completely depolarize all cells of the preparations, relaxation by ACh can apparently occur independently of membrane potential changes of the smooth muscle cells.

The fact that rubbing of the intimal surface, but not the adventitial surface, removed the capacity of aortic preparations to relax in response to ACh strongly suggested that the endothelial cells were necessary for the relaxation and that they were removed by the rubbing. To investigate this possibility, the intimal surfaces of variously treated preparations were examined microscopically *en face* after application of a silver staining procedure<sup>8</sup> which delineates endothelial cell borders, and also stains the subendothelial layer in areas where endothelial cells have been lost. Some typical photomicrographs are shown in Fig. 2. Unrubbed preparations in which ACh produced 80–100% relaxation of moderate tone had usually retained 60–75% of the endothelial cells by the end of an experiment. In 'inadequately' rubbed preparations it was not unusual to observe about 20% relaxation of moderate tone when only a few per cent of the endothelial cells were retained. When rubbing resulted in the complete loss of the relaxing response to ACh, there was always virtually a complete loss of endothelial cells. Thus, the staining procedure clearly showed that endothelial cells were required for relaxation by ACh. Preparations were



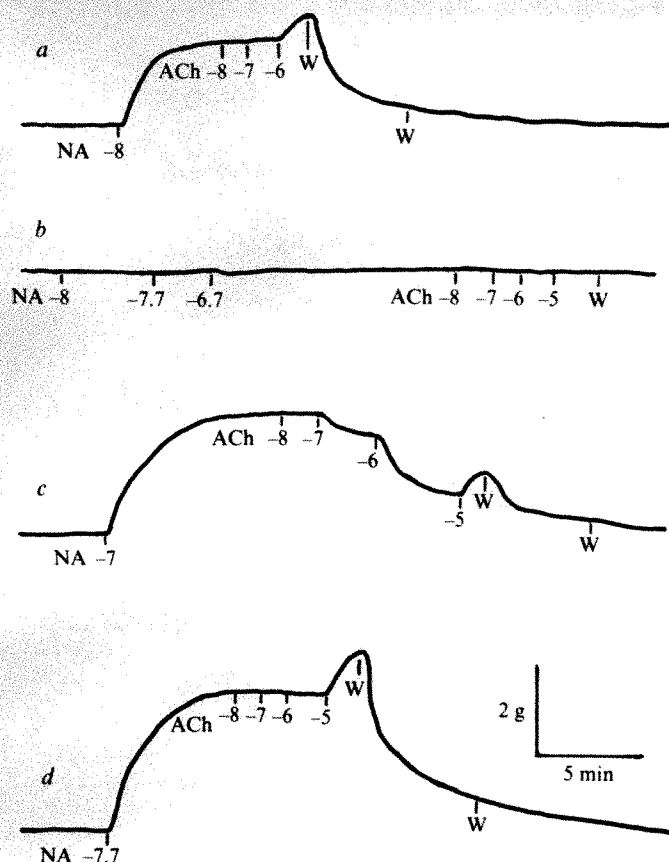


**Fig. 1** Loss of relaxing response of preparations of rabbit aorta to ACh after rubbing of the intimal surface or exposure to collagenase. Rings and transverse strips were mounted in all-glass 20-ml muscle chambers at 37 °C. The bathing fluid was Krebs solution of the following composition (mM): NaCl 118, KCl 4.8, CaCl<sub>2</sub> 2.5, MgSO<sub>4</sub> 1.2, KH<sub>2</sub>PO<sub>4</sub> 1.2, NaHCO<sub>3</sub> 24, glucose 11 and Na<sub>2</sub>-EDTA 0.03. It was continuously gassed with 95% O<sub>2</sub>-5% CO<sub>2</sub>. Two hooks of stainless steel wire (0.6-mm diameter), bent in a modified L-shape, were used to mount each ring. The short straight portion of each hook passed through the lumen of the ring. The lower hook was attached to the base of the muscle chamber, the upper to a strain gauge. For mounting each strip, two small lucite clips with jaws under spring tension were used. Hooks connected the lower clip to the base of the muscle chamber, and the upper clip to a strain gauge. All preparations were first equilibrated for at least 2 h, and basal tension was set to 2 g before drug additions. The records show the point at which each drug addition was made, and the corresponding cumulative concentration of the drug in the chamber after the addition, expressed as the log of the molar concentration. NA indicates noradrenaline; W indicates washout of the chamber. *a*, Recordings from the same ring before and after rubbing of its intimal surface. After the record on the left had been obtained, the ring was removed from the chamber on its mounting hooks. While it was kept under tension and moist with Krebs solution, its intimal surface was gently rubbed for 1 min with a small, wooden applicator stick that had been shaved down to permit easy insertion through the lumen. The ring was then resuspended in the muscle chamber and retested about 30 min later. A matched ring that was rubbed for the same time on its adventitial surface exhibited no loss of its capacity for relaxation by ACh (not shown). *b*, Simultaneous recordings from an unrubbed (left) and rubbed (right) transverse strip from the same aorta. Before being placed in clips for mounting, the latter strip had been dragged slowly for 1 min with intimal surface down, over a sheet of filter paper wetted with Krebs solution. A third strip, that had been similarly dragged with adventitial surface down, exhibited no loss of relaxation capacity (not shown). *c*, Simultaneous recordings from rings made from the same aorta before and after exposure of the intimal surface to a solution of collagenase, similar to that used by Jaffe *et al.*<sup>9</sup>, and containing 0.2% of the CLS-type enzyme preparation (Worthington) in a phosphate-buffered saline solution (PBS). The control ring (left) was cut first and incubated for 25 min in PBS alone at 37 °C. The remaining segment of aorta was cannulated at its upper end and closed with a clip at its lower end. It was then filled with collagenase solution and immediately immersed in PBS at 37 °C. After the desired exposure time, a ring was cut from near the lower end of the segment. The record on the right is for a ring whose intimal surface had been exposed to the collagenase solution at 37 °C for 15 min. Similar results were obtained in three other experiments. Rings whose intimal surfaces had been exposed for only 7 min showed about a 50% reduction in maximal relaxing response to ACh (not shown). A 15-min exposure to collagenase did not interfere with contraction elicited by high concentrations of ACh nor with relaxation by other agents such as isoprenaline, sodium nitrate and 5'-AMP.



**Fig. 2** Photomicrographs of the intimal surface of aortic preparations after various treatments. A preparation, cut open in strip form, was laid adventitia-side down on a small piece of paper towel, to which it adhered well during exposure to each solution in the silver staining procedure. The procedure was that of Poole *et al.*<sup>8</sup>, with the modification that the blood vessel preparation moved about in each solution for the recommended time, while on the paper-towel backing. After final fixation in 5% formalin, the preparation could be examined microscopically *en face* in the wet state, or it could be dehydrated and imbedded in a permanent mount. The photomicrographs here are of preparations after imbedding. Magnification is  $\times 218$ . *a*, Strip that was stained immediately after being cut from freshly excised and trimmed aorta. Almost all the intimal surface was covered by endothelial cells. *b*, Strip made from an unrubbed ring at the end of an experiment on drug testing. During the experiment ACh at  $10^{-6}$  M relaxed moderate NA-induced tone in this ring by about 95%. Only about 70% of the intimal surface (excluding those parts that had been apposed to the surface of the metal mounting hooks) was covered by endothelial cells. It was rare to find more than 80% retention of endothelial cells in unrubbed preparations examined at the end of an experiment. *c*, Strip that had had its intimal surface rubbed on filter paper for 1 min before being used in an experiment in which it gave no relaxation in response to ACh (similar to Fig. 1*b*). The surface was devoid of endothelial cells. *d*, Strip made from a ring from a segment of aorta that had been exposed intraluminally to 0.2% collagenase for 15 min at 37 °C. During the experiment the ring gave no relaxation in response to ACh (similar to Fig. 1*c*). No endothelial cells were left on the intimal surface.





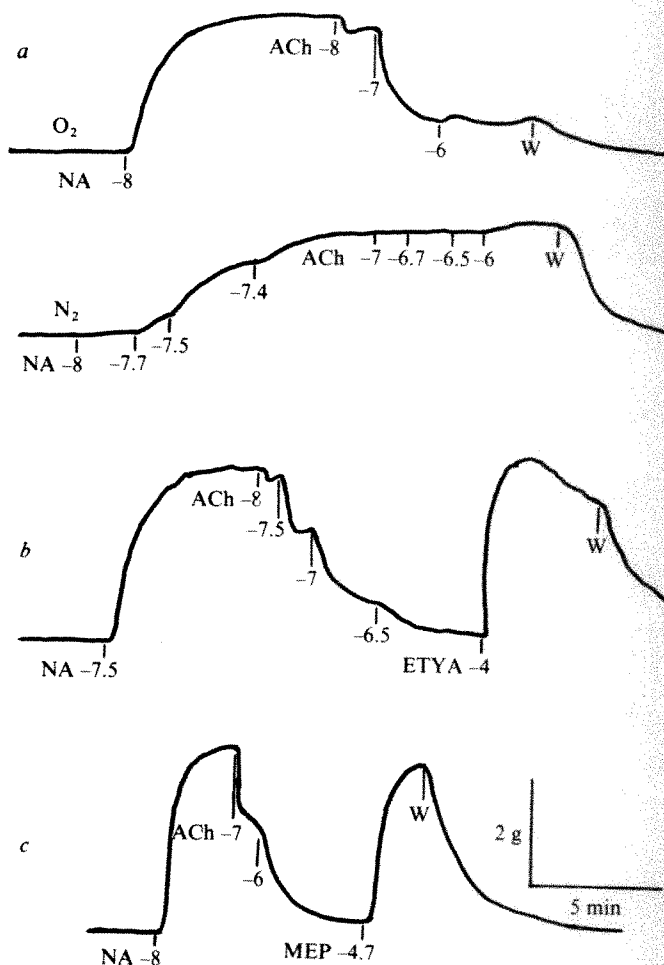
**Fig. 3** Demonstration of release of a relaxing substance (or substances) from endothelial cells by ACh. Rings of uniform width (2.5 mm) were cut from a segment of descending thoracic aorta, and then cut across to yield transverse strips. Before the strips were mounted in muscle chambers, the intimal surfaces of three of them were rubbed on filter paper (as in Fig. 2b) to remove their endothelial cells. A second segment of aorta was incubated without tension in Krebs solution at 37 °C, and from it longitudinal strips (strips running parallel to the long axis) were cut as needed in the same dimensions as the transverse strips. Initially, all strips mounted for recording were mounted singly with plastic clips. Later, certain pairs of strips were mounted together in sandwich form, with their entire intimal surfaces apposed. *a*, NA and ACh on a transverse strip with endothelium removed. ACh did not relax NA-induced tone, and evoked additional contraction at  $1 \mu\text{M}$ . *b*, NA and ACh on a longitudinal strip with endothelium present. Only trivial changes in tension were exerted on the transducer (because of the orientation of the smooth muscle cells). *c*, NA and ACh on a sandwich made from the transverse strip without endothelium (same strip as in *a*) and a longitudinal strip with endothelium. The latter strip was cut from the incubated but unmounted segment of aorta in a region adjacent to that from which the strip that gave record *b* was cut. The sandwich was allowed to equilibrate for about 30 min after mounting. Note the relaxation at  $10^{-7}$  and  $10^{-6}$  M ACh. This was relaxation of the transverse strip, as it was this strip in the sandwich that gave the recorded tension increase on addition of NA. *d*, Test of NA and ACh on the transverse strip without endothelium after removing the longitudinal strip with endothelium. As in *a*, it now again gave no relaxation in response to ACh. In this experiment relaxation by ACh was also demonstrated in a second transverse strip without endothelium only when it was mounted in a sandwich preparation with a longitudinal strip with endothelium. However, in a sandwich preparation made with a longitudinal strip that had also been freed of endothelium (by rubbing) and a transverse strip without endothelium, the latter failed to relax in response to ACh. The results in this experiment were replicated in four similar experiments.

also studied in which endothelial cells had been removed by exposing the intimal surface to commercial collagenase<sup>9</sup>. Figure 1c shows that a ring from a collagenase-treated segment failed to relax in response to ACh, and Fig. 2d shows that the intimal surface of such a ring was completely free of endothelial cells.

To explain the obligatory role of endothelial cells in the relaxation, it was postulated that ACh acting on a muscarinic receptor in these cells stimulates them to release a substance (or substances) which in turn acts on the smooth muscle cells in the media to activate relaxation. Direct evidence for this hypothesis

was obtained in experiments in which a regular transverse strip freed of endothelial cells was tested when mounted separately and also when mounted, intimal surface against intimal surface, with a longitudinal strip of the same width and length with endothelial cells present (Fig. 3). Because of the orientation of its muscle cells, the longitudinal strip could contribute only trivial increases in tension on the strain gauge during contraction. As shown in Fig. 3, ACh, which failed to relax contraction of the transverse strip mounted separately, gave good relaxation of contraction of the same strip when it was mounted as a 'sandwich' with the longitudinal strip.

Although we have not identified the released relaxing substance(s), we have ruled out bradykinin, prostacyclin, cyclic AMP and cyclic GMP (no relaxation or only slight relaxation of



**Fig. 4** Inhibition of the relaxing action of ACh by anoxia, ETYA and mepacrine (MEP). *a*, Response of an aortic ring to ACh under oxygen (upper record) and under anoxia (lower record). About 30 min before making the lower record, 95%  $\text{N}_2$ -5%  $\text{CO}_2$  was substituted for 95%  $\text{O}_2$ -5%  $\text{CO}_2$ , and was bubbled rapidly through the solution in the muscle chamber. To minimize the chance of significant traces of  $\text{O}_2$  from air getting into the solution, the top of the chamber was covered with a plastic cap containing only two small holes, one for passage of the thread to the transducer and the other for introduction of needles of Hamilton syringes in adding drugs. In this and three similar experiments, the relaxing response to ACh was completely lost under anoxia. It was completely restored on return of the preparation to  $\text{O}_2$  (not shown). *b*, Acute inhibition by ETYA of ACh-induced relaxation. The ETYA was added as a solution in ethanol in a volume of  $60 \mu\text{l}$  to the 20 ml of Krebs solution in the muscle chamber. The addition of  $60 \mu\text{l}$  of ethanol alone in control experiments gave only small variable increases in tone (not shown). The ETYA concentration of  $10^{-4}$  M represents the concentration that would have been obtained if all ETYA had stayed in solution in the muscle chamber; however, some always came out of solution. The fall in tone that began about 2 min after the addition of ETYA and before washout (W) is the result of a marked (but reversible) depression of responsiveness to contractile agents that develops in aortic preparations on exposure to ETYA. *c*, Acute inhibition by mepacrine of ACh-induced relaxation. Mepacrine inhibition was readily reversed by washout.



aortic preparations), and also adenosine and 5'-AMP (maximal relaxation much less than with ACh in some experiments). In addition to prostacyclin, other products of cyclo-oxygenase activity were ruled out because inhibitors of that enzyme, indomethacin (40  $\mu$ M) and aspirin (100  $\mu$ M), had no effect on the relaxing action of ACh.

When aortic preparations were made anoxic, ACh produced very little or no relaxation (Fig. 4a). In the same conditions, agents like sodium nitrite, glyceryl trinitrate and isoprenaline still produced good relaxation. Inhibition of ACh-induced relaxation by anoxia has been reported previously for rings of dog femoral artery<sup>10</sup>. Furthermore, when 5, 8, 11, 14-eicosatetraenoic acid (ETYA) was added in sufficient concentration, it rapidly (<1 min) and often completely antagonized an ACh-induced relaxation (Fig. 4b). Moreover, exposure of preparations to 100  $\mu$ M ETYA for 30–60 min completely and irreversibly inhibited relaxation by ACh. Mepacrine at 20  $\mu$ M almost completely inhibited relaxation by ACh, whether it was added before or after the ACh. As ETYA is an inhibitor of lipoxygenase and cyclo-oxygenase<sup>11</sup> and as mepacrine inhibits the release of arachidonic acid from certain phosphatides (possibly by inhibiting phospholipase A<sub>2</sub> (ref. 12), these results suggest that ACh acting on the muscarinic receptor of the endothelial cells somehow activates a reaction sequence in which arachidonic (or some other unsaturated fatty acid) is liberated and then oxidized by lipoxygenase to a product that is responsible for the relaxation of the smooth muscle cells. The involvement of lipoxygenase is attractive despite negative results with the lipoxygenase inhibitor BW755C (ref. 13).

In experiments on other arteries, we have found that rings from the following exhibit ACh-induced relaxation before, but not after, rubbing of the intimal surface: rabbit superior mesenteric, pulmonary and ear arteries; rat thoracic aorta; guinea pig thoracic aorta, cat thoracic and abdominal aortae, superior mesenteric, pulmonary and external iliac arteries, dog circumflex and left anterior descending coronary arteries.

In relating the present *in vitro* findings to the vasodilating effect of ACh *in vivo*, it should be remembered that vasoconstriction of isolated blood vessels produced by stimulation of adrenergic nerves can be antagonized by ACh acting on pre-junctional muscarinic receptors of the nerve terminals<sup>14–17</sup>. As this antagonism depends on inhibition of the stimulation-evoked release of the adrenergic neurotransmitter NA<sup>16–18</sup>, it is a mechanism for vasodilatation by ACh only in blood vessels that are vasoconstricted by nerve stimulation. The endothelium-requiring mechanism explored here would be effective whether or not the vasoconstriction was caused by nerve stimulation. We propose that this mechanism applies in the case of smaller resistance vessels as well as for the larger arteries used in this study, and that it is one of the principal mechanisms responsible for the very potent vasodilating effect of ACh and other muscarinic agonists in intact animals.

We thank David Davidson and Peter Cherry for technical assistance, and Dr S. Moncada for supplying BW755C. The work was supported by USPHS grant NL 21860.

Received 21 July; accepted 18 September 1980.

1. Furchgott, R. F. *Pharmac. Rev.* **7**, 183–265 (1955).
2. Furchgott, R. F. & Bhadrakom, S. *J. Pharmac. exp. Ther.* **108**, 129–143 (1953).
3. Furchgott, R. F., Davidson, D. & Lin, C. I. *Blood Vessels* **16**, 213 (1979).
4. Furchgott, R. F. & Zawadzki, J. V. *Pharmacologist* **21**, 271 (1979).
5. Jelliffe, R. W. *J. Pharmac. exp. Ther.* **135**, 349–353 (1962).
6. Furchgott, R. F. & Zawadzki, J. V. *Fedn Proc.* **39**, 581 (1980).
7. Furchgott, R. F., Ehrlich, S. J. & Greenblatt, E. J. *gen. Physiol.* **44**, 499–519 (1961).
8. Poole, J. C. F., Sanders, A. G. & Florey, H. W. *J. Path. Bact.* **75**, 133–143 (1958).
9. Jaffe, E. A., Nachman, R. L., Becker, C. G. & Minick, C. R. *J. clin. Invest.* **52**, 2745–2756 (1973).
10. DeMey, J. G. & Vanhoutte, P. M. *Archs int. Pharmacodyn. Théor.* **234**, 339 (1978).
11. Flower, R. J. *Pharmac. Rev.* **26**, 33–67 (1974).
12. Flower, R. J. & Blackwell, G. C. *Biochem. Pharmac.* **25**, 285–291 (1976).
13. Higgs, G. A. *et al. Abstr. 7th int. Congr. Pharmac.*, 334 (Pergamon, Oxford, 1978).
14. Rand, M. J. & Varma, B. *Br. J. Pharmac.* **38**, 758–770 (1970).
15. Hume, W. R., DeLalande, I. S. & Waterson, J. G. *Eur. J. Pharmac.* **17**, 227–233 (1972).
16. Steinstand, O. S., Furchgott, R. F. & Kirpekar, S. M. *J. Pharmac. exp. Ther.* **184**, 346–356 (1973).
17. Vanhoutte, P. M. *Circulation Res.* **34**, 317–326 (1974).
18. Löffelholz, K. & Muscholl, E. *Naunyn-Schmiedeberg's Arch. exp. Path. Pharmac.* **265**, 1–15 (1969).

## Cholecystokinin octapeptide in the rat hypothalamo-neurohypophyseal system

Margery C. Beinfeld\*†, Dieter K. Meyer† & Michael J. Brownstein†

\* Department of Psychiatry, Washington University Medical School, St Louis, Missouri 63110

† Laboratory of Clinical Science, National Institute of Mental Health, Bethesda, Maryland 20205

**Gastrin-cholecystokinin (CCK)-like immunoreactivity has been visualized by immunohistochemistry in the vasopressin-oxytocin neurosecretory system comprising the posterior lobe of the pituitary, the supraoptic and paraventricular nuclei of the hypothalamus<sup>1</sup>. This CCK-like substance has not been chemically identified in the rat, but has been reported to be gastrin 17 in the swine pituitary<sup>2</sup>. We report here that this CCK-like immunoreactive substance co-chromatographs with CCK8 sulphate on Sephadex G-50 and two HPLC chromatographic systems. No gastrin 17 was detected in rat pituitary or brain. We further report that about 60% of the CCK in posterior lobe originates in cell bodies in the paraventricular nucleus of the hypothalamus. The CCK content of posterior pituitary is dramatically decreased by physiological perturbations which stimulate vasopressin or oxytocin release. We propose that CCK may either be co-secreted with vasopressin and oxytocin to act on peripheral targets or may be involved in the regulation of vasopressin or oxytocin neurosecretion.**

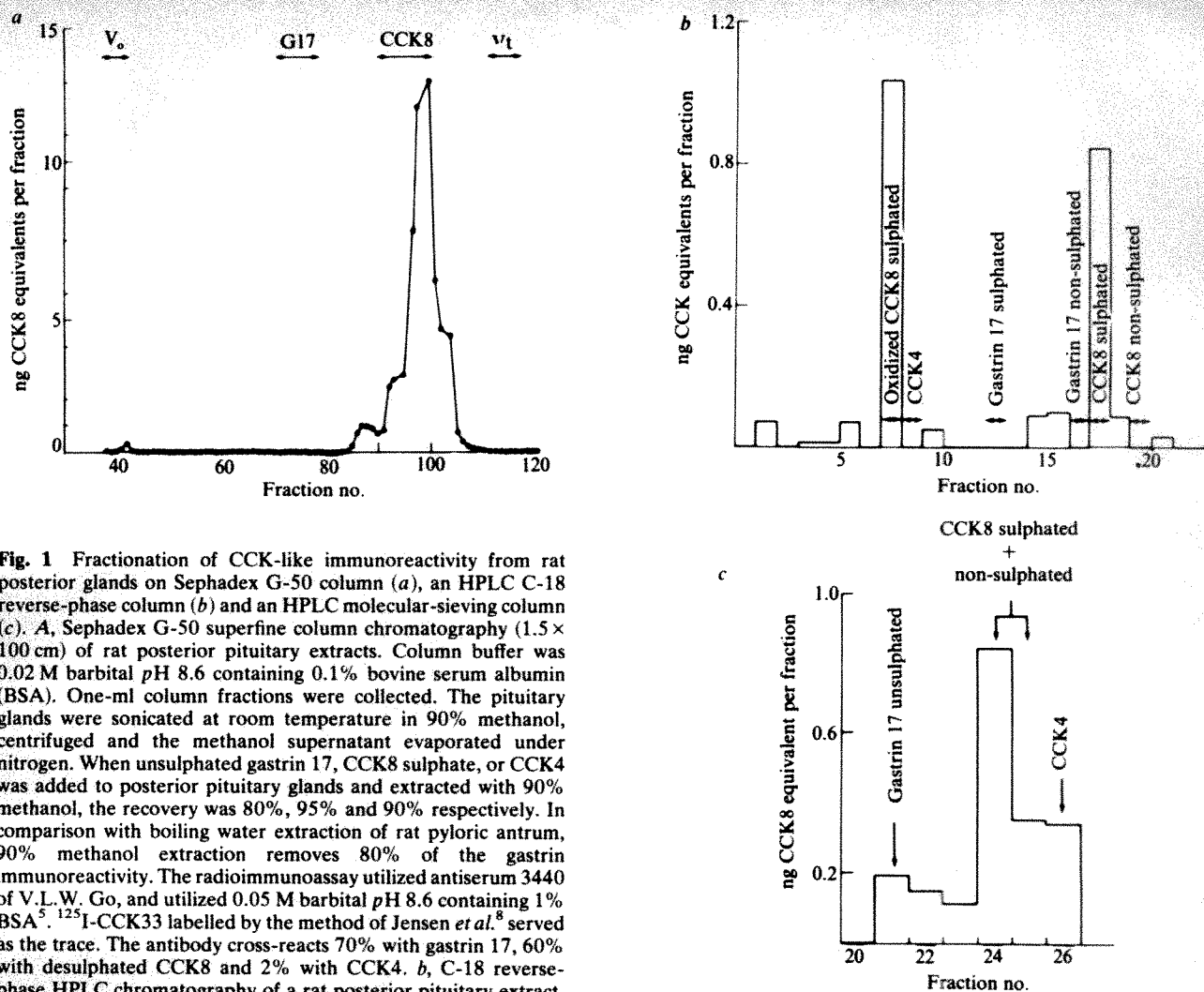
The CCK-like substance extracted with 90% methanol from rat posterior pituitary glands was fractionated on three chromatographic columns which separate CCK8 from gastrin: a Sephadex G-50 column, a HPLC reverse-phase C-18 column, and a HPLC molecular-sieving column. The pattern of elution of pituitary CCK immunoreactive material from these chromatographic columns was measured with a radioimmunoassay (RIA) which displayed 70% cross-reactivity with gastrin.

When a rat posterior pituitary extract was chromatographed on Sephadex G-50 the immunoreactivity emerged in one peak that had the same elution volume as synthetic sulphated CCK8 (Fig. 1a). Sephadex chromatography coupled with RIA has been used in the past to separate the molecular forms of CCK in central and peripheral nerves<sup>3</sup> and was, therefore, the first method applied in this study. However, as HPLC offers better

**Table 1** CCK content of posterior lobe in control and paraventricular lesioned rats

|                                      | CCK<br>(pg per lobe) |
|--------------------------------------|----------------------|
| Control (6)                          | 219 ± 46             |
| Paraventricular (6) nucleus lesioned | 89 ± 40              |

Bilateral paraventricular nucleus lesions were made under ether anaesthesia. Animals were placed in a Kopf stereotaxic device, 5° nose down. The electrode tips were positioned 6.4 mm rostral to the interauricular line, 0.4 mm lateral to the midline, 7.5 mm ventral to the dural surface. A current of 3 mA was passed through each electrode for 30 s. The lesions destroyed both paraventricular nuclei and damaged adjacent structures (anterior hypothalamic nuclei, ventral thalamus, perifornical area) to varying degrees. One week after the paraventricular nucleus lesions, the posterior lobe CCK content of lesioned Osborne-Mendel female rats and age-matched controls was determined. Note that strain differences exist in posterior pituitary CCK levels. Zivic-Miller rats have higher levels than Osborne-Mendel animals. Values are given as mean ± s.e.m.



**Fig. 1** Fractionation of CCK-like immunoreactivity from rat posterior glands on Sephadex G-50 column (a), an HPLC C-18 reverse-phase column (b) and an HPLC molecular-sieving column (c). **A**, Sephadex G-50 superfine column chromatography ( $1.5 \times 100$  cm) of rat posterior pituitary extracts. Column buffer was 0.02 M barbital pH 8.6 containing 0.1% bovine serum albumin (BSA). One-ml column fractions were collected. The pituitary glands were sonicated at room temperature in 90% methanol, centrifuged and the methanol supernatant evaporated under nitrogen. When unsulphated gastrin 17, CCK8 sulphate, or CCK4 was added to posterior pituitary glands and extracted with 90% methanol, the recovery was 80%, 95% and 90% respectively. In comparison with boiling water extraction of rat pyloric antrum, 90% methanol extraction removes 80% of the gastrin immunoreactivity. The radioimmunoassay utilized antiserum 3440 of V.L.W. Go, and utilized 0.05 M barbital pH 8.6 containing 1% BSA<sup>5</sup>.  $^{125}$ I-CCK33 labelled by the method of Jensen *et al.*<sup>8</sup> served as the trace. The antibody cross-reacts 70% with gastrin 17, 60% with desulphated CCK8 and 2% with CCK4. **b**, C-18 reverse-phase HPLC chromatography of a rat posterior pituitary extract. Chromatography was through a Supelco LC-18 HPLC column<sup>9</sup>. Elution buffer was 22% acetonitrile-78% triethylamine-phosphoric acid buffer pH 6.5. The position of partially and completely oxidized CCK and gastrin was determined by deliberately oxidizing the peptide with hydrogen peroxide and following the time course of the oxidation with the HPLC. **c**, Varian 2000 molecular-sieving HPLC column chromatography<sup>9</sup> of a rat posterior pituitary extract. Elution buffer was phosphate-buffered saline (PBS) pH 6.5. Before radioimmunoassay the fractions were passed through and eluted from a Waters C-18 Sep-pack to remove the PBS.

resolution of CCK peptides than Sephadex, two HPLC systems were also utilized to chromatograph rat posterior pituitary extracts.

In Fig. 1b the elution of a rat posterior pituitary extract from a HPLC reverse-phase C18 column is shown. All of the immunoreactivity emerges in two column fractions, one of which coincides with partially oxidized sulphated CCK8 and the other with reduced (that is, native) sulphated CCK8. No immunoreactivity co-migrates with sulphated or unsulphated gastrin 17 (in either their native or oxidized forms) or with CCK4 (Trp-Met-Asp-Phe-NH<sub>2</sub>). However, although 90% methanol can efficiently extract CCK4, the cross-reactivity of the antibody with CCK4 is sufficiently low that the existence of some CCK4 cannot be excluded.

In Fig. 1c the elution pattern of a rat pituitary extract from an HPLC molecular-sieving column is shown. The bulk of the immunoreactivity elutes with sulphated and desulphated CCK8; little material elutes with gastrin 17. Thus, sulphated CCK8 is the dominant CCK-like immunoreactive substance in the posterior pituitary of the rat, as it is in rat brain<sup>3-5</sup>. The presence of large amounts of gastrin 17 in the pig pituitary<sup>2</sup> may reflect species differences.

The distribution of CCK in the hypothalamus and pituitary resembles the distributions of vasopressin and oxytocin. As mentioned above, CCK-containing cell bodies have been visualized in the supraoptic and paraventricular nuclei by means of immunocytochemistry, and a dense collection of CCK fibres is

found in the median eminence and posterior pituitary<sup>1,6</sup>. Considerable CCK was detected by RIA in Osborne-Mendel female rats in paraventricular and supraoptic nuclei ( $0.86 \pm 0.1$  and  $1.5 \pm 0.4$  ng CCK8 equivalents per mg protein ( $n = 3$ ), respectively), more CCK in median eminence ( $2.3 \pm 0.5$  ng per mg protein) and still more in posterior pituitary ( $4.4 \pm 1.3$  ng per mg protein or 200–300 pg per lobe). CCK was undetectable ( $<10.0$  pg per pituitary) in the intermediate and anterior lobes of the pituitary.

To determine whether the CCK in the posterior pituitary is intrinsic to it, the CCK content was measured in pituitaries of stalk sectioned Zivic-Miller rats. One week after the stalk sections were performed the CCK content of the posterior pituitaries was undetectable. This indicates that all of the CCK in the posterior pituitary has an extrapituitary origin. The paraventricular nucleus contributes a substantial portion of the posterior lobe's CCK as paraventricular nucleus lesions reduced the CCK content of the posterior pituitary by 60% (Table 1).

To determine whether CCK might be secreted in parallel with vasopressin and/or oxytocin, the posterior pituitary CCK content was determined in lactating rats and rats given 2% saline to drink. The results are shown in Table 2. In lactating animals whose oxytocin release is increased, the CCK content in the posterior pituitary was reduced to 17% of control. In rats given 2% saline to drink for 5 days, a treatment which is known to reduce vasopressin by 80% (ref. 7), the pituitary CCK content was about 20% of control.



**Table 2** CCK in posterior lobe in lactating and salt-treated rats

|                  | CCK<br>(pg per lobe) |
|------------------|----------------------|
| Controls (9)     | 257 ± 36             |
| Salt treated (6) | 56 ± 20              |
| Lactating (3)    | 43 ± 4               |

Osborne-Mendel female rats (250 g) which were given 2% NaCl for 5 days were compared with controls given tap water. Lactating Osborne-Mendel rats were separated from their pups and compared with age-matched female controls. The CCK concentrations of both control groups were the same so the data were pooled. Numbers in parentheses refer to the number of animals tested. This experiment was repeated once with similar results. Values are mean ± s.e.m.

The CCK content of posterior pituitary is thus dramatically decreased by physiological perturbations which stimulate the release of vasopressin and oxytocin. We propose that CCK may either be co-secreted with vasopressin and oxytocin to act on peripheral targets, or may be involved at the pituitary level in the regulation of vasopressin or oxytocin secretion. Whether CCK is found in the same or different neurones as vasopressin or oxytocin remains to be determined.

Received 9 June; accepted 17 September 1980.

1. Vanderhaegen, J. J., Lotstra, F., DeMay, J. & Gilles, C. *Proc. natn. Acad. Sci. U.S.A.* **77**, 1190-1194 (1980).
2. Rehfeld, J. F. *Nature* **271**, 771-773 (1978).
3. Rehfeld, J. F. *J. biol. Chem.* **253**, 4022-4033 (1978).
4. Dockray, G. J. *Brain Res.* **188**, 155-165 (1980).
5. Beinfeld, M. C., Meyer, D. K., Eskay, R. L., Jensen, R. T. & Brownstein, M. J. *Brain Res.* (in the press).
6. Loren, I., Alums, J., Hakanson, R. & Sundler, F. *Histochemistry* **59**, 249-257 (1979).
7. Vaitin, H., Sokol, H. W. & Sundel, D. *Rec. Prog. Horm. Res.* **31**, 447-486 (1975).
8. Jensen, R. T., Lemp, G. F. & Gardner, J. D. *Proc. natn. Acad. Sci. U.S.A.* **77**, 2079-2083 (1980).
9. Beinfeld, M. C., Jensen, R. T. & Brownstein, M. J. *J. Liquid Chromat.* (in the press).

## VIP as a possible neurotransmitter of non-cholinergic non-adrenergic inhibitory neurones

Raj K. Goyal & Satish Rattan\*

Department of Internal Medicine, University of Texas Health Center, 7703 Floyd Curl Drive, San Antonio, Texas 78284

Sami I. Said

Department of Internal Medicine, Veterans Administration Medical Center, 4500 Lancaster, Dallas, Texas 75216

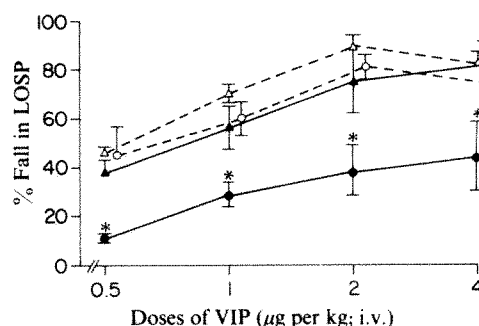
Many peripheral autonomic nerves are neither cholinergic nor adrenergic. Such nerves are widely distributed in the gastrointestinal, urogenital and respiratory tracts, and in blood vessels<sup>1,2</sup>. The nature of their neurotransmitter is not known. We have previously reported that vasoactive intestinal polypeptide (VIP) is a potent inhibitor of opossum lower oesophageal sphincter (LOS) and that its inhibitory effect is exerted directly on the sphincter muscle<sup>3</sup>. Subsequent studies have confirmed the inhibitory effect of VIP on LOS in other species<sup>4-6</sup>. Recently, very high tissue levels of VIP have been reported in the LOS and other gastrointestinal sphincters<sup>7</sup>. Furthermore, VIP has been localized to intramural neurones and is released upon electrical stimulation of the vagus nerve<sup>8,9</sup>. We report here that immunoantagonism of VIP with a high-titre antiserum antagonized inhibitory neuromuscular transmission in the LOS. These findings provide evidence of a role for VIP as an inhibitory neurotransmitter.

\* To whom correspondence should be addressed.

Experiments were performed in opossums (*Didelphis virginiana*) anaesthetized with pentobarbital (40 mg per kg). Opossum LOS is suitable for these studies because it maintains a resting tone independent of tonic neural activity and the vagus nerves carry predominantly inhibitory influences to the LOS<sup>10</sup>. Moreover, the inhibitory neurones that lie in the vagal pathway have been shown to be non-cholinergic and non-adrenergic in nature<sup>11</sup>.

The lower oesophageal sphincter pressures (LOSP) were monitored with water-filled, continuously perfused catheters that were anchored in the LOS as described elsewhere<sup>12</sup>. Ringer's solution, control serum (non-immune serum from an unimmunized rabbit), VIP antiserum or VIP antiserum preabsorbed *in vitro* with native VIP, were infused into the branch of left gastric artery that supplies the sphincter<sup>13</sup>. VIP antiserum no. 89N was raised in a rabbit immunized with a conjugate of natural porcine VIP and bovine serum albumin. Using the antiserum in a dilution of 1:300,000 at 4°C, the equilibrium constants of association were found to be  $K_{a1} = 6.7 \times 10^{10} \text{ M}^{-1}$  and  $K_{a2} = 2.3 \times 10^9 \text{ M}^{-1}$ . The binding capacity of the undiluted antiserum was calculated to be 57 µg VIP per ml of antiserum. *In vitro* assay showed no cross-reactivity with gastric inhibitory polypeptide, glucagon, secretin, substance P, porcine pancreatic polypeptide, cholecystokinin or gastrin. The antiserum from the same batch was neutralized by addition of VIP (57 µg VIP per ml of antiserum). The mixture was kept overnight and then centrifuged to remove any precipitate before its use.

The brachial vein was used for intravenous (i.v.) administration of VIP. Vagal efferent stimulation was provided by electrical stimulation of the peripheral end of the cut vagus nerve in the neck<sup>10</sup>. Stimulation of intramural neurones was achieved with electrodes inserted into the wall of the sphincter as described elsewhere<sup>12</sup>. Nicotine (40 µg per kg) was administered intravenously<sup>14</sup>.



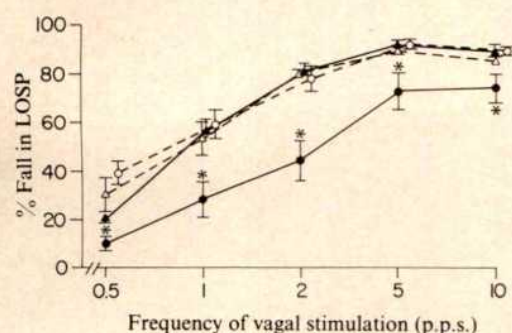
**Fig. 1** The influence of intra-arterial VIP antiserum on the inhibitory effect of intravenously administered VIP on the LOSP. The corresponding Ringer controls for control serum (○, 1:12.5) and VIP antiserum (●, 1:12.5) are represented by △ and ▲ respectively. VIP antiserum significantly (\*) antagonized the effect of all doses of VIP studied. This antagonism was significant ( $P < 0.05$ ) when compared to either control serum or the Ringer's infusion. Each point is mean ± s.e. of four observations.

Two separate groups, each of four animals, were studied. One group received an infusion of Ringer's solution followed by control serum. The second group received Ringer's solution followed by VIP antiserum. All infusions were made at the rate of 5 ml h<sup>-1</sup>. The pressure recording was coded and results were analysed blindly. Intravenous administration of VIP produced a dose-dependent fall in LOSP, which was not modified by control serum (1:12.5 dilution). In contrast, VIP antiserum (1:12.5) significantly ( $P < 0.05$ ) antagonized the inhibitory effect of VIP at all dose levels (Fig. 1). Thus the antiserum was effective in partially antagonizing the effect of exogenous VIP. Higher dilutions of antiserum 1:50 were ineffective and the dilution of 1:25 produced inconsistent effects.

Electrical stimulation of vagal efferents produced a frequency-dependent fall in the sphincter pressure. Other



parameters of stimulation were 10 V, 0.5 ms square pulses for 2-s train duration. Infusion of control serum did not modify vagal-stimulated sphincter relaxation at any of the frequencies of stimulation examined ( $P > 0.05$ , Fig. 2).



**Fig. 2** The influence of VIP antiserum on the vagal-stimulated fall in LOSP. Note that vagal stimulation produced frequency-dependent fall in LOSP. VIP antiserum significantly (\*) antagonized the inhibitory effect of vagal stimulation at all the frequency levels studied ( $P < 0.05$ ). Control serum did not modify the effect of vagal stimulation. The corresponding Ringer controls in two different groups for control (○) and VIP antiserum (●) are represented by △ and ▲ respectively. Each point is mean  $\pm$  s.e. of 9–12 observations. p.p.s., Pulses per s.

As the vagal pathway to the LOS muscle consists of pre-ganglionic fibres that synapse with postganglionic inhibitory neurones<sup>11</sup>, the effect of VIP antiserum on vagal-stimulated sphincter relaxation could be exerted at the preganglionic or at the postganglionic level. To examine these alternatives we investigated the effect of postganglionic neuronal activation with intramural electrical stimulation. We have previously shown that intramural stimulation in this preparation activates postganglionic neurones as the effect of such a stimulation is not antagonized by synaptic block with a combination of hexamethonium and atrophine<sup>15</sup>. Effect of ganglionic stimulant nicotine<sup>14</sup> was also examined.

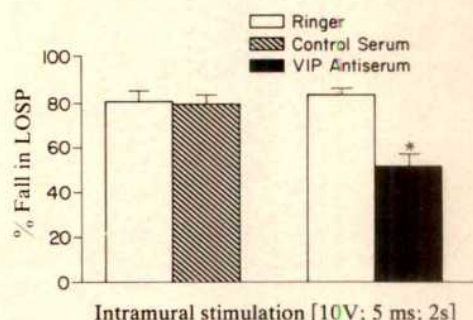
LOS relaxation induced by intramural stimulation was significantly antagonized by VIP antiserum but was unaffected by control serum (Fig. 3). Likewise, the fall in LOSP induced by nicotine was antagonized by VIP antiserum but not by control serum. Nicotine (40  $\mu$ g per kg) caused  $83.4 \pm 3.2$  (s.e.) per cent fall in LOSP during control serum and  $58.7 \pm 5.9$  per cent during VIP antiserum infusion ( $P < 0.05$ ,  $n = 5$ ). These results suggest that the VIP antiserum acted at the postganglionic neuromuscular site.

The effect of VIP antiserum on all the stimuli studied above could theoretically be due to its non-selective action on the LOS

smooth muscle. To examine this, we studied the effect of a direct-acting inhibitory agent, isoproterenol. VIP antiserum did not modify its inhibitory action. Isoproterenol (2.5  $\mu$ g per kg) caused  $84.7 \pm 3.1$  per cent fall in LOSP during the infusion of control serum and  $85.0 \pm 2.6$  per cent during the VIP antiserum infusion ( $P > 0.05$ ,  $n = 5$ ).

The control serum used in these studies was not obtained from the same animal that provided the VIP antiserum. Theoretically the observed influence of the VIP antiserum could have been due to an unknown inhibitor other than the VIP antibody. To test this, we examined the influence of VIP antiserum that was preabsorbed with VIP before administration. As summarized in Table 1, preabsorbed VIP antiserum did not modify the effects of exogenous VIP, vagal or transmural stimulation in the same animal. These observations support the view that the inhibitory effect of VIP antiserum was due to the VIP antibody.

These immunopharmacological studies provide evidence for the role of VIP as a neurotransmitter of the inhibitory neurones in the LOS. This conclusion is supported by immunohistochemical demonstration of VIP in the intramural neurones and its release upon electrical stimulation of vagus nerves<sup>9,16–19</sup>.



**Fig. 3** Influence of VIP antiserum on the effect of intramural stimulation on LOSP. Note that VIP antiserum significantly (\*) antagonized the inhibitory effect of intramural stimulation ( $P < 0.05$ ). Control serum, however, failed to modify the effect of intramural stimulation. Each point is mean  $\pm$  s.e. of 12 observations.

The VIP antiserum in the dilution of 1:12.5 did not fully antagonize the effect of exogenous VIP or of inhibitory neurone stimulation. This may be because the large size of the antibody makes it difficult for the antibody molecule to achieve sufficiently high concentrations in the extracellular space at the site of neuromuscular transmission. Moreover, the time course and the affinity of binding of the released VIP with the antiserum compared to that with the muscle receptors may also influence the degree of the antagonism. Higher concentration of antiserum could further antagonize the inhibitory response to exogenous or neurally-released VIP. Further studies are needed to resolve these issues. Alternatively, VIP may be only one of two or more neurotransmitters that are released by non-adrenergic, non-cholinergic inhibitory neurones<sup>20</sup>. Burnstock originally suggested that ATP or a related nucleotide is the neurotransmitter of the non-cholinergic, non-adrenergic neurones, which he termed 'purinergic' neurones<sup>1</sup>. Recent studies, however, do not support the view of purinergic nature of the inhibitory neurotransmitter in the opossum LOS<sup>21</sup>.

This work was supported by Public Health Services grant AM25609 from NIAMDD, and Center awards HL-17187 and CA-21570. We thank Laine Brainard and Melinda Grady for technical help.

Received 23 June; accepted 22 September 1980.

1. Burnstock, G. *Pharmac. Rev.* **24**, 509–581 (1972).
2. Chesrown, S. E., Venugopalan, C. S., Gold, W. M. & Drazen, J. M. *J. clin. Invest.* **65**, 314–320 (1980).
3. Rattan, S., Said, S. I. & Goyal, R. K. *Proc. Soc. exp. Med.* **155**, 40–43 (1977).

**Table 1** Influence of preabsorbed VIP antiserum on the effect of exogenous VIP or neurally stimulated LOS relaxation

|                              |                     | Per cent fall in LOSP |                           |                |
|------------------------------|---------------------|-----------------------|---------------------------|----------------|
|                              | No. of observations | Ringer's solution     | Preabsorbed VIP antiserum | <i>P</i> value |
|                              |                     | (Mean $\pm$ s.e.)     | (mean $\pm$ s.e.)         |                |
| VIP (4 $\mu$ g per kg; i.v.) | 3                   | 72.3 $\pm$ 3.5        | 75.0 $\pm$ 2.9            | >0.05          |
| Vagal stimulation            |                     |                       |                           |                |
| 0.5 Hz                       | 5                   | 23.8 $\pm$ 4.4        | 20.8 $\pm$ 4.8            | >0.05          |
| 1 Hz                         | 5                   | 45.8 $\pm$ 3.1        | 42.2 $\pm$ 7.5            | >0.05          |
| 2 Hz                         | 5                   | 61.7 $\pm$ 7.5        | 58.2 $\pm$ 3.1            | >0.05          |
| 5 Hz                         | 5                   | 73.6 $\pm$ 3.5        | 81.5 $\pm$ 5.0            | >0.05          |
| 10 Hz                        | 5                   | 69.5 $\pm$ 7.9        | 75.7 $\pm$ 7.2            | >0.05          |
| Intramural stimulation       | 5                   | 75.3 $\pm$ 4.9        | 82.8 $\pm$ 4.6            | >0.05          |



4. Uddmann, R., Alumets, J., Edvinson, L., Häkanson, R. & Sundler, F. *Gastroenterology* **75**, 5-8 (1978).
5. Behar, J., Field, S. & Marin, C. *Gastroenterology* **77**, 1001-1007 (1979).
6. Siegel, S. R., Brown, F. C., Castell, D. O., Johnson, L. F. & Said, S. I. *Dig. Dis. Sci.* **24**, 345-359 (1979).
7. Alumets, J. *et al. Nature* **280**, 155-156 (1979).
8. Bryant, M. G. *et al. Lancet* **i**, 991-993 (1976).
9. Fahrenkrug, J., Galbo, H., Holst, J. J. & Schaffalitzky de Muckadell, O. B. *J. Physiol., Lond.* **280**, 405-422 (1978).
10. Rattan, S. & Goyal, R. K. *J. clin. Invest.* **54**, 889-906 (1974).
11. Goyal, R. K. & Rattan, S. *J. clin. Invest.* **55**, 1119-1126 (1975).
12. Goyal, R. K. & Rattan, S. *Gastroenterology* **71**, 62-67 (1976).
13. Goyal, R. K. & Rattan, S. *J. clin. Invest.* **52**, 337-342 (1973).
14. Rattan, S. & Goyal, R. K. *Gastroenterology* **61**, 154-159 (1975).
15. Rattan, S. & Goyal, R. K. *Am. J. Physiol.* **234**, E273-E276 (1978).
16. Larsson, L. I. *et al. Proc. natn. Acad. Sci. U.S.A.* **73**, 3197-3200 (1976).
17. Schaffalitzky de Muckadell, O. B., Fahrenkrug, J. & Holst, J. J. *Gastroenterology* **72**, 373-375 (1977).
18. Fahrenkrug, J. *Digestion* **19**, 149-169 (1979).
19. Lundberg, J. M. *et al. Gastroenterology* **77**, 468-471 (1979).
20. Burnstock, G. *Neuroscience* **10**, 239-248 (1979).
21. Rattan, S. & Goyal, R. K. *Gastroenterology* **78**, 898-904 (1980).

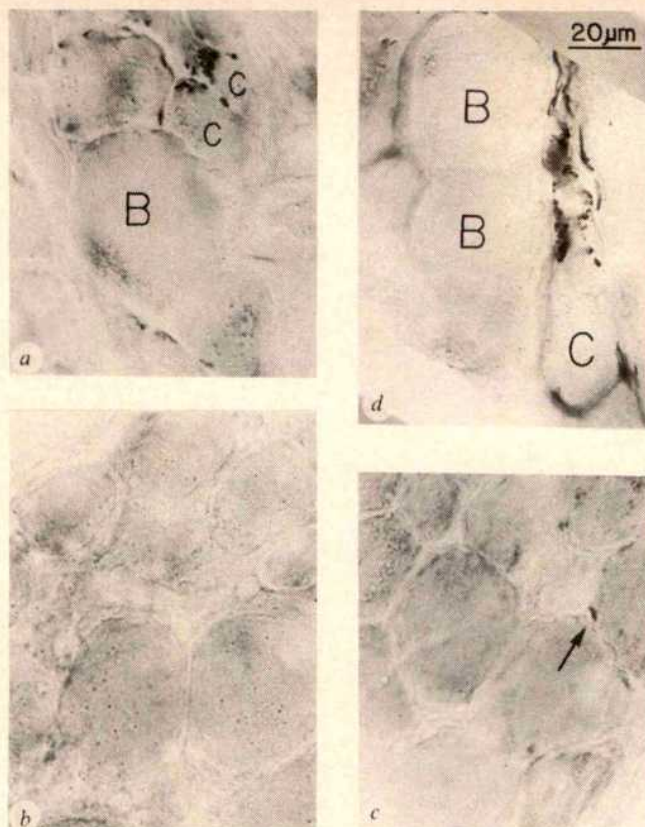
## Peptidergic transmitters in synaptic boutons of sympathetic ganglia

L. Y. Jan, Y. N. Jan & M. S. Brownfield

Department of Physiology, University of California, School of Medicine, San Francisco, California 94143

In sympathetic ganglia of the bullfrog, a slow synaptic potential lasting for minutes—the late slow excitatory postsynaptic potential (e.p.s.p.)—was discovered<sup>1</sup>. This slow response, unlike other previously known synaptic potentials in the autonomic nervous system, is not mediated by acetylcholine or monoamines. Similar non-cholinergic, non-adrenergic slow synaptic potentials have since been found in several other vertebrate autonomic ganglia<sup>2</sup>. We found that the late slow e.p.s.p. is probably mediated by a peptide that is identical to, or closely resembles, mammalian luteinizing hormone releasing hormone (LHRH)<sup>3</sup>, because (1) when applied directly to sympathetic neurones, LHRH and its agonists elicit a slow depolarization, associated with similar changes in membrane conductance and excitability as those occurring during the late slow e.p.s.p. Furthermore, both peptide-induced and nerve-evoked responses are blocked by antagonists of LHRH; and (2) radioimmunoassays indicate that a chain of sympathetic ganglia contains 100–800 pg of a LHRH-like peptide. Its distribution among spinal nerves, the great reduction of this substance following denervation, and its release from ganglia following isotonic KCl treatment or nerve stimulation suggest that the LHRH-like material is contained in preganglionic nerve fibres. Here we report that immunohistochemical staining of sympathetic ganglia shows that LHRH-like immunoreactivity is indeed present in synaptic boutons. We also show that the two types of ganglion cells (B cells and C cells) receive strikingly different patterns of peptidergic innervation.

The ninth and tenth ganglia of the bullfrog, the two most caudal ones in the paravertebral sympathetic chain, were used in these experiments because extensive electrophysiological studies have used them. By using several anti-LHRH sera raised in different laboratories, and the peroxidase–antiperoxidase (PAP) technique of Sternberger and co-workers<sup>4</sup>, we stained many boutons on the ganglion cell soma, particularly around the axon hillock region (Fig. 1a). To ensure that the staining was specific for LHRH-like immunoreactivity, we used the same anti-LHRH sera preadsorbed with LHRH in control experiments. Figure 1b shows that preadsorption completely abolishes the staining. Thus, the immunohistochemical procedure shows that the LHRH-like immunoreactivity is confined to synaptic boutons in sympathetic ganglia.



**Fig. 1** Vibratome-sectioned sympathetic ganglia treated with *a*, anti-LHRH sera, or *b*, same anti-LHRH sera preadsorbed with excess synthetic LHRH ( $40 \mu\text{g ml}^{-1}$ ), according to the PAP procedure of Sternberger<sup>4</sup>. In *c*, the seventh and eighth rami had been cut 5 days before the ganglia were stained with anti-LHRH sera (arrow indicates residual staining). In all cases, bullfrogs were anaesthetized with ethyl *m*-aminobenzoate and perfused through the ventricle with 4% paraformaldehyde, 0.1% glutaraldehyde in 0.15 M phosphate buffer at pH 7.4. The sympathetic chains were removed, postfixed in the same fixative for 30 min, and cut into 50- $\mu\text{m}$  sections on a vibratome. Rabbit antisera to LHRH were diluted 1:1,000 with 0.05 M Tris-buffered saline, pH 7.6, containing 1 mg  $\text{ml}^{-1}$  bovine serum albumin, 1% normal sheep serum, and 0.4% Triton X-100 and used to treat sections of ganglia for 24 h at 4°C. This incubation with primary rabbit antisera was followed sequentially by an incubation with sheep antisera specific for rabbit gamma immunoglobulins (IgG) and an incubation with rabbit PAP complex. Sheep antisera against rabbit IgG and rabbit PAP were used at 1:20 dilution in Tris-buffered saline containing 1% normal sheep serum and 0.02% Triton X-100. In each case, the incubation lasted 1 h at room temperature. Between incubations, vibratome sections were first washed for 2 h or longer in the same solution as that used in diluting the antisera for the previous incubation and then treated for 30 min with 5% normal sheep serum in the same solution as that used in diluting the antisera for the following incubation. *d*, HRP-filled terminals in partially denervated sympathetic ganglia. The sympathetic chain was severed above the seventh ganglion 5 days before preganglionic fibres were filled orthodromically with HRP. This denervation procedure removes cholinergic terminals around B cells, but leaves intact cholinergic terminals on C cells and peptidergic terminals for the late slow e.p.s.p. Note that very few terminals are found near B cells. To fill preganglionic fibres, a fresh cut was made in the chain below the seventh ganglion and the cut end was taken up in a suction electrode containing 30% HRP and 3% lysocleithin in  $\text{dH}_2\text{O}$ . Sixteen h later, the ganglia were fixed with 2% glutaraldehyde in 0.1 M phosphate buffer, pH 7.4, for 1 h, cut into 50- $\mu\text{m}$  sections on a vibratome, and reacted in a mixture of 0.5 mg  $\text{ml}^{-1}$  DAB and 0.0009%  $\text{H}_2\text{O}_2$  in 0.1 M phosphate-buffered saline for 10–15 min. B and C in *a*, *d* indicate B cells and C cells respectively, as judged from their sizes. In all cases, the sections were unstained, apart from the end-product of the peroxidase reactions.



**Table 1** Distribution of LHRH-positive boutons in sympathetic ganglia

|                         | Small cells<br>( $<28\ \mu\text{m}$ in diameter) |           |           | Medium cells<br>( $>28\ \mu\text{m}$ , $<42\ \mu\text{m}$ in diameter) |           |           | Large cells<br>( $>42\ \mu\text{m}$ in diameter) |           |           |
|-------------------------|--|-----------|-----------|--|-----------|-----------|--|-----------|-----------|
|                         | No. stained                                      | Total no. | % Stained | No. stained  | Total no. | % Stained | No. stained                                      | Total no. | % Stained |
| Normal                  | 640  | 792       | 81        | 307  | 653       | 47        | 14   | 203       | 7         |
| Unilaterally denervated | 84   | 451       | 19        | 164  | 557       | 29        | 177  | 356       | 50        |
| Bilaterally denervated  | 13   | 502       | 2.6       | 85   | 508       | 17        | 55   | 203       | 27        |

50- $\mu\text{m}$  thick sections of ganglia stained immunohistochemically with PAP and Sternberger's antisera for mammalian LHRH (see Fig. 1 legend) were examined with a Zeiss microscope and a  $\times 40$  water immersion lens. Diameters of cells surrounded with LHRH-positive boutons were measured, as were diameters of cells which clearly had no staining in their vicinity. (Using such criteria, the latter cell type is probably somewhat under-represented.) 'Diameters' for oblong cells were estimated as the geometric mean of the length and width of each cell. No corrections were made on account of the thickness of the sections. 'No. stained', number of cells surrounded by LHRH-positive terminals; 'Total no.', the sum of the number of cells surrounded by LHRH-positive terminals and the number of cells clearly void of stained terminals in their vicinity; '% Stained', the ratio of no. stained to total no. 'Normal' includes sections of ninth and tenth ganglia from five frogs; 'Unilaterally denervated' includes sections of ninth and tenth ganglia with their ipsilateral input from the seventh and eighth spinal nerves removed for 10 days (three frogs); and 'Bilaterally denervated' includes sections of ninth and tenth ganglia from two frogs whose seventh and eighth rami on both sides had been cut for 10 days.

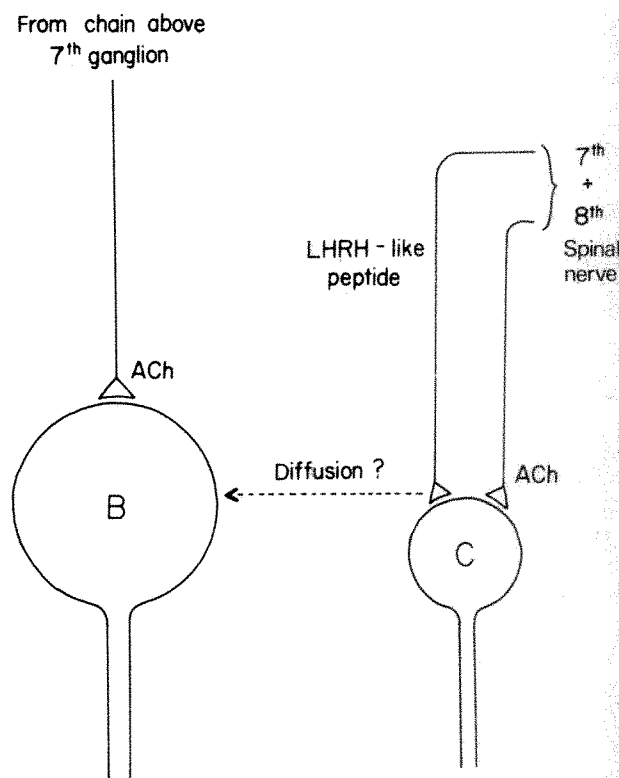
The principal neurones in the ninth and tenth ganglia can be divided into two groups<sup>5</sup>: B cells and C cells. B cells are larger (with diameters from  $\sim 30$  to  $\sim 70\ \mu\text{m}$ ). They send out axons that conduct at velocities of about  $2\ \text{m s}^{-1}$ . C neurones are smaller (with diameters from  $\sim 20$  to  $\sim 45\ \mu\text{m}$ ) and their axons conduct at speeds  $\sim 0.2\ \text{m s}^{-1}$ . Both B and C cells give late slow e.p.s.ps on stimulation of the seventh and eighth spinal nerves, which carry most of this non-cholinergic input. Cholinergic inputs to these cells, however, are segregated anatomically<sup>6</sup>. B cells are innervated by cholinergic fibres from the chain above the seventh ganglion whereas C cells receive cholinergic input through the seventh and eighth spinal nerves (Fig. 2).

Although physiological studies have shown that most B and C cells give late slow e.p.s.ps on stimulation of the seventh and eighth spinal nerves<sup>3,6</sup>, immunohistochemical experiments reveal that LHRH-positive synaptic boutons are mainly around C cells (14 frogs). Cell counts on 50- $\mu\text{m}$  thick sections of ganglia from five frogs showed that 640 out of 792 small cells (with diameters  $<28\ \mu\text{m}$ ) were surrounded by LHRH-positive synaptic boutons, whereas only 14 out of 203 large cells (with diameters  $>42\ \mu\text{m}$ ) were surrounded by LHRH-positive terminals (Table 1). As physiological studies have shown that almost all cells larger than  $45\ \mu\text{m}$  in diameter are B cells, whereas cells smaller than  $30\ \mu\text{m}$  in diameter are most likely C cells, it seems that most, if not all, LHRH-positive nerve terminals are apposed to C cells.

This preferential staining of synaptic boutons around C cells was confirmed with two different approaches. First, we eliminated the cholinergic input to B cells by cutting the sympathetic chain above the seventh ganglion, identified B cells which gave the late slow e.p.s.p. but no cholinergic synaptic potentials, and serial-sectioned through those cells to look for remaining terminals using an electron microscope. Of the three B cells studied, none had terminals directly apposed to its membrane. Second, we again cut the chain above the seventh ganglion to remove the cholinergic innervation to B cells, leaving intact the cholinergic innervation to C cells plus peptidergic inputs to both B and C cells (Fig. 2). Then we used horseradish peroxidase (HRP) to fill terminals of preganglionic fibres arising from the seventh and eighth spinal nerves. Again, HRP-filled terminals were found around C cells, but hardly any filled terminals were found on B cells (Fig. 1d). Together, these anatomical approaches suggest that synaptic boutons containing LHRH-like immunoreactivity are almost exclusively around C cells. The similarity between the pattern of distribution of LHRH-positive boutons and that of HRP-filled terminals around C cells raises the question of whether acetylcholine and LHRH might exist in the same synaptic boutons, as has been suggested in some systems<sup>7</sup>.

To test further whether these LHRH-positive boutons arise from preganglionic fibres responsible for the late slow e.p.s.p., we removed most of those fibres from the ganglia by cutting the

seventh and eighth rami (Fig. 2). Previous physiological and anatomical studies have shown that after the preganglionic fibres are cut, synaptic transmission fails and nerve terminals of cut axons degenerate in a few days, but the ganglion cells retain their membrane potentials and give impulses. As expected, immunohistochemical staining of denervated ganglia showed that the staining for LHRH-like immunoreactivity was



**Fig. 2** Scheme of innervation of principal cells in ninth or tenth ganglia, the last two ganglia in the sympathetic chain. B cells are larger ( $\sim 30$  to  $\sim 70\ \mu\text{m}$  in diameter), whereas C cells are generally smaller (with diameters from  $\sim 20$  to  $\sim 45\ \mu\text{m}$  possibly down to  $10$ – $15\ \mu\text{m}$ ). Cholinergic axons for B neurones reach these ganglia through the sympathetic chain above the seventh ganglion, whereas preganglionic fibres for C neurones come through the seventh and eighth spinal nerves. The majority of LHRH-positive preganglionic axons for all neurones in the ninth and tenth ganglia also enter through the seventh and eighth nerves. Peptidergic input to B neurones is represented by dotted lines, because very few LHRH-positive boutons are found near large B neurones. It is not yet known whether acetylcholine and the LHRH-like peptide exist in the same nerve terminals around C cells.



essentially normal in the ninth and tenth ganglia after the chain was severed above the seventh ganglion (three frogs). On the other hand, cutting the seventh and eighth rami greatly reduced the staining (Fig. 1c). Rather unexpectedly, the distribution of staining in these denervated ganglia turned out to be drastically different from the normal pattern. Most of the cells surrounded by LHRH-positive boutons are large B cells (Table 1). The residual staining around C cells may be accounted for by a small percentage of peptidergic input from the contralateral seventh and eighth spinal nerves, as from previous electrophysiological experiments we knew that such contralateral contributions normally exist and that they increase after the ipsilateral input is removed, possibly as a result of sprouting<sup>8</sup>. Indeed, in two frogs whose seventh and eighth rami were cut on both sides, only 2.6% of small cells were surrounded by LHRH-positive boutons (Table 1), compared with 19% in unilaterally denervated frogs or 81% in the unoperated frog. Therefore, cutting preganglionic fibres from the seventh and eighth rami almost completely removed staining around C cells. The staining around large cells after denervation could be due to sprouting of the remaining few LHRH-positive fibres, which occasionally arise from the ninth spinal nerve, uptake of LHRH-positive materials into cholinergic nerve terminals, or other factors. Further studies are necessary to answer this question.

LHRH-like immunoreactivity has been found in synaptic boutons, as seen by light microscopy, in sympathetic ganglia. Further, denervation experiments suggest that these LHRH-positive synaptic boutons are probably the preganglionic nerve terminals for the late slow e.p.s.p. This considerably strengthens our hypothesis that the transmitter for the late slow e.p.s.p. in frog sympathetic ganglia is a LHRH-like peptide. Although the late slow e.p.s.p. is present in both B and C cells, LHRH-positive synaptic boutons are mainly around C cells. Therefore, whereas C cells may receive peptidergic transmitters from synaptic boutons in the vicinity of their cell bodies, the late slow e.p.s.p.s. recorded in B cells must be largely due to diffusion of the LHRH-like peptides from terminals around C cells. The delayed and variable onset of the late slow e.p.s.p. recorded in different B cells is compatible with the suggestion that B cells receive peptidergic transmitters that are released at a distance. This result implies that inactivation of this peptidergic transmitter must be relatively slow. Indeed, if an antagonist of LHRH is ejected by pressure on to a B cell anytime during a late slow e.p.s.p., the slow synaptic potential is truncated right away<sup>8</sup>, suggesting that the slowness of this response is partly due to the prolonged presence of transmitters after they are released on nerve stimulation. The fact that sympathetic ganglia contained two anatomically distinct types of peptidergic innervation, together with their relative structural simplicity and easy access, makes them a promising model for detailed analysis of peptidergic transmission.

We thank Drs W. Vale and J. Rivier of the Salk Institute for peptides and rabbit antisera, Drs L. A. Sternberger and G. P. Kozlowski for rabbit antisera, and Louise Evans for photography. This research was supported by NIH Training Grant AM 07265 and grant 1 R01 NS 15757-01 from NIH to Y.N.J., who is a McKnight Scholar. L.Y.J. is a Sloan Fellow and an established investigator of the American Heart Association. M.S.B. is a Giannini Fellow.

Received 18 July; accepted 23 September 1980.

1. Nishi, S. & Koketsu, K. *J. Neurophysiol.* **31**, 109–121 (1968).
2. Burnstock, G. & Hökfelt, T. *Neurosci. Res. Prog. Bull.* **17**, No. 3, 379–519 (MIT Press, Cambridge, Massachusetts, 1979).
3. Jan, Y. N., Jan, L. Y. & Küffer, S. W. *Proc. natn. Acad. Sci. U.S.A.* **76**, 1501–1505 (1979); **77**, 5008–5012 (1980).
4. Sternberger, L. A., Hardy, P. H., Cuculus, J. J. & Meyer, H. G. *J. Histochem. Cytochem.* **18**, 315–333 (1970).
5. Nishi, S., Soeda, H. & Koketsu, K. *J. Cell comp. Physiol.* **66**, 19–32 (1965).
6. Libet, B. & Kobayashi, H. *J. Neurophysiol.* **8**, 805–814 (1974).
7. Hökfelt, T. *et al. Nature* **284**, 515–521 (1980).
8. Jan, Y. N. & Jan, L. Y. (in preparation).

## Do human platelets have opiate receptors?

A. Reches\*, A. Eldor†, Z. Vogel‡ & Y. Salomon§

Departments of Neurology\* and Hematology†, Hadassah University Hospital, Jerusalem, Israel

Departments of Neurobiology‡ and Hormone Research§, The Weizmann Institute of Science, Rehovot, Israel 76100

In their study of prostaglandin E<sub>1</sub> (PGE<sub>1</sub>)-sensitive adenylate cyclase (AC) in rat brain homogenates, Collier and Roy<sup>1</sup> claimed that the activity of this enzyme is inhibited by opiates. They also proposed that opiates exert their analgesic and allied effects by inhibiting AC of neurones that are normally stimulated by E prostaglandins<sup>2</sup>. Studies using neuroblastoma × glioma hybrid cells<sup>3,4</sup> supported this hypothesis. However, subsequent studies with the mammalian brain<sup>5,6</sup> and rat brain tissue slices<sup>7,8</sup> yielded conflicting results. PGE<sub>1</sub> also inhibits platelet aggregation<sup>9</sup>, probably through activation of platelet AC<sup>10</sup>. Gryglewski *et al.*<sup>11</sup> showed that morphine inhibits the anti-aggregating effect of PGE<sub>1</sub> on ADP- and adrenaline-induced platelet aggregation, and suggested that the inhibition by morphine is mediated through platelet AC activity. We report here our attempts to reproduce the results of Gryglewski *et al.* and our examination of the effect of morphine on PGE<sub>1</sub>-sensitive AC activity in platelet lysates and on PGE<sub>1</sub>-induced accumulation of cyclic AMP in intact platelets. The possible existence of opiate receptors in platelets was also assessed by direct binding studies with <sup>3</sup>H-etorphine. In contrast to Gryglewski *et al.*<sup>11</sup>, we could not detect any effect of opiates on the aggregation of human platelets, nor did we find any other evidence supporting the presence of opiate receptors in these cells. Thus we conclude that the presence of opiate receptors in human platelets is unlikely.

Blood collection and preparation of citrated platelet-rich and platelet-poor plasmas were done according to Han and Ardlie<sup>12</sup>. Platelet aggregation was measured by the turbidometric technique of Born<sup>13</sup>, as described previously<sup>14</sup>. Human platelet lysates were prepared by a modification of the method of Jakobs *et al.*<sup>15</sup>, as described previously<sup>14</sup>. Homogenates of rat corpus striatum (10% w/v in 0.32 M sucrose 10 mM Tris-HCl pH 7.6) and P<sub>2</sub>-pellets were prepared according to Gray and Whittaker<sup>16</sup>.

Adenylate cyclase activity in platelet lysates was determined as described previously by measuring the conversion of [ $\alpha$ -<sup>32</sup>P]ATP (Amersham) to <sup>32</sup>P-cyclic AMP by the method of Salomon<sup>17</sup>. Cyclic AMP accumulation in intact <sup>3</sup>H-adenine (Negev)-prelabelled platelets was as described previously<sup>17</sup>.

**Table 1** The effect of PGE<sub>1</sub> and morphine on PGE<sub>1</sub>-sensitive AC activity in platelet lysates

| Additions       | None            | Morphine<br>(13.3 $\mu$ M) | PGE <sub>1</sub><br>(0.35 $\mu$ M)       | PGE <sub>1</sub> +<br>morphine<br>(0.35 $\mu$ M<br>+ 13.3 $\mu$ M) |
|-----------------|-----------------|----------------------------|--|--|
|                 |                 |                            | cAMP (pmol per mg<br>protein per 10 min) |  |
| Donor 1         | 86              | 110                        | 2,103                                    | 2,108  |
| Donor 2         | 116             | 110                        | 2,122                                    | 2,046  |
| Donor 3         | 106             | 87                         | 684                                      | 643  |
| Donor 4         | 65              | 71                         | 1,395                                    | 1,152  |
| Mean $\pm$ s.d. | 93.2 $\pm$ 13.0 | 94.5 $\pm$ 11              | 1,576 $\pm$ 395                          | 1,487 $\pm$ 411  |
| P value         |                 | NS                         |  | NS   |

Each value is the average of duplicate determinations. NS, not significant by paired *t*-test.

Binding of  $^3\text{H}$ -etorphine (Amersham) to platelet lysates was measured as described for rat brain homogenates<sup>18</sup>. The amount of lysate protein was 0.05–0.45 mg per assay.  $^3\text{H}$ -etorphine concentration was 3.0 nM and incubations were performed in a final volume of 250  $\mu\text{l}$  for 30 min at 37 °C. The experiments were repeated 3–5 times with platelet preparations derived from several healthy volunteers who had not taken any drugs for at least 1 week before blood collection.

$\text{PGE}_1$ , 0.02–0.34  $\mu\text{M}$ , inhibited ADP-induced aggregation in a dose-dependent manner. In five experiments we used 0.14  $\mu\text{M}$   $\text{PGE}_1$  (the concentration used by Gryglewski *et al.*<sup>11</sup>). At this concentration  $\text{PGE}_1$  inhibited ADP-induced platelet aggregation by  $70.5\% \pm 1 \text{ s.e.m.}$  In these conditions we tested a wide range of morphine concentrations (13.2–53  $\mu\text{M}$ ). No significant effect on the anti-aggregating properties of  $\text{PGE}_1$  could be demonstrated.

Stimulation of platelet AC by  $\text{PGE}_1$  in the concentration range of 0.01–0.35  $\mu\text{M}$  was dose dependent. At the highest concentration (0.35  $\mu\text{M}$ ),  $\text{PGE}_1$  stimulated AC activity by about 6–20-fold (Table 1). We tested platelet preparations from four donors but could not demonstrate any inhibitory effect of morphine (13.3  $\mu\text{M}$ ) on basal (unstimulated) or  $\text{PGE}_1$ -sensitive AC activity (Table 1). The concentration of morphine selected for this experiment was that reported by Gryglewski *et al.*<sup>11</sup> to be optimal in their experiments.

**Table 2** The effect of  $\text{PGE}_1$  and morphine on the intracellular accumulation of  $^3\text{H}$ -cyclic AMP in intact platelets prelabelled with [ $2\text{-}^3\text{H}$ ]adenine

| Additions                            | Morphine ( $\mu\text{M}$ )        |              |              |
|--------------------------------------|-----------------------------------|--------------|--------------|
|                                      | 0                                 | 13.3         | 26           |
|                                      | $^3\text{H}$ -cyclic AMP (c.p.m.) |              |              |
| None                                 | $85 \pm 2$                        | $93 \pm 5$   | $98 \pm 2$   |
| $\text{PGE}_1$ (0.14 $\mu\text{M}$ ) | $496 \pm 25$                      | $525 \pm 19$ | $540 \pm 28$ |

Results are given in c.p.m., mean  $\pm$  s.d. ( $n = 4$ ).

To eliminate the possibility that the inhibitory effect of morphine may not be demonstrable at saturating  $\text{PGE}_1$  concentrations, we also tested its effect at submaximal concentrations of  $\text{PGE}_1$ . At 0.04  $\mu\text{M}$   $\text{PGE}_1$ , AC activity was stimulated over 65–490 pmol cyclic AMP per mg protein per 10 min. Addition of a wide range of morphine concentrations (1.33–79.8  $\mu\text{M}$ ) did not inhibit the basal or the  $\text{PGE}_1$ -stimulated enzyme activity. The same results were obtained with lysates preincubated with morphine (2 min, 30 °C) before the AC assay.

Similar negative observations were also made with intact platelets.  $\text{PGE}_1$  (0.14–0.7  $\mu\text{M}$ ) stimulated cyclic AMP accumulation by 1.8- to 10.1-fold over the unstimulated controls. The addition of morphine (2.6–26  $\mu\text{M}$ ) did not affect the unstimulated controls. The addition of morphine (2.6–26  $\mu\text{M}$ ) did not affect the stimulatory action of  $\text{PGE}_1$ . A typical experiment in which the lowest concentration of  $\text{PGE}_1$  (0.14  $\mu\text{M}$ ) was used in combination with 13.3 or 26  $\mu\text{M}$  morphine is given in Table 2.

In direct binding studies of  $^3\text{H}$ -etorphine to platelet lysate preparations, we failed to demonstrate any specific binding. The difference between the amount of  $^3\text{H}$ -etorphine bound in the absence or presence of 10  $\mu\text{M}$  levorphanol was not significantly different from zero (four duplicate determinations performed on each platelet preparation obtained from four donors). Simultaneously with these determinations, and in identical experimental conditions, we also measured the binding of  $^3\text{H}$ -etorphine to a particulate fraction derived from rat corpus striatum as a control tissue. The content of  $^3\text{H}$ -etorphine binding sites in this brain preparation was  $315 \pm 45 \text{ fmol per mg protein}$  ( $n = 4$ ). Binding of  $^3\text{H}$ -etorphine in the presence of 10  $\mu\text{M}$  levorphanol did not exceed 25–40% of the amount bound in the absence of the unlabelled competing ligand.

In conclusion, the inverse relationship of cyclic AMP levels and aggregability of human platelets is now well documented<sup>19</sup>, as  $\text{PGE}_1$ , which stimulates platelet AC<sup>10</sup>, also antagonizes ADP-

induced aggregation<sup>9</sup>. Furthermore, this relationship also seems to hold for nonspecific agents such as heparin and dextran sulphate, recently demonstrated by us to inhibit  $\text{PGE}_1$ -stimulated AC on the one hand and to augment platelet aggregation on the other<sup>14,20–22</sup>. Although opiates act as inhibiting agonists of AC in some cell types of neural origin, we are so far unable to support the suggestion made by Gryglewski *et al.*<sup>11</sup> that 'AC is the common target for  $\text{PGE}_1$  and morphine in platelets as it is in neurones'. We therefore suggest that the presence of opiate receptors in human platelets remains questionable.

This work was supported by grants to A.R. from the Charles E. Smith Family Foundation, the Israel Center for Psychobiology and from the joint research fund of the Hebrew University and Hadassah, the Dr Leon Deutsch Memorial Endowment Fund; to Y.S. from the US-Israel Binational Science Foundation, and to Professor H. R. Lindner by the Ford Foundation and Population Council. Y.S. is the incumbent of the Charles and Tillie Lubin Career Development Chair. We thank Professor H. R. Lindner for helpful discussions and Mrs E. Epstein and M. Kopelowitz for secretarial assistance.

Received 27 May; accepted 15 October 1980.

- Collier, H. O. J. & Roy, A. C. *Nature* **248**, 24–27 (1974).
- Collier, H. O. J. & Roy, A. C. *Prostaglandins* **7**, 361–376 (1974).
- Sharma, S. K., Nirenberg, M. & Klee, W. A. *Proc. natn. Acad. Sci. U.S.A.* **72**, 590–594 (1975).
- Traber, J., Fischer, K., Latzin, S. & Hamprich, B. *Nature* **253**, 120–122 (1975).
- Tell, G. P., Pasternak, G. W. & Cuatrecasas, P. *FEBS Lett.* **51**, 242–245 (1975).
- van Inwegen, R. G., Strada, S. J. & Robison, G. A. *Life Sci.* **16**, 1875–1876 (1976).
- Katz, J. B. & Catravas, G. N. *Brain Res.* **120**, 263–268 (1977).
- Havemann, V. & Kuschinsky, K. *Arch. Pharmac.* **302**, 103–106 (1978).
- Kloze, J. in *Prostaglandins, Proc. 2nd Nobel Symp.*, Stockholm (eds Bergstrom, S. & Samuelson, B.) 241 (Interscience, New York, 1976).
- Wolfe, S. M. & Shulman, N. R. *Biochem. biophys. Res. Commun.* **35**, 265–272 (1969).
- Gryglewski, R. J., Szczeklik, A. & Bierson, K. *Nature* **256**, 56–57 (1975).
- Han, P. & Ardlie, N. G. *Br. J. Haemat.* **26**, 331–356 (1974).
- Born, G. V. R. *Nature* **194**, 927–929 (1962).
- Reches, A., Eldor, A. & Salomon, Y. *J. Lab. clin. Med.* **93**, 638–644 (1979).
- Jakobs, K. H., Saur, W. & Schultz, G. *J. Cyclic Nucleotide Res.* **2**, 381–392 (1976).
- Gray, E. G. & Whittaker, V. P. *J. Anat.* **96**, 79–87 (1962).
- Salomon, Y. *Adv. Cyclic Nucleotide Res.* **10**, 35–55 (1979).
- Vogel, Z. & Alstein, M. *FEBS Lett.* **98**, 44–48 (1979).
- Salzman, E. W. *New Engl. J. Med.* **286**, 358–363 (1972).
- Reches, A., Eldor, A. & Salomon, Y. *Israel J. med. Sci.* **14**, 990 (1978).
- Reches, A., Eldor, A. & Salomon, Y. *Israel J. med. Sci.* **15**, 81 (1979).
- Reches, A., Eldor, A. & Salomon, Y. *Thromb. Res.* **16**, 107–116 (1979).

## Induction of diabetes by cumulative environmental insults from viruses and chemicals

Antonio Toniolo, Takashi Onodera, Ji-Won Yoon & Abner Louis Notkins

Laboratory of Oral Medicine, National Institute of Dental Research, National Institutes of Health, Bethesda, Maryland 20205

Encephalomyocarditis virus (EMC) induces diabetes in certain inbred strains of mice by infecting and destroying pancreatic  $\beta$  cells<sup>1,2</sup>, the severity of the diabetes depending on the number of  $\beta$  cells destroyed<sup>3</sup>. In strains of mice resistant to EMC-induced diabetes, insufficient  $\beta$  cells are damaged to alter glucose homeostasis<sup>3,4</sup>. However, diabetes can be produced in many species by streptozotocin, a highly specific  $\beta$ -cell toxin<sup>5</sup>. Here, we used concentrations of streptozotocin that did not produce diabetes, but reduced the  $\beta$ -cell reserve. When strains of mice normally resistant to EMC-induced diabetes were first treated with sub-diabetogenic doses of streptozotocin, then infected with EMC virus, diabetes developed. Furthermore, when mice were infected with viruses such as Coxsackie B3 and B5, which ordinarily produce little if any  $\beta$ -cell damage<sup>6</sup>, diabetes developed if the mice were first treated with sub-diabetogenic doses of streptozotocin. These findings suggest that diabetes may result from cumulative  $\beta$ -cell damage induced by sequential environmental insults.



Male mice, 4–6 weeks old, weighing 20–25 g (Jackson Laboratories or NIH), were used in these experiments. A highly diabetogenic variant of EMC virus, designated D, and a non-diabetogenic variant, designated B, were prepared in secondary mouse embryo cells as described elsewhere<sup>7</sup>. Unless otherwise indicated, the D variant was used in all experiments. Coxsackieviruses B3 (Nancy strain) and B5 (Faulkner strain) (both from American Type Culture Collection) were passaged in cultures enriched with murine pancreatic  $\beta$  cells<sup>8</sup>. The preparation of fluorescein-labelled anti-EMC antibody and the detection of infected islet cells were carried out as described elsewhere<sup>3,4</sup>.

Mice were injected intraperitoneally with a sub-diabetogenic dose of streptozotocin (1 mg per mouse, mixed anomers, Sigma lot 29C-0009), which did not significantly alter glucose homeostasis in preliminary experiments. Twelve days after administration of streptozotocin, mice were infected intraperitoneally with virus. Each animal was then bled four times; glucose from non-fasting animals was measured 7 and 14 days after infection and single-point 60-min glucose tolerance tests were performed 10 and 17 days after infection. Uninfected animals and animals given only streptozotocin were bled at the same time. The weighted results were expressed as the glucose index<sup>9</sup>. An animal was considered diabetic if its glucose index was equal to or exceeded 3 s.d. above the mean of 124 uninfected mice (mean  $\pm$  s.d. =  $163 \pm 23$ ).

Table 1 shows that the glucose index and percentage of animals developing diabetes was increased if diabetes-prone strains of mice<sup>4,10</sup> were treated with sub-diabetogenic doses of streptozotocin before infection with EMC virus. The most striking results were obtained with NIH/Swiss mice in which the glucose index increased from 223 in mice receiving only EMC virus to 442 in mice receiving both streptozotocin and EMC virus, and the percentage of animals developing diabetes rose

from 28 to 92. Increases in the glucose index were also observed in SJL/J and NFS/N mice. The enhancement in diabetes-prone mice suggested that strains of mice which were ordinarily resistant to EMC-induced diabetes<sup>4,10</sup> might become diabetic if first treated with sub-diabetogenic doses of streptozotocin. As seen in Table 1, 18%, 30%, 53% and 100% of C3H/HeJ, C57BL/6J, CBA/J and AKR/J mice, respectively, developed diabetes when treated with streptozotocin and infected 12 days later with EMC virus.

Treatment of mice with a low dose of streptozotocin also led to the induction of diabetes by viruses which ordinarily did not elevate blood glucose levels. Table 2 shows that Coxsackieviruses B3 and B5 produced diabetes in animals which had been treated with a sub-diabetogenic dose of streptozotocin, whereas in untreated animals these viruses produced little if any diabetes. However, the non-diabetogenic B variant of EMC virus<sup>7</sup> did not produce diabetes in either streptozotocin-treated or untreated mice.

To determine whether streptozotocin enhanced virus-induced diabetes by increasing the susceptibility of islet cells (for example, by immunosuppressing the host)<sup>11</sup>, the number of EMC-infected islet cells was determined by staining sections of pancreas with fluorescein-labelled anti-EMC virus antibody<sup>3,4</sup>. Table 3 shows that approximately the same or slightly fewer islet cells were infected in streptozotocin-treated mice as in untreated mice. This suggests that streptozotocin is acting by decreasing the  $\beta$ -cell reserve rather than by increasing the susceptibility of  $\beta$  cells to infection. In fact, microscopic examination of sections of pancreas from mice treated with streptozotocin (1 mg per mouse) showed that some  $\beta$  cells had been destroyed. Furthermore, quantification by radioimmunoassay revealed that the insulin content of the pancreas of mice treated with 1 and 2 mg of streptozotocin was reduced by 15% and 48%, respectively, 12 days later.

**Table 1** Enhancement of virus-induced diabetes by treatment with sub-diabetogenic doses of streptozotocin

| Mouse strain              | Streptozotocin |               | EMC virus     |              | Streptozotocin and EMC virus |              |
|---------------------------|----------------|---------------|---------------|--------------|------------------------------|--------------|
|                           | Glucose index* | Diabetic (%)† | Glucose index | Diabetic (%) | Glucose index                | Diabetic (%) |
| <b>Diabetes-prone</b>     |                |               |               |              |                              |              |
| NIH/Swiss                 | 142 $\pm$ 29   | 0             | 223 $\pm$ 89  | 28           | 442 $\pm$ 153                | 92           |
| SJL/J                     | 166 $\pm$ 16   | 0             | 333 $\pm$ 113 | 76           | 466 $\pm$ 126                | 89           |
| NFS/N                     | 172 $\pm$ 15   | 0             | 358 $\pm$ 47  | 100          | 448 $\pm$ 80                 | 100          |
| <b>Diabetes-resistant</b> |                |               |               |              |                              |              |
| C3H/HeJ                   | 186 $\pm$ 18   | 0             | 151 $\pm$ 23  | 0            | 202 $\pm$ 30                 | 18           |
| C57BL/6J                  | 126 $\pm$ 24   | 0             | 152 $\pm$ 33  | 6            | 203 $\pm$ 89                 | 30           |
| CBA/J                     | 185 $\pm$ 17   | 0             | 183 $\pm$ 24  | 0            | 234 $\pm$ 38                 | 53           |
| AKR/J                     | 189 $\pm$ 39   | 13            | 172 $\pm$ 29  | 0            | 345 $\pm$ 95                 | 100          |

Each mouse was given 1 mg of streptozotocin and 12 days later infected with  $1.0 \times 10^4$  plaque-forming units (PFU) of the D variant of EMC virus.

\* Approximately 20 mice were tested in each group (mean  $\pm$  s.d.).

† Percentage of mice with a glucose index 3 s.d. above the mean of uninfected controls.

**Table 2** Induction of diabetes by Coxsackieviruses in mice treated with sub-diabetogenic doses of streptozotocin

| Mouse strain | Virus  | Streptozotocin |               | Virus         |              | Streptozotocin and virus |              |
|--------------|--------|----------------|---------------|---------------|--------------|--------------------------|--------------|
|              |        | Glucose index* | Diabetic (%)† | Glucose index | Diabetic (%) | Glucose index            | Diabetic (%) |
| SJL/J        | Cox B3 | 149 $\pm$ 35   | 0             | 198 $\pm$ 28  | 18           | 241 $\pm$ 43             | 59           |
| NFS/N        | Cox B3 | 180 $\pm$ 22   | 0             | 158 $\pm$ 18  | 0            | 285 $\pm$ 76             | 76           |
| NFS/N        | Cox B5 | 180 $\pm$ 22   | 0             | 166 $\pm$ 13  | 0            | 267 $\pm$ 58             | 67           |
| SJL/J        | EMC(B) | 177 $\pm$ 12   | 0             | 175 $\pm$ 14  | 0            | 191 $\pm$ 17             | 0            |

Each mouse was given 1 mg of streptozotocin and 12 days later infected with  $1.0 \times 10^5$  PFU of Coxsackievirus B3 or B5, or  $1.0 \times 10^6$  PFU of the B variant of EMC virus.

\* Approximately 20 mice were tested in each group (mean  $\pm$  s.d.).

† Percentage of mice with a glucose index 3 s.d. above the mean of uninfected controls.

In the normal animal there are enough  $\beta$  cells to maintain glucose homeostasis—only when the  $\beta$ -cell reserve is sufficiently depleted does hyperglycaemia develop<sup>5</sup>. Our experiments show that, by reducing the  $\beta$ -cell reserve with a sub-diabetogenic dose of streptozotocin, it is possible to produce diabetes in strains of mice which are usually resistant to EMC-induced diabetes. In previous experiments with EMC virus, we found that over 40% of the  $\beta$  cells in the pancreas of diabetes-prone SJL/J mice contained viral antigens, as opposed to less than 12% of  $\beta$  cells from diabetes-resistant CBA/J, AKR/J and C57BL/6J mice<sup>4</sup>.

**Table 3** Percentage of cells in islets of Langerhans containing viral antigens

| Mouse strain | Pretreatment with streptozotocin* | (% infected islet cells)<br>(days after infection) <sup>†</sup> |     |     |
|--------------|-----------------------------------|---|-----|-----|
|              |                                   | (2)   | (3) | (4) |
| C57BL/6J     | +                                 | 2   | 12  | 7   |
| C57BL/6J     | —                                 | 2   | 12  | 9   |
| SJL/J        | +                                 | 30  | 36  | 10  |
| SJL/J        | —                                 | 41  | 44  | 12  |

\* Each mouse received 1 mg of streptozotocin intraperitoneally 12 days before infection with  $1.0 \times 10^4$  PFU of the D variant of EMC virus.

<sup>†</sup> At 2, 3 and 4 days after infection, sections of pancreas from groups of three mice were stained with fluorescein-labelled anti-EMC antibody and the approximate number of cells containing viral antigens determined. At each time point, an average of 40 islets and over 2,000 cells were counted.

It was concluded that the latter strains did not develop diabetes because  $\beta$ -cell damage was insufficiently extensive. The experiments reported here show that neither a low dose of streptozotocin alone nor EMC virus alone produced diabetes, but the combined insult resulted in diabetes. Similarly, Coxsackieviruses B3 and B5 produced relatively little  $\beta$ -cell damage in untreated animals, but when the  $\beta$ -cell reserve was reduced by a low dose of streptozotocin, the animals developed diabetes.

Depletion of  $\beta$  cells in mice by sub-diabetogenic doses of streptozotocin may provide a useful model for identifying other diabetogenic viruses, especially those which infect and destroy only minimal numbers of  $\beta$  cells. The enhancement of virus-induced diabetes by low doses of streptozotocin also raises the possibility that in humans a series of viral infections or other environmental insults (for example, chemicals, drugs, toxins), each producing some  $\beta$ -cell damage, finally results in overt insulin-dependent diabetes once the  $\beta$ -cell reserve has been sufficiently depleted.

Genetic factors are also known to play an important role in the development of insulin-dependent diabetes<sup>2</sup>, but precisely how is not clear. If the result is a relative deficiency of  $\beta$  cells or an impaired capacity to regenerate damaged  $\beta$  cells, then viruses, chemicals or drugs might more readily produce diabetes in these already deficient individuals.

We thank Tecolia Brown and Royd Ellis for technical assistance.

Received 28 April; accepted 30 September 1980.

1. Craighead, J. E. *Prog. med. Virol.* **19**, 161–214 (1975).
2. Notkins, A. L. *Scient. Am.* **241**, 62–73 (1979).
3. Hayashi, K., Boucher, D. W. & Notkins, A. L. *Am. J. Path.* **75**, 91–102 (1974).
4. Yoon, J. W., Onodera, T. & Notkins, A. L. *J. gen. Virol.* **37**, 225–232 (1977).
5. Junod, A., Lambert, A. E., Stauffacher, W. & Renold, A. E. *J. clin. Invest.* **48**, 2129–2139 (1969).
6. Ross, M. E., Hayashi, K. & Notkins, A. L. *J. infect. Dis.* **129**, 669–676 (1974).
7. Yoon, J. W., McClintock, P. R., Onodera, T. & Notkins, A. L. *J. exp. Med.* **152**, 878–892 (1980).
8. Yoon, J. W., Onodera, T. & Notkins, A. L. *J. exp. Med.* **148**, 1068–1080 (1978).
9. Ross, M. E., Onodera, T., Brown, K. S. & Notkins, A. L. *Diabetes* **25**, 190–197 (1976).
10. Boucher, D. W., Hayashi, K., Rosenthal, J. & Notkins, A. L. *J. infect. Dis.* **131**, 462–466 (1975).
11. Saiki, O., Negoro, S., Tsuyugueshi, I. & Yamamura, Y. *Infect. Immun.* **28**, 127–131 (1980).

## Tolerance as an active process

Judy M. Teale & Norman R. Klinman

The Department of Cellular and Developmental Immunology, Scripps Clinic and Research Foundation, La Jolla, California 92037

The clonal deletion model proposed by Burnet<sup>1</sup> and Lederberg<sup>2</sup> and expanded by Nossal<sup>3</sup> was one of the first theories concerning the nature of tolerance to self constituents. The model proposed that during the maturation of lymphocytes into immunocompetent cells, there is a sensitive differentiation stage whereby contact with antigen results in specific inactivation of the cell. Experimental evidence indicates that neonatal or immature B lymphocytes are indeed different from adult lymphocytes in their extreme sensitivity to tolerance induction even at low antigen concentrations and with antigens that are normally immunogenic<sup>3–9</sup>. The present study examines the mechanism of this tolerance phenomenon by determining whether or not tolerance of immature B cells is an active process and what specific interactions can induce this event. We used various putative inhibitors of tolerance induction in the splenic focus assay<sup>4</sup> which examines the tolerance susceptibility of individual B cells. The results suggest that tolerance requires protein synthesis and that this process is initiated only after a minimum threshold affinity of binding occurs between antigen and cell-surface receptor with subsequent receptor interlinkage.

Nonimmune neonatal or adult spleen cells were injected intravenously into irradiated (1,300R) BALB/c recipients that had been primed with 0.1 mg of *Limulus polyphemus* haemocyanin(Hy) 6–12 weeks previously. At 16–18 h after transfer, fragment cultures derived from the recipient spleens were prepared and incubated for 18 h in Dulbecco's modified Eagle's medium (DMEM) with or without the presence of the tolerogen dinitrophenol-ovalbumin (DNP<sub>10</sub>-OVA) at  $10^{-6}$  M DNP<sup>4</sup>. To study the inhibition of tolerance induction, concentrations of putative inhibitors were chosen which, if removed after the first 18 h of culture and before antigenic stimulation, had no inhibitory effect on stimulation. Thus, by adding DNP<sub>10</sub>-OVA in the presence or absence of the inhibitors for the first 18 h of culture, the effect of each inhibitor on tolerance could be determined. The DNP<sub>10</sub>-OVA and/or inhibitors were washed out after 18 h and DMEM containing the antigen DNP<sub>10</sub>-Hy ( $10^{-6}$  M DNP)<sup>4</sup> was added. Culture supernatants were collected on days 10, 13 and 17 and analysed for the presence of anti-DNP antibody by a

**Table 1** A requirement for protein synthesis during tolerance induction

| Age of donor cells | Experimental group                 | % Of control response* |
|--------------------|------------------------------------|------------------------|
| 1–3 day neonatal   | Tolerogen (DNP <sub>10</sub> -OVA) | 28.5 ± 7.0             |
| 1–3 day neonatal   | Puromycin alone                    | 87.5 ± 12.7            |
| 1–3 day neonatal   | Tolerogen + puromycin              | 92.1 ± 3.8             |
| 10–12 week adult   | Tolerogen (DNP <sub>10</sub> -OVA) | 100                    |
| 10–12 week adult   | Puromycin alone                    | 77.0                   |
| 10–12 week adult   | Tolerogen + puromycin              | 77.0                   |

Adult or neonatal spleen cells were transferred to carrier-primed recipients ( $4\text{--}6 \times 10^6$  donor cells per recipient). Fragment cultures were incubated for 18 h in the presence or absence of the tolerogen DNP<sub>10</sub>-OVA and in the presence or absence of the inhibitor puromycin ( $25 \mu\text{g ml}^{-1}$  for adult groups,  $20 \mu\text{g ml}^{-1}$  for neonatal groups). The tolerogen and/or inhibitor was/were washed out after 18 h and stimulated for 3 days with DNP-Hy ( $10^{-6}$  M DNP). Supernatants were collected on days 10, 13 and 17 and the frequency of anti-DNP-secreting clones was detected by RIA. Data are expressed as per cent of control response.

\* Neonatal groups represent the means of three experiments ± s.e.m. Adult groups represent the average of two experiments.



solid-phase radioimmunoassay (RIA). The anti-DNP antibody was detected in RIA through the use of rabbit anti-mouse immunoglobulin followed by  $^{125}\text{I}$ -labelled purified goat anti-rabbit immunoglobulin<sup>10</sup>.

To determine if tolerance of neonatal B cells represents an active process which would require a trigger, the effect of the protein biosynthesis inhibitor, puromycin, was studied. It was assumed that any effect on tolerance observed would be due to the effect of puromycin on the neonatal donor B cells, although there is a remote possibility that the highly irradiated cells also present in the fragment are involved in tolerance and, therefore, would be affected by puromycin. Table 1 shows that puromycin substantially inhibits the induction of tolerance by DNP<sub>10</sub>-OVA resulting in stimulation and production of anti-DNP-secreting clones at a frequency close to that observed in control cultures. On the other hand, when adult B cells were assayed using the same experimental procedure, they were found to be resistant to tolerance induction as reported elsewhere<sup>4,5</sup> and the addition of puromycin was, therefore, inconsequential. The requirement for protein biosynthesis during tolerance induction of neonatal B cells provides compelling evidence that tolerance is an active process and cannot be explained simply by passive phenomena such as receptor blockade<sup>11,12</sup>.

Our next concern was the mechanism by which immature B cells are induced into the tolerance mode, including the antigen-binding prerequisites of the tolerance trigger. Although previous studies had indicated that multivalent antigens maximize tolerance induction<sup>4,13</sup>, a requirement for multivalent interactions during tolerance had not been tested directly. Thus, the effect of various concentrations of DNP-L-lysine on DNP<sub>10</sub>-OVA-induced tolerance was ascertained. Table 2 indicates that a 10-fold higher molar concentration of DNP-L-lysine as compared with the molar concentration of DNP present on DNP<sub>10</sub>-OVA markedly inhibits tolerance induction. Inhibitory effects of equal molar concentrations and 10-fold lower concentrations of DNP-L-lysine can also be seen. This finding demonstrates the necessity for multivalent interactions between tolerogen and cell-surface receptors. As DNP-L-lysine can bind receptors with a high enough affinity to inhibit tolerance induced by DNP presented multivalently, it is inferred that binding alone is not sufficient to trigger tolerance but that receptor interlinkage must be achieved.

It is well known that the antibody products from most DNP-specific B cells can bind to the hapten trinitrophenol (TNP)<sup>14,15</sup>. However, TNP antigens seem incapable of stimulating primary DNP-specific B cells<sup>14,15</sup> or of tolerizing DNP-specific immature B cells<sup>4</sup>. Therefore, it was of interest to determine if various concentrations of TNP-L-lysine could inhibit tolerance induction by DNP<sub>10</sub>-OVA (Table 2). Similar to the experiments using DNP-L-lysine, a 10-fold higher molar concentration of TNP-L-lysine as compared with the molar concentration of DNP on DNP<sub>10</sub>-OVA resulted in almost complete inhibition of tolerance. However, equal and 10-fold lower concentrations of TNP-L-lysine resulted in little or no

inhibition of tolerance induction, indicating that a higher ratio of TNP to DNP is necessary to inhibit tolerance than when the homologous hapten is used as an inhibitor. This suggests that TNP-L-lysine binds to DNP-specific B cells but at a lower affinity than DNP-L-lysine. As TNP-L-lysine does bind to the receptors of DNP-specific B cells, the failure of TNP antigens to trigger DNP-specific B cells is probably directly related to the affinity with which it is bound by the cell's receptors.

**Table 3** Inhibition of DNP<sub>12</sub>-OVA-induced tolerance with TNP<sub>17</sub>-BSA

| Experimental treatment  | % Of control response* |
|---|------------------------|
| DNP response  |                        |
| Tolerogen alone (DNP <sub>10</sub> -OVA, $10^{-6}$ M)                                   | 27.8 ± 7.8             |
| Tolerogen (DNP <sub>10</sub> -OVA, $10^{-6}$ M) + TNP <sub>17</sub> -BSA ( $10^{-5}$ M) | 89.6 ± 10.5            |
| TNP <sub>17</sub> -BSA ( $10^{-5}$ M)   | 100                    |
| TNP response  |                        |
| Tolerogen (TNP <sub>17</sub> -BSA, $10^{-6}$ M)   | 33.3                   |

For the DNP response, the same procedure was used as described in Table 1 legend except TNP<sub>17</sub>-BSA was used as inhibitor. For the TNP response, TNP<sub>17</sub>-BSA was used as tolerogen and TNP<sub>10</sub>-Hy ( $10^{-6}$  M) as antigen.

\* Results represent the mean ± s.e.m. of three experiments. The results represent the average of two experiments where the s.e.m. is omitted.

To test directly the postulate that TNP antigens bind to DNP-specific B cells but fail to trigger these cells because the affinity of such binding is too low, an excess of TNP presented multivalently with bovine serum albumin (TNP<sub>17</sub>-BSA) was tested for its ability to inhibit DNP<sub>10</sub>-OVA-induced tolerance. As shown in Table 3, TNP<sub>17</sub>-BSA inhibits DNP<sub>10</sub>-OVA-induced tolerance demonstrating its ability to bind to DNP-specific B cells yet its inability to tolerize these cells. Also included in Table 3 are data which show that the same preparation of TNP<sub>17</sub>-BSA is an effective tolerogen for TNP-specific cells. The ability to distinguish between two closely related haptens demonstrates that the tolerance trigger is an extremely specific one and that this specificity apparently depends on a minimum threshold affinity of binding between tolerogen and receptor. Below this threshold the tolerogen may not bind to the receptor long enough to achieve stable interlinkage of receptors<sup>16</sup>.

If one compares the analyses of the apparent binding requisites of stimulation with the present findings on tolerance, obvious parallels can be drawn between the two processes. First, despite a few reports to the contrary<sup>17-19</sup>, monovalent haptens seem unable to induce stimulation<sup>13,20,21</sup>, and in fact, can inhibit stimulation induced by the same hapten presented multivalently<sup>16</sup>. Thus, stimulation, like tolerance, apparently requires multivalent determinant presentation and receptor interlinkage<sup>13,16,20-22</sup>. Whether or not this is analogous to the receptor patching-capping-endocytosis cycle induced by anti-immunoglobulin<sup>23</sup> or some antigens<sup>23-25</sup> is unclear as considerably greater concentrations of either anti-immunoglobulin or antigen are required to induce this cycle than are required to induce either stimulation or tolerance<sup>25</sup>. In any event, more than receptor modulation is required to achieve both stimulation and tolerance as protein synthesis is required (ref. 26 and this work), a requirement not found necessary for the patching-capping-endocytosis cycle<sup>23</sup>.

Similarly, both the tolerance and the stimulation seem to be dependent on a minimum threshold affinity of binding between antigen and receptor. Earlier studies demonstrating the affinity dependence of stimulation showed that increasing concentrations of antigen above  $5 \times 10^{-7}$  M did not stimulate a higher frequency of cells nor did it stimulate more cells producing lower-affinity antibody<sup>15,16</sup>. Clearly, antigen-binding cells did not correlate with cells capable of being triggered. Correspondingly, as mentioned previously, it was found that TNP on an

**Table 2** Inhibition of the tolerance trigger by monovalent haptens

| Experimental treatment                                    | % Of control response* |            |
|---|------------------------|------------|
|   | Neonates               | Adult      |
| Tolerogen alone (DNP <sub>10</sub> -OVA, $10^{-6}$ M DNP) | 27.8 ± 9.3             | 100 ± 0    |
| Tolerogen + $10^{-7}$ M DNP-L-lysine                      | 60.4                   | 77.0       |
| Tolerogen + $10^{-6}$ M DNP-L-lysine                      | 77.3 ± 9.1             | 100 ± 0    |
| Tolerogen + $10^{-5}$ M DNP-L-lysine                      | 95.8 ± 3.4             | 85.2 ± 8.7 |
| Tolerogen + $10^{-7}$ M TNP-L-lysine                      | 25.0                   | Not done   |
| Tolerogen + $10^{-6}$ M TNP-L-lysine                      | 53.5 ± 10.4            | 100        |
| Tolerogen + $10^{-5}$ M TNP-L-lysine                      | 94.3 ± 2.9             | 100        |

The same procedure was used as described in Table 1 legend except that the indicated concentrations of monovalent haptens were used as inhibitors.

\* Results of three experiments ± s.e.m. Results represent the means of two experiments where s.e.m. is omitted.

appropriate carrier could not activate DNP-specific cells even though the antibody products cross-react<sup>13,14</sup>. Therefore, the stimulation trigger, like the tolerance trigger, is an extremely specific one that seems to be a consequence of the requirement for a minimum affinity of binding between the antigen and receptor. It should be emphasized that stimulation is a more complex process than tolerance. Stimulation involves not only antigen-receptor interaction but also interactions with other cell-surface receptors and/or cell types (for example, macro-

phages, T cells). Thus, these experiments on stimulation are open to other interpretations. In comparison, the tolerance trigger seems to be relatively simple, involving only antigen-receptor interactions. Thus, for the first time it has been possible to affix a requirement for both multivalency and a minimum binding affinity to the triggering of B cells by antigen.

This work was supported by the USPHS grant AI 15797 from the NIH. J.M.T. is supported by NIH Postdoctoral Fellowship AI 06038. We thank Miss Robin Eskoz for technical assistance.

Received 31 July; accepted 26 September 1980.

1. Burnet, F. M. in *The Clonal Selection Theory of Acquired Immunity* (Cambridge University Press, New York, 1959).
2. Lederberg, J. *Science* **129**, 1649-1651 (1959).
3. Nossal, G. J. V. & Pike, B. L. *J. exp. Med.* **141**, 904-917 (1975).
4. Metcalf, E. S. & Klinman, N. R. *J. exp. Med.* **143**, 1327-1340 (1976).
5. Teale, J. M., Layton, J. E. & Nossal, G. J. V. *J. exp. Med.* **150**, 205-217 (1979).
6. Teale, J. M. & Mandel, T. E. *J. exp. Med.* **151**, 429-445 (1980).
7. Scott, D. W., Venkataraman, M. & Jandinski, J. *J. Immun. Rev.* **43**, 241-280 (1979).
8. Kay, T. W., Pike, B. L. & Nossal, G. J. V. *J. Immun.* **124**, 1579-1584 (1980).
9. Etlinger, H. M. & Chiller, J. M. *J. Immun.* **122**, 2558-2563 (1979).
10. Pierce, S. K. & Klinman, N. R. *J. exp. Med.* **144**, 1254-1262 (1976).
11. Aldo-Benson, M. A. & Borel, Y. *J. Immun.* **122**, 1793-1803 (1974).
12. Diener, E. & Armstrong, W. D. *J. exp. Med.* **129**, 591-603 (1969).

13. Feldman, M. *J. exp. Med.* **135**, 735-753 (1972).
14. Klinman, N. R., Press, J. L. & Segal, G. P. *J. exp. Med.* **138**, 1276-1281 (1973).
15. Klinman, N. R. & Press, J. L. *Transplant. Rev.* **24**, 41-83 (1975).
16. Klinman, N. R. *J. exp. Med.* **136**, 241-260 (1972).
17. Watson, J., Trenker, E. & Cohn, M. *J. exp. Med.* **138**, 699-714 (1973).
18. Trenker, E. *J. Immun.* **113**, 918-924 (1974).
19. Schrader, J. W. *J. exp. Med.* **137**, 844-849 (1973).
20. Waldman, H. & Munro, A. *Transplant. Rev.* **23**, 213-222 (1975).
21. Vidal-Gomez, J. *Scand. J. Immun.* **8**, 313-321 (1978).
22. Dintzis, H. M., Dintzis, R. Z. & Vogelstein, B. *Proc. natn. Acad. Sci. U.S.A.* **73**, 3671-3675 (1976).
23. Schreiner, G. F. & Unanue, E. R. *Adv. Immun.* **24**, 37-165 (1976).
24. Ault, K. A. & Unanue, E. R. *J. exp. Med.* **139**, 1110-1124 (1974).
25. Nossal, G. J. V. & Layton, J. E. *J. exp. Med.* **143**, 511-528 (1976).
26. Van den Berg, K. J. & Betal, I. *Expt Cell Res.* **84**, 412-418, (1974).

## Major anti-paternal alloantibody induced by murine pregnancy is non-complement-fixing IgG1

Stephen C. Bell & W. David Billington

Reproductive Immunology Group, Department of Pathology, The Medical School, University of Bristol, Bristol BS8 1TD, UK

Maternal humoral immune responses against antigens of the genetically alien embryo have been reported in several mammalian species, including man, although little is known of the biological relevance of this phenomenon. In the mouse, only females of certain inbred strains mated repeatedly with an allogeneic male produce antibody directed against paternally inherited fetal histocompatibility antigens, as assessed by haemagglutination techniques<sup>1-4</sup>. It has been suggested that this characteristic of the female is associated with the H-2<sup>b</sup> haplotype<sup>3</sup>, although some reports indicate that it also extends to other H-2 types<sup>5</sup>. Potentially deleterious complement-dependent cytotoxicity, albeit at low levels, has been claimed to be associated with this alloantibody, but we have been unable to detect any such activity in a large number of maternal sera<sup>6</sup>. Four IgG isotypes (IgG1, IgG2a, IgG2b and IgG3) have been identified and shown to occur in the serum of normal animals<sup>7,8</sup>. Despite their similar physicochemical properties, which complicate purification procedures, the availability of immunoglobulin-secreting plasmacytomas has made possible the preparation of isotype-specific antisera<sup>9,10</sup>. Using these antisera in a modified haemadsorption assay<sup>11</sup>, we have now demonstrated that the major alloantibody response induced by murine pregnancy involves the non-complement-fixing IgG1 subclass. This is a noncytotoxic antibody with potentially protective (enhancing) properties<sup>12</sup>.

Mature C57BL (H-2<sup>b</sup>) inbred female mice were caged with fertile CBA/Ca (H-2<sup>k</sup>) males and pregnancies recorded following observation of vaginal plugs. Between 1 and 7 days after birth of their third litter, females were bled by cardiac puncture and the serum stored at -20°C. A group of C57BL animals were injected intraperitoneally (i.p.) with 3 × 10<sup>7</sup> spleen cells from CBA/Ca males in 0.2 ml of saline, at weekly intervals for 5 weeks. Fourteen days after the final injection, animals were bled by cardiac puncture and serum stored at -20°C. The IgG subclass of the alloantibody response was determined by a modified haemadsorption assay<sup>11</sup>, using sheep red blood cells (SRBCs) coated with rabbit anti-immunoglobulin, anti-IgG1 or

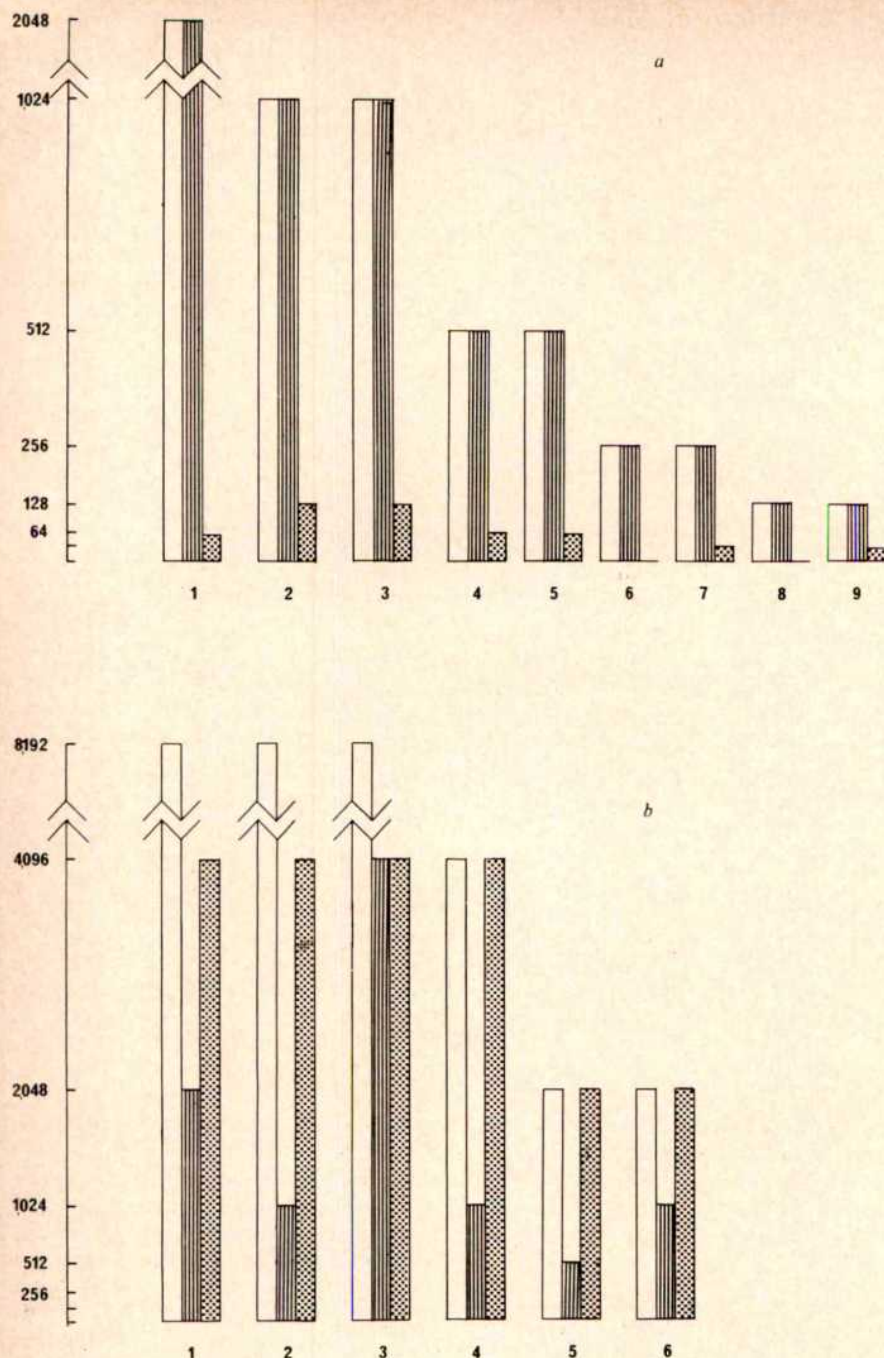
anti-IgG2 (Bionetics). Fibroblasts obtained by trypsinization of CBA/Ca 14-day embryos were cultured in immunofluorescence trays (Sterilin). After incubation with serial double dilutions of sera, plates were incubated with coated SRBCs. The presence of alloantibody was indicated by SRBC binding to the fibroblasts.

The sera from all nine multiparous females exhibited titres of alloantibody of the IgG1 subclass equivalent to the titres obtained with total immunoglobulin reagent (Fig. 1a). This indicates that approximately all the alloantibody present can be accounted for by IgG1 alloantibody. Although IgG2 alloantibody was detected in seven of the sera, this was present at only 1/32 to 1/8 of the levels of the IgG1 alloantibody. To compare this response with one induced by a well-documented route of immunization, sera from animals injected i.p. with allogeneic spleen cells were analysed. As shown in Fig. 1b, in three of the six sera the immunoglobulin levels could largely be accounted for by the IgG2 alloantibody (sera nos 4-6). In all cases, alloantibody of the IgG1 subclass was also detected, ranging from titres equal to those of the IgG2 alloantibody down to 1/4 of these levels. The finding in pregnancy of IgG1 alloantibody levels largely equivalent to those of the total immunoglobulins made it unnecessary, for the present purposes, to assess the precise level of any IgG3 response, especially as this is also believed to be a non-complement-fixing subclass. No cytotoxic activity was detected in any of the maternal sera.

The finding that the major alloantibody response directed against the paternally inherited fetal histocompatibility antigens in multiparous females is of the IgG1 subclass, and that no complement-dependent cytotoxicity is detectable in these sera, suggests that it represents a non-complement-fixing IgG1 subclass. All IgG1 antibodies have been assumed to be unable to fix complement<sup>10,13</sup>, although a cytotoxic complement-fixing IgG1 antibody has recently been demonstrated in mice injected intravenously with SRBCs<sup>14</sup>. The alloantibody induced by i.p. immunization was cytotoxic, and this seems attributable to the predominance of IgG2 alloantibody. Although seven of the multiparous females also produced IgG2 alloantibody the levels were clearly too low to effect cytotoxicity. It is interesting that the levels of IgG1 antibody in the immunized mice were similar to those in the pregnant females, for this suggests there may be a selective suppression of complement-fixing IgG2 antibody in pregnancy.

We know of no comparable data on antibody subclass distribution in pregnancy for other species. In the human, it is well established that antibodies with cytotoxic activity (which are used as HLA-typing reagents) may be detected in up to 15% of primiparous and 60% of multiparous women. However, in almost all cases the titre of such cytotoxic antibody is very low





**Fig. 1** Levels of anti-CBA/Ca ( $H-2^k$ ) alloantibody as total immunoglobulin, IgG1 and IgG2 subclasses in sera from nine multiparous C57BL ( $H-2^b$ ) females mated with CBA/Ca males (a) and six C57BL animals repeatedly immunized i.p. with CBA/Ca spleen cells (b). CBA/Ca fibroblasts ( $1 \times 10^5$  cells per well of immunofluorescence tray) were cultured for 24 h and, after removal of culture medium, serial double dilutions of test sera were incubated with the monolayer for 30 min. Sera were diluted with culture medium. Monolayers were then incubated for 30 min with SRBCs coated sequentially with mouse anti-SRBC sera and rabbit anti-mouse immunoglobulin, IgG1 or IgG2. After washing, monolayers were examined for SRBC binding. The final dilution of sera with which binding was obtained was considered to represent the alloantibody titre. Results shown are the reciprocal of the alloantibody titre obtained with □ anti-immunoglobulin; ■ anti-IgG1; ▨ anti-IgG2.

(usually less than 1/32) and it is quite possible that this does not represent the major alloantibody response. Further studies with different assay systems are required to determine whether there is a significant non-complement-fixing antibody response as in the mouse.

The factors responsible for regulation of the type of antibody response have not been fully defined, although the nature of the antigen and the route of immunization are certainly major determinants. In allogeneic murine pregnancy much information is available on the ontogeny and tissue distribution of  $H-2$  antigens on the fetus and placenta<sup>11</sup>, but the precise source of the stimulatory antigen and the timing and route of maternal immunization are unknown. If the factors that favour a predominantly non-complement-fixing IgG1 antibody response could be determined, this would throw light on the mechanisms responsible for the survival of the fetus as an intra-uterine allograft, especially those directly implicating maternal alloantibody or antigen-antibody complexes in the blocking of cell-mediated immune reactions. The present findings also caution

against the use of experimentally hyperimmunized female mice in studies on the role of pregnancy-induced maternal alloantibody in other feto-maternal immunological interactions.

We thank Mrs Sue Watts for technical assistance and the Rockefeller Foundation for financial support.

Received 27 May; accepted 9 October 1980.

- Goodlin, R. C. & Herzenberg, L. A. *Transplantation* **2**, 357-361 (1964).
- Kaliss, N. & Dagg, M. K. *Transplantation* **2**, 416-425 (1964).
- Kaliss, N. in *Immunology of Reproduction* (ed. Bratanov, K.) 495-511 (1973).
- Mishell, R. I., Herzenberg, L. A. & Herzenberg, L. A. *J. Immun.* **90**, 628-633 (1963).
- Chaouat, G., Voisin, G. A., Escalier, D. & Robert, P. *Clin. exp. Immun.* **35**, 13-24 (1979).
- Bell, S. C. & Billington, W. D. *J. Reprod. Immun.* (in the press).
- Fahey, J. L., Wunderlich, J. & Mishell, R. J. *exp. Med.* **120**, 223-240, 243-251 (1964).
- Grey, H. M., Hirst, J. W. & Cohn, M. *J. exp. Med.* **133**, 289-304 (1971).
- Potter, M. *Physiol. Rev.* **52**, 631-719 (1972).
- Nisonoff, A., Hopper, J. E. & Spring, S. B. *The Antibody Molecule*, 333-337 (Academic, New York, 1975).
- Sellens, M. H., Jenkinson, E. J. & Billington, W. D. *Transplantation* **25**, 173-179 (1978).
- Voisin, G. A. *Immun. Rev.* **49**, 3-59 (1980).
- Spiegelberg, H. L. *Adv. Immun.* **19**, 259-294 (1974).
- Ey, P. L., Prowse, S. J. & Jenkin, C. R. *Nature* **281**, 492-493 (1979).

## Spontaneous remission of autoimmune encephalomyelitis is inhibited by splenectomy, thymectomy or ageing

Avraham Ben-Nun, Yacov Ron & Irun R. Cohen

Department of Cell Biology, The Weizmann Institute of Science, Rehovot, Israel

**Experimental autoimmune encephalomyelitis (EAE) can be induced in genetically susceptible animals by injecting them with basic protein of myelin (BP) in a suitable adjuvant<sup>1</sup>. EAE in adult Lewis rats is expressed clinically by acute paralysis and histologically by mononuclear cell infiltration of the central nervous system. Most rats spontaneously recover from EAE and show little or no damage to myelin<sup>2</sup>. We report here that chronic progressive EAE with marked myelin lesions can be induced by a single injection of BP in complete Freund's adjuvant in intact 13-month old rats, or in 4-month old rats provided they have been splenectomized. Juvenile 2½-month old rats recover spontaneously despite splenectomy. Thymectomy of young adult rats leads to relapsing EAE. These results illustrate that the clinical course of EAE is markedly influenced by age and integrity of immune organs. Furthermore, they provide an experimental model with features similar to those of chronic relapsing disease of the nervous system of man.**

Eleven to twelve days following a single injection of BP emulsified in complete Freund's adjuvant, young adult Lewis rats develop paralysis, primarily of the tail and hind legs. Histological examination of the brain typically shows perivascular infiltration of mononuclear cells. The myelin is usually intact, or only slightly damaged, and within 5–6 days most rats spontaneously recover. A proportion of female rats has been reported to relapse after recovery<sup>3</sup> and the incidence of relapses can be increased by adrenalectomy after the onset of EAE<sup>4</sup>. Past experience<sup>2</sup> shows that relapses of EAE in young rats are not frequent and chronic EAE is rare.

EAE has been proposed as a model of human demyelinating diseases, such as multiple sclerosis<sup>5</sup> but this condition is characterized by a relapsing clinical course and extensive damage to myelin. Therefore rat EAE, as an acute monophasic disease, with little evidence of demyelination, is not a very faithful model of multiple sclerosis. The mechanisms responsible for recovery from EAE have not been identified. The thymus and spleen are organs which function in regulating some aspects of immune reactions<sup>6,7</sup>. To investigate the possible role of these organs in recovery we surgically removed the thymus from 6-week old Lewis rats and splenectomized 3-month old rats. When these rats were 4 months old we injected them with BP in adjuvant.

Untreated rats, or controls that underwent sham thymectomy or sham splenectomy, all developed EAE, judged by overt paralysis (see Table 1), and 10% of the rats died acutely. The remaining 90% were kept alive by individual supportive care with food and water, and all had a full clinical recovery. Histological examination of the brains 32 days after induction of EAE revealed perivascular infiltration of mononuclear cells. There was no evidence of myelin damage in these rats.

Four month old rats which had undergone thymectomy before induction of EAE demonstrated a different type of disease. Of the eight rats which survived the acute onset of EAE, three showed persistent paralysis. The other five recovered at about day 17, but all showed a relapse of clinical paralysis 3 days later, on day 20. Four of these five rats recovered from this relapse on day 24 but one had persistent paralysis. All the rats had marked perivascular infiltrates and all showed severe disruption of myelin.

Rats which had been splenectomized before induction of EAE developed acute disease, from which 2 out of 10 died. The remaining eight rats did not recover and showed persistent paralysis of the hind limbs until they were killed on day 32. The brains showed severe perivascular infiltration and myelin damage. Rats which had been thymectomized at 6 weeks then splenectomized at 3 months behaved about the same as those which had been splenectomized but not thymectomized.

It has been reported that spontaneous relapses are more common in 6-month old than in 3-month old rats<sup>8</sup>. Table 2 shows the results of an experiment in which we compared the responses of groups of rats which were splenectomized at 1½, 3 or 12 months. EAE was induced 1 month later. Rats aged 2½ months that had not died of acute EAE recovered, and no

**Table 1** Chronic or relapsing EAE in 4-month old Lewis rats following splenectomy or thymectomy

| Treatment     | Day of onset | Acute EAE |             | Recovery Day | Recovery Incidence | Chronic EAE Incidence | Relapse |           | Recovery from relapse |           | Grade of pathology |
|---------------|--------------|-----------|-------------|--------------|--------------------|-----------------------|---------|-----------|-----------------------|-----------|--------------------|
|               |              | (Total)   | (Mortality) |              |                    |                       | Day     | Incidence | Day                   | Incidence |                    |
| None          | 12           | 40/40     | 4/40        | 18           | 36/36              | 0/36                  | —       | 0/36      | —                     | —         | ++                 |
| Sham          |              |           |             |              |                    |                       |         |           |                       |           |                    |
| thymectomy    | 12           | 10/10     | 1/10        | 16           | 9/9                | 0/9                   | —       | 0/9       | —                     | —         | ++                 |
| Thymectomy    | 11           | 10/10     | 2/10        | 17           | 5/8                | 3/8                   | 20      | 5/5       | 24                    | 4/5       | ++++               |
| Sham          |              |           |             |              |                    |                       |         |           |                       |           |                    |
| splenectomy   | 11           | 10/10     | 1/10        | 17           | 9/9                | 0/9                   | —       | 0/9       | —                     | —         | ++                 |
| Splenectomy   | 10           | 10/10     | 2/10        | —            | 0/8                | 8/8                   | —       | —         | —                     | —         | ++++               |
| Thymectomy    |              |           |             |              |                    |                       |         |           |                       |           |                    |
| + splenectomy | 10           | 10/10     | 3/10        | —            | 0/7                | 7/7                   | —       | —         | —                     | —         | ++++               |

Thymectomy and splenectomy of female Lewis rats were performed under Nembutal anaesthesia (Veterinary Nembutal; Abbot), 60 mg per kg body weight. Thymectomies were done when rats were 6 weeks old and splenectomies when they were 3 months old. The animals were injected to induce EAE at the age of 4 months. Basic protein (500 µg ml<sup>-1</sup>) extracted from guinea pig spinal cords was emulsified with an equal volume of Freund's adjuvant containing 4 mg ml<sup>-1</sup> H37Ra *Mycobacterium tuberculosis* (Difco). Each rat was injected with a total volume of 0.1 ml emulsion, containing 25 µg of basic protein, equally divided between the two hind footpads. The animals were examined daily for unequivocal signs of EAE which we considered to be overt paralysis of the tail and hind legs. Chronic EAE refers to paralysis that was unremitting from its onset until the experiment was terminated 32 days after injection. The surviving rats were killed and their brains and segments of spinal cord fixed for histological examination in 10% formalin, processed and embedded in paraffin for staining by haematoxylin and eosin, or by Luxol fast blue-periodic acid Schiff, to detect myelin damage. Pathology was scored on a scale + to +++++. (++++ Indicates disruption of myelin and severe mononuclear cell infiltrates in perivascular and periventricular areas, and in the parenchyma of the nervous tissue: spinal cord, brain stem, cerebellum and cerebrum. +++ Indicates no damage to myelin but severe and extensive infiltration as above. ++ Indicates moderate infiltration limited to perivascular areas with a spotty distribution. + Indicates mild perivascular infiltrates observed in at least one area.)



Table 2 Chronic or relapsing EAE as a function of age or splenectomy

| Age (months) | Treatment   | Day of onset | Acute EAE |             | Recovery Day | Recovery Incidence | Chronic EAE Incidence | Relapse |           | Recovery from relapse Incidence | Grade of pathology |
|--------------|-------------|--------------|-----------|-------------|--------------|--------------------|-----------------------|---------|-----------|---------------------------------|--------------------|
|              |             |              | (Total)   | (Mortality) |              |                    |                       | Day     | Incidence |                                 |                    |
| 2½           | None        | 11           | 8/8       | 2/8         | 17           | 6/6                | 0/6                   | —       | 0/6       | —                               | ++                 |
|              | Sham        |              |           |             |              |                    |                       |         |           |                                 |                    |
|              | splenectomy | 12           | 8/8       | 2/8         | 16           | 6/6                | 0/6                   | —       | 0/6       | —                               | ++                 |
| 4            | Splenectomy | 11           | 8/8       | 3/8         | 17           | 5/5                | 0/5                   | —       | 0/5       | —                               | ++                 |
|              | None        | 12           | 8/8       | 1/8         | 17           | 7/7                | 0/7                   | —       | 0/7       | —                               | ++                 |
|              | Sham        |              |           |             |              |                    |                       |         |           |                                 |                    |
| 13           | splenectomy | 12           | 10/10     | 1/10        | 17           | 9/9                | 0/9                   | —       | 0/9       | —                               | ++                 |
|              | Splenectomy | 11           | 10/10     | 2/10        | —            | 0/8                | 8/8                   | —       | —         | —                               | +++                |
|              | None        | 11           | 10/10     | 3/10        | 20           | 2/7                | 5/7                   | 24      | 2/2       | 0/2                             | ++++               |
|              | Sham        |              |           |             |              |                    |                       |         |           |                                 |                    |
|              | splenectomy | 12           | 10/10     | 4/10        | 19           | 2/6                | 4/6                   | 24      | 2/2       | 0/2                             | ++++               |
|              | Splenectomy | 11           | 10/10     | 4/10        | —            | 0/6                | 6/6                   | —       | —         | —                               | ++++               |

Splenectomy of female Lewis rats was carried out at 1½, 3 or 12 months of age and EAE was induced 1 month later, as described in the legend to Table 1. Each age group was studied in a separate experiment. Repeat experiments involving rats of these ages all produced essentially the same results.

relapses were observed, whether or not the rats had been splenectomized a month earlier. Untreated or sham splenectomized 4-month old rats all developed acute EAE with about 10% mortality. All the surviving rats recovered without relapsing and their brains showed perivascular infiltrates with no damage to myelin. Similar to results shown in Table 1, the splenectomized rats that survived acute EAE all developed chronic paralysis and showed disruption of myelin on histological examination.

The 13-month old Lewis rats that were untreated or sham-splenectomized showed a relapsing or chronic course of EAE. Of the 13 rats that survived acute EAE in both of these groups 9 had unremitting, chronic paralysis. The four rats that recovered all suffered a relapse from which none recovered. Thirteen month old rats that had been splenectomized developed a chronic form of EAE similar to that of 3-month old splenectomized rats. These all had severe perivascular infiltrates and myelin damage.

EAE was also induced in unsplenectomized 15-month old rats. Of 14 rats inoculated, 5 died with acute EAE and 9 had chronic unremitting paralysis of the hind legs for 45 days, at which time the experiment was terminated.

It has been reported that male Lewis rats are more resistant to relapse of EAE than females<sup>3</sup>, but we have not yet had the opportunity to study the influence of sex on the effects of age or splenectomy.

In contrast to EAE in rats, EAE induced in guinea pigs is usually acutely fatal. However, injection of very young (2–4-week old) guinea pigs with guinea pig spinal cord in adjuvant produced a chronic or relapsing form of EAE after a relatively long latent period<sup>9,10</sup>. Although there are differences between the rat and guinea pig models of EAE, these results emphasize the importance of an animal's age to the clinical course of EAE. The mechanisms by which age affects expression of EAE are probably complex, because age modifies the functions of organ systems which influence EAE, such as the immune and endocrine systems. It is conceivable that changes in the expression of EAE with age are related to changes in the function of the spleen.

Age also seems to have an important influence on the outcome of thymectomy. As we have shown (Table 1), thymectomy of 4-month old rats increases the severity of EAE. This contrasts with the effect of neonatal thymectomy, which has been observed to decrease markedly susceptibility to induction of EAE<sup>11</sup>.

The effects of thymectomy and splenectomy indicate the importance of immune physiology in the clinical course of EAE. We have found (in preparation) that recovery from acute EAE is associated with suppression, in the draining lymph nodes, of the

proliferative response of T lymphocytes to a particular determinant of BP. The reactivity to other determinants on the BP molecule is undiminished during recovery. This suggests that the spleen and thymus may be involved in the physiological suppression of the immune response to a critical determinant on BP. However, splenectomy of 1½-month old rats failed to interfere with recovery from EAE induced a month later (Table 2). We have also observed that splenectomy of 3-month old rats 1 week rather than 4 weeks before induction of EAE did not prevent recovery from acute EAE (data not shown). Therefore, the task of the spleen is modified by the age of the subject and the timing of EAE induction. This suggests that the populations of cells mediating recovery are not always resident in or dependent on the spleen.

Our results suggest that defects in regulation of an immune response can transform what might otherwise be a self-limited insult into a chronic or relapsing disease of the nervous system. It is conceivable that multiple sclerosis or other progressive or relapsing diseases could be triggered acutely by a virus or some other noxious agent and be perpetuated by a defect in immune regulation. Subacute sclerosing panencephalitis, a chronic degeneration of the brain associated with infection by measles virus, has been suggested as an example of diseases involving irregularity of the immune response<sup>12</sup>. It is possible that our experimental models of chronic or relapsing EAE might provide a means of identifying immune mechanisms regulating recovery from an autoimmune process and thus, a useful experimental approach to certain clinical problems such as multiple sclerosis.

We thank Mr H. Otmi and Mr M. Margalit for their technical assistance, and Professor M. Feldman for his support. This study was supported by a grant from the Stiftung Volkswagenwerk, Hannover.

Received 6 April; accepted 6 October 1980.

1. Paterson, P. Y. *Adv. Immun.* **5**, 131 (1966).
2. Paterson, P. Y. & Harwin, S. M. *J. exp. Med.* **117**, 755–774 (1963).
3. Keith, A. B. *Nature* **272**, 824–825 (1978).
4. Levine, S. & Sowinski, R. *Proc. Soc. exp. Med.* **149**, 1032–1035 (1975).
5. Wolgram, F., Ellison, G. W., Stevens, J. W. & Andrews, J. M. (eds) *Multiple Sclerosis: Immunology, Virology and Ultrastructure* 127–142 (Academic, New York, 1972).
6. Okumura, K. & Tada, T. *J. Immun.* **106**, 1019–1025 (1971).
7. Gershon, R. K., Lance, E. M. & Kondo, K. *J. Immun.* **112**, 546–554 (1974).
8. McFarlin, D. E., Blank, S. E. & Kibler, R. J. *J. Immun.* **113**, 712–715 (1974).
9. Raine, C. S., Snyder, D. H., Valsamis, M. P. & Stone, S. H. *Lab. Invest.* **31**, 369–380 (1974).
10. Wisniewski, H. M. & Keith, A. B. *Ann. Neurol.* **1**, 144–148 (1977).
11. Arnason, B. G., Janković, B. D., Waksman, B. H. & Wennersten, C. *J. exp. Med.* **116**, 177–186 (1962).
12. Saunders, M. et al. *Lancet* **i**, 72–77 (1969).

## Precursor and effector phenotypes of activated human T lymphocytes

L. Fainboim, C. Navarrete & H. Festenstein

Department of Immunology, London Hospital Medical College, Turner Street, London E1 2AD, UK

In mice, thymus-derived lymphocytes are differentiated into functional subclasses by their cell surface antigens. The Ly 1 determinants are present on T cells with a helper function, whereas Ly 2 and Ly 3 antigens are expressed on the surface of lymphocytes with suppressor or cytotoxic functions<sup>1-6</sup>. In man also, T-cell subsets have been identified using allo- and heteroimmune sera and, more recently, using monoclonal antibodies, which seem to identify helper and suppressor or cytotoxic subpopulations<sup>7-9</sup>. The major histocompatibility system (MHS)-encoded Ia antigens belong to several polymorphic families of membrane associated glycoproteins originally found on B lymphocytes<sup>10,11</sup>; however, they have also been shown to be markers for suppressor T cells in mice<sup>12,13</sup>. Recent studies have shown that in both mouse and man, T cells activated by a mixed lymphocyte reaction or by mitogens become Ia<sup>+</sup><sup>14-18</sup>. Furthermore, some human T lymphoid cells, either freshly isolated from peripheral blood or after *in vitro* activation by lectins<sup>19-21</sup> or alloantigens<sup>22-24</sup>, possess suppressor properties. We report here the phenotype of a T suppressor-cell subpopulation which was induced in long-term culture of lymphoid cells after activation with phytohaemagglutinin (PHA). Our results suggest that a subset of T cells was progressively expanded over a period of 8 days in culture and that, with the expression on the surface of these cells of 'Ia-like' antigens, they acquired the capacity to suppress the proliferative response of syngeneic or allogeneic lymphocytes to alloantigens or mitogens.

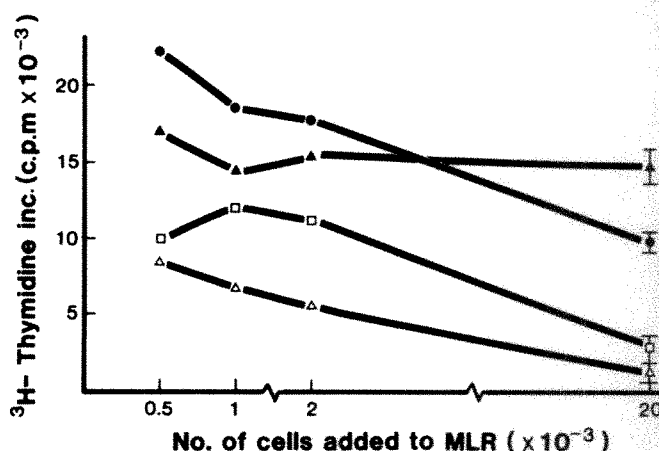
Peripheral blood lymphocytes (PBL) from six healthy donors were stimulated *in vitro* with PHA. The cultures were maintained for 30 days by repeatedly changing the culture medium. After 3, 8, 11, 18 and 23 days,  $5 \times 10^6$  activated cells were taken from the suspension cultures and divided into two aliquots—one for assaying the suppressor activity in culture experiments, and the other for serological investigation of surface antigens on the activated cells.

To study their influence on syngeneic cells, activated cells were irradiated and mixed with equal numbers of syngeneic lymphocytes. Three of these mixed syngeneic/activated cell (SAC) cultures gave similar kinetic patterns with an exponential decline in stimulation: in donor V.A., SACs dropped to background stimulation by day 11, and in donors R.H. and J.A. by day 18 (Table 1). These results suggest that the decline of DNA synthesis in the SACs could be due to the development of suppressor cells. To test this, activated cells were added to cultures of normal lymphocytes stimulated either by purified protein derivative (PPD) or alloantigens. In SACs, reactions were prominent up to day 11, so that potential suppressor activity by J.A.- and R.H.-irradiated peripheral activated lymphocytes (IPALs) on PPD transformation could only be tested with '18-day' IPALs. Syngeneic PBL cultures mixed with '18-day' IPALs then stimulated with PPD were clearly suppressed by R.H., J.A. and V.A., but the suppressor V.A. IPALs were already present on day 8 after activation (Table 1).

Results from mixed lymphocyte culture (MLC) experiments designed to test the suppressor properties of '18-day' (experiment 1) and '23-day' (experiment 2) IPALs are shown in Table 2. These experiments have been repeated several times using frozen cells from '23-day' IPALs, with similar results. The suppressor effects of the IPALs were effective on syngeneic

R.H. and V.A., and also on allogeneic normal lymphocytes (LF).

The resting cells from three different donors were typed for the expression of DR antigens using the method of van Rood *et al.*<sup>25</sup>, and the PHA-activated cells were typed using acridine orange and ethidium bromide at the end of the incubation period. Typings were done using alloantisera from the 7th and 8th International Workshops. Activated T cells were negative for DR antigens when tested on days 3 and 4 after activation, but were positive on day 8. In agreement with a previous report<sup>15</sup>, they expressed the same DR specificities present on the B cells of their resting lymphocytes. When the number of Ia<sup>+</sup> cells was scored using two different anti-Ia monoclonal antibodies (McAB)—DA2 and 62-3-34 (ref. 26)—the number of donor RH Ia<sup>+</sup> cells dropped from 28% on day 0 to become negative on day 3, and from day 8 progressively expanded to 83% on day 23 (Table 3). Similar patterns were observed with donors N.Y. (65% Ia<sup>+</sup>) and A.A. (51% Ia<sup>+</sup>).



**Fig. 1** Suppressor effect on an MLC by different cell numbers of an activated T cells subset.  $20 \times 10^7$  day 23 activated cells were treated with 1:25 (final dilution) of DA2 for 30 min at room temperature, washed twice and incubated with 1:20 dilution of a rabbit anti-mouse FITC conjugated IgG. The cells were fractionated into weakly reactive (the lower 20% of fluorescence Ia<sup>-</sup>) and strongly reactive (the upper 60% of fluorescence Ia<sup>+</sup>) in a fluorescence-activated cell sorter (FACS-1). The MLC was carried out as described in the legend to Table 2. RH was used as responder and irradiated LF as stimulator. Different concentrations of irradiated normal syngeneic cells (▲), Ia<sup>+</sup> (□), Ia<sup>-</sup> (●) or total unfractionated activated cells (Δ) were added to the MLC.

The activated cells were then typed for the expression of the TH2 marker, which had previously been reported to react with a small subset of T peripheral blood lymphocytes with suppressor properties<sup>8</sup>. The number of TH2<sup>+</sup> cells from the responder N.Y. increased from 31% for the resting cells to 68% on day 23 after activation; cells from responder A.A. increased from 20% to 51% and R.H. from 17% to 71%. It was then important to establish if the expanded TH<sup>+</sup> population also expressed the Ia antigens. The activated and resting cells were tested with two fluorescent labels for the simultaneous expression of Ia and TH2 (see Table 4). On day 11, 41 out of 45 (91%) R.H. TH2 T cells expressed the Ia antigen, compared with 12 out of 41 'day 7' A.A. cells (28%).

In another series of experiments, 7- and 23-day activated cells were separated into Ia<sup>+</sup> and Ia<sup>-</sup> by means of a fluorescence activated cell sorter (FACS-1) with an anti HLA-DR (non-polymorphic) monoclonal antibody (DA2). The 7-day unseparated population contained 36% TH2<sup>+</sup> cells and 12% Ia<sup>+</sup>. When separated into subpopulations, the Ia<sup>+</sup> cells were



**Table 1** Time course response to PPD of Ly from normal donors in presence of syngeneic irradiated normal or activated lymphocytes

|      |     | Day 3          |                  | Day 8         |                 |
|------|-----|----------------|------------------|---------------|-----------------|
|      | PPD | Normal cells   | Activated cells  | Normal cells  | Activated cells |
| R.H. | -   | 8,070 ± 1,415  | 116,426 ± 4,637  | 1,390 ± 907   | 45,600 ± 3,215  |
| R.H. | +   | 20,429 ± 1,571 | 170,569 ± 8,144  | 7,245 ± 1,640 | 30,684 ± 293    |
| J.A. | -   | 3,123 ± 1,397  | 115,578 ± 10,963 | 1,390 ± 907   | 123,990 ± 9,090 |
| J.A. | +   | 9,027 ± 1,733  | 118,481 ± 2,962  | 6,668 ± 2,292 | 108,069 ± 7,113 |
| V.A. | -   | 5,175 ± 1,694  | 108,814 ± 18,665 | 3,489 ± 1,128 | 11,580 ± 6,282  |
| V.A. | +   | 31,813 ± 9,990 | 74,334 ± 10,738  | 12,173 ± 611  | 7,055 ± 894     |

|      |     | Day 11         |                     | Day 18         |                 |              |
|------|-----|----------------|---------------------|----------------|-----------------|--------------|
|      | PPD | Normal cells   | Activated cells     | Normal cells   | Activated cells | % Inhibition |
| R.H. | -   | 2,007 ± 647    | 31,109 ± 7,585      | 5,141 ± 22     | 5,321 ± 558     |              |
| R.H. | +   | 7,174 ± 1,586  | 17,558 ± 6,388      | 15,408 ± 2,505 | 7,862 ± 2,277   | (76%)        |
| J.A. | -   | 3,501 ± 3,263  | 55,433 ± 3,160      | 2,607 ± 1,103  | 5,197 ± 826     |              |
| J.A. | +   | 9,944 ± 3,838  | 34,363 ± 7,818      | 12,312 ± 4,026 | 6,584 ± 1,286   | (86%)        |
| V.A. | -   | 4,703 ± 1,576  | 3,429 ± 2,094       | 4,762 ± 1,690  | 5,237 ± 1,719   |              |
| V.A. | +   | 12,358 ± 2,801 | 6,176 ± 1,507 (36%) | 18,105 ± 3,176 | 7,895 ± 1,942   | (81%)        |

PBL from donors R.H., J.A. and V.A. were stimulated in culture ( $1 \times 10^6$  cells per ml) with 1:100 final dilution of PHA for 36 h. The supernatant (conditioned medium, CM) was decanted and the cells resuspended in fresh medium (RPMI 1640 plus 10% AB serum) containing 30% CM (v/v final dilution). The cultures were maintained for up to 30 days by changing the medium with CM every 3-4 days. The suppressor effect of the activated T cells (>95% E-rosetting positive cells) on the response of resting cells to PPD was studied as follows: At 3, 8, 11 and 18 days after PHA activation,  $5 \times 10^4$  activated cells in 50  $\mu$ l of medium (without CM) were irradiated with 4,000 rad and mixed with  $5 \times 10^4$  syngeneic resting lymphocytes (50  $\mu$ l) in the presence or absence of 0.6  $\mu$ g of PPD (50  $\mu$ l). As a control,  $5 \times 10^4$  resting cells were mixed with an equal number of syngeneic irradiated resting cells, in the presence or absence of PPD. Kinetic studies of DNA synthesis measured by the addition of  $^3$ H-thymidine between days 3 and 6 showed that the peak of incorporation of isotope was on day 4.5.  $^3$ H-thymidine uptake was measured on day 4.5 and percentage inhibition calculated as follows:

$$1 - \frac{\text{c.p.m. SAC(with PPD)} - \text{c.p.m. SAC(without PPD)}}{\text{c.p.m. resting cells(with PPD)} - \text{c.p.m. resting cells(without PPD)}} \times 100$$

**Table 2** Suppressor capacity of activated T cells in MLC

|  |                             | Stimulator cells*                           |       |   |  |      |                |
|--|-----------------------------|---|-------|---|--|------|----------------|
| HLA phenotype<br>Normal responder<br>(50,000 cells per well) |                             | Allogeneic cells<br>(50,000 cells per well) |       | Normal<br>autologous<br>(20,000 cells<br>per well | Activated cells<br>(20,000 cells per well) |      | c.p.m.         |
|  |                             | L.F.  | K.H.† |   | R.H.                                       | V.A. |                |
| Experiment 1   |                             |   |       |   |  |      |                |
| Donor  | R.H. A1, AX/B8, BX/DR3, DR7 | +   |       | +   | -  | -    | 57,813 ± 6,065 |
|  |                             | +   |       | -   | +  | -    | 3,111 ± 817    |
|  |                             | -   |       | +   | -  | -    | 8,536 ± 2,026  |
| V.A.   | A2, A3/B35, B44/DR1, DR2    | +   |       | +   | -  | -    | 20,523 ± 2,048 |
|  |                             | +   |       | -   | -  | +    | 2,229 ± 738    |
|  |                             | -   |       | +   | -  | -    | 2,363 ± 443    |
| Experiment 2   |                             |   |       |   |  |      |                |
| R.H.   | A1, AX/B8, BX/DR3, DR7      | +   |       | +   | -  |      | 25,718 ± 4,296 |
|  |                             | +   |       | -   | +  |      | 2,158 ± 185    |
|  |                             | -   |       | +   | -  |      | 6,619 ± 514    |
| L.F.   | A26, AX,/B38, BX/DR4, DR5   | -   | +     | +   | -  |      | 27,930 ± 1,623 |
|  |                             |   | +     | -   | +  |      | 3,240 ± 1,097  |
|  |                             |   | -     | +   | -  |      | 2,370 ± 2,132  |

50  $\mu$ l of autologous PBL ( $5 \times 10^4$ ) were cultured in quadruplicate on microtitre V-well plates in RPMI 1640 plus 10% AB serum, then  $2 \times 10^4$  irradiated autologous normal PBL or '23 day' activated cells were added in 50  $\mu$ l of the same medium.  $5 \times 10^4$  allogeneic cells were added to each well of this mixture. For each experiment, the cultures were pulsed for 16 h with 1  $\mu$ Ci of  $^3$ H-thymidine after 2, 3, 4 and 5 days of culture, and results expressed in c.p.m. on the peak stimulation on day 5.5.

\* Irradiated.

† HLA phenotype = A3,A11/B12,B35/DR2,DR4.

48% and the Ia<sup>-</sup> cells were 32% TH2<sup>+</sup>. The 23-day activated population contained >90% Ia<sup>+</sup> TH2<sup>+</sup> cells.

Subsequently, the populations (Ia<sup>+</sup> and Ia<sup>-</sup>) from 7- and 23-day activated cells were assayed for suppressor properties. With 23-day activated cells, most of the suppressor effect was confined to the Ia<sup>+</sup> population (Fig. 1). However, when irradiated Ia<sup>+</sup> or Ia<sup>-</sup> 7-day activated cells were added to syngeneic responders and stimulated by a third party, both Ia<sup>+</sup> and Ia<sup>-</sup> cells stimulated strongly compared with controls (the cultures were assayed on day 4.5). These results suggest a carry-over of PHA although a helper effect of the activating cells cannot be ruled out completely, especially since 50% of the Ia<sup>+</sup> population is not TH2<sup>+</sup>. Because both Ia<sup>+</sup> and Ia<sup>-</sup> populations were stimulators, no conclusions can be drawn about the relative suppressor properties of the various cell subpopulations in these 7-day cultures.

**Table 3** Kinetic expression of TH2 and Ia antigens on activated T cells

| Donor | Days after activation | TH2 | Anti-Ia |
|-------|-----------------------|-----|---------|
| N.Y.  | 0                     | 31% | 17%     |
|       | 14                    | 50% | 42%     |
|       | 22                    | 68% | 65%     |
| A.A.  | 0                     | 20% | 15%     |
|       | 7                     | 42% | 16%     |
|       | 14                    | 45% | 48%     |
|       | 22                    | 48% | 51%     |
| R.H.  | 0                     | 17% | 28%     |
|       | 4                     | 30% | <1%     |
|       | 9                     | 40% | 42%     |
|       | 14                    | 55% | 51%     |
|       | 22                    | 71% | 83%     |

Indirect immunofluorescence was used to analyse cell surface markers. Resting or activated cells ( $1 \times 10^6$ ) were treated with 1:50 (final dilution) of horse anti-human TH2 and with two anti-Ia McAB (DA2 and 62-3-34, both mouse anti HLA-DR non-polymorphic antibodies) at 1:25 (final dilution). The TH2 antibody was obtained from G. Janosy who prepared it from a batch of ATG (lot no. 17923, Upjohn) which was originally shown to have anti TH2 activity, and purified it according to the method of Reinherz and Schlossman<sup>8</sup>. The specificity was validated by comparing the prepared antibody with the Reinherz and Schlossman antibody on lymphocytes from a panel of 26 unrelated individuals and the reactions of the two antibodies were in complete agreement. After 20 min of incubation, 1:25 swan anti-horse FITC-labelled or 1:10 goat anti-mouse rhodamine conjugate antibodies were added to the second layer. Observations were made using a standard 14 Zeiss photomicroscope with epi-illumination (iv F1 epi-fluorescence condenser) and 2F1 reflector sleeve, equipped with exciter and barrier filters, for selective excitation and observation of fluorescence and rhodamine.

The changing antigenic profile of the activated T lymphocytes from Ia<sup>-</sup> into Ia<sup>+</sup> in a population of TH2<sup>+</sup> cells is in sharp contrast to the profile of the resting population, in which there are less than 1% of TH2<sup>+</sup> cells which are also Ia<sup>+</sup>. This implies either that this small sub-population had been expanded over 7 days of culture, or alternatively that the TH2<sup>+</sup> Ia<sup>-</sup> population, already expanded on day 4, became Ia<sup>+</sup> after 8 days of culture. These data strongly suggest that cells with this phenotype are the active suppressors, although there is no direct evidence for this. Ideally one would like to be able to separate the cells into Ia<sup>+</sup> TH2<sup>+</sup> and Ia<sup>-</sup> TH2<sup>+</sup> cells, but the 23-day cells are practically all Ia<sup>+</sup>, whereas the 7-day cultures are all stimulatory, therefore such experiments are uninformative.

These findings may also have functional implications and may be important in the pathogenesis of certain diseases. For example, the increase of the Ia<sup>+</sup> T cells *in vivo* could reflect the efforts

of the immune system to control the autoimmune reaction, for example in rheumatoid arthritis and systemic lupus erythematosus, where a disproportionate increase of Ia<sup>+</sup> T cells in the peripheral blood has been reported<sup>27</sup>. These alloantigens could be central to immunoregulation, and changing proportions of cells carrying one kind of alloantigen or another following stimulation by microorganisms or tumour-associated transplantation antigens may result in the production of suppressor/helper sub-populations.

**Table 4** Simultaneous expression of TH2 and Ia<sup>+</sup> antigens on the surface of PHA-activated cells

| Responder | Days after activation | TH2 <sup>+</sup> | Ia <sup>+</sup> | Ia <sup>+</sup> and TH2 <sup>+</sup> |
|-----------|-----------------------|------------------|-----------------|--------------------------------------|
| A.A.      | 0                     | 20%              | 15%             | 1%                                   |
| A.A.      | 7                     | 42%              | 16%             | 12%                                  |
| R.H.      | 0                     | 17%              | 38%             | 1.7%                                 |
| R.H.      | 11                    | 45%              | 53%             | 41%                                  |

| 2 × 2 contingency table: |                       |    |    |    |    |                        |
|--------------------------|-----------------------|----|----|----|----|------------------------|
| Responder                | Days after activation | ++ | +- | -+ | -- | $\chi^2$ <sup>12</sup> |
| A.A.                     | 0                     | 1  | 19 | 15 | 65 | -3.39                  |
|                          | 7                     | 12 | 26 | 4  | 58 | 9.27                   |
| R.H.                     | 0                     | 2  | 16 | 36 | 46 | -8.20                  |
|                          | 11                    | 41 | 4  | 12 | 43 | 44.90                  |

See legend to Table 3 for experimental details. The contingency table shows number of TH2 positive versus number of monoclonal Ia positive cells.

We acknowledge the financial support of the Leukaemia Research Fund, the World University Service, the Cancer Research Campaign of Great Britain, and the Locally Organised Research Scheme (DHSS). We also thank M. Greaves, D. Delia and A. Edwards for the use of the FACS-1, G. Janosy and N. Tidman for TH2, and J. and W. Bodmer for DA2 and 62-3-34 monoclonal antibodies.

Received 11 June; accepted 25 September 1980.

- Kisielow, P. *et al.* *Nature* **253**, 219-220 (1975).
- Cantor, H. & Boyse, E. A. *J. exp. Med.* **141**, 1376-1389 (1975).
- Cantor, H. & Boyse, E. A. *J. exp. Med.* **141**, 1390-1399 (1975).
- Feldman, M., Beverley, P. C. L., Dunkley, M. & Kontinen, S. *Nature* **258**, 614-616 (1975).
- Beverley, P. C. L., Woody, J., Dunkley, M., Feldman, M. & McKenzie, I. *Nature* **262**, 495-497 (1976).
- Cantor, H., Shen, F.-W. & Boyse, E. A. *J. exp. Med.* **143**, 1391-1401 (1976).
- van Leeuwen, A., Festenstein, H. & van Rood, J. J. *J. exp. Med.* (in the press).
- Reinherz, E. L. & Schlossman, S. F. *J. Immun.* **122**, 1335-1341 (1979).
- Reinherz, E. L., Kung, P., Goldstein, G., Levey, R. & Schlossman, S. F. *Proc. natn. Acad. Sci. U.S.A.* **77**, 1588-1592 (1980).
- Sachs, D. H. & Cone, J. L. *J. exp. Med.* **138**, 1289-1304 (1973).
- van Rood, J. J., van Leeuwen, A., Termijtelen, A. & Keuning, J. J. *Transplant. Rev.* **30**, 122-136 (1976).
- Murphy, D. B., Herzenberg, C. A., Okumura, K., Herzenberg, L. A. & McDevitt, H. O. *J. exp. Med.* **144**, 699-711 (1976).
- Okumura, K., Takemori, T., Tokuhisa, T. & Tada, T. *J. exp. Med.* **146**, 1234-1245 (1977).
- Schirmacher, V. & Festenstein, H. *J. Immunogenet.* **2**, 337-349 (1975).
- Greaves, M. F. *et al.* *Eur. J. Immun.* **9**, 356-362 (1979).
- Fu, S. M. *et al.* *J. exp. Med.* **148**, 1423-1428 (1978).
- Metzgar, R. S., Bertoglio, G., Anderson, J. K., Bonnard, G. D. & Ruscetti, F. W. *J. Immun.* **122**, 949-953 (1979).
- Reinherz, E. L. *et al.* *J. exp. Med.* **150**, 1472-1482.
- Shou, L., Schwartz, S. A. & Good, R. A. *J. exp. Med.* **143**, 1100-1110 (1976).
- Kurnick, J. T., Bell, C. & Grey, H. M. *Scand. J. Immun.* **5**, 771-778 (1976).
- Maca, R. D., Bonnard, G. D. & Herberman, R. B. *J. Immun.* **123**, 246-251 (1979).
- Hirschberg, H. & Thorsby, E. *Scand. J. Immun.* **6**, 809-815 (1977).
- Engleman, E. G., McMichael, A. J., Batey, M. E. & McDevitt, H. O. *J. exp. Med.* **147**, 137-146 (1978).
- Bean, M. A., Kodeva, Y., Cummings, K. B. & Bloom, B. R. *J. exp. Med.* **146**, 1455-1460 (1977).
- van Rood, J. J., van Leeuwen, A. & Ploem, J. S. *Nature* **262**, 795-797 (1976).
- Brodsky, F. M., Parham, P., Barnstable, C. J., Crumpton, M. J. & Bodmer, W. F. *Immun. Rev.* **47**, 3-61 (1979).
- Yu, D. T. Y. *et al.* *J. exp. Med.* **151**, 91-96 (1980).



# Monoclonal antibodies which distinguish between human NK cells and cytotoxic T lymphocytes

Joyce M. Zarling

Immunobiology Research Center, Department of Laboratory Medicine and Pathology, University of Minnesota, Minneapolis, Minnesota 55455

Patrick C. Kung

Immunobiology Division, Ortho Pharmaceutical Corporation, Raritan, New Jersey 08869

Although it is widely accepted that T cells have a major role in specific tumour immunity, there is now much evidence that natural killer (NK) cells, which exist in many species and spontaneously lyse certain tumour cells *in vitro*, provide early resistance against tumour growth<sup>1-4</sup>. Human NK-cell activity can be augmented *in vitro* by interferon<sup>5-7</sup> and its inducers, including polyinosinic:polycytidylic acid (poly I:C)<sup>8</sup>; furthermore, NK-like activity is generated in mixed leukocyte cultures (MLCs) as is specific cytotoxic T-cell (T<sub>c</sub>) activity<sup>9-11</sup>. When effector cells generated in human MLCs lyse allogeneic or autologous virus-transformed or tumour cells<sup>9-13</sup>, it has been difficult to evaluate the relative contributions of T<sub>c</sub> and NK-like cells to the lysis because the latter, like T cells, can form rosettes with sheep erythrocytes<sup>14</sup> and react with xenogeneic anti-human thymocyte serum<sup>15</sup>. We report here that monoclonal antibodies against human mononuclear cell subpopulations can distinguish T<sub>c</sub> from NK and NK-like cells. OKT3 or OKT8 monoclonal antibodies (reactive with virtually all or a subset of T cells, respectively<sup>16,17</sup>) with complement (C') ablate MLC-generated T<sub>c</sub> activity against allogeneic normal cells but do not decrease lysis of HLA-negative, NK-sensitive K562 leukaemia cells by NK, poly I:C-activated NK or MLC-activated NK-like cells. In contrast, OKM1 monoclonal antibody (reactive with a low proportion of non-adherent mononuclear cells as well as macrophages<sup>18</sup>) with C' causes marked diminution of NK and poly I:C-activated NK-cell activity.

The production and characterization of the monoclonal antibodies used in this study have been reported elsewhere<sup>16-19</sup>; all are ascites fluid preparations from mice inoculated with hybridoma cells producing antibodies of the IgG2 subclass, which fix rabbit C'. However, it had not been determined which, if any, of the antibodies with C' would eliminate cytotoxic effector cells. Thus, peripheral blood mononuclear cells, stimulated in MLC for 7 days with X-ray irradiated normal cells pooled from 20 unrelated individuals (pool<sub>x</sub>), were treated with anti-human T-cell antibodies OKT3, OKT8, OKT4 or control ascites fluid, followed by the addition of C', as detailed in Table 1 legend. Cytotoxic activities of the treated effector cell populations were compared against <sup>51</sup>Cr-labelled allogeneic normal lymphocyte targets which are lysed by T<sub>c</sub> but not by fresh or activated NK cells<sup>7</sup>. Typical results of one of five experiments, shown in Table 1, indicate that treatment of MLC-generated effector cells with OKT3 or OKT8 and C' totally ablated T<sub>c</sub> activity against the normal allogeneic cells. OKT4 and C' did not decrease T<sub>c</sub> activity; however, it is unclear why enrichment of cytotoxicity was not observed following removal of the 33% cells killed by this antibody, because previous results, obtained using the fluorescence-activated cell sorter, showed that OKT4 reacts with a subset of T cells lacking T<sub>c</sub> activity<sup>19</sup>.

Experiments were carried out to determine whether the monoclonal anti-T-cell antibodies would decrease either non-augmented or poly I:C-augmented NK-cell activity against

NK-sensitive K562 cells. Representative results (Fig. 1) confirm our previous report<sup>8</sup> that poly I:C augments human NK-cell activity against K562 cells by approximately 2.5-fold (44.6 lytic units (LU) compared with 106 LU). Exposure of untreated or poly I:C-treated non-adherent mononuclear cells to OKT3 or OKT8 and C', which deplete T<sub>c</sub> activity, did not decrease NK or poly I:C-augmented NK activity against K562 cells in this or in two similar experiments; additionally, OKT4 and C' failed to decrease NK-cell activity. The increase in lytic units per 10<sup>6</sup> cells, following treatment with the anti-T-cell antibodies and C', can be accounted for primarily by enrichment for NK cells resulting from lysis of T cells; this is because the total LU recovered following antibody or control ascites treatments were similar, except for the less than twofold increase in LU recovered following treatment of poly I:C-activated cells with OKT3 and C' (Fig. 1b). In contrast, OKM1 and C' (which lysed 11-14% of the cells) reduced NK and poly I:C-augmented NK-cell activity against K562 cells by at least 75% in this and in two other experiments. It thus seems that the majority of NK and poly I:C-activated NK cells are OKM1<sup>+</sup> and OKT3<sup>+</sup>.

**Table 1** Depletion of MLC-generated T<sub>c</sub> against allogeneic normal cells by monoclonal antibodies OKT3 and OKT8

| Treatment of A pool <sub>x</sub> effector cells | % Specific <sup>51</sup> Cr release from B ± s.d. |            |
|---|---|------------|
|   | 30:1  | 10:1       |
| Control ascites + C'                            | 56.8 ± 8.9  | 38.7 ± 7.5 |
| OKT4 + C'                                       | 50.7 ± 8.4  | 37.2 ± 4.8 |
| OKT8 + C'                                       | 3.7 ± 3.9   | 2.7 ± 3.6  |
| OKT3 + C'                                       | 7.0 ± 4.3   | 5.6 ± 4.0  |

Ficoll-Hypaque-isolated mononuclear cells from individual A were washed and resuspended in culture medium consisting of RPMI 1640 (Gibco) supplemented with 25 mM HEPES buffer and 15% heat-inactivated normal human serum. 9 × 10<sup>6</sup> responding cells from individual A were incubated in a final volume of 10 ml culture medium in Falcon T25 tissue culture flasks with 9 × 10<sup>6</sup> X-ray irradiated (2,500R) allogeneic normal lymphocytes, pooled in equal numbers from 20 unrelated individuals (pool<sub>x</sub>) as previously described<sup>12</sup>. On day 7 after the onset of MLC, the non-adherent A pool<sub>x</sub> effector cells were collected from flasks, washed once and treated in culture medium with control ascites from mice inoculated with the parental myeloma cell line or ascites fluid containing monoclonal antibodies OKT4, OKT8 or OKT3 (produced as described elsewhere<sup>16-19</sup>), at a final dilution of 1:100 for 1 h at 4 °C. Rabbit complement (C') (Pel-Freez Biologicals) was added at a final dilution of 1:2. Following a 1-h incubation at 37 °C, the % viable cells, determined by trypan blue dye exclusion, was 98, 67, 57 and 26% for cells treated with control ascites, OKT4, OKT8 and OKT3, respectively. The treated cells were layered on Ficoll-Hypaque gradients to remove dead cells and the viable cells isolated from the interfaces were washed and resuspended in complete medium before their use as effector cells. Effector cells were added to round-bottom wells of microtitre trays (0.8-2.4 × 10<sup>5</sup> per well) followed by the addition to each well of 8 × 10<sup>3</sup> <sup>51</sup>Cr-labelled allogeneic normal lymphocytes from individual B; the resulting effector to target cell ratios were 30:1 and 10:1. Following a 7-h <sup>51</sup>Cr-release assay at 37 °C, a constant amount of supernatant was removed from each well and transferred to tubes for counting in a γ-counter. The % specific <sup>51</sup>Cr release from target cells was calculated as follows:

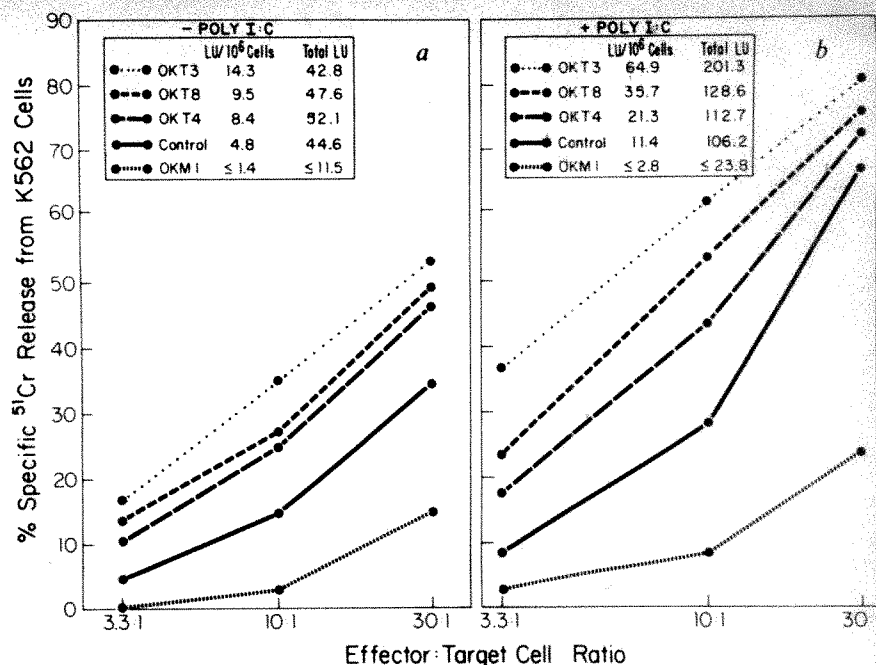
$$\frac{(\text{c.p.m. test release} - \text{c.p.m. spontaneous release})}{(\text{c.p.m. maximal release} - \text{c.p.m. spontaneous release})} \times 100$$

where spontaneous release = c.p.m. release from target cells in medium alone, and maximal release = c.p.m. release from target cells in detergent. Spontaneous <sup>51</sup>Cr release was 13.2% of the maximal release. The values shown are the mean specific % <sup>51</sup>Cr released from four replicate wells ± s.d. The % specific <sup>51</sup>Cr released from the cells by mononuclear cells from individual A cultured for 7 days without stimulating cells was 4.2 ± 1.3%. The % specific <sup>51</sup>Cr released from the target cells by A pool<sub>x</sub> effector cells treated with control ascites and C', control ascites alone, C' alone or antibodies in the absence of C' did not differ from that released by untreated effector cells.

OKT4<sup>+</sup> and OKT8<sup>+</sup>. This finding firmly supports a recent hypothesis that NK cells might be OKM1<sup>+</sup>, which was based on data showing that OKM1 antibody reacts in immunofluorescence assays with the majority of non-adherent cells having surface characteristics of NK cells<sup>20</sup>, that is, receptors for sheep erythrocytes<sup>14</sup> and for the Fc portion of IgG (refs 7, 11, 14). Our failure to ablate NK-cell activity totally by OKM1 and C' (Fig. 1) suggests that either a small percentage of NK cells are OKM1 or that they express a very low density of OKM1 antigen.

Effector cells generated in MLC can lyse certain allogeneic and autologous lymphoblastoid cell lines and leukaemia

**Fig. 1** Effect of monoclonal antibodies on NK and poly I:C-augmented NK-cell activities.  $10 \times 10^6$  Ficoll-Hypaque isolated mononuclear cells were cultured in Falcon T25 tissue cultured flasks containing 5 ml RPMI 1640 medium supplemented with 25 mM HEPES buffer, 15% normal human serum and 0 (a) or 100  $\mu$ g (b) poly I:C ml $^{-1}$ . Following a 16-h incubation at 37°C, the non-adherent cells (containing <1% macrophages, as judged by nonspecific esterase staining) were collected and treated with antibodies or control ascites and C' as detailed in Table 1; OKM1 was used at a dilution of 1:10. The numbers of viable cells recovered after treating  $10^7$  cells with OKT3, OKT8, OKT4, control ascites or OKM1 and C' were 3.0, 5.0, 6.2, 9.3 or  $8.2 \times 10^6$ , respectively (a), and 3.1, 3.6, 5.3, 9.3 or  $8.5 \times 10^6$ , respectively (b). The washed effector cell populations were tested for cytotoxicity against  $^{51}$ Cr-labelled K562 cells in a 5-h  $^{51}$ Cr release assay. The data points represent the mean % specific  $^{51}$ Cr released from K562 cells in four replicate wells, calculated as in Table 1; the s.d. values were <12% of the mean values. Spontaneous  $^{51}$ Cr release was 11.2% of maximal release. 1 LU (lytic unit) was defined as the number of effector cells required to cause 35% specific  $^{51}$ Cr release from  $8 \times 10^3$  target cells. Total LU recovered after treating  $10^7$  cells was calculated as follows: LU per  $10^6$  cells  $\times$  no. of viable cells recovered.

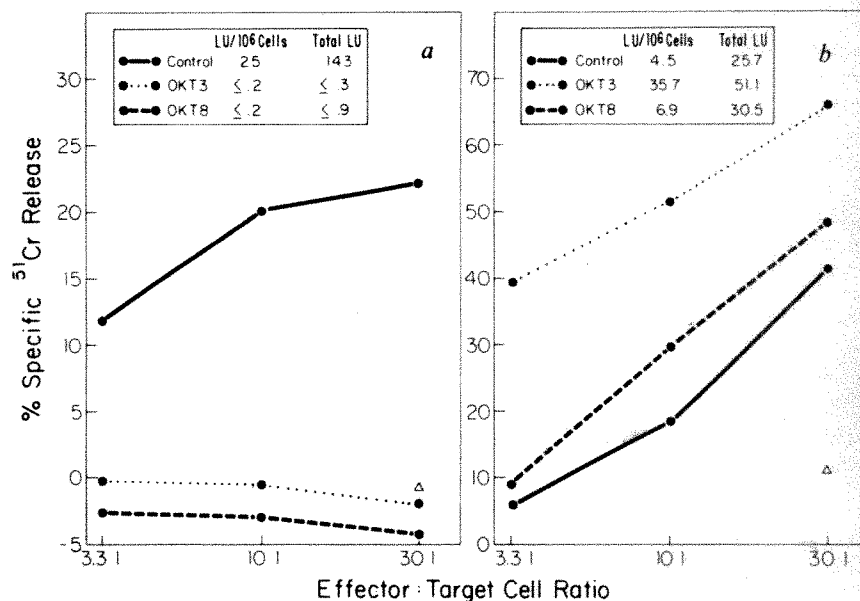


cells<sup>9-13</sup>, which may be sensitive to lysis by NK or activated NK cells<sup>7</sup>. It is difficult to determine the proportion of such cytotoxicity that is mediated by T<sub>c</sub> or NK-like cells; the mere observation that NK-sensitive target cells are lysed is insufficient to exclude participation by T<sub>c</sub> in the lytic reaction. In attempts to distinguish T<sub>c</sub> from NK-like cells, effector cells generated in MLC by stimulation with pooled allogeneic normal cells, were treated with OKT3 or OKT8 and C' and were then tested for their ability to lyse allogeneic normal lymphocytes and HLA-negative K562 cells. Results shown in Fig. 2a, similar to those shown in Table 1, indicate that OKT3 or OKT8 plus C' depletes T<sub>c</sub> activity against allogeneic normal lymphocytes; in contrast, treatment of the stimulated cells with OKT3 or OKT8 and C' did not decrease cytotoxicity against the NK-sensitive K562 leukaemia cells (Fig. 2b). Similar results were obtained in four other experiments; however, the total LU recovered against K562 cells from OKT3-treated cells was not consistently higher than that recovered from control ascites-treated cells. Our results thus demonstrate that T<sub>c</sub> can be distinguished from MLC-activated NK-like cells by use of monoclonal OKT3 or OKT8 antibodies and C'.

Although we observed that OKM1 plus C' caused marked diminution of fresh and poly I:C-activated NK cells (Fig. 1), we have failed, with such a treatment, to eliminate cytotoxic activity of effector cells generated in MLC against allogeneic normal cells or K562 cells (data not shown). This finding is reminiscent of observations that NK as well as interferon- and poly I:C-augmented NK-cell activities are depleted by removing cells expressing receptors for the Fc portion of IgG (refs 7, 8, 11, 14); however, both NK-like cells and T<sub>c</sub> generated in MLC seem to lack Fc receptors<sup>11,21</sup>. The relationship between OKM1 antigen and the Fc receptor on NK cells remains to be elucidated. It is possible that MLC-activated NK-like cells are derived from OKM1<sup>+</sup> cells but that following several days in MLCs, the OKM1 antigen may not continue to be expressed on these cells; alternatively, the NK-like cells generated in MLCs may originate from a phenotypically different precursor cell.

As monoclonal antibodies directed against human mononuclear cell subpopulations can distinguish T<sub>c</sub> from NK and NK-like cells, it is now possible to delineate the effector cells that are cytotoxic for a variety of cell lines and autologous malignant cells.

**Fig. 2** Distinction between T<sub>c</sub> and NK-like cells generated in MLC by monoclonal anti-T-cell antibodies. Peripheral blood mononuclear cells were stimulated for 7 days in MLC with X-ray irradiated pooled allogeneic normal cells and collected and treated with monoclonal antibodies OKT3 or OKT8 and C' as detailed in Table 1 legend. The numbers of viable cells recovered after treating  $10^7$  cells with control ascites, OKT3 or OKT8 with C' were 5.7, 1.4 or  $4.4 \times 10^6$ , respectively. The effector cells were then tested for cytotoxicity against allogeneic normal lymphocyte targets (a) and HLA-negative K562 leukaemia cells (b) in 7-h and 5-h  $^{51}$ Cr release assays. The % specific  $^{51}$ Cr released from targets by responding cells cultured in the absence of stimulating cells is designated by  $\Delta$ . Negative % specific  $^{51}$ Cr release values indicate that less  $^{51}$ Cr was released from target cells in the presence of effector cells than that which was released spontaneously in medium alone. Spontaneous  $^{51}$ Cr release from allogeneic normal cells and K562 cells was 14.8 and 10.2% of maximal  $^{51}$ Cr release. LU per  $10^6$  cells and total LU recovered from  $10^7$  cells were calculated as shown in Fig. 1. One lytic unit was defined as the number of effector cells required to cause 15% or 40% specific  $^{51}$ Cr release from  $8 \times 10^3$  labelled allogeneic normal cells or K562 cells, respectively.





We thank Ms M. S. Dierckins and Ms M. Cunanan for assistance and Dr G. Goldstein for valuable discussions. This work was supported by NIH grant CA26738 and a grant from the Minnesota Medical Foundation to J.M.Z. who is a Scholar of Leukemia Society of America.

Received 25 June; accepted 22 September 1980.

- Herberman, R. B. & Holden, H. T. *Adv. Cancer Res.* **27**, 305-377 (1977).
- Haller, O., Hansson, M., Kiessling, R. & Wigzell, H. *Nature* **270**, 609-611 (1977).
- Karre, K., Klein, G. O., Kiessling, R., Klein, G. & Roder, J. C. *Nature* **284**, 624-626 (1980).
- Talmadge, J. E., Meyers, K. M., Prieur, D. J. & Starkey, J. R. *Nature* **284**, 622-624 (1980).
- Trinchieri, G. & Santoli, D. *J. exp. Med.* **147**, 1314-1333 (1978).
- Herberman, R. B., Ortaldo, J. R. & Bonnard, G. D. *Nature* **277**, 221-223 (1979).
- Zarling, J. M., Eskra, L., Borden, E. C., Horoszewicz, J. & Carter, W. A. *J. Immun.* **123**, 63-69 (1979).
- Zarling, J. M. *et al. J. Immun.* **124**, 1852-1857 (1980).
- Ortaldo, J. R. & Bonnard, G. D. *Fedn Proc.* **35**, 1325 (1977).
- Callewaert, D. M. *et al. J. Immun.* **122**, 81-85 (1978).
- Seeley, J. K., Masucci, G., Poros, A., Klein, E. & Golub, S. H. *J. Immun.* **123**, 1303-1311 (1979).
- Zarling, J. M. & Bach, F. H. *J. exp. Med.* **147**, 1334-1340 (1978).
- Zarling, J. M., Robins, H. L., Raich, P. C., Bach, F. H. & Bach, M. L. *Nature* **274**, 269-271 (1978).
- West, W. H., Cannon, G. B., Kay, H. D., Bonnard, G. D. & Herberman, R. B. *J. Immun.* **118**, 335-361 (1977).
- Kaplan, J. & Callewaert, D. M. *J. natn. Cancer Inst.* **60**, 961-964 (1978).
- Kung, P. C., Goldstein, G., Reinherz, E. L. & Schlossman, S. F. *Science* **206**, 347-349 (1979).
- Kung, P. C. *et al. Transplant Proc.* **12**, 141-146 (1980).
- Breard, J., Reinherz, E. L., Kung, P. C., Goldstein, G. & Schlossman, S. F. *J. Immun.* **124**, 1943-1948 (1980).
- Reinherz, E. L., Kung, P. C., Goldstein, G. & Schlossman, S. F. *Proc. natn. Acad. Sci. U.S.A.* **76**, 4061-4065 (1979).
- Reinherz, E. L. *et al. J. exp. Med.* **151**, 969-974 (1980).
- Shaw, S., Pichler, W. J. & Nelson, D. L. *J. Immun.* **122**, 599-604 (1979).

## H-2-linked genes control immune response to V-domains of myeloma protein 315

Trond Jørgensen & Kristian Hannestad

Institute of Medical Biology, University of Tromsø School of Medicine, Tromsø, Norway

**Immunoglobulins function as antigen receptors of B lymphocytes and as effector molecules for elimination of foreign antigens. Recently, other functions have been revealed: for example, idiotypes (antigenic sites of variable (V) domains) bound on the surface of plasmacytomas<sup>1,2</sup> can act as tumour-specific transplantation antigens<sup>3</sup>. Moreover, optimal maturation of B lymphocytes of a given idio type into antibody-secreting cells seems to require assistance from two different kinds of helper T cells (Th), one bearing receptors complementary or similar to that idio type, and another that recognizes the antigen<sup>4-6</sup>. To learn more about recognition of V regions by Th, we have used V-domains of the immunoglobulin A (IgA) (A2) myeloma protein M315 produced by the BALB/c plasmacytoma MOPC 315 (ref. 7) as carriers for anti-hapten responses. We report here that the Th response to the V-domain of the heavy chain (V<sub>H</sub>) and the light chain (V<sub>L</sub>) of M315 seems to be under H-2-linked immune response (IR) gene control.**

Varibus strains of mice were injected separately with 100 µg of V<sub>H</sub><sup>315</sup> and V<sub>L</sub><sup>315</sup> (carrier) and 200 µg of hapten coupled to bovine serum albumin (BSA). The hapten was the (4-hydroxy-5-iodo-3-nitrophenyl)acetyl (NIP) group. The Th responses to the two carrier antigens were determined by transferring the carrier-primed spleen cells to irradiated (500R X-ray) syngeneic recipients together with hapten-primed B cells. We concluded that those strains in which a pronounced anti-NIP response was observed 10-12 days following boost with 200 µg of NIP<sub>3</sub>-Fab<sup>315</sup> in saline had responder Th, whereas those strains in which the anti-NIP response was very low had non-responding Th. Previous studies had established that the BALB/c anti-NIP antibody response in this adoptive transfer system is Th dependent<sup>8,9</sup>. For example, BALB/c spleen cells primed with minimal essential medium (MEM) or BSA have never evoked a secondary anti-NIP response above 7.5% (see Table 1).

This analysis revealed that for each antigen the various mouse strains could be clearly distinguished into high responders and non-responders (Table 1). Thus, mice of the d (BALB/c and DBA/2), b (C57BL) and s (SJA, SJL) haplotypes made strong anti-NIP antibody responses when they received Th primed with V<sub>L</sub><sup>315</sup>. Mice of the k (CBA, C3H and AKR) haplotype made no or poor anti-NIP responses. For unknown reasons, CBA mice from Gl. Bomholtgaard gave a higher response to V<sub>L</sub> than the other H-2<sup>k</sup> strains (Table 1, expt A), including CBA from the Jackson Laboratory (Table 1, expt B).

A different genetic pattern was observed for Th responses to V<sub>H</sub><sup>315</sup>. Mice of the k and s haplotypes made strong anti-NIP responses, whereas mice of the b and d haplotypes made no or weak responses (Table 1). The Th of (C3H × BALB/c)F<sub>1</sub> mice responded to both V<sub>H</sub> and V<sub>L</sub> priming (Table 1), showing that the responder phenotypes are inherited in a dominant fashion.

Mice of the b (C57BL/6), d(BALB/c) and k (C3H, CBA, AKR) haplotypes were also primed with the Fv fragment of M315 which contains both the V<sub>H</sub> and the V<sub>L</sub> domains. In contrast to the distinct response patterns observed with the isolated V-domains, all strains were responders to Fv (Table 1, expt C). We have been unable to demonstrate suppressor activity in spleen cells of V<sub>H</sub><sup>315</sup>-primed BALB/c mice. Thus, the anti-NIP responses of recipients that received a mixture of 20 × 10<sup>6</sup> V<sub>L</sub>- and 80 × 10<sup>6</sup> V<sub>H</sub>-primed spleen cells were equivalent to the responses of animals receiving only V<sub>L</sub>-primed cells (data not shown).

The importance of the major histocompatibility complex (MHC) genes in these responses is shown by the correlation between MHC type and ability to respond to either V<sub>H</sub> or V<sub>L</sub> (Table 1). Furthermore, the congenic strain BALB.K (H-2<sup>k</sup>), which only differs from BALB/c at the H-2 complex, responds like mice of the k haplotype (Table 2). Thus, it is a non-responder to V<sub>L</sub><sup>315</sup>, although BALB/c responds, and it is a responder to V<sub>H</sub><sup>315</sup>, although BALB/c does not respond. There was no correlation between Igh-C allotypes and response patterns (Table 1). These results provide strong evidence that distinct genes within the MHC control the Th responses to these V-domains.

What is the nature of the V-domain epitopes recognized by the Th of this study? The genetic background of the mouse in which MOPC-315 arose was the seventh generation of successive backcrosses to inbred BALB/c mice, starting with the F<sub>1</sub> progeny of a BALB/c × C57BL/Ka cross. The progeny selected for each backcross with BALB/c had both BALB/c and C57BL/Ka allotypic Igh-C markers<sup>10</sup>. As M315 bears the same Igh-C allotypes (A<sup>12,13,14</sup>) as BALB/c IgA myeloma proteins<sup>7</sup>, the BALB/c origin of C<sub>H</sub><sup>315</sup> is established. It has not been possible to prove the BALB/c origin of L<sup>315</sup> because no allotypic markers have been found on the λ2 chain. However, the probability that L<sup>315</sup> is the product of C57BL genes is only 1/256 (ref. 10). As both BALB/c and C57BL mice have on average 11-14 µg per ml of protein immunochemically related to V<sub>L</sub><sup>315</sup> (ref. 11) and are responders to V<sub>L</sub><sup>315</sup> (this work), it is unlikely that the antigenic determinant is an allotype. Hence we conclude that it is related to idiotypes. For V<sub>H</sub><sup>315</sup> one cannot rule out allotype as both BALB/c and C57BL are non-responders.

These experiments demonstrate that complete immunoglobulins may be unsuitable for priming Th in studies of MHC-linked IR gene control of immune responses to V-regions because complete immunoglobulins may, as with M315, bear more than one genetically controlled V-region determinant. This is illustrated by the uniform high responsiveness of all strains to the Fv-315 fragment. In addition, new epitopes formed when V<sub>H</sub> and V<sub>L</sub> are assembled, as in Fv, may also contribute to these high responses. Therefore, the lesser antigenic complexity of individual domains offers certain advantages in the dissection of the immunogenicity of complete immunoglobulins. Second, a significant set of Th present in many mouse strains recognize the V-domains of M315 in another way than most B lymphocytes. Thus, the anti-idiotypic antibodies raised in isogenic mice against M315 usually bind to

**Table 1** Separate genetic control of helper T-cell (Th) responses to  $V_H^{315}$  and  $V_L^{315}$ 

| Strain*<br>immunized | H-2<br>type | Igh-C<br>type | Secondary anti-NIP response in recipients of Th primed with: |            |                 |              |
|----------------------|-------------|---------------|--|------------|-----------------|--------------|
|                      |             |               | Expt A<br>$V_H$  | $V_L$      | Expt B<br>$V_H$ | Expt C<br>Fv |
| BALB/c               | d           | a             | 3.4 (3.0)  | 64.3 (2.8) | 0.0             | 67.7 (1.0)   |
| DBA/2                | d           | c             | 5.6 (0.9)  | 60.8 (1.8) | 4.8 (0.8)       | 29.6 (5.9)   |
| NZB                  | d           | e             | 3.6 (1.3)  | 30.9 (1.5) |                 |              |
| C57BL <sup>†</sup>   | b           | b             | 7.7 (1.1)  | 33.3 (4.6) | 0.9 (0.9)       | 34.4 (1.1)   |
| C3H                  | k           | a             | 39.9 (2.4)   | 7.9 (2.2)  | 52.5 (3.5)      | 8.0 (2.9)    |
| CBA                  | k           | a             | 52.6 (3.2)   | 22.8 (7.3) | 49.4 (2.6)      | 1.5 (0.6)    |
| AKR                  | k           | d             |  |            | 52.7 (1.1)      | 5.1 (1.7)    |
| (C3H × BALB/c)       | k × d       | a             |  |            | 41.1 (6.1)      | 32.7 (6.0)   |
| SJL                  | s           | b             | 45.5 (5.2)   | 66.4 (2.0) | 50.1 (3.7)      | 54.9 (5.5)   |
| SJA                  | s           | a             | 26.1 (3.3)   | 43.2 (4.3) |                 |              |

Each irradiated (500R X ray) recipient was given  $\frac{1}{2}$  spleen equivalent of NIP-BSA- and carrier-primed cells<sup>9</sup>. The values represent per cent of  $1.2 \times 10^{-6}$  mol of N-[<sup>125</sup>I]P-caproic acid bound by 20  $\mu$ l serum collected 10 days (expts A and B) and 13 days (expt C) after boost with NIP<sub>3</sub>-Fab<sup>315</sup>. BALB/c spleen cells primed with MEM or BSA have never evoked a secondary anti-NIP response above 7.5% in this assay system. The numbers in parentheses are s.e.

\* Mice of expts A and C were from Gl. Bomholtgaard, and of expt B from the Jackson Laboratory. The SJA strain was from Institute of Cancer Research, Philadelphia.

<sup>†</sup> C57BL/6 in expts A and C; C57BL/10 in expt B.

'neo' antigenic idiotype determinants that form when the  $V_H$  and  $V_L$  domains assemble<sup>12</sup>. We propose that the Th primed with individual  $V^{315}$  domains encounter and recognize the same domains in an assembled form when the animals are boosted with NIP<sub>3</sub>-Fab<sup>315</sup>, and that these Th focus on immunogenic sites shared by free and assembled V-regions. According to this hypothesis each member of the M315 pair of V-domains contains sufficient structural information by itself to be recognized by Th. This interpretation is in line with Edelman's proposal that each of the compact domains of immunoglobulin chains has evolved to perform a special function<sup>13</sup>, and contrasts with the combined contribution of  $V_H$  and  $V_L$  domains to the construction of the antigen-binding sites of complete antibodies<sup>14,15</sup> and many, but not all, serologically defined idiotypes.

The broader implications for the idiomotype network<sup>16</sup> concept are that the V-region-specific Th of the present study, detected by a conventional hapten-carrier system, may be envisaged to be able to operate directly on the immunoglobulin receptors of B lymphocytes like the idiomotype-specific set of Th (refs 4–6). Hence,  $V_H$  and  $V_L$  may also function as independent targets in the idiomotype network and the same Th may be able to perform both carrier- and idiomotype-specific help.

An objection to this interpretation is that the immunoglobulin receptors of B cells presumably are not subject to antigen processing before recognition by idiomotype-specific Th whereas such processing may have taken place with the antigens of the present study. Evidence against this objection derives from an earlier experiment where  $L^{315}$  priming of Th from BALB/c mice not only augmented the anti-NIP responses but also the antibody responses to the M315 idiomotype of recipients boosted with M315 (ref. 8). As the serologically defined idiomotype of M315 requires assembled ( $V_H + V_L$ ) domains for its expression, and as the determinants recognized by collaborating B and Th cells must be present on the same molecular complex<sup>17</sup>, this result suggests that the V-domains of M315 used in the present

experiments were recognized as intact during priming and assembled during the boost.

This work was supported by the Norwegian Research Council for Science and the Humanities, the Norwegian Cancer Society and the Norwegian Society for Fighting Cancer.

Received 17 July; accepted 26 September 1980.

- Hannestad, K., Kao, M. S. & Eisen, H. N. *Proc. natn. Acad. Sci. U.S.A.* **69**, 2295–2299 (1972).
- Hannestad, K. & Gaudernack, G. *Scand. J. Immun.* **6**, 59–76 (1977).
- Lynch, R. G., Graff, R. J., Sirisinha, S., Simms, E. S. & Eisen, H. N. *Proc. natn. Acad. Sci. U.S.A.* **69**, 1540–1544 (1972).
- Woodland, R. & Cantor, H. *Eur. J. Immun.* **8**, 600–606 (1978).
- Hetzlberger, D. & Eichmann, K. *Eur. J. Immun.* **8**, 846–852 (1978).
- Eichmann, K., Falk, I. & Rajewsky, K. *Eur. J. Immun.* **8**, 853–857 (1978).
- Eisen, H. N., Simms, E. S. & Potter, M. *Biochemistry* **7**, 4126–4134 (1968).
- Jørgensen, T. & Hannestad, K. *Eur. J. Immun.* **7**, 426–431 (1977).
- Jørgensen, T. & Hannestad, K. *Scand. J. Immun.* **10**, 317–323 (1979).
- Schulenburg, E. P., Simms, E. S., Lynch, R. S., Bradshaw, R. A. & Eisen, H. N. *Proc. natn. Acad. Sci. U.S.A.* **68**, 2623–2626 (1971).
- Cotner, T. & Eisen, H. N. *J. exp. Med.* **148**, 1388 (1978).
- Sirisinha, S. & Eisen, H. N. *Proc. natn. Acad. Sci. U.S.A.* **68**, 3130–3135 (1971).
- Edelman, G. M. *Biochemistry* **9**, 3197–3204 (1970).
- Amzel, L. M., Poljak, R. J., Saul, F., Varga, J. M. & Richards, F. F. *Proc. natn. Acad. Sci. U.S.A.* **71**, 1427–1430 (1974).
- Segal, D. M. *et al. Proc. natn. Acad. Sci. U.S.A.* **71**, 4298–4302 (1974).
- Jerne, N.-K. *Ann. Immun., (Paris)* **125C**, 373–389 (1974).
- Mitchison, N. A. *Eur. J. Immun.* **1**, 18–27 (1971).

## Sperm-specific surface antigenicity common to seven animal phyla

Alina C. Lopo\*

Department of Zoology, University of California, Davis, California 95616

Victor D. Vacquier

A-002, Marine Biology Research Division, Scripps Institution of Oceanography, University of California, San Diego, La Jolla, California 92093

**While studying the plasma membrane of sperm of the sea urchin *Strongylocentrotus purpuratus*, we developed an antiserum that exhibits unusual reactivity—it cross-reacts with the surfaces of spermatozoa of 28 species representing seven phyla of the animal kingdom. A negative cross-reaction has not been found. This suggests the possible existence of common antigenic determinants on the surface of all animal sperm. We report these preliminary results here because of the broad implications common sperm-surface antigenicity has for the potential development of immunocontraceptive methods.**

\* To whom correspondence should be addressed at Anatomy Department, University of California, San Francisco, California 94143.

**Table 2** T-helper cell recognition of  $V_H^{315}$  and  $V_L^{315}$  is regulated by genes within the MHC complex

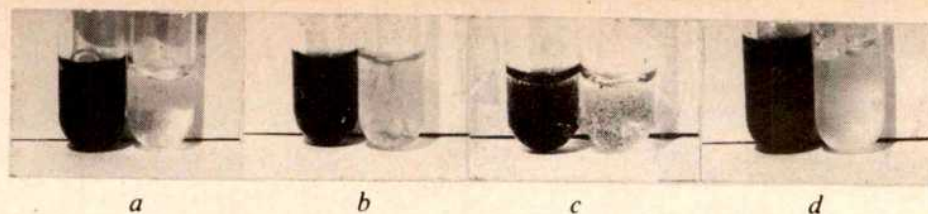
| Strain*<br>immunized | H-2<br>type | Secondary anti-NIP response<br>in recipients of Th primed with: |                         |
|----------------------|-------------|---|-------------------------|
|                      |             | $V_H$   | $V_L$                   |
| BALB/c               | d           | 5.9 (2.3)   | 57.8 (1.0) <sup>†</sup> |
| C3H                  | k           | 61.3 (0.6)  | 8.5 (1.1)               |
| BALB.K               | k           | 27.1 (2.9)  | 2.0 (0.2)               |

\* The strains BALB/c and C3H were purchased from Gl. Bomholtgaard. BALB/K mice were from Olac 1976.

<sup>†</sup> Values expressed as in Table 1. The serum was collected 11 days after boost with NIP<sub>3</sub>-Fab<sup>315</sup>.



**Fig. 1** Cross-reactivity of SSA with sperm of four species visualized by the immunoperoxidase procedure. Approximately equal numbers of spermatozoa ( $5 \times 10^8 \text{ ml}^{-1}$ ) were used for each reaction (tube on left, SSA; tube on right, preimmune serum). a, *S. purpuratus* (sea urchin); b, *Rattus norvegicus* (rat); c, *Salmo* sp. (salmon); d, *Metridium senile* (*fibriatum*) (sea anemone). To prepare SSA, sperm of the sea urchin *S. purpuratus* were washed by sedimentation (1,000 g, 10 min) in filtered sea water to remove seminal fluid, fixed 1 h in 3% glutaraldehyde-sea water, then washed to remove the fixative. They were resuspended in phosphate-buffered saline (PBS, pH 7.2, 0.5 mg per ml sperm protein), mixed with Freund's complete adjuvant (1 Freund's: 2 sperm) and a virgin female New Zealand rabbit was immunized by direct injection into the popliteal lymph nodes<sup>14</sup>. After 4 weeks a second injection was given subcutaneously and the rabbit bled 10 days later. Serum was removed following clot retraction and heated to 56 °C for 30 min. To eliminate non-sperm-specific activities, antiserum was absorbed with minced sea urchin ovary and non-gametic male tissues (coelomocytes and tube feet) by incubating the tissues in antiserum, then clarifying by centrifugation. To obtain a 1% TX-100 extract, sperm were washed and resuspended in sea water containing 10 mM TAME (*p*-tosyl-1-arginine-methyl ester) and 10% TX-100 in sea water added to a final concentration of 1%. After 30 min the soluble extract was collected by centrifugation at 30,000 g for 30 min. To perform the immunoperoxidase localization, sperm were fixed for 1 h in 3% glutaraldehyde- or formaldehyde-sea water (or PBS), washed and then incubated for 30 min in 10% normal swine serum (NSS). Following removal of excess NSS, the cells were incubated 1 h in preimmune serum (1/80) or SSA (1/80), washed three times in 1% NSS-PBS, incubated 15 min in horseradish peroxidase-conjugated swine anti-rabbit IgG (1/50; Bio-Rad Laboratories) and washed three times in 1% NSS-PBS over a 12-h period. The cells were then resuspended in 1 ml reaction mixture, containing 0.75 mg Hanks-Yates reagent (Polysciences), 0.1 M Tris-HCl, pH 7.6, and 0.01%  $\text{H}_2\text{O}_2$  (ref. 15). After 15 min the cells were washed in PBS, transferred to a clean tube and the presence or absence of reaction product determined by direct visual observation or phase-contrast microscopic observation of the cell suspension. The precipitate was visible over the entire cell surface. No free precipitate was observed in the suspension. Preimmune serum did not react. Hanks-Yates reagent was used in place of diaminobenzidine because the latter is a potent carcinogen.



The antiserum was prepared using whole, glutaraldehyde-fixed *S. purpuratus* sperm as the immunogen. Fixed cells may be a better immunogen than their unfixed counterparts because they are not cleared by macrophages as readily as unfixed ones, thus creating an artificial booster effect<sup>1</sup>. The antiserum to the fixed sperm produced several precipitin lines when diffused in agar against a Triton X-100 (TX-100) extract of sea urchin sperm. Following absorption of the whole antiserum with sea urchin ovary and non-gametic male tissues, only one precipitin line appeared in the agar plate. However, we recognize that minor antigenic activities may remain undetected by simple immunodiffusion assay (the number of antigenicities present in the absorbed serum is not the point of this letter). This absorbed antiserum is hereafter designated 'sperm-specific antiserum' (SSA). The sperm-specific activity of SSA could be completely eliminated by absorption with fixed or living sperm [as determined by immunodiffusion, immunoperoxidase and indirect immunofluorescence (IIF)]. The SSA inhibited the egg jelly-induced acrosome reaction in living *S. purpuratus* sperm.

When the SSA was tested for cross-reactivity (using immunoperoxidase and IIF) with sperm of other species, we found that every species gave a positive reaction (Figs 1 and 2, Table 1). Rat sperm (Figs 1b and 2d), salmon sperm (Fig. 1c) and coelenterate sperm (Fig. 1d) reacted as strongly as sea urchin sperm (Figs 1a and 2b). We stress that this is a qualitative assay and that we have not determined the number of binding sites for the SSA on a per cell basis. The results obtained with IIF (Fig. 2) and phase-contrast and bright-field observations of immunoperoxidase-reacted cells showed that the activity is distributed over the entire surface of the sperm. Controls on the immunoperoxidase procedure (Fig. 3) showed that the deposition of the coloured reaction product depended on the reaction of the SSA with the sperm surface. A variety of cell types were tested to determine that the activity was indeed sperm specific; no non-sperm cell types reacted with the SSA (Table 2).

The unusual reactivity of this antiserum led us to perform an extensive series of controls to establish that the sperm-specific activity was not artefact. Because glutaraldehyde-fixed sperm were used as the immunogen, we examined whether the activity of the SSA might be due to a glutaraldehyde-hapten effect. This has been ruled out by the following findings: (1) The SSA raised against the glutaraldehyde-fixed sea urchin sperm reacted with both living sperm and formaldehyde-fixed sperm. (2) Another antiserum, raised by injecting unfixed, whole sea urchin sperm into a rabbit, had the same reactivity as the serum to glutaraldehyde-fixed sperm. (3) A third antiserum produced by

using a 1% TX-100 extract of sea urchin sperm as the immunogen also had the same specificity. (4) The activity of the SSA was completely eliminated by absorbing the antiserum with either living or glutaraldehyde-fixed sperm, also showing that the activity was directed against surface molecules.

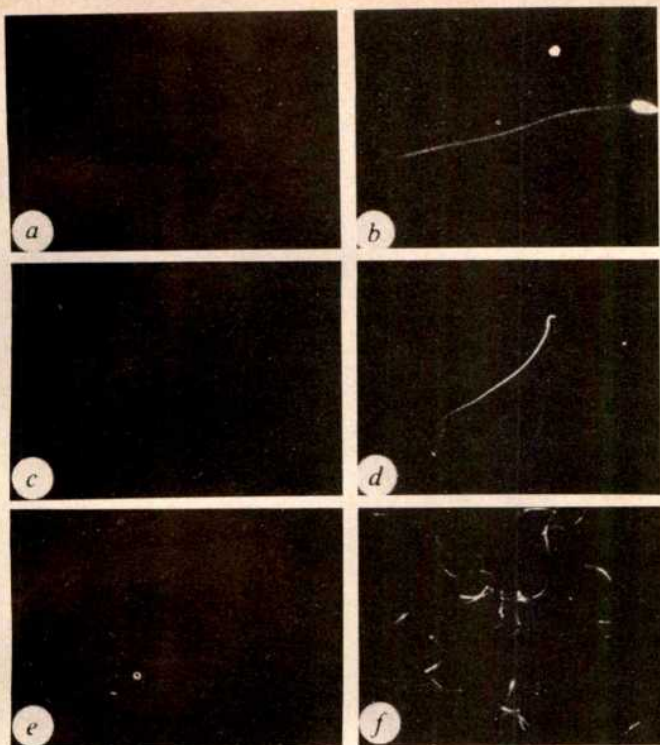
Because there are carbohydrate sequences in complete Freund's adjuvant that might elicit the production of antibodies that cross-react with some mammalian sperm<sup>2</sup>, two experiments were performed to show that the activity of the SSA was not the result of this phenomenon. First, a rabbit was injected with complete Freund's adjuvant only from the same vial of adjuvant that had been used in production of the SSA. Both the pre-injection and post-injection sera from this rabbit showed no reactivity with sperm. Second, a rabbit was immunized with

**Table 1** Reaction of SSA prepared against *S. purpuratus* sperm (sea urchin) with sperm of other species

| PHYLUM COELENTERATA               | PHYLUM ECHINODERMATA           |
|-----------------------------------|--------------------------------|
| Class Anthozoa                    | Class Echinoidea               |
| <i>Metridium senile fibriatum</i> | <i>S. purpuratus</i>           |
| PHYLUM ANNELIDA                   | <i>S. franciscanus</i>         |
| Class Polychaeta                  | <i>S. pallidus</i>             |
| Fam. Spionidae (1 species)        | <i>S. droebachiensis</i>       |
| Fam. Polynoidae (1 species)       | <i>Lytechinus pictus</i>       |
| PHYLUM MOLLUSCA                   | <i>Arbacia punctulata</i>      |
| Class Amphineura                  | <i>Tridacna striatula</i>      |
| <i>Cryptochiton stelleri</i>      | <i>Dendroaster excentricus</i> |
| Class Gastropoda                  | Class Ophiuroidea              |
| <i>Acmaea</i> sp.                 | <i>Ophioplocus esmarkii</i>    |
| Class Pelecypoda                  | Class Asteroidea               |
| <i>Macoma nasuta</i>              | <i>Patiria miniata</i>         |
| PHYLUM ECHIUROIDEA                | PHYLUM CHORDATA                |
| <i>Urechis caupo</i>              | Class Urochordata              |
| PHYLUM ARTHROPODA                 | <i>Styela clava</i>            |
| Class Crustacea                   | <i>S. plicata</i>              |
| <i>Cancer antennarius</i>         | <i>Ciona intestinalis</i>      |
| <i>Pinnixa tubicola</i>           | Class Osteichthyes             |
| Class Merostomata                 | <i>Salmo</i> sp.               |
| <i>Limulus polyphemus</i>         | Class Amphibia                 |
|                                   | <i>Rana pipiens</i>            |
|                                   | Class Aves                     |
|                                   | <i>Meleagris gallopavo</i>     |
|                                   | Class Mammalia                 |
|                                   | <i>Mesocricetus auratus</i>    |
|                                   | <i>Rattus norvegicus</i>       |

Reactivity of the SSA was assayed by IIF or by the immunoperoxidase procedure. The sperm were fixed in either 3% glutaraldehyde or formaldehyde. Preimmune serum did not react. See Figs 1 and 2 legends for methods.



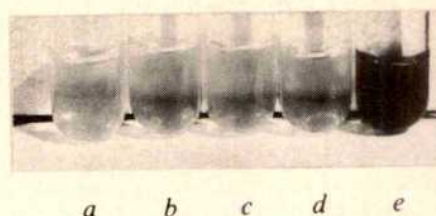


**Fig. 2** Reactivity of SSA with sperm of three species visualized by IIF *a* and *b*, sea urchin; *c* and *d*, rat; *e* and *f*, turkey. *a*, *c* and *e*, preimmune serum; *b*, *d* and *f*, SSA. Sperm were fixed and washed as in Fig. 1 legend, then incubated for 1 h in preimmune serum (1/100) or SSA (1/100), washed three times in 1% normal rabbit serum in PBS, incubated 15 min in 1:10 fluorescent goat anti-rabbit antiserum (Antibodies Incorporated), and washed three times in PBS over a 30-min period. The cells were then resuspended in PBS and observed and photographed on GAF 500 film with a Zeiss fluorescent microscope equipped with an Osram mercury lamp. The fluorescence appears over the entire cell surface. Pre-immune serum did not react.

unfixed sperm without adjuvant, and this antiserum, after absorption, had the same specific reactivity as the SSA.

The possibility existed that the supposedly sperm-specific activity was not due to the recognition of a surface antigen but resulted from the cross-reactivity of male accessory gland secretions. However, no reactivity was detected when sea urchin seminal fluid was diffused in agar against the SSA. Another possibility was that the SSA was recognizing H-Y antigen, the male sex-determining antigen present on the sperm (and all other cells) of all species in which the male is the heterogametic sex<sup>3,4</sup>. To answer this question the following experiments were performed. First, the serum was extensively absorbed using sea urchin male non-gametic tissues (coelomocytes and tube feet); the activity of the SSA was not affected. Second, the antiserum

was extensively absorbed using splenocytes from two male rats (the standard procedure for absorbing H-Y antibodies<sup>5</sup>); there was no loss of activity of the SSA. It has been reported that H-Y activity is limited in distribution to the region of the acrosomal cap in mammalian sperm<sup>6</sup>. We found, however, that SSA activity was distributed over the entire surface of rat and hamster sperm, as judged by immunoperoxidase localization using phase-contrast microscopy at  $\times 1,000$  magnification and by IIF. Finally, the serum reacted with turkey sperm by both the immunoperoxidase and IIF (Fig. 2*e*, *f*) procedures, proving conclusively that the SSA is not recognizing H-Y activity, because in birds the heterogametic sex, and hence the bearer of H-Y (H-W in birds), is the female<sup>3,4</sup>.



**Fig. 3** No reaction product was deposited when the immunoperoxidase procedure was performed using sea urchin sperm in the absence of one of the following reactants: *a*, hydrogen peroxide; *b*, SSA; *c*, horseradish peroxidase. *d*, Preimmune serum, and *e*, SSA, all reagents included.

In mammals, cross-reacting antigens exist among nervous tissue, sperm and preimplantation embryos<sup>7</sup>. However, we found that the SSA did not react with fixed or unfixed rat brain. Some sperm, such as those of the rabbit, nonspecifically bind the Fc region of antibodies<sup>8</sup>. To exclude this as a possibility for the activity of our SSA, we tested two other antisera raised against two different genus-specific sea urchin sperm surface glycoproteins (*S. purpuratus*<sup>9</sup>). Sperm of 16 species, representing four phyla, did not react with these other antisera, showing that the activity of the SSA did not result from nonspecific binding of the Fc region of the rabbit immunoglobulins. To investigate the possibility that the SSA was reacting with cell-surface tubulin, we reacted it with *Chlamydomonas reinhardtii* cells and mussel gill tissue (*Mytilus californicus*), two cell types reported to have tubulin on their outer surface<sup>10-13</sup>. Both cell types gave a negative reaction by the immunoperoxidase assay. The results here suggest that common cross-reactive antigenic determinant(s) exist which are specific to the surface of animal sperm.

We thank Drs B. S. Dunbar, R. P. Erickson, E. Goldberg, and S. Sarkar for discussions, G. W. Moy for technical assistance, and Drs P. G. Calarco and C. L. Banka for use of the fluorescent microscope and assistance with the immunofluorescence assay. This work was supported by NIH HD 12986 to V.D.V. A.C.L. was a 1977-78 American Association of University Women predoctoral fellow.

Received 21 July; accepted 2 September 1980.

**Table 2** Cells and tissues which did not react with SSA as assessed by immunoperoxidase

|  |
|--|
| 1. Cell lines  |
| DS8 = Mouse mammary tumour   |
| A549 = Human lung tumour   |
| ATC103 = Iguana heart  |
| B104 = Rat neuroblastoma   |
| DC2 = <i>Drosophila</i> Schneider cells  |
| 2. <i>Chlamydomonas reinhardtii</i> cells  |
| 3. Mussel gill tissue ( <i>Mytilus californicus</i> )                              |
| 4. Sliced rat brain tissue   |
| 5. Dissociated blastomeres of sea urchin hatched blastula ( <i>S. purpuratus</i> ) |

See Fig. 1 legend for methods.

- Dewey, M. J., Gearhart, J. D. & Mintz, B. *Dev Biol.* **55**, 359-374 (1977).
- Russo, J., Metz, C. B. & Dunbar, B. S. *Biol. Reprod.* **13**, 136-141 (1975).
- Wachtel, S. S. *Science* **198**, 797-799 (1977).
- Silvers, W. K. & Wachtel, S. S. *Science* **195**, 956-960 (1977).
- Goldberg, E. H., Boyse, E. A., Bennett, D., Scheid, M. & Carswell, E. A. *Nature* **232**, 478-480 (1971).
- Koo, G. C., Stackpole, C. W., Boyse, E. A., Hammerling, U. & Lardis, M. P. *Proc. natn. Acad. Sci. U.S.A.* **70**, 1502-1505 (1973).
- Solter, D. & Schachner, M. *Dev Biol.* **52**, 98-104 (1976).
- Allen, G. J. & Bourne, F. J. *J. exp. Zool.* **203**, 271-276.
- Lopo, A. C. & V. D. Vacquier *Dev Biol.* **79**, 325-333 (1980).
- Adair, W. S. & Goodenough, U. W. *J. Cell Biol.* **79**, 54a (1978).
- Dentler, W. L. *J. Cell Biol.* **84**, 364-380 (1980).
- Dentler, W. L., Pratt, M. M. & Stephens, R. E. *J. Cell Biol.* **84**, 381-403 (1980).
- Stephens, R. E. *Biochemistry* **16**, 2047-2058 (1977).
- Goudie, R. B., Horne, C. H. W. & Wilkinson, P. C. *Lancet* **ii**, 1224-1228 (1966).
- Hanker, J. S., Yates, P. E., Metz, C. B. & Rustioni, A. *Histochem. J.* **9**, 789-792 (1977).



## Retroviral antigens on $gs^- chf^-$ leukocytes

P. Jurdic, J. Huppert & T. Greenland

Unité de Virologie Fondamentale et Appliquée, INSERM U.51, Groupe de Recherche CNRS 33, 1, Place Pr Joseph Renaut, 69371 Lyon Cedex 2, France

E. Heller

Hebrew University-Hadassah Medical School, Jerusalem, Israel

It has recently been suggested that the endogenous retroviruses present in many different species might be involved during stimulation of the immune system of their hosts<sup>1-3</sup>. We have now studied the expression of two avian retroviral antigens p27 and gp85 in chicken lymphoid cells by indirect immunofluorescence (IIF) and by complement-dependent microcytotoxicity (CDM). We have now found that these viral antigens are expressed in peripheral blood leukocytes of adults and embryos and in splenic and bursal lymphocytes of Spafas  $gs^- chf^-$  chickens but they are not expressed in fibroblasts cultured from the feather follicles of the same individual adult birds nor in fibroblasts cultured from embryos of the same flock. The differential expression of viral antigens in leukocytes may be related to a specific property or function of these cells.

We wished to study the possible modifications of the expression of avian retroviral antigens by chicken lymphoid cells during the immune response, but, using outbred  $gs^+ chf^+$  birds, we observed that their lymphoid tissues frequently expressed considerable quantities of p27 and gp85 as estimated by IIF (see Table 1). Splenic cells from some 20 birds of ages ranging from 3 weeks to 6 months were 30–100% positive for either antigen; bursal cells from the same birds were more variable, some samples being negative for one or both of the antigens, others consisting of 100% positive cells. Only a few samples of peripheral blood leukocytes from these birds were examined but they were uniformly strongly positive ( $\geq 80\%$ ) for both antigens. These results agree with those of Chen and Hanafusa<sup>4</sup> who used radioimmunoassay techniques to show that p27 was expressed in greater amounts by the lymphocytes of such chickens than by any other tissue. We therefore decided to use Spafas chickens which, although they contain the endogenous viral genome, do not usually express the corresponding antigens<sup>5-7</sup>.

In an initial experiment, leukocytes from peripheral blood of adult Spafas chickens were examined by IIF for expression of viral antigens (see Table 1). A considerable proportion of peripheral blood leukocytes from all four of the birds reacted with the anti-gp85 serum (50–90%) and with the anti-p27 serum (40–70%) and these percentages remained fairly stable for the individual birds over the experimental period. The birds were killed and smears prepared from mechanically disrupted splenic and bursal tissue and compared with the peripheral blood samples. The percentage of positive cells was never higher in these tissues than in the corresponding blood.

These results were confirmed using a CDM assay as described by Mohanakumar *et al.*<sup>8</sup>. A series of Spafas chickens were the source of peripheral blood leukocytes and these were examined by the CDM test using the same antisera as used in the IIF.

In these conditions, the anti-p27 serum caused a specific cytotoxicity of 50–80% of Spafas peripheral blood leukocytes at a dilution of 1:20 and had an end point titre of 80–160. The anti-gp85 serum showed greater reactivity, regularly killing some 90% of the target cells at dilutions up to 1:5,000 and having an end point titre of 20,000–40,000 (Fig. 1). The specificity of this reaction was verified by absorption of the serum against cells with known expression of viral antigens. This

activity could be absorbed by Spafas blood leukocytes or by mammalian cells transformed by Rous sarcoma virus and expressing viral antigens but not by analogous untransformed cells nor by Spafas fibroblasts even after 5-bromodeoxyuridine (BUdR) treatment. Similar results, although at lower titre, were obtained with antisera raised in rabbits using a different preparation of p27 and gp85 antigens.

As a further control, the reactivity of the sera towards Spafas embryo fibroblasts was tested by IIF. Neither p27 nor gp85 was ever expressed over 12 culture passages, even after culturing the cells for 6 days in the presence of BUdR ( $4 \mu\text{g ml}^{-1}$ ). We also cultivated fibroblasts from the feather follicles<sup>9</sup> of individual Spafas chickens which provided the blood leukocytes for comparisons over the culture period. These fibroblasts also showed no reactivity by IIF for either antigen even after BUdR treatment and were incapable of absorbing the reactivity of the sera for leukocytes of the same individual chicken (Fig. 1).

The expression of these antigens by peripheral blood leukocytes has regularly been observed at all ages from newly hatched chicks to birds of over 1 year old. We have also tested some samples from chick embryos, and have found by IIF that white blood cells are already positive for both antigens in 10-day-old embryos, the earliest date at which we could obtain adequate samples. An additional technique has been used to detect these viral antigens in Spafas lymphocytes. This consisted of competitive radioimmune assays using 'purified' labelled antigens and competition with 'cold' antigens from cells. For p27, lymphocytes showed weak activity and muscle, heart, liver, kidney and lung were negative. For gp85, lymphocytes showed greater activity than transformed mammalian cells used as positive controls, other tissues being negative.

The difference in expression of retroviral antigens between Spafas fibroblasts and lymphocytes, although both cell types contain the endogenous viral genome, indicates that some control over this expression must be exerted at the transcriptional or post-transcriptional level. Our results suggest that this regulation acts differently in different tissues of the same bird, as fibroblasts from a given individual can be totally negative whereas the leukocytes from the same bird express considerable quantities of both p27 and gp85. A similar observation has been reported for BALB/Mo mice infected at an early embryonic stage with Moloney leukaemia virus. After birth, viral antigen was found to be strongly expressed by splenic and thymic cells, but not by those of other tissues tested (liver, kidney and brain), although the viral genome was present in the DNA of all these organs<sup>10</sup>. This system is, however, not a natural

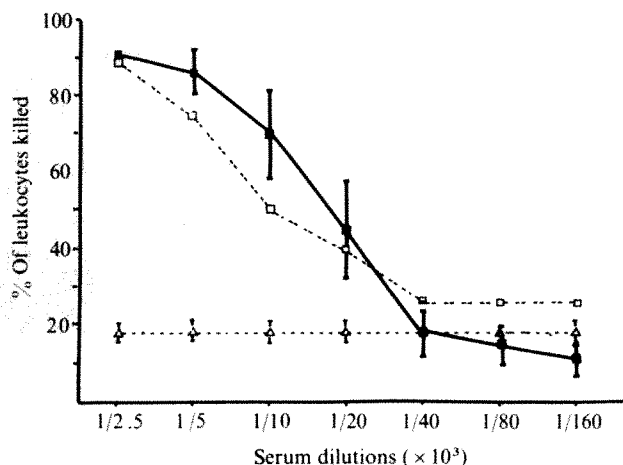


Fig. 1 Complement-dependent microcytotoxicity assay of anti-gp85 (AMV) serum against Spafas peripheral blood leukocytes. ■, Unabsorbed serum ( $n = 12$ ); □, serum absorbed on feather follicle fibroblasts from the same chicken (duplicate measures); △, serum absorbed on Spafas leukocytes ( $n = 4$ ). Bars represent s.d. In the absence of complement or with control negative sera the percentage of leukocytes killed is always  $\leq 20\%$ .

**Table 1** Expression of endogenous viral antigens in  $gs^- chf^-$  chicken lymphocytes

| Chicken                                     | Age                                | Tissue  | Antiserum       | Test | Reactivity |
|---|------------------------------------|---|-----------------|------|------------|
| Outbred<br>gs <sup>+</sup> chf <sup>+</sup> | 3 weeks-<br>6 months               | Spleen<br>bursa<br>blood                          | Anti-p27<br>and | IF   | +30-100%   |
|   |                                    |   | Anti-gp85       |      | +10-100%   |
| Spafas<br>gs <sup>-</sup> chf <sup>-</sup>  | 4 months                           | Spleen<br>bursa<br>blood                          | Anti-p27        | IF   | +40-70%    |
|   |                                    |   | Anti-gp85       |      | +50-90%    |
|   |                                    |   | Anti-p27        | CDM  | +50-80%    |
|   |                                    |   | Anti-gp85       |      | +90%       |
| Spafas<br>gs <sup>-</sup> chf <sup>-</sup>  | 0-1 yr                             | Blood   | Anti-p27        | IF   | +          |
|   |                                    |   | Anti-gp85       |      |            |
| Spafas<br>gs <sup>-</sup> chf <sup>-</sup>  | 10-18-day-<br>old embryo<br>Embryo | Blood   | Anti-p27        | IF   | +          |
|   |                                    |   | Anti-gp85       |      |            |
|   |                                    |   | Anti-p27<br>and | IF   | -          |
|   |                                    |   | Anti-gp85       |      |            |
|   | Adult                              | Fibroblast<br>cultures<br>12<br>passages<br>±BUdR | Anti-p27<br>and | IF   | -          |
|   |                                    |   | Anti-gp85       |      |            |

For IIF testing, blood samples were taken from four adult (4-month-old) Spafas chickens at 2-3-day intervals over a 15-day period. The blood was taken from the wing vein and collected into citrate. The leukocytes were separated either by allowing the cells to settle at 37°C and recovery of the buffy coat, or by centrifugation through Ficoll-paque (Pharmacia) at 1,500 r.p.m. for 15 min. Identical results were obtained using either method. After washing with phosphate-buffered saline (PBS), pH 7.4, the cells were smeared on to microscope slides, air dried, fixed in buffered formaldehyde (3.7% w/v) for 3 min, rinsed and postfixed in dry acetone for 10 min. Dilutions of antisera to p27 or gp85 raised in rabbits to purified polypeptides from avian myeloblastosis virus or control sera were then allowed to react with the fixed smears for 45 min at 37°C. After washing with PBS, the reaction was visualized by a further incubation with fluorescein-labelled goat anti-rabbit immunoglobulin serum (Behring, dilution 1:50) for 30 min at room temperature. The washed specimens were then examined under a Zeiss Ultraphot II fluorescence microscope. In some cases the surface expression of the antigens was estimated by the use of unfixed cell suspensions in a similar protocol. Control samples of cultured cell lines with known expression of the viral antigens were always included in each series. For cytotoxicity testing, the separated leukocytes were resuspended at  $6 \times 10^6$  cells  $ml^{-1}$  in RPMI 1640 medium supplemented with 10% inactivated fetal calf serum. This suspension (1  $\mu$ l) was introduced under liquid paraffin into each well of a 60-well Falcon microtitre plate together with 1  $\mu$ l of diluted antiserum. After 30 min at room temperature, 5  $\mu$ l of rabbit complement (Gibco), previously absorbed on adult chicken erythrocytes and brought to a dilution of 1:3, was added to each well and the incubation continued for 45 min. After this the dead cells were stained by the introduction of 5  $\mu$ l of a solution of eosin to each well, then, 2 min later, the cells were fixed by the introduction of 2  $\mu$ l of buffered formaldehyde (30% w/v, pH 7.0). The reactions were read under the phase-contrast microscope.

transmission of a strictly endogenous virus. In the same system there was no stimulation of viral expression in actively proliferating hepatocytes<sup>11</sup>, arguing against the hypothesis that endogenous virus expression might be simply associated with cellular proliferation.

The association of the expression of endogenous viral antigens with cells intimately involved in the animal's immune responses suggests some relationship between these molecules and the cell-surface (glyco)proteins implicated in immune reactions. The fact that viral antigens are expressed on most leukocytes suggests that these molecules may be involved in a general function of these cells rather than affecting only those cells and their clones specifically sensitized by antigen. Recently, Astrin *et al.*<sup>12</sup> have successfully reared to breeding age a healthy cockerel that has no endogenous viral DNA in its genome. It would be of interest to test the immune response of such birds and to compare it with that of birds carrying the endogenous virus.

Possibly the observed effect can be explained on the basis of artefact due to the culturing procedure itself. Fibroblasts might be negative for virus expression because of trypsinization or culturing. This explanation is, however, improbable as  $gs^- chf^-$  fibroblasts in these same conditions retain viral expression suggesting that  $gs^- chf^-$  fibroblasts are inherently negative. A more likely reason for the differential viral antigen expression may involve one of several control levels. For example, viral

RNA may be constitutively expressed in lymphocytes whereas it may require induction in fibroblasts.

Our results suggest that p27 expression takes place on the surface of lymphocytes. Although the 'usual' mode of expression of p27 is intracellular, a large precursor polypeptide containing the sequence of p27 has been shown to be present on the surface of cells infected by RSV, although in this case p27 antigenicity could not be demonstrated<sup>13</sup>. Alternatively, the lymphocyte plasma membrane might permit the insertion of p27 although that of fibroblasts does not.

These studies were supported by DGRST grant 78 7 2647 and by an INSERM fellowship to E.H. Some of the p27 and gp85 antisera, and the avian myeloblastosis virus antigens were gifts from Dr H. Diggelman and D. P. Bolognesi respectively.

Received 28 July; accepted 22 September 1980.

- Schumann, G. & Moroni, C. *J. Immun.* **120**, 1913-1916 (1978).
- Moroni, C. & Schumann, G. *J. gen. Virol.* **38**, 497-503 (1978).
- Phillips, S. M., Stephenson, J. R. & Aaronson, S. A. *J. Immun.* **118**, 662-666 (1977).
- Chen, J. H. & Hanafusa, H. *J. Virol.* **13**, 340-346 (1974).
- Tereba, A., Skoog, L. & Vogt, P. K. *Virology* **65**, 524-534 (1975).
- Hanafusa, T., Hayward, W. S. & Hanafusa, H. in *Virus Research* (eds Fox, C. F. & Robinson, W. S.) 387-402 (Academic, New York, 1973).
- Hayward, W. S., Wang, S. Y., Urm, E. & Hanafusa, H. in *Animal Virology* (eds Baltimore, D., Huang, A. S. & Fox, C. F.) 21-35 (Academic, New York, 1976).
- Mohanakumar, T., Metzgar, R. S. & Miller, D. S. *J. nat. Cancer Inst.* **52**, 1435-1444 (1974).
- Crittenden, L. B., Wendel, E. J. & Ratzsch, D. *Avian Dis.* **15**, 503-507 (1971).
- Jaenisch, R. *Virology* **93**, 80-90 (1979).
- Jaenisch, R. & Hoffmann, E. *Virology* **98**, 289-297 (1979).
- Astrin, S. M., Buss, E. G. & Hayward, W. S. *Nature* **282**, 339-341 (1979).
- Buetti, E. & Diggelman, H. *Virology* **102**, 251-261 (1980).

## Genes which control cell proliferation in the yeast *Saccharomyces cerevisiae*

Peter E. Sudbery & Andrew R. Goodey\*

Department of Genetics, University of Sheffield, Sheffield S10 2TN, UK

Bruce L. A. Carter

Department of Genetics, Lincoln Place Gate, Trinity College, Dublin 2, UK

In many eukaryotes it is thought that cell proliferation is regulated at a point in  $G_1$  close to the initiation of DNA synthesis<sup>1</sup>. Hartwell<sup>2,3</sup> and his colleagues have shown such a point in  $G_1$  phase in the budding yeast, *Saccharomyces cerevisiae*, defined by the *cdc 28* mutation. He has termed this point 'start' and showed that for cells to proceed beyond start, initiate DNA synthesis and produce a bud, various conditions must be met. Two of these conditions are the presence of adequate nutrients in the medium and the attainment of a critical size. We identify here some of the genes controlling start by isolating mutants which are altered with respect to the conditions in which start occurs. Two types of mutant have been isolated. One results in bud initiation when the parent cell is only half the size at which bud initiation occurs in wild-type cells. Such mutants define a single gene, *whi-1*, and they are apparently analogous to the size mutants isolated by Nurse and his colleagues<sup>4-6</sup> in *Schizosaccharomyces pombe*. A second type of mutation affects a second gene, *whi-2*, which is involved in the mechanism whereby cells arrest in  $G_1$  in stationary phase. *whi-2* cells growing exponentially initiate buds at the same size as wild-type cells. In stationary phase, however, *whi-2* cells, unlike wild-type cells, are predominantly budded and are smaller than wild-type cells.

\* Present address: The Brewing Research Foundation, Lyttel Hall, Nutfield, Redhill, Surrey RH1 4HY, UK.



Small cell-size mutants of strain X2180-1A were isolated by a procedure involving cell size separation by zonal centrifugation together with the use of the mating hormone  $\alpha$  factor. This procedure is described in detail elsewhere<sup>7</sup>. Three mutants, designated *whi A1*, *whi C7* and *whi D3*, which were recovered from different mutagenized cultures and are therefore independent mutations, were examined in detail. Parent cell volume of these mutants is shown in Table 1, together with dry mass measurements obtained by scanning interferometry and cell protein content for the wild type and the mutant *whi-A1*. Mutant cell size, whether measured by volume, protein content or dry mass, is approximately one-half that of the wild type. Volume was routinely measured as a parameter of cell size in further determinations.

**Table 1** Cell sizes of wild type and *whi-1*<sup>-</sup> mutants in exponential growth phase

| Strain        | Mother cell volume* ( $\mu\text{m}^3$ ) | Total cell protein† ( $\text{g} \times 10^{13}$ ) | Dry mass‡ at bud initiation (arbitrary units) |
|---------------|---|---|---|
| X2180-1A      | 47 ± 2                                  | 7.5   | 11.45 ± 0.38                                  |
| <i>whi-A1</i> | 25 ± 1                                  | 4.7   | 5.39 ± 0.48                                   |
| <i>whi C7</i> | 26 ± 2                                  | —   | —   |
| <i>whi D3</i> | 20 ± 1                                  | —   | —   |

\* Cells were inoculated from a YEPD plate into 2.5 ml YEPD medium in a 50 ml Erlenmeyer flask. The culture was shaken overnight at 25°C. The next day 0.1 ml of the late log phase culture was re-inoculated into 2.5 ml fresh medium and cultured in the same conditions for a further 5 h. Photomicrographs were prepared with a phase-contrast microscope at +400 magnification. Cells were concentrated by centrifugation if necessary. The negatives were projected and the major (a) and minor (b) axis of budded mother cells measured. The final magnification was measured using a photomicrograph of a stage graticule. Volume was calculated assuming a prolate spheroid shape according to the formula  $4/3\pi ab^2$ . Sufficient cells were measured so that the s.e.m. shown, was below 5% of the mean. This involved a minimum of 25 cells.

† Cells were cultured as above. Cell number per ml was measured with a Coulter counter following 10-s sonication to separate clumped cells. To measure protein per ml the cells were washed twice in distilled water and dissolved in 1 M NaOH at 100°C. Protein was estimated using the Folin test<sup>14</sup>.

‡ Unbudded stationary phase cells were diluted into fresh YEPD medium. At intervals samples were removed and mounted in a thin layer of gelatin on a slide<sup>15</sup>. Using a scanning interferometer<sup>16</sup>, the dry mass of cells which had just produced buds was measured. Measurements were continued until over 95% of the cells were budded. The errors are s.e.m.

Each mutant was crossed with XJB17-1 (*arg 9*, *his 4*, *ura 1*, *ilv 3*) and AN 33 (*arg thr*) both of which are  $\alpha$  mating type and produce buds at the same parent cell volume as X2180-1A. The parent cell volume for wild-type diploid cells is 81  $\mu\text{m}^3$  (Table 2). (A similar pattern of results is obtained if only zero bud scar class cells are considered.) The heterozygous diploids had cell volumes intermediate between those of wild-type haploid cells and diploid cells (Table 2). Thus the three mutant alleles are semi-dominant to the wild-type allele.

The heterozygous diploids were sporulated and tetrads dissected. The small phenotype segregated 2:2 in all tetrads showing that in each mutant it was due to a single nuclear mutation. Small progeny with appropriate combinations of mating type and auxotrophic markers were crossed together and diploids selected by prototrophic selection. These diploids all had a parent cell volume similar to that of wild-type haploids (Table 2).

Heteroallelic mutant diploids were sporulated and cell volume at bud initiation measured in the individual spore clones of the resulting tetrads. At least 20 tetrads were analysed in each of the three combinations but no wild-type recombinant pro-

geny were observed. Thus, the mutations probably affect the same gene, *whi-1*, although two closely linked genes could be involved.

If more than one gene is involved sequentially in the synthesis of a product controlling cell size, then the data shown in the last three lines of Table 2 may be used for complementation tests. Although the alleles are apparently showing dosage effects, if two alleles are in the same cistron then the heteroallelic diploid should be the same size as the homozygous diploid. If the alleles are in different cistrons then the heteroallelic diploid should be intermediate in size between the homozygous and heterozygous diploid. The data show the heteroallelic to be the same size as the homozygous diploid, showing the alleles to be in the same cistron. However, the predicted difference is small and may not be resolvable in the tests.

An alternative interpretation of the data, precluding the use of complementation tests, arises from the observation that the homozygous diploid is still twice the size of the mutant haploid even though neither will be producing any normal product from the *whi-1* gene. There is clearly an element of size control remaining which could be explained if there was a second gene so far undefined by mutation. The product of a second gene would act in parallel to that of the *whi-1* gene so that each would affect cell size directly. The size of the cell at bud initiation would therefore be proportional to the combined number of these two genes. The wild-type haploid would thus contain two genes and the wild-type diploid, four. The *whi-1*<sup>-</sup> haploid retains one gene, the homozygous diploid two and the heterozygous diploid three. The observed sizes of 20–25  $\mu\text{m}^3$  (*whi-1*<sup>-</sup> haploid), 45–50  $\mu\text{m}^3$  (wild-type haploid and homozygous mutant diploid), 60–65  $\mu\text{m}^3$  (heterozygous diploid) and 81  $\mu\text{m}^3$  (wild-type diploid) agree well with this interpretation. The results also predict that a second class of mutant, if isolated, could only be distinguished from *whi-1* mutants by recombination. Complementation could not be used, because the heteroallelic diploid would contain two functional genes whether or not the alleles were in the same or different genes.

The mutation *whi-2* apparently occurred spontaneously in strain M11. Whereas *whi-1* cells are smaller than wild type in both exponential growth and stationary phases, *whi-2*<sup>-</sup> mutants are approximately one-half the size of wild-type cells only in stationary phase (Table 3). In stationary phase these cells also differ from wild-type cells as: (1) the budding index is 24% compared with 1.6% of wild-type cells (Table 3). (2) The final cell density is approximately twice that of wild-type cells. (3) The cells have the phase-dark appearance characteristic of exponentially growing cells rather than the normal phase-bright appearance of stationary-phase cells (Fig. 1).

This phenotype suggests a lesion causing defective G<sub>1</sub> arrest. The cells undergo at least one more cycle of division in the absence of growth and consequently become smaller than wild-type cells.

*whi-2*<sup>-</sup> cells were crossed with 4/4D, a wild-type strain. In stationary phase the resulting diploid was phase-bright,

**Table 2** Mother cell volumes of *whi-1*<sup>-</sup> heterozygous and homozygous diploids growing in exponential phase

| Strain                              | Constitution  | Volume |
|-------------------------------------|---|--------|
| XJB17.1                             | <i>whi-1</i> <sup>+</sup>                               | 50 ± 3 |
| C276                                | <i>whi-1</i> <sup>+</sup> / <i>whi-1</i> <sup>+</sup>   | 81 ± 3 |
| <i>whi A1</i> × XJB17.1             | <i>whi-A1</i> <sup>-</sup> / <i>whi-1</i> <sup>+</sup>  | 60 ± 2 |
| <i>whi C7</i> × XJB17.1             | <i>whi C7</i> <sup>-</sup> / <i>whi-1</i> <sup>+</sup>  | 64 ± 2 |
| <i>whi D3</i> × XJB17.1             | <i>whi D3</i> <sup>-</sup> / <i>whi-1</i> <sup>+</sup>  | 65 ± 3 |
| <i>whi A1.1a</i> × <i>whi A1.1b</i> | <i>whi A1</i> <sup>-</sup> / <i>whi A1</i> <sup>-</sup> | 45 ± 2 |
| <i>whi C7 7d</i> × <i>whi C7 8d</i> | <i>whi C7</i> <sup>-</sup> / <i>whi C7</i> <sup>-</sup> | 50 ± 2 |
| <i>whi D3 4b</i> × <i>whi D3 9c</i> | <i>whi D3</i> <sup>-</sup> / <i>whi D3</i> <sup>-</sup> | 47 ± 2 |
| <i>whi A1.1b</i> × <i>whi C7.6c</i> | <i>whi A1</i> <sup>-</sup> / <i>whi C7</i> <sup>-</sup> | 51 ± 2 |
| <i>whi C7 5b</i> × <i>whi D3-22</i> | <i>whi C7</i> <sup>-</sup> / <i>whi D3</i> <sup>-</sup> | 44 ± 2 |
| <i>whi A1 5d</i> × <i>whi D3-22</i> | <i>whi A1</i> <sup>-</sup> / <i>whi D3</i> <sup>-</sup> | 46 ± 3 |

Culture conditions are described in Table 1 legend.



**Table 3** Cell size, final number per ml, percentage budding and percentage viable cells in stationary-phase cultures

| Strain                        | Constitution   | Cell volume ( $\mu\text{m}^3$ ) | Final cell no. $\text{ml}^{-1} (\times 10^9)$ | % Budding | % Viable cells |
|-------------------------------|--|---------------------------------|---|-----------|----------------|
| X2180-1A                      | <i>whi 1<sup>+</sup> whi 2<sup>+</sup></i>                                       | $36 \pm 3$                      | 1.1   | 2         | 55             |
| C276                          | <i>whi 1<sup>+</sup> whi 2<sup>+</sup> / whi 1<sup>+</sup> whi 2<sup>-</sup></i> | $68 \pm 2$                      | 0.49  | 10        | 65             |
| M11                           | <i>whi 1<sup>+</sup> whi 2<sup>-</sup></i>                                       | $24 \pm 1$                      | 1.97  | 24        | 30             |
| S673a                         | <i>whi 1<sup>-</sup> whi 2<sup>+</sup></i>                                       | $15 \pm 1$                      | 1.98  | 13        | 21             |
| XJB.9d.4a                     | <i>whi 1<sup>-</sup> whi 2<sup>-</sup></i>                                       | $8 \pm 1$                       | 3.60  | 31        | 10             |
| XJB.9d.4a $\times$ M11.13d.5d | <i>whi 1<sup>-</sup> whi 2<sup>-</sup> / whi 1<sup>-</sup> whi 2<sup>-</sup></i> | $19 \pm 1$                      | 1.95  | 47        | 5              |

Cells were inoculated from a YEPD plate into 2.5 ml YEPD medium in a 50-ml Erlenmeyer flask. They were cultured for 48 h at 25 °C, by which time cell number had stopped increasing and the culture considered to be in stationary phase. Cell volume of all cells was measured as described in Table 1 legend. After 10 s sonication, cell number was determined using a Coulter counter, percentage budding by microscopic examination, and per cent viable cells by plating out on YEPD plates at a suitable dilution and counting colonies that had appeared after 3 days.

unbudded and the mean cell volume was  $62 \pm 4 \mu\text{m}^3$ , only slightly less than the wild-type diploid in stationary phase ( $68 \mu\text{m}^3$ , Table 3). The mutation is therefore recessive. The diploid was sporulated and tetrads dissected; the phenotype segregated 2:2 in all 30 tetrads examined and therefore results from a single nuclear mutation.

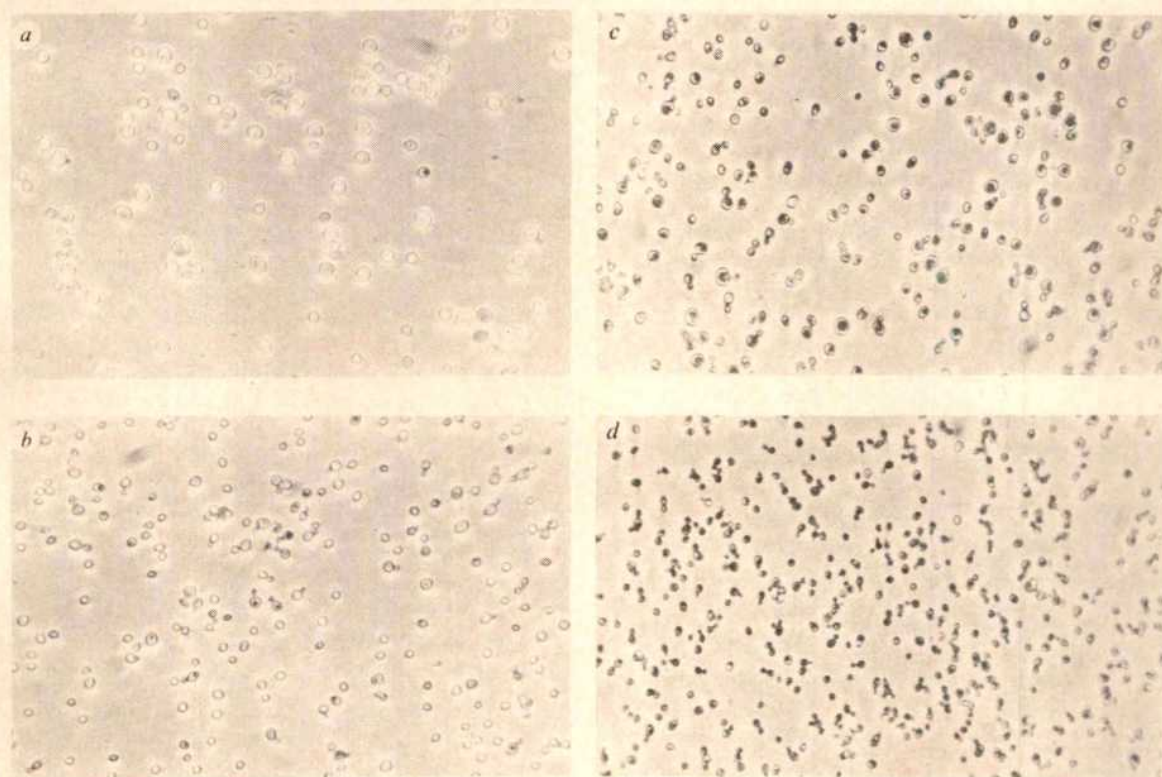
M11 is a strain derived from DR19/T7 which<sup>7</sup> lacks the 2- $\mu\text{m}$  plasmid<sup>8</sup>. This trait is not associated with its absence. First, the trait segregates as a nuclear gene whereas the 2- $\mu\text{m}$  plasmid is inherited cytoplasmically. Second, *whi-2<sup>-</sup>* segregants from the above cross were shown to have received the 2- $\mu\text{m}$  plasmid when they were screened for its presence by buoyant density centrifugation.

A strain carrying the *whi-2* mutation was crossed with one carrying the *whi-1* mutation, the resulting diploid was sporulated and spore clones were grown to stationary phase and analysed for parent cell size. Wild-type recombinants were observed in some tetrads, which also contained spore clones

smaller in stationary phase than either *whi-1<sup>-</sup>* or *whi-2<sup>-</sup>* cells (Table 3). These are the reciprocal recombinant *whi-1<sup>-</sup> whi-2<sup>-</sup>*. The numbers of complete tetrad types was 1 Pd: 3 NPds: 13 Ts indicating unlinked genes. That the putative *whi-1<sup>-</sup> whi-2<sup>-</sup>* was a double mutant was confirmed in a further cross with wild type where the expected single mutant recombinants were recovered.

The stationary-phase appearance of wild-type, *whi-1<sup>-</sup>*, *whi-2<sup>-</sup>* and *whi-1<sup>-</sup> whi-2<sup>-</sup>* cells is shown in Fig. 1. *whi-1<sup>-</sup> whi-2<sup>-</sup>* mutants are much smaller than wild-type cells (Table 3). The high budding index (31%, Table 3), high final cell density (Table 3) and phase-dark appearance suggest continuing division. Cell size is only  $8 \mu\text{m}^3$  (Table 3) compared with the  $38\text{--}50 \mu\text{m}^3$  cell volume of wild-type cells in stationary phase and  $50 \mu\text{m}^3$  at which wild-type cells produce buds. Clearly, *whi-1<sup>-</sup> whi-2<sup>-</sup>* cells have lost much of their control over cell division.

The sizes of strains containing the *whi-2<sup>-</sup>* allele growing in exponential phase are shown in Table 4. The sizes are the same as the corresponding *whi-2<sup>+</sup>* strain indicating an abnormal



**Fig. 1** Phase-contrast pictures of stationary-phase haploid cells. *a*, Wild-type cells; *b*, *whi-1<sup>-</sup>*; *c*, *whi-2<sup>-</sup>*; *d*, *whi-1<sup>-</sup> whi-2<sup>-</sup>*. Stationary-phase cultures were prepared as described in Table 3 legend and photographed with a phase-contrast microscope. Final magnification  $\times 420$ .



phenotype is only expressed in stationary phase. This suggests that *whi-2* is not the gene whose existence was inferred from the size of *whi-1* strains. However, to investigate this further, the diploid *whi-1<sup>-</sup> whi-2<sup>-</sup>/whi-1<sup>-</sup> whi-2<sup>-</sup>* was isolated by mating double mutant haploids carrying complementary auxotrophic requirements. In stationary phase this diploid was extremely small ( $19 \mu\text{m}^3$ ), only 52% of the size of the wild-type haploid in similar condition. The doubly homozygous mutant diploid had the additional characteristic of the double mutant haploid—a high budding index. Furthermore, the size increased to that of a *whi-1<sup>-</sup>/whi-1<sup>-</sup>* strain when inoculated into fresh medium. In stationary phase the *whi-1<sup>-</sup> whi-2<sup>-</sup>/whi-1<sup>-</sup> whi-2<sup>-</sup>* homozygous diploid is larger than the *whi-1<sup>-</sup> whi-2<sup>-</sup>* haploid. Therefore, either an element remains which ensures an increase in cell size in the diploid, or no active size regulation remains and size increase is a result of a physical requirement for the accommodation of cellular organelles.

**Table 4** Cell volumes of *whi-2<sup>-</sup>* strains growing in exponential phase

| Strain     | Constitution                               | Cell size  |
|------------|--|------------|
| M11        | <i>whi-2<sup>-</sup></i>                   | $45 \pm 2$ |
| M11/44D    | <i>whi-2<sup>-</sup>/whi-2<sup>+</sup></i> | $90 \pm 4$ |
| XJB.9d.4a  | <i>whi-1<sup>-</sup> whi-2<sup>-</sup></i> | $18 \pm 1$ |
| XJB.9d.4a/ | <i>whi-1<sup>-</sup> whi-2<sup>-</sup></i> | $40 \pm 2$ |
| XJB.9d.10a | <i>whi-1<sup>-</sup> whi-2<sup>-</sup></i> |            |

Cells were grown in exponential phase as described in Fig. 1 legend.

The loss of size control and/or  $G_1$  arrest would reduce cell viability. Thus, wild-type cells are more viable than either *whi-1<sup>-</sup>* or *whi-2<sup>-</sup>* cells, which in turn are more viable than the *whi-1<sup>-</sup> whi-2<sup>-</sup>* double mutants (Table 3). However, many cells remain viable, possibly due to the action of the, as yet, undefined gene which may act in a similar manner to *whi-1*.

These studies show that cell size and  $G_1$  arrest are under separate genetic control. One gene, *whi-1*, controls cell size and its action is dose-dependent, as might be expected if cell size is normally proportional to ploidy<sup>9-13</sup>. This gene may correspond to the *wee-1* gene described by Nurse<sup>6</sup> in *S. pombe* and the conclusion that this gene codes for an inhibitor of cell division is consistent with our findings. Fantes *et al.*<sup>9</sup> concluded that elements must exist on the DNA exerting their influence on cell size according to their number. It was not clear how many such elements exist to a genome. The present study indicates that cell size is controlled by one or a small number of genes.

The second gene, *whi-2*, ensures that the cell cycle arrests in  $G_1$  when nutritional conditions no longer support growth. A *whi-1<sup>-</sup> whi-2<sup>-</sup>* double mutant is defective in both functions and has lost much of the control over cell division exhibited by wild-type cells.

P.E.S. and A.R.G. were supported by a SRC grant, B.L.A.C. by a grant from the Irish MRC. We thank Mr E. Gilmartin, Mrs D. Parkinson and Miss A. Watson for technical assistance, and the Berkeley Yeast Stock Centre for many of the strains used.

Received 3 June; accepted 18 September 1980.

- Prescott, D. M. *Adv. Genet.* **18**, 100-178 (1976).
- Hartwell, L. H. *Bact. Rev.* **38**, 164-198 (1974).
- Johnston, G. S., Pringle, J. R. & Hartwell, L. H. *Expl Cell Res.* **105**, 79-98 (1977).
- Nurse, P. *Nature* **256**, 547-551 (1975).
- Nurse, P. & Thuriaux, P. *Expl Cell Res.* **107**, 365-375 (1977).
- Thuriaux, P., Nurse, P. & Carter, B. L. A. *Molec. gen. Genet.* **161**, 215-220 (1978).
- Carter, B. L. A. & Sudbery, P. E. *Genetics* (in the press).
- Guerineau, M., Slonimski, P. P. & Avner, P. R. *Biochem. biophys. Res. Commun.* **61**, 462-469 (1974).
- Fantes, P. A., Grant, W. D., Pritchard, R. H., Sudbery, P. E. & Wheals, A. E. *J. theor. Biol.* **50**, 213-244 (1975).
- Harris, M. *Expl Cell Res.* **66**, 329-336 (1971).
- Lorincz, A. & Carter, B. L. A. *J. gen. Microbiol.* **113**, 287-296 (1979).
- Adams, J. *Expl Cell Res.* **106**, 267-275 (1977).
- Weiss, R. L., Kukora, J. R. & Adams, J. *Proc. natn. Acad. Sci. U.S.A.* **72**, 794-798 (1975).
- Layne, E. *Meth. Enzym.* **3**, 447-462 (1957).
- Mitchison, J. M. *Expl Cell Res.* **13**, 244-262 (1957).
- Goldstein, D. in *Analytical and Quantitative Methods of Microscopy* (eds Meek, G. A. & Elder, H. Y.) 137-158 (Cambridge University Press, 1977).

## Conservation and rearrangement of mitochondrial structural gene sequences

G. Macino

Istituto di Fisiologia Generale, Università di Roma, Italy

C. Scazzocchio\*, R. B. Waring, M. McPhail Berks & R. Wayne Davies\*

University of Essex, Department of Biology, Wivenhoe Park, Colchester CO4 3SQ, UK

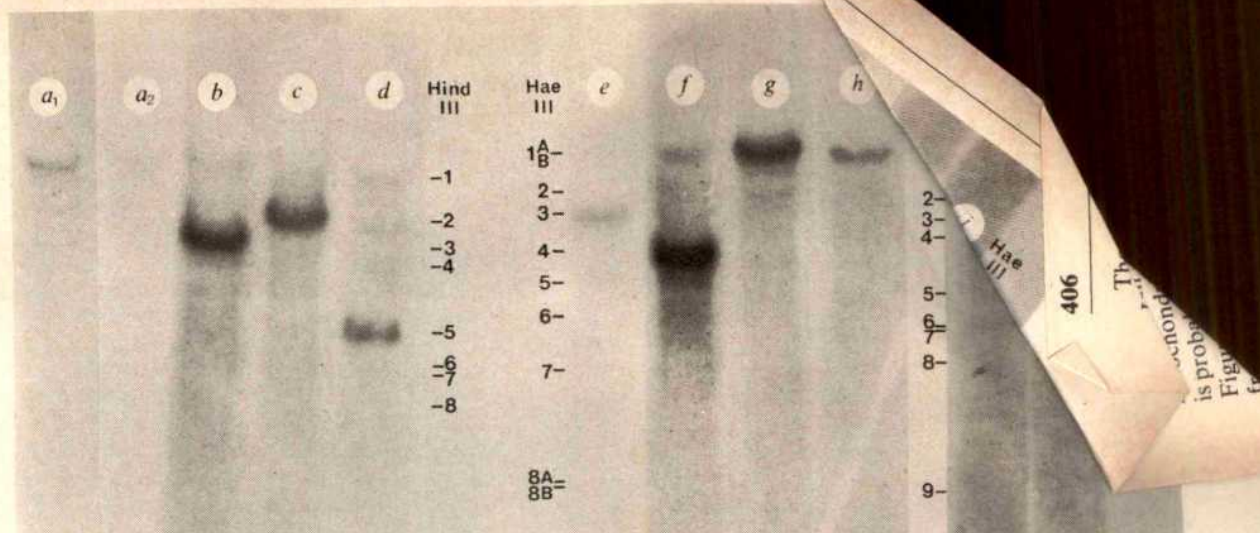
Mitochondria contain the simplest DNA molecules that are present in eukaryotes. Mitochondrial DNA (mtDNA) is easily purified, and is an important model system for studying eukaryote gene structure and basic molecular processes. The protein sequences of mitochondrial gene products have been shown to be conserved from yeast<sup>1-3</sup> to man<sup>4</sup>, and there are definite similarities at the DNA sequence level. In contrast, the overall organization of the mitochondrial genome is drastically different in these organisms. To understand this, we need to extend work on mtDNA to a wider range of species. We have chosen to study the mtDNA of *Aspergillus nidulans* because a particularly comprehensive analysis of this system can be achieved using genetics as well as biochemistry, and like most eukaryotes it is an obligate aerobe, whereas *Saccharomyces cerevisiae* is not. We have investigated whether defined pieces of particular yeast mitochondrial genes show enough homology to *Aspergillus* mtDNA fragments to enable the corresponding *Aspergillus* genes to be located on the physical map. The results reported here show that this is the case for all five genes tested, and present the first data on the physical organization of the structural genes in the mitochondrial genome of *A. nidulans*.

The yeast DNAs that we have used to locate homologous *Aspergillus* sequences by hybridization are derived from the mtDNA of particular well defined *petite* ( $p^-$ ) deletion mutants of yeast. The deletion is usually large and sometimes leaves as little as 0.1% of the mitochondrial genome intact, so that single genes or fragments of genes may be the only sequences remaining. The molecules actually used as probes for homology were 5'-end-labelled single strands of defined restriction fragments prepared as described in Fig. 1 legend. The five *petite* strains and the restriction fragments used are shown in Fig. 2.

*A. nidulans* mtDNA was cut with the restriction endonucleases *Hind*III or *Hae*III, and the fragments separated in an agarose gel and transferred to diazobenzyloxymethyl (DBM) paper<sup>5,6</sup>. After hybridization and autoradiography, we were able to show that specific yeast gene probes hybridized preferentially to particular restriction fragments from *A. nidulans* mtDNA (Fig. 1). This indicates a high degree of homology at the DNA sequence level between mitochondrial genes of these species.

We used this homology with yeast sequences to locate five *Aspergillus* mitochondrial structural genes on the physical map; the genes coding for subunits I, II and III of the cytochrome *c* oxidase complex, which we name [*oxiA*], [*oxiB*] and [*oxiC*], respectively, the gene coding for apocytochrome *b*, which we name [*cobA*], and a gene coding for subunit VI of the ATPase complex, which probably corresponds to the gene [*oliA*], previously identified genetically as giving rise to oligomycin-resistant mutants<sup>7</sup>. The parts of the yeast genes to which the five probes correspond are shown in Fig. 2. A restriction map of *Aspergillus* mtDNA is given in Fig. 3.

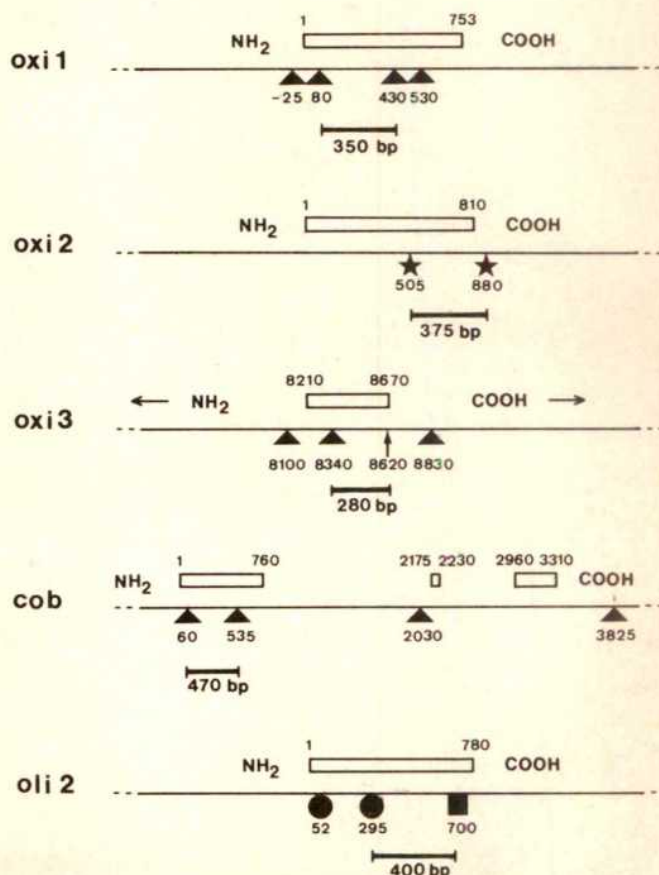
\* To whom reprint requests should be addressed.



**Fig. 1** Autoradiographs of Southern transfers of restriction endonuclease digests of *A. nidulans* mtDNA after hybridization to yeast mtDNA fragments. Mitochondrial DNA of *A. nidulans* strain *bi* A-1 was prepared by a modification of the method of Cummings *et al.*<sup>19</sup>. After restriction endonuclease digestion in 6.6 mM Tris-HCl pH 7.4, 6.6 mM MgCl<sub>2</sub>, 50 mM NaCl and 1 mM dithiothreitol, 2 µg of DNA was loaded per track of an 0.8% agarose gel<sup>20</sup>. After electrophoresis the gel was stained in ethidium bromide and photographed, then transferred to DBM paper<sup>6</sup> by the method of Southern<sup>7</sup>. Yeast mitochondria were prepared as described by Faye *et al.*<sup>21</sup>, and mitochondrial DNA purified as in Sanders *et al.*<sup>22</sup>. Restriction enzyme digests (all enzymes from Bethesda Research Laboratories) of yeast mtDNA were 5' end-labelled with [ $\gamma$ -<sup>32</sup>P]ATP (NEN)<sup>23</sup> using polynucleotide kinase (Bethesda Research Laboratories). The labelled fragments were denatured in 90% formamide and run into a 6% polyacrylamide gel to separate the strands of each fragment. The area of gel containing the strand to be used as a hybridization probe was cut out after identification by autoradiography and the DNA eluted from the gel and ethanol precipitated<sup>23</sup>. Preparation of the DBM paper and hybridization of labelled yeast mtDNA fragment single strands to the Southern transfer were carried out following Wahl *et al.*<sup>6</sup>, using 10% dextran sulphate in the hybridization mixture to improve the efficiency of hybridization<sup>6</sup>. The fragments used as probes for the various tracks, identified by their gene of origin, are *a*<sub>1</sub>, *a*<sub>2</sub> and *e*, *oxi*1; *b* and *f*, *oxi*2; *c* and *g*, *cob*; *d* and *h*, *oli*2; *i* and *j*, *oxi*3. *a*<sub>1</sub> and *a*<sub>2</sub> were from different series of experiments using formamide from Fluka and Merck, respectively. Tracks *a*<sub>1</sub>-*d* and *i* are of Southern transfers of *Hind*III digests, tracks *e*-*h* and *j* of Southern transfers of *Hae*III digests. The positions where DNA bands were present in the ethidium bromide-stained agarose gels before the Southern transfers are marked and numbered.

The yeast genes for cytochrome *c* oxidase subunits I, II and III are *oxi*3, *oxi*1 and *oxi*2, respectively. The probes for both *oxi*3 and *oxi*1 can be seen in Fig. 1 to hybridize to the large *Aspergillus* *Hind*III fragment 1 and to the 3,500-base pair *Hae*III fragment 3. This places the promoter-proximal half of [*oxi*B] (= *oxi*1) and the promoter-distal half of [*oxi*A] (= *oxi*3) within this *Hae*III fragment. The *oxi*2 probe hybridizes with *Aspergillus* mtDNA *Hind*III fragment 3 and *Hae*III fragment 4, placing the [*oxi*C] gene in the 2,500-base pair region between the large and small mitochondrial ribosome RNAs, together with a cluster of tRNA genes<sup>8</sup>.

**Fig. 2** Restriction fragments used as hybridization probes. The *petite* mutant strains used are named according to the yeast gene that they contain; they were DS200A1 (*oxi*1)<sup>2</sup>, DS40 (*oxi*2)<sup>24</sup>, DS6/A407 (*oxi*3) (unpublished), DS400/A12 (*cob*)<sup>25</sup> and DS14 (*oli*2)<sup>3</sup>. The bar above the line indicates the position of coding regions of the gene in each case; the numbers indicate base pairs starting from the NH<sub>2</sub>-terminal coding end. Arrows show the direction in which NH<sub>2</sub> or COOH terminal-coding regions would lie if they were in the *petite*. The *Hin*II-TaqI *oxi*3 ([*oxi*A]) probe contains only exon 5, which is towards the promoter-distal end of the *oxi*3 split gene. The *oxi*1 ([*oxi*B]) probe corresponds essentially to the promoter-proximal coding half of the gene, the *oxi*2 ([*oxi*C]) probe to the promoter-distal half of the gene. The *cob* gene probe is part of the first exon of this split gene and the *oli*2 ([*oli*A]) probe corresponds to the promoter-distal two-thirds of this gene. All *petites* have been completely sequenced<sup>2,3,24,25</sup>. The solid bar below the line gives the position and length in base pairs of the restriction fragment used as a probe. Other symbols show the position of restriction endonuclease recognition sites. ▲, *Hin*II; ★, *Hind*III; ↑, *Taq*I; ●, *Mbo*I; ■, *Eco*RI; bp, base pairs.





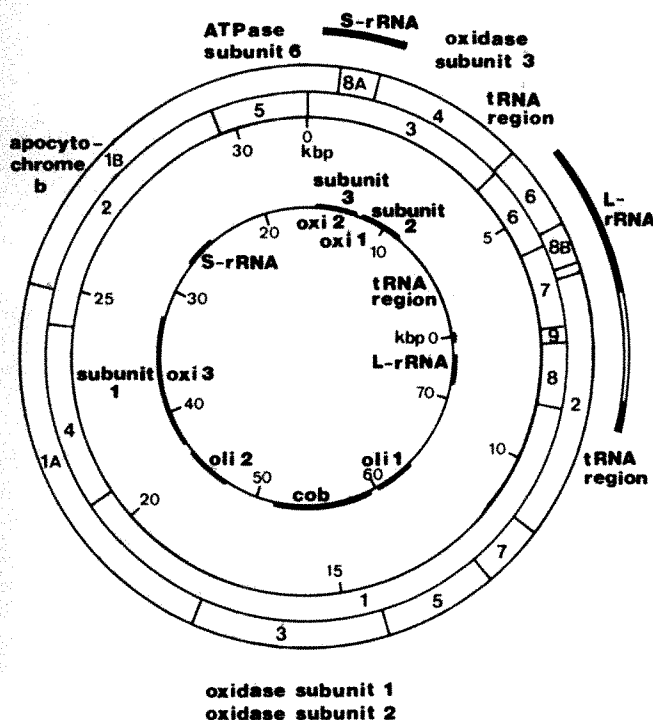
*Aspergillus* mtDNA. The *oli1* gene maps to the *Hae*III fragment 1A or 1B. The *oli2* gene maps to the *Hind*III fragment 5 at the [*cobA*] gene lies in this region (Fig. 1). Mutations in mitochondrial genes can give rise to a growth defect phenotype. Both genes code for subunits of the cytochrome *c* oxidase complex; the *oli1* gene codes for the cytochrome *c* oxidase subunit I, the *oli2* gene for subunit VI of the cytochrome *c* oxidase complex. Previous genetic work on oligomycin resistance in *Aspergillus* has shown that one gene maps in the mitochondrial genome ([*oliA*]<sup>10</sup>; the [*oliB*] group of mutations maps to a small part of [*oliA*]) and one in the nuclear genome [*oliC*]. Figure 1 shows that a yeast *oli2* gene probe hybridizes to *Hind*III fragment 5 of *Aspergillus* mtDNA and to *Hae*III fragment 1A or 1B (presumably to 1B). An *Aspergillus* mitochondrial gene thus corresponds to the *oli2* gene of yeast, maps between the [*cobA*] gene and the small rRNA and probably corresponds to the [*oliA*] gene.

which is a mitochondrially inherited suppressor of [*cs-67*]. Genetic mapping<sup>11</sup> has shown [*camA*], [*cs-67*] and [*sumD*] to be linked in the order given; [*oliA*] is unlinked to these genetically. We can locate [*oliA*] precisely on the physical map. All the other mutations probably affect the mitochondrial ribosome and thus represent mutations either in mitochondrial rRNA or in a gene coding for a ribosomal protein, analogous to the yeast *var-1* gene<sup>16</sup>.

The overall plan of the mitochondrial genome of *Aspergillus nidulans* has some similarity to that of *S. cerevisiae*, although they differ considerably in size (*A. nidulans* 31.5 kilobase pairs, *S. cerevisiae* 75 kilobase pairs) and gene arrangement. In both organisms the mitochondrial rRNA genes are not contiguous, and the large rRNA gene is split by an intron<sup>17</sup>. The space between them is very large (25 kilobase pairs) in *S. cerevisiae*, and contains the *oxi1* and *oxi2* genes and a cluster of tRNA genes<sup>1</sup>, whereas in *A. nidulans* they are separated by only 2.5 kilobase pairs containing the [*oxiC*] (= *oxi2*) gene and part of the tRNA gene cluster. The two rRNA genes, [*oxiC*] (= *oxi2*), [*cobA*] (= *cob*) and [*oliA*] (= *oli2*) have the same positions relative to one another in the two organisms, although the distances between them are quite different. The *Aspergillus* equivalent of the yeast mitochondrial *oli1* gene is in the nucleus<sup>18</sup>. The [*oxiA*] (= *oxi3*) and [*oxiB*] (= *oxi1*) genes are in the mitochondrial genome in both organisms, but in very different positions. The coding sequences of all five genes must be remarkably strongly conserved to show such clear hybridization specificity. In coding regions that have been sequenced, up to 60% of the amino acids and 72% of the base pairs are the same in *S. cerevisiae* and *A. nidulans* (R.W.D. *et al.*, unpublished).

All the differences between the mitochondrial genome of *A. nidulans* and *S. cerevisiae* reported here can be explained by a series of inversion or translocation events. The comparatively small size of *Aspergillus* mtDNA is due to the loss of large tracts of A + T-rich noncoding sequences, and of (at least) one gene to the nucleus. We do not know if any of these changes have any relationship to the switch from facultative to obligate aerobiosis. The technique used here provides a quick and convenient method for mapping mitochondrial genes at least in other lower eukaryotes and potentially allows us to follow gross changes in mitochondrial genome structure throughout the evolutionary process.

This work was supported by MRC project grant G979/429/C to R.W.D. and C.S.



**Fig. 3** Location of mitochondrial structural genes of *A. nidulans* on the physical map. Circular physical maps of *S. cerevisiae*<sup>1</sup> and *A. nidulans* mtDNA<sup>17</sup> are given, arranged so that the large and small rRNA (L- and S-rRNA) genes of the two organisms are in similar positions. Distances are given in kilobase pairs (kbp). In the *A. nidulans* map the inner circle shows the *Hind*III fragments, the outer circle the *Hae*III fragments<sup>17</sup>. The restriction map was confirmed by us for the strains used in this work. The positions of the rRNA genes and the tRNA cluster are based on refs 17 and 18, respectively. In terms of *Aspergillus* gene symbols, apocytochrome *b* = [*cobA*], ATPase subunit 6 = [*oliA*], oxidase subunit 1 = [*oxiA*], 2 = [*oxiB*], 3 = [*oxiC*].

The hybridization results are summarized in Fig. 3. Previous information about the nature and relative positions of *Aspergillus* mitochondrial genes has come from recombinational mapping<sup>11,12</sup> of mitochondrially inherited mutations<sup>13</sup>. Five classes of such mutations are known in *Aspergillus*: [*oliA*]<sup>10</sup>, conferring oligomycin resistance, [*camA*] and [*camB*] (probably in the same gene), conferring chloramphenicol resistance<sup>7,14</sup> [*cs-67*], which is a cold-sensitive mutation<sup>15</sup> and [*sumD*]<sup>13</sup>,

1. Borst, P. & Grivell, L. A. *Cell* **15**, 705-723 (1978).
2. Coruzzi, G. & Tzagoloff, A. *J. biol. Chem.* **254**, 9324-9330 (1979).
3. Macino, G. & Tzagoloff, A. *Cell* (in the press).
4. Barrell, B. G. *et al. Proc. natn. Acad. Sci. U.S.A.* **77**, 3164-3166 (1980).
5. Southern, E. M. *J. molec. Biol.* **98**, 503 (1975).
6. Wahl, G. M., Stern, M. & Stack, G. R. *Proc. natn. Acad. Sci. U.S.A.* **76**, 3683-3687 (1979).
7. Lazarus, C. M. & Turner, G. *Molec. gen. Genet.* **156**, 303-311 (1977).
8. Küntzel, H. in *Organisation and Expression of the Mitochondrial Genome* (eds Kroon, A. M. & Saccone, C.) (Elsevier, Amsterdam, in the press).
9. Wachter, E. & Sebald, W. in *Mitochondria 1977, Genetics and Biogenesis of Mitochondria* (eds Bandlow, W., Schweyen, R. J. Wolf, K. & Kaudewitz, F.) 441-449 (de Gruyter, Berlin, 1977).
10. Rowlands, R. T. & Turner, G. *Molec. gen. Genet.* **126**, 201-216 (1973).
11. Waring, R. B. & Scazzocchio, C. *Genetics* (submitted).
12. Rowlands, R. T. & Turner, G. *Molec. gen. Genet.* **141**, 69-79 (1975).
13. Waring, R. B. & Scazzocchio, C. *J. gen. Microbiol.* **119**, 297-311 (1980).
14. Gunatilleke, I. A. U. N., Scazzocchio, C. & Arst, H. N. Jr *Molec. gen. Genet.* **137**, 269-276 (1975).
15. Waldron, C. & Roberts, C. F. J. *gen. Microbiol.* **78**, 379-381 (1973).
16. Butow, R. A., Vincent, R. D., Strausberg, R. L., Zanders, E. & Perlman, P. S. in *Mitochondria 1977, Genetics and Biogenesis of Mitochondria* (eds Bandlow, W., Schweyen, R. J., Wolf, K. & Kaudewitz, F.) 317-335 (de Gruyter, Berlin, 1977).
17. Lazarus, C. M., Lünsdorf, H., Hahn, U., Stepien, P. & Küntzel, H. *Molec. gen. Genet.* **177**, 389-397 (1980).
18. Turner, G., Imam, G. & Küntzel, H. *Eur. J. Biochem.* **97**, 565-571 (1979).
19. Cummings, D. J., Belcour, L. & Grandchamp, C. *Molec. gen. Genet.* **171**, 229-238 (1979).
20. Peacock, A. D. & Dingman, C. W. *Biochemistry* **7**, 668-674 (1968).
21. Faye, G., Kujawa, C. & Fukuhara, H. *J. molec. Biol.* **88**, 185-203 (1974).
22. Sanders, J. P. M., Borst, P. & Weigers, P. J. *Molec. gen. Genet.* **143**, 53-64 (1975).
23. Maxam, A. M. & Gilbert, W. *Proc. natn. Acad. Sci. U.S.A.* **74**, 560-564 (1977).
24. Thelefeld, B. E. & Tzagoloff, A. *J. biol. Chem.* (in the press).
25. Nohrega, F. & Tzagoloff, A. *J. biol. Chem.* (in the press).

## Comparison of benzo(a)pyrene metabolism and sister chromatid exchange induction in mice

Rhona R. Schreck & Samuel A. Latt

Division of Genetics and Mental Retardation Center, Children's Hospital Medical Center and Department of Pediatrics, Harvard Medical School, Boston, Massachusetts 02115

**Genetic differences in the inducible arylhydrocarbon hydroxylase (EC 1.14.14.2) (AHH) system, which is involved in the multi-step metabolism of hydrocarbons, are known to exist in both humans and mice<sup>1-4</sup>. However, the predictive value of AHH activity in human or murine tissues, assayed as benzo(a)pyrene hydroxylation, as an index of individual susceptibility to mutagens and carcinogens, remains unclear<sup>5-8</sup> because of apparent inconsistencies between results obtained from different *in vitro* and *in vivo* systems. This situation may in part reflect the complexity of the pathways involved in drug metabolism, which combine both activation and detoxification. To determine the relationship of metabolic potential to an easily quantified, short-term *in vivo* end point of genetic damage, we compared the ability of AHH inducible and uninducible mice to metabolize a procarcinogen, benzo(a)pyrene (BP), with the *in vivo* induction by BP of sister chromatid exchanges (SCEs). SCE induction has been shown to correlate with mutagenesis<sup>9,10</sup>. We report here that although BP did cause an increase in SCEs in test animals, the extent of this increase did not differ between the inducible C57BL/6 mice and the uninducible DBA/2 mice. Moreover, prior exposure to an AHH inducer, 3-methylcholanthrene (3-MC), did not increase the number of BP-induced SCEs in C57BL/6 mice. This lack of correlation between benzo(a)pyrene hydroxylase (BP-OH) inducibility and SCE response reinforces the idea that other metabolic steps, such as detoxification or DNA repair, may influence the overall genetic impact of a drug.**

Mice were examined for their ability to convert BP to the fluorescent product 3-hydroxybenzo(a)pyrene, as a measure of the early metabolism of this drug by the AHH system<sup>11</sup> (Fig. 1). C57BL/6 was used as the inducible strain as these mice show BP-OH induction in both the liver (Fig. 1a, b) and bone marrow (Fig. 1c) in response to prior administration of 3-MC. DBA/2 was used as the uninducible strain as these mice showed no hepatic enzyme induction (Fig. 1d, e) in response to 3-MC and only minimal enzyme induction in peripheral tissues (Fig. 1f).

The same mouse strains were also tested for epoxide hydrolase (EC 4.2.1.63) activity, the second enzyme in the proposed metabolic pathway of BP to its ultimate carcinogenic form<sup>12</sup> (Table 1). There was no significant difference in epoxide hydrolase activity between the two strains, and neither strain showed 3-MC inducibility for this enzyme.

Having confirmed differences in AHH activity between the two strains, these mice were used for *in vivo* SCE analysis following partial hepatectomy as previously described<sup>13</sup> with or without prior 3-MC induction. BP-induced SCEs were scored in both liver and bone marrow cells and the results from multiple animals pooled (Fig. 2). The data were compared by a two-tailed *t*-test which took into account differences in baseline SCE frequencies.

Although prior 3-MC treatment produced a 6.8-fold increase in BP-OH activity in regenerating liver of the inducible C57BL/6 mice (Fig. 1b), this pretreatment did not alter the number of BP-induced SCEs in either the liver or bone marrow of this strain (Fig. 2a, b). A small increase in baseline SCE frequencies was observed with induction, attributable to the 3-MC itself, which is metabolized by the AHH system and known to induce SCEs when activated<sup>14</sup>. However, there was no statistically significant difference in BP-induced SCEs above this

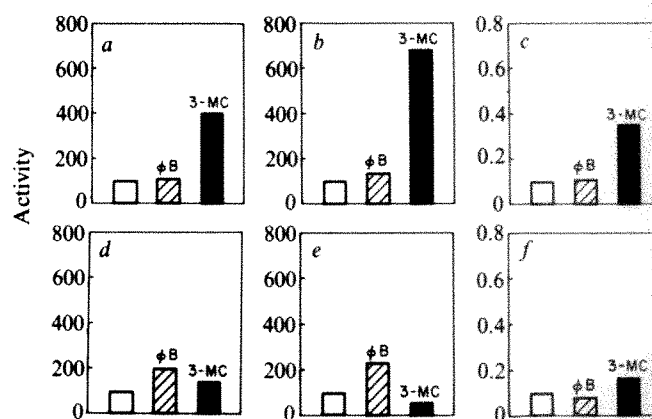
baseline effect with and without prior BP-OH induction by 3-MC.

Both the inducible and uninducible strains, in the absence of enzyme induction, showed fairly similar SCE induction in liver cells in response to BP (Fig. 2a, c;  $P > 0.1$  at 50 and 200 mg per kg BP), although the DBA mice showed a slightly larger SCE response to BP in bone marrow (Fig. 2b, d;  $P < 0.01$ ) than did C57BL/6 mice. Our previous observation that reduced liver function can lead to an enhanced response to clastogens in peripheral tissues<sup>13</sup> may account for this effect, as well as the observation of Nebert<sup>15</sup> that nonresponsive mouse strains exhibit larger drug-induced effects in distant tissues than do responsive mice.

In contrast to the results in BP, the induction of SCEs in response to 3-MC differed markedly between the two mouse strains. In C57BL/6 mice, 3-MC caused only a small increase in SCE frequencies (from 6.2 to 8.7 SCEs per cell, Fig. 2a, b), but effected a marked increase in enzyme activity (Fig. 1b, c). In contrast, in the DBA/2 mice, 3-MC does not induce AHH activity, but it produces a large increase in SCE frequencies (from 5.1 to 15.9 SCEs per cell, Fig. 2c, d), even 2 days after its administration. This result may be due to the prolonged persistence of 3-MC in the strain with the lower metabolic capabilities.

The inability of BP to induce additional SCEs over the heightened baseline level in 3-MC-treated DBA mice (Fig. 2c, d) remains unexplained. It does not reflect a saturation of the SCE response, because higher levels of SCEs per cell can be obtained with other drugs<sup>13,16</sup>. The lack of additional SCE induction might instead reflect some form of competition (between the two hydrocarbons, 3-MC and BP), perhaps for limited metabolic enzymes or the cytoplasmic receptor known to be deficient in DBA mice<sup>15</sup>.

The metabolism of BP can involve multiple pathways leading to a variety of products, many of which are capable of reacting with DNA. 3-MC treatment of inducible mouse strains has been reported to induce a distinct class of cytochromes that activate hydrocarbons such as BP to their ultimate carcinogenic form, in this case the 7,8-diol-9,10 epoxide<sup>17</sup>. In the present



**Fig. 1** Benzo(a)pyrene hydroxylase activity in intact liver (a, d), regenerating liver (b, e) and bone marrow (c, f) of C57BL/6 (a, b, c) and DBA/2 (d, e, f) mice. Activity expressed as percentage of control activity (open bars) seen with either phenobarbital (PB) (hatched bars) or 3-methylcholanthrene (3-MC) (solid bar) induction. Hepatectomy, when done, immediately preceded induction. Bone marrow was collected from non-hepatectomized mice. Animals received either three daily injections of 80 mg phenobarbital (Sigma) per kg in 8% ethanol or 80 mg 3-MC (Sigma) per kg in corn oil. Controls received no injection. Tissue was collected at 72 h after induction from PB-treated animals, at 50 h from 3-MC-treated animals and 67 h from control animals (times reported to be maximal for enzyme induction)<sup>28-30</sup>. Livers were homogenized and bone marrow cells sonicated in 0.15 M KCl and the 9,000g supernatant (S-9) material used in the enzyme assays. Liver S-9 was incubated for 5 min and bone marrow for 20 min in 56 mM Tris, 2.8 mM MgCl<sub>2</sub>,  $3.7 \times 10^{-4}$  M NADPH,  $4.3 \times 10^{-4}$  M NADH, 0.6 mg ml<sup>-1</sup> albumin with  $8.5 \times 10^{-5}$  M BP ( $\epsilon_{384.5} = 27,542$  in methanol). The reaction was stopped with hexane/acetone (3.75:1 v/v). After mixing, the organic phase was extracted with 1 M NaOH and the fluorescence read with a Perkin-Elmer MPF-3 (excitation 396 nm; emission 522 nm)<sup>11</sup>. This fluorescence was compared with that of pure 3-hydroxy-benzo(a)pyrene ( $\epsilon_{380} = 36,300$  in alcohol) and activity expressed as pmol 3-OH-BP formed per mg S-9 per min. Bone marrow activity was 1/1,000th of that in liver.



Table 1 Epoxide hydase activity in regenerating mouse liver

| Induction            | C57BL/6  | DBA/2     |
|----------------------|----------|-----------|
| None                 | 245 ± 72 | 243 ± 80  |
| Phenobarbital        | 523 ± 41 | 354 ± 138 |
| 3-Methylcholanthrene | 292 ± 81 | 262 ± 109 |

Activity is expressed as pmol <sup>3</sup>H-styrene glycol formed per min per mg S-9, measured by the conversion of <sup>3</sup>H-styrene oxide (Amersham, specific activity 88 mCi mmol<sup>-1</sup>) to styrene glycol<sup>27</sup>. Approximately 2.5 mg liver S-9 was incubated with 125 mM Tris (pH 9.0, with 0.025% Tween) and 1 mM styrene oxide (diluted with cold reagent to 190,000 c.p.m.) for 30 and 60 min. After two extractions with *n*-hexane, the reagent mixture was extracted with 2 ml ethyl acetate and 200-μl aliquots counted in a Beckman LS8000 scintillation counter. Each value represents the mean of four trials ± s.d.

experiments, the number of SCEs induced by BP *in vivo* was independent of the AHH inducibility of the mouse strain used or the exposure of inducible mice to 3-MC. The lack of correlation between AHH inducibility and SCE induction suggests either that constitutive AHH activities and products thus formed are responsible for the SCE induction observed or that the involvement of other enzymes in the metabolic pathway, such as epoxide hydase, obscures any differences which may exist in the AHH system.

This lack of correlation between metabolic potential expressed as AHH activity and biological end points has been observed previously. For example, no relationship was observed between AHH inducibility and the *in vitro* induction of SCEs by BP<sup>18</sup>, the activation of BP by S-9 fractions to a mutagen in the Ames test<sup>19,20</sup>, the induction by hydrocarbons of tumorigenesis in humans<sup>6</sup> or in mice<sup>8</sup>, or the extent of covalent binding of BP metabolites to DNA<sup>21</sup>. Several of these effects can, however, be enhanced by inhibiting epoxide hydase activity<sup>22,23</sup>, suggesting that this enzyme, which shows no variability between the two strains examined, may have a critical role. Developmental differences in epoxide hydase levels<sup>24</sup> or in other metabolic enzymes<sup>25</sup> may explain a recent study<sup>26</sup> of the effect of BP on isolated early mouse embryos, in which AHH activity was not measurable, and a larger SCE increment was observed in inducible strains than in noninducible strains.

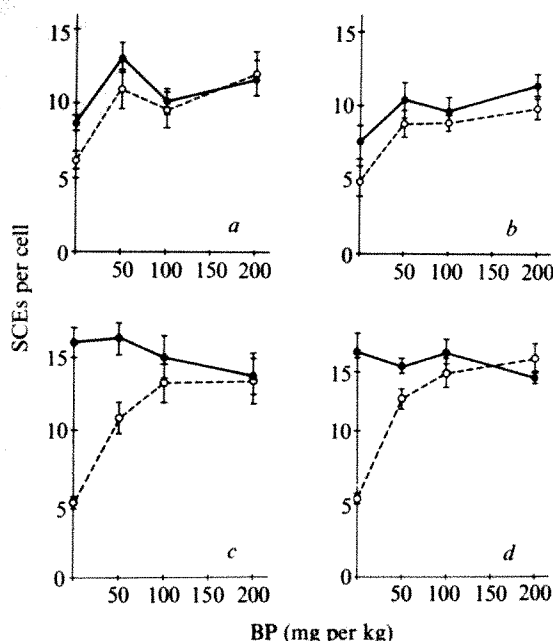


Fig. 2 Induction of SCEs by benzo(a)pyrene (BP) in the liver (a, c) and bone marrow (b, d) of partially hepatectomized (two-thirds removal of liver) C57BL/6 (a, b) and DBA/2 (c, d) young (7-9 weeks) female mice (Charles River) with (solid line) and without (broken line) prior 3-MC treatment (as in Fig. 1). Animals received BP by intraperitoneal injection (53 h post-hepatectomy) followed by a series of 10<sup>-2</sup> M bromodeoxyuridine injections. The following day the animals received two 0.4-ml injections of colchicine (0.2 mg ml<sup>-1</sup>) and liver and bone marrow cells were collected from each animal. Each point on the graph represents the mean of three to six animals (a minimum of 20 cells was examined per animal) and the error bars indicate s.e.

The inability to demonstrate clear and consistent relationships between AHH inducibility and a variety of genetic responses, including SCE induction, suggests that other biological pathways including alternative activation and detoxification, and perhaps DNA repair, influence the end points obtained. The complexity of steps involved in reaching a biological end point thus makes measurement of a single enzyme in the metabolic pathway unreliable as a predictor of an individual's susceptibility to the *in vivo* effects of a procarcinogen.

This work was supported by NIH grant HD 04867 and American Cancer Society grant CD-36E. We thank Dr I. J. Paika and Mr M. E. Eisenhard for their assistance, Dr J. Felton for providing details of the BP-OH assay and the NCI Chemical Repository (ITT Research Institute, Chicago) for providing the 3-hydroxybenzo(a)pyrene.

Received 16 June; accepted 15 September 1980.

1. Nebert, D. W., Robinson, J. R., Niwa, A., Kumaki, K. & Poland, A. P. *J. cell. Physiol.* **85**, 393-414 (1975).
2. Nebert, D. W., Atlas, S. A., Guenther, T. M. & Kouri, R. E. in *Polycyclic Hydrocarbons and Cancer* Vol. 2 (eds Gelboin, H. & T'so, P.) 345-390 (Academic, New York, 1978).
3. Gelboin, H. V. & Blackburn, N. R. *Cancer Res.* **24**, 356-360 (1964).
4. Wiebel, F. J., Leutz, J. C. & Gelboin, H. V. *Archs Biochem. Biophys.* **154**, 292-294 (1973).
5. Kellermann, G., Shaw, C. R. & Luyten-Kellermann, M. *New Engl. J. Med.* **289**, 934-937 (1973).
6. Paigen, B. H. et al. in *Polycyclic Hydrocarbons and Cancer* Vol. 2 (eds Gelboin, H. & T'so, P.) 391-408 (Academic, New York, 1978).
7. Kouri, R. E., Salerno, R. A. & Whitmire, C. E. *J. natn. Cancer Inst.* **50**, 363-368 (1973).
8. Benedict, W. F., Considine, N. & Nebert, D. W. *Molec. Pharmac.* **6**, 266-277 (1973).
9. Perry, P. & Evans, H. J. *Nature* **258**, 121-125 (1975).
10. Carrano, A. V., Thompson, L. H., Lindl, P. A. & Minkler, J. L. *Nature* **271**, 551-553 (1978).
11. Nebert, D. W. & Gelboin, H. V. *J. biol. Chem.* **243**, 6242-6249 (1968).
12. Holder, G. et al. *Proc. natn. Acad. Sci. U.S.A.* **71**, 4356-4360 (1974).
13. Schreck, R. R., Paika, I. J. & Latt, S. A. *Mutat. Res.* **64**, 315-328 (1979).
14. Popescu, N. C., Turnbull, D. & DiPaolo, J. A. *J. natn. Cancer Inst.* **59**, 289-293 (1977).
15. Nebert, D. W. *J. natn. Cancer Inst.* **64**, 1279-1290 (1980).
16. Vogel, W. & Bauknecht, T. *Nature* **260**, 448-449 (1976).
17. Thakker, D. R. et al. *Proc. natn. Acad. Sci. U.S.A.* **10**, 3381-3385 (1976).
18. Rudiger, H. W. et al. *Nature* **262**, 290-292 (1976).
19. Felton, J. S. & Nebert, D. W. *J. biol. Chem.* **250**, 6769-6778 (1975).
20. Tucker, A. N. & Tang, T. *J. envir. Path. Tox.* **2**, 613-623 (1979).
21. Phillips, D. H., Grover, P. L. & Sims, P. *Int. J. Cancer* **22**, 487-494 (1978).
22. Bresnick, E. in *In Vitro Metabolic Activation in Mutagenesis Testing* (eds de Serres, F. J., Fouts, J. R., Bend, J. R. & Philpot, R. M.) 91-104 (Elsevier, Amsterdam, 1976).
23. Nebert, D. W., Thorgeirsson, S. S. & Felton, J. S. in *In Vitro Metabolic Activation in Mutagenesis Testing* (eds de Serres, F. J., Fouts, J. R., Bend, J. R. & Philpot, R. M.) 105-124 (Elsevier, Amsterdam, 1976).
24. Oesch, F. *J. biol. Chem.* **251**, 79-87 (1976).
25. Hales, B. F. & Neims, A. H. *Biochem. J.* **160**, 231-236 (1976).
26. Galloway, S. M., Perry, P. E., Meneses, J., Nebert, D. W. & Pedersen, R. A. *Proc. natn. Acad. Sci. U.S.A.* **77**, 3524-3528 (1980).
27. Oesch, F., Jerina, D. M. & Daily, J. *Biochim. biophys. Acta* **227**, 685-691 (1971).
28. Boobis, A. R., Reinhold, C. & Thorgeirsson, S. *Biochem. Pharmac.* **26**, 1501-1505 (1977).
29. Boobis, A. R., Nebert, D. W. & Felton, J. S. *Molec. Pharmac.* **13**, 259-268 (1976).
30. Gielen, J. E., Goujon, F. M. & Nebert, D. W. *J. biol. Chem.* **247**, 1125-1137 (1972).

## Chemical cross-linking restrictions on models for the molecular organization of the collagen fibre

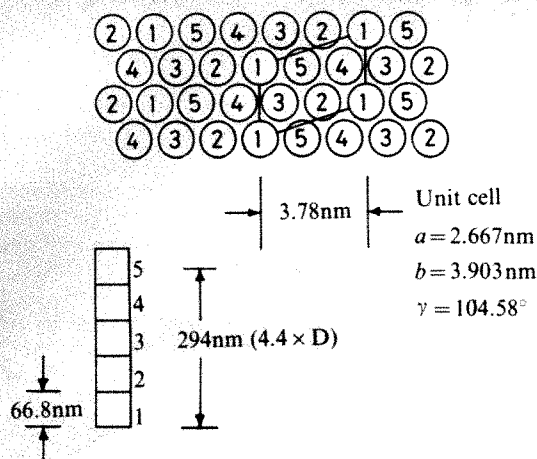
A. J. Bailey\*, N. D. Light† & E. D. T. Atkins‡

\* Agricultural Research Council, Meat Research Institute, Langford, Bristol BS18 7DY, UK

† Department of Animal Husbandry, University of Bristol, Langford, Bristol BS18 7DU, UK

‡ Department of Physics, University of Bristol, Bristol BS8 1TH, UK

The nature of the precise packing of collagen molecules into a collagen fibril, producing the characteristic regular banding, is still debatable. The problem has been approached using electron microscopy and X-ray diffraction techniques, and several models have been proposed, including hexagonal packing, an octafibril structure, a two-strand rope and a five-strand rope (for review, see ref. 1). For the past decade the penta-fibrillar model, originally proposed by Smith<sup>2</sup>, has been widely accepted as the fundamental building unit. This model, based on the quarter-stagger end-overlap hypothesis of Hodge and Petruska<sup>3</sup>, was



**Fig. 1** Projection of the hexagonally packed collagen molecules along their axis. The small distortions of the lattice<sup>5</sup> and the slight ( $4^\circ$ ) tilting of the collagen molecules are not shown. The numbers 1–5 refer to the molecular segments (see lower left) in one 66.8-nm (D) thick transverse section. The packing arrangement may be considered as horizontal layers of the quarter-stagger end-overlap<sup>3</sup> system, running 1 to 5 from right to left, with successive layers displaced from left to right by 3.78 nm, thus generating the unit cell<sup>5</sup> outlined.

supported by the X-ray diffraction data of Miller and Wray<sup>4</sup>. These X-ray data have now been reinterpreted by Hulmes and Miller<sup>5</sup> in terms of a quasi-hexagonal packing of collagen molecules. We argue here that until other characteristic parameters are taken into account, in particular the chemical cross-linking evidence, the packing problem is still unresolved.

The recently proposed model<sup>5</sup> involves the juxtaposition of the collagen molecules in a slightly distorted two-dimensional hexagonal lattice, having a specific tilt of about  $4^\circ$  between the collagen molecules and the normal to the basal lattice plane, together with some longitudinal shear. The model is a development of the packing arrangement proposed by McFarlane<sup>6</sup>. The apparent advantage of this model is that it provides a better fit with the X-ray diffraction data compared with other models. Note that both models (the penta-fibrillar rope and the quasi-hexagonal arrangement) rely essentially on the same X-ray diffraction data.

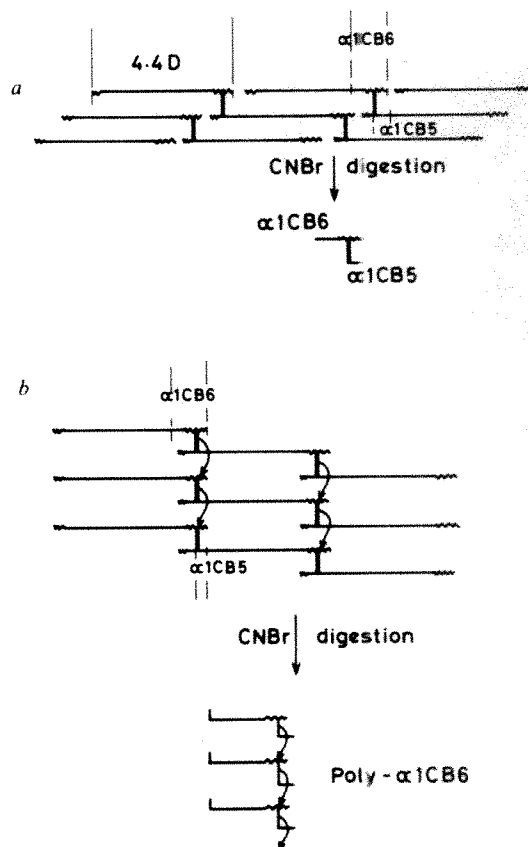
These three-dimensional structures must incorporate the quarter-stagger end-overlap array<sup>3</sup> to generate the banding pattern observed by electron microscopy. However, none of these models considers the characteristic chemical cross-linking evidence of collagen. In particular, the new quasi-hexagonal model does not account for the restrictions on proposed molecular arrangements imposed by the known location of the intermolecular cross-links.

A cross-section through the proposed quasi-hexagonal model perpendicular to the collagen fibrillar axis is shown schematically in Fig. 1. The numbers 1–5 represent specific distances along the collagen molecules commensurate with the D-stagger in the end-overlap model<sup>3</sup>. To fit the basic features of the X-ray diffraction pattern<sup>4</sup>, Hulmes and Miller<sup>5</sup> stagger successive layers laterally (see Fig. 1) by 3.78 nm relative to each other, generating the 3.78-nm row lines observed in the X-ray fibre diffraction patterns<sup>4</sup> and developing a two-dimensional lattice defined by  $a = 2.607$  nm,  $b = 3.903$  nm with  $\gamma = 104.58^\circ$  (Fig. 1).

The location of the bifunctional cross-links has been established by biochemical techniques for the fibrous types of collagen, type I<sup>7,8</sup>, type II<sup>9,10</sup> and type III<sup>11,12</sup>, as only occurring between the telopeptide lysine-aldehyde and the  $\epsilon$ -NH<sub>2</sub> group of specific lysine or hydroxylysine residues 25 nm from either end of the molecule, that is, the end of the overlap region (Fig. 2a). We have now extended these observations to mature tissue and have demonstrated that cross-linking occurs through polymeric interactions involving the C-terminal non-helical

region of  $\alpha 1CB6$  and the helical peptide  $\alpha 1CB5$ . This polymeric cross-linked material, poly- $\alpha 1CB6$ , has been isolated from mature bovine tendon and partially characterized<sup>13,14</sup>. The important factor relating to the molecular structure of the fibres is that this cross-linking arrangement can only occur if the C-terminal ends of the molecule are in register. In terms of the numerical notation of the D-stagger of the molecules, the  $\alpha 1CB6$ - $\alpha 1CB5$  dipeptide is classified as 1, 5—the molecules align in the lattice such that 1's are adjacent to 5's and vice versa. In the fibre structure, individual collagen molecules must experience neighbours staggered by D and have at least one neighbour aligned in longitudinal register to generate limited interconnections of the type 1, 5; 1, 5; 1, 5 within the fibre, thereby generating poly- $\alpha 1CB6$  (Fig. 2b).

Analysis of the new structure proposed by Hulmes and Miller<sup>5</sup> shows that such a cross-link scheme is unattainable. Furthermore, if to accommodate this packing restriction the molecules in the structure are moved longitudinally or laterally, then the proposed unit cell on which the X-ray argument is based will have to change. This model must therefore be adapted to fit the cross-linking data. This can readily be achieved if C-terminals in successive layers are juxtaposed with reducible cross-links between  $\alpha 1CB6$  and  $\alpha 1CB5$  (or 1, 5 in quarter-stagger nomenclature) to form a polymer containing 1:1 proportions of  $\alpha 1CB6$  and  $\alpha 1CB5$ . Analysis of poly- $\alpha 1CB6$  did indeed show an approximate 1:1 ratio of these two peptides<sup>14</sup>. Hence, by using the cross-linking data to modify the model suggested by the physical data, a detailed and more accurate quasi-hexagonal model could be postulated.



**Fig. 2** a, Schematic quarter-staggered array of collagen molecules showing the location of a reducible cross-link between  $\alpha 1CB6$  and  $\alpha 1CB5$  peptides and the resultant 'H' peptide derived from a cyanogen bromide digest. b, Diagrammatic representation of the proposed formation of poly- $\alpha 1CB6$ . Layers of quarter-staggered collagen molecules are shown in register, that is, layer 1 is in register with layer 2 which is in register with layer 3. Each reducible cross-link between  $\alpha 1CB6$  and  $\alpha 1CB5$  is aligned and closely packed with a reactive residue in the adjacent  $\alpha 1CB6$  peptide in the molecule in the next layer, thus several layers can be interlinked by repeating this simple additive process.



Recent evidence on variations in fibre size from electron microscopy has suggested that there is a basic building fibril of about 8.0 nm<sup>15</sup>. Similarly, the X-ray evidence of Nemetschek<sup>16</sup> using stained fibres provides strong evidence for a unit cell of 8.0 nm, contrasting with the 4.0-nm cell of the other pentafibril and hexagonal models. These data have received recent support from the electron diffraction studies of Squire and Freundlich<sup>17</sup>. Fraser's group suggests<sup>18</sup> that four pentafibrils align in register to form such an 8.0-nm unit, which they term the tetragonal cell or unit. Considering the restrictions that such a structure puts on the possible extent of formation of polymeric cross-linked material, this model similarly, in its simplest form, cannot readily be adapted to fit the chemical evidence. Intrapentafibrillar reducible cross-links can be formed relatively easily so that the unit itself is stabilized. However, when these cross-links are stabilized by addition reactions with other aligned C-terminals in other pentafibrils, only internal interactions within the tetragonal unit seem possible due to the large interatomic distances between sites in different units. This would seem to limit the maximum molecular weight of the resultant polymeric cross-linked material to a much lower range than that actually observed. A further difficulty with this model concerns the discrepancy between observed and calculated densities, as discussed by Hulmes and Miller<sup>5</sup>.

It might be profitable to view the hexagonal models<sup>6,5</sup> as being built up from groups of five collagen molecules (or multiples as favoured by the larger unit cells suggested by the more recent X-ray evidence of Nemetschek<sup>16</sup>), each lying on a hexagonal lattice site (or a slightly distorted hexagonal lattice in the final analysis) so that they form a collapsed pentafibril which in turn aligns with other such units to complete a full two-dimensional array. Certainly, between the extremes of the McFarlane model<sup>6</sup> and the Hulmes and Miller model<sup>5</sup>, there might be scope for organizing limited runs of 1, 5 interconnections.

The parameters which govern the organization of such interactions may be determined by considering the precise restrictions imposed on the structure of the collagen fibril by the known characteristics of poly- $\alpha$ 1CB6 as follows. (1) The bifunctional cross-links formed between staggered molecules to give the 1, 5 interactions must limit the movement of the non-helical region involved. (2) Chemical evidence strongly suggests that the stable cross-link is produced by an addition reaction of a reactive group in an adjacent molecule with the bifunctional cross-link. An exogenous molecule (such as a lipid) could be involved as a chemical bridge in this reaction, in which case the intermolecular distances of the collagen molecules need not be restricted. However, no evidence exists for such a mechanism and, given the precise collagen molecule packing, this pathway is extremely unlikely. The most feasible mechanism would involve a reactive side chain in the nearest-neighbour collagen molecule. This prediction limits the possible intermolecular distance to a maximum of the length of the longest amino acid side chain. (3) The experimental data suggest that the range of poly- $\alpha$ 1CB6 polymers characterized would be formed from the interactions of molecules in 5–10 layers of close-packed collagen sheets.

Clearly, the rigorous application of the chemical evidence can profoundly affect the types of model constructed to explain the physical data. Model building is of considerable value but has severe limitations, particularly if all lines of evidence are not accounted for. Definitive chemical evidence on cross-linking is now available and should be regarded as at least as important as the physical data and may, indeed, ultimately prove to be the most crucial criterion for unravelling higher molecular organization in the collagen matrix.

After submission of this paper various arrangements of the collapsed pentafibril model similar to that proposed by us was postulated by Trus and Piez<sup>19</sup>, but without consideration of the chemical cross-linking evidence.

Received 20 June; accepted 3 October 1980.

1. Miller, A. in *The Biochemistry of Collagen* (eds Ramachandran, G. N. & Reddi, A. H.) (Academic, New York, 1976).
2. Smith, J. W. *Nature* **219**, 157–159 (1968).

3. Hodge, A. J. & Petraska, J. A. in *Aspects of Protein Structure* (ed. Ramachandran, G. N.) 289–300 (Academic, New York, 1963).
4. Miller, A. & Wray, J. S. *Nature* **230**, 437–439 (1971).
5. Hulmes, D. J. S. & Miller, A. *Nature* **282**, 878–880 (1979).
6. McFarlane, E. F. *Search* **2**, 171–172 (1971).
7. Kang, A. H. *Biochemistry* **11**, 1828–1835 (1972).
8. Henkel, W., Rauterberg, J. & Stirtz, T. *Eur. J. Biochem.* **69**, 223–231 (1976).
9. Miller, E. J. *Biochem. biophys. Res. Commun.* **45**, 444–451 (1971).
10. Miller, E. J. & Robertson, P. B. *Biochem. biophys. Res. Commun.* **54**, 432–439 (1973).
11. Nicholls, A. C. & Bailey, A. J. *Biochem. J.* **185**, 195–201 (1980).
12. Henkel, W., Rauterberg, J. & Glanville, R. W. *Eur. J. Biochem.* **96**, 249–256 (1979).
13. Light, N. D. & Bailey, A. J. *Biochem. J.* **185**, 373–381 (1980).
14. Light, N. D. & Bailey, A. J. *Biochem. J.* **189**, 111–124 (1980).
15. Parry, D. A. D. & Craig, A. S. *Nature* **282**, 213–215 (1979).
16. Nemetschek, Th., Riedk, H. & Jonar, R. *J. molec. Biol.* **133**, 67–83 (1979).
17. Squire, J. M. & Freundlich, A. *Nature* **288**, 410–413 (1980).
18. Fraser, R. D. B., Macrae, T. P. & Suzuki, E. *J. molec. Biol.* **129**, 463–481 (1979).
19. Trus, B. L. & Piez, K. A. *Nature* **286**, 300–301 (1980).

## Direct observation of a transverse periodicity in collagen fibrils

John M. Squire & Alan Freundlich

Biopolymer Group, Department of Metallurgy and Materials Science, Imperial College, London SW7 2BP, UK

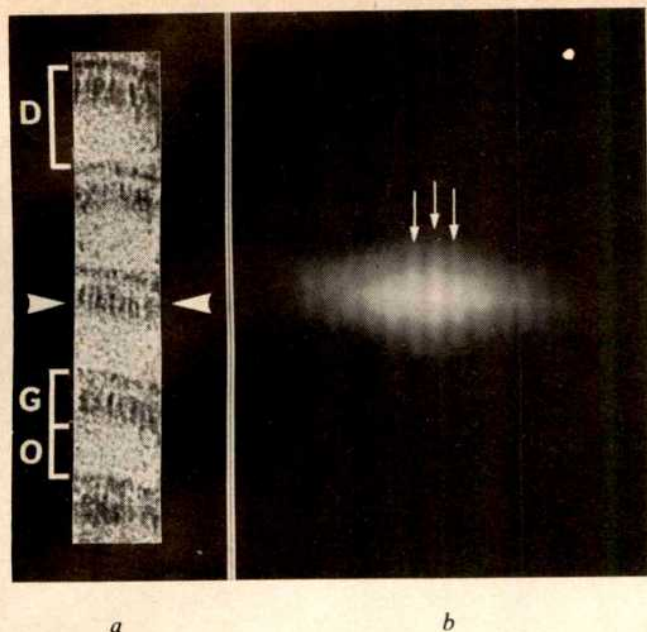
Collagen fibrils have been extensively studied by electron microscopy, but only scant evidence has yet been obtained about their transverse structure. A transverse periodicity of about 40 or 80 Å might be expected if the microfibril model (until recently the common preference) is correct<sup>1–9</sup>, but little direct evidence for such a periodicity has been obtained so far. We have studied electron micrographs of longitudinal cryosections of rat tail tendon. These appear very fibrous when studied by eye, but they produce at best only weak diffuse equatorial peaks in optical diffraction patterns. Nevertheless, we show here that like other fibrous protein structures, they do possess a strong transverse periodicity as revealed by their self-convolution functions (or auto-correlation functions)<sup>10–12</sup>. The observed periodicity is consistent with the presence of an 80 Å structural unit in collagen fibrils *in vivo*.

Many aspects of the structure of collagen fibrils have been satisfactorily accounted for in recent years. The chain conformation in tropocollagen molecules has recently been refined by Fraser *et al.*<sup>13</sup>, and the axial striation patterns in positively stained aggregates of collagen have been correlated well with the known amino acid sequence of the  $\alpha$ 1 collagen chains<sup>14–21</sup>. The sequence studies show that the characteristic *D*-period of about 670 Å in collagen fibrils is due to the 670 Å axial stagger between molecules and that this stagger, or a multiple of it, is such that the number of polar and apolar interactions between adjacent molecules is maximized.

However, considerable controversy remains about the arrangement of collagen molecules in a transverse view of a collagen fibril. For several years the favoured model was one in which fibrils were formed from an ordered near-tetragonal array of microfibrils of diameter ~38 Å and probably containing five strands of tropocollagen molecules. Four such microfibrils, each twisted to have 4<sub>1</sub> helical symmetry, would then be related by an approximate 4<sub>3</sub> screw axis to give a repeating unit about 80 Å square<sup>1,3,6,9</sup>. Other published models also have microfibrils 38 Å in diameter but containing differing numbers of strands<sup>4,5,7,8</sup>. In support of such structures there have been several observations of individual filamentous elements about 40 Å in diameter in electron micrographs of collagen preparations (see refs 22 and 23). In addition, Parry *et al.*<sup>24,25</sup> have recently reported that in many types of connective tissue the fibril diameters are always multiples of about 80 Å; a result clearly favouring the existence of an 80 Å structural unit.

But a radically different model for collagen structure has recently been proposed by Hulmes and Miller<sup>26,27</sup>. This model explains the observed X-ray diffraction data on collagen<sup>2</sup> not in terms of a near-tetragonal lattice of microfibrils, but rather in





**Fig. 1** *a*, Electron micrograph of part of a negatively stained, fixed collagen fibril from rat tail tendon (fibril axis vertical) showing the characteristic pattern of alternating dark (stain filled) and light (stain excluding) bands which together define one *D*-period (*D*). In molecular terms the dark band (*G*) is the gap region in the modified quarter-stagger model of Hodge and Petruska<sup>38</sup>, and the light band (*O*) is the region of molecular overlap. Within the dark band between the arrowheads thin vertical strands of protein (white) can be seen. The self-convolution function of this single dark band is shown in *b*. As indicated by the arrows, regularly spaced vertical white lines can be seen in the convolution indicating that the strands in *a* have a well-defined average lateral separation. In *a*, *D* is 708 Å and in *b*, *s* (the lateral period between adjacent arrowed lines) is 55 to 60 Å. Note that the convolution *b* is enlarged relative to *a*.

terms of a molecular crystal<sup>28</sup> in which straight collagen molecules, somewhat tilted to the fibril axis, pack in a quasi-hexagonal lattice<sup>29</sup>. Miller<sup>27</sup> has shown that such a model can account well for the intensity distribution in the equatorial and near-equatorial regions of the observed X-ray diffraction pattern and it explains some features not accounted for by the tetragonal lattice.

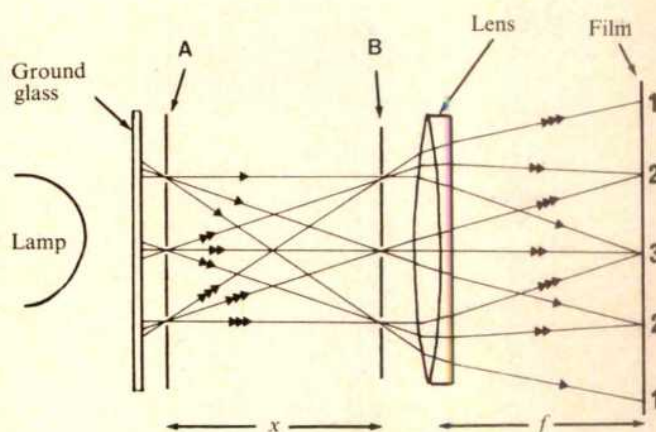
It is by no means clear, however, that this new model could explain the 80 Å increments in fibril diameter observed by Parry *et al.*<sup>24-25</sup>. On the other hand, one might expect from these observed diameters that it should be possible to see an 80 Å lateral periodicity in electron micrographs of collagen fibrils. But only in one reported case<sup>30</sup> have sections of collagen fibrils revealed the presence of an 80 Å periodicity. The fibrils, which were very different in character from those in tendon, were from the inner layers of the dogfish egg capsule and they showed a square lattice of side 80 Å in transverse sections. No such structure has yet been reported in connective tissue from higher vertebrates.

In an attempt to study the transverse structure in rat tail tendon, we are using the relatively novel cryosectioning technique, which we have successfully applied to muscle<sup>31,32</sup>, to obtain both transverse and longitudinal frozen sections of tendon. Briefly, ultra-thin longitudinal sections, which are not as difficult to obtain as transverse cryosections, have already provided direct evidence for a prominent transverse periodicity larger than the unit cell dimensions in the hexagonal model of Hulmes and Miller<sup>26</sup> but compatible with the presence of an 80 Å structural unit.

Fresh rat tail tendon was fixed for 60 min in 2.5% glutaraldehyde at 4 °C, soaked for 45 min in 30% glycerol in water (which

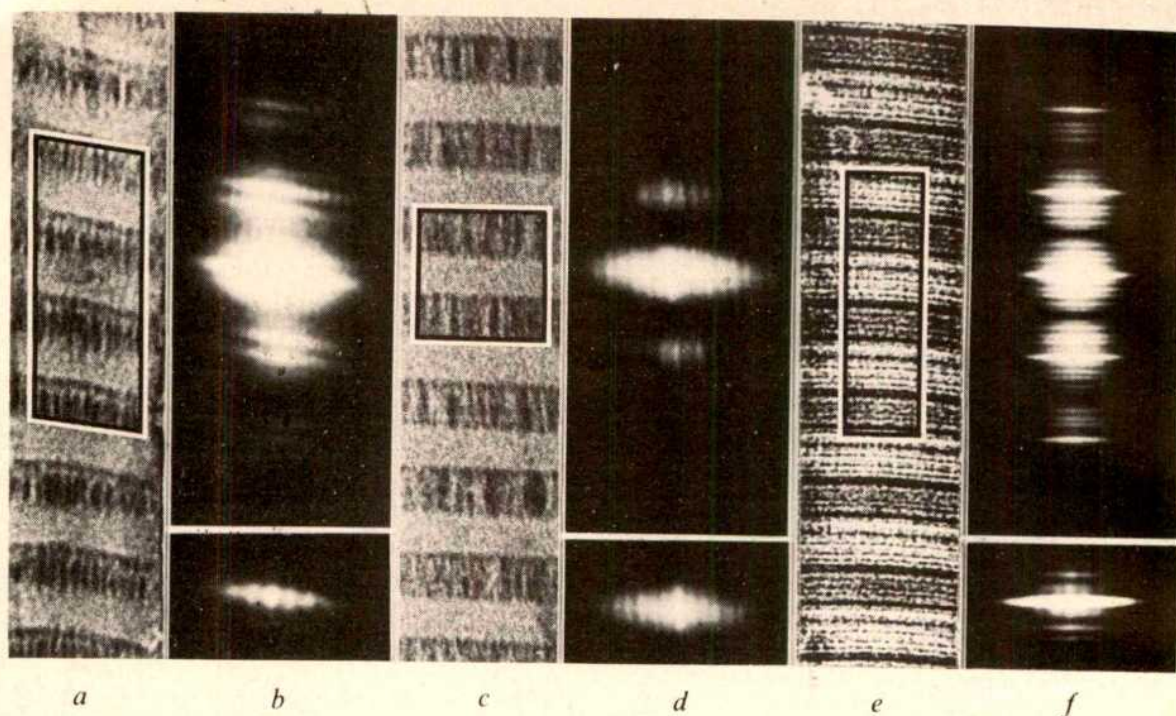
acts as an antifreeze agent), dissected into small pieces (1 mm cube at most) and frozen rapidly by immersion in Freon 12 cooled by liquid nitrogen. The frozen tissue, held at about -110 °C, was sectioned, using an LKB ultramicrotome and Cryokit, with a glass knife at -45 °C, onto a trough containing 50% dimethylsulphoxide. Sections or section fragments (sections tended to tear because of the very fibrous nature of the tendon) were collected on formvar/carbon coated grids and either negatively stained with 2% ammonium molybdate or positively stained with 2% uranyl acetate and Reynolds lead citrate. In some preparations the initial fixation step in glutaraldehyde was omitted.

Electron micrographs of these various preparations often showed remarkably clear structure (as in Fig. 1*a*); they were comparable to or better than the best published micrographs of negatively stained or positively stained isolated fibrils obtained by homogenization (see for example refs 33 and 34). Stereo-pair electron micrographs also showed that in many of these preparations only surface negative staining was present and in such cases, despite the low inherent contrast, there was a considerable enhancement of detail and clarity. In addition to the marked *D*-periodicity along these fibrils (*D* in Fig. 1*a*) many seemed to show some evidence of transverse structure. They were frequently very fibrous in appearance, as noted previously by others<sup>33,34</sup>, but optical diffraction analysis showed little tangible trace of any equatorial spacings (other than diffuse and



**Fig. 2** Schematic ray diagram of the convolution camera<sup>10,11</sup>. The lamp and ground glass (or opal glass) screen provide an extended diffuse light source which evenly illuminates a transparency (*A*) of the micrograph to be studied. An identical transparency (*B*) at a distance *x* from *A* is positioned close to a lens which is set to focus parallel light in the plane of the film (right). The film is conveniently held in a reflex camera body. While viewing the image in the focal plane using the camera viewfinder, the transparency *B* is rotated in its own plane until the images in *A* and *B* are exactly parallel. This can be judged by making the central spot in the image plane as small and symmetrical as possible. When this has been done, the image is the self-convolution of the micrograph in *A* (or *B*). The ray diagram illustrates the light paths for a model micrograph containing three equidistant transparent objects (here shown as holes). Each hole in *B* acts as a pinhole camera and transmits light from *A* to form an inverted image of *A* in the film plane. But since the holes in *B* are periodically displaced, so are the images of *A* in the film plane. It will be seen that the central feature in this plane has light reaching it from each hole in *A*; it is an average of the features in *A*. Similarly further rays reach the film on each side of the centre and are separated from the centre by the periodicity in *A* (or *B*). Thus the self-convolution is a particular form of average of the structure in *A* (or *B*) and any regularities in the micrograph tend to be enhanced in the self-convolution. If *x* = *f* then the convolution has the same magnification as the micrograph, otherwise the magnification is *f*/*x*. Note that *f* is the focal length of the lens and must be fixed, whereas *x* can be varied at will. Full details of the convolution technique will be given elsewhere (ref. 12 and manuscript in preparation).





**Fig. 3** *a*, *c* and *e* are electron micrographs of collagen fibrils which were *a* fixed and negatively stained; *b*, unfixed and negatively stained and *e*, fixed and positively stained. The self-convolution functions of the outlined areas are shown in *b*, *d* and *f* respectively. In each case the whole self-convolution is shown at the top and just the central region is shown at the bottom. In *b* and *f*, the lower prints are at twice the magnification of the upper prints. Note that the whole outlined areas in *a* and *e* were used to give *b* and *f*, but that in *c*, the central light band in the outlined area on the convolution negative was blacked out using Indian ink (without doing this the light from the highly transparent but, in negatively stained preparations, relatively structureless overlap regions tends to swamp the convolution and to obscure the features of interest in the gap regions). The convolution in *d* therefore reveals the structure of the dark bands only. Clear lateral periods can be seen in *b*, *d* and *f* and the spacings measured from these were respectively,  $s = 75\text{--}80 \text{ \AA}$  ( $D = 583 \text{ \AA}$ ),  $s = 95\text{--}100 \text{ \AA}$  ( $D = 625 \text{ \AA}$ ) and  $s = 55\text{--}60 \text{ \AA}$  ( $D = 598 \text{ \AA}$ ).

unmeasurable regions barely perceptible above the noise level) out to a reciprocal spacing of about  $1/20 \text{ \AA}^{-1}$ . However, similar negative results using optical diffraction have been obtained from other fibrous protein structures such as isolated paramyosin filaments<sup>10</sup> and synthetic tactoids of tropomyosin<sup>11</sup>. In both cases some trace of a transverse periodicity seemed to be apparent from visual inspection, and despite the failure of the optical diffraction method, the existence of a strong lateral periodicity (about  $35$  to  $40 \text{ \AA}$  in each case) was confirmed by means of the so-called convolution camera<sup>10,11</sup>. In this camera (Fig. 2) the self-convolution function (or auto-correlation function) of an image is generated by a simple optical system<sup>10-12</sup> comprising a diffuse light source, two identical negative transparencies (A and B) of the image to be analysed, a lens and a film holder. If periodicities are present in the micrograph, then they will become very much enhanced in the self-convolution. The extent of the order can also be deduced. Just like the Patterson function in X-ray crystallography, to which it is analogous, the self-convolution function reveals the presence of strong inter-object vectors in the image being studied.

Application of the self-convolution technique to collagen fibrils such as that in Fig. 1*a* has revealed directly that a strong transverse periodicity is often present. Other examples are shown in Fig. 3. The spacing of the periodicity was in each case related to the  $D$ -period of the same fibril which in turn was deduced from the known calibration of the electron microscope. It was found that the  $D$ -spacing varied between different preparations and even between different fibrils in the same electron micrograph, the observed  $D$ -spacings generally being in the range  $580\text{--}710 \text{ \AA}$ . A wide variation of this period as a function of moisture content has previously been observed in X-ray diffraction studies of tendon<sup>35</sup> and presumably this behaviour is

being mimicked here by a variable stain content in our preparations.

It can be seen in the self-convolution in Fig. 1*b* that there are strong regularly spaced lines of density (white) running parallel to the fibril axis in Fig. 1*a*. Similarly in Fig. 3*b*, *d* and *f* it is clear that the lines running from left to right (that is, perpendicular to the fibril axis) are composed of discrete blobs of density (white) with a fairly uniform spacing. These appearances are direct evidence that there is regular transverse structure within the fibrils which gave rise to the convolutions. However it was found that not all fibrils or even all areas of the same fibril gave equally regular convolution patterns. But, whenever the lateral periodicity could be seen clearly, it always had a measured spacing ( $s$ ) of about the same size. Most of the fibrils which were studied were from fixed and negatively stained preparations (for example Figs 1*a* and 3*a*) and the observed range of side-spacing was  $s = 55\text{--}80 \text{ \AA}$ . Preliminary examination of unfixed fibrils (Fig. 3*c*) or fixed positively stained fibrils (Fig. 3*e*) has given  $s$  values of about  $90\text{--}100 \text{ \AA}$  and  $55\text{--}60 \text{ \AA}$  respectively.

Despite the apparent lack of order in some fibrils, it is clear in others (for example Fig. 3*a*) that the order is very good. In some cases the transverse order has been seen up to eight to ten  $s$  periods from the centre of the convolution, indicating a correlation of lateral structure over a range of about  $500$  to  $800 \text{ \AA}$ . This would represent most or all of the width of many collagen fibrils<sup>24,25</sup>. Similarly the presence of obvious structure along the strong transverse lines above and below the central line through a convolution such as Fig. 3*b*, shows that the lateral structure in one  $D$ -period correlates well with that in the adjacent  $D$ -periods along the fibril. We have observed similar correlation over an axial range of at least four  $D$ -periods, indicating that in some preparations there is a very high degree of structural regularity.



along the fibrils. It is not yet clear whether the observed differences in regularity within or between fibrils are a result of the preparative procedure, or are an inherent feature of the fibrils *in vivo*.

The observation of a transverse periodicity of 55–100 Å implies that there is some form of molecular organization of intermediate size within collagen fibrils; this, clearly, is incompatible with the model of Hulmes and Miller<sup>26</sup> as it stands. Recently Bailey *et al.*<sup>36</sup> have also questioned the validity of this model on the basis of cross-linking data. On the other hand our results tie in well with the observations of Parry *et al.*<sup>24,25</sup> on fibril diameters and they are consistent with the presence of an 80 Å molecular aggregate. However, it remains to be seen whether the molecular organization takes the form of microfibrils as previously described<sup>1–9</sup> or is related to some form of superlattice structure based on an underlying quasi-hexagonal lattice<sup>37</sup>. Although the observed variability in the side spacing could be due to variable distortion of a single structural repeat, it could also be a result of viewing a superlattice structure along different lattice planes.

In order to clarify some of these points, we are carrying out a further analysis of longitudinal cryosections of tendon and we also hope to develop the transverse cryosectioning technique so that the transverse ultrastructure of collagen fibrils can be seen in two dimensions. In the mean time the early results reported here provide direct support for some form of intermediate molecular aggregate within collagen fibrils and they emphasize once again the power of the convolution camera in studying elusive features in the transverse structure of fibrous protein assemblies.

We thank Dr D. A. D. Parry for suggesting this project, and the SRC for a project grant.

Received 9 June; accepted 26 September 1980.

## Salt-dependent dynamic structure of poly(dG-dC) . poly(dG-dC)

Jean Ramstein & Marc Leng

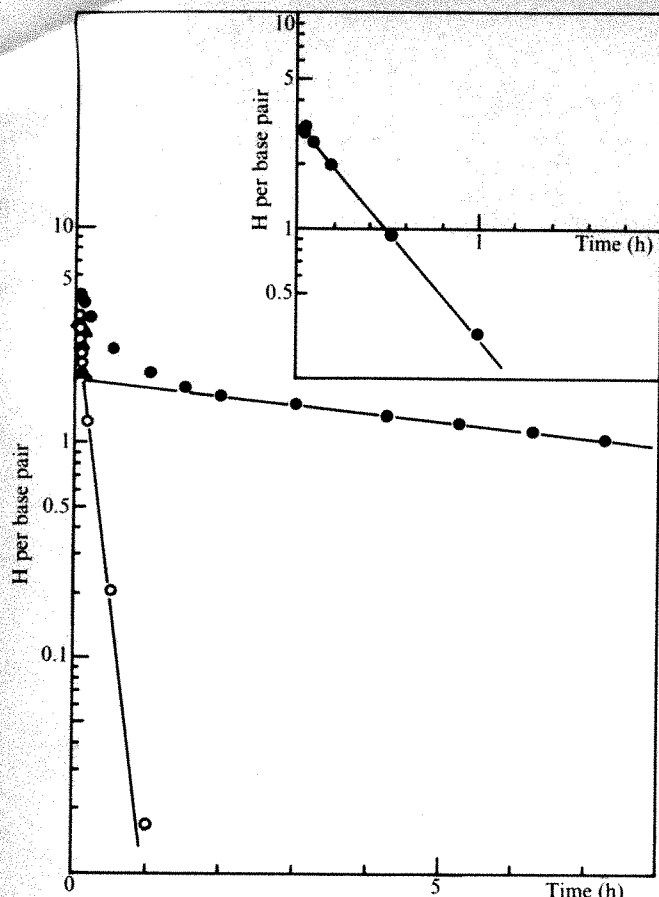
Centre de Biophysique Moléculaire, CNRS, 1A, avenue de la Recherche Scientifique, 45045 Orléans Cedex, France

Until recently, all known nucleic acid duplex helices were thought to be conformationally related to A DNA or B DNA, these right-handed helices being characterized by C(3') *endo* or C(2') *endo* pucker for the respective sugar residues and by an antiligandic bond<sup>1</sup>. This situation has since drastically changed, for X-ray studies on crystals of alternating d(CpG) DNA fragments have demonstrated the existence of a left-handed double helix, termed Z DNA (ref. 2). In this novel double helix the base-pairing is of Watson-Crick type, but the cytidine and guanosine residues have the *anti* and *syn* conformations, respectively, and thus the repeating unit is two base pairs. Such a left-handed helix can also account for the X-ray diffraction pattern of alternating poly(dG-dC) . poly(dG-dC) fibres<sup>3</sup>. However, Pohl and Jovin have shown that in solution poly(dG-dC) . poly(dG-dC) undergoes a salt-induced cooperative transition<sup>4</sup>. It is very likely that the left-handed double helix is relevant to the high-salt conformation of poly(dG-dC) . poly(dG-dC) and that the low-salt conformation of poly(dG-dC) . poly(dG-dC) belongs to the B-DNA family<sup>3,5</sup>. The techniques previously used to study the salt-induced transition of poly(dG-dC) . poly(dG-dC) in solution—circular dichroism (CD), absorption spectroscopy<sup>4</sup> and nuclear magnetic resonance<sup>5</sup>—give essentially a static picture of the conformation of the molecule. Such information, although fundamental, is incomplete because double-helical nucleic acids in solution are known to be subjected to thermal fluctuations resulting in transient conformations with opened base pairs<sup>6,7</sup>. A particularly useful probe of the dynamic aspects of nucleic acid structure is the tritium exchange technique largely developed by Englander and colleagues<sup>10</sup>. We have now used this technique to study the dynamic structure of poly(dG-dC) . poly(dG-dC) and have found that this varies depending on whether high or low salt conditions are used.

The exchange rate of the five protons involved in the hydrogen bonds between guanosine and cytosine residues in poly(dG-dC) . poly(dG-dC) were measured at two different ionic strengths (1 M NaClO<sub>4</sub> and 3 M NaClO<sub>4</sub>). As Fig. 1 shows, there is dramatic difference between the two hydrogen exchange curves, the overall exchange in high salt conditions being much slower than in low salt conditions. In 1 M NaClO<sub>4</sub>, four protons are measured and they all exchange with the same rate characterized by an exchange half-time of 6 min. Identical results were obtained by Teitelbaum and Englander for poly(rG) . poly(rC) in the same pH conditions<sup>7</sup>. These four protons were assigned to the exocyclic amino protons of the guanine and cytosine whereas the missing proton corresponds to the guanine imino proton, whose exchange rate is too fast to be measured by this technique<sup>7</sup>. In contrast, all five protons of the (GC) hydrogen bonds are measured in 3 M NaClO<sub>4</sub>. The exchange of two of these protons is surprisingly slow, the exchange half-time being about 7 h. Subtraction of these protons from the total exchange curve reveals that the remaining three protons have the same exchange half-time of about 20 min (Fig. 1 inset). To rule out any possible effect of the difference in NaClO<sub>4</sub> concentration on the chemistry of the exchange process, we have studied the exchange in 2.5 M NaClO<sub>4</sub> of poly(dG-dC) . poly(dG-dC) trapped in its low-salt conformation (this is possible because the kinetics of the transition between high and low salt conformation is very slow, with a relaxation time of 2 h in 2.5 M NaClO<sub>4</sub> (ref. 3)). All the measured points fall on the exchange curve obtained in 1 M NaClO<sub>4</sub>, showing clearly that there are no measurable salt effects on the chemistry of the exchange process.

- Smith, J. W. *Nature* **219**, 157–158 (1968).
- Miller, A. & Wray, J. S. *Nature* **230**, 437–439 (1971).
- Miller, A. & Parry, D. A. D. *J. molec. Biol.* **75**, 441–447 (1973).
- Nemetschek, Th. & Hosemann, R. *Kolloid-Z. u. Z. Polymere* **251**, 1044–1056 (1973).
- Hosemann, R., Dreissig, W. & Nemetschek, Th. *J. molec. Biol.* **83**, 275–280 (1974).
- Fraser, R. D. B., Miller, A. & Parry, D. A. D. *J. molec. Biol.* **83**, 281–283 (1974).
- Woodhead-Galloway, J., Hukins, D. W. L. & Wray, J. S. *Biochem. biophys. Res. Commun.* **64**, 1237–1244 (1975).
- Veis, A. & Yuan, L. *Biopolymers* **14**, 895–900 (1975).
- Fraser, R. D. B. & MacRae, T. P. *J. molec. Biol.* **127**, 129–133 (1979).
- Elliot, A., Lowy, J. & Squire, J. M. *Nature* **219**, 1224–1226 (1968).
- Parry, D. A. D. & Squire, J. M. *J. molec. Biol.* **75**, 33–55 (1973).
- Squire, J. M. *The Structural Basis of Muscular Contraction* (Plenum, New York, in the press).
- Fraser, R. D. B., MacRae, T. P. & Suzuki, E. *J. molec. Biol.* **129**, 463–481 (1979).
- Hulmes, D. J. S., Miller, A., Parry, D. A. D., Piez, K. A. & Woodhead-Galloway, J. *J. molec. Biol.* **79**, 137–148 (1973).
- Doyle, B. B. *et al. Proc. R. Soc. B* **187**, 37–46 (1974).
- Walton, A. G. *J. Biomed. Mater. Res.* **8**, 409–425 (1974).
- Chapman, J. A. & Hardcastle, R. A. *Connective Tissue Res.* **2**, 151–159 (1974).
- Hulmes, D. J. S., Miller, A., Parry, D. A. D. & Woodhead-Galloway, J. *Biochem. biophys. Res. Commun.* **77**, 574–580 (1977).
- McLachlan, A. D. *Biopolymers* **16**, 1271–1297 (1977).
- Bear, R. S., Adams, J. B. & Poulton, J. W. *J. molec. Biol.* **118**, 123–126 (1978).
- Meek, K. M., Chapman, J. A. & Hardcastle, R. A. *J. biol. Chem.* **254**, 10710–10714 (1979).
- Miller, A. in *Biochemistry of Collagen* (eds Ramachandran, G. N. & Reddi, A. H.) 85–136 (Plenum, New York, 1976).
- Fraser, R. D. B., MacRae, T. P. & Suzuki, E. in *Fibrous Proteins: Scientific, Industrial and Medical Aspects* Vol. 1 (eds Parry, D. A. D. & Creamer, L. K.) 179–206 (Academic, London 1979).
- Parry, D. A. D. & Craig, A. S. *Nature* **282**, 213–215 (1979).
- Parry, D. A. D., Craig, A. S. & Barnes, G. R. G. in *Fibrous Proteins: Scientific, Industrial and Medical Aspects* Vol. 2 (eds Parry, D. A. D. & Creamer, L. K.) 77–88 (Academic, London, 1980).
- Hulmes, D. J. S. & Miller, A. *Nature* **282**, 878–880 (1979).
- Miller, A. *New Scientist* **85**, 470–473 (1980).
- Woodhead-Galloway, J. *Acta crystallogr.* **B33**, 1212–1218 (1977).
- McFarlane, E. F. *Search* **2**, 171–172 (1971).
- Knight, D. P. & Hunt, S. *Nature* **249**, 379–380 (1974).
- Sjostrom, M. & Squire, J. M. *J. Microscopy* **111**, 239–278 (1977).
- Freundlich, A. & Squire, J. M. in *Fibrous Proteins: Scientific, Industrial and Medical Aspects* Vol. 2 (eds Parry, D. A. D. & Creamer, L. K.) 11–21 (Academic, London, 1980).
- Cox, R. W., Grant, R. A. & Horne, R. W. *J. R. microsc. Soc.* **87**, 123–142 (1967).
- Grant, R. A., Cox, R. W. & Horne, R. W. *J. R. microsc. Soc.* **87**, 143–155 (1967).
- Rougvié, M. A. & Bear, R. S. *J. Amer. Leather Chem. Ass.* **48**, 735–751 (1953).
- Bailey, A. J., Light, N. D. & Atkins, E. D. T. *Nature* **288**, 408–410 (1980).
- Trus, B. L. & Piez, K. A. *Nature* **286**, 300–301 (1980).
- Hodge, A. J. & Petruska, J. A. in *Aspects of Protein Structure* (ed. Ramachandran, G. N.) 289–300 (Academic, New York, 1963).





**Fig. 1** Hydrogen-tritium exchange curves at 0°C for poly(dG-dC). poly(dG-dC) (PL-Biochemicals, lot 658-5) in 3 M NaClO<sub>4</sub> (●), 1 M NaClO<sub>4</sub> (○) and 2.5 M NaClO<sub>4</sub> (▲). The salt solutions were adjusted to pH 7.5 and phosphate buffer pH 7.5 then added to a final molarity of 10 mM. It was checked that the CD (circular dichroism) spectrum of poly(dG-dC). poly(dG-dC) in 1 M NaClO<sub>4</sub> was almost an inversion of the one in 3 M NaClO<sub>4</sub>, in agreement with previous results<sup>4</sup>. The tritium Sephadex method of Englander was used<sup>10</sup>. All exchange experiments were carried out at 0°C. Exchangeable protons were labelled with tritium by incubating 0.5 ml of the nucleic acid solution (2 mg ml<sup>-1</sup>) with tritiated water (10 μl, 1 Ci ml<sup>-1</sup>) for 21 h. In all experiments the incubation solvent was identical to the exchange solvent except for the exchange experiment in 2.5 M NaClO<sub>4</sub>, for which the incubation solvent was 1 M NaClO<sub>4</sub>. To initiate the exchange of nucleic acid-bound tritium the incubation sample was passed through a Sephadex column (G-25 fine grade, 8 cm × 1 cm) previously equilibrated with the exchange buffer. This column removed the free tritium and the nucleic acid peak was collected in a test tube. To measure the amount of tritium still bound at any given time *t*, 300-μl aliquots were passed through a second Sephadex column (G-25 fine grade, 5 cm × 1 cm) previously equilibrated with the exchange buffer. This column removed the tritiated water formed during time *t*. The nucleic acid peak was collected in four test tubes which were analysed for radioactivity and nucleic acid concentration. The latter was determined by optical density at 260 nm, using a Zeiss PMQ II spectrometer and an extinction coefficient of 7 × 10<sup>3</sup> and 6.3 × 10<sup>3</sup> mol<sup>-1</sup> cm<sup>-1</sup> in 1 M and 3 M NaClO<sub>4</sub>, respectively<sup>4</sup>. Tritium was measured in 0.5-ml aqueous samples with 6 ml of dioxan-based liquid scintillation mixture by counting in an Inter technique SL 30 liquid scintillation counter. From the ratio of tritium counts per base pair, protons remaining unexchanged at *t* can be evaluated<sup>10</sup>. The gramme-atom concentration of protons in water was not corrected for the presence of NaClO<sub>4</sub> and was set equal to 111. For measurements of early time points (*t* < 5 min), a one-column procedure was used<sup>10</sup>. The exchange of the nucleic acid-bound tritium was initiated by passing 0.2 ml of incubation solution half-way down a column (8.5 cm × 1 cm). The flow was stopped to allow exchange to take place in the column during a suitable time interval; elution was then continued to complete separation of labelled nucleic acid and newly exchanged tritium. Fractions were collected and assayed as above. All necessary time corrections as indicated by Englander<sup>10</sup> have been made.

It is not possible to decide whether the two protons are the cytosine or the guanine amino protons, although the latter are the more likely candidates. Indeed, X-ray crystal studies of d(GpC) oligonucleotides show that a hydrogen bond is formed between the guanine amino group and a water molecule which is also hydrogen bonded to a phosphate oxygen<sup>2</sup>. Whatever the exact assignment of these five protons, our results show clearly

that the exchange rate of the protons is dependent on the conformation of poly(dG-dC). poly(dG-dC), which in turn means that the dynamic structure of the high and low salt conformations must be different.

Finally, we emphasize that this technique might be very useful for detecting the presence of the poly(dG-dC). poly(dG-dC) high-salt conformation in natural DNA. As already pointed out with respect to hydrogen exchange, the high-salt conformation is essentially characterized by the presence of two very slowly exchanging protons with a half-time at least 50 times greater than that measured for protons in double-stranded polynucleotides<sup>6,7</sup>. The existence of these two protons together with the high sensitivity of the tritium-labelling technique should enable the presence of small amounts of high-salt poly(dG-dC). poly(dG-dC) conformation to be detected in natural DNA.

We thank Professor C. Hélène for his interest and encouragement throughout this work and Dr E. Sage for her help. This work was supported in part by the Delegation Générale à la Recherche Scientifique et Technique (contract 79-7-06641).

Received 15 August; accepted 22 September 1980.

1. Crick, F. H. C., Wang, J. C. & Bauer, W. R. *J. molec. Biol.* **129**, 449-461 (1979).
2. Wang, A. H. J. *et al. Nature* **282**, 680-686 (1979).
3. Arnott, S., Chandrasekaran, R., Birdsall, D. L., Leslie, A. G. W. & Ratliff, R. L. *Nature* **283**, 743-745 (1980).
4. Pohl, F. M. & Jovin, T. M. *J. molec. Biol.* **67**, 375-396 (1972).
5. Patel, D. J., Canuel, L. L. & Pohl, F. M. *Proc. natn. Acad. Sci. U.S.A.* **76**, 2508-2511 (1979).
6. Teitelbaum, H. & Englander, S. W. *J. molec. Biol.* **92**, 55-78 (1975).
7. Teitelbaum, H. & Englander, S. W. *J. molec. Biol.* **92**, 79-92 (1975).
8. McConnel, B. & Von Hippel, P. H. *J. molec. Biol.* **50**, 297-316 (1970).
9. McConnel, B. & Von Hippel, P. H. *J. molec. Biol.* **50**, 317-332 (1970).
10. Englander, S. W. & Englander, J. J. *Meth. Enzym.* **26C**, 406-413 (1972).

## Neutron diffraction identifies His 57 as the catalytic base in trypsin

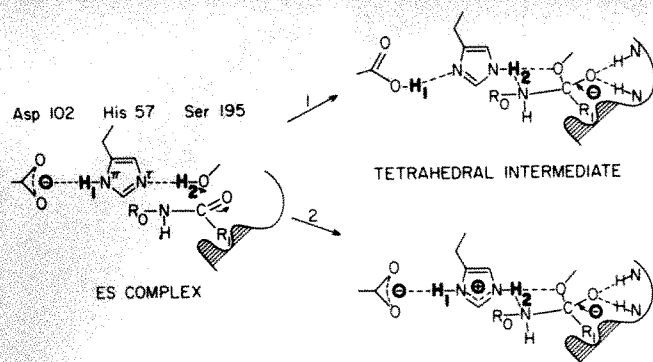
A. A. Kossiakoff & S. A. Spencer

Biology Department, Brookhaven National Laboratory, Upton, New York 11973

The mechanism of action of trypsin and other serine proteases has been widely debated<sup>1-5</sup>, particularly with regard to the identification of the group at the active site which functions as the chemical base during the catalytic process. Attempts to resolve this question by a number of indirect techniques, including NMR, isotope exchange, difference IR and quantum mechanical calculations, have resulted in different identifications of this group<sup>6,7</sup>. Neutron diffraction, because of its ability to locate hydrogen atoms experimentally, offers the most direct way of resolving this issue. Results are presented here from a 2.2-Å neutron data set for bovine trypsin covalently inhibited by a transition-state analogue, the monoisopropylphosphoryl (MIP) group. His 57 is clearly identified as the base in the catalytic process.

The catalytic site of the serine proteases is characterized by three invariant residues, a histidine (57), an aspartic acid (102) and a serine (195). The mechanism by which these enzymes hydrolyse peptide bonds can be described as a general base-catalysed nucleophilic attack on the carbonyl carbon of the substrate by the hydroxyl oxygen of Ser 195 (refs 8, 9). Coincident with this attack, the hydroxyl proton of the serine is transferred to the imidazole of His 57. The primary unresolved mechanistic question has been whether His 57 is the actual chemical base in the hydrolysis reaction (intermediate 2, Fig. 1) or whether the histidine acts as an intermediary through which Asp 102 functions as the base (intermediate 1). The neutron studies of myoglobin by Schoenborn and his co-workers<sup>10-12</sup>, which have shown that well ordered hydrogen and deuterium atoms can be located in Fourier maps of approximately 2.0 Å resolution, suggested that neutron diffraction would be the most direct technique to resolve the question.

The trypsin used in this study was initially inhibited with diisopropylfluorophosphate, an inhibitor which specifically and

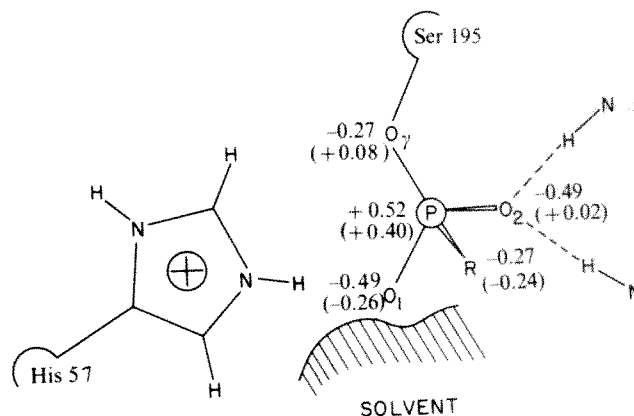


**Fig. 1** The two different locations proposed for proton H-1 in the tetrahedral intermediate (TI) structure. In the formation of TI(1), H-1 shifts from  $N^{\pi}$  to Asp 102 ( $O-\delta 2$ ) as proton H-2 transfers from the serine hydroxyl group to  $N^{\pi}$  of the imidazole. His 57 remains neutral throughout the reaction. In TI(2), proton H-1 remains on the imidazole as H-2 transfers. The imidazole becomes charged and forms a zwitterion with the carboxylate of Asp 102. The intermediate pictured here corresponds to that formed during acylation and differs from the deacylation intermediate (which MIP mimics) only by the replacement of the leaving group ( $R_0-NH_2$ ) with a hydroxyl group.

covalently binds to the hydroxyl group of Ser 195 in serine proteases<sup>13</sup>. However, it was determined both chemically and crystallographically (R. M. Stroud, personal communication) that during the period of crystallization, this triester hydrolysed to the more stable diester form, producing MIP trypsin (Fig. 2). The geometry of this inhibitor closely resembles that of the tetrahedral intermediate<sup>14</sup>, which is believed to be the transition-state configuration for the hydrolytic reaction<sup>15-17</sup>. Analysis of this complex consequently allows the direct determination of the protonation states of the catalytically important residues at the crucial step in the hydrolysis.

Neutron data to 2.2 Å were collected at the single-crystal station at the Brookhaven High Flux Beam Reactor<sup>18</sup>. The

crystal of bovine trypsin was grown from  $MgSO_4$  at pH 7 (ref. 14) and had a volume of 1.5 mm<sup>3</sup>. It was soaked for approximately 1 month in  $D_2O$  solution containing 8%  $MgSO_4$  (pD 6.2, uncorrected) to replace most of the exchangeable hydrogen atoms with deuterium. This exchange greatly reduces the background component in the data produced by the large, incoherent scattering effects of hydrogen. In all, 8,700 independent reflections were collected using normal-beam rotation geometry. The initial phasing model was calculated by applying the appropriate neutron-scattering lengths<sup>19</sup> to the refined trypsin X-ray coordinates of Chambers and Stroud<sup>20</sup>. The first structure-factor calculation for the neutron data, excluding all hydrogen atoms and water molecules, gave an  $R$  of 0.304. The current model is refined to an  $R$  of 0.187. Table 1 summarizes the structure refinement statistics.



**Fig. 2** Schematic diagram showing the orientation of the MIP group with respect to the imidazole of His 57. The MIP group resembles the deacylation intermediate of the reaction. In the real intermediate, the phosphorus is replaced by a carbon atom and oxygen O-1 by a hydroxyl group. Ligand R corresponds to the amino acid side chain, which in MIP is an isopropyl group. The individual charges on the atoms in the MIP group are given<sup>25</sup>. The numbers in parentheses represent the computed differences in charge between corresponding atoms in the MIP group and the tetrahedral intermediate. The charges for the tetrahedral intermediate were obtained from a model reaction study (using methoxide ion and formamide) of the acylation step of the reaction<sup>26</sup>. The charge on the hydroxyl group was assumed to be approximately the same as that on  $NH_2$  in the methoxide-formamide intermediate<sup>27</sup>. Electrostatic potential energies were calculated using the expression  $E = \sum (q_i q_j) / (\epsilon_0 r)$ .  $\epsilon_0$ , the dielectric constant, was 3.0;  $r$  is the distance between charges  $q_i$  and  $q_j$ .

As a major objective was to identify conclusively the group acting as the base, it was necessary to ascertain that the identification of the proton positions in the catalytic site was unambiguous. Three methods were used to test the preferred location of proton H-1 (Fig. 1). In method 1, the deuterium (proton H-1 was exchanged for deuterium during the soaking procedure) was omitted from the model and the full structure refined through one cycle of coordinate shifts and model reidealization. This refinement cycle was run to eliminate any bias in the phases that might have been introduced by a previous placement of this atom in the model. As seen in Fig. 3a, the difference synthesis calculated from these structure factors shows a distinct preference for the deuterium to reside on the imidazole.

In method 2, a deuterium atom was placed by stereochemistry on the  $\pi$  nitrogen of the imidazole and its position refined. After two cycles, the deuterium exhibited stable refinement characteristics and a relatively low temperature factor, indicating that it was tightly bound to the parent  $N^{\pi}$  atom. This process was then repeated with the deuterium placed in the proposed alternative position on the O-δ2 of the Asp 102 side chain. In this case, the refinement was quite unstable, and the deuterium atom

**Table 1** Refinement of monoisopropylphosphoryl trypsin

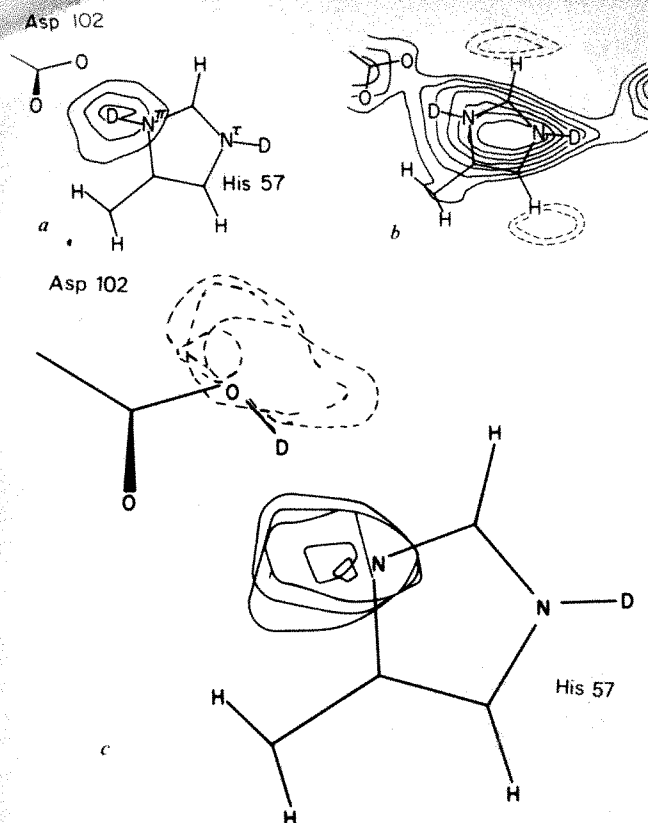
| Prerefinement models  | Source  | Statistics                                |
|---|---|---|
| Model   |   | $R = \frac{\sum  F_o - F_c }{\sum  F_o }$ |
| Starting model*   | Chambers-Stroud X-ray model <sup>20</sup> with neutron scattering lengths <sup>19</sup> | $R = 0.304$                               |
| Initial neutron model†                                      | Hydrogen and deuterium atoms placed in model by inspection of difference maps           | $R = 0.255$                               |
| Refinement Function   | Approach  |   |
| Shifts in atom positions                                    | Difference maps (curvature/gradient) <sup>23</sup>                                      |   |
| Reidealization of model coordinates and energy minimization | Model building and energy refinement <sup>24</sup>                                      |   |
| Current status‡   | Nine cycles of refinement   | $R = 0.187$                               |

\*Model contained no hydrogen or deuterium atoms.

† About three-quarters of the total hydrogen/deuterium atoms were located. 55 water molecules were also located and included in the phasing model.

‡ The current model is highly constrained, with r.m.s. deviations of bond lengths <0.015 Å and angles (bond and dihedral) <2.6° from the ideality. Nonbonded energy terms (van der Waals attraction-repulsion forces, electrostatic and torsional energies) have been refined.





**Fig. 3** *a*, A difference map  $((F_o - F_c) \exp(i\phi_o))$  calculated with only the deuterium (H-1) between the His 57 and Asp 102 side chains left out of the phases. The difference peak is approximately  $5.5\sigma$  above the background level and shows the deuterium to be bound to the imidazole nitrogen. *b*, A Fourier map computed with terms  $(2F_o - F_c) \exp(i\phi_o)$ . In this map, both of the catalytically important deuteriums (corresponding to H-1 and H-2 in Fig. 1) were omitted from the phases. This map clearly shows that both are located on the imidazole. (Hydrogen atoms appear as negative density because of their negative neutron-scattering length. The peaks for the ring hydrogens seem to be displaced from their true positions due to the limited resolution of the map. At  $2.2 \text{ \AA}$ , a portion of the negative density peak of a ring hydrogen overlaps the positive peak of the parent atom, effectively cancelling density between the atoms and giving the illusion that the peak has been translated.) *c*, A difference map in which the deuterium was placed by stereochemistry on atom O- $\delta_2$  of Asp 102 (if there were a proton coordinated to Asp 102, it would be on O- $\delta_2$ ). The difference density peak clearly indicates that the preferred location of the deuterium is on the imidazole of His 57.

resided along a distinct gradient, giving a clear indication of misplacement.

Method 3 involved the qualitative examination of two independent difference maps. For the first map, structure factors were calculated with the deuterium atom on the N $^{\pi}$  of His 57. In agreement with the refinement results, a nearly featureless map was produced, signifying that this placement was in close accord with the data. In contrast, placement of the deuterium on the O- $\delta_2$  of Asp 102 resulted in the interpretable difference map shown in Fig. 3c. The difference peak clearly indicates that a substantial shift towards the imidazole ring is warranted.

The results from each of these three techniques independently support the conclusion that the mechanistically important proton is coordinated to the imidazole of His 57. Taken together, we believe they offer compelling evidence that, at physiological pH, the protonated species in the tetrahedral intermediate is the imidazole of His 57 rather than the carboxylate of Asp 102.

To eliminate any possibility that the protonation states of the aspartate and histidine observed in this neutron diffraction study were artefacts due to the substitution of a MIP group for a real tetrahedral intermediate, a series of calculations was performed

to establish that the phosphate ester in trypsin also models the structure of the tetrahedral intermediate with respect to the location of the critical atom (H-1 in Fig. 1). Although both the phosphate ester (MIP) and the tetrahedral intermediate (TI) possess a net charge of  $-1$ , the centres of their charge distributions, with respect to the centre of the positively charged imidazole, differ somewhat ( $R_{\text{MIP}} = 4.3 \text{ \AA}$ ,  $R_{\text{TI}} = 4.6 \text{ \AA}$ ). However, energy calculations suggest that this difference of  $0.3 \text{ \AA}$  in the centres of the distributions is unlikely to be large enough for the MIP group to promote an interchange of the protonation states of His 57 and Asp 102 (from TI(1) to TI(2) in Fig. 1), as the calculated electrostatic potential energy (Fig. 2) derived from the interaction between the imidazole and the MIP group differs by only  $\sim 6\%$  from that obtained with a model of the expected tetrahedral intermediate.

Possible changes in the  $pK_a$  of His 57 were also explored by the method of Gurd *et al.*<sup>21,22</sup> Assuming no attenuation due to solvation, it was estimated that the MIP group can increase the  $pK_a$  of His 57 by, at most,  $0.8 \text{ pK}$  units, whereas the tetrahedral intermediate was estimated to increase it by about  $0.6 \text{ pK}$  units. In addition, the phosphoryl oxygen adjacent to the imidazole (O-1, Fig. 2), the largest contributor to the calculated  $pK$  effect, is solvent accessible; therefore, the influence of this oxygen should be significantly attenuated by solvation. If the assignment of  $pK$ 's by Hunkapiller *et al.*<sup>2</sup> were correct, the  $pK_a$  of His 57 would have to be raised by about  $3.0 \text{ pK}$  units to interchange the protonation states. As the calculated electrostatic effects due to the MIP group are much too small to accomplish this, it can be stated with confidence that the protonation states observed in the neutron diffraction experiment correspond to those in a true transition state.

The implications of the neutron diffraction results for the understanding of the mechanism of action of the serine proteases are twofold: (1) Those mechanisms which assigned Asp 102 as the base can now be eliminated from consideration and (2) the conclusive assignment of His 57 as the base will allow the major experimental emphasis of future work to focus on other important aspects of the mechanism. A more detailed description of the crystallographic results will be published elsewhere.

This research was carried out at Brookhaven National Laboratory under the auspices of the US Department of Energy. We thank Drs B. Schoenborn and J. Cain, who designed and developed the crystallographic station at the Brookhaven High Flux Beam Reactor, for their help and suggestions, Dr R. Stroud for donating the trypsin crystal and Dr J. Hanson for help with the computer graphics.

Received 10 July; accepted 3 October 1980.

- Blow, D. M., Birktoft, J. J. & Hartley, B. S. *Nature* **211**, 337–340 (1969).
- Hunkapiller, M. W., Smallcombe, S. H., Whitaker, D. R. & Richards, J. H. *Biochemistry* **12**, 4732–4743 (1973).
- Stroud, R. M., Krieger, M., Koeppe, R. E., Kossiakoff, A. A. & Chambers, J. L. in *Proteases and Biological Control* (eds Reich, E., Rifkin, D. B. & Shaw, E.) 13–22 (Cold Spring Harbor Laboratory, New York, 1975).
- Bachovchin, W. W. & Roberts, J. D. *J. Am. chem. Soc.* **100**, 8041–8047 (1978).
- Markley, J. L. & Ibanez, I. B. *Biochemistry* **17**, 4627–4640 (1978).
- Blow, D. M. *Acc. chem. Res.* **9**, 145–152 (1976).
- Kraut, J. A. *Rev. Biochem.* **46**, 331–358 (1977).
- Bender, M. L. & Kezdy, F. J. *J. Am. chem. Soc.* **86**, 3704–3714 (1964).
- Inward, P. W. & Jencks, W. P. *J. biol. Chem.* **240**, 1986–1996 (1965).
- Schoenborn, B. P. *Nature* **224**, 143–146 (1969).
- Schoenborn, B. P. *Cold Spring Harb. Symp. quant. Biol.* **36**, 569–575 (1971).
- Norvell, J. C. & Schoenborn, B. P. *Brookhaven Symp. Biol.* **27**, 11, 12–23 (1975).
- Jansen, E. F., Nutting, M. D. F. & Balls, A. K. *J. biol. Chem.* **179**, 201–204 (1949).
- Stroud, R. M., Kay, L. & Dickerson, R. E. *J. molec. Biol.* **83**, 185–208 (1974).
- Hunkapiller, M. W., Forgac, M. D. & Richards, J. H. *Biochemistry* **15**, 5581–5588 (1976).
- Caplow, M. J. *J. Am. chem. Soc.* **91**, 3639–3645 (1969).
- Fersht, A. R. & Requena, Y. *J. Am. chem. Soc.* **93**, 7079–7087 (1971).
- Cain, J. E., Norvell, J. C. & Schoenborn, B. P. *Brookhaven Symp. Biol.* **27**, VIII, 43–50 (1975).
- Bacon, G. E. in *Neutron Diffraction*, 39–41 (Clarendon, Oxford, 1975).
- Chambers, J. L. & Stroud, R. M. *Protein Data Bank* (Brookhaven National Laboratory, New York, 1977).
- Shire, S. J., Hanania, G. I. & Gurd, F. R. *Biochemistry* **13**, 2967–2979 (1974).
- Matthew, J. B., Hanania, G. I. & Gurd, F. R. *Biochemistry* **18**, 1919–1928 (1979).
- Chambers, J. L. & Stroud, R. M. *Acta crystallogr. B* **33**, 1824–1837 (1977).
- Hermans, J. & McQueen, J. E. *Acta crystallogr. A* **30**, 730–739 (1974).
- Perahia, D., Pullman, A. & Berthod, H. *Theor. chim. Acta* **40**, 47–60 (1975).
- Kleier, D. A., Scheiner, S. & Lipscomb, W. N. *Int. J. Quantum Chem. Quantum Biol. Symp.* **3**, 161–169 (1976).
- Alagona, G., Scrocco, E. & Tomasi, J. *J. Am. chem. Soc.* **97**, 6976–6983 (1975).



## BOOK REVIEWS

## Archaeologist extraordinary

Gordon R. Willey

V. GORDON Childe (1892–1957), an Australian by birth, who became, successively, the Abercromby Professor of Archaeology at the University of Edinburgh and the Director of the Institute of Archaeology at the University of London, was the foremost prehistoric archaeologist of his time. His influence on the archaeological profession, both in English-speaking countries and elsewhere, was profound and continues to be felt; and his best-known writings, although by no means "popular" in an ordinary sense, have been read in circles far beyond those of the profession.

Numerous articles, reviews and commentaries about Childe and his work have appeared over the years, but this study by Professor Bruce G. Trigger, of McGill University, is the first book-length intellectual and professional biography of this extraordinary man and scholar. Trigger is well-prepared for and suited to the task. As a Canadian he is familiar with both American and Old World archaeological histories, and his own research has spanned both archaeology and ethnology.

The biography begins with a brief consideration of Childe the controversial figure — "Man and Myth", as Trigger terms it — the conceptions and misconceptions about Childe that have developed in the archaeological community since the 1930s and 1940s and the publication of his two most widely read books, *Man Makes Himself* (Watts, 1936) and *What Happened in History* (Penguin, 1942). Trigger follows this with a review of European archaeology and archaeological thinking before Childe and indicates just how the latter both learned from and began to change this thinking. Subsequent chapters carry the story forward in time, although as the author's primary intention is to trace Childe's intellectual development there are, of necessity, many retrospective and anticipatory observations in his skilful analysis.

In such early works as *The Dawn of European Civilization* (Kegan Paul, 1925) Childe built on the artifact typologies and synchronisms of his predecessors, but he did it better, presenting the most complete and satisfactory synthesis of European prehistory up to that time. He accepted Kossinna's "archaeological culture" concept as a useful working device but rejected its racist grounding; while he abjured rigid unilinear evolutionism he

*Gordon Childe: Revolutions in Archaeology.* By Bruce G. Trigger. Pp.207. (Thames and Hudson/Columbia University Press: 1980.) £10, \$22.50.



Gordon Childe: "the foremost prehistoric archaeologist of his time".

then began his life-long attempt to develop a more sophisticated set of cultural evolutionary theories, doing so in conjunction with diffusionist thinking more akin to that of Montelius than to the extravagances of Eliot-Smith and Perry. This was followed up directly in the 1920s and 1930s with those great books, *The Danube in Prehistory* (Oxford University Press, 1929), *The Most Ancient East* (Kegan Paul, 1928), *The Bronze Age* (Cambridge University Press, 1930) and *New Light on the Most Ancient East* (Kegan Paul, 1934), all of which trace the course of development of Neolithic life and subsequent civilization from the Near and Middle East into Europe. In doing this, Childe's consideration of such processes of civilization as the stabilization of institutions, the widening of trade horizons, the capitalization of surplus wealth and the consolidation of smaller communities into urban settlements clearly foreshadowed present-day archaeological concerns. The same is also true of Childe's pioneer

settlement pattern studies in Scottish archaeology. Indeed, the last sentence of Trigger's biography sums this up forcefully and succinctly:

It is surely a measure of Childe's intellectual stature that, in spite of the buffeting of two decades, the major questions that he dealt with at the end of his career are now more critical to the future of archaeology than they were when he first raised them.

Here Trigger is referring primarily to some of Childe's later, more explicitly theoretical works of the 1940s and 1950s; but even in these earlier writings which were addressed to the data contexts of prehistory it is obvious that Childe had a sense of problem that overreached that of most of his contemporaries.

Childe is, of course, best known as a theoretician, and, cognizant as he was of the changing nature of the archaeological record, it was his own opinion that it was in this sphere that he would be best remembered; nevertheless, it cannot be overstressed that Childe was "data bound" in the very best sense of that term. This comes out, again and again, in all of his publications, as Trigger has demonstrated so tellingly. He was committed to the idea that the archaeologist should be concerned with the explaining of society, human behaviour and ideas, but he did not believe that this could be done successfully and satisfactorily out of the context of the facts of prehistory and history.

Much has been made of Childe as a Marxist thinker; but as Trigger shows us in his chapters "Human Progress and Decline", "Archaeology and Scientific History" and "Societal Archaeology", Childe was highly ambivalent about Marxist doctrine. Marxist dialectics presented to him a way of thinking, but there was always a tension, a conflict within himself as he measured the realities of the archaeological data in and on the ground with Marxist doctrines. In doing so he was cautious, critical, even pessimistic. He was a materialist but he was also a humanist. Out of these complexities and contradictions came the most creative archaeological writing of the mid-twentieth century.

No treatment of Childe would be, or could be, complete without some reference to the "new archaeology" of the 1960s and 1970s, and Trigger has provided this in a final chapter, "Beyond the New Archaeo-



logy". While Childe was not an immediate intellectual prototype for it, it cannot be denied that his writings have helped prepare the way. Childe was ever interested in the search for regularities, "laws" in human cultural and social behaviour. Trigger makes the point, however, that Childe differed from the "new archaeologists" in seeing human behaviour as changing, not immutable. In this he was Marxist for he believed that behaviour changed as social context changed. For him the search for "laws" was a legitimate but not the primary objective of archaeology. The primary objective and the future of archaeology lay, in his mind, with history — in the full context of social and cultural history. With this conviction, as Trigger says, he would have had little sympathy with archaeological examinations of "fragmentary" behaviour, behaviour out of context.

It is redundant or over-obvious to say that archaeology is "as large as life" — but, indeed, it is; or at least it may legitimately encompass all aspects of human life in the past. Gordon Childe was very much aware of this. Those who view him as a special pleader or partisan adherent of limited theoretical views overlook the facts of his devotion to and masterly control of the data, the traditional data of form, time and space. What he did was to ask new questions and in attempting to answer these questions — all of which were of importance in understanding mankind's past — he made us aware of how much of the potential record remained to be discovered. This was disturbing — and exciting — but it raised the discipline of archaeology to a whole new level of consciousness. □

Gordon R. Willey is Bowditch Professor of Mexican and Central American Archaeology and Ethnology at Harvard University.

## Red bed diversity

J.R.L. Allen

*Continental Red Beds. Developments in Sedimentology*, Vol. 29. By P. Turner. Pp. 562. (Elsevier Scientific: 1980.) Dfl. 145, \$70.75.

THIS is an important and original book in which the author sets out to synthesize and review what we currently know of the nature, depositional environments and processes, and diagenesis of continental red beds. Continental red beds and the "red-bed problem" have fascinated sedimentary geologists for many years, and in the minds of some investigators have seemed of particular petrogenetic significance. Dr Turner's book illustrates the variety of the issues raised by investigation of continental red beds and shows that it is

naïve to conceive of a single red-bed problem. Its value is rather to illustrate the remarkable diversity of continental red beds, a diversity of diagenetic environments and history as much as of depositional environment.

There are four sections in the book. The first considers the tectonic and climatic setting of ancient red beds and leads to a preliminary assessment of the question of the origin of red coloration. A practical classification of red beds is advanced, based on depositional environment, colour characteristics and diagenesis. The second and longest section is a thorough review of the depositional processes and environments of modern continental sediments and of ancient reddened counterparts, such as the European Lower Permian, the Upper Coal Measures of South Wales, and the Old Red Sandstone of the British Isles. The third section is concerned with the diagenesis, mineralogy and geochemistry of continental red beds. The fourth comprises two chapters, of which the first is a general account of the magnetization of continental red beds, and the second a study of magnetization case-histories (Proterozoic basins of western Canada,

Late Precambrian of Scotland, Moenkopi Formation of western USA, late Cenozoic red beds of Baja California). These clearly illustrate the complex controls on the magnetization histories of continental red beds and the difficulties of interpreting palaeomagnetic data, even when a wide variety of supporting field, petrographic and geochemical information is available.

Dr Turner's book is a carefully researched and well-written account of the sedimentology of continental red beds, the author moving confidently from large-scale phenomena to problems on the smallest of scales. The book was prepared from camera-ready typescript (there are a few small errors) and is well-illustrated by line drawings and photographs. There is an extensive and up to date list of references. The book is expensive but no sedimentologist concerned with continental sediments can afford to neglect it. □

J.R.L. Allen is Professor of Geology at the University of Reading. His research interests include the sedimentology of the Old Red Sandstone (a series of continental red beds of Devonian age) in southern Britain.

## Introduction to liposome research

Timothy D. Heath

*Liposomes in Biological Systems*. Edited by G. Gregoriadis and A. C. Allison. Pp. 424. (Wiley: 1980.) £23, \$69.

*Liposomes in Biological Systems* is the first book to be devoted completely to this aspect of liposomes. Its publication reflects the considerable expansion which has recently occurred in liposome research.

The book begins with a contribution by A.D. Bangham who traces the history of liposomes as he and others first characterized them, and their subsequent use by biologists. Following this, Dr Gregoriadis summarizes the potential applications of liposomes as drug carriers, and expresses his hopes for the future.

In the subsequent chapters various specialist authors concentrate largely on their own contributions to the field. J.H. Fendler describes the various factors concerned with encapsulation of drugs. G. Poste gives a critical review of liposome-cell interactions, which will enlighten those who may still believe the predominant mode of vesicle-cell interaction to be fusion. This area of liposome research in particular has been the subject of much recent reconsideration. Several chapters are devoted mainly to the *in vivo* fate of liposomes and their contents, including the uptake of enzyme-bearing liposomes by G. Weissmann and M. Finkelstein. G. Scherphof *et al.* have described their efforts to elucidate the interaction of

liposomes with serum components, and H. Kimelberg discusses his work on the *in vivo* fate of encapsulated methotrexate. I. H. Shaw and J. T. Dingle describe the interarticular injection of steroid-containing liposomes which is indeed one of the most promising applications of liposomes so far developed. (It would also have been appropriate had this volume included a chapter on the work of C. D. V. Black, R. R. C. New and C. R. Alving on the use of liposome-encapsulated antimonials in the treatment of visceral Leishmania, which clearly may be one of the first successful therapeutic applications of liposomes.) The final specialist chapter, by G. M. K. Humphries, covers the use of liposomes for studying *in vitro* immune reactions, which will undoubtedly become a major area of liposome research.

The contents of this volume are very similar to those of Vol. 308 of the *Annals of the New York Academy of Sciences* (1978), and most of the contributions appear to have been written between 1976 and 1978. The delay in publication is unfortunate, although Dr Gregoriadis has added a short chapter which summarizes much of the more recent literature.

In conclusion, this volume will provide a useful introduction for those unfamiliar with the field. □

Timothy D. Heath is a research fellow at the Cancer Research Institute, University of California, San Francisco.



# Telescopes of the future: heading for the supergiants

V.C. Reddish

*Optical and Infrared Telescopes for the 1990s.* Edited by Adelaide Hewitt. Two volumes, pp.1260. (Kitt Peak Observatory: Tucson, Arizona, 1980.) \$35 + \$15 airmail.

AT A time when the financial outlook for fundamental science may appear bleak, these two volumes should raise the spirits even of the pessimistic. Undaunted, more than 200 scientists and engineers gathered at Tucson, Arizona, in January 1980 to discuss how best to apply the latest technologies to the design and construction of very large optical and infrared telescopes, and what further technological research and development is needed for that purpose in the immediate future. This record of their deliberations makes exciting reading.

A wide range of possibilities was considered for telescopes with apertures mostly in the range 7m to 30m; the pros and cons of monolithic versus segmented mirrors, multi-mirror versus multi-telescope, single telescope versus arrays, were argued. Everyone, it seems, accepts that mirrors will be thin whatever configurations are adopted; the UK Infrared Telescope has proved that they can give optical performance and major cost savings.

Although various kinds of mountings were mentioned — alt-az, inverted alt-az, siderostat, steerable dish — not a lot of consideration was given to this aspect of telescope construction, and even less to the problems of domes and buildings. These are areas where major cost savings may be made and it could be worthwhile having a follow-up conference on the topic of housing very large telescopes. A radical breakaway from historical approaches (even recent ones such as the MMT building and the CERGA concept) may be possible and desirable if large economies are to be made, sufficient to make the construction of very large telescopes acceptable propositions. Do we really need to erect large concrete towers with rotating domes on top, or even rotating buildings, to protect the telescope from the weather and to provide a satisfactory working environment for engineers when it is not being used, and to shield it from the wind when it is? The cost is high not only in financial terms but in the deleterious effect which the building usually has on the astronomical seeing. I think that far more satisfactory structures could be made at costs one to two orders of magnitude less than those current.

A heartening feature of the discussions, however, was the recognition of the need to pay attention to the relationship between the design and aperture of the telescope, and the effects of the atmosphere on the image. These are of course functions of the

wavelengths at which the telescope is to be used and therefore relate to the astronomical research objectives and to the instrumentation — spectrometers and detectors — to be employed. This chain forms a recurring theme throughout the discussions; repeated attention was drawn to astronomical objectives and to the need to make the whole telescope system efficient. Considerable further advances in computer control are possible and substantial gains in efficiency can result from more extensive use of photoelectric autoguiders. It is surprising, as one participant pointed out, that autoguiders are still so little used. Every telescope built by the Royal Observatory Edinburgh since 1962 has been autoguided and that has been a major factor in the high quality of photographs produced by the UK Schmidt Telescope in Australia which was equipped with one from the outset; if it can be done for a Schmidt telescope, it can be done for any telescope.

There were so many contributions that it is impossible to mention more than a few. The experimental data on deformable mirrors by J.W. Hardy I found fascinating; also the discussion of (iso)thermally invariant structures by F.D. Drake and the paper on imaging by C.H. Townes. The most important technological papers, however, were probably those concerned with the matter stated succinctly by T.S. Mast and J.E. Nelson:

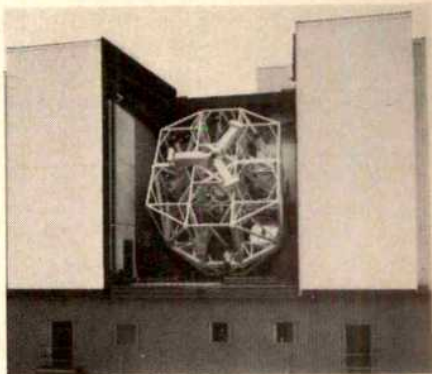
The central problem with a segmented mirror is to assemble the small mirrors and maintain their orientations and positions so they form the figure of a single large optical quality mirror.

## Between the sheets

J.M. Thomas

*Intercalated Layered Materials.* Edited by F. A. Levy. Pp.562. (Reidel: 1979.) Dfl.150, \$78.

WHEN a sheet-like structure assimilates guest species into its interlamellar spaces the phenomenon is known as intercalation. The uptake of ammonia by clay minerals in soil, first identified in 1850, is an example of such a process, so also is the swelling of clay when immersed in water, an effect known to the potters and ceramicists of antiquity. When transition-metal chalcogenides (such as niobium diselenide or molybdenum disulphide) take up alkali metals, the intercalation may dramatically alter the electronic properties of the parent solid: semiconductors become metals and metals semiconductors, purely as a con-



A telescope of today: the multi-mirror telescope on Mount Hopkins, Arizona.

Much effort, study and experiment will be devoted to this problem in many observatories around the world during this decade. It will be a happily competitive business, a race to be the first with the biggest and the best. It is difficult not to believe that the problem will be solved and the 1990s will see giant telescopes with apertures of 25m or more probing the outer half, the earlier half, of the Universe, intent upon discovering its structure, chemistry and evolution. The prizes in new knowledge in one of the most fundamental of our sciences could be immense, a just and proper reward for the supergiant telescope builders.

V. C. Reddish was until recently Director of the Royal Observatory Edinburgh and Professor of Astronomy in Edinburgh University. The UK Schmidt Telescope in Australia, the UK Infrared Telescope in Hawaii and the COSMOS measuring machine at Edinburgh were built under his direction.

sequence of the donation of electrons into empty or partially filled bands. Moreover, the addition of a wide range of organic materials (amines, amides, acids, pyrimidines and numerous heterocyclics and their derivatives) changes the superconducting transition temperature of the chalcogenide. When graphite, the best known and most widely studied of layered solids, assimilates certain electron-donating or electron-accepting guests, the process is accompanied by many significant structural, chemical and electronic changes. Alchemists would doubtless have been aroused to discover that when graphite is exposed to the vapour of potassium the glistening black solid is "transmuted" into a specular, golden mass. Intercalated species generally carry a residual charge and they usually take up



well-defined positions in directions parallel and perpendicular to the sheets. For graphite, but not, in general, for all other layered hosts, there is also the phenomenon of staging: the guests enter only some of the available interlamellar spaces and in an ordered fashion. The resulting range of structural possibilities is bewildering.

In this, the sixth volume in a worthwhile series devoted to the physics and chemistry of materials with layered structures, there are some outstanding chapters which elegantly combine both comprehensive coverage and critical assessment. All of the chapters are, to a greater or lesser degree, useful, but one or two lapse into the kind of language which scientists, in their quests for funding, inflict upon grant-awarding committees. Thus we read "... graphite intercalation compounds provide a near-ideal training vehicle in electronic materials science ... The frequent observation of surprising or dramatic results provides a beneficial stimulating effect, and the ever-present potential for gross error instills [sic] a healthy caution". Such sentiments could equally justify a reinterpretation of the Egyptian Book of the Dead or the factors that led to the emergence of Sufism.

Solid-state physicists, chemists and materials scientists will find much that is stimulating and rewarding in this monograph. I know of no more comprehensive survey of the intercalates of transition metal chalcogenide,  $\text{MX}_2$ , than that provided here by G. V. Subba Rao and Shafer, and no superior summary of the exciting developments that have occurred in studies of graphite intercalates since they were discovered by Schaufhault in 1841 than the chapter by Herold. The former deals admirably with, *inter alia*, the analogy between "solvated" intercalates (such as  $\text{Na}_x^+(\text{sol.})_y$ ,  $(\text{MX}_2)_x^-$  where solv. can be water, formamide, glycol, ethers, amines or amine oxides) and classical polyelectrolytes, well-known to colloid scientists. The latter covers all relevant aspects of graphite intercalate including two tentative schematic models for "interpenetrating stages" and "residue compounds" (where guest species are well and truly enclathrated up to quite high temperatures), the correctness of each of which has recently been confirmed by electron microscopic studies.

Ubbelohde's opening chapter summarizes his own well-known contributions to graphite intercalates, which receive further attention in this volume by M. S. and G. Dresselhaus, who review lattice mode structures explored principally by the Raman effect, and by Fischer, who assesses their electronic properties. Other chapters, devoted to chalcogenides, include an informative, closely argued contribution by Acrivos on the actual process of intercalation (its kinetic, mechanistic and thermodynamic aspects as well as likely bonding modes); a neat appraisal, by Beal, of the transition-metal intercalates of Group VA dichalco-

genides; a similar account by Rouxel of alkali-metal intercalates of hosts such as  $\text{MX}_2$ ,  $\text{MX}_3$  and  $\text{MX}_4$ ; and a rather telegraphic account by Samoana and Wollam of some intercalates of  $\text{MoS}_2$ .

The final chapter, entitled "Applications of Intercalation Compounds", by Whittingham and Ebert, though it covers thoroughly the electrochemistry of the various intercalates discussed elsewhere in this volume and touches upon the utility of variants of beta alumina as solid electrolytes and on  $\text{Li}_x\text{TiS}_2$  as typical, reversible, solid cathode material for commercially viable "solid-state" batteries, is rather brief in its attention to other chemical applications. True, when this book was written, which I estimate to be nearly three years prior to publication, not a great deal had been unearthed from the laboratory (or from existing literature!) about the range of chemical reactions that are "catalyzed" by various intercalates (for example the Fischer-Tropsch reaction and the ammonia synthesis). But it seems odd that, apart from the very last sentence in the book, there is no mention of one of the largest families of intercalates yet discovered — those formed by kaolinite, montmorillonite, hectorite and vermiculite. These so-called kandites and smectites form more or less stable intercalates with a wide range of polar and non-polar

molecules (including alcohols, hydrocarbons, amines, amino acids, ketones, purines and so on). Although the structures of these insulating, clay-based intercalates, are, with a few notable exceptions, no better elucidated than the structures of many of the intercalates discussed in this volume, what is abundantly clear is that the range of highly selective organic chemical conversions — dimerizations, etherification, lactonization, hydrogen transfer, ester and amine syntheses — that may be effected through their agency is already impressive and continues to grow. Recently, Weiss and others demonstrated that intercalated amino acids may be stimulated to produce peptides inside a sheet silicate, thus vindicating Bernal's well-known speculation about the role of clay minerals in the origin of life. Reflecting on these thoughts, one recalls that in the Biblical account of Creation the Hebrew verb "to form" in Genesis 2:7 is also the technical word used for the potter forming the clay into a vessel.

This book can be unreservedly recommended, despite a few minor errors such as the omission of many of the references given in the main text from the index of names. □

*J. M. Thomas is Professor and Head of the Department of Physical Chemistry at the University of Cambridge.*

## The biology of potassium

Clive Ellory

*Cell Potassium.* By Roderick P. Kerner. Pp.200. (Wiley-Interscience: 1980.) £17.30, \$40.65.

CONTROL of potassium, the dominant intracellular cation, is of fundamental interest and an obvious topic for a monograph. Appearing 15 years after its modest ancestor, *Cell K* (Butterworths, 1965), *Cell Potassium* is a more authoritative work, increased in breadth and depth. The author has retained the general framework, and certain figures and anecdotes are familiar (including the curiously obscure story about the *Discovery's* dredge of sharks' teeth). Plants and geology are discussed first, followed by a useful chapter on measuring techniques, which surprisingly omits any reference to micro-probe analysis. The author is clearly at his happiest dealing with nerve and muscle, providing a good account of anomalous rectification, action potentials and gating currents. The sodium pump is treated competently, at a level high enough to include the occluded K form and conformational states, but without some of the more byzantine complexities of this system (and, thank goodness, no mention of vanadate). LK cells receive flatteringly extensive treatment, which makes the omission of KCl co-transport in avian

erythrocytes and Ehrlich cells more surprising. Similarly, the Gardos effect gets short shrift.

Mitochondrial K movements and the chemiosmotic hypothesis are adequately covered, although a basic revision to refresh the amateur's memory on mitochondrial structure would be of value. This comment applies to other sections of the book; to some extent it appears to be addressed to the already informed, in that a working knowledge of the specific subject being covered is often assumed.

A short chapter is devoted to the important yet neglected role of K as a co-factor in many biochemical systems, before the book closes with a consideration of K in epithelial transport. Extended treatment of the Koefoed-Johnsen-Ussing model is tempered by discussion of other interesting epithelia like that of the cochlea, but the final brief chapter on interactions between body K and pH sits rather uneasily.

Nevertheless this is a scholarly work which, in the most fluent chapters, on excitable tissues, sets a high standard. With its unique thematic approach, it should serve as a useful reference work. □

*Clive Ellory is a Lecturer in the Department of Physiology, University of Cambridge.*

## BOOKS RECEIVED

## Astronomy

- BÖHME *et al.* (eds). *Astronomy and Astrophysics Abstracts*. Vol. 26, Literature 1979, Part 2. Pp.794. ISBN 3-540-10134-9. (Springer-Verlag: 1980.) DM118, \$69.70.
- HÖGNER, W. and RICHTER, N. *Isophotometric Atlas of Comets, Part 1*. Pp.90 (loose-leaf binder). ISBN 3-540-09171-8. (Springer-Verlag: 1980.) DM106, \$62.60.
- HÖGNER, W. and RICHTER, N. *Isometric Atlas of Comets, Part 2*. Pp.55 (loose-leaf binder). ISBN 3-540-09172-6. (Springer-Verlag: 1980.) DM88, \$52.
- WILLIAMS, R.H. (ed.). *Toward a Solar Civilisation*. Pp.251. Flexi ISBN 0-262-23089-5. (MIT Press: 1980.) \$6.95.
- HANES, D. and MADORE, B. (eds). *Globular Clusters*. Based on the Proceedings of a NATO Advanced Study Institute held at the Institute of Astronomy, University of Cambridge, August 1978. Pp.390. ISBN 0-521-22861-1. (Cambridge University Press: 1980.) £27.50.
- ROSSANO, G.S. and CRAINE, E.R. *Near Infrared Photographic Sky Survey: A Field Index*. *Astronomy and Astrophysics Series*, Vol.8. Pp.202. ISBN 0-912918-11-X. (Pachart Publishing: Tucson, Arizona, 1980.) \$38.
- SZOKOLAY, S.V. *World Solar Architecture*. Pp.278. ISBN 0-85139-595-3. (Architectural Press: London, 1980.) £29.95.

## Physics

- ALCÁCER, L. (ed.). *The Physics and Chemistry of Low Dimensional Solids*. Proceedings of the NATO Advanced Study Institute held at Tomar, Portugal, August 1979. NATO Advanced Study Institutes Series C, Vol.56. Pp.436. ISBN 90-277-1144-5. (Reidel: 1980.) Dfl. 95, \$50.
- BARBE, D.F. (ed.). *Very Large Scale Integration (VLSI) Fundamentals and Applications*. *Springer Series in Electrophysics*, Vol.5. Pp.279. ISBN 3-540-10154-3. (Springer-Verlag: 1980.) DM52, \$30.70.
- BASS, R. *Nuclear Reactions with Heavy Ions*. Pp.410. ISBN 3-540-09611-6. (Springer-Verlag: 1980.) DM88, \$52.
- CROXTON, C.A. *Statistical Mechanics of The Liquid Surface*. Pp.345. ISBN 0-471-27663-4. (Wiley-Interscience: 1980.) £25.
- EHRENREICH, H., SEITZ, F. and TURNBULL, D. (eds). *Solid State Physics: Advances in Research and Applications*, Vol.35. Pp.404. ISBN 0-12-607735-5. (Academic: 1980.) \$39.50.
- FISCHER, H. and HELLWEGE, K.-H. (eds). *Magnetic Properties of Free Radicals*. *Atomic and Molecular Physics* Vol.9. Pp.369. ISBN 3-540-09666-3. (Springer-Verlag: 1980.) DM 470, \$277.30.
- GRUBER, B. and MILLMAN, R.S. (eds). *Symmetries in Science*. Proceedings of the Einstein Centennial Celebration Science Symposium held at Southern Illinois University, February 1979. Pp.495. ISBN 0-306-40541-5. (Plenum: 1980.) \$49.50.
- HELLWEGE, K.-H. and HELLWEGE, A.M. (eds). *Magnetic and Other Properties of Oxides and Related Compounds*. *Crystal and Solid State Physics*, Vol.12. Pp.758. ISBN 3-540-09421-0. (Springer-Verlag: 1980.) DM 790, \$466.10.
- HULST, H.C. van de. *Multiple Light Scattering*. Tables, Formulas, and Applications, Vol.2. Pp.739. ISBN 0-12-710702-9. (Academic: 1980.) \$46.50.
- KUBO, R. and HANAMURA, E. *Relaxations of Elementary Excitations*. Proceedings of the Taniguchi International Symposium, Susono-shi, Japan, October 1979. Pp.285. ISBN 3-540-10129-2. (Springer-Verlag: 1980.) DM 72, \$42.50.

## Chemistry

- SCHLUNEGGER, U.P. *Advanced Mass Spectrometry: Applications in Organic and Analytical Chemistry*. Pp.143. ISBN 0-08-023842-4. (Pergamon: 1980.) £12.50.
- THOMAS, J.D.R. (ed.). *Ion-Selective Electrode Reviews*, Vol.1. Pp.279. ISBN 0-08-026044-6. (Pergamon: 1980.) \$43, £19.
- WADE, L.G. Jr and O'DONNELL, M.J. (eds). *Annual Reports in Organic Synthesis-1979*. Pp.461. Flexi ISBN 0-12-040810-4. (Academic: 1980.) Np.

## Technology

- BOCKRIS, J. O'M. *Energy Options: Real Economics and the Solar-Hydrogen System*. Pp.441. ISBN 0-85066-204-4. (Taylor & Francis: 1980.) Np.
- CAPPELLINI, V. and CONSTANTINIDES, A.G. (eds). *Digital Signal Processing: Selected Papers from the International Conference held at the Università di Firenze, Italy, August 1978*. Pp.292. ISBN 0-12-159080-1. (Academic: 1980.) £22.80, \$52.50.
- CRONAN, D.S. *Underwater Minerals*. Pp.362. ISBN 0-12-197480-4. (Academic: 1980.) \$57.50, \$24.80.
- ENGLE, E. and LOTT, A.S. *Man in Flight: Biomedical Achievements in Aerospace*. Pp.396. ISBN 0-915268-28-8. (American Astronautical Society: 1980.) \$20.
- HOLM, H.H. and KRISTENSEN, J.K. (eds). *Ultrasonically Guided Puncture Technique*. Pp.128. ISBN 87-16-8459-4. (Munksgaard: Copenhagen, 1980.) D.kr. 150.
- LEE, K.N., KLEMK, D.L. and MARTS, M.E. *Electric Power and the Future of the Pacific Northwest*. Pp.331. ISBN 0-295-95720-4. (University of Washington Press: 1980.) £10.20.

- LEONDES, C.T. (ed.). *Control and Dynamic Systems. Advances in Theory and Application*, Vol. 16. Pp.371. ISBN 0-12-012716-4. (Academic: 1980.) \$27.50.
- MUJUMDAR, A.S. (ed.). *Advances in Drying*, Vol. 1. Pp.301. ISBN 0-89116-185-6. (Hemisphere: 1980.) \$55.
- MUJUMDAR, A.S. (ed.). *Drying '80*. Vol. 1, *Developments in Drying*. Pp.518. ISBN 0-89116-201-1. (Hemisphere: 1980.) \$62.
- MUJUMDAR, A.S. (ed.). *Drying '80*. Vol. 2, *Proceedings of the Second International Symposium*. Pp.532. ISBN 0-89116-188-0. (Hemisphere: 1980.) \$58.
- O'HANLON, J.F. *A User's Guide to Vacuum Technology*. Pp.402. ISBN 0-471-01624-1. (Wiley-Interscience: 1980.) £13.75.
- WHITEHURST, D.D., MITCHELL, T.O. and FARCASIU, M. *Coal Liquefaction: The Chemistry and Technology of Thermal Processes*. Pp.378. ISBN 0-12-747080-8. (Academic: 1980.) \$19.50.
- WILLIAMSON, R. *Fluorescent Brightening Agents*. *Textile Science and Technology*, 4. Pp.148. ISBN 0-444-41914-4. (Elsevier Scientific: 1980.) £46.25, Dfl.95.

## Computer Science

- DIAMOND, R., RAMASESHAN, S. and VENKATESAN, K. (eds). *Computing in Crystallography*. Lectures delivered at the International Winter School on Crystallographic Computing, Bangalore, India, January 1980. Pp.522. (Indian Academy of Sciences: Bangalore, 1980.) Np.
- HENNEL, M.A. and DELVES, L.M. (eds). *Production and Assessment of Numerical Software*. Based on the Proceedings of the Conference (NS79) held in Liverpool in April 1979. Pp.386. ISBN 0-12-340940-3. (Academic: 1980.) £15, \$34.50.
- HOWARD, J.C. *Practical Applications of Symbolic Computation*. Pp.394. ISBN 0-86103-036-2. (IPC Science and Technology Press: Guildford, 1980.) £20, \$52.
- KAHN, P.M. (ed.). *Computational Probability*. Proceedings of the Conference held at Brown University, Rhode Island, August 1975. Pp.340. ISBN 0-12-394680-8. (Academic: 1980.) \$21.
- PAKER, Y. *Minicomputers: Guidelines for First Time Users*. Pp.250. ISBN 0-85626-184-X. (Abacus: Tunbridge Wells, 1980.) £12.
- YOVITS, M.C. (ed.). *Advances in Computers*, Vol. 19. Pp.351. ISBN 0-12-012119-0. (Academic: 1980.) \$36.50.

## Earth Sciences

- GOWER, A.M. (ed.). *Water Quality in Catchment Ecosystems*. Pp.335. ISBN 0-471-27692-8. (Wiley: 1980.) £18.
- IVES, J.D. (ed.). *Geocology of the Colorado Front Range: A Study of Alpine and Subalpine Environments*. Pp.484. ISBN 0-89158-993-7. (Westview: Boulder, Colorado, 1980.) \$25.
- MARTINEZ, C. *Géologie Des Andes Boliviennes*. Pp.352. Pbk ISBN 2-7099-0565-5. (ORSTOM: Paris, 1980.) Np.
- RONA, P.A. *The Central North Atlantic Ocean Basin and Continental Margins: Geology, Geophysics, Geochemistry and Resources, including The Transatlantic Geotraverse (TAG)*. NOAA Atlas 3. Pp.102. Publication Number: S/N 003-017-00475-9. (US Government Printing Office: Washington DC, 1980.) \$17 (US), \$21.25 (elsewhere).
- THACKRAY, J. *The Age of the Earth*. Pp.36. Flexi ISBN 0-11-884077-0. (HMSO: 1980.) £0.90.

## Biological Sciences

- BRONNER, F. and KLEINZELLER, A. (eds). *Current Topics in Membranes and Transport*, Vol. 14. *Carriers and Membrane Transport Proteins*. Pp.477. ISBN 0-12-153314-X. (Academic: 1980.) \$49.50.
- COLD SPRING HARBOR SYMPOSIA. *Quantitative Biology*, Vol. XLIV. *Viral Oncogenes*. Pp.1322. Two-book set. ISBN 0-87969-043-7. (Cold Spring Harbor Laboratory: New York, 1980.) \$130 (US), \$156 (elsewhere).
- CROSBY, T. K. and POTTINGER, R. P. (eds). *Proceedings of the 2nd Australasian Conference on Grassland Invertebrate Ecology*. Pp.294. Pbk ISBN 0-477-06654-2. (Department of Scientific and Industrial Research: Auckland, New Zealand, 1980.) NZ \$12.
- DAVSON, H. and SEGAL, M. B. *Introduction to Physiology*, Vol. 5. *Control of Reproduction*. Pp.602. ISBN 0-12-206805-X. (Academic/Grune & Stratton: 1980.) £19.20, \$44.50.
- ESSEX, M., TODARO, G. and HÄUSEN, H. Z. (eds). *Viruses in Naturally Occurring Cancers*, Books A & B. *Cold Spring Harbor Conferences on Cell Proliferation*, Vol. 7. Pp.1284. ISBN 0-87969-131-X. (Cold Spring Harbor Laboratory: New York, 1980.) \$125 (US), \$150 (elsewhere).
- FRISTROM, J. W. and SPIETH, P. T. *Principles of Genetics*. Pp.687. ISBN 0-632-00647-1. (Blackwell Scientific: 1980.) \$21.95.
- GOODFELLOW, M. and BOARD, R. G. (eds). *Microbiological Classification and Identification*. The Society for Applied Bacteriology Symposium Series, No. 8. Pp. 396. ISBN 0-12-289660-2. (Academic: 1980.) \$46, £20.
- HARTMAN, W. D., WENDT, J. W. and WIEDENMAYER, F. *Living and Fossil Sponges: Notes for a Short Course*. *Sedimenta VIII*. Pp.274. (Comparative Sedimentology Laboratory: University of Miami, 1980.) Pbk \$11.



LARKIN, P. Pacific Salmon: Scenarios for the Future. Donald L. McKernan Lectures in Marine Affairs. Pp.23. (Washington Sea Grant Publication in cooperation with the Institute for Marine Studies, University of Washington: 1980.) Pbk \$3.

LI, H.-L. Nan-fang ts'ao-mu chuang. A Fourth Century Flora of Southeast Asia. Pp.168. ISBN 962-201-162-2. (University of Washington Press: 1980.) £9.

MAUVIS-JARVIS, P., VICIERS, C. F. H. and WEPIERRE, J. (eds). Percutaneous Absorption of Steroids. Pp.294. ISBN 0-12-480680-5. (Academic: 1980.) £15.60, \$36.

McLOUGHLIN, J. C. Synapsida: A New Look into the Origin of Mammals. Pp.148. ISBN 0-670-68922-X. (Viking: New York, 1980.) \$14.95.

OLSEN, E. G. J. The Pathology of the Heart. 2nd Edn. Pp.402. ISBN 0-333-24265-3. (Macmillan Press: London, 1980.) £35.

PRESCOTT, D. M. and GOLDSTEIN, L. (eds). Cell Biology: A Comprehensive Treatise, Vol. 4. Gene Expression: Translation and the Behavior of Proteins. Pp.496. ISBN 0-12-289504-5. (Academic: 1980.) \$49.

SIGEL, H. (ed.). Metal Ions in Biological Systems Vol. 10. Carcinogenicity and Metal Ions. Pp.408. ISBN 0-8247-6980-5. (Dekker: 1980.) Sw Fr. 115.

STRAULI, P., BARRET, A. J. and BAICI, A. (eds). Proteinases and Tumor Invasion. Monograph Series of the European Organization for Research on Treatment of Cancer, Vol.6. Pp.227. ISBN 0-89004-515-1. (Raven: 1980.) \$21.

TOATES, F. M. Animal Behaviour — A Systems Approach. Pp.299. Hbk ISBN 0-471-27724-X; pbk ISBN 0-471-27723-1. (Wiley: 1980.) Hbk £17; pbk np.

USDIN, E., SOURKES, T. L. and YODIM, M. B. H. (eds). Enzymes and Neurotransmitters in Mental Disease. Based on a Symposium held at the Technion Faculty of Medicine, Haifa, August 1979. Pp.650. ISBN 0-471-27791-6. (Wiley-Interscience: 1980.) £33.50.

WARING, R. H. (ed.). Forests: Fresh Perspectives from Ecosystem Analysis. Pp.210. Pbk ISBN 0-87071-179-2. (Oregon State University Press: 1980.) \$12.

WILDENTHAL, K. (ed.). Degradative Processes in Heart and Skeletal Muscle. Research Monographs in Cell and Tissue Physiology, Vol. 3. Pp.461. ISBN 0-444-80235-5. (Elsevier/North-Holland Biomedical: 1980.) \$95, Dfl. 195.

WILLIAMS, P. L. and WARWICK, R. (eds). Gray's Anatomy. 36th Edn. Pp.1578. ISBN 0-443-01505-8. (Churchill Livingstone: 1980.) £32.

## Applied Biological Sciences

AMES, B., INFANTE, P. and REITZ, R. (eds). Ethylene Dichloride: A Potential Health Risk? Banbury Report, 5. Pp.325. ISBN 0-87969-204-9. (Cold Spring Harbor Laboratory: New York, 1980.) \$45 (US), \$150 (elsewhere).

FINK, B. R. (ed.). Progress in Anesthesiology, Vol. 2. Molecular Mechanisms of Anesthesia. Pp.528. ISBN 0-89004-456-2. (Raven: 1980.) \$48.50.

HENNINGSEN, B., LINDER, F. and STEICHELE, C. (eds). Endocrine Treatment of Breast Cancer: A New Approach. Recent Results in Cancer Research, 71. Pp.225. ISBN 3-540-09781-3. (Springer-Verlag: 1980.) DM 80, \$47.20.

HERBERMAN, R. B. (ed.). Natural Cell-Mediated Immunity Against Tumors. Pp.1321. ISBN 0-12-341350-8. (Academic: 1980.) \$65.

HURD, R. G., BISCOE, P. V. and DENNIS, C. (eds). Opportunities for Increasing Crop Yields. From Proceedings of a Meeting held at the University of Reading, September 1979. Pp.410. ISBN 0-273-08481-X. (Pitman Advanced Publishing Program: 1980.) Np.

McCONNELL, P. S. *et al.* (eds). Adaptive Capabilities of the Nervous System. Progress in Brain Research, Vol. 53. Proceedings of the 11th International Summer School of Brain Research, held at the Royal Netherlands Academy of Sciences, 1979. Pp.445. ISBN 0-444-80207-X. (Elsevier/North-Holland Biomedical: 1980.) \$92.25, Dfl. 189.

SANDLER, J. Psychopharmacology of Alcohol. Pp.294. ISBN 0-89004-506-2. (Raven: 1980.) \$27.

SOKOL, G. H. and MAICKEL, R. P. (eds). Radiation-Drug Interactions in the Treatment of Cancer. Pp.235. ISBN 0-471-04697-3. (Wiley: 1980.) \$16.

ZADUNAISKY, J. A. and DAVSON, H. (eds). Current Topics in Eye Research, Vol. 3. Pp.336. ISBN 0-12-153003-5. (Academic: 1980.) \$35.

## Psychology

BROOKS-GUNN, J. and MATTHEWS, W. S. He and She: How Children Develop Their Sex-Role Identity. Pp.338. Hbk ISBN 0-13-384388-2; pbk ISBN 0-13-384370-X. (Prentice-Hall International: 1980.) Hbk £8.40; pbk £4.50.

FOSTER, M. L. and BRANDES, S. H. (eds). Symbol as Sense: New Approaches to the Analysis of Meaning. Pp.416. ISBN 0-12-262680-X. (Academic: 1980.) \$35.

MENDLEWICZ, J. and VAN PRAAG, H. M. (eds). Psychoneuroendocrinology and Abnormal Behavior. Advances in Biological Psychiatry, Vol. 5. Pp.130. Flexi ISBN 3-8055-0599-X. (Karger: Basel, 1980.) Sw Fr. 58, DM 69, \$34.75.

## Sociology

AUSUBEL, J. and BISWAS, A. K. (eds). Climatic Constraints and Human Activities. Task Force on the Nature of Climate and Society Research, February 1980. IASA Proceedings Series, Vol. 10. Pp.205. ISBN 0-08-026721-1. (Pergamon: 1980.) £13, \$30.

VEROFF, J. and VEROFF, J. B. Social Incentives: A Life-Span Developmental Approach. Pp.311. ISBN 0-12-718750-2. (Academic: 1980.) \$23.

## History of Science

CAMERON, I. To the Farthest Ends of the Earth: The History of the Royal Geographical Society, 1830-1980. 150 years of World Exploration. Pp.288. ISBN 0-354-04478-8. (MacDonald & Jones: London, 1980.) £10.95.

GURZADYAN, D. A. Flare Stars. International Series in Natural Philosophy. Volume 101. Pp.xiv + 344. ISBN 0-08-023035-0. (Pergamon Press: Oxford and New York, 1980.) \$50 (approx. £25).

HOWSE, D. Greenwich Time, and the Discovery of Longitude. Pp.254. ISBN 0-19-215948-8. (Oxford University Press: Oxford, 1980.) £7.95.

STEGMÜLLER, W. Neue Wege der Wissenschafts-philosophie. Pp.vi + 198. ISBN 3-540-09668-X. (Springer-Verlag: New York, 1980.) DM49, \$27.50.

TRUSTED, J. The Logic of Scientific Inference: An Introduction. Pp.145. ISBN 0-333-26669-2. (Macmillan: London, 1980.) Hbk £8.00; pbk £3.95.

## Anthropology

ALTMAN, I., RAPOPORT, A. and WOHLWILL, J. F. (ed.) Human Behavior and Environment. Advances in Theory and Research Volume 4. Environment and Culture. Pp.xvi + 351. ISBN 0-306-40367-6. (Plenum: New York and London, 1980.) £25.

## General

ABRECHT, P. Faith and Science in an Unjust World. Report of the World Council of Churches' Conference on Faith, Science and the Future. Vol. 2, Reports and Recommendations. Pp.214. Flexi ISBN 0-8006-1391-0. (Fortress Press: Philadelphia, 1980.) £6.95.

ALLABY, M. and BUNYARD, P. The Politics of Self-sufficiency. Pp.242. Hbk ISBN 0-19-217695-1; pbk ISBN 0-19-286005-4. (Oxford University Press: 1980.) Hbk £7.95; pbk £3.95.

BACH, W. *et al.* (ed.) Renewable Energy Prospects. Pp.340. ISBN 0-08-024252-9. (Pergamon: Oxford and New York, 1980.) £18, \$50.

BOUTH, B. and FITCH, F. Earth Shock: Can the Earth Survive its Natural Catastrophes? Pp.327. ISBN 0-7221-1778-9. (Sphere: London, 1980.) £1.50.

CONNORS, C. K. Food Additives and Hyperactive Children. Pp.xv + 167. ISBN 0-306-40400-1. (Plenum: New York and London, 1980.) \$18.50.

DODGSON, R. A. The Origin of British Field Systems: An Interpretation. Pp.164. ISBN 0-12-219260-5. (Academic: 1980.) £9.40, \$22.

DYKE, B. and MORRILL, W. T. (eds). Genealogical Demography. Population and Social Structure. Advances in Historical Demography. Pp.255. ISBN 0-12-226380-4. (Academic: 1980.) \$19.50.

EMERSON, V. J. *et al.* The Measurement of Breath Alcohol: The Laboratory Evaluation of Substantive Breath Test Equipment and the Report of an Operational Police Trial. Pp.70. ISBN 0-9502425-78. (Forensic Science Society: Harrogate, 1980.) £10, \$25.

FOSTER, D. W. A Layman's Guide to Modern Medicine. Pp.398. ISBN 0-671-23466-7. (Simon & Schuster: New York, 1980.) \$14.95.

FOX, M. W. Returning to Eden: Animal Rights and Human Responsibility. Pp.281. ISBN 0-670-12722-1. (Viking: New York, 1980.) \$13.95.

KAPLAN, H. B. Deviant Behavior in Defense of Self. Pp.255. ISBN 0-12-396850-X. (Academic: 1980.) \$22.

LI, A. K. C., WILLS, M. R. and HANSON, G. C. Fluid, Electrolytes, Acid-Base and Nutrition. Pp.80. Flexi ISBN 0-12-448150-7. (Academic: 1980.) £3.40, \$8.

LONNROTH, M., STEEN, P. and JOHANSSON, T. B. Energy in Transition: A Report on Energy Policy and Future Options. Pp.197. ISBN 0-520-03881-9. (University of California Press: California, 1980.) \$10.95.

LOXTON, J. Practical Map Production. Pp.137. Hbk ISBN 0-471-27782-7; pbk ISBN 0-471-27783-5. (Wiley: 1980.) Hbk £8.50; pbk np.

MCLACHLAN, G. (ed.). The Planning of Health Services. Studies in Eight European Countries. Pp.252. Flexi ISBN 92-9020-195-9. (WHO: Copenhagen, 1980.) SW Fr. 20.

MEDVEDEV, R. On Soviet Dissent. Pp.158. ISBN 0-09-463870-5. (Constable: London, 1980.) £5.95.

MOORE, Tui De Roy. Galapagos: Islands Lost in Time. Pp.160. ISBN 0-670-33361-1. (Viking: New York, 1980.) \$25.

PALMORE, E. (ed.). International Handbook on Ageing: Contemporary Developments and Research. Pp.529. ISBN 0-333-27823-3. (Macmillan Press: London, 1980.) £30.

PAYNE, J. P. and BUSHMAN, J. A. (eds). Artificial Ventilation: Technical, Biological and Clinical Aspects. Based on the Proceedings of a Symposium held at Chartridge, June 1978. Pp.164. ISBN 0-12-547960-3. (Academic: 1980.) £13.40, \$31.

SHINN, R. L. Faith and Science in an Unjust World. Report of the World Council of Churches' Conference on Faith, Science and the Future. Vol. 1, Plenary Presentations. Pp.392. Flexi ISBN 0-8006-1390-2. (Fortress Press: Philadelphia, 1980.) \$12.95.

SIMON, J. Middle East Health: The Outlook After 30 Years of WHO Assistance in a Changing Region. Pp.133. (WHO: Alexandria, Egypt, 1980.) Flexi np.

SPENCE, C. C. The Rainmakers: American "Pluviculture" to World War II. Pp.181. ISBN 0-8032-4117-8. (University of Nebraska Press: 1980.) £9.60.

ZORZA, R. and M. A Way to Die; Living to the End. Pp.254. ISBN 0-233-97355-9. (André Deutsch: 1980.) £5.95.

4 December 1980

# Harvard backs off recombinant DNA

Harvard University's decision (see *Nature* 27 November) not to become a minority partner in a commercial venture to exploit recombinant DNA technology will have more than merely parochial consequences. Although it is probably no longer the case that universities in the United States and even elsewhere take their cues from what Harvard does, the public agony in which the university has come to its decision cannot fail to be instructive. Naturally, different universities will interpret events since the beginning of the term in October in different ways. Some will say that what has happened only goes to show that Harvard is the stuffy, or indecisive, place they have always supposed it to be. Others will be confirmed in their conviction that commerce does not mix with academic life. Harvard itself may be surprised to discover that the issue which it has been debating for the past two months has stirred up other and less tractable issues that will themselves keep both the administration and the faculty on tenterhooks for some time to come. What are the circumstances in which academic institutions may properly take a commercial interest in the academic research of members of their faculties? What limits should there be on the entrepreneurial interests of members of university staffs? And what arrangements do universities need for regulating these questions? Plainly there is a long agenda ahead.

The events of the past few months at Harvard are not without interest in themselves. The tale goes back to the beginning of this year, when small companies for the exploitation of recombinant DNA were springing up all over the place. One of the Harvard faculty, Professor W. Gilbert, was already a prominent member of the company called Biogen which held a press conference in Boston to make public its plans for using cloning techniques for the manufacture of interferon. Some of Gilbert's Harvard colleagues were even then disturbed at the implications of his involvement with a commercial company in such a prominent way. For although Harvard is probably more rigorous than most other distinguished universities in making sure that members of the faculty do not spend more than a limited proportion of their time on extramural activities, people were concerned that the work of one of their most creative colleagues (Gilbert shared this year's Nobel prize for chemistry) might in future be less freely shared within the university. The proposal that the university should become a minority shareholder (without paying for its shares) in a commercial company to exploit recombinant DNA techniques was at least in part inspired by the hope of doing the same thing while benefiting the university in some tangible way. The plan was that research carried out in Professor Mark Ptashne's laboratory should be exploited by a new company financed by venture capital, managed and housed separately from the university but from which the university would derive a substantial income. The university administration seems from the beginning to have been keen on the prospect of an alternative source of income. If it had seemed less greedy, the Faculty of Arts and Sciences might have been less quick to take fright. But, in the end, the proposal foundered on the faculty's misgivings. For a time, Cambridge (Massachusetts) seems to have been thick with anxiety about secrecy, academic freedom and the like, but perhaps the clinching argument against the commercial venture was that the university could not, in the arrangements proposed, avoid discriminating in favour of those on whose research its financial prospects seemed to depend. In a college of supposed equals, some would be more equal than others.

Such issues are familiar stimulants of cant, and even Harvard's

internal argument appears not to have been entirely blameless in this respect. Talk of academic freedom jeopardized would have been more persuasive if those professing concern for this lofty cause had been able to specify what specific freedom might be lost. It is also important to acknowledge that both Gilbert and Ptashne have been entirely open with their colleagues (and with outsiders) about their motives. Indeed, it is ironical that Ptashne, the latecomer in commercial matters, should now be widely identified with a project which the university has flirted with but dropped. Meanwhile, the serious questions the Harvard faculty has been asking about the entrepreneurial role of universities, or of members of their faculties, remain unanswered.

There is one important respect in which the issue is already decided. Since 1975 and the change in that year in the rules for the ownership of patents deriving from research carried out with research grants from the National Institutes of Health, Harvard (like other American universities) has become a substantial patent holder. The new rule is that universities can acquire the rights in patentable inventions arising within their laboratories if they can somehow persuade those responsible to apply for legal protection. Experience, not only at Harvard, has shown that little benefit accrues to anybody — the university or even the public — if a patent holder simply sits on his patent. Exploitation requires flair, finance and a keen sense for dollar bills (or for whatever other currency may be concerned). Even well organized universities in the United States are probably less commercially effective at making money out of patents than would be strictly commercial organizations. (In Britain, where the National Research Development Corporation is the public patent holder on behalf of academics and their universities, complaints are common that more might be done to make money out of people's cleverness.) In a sense, Harvard's proposed venture into biotechnology was merely an extension of its established role as a patent holder. On the face of things, moreover, the university was not being asked to back the new company with funds of its own. Yet there is a difference of principle between earning royalties on a set of patents and being a shareholder in a company. Substantial shareholders, however cheaply acquired their equity, must take a serious interest in the management of their companies — and must be prepared, when things go wrong, to step in quickly with extra funds. There is no reason to suppose that Harvard would be any more able to shoulder these responsibilities than other universities. Indeed, given the way in which at Harvard the administration's power of decision is rightly blunted by the veto powers distributed among the several faculties, Harvard is not everybody's favourite business partner.

There is also force in the argument, much canvassed in the past two months, that a university cannot enter into a risk-taking business partnership with some section of its own faculty without resolving the obvious difficulties in advance. Whatever the terms of the partnership, success is certain to engender a pattern of importance within the faculty that reflects considerations other than academic merit. Ptashne, no doubt, would argue that arrangements could have been made for avoiding such problems; a faculty as vigilant as that at Harvard is unlikely to have allowed the university administration to favour him and his immediate colleagues with extra space and resources, however successful the new venture. The more serious problems would have arisen if the venture seemed to be failing. Would it then have been possible for either partner to have behaved as if only academic business mattered? This is the sense in which joint involvement in a



commercial company differs from the sale and exploitation of patent rights, however profitable. The circumstances in which universities may properly set up commercial companies to exploit work of their faculty members are thus easily defined. Success must not depend on future promise, and there must be no foreseeable circumstances in which an academic will feel compelled to function as the research or even marketing director of a company if things should start going wrong. The academic freedom most at risk is that of the academics who are most directly involved.

A further difficulty, which persists even though the university has said no to its commercial venture, is that the laboratories of individual professors will continue to be sources of research with entrepreneurial potential. Even if Ptashne decides not to go ahead independently of the university, Gilbert as a member of Biogen will no doubt remain on the lookout for ideas that can be exploited commercially. No doubt he will be as anxious as his academic colleagues that he should never be open to the charge of making inequitable use of his position, and of his access to university facilities. The most immediate cause for concern must be the graduate students working in his and other people's laboratories. Graduate students are called students because the university to which they belong is responsible for their further education, and the formalities of registration for higher degrees reflect that understanding. There is, however, an obvious danger that in the present excitement about recombinant DNA, the Gilberts and Ptashnes of this world, but also their graduate students, will put commerce before education. Having said no to the university's proposal, the Harvard faculty now has no choice

but to make more explicit its corporate responsibility for graduate students.

In the long run, Harvard will find it necessary to take a further and more painful step. A university is a kind of club of academics, kept together by mutual respect. Academics' external interests are by no means always destructive of that spirit. Academics who serve their governments, who write good literature or who add to the public enlightenment in other ways, often by doing so enhance the esteem in which they are held by their colleagues and in which their university is held by the wider public. Naturally, most universities have explicit rules for making sure that academics are not so caught up in extramural activities that they have insufficient time for their students, but there are other less formal constraints to be reckoned with. The worst offence an academic can commit against his colleagues is to abuse his position as a member of his academic club.

Yet universities (like other kinds of clubs) differ in their unspoken definitions of what constitutes abuse. Even at Harvard, it seems to be accepted that within reason people should be able to advise commercial companies. The problem of the faculty member as entrepreneur in the exploitation of his own research seems not previously to have arisen as sharply as in the past few months. (At some other universities, it is commonplace.) The Harvard faculty seems to have been taken by surprise. It has only itself to blame for not having made its unspoken rules explicit long ago. What it needs now is a general understanding that people's extramural activities and the financial gains therefrom are fully disclosed within the faculty, and are proper material for faculty discussion and even decision.

## How not to run a public monopoly

The British government's proposals for the reorganization of the British Post Office (see *Nature* 27 November) seem calculated to win the worst of all possible worlds for everybody concerned, but the hapless users of telecommunications systems in particular. The chief purpose of the bill soon to begin its passage through the House of Commons is to separate the postal service from the rest of this nationalized industry, and there is no argument about the wisdom of that course. Indeed, for more than a decade the Post Office has been organized internally as if it were two organizations — a loss-making postal service and a money-making telecommunications service. Three years ago, Sir Charles Carter's committee on the problem told the government that it should go the whole way along this road, and formally split the two parts of the business. Everybody agrees that this should be done. But how?

The issue is important for several reasons, but not least because of the technical importance of the telecommunications industry to the wealth (and even the health) of a modern state. For far too long, Britain has been badly served by the electronic half of the Post Office. When other countries were installing modern and increasingly versatile telephone systems, would-be British users were forced to wait, often for more than a year, for the privilege of renting an antiquated handset. From time to time, bursts of excitement would nevertheless filter out of the British government's public relations network, explaining that this or that new miracle was about to be brought into service. In the late 1950s, for example, the "world's first" electronic exchange was being praised to the skies. Unfortunately, it never worked. More recently, with the new internal arrangements at the Post Office, there has been discerned a sense of realism. The managers of the telecommunications network have plainly begun to come to grips with the nature of their business. Keeping up with the Joneses (or the Japanese) technically is much more difficult than it seemed in the old days, when the Post Office would draft a specification for some new system and farm out the development and manufacture of the equipment to a cosy cartel of manufacturers. But the technical problems are not even half the battle. Managing a complicated telecommunications network is hair-raising.

Meeting the cost of developing a modern network is an exercise in high finance.

In all the recent discussions about the British Post Office, it has been plain that the crucial question to decide is where the line should be drawn between the public monopoly and private enterprise. Again, there is no dispute about the good sense of monopoly ownership and management of the telecommunications network. Every modern state has been driven to recognize as much. The questions that arise concern the definition of the monopoly at its margins, and the arrangements for its regulation. In Britain, there has been a lot of excited talk (encouraged by Sir Keith Joseph the industry minister) about the shading of the telecommunications monopoly. There are two respects in which this might with advantage be done. There is a need that those who rent access to telephone lines or other channels of communication should be allowed to attach to them whatever terminal equipment they choose, provided it is technically compatible with the network (and also legal). For no single organization, however competent (and British Telecom has a great deal of depressing history to live down), can hope itself to supply everything that users of the network are likely to need in the decades ahead. But the network (whatever it is) should also be usable by people prepared to offer services that the monopolists themselves choose not to offer.

Sir Keith Joseph's reorganization bill fudges both these issues. British Telecom will not have an exclusive right to supply all terminal equipment, but it will be dragged in if an attachment has to be serviced, while the minister's own civil service will assume some of the responsibility for telling what attachments can be attached. And yes, there will be arrangements for letting private people use the network for providing novel services, but again the details are not worked out and the minister's civil servants will again decide. The consequences of these un-Tory compromises are potentially disastrous. Neither British Telecom, the users of the network nor manufacturers of equipment will know where they stand, but crucial decisions about the development will return from whence they came several years ago — to the civil service.

# Anti-trust waiver for industrial research

## Justice blesses inter-company collaboration

Washington

The US Department of Justice has given the green light to research programmes jointly sponsored by two or more private companies, arguing that in general — and provided certain criteria are respected — these should not conflict with the country's strict anti-trust legislation.

Uncertainty about the implications of anti-trust laws is often cited by US business as an obstacle to greater cooperation in research. Their concern is that, once a joint research project has been agreed and set up, they may be accused of violating legislation developed to ensure maximum competitiveness between rival companies.

As a result, anti-trust legislation was closely studied during last year's domestic policy review of industrial innovation, carried out under the auspices of the Office of Science and Technology Policy (OSTP) and the Department of Commerce.

Announcing the results of this review last November, President Carter said that by spurring competition, anti-trust policies could provide a stimulant to innovation, but he added that in some cases — such as research — industrial cooperation might have clear social and economic benefits for the country.

"Unfortunately our anti-trust laws are often mistakenly viewed as preventing all cooperative activity", Mr Carter said. And, rather than proposing any change to the law, he instructed the Department of Justice to publish a guide explaining its interpretation of the laws that already exist.

The guide was finally published in Washington last week. It is now being closely studied by companies and research associations contemplating joint research ventures, since, although not a legally binding document, it indicates how the department is likely to react to particular arrangements.

The guide should also help to clear the way for the creation of so-called Cooperative Generic Technology (COGENT) centres. These have been proposed by the Department of Commerce and the National Science Foundation, jointly funded by government and various industrial companies in fields such as welding, lubrication and powdered metal processing. The idea was approved by Congress in recently passed legislation.

The guide points out that there are various ways in which joint research

ventures could involve anti-trust considerations. For example, they could lead to market-dominating technology, to unfair collaboration between commercial competitors or to restrictive agreements on the use of research results.

Each of these might restrict open competition. At the same time, the guide says, competitiveness is a source of increased innovation — while innovation itself is a basis for commercial competitiveness — so that to discourage the one is to discourage the other.

So the challenge is to develop an arrangement that will maximize the rate of innovation (and hence competitiveness) by permitting research that would not otherwise be carried out, but in a way that does not give one or more companies an

unfair advantage over others in the same field.

Rather than providing any hard and fast rules on how this should be done, the Department of Justice offers general guidance on how it would probably interpret existing statutes in particular situations. And it includes eight hypothetical case studies intended to illuminate its position.

As far as basic research is concerned, the department says that cooperation is unlikely to be much of a problem, since the competitive significance of the research is likely to be largely speculative and, as the results would be published in the open literature, there should be few problems about equal access by other companies.

David Dickson

## Science foundation all set at last

Washington

As widely expected, the US National Science Foundation (NSF) has announced its intention to set up a new directorate for engineering, and to distribute responsibility for applied science — at present administered jointly with engineering — across the foundation's basic science directorates.

Announcing the planned reorganization to members of the National Science Board last week, NSF's director-designate, Dr John Slaughter, said that creating the new directorate meant that the foundation intended to seek more resources for the engineering disciplines.

The reorganization is the result of discussions that have been taking place within NSF since early in the summer, and are partly in response to outside criticism that NSF has not been doing enough to encourage engineering research, with the result that engineering has suffered in comparison with more traditional basic science disciplines.

At the same time, NSF has dropped a proposal that had also been under discussion to set up a new directorate for social science, at present linked with the biological and behavioural sciences. Although many researchers had argued that such a move could help to enhance the academic status of social science research, administrators had voiced fears that it might increase the visibility of the social science research budget — and hence its vulnerability to congressional budget cuts.

According to Dr Slaughter, the new reorganization means that although basic research remains the central mission of NSF, the base of support for applied research will be broadened, since all research directorates will now support applied research projects while keeping their basic research programmes more or less in being.

In addition, the reorganization would

give new emphasis to engineering research and education, Dr Slaughter told the members of the National Science Board, which is formally responsible for the activities of NSF and had previously endorsed the reorganization proposals.

NSF officials hope that, by giving engineering research a new emphasis, they will be able to head off plans to set up a National Technology Foundation, contained in a bill introduced to the House of Representatives by Mr George Brown, chairman of the House Science and Research Subcommittee.

In a letter to Dr Donald Langenberg, acting NSF director, Mr Brown said that Congress might conclude, in studying the technology foundation concept, that "existing mechanisms to improve the state of technology are not able to handle current challenges, and that major programme dislocations are not too high a price to pay for a fundamental programme reorientation".

Several members of the engineering research community, while welcoming NSF's greater emphasis on engineering, have been saying that this will only improve the situation for engineering research, which now receives only about 10 per cent of the NSF's budget, if it results in more money being made available by Congress.

David Dickson

## Nuclear power

## Border problems

Brussels

France's policy of siting nuclear power stations on its frontiers has aroused antagonism both in the European Parliament and among environmental groups. The European parliament met on 19 November to discuss a report by Mechthild von Alemann (German, Liberal) which reflected the concern over the French government's plans to build



further power stations at Chooz and Cattenoom, close to the Luxembourg and Belgian borders.

The previous day, environmental groups from Luxembourg, France and Belgium had called a press conference in Luxembourg and denounced the French government's total disregard for the principles and rules of international law. The French, however, are not the only culprits. Of the 120 or so nuclear power stations at present in operation, under construction or planned in the European Community, 33 are less than 25 miles from national borders and another 15 are less than 6 miles from borders.

Von Alemann's report urges the introduction of Community safety norms and the implementation of a Community consultation procedure, bolstered by an EEC regulation. During the debate many speakers called for a broader interpretation of Articles 37 and 41 of the Euratom Treaty. These relate to the obligation of member states to supply the European

Commission with all data on radioactive effluent capable of causing pollution and details of all future plans for nuclear power stations.

French parliamentarians of all political hues united against the attack, claiming that it compromised national sovereignty. Pierre Calvez (French, Liberal) said he was opposed to any Community decision which transcended national policy. He added that all new power stations were subject to bilateral agreements and international regulations.

Speaking on behalf of the European Commission, acting Energy Commissioner Etienne Davignon declared that France had not infringed the Euratom Treaty and that the treaty could not be interpreted in such a light as to give the Commission the right to interfere.

Stanley Johnson (UK, Conservative) reminded the parliament of the fate of the so-called Sèvres Directive at the last meeting of the Environment Council in June. The draft directive on the prevention of major accidents was not adopted because the French objected to the provisions for transboundary notification procedures. A compromise formula over this problem is now being thrashed out and it is hoped that the next council meeting on 12 December will adopt the text.

The EEC's energy ministers, when they met in Brussels on 27 November, briefly discussed the problems associated with the siting of nuclear power stations near boundaries. The draft regulation on the Community consultation procedure for electricity power stations that affect the territory of another member state has been held up in the council for several years. It now seems likely that this regulation will be looked at more seriously and its progress accelerated.

**Jasper Becker**

### Soviet health

## More research

A high-level cooperation programme between Soviet scientists and doctors will be an important feature of the next Five Year Plan for public health. This was decided by a joint session of the Academy of Sciences and the Academy of Medical Sciences last month. An interdepartmental scientific council is to be established, and a joint research programme is being drawn up. This says Academician Anatolii Aleksandrov, president and chairman of the new council of the Academy of Sciences, will reflect the main problems in public health and take into account the potential of the country's scientific institutes.

Aleksandrov reported that cooperation between scientists and medical teams has already led to some major advances, including medical applications of ultrasonics, cryogenics and laser technology. The Minister of Public Health, Boris Petrovskii, spoke warmly of the raised standards of diagnosis and

treatment made possible by the introduction of new techniques in cardiology, oncology, surgery, paediatrics and pharmacology.

Molecular biology, which until the mid-1970s was neglected in the Soviet Union, received a glowing tribute from Dr. Nikolai Blokhin, President of the Academy of Medical Sciences. Recent results, he said, opened up prospects for the establishment of new ideas about the nature of viruses, malignant changes in cells, human heredity and the development of genetic engineering techniques. Other innovations are less welcome. The Marxist-Leninist world outlook, said Blokhin, protected Soviet medicine from mysticism, parapsychology, the psychosomatic theories of Freud, various types of neo-Freudianism and other "views that could lead medicine astray". He called therefore for greater cooperation between medical workers and representatives of the philosophical institutes of the Academy of Sciences.

**Vera Rich**

### Polish science

## Advice not taken

The Gierek regime consistently "torpedoed or disavowed" constructive criticisms from its nine-person team of scientific advisers. So claims Professor Alojzy Melich, a member of the team since its inauguration in 1977, in an interview in *Trybuna Robotnicza*, the daily paper of Katowice (Mr Gierek's home power-base).

Professor Melich said that during the past three years, the team had prepared about a dozen comprehensive surveys on the main problems facing the country, as well as numerous smaller papers and analysis. These, however, were rejected by the government and the planning commission, simply because they attacked current policies. In the end, Professor Melich said, the government simply stopped providing its scientific advisers with any information at all.

This is not the first such accusation to be levelled in recent months. In August, an *ad hoc* farmers' committee which has since become the nucleus of the farmers' campaign for trade union representation, accused the authorities of suppressing expert reports on the deterioration of Polish agriculture. Unlike most critics, however, Professor Melich did not condemn Mr Gierek's policy of obtaining massive foreign loans to back his investment projects; these, said Melich, had provided an important stimulus for the economy.

The current economic crisis, however, has meant that the future of many major investment projects has become doubtful. Even the much hailed Programme-Wisla is liable to suffer some cutbacks at least for the present. This scheme, which was envisaged as a major contribution to Poland's economy in the twenty-first century, consists of a broad range of water-

### French take Manhattan

A French firm has stormed the US optical communications market — and installed a 6.5-km optical fibre system in Manhattan. CIT-Alcatel, the leading French telecommunications company, announced last week that it had beaten off competition — including the giant ITT — to supply the link to Western Union cable and telegraph company. They system will be the first fully operational optical fibre link in the United States CIT officials believe.

CIT will also supply the second such link, an experimental one which the company sold to Western Union a year ago. When the new link, which uses light emitting diodes to convert electrical signals into light, goes into operation in January, the experimental link (which uses laser diodes) will also be put into regular use. CIT will thus gain operating experience with the two principal competing technologies for optical fibre input.

The great advantage of optical fibre systems for Manhattan is that available cable ducts under the city are physically crammed to capacity, and it is now almost impossible to feed through standard electrical links. Optical fibre links, however, can be made on cables 10 times smaller in outer diameter — allowing a hundredfold increase in channel capacity for the same duct cross-section.

The CIT system uses cables, supplied by another company, of 1 cm outer diameter to carry 44 megabits per second (672 telex channels). CIT supplied the input-output devices and the data management systems for the link. CIT considers that this first step in the US market is "fundamental" and that the potential scale of the market is "huge".

**Robert Walgate**

## Cable of protest

One hundred and six Fellows of the Royal Society, including four Nobel Prize Winners, (Sir Nevill Mott, Sir Max Perutz, Sir George Porter, and Dr Fred Sanger) have sent the following telegram to the Soviet Delegation to the Madrid Review Conference.

"The arrest of Dr Brailovskii is a cause of great concern which can only harm further scientific exchange between our countries."

Viktor Brailovskii, arrested on 13 November, the day after the opening of the Madrid Conference, is thought to be facing charges under Article 191/1 of the Soviet Penal Code: Disseminating information known to be false and detrimental to the Soviet Union and socialist system. His detention, however, seems to be linked with his activity as host to the Sunday seminars for Jewish refusenik scientists in Moscow. Last week, his wife was warned by the security authorities not to try to go ahead with the seminar. When, on Sunday, she attempted to hold the seminar, intending participants were prevented by the police from entering the apartment.

In Washington last Sunday, the Committee of Concerned Scientists organized a seminar on the style of the Moscow seminar. A paper was read by Dr Maxine Singer who earlier this year was refused a visa to visit Moscow, where she had intended to visit the Brailovskii seminar. Several of the participants had read papers at the Brailovskii seminar during professional visits to Moscow. It is hoped to hold such seminars every Sunday in various US academic centres.

An international delegation of scientists, led by the French Nobel Laureate Andre Lwoff, who is a corresponding member of the Soviet Academy of Medical Sciences, is seeking a meeting with Ilichev, head of the Soviet delegation in Madrid, to discuss the Brailovskii case.

Vera Rich

managed developments, ranging from recreation to heavy transport, with canal links through the Soviet Union and East Germany. Such a major project cannot, of course, be simply abandoned, but as the press spokesman for the programme recently pointed out, it is a complex plan, the implementation of one part does not necessarily depend on that of another, and, in any case, the announced completion deadline of the year 2000 had rather "symbolic" significance. Nevertheless, he said, the country simply cannot afford *not* to implement some parts of the scheme as soon as possible — the anti-pollution and water-storage proposals which will be vital in the next few years if the country's agriculture and industry are to recover.

A similar stance was adopted recently in the *Sejm* (Parliament) by Deputy Zbigniew Kledecki. Speaking on the pollution of the

Krakow area by the Nowa Huta steel mills and the Skawina aluminium plant, he stated that the cost of installing modern, non-polluting equipment would be 120 million zloty (£2 million) at Nowa Huta and 7,500 million zloty (£125 million) at Skawina. Nevertheless, he said, in view of the grave pollution hazards and the "critical attitude of community scientists and journalists in Krakow", preparatory work on modernizing the plants would begin next year.

Important as such major investments still may be, the most immediate investment problem is that of agriculture. Recent pledges by the Minister of Agriculture, Leon Klonica, include an increase in the production of plant protection chemicals, and fertilizers, investments in land-improvement, development of an intermediate technology suitable for small farms, changes in the supply and pricing system to aid the private farmer, and a relaxation of central arbitrary planning in agriculture. These last points, which are a considerable reversal of recent policy, have been welcomed by the farmers with cautious approval.

Vera Rich

## Brazilian universities

### No cash ahead

Sao Paulo, November

Inflation and a lack of sympathy from the state government have forced the University of São Paulo (USP), Brazil's oldest university and one of its best, into a serious crisis. But the crisis is not confined to São Paulo. All government-supported universities face difficulties over dwindling budgets. Academics throughout Brazil have been protesting about the lack of resources by holding a series of one or two-day stoppages, the latest at the beginning of this month.

The academics' complaint is that the state and federal governments have made the universities take an unfair share of public expenditure cuts and have thus neglected the country's long-term future in the panic to service Brazil's massive foreign debt and oil import bill. This results in the universities having virtually no money for new building and very little for buying and maintaining equipment.

The most serious complaint, however, is the effect of inflation on academic salaries, which have recently been increasing at only about half the rate of inflation and which are corrected only once a year. (The academics are asking for termly readjustment.) The lack of money available for salaries has meant that some academics have to turn to part-time and piecemeal teaching. Many academics can get contracts for only 20 hours a week and have to eke out a living by other means. But even those with 40-hour contracts are finding it necessary to look for ways of topping up their incomes.

Salary problems seem to vary from one

university to another and depend on how individual funds are administered. Some federal universities, called *fundações*, are allowed to keep their own trust funds which are being used to top up salaries, but others, the *autarquias*, are strictly limited to paying agreed government salaries only. For those in the humanities in the *autarquias*, the outlook is bleak, but for scientists there is a chance of extra support from the national research councils, which have recently started to top up researchers' salaries as well as making research grants. The budgets of the research councils have not, however, stretched to helping every scientist worthy of support.

The number of applications made to the main research council, the Conselho Nacional de Desenvolvimento Científico e Tecnológico (CNPq), for grants to supplement salaries increased dramatically in 1980. The CNPq estimates that it is now supplementing about 2,200 scientists' salaries and that its sister organizations may be supplementing as many as 3,000. Most notable, says the CNPq, is the large increase in applications from the University of São Paulo.

For federal universities, the CNPq is confident that the problem is only temporary and that the salaries problem will be alleviated by the beginning of the next academic year in March. The University of São Paulo, however, cannot necessarily expect such a reprieve. Its finances are controlled by the government of the state of São Paulo which allocates the budget annually — the most serious deterioration in the university's finances has occurred over the past few years, since a change in the state government.

If São Paulo has been hit more severely than most of the federal universities, it may be — according to one administrator — that the university had more to lose. But many academics and newspaper reports blame the crisis on the governor of São Paulo state, Paulo Maluf, who is keener on oil exploration projects than on the university.

The university's teachers' association says that its share of the state budget decreased from 3 per cent in 1975 to 1.89 per cent in 1980, and that the share taken by higher education generally decreased from 5.1 per cent to 3.3 per cent over the same period. The same figures put the average salary of a full-time professor at about 80,000 cruzeiros a month (£6,000 a year), less than half of its maximum real value in the past decade. But budgets are not the only problem afflicting Brazilian universities. Their rapid expansion from 500,000 students in 1968 to 1.5 million now has led to unwieldy bureaucracies which changes of government have only aggravated. At São Paulo, the seat of university unrest in 1968, academics say that even relatively small items of expenditure have to be approved by the rector, who in turn has to argue for funds with the state government.

Judy Redfearn



## High-energy physics

# Machines shut down

A rise in electricity prices of nearly 50 per cent has forced the West Germany high-energy physics laboratory, DESY in Hamburg, to close down its accelerators until the end of 1980. The federal government in Bonn has asked the regional Hamburg government to foot the bill, but Hamburg refused — so DESY had to shut, losing three weeks of accelerator time.

Electricity costs have risen because of a recent agreement between the utilities, coal mining companies and the government. Under the agreement, coal used in electricity production will be raised from its present 33 million tonnes a year to 45 million tonnes by 1985. The utilities will thus have to invest in new power stations and the federal government has allowed them to raise the necessary cash from the consumer.

DESY will have to find another DM 5–10 million (£1–2 million) in 1981 to cover the increased electricity charges. If the money is not forthcoming, the accelerators will have to be run at two-thirds mean power. This would mean either low-energy experiments or relatively few runs at high energy. For example, Nobel laureate Samuel Ting's experiment to find interference between the weak and electromagnetic interactions, as evidence for the intermediate vector boson, requires the highest energies and long data runs and may be threatened unless one or other government pays the increased bill.

The federal government in Bonn, however, which through the Bundesministerium für Forschung und Technologie (BMFT) provides 90 per cent of DESY's budget, is in the red, and has been asking all public institutions to find savings. DESY's DM 143 million budget for 1980 has already suffered two cuts — DM 10.5 million in its DM 50 million "capital projects" budget (achieved by delays) and DM 1.5 million in running costs. BMFT also seems set not to grow this year, its provisional increase for 1981 being slightly less than the current 5.3 per cent annual growth in the cost of living in Germany.

In principle, the Hamburg government could increase its 10 per cent contribution to DESY, as it already benefits from DESY's policy of placing many of its equipment contracts with local industry, and it owns the electricity company which is now charging the laboratory so highly. So far, however, it has not done so.

The DESY crisis may prove to be a test of the new science minister's faith in basic science. Dr von Bülow announced at a press conference last week that he was in favour of "full government financing" for basic research, whereas in energy research, for example, industry must make a contribution.

In the long run, physicists have pinned DESY's future on the construction of

HERA, a DM 600 million machine to collide electrons with protons at high energy and so probe proton and quark structure; the project is being weighed against other big science projects by a committee of BMFT, and no doubt electricity costs will be taken into account. DESY's electricity bill this year will be about DM 22 million, with the full HERA, at current prices, about DM 43 million. So DESY is making a great effort to develop superconducting bending magnets for the proton ring to keep down the bill. It has two designs, one based on the successful dipole constructed at Fermilab in the United States and another under construction at Saclay in France.

Moreover, it is still planned to build HERA in two stages, the first involving 35 GeV electrons and positrons alone and costing DM 290 million. This stage could be ready 5½ years after approval (at the end of 1986 at the earliest) and still offers some competition for the large electron-positron ring (LEP), the next major project of the European nuclear research centre CERN at Geneva. LEP's electricity costs for the same energy would, however, be lower as its ring would be much larger, and it would radiate less synchrotron radiation (the major energy sink in a circular electron machine).

Robert Walgate

## Third World

# Consumers arise

Kuala Lumpur, November

At a time when the new Administration in the United States seems likely to ease up on the stringent regulation of technological products, consumer groups in the Third World are beginning to voice demands for protection against potentially harmful substances and goods like that already adopted by more affluent societies.

A principal target of such groups in the alleged "dumping" in developing countries of products, such as drugs and pesticides, which have been banned in one or more of the industrialized nations.

Three weeks ago, for example, individuals from twelve developing nations attending a conference in Malaya organized by the International Organization of Consumer Unions (IOCU) signed a declaration urging that there should be no distinction between domestic and foreign consumers in export control programmes for hazardous substances and production facilities.

But the concerns of the embryonic consumer groups in the Third World go much further, ranging from the conventional complaints about the quality of consumer goods to criticism of low-standard imitations of Western goods (for example a drug named "Panadol", easily confused with "Panadol").

Malaya's Finance Minister, Tangku Razaleigh Hamzah, has called on university scientists and other faculty

members to put their efforts behind work of such consumer associations, should be "watchdogs of the people veying the unfair practices of business".

Tengku Razaleigh was speaking at a seminar on economics and development organized by one of the largest and active of Third World consumer groups, the Consumer Association of Penang (CAP).

Formed more than ten years ago on a Malayan island of Penang, CAP now has a full-time staff of 60. Its activities cover a range of issues familiar to pressure groups in industrialized countries, from assisting fishermen whose livelihood was threatened by the discharge of wastes from a new factory, to working with local labour unions to identify occupational carcinogens, to developing courses and teaching materials on consumer rights for use in school and universities.

One of the successes claimed by CAP was the Malay government's decision to accept explicit responsibility for environmental issues by expanding its portfolio of the Ministry of Science and Technology. Various controls on pollution sources have since been introduced, but less progress has been made on efforts to curb the rapid exploitation of Malaya's diminishing natural resources. As with tin and petroleum, these include wood forests which may disappear completely in ten to twelve years if the rate of cutting continues at the present pace.

Taking a lead from CAP, and in line with widespread concern among the developing nations, many universities have introduced courses in environmental sciences in the past decade in Malaya. The University of Malaya in Kuala Lumpur has recently introduced a course in consumer law as part of its law degree, taught by one of CAP's founders in Penang.

But both CAP and IOCU — with its current president, Mr Anwar Fazal — argue that Western concepts of environmental consumer protection should be expanded to include concern for all aspects of industrial production, from factory working conditions to community health.

Even though Malaya has in recent years passed a variety of laws covering all areas, CAP claims that government authorities are frequently slow or reluctant to put these laws into effect. Officials that the magnitude of the task that faces them, and the continued pressure for economic growth, make it difficult to do any faster.

In a country where opportunities for political dissent remain limited — recently moved its Asian headquarters from Singapore to Malaysia — officials tread warily on the boundaries of legitimacy, aware that their requests for registration as a society could be questioned if their activities become overtly political.



But given the relative weakness of labour unions and official opposition parties, the consumer movement has become one of the few direct routes for attempting to influence government policies. "We create pressures within the bureaucracy" says Martin Khor Khok Peng, CAP's research director. "If we educate the public, the bureaucrats will have to listen."

David Dickson

## Conservation

### Bill of rights

The British government is hoping that its new Wildlife and Countryside Bill, introduced in the House of Lords last week, will be law by the end of next summer. Its passage through parliament, however, may not be easy. The bill has taken a long time to compile, preliminary consultation papers having aroused considerable opposition from conservation groups which do not feel that all inadequacies have been ironed out in the latest draft.

The chief effect of the bill is to bring British law in line with that of Europe, but Mr Tom King, minister for local government and environmental services, stresses that many of the new measures are badly needed anyway. The clauses in the bill on the protection of birds, methods of killing wild animals and the introduction of exotic species fulfil European requirements while those relating to nature conservation, the countryside and national parks are designed to improve wildlife management.

Mr King is especially pleased with the clauses relating to the management of areas designated as sites of special scientific interest (SSSIs). The conservation groups, however, say that these clauses are amongst the most worrying in the bill. Under them,

owners of some SSSIs will have a statutory obligation to inform the Nature Conservancy Council (NCC) of any planned operations which may affect the physical or biological features of the site and to wait for up to a year for the consent of NCC. Failure to notify would carry a penalty of up to two years imprisonment and a fine of £1,000 or both.

The conservationists will be seeking to amend these clauses to include all SSSIs, not just those singled out for special treatment, and to include some statutory obligation on the landowner to carry out the management recommendations of NCC. Under the bill, if agreement on management of a site is not reached within one year of notification, the landowner is free to carry out his original plan, although he may risk compulsory purchase by NCC.

On the whole, conservationists welcome clauses in the bill relating to the protection of wild birds, animals and plants, seeing them as a major improvement over existing legislation. The bill will tighten up the laws on the import and export of endangered species, methods of killing wild animals, keeping birds in captivity and selling them either dead or alive. Most of these amendments are in line with the European Community Directive on Wild Birds. The bill also seeks to protect "rare" creatures, such as the otter in Scotland, before they reach the endangered list.

A serious omission in these clauses, however, say the conservationists, is the lack of adequate provision for enforcement. They will be lobbying for the creation of a small investigation unit, probably under the aegis of the NCC, to give support and expert advice to customs officials and police who often miss infringements in the law because of unfamiliarity with wildlife.

Recent controversies about the main-

## Fallout from China

China's latest nuclear test on 16 October was "dirty" — according to the official Polish news agency PAP. The dust cloud had previously been monitored in Japan and New York, but the Polish agency reports of work from the Central Laboratory of Radiological Protection outside Warsaw is an example of the new policy of openness adopted by the Polish press. The laboratory has been working in the field since about 1973 with little publicity in Poland.

The Polish team, in the person of its leader, Dr Zbigniew Jaworowski, says that it has observed a significant amount of radioactivity at a height of 15 km. The Polish monitoring method is novel. A converted Mig-18 fighter flies horizontally through the dust cloud, opening a collecting duct at a predetermined altitude. The results suggested a fission-fusion-fission device, and this information was made available to the American group at the Environmental Protection Agency in Washington.

These aerial activities are not Dr Jaworowski's main interest, however. He is principally concerned with monitoring background levels of radioactivity — both natural and that produced by discharge of radioactivity into the atmosphere by "conventional" means — in Poland, largely from the combustion of coal. In September of this year Dr Jaworowski was appointed head of a United Nations commission on fallout, directly responsible to the General Assembly. His measurements of radioactivity levels in glaciers and icecaps throughout the world have met with some controversy, as he says that apart from a few black spots, the global build-up of radioactive fallout over the last century is far less than is claimed by the powerful "doomwatch lobby".

Vera Rich

English floodmeadows: threatened by ditch or protected by bill?



Photo: RSPB

tenance and safety of public footpaths are only partly dealt with in the bill. Although the rights of farmers to keep bulls in fields crossed by public footpaths will be restricted to some extent, beef bulls will be allowed if they are accompanied by cows. Ramblers will be no happier with that provision than with the transfer of general powers over footpaths from central to local government. Ramblers fear that local bias will mean that many paths are lost.

Although many conservationists agree that the bill improves on existing legislation, they consider it far from ideal. The opportunity to revise wildlife and conservation legislation comes up only about every five years so some hard fighting seems inevitable. The bill may have to take more blows than the government seems to have anticipated.

Judy Redfearn



## CORRESPONDENCE

## Museum pieces

SIR — Halstead's progress report on the death of scholarship and the rise of Marxism in the Natural History Museum (*Nature* 20 November<sup>1</sup>) mixes too many different issues for a full reply. I will concentrate on his attack on scholarship in this institution. To Halstead, the symptom of decay is advocacy, in the public galleries, of cladistics, a method which he believes is being forced down the public throat by a Public Services Department which has overridden the views of scientists in the Museum.

Cladistics, as presented in the "Dinosaur" and "Fossil man" exhibits, may indeed seem oversimplified to some, or not fully thought through to others. But Halstead's alternative approach, as detailed in his comments on fossil man, seem to me far more grievously mistaken. In accusing us of lack of scholarship, he offers instead "the well attested sequence of human fossils representing samples of succeeding populations has . . . been taken as a classic example of the gradual evolution of a single gene pool. Certainly there is not any serious doubt about *Homo erectus* being directly ancestral to *Homo sapiens*". Confronted with these statements, one must either bow to Halstead's scholarship, or ask "attested" by whom? "been taken" by whom? "not any serious doubt" by whom? Halstead's answer might be, to quote the Museum handbook to the old exhibit on fossil man which was removed to make way for the dinosaurs, "the evolution of Man has come to be regarded as fact rather than hypothesis by all persons qualified to judge the evidence"<sup>2</sup>. In other words, we (scientists, experts, authorities) tell you it is so.

The radical departure in the exhibit reviled by Halstead is that the voice of authority is less strident. The visitor is encouraged to understand, and to take part in, the reasoning that underpins the story of human evolution; to become one of those "persons qualified to judge the evidence". And cladistics is the logical entry to that reasoning.

Amongst scientists in the Museum there are many different viewpoints on the value and generality of cladistic methods. Those viewpoints are a symptom of activity and debate. Halstead opts out of the debate, deferring instead to the authority of Mayr and Simpson, of books published 30 or 40 years ago, "and indeed of Charles Darwin himself". From his "reading of the literature of cladistics" Halstead concludes that cladists form the opposition "to the concept of gradualism and to the idea that the processes that can be observed at the present day, when extrapolated into the past, are sufficient to explain changes observed in the fossil record". This last idea, of extrapolating the present into the past as sufficient explanation, is usually attributed to Charles Lyell under the name uniformitarianism. Lyell's uniformitarian explanation of the changes observed in the fossil record was piecemeal extinction and creation<sup>3</sup>, an explanation invoking "qualitative leaps". Indeed, T.H. Huxley himself was unable fully to accept Darwin's gradualism, and preferred the saltationist camp. In short, Halstead's equation of cladistics and saltation is simply mistaken.

Recent advocates of saltation, and critics of extrapolation from population genetics to macroevolution, such as Gould<sup>4</sup> and Stanley<sup>5</sup>, are not cladists. Whether they are Marxists is another matter, in my view an irrelevant one.

More relevant is Halstead's confusion over the relation between cladistics, a method of systematics, and questions of process — modes of speciation or transformation of species. He sees a necessary connection between cladistics and one view of the evolutionary process, but as cladistic literature makes plain<sup>6-8</sup>, there is no such connection. Cladistics is not about evolution, but about the pattern of character distribution in organisms, or the recognition and characterization of groups. Halstead might direct his search for Marxist propaganda towards the Nuffield Biology texts and guides, for the teacher is urged "to develop a common vocabulary (and possibly notation) in biology and mathematics" by teaching the elements of systematics through Venn diagrams, which are logically synonymous with cladograms<sup>8</sup>. All that seems to lie behind Halstead's complaint is his failure to grasp the distinction between pattern (systematics) and process (explanation of the pattern)<sup>9</sup>. Hence his mistaken belief that he knows how evolution works, and that we are unwittingly committed to Marxist historicism.

COLIN PATTERSON

Department of Palaeontology,  
British Museum (Natural History),  
London SW7, UK

1. Halstead, L.B. *Nature* 288, 208 (1980).
2. de Beer, G.R. *Evolution* 4th edn (British Museum (Natural History) London, 1970).
3. Oldroyd, D.R. *Darwinian Impacts* (Open University Press, Milton Keynes, 1980).
4. Gould, S.J. *Paleobiology* 6, 119-130 (1980).
5. Stanley, S.M. *Macroevolution* (Freeman, San Francisco, 1979).
6. Platnick, N.I. *Syst. Zool.* 26, 438-442 (1977).
7. Platnick, N.I. *Syst. Zool.* 28, 537-546 (1980).
8. Patterson, C. *Biologist* 27, 234-240 (1980).
9. Eldredge, N. & Cracraft, J. *Phylogenetic Patterns and the Evolutionary Process* (Columbia University Press, New York, 1980).

SIR — In Dr Halstead's pleas for traditionalism in the Natural History Museum's exhibitions (*Nature* 20 November, p.208) he makes an assumption that lends much potential support to those whose policies he is so "fervently dedicated" to trying to discredit.

It is true that Marxists have attempted to equate the idea of punctuated equilibria (in its many guises) with the principles of dialectic, the head-on collision between changed environment and less well adapted organisms giving rise, by dialectic confrontation, to the new 'adapted' order, exactly as Marx envisaged the clash of the bourgeoisie and the proletariat, though Marx himself was somewhat vague in this area. Gradualism has been called on as evidence for other political persuasions. Politicians of all colours of the political spectrum have found things in Darwinism to support their political positions. As Shaw says of Darwin, "He had the luck to please everybody who had an axe to grind".

Unfortunately Dr Halstead is himself supporting the tenuous link between change in historical and present day human societies; between so-called "cultural

evolution" (which is a true Lamarckian system in any case) and the far slower and partially understood process of biological evolution, he is approving the idea that supposed historical events in evolution can be used as "scientific" evidence to predict and explain cultural evolution. Dr Halstead has only got under the surface of the argument, not to its core; he would surely be far better off questioning this primary assumption, rather than unintentionally lending support to biologically naive political thinkers. If he could do this, the problem he feels so strongly about would evaporate and he could escape. As it is, he is in great danger of being trapped by his position; his gradualist evidence is more tenuous than he implies, and since the recent Chicago conference it is probable that punctuated equilibria will indeed become a new orthodoxy. How will Dr Halstead free himself? With a "mighty leap" — a method some orthodox neo-Darwinians have been known to use?

The confirmation of his superficial attitude is given by his statement that, "Marxism will be able to call upon the scientific laws of history in its support". Dr Halstead clearly believes, as, of course, Marx did, that such "scientific laws of history" exist, but their emptiness has been elegantly demonstrated by Sir Karl Popper in *The Poverty of Historicism*, and *The Open Society and its Enemies*.

Having read Dr Halstead's views on Popper elsewhere I am not surprised at all by his confusion.

M. J. HUGHES-GAMES

Clifton,  
Bristol, UK

SIR — L.B. Halstead's letter (*Nature* 20 November, p.208) is misguided and, if his arguments were generally accepted, dangerous to the unfettered development of science. Whatever the scientific merits and demerits of the "cladist" theories behind the Natural History Museum's "Dinosaur" and "Fossil man" exhibits, it is most certainly wrong to attack them on the grounds that they might provide support for "a fundamentally Marxist view of the history of life". Indeed, it is ironic that Halstead should quote J.V. Stalin, for it was precisely his policy of encouraging the application of political criteria, rather than scientific ones, to assess scientific theories that ruined so much Soviet science for a generation.

It is really quite silly of Halstead to argue that because Marxist philosophers believe in revolutionary leaps (and, incidentally, so do several other, and quite different, philosophical and sociological schools of thought) then we ought to reject any scientific theory that explains changes in specific phenomena by way of "an abrupt leap from one state to another". How far is Halstead prepared to go with this "critique"? Should cosmologists now be called upon to reject the "big bang theory", topologists "catastrophe theory" or historians of science "paradigm breaks" because they might be construed as support for a law of Marxist dialectics?

HARRY ROTHMAN

Technology Policy Unit,  
University of Aston,  
Birmingham, UK

## NEWS AND VIEWS

## Open debate

From M.G. Edmunds

THE simplest questions are often the hardest. It might be thought that 'What is most of the mass in the Universe?' should have been answered long ago, but a conclusive statement still eludes us. It is not too difficult to determine the radiation output of the galaxies, stars and interstellar material that we can actually see — with 'seeing' including radio, X-rays, infrared or ultraviolet, as well as visible light. From the amount of radiation we can infer the amount of radiating mass present. The resultant mass density of the Universe is comparatively modest, being only about one-fortieth of the 'closure' density required to exert sufficient gravitational pull to eventually halt the Hubble expansion and cause a re-collapse. The consequences of a closed or open Universe are rather remote on human timescales, but the problem exerts a strong philosophical attraction. Hence it is of considerable interest that there is growing evidence for a large amount of mass which does not radiate enough to have been seen, yet which might go a long way to making up the density required for closure.

The idea of 'missing mass' — mass that is present but not detected apart from its gravitational influence — is not a new one, and dates back to investigations of the dynamics of clusters of galaxies in the 1930s. In giant clusters, the rapid motions of the galaxies imply the existence of a gravitational potential well that is much deeper than can be explained by adding up the assumed masses of the visible galaxies. For many years there existed a feeling among astronomers that the 'missing mass' problem would eventually just go away when better observational data, or more appropriate theoretical treatment of that data, became available. But the problem has not gone away, and improved observations have all pointed to an upward revision of the mass density.

The most persuasive evidence for non-luminous matter comes from observations of the rotational velocities of spiral galaxies out to quite large distances from their centres (see, for example, Rubin, Ford & Thonnard *Ap. J.* **238**, 471; 1980). In many cases the velocities do not fall off with

distance from the nucleus but stay constant. A little elementary physics indicates this implies that the total mass inside a given radius increases linearly with radius. Yet the light output decreases exponentially with distance from the centre, so the matter in the outer parts must be many times less luminous per unit mass than the material in the inner parts. Since there is no evidence for a large amount of hidden material in the disk of our own Galaxy, it is likely that the dark mass in spirals has an extended, or 'halo', structure. Again from our own Galaxy, there is no evidence that the mass is in the form of faint stars.

It is obviously important to know how far the dark haloes extend, and how much they contribute to the total mass of a galaxy. Some evidence comes from the dynamics of small groups and binary pairs of galaxies, although the interpretation is difficult (see, for example, the excellent review of the whole question of galaxy masses by Faber & Gallagher *Ann. Rev. Astron. Astrophys.* **17**, 135; 1979; although considerably more galaxy masses have been published since this review, the general picture remains the same). Widely separated galaxies should sample the whole of each others' gravitational field, and such evidence as there is suggests the haloes could extend to 100 kpc, which is five or ten times the nominal visible extent of a typical galaxy. The dark material contributes as much, and probably several times as much, mass as the visible material.

If galaxies are considerably more massive than previously supposed, then this goes some way towards explaining the high dynamical mass implied for giant clusters of galaxies — but probably not all the way. There may still be several times more mass in the cluster than can be explained by adding up the (now heavier) individual galaxies. A new method of illustrating the presence of hidden material on an even larger size scale has been recently proposed (Davis, Tonry, Huchra & Latham *Ap. J. Lett.* **238**, L113; 1980),

*M.G. Edmunds is in the Department of Applied Mathematics and Astronomy, University College, Cardiff.*

which uses the motion of our local group of galaxies against the reference frame of the cosmic microwave background radiation. When this motion was first detected its direction was something of a surprise since it did not coincide with previous determination of the local group motion relative to other galaxies. Although the differences between the two motions are not fully understood, Davis *et al.* suggest that the component of motion towards the Virgo supercluster of galaxies, as determined in the microwave data, can be used to estimate the mean mass density of the Universe. They do this by considering the peculiar motions induced by perturbations of density (such as the Virgo superclustering) on an expanding Hubble flow. Their derived mean density is as high as four-tenths of the critical density required for closure. Thus the relative amount of mass which is hidden from view appears to increase with the linear size of the system — it is barely noticeable in the inner regions of galaxies, but becomes apparent at the outsides, it markedly influences groups and pairs, then dominates clusters and superclusters.

So what form is the dark mass in? The question is now a very important one since the dark mass is considerably greater than the visible mass. A population of low-mass objects can be imagined — interstellar material which condensed, became electron degenerate and is able to support itself without nuclear reaction. Such objects would have to be individually less than about one-twentieth of a solar mass. Large numbers of black holes or neutron stars are another possibility. But, apart from the difficulty of inventing a coherent picture to account for the formation of such objects without violating other constraints (notably limits to the amount of synthesis of heavy elements), there remains a fundamental problem if the missing mass is to be in conventional nucleon form. The dilemma comes from the effect of the extra mass on the nuclear reactions which synthesized helium and deuterium in the Big-Bang fireball at the beginning of the Hubble expansion. Putting the missing mass into nucleons



causes increased synthesis of helium and decreased synthesis of deuterium (see, for example, Yang, Schramm, Steigman & Rood *Ap.J.* **227**, 697; 1979). It might be possible to account for the observed deuterium in the Universe by production in other sites — perhaps supernova envelopes, although nobody has been able to think up an efficient enough mechanism. But overproduction of helium is a much more difficult problem, since it is not significantly destroyed (but rather added to) in normal stellar evolution and the observational limits on the maximum amount which could have been produced in the Big-Bang are now quite good.

The nuclear arguments would imply that the mass of nucleons in the Universe is not more than a tenth, and probably not more than a twentieth, of that required for closure. This corresponds to what we see in galaxies, although the error bars might just allow us to squeeze in the extra mass in galactic dark haloes as nucleons. The hidden mass in clusters, or that implied by Davis *et al.*'s Virgo supercluster argument would cause too much primordial helium production and far too little deuterium. A possible solution lies in the existence of a sea of massive neutrinos, left over from the Big Bang. The case for such a sea has been eloquently argued by D.N. Schramm and G. Steigman in this year's Gravity Research Foundation first-prize essay (to be published in *General Relativity and Gravitation*. See also Sybailis, Yang & Schramm *Nature* **288**, 143; 1980). They argue, on the basis of consideration of the clustering properties of massive neutrinos (see Tremaine & Gunn *Phys. Rev. Lett.* **42**,

407; 1979) that the most likely neutrino mass would be  $3\text{eV} \leq m \leq 10\text{eV}$ . The extra mass of these neutrinos would allow the missing mass in galaxy clusters to be explained, but problems would still remain if Davis *et al.*'s (albeit indirect, and somewhat uncertain) mass density is correct, or if closure is desired. The difficulty is that putting more and more neutrinos into the Universe will eventually cause degeneracy of the neutrino sea, which would again affect primordial element production. At one-tenth closure density, this does not appear to be a problem, but at much higher densities a more massive neutrino would be required, and it is not clear that such a neutrino would cluster in the right way to provide the increase of missing mass fraction with linear scale of the system considered. Astrophysicists will be eagerly awaiting experimental evidence of neutrino masses (see *Nature* **286**, 755; 1980), and further investigation of the clustering of neutrinos would seem important.

Whether the majority of mass in the Universe really is a sea of neutrinos, or whether it is conventional nucleon matter, remains to be decided. But the existence of considerable dark matter has been demonstrated. It is not so long ago that a headline appeared in a North American newspaper reporting "Caltech astronomers declare Universe open". Although the evidence still remains in favour of openness, one cannot help wondering if (in apparent obedience to current financial stringencies) the Universe may not be all that far from closing again. □

expanded the structural details along more speculative lines to propose evolutionary trees based on the variations between polypeptide subunits in ATPases.

The argument still rages in mitochondrial bioenergetics as to how many protons are translocated at each energy conservation site in the electron transport chain, S. Papa (Bari) favouring two whilst other groups favour three or four. Unfortunately, experimental measurements show little prospect of resolving this problem. Since extensive research has failed to implicate any quinone in the transfer of electrons from cytochrome *b* to cytochrome *a*, there is speculation about an alternative mechanism of proton translocation, possibly involving multiple  $\text{H}^+/\text{e}^-$  ratios. In contrast, research using chromatophores has provided strong evidence for the involvement of a specific quinone (Z) between cytochromes *b* and *c*, and the requirement for a quinone pool for ATP synthesis.

New evidence for the role of quinones in electron gating was discussed by A. R. Crofts (Urbana). In both chloroplasts and photosynthetic bacteria there is evidence that a quinone reduces cytochrome *b* only on even flashes of light, that is, only after the formation of  $\text{QH}_2$ , which would fit with the original ideas of a Q cycle. As Z has been identified as different from  $\text{Q}_2$  however, this must be rejected and an alternative mechanism of quinone oxidation invoked, although the proponents of a linear chain model have not explained how it copes with two electrons simultaneously. The concept of gating raises many problems, not least being the interpretation of the results of repetitive flash experiments used to measure rates of electron transport in photosynthetic systems. In mitochondria, although much evidence now points away from a classical Q cycle, no real alternative was put forward.

A system for examining an alternative non-Mitchellian mechanism of proton translocation is the bacteriorhodopsin proton pump from halobacteria. However, it was evident from the discussion that this apparently simple system is resistant to experimental analysis and is still a long way from providing a useful model. One recent, interesting development is the discovery that there is also a light-driven sodium pump in these organisms, possibly using a second retinal protein (J.K. Lanyi, Max-Planck-Institute, Munich).

Calcium transport was covered extensively but no new theories were presented and the sessions were devoted to discussing the alternative mechanisms for calcium release from mitochondria which are sodium insensitive. There is still no consensus as to which of three different methods is the more probable, polyunsaturated fatty acid induced-efflux, oxidation of mitochondrial pyridine nucleotides or an indirect inorganic phosphate-induced pathway.

## Bioenergetics in Europe

from Judith Armitage

THE First European Bioenergetics Conference, held in July in Italy, showed that, with the general acceptance of the chemiosmotic concept of energy transduction, interest has moved from the gross theory to the finer, molecular and genetic details.

The problem of elucidating the functional, *in vivo* structure of the membrane-bound energy-transducing proteins using isolated systems and physical techniques was one of the basic themes of the conference. This problem was well illustrated by the many discussions on the possible structure of cytochrome oxidase, and its relation to function. R. Capaldi (Oregon) using X-ray diffraction and image reconstruction on the isolated enzyme described the possible functional

arrangement of the seven polypeptides across the membrane. Although local interactions *in vivo* and the precise role of each subunit is still unknown, the experimental data and *in vitro* structural studies were used by M. Wikström (Helsinki) to speculate on the possible mechanism of proton translocation by the protein and its relationship to the conservation of the membrane potential, emphasizing the need to consider both molecular and electrical topography within the protein.

Using very similar *in vitro* techniques on the crystallized  $\text{F}_1\text{-ATPase}$  M. Amzel and coworkers (Johns Hopkins) proposed a model for the structure of  $\text{F}_1\text{-ATPase}$  as a functional dimer, rather than the previous triple/single structure. There are, however, at least two arrangements of the subunits which would yield a dimer and fit *in vivo* experimental data. Some speakers

Judith Armitage is in the Department of Botany and Microbiology, University College London.





### 100 years ago

The recently-presented budget of Prussia shows that, despite the financial straits of the kingdom, no considerations of economy are allowed to hamper the growth of its scientific and educational system. First on the list come the nine universities with an allotment of 7,050,000 marks (352,500/). Berlin receives the lion's share, 1,378,348 marks, an increase of about 37,000 marks on its last annual subvention. Bonn and Königsberg each have 740,000 marks, Breslau 600,000, Kiel 404,000, Marburg and Halle each 430,000, Göttingen 201,000, and Greifswald 136,000. Of the above-mentioned sum about 1,306,000 marks are appropriated for extraordinary expenses in connection with the construction of university

buildings, and of this amount Berlin absorbs over one-half, viz., 766,000 marks. The other chief items in the Budget of Public Instruction are: Gymnasias and Realschulen, 5,000,000 marks; primary schools, 14,500,000; orphanages, schools for the blind, deaf and dumb, &c., 300,000; technical schools, and for the general furtherance of science and art, 3,000,000 marks.

The number of pupils of Lycées and Colleges in the French Republic is 87,000 (46,500 for Lycées and 40,500 for Colleges). Last year it was only 84,700. These establishments may be considered as analogous to the English grammar-schools.

Mr. Mundella has been speaking on education again, repeating essentially the old story, that our country must lose in the race unless, as in other countries, education in science is made an imperative part of elementary education. We have many natural and traditional advantages over other countries, but all these must in the long run succumb to scientific training.

From *Nature* 22, 2 December, 106 & 115, 1880.

Historically, Heuser had been interested in the use of rapid freezing to study exocytosis in neurotransmission. To trap exocytosis during membrane fusion and allow examination by freeze fracture techniques, Heuser and his colleagues devised an apparatus for the very rapid freezing of nerve-muscle preparations in liquid helium a few milliseconds after electrical stimulation (*J. Cell Biol.* 81, 275 1979). From here it was a small step to apply this rapid freezing, platinum replica technique to other preparations such as fibroblast cytoskeletons.

What advantages does this approach have? Heuser suggests that it avoids the use of chemical fixation of whole cells, a procedure which, by definition, is denaturing and which may, therefore, be a source of artefacts. Heuser and Kirschner compare the images of triton cytoskeletons that were prepared before or after fixation with glutaraldehyde. The filaments in cytoskeletons prepared from fixed cells appeared with variable thickness, partially agglutinated and covered with irregular deposits while those prepared from unfixed cells were more discrete entities, had more regular and consistent dimensions, and were frequently recognizable, for example, as actin filaments or intermediate filaments. The general appearance of the cytoskeletons prepared from fixed cells resembled the 'microtrabeculae' described by Wolosowick and Porter (*Am. J. Anat.* 147, 303; 1976; *J. Cell Biol.* 82, 114; 1979), who have described this structural matrix in whole cells fixed with glutaraldehyde and viewed by high voltage electron microscopy. The similarity of the cytoskeletal preparations from fixed cells has led Heuser and Kirschner not to question the existence of the microtrabecular lattice but to suggest that its appearance, with irregular dimensions and anastomosing filaments may result from the use of glutaraldehyde and the consequent cross-linking of filaments and

## A new view inside cells

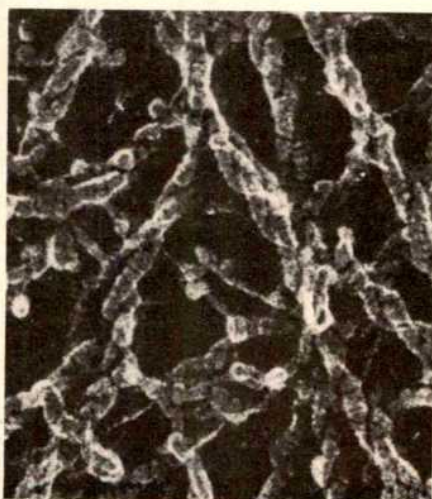
from Keith Burridge

LIKE so many areas of science, electron microscopy does not advance smoothly but in quantal jumps which are often the result of the introduction of a new technique. The use, for example, of glutaraldehyde as a fixative by Sabatini and his colleagues in 1963 made possible the visualization of the cytoplasmic filaments that are so much studied today.

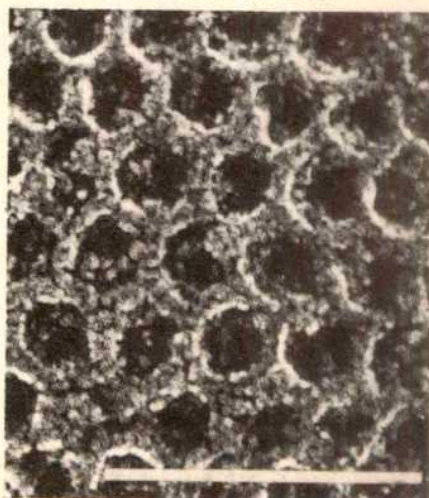
Perhaps the most recent and exciting advance in electron microscopy, gracing the pages of the *Journal of Cell Biology* with dramatic images, has come from J. Heuser and his colleagues (*J. Cell Biol.* 84, 560; 1980; Heuser & Kirschner *J. Cell Biol.* 86, 212, 1980). Heuser's approach differs

greatly from the conventional method of examining thin sections of cells that have been fixed (with agents such as glutaraldehyde and osmium tetroxide), dehydrated, embedded, sectioned and stained with heavy metals. Instead, Heuser and his colleagues have rapidly frozen either whole cells or cytoskeletal preparations (cells extracted with nonionic detergents), opened the cells by freeze fracture, removed the volatile components by freeze drying, and rotary shadowed the remaining structures with platinum. These platinum replicas are then examined by transmission electron microscopy (TEM) (Figures 1 and 2).

**Figure 1** Two views of cytoskeletal elements. *a* is a tangle of filaments from the perikaryal region of a freshly plated cell which would stain diffusely for actin by light-microscope immunocytochemistry. The filaments display a 5.5nm repeat or graininess that appears to be characteristic of actin filaments as revealed by this technique. *b* shows filaments from a similar area but after decoration with the S1 fragment of myosin. (From J. Heuser and M. W. Kirschner *J. Cell Biol.* 86, 226, 1980.)



**Figure 2** High magnification of a coated pit area on the cytoplasmic face of the plasma membrane of a fibroblast. Bar =  $\mu\text{m}$ . (From J. Heuser *J. Cell Biol.* 84, 564; 1980.)





adsorption of cytoplasmic proteins to them during fixation.

Although this may be true, it is important to realize that when Heuser and Kirschner make a cytoskeleton without fixation, many proteins are extracted and these most probably include a number that bind to or cross-link the filaments such as the actin-binding proteins (filamin,  $\alpha$ -actinin, myosin, etc.). Whereas the cellular images obtained by Wolosowick and Porter may contain fixation artefacts that contribute to the microtrabecular appearance, equally the images of Heuser and Kirschner may be oversimplified by the extraction of many of the bridging elements. Perhaps a more accurate image lies somewhere between these two.

A second advantage of Heuser's approach is that the image comes from the platinum replica. With conventional thin sections and most whole mounts viewed by TEM the final image is due to the selective binding or deposition of heavy metals, such as osmium, uranium and lead. Since the chemistry of this selective staining has not been fully worked out, there is a degree of uncertainty in the interpretation of the final image. In particular, if a cytoplasmic structure is not stained, it will not be seen. On the other hand, the replica technique should mirror the surface of the cytoplasm, cytoskeleton, or intact cell very closely. However, herein lies a problem and a limitation of the technique. When unfixed cells are rapidly frozen and then fractured so as to reveal the cytoplasm, it is difficult to reveal any structure other than a complex granularity. To obtain unimpeded views of cytoplasmic structures such as the various filaments, this granularity must be extracted or diluted. Hence cytoskeletons are excellent material for this approach but whole cells present problems. These may be partially overcome by swelling the cell briefly in distilled water or by fixing a cell first and then washing it in distilled water. Presumably, both procedures eliminate the salts and other unetchable components, but the one method reintroduces the problem of chemical fixatives whereas the other exposes cells to an osmotic shock. Although these approaches do not appear suitable for examining the cytoplasm of whole cells, they have generated some very interesting views of the cytoplasmic face of the plasma membrane (*J. Cell Biol.* **84**, 560, 1980). Indeed, the ability to view the cytoplasmic face of the membrane may be one of the most valuable contributions of this whole technique.

Part of the appeal of the images achieved by Heuser's technique comes from the depth of the three-dimensional view (similar in appearance to scanning electron micrographs). Viewing only the surface of structures avoids superimposing their upper and lower faces which occurs with thin objects in conventional thin sections.

Examining the platinum replicas of microtubules after rapid freezing and fracture, it is possible to discern the tubulin subunits in a 3-start helix, something that has only previously been seen after optically filtering electron micrographs of negatively stained preparations. Similarly, the geometry of coated pits and vesicles is particularly clear in Heuser's pictures since the upper and lower faces of these structures are not superimposed (Figure 2).

The resolution of the technique as used by Heuser is about 2nm and easily picks up, for example, the 4nm repeat of tubulin monomers in microtubules. The resolution is sufficient to distinguish the different filament types by their surface

substructure, although the resolution is less than with negative stain. When actin is decorated with the S1 subfragment of myosin, the image of an actin filament is transformed into a double-stranded rope-like structure. Like the underlying actin filament, this reveals a 5.5nm axial periodicity (Figure 1). Heuser and Kirschner also demonstrate that the technique has sufficient resolution to visualize IgG molecules directly without additional electron-dense labels. This application is particularly exciting and may permit the ultrastructural localization of accessory proteins which previously have been seen in the filament systems only by immunofluorescence.

## Pathways of endocytosis

from Michael Geisow

ENDOCYTOSIS is an elegant biological solution to two related needs of living cells — the need to retrieve material bound to the plasma membrane and the need to recover the membrane itself. But what components of the membrane enter the cell and what happens to them?

Exogenous ligands — nutrients or effectors — bound by receptors at the plasma membrane collect within differentiated regions known as coated pits. The cytoplasmic coat is thought to be composed of clathrin and, provided that the temperature is above 10°C, bound ligands are cleared from the coated pits, to lodge [ultimately] in cytoplasmic structures containing hydrolytic enzymes.

The composition of coated pits is of some interest. It has been presumed that coated pits are enriched in the appropriate receptors which enter the cells together with bound ligand. Naturally, this assumes the continued fidelity of the receptor part of the labelled ligand complex. What other components of the plasma membrane also disappear into the pit?

In the fibroblastic cell at least two intrinsic membrane polypeptides appear to stay clear of coated pits. Ferritin markers linked via specific antibodies to these two membrane proteins (the  $\theta$  and H63 antigens) were found by Mark Bretscher and colleagues to be excluded from pits<sup>1</sup>. In contrast, ferritin and other labels conjugated to low density lipoprotein<sup>2</sup> and epidermal growth factor<sup>3</sup> clustered selectively in these regions. The coated pit may also control some selection of its own lipid components as suggested by the apparent exclusion of cholesterol<sup>4</sup>.

Since all components of the plasma membrane of fibroblasts can be renewed the observations on the  $\theta$  and H63 antigens means that such proteins must be taken up by other routes — otherwise the plasma membrane would act as a dead end for

redundant copies of the proteins. Perhaps the alternative route in this case is via uncoated membrane invaginations seen to sequester ferritin-labelled HLA antigens<sup>5</sup>. Coated pits observed in the same cells were free of marker.

The majority of proteins or peptides which enter the cell by endocytosis appear to be deposited in secondary lysosomes or multivesicular bodies (essentially the same thing). Do the associated receptors coincidentally suffer the same fate? At least one well-studied receptor<sup>6</sup> — for epidermal growth factor — does appear to be destroyed together with its bound hormone<sup>6</sup>. For a number of other receptors, there is evidence of efficient recycling. Results obtained from studies of the hepatocyte galactose receptor and low density lipoprotein receptors in fibroblasts are exemplified by recent observations<sup>7</sup> of the mannose/N-acetyl glucosamine receptor (macrophages).

Only a small fraction of the total cellular pool of sugar receptors are present on the macrophage surface at any time. However, if the accessible copies are destroyed enzymically at low temperature they can be rapidly and repeatedly replaced upon warming the cells, even in the absence of protein synthesis. Similar treatment of cells at 37°C quickly destroys the entire receptor stockpile suggesting that receptor turnover is fast and continues even in the absence of specific ligand. The galactose receptor in hepatocytes has a long intracellular half-life, of several days — an observation obtained after challenge with saturating amounts of specific ligand<sup>8</sup>.

For these receptors it is necessary to envisage recycling and to postulate that receptor and ligand part company somewhere between coated pit and secondary lysosome. Two recent articles describing the route of ligands entering cells via coated pits provide a new structural context for biochemical approaches to this problem.

In hepatic cells, Wall *et al.*<sup>9</sup> have traced

Keith BurrIDGE is in the Cold Spring Harbour Laboratory, New York.

Michael Geisow is in the National Institute for Medical Research, Mill Hill, London.

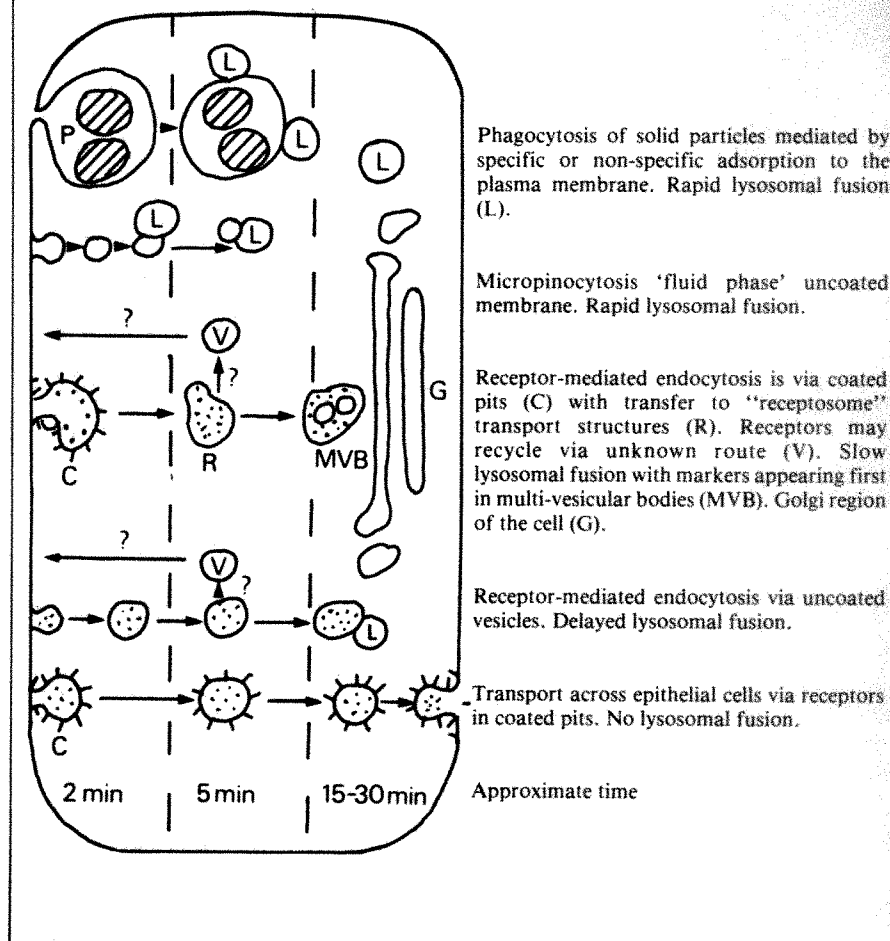
the route of ligands expressing galactose residues. Numerous coated pits were seen in the absorptive membranes of cells before exposure to ligand. Coated vesicles close to the membrane were almost invariably shown to be pits lying with their principal axes roughly parallel to the plasma membrane as recently observed by others<sup>1,12</sup>. Ligand first seen in these pits was found one and a half minutes later inside irregular structures (vesicles and tubules) lacking coats. After five minutes ligand appeared in the Golgi-lysosome region of the cell inside a heterogeneous population of uncoated structures. The appearance of ligand in association with lysosomal enzymes was first apparent at fifteen and complete at sixty minutes. Another recent report<sup>10</sup> suggests the delay in fusion of pinocytic vesicles with lysosomes has a half-time of only seven minutes. Nevertheless, there does appear to be some agreement that ligand entering cells via coated pits takes longer to complete this standard journey than by other uptake routes<sup>11</sup>.

Willingham and Pastan<sup>12</sup> present findings with strikingly similar features. In addition to electron microscopy, a system of image-intensified fluorescence microscopy permitted continuous observation of their ligand —  $\alpha_2$ -macroglobulin — as it was taken up by fibroblasts. They found no evidence of coated transport structures other than the initial coated pit. Instead the ligand transferred from pits to uncoated, irregular vesicles apparently like those described by Wall *et al.*<sup>9</sup> with no clear transitional stage. The cytoplasmic structures were highly mobile and did not combine with anticlathrin antibodies; nor did they show any affinity for antibodies to the major microtubule or microfilament proteins. One more point of similarity between the Wall and the Willingham articles concerns timing. Label was in uncoated structures after five minutes, in the Golgi-lysosome region in fifteen minutes and in lysosomes after thirty minutes. To distinguish the uncoated vesicles arising as a result of endocytosis through coated pits from other pinocytic vesicles, Willingham and Pastan have coined the term 'receptosome'.

Concerning the new nomenclature, one might comment that the name would be even more appropriate if one could be sure that the receptors were still there. In the structures described by Willingham, the reaction product of their marker — conjugated peroxidase — did seem to be associated with the limiting membrane. However, the higher resolution marker employed by Wall *et al.* — conjugated ferritin — appeared throughout the lumen of the transporting vesicles at this stage. They speculate that dissociation of receptor and ligand might have already occurred.

Each of these recent articles emphasise the role of the clathrin-coated pit as a

# PATHWAYS OF ENDOCYTOSIS IN CELLS



structure specialising in receptor transfer across the plasma membrane. Strong evidence for a similar role has been reported for coated regions in endoplasmic reticulum membranes<sup>13</sup>. On the other hand direct evidence for coated vesicles as putative transport structures is as rare as coated pits are common. Recent reports either state or imply that the existence of coated vesicles, is extremely transient. Instead, the transport structures themselves appear to be smooth-membraned vesicles. It's worth noting that the isolation of coated vesicles containing ligand<sup>13</sup> does not prove their independent existence as cytoplasmic entities, since homogenisation of plasma or Golgi membrane containing coated pits is very likely to produce closed vesicles when the membranes rupture.

The irregular appearance of the uncoated transport structures<sup>9,11</sup> may imply intense membrane fusion activity — secondary lysosomes and Golgi condensing vacuoles are two examples of this. The 'receptosomes' of Willingham and Pastan might well act as a short limbo for incoming receptor-ligand bearing vesicles and, in the case of receptors which recycle, for

departure of vesicles bearing receptor alone. The delay in lysosomal sequestration of label entering cells by receptor-mediated endocytosis accords with the requirement for prior dissociation of ligand and receptor. However, entry via coated pits does not appear to be mandatory for a delay in lysosomal fusion, since HLA antigen complexes which are endocytosed in uncoated structures<sup>14</sup> are also slow to appear in multi-vesicular bodies. The key to fusion or complete absence of fusion (as in the case of epithelial cells mediating transport across the cell layer) may lie in the proteins expressed upon the surface of the (uncoated?) transport structures.

I now anticipate the characterisation of 'Charonosomes' named after Charon who was able to return in his ferry after his passenger had crossed the point of no return into the underworld to face dissolution or immortality. But even more I await the direct, covalent labelling of a surface receptor. Surely, only a technique of this kind will enable the current models of receptor recycling and receptor-mediated endocytosis to achieve the elegance of the biological processes they seek to explain.



1. Bretscher, M.S. Thomson, J.N. & Pearce, B.M.F. *Proc. natn. Acad. Sci. U.S.A.* 77, 4156 (1980).
2. Anderson, R.G.W., Brown, M.S. & Goldstein, J.L. *Cell* 10, 351 (1977).
3. Willingham, M.C., Maxfield, F.R. & Pastan, I.H. *J. Cell Biol.* 82, 614 (1979).
4. Montanese, R., Perrelet, A., Vassalli, P. & Orci, L. *Proc. Natn. Acad. Sci. U.S.A.* 76, 6391 (1979).
5. Hopkins, C.R. *Nature* 285, 205 (1980).
6. Das, M. & Fox, C.F. *Proc. natn. Acad. Sci. U.S.A.* 75, 2644, (1978).
7. Stahl, P., Schlesinger, P.H., Sigardson, E., Rodman, J.S. & Lee, Y.C. *Cell* 19, 207 (1980).
8. Tanabe, T., Pricer, W. & Ashwell, G. *J. Biol. Chem.* 255, 5971 (1980).
9. Wall, D.A., Wilson, G. & Hubbard, A.L. *Cell* 21, 79 (1980).
10. Dunn, W.A., Hubbard, A.L. & Aronson, N.N. *J. Biol. Chem.* 255, 5971 (1980).
11. Willingham, M.C. & Yamada, S.S. *J. Cell Biol.* 78, 480, (1978).
12. Willingham, M.C. & Pastan, I. *Cell* 21, 67 (1980).
13. Rothman, J.E. & Fine, R.E. *Proc. natn. Acad. Sci. U.S.A.* 77, 780 (1980).
14. Huet, C., Ash, J.F. & Singer, S.J. *Cell* 21, 429 (1980).

## The slow process of succession

from Peter D. Moore

THERE are certain areas of ecology which are made more difficult to investigate by the current tendency to limit research grants to three years. Take the long-term study of plant competition between bracken (*Pteridium aquilinum*) and heather (*Calluna vulgaris*) on the Brecklands of East Anglia. If Alex Watt (*J. Ecol.* 43, 490; 1955) had been restricted to a three-year study period, plant ecology would be much the poorer. Then there is the study of successional processes, which may take several hundred years to reach completion. The subject is of considerable interest to both pure and applied ecologists but short-term studies have considerable weaknesses.

Some brief research projects concerning succession have been undertaken, such as that of Tramer (*Ecology* 56, 905; 1975) who observed abandoned agricultural plots over a three-year period. But it is difficult to derive general statements concerning the nature of the process from such a restricted view. Many researchers have tried to solve this problem by observing the extant stages in successions which have been proceeding for different lengths of time. Classical studies such as those of Crocker and Major (*J. Ecol.* 43, 427; 1955) on a glacial retreat recolonization and Olson (*Bot. Gaz.* 119, 125; 1958) on the sand dunes of the Great Lakes region are of this type. Similar studies have used abandoned agricultural land of known history, such as those of Bazzaz (*Ecology* 56, 485; 1975) and Nicholson and Monk (*Ecology* 55, 1075; 1974). This approach suffers from the disadvantage that one must assume that study sites are alike in all but the developmental time factor. Naturally, this is hardly ever the case.

Ideally, one would like to take a single location and study the changes in plant and animal populations over many decades, or even centuries. In Britain we are fortunate in that one such experiment has been in progress for over a century, and some of the resulting data has now been analysed by Silvertown (*J. appl. Ecol.* 17, 491; 1980).

This is the Park Grass Experiment at Rothamsted Experimental Station, which was begun in 1856 and which was originally intended to study the effects of various fertilizer regimes on grassland composition and productivity. The subdivision and replication of treatment plots was improved in 1964, but the data analysed by Silvertown covers only the period up to this revision.

From 1862, samples were cropped from the plots, were separated into species, dried and weighed. Plots which had received regular applications of ammonium sulphate were of lower pH and lower diversity (Shannon function), and all plots showed a negative relationship between overall biomass and diversity (and species richness).

The succession at Rothamsted has reached an equilibrium condition, under the constraints of harvesting imposed upon it. It is essentially a plagioclimax in the Tansley sense. Yet the variation of the equilibrium point in relation to nutrient capital and therefore biomass is of considerable interest for the theory of succession.

It adds considerable weight to the ideas of Green (*Biol. Conserv.* 4, 378; 1972) who regarded the successional process in chalk grassland to be an accretion of nutrients in the biomass and litter, resulting in increased dominance and consequently reduced diversity among the plants. The results also fit well into the Grime model (*Nature* 242, 344; 1973) if one regards increased fertilization as 'reduced stress', but the term over-simplifies the complexity of the system by reducing it to one dimension.

One of the particularly interesting features of the development of short turf into tall turf (increasing biomass) in grassland succession is that its influence upon invertebrate diversity is the reverse of that found in plants. As plant diversity falls, invertebrate diversity increases. This is considered by Morris (In *The Scientific Management of Plant and Animal Communities for Conservation*, ed. E. Duffey and A.S. Watt, Blackwell, Oxford, 527; 1971) to be a consequence of the increased opportunities for herbivorous grazers in the structurally and

microclimatically more complex environment offered by tall grassland plants. This, of course, will increase diversity at higher trophic levels also.

An Australian experiment has recently confirmed this relationship by monitoring the invertebrate faunas associated with different stock density of sheep. Hutchinson and King (*J. appl. Ecol.* 17, 369; 1980) sampled sites over a three year period which were grazed at densities of 10 sheep ha<sup>-1</sup>, 20 ha<sup>-1</sup> and 30 ha<sup>-1</sup>. Apart from Scarabaeid beetle larvae and Oligochaeta, which showed greatest mean abundance (no. m<sup>-2</sup>) and biomass in intermediate grazing levels, other groups showed a reduction in biomass and density as the grazing pressure increased. Here again, grazing pressure can be considered as a controlling influence upon habitat structure.

But what of vertebrates? Small mammals, like invertebrates, are more abundant in taller, undisturbed turf (Duffey, *J. Anim. Ecol.* 31, 571; 1962), but birds, particularly those which use grassland for feeding, seem to prefer short turf. In Sweden, Larsson (*Oikos* 20, 136; 1969) has shown a considerable decrease in the numbers and diversity of birds frequenting the grassland areas around some Swedish lakes, following the removal of cattle grazing, and the consequent increase in vegetation cover.

This change in avifaunal diversity and density with the successional development from short to long turf has some interesting implications for applied ecology. A survey by Brough and Bridgman (*J. appl. Ecol.* 17, 243; 1980) of thirteen airfields in Britain has shown very considerable differences in the density of feeding birds in short and long turf. The total counts over a two year period showed that three times as many birds overall used the short turf sites (which was defined as being a grass height of 5-10cm) when compared to long turf sites (grass height 15-20cm). In the case of gulls, the numbers feeding in long grass were only one fifth of those in short turf habitats. Their distaste for long turf may be associated with a greater difficulty in feeding upon soil invertebrates, coupled with a lack of visibility which might allow the approach of predators.

There thus seems to be a strong case for allowing the grassland succession on airfields to proceed beyond the short-turf stage and thus reduce the risk of bird strikes for aircraft. As Brough and Bridgman point out, however, there is one snag. The increased small mammal populations of the long grass may attract avian predators, such as kestrels and short-eared owls. But the data which they present suggests that these species are unlikely to reach seriously high population levels.

It would be pleasant to think that such a practical application of the study of what are essentially successional processes might encourage further and longer term studies.

Peter D. Moore is in the Department of Plant Sciences, University of London King's College.

# Actin assembly

from Sarah E. Hitchcock-DeGregori

A survey of the literature shows that the study of actin filament assembly is positively booming although it is one of the older areas in the contractile protein field.

Understanding of the polymerization of many protein polymers grew out of biophysical studies begun in the 1960s on the mechanism of actin polymerization<sup>1</sup>. The conversion of monomeric actin (G-actin) into filamentous actin (F-actin) has been viewed as a two-step condensation-polymerization process: condensation of a few actin monomers to form nuclei (the rate limiting step), followed by addition of monomers to form actin filaments (elongation). At steady-state, the F-actin is in equilibrium with a critical concentration of G-actin. Wegner<sup>2</sup> has proposed that actin elongates by a 'head-to-tail' mechanism, with a net addition of monomers to one end of the filament and a net depolymerization at the other end. While experimental work has supported the Wegner model, recent work suggests that the mechanism of actin assembly and disassembly may be more complex in detail<sup>3-5</sup>. The 'polymerizing' end of the filament has been shown to be the end that appears barbed in filaments decorated with myosin HMM or S<sub>1</sub><sup>6,7</sup>. It is also the end that is attached to the Z-line in muscle, to dense bodies and to microvilli.

The model seemed particularly suitable to those working on muscle as in rabbit and frog skeletal muscle actin is in 1  $\mu$  long thin filaments, and once assembled with tropomyosin and troponin to this miraculously constant length, it seems to stay there until it needs to be turned over for new protein. Although many questions remained unanswered, other aspects of muscle contraction, such as regulation and myosin kinetics, received more attention in the 1970's.

This situation has now changed with the new emphasis on non-muscle motility. Bray and Thomas<sup>8</sup> showed that a substantial amount of actin from cells is in a non-filamentous form. In addition, there have been numerous reports of changes in the state of actin which correlate with changes in cell shape and function.

It is now believed that the state of actin assembly is specifically regulated at a number of points, including (at a minimum) nucleation, addition of monomers at the net polymerizing end, loss of monomers at the net depolymerizing end (or other sites of depolymerization), and association of filaments to form bundles and networks. Nature has aided studies of these problems by supplying ready-made poisons, the cytochalasins and phalloidin, which interfere with one or more of these processes.

Sarah E. Hitchcock-DeGregori is in the Department of Biological Sciences, Carnegie-Mellon University, Pittsburgh.

First, the problem of nucleation. Although ionic conditions in the cell are highly favourable for polymerization of actin, much of it is non-filamentous. A protein called profilin that prevents the polymerization of actin has been isolated from a variety of sources<sup>9,14</sup>. Profilin combines with G-actin and inhibits the formation of nuclei. The dissociation of profilin from actin is promoted by agents that are known to form sites of attachment for actin filaments in cells. For example,  $\alpha$ -actinin is found in the Z-line and at other sites of filament attachment such as dense bodies in smooth muscle and adhesion plaques of stress fibers in cultured cells. Long suspected to be a promoter of actin polymerization,  $\alpha$ -actinin has now been shown to dissociate profilin from actin, thereby allowing polymerization<sup>16</sup>. Similar results are found with spectrin-actin complex from erythrocyte membranes and with nuclei of purified actin<sup>12,17,18</sup>. Once nucleation has taken place, elongation ensues, resulting in filament growth.

Assuming nucleating sites exist at all times in cells, an obligatory site of regulation is the elongation step. Cytochalasins and proteins with properties resembling cytochalasin are believed to regulate elongation. Research has focussed on the effect of cytochalasins on actin polymerization<sup>19</sup>. Cytochalasin binds to F-actin and spectrin-actin complex and inhibits polymerization, presumably by competing with the G-actin for the nucleating site. There is general agreement that, in terms of Wegner's head-to-tail model of elongation, cytochalasin inhibits polymerization by preventing addition of monomers to the preferred polymerization end, the barbed end of decorated actin filaments<sup>20,27</sup>. This results in net depolymerization and shortening of existing actin filaments. In addition, some investigators believe cytochalasin may also alter or fragment filaments<sup>28,30</sup>. It is probable that in the final analysis the mechanism of cytochalasin will be complex.

Recently, there have been reports of proteins with cytochalasin-like activities: from platelets<sup>31</sup> and *Acanthamoeba*<sup>32</sup>. The platelet factor competes with cytochalasin B for spectrin-actin complexes, inhibits polymerization of G-actin on to these complexes or on to actin nuclei, and when added to preformed actin filaments causes a slow loss of viscosity. The *Acanthamoeba* factor appears both to promote nucleation and to inhibit the rate of elongation. There is electron microscopic evidence that in the presence of this protein, actin monomers are added at the pointed end but not at the barbed end of the filament. When the factor is added to filamentous actin, some depolymerization is observed. Isenberg *et al.* have interpreted these results to suggest

that their factor, which they call capping protein, may promote nucleation by stabilizing actin dimers and then inhibiting elongation by allowing growth only in the 'slow' or pointed direction. Capping protein (see this issue of *Nature*, p 455) and the platelet protein<sup>33</sup>, like cytochalasin B, reduce the low shear viscosity believed to result from interactions between ends and sides of filaments and between filaments and other actin binding proteins<sup>27,28,34</sup> and gelation factors<sup>35,37</sup>. A factor with similar properties to capping protein has been isolated from conventional muscle actin preparations<sup>38</sup>. These proteins may have a role in regulating the consistency of the cytoplasm.

From these reports it seems highly likely that capping or cytochalasin-like proteins may regulate the elongation of actin filaments on existing nucleating sites. This leaves us the problem of depolymerization of actin. Change in cell shape involves, in some cases, rapid dissolution of filamentous structures. From *in vitro* studies, it appears unlikely that factors blocking the net polymerizing end of actin (if this is the correct interpretation) or nucleation (profilin) could cause rapid depolymerization, since the ionic conditions of the cytoplasm are highly favourable for polymerization. Rather, it seems likely that there will be factors that actively depolymerize actin. DNase I depolymerizes actin rapidly, apparently by acting directly on the filament<sup>3,39</sup>. Other factors that depolymerize actin in seconds or minutes *in vitro* have been isolated from plasma and serum<sup>40,42</sup> and the presence of depolymerizing factors in cells has been reported<sup>42,43</sup>. The detailed mode of action of these factors is the next problem that will have to be elucidated.

1. Oosawa, F. & Asakura, S. *Thermodynamics of Polymerization of Proteins*, Academic Press, New York (1975).
2. Wegner, A. *J. molec. Biol.* **108**, 139 (1976).
3. Hitchcock, S.E. *J. biol. Chem.* **255**, 5668 (1980).
4. Simpson, P.A. & Spudich, J.A. *Proc. natn. Acad. Sci. U.S.A.* **77**, 4610 (1980).
5. Simpson, P.A. & Spudich, J.A. *J. Cell Biol.* **87**, 227a (1980).
6. Woodrum, D.T., Rich, S.A. & Pollard, T.D. *Biol. Bull.* **147**, 503 (1975).
7. Kondo, H. & Ishiwata, S. *J. Biochem. (Tokyo)* **79**, 159 (1976).
8. Bray, D. & Thomas, C. *Biochem. J.* **147**, 221 (1975).
9. Carlsson, L., Nyström, L.-E., Sundkvist, I., Markey, F. & Lindberg, J. *molec. Biol.* **115**, 465 (1977).
10. Harris, H.E. & Weeds, A.G. *FEBS Lett.* **90**, 84 (1978).
11. Markey, F. & Lindberg, U. *FEBS Lett.* **88**, 78 (1978).
12. Reichstein, E. & Korn, E.D. *J. biol. Chem.* **254**, 6174 (1979).
13. Blikstad, I., Sundkvist, I. & Eriksson, S. *Eur. J. Biochem.* **105**, 425 (1980).
14. Fattoum, A., Roustan, C., Feinberg, J. & Pradel, L.-A. *FEBS Lett.* **118**, 237 (1980).
15. Maruyama, K. & Ebashi, S. *J. Biochem.* **58**, 13 (1965).
16. Blikstad, I., Eriksson, S. & Carlsson, L. *Eur. J. Biochem.* **109**, 317 (1980).
17. Brenner, S.L. & Korn, E.D. *J. biol. Chem.* **255**, 1670 (1980).
18. Grumet, M. & Lin, S. *Biochem. biophys. Res. Commun.* **92**, 1327 (1980).
19. Bray, D. *Nature* **282**, 671 (1979).
20. Brenner, S.L. & Korn, E.D. *J. biol. Chem.* **254**, 9982 (1979).
21. Brown, S.S. & Spudich, J.A. *J. Cell Biol.* **83**, 657 (1979).
22. Howard, T.H. & Lin, S. *J. Supramol. Str.* **11**, 283 (1979).
23. Lin, D.C. & Lin, S. *Proc. natn. Acad. Sci. U.S.A.* **76**, 2345 (1980).
24. Brenner, S.L. & Korn, E.D. *J. biol. Chem.* **255**, 841 (1980).
25. Flanagan, M.D. & Lin, S. *J. biol. Chem.* **255**, 835 (1980).



26. Lin, P.C., Tobin, K.D., Grumet, M. & Lin, S. *J. Cell Biol.* **84**, 455 (1980).
27. MacLean-Fletcher, S. & Pollard, T.D. *Cell* **20**, 329 (1980).
28. Hartwig, J.H. & Stossel, T.P. *J. molec. Biol.* **134**, 539 (1979).
29. Morris, A. & Tannenbaum, J. *Nature* **287**, 637 (1980).
30. Selden, L.A., Gershman, L.C. & Estes, J.E. *Biochem. biophys. Res. Commun.* **95**, 1854 (1980).
31. Grumet, M. & Lin, S. *Cell* **21**, 439 (1980).
32. Isenberg, G., Aebi, U. & Pollard, T.D. *Nature* this issue, p.455.
33. Grumet, M., Loonsk, J. & Lin, S. *J. Cell Biol.* **87**, 217a (1980).
34. Lin, D.C. & Lin, S. *J. Cell Biol.* **87**, 213a (1980).
35. Yin, H.L. & Stossel, T.P. *Nature* **281**, 583 (1979).
36. MacLean-Fletcher, S. & Pollard, T.D. *J. Cell Biol.* **85**, 414 (1980).
37. Pollard, T.D., Levy, J., Isenberg, G. & Aebi, U. *J. Cell Biol.* **87**, 223a (1980).
38. MacLean-Fletcher, S. & Pollard, T.D. *Biochem. biophys. Res. Commun.* **96**, 18 (1980).
39. Hitchcock, S.E., Carlsson, L. & Lindberg, U. *Cell* **7**, 531 (1976).
40. Chaponnier, C., Borgia, R., Rungger-Brändle, E., Weil, R. & Gabbiani, G. *Experientia* **35**, 1039 (1979).
41. Norberg, R., Thorstenson, R., Uter, G. & Fagraeus, A. *Eur. J. Biochem.* **100**, 575 (1979).
42. Harris, H.E. & Weeds, A.G. *Cell Biol. Int. Reports* **4**, 741 (1980).
43. Brown, S.S. & Spudich, J.A. *J. Cell Biol.* **87**, 224a (1980).

## Where do cosmic rays come from?

from a Correspondent

ABOUT once a second a single atomic nucleus carrying on its own at last 10 Joules of energy from Space hits an air nucleus in the Earth's atmosphere. It thereby initiates an enormous shower of secondary particles which builds up to an extensive air shower (EAS) of  $10^{10}$  particles by the time it reaches sea-level. Such a primary cosmic ray particle has been accelerated somewhere in the Universe through the equivalent of a voltage difference of  $6 \times 10^{19}$  volts. How and where this acceleration takes place remain among the major unsolved questions of high energy astrophysics.

The origin of cosmic ray particles has been a subject of controversy for more than 50 years and has resulted in something of an East-West divide amongst astrophysicists. On the one side V. L. Ginzburg (P. N. Lebedev Institute of Physics, Academy of Science of the USSR, Moscow) and others have argued consistently that these cosmic ray nuclei originate mainly in our own Galaxy. On the other side, British theoretical astronomers, such as G. R. Burbidge (University of California), have maintained that the sources must be extragalactic. Whichever viewpoint is held, however, there is general agreement that supernovae explosions play a significant part in cosmic ray particle acceleration.

Most cosmic rays, of course, have energies far less than the highest energy particles; the spectrum at the Earth peaks at energies of  $10^9$  eV per nucleus and falls rapidly to energies greater than  $10^{20}$  eV per nucleus ( $1 \text{ eV} = 1.6 \times 10^{-19}$  Joules). At the highest energies ( $>10^{18}$  eV per nucleus) astrophysicists have so far failed to produce a satisfactory model for the acceleration mechanism. Almost by a process of elimination, however, the net seems to be closing in on possible source regions. Briefly the case is as follows. The ultra-high energy particles cannot originate and remain captured in the Galactic disc because the Galactic magnetic field is not strong or extensive enough to contain the particles. For a Galactic origin it is generally thought that strong anisotropy in the particle arrival directions should exist — presumably from the centre of the Galaxy. Again, the particles cannot come

from the deep depths of space. They could not travel that far without colliding with the Universal  $2.7^\circ \text{ K}$  microwave background photons and undergoing strong absorption through pion production at energies greater than  $10^{19}$  eV per nucleus. The experimental evidence shows that rather than a cut-off in the cosmic ray energy spectrum occurring at  $10^{19}$  eV, it is just at this point that a flattening of the spectrum appears to occur. So where does that leave us?

The latest East-West confrontation took place recently in the beautiful old Russian capital of Leningrad where the VIIth European Cosmic Ray Symposium was held from September 15th-19th. Here A. W. Wolfendale (University of Durham) suggested that the problem could be resolved by a model in which those ultra-high energy particles reaching the Earth come predominantly from the nearby local supercluster of galaxies in Virgo. The actual sources would be active galaxies within the cluster of 2,500 galaxies. Wolfendale and his colleagues have developed their model to explain the available experimental data and it predicts an obvious anisotropy in the particles arrival direction at the Earth. Such an anisotropy in the general direction of Virgo is indeed observed for the highest energy particles detected by the Haverah Park EAS Detector Array in Yorkshire (*16th Int. Cosmic Ray Conf. Kyoto* **13**, 130; 1979).

At Leningrad J. Lloyd-Evans (University of Leeds) presented the latest data on the anisotropy analysis from the Haverah Park Group. These indeed confirm a sharp and significant change in the phase of preferred arrival direction from low Galactic latitudes to high positive latitudes as the primary energy increases above  $10^{19}$  eV in EAS detected at Haverah Park. This change occurs sharply at  $10^{19}$  eV per nucleus, just where the flattening in the energy spectrum is observed. So the Wolfendale model fits in well with the latest experimental data.

However, the 'extragalactic' Western scientists were not allowed to have it all their own way in Leningrad. D. D. Krasilnikov (Inst. of Cosmophysical Research and Astronomy, Yakutsk, USSR), presented a paper entitled

'Intensity Anisotropy of Highest Energy Cosmic Rays, its Energy Dependence'. In this the author considers the distribution on the celestial sphere of all the 313 cosmic ray particles with energies above  $10^{19}$  eV detected by the four large EAS detector arrays in England, Australia, US and the USSR. Krasilnikov too demonstrates that the anisotropy increases and changes phase as the primary energy increases. In particular, he selects out for special treatment the particles with energy/  $3 \times 10^{19}$  eV/nucleus. He splits the data in half in four different ways: (a) those coming from below and those above the Galactic equatorial belt of  $\pm 30^\circ$  latitude; (b) those coming from inside and those outside the Galactic equatorial belt of  $\pm 30^\circ$  from the Galactic centre; (c) those coming from opposite hemispheres pointing towards and away from the Galactic centre; and (d) those coming from opposite hemispheres pointing towards and away from the centre of the Virgo cluster. Taking the ratios of the intensities from the two groups in each of the four cases, Krasilnikov finds that only in case (c) does the intensity ratio ( $= 0.43 \pm 0.14$ ) differ significantly from unity. Thus he claims the measured anisotropy is associated with Galactic co-ordinates. The author therefore concludes that these results point to a Galactic source for the particles and infer a mass composition of heavy or middle mass nuclei and a modulation of their propagation directions by Galactic disc and halo magnetic fields. He argues that although supernovae can only directly accelerate the particles up to  $\sim 10^{17}$  eV per nucleus, further acceleration can be achieved by the magnetic fields of the Galaxy, both disc and halo, over time scales of  $10^7$  to  $10^8$  years.

Significantly, Krasilnikov needs heavy primary nuclei to support his theory. Unfortunately, as yet, there is little experimental guide as to the primary mass composition at these energies. What there is suggests that protons are still abundantly present as at lower energies. The East v West battle is thus still alive. We must now await the next round, to take place at the 17th IUPAP Conference in Paris next July.

The Leningrad symposium was, not unexpectedly, dominated by the Russians, since they combined the biannual European Symposium with an annual national cosmic ray meeting. The great magnitude of the Russian effort showed up forcefully in the special workshop session devoted to cosmogenic nuclides — that is the study of individual nuclear isotope concentration in meteorites. The analysis and interpretation of such data is now reaching a very high degree of sophistication.

### ERRATUM

In the News and Views article "Lessons from a peptidergic neurone" by B. T. Pickering (13 November, **288**, 117; 1980) the molecular weights quoted were incorrectly altered by the insertion of 'K' and should instead be read in Daltons.

## ARTICLES

## First Voyager view of the rings of Saturn

Stewart A. Collins\*, Allan F. Cook II†, Jeffrey N. Cuzzi‡, G. Edward Danielson§, Garry E. Hunt||, Torrence V. Johnson\*, David Morrison¶, Tobias Owen#, James B. Pollack‡, Bradford A. Smith\*\* & Richard J. Terrile\*

\* Jet Propulsion Laboratory, Pasadena, California 91109

† Harvard-Smithsonian Center for Astrophysics, Cambridge, Massachusetts 02138

‡ NASA/Ames Research Center, Moffett Field, California 94035

§ Division of Geological and Planetary Sciences, California Institute of Technology, Pasadena, California 91125

|| Department of Physics and Astronomy, University College London, London WC1E 6BT, UK

¶ Institute for Astronomy, University of Hawaii, Honolulu, Hawaii 96822

# State University of New York, Stony Brook, New York 11790

\*\* Department of Planetary Sciences, University of Arizona, Tucson, Arizona 85721

*Pictures taken from Voyager 1 between 3 September and 13 October 1980 at a resolution of ~1,000 km/lp reveal new data on Saturn rings.*

THE Voyager 1 spacecraft was launched on 5 September 1977 and successfully flew past Jupiter on 5 March 1979, assuming a trajectory to encounter Saturn on 12 November 1980. By mid-summer of 1980, at a range from Saturn of ~1 AU ( $1.5 \times 10^8$  km), the resolution of the Voyager Imaging System<sup>1</sup> had equalled that achieved in excellent seeing conditions with ground-based telescopes. Since then, pictures of the planet and its rings have revealed steadily increasing detail. We present here a preliminary discussion of imaging data for the rings at a resolution of about 1,000 kilometres per line pair (km/lp), corresponding to approximately 0.1 arcs as seen from Earth.

During the Voyager approach the spacecraft has viewed the planet from above (north of) the ecliptic plane, showing the rings open at an angle of ~9°. When seen from Earth at a similar opening angle, the surface brightness of the rings (illuminated by the Sun at about the same angle) is comparable to that of the planet. However, the rings as seen by Voyager are much darker, being illuminated at a low solar angle; the inclination to the Sun increased from zero on 3 March 1980 to 3.4° on 1 October.

The images we are using for the present analysis were obtained during the Voyager 1 Observatory Phase between 3 September and 13 October 1980. During that period the range to Saturn decreased from  $92 \times 10^6$  to  $40 \times 10^6$  km, and the resolution improved from 1,700 to 800 km/lp. The details of the ring are best shown in 3-s exposures with the clear filter (~300–650-nm bandpass). The photometric calibration of the Voyager cameras has been discussed in detail elsewhere<sup>2</sup>. We follow the traditional nomenclature for the rings of Saturn given by Alexander<sup>3</sup> and Cook *et al.*<sup>4</sup>, reserving the problem of naming recently observed structures within the rings until all of these features have been adequately defined.

### Appearance of the rings

As the spacecraft has approached Saturn, finer radial structure in the rings has become apparent. At a range of ~1 AU (~3,000 km/lp), the Encke Division in the A ring was first clearly visible. At ~0.5 AU, the existence of a separate maximum within the Cassini Division was apparent, and two prominent minima in the C ring became visible. By the time the resolution was 1,000 km/lp, considerable fine structure between the major divisions was apparent, and the first evidence of azimuthal structure appeared in the central parts of the B ring. Figure 1 illustrates the ring as seen at this level of resolution.

Table 1 lists the radial features of the rings that can be seen at a resolution of 1,000 km/lp. The terms maximum and minimum refer to features, possibly unresolved, in the radial brightness distribution. At higher resolution it may be possible to deter-

mine if these relative minima are clear regions with widths below our 1,000-km resolution limit, or are simply zones of lower particle density. Similarly, the features we now describe as relative maxima may reveal internal structure (for example, zones of lower brightness) at higher resolution.

The most dramatic discovery from images at 1,000-km/lp resolution has been extensive azimuthal structure within the B ring, at distances of ~104,000–116,000 km from the centre of Saturn. These non-axisymmetric features take the form of lanes, which are seen near the ring ansae, approximately radial to the planet, and 5–10% darker than surrounding areas. The time resolution during Observatory Phase (one observation each 2h) is insufficient to follow the evolution of any particular marking, so we do not know the lifetimes of these features, except that some persist for at least 3 h. A more detailed discussion of the non-axisymmetric features will be given elsewhere.

### Individual features

The centre of the Encke Division is at a distance of 133,400 km from the centre of Saturn ( $2.21 R_s$ , where  $R_s = 60,330$  km<sup>5</sup>). It is barely resolved in the Voyager images, indicating a width of 1,000–2,000 km. The position agrees well with that measured in transmission by Gehrels *et al.*<sup>6</sup> whereas the width seems somewhat greater than Gehrels' measurement (876 km).

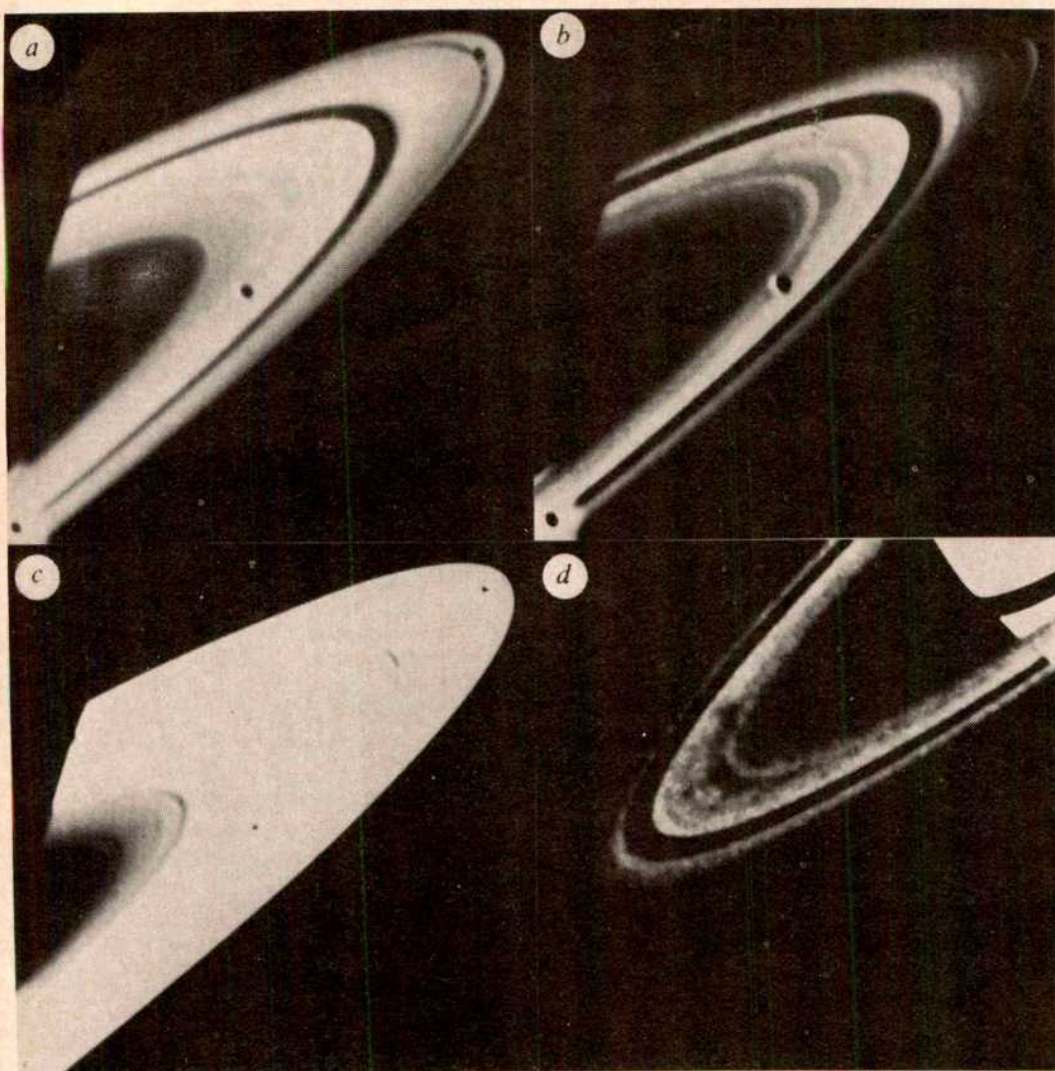
The Cassini Division has a width of about 4,000 km and is centred at 118,900 km ( $1.97 R_s$ ). It shows a nearly symmetrical brightness profile, as illustrated in Fig. 2. In the centre is a narrow ring, clearly separated from the A and B rings on either side. At current resolution this ring appears to be ~2,000-km wide. This ring also was seen by Pioneer, where it showed as a dark core in the bright Cassini Division; however, in diffuse transmission, as seen by Pioneer 11, it was ambiguous whether this feature corresponded to a local maximum or minimum in particle density. We now see that it is a maximum.

The most prominent features in the B ring, at this resolution, aspect and epoch, are three bright bands in the outer half of the ring, at distances of 102,300 km, 108,000 km and 116,300 km (see Fig. 2). Just outwards of the innermost bright feature is a minimum whose amplitude is time variable, which forms the inner boundary of the non-axisymmetric dark features that extend outwards almost as far as the outer edge of the B ring.

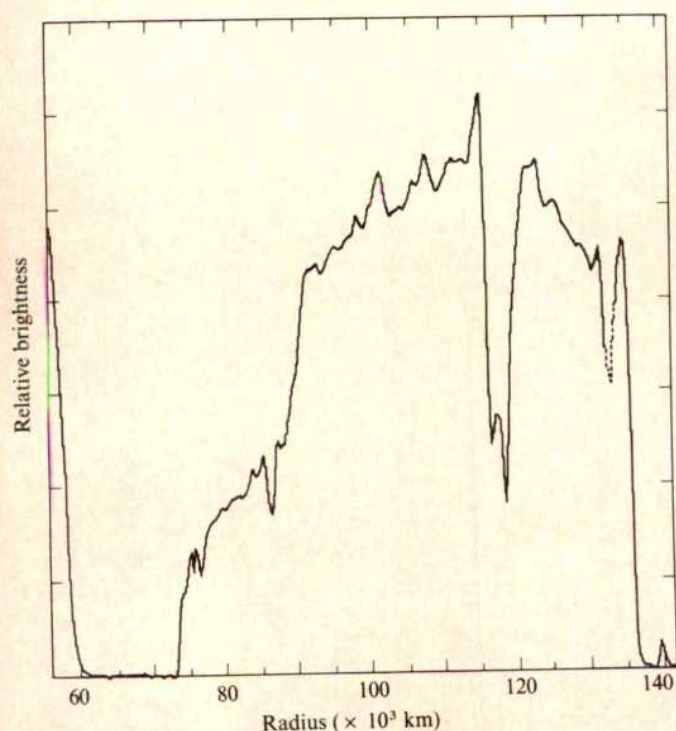
Inwards from the bright band (at 102,300 km) is a darker lane, followed by a fairly smooth decline in brightness to the edge of the B ring at 92,200 km. There is no indication of the deep minimum and prominent maximum near the inner edge reported by Dollfus<sup>7</sup>.

There are two prominent minima within the C ring, one at





**Fig. 1** *a*, *b* and *c* are three separate enhancements of a single Voyager 1 clear exposure (34032.33), taken on 13 October 1980 at a range of  $40.5 \times 10^6$  km (resolution 750 km/lp). *a* is enhanced to show the relative brightness of the major ring features: the C ring, B ring, Cassini Division (and material therein), A ring and Encke Division. *b* has been enhanced to show radial structure within the A and B rings. In *c*, the darker C ring has been enhanced. *d* is an image which was taken on 4 October 1980 from a distance of  $52 \times 10^6$  km (resolution 960 km/lp) and illustrates the non-axisymmetric structure that has been discovered in the outer part of ring B.



86,700 km and one at 77,300 km. Because neither is fully resolved at 1,000-km resolution, we do not know how dark these gaps are. The inner minimum (77,300 km) has not been previously reported whereas the outer minimum corresponds closely to a feature observed by the Pioneer 11 IR investigation<sup>8</sup> and apparently accounts for a feature seen in a Pioneer photograph of the ring shadow on the disk of Saturn. Gehrels *et al.*<sup>6</sup> erroneously assumed that this minimum was at the boundary between the B and C rings and identified it with the brightness maximum in diffusely transmitted light at the outer edge of the C ring, at 90,000 km. We now see that there is no prominent minimum between these two rings, and the minimum observed by Voyager is  $\sim 5,000$  km inwards of the B-C boundary.

The dimensions we obtain at a Voyager resolution of 1,000 km for the boundaries of the A, B, and C rings agree well with those obtained from ground-based observations<sup>4,9</sup> and from Pioneer 11 (ref. 6).

### Ring structure and satellite resonances

The radial structure in the rings has long been believed to result from the effects of gravitationally induced perturbations in ring

**Fig. 2** The brightness profile of the rings at 750-km/lp resolution is shown here, using the same image as Fig. 1*a-c*. On the left is Saturn's terminator. The dotted line in the Encke Division (133,500 km) indicates the location of a reseau mark in the original data; here the profile is taken from an adjacent trace (that is, one just removed from the image's semi-major axis) through the data. The small peak at 140,000 km is the F ring.

particle orbits resulting from resonances with the inner satellites, particularly Mimas (see, for example, ref. 10). The satellites S10 and S11 (refs 11, 12), both orbiting near the edge of the ring at  $1.51 \times 10^5$  km, provide potentially stronger perturbations than does Mimas. Other satellites may also have an influence on radial structure, particularly in view of the complex ring structure shown in the Voyager images. Because the difference in orbital longitude varies slowly for the two co-orbital satellites, S10 and S11 (ref. 13), ring structure may also have time-variable components.

Table 1 lists the assigned resonances for the various features in the rings. Table 2 lists all members of two types of resonance which fall within the rings. The satellites S10, S11, Mimas, Titan, Hyperion and Iapetus are the only ones which generate resonances of these two types within the rings. The resonances are characterized by multipliers of the mean orbital longitudes of the satellite,  $j'$ , and the particle in the ring,  $j$ . Resonances of Type I appear to the zeroth power in the orbital eccentricity of the satellite and involve  $j' - j = 1$ . Resonances of Type II, which are generally weaker, appear to the first power in the orbital eccentricity of the satellite and involve  $j' - j = 2$ . Note that resonances of Type I at  $j' = 1, j = 0$  involve an equality of the rate of advance of the line of apsides of a ring particle and of the mean motion of the satellite. The motions of the apsides are those induced by Saturn's oblateness.

Table 1 Ring features

| Feature  | Position*<br>( $\times 10^3$ km) | Position*<br>( $R_s$ ) | Resolved | Possible<br>resonance†                               |
|----------|----------------------------------|------------------------|----------|--|
| Saturn   | 60.33                            | 1.00                   | —        | —  |
| Inner C  | 73.2                             | 1.21                   | —        | S10, S11 (II, I)                                     |
| Maximum  | 74.5                             | 1.23                   | No       | —  |
| Minimum  | 75.0                             | 1.24                   | No       | None   |
| Maximum  | 75.5                             | 1.25                   | No       | —  |
| Minimum  | 76.0                             | 1.25                   | No       | None   |
| Maximum  | 76.3                             | 1.26                   | No       | —  |
| Division | 77.3                             | 1.28                   | Yes?     | Titan (I, 0)   |
| Diffuse  | 83.0                             | 1.38                   | Yes      | Hyperion (I, 0)                                      |
| Minimum  |                                  |                        |          |  |
| Maximum  | 84.5                             | 1.40                   | No       | —  |
| Minimum  | 85.3                             | 1.42                   | No       | None   |
| Maximum  | 86.0                             | 1.43                   | Yes      | —  |
| Division | 86.7                             | 1.44                   | Yes?     | None   |
| Maximum  | 88.3                             | 1.46                   | No       | —  |
| Minimum  | 89.6                             | 1.48                   | No       | None   |
| Maximum  | 90.1                             | 1.49                   | No       | —  |
| Inner B  | 92.2                             | 1.53                   | —        | S1 (II, 2)?  |
| Minimum  | 97.0                             | 1.61                   | ?        | S10, S11 (I, 2)                                      |
| Maximum  | 102.3                            | 1.70                   | No       | —  |
| Minimum  | 104.6                            | 1.73                   | Yes      | None   |
| Maximum  | 108.0                            | 1.79                   | Yes      | —  |
| Minimum  | 111.0                            | 1.84                   | Yes      | None   |
| Maximum  | 114.0                            | 1.88                   | No       | —  |
| Minimum  | 115.0                            | 1.90                   | No       | None   |
| Maximum  | 116.3                            | 1.93                   | No       | —  |
| Inner    | 117.5                            | 1.95                   | —        | Mimas (II, 2)  |
| Cassini  |                                  |                        |          |  |
| Center   | 118.9                            | 1.97                   | —        | —  |
| Cassini  |                                  |                        |          |  |
| Outer    | 121.0                            | 2.01                   | —        | S10, S11 (II, 5)<br>Iapetus (I, 0)                   |
| Cassini  |                                  |                        |          |  |
| Maximum  | 124.5                            | 2.06                   | Yes      | —  |
| Minimum  | 126.6                            | 2.10                   | No       | S10, S11<br>(II, 6; I, 3; II, 7)                     |
| Minimum  | 131.0                            | 2.17                   | No       | S10, S11<br>(II, 8; I, 4)                            |
| Encke    | 133.5                            | 2.21                   | Yes      | S10, SS11<br>(II, 9; II, 10; I, 5);<br>Mimas (II, 4) |
| Division |                                  |                        |          |  |
| Outer A  | 136.2                            | 2.26                   | —        | S10, S11<br>(II, 12; I, 6)                           |

Region of azimuthal structure ranges from 1.72 to  $\sim 1.92 R_s$ .

\* All  $\pm 500$  km, except those underlined, which are  $\pm 1,000$  km.

† Notation for resonances consists of Type (I or II) and multiplier  $j$  of longitude of ring particle in argument of libration (see Table 2).

Table 2 Resonances with known satellites

| Satellites | Type | $j'$ | $j$ | Distance<br>( $R_s$ ) | Comments                                    |
|------------|------|------|-----|-----------------------|---|
| S10, S11   | II   | 3    | 1   | 1.227                 | Inner edge, C                               |
| Titan      | I    | 1    | 0   | 1.289                 | Gap (1.28)                                  |
| Hyperion   | I    | 1    | 0   | 1.396                 | Seen? (1.38)                                |
| Mimas      | II   | 3    | 1   | 1.495                 | Not seen                                    |
| S10, S11   | II   | 4    | 2   | 1.591                 | Not separable from next                     |
|            | I    | 2    | 1   | 1.595                 | See (1.61)                                  |
|            | II   | 5    | 3   | 1.792                 | Not seen                                    |
|            | II   | 6    | 4   | 1.921                 | Not separable from next                     |
| Mimas      | I    | 3    | 2   | 1.922                 | Not seen                                    |
|            | II   | 4    | 2   | 1.945                 | Not separable from next                     |
|            | I    | 2    | 1   | 1.948                 | Inner part of Cassini Division (inner edge) |
| S10, S11   | II   | 7    | 5   | 2.010                 | Not separable from next                     |
| Iapetus    | I    | 1    | 0   | 2.010                 | Outer part of Cassini Division (outer edge) |
| S10, S11   | II   | 8    | 6   | 2.075                 | Not separable from next                     |
|            | I    | 4    | 3   | 2.076                 |   |
|            | II   | 9    | 7   | 2.125                 | Seen (2.10)                                 |
|            | II   | 10   | 8   | 2.166                 | Not separable from next                     |
| Mimas      | I    | 5    | 4   | 2.166                 | Seen (2.17)                                 |
|            | II   | 5    | 3   | 2.193                 | In Encke Division                           |
| S10, S11   | II   | 11   | 9   | 2.199                 | In Encke Division                           |
|            | II   | 12   | 10  | 2.225                 | Not separable from next                     |
|            | I    | 6    | 5   | 2.225                 | In Encke Division                           |
|            | II   | 13   | 11  | 2.247                 | Not seen                                    |
| S10, S11   | II   | 14   | 12  | 2.267                 | Not separable from next                     |
|            | I    | 7    | 6   | 2.267                 | Outer edge, A                               |

Tables 1 and 2 show that as the density of matter in ring C increases outward, the divisions due to S10 and S11 disappear; this happens first for resonances of Type II, then for those of Type I. Those of Type I reappear outside the Cassini Division and may form the outer edge of ring A. For Mimas there is good evidence only for resonances of Type I. The Type I apsidal resonance from Iapetus may contribute to structure within the Cassini Division. Hyperion's small size casts doubt on the assignment listed.

It is clear from Tables 1 and 2 that the classical satellite resonances do not explain most of the fine structure seen in the rings. Some of the structure may be generated by the presence of small, as yet undiscovered satellites within the rings, for example, at the edges of major divisions. These satellites may produce additional maxima and minima through their orbital resonances; they may also serve as sources for some of the ring material. The presence of the spoke-like azimuthal structures in the B ring reminds us that other dynamical processes may also be important in producing observed features.

### Preliminary ring photometry

The ring brightness is of great interest, as it contains implications as to the constituent particle albedos and phase functions. Several previous studies<sup>14,15</sup> have been conducted to determine these parameters. We have made preliminary model calculations of ring brightness using a doubling-adding radiative transfer code<sup>16</sup> for the geometry of these observations. Although the data reduction is as yet preliminary, certain overall conclusions may be drawn.

Due to the low Sun angle ( $\sim 3^\circ$ ), the dependence of observed brightness on layer optical depth is small. We find that the constituent particles of the A and B rings are characterized by a greater degree of diffuse backscattering ability than previously



suspected. In fact, particles behaving like Lambert spheres provide quite a good fit to the observed A- and B-ring brightness.

However, the C ring has noticeably different properties. For an optical depth  $\sim 0.1$  (refs 15, 17), the C ring would be nearly as bright as the A and B rings at the present epoch, if the constituent particles were identical. However, Voyager observations show it to be less than half of the A and B brightness. Fuller phase-angle coverage, obtained subsequently in the mission, will be required for a distinction to be made between albedo and phase-function effects. However, the unambiguous implication is that the C-ring particles are different, either darker or more highly forward scattering than the A- and B-ring particles. This qualitative conclusion is consistent with the conclusions of recent analyses of Pioneer Saturn data<sup>15,18</sup>. This observation argues very strongly for a different particle population in the C

ring as compared with the main rings. More data and analysis will refine these preliminary conclusions.

The figures and much of the data reduction for this article were provided by the Image Processing Laboratory at the Jet Propulsion Laboratory. We particularly thank G. W. Garneau and L. R. Doyle for assistance. G. E. Hunt is supported by the SRC. This report presents the results of one phase of research carried out at JPL under NASA contract NAS7-100.

*Note added in proof:* Subsequent Voyager observations have shown the azimuthal features which appear dark in back-scattered light reverse contrast and appear bright against the background B ring in forward-scattered illumination. This behaviour indicates that these features result from concentrations of small particles (a few micrometres) and not from variations in the B-ring particle density.

Received 31 October; accepted 17 November 1980.

1. Smith, B. A. *et al. Space Sci. Rev.* **21**, 103 (1977).
2. Danielson, G. E. *et al.* (in preparation).
3. Alexander, A. F. O'D. *The Planet Saturn* (Faber and Faber, London, 1962).
4. Cook, A. F. II, Franklin, F. A. & Palluconi, F. D. *Icarus* **18**, 317 (1973).
5. Klore, A. J. *et al. J. geophys. Res.* (in the press).
6. Gehrels, T. *et al. Science* **207**, 434 (1980).
7. Dollfus, A. *Icarus* **12**, 101 (1970).
8. Ingersoll, A. P. *et al. Science* **207**, 439 (1980).
9. Reese, E. J. *Icarus* **15**, 466 (1971).
10. Franklin, F. A. & Colombo, G. *Icarus* **12**, 338 (1970).
11. Dollfus, A. *IAU Circ. No.* 1995 (1967).
12. Fountain, J. W. & Larson, S. M. *Icarus* **36**, 92 (1978).
13. Smith, B. A. *et al. Bull. Am. astr. Soc.* **12**, 727 (1980).
14. Kawata, Y. & Irvine, W. M. in *The Exploration of the Solar System* (eds Wozniak & Iwaniszewska) (Reidel, Boston, 1974).
15. Esposito, L., Dilley, J. P. & Fountain, J. W. *J. geophys. Res.* (in the press).
16. Hansen, J. E. *Astrophys. J.* **155**, 565 (1969).
17. Cuzzi, J. N. in *The Saturn System* (eds Hunten, D. M. & Morrison, D.) (NASA CP-2068, 1978).
18. Gehrels, T. *J. geophys. Res.* (in the press).

## Planform of mantle convection beneath the Pacific Ocean

Dan McKenzie\*, Anthony Watts†, Barry Parsons‡ & Micheline Roufosse§

\* Bullard Laboratories, Department of Earth Sciences, University of Cambridge, Madingley Road, Cambridge CB3 0EZ, UK

† Lamont-Doherty Geological Observatory and Department of Geological Sciences of Columbia University, Palisades, New York 10964

‡ Department of Earth & Planetary Sciences, MIT, Cambridge, Massachusetts 02139

§ Smithsonian Astrophysical Observatory, Cambridge, Massachusetts 02138

*The correlation between variations of the bathymetry and of the geoid in the Pacific Ocean suggests that both are the surface expression of mantle convection. The planform of the convection which is required to generate the observed anomalies does not consist of rolls but is three dimensional, with rising and sinking jets elongated in the direction of motion of the Pacific plate relative to the frame of reference defined by the hot spots. The spacing between the maxima and minima of the geoid is between 1,500 and 2,000 km and hence favours a model of mantle convection with multiple scales of circulation.*

ALTHOUGH most geophysicists agree that plate motions are maintained by mantle convection, there is little agreement about the geometry of the motion which converts heat into work. One of the principal difficulties is that the motion of the plates themselves provides a few restrictions on the form of the flow, because their motion can be described by rigid body rotations. Runcorn<sup>1</sup> recognized that long-wavelength gravity anomalies should be directly related to the fluid motion, and McKenzie *et al.*<sup>2</sup> showed that upper surface of the convecting region with constant viscosity was elevated, producing a positive gravity anomaly, over the rising region of the flow. The influence of the elastic forces within the plate on the magnitude and sign of the anomalies of gravity and bathymetry above a convecting region<sup>3,4</sup> is small if their wavelength is  $> 500$  km and the elastic thickness of the plates is  $\leq 30$  km (ref. 5). The wavelengths are expected to be at least twice the depth of the convecting region, or  $> 1,400$  km, if the convection is confined to the upper mantle. The amplitudes of the gravity and bathymetry anomalies obtained from the numerical calculations are about 20 mGal and 500 m respectively. Hence the anomalies should be easily observed, correlated with each other, and be little affected by the elastic behaviour of the plates. Two difficulties must be overcome before geophysical observations can be used to examine the convective planform. The first involves corrections to the observed bathymetry to remove the effects of lithospheric

age, determined from the magnetic anomalies, and of sediment loading. Both of these can now be calculated with reasonable accuracy, and the depth obtained after these corrections has been applied is known as the residual depth. Only that part of the residual depth which is not produced by variations in crustal thickness and whose wavelength is longer than  $\sim 500$  km is dynamically maintained by the convection. The other difficulty concerns the gravity field. Surface observations contain large amplitude short wavelength anomalies, and long wavelength errors are produced by drift of the instrument and calibration errors. For these reasons the long wavelength gravity anomalies can only be reliably obtained from surface ship observations in areas where there is dense coverage.

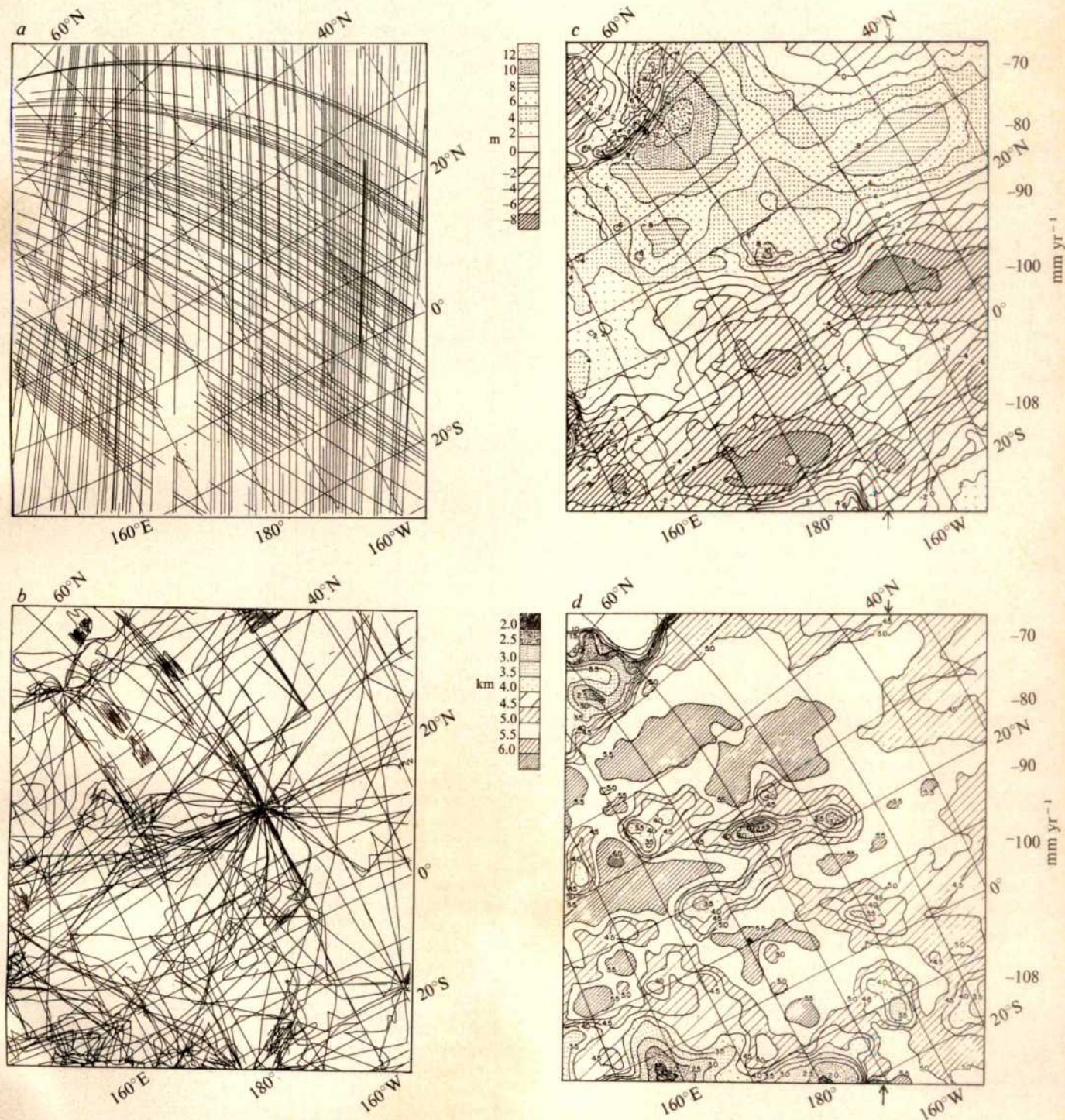
### Historical techniques

The first attempt to use these arguments to investigate mantle convection<sup>6</sup> used the depth of the ridge axis and a satellite-derived gravity field. The procedure avoided the use of depth corrections, as the age of the ridge axis is the same everywhere and the sediment cover is very thin. Although the correlation between gravity and residual depth was clear in the North Atlantic, where it agreed with the numerical calculations, it was much less convincing in the other oceans. This behaviour was probably produced by errors in the satellite gravity field, whose



higher harmonics were poorly determined. Extensive two-dimensional investigations of gravity and residual depth anomalies in the North Atlantic<sup>4</sup> and the Pacific around Hawaii<sup>7</sup> using surface gravity observations showed good agreement with the numerical models but neither covered a large enough area to demonstrate the convective planform. Cochran and Talwani<sup>8</sup> considered a larger region but failed to find a global relationship between gravity and residual depth similar to that found in the smaller regions<sup>4,7</sup>. Their lack of success was probably due to the poor sampling of the long-wavelength part of the gravity field due to the wide spacing of the ship tracks. Figure 3 shows that the amplitude of the gravity anomalies corresponding to 10 m variations in geoid height is only  $\sim 20$  mGal. Such gravity

anomalies will be difficult to detect in the presence of short wavelength anomalies of hundreds of mGal produced by seamounts, and measurement errors of at least 10 mGal. Menard and Dorman<sup>9</sup> attempted to use the bathymetry alone to examine the convective planform. Because long-wavelength variations in bathymetry may be isostatically compensated, and hence be unrelated to mantle convection, it is not obvious what constraints a study of the bathymetry alone imposes on the form of the circulation (see Fig. 2). An attempt<sup>10</sup> to obtain a gravity field over the Pacific from satellite orbits and surface gravity seems to have produced spurious anomalies, due to lack of sufficient surface observations and an instability caused by downward continuation<sup>11</sup>.



**Fig. 1** Satellite altimeter (a) and ship (b) tracks used to obtain contour maps of geoid (c) and bathymetry (d) in the North and Central Pacific. The projection is an oblique mercator projection with axis  $61.7^\circ\text{N}$ ,  $-82.8^\circ\text{E}$ . Contour intervals are 2 m for (c) and 0.5 km for (d). The grid spacing in both cases is 100 km at the equator of the projection, and the gaussian half width for interpolation is 110 km for (c), 150 km for (d). The velocities shown on the right of (c) are those of the Pacific plate, moving from right to left, relative to the hot spot frame<sup>15</sup>, and is  $108 \text{ mm yr}^{-1}$  at the equator of the projection.



A detailed analysis of the gravity field and surface deformation above different types of convection<sup>12</sup> showed that their ratio depends little on the form of the heating, the Rayleigh number, or the boundary conditions. Hence little further progress could be made until more accurate estimates of gravity anomalies between wavelengths of 500 km and 5,000 km became available over large areas of the oceans. GEOS 3 has now provided such estimates by direct determination of the geoid.

### GEOS 3 measurements

The GEOS 3 satellite contains a radar altimeter which measures the distance from the satellite to the sea surface. If the orbit of the satellite and oceanographic corrections are known the geoid can be obtained directly. In practice, the precision of the altimeter is between 0.5 and 1 m, and analysis of the cross-over errors between different tracks shows errors of  $\sim 10$  m (ref. 13) due to orbit errors. The orbit errors can be reduced to about 0.6 m by adjusting the orbits to minimize the cross-over errors<sup>13</sup>. We used these adjusted heights. Oceanographic corrections consist of tides and both time-dependent and steady-state variations produced by currents. These corrections are poorly known, but are probably  $< 1$  m in most parts of the ocean and were therefore ignored. The heights  $h_i$  corrected for bias and trend<sup>13</sup>, at points described by radial unit vectors  $\mathbf{a}_i$  were then filtered with a gaussian filter to give a smoothed height  $H_i$  at position  $\mathbf{b}_i$ ,

$$H_i = \sum_j h_j \omega_j / \sum_j \omega_j, \quad \mathbf{b}_i = \sum_j \mathbf{a}_j \omega_j / \sum_j \omega_j$$

$$\omega_j = \exp(-d_j^2/\sigma^2) \quad (1)$$

where  $d_j$  is the distance between a chosen point on the profile and  $\mathbf{a}_j$ , and  $\sigma$  is the half width of the gaussian filter, chosen to be 100 km. In addition a weight  $W_i$  was obtained from the ratio of the rectangular approximation to the integral of the filter to the true integral

$$W_i = S \sum_j \omega_j / \sigma \sqrt{\pi}$$

where  $S$  is the spacing between successive points on the profile. If  $W_i < 0.3$  the point was rejected. This processing reduced the number of data points while leaving unchanged longer wavelength features of the geoid. Because the geoid is dominated by long wavelength anomalies ( $\lambda > 5,000$  km) and we are principally interested in those of intermediate wavelength, we subtracted the GEM7 geoid<sup>14</sup> up to and including  $l = m = 10$ . GEM7 was used because this geoid was determined from satellite orbits alone, and because the coefficients of degree and order  $< 10$  agree excellently with those of more recent determinations. The points  $\mathbf{b}_i$  were projected onto a plane to give a position  $\mathbf{x}_i$ , and  $H_i$  then interpolated onto a square mesh using equation (1) with  $\sigma = 110$  km,  $d_i$  being the distance between a mesh point and  $\mathbf{x}_i$  in the plane of the projection, provided  $d_i < 4\sigma$ . Otherwise  $\omega_i$  was set to zero. Finally the grid values were machine contoured. The bathymetry obtained from digitized profiles of more than 400 cruises in the Pacific Ocean treated similarly, except for the interpolation onto a square mesh where  $\sigma = 150$  km was used.

### Results

Figure 1 shows contour maps of the geoid and bathymetry, together with the satellite and ship tracks used. The area was chosen because it is large and well studied. Except in the upper right-hand corner of Fig. 1 sediment thicknesses are thin and uniform, and hence sediment loading corrections, which were not made, will produce little change in Fig. 1d. The depths in Fig. 1 have also not been corrected for subsidence as the lithosphere cools. Such corrections are also only important in the upper right-hand corner of Fig. 1, because the remainder of the area studied is underlain by lithosphere older than 60 Myr. The projection is an oblique mercator projection with the pole of relative motion between the Pacific plate and the hot spot frame

as an axis<sup>15</sup>, and the mesh spacing in Fig. 1c,  $d$  is 100 km on the equator of the projection. The region shown in Fig. 1 covers most of the North and Central Pacific. An accurate short wavelength anomaly produced by the Aleutian Island Arc is clearly visible at the top left of Fig. 1c, the anomaly on the left-hand edge is produced by the Mariana Island Arc, and those along the bottom by the Solomon and Tonga arcs. The geoid contours show the existence of elliptical maxima and minima whose amplitude is about 8 m and whose separation is between 1,500 and 2,000 km. One of the largest of these anomalies is associated with the Hawaiian Swell and has already been mapped using ship profiles<sup>5</sup>. The anomalies in Fig. 1c are too large and their separation is too great to be supported by the elastic part of the lithosphere, and therefore they must be dynamically maintained by mantle convection. Figure 1d shows that many of the geoid anomalies in Fig. 1c are associated with bathymetric anomalies. Figure 2 shows two profiles obtained from the values of the geoid and the bathymetry on the mesh points and plotted against distance in the oblique mercator projection to show the correlation more clearly. These two profiles are in the eastern part of the Pacific, where the geoid anomalies are large. The shoal region at the northern end of the profile is produced by the young lithosphere near the Gorda and Juan da Fuca ridge crests. This bathymetric anomaly does not correlate with the geoid and will be removed by the age corrections which have not yet been applied. Such corrections will not remove depth variations which are maintained by variations in crustal thickness, produced by vulcanism either on ridge axes or within plate interiors. Two such features, the Line Islands ridge and the Manihiki Plateau, are crossed by the profiles in Fig. 2 and both were produced by ridge axis vulcanism. Neither the crustal thickness nor the density of such ridges is well known, and therefore corrections are hard to apply. Towards the trench systems in the west the geoid is flatter than in the east, and several small anomalies of 2 and 4 m are associated with some of the large aseismic plateaus, such as the Shatsky and Hess Rises. Ridge axis vulcanism, which builds aseismic ridges at or above sea level on thin lithosphere, gives rise to anomalies of this magnitude, and there are many such features in the western Pacific<sup>16</sup>.

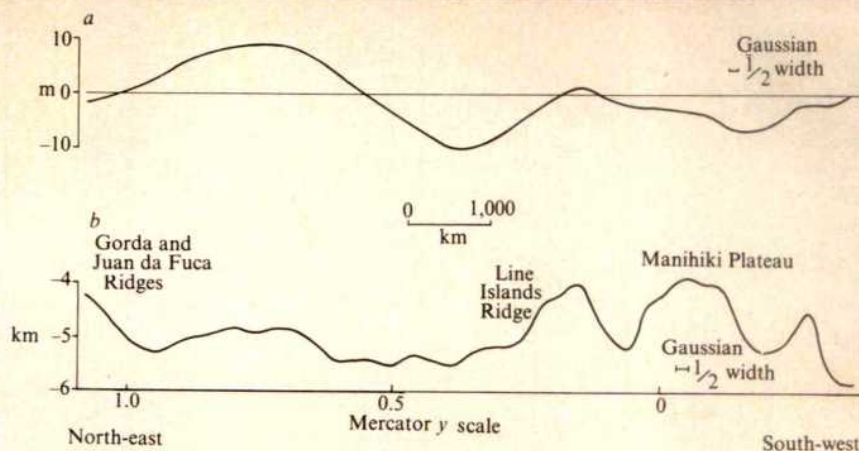
The geoid anomalies in Fig. 1c are mostly elliptical, with the long axes of the ellipses approximately parallel to the  $x$  axis of the plot. As the projection is an oblique mercator projection whose axis is the pole of relative motion between the Pacific plate and hot spot frame, the rigid motion of the Pacific plate in Fig. 1c corresponds to a translation in the  $x$  direction. The relative velocity in this projection is  $v_0 \operatorname{sech} y$ , where  $v_0$  is the equatorial velocity and  $y$  is the vertical coordinate of the mercator projection, and is shown on the right of Fig. 1c. The ellipticity suggests that the convective pattern is elongated in the direction of motion. The contours provide evidence that the elongation increases with increasing velocity.

### Discussion

The above observations provide various constraints on models of mantle convection. Perhaps the most important is that the geoid strongly suggests the existence of mantle convection whose horizontal scale is considerably smaller than that of the plates themselves, and that the elongation of the anomalies in one direction results from the shearing of the circulation by plate motions. Such a model has previously been proposed on theoretical grounds<sup>3,17</sup>; where it was argued that the spacing between the rising and sinking regions should be similar to the depth of the convecting layer, and that the planform of the flow would probably consist of rolls aligned with their axes in the direction of motion, at least beneath rapidly moving plates such as the Pacific. This conclusion was qualified by Skilbeck and McKenzie<sup>18</sup> who used an approximate method to examine the stability of a model suggested by Richter and McKenzie<sup>19</sup>, which possessed a low viscosity zone beneath the plates which decoupled the horizontal movement of the plates from that of the mantle below. The calculations suggested that even the Pacific



**Fig. 2** Profiles of the geoid (*a*) and bathymetry (*b*) between the arrows on Fig. 1c, d. The horizontal axis shows the *y* coordinate in the oblique mercator projection, and the scale applies at *y* = 0.



was unlikely to be moving sufficiently fast to stabilize rolls, and that the small scale flow would probably be three dimensional. An alternative explanation is suggested by the experiments of Richter and Parsons<sup>17</sup> on the evolution of sheared convection. As the geometry of the Hawaiian Ridge requires the motion of the Pacific plate in the hot spot frame to have changed ~40 Myr ago, the present direction of motion may not have existed for long enough to have established rolls. It is obviously of interest to extend the observations of Richter and Parsons<sup>17</sup> to slower shearing rates.

Figure 3a, b and c shows the geoid, bathymetry and gravity produced by the convective flow in Fig. 3d, e. The depth of the convective layer is 700 km, the Rayleigh number is  $1.4 \times 10^6$ , and the flux is fixed at  $58.5 \text{ mW m}^{-2}$  on both boundaries (see refs 2 and 20 for details). Both horizontal and vertical scales are the same as those in Fig. 2 at the equator of the projection. Both the horizontal scale and the amplitude of the bathymetry and geoid in Fig. 3 are similar to those in the Pacific. Superimposed on the cellular circulation is a time-dependent flow driven by hot and cold blobs detaching from the boundaries. This flow produces obvious bathymetric and gravity anomalies, but the wavelength is too small to produce more than 1 m anomalies in the geoid. Similar numerical experiments with the more realistic boundary condition of a plate superimposed on top of the convecting region also show that the spacing is often considerably greater than the layer depth (G. Houseman, personal communication). Hence the geometry suggested by Fig. 1 is to be expected, and is not evidence for whole mantle convection.

An unexpected feature of the geometry of the geoid anomalies is that they are larger in the east where the plate is young than they are in the west where it is old. This distribution suggests that they are not the result of instabilities beneath the cooling plate, and hence are not related to the flow postulated by Parsons and McKenzie<sup>21</sup> to account for the observed relation between depth and age. The anomalies are better explained by instabilities of a lower hot boundary layer, perhaps at the base of the upper mantle. Near the trenches, where cold material is returned to the base of the convecting layer, the lower boundary layer is stable. As this material moves towards the east it is warmed by heat conducting into the upper mantle from the lower mantle, and becomes unstable. The same behaviour is clearly seen in the right-hand cell in Fig. 3d. The geoid anomalies are the surface expression of these instabilities.

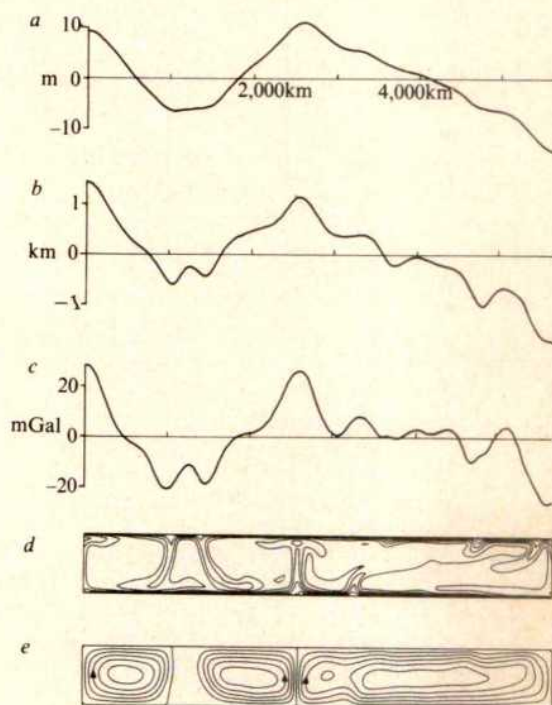
Transfer of heat to the base of old lithosphere could still be produced by small cold blobs detaching from its base, similar to those on the right of Fig. 3d, because the geoid anomalies they would produce would be similar in magnitude to the noise (Fig. 3a). Such blobs would, however, produce obvious anomalies in the gravity field (Fig. 3c).

Some of the existing models of the return flow on a spherical Earth<sup>22-24</sup> show that the return flow is approximately antiparallel to the plate motion, and therefore can account for the elongation of the geoid anomalies in Fig. 1. All these models, however, neglect the thermal buoyancy forces in the interior of

the convecting region. As such forces are dominant within large aspect ratio convective cells, such as that on the right in Fig. 3, the direction of flow obtained from the model calculations may not agree well with that in the mantle.

## Conclusions

The observations discussed above have little relevance to whether the convective circulation involved in plate movements is confined to the upper mantle or extends throughout the whole mantle. If the whole mantle is convecting its Rayleigh number must be  $10^9$ – $10^{10}$  and the flow must be principally driven by internal heating. In these conditions the horizontal scale is



**Fig. 3** Profiles of the geoid (*a*), bathymetry (*b*) and gravity (*c*) above a convecting fluid where the planform of the convection consists of two-dimensional rolls normal to the plane of the page. In all three cases the surface deformation obtained by the method outlined in ref. 12 has been convolved with the response of an elastic plate 30 km thick<sup>3</sup>. The horizontal scales are the same as those in Fig. 2 at the equator of the projection, and the vertical scales are the same. The temperature (*d*) contoured at 100°C intervals and the stream function (*e*) at 0.1 intervals are for a Rayleigh number of  $1.4 \times 10^6$  with both upper and lower boundaries stress free and deformable. All the heat is supplied from below and the heat flux, not the temperature, is fixed on both boundaries (see ref. 20 for details).



controlled by the thickness of the boundary layer, and may be much smaller than the depth of the layer itself. In contrast, if the circulation is restricted to the upper mantle the boundary conditions<sup>20</sup> may produce a circulation whose horizontal scale is considerably greater than its depth (Fig. 3). Hence the horizontal scale is very little guide to the vertical extent of the flow. Nonetheless, the geometry of the anomalies is more easily explained by instabilities of hot lower boundary layer, which exists only if heat is supplied from below. Although the existence of such a boundary layer is required by models in which the flow is confined to the upper mantle, it is possible, though unlikely,

that the unstable layer is as deep as the core-mantle boundary and that a considerable fraction of the heat is supplied from within the core. There is some evidence that models in which all the heat is supplied by internal heating are not compatible with the anomaly distribution, because instabilities can only originate in the upper boundary layer. The presence of large anomalies over the younger but not the older part of the Pacific suggests that the instabilities arise in the lower, not the upper, boundary layer.

We thank R. Rapp for providing the corrected altimetry profiles, and NASA, the Office of Naval Research, the NERC, and the Smithsonian Institution, for grants.

Received 13 June; accepted 19 September 1980.

1. Runcorn, S. K. *Phil. Trans. R. Soc. A* **258**, 228 (1965).
2. McKenzie, D. P., Roberts, J. M. & Weiss, N. O. *J. Fluid Mech.* **62**, 465 (1974).
3. McKenzie, D. P. & Weiss, N. O. *Geophys. J. R. astr. Soc.* **42**, 131 (1975).
4. Sclater, J. G., Lawver, L. A. & Parsons, B. *J. geophys. Res.* **80**, 1031 (1975).
5. Watts, A. B. *J. geophys. Res.* **83**, 5989 (1978).
6. Anderson, R. N., McKenzie, D. P. & Sclater, J. G. *Earth planet. Sci. Lett.* **18**, 391 (1973).
7. Watts, A. B. *J. geophys. Res.* **81**, 1533 (1976).
8. Cochran, J. R. & Talwani, M. *Geophys. J. R. astr. Soc.* **50**, 495 (1977).
9. Menard, H. W. & Dorman, L. M. *J. geophys. Res.* **82**, 5329 (1977).
10. Marsh, B. D. & Marsh, J. G. *J. geophys. Res.* **81**, 5267 (1976).
11. Watts, A. B. *J. geophys. Res.* **83**, 3551 (1978).
12. McKenzie, D. P. *Geophys. J. R. astr. Soc.* **48**, 211 (1977).
13. Rapp, R. H. *J. geophys. Res.* **84**, 3784 (1979).
14. Wagner, C., Lerch, F., Brown, J. & Richardson, J. *J. geophys. Res.* **82**, 901 (1977).
15. Minster, J. B. & Jordan, T. H. *J. geophys. Res.* **83**, 5331 (1978).
16. Watts, A. B., Bodine, J. H. & Ribe, N. M. *Nature* **283**, 532 (1980).
17. Richter, F. M. & Parsons, B. *J. geophys. Res.* **80**, 2529 (1975).
18. Skilbeck, J. N. & McKenzie, D. P. *Pageophysics* **117**, 958 (1979).
19. Richter, F. & McKenzie, D. *J. Geophys.* **44**, 441 (1979).
20. Hewitt, J. M., McKenzie, D. P. & Weiss, N. O. *Earth planet. Sci. Lett.* **51** (in the press).
21. Parsons, B. & McKenzie, D. P. *J. geophys. Res.* **83**, 4485 (1978).
22. Parmentier, E. M. & Oliver, J. E. *Geophys. J. R. astr. Soc.* **57**, 1 (1979).
23. Chase, C. G. *Geophys. J. R. astr. Soc.* **56**, 1 (1979).
24. Hager, B. H. & O'Connell, R. J. *J. geophys. Res.* **84**, 1031 (1979).

# Vesiculation of mafic magma during replenishment of silicic magma reservoirs

J. C. Eichelberger

Sandia National Laboratories, Albuquerque, New Mexico 87185

*Mafic inclusions are lower in bulk density than the andesitic and dacitic lavas in which they occur, and apparently represent a foam inflated during rapid cooling of wet mafic magma in contact with cooler, more silicic reservoir magma. This process occurs as mafic magma enters the base of the reservoir, so that the mafic/silicic interface becomes unstable in Rayleigh-Taylor fashion. Mixing in these reservoirs thus depends on water content of mafic magma and pressure.*

MAFIC inclusions in andesitic and dacitic lavas and in equivalent plutonic rocks have been interpreted as cumulates from fractional crystallization<sup>1</sup>, restites from deep crustal melting<sup>2</sup> and rapidly crystallized mafic magmatic material generated during magma mixing<sup>3</sup>. The implications of these interpretations for both magmatic and crustal evolution differ dramatically. I have previously argued that the inclusions result from magma mixing on the basis of their texture, bulk composition and phase composition<sup>4-6</sup>. A new observation is that the inclusions exhibit high vesicularity and consequently have a lower bulk density than their hosts. This property is consistent with generation of the inclusions by magma mixing, and may play an important part in the evolution of large magma reservoirs within the upper crust.

## Origin of mafic inclusions

Intermediate composition calc-alkaline volcanic and plutonic rocks commonly contain fine-grained mafic inclusions which appear as dark clots or blobs ranging from a few millimetres to a few tens of centimetres in diameter. Despite differing geological settings of the igneous complexes in which they occur, these inclusions display remarkably uniform textures, compositions and physical properties. In volcanic rocks the inclusions are dominantly plagioclase + hornblende + glass or plagioclase + pyroxene + glass. In plutonic rocks, a felsic matrix is present instead of glass and the dominant mafic phase is usually hornblende or biotite. Several observations indicate that the

inclusions represent mafic magma injected into and chilled within cooler, more silicic magma reservoirs.

(1) Most inclusions are subspherical in shape, unlike accidental xenoliths derived from solid or nearly solid wall rock.

(2) In bulk composition and phenocryst content (typically calcic plagioclase and magnesian olivine) inclusions resemble associated mafic lava. This should not be the case for cumulates, the composition of which is controlled by the crystallizing magma and physical properties of the precipitating phases.

(3) Inclusions have an igneous texture characterized by abundant, elongated, strongly zoned, euhedral crystals in residual glass, indicative of rapid cooling and crystallization to just above solidus. This texture differs from the glassy or micro-crystalline groundmass characteristic of mafic magma quenched at the surface. It also differs from the partial melt texture to be expected in restites.

(4) Some large inclusions exhibit outwards decrease in grain size, increase in elongation of grains, and/or an outer hybrid rind containing reacted or resorbed phenocrysts from the host lava. These observations indicate that the inclusions were chilled against the host, but that both host and inclusions were molten at the same time.

(5) Phenocrysts in the host lava are reacted or resorbed, consistent with heating of reservoir magma during cooling and crystallization of the inclusions.

These observations are further discussed elsewhere<sup>4-6</sup>. Important implications are that crustal magma reservoirs are



**Table 1** Densities of some mafic inclusions and their host lavas\*

| Volcano                                   | Sample description                               | Inclusions ( $\text{g cm}^{-3}$ ) |                    | Nonvesicular host lava ( $\text{g cm}^{-3}$ ) |
|---|--|-----------------------------------|--------------------|---|
|   |  | Bulk ( $\rho_x$ )                 | Grain ( $\rho_B$ ) |   |
| Medicine Lake Highland, California        | Rhyolite to pyroxene dacite, Glass Mountain flow | $2.15 \pm 0.04^\dagger$           | $2.79 \pm 0.01$    | $2.38 \pm 0.01^\ddagger$                      |
| Crater Lake, Oregon                       | Hornblende dacite, Llao Rock flow                | $1.87 \pm 0.03$                   | $2.79^\S$          | $2.38 \pm 0.01$                               |
| Lassen Volcanic National Park, California | Hornblende dacite, Chaos Crag domes              | 2.16                              | 2.75               | 2.47 $\parallel$                              |
| Jemez Mountains, New Mexico               | Hornblende dacite, Chicoma Mtn                   | $2.07 \pm 0.01$                   | 2.76               | $2.46 \pm 0.04$                               |

\* To obtain bulk density, 0.5–1.0-kg samples of inclusions were separated from host lavas and weighed in air and water. To obtain grain density, these samples were dried and crushed to destroy at least 99% of voids, as indicated by inspection of polished grain mounts. The powder was then weighed in air and water, with the wet measurement made following subjection of the powder to a vacuum for 20 min and addition of water while under vacuum.

$^\dagger$  Standard deviation given where  $N \geq 3$ .

$^\ddagger$  Rhyolitic portion of flow.

$^\S$  Estimated from  $\rho_x$  and point count of voids. Voids were too small to remove by crushing.

$\parallel$  Grain density of vesicular surface phase.

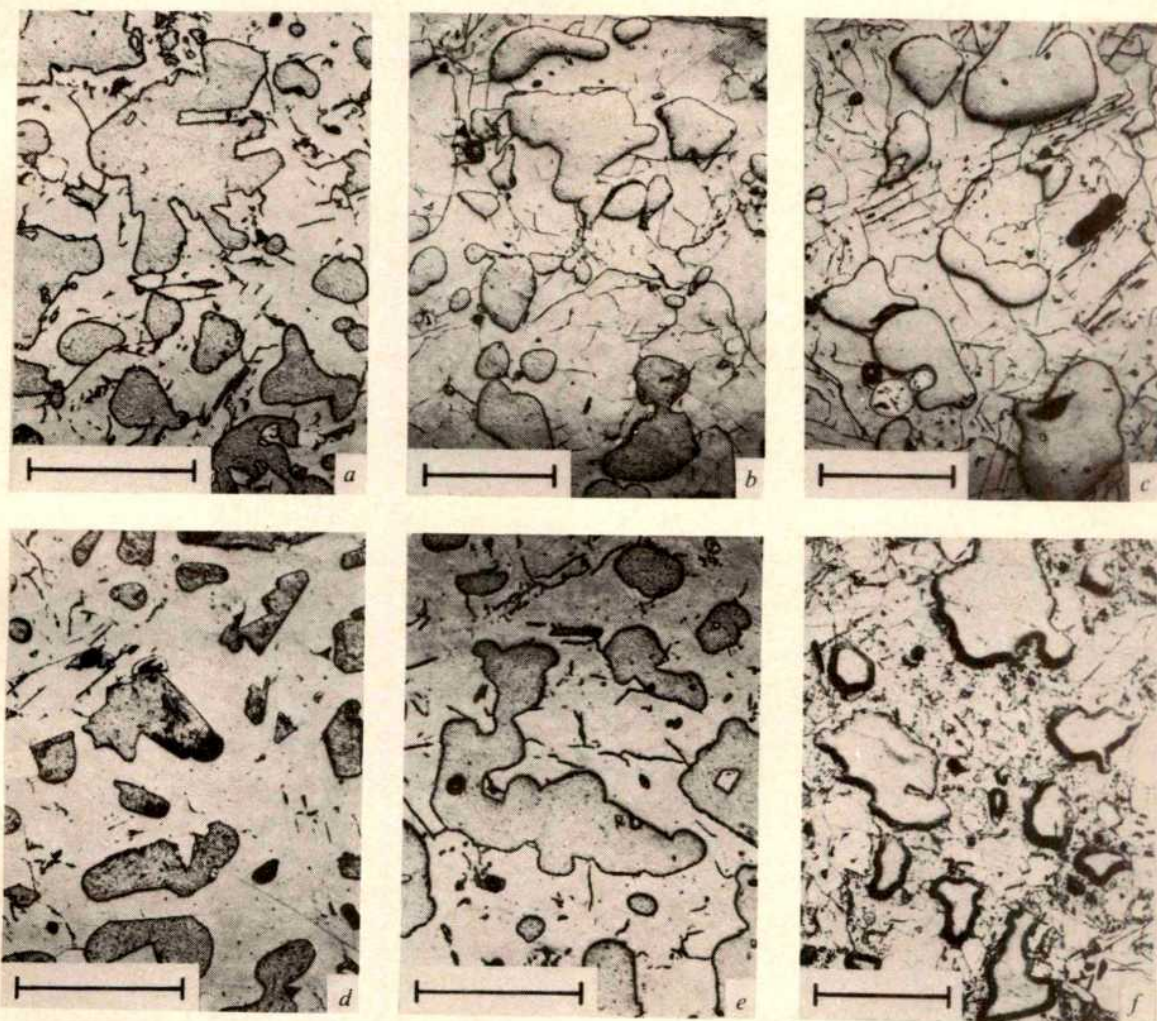
maintained by convective transport of heat from the mantle and contain a mixture of components of crustal and mantle derivation<sup>5</sup>.

### Vesicularity of inclusions

Inclusions in lavas contain abundant, fine, evenly distributed vesicles (Figs 1 and 2), even where the host lava contains virtually no vesicles (Fig. 2). Where vesicularity varies within a volcanic unit, as in lava flows with a dense interior and pumiceous surface, vesicularity of inclusions seems to be nearly independent of vesicularity of the host<sup>7</sup>.

Although vesicles are common in extrusive materials, the uniformity in vesicular texture of the inclusions is remarkable. Vesicles in tephra and lavas vary greatly in size and shape (spherical, elongate or irregular) and are sometimes unevenly distributed over distances of 1 cm or less. Vesicles are generally not present in accidental xenoliths. In contrast, vesicular textures in mafic inclusions are consistent not only within a single flow, but among flows of completely unrelated volcanoes (Fig. 1).

Measurement of bulk and grain density of the inclusions (Table 1) shows that this textural similarity is also reflected in



**Fig. 1** Reflected light photomicrographs of mafic inclusions in some andesitic lavas, showing the large proportion of vesicles. *a*, Llao Rock dacite, Crater Lake (Oregon). *b*, Mt Hood andesite (Oregon). *c*, Glacier Peak dacite (Washington). *d*, Chaos Crag dacite, Lassen Volcanic National Park (California). *e*, Nevada Antizana dacite (Ecuador). *f*, Chicoma Mountain dacite, Jemez Mountains (New Mexico). Scale bars: *a*, *d* and *e*, 0.2 mm; and *b*, *c* and *f*, 0.5 mm. Only the vesicles in sample *f* are not filled with epoxy resulting in greater apparent relief. Density data for inclusions *a*, *d* and *f* are reported in Table 1. Transmitted light views are presented in ref. 5.



physical properties. All inclusion samples have a grain density near  $2.8 \text{ g cm}^{-3}$ , because they consist largely of plagioclase and hornblende or pyroxene. Bulk densities are very consistent within a single volcanic unit, and show only a 10% variation from an average for the four volcanoes of  $2.1 \text{ g cm}^{-3}$ . Porosity of the samples ranges from 21 to 33%. Inclusions always have a lower bulk density than their nonvesicular hosts.

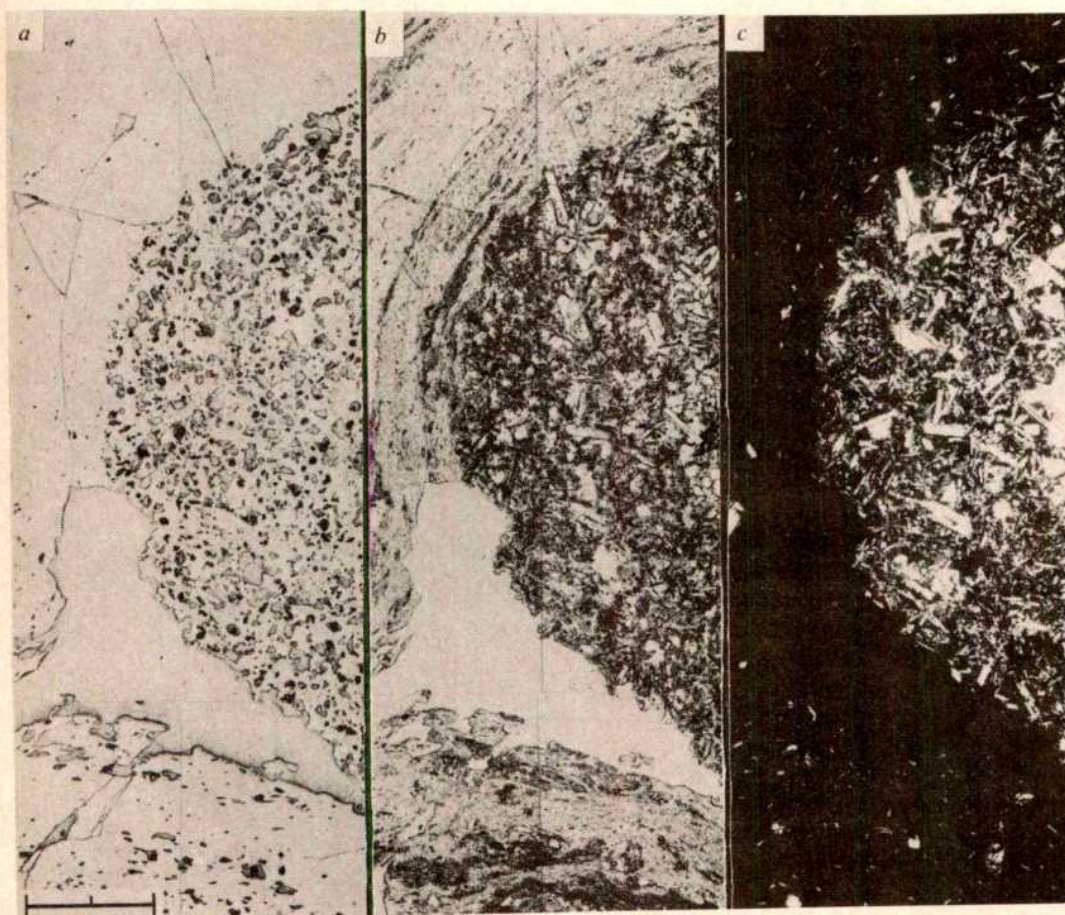
Consistency in texture and density relationships suggests that vesicularity of the inclusions may be a primary feature related to their formation and/or incorporation in the host magma. If this is the case and the vesicles, on formation, occupy half or more of the volume fraction observed in the samples, then the inclusions would be buoyant within the magma reservoir. The effect of this phase change on magmatic flow could easily exceed the effect of thermal expansion by an order of magnitude.

### Vesiculation during crystallization

The potential importance of the inclusions to flow within the reservoir means we should evaluate conditions in which the vesicles could be primary. Consider a hot mafic magma which is suddenly brought into contact with a large volume of cooler silicic magma, so that the two magmas are initially in thermal and chemical disequilibrium. The rate at which temperature and concentration of water change towards equilibrium values is proportional to thermal diffusivity ( $K$ ) and chemical diffusivity of water ( $D_{\text{H}_2\text{O}}$ ), respectively. As  $K$  is several orders of magnitude larger than  $D_{\text{H}_2\text{O}}$  (ref. 8), mafic magma quickly reaches thermal equilibrium but not chemical equilibrium with the reservoir, and, therefore, can be regarded as a system open to extraction of heat but initially closed to extraction (or addition) of water. The response of this system to extraction of heat is crystallization. However, only the melt phase can contain

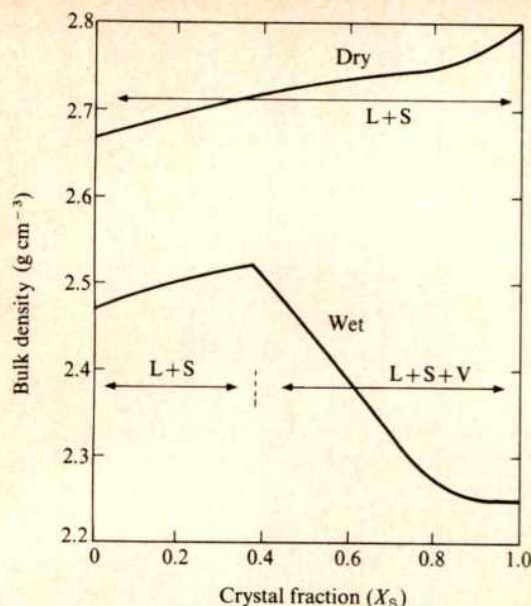
significant amounts of water. The decrease in melt fraction of this system from nearly 1.0 to  $\sim 0.1$  ( $\sim 10\%$  glass by volume observed in inclusions, recalculated vesicle-free) raises the concentration of water in the melt by an order of magnitude. Even for low initial concentrations of water in mafic magma, this enrichment will cause exsolution of a vapour phase at crustal pressures, forming a foam of reduced bulk density. Similar conclusions apply to other possible volatile components, but only water will be considered here, as it is believed to be the dominant volatile component in calc-alkaline volcanism<sup>9,10</sup>.

Cooling can thus cause vesiculation, but the depth at which such a process will be significant strongly depends on volatile content of mafic magma. Bulk density of the mafic foam can be estimated for the water contents and magmatic conditions of interest, because the densities of crystals, melt and water vapour as a function of pressure and temperature, and the solubility of water in melt as a function of pressure, are known or approximately known. Analyses of mafic inclusions and closely associated mafic lavas indicate that the type of mafic magma involved is high alumina basalt or basaltic andesite<sup>1,11,12</sup>. Explosive eruption style, common presence of hornblende phenocrysts, and inferred water content of glass inclusions in phenocrysts indicate that such magmas are volatile-rich, with an estimated water content<sup>13,14</sup> of 3–5 wt% (although some estimates are lower<sup>15</sup>). Figure 3 contrasts bulk density of high alumina basaltic magma containing 3 wt%  $\text{H}_2\text{O}$  during crystallization at 1.5 kbar with the bulk density of similar anhydrous magma. Both systems initially become more dense in response to growth of crystals. However, once vapour saturation occurs in the wet system, continued crystallization causes bubble growth which dramatically lowers bulk density of the magma. Figure 4 shows bulk density of foam formed from basalts with various water contents as a function of pressure at 90% crystallization, the degree of



**Fig. 2** Photomosaics of mafic inclusion in rhyodacitic lava from the Glass Mountain flow, Medicine Lake Highland Volcano, California. The inclusion is predominantly plagioclase and pyroxene with lesser amounts of glass, olivine, and oxides. The host lava is rhyolitic glass with varying amounts of basaltic debris. Scale bar, 1.0 mm. *a*, Reflected light, reveals the abundance of 0.1 mm-diameter vesicles in the inclusion and their scarcity in the host lava. A large vesicle is present at the lava/inclusion interface in the lower portion of *a*. *b*, Transmitted light, shows the mafic character of the inclusion in contrast to the host. Plagioclase crystals within the inclusion and the large vesicle at the interface are apparent. *c*, Taken with transmitted light and crossed polars, shows the crystal-rich character of the inclusion. Density data for these materials are presented in Table 1.





**Fig. 3** Calculated bulk density plotted against degree of crystallization for wet and dry high alumina basaltic magma. The wet curve is for basalt with 3 wt% water at 1.5 kbar. Crystal fraction ( $X_s$ ) is the ratio of crystals to crystals plus melt, by volume:  $X_s = 0$  at the liquidus and  $X_s = 1$  at the solidus. When mafic magma enters a cooler silicic reservoir,  $X_s$  increases with time from near zero until thermal equilibrium is reached near 1. To calculate bulk density as a function of  $X_s$ , the density of the crystal fraction was assumed to be constant at  $2.80 \text{ g cm}^{-3}$ , based on measured values of grain density of inclusions (Table 1) and allowance for thermal expansion<sup>16</sup>. Melt composition was calculated assuming constant crystal fraction composition such that the anhydrous melt composition is rhyolitic<sup>6</sup> at  $X_s = 0.9$ , using an average high alumina basaltic composition<sup>11</sup> for the bulk system. Temperature was assumed to decrease linearly with increasing crystallization ( $X_s$ ) so that  $T = 1,200^\circ\text{C}$  at  $X_s = 0$  and  $T = 900^\circ\text{C}$  at  $X_s = 0.9$ . Melt density was then calculated from melt composition at appropriate temperature and pressure<sup>17</sup>. Vapour fraction of the system was calculated from solubility of water in melt<sup>18</sup> and density of the vapour phase<sup>19</sup>. The calculated bulk density at low to moderate crystallization has uncertainties in assumed conditions, compositions and density of hydrous melt. However, the form of the curve and the bulk density near complete crystallization, which depends mostly on the measured grain density (Table 1) and vapour density, are not significantly affected by these uncertainties. Higher water content or lower pressure result in vapour saturation at lower crystal fraction and greater reduction in bulk density at advanced crystallization.

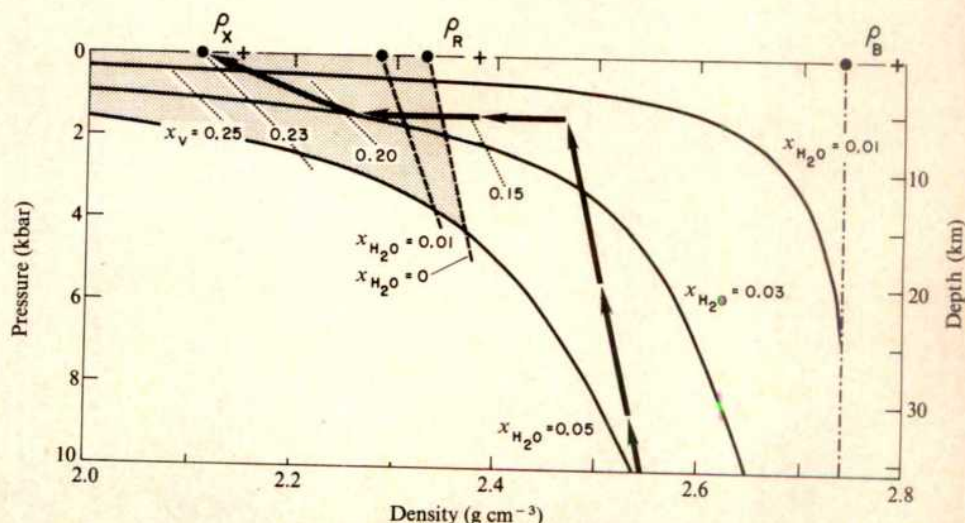
crystallization observed in the inclusions. Within the range of water contents estimated for high alumina basalts, a significant density decrease accompanies crystallization at mid- to upper-crustal pressures.

## Flotation of foam

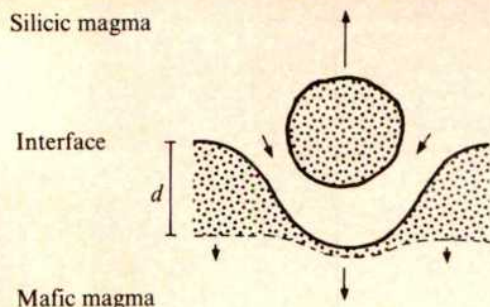
It has been argued that the arrangements of vents in andesitic and bimodal volcanic fields, as well as the history and petrology of these fields, indicate episodic replenishment of crustal magma systems by mafic magma from the mantle<sup>5,21-30</sup>. Such magma should initially fill the base of the crustal reservoir, resulting in a stratified system of two fluids. Direct evidence of such stratification, which has been suggested for other types of magma reservoirs<sup>31</sup>, is provided by the compositional zonation of some large tephra sheets, as at Crater Lake<sup>12,32</sup>. The stratification of two fluids is stable if the denser layer is on the bottom. However, Rayleigh-Taylor instability results if the denser layer is on top<sup>33</sup>. Thus, if conditions (volatile content, pressure) permit formation of a mafic foam less dense than the reservoir magma, the interface becomes unstable in Rayleigh-Taylor fashion and blobs of foam will rise into the reservoir magma. Large-scale convection in the reservoir magma driven by heating<sup>8,26,34-36</sup> of, and addition of low density material to, its base would contribute to dispersal of the mafic foam.

From the time that mafic magma enters the reservoir, a foam layer will form at the interface and thicken downwards. The rate of thickening by foam generation is controlled by the thickness of the layer and the rate of removal of foam is controlled by the rise of blobs from the interface (Fig. 5). Inclusion textures indicate that the foam has sufficient crystal content to be cohesive, so it is likely that separation of blobs from underlying material occurs at the base of the foam layer. Furthermore, if the blobs were derived from disaggregation of a large mass many diameters thicker than the inclusions, then a large range of textures representing a large range of cooling rates would be observed. Thus, layer thickness may be comparable with blob diameter. These considerations suggest a dynamic process, in which foam is continually added to a thin layer by downward propagation of a cooling wave and removed from the layer by flotation. For this to be the case, thickening of the foam layer by conduction must approximately balance thinning of the layer by flotation of blobs. A 20-cm layer, the maximum common diameter of inclusions, would thicken at a rate of the order of  $10^{-4} \text{ cm s}^{-1}$  (Fig. 5), close to the rate at which material in the form of blobs 20 cm in diameter and  $2.1 \text{ g cm}^{-3}$  in density ( $\Delta\rho = 0.3 \text{ g cm}^{-3}$ ) would be removed by flotation in  $10^8 \text{ P}$  reservoir magma. Cooling rates for the mafic magma would be of the order of  $10^\circ\text{C h}^{-1}$ . Basalt crystallization experiments have produced textures similar to those of the inclusions, characterized by acicular and skeletal plagioclase, at comparable cooling rates<sup>39,40</sup>. Thus, both the size and texture of the inclusions seem to be consistent with this hypothesized origin.

**Fig. 4** Calculated density plotted against pressure (depth) for mafic foam ( $X_s = 0.9$ ) of various water contents, and measured densities for materials from Medicine Lake lava.  $\rho_x$  and  $\rho_B$  are bulk and grain density of mafic foam, respectively, and  $\rho_R$  denotes density of reservoir magma.  $X_{\text{H}_2\text{O}}$  is weight fraction of water in magma and  $X_V$  is volume fraction of vapour in magma (that is, porosity). Density of reservoir magma ( $\rho_R$ ) with 0 and 1 wt% water<sup>11</sup> at  $T = 900^\circ\text{C}$  was calculated from measured density of lava using data for thermal expansion and compressibility of silicate melt<sup>20</sup>. The possible region for the Medicine Lake volcano magma chamber is shaded, constrained by the conditions that  $\rho_x < \rho_R$  and  $X_{\text{H}_2\text{O}} < 0.05$ . A possible path for magma feeding the chamber is indicated by arrows. —,  $\rho_x$  at constant  $X_{\text{H}_2\text{O}}$ ; ···,  $\rho_x$  at constant  $X_V$ ; ---,  $\rho_R$  at constant  $X_{\text{H}_2\text{O}}$ ; +, measured  $\rho$ ,  $T = 20^\circ\text{C}$ ; ●, calculated  $\rho$ ,  $T = 900^\circ\text{C}$ .







**Fig. 5** Formation of mafic foam (patterned) in the region of the interface between mafic and silicic magma. A cooling wave advances downwards into the mafic magma while foam is removed from the interface by flotation. Within the mafic magma there is an upward transition from mafic liquid below the cooling wave, through less mafic liquid + crystals, to the foam layer, consisting of silicic liquid + crystals + vapour, below the interface. Within the reservoir magma, resorption or reaction of phenocrysts occurs near the interface. The base of the foam layer will be near the isotherm representing  $1/2\Delta T$ . If the interface is kept approximately isothermal by flow of silicic magma (upper limit case for rate of foam formation), then the thickness of the foam layer is  $(Kt)^{1/2}$  and the rate at which it thickens is  $K/2d$  (ref. 37). Using thermal conductivity data<sup>38</sup> and including the effect of crystallization gives  $K = 3 \times 10^{-3} \text{ cm}^2 \text{ s}^{-1}$  so that a 20-cm layer thickens at  $10^{-4} \text{ cm s}^{-1}$ . When the foam layer has grown to this thickness, removal of foam by flotation approximately balances growth of the layer by conduction.

The field of Rayleigh–Taylor instability and hence mixing of mafic material into a silicic reservoir can be defined in terms of water content of basaltic magma and pressure. Much more water is required for flotation of foam at higher pressure because both density of water vapour and solubility of water in melt increase with pressure. Figure 4 shows the possible conditions for mixing in the magma reservoir from which the Medicine Lake dacite of Table 1 erupted. The inference that the inclusions floated constrains depth of the reservoir to  $\leq 15$  km for basalt with 5 wt% water, or 7 km for basalt with 3 wt% water. Data from the other volcanoes studied give similar results. Although volatile content of basalt is a major unknown, the flotation process is clearly limited to magma reservoirs in the upper crust. This conclusion is consistent with the association of foam-bearing lavas with calderas or caldera-like structures, and with the occurrence of analogous intrusive rocks as large, shallowly emplaced plutons.

A possible path of mafic magma feeding such a reservoir is also shown in Fig. 4. The basalt ascends through the crust, slowly becoming less dense with decreasing pressure. As it enters the magma reservoir at 1.5 kbar it is still water unsaturated. As it fills the base of the reservoir, heat is quickly transferred to silicic magma across the large area of the interface so that the mafic magma undergoes rapid crystallization (following the curve in Fig. 3) forming a foam with a bulk density of  $2.25 \text{ g cm}^{-3}$ , and

porosity of 0.19. If this foam remains rigid but leaks after formation, it will follow a constant porosity curve as it flows upwards. If it maintains an equilibrium pore pressure and does not leak, it will follow a constant water curve and blow up during ascent. Obviously, the foam does expand infinitely. As with silicic tephra<sup>41</sup>, growth of vesicles is retarded by increasing viscosity of the residual melt and interference from neighbouring crystals and vesicles. That the inclusions do leak water after their formation is suggested by the common presence of large vesicles at the inclusion/lava interface, as shown in Fig. 2.

## Petrological implications

An important aspect of the problem of silicic magma reservoirs open to replenishment is the stability of the stratification induced by replenishment. In the stable case, any mixing is limited to the very slow process of diffusion across the interface between the two separately convecting magmas. Magma in the reservoir is heated by injection of mafic magma and may, therefore, grow by crustal melting, but it evolves in a manner chemically independent of the primitive magma feeding the chamber. In the unstable case, mixing occurs by rapid transport of mafic material across the mafic/silicic interface and into the convecting reservoir magma. The composition of magma in the reservoir reflects the combined effects of mixing, which makes the magma more mafic, and crustal melting and/or differentiation, which make it more silicic. I suggest that bimodal volcanism represents the stable case, while an important stage in the evolution of andesitic volcanoes and granodioritic batholiths represents the unstable case.

Although these conclusions are based primarily on investigation of certain volcanic rocks of the andesite family, their most important application in terms of volume is to granodioritic batholiths, in which mafic inclusions are a nearly ubiquitous feature. Recent work suggests that most of these inclusions are the plutonic equivalent of the extrusive materials described here<sup>42,43</sup>. If so, these large magma bodies may initially evolve as bimodal systems in the deeper crust, with formation and accumulation of granitic crustal melt in response to basaltic volcanism<sup>44–46</sup>. Subsequent rise of granitic magma bodies into the upper crust within regions of upward flux of wet basaltic magma would result in mixing driven by vapour exsolution, with generation of granodioritic bulk compositions. Direct exsolution of a vapour phase from basaltic magma within upper crustal reservoirs may also play a part in formation of ore deposits, which are sometimes associated with granodioritic intrusives<sup>47</sup>.

I thank B. Daly and F. Harlow of Los Alamos Scientific Laboratory for their help in developing these ideas. This work was conducted at LASL and Sandia National Laboratories (USDOE facilities) with support from the US Department of Energy under contracts W-7405-ENG-36 and DE-AC04-76DP00789, respectively.

Received 21 April; accepted 17 September 1980.

- Williams, H. *Am. J. Sci.* **222**, 385–403 (1931).
- Presnall, D. C. & Bateman, P. C. *Bull. geol. Soc. Am.* **84**, 3181–3202 (1973).
- Walker, G. P. L. & Skelhorn, R. R. *Earth-Sci. Rev.* **2**, 93–109 (1966).
- Eichelberger, J. C. & Gooley, R. *Geophys. Monogr. Ser.* **20**, 57–77 (1977).
- Eichelberger, J. C. *Nature* **275**, 21–27 (1978).
- Heiken, G. & Eichelberger, J. C. *J. Volcan. Geothermal Res.* **7**, 443–481 (1980).
- Eichelberger, J. C. *U. S. Geol. Surv. Circ.* (in the press).
- Shaw, H. R. *Yb. Carnegie Instn Wash.* **634**, 139–170 (1974).
- Anderson, A. T. Jr *Rev. Geophys. Space Phys.* **13**, 37–54 (1975).
- Mysen, B. O. *Rev. Geophys. Space Phys.* **15**, 351–361 (1977).
- Anderson, C. A. *Univ. Calif. Publ. geol. Sci.* **25**, 347–422 (1941).
- Williams, H. *Yb. Carnegie Instn Wash.* **540**, 1–162 (1942).
- Anderson, A. T. Jr *Bull. volcan.* **37**, 530–552 (1974).
- Rose, W. I. Jr, Anderson, A. T. Jr, Woodruff, L. G. & Bonis, S. B. *J. Volcan. Geothermal Res.* **4**, 3–52 (1978).
- Marsh, B. D. *J. Geol.* **84**, 27–45 (1976).
- Skinner, B. J. *Geol. Soc. Am. Mem.* **97**, 78–96 (1966).
- Bottinga, Y. & Weill, D. F. *Am. J. Sci.* **269**, 169–182 (1970).
- Burnham, C. W. & Jahns, R. H. *Am. J. Sci.* **260**, 721–745 (1962).
- Burnham, C. W., Holloway, J. R. & Davis, N. F. *Geol. Soc. Am. Spec. Pap.* **132**, 1–96 (1969).
- Burnham, C. W. & Davis, N. F. *Am. J. Sci.* **270**, 54–79 (1971).
- Thorarinnsson, S. in *The Eruption of Hekla 1947/1948* (eds Einarsson, T., Kjartansson, G. & Thorarinnsson, S.) (Societas Scientiarum Islandica, Reykjavik, 1967).
- Smith, R. L. & Shaw, H. R. *U. S. Geol. Surv. Circ.* **726**, 58–83 (1975).
- Eaton, G. P. *et al. Science* **188**, 787–796 (1975).
- Walker, G. P. L. *J. geol. Soc. Lond.* **131**, 121–141 (1975).

- Anderson, A. T. Jr *J. Volcan. Geothermal Res.* **1**, 3–33 (1976).
- Sparks, R. S. J., Sigurdsson, H. & Wilson, L. *Nature* **267**, 315–318 (1977).
- Yanagi, T. & Ishizaka, K. *Earth planet. Sci. Lett.* **40**, 252–262 (1978).
- Sakuyama, M. *J. Volcan. Geothermal Res.* **5**, 197–208 (1979).
- Newhall, C. G. *J. Volcan. Geothermal Res.* **6**, 61–83 (1979).
- Smith, R. L. *Geol. Soc. Am. Spec. Pap.* **180**, 5–27 (1979).
- Huppert, H. E. & Sparks, R. S. J. *Nature* **286**, 46–48 (1980).
- Eichelberger, J. C. & Crowe, B. *Geol. Soc. Am. Abstr.* **10**, 104 (1978).
- Chandrasekhar, S. *Hydrodynamic and Hydromagnetic Stability* (Oxford University Press, London, 1970).
- Shaw, H. R. *Am. J. Sci.* **263**, 120–152 (1965).
- Bartlett, R. W. *Am. J. Sci.* **267**, 1067–1082 (1969).
- Rice, A. & Eichelberger, J. C. *EOS* **57**, 1024 (1976).
- Carlsaw, H. S. & Jaeger, J. C. *Conduction of Heat in Solids* (Clarendon, Oxford, 1959).
- Murase, T. & McBirney, A. R. *Bull. geol. Soc. Am.* **84**, 3563–3592 (1973).
- Lofgren, G. *Am. J. Sci.* **274**, 243–273 (1974).
- Lofgren, G., Donaldson, C. H., Williams, R. J., Mullins, O. Jr & Usselman, T. M. *Geochim. cosmochim. Acta* **1**, 549–567 (1974).
- Sparks, R. S. J. *J. Volcan. Geothermal Res.* **3**, 1–37 (1978).
- Reid, J. B. Jr, Evans, O. C. & Fates, D. G. *Geol. Soc. Am. Abstr.* **12**, 507 (1980).
- Reid, J. B. Jr *EOS* (in the press).
- Lachenbruch, A. H., Sass, J. H., Munroe, R. J. & Moses, T. H. Jr *J. geophys. Res.* **81**, 769–784 (1976).
- Younker, L. W. & Vogel, T. A. *Can. Miner.* **14**, 238–244 (1976).
- Lachenbruch, A. H. & Sass, J. H. *Geol. Soc. Mem.* **152**, 209–250 (1978).
- Burnham, C. W. in *Geochemistry of Hydrothermal Ore Deposits* (ed. Barnes, H. L.) (Wiley, New York, 1979).



# Specific high affinity cell membrane receptors for biologically active phorbol and ingenol esters

Mohammed Shoyab & George J. Todaro

Laboratory of Viral Carcinogenesis, National Cancer Institute, National Institutes of Health, Bethesda, Maryland 20205

*A variety of normal and transformed avian and mammalian cells and tissues contain high affinity specific receptors on their membranes which interact with biologically active phorbol and ingenol esters in a reversible and saturable manner. The binding of labelled phorbol-12,13-dibutyrate (PDBu) to live or glutaraldehyde-fixed cells is dose-, time- and temperature-dependent. Those phorbol or ingenol esters which stimulate cell growth in culture and have tumour-promoting activity in vivo inhibit the binding of labelled PDBu, while the biologically inactive derivatives fail to do so. Other non-diterpene tumour-promoting agents, epidermal growth factor (EGF), retinoids and prostaglandins do not compete for the binding of labelled PDBu to its specific membrane receptors.*

TUMOUR promoters are compounds which are themselves non-carcinogenic but which can induce tumours in animals previously treated with a suboptimal dose of certain chemical carcinogens<sup>1-5</sup>. Most of the experimental work on tumour promotion has been carried out with phorbol esters, especially 12-*O*-tetradecanoylphorbol esters (TPA), initially isolated from croton oil derived from the seed of the plant *Croton tiglium*<sup>4,6</sup>. TPA and other biologically active phorbol esters elicit and modulate a variety of biochemical and biological responses in mouse skin, including stimulation of macromolecular synthesis, histone phosphorylation, synthesis of phospholipids and modulation of the metabolism of polyamines and cyclic nucleotides<sup>1-5,7-13</sup>. In addition, these compounds induce ultrastructural changes in and affect the differentiation of murine epidermis<sup>7,14</sup>. Tumour-promoting phorbol esters also evoke pleiotypic responses in cultured cells, including the stimulation of macromolecular synthesis and cell proliferation, induction of plasminogen activator and ornithine decarboxylase, loss of surface-associated fibronectin, alterations in the metabolism of cyclic nucleotides and polyamines, stimulation of prostaglandin synthesis, either the inhibition or stimulation of differentiation, and alterations in cell morphology and cell permeability, and elevation in the level of  $[Na^+K^+]ATPase$  activity<sup>1-5,15-23</sup>.

Several biochemical and biological studies provide evidence that the initial site of action of tumour-promoting phorbol esters may be the membrane of target cells<sup>3-5,21,23-26</sup>. The tumour-promoting phorbol esters have been found to modulate the interaction between epidermal growth factor (EGF) and its membrane receptors in a variety of cells in culture<sup>27-29</sup>. The pleiotypic effects of TPA and related tumour promoters *in vivo* as well as *in vitro* seem to mimic the several actions of growth-stimulating polypeptide hormones such as EGF<sup>30</sup> and sarcoma growth factor (SGF)<sup>31</sup>. However, the effect, though rapid in modulating the EGF receptors, is indirect as it cannot be shown using low temperatures<sup>26</sup> and/or fixed cells or in isolated cell membranes (unpublished results). This would suggest that TPA produces its membrane effects through an interaction distinct from the EGF receptor interaction.

<sup>3</sup>H-TPA has been reported to bind to HeLa cells in a non-saturable, noncompetitive and nonspecific fashion<sup>32</sup>. We find that <sup>3</sup>H-TPA binds to a variety of fibroblastic and epithelioid cells in saturable and reversible manner but these binding sites for TPA seem to be numerous ( $30 \times 10^6$  per cell) and of low affinity ( $K_d = 10^{-7}$  M). We have used <sup>3</sup>H-PDBu to characterize the binding sites of phorbol and ingenol esters. PDBu is a phorbol ester which is highly active *in vivo* and *in vitro* but is

comparatively less lipophilic than TPA<sup>4,33</sup>. Thus, PDBu would partition in membrane lipids much less than TPA and lead to less nonspecific binding. Recently, <sup>3</sup>H-PDBu binding to a particulate fraction of chicken embryonic fibroblasts has been reported<sup>34</sup>.

## Binding of PDBu to Cells

Figure 1 describes the binding of <sup>3</sup>H-PDBu ( $19.7 \text{ ng ml}^{-1}$ , specific activity  $6.4 \text{ Ci mmol}^{-1}$ , Life System Co., Newton, Massachusetts) to live and fixed mink lung cells (CCL 64)<sup>35</sup> and BALB/3T3 clone A31 cells (CLL 163)<sup>36</sup> at 23 °C, and the competition of binding of labelled PDBu to cells with unlabelled PDBu. The live and the fixed mink cells bound 2,155 and 1,987 c.p.m., respectively, whereas live and fixed A31 cells bound 3,605 and 3,419 c.p.m., respectively, of <sup>3</sup>H-PDBu per  $10^6$  cells in the absence of unlabelled PDBu. As the concentration of unlabelled PDBu was increased, the binding of <sup>3</sup>H-PDBu to both types of cells decreased. Figure 1 shows that viable and glutaraldehyde-fixed mink cells required 30–35  $\text{ng ml}^{-1}$  of PDBu for 50% inhibition of binding; the A31 showed  $ID_{50}$ s of 65–70  $\text{ng ml}^{-1}$  and, again, no difference between viable and fixed cells.

Figure 2a shows the extent of binding of <sup>3</sup>H-PDBu to mink lung cells at various temperatures, as a function of incubation time. The binding increased linearly for 15 min at 4 °C, whereas binding at 23 °C and 37 °C was linear for only a few min. Maximal binding was achieved within 7.5 min at 37 °C and started to decrease with increasing incubation time. The saturation of the binding of labelled PDBu to cells at 23 or 4 °C was observed between 20–40 and 90–120 min, respectively. When <sup>3</sup>H-PDBu-labelled mink lung cells (23 °C, 30-min incubation) containing bound <sup>3</sup>H-PDBu were incubated in only binding buffer at 4, 23 or 37 °C, bound radioactivity dissociated from cells and was released into the medium in a time- and temperature-dependent manner (Fig. 2b).

Optimum binding of PDBu was achieved at pH 6.7. The binding was found to be linear up to  $12 \times 10^6$  cells  $\text{ml}^{-1}$  (23 °C, 20-min incubation). It was not significantly affected by hydroxyurea (10 mM), actinomycin D ( $10 \mu\text{g ml}^{-1}$ ), cycloheximide ( $10 \mu\text{g ml}^{-1}$ ) or sodium fluoride (1 mM). Thus, it seems that PDBu binding to its receptors does not require DNA, RNA or protein synthesis, or metabolic energy. We did not find any absolute requirements of metal ions for PDBu binding to cells; however, metal chelating agents (EDTA and EGTA) at 5 mM concentration reduced the binding to approximately 50%.  $Mg^{2+}$ ,  $Co^{2+}$ ,  $Na^+$  and  $K^+$  did not significantly affect the binding



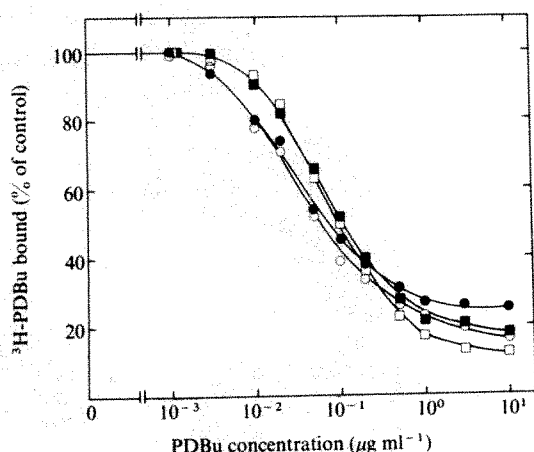
although  $Mn^{2+}$ ,  $Ca^{2+}$  and  $Zn^{2+}$  significantly stimulated the binding of  $^3H$ -PDBu to mink cells.

Sub-cellular distribution of bound  $^3H$ -PDBu to mink cells ( $4^\circ C$  for 30 min or  $23^\circ C$  for 10 min) revealed that approximately 80% of labelled PDBu bound to the membranous fraction. This result and the comparable binding of  $^3H$ -PDBu to fixed or live cells suggest that the binding sites are located on the plasma membranes of cells.

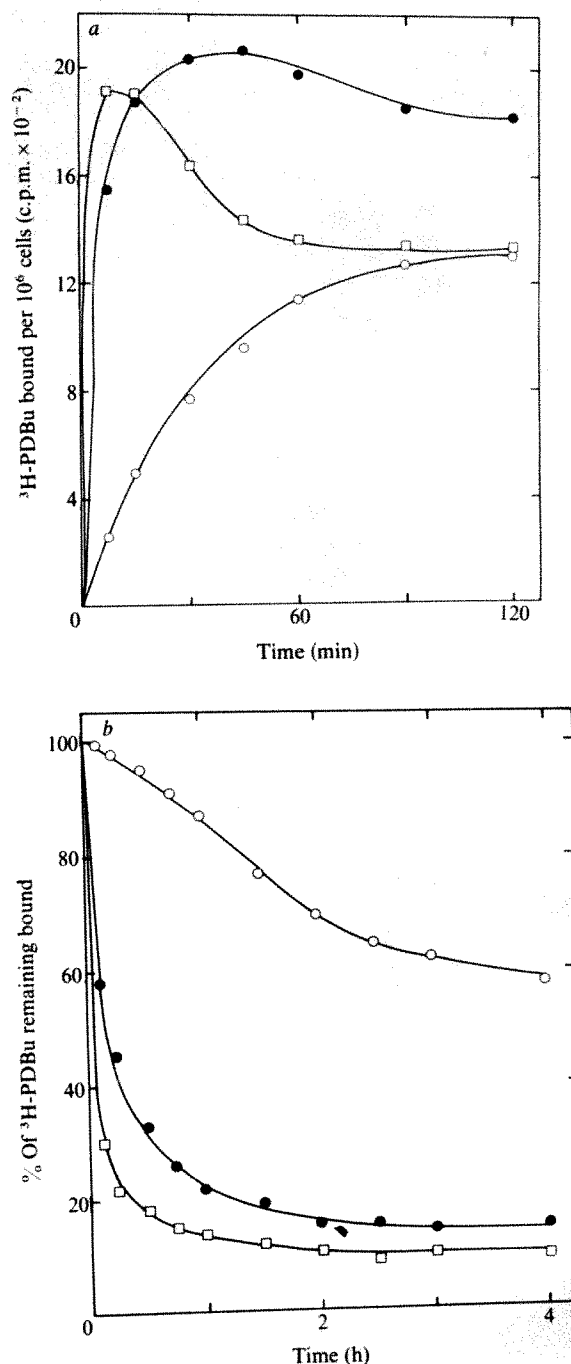
### Wide distribution of PDBu binding sites in cell cultures and various murine tissues

Table 1 shows the specific binding of  $^3H$ -PDBu to various normal cell lines from different species in culture and murine cell lines transformed by RNA tumour viruses, DNA tumour viruses, SV40 and polyoma or by chemical carcinogens, benzo-pyrene (BP) and methylcholanthrene (MC). PDBu bound to murine (normal or transformed), rat, cat, mink, hamster, rabbit, bat, dog, monkey, human and chicken cells. The transformed murine cells were found to bind more PDBu than their normal counterparts.  $^3H$ -PDBu also bound to Kirsten sarcoma virus transformed murine cells as well as to Swiss/3T3 clone NR-6; both cell lines lack EGF receptors<sup>37,38</sup>. The specific binding sites are also present in murine brain, spleen, thymus, lung, skin, kidney, heart, thigh muscle, liver and intestine in decreasing order. The murine brain which lacks EGF receptors and spleen

has an exceptionally high number of receptors for PDBu. Neither human nor mouse erythrocyte bound detectable amounts of  $^3H$ -PDBu. Thus, the PDBu binding sites are widely distributed and are distinct from EGF binding sites.



**Fig. 1** Binding of  $^3H$ -PDBu to live and fixed cells and inhibition of  $^3H$ -PDBu binding by unlabelled PDBu. The cells were grown in 850 cm<sup>2</sup> roller culture bottles (RCB) in Dulbecco's minimum essential medium (DMEM) containing 10% calf serum (CS). Approximately 70% confluent cells were used for the binding assays. The medium was aspirated from bottles, cells were washed twice with 50 ml of binding buffer (BB) consisting of DMEM containing bovine serum albumin (BSA, 1 mg ml<sup>-1</sup>) and *N,N*-bis-(2-hydroxyethyl)-2-amino-ethane-sulphonic acid (BES, 5 mM), adjusted to pH 6.8. The cells were scraped in 25 ml of BB per RCB and transferred to plastic tubes and pelleted in a refrigerated centrifuge. The cell pellets were suspended in BB and an aliquot used to determine cell number in a Coulter counter. The binding assays were performed in duplicate in 12 × 75 mm disposable glass culture tubes (Kimax). The binding mixture contained 5 ng  $^3H$ -PDBu ( $\sim 4 \times 10^4$  c.p.m.), 0–5  $\mu$ g of unlabelled PDBu, 0.5% final concentration of dimethyl sulphoxide (DMSO) and  $1 \times 10^6$  cells in a total volume of 0.25 ml BB. After incubation for 30 min at  $23^\circ C$ , 4 ml cold BB was added to each tube, the contents mixed and tubes were centrifuged for 4 min at  $4^\circ C$  at 1,000g to pellet the cells. The supernatant solution was carefully drained off, the pellet was suspended in 4 ml of cold BB and transferred to other tubes. Tubes were again centrifuged as earlier, supernatant solution was removed and cell pellets solubilized in 0.7 ml of lysing buffer (0.01 M Tris-HCl, pH 7.4, containing 0.5% SDS and 1 mM EDTA). The mixture was transferred to counting vials and 10 ml of Optigel (Melay Laboratories) was added to each vial. The vials were vigorously shaken and radioactivity determined using a Beckman beta counter. For binding assays with fixed cells, the medium was aspirated, cells were washed twice with cold PBS and scraped from RCB and transferred to plastic tubes and pelleted. The pellet was suspended in 2% glutaraldehyde, pH 7.4 (1 ml per  $10^6$  cells) for 2 h at  $4^\circ C$ . After this period, cells were pelleted and washed twice with cold PBS and the final pellet was suspended in BB. The binding with fixed cells was performed as described for the live cells.  $\circ$ , Live mink lung cells;  $\bullet$ , fixed mink lung cells;  $\square$ , BALB/3T3-A31 cells;  $\blacksquare$ , fixed BALB/3T3-A31 cells.



**Fig. 2** a, Effect of incubation time and temperature on  $^3H$ -PDBu binding to mink lung cells. The binding assays were performed in duplicate as in Fig. 1 legend, in the presence or absence of  $20 \mu$ g ml<sup>-1</sup> unlabelled PDBu. The radioactivity bound to cells in the presence of  $20 \mu$ g ml<sup>-1</sup> unlabelled PDBu was considered to be nonspecific binding and all data were corrected accordingly.  $\circ$ ,  $4^\circ C$ ;  $\bullet$ ,  $23^\circ C$ ;  $\square$ ,  $37^\circ C$ . b, Dissociation of bound  $^3H$ -PDBu from mink lung cells. Binding of  $^3H$ -PDBu (30 min at  $23^\circ C$ ) was performed as described in Fig. 2a legend. After the final washing, cells were suspended in BB (0.25 ml per  $10^6$  cells) and duplicate mixtures were incubated at each indicated temperature for each indicated time. After incubation, 4 ml of cold BB was added to each tube, cells were mixed and pelleted as described in Fig. 1 legend. The supernatant solutions were removed, pellets suspended in the lysing buffer and counted as in Fig. 1 legend. The nonspecific binding was corrected as in a.  $\circ$ ,  $4^\circ C$ ;  $\bullet$ ,  $23^\circ C$ ;  $\square$ ,  $37^\circ C$ . The released labelled material was analysed by HPLC and was found to be PDBu.

**Table 1** Binding of  $^3\text{H}$ -PDBu to cells of various species

| Species | Cells                                   | $^3\text{H}$ binding<br>(c.p.m. per<br>$10^6$ cells) |
|---------|---|--|
| Chicken | Embryo fibroblasts                      | 4,273  |
| Mouse   | BALB/3T3-A31                            | 3,506  |
|         | Murine sarcoma virus transformed A31    | 4,995  |
|         | Benzo[a]pyrene transformed A31          | 5,790  |
|         | SV40 transformed A31                    | 5,505  |
|         | Methylcholanthrene transformed A31      | 7,983  |
|         | NIH/3T3 Cl 142                          | 3,285  |
|         | Polyoma virus transformed NIH/3T3 Cl 4A | 6,729  |
|         | Swiss/3T3 Cl 8                          | 3,635  |
|         | Swiss/3T3-NR6 (no EGF receptors)        | 3,342  |
|         | Swiss/3T3 Cl LI (preadipocytes)         | 1,560  |
|         | 129/J F9 (teratocarcinoma)              | 487  |
|         | Swiss mouse erythrocytes (fresh)        | 6  |
| Rat     | NRK (fibroblasts) clone 49F             | 2,824  |
|         | NRK (epithelial) VB-4                   | 1,928  |
| Hamster | Ovary CHO                               | 3,357  |
| Mink    | Lung (epithelial) Mv1Lu (CCL 64)        | 2,074  |
| Bat     | Lung (fibroblastic) TblLu (CCL 88)      | 2,498  |
| Cat     | Embryo (FEC) Cl 60                      | 3,362  |
| Dog     | Thymus cf2Th                            | 1,626  |
| Monkey  | Rhesus RBS                              | 1,407  |
| Human   | Fibroblast (CCL 1553)                   | 4,360  |
|         | Cervical carcinoma HeLaS3               | 864  |
|         | Epidermal carcinoma of vulva A431       | 2,250  |
|         | Acute myelogenous leukaemia HL60        | 2,114  |
|         | Erythrocytes                            | 12   |

The binding assays were performed as in Fig. 1 legend. The nonspecific binding was corrected as described in Fig. 2 legend.

### Saturability of PDBu Binding

The effect of PDBu concentration on PDBu binding to mink lung cells and murine BALB/3T3-A31 cells is shown in Fig. 3. PDBu binding was found to be linear up to a PDBu concentration of about  $5 \text{ ng ml}^{-1}$  for both cell types. As the concentration of PDBu was increased beyond  $5 \text{ ng ml}^{-1}$ , the binding of PDBu to cells gradually began to deviate from linearity and started to level off. PDBu binding sites were almost saturated at a PDBu concentration of  $200 \text{ ng ml}^{-1}$  (Fig. 3, insets). Figure 3 also includes Scatchard plots of PDBu binding to mink lung cells and to BALB/3T3 cells. These data produced almost linear plots for both cell types. At saturating concentration of PDBu, approximately  $2.0 \times 10^5$  molecules bound to mink lung cells and  $5.1 \times 10^5$  molecules to BALB/3T3 cells. The apparent  $K_d$  values were calculated to be  $1.3 \times 10^{-9} \text{ M}$  for mink lung cells (Fig. 3a) and  $0.9 \times 10^{-9} \text{ M}$  for BALB/3T3 cells (Fig. 3b). The apparent  $K_d$  value for EGF interaction to its receptors on both cell types has been reported to be  $0.5 \times 10^{-9} \text{ M}$  (ref. 28). Thus, the affinity of PDBu for its receptors is in the same range as that of EGF receptors for its ligands and other ligands for their receptors<sup>28</sup>.

### Relationships between structure of phorbol and ingenol derivatives and binding to mink lung cells

There are now available several natural and synthetic analogues of phorbol and ingenol with various degrees of promoting activity in the two-stage tumorigenesis model<sup>1-5</sup>. We studied their effects on inhibiting the binding of  $^3\text{H}$ -PDBu to mink lung cells (Fig. 4 and Table 2). TPA was the most potent competitor of PDBu binding among the phorbol, ingenol and mezerein derivatives tested. The dose required for 50% inhibition of PDBu binding to cells for TPA, PDBu, phorbol-12,13-didecanoate (PDD), phorbol-12,13-dibenzoate (PDB), 12-deoxyphorbol-13-tetradecanoate (DPTD), ingenol-13-hexadecanoate (IHD), mezerein (MZ), phorbol-12,13-diacetate (PDA) and ingenol 3,5,20-triacetate (ITA) were  $9.6 \times 10^{-9} \text{ M}$ ,  $9.9 \times 10^{-8} \text{ M}$ ,  $13.4 \times 10^{-8} \text{ M}$ ,  $18.2 \times 10^{-8} \text{ M}$ ,  $2.4 \times 10^{-8} \text{ M}$ ,  $5.8 \times 10^{-8} \text{ M}$ ,  $7.2 \times 10^{-8} \text{ M}$ ,  $6.4 \times 10^{-6} \text{ M}$  and  $9.8 \times 10^{-6} \text{ M}$ , respectively; 4  $\alpha$ -PDD, 4-O methyl-TPA (MeTPA), phorbol and ingenol had negligible effects on PDBu binding (Fig. 4a, b). The relative potency of these agents in competing EGF binding was: TPA > DPTD > IHD > MZ > PDBu > PDD > PDB > PDA > ITA > Me-TPA > 4  $\alpha$ -PDD > phorbol > ingenol (Table 2). The inhibition of PDBu binding to its receptors by different phorbol and ingenol derivatives correlated very well with their tumour-promoting activity. Table 2 also summarizes the dose required for 50% inhibition of EGF binding for various phorbol derivatives (data taken from ref. 28) and for ingenol derivatives and MZ (unpublished data).  $2 \text{ ng ml}^{-1}$  of  $^{125}\text{I}$ -EGF and  $19.7 \text{ ng ml}^{-1}$  of  $^3\text{H}$ -PDBu were used in these binding experiments. Table 2 shows that ID values for PDBu binding and for the indirect effect on EGF binding, as well as calculated  $K_i$  values for PDBu binding and EGF binding for the various agents correlated very well with each other and with their tumour-promoting potential. The relative values ( $\text{ID}_{50}/K_i$ ) for various agents were found to be almost similar.

### Lack of competition of PDBu binding by non-diterpene ester tumour promoters and by certain other compounds

Non-diterpene ester tumour promoting agents such as phenol, iodoacetic acid, iodoacetamide, bile acids, barbiturate, oleate, laurate, limonene, canthradin, anthradin, saccharin, or cyclamate<sup>1-5</sup>, did not affect the binding of  $^3\text{H}$ -PDBu to its receptors even up to a concentration of  $10 \mu\text{g ml}^{-1}$ . However, anthralin, another tumour promoter, actually enhanced the binding of PDBu to mink lung cells (Table 3). Thus, it seems that non-diterpene ester tumour promoting agents do not exert their biological effect through these membrane receptors. Retinoic

**Table 2** Correlation between the potency of phorbol and ingenol derivatives for promoting skin tumours and their ability to inhibit the binding of  $^3\text{H}$ -PDBu or  $^{125}\text{I}$ -EGF to cells

| Compounds   | Dose required for 50% inhibition ( $\text{ng ml}^{-1}$ ) |  | $K_i$ values ( $\text{M}$ ) <sup>‡</sup> |                              | Tumour-promoting activity <sup>1-5</sup> |
|---|--|--|--|------------------------------|--|
|   | PDBu binding to its receptor*                            | EGF binding to its receptor <sup>†</sup> | PDBu binding to its receptors            | EGF binding to its receptors |  |
| 12-O-tetradecanoylphorbol-13-acetate (TPA)              | 5.9  | 1.8                                      | $2.3 \times 10^{-10}$                    | $1.8 \times 10^{-9}$         | +++                                      |
| Phorbol-12,13-dibutyrate (PDBu)                         | 50.2   | 32.8                                     | $2.4 \times 10^{-9}$                     | $3.9 \times 10^{-8}$         | ++                                       |
| Phorbol-12,13-didecanoate (PDD)                         | 83.5   | 53.8                                     | $3.2 \times 10^{-9}$                     | $5.2 \times 10^{-8}$         | ++                                       |
| Phorbol-12,13-dibenzoate (PDB)                          | 104.0  | 105.0                                    | $4.4 \times 10^{-9}$                     | $1.1 \times 10^{-7}$         | +  |
| 4 $\alpha$ -Phorbol-12,13-didecanoate (4 $\alpha$ -PDD) | >100,000   | >10,000                                  | $>1.6 \times 10^{-4}$                    | $>9.6 \times 10^{-6}$        | Non-promoter                             |
| Phorbol-12,13-diacetate (PDA)                           | 3,100  | >10,000                                  | $>1.5 \times 10^{-4}$                    | $>12.4 \times 10^{-6}$       | Non-promoter                             |
| 4-O-methyl-TPA (Me-TPA)                                 | >100,000   | >10,000                                  | $>1.7 \times 10^{-4}$                    | $>9.5 \times 10^{-6}$        | Non-promoter                             |
| Phorbol   | >100,000   | >10,000                                  | $>2.7 \times 10^{-4}$                    | $>16.5 \times 10^{-6}$       | Non-promoter                             |
| 12-deoxyphorbol-13-tetradecanoate (DPTD)                | 13.8   | 21.1                                     | $5.7 \times 10^{-9}$                     | $2.3 \times 10^{-8}$         | ++                                       |
| Mezerein  | 42.5   | 9.8                                      | $1.7 \times 10^{-9}$                     | $9.9 \times 10^{-8}$         | ?  |
| Ingenol-13-hexadecanoate (IHD)                          | 34.2   | 101.0                                    | $1.4 \times 10^{-9}$                     | $10.3 \times 10^{-8}$        | +  |
| Ingenol-3,5,20-triacetate (ITA)                         | 3,400  | 3,000                                    | $2.3 \times 10^{-7}$                     | $3.6 \times 10^{-6}$         | Non-promoter                             |
| Ingenol   | >100,000   | >10,000                                  | $>2.8 \times 10^{-4}$                    | $>17.2 \times 10^{-6}$       | Non-promoter                             |

\* Values derived from Fig. 4.  $19.7 \text{ ng ml}^{-1}$  of  $^3\text{H}$ -PDBu was used for binding.

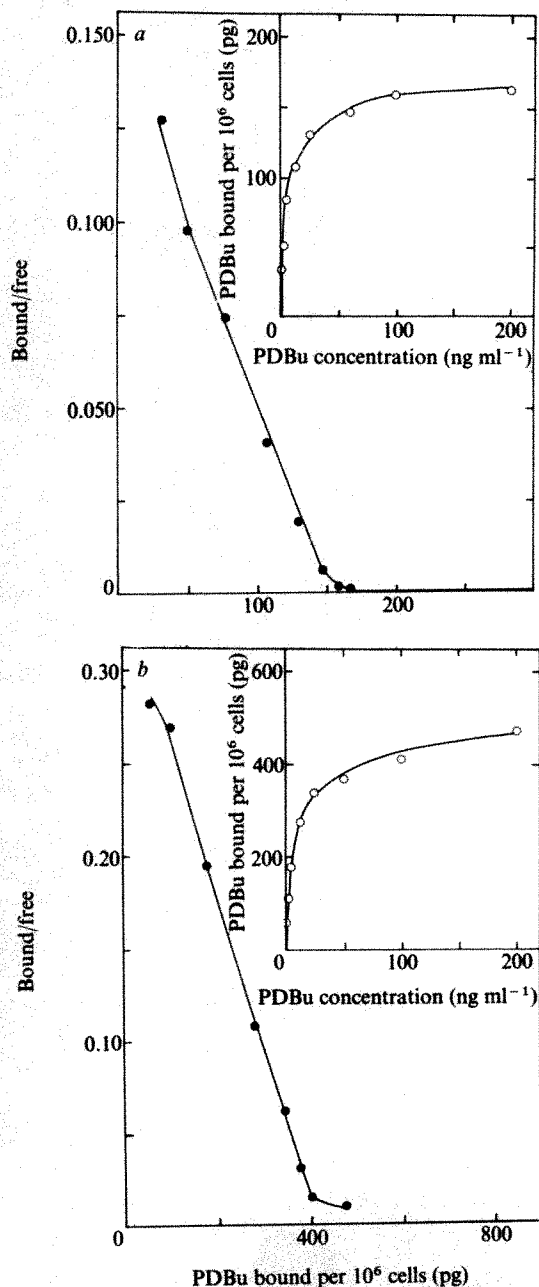
<sup>†</sup> Values for phorbol derivatives are taken from ref. 28. The values for DPTD, MZ and ingenol derivatives are from our unpublished results.  $2 \text{ ng ml}^{-1}$  of  $^{125}\text{I}$ -EGF were used for binding.

<sup>‡</sup>  $K_i$  values were calculated according to method of Cheng and Prusoff<sup>42</sup>, using the equation  $K_i = \text{ID}_{50} \times 1/(1 + L/K)$ , where  $L$  and  $K$  denote concentration and affinity of labelled probe.

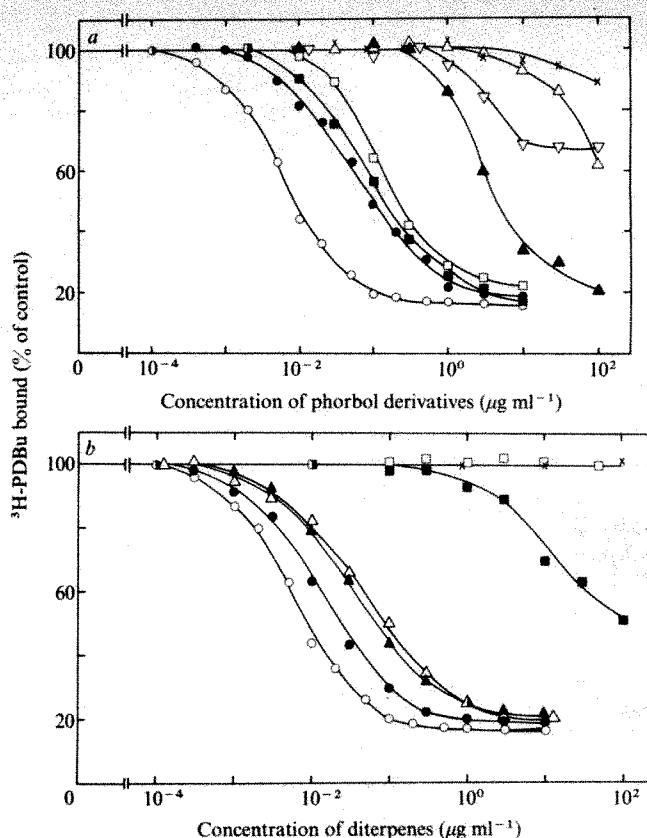


acid, dexamethasone, prostaglandins and disulfiram are reported to inhibit tumour promotion<sup>1-5</sup>. None of these reagents significantly modulated the binding of PDBu to mink lung cells (Table 3). These results suggest that these reagents inhibit tumour promotion by acting at some site other than the receptors for phorbol or ingenol esters. In addition, cholera toxin, diphtheria toxin, oxytocin, vasopressin, gramicidin, monensin, melittin, digitonin, filipin, amphotricin, kanacidin, ganglioside, nystatin, cholesterol and lysophosphocholine, up to a concentration of  $10 \mu\text{g ml}^{-1}$ , did not significantly affect the binding of labelled PDBu to its receptors.

The binding of PDBu to mink cells is not inhibited by EGF even up to a concentration of  $10 \mu\text{g ml}^{-1}$  (Table 3). Although biologically active diterpene esters efficiently modulate EGF



**Fig. 3** *a*, Effects of PDBu concentration on binding to mink lung cells and Scatchard plot. The binding assays were performed as in Fig. 1 legend. The indicated concentrations of  $^3\text{H}$ -PDBu were used. The nonspecific binding was corrected as in Fig. 2.  $\circ$ , PDBu binding as a function of PDBu concentration;  $\bullet$ , Scatchard plot of the data in inset. *b*, Effect of PDBu concentration on PDBu binding to BALB/3T3-A31 cells and Scatchard plot. Experiment was performed as in *a*.  $\circ$ , PDBu binding as function of PDBu concentration;  $\bullet$ , Scatchard plot of the data in inset.



**Fig. 4** *a*, Competition of the binding of  $^3\text{H}$ -PDBu to mink lung cells by various derivatives of phorbol. The binding assays were performed in the presence of  $^3\text{H}$ -PDBu ( $19.7 \text{ ng ml}^{-1}$ ) and the indicated concentrations of various derivatives of phorbol as described in Fig. 1 legend.  $\circ$ , TPA;  $\bullet$ , PDBu;  $\square$ , PDB;  $\blacksquare$ , PDD;  $\triangle$ , 4  $\alpha$ -PDD;  $\blacktriangle$ , PDA;  $\nabla$ , Me-TPA;  $\times$ , phorbol. *b*, Competition of the binding of  $^3\text{H}$ -PDBu to mink lung cells by various derivatives of ingenol, mezerein, DPTD and retinoic acid. Experiment was performed as in *a*.  $\circ$ , TPA;  $\bullet$ , DPTD;  $\triangle$ , MZ;  $\blacktriangle$ , IHD;  $\square$ , ingenol;  $\blacksquare$ , ITA;  $\times$ , retinoic acid.

**Table 3** Effect of tumour promoters and other compounds on the binding of  $^3\text{H}$ -PDBu to mink lung cells

| Compounds                    | Concentration ( $\mu\text{g ml}^{-1}$ ) | Binding (c.p.m. per $10^6$ cells) | Inhibition of binding (%) |
|------------------------------|---|-----------------------------------|---------------------------|
| None                         | —                                       | 2,049                             | 0                         |
| TPA                          | 10                                      | 62                                | 97                        |
| Phorbol                      | 10                                      | 2,039                             | 0                         |
| Phenol                       | 10                                      | 2,018                             | 2                         |
| Iodoacetic acid              | 10                                      | 1,967                             | 4                         |
| Lithocholic acid             | 10                                      | 2,070                             | -1                        |
| Na-barbituate                | 10                                      | 2,002                             | 2                         |
| Na-oleate                    | 10                                      | 2,072                             | -1                        |
| Limonene                     | 10                                      | 2,011                             | 2                         |
| Anthradin                    | 10                                      | 2,004                             | 2                         |
| Anthralin                    | 1                                       | 2,449                             | -20                       |
| Anthralin                    | 5                                       | 3,133                             | -53                       |
| Anthralin                    | 10                                      | 4,180                             | -104                      |
| Saccharin                    | 10                                      | 2,041                             | 0                         |
| Cyclamate                    | 10                                      | 2,065                             | 1                         |
| Vitamin K <sub>3</sub>       | 10                                      | 2,079                             | -1                        |
| Disulfiram                   | 10                                      | 1,997                             | 3                         |
| Retinoic acid                | 50                                      | 2,088                             | -2                        |
| EGF                          | 10                                      | 2,075                             | -1                        |
| Dexamethasone                | 10                                      | 2,045                             | 1                         |
| Insulin                      | 50                                      | 2,155                             | -5                        |
| Prostaglandin E <sub>1</sub> | 50                                      | 2,106                             | -3                        |
| Prostaglandin F <sub>2</sub> | 50                                      | 1,905                             | -7                        |

The binding assays were performed as in Fig. 1 legend. The nonspecific binding was corrected as in Fig. 2 legend.

receptor interaction in this cell<sup>28</sup>, PDBu binds to cells lacking EGF receptors (Table 1). The binding of PDBu to cells does not correlate with their EGF receptor numbers. These experiments clearly demonstrate that membrane receptors which specifically interact with phorbol or ingenol diterpene esters are structurally and functionally distinct from EGF membrane receptors.

## Discussion

These experiments demonstrate the existence of high affinity sites on avian, mammalian and primate cells in culture which specifically interact with biologically active phorbol and ingenol derivatives but not with biologically inert analogues of these diterpenes. PDBu binding to its receptors exhibits specificity, saturability, and reversibility. PDBu-binding sites in cell membranes are different from EGF membrane receptors as PDBu also binds to cells which lack EGF receptors. In contrast to the modulation of EGF binding to its receptors by biologically active phorbol or ingenol esters, EGF does not influence the interaction between PDBu and its membrane receptors. These membrane receptors specifically bind biologically active phorbol and ingenol esters but not other non-diterpene ester tumour promoters. Potent inhibitors of tumour promotion such as retinoids, anti-inflammatory steroids, prostaglandins and cyclic nucleotides do not interact with these receptors. Inter-

tingly, anthralin, a non-diterpene tumour promoter, increases the binding of PDBu to mink cells in a dose-dependent manner. We do not know whether anthralin exhibits this effect by increasing the binding capacity or the binding affinity or both, or acts by some other mechanism. Whether anthralin enhances the tumour-promoting activity of PDBu and other related compounds should be investigated.

Thus, why should mammalian cells have specific receptors for biologically active phorbol and ingenol ester compounds of plant origin? TPA and certain analogues may have some structural resemblance to the endogenous growth-promoting and/or differentiation-modulating substance(s) (agonists and/or antagonists) that have specific membrane receptors. These compounds recognize and interact with the receptors, mimicking the action of the putative substance(s). Azaserine, cordycepin, curare, opiate, physostigmine, plant lectins, puromycin and tubercidin appear to exert their action by such biological mimicry<sup>39-41</sup>. Rohrschneider and Boutwell have suggested that TPA bears some similarity to a polyunsaturated fatty acid ester (PUFA), or a metabolite of it, and might exert its effects by interacting with PUFA receptors<sup>39</sup>. The binding of PDBu to fixed cells suggests that it interacts with the cellular components (receptors) located on the plasma membranes of the cells. The isolation and further characterization of PDBu receptors and putative endogenous ligand(s) should help in understanding tumour promotion.

Received 4 May; accepted 25 July 1980.

1. Van Duuren, B. L. *Prog. exp. Tumour Res.* **11**, 31 (1969).
2. Hecker, E. *Meth. Cancer Res.* **6**, 439 (1971).
3. Boutwell, R. K. *Crit. Rev. Tox.* **2**, 419 (1974).
4. Slaga, T. J., Sivak, A. & Boutwell, R. K. (eds) *Mechanisms of Tumor Promotion and Cocarcinogenesis* (Raven, New York, 1978).
5. Sivak, A. *Biochim. biophys. Acta* **560**, 67 (1979).
6. Hecker, E. & Schmidt, R. *Fortschr. Chem. org. Natstoffe* **31**, 377 (1974).
7. Raick, A. N. *Cancer Res.* **32**, 269 (1973).
8. Paul, D. L. & Hecker, E. *J. Krebsforsch.* **73**, 149 (1969).
9. Balmain, A., Alonso, A. & Fisher, S. *Cancer Res.* **37**, 1548 (1977).
10. Mufson, R. A., Astrup, E. G., Simsiman, R. C. & Boutwell, R. K. *Proc. natn. Acad. Sci. U.S.A.* **74**, 657 (1977).
11. Mufson, R. A., Simsiman, R. C. & Boutwell, R. K. *Cancer Res.* **37**, 665 (1977).
12. Murray, A. W. & Frosio, M. *Cancer Res.* **37**, 1360 (1977).
13. O'Brien, T. G., Simsiman, R. C. & Boutwell, R. K. *Cancer Res.* **35**, 2426 (1975).
14. Balmain, A. *J. invest. Derm.* **67**, 246 (1976).
15. Whitfield, J. F., McManus, J. P. & Gillan, D. J. *J. cell. Physiol.* **82**, 151 (1973).
16. Boyton, A. L., Whitfield, J. F. & Issacs, R. J. *J. cell. Physiol.* **87**, 25 (1976).
17. Sivak, A. *J. cell. Physiol.* **80**, 167 (1972).
18. Wigler, M. & Weinstein, I. B. *Nature* **259**, 232 (1976).
19. Yuspa, S. H. *et al. Nature* **262**, 402 (1976).
20. Blumberg, P. M., Driedger, P. E. & Rossow, P. W. *Nature* **264**, 446 (1976).
21. Wenner, C., Hackney, J., Kimelberg, H. & Mayhew, E. *Cancer Res.* **34**, 1732 (1973).
22. Ohuchi, K. & Levine, L. *J. biol. Chem.* **13**, 4783 (1978).
23. Sivak, A., Mossman, B. F. & Van Duuren, B. L. *Communications* **46**, 605 (1972).
24. Sivak, A. & Van Duuren, B. L. *Chem. biol. Interactions* **3**, 401 (1971).
25. Suss, R., Kinzel, V. & Kreebier, G. *Experientia* **27**, 46 (1971).
26. Rohrschneider, L. R., O'Brien, D. H. & Boutwell, R. K. *Biochim. biophys. Acta* **280**, 57 (1972).
27. Lee, L. S. & Weinstein, I. B. *Science* **202**, 313 (1978).
28. Shoyab, M., De Larco, J. E. & Todaro, G. J. *Nature* **279**, 387 (1979).
29. Brown, K. D., Dicker, P. & Rozengurt, E. *Biochem. biophys. Res. Commun.* **86**, 1037 (1979).
30. Cohen, S. & Taylor, J. M. *Recent Prog. Hormone Res.* **30**, 533 (1974).
31. De Larco, J. E. & Todaro, G. J. *Proc. natn. Acad. Sci. U.S.A.* **75**, 4001 (1978).
32. Lee, L. S. & Weinstein, I. B. *J. Envir. Path. Toxic.* **1**, 627 (1978).
33. Kubinyi, H. *Arzneim. Forsch.* **26**, 1991 (1976).
34. Driedger, P. E. & Blumberg, P. M. *Proc. natn. Acad. Sci. U.S.A.* **77**, 567 (1980).
35. Henderson, I. C., Lieber, M. M. & Todaro, G. J. *Virology* **60**, 282 (1974).
36. Aaronson, S. A. & Todaro, G. J. *J. cell. Physiol.* **72**, 141 (1968).
37. Todaro, G. J., De Larco, J. E. & Cohen, S. *Nature* **264**, 26 (1976).
38. Pruss, R. W. & Herschmann, H. R. *Proc. natn. Acad. Sci. U.S.A.* **74**, 3918 (1977).
39. Rohrschneider, L. R. & Boutwell, R. K. *Nature new Biol.* **243**, 212 (1973).
40. Goldstein, A., Cox, B. M., Gentleman, S., Lowney, L. I. & Cheung, A. L. *Ann. N.Y. Acad. Sci.* **297**, 108 (1978).
41. Sharon, N. & Lis, H. *Science* **177**, 949 (1972).
42. Cheng, C. Y. & Prusoff, W. H. *Biochem. Pharmac.* **22**, 3099 (1973).

# An actin-binding protein from *Acanthamoeba* regulates actin filament polymerization and interactions

Gerhard Isenberg, Ueli Aebi & Thomas D. Pollard

Department of Cell Biology and Anatomy, The John Hopkins University School of Medicine, Baltimore, Maryland 21205

*A protein has been purified from Acanthamoeba which, like cytochalasin B, caps the end of actin filaments normally favoured for monomer addition and inhibits the interactions of actin filaments. In addition, this 'capping' protein nucleates the polymerization of actin monomers and blocks the annealing of actin filament fragments.*

REGULATION of actin filament polymerization and actin filament interactions seems to be essential for cellular motility and the maintenance of cytoplasmic consistency. Thus, cells must have mechanisms to specify actin filament number, length, stability and sites of formation, in addition to mechanisms which regulate the interactions of the filaments with each other, with membranes and with other cellular structures such as microtubules. These mechanisms are just beginning to be understood<sup>1</sup>.

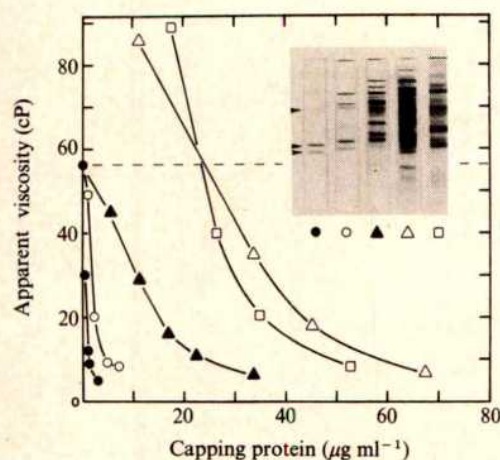
The number and length of the actin filaments could be limited partly by the concentration of polymerizable monomer and the number of filament nucleating sites. The concentration of actin monomer may be controlled by profilin<sup>2</sup>, a ubiquitous small protein which binds actin monomer and inhibits polymerization<sup>2,3</sup>, or by other unrecognized mechanisms which also sequester actin monomers. Even less is known about cellular nucleating mechanisms, because nucleating molecules have not previously been identified. However, electron microscopy



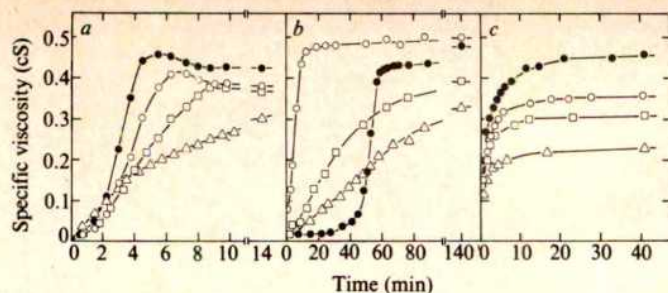
clearly shows that there are structures, such as the dense tips of microvilli<sup>4</sup> and sperm actomeres<sup>5</sup>, which can specify both the site and polarity of polymerization.

A more specific mechanism for controlling filament length would be to cap one or both ends with specific proteins. In striated muscle a protein named  $\beta$ -actinin may block the 'pointed' end of the thin filaments<sup>6</sup>. (The terms 'barbed' and 'pointed' are used to specify the polarity of actin filaments which is revealed by the arrowhead-shaped complexes formed when myosin binds to the filament<sup>7</sup>. The barbed end is the fast, and the pointed end the slowly polymerizing end<sup>8</sup>.) There have been disagreements about the identification of the molecule<sup>6,9</sup>, but a preparation consisting of polypeptides of molecular weights (MWs) 34,000 and 37,000 is a potent inhibitor of the annealing of sonicated actin filament fragments<sup>6</sup>. Non-muscle cells also have proteins which can limit actin filament length, presumably by acting on the end(s) of the filaments. In *Physarum* the protein is called plasmodium actinin and has a molecular weight of 43,000 (refs 10, 11). In macrophages the length-regulating protein, gelsolin, is calcium sensitive and has a MW of 90,000 (ref. 12).

Actin filaments can interact with each other by both cytochalasin-insensitive connections by multivalent actin-binding proteins<sup>13-16</sup> and by cytochalasin-sensitive direct associations between filaments<sup>17,18</sup>. Gels consisting of random networks of filament form when the number of cross-links is low<sup>16</sup>, whereas bundles of aligned filaments form when the number of cross-links is high<sup>15</sup>. The regulation of these interactions could, in principle, occur at three levels: the formation and breakdown of



**Fig. 1** Purification of the actin filament capping protein from *Acanthamoeba*. The material obtained at each step of the purification was assayed for its ability to inhibit the low-shear apparent viscosity<sup>16</sup> of pure actin filaments and for polypeptide composition by gel electrophoresis in 7.5% polyacrylamide with 0.1% sodium dodecylsulphate<sup>16</sup>. The viscometric assay was carried out by polymerizing a mixture of 0.5 mg ml<sup>-1</sup> gel-filtered muscle actin monomers<sup>18</sup> with the material to be tested in a buffer consisting of 10 mM imidazole, 2 mM MgCl<sub>2</sub>, 1 mM EGTA, 1 mM ATP, pH 7.5, in a 1.2-mm inside-diameter capillary tube for 10 min at 25°C. A 0.64-mm outside-diameter stainless steel ball was then rolled down the wall of the capillary tilted at 50° from horizontal. The apparent viscosity was calculated from the ball velocity by comparison with newtonian standards<sup>16</sup>. The horizontal dashed line is the viscosity of actin filaments alone. Actomyosin supernatant (□) was obtained as described<sup>22</sup> and the fraction precipitating between 1.5 and 2.5 M ammonium sulphate (Δ) collected and dialysed against ID buffer (20 mM imidazole, 0.5 mM dithiothreitol (DTT), pH 7.5) with 1 mM EGTA. The ammonium sulphate fraction was further purified by gel-permeation chromatography on a 4 × 95-cm column of Sephadex G-150 in the same buffer. The peak of the viscosity-inhibiting activity (▲) was then applied to a 2.5 × 19-cm column of hydroxylapatite equilibrated with ID buffer and eluted with a concave 0–250 mM phosphate gradient. The peak of viscosity-inhibiting activity (○) was dialysed against ID buffer and finally purified by chromatography on a 1.5 × 7.5-cm column of DEAE-cellulose equilibrated with ID buffer and eluted with a linear 50–300 mM KCl gradient. The purified capping protein eluted at 200 mM KCl (●) and consisted of two major polypeptides (of MWs 28,000 and 31,000) and a minor 60,000-MW polypeptide (arrowheads).



**Fig. 2** Effect of filament capping protein on the polymerization kinetics of pure actin. Polymerization was monitored by measuring the high-shear viscosity in an Ostwald capillary viscometer<sup>18</sup>. *a*, Gel-filtered pure actin monomer (0.5 mg ml<sup>-1</sup>) was mixed with 0 (●), 0.44 μg ml<sup>-1</sup> (○), 1.54 μg ml<sup>-1</sup> (□) or 3.08 μg ml<sup>-1</sup> (Δ) of capping protein and polymerized in 2 mM MgCl<sub>2</sub>, 10 mM imidazole, 1 mM EGTA, 1 mM ATP, pH 7.5, at 25°C. *b*, Gel-filtered actin monomer (0.5 mg ml<sup>-1</sup>) (●) was mixed with 2.2 μg ml<sup>-1</sup> capping protein (Δ), 30 μg ml<sup>-1</sup> actin filaments (○) or 2.2 μg ml<sup>-1</sup> capping protein plus 30 μg ml<sup>-1</sup> actin filaments (□) and polymerized in 20 mM KCl, 10 mM imidazole, 0.7 mM Tris, 0.07 mM ATP, 0.2 mM DTT, 0.07 mM CaCl<sub>2</sub>, pH 7.5, at 25°C. *c*, Steady-state samples of 0.5 mg ml<sup>-1</sup> actin filaments in the buffer described in *b* were mixed with 0 (●), 2.2 μg ml<sup>-1</sup> (○), 4.4 μg ml<sup>-1</sup> (□) or 8.8 μg ml<sup>-1</sup> (Δ) of capping protein and sonicated for 15 s at setting 1 of a Branson sonicator. The recovery of viscosity was followed at 25°C.

the actin filaments<sup>19</sup>; the cross-linking of filaments by actin-binding proteins<sup>13-16</sup>; and the modulation of actin filament self-associations<sup>16</sup>. This last possibility has not been considered seriously before, but the cell might well need to regulate actin filament self-associations, because they are sufficiently strong for the viscosity of pure actin filament solutions to approach infinity at the low shear rates found in cells<sup>20</sup>. The existence of an endogenous cytochalasin-like factor could explain why cytoplasm is not solid. Such a protein factor contaminates conventional muscle actin preparations<sup>18,21</sup>. This unpurified factor strongly inhibits actin filament self-associations without inhibiting polymerization<sup>21</sup>.

We have purified and characterized an actin filament 'capping protein' from *Acanthamoeba* and suggest that it may play a central role in the regulation of both actin filament polymerization and cross-linking.

## Purification of the capping protein

As the capping protein inhibits the low shear viscosity of pure actin filaments, we used a low-shear (<10 s<sup>-1</sup>) falling-ball viscometer<sup>16</sup> to assay the capping protein during purification. As the first step, crude *Acanthamoeba* extracts were fractionated on DEAE-cellulose as described previously<sup>16</sup>. The fractions containing the overlapping peaks of viscosity-inhibiting activity<sup>16</sup>, myosin-2 and actin were pooled and actomyosin-2 precipitated<sup>22</sup>. The resulting supernatant, which contained most of the viscosity-inhibiting activity, was used as the starting material to purify capping protein to near homogeneity. The purification steps included ammonium sulphate precipitation, and gel permeation, hydroxylapatite and ion-exchange chromatography (Fig. 1). The small amount of capping protein which precipitated with the actomyosin-2 could be recovered as a by-product of myosin-2 purification by the method of Pollard *et al.*<sup>22</sup>.

The purified protein from four different preparations consisted of two major polypeptides with MWs 28,000 and 31,000 and a variable minor polypeptide of MW 60,000. The inhibitory activity is probably associated with the polypeptides of MWs 28,000 and 31,000 because they were present in proportion to inhibitory activity over the final DEAE peak, and because the minor contaminants including the 60,000-MW polypeptide



were also present in neighbouring fractions without inhibitory activity.

As shown in Fig. 1, the specific inhibitory activity of the fractions increased about 50-fold during purification of the two polypeptides by more than 100-fold, suggesting that the protein was partially inactivated during purification. The presence of some gelation-factor activity in the crude fractions (Fig. 1) made calculation of yields somewhat difficult, but we estimated the overall yield to be ~10%. In terms of mass, we obtained ~4  $\mu\text{g}$  of purified capping protein per g of wet cells.

### Physical properties of the capping protein

The two polypeptides constituting the purified protein were present in the ratio of 1.5 (31 K) to 1 (28 K) judging from the intensities of the two bands on Coomassie blue-stained electrophoretic gels. In addition there was ~10% of a 60 K polypeptide. The Stokes' radius of native capping protein was 4.0–4.4 nm measured by the method of Ackers<sup>23</sup> using gel-permeation chromatography in either 20 mM imidazole or 0.6 M KCl. A spherical protein of this size would have a molecular weight of about 120,000 to 160,000. Thus the native protein could consist of up to two copies each of the two polypeptides. The capping protein is soluble in both low and high ionic strength buffers at neutral pH, but its activity is more stable in 50 mM KCl than in 20 mM imidazole alone. The absorption spectrum of the capping protein has a maximum at 277 nm and a minimum at 250 nm. The extinction coefficient at 280 nm is ~0.86  $\text{cm}^{-1} \text{ml mg}^{-1}$ .

### Binding of capping protein to actin filaments

Capping protein does not pellet by itself, but binding to actin filaments was demonstrated in experiments where 4.8  $\mu\text{g}$  capping protein (6  $\mu\text{g}$  total) pelleted at 150,000g for 45 min with 500  $\mu\text{g}$  of actin filaments in 2 mM  $\text{MgCl}_2$ . Although binding has not been studied in any detail, this did not represent saturation of capping protein binding sites, because 7.2  $\mu\text{g}$  capping protein (12  $\mu\text{g}$  total) pelleted with the same amount of actin.

### Effect of capping protein on actin filament polymerization

The polymerization of purified actin monomers consists of a slow nucleation step followed by a rapid elongation step<sup>24</sup>. We measured the rate and extent of polymerization in an Ostwald capillary viscometer with a high shear rate ( $>1,000 \text{ s}^{-1}$ ) which disrupts weak associations between the filaments, making the observed viscosity largely a function of polymer concentration and length distribution. In 20 mM KCl the nucleation step was very slow as shown by the 40-min lag in the time course of the viscosity change for actin monomer alone (Fig. 2b). The elimination of this lag by added actin filaments confirmed that it was due to nucleation (Fig. 2b). The rapid rise in viscosity after nucleation was due to elongation of the filaments. In 2 mM  $\text{MgCl}_2$  both of these steps were faster (Fig. 2a).

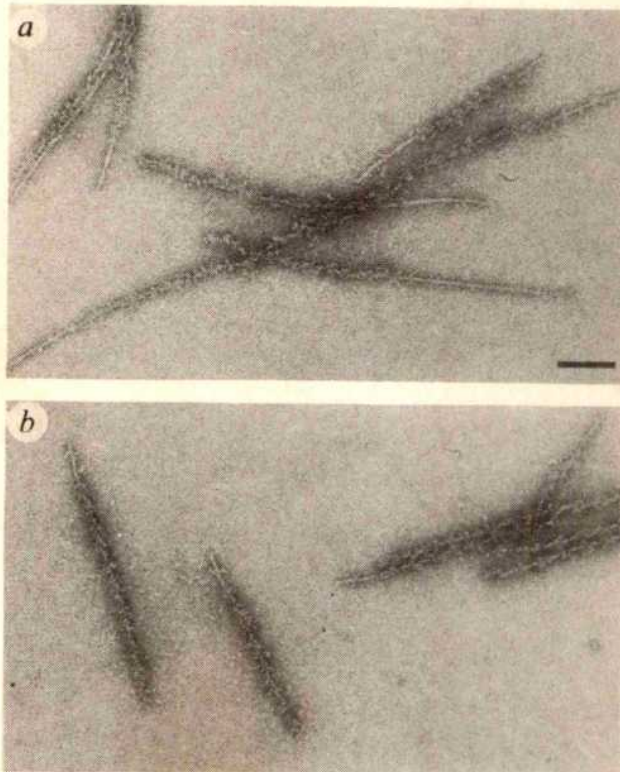
Purified capping protein had a complex effect on actin polymerization. Paradoxically, it both promoted nucleation and inhibited the rate of growth of actin filaments (Fig. 2a,b). These effects were most apparent in conditions where polymerization was slow, such as 20 mM KCl, where very low concentrations of capping protein eliminated the lag phase (Fig. 2b). This demonstrated stimulation of nucleus formation. In 2 mM  $\text{MgCl}_2$  the lag was short, but high concentrations of capping protein clearly increased the initial rate of the viscosity change and altered the shape of the curve from sigmoidal to hyperbolic (Fig. 2a).

Although capping protein promoted nucleus formation, it was, at the same time, a potent inhibitor of the rate of actin filament elongation. This inhibition was seen in mixtures of capping protein with pure actin monomers (Fig. 2a,b), but is best illustrated by experiments in which actin monomer polymerization was nucleated by actin filament fragments. The rate

of the viscosity change in the absence of capping protein was much greater than the rate in the presence of capping protein (Fig. 2b).

By observing the direction and extent of actin filament growth at the ends of decorated nuclei (Fig. 3), we found that capping protein inhibited filament elongation by blocking monomer addition at the barbed end of the filaments (Fig. 3). As established previously<sup>8</sup> actin filaments normally grow bidirectionally with a strong bias for the barbed end (Fig. 3a). In the presence of low concentrations of capping protein, monomer added to the pointed end, but there was no growth at the barbed end (Fig. 3b). Capping protein also blocked monomer addition to the barbed end of actin filaments in the presence of 5 mM  $\text{MgCl}_2$ , 75 mM KCl and 0.16 mM ATP. This was shown in monomer addition experiments using demembrated microvillus cores<sup>25</sup>. The rates of growth at the pointed end with capping protein were 1 molecule per s in 20 mM KCl and 6  $\mu\text{M}$  actin, and 6 molecules per s in Mg-KCl and 3  $\mu\text{M}$  actin. These rates were similar to normal growth rates at the pointed end.

The capping protein also inhibited the extent of annealing of actin filaments fragmented by sonication (Fig. 2c). The steady-state viscosity is reduced in a concentration-dependent fashion, but the rate of the approach of the viscosity to the steady state was hardly affected.



**Fig. 3** Effect of filament capping protein on the polarity of actin filament polymerization in 20 mM KCl. The direction of polymerization was determined electron microscopically by adding actin monomers to short actin filaments decorated with an equimolar amount of muscle myosin subfragment-1 which acted as nuclei. These decorated nuclei were reduced in length by passage through a syringe needle. Samples for electron microscopy were negatively stained with 0.75% uranyl formate, pH 4.3. Scale bar, 100 nm. *a*, Control. 50  $\mu\text{g ml}^{-1}$  decorated actin nuclei were incubated for 5 min at 22 °C with 100  $\mu\text{g ml}^{-1}$  actin monomer freshly prepared by gel filtration in ATP-free buffer<sup>18</sup>. The bare filament growth is predominantly from the barbed end of the decorated nuclei. *b*, Effect of capping protein. 50  $\mu\text{g ml}^{-1}$  decorated nuclei were incubated with 150  $\mu\text{g ml}^{-1}$  ATP-free monomer and 2.2  $\mu\text{g ml}^{-1}$  capping protein for 30 min at 22 °C. Note the absence of barbed-end growth and the short bare filaments at the pointed end.



**Table 1** Effect of filament capping protein on the steady-state polymer concentration

| Capping protein ( $\mu\text{g ml}^{-1}$ ) | Supernate actin monomer ( $\mu\text{g ml}^{-1}$ ) | Calculated polymer ( $\mu\text{g ml}^{-1}$ ) | Specific viscosity (cS) | Reduced viscosity (cS per mg polymer per ml) |
|---|---|--|-------------------------|--|
| 0   | 34  | 466  | 0.42                    | 0.90   |
| 0.44                                      | 59  | 441  | 0.38                    | 0.86   |
| 1.54                                      | 128   | 372  | 0.37                    | 0.99   |
| 3.08                                      | 136   | 364  | 0.32                    | 0.88   |

Steady-state polymerized actin samples from the experiment in Fig. 2a were centrifuged for 20 min at  $10^5$  r.p.m. in a Beckman Airfuge at 22 °C. Actin filaments pellet in 5 min in these conditions. The fraction of unpolymerized actin in the supernate was determined by quantitative gel electrophoresis. The concentration of polymer was calculated by difference.

The filament capping protein reduced the steady-state high-shear viscosity in a concentration-dependent fashion (Fig. 2). This seemed to be due primarily to a reduction in polymer concentration (Table 1), because the reduced viscosity per mg polymer was not altered significantly by the presence of the capping protein. We also used electron microscopy of negatively stained specimens to measure the lengths of actin filaments formed in the presence or absence of the capping protein. Although the weight-average filament length of samples with capping protein was about 25% less than controls in two different experiments, we were not convinced that the observed difference was meaningful. One problem was that the extent of the reduction in length was not proportional to the reduction in viscosity. Another was that the measured weight-average lengths of identical samples can differ by more than 25% (ref. 18).

### Effect of the capping protein on actin filament structure

Visual inspection of negatively stained actin filaments in the absence or presence of enough capping protein to inhibit the low-shear viscosity by more than 95% did not reveal any qualitative structure differences; nor was it possible to detect capping protein at the ends of the filaments. To assess possible structural differences in a more quantitative way, we prepared  $\text{Mg}^{2+}$ -paracrystals from pure actin filaments (Fig. 4a) and capping protein-actin filaments (Fig. 4c) and analysed electron micrographs of these specimens by optical diffraction (Fig. 4c,d). (Although 50 mM  $\text{MgCl}_2$  was used to make actin filament paracrystals, approximately the same amount of capping protein is bound to actin filaments in 2 mM or 50 mM  $\text{MgCl}_2$ .) In both cases we selected the 10 best diffraction patterns which showed diffraction spots to at least  $(3 \text{ nm})^{-1}$ . We measured the layer-line altitudes corresponding to the axial and structural repeats of the actin double helix (see, for an example, ref. 26). The average helix parameters for the two data sets did not differ significantly from each other: the axial repeat was  $5.5 \pm 0.1$  nm and the structural repeat was  $35.5 \pm 1$  nm in both cases. Furthermore the centre-to-centre spacing of the filaments measured directly on electron micrographs was  $6.5 \pm 0.3$  nm for both samples. Qualitatively the intensity distribution along corresponding layer lines was the same. This low-resolution structural analysis suggested that capping protein bound to actin filaments does not alter the helical structure of the filaments substantially.

### Effect of the capping protein on actin filament networks

Capping protein inhibited the low-shear viscosity of pure actin filaments (Fig. 5 inset) much more strongly than the high-shear viscosity (Fig. 2a). One microgramme of capping protein reduced the low-shear viscosity of 500  $\mu\text{g}$  actin by 90%. This inhibition of the low-shear viscosity was identical in EGTA and

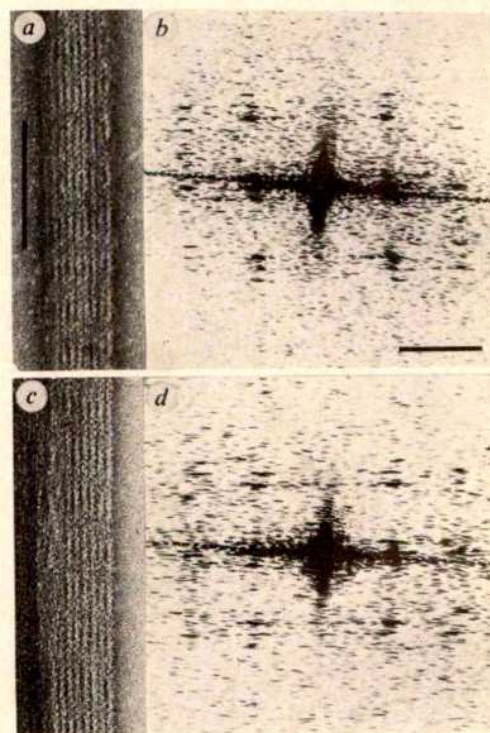
in 0.1 mM  $\text{CaCl}_2$ , so the capping protein was not regulated directly by calcium. Cytochalasin B and capping protein have an additive inhibitory effect on pure actin filament low-shear viscosity; 0.1  $\mu\text{M}$  cytochalasin B reduced the viscosity by about the same amount as 0.5  $\mu\text{g ml}^{-1}$  ( $\sim 0.0003 \mu\text{M}$ ) capping protein.

Capping protein also decreased the low-shear viscosity of mixtures of actin filaments with a new 85,000-MW  $\text{Ca}^{2+}$ -sensitive gelation factor from *Acanthamoeba*<sup>27</sup> (Fig. 5) or with aldolase, a nonspecific actin cross-linker. Low concentrations of capping protein increased the concentration of cross-linker required to form a gel and concentrations of capping protein greater than 1.1  $\mu\text{g ml}^{-1}$  prevented gelation by the *Acanthamoeba* gelation factor entirely (Fig. 5).

### Interpretation

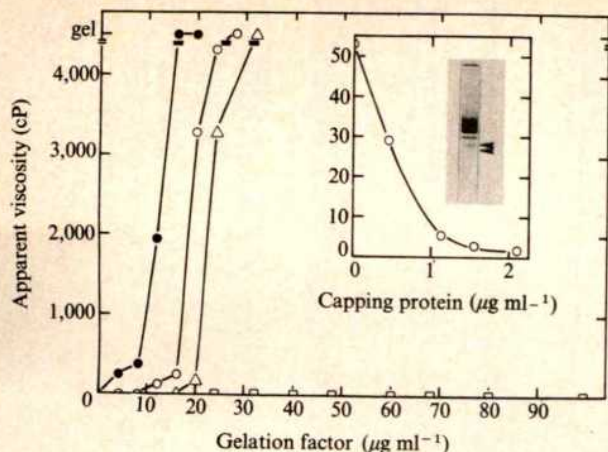
We suggest that actin filament capping protein has the following mechanism: it binds to the two actin molecules at the barbed end of actin filaments or it binds to two actin monomers at their barbed poles. In this way it might both promote nucleation, by stabilizing actin dimers, and also inhibit filament elongation by allowing growth in only the slow pointed direction. The formation of networks by pure actin filaments might be affected if the presence of capping protein at the barbed ends of filaments eliminates the cytochalasin-sensitive interactions, postulated<sup>18</sup> to be between the ends and the sides of the filaments. A second but less likely possibility for the effect of capping protein on actin filament networks is that it simply reduces the length of the filaments, as others have suggested for the action of cytochalasin B (ref. 17) and gelsolin<sup>12</sup>.

Capping protein is similar to cytochalasin B in that both block actin monomer addition at the barbed end of actin filaments<sup>18</sup> and both strongly inhibit the formation of networks by actin



**Fig. 4** Electron micrographs (a, c) and optical diffraction patterns (b, d) of actin (a, b) and capping protein-actin (c, d) paracrystals. Gel-filtered actin, 0.5  $\text{mg ml}^{-1}$ , was first polymerized for 10 min at 22 °C in 50 mM KCl, 2 mM  $\text{K}_2\text{S}_2\text{O}_8$ , 10 mM imidazole, pH 7.5, either alone or with 3  $\mu\text{g ml}^{-1}$  of capping protein.  $\text{MgCl}_2$  was then added to a concentration of 50 mM for 10 min to induce paracrystal formation. Samples diluted to 50  $\mu\text{g ml}^{-1}$  were applied to glow-discharged carbon-coated grids and stained with 0.75% uranyl formate, pH 4.3. Optical diffraction patterns were recorded from selected areas of electron micrographs of the paracrystal, typically four to six filaments wide and six to 12 structural repeats long. Scale bars, 100 nm (a, c),  $(5 \text{ nm})^{-1}$  (b, d).





**Fig. 5** Effect of filament capping protein on actin gel formation, and on the low-shear viscosity of actin filaments. Samples consisting of  $0.5 \text{ mg ml}^{-1}$  actin with 0 (●),  $0.44 \text{ μg ml}^{-1}$  (○),  $0.88 \text{ μg ml}^{-1}$  (△) or  $1.1 \text{ μg ml}^{-1}$  (□) capping protein were mixed with various concentrations of an 85,000-MW gelation protein from *Acanthamoeba*<sup>27</sup> and polymerized in capillary tubes for 10 min in 2 mM  $\text{MgCl}_2$ , 1 mM ATP, 1 mM EGTA, 10 mM imidazole, pH 7. The low-shear apparent viscosity was measured with the falling-ball device. Inset: actin alone or with several concentrations of capping protein was polymerized in capillary tubes in the conditions of Fig. 2a legend for 10 min after which the apparent viscosity was measured with the falling-ball device. Incubation for up to 40 min did not change the viscosity of actin plus  $2.2 \text{ μg ml}^{-1}$  capping protein. The electrophoretic gel illustrates the composition of a sample with  $0.5 \text{ mg ml}^{-1}$  actin with  $1.1 \text{ μg ml}^{-1}$  capping protein.

filaments<sup>17,18</sup>. In contrast, capping protein, but not cytochalasin B, promotes the formation of filament nuclei by actin monomers and inhibits annealing of actin filaments.

Both the *Acanthamoeba* capping protein and muscle  $\beta$ -actinin<sup>6</sup> inhibit polymerization rates and annealing, but they seem to be different molecules. The subunit molecular weights and Stokes' radii differ, the two proteins may be bound at opposite ends of the filament, and  $\beta$ -actinin is not a potent inhibitor of the low-shear viscosity of pure actin filaments<sup>6</sup>.

Although physiological functions cannot be proven by our purely biochemical experiments, the properties of the capping

protein molecule suggest several functions. For example, capping protein could prevent actin filament self-associations and thereby permit regulation of cytoplasmic consistency solely by variation of the extent of filament cross-linked by gelation factors<sup>14,16,27</sup>. This could be accomplished without changing the extent of actin filament polymerization or the size of the filaments. Second, the concentration of capping protein could determine the number of actin filaments in the cell. This would occur if filaments with blocked barbed ends are more stable than filaments with free barbed ends, or if spontaneous nucleation is prevented by the binding of profilin to actin monomers<sup>3</sup>. Finally, and perhaps most interestingly, capping protein could provide a link between the barbed end of actin filaments and various cellular structures to which they are attached, such as membranes.

We thank Janelle Levy, Dan Kiehart, Linda Griffith and Mark Mooseker for help. This work was supported by NIH grant GM-26338 to T.D.P. and GM27765 to U.A. G.I. is supported by a Heisenberg fellowship from Deutsche Forschungsgemeinschaft.

Received 23 May; accepted 10 September 1980.

1. Taylor, D. L. & Condeelis, J. S. *Int. Rev. Cytol.* **56**, 57–144 (1979).
2. Carlsson, L., Nystrom, L. E., Sundkvist, L., Markey, F. & Lindberg, U. *J. molec. Biol.* **115**, 465–483 (1977).
3. Reichstein, E. & Korn, E. D. *J. biol. Chem.* **254**, 6174–6179 (1979).
4. Tilney, L. G. & Cardell, R. R. *J. Cell Biol.* **47**, 408–419 (1970).
5. Tilney, L. G. & Kallenbach, N. *J. Cell Biol.* **81**, 608–623 (1979).
6. Maruyama, K. *et al. J. Biochem.* **81**, 215–232 (1977).
7. Huxley, H. E. *J. molec. Biol.* **7**, 281–308 (1963).
8. Woodrum, D. T., Rich, S. & Pollard, T. D. *J. Cell Biol.* **67**, 231–237 (1975).
9. Heizmann, C. & Hauptle, M. *Eur. J. Biochem.* **80**, 443–451 (1977).
10. Hatano, S. *et al. in Cell Motility: Molecules and Organization* (eds Hatano, S., Ishikawa, H. & Sato, H.) 87–104 (University of Tokyo Press, 1979).
11. Hinssen, H. *in Cell Motility: Molecules and Organization* (eds Hatano, S., Ishikawa, H. & Sato, H.) 59–85 (University of Tokyo Press, 1979).
12. Yin, H. L. & Stossel, T. P. *Nature* **281**, 583–586 (1979).
13. Hartwig, J. H. & Stossel, T. P. *J. Cell Biol.* **71**, 295–302 (1976).
14. Maruta, H. & Korn, E. D. *J. biol. Chem.* **252**, 399–402 (1977).
15. Bryan, J. & Kane, R. E. *J. molec. Biol.* **125**, 207–224 (1978).
16. MacLean-Fletcher, S. & Pollard, T. D. *J. Cell Biol.* **85**, 414–428 (1980).
17. Hartwig, J. H. & Stossel, T. P. *J. molec. Biol.* **134**, 539–553 (1979).
18. MacLean-Fletcher, S. & Pollard, T. D. *Cell* **20**, 329–341 (1980).
19. Isenberg, G. & Wohlfarth-Bottermann, K. E. *Cell Tissue Res.* **173**, 495–528 (1976).
20. Maruyama, K., Kaibara, M. & Fukada, E. *Biochim. biophys. Acta* **271**, 20–29 (1974).
21. MacLean-Fletcher, S. & Pollard, T. D. *Biochem. biophys. Res. Commun.* **96**, 18–27 (1980).
22. Pollard, T. D., Stafford, W. F. & Porter, M. E. *J. biol. Chem.* **253**, 4798–4808 (1978).
23. Ackers, G. K. *J. biol. Chem.* **242**, 3237–3238 (1967).
24. Oosawa, F. & Asakura, S. *Thermodynamics of the Polymerization of Protein* (Academic, New York, 1975).
25. Pollard, T. D. & Mooseker, M. *J. Cell Biol.* (submitted).
26. Moore, P. B., Huxley, H. E. & DeRosier, D. J. *J. molec. Biol.* **50**, 279–295 (1970).
27. Pollard, T. D., Levy, J., Isenberg, G. & Aebi, U. *J. Cell. Biol.* **87**, 223a (1980).

## LETTERS

### B2 1141+37: a giant radio galaxy with remarkable radio and optical properties

M. H. Ulrich\*, H. Butcher† & D. L. Meier‡

\* European Southern Observatory, Karl-Schwarzschild-Strasse 2, D-8046 Garching bei München, FRG

† Kitt Peak National Observatory, Tucson, Arizona 85726

‡ Jet Propulsion Laboratory, Pasadena, California 91103

The radio galaxy B2 1141+37 is remarkable for both its radio and optical properties. The radio source has a double structure for which the ratio of the separation between the components to their dimension is exceptionally large. Moreover, our recent measurement of the redshift gives  $z = 0.115$  giving a separation between the components of 1.0 Mpc. This makes 1141+37 one of the largest radio structures known. The optical identification which has been proposed is a tight chain of galaxies which are

probably gravitationally bound. If this is the case, the radio galaxy must have some precession and/or rotation motion around the centre of mass of the group with important consequences on the structure and evolution of the radio source. We report here on the redshift measurement and on some VLA observations at 4.9 GHz.

The radio source is formed by the two sources of the Bologna Catalogue B2 1141+37 A and B, and is also 4C37.42. It is one of the objects in the sample of radio galaxies which was analysed by Meier *et al.*<sup>1</sup> to obtain the luminosity function of radio galaxies, and it is the only object in that sample for which the redshift was not measured.

The map<sup>2</sup> of B2 1141+37 obtained at 1,415 MHz with the Westerbork Synthesis Radio Telescope shows two intense components of nearly equal intensity separated by 264 arc s and with dimensions of  $65 \times (<30)$  arc s for the NE component and  $20 \times (<30)$  arc s for the SW component. No third component was detected along the line joining the two bright components. Polarization of 4% and 3% at 1,415 MHz has been detected in the SW and NE components respectively<sup>7</sup>.

The radio source was re-observed at 4,900 MHz with the VLA in August 1978 during observations of the central sources



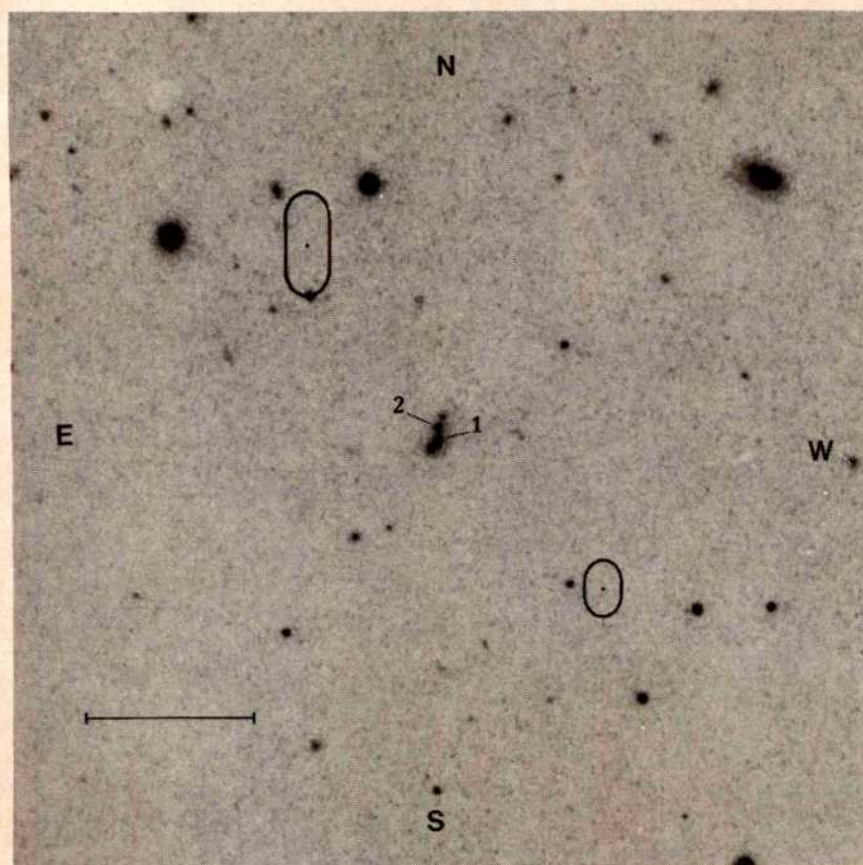


Fig. 1 Radio lobes observed at 1,415 MHz (ref. 2) on a print of the Blue Sky Survey photograph. Scale bar, 100 arc s.

of several radio galaxies from the Bologna Catalogue<sup>3</sup>. Five integrations of 5 min were done, but after removing the scans affected by phase shifts due to stormy weather, the effective integration time was 17 min. The map obtained with a grid of  $3 \times 3$  arc s and a gaussian taper falling to 50% at 2.5 km in the  $(u, v)$  plane shows two radio lobes with maxima at the positions indicated in Table 1 and exactly coinciding with the maxima in the 1,415 MHz map<sup>2</sup>. The intensities of the NE and SW lobes at

Table 1 Parameters relative to B2 1141 + 37 A, B

|  | NE                              | SW                              |
|--|---------------------------------|---------------------------------|
| Coordinates of the peak at 4.9 GHz: (1950) | 11 h 41 min 57.2 s<br>37°26'58" | 11 h 41 min 41.6 s<br>37°23'42" |
| Radio power of the two components (Jy):    |                                 |                                 |
| 408 MHz                                    | 2.79                            | 2.35                            |
| 1,415 MHz                                  | 0.97                            | 0.84                            |
| 5,000 MHz                                  | 0.23                            | 0.18                            |

Table 2 Comparison of 3C236, Cyg A, and B2 1141 + 37 A, B

| Source  | 3C236†                | Cyg A‡               | B2 1141 + 37 A, B‡    |
|---|-----------------------|----------------------|-----------------------|
| Distance* (Mpc)                                   | 554                   | 320                  | 687                   |
| Linear size (Mpc)                                 | 5.7                   | 0.16                 | 1.0                   |
| Radio power (WHz <sup>-1</sup> sr <sup>-1</sup> ) | $2.6 \times 10^{25}$  | $2.7 \times 10^{27}$ | $1.8 \times 10^{25}$  |
| Component properties                              |                       |                      |                       |
| Volume (cm <sup>3</sup> )                         | $3.5 \times 10^{72}$  | $3.3 \times 10^{65}$ | $4.7 \times 10^{70}$  |
| Minimum energy (erg)                              | $5.4 \times 10^{59}$  | $8.9 \times 10^{57}$ | $1.6 \times 10^{59}$  |
| Energy density (erg cm <sup>-3</sup> )            | $1.6 \times 10^{-14}$ | $2.7 \times 10^{-8}$ | $3.4 \times 10^{-12}$ |
| Equipartition magnetic field (G)                  | $6.3 \times 10^{-7}$  | $8.2 \times 10^{-4}$ | $9.3 \times 10^{-6}$  |

\*Assuming  $H_0 = 50 \text{ km s}^{-1} \text{ Mpc}^{-1}$ .

†Ref. 5.

‡See text.

4,900 MHz are 0.23 and 0.18 Jy, respectively. These values are both  $\sim 1.5$  times smaller than the values obtained by extrapolating to 4,900 MHz the spectrum defined by the flux density at 408 and 1,415 MHz,  $f_\nu \propto \nu^{-0.84}$ , of the two radio lobes. This suggests that some flux is missing in the 4,900-MHz map, and this is probably caused by the fact that the shortest baseline spacing of the VLA observations was 480 m. No central source brighter than 0.03 Jy has been detected at the location of the optical identification.

A tight chain of four galaxies located very close to the mid-point between the two radio components has been proposed as the optical identification<sup>2</sup>. We have recently measured the redshifts of the two brightest galaxies in the chain, galaxies 1 and 2 in Fig. 1, with the image intensified dissector scanner of the 4 m telescope at Kitt Peak National Observatory. Galaxy 1 shows the *K*, *H*, and *G* features and the [O II]  $\lambda 3,727$  emission line at a redshift  $z = 0.1145 \pm 0.0005$ . The scan of galaxy 2 shows the *K* and *H* lines at  $z = 0.1155 \pm 0.005$ . Galaxy 1, being the brightest and having a spectrum with at least one emission line, is likely to be the radio galaxy among the four members of the chain. Taking  $H = 50 \text{ km s}^{-1} \text{ Mpc}^{-1}$ , the distance to the radio source is 687 Mpc and 1 arc s corresponds to 3.3 kpc. The distance between the edges of the two radio lobes is, therefore, 1.0 Mpc making it one of the largest radio sources known. The minimum energy in the radio lobes, the energy density, and the equipartition magnetic field have been calculated following the procedure of McDonald *et al.*<sup>4</sup> and making no allowance for the presence of high energy protons. The calculations are based on the flux density at 604 MHz which is calculated by interpolating the radio spectrum defined by the flux density at 408 and 1,415 MHz,  $f_\nu \propto \nu^{-0.84}$ . The values corresponding to the NE component are listed in Table 2 together with the values of the same parameters for the E component of 3C236 (ref. 5) and for the outer compact component in the W lobe of Cyg A (component 'D' in ref. 6). For Cyg A we have calculated the energy from the flux measured<sup>6</sup> at 5 GHz extrapolated to 604 MHz with a power law spectrum  $f_\nu \propto \nu^{-1}$  and assuming that this flux comes from a region which has the same dimensions as



those measured<sup>6</sup> at 5 GHz. Comparison of the values of the energy density in the radio lobes of 1141+37 and in the outer compact component of Cygnus A indicates that 1141+37 is in a more relaxed state.

A full synthesis map of 1141+37 would be particularly interesting for several reasons. First, there are very few radio galaxies with comparable dimensions. Second, the inner radio structure should contain information related to the motion of the parent radio galaxy in its group. The closeness in redshifts of galaxy 1 and 2 and the tight group which they form in the plane of the sky with the other two smaller galaxies suggest that this is a gravitationally bound group. If this is the case, the radio galaxy, probably galaxy 1, has some precession motion and/or rotation motion around the centre of mass of the group. The direction of the beam along which the particles have been ejected must, therefore, have recently undergone some changes influencing the shape and the evolution of the radio structure between the outer lobes and the parent radio galaxy.

M.H.U. is a Visiting Astronomer at Kitt Peak National Observatory, which is operated by AURA Inc. under contract with NSF.

Received 11 August; accepted 11 September 1980.

1. Meier, D. L., Ulrich, M. H., Fanti, R., Gioia, I. & Lari, C. *Astrophys. J.* **229**, 25 (1979).
2. Fanti, R., Gioia, I., Lari, C. & Ulrich, M. H. *Astr. Astrophys. Suppl.* **34**, 341 (1978).
3. Meier, D. L. & Ulrich, M. H. (in preparation).
4. McDonald, G. H., Kenderdine, S. & Neville, A. C. *Mon. Not. R. astr. Soc.* **138**, 259 (1968).
5. Willis, A. G., Strom, R. G. & Wilson, A. S. *Nature* **250**, 625 (1974).
6. Hargrave, P. J. & Ryle, M. *Mon. Not. R. astr. Soc.* **166**, 305 (1974).
7. Gioia, I. M. & Gregorini, L. *Astr. Astrophys. Suppl.* **36**, 347 (1979).

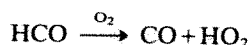
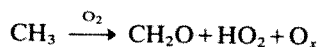
## Two-dimensional model calculations of stratospheric HCl and ClO

C. Miller\*, J. M. Steed†, D. L. Filkin\* & J. P. Jesson†

\* Engineering Department and † Central Research and Developments, El du Pont de Nemours and Company, Experimental Station, Wilmington, Delaware 19898

Most previous attempts to estimate the effects of atmospheric contaminants on stratospheric ozone have involved one-dimensional models of the troposphere and stratosphere. Estimates of the distribution of HCl and ClO with height have, however, failed to match the measured concentration profiles<sup>1</sup>. Hence, there has been much interest in the development of two-dimensional atmospheric models which, by including variations with latitude and seasonal effects, might remove these discrepancies. We have developed such a two-dimensional model which incorporates the refinements of the most advanced one-dimensional models; we now report that, contrary to expectation, the calculated profiles of HCl and ClO are insignificantly different from those of comparable one-dimensional models.

Our model includes 30 active chemical species ( $\text{H}_2\text{O}$ ,  $\text{CH}_4$ ,  $\text{H}_2$ ,  $\text{CO}$ ,  $\text{CH}_2\text{O}$ ,  $\text{NO}$ ,  $\text{NO}_2$ ,  $\text{HNO}_3$ ,  $\text{N}_2\text{O}$ ,  $\text{NO}_3$ ,  $\text{N}_2\text{O}_5$ ,  $\text{HO}_2\text{NO}_2$ ,  $\text{N}$ ,  $\text{HCl}$ ,  $\text{ClO}$ ,  $\text{Cl}$ ,  $\text{ClONO}_2$ ,  $\text{HOCl}$ ,  $\text{O}(^3\text{P})$ ,  $\text{O}(^1\text{D})$ ,  $\text{O}_3$ ,  $\text{H}_2\text{O}_2$ ,  $\text{OH}$ ,  $\text{HO}_2$ ,  $\text{H}$ ,  $\text{CFCl}_3$ ,  $\text{CF}_2\text{Cl}_2$ ,  $\text{CCl}_4$ ,  $\text{CH}_3\text{Cl}$ ,  $\text{CH}_3\text{CCl}_3$ ) and all chemical reactions and reaction rates from the current NASA kinetics documentation<sup>2</sup> applicable to these species, except that a single pair of reactions in the model methane oxidation sequence is assumed to describe the instantaneous fate of  $\text{CH}_3$  and  $\text{HCO}$  radicals:



More recent reaction rates for  $\text{OH} + \text{H}_2\text{O}_2$  (refs 3, 4) and  $\text{HO}_2\text{NO}_2$  photolysis<sup>5</sup> have, however, been used.

In this model, the transport of all chemical species is calculated separately, except in the odd-oxygen family ( $\text{O}_3$ ,  $\text{O}(^3\text{P})$  and  $\text{O}(^1\text{D})$ ) and H and N atoms (the latter two are assumed to be in photochemical equilibrium). The domain of the model is from pole to pole and from 0 to 55 km. Solar declination angle, temperature field, number density field and transport coefficients are specified for quarter-year intervals to allow for seasonal variations. The treatment of diurnal effects and the approach used for Rayleigh scattering of solar radiation are described by Miller *et al.*<sup>6</sup>. Rainout of soluble species occurs below 10 km with a 5-day time constant.

Mean meridional circulation is parameterized using the advective circulation field of Murgatroyd and Singleton<sup>7</sup>, with a scale factor of 0.4. Dunkerton<sup>8</sup>, Matsuno<sup>9</sup> and Schoeberl (personal communication) have indicated that, with downward scaling to account for improvements in calculated stratospheric heating rates<sup>10</sup>, this field should reasonably approximate the so-called lagrangian mean motion. The lagrangian mean, which resembles a simple Brewer–Dobson<sup>11,12</sup> cell, combines the zonal eulerian mean motion with a meridional advective contribution arising from planetary waves<sup>9</sup>. This is the first attempt in a complete two-dimensional chemical model to simulate directly the effects of the lagrangian mean circulation.

The eddy diffusion parameterization is basically that of Luther<sup>13</sup>, with the latitudinal coefficient  $K_{yy}$  adjusted below 10 km to give a realistic interhemispheric mixing time of ~14 months (ref. 14). This adjustment produces negligible changes in calculated stratospheric profiles of HCl and ClO. The vertical eddy diffusion coefficient  $K_{zz}$  is the most uncertain aspect of Luther's parameterization, and has been replaced by that of Hunten<sup>15</sup> for all seasons throughout the model stratosphere.

Spatial derivatives for transport are approximated by a second-order finite difference representation that automatically conserves mass. Grid resolution is 5 km vertically and 0.2 in the sine of latitude. Fluxes across upper (55 km) and polar boundaries are set to zero for all species. Ground-level species mixing ratios and fluxes are provided as a function of latitude.

The time-dependent integration uses an implicit finite difference formula, second order in the time increment with respect to transport, and first order for chemistry. At each integration step, the finite difference formula is solved by a Newton–Raphson iteration until convergence is achieved. The calculations are performed on a CRAY 1 computer.

Figure 1 compares the calculated latitudinal variations of the  $\text{N}_2\text{O}$  volume mixing ratio with a selection of the available measurements<sup>16–21</sup>. Agreement is excellent in all latitude bands examined. Results for other upward-moving species such as  $\text{CFCl}_3$ ,  $\text{CF}_2\text{Cl}_2$  and  $\text{CH}_4$  are similar. The vertical gradient in  $\text{N}_2\text{O}$  mixing ratio is steeper towards the poles than towards the equator, indicating that tropical upwelling associated with the Hadley cell is reproduced qualitatively by the prescribed lagrangian circulation.

Model results for column ozone are consistent with measurements by Wilcox *et al.*<sup>22</sup> at all latitudes, as shown by the mid-spring comparison in Fig. 2. Column  $\text{HNO}_3$  is considerably improved relative to previous two-dimensional simulations<sup>23,24</sup>, which typically exceed the measurements of Murcray *et al.*<sup>25</sup> by factors of 2–3 at latitudes below 30°. Present calculations fall within the data range in this region, an improvement largely attributable to the use of a lagrangian mean velocity field.

The calculated daytime average vertical profiles for HCl and ClO in May 1977 vary considerably with latitude (Fig. 3). Short-term temporal and local variations might be expected in regions of large spatial gradients. Where the spatial gradient is high for HCl, for example, local variability might be expected below ~30 km, possibly accounting for the observed 'dips' in measured HCl profiles. The seasonal variations suggested by these profiles (for example, 30°N versus 30°S) are, to a first approximation, chemical consequences of changes in the solar



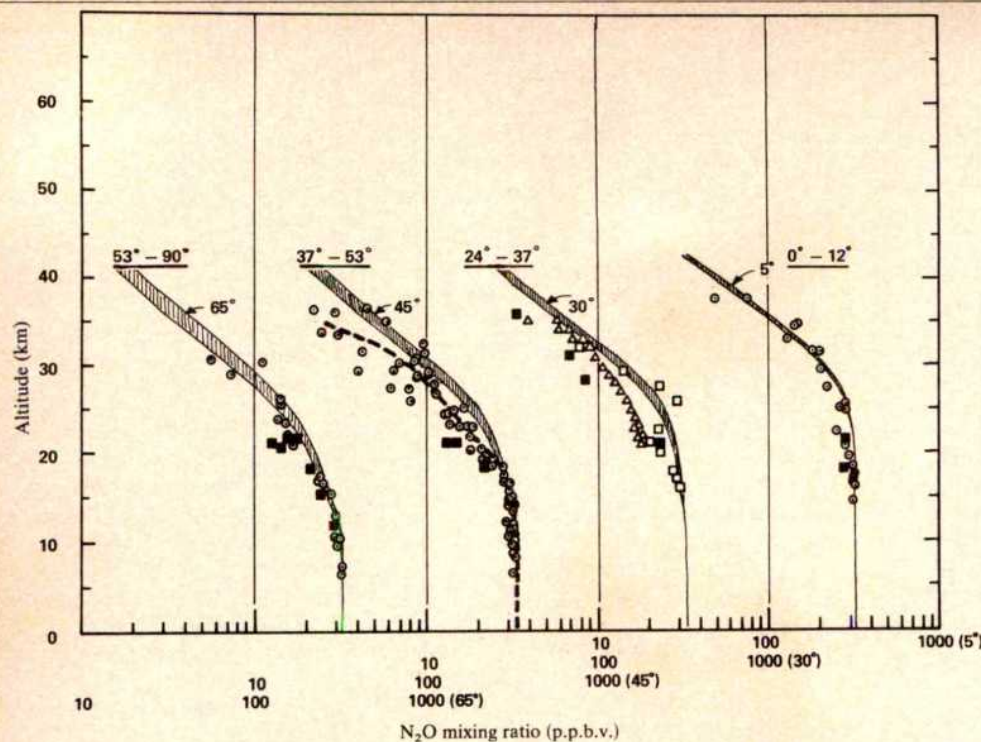


Fig. 1 Calculated vertical profiles of the  $N_2O$  volume mixing ratio for several latitudes are compared with a selection of measurements (refs 16–21).  $\circ$ , Golden *et al.* (1979);  $\blacksquare$ , NASA Ames Group: Vetter *et al.* (1978), Tyson *et al.* (1978); ----, Fabian *et al.* (1979);  $\square$ , Ehhalt *et al.* (1975);  $\triangle$ , Farmer *et al.* (1980);  $\blacksquare$ , model range over a year.

declination angle rather than of total transport of CIX ( $= HCl + ClO + ClONO_2 + Cl + HOCl$ ). Below 20 km, seasonal variability is small because  $HCl \approx CIX$ , but latitudinal variations are quite large.

The range of model-calculated profiles during 1977 for HCl at  $30^\circ N$  latitude (for  $\sim 1.8$  p.p.b. (parts per  $10^9$ ) total CIX) is plotted in Fig. 4 together with spectroscopic experimental profiles (from refs 26–30 and Zander, personal communication, 1979), which were obtained between late 1975 and late 1978 at a comparable latitude ( $\sim 32^\circ N$ ). The *in situ* base-coated filter measurements of Lazrus *et al.*<sup>31</sup> are believed to include  $ClONO_2$  and  $HOCl$ , in addition to HCl, and are therefore not included in Fig. 4. Also, these measurements lie consistently below not only the sum of calculated acidic chloride species, but also virtually all

spectroscopically measured HCl profiles in the region above 28 km.

The calculated HCl profiles in Fig. 4 fall within the envelope of the measurements, exhibiting a qualitatively similar trend of monotonically increasing mixing ratio with increasing altitude. Some measurements also indicate dips that may be due to local variability. The average slope of the calculated profile differs quantitatively from the measurements, with the calculated mixing ratios below 25 km falling at the high end of the measurement envelope, and the values above 25 km deviating towards the low end. These differences are similar to deviations in slope which are observed for HCl in one-dimensional model calculations<sup>32</sup>.

Figure 5 plots the range of two-dimensional model calculations for daytime average ClO over 1977 at  $30^\circ N$  latitude and the measurements of Anderson *et al.*<sup>33</sup> by *in situ* resonance fluorescence and Menzies<sup>34</sup> by laser heterodyne radiometer. If the 28 July 1976 and 14 July 1977 ClO profiles of Anderson are excluded as being unrepresentative of the 'normal' range for that species, then, according to the figure, the model significantly overestimates the abundance of ClO between 25 and 30 km. This overestimation of lower stratospheric ClO is an important problem<sup>35</sup>, because a major part of the calculated ozone depletion by chlorofluorocarbons occurs below  $\sim 30$  km in the current chemical scheme. Furthermore, it suggests that there may be a problem with CIX partitioning in this altitude region, because ClO represents only a small fraction of total CIX and because calculated HCl is in reasonable agreement with the spectroscopic measurements between 25 and 30 km.

The discrepancy between the calculated and observed ClO profiles in the lower stratosphere is also a feature of one-dimensional modelling calculations. Relative to the one-dimensional case, the present two-dimensional result represents only a minor improvement in agreement between experiment and theory<sup>32</sup>. Although the pioneering two-dimensional modelling results of Pyle<sup>36</sup> have been interpreted as suggesting that the discrepancy would be removed in other two-dimensional simulations<sup>1</sup>, this improvement is not found in the present calculation. Other multi-dimensional model results reported by the UK Department of the Environment corroborate this conclusion<sup>37</sup>. The improved agreement in the calculations of Pyle is related partly to his lower calculated abundance of total CIX in the lower stratosphere and partly to his use of a slower rate for the reaction  $HO_2 + NO$ .

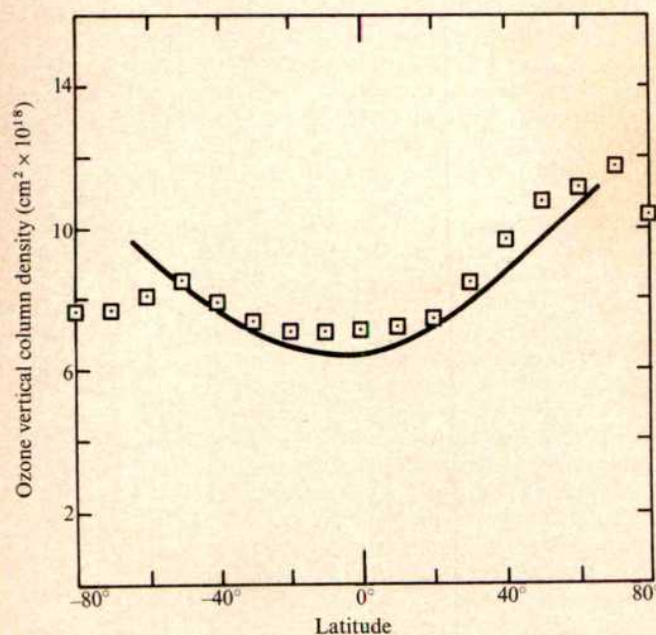
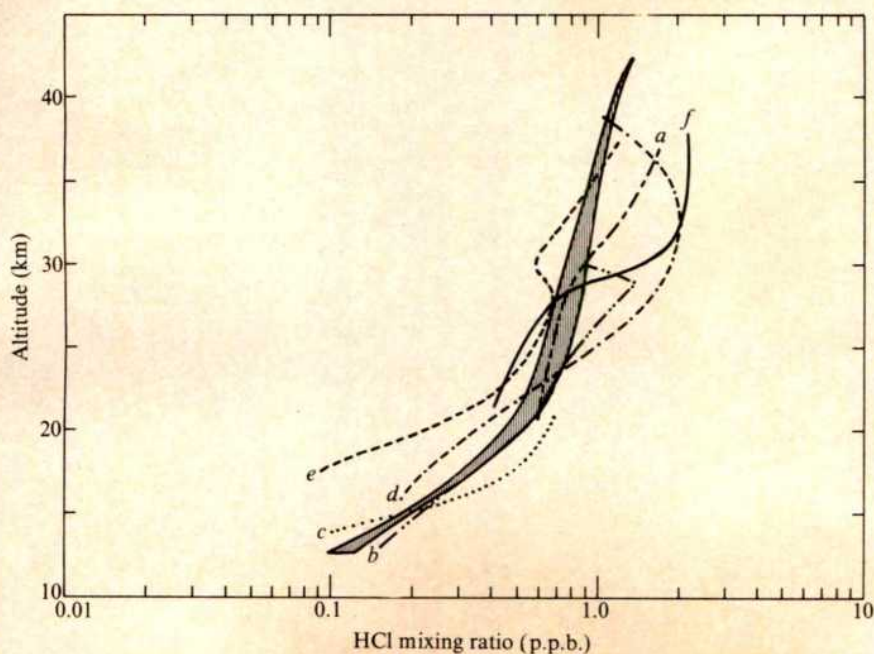
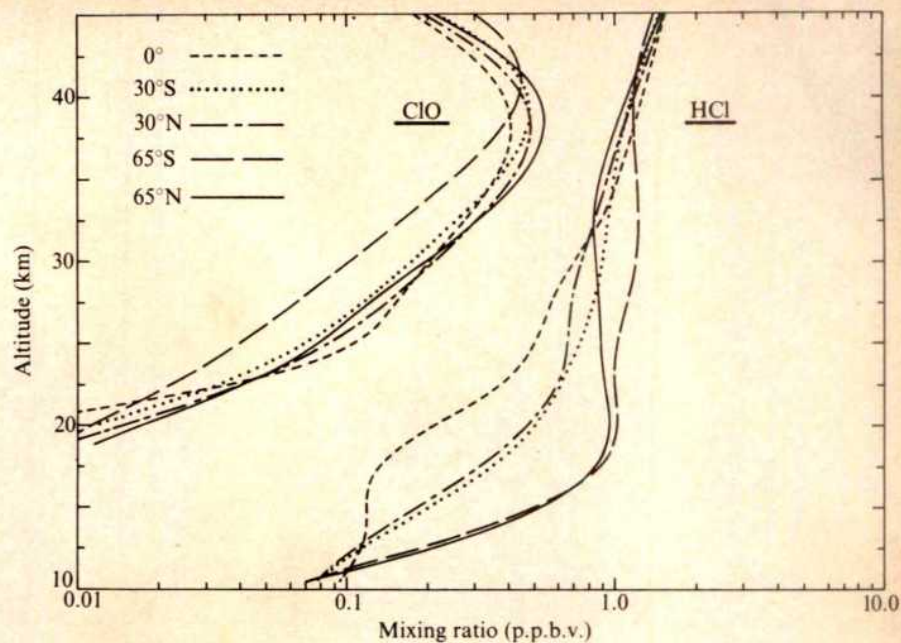


Fig. 2 Model-calculated column ozone as a function of latitude during Northern Hemisphere spring (solid line) is compared with measurements by Wilcox *et al.*<sup>22</sup> ( $\square$ ).

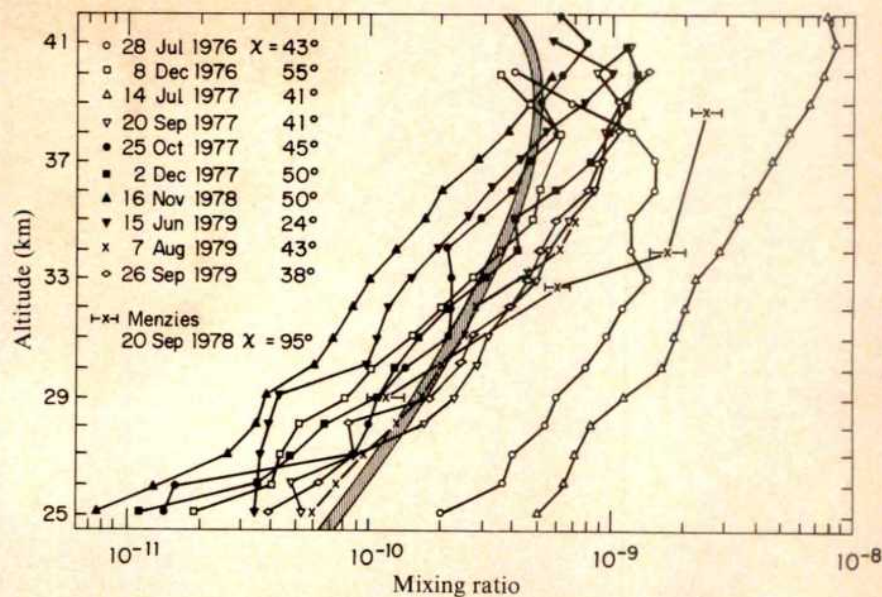


**Fig. 3** Calculated vertical mixing ratio profiles of HCl and ClO (daytime average) for several latitudes in May 1977.



**Fig. 4** The range of model-calculated HCl profiles during 1977 at 30°N (■) plotted together with a selection of experimental measurements; a, ref. 30; b, ref. 27; c, ref. 28; d, ref. 29; e, ref. 26; f, Zander, personal communication; made in the same year.

**Fig. 5** The range of model-calculated ClO profiles (daytime average) during 1977 at 30°N (■) is plotted together with the *in situ* resonance fluorescence profiles of Anderson *et al.*<sup>33</sup> and the laser heterodyne radiometer measurement of Menzies<sup>34</sup>.





In the 30–40-km region the agreement between calculated and measured HCl values could be improved considerably by an increase in the maximum ClX mixing ratio from ~1.8 to ~2.5 p.p.b. for 1977. However, such an adjustment would also increase the calculated abundances of both HCl and ClO at altitudes below 30 km, and would therefore produce larger deviations from experiment in the lower stratosphere, given the current chemistry. Furthermore, a mixing ratio of ~2.5 p.p.b. ClX for 1977 would be difficult to reconcile with currently identified source strengths.

Consideration of the behaviour of both HCl and ClO in Figs 4 and 5 suggests that the calculated ratio of ClO/HCl exceeds measurements at all altitudes below 40 km, with the largest deviations occurring in the lower stratosphere. This implies that problems may exist in partitioning of ClX, not merely in the 25–30-km region, but also at altitudes up to 40 km.

The present ClX profiles from a two-dimensional chemical model with advanced treatment of both chemistry and transport indicate that, at 30°N, the comparison with measurements is similar to that obtained with one-dimensional models. In particular, the overestimation of ClO in the lower stratosphere, present in both one- and two-dimensional calculations, is directly related to the large ozone reductions calculated in that region for the fluorocarbon perturbation. As this is also the region where both transport and chemistry are most uncertain, these discrepancies may be reconciled by future revisions to accepted input parameters. At present, discrepancies in total ClX and in partitioning among ClX species imply that the problems are not unique to one-dimensional models and that a reasonable treatment of meridional transport and chemistry does not remove the current disagreements.

Received 24 June; accepted 25 September 1980.

1. US National Academy of Sciences *Stratospheric Ozone Depletion by Halocarbons: Chemistry and Transport* 161–164 (1979).
2. DeMore, W. B. *et al. J. Phys. Chem.* **84**, 1659–1663 (1980).
3. Keyser, L. F. *J. Phys. Chem.* **84**, 1659–1663 (1980).
4. Sridharan, U. C., Reimann, B. & Kaufman, F. *J. Chem. Phys.* **73**, 1286–1293 (1980).
5. Molina, L. T. & Molina, M. J. *14th Informal Conf. on Photochemistry*, California (1980).
6. Miller, C., Filkin, D. L. & Jesson, J. P. *Atmos. Envir.* **13**, 381–394 (1979).
7. Murgatroyd, R. J. & Singleton, F. Q. *J. R. Met. Soc.* **87**, 125–135 (1961).
8. Dunkerton, T. *J. Atmos. Sci.* **35**, 2325–2333 (1978).
9. Matsuno, T. *Pure appl. Geophys.* **118**, 189–216 (1980).
10. Dopplick, T. G. *J. Atmos. Sci.* **29**, 1278–1294 (1972).
11. Brewer, A. W. Q. *J. R. Met. Soc.* **75**, 351–363 (1949).
12. Dobson, G. M. B. *Proc. R. Soc. A* **236**, 187–192 (1956).
13. Luther, F. M. in *Lawrence Livermore Lab. 2nd A. Rep.* 66–73 (DOT-CIAP Program, UCRL-51336-74, 1974).
14. Czeplak, G. & Junge, C. *Adv. Geophys.* **18B**, 57–72 (1974).
15. Hunten, D. M. *Atmospheres of Earth and the Planets* 59–72 (ed. McCormax, B. M.) (Reidel, Dordrecht, 1975).
16. Gordan, P. D., Kuster, W. C., Albritton, D. L. & Schmeltekopf, A. L. *J. geophys. Res.* **85**, 413–423 (1980).
17. Ehhalt, D. H., Heidt, L. E., Lueb, R. H. & Pollock, W. *Pure appl. Geophys.* **114**, 389–402 (1975).
18. Vedder, J. F., Tyson, B. J., Brewer, R. B., Boitnott, C. A. & Inn, E. C. Y. *Geophys. Res. Lett.* **5**, 33–36 (1978).
19. Tyson, B. J., Vedder, J. F., Arvesen, J. C. & Brewer, R. B. *Geophys. Res. Lett.* **5**, 369–372 (1978).
20. Fabian, P. *et al. J. geophys. Res.* **84**, 3149–3154 (1979).
21. Farmer, C. B., Raper, O. F., Robbins, B. D., Toth, R. A. & Muller, C. *J. geophys. Res.* **85**, 1621–1632 (1980).
22. Wilcox, R. W., Nastrom, G. D. & Belmont, A. D. *J. appl. Met.* **16**, 290–298 (1977).
23. Widhopf, G. F. & Glatt, L. *Rep. to U.S. Dept Transp.* (FAA-EE-79-07, 1979).
24. Whitten, R. C. *Pap. NASA Stratospheric Workshop*, Harpers Ferry (1979).
25. Murcray, D. G., Barker, D. B., Brooks, J. N., Goldman, A. & Williams, W. J. *Geophys. Res. Lett.* **2**, 223–225 (1975).
26. Kendall, D. J. W. & Buijs, W. H. *Rep. to Chemical Manufacturers Association* (December 1979).
27. Williams, W. J., Kostus, J. J., Goldman, A. & Murcray, D. G. *Geophys. Res. Lett.* **3**, 383–385 (1976).
28. Farmer, C. B., Raper, O. F. & Norton, R. H. *Geophys. Res. Lett.* **3**, 13–16 (1976).
29. Eyre, J. R. & Roscoe, H. K. *Nature* **226**, 243–244 (1977).
30. Raper, O. F., Farmer, C. B., Toth, R. A. & Robbins, B. D. *Geophys. Res. Lett.* **4**, 531–534 (1977).
31. Lazrus, A. L. *et al. Geophys. Res. Lett.* **4**, 587–589 (1977).
32. Miller, C., Steed, J. M., Filkin, D. L. & Jesson, J. P. *Atmos. Envir.* (in the press).
33. Anderson, J. G., Grassl, H. J., Shelter, R. E. & Margitan, J. J. *J. geophys. Res.* **85**, 2869–2887 (1980).
34. Menzies, R. T. *Geophys. Res. Lett.* **6**, 151–154 (1979).
35. Hudson, R. D. & Reed, E. I. (eds) *NASA Rep.* 1049, 175–176 (1979).
36. Pyle, J. A. *Pure appl. Geophys.* **118**, 355–377 (1980).
37. UK Department of the Environment *Pollut. Pap.* No. 15, 115 (1979).

## Large rain drops in the bright band

Edward E. Altshuler

Rome Air Development Center, Electromagnetic Sciences Division, Hanscom AFB, Bedford, Massachusetts 01731

It has recently been suggested<sup>1–3</sup>, based on dual-polarized radar measurements, that in the bright-band region, melting snow exhibits the characteristics of rain drops having very large effective drop diameters. It is postulated that snow flakes falling below the 0 °C isotherm melt slowly with small water droplets first forming on the outer edges of the flakes; as the snow continues to melt water forms on the surface of the flake, thus it takes on the behaviour of a large rain/ice drop; in the final stages of melting the particles start to collapse into smaller drops. Here another technique for inferring rain-drop sizes<sup>4</sup> is described which produces results which, being consistent with those above, support the bright-band model.

Based on calculations by Medhurst<sup>5</sup>, rain attenuation can be shown to be a strong function of frequency and drop diameter. In Fig. 1, the ratio of the attenuation at 35 GHz to that at 15 GHz is plotted as a function of drop diameter and it is seen that for small drops, the ratio of the attenuations may be very large but as the drop size increases, the ratio decreases. Although Medhurst's calculations assume hypothetical distributions of rain in that they are for spherical drops all having the same size and temperature, his results are of qualitative value and enable the average drop diameter of the rain to be estimated from measurements of attenuation at two widely separated frequencies. Unfortunately, with the radiometric technique for measuring attenuation, it is not possible to obtain attenuation as a function of distance along the path directly, as

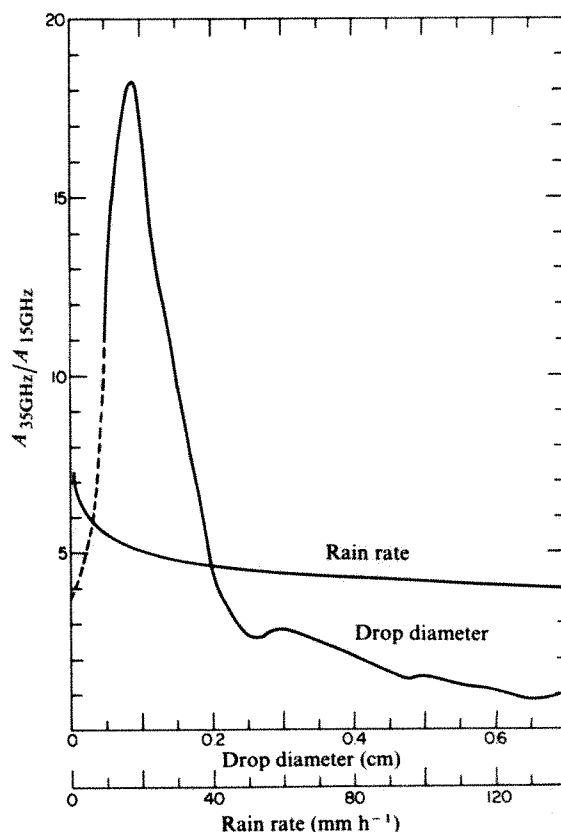


Fig. 1 Ratios of 35-GHz to 15-GHz attenuations as a function of rain-drop diameter and rain rate.



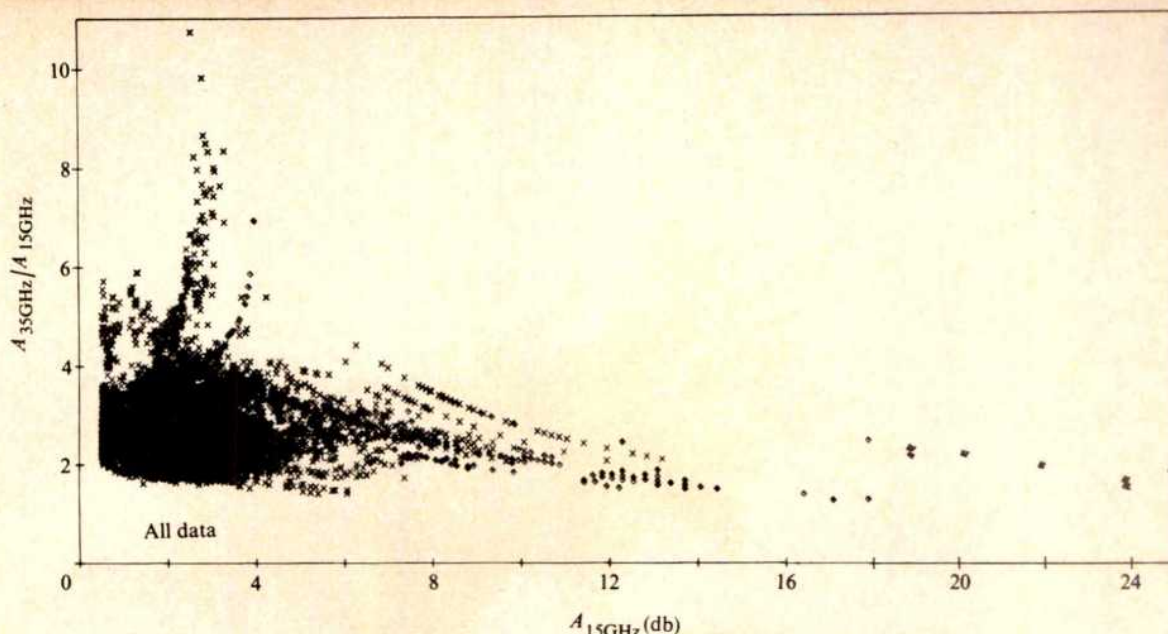


Fig. 2 Ratios of measured 35-GHz to 15-GHz attenuations as a function of 15-GHz attenuation.

can be done with radar. Drop size distributions of rain have been measured at ground level<sup>6</sup> and a strong correlation between rain rate and the average drop size has been shown; light rain typically consists of small drops of 1- or 2-mm diameter, whereas heavy rain has larger-diameter drops of 3–5 mm. The attenuations corresponding to these drop size distributions can be calculated so the attenuation ratio can also be expressed as a function of rain rate as shown in Fig. 1. Note that the attenuation ratios of ground-level rain would be expected to fall in the range 4–7.

Slant-path attenuation measurements at frequencies of 15 and 35 GHz were conducted in the Boston area, during eight rainstorms with various rain-fall intensities, using the Sun as a source<sup>4</sup>. A dual-frequency radiometer mounted in an 8.8-m paraboloidal antenna was the detector. Antenna beamwidths were approximately 9 and 4 arc min respectively and the centre of the Sun was tracked with an accuracy of at least 0.5 arc min. Over 10,000 simultaneous measurements of attenuations at 15 and 35 GHz were recorded during a year. The ratios of these attenuations are plotted against the 15-GHz attenuations in Fig. 2. Data points corresponding to 15-GHz attenuations below 0.5 dB were not included because they were probably too low to be due to rain and also the measurement accuracy at these low attenuations is poor. If the rain-drop size distributions along the slant path were similar to those which have been measured on the ground, then one would expect the attenuation ratios to be of the order of 6 or 7 for low rain rates (low 15-GHz attenuations) and decrease to about 4 or 5 for the higher rain rates which would correspond to higher 15-GHz attenuations. Of the points which are plotted, the bulk of these have ratios between 2 and 4 and occur for low 15-GHz attenuations. Therefore, these results are not consistent with ground-level rain-drop size distributions but suggest instead that somewhere along the slant path there is a significant contribution to the attenuation which results from precipitation, with characteristics of rain drops having very large effective drop diameters, as noted in the drop-diameter curve of Fig. 1. Because most of the rain along the path occurs below the bright band, the attenuation contribution from the bright band would be expected to be relatively small. Yet, the fact that the attenuation ratios are so low means that there must be very large drops in the bright-band region and therefore drop diameters of the order of 10–20 mm, as suggested by Humphries and Barge<sup>2</sup>, are certainly possible.

Note that it may be advantageous to conduct both dual-frequency attenuation and dual-polarized reflectivity measurements to differentiate between rain and ice. The

attenuation measurement easily distinguishes rain from ice particles as losses due to ice are much smaller; this is not always the case with radar because both ice and rain have high reflectivity. In addition, if the attenuation through the absorbing medium is known, the radar can be more accurately calibrated.

I thank Dr Robert K. Crane for helpful discussions.

Received 30 June; accepted 3 October 1980.

1. Hall, M. P. M., Cherry, S. M., Goddard, J. W. F. & Kennedy, G. R. *Nature* **285**, 195–199 (1980).
2. Humphries, R. G. & Barge, B. L. *IEEE Trans. Geomagn. Elect.* **GE-17**, 190–195 (1979).
3. Crane, R. K. *Air Force Geophys. Lab. TR 78-0118* (1978).
4. Alshuler, E. E. & Telford, L. E. *Radio Sci.* **15**, 781–796 (1980).
5. Medhurst, R. G. *IEEE Trans. Ant. Propul.* **AP-13**, 550–564 (1965).
6. Laws, J. O. & Parsons, D. A. *EOS* **24**, 452–460 (1943).

## Proton mobility in ice

Marinus Kunst & John M. Warman

Interuniversitair Reactor Instituut, Mekelweg 15, 2629 JB Delft, The Netherlands

Ice is frequently taken as a model when factors controlling proton transport in hydrogen-bonded molecular networks are discussed. Such discussions have increased with the acknowledgement that proton transfer across cell membranes may play a significant part in energy conversion and storage in biological systems<sup>1–4</sup> and that this transfer may involve hydrogen-bonded chains spanning the membrane<sup>5,6</sup>. However, there is still much uncertainty about the basic mode of proton displacement and the external factors which effect bulk proton transport in ice itself. We present here results of a microwave conductivity pulse radiolysis technique which has been used to determine the mobility of bare protons in ice, and thus reduce some of the uncertainty over proton mobility.

The displacement of protons through a Grotthuss-type mechanism can only occur if a subsidiary mechanism is available to wipe out the polarization field produced by dipole reversals which accompany proton jumps. This led Bjerrum to introduce *L* and *D* orientation defects. For a sufficiently high concentration of Bjerrum defects, resistance to proton motion due to bulk polarization should become negligible. In these conditions, therefore, the net drift mobility of protons in an applied field,  $\mu(H^+)_{\infty}$ , should be equal to the microscopic or virtual mobility,



$M(H^+)$ . The latter parameter is of considerable interest because it reflects the basic mode of proton displacement.

However, the situation may be complicated<sup>7,8</sup> by the formation of immobile complexes between protons and the net negatively charged  $L$  defects.



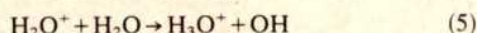
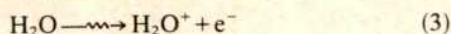
The net drift mobility, even for high concentrations of orientational defects, will, therefore, give only a lower limit to  $M(H^+)$ :

$$\mu(H^+)_{\infty} = M(H^+) \frac{[H_3O^+]}{[H_3O^+] + [H_3O^+L]} \quad (2)$$

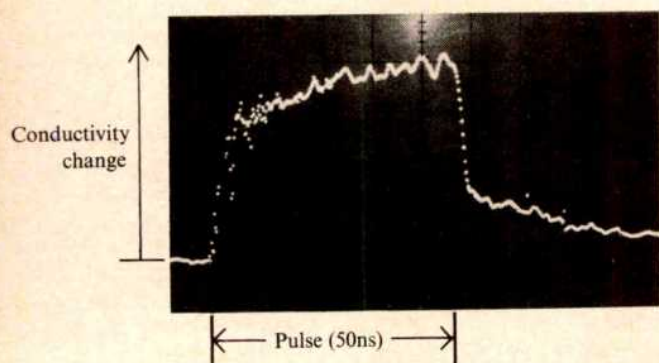
The presently accepted values of the proton mobility in ice at close to the melting point are considerably lower than the estimate of  $7.5 \times 10^{-2} \text{ cm}^2 \text{ V}^{-1} \text{ s}^{-1}$  by Eigen *et al.*<sup>9</sup> and tend to lie within the range  $(0.5-5) \times 10^{-3} \text{ cm}^2 \text{ V}^{-1} \text{ s}^{-1}$  (ref. 11). The temperature dependence of the mobility is not accurately known. There are indications of increasing mobility with decreasing temperature<sup>12,13,15</sup>. However, zero activation energy for the mobility is frequently assumed even in recent theoretical models of the dielectric properties of ice<sup>17</sup>.

We have studied the change in conductivity which results from pulsed ionization of ice using 3-MeV electrons from a Van de Graaff accelerator. The present results were obtained in the temperature range  $-5$  to  $-30^\circ \text{C}$  using 50-ns long pulses with a total dose per pulse of  $\sim 1 \text{ krad}$  ( $\sim 5 \times 10^{16} \text{ eV cm}^{-3}$ ). The concentration of ions formed was  $\leq 1 \times 10^{-6} \text{ M}$ . The experimental set-up and background to the microwave conductivity technique used have been described elsewhere<sup>18,19</sup>. Figure 1 shows the conductivity transient observed in  $\text{H}_2\text{O}$  ice at  $-7^\circ \text{C}$ .

The results can be discussed in terms of the main ionic processes occurring on irradiation:



The highly mobile ( $\sim 10 \text{ cm}^2 \text{ V}^{-1} \text{ s}^{-1}$ ) conduction electrons,  $e^-$ , have a mean lifetime towards localization at pre-existing lattice-defect sites,  $T$ , of 100 ps at  $-5^\circ \text{C}$  (ref. 18). This process is responsible for the initial, very rapid decay of the conductivity on termination of the pulse. Further relaxation to give the deeply trapped ( $\lambda_{\text{max}} = 680 \text{ nm}$ ) (refs 20-22), 'solvated' state of the electron,  $e_{\text{sol}}^-$ , occurs with a mean time of 400 ps (C. D. Jonah and our unpublished results). The relatively slowly decaying



**Fig. 1** Transient digitizer trace of the change in conductivity of  $\text{H}_2\text{O}$  ice at  $-7^\circ \text{C}$  which results on pulsed ionization using a 50-ns pulse of 3-MeV electrons (beam charge 60 nC). The maximum signal height corresponds to a conductivity of  $\sim 2 \times 10^{-4} \Omega^{-1} \text{ m}^{-1}$ . The signal during the pulse is due mainly to the steady-state concentration of highly mobile conduction electrons which undergo trapping in  $\sim 0.1 \text{ ns}$  at this temperature. This electron component is seen to decay very rapidly on termination of the pulse but an appreciable, relatively slowly decaying conductivity transient remains. This transient is attributed to proton conduction.

conductivity transient apparent in Fig. 1 cannot therefore be attributed to the migration of weakly localized electrons through the conduction band or by trap-to-trap hopping.

Because the formation of  $\text{H}_3\text{O}^+$  through the proton-transfer reaction (5) is expected to take place within a few O-H vibrations<sup>23</sup> or  $\text{H}_2\text{O}^+$  displacements<sup>24</sup> and should certainly be complete well within the nanosecond time scale of the present experiments, we conclude that the slowly decaying conductivity is due to mobile protons.

The present measurements were carried out using microwaves, so that effects on the proton mobility due to polarization of the medium can be neglected. The initial after-pulse conductivity should then be proportional to the product of the proton yield and the virtual mobility  $M(H^+)$ . Using the known dosimetry, the parameter  $G(H^+)M(H^+)$ , where  $G(H^+)$  is the yield in ions per 100 eV absorbed, can be determined from the conductivity signal after correction for a certain amount of decay during the pulse. At  $-5^\circ \text{C}$ , the yield times mobility product is determined to be  $6.4 \times 10^{-3}$  and  $2.4 \times 10^{-3} \text{ cm}^2 \text{ V}^{-1} \text{ s}^{-1} (100 \text{ eV})^{-1}$  for  $\text{H}_2\text{O}$  and  $\text{D}_2\text{O}$  ice respectively.

From optical absorption pulse radiolysis studies<sup>20,22</sup>, the yield of solvated electrons is found to be  $1.0 \pm 0.2 (100 \text{ eV})^{-1}$  for  $\text{H}_2\text{O}$  and  $\text{D}_2\text{O}$  ice at  $-5^\circ \text{C}$ . Taking the yield of protons to be equal to the yield of solvated electrons results in estimates of virtual mobilities of  $\text{H}_3\text{O}^+$  and  $\text{D}_3\text{O}^+$  of  $6.4 \times 10^{-3}$  and  $2.4 \times 10^{-3} \text{ cm}^2 \text{ V}^{-1} \text{ s}^{-1}$ . As expected on the basis of the initial discussion, the value of  $M(H^+)$  lies above the range of drift-mobility values determined from low-frequency dielectric measurements on ice at equilibrium.

Of considerable importance to theoretical models of proton transport is the temperature dependence of  $M(H^+)$ . For both  $\text{H}_2\text{O}$  and  $\text{D}_2\text{O}$ , the yield times mobility product is found to remain almost unchanged between  $-5$  and  $-30^\circ \text{C}$  with a slight,  $\sim 10\%$ , increase being indicated for  $\text{H}_2\text{O}$ . Over this same temperature range, the yield of ions formed, as measured by the solvated electron absorption, decreases considerably<sup>20-22,25</sup>. A pronounced increase in the virtual mobility with decreasing temperature is therefore indicated.

The electron yield at  $-30^\circ \text{C}$  is quite sensitive to the conditions of pulse width and total dose used<sup>20,26</sup>. It can be concluded, however, that the ion yield is at least a factor of 2 lower at the lower temperature. It may then be concluded that the virtual mobility has a negative activation energy of at least 0.15 eV which corresponds to an inverse sixth-power dependence on temperature in the present range.

Such a large negative energy of activation is incompatible with simple theoretical models involving hopping or tunnelling of protons between isoenergetic states separated by a potential energy barrier. A more complex approach, in which interaction between the charged particle as a whole and lattice vibrations is taken into account, has been shown by Gosar and Pintar<sup>27</sup> to predict a mobility which sharply decreases with increasing temperature. Fischer and Hofacker<sup>28</sup> pointed out that proton conduction can be treated in an analogous way to that used for narrow-band polaron transport. In the low-temperature regime, the narrow-band polaron mobility is given by<sup>29</sup>

$$\mu = \frac{ea^2}{kT} \pi^{1/2} \nu_0 F(T)^{1/2} \exp[-F(T)] \quad (6)$$

with

$$F(T) = \frac{2W_p}{h\nu_0} \text{cosech} \frac{h\nu_0}{2kT} \quad (7)$$

In equations (6) and (7),  $a$  is the intermolecular distance ( $2.76 \text{ \AA}$  in the present case),  $\nu_0$  is the unperturbed natural frequency of the vibrational mode interacting with the charge, and  $W_p$ , the polaron binding energy, is the potential energy gained by the charge due to lattice distortion.

In the case of ice, strong interactions of  $\text{H}_3\text{O}^+$  with both the oxygen-oxygen lattice mode,  $h\nu_0 = 0.025 \text{ eV}$ , and the restricted rotation or libration mode,  $h\nu_0 = 0.1 \text{ eV}$ , have been suggested<sup>28</sup>.



The measured value of  $M(H^+)$  of  $6.4 \times 10^{-3} \text{ cm}^2 \text{ V}^{-1} \text{ s}^{-1}$  at  $-5^\circ \text{C}$  is obtained using equation (6) with  $W_p/h\nu_0 = 1.72$  or  $16.6$  for  $h\nu_0 = 0.025$  or  $0.1 \text{ eV}$  respectively. Using the same combinations of parameters, an increase in mobility by factors of 1.9 and 4.6 respectively would be predicted on decreasing the temperature to  $-30^\circ \text{C}$ . The predicted effect of temperature is of the same magnitude as found. However, because of the large uncertainty in the value of the ion yield at  $-30^\circ \text{C}$ , the temperature dependence alone cannot be used to specify which lattice interaction predominates. The isotope effect of a factor of 2.7 in the mobility, however, favours the lower energy mode, if the polaron binding energy is assumed to be the same for both isotopes. Thus the decrease in frequency of  $\sim 5\%$  for the oxygen-oxygen vibration corresponds to a decrease in mobility using equation (6) by a factor of 1.9. For the librational mode the shift in frequency is  $\sim 30\%$  (ref. 30), which would result in the prediction of a mobility a factor of almost  $10^4$  lower for the heavier isotope.

An interesting aspect of the general narrow-band polaron theory is the prediction of a sharp changeover to a thermally activated hopping motion at higher temperatures<sup>29,31,32</sup> with, however, an activation energy which decreases with increasing temperature. At sufficiently elevated temperatures, a maximum in the mobility is predicted<sup>29</sup>. This behaviour is descriptive of the temperature dependence of the excess mobility of protons in liquid  $\text{H}_2\text{O}$  (refs 33, 34).

The proton conductivity signal is found to decay over a period of a few hundred nanoseconds to a much lower level (10–20% of the initial signal) which then further decreases over many microseconds. The slow decay occurs on the same time scale as observed for the solvated electron disappearance in optical studies<sup>22</sup> for similar dose conditions and is therefore ascribed to the recombination reaction



The initial relatively rapid decay is attributed to a pseudo first-order reaction of bare protons with  $L$  defects, present at a concentration of  $\sim 10^{-5} \text{ M}$  (ref. 35) resulting eventually in a considerably lower equilibrium concentration of  $\text{H}_3\text{O}^+$ .

The ratio between the initial conductivity and the low-level, slowly decaying component is equal to the concentration ratio  $([\text{H}_3\text{O}^+] + [\text{H}_3\text{O}^+L])/[\text{H}_3\text{O}^+]$  at equilibrium. The ratios found at  $-5^\circ \text{C}$  are 8 and 10 for  $\text{H}_2\text{O}$  and  $\text{D}_2\text{O}$  respectively. Combining these ratios with the above values of the virtual mobilities gives the effective drift mobilities  $\mu(H^+)_{\infty} = 8 \times 10^{-4}$  and  $\mu(D^+)_{\infty} = 2 \times 10^{-4} \text{ cm}^2 \text{ V}^{-1} \text{ s}^{-1}$ . The value of  $\mu(H^+)_{\infty}$  lies close to the lower limit of the range of mobility values derived from low-frequency dielectric measurements. Drift mobility estimates larger than  $\mu(H^+)_{\infty}$  could be due to perturbation of equilibrium (1) by excessive applied fields.

In summary, using a nanosecond pulse radiolysis microwave conductivity technique, the virtual mobility of protons in  $\text{H}_2\text{O}$  ice has been determined to be  $6.4 \times 10^{-3} \text{ cm}^2 \text{ V}^{-1} \text{ s}^{-1}$ , and of deuterons in  $\text{D}_2\text{O}$  ice to be  $2.4 \times 10^{-3} \text{ cm}^2 \text{ V}^{-1} \text{ s}^{-1}$  at  $-5^\circ \text{C}$ . These values increase by a factor of at least 2 on decreasing the temperature to  $-30^\circ \text{C}$ . This corresponds to a negative activation energy of at least  $0.15 \text{ eV}$ . The narrow-band polaron theory is capable of describing the data with the main charge interaction apparently involving the  $200 \text{ cm}^{-1}$  oxygen-oxygen lattice vibration. Temporary complexing of protons with  $L$  defects reaches equilibrium within a few hundred nanoseconds and results in effective drift mobilities of  $8 \times 10^{-4}$  and  $2 \times 10^{-4} \text{ cm}^2 \text{ V}^{-1} \text{ s}^{-1}$  for  $\text{H}_3\text{O}^+$  in  $\text{H}_2\text{O}$  and  $\text{D}_3\text{O}^+$  in  $\text{D}_2\text{O}$  respectively at  $-5^\circ \text{C}$ .

Kinetic and thermodynamic parameters will be discussed elsewhere.

Received 14 July; accepted 8 October 1980.

- Mitchell, P. *Nature* **191**, 144 (1961).
- Mitchell, P. *Biol. Rev.* **41**, 445 (1966).
- Henderson, R. A. *Rev. Biophys. Bioengng* **6**, 87 (1977).
- Stoeklenius, W., Lozier, R. H. & Bogomolni, R. A. *Biochim. biophys. Acta* **505**, 215 (1979).

- Knapp, E.-W., Schulten, K. & Schulten, Z. *Chem. Phys.* **46**, 215 (1980).
- Nagle, J. F., Mille, M. & Morowitz, H. J. *J. chem. Phys.* **72**, 3959 (1980).
- Onsager, L. & Dupuis, M. *Electrolytes*, 27 (Pergamon, Oxford, 1962).
- Bilgram, J. H. & Gränicher, H. *Phys. Cond. Matter* **18**, 275 (1974).
- Eigen, M., de Maeyer, L. & Spatz, H. C. *Ber. Buns. Phys. Chem.* **68**, 19 (1964).
- Whalley, E., Jones, S. J. & Gould, L. W. (eds) *Proc. int. Symp. Phys. Chem. Ice* (Royal Society of Canada, 1973).
- Onsager, L. in *Proc. int. Symp. Phys. Chem. Ice* (eds Whalley, E., Jones, S. J. & Gould, L. W.) **10** (Royal Society of Canada, 1973).
- Jaccard, C. in *Water and Aqueous Solutions* (ed. Horne, R. A.) (Wiley, London, 1972).
- Eckener, U., Helmreich, D. & Engelhardt, H. in *Proc. int. Symp. Phys. Chem. Ice* (eds Whalley, E., Jones, S. J. & Gould, L. W.) **242** (Royal Society of Canada, 1973).
- Riehl, N., Bullemer, B. & Engelhardt, H. (eds) *Proc. int. Symp. Phys. Chem. Ice* (Plenum, New York, 1969).
- Engelhardt, H., Bullemer, B. & Riehl, N. (eds) in *Proc. int. Symp. Phys. Chem. Ice*, 430 (Plenum, New York, 1969).
- J. Glaciol.* **21** (1978).
- Camplin, G. C., Glen, J. W. & Paren, J. G. *J. Glaciol.* **21**, 123 (1978).
- Warman, J. M., de Haas, M. P. & Verberne, J. B. *J. phys. Chem.* **84**, 1240 (1980).
- Infelta, P. P., de Haas, M. P. & Warman, J. M. *Radiat. phys. Chem.* **10**, 353 (1977).
- Gillis, H. A., Teather, G. G. & Ross, C. K. *J. phys. Chem.* **84**, 1248 (1980).
- Taub, I. A. & Eiben, K. *J. chem. Phys.* **49**, 2499 (1968).
- Nilsson, G., Christensen, H., Pagsberg, P. & Nielsen, S. O. *J. phys. Chem.* **76**, 1000 (1972).
- Henglein, A. *Einführung in die Strahlenchemie*, 133 (Chemie, Berlin, 1969).
- Hamill, W. H. *J. phys. Chem.* **73**, 1341 (1969).
- Buxton, G. V., Gillis, H. A. & Klassen, N. V. *Can. J. Chem.* **55**, 2385 (1977).
- Nilsson, G. & Pagsberg, P. *Chem. Phys. Lett.* **74**, 119 (1980).
- Gosar, P. & Pintar, M. *Phys. Status Solidi* **4**, 675 (1964).
- Fischer, S. F. & Hofacker, G. L. in *Proc. int. Symp. Phys. Chem. Ice* (eds Riehl, N., Bullemer, B. & Engelhardt, H.) **369** (Plenum, New York, 1969).
- Roberts, G. G., Apsley, N. & Munn, R. W. *Phys. Rep.* **60**, 59 (1980).
- Hobbs, P. V. *Ice Physics*, 237 (Clarendon, Oxford, 1974).
- Silbey, R. & Munn, R. W. *J. chem. Phys.* **72**, 2763 (1980).
- Gosar, P. *Phys. Rev.* **B3**, 1991 (1971).
- Bockris, J. O' M. & Reddy, A. K. N. *Modern Electrochemistry*, 473 (Plenum, New York, 1970).
- Franck, E. U., Hartmann, D. & Hensel, F. *Disc. Faraday Soc.* **39**, 200 (1965).
- Fletcher, N. H. *Chemical Physics of Ice*, 156 (Cambridge University Press, 1970).

## Evidence against a crystal instability in melting

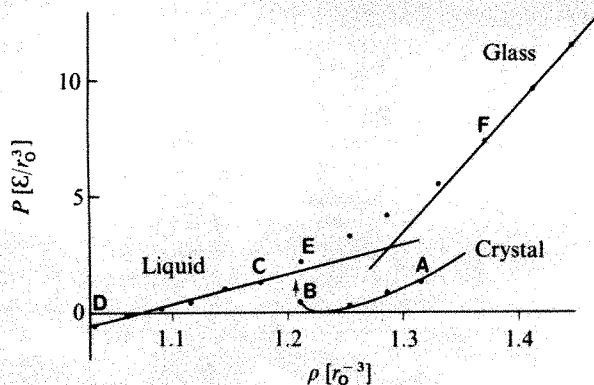
R. M. J. Cotterill & J. U. Madsen

Department of Structural Properties of Materials, The Technical University of Denmark, Building 307, DK-2800 Lyngby, Denmark

Since Born's original suggestion<sup>1</sup>, melting has frequently been attributed to a crystal instability although its one-phase approach has been objected to. Using a molecular dynamics computation of the behaviour of a 336-atom Lennard-Jones system, and exploiting the inherent limitations on model size and simulation time, we have found a crystal-liquid instability. It falls outside the density interval for thermodynamic melting, however, and we conclude that it is not true melting. We have also discovered an isothermal liquid-glass transition on compressing the liquid, and this occurs at a density within the transition interval. The results reported here are consistent with the first-order nature of melting and provide new insight into the difference between the crystalline and liquid states.

A sufficiently large system, given enough time, would melt by traversing the two-phase region, whereas a limited model like ours can explore nonequilibrium states. A similar model has, for example, probed the van der Waals loop of the liquid-gas transition (S. Toxvaerd, personal communication). Our three-dimensional system, with periodic boundaries, has been investigated at various densities in the melting region. The studies extended those of Damgaard Kristensen<sup>2</sup>, using the same model and the same reduced units. (The diatomic Lennard-Jones interaction energy is  $V_{LJ} = \epsilon((r_0/r)^{12} - 2(r_0/r)^6)$ ; reduced units are used throughout—lengths in units of  $r_0$ , energies  $\epsilon$ , temperatures  $\epsilon/k_B$ , densities  $\rho/\rho_0^*$ , pressures  $\epsilon/r_0^3$ .) An equation of state was first established for the face-centred cubic (f.c.c.) phase for densities 1.20–1.35 and temperatures 0.5–1.0. All state points were derived on the basis of 5,000 computational time steps, each of duration 0.003 in reduced units ( $2 \times 10^{-14} \text{ s}$ ). The zero-pressure and higher-pressure isobars all displayed divergence of the isobaric volume expansion coefficient for the (metastable) f.c.c. phase, as implied by the vertical tangent of each isobar, and this defined an unequivocal





**Fig. 1** The  $T = 0.77$  isotherms of crystal, liquid and glass with the experimental points indicated. The arrow indicates the position of the crystal instability, and the intersection of the extrapolated lines locates a formal glass transition density. A–F, The expansion and compression sequence of states described in Fig. 2.

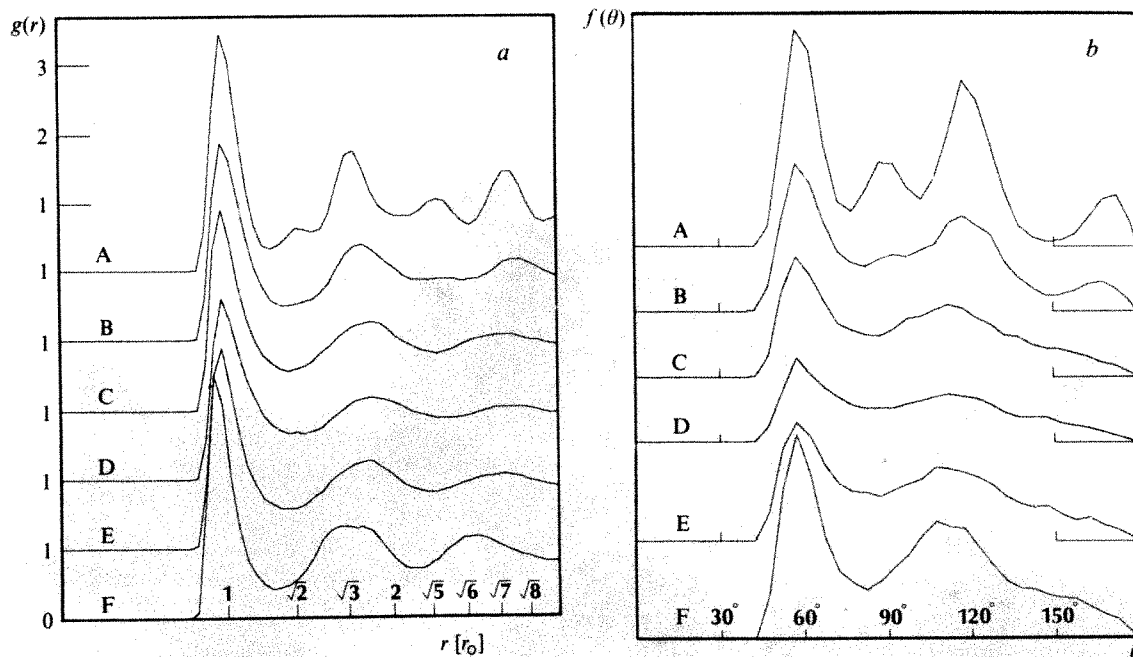
thermodynamic stability limit<sup>3</sup>; however, for the small system investigated the limit can be bypassed slightly<sup>4</sup>. A typical isotherm for  $T = 0.77$ , starting with the f.c.c. state is shown in Fig. 1. A discontinuous jump in pressure is observed at a density of 1.22. (All isotherms exhibited discontinuities which were sharp within computational limits, the discontinuity density increasing with temperature.) Beyond the discontinuity, pressure again decreased with density. The isotherm was retraced if the density was then increased, but the pressure rose continuously and passed the discontinuity with no detectable change of slope. A change in slope was encountered, however, at a higher density, as shown in Fig. 1.

The pair distribution function,  $g(r)$ , and a bond-angle distribution function,  $f(\theta)$ , defined elsewhere<sup>5</sup>, were monitored for all the states indicated in Fig. 1. These functions are shown in Fig. 2. For  $g(r)$ , the  $\sqrt{2}$ -peak, a signature of the f.c.c. structure, a remnant flat portion at B, was totally absent at C. States C to F had liquid-like  $g(r)$ , with the suggestion of second-peak splitting present at F. The well defined second-peak splitting reported for hard sphere model glasses<sup>6</sup> was smeared out, presumably by

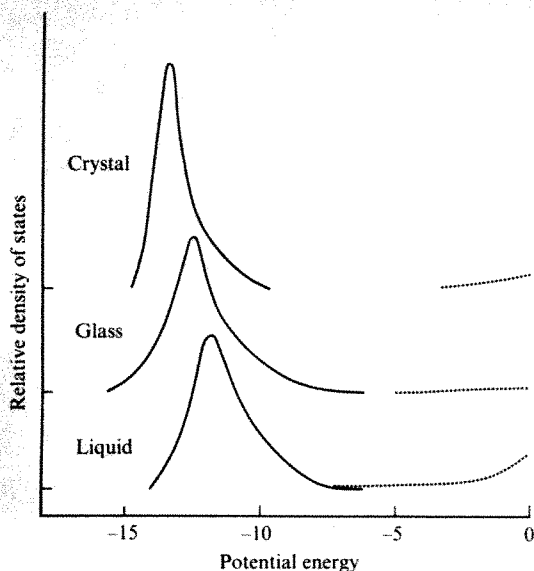
thermal vibrations. We conclude that the discontinuity is associated with a crystal–liquid transition and that a liquid–glass transition is obtained by compressing the liquid. The glass transition density increased slightly with increasing pressure and temperature relative to the zero-pressure transition density located by Damgaard Kristensen<sup>2</sup>. For  $f(\theta)$ , there were more pronounced differences between B and C: the  $90^\circ$  peak and the  $150^\circ$  depression, still both seen in B, were absent in C. Because the  $90^\circ$  bond angle is a characteristic of the f.c.c. structure, this supports our conclusion that the discontinuity corresponds to crystal breakdown. Here too, E and F differed markedly: the  $60^\circ$  and  $110$ – $120^\circ$  peaks were much sharper in F, and the shoulder at  $150^\circ$  more pronounced, both features are glassy-state characteristics<sup>7</sup>.

Using a Monte-Carlo technique to locate free energy equality, and hence melting pressures for given melting temperatures, Hansen and Verlet<sup>8</sup> derived the fluid and solid densities at melting. Because their model presumably had similar limitations, such as the suppression of long-wavelength fluctuations, imposed by the periodic boundaries, comparison of their results with our own seems reasonable. Clearly, however, both approaches should be applied to larger models when this becomes computationally feasible. For the melting temperature 0.75, which is within computational limits of our  $T = 0.77$ , they found  $\rho_{\text{cryst}} = 1.38$  and  $\rho_{\text{liq}} = 1.24$  in our units. Our instability lies at  $\rho_{\text{inst}} = 1.22$  for  $T = 0.77$ . Moreover, their  $\rho_{\text{cryst}}$  and  $\rho_{\text{liq}}$  values rise with temperature much faster than does our  $\rho_{\text{inst}}$ , so the latter would become progressively further removed from Hansen and Verlet's melting interval. This indicates that the observed instability density is not connected with the density at which the critical liquid nucleus becomes comparable in size to the system; if that were so,  $\rho_{\text{cryst}} - \rho_{\text{inst}}$  would be expected to be approximately constant. Furthermore, nucleation, albeit of crystal, has been observed<sup>9</sup> in a system of size comparable with ours. We suggest therefore that there is no essential connection between crystal instability and thermodynamic melting. The observed hysteresis, however, is consistent with approaches to melting which assume no intrinsic correlation between the properties of the crystalline and liquid phases, as discussed recently by Ziman<sup>10</sup>.

Two important variants of the crystal instability approach have involved free volume<sup>11</sup> and dislocations<sup>12</sup>. The present study allows the relative merits of these models to be evaluated.

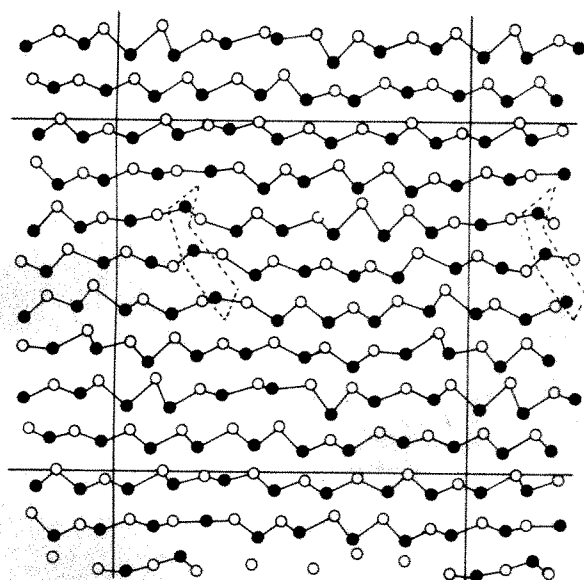


**Fig. 2** *a*, Pair correlation functions,  $g(r)$ , for the six states indicated in Fig. 1. *b*, Bond-angle distribution functions,  $f(\theta)$ , for the six states indicated in Fig. 1.



**Fig. 3** Potential energy density of states spectra for the normal (solid curve) and hole (dotted curve) states. The three situations (shifted vertically with respect to one another, for clarity) correspond to states A (crystal), F (glass) and E (liquid) indicated in Fig. 1, and the curves extend over the ranges for which states were detectable. For the liquid, the maximum of the normal spectrum lies at  $-5.97$ , while the minimum of the hole spectrum occurs at  $-7.09$ . The curves all have the same (arbitrary) ordinate scale.

The existence of a virtual glass point, located in the thermodynamic density interval for melting, suggests that this transition occurs when the free-energy loss in disordering is just offset by the free-energy gain due to increased atomic mobility. Survival of the crystal at a density lower than  $\rho_{\text{liq}}$  shows that disorder is a prerequisite for such higher mobility, while the isothermal liquid-glass transition reveals the connection between mobility and density in the disordered state. Stimulated by the recent local free-volume approach of Cohen and Grest<sup>13</sup>, we have computed two potential energy spectra: one for actual energies



**Fig. 4** Atomic positions in two adjacent close-packed layers, corresponding to state B of Fig. 1. Linkage reversal, in which the angle subtended at an atom by its immediate neighbours passes through  $180^\circ$  (changing the zig-zag pattern to zag-zig), permits detection of (Shockley partial) dislocations<sup>12</sup>. The dotted line indicates the approximate position of a dislocation loop found in this manner. The long straight lines indicate the periodic boundaries.

of the atoms during the simulation, and one for the energies that atoms would have if moved to the centres of the closest and largest regions of local free volume. These 'normal' and 'hole' spectra for states A (crystal), E (liquid) and F (glass) are shown in Fig. 3. Only for the liquid do the two spectra overlap. In this case, atoms seem to have sufficient energy to take advantage of the choice of position provided by local free volume, and the distinction between normal and hole states is no longer well defined. This is presumably the origin of the enhanced atomic mobility. Finally, using an earlier dislocation-detection procedure<sup>12</sup>, we find that the observed crystal-liquid instability is dislocation mediated. No dislocations were observed at densities above state B, but these defects appeared (and rapidly proliferated) on reaching B, as shown in Fig. 4. This result is in conflict with the dislocation theory of melting.

We thank W. Damgaard Kristensen for stimulating discussions, and the Danish Natural SRC for support.

Received 23 June; accepted 8 October 1980.

1. Born, M. *J. chem. Phys.* **7**, 591-603 (1939).
2. Damgaard Kristensen, W. *J. Non-Crystal. Sol.* **21**, 303-318 (1976).
3. Landau, L. D. & Lifshitz, E. M. *Statistical Physics* 60 (Pergamon, Oxford, 1969).
4. Cotterill, R. M. J. & Madsen, J. U. *Phys. Scr.* (in the press).
5. Jacobaeus, P., Madsen, J. U., Kragh, F. & Cotterill, R. M. *J. Phil. Mag.* **B41**, 11-20 (1980).
6. Finney, J. L. *Proc. R. Soc.* **319A**, 479-493 (1970).
7. Hansen, J.-P. & Verlet, L. *Phys. Rev.* **184**, 151-161 (1969).
8. Hansen, J.-P. *Phys. Rev.* **A2**, 221-230 (1970).
9. Hsu, C. S. & Rahman, A. *J. chem. Phys.* **70**, 5235-5240 (1979).
10. Ziman, J. M. *Models of Disorder* 239 (Cambridge University Press, 1979).
11. Turnbull, D. in *Liquids: Structure, Properties, Solid Interactions* (ed. Hughel, T. J.) 6-24 (Elsevier, Amsterdam, 1965).
12. Cotterill, R. M. J., Damgaard Kristensen, W. & Jensen, E. *J. Phil. Mag.* **30**, 245-263 (1974).
13. Cohen, M. H. & Grest, G. S. *Phys. Rev.* **B20**, 1077-1098 (1979).

## Low-temperature preparation of refractory alloys

A. K. Cheetham

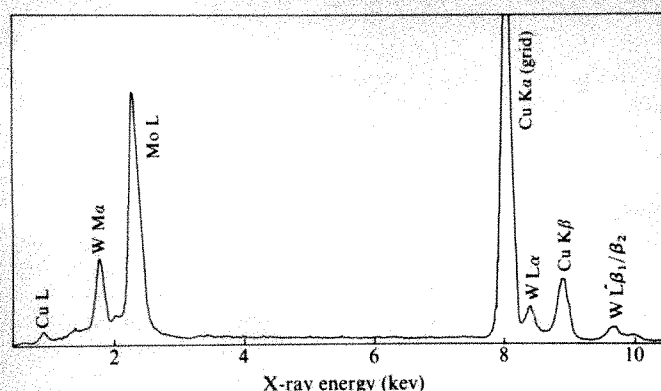
Chemical Crystallography Laboratory, University of Oxford,  
9 Parks Road, Oxford OX1 3PD, UK

The escalating cost of energy has stimulated interest in the preparation of refractory and ceramic materials by low-temperature methods. Such methods are particularly attractive for the preparation of catalysts because the products are more finely divided than those obtained from conventional solid-state reactions, and they are also of academic interest because they provide the opportunity to examine some previously inaccessible low-temperature areas of phase diagrams. So far, interest has focused mainly on the synthesis of mixed metal oxides by the ignition of precursors which have been precipitated from aqueous solution<sup>1</sup> or freeze dried<sup>2</sup>, although platinum metal alloys have also been prepared, for example by the reduction of salts which have been impregnated on a silica support<sup>3</sup>. I report here the low-temperature synthesis of the refractory alloy Mo-W by precipitation from aqueous solution followed by hydrogen reduction.

The melting points of Mo and W are  $2,610^\circ\text{C}$  and  $3,410^\circ\text{C}$  respectively. They form a continuous body-centred cubic solid solution in which the lattice parameter varies linearly with composition<sup>4</sup> between  $3.1472\text{ \AA}$  (Mo) and  $3.1648\text{ \AA}$  (W). The alloys are typically prepared from the melt or by sintering the metals in a powder form at  $\sim 2,300^\circ\text{C}$ .

In the present experiments, ammonium paramolybdate,  $(\text{NH}_4)_6\text{Mo}_7\text{O}_{24}\cdot 4\text{H}_2\text{O}$ , and ammonium paratungstate,  $(\text{NH}_4)_{10}\text{W}_{12}\text{O}_{41}\cdot 5\text{H}_2\text{O}$ , were dissolved in hot water and then precipitated by adding the cooled solution to a large excess of ethanol. Examination of individual particles of the precipitates by X-ray emission analysis in a Jeol 100CX TEMSCAN analytical electron microscope revealed a surprising degree of homogeneity in the Mo-W distribution at this stage. The alloys

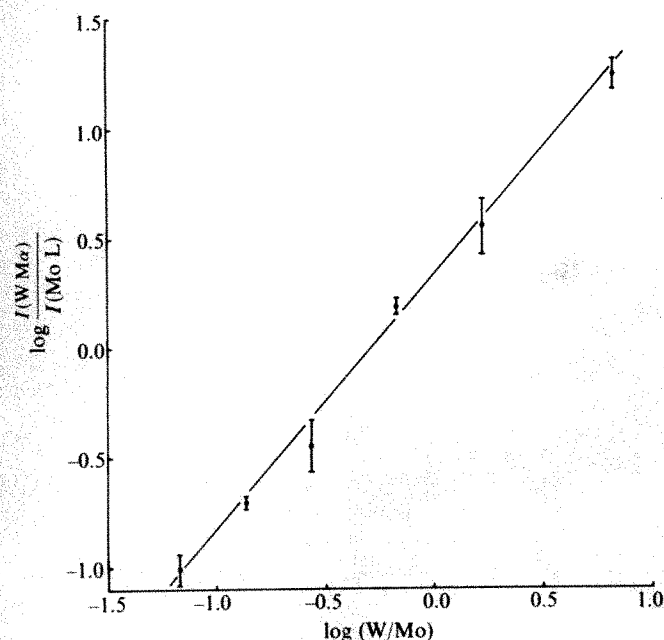




**Fig. 1** X-ray emission spectrum from a thin crystal of  $\text{Mo}_{0.6}\text{W}_{0.4}$  supported on a copper grid. Operating voltage, 100 keV.

were obtained by reducing the precipitates in hydrogen for  $\sim 5$  h at  $700^\circ\text{C}$ ; reduction can even be effected at  $500^\circ\text{C}$  but the product is pyrophoric. The thermal decomposition of the precipitates in air at  $500^\circ\text{C}$  led to the formation of mixed metal oxides in the system  $\text{MoO}_3\text{--}\text{WO}_3$ . The preparation of these oxides has previously been carried out by a solid-state reaction between  $\text{MoO}_3$  and  $\text{WO}_3$  at temperatures up to  $1,100^\circ\text{C}$  for 3 days<sup>5</sup>.

The chemical composition of the alloy may be controlled by changing the composition of the starting solution and samples were prepared at the following compositions: 13, 37, 60, 79, 88 and 94 atom % Mo. Individual alloy particles were examined in the analytical electron microscope to monitor the composition and homogeneity, and Fig. 1 shows a typical X-ray emission spectrum. In the thin-crystal limit, the W:Mo ratio is directly proportional to the ratio of appropriate X-ray emission intensities<sup>6</sup>, for example  $\text{WM}\alpha : \text{MoL}$ , and the results obtained from an examination of several thin crystals at each composition are presented in Fig. 2. The error bars represent the range of  $\text{WM}\alpha : \text{MoL}$  ratios observed at each composition. Two of the alloys, at 37 and 79% Mo, are noticeably less homogeneous ( $\pm 4\text{--}5\%$  Mo) and this is reflected in their X-ray powder patterns which exhibit broader lines. However, the results clearly



**Fig. 2** The measured  $\text{WM}\alpha : \text{MoL}$  intensity ratio for the alloys versus the W:Mo ratio in the starting solution. Use of a log-log plot distributes the points more evenly.

indicate the preparation of alloys across the complete composition range and are in accord with the thin-crystal approximation. The electron optical study also revealed a small particle size in the range  $0.1\text{--}10\ \mu\text{m}$ .

The alloys containing 13, 60, 88 and 95% Mo gave sharp Guinier X-ray patterns with bcc cell constants of  $3.165(1)$ ,  $3.152(1)$ ,  $3.149(1)$  and  $3.147(1)\ \text{\AA}$  respectively. These values agree well with the expected cell constants ( $3.163$ ,  $3.154$ ,  $3.149$  and  $3.148\ \text{\AA}$ ) and confirm that true alloys, rather than biphasic mixtures of Mo and W, have been formed.

It is surprising that the degree of homogeneity observed in the precipitate can be obtained by precipitating two ammonium salts which apparently contain polyanions of different stoichiometries, that is  $\text{Mo}_7\text{O}_{24}^{6-}$  and  $\text{W}_{12}\text{O}_{41}^{10-}$ . However, a modification of sodium tungstate containing the  $\text{W}_7\text{O}_{24}^{6-}$  ion has been prepared by boiling aqueous solutions of sodium paratungstate<sup>7</sup> and it is possible that the initial heating step in the procedure described above results in the formation of heteropolyanions of the type  $(\text{Mo}_{7-n}\text{W}_n\text{O}_{24})^{6-}$  so that a rather homogeneous distribution of the metals is frozen in before precipitation.

The alloy synthesis described here may be adapted for the preparation of a wide range of alloys containing metals which can normally be obtained by hydrogen reduction of an appropriate compound. This group comprises almost all the metallic elements to the right of molybdenum and tungsten in the Periodic Table. The method of precipitation will clearly depend on the particular elements involved and, in some cases, milder reducing conditions may be appropriate. The most exciting application of the procedure is likely to be in catalysis where the small particle size obtained in a low-temperature synthesis is particularly advantageous.

I thank Dr Michael Pope for a useful discussion, Mrs Ann Stoker for technical assistance and the SRC for grant GR/A/3320 towards an electron microscope.

**Note added in proof:** My coworkers and I have recently demonstrated that alloys in the systems W-Re, Pt-Ru and Fe-Ni can be prepared by related methods.

Received 4 August; accepted 10 October 1980.

1. Horowitz, H. S. & Longo, J. M. *Mater. Res. Bull.* **13**, 1359-1369 (1978).
2. Kim, Y. S. & Monforte, F. R. *Bull. Am. ceram. Soc.* **50**, 532-535 (1971).
3. Sinfelt, J. H. & Via, G. H. *J. Catal.* **56**, 1-11 (1979).
4. Bückle, H. Z. *Metallk.* **37**, 53-59 (1946).
5. Salje, E., Gehlig, R. & Viswanath, K. *J. Solid State Chem.* **25**, 239-250 (1978).
6. Cliff, G. & Lorimer, G. W. *J. Microsc.* **103**, 203-207 (1975).
7. Petrun'kov, P. P., Burtseva, K. G. & Semchenko, D. P. *Russ. J. inorg. Chem.* **21**, 1308-1310 (1976).

## Geometry of transform zones

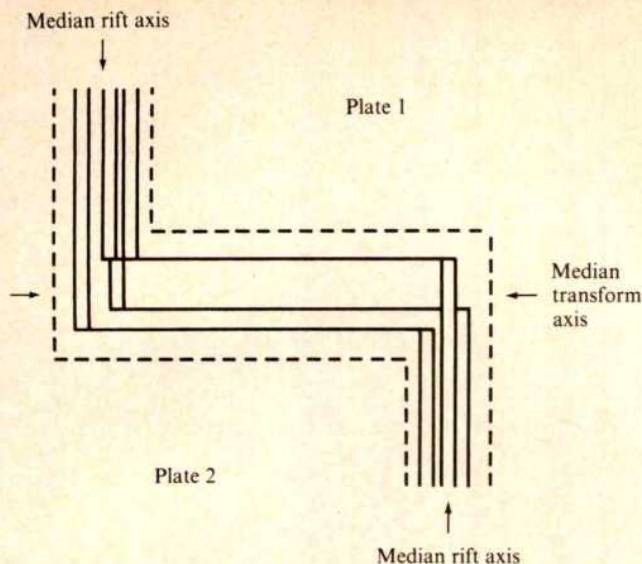
Hans Schouten, Jeff Karson & Henry Dick

Department of Geology and Geophysics, Woods Hole Oceanographic Institution, Woods Hole, Massachusetts 02543

**Asymmetric sea-floor formation at oceanic spreading centre/transform fault intersections is predicted by the steady-state (average) geometry of finite-width transform fault zones. In the central North Atlantic, geological and geophysical data near both small-offset (FAMOUS Fracture Zone B) and large-offset (Kane Fracture Zone) transforms support this geometry. We report here observations made on both regional and local scales which suggest predictable systematic development of asymmetric features in these areas.**

Sea-floor spreading occurs along mid-ocean ridges<sup>1</sup>. These oceanic rift zones form the continuous boundaries between diverging lithospheric plates. To a first approximation, the plates are rigid—major deformation occurs only at their boundaries<sup>2</sup>. The diverging or accreting boundary between two plates consists of a string of discontinuous elongate spreading-centre segments





**Fig. 1** Three successive transform fault events on a divergent plate boundary. The dashed lines mark the 95% width of the active plate boundary. Successive strike-slip faults and corresponding rifts (heavy double lines) are randomly distributed about their respective median axes. Half the time rifting will extend beyond the median axis of the transform fault zone. The steady-state (average) geometry of a transform zone formed by a succession of these events is shown in Fig. 2.

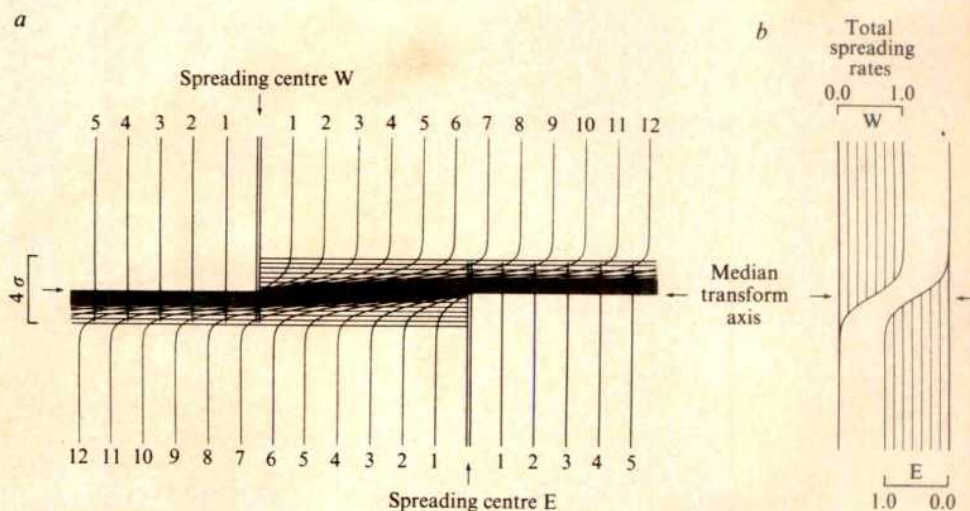
where young oceanic crust is accreted in a predominantly extensional regime. The extensional segments are joined by transform fault zones<sup>3</sup> which represent a regime of predominant shear displacement, parallel to the direction of spreading. Spreading centres have a typical width of 2–10 km (refs 4, 5) over which most of the volcanic emplacement of oceanic crust occurs, whereas extensional tectonic deformation may be active over a broader zone<sup>4</sup>. Based on observations from manned submersibles and deep-towed instruments, the time-integrated width of crust affected by tectonic deformation in Atlantic transform fault zones may be as much as a few tens of kilometres<sup>6–8</sup>. At a given time, however, strike-slip activity in a transform zone may be restricted to a single fault<sup>9</sup> but averaged over a longer period of time (steady state), strike-slip deformation will have affected a zone of finite width (see Fig. 1).

We consider now the steady-state (average) configuration of a finite-width transform zone. Let the strike-slip activity be randomly distributed about the median axis of the transform zone. The assemblage of strike-slip faults constitute transform faults which, as Wilson<sup>3</sup> pointed out, provide the continuity of the active plate boundary between spreading-centre segments on either side of the transform. Following Wilson's definition, strike-slip transform activity terminates in extensional activity at both ends. Thus, if transform fault deformation occurs over a zone of finite width, then, logically, half the time the rift termination will extend beyond the median axis of the transform zone (see Fig. 1).

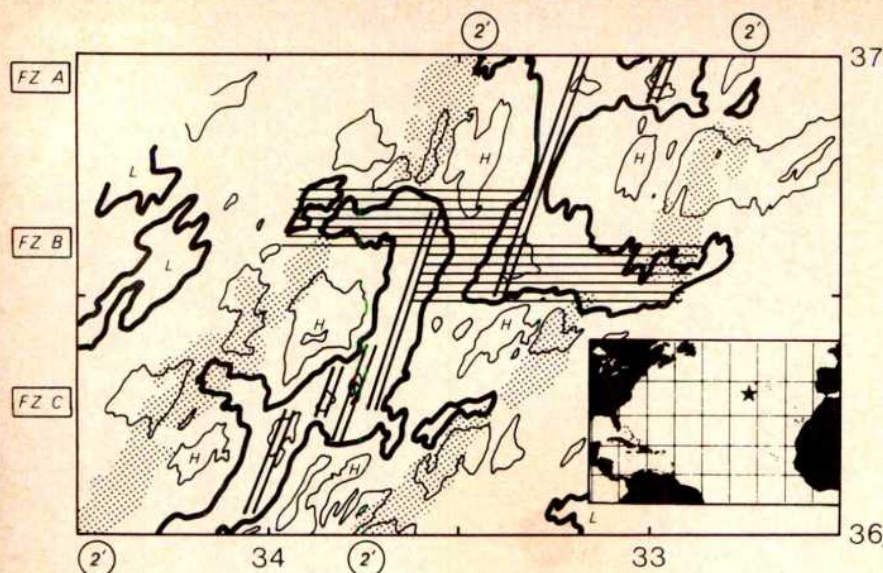
Figure 2a shows the steady-state model of a finite-width transform zone that offsets two spreading-centre segments. The numbered isochrons illustrate the steady-state geometry and asymmetric evolution of the sea floor in a transform zone. Consecutive isochrons describe progressive stages of strike-slip deformation of the linear isochrons formed originally in the spreading centres of Fig. 2a. This geometry has been computed for strike-slip transform activity that is normally distributed about the median axis of the transform zone with standard deviation  $\sigma$ . Thus, 95% of the strike-slip activity occurs within  $4\sigma$ , or there is a 95% probability that strike-slip activity will occur within  $\pm 2\sigma$  from the median axis. The total spreading rates in the individual spreading centres are shown in Fig. 2b. The rigid-plate geometry requires that the sum of the total spreading rates in the direction of spreading is a constant everywhere on the accreting boundary. At the median transform axis, the contribution to the total spreading for both spreading-centre segments is equal. Thus, up to the median transform axis, the spreading velocity must remain constant on one side of the spreading centre (outside the active transform zone) while on the other side, spreading decreases to zero at the median axis (Fig. 2a). In other words, at the intersection of a spreading centre with a transform zone, accretion of sea floor should become progressively asymmetric until it is fully asymmetric at the median axis. Beyond the median transform axis, extension and magmatism could propagate into crust that was formed originally at the other spreading centre, resulting in mixing of young crustal material with older crust that has a transform-deformation history.

The steady-state geometry in Fig. 2a predicts that the average age of the sea floor in the transform zone will be older than that of the surrounding sea floor. The inactive trace of the transform zone will be only half the width of the active transform and will consist of mixed-age oceanic crust. Sea floor formed in the transform-zone segment of the spreading centres will have no

**Fig. 2** a, Steady-state (average) geometry of a finite-width transform zone that offsets two spreading centres (heavy double lines). This geometry has been computed for strike-slip transform fault activity that is normally distributed about the median axis of the transform zone with standard deviation  $\sigma$ . The numbered isochrons illustrate the asymmetric evolution of the sea floor in a finite-width transform zone. Note the mixed-age isochrons in the inactive parts of the transform. Hachures indicate sea floor with transform deformation history. b, Total spreading rates in each spreading centre. Rigid-plate geometry requires that the sum of these total spreading rates is a constant everywhere along the plate boundary.







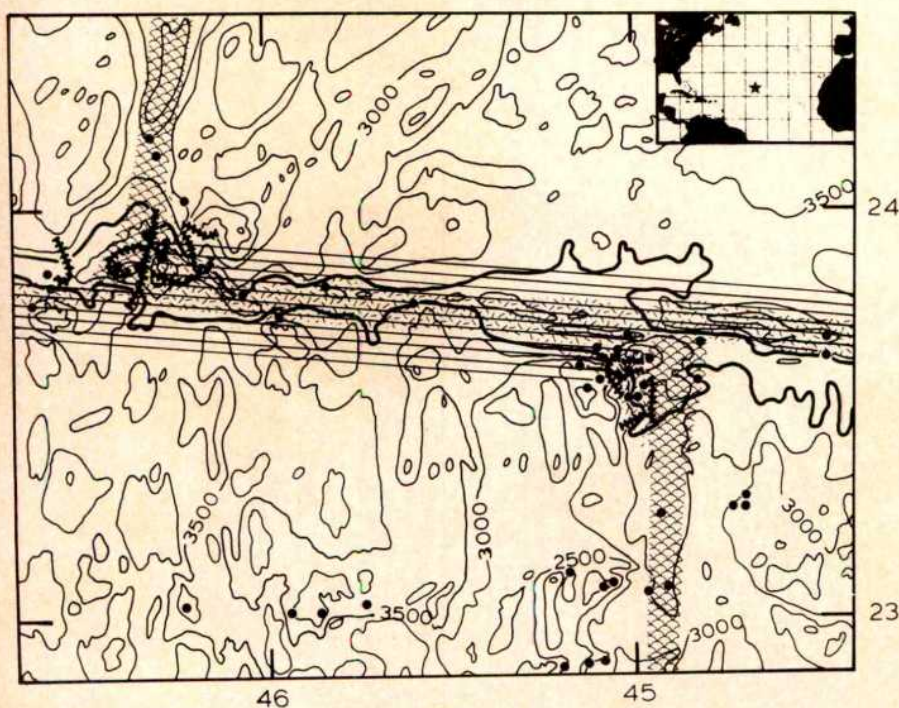
**Fig. 3** Asymmetric bathymetry and marine magnetic anomalies 2' (stipples, after ref. 11) in FAMOUS Fracture Zone B. Depth contours are in fathoms. Active spreading axes (after ref. 11) are indicated by heavy double lines. The asymmetric transform zone geometry of Fracture Zone B is illustrated by a pattern of hachures explained in Fig. 2. Similar geometries can be drawn for Fracture Zones A and C.

matching counterpart on the opposite plate—the distribution of youngest volcanics at the transform intersection will be highly asymmetric and marine magnetic anomalies (isochrons) will not match.

Although this model may not be applicable to all classes of ridge-ridge transform faults, geological and geophysical data from two separate areas agree with this geometry. The first is the FAMOUS detailed survey located at latitude 36.5°N on the Mid-Atlantic Ridge crest between the Azores and the Oceanographer Fracture Zone. The bathymetry<sup>10</sup> and segments of marine magnetic anomaly 2' (stipples)<sup>11</sup> around FAMOUS Fracture Zone B are shown in Fig. 3. The active transform section of Fracture Zone B offsets the Mid-Atlantic Ridge ~20 km in a right-lateral sense. Focal mechanism solutions of earthquakes and structural trends in the FAMOUS fracture zones suggest an east-west direction of relative plate motion in the central North Atlantic<sup>12,13</sup>. We assume the east-west direction of spreading has been active since magnetic anomaly 2' (3 Myr BP). A relevant feature of the bathymetry (Fig. 3) is the

existence of parallel extensions of the adjacent spreading centres in Fracture Zone B and an asymmetric distribution of the fracture zone valleys<sup>11,14</sup>. In the magnetic anomaly pattern, northwestern anomaly 2' terminates at the (steepest) northern wall of the western fracture-zone valley whereas northeastern anomaly 2' continues across the eastern fracture zone and terminates at the (steepest) southern wall of the valley.

These observations of Fracture Zone B suggest a 20-km wide transform-zone geometry (hachures in Fig. 3) that has been active during the past 3 Myr of central North Atlantic sea floor spreading. The transform-zone segment of northeastern anomaly 2' has no matching counterpart on the western plate. According to the model, young sea floor formed in the transform zone at the northern spreading centre will be transported to the east undeformed, but to the west it will be deformed in the active transform zone and then overprinted when it passes through the southern spreading centre. In this small-offset transform zone, spreading-centre activity seems to extend well beyond the median transform axis as indicated by the echelon rift valley



**Fig. 4** Generalized geology of the Kane Fracture Zone. Bathymetric contours in metres, 500-m interval (after ref. 16). ●, Dredge haul locations; bold hachured lines, Angus camera runs (after ref. 8); scalloped pattern, young pillow basalts with negligible pelagic cover; dashed pattern, transform zone lithologies including basalt, metabasalt, greenstone, gabbro, metagabbro, serpentinite and various breccias; no pattern, areas of older basalts with variable cover of carbonate ooze. Asymmetric pattern of hachures (as in Figs 2 and 3) indicates the inferred extent of crust affected by transform tectonics.



extensions and the northeastern segment of anomaly 2'. This suggests that the physical properties of the deformed lithosphere within the transform zone at the ridge intersections are not significantly different from the physical properties of the lithosphere in spreading centres outside of transform zones and that spreading may occur in both areas.

The active transform section of the Kane Fracture Zone offsets the Mid-Atlantic Ridge approximately 160 km in a left-lateral sense near latitude 24° N (see Fig. 4)<sup>15-18</sup>. The fracture-zone valley is outlined by the 4,000-m contour in Fig. 4 and has a width of 10–20 km over most of its length. Combined dredging and acoustically navigated bottom camera *Angus* surveys in the fracture zone reveal an asymmetric distribution of young pillow basalts with respect to highly altered and faulted lithologies as well as the major tectonic features at the ridge intersections<sup>16</sup>.

Fresh pillow basalts with negligible pelagic cover are exposed in the median rift valley floors and at the base of the older walls in the transform zone opposite both ridge intersections (scaloped pattern in Fig. 4). Fissures and faults in the young pillow lavas at the intersections indicate extension normal to the regional trend of the spreading centre<sup>8</sup>. Thus, sea-floor spreading seems to be continuous across the Kane Fracture Zone valley at the ridge intersections.

Pillow basalts with a variable cover of calcareous ooze occur along the median rift valley walls and marginal highs north and south of the fracture zone. Pillow basalts are also found on the floor and up the younger walls of the fracture zone outside the transform region (no pattern in Fig. 4). However, the walls of the active transform zone, the older fracture zone walls outside the transform, and oblique-trending median valley walls near the intersection provide exposures of a variety of lithologies including basalt, metabasalt, greenstone, gabbro, metagabbro, serpentinite and various breccias (dashed pattern in Fig. 4). Most of these lithologies are variably fractured and covered with ferromanganese crusts.

The asymmetric distribution of pillow basalts is best documented at the western Kane intersection where *Angus* coverage is more extensive (see Fig. 4). Relatively fresh pillow lavas extend down the fracture-zone valley a considerable distance to the west. Immediately to the east of the western intersection, the floor of the transform is largely covered with sediments and a few older appearing outcrops of brecciated rock. *Angus* coverage of transform zone lithologies immediately to the west of the eastern Kane intersection and fresh basalts dredged at the base of the older wall in the transform zone opposite the eastern ridge intersection suggests a similar asymmetry. We indicate the proposed transform zone geometry with hachures in Fig. 4. The relative abundance of plutonic and metamorphic rocks dredged from the older walls in the transform zone opposite the ridge intersections indicates little if any recent volcanism in these areas. The young volcanics in the fracture-zone valley terminate abruptly against old deformed crust that is passing out of the active Kane transform zone. In contrast to the small-offset FAMOUS Fracture Zone B, extension and magmatism do not seem to continue across the width of the large-offset Kane transform zone, but presumably terminate near the median transform axis. The age contrast across transform zones probably controls the nature and extent of the rifting that propagates into older crust at ridge-transform intersections.

In conclusion, these studies show that various asymmetric aspects of some ridge-transform intersections on the Mid-Atlantic Ridge can be explained by a steady-state geometry of transform fault zones that are a few tens of kilometres wide. The agreement between observations and steady-state model suggests that even on a 10-km scale, the process of sea-floor formation along an accreting boundary can be considered more uniform than random.

We thank Bill Bryan and Jim Heirtzler for their comments. H.S. acknowledges support from the NSF grant OCE-7622512 A01. J.K. acknowledges support from a WHOI Postdoctoral Scholarship and NSF grant OCE-26842 (J.K. and H.D.).

Received 2 June; accepted 8 October 1980.

1. Vine, F. J. & Matthews, D. M. *Nature* **199**, 947–949 (1963).
2. Oliver, J. & Isacks, B. *J. geophys. Res.* **72**, 4259–4275 (1967).
3. Wilson, J. T. *Nature* **207**, 343–347 (1965).
4. Macdonald, K. C. & Luyendyk, B. P. *Bull. geol. Soc. Am.* **88**, 621–636 (1977).
5. Schouten, H. & Denham, C. R. in *Deep Drilling Results in the Atlantic Ocean: Ocean Crust* (eds Talwani, M., Harrison, C. G. & Hayes, D. E.) 151–159 (American Geophysical Union, Maurice Ewing Ser. 2, Washington, 1979).
6. ARCYANA *Science* **190**, 108–116 (1975).
7. Searle, R. C. *J. geol. Soc. Lond.* **136**, 283–291 (1979).
8. Bryan, W. B. *et al.* (in preparation).
9. Eittreim, S. & Ewing, J. *Geology* **3**, 555–558 (1975).
10. Phillips, J. D. & Fleming, H. S. *Map and Chart Ser. MC-19* (Geological Society of America, 1978).
11. Ramberg, I. B., Gray, D. F. & Reynolds, R. G. H. *Bull. geol. Soc. Am.* **88**, 609–620 (1977).
12. Reid, I. & Macdonald, K. C. *Nature* **246**, 88–90 (1973).
13. Spindel, R. C., Davis, S. B., Macdonald, K. C., Porter, R. P. & Phillips, J. D. *Nature* **248**, 557–559 (1974).
14. Bryan, W. B. *J. Petrol.* **20**, 293–325 (1979).
15. Purdy, G. M. *et al. Init. Rep. DSDP Leg 45*, 119–128 (1979).
16. Purdy, G. M. & Rabinowitz, P. D. *Init. Rep. DSDP Leg 45* (Colour Map Suppl., 1979).
17. Sykes, L. R. *J. geophys. Res.* **72**, 2131–2153 (1967).
18. Fox, P. J. *et al. Science* **165**, 487–489 (1969).

## Subduction of the Iapetus Ocean crust beneath the Møre Gneiss Region, southern Norway

S. Mykkeltveit\*, E. S. Husebye\*† & C. Oftedahl‡

\* NTNF/NORSAR, Box 51, N-2007 Kjeller, Norway

† Institutt for geologi, Universitetet i Oslo, Norway

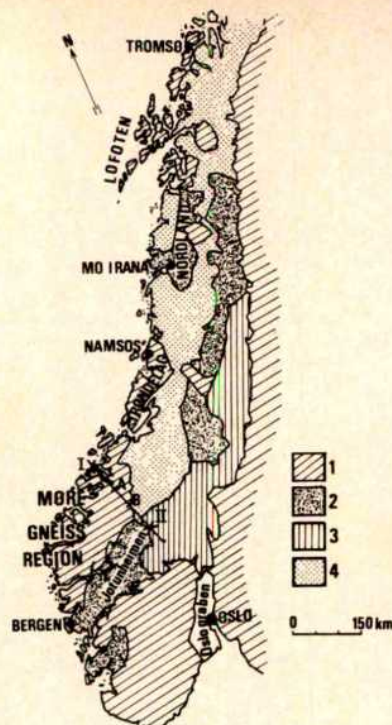
‡ Geologisk institutt, Norges Tekniske Høgskole, N-7034 Trondheim NTH, Norway

**Basement–cover relations between Caledonian nappes and underlying Precambrian basement along the western coastline of southern Norway have long intrigued geologists and considerable progress has recently been made in understanding the Caledonian geology<sup>1–3</sup>, geochronological studies proving particularly useful. For example, the Precambrian gneisses along the coast from Bergen to Namsos yield ages up to 1,700 Myr, supposedly the age both of the formation of the rocks and the main metamorphism and deformation phases<sup>4</sup>. The Lofoten–Tromsø archipelago is a presumed continuation of this basement block once sandwiched between the Caledonides of Norway and Greenland. An important phase of rock formation and metamorphism affected the gneisses here at around 1,800 Myr, whereas subsequent orogenies at 1,100 and 400 Myr (Grenville–Sveco-Norwegian or Dalslandian, and late Caledonian orogenies, respectively) had little effect. COCORP reflection profiling in the southern Appalachians<sup>5</sup> has demonstrated that crystalline ‘basement’ has been thrust for a large distance over autochthonous early Palaeozoic sediments of the proto-Atlantic continental margin. Data from a seismic profile<sup>6</sup> across the Møre Gneiss Region (often called the northwestern basal gneisses of southern Norway) show evidence of P-wave velocity reversal at a depth of about 14 km, and the associated low-velocity layer (LVL) has a thickness of 4 km. As there is no excess of heat flow to account for the LVL, we consider here the hypothesis that oceanic crust and accompanying sediments have been subducted under the gneisses.**

The refraction–wide-angle reflection seismic profile is indicated in Fig. 1, together with the two shot-point locations I and II. Five 3-component seismometers were moved along the profile at an average spacing of 2.5 km, while explosive charges of 25–300 kg were fired in water depths of ~20 m at the shot points. Altogether 145 seismic field records were obtained, but many of them were not suitable for detailed digital analysis, although several poorer-quality records were used for extracting first arrival travel times.

After the necessary elevation corrections had been made, a Herglotz–Wiechert inversion procedure was applied to the first





**Fig. 1** Simplified tectonic map of Norway redrawn after Reymer<sup>7</sup>, showing shot points I and II of the seismic profile crossing the Møre Gneiss Region. 1, Precambrian basement, including the generally presumed autochthonous Møre Gneiss Region, with radiometric ages in the range 1,900–1,200 Myr; 2, mostly Precambrian nappes (1,200–850 Myr) also including structures of Caledonian ages; 3, Lower Palaeozoic elements, (par)-autochthonous-allochthonous structures of mostly Cambrian–Silurian ages; 4, Lower Palaeozoic elements, typical nappe substructures having a presumed south-eastern direction of thrusting.

arrival observations (see Fig. 2a). The continuously increasing velocity distribution obtained (Fig. 2b) was truncated at 12–14-km depth, because the pronounced offset in the travel-time curves suggests the existence of a LVL in the upper crust. Note that strong lateral inhomogeneity effects are ruled out by detailed comparison of records from the two shot points.

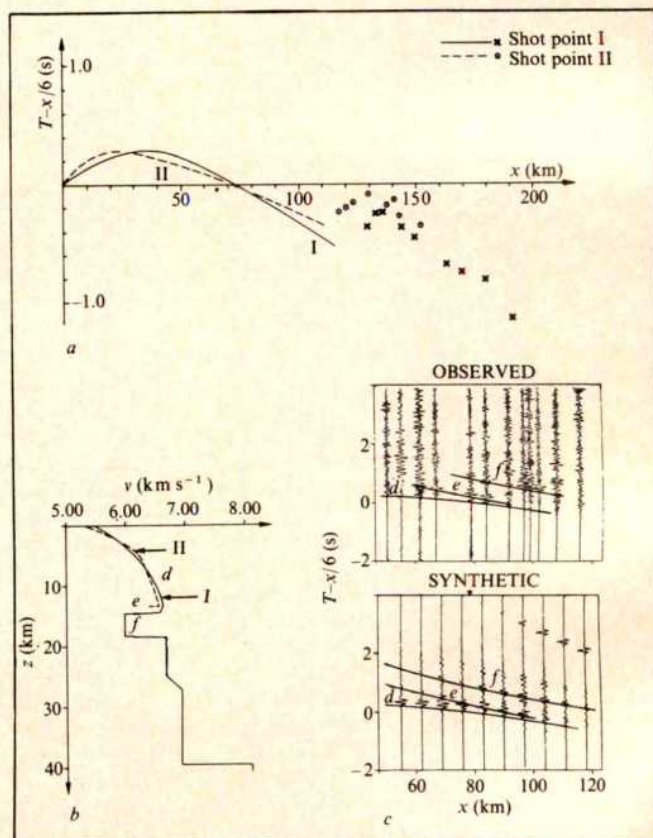
Modelling of the lower crust is relatively uncertain in view of a maximum shot-detector separation of 190 km. The outstanding feature, however, of the velocity model obtained is the roughly 4-km thick LVL in the upper crust. Because of objections to such a feature on the grounds of both realistic heat-generation mechanisms and limited resolving power of our data, we have undertaken extensive synthetic seismogram analyses. These experiments demonstrate that the most appropriate model for reconciling discontinuous travel-time data and amplitude distributions of primary and secondary phases involves the introduction of a LVL, which can generally be recognized best from reflections from the top of it. Characteristics of these arrivals are: (1) a 180° phase shift relative to the first arrivals; (2) the travel time and apparent velocity; and (3) absence of associated head-wave arrivals<sup>8</sup>. Figure 2c shows an extract from both the observed record section (shot point I) and a synthetic section computed from the model in Fig. 2b, covering the distance interval over which the LVL reflections are observed. The upper-crustal first arrivals (d) and the reflections from the top and bottom (e and f respectively) of the LVL are well modelled by the synthetic section.

From our data it is impossible to estimate accurately the actual horizontal extent of the LVL, even in the direction of the profile. Our modelling experiment here demonstrates that, even if the LVL were present under the entire profile, the reflections would

be observable only where they are actually seen in the record section. However, a minimum extent of the LVL can be estimated and is indicated by AB in Fig. 1. The data also suggest that the LVL is rather flat-lying. The two velocity–depth curves of Fig. 2b can be taken to be representative at points A (curve I) and B (curve II) of Fig. 1, some 50-km apart, yielding a westward dip of the upper LVL interface of <2°.

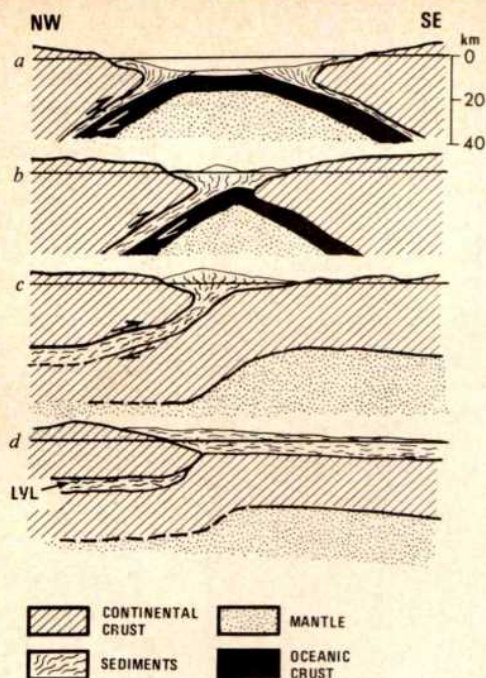
The nature and significance of low-velocity zones are still not well understood. Extensive laboratory experiments have been undertaken to investigate the possibility of crustal velocity reversals. The main prerequisite for such phenomena is either anomalously high temperatures and/or profound compositional changes. Typical examples are areas of exceptionally high heat flow such as rift zones and areas, where high-velocity crystalline rocks have been thrust over 'soft' material of lower velocity<sup>9,10</sup>. Within the Møre gneisses there is no evidence of high heat flow<sup>11</sup>, so the postulated LVL must be associated with compositional changes. Further to the north near Mo i Rana, a trans-Scandinavian profile<sup>12</sup> also gives evidence of an upper-crustal velocity reversal under the Caledonides only (see Fig. 1).

We suggest that the crustal structure in the Møre Gneiss Region is explained by a doubling of the crust, which occurred during the final continent–continent collision of the Caledonides towards the end of the Silurian. As low-velocity rocks, sandwiched between continental rocks from two opposing continents, two types must be considered: (1) serpentinites, and (2) eugeosynclinal sedimentary rocks of relatively low metamorphic grade. It is impossible to discriminate between types (1) and (2) from the geophysical data only. Type (1) is, however, discarded because of the geological improbability of having serpentinite from the lower oceanic crust as a surface layer on top of the lower continental mass. Logically the



**Fig. 2** a, First arrival travel times for both shot points. The continuous curves represent a slight smoothing of travel-time observations. b, Velocity–depth distribution derived from shot point I data. Dashed curve, shot point II data. c, Detail of record section (top) for shot point I and corresponding synthetic section (bottom). Selected segments of the travel-time curves as computed from the model of b (curve I) are inserted.





**Fig. 3** Simplified cross-sections through the Møre Gneiss Region, with the closing of the Iapetus Ocean, illustrating our hypothesis for the LVL. *a*, Late stage in the closing of the Iapetus Ocean. *b*, Situation before the continents collide, with a westerly dipping subduction zone along which orogenic sediments are dragged down. *c*, The continental collision resulting in doubling of crustal thickness with sediments constituting the LVL sandwiched between the two crustal blocks. *d*, A westerly Himalayan-type mountain chain resulting from isostatic uplift, off which the nappes glide to the east.

incorporation of eogeosynclinal sediments during subduction should occur during a subduction process<sup>13</sup>. This hypothesis contrasts with the current thinking of many geologists working with the basement-cover relations of the Caledonides in southern Norway, who favour the view that the Møre gneisses represent an autochthonous area above which Caledonian nappes to the east have been thrust from a westerly location in the Lower Palaeozoic proto-Atlantic (Iapetus) ocean<sup>4,14</sup>.

Our hypothesis relies on the general features of the Bergen-Namsos area, which exhibits a lithological and structural development clearly different from that of southeastern Norway<sup>3</sup>. This area may either be classed as a separate Precambrian block<sup>15</sup>, or may represent an overthrusting part of the American block over the Eurasian one. In the latter case, a last deformation of the Precambrian gneisses has to be of Caledonian age. This possibility is permitted by a recent Sm/Nd age study<sup>16</sup> of eclogite lenses located in granitic gneisses in the coastal Møre area, which are found to be late Ordovician-Silurian.

A mechanism envisaging a Himalayan-type doubling in thickness of the crust of the mid-Scandinavian Caledonides is sketched in Fig. 3, based on recent suggestions for the Grenville collision<sup>17</sup> and the Sunda trench subduction<sup>13</sup>. The allochthonous overthrust block of the Møre gneisses may not be restricted to the Bergen-Namsos area, but may include the basement of the whole Nordland coast as well as the Precambrian of the Lofoten-Tromsø coastal area. The buoyancy of the doubled continental crust would have produced a Himalayan-type mountain chain, off which slid the soft Cambro-Silurian orogenic rocks as nappes travelling far to the east—250–500 km, possibly even further<sup>18,19</sup>. The weathered core of this chain now exhibits the eclogites. The postulated collision zone to the east of the Møre Gneiss Region (the 'Jotunheimen suture') is supported by recent detailed geological field work<sup>20</sup>. Also, a recent Fennoscandian study<sup>21</sup> supports the idea of a relatively thick crust (~40 km) in the coastal areas of

western and northern Norway, as opposed to southeastern Norway (Oslofjord), where the Moho depth is only around 30 km. Finally, some features of our model have earlier been hinted at<sup>3</sup> and also used to explain the surprisingly young age of the Møre eclogites<sup>16</sup>.

Although our interpretations of the LVL beneath the Møre Gneiss Region may be considered premature, we conclude that the identification and interpretation of similar crustal velocity reversals will have an important application to the problem of unravelling continental collisions and locating the sutures between them.

We thank R. Kanestrøm, M. A. Sellevoll and B. A. Sturt for helpful discussions and D. K. Smythe for helpful comments. This research was partly supported by the Advanced Research Projects Agency of the US Department of Defence.

Received 9 July; accepted 7 October 1980.

1. Tozer, E. T. & Schenk, P. E. (eds) *IGCP Prof. 27. Caledonian-Appalachian Orogen of the North Atlantic Region* (Geological Survey of Canada, Paper 78-13, 1978).
2. Furnes, H., Roberts, D., Sturt, B. A., Thon, A. & Gale, G. H. *Proc. int. Ophiolite Symp.*, Nicosia (in the press).
3. Oftedahl, C. *Norges. geol. Unders.* **356**, 3–114 (1980).
4. Råheim, A. *Norsk. geol. Tidsskr.* **57**, 193–204 (1977).
5. Cook, F. A., Albaugh, D. S., Brown, L. D., Kaufman, S. & Oliver, J. E. *Geology* **7**, 563–567 (1979).
6. Mykkeltveit, S. *Pure appl. Geophys.* (in the press).
7. Reymer, A. P. S. thesis, Univ. Leiden (1979).
8. Braile, L. W. & Smith, R. B. *Geophys. J. R. astr. Soc.* **40**, 145–176 (1975).
9. Christensen, N. I. *Tectonophysics* **47**, 131–157 (1978).
10. Christensen, N. I. *J. geophys. Res.* **84**, 6849–6857 (1979).
11. Haenel, R., Grönlie, G. & Heier, K. S. in *Terrestrial Heat Flow in Europe* (eds Cermak, V. & Rybach, L.) 232–239 (Springer, Berlin, 1979).
12. Lund, C.-E. *Geol. För. Stockh. Förh.* **101**, 191–204 (1979).
13. Kieckhefer, R. M., Shor, G. G., Curran, J. R., Sugiarta, W. & Hekuwat, F. J. *J. geophys. Res.* **85**, 836–890 (1980).
14. Roberts, D. & Gale, G. H. in *Evolution of the Earth's Crust* (ed. Tarling, D. H.) 255–324 (Academic, New York, 1978).
15. Berthelsen, A. *Int. Geol. Congr. Colloq. C6*, Paris (1980).
16. Griffin, W. L. & Brueckner, H. K. *Nature* **285**, 319–321 (1980).
17. Seyfert, C. K. *Bull. geol. Soc. Am.* **91**, 118–120 (1980).
18. Oftedahl, C. *Norsk. geol. Tidsskr.* **46**, 237–244 (1966).
19. Gee, D. G. *Tectonophysics* **47**, 393–419 (1978).
20. Banham, P. H., Gibbs, A. D. & Hopper, F. W. M. *Nature* **277**, 289–291 (1979).
21. Bungum, H., Pirhonen, S. E. & Husebye, E. S. *Geophys. J. R. astr. Soc.* (in the press).

## Guidance system used in moth sex attraction

J. S. Kennedy\*, A. R. Ludlow & C. J. Sanders†

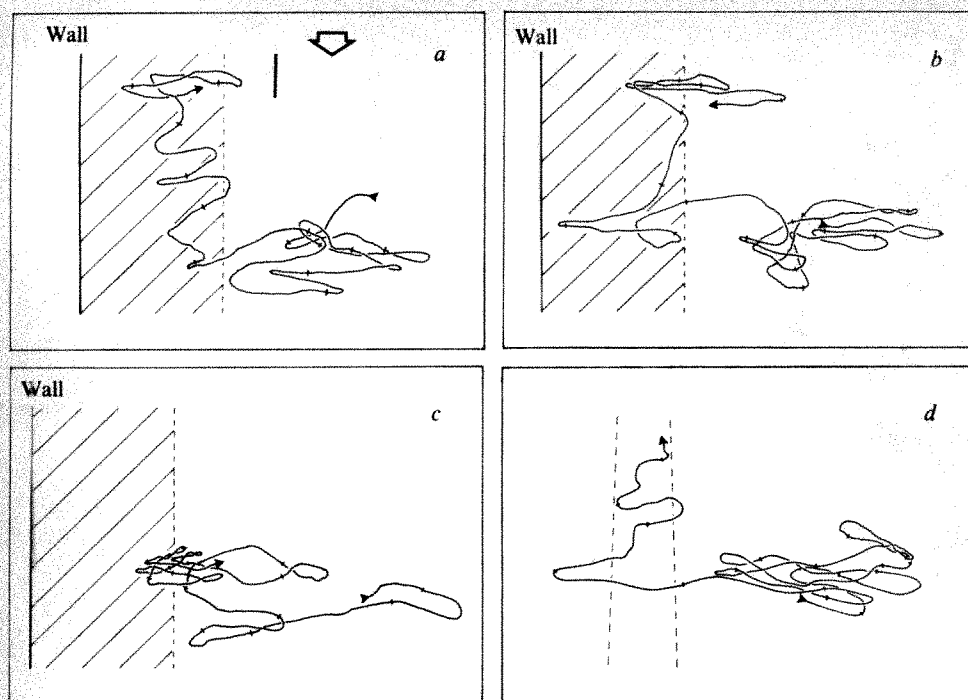
ARC Insect Physiology Group, Department of Zoology and Applied Entomology, Imperial College of Science and Technology, London SW7 2AZ, UK

It has been proposed<sup>1–4</sup> that a flying male moth finds its way to a 'calling' female or other small, distant source of wind-borne sex pheromone using two contrasting anemotactic manoeuvres: (1) upwind flight in response to the onset or increase of the pheromone stimulus, maintained as long as the stimulus continues, and (2) cross-wind flight with switching between left and right of the wind line (the so-called 'track reversals'<sup>4</sup> or 'tack reversals'<sup>5</sup> seen in casting or zig-zagging) which occurs only in response to the loss or decrease of the pheromone stimulus. A simpler system can now be proposed in the light of wind-tunnel experiments on male summerfruit tortrix moths (*Adoxophyes orana*) entering homogeneous pheromone clouds. The moths did not fly persistently upwind with continuous pheromone stimulation, and their programmed left-right track reversals occurred in response to pheromone onset, not loss, and continued after pheromone loss but with widening cross-wind excursions between reversals.

\* To whom correspondence should be addressed at Imperial College at Silwood Park, Ashurst Lodge, Ascot, Berks SL5 7DE, UK.

† Present address: Great Lakes Forest Research Centre, PO Box 490, Sault Ste. Marie, Ontario, Canada PLA 5M7.





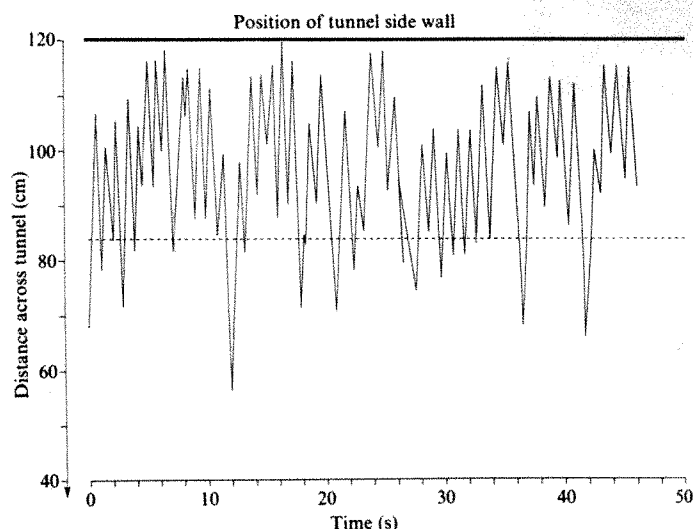
**Fig. 1** Samples of flight tracks in the wind tunnel. Time marks at 0.5 s intervals. 0.1-m scale bar and wind direction arrowhead in *a* apply to all tracks. *a, b*, Cross-wind casting after removal of a pheromone plume, leading to entry into the pheromone corridor (hatched) and a brief upwind advance, followed by resumed casting. *c*, Same as above but entry into the pheromone corridor followed only by narrowed casting without upwind progress. *d*, A normal, structured, pheromone plume (broken lines indicate its smoke-simulated, time-averaged outer envelope) added to a pheromone cloud filling the entire tunnel—on encountering this plume the casting moth 'locks-on' to it and advances upwind along it as if the plume were in clean air.

The male moths were held in constant light without females for 3–4 days from emergence and then in darkness for ~2 h before transfer to the wind-tunnel<sup>4</sup> (working section  $1.9 \times 1.2 \times 0.45$  m) in ~12 lx from overhead fluorescent lamps and a smooth air flow of  $\sim 0.24 \text{ m s}^{-1}$ . The pheromone was not presented to the flying moths in the normal form of a broken, filamentous plume because it is then impossible to say when the flier is and is not meeting pheromone, and stimulus-response relations cannot be identified. In these experiments, therefore, the pheromone was presented as a homogeneous cloud. The pheromone cloud filled a floor-to-ceiling 'corridor' about 0.36 m wide against one wall of the tunnel, and smoke simulation showed a sharp boundary with negligible mixing between this 'corridor' air and the contiguous body of clean air moving in parallel down the rest of the tunnel.

The following procedure was used to select only responsive moths and to ensure they received the pheromone test-stimulus (by entering the corridor) in a standard and observable manner. Each moth was first exposed to the normal type of plume from a small pellet of polyvinyl chloride containing synthetic pheromone (a 9:1 mixture of *trans*- and *cis*-11-tetradecenyl acetate) in the clean part of the tunnel. Moths were discarded unless they responded by taking off, 'locking-on' to the plume (that is, heading into wind and restricting their cross-wind movements to the immediate vicinity of the plume) and then advancing up it for more than 1 m, keeping away from the side corridor of diffuse pheromone. Each moth that responded in this way was then induced, by suddenly removing the pheromone plume, to stop advancing upwind and to cast across wind increasingly widely<sup>2,4</sup> and so enter the side pheromone corridor within a few seconds. A control set of moths were treated in the same way in the absence of pheromone corridor. The horizontal component of the flier's movements was recorded on videotape, and the position and time of each track reversal (switching from one side of the wind-line to the other) were later read to provide data on the cross-wind extent, duration and net direction of each inter-reversal leg of the track. The tracks were also traced frame by frame to determine the incidence of upwind advances. For this purpose an upwind advance was defined as a section of the flight track that continued with no downwind movement at all until upwind progress of at least 0.2 m had been made. Such advances often comprised zig-zags (Fig. 1*a*) but without the track deviating from due upwind by more than 90°.

Twenty-nine moths were recorded with the side pheromone corridor present. They flew in and out of it repeatedly and 40 of

their entries were made after they had spent more than 2 s outside it. 35% (14) of these entries were followed directly by an upwind advance as defined, as against 5% (5) of 93 equivalent legs in the control series without any pheromone cloud ( $P < 0.001$ ). The time from crossing the border into the pheromone corridor to the next track reversal averaged about 0.2 s, and an upwind turn was already evident in the mean angle to wind of the 40 legs starting then. Taking due upwind as 0°, this angle was  $70.0 \pm 4.2$  (30% of legs at  $< 60^\circ$ ) as against  $87.0 \pm 1.1^\circ$  (all legs  $> 60^\circ$ ) in the controls. By contrast, there was no significant upwind response when the moths entered the pheromone corridor after spending less than 2 s outside it. Only 2% (7) of these 438 entries were followed by an upwind advance, significantly less than the figure of 35% after more than 2 s outside ( $P < 0.001$ ).



**Fig. 2** The cross-wind component of one moth's flight track in the wind tunnel, plotted against time. Only the positions at which the track reversed across wind were measured, the straight lines joining these reversal points being interpolations. The broken line marks the approximate position of the border between the 'clean' part of the airflow and the pheromone 'corridor' extending to the tunnel wall at 120 cm. Note frequent track reversals inside the pheromone corridor, which cannot be attributed to any change in pheromone stimulation.

The lack of response on re-entering the pheromone after less than 2 s outside it implies that the moths were then adapted (*sensu lato*) to the given pheromone stimulus, at least in respect of the upwind flight response, and that substantial disadaptation required more than 2 s in clean air. A second indication of adaptation was that the upwind advances were mostly brief, of the order of 1 s, the moth then reverting to cross-wind casting and 'keeping station' against the wind as in Fig. 1a and b. This arrest of upwind progress could not be attributed entirely to a high pheromone concentration in the corridor although high concentrations are known to retard upwind flight along pheromone plumes<sup>4-6</sup>. These same moths had all progressed freely up the broken plume from the single-pellet pheromone source shortly before, and the pheromone concentration in the individual filaments of the plume will have been higher than in the corridor cloud. In a parallel treatment, 26 moths, casting widely after plume removal as before, were engulfed by a wind-borne, homogeneous pheromone cloud that was not confined to a side corridor but filled the entire tunnel. Again there were brief upwind advances with reversion to cross-wind casting, although the cloud concentration was at least 30 times less than the mean concentration in the plume up which these same moths had progressed freely just before. Furthermore on several occasions when moths had been casting and making no progress for many seconds within such a ubiquitous pheromone cloud, they were also presented with a normal, broken, pheromone plume from a single pellet. On encountering this superimposed plume the moths promptly 'locked on' to it and advanced up it in zig-zags (Fig. 1d) in the same manner as they had done when presented with the same plume in otherwise clean air. Evidently the moths were adapted to the pheromone concentration in the cloud but still fully responsive to increases above that level.

Entries into the side pheromone corridor, or the ubiquitous pheromone cloud, led not only to some upwind advances but also, and much more predictably, to a restriction of cross-wind movement. This was not mainly due to turning upwind although that, of course, enhanced the effect. When combined with an upwind advance, the restriction produced narrow upwind zig-zagging as in Fig. 1a. More frequent was a simple narrowing of the cross-wind casting already in train, without upwind progress, as in Fig. 1c. The narrowing was due mainly to a reduction of flight speed rather than time interval between track reversals, and it persisted for at least 2 s in clean air after emergence from the pheromone corridor. As a result of this persistent, pheromone-induced narrowing the moths' movements became concentrated around the free border of the pheromone corridor and often crossed it in both directions (Figs 1a-c, 2). Thus there were many instances of turning back into the pheromone corridor after leaving it, but there were also many cases of two or more consecutive track reversals entirely inside the pheromone corridor (Figs 1a, 2). This contradicts the above theory that track reversal is a response to losing the scent. There were a total of 224 cases of moths moving across the inside of the pheromone corridor towards its free border with the clean air, but then turning back well before reaching the border. Furthermore the 26 moths engulfed in the ubiquitous pheromone cloud already mentioned made an average of 27 (3-59) consecutive track reversals each, all without any pheromone decrease.

We conclude that persistent upwind flight requires decreases as well as increases of the pheromone stimulus and that the programmed switching of the flight track between left and right of the wind-line, seen in zig-zagging and casting flight, is not a response to loss of pheromone. It is initiated by pheromone, and then modulated by pheromone changes, the amplitude of these cross-wind movements changing inversely with the strength of the pheromone stimulus. This would provide a simpler guidance system than those previously proposed.

We thank Dr P. Gruys for the regular supply of moth pupae, Dr S. Voerman for the synthetic pheromone and Mr J. G. Ions for technical support.

Received 18 August; accepted 30 October 1980.

1. Farkas, S. R. & Shorey, H. H. in *Pheromones* (ed. Birch, M. C.) 81-95 (North-Holland, Amsterdam, 1974).
2. Kennedy, J. S. & Marsh, D. *Science* **184**, 999-1001 (1974).
3. Kennedy, J. S. in *Chemical Control of Insect Behaviour: Theory and Application* (eds Shorey, H. H. & McKelvey, J. J.) 67-91 (Wiley, New York, 1977).
4. Marsh, D., Kennedy, J. S. & Ludlow, A. R. *Physiol. Ent.* **3**, 221-240 (1978).
5. Cardé, R. T. & Hagaman, T. E. *Envir. Ent.* **8**, 475-484 (1979).
6. Farkas, R., Shorey, H. H. & Gaston, L. K. *Ann. ent. Soc. Am.* **67**, 633-638 (1974).

## Environmentally dependent sensitive periods for avian vocal learning

Donald E. Kroodsma\* & Roberta Pickert

Rockefeller University Field Research Center, Millbrook, New York 12545

**Experience during brief periods of development can exert a profound influence on later life<sup>1</sup>. Among songbirds, experimental evidence for enhanced vocal learning during a relatively brief period early in life is well documented<sup>2,3</sup>. The timing of vocal learning with respect to dispersal is fundamental to our understanding of many population processes, yet the significance of the sensitive period remains unclear. We report here that in our study of the marsh wren (*Cistothorus palustris*), a North American songbird, we found that the sensitive period for song learning is not rigidly programmed with respect to dispersal and/or migration; two environmental factors, the photoperiod and the amount of adult song heard during the hatching year, influence the nature of the sensitive period during the hatching year, the ability to learn further the next spring, and the relative dates at which young males develop their adult songs.**

In our Hudson River marsh, nestling wrens hatch from mid-June to late August. Young hatched early in the year hear many adult songs and experience long days through June and July, and two previous laboratory experiments had indicated that song learning in these conditions seemed restricted to the first 60-80 days of life<sup>4</sup>. Young hatched late in the year, however, hear few if any adult songs<sup>5</sup> and experience relatively short days during the first couple of months. If these late-hatched young are to sing and breed the next year, their learning period must also be delayed until the following spring.

To test the possible effects of the photoperiod and exposure to song on the timing of the sensitive period, during early July we collected 18 nestling males from our Hudson River marsh at 41° north latitude. These were placed in sound isolation chambers; 10 males (hereafter called June males) were placed on a photoperiod simulating an early June hatching, whereas the remaining 8 males (August males) were on a photoperiod simulating an early August hatching. Thus, mean ages for the two groups were the same, and subsequent changes in daylength for each photoperiod group matched that of the home latitude. Each photoperiod group was further subdivided into three experience treatments: from roughly days 20 to 100 (Fig. 1), some males were tutored with two different song types every 5 days (a total of 32 song types; three June and two August males), some with one song type every 5 days (16 song types, four June and four August males), and some heard no songs during their hatching year (three June and two August males). During development of their adult songs the next spring all 18 males were exposed daily to 12 additional song types.

The physiological effects of the two photoperiod treatments were substantial (Fig. 1). Median ages for onset and termination of moult in the August males were 45 and 71 days compared with 62.5 and 95 days for the June males. Early morning practice singing (subsinging) also revealed that the autumn period of

\* Present address: Department of Zoology, University of Massachusetts, Amherst, Massachusetts 01003.



subsong was sharply curtailed in the August males; thus, between days 70 and 140, 72-min recordings from each male revealed subsong for a median period of only 11 min for August males but 54 min for June males. The quality of this subsong during the autumn period differed substantially between groups: the August males never passed a very rudimentary rambling characteristic of the very earliest stages of song development, but many of the June males developed more advanced and stable songs. Finally, the 'migratory restlessness' of the August males began and ended much earlier than that of the June males.

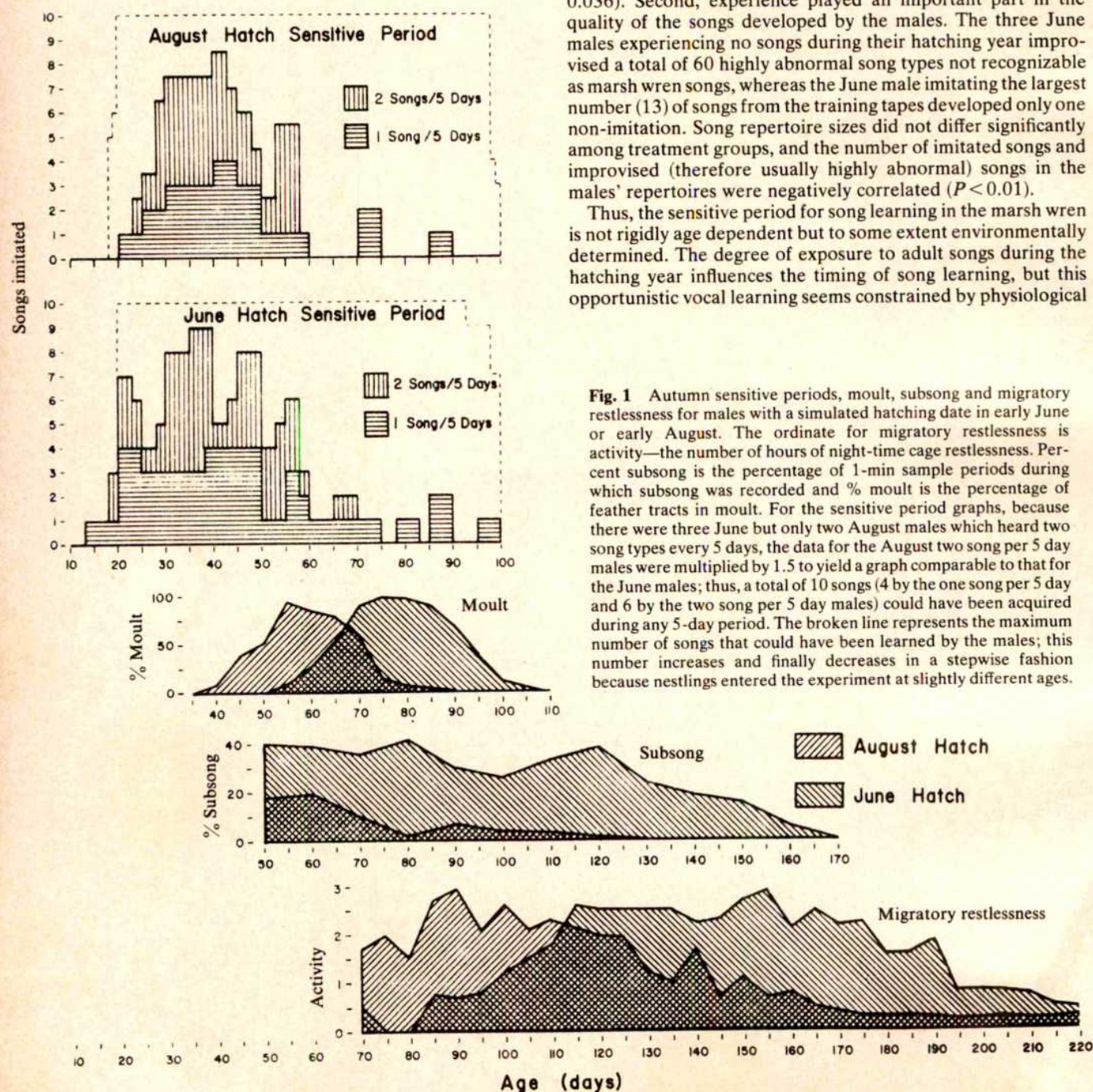
Despite the photoperiodic effects on moult, subsong and migratory activity, the sensitive periods for vocal learning during the autumn did not differ significantly between the two groups; June males seemed to learn<sup>4</sup> more songs and learn them at a later age than August males ( $P=0.1$  in both cases; 1-tailed Mann-Whitney  $U$ -test). August males acquired appreciable repertoire sizes in daylengths when songs in the wild would not normally be available to them. There was a significant difference the next spring, however, as four of the eight August males

imitated songs from the spring training tapes, whereas none of the 10 June males did; the probability of all four of the spring imitators being August males by chance alone is only 0.023.

Those four August males which learned spring songs included two males with no autumn tutoring and two males hearing only one song every 5 days during autumn. The spring learners tended to be the August males which had acquired the fewest imitations during their hatching year ( $P=0.06$ ). In addition, in both photoperiod treatment groups, those males experiencing no songs during their hatching year were the last to develop their final songs the next spring ( $P=0.018$  and  $0.05$  for June and August males, respectively), indicating that lack of exposure to songs can actually delay song development.

Experience with tutor songs during the autumn affected two other features of vocal learning; first, the autumn sensitive period was extended in males hearing fewer songs, as males hearing only one song every 5 days acquired their autumn imitations at a slower rate than the males hearing two songs every 5 days. By day 60, there was a significant difference in the fraction of the final repertoire which had been learned ( $P=0.036$ ). Second, experience played an important part in the quality of the songs developed by the males. The three June males experiencing no songs during their hatching year improvised a total of 60 highly abnormal song types not recognizable as marsh wren songs, whereas the June male imitating the largest number (13) of songs from the training tapes developed only one non-imitation. Song repertoire sizes did not differ significantly among treatment groups, and the number of imitated songs and improvised (therefore usually highly abnormal) songs in the males' repertoires were negatively correlated ( $P<0.01$ ).

Thus, the sensitive period for song learning in the marsh wren is not rigidly age dependent but to some extent environmentally determined. The degree of exposure to adult songs during the hatching year influences the timing of song learning, but this opportunistic vocal learning seems constrained by physiological



**Fig. 1** Autumn sensitive periods, moult, subsong and migratory restlessness for males with a simulated hatching date in early June or early August. The ordinate for migratory restlessness is activity—the number of hours of night-time cage restlessness. Percent subsong is the percentage of 1-min sample periods during which subsong was recorded and % moult is the percentage of feather tracts in moult. For the sensitive period graphs, because there were three June but only two August males which heard two song types every 5 days, the data for the August two song per 5 day males were multiplied by 1.5 to yield a graph comparable to that for the June males; thus, a total of 10 songs (4 by the one song per 5 day and 6 by the two song per 5 day males) could have been acquired during any 5-day period. The broken line represents the maximum number of songs that could have been learned by the males; this number increases and finally decreases in a stepwise fashion because nestlings entered the experiment at slightly different ages.



consequences of the photoperiod; irrespective of early song treatment, only males which were raised under daylengths simulating a late season (August) hatching learned songs the next spring. Nottebohm<sup>6</sup> may have simulated this late season effect to an extreme degree when he castrated a young chaffinch (*Fringilla coelebs*) and delayed the sensitive period for song learning until administration of exogenous testosterone. Thus, in late hatching males low levels of testosterone and/or reduced singing, controlled by the photoperiod, are undoubtedly important factors in delaying the sensitive period.

Among songbird populations, late-hatched young necessarily hear fewer adult songs during the hatching year<sup>5</sup> and often disperse further to the first breeding territory than the early hatched young<sup>7</sup>. A sensitive period which is in part environmentally determined will allow the dispersing juvenile some flexibility in when and where it learns a local song dialect and establishes its territory. Marsh wren juveniles can disperse over considerable distances<sup>8</sup>, and the timing of vocal learning has undoubtedly co-evolved not only with juvenile dispersal strategies but also with adult site-fidelity and habitat stability, large song repertoires, the highly complex male-male vocal interactions<sup>9,10</sup> and other life-history parameters of marsh wren breeding populations. These parameters vary between populations, both within and among species<sup>11,12</sup>, and will, through natural selection, influence the nature of the sensitive period for song learning.

This work was supported by NSF grants BNS 76-07704A02 and BNS 7802753. We thank P. Marler, F. Nottebohm and K. Yasukawa for helpful comments on the manuscript.

Received 28 January; accepted 24 September 1980.

1. Bateson, P. *Anim. Behav.* **27**, 470-486 (1979).
2. Marler, P. *J. comp. physiol. Psychol.* **71**, 1-25 (1975).
3. Thorpe, W. H. *Ibis* **100**, 535-570 (1958).
4. Kroodsma, D. E. in *Ontogeny of Behavior* (eds Burghardt, G. & Bekoff, M.) 215-230 (Garland, New York, 1978).
5. Welter, W. A. *Wilson Bull.* **47**, 3-34 (1935).
6. Nottebohm, F. *Ibis* **111**, 386-387 (1969).
7. Dhondt, A. A. & Huble, J. *Bird Study* **15**, 127-134 (1968).
8. Verner, J. *Bird-Banding* **42**, 92-98 (1971).
9. Verner, J. *Living Bird* **14**, 263-300 (1975).
10. Kroodsma, D. E. *Auk* **96**, 506-515 (1979).
11. Göttinger, H. R. *J. Orn.* **115**, 321-337 (1974).
12. Kroodsma, D. E. & Verner, J. *Auk* **95**, 703-716 (1978).

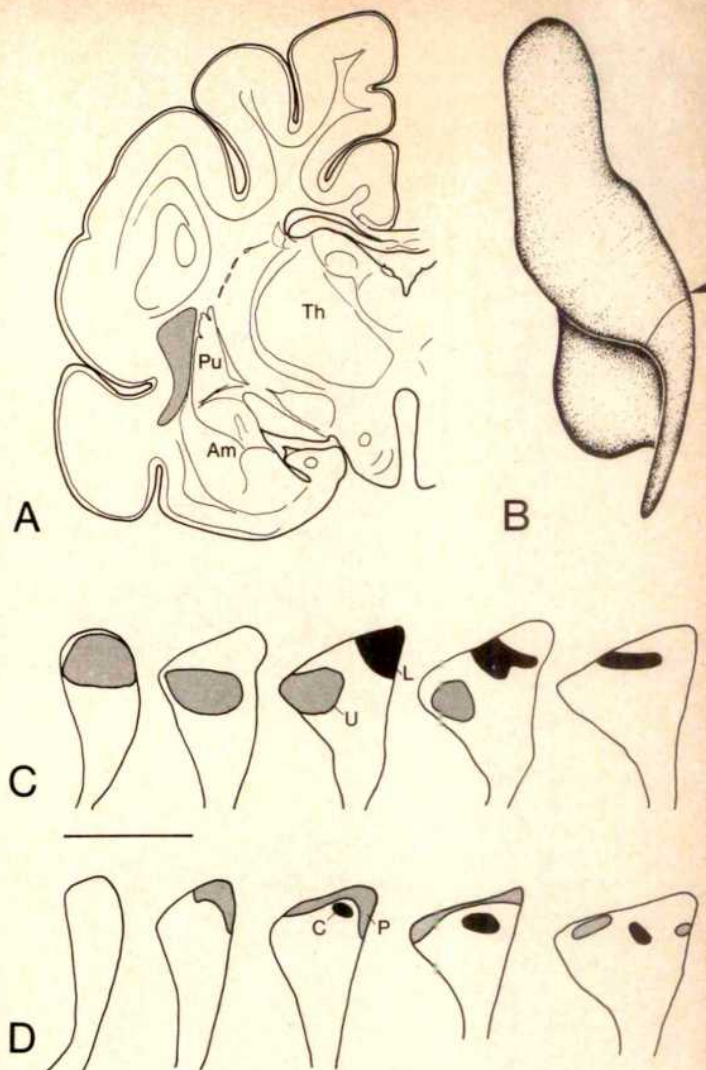
## Sensory maps in the claustrum of the cat

C. R. Olson & A. M. Graybiel

Department of Psychology and Brain Science, Massachusetts Institute of Technology, Cambridge, Massachusetts 02139

The claustrum is a telencephalic cell group (Fig. 1A, B) possessing widespread reciprocal connections with the neocortex<sup>1-5</sup>. In this regard, it bears a unique and striking resemblance to the thalamus. We have now examined the anatomical ordering of pathways linking the claustrum with sensory areas of the cat neocortex and, in parallel electrophysiological experiments, have studied the functional organization of claustral sensory zones so identified. Our findings indicate that there are discrete visual and somatosensory subdivisions in the claustrum interconnected with the corresponding primary sensory areas of the neocortex and that the respective zones contain orderly retinotopic and somatotopic maps. A third claustral region receiving fibre projections from the auditory cortex in or near area Ep was found to contain neurones responsive to auditory stimulation. We conclude that loops connecting sensory areas of the neocortex with satellite zones in the claustrum contribute to the early processing of exteroceptive information by the forebrain.

Areas 17, 18 and 19 of visual cortex are known to have overlapping fibre connections with a small dorsocaudal sector of the claustrum<sup>6</sup> and the pathway from areas 17 has a rostrocaudal topography<sup>5</sup>. To analyse the claustral origins and terminations of these visual pathways in detail, we carried out neuroanatomical experiments with the tracers horseradish peroxidase<sup>7</sup>



**Fig. 1** A, Representative frontal section through left hemisphere ~2 mm ahead of the caudal tip of the claustrum. The claustrum is set off by cross-hatching. Am: amygdala. Pu: putamen. Th: thalamus. B, Three-dimensional reconstruction of left claustrum as viewed from a point above, behind and lateral to the structure. Total rostrocaudal extent is ~12 mm. Arrow indicates transverse level of section shown in A. C, D, Patterns of tracer labelling in the claustrum elicited by injections of HRP and NY in parts of area 17 representing vertically separated (U = upper, L = lower) and horizontally separated (C = central, P = peripheral) areas in the visual field. Transverse sections are shown at 0.5-mm intervals beginning 0.75 mm ahead of caudal tip (lateral is to the left). Scale bar, 2 mm. In each cat, HRP (25% solution in saline, 0.2  $\mu$ l) and NY (10% suspension in saline, 0.2  $\mu$ l) were injected into separate parts of area 17, with some encroachment into retinotopically overlapping parts of area 18. The brains were fixed by perfusion with 10% formalin, 0.25% glutaraldehyde and 3% sucrose in 0.1 M phosphate buffer and cut at 50  $\mu$ m. Serial sections were processed for HRP by the TMB method<sup>7</sup>. Retrograde and anterograde HRP-labelling was charted under dark- and light-field illumination and nuclei labelled with NY were identified by intense fluorescence exhibited under 360 nm illumination. The part of the area 17 contralateral visual-field map covered by each injection was estimated from the distribution of label in the lateral geniculate body as follows<sup>17</sup>: C, Dark stipple: HRP: vertical -15° to -40°; horizontal 0° to 30°. Light stipple: NY: vertical +5° to 0°; horizontal 0° to 10°. D, Dark stipple: HRP: vertical -5° to 15°; horizontal 0° to 10°. Light stipple: vertical -5° to -20°; horizontal 30° to 60°.

(HRP) and nuclear yellow<sup>8</sup> (NY), and with isotopically labelled amino acids<sup>9</sup>. In 11 cats, distinguishable tracers were deposited in separate cortical sites under electrophysiological guidance. This approach allowed us, in single animals, to compare patterns of claustral uptake elicited by injections in retinotopically identical parts of two areas or in retinotopically distinct parts of the same area. The findings suggest that projections to and from areas 17 and 18 are organized retinotopically and in register, with the upper-to-lower axis of the visual field represented caudorostrally in the claustrum and the central-to-peripheral axis



represented ventrodorsally (Fig. 1C, D). The same pattern is observed in cases (not illustrated) of injections involving area 19. The ventral core of the claustrum, related to the midline of the visual field, is exceptional in having connections with visual cortical areas in both hemispheres (Fig. 2D).

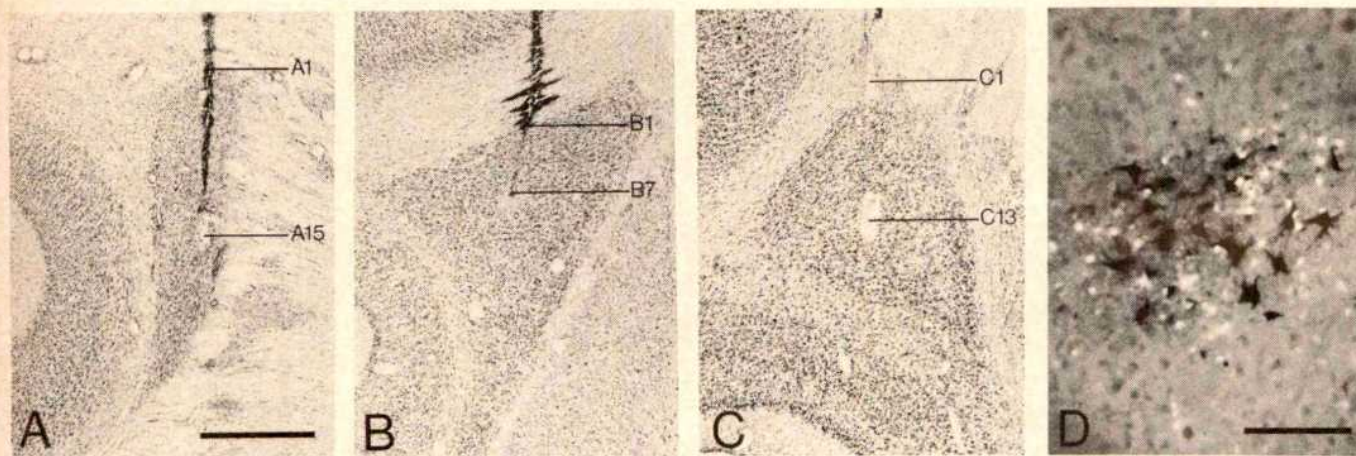
Guided by these anatomical findings, we performed microelectrode-recording experiments in the caudal claustrum of eight cats. Our results demonstrate the existence of a circumscript zone of visually responsive cells closely co-extensive with the region delineated anatomically. Units and unit clusters were exclusively visual, responded best to moving bars and spots and had receptive fields ranging in area from a few degrees square to a few hundred degrees square. Most cells could be driven through either eye and some seemed to be broadly tuned for bar orientation or axis of motion. Responses were weaker and more variable than in area 17 of the same preparation. There was clear evidence for detailed retinotopy in this zone. As shown in Figs 2A, B and 3A, B, receptive fields moved downward systematically as the electrode was moved rostrally and towards the midline as the electrode was advanced ventrally.

To test the generality of the finding of topographic sensory mapping in the claustrum, we studied the slightly more rostral claustral region interconnected with primary somatosensory cortex, SI<sup>10</sup>. Restricted deposits of tracers placed under electrophysiological guidance in parts of SI representing caudal and rostral body parts labelled, respectively, dorsal and ventral sectors in this claustral zone. The pattern of connections was analysed only with respect to the longitudinal body axis because the circumferential axes of the body are not simply represented

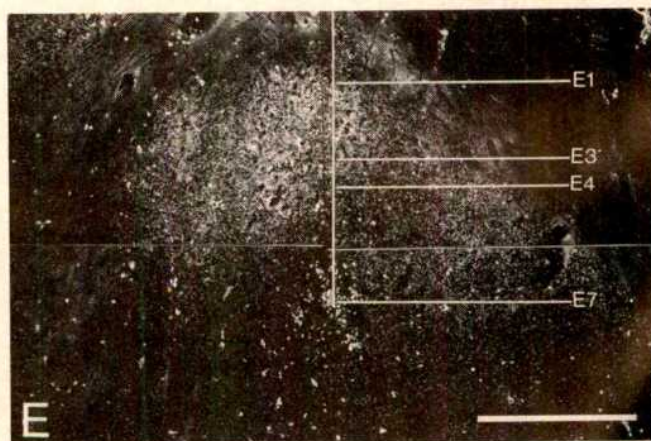
in SI<sup>10</sup>. In electrophysiological experiments, we encountered, throughout this region, neurones with large somatosensory receptive fields occupying parts of the contralateral body (Fig. 3). All could be driven effectively by firm pressure or sharp taps and some also responded to light cutaneous stimulation. During downward traverses, receptive fields shifted gradually from the hindparts to the face (Figs 2C, 3C). This pattern of organization, though not noted in previous physiological studies<sup>11</sup>, is in accord with the demonstration of somatotopy based on the anatomy (Fig. 2E).

In contrast to the findings for visual and somatosensory cortex, injections of HRP confined to the primary auditory cortex have not, in our hands, consistently produced labelling in the claustrum (compare with ref. 4). However, injections encroaching on or centred in area Ep of the posterior ectosylvian gyrus, a region of known auditory affiliations<sup>12,13</sup>, have produced anterograde and retrograde labelling of a claustral zone lying beneath the somatosensory division and approximately co-extensive with it rostrocaudally. Guided by this observation, we searched for and found a region of exclusive auditory responsiveness in the claustrum. During downward passes of the electrode, this region typically was encountered within a few 100  $\mu$ m of the most ventral somatosensory activity, and was lost again within 100–200  $\mu$ m (Fig. 3, C11). Cells recorded at this depth characteristically responded to clicks or tone bursts delivered to either ear, as well as to a variety of free-field stimuli. We have not mapped the auditory zone through its full extent.

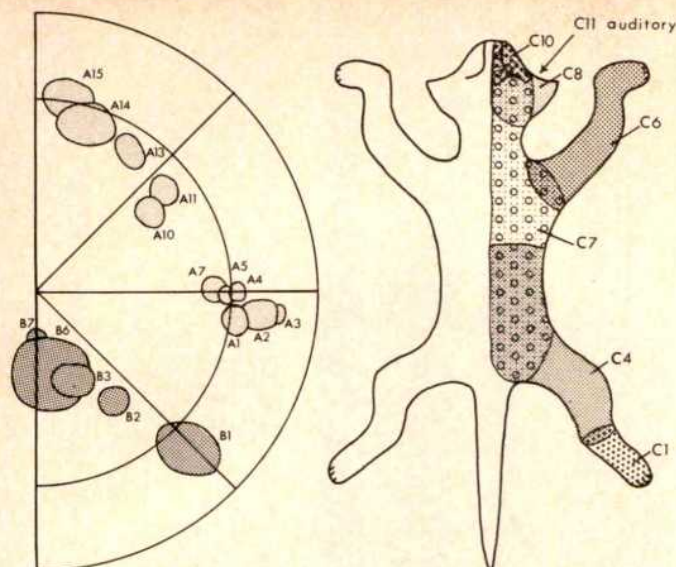
The connections of the neocortex with the claustrum are organized not only by cortical area but also by cortical layer. In



**Fig. 2** A–C, Transverse sections stained by the Nissl method illustrating vertical electrode penetrations through the claustrum. Along tracks shown in A and B, the units recorded had the visual receptive fields plotted to the left in Fig. 3. C shows, from another experiment, a more rostral track along which units were driven by somatosensory stimuli as plotted to the right in Fig. 3, except for the most ventral unit (C11), which responded to auditory stimulation. Cats were prepared for single-unit recording by standard methods<sup>18</sup> and were maintained under Flaxedil paralysis on N<sub>2</sub>O anaesthesia supplemented with barbiturates. The microelectrode was advanced in 100- $\mu$ m steps and successive recording sites were numbered sequentially beginning at the top of the claustrum. Electrolytic marking lesions (10  $\mu$ m, 10 s, tip negative) were made at A15, B7, C1 and C13. The tracks of A, B and C were placed, respectively, 0.4, 2.4 and 6.0 mm in front of the caudal tip of the claustrum. Scale bar, 1 mm. D, Photomicrograph illustrating intermingled cell populations labelled in the claustrum by HRP injected into the ipsilateral area centralis representation of areas 17 and 18 and NY injected into the homotopic locus in the contralateral hemisphere. From a 50- $\mu$ m frontal section 1.1 mm ahead of the caudal tip of the claustrum and viewed under 360 nm illumination; dark cytoplasmic reaction product indicates HRP labelling and bright nuclear fluorescence indicates NY labelling. Scale bar, 200  $\mu$ m. The most dorsal HRP-positive neurones lie 300  $\mu$ m below the dorsal border of the claustrum. E, Dark-field photomicrograph of a transverse section through the somatosensory claustrum shows the results of a combined electrophysiological-neuroanatomical experiment. As the electrode was lowered along the track marked by the vertical white line, cells with receptive fields containing the hindleg were encountered first (E1–E3), followed by cells with receptive fields restricted to more rostral body parts (E4–E7). Subsequently, HRP was injected under electrophysiological guidance into the area of primary somatosensory cortex (SI) representing the hindleg. The dorsal zone of dust-like reaction product, indicative of HRP transported along corticofugal axons, overlaps closely the stretch of the track (E1–E3) along which hindleg responses were recorded. The track was placed 5.9 mm rostral to the caudal tip of the claustrum and a marking lesion was made at the bottom of the track (E7) (note erythrocytes at the site of the lesion labelled because of their endogenous peroxidase activity). Scale bar, 0.5 mm.







**Fig. 3** Visual and somatosensory receptive fields of selected units recorded along the tracks shown in A, B and C of Fig. 2. The electrode was advanced in 100- $\mu$ m steps and recording sites were numbered consecutively in downward succession from the claustral surface. Visual receptive fields were plotted on a hemispheric screen, here shown in frontal projection with concentric circles representing 45° and 90° isodeviation lines. The pronounced upward progression of fields plotted during track A confirms anatomical evidence (not shown here) indicating that the extreme upper visual periphery is represented ventrocaudally in the claustrum, as in the cortex. The figurine map to the right illustrates the systematic caudorostral progression of receptive fields observed as units recorded at successively deeper sites along track C in the somatosensory claustrum. For clarity, only selected representative somatic fields are shown here. The unit at C11, recorded just below the region of somatic responsiveness, was excited by clicks or tone bursts delivered to either ear.

tree shrew area 17, the claustral projection arises in neurones of layer VI whereas the return pathway terminates in a number of layers including I and IV<sup>5</sup>. We have confirmed and extended these results in the cat, first, by injecting anterograde and retrograde tracers into the caudal claustrum and observing patterns of transported label in area 17, and, second, by comparing the cell populations in area 17 projecting, respectively, to the claustrum and to the lateral geniculate body (LGd). The anterograde results suggest that in the cat the claustrum projects densely to layer I, but there was also heavy labelling of deeper layers, including IV. The retrograde results indicate that the projection to the claustrum arises from cells in layer VI. These cells seem to be distinct from those projecting to the LGd<sup>14</sup>, for in two cases intermingled but separate layer-VI populations were labelled following placement of distinguishable retrograde tracers (NY and HRP) in retinotopically matched parts of the claustrum and the LGd.

The claustrum bears a unique resemblance to the thalamus by virtue of its extensive reciprocal connections with the neocortex. We have extended this parallel by showing that the claustrum, like the thalamus, contains discrete subdivisions that are tightly interlinked with sensory cortex and are organized topographically. However, in lacking major ascending sensory connections, the claustrum fails to share at least the relay functions of the thalamus and seems, in its sensory afference, to be a satellite of the neocortex. This is a rare pattern, a second instance being the almost exclusive dependence of the parabigeminal nucleus on the superior colliculus<sup>15</sup>. Like the sensory divisions of the claustrum, the parabigeminal nucleus is a small cell group receiving a topographic projection from a subset of cells in a much larger structure to which it returns a topographically organized projection<sup>15,16</sup>. Why either cell group should exist as a satellite and not as a set of interneurons within the parent structure is an intriguing question to which no satisfactory answer has been obtained.

We thank Drs H. G. J. M. Kuypers, O. Dann and J. Loewe for fluorescent tracers used in this study. The work was supported

by NIH R01EY02866-02, NIH EY05316-01 and NSF 5T32GM07045.

**Note added in proof:** Since submission of this paper, the existence of retinotopic organization in the claustrum has been reported independently<sup>19</sup>.

Received 14 July; accepted 9 October 1980.

1. Carmen, J. B., Cowan, W. M. & Powell, T. P. S. *J. Neurol. Neurosurg. Psychiat.* **27**, 46–51 (1964).
2. Narkiewicz, O. *J. comp. Neurol.* **123**, 335–356 (1964).
3. Druga, R. *Folia morph.* **14**, 391–399 (1966); **16**, 142–149 (1968).
4. Norita, M. *Arch. histol. jap.* **40**, 1–10 (1977).
5. Cary, R. G., Bear, M. F. & Diamond, I. T. *Brain Res.* **184**, 193–198 (1980).
6. Jayaraman, A. & Updyke, B. V. *Brain Res.* **178**, 107–115 (1979).
7. Mesulam, M. M. *J. Histochem. Cytochem.* **26**, 106–117 (1978).
8. Bentivoglio, M., Kuypers, H. G. J. M., Catsman-Berresvoets, C. E., Loewe, H. & Dann, O. *Neurosci. Lett.* **18**, 25–30.
9. Cowan, W. M., Gottlieb, D. I., Hendrickson, A. E., Price, J. L. & Woolsey, T. A. *Brain Res.* **37**, 21–51 (1972).
10. Dykes, R. W. *Prog. Neurobiol.* **10**, 33–83 (1978).
11. Spector, I., Hassmannova, J. & Albe-Fessard, D. *Brain Res.* **66**, 39–65 (1974).
12. Rose, J. E. & Woolsey, C. N. *J. comp. Neurol.* **91**, 441–466 (1949).
13. Winer, J. A., Diamond, I. T. & Raczkowski, D. *J. comp. Neurol.* **176**, 387–418 (1977).
14. Gilbert, C. D. & Kelly, J. P. *J. comp. Neurol.* **163**, 81–106 (1975).
15. Graybiel, A. M. *Brain Res.* **145**, 365–374 (1978).
16. Sherk, H. *J. Neurophysiol.* **42**, 1656–1668 (1979).
17. Sanderson, K. J. *J. comp. Neurol.* **143**, 101–118 (1971).
18. Olson, C. R. & Freeman, R. D. *J. Neurophysiol.* **41**, 65–74 (1978).
19. Sherk, H. & LeVay, S. *Soc. Neurosci. Abstr.* **6**, 482 (1980).

## Dorsal column input into the reticular formation

N. A. Salibi\*, N. E. Saadé†, N. R. Banna† & S. J. Jabbur\*‡

\* Department of Physiology, American University of Beirut, Beirut, Lebanon

† Comparative Physiology Laboratory, Faculty of Sciences, Lebanese University, Hadath-Beirut, Lebanon

Somatic sensory information, such as touch, pressure, pain and body position, is conveyed to the mammalian thalamus and ultimately the cerebral cortex along three major ascending pathways in the spinal cord: (1) the dorsal column medial lemniscal (DCML) system, (2) the ventral column (VC) system, including the 'neospinothalamic', 'palaeospinothalamic' and spinothalamic tracts, and (3) the spino-cervico-lemniscal (SCL) system<sup>1,2</sup>. The phylogenetically recent DCML system has been traditionally viewed as an exclusive and homogeneous one-to-one relay of somatic sensory information to the thalamic ventralis posterolateralis nucleus. The emerging evidence, however, shows the gracile and cuneate nuclei as non-homogeneous structures which contain neurones that are subject to many kinds of central and peripheral influences, and which include neurones that do not project to the thalamus<sup>3</sup>. The relation of the ascending spinal pathways to the brain stem reticular formation (RF) is of particular interest in view of the numerous important functions subserved by this region. The spinal input into the RF is generally considered to reach it exclusively through the VC<sup>4</sup>. In view of their intraspinal connections<sup>5–8</sup>, it is difficult to separate and interact the three ascending spinal pathways. We now demonstrate a DCML input into the gigantocellular nucleus (Rgc) of the medial medullary RF in cats, and show inhibitory as well as excitatory interactions between DCML and VC tracts in RF cells. We used a combination of careful spinal surgical lesions aimed at disconnecting the DCML from the other afferent systems and of localized spinal and peripheral stimulations. Persistence of the response of Rgc neurones to DCML stimulation in decerebrate and decerebellate cats rules out the possibility of descending activation via a feedback loop from the cerebral and cerebellar cortices. In view of the possible involvement of Rgc in processing nociceptive input, these findings are of interest to our understanding of the DCML system in somatosensory function and, in particular, pain mechanisms.

‡ To whom correspondence should be addressed.



Experiments were carried out on 17 adult cats, anaesthetized with 30 mg per kg pentobarbitone sodium (9 cats) or 70 mg per kg chloralose (3 cats), or decerebrated just rostral to the superior colliculus following induction of anaesthesia with ether (5 cats). All animals were subsequently paralysed with gallamine triethiodide and artificially respired. Body temperature, blood pressure and end-tidal  $\text{CO}_2$  were maintained within physiological levels. Laminectomy was performed from  $\text{C}_1$  to  $\text{C}_5$  followed by suboccipital craniectomy and bilateral exposure of the sensorimotor cortex. A coaxial electrode was placed stereotactically in the medial lemniscus at coordinates A 5, L 4.5, V 1.8.

In all cats, the cerebellar connections to the brain stem were interrupted and one of two types of spinal lesion was performed. In the first, the 'dorsal-cut' (d-cut) preparation, the dorsal half of the spinal cord was completely severed at the level of  $\text{C}_1$  or  $\text{C}_3$  (in the latter case, the upper three cervical dorsal roots were also cut) or at both levels. The completeness of the cut was tested electrophysiologically. This preparation eliminates DCML and SCL inputs but allows VC inputs to reach RF following peripheral cutaneous stimuli. In the second, the 'ventral-cut' (v-cut) preparation, the entire spinal cord, except for dorsal columns on both sides, was severed at  $\text{C}_1$  or  $\text{C}_3$ . This preparation leaves the dorsal columns (DC) as the sole connection between the periphery and the brain. At the end of each experiment, the cat was perfused with a 10% formaldehyde solution through the aorta. The whole brain (in non-decerebrate cats) and spinal cord were removed and Nissl-stained. All the lesions were later verified for completeness and accuracy. Experiments where histological lesions were imperfect were discarded.

Electrical stimuli were delivered at the rate 0.5–1 Hz to the DC or ventrolateral tracts of VC through stainless steel bipolar electrodes with 1-mm tip separation and to the central footpad of each limb through needle electrodes. Stimuli consisted of single pulses of 0.05–0.1 ms duration. Occasionally, a train of three pulses was delivered to the VC or the paws. The current pulse strength (peak intensities of 0.5–2.5 mA) and the special precautions to insure that the spinal cord stimuli were localized to the stimulated tracts are described elsewhere<sup>9</sup>. Peripheral stimuli would be expected to be carried into the brain along VC tracts in d-cut cats and along DC tracts in v-cut cats.

We studied 160 Rgc units through microelectrodes at coordinates P 3 to 7, L 1.5 and V –7 to –11. Microelectrode recording sites were marked by the electrocoagulation technique. Most (154) of the units were initially isolated after a DC searching stimulus and 6 units after VC stimulation. DCML-activated cells were widely distributed in Rgc and their occurrence correlated

well with the amplitude of the gross potential evoked by DC stimulation. These cells responded to contralateral DC (CDC), ipsilateral medial lemniscal and, most interestingly, to peripheral stimulation in v-cut cats (Fig. 1). The CDC activation pattern consisted of one or more spikes per discharge. Spontaneous activity, when present, was also modified. CDC stimulation (just above  $\text{C}_1$  cut) evoked a response which ranged in latency between 2 and 14 ms. The shorter latency units showed a frequency following up to 50 Hz (but usually less than 25 Hz). Medial lemniscal stimulation was tested in 91 units in non-decerebrate cats, 66 of which responded, usually with latencies and frequency following characteristics similar to those evoked by CDC stimulation.

Of 82 units studied in v-cut cats, most (79 units) responded to DC stimulation and 53 responded to electrical stimulation of the footpads (Fig. 1c, d). The natural receptive fields could be determined in 20 of these cells (18 responded to touch, 2 to hair stimulation). Such fields were usually well defined and circumscribed.

Of the total 160 units studied, 110 were activated through the VC following stimulation of either the VC directly along the ventrolateral tracts or the peripheral paws in d-cut cats. In the latter, unit responses evoked by direct VC stimulation were similar to those evoked by peripheral stimulation, except for slightly shorter latencies. These units were activated by electrical stimuli to all four paws and, in some instances, by acoustic stimuli as well. Some of these units were stimulated or inhibited by noxious pinch at several peripheral sites. Thus, compared with units responding to CDC stimulation in v-cut cats, these units showed more diffuse receptive fields and somewhat longer initial spike latencies.

Interactions between DC and VC inputs on Rgc neurones were studied using conditioning-testing techniques in 79 units discharging to both DC and VC inputs and 32 units discharging to one input only. All (except two) units demonstrated an interaction between the two inputs which took the form of inhibition (48 units) or initial facilitation for 30–40 ms followed by inhibition (61 units). Inhibition lasted up to 200–600 ms.

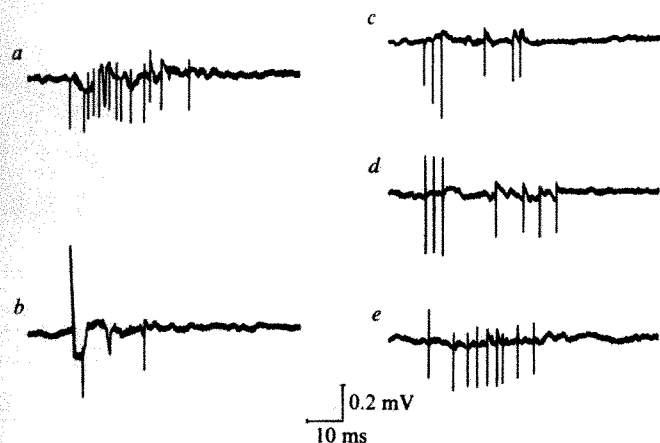
These results strongly support the existence of an input from the DCML system into the RF which also interacts with the well known VC inputs. We cannot explain the failure of recent physiological studies<sup>10–12</sup> to observe these connections. The neuroanatomical substrate for this DC–RF route also remains unclear except perhaps for the brief description of sparse projections from the DC nuclei into the RF with silver degeneration stains<sup>13–15</sup> or in Golgi-stained serial sections<sup>16</sup>. Similar sparse projections have been described from the dorsal roots (presumably through the DC) to the RF<sup>17</sup>. It is difficult to ascertain whether the dense DC nuclear projection to the inferior olive<sup>18</sup>, which in turn connects reciprocally to the RF<sup>19</sup>, could mediate the DC influences on the RF described here. However, RF projections into DC nuclei have recently been described<sup>20–23</sup>.

The above DC–RF connection could be part of a 'palaeolemniscal' subsystem of the DCML system recently shown to originate from distinct parts of the DC nuclei, to possess a significant number of post-primary DC fibres, and to be characterized by a more diffuse arrangement of neurones with widespread efferents into thalamic (other than VPL) and brain stem areas<sup>24</sup>. The DC–Rgc route and the DC–VC interactions on Rgc neurones described here support the hypothesis, reviewed by Dennis and Melzack<sup>25</sup>, implicating the palaeolemniscal component of the DCML system in pain mechanisms.

This investigation was supported by two grants from the Lebanese National Research Council. We thank Professor P. D. Wall for reading and commenting on the manuscript, and M. Shakarji for technical assistance.

Received 19 June; accepted 9 September 1980.

1. Ruch, T. C. in *Physiology and Biophysics. The Brain and Neural Function* (eds Ruch, T. C. & Patton, H. D.) 201–271 (Saunders, Philadelphia, 1979).
2. Wall, P. D. & Dubner, R. A. *Rev. Physiol.* **34**, 315–335 (1972).



**Fig. 1** Sample records showing the responses of an Rgc neurone in a v-cut preparation to electrical stimulation of the following sites. *a*, Contralateral dorsal column; *b*, ipsilateral medial lemniscus; *c*, contralateral forepaw; *d*, ipsilateral forepaw; *e*, ipsilateral ventrolateral column. Single pulses were used in *a*, *b* and *e*, and a train of three pulses at 300 Hz was used in *c* and *d*.



3. Norton, A. C. & Kruger, L. *The Dorsal Column System of the Spinal Cord. Its Anatomy, Physiology, Phylogeny and Sensory Function* (Brain Information Service, Los Angeles, 1973).
4. Mehler, W. R. *Ann. N.Y. Acad. Sci.* **167**, 424-468 (1969).
5. Brown, A. G. & Martin, H. F. *J. Physiol., Lond.* **224**, 34P-35P (1972).
6. Dart, A. M. & Gordon, G. *Brain Res.* **58**, 61-68 (1973).
7. Gordon, G. & Grant, G. *Acta physiol. scand.* **84**, 30A-31A (1972).
8. Foreman, R. D., Beall, J. E., Applebaum, A. E., Coulter, J. D. & Willis, W. D. *J. Neurophysiol.* **39**, 534-546 (1976).
9. Jabbur, S. J., Baker, M. A. & Towe, A. L. *Expl Neurol.* **36**, 213-238 (1972).
10. Casey, K. L. *Expl Neurol.* **25**, 35-56 (1969).
11. Pearl, G. S. & Anderson, K. V. *Expl Neurol.* **57**, 307-321 (1977).
12. Schetter, A. G. & Atkinson, J. R. *Expl Neurol.* **54**, 185-198 (1977).
13. Hand, P. & Liu, C. N. *Anat. Rec.* **154**, 353-354 (1966).
14. Hazlett, J. C., Dom, R. & Martin, G. F. *J. comp. Neurol.* **146**, 95-118 (1972).
15. Jane, J. A. & Schroeder, D. M. *Expl Neurol.* **30**, 1-17 (1971); Schroeder, D. M. & Jane, J. A. *J. comp. Neurol.* **142**, 309-350 (1971).
16. Valverde, F. *J. comp. Neurol.* **116**, 71-99 (1961); *Anat. Rec.* **151**, 496 (1965); *Z. Zellforsch. mikrosk. Anat.* **71**, 297-363 (1966).
17. Rustioni, A. & Macchi, G. *J. comp. Neurol.* **134**, 113-126 (1968).
18. Berkley, K. J. & Worden, I. G. *J. comp. Neurol.* **163**, 285-304 (1975).
19. Crosby, E. C., Humphrey, T. & Lauer, E. W. *Correlative Anatomy of the Nervous System* (Macmillan, New York, 1962).
20. Blomqvist, A. & Westman, J. *Brain Res.* **111**, 407-410 (1976).
21. Odutola, A. B. *Expl Neurol.* **54**, 54-59 (1977).
22. Sotgiu, M. L. & Margnelli, M. *Brain Res.* **103**, 443-453 (1976).
23. Sotgiu, M. L. & Marini, G. *Brain Res.* **128**, 341-345 (1977).
24. Hand, P. J. & Van Winkle, T. *J. comp. Neurol.* **171**, 83-110 (1977).
25. Dennis, S. G. & Melzack, R. *Pain* **4**, 97-132 (1977).

## Adult tissues contain chemo-attractants for vascular endothelial cells

Bert M. Glaser & Patricia A. D'Amore

Wilmer Ophthalmologic Institute, The Johns Hopkins University School of Medicine and The Johns Hopkins Hospital, Baltimore, Maryland 21205

Heikki Seppa, Silja Seppa & Elliott Schiffmann

Laboratory of Development Biology and Anomalies, National Institute of Dental Research, National Institutes of Health, Bethesda, Maryland 20205

New blood vessel formation, or angiogenesis, occurs through the migration of endothelial cells in elongated sprouts. These sprouts are directed preferentially towards the inciting stimulus<sup>1-3</sup>. Several studies have demonstrated that certain chemical substances can stimulate angiogenesis<sup>4-7</sup>. In these cases, endothelial cell migration towards the chemical stimulus may be due to a preferential migration of cells from lower to higher concentrations of the mediator. Such concentration gradient-dependent cellular migration has been termed chemotaxis<sup>8</sup>. Using a modification of the Boyden chamber technique<sup>9</sup> to measure chemotaxis *in vitro*, we have now found that extracts of various adult bovine tissues have potent chemotactic activity for vascular endothelial cells. Adult bovine serum lacks similar chemotactic activity.

The blind well Boyden chamber<sup>9</sup>, commonly used for studying chemotaxis, consists of two wells (an upper well and a lower well) separated by a porous membrane. A known concentration of the chemoattractant to be tested is placed in the lower well. The upper well receives a predetermined number of cells and, in some experiments, a known concentration of chemoattractant. The cells we used were fetal bovine aortic endothelial cells, prepared as described previously<sup>7,10</sup>. The cells attach to the upper surface of the membrane, migrate through the pores and then attach to the lower surface of the membrane (Fig. 1). We have found that, unlike some other cell types<sup>11,12</sup>, less than 5% of the vascular endothelial cells detach from the lower surface of the membrane during the experiment. Therefore, the number of cells found on the lower surface of the membrane accurately reflects the number of endothelial cells which have migrated through the pores. The relationship between the number of cells migrating through the porous membrane and the concentration gradient of attractant across the membrane can then be

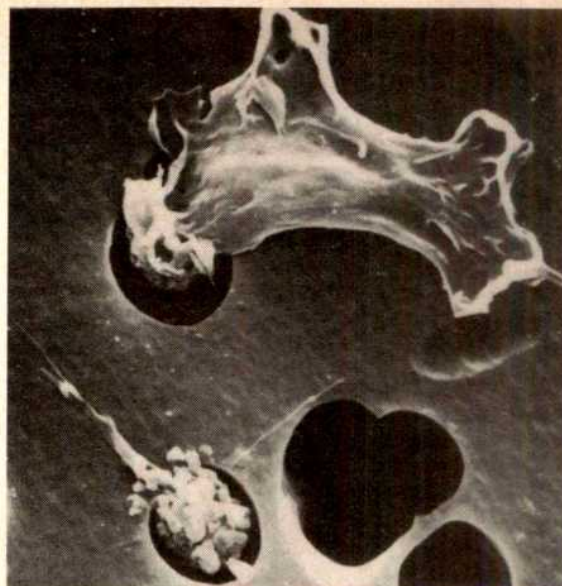


Fig. 1 Scanning electron micrograph of the lower surface of a porous membrane, showing two successive stages of endothelial cell migration through the membrane. The cell shown in the lower half of the field has extended only a slender cell process to attach to the undersurface of the membrane. The cell in the upper half of the field has extended a large pseudopod through a pore to attach to the undersurface of the membrane.  $\times 4,900$ .

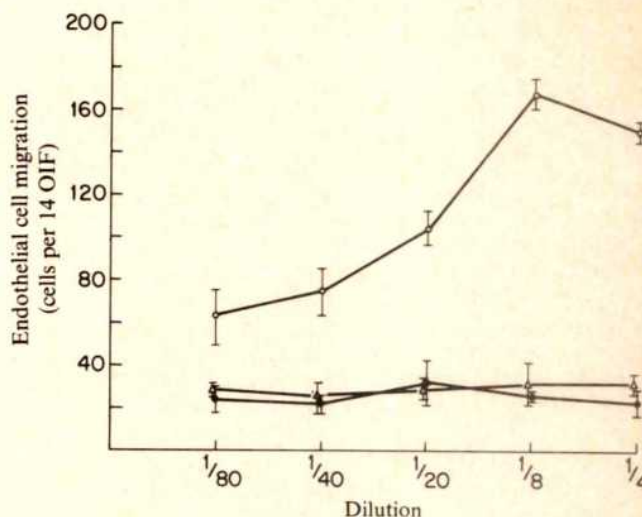


Fig. 2 Effect of bovine retinal extract on vascular endothelial cell migration. Migration is measured using blind well chambers (Neuroprobe, no. 200-312) and polyvinylpyrrolidone-free polycarbonate membranes with 5- $\mu$ m pores (Nucleopore). Retinal extract is prepared by incubating bovine retinas in BSS at room temperature for 3 h (ref. 7). The suspension is centrifuged and the supernatant used immediately or stored at  $-20^{\circ}\text{C}$  (ref. 7). The lower wells receive retinal extract (○), BSS (●) or ABS (△) (Sterile Systems) diluted in minimal essential medium with 10% fetal bovine serum (MEM/10). The upper wells receive 175,000 fetal bovine aortic endothelial cells in 0.8 ml MEM/10 without added retinal extract, salt solution or adult serum. The migration chambers are then incubated at  $37^{\circ}\text{C}$  in 5%  $\text{CO}_2$  with 85% relative humidity for 7 h. The cells on the upper surface of the membranes are then removed with a cotton swab. The cells which have migrated through the membrane on to the lower surface are fixed in a 10% neutral buffered formalin and stained with Wright's stain. Migration is quantified by counting the number of cell nuclei on the lower surface in 14 oil immersion fields (OIF). Each point represents the mean of three experiments  $\pm$  s.e.m. To measure cell attachment to the membranes, each membrane is rinsed in BSS, treated with 0.3 ml of 0.1% trypsin for 5 min, and the trypsin activity quenched by the addition of 0.7 ml MEM/10. The cell number and Trypan blue exclusion are then determined using a haemocytometer. Attachment and viability are measured at hourly intervals during the experiment.



**Table 1** Vascular endothelial cell chemotaxis induced by retinal extract

| % Retinal extract below membrane | % Retinal extract above membrane |          |          |          |
|----------------------------------|----------------------------------|----------|----------|----------|
|                                  | 0                                | 2.5      | 5        | 10       |
| 0                                | 46 (9)                           | 71 (9)   | 56 (4)   | 77 (10)  |
| 2.5                              | 107 (13)                         | 90 (6)   | 89 (5)   | 106 (15) |
| 5                                | 175 (12)                         | 157 (5)  | 124 (3)  | 140 (10) |
| 10                               | 214 (18)                         | 208 (13) | 183 (13) | 142 (13) |

The chemotactic activity of retinal extract was determined using the migration assay as described in Fig. 2 legend, except that various amounts of retinal extract are added to both upper and lower wells to produce a series of concentration gradients across the membranes. Migration is quantified by counting the number of cell nuclei on the lower surface of the membrane in 14 oil immersion fields. Each number represents the mean of three experiments ( $\pm$ s.e.m.). The values in the diagonal, where there is no gradient, show the chemokinetic effects of retinal extract.

determined, thus providing a measure of the chemotactic activity of that substance for vascular endothelial cells *in vitro*.

To investigate the stability of the concentration gradients across the membranes, various amounts of the tricarbocyanine dye indocyanine green (ICG) (maximum final concentration of  $0.5 \mu\text{g ml}^{-1}$ ) were added to the upper and lower wells of the migration chambers. (ICG binds rapidly to serum proteins, mainly albumin (95%)<sup>13</sup>.) The migration assay was then carried out as described in Fig. 2 legend. The concentration of ICG in the upper and lower wells was determined at various times by spectrophotometry. After 4 and 7 h the concentrations varied from their initial values by less than 10% and 20%, respectively. Although we cannot determine the concentration gradient of chemoattractant in the immediate area of the porous membrane, the relative stability of the concentration gradients of ICG-labelled proteins suggests that the initial gradient is a good estimate of the gradient that affects the cells.

Extracts of adult retinas from several mammalian species have been found to be potent stimulators of angiogenesis<sup>7</sup>. We therefore studied their effect on vascular endothelial cell migration to establish that vascular cells could be stimulated to migrate through the porous membranes. The addition of adult bovine retinal extract to the lower well of the migration apparatus results in a marked, dose-dependent increase in the number of endothelial cells moving through the porous membrane as compared with control wells to which balanced salt solution (BSS) is added (Fig. 2). In contrast, adult bovine serum (ABS) does not stimulate endothelial cell migration. The presence of retinal extract, BSS or ABS in the concentrations tested does not affect the rate of endothelial cell attachment or the absolute number of viable cells attaching to the porous membranes (Fig. 2 legend).

These results demonstrate that retinal extract is a potent stimulator of vascular endothelial cell migration but do not indicate whether the effects of the extract are chemotactic or chemokinetic (that is, due to chemically stimulated migration not dependent on concentration gradients). To investigate this,

**Table 2** Vascular endothelial cell chemotaxis induced by various tissue extracts

| % Extract below membrane | % Extract above membrane |         |          |         |
|--------------------------|--------------------------|---------|----------|---------|
|                          | 0                        | 2.5     | 5        | 10      |
| 0                        | 46 (10)                  | 73 (2)  | 91 (12)  | 119 (7) |
| 2.5                      | 159 (17)                 | 154 (3) | 158 (3)  | 139 (6) |
| 5                        | 226 (16)                 | 191 (5) | 153 (3)  | 139 (5) |
| 10                       | 256 (12)                 | 215 (2) | 178 (12) | 149 (8) |

The chemotactic activity of extracts of adult bovine liver, kidney, heart and skeletal muscle was determined as described in Table 1 legend. These extracts were prepared in the same manner as retinal extract (Fig. 2). The chemotactic activity of liver extract is shown above; extracts of the other tissues have similar activity.

we varied the concentration gradient of retinal extract across the membranes and noted the effect on endothelial cell migration. The results shown in Table 1 demonstrate that vascular endothelial cells *in vitro* migrate preferentially from a lower to a higher concentration of bovine retinal extract, and that the extract thus has a chemotactic effect on these cells.

Recent studies on the ability of other adult tissues to stimulate and support new blood vessel growth<sup>7,14-16</sup> have occasionally produced conflicting results. We prepared extracts of adult bovine liver, kidney, heart and skeletal muscle as previously described<sup>7</sup> and found that all have chemotactic activity for vascular endothelial cells *in vitro* (Table 2). These extracts have no effect on the adherence of endothelial cells to the membranes or on endothelial cell viability. The chemotactic activities of all tissue extracts tested are nondialysable (molecular weight cut-off 10,000-12,000), are not retained by an Amicon XM-100 filter (molecular weight cut-off 100,000) and are inactivated by boiling for 2 min.

As vascular endothelial cell migration and chemotaxis seem to be essential for angiogenesis, it is important to study these phenomena in a quantitative *in vitro* system where various parameters can be readily controlled. We have developed a simple, rapid (6-8 h), reproducible and quantitative assay of vascular endothelial cell chemotaxis *in vitro*, and have used it to demonstrate significant chemotactic activity in extracts of various adult bovine tissues. Further study of tissue-derived chemotactic activity should improve our understanding of neo-vascularization. Furthermore, it is reasonable to assume that chemotactic behaviour in endothelial cells has a crucial role in developmental events.

We thank Sandie K. Brunson for technical assistance, and Allan Fenselau and Arnall Patz for support. This work was supported by NIH grants EYO2603 and EYO3510.

Received 18 August; accepted 22 September 1980.

- Schoeff, G. I. *Virchows Arch. path. Anat. Physiol.* **337**, 97-141 (1963); *Ann. N.Y. Acad. Sci.* **116**, 789-802 (1964).
- Yamagami, I. *Jap. J. Ophthalmol.* **14**, 41-58 (1970).
- Ausprunk, D. H. & Folkman, J. *Microvascular Res.* **14**, 53-65 (1977).
- Folkman, J. *Cancer Res.* **34**, 2109-2113 (1974).
- Ben Ezra, D. *Am. J. Ophthalmol.* **86**, 455-461 (1978).
- Weiss, J. B., Brown, R. A., Kumar, S. & Phillips, P. *Br. J. Cancer* **40**, 493-496 (1979).
- Glaser, B. M., D'Amore, P. A., Michels, R. G., Patz, A. & Fenselau, A. *J. Cell Biol.* **84**, 298-304 (1980).
- Schiffmann, E. & Gallin, J. I. *Curr. Topics Cell Regulation* **15**, 203-261 (1979).
- Boyden, S. J. *exp. Med.* **115**, 453-466 (1962).
- Fenselau, A. H. & Mello, R. J. *Cancer Res.* **36**, 3269-3273 (1976).
- Keller, H. U., Borel, J. F., Wilkinson, P. C., Hess, M. W. & Bottier, J. J. *Immun. Meth.* **1**, 165-168 (1972).
- Zigmond, S. H. & Hirsch, J. G. *J. exp. Med.* **137**, 387-410 (1973).
- Fox, I. J. & Wood, E. H. *Proc. Staff Meet. Mayo Clinic* **35**, 732-744 (1960).
- Eisenstein, R., Sorgente, N., Soble, L. W., Miller, A. W. & Kuettner, K. E. *Am. J. Path.* **73**, 765-774 (1973).
- Ausprunk, D. H., Knighton, D. R. & Folkman, J. *Am. J. Path.* **79**, 597-618 (1975).
- Federman, J. L., Brown, G. C., Felberg, N. T. & Felton, S. M. *Am. J. Ophthalmol.* **89**, 231-237 (1980).

## Leukotrienes are potent constrictors of human bronchi

Sven-Erik Dahlén\*, Per Hedqvist\*, Sven Hammarström† & Bengt Samuelsson†

Departments of \*Physiology and †Chemistry, Karolinska Institutet, Stockholm S-104-01, Sweden

Slow reacting substance of anaphylaxis (SRS-A) is released by various stimuli, including immunological challenge, and has long been considered an important mediator of immediate hypersensitivity reactions, such as bronchoconstriction in allergic asthma<sup>1-3</sup>. Recently, slow reacting substances from several tissues have been identified and characterized as members of a newly discovered group of substances, the leukotrienes<sup>4</sup>. Leukotrienes are generated from arachidonic acid and other polyunsaturated fatty acids in a pathway initially involving a lipoxygenase-catalysed oxygenation at C-5 (Fig. 1). This differs

from the synthesis of prostaglandins and thromboxanes, where the initial transformation of arachidonic acid is catalysed by a cyclo oxygenase (Fig. 1). Recently, leukotriene  $C_4$  ( $LTC_4$ : 5(*S*)-hydroxy, 6(*R*)-*S*- glutathionyl-7,9-*trans*, 11,14-*cis*- eicosatetraenoic acid) and  $D_4$  ( $LTD_4$ : 5(*S*)-hydroxy, 6(*R*)-*S*-cysteinylglycyl-7,9-*trans*, 11,14-*cis*-eicosatetraenoic acid) were found to have biological effects in several bioassay systems, which are strikingly similar to those previously reported for impure extracts of SRS-A<sup>5,6</sup>. Here we report the remarkable contractile activity of both  $LTC_4$  and  $LTD_4$  on isolated human bronchi, which further emphasizes the possibility that leukotrienes are potent mediators of bronchoconstriction in man.

Macroscopically normal parts were selected from human lung parenchyma excised because of carcinoma, and immediately after removal placed in ice-cold Tyrode solution. Bronchi with a diameter of 2–4 mm were cut into helical strips and suspended in a 5-ml organ bath filled with Tyrode solution containing (mM): NaCl 149, KCl 2.7,  $NaHCO_3$  11.9,  $CaCl_2$  1.8,  $MgCl_2$  0.5,  $NaH_2PO_4$  0.4 and glucose 5.5, kept at 37°C gassed with 5%  $CO_2$  in  $O_2$ . Contractions were recorded on a Grass Model 7 Polygraph using an isometric Grass FT 03C force displacement transducer (resting tension 5 mN). Drug concentrations are expressed as final concentration in bath fluid surrounding the tissue. Leukotrienes  $C_4$  and  $D_4$  were generated biosynthetically, as described previously<sup>7–9</sup>.  $LTA_4$  was obtained by hydrolysis of its methyl ester, and was dissolved in ethanol whereas  $LTC_4$  and  $LTD_4$  were dissolved in 0.9% NaCl:ethanol (5:1). Care was taken to avoid ethanol concentrations in the bath above 0.05%, because ethanol can itself act on the preparation.

$LTC_4$  and  $LTD_4$ , as well as histamine, caused dose-dependent and long-lasting contractions of human bronchial strips (Fig. 2). The contraction induced by histamine readily disappeared after changing of the bath fluid, whereas the response to both  $LTC_4$  or  $LTD_4$  vanished only very slowly even after repeated washing. In fact, a contraction obtained by a high dose of  $LTC_4$  (100 nM), although reversible by isoprenaline (1  $\mu$ M), reappeared when added drugs were washed out.

The proposed SRS-A antagonist FPL 55 712 (1–10  $\mu$ M) reversed the contraction induced by  $LTC_4$  or  $LTD_4$ , whereas the

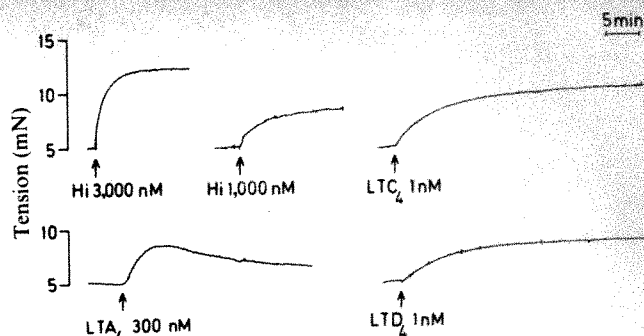


Fig. 2 Contraction responses to histamine (Hi),  $LTC_4$ ,  $LTD_4$  and  $LTA_4$  in isolated human bronchi. Drugs added at arrows, wash indicated by broken curve.

histamine response was largely unaffected (not shown). Blockade of muscarinic and histamine-1 receptors by atropine (1  $\mu$ M) and mepyramine (1  $\mu$ M), respectively, had no effect on the  $LTC_4$ -contraction.

Because repeated administration of leukotrienes seemed to cause tachyphylaxis, we used non-cumulative administration of drugs to assess their potency. The log dose-response curves thus obtained for histamine and  $LTC_4$  almost paralleled and had similar maximal values, but the  $LTC_4$  curve was markedly to the left of histamine. The regression lines calculated from the dose-response relationships of the two compounds showed a 100% increase in resting tension of the preparation ( $ED_{100\%}$ ) obtained with 6.3 nM  $LTC_4$  and 10  $\mu$ M histamine (Fig. 3). This indicates that, on a molar basis,  $LTC_4$  is at least 1,000 times more potent than histamine in causing contraction of isolated human bronchi.

In some experiments, the contractile effect of  $LTC_4$  was compared with that of  $LTD_4$  (Fig. 2). There were no large differences in potency between the two compounds in either the low or high concentration range. However,  $PGF_{2\alpha}$ , recognized as an effective bronchoconstrictor<sup>10</sup>, was always more than 500 times less potent than  $LTC_4$ . The close similarity between  $LTC_4$  and  $LTD_4$  in causing contraction of the human bronchi agrees well with their equipotency as bronchoconstrictors in the guinea pig lung both *in vitro* and *in vivo*<sup>5</sup>, although it has been suggested that  $LTD_4$  is more potent than  $LTC_4$  in the guinea pig parenchymal strip<sup>11</sup>. Whether the observed similarity in potency between  $LTC_4$  and  $LTD_4$  is due to a rapid conversion of administered  $LTC_4$  into  $LTD_4$  by the enzyme  $\gamma$ -glutamyl transpeptidase (GGTP)<sup>8,12</sup>, tissue catabolism of  $LTD_4$ , or a true equipotency as contractile agents on bronchial smooth muscle, remains to be established.

$LTA_4$ , the unstable epoxide intermediate formed from 5-hydroperoxy-6,8,11,14-eicosatetraenoic acid (5-HPETE)<sup>4</sup> (Fig. 1), was less potent than both  $LTC_4$  and  $LTD_4$ , but almost as potent as histamine in causing contraction of the bronchial strip (Fig. 2). The effect of  $LTA_4$  seemed to be more short-lived than that of  $LTC_4$  or  $LTD_4$  and sometimes the contraction faded before washing. This could be due to spontaneous breakdown of  $LTA_4$  in the organ bath or enzymatic transformation of the substance in the tissue.

It has been shown that SRS-A consists of a mixture of leukotrienes<sup>11,13</sup>, with  $LTC_4$  as the primary product, and depending on the type of tissue and experimental conditions, varying amounts of  $LTD_4$ , and other leukotriene metabolites are formed<sup>12,14</sup>. It has not been established whether  $LTC_4$  or  $LTD_4$  is predominantly formed in human lung tissue *in vivo* but both compounds are highly potent bronchoconstrictors. They both increase the vascular permeability in guinea pig skin<sup>5</sup>; thus leukotrienes must seriously be considered as possible pathophysiological agents causing both the bronchospasm and mucosal oedema of bronchial asthma.

The finding that arachidonic acid can be transformed into leukotrienes might explain the failure of aspirin, and other non-steroidal anti-inflammatory drugs, to alleviate allergic

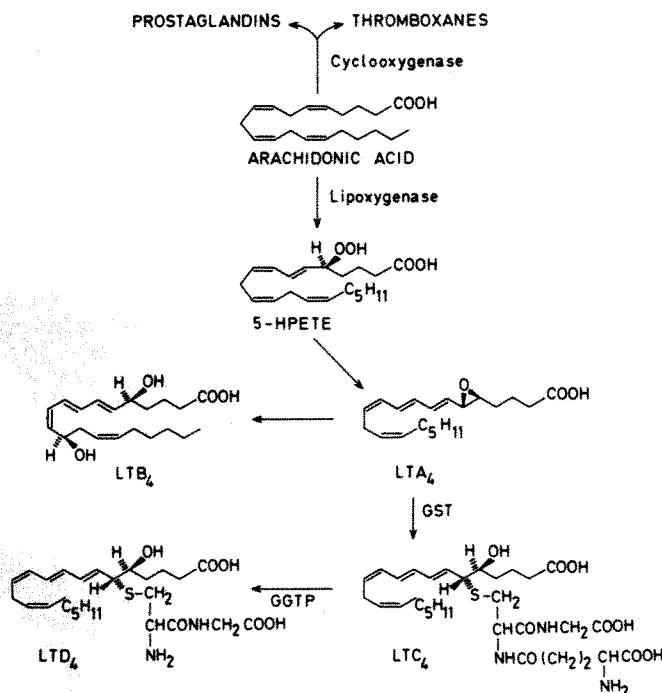
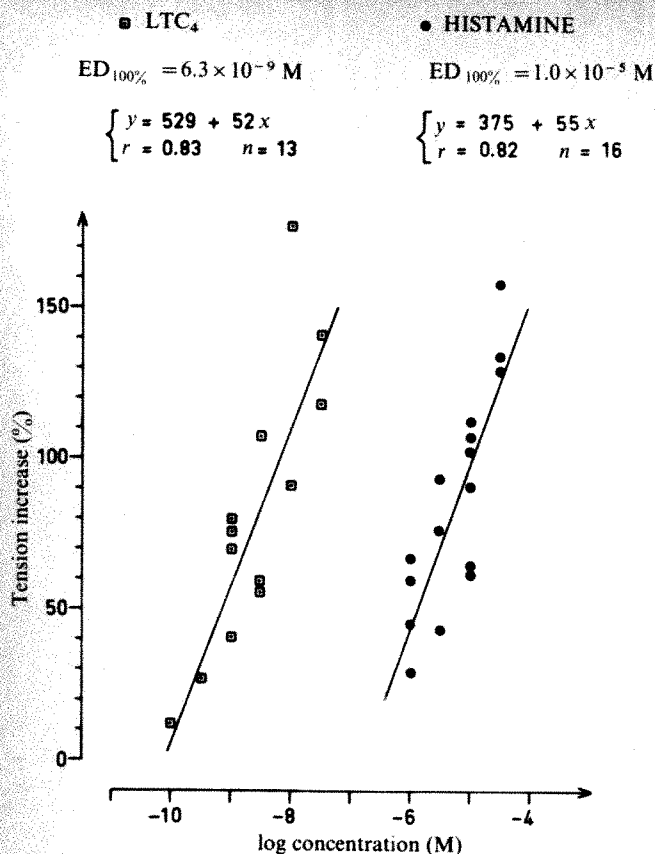


Fig. 1 Conversions of arachidonic acid into oxygenated derivatives.  $LTA_4$ : leukotriene  $A_4$ , etc. (subscript denotes number of double bonds)<sup>17</sup>. 5-HPETE: 5-hydroperoxy-6,8,11,14-eicosatetraenoic acid. GST: glutathione *S*-transferase. GGTP:  $\gamma$ -glutamyl transpeptidase.





**Fig. 3** Contraction responses to histamine (●,  $n = 16$ ) and LTC<sub>4</sub> (□,  $n = 13$ ) plotted on a semilogarithmic scale. Regression lines calculated according to the method of least squares. ED<sub>100%</sub>, dose of agonist increasing tension 100% above resting level (5 mN). Results for 13 strips obtained from eight subjects.

bronchoconstriction, because these drugs block the cyclooxygenase, but not the lipoxygenase<sup>15</sup> (Fig. 1). It is even possible that in 'aspirin-sensitive' asthma, inhibition of the cyclooxygenase by aspirin could contribute to the symptoms by diverting arachidonic acid metabolism into formation of the potent leukotriene bronchoconstrictors, while formation of prostaglandins inhibiting mediator release<sup>16</sup> is decreased. In addition, the ability of LTC<sub>4</sub> and LTD<sub>4</sub> to cause release of the potent bronchoconstrictor and cyclooxygenase product, thromboxane A<sub>2</sub> (Folco *et al.*, personal communication), further illustrates the complex situation concerning the formation of arachidonic acid-derived products with biological effects relevant to bronchial asthma. The interrelationship between prostaglandins, thromboxanes and leukotrienes in immediate hypersensitivity reactions obviously requires further study. The results presented here demonstrate that the leukotrienes C<sub>4</sub> and D<sub>4</sub> could be of considerable importance in the pathophysiology of human asthma.

We thank all personnel at the Department of Thoracic Surgery, Karolinska Sjukhuset, for help in obtaining tissue specimens, and Dr E. J. Corey for providing the methylester of LTA<sub>4</sub>. This work was supported by Swedish MRC grants 04X-4342, 03X-217, 03X-5914, the Karolinska Institutet, the National Association against Chest and Heart Diseases, and the MRC of the Swedish Life Insurance Companies.

Received 11 September; accepted 15 October 1980.

1. Feldberg, W., Holden, H. F. & Kellaway, C. H. *J. Physiol., Lond.* **94**, 232-248 (1938).
2. Kellaway, C. H. & Trethewie, E. R. *Q. J. exp. Physiol.* **30**, 121-145 (1940).
3. Brocklehurst, W. E. *J. Physiol., Lond.* **151**, 416-435 (1960).
4. Samuelsson, B., Hammarström, S., Murphy, R. C. & Borgeat, P. *J. Allergy* **35**, 375-381 (1980).
5. Hedqvist, P., Dahlén, S.-E., Gustafsson, L., Hammarström, S. & Samuelsson, B. *Acta physiol. scand.* **110**, 331-333 (1980).
6. Orange, R. P. & Austen, F. K. *Adv. Immun.* **10**, 105-144 (1969).

7. Murphy, R. C., Hammarström, S. & Samuelsson, B. *Proc. natn. Acad. Sci. U.S.A.* **76**, 4275-4279 (1979).
8. Örnberg, L., Hammarström, S. & Samuelsson, B. *Proc. natn. Acad. Sci. U.S.A.* **77**, 2014-2017 (1980).
9. Hammarström, S. *et al. Biochem. biophys. Res. Commun.* **91**, 1266-1272 (1979).
10. Hedqvist, P. & Mathé, A. A. in *Asthma, Physiology, Immunopharmacology and Treatment* (eds Lichtenstein, L. M. & Austen, F. K.) 131-146 (Academic, New York, 1977).
11. Lewis, R. A. *et al. Proc. natn. Acad. Sci. U.S.A.* **77**, 3710-3714 (1980).
12. Örnberg, L. & Hammarström, S. *J. biol. Chem.* **255**, 8023-8026 (1980).
13. Bach, M. K., Brashier, J. R., Hammarström, S. & Samuelsson, B. *J. Immun.* **125**, 115-118 (1980); *Biochem. biophys. Res. Commun.* **93**, 1121-1126 (1980).
14. Morris, H. R., Taylor, G. W., Piper, P. J. & Tippins, J. R. *Nature* **285**, 104-106 (1980).
15. Hamberg, M. & Samuelsson, B. *Proc. natn. Acad. Sci. U.S.A.* **71**, 3400-3404 (1974).
16. Lichtenstein, L. W. in *Asthma, Physiology, Immunopharmacology and Treatment* (eds Lichtenstein, L. M. & Austen, F. K.) 93-110 (Academic, New York, 1977).
17. Samuelsson, B. & Hammarström, S. *Prostaglandins* **19**, 645-648 (1980).

## Monoclonal antibodies to lymphocytic choriomeningitis virus react with pathogenic arenaviruses

Michael J. Buchmeier\*, Hanna A. Lewicki\*,  
Oyewale Tomori† & Karl M. Johnson†

\* Scripps Clinic and Research Foundation, Department of Immunopathology, La Jolla, California 92037

† Special Pathogens Branch, Center for Disease Control, Atlanta, Georgia 30333

Certain arenaviruses have become widely recognized as important human pathogens<sup>1-3</sup>, the most notable among these being Lassa virus, the causative agent of Lassa fever<sup>4</sup>. Two other members of the group, Junin and Machupo virus, are the aetiological agents of Argentine and Bolivian haemorrhagic fevers, respectively<sup>2</sup>. All these agents share both morphological features and to varying degrees serological cross-reactivity with other non-pathogenic arenaviruses<sup>3,5,6</sup>. Despite the evident clinical importance of these viruses, work to define their physicochemical structure and to develop rapid and precise diagnostic techniques has been slow. Consequently, the definitive relationships among West African Lassa strains, strains of a related agent from Mozambique and of an Old World arenavirus, lymphocytic choriomeningitis (LCM), have not been established. This problem is of more than simple taxonomic importance in view of the fact that a Mozambique virus strain produced subclinical infection in experimental monkeys which were then resistant to challenge with monkey and human virulent Lassa virus from Sierra Leone<sup>7</sup>. We have explored the use of monoclonal hybridoma antibodies generated against relatively less hazardous arenaviruses to define antigens cross-reactive with the important human pathogens of the group. Here we describe the use of monoclonal antibodies directed against LCM virus to define antigenic specificities shared among LCM, Lassa and Mozambique viruses.

Hybridoma cell lines were generated by fusion of spleen cells from immunized mice with P3 × 63 Ag8 mouse myeloma cells, and selected in hypoxanthine-aminopterin-thymidine (HAT) medium as described elsewhere<sup>8,9</sup>. Immunization of spleen cell donor mice was accomplished by intraperitoneal (i.p.) inoculation of BALB/c mice with 10<sup>4</sup> plaque-forming units of LCM virus (Armstrong Strain, CA 1371) followed by a second inoculation of 3-7 µg of purified LCM virus given intravenously 3 days before fusion. The spleen cells obtained were fused at a ratio of 10 spleen cells per myeloma cell using polyethylene glycol 1000. Cells were placed in microtitre wells in HAT medium, and wells showing growth were screened for antibody to LCM virus by indirect immunofluorescence<sup>10</sup>. Wells showing evidence of specific antibody were cloned by limiting dilution and the resultant clones again screened for specific antibody either by indirect immunofluorescence or by solid-phase radioimmune assay. Final determination of specificity of the cloned antibodies was made by radioimmune precipitation assay

**Table 1** Cross-reactivity of LCMV hybridoma antibodies with Lassa and Mozambique viruses

| Hybridoma antibody | Immunoglobulin isotype | LCMV polypeptide specificity | Indirect immunofluorescence titre ( $\times 10^{-1}$ ) against: |        |            |
|--------------------|------------------------|------------------------------|---|--------|------------|
|                    |                        |                              | LCMV  | Lassa  | Mozambique |
| 1-1-3 (MAF)        | IgG2A                  | NP                           | 12,800  | 200    | 3,200      |
| 24A-21 (MAF)       | IgG2A                  | NP                           | 51,200  | 51,200 | 51,200     |
| 25-39 (MAF)        | IgG2A                  | NP                           | 12,800  | 6,400  | 6,400      |
| 24 B-2 (TCF)       | IgG1                   | NP                           | 100   | 100    | 100        |
| 3-3 (TCF)          | ND                     | ND                           | 8   | 8      | 8          |
| 9-7-5 (MAF)        | IgG2A                  | GP-2                         | 800   | <2     | 400        |

MAF: mouse ascites fluid; TCF: tissue culture fluid; ND: not done; NP: 63,000 molecular weight nucleocapsid protein of LCM virus; GP-2: 35,000 molecular weight glycoprotein of LCM virus<sup>11</sup>.

as described elsewhere<sup>11</sup>. Ascites fluids were obtained by inoculation of  $5 \times 10^6$  to  $10^7$  hybridoma cells i.p. into pristane-primed BALB/c mice.

Cross-reactivity was assessed by indirect immunofluorescent staining of spot slides of cells infected with Lassa or Mozambique viruses<sup>12</sup>. These slides were prepared in the maximum containment facility at CDC, Atlanta, and were fixed in acetone. Fluorescein isothiocyanate-conjugated goat antibody to mouse IgG was prepared in this laboratory. Infected cells stained with serial twofold dilutions of culture fluid or ascites from individual hybridoma cultures were examined using a Zeiss fluorescence microscope equipped with a 100-W mercury lamp and epilluminator. The results reported are the highest dilution giving positive staining. Controls included LCM virus-infected cell preparations (positive control) as well as uninfected cells. Control hybridoma culture fluids directed against unrelated viral (Pichinde virus, measles) and non-viral antigens (P3  $\times$  63 Ag8 culture fluid) were used.

Forty-six monoclonal antibody-producing hybridoma cell lines with specificity for LCM virus were analysed for cross-reactivity with Lassa and Mozambique viruses. Of these, 9 reacted against virus-specific determinants expressed at the surface of the LCM-infected cell (M. J. B., unpublished observations). Of the remaining 37 antibodies, most recognized determinants on the viral nucleocapsid protein, although some remain uncharacterized.

To assess the fine specificity of these monoclonal antibodies, we reacted each against two strains of LCM virus differing in their pathogenicity for guinea pigs. These viruses, LCMV Armstrong (ARM)<sup>13</sup> strain and LCMV-WE<sup>14</sup> strain, have not been previously observed to differ serologically. When our panel of nine monoclonal antibodies which reacted at the surface of infected cells was tested against target cells infected with either virus, six antibodies were found to be cross-reactive, two defined determinants unique to LCMV-ARM and one reacted only with LCMV-WE. These results are also of interest because of the low pathogenicity of LCMV-ARM in humans when compared with LCMV-WE. Thus, differences in the virus-specific surface antigens, previously unknown using conventional reagents, were resolved. Similar strain-specific antigenic determinants were not observed in the nucleocapsid protein using our panel of reagents, presumably indicating conservation of this viral polypeptide.

Lassa virus had previously been shown to cross-react with LCM virus by complement fixation<sup>1,7,15</sup> and indirect immunofluorescence<sup>16</sup> tests. We therefore assayed target cells infected with Lassa and Mozambique viruses with our panel of monoclonal antibodies directed against LCM virus, to identify cross-reactive determinants. A panel of 46 monoclonal antibodies was screened. The results summarized in Table 1 showed that five cross-reacted with both viruses and a sixth reacted only with Mozambique virus. Cross-reactivity with Lassa virus was limited to antibodies which recognize determinants on the nucleocapsid protein of LCM virus.

Such antibodies, notably 1-1-3 and 24A-21 (Table 1), did not react at 1:10 dilution to any of the antigens prepared with all

eight New World arenaviruses of the Tacaribe antigenic complex. This pattern suggests that Old World and New World arenaviruses have evolved independently over a long period. These antibodies also provide a convenient method for initial screening of candidate Old World arenaviruses.

Of particular interest was antibody 9-7-5, which reacted with the Mozambique agent but not West African Lassa virus. This antibody, which recognizes the GP-2 glycoprotein on LCM virus-infected cells (M.J.B., unpublished observations), thus enables Mozambique strains to be specifically segregated by serological test. In further tests, we found that antibody 9-7-5 reacted with each of nine 'Mozambique' strains recovered from *Mastomys natalensis* rodents in that country and in Zimbabwe, whereas it failed to detect antigens produced by six West African Lassa strains of human and rodent origin obtained from Nigeria, Liberia and Sierra Leone.

Monoclonal antibodies have proved to be useful tools in analysing virus-specific antigens. The present study demonstrates that antibodies raised *in vitro* against LCM virus, the prototype virus of the arenavirus group, can be used to analyse cross-reactive viruses in the group. This ability to raise useful cross-reactive monoclonal antibodies may make it possible to circumvent the need to grow dangerous pathogens such as Lassa virus yet still produce useful and precise clinical reagents. Such reagents would be expected to facilitate the rapid and accurate identification of virus isolates. In particular, the reaction of the anti-glycoprotein monoclonal antibody 9-7-5, which specifically cross-reacts with Mozambique virus but not Lassa virus, suggests that Mozambique virus shares homology in the envelope glycoprotein with LCM virus. We are now expanding our panel of monoclonal reagents both to facilitate the precise identification of clinical isolates and to analyse further the antigenic relatedness among arenaviruses.

We thank Richarda deFries for technical assistance and Michael B. A. Oldstone for comments. This work was supported by USPHS grants AI-16102, AI-09484 and NS 12428 and was done during the tenure of American Heart Association Established Investigatorship 79-102 granted to M.J.B. O.T. is a recipient of a Fogarty Foundation Fellowship awarded by the Fogarty International Center-NIH, Bethesda, Maryland.

Received 28 July; accepted 15 October 1980.

- Casals, J. *Yale J. Biol. Med.* **48**, 115-140 (1975).
- Johnson, K. M., Webb, P. A. & Justines, G. in *Lymphocytic Choriomeningitis Virus and Other Arenaviruses* (ed. Lehmann-Grube, F.) 241-258 (Springer, Berlin, 1973).
- Rowe, W. P. *et al. J. Virol.* **5**, 561-652 (1970).
- Carey, D. E. *et al. Trans. R. Soc. trop. Med. Hyg.* **66**, 402-408 (1972).
- Murphy, F. A., Webb, P. A., Johnson, K. M., Whitfield, S. G. & Chapple, W. A. *J. Virol.* **6**, 507-518 (1970).
- Rowe, W. P., Pugh, W. F., Webb, P. A. & Peters, C. J. *J. Virol.* **5**, 289-292 (1970).
- Kiley, M. P., Lange, J. V. & Johnson, K. M. *Lancet* **ii**, 738 (1979).
- Kohler, G. & Milstein, C. *Nature* **256**, 495-497 (1975).
- Koprowski, H., Gerhard, W. & Croce, C. *Proc. natn. Acad. Sci. U.S.A.* **74**, 2985-2988 (1977).
- Buchmeier, M. J. & Oldstone, M. B. A. *J. Immun.* **120**, 1297-1303 (1978).
- Buchmeier, M. J. & Oldstone, M. B. A. *Virology* **99**, 111-120 (1979).
- Peters, C. J., Webb, P. A. & Johnson, K. M. *Proc. Soc. exp. Biol. Med.* **142**, 526-531 (1973).
- Rowe, W. P., Black, P. H. & Levey, R. H. *Proc. Soc. exp. Biol. Med.* **114**, 248-251 (1963).
- Scott, T. F. M. & Rivers, T. M. *J. exp. Med.* **63**, 397-414 (1936).
- Buckley, S. M. & Casals, J. *Am. J. trop. Med. Hyg.* **19**, 680-691 (1970).
- Wulff, H., Lange, J. V. & Webb, P. A. *Intervirology* **9**, 344-350 (1978).



## Production of human hybridomas secreting antibodies to measles virus

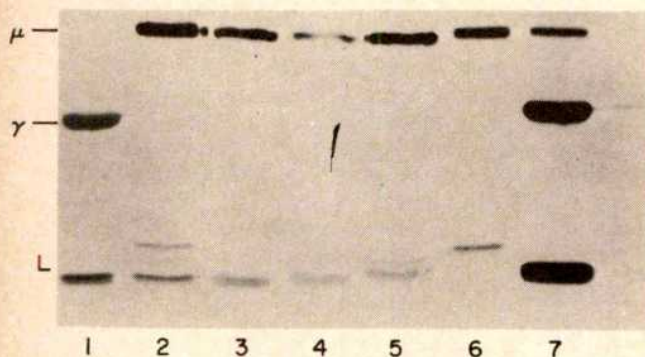
Carlo M. Croce\*, Alban Linnenbach\*, William Hall†, Zenon Steplewski\* & Hilary Koprowski\*

\* The Wistar Institute of Anatomy and Biology, 36th Street at Spruce, Philadelphia, Pennsylvania 19104

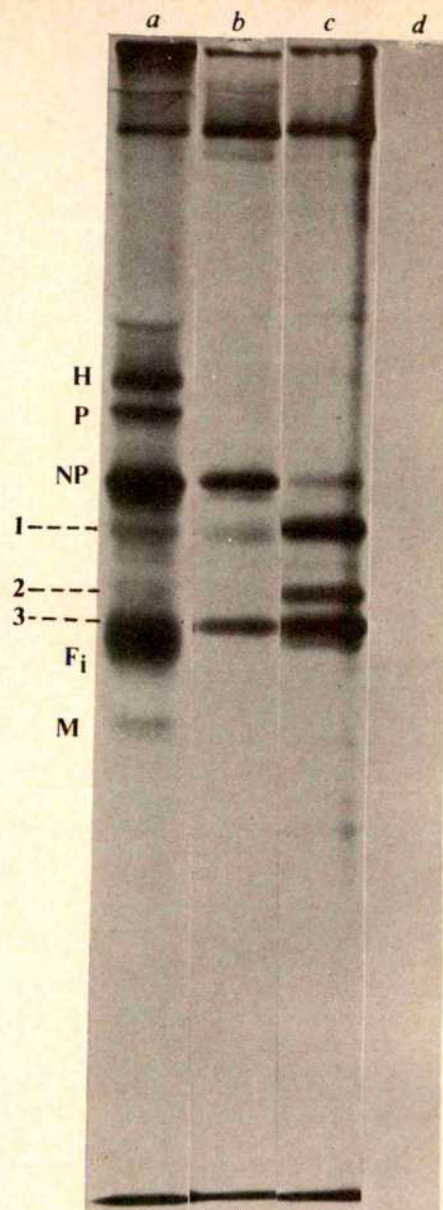
† Rockefeller University, New York, New York 10021

Monoclonal antibodies against a variety of antigens can be produced using techniques of somatic cell hybridization between cells of rodent myeloma lines and B cells derived from animals immunized against a given antigen<sup>1,2</sup>. However, because the monoclonal antibodies secreted by these hybridomas are of rodent origin, their use in human immunotherapy is limited. Thus the production of B-cell hybrids that secrete human monoclonal antibodies may be of considerable value. We have hybridized a hypoxanthine phosphoribosyl transferase (HPRT)-deficient human B-cell line derived from a patient suffering from multiple myeloma with peripheral lymphocytes obtained from a patient with subacute sclerosing panencephalitis (SSPE). These hybridomas were found to secrete human IgM specific for measles virus nucleocapsids.

As human chromosomes are lost in mouse × human hybridomas<sup>3,4</sup> it is difficult to obtain interspecies hybridomas that secrete human antibodies, because such hybrids must retain both of the two human chromosomes that carry the rearranged genes for the human light and heavy immunoglobulin chains<sup>3,4</sup>. The chromosomal constitution of intraspecific human hybrids is much more stable<sup>5</sup>; therefore we decided to use a HPRT-deficient human B-cell line derived from a patient with multiple myeloma to produce human × human hybridomas. We mutagenized human B-cell line GM 1500 (obtained from the Human Cell Depository, Camden, New Jersey)<sup>3</sup> with ethylmethane sulphonate (EMS) and selected the mutagenized cells in the presence of 30 µg ml<sup>-1</sup> 6-thioguanine. Two independent mutants, GM 1500 6TG-A1 1 and GM 1500 6TG-A1 2, were obtained. They did not express HPRT activity and died in

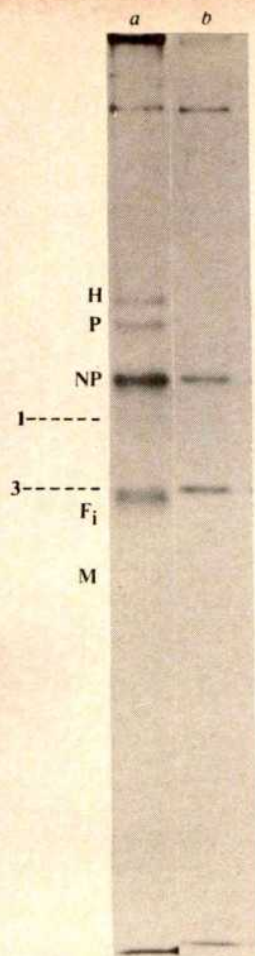


**Fig. 1** Immunoprecipitation and 10% SDS-polyacrylamide gel electrophoresis of secreted human immunoglobulin chains produced by human hybridomas. Hybridoma cultures were labelled with 100 µCi <sup>3</sup>H-leucine (70 Ci per mmol) per ml for 12 h. The human immunoglobulin chains were immunoprecipitated with rabbit anti-human heavy chain antigen using established procedures<sup>3,4</sup>, then separated by 10% SDS-polyacrylamide gel electrophoresis as described elsewhere<sup>3,4</sup>. Lane 1, immunoprecipitates of the immunoglobulin produced by GM 1500 6TG-A1 2 cells after reaction with an anti-human γ antiserum; lanes 2–6, immunoprecipitates of immunoglobulin chains secreted by human × human hybridomas after reaction with anti-human μ antiserum; lane 7, immunoprecipitate of immunoglobulin chains secreted by hybridoma D3 after reaction with anti-human μ and γ antiserum.



**Fig. 2** Polyacrylamide gel electrophoretic analysis of the measles virus polypeptides precipitated by the various monoclonal antibodies. *a*, Virus polypeptides precipitated by convalescent serum of a patient with atypical measles were used as markers. The polypeptides are as follows: H, the virus haemagglutinin; P, a polypeptide associated with the internal nucleocapsid structure; NP, the major structural polypeptide of the nucleocapsid; F, the polypeptide responsible for cell fusion and haemolytic activities; M, the non-glycosylated membrane polypeptide. Bands 1, 2 and 3 are not unique virus polypeptides, but represent proteolytic cleavage fragments of the NP polypeptide<sup>8</sup>. *b*, Virus polypeptides precipitated by antibody D3. *c*, Polypeptides precipitated by antibody C5. *d*, Culture fluid from the human GM 1500 6TG-A1 2 cell line. Culture fluids of *b*, *c* and *d* were concentrated 20-fold by freeze-drying before use. The procedures used in immunoprecipitation, similar to those described elsewhere<sup>1</sup>, were as follows: lysates of virus-infected CV1 cells labelled with <sup>35</sup>S-methionine were used as antigen. Aliquots (25 µl) were mixed with 100 µl concentrated culture fluid and incubated at 37 °C for 90 min then at 4 °C for 4 h. Rabbit total anti-human antibody (25 µl) was then added and the incubation period repeated. Precipitated polypeptides were collected by centrifugation in an Eppendorf centrifuge for 20 min at 10,000 r.p.m. The visible pellet was resuspended and washed three times. After the final washing, the pellet was suspended in lysis buffer, boiled for 3 min and electrophoresed on a 10% SDS-polyacrylamide gel in conditions described elsewhere<sup>1</sup>. After fluorography, dried gels were exposed to Cronex X-ray film.





**Fig. 3** Lane *a* represents the virus polypeptides precipitated by the same atypical measles serum as in Fig. 2*a*. *b*, Polyacrylamide gel electrophoretic analysis of the measles virus polypeptides precipitated by culture fluid from subclone D3M2. The conditions of the experiments were as described in the legend to Fig. 2, except that culture fluid was unconcentrated.

hypoxanthine-aminopterin-thymidine (HAT)<sup>6</sup> selective medium (data not shown). The mutant cells were found to secrete human IgG ( $\gamma 2$ ,  $\kappa$ ), as did the parental GM 1500 cells (Fig. 1, lane 1)<sup>3</sup>.

Heparinized blood plasma was obtained from a patient suffering from SSPE. This patient was a 19-yr-old female who had first developed SSPE at age 9—the disease lasted for 2 yr, leading ultimately to recovery with the persistence of only some residual symptoms. At the age of 18 yr, she married and became pregnant, then in the fourth month of pregnancy SSPE recurred with great severity and she is now in a chronic vegetative state. Measles virus was isolated from a brain fragment during the first tissue culture. Serum from the patient, diluted 1:10<sup>6</sup>, bound in radioimmunoassay (RIA) with measles-infected target cells. These data, as well as typical histological lesions of the brain, confirmed the clinical diagnosis of SSPE.

Using established procedures<sup>3,4</sup>, we fused 10<sup>7</sup> GM 1500 6TG-A1 2 cells with Ficoll-purified lymphocytes derived from peripheral blood (10 ml) taken from the patient in the presence of polyethylene glycol 1000 (ref. 7). The fused cells were distributed into 24 wells of a Linbro FB-16-24 TC plate in the presence of HAT selective medium. Growth of hybrids was detected in 20 of the 24 wells. These hybrids were propagated in HAT-RPMI 1640 medium and cloned by limiting dilution. Each independent clone (derived from an independent well) was tested for the expression of human immunoglobulin chains and for the ability to immunoprecipitate measles virus proteins<sup>8</sup>.

As shown in Fig. 1, six hybrid clones, including the two that reacted with measles virus (see Fig. 2), expressed the human  $\mu$  chains, as determined by immunoprecipitation of the immunoglobulins secreted by the hybrids with rabbit anti-human  $\mu$  antiserum<sup>3,4</sup>. Some hybridomas also expressed a light chain (L) that migrated differently from the light chain expressed by the GM 1500 line. The clone of the hybridoma illustrated in lane 6 (Fig. 1) lost the ability to produce the light chain expressed by

GM 1500. The hybridoma culture fluid in lane 7 was immunoprecipitated with both anti-human  $\mu$  and anti-human  $\gamma$  chain antisera—the hybrid expressed two heavy chains, the  $\gamma$  chain of the GM 1500 parent and the  $\mu$  chain of the human SSPE B-cell parent.

The specificity of the antibodies for measles virus was determined by immunoprecipitation using methods similar to those described elsewhere<sup>8</sup>. Culture fluids from cultures D3 and C5 only precipitated the virus nucleocapsid polypeptide (NP) and varying amounts of its cleavage fragments (Fig. 2). The antibodies in the culture fluids seemed to be specific for this one polypeptide which is the major polypeptide of the virus nucleocapsid<sup>8</sup>. NP is extremely sensitive to proteolytic cleavage<sup>8</sup>, thus the long incubation periods used in the immunoprecipitation procedure could be partly responsible for the high level of cleavage of the polypeptide. The level of cleavage is particularly evident in Fig. 2*c*. The specificity of the antibodies for NP was confirmed by the demonstration that subclones of hybrid clone D3 could also precipitate this polypeptide (Fig. 3*b*).

These results indicate that it is possible to obtain human B-cell hybrids which continuously secrete human antibodies, particularly antibodies specific for a human pathogenic virus. The availability of a human continuous B-cell line with appropriate drug resistance markers represents a breakthrough in work towards the possible application of this technology to human immunotherapy. In addition, lymphocytes from patients with human autoimmune diseases such as myasthenia gravis and Graves' disease could be fused with human B-cell lines to produce hybridomas that secrete the autoantibodies responsible for the disease. Once such monoclonal autoantibodies are available, the production of anti-autoantibodies could provide a cure for patients with autoimmune diseases.

This work was supported by NIH grants CA-10815 and CA-23568 and by grant 1-522 from the National Foundation-March of Dimes. We thank Mr Jan Erickson for technical assistance.

Received 24 September; accepted 21 October 1980.

1. Kohler, G. & Milstein, C. *Nature* **256**, 495–497 (1975).
2. Koprowski, H., Gerhard, W. & Croce, C. M. *Proc. natn. Acad. Sci. U.S.A.* **74**, 2895–2988 (1977).
3. Croce, C. M. *et al. Proc. natn. Acad. Sci. U.S.A.* **76**, 3416–3419 (1974).
4. Croce, C. M. *et al. Eur. J. Immun.* **10**, 486–488 (1980).
5. Croce, C. M. & Koprowski, H. *Science* **184**, 1288–1289 (1974).
6. Littlefield, J. W. *Science* **145**, 709–710 (1964).
7. Pontecorvo, G. *Somatic Cell Genet.* **1**, 397–400 (1975).
8. Hall, W. W., Lamb, R. A. & Choppin, P. W. *Proc. natn. Acad. Sci. U.S.A.* **76**, 2047–2051 (1979).

## Surface phenotypes in T-cell leukaemia are determined by oncogenic retroviruses

Christoph C. Zielinski, Samuel D. Waksal, Laurence D. Tempelis, Raman H. Khirany & Robert S. Schwartz

Departments of Medicine and Pathology and the Tufts Cancer Research Center, Tufts University School of Medicine, Boston, Massachusetts 02111

Spontaneous thymic leukaemia in experimental mice is the result of a complex series of genetically controlled events<sup>1</sup>. An important step in this process involves the production by thymocytes of recombinant polytropic retroviruses (MCF viruses)<sup>2,3</sup>. These leukaemogenic agents arise by recombination of genes from the *env* regions of endogenous precursor viruses<sup>4,5</sup>. Sequences in these regions encode the envelope glycoprotein gp70 (ref. 6). Thus far, each cloned isolate of recombinant virus from AKR and HRS/J mice has been found to possess unique oligonucleotide sequences in its *env* region, as well as clone-specific peptides in its gp70 (refs 7, 8). Therefore, the polytropic viruses of these leukaemia-susceptible mice are

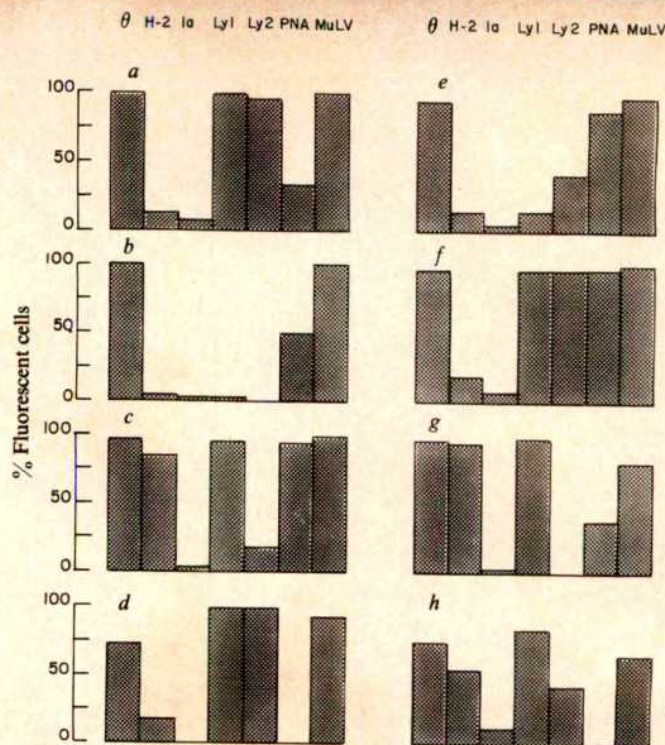


extremely diverse. These findings suggest that random recombination of *env* genes gives rise to leukaemogenic polytropic viruses. McGrath and Weissman<sup>9</sup> have proposed that thymocytes with cell surface receptors for the gp70 of a particular leukaemogenic virus are the target cells for malignant transformation by that specific virus. In view of the diversity of polytropic viral gp70, their hypothesis would predict extensive phenotypic diversity among spontaneous thymic leukaemias. In contrast, leukaemias induced by a particular leukaemogenic recombinant virus would always have the same phenotype. Here we verify these predictions experimentally.

We studied thymomas that arose spontaneously in HRS/J mice, or that were induced in HRS/J or CBA/J mice by neonatal inoculation of cloned polytropic viruses of HRS/J origin<sup>8</sup>. The surface phenotypes of these tumours were characterized by fluorescent staining of the cells with monoclonal antisera and other reagents, followed by analyses on a fluorescence-activated cell sorter (FACS IV, Becton Dickinson). The surface phenotypes of thymocytes obtained from normal HRS/J and CBA/J mice were also studied with these reagents.

The results obtained with normal thymocytes were similar to those already published<sup>10</sup>, that is, consistently high Thy-1, low H-2K<sup>k</sup> and Ia<sup>k</sup>, and consistently high Lyt-1 and Lyt-2 (Table 1). The percentage of cells that stained with fluorescein isothiocyanate (FITC)-conjugated peanut agglutinin (PNA), a marker of immature thymocytes<sup>11</sup>, was high in all cases. The expression of murine leukaemia virus (MuLV) antigen was low except in old (40-week) HRS/J mice, in which an increase in this antigen is expected<sup>3</sup>.

In comparison, the surface phenotypes of thymocytes from eight spontaneous HRS/J thymomas had no consistent pattern. The thymic tumours were taken from mice that were chosen at random from our animal colony. The sole criterion for the selection was clinical evidence of a tumour. Figure 1 shows that each tumour had a distinctive phenotype, although several features were shared by all of them. All tumours expressed Thy-1.2, although in two cases (*d* and *h*) the percentage of thymocytes that were positive for this marker was lower than in the other six. Moreover, all the neoplasms contained a high percentage of thymocytes that expressed MuLV antigen. All the



**Fig. 1** Thymocyte surface markers of randomly selected spontaneously occurring thymomas in HRS/J mice. All reagents and techniques were the same as for experiments in Table 1. *a*, Thy-1.2; H-2, H-2K<sup>k</sup>; Ia, Ia<sup>k</sup>; Ly1, Lyt-1; Ly2, Lyt-2. Note that each tumour has a distinctive phenotype.

thymomas were low in Ia<sup>k</sup>, which may be characteristic of the HRS/J strain because thymomas from AKR mice express increased amounts of this antigen<sup>12</sup>. Other surface markers (H-2K<sup>k</sup>, Lyt-1, Lyt-2) and the percentage of cells with receptors for PNA varied independently.

The phenotypes of thymomas that were induced by cloned isolates of two HRS/J polytropic viruses (PTV 1 and PTV 2) were examined next. These viruses have been characterized biochemically and each has distinctive oligonucleotides in the *env* region as well as distinctive gp70 peptides<sup>8</sup>. They are highly thymotropic and leukaemogenic in both HRS/J and CBA/J mice<sup>8</sup>. The surface phenotypes of thymomas induced by injection of neonatal mice with PTV 1 or PTV 2 are shown in Table 2. Each cloned virus regularly produced thymomas with phenotypes characteristic of that particular clone. Thus, the neoplasms induced by PTV 1 were low in Thy-1.2, high in H-2K<sup>k</sup>, increased in Ia<sup>k</sup>, high in Lyt-1 and low in Lyt-2. Expression of MuLV by these cells was always high. The percentage of thymocytes with receptors for PNA varied; four thymomas had many and four had few PNA<sup>+</sup> cells. In contrast, PTV 2 induced the development of malignant thymocytes with high expression of Thy-1.2, H-2K<sup>k</sup>, and Lyt-1, whereas the expression of Lyt-2 and Ia<sup>k</sup> was low. MuLV antigen was again expressed by a high percentage of cells. PNA receptor-bearing thymocytes were low in four of five cases. The surface phenotypes of leukaemic cells induced by PTV-1 were similar in CBA, HRS/J and (CBA × HRS/J)<sub>F1</sub> recipients.

These results demonstrate that the surface phenotypes of spontaneously occurring thymomas are apparently random, whereas the phenotypes of thymomas induced by cloned leukaemogenic viruses are predictable and characteristic of a given clone. The PTV 1- and PTV 2-induced leukaemias produce the specific recombinant virus which induced them<sup>8</sup>, so it is unlikely that a new recombinant virus caused these leukaemias. Pepersack *et al.*<sup>13</sup> found phenotypic heterogeneity among thymomas induced by Moloney leukaemia virus. Stocks of this agent contain recombinant viruses<sup>14</sup> which might vary

**Table 1** Expression of cell surface markers and MuLV antigen by normal CBA/J and HRS/J mice of different ages

| Strain | Age (weeks) | Age      |                   |                 |       |       |      |      |
|--------|-------------|----------|-------------------|-----------------|-------|-------|------|------|
|        |             | Thy-1.2* | H-2K <sup>k</sup> | Ia <sup>k</sup> | Lyt-1 | Lyt-2 | PNA  | MuLV |
| CBA    | 8           | 97.7     | 9.3               | 1.5             | 90.0  | 88.6  | 82.7 | 0.8  |
| CBA    | 20          | 97.9     | 8.6               | 3.2             | 93.9  | 89.6  | 84.9 | 1.4  |
| CBA    | 28          | 97.8     | 6.5               | 1.6             | 86.4  | 90.0  | 85.4 | 0.6  |
| CBA    | 28          | 96.7     | 7.8               | 1.3             | 87.0  | 91.0  | 85.0 | 1.0  |
| CBA    | 40          | 95.1     | 8.5               | 1.9             | 89.8  | 90.0  | 87.6 | 1.2  |
| CBA    | 40          | 85.1     | 11.0              | 7.6             | 92.2  | 81.2  | 75.7 | 4.7  |
| CBA    | 40          | 92.4     | 6.4               | 2.6             | 90.3  | 88.0  | 87.7 | 1.7  |
| hr/hr  | 8           | 93.5     | 8.9               | 3.7             | 90.5  | 89.5  | —    | 0.8  |
| hr/+   | 8           | 91.8     | 8.7               | 5.9             | 98.8  | 85.0  | —    | 1.1  |
| hr/+   | 20          | 95.7     | 10.3              | 4.0             | 91.2  | 84.6  | —    | 18.9 |
| hr/hr  | 24          | 99.2     | 14.0              | 4.1             | —     | —     | —    | 10.9 |
| hr/hr  | 28          | 98.3     | 16.2              | 2.9             | 87.4  | 81.7  | 83.8 | 24.0 |

Suspensions of thymocytes were prepared in phosphate-buffered saline (PBS) supplemented with 5% heat-inactivated fetal calf serum (iFCS) and 0.1% sodium azide.  $1 \times 10^6$  thymocytes were incubated with the following monoclonal antisera for 30 min on ice: anti-Thy-1.2 (NEN, dilution 1:1,000), biotinylated anti-H-2K<sup>k</sup> (1:50) and anti-Ia<sup>k</sup> (1:50), directly fluoresceinated anti-Lyt-1 and -Lyt-2 (Becton-Dickinson); both at a dilution of 3  $\mu$ l antiserum per 100  $\mu$ l diluent. Also used were FITC-PNA (Pharmindustrial, 1:50), and FITC-goat antiserum prepared against Tween-ether disrupted Moloney MuLV (1:1,000). The cells were washed through FCS and incubated, when necessary, with the appropriate second-step reagent—FITC-rabbit anti-mouse immunoglobulin (1:40) or fluorescein-avidin D (Vector Laboratories, 1:50) for another 30 min on ice. The percentages of fluorescent cells were determined and recorded on a FACS.

\* Percentage of fluorescent cells.



from one preparation to another. Studies in AKR/J mice also indicate heterogeneity of spontaneous thymomas<sup>15-17</sup>. Thus, these tumours may be considered as an example of genetically determined neoplasms with a randomly specified phenotype. The diverse phenotypic patterns of these spontaneous leukaemias are consistent with the concept that the causative leukaemogenic viruses arise by random genetic recombination<sup>18</sup>.

The results with cloned viruses demonstrate the induction of neoplasms with virus-specific phenotypes. The mechanism whereby cloned viruses induce leukaemias with a specific phenotype is unknown, but a reasonable conjecture is that this process is related to gp70 because the only major difference between PTV 1 and PTV 2 is in the structure of this glycoprotein<sup>8</sup>. Elder *et al.*<sup>18</sup> have proposed that gp70 may be a transforming protein. We think it unlikely that gp70 contains the information that would be required to specify the distinctive and characteristic leukaemia cell phenotypes we observed. Alternatively, the type of cell that is programmed to undergo transformation by a given retrovirus might be selected by the fortuitous affinity of its receptor for the gp70 of that virus. This hypothesis predicts that certain recombinant retroviruses will not be leukaemogenic because their gp70 cannot bind with sufficient affinity to the receptor of any thymocyte. Moreover, genetic variants of these receptors would explain why a particular recombinant virus is leukaemogenic in some inbred strains of mice, but not in others<sup>7,8</sup>. McGrath and Weissman<sup>9</sup> have argued that recombinant viral gp70 acts via such receptors to stimulate thymocytes immunologically. This persistent immunological stimulation, they propose, leads to malignant transformation of the cell. Their concept implies that the receptor for gp70 is antigen-specific and encoded by V<sub>H</sub> genes. Whereas experimental evidence supports the idea that persistent immunological stimulation can lead to lymphoid malignancy<sup>19</sup>, the receptors being discussed need not have an immunological function. These hypothetical receptors may act in leukaemogenesis simply as points of attachment and penetration by the leukaemogenic agent. If the thymomas we studied represent neoplastic counterparts of various stages of thymocyte differentiation, then the receptors may be differentiation structures on the cell surface rather than antigen-specific receptors.

**Table 2** Surface phenotypes of thymic tumours that developed after intraperitoneal injection of newborn mice with recombinant viruses PTV 1 and PTV 2

| Strain                    | Thy-1.2* | H-2K <sup>k</sup> | Ia <sup>k</sup> | Lyt-1 | Lyt-2 | PNA  | MuLV |
|---------------------------|----------|-------------------|-----------------|-------|-------|------|------|
| <i>a</i> PTV 1            |          |                   |                 |       |       |      |      |
| CBA                       | 75.6     | 80.4              | 17.7            | 88.6  | 22.3  | 82.0 | 82.5 |
| CBA                       | 80.1     | 86.6              | 16.0            | 84.3  | 7.3   | 64.6 | 90.1 |
| HRS                       | 77.7     | 98.8              | 8.1             | 97.0  | 3.5   | 37.0 | 88.4 |
| HRS                       | —        | 98.7              | 11.3            | 99.1  | 4.4   | 98.7 | 98.6 |
| HRS                       | —        | 85.3              | 9.3             | 96.6  | 7.5   | 44.0 | 99.1 |
| (CBA × HRS)F <sub>1</sub> | 86.1     | 98.0              | 12.0            | 97.1  | 39.6  | 94.1 | 51.1 |
| (CBA × HRS)F <sub>1</sub> | 52.2     | 96.8              | 32.8            | 97.1  | 4.5   | 98.2 | 99.2 |
| (CBA × HRS)F <sub>1</sub> | 75.0     | 96.0              | 9.0             | 94.6  | 19.6  | 19.6 | 70.0 |
| <i>b</i> PTV 2            |          |                   |                 |       |       |      |      |
| CBA                       | 98.5     | 76.2              | 27.1            | 89.0  | 25.9  | 9.1  | 96.7 |
| (CBA × HRS)               | 98.4     | 78.4              | 3.0             | 88.9  | 4.2   | 26.9 | 83.6 |
| (CBA × HRS)F <sub>1</sub> | 98.6     | 74.9              | 2.0             | 84.0  | 1.9   | 19.0 | 60.3 |
| (CBA × HRS)F <sub>1</sub> | 95.0     | 87.0              | 6.6             | 90.0  | 9.0   | 84.1 | 93.1 |
| (CBA × HRS)F <sub>1</sub> | 99.1     | 65.3              | 1.5             | 95.5  | 3.5   | 7.4  | 71.5 |

In the group injected with PTV 1 were two CBA, three HRS/J and three (CBA × HRS)F<sub>1</sub> mice (the latter were bred in our animal facility), and in the group injected with PTV 2 were one CBA and four (CBA × HRS)F<sub>1</sub> mice. The viruses were isolated, cloned and characterized according to previously described methods<sup>8</sup>. The latent period between virus injection and the occurrence of thymoma, and the incidence of thymomas did not differ from previous observations<sup>8</sup>. The dose of virus administered to the mice was about  $1 \times 10^5$  focus-forming units. All reagents and techniques were the same as for experiments in Table 1.

\* Percentage of fluorescent cells.

We cannot exclude the possibility that the clones of viruses we studied possess a relevant transforming function that has not been revealed by the previous biochemical analyses of their genomes and major structural proteins. With certain oncogenic avian retroviruses, for example, transforming genes that are specific for certain types of haematopoietic cells have been demonstrated<sup>20</sup>. Clarification of the mechanisms whereby cloned recombinant retroviruses induce characteristic clones of leukaemic cells is therefore in progress. Finally, note that the diversity of cell-surface phenotypes in mouse T-cell leukaemias of viral aetiology, as shown here, resembles a similar heterogeneity in human T-cell leukaemia<sup>21</sup>.

This work was supported in part by grants CA24530 and CA09351 and contract N-01CB-74150. C.C.Z. is on leave from the II Department of Medicine, University of Vienna; S.D.W. is a scholar of the Leukaemia Society of America; L.D.T. is a Damon Runyon-Walter Winchell Cancer Fund Fellow. The authors thank Ms Nancy Bond and Mr Joseph Gabriels for technical assistance. FITC-goat antiserum against Moloney MuLV was supplied by Dr J. Gruber; FITC-rabbit anti-mouse immunoglobulin was a gift from Dr R. Stout.

Received 15 July; accepted 1 October 1980.

- Schwartz, R. S., Datta, S. K., Hiai, H., Morrissey, P. J. & Waksal, S. D. in *Viruses in Naturally Occurring Cancers* (Cold Spring Harbor Conf. on Cell Proliferation) Vol. 7 (1980).
- Hartley, J. W., Wolford, N. K., Old, L. J. & Rowe, W. P. *Proc. natn. Acad. Sci. U.S.A.* **74**, 789–792 (1977).
- Hiai, H., Morrissey, P., Khirya, R. & Schwartz, R. S. *Nature* **270**, 247–249 (1977).
- Elder, J. H. *et al. Proc. natn. Acad. Sci. U.S.A.* **74**, 4676–4680 (1977).
- Rommelaere, J., Faller, D. V. & Hopkins, N. in *Differentiation of Normal and Neoplastic Hematopoietic Cells* (Cold Spring Harbor Conf. on Cell Proliferation) Vol. 5 (New York, 1978).
- Rommelaere, J., Faller, D. V. & Hopkins, N. *Proc. natn. Acad. Sci. U.S.A.* **75**, 495–499 (1978).
- Cloyd, M. W., Hartley, J. W. & Rowe, W. P. *J. exp. Med.* **151**, 542–552 (1980).
- Green, N. *et al. J. exp. Med.* **152**, 249–264 (1980).
- McGrath, M. & Weissman, I. L. *Cell* **17**, 65–75 (1978).
- Mathieson, B. J., Sharrow, S. O., Campbell, P. S. & Asofsky, R. *Nature* **277**, 478–480 (1979).
- Reisner, Y., Linker-Israeli, M. & Sharon, N. *Cell Immun.* **25**, 129–134 (1976).
- Zielinski, C. C., Datta, S. K. & Waksal, S. D. *Immunogenetics* (in the press).
- Pepersack, L., Lee, J. C., McEwan, R. & Ihle, J. N. *J. Immun.* **124**, 279–285 (1980).
- Shih, T. Y., Weeks, M. O., Troxler, D. H., Coffin, J. M. & Scolnick, E. M. *J. Virol.* **26**, 71–83 (1978).
- Mathieson, B. J., Campbell, P. S., Potter, J. & Asofsky, R. *J. exp. Med.* **147**, 1267–1279 (1978).
- Krammer, P. J., Citronbaum, R., Read, S. E., Forni, L. & Lang, R. *Cell. Immun.* **21**, 97–111 (1976).
- Zielinski, C. C., Waters, D. L., Datta, S. K. & Waksal, S. D. *Cell. Immun.* (in the press).
- Elder, J. H., Gautsch, J. W., Jensen, F. C. & Lerner, R. A. *J. natn. Cancer Inst.* **61**, 625–638 (1978).
- Schwartz, R. S. & Beldotti, L. *Science* **149**, 1511–1513 (1965).
- Roussel, M. *et al. Nature* **281**, 452–455 (1979).
- Reinherz, E. L. & Schlossman, S. F. *Cell* **19**, 821–827 (1980).

## Is myosin in the cochlea a basis for active motility?

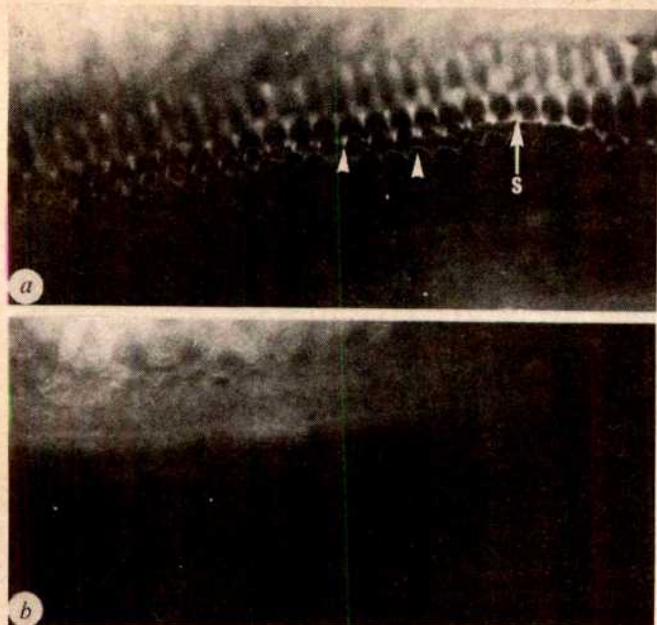
J. C. Macartney\*, S. D. Comis & J. O. Pickles

Department of Pathology\* and Neurocommunications Research Unit, Birmingham University, Birmingham B15 2TJ, UK

**Recent evidence suggests that the stereocilia of cochlear hair cells contain actin filaments<sup>1-3</sup>. The experiments reported here demonstrate the presence of myosin, suggesting that the mechanical properties of the hair cells may be actively modifiable by actin-myosin interactions as in muscle cells.**

Myosin was detected in the hair cells of the guinea pig cochlea by indirect immunofluorescence using an antiserum raised against human smooth muscle myosin<sup>4</sup>. Immunofluorescence was visible in very specific areas of the organ of Corti. The stereocilia fluoresced strongly along their length (Fig. 1a). It is possible that the bright spots of fluorescence seen in one row of stereocilia in Fig. 1a indicate a concentration of myosin near the roots of the stereocilia, perhaps due to the many rows of short





**Fig. 1** Anti-myosin immunofluorescence (a), and control section using myosin-absorbed antiserum (b) in the outer hair cells of the guinea pig cochlea, seen from above ( $\times 512$ ). The stereocilia of two rows of outer hair cells are in focus at different depths (white arrows, a). Fluorescence is also seen in the apical ends of the supporting cells, in between the hair cells (S). Guinea pig cochleas were fixed briefly in buffered formalin glutaraldehyde<sup>9</sup> and the organ of Corti rapidly dissected out and washed in tris saline buffer (pH 7.6). The intact organs of Corti were fixed in cold acetone ( $-10^{\circ}\text{C}$ ) for 10 min followed by brief air drying and further washing in buffer. Following removal of the buffer the organs of Corti were incubated in a rabbit antiserum raised against smooth muscle myosin<sup>4</sup> diluted 1:20 with tris saline buffer for 60 min, followed by washing in three changes of buffer. The second stage antiserum was a fluorescein-labelled swine anti-rabbit immunoglobulin (Dako-Immunoglobulins 52190) diluted 1:20 in buffer. After washing the specimens were orientated and mounted in glycerol-phosphate buffered saline. They were viewed using a Leitz SM-Lux microscope fitted with a fluorescence vertical illuminator for incident light excitation. Controls included the use of preimmune rabbit serum and myosin-absorbed antiserum in place of the first stage anti-myosin serum.

stereocilia. A similar pattern of fluorescence was seen in inner and outer hair cells. In transverse sections faint immunofluorescence was also seen in the cuticular plate at the apex of the hair cells. Therefore in contrast to the microvilli of the intestinal brush border, most of the immunofluorescence was associated with the cilia rather than any terminal web. It is possible that actin-myosin interactions in such areas could lead to a shortening or a change in stiffness of the stereocilia. Although there is little information on the amount of movement possible, the results of Tilney *et al.*<sup>2</sup> strongly suggest that it may be limited, perhaps due to the large numbers of cross-bridges between the actin filaments<sup>3</sup>. In both transverse and surface preparations immunofluorescence was also visible in the supporting cells between the apical ends of the hair cells (Fig. 1a). It is very unlikely that such structures deform, even passively, thus although these experiments indicate that the molecular basis of actin-myosin interactions exists in the cochlea, they do not indicate that motility must necessarily occur.

These results have the following implications: (1) it has been suggested that the cochlear transducer can produce sound<sup>5</sup>, which may be the result of actin-myosin motility; (2) the changes in the mechanical properties of the cochlea seen after death<sup>6</sup> or the loss of rigidity of the stereocilia, which is an early sign of sound-induced damage<sup>7</sup>, may result from changes in the actin-

myosin linkage; (3) similarly, in physiological conditions the stereocilia may not be as stiff as demonstrated by Flock<sup>1</sup> in the excised organ; (4)  $\text{Ca}^{2+}$ , which is essential for the transduction process<sup>8</sup>, may enter the stereocilia as a result of sound stimulation and so affect the mechanical properties of the hair cells; (5) the nonlinear growth of basilar membrane movement with stimulus intensity<sup>6</sup> may be due to the progressive activation of the actin-myosin linkage as a result of sound stimulation; and (6) the fibres of the olivocochlear bundle may affect the mechanical properties of the hair cells by altering the actin-myosin linkage, perhaps as a result of changed  $\text{Ca}^{2+}$  influx.

Received 30 June; accepted 7 October 1980.

1. Flock, A. in *Psychophysics and Physiology of Hearing* (eds Evans, E. F. & Wilson, J. P.) 15-25 (Academic, London, 1977).
2. Tilney, L. G., DeRosier, D. & Mulroy, M. J. *Cell Biol.* **86**, 244-259 (1980).
3. DeRosier, D. J., Tilney, L. G. & Egelman, E. *Nature*, **287**, 291-296 (1980).
4. Macartney, J. C., Trevithick, M. A., Kricka, L. & Curran, R. C. *Lab. Invest.* **41**, 437-445 (1979).
5. Kemp, D. T. *Hearing Res.* **2**, 533-548 (1980).
6. Rhode, W. S. *J. acoust. Soc. Am.* **64**, 158-176 (1978).
7. Liberman, M. C. & Beil, D. G. *Acta otolar.* **88**, 161-176 (1979).
8. Sand, O. *J. comp. Physiol.* **102**, 27-42 (1975).
9. Comis, S. D., Hayward, T. L. & Pratt, S. R. *J. Physiol., Lond.* **301**, 4P-6P (1980).

## $\text{Ca}^{2+}$ -activated ATPase and ATP-dependent calmodulin-stimulated $\text{Ca}^{2+}$ transport in islet cell plasma membrane

Harrihar A. Pershadsingh\*, Michael L. McDaniel, Michael Landt, Cheryl G. Bry, Paul E. Lacy & Jay M. McDonald

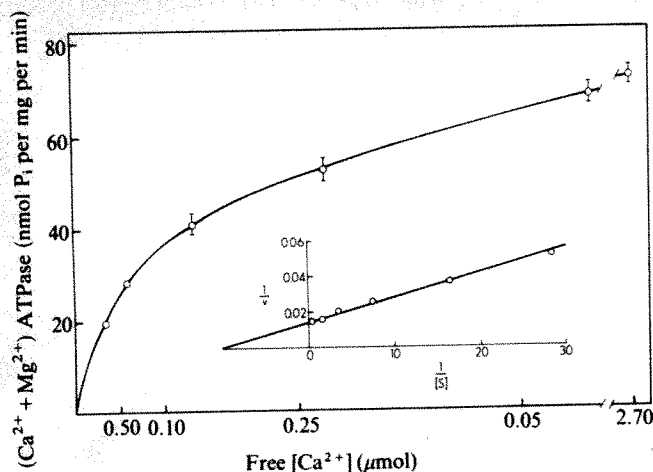
Division of Laboratory Medicine, Departments of Pathology and Medicine, Washington University School of Medicine, St Louis, Missouri 63110

Calcium is known to play an essential part in the regulation of insulin secretion in the pancreatic  $\beta$  cell<sup>1,2</sup>. Calcium influx/efflux studies indicate that glucose promotes an accumulation of calcium by the  $\beta$  cell<sup>2</sup>. However, interpretation of such data is particularly difficult due to the complex compartmentalization of calcium within the cell. Although indirect evidence using chlorotetracycline suggests that control of calcium homeostasis at the plasma membrane may be central to insulin secretion<sup>3</sup>, the mechanism by which secretagogues influence the handling of calcium remains unknown. Despite its continuous diffusive entry, intracellular calcium is maintained in the submicromolar range<sup>4,5</sup> by energy-dependent mechanisms<sup>5-9</sup>. One such process which has been well characterized in erythrocytes is a plasma membrane calcium extrusion pump whose enzymatic basis is a high affinity ( $\text{Ca}^{2+} + \text{Mg}^{2+}$ )ATPase<sup>9</sup>. A similar mechanism<sup>10,11</sup> regulated by insulin<sup>12,13</sup> has recently been identified in adipocyte plasma membranes. We report here the presence of a high affinity ( $\text{Ca}^{2+} + \text{Mg}^{2+}$ )ATPase and ATP-dependent calmodulin-stimulated calcium transport system in rat pancreatic islet cell plasma membranes<sup>14</sup>.

Calcium-stimulated ATPase activity was demonstrated in the plasma-membrane enriched fraction from pancreatic islets. The dependence of ATPase activity on calcium concentration revealed the presence of two saturable components similar to those observed in erythrocyte<sup>15</sup> and adipocyte<sup>10</sup> plasma membranes. One had a high affinity for calcium, designated ( $\text{Ca}^{2+} + \text{Mg}^{2+}$ )ATPase, and achieved saturation at submicro-

\* Present address: University of Missouri-Columbia, School of Medicine, Columbia, Missouri 65212.





**Fig. 1** Calcium dependence of the high affinity ( $\text{Ca}^{2+} + \text{Mg}^{2+}$ )ATPase in pancreatic islet cell plasma membranes. Islets were isolated from male Sprague-Dawley rats by the method of Lacy and Kostianovsky<sup>37</sup> and the plasma membrane-enriched fraction (band I) was obtained by the method of Naber *et al.*<sup>20,43</sup> with the modification that EDTA was omitted from the homogenization and fractionation buffers. Omission of EDTA does not modify the distribution of organelles among the subcellular fractions<sup>20,43</sup>. The plasma membranes were frozen immediately and were used within 2 days of storage at  $-70^\circ\text{C}$ . ( $\text{Ca}^{2+} + \text{Mg}^{2+}$ )ATPase activity was quantitated by monitoring the release of  $^{32}\text{P}_i$  from  $[\gamma\text{-}^{32}\text{P}]\text{ATP}$  and is expressed as nmol  $\text{P}_i$  per mg protein per min (ref. 38). Protein was determined as described elsewhere<sup>39</sup>. The assay medium contained 1–2  $\mu\text{g}$  protein per ml with 2 mM EGTA, 1.4–2 mM  $\text{CaCl}_2$  (equivalent to 0.035–2.7  $\mu\text{M}$  free  $\text{Ca}^{2+}$ ), 1–2  $\mu\text{Ci}$   $[\gamma\text{-}^{32}\text{P}]\text{ATP}$ , 0.25 mM ATP (Tris salt), 20 mM  $\text{Na}_2\text{S}_2\text{O}_8$  and 10 mM Tris-PIPES, pH 7.5 at  $37^\circ\text{C}$ . The incubation volume was 1.0 ml. Reaction times were 30 or 60 min. The ATPase reaction rates were linear over the assay period and directly proportional to the amount of tissue added. The amount of ATP hydrolysed was always less than 5% of the total ATP present over the incubation period. Calcium-stimulated activity was determined by subtracting values obtained with chelator alone (background activity) from those obtained with calcium plus chelator. The background ATPase was  $18 \pm 4\%$  ( $n=6$ ) of the maximum velocity of the high affinity ( $\text{Ca}^{2+} + \text{Mg}^{2+}$ )ATPase. Total endogenous calcium and magnesium in the assay medium were 2.0–2.5 and 8.5–9.0  $\mu\text{M}$ , respectively, as measured by atomic absorption spectroscopy. Each point represents the mean  $\pm$  s.e.m. of triplicate determinations. The inset represents a double-reciprocal plot of the data. Free calcium was calculated using an apparent  $\text{Ca}$ -EGTA association constant of  $10^{7.832} \text{ M}^{-1}$  which was determined for pH 7.5 as described by Portzehl *et al.*<sup>4</sup>. The high affinity ( $\text{Ca}^{2+} + \text{Mg}^{2+}$ )ATPase was studied at free calcium concentrations  $< 2.7 \mu\text{M}$ —in these conditions ATP has a negligible effect on free calcium in a  $\text{Ca}$ -EGTA buffer system because the apparent  $\text{Ca}$ -ATP association constant ( $10^{3.390} \text{ M}^{-1}$  at pH 7.5) is four orders of magnitude less than that of  $\text{Ca}$ -EGTA. All cation-ligand association constants were obtained from Sillén and Martell<sup>24</sup>.

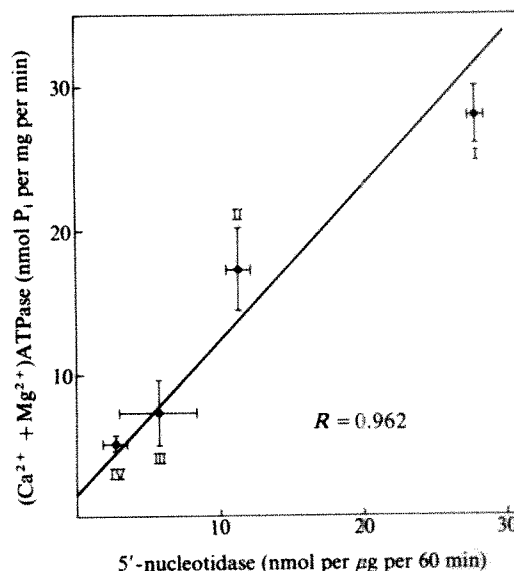
molar concentrations of free calcium (Fig. 1). Data from five separate preparations yielded a  $K_m$  of  $0.093 \pm 0.010 \mu\text{M}$  free calcium and a Hill coefficient of  $1.5 \pm 0.2$ , both similar to values obtained for erythrocyte<sup>16</sup> and adipocyte<sup>10</sup> plasma membranes. The value of  $V_{\text{max}}$  was  $54.8 \pm 10.1$  nmol of  $\text{P}_i$  released per mg protein per min. The second saturable component which was observed above 10  $\mu\text{M}$  had a comparatively low affinity for free calcium (data not shown).

It is important to demonstrate that the ( $\text{Ca}^{2+} + \text{Mg}^{2+}$ )ATPase reported here originates from the plasma membrane, because the endoplasmic reticulum of other tissues (and therefore probably the  $\beta$  cell) has a high affinity ( $\text{Ca}^{2+} + \text{Mg}^{2+}$ )ATPase<sup>17,18</sup> which also drives a calcium pump<sup>18,19</sup>. Three lines of evidence support a plasma membrane location: first, the distribution of the high affinity ( $\text{Ca}^{2+} + \text{Mg}^{2+}$ )ATPase amongst the four islet-

cell subcellular fractions was shown to parallel directly the distribution of the plasma membrane-specific marker enzyme 5'-nucleotidase with a highly significant degree of correlation (Fig. 2). Second, the ( $\text{Ca}^{2+} + \text{Mg}^{2+}$ )ATPase activity was inversely related to the distribution of NADH cytochrome *c* reductase (an endoplasmic reticulum-specific marker enzyme) amongst the four subcellular fractions<sup>20,43</sup> and third, both endoplasmic<sup>17</sup> and sarcoplasmic<sup>21</sup> reticulum ( $\text{Ca}^{2+} + \text{Mg}^{2+}$ )ATPases from other cells are strongly stimulated by potassium ( $K_m = 10 \text{ mM}$ ), whereas the ( $\text{Ca}^{2+} + \text{Mg}^{2+}$ )ATPase reported here was slightly inhibited ( $17 \pm 5\%$ ,  $n=3$ ) by 20 mM potassium. Also, as in the erythrocyte<sup>9</sup> and adipocyte<sup>10</sup>, 0.8 mM ouabain had no effect on the ( $\text{Ca}^{2+} + \text{Mg}^{2+}$ )ATPase.

A calcium-activated ATPase has been identified in subcellular fractions from mouse pancreatic islets by Formby *et al.*<sup>22</sup>. They reported a high affinity activity ( $K_m = 0.18 \mu\text{M}$ ) which seems similar to the high affinity enzyme reported here. However, there is no reason to believe that their high affinity activity represents a plasma membrane enzyme because it is detectable in all subcellular fractions. Indeed, the authors suggested that mitochondria and secretory granules were mostly responsible for their high affinity  $\text{Ca}^{2+}$ -ATPase<sup>22</sup>, but it is possible that it originated from a plasma membrane contamination of the subcellular fractions. We also observed a small inhibitory effect ( $17 \pm 6\%$ ,  $n=3$ ) of sodium (20 mM  $\text{NaCl}$ ) similar to that observed by Formby *et al.*<sup>22</sup> at high ATP concentration. In these experiments 1 mM dicyclohexylcarbodiimide instead of 20 mM sodium azide was used to block the mitochondrial ATPase<sup>23</sup>.

Although magnesium *per se* was not added to the assay medium, it seemed to be necessary for activity, a requirement apparently common to all ion-transporting enzymes. This was shown using the chelator, cyclohexane-1,2-diamine- $N,N,N',N'$ -tetraacetic acid (CDTA, Sigma) which has high affinities for calcium and magnesium whereas EGTA has a high affinity for calcium alone<sup>24</sup>. In the  $\text{Ca}^{2+}$ -CDTA buffer system,  $>99\%$  of the magnesium present in the assay medium (8.5–9.0  $\mu\text{M}$  as measured by atomic absorption spectroscopy) was complexed. When free calcium was maintained at 0.283  $\mu\text{M}$

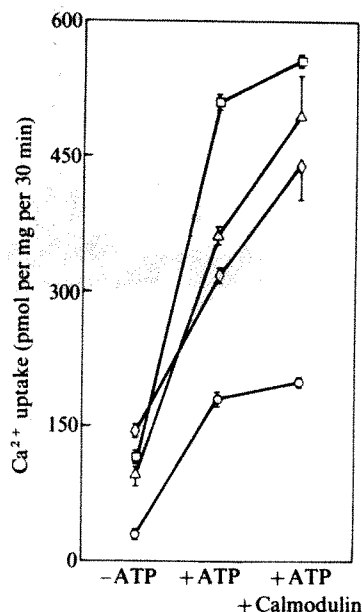


**Fig. 2** Distribution of the high affinity ( $\text{Ca}^{2+} + \text{Mg}^{2+}$ )ATPase relative to 5'-nucleotidase amongst pancreatic islet subcellular fractions. The plasma membrane-specific marker enzyme, 5'-nucleotidase<sup>40</sup>, was assayed by the method of Avruch and Wallach<sup>41</sup>. Bands I, II, III and IV as designated by Naber *et al.*<sup>20,43</sup> are shown. Free  $[\text{Ca}^{2+}] = 0.283 \mu\text{M}$ . Other assay conditions were as described in Fig. 1 legend. Each point represents the mean  $\pm$  s.e.m. of triplicate determinations for both enzyme activities. Band I, which had the highest activities of both enzymes, was the plasma membrane-enriched fraction used throughout these studies.



using this system, 98% of the  $(\text{Ca}^{2+} + \text{Mg}^{2+})\text{ATPase}$  activity was lost as compared with the activity obtained in a  $\text{Ca}^{2+}$ -EGTA buffer at the same free calcium concentration. Therefore, like the adipocyte enzyme<sup>10</sup>, both calcium and magnesium seem to be required simultaneously for high affinity  $(\text{Ca}^{2+} + \text{Mg}^{2+})\text{ATPase}$  activity. Calcium or magnesium alone cannot produce significant ATPase activity below 10  $\mu\text{M}$ .

$(\text{Ca}^{2+} + \text{Mg}^{2+})\text{ATPase}$  activity gave a complex relationship with varying ATP concentration. Two apparent saturable components with low ( $K_{0.5} = 2.1 \mu\text{M}$ ) and high ( $K_{0.5} = 70 \mu\text{M}$ ) affinities were observed, and were obtained by fitting the Hill equation to the data using the computer program developed by Atkins<sup>25</sup>. (The estimated  $V_{\text{max}}$  for the high affinity component was subtracted from the total activity to obtain data for the low affinity component.) Similar observations have been reported for the high affinity  $(\text{Ca}^{2+} + \text{Mg}^{2+})\text{ATPases}$  of erythrocyte<sup>26,27</sup> and adipocyte<sup>10</sup> plasma membranes.



**Fig. 3** Calmodulin stimulation of ATP-dependent calcium uptake in pancreatic islet cell plasma membranes. Transport was assayed as uptake of  $^{45}\text{Ca}^{2+}$  from a medium containing: 200 mM sucrose, 20 mM  $\text{Na}_2\text{S}_2\text{O}_8$ , 2.5 mM  $\text{MgCl}_2$ , 1.5 mM  $\text{Na}_2\text{ATP}$ , 10 mM Tris-oxalate, 2 mM Tris-EGTA, 1.8 mM  $\text{CaCl}_2$  ( $0.134 \mu\text{M}$  free  $[\text{Ca}^{2+}]$ ), 4–8  $\mu\text{Ci}$   $^{45}\text{CaCl}_2$  and 10 mM Tris-PIPES, pH 7.5 at 37 °C. Magnesium (2 mM) was added to the transport assay medium because it seems to be necessary for ATP-coupled calcium transport<sup>27</sup>. The reaction was initiated by addition of 10–15  $\mu\text{g}$  tissue and incubated for 30 min at 37 °C. The incubation volume was 0.5 ml and the reaction was terminated by rapid filtration of a 0.4-ml aliquot on 0.45- $\mu\text{m}$  Millipore HAWP filters and washed with 30 volumes of isotonic sucrose. Calcium uptake is shown in the absence (far left) and presence of ATP (middle) and with ATP plus calmodulin (far right). Uptake was not linear with time but was directly proportional to the amount of tissue added and is reported as the level attained after 30 min. The presence of ATP and/or calmodulin did not affect the amount of radioactivity bound to the filters. Furthermore, calmodulin did not affect the amount of  $^{45}\text{Ca}^{2+}$  associated with the membranes in the absence of ATP. The data represent results from four separate experiments and are presented as the mean  $\pm$  s.e.m. Each symbol type represents a different preparation. Purified calmodulin was prepared from Sprague-Dawley rat brains by a previously described method<sup>42</sup> and was added to a final concentration of 43 nmol ( $0.72 \mu\text{g ml}^{-1}$ ) assuming a molecular weight of 16,723 (ref. 36). Purity of the calmodulin preparation was established by resolution into a single homogeneous band by SDS-polyacrylamide gel electrophoresis. The ability to stimulate calmodulin-dependent cyclic nucleotide phosphodiesterase and erythrocyte plasma membrane  $(\text{Ca}^{2+} + \text{Mg}^{2+})\text{ATPase}$  were the criteria used to establish the protein's identity<sup>36</sup>. The preparations used in transport experiments contained EDTA in the homogenization buffers. The chelator was required during fractionation to dissociate endogenous calmodulin from the membranes<sup>35</sup>.

To ascertain whether or not the high-affinity plasma membrane  $(\text{Ca}^{2+} + \text{Mg}^{2+})\text{ATPase}$  served as the enzymatic basis of an active transport system, we assayed the preparation for  $^{45}\text{Ca}^{2+}$  transport. ATP-dependent uptake was observed in the islet cell plasma membranes (Fig. 3) and seems to represent accumulation of calcium in vesicles spontaneously formed during fractionation. The ATP-dependent component does not seem to represent binding of calcium to protein or lipids<sup>28</sup> as it was abolished when the vesicles were made freely permeable to calcium with ionophore A23187 ( $2 \mu\text{M}$ )<sup>29</sup>. In this system, the presence of azide excluded any possible participation of energy-dependent sequestration of calcium by contaminating mitochondria<sup>30,31</sup> and the persistence of calcium uptake activity in the absence of potassium suggests that uptake is not derived from the endoplasmic reticulum, which has been shown in adipocytes to be potassium dependent<sup>19</sup>.

The calcium-dependent regulatory protein, calmodulin, which stimulates ATP-dependent calcium uptake across red cell<sup>32</sup> and adipocyte<sup>11</sup> plasma membranes, had a similar effect in pancreatic islet cell plasma membrane vesicles (Fig. 3). In each of four experiments, calmodulin produced a significant ( $P < 0.05$  in a paired  $t$ -test) stimulation of ATP-dependent uptake (Fig. 3), ranging from 10 to 74% with a mean of  $36 \pm 15\%$ . Evaluation of a direct effect of calmodulin on the  $(\text{Ca}^{2+} + \text{Mg}^{2+})\text{ATPase}$  may require the presence of millimolar concentrations of magnesium (H.A.P. and J.M.McD., unpublished observations). Interpretation of the data is therefore complicated by the low affinity magnesium-stimulated ATPase and we are now investigating procedures to resolve this problem.

The demonstration of this high affinity  $(\text{Ca}^{2+} + \text{Mg}^{2+})\text{ATPase}$  associated with a calmodulin-stimulated active calcium transport system in pancreatic islet cell plasma membranes implies the presence of a mechanism capable of fine control of cytoplasmic free calcium concentration at the level of the plasma membrane. Calmodulin, which is present in pancreatic islets<sup>33</sup>, has been shown to activate adenylate cyclase<sup>34,35</sup> in this tissue, a mechanism which may serve to amplify the secretory response<sup>34</sup>. Activation of a calcium extrusion pump by calmodulin would provide a powerful means of negative feedback control of calcium and calcium plus calmodulin mediated effects on intermediary metabolism. Studies with intact islets using the calmodulin inhibitor, trifluoperazine, have suggested that calmodulin may play an important part in insulin secretion<sup>33</sup>. However, calmodulin regulates many diverse cellular metabolic events<sup>36</sup>, and thus its exact role in insulin secretion remains to be determined.

Whether or not the  $(\text{Ca}^{2+} + \text{Mg}^{2+})\text{ATPase}/\text{Ca}^{2+}$  pump complex is responsible for increased levels of cellular calcium in response to glucose stimulation is unknown, but this possibility can be easily tested using the model system described here. This cell-free system may provide a means of investigating the effects of other secretagogues and agents on calcium homeostasis at the level of the plasma membrane.

This work was supported in part by USPHS grants AM25897, AM06181, AM03373 and a grant from the Juvenile Diabetes Foundation. H.A.P. is the recipient of a Juvenile Diabetes Foundation Research Fellowship. We thank Becca Hokanson and Nancy Klaven for technical assistance.

Received 28 April; accepted 29 September 1980.

- Grodsky, G. M. & Bennett, L. L. *Diabetes* **15**, 910–913 (1966).
- Malaisse, W. J. et al. *Ann. N.Y. Acad. Sci.* **307**, 562–582 (1978).
- Täljedal, I.-B. *Biochem. J.* **178**, 187–193 (1979).
- Portzehl, H., Caldwell, P. C. & Rüegg, J. C. *Biochim. biophys. Acta* **79**, 581–591 (1966).
- Baker, P. F. *Ann. N.Y. Acad. Sci.* **307**, 250–268 (1978).
- Carafoli, E. & Crompton, M. *Curr. Topics Membrane Transport* **10**, 151–216 (1978).
- Dipolo, R. *Nature* **274**, 390–393 (1978).
- Dipolo, R. & Beaugé, L. *Nature* **278**, 271–273 (1979).
- Schatzmann, H. J. *Curr. Topics Membrane Transport* **6**, 125–168 (1974).
- Pershad Singh, H. A. & McDonald, J. M. *J. biol. Chem.* **255**, 4087–4093 (1980).
- Pershad Singh, H. A., Landt, M., & McDonald, J. M. *J. biol. Chem.* **255**, 8983–8986 (1980).
- Pershad Singh, H. A. & McDonald, J. M. *Nature* **281**, 495–497 (1979).
- Pershad Singh, H. A. & McDonald, J. M. *Diabetes* **28**, 366 (1979).
- McDonald, J. M., Pershad Singh, H. A., Bry, C. G., McDaniel, M. L. & Lacy, P. E. *Fedn Proc.* **39**, 3628 (1980).
- Quist, E. E. & Roufogalis, B. D. *J. supramolec. Struct.* **6**, 375–381 (1977).

16. Schatzmann, H. J. & Roelofsen, B. in *Biochemistry of Membrane Transport* (eds Semenza, G. & Carafoli, E.) 121–130 (Springer, Berlin, 1977).
17. Black, B. L., McDonald, J. M. & Jarett, L. *Archs Biochem. Biophys.* **199**, 92–102 (1980).
18. Blaustein, M. P., Ratzlaff, R. W., Kendrick, N. C. & Schweitzer, E. S. *J. gen. Physiol.* **72**, 15–41 (1978).
19. Black, B. L., Jarett, L. & McDonald, J. M. *Biochim. biophys. Acta* **596**, 359–371 (1980).
20. Naber, S. P., Jarett, L. & Lacy, P. E. *Diabetes* **26**, 409 (1977).
21. Duggan, P. F. *J. biol. Chem.* **252**, 1620–1627 (1977).
22. Formby, B., Capito, K., Egeberg, J. & Hedeskov, C. J. *Am. J. Physiol.* **230**, 441–448 (1976).
23. Beechey, R. B., Robertson, A. M., Holloway, C. T. & Knight, I. G. *Biochemistry* **6**, 3867–3879 (1967).
24. Sillén, L. G. & Martell, A. E. *Chem. Soc. Spec. Publ.* **25** (1971).
25. Atkins, G. L. *Eur. J. Biochem.* **33**, 175–180 (1973).
26. Mualem, S. & Karlisch, S. J. D. *Nature* **277**, 238–240 (1979).
27. Richards, D. E., Rega, A. F. & Garrahan, P. J. *Biochim. biophys. Acta* **511**, 194–201 (1978).
28. Duffy, M. J. & Schwarz, V. *Biochim. biophys. Acta* **330**, 294–301 (1973).
29. Mollman, J. E. & Pleasure, D. E. *J. biol. Chem.* **255**, 569–574 (1980).
30. Mitchell, P. *Biochem. J.* **81**, 24 (1961).
31. Sehlin, J. *Biochem. J.* **156**, 63–69 (1976).
32. Larsen, F. L. & Vincenzi, F. F. *Science* **204**, 306–308 (1979).
33. Sugden, M. C., Christie, M. R. & Ashcroft, S. J. H. *FEBS Lett.* **105**, 95–100 (1979).
34. Valverde, I., Vandermeers, A., Anjaneyulu, R. & Malaisse, W. J. *Science* **206**, 225–227 (1979).
35. Sharp, G. W. G., Wiedenkel, D. E., Kaelin, D., Siegel, E. G. & Wollheim, C. B. *Diabetes* **29**, 74–77 (1980).
36. Wolff, D. J. & Brostrom, C. O. *Adv. Cyclic Nucleotide Res.* **11**, 27–88 (1979).
37. Lacy, P. E. & Kostianovsky, M. *Diabetes* **16**, 35–39 (1967).
38. Seals, J. R., McDonald, J. M., Bruns, D. E. & Jarett, L. *Analyt. Biochem.* **90**, 785–795 (1978).
39. Lowry, O. H., Rosebrough, N. J., Farr, A. L. & Randall, R. J. *J. biol. Chem.* **193**, 265–275 (1951).
40. Brake, E. T., Will, P. C. & Cook, J. S. *Membrane Biochem.* **2**, 17–46 (1978).
41. Avruch, J. & Wallach, D. F. H. *Biochim. biophys. Acta* **233**, 334–337 (1971).
42. Charbonneau, H., McRorie, R. A. & Cormier, M. J. *Fedn Proc.* **38**, 232 (1979).
43. Naber, S. P., McDonald, J. M., Jarett, L., McDaniel, M. L., Ludvigsen, C. & Lacey, P. E. *Diabetologia* (in the press).

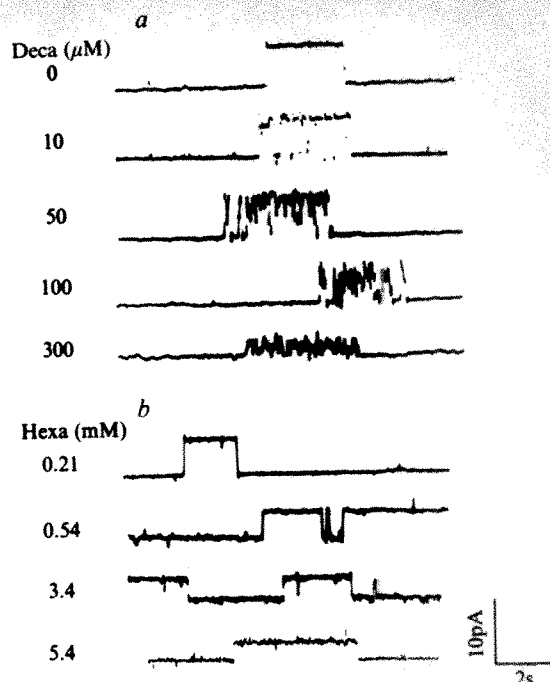
## Decamethonium and hexamethonium block $K^+$ channels of sarcoplasmic reticulum

Roberto Coronado\* & Christopher Miller†

Graduate Program in Biophysics and Graduate Department of Biochemistry, Brandeis University, Waltham, Massachusetts 02254

The sarcoplasmic reticulum membrane (SR) of skeletal muscle contains cation-selective channels which have been detected by isotope fluxes in fragmented SR vesicles<sup>1</sup>, fluorimetric dyes<sup>2</sup> and direct incorporation of SR vesicles to planar phospholipid bilayers<sup>3–5</sup>. SR channels incorporated in bilayers have a single open-state conductance of 140 pS in 0.1 M  $K^+$  (refs 4, 5). We have previously reported blockade of the SR channel by  $Cs^+$ , a low-affinity blocker with a zero-voltage dissociation constant of 40 mM (ref. 6). We showed that increasing  $Cs^+$  concentrations reduced the open-channel conductance, increased the mean open time and conferred voltage dependence on the open-state conductance<sup>6</sup>. Here we report on the blockade induced by the cholinergic drugs decamethonium and hexamethonium<sup>7</sup> on the SR channel. Although blockade by hexamethonium is similar to that of  $Cs^+$ , decamethonium blocks with a much higher affinity and induces flickering events which are probably due to the interaction of single drug molecules with the open state.

Figure 1 shows oscilloscope traces of single channel openings at  $-40$  mV for different concentrations of blocker. Addition of 10  $\mu$ M decamethonium induces flickering noise that is observed only when the channels are open. Higher concentrations increase the flickering rate, until at very high concentrations the flickering becomes faster than the amplifier time response; this results in an apparent reduction in the open-state conductance. At 300  $\mu$ M decamethonium this time-averaged conductance is about 10% of the control value. Figure 1 also shows that channels blocked with hexamethonium do not flicker, but rather undergo a smooth reduction in open-state conductance as drug concentration is increased. The amount of blocker necessary to reduce the open-state conductance to 50% of its original value is



**Fig. 1** Lipid bilayers were formed on polystyrene cups with 0.5-mm diameter holes using a 30 mM solution of Soy PE in decane. The aqueous phase was composed of symmetrical solutions of 50 mM  $K_2SO_4$  buffered with 1 mM HEPES-Tris/10  $\mu$ M EDTA, pH 7.2. Electrical measurements were made in voltage-clamp conditions using a Burr-Brown 3528CM amplifier. Output current was filtered using a low-pass active filter (Khron-Hite 3202) set at 20 Hz in all experiments except in the fast traces of Fig. 2c, where the cutoff was at 200 Hz. Current traces were taken from a storage oscilloscope and simultaneously recorded on chart paper. The *trans* chamber (side opposite to where SR vesicles are added) is defined as zero voltage. Incorporation of single SR vesicles was accomplished as described elsewhere<sup>4,5</sup>. Hexamethonium,  $(CH_3)_3N^+-(CH_2)_6-N^+(CH_3)_3$  and decamethonium,  $(CH_3)_3N^+-(CH_2)_{10}-N^+(CH_3)_3$  (bromide salts, Sigma) were added as glucuronate salts to the *trans* chamber in 50 mM  $K_2SO_4$  buffer. *a*, Traces of individual opening events at  $-40$  mV from the same membrane and at the concentrations of *trans* decamethonium (Deca) indicated. *b*, Channel openings from the same membrane at  $-40$  mV and concentrations of hexamethonium (Hexa) indicated. Experiments were done at room temperature, 21–22 °C.

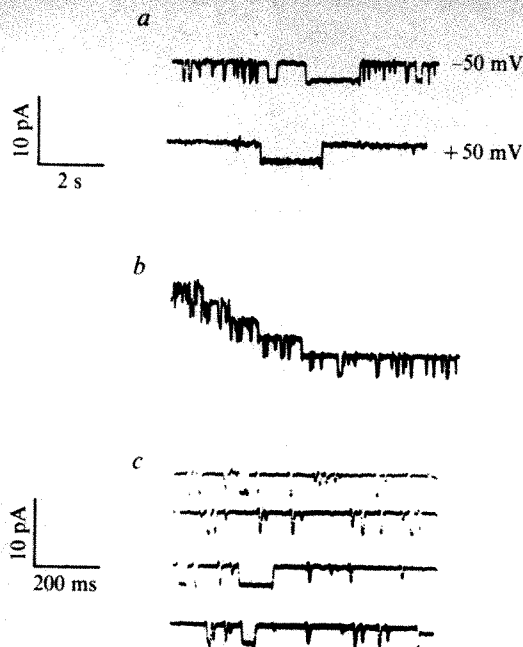
120  $\mu$ M for decamethonium and 3.5 mM for hexamethonium at  $-40$  mV. Three important features of the block induced by decamethonium are shown in Fig. 2. Figure 2a shows that the flickering is voltage dependent. Flickering is observed only at voltages that drive the drug inside the channel (negative voltages). Figure 2b shows that flickering does not interfere with the gating process (that is, the voltage dependence of the open state<sup>4,5</sup>). A positive voltage was applied to open the channels and then returned to  $-50$  mV to observe the closing events. Repetitive flickering is observed but channels are still able to close at voltages that make the open state less probable<sup>4,5</sup>. The higher rate of flickering observed in Fig. 2 when five channels are open and its decrease as channels close strongly suggest that the drug blocks each channel independently. In Fig. 2c individual flickering events are displayed on a faster time scale. Traces were taken while a single channel was open. In the conditions specified the mean open time for this experiment was 3.5 s and the mean closed time 18–20 s. Addition of 20  $\mu$ M decamethonium segments the open state into much shorter dwell times ( $\sim 200$  ms). The individual flickering events, when they could be resolved, were square pulses that dropped the conductance from its open state value to zero and lasted less than 200 ms (see Fig. 2 legend).

We have recently concluded that conduction of cations through the SR channel occurs by movement of the ions across

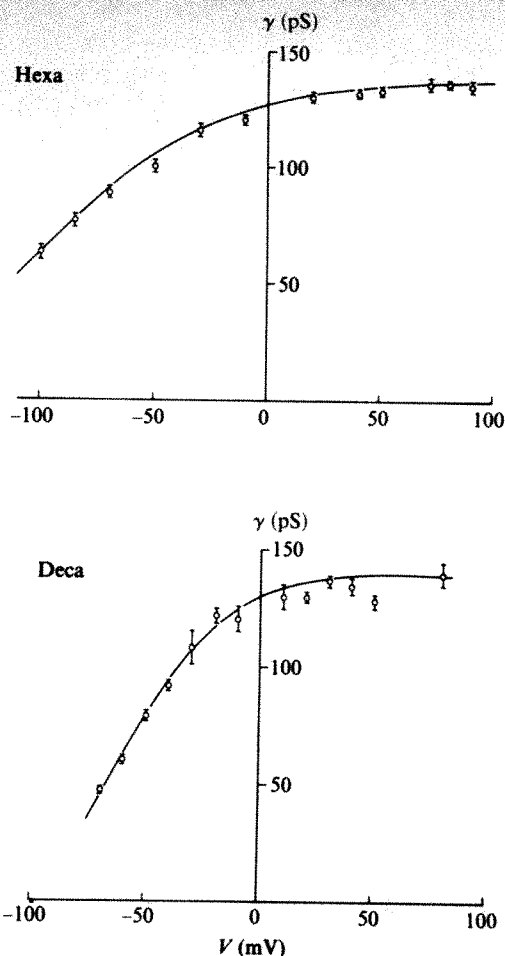
\* Present address: Department of Biochemistry, Cornell University, Ithaca, New York 14854.

† To whom correspondence should be addressed.





**Fig. 2** Channels at low temperature in the presence of 20  $\mu$ M decamethonium added *trans*. Temperature was maintained at 7 °C using an ice-water bath. *a*, Recordings from the same membrane at -50 and +50 mV. *b*, Closing events at -50 mV after channels were open by holding the voltage at +50 mV (refs 4, 5). *c*, Recordings while a single channel opens at -50 mV and undergoes repetitive flickering. The mean open time of the open state in this experiment was 3.5 s and the mean closed time was 19.3 s (measurements done before addition of drug). The conductance drop during individual blocking events, measured in the cases where they could be resolved, was  $72 \pm 2$  pS ( $n = 10$ ) whereas the open-state conductance, measured in between flickering, was  $71 \pm 0.5$  pS ( $n = 20$ ). Blocking events were defined as apparent 'closed' states lasting less than 100 ms. These short-lived "closed" dwell times were observed only when the drug was present.



**Fig. 3** Voltage-dependent single-channel conductance in symmetrical solutions of 50 mM  $K_2SO_4$  buffer plus 100  $\mu$ M decamethonium or 1 mM hexamethonium. To obtain reliable measurements of the time-average conductance of channels with decamethonium, flickering was filtered using the amplifier with a time resolution of 0.5 s. This allowed measurement of a smooth d.c. value for the average open-state conductance. A total of 169 determinations from 4 membranes for decamethonium and 135 determinations from 7 membranes for hexamethonium were used to fit the curves. Bars indicate s.e.m.; the solid lines correspond to the single-site blocking equilibria<sup>6,9</sup> described by equation (1) below and the parameters given in the text

$$\langle \gamma \rangle / \gamma_0 = [1 + (B/K_0) \exp(z\delta FV/RT)]^{-1} \quad (1)$$

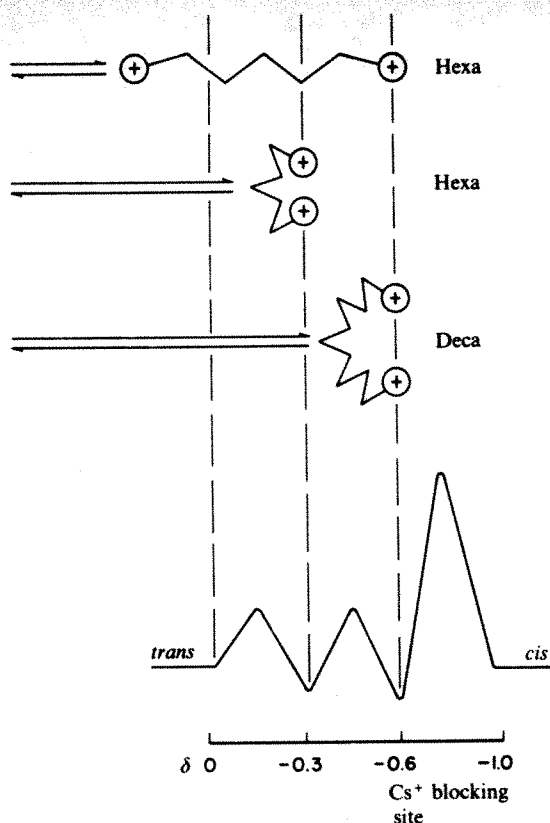
Where  $\langle \gamma \rangle$  is the time-averaged conductance in the presence of constant blocker at concentration  $B$ ;  $\gamma_0 = 140$  pS is the unblocked open-state conductance;  $K_0$  is the dissociation constant of the blocking reaction at zero volts;  $z$  is the valence of the blocking ion;  $\delta$  is the fraction of the total electric potential drop across the membrane found at the blocking site;  $V$  is the applied voltage;  $R$ ,  $T$ ,  $F$  have their usual meanings. Parameters for the fitted curves were obtained from a linearized form of equation (1) as described previously<sup>6</sup>. These parameters are  $K_0 = 11 \pm 0.5$  mM,  $z\delta = -0.66 \pm 0.02$  for hexamethonium and  $K_0 = 1.2 \pm 0.2$  mM,  $z\delta = -1.22 \pm 0.08$  for decamethonium.

three kinetic barriers and that the channel can accommodate at most one ion at a time (two sites, three barriers, one-ion Eyring model)<sup>12</sup>. The one-ion condition implies that the channel can accommodate a blocker ion or a conducting ion but not both simultaneously. Thus, we propose that the short-lived non-conducting dwell times observed in the presence of decamethonium correspond to blocking events generated by single drug molecules as they bind to the conducting channel. Flickering would then be the consequence of the reversible equilibrium of the blocking reaction. A one-site one-blocker model predicts that the time-averaged open-state conductance should decrease in the presence of the drug and that this average should be voltage dependent<sup>6,9-11</sup>.

An expression that combines the single-site binding with the voltage dependence of the dissociation constant is given by equation (1) shown in Fig. 3 legend. In Fig. 3 we measured the time-averaged conductance  $\langle \gamma \rangle$  as a function of voltage at constant and symmetrical concentration of blocker. Starting from the unblocked open-state conductance of 140 pS at positive voltages, the conductance falls steeply at negative voltages for both hexamethonium and decamethonium. Thus, these drugs block only from the *trans* side of the membrane. The solid lines correspond to equation (1) with  $K_0 = 11$  mM,  $z\delta = -0.66$  for hexamethonium and  $K_0 = 1.2$  mM,  $z\delta = -1.22$  for decamethonium (see Fig. 3 legend for explanation of symbols). The fit is consistent with the one-site blocking model within the voltage range measured.

The qualitative difference between the two blockers (flickering compared with 'quiet' channels) would be attributable to differences in the lifetime of the blocked state. If a blocker molecule forms blocked states that are short lived with respect to

the time response of the amplifier (5 ms), we would observe only an average apparent open-state conductance equal to the time-average of true open and true blocked conductances<sup>11</sup>. This seems to be the case for hexamethonium and caesium<sup>6</sup> in this channel. Molecules forming long-lived blocked states would generate flickering of the open-state conductance. This seems to be the case for lidocaine derivatives in the acetylcholine-receptor channel<sup>10</sup>, for tetraalkylammonium ions in the amphotericin channel<sup>8</sup>, and for decamethonium, as described here.



**Fig. 4** One or two blocking site models for methonium derivatives. In the same spirit of the two-site conduction model proposed for the SR channel recently<sup>12</sup>, we propose that both molecules can block at the  $\text{Cs}^+$  site but in different conformations to account for  $z\delta$  values measured (upper part). The alternative, of block at different sites, implies that hexamethonium would also act in a bent conformation. We envision that for methonium molecules at least one of the energy barriers (the *cis*-facing barrier) must be higher than the rest because they block only from the *trans* side. This is shown at the energy profile at the bottom. The  $\text{Cs}^+$ -blocking site was determined previously<sup>6</sup> and corresponds to  $\delta = 0.37 \pm 0.01$  measured from the *cis* side;  $\delta$ , when measured from the *trans* side is equal to  $1 - \delta$  measured from the *cis* side.

We suggest two possible explanations for the different voltage dependences found for the two methonium blockers. As shown in Fig. 4, both molecules could possibly bind to the same site in the channel if hexamethonium blocks in a linear conformation with one charge inside the field and decamethonium in a bent conformation with both charges inside the field. In this case, the long-lived blocked states could be due to stabilization of the two charges of the molecules at the binding site. Alternatively, if both blockers act in bent conformations, the blocking site would be more external for hexamethonium than for decamethonium.

It is necessary to propose the unusual bent-over conformation for decamethonium (Fig. 4), with the two positively charged quaternary ammonium groups located in close proximity, both inside a channel structure, because of the following observations: (1) the channel seems to accommodate only one ion at a time<sup>12</sup>; (2) decamethonium blocks with an 'effective valence' of 1.2, indicating that more than one charge enters the field; (3) at least 18 different monovalent organic cations (decyltrimethylammonium among them) block the channel from the *trans* side with  $z\delta = -0.62 \pm 0.03$  (R.C., unpublished results). Fortunately, decamethonium is a simple molecule, and it will be possible to synthesize several analogues with locked-in conformations which should reveal the molecular requirements for block with high affinity, long-lived blocked states and strong voltage dependence.

We thank Dr Eve Marder for providing us with the methonium blockers, and Mr Jeff Stern for comments on the

manuscript. This work was supported by NIH grants R01-AM-19826-03, K04-AM-00354-02 and by a Dretzin fellowship of Brandeis University.

Received 4 July; accepted 22 September 1980.

- McKinley, D. & Meissner, G. *FEBS Lett.* **82**, 47-50 (1977).
- McKinley, D. & Meissner, G. *J. Membrane Biol.* **44**, 159-186 (1978).
- Miller, C. *J. Membrane Biol.* **40**, 1-23 (1978).
- Miller, C. & Rosenberg, R. *J. gen. Physiol.* **74**, 457-478 (1979).
- Labarca, P., Coronado, R. & Miller, C. *J. gen. Physiol.* **76**, 397-424 (1980).
- Coronado, R. & Miller, C. *Nature* **280**, 807-810 (1979).
- Adams, P. R. & Sakmann, B. *Proc. natn. Acad. Sci. U.S.A.* **75**, 2994-2998 (1978).
- Borisova, M. P., Ermishkin, L. N. & Silberstein, A. Ya. *Biochim. biophys. Acta* **553**, 450-459 (1979).
- Adelman, J. & French, R. *J. Physiol., Lond.* **276**, 13-25 (1978).
- Neher, E. & Steinbach, J. H. *J. Physiol., Lond.* **277**, 153-176 (1978).
- Woodhull, A. M. *J. gen. Physiol.* **61**, 687-708 (1973).
- Coronado, R., Rosenberg, R. & Miller, C. *J. gen. Physiol.* **76**, 425-446 (1980).

## Defective synthesis of HbE is due to reduced levels of $\beta^E$ mRNA

Joanne Traeger, W. G. Wood\*, J. B. Clegg & D. J. Weatherall

MRC Molecular Haematology Unit and Tropical Medicine Research Unit, University of Oxford, Nuffield Department of Clinical Medicine, John Radcliffe Hospital, Oxford OX3 9DU, UK

P. Wasi

Division of Haematology, Siriraj Hospital Bangkok, Thailand

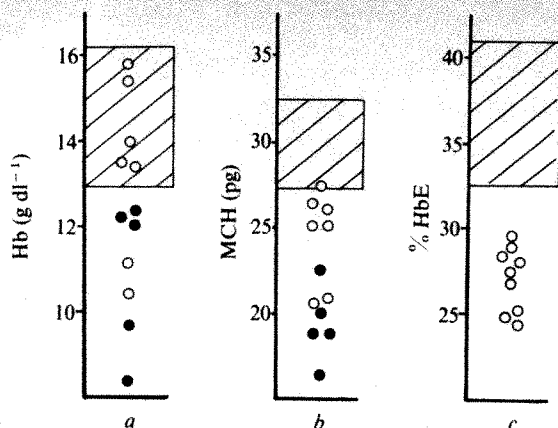
**Haemoglobin E ( $\alpha_2\beta_2^{26\text{Glu} \rightarrow \text{Lys}}$ )** is one of the commonest haemoglobin variants. There are an estimated 30 million carriers of the  $\beta^E$  gene in South-East Asia, where they comprise more than 50% of the population in some areas<sup>1,2</sup>; however, the reasons for this high frequency have never been adequately explained. Homozygotes for HbE may be mildly anaemic, but they do not have any clinical disability<sup>3,4</sup>. However, individuals heterozygous for both  $\beta^E$  and  $\beta$  thalassaemia (HbE/ $\beta$  thalassaemia) have a severe clinical disorder which in some cases may approach that seen in homozygous  $\beta$  thalassaemia<sup>3,5,6</sup> and which is by far the commonest form of symptomatic thalassaemia in the Indian subcontinent and South-East Asia. Haemoglobin E is the only common structural variant which interacts with  $\beta$  thalassaemia to produce such a severe disorder and the underlying mechanism of the interaction is not known. We have studied several homozygotes and heterozygotes for HbE and show here that the  $\beta^E$  chain is inefficiently synthesized and produces the phenotype of a mild form of  $\beta$  thalassaemia; hence, when inherited together with  $\beta$  thalassaemia it causes a marked  $\beta$ -chain deficit. Furthermore, the mechanism for the defective production of  $\beta^E$  chains seems to be a reduction of  $\beta^E$  mRNA, a most unexpected finding in a disorder caused by a single amino acid substitution and presumably by a single nucleotide change in the DNA of the  $\beta$  globin gene.

Five HbE homozygotes and nine heterozygotes were studied, all of South-East Asian origin. The presence of HbE was confirmed by peptide analysis in two cases and by a positive DCIP precipitation test<sup>7</sup> in the remainder. The  $\alpha$  gene status of all the cases was examined by restriction endonuclease mapping<sup>8</sup> and, with the exception of a single  $\alpha$  gene deletion in one of the HbE heterozygotes, normal  $\alpha$  gene maps were obtained.

All the homozygotes showed a reduced haemoglobin level and microcytic, poorly haemoglobinized red cells (Fig. 1). The heterozygotes also had a reduced amount of haemoglobin per cell, as reported previously<sup>9</sup>, and the proportion of HbE was only 25-30% (Fig. 1), significantly less than the 35-45% normally observed in heterozygotes for stable  $\beta$  chain

\* To whom correspondence should be addressed.



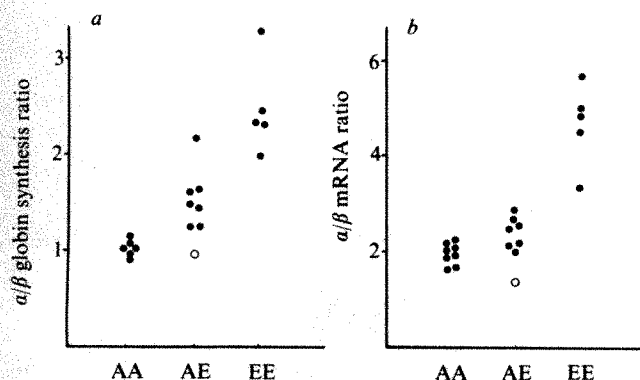


**Fig. 1** Haemoglobin level (a), mean cell haemoglobin (b) and % HbE (c) in homozygous (●) and heterozygous (○) carriers of the  $\beta^E$  gene. The hatched area shows the normal range; in c this represents the % abnormal haemoglobin in a series of 16 heterozygotes for HbS, HbC and HbD, as measured in our laboratory.

variants<sup>10</sup>. Separation of peripheral blood erythrocytes according to age, by high-speed centrifugation, showed no change in the proportion of HbE between old and young cells, demonstrating that there is no preferential loss of HbE as the cells age.

The measurement of globin chain synthesis in peripheral blood reticulocytes of five HbE homozygotes showed a marked deficit of  $\beta^E$  chain synthesis (Fig. 2a), with  $\alpha/\beta$  chain synthesis ratios similar to, or greater than, those normally observed in  $\beta$  thalassaemia heterozygotes. The synthesis of excess  $\alpha$  chains in these cells was confirmed by gel filtration of the  $^3\text{H}$ -leucine-labelled reticulocyte lysates<sup>11</sup>, where a pool of radioactive free  $\alpha$  chains could be easily demonstrated. Furthermore, fine precipitates, typical of the free  $\alpha$  chain precipitates found in  $\beta$  thalassaemia, were observed in the bone marrow normoblasts of two of these patients by electron microscopy (S. Wickramasinghe, personal communication).

Among the HbE heterozygotes, the  $\alpha/\beta^A + \beta^E$  ratios ranged from 1.03 to 2.19 (Fig. 2a), which, with the exception of the individual who also had  $\alpha$  thalassaemia, were always greater than those for the normal control incubation run in parallel. The mean  $\beta^A/\beta^E$  specific activity (c.p.m. per mg) ratio obtained after

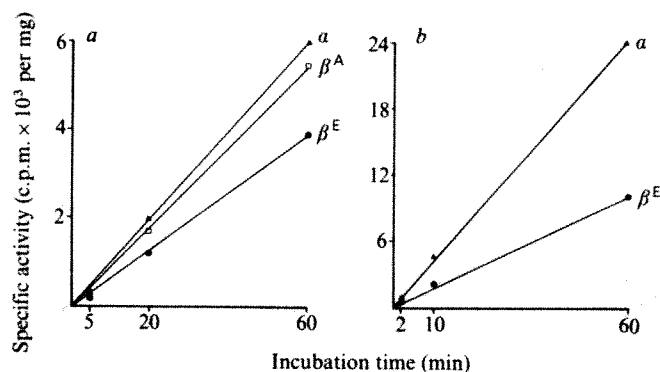


**Fig. 2** a, Globin chain synthesis ratios in peripheral blood reticulocytes in normal (AA), heterozygous HbE (AE) and homozygous HbE (EE) individuals measured after 60 min incubation with  $^3\text{H}$ -leucine<sup>11</sup>. b, Ratios of  $\alpha/\beta$  globin RNA in the same individuals using the method described in ref. 14. The open symbols are the results from the individual shown by gene mapping to have one (out of four)  $\alpha$  gene deleted.

60 min incubation was  $1.24 \pm 0.20$ ; this provides further evidence that HbE is not an unstable haemoglobin, because if that were the case, such ratios would be less than 1.0.

The time course of globin chain synthesis was studied in three homozygotes and three heterozygotes (Fig. 3). Even at the earliest time point (2 min) there was no evidence that the specific activity of the  $\beta^E$  chains exceeded those of the  $\alpha$  and  $\beta^A$  chains, and in the heterozygotes the  $\beta^A/\beta^E$  chain synthesis ratios remained constant throughout the incubation period. This argues against rapid destruction of the newly synthesized  $\beta^E$  chains.

Globin chain synthesis was also measured in bone marrow aspirates from three homozygotes and two heterozygotes and in each case the  $\alpha/\text{non-}\alpha$  chain synthesis ratio was more balanced than in the corresponding peripheral blood sample (Fig. 4). This must in part reflect the proteolytic destruction of some of the excess  $\alpha$  chains, as has been shown to occur in  $\beta$  thalassaemia heterozygotes<sup>12,13</sup>. In the marrow of one of the heterozygotes the  $\beta^A/\beta^E$  synthesis ratio remained constant throughout a 60 min incubation, but in both heterozygotes this ratio was lower in the bone marrow (1.23, 0.91) than in the reticulocytes (1.51, 1.15) after a 60-min incubation.



**Fig. 3** a, The incorporation of  $^3\text{H}$ -leucine into the globin chains of a HbE heterozygote during a 60-min incubation of peripheral blood reticulocytes. b, A similar experiment with blood from a HbE homozygote.

These experiments produce clear evidence for the defective synthesis of  $\beta^E$  chains. To determine whether this occurs at, or before, the translational level, the amounts of  $\alpha$  or  $\beta$  globin mRNA in the reticulocytes of these individuals were measured. We have reported previously<sup>14</sup> that in carefully standardized conditions the  $\alpha/\beta$  globin mRNA ratios fall into non-overlapping groups of normal individuals and those with various forms of  $\alpha$  and  $\beta$  thalassaemia. The values obtained do not represent absolute mRNA values, but the results are valid for comparative purposes<sup>14</sup>. In the present study the  $\alpha/\beta$  mRNA ratios in five HbE homozygotes (Fig. 2b) ranged from 3.29 to 5.81. This is two- to threefold higher than the range of 1.62–2.22 (mean 1.98) found in eight normal individuals studied at the same time, and similar to the values of 3.7 and 3.9 obtained in two  $\beta$  thalassaemia heterozygotes examined in this laboratory. Clearly, the deficit of  $\beta^E$  chain synthesis is reflected by a similar deficit of  $\beta^E$  mRNA production. Furthermore, in seven HbE heterozygotes the  $\alpha/\beta^A + \beta^E$  mRNA ratios were significantly higher than in the normal controls (Fig. 2b).

These experiments demonstrate, therefore, that the low level of HbE is not primarily due to instability of the  $\beta^E$  chain<sup>15</sup>, or to incomplete association into tetramers<sup>16</sup>, as previously suggested, but results from deficient synthesis of  $\beta^E$  chains, as suggested by previous studies on isolated cases<sup>4,16,17</sup>. The reduced synthesis of HbE (to approximately half normal levels) means that the  $\beta^E$  gene acts like a mild form of  $\beta$  thalassaemia and explains why, in the homozygous state, it produces a phenotype

similar to  $\beta$  thalassaemia minor, and why on interaction with a  $\beta$  thalassaemia gene, it produces a severe clinical disorder. The demonstration that deficient synthesis of the  $\beta^E$  chain results from lowered amounts of  $\beta^E$  mRNA is completely unexpected for a structural globin chain variant which results from a single amino acid substitution and hence presumably from a single nucleotide change. It is difficult to see how this single base change could alter globin gene transcription, but it is possible that its position at codon 26, close to the boundary of coding

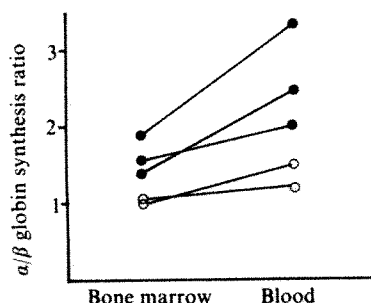


Fig. 4 Comparison of the  $\alpha/\beta$  globin chain synthesis ratios in peripheral blood reticulocytes and bone marrow in three HbE homozygotes (●) and two HbE heterozygotes (○).

and intervening sequences after codon 30, might interfere with nuclear RNA processing. It is also possible that this particular nucleotide is involved in the secondary structure of the mRNA and that its substitution results in mRNA instability. The finding that the specific activity of  $\beta^E$  chains is lower than that of  $\beta^A$  chains in the reticulocyte incubations and the increase in the  $\beta^A/\beta^E$  globin synthesis ratios from bone marrow to reticulocytes would be consistent with this mechanism but this is very indirect evidence and could only be confirmed by measurements of bone marrow cytoplasmic mRNA ratios.

The remaining possibility is that the base substitution is not the cause of the decreased  $\beta^E$  chain synthesis but that there is a mild  $\beta$  thalassaemia mutation in *cis* to the  $\beta^E$  mutation. This could have arisen by sequential mutations in the same  $\beta$  globin gene, in either order, or by recombination between genes carrying the  $\beta^E$  and  $\beta$  thalassaemia lesions. If this were the case, the high frequency of the  $\beta^E$  gene in South-East Asia may be the result of selection for the  $\beta$  thalassaemia phenotype and the presence of the structural variant may be incidental.

**Note added in proof:** Reduced amounts of  $\beta^E$  mRNA have also been observed in patients with HbE/ $\beta$  thalassaemia, as reported in abstract form by Berman *et al.*<sup>18</sup>.

Received 5 August; accepted 27 October 1980.

1. Platz, G. *Humangenetik* **3**, 189–234 (1967).
2. Sicard, D., Lieuzou, Y., Lapoumeroulie, C. & Labie, D. *Hum. Genet.* **50**, 327–336 (1979).
3. Chernoff, A. I. *et al. J. Lab. clin. Med.* **47**, 455–489 (1956).
4. Fairbanks, V. F., Oliveros, R., Brandabur, J. H., Willis, R. R. & Fiester, R. F. *Am. J. Hemat.* **8**, 109–121 (1980).
5. Bamapravati, N., Na-Nakorn, S., Wasi, P. & Tuchinda, S. *Am. J. clin. Path.* **47**, 745–753 (1967).
6. Wasi, P. *et al. Ann. N.Y. Acad. Sci.* **165**, 60–82 (1969).
7. Frischer, H. & Bowman, J. J. *Lab. clin. Med.* **85**, 531–538 (1975).
8. Higgs, D. R. *et al. Lancet* **ii**, 272–276 (1979).
9. Fairbanks, V. F., Gilchrist, G. S., Brimhall, B., Jereb, J. A. & Goldston, E. C. *Blood* **53**, 109–115 (1979).
10. Nute, P. E. *Ann. N.Y. Acad. Sci.* **241**, 39–60 (1974).
11. Weatherall, D. J., Clegg, J. B., Na-Nakorn, S. & Wasi, P. *Br. J. Haemat.* **16**, 251–267 (1969).
12. Wood, W. G. & Stamtoyannopoulos, G. *J. clin. Invest.* **55**, 567–578 (1975).
13. Chalevalakis, G., Clegg, J. B. & Weatherall, D. J. *Proc. natn. Acad. Sci. U.S.A.* **72**, 3835–3857 (1975).
14. Hunt, D. M. *et al. Br. J. Haemat.* **45**, 53–64 (1980).
15. Feldman, R. & Rieder, R. F. *Blood* **42**, 783–791 (1973).
16. Pagnier, J., Wajcman, H. & Labie, D. *FEBS Lett.* **45**, 252–255 (1974).
17. Testa, U. *et al. Acta haemat.* **64**, 42–52 (1980).
18. Berman *et al. Clin. Res.* **28**, 350A (1980).

## Amino acid sequence homology between cholera toxin and *Escherichia coli* heat-labile toxin

Walter S. Dallas\* & Stanley Falkow

Department of Microbiology and Immunology, University of Washington, Seattle, Washington 98195

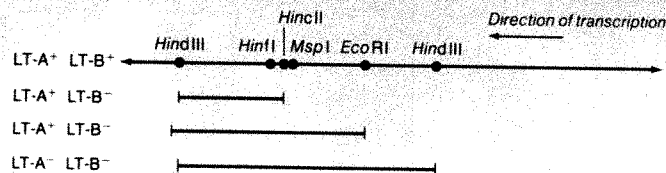
Cholera toxin (CT) and the *Escherichia coli* heat-labile toxin (LT) are functionally, structurally and immunologically similar enterotoxins. Both toxins cause the elevation of cyclic AMP levels in gut epithelial cells<sup>1,2</sup> by catalysing the NAD-dependent ADP ribosylation of membrane proteins<sup>3–6</sup>. Each toxin is composed of two dissimilar subunits<sup>7,8</sup>. The A subunit has an enzymatic activity and is the adenylate cyclase-activating component of the enterotoxin<sup>4–11</sup>. The B subunit recognizes membrane components and binds the holotoxin to the target cell juxtaposing the A subunit with its substrates<sup>9,12</sup>. Binding studies and competition experiments indicate that the membrane receptors for cholera toxin B subunit (CT-B) and LT-B are similar but not identical<sup>13</sup> (these studies were performed before LT was purified to homogeneity). The monosialoganglioside GMI has been shown to be the receptor for the cholera toxin<sup>14</sup>, and it probably composes part of the receptor for LT. Gyles and Barnum<sup>15</sup> first reported that LT and cholera toxin were immunologically related, and it has subsequently been shown that they share common antigenic determinants in both A and B subunits<sup>16</sup>. The primary structure of CT-B has been determined<sup>17,18</sup>. We report here a comparison between the amino acid sequences of LT-B and CT-B. The nucleotide sequence of the LT-B cistron (*eltB*) was determined using a recombinant plasmid encoding LT<sup>9</sup>. Translation of this sequence revealed that LT-B and CT-B show significant amino acid sequence homology. In addition, several features of the *eltB* cistron were revealed by the sequence analysis.

Previously, we described the cloning of the LT genetic determinant<sup>19</sup>. Analysis of *in vitro* generated deletions in the LT gene showed that the gene was composed of two cistrons and established an approximate locus for both *eltA* (encoding LT-A) and *eltB* (encoding LT-B)<sup>9</sup>. The LT phenotypes encoded by various deletion plasmids indicated that *eltB* was located on a DNA fragment bounded by *Hind*III sites (Fig. 1). If *eltA* and *eltB* were adjacent cistrons, then the data further suggested that the N-terminus of LT-B would be coded by the smaller DNA fragment between the *Hind*III site and the *Eco*R1 site. Figure 2 shows the nucleotide sequence around the *Eco*R1 site. In most instances the nucleotide sequence of both strands was ascertained. The largest protein that could be encoded in this region was found to be 124 amino acids in length. The initiation codon for this protein was located 10 base pairs from the *Eco*R1 site, but not in the small DNA fragment as initially speculated.

The nucleotide sequence encoding this protein was translated into an amino acid sequence which was compared with the sequence of CT-B (Fig. 3). The N-terminus of mature CT-B is threonine and the C-terminus is asparagine. The putative LT-B amino acid sequence also had asparagine as the C-terminal amino acid. If one compares the next 102 amino acid residues starting from the C-terminus, 80 of the LT-B residues are identical to those of CT-B. This result represents 79% homology. Of the 22 amino acid residues that differ, a single base change in the *eltB* codon could account for 20 of the changes. The other two nonhomologous amino acids would require a minimum of two base changes in the *eltB* codon to result in the homologous amino acid as found in CT-B. There are no regions in which the nonhomologous amino acids are concentrated, but rather they seem to be scattered throughout the primary sequence, except for a run of 23 residues (47–69) that are identical between the two proteins. A mature LT-B

\* Present address: Cetus Corporation, 600 Bancroft Way, Berkeley, California 94710.





**Fig. 1** Schematic diagram of the LT DNA region. Bars indicate plasmid DNA that was deleted<sup>9</sup>. The effect of each deletion on LT-A and LT-B expression is shown. Restriction enzyme recognition sequences used for DNA sequencing are also shown.

would have three more acidic amino acid residues than CT-B, whereas CT-B would have two more basic residues than does LT-B. CT-B has a compositional molecular weight of 11,590, whereas that of mature LT-B is 11,780, the difference corroborating our earlier reports that LT-B was slightly larger than CT-B (see note added in proof)<sup>8,9</sup>.

The 21 additional amino acid residues encoded at the N-terminus of *eltB* are undoubtedly a leader sequence that directs the nascent protein through (into) the cell membrane(s) and is eventually cleaved from the molecule. This is suggested by: (1) A few prokaryotic leader sequences have been characterized and these sequences range from 20 to 23 residues in length<sup>20</sup>; the LT-B leader sequence would be 21 amino acids in length. (2) Like prelipoprotein, the LT-B leader sequence would be cleaved after a glycine residue<sup>21</sup>. (3) The leader sequence of LT-B resembles the leader sequence of prelipoprotein in that both polypeptides have several charged amino acid residues at the N-terminus followed by a region, ~60%, composed of hydrophobic amino acids. (4) There is evidence that LT is either a periplasmic protein<sup>22</sup> or an outer membrane-associated protein<sup>11</sup> and, therefore, it would be expected to possess a leader sequence.

One hundred and eighty nucleotides proximal to *eltB* have also been determined. None of these sequences has a Pribnow box-like structure which is characteristic of an RNA polymerase binding site. This result supports our earlier data which suggested that *eltA* and *eltB* are transcribed as a single polycistronic mRNA and that *eltA* was located next to the promoter<sup>9</sup>. There is a Shine-Dalgarno sequence<sup>23</sup> three nucleotides from the initiation codon of *eltB*. Five nucleotides in this region are complementary with five of the first 12 nucleotides at the 3' end of the 16S ribosomal RNA. The nucleotide adjacent to the initiation codon *eltB* is an A which has been reported to enhance ribosome

| LT  | CT  | LT  | CT  | LT | CT  | LT  | CT  | LT  | CT  |
|-----|-----|-----|-----|----|-----|-----|-----|-----|-----|
| Met | Asn | Ile | Ile | 30 | Ser | Ser | Ser | 80  | Thr |
| Asn | Lys | Thr | Thr |    | Met | Leu | Gln | Gln | Ala |
| Lys | Val | Glu | Asp |    | Ala | Ala | His | His | Ile |
| Val | Lys | Leu | Leu |    | Gly | Gly | Ile | Ile | Asp |
| Lys | Cys | Cys | Cys |    | Lys | Lys | Asp | Asp | Lys |
| Cys | Tyr | Ser | Ala | 10 | Arg | Arg | 60  | Ser | Ser |
| Tyr | Val | Glu | Glu |    | Glu | Glu | Gln | Gln | Lys |
| Val | Leu | Tyr | Tyr |    | Met | Met | Lys | Lys | Cys |
| Leu | Phe | Arg | His |    | Val | Ala | Lys | Lys | Val |
| Phe | Thr | Asn | Asn |    | Ile | Ile | Ala | Ala | Trp |
| Thr | Ala | Thr | Thr | 40 | Ile | Ile | Ile | Ile | Asn |
| Ala | Leu | Gln | Gln |    | Thr | Thr | Glu | Glu | Asn |
| Leu | Ser | Ile | Ile |    | Phe | Phe | Arg | Arg | Lys |
| Leu | Ser | Tyr | His |    | Met | Met | Met | Met | Thr |
| Ser | Ser | Thr | Thr |    | Ser | Asn | Lys | Lys | Pro |
| Ser | Leu | Ile | Leu | 20 | Gly | Gly | 70  | Asp | Asn |
| Tyr | Ala | Asn | Asn |    | Glu | Ala | Thr | Thr | Ile |
| Ala | His | Lys | Lys |    | Thr | Thr | Leu | Leu | Ala |
| Gly | Ala | Ile | Ile |    | Phe | Phe | Arg | Arg | Ile |
|     |     | Leu | Phe | 50 | Gln | Gln | Ile | Ile | Ala |
| Thr | Pro | Ser | Ser |    | Val | Val | Thr | Ala | 100 |
| Pro | Gln | Tyr | Tyr |    | Glu | Glu | Tyr | Tyr | Ser |
| Gln | Thr | Thr | Thr |    | Val | Val | Leu | Leu | Met |
| Thr | Asn | Glu | Glu |    | Pro | Pro | Thr | Thr | Lys |
|     |     |     |     |    | Gly | Gly | Glu | Glu | Asn |

**Fig. 3** Comparison of the amino acid sequence of LT-B and CT-B. The arrows indicate nonhomologous amino acids. Amino acids are numbered starting with the proposed N-terminal residue of mature LT-B.

binding<sup>24</sup>. The presence of a ribosome binding site adjacent to *eltB* may explain the observation that LT-B is present in at least 5 M excess compared with LT-A, even though *eltA* is closer to the promoter<sup>9</sup>. This could be accounted for if the *eltB* ribosome binding site is more efficient than the *eltA* ribosome binding site and/or if the secondary structure of the mRNA enhances translation of *eltB* compared to *eltA*. Interestingly, no sequences characteristic of mRNA termination signals have been found in the DNA sequences distal to *eltB*. Preliminary sequencing information does suggest, however, that an additional protein may be encoded by the LT operon, but additional sequencing will be necessary to confirm or reject this conjecture.

Our sequencing information confirms the similarities between LT and CT. Knowledge of the nucleotide sequence of *eltB* should enable substitution of single amino acids by site-specific mutagenesis of a nucleotide in a codon and observation of the effect on protein function. The structural similarities shared by the adsorption proteins makes it tempting to speculate that immunity to LT-B might result in immunity to CT and neutralization of the toxin. In this regard, LT-B-producing *E. coli* might be potential live, oral vaccine candidates, both for LT-mediated diarrhoeal disease (in man and animals) and cholera.

We have successfully cloned *eltB* in such a way that it is being transcribed through the *lac* promoter and a protein is being made from this transcript that is structurally, functionally, and immunologically indiscernible from LT-B (manuscript in preparation). Using a strain harbouring this gene, we are pursuing the idea of an LT-B vaccine.

We thank Donna Montgomery and Jeff Bennetzen for technical assistance. This work was supported by Public Health Service grant AI-10885-09 from the National Institute of Allergy and Infectious Diseases. W.S.D. was supported by the Biological Infections grant T32A1079-02 from the NIH.

**Note added in proof:** Clements *et al.*<sup>25</sup> have reported the first 20 amino acids of LT-B isolated from *E. coli* K-12 carrying one of our LT plasmids. These amino acids are identical with the first 20 amino acids of our predicted mature LT-B amino acid sequence.

Received 11 July; accepted 25 September 1980.

- Evans, D. J., Chin, L. C. & Evans, D. G. *Nature new Biol.* **236**, 137-138 (1972).
- Chen, L., Rhode, J. E. & Sharp, G. W. G. *J. clin. Invest.* **51**, 731-740 (1972).
- Gill, D. M., Evans, D. J. Jr & Evans, D. G. *J. infect. Dis. Suppl.* **133**, S103-107 (1976).
- Gill, D. M. & King, C. A. *J. biol. Chem.* **250**, 6424-6432 (1975).
- Cassel, D. & Pfeuffer, T. *Proc. natn. Acad. Sci. U.S.A.* **75**, 2669-2673 (1978).
- Moss, J. & Richardson, S. H. *J. clin. Invest.* **62**, 281-285 (1979).
- Lonnroth, I. & Holmgren, J. *J. gen. Microbiol.* **76**, 417-427 (1973).
- Dallas, W. S. & Falkow, S. *Nature* **277**, 406-407 (1979).
- Dallas, W. S., Gill, D. M. & Falkow, S. *J. Bact.* **139**, 850-858 (1979).
- Dorner, F., Hughes, C., Nahler, G. & Hogenauer, G. *Proc. natn. Acad. Sci. U.S.A.* **76**, 4832-4836 (1979).
- Kunkel, S. L. & Robertson, D. C. *Infect. Immun.* **25**, 586-596 (1979).
- Cuatrecasas, P., Parikh, I. & Hollenberg, M. D. *Biochemistry* **12**, 4253-4264 (1973).
- Holmgren, J. *Infect. Immun.* **8**, 851-859 (1973).

HinfI EcoRI  
 5' GTTGACATATATAACAGAAATTCGGATGAATT ATG AAT AAA GTA AAA TGT TAT GTT TTA  
 Met Asn Lys Val Lys Cys Tyr Val Leu  
 5' TTT ACG GCG TTA CTA TCC TCT CTA TAT GCA CAC GGA GCT CCC CAG ACT ATT  
 Phe Thr Ala Leu Leu Ser Ser Leu Tyr Ala His Gly Ala Pro Gln Thr Ile  
 5' ACA CAA CTA TGT TCG GAA TAT CGCAAC ACA CAA ATA TAT ACG ATA AAT GAC  
 Thr Glu Leu Cys Ser Glu Tyr Arg Asn Thr Gln Ile Tyr Thr Ile Asn Asp  
 5' AAG ATA CTA TCA TAT ACG GAA TCG ATG GCA GGC AAA AGA GAA ATG GTT ATC  
 Lys Ile Leu Ser Tyr Thr Glu Ser Met Ala Gly Lys Arg Glu Met Val Ile  
 5' ATT ACA TTT ATG AGC GGC GAA ACA TTT CAG GTC GAA GTC CCG GGC AGT CAA  
 Ile Thr Phe Met Ser Gly Glu Thr Phe Gln Val Glu Val Pro Gly Ser Gln  
 5' CAT ATA GAC TCC CAG AAA AAA GCC ATT GAA AGG ATG AAG GAC ACA TTA AGA  
 His Ile Asp Ser Gln Lys Lys Ala Ile Glu Arg Met Lys Asp Thr Leu Arg  
 5' ATC ACA TAT CTG ACC GAG ACC AAA ATT GAT AAA TTA TGT GTA TGG AAC AAT  
 Ile Thr Tyr Leu Thr Glu Thr Lys Ile Asp Lys Leu Cys Val Trp Asn Asn  
 5' AAA ACC CCC AAT TCA ATT GCG GCA ATC AGT ATG AAA AAC TAG  
 Lys Thr Pro Asn Ser Ile Ala Ala Ile Ser Met Lys Asn STOP

**Fig. 2** Nucleotide sequence of *eltB*. The nucleotide sequence was determined using the chemical method of Maxam and Gilbert<sup>26</sup>. DNA strands were radiolabelled by a kinase reaction or by end repair using DNA polymerase I Klenow fragment. The five underlined nucleotides are complementary with five of the first 12 nucleotides of the 16S ribosomal RNA. The amino acid labelled 1 is the proposed N-terminal amino acid residue of mature LT-B. Several restriction enzyme recognition sites are shown.

14. Bennett, V. & Cuatrecasas, P. in *The Specificity and Actions of Animal, Bacterial, and Plant Toxins* (ed. Cuatrecasas, P.) 3-66 (Halsted, London, 1977).
15. Gyles, C. L. & Barnum, D. A. *J. infect. Dis.* **120**, 419-426 (1978).
16. Clements, J. D. & Finkelstein, R. A. *Infect. Immun.* **21**, 1036-1039 (1978).
17. Kurosky, A., Markel, D. E., Peterson, J. W. & Fitch, W. M. *Science* **195**, 299-301 (1977).
18. Lai, C. J. *biol. Chem.* **252**, 7249-7256 (1977).
19. So, M., Dallas, W. S. & Falkow, S. *Infect. Immun.* **21**, 405-411 (1978).
20. Selker, B. D. & Tai, P. C. *Nature* **283**, 433-438 (1980).
21. Inouye, S., Wan, S., Sekizawa, J., Halegoua, S. & Inouye, M. *Proc. natn. Acad. Sci. U.S.A.* **74**, 1004-1008 (1977).
22. Evans, D. J. Jr, Evans, D. E., Richardson, S. H. & Gorbach, S. L. *J. infect. Dis. Suppl.* **133**, S97-108 (1976).
23. Shine, J. & Delgarno, L. *Proc. natn. Acad. Sci. U.S.A.* **71**, 1342-1346 (1974).
24. Selker, B. D. & Yanofsky, C. *J. molec. Biol.* **130**, 135-143 (1979).
25. Clements *et al.* *Infect. Immun.* **29**, 91-97 (1980).
26. Maxam, A. M. & Gilbert, W. *Proc. natn. Acad. Sci. U.S.A.* **74**, 560-564 (1977).

## Freezing induced change in ligand orientation in oxycobalt-myoglobin

Hiroshi Hori, Mássao Ikeda-Saito & Takashi Yonetani\*

Department of Biochemistry and Biophysics, University of Pennsylvania School of Medicine, Philadelphia, Pennsylvania 19104 and INSERM Laboratory Unit 128, 34033 Montpellier, France

Single crystals of oxycobalt-myoglobin were examined by electron paramagnetic resonance (EPR) spectroscopy at ambient and cryogenic temperatures. The principal values and eigenvectors of the  $g$ -tensor and the hyperfine coupling tensor were determined. The Co—O—O bond angle was estimated to be  $125^\circ$  at ambient temperature. The single crystal EPR data of oxycobalt myoglobin at 77 K showed two sets of the principal values for  $g$  and hyperfine coupling tensors and eigenvectors, indicating that the bound oxygen molecule takes two distinct orientations. The result has demonstrated for the first time that the well defined change in the molecular orientation is induced upon freezing the biological macromolecule.

Oxycobalt-myoglobin (oxyCoMb) was prepared by recombination of globin from sperm whale myoglobin and cobaltous protoporphyrin IX, followed by CM-cellulose column chromatography according to the method of Yonetani *et al.*<sup>1</sup>. OxyCoMb was crystallized from ammonium sulphate-phosphate at pH 6.1 (refs 2, 3) in a space group  $P_2$ , with unit cell dimensions  $a = 64.51 \text{ \AA}$ ,  $b = 31.03 \text{ \AA}$ ,  $c = 34.82 \text{ \AA}$ ,  $\beta = 105.84^\circ$ , and a  $Z$  value of 2 (ref. 3). EPR measurements were performed with a Varian E-109 X-band spectrometer with 100 kHz field modulation, interfaced with a PDP 11/40 digital computer system for data acquisition and analysis. OxyCoMb crystals were mounted with a small amount of grease on a home-built two-circle Teflon goniometer<sup>4</sup> and held in a Varian immersion Dewar flask for 77 K measurements or in a Varian variable temperature Dewar for higher temperature measurements. The crystal on the goniometer was manually rotated every  $5^\circ$  and/or  $10^\circ$  around its crystallographic axes with a reproducibility of  $\pm 5^\circ$ . The EPR data of the resonance positions versus the angle of rotation were computer-fitted to Schonland's equation<sup>5</sup> to determine the angular dependence of  $g^2$  and  $A^2$  (the squares of the  $g$  values and hyperfine coupling-constants, respectively). The signs of the non-diagonal elements of  $g^2$  and  $A^2$  tensor were determined by measuring the angular dependence of  $g$  and  $A$  values around any direction in a single crystal with respect to its crystallographic axes. The principal values for these tensors and the eigenvectors with respect to the crystallographic axes, determined according to Schonland<sup>5</sup>, are summarized in Table 1.

At room temperature (300 K), oxyCoMb exhibits one unique set of  $g$  and  $A$  tensors, indicating that the paramagnetic centre or the metal-bound oxygen maintains a definitive molecular orientation relative to the crystallographic axes. The  $g$  and  $A$  tensors of oxyCoMb, however, do not share the same principal axis system with each other. The  $A$  tensors are principally determined by the 3d orbital of the cobalt ion. The EPR results

obtained at room temperature are compared with the X-ray structure of oxyCoMb, which was determined in an unfrozen state at  $-15^\circ\text{C}$  (ref. 3), and schematically illustrated in Fig. 1. The  $\xi$  axis associated with  $g_{\xi\xi} = 2.056$  does not lie along the O—O axis. Among the three principal axes of the  $g$ -tensor, the  $\zeta$  axis associated with  $g_{\zeta\zeta} = 2.003$  ( $\approx g_e$  or the  $g$  value of free electron) appears to be the nearest direction to the O—O axis. From the directional cosines of  $z$  and  $\zeta$  axes, the Co—O—O bond angle is calculated to be  $125^\circ$ , in good agreement with the results of the X-ray structural analysis<sup>3</sup>, in which the bound oxygen is shown to be oriented in the Pauling geometry with the Co—O—O bond angle of  $129^\circ$ . Note that the direction of the maximal  $A$  value, or  $A_{xx} = 18.12 \text{ G}$ , is parallel to the imidazole plane ( $C_\delta - C_\epsilon$ ) of the proximal histidine. Thus, the interaction between the  $p$  orbital of the imidazole ring of the proximal histidine and the 3d orbital of the cobalt ion, which has been previously proposed, cannot be verified from these results. The direction of  $A_{zz}$  is very close to the normal of the porphyrin plane within  $5^\circ$ , thus it is reasonable to assign  $A_{zz}$  to the direction of the Co—O<sub>1</sub> axis. However, the Co—O<sub>1</sub> bond is not strictly perpendicular to the porphyrin plane, but inclines approximately  $8^\circ$  from the normal of the porphyrin plane. On the other hand, the nearest axis to the direction of the O<sub>1</sub>—O<sub>2</sub> axis is the  $\zeta$  axis, which inclines about  $20^\circ$  from the direction of the O<sub>1</sub>—O<sub>2</sub> axis. These angles are larger than our experimental error of  $5^\circ$ .

The unpaired electron, which is responsible for EPR in oxygen adducts of cobaltous chelates including cobaltous porphyrins has been generally assigned to the  $\pi^*$  orbital of the bound oxygen and the bound oxygen molecule has been oriented in such a way that its orbital overlaps maximally with the 3d orbitals of the cobalt ion in previous EPR studies of these compounds. The interaction between the  $\pi^*$  orbital of O<sub>2</sub> and the 3d<sub>z<sup>2</sup></sub> orbital of Co<sup>2+</sup> (ref. 6) and the molecular orbital involving the  $\pi^*$  orbital of O<sub>2</sub> and the 3d<sub>z<sup>2</sup></sub> orbital of Co<sup>2+</sup> (ref. 7) have been proposed. In these theoretical treatments, which assume the unpaired electron in the  $\pi^*$  orbital of O<sub>2</sub>, the direction of the maximal  $g$  value ( $g_{\xi\xi}$ ) should inevitably lie along the O—O axis<sup>7</sup>. Contrary to this assumption, our single-crystal EPR results at room temperature suggest that the direction of  $g_{\xi\xi}$  ( $\approx g_e$ ) does lie along the O—O axis. This suggests the possible contribution of the antibonding orbital of  $\sigma$  bond of O<sub>2</sub> to the metal-oxygen bond, although we could not exclude that of the  $\pi^*$  orbital. We believe that steric interaction of the distal residues such as E7 His, E11 Val, and CD1 Phe as well as the proximal histidine (F8 His) would contribute significantly to the stereochemistry of the Co—O<sub>2</sub> bond and should be

**Table 1** The principal  $A^{\text{Co}}$  and  $g$  values and the directions in a single crystal

| Complex               | Temperature (K) | Principal values         | †Angle to: |            |       |
|-----------------------|-----------------|--------------------------|------------|------------|-------|
|                       |                 |                          | $a$        | $b$        | $c^*$ |
| O <sub>2</sub> CoMb   | 300             | $A_{xx} = 18.12$         | 85.4       | $\pm 50.2$ | 40.1  |
|                       |                 | $A_{yy} = 11.12$         | 67.6       | $\pm 46.4$ | -51.9 |
|                       |                 | $A_{zz} = 7.30$          | 22.9       | $\mp 70.1$ | 79.2  |
|                       |                 | $g_{\xi\xi} = 2.056$     | 56.3       | $\pm 48.3$ | 60.0  |
|                       |                 | $g_{\eta\eta} = 2.011$   | 66.1       | $\mp 42.2$ | 57.6  |
|                       |                 | $g_{\zeta\zeta} = 2.003$ | 43.4       | $\mp 84.6$ | -47.1 |
| O <sub>2</sub> CoMb I | 77              | $A_{xx} = 7.2$           | -62.3      | $\mp 33.1$ | 73.3  |
|                       |                 | $A_{yy} = 23.2$          | 81.3       | $\pm 75.9$ | 16.7  |
|                       |                 | $A_{zz} = 11.6$          | 29.9       | $\mp 60.1$ | -89.2 |
|                       |                 | $g_{\xi\xi} = 2.08$      | 59         | $\pm 82$   | 32    |
|                       |                 | $g_{\eta\eta} = 2.03$    | 45         | $\mp 50$   | -72   |
|                       |                 | $g_{\zeta\zeta} = 1.98$  | 60         | $\pm 41$   | -65   |
|                       | II 77           | $A_{xx} = 17.3$          | -76.2      | $\mp 22.0$ | 73.2  |
|                       |                 | $A_{yy} = 8.2$           | 77.6       | $\mp 70.1$ | -23.7 |
|                       |                 | $A_{zz} = 7.2$           | -18.8      | $\pm 81.0$ | -73.6 |
|                       |                 | $g_{\xi\xi} = 2.085$     | -83.1      | $\pm 11.0$ | -81.6 |
|                       |                 | $g_{\eta\eta} = 2.008$   | -9.4       | $\mp 84.1$ | 82.8  |
|                       |                 | $g_{\zeta\zeta} = 1.983$ | 83.8       | $\pm 80.8$ | 11.1  |

†Upper sign refers to site A, lower to site B in unit cell<sup>2-4</sup>.

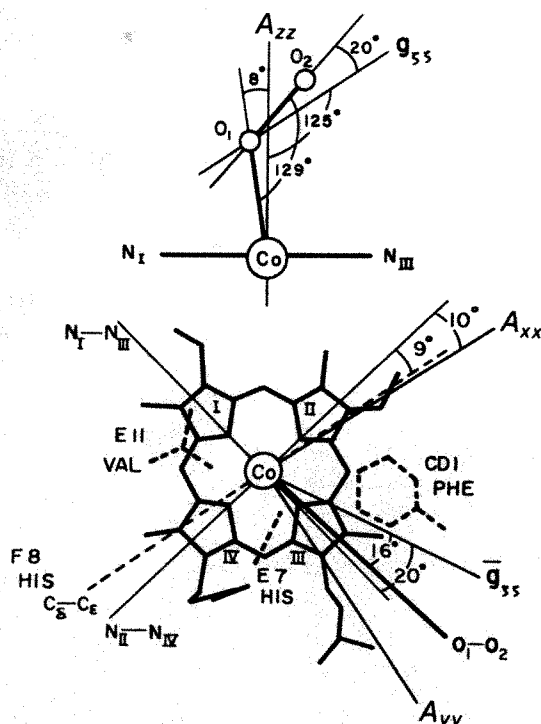
\*Present address: Abteilung Biochemie, Biozentrum der Universität Basel, Klingelbergstrasse 70, CH-4056, Basel, Switzerland.



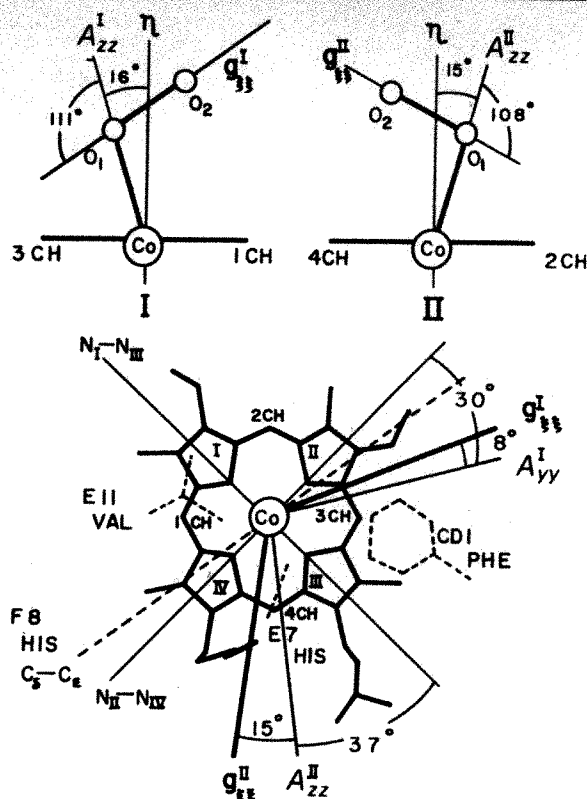
incorporated in the theoretical calculation of the Co—O<sub>2</sub> bonding.

The single-crystal EPR data of oxyCoMb at 77 K are much more complex: two sets of the principal values for  $g$  and  $A$  tensors and eigenvectors are found, indicating that the bound oxygen molecule takes two distinct orientations (species I and II), confirming the previous observation of Chien and Dickinson<sup>8</sup>. However, these workers report different principal values and eigenvectors of  $A$  and  $g$  tensors from our own. The origin of these differences is not clear. However, there are two solutions for selecting the signs of the non-diagonal elements of  $g^2$  or  $A^2$  tensors, only one of which is correct. Figure 2 illustrates the Co—O—O bonding structure and the projections of the directions of  $A_{xx}$ ,  $A_{yy}$ , and  $g_{zz}$  onto the porphyrin plane, together with those of proximal and distal residues, which are determined from our single-crystal EPR measurements at 77 K. If we assume that the direction of  $A_{zz}$  is fixed approximately to the normal of the porphyrin plane, the directions of the maximal  $A$  values for species I and II produce an angle of about 90° in the porphyrin plane. If the axis associated with its  $g$  values nearest to  $g_e$  is taken as the O—O axis, in accordance with the room temperature data, the Co—O—O bond angle becomes 93° ( $g_{zz} \wedge A_{zz}^I$ ) for species I and 163° ( $g_{zz} \wedge A_{zz}^{II}$ ) for species II, respectively. These two directions of the O—O axis nearly coincide with the direction of the imidazole plane ( $C_\delta$ — $C_\epsilon$ ) of the distal histidine. On the other hand, if the  $\xi$  axis (the direction of the maximal  $g$  value) is taken to be the O—O axis, the Co—O—O bond angle becomes 111° for species I and 108° for species II, and each  $\xi$  axis is oriented almost in the direction of its maximal  $A$ -value, respectively. However, it cannot be determined which axis should be the O—O axis in the 77 K EPR conditions. Whichever one is taken as the O—O axis, the direction of the O—O axis at 77 K is definitely different from that observed at room temperature.

In a previous single-crystal EPR study at 77 K (ref. 8), it was concluded that the bound oxygen molecule in oxyCoMb takes two types of orientation (species I and II) which are more or less in the Griffith parallel geometry. However, we find that the two orientations of oxygen in oxyCoMb at 77 K are best described



**Fig. 1** The bonding structure of Co—O<sub>2</sub> and the directions of  $g$  and  $A$  tensor (room temperature): Co—O—O bond angle and the directions of  $A_{zz}$  and  $g_{zz}$  are shown (upper). The projections of  $A_{xx}$ ,  $A_{yy}$ ,  $g_{zz}$ , and O—O axis onto the porphyrin plane are shown (lower), from the proximal-side view. The projections of the distal residues are shown by dotted lines.



**Fig. 2** The bonding structure of Co—O<sub>2</sub> (77 K); the directions of the maximal  $A$ -values for species I ( $A_{yy}^I$ ) and for species II ( $A_{xx}^{II}$ ) are shown (lower).  $\xi$ -axis is assumed to be fixed on the O—O axis. The two species (I and II) are oriented about 90° to each other in the crystal (upper).

by Pauling bent geometry, neither of which is identical to its Pauling orientation at room temperature (see Figs 1 and 2). EPR measurements at different temperatures indicated that the transition between one potential-well at room temperature and two potential-wells at 77 K for the oxygen binding in CoMb is a reversible process and takes place at/near the freezing point of crystals.

Adverse effects of solvent freezing on biological compounds are well recognized but only limited data are currently available. Examples are abrupt changes in the paramagnetic susceptibility in haemoglobin near freezing point<sup>9</sup> and the loss of the ordered intermolecular arrangement in crystals of cytochrome *c* peroxidase on freezing<sup>10</sup>. The present single-crystal EPR study shows for the first time that a well defined change in the molecular orientation is induced by freezing of a biological macromolecule. Since magnetic and spectroscopic measurements of biological macromolecules, particularly metalloproteins, are by necessity carried out in a wide range of ambient and cryogenic temperatures, it is important to recognize that the analyses of experimental data and theoretical interpretation of such data must take into account the possible adverse effects of freezing, as demonstrated here.

We thank Dr G. Petsko for the coordinates of the X-ray structure of oxyCoMb and Drs G. Petsko, P. Douzou, and T. Inubushi for stimulating discussions. This work was supported by research grants from the National Heart, Lung, and Blood Institute (HL 14508) and the NSF (PCM79-22841).

Received 20 May; accepted 17 September 1980.

- Yonetani, T., Yamamoto, H. & Woodrow, G. V. *J. biol. Chem.* **249**, 682–690 (1974).
- Kendrew, J. C. & Parrish, R. G. *Proc. R. Soc. A* **238**, 305–324 (1956).
- Petsko, G. A., Rose, D., Tsernoglou, D., Ikeda-Saito, M. & Yonetani, T. in *Frontiers of Biological Energetics* (eds Dutton, P. L., Scarpa, A. & Leigh, J. S.) 1011–1016 (Academic, New York, 1978).
- Hori, H. *Biochim. biophys. Acta* **251**, 227–235 (1971).
- Schonland, D. S. *Proc. phys. Soc. Lond.* **73**, 788–792 (1959).
- Dedieu, A., Rohmer, M.-M. & Veillard, A. *J. Am. chem. Soc.* **98**, 5789–5800 (1976).
- Hoffman, B. M., Diemente, D. L. & Basolo, F. *J. Am. chem. Soc.* **92**, 61–65 (1970).
- Chien, J. C. W. & Dickinson, L. C. *Proc. natn. Acad. Sci. U.S.A.* **69**, 2783–2787 (1972).
- Iizuka, T. & Kotani, M. *Biochim. biophys. Acta* **194**, 351–363 (1969).
- Yonetani, T. & Schleyer, H. *J. biol. Chem.* **242**, 3919–3925 (1967).





# CHRISTMAS BOOKS SUPPLEMENT

## From Dan to Beersheba, and beyond

P.J. Parr

THERE was a time, in the late nineteenth and early twentieth centuries, when a desire to illuminate, explain and even to vindicate the Bible provided the chief motive force behind much of the archaeological exploration of the Near East — of Mesopotamia and Egypt, and of Palestine itself. Archaeology has changed in recent years, however, both in its goals and its methods, and its practitioners in the Holy Land today are likely to be as concerned with such problems as the diet of Neolithic man or the mechanisms of Bronze Age trade as they are with the date of the Exodus, the design of Solomon's temple or the location of the tomb of Christ. In academic circles Biblical archaeology has certainly lost much of its former prestige; which is, on the whole, not a bad thing. Nevertheless, it remains probably the most popular branch of the subject amongst the educated lay public, for the simple reason that Palestine — as Moshe Pearlman admirably puts it in his book *Digging up the Bible* (Morrow/Weidenfeld & Nicolson, \$19.95/£8.95) — “is the only region of antiquity of which there is a written historical record that has been familiar to so many people in every generation for so long”. The writer of a book catering for this interest has a duty to be readable, accurate and reliable, and to add something new to the already vast literature available, and it is by these criteria that all of the three new books reviewed here should be judged.

Pearlman's volume is certainly the least satisfactory, despite the fact that it is well-written and produced, with many pertinent and attractive illustrations and a lively text. His re-telling of the “stories behind the great archaeological discoveries of the Holy Land” is substantially accurate, though they have all been told before. It is a pity that, as the account nears the present day, there is a definite over-emphasis on



Erosion features in the Sinai

Israeli research at the expense of that carried out by foreign scholars; for example, the important work of Kathleen Kenyon at Jerusalem just before the Six Day War receives scant mention, while the excavations of Roland de Vaux (one of France's most outstanding Biblical archaeologists) at Qumran, where the Dead Sea Scrolls were written, are not referred to at all, although the Scrolls themselves are given a dozen pages of text. The book's chief fault lies in the dubious nature of some of its archaeological statements, however. Thus (at random) the Hyksos are no longer seen as a “northern people” by most scholars (p.146); the date of the Exodus has not been proved just by the discovery of a few pieces of Mycenaean pottery at Hazor (pp.71–72) — it has, in fact, not yet been satisfactorily established that there really was an Exodus; the date of the Neolithic tower at Jericho has been known for over a decade to be at least a thousand years earlier than the date of 6850 BC quoted on p.141. Even a popular book has to be less misleading and simplistic than this.

Father Murphy O'Connor's *The Holy Land: An Archaeological Guide from Early Times* (Oxford University Press; hbk

£8.50, \$15; pbk £3.95, \$5.95) is much more reliable, though it too has its faults. Almost everything written on the dust jacket is true: it is “concise, readable and wittily erudite . . . its scope is wide . . . it gives clear directions [and has] numerous detailed plans”. It differs from — and adds to — most comparable books by giving a prominent place to many of the less well known and accessible sites and monuments, especially of the Byzantine and Crusader periods, with which the author — who is Professor of New Testament at the Ecole Biblique in Jerusalem — is clearly most familiar. It is, conversely, perhaps a little thin on some of the pre-Israelite remains (the important Canaanite temples of Area H at Hazor, for example), and the brief discussion in the opening pages of the early history of the country is really much too short to be useful to anyone, and includes some statements (for instance, the date of the Neolithic Revolution; the date and nature of Abraham's journey from Mesopotamia) which are as simplistic and inaccurate as some of Pearlman's. But this is the only flaw in an otherwise excellent guide, which should be in the luggage of every visitor to the Holy Land.

P. J. Parr is Senior Lecturer in the Archaeology of Western Asia at the Institute of Archaeology, University of London.

Simon McBride



The third volume, *Sinai* (Kümmerly and Frey, Berne, SF88), edited by Beno Rothenberg, is remarkable for achieving a very successful synthesis of attractive coffee-table format and serious academic text between the same two covers. Its hundred-odd colour photographs, by Helfried Weyer, are outstandingly beautiful, and the only danger is that they will distract the reader from the text. This would be a pity. It consists of a number of concise but scholarly chapters not only on the archaeology and history (ancient and modern) of the peninsula, but also on the environmental background (geology,

mineral resources, flora, fauna) essential for an appreciation of that history. The archaeological chapters are based mainly on the fieldwork of Rothenberg himself, and present some of the results for the first time in English. Rothenberg does not avoid technicalities and sometimes indulges in jargon; but the terms are usually explained, the arguments logically presented and the accompanying plans and diagrams attractively informative — all in the best traditions of popularization. These archaeological discoveries in Sinai are mostly related to periods long pre-dating the Israelites, and have little direct bearing on Biblical archaeology, in its narrow sense. But the book provides a vivid and reliable demonstration of the sorts of problems and categories of evidence now engaging the attention of archaeologists in Palestine, and as such is to be warmly recommended.

*Sinai* is available in the UK from The Museum Bookshop, 36 Great Russell St, London WC1 3PP, price £20, and in the US from J.J. Binns, 6919 Radnor Rd, Bethesda, Maryland.

reproduced are fuzzy and faint, and are plainly failures which a critical photographer normally consigns to the waste-paper basket. They do not captivate and entrance us, as the author surmises. For her they represent "a dream world of symbols and queer relationships . . . that naively ask questions pertaining to life and death, time and motion". The author slips quite easily from science to poetic flights, a nice feature but we have to come back to the ground. The poor reproduction of the photographs is due to a cardinal mistake in this American production in printing them on text instead of art paper. Neither in colour nor in contrast do the sepia reproductions approach the quality of the originals. Only those few examples printed in red, purple and primrose — colours imparted to the calotypes by use of different fixing salts — fulfil this expectation, and they are beautiful.

In any new edition I would recommend the correction of a few statements; I will mention just three. Talbot's discovery of the latent image was a vital element in his calotype process. Yet Daguerre had made the same discovery five years earlier in his. It is therefore wrong to use the term "photography" which covers both methods. Talbot's wife Constance was not the first woman photographer. Madame Giroux, wife of the manufacturer of the official Daguerre camera, in 1839–1840 supplied each outfit with a sample daguerreotype taken by herself. *The Pencil of Nature* was published in six parts over a period of two years, the last appearing in April 1846 (not 1845).

The history of photography has been enriched by two recent biographies of one of the inventors of the process. Both of them are valuable additions to the literature, but neither is objective enough to be considered definitive. Hero worship is a poor partner of truth.

*Helmut Gernsheim is a photohistorian and Distinguished Visiting Professor at the Universities of Texas and Arizona. In 1959 he was the first recipient of the Kulturpreis for photography.*

## Negative and positive of Fox Talbot

Helmut Gernsheim

*Fox Talbot and the Invention of Photography.* By Gail Buckland. Pp.216. (Scolar/David Godine: 1980.) £20, \$50.

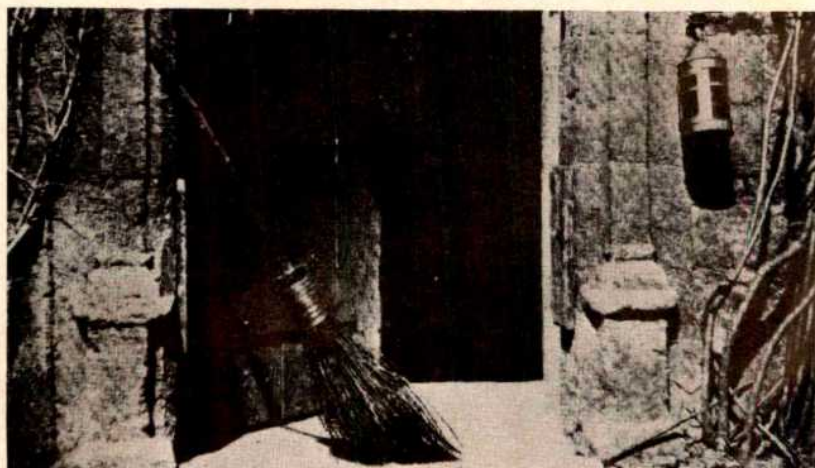
WILLIAM Henry Fox Talbot FRS, inventor of the negative/positive method of photography on which modern photography is based, patentee of halftone photo-engraving, of electric flash photography and a number of other important contributions to the development of photography, was a brilliant scholar in several fields of science. Yet an unfortunate mania for pursuing patents, for commercial enterprises and for law suits earned him more animosity than cash the impoverished owner of the ancient abbey and village of Lacock needed to rebuild the family fortunes.

In his belief that every photographic process with the exception of the daguerreotype was only a variation of his own, Fox Talbot effectively prevented important improvements, freely published by others, from becoming common property in England, thus severely impeding the progress of photography. However, his claim to Frederick Scott Archer's collodion process on glass, which was about to oust his own method on paper, outraged English photographers, fellow scientists and editors of journals and they combined to defend photography from further interference; Talbot lost the case in December 1854. With the new-won freedom to compete with other countries, a golden age of invention and creativity set in giving Britain a leading position with France in the latter half of the nineteenth century. As neither Daguerre's nor Talbot's patents included Scotland the position there was quite different. The finest calotype portraits and some of the

best waxed-paper photographs in existence were produced in Edinburgh in the 1840s and early 1850s.

Probably out of a false respect for her hero, little of this strangulation of English photography in its early formative period (1841–1854) emerges in Mrs Buckland's book. Similarly, H. J. P. Arnold, in his biography of Talbot (Hutchinson, 1977) which preceded hers by three years, tried hard to belittle the strong contemporary evidence of Talbot's machinations. Anyone interested in a rather different view of Talbot can find it in my *History of Photography* (Oxford University Press, 2nd Edn 1969) and in R. Derek Wood's detailed study of Talbot's law suits (*Annals of Science* 1971 and 1975).

The 230 photographs partly integrated with Mrs Buckland's text, and partly added to it in album fashion, plus the many interesting excerpts from letters and journals, make her monograph particularly valuable. Yet many of the calotypes



"The Open Door", March 1843. The picture that made Talbot "certain that he could give form to his creative instincts . . .".

Science Museum, London



## More variations on a biological theme

Ashley Montagu

*The Panda's Thumb.* By Stephen Jay Gould. Pp.343. (W.W. Norton: 1980.) \$11.95. To be published in the UK in spring 1981, £6.95.

RECENTLY a young student of mine, having ably presented a seminar on Stephen Jay Gould's admirable book, *Ontogeny and Phylogeny* (Harvard University Press, 1977), asked me what Gould's specialty was. Only one answer was possible: versatility. Gould is a professor at Harvard and lectures on geology and palaeontology; he also teaches courses in biology and the history of science, and writes on physical and biological anthropology, growth and development, evolutionary theory, human nature, intelligence testing and sociobiology, to name but a few areas of his competence. In addition he is a highly regarded reviewer in scientific and literary journals and magazines. To cap it all, he writes a monthly column, "This View of Life", in the magazine *Natural History*.

It is from the column that this anthology, lightly edited, has been put together. Gould's earlier collection of essays from the same source, *Ever Since Darwin* (W.W. Norton), appeared in 1977. That volume immediately established him as perhaps the best of our natural history essayists. As a friend remarked the other day, "Whatever he writes is a gift".

In the prologue to the 31 pieces which make up this new volume, Gould expresses the hope that he has avoided that incubus of essay collections: diffuse incoherence. Neither author nor reader need have any qualms on that or any other score: the essays are consistently coherent and follow naturally, one upon the other, as if they were chapters on a single theme. There is a continuity which runs through this eminently readable book like a red thread, giving it a unity behind which an unusual mind is at work trying to figure out, among other things, how multicellular creatures regulate the timing involved in the complex orchestration of their embryonic growth, in the hope that developmental biology might one day unite molecular genetics with natural history to form a unified science of life. In one way or another these essays are mostly directed toward illuminating the routes to be taken to solve that problem.

The book plays variations upon this theme most delightfully, for in addition to being the best-informed of writers, Gould is also one of the most elegant. He is unfailingly interesting, for he has the rare gift of communicating the excitement he feels about whatever his fertile brain encounters. The reader comes away enriched and entertained at the same time. From the first essay, from which the book takes its title, in which the author discusses

the manner and the method of evolution, to the last, in which he shows, by way of the chambered nautilus, how the palaeontologist has come to the rescue of the geophysicist and mathematician in arriving at a sound estimate of the rotational slowing of our planet, Gould holds the general principle of evolution steadily in view.

In an essay on Darwin and Wallace, Gould shows how the latter, one of the most remarkable and underestimated of thinkers, ultimately became an intellectual victim of his own hyperselectionism, in arguing that the excessive complexity of the human brain could not have been produced by selection. In another essay, "Darwin's Middle Road", the author writes revealingly of the fibs that the great man told about his insights. Here it is good to see Gould recognizing what few ever do in discussing the historical background of the Wallace-Darwin theory, namely, the role played by sociopolitical ideas, a fact clarified by Patrick Geddes in the late

nineteenth century and by Charles Sanders Peirce almost as long ago.

In this essay Gould errs in saying that what was presented at the famous Linnean Society meeting of 1858 was "a joint paper". Though this is often stated, the truth is that what was presented, in the absence of both men, was an extract communicated in 1844 to Lyell and a letter to Asa Gray of 1857 (both by Darwin) and at the same time, but separately, Wallace's 1858 essay "On The Tendency of Variations to Depart from the Original Type". The communications were presented *together*. There was no joint paper as such.

But Gould rarely nods. On the few occasions on which he does he challenges one furiously to think. His book is a treasure. □

Ashley Montagu is a biological and cultural anthropologist. He is editor of the recently published *Sociobiology Examined* (Oxford University Press).

## Contrary natures

Richard Mabey

THE ideal countryside of the book-packager is all things to all possible buyers: visible, walkable, edible, amenable to identification and to technicolour display, wonderfully awesome without ever being fundamentally mysterious. When Felix Gluck Press put together *Nature Through the Seasons* and *Nature Day and Night* for Penguin/Viking (now issued as paperbacks at £1.95/\$4.95 and £2.50/\$7.95 respectively) they took this principle to its depressingly logical conclusion and interweaved quite separate contributions by a writer, an artist and a scientist — the days being long past, presumably, when one person could be expected to be all three. The series of cameos in each book begins with an imaginative scene setter ("A Rocky Coast by Day", for example), continues with a "science text" ("Tides and Internal Clocks"), and is rounded off by one of those breathless habitat collages which look as if they are depicting local assembly points for the Ark.

Max Hooper's science notes are, as you would expect, lively and entertaining; David Goddard's set-pieces — all sharp edges and precise little tessellations of colour — are meant, I suppose, to be some kind of half-way stage between the scientific and poetic visions, but end up looking as stiffly unnatural as paintings-by-numbers. Neither seem to grow in any convincing way out of Richard Adams's wonderfully evocative introductory essays. For anyone who finds his fiction a little

indigestible these are a revelation. He meanders through his favourite landscapes, sniffing, listening, exulting, reflecting, but without being intrusive in any way, and succeeds in capturing the exact flavour of *moments* in nature, from the small hint of spring in the first brimstone butterfly, to the flowing away of the whole year in a leafless winter wood.

The ingredients which have been sandwiched together in Hodder and Stoughton's series *The Natural History of Britain and Northern Europe* are a lightning guide to the ecology of each habitat and a European field guide. The latest volume by Brian Whitton, *Rivers, Lakes and Marshes* (£5.50), ends up being rather unsatisfying on both counts. It was surely a mistake to try and produce a digest of the aquatic flora and fauna of half a continent, couched in scientific language yet marketed for tourists. What would your botanically-inclined riverside picnicker make, I wonder, of a branched bur-reed whose description reads "Lvs erect, <15mm wide, keeled, triangular in section, ♂ and ♀ fls in separate, spherical heads; in branched inflo., ♂ above, ♀ below"? A bee-line for the sandwiches rather than the glossary, I would imagine.

At least *Nature Detective* by Hugh Falkus (Penguin, £2.95) takes the view that there is more to the study of nature than the naming of parts, and presents an entertaining guide to forensic field biology. The countryside is littered with physical clues



about animal encounters: tracks, scratchings, suspicious mounds, discarded skins, decapitated corpses, each one with its distinctive "MO" as they call it in Criminal Records. Again, it is a rather narrowly materialistic view of the natural world, but at least the tone of the writing — and of the captions in particular — encourages you to go sleuthing with a light heart. The photographs, mostly by Niko Tinbergen, are superb, and take this book beyond the purely anecdotal. One, of the heraldic print of a raven's wings in deep snow, suggests an ancient survival myth way outside admissible evidence.

One needs to be something of a nature detective to work out what on Earth is going on in the anonymous *The Twelve Months of the Year* (David and Charles; hbk £5.95, £16.95; pbk £3.95, \$11.50) so scrappy, inaccurate and disorganized are its contents. But clues to the conspiracy (and the motivation) are plain enough: a photograph of a red-backed shrike with young (in the February section!) mislabelled as a great grey shrike; common mouse-ear equated with chickweed — rather alarmingly, since a few pages later you are encouraged to eat it; those habitat collages again, with crows cohabiting with cranes, black woodpeckers in the beechwoods and hamsters in the corn. This is a world we have never encountered naturally in Britain, and you do not need to check in the picture credits to realize that this was originally a Dutch volume which has been hurriedly adapted, entirely unexplained, for a British audience. It is as cynical an exercise in book-making as I have ever seen, and I feel rather sorry for the British author who has translated or added to parts of the text (unacknowledged, even though he or she writes in the first person) as these fragments are really rather good.

Gordon Benningfield has provided (and signed) both text and pictures for *Benningfield's Countryside* (Allen Lane/Viking, £7.95/\$19.95). His paintings are as accomplished and idyllic as usual.

What is the surprise in this book is the quality of his prose, which has a mixture of unaffected strength and personal vision that is now sadly rare in English country literature. He writes uncompromisingly about the devastation wrought to his childhood countryside, about the forces that draw him to painting, and best of all about the business of putting a picture together. I must confess that I like his big soft, pastoral landscapes least of all his work, but his notes on why they were composed just so at least made me look at them with a new curiosity:

I have also put a glimpse of deer into my large painting of a typical piece of Ashridge [in Hertfordshire] at bluebell time, in May . . . The deer have just seen me and are about to move off; in a moment, they will have disappeared altogether. I wanted to convey the feeling that wildlife is not at all obvious in the countryside, that it is just a piece of luck that it has appeared at this moment.

Along with his prose, I think Benningfield's strengths lie in his detailed portraits, quite unidealized, of butterflies and gates and mucky field corners. It would be exciting, then, to see some of the outrage he expresses in his writing worked out in his painting.

Compartmentalization of the ways we look at and talk about the natural world is now dangerously endemic. Gordon

Benningfield is a man of sufficient popular appeal and broad-based skills to be able to make the kind of coherent personal statements that are normally anathema to contemporary publishers.

*Richard Mabey is a writer specializing in conservation and countryside matters. His most recent book is The Flowering of Britain, published by Hutchinson.*

## In the wake of the *Beagle*

Arthur Bourne

*The Yachtsman's Naturalist.* By Maldwin Drummond and Paul Rodhouse. Pp.270. (Angus & Robertson: 1980.) £8.95.

NOSING about the coastlines of western and north-western Europe covered by this book is one of the most rewarding occupations open to the yachtsman. These rewards are greatly increased if the navigator combines his art with an understanding of and a curiosity about the natural world around and beneath him. If his curiosity extends to exploring that world, then it requires only a small push to hook him into doing some real science.

The push can come in many guises, most often through the infectious enthusiasm of a friend or a book. There used to be an excellent book but it is now long out of print and most of us have had to rely on the enthusiastic friend. So there is a need for a guide designed especially for the amateur marine biologist and oceanographer and the present volume is intended to fill that need. The question is does it do so?

In Part one, which consists of three chapters, the authors describe the ecology of the coastal zone, from the land, down the shore to the water column itself. This part of the book is excellent and one could not wish for a better introduction to the subject. Part two, covering seamanship and equipment, has only two chapters and is more condensed. It is less satisfactory and gives the feeling that the authors were in a hurry and used scissors and paste in an attempt to finish quickly.

The chapter on seamanship and long-shoremanship begins with an interesting and informative description of the sort of seamanship required of the yachtsman if he is to navigate and lie safely close in to the shore — necessary if he is to observe the natural scene to best advantage. Such matters as the most effective way of anchoring, types of anchors and their weights, lengths of warp are dealt with in some detail, including the all-important — and often neglected — subject of drying out. Unfortunately little else! The equipment needed for the yachtsman/naturalist (now, by the way, called the sailor/naturalist), including the yacht

itself, comes in the final chapter. My own preference would have been to have placed choosing a yacht right at the start of Part two and I would have liked to have seen some more detail. The authors give only two pages to what is not only the most expensive piece of equipment but the most important. The rest of the equipment and its use is covered reasonably comprehensively, though the amount of detail varies and reflects, probably, the interests of the authors.

A feature of the book is the colour plates, illustrating animals and plants of the coast and sea, which are slotted into the book in six groups of two. The names of the organisms are provided on the backs of the plates and a numbered key aids rapid identification. The same key is used in the text where the organisms are mentioned. This arrangement works well. The plates themselves are adequate; one can recognize the organisms and perhaps that is all one requires. They do make the book colourful but I cannot agree with the authors that the plates make the book. They do not. What makes the book is the writing and the obvious enthusiasm of the writers. There are also large numbers of line drawings but these are poor except for those showing equipment and boats where the artist is particularly good at portraying yachts in the transparent shorescapes.

These are only small criticisms and perhaps we should go back to the question as to whether the book fills the need? Yes and no. As a personal preference I would like to have seen Part two as well developed as Part one, but, overall, the authors have provided a sound, useful and stimulating volume. I suppose one should ask of this sort of book whether it works, given its limitations, often dictated by constraints of size and costs. Would a yachtsman with this book be able to increase his knowledge of the natural scene about him? I believe the answer must be an unqualified yes. I hope it will find a place on the shelves of yachtsmen and naturalists alike. □

*Arthur Bourne has a special interest in coastal zone ecology and has been a member of many shipborne expeditions from the tropics to the higher latitudes.*



## Rare gifts of botanical illustration

Peter D. Moore

THE art of botanical illustration has presented a great challenge to many who have been fascinated by the structure and colour of flowers, and who have sought to represent these in two dimensions. Science is itself an attempt to describe with precision the world in which we live, and the graphic arts have proved a valuable consort to the physical sciences and mathematics in achieving this end. In no area of science is this more true than in botany, where much early, observational work was assisted by the skills of artistic illustration. The three books reviewed here are splendid examples of the contribution which art makes to the understanding, appreciation and enjoyment of plants and, indeed, the contribution made by the plant to art.

The life and work of Marianne North, set out in *A Vision of Eden* (Holt, Rinehart and Winston/Webb and Bower, \$22.50/£8.95), is a prime example of the mixing of art and science. It is the autobiography of an unmarried Victorian lady who, at the age of 40 and on the death of her father, took to a life of travel, and recorded in paintings the vegetation of the areas she visited. It is a story of amazing courage, for the hazards of travel in the 1870s were quite formidable, but she tackled both these and her art with devotion and fortitude. The result was a large collection of botanical illustrations from many areas of the world and an extensive selection of these is presented in this book.



Marianne North, 1886

An interesting aspect of Marianne North's work is the varied way in which she presented her botanical subjects. Some illustrations are entirely devoted to a single plant, in which close detail of structure is represented. Some take the form of still-life groups in delicate arrangements. Other plants are shown in natural settings, with birds and butterflies and other insects in

attendance. But, to my mind, her most artistically appealing works are those in which the plant becomes the foreground to a landscape. Her paintings from northern India, for example, together with her vivid descriptions of the dust, the heat and the inevitable sickness, rival the works of Forster and Masters in conveying the unique atmosphere of that part of the world. As a book of travel stories from a century ago, this book is particularly valuable, for it provides us with botanically detailed descriptions of many areas which, like the Himalayas, are now greatly changed under the impact of increasing human exploitation.

Among our modern painters of flowers, the name of Marjorie Blamey is outstanding. In her latest book, *Flowers of the Countryside*, produced in cooperation with Philip Blamey (Collins/Morrow, £8.95/\$25) she has assumed the role of author as well as illustrator. The text is something of a botanical scrapbook, parts autobiographical, parts historical and parts anecdotal. It is in no way a botanical textbook and it is unclear what purpose it is intended to serve. A large portion of the book consists of a survey of the major British plant families, of which selected species are illustrated and described; yet this cannot be regarded as a field guide. The paintings are both accurate and pleasing, and I am sure that many who buy this book will be motivated by an admiration of these pictures, which are generally well produced and whose colours are more realistic and less garish than some recent efforts by Collins to reproduce Marjorie Blamey's work.

Another collection of botanical jottings which is rather more tightly packed with interesting items of science and folk-lore, is Richard Mabey's book, *The Flowering of Britain* (Hutchinson, £9.95). The style is informal and will appeal to those who find information easier to accept and assimilate when presented in a chatty manner. No scientist should object to this whilst accuracy is retained. The historical and other tales in this book make very good reading and deserve to be read widely.

On the art side, Richard Mabey has found a very able associate in Tony Evans, whose colour photographs are superior to any I have previously seen in print. The atmosphere of his photographs is brilliantly conveyed by the careful setting of the plant subject in its surroundings. The unity of plant and habitat which results is reminiscent of the paintings of Marianne North and is equally striking. The camera may have replaced the brush in the equipment of the latter-day botanist, but the art of composition is still a rare gift: Tony Evans, in my opinion, has provided a new dimension to the art of botanical illustration.



Lords and ladies, by Marjorie Blamey

Peter D. Moore is Senior Lecturer in the Department of Plant Sciences, King's College, London. His most recent book is *The Mitchell Beazley Pocket Guide to Wild Flowers*, published in October of this year.

From *A Vision of Eden*

From *Flowers of the Countryside*, by Marjorie and Philip Blamey



## Ornithology in art and art in ornithology

T. R. Halliday

IT IS one of the finer traditions of publishing that books on natural history have been illustrated by artists, some of whom have gained recognition within a wider artistic world. Three new books are richly endowed with the work of three of Britain's finest bird painters: Peter Scott, Charles Tunnicliffe and George Lodge. Peter Scott's autobiographical *Observations of Wildlife* (Phaidon/Cornell, £7.95/\$19.95) contains four chapters which deal with his major lifetime preoccupations as a painter and naturalist, as creator of the Wildfowl Trust, as a leading figure in conservation, and as a traveller and ambassador for the conservationist cause. Peter Scott himself draws attention to a feature of his work that some critics have deplored, that many of his paintings are just variations on the theme of a flight of birds against a dramatic sky. He attributes this to the demands of his market which have led him to paint to a "formula which guarantees sales but limits invention and innovation". Happily, this book bears testament to an artist of very diverse talents. The sketches from his diaries, which include studies of insects and fish as well as birds, are unexpected and exquisite. Peter Scott's text reminds us of the many important ways in which he has contributed to a greater understanding of nature and of conservation in particular, and it is understandable that his art has not been as varied and innovative as it might have been.

In contrast, Charles Tunnicliffe was an artist who devoted his entire life to his craft and Ian Niall's affectionate biography *Portrait of a Country Artist* (Gollancz, £10) contains vivid evidence of his many and varied skills. Here we find a rich variety



Charles Tunnicliffe at work, January 1952

of both subject matter and technique. Some of his oil paintings on unprimed cloth have a distinctly oriental flavour, while his woodcuts and etchings remind one of Durer. Sadly, Tunnicliffe's paintings sometimes seem over-posed and excessively pretty and have lost the life and vigour that he captured so brilliantly in his sketches. The basis of his work was a meticulous attention to detail which is best seen in his beautiful post-mortem studies of birds. The visual feast that his book provides is admirably complemented by Ian Niall's informative and interesting portrait of an exceptionally talented and self-effacing man.

*A Season of Birds* (Weidenfeld & Nicolson/A&W, £7.50/\$14.95) is a less successful book. The text consists of a diary kept by Jim Vincent in 1911 on the

wildlife of Hickling Broad, Norfolk, for which Edwin Montague commissioned illustrations from G.E. Lodge. The text is likely to be of interest only to the most ardent bird-watcher as much of it consists simply of a list of species seen on each day. Lodge's watercolours are reminiscent of Thorburn's work but are not nearly as successful at capturing the essential characters of their subjects. Lodge's reputation is mainly based on his painting of birds of prey and it is clear from this book that he was not nearly as good at portraying other kinds of bird.

T. R. Halliday is a Lecturer in Biology at the Open University and an author and illustrator of a number of books on natural history. His most recent volume is *Sexual Strategy*, published by Oxford University Press in October of this year.

## There was a young artist called Lear . . .

M. A. Ogilvie

*Edward Lear's Birds*. By Susan Hyman. Pp. 96. (Weidenfeld & Nicolson/Morrow: 1980.) £18.50, \$37.95.

THERE was an old man who said 'Hush!  
I perceive a young bird in this bush!'  
When they said - 'Is it small?' He replied -  
'Not at all!  
It is four times as big as the bush!'

Who else could have written that but Edward Lear? He did not invent limericks, but he certainly wrote some of the best there are, and illustrated them with his inimitable line drawings. To these add his nonsense verses ('The Owl and the Pussycat', 'The Dong with the Luminous Nose'), and one probably has the sum of most people's knowledge of him. This handsomely produced and lavishly illustrated book demonstrates just how restrict-

ed that knowledge is. The limericks and nonsense verses were not published until Lear was nearly 60, but by that time he had proved himself firstly as one of the finest natural history artists of all time, and then, abandoning this field before he was 30 because of failing eyesight and a lack of financial success, he became a highly talented landscape artist, producing several illustrated travel books from around Europe.

Susan Hyman, an American art historian, has concentrated on Lear as a natural history artist, and in particular on his bird portraits. And these were something special; Lear was an innovator and a precocious one. Ceasing formal education at 15, he began visiting the newly-opened Zoological Gardens in Regent's Park, sketching the birds and

animals. Within two years he was contributing drawings for the first visitors' guidebook, and the following year, when still only 18, he began work on a most ambitious undertaking, a series of 42 large (folio) plates of parrots. The most important difference between Lear and his contemporaries - and many of his successors - was that he drew from living birds. Instead of relying solely on the stuffed skin, with the resulting unnatural and angular postures on the plate, he worked in the Zoo, persuading the keepers to catch the birds for him to make detailed notes and measurements. Not content with painting more lifelike birds than anyone else, Lear also engraved his own stones for the lithographic reproduction, rather than handing over his plates to an engraver with the inevitable loss from the artist's



intentions. It is perhaps this, above all, which gives Lear's parrots their individuality and their character, as they peer out at one with beady eye and knowing look.

Several plates from *Illustrations of the Family Psittacidae, or Parrots* are reproduced here, together with, and adding greatly to the interest, sketches and preliminary studies, showing Lear's pencil notes on colour details and shape, instructions to the colourists, and charming vignettes of different postures. And, just once or twice, somewhat disparaging sketches of visitors to the Zoo who gathered round him to watch.

Lear contributed plates to books by many famous nineteenth-century naturalists, including Jardine, Selby, Eyton and Gould. This last-named ruthlessly exploited Lear, paying him little and even erasing his name from the plates and substituting his own. That Lear knew what was happening is perhaps revealed by a sentence in a letter written to Gould from abroad some years later: "I often think of

you when I see the large kites and falcons which are so numerous in the mountains where I have been residing".

The many sides to Lear's character and his varied talents are all brought out in this book. As well as the superbly reproduced colour plates there are many in black and white, including drawings from his nonsense books and a few from his period as a landscape artist. Lear was indeed a most remarkable man, and if, for the many, his memorial is made up of the limericks and verses of nonsense, then this book should certainly add to the few for whom Lear is quite simply the finest of bird artists.

In his own words:

How pleasant to know Mr Lear!  
Who has written such volumes of stuff!  
Some think him ill-tempered and queer,  
But a few think him pleasant enough.

*M.A. Ogilvie is a Research Officer at the Wildfowl Trust, Slimbridge, working on population and migration studies, and the author of several books on ornithology.*

## Photographic atlas of alpine flowers

G. Pontecorvo

*I Fiori delle Alpi.* By F. Rasetti. Pp.316. (Accademia Nazionale dei Lincei: Rome, 1980.) £19,500.

THIS monumental work, aimed at the naturalist, is the outcome of 20 summers of one man's intense botanizing throughout the Alps. The 572 excellent colour illustrations reproduced here — selected from some 8,000 photographs taken by the author in the wild — are one of the two major outcomes of that activity. The illustrations cover practically every species of angiosperm that has its altitudinal centre of distribution above the tree line. They include, as a most welcome but unusual feature, all 61 of the high-altitude Gramineae, Cyperaceae and Juncaceae; in fact the plates of these three families, usually neglected in illustrated field floras, are of an even higher quality than the rest.

The standard of the photographs and of their reproduction in this book disposes for good of the myth that preliminary identification from colour plates is easier if they are reproductions from paintings rather than photographs. The idea is that it is only in paintings that relevant diagnostic features can be emphasized and shown to best effect. Yet, of course, it all depends on the knowledge of the photographer and his ability to bring out what is botanically desirable. Rasetti includes an interesting discussion of this matter in a chapter on alpine plant photography.

The second upshot of the author's devoted and painstaking work on the Alpine flora lies in the longest and by far the most valuable chapter in his book. In

this, the botany of individual valleys and massifs is considered. For each, a short geological outline is followed by a discussion of the distinctive species of the area and their distribution. Becherer, in his *Führer durch die Flora der Schweiz* (Schwabe: Basel, 1972), has already attempted something of this kind, but limited to Switzerland and a few contiguous areas. Rasetti covers all of the Alps, north to south and from the Maritimes to the Schneeberg. Furthermore, in limiting himself to the alpine and nival plants, he has been able to deal with the subject much more extensively and in great detail. This section of Rasetti's book will be of great help to botanists, ecologists and amateur orophytologists who wish to know what grows where. Even the local wizard having a very detailed knowledge of the flora of his valley — and there are many — will find how and why his local haunts differ from those of the next valley.

It is a pity that a book with these two outstanding features — and many more minor ones — should be marred by a number of editorial shortcomings. To mention four: the format and weight are such that it cannot be carried for field identification, for which, presumably, the pictures were meant; the scale of a subject must be inferred by going from the picture to the index and then to the description of the species; there is no indication, with each picture, of time, altitude and locality; the description in great detail of the topography of the Alpine Range (with some new and valuable suggestions as to subdivision) is not supported by a sketch.

No doubt this major contribution to the

literature on the flora of the Alps will be translated into English and German, at least. These drawbacks can then be rectified. In the meantime, this Italian edition, besides being an essential acquisition for botanical libraries, will give much added interest to those carrying in their car Bacon's *Mountain Flower Holidays in Europe* (Alpine Garden Society, 1979).

*G. Pontecorvo retired in 1975 as a member of the research staff of the Imperial Cancer Research Fund, London.*

## Prayer for Shetland

H.N. Southern

*The Natural History of Shetland.* By R.J. Berry and J.L. Johnston. Pp.380. (Collins: 1980.) £8.50.

THE first author of this book is well known as a professional biologist; the second, since he is resident in Shetland and was previously the Nature Conservancy Council's representative there, has an intimate knowledge of the islands. Theirs is an unusual book because it is a mixture of a massive amount of raw data and an interpretation of some only of it, and because — in spite of this mixture — some important principles emerge from the illumination shed on the whole subject by the senior author.

Professor Berry has already shown in his previous book in this series — *Inheritance and Natural History* (Collins, 1977) — the significance, for tracking small-scale evolutionary processes, of studying the faunas and floras of archipelagoes. Shetland is such an archipelago, right on our doorstep, and he has used the information amassed, both by individual researchers and by the extensive surveys, funded by the government and the big oil companies, to further this interpretation of how the Shetland fauna and flora have evolved. The intensive investment in the extraction of North Sea oil has aroused fears of the possibility of disasters being inflicted upon a fragile environment and money has been provided to lay a base-line survey from which effects on the habitats can be measured. This survey of the fauna and flora has been a tremendous effort and its achievements can be judged from the full appendices to this book which comprise checklists for all of the groups of animals and plants that have been studied.

The text of the book is heterogeneous, as would be expected from the many authors who have taken part in the survey. Some aspects receive much fuller treatment than others (83 pages on birds and 9 on invertebrates, for example), again as might be expected. The chapters on vegetation and geology are solid stuff, though the maps illustrating the latter are reduced to the extent of needing a magnifying glass to



discern the details. Professor Berry, however, has made a great effort to produce some unification in this pot-pourri. His general introductory chapters, together with those he has written on the mammals (including Shetland man) and other groups (whose composition and distribution shed light, under his guidance, on what Darwin called "that mystery of mysteries — the first appearance of new beings on this earth"), have a vitality that leavens the lump.

The final chapters on the practicalities of

the extraction of the oil and the precautions that have been taken against disasters and on the potential problems which conservationists, and the Shetlanders themselves, have faced and are facing are cagey. We are left with the feeling that a good deal of what could be done has been done — as for the rest, we must just pray.

*H. N. Southern was formerly Senior Research Officer of the Animal Ecology Research Group in the Department of Zoology, University of Oxford.*

## Evolution of thinking on evolution

John Lawton

*Evolution for Naturalists: The Simple Principles and Complex Reality.* By P.J. Darlington, Jr. Pp.262. (Wiley-Interscience: 1980.) £12.75, \$27.50.

THIS is a lovely book — easy and enjoyable to read, outspoken, tart, philosophical and wise. In it, at all times and in whatever mood, Darlington displays a deep personal understanding of the living world, acquired by a life-time of study in the best traditions of scientific natural history, combining accurate observations with acute curiosity and a love for obscure corners of the living world, in his case carabid beetles.

It is not, or rather I did not find it, a straight-forward account of biological evolution written for interested laymen (that is, naturalists without a scientific training). Rather, it is an extremely personal view of evolution that might profitably be read by professional biologists and laymen alike.

It is perhaps trite, but it struck me forcefully whilst reading *Evolution for Naturalists* how human views of biological evolution have themselves evolved, and how they continue to do so. In the book, Darlington traces the early history of evolutionary thought, and explains carefully and precisely why Darwin's ideas are now favoured at the expense of others. Although the central theme is familiar, I was not aware of the clear and accurate statements of a theory of evolution by natural selection made by Scottish land-owner and forester Patrick Matthew, 28 years before the publication of the *Origin*. Even the best ideas are not always favoured by selection until the time and place are right!

Contemporary views on evolution range from the extremely primitive (of the "it doesn't happen" fundamental religious school), to the very sophisticated — with the whole gamut scrambling for attention, acceptance and success. Darlington has his own clear ideas about which should fail and which should succeed. There are the sound principles of the modern synthesis, carefully explained: sadly, whilst finding "great flaws in it", I doubt that President-elect Ronald Reagan would have the time or inclination to inform himself properly, even if he finds the book in his stocking on Christmas morning.

Amongst those who are better informed, Darlington himself sees "hopeful monsters" rampaging through the collective consciousness: most mathematical models of evolution, for example, he assigns firmly to this pedigree. I disagree; partly because I think he misunderstands some of the models, and partly because models force people to state their assumptions. They can therefore be useful, not monstrous, even if eventually proved wrong.

Other ideas he positions explicitly or implicitly at different points along the path of scientific appraisal and selection. Some, such as the strong group-selection theme permeating the book at all levels, are not to my taste either, but look set to enjoy a period of rapid growth and attention, despite strong initial selection against them. Those falling under the broad mantle of "sociobiology" have recently grown explosively, and are now subject to hard testing on many fronts; not all of this testing, in Darlington's opinion, is either ethical or scientific. Still more ideas are murmurings in the minds of a few: Darlington firmly believes, for example, that many adaptations are far from perfect, a heretical notion if ever there was one, but cogently argued.

Philip Darlington is retired. He wrote the book because he wanted to, not because he had to. He finds it neither far-fetched nor funny that Darwin might not be allowed a first-class college education today because he was bad at mathematics and worse at languages. He writes with affection about carabid beetles on mountain tops; the role of stone-throwing in the evolution of human co-ordination, perception and intelligence; and why evolution drives a progressive increase in organic diversity. And through all this detail, he writes directly, simply and with conviction. The book often made me pause; it sometimes made me cross; but above all it made me think again about evolution in all sorts of ways. If you are interested in evolution, and if you do not get *Evolution for Naturalists* in your stocking, buy it, or borrow the new President's — he won't have time to read it, though I wish he would.

*John Lawton is a Senior Lecturer in Ecology in the Department of Biology at the University of York.*

## SCIENTIFIC BOOKSHOP

H.K. LEWIS can supply works in all branches of Pure and Applied Science. Catalogues on request. Please state interests.

## SCIENTIFIC LENDING LIBRARY

Annual Subscription from £7.50.  
(Available in U.K. only)

Reduced rates for multiple subscriptions.

Prospectus post free on request.

Quarterly List of New Books and new editions added to the Library sent post free to subscribers regularly.

**H.K. LEWIS  
& Co. Ltd.**  
136 GOWER STREET,  
LONDON, WC1E 6BS

Telephone: 01-387 4282  
Telegrams: "Publicavit,  
London, WC1E 6BS."

Circle No. 14 on Reader Enquiry Card.

## Abroad migration

John Krebs

*The Mystery of Migration.* Chief editor Robin Baker. Pp.256. (Macdonald-Futura/Viking: 1980.) £13.95, \$29.95.

AT FIRST glance this appears to be a straightforward popular book about migration in plants and animals. However I suspect that many lay readers might find parts of the first two chapters sufficiently difficult to dissuade them from reading the rest.

The first chapter is an introduction consisting largely of an historical survey of ideas about bird migration. It includes two especially charming engravings from sixteenth- and seventeenth-century natural history books. One shows Swedish fishermen on the ice hauling in nets loaded with swallows; at that time it was thought that swallows spent the winter months

underwater. The other describes the ontogeny of a barnacle goose, showing how it develops from a goose barnacle through a series of gradual transitions in an illustration worthy of M. C. Escher.

After this the going gets a bit tough. Chapter 2 works through a series of definitions — lifetime track, familiar area, exploratory instinct, preferred direction, partial migration, navigation, orientation and pilotage — and develops some quite complicated arguments that would be more appropriate to a textbook than a popular account. An example is the section on the arbitrariness of various definitions of habitat. Although the diagrams here and elsewhere in the book are outstanding, the absence of labelling often leaves the reader confused — I struggled for some time, without success, to understand the graph about prairie dog migration on p.29.

The reward for persisting beyond the second chapter is a taxonomically arranged survey of migration (plants, invertebrates, insects, fish, amphibians and reptiles, various mammals and Man). The pages are full of interesting information and many are illustrated by some fine photographs and diagrams. My personal favourite is a photo of the trunk of a pine tree completely clothed in roosting monarch butterflies. The term "migration" is used in its broadest possible sense in the book so that it includes, in addition to "conventional" examples such as salmon, birds and butterflies, "migration" by potatoes or shallots as a result of forming swollen underground stems. The rationale for this extraordinarily broad definition is developed in Baker's earlier book (*The Evolutionary Ecology of Animal Migration*; Hodder and Stoughton, 1978). He argues that all forms of movement serve the same function (to transfer the organism from one site to another, even if sites are separated only by centimetres), so all should be labelled as migration.

The book has been written by a team of authors, and this may have contributed to some problems in continuity. For example, on p.32 the point is made that tracking radar allows an observer to follow individual birds of known species on their migration, while on p.135 we are told that radar studies are limited by their inability to distinguish between species of migrating birds. The possibility that pigeons might find their way home by infrasound is referred to in a general chapter on p.27, but warrants no mention at all in the section devoted to a detailed discussion of navigation and homing in birds on pp.161–165.

An inexperienced reader may find the text a bit difficult, but beginners and old hands alike cannot fail to admire and enjoy the photographs and — lack of labelling apart — the diagrams.

John Krebs is a Lecturer in Zoology at the Edward Grey Institute of Field Ornithology, Department of Zoology, University of Oxford.

## Companions for the fungal foray

Clark T. Rogerson

*Mushrooms of Western North America.* By R.T. Orr and D.B. Orr. Pp.293. (University of California Press: 1980.) \$6.95. *Mushrooms Wild and Edible.* By Vincent Marteka. Pp.290. (W.W. Norton: 1980.) \$15.95.

*Mushrooms of Western North America* is only the second guide to cover an area until now without much published information on its fungi. The area dealt with is the Rocky Mountains west to the Pacific Coast and from the Mexican boundary north to include Alaska. It is an introductory book written primarily for the novice in mushroom lore and identification, and treats only some of the commonest species. The introduction gives concise information on characteristics of fungi, seasonal occurrence and habitat, mycorrhizal associations, collecting fungi, and on edible, toxic and hallucinogenic species. The scientific nomenclature follows modern usage, about 30 of the larger ascomycetes, 100 non-gilled basidiomycetes and 200 or more gilled mushrooms being included. The descriptions are brief, appear to be accurate and include microscopic details. Information on edibility is given. Keys are given for the larger genera. Perhaps the major fault is that less than a third of the species are illustrated in colour, making the identification of the others by descriptions alone difficult for the beginner.

As an introductory field guide to the commonly found species, the Orrs' book will be useful and certainly should stimulate a greater interest in the fungi of the western United States and Canada.

Marteka's book, which deals with some common and easily recognized mushrooms, has several attributes that make it unique amongst the recent crop of mushroom books. First, it is arranged by seasons during which the mushrooms occur in the wild — not by a system of classification of those fungi included; second, it contains a wealth of information on folklore, first-hand field observations, environmental variations, case histories of experiences in eating mushrooms — much more than is typically found in books of this kind; third, it includes up-to-date and new information on preparing mushrooms for eating, both fresh and preserved, stalking wild and not so wild mushrooms in stores, growing your own mushrooms, and a good section on further reading. Only 30 species are treated in detail; they are described briefly but correctly, and all are illustrated with good colour photographs and additional black-and-white photographs and drawings are provided for some species.

The book is well written and organized: it really is enjoyable to read and browse through. While written primarily for

mushroom hunters in the United States, the choice of species will also make it useful in other parts of the world. For an introduction to the mushrooms and for a companion book to others which cover more species, it can be recommended to all who are interested in the subject.

Clark T. Rogerson is at The New York Botanical Garden, Bronx, New York.

## Love of hands

Bernard Wood

*Hands.* By John Napier. Pp.176. (George Allen & Unwin/Pantheon: 1980.) £12.50, \$13.95.

AS FAR as I am concerned there are two categories of books, "work" books and "non-work" books. I wish I could say that I read too many "work" books and too few "non-work" books, but the truth is that I don't read enough of either kind. Reviewing "work" books is simple in theory. They are either research monographs, symposium volumes or textbooks. The criteria are usually clear. Do they advance the subject? Are they comprehensive? Are they up to date? Mercifully, I am never called upon to review "non-work" books, but to take me past the first few pages they have to be entertaining, in the broadest sense, or illuminating, and preferably a combination of the two. John Napier's new book *Hands* straddles my literary boundary in an interesting way.

The book is presented in two nearly equal parts. The first deals with the structure and evolution of the hand. It sets out to explain what human hands are like, what they can do and how they came to be the way they are. The second part is devoted to four separate aspects of the hand. It covers how we use our hands, and considers tool-using and gestures. It also examines the forensic use of fingerprints, and "handedness". The author's aim is made clear in the first chapter. He wants to pass on to the reader something of the fascination and beauty of the hand, and he seeks to communicate some of the wonder we all feel when we come across any example of near-perfect harmonization of structure and function.

John Napier is less than fair to himself in the opening pages. He declares that he is

*The Image of Eternity: Roots of Time in the Physical World* by David Park, reviewed in *Nature* 288, 305; 1980, is available in the UK through Transatlantic Book Service, 24 Red Lion Street, London WC1, price £8.



infatuated with the hand. In my dictionary infatuation is defined as "an extravagantly foolish or unreasoning passion". I think his treatment neither extravagant or unreasoning, but, like all lovers, he occasionally fails to appreciate that what interests him may not always interest those not so closely involved, and vice versa. For non-anatomists, particularly, the section on morphology and evolution may be too dense, but elsewhere it is difficult to avoid making the charge that some subjects are treated too superficially. Again and again, just when I was beginning to be fascinated, the chapter was drawn rapidly to a close and my curiosity was left unsatisfied. The sections on fingerprints and handedness, for example, left me wanting more. The discussion of handedness hardly touches upon the neurological concomitants and there was no discussion of lateralization or speech. The neurological control of the hand is dealt with in the book, but very briefly. Too many questions are left unanswered. For example, does the brain deal with individual muscles, or whole movements? I was excited by the broader perspectives offered by his treatment of topics such as palimetry, the etymology of vernacular and anatomical terms, and the problems besetting a nail-brush designer! I am only sorry that he chose to explore so few of these general fields of interest.

On a more academic level, there are, of course some points of detail where I would take issue with the author, but these are few. I wonder why he discounts the pisiform as a carpal bone (p.35), and the course of the radial artery depicted in Fig.20 is an unusual one to say the least. Stone artefacts are found with the fossil remains of *Australopithecus* (p.113), and the mean brain sizes quoted for early hominids are confusing in their exactness (p.166). These minor points of detail, however, do not detract from a text which is generally of a high standard. The use of technical terms is sometimes uneven, and perhaps the publishers could have served the author better if they had encouraged him to include a glossary. I was disappointed, too, by the illustrations; they seemed predictable and rather dull.

For some years now there has been a steady buzz on the anatomical/anthropological "grapevine" to the effect that John Napier was writing a monograph on the hand. Many of us were eager to see Wood Jones's classic monograph of the 1920s updated. Unfortunately, while *Hands* will entertain a much wider audience, it will disappoint the professional fraternity. Not because it is not a good book in its own way, but because it is not the sort of book we were hoping for. I only hope that *Hands* will have whetted the author's appetite sufficiently for him to go on and produce the book we are still waiting for, and which he is particularly well equipped to write. □

Bernard Wood is Reader in Anatomy at The Middlesex Hospital Medical School, London.

## Flair for fossils

John C. W. Cope

*The Natural History of Fossils*. By C. R. C. Paul. Pp.292. (Weidenfeld & Nicolson/Holmes & Meier: 1980.) Hardback £15, \$37.50; paperback £6.95.

WHEN an experienced palaeontologist draws upon his knowledge and adds his own views on diverse aspects of modern palaeontology, the result promises to be interesting. When this is combined with a flair for imparting information to the uninitiated such as Dr Paul has, the result is a book which is informative, clearly presented and easy to read.

This is no textbook of palaeontology — nor does it profess to be such. Rather, it explains what palaeontology is concerned with — the uses of fossils, their palaeobiology, their ecology, their evolution and so on. Those who seek any sort of taxonomic treatment of fossils must look elsewhere.

In his discussion of each new concept, the author makes sure his readers are never left behind; there is careful exposition of many non-palaeontological topics, including "way-up" criteria, cyclothem, radiometric dating, palaeomagnetism, osmosis. Although, therefore, the book is readily accessible to the layman, it contains much that any aspiring palaeontologist should know.

From his introduction, the author goes on to discuss fossilization, with a useful review of trace fossils. Then follows treatment of sediments, fossil communities and associations. Consideration of faunal provinces and continental drift brings in palaeotemperature studies. The chapter on growth studies covers moult stages and modern work on growth-line studies of bivalves and corals. There is a useful

assessment of the adequacy of the fossil record and subjects such as the origin of life, evolution and the development of life on land are clearly discussed.

In his attempt to make the book comprehensible to the layman, Dr Paul has sacrificed some of the information which would make the volume more compulsory reading for undergraduates. Thus some diagrams are used to illustrate basic non-palaeontological concepts, whereas the space available and the subject really merit the imparting of additional and more advanced information through the medium of the diagrams. Incidentally, the reproduction of those diagrams included is not of the highest standard — how much the rough textured paper is responsible for this is difficult to judge.

There are 40 photographs which illustrate some of the subjects covered in the text. Their quality varies and they seem rather an afterthought — I do not feel that they contribute greatly to the book, but a layman unused to seeing fossils might well disagree.

In a book which is so stimulating and in which the author has clearly taken considerable care in presentation of his material, it is strange to find some words consistently spelt incorrectly. I found particularly jarring the mis-spellings of "Trias", "Lias", "Gault" and "isostasy".

The other titles in the *World Naturalist Series* suggest that this is primarily a book for the layman. As such, an introduction to modern ideas in palaeontology, it is a clearly presented exposition of the subject which deserves to succeed.

John C. W. Cope is a Senior Lecturer in Geology at the University College, Swansea.

## Geological tour de France

John Sutton

*Geology of France (with twelve itineraries)*. By Ch. Pomerol *et al.* Pp.256. (Masson: 1980.) £8, \$25.

GEOLOGY came into existence as a science in large part through the travels across France and Britain of some remarkable observers who were active more than 150 years ago. The founding fathers of geology are long since dead, but the rocks from which they learnt survive; with modern motorways we can cross in an afternoon what Smith, Murchison, de Beaumont and Cuvier took weeks to explore on horseback or on foot.

Geological traverses, though no substitute for painstaking mapping, can be great fun. Over there we see the hilltop of

Jurassic rock that Vercingetorix held against the Romans; here we find the Tertiary deposits overlying the Chalk from which all authentic Champagne is produced; and down there huge blocks of rock were displaced in the geological past to open the caves where Roquefort cheese now matures. This is what this book is about. It is not a geology of France as the English title wrongly states; it provides an account, prefaced by a summary of the geological structure of France, of what one can find of geological interest and much else besides on 12 journeys through the French countryside. "France géologique, grands itinéraires", as the original has it, puts the matter much better. Professor Pomerol assumes a knowledge of geology



on the part of the reader and uses technical terms freely. This and the remarkably bad indexes — erratic to the point of fascination — may restrict use of the book to those who already have a pretty good idea of what they are looking for and who know the jargon. This is a pity, for this guide is laid out in a way which could reward more than the committed geologist and could enliven a long journey across the country or contribute to an enjoyable leisurely holiday tour. Of the 12 itineraries, five radiate from Paris, though none reaches the Channel coast, so the English-speaking visitor descending at Charles de Gaulle airport fares better than the cross-Channel sailor. Other routes take in the French Alps, the Pyrenees and the Massif Central.

Instructions are specific, give route numbers, indicate good spots to park and are thoroughly practical. With their aid the

traveller can take in the general geology of the passing countryside and supplement this with stops to see outcrops at first hand.

This is a book to have handy in the car or to read by the Christmas fireside in anticipation or in retrospect. The translation is adequate but no more. With a little more trouble, fewer technical terms, an accurate index, a route or two for the traveller entering France at the Channel coast and some reference to relevant books in English the translation could be much improved. The Anglo Saxon critic must in fairness reflect that, Canada apart, geological guides in French to North America and Britain are rare birds. In this spirit we should welcome this migrant from the south and hope it reappears in finer plumage. □

John Sutton is Prorector and Professor of Geology at Imperial College, London.

## Seismology explained

Peter J. Smith

*Earthquakes.* By G. A. Eiby. Pp.209. (Heinemann Educational/Van Nostrand: 1980.) £7.50, \$14.95.

AT SCHOOL more than 20 years ago, I was pleased to come across a newly-published little book on earthquakes, written by G. A. Eiby of the Seismological Observatory in Wellington, New Zealand. Like most popular science books of the time — what few there were, that is — it was visually rather less appealing than the back of the local gasworks; and despite its dealing with the Earth, an international body if ever there was one, it had an irritatingly parochial emphasis in its chosen seismic examples, clearly reflecting the author's chief area of study. Still, earthquake-curious beggars in those days had little opportunity to be choosers as far as popular expositions were concerned and, for all its (really rather minor) faults, the Eiby of 1957 was a godsend to seekers of extra-curricula science.

By contrast, the 1967 revised edition of *Earthquakes* was a bit of a disappointment. It came at a bad time, of course, for never before had there been a period during which geophysics had undergone such rapid change. It must have appeared to Eiby at the time that the seismological advances of the early 1960s warranted an enlarged volume; but in retrospect it was not very wise to try to set down the state of knowledge about earthquake phenomena during a revolution in thinking in which seismics were to play an important part. Thirteen years on from there, however, things are quite different. Geophysics in general and seismology in particular continue to advance, but much more

slowly. It is now possible to take a more sober look at what the revolution of the 1960s and early 1970s threw up.

Those familiar with Eiby's two earlier volumes will be inclined to see the 1980 version as a third edition under a new publisher; and indeed there are some minor echoes of the past in chapter headings, the occasional diagram and the odd turn of phrase. In general, however, Eiby Mark 3 is really a new book — largely rewritten, glossier than its predecessors, fatter and with pages double the size. There is still a tendency to overemphasize the seismic position of New Zealand; but the context in which earthquakes may be discussed is now so much wider and more varied that this hardly matters. What does matter is that the end product, though obviously not scientifically complete in the sense that it records everything known about earthquakes, is comprehensive in that it covers authoritatively all those aspects of the subject likely to interest the non-seismologist.

So how does the new Eiby compare with its competitors? Very well. Although the layperson now has access to more material on earthquakes than ever before, most of it is tied up in wider ranging books on catastrophic phenomena — books with such exotic titles as *Disasters*, *Geological Hazards*, *Forces of Nature*, *Catastrophe* and *Earthquake*. Popular books devoted solely to earthquakes are still surprisingly rare. Of the two most recent volumes within this genre, the less said the better about *The Earthquake Handbook* by Peter Verney (Paddington Press, 1979). But much more importantly there is Bruce Bolt's *Earthquakes: A Primer* (Freeman,



Earthquake damage in Concepción, Chile, May 1960.

1978), a curiously underproduced book but splendid in content. Bolt's primer is likely to remain the natural resort of the non-seismological Earth scientist wanting to swot up on basic seismic matters; but the genuine layperson will probably find the 1980 Eiby the more attractive. □

Peter J. Smith is Reader in the Department of Earth Sciences at the Open University, Milton Keynes.



# To the planets and beyond

David W. Hughes

ASTRONOMY has always been a subject that can be tackled at many different levels. Diversity is one of its fascinations and is illustrated perfectly by the first two books in this year's Christmas collection. Both are about planets, both consider planets in considerable detail, but amazingly there is virtually no overlap between them.

Let us start with *Planetary Geology* by John Guest with Paul Butterworth, John Murray and William O'Donnell (David and Charles, £7.95). Half of the book is made up of photographs, half of text. I state this with some certainty because throughout the volume there are photographs from the United States National Aeronautics and Space Administration on the right-hand pages and a descriptive text on the left. The Moon, Mars and Mercury are dealt with in detail and there is a brief discussion of the features of Phobos, Deimos, Venus and the satellites of Jupiter. This format is most useful as you are invariably reading about surface features which are illustrated on the opposite page and which can be seen by a flick of the eye. The text stresses the physical and chemical processes that produce rocks and landforms, and also the evolution of planetary surfaces as a function of time. Each double-page spread covers a specific topic, a few *ad hoc* examples being crater rays, faulting, lava channels and tubes, graben, fretted terrain and so on. The book is fascinating; anyone interested in planetary science will find it most rewarding. Astronomers have suffered an invasion of geologists; our cohabitation is reasonably harmonious and this book will go a long way to make the relationship even more beneficial.

The systematic pattern of planetary exploration started with the ground-based telescope and progressed by using imaging systems on flyby and orbiting spacecraft, unmanned soft landers and, in the case of the Moon, a manned landing and return of samples. Paul Doherty, in his *Atlas of the Planets* (Hamlyn/McGraw-Hill, £6.95/\$16.95), has taken us back to the beginning and gives us a succession of drawings of the planets as seen by him through his 419mm and 254mm reflecting telescopes. Doherty derives an enormous satisfaction from planet-watching and this enjoyment and enthusiasm radiates from every page of his book. The great beauty of the planets is graphically described. This is an ideal book for the amateur astronomer and is a superb introduction to the problems, joys and possibilities of studying planets with small telescopes.

The next book takes us to the boundaries of the Solar System. *Out of the Darkness: the Planet Pluto* by Clyde W. Tombaugh and Patrick Moore (Stackpole: Harrisburg/Lutterworth, \$14.95/£7.95) describes one of the most painstaking

searches in the history of astronomy, the 25-year quest for Percival Lowell's "Planet X". Tombaugh gives an autobiographical account of his childhood on the farm, his first telescopes, his amateur telescope making, and the way he approached V.M. Slipher at Flagstaff and got a job at the Lowell Observatory. We then read of the planet hunting ("a slippery business" according to Tombaugh), the life at the observatory, the new 33cm objective lens, the hours of careful telescope guiding, the succession of 35.6 by 43.2cm photographic plates, the work at the Blink-Comparator, and the search for the ninth planet. The discovery of Pluto on February 18th 1930 and its aftermath is described vividly. After the excitement dies away, comes the slow realization that Pluto is not Planet X. The search continues. More plates, more stars, more comparisons, all to no avail. In the words of Kuiper: "What Tombaugh did not find out there was even more important than what he did discover". A Jupiter-like planet, if it exists, would have been detected out to a distance of 470 astronomical units, Earth could have been detected out to 100AU, other planets like Pluto do not appear to exist out to 60AU. If Pluto isn't Planet X and there are no more planets what did Lowell do wrong? How do we explain the perturbations of Neptune? This is a great story, told by a great astronomer and makes compulsive reading.

Beyond the planets we have the stars and again two completely different books aimed at the amateur star gazer. *Star Maps for Beginners* (Simon and Schuster; \$4.95, £2.95) by I.M. Levitt and Roy K. Marshall is a competent introduction to the splendours of the night sky which is now in its twenty-sixth printing. The kernel of the book is a sequence of monthly evening star charts

drawn for a latitude of 40 degrees North (Philadelphia, Denver, Peking and Madrid). The message of the book is "get outside and star gaze". For the more armchair-minded astronomer who specifically wishes to know the mythological associations of the constellations we have *The Constellations: How They Came To Be*, by Roy A. Gallant (Four Winds: New York/Scholastic: London, \$11.95/£5.25) published in late 1979. Gallant takes us on a legendary tour of the star lore of ancient civilizations and reveals the details behind the names of stars and star groups.

Turning to the more active amateur we have *The Pocket Guide to Astronomy* (Simon and Schuster/Mitchell Beazley, \$5.95/£3.95) by Patrick Moore and *An Amateur Radio Telescope* (Pachart Publishing: Tucson, \$6.95) by G.W. Swenson Jr. Moore's handy little book is ideal for the observer in a hurry. It has a full series of star and moon maps and a guide to the accessible double stars, variable stars, open clusters, globular clusters, nebulae and galaxies to be seen from both hemispheres.

Have you ever wanted to build your own radio telescope? If you haven't, read Swenson's book and you probably soon might; if you have, read it again and it tells you how. Swenson is thorough, all the information is there for the construction of an instrument relying on solid state circuitry. The book is made up of a series of articles originally published in *Sky and Telescope*. If you want to add words such as superheterodynes, baluns, yagis, impedance bridges and radio spectral pollution to your vocabulary it is just the book for you.

David W. Hughes is a Lecturer in the Department of Physics and Astronomy at the University of Sheffield.

## Cosmic contemplation

John Maddox

*Cosmos*. By Carl Sagan. Pp.416. (Random House: 1980.) \$19.95. To be published in the UK in spring 1981 by Macdonald-Futura, £12.50.

CARL Sagan is professor of astronomy at Cornell University and has for the past two years been working on a series of television films being shown, or to be shown, by English-language television stations on both sides of the Atlantic.

With the title *Cosmos*, the films add up to what the television people describe as a "blockbuster". The model seems to be that of Dr Jacob Bronowski's series *The Ascent of Man* — one man's view of an important theme.

This is very much the book of the television series. In a curious way, it reads like television. It is a series of purple passages linked together, so to speak, with magenta. Those who read the book — and there will be a great many readers, for it is a popular book — learn much less than they might have expected about the way in which the real Universe is constructed and much more than they need to know about Carl Sagan's own way of regarding the phenomenon of his own place in the scheme of things, nicely summarized by the opening sentences:

The Cosmos is all that is or ever was or ever will be. Our feeblest contemplations of the Cosmos stir us — there is a tingling in the spine, a catch in the voice, a faint



sensation, as if a distant memory, of falling from a height. We know we are approaching the greatest of mysteries.

As if in a distant memory, you can hear the television producer shouting "Fade music; voice over!"

The theme is thus that the Universe is very large, too large for the human imagination to comprehend. By great feats of imagination, humans (Sagan's word; mercifully, he is sparing with "Man") have nevertheless been able to comprehend a little. Yet the mystery remains.

The plan of the book is simple, but conditioned by its link with a sequence of film scripts. It is an explanation of the Cosmos, only partly a history of it. Sagan's special twist is his repeated statement of his well-known position on extraterrestrial life — there are living things out there somewhere but they won't look like plants or people.

For my taste, too many of the tales that Sagan tells have obvious origins in television's insatiable need for visuals. The Japanese legend of the Heike, the belief that the warriors killed in battles fought in antiquity now walk the sea bottom as crabs, is a nice way of illustrating how artificial selection works. I haven't seen the films, but would bet that Sagan and a film crew spent some time filming the carapaces of crabs in Japan.

As the title suggests, the book touches all the bases — indeed it does so economically, packing into its 400-odd pages an account of stellar evolution, galaxy formation, quasars, nucleogenesis, the origin of life, evolution and the question "Where will it all end?". In passing, Sagan gives thumbnail sketches of the contributions of people as different in character and time as Thales, Democritus, Leuwenhoek and Darwin to the progress of science.

Occasionally he uses the technique of lapsing into fiction: "Sometimes in my fantasies I imagine there was someone who thought like this . . .". There follows a soliloquy by a creature living in the "childhood of the genus *Homo*" on such matters as the economy (and the danger) of the hunter/gatherer society, the discovery of fire and the meaning of the stars.

I don't know if the stars are camp fires in the sky or holes in a skin through which the flame of power looks down on us. Sometimes I think one way, sometimes I think a different way.

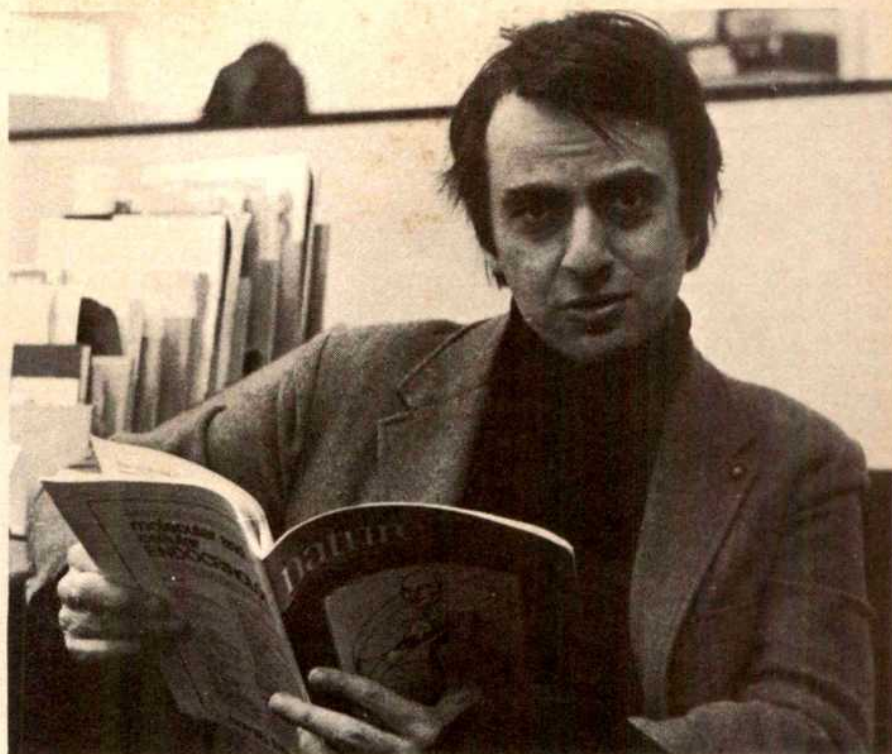
Sagan's fantasy is fair enough, I suppose, even when he has this early hominid say that he would like to visit those camp fires in the sky. But the technique is a trick for making the tale more vivid, not for making it complete.

As an exercise in popularization, *Cosmos* courageously aims at the widest audience. Its readers will come away with a vivid impression that the Cosmos is an interesting place, the exploration of which has hardly begun, with a rich store of

anecdotal information about a variety of topics and with "a tingling in the spine". Some of the images are nevertheless unhelpful — is "an explosion in a spaghetti factory" the best image for the interior of a

cell, for example? I'm not sure, but I'd quite like to see how the film crew tackled that.

John Maddox is Editor of Nature.



Carl Sagan

## Heavenly images

Philip Campbell

*Galaxies.* By Tim Ferris. Pp.192 (Thames & Hudson/Sierra Club: 1980.) £20, \$75.

THIS book has been written for a popular audience, though professional astronomers — including galactic specialists — will probably derive some interest and not a little pleasure from it. In particular, it contains the most beautiful set of astronomical coloured photographs that I have encountered.

Tim Ferris, a science writer by profession, presents a clear and comprehensive discussion of the current understanding of his subject, working outwards, as it were, from our own neighbourhood. He discusses the structure and the constituents of our own galaxy — the stars, globular and open clusters, supernova remnants, interstellar clouds — before proceeding to the local group of galaxies and then to a more general discussion of galactic structure and evolution. Chapters are also devoted to interacting galaxies and to clusters of galaxies. The book ends with a brief and fairly standard introduction to big-bang cosmology.

In his style of writing, Ferris attempts to stimulate the reader's visual imagination to the full. A particular example of this is the

imaginary journey through the Universe with which he prefaces and parallels his chapters. Picturing the reader in a spacecraft constantly accelerating from the Earth at 1g, the author introduces the notions of relativistic time-dilation and cosmological space-time distances, his narrative occasionally tinged with wit.

At times, however, the style becomes obtrusive. Although uncluttered by references and mathematical or quantitative details, the text is scattered with similes and metaphors, at times laboured. Occasionally, astrophysical processes are described in the active present tense with anthropomorphized stars, for example, as protagonists. There is also a tendency to gush; the Andromeda galaxy M31, for instance, is described as "heart-rendingly" beautiful.

Such excesses apart, the informative text and superb illustrations make this an unusually fine book. The author makes full use of the large format (13" × 14") and the price of £20, though high, is for once not unreasonable. □

Philip Campbell is an Assistant Editor of Nature.



## Beauty in the tools of science

Silvio A. Bedini

*Antique Scientific Instruments.* By Gerard L'E. Turner. Pp.168. (Blandford/Sterling: 1980.) Hardback £3.95, \$12.95; paperback \$6.95.

SCIENTIFIC instruments were once the prized possessions only of Renaissance princes and prelates, acquired for their cabinets of curiosities. Generally they were masterworks of the goldsmith and engraver, more decorative than practical, for it was not until the early seventeenth century that instruments became functional as tools of measure and observation. It was with the emergence of the mathematical practitioners and the practical sciences of mapmaking, navigating, surveying and science teaching that the craft of the instrument maker developed

and flourished. With the advent of the scientific revolution other scientific apparatus and instruments of increasing precision were required, and played an important role in the advancement of the sciences.

Now, centuries later, these early instruments are eagerly sought by museums and collectors alike. In museum exhibitions they represent the work of important artists and craftsmen, and reflect the state of the sciences as part of national history. For the collector they are evidence of romantic aspects of the past and are tangible reminders of pioneering scientists. Instruments are sought and collected by some because of their beauty, by others through intellectual curiosity.

Until the past decade, few books had been published about instruments. Then, one by one, popular works started to appear, some describing and illustrating only pieces of the finest museum quality as examples of art, and others reflecting the role of the instruments as tools of the sciences. Only one or two have been designed to inform the collector.

In *Antique Scientific Instruments* Gerard Turner addresses himself specifically to the collector and has produced the first practical handbook on the subject. He has adopted the three broad categories into which the instrument-makers themselves divided their products — mathematical, optical and philosophical — and has further segmented the mathematical instruments into five groups based on their functions — astronomy and time-telling, navigating, surveying, drawing and calculating, and weights and measures.

The instruments categorized in each of these groups are briefly described as regards their history, function and physical appearance. Under optical instruments are included microscopes, telescopes and a whole range of optical "toys" such as mirrors, camera lucida, magic lanterns, zygoscopes, stereoscopes, kaleidoscopes and cameras. The philosophical instruments covered are basically teaching devices related to mechanics, magnetism, pneumatics, hydraulics, electricity, heat and meteorology. Each of the sciences to which each group relates is described in a short history. Also included are a chapter on "Practical Advice on Collecting", a useful bibliography for further reading, a list of museums having collections of instruments and a comprehensive index.

The author is particularly well qualified to produce such a book. The Senior Assistant Curator of the Museum of the History of Science at Oxford University, which contains what is considered to be the finest collection of scientific instruments in the world, Turner is internationally recognized as an authority on the subject. He

is the author of numerous articles and several books on the subject.

This handbook is equally useful for historians and students of science, as well as for the collector and the dealer in antiquities. □

*Silvio A. Bedini is Keeper of Rare Books at the Smithsonian Institution, Washington DC, and specializes in the history of scientific instrumentation and horology.*

## Doing time

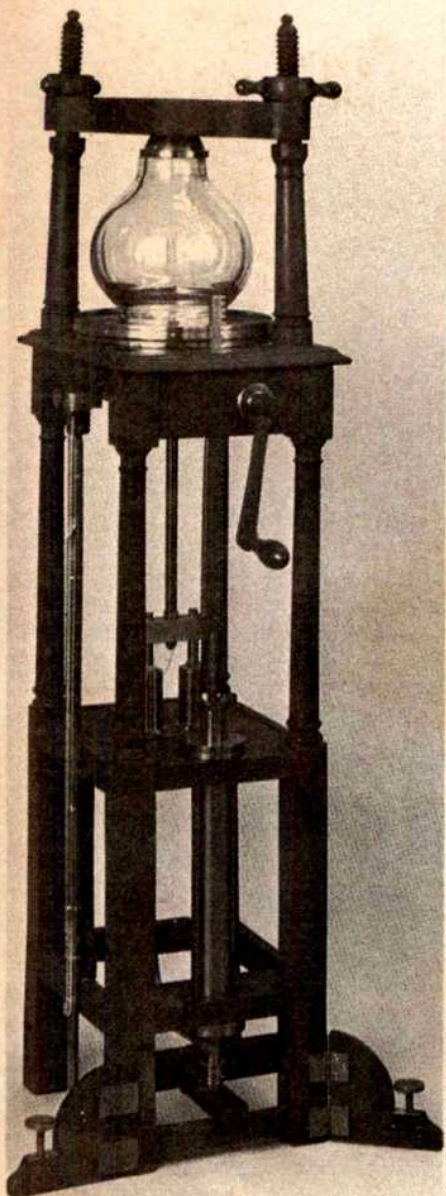
Derek de Solla Price

*Greenwich Time.* By Derek Howse. Pp. 254. (Oxford University Press: 1980.) £7.95, \$24.95. *The Book of Time.* Consulting editor Colin Wilson. Pp. 320. (Westbridge Books/David and Charles: 1980.) £10.50, \$24.95.

SINCE the dawn of mankind time has had such a fascination for us that it is not much of an exaggeration to say that it has been the ultimate cause of Babylonian, Greek, and therefore of all modern science. Sheer workaday astronomical time has an exciting and crucial institutional history, and it is quite a feather in the cap of the British that Greenwich rather than Paris Observatory time became a world standard and the prime point of reference, not just for astronomers, but also for navigation and world geographers as well as the standard for the railroad age.

Derek Howse, an accomplished scholar and historical sleuth of the National Maritime Museum in Greenwich, has told the fascinating story of how it all happened in the international meetings and councils that had to deliberate the issues and resolve the intense international rivalries. The story of the International Meridian Conference, Washington 1884, is especially interesting for an analysis of the power play as convoluted as anything in the UN today. He has taken the matter right up to the present-day technologies that enable us to chide the wobbly earth for its non-uniform meanderings and institute "leap seconds" to correct it. A very pleasing book this is, written by somebody who really knows something. Not so with *The Book of Time*.

I imagine it all must have started with consultant editor Colin Wilson, a well-known novelist and author, being excited (as was J. B. Priestley) with the psychic mysteries of time and precognition. Unlike Priestley he did not write all of the book himself, but seems to have sold the publisher and editor on the idea of getting together a team of science writers to take on the merely scientific aspects of time, such



A double-barrelled air pump of about 1785, signed I.B. Haas Invt, By the King's Patent Made & Sold by J.H. Hurter, London.

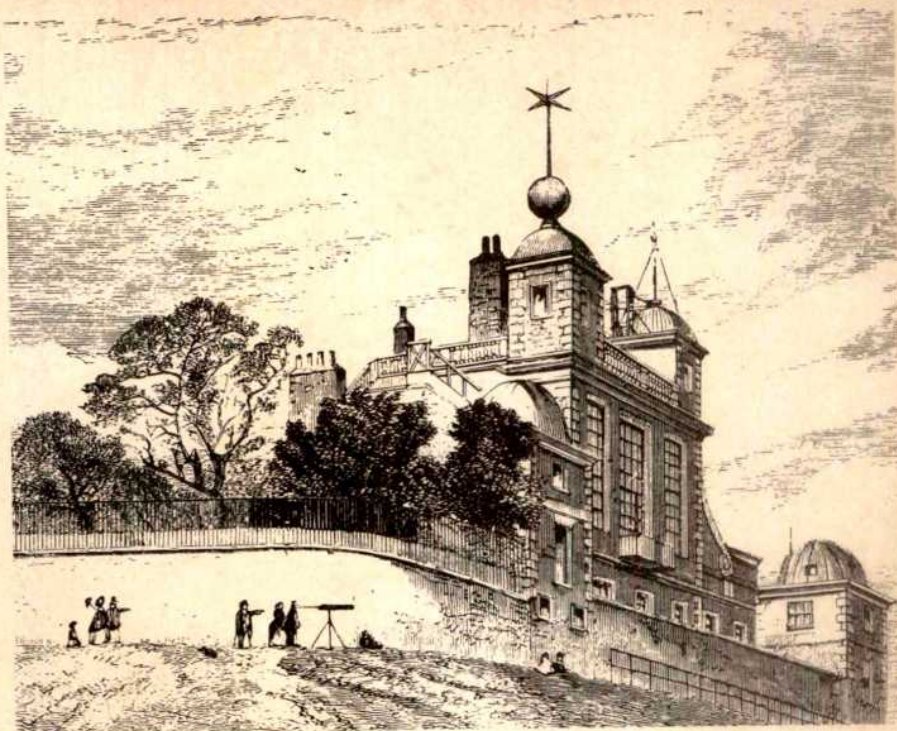
Royal Swedish Academy of Sciences, Stockholm



as historico-theological, horological, biological, physical and geological. They are all covered passably well, except perhaps the one on the history of sundials and clocks which is trite, but one misses the passion of somebody who cares and really knows their stuff. Science writing is a tricky business and needs a certain genius to pull off with distinction, and evidently nobody cared enough to do more than get this book together as prescribed.

Since I cannot recommend it, let me say that if you are interested in the philosophical and psychological problems of time you might go back to an old but splendid thesis by M. F. Cleugh, *Time and its Importance in Modern Thought* (Methuen, 1937). And if you want something more modern than her book, you might wade through the scholarly chapters in the series *The Study of Time*, edited by J. T. Fraser and others of the International Society for the Study of Time (Springer-Verlag, Vol. 2 1975), or the fine and authoritative treatment by G. J. Whitrow, *Nature of Time* (Penguin, 1976).

Derek de Solla Price is Avalon Professor of History of Science at Yale University.



The Royal Observatory, Greenwich, with the time-ball on the east turret.

Mary Evans

## Mind-bending and the paranormal

David Davies

*Science and the Supernatural*. By John Taylor. Pp.180. (Maurice Temple Smith/Dutton: 1980.) £7.50, \$10.95.

THE late Chris Evans, a seasoned hunter of the paranormal, had one inflexible rule when in pursuit of unusual phenomena: do not pronounce on what you have seen for 24 hours — the excitement of the moment may cause you to say something that you would find difficult to retract later. Probably unaware of this rule, John Taylor went on television "live" in 1973 to act as (in his own words) "scientific hatchet man on Uri Geller". Before an audience of millions Taylor was bowled over by the metal-bending spectacular that unfolded in front of him (though he had apparently also seen it the previous evening) and has since devoted a substantial amount of time to pursuit of the paranormal.

In 1975 he published a book, *Super-minds* (Macmillan) which extolled the "Geller effect". He wrote "I have been convinced that such supernormal abilities [as Geller and some others generate] do actually occur . . . the total available evidence puts the Geller phenomenon truly into the class of the supernatural", and much more. In 1980 he tells a different story. Now, "the paranormal is totally normal. ESP is dead . . . I started my investigations with an open mind . . . on the evidence presented in this book, science has won". What manner of investigation,

what kind of evidence could cause such a complete about-face? For myself, in late 1973 I felt that maybe there really could be something that merited examination by scientists. Three years later I felt it was probably all bunk. This was a journey of steadily growing awareness that magicians have remarkable "paranormal" deceptions up their sleeves (as James Randi has continually demonstrated), that children are not averse to playing quite sophisticated tricks on grown-ups — particularly if it gets them attention — and that scientists, whilst detached observers of experiments under their own control, may have no special abilities in observing the much more complex goings-on that generally surround allegedly paranormal happenings. In short I learnt a lot about people.

John Taylor's route was very different. He argued that electromagnetism was the only possible explanation for unusual phenomena and therefore that electromagnetic measurements should be made and electromagnetic theories sought. And when nothing turned up (except from some fairly simple electrostatic explanations of the odd phenomenon) Taylor found himself forced to the conclusion that the phenomena were without substance. It is, for my taste, a circuitous and intellectually unsatisfying argument. For all that I believe his final conclusion is correct, I'm not sure that one is allowed to pronounce a subject dead simply because one's own

intellectual skills and measuring equipment cannot come to grips with it.

The consequence of Taylor's conclusion that the paranormal does not exist is that people have deceived him left, right and centre. But this book, which wanders anecdotally through the whole gamut of strange happenings, barely comes to grips at all with the question of why some people deceive and why others are deceived. Indeed, Taylor, now back in the anti-paranormal camp, is hard and unforgiving of those who adduce the sort of evidence which until recently he would have taken seriously: "There is a high level of gullibility where seeming inexplicable events are concerned. Even apparently sober people appear to become very naive after witnessing something in the heavens [UFOs] which they cannot readily explain". Five years ago, Taylor himself was writing: "Puharich has observed Geller enter an unidentified flying object . . . unhappily the film cartridge containing the essential record of this event was lost, having dematerialised within a few minutes". It surely needs more than a few null results from electromagnetic equipment to reverse positions quite so dramatically.

David Davies was Editor of Nature from 1973–1979. He is now director of Dartington North Devon Trust, a charity dedicated to rural development.



## Avian delights: on the wing and on the water

John Andrews

PROFESSIONAL ornithology in the UK is fortunate in benefiting from substantial skilled amateur assistance and from a rapidly expanding public interest in birds and their place in nature. One result of this has been a steady increase in the funding available for research to determine the effects on birds of land-use changes and of individual development schemes. This is certainly the case with work on waders. Moving south from their breeding grounds each autumn, many species overwinter in our relatively mild, unfrozen estuaries, which are subject to threats from a great diversity of uses and abuses. In *Waders* (Collins, £9.50), Professor W.G. Hale draws together current knowledge on the biology of those species which occur in Britain, much of it either collected by amateurs or as a response to pressure from them, expressed through the conservation organizations.

Commencing with a general introduction to the species concerned, the author moves on to deal with habitats and adaptations, geographical distribution, mortality and evolution, breeding biology, migration and various aspects of wintering

ecology, including the important subject of estuarine carrying capacities which arises wherever a public inquiry asks the question "why can't these birds go somewhere else?" The author is particularly known for his own work on redshank, largely undertaken on the Ribble saltmarshes, themselves recently threatened by a scheme to embank and convert them to arable farmland. Complete with a substantial bibliography and index, the book is illustrated and presented to the high standard one expects from the *New Naturalist* series.

It is pleasing to find another publishing house aiming to produce works of similar quality. Some years ago Hamlyn produced a volume which came up to *New Naturalist* standards but was a little more adventurous in presentation and ventured outside the latter's self-imposed limits of the United Kingdom to look at birds of prey worldwide. Now they have produced a volume on *Seabirds: Their Biology and Ecology* (£7.50, \$14.95) written with evident enthusiasm by Dr Bryan Nelson of Aberdeen University and illustrated generously throughout the text not only with well-chosen colour and black-and-white photographs, but also with delightful drawings by John Busby. The author has put together an authoritative summary of the biology and ecology of seabirds worldwide in a relaxed and fluent style, without wasting words or taking the non-scientist out of his depth. After a general chapter which indicates the diversity of seabird species and of their biology, the reader is led to consider the problems and opportunities presented by their vast, rich and complex habitat, the oceans of the world. From there, the book turns to food resources and feeding methods and thence to breeding behaviour and biology, concluding with sections on movements and distribution, populations and human impact. Unlike waders, seabirds are known mostly at their breeding sites and so this aspect of their lives occupies about half the book as against one-twentieth of the text of *Waders*. All concerned deserve congratulations for producing a thoroughly enjoyable and instructive work at such a relatively modest price.

Because of their importance as quarry, geese have always attracted a good measure of interest in their distribution and numbers. Latterly, linked to a growing concern for their conservation, they have enjoyed a relatively large share of the bird research effort in both Europe and North America. For the last 13 years Dr Myrfin Owen has been working on goose ecology at the Wildfowl Trust and in *Wild Geese of the World* (Batsford, £15) he presents and discusses current knowledge of all 15 species and 23 sub-species. The first third of the book is occupied by species' accounts and the bulk of the very readable

text is reserved for discussion of social behaviour, movements and migration, summer and winter biology, population dynamics, and conservation and exploitation. Thanks to the research effort devoted to them, some aspects of the complex biology of geese are now understood, but much still remains to be worked out and the author ventures some stimulating speculation in these areas. The book is helpfully supplemented by line illustrations, accurate colour plates and a substantial bibliography.

Knowing what to leave out of any book is part of the art of writing and one most relevant to any book on general bird biology where there is a risk of taking all the information available, much of it pre-digested by other authors, and piling it into convenient heaps too large and generalized for comfort. The basic form of *Birds* (W.H. Freeman; hbk \$17.95, £10.60; pbk \$8.95, £4.90) is much the same as usual — geography, flight, migration and navigation, evolution, behaviour, physiology and song. The refreshing difference is that, while each is introduced by a crisp article summarizing the topic in very broad terms, there then follow several papers by different authors, focusing on one or another aspect of the subject. The papers — 25 in all — are selected from about 40 which have been published in *Scientific American* over the past 30 years. Despite the time span in which they were written and the many different authors, the whole book works well. It is surprisingly cohesive and easy to read.

Another imaginative, but less successful venture into natural history publishing is Derek Bromhall's *Devil Birds: The Life of the Swift* (Hutchinson; hardback £8.95, paperback £5.95). In 1948 Dr David Lack installed swift nest boxes in the roof of the tower of Oxford University Museum of Science to accommodate what has since become the best-known swift colony in the world. In 1975 Derek Bromhall decided to make a film of the same colony and this book is set against the background of its making. Swifts are fascinating birds by any standards. At about six weeks the youngsters leave their dark nest, plunging into sunlight and space at the beginning of a flight which may last for three years or more before they return to the colony to breed. Adapted to life on the wing, feeding on aerial plankton, swifts casually undertake movements of hundreds of kilometres to avoid bad weather, sleep in the air and sometimes even mate in flight. The fairly short text is an unpretentious and readable presentation of interesting information but the book is irritatingly over-illustrated by photographs many of which are of poor quality and add nothing to one's understanding of the subject. A pity because the idea is a good one and any attempt to



Passage peregrine, painted by Mary-Clare Critchley-Salmonson

From *Falconry in Arabia*, by Mark Allen



MAZLIAK, P. *et al.* (eds). *Biogenesis and Function of Plant Lipids. Developments in Plant Biology*, Vol. 6. Proceedings of the Symposium, held in Paris, June 1980. Pp. 451. ISBN 0-444-80273-8. (Elsevier/North-Holland Biomedical: 1980.) \$63.50, Dfl. 130.

MILTON, K. *The Foraging Strategy of Howler Monkeys: A Study in Primate Economics*. Pp. 165. ISBN 0-231-04850-5. (Columbia University Press: 1980.) \$20.

PREISS, J. (ed.). *The Biochemistry of Plants: A Comprehensive Treatise*. Vol. 3, *Carbohydrates: Structure and Function*. Pp. 643. ISBN 0-12-675403-9. (Academic: 1980.) Np.

ROBERT, A.M. and ROBERT, L. (eds). *Biology and Pathology of Elastic Tissues. Frontiers of Matrix Biology*, Vol. 8. Pp. 232. ISBN 3-8055-3078-1. (Karger: Basel, 1980.) SwFr. 124, DM 148, \$74.25.

ROLAND, J.-C. and ROLAND, F. *Atlas of Flowering Plant Structure*. Pp. 103. Flexi ISBN 0-582-45589-8. (Longman: 1980.) £6.25.

SUCKLING, K.E. and SUCKLING, C.J. *Biological Chemistry: The Molecular Approach to Biological Systems*. Pp. 381. Hbk ISBN 0-521-22852-2; pbk ISBN 0-521-29678-1. (Cambridge University Press: 1980.) Hbk £25; pbk £9.95.

WILSON, P.J. *Man, The Promising Primate: The Conditions of Human Evolution*. Pp. 185. ISBN 0-300-02514-9. (Yale University Press: 1980.) £8.80.

## Applied Biological Sciences

OSOL, A. *et al.* (eds). *Remington's Pharmaceutical Sciences*. 16th Edn. Pp. 1928. ISBN 0-912374-02-9. (Wiley: 1980.) £35.

PERRY, T.W. *Beef Cattle Feeding and Nutrition*. Pp. 383. ISBN 0-12-552050-6. (Academic: 1980.) \$35.

## Psychology

ARGYRIS, C. *Inner Contradictions of Rigorous Research: Organizational and Occupational Psychology*. Pp. 203. ISBN 0-12-060150-8. (Academic: 1980.) \$16.

HANSEL, C.E.M. *ESP and Parapsychology: A Critical Re-evaluation*. Pp. 325. Hbk ISBN 0-87975-119-3; pbk ISBN 0-87975-120-7. (Prometheus: Buffalo, New York, 1980.) Np.

McMILLAN, J.H. (ed). *The Social Psychology of School Learning*. Pp. 262. ISBN 0-12-485750-7. (Academic: 1980.) \$21.

VAN PRAAG, H.M. *et al.* (eds). *Handbook of Biological Psychiatry, Part III. Brain Mechanisms and Abnormal Behaviour — Genetics and Neuroendocrinology*. Pp. 400. ISBN 0-8247-6965-1. (Dekker: 1980.) SwFr. 62.

## Sociology

KAHN, J. and WRIGHT, S.E. *Human Growth and the Development of Personality*. 3rd Edn. Pp. 227. Hbk ISBN 0-08-023383-X; flexi ISBN 0-08-023382-1. (Pergamon: 1980.) Hbk £14.95, \$33.50; flexi £6.95, \$15.50.

MALMBERG, T. *Human Territoriality. Survey of Behavioural Territories in Man with Preliminary Analysis and Discussion of Meaning*. New Babylon. Studies in the Social Sciences, 33. Pp. 346. Flexi ISBN 90-279-7948-0. (de Gruyter: Berlin and New York, 1980.) DM 75.

## History of Science

FINOCCHIARO, M.A. *Galileo and the Art of Reasoning. Rhetorical Foundations of Logic and Scientific Method*. Boston Studies in the Philosophy of Science, Vol. 61. Pp. 478. Hbk ISBN 90-277-1094-5; pbk ISBN 90-277-1095-3. (Reidel: 1980.) Hbk Dfl. 80 \$42; pbk Dfl. 40 \$21.

FROMM, E. *Greatness and Limitations of Freud's Thought*. Pp. 147. ISBN 0-224-01875-2. (Cape: 1980.) £4.95.

## Anthropology

CHARLES-DOMINIQUE, P. *et al.* *Nocturnal Malagasy Primates: Ecology, Physiology, and Behaviour*. Pp. 215. ISBN 0-12-169350. (Academic: 1980.) \$27.50.

WENDORF, F. and SCHILD, R. *Prehistory of the Eastern Sahara*. Pp. 414. ISBN 0-12-743960-9. (Academic: 1980.) \$65.

## General

ALFONSECA, M. *Human Cultures and Evolution*. Pp. 136. ISBN 533-03747-6. (Vantage Press: New York, 1979.) Np.

CRAWFORD, P. *In the Country*. Pp. 202. ISBN 0-333-29325-8. (Macmillan: London, 1980.) £7.95.

DUBOS, R. *Man Adapting*. (With a new chapter by the author.) Pp. 538. Hbk ISBN 0-300-02580-5; pbk ISBN 0-300-02581-5. (Yale University Press: 1980.) Hbk £19.10; pbk £5.

HARMES, J. *The Magic of Herbs and Flowers. An Illuminated Manuscript Celebrating their Healing Properties*. Pp. 70. ISBN 0-333-29375-4. (Macmillan: London, 1980.) £2.95.

ISAACS, J. (ed.). *Australian Dreaming: 40,000 Years of Aboriginal History*. Pp. 304. ISBN 0-7018-1330-X. (Mereweather; New York, 1980.) Np.

LURKER, M. *The Gods and Symbols of Ancient Egypt: An Illustrated Dictionary*. Pp. 142. (Thames & Hudson: 1980.) £8.95.

NARENDRA, K.S. and MONOPOLI, R.V. (eds). *Applications of Adaptive Control. Papers presented at the International Workshop held at Yale University, August 1979*. Pp. 554. ISBN 0-12-514060-6. (Academic: 1980.) \$39.50.

O'RIORDAN, T. and TURNER, R.K. (eds). *Progress in Resource Management and Environmental Planning, Vol. 2*. Pp. 246. ISBN 0-471-27747-9. (Wiley: 1980.) £16.75.

PAULY, M.V. (ed.). *National Health Insurance: What Now, What Later, What Never? A Conference Sponsored by the American Enterprise Institute for Public Policy Research*. Pp. 381. Hbk ISBN 0-8447-2184-0; pbk ISBN 0-8447-2185-9. (AEIPPR: 1150 17th Street, NW, Washington DC, 1980.) Pbk \$8.25.

SALT, B. *Rural Science 2. Cassell's Rural Science Series*. Pp. 153. Flexi ISBN 0-304-30425-5. (Cassell: 1980.) £2.50.

TORRANCE, F. (ed.). *Belief in Science and Christian Life: The Relevance of Michael Polyanyi's Thought for Christian Faith and Life*. Pp. 150. ISBN 0-905312-11-2. (Hansel Press: Edinburgh, 1980.) £5.25.

UNITED NATIONS INDUSTRIAL DEVELOPMENT ORGANIZATION. *Stone in Haiti*. Pp. 64. (UN Industrial Development Organization: Vienna, 1980.) Flexi Np.

WHITTOW, J. *Disasters. The Anatomy of Environmental Hazards*. Pp. 411. Flexi ISBN 0-14-02-2114-X. (Penguin: 1980.) £4.50.

WINTER, R. *The Scientific Case Against Smoking*. Pp. 125. Hbk ISBN 0-517-539470; pbk ISBN 0-517-541416. (Crown: New York, 1980.) Hbk np; pbk \$4.95.

## GUIDE TO AUTHORS

● Review articles should be aimed at a relatively wide readership. Many reviews are invited, but submitted articles may also be accepted; it is advisable to consult us before writing a review article.

● Articles may be up to 3,000 words long with at most six displayed items (figures and tables); they are reports of major research developments.

● Letters are brief reports of original research of unusual and wide interest, not in general longer than 1,000 words; they have at most three or four displayed items.

● 'Matters Arising' permits short discussion (up to 300 words) of papers that have recently appeared in *Nature*.

Articles should be accompanied by an abstract of not more than fifty words. Letters should begin with a paragraph giving the background and main conclusion in terms intelligible to as wide a readership as possible.

**Manuscripts** may be submitted either to London or New York. Three typed copies should be submitted, each including lettered copies of figures. Typing (including references) should be double spaced. The title should be brief and informative. Pages should be numbered. References, tables and figure legends should start on separate pages. Experimental detail vital to the paper yet which would interrupt the narrative is best placed in the figure legends. Units should be identified in the margin on their first appearance. Equations should occupy single lines if possible:  $\exp(a)$  is preferred to  $e^a$  if 'a' is more than one character.

**References** are indicated by superscripts in the text. See any contemporary *Nature* for style, but note:

(i) only one reference number need be used if the reference is to several papers by identical authors.

(ii) first and last pages of references should be cited.

Abbreviations should follow the *World List of Scientific Periodicals*, fourth edn (Butterworth, 1963-65). Symposia are often difficult to refer to and only published or soon-to-be-published volumes should be mentioned in references. Their publisher and place of publication should be clearly indicated 'Personal communication' and 'unpublished' should be incorporated in text.

**Artwork** should be sent with the manuscript and clearly marked with author's name and the figure number. Line drawings should be either photographic prints or in Indian ink on heavy cartridge paper, tracing paper or similar materials. Most figures are reduced to one column width so originals should be about as wide as a page of *Nature*. To enable figures, particularly maps, to be edited in the same style as the text, they should contain only essential material. Ideally, an unlettered original and three lettered copies should be provided; labelling on halftones should, if possible, be avoided entirely. Magnifications quoted should be for the figures as submitted. We are always glad to see artwork for possible use on the cover, but cannot guarantee its return.

In order to save on postal expenses we return only the top copy and artwork of manuscripts that we cannot publish.

*Nature's* publishing policy is outlined in 258, 1 (1975) and 264, v, 11 Nov. (1976).



# A F O U R C E M E T S

## Awards

**Georges Köhler** (Basle Institute of Immunology) has been awarded the Albion O. Bernstein M. D. Prize for 1980 by the New York Medical Association.

**Dr Günther Ohloff** (Switzerland) is to receive the 1980 Hackforth-Jones Award for his work in perfumery chemistry.

**Dr Arthur Kornberg**, (Stanford University) has been awarded the 1981 Forteza Gold Medal by the Institute for Cell Research of the Caja de Ahorros of Valencia, Spain.

In the Chemical Writers' Awards BASF in association with the SCI have announced that **Peter Grange** (technical editor of *British Plastics & Rubber*); is Chemical Writer of the Year; **Mike Hyde** (editor, *Chemical Insight*) is Chemical Reporter of the Year; **John Murphy** (editor, *Plastics Industry Europe*) is Chemical Application Writer of the Year; and **David McDonald** (editor, *International Pest Control*) is Agrochemical Writer of the Year.

## Appointments

**Trevor W. Cole** has been appointed the P. N. Russell Professor of Electrical Engineering at the University of Sydney, Australia.

**Dr J. L. Hall**, reader in plant physiology in the University of Sussex has been appointed to a Chair of Biology in the University of Southampton with effect from 1 April 1981.

New members of the Directorate of the CERN Laboratory in Geneva include: director general, **Professor H. Schopper**; research directors, **Professor R. Klapisch** (France), **Dr Erwin Gabathuler** (UK); technical director, **Dr G. Brianti** (Italy); LEP Project Leader, **Dr E. Picasso** (Italy); administrative director, **Dr R. F. Heyn** (Netherlands).

## Meetings

13-16 April, **88th Health Congress**, London (Royal Society of Health, 13 Grosvenor Place, London SW1, UK).

29-30 April, **Gauge Theories of the Fundamental Interactions**, London (The Royal Society, 6 Carlton House Terrace, London SW1, UK).

4-7 May, **Emerging Environmental Solutions for the Eighties**, Los Angeles (Institute of Environmental Sciences, 940 East Northwest Highway, Mt Prospect, Illinois 60056).

6-7 May, **Monoclonal Antibodies and Ultrasensitive Immunoassay in Human Diagnosis and Monitoring of Therapy**, Gardone Riviera (RIA 81, Fondazione Giovanni Lorenzini, Via Monte Napoleone, 23, 20121 Milan, Italy).

8-9 May, **Calcitropic Hormones Methods and Clinical Applications**, Gardone Riviera (RIA 81, Fondazione Giovanni Lorenzini, Via Monte Napoleone, 23, 20121 Milan, Italy).

10-16 May, **The Structure and Development of the Greenland — Scotland Ridge**, Bressanone (Prof. Svend Saxov, Laboratory of Geophysics, Aarhus University, Finlandsgade 6-8, DK-8200 Aarhus N, Denmark).

14 May, **Ores in Sediments: Mineralising Fluids**, London (Geological Society of London, Burlington House, London W1, UK).

11-15 May, **Remote Sensing of Environment** Ann Arbor (Ann Arbor Conference & Visitors Bureau, 207 East Washington St, Ann Arbor, Michigan 48106).

14-18 May, **Reproductive Immunology**, Banff (Dr T. G. Wegmann, Division of continuing Medical Education, 12-103 Clinical Sciences Bldg, University of Alberta, Edmonton, Alberta, Canada T6G 2G3).

18-22 May, **Ground based Spacecraft Flight Dynamics Operations**, Darmstadt (R. E. Münch, esoc, Robert-Bosch-Strasse 5, 6100 Darmstadt, FRG).

19-21 May, **Telecommunications Energy Conference**, London (IEE, Savoy Place, London WC2, UK).

1-13 June, **Methods of Immunological Research and Diagnosis**, Buffalo (James F. Mohn, The Ernest Witebsky Center for Immunology, State University of New York at Buffalo, 210 Sherman Hall, Buffalo, New York 14212).

2 June, **Geothermal Studies**, Southampton (Geological Society of London, Burlington House, London W1, UK).

8 June, **High Pressure as a Reagent and an Environment**, Washington DC (Dr Robert S. Shane, 7821 Carreigh Parkway, Springfield, Virginia 22152).

10-12 June, **Leukotrienes and Other Lipooxygenase products**, Florence (Fondazione Giovanni Lorenzini, Via Monte Napoleone 23, 20121 Milan, Italy).

16-17 June, **Chromatography in Biochemistry, Medicine and Environmental Research**, Venice (Dr A. Frigerio, Mario Negri Institute for Pharmacological Research, Via Eritrea, 62-20157 Milan, Italy).

18-19 June, **Mass Spectrometry in Biochemistry, Medicine and Environmental Research**, Venice (Dr A. Frigerio, Mario Negri Institute for Pharmacological Research, Via Eritrea, 62-20157, Milan Italy).

## New ventures

A new service has been launched by Harwell which makes the Laboratory's neutron beam facilities available to industry for research into materials problems. The service, based on Harwell's DIDO and PLUTO materials testing reactors, provides a range of techniques — radiography, crystal diffraction, small angle scattering and vibrational spectroscopy — for the investigation of materials properties. Further details from: Peter Schofield, Materials Physics Division, AERE Harwell, Didcot, Oxon OX11 0RA, UK.

A new company Merseyside Laboratories has been formed to manufacture and distribute peptides, amino acid derivatives, resins, anti-sera and reagents and catalysts for asymmetric synthesis. Merseyside Laboratories also has a custom peptide synthesis service. This company is the UK and European distributor of peptides manufactured by Peninsula Laboratories, California. Further information from: Merseyside Laboratories, PO Box 62, 21 Aston Court, Kingsland Grange, Woolston, Warrington WA1 4SL, UK.

London-based Scientific and Technical Book Services Ltd have acquired world distribution rights in English for two Chinese scientific journals. *Science in China* (Scientia Sinica) and *Science Bulletin* (Kexue Tongbao). Further information from: Jennifer Clarkson, Gordon & Breach, 41/42 William IV St, London WC2N 4DE, UK.

The *Journal of Psychophysical Systems* commences publication shortly, with the object of promoting research into the behaviour of systems in which the presence of psychic factors cannot be ignored. Further information from: Prof. D. F. Lawden, Dept of Mathematics, University of Aston, Gosta Green, Birmingham B4 7ET, UK.

Elsevier announces a new bi-monthly publication *Applied Catalysis*, an international journal devoted to catalytic science and its applications. Sample copies from: Elsevier Scientific Publishing Company, PO Box 330, 1000 AH Amsterdam, The Netherlands.

11 December 1980

# Code of conduct for national academies

The national academies of science throughout the world are a mixed bag. Some of them, and certainly the oldest among them, exist more or less by accident. The *Accademia dei Lincei* began in 1603 as a kind of club for cultivated Roman noblemen interested in the doings of those scientists whom they chose to maintain by patronage. The Royal Society in London, also very much a club of enthusiasts, nevertheless won the blessing of Charles II on the strength of its promise that science might help with some of the British government's problems, how most effectively to navigate the oceans for example. Unlike the *Lincei*, the Royal Society has had the good fortune of an uninterrupted history. Elsewhere, national academies have more formal origins. The National Academy of Sciences in the United States, now just over a century old, was set up by the US Congress explicitly to provide advice on scientific and technical questions. Since then, it has become the custom to build in an academy to every new constitution — this, for example, is how the Academy of Sciences of the USSR came formally to be responsible for the administration of a substantial part of the Soviet government's research and development. With the passage of time, the notion has taken hold that national academies, while remaining clubs in the sense that only the membership has a voice in its succession, also have important functions in relation to their national governments.

On the face of things, this relationship is anomalous. What benefits can governments hope to derive from relationships with self-perpetuating societies of scientists? And why should clubs of scientists, having elected each other on the grounds of their achievements in research, then look for a special influence in public affairs for which their scientific work will not have prepared them? These are the questions implicit in Lord Todd's address to the anniversary meeting of the Royal Society last week, at which his five year stint as president of the society came to an end.

Breaking with the customs of gentility that mark these occasions, Todd openly complained that his immediate predecessors had spoiled the relationship between the society and the British government. "From 1950 under three successive presidents", he said, "the society gradually lost influence and drifted away from matters of public policy." The references are to Lord Adrian, Sir Cyril Hinshelwood and Lord Florey, presidents in succession between 1950 and 1965. Todd's analysis is fair, although, in Florey's case, the decision to disengage from government was deliberate. (Instead, Lord Florey tried, without much success, to interest the Royal Society as a whole in matters such as the rate of population growth.) Todd was also right to complain last week that the Royal Society was, as a result, far less able than it might have been to influence the upheavals of the early 1960s — the Robbins expansion of the universities ("ill-considered"), the abolition of the Advisory Council on Scientific Policy, the separation of technology from science and the transfer of the latter to the Ministry of Education (now the Department of Education and Science). But from 1965 until 1970, according to Lord Todd, Lord Blackett's personal commitment to the then new Labour government compromised the independence of the Royal Society and thus further diminished its influence.

The issue here is complicated. Blackett's own influence on the Labour government's policy was immense. Respected as he was by the then Prime Minister, Mr (now Sir) Harold Wilson, Blackett lent his support to some of the favourite policies of the Labour government, for example the Industrial Reconstruction Corporation which acted as midwife to the string of injudicious

industrial mergers of the late 1960s. There can never have been so influential a president. The fact that many of the then Labour government's policies are now recognized to have been mistaken is presumably irrelevant to Todd's implicit definition of how an academy should conduct itself. To be identified with government is to be compromised, even if government policy shows the wisdom of Solomon. But to offer independent advice and even help is not merely common patriotism but in the interests of science and its effective application. This, however, is not an easy balance to strike, if only because of the notorious reluctance of governments to take advice that does not suit them.

Lord Todd's account last week of his own presidency shows what the problems are. He made no secret of his fondness for the Advisory Council on Scientific Policy, which used to publish an annual commentary on the evolution of government policy on subjects as varied as the recruitment of scientific manpower and the conditions (always parlous) of the national scientific libraries. The modern equivalent is the Advisory Council on Applied Research and Development which puts out reports on subjects such as the economic and social consequences of the microprocessor. Todd said last week that the existence of this committee, like the presence of a scientist in the part of the Cabinet Office known popularly as the "think tank", owes something to his own intervention in his role as president. One obvious snag is that, in these respects, the Royal Society has been concerned with mechanisms and not with content and that the arrangements devised fall far short of what Todd himself said last week that he would prefer — the separation of the research councils from the Department of Education and Science and the restoration of the old advisory council. Another, perhaps more serious, difficulty is that the Royal Society has no means by which it can reach a corporate opinion on any substantial issue of public policy. Although, in the past few years, there has been a modest growth of the society's efforts at providing government and parliamentary committees with written evidence on questions such as secondary education or the environment, the process is slow and the outcome is often a muffled recommendation, not a clarion call. The Royal Society would be unable, even if asked, to arrive at anything like a corporate view on, say, government policy on nuclear power stations or whether manufacturers of drugs should in future be liable for side-effects even if there are no known ways of telling in advance what these might be.

To be fair, in this respect even the United States academy is no better off. Congress may commission studies of the hazards of low-level radiation or of climatic change, and the academy will dutifully recruit a panel to do the work without committing each of its members to the conclusions. But neither Congress nor the Administration would welcome the academy's unsolicited opinion on, say, the proper organization of federal research agencies or on the zany procedures followed by Congress in settling the annual research budget. It may be luck for all concerned that the academy would be likely to have as many conflicting opinions on such questions as it has members. Thus even the United States academy, corporately, is not nearly as influential as it likes to think. Its members, especially its president, may often be powers in the land, but almost always on personal grounds — and by personal means, back-slapping and arm-twisting, if it comes to that.

How, then, should academies set out towards Todd's two domestic goals — "to protect and encourage science in all its aspects" and to advise on and help with bringing science and



technology "fully to bear on the formulation of national policy"? The first need is that they should acknowledge their own limitations. They cannot hope too often to bite the hands that feed them without being fed less well. Yet there are some issues on which the academies' unprompted advice would be helpful and even welcome. Both in Britain and in the United States, there is thus a need just now for an independent examination of the relationship between academic research and commercial exploitation. Harvard's problems with genetic manipulation (see *Nature* 4 December) are likely to crop up elsewhere, and in

different fields. The academies are better placed than either universities or governments to say what should be done, but they have been slow to devise an agenda for discussion. (Are they, by any chance, afraid of offending their members?) Similarly, there is an urgent need (and not only in Britain and the United States) for an independently formulated policy on higher education in science, and on the problems of professional people thrown on the scrap-heap before retirement age because of chopping and changing of government policy. If they chose, the academies could be more directly influential than they are.

## Further nonsense on product liability

The United States Supreme Court, which does not often make an ass of itself, handed down a decision in October which will already have denied sleep to a host of manufacturers, especially to pharmaceutical manufacturers. The Supreme Court had been asked to rule on the legality of a decision made last March by the Supreme Court of California in the preliminary stages of a suit for damages. Two Californian litigants were suing because of the congenital damage they had suffered because their mothers took diethylstilbestrol during pregnancy. The original claims were faulty in that the plaintiffs did not specify the manufacturers of the diethylstilbestrol from whom they sought damages, but the Californian court helped out by suggesting that any damages eventually awarded might be shared among the suppliers of diethylstilbestrol in proportion to the various manufacturers' shares of the Californian market. The United States Supreme Court has now confirmed that this device is permissible, at least at this early stage. Whether the original suit (which has not yet been heard) will succeed, and will then survive the inevitable circuit of the appeal courts, remains to be seen. But the law on product liability, more stringent in California than elsewhere, is in danger of being made a nonsense. It also promises to be a serious impediment of innovation.

The issues are not complicated, even though the law may be. A manufacturer designs a product, say a mousetrap, sells several copies to the public and makes himself a profit in the process. As time goes on, the mousetraps are used to catch a host of mice, a benefit to the purchasers. But, sooner or later, a clumsy user will impale a finger on a piece of metal or have it broken because the trap goes off prematurely. Who, then, is to blame? In the old days, the law in most countries coincided with commonsense. A person buying a mousetrap intended to injure mice who managed to injure only himself had no cause to sue the mousetrap manufacturer. If he did so, the manufacturer would have been able to plead "contributory negligence" or something of the sort, and the only beneficiaries would have been the lawyers. In future (but already in California), the hapless mousetrap manufacturer will not be able to rely on that defence. First, he must design his mousetrap so that foreseeable accidents cannot take place. Mousetraps that cannot catch fingers will be more expensive and may be less efficient at catching mice, part of the price of product liability. What will keep manufacturers awake at night, however, is the fear that their designers have not thought of every accident. Is there a risk that in emptying the trap of mice, an innocent user may suffer some unsuspected damage? May he contract cancer, for example? For, if that happens, the manufacturer will be liable for damages under the law of strict product liability.

The Supreme Court's decision shows that the vigorous application of this principle offends against natural justice. If all manufacturers of diethylstilbestrol are to be joined in the suit in proportion to their sales revenue in the 1950s from the synthetic hormone, the implication is that no aspect of their behaviour can diminish their share of the liability. Yet some may have been more diligent than others in seeking out unwanted side-effects. Some may have made more profit than others. And some may have gone out of business, leaving the others to carry a greater share of the liability. The reasons why the drug manufacturers are especially

alarmed is clear — identifying unknown side-effects is an open-ended problem, for which reason it seems unfair that virtue is no defence. Strict product liability thus seems inequitable as between individuals. It is too soon to know how many drug manufacturers will turn to making mousetraps because the risks are better known, but strict product liability is a deterrent from doing anything for the first time. The community at large will not in the long run benefit.

This is the manufacturers' case against strict product liability. The other side of the argument is also telling. In the past thirty years, all kinds of manufactured products have turned out to be less safe in use than their salesmen promised. Motor cars have caught fire without warning, or have careered off highways. Aircraft have fallen from the skies unexpectedly, for reasons attributable (with hindsight, easily enough) to faulty design. Electrical appliances have electrocuted their users. And drugs have caused damage as well as bringing benefit, often in the most tragic ways. The wave of product liability legislation springs from the fund of reasonable grievance by innocent consumers against manufacturers who have frequently been slipshod in design or even guilty of telling lies. Manufacturers should not think their troubles will go away spontaneously. In Britain, for example, in the past three years, one royal commission (the Pearson Commission) and two law commissions (one for Scotland, one for England and Wales) have advocated the principle of product liability. How is a line to be drawn between the interests of manufacturers and consumers?

In Europe, the issue is lively just now because of the draft directive on product liability promulgated by the European Commission, and likely to compel national legislation in the next few years. The question is obviously within the interest of the European Commission, for without common legal principles, member states could use product legislation as a way of favouring their own manufacturers. But what should be the common standards? In the past few weeks, the British government (which accepted the principle of strict liability two years ago) has said that it will press the European Commission to allow as a defence by manufacturers the plea that a new product is as safe as the "state of the art" allows. The diethylstilbestrol manufacturers of California would be delighted with such a lifeline in their own case, but it is unlikely to satisfy either the European Commission or European consumers. The snag is that such a defence does not provide manufacturers, either collectively or singly, with an incentive for investing in research and development intended to improve the safety of their products. Indeed, used mischievously, the state of the art defence could become a refuge for the complacent. But is it entirely beyond the lawyers' wit to design a form of words that would allow a manufacturer to defend himself, if something goes wrong with a new product, by pointing to steps prudently taken in the research laboratory to investigate the safety of what he makes? Unless some such device can be found, there is a serious risk that innovation, especially adventurous innovation, will be inhibited. Whatever happens, the drug industry is bound to feel unfairly put upon because its new products have to be tested under government supervision. Should not such a procedure in itself be a defence against a product liability suit?

# Congress shares out patent licences

## Universities, business, given wider rights

Washington

After several years of intensive lobbying, US universities have persuaded Congress to pass a bill which will enable them to profit directly from the commercial exploitation of any research carried out with federal funds.

The bill was passed hurriedly by both the Senate and the House of Representatives in the last days of the session, and is expected to be signed into law by President Carter before the end of the month.

It makes uniformly applicable across all government agencies an arrangement which universities are already able to make with some departments, giving them the right to license patents arising from the work of federally-sponsored scientists provided that all profits made by the university are ploughed back into teaching or research.

The bill has been strongly advocated by university administrators and patent officers, who have claimed that it will reinforce their efforts to get the results of research onto the marketplace. The bill does not, however, go as far as some would have liked, as it awards patent rights only to small businesses and non-profit institutions, and is therefore not applicable to large companies which receive federal research support.

An alternative version of the bill originally passed by the House of Representatives included comparable coverage of large business. But this provision was fiercely opposed in the Senate, where several members argued that it would result in a "massive give-away" of public resources (*Nature* 6 March 1980).

Rather than prejudice the agreement between the two legislative bodies which is necessary before a bill can become law, members of the House agreed to limit the scope of the bill. They have, however, promised that there will be further attempts to introduce additional legislation covering large companies when the new Congress convenes next year.

In the past, the rights to any patent arising from publicly-funded research have remained the property of the federal government, on the basis that the results of research should be made available to anybody who wants to use them, and that any profits should go towards covering the costs of the original research.

With nobody actively pushing the commercial development of the patents, however, the take-up has been small. Of

the 30,000 patents that have been awarded to the federal government, no more than 5 per cent have been licensed.

In an attempt to give universities a greater incentive to find or create markets for their research results, both the National Science Foundation and the Department of Health, Education and Welfare have recently permitted research institutions to enter into an Institutional Patent Agreement.

Under such arrangements, which have been agreed with more than 30 leading US universities, the institution is allowed to retain patent rights provided that it can present evidence that it will press vigorously to license such patents as it is awarded. (Such an arrangement, for example, has given Harvard University the rights to the results of recombinant DNA research carried out with funds from the National Institutes of Health.)

Even this arrangement has come under fire from some scientists. Two years ago, for example, Professor Joshua Lederberg, now president of Rockefeller University in New York, wrote to a Senate committee suggesting that universities should stay out of the patent business, and suggesting some form of holding institution along the line of Britain's National Research Development Corporation to which patent rights should be allocated.

But support for expanding the principle to cover all federal research came both from the universities, who see royalties as a potentially fruitful source of additional income, and from the Carter Administration, which had made patent law reform a major recommendation in last

year's domestic policy review of industrial innovation.

Under the terms of the new law, all federal research agreements with small businesses and non-profit institutions will carry a clause stating that the institution carrying out the research will own the 17-year rights to any patents provided certain conditions are met.

In the case of universities, all licensing agreements must be approved by the funding agency; exclusive licences can only be awarded to large companies for between 5 and 8 years, after which they must be made generally available; royalties must be shared with the inventor; and the balance of royalties or other income made after the deduction of reasonable expenses must be used to support scientific research or education.

In addition, the federal government retains "march-in" rights to direct the university to award licences if it feels these are being inadequately handled. Any products or processes arising from the patent for the domestic market must be produced "substantially" in the United States. The earlier requirement that universities should share their profits with the government has, however, been dropped.

The bill also included a separate section extending the copyright laws to cover computer software. At present, software compilers have no way of protecting their programs from being copied and used without their permission. Now a software program which has been copied can be used only where permission has been granted, or for archival purposes. **David Dickson**

## Stanford and UCLA plasmid patent

Washington

A patent was awarded last week covering some of the fundamental techniques used in recombinant DNA research and developed by Dr Herbert Boyer of the University of California, San Francisco, and Dr Stanley Cohen of Stanford University.

The patent covers a process developed in the early 1970s for inserting foreign genetic material into a bacterial plasmid. The method has since become widely used by almost all of the companies engaged in recombinant DNA research. These companies will now have to obtain a licence to use the techniques.

The patent, covering the United States only, was issued to Dr Boyer and Dr Cohen as inventors, but they have already agreed to assign the rights and royalties that may ensue to their respective institutions. Mr Niels Reimers, director of Stanford's technology licensing office, said, however, that any royalties demanded would be

"reasonable", and stressed that, at least initially, it was not expected to make a large amount of money from the patent. Also the techniques developed by Boyer and Cohen can still be used freely by scientists for research purposes.

The question of payment is sensitive. If the patent turns out to be lucrative for the two universities, it could be challenged on the grounds that the patent application did not acknowledge the contribution which scientists other than the two named inventors had made to the techniques described (*Nature*, 3 April 1980).

Several scientists said last week that they were waiting to read the details of the patent — and to see what licence fee Stanford and the University of California, San Francisco were likely to demand from private companies — before deciding whether to take any further action.

The terms of the patent, No.4237224, are intentionally broad. They cover "a method for replicating a biologically



functional DNA", and describe the various steps used to cleave viral or circular plasmid DNA, insert a separate DNA fragment, and grow up and separate unicellular organisms containing the altered DNA.

Still awaited is a decision from the Patent and Trademark Office on a second application made by the two universities on behalf of Dr Cohen and Dr Boyer, which covers any organism produced with the techniques covered in the first patent.

Mr Reimers said last week that, from the universities' point of view, this was likely to be the more important patent, since without its protection companies could manufacture products abroad using the recombinant DNA techniques, and subsequently sell them in the United States without having to pay royalties.

The Patent Office's decision on the second application is expected within a year. All such patent applications covering microorganisms had previously been held up pending a ruling from the Supreme Court, which decided in the summer that there is nothing in existing patent law which denies microorganisms protection.

Meanwhile, the University of California has filed a suit against the pharmaceutical company Hoffman LaRoche and the San Francisco firm Genentech, claiming that the two companies must pay damages to the university for the use of a cell line produced by university scientists which the companies have been developing as a potential commercial source of interferon.

The scientists at the University of California, Los Angeles who produced the cell line claim that it was passed to Hoffman LaRoche without their permission. But in the counter-claim Hoffman LaRoche is arguing that there were no conditions attached to the cell line when it was obtained indirectly through a researcher at the National Cancer Institute, and that the company therefore has no obligation to the university.

David Dickson

## Genetic engineering

### Hormone growth

Genentech, the California-based biotechnology company, will begin clinical trials of its latest genetically-engineered product, human growth hormone (HGH), in London this January. But Genentech's industrial partners in the venture, Kabi Vitrum AG of Sweden, are somewhat ambivalent about the development.

Kabi Vitrum is the major world producer of HGH, made at present from cadaver pituitaries. The hormone is used to treat HGH-deficient children, reckoned to be some 7-10 per million of population. But the nature of the source naturally limits production, and Kabi estimates the true market to be three times the present supply; so the firm searched for other sources. Genetic engineering was an obvious possibility, as HGH is a small

peptide, about the size of insulin.

So in 1978 Kabi asked Genentech to produce a strain of *Escherichia coli* containing the HGH gene. Under the contract, Kabi would have sole world production rights, except in the United States and Canada, where they would be shared with Genentech. But Genentech was successful sooner than Kabi expected, and further surprised the firm by making rapid preparations for commercial production. Genentech had been expected to stick to research.

Now Genentech is well ahead with pilot tests in 700-litre fermenters, while Kabi has been restricted to 10 litres by Swedish limits on scale-up of genetic engineering experiments; and Genentech plans clinical trials at Great Ormond Street Hospital for Sick Children starting in January 1981. Kabi, meanwhile, would wish to be more cautious. "We do not know about Genentech's toxicological testing" said Dr Bengt Karlsson, Kabi's managing director, "but we would not wish to put the product on clinical trial for at least six months". Nor is Kabi's caution due to lack of material, for they have access to Genentech's supply.

However, in London, where Dr James Tanner at Great Ormond Street will conduct the trial, it is felt that Genentech's toxicity testing has been quite sufficient. There have been plenty of animal and monkey tests, says Dr Tanner, and the UK Department of Health has passed the material for clinical trials. The Genentech HGH will be given to 20 patients for a year, 10 of them first treatments, and the other 10 already three years into a course of pituitary HGH. The main contaminant will be 1-2 per cent of bacterial protein; and the danger is that HGH-like proteins in this material may induce antibody formation to true HGH.

Dr Tanner welcomes the new source of the hormone. In the United Kingdom there are 100 new cases a year of HGH deficiency, and just enough pituitary HGH to go round (produced from 60,000 cadavers a year). But it is always "touch and go" each year whether sufficient cadavers will be made available. Moreover, if there were more HGH around, it could be tried out on more marginal cases of delayed growth, or slow bone healing after fractures.

Ultimately, Genentech will not be the source of HGH in Britain. Kabi announced last week that it has concluded a deal with the Department of Health for the Centre for Applied Microbiological Research at Porton Down to conduct scale-up trials on the Genentech bacterium. In exchange, Kabi will offer the product at a preferential price to the Department of Health, and assist Porton with its present production of HGH from pituitaries. (Kabi believes it has a more efficient extraction system.)

The centre is seeking permission from the Genetic Manipulation Advisory Group to ferment the engineered *E. coli* in

400-litre vats; and to satisfy GMAG, it must show that the organism is killed in the closed fermenter before the material is extracted.

Despite early misgivings, the Department of Health has begun to encourage Porton to become involved with industrial applications of the recombinant DNA technique — Unfortunately nothing has yet come forward in the United Kingdom that fits the bill. Dr Peter Sutton, director of Porton, is delighted at the deal with Kabi: "It means we can get our feet wet" with commercial scale genetic engineering, he said last week.

Robert Walgate

## US Administration

### Reagan's men?

Washington

President-elect Ronald Reagan's transition staff is sifting through the list of candidates for top-level positions in the new Administration, and the names of the first cabinet appointments should be announced this week. Potential choices have been widely discussed in the press — often names intentionally leaked to gauge public reaction — so few major surprises are expected.

Top candidate for the renamed Department of Health and Human Services (DHHS), responsible for the biomedical research budget of the National Institutes of Health (NIH), is Senator Richard Schweiker, Mr Reagan's running mate in his bid for the 1976 Republican nomination.

Mr Schweiker gave up his Senate seat earlier this year to work for Mr Reagan's election. In the Senate he was an active member of the Labor Committee's health and scientific research subcommittee, and as ranking minority member often supported the initiatives of the committee's present chairman, Senator Edward Kennedy.

Mr Schweiker is "definitely pro-science", one NIH official said last week, although adding that he had received some criticism for inserting in the institutes' funding legislation a clause that requires special arrangements for supporting research in diabetes and digestive diseases — the type of constraint that NIH prefers to work without.

The appointment would be less popular with labour unions, since Mr Schweiker is the sponsor of a bill designed to restrict the activities of the Occupational Safety and Health Administration.

As DHHS Secretary, Mr Schweiker would be responsible for the budget and activities of the National Institute of Occupational Safety and Health, part of the Center for Disease Control.

A predecessor in that post, Mr Caspar Weinberger, is widely tipped as next Secretary of Defense. He was director of the Office of Management and Budget under President Nixon, where his financial

stringency earned him the nickname "Cap the Knife". He was later promoted to Secretary of the then-named Department of Health, Education and Welfare at a period when biomedical research was becoming dominated by a congressional "disease of the month" approach.

Various names are being discussed for the position of Under-Secretary of Defense for Research and Technology, responsible for the Pentagon's massive research budget. They include Mr William van Cleave, at present head of Mr Reagan's defence transition team, and Mr Benjamin T. Plymale of the Boeing Corporation, who was the source of controversy last year when his security clearance was temporarily revoked.

No clear candidate has yet emerged to head the Department of Energy. One suggestion, Mr Michel Halbouty, a Houston oilman and geologist who was Reagan's chief energy strategist during the campaign, is being opposed by some influential Republicans because of his lack of government experience. Others have opposed the nomination of Mr Frank Zarb, a top energy official in the Nixon and Ford administrations, because of his involvement in setting up the present system of price controls on crude oil and gasoline. Two possible contenders are Dr John Sununu, professor of engineering at Tufts University, Massachusetts; and Representative Clarence Brown of Ohio.

Appointments at a lower level, including the heads of independent agencies such as the National Aeronautics and Space Administration, are not likely to be announced until the main cabinet posts have been filled.

In the science field, these appointments will also depend on the report of the science and technology transition team under Dr Simon Ramo of TRW and Dr Art Bueche of General Electric.

Dr William A. Nierenberg, director of the Scripps Institute of Oceanography, is widely mentioned as possible director of the Office of Science and Technology Policy (OSTP), as is Dr Guyford Stever, ex-director of the National Science Foundation, who held the OSTP job for a few months at the end of the Ford administration.

At the National Science Foundation (NSF) itself, the Reagan administration seems unlikely to overturn the appointment of Dr John Slaughter as director. Dr Slaughter was sworn in two weeks ago, and that the emphasis that he is keen to put on the development of engineering and applied research should match Republican goals for science.

Finally, the appointment of Dr Frank Press, the present director of OSTP and President Carter's Science Advisor, was assured as the next president of the National Academy of Sciences when nominations for the post closed last Monday without any other names having been put forward.

David Dickson

## Soviet plans

### Science on tap

Soviet science is to be geared even more closely to the needs of the economy, according to the guidelines for the 11th Five Year Plan, published last week. The plan calls for a substantial reduction in the time taken to disseminate research results, strengthening of the links between research and production, better coordination between scientific establishments and an improved basis for scientific planning.

Individual research priorities specified by the guidelines range from the immediately practical (the improvement of computer technology and software) to the long-term (creation of the bases for thermonuclear power engineering), and from the further conquest of space to greater environmental protection and economic utilization of the biosphere. Biotechnology to produce new compounds with tailor-made properties, particle physics and immunology all receive special mention.

At this stage of planning, however, no specific targets are mentioned, nor is the financing of science discussed. The emphasis on closer links between science and industry, however, and the statement that ministries and departments are to bear increased responsibility for industrial research may have some financial implications. Their responsibility will presumably also include the planning of research in institutes under their control. One of the main complaints of Soviet scientists in recent years has been the inflexibility of research plans once approved. The new guidelines, however, urge that the direction of research and development should be "determined in good time . . . and changed to meet the demands of the scientific-technological revolution".

All this, however, depends on an overall increase of labour productivity. In industry, this increase is specified as 23–25 per cent, which is to account for more than 90 per cent of the increase in output. For the scientists no such target is set, perhaps because the recent "press debate" in *Literaturnaya Gazeta* has revealed only too clearly how much scientists resent having their intellectual performance monitored.

Vera Rich

## DNA guidelines

### Bowing out

The US National Institutes of Health (NIH) are facing a virtual revolt from local Institutional Biosafety Committees (IBCs) over whether there is still a need for strict surveillance of research using recombinant DNA techniques.

At a meeting in Washington organized by the National Institute of Allergy and Infectious Diseases, the predominant view

of the chairpersons and representatives from more than 150 IBCs throughout the country was that the prime role of the IBCs has become largely a public relations exercise.

Few of those attending the meeting were prepared to accept that recombinant DNA research presented any greater health or environmental hazard than work with unaltered organisms not covered by the NIH guidelines.

Many complained of the amount of paperwork they are required to carry out, particularly in the light of recent revisions of the guidelines, which have shifted most of the responsibility for reviewing research protocols from the NIH's Office of Recombinant DNA Activities to the local level.

The Washington meeting had originally been called for IBC chairpersons to discuss how their committees were operating. But the main focus of the two-day meeting rapidly became whether the IBCs — or even specific regulations covering recombinant DNA research — were any longer needed in their present form.

According to one NIH official, the mood of the meeting was that the amount of time that IBCs put into DNA issues was out of proportion to all sorts of other bio-hazards.

One recommendation being forwarded to next month's meeting of the NIH's Recombinant DNA Advisory Committee is that all experiments using the disabled K12 strain of the bacterium *Escherichia coli*, or the yeast *Saccharomyces cerevisiae*, as host-vector systems should be totally exempt from the guidelines.

In the case of *E. coli*, the same suggestion was made last year, but the advisory committee then recommended — and NIH director Dr Donald Fredrickson agreed — that although prior approval was no longer necessary for such experiments, the requirement that the experiments be carried out under P1 physical containment conditions should remain.

Members of biosafety committees also complained about the additional paperwork resulting from NIH's requirement that, although details of all approved experiments no longer have to be registered, they must keep detailed records of all recombinant DNA work carried out in their institutions.

The latter requirement was partly the result of a survey at Stanford University in California which showed a discrepancy between the rate at which different committees required experiments to be reclassified, possibly indicating that some were interpreting the guidelines more strictly than others.

But the IBC members balked at yet more paperwork.

A straw vote taken during the final plenary session of the meeting revealed little support for the proposal that NIH should keep a record of all recombinant DNA research carried out under the guide-



lines, a small majority for recording research carried out under P2 containment conditions and above, and a larger majority for keeping a record merely of all research in P3 and P4 containment conditions, the two strictest categories.

Reflecting their general belief that recombinant DNA research no longer represents a greater hazard than ordinary research with microorganisms, many committee members were sceptical about the value of a broad study of the effectiveness of IBCs which NIH is now preparing.

If the committees had any value, it was felt, it had been in calming public fears about the health implications of such research. Mr Ray Thornton, for example, recently appointed chairman of the advisory committee, said that the careful supervision of experiments had been largely responsible for the general development of public confidence.

Other speakers suggested that, even if no extra hazards had been identified, the public discussion raised by initial fears had helped to generate a consciousness about the need to watch for biohazards in general.

David Dickson

## Yugoslavia now

### Supek's worry

Yugoslavia could shortly face economic collapse if the planners fail to make proper use of the country's scientific personnel. This is the opinion of Dr Ivan Supek, the Yugoslav physicist and philosopher, in London this week for a Pugwash meeting.

Yugoslav scientific and academic life, says Dr Supek, has almost completely lost the impetus of 20 years ago. The financing of basic research is hampered by a bureaucratic system which allegedly subordinates research to consumer control. But reliance on foreign licences (usually purchased when already obsolescent) means that the technological base required by Yugoslav industry and agriculture is either inappropriate or altogether absent.

The chief factor in the decline, according to Dr Supek, is excessive party and state control over science. After the hardliners' coup of 1971, the universities lost much of their autonomy, including the right to elect their own deputies to parliament. (Dr Dupek himself was a non-party deputy from 1963 to 1967.)

At the same time, the university structure was decentralized. The University of Croatia, for example, was divided into four separate universities (Zagreb, Split, Rijeka and Osijek) and the individual faculties, rather than the university as a whole, became the basis of planning and financing. Frequently, said Dr Supek, decision-making fell into the hands of party members with no particular academic background.

Under these arrangements, "censorship by budget" was made easier. Among the

victims of this process was the *Encyclopedia Moderna*, a philosophy of science journal edited by Dr Supek himself.

Dr Supek stresses that it is not the "self-management" process — Yugoslavia's special contribution to socialism — which is at fault. If the current trend towards bureaucratic centralism could be reversed, he said, and "self-management" restored to scientists, both basic and applied research would benefit. At present, however, self-management is simply a slogan.

Such official duplicity, said Dr Supek, is nothing new in Yugoslav science. In 1956, when Yugoslavia began a nuclear research programme, Dr Supek, as director of the prestigious Rudjer Boskovic Physics Research Institute, found himself *ex officio* on the country's atomic energy commission. Although the programme had, officially, a purely scientific and peaceful orientation, its members included the Minister of Defence Ivan Gosrjak and



Supek (right) and defence minister, 1956

Minister of Internal Affairs Alexander Rankovic. Their presence made Dr Supek extremely sceptical of the true aim of the programme, and made him a fervent opponent not only of nuclear weapons but of all applications of nuclear energy.

The duplicity, which, in Dr Supek's words, is allowing self-management to be killed in the name of self-management, will be a major obstacle to any move by the scientists to regain their pre-1971 position. The recent ban of the proposed cultural and sociological journal *Javnost* was justified by the Belgrade authorities on the grounds that the journal was meant to be a front for a would-be cultural elite. Dr Supek, however, is strongly opposed to elitism, and would claim for science only that right of self-government which is constitutionally guaranteed to all Yugoslav workers. The Party hardliners, however, are not prepared to yield without a struggle. Recently agronomists working on the forthcoming five year plan proposed that, for modern farming methods to be introduced, the maximum peasant holding should be increased from 10 to 50 hectares. But in spite of the deteriorating state of Yugoslav agriculture, the proposal was rejected as liable to cause class conflict.

Vera Rich

## Agricultural research

### Ministry at top

An impending change in the relationship between the Agricultural Research Council and the Ministry of Agriculture, Fisheries and Food (MAFF) now seems likely. Most probably, the council will in future be more directly subject to the ministry. In this respect, it is likely to be worse off than the Medical Research Council, which in October reached an arrangement with its chief sponsoring department of government, the Department of Health and Social Security, that some £12 million of "Rothschild money" should be transferred back to its own annual budget.

Change has been in the air since the publication of a report of the Public Accounts Committee in July 1979 which suggested that the government should consider transferring a further slice of the ARC budget to the agriculture ministry. The underlying principle is that put forward in 1971 by Lord Rothschild, who advocated giving control of research budgets to the chief users of the results of research — the ministerial "customers". At present, some 40 per cent of the research council's spending derives from the ministry, and the Public Accounts Committee was asking why the balance should not be shifted further.

For the past year, a committee under the chairmanship of Sir Brian Hayes, permanent secretary at the ministry, has been trying to decide what should be done. The alternative to a further transfer of funds is a more direct influence by the ministry on the policy of the council. Although a decision has not yet been reached, the second course is the more likely. Either way, the council is unlikely to be overjoyed.

Like many government-supported institutions, the council (ARC) has been hard-pressed to operate within its cash limits during the financial year 1979-80. Nevertheless, by the end of that year, says its annual report published last week, it had managed to plan a reasonable research programme for 1980 and beyond by concentrating its efforts on high priority research.

The council's choice of priorities was effectively made by MAFF which has cut the amount of research it is prepared to buy in some of the ARC's research institutes while increasing it in others. MAFF currently pays for about half of the work conducted in ARC institutes under the Rothschild customer-contractor principle.

MAFF is particularly keen to encourage food research, interest which has proved lucky for the ARC's Meat Research Institute whose grant of £370,000 from the Meat and Livestock Commission was cut last September. MAFF has stepped in to make up some of the loss. It has also increased its contribution to the budget of the Food Research Institute in Norwich.



the extra support going mainly to research on biopolymers, nutrition and biotechnology. This new emphasis coincides with a reorganization of the Food Research Institute and the setting up of a joint ARC-Medical Research Council working party on food research policy.

Irrespective of MAFF, ARC has been increasing support for research in priority areas, in particular by introducing a new scheme for supporting work in universities outside the normal research grant system. ARC research groups in photosynthesis have been set up at the universities of Leeds and Sheffield and at Imperial College, London; and at the University of Bristol a group has been established in the neurobiology of animal behaviour and reproduction. The ARC's plans for the forthcoming year include the establishment with the Medical Research Council of a new unit at Edinburgh on neuropathogenesis.

Judy Redfearn

## British dentists

### Broader, better

The proposal that dentists newly qualified from British dental schools should not be allowed to practise without first spending a year in supervised practice is the chief recommendation of an inquiry into dental education, commissioned by the Nuffield Foundation and published earlier this week. The inquiry was directed by Sir Gordon Wolstenholme and supervised by a steering committee under Professor T. C. Thomas, previously vice-chancellor of the University of Liverpool.

British dentistry, long saddled with an international reputation not very different from that of the British motor car industry, is offered a cheerful future in the report (to be had from the Nuffield Foundation at £4.50). The incidence of caries among children is decreasing, dramatically so in cities such as Birmingham where there has been fluoridation of water supplies for some time. In the ten years from 1968, the proportion of the British population entirely without teeth (described in the report as "the edentulous state") decreased from 36 per cent to 29 per cent.

Part of the stimulus for the inquiry was the recognition that dentists now being trained would still be in practice when the state of British dental health has been further transformed, so that the pattern of practice will have changed, and when novel dental technology will be available.

The theme of the inquiry's report is that dentists should be trained for flexibility. The dental schools are told that their present output of professionals is likely to be sufficient for the future, but that British dentists should rely more than is their present habit on ancillaries, especially hygienists and therapists, all of whom are in need of more explicit training and career structures.

On the curriculum of the dental schools,

the report argues for greater attention to basic science and the early introduction of students to clinical work. Present dental courses are too narrowly vocational, and should be broadened but not lengthened (at present training lasts four or five years). Instead, the argument goes, there should be a pre-registration year.

But where? Newly qualified physicians spend their pre-registration years in hospitals, but dentists have no comparable places of supervised work. The committee suggests a system of supervision in practice organized by the dental schools and based on the Community Dental Service or on the dental services provided for the forces. It also wants to see a period of vocational training in the first two years of a dentist's regular practice and more opportunities for in-service training than there are at present.

The committee of inquiry also asks that steps should be taken to increase the present scale of dental research in Britain, including the setting up of a national research centre. One obvious present difficulty is that most dental research is at present undertaken on short-term research grants.

The committee neatly skirts around the most contentious problems in British dentistry — how should dentists be paid? It echoes the general discontent (shared by some dentists and most National Health Service patients) that the present system of piecemeal payments is unsatisfactory, but judiciously recommends that professional organizations "should seek a system of payment . . . other than that existing at present".

## Israeli science

### Crisis at Weizmann

Financial crisis threatens the "very existence" of the Weizmann Institute of Science, Israel's private and principal research institution — or at least that is what Weizmann president, Professor Michael Sela, told the governing body recently. But according to the Weizmann Institute Foundation in London, which helps to raise money in the United Kingdom for the institute in Israel, the Weizmann finances have never been better.

Somewhere between these two statements lies the true position — that the Israeli government, which provides 45 per cent of the institute's running costs, has announced government spending cuts which will reduce its contribution to the Weizmann Institute by 7½ per cent (in real terms) compared with last year; and that Professor Sela was painting a grim picture to drum up support from the Weizmann's foreign friends, who are strongly represented on the governing body.

Foreign endowments and bequests from Europe as well as the United States contribute around 20 per cent of the Weizmann's funds. While these contri-

butions have been increasing, they have not kept up with inflation outside Israel — except for the United Kingdom, whose donation has increased by two-thirds in the past two years. This is due to the encouragement of Lord Sieff, chairman of the major British chain store Marks and Spencer, and also chairman of the Weizmann Institute board of governors.

The net result is that the Weizmann budget will be static this year (October 1980 to September 1981) in dollar terms at about \$30 million, whereas institute officials would have liked to see a small growth to take into account inflation abroad (where scientific equipment, for example, must mostly be bought).

Nevertheless, in 1980 funds were sufficient to establish, on a scientific staff of 300, five new "career development



Sela, crying wolf??

chairs", as an exercise to introduce new talent to the campus, and 10 professorial chairs. Money for these came mostly from the United States, but also from France and South Africa. Two new research centres were also established within the institute: the K. B. Weissman Institute of Physical Sciences and the Melvyn A. Dobrin Centre of Plant Research. Moreover, the Yeda Research and Development Company, which acts as a link between the institute and industry, increased its turnover to \$4.5 million in 1980, compared with \$1 million three years ago. (One recent venture, Inter-Yeda, manufactures human fibroblast interferon for use in clinical trials.) The government cuts must therefore be seen in the context of a recent very healthy spending pattern at the Weizmann.

Nevertheless, 70 per cent of the institute's budget is spent on salaries; so the effect of a cut in total budget is magnified when compared with the 30 per cent the institute has to spend on books, equipment and fuel. Bequests on the whole do not provide these items; so cuts are, in the end, having to be made in these financially marginal but scientifically significant areas. Because a potential donor is not likely to want his name on a batch of test tubes or even a spectrophotometer, the Weizmann may find it more difficult to raise this kind of small change abroad.

Robert Walgate



## CORRESPONDENCE

## Medical schools

SIR — Although your editorial of 27th November 1980 on the reorganization of London Medical Schools has some hard things to say about London University in general and some of its senior members in particular, for these your writer may perhaps be forgiven, since they are largely matters of opinion. Less forgivable, however, are the errors of fact that spice the article. I wish to draw attention to only two of these. You refer to "two preclinical schools (at King's College and Westminster Hospital)". The Westminster Medical School has no preclinical departments of its own: King's College is a preclinical school for both King's College Hospital Medical School and the Westminster Medical School. More important, you continue "... the effect of the Senate's decision is that the preclinical schools at King's College and Westminster Hospital (sic) should be closed ...". The Senate's decision implies nothing of the sort: all preclinical schools of the University, including that at King's College, are to be reinvestigated in the next few months. Which school, if any, is to be recommended for closure is still a matter of speculation, even for members of the new Working Party. The article does contain one germ of good sense, where it refers to planning. If there is or ever has been a plan, would that the hewers of wood and drawers of water could be told it.

K.E. WEBSTER

Department of Anatomy,  
University of London, King's College,  
London WC2, UK

## Badgers and TB

SIR — Following public criticism of the policy of the Ministry of Agriculture, Fisheries and Food (MAFF) for dealing with badgers infected with tuberculosis (TB) the Minister of Agriculture asked Lord Zuckerman to take an objective look at the relationship between badgers, cattle and bovine TB, and to advise on how the problem should be tackled in the future. This is a complex question. The Mammal Society agrees with Lord Zuckerman's basic conclusion that the badger is a major reservoir of bovine TB in certain limited areas of South West England, and hence is a potential danger to the cattle in those areas. However, we feel that the report gives a biased interpretation of the evidence, and that many of Lord Zuckerman's conclusions were not justified from the data presented in the report. We would like to correct some of the factually misleading statements.

During the period of the moratorium on gassing, the percentage incidence of TB in badgers from Gloucestershire and Avon increased, an observation that Lord Zuckerman took to imply that the disease has "spread". The fact that the percentage incidence declined slightly in Cornwall during the same period was overlooked (p. 63). Also, Lord Zuckerman's statement (p. 40) that at

least one in five to one in ten badgers in affected areas is now infected with TB is misleading. The incidence quoted relates largely to samples taken in the vicinity of TB outbreaks in cattle, and there is no reason to believe that such high levels of TB are to be found except in very small pockets of infection. Certainly there is no scientific evidence to justify Lord Zuckerman describing badgers in the South West as a "highly-infected population" spreading TB to badgers in other areas.

Since TB in badgers appears to be confined largely to limited areas of the South West, and since the evidence to suggest that the disease is spreading is equivocal, we strongly contest Lord Zuckerman's view that bovine TB is a major hazard to the survival of the badger.

Lord Zuckerman stated (p. 27) that the gassing of badgers was accompanied by a decline in the number of reactors in the cattle herds concerned, and that the two events were related. However, the rate of decline in the incidence of TB in badgers in the South West was paralleled by a decline in the incidence of reactors in cattle herds not only in the South West but also in the rest of England. The timing and rate of decline were similar in all three samples. Lord Zuckerman offered no explanation for this. One possible interpretation is that the incidence of TB in both badgers and cattle underwent a decline throughout the country, and that the badger gassing campaign had little significant effect on the overall timing or rate of decline, though gassing may have affected the situation locally.

Lord Zuckerman concluded that the appearance of the disease in cattle in the South West reflected a high local prevalence of TB in badgers (p. 41). This is manifestly untrue; in Cornwall only 15 per cent (51/340) of herd infections were definitely attributable to badgers (p. 57).

Lord Zuckerman stated that "population density is a major factor in the spread of TB". Certainly it is probable that population density is a factor in the spread of disease, but other more subtle factors may be significant. Badger and cattle densities<sup>2</sup> in parts of Dorset and Somerset are as high or higher than in Gloucestershire, Avon and Wiltshire, yet the incidence of TB is very much lower. Why? Also, the presence of infected badgers does not always result in reactors in nearby cattle herds (p. 21). Why?

Lord Zuckerman speculated that badgers all over the country once suffered and died from TB, and that the prevalence of TB in badgers had declined in parallel with the decrease in the incidence of TB in humans and cattle (p. 41). But since badgers are a self-perpetuating reservoir of tuberculosis (p. 95), it is difficult to see why, when the incidence of TB was reduced in cattle, it should also have declined in the badger. This is particularly inexplicable in areas such as parts of South East England and North Wales, where badger densities are comparable to those in the South West (p. 68). In the absence of any evidence to support Lord Zuckerman's view, it seems more logical to speculate that TB was never as prevalent in badgers in the rest of England. So what factors make the situation so different in parts of the South West?

There are many anomalies in the data presented in the report; we have only mentioned a few. Clearly many issues remain unresolved, and there are likely to be many subtle factors involved in the process of transmission of TB from badgers to cattle which are not yet understood. We believe that the continuation of the badger gassing campaign should only be regarded as a short-term expedient. Lord Zuckerman accepted that eradication of TB in badgers is probably impossible (p. 27). In that case, there is every reason to suppose that if/once gassing operations cease, and the badger population builds up again, the incidence of TB in the badger will also increase. In order to achieve an acceptable long-term solution we believe that it is imperative that further research is undertaken to (1) explain some of the many anomalies in the data available and (2) understand the factors involved in the transmission of TB from badgers to cattle.

STEPHEN HARRIS

The Mammal Society,  
Reading, Berks, UK

1. Zuckerman, Lord. *Badgers, Cattle and Tuberculosis: Report to The Right Honourable Peter Walker, MBE, MP* (HMSO, London, 1980).
2. Ministry of Agriculture, Fisheries and Food — *Agricultural Returns — England and Wales, Regions and Counties — Final Results of the June 1979 Census* (HMSO, London, 1980).

## Court feasibility

SIR — Your United States election scoreboard of plusses and minuses (*Nature* 13 November, p. 107) scores the President-elect's statement that he would explore the feasibility of a "science court" as a "plus". This seems only justifiable if one regards a statement that feasibility will be explored as preferable to one that the concept will be implemented. At the risk of making a hackneyed point that is, however, evidently unfamiliar to your reporter, it cannot be too strongly emphasized that the procedures of science and a court of law are necessarily different. To take only the best known example: the verdict of a court of law can take only one of two values — guilty or not guilty. In science, there are no probabilities that are equal to zero or one.

C.R.B. JOYCE

Ciba-Geigy AG,  
Basle, Switzerland

## Plusses and losses

In the article by David Dickson on the likely consequences of the election of Mr Ronald Regan as President of the United States, published on 13 November, the likely changes in US science policy were described as "Plusses" and "Minuses", not as "Winners" and "Losers" as in the original article. The complaints of Messrs Noble, Klimowsky, Volliamy, Price and Joyce (*Nature* 27 November) therefore lie against the London office and not against Mr Dickson.

EDITOR, *Nature*

## NEWS AND VIEWS

# Conflict and commitment in neural development

from Miranda Robertson

Two controversial questions dominate research on the development of the nervous system. The first, which has the longer history of controversy, is that of how growing nerve fibres make specific connections with their targets. The second is that of the extent to which neurotransmitter specificity is induced by the micro-environment of the nerve cell or its axon during development. It was clear from the collision of views at the annual Symposium of the British Society for Developmental Biology\* that both issues remain contentious, but for different reasons.

## Specification of connections

The principal difficulty with research on the specificity of connections (or Sperry-ficity, as one participant nicknamed it) is that the complex results of manipulating an embryo have too often been interpreted on the basis of too limited an investigation. One of Sperry's own first contributions to the field was to reinvestigate in detail the effects on the motor performance of adult animals of crossing their motor nerves, which was said at the time to lead to central respecification and the reestablishment of normal movement. Sperry showed that no such respecification occurred and the 'normal' movements resulted from a good, but imperfect adaptation on the part of the animal to the handicap. It is therefore somewhat ironic that one of the more recent contretemps in the field, which also concerns the respecification of connections, though in embryos, not adults, has in its turn recently been resolved by close attention to anatomy. The argument, recapitulated by J. Feldman (London), was over Jacobson's elegant experiments apparently showing respecification of the dorso-ventral and antero-posterior polarity of frogs' eyes after very early rotation of the eye cup<sup>1</sup>. Feldman and others working in M. Gaze's laboratory consistently failed to replicate Jacobson's electrophysiological evidence for normal retinotectal maps in the adult animals, and the conflict was resolved only when an examination of the eye itself revealed that rotated eyes are usually replaced gradually by new eyes which regenerate from residual unrotated tissue<sup>2,3</sup>. Gaze and his colleagues examined their animals early, before

regeneration was complete; Jacobson examined his later: hence the conflicting results. In fact, the balance of the evidence now suggests that the polarity of neural tissue is irreversibly determined very early in development and rotation of embryonic tissue is one of the few manipulations that does not result in respecification: instead, the nerves tend to re-rotate *en route* to their targets.

The focus of controversy has now switched to the question of how far general properties such as polarity can account for the precision of individual connections between one array of nerve cells and another. There are two extreme positions on this. One is that given a fixed polarity and a chemical signal that determines the general direction of growth, the orderliness of connections can be ensured simply by the strict preservation of neighbour relations, possibly by general adhesiveness between growing fibres. The other is that nerve fibres are guided to their destinations by specific chemoaffinity between an individual innervating neurone and its target. Neither of these mechanisms however can account for the flexibility shown by growing nerve fibres in response not only to experimental manipulation but to the demands of normal growth.

For example, both the retina and the visual tectum of the frog *Xenopus* grow continuously throughout life. But the retina grows concentrically, whereas the tectum grows from rostral-lateral to caudomedial; so in order to maintain an orderly map, connections between the two must be continuously broken and re-established (M. Keating, NIMR London). This rules out strict chemoaffinity and implies that incoming nerve fibres are ordered relatively rather than absolutely. That the ordering is relative with respect to the other nerve fibres as well as to the target follows from the results of removing either half of the retina, or half of the tectum in developing fish, amphibia or hamsters<sup>4</sup>. When the optic nerve fibres arrive at the tectum, they spread out over the whole tectum, or squeeze up into half of it, respectively, in an orderly fashion.

On the other hand, there is evidence against the preservation of neighbour relations by general adhesiveness. The ordering of nerve fibres is not always reflected in their physical relationships to one another: in both *Xenopus* and cat,

nerve fibres leave the retina in an orderly manner, become increasingly disordered on the way to the tectum (or in the case of the cat, the lateral geniculate), and re-establish order once more just before arrival<sup>5,6</sup>. It is thus more as though fibres are assigned intrinsic positional values which govern their actual positions only in response to local cues, for example at the target. Furthermore, it is clear that the response may not result in the simple establishment of linear order. For example, in the optic chiasm of mammals, half the fibres of each eye follow a course to the contralateral side of the brain while the other half turn to make connections on the ipsilateral side. Similarly, even in the ribbon nerve of the cichlid fish, in which neighbour relations are rigidly maintained over most of the pathway, the fibres undergo systematic piecemeal rearrangement at the point of their entry to the tectum (J. Scholes, Kings College London)<sup>7</sup>.

The one system in which neighbour relations do seem to be rigidly maintained throughout is the retino-tectal map of the chick. Not only does the retino-tectal projection remain orderly throughout its course, but, unlike those of hamsters and frogs, it fails to compensate for ablation: removal of part of the developing retina results in a corresponding area of denervated tectum (W.M. Cowan, Salk Institute)<sup>8</sup>. This inflexible behaviour on the part of the chick optic nerve has been the main support for the school of thought favouring a simple neighbour-relations mechanism for the specification of connections. The alternative point of view is that the chick retino-tectal projection is a less plastic manifestation of the same mechanisms that operate in fish, frogs and mammals.

This point of view is certainly easier to reconcile with other aspects of neural development in the chick itself. Nearest-neighbour guidance is plainly inadequate to explain the pattern of connections between spinal motor neurones and the muscles of the chick limb, which have been investigated in considerable detail in the laboratory of L. Landmesser (Yale University).

Like the eye, the spinal cord seems to

Miranda Robertson is associate editor of Nature.

\*The Symposium of the British Society for Developmental Biology on Development in the Nervous System was held in Southampton on September 9-11 1980.



acquire an irreversible polarity very early in embryogenesis. If small sections of chick spinal cord are reversed before the outgrowth of motor nerve fibres, the axons will correct for the reversal and adjust their paths so as to connect with the muscles appropriate to their original position<sup>9</sup>. This is at first sight inconsistent with the results of Stirling and Summerbell<sup>10</sup>, who reversed the limb bud instead of the spinal cord and found that ingrowing motor neurones failed to correct for the reversal. Landmesser and her colleagues have suggested two ways in which this failure could be explained without abandoning the principle of early determination of polarity. The first is to postulate that because there is no conflict between the polarity of the nerve fibres and that of their environment until they actually enter the limb, nerve fibres growing into a reversed limb bud are simply not alerted to the reversal until it is too late for them to change their paths. Landmesser finds that nerve fibres from reversed segments of cord begin to adjust their courses soon after they have left the spinal cord, which suggests that the fibres are guided at least partly by morphogenetic signals that operate before they enter the limb. The second explanation for the conflict between Landmesser and Stirling is that there are limits to the extent of the reversal a nerve fibre can correct. Landmesser finds that after cord reversal limited to 2 or 3 segments, motor nerves can always correct their paths, whereas reversals involving 4–6 segments may defeat them. Her detailed investigations on the innervation pattern resulting from reversal of 4–6 lumbosacral segments suggest that the nerve plexus at the base of the limb may be crucial in sorting out the branching pattern of the ingrowing nerves, and that nerves that fail to enter the correct bundle at the plexus are usually the ones that innervate the wrong muscles. Even then, however, some nerves reach their own muscles by taking novel pathways in the limb.

These results plainly imply relatively specific local signals; but a recent ingenious attempt by Lewis to test for the presence of specific chemoaffinities in the chick wing raises the possibility of other interpretations. Lewis traced the fate of the brachialis longus inferior nerve in the wings of chicks in which one wing bud had been grafted onto the end of another before the outgrowth of motor axons<sup>11</sup>. In a normal wing, this nerve branches into three at the elbow, the median nerve proceeding to the wing tip. In the experimental wings, however, the median nerve on arriving at the wing tip is confronted with a second elbow. But instead of growing onto the second wing tip, as would be predicted on the basis of chemoaffinity, the nerve branches again exactly as the brachialis branched at the first elbow.

There are three ways of explaining this result. Perhaps the growing median nerve contains components of the other two

branches which would normally be eliminated once the nerve reached its target, but which given a second chance home to their own muscles. This could be tested by tracing their central connections. The second possibility is that purely mechanical factors determine the branching, and chemoaffinity operates only very close to the target. The third possibility is that the median nerve is behaving like the optic nerve of an amphibian half of whose retina has been removed, and spreading out according to its relative positional values to innervate the entire limb. More detailed investigations will be needed to resolve these ambiguities.

### Neurochemical differentiation

By contrast with the resistance shown by nerves to respecification after tissue rotation, developing neurones show a surprising degree of flexibility in the face of simple transfer up or down the antero-posterior axis. Most strikingly, Le Douarin and her colleagues (CNRS, Nogent-Sur-Marne) have shown that autonomic neurones from differentiated adrenergic ganglia of chick embryos can be induced by back-transplantation into an earlier host at a different position to express cholinergic functions, with appropriate changes in connectivity. One possibility that has excited a great deal of interest is that the switch in neurotransmitter specificity may be the consequence of the change in connectivity: that is, that it is induced by the target organ. An important source of support for this idea has been the work of Patterson and his colleagues on the neurochemical differentiation of rat sympathetic ganglion cell *in vitro*.

They have shown that in the absence of other tissues, the dissociated neurones develop adrenergic properties, but cholinergic differentiation can be induced by co-culture with certain non-neuronal tissues, such as heart, or by soluble factors released by them. The main argument against an induced switch in neurotransmitter synthesis rests on the alternative possibility that environmental factors, or target organs, are selectively enhancing the survival of cholinergic neurones from a heterogeneous population. (This argument will be discussed in greater detail in a later report of a CIBA symposium on the development of the autonomic nervous system.) While selective cell death is without doubt an important mechanism in neural development, it cannot in fact account for the phenomena described by the Harvard group, which have now been followed at the single-cell level *in vitro*. The real question is whether they play any part in normal embryonic development. Thus one of the most important advances reported at the Symposium was the morphological investigation of sweat glands in the rat foot pad, which show evidence of a change from adrenergic to cholinergic innervation between 7 and 14

days after birth (S. Landis, Harvard University). At the 7th postnatal day, the neural network surrounding the developing glands stains brightly with fluorescent markers for endogenous catecholamines; thereafter, catecholamine fluorescence wanes and acetylcholinesterase staining increases. These changes are paralleled by corresponding changes in the appearance of the vesicles in the nerve endings: predominantly small granular adrenergic vesicles give way to larger, clear cholinergic vesicles.

It is possible to quibble about these results: the interpretation of vesicle morphology is not easy, and in this case it is complicated by the fact that although the endogenous catecholamines disappear, a specific uptake system for exogenous ones remains. However the observations are at the very least consistent with a transition from adrenergic to cholinergic function during normal development *in vivo*, even if it has not been possible yet strictly to rule out the retraction of early adrenergic fibres and their replacement by new cholinergic ones.

### Differentiation of glia

If experiments *in vivo* are essential for establishing the relevance of phenomena *in vitro*, experiments *in vitro* are equally important for dissecting the bewilderingly complex interactions that take place *in vivo*. An important prerequisite for such dissection is a battery of specific markers for distinguishing between interacting cell types; and progress in the development of cell-type specific antibodies has recently been responsible for some interesting advances in the study of neurone-glia interactions. M. Raff and his colleagues (University College London) have been able to demonstrate that astrocytes, ciliated ependymal cells and oligodendrocytes differentiate in dissociated cell cultures of 10-day-old embryonic rat brain with exactly the same timing as they do *in vivo*, showing that the events that lead to their differentiation are already determined by 10 days' gestation and are not disturbed by the subsequent disruption of their positional relationship.

J. Brookes (California Institute of Technology), investigating later stages in the differentiation of peripheral glia, has established the existence of two inducible biosynthetic systems in Schwann cells. Contact with large axons (that is, axons which they would normally myelinate) induces an increase by at least 1,000 fold in the synthesis of the principal myelin protein P<sub>0</sub>. More surprisingly, purified Schwann cells can be induced by co-culture with primary muscle cells to synthesize acetylcholine. The observation that Schwann cells can synthesize acetylcholine is not new: after denervation of vertebrate muscle *in vivo*, they have been shown to migrate into the region of the endplate where they secrete acetylcholine<sup>12</sup>. The new contribution of Brookes's experiment is



# Cretaceous ammonites

from M. K. Howarth

AMMONITES are an extinct group of Cephalopods that flourished during the Mesozoic era 240 to 65 million years ago. Their world-wide distribution and speed of evolution, reflected in distinctive shell features, makes them the most useful macrofossils in the Mesozoic for relative dating of rocks. Rock divisions representing time intervals as small as about one-third of a million years can be recognized.

Ammonites from coastal exposures of Upper Cretaceous rocks in Zululand and Pondoland in South Africa are splendidly illustrated in a recent work by Klinger & Kennedy\*. Abundant representatives of

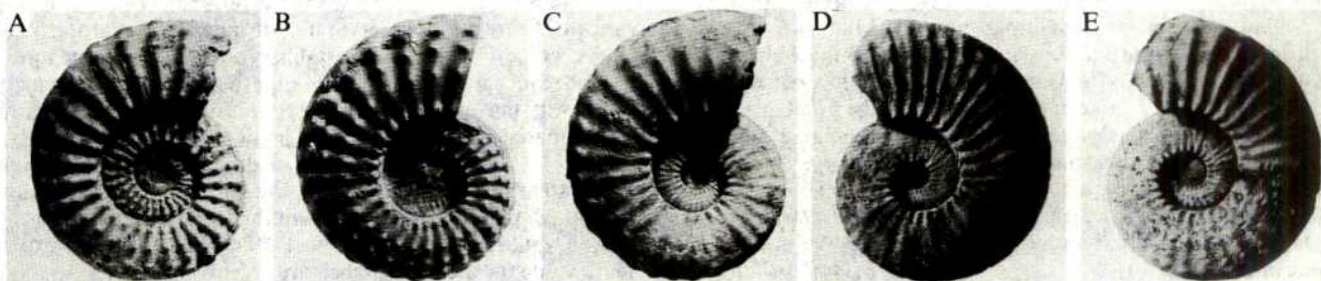
M.K. Howarth is in the Department of Palaeontology, British Museum (Natural History), London.

the subfamily Texanitinae were found in two areas 350 miles apart. Careful stratigraphical collecting showed that in each case there are complete series of transitions between the same four successive species, two of the ancestral *Texanites*, two of the successor *Submortonicerases*. Although the four species showed very high variability in both areas, there are small consistent differences between the same species in the two areas that are held to be of subspecific rank. It seems that the two populations were sufficiently isolated geographically to maintain these subspecific differences, but contact between them was enough to ensure that they evolved in parallel in specific and generic characters.

In the past ammonite systematics became unnecessarily complicated as generic and specific divisions were multiplied without any agreed method of control. This description of South African Upper Cretaceous ammonites is a good example of the new methods that have been applied during the past 25 years, involving accurate stratigraphical collecting and the use of single bed assemblages as a control to the species classification. It has been found repeatedly that the considerable morphological variation that has to be admitted to ammonite species, embraces many species and even genera of past ammonite systematists.

\*H.C. Klinger and W.J. Kennedy *Annals of the South African Museum* 80, 1980.

A — *Texanites presoutoni* sp. nov.; B — *Texanites soutoni* (Baily); C — *Submortonicerases woodsii* (Spath); D — *Submortonicerases condami* (Collignon); showing progressive evolution from A, the oldest, to D, the youngest. E — *Submortonicerases woodsii* (Spath).



show that it is almost certainly the muscle that induces acetylcholine synthesis in the Schwann cell. The identity of the inducing factor(s) is, here, as elsewhere, unknown.

It is an exasperating fact that while the chemical mediators of induction in embryos remain unknown, most of the known and characterized growth factors discovered through assays *in vitro* have no well established role *in vivo*. The most recently discovered of these factors is a component of the brain and pituitary that causes proliferation of Schwann cells and astrocytes *in vitro*<sup>14</sup>. Brookes has now raised a monoclonal antibody against it, which will make it possible to purify and sequence it; and to discover what, if any, its function is *in vivo*. □

## Solar oscillations

from H.B. van der Raay

KNOWLEDGE of the Sun, our closest star, is based on observations of its surface properties. The temperature, magnetic field and constituents of the outer layers can be deduced by spectroscopy and, combining these data with estimates of size and mass, a model of the Sun's properties can be formulated. The model fits not only the observed surface properties but also predicts interior characteristics such as density and temperature. From these parameters and rates for the nuclear fusion reaction which converts hydrogen to helium and provides the energy output of the Sun the number of solar neutrinos associated with the nuclear burning may be readily found. An experimental verification of the standard solar model thus became possible. Unfortunately, as is well known, the experiment designed to detect these solar neutrinos failed to record the numbers predicted.

An alternative way to probe the solar interior is by the detection of solar oscillations in a manner analogous to terrestrial seismology. The pressure waves associated with the oscillations, especially if of long period, penetrate deeply into the

solar interior and convey information about the internal structure. Here again observations and predictions from the standard model appear contradictory. Does this imply that the theory is incorrect or is it the interpretation of the observations that is at fault?

Long period oscillations of the sun were discovered by Birmingham<sup>1</sup> and Crimean<sup>2</sup> groups, working independently, in 1976. Both groups measured the line of sight Doppler shifts of certain Fraunhofer absorption lines and, since observations were made on the integral solar disk, concluded that these observations corresponded to simple radial oscillations of the sun. The measured period of 160 minutes raised an immediate conflict with the standard solar model since if these were simple radial oscillations the longest period predictable was approximately 60 minutes. The Cambridge theorists<sup>3</sup>, however, pointed out that the observations could be interpreted in terms of more complex g mode oscillations.

Since these early observations, studies of line of sight velocities of the solar surface have continued. The Crimean group have found evidence that the 160 minute oscillation has persisted to the present day

- Jacobson, M. *Science* 155, 1106 (1967).
- Gaze, R.M., Feldman, J.D., Cooke, J. & Chung, S.-H. *J. Embryol. exp. Morph.* 53, 39 (1979).
- For brief summary see Robertson, M. *Nature* 278, 778 (1979).
- Neurosci. Res. Prog. Bull. 17, (1979).
- Fawcett, J.W. *J. Physiol.* 306, 32P (1980).
- Horton, J.C., Greenwood, M.M. & Hubel, D.H. *Nature* 282, 720 (1979).
- Scholes, J.H. *Nature* 278, 620 (1979).
- Cowan, W.M., Rogers, L.A. & Kelly, P.J. *J. comp. Neurol.* 155, 127 (1974).
- Lance-Jones, C. & Landmesser, L. *J. Physiol.* in the press.
- Stirling, R.V. & Summerbell, D. *Nature* 282, 640 (1979).
- Lewis, J. *Zoon* 6, 175 (1980).
- Le Douarin, N.M. *Nature* 286, 663 (1980).
- Miledi R. & Slater, C.R. *Proc. R. Soc. Lond. B* 169, 289 (1968).
- Brookes, J.P., Lemke, G.E. & Balzer, D.R. *jun. J. biol. Chem.* 255, 8374 (1980).

H.B. van der Raay is in the Department of Physics, University of Birmingham UK.



with the same phase, although with a substantially decreased amplitude. This is confirmed by a group working at Stanford<sup>4</sup>. The Birmingham group have, however, failed to confirm this result and find many long period oscillations which vary in period, phase and amplitude from one day to the next<sup>5</sup>.

All these observations necessarily suffer from the fact that the sun is only visible for part of the day and, as a consequence, the data sets are modulated by a 24 hour period. Any periods found which are harmonics of a day thus need to be considered most critically. 160 minutes is exactly 1/9 of a day — could this oscillation appear simply as the result of the method of analysis? The Crimean and Stanford groups, aware of this possibility, point out that the period is now found to be 160.01 minutes.

At the other end of the time scale are the five minute oscillations first discovered by Leighton in 1960. A detailed study of this region over some three years by the Birmingham group<sup>6</sup>, showed that these five-minute ( $\sim 3$  mHz) oscillations had a well defined structure and consisted of  $>20$  well defined discrete frequencies with a mean spacing of alternate lines of 135.6  $\mu$ Hz. Interpreting these data in terms of the then current solar models Iben and Mahaffy<sup>7</sup> and Christensen-Dalsgaard *et al.*<sup>8</sup> suggested a heavy element abundance  $z \approx 0.004$  in contrast to the standard model value of  $z = 0.02$ .

The solution to the 24 hour modulation problem may be found in three ways: (a) by placing many observation stations around the globe, (b) by observing at one of the earth's poles, (c) by operating from a suitable space satellite. Each of these solutions have both advantages and disadvantages: (a) would require redundancy at any given longitude to overcome weather problems, (b) is subject to atmospheric effects as the sun is always close to the horizon, (c) includes all the technical problems associated with a space program. Also the costs involved increase rapidly as one proceeds from (a) to (c).

The polar solution has been taken by Grec *et al.* and is described in this issue of *Nature* (see p.541). The stresses of an austral summer were amply rewarded by the results of an excellent experiment which resulted in 120 hours of uninterrupted

observations. The preliminary analysis confirms the detailed structure and spacing found in the five-minute oscillation. However, those data relating to the longer periods do not show convincing evidence for the existence of a 160 minute oscillation. It is only when a superposed epoch analysis similar to that used by the Crimean and Stanford groups is used that the 160 minute period emerges. Admittedly the 24 hour modulation associated with daytime observation is no longer present in these data, but the earth does still rotate about its axis once every 24 hours, even at the pole. Hence any instrumental or atmospheric effects would have to be clearly eliminated.

Interpretation of the five-minute structure depends on the assignment of the modes observed. All the Doppler shift measurements are strongly biased to low order modes since the integral disk is observed. Hence it is customary to assume  $l_0, l_1 \dots$  modes, where  $l_0$  is the simple radial oscillation  $l_1$  alternate radial and axial expansions and contractions and higher  $l$  values correspond to more complex shape deformations. Once  $l$  has been assumed then for a given frequency  $\nu$ , the number of radial overtones,  $n$ , may be estimated and the results compared with theory.

In a revival of the standard solar model Christensen-Dalsgaard and Gough present a paper in the present issue of *Nature* (see p.544), in which the standard value for the

heavy element abundance is retained,  $z = 0.02$ , and the observational structure of the five-minute oscillations is fitted by taking into account the effect of the solar atmosphere. However it is clear from the models listed that these are very insensitive to the observed frequency separation. Indeed it appears that the only significant change in  $\Delta\nu$ , the frequency separation, occurs when low  $z$  values are considered. At the recent Eslab symposium<sup>9</sup> a mean spacing of  $135.2 \pm 0.2 \mu$ Hz was reported which would still appear to favour the  $z = 0.004$  value. A direct comparison of the predicted frequencies with the 25 which have now been measured to an accuracy of  $1:10^3$  may yield a more conclusive test as to which model to use.

All interpretation of the data depends critically on the correct identification of the mode concerned. This may be experimentally determined by considering two dimensional observations of the solar disk. Such work is at present in progress<sup>10</sup> and will hopefully resolve any mode identification problems. The experimental observations of independent groups have firmly established the discrete structure of the five-minute oscillations although the mode identification and reconciliation with theory is still unsatisfactory.

Clearly if we do not understand our own closest star, the implications on the whole field of cosmology are enormous, and continued efforts by both theorists and experimentalists are urgently required.

## Coronavirus come of age

from B.W.J. Mahy

ALMOST thirty years after the pioneering work of A.W. Gledhill and C.H. Andrewes at the Mill Hill laboratories established the essential features of murine hepatitis virus (MHV) infection (*Brit. J. exp. Pathol.* **32**, 559) the first international conference on the coronavirus group, of which MHV is the best studied member, has been held in Germany\*. The meeting consolidated much new and interesting data on a group of viruses responsible for a wide range of acute and chronic diseases. These presently include respiratory and enteric disease in humans, bronchitis in birds, transmissible gastroenteritis and encephalitis in pigs, diarrhoea in calves and dogs, peritonitis in cats, and both demyelinating encephalitis and hepatitis in rodents. A recent report of the isolation of coronaviruses from the brains of multiple sclerosis patients (Burks *et al.* *Science* **209**, 933; 1980) has intensified interest in the group.

During the first half of the meeting, on

structure and replication, it became clear that, in addition to the characteristic morphological features of the group, coronaviruses from whatever species are unified by the possession of a large infectious single-stranded genome of  $6$  to  $7 \times 10^6$  molecular weight. Both the mechanism of expression of this genome, and the protein products, have unique features. M.C. Lai (Los Angeles) for a murine coronavirus and S.I.T. Kennedy (La Jolla) working with avian infectious bronchitis, each presented evidence that the genome is positive-stranded, with a capped (m<sup>7</sup>G) 5'-terminus and a stretch of poly(A) at the 3'-terminus. In infected cells six virus-specific RNA species are consistently found, ranging in molecular weight from  $0.6 \times 10^6$  up to genome size. T<sub>1</sub> ribonuclease mapping studies (S.I.T. Kennedy and J.L. Leibowitz, La Jolla) show that these RNAs form a 'nested set', the sequence of each RNA being contained

1. Brookes, J.R., Isaak, G.R. & van der Raay, H.B. *Nature* **259**, 92 (1976).
2. Severny, A.B., Kotov, V.A. & Tsap, T.T. *Nature* **259**, 87 (1976).
3. Christensen-Dalsgaard, J. & Gough, D.O. *Nature* **259**, 89 (1976).
4. Scherrer, P.M., Wilcox, J.J., Kotov, V.A., Severny, A.B. & Tsap, T.T. *Nature* **277**, 635 (1979).
5. Brookes, J.R., Isaak, G.R. & van der Raay, H.B. *Mon Not R. astr. Soc.* **185**, 1 (1978).
6. Claverie, A., Isaak, G.R., McLeod, C.P., van der Raay, H.B. & Roca Cortes, T. *Nature* **282**, 591 (1979).
7. Iben, I. & Mahaffy, J. *Astrophys. J.* **209**, 39 (1976).
8. Christensen-Dalsgaard, J., Gough, D.O. & Morgan, J.G. *Astr. Astrophys* **73**, 121 (1979).
9. Claverie, A., Isaak, G.R., McLeod, C.P., van der Raay, H.B. & Roca Cortes, T. *XIV Eslab Symposium* (1980).
10. Brookes, J.R., Isaak, G.R. & van der Raay, H.B. *XIV Eslab Symposium* (1980).

B.W.J. Mahy is Huddersfield Lecturer in Special Pathology at the University of Cambridge.

\*An international symposium on the 'Biochemistry and Biology of Coronaviruses' sponsored by the Deutsche Forschungsgemeinschaft was held in the Institut für Virologie und Immunobiologie, University of Würzburg from October 15th to 18th, 1980.

within the sequences of all larger RNAs; the 3'-termini of all the RNAs are common, and they all extend inward from the 3' end of the genome. *In vitro* translation experiments by S. Siddell (Würzburg) and B. van der Zeijst (Utrecht) showed that each subgenomic RNA is a messenger species which specifies a single primary protein product translated from its unique 5'-terminal sequence. Nothing is known at present as to the mechanism by which these subgenomic RNAs are synthesised, although UV target size measurements suggest that each is independently initiated on a negative strand template, and not derived by processing from a larger species (van der Zeijst). A membrane-bound RNA-dependent RNA polymerase activity present in cells infected with a porcine coronavirus was described by D. Brian (Knoxville), but as yet no evidence as to the nature of replicative intermediate molecules has been obtained.

Of the three well-defined virion proteins, one is a 60K nucleocapsid protein phosphorylated by a virion-bound protein kinase, and the others are envelope glycoproteins. The largest (90K) forms the petal-like structures (peplomers) of the 'crown' (from which the group derives its names), and apparently has a conventional mode of synthesis similar to the glycoproteins of other enveloped viruses. The smaller glycoprotein (23K) is embedded in the envelope lipid bilayer, and is largely unaltered by treatment of the virus particle with bromelain, which removes the peplomers; this protein thus fulfils a similar role to that of the membrane protein of other enveloped viruses such as influenza. Glycosylation of this coronavirus membrane protein has unique features. R. Rott (Giessen) showed for a bovine coronavirus that the 23K protein contains no fucose or mannose. H. Niemann and H. Klenk (Giessen), P. Rottier (Utrecht) and K. Holmes (Bethesda) all reported that synthesis of the 23K glycoprotein is not inhibited by tunicamycin; this indicates that, in contrast to all other virus glycoproteins studied so far (including the 90K corona-virus protein) dolichol-linked N-acetylglucosamine plays no part in biosynthesis. L. Sturman (Albany) showed that in the presence of tunicamycin virus particles still matured, but were released from the cells as 'spikeless' virions lacking the 90K protein.

Comparisons between the genomic and subgenomic RNAs of coronaviruses differing in pathogenic potential or species of origin were reported by several workers. T<sub>1</sub> ribonuclease mapping studies by B. Lomniczi (Budapest) gave rise to at least 11 different genome RNA fingerprints within 13 isolates of avian coronavirus originally classified as infectious bronchitis by pathological criteria. However it is likely that this technique provides too fine an analysis of genome structure for useful strain comparisons. S. Weiss (Philadelphia) described the *in vitro*

## Molecular lines in the red

from a correspondent

THE FIRST OBSERVATIONS of molecular emission in the far infra-red (IR) from an interstellar cloud have been made by a team at the University of California (D.W. Watson, J.W.V. Storey, C.H. Townes, E.E. Haller and W.L. Hansen *Astrophys. J.* 239, L129; 1980). These observations were made from the NASA Kuiper Airborne Observatory in January 1980 at an altitude of 12.5 km, using a liquid helium-cooled Ge:Sb photodetector in a metal-mesh, scanning Fabry-Pérot interferometer. The two  $J = 21 \rightarrow 20$  and  $J = 22 \rightarrow 21$  rotational lines of CO were observed in emission at 124 and 119  $\mu\text{m}$  from the Kleinmann-Low region of the Orion molecular cloud. The CO molecule in interstellar clouds has previously been observed in the millimetre and submillimetre regions of the spectrum, where it has been shown to be one of the principal molecular species containing carbon in dense molecular clouds such as Orion. The significance of the new 124- and 119- $\mu\text{m}$  observations is that for these rotational transitions to be observable at all, the CO must be much

hotter (500–1,000K) than the temperature of the CO molecules observed in the microwave ( $\sim 100\text{K}$ ). These high temperatures indicate that the CO observed in the far IR is present in a post-shock gas, corroborating earlier evidence obtained from H<sub>2</sub> observations that a shock wave is propagating into the Orion cloud.

This observational technology opens up an entire new spectral range for observations of molecular species in the interstellar medium. Until now observations of interstellar clouds have been limited mainly to the microwave and radio regions at the long-wavelength end of the spectrum, and to the visible and near ultra-violet regions at the short end of the spectrum. The IR region of the spectrum is a rich arena for remote-sensing applications, but it has been essentially closed to interstellar observations by a combination of detector problems and atmospheric absorption. The development of far-IR techniques for observation of the interstellar medium increases the potential for new discoveries concerning the structure, dynamics, chemistry and evolution of interstellar clouds.  $\square$

synthesis of a representative DNA copy of the genome of MHV strain A59. Using this cDNA probe, she found considerable sequence homology with other murine coronaviruses and a low level of homology with 229E virus, a human coronavirus. Extension of such studies to the virus isolates from multiple sclerosis brain tissue, which were obtained by passage of the tissue in mice, should help to identify the origin of these agents.

The second half of the meeting was devoted to persistency and pathogenesis. Although little is known of the molecular mechanisms underlying organotropism and pathogenesis following coronavirus infection, some advances were reported. Coronavirus-induced disease is very dependent upon the age at infection, genetic background, and route of inoculation of the host. K. Pickel (Würzburg) showed that mice were fully susceptible to fatal JHM virus infection up to the age of 21 days, but thereafter became fully resistant. Resistance could be induced by transfer of immune spleen cells from adult mice to baby mice, or by priming of adult non-immune spleen cells in baby mice with UV-inactivated JHM virus, but not by non-immune spleen cells alone. R. Knobler (La Jolla) confirmed that fatal encephalomyelitis induced by JHM virus is an autosomal dominant trait; the ability of the virus to induce demyelinating lesions

depended upon the cell tropism of selected mutants to replicate in oligodendroglial cells. H. Wege (Würzburg) reported that injection of JHM *ts* mutants into preimmunised rats by the intracerebral route causes a high rate of subacute to chronic demyelinating disease with similarities to virus-induced demyelination in man. Rats survive normally after intraperitoneal injection of similar virus doses.

Several investigators have studied the mechanism of resistance at the cellular level. F. Bang (Baltimore), who had shown as early as 1960 that peritoneal macrophages taken from MHV resistant mice were also resistant to infection *in vitro*, now reported that macrophage resistance is also dependent upon associated lymphocyte action and may also involve interferon. Extension of these studies from macrophages to primary mouse hepatocyte monolayer cultures by H. Arnheiter (Zürich) confirmed that the hepatocytes were genetically resistant to virus infection as were the mice themselves. Although interferon treatment reduced virus titres in susceptible cell cultures, addition of anti-interferon antiserum did not augment the susceptibility of resistant hepatocyte cultures. Thus it can be concluded that such cells are intrinsically resistant to virus infection, though by what mechanism remains to be determined.



In contrast to other positive strand RNA viruses, the corona-viruses readily establish persistent infections in the host. For example, chronic hepatitis or chronic demyelination of the central nervous system occur with certain virus-host combinations. Not surprisingly, persistent infections are relatively easy to establish in cell culture *in vitro*, and such model systems have some unusual features. K. Holmes (Bethesda), N. Hirano (Morioka) and S. Stohman (Los Angeles) each reported that in cloned cell cultures persistently infected with MHV only 10–20 percent of the cells express coronavirus antigens detectable by immunofluorescence, but 100 percent are resistant to superinfection with homologous virus. G. Chaloner-Larsson (Ottawa) has obtained very similar results with a human

coronavirus (229E) persistent infection of L 132 cells. Further characterisation of such *in vitro* systems is sure to provide much-needed insight into the way these viruses establish such an intimate relationship with the host. Summing up the meeting, D. Tyrrell (Harrow) emphasised the very wide range of diseases now known to be caused by these viruses, and the value of their study as models of virus pathogenesis. As the meeting convener, V. ter Meulen (Würzburg) pointed out, virtually every laboratory currently working with coronaviruses was represented amongst the seventy participants, and the collective presentation of their data undoubtedly served to strengthen and unify their purpose in unraveling the molecular biology of this unique group of viruses.

transposition is reasonably low, it should be possible to build a *Drosophila* strain that lacks copia sequences. Young has made a start to this interesting, but very tedious experiment: at the time of the meeting a strain with only six copia sequences had been made and the flies were apparently no worse for their experience. Only time, and hard work, will tell whether or not copia sequences are necessary for some aspect of *Drosophila*'s existence.

The second genetic approach stems from the exciting discovery that at least one well known mutation (white-apricot) is associated with an insertion of copia into the white gene. B. Judd and P. Bingham (Research Triangle) have mapped this copia element within white to the same region as maps the *w<sup>ad</sup>* allele and W. Gehring's laboratory (Basel) has found that revertants of *w<sup>ad</sup>* may be accompanied by loss of the copia element from this site.

The role of the insertion of nomadic middle repeat sequences into genes as a cause of spontaneous mutation in *Drosophila* was also highlighted by the molecular study of the bithorax region. W. Bender (Caltech) has now cloned over 145 kilobase pairs of this region and has used these clones to analyse the nature of some of the many mutant bithorax genes. Two (*bxd<sup>1</sup>* and *bxd<sup>5</sup>*), both spontaneous in origin, result from large insertions (of about 10 kb) into the gene. Although the insertion sites are not identical they are reasonably close together and each insertion is a repetitive DNA sequence. A spontaneous reversion of *bxd* turns out to have lost most, though not all, of its insertion. It must be most gratifying to E. B. Lewis, who is responsible for the very detailed genetic analysis of this complex locus, to see how well the molecular analysis of these mutations is confirming the genetic data. For example, the dominant mutation *Chx* was recovered, after X-ray mutagenesis, together with a recessive *pbx* allele: Bender has now shown that *pbx* is a deletion and that the sequence removed from the *pbx* site has been inserted some kilobase pairs away in reverse orientation to give the *Chx* mutation. Reversion of *Chx* has been accompanied by an inversion broken within this inserted sequence.

It is to be hoped that the molecular analysis of long regions of the genome will throw some light on the old question of the relationship between genetic organisation and chromosome structure. P. Spierrer (Geneva) recounted his latest travels along the chromosome in the region of the genes coding for xanthine dehydrogenase (*rosy*) and acetyl cholinesterase. Over 300 kb of DNA (three 'Benders') have been covered and this spans eight polytene chromosome bands and as many characterised genes. As dramatically as any other this experiment demonstrates the variation in location of middle repeat DNA sequences. The DNA cloned for this walk came from two different 'wild type' stocks of *D.*

## Drosophila at Kolymbari

from M. Ashburner

FOR the second time the Greek Orthodox Academy at Kolymbari, on the northern shores of Crete, was host to a meeting of *Drosophila* biologists\*. Not surprisingly, the scientific sessions were dominated by discussions of the molecular structure of the *Drosophila* genome. Restriction maps and nucleotide sequences were so common that I am sure more than one participant considered that his colleagues, but naturally not himself, had fallen into the trap so carefully avoided by Dr Watson, of confusing hard work with hard thinking. Nevertheless some very interesting facts were brought to our attention: interesting if only for the reason that they were quite unexpected.

There can be little doubt that the major challenge to conventional genetic wisdom revealed by the molecular analysis of the genome of *Drosophila*, and other eukaryotes, has been the discovery of repeated DNA sequences of no fixed abode. The 'type' of these sequences, as far as *Drosophila* is concerned, is that dubbed 'copia', a sequence of some 5 kilobase pairs which is present, in the typical strain of *D. melanogaster*, roughly 30 times. Comparison of the chromosomal locations of this sequence in different strains of *D. melanogaster* has shown that these differ between, and even within, strains.

Studies on the sequence organisation of copia, and similar elements, by G. Rubin's laboratory (Harvard Medical School) have revealed striking similarities between copia, a dispersed middle repeat sequence of yeast known as Tyl, and integrated vertebrate retroviruses. Copia is flanked by

a direct terminal repeat of 276 base pairs and a comparison of the nucleotide sequence of sites into which copia has inserted reveal that insertion is accompanied by a direct duplication of five base pairs of the 'target' sequence. Other nomadic middle repeat sequences of *Drosophila* appear to have a similar overall organisation to copia but to generate duplications of the insertion site of different sizes (for example four or seven base pairs). The similarities between these elements and bacterial IS sequences are striking; whether these similarities reflect the mechanisms IS sequences and the nomadic eukaryotic elements use for transposition is not yet known.

Copia, and some other nomadic middle repeat sequences of *Drosophila*, were originally cloned by virtue of the fact that their RNA transcripts are particularly abundant, at least in tissue culture cells. Work in both M. Young's laboratory (Rockefeller University) and in Rubin's has now shown that several different transcripts complementary to copia can be found in cells: whether these can all come from any single copia sequence is not known. For many years the function of RNAs complementary to copia has been the subject of some considerable discussion. They are clearly not translated in proportion to their mass yet, as work by both Rubin and J. Lengyel (University of California, Los Angeles) has shown, these RNAs can be translated into polypeptides in a cell free system.

Two genetic approaches to understanding the function of these nomadic sequences were discussed at Kolymbari. Since different stocks of *D. melanogaster* differ in the location of their copia sequences, and since the frequency of copia

M. Ashburner is in the Department of Genetics, University of Cambridge.



*melanogaster*: Oregon-R and Canton-S. Overall seven different insertions of middle repeat DNA were found but none were in the same location in both stocks: indeed many were polymorphic within a stock. Yet for non-repetitive DNA these two stocks show only a fraction of a percent divergence in sequence.

A rather different type of transposable element in *Drosophila* was described by G. Ising (Lund). This element, called TE1, is huge, it carries at least two genes (white and roughest) normally adjacent in the X. It arose spontaneously some years ago as a transposition of  $w^a$  and  $rst^+$  from the X chromosome to chromosome two and, since then, has been merrily hopping around the genome with a frequency of about  $1:10^4$ . Ising has mapped over 150 different sites into which it has inserted, insertion often being accompanied by mutation of the 'target' gene. Just how TE1 moves, or how it can be lost altogether from the genome, is rather mysterious but there is hope that the cloning of one end of TE1 fortuitously inserted very near one of the heat shock genes (M. Goldberg, Basel) will help to solve this mystery.

As at Kolymbari two years ago the analysis of genes of known function, known at least in terms of their protein products, continues to give great pleasure to participants and onlookers alike. Those few genes in *Drosophila* whose activity is so dramatically induced by heat shock are by far the best known. Cloning has confirmed earlier genetic conclusions that those coding for the four small heat shock proteins are very closely linked. R. Morimoto (Harvard) described that their coding sequences are all contained within a 13 kb fragment. Detailed comparison of

the DNA sequences upstream of the 5' ends of these genes with those of genes coding for three other heat shock proteins is revealing homologies some 125 bases upstream from the 'TATA box' sequence.

The clones of the 'major' heat shock gene (Hsp70), a gene that is repeated at each of two different loci in *D. melanogaster*, are now beginning to be used for a number of quite different studies, for example of gene evolution (D. Ish-Horowicz, ICRF, London), nucleosome spacing (M. Noll, Basel) and chromatin organisation revealed in the pattern of sensitivity to nucleases (S. Elgin and C. Wu, Harvard). Yet early hopes that a comparison of the sequences adjacent to different Hsp70 copies would quickly reveal those sequences important for the control of transcription appear to have been too optimistic, since variant Hsp70 genes have been isolated that can be shown to be functional, yet lack a characteristic class of sequences normally found 5' to the coding region (M. E. Mirault, Geneva). On the other hand the conference heard from J. Liss (Cornell) that the insertion of a small (406 base pair) sequence, which includes the first 63 base pairs of the translated Hsp70 gene and material 5' to it, into a particular repetitive DNA sequence found adjacent to some Hsp70 genes results in the induction, by heat shock, of transcription of the middle repeat sequence.

Unfortunately, the function of the heat shock proteins remains unknown. Their importance for the cell in the recovery of normal protein synthesis after the heat shock was shown by S. Lindquist (Chicago). The incorporation of certain amino acid analogues into the heat shock

proteins apparently blocks their post-transcriptional processing and normal accumulation in the nucleus; it also blocks the recovery of normal protein synthesis after the heat shock. Lindquist suggests that normally these proteins may be nucleic acid binding proteins. Recently, rather similar responses to environmental shock have been found in organisms as different as yeast and man. A. Tissières (Geneva) discussed evidence from fingerprints of 'heat shock' proteins from different animals that indicates that at least Hsp70 may be conserved.

Progress is also slow in discovering the mechanisms of induction of heat shock protein synthesis. T. Kornberg (University of California, San Francisco) has characterised an *in vitro* system using isolated *Drosophila* tissue culture cell nuclei in which the *E. coli* RNA polymerase directed transcription of the heat shock genes is responsive to the addition of factors from heat shocked, but not control, cells. The nature of these factors (or factor) is yet to be elucidated.

Other genes that attracted attention at Kolymbari were those coding for the salivary gland 'glue' proteins and the proteins of the egg shell of *Drosophila*. Each had their surprises. A component of the salivary gland glue, known as SGS-4, is coded for by a gene on the X chromosome and is of interest for several reasons. G. Korge (Munich) has characterised mutations that normally fail to express this gene yet will do so when the mutant gene is made heterozygous with a wild type allele, at least under certain conditions. This is rather similar to the transvection affect described for the bithorax locus by E. B. Lewis 25 years ago. The coding region for SGS-4 has

## 100 years ago



Fanduri — a Dorey papuan



Epa — a Village of the Mahori papuans.

Pictures from "New Guinea: What I did and what I saw" by L. M. D'Alberty reported in *Nature* 23, 16 December, 153, 1880.



been cloned in Stanford and is being used for the analysis of this entire region of the genome by S. Beckendorf (University of California, Berkeley) and for detailed studies of the gene itself by M. Muskavitch (Stanford). A surprising result is that the transcript of SGS-4 differs in size in different strains of *Drosophila*. This results, it would appear, from the fact that within the coding sequence there is a 21 base pair sequence whose repetition frequency can vary between different SGS-4 alleles. Although nothing is known of the chemistry of the protein this must reflect a sequence of seven amino acids repeated a varying number of times.

The mutation characterised by Korge, that fails to make SGS-4 protein when homozygous turns out to be a small deletion, but of a sequence over 200 base pairs away from the 5' end of the messenger RNA. The importance of this region is indicated by the fact that two different expressed alleles of SGS-4 differ by a single

base pair substitution in this region and by a factor of two in the abundance of their mRNAs.

The egg shell protein genes, under study by A. Spradling (Carnegie Institution, Washington) and in F. C. Kafatos' laboratory (Harvard) also surprised us for they are amplified in the tissue in which they are expressed. Spradling has found that the amount of DNA amplified extends at least 30 kb on each side of the genes themselves, but the degree of amplification falls off, from a peak of some 60 fold, in both directions away from the coding sequences. This, and the fact that the amplified DNA has an identical restriction pattern to non-amplified DNA, may indicate that the process is chromosomal, rather than extra-chromosomal as in oocyte ribosomal genes in many organisms. Yet the Harvard laboratory (G. Thiroes and R. Griffin-Shea) have found that amplification of another pair of egg shell protein genes is accompanied by their

premature transcription; but that these early transcripts are not translated and, indeed, decay as development gets under way. Only at the appropriate developmental stage several hours later does transcription resume to produce mRNAs that are subsequently translated.

What is the meaning of this? It implies some relationship between amplification and early transcription and also indicates the existence of a translational control at the early developmental stage.

Like all good meetings, at the end there were far more questions than answers. As is right and proper we were treated to many very preliminary data whose place in the jigsaw puzzle is yet undiscovered. The great success of the Kolymbari meeting was in bringing together molecular and classical *Drosophila* biologists to discuss their data from their different perspectives and we can only hope that some of today's mysteries will be clearer to us when we next meet.

## Comets and the origin of life

from N.J. McNaughton and C.T. Pillinger

COMETS are the most spectacular bodies in our solar system and the anticipated return of Halley's Comet in 1985-6 has already proved a catalyst for increased cometary research. As the comet nucleus contains, perhaps with the exception of phosphorus, the necessary ingredients for life on this planet, the pundits of earthbound chemical evolution and cometary science found common ground at a recent colloquium\* entitled 'Comets and the origin of life'.

Although almost all of our observations of comets have been obtained from or near the Earth, the accumulated data yields a basic understanding of the structure, chemistry and physics of the comet nucleus and tails. Perhaps the most significant point to emerge from new observations is the apparent constancy of comet's chemical composition.

A'Hearn (University of Maryland) observed that the rate of production of certain chemical species, particularly CN, C<sub>2</sub>, C<sub>3</sub> and OH, from the comet nucleus near the sun is uniform irrespective of the type of comet and its gas to dust ratio. The spectroscopic continuums of comets of different ages are also strikingly similar (Donn, NASA-Goddard). It is not yet clear whether this uniformity is due to the nature of the chemical reactions in the coma or if it implies that comets are derived from a constant composition reservoir. How the latter interpretation fits with a recently announced theory for the origin of comets (Biermann *Royal Society Meeting on Planetary Exploration*, Munich, Nov. 4-5, 1980) is not clear. Biermann's new hypothesis predicts cometisimals as the

possible end product of a fragment of protosolar nebula collapsing in a relatively low magnetic flux. According to the same theory, planetary systems would be produced in a large magnetic flux and there seems to be no way for both planets and comets to be produced together.

The current interest in comets has promoted a shift in emphasis among the prebiotic synthesis investigators — low temperatures and photon or proton irradiation appear to be the order of the day. Reproducing cometary compositions and environments in the laboratory, the Maryland group and Greenberg (Leiden University, Netherlands) have synthesised 'life-like' organic molecules. Long chain hydrocarbons, nitrogenous compounds and carboxylic acids have been identified spectroscopically among the products of reactions carried out at temperatures as low as 15°K. Given that similar molecules could only be produced on the Earth under a strongly reducing protoatmosphere (which the Levine group from Virginia calculate would be short-lived due to the high reactivity and abundance of OH), the introduction of such molecules via comets into a less drastic protoatmosphere offers a real, and in some cases preferred, mechanism for the beginning of life on Earth. Speculations on this theme range from the controversial — Wickramasinghe (University of Cardiff) envisaging comets as the carriers of already living organisms — to efforts to calculate possible mass inputs (Lizcano-Aranjo, Houston).

Definitive evidence on the relationship between comets and the origin of life must

await the eventual laboratory analysis of cometary material. The identification of microscopic stratospheric and deep-sea particles of extraterrestrial origin by Brownlee (University of Washington) offers, however, the first real samples of probable cometary debris. The minute size and rarity of unaltered Brownlee particles preclude the use of most conventional analytical procedures, and substantial refinements to existing or even new techniques (such as the CD<sub>4</sub> carbon isotopic method pioneered at the University of Cambridge), are required before even the Brownlee particles can be fully exploited.

The alternative to analysing cometary material found in the terrestrial environment is *in situ* measurements from spacecraft. The planned NASA/ESA international mission to rendezvous with Halley's Comet which would have allowed analyses as sophisticated as those needed for origin of life studies will now not take place. ESA's fast flyby of Halley (the Giotto mission) will undoubtedly produce information on the composition of the gas and solid phases to fuel further laboratory based studies but is unlikely to provide definite answers to the question of whether comets were involved in the origin of life on Earth.

### CORRIGENDUM

Edward Herbert would like to point out that he was not the sole author of *Biosynthesis and processing of cellular and viral polypeptides* (News and Views, 13 November, 288, 115, 1980) and would like to acknowledge the co-authorship of Gunther Kreil (Salzburg) and the help of Carolyn Carter and Eckard Wimmer (Stoneybrook, New York).

N.J. McNaughton and C.T. Pillinger are in the Department of Earth Sciences, University of Cambridge.

\*The Fifth College Park Colloquium on Chemical Evolution was organized by Cyril Ponnamperna and held at the University of Maryland, Oct 29-31, 1980.

## ARTICLES

# Solar oscillations: full disk observations from the geographic South Pole

Gérard Grec\*, Eric Fossat† & Martin Pomerantz‡

\* Département d'Astrophysique de l'IMSP, ERA 669 du CNRS, Université de Nice, Parc Valrose, F-06034 Nice Cedex, France

† Observatoire de Nice, BP 252, F-06007 Nice Cedex 2, France

‡ Bartol Research Foundation of the Franklin Institute, University of Delaware, Newark, Delaware 19711

*Observing conditions at the geographic South Pole enable modes of global solar oscillations and theoretical models of the internal solar structure to be identified.*

THERE are only two methods available for probing the interior of the Sun to test the theoretical models of the internal solar structure. Such calculations have been based on externally observable parameters ( $M_{\odot}$ ,  $L_{\odot}$ ,  $R_{\odot}$ ,  $t_{\odot}$ ) plus some speculations regarding the relative abundances of certain elements, such as metals and helium<sup>1</sup>.

The first technique requires the exceedingly difficult measurement of neutrinos emanating from thermonuclear reactions in the solar core. After much effort, Davis<sup>2</sup> established an upper limit of the solar neutrino flux ( $1.75 \pm 0.4$  SNU) that is somewhat below original expectations. These neutrinos convey information only about the central region of the Sun, where the time scale of temporal variations is enormous ( $\sim 3 \times 10^7$  yr).

The second approach attempts to detect and identify normal modes of global solar oscillations arising from internal processes. These pulsations characterize phenomena in the layers in which dynamical processes can cause effects that produce visible manifestations on the solar surface<sup>3</sup>.

Efforts to detect global solar oscillations through observation of luminosity variations<sup>4-7</sup> were unsuccessful because the amplitudes are far smaller than the transparency fluctuations of the Earth's atmosphere.

Another technique utilizes continuous determinations of the apparent solar diameter<sup>8-12</sup>. These experiments have produced positive results which have been attributed to underestimates of the effects of atmospheric fluctuations<sup>13-16</sup>.

Finally, various Doppler shift measurements of large-scale velocity fields have been carried out either with spatial resolution or with integral light from the entire visible disk. These have usually involved continuous observations of various spectral lines by optical resonance techniques.

Fifteen years after the discovery of 5-min oscillations by Leighton<sup>17</sup> came the first incontrovertible observations of global solar pulsations by Deubner<sup>18</sup> who succeeded in resolving the diagnostic  $\kappa$ - $\omega$  diagram (or spatiotemporal power spectrum) into discrete lines. The periods were  $\sim 5$  min and the horizontal wavelengths typically  $1-3 \times 10^4$  km corresponding to spherical harmonics with high  $l$  values (typically a few hundred). These results subsequently proved that solar seismology is an exceedingly powerful diagnostic tool for investigating the solar interior<sup>19</sup>. The modes discovered by Deubner have provided information on layers located several thousand kilometres below the photosphere. The detection of lower-order modes is required for probing greater depths.

Thus, there is general agreement over the occurrence of solar pulsations with periods in the range of  $\sim 5$  min. In fact, a recent study has resolved some low-angular ( $l$ ), high-radial ( $n$ ) overtones into discrete lines of amplitudes  $0.1-0.3$  m s<sup>-1</sup> separated by an average uniform spacing of 67.8  $\mu$ Hz (ref. 20). However, for various reasons (including possible solar noise, interference

by the Earth's atmosphere and other local considerations and the severe problems in conducting these difficult observations at normal mid-latitude locations), the validity of reports of longer period global solar pulsations, especially one at 2 h 40 min (refs 21, 22), has not been universally accepted<sup>23-25</sup>.

## The polar solar observatory

The advantages of undertaking certain types of astronomical observations at the geographic South Pole became apparent<sup>26</sup> during a program of cosmic ray research in Antarctica<sup>27</sup>. More recently, we recognized that the South Pole enabled us to pursue the solar oscillation problem in conditions that cannot be duplicated anywhere else on Earth:

- (1) during the austral summer, the Sun remains essentially at a constant angular altitude, thereby eliminating the difficulties introduced by the day-night cycle;
- (2) uninterrupted data runs appreciably longer than those attainable elsewhere are feasible, thus significantly improving both the  $\omega$ -resolution and the potential for detecting long-period oscillations;
- (3) the Amundsen-Scott Station at the South Pole is, in fact, at an elevation corresponding to a pressure altitude of  $\sim 3,400$  m;
- (4) the atmosphere is colder than elsewhere, hence the precipitable water vapour content is exceedingly low, and the transparency is good, providing extended periods of coronal seeing;
- (5) the polar plateau constitutes an absolutely uniform terrain (a desert of snow) out to great distances in all directions;
- (6) the large trend due to the Earth's rotation, which can never be removed as perfectly as is required, is absent at the planet's rotational axis.

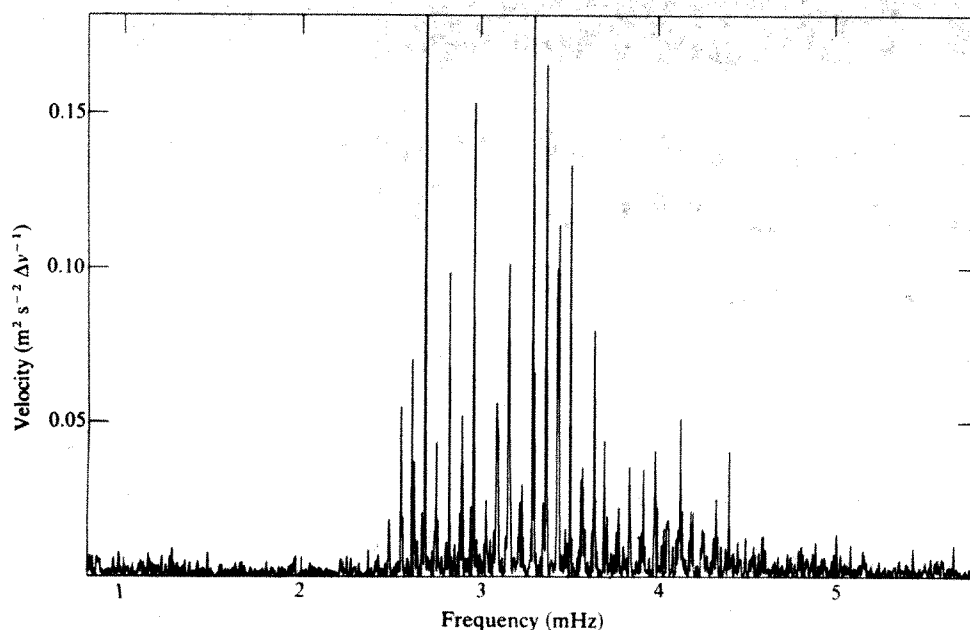
Consequently, an American-French programme was organized to conduct this experiment during the austral summer 1979-80. Only the main characteristics of the apparatus constructed for obtaining the required observations in the hostile polar environment ( $T \leq -30^\circ\text{C}$ ) will be summarized here.

A sodium optical resonance photoelectric spectrophotometer developed at Nice (France) for full disk measurements of the Doppler shifts in the 5,896-Na D1 line<sup>28</sup> was modified to operate in the rigorous conditions at the South Pole. A vertical telescope (8 cm,  $f/18$ ), specifically designed and constructed for this experiment at Bartol, provided two nonrotating solar images, one of which was focused on the guiding sensor array, the other on the spectrophotometer.

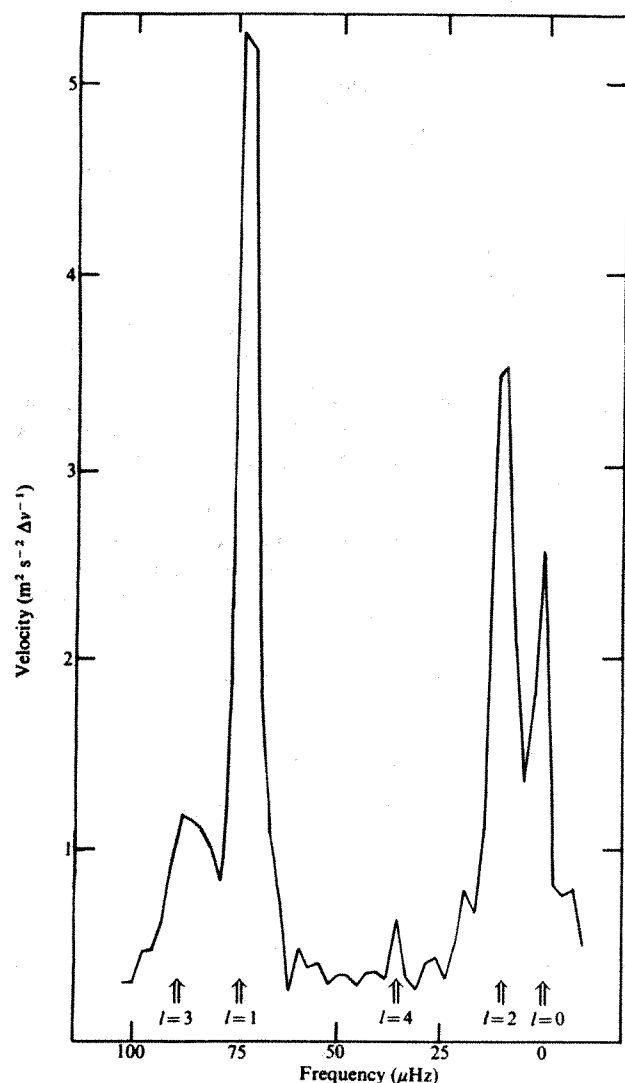
Extensive photography in H $\gamma$  during the preceding austral summer<sup>29</sup> revealed that the telescope completely satisfied the requirements for the present programme.

We attempted to create the best conditions possible by eliminating all potential man-made sources of spurious effects such as the local source of thermal turbulence arising from the





**Fig. 1** Power spectrum of the continuous 5-day full-disk Doppler shift measurements recorded at the South Pole from 31 December, 1979 to 5 January, 1980. The resolution of the power in the 3-mHz range into many discrete equidistant lines separated by  $68 \mu\text{Hz}$  indicates that global  $p$ -modes corresponding at least to  $l$  values of 0 and 1 are observed. Note that the small peaks around 2.4 mHz represent global oscillations with an amplitude  $<10 \text{ cm s}^{-1}$ , corresponding to motion of the solar radius  $<5 \text{ m}$ , or  $7 \times 10^{-6}$  arc s.



**Fig. 2** A superposed frequency analysis of the frequency range between 2.4 and 4.8 mHz reveals the average shape of spectral lines displayed in the power spectrum of Fig. 1. The horizontal axis indicates where the theory predicts the positions of  $l = 1, 2, 3$  and 4 modes if the one on the extreme right is assumed to be  $l = 0$ . The good agreement leaves no room for doubt. Note that the natural width of each separate mode indicates a  $Q$  value of the order of 600.

Amundsen-Scott station complex which would be seen at the same time every day, a site 8.1-km upwind from the base was selected. There, the well insulated  $3.5 \text{ m} \times 2.5 \text{ m}$  laboratory building mounted on a sled was installed in a deep trench. The wanigan was then enclosed by a plywood roof and vestibule walls fore and aft, and was buried in the snow. The telescope and instrument package were mounted on the surface 30 m away. A 300-m cable connected the observatory to the diesel-powered electrical generator positioned downwind with respect to the prevailing wind direction. The exhaust emerged practically at ambient temperature, and neither the generator nor the track vehicle utilized for transport produced any detectable atmospheric disturbance.

## Observations

Historical meteorological records and experience gained during 1978–79 made us hope for one 5-day period of uninterrupted optimal seeing during December–January. In fact, this did materialize, and the 5-day interval was extended to  $\sim 7$  days by remaining on the air during two brief cloudy periods, which did not interrupt the tracking. In addition, clean data (cloud free) were recorded during intervals of additional hours ranging from 5 to 10, yielding high-quality tape recordings covering more than 200 h.

## Data analysis and results

The definitive results of the analyses so far completed use part of the available data—basically the 5-day continuous run. The results mostly concern: (1) whether the widely discussed oscillation of period 160 min could be confirmed in the ideal conditions that prevail at South Pole; and (2) the investigation of the theoretically expected line spectrum of the 5-min oscillation.

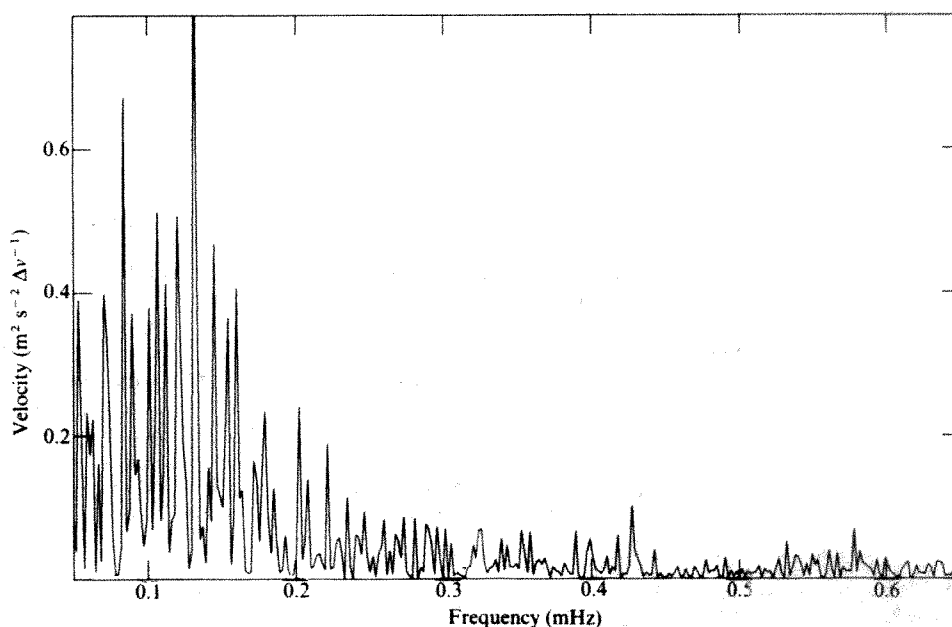
Note that the noise level at all frequencies was significantly lower than has ever been attained previously, by about an order of magnitude.

## The 5-min range

Figure 1 shows the power spectrum of the 5-day data sample. It reveals that the power in the 3-mHz range is resolved into many equidistant peaks, separated by  $68.0 \mu\text{Hz}$ . This confirms the result published by Isaak's group<sup>20</sup>. This constant displacement of  $68 \mu\text{Hz}$  clearly indicates that modes of low degree with both odd and even values of  $l$  are observed, because the frequency separation between modes of high order with the same value of  $l$  is expected to be around  $130\text{--}145 \mu\text{Hz}$  (depending on the theoretical model)<sup>31</sup>.

Modes with values of  $l$  between 0 and 3 may possibly contribute substantially to the observed line spectrum. Each line

**Fig. 3** The low-frequency part of the power spectrum shown in Fig. 1. Its spiked structure is consistent with statistical departure around a broad, continuous spectrum. A spiked spectrum of oscillatory  $g$ -modes, a broad-band solar convective spectrum as well as a broad-band telluric spectrum could separately be responsible for this result.



would then contain contributions from modes with even  $l$  or odd  $l$  with almost coincident frequencies. The frequency separation between neighbouring modes with  $l = 0$  and  $l = 2$ , and with  $l = 1$  and  $l = 3$  is expected to be  $\sim 10 \mu\text{Hz}$  and  $16 \mu\text{Hz}$  respectively<sup>31</sup>. Indeed, many peaks in Fig. 1 seem to be split into two or more components. To verify the significance of this splitting, we have used the equidistance to obtain the average shape of odd and even peaks by a 'superposed frequency analysis' of the spectrum between 2.4 and 4.8  $\mu\text{Hz}$  for an interval equal to 136.0  $\mu\text{Hz}$ . Figure 2 shows the result of this analysis, and clearly indicates that all modes between  $l = 0$  and  $l = 3$  and possibly even  $l = 4$  contribute to the power spectrum. It is quite reassuring that the  $l = 3$  modes display a significantly lower amplitude due to the smearing effect of the full disk integration.

In addition to the identification of the spherical harmonics associated with the spectral peaks, another important result emerges from Fig. 2. The width of the four main peaks indicates a  $Q$  value of about 600, or a typical damping time of 2 days. Indeed, if shorter data samples, of, say, 12 h, are Fourier analysed, the energy present in a given spectral peak does not seem to be constant in time or regularly modulated as would be expected from overstable beating pulsations. Rather, an individual peak seems to be suddenly excited and then slowly damped over a 2-day interval, unless it is re-excited before this time. A more complete statistical analysis of this temporal behaviour, embracing the total amount of data, will be necessary, but it is already clear that these modes around the 5-min period have a damping time of about 2 days and are spasmodically excited.

### The intermediate frequency range

Figures 1 and 2 show the asymptotic behaviour of low degree global modes that must be predicted by solar models. Between 2.4 and 5 mHz the order  $n$  (the number of nodes along a solar radius in the vertical component of the displacement eigenfunction) must typically be between  $\sim 15$  and 35 for these peaks<sup>31</sup>. To be able to identify each peak with one given order would require the detection of  $p$  modes with longer periods, and if possible all modes until the fundamental, the period of which is expected to be of the order of 1 h. Figure 1 shows that peaks with approximately uniform separation can be followed, with the limit of noise, towards low frequencies below 1 mHz. The same type of superposed frequency analysis, described above, over the range 0.8–2.4 mHz, demonstrates that  $l = 0$ ,  $l = 1$  and  $l = 2$  normal modes may be present in this frequency interval, with a mean amplitude of less than  $3\text{--}5 \text{ cm s}^{-1}$ . Comparing this information with theoretical model predictions, one can be assured that, for example, the first peak which emerges significantly above the noise level near 2.23 mHz must be an

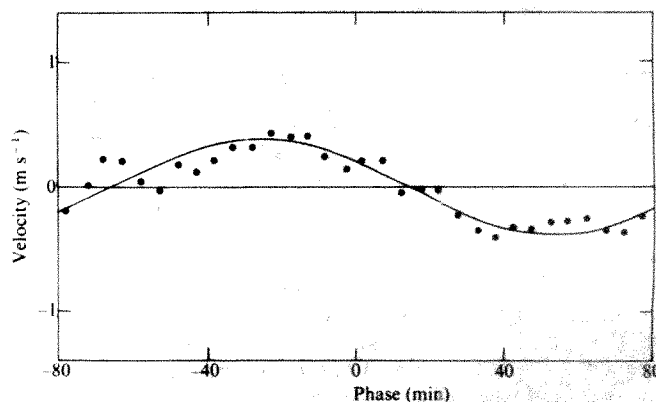
$l = 0\text{--}2$  pair with  $n = 15 \pm 1$ . To suppress the indicated uncertainty of the  $n$ -number definitely, the first four or five spherical harmonics must be identified, and this is more difficult because the asymptotic frequency equidistance prediction is no longer valid in the frequency range 0.3–0.8 mHz. We hope to be able to eliminate this ambiguity eventually by including the totality of recorded data.

### The long period range

For periods longer than 1 h, we obtain an increasing power spectrum with decreasing frequency. Figure 3 shows this long-period power spectrum, for periods between roughly 30 and 300 min. Its spiked structure is consistent with pure statistical fluctuations around a broad, continuous curve. Although it may contain some solar information from oscillatory gravity wave or broad-band convective spectrum, this result alone does not allow us to conclude that any spectral peak is characteristic of a long-period solar oscillation.

### The 160-min period

The presence of the 160-min solar oscillation originally discovered in the Crimea and observed in phase coherence during the past few years both in the Crimea and at Stanford was looked for using a superposed epoch analysis of the data processed thus far (5 days). Figure 4 shows the result of this analysis, together with the sine wave which would be expected by extrapolating the phase and amplitude according to the average of the Crimean



**Fig. 4** The superposed epoch analysis of a data sample extending over 5 days (45 periods of 160 min). The points represent the South Pole data, and the solid line is the average based upon the observations obtained at the Crimean Observatory and Stanford.



and Californian results. The present result seems to be consistent with the latter. However, note that following a recent study of error analysis of superposed epoch procedure by Forbush *et al.*<sup>30</sup>, standard methods of assigning statistical uncertainties may be not valid in this case.

## Discussion

As we have analysed only part of the data processed so far, it would be premature to undertake a comprehensive discussion of theoretical implications concerning, for example, the depth of the convective zone, helium abundance, or other solar parameters. We have, therefore, only presented observational results which can be regarded as definitive:

(1) Although the 160-min oscillation, in phase with the wave expected from the latest Russian and American results, has been detected, further analysis is required to determine its significance.

(2) The power in the 5-min range is resolved into many equidistant peaks separated by 68  $\mu\text{Hz}$ . The splitting of these peaks,

which is different for even and odd lines, indicates that global modes with  $l$  values of 0, 1, 2 and 3 have been identified.

(3) These global solar oscillations are not overstable, but are spasmodically excited, with a damping time of about 2 days ( $Q = 600$ ).

(4) Comparison between theoretical and observed frequencies of a large number of different modes has made it possible to reduce the uncertainty in the specification of the order of the spherical harmonics to unity.

These results are very encouraging for future astronomical research at the South Pole.

This work was supported by the NSF's Division of Polar Programs under grant DPP-7822267. Assistance in the field was provided by Lyman Page Jr and Jon Towle. Numerous individuals associated with the US Antarctic Research Program in different capacities provided logistical help. We especially thank Robert Pfeiffer, Arthur Smith, Don McCauley, Max Azouit, Jean-Francois Manigault and Alex Robini for technical assistance and Dermott Mullan for helpful discussions.

Received 30 September; accepted 6 November 1980.

1. Mazzitelli, J. *Astr. Astrophys.* **79**, 251 (1979).
2. Davis, R. Jr, Evans, J. C. & Cleveland, B. T. *Proc. Conf. Neutrinos 53 Lafayette* (1978).
3. Gough, D. O. *2nd Assemblée Générale Européenne de Physique Solaire*, 81 (CNRS, Paris, 1978).
4. Musman, S. & Nye, A. N. *Astrophys. J. Lett.* **212**, L95 (1977).
5. Livingston, W. D., Milkey, R. & Slaughter, C. *Astrophys. J.* **211**, 281 (1977).
6. Beckers, J. M. & Ayres, T. R. *Astrophys. J. Lett.* **217**, L69 (1977).
7. Deubner, F. L. *Astr. Astrophys.* **57**, 317 (1977).
8. Hill, H. A. & Stebbins, R. T. *Astrophys. J.* **200**, 471 (1975).
9. Hill, H. A., Stebbins, R. T. & Brown, T. M. *Atomic Masses and Fundamental Constants Vol. 5*, 622 (Plenum, New York, 1976).
10. Brown, T. M. thesis, Univ. Colorado (1977).
11. Brown, T. M., Stebbins, R. T. & Hill, H. A. *Astrophys. J.* **223**, 325 (1978).
12. Hill, H. A. & Caudell, T. P. *Mon. Not. R. astr. Soc.* **186**, 327 (1979).
13. Fossat, E., Harvey, J. W., Hausman, M. & Slaughter, C. *Astr. Astrophys.* **59**, 279 (1977).
14. KenKnight, C., Gatewood, G. D., Kipp, S. L. & Black, D. *Astr. Astrophys.* **59**, L27 (1977).
15. Clarke, D. *Nature* **274**, 670 (1978).
16. Fossat, E., Grec, G. & Harvey, J. W. *Astr. Astrophys.* (in the press).
17. Leighton, R. B. *Nuovo Cimento Suppl.* **22** (1961).
18. Deubner, F. L. *Astr. Astrophys.* **44**, 371 (1975).
19. Deubner, F. L., Ulrich, R. K. & Rhodes, E. D. *Astr. Astrophys.* **72**, 177 (1979).
20. Claverie, A., Isaak, G. R., McLeod, C. P., Van der Raay, H. B. & Roca Cortes, T. *Nature* **282**, 591 (1979).
21. Severny, A. B., Kotov, V. A. & Tsap, T. T. *Nature* **259**, 8 (1976).
22. Scherrer, P. M., Wilcox, J. J., Kotov, V. A., Severny, A. B. & Tsap, T. T. *Nature* **277**, 635 (1979).
23. Fossat, E. & Grec, G. *2nd Assemblée Générale Européenne de Physique Solaire*, 151 (CNRS, Paris, 1978).
24. Grec, G. & Fossat, E. *Astr. Astrophys.* **77**, 351 (1979).
25. Worden, S. D. & Simon, G. W. *Astrophys. J. Lett.* **210**, L1 (1976).
26. Willer, A. A. *Polar Research, A Survey*, 170 (National Academy of Sciences, Washington DC, 1970).
27. Pomerantz, M. A. *Antarctic Research Series Vol. 29*, 12 (American Geophysical Union, Washington DC, 1978).
28. Grec, G., Fossat, E. & Vernin, J. *Astr. Astrophys.* **50**, 221 (1976).
29. Kusoffsky, U. & Pomerantz, M. A. *Proc. IAU General Assembly*, Montreal (1979).
30. Forbush, S. E., Pomerantz, M. A. & Duggel, S. P. (in preparation).
31. Christensen-Dalsgaard, J. & Gough, D. O. *Nature* **288**, 544–547 (1980).

# Is the Sun helium-deficient?

J. Christensen-Dalsgaard\* & D. O. Gough†

\* Institut d'Astrophysique, Université de Liège, 4200 Cointe Ougrée, Belgium

† Institute of Astronomy, and Department of Applied Mathematics and Theoretical Physics, University of Cambridge, Silver Street, Cambridge CB3 9EW, UK

*The recent observations of solar 5-min oscillations of low degree agree approximately with the predictions of a standard solar model with normal abundances of helium and heavy elements. Much of the apparent discrepancy noticed when the observations were first announced was a result of having neglected the influence of the Sun's atmosphere in the normal mode analysis of the theoretical models. Our standard solar models are not in perfect agreement with observation, but it seems that major modifications will not be necessary to remove the remaining small discrepancies.*

CLAVERIE *et al.*'s<sup>1</sup> announcement of the resolution of a sequence of peaks in the power spectrum of whole-disk Doppler observations of the Sun, with frequencies in the range 2–4 mHz, produced an immediate discussion of the implications regarding the Sun's internal structure<sup>2</sup>. The peaks were interpreted as being the result of groups of  $p$  modes of high order, of alternately odd and even degree<sup>2</sup>. Direct comparison of the observed mean spacing between the peaks with predictions from a sequence of three solar models having different internal compositions<sup>3</sup> gave precise agreement only when the internal abundances  $Y$  and  $Z$  of helium and heavy elements were rather low ( $Y = 0.19$ ,  $Z = 0.004$ ). A similar result seemed to be true of a sequence of models studied earlier by Iben and Mahaffy<sup>4</sup>, although in this case it was necessary to extrapolate the composition. However, the discrepancy between observation and the 'standard' models, with  $Z = 0.02$  and  $Y = 0.25$ , was  $< 2\%$ , and without careful consideration of the uncertainties in both theory and observation it could not be concluded that the Sun is necessarily deficient in helium and heavy elements.

Nevertheless, there has already been some discussion of the implications of such a postulate<sup>5</sup>.

The observations of Grec *et al.*<sup>6</sup> have confirmed the original results and have provided us with more accurate and detailed knowledge of the oscillation frequencies. We report here a further theoretical study of the 5-min modes, in the adiabatic approximation, and compare the results with the new observations. Although agreement is not perfect, we find no reason to conclude that the abundances  $Y$  and  $Z$  are surprisingly low.

## Observations

Both Claverie *et al.* and Grec *et al.* measured the shift in a spectrum line in integrated sunlight, and the time dependence of the shift was analysed. In particular, power spectra of the data revealed almost uniformly spaced peaks in the range 2–5 mHz. Similar observations had been made before<sup>7–9</sup>, and although there is a strong hint of discrete peaks in the results of Grec and Fossat<sup>8</sup>, they were never unambiguously resolved, partly because the periods of observation were too short<sup>10</sup>.

The most accurate observations are those of Grec *et al.*<sup>6</sup>. These were made at the South Pole, where the Sun can be seen continuously for long periods of time. The results have not yet been fully analysed, but a power spectrum of 120 h of continuous data is available. In agreement with previous observations<sup>1,7-9,11</sup>, there is a concentration of power near 3 mHz. Moreover, almost all that power is contained in discrete peaks, whose mean spacing in the range 2.4–4.7 mHz is half of 136.0  $\mu$ Hz.

### Interpretation of the observations

We accept that the direct cause of much of the observed power is an oscillation of the Sun that can be represented well by a superposition of linear normal modes. Because the observations integrate light from the entire solar disk, the measurements are sensitive only to modes of low degree. Consequently the modes are probably  $p$  modes of high order, because no solar  $f$  or  $g$  mode of low degree has a frequency as high as 2 mHz.

The frequencies of adiabatic  $p$  modes of low degree  $l$  and high order  $n$  are given approximately by<sup>12</sup>

$$\nu_{n,l} \approx (n + \frac{1}{2}l + \varepsilon)\nu_0 - [l(l+1) + \delta]A\nu_0^2\nu_{n,l}^{-1} \quad (1)$$

where

$$\nu_0 = \left(2 \int_0^R c^{-1} dr\right)^{-1} \quad (2)$$

and  $\varepsilon$ ,  $\delta$  and  $A$  are other constants of the equilibrium solar model. Here  $c$  is the adiabatic sound speed in the equilibrium model,  $r$  is a radial coordinate and  $R$  is the radius of the Sun. The approximation was derived assuming that  $l \ll n$ , and for such modes it provides a good representation of the numerical calculations<sup>10</sup>. The second term is a relatively small correction to the first. It therefore follows that sequences  $\nu_{n,l}$  with fixed  $l$  and varying  $n$  are approximately uniformly spaced with separation close to  $\nu_0$ , that two such sequences with different  $l$  have almost coincident frequencies provided both values of  $l$  are either odd or even, and that the frequencies of modes with odd  $l$  lie approximately midway between those of modes with even  $l$ . The frequencies thus fall into almost uniformly spaced groups, which we label with  $i = 2n + l$ .

Theoretically one would expect modes with high  $n$  and low  $l$  to be excited to amplitudes that on average are roughly independent of  $l$  at fixed  $\nu_{n,l}$  and there is some observational evidence that this is so<sup>10</sup>. Consequently each peak in the observed power spectra should contain contributions from several modes with almost identical frequencies. Thus the value of 136.0  $\mu$ Hz reported by Grec *et al.*<sup>6</sup> for twice the mean spacing between the peaks in their power spectrum represents approximately the spacing between a sequence of eigenfrequencies at fixed  $l$  and varying  $n$ . As  $l$  increases, so does the second term in equation (1), which destroys the correspondence between frequencies of modes with different  $l$ . However, once  $l$  is large enough for the divergence to be substantial, the sensitivity of the observations is too low for it to matter. Indeed, theoretical estimates<sup>10</sup> suggest that the observed signal is dominated by contributions from only those modes with  $l \leq 3$ , and that the expectation  $\bar{\nu}_i$  of the peak frequencies is approximately

$$\bar{\nu}_i = \begin{cases} 0.51 \nu_{n,0} + 0.49 \nu_{n-1,2} & i \text{ even} \\ 0.87 \nu_{n,1} + 0.13 \nu_{n-1,3} & i \text{ odd} \end{cases} \quad (3)$$

The observations of Grec *et al.*<sup>6</sup> confirm this interpretation. It has been possible to resolve structure in the major peaks, which presumably arises from the presence of modes with slightly different frequencies. To reduce noise and the effects of interference, Grec *et al.*<sup>6</sup> performed a superposed frequency analysis on the spectrum, by dividing the spectrum into segments of length 136.0  $\mu$ Hz and adding the segments of spectrum. The result is shown in their Fig. 2. Although this procedure does not take account of the nonlinearity of the dependence of  $\nu_{n,l}$  on  $n$ , the separation of each peak into two main components is clear and the relative power within each of those components is roughly in accordance with theoretical predictions.

### Oscillation eigenfrequencies and the influence of the atmosphere

Oscillation eigenfrequencies of the solar models discussed in ref. 3 and some models of Christensen-Dalsgaard<sup>13</sup> have been computed as described in ref. 10. The most important difference between these computations and those discussed in ref. 3 is that here some account has been taken of the solar atmosphere.

The influence of the atmosphere is important only when the oscillation frequency  $\nu$  is comparable with Lamb's<sup>14</sup> acoustical cutoff frequency  $\nu_c = \gamma g/4\pi c$ , which is the minimum frequency at which acoustic waves can propagate vertically in the atmosphere. Here  $\gamma$  is the adiabatic exponent ( $\partial \ln p / \partial \ln \rho$ ), where  $p$ ,  $\rho$  and  $g$  are pressure, density and specific entropy, and  $g$  is the gravitational acceleration. In the solar atmosphere,  $\nu_c \approx 5$  mHz. Provided  $\nu < \nu_c$ ,  $p$  modes are reflected by an evanescent region that includes the atmosphere, and are thus confined to the solar interior. The lower the frequency, the deeper the level at which reflection takes place. Thus when  $\nu < \nu_c$ , reflection occurs so deep in the Sun that the modes are almost unaffected by the presence of the atmosphere. Neglecting the atmosphere in the computations reported in ref. 3, for example, introduces errors in the frequencies stated explicitly in that paper that are no more than about a part in  $10^5$ .

When  $\nu$  is comparable with  $\nu_c$ , the inertia of the atmosphere is an appreciable fraction of the total mass above the reflecting region. In this case the atmosphere introduces a phase shift in the spatial oscillation of the eigenfunction, and so changes the frequency. It is only when  $\nu$  is quite close to  $\nu_c$  however, that the detailed structure of the atmosphere is important. Otherwise the atmosphere moves almost hydrostatically, and its influence on the phase shift depends only on its mass, which is directly related to the equilibrium photospheric pressure.

We substantiate the discussion above by considering a plane-parallel polytropic layer under constant gravity, supporting an isothermal atmosphere of the same composition. The polytrope is taken to have the structure

$$p = p_0 z^{m+1}, \quad \rho = \rho_0 z^m, \quad z_{ph} \leq z \leq Z \quad (4)$$

where  $z$  is a vertical coordinate measured downwards, and  $p_0$ ,  $\rho_0$  and  $m$  are constants. The isothermal atmosphere in  $(-\infty, z_{ph})$  is determined by requiring that temperature and pressure, and hence density, are continuous at the photosphere  $z = z_{ph}$ .

The horizontal wavelengths of the solar modes of low degree are much greater than the scale height in the atmosphere. Therefore, to determine the influence of the atmosphere on the eigenfrequencies, we need only consider purely vertical oscillations. We assume a rigid base at  $z = Z$ , and select those modes with an energy density that tends to zero as  $z \rightarrow -\infty$ . Thus we are ignoring the potential influence of the corona, or nonlinearities in the upper atmosphere<sup>15-17</sup>.

The analysis is a straightforward generalization of that presented by Lamb<sup>14</sup>. The eigenfrequencies  $\nu_n$  of high order  $n$ , satisfying  $2\pi n \gg m^2$ , are given by

$$\nu_n \approx (n + \frac{1}{2}m - \frac{1}{2})\nu_0 - \frac{(4m^2 - 1)\nu_0^2}{8\pi^2\nu_n} - \frac{\nu_0}{\pi} \tan^{-1} \Phi_m(\alpha_n \lambda_n), \quad (5)$$

where

$$\Phi_m(\alpha, \lambda) = \frac{J_{m+1}(\lambda) - \alpha J_m(\lambda)}{Y_{m+1}(\lambda) - \alpha Y_m(\lambda)}$$

$$\lambda_n = (m+1)x_n, \quad \alpha_n = x_n^{-1} - (x_n^{-2} - 1)^{1/2}, \quad x_n = \nu_n/\nu_0 \quad (6)$$

and the characteristic frequency  $\nu_0$  is now defined by

$$\nu_0^{-1} = 2 \int_0^Z \left( \frac{\rho_0}{\gamma p_0 z} \right)^{1/2} dz; \quad (7)$$

$J_m$  and  $Y_m$  are Bessel functions of order  $m$ . If the isothermal atmosphere were replaced by a rigid lid of the same mass, the



Table 1 Properties of solar models

| Model | Opacity | $M$ | $Z$   | $Y$   | $D$<br>( $10^5$ km) | $\Delta\nu$<br>( $\mu$ Hz) | $\nu_{16,1}$<br>(mHz) | $\nu_{28,1}$<br>(mHz) | $\nu_{n,0} - \nu_{n-1,2}$<br>( $\mu$ Hz) | $\nu_{n,1} - \nu_{n-1,3}$<br>( $\mu$ Hz) |
|-------|---------|-----|-------|-------|---------------------|----------------------------|-----------------------|-----------------------|--|--|
| A     | CS/L    | 200 | 0.02  | 0.251 | 1.67                | 136.6                      | 2.404                 | 4.041                 | 10                                       | 16                                       |
| B     | CS/L    | 200 | 0.004 | 0.187 | 1.20                | 134.8                      | 2.353                 | 3.970                 | 13                                       | 17                                       |
| C     | CS/L    | 200 | 0.001 | 0.160 | 0.29                | 129.9                      | 2.336†                | 3.895†                | 13                                       | 18                                       |
| A*    | CS/L    | 200 | 0.02  | 0.251 | 1.67                | 138.1                      | 2.412                 | 4.069                 |  |  |
| 1     | CT/S    | 201 | 0.02  | 0.247 | 1.97                | 136.7                      | 2.417                 | 4.056                 |  |  |
| 2     | CT/S    | 401 | 0.02  | 0.247 | 1.97                | 136.5                      | 2.416                 | 4.053                 |  |  |
| 3     | CT/L    | 201 | 0.02  | 0.253 | 1.91                | 136.5                      | 2.415                 | 4.053                 |  |  |
| 4     | CRS/S   | 201 | 0.02  | 0.249 | 1.75                | 135.9                      | 2.409                 | 4.039                 |  |  |
| H     | CT/S    | 201 | 0.02  | 0.266 | 1.42                | 136.5                      | 2.398                 | 4.035                 |  |  |

$Y$  and  $Z$  are the initial abundances by mass of helium and heavy elements;  $D$  is the present depth of the convection zone. CS refers to the tables of Cox-Stewart<sup>23</sup>, CRS to Carson (unpublished, but see ref. 24) and CT to Cox-Tabor<sup>25</sup>; the L or S refers to linear or spline interpolation in the tables.  $M$  is the number of mesh points between the centre and the photosphere of the model. Electron screening was taken into account in computing nuclear reaction rates only in models 1–4 and H. An evolutionary calculation was not performed for the chemically homogeneous model H; the initial helium abundance of that model was estimated by homology scaling from its present value of 0.303. The mean frequency separation  $\Delta\nu$  is twice the mean separation, in the range 2.3–4.1 mHz, between the peaks in the power spectrum of an ensemble of all the modes. The mean separations between neighbouring  $l=0$  and  $l=2$  eigenfrequencies and between neighbouring  $l=1$  and  $l=3$  eigenfrequencies of models A, B and C are listed in the last two columns, and are averaged over the same frequency range as  $\Delta\nu$ . The mean separation between neighbouring  $l=0$  and  $l=4$  eigenfrequencies of model A in that range is 35  $\mu$ Hz. The expectations of the relative power in the peaks of a power spectrum produced by modes of different degree can be obtained from ref. 10. These are 0.56, 1.0, 0.54, 0.06 and  $2 \times 10^{-3}$  for  $l=0, 1, 2, 3$  and 4 respectively. Frequencies of dipole modes with frequencies near 2.4 and 4.0 mHz are listed in columns 8 and 9. For model C these frequencies† are  $\nu_{17,1}$  and  $\nu_{29,1}$ .

eigenfrequencies would still be given by equation (5), but with  $\alpha_n = \frac{1}{2}x_n$ . If the atmosphere were ignored entirely, and the lagrangian pressure perturbation were assumed to vanish in the photosphere, then  $\alpha_n = 0$ . Replacing the atmosphere by a polytrope of index  $m$  reduces the equilibrium model to a complete polytrope; in that case the last term in equation (5) is removed, yielding what is essentially Lamb's<sup>14</sup> result. Note that in the limit of small  $x_n$ ,  $\alpha_n = \frac{1}{2}x_n$  and the leading terms in the expansions of  $J_{m+1}(\lambda_n)$  and  $\alpha_n J_m(\lambda_n)$  cancel in equation (6). Thus to leading order, the isothermal and polytropic atmospheres and the rigid lid all yield the same eigenfrequencies.

The result of ignoring the atmosphere entirely is to overestimate the eigenfrequencies by

$$\delta\nu_n = \pi^{-1} \nu_0 [\tan^{-1} \Phi_m(\alpha_n, \lambda_n) - \tan^{-1} \Phi_m(0, \lambda_n)] \quad (8)$$

When  $x_n$  is small this reduces to

$$\delta\nu_n \approx \nu_0 [\Gamma(m+1)\Gamma(m+2)]^{-1} (\frac{1}{2}\lambda_n)^{2(m+1)} \quad (9)$$

where  $\Gamma$  is the gamma function, which shows the increasing importance of the atmosphere as the frequency rises.

We can use equation (8) to obtain a rough estimate of the error in the mean frequency separation introduced by ignoring the atmosphere. If the mean is evaluated between  $\sim 2$  and 4.5 mHz, and  $m \geq 2$ , the result is  $\sim 1$   $\mu$ Hz, and depends only weakly on  $m$  and the precise frequency range over which the mean is evaluated. This estimate is comparable with the difference between the mean separation originally obtained by Claverie *et al.*<sup>1</sup> and the mean that can be deduced from equations (3) and the values quoted for the standard solar model in ref. 3. This justifies our repeating the theoretical eigenfrequency analysis with the atmosphere included.

Equation (8) cannot be used to correct the frequencies in refs 3 and 4, because the Sun is neither plane parallel nor polytropic. It is easy to show that even though the solar atmosphere is thin compared with its radius, in the limit  $x_n \rightarrow 0$  a geometrical correction is introduced into equation (9) which is of the same order as the value derived here. Indeed, the difference between our new results and those of ref. 3 obey a power law when  $\nu \leq 2$  mHz, with exponent  $2(m+1) = 8.6$ , but with a coefficient considerably greater than that given by equation (9). For higher values of  $\nu$ , the numerical results and the plane-parallel theory agree more closely.

## Mean frequency separation of modes

The mean frequency separation between groups of modes was computed in the range 2.3–4.1 mHz, using equation (3) to determine the mean peak positions. The frequency range was chosen to correspond approximately to that within which

Claverie *et al.*<sup>11</sup> could resolve discrete peaks. The mean separations between the peaks with odd  $l$  and with even  $l$  were computed separately; in all the cases we investigated the two values differed by no more than 2 parts in  $10^4$ . The values in Table 1 are averages of the two values and therefore represent twice the mean spacing of the peaks in a power spectrum of an ensemble of all the oscillations.

Model A was computed in the standard way from the zero-age main sequence. In models B and C, which have low initial abundances of heavy elements, the surface was assumed to have been contaminated continuously by accreted material during evolution, at a rate chosen to give  $Z = 0.02$  throughout the convection zone at present. In all cases an atmosphere in hydrostatic equilibrium with the  $T$ - $\tau$  relation of the Harvard-Smithsonian Reference Atmosphere<sup>18</sup> out to  $\tau = 10^{-4}$  was added, as described in ref. 10. The outer boundary condition—that the lagrangian pressure perturbation vanishes—was applied at  $\tau = 10^{-4}$ . Included for comparison is model A\*, which is simply model A with the outer oscillation boundary condition applied at the photosphere, as in ref. 3.

Four other so-called standard models are included in Table 1, to give some idea of the sensitivity of the results to uncertainties in the theory. These are models 1–4 of ref. 13. They all have  $Z = 0.02$ , and differ from each other through the use of different opacity tables, or a different number of mesh points. Electron screening was taken into account in computing the nuclear reaction rates, which was not the case for models A, B and C, and a more accurate numerical scheme was used.

## Comparison of theory with observation

Given a sequence of solar models, one can attempt to find by interpolation a model which best fits the data. First, the frequency separation is interpolated, which should give sufficient information to identify the modes, and then the frequencies themselves can be used.

The original attempt to do this<sup>2</sup> took account of only the frequency separation, because the observed frequencies were not available<sup>1</sup>. Interpolation was essentially between models A, B and C, except that the oscillation boundary condition had been applied at the photosphere. This overestimated the mean theoretical separations by  $\sim 1.5$   $\mu$ Hz for models A and B and 1  $\mu$ Hz for model C, and led to the tentative conclusion that a model close to model B was preferred. However, the reduction of the theoretical eigenfrequencies that has resulted from including the atmosphere, and the slight upward revision of the estimate of the actual frequency separation by the South Pole measurements<sup>6</sup>, have now brought the standard model into closer agreement with observation. Interpolation with respect to

frequency separation alone suggests a model between models A and B, but closer to model A.

The superposed frequency analysis of Grec *et al.*<sup>6</sup>, summarized in their Fig. 2, enables us to identify the modes. By comparison of the relative power within the peaks and the peak separations with the theory summarized in ref. 10 and Table 1, it is evident that the peaks on the left result from modes of odd degree and those on the right from modes of even degree. Note that there is even a hint of the  $l=4$  modes about 35  $\mu\text{Hz}$  below the radial modes. Thus it has been possible to identify the peaks in the power spectrum of the observations at, for example,  $\nu=2.426$  and 4.057 mHz, as modes with  $l=1$  (E. Fossat, personal communication); and we deduce that these modes are of the order of  $n=16$  and 28 respectively. Note, however, that the frequencies of these modes cannot be reproduced by interpolation between models A and B. Extrapolation beyond the standard model to one slightly richer in helium and heavy elements reduces the discrepancies, but perfect agreement is not possible.

### Other solar models

It is not possible to fit all the observations with the eigenfrequencies of a model interpolated in or extrapolated from the sequence A, B, C. However the variations amongst models 1–4 seem to be sufficiently great to suggest that agreement could be achieved with a model that does not differ substantially from our standard. That does not necessarily imply that such a model is a good representation of the Sun. There may be other quite different models which could reproduce the observed frequencies equally well.

In particular, we consider the transient-mixed model that was discussed by Dilke and Gough<sup>19</sup> as a potential explanation for terrestrial glaciation and the low solar neutrino flux. Unfortunately we do not have sufficient information to calculate eigenfrequencies, but we do have the integral in equation (2) evaluated between  $r=0$  and the radius in the radiative interior within which 98% of the mass is contained. Though  $\nu_0$  is not equal to the frequency separation  $\Delta\nu$ , we have found in other models that its variation follows that of  $\Delta\nu$  quite closely. Therefore we have estimated  $\nu_0$  for the transient models as follows.

We selected three values of the time  $t$ . The first,  $t_1$ , was 4,700 Myr, immediately before a phase of mixing; the second,  $t_2$ , was 2 Myr later, which is near to the luminosity minimum; and the third,  $t_3$ , was 5 Myr after  $t_1$ , which is roughly when the luminosity and radius first return to values close to those at  $t_1$ . At each time the radiative interior was scaled homologously, varying  $Y$  at fixed  $Z$  by such an amount as to bring the model to the current solar luminosity. Model envelopes with the solar photospheric radius and the same composition as the unburnt region of the scaled interior were then fitted to the interior, by insisting that the mass and temperature be continuous at the fitting radius. A further small homologous scaling was then necessary to bring the total mass of the entire model to the solar value. The remainder of the integral in equation (2) could then be computed.

During the transient mixing phase of a single model, the luminosity and radius vary. The decrease in temperature, and consequently sound speed, outweighs the smaller relative

decrease in radius, and causes  $\nu_0$  to decrease. However, when three different models each having the same luminosity and radius at the different epochs  $t_1$ ,  $t_2$ , and  $t_3$  are compared, the reverse is true. The values of  $\nu_0$  at  $t_2$  and  $t_3$  were found to be 1.2 and 0.7% greater than the value at  $t_1$ . We conclude that the frequency separation  $\Delta\nu$  has a similar variation.

As a second example we consider a chemically homogeneous solar model in thermal balance, model H. We computed this model to see whether  $g$  modes of low degree and low order could have periods close to 160 min. This particular model, whose properties are summarized in Table 1, has modes  $g_2(l=1)$  and  $g_4(l=2)$  both with periods close to 150 min, and a relatively minor change of parameters could no doubt change them to 160 min. The low degree 5-min  $p$  mode eigenfrequencies are hardly distinguishable from those of model A.

### Conclusion

Approximate agreement between the eigenfrequencies of a standard solar model and the observations of Grec *et al.*<sup>6</sup> has been found in the frequency range 2.3–4.1 mHz. Thus there seems to be no evidence from the whole-disk observations of 5-min oscillations that the solar structure is very different from that of a standard model. Moreover, models with low abundances of helium and heavy elements are incompatible with observation.

The frequencies discussed here contain enough information to differentiate between the models in Table 1 and the real Sun. Therefore we know that none of our models is exact. Small changes in the physics could possibly improve the agreement. In particular, our equation of state may be too inaccurate. Moreover, there have been revisions in opacities and nuclear reaction rates since the models were computed<sup>20</sup>, and when these are taken into account the discrepancies may disappear. Nevertheless, the relative insensitivity of the frequencies to considerable changes in structure, as illustrated by the properties of the mixed models, has suggested that agreement might also be achieved with models rather different from the standard.

To differentiate between the models it may be necessary to seek other measures. For example, only those models with convection zones as deep as  $\sim 2 \times 10^5$  km are compatible with observations of the 5-min oscillations of high degree<sup>21,22</sup>. Thus the chemically homogeneous model H seems to be ruled out. Another quantity that might be measurable is the buoyancy frequency  $N$  beneath the convection zone which controls the  $g$  mode frequencies. Unfortunately, no solar  $g$  mode has yet been identified. However, there is some influence of  $N$  on the  $p$  modes of low degree, especially those that are of low order and which do seem to be present in the whole-disk power spectrum<sup>6</sup>. The data currently available are too noisy to determine the frequencies of the low-order modes precisely, but further analysis of the data obtained by Grec *et al.*<sup>6</sup>, and possibly longer observations of the same type, may make it possible. Then we shall be in a better position to judge the models.

We thank E. Fossat and A. B. Severny for conversations and correspondence. J. C.-D. thanks Aarhus Universitet and Statens naturvidenskabelige Forskningsraad of Denmark for financial support.

Received 26 September, accepted 6 November 1980.

- Clavero, A., Isak, G. R., McLeod, C. P., van der Raay, H. B. & Roca-Cortés, T. *Nonradial and Nonlinear Stellar Pulsation* (eds Hill, H. A. & Dziembowski, W. A.) 181–183 (Springer, Heidelberg, 1980).
- Christensen-Dalsgaard, J. & Gough, D. O. *Nonradial and Nonlinear Stellar Pulsation* (eds Hill, H. A. & Dziembowski, W. A.) 184–190 (Springer, Heidelberg, 1980).
- Christensen-Dalsgaard, J., Gough, D. O. & Morgan, J. G. *Astr. Astrophys.* **73**, 121–128; 79, 260 (1979).
- Iben, I. Jr & Mahaffy, J. *Astrophys. J. Lett.* **139**, L43 (1976).
- Isak, G. R. *Nature* **283**, 644–645 (1980).
- Grec, G., Fossat, E. & Pomerantz, M. *Nature* **288**, 541–544 (1980).
- Fossat, E. & Rieutort, G. *Astr. Astrophys.* **43**, 243–252 (1975).
- Grec, G. & Fossat, E. *Astr. Astrophys.* **88**, 411–420 (1977).
- Dittner, P. H. *Astrophys. J.* **224**, 265–275 (1978).
- Christensen-Dalsgaard, J. & Gough, D. O. *Mem. Not. R. astr. Soc.* (in the press).
- Clavero, A., Isak, G. R., McLeod, C. P., van der Raay, H. B. & Roca-Cortés, T. *Nature* **283**, 591–594 (1979).
- Tassoul, M. *Astrophys. J. Suppl.* **43**, 469–490 (1980).

- Christensen-Dalsgaard, J. *Mem. Not. R. astr. Soc.* (in the press).
- Lamb, H. *Proc. Lond. Math. Soc.* **7**, 122–141 (1909).
- Rosenwald, R. D. & Hill, H. A. *Nonradial and Nonlinear Stellar Pulsation* (eds Hill, H. A. & Dziembowski, W. A.) 404–412 (Springer, Heidelberg, 1980).
- Libun, J. D., Hill, H. A., Puccio, P. & Rosenwald, R. D. *Nonradial and Nonlinear Stellar Pulsation* (eds Hill, H. A. & Dziembowski, W. A.) 413–428 (Springer, Heidelberg, 1980).
- Gough, D. O. *Nonradial and Nonlinear Stellar Pulsation* (eds Hill, H. A. & Dziembowski, W. A.) 273–299 (Springer, Heidelberg, 1980).
- Gingrich, O., Noyes, R. W., Kalkofen, W. & Cony, Y. *Solar Wind* **18**, 347–365 (1971).
- Dilke, F. W. W. & Gough, D. O. *Nature* **240**, 262–264; 293–294 (1972).
- Baball, J. N. *et al. Phys. Rev. Lett.* **45**, 945–948 (1980).
- Labov, S. H., Rhodes, E. J. Jr & Ulrich, R. K. *Nonradial and Nonlinear Stellar Pulsation* (eds Hill, H. A. & Dziembowski, W. A.) 300–306 (Springer, Heidelberg, 1980).
- Berthomieu, G. *et al. Nonradial and Nonlinear Stellar Pulsation* (eds Hill, H. A. & Dziembowski, W. A.) 307–312 (Springer, Heidelberg, 1980).
- Cox, A. N. & Stewart, J. N. *Astrophys. J. Suppl.* **19**, 243–279 (1970).
- Carmichael, T. R. *A. Rev. Astr. Astrophys.* **14**, 95–117 (1976).
- Cox, A. N. & Tabor, J. E. *Astrophys. J. Suppl.* **31**, 271–312 (1976).



# The constancy of the solar diameter over the past 250 years

John H. Parkinson\*, Leslie V. Morrison† & F. Richard Stephenson‡

\* Mullard Space Science Laboratory, University College London, Holmbury St Mary, Dorking, Surrey RH5 6NT, UK

† Royal Greenwich Observatory, Herstmonceux Castle, Hailsham, East Sussex BN27 1RP, UK

‡ Department of Geophysics, University of Liverpool, Liverpool L69 3BX, UK

*Reconsideration of meridian circle observations with analysis of transits of Mercury and durations of total solar eclipses indicate that there has been no detectable secular change in the solar diameter during the past 250 yr.*

ALTHOUGH the output of energy by the Sun is generally assumed to be produced entirely by nuclear processes in the core, experiments to detect the neutrino flux yield only about one-third of the expected value. Among the many ingenious suggestions that have been made to resolve this apparent discrepancy<sup>1</sup> is the recent claim that observational evidence from about 1840 suggests that the Sun's radius is shrinking at the considerable rate of about 0.1% per century<sup>2</sup>. The gravitational energy released in this contraction of the Sun, or at least of the outer layers, would then supplement the Sun's luminosity from nuclear reactions.

The brightness of the Sun depends principally on the core temperature so that, in contracting models of the Sun, the core temperature would need to be reduced to bring the predicted brightness of the Sun into agreement with observation. Such a change would also lower the predicted neutrino emission, possibly to the extent of being consistent with the observed rate. This would remove a major stumbling block in modern astrophysics. Only a small fraction of the Sun's mass could be involved in such a gravitational contraction as a uniform contraction of the entire Sun at the rate suggested would increase the luminosity to  $10^2$ – $10^3$  times its present value.

Here we investigate the reality of the observed contraction of the solar diameter and show that it is based on a misinterpretation of the meridian circle observations used. A more careful analysis, combined with two other methods of investigation, show that there has been no detectable secular change in the Sun's diameter since at least AD 1700.

## Meridian circle measurements

One of the earliest tasks of the Royal Observatory at Greenwich was to measure the position of the Sun in the sky. Using a meridian circle, the times at which the leading and following edges crossed the meridian were noted and the angles from the zenith to the upper and lower limbs were measured. By averaging these pairs of measurements the Sun's position could be obtained, whereas subtraction gives the apparent horizontal and vertical solar diameters.

Analyses of meridian transit measurements for periodic changes in the diameter have produced inconclusive results<sup>3</sup>. There have, however, been reports of secular trends found in the measurements; for example, a horizontal semi-diameter decrease of 0.01 arcs per year from 1890 onwards has been reported<sup>4</sup>. Recently Eddy and Boornazian<sup>2</sup> claimed to find a

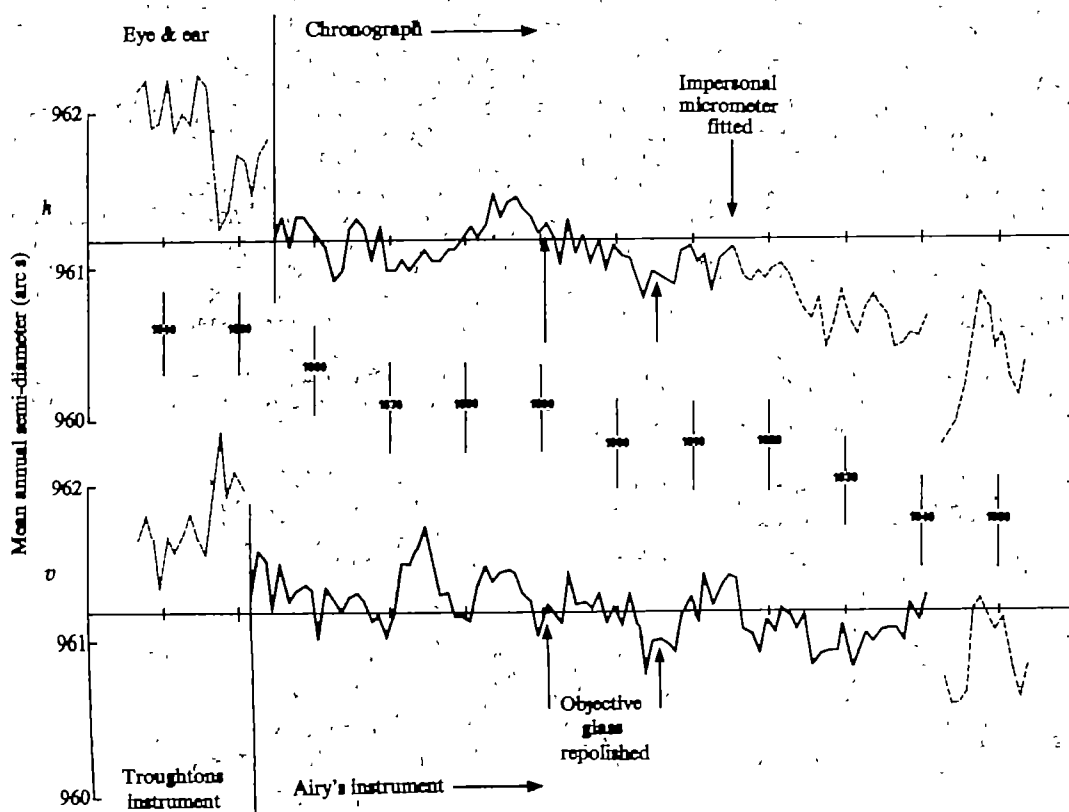
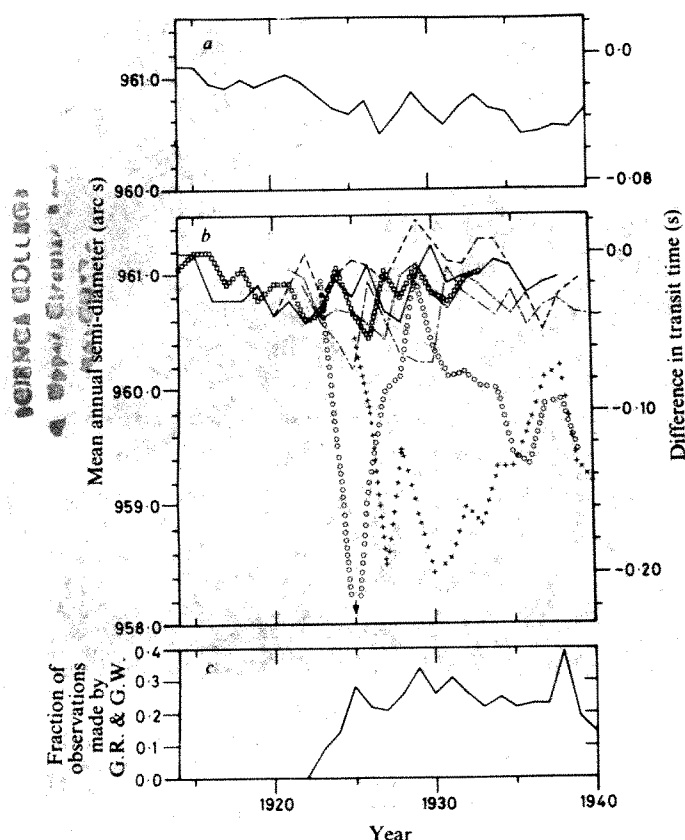


Fig. 1 Annual mean values of the Sun's horizontal ( $h$ ) and vertical ( $v$ ) semi-diameters derived from meridian circle observations made at Greenwich<sup>2</sup>. The most reliable results are joined by solid lines and the less reliable ones by dashed lines.



**Fig. 2** *a*, Mean horizontal semi-diameter for the seven regular observers between 1915 and 1940 showing an apparent decrease of 0.01 arc s per year. *b*, Individual annual means for the seven regular observers. Five observers: W,  $\square$ ; H.A., —; R.C., ---; L.S., - - -; H.B.,  $\Delta$  give consistent results, whereas G.R.,  $\circ$  and G.W., + show erratic changes. *c*, The fraction of measurements made each year by G.R. and G.W. As the fraction increased, so the semi-diameter seemed to decrease.

similar trend in the horizontal diameter and about half that rate in the vertical diameter, the evidence for both trends commencing in 1836. As such a significant change would have profound implications for the evolution of the Sun, it warrants further study using other techniques.

Such analyses must be complicated by the instrumental changes at Greenwich since 1836. In 1851, 'Airy's telescope' replaced Troughton's instrument<sup>5</sup>. Figure 1 shows the variation in the annual mean horizontal and vertical semi-diameters derived by Eddy and Boornazian. There is a clear discontinuity in the measurements of the vertical semi-diameter coinciding with the change of telescope showing that the measured

diameter depends crucially on the instrument used. After Airy's instrument had been in service for only one year, it was stated that "no other instrument... can be compared with this for steadiness and accuracy of adjustments or for the accuracy of results"<sup>6</sup>.

As the horizontal measurements were made by noting the length of time taken for the Sun to cross a wire in the eyepiece of the telescope, the measured horizontal diameter depends on both the clarity of the image formed and the accuracy with which the transit time could be measured. Before 1854 the observer watched the Sun while listening to the ticking of a pendulum clock. The precise time at which the Sun crossed the meridian was then interpolated mentally between two successive ticks. In 1854 this crude 'eye and ear' method was replaced by a chronograph, which had the advantage of recording the time automatically. Again, after only one year the observations were judged to be "... indisputably of a higher order of excellence than those formerly made by the ordinary method of eye and ear"<sup>7</sup>. The horizontal semi-diameters in Fig. 1 show a clear discontinuity when the observing method was changed.

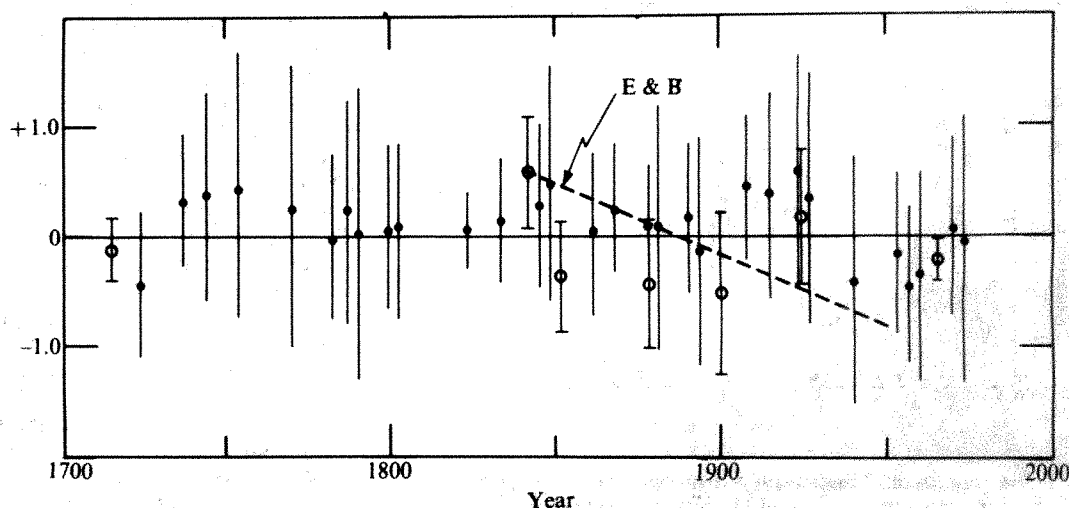
The telescope objective glass was repolished in 1891 and again in 1906 (ref. 8) which may have altered the definition of the image and hence the apparent diameter of the Sun. In 1915 the 'impersonal micrometer' was fitted and again this may have affected the horizontal diameter measurements. Observations with Airy's telescope ceased in 1953 when the reversible transit instrument came into operation at Herstmonceux.

A high degree of skill and dexterity were required to operate Airy's meridian circle, and, from its early days, the influence of observer bias was recognized<sup>3,9-11</sup>. In particular, Thackeray demonstrated that each observer had a personal bias which was maintained consistently throughout his observing career. For the nine observers in the period 1861-83, the range of career means was as much as 4.8 arc s for the vertical diameter and 2.2 arc s for the horizontal diameter.

Generally, such personality effects would be expected to increase the scatter in the results, as happens for the data after World War II when as many as 14 observers, most with little or no previous experience, made measurements. The period from the introduction of the impersonal micrometer to 1940 shows a decrease of  $\sim 0.02$  arc s  $\text{yr}^{-1}$  in the mean horizontal semi-diameter. During this time there were seven regular observers, five of whom reported self-consistent annual means with no apparent trends. The other two observers exhibited strong, erratic personal biases, as shown in Fig. 2. As the number of observations made by these two individuals increased through the early 1920s, so the resultant mean diameter based on all the observers decreased, giving a spurious trend.

The observational reports from Greenwich show that weather and seeing conditions were often far from ideal with many comments such as 'through cloud', 'unsteady', 'ill defined', 'poor image', 'limbs boiling', 'definition extremely bad', and so on.

**Fig. 3** Apparent changes in the semi-diameter of the Sun (arc s) deduced from transits of Mercury ( $\bullet$ ) and total solar eclipses ( $\circ$ ). The zero point corresponds to 959.63 arc s. The half-bar lengths are the standard deviations of the distributions, the standard errors of the means lie in the range  $\pm 0.1$  to  $\pm 0.2$  arc s. The dashed line was deduced by Eddy and Boornazian<sup>2</sup> from horizontal meridian circle observations in the period 1836-1953 and has been adjusted for irradiation.





These grave difficulties show that meridian circle observations are unsuitable for investigating possible changes in the solar diameter. We now discuss other, more accurate methods which have the advantage of covering a longer time span and are not so dependent on the defects of the instrument used.

## Transits of Mercury

Observations of the time taken for the planet Mercury to transit across the face of the Sun provide one of the most accurate methods of detecting long-term changes in the solar diameter. These observations are spread over some 300 yr. Due to the particular geometry of the orbits of the Earth and Mercury, transits occur only in May or November, and there are ~14 in a century. The maximum duration of a central transit in May is ~8 h and in November it is ~6 h. Thus, if the instants at which Mercury seemed to touch the rim of the Sun were timed to a precision of 1 s, the resolution obtained for the solar diameter would be ~0.1 arcs. However, due to the observational difficulty of discerning when Mercury first touches the limb of the Sun, the standard deviation of the observations of each transit are typically in the range 0.5–1.0 arc s. It is also necessary to restrict observations to timings of the first and last instants (contacts 2 and 3) at which Mercury appears completely inside the limb of the Sun; these internal contacts are more definite than the external ones.

Over 2,000 timings of the internal contacts of 30 transits of Mercury spread over the past 250 yr have been used in this analysis. The observations of these transits have been collected by Morrison and Ward<sup>12,13</sup> mainly to determine fluctuations in the Earth's rate of rotation and the relativistic advance in the perihelion of Mercury's orbit. When allowance has been made for these and other orbital parameters (see solution 2, Table III of ref. 13), the angular separation between the centres of the Sun and Mercury, calculated from the observed times of internal contact, should be equal to the difference of their semi-diameters.

The residual angular separation for each observation has been calculated using values of 959.63 and 3.37 arcs for the semi-diameters of the Sun and Mercury at unit distance. The means and standard deviations of the distributions of the residuals for 30 of the transits in the period 1723 to 1973 are plotted in Fig. 3 where they are compared with the meridian circle trend claimed by Eddy and Boornazian<sup>2</sup>. To make this comparison we have subtracted 1.55 arcs from the meridian circle observations, this being the generally accepted value used to account for the somewhat arbitrary effect of irradiation<sup>14</sup>.

The results from the transits shown in Fig. 3 are at variance with the change in the semi-diameter claimed by Eddy and Boornazian between 1836 and 1953 and rule out any extrapolation of this trend to other epochs. A linear regression analysis of the Mercury transits produces a secular trend of  $-0.14 \pm 0.08$  arcs per century in the solar semi-diameter, broadly agreeing with Shapiro<sup>15</sup>, who reported a decrease of less

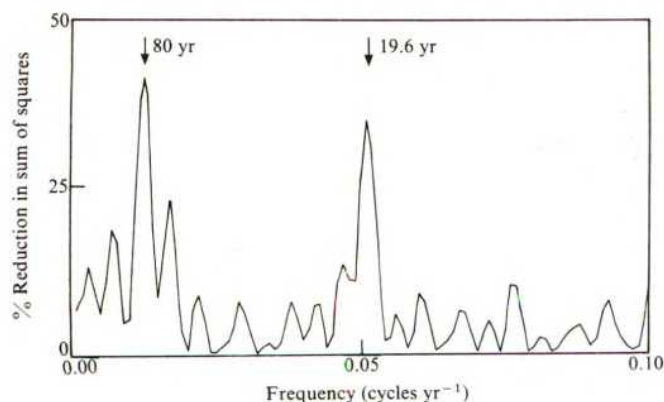


Fig. 4 Spectrum of the apparent changes in the semi-diameter deduced from transits of Mercury shown in Fig. 3.

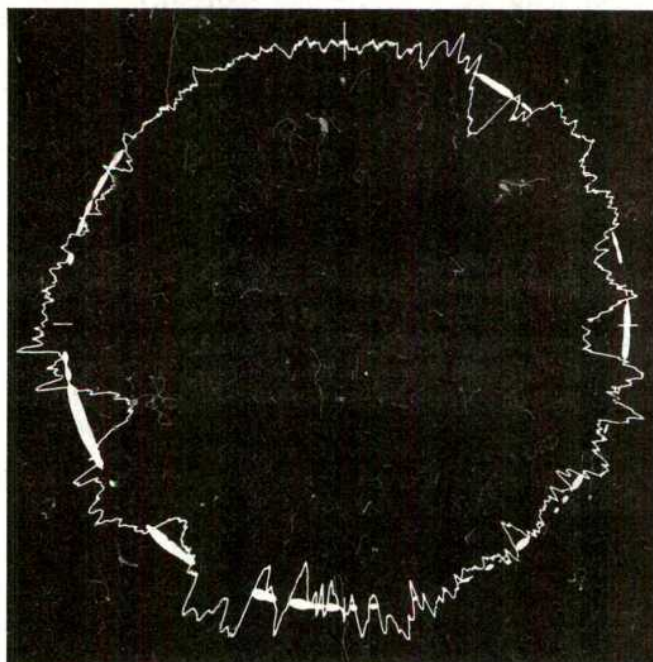


Fig. 5 An enlargement of a frame from J. H. Mathers' 16-mm cine film of the solar eclipse of 20 May 1966 taken on the island of Lesbos in Greece. The jagged outline of the Moon, exaggerated by a factor of 60, is shown superimposed on the frame. Baily's beads can be seen in the lunar depressions.

than 0.15 arcs per century with >90% confidence from a smaller set of Mercury transit observations.

We have also examined the data for possible periodic changes using a least-squares frequency analysis. Sine curves were fitted to the data by least squares and the percentage reduction in the sum of the squares is shown in Fig. 4. There are significant peaks at 80 yr and 19.6 yr. Removal of one of these sinusoids from the data reduces the other to the level of the noise. One is therefore the alias of the other, and is caused by the particular spacing of the transits. Because the 80-yr peak is the higher of the two, it is more likely to be the basic causal period, but we cannot be certain of this<sup>16</sup>.

The amplitude, phase and standard errors of the 80-yr sinusoid were found to be given by:

$$\begin{aligned} \text{change in semi-diameter (arc 2)} = \\ 0.24(\pm 0.08) \sin 2\pi[(t-1700)/80 + 0.43(\pm 0.04)] \end{aligned}$$

where  $t$  is the year of the observation.

## Total solar eclipses

The observed durations of total solar eclipses, typically a few minutes, present an alternative method of detecting possible long-term changes in the solar diameter. The timing of such a duration to a precision of 1 s would give a measure of the Sun's semi-diameter to an accuracy of ~0.2 arcs assuming that the profile of the Moon were known accurately. In practice observations need to be restricted to the timing of the interval between the disappearance of the last and the reappearance of the first beads of light, which are seen at the irregular edge of the Moon at the beginning and end of total eclipses.

The edge of the solar photosphere is extremely well defined and eclipse observers have shown that, until the last bead of light shining down one of the depressions on the lunar limb has disappeared, then totality has not yet started. Perhaps the best test is the internal consistency of timings of totality by independent observers, which is typically a few seconds of time. Although the absolute times of the contacts might well be in error, only the duration of totality is important in determining the diameter and even in the early eighteenth century it was possible to time such durations to within a second or two by counting the beats of a pendulum clock.



In our investigation of solar eclipses, we have used visual observations of the durations of the total eclipses of 1715, 1842, 1851, 1878, 1900 and 1925. We have also analysed photographs of the eclipse of 1966, which was intermediate between total and annular.

After Halley<sup>17</sup> had carefully organized timings of the 1715 eclipse, there are no comparable timings until 1842. From then until 1925, eclipses were chosen that were reasonably uniformly spaced in time and also the individual reports are fairly easily accessible. References are too numerous to cite here. After 1925 only scattered timings are available and we have accordingly ended our investigation of such material at that date.

In analysing these eclipse observations we have adopted the values of 959.63 and 932.58 arc s for the solar and lunar semi-diameters at mean distance and applied lunar limb profile corrections for each individual observation<sup>18</sup>, the errors of which are unlikely to exceed 0.2 arc s at any point. Many of the observations were made quite close to the central line of the shadow path, where the duration was greatest. We have rejected all observations for which the duration was less than ~1 min because the location would be very close to either of the edges of the zone of totality. In these circumstances it becomes difficult to identify exactly which depressions on the Moon's limb permit the appearance of the last and first beads of light. The results of this analysis are plotted in Fig. 3 alongside the Mercury transit data. For each eclipse, the mean correction to the Sun's semi-diameter and the standard deviation of the individual observations is shown.

During the eclipse of 20 May 1966, Mathers took a 16-mm cine film of the central phase from the island of Lesbos in Greece. From this point in the path of the eclipse, the calculated solar semi-diameter was only 0.07 arc s greater than that of the Moon. Mathers positioned himself almost exactly on the central line and at the time of maximum eclipse the Sun was seen to be

reduced to a broken circle of light composed of ~50 individual beads (see Fig. 5). On the eight frames nearest to the time of greatest phase we have been able to identify each bead of light with a depression of the lunar limb as plotted by Duncombe<sup>18</sup>. From a consideration of the visibility of the various beads, we deduce a correction of  $-0.22 \pm 0.20$  arc s to the adopted semi-diameter of the Sun. This provides a valuable additional point on Fig. 3.

Figure 3 shows that, in general, the accuracy of the eclipse results is similar to that of the Mercury transit data. If we include the eclipses with the transits in a linear regression analysis, the secular trend in the semi-diameter reduces to  $-0.08 \pm 0.07$  arc s per century. This corresponds to a change of  $-0.008 \pm 0.007\%$  per century, well over an order of magnitude smaller than the rate claimed by Eddy and Boornazian.

## Conclusion

The combined data sets of the Mercury transit and total solar eclipse observations, which cover a much longer time span than the material used by Eddy and Boornazian, demonstrate that there has been no detectable secular change in the solar diameter over the past 250 yr or so. However, there is some evidence that periodic changes of about 0.02% on a time scale of 80 yr may have occurred. The findings of Eddy and Boornazian are the result of instrumental and observational defects rather than real changes, hence the problem of the missing solar neutrinos still remains.

We thank Mr J. H. Mathers for use of his unique eclipse film. *Note added in proof:* In a recent preprint by Dunham *et al.*<sup>19</sup> they deduce, from observations made near the limits of the total eclipses of 1715 and 1976–79, that the Sun's semi-diameter decreased by  $0.34 \pm 0.2$  arc s in this interval. Their result depends critically on the interpretation put on the only observation made near the northern limit of the 1715 eclipse.

9. Dunkin, E. *Mon. Not. R. astr. Soc.* **35**, 91–97 (1874).
10. Thackeray, W. G. *Mon. Not. R. astr. Soc.* **45**, 389–399, 464, 467–469 (1885).
11. Cullen, R. T. *Mon. Not. R. astr. Soc.* **86**, 344–349 (1926).
12. Morrison, L. V. & Ward, C. G. *R. Gr. Obs. Bull. No.* 181 (1975).
13. Morrison, L. V. & Ward, C. G. *Mon. Not. R. astr. Soc.* **173**, 183–206 (1975).
14. *Explanatory Supplement to the Astronomical Ephemeris*, 103 (HMSO, London, 1961).
15. Shapiro, I. I. *Science* **208**, 51–52 (1980).
16. Lomb, N. R. *Astrophys. Space Sci.* **39**, 447–462 (1976).
17. Halley, E. *Phil. Trans. R. Soc.* **29**, 245–262 (1715).
18. Duncombe, J. S. *U.S. Naval Obs. Circ. No.* 141 (1973).
19. Dunham, D. W. *et al. Science* (submitted).

Received 30 June; accepted 15 October 1980.

1. Bahcall, J. N. *Space Sci. Rev.* **24**, 227–251 (1979).
2. Eddy, J. A. & Boornazian, A. A. *Bull. Am. astr. Soc.* **11**, 437 (1979); *Sci. News* **115**, 420 (1979); *Phys. Today* **35**, 17 (1979).
3. Gething, T. J. D. *Mon. Not. R. astr. Soc.* **115**, 558–570 (1955).
4. Gianuzzi, M. A. *Mem. Soc. astr. Ital.* **24**, No. 3 (1953).
5. Howse, D. *Greenwich Observatory Vol.* 3, 43–48 (Taylor & Francis, London, 1975).
6. *Mon. Not. R. astr. Soc.* **12**, 97 (1852).
7. *Mon. Not. R. astr. Soc.* **15**, 122–123 (1855).
8. Wittichell, W. M. *Occ. Not. R. astr. Soc.* **14**, 147–159 (1952).

# Angiogenesis *in vitro*

Judah Folkman\* & Christian Haudenschild

The Department of Surgery, Children's Hospital Medical Center and The Harvard Medical School and The Mallory Institute of Pathology, Boston, Massachusetts 02115

*Cloned capillary endothelial cells, cultured in tumour-conditioned medium, form capillary tubes. By light and electron microscopy these tubes resemble capillaries in vivo. This first demonstration of angiogenesis in vitro: (1) shows that all the information necessary to develop an entire capillary network in vitro is expressed by one cell type; (2) suggests a mechanism for lumen formation; and (3) offers a possibility of distinguishing between direct and indirect angiogenesis factors.*

MOST, if not all, solid tumours are capable of continuously inducing the proliferation of new capillary blood vessels from the host vascular bed. There is accumulating evidence that this property, angiogenesis, is important for the progressive growth of solid tumours<sup>1–3</sup>. Previous studies have described the growth and regression of new capillaries *in vivo*<sup>4,5</sup> but there is little understanding of how a capillary grows. It is not known how a lumen develops in a capillary sprout, how branches arise, or how

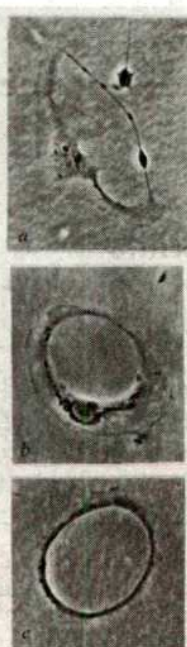
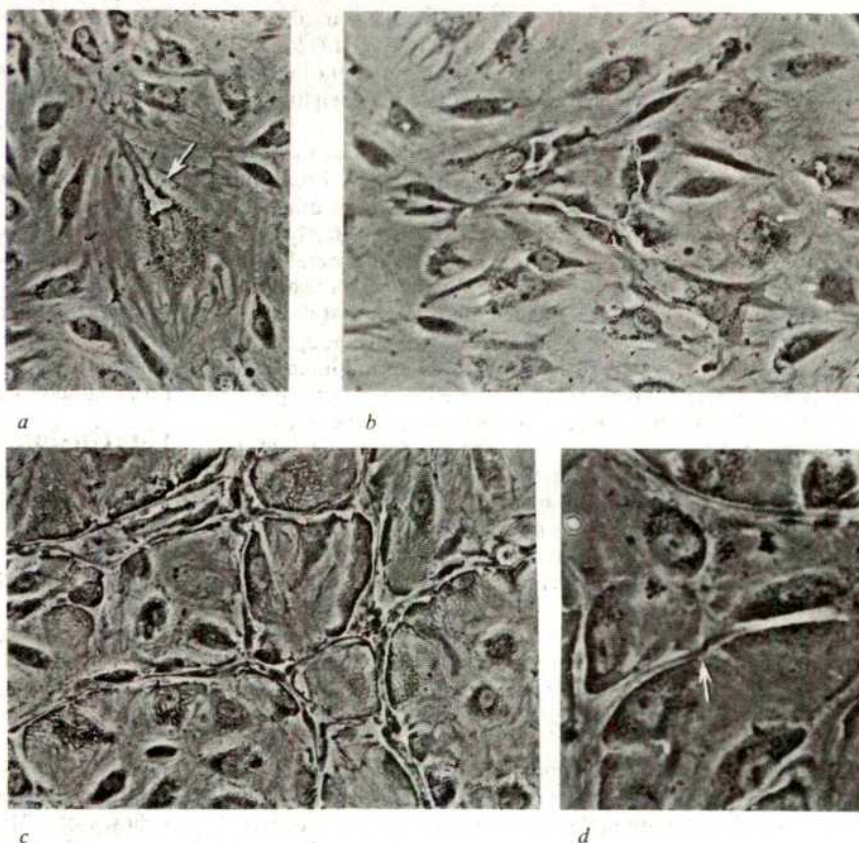
anastomoses are made between one capillary loop and another. Until now, angiogenesis could be studied only in animal models<sup>6,7</sup> or in the chick embryo<sup>8</sup>. Lack of an *in vitro* model has made the investigation of angiogenesis as difficult as the study of blood coagulation would be without *in vitro* methods.

In a previous report, bovine capillary endothelial cells were cloned, and bovine and human capillary endothelial cells were carried in long-term culture<sup>9</sup>. We show here that in appropriate conditions, these capillary endothelial cells will form tubular networks *in vitro* which are almost identical, by light and electron microscopy, to capillary vascular beds *in vivo*.

\* Present address: Children's Hospital Medical Center, 300 Longwood Avenue, Boston, Massachusetts 02115.



**Fig. 1** Human capillary endothelial cells forming 'capillary' tubes (phase contrast). *a*, A cylindrical 'keyhole' vacuole (arrow) is the first evidence of tube formation. Capillary endothelial cells from Sertoli-Leydig ovarian tumour in a 16-yr-old girl. Third passage.  $\times 115$ . *b*, Same field 3 days later showing tubes that traverse the entire length of some cells, and connect with tubes of neighbouring cells.  $\times 115$ . *c*, Network of tubes formed by capillary endothelial cells from human foreskin. Tubes began to form 1 month after the primary cells were plated.  $\times 115$ . *d*, The junction of the capillary tube of one cell with another (arrow). String-like material within the lumen ('mandril') traverses the anastomosis between the two cells.  $\times 230$ . Capillary endothelial cells were isolated as described elsewhere<sup>9</sup> except that 0.75% collagenase (Worthington type II) with 0.5% bovine serum albumin (BSA) was used for digestion of tissue. Human capillary endothelial cells were grown in tumour-conditioned medium<sup>9</sup> mixed 1:1 with aortic-conditioned medium, 15% human serum and endothelial cell growth supplement (ECGS)  $5.4 \text{ mg ml}^{-1}$  (Collaborative Research). Aortic-conditioned medium was obtained from cloned bovine aortic endothelial cells grown to confluence in T-75 flasks. Dulbecco's minimal essential medium (MEM) with 10% calf serum was changed every 48 h, centrifuged (2,000 r.p.m. for 10 min), passed through a Millipore filter ( $0.22 \mu\text{m}$ ), and stored at  $-30^\circ\text{C}$ . It was thawed and centrifuged immediately before use (A growth factor has been derived from aortic endothelial cells by Gajdusek *et al.*<sup>11</sup>). Human serum was heat-inactivated at  $56^\circ\text{C}$  for 30 min before use. It was convenient to make up the media before use in 50-ml polyethylene tubes (35 ml tumour-conditioned medium, 35 ml aortic-conditioned medium, 11.5 ml human serum and 15 mg ECGS). Unused media were stored at  $4^\circ\text{C}$  for a few days. Cultures were re-fed every 48 h. Bovine capillary cells will form capillaries optimally in a mixture of 60 ml tumour-conditioned medium + 30 ml aortic-conditioned medium + 10% calf serum and 15 mg ECGS. Occasionally bovine cells will form capillaries in tumour-conditioned medium mixed 1:1 with alpha MEM or with Dulbecco's MEM with 10% calf serum (especially late passage cells). Both bovine and human cells survive freezing in dimethyl sulphoxide (DMSO) and will form capillaries after thawing. Bovine cells have been carried in culture for up to 9 months and human cells for up to 5 months. During early passage, human capillary cells must pass at high density. When Falcon (3001) plates were used (for easier weeding of non-endothelial cells<sup>9</sup>) the capillary cells were plated into a glass cloning ring (6 mm i.d.) placed in the centre of the dish.



**Fig. 2** Ring formation by single capillary endothelial cells (phase contrast). Human foreskin capillary endothelial cells without any neighbours, but stimulated by tumour-conditioned medium, seem unable to form a tube in three dimensions. Instead, they move cytoplasmic extensions along the bottom of the culture dish, until the tips of these extensions join to form a flat, two-dimensional 'ring'. *a*, *b* and *c* show different stages of this process.  $\times 230$ .

### Isolation and culture of capillary endothelial cells

Capillary segments were isolated from bovine adrenal cortex, human foreskin, human spleen, an ovarian tumour, a neuroblastoma and a rhabdomyoma of the heart as described elsewhere<sup>9</sup> (except for the modifications described in Fig. 1 legend). The amount of starting tissue need not be more than 0.1–0.5 g. Experience has shown that even a small tumour biopsy yields capillary segments in culture provided the biopsy is taken from the vascular, non-necrotic portion of the tumour. The capillary segments were cultured in tumour-conditioned medium on gelatin-coated plates<sup>9</sup>. The bovine cells were cloned, whereas endothelial cells from other tissues, also derived from a single capillary segment (2–4 capillary endothelial cells), were not cloned.

The evidence that these cultured cells are capillary endothelial cells, detailed elsewhere<sup>9,10</sup>, is as follows: (1) each culture is initiated from one capillary segment of ~2–4 capillary endothelial cells. With experience, it is possible to distinguish capillary segments from arterioles or venules. (2) The capillary endothelial cells of different organs from the same animal and from different species seem to be almost identical by phase-microscopy. (3) Both human and bovine capillary endothelial cells contain factor VIII antigens<sup>9</sup>. (4) Cultured capillary endothelial cells have a similar ultrastructure to the capillary endothelial cells of their organ of origin: human cells contain Weibel-Palade bodies—bovine cells do not. (5) Both human and bovine capillary endothelial cells form 'rings' when they are in sparse culture (Fig. 2). (6) Early passage bovine capillary endothelial cells, and human capillary endothelial cells at any passage



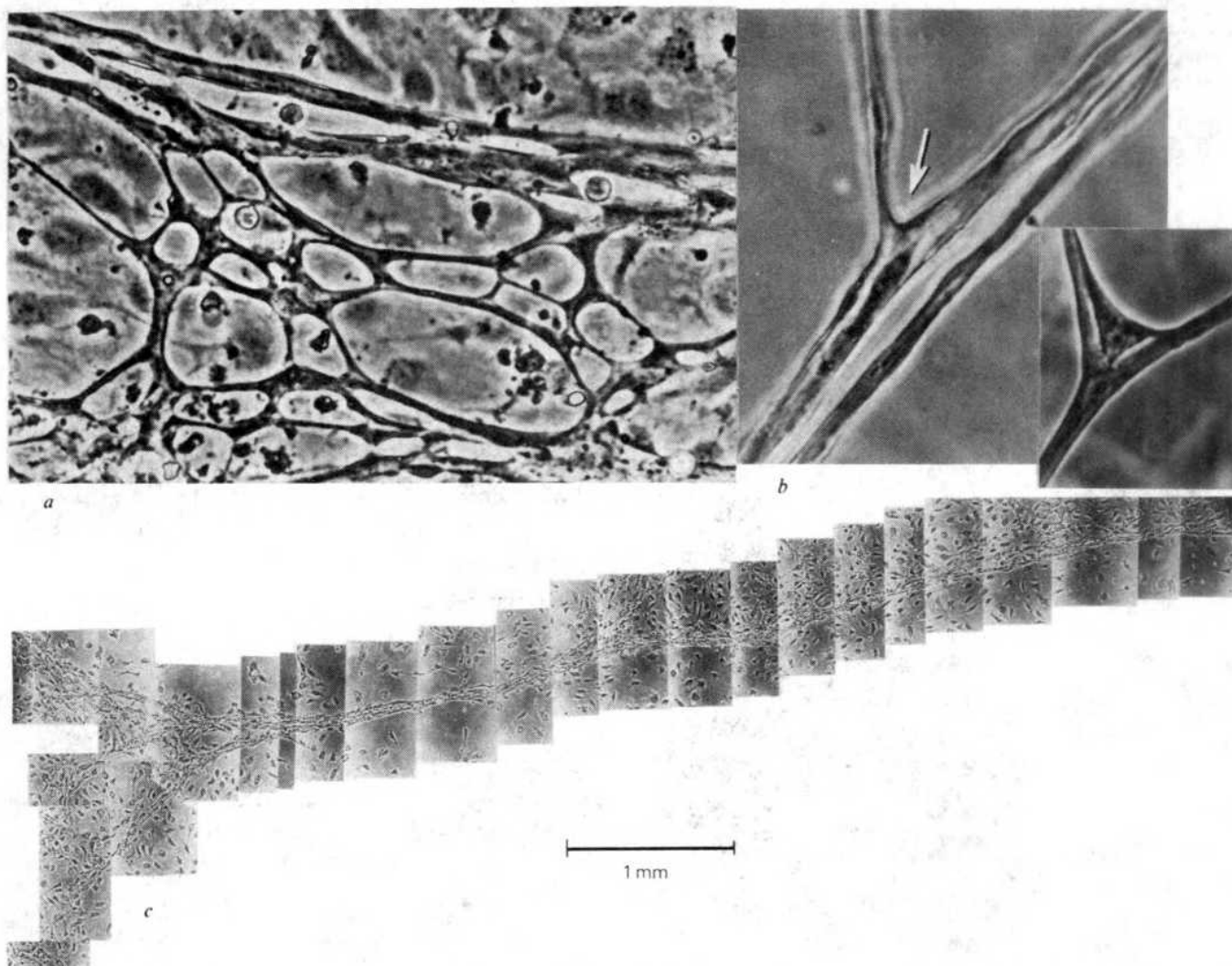
require conditioned medium, and grow best in tumour-conditioned medium. However, endothelial cells from aorta and umbilical vein do not require conditioned medium for growth<sup>9</sup>. (7) Capillary endothelial cells increase their rate of migration in a dose-dependent manner when increasing concentrations of tumour-conditioned medium or tumour-derived factors are added<sup>10</sup>. In contrast, the migration of aortic endothelium is not affected by tumour-conditioned medium. (8) Capillary endothelial cells have a special matrix requirement (for example, gelatin<sup>9</sup> or collagen<sup>11</sup>) for their survival.

### Development of capillary tubes *in vitro* and the origin of branches

When the endothelial cells of a single human capillary are allowed to proliferate, they form a small colony which enlarges gradually. When the colony reaches 3–5 mm, the centre approaches confluence. In ~50% of the cultures, capillary tubes begin to form in the middle zone of the colony, between the deeply confluent centre and the sub-confluent periphery. In

primary cultures of most human and bovine capillary cells, the earliest appearance of tubes is 20 days and the latest, 40 days. Capillary endothelial cells from a rhabdomyoma formed tubes 10 days after the primary culture was started. However, once tubes have formed in the primary culture, they appear earlier in subsequent passages. In the fourth passage, tubes developed in 5–10 days.

The first evidence of tube formation is the appearance (by phase contrast) of a cylindrical vacuole within an endothelial cell, which resembles a 'keyhole' (Fig. 1a). After 48 h, contiguous cells develop similar vacuoles which form a long tube connecting one cell to another (Fig. 1b). These tubes do not arise from cleavage planes between cells, but in fact traverse the cytoplasm, or the nucleus, so that the nucleus sometimes seems to be split into two parts (Fig. 1d). Electron micrographs taken at these locations always show a single nucleus which has a portion close to the lumen deformed into a thin plate positioned either at the bottom or the roof of the tube. Branches begin to appear after four or five cells have become connected, and within 5–10 days an entire network of tubes replaces the dense regions of the colony (Fig. 1c).



**Fig. 3** Organization of a second layer of capillary tubes on the dorsal surface of the original monolayer of capillary endothelial cells (phase contrast). *a*, A network of tubes began to form in the original monolayer of these 11th-passage bovine capillary endothelial cells, after 2 weeks in the same plate. A branch that was directed out of the plane of the substratum led to the formation of a second layer of tubes. This photograph shows only the second layer in focus. The first cell layer (lying directly on the gelatin) is out of focus.  $\times 115$ . *b*, Branches formed *in vitro* by capillary endothelial cells derived from human foreskin. Note the position of the endothelial cell (arrow) that lies at the intersection of two limbs. Inset shows another branch bridged by the endothelial cell from which the branch was formed. These tubes formed in a second layer of capillary endothelial cells after they had been plated into the microwells of a gelatinized Cuprak dish. Monolayers formed in the wells that contained more than one cell. When tubes appeared in these monolayers, many branches were directed out of the plane of the substratum, presumably because of the curvature of the wells. The first layer is not visible here because it is out of focus. *c*, A capillary tube, 7.5 mm long, that grew *in vitro* from fourth-passage capillary endothelial cells from human foreskin.



A branch in the tubular network always originates within a single cell. Before a branch appears, the cylindrical vacuole within a cell forms a 'Y' or a 'T', each arm of which then aligns with the vacuole of another cell. An entire capillary network develops in this way. After a branch has matured, the original endothelial cell can usually be found at the intersection of three tubes (Fig. 3b). Occasionally, a branch will be directed out of the plane of the substratum—then a second layer of capillaries organizes on the dorsal surface of the cells that were originally plated. This three-dimensional growth results in a capillary network of multiple layers (Fig. 3a, c).

### Remodelling and regression of capillary tubes

Time-lapse, phase contrast pictures (2 frames per min) taken continuously for 1 week, showed that established tubes undergo remodelling. New branches appear and others are contracted into the parent vessel within a period as short as 12 h. Once a tube has formed by the alignment of 5–10 endothelial cells, it presents a thin, phase-dense lining. The endothelial cells that embrace it also migrate along the tube and out to the tips of its branches. Tumour-conditioned medium has been shown to cause a 500% increase in migration of capillary endothelial cells *in vitro*<sup>10</sup>. Remodelling seems to be carried out primarily by migratory activity of capillary endothelial cells and not by mitosis. Furthermore, when cultures were incubated with <sup>3</sup>H-thymidine ( $4 \mu\text{Ci ml}^{-1}$  for 48 h), endothelial cells lining the tubes were not labelled, but those at the periphery of the colony were.

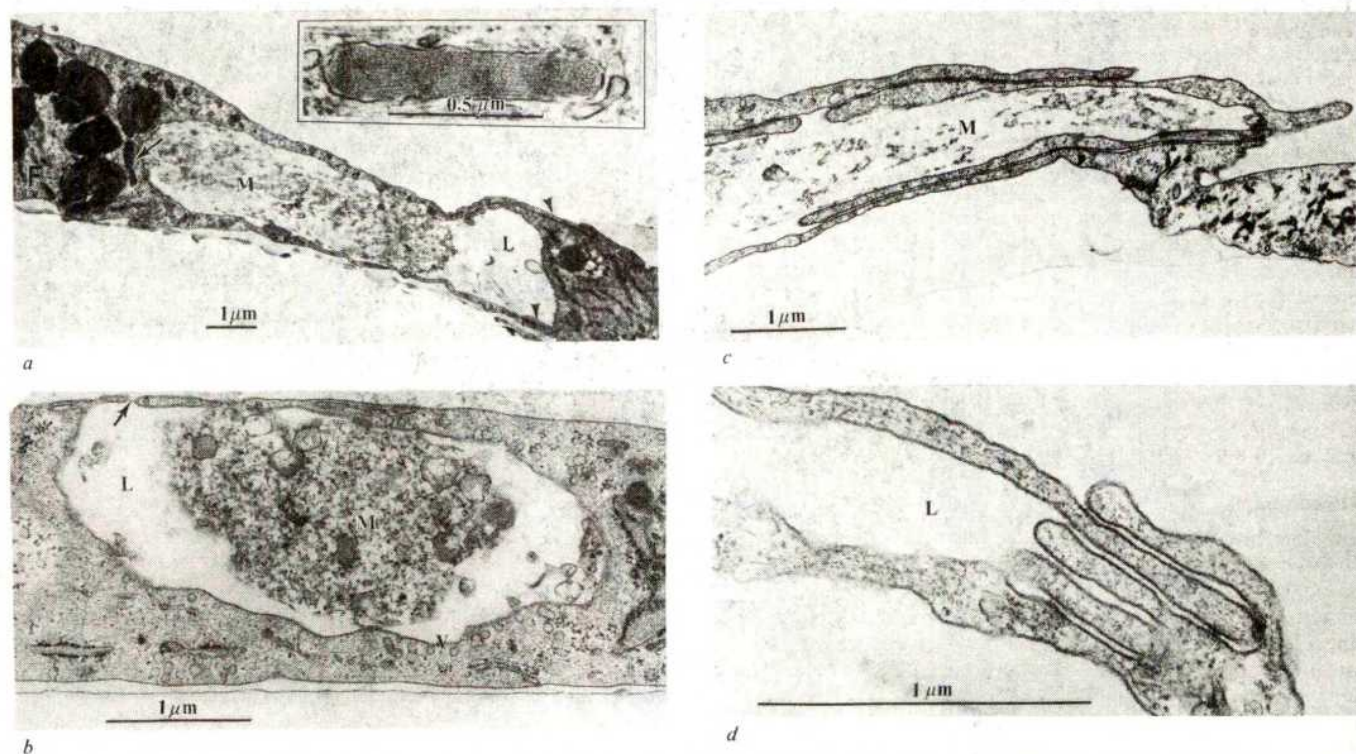
When the cells in a capillary network were trypsinized and re-plated, new capillary tubes formed. There was no obvious difference between the capillary networks formed by capillary endothelial cells isolated from normal or malignant human tissue.

### Ultrastructure of capillary tube formation

Transmission electron micrographs taken perpendicular and parallel to the plane of the culture dish prove that these aligned, phase-optically transparent structures are continuous lumina bordered by cell cytoplasm and membranes (plasmalemma), and that they form a network of tubes (Fig. 4a). The origin of a tube seems to be a true vacuole surrounded by one uninterrupted membrane (Fig. 4b). Later, the vacuole seems to become an extracellular tube surrounded by an extremely thin wall of cytoplasm of the endothelial cell. The tubular wall of one cell will connect to the tubular wall of another cell (Fig. 4c, d). Although we have been unable to observe the exact transition from an intracellular vacuole of one cell to an intercellular tube girdled by several cells, we have seen intermediate stages. For example, at one stage, the initially intracellular vacuole opens to form two cytoplasmic sheets (Fig. 5a) which are capable of joining with similar cytoplasmic extensions of a neighbouring cell, or with themselves (Fig. 5b). At these connections the structure resembles a junctional complex. (However, freeze-fracture and other studies to characterize these junctions formed *in vitro*, remain to be done).

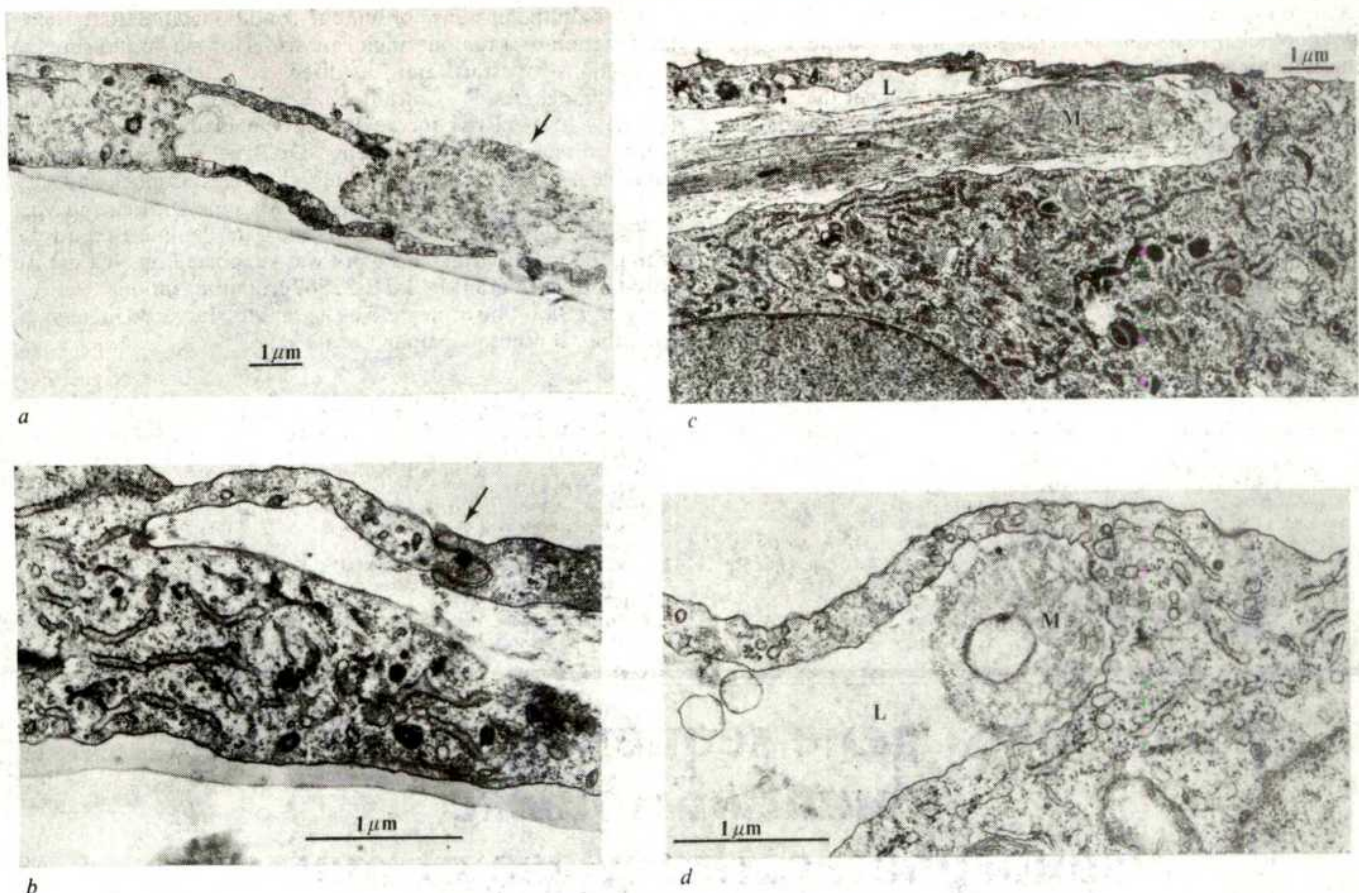
Early in their development, the tubes are filled with a partially fibrillar, partially membranous and amorphous material of undetermined nature that apparently originates from the endothelial cells (Fig. 5c). In some areas, this material resembles basement membrane, and is also found outside the lumen in direct contact with the gelatin substratum. This material may serve as a guide or 'mandril' for the alignment of tubes from cell to cell. Later the material apparently dissolves, or is cleared from the lumen in some other way (Fig. 5a), because the tubes become hollow as the capillary network matures (Fig. 5d).

To control for the possibility that the tumour-conditioned medium and the gelatin-coated plates might induce tube



**Fig. 4** Transmission electron micrographs of capillary formation. *a*, Micrograph taken in a plane perpendicular to that of the culture dish, showing the formation of a tube by human capillary endothelium. Note the amorphous and fibrillar material (M) within the lumen (L), the Weibel-Palade body (arrow), some myelinated figures (F) and the junction between the two cells (arrowheads). Insert shows higher magnification of Weibel-Palade body from another tube-forming human capillary endothelial cell. *b*, Earliest phase of tube formation within one cultured capillary endothelial cell derived from bovine adrenal. The micrograph is taken in a plane perpendicular to the culture dish and demonstrates the thin cytoplasmic plate which covers the lumen (L) and which shows structures resembling fenestrations (arrow). Note the intraluminal material (M) and the pinocytotic vesicles (V). *c*, Thin cytoplasmic plates surround the lumen of a tube formed *in vitro* by capillary endothelial cells derived from human foreskin. The intraluminal material (M) is disappearing. Micrograph taken in a plane perpendicular to the culture dish. *d*, Junctional complex formed *in vitro* by two capillary endothelial cells derived from an ovarian (Sertoli-Leydig) tumour. The lumen (L) is empty. Micrograph taken in a plane perpendicular to the dish.





**Fig. 5** Transmission electron micrographs of capillary formation. *a*, Section (perpendicular to the plane of the culture dish) of a human capillary endothelial cell showing two cytoplasmic extensions at the open end of a tube partially filled with extracellular material (arrow). *b*, Human capillary endothelial cell (cross-section perpendicular to the plane of the dish). A cytoplasmic extension forms a connection resembling a junctional complex (arrow) with another cytoplasmic extension from the same cell. *c*, Micrograph taken parallel to the plane of the culture dish, showing lumen (L) beginning to form within one capillary endothelial cell derived from human foreskin. Note the fibrillar nature of the intraluminal material (M) appearing like a 'mandril' within the lumen. N, nucleus. *d*, Lumen formation by human capillary cells derived from an ovarian tumour. Note the increased number of pinocytotic vesicles in the vicinity of the sparse material (M) remaining in the lumen (L).

formation by other cells, the following non-capillary cells were cultured in the same conditions that caused tube formation by human and bovine capillary endothelial cells—human foreskin fibroblasts obtained during the isolation of endothelial cells from foreskin were cultured for 4 months. Primary cultures of human kidney epithelium and umbilical vein endothelium were maintained for 4 months and human chondrocytes for 2 months. Also, WI-38 cells, BALB/c 3T3 fibroblasts, MDCK canine kidney cells and bovine aortic endothelial cells were cultured for up to 4 months. No tubes formed in any of these cultures.

## Discussion

Our experiments show that all the information necessary to construct a 'capillary' tube, make branches and assemble an entire 'capillary' network *in vitro* can be expressed by a single cell type, the capillary endothelial cell. Other cell types are unnecessary. Therefore, mast cells and pericytes so frequently associated with capillaries *in vivo*, may have functions other than the formation and remodelling of the lumen. The unexpected finding is that cultured cells can be induced to mould into a tissue by themselves building a complex three-dimensional matrix. A further implication is that blood flow and hydrostatic pressure are not required for the organization of a vascular bed.

A general mechanism of microvascular lumen formation is suggested by the formation of an autolytic vacuole within a capillary endothelial cell, the conversion of this vacuole to a tube, the connection of one tube to another, the girdling of the tube by capillary endothelial cells that form special junctions with themselves and with each other and the ability of these cells to glide along the tube once it has formed. If these *in vitro*

observations are a valid model for growing capillaries *in vivo*, our understanding of how capillaries regenerate in wounds, proliferate at the edge of a tumour or arise from blood islands in the embryo may be enhanced.

We do not know why capillaries take so long to appear in primary cultures. One possibility is that gelatin is not the optimum substratum and the cultured capillary endothelial cells must lay down their own matrix<sup>12,13</sup>. In addition, selection may be occurring, because capillary tubes arise earlier after passage of the endothelial cells. It is highly probable that the culture medium is not optimal. The medium used in this study was found empirically after several years of failure to grow capillary endothelium. Once we observed the first tube formation, the composition of the medium was not varied. The nature of the contents of the early vacuoles, the fibrils within the 'mandril', and the mechanisms of the removal of the material from within the tubes are unknown.

These experiments do not imply that only capillary endothelial cells are the source of new capillaries. We have limited our primary cultures to capillary segments. It is well known, however, that *in vivo* new capillaries arise from venules as well as from other capillaries.

This is the first report of angiogenesis *in vitro*. Because a variety of angiogenesis factors have been reported, based on *in vivo* assays<sup>8,14-20</sup>, it will become critical to be able to distinguish between an indirect and a direct angiogenesis factor. By indirect, we mean compounds (for example formic acid and silica) that have in common the ability to attract macrophages or other white cells which might subsequently secrete a direct angiogenesis factor<sup>18,19</sup>. An indirect angiogenesis factor would be



unable to induce capillary formation *in vitro*, where only capillary endothelial cells were present. By contrast, a direct angiogenesis factor should be capable of inducing angiogenesis *in vivo* or *in vitro* independently of other cell types. As yet there is no way to make this distinction. In the future, capillary endothelial cell cultures may be used to discriminate between indirect and direct angiogenesis factors. Furthermore, this approach may be used to screen for angiogenesis inhibitors.

A better understanding of angiogenesis in general, and tumour angiogenesis in particular, will be achieved if the various components of this phenomenon can be studied *in vitro*. At least one new concept is immediately apparent. If capillary endothelial cells have the capacity to generate a whole capillary

network (in the presence of tumour-conditioned medium) then the function of a tumour angiogenesis factor may be to supply instructions for 'start' and for 'direction' of capillary growth.

We thank Drs R. Cotran, N. LeDouran, G. Majno, A. Pardee and R. Ross for reviewing the manuscript and for helpful discussion and comments, Dr Bruce Zetter for many valuable discussions, Mrs C. Butterfield, Ms N. Connell and Mr A. Wallstrom for technical assistance, Ms Jane Dittrich and Mr Carl Cobb for editorial assistance and Mrs Pauline Breen for typing the manuscript. This work was supported by NCI grant R01-CA14019, grant R01-HL23567 from the National Heart, Lung and Blood Institute, and by a grant to Harvard University from the Monsanto Company.

Received 22 July; accepted 15 October 1980.

1. Gimbrone, M. A. Jr, Leapman, S. B., Cotran, R. S. & Folkman, J. *J. exp. Med.* **136**, 261–276 (1972).
2. Folkman, J. *Ann. intern. Med.* **82**, 96–100 (1975).
3. Folkman, J. & Cotran, R. S. *Int. Rev. exp. Path.* **16**, 207–248 (1976).
4. Ausprunk, D. H. & Folkman, J. *Microvasc. Res.* **14**, 53–65 (1977).
5. Ausprunk, D. H., Falterman, K. & Folkman, J. *Lab. Invest.* **38**, 284–294 (1978).
6. Folkman, J., Merler, E., Abernathy, C. & Williams, G. *J. exp. Med.* **133**, 275–288 (1971).
7. Gimbrone, M. A. Jr, Cotran, R. S., Leapman, S. B. & Folkman, J. *J. natn. Cancer Inst.* **52**, 413–427 (1974).
8. Klagsbrun, M., Knighton, D. & Folkman, J. *Cancer Res.* **36**, 110–114 (1976).
9. Folkman, J., Haudenschild, C. C. & Zetter, B. R. *Proc. natn. Acad. Sci. U.S.A.* **76**, 5217–5221 (1979).

10. Zetter, B. R. *Nature* **285**, 41–43 (1980).
11. Gajdusek, C., Dicorlet, P. & Ross, R. *J. Cell. Biol.* **85**, 467–472 (1980).
12. Howard, B. V., Macarak, E. J., Gunson, D. & Kefalides, N. A. *Proc. natn. Acad. Sci. U.S.A.* **73**, 2361–2364 (1976).
13. Birdwell, C. R., Gospodarowicz, D. & Nicolson, G. L. *Proc. natn. Acad. Sci. U.S.A.* **7**, 3273–3277 (1978).
14. Brown, R. A., Weiss, J. B. & Tomlinson, I. W. *Lancet* **i**, 682–685 (1980).
15. Fenselau, A. & Mello, R. J. *Cancer Res.* **36**, 3269–3273 (1976).
16. Fenselau, A. *et al. Fedn Proc.* **39**, 1615 (1980).
17. Ryan, T. J. *Br. J. Derm.* **82**, Suppl. 5, 99–111 (1970).
18. Polverini, P. J., Cotran, R. S., Gimbrone, M. A. Jr & Unanue, E. R. *Nature* **269**, 804–806 (1977).
19. Auerbach, R. & Sidky, Y. A. *J. Immun.* **123**, 751–754 (1979).
20. Schor, A. M., Schor, S. L. & Kumar, S. *Br. J. Cancer* **40**, 302 (1978).

# Chloroplast gene sequence for the large subunit of ribulose biphosphatocarboxylase of maize

Lee McIntosh, Carsten Poulsen & Lawrence Bogorad

The Biological Laboratories, Harvard University, Cambridge, Massachusetts 02138

*The chloroplast gene coding for the large subunit of ribulose 1,5-biphosphatocarboxylase in Zea mays has been sequenced. It contains neither a 'classical' prokaryotic promoter sequence nor its proposed eukaryotic counterpart but does have a typical prokaryotic ribosome binding site close to the site at which translation is initiated. Almost all possible codons occur and are translated by the 'universal code' rather than by the variation of it found in mitochondria.*

THE enzyme ribulose biphosphatocarboxylase (RuBPCase) fixes CO<sub>2</sub> in plants and is the most abundant soluble leaf protein; it is also thought to be the most abundant protein on earth<sup>1</sup>. It is an aggregate of eight identical 12,000–14,000 molecular weight (MW) 'small' subunits together with eight identical 'large' subunits (LS) of 50,000–55,000 MW (ref. 2). The small subunit of RuBPCase is inherited biparentally in *Nicotiana* and thus appears to be coded for by a nuclear gene<sup>3</sup> which, in peas, is found among the population of unique or low copy sequences of the nuclear genome<sup>4</sup>. The large subunit, however, is encoded by chloroplast DNA for not only is it inherited maternally in *Nicotiana*<sup>5</sup> but it can also be physically mapped on chloroplast DNA in *Zea mays*<sup>6–8</sup> and in *Chlamydomonas reinhardtii*<sup>9</sup>. This distribution of the genes for the two subunits of RuBPCase between the nuclear and chloroplast genomes is an example of the widespread phenomenon of the dispersal of genes for the components of multimeric proteins of subcellular organelles<sup>10</sup>.

We report here the complete DNA sequence of the gene for the LS of *Z. mays* RuBPCase contained in a fragment of the chloroplast genome that has been cloned in *Escherichia coli*<sup>6–8</sup> and mapped on the cloned fragment<sup>7,8</sup>. The transcribed portion of the DNA sequence has some features in common with genes of other groups of organisms but overall is unique. The codons used for translation of LS mRNA include most of those possible, which has led us to consider the kinds of tRNA genes that may be found in the maize chloroplast chromosome. Furthermore, the amino acid sequence deduced from the DNA sequence has been compared and aligned with amino acid sequences obtained

earlier for some cyanogen bromide (CNBr) fragments of barley LS<sup>11</sup> and with sequences of tryptic peptides of the spinach enzyme, believed to be in or near the catalytic sites<sup>12</sup>. Stretches of the deduced amino acid sequence of maize LS are remarkably similar to the known amino acid sequences in the barley and spinach polypeptides, with the putative catalytic sites widely separated along the polypeptide.

## Features of DNA sequence for LS RuBPCase mRNA

A physical map of the maize chloroplast DNA fragment that includes the structural gene for the LS of RuBPCase is shown in Fig. 1 together with the strategy used for sequencing the region complementary to the LS mRNA. The nucleotide sequence is shown in Fig. 2.

The 5' terminus of LS mRNA was previously estimated to be complementary to the DNA for about 40 nucleotides upstream from a mapped *EcoRI* restriction site<sup>8</sup> (nucleotide –34 to –29 in Fig. 2). We have now placed the terminus more precisely using a modification<sup>13</sup> of the Berk–Sharp technique<sup>14</sup>. The 5' terminus of the transcript was previously mapped within a 196-base pair *EcoRI* fragment that is part of a larger 480-base pair *HinfI* fragment (Fig. 1). This fragment was isolated and labelled with <sup>32</sup>P at its 5' ends by polynucleotide kinase<sup>15</sup> and then digested with *HincII* endonuclease. The resulting radioactive 443-base pair *HinfI/HincII* fragment was purified by polyacrylamide gel electrophoresis and used for DNA:RNA hybridization and DNA sequencing (Fig. 3).

The radioactive segment recovered from the hybrid should represent the DNA protected from  $S_1$ -nuclease digestion by hybridization with LS mRNA. Determination of its length should establish the precise beginning of the LS transcript. Protected fragments of 219, 220, 224 and 225 bases were detected as a set of two bands. This places the 5' end of the LS mRNA 59 to 63 nucleotides from the start of the codon for the N-terminal methionine residue (nucleotide 1 in Fig. 2). Removal of a 3'-terminal phosphate by the  $S_1$  nuclease increases the electrophoretic mobility of the fragment by about 1/2 base in relation to the sequence ladder<sup>13</sup>.

Five nucleotides upstream from the N-terminal methionine codon on the LS mRNA is the sequence 5'-GGAGG-3' that is complementary to a sequence at the 3' terminus of maize chloroplast 16S rRNA<sup>16</sup>. A sequence identical with the latter is found at the 3' terminus of 16S rRNA in *E. coli* and a complementary sequence is generally found on bacterial mRNAs, about three to seven nucleotides upstream from the initiator codon. The suggestion by Shine and Dalgarno<sup>17</sup> that this complementary mRNA sequence is a translation signal was later confirmed by identification of hybrids between mRNA and sequences at the 3' terminus of 16S rRNA<sup>18</sup>. The entire 'Shine and Dalgarno' nine-nucleotide sequence of *E. coli* 16S rRNA is present in maize chloroplast 16S rRNA but only seven of the nine nucleotides at positions 5-13 upstream from the initiator codon on the LS mRNA are complementary to the maize chloroplast 16S rRNA Shine-Dalgarno sequence (Fig. 2). Another partially complementary sequence has been detected on a different maize chloroplast DNA fragment upstream of a putative translation start site for an unidentified polypeptide. (Z. Schwarz, A. Steinmetz and L. Bogorad, unpublished). Partially complementary sequences have also been seen in the *cro* gene (5'-A-A-G-G-A-G-G-3'), the *O* gene (5'-A-G-G-A-G-3') and in the *CII* gene (5'-A-A-G-G-A-3') of  $\lambda$  phage<sup>19</sup>.

### Amino acid sequence of maize LS RuBPCase

The amino acid sequence deduced from the nucleotide sequence of the structural region of the LS gene is shown in Fig. 2. The polypeptide comprises 475 amino acid residues and has a molecular weight of 52,682. This number of residues is lower than previously estimated from electrophoretic and amino acid analyses of LS of RuBPCase from species other than maize.<sup>20</sup>

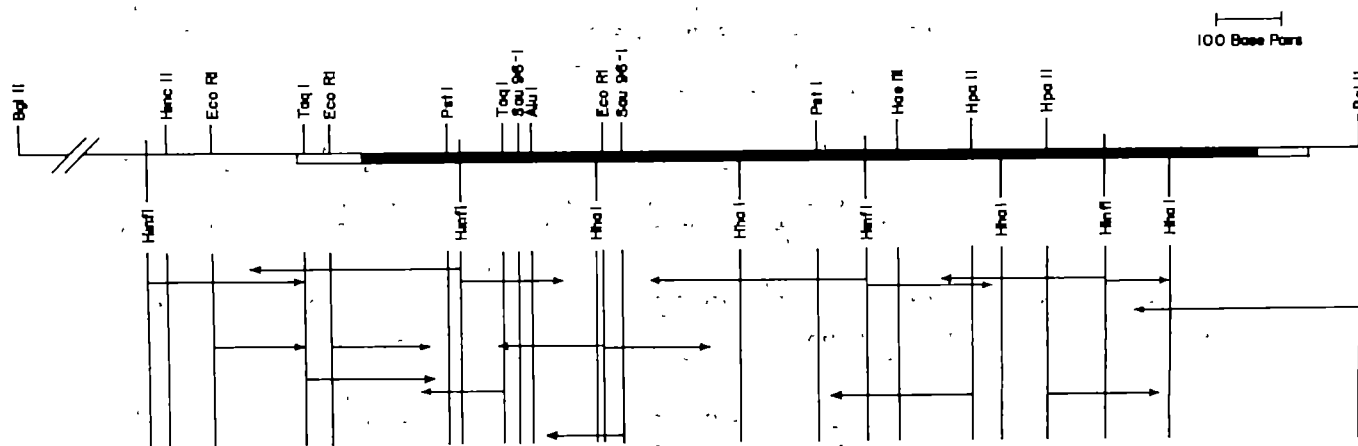
The availability of the DNA sequence for the maize LS RuBPCase gene has permitted the alignment of amino acid sequences totalling 244 residues known for fragments of the barley and spinach LS polypeptides<sup>11,12</sup> with the predicted maize LS sequence (Fig. 2). There are few differences. Seven positions in the maize sequences have amino acid replacements due to single nucleotide substitutions and five of these (positions 36,

43, 282, 394 and 460) must be considered neutral replacements. The proline residues at positions 46 and 415 in the barley LS primary structure are replaced by leucine and histidine respectively. The application of methods for secondary-structure prediction<sup>21</sup> to these domains in the sequences suggest that they are not likely to have any drastic effect on secondary structure. The eighth difference, at amino acid residue 215, may be the result of an error in identification of that residue in the barley polypeptide.

Compared with the barley polypeptide<sup>20</sup>, the maize LS mRNA seems to contain a sequence for 14 amino acid residues that extends beyond the N-terminus of the barley LS sequence. This difference could be due to variation in the DNA sequences, but it seems more likely that the difference is an artefact. After SDS polyacrylamide gel electrophoresis of fragments produced by CNBr-cleavage of the large subunits from maize and from rapidly isolated barley RuBPCase, we found N-terminal fragments of identical size (MW 14,000–15,000, data not shown). The N-terminal alanine, which has previously been reported for the LS of barley<sup>11</sup>, was not found among the CNBr-fragments of either maize or barley. The N-terminal amino acid could not be identified for intact maize or barley LS polypeptides, which suggests that these are blocked, possibly by N-formyl-methionine. N-terminal blocking has now been observed for large subunits from a number of species<sup>11</sup>. It is possible that the 14 N-terminal residues of the barley LS are removed by an endo-protease present in the barley leaf extracts during the slower large-scale preparations of the enzyme<sup>11</sup>.

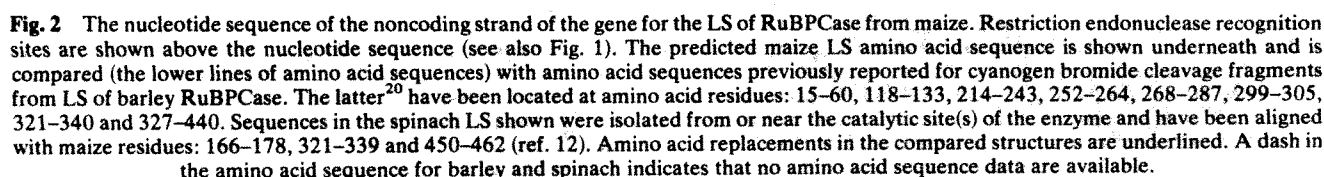
The amino acid sequences of spinach LS that have been proposed to be in or near the catalytic site of RuBPCase<sup>12</sup> are widely separated along the maize polypeptide, corresponding to positions 166-178, 321-340 and 450-462, and are well conserved. The only exceptions are neutral replacements at positions 330 and 460. Note that nine histidines are clustered among residues 268-327 and that this is just on the N-terminal side of one of the proposed catalytic site sequences. Four of these histidines are found in two His-Ile-His sequences (292-294 and 325-327). Whether any of the clustered imidazole groups are used for chelation of  $Mg^{2+}$ , which is required for enzyme activity, is not known. Note also that many lysine, arginine and cysteine residues are in the middle of the sequence and close to the C-terminus. Some side chains of these residues are thought to have important roles in binding to, or acting on, the substrates<sup>12,21,22</sup>. The positions in which they have been found might be close to the three proposed catalytic site sequences.

The complete amino acid sequence deduced for the maize LS polypeptide clarifies some ambiguities in previously published data<sup>20</sup> on the amino acid sequence of the barley LS: (1) An



**Fig. 1** Fine restriction endonuclease map and the strategy followed for sequencing the maize-chloroplast DNA sequence containing the gene for LS RuBPCase. The recombinant plasmid pZmc 3711 is comprised of a 2.7-kilobase pair maize chloroplast DNA fragment bearing the LS gene<sup>7</sup> incorporated into resistance plasmid RSF 1030 (ref. 8). The double-lined region indicates the boundaries of the mature LS transcript and the solid rectangle within represents the amino acid coding part of the sequence. The sequencing strategy is indicated by the arrows which originate from specific endonuclease restriction sites that were labelled at their 5' ends with [ $\gamma$ -<sup>32</sup>P]ATP. DNA sequence determination, end labelling and electrophoresis were according to the procedures of Maxam and Gilbert.<sup>15</sup>





amino acid sequence corresponding to residues 118–113 has previously been reported as arising from the barley small subunit<sup>23</sup> but the absence of a similar sequence from the spinach small subunit<sup>24</sup> and the presence of this sequence in the maize LS primary structure indicate that it was a contaminant from the large subunit. (2) An undecapeptide corresponding to amino acid positions 310–320 of maize LS was not detected on isolation of CNBr-fragments from the barley LS although the two surrounding CNBr fragments were found<sup>20</sup>. Failure to identify this undecapeptide in the course of the work on the barley enzyme might have confused the conclusions drawn from the sequencing of the peptide fragment 298–309. Although differences at one or two positions cannot be excluded, it seems likely that the two sequences are similar in this region. (3) The size of the fragment 252–267 was earlier over-estimated<sup>20</sup> due to abnormal chromatographic behaviour and the presence of a larger contaminating peptide. (4) The extra tryptophan thought to be present in the sequence 368–383 of the LS in barley<sup>20</sup> seems to be absent. (5) The assignment of isoleucine instead of tryptophan to a position in the barley LS corresponding to residue 215 in the maize LS does not comply with the simple nucleotide substitution patterns observed for the eight replacements described above. However, phenylthiohydantoin derivatives of isoleucine and tryptophan may have been confused in the HPLC system used for their identification<sup>23</sup>. Tryptophan has been detected in the sequence 214–243 in a Trp-Arg peptide after tryptic digestion of the corresponding barley CNBr fragment<sup>20</sup>. Because no other tryptophans in this sequence can be deduced from the nucleotide sequence, tryptophan is the most likely residue at this position in the barley LS.

The major difference in the amino acid sequence seems to be that between the C-termini of the barley and maize large subunits—the barley LS showed Leu-Ala-Val-COOH as C-terminal residues. This sequence cannot be obtained from the maize LS C-terminus by nucleotide sequencing. It is possible that this discrepancy is an artefact of the same type as described for the N-terminus and further study of the barley LS gene may clarify this.

### Codon usage in the LS gene

Figure 4 shows the frequency with which amino acid codons are used in the synthesis of the LS of maize RuBPCase. All 20 amino acids are used and all codons except for three which may be used in other chloroplast genes. There is a strong bias towards having adenine and thymine bases in the third position of the codons used. In the maize LS gene 178 thymine, 145 adenine, 78 cytosine and 75 guanine bases occur in the third position of the codon. These distributions are similar to those found for codon usage in the human mitochondrial gene for cytochrome oxidase subunit II<sup>25</sup>. However, we did not find the stop codon, UGA, used for tryptophan as it is in the mRNA for cytochrome oxidase II from human<sup>25</sup> and yeast mitochondria<sup>26</sup>.

The use of almost all codons possible in the LS mRNA seems to be inconsistent with earlier results for the number of tRNA genes in maize chloroplasts. Saturation-hybridization studies conducted with maize cpDNA and chloroplast tRNAs gave an estimate of 20–26 tRNA genes on the maize chloroplast chromosome<sup>27</sup>. Similar types of hybridization experiments have given estimates of 18–25 chloroplast tRNA genes for *Euglena*<sup>28</sup> and 30–40 tRNA genes for pea<sup>29</sup>.

Recently these hybridization data have been complemented by separation of chloroplast 4S RNAs in two-dimensional gel electrophoresis and identification of the individual tRNAs by charging them using *E. coli* and chloroplast aminoacyl tRNA synthetases<sup>30,31</sup>. Maize chloroplast tRNAs separated in this manner yielded approximately 28 spots of which 25 were charged by 17 amino acids.

If, as predicted by the LS gene, almost all codons were used, a minimum of 32 tRNAs are required if the G–U wobble hypothesis is followed<sup>32</sup>. This is inconsistent with the saturation-hybridization data<sup>27</sup> but the conditions in those experiments may not have favoured hybridization of all the tRNAs. In



**Fig. 3** Localization of the 5' terminus of the LS mRNA on the coding strand of the LS gene. This experiment was carried out using a modification of the method of Berk and Sharp<sup>14</sup>. A <sup>32</sup>P 5'-terminally labelled DNA fragment was denatured and hybridized with RNA samples, digested with S<sub>1</sub> nuclease, and the length of the protected fragment was measured by polyacrylamide gel electrophoresis in 8.3 M urea. Total maize chloroplast RNA was obtained from isolated chloroplasts<sup>8</sup>. The DNA probe was a 443 base pair *HinfI/HincII* DNA fragment (see Fig. 1) with the 5' end labelled at the *HinfI* restriction endonuclease site, that is, on the coding strand of DNA for the LS gene. The *HinfI/HincII* fragment was denatured at 65 °C in flame-sealed 10-μl siliconized glass capillary pipettes. The 10-μl hybridization mixture was composed of 80% w/v deionized formamide, 0.4 M NaCl, 0.04 M PIPES (pH 6.4), 1 mM EDTA, 20–50 ng DNA probe and 30 μg of total chloroplast RNA<sup>8,14</sup>. Digestion was carried out with 20 units of S<sub>1</sub> nuclease in a total volume of 110 μl of dilution buffer (0.25 M NaCl, 0.02 M NaOAc, 1 mM ZnSO<sub>4</sub>, 20 μg ml<sup>-1</sup> freshly denatured calf thymus DNA) for 20 min at 40 °C. The S<sub>1</sub>-resistant material was precipitated with ethanol and resuspended in 80% formamide, 50 mM Tris-borate (pH 8.3), 1 mM EDTA, and electrophoresed on 6% polyacrylamide 8.3 M urea gels. Results are shown in the autoradiograph. The sample in lane a was probe DNA treated with S<sub>1</sub> nuclease in the absence of chloroplast RNA—the only DNA band seen is a residual amount of double-stranded (therefore S<sub>1</sub> nuclease resistant) probe. The DNA used in lane c was subjected to hybridization incubation without RNA. It was not treated with S<sub>1</sub> nuclease. The DNA in lane b was from the reaction mixture in which RNA was present during hybridization incubation and treatment. Two wide bands are seen representing four DNA fragments protected from digestion by hybridization with LS mRNA. Their sizes and positions in the DNA sequence were determined by comparison with the G-reaction for the original DNA fragment, shown in lane d.



|              |     | Second letter |     |    |       |    |      |    |   |
|--------------|-----|---------------|-----|----|-------|----|------|----|---|
| First letter |     | U             |     | C  |       | A  |      | G  |   |
|              |     |               |     |    |       |    |      |    |   |
| U            | Phe | 12            | Ser | 6  | Tyr   | 9  | Cys  | 6  | U |
|              | Phe | 9             | Ser | 4  | Tyr   | 8  | Cys  | 5  | C |
|              | Leu | 11            | Ser | 5  | ochre | 1  | opal | 0  | A |
|              | Leu | 12            | Ser | 1  | amber | 0  | Trp  | 8  | G |
| C            | Leu | 5             | Pro | 6  | His   | 11 | Arg  | 11 | U |
|              | Leu | 1             | Pro | 2  | His   | 4  | Arg  | 9  | C |
|              | Leu | 7             | Pro | 9  | Gln   | 11 | Arg  | 3  | A |
|              | Leu | 1             | Pro | 4  | Gln   | 2  | Arg  | 0  | G |
| A            | Ile | 11            | Thr | 17 | Asn   | 6  | Ser  | 3  | U |
|              | Ile | 9             | Thr | 7  | Asn   | 7  | Ser  | 0  | C |
|              | Ile | 4             | Thr | 6  | Lys   | 18 | Arg  | 4  | A |
|              | Met | 1 + 11        | Thr | 0  | Lys   | 8  | Arg  | 2  | G |
| G            | Val | 12            | Ala | 18 | Asp   | 24 | Gly  | 21 | U |
|              | Val | 1             | Ala | 6  | Asp   | 6  | Gly  | 1  | C |
|              | Val | 14            | Ala | 18 | Glu   | 20 | Gly  | 13 | A |
|              | Val | 3             | Ala | 5  | Glu   | 8  | Gly  | 9  | G |

**Fig. 4** Use of codons in the translation of the maize LS mRNA. All codons but three are used. The three codons not used, ACG(Thr), CGG (Arg) and AGC (Ser), may be used for other chloroplast proteins.

addition, too few tRNAs are revealed by two-dimensional separation of chargeable tRNAs<sup>31</sup>. It is possible that specific tRNAs are preferentially lost and/or degraded during isolation, that some may be present in amounts below the level of detection, or that chloroplast tRNAs may not all be chargeable with the *E. coli* tRNA aminoacyl synthetases usually used<sup>31</sup>. Another possibility is that tRNAs are superimposed on one another in two-dimensional electrophoresis. The latter has occurred in one case, where a tRNA<sup>Leu</sup> spot contains two isoacceptors (A. Steinmetz, personal communication).

There is no firm evidence that RNA is transported into higher-plant chloroplasts. It may therefore be reasonable to assume that chloroplasts contain a full complement of tRNAs, some of which have not been detected. However, it is possible that chloroplasts of some species contain only a limited set of tRNAs and use a different protein synthesizing system, or an alternative codon reading method such as the 'two out of three' system<sup>33</sup> could be used. This mechanism requires that only the first two bases be read in codon recognition and thus only 24 tRNAs be required.

## Conclusions

A number of features of transcribed and adjacent non-transcribed portions of the maize gene for LS of RuBPCase can be enumerated: (1) The two ribonucleotides at the 5' terminus of LS mRNA are most probably adenosines (AA, see Fig. 3)—other experiments (S. O. Jolly, L. McIntosh and L. Bogorad, unpublished) show that maize chloroplast DNA-dependent RNA polymerase initiates transcription *in vitro* at a position equivalent to the 5' end of the LS mRNA in the presence of the S factor described by Jolly and Bogorad<sup>34</sup>. Thus, the 5'-terminus

of LS mRNA is very likely to be at the site of initiation of transcription and is not processed. (2) The mRNA transcript carried an almost complete Shine-Dalgarno sequence a few nucleotides upstream from the translation initiation codon. Preliminary evidence (Z. Schwarz, A. Steinmetz and L. Bogorad, unpublished) indicates that at least one other mRNA in the chloroplast may carry this type of prokaryotic signal sequence. (3) It is not known whether chloroplast mRNAs are capped, as are eukaryotic and viral mRNAs<sup>35</sup>, but the LS DNA sequence shows no apparent homology to identified capping sequences<sup>36,37</sup>. Thus, unless some entirely different signal sequence is recognized by a chloroplast capping enzyme, LS mRNA is similar to prokaryotic messages in lacking a cap. (4) No DNA sequence homologous to a classical bacterial promoter<sup>38</sup> nor its presumed eukaryotic counterpart, the 'Hogness' box<sup>39</sup>, is found upstream from the transcribed portion of the maize LS gene. (5) The colinearity of LS mRNA with the DNA sequence is confirmed. (6) Almost all possible codons are used in the LS gene. (7) Analysis of the codon usage by the LS mRNA indicates that, unlike fungal<sup>26</sup> and mammalian<sup>25</sup> mitochondria, the universal genetic code is used in chloroplasts.

It is not known how many of the features listed will prove to be universal for chloroplast mRNAs although it would not be surprising if many were general. Another characteristic which may be universal is the striking conservation of amino acid sequences between the LS polypeptides of maize, barley and spinach. Only seven or eight amino acid substitutions have been detected among 228 (of 475) amino acids sequenced for LS in barley<sup>20</sup> and corresponding portions of the deduced amino acid sequence in maize. It is possible that sequence conservation of multimeric enzymes, especially those whose components are dispersed in two different genomes<sup>10</sup>, will prove to be common.

In understanding the three-dimensional structure of this polypeptide and the mechanism of its enzymatic action, it is interesting that the active site sequences are widely separated in the maize polypeptide; thus, extensive folding must be required to bring these sequences close together.

The hypothesis that chloroplasts and mitochondria evolved from prokaryotic symbionts in pro-eukaryotic cells has been well received. Evidence to support this view has been mainly the presence of 'prokaryotic features' in organelle nucleic acids and proteins and the 'retention' of presumed biochemical relics. The alternative genetic code used by mitochondria, that is, UGA coding for tryptophan<sup>25,26</sup>, and the failure to detect prokaryotic-type promoter sequences adjacent to chloroplast genes emphasize that organelles—regardless of their origin—are unique.

This research was supported in part by research grants from the USDA Competitive Research Grants Program, the NSF, and the Maria Moors Cabot Foundation of Harvard University. L.M. is a post-doctoral fellow of the Maria Moors Cabot Foundation. C.P. is a research fellow of the Department of Physiology, The Carlsberg Laboratory, Copenhagen. We are indebted to Professor D. von Wettstein of the Carlsberg Laboratory for his cooperation in this project.

Received 13 August; accepted 10 October 1980.

- Kung, S.-D. *Science* **191**, 429–434 (1976).
- Kawashima, N. & Wildman, S. G. *A. Rev. Pl. Physiol.* **21**, 325–358 (1970).
- Kawashima, N. & Wildman, S. G. *Biochim. biophys. Acta* **262**, 42–49 (1972).
- Cashmore, A. R. *Cell* **17**, 383–388 (1979).
- Chan, P. H. & Wildman, S. G. *Biochim. biophys. Acta* **277**, 677–680 (1972).
- Coen, D. M., Bedbrook, J. R., Bogorad, L. & Rich, A. *Proc. natn. Acad. Sci. U.S.A.* **74**, 5487–5491 (1977).
- Bedbrook, J. R., Coen, D. M., Beaton, A. R., Bogorad, L. & Rich, A. *J. biol. Chem.* **254**, 905–910 (1979).
- Link, G. & Bogorad, L. *Proc. natn. Acad. Sci. U.S.A.* **77**, 1832–1836 (1980).
- Malnoe, P., Rochaix, J.-D., Chua, N. H. & Spahr, P.-F. *J. molec. Biol.* **133**, 417–434 (1979).
- Bogorad, L. *Science* **188**, 891–898 (1975).
- Poulsen, C., Martin, B. & Svendsen, I. *Carlsberg Res. Commun.* **44**, 191–199 (1979).
- Hartman, F. C., Norton, I. L., Stringer, C. D. & Schloss, J. V. in *Photosynthetic Carbon Assimilation* (eds Siegelman, H. W. & Hind, G.) 245–269 (Plenum, New York, 1978).
- Moss, T. & Birnstiel, M. L. *Nucleic Acids Res.* **7**, 3733–3743 (1979).
- Berk, A. J. & Sharp, P. A. *Cell* **11**, 721–732 (1977).
- Maxam, A. & Gilbert, W. *Proc. natn. Acad. Sci. U.S.A.* **74**, 560–564 (1977).
- Schwarz, Zs. & Kossel, H. *Nature* **279**, 520–523 (1979).
- Shine, J. & Dalgarno, L. *Proc. natn. Acad. Sci. U.S.A.* **71**, 1342–1346 (1974).
- Steitz, J. A. & Jakes, K. *Proc. natn. Acad. Sci. U.S.A.* **72**, 4734–4738 (1975).
- Schwartz, E., Scherer, G., Hobom, G. & Kossel, H. *Nature* **272**, 410–414 (1978).
- Poulsen, C. *Carlsberg Res. Commun.* **44**, 163–189 (1979).
- Paech, C., McCurry, S. D., Pierce, J. & Tolbert, N. E. in *Photosynthetic Carbon Assimilation* (eds Siegelman, H. W. & Hind, G.) 227–243 (Plenum, New York, 1978).
- Sugiyama, T., Nakayama, N., Ogawa, M., Akazawa, T. & Oda, T. *Archs Biochem. Biophys.* **125**, 98–106 (1968).
- Poulsen, C., Strobaek, S. & Haslett, B. G. in *Genetics and Biogenesis of Chloroplasts and Mitochondria* (eds Bucher, Th., Neupert, W., Sebald, W. & Werner, S.) 17–24 (1976).
- Martin, P. G. Aust. *J. Pl. Physiol.* **6**, 401–408 (1979).
- Barrell, B. G., Bankier, A. T. & Drouin, J. *Nature* **282**, 180–194 (1979).
- Fox, T. D. *Proc. natn. Acad. Sci. U.S.A.* **76**, 6534–6538 (1979).
- Haff, L. A. & Bogorad, L. *Biochemistry* **15**, 4105–4109 (1976).
- McCreary, J. M. & Herschberger, C. L. *Nucleic Acids Res.* **3**, 2005–2018 (1976).
- Tewari, K. K., Kolodner, R., Chu, N. M. & Meeker, R. R. in *Nucleic Acids and Protein Synthesis in Plants* (eds Bogorad, L. & Weil, J.-H.) 15–36 (Plenum, New York, 1977).
- Driessell, A. J. *et al. Gene* **6**, 285–306 (1979).
- Mubumbila, M. *et al. Biochim. biophys. Acta* (in the press).
- Crick, F. H. J. *molec. Biol.* **19**, 548–555 (1966).
- Lagerkvist, U. *Proc. natn. Acad. Sci. U.S.A.* **75**, 1759–1762 (1978).
- Jolly, S. O. & Bogorad, L. *Proc. natn. Acad. Sci. U.S.A.* **77**, 822–826 (1980).
- Shatkin, A. J. *Cell* **9**, 645–653 (1976).
- Lai, E. C. *et al. Cell* **18**, 829–842 (1979).
- Ziff, E. B. & Evans, R. M. *Cell* **15**, 1463–1474 (1978).
- Pribnow, D. *Proc. natn. Acad. Sci. U.S.A.* **72**, 784–788 (1975).
- Busslinger, M., Portmann, Irminger, T. C. & Birnstiel, M. L. *Nucleic Acids Res.* **8**, 957–977 (1980).

# Recognition sequence of bacteriophage $\Phi$ X174 gene A protein—an initiator of DNA replication

A. D. M. van Mansfeld<sup>\*†</sup>, S. A. Langeveld<sup>\*</sup>, P. D. Baas<sup>\*†</sup>, H. S. Jansz<sup>\*†</sup>,  
G. A. van der Marel<sup>‡</sup>, G. H. Veeneman<sup>‡</sup> & J. H. van Boom<sup>‡</sup>

<sup>\*</sup> Institute of Molecular Biology and <sup>†</sup> Laboratory for Physiological Chemistry, State University of Utrecht, Utrecht, The Netherlands  
<sup>‡</sup> Department of Organic Chemistry, State University of Leiden, Leiden, The Netherlands

*Gene A protein, the initiator protein of bacteriophage  $\Phi$ X174 DNA replication, cleaves synthetic single-stranded oligodeoxyribonucleotides at the same site as the corresponding sequence at the  $\Phi$ X origin. The results identify the recognition sequence within the decamer CAACTTGATA which is cleaved next to the G residue. Further requirements for cleavage of double-stranded DNA by the gene A protein are supercoiling and an A + T-rich domain adjacent to the recognition sequence.*

THE single-stranded circular  $\Phi$ X DNA replicates via a double-stranded circular intermediate, the replicative form (RF)<sup>1</sup>.  $\Phi$ X DNA replication is initiated by the introduction of a single nick in one strand, the viral strand, of the RF DNA by the virus-coded gene A protein<sup>2</sup>. *In vivo*<sup>3</sup> and *in vitro* studies<sup>4-6</sup> have shown that this nick resides at a unique site of the  $\Phi$ X RF DNA molecule and that  $\Phi$ X DNA replication starts at this nick. Therefore, the site of the gene A protein nick in  $\Phi$ X RF DNA is the origin of DNA replication. Because only two macromolecular components—the DNA and the gene A protein—are involved, the  $\Phi$ X system is particularly favourable for studying the initiator–origin interaction at the molecular level.

Previous studies from our laboratory<sup>4</sup> have shown that the purified gene A protein nicks the viral strand of  $\Phi$ X RFI DNA,

creating a 3'OH-G residue at position 4,305 of the  $\Phi$ X DNA sequence<sup>7</sup>. After nicking, the gene A protein remains covalently bound at the 5'-end of the nick<sup>4,6,8</sup>. Further studies have shown that the RFI DNAs of the bacteriophages G4, St-1, U3, G14 and  $\alpha$ 3 are also nicked by the  $\Phi$ X gene A protein<sup>9-11</sup>. Comparison of the sequences around the nick sites in  $\Phi$ X, G4 and St-1 shows that the three phages have an uninterrupted stretch of 10 nucleotides, CAACTTGATA, in common<sup>10</sup>. This suggests that the recognition site of the  $\Phi$ X gene A protein lies within this 10-nucleotide sequence.

The present study is concerned with the further elucidation of the recognition nucleotide sequence of the  $\Phi$ X gene A protein, and used synthetic oligodeoxyribonucleotides as substrates for the purified gene A protein. This approach was suggested by the

**Table 1** Oligonucleotides obtained by partial digestion of CAACTTGATATTAATA with snake venom (a) and spleen (b) phosphodiesterase and incubation with or without gene A or A\* protein

| a<br>Length | % Of total*     |                 | b<br>Length | % Of total*           |                 |                  |
|-------------|-----------------|-----------------|-------------|-----------------------|-----------------|------------------|
|             | -Gene A protein | +Gene A protein |             | -Gene A or A* protein | +Gene A protein | +Gene A* protein |
| 16          | 7.9             | 1.5             | 16          | 25.5                  | 7.7             | 6.9              |
| 15          | 8.1             | 1.0             | 15          | 18.7                  | 12.3            | 6.3              |
| 14          | 4.2             | —               | 14          | 24.6                  | 19.3            | 7.4              |
| 13          | 2.7             | —               | 13§         | 21.3                  | 15.4            | 15.2             |
| 12          | 1.7             | —               | 12§         | 10.1                  | 6.0             | 5.7              |
| 11          | 2.9             | —               | 11          | —                     | 2.2             | 2.0              |
| 10          | 3.1             | 1.9‡            | 10          | —                     | 3.0             | 5.7              |
| 9           | 5.2             | 5.3             | 9           | —1                    | —               | —                |
| 8           | 9.0             | 9.8             | 8           | —                     | 2.3             | —                |
| 7           | 12.6            | 37.8            | 7           | —                     | 21.2            | 17.6             |
| 6           | 8.9             | 10.2            | 6           | —                     | 4.5             | 11.1             |
| 5           | 10.1            | 10.1            | 5           | —                     | 3.4             | 19.9             |
| 4           | 8.1             | 7.0             | 4           | —                     | 0.4             | 27               |
| 3           | 4.0             | 3.7             | 3           | —                     | —               | —                |
| 2           | 1.9             | 1.7             |             |                       |                 |                  |
| 1           | 9.7             | 7.2             |             |                       |                 |                  |
| 11†         | —               | 2.6             |             |                       |                 |                  |

For the incubation with the A\* protein values for a were not determined.

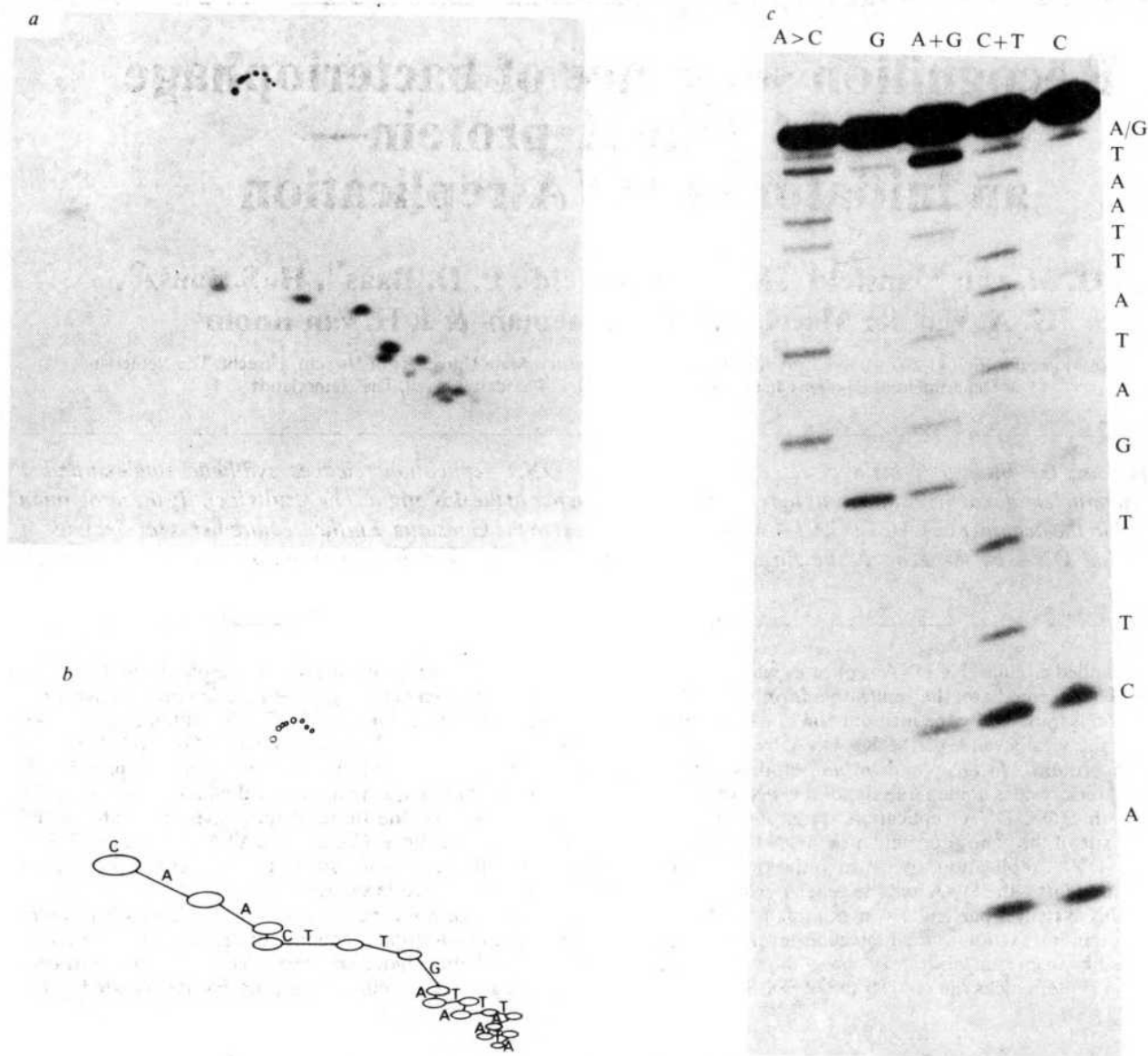
\* 100% in parts a and b is the sum of the radioactivity present in bands 1–16 and 3–16, respectively.

† This material represents unknown minor component which is also seen in Fig. 2, lane b.

‡ This value is relatively high, because an unknown minor component which is also seen in Fig. 2, lane b, also migrates at this position.

§ Although the oligonucleotides with chain lengths 13 and 12 are also degraded by incubation with the gene A protein or the A\* protein, there is no corresponding appearance of <sup>32</sup>P-labelled tetra- and trinucleotide cleavage products. The most likely explanation for this is that during incubation with spleen phosphodiesterase, some degradation from the 3' end of the hexadecamer also occurs. This yields oligonucleotides shorter than 16 residues, all of which give rise to a <sup>32</sup>P-labelled cleavage product seven residues long.





**Fig. 1** Characterization of the synthetic hexadecamer. The synthetic hexadecamer was labelled at the 5' end with radioactive phosphate according to the protocol of Maxam and Gilbert<sup>19</sup>. [ $\gamma$ - $^{32}$ P]ATP,  $\sim 2,000$  Ci mmol<sup>-1</sup>, was from the Radiochemical Centre and T4-induced polynucleotide kinase was from Boehringer Mannheim. The labelled oligonucleotide (0.18 pmol) was partially digested with snake venom phosphodiesterase (32 pg Worthington) by incubating for 1 or 20 min at 37 °C in 10 mM Tris-HCl (pH 7.5), 1 mM EDTA, 10 mM MgCl<sub>2</sub> and 5 mM dithiothreitol (DTT) in a volume of 20  $\mu$ l. The reaction was stopped by addition of 50  $\mu$ l phenol and vigorous mixing. After separating the phenol and water phase, the water phase was extracted with ether to remove residual phenol. The water phases of the different incubations (1 min and 20 min) were mixed. Aliquots (1.25  $\mu$ l) of this mixture were applied to a cellulose-acetate strip and the radioactive products were separated by electrophoresis (1st direction) and homochromatography (2nd direction) on a PEI-cellulose thin layer using a 3% 'homomix' and visualized by autoradiography as described before<sup>15</sup>. The 5'-labelled oligonucleotide was also subjected to the chemical method for sequencing DNA devised by Maxam and Gilbert<sup>18</sup>, with modifications as described recently<sup>19</sup>. The digonucleotide was treated with alkali (the so-called A > C reaction), dimethylsulphate (G), piperidinium formate (A + G), hydrazine (C + T), and hydrazine in the presence of salt (C). To obtain a higher recovery of this short DNA fragment at the ethanol precipitations, the ethanol to water ratio was raised to 4:1 (instead of 3:1). After the modifications the cleavage reactions were performed with 1 M piperidine. The samples were then lyophilized repeatedly, dissolved in 7.5  $\mu$ l 98% formamide containing 0.05% bromophenol blue (BPB) and 0.05% xylene cyanol F (XFC) and applied onto a thin (0.45 mm) 25% polyacrylamide gel containing 50 mM Tris-borate (pH 8.35), 1 mM EDTA (TBE buffer) and 7 M urea. Electrophoresis was performed at 30 W until the XCF marker had migrated 9 cm. *a*, The autoradiograph of the radioactive products separated by electrophoresis and homochromatography. *b*, The interpretation of the autoradiograph. The capitals indicate which nucleotide causes the shift of an oligonucleotide to the next longer one. *c*, The autoradiograph of the sequencing gel, aligned with the sequence deduced from the successive bands.

finding that the gene A protein nicks single-stranded  $\Phi$ X DNA only once and at exactly the same position as  $\Phi$ X RFI DNA<sup>12</sup>.

The gene A of bacteriophage  $\Phi$ X not only codes for the gene A protein (molecular weight (MW) 55,000), but also for the A\* protein (MW 37,000) which is formed from a natural internal initiator site within gene A<sup>13</sup>. The function of the A\* protein is unknown. It does not nick  $\Phi$ X RFI DNA. However, the purified A\* protein can cleave the single-stranded viral DNA of  $\Phi$ X at many different sites<sup>12</sup>. Gene A protein and A\* protein were purified as described recently<sup>14</sup>. Both proteins were available in pure form, and therefore we also tested the action of the A\* protein on the synthetic oligonucleotides.

### Characterization of the hexadecadeoxyribonucleotide

The hexadecamer CAACTTGATATTAATA was synthesized using the phosphotriester method<sup>15,16</sup>. This sequence corresponds to nucleotides 4,299–4,314 in the  $\Phi$ X DNA sequence<sup>7</sup>. It contains the gene A protein cleavage site (at the 3' side of the G residue) in  $\Phi$ X DNA and the remarkable self-complementary sequences left (CAACTTG) and right (TATTAATA) of this site. It was thought that these self-complementary structures might have a role in the recognition between the gene A protein and the DNA.



**Fig. 2** The nicking activity of the gene A protein and A\* protein on the hexadecamer and derivatives. 5'-Labelled oligonucleotide (0.045 pmol) was incubated with gene A protein (0.9 pmol) or A\* protein (0.72 pmol) in 50 mM Tris-HCl (pH 7.5), 1 mM EDTA, 10 mM MgCl<sub>2</sub>, 5 mM DTT and 150 mM NaCl for 45 min at 37 °C in a volume of 12 µl. Then 1 µl 150 mM EDTA (pH 8.0) and 1 µl of a solution of proteinase K (Merck Darmstadt), 2 mg ml<sup>-1</sup> in 1 mM Tris-HCl (pH 7.5), 0.1 mM EDTA, preincubated for 30 min at 37 °C, were added and the incubation was continued for 30 min at 37 °C. Then 15 µl 98% formamide containing 0.05% XCF and 1 µl 1% sarkosyl (Ciba-Geigy) were added, the sample was heated for 30 s at 100 °C and applied to a 25% polyacrylamide gel in TBE buffer containing 7 M urea. Electrophoresis was carried out at 35 W until the XCF marker had migrated 9 cm. Autoradiography was performed at -20 °C. Instead of the hexadecamer, the mixture of oligonucleotides, obtained by shortening the hexadecamer from the 3' end by digestion with snake venom phosphodiesterase as described in Fig. 1 legend, was used. A third series of incubations was carried out with a mixture of oligonucleotides that had been obtained by shortening the hexadecamer from the 5' end; 150 pmol hexadecamer was incubated with 7.5 µg spleen phosphodiesterase (Boehringer Mannheim) in 20 µl 10 mM Tris-HCl (pH 7.5), 1 mM EDTA for 10 min at 37 °C. Phenol was added to stop the reaction. After vigorous mixing and separation of the phenol and water phase, the water phase was extracted with ether and the oligonucleotides were labelled at their 5' end as described in Fig. 1 legend. The oligonucleotide mixture (0.05 pmol) was used in the different incubations. Lanes a, b, c: the hexadecamer incubated without (a), with gene A protein (b) or with A\* protein (c). Lanes d, e, f: the mixture of oligonucleotides obtained after partial digestion with snake venom phosphodiesterase and incubation without (d), with gene A protein (e) or with A\* protein (f). Lanes g, h, i: the mixture of oligonucleotides obtained after partial digestion with spleen phosphodiesterase and labelling at the 5' end, followed by incubation without (g), with gene A protein (h) or with A\* protein (i).

The nucleotide sequence of the synthetic DNA was confirmed using two different methods. The DNA was labelled at the 5' end with <sup>32</sup>P and partially digested with snake venom phosphodiesterase from the 3' end. The resulting oligonucleotides were separated by the standard two-dimensional system<sup>17</sup>. From the shifts in mobility of the successive radioactive products, a nucleotide sequence can be deduced (Fig. 1a, b) which is consistent with the one expected. The 5'-labelled synthetic DNA was also subjected to the chemical method for sequencing DNA<sup>18,19</sup>. Again the sequence deduced from the successive bands in the autoradiograph (Fig. 1c) is consistent with that expected. However, from the intensities of the second slowest bands in the five lanes it can be inferred that a minor part of the hexadecamer has a deoxyguanosine instead of a deoxyadenosine as the 3'-terminal building block.

### The ΦX gene A protein and A\* protein nick the hexadecamer

The 5'-<sup>32</sup>P-labelled hexadecamer was incubated with the purified ΦX gene A protein or the A\* protein. Analysis of the reaction mixtures by polyacrylamide gel electrophoresis (Fig. 2, lanes a-c) shows that the mobility of a large portion of the labelled DNA is now present at a position corresponding to an oligonucleotide with a chain length of 7. This indicates that the gene A protein as well as the A\* protein cleave the hexadecamer at the 3' side of the G residue, that is, at the same site at which gene A protein cleaves ΦX RFI DNA<sup>4</sup> as well as ΦX single-stranded DNA<sup>12</sup>. The A\* protein also cleaves ΦX single-stranded DNA at this site although other sites are also cleaved<sup>12</sup>. Some minor products with mobilities corresponding to chain lengths between 11 and 10 and between 10 and 9 nucleotides can also be observed (Fig. 2, Table 1a). We do not know how these minor products arise nor what they represent. To obtain extensive cleavage, the same high molar ratio (10-20:1) of enzyme to substrate is required as in the reaction with ΦX RFI DNA<sup>4-6,12</sup>.

### Which part of the hexadecamer is required for cleavage by gene A protein or A\* protein?

First, it was determined which nucleotides from the 3' end of the hexadecamer are dispensable for cleavage by the gene A protein or the A\* protein. Therefore, the synthetic DNA was labelled with <sup>32</sup>P at the 5' end and partially degraded by snake venom phosphodiesterase to form a mixture of oligonucleotides ranging from 1 to 16 nucleotides in length, all having the same 5' end.



This mixture was exposed to the gene A protein or the A\* protein, respectively, and the products were analysed by polyacrylamide gel electrophoresis. The results (Fig. 2) show that a clear separation of the 16 oligonucleotides is obtained (lane d, control), and that both the gene A protein (lane e) and the A\* protein (lane f) cleave the DNAs containing 16 to 10 nucleotides whereas the DNAs containing ≤9 nucleotides remain intact. The increase of DNA containing seven nucleotides (lanes e, f) indicates that cleavage occurs at the 3' side of the G residue in all oligonucleotides which are susceptible to cleavage by the gene A protein and the A\* protein, respectively. These conclusions were confirmed by the determination of Cerenkov counts in the radioactive bands of the polyacrylamide gel (Fig. 2). As shown in Table 1a, the radioactivity of the oligonucleotides with lengths of 16 to 10 nucleotides decreases after incubation with gene A protein. The only significant increase in radioactivity is observed for the oligonucleotide containing seven nucleotides. The radioactivity of the other oligonucleotides does not differ significantly after incubation with or without gene A protein.

From the results in Fig. 2 and Table 1a, we conclude that the decamer CAACTTGATA is still cleaved, next to the G residue, by the gene A protein or the A\* protein. Cleavage no longer takes place on further degradation from the 3' end, indicating that cleavage is specified by no more than the three nucleotides ATA behind the cleavage site.

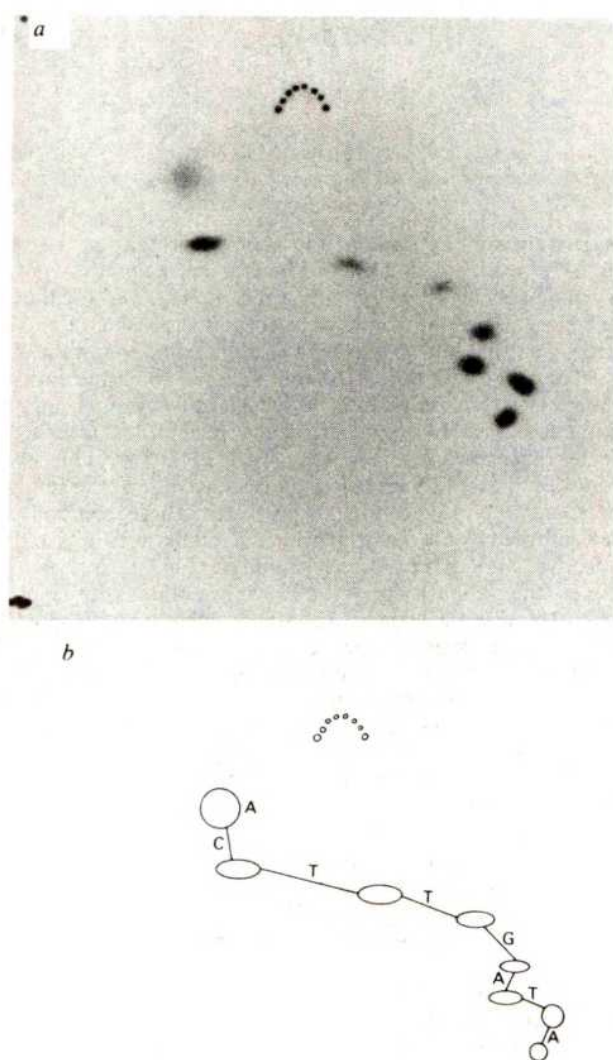
The following experiment established which nucleotides from the 5' end of the hexadecamer are dispensable for cleavage by the gene A protein or A\* protein. The synthetic DNA was degraded partially from the 5' end by incubation with spleen phosphodiesterase. In the resulting mixture the oligonucleotides have different 5' ends but the same 3' end. They were then <sup>32</sup>P-labelled at their 5' ends and incubated with gene A protein or A\* protein. The radioactive products of these reactions were analysed by electrophoresis on a polyacrylamide gel and compared with the undigested mixture of oligonucleotides



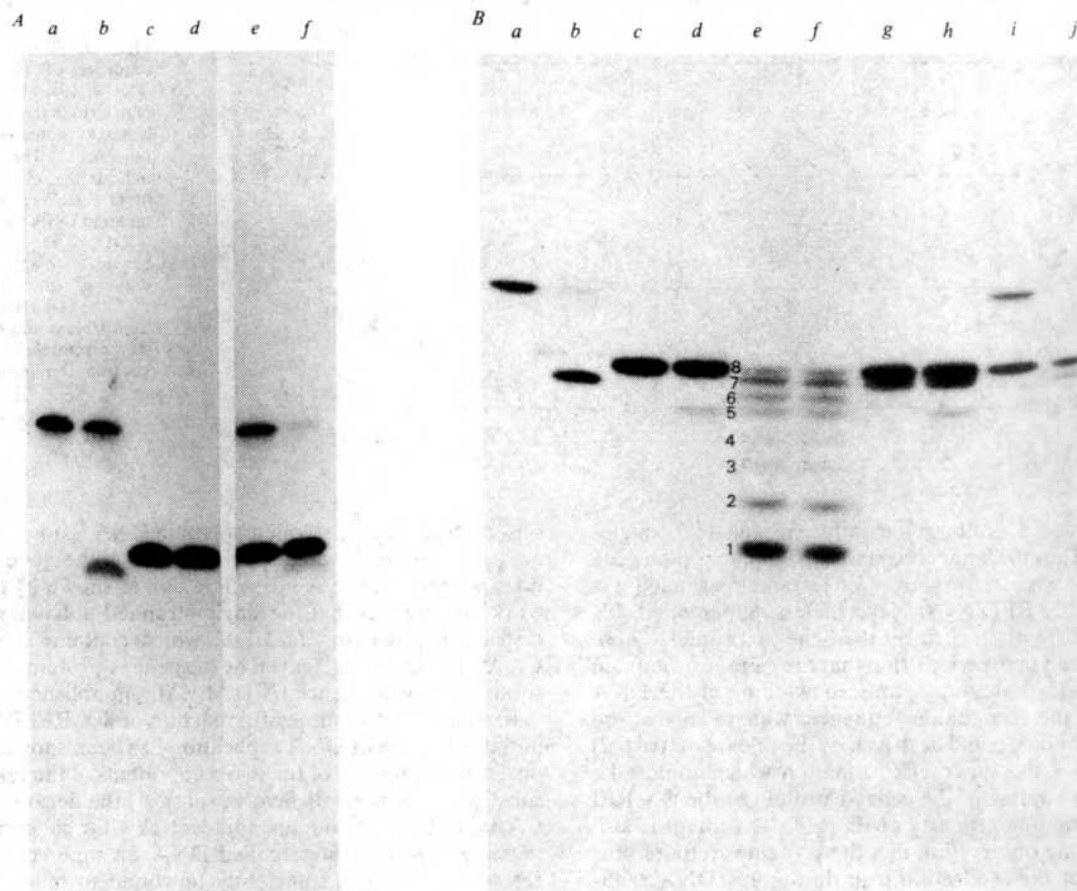
Fig. 2, lanes *g-i*). The Cerenkov radiation from the radioactive bands was determined and the relative amounts were calculated (Table 1*b*). The results show that  $^{32}\text{P}$ -labelled oligonucleotides with chain lengths of seven, six and five nucleotides are formed after incubation with the gene *A* protein or the *A\** protein (Fig. 2, lanes *g-i*). Assuming that cleavage always occurs next to the G residue, these results indicate that not only is the hexadecamer cleaved, but also the oligonucleotides which are shorter at their 5' ends by one and two nucleotides, respectively. The quantitative results (Table 1*b*) show that the oligonucleotides with 16, 15 and 14 residues are cleaved with equal efficiency by the *A\** protein. In all three cases, ~70% of the  $^{32}\text{P}$  disappears from the original position and appears at the corresponding position of the  $^{32}\text{P}$ -labelled cleavage product. However, in the reaction with the gene *A* protein, 69% of the hexadecamer disappears and is associated with the corresponding appearance of the oligonucleotide with 7 residues, whereas only 35% and 22% of the oligonucleotides with 15 and 14 residues disappear, respectively. Therefore, among the products which had been shortened from the 5' end, the hexadecamer is clearly the best substrate for the gene *A* protein. The possibility that the observed small cleavage effect on the oligonucleotides with 15 and 14 residues by the gene *A* protein is due to a slight contamination of the gene *A* protein preparation by *A\** protein has not been excluded.

The results show, however, that at least the five nucleotides ACTTG before the cleavage site, are necessary for cleavage. Together with the observation that the three nucleotides ATA after the cleavage site are indispensable, this suggests that the minimal substrate for gene *A* protein and *A\** protein is the octamer ACTTGATA.

This octamer was synthesized using the phosphotriester method<sup>15,16</sup>. It was labelled at the 5' end and the nucleotide sequence determined using the two different methods as described for the hexadecamer (Fig. 3*a-c*). The sequence deduced from both analyses is consistent with that expected: ACTTGATA. Incubation of the octamer with the gene *A* protein did not result in an altered migration of the radioactive starting material (Fig. 4*A*, lanes *c, d*). Control experiments with the hexadecamer (Fig. 4*A*, lanes *a, b*) and a mixture of the hexadecamer and the octamer (Fig. 4*A*, lanes *e, f*) clearly show that the gene *A* protein was active and cleaves the hexadecamer. Analysis after incubation of the octamer with the *A\** protein (Fig. 4*B*, lanes *c, d*) shows that the *A\** protein cleaves the octamer. The resulting product is five nucleotides long, so *A\** protein cleaves the octamer as expected, at the 3' side of the G residue. Control experiments with the hexadecamer (Fig. 4*B*, lanes *a, b*) and a mixture of the hexadecamer and the octamer (Fig. 4*B*, lanes *i, j*) show that the hexadecamer is a much better substrate for the *A\** protein than the octamer. In the mixture of



**Fig. 3** Characterization of the synthetic octamer. The synthetic octamer was labelled at the 5' end and subjected to the different sequence analyses as described for the hexadecamer in Fig. 1 legend. *a*, The autoradiograph of the radioactive products obtained by partial digestion with snake venom phosphodiesterase and separated by electrophoresis and homochromatography. *b*, The interpretation of the autoradiograph. The capitals indicate which nucleotide causes the shift of an oligonucleotide to the next longer one. *c*, The autoradiograph of the sequencing gel, aligned with the sequence deduced from the successive bands.



**Fig. 4** The nicking activity of the gene A protein and A\* protein on the octamer. 5'-Labelled octamer or hexadecamer (0.045 pmol) was incubated with gene A protein or A\* protein as described in Fig. 2 legend. The mixtures of oligonucleotides, which had been shortened from the 3' end, or the 5' end, were prepared with snake venom phosphodiesterase or spleen phosphodiesterase as described in Figs 1 and 2 legends respectively. **A**, Lanes a, b: the hexadecamer after incubation without (a) and with (b) gene A protein. Lanes c, d: the octamer after incubation without (c) and with (d) gene A protein. Lanes e, f: the mixture of the hexadecamer and the octamer after incubation without (e) and with (f) gene A protein. **B**, Lanes a, b: the hexadecamer after incubation without (a) and with (b) A\* protein. Lanes c, d: the octamer after incubation without (c) and with (d) A\* protein. Lanes e, f: the mixture of oligonucleotides after partial digestion with snake venom phosphodiesterase after incubation without (e) and with (f) A\* protein. Lanes g, h: the mixture of oligonucleotides obtained after partial digestion with spleen phosphodiesterase and labelling of the 5' end after incubation without (g) and with (h) A\* protein. Lanes i, j: the mixture of the hexadecamer and the octamer after incubation without (i) and with (j) A\* protein.

oligonucleotides obtained after partial digestion of the octamer from the 3' end with snake venom phosphodiesterase, the A\* protein did not cleave a significant amount of any of the oligonucleotides shorter than eight nucleotides (Fig. 4B, lanes e, f). The two products obtained after partial digestion with spleen phosphodiesterase and labelling of the different 5' ends show that only the octamer is cleaved, resulting in the simultaneous appearance of an oligonucleotide with a chain length of five. The heptamer is not nicked by A\* protein (Fig. 4B, lanes g, h).

## Conclusions

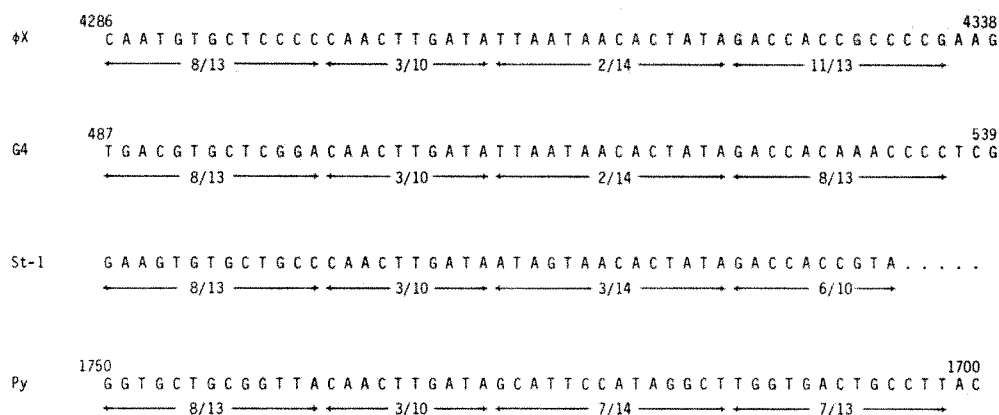
The gene A protein cleaves the synthetic hexadecamer CAACTTGATATTAATA at the 3' side of the G residue, at which site the corresponding sequences in  $\Phi$ X single-stranded DNA<sup>12</sup> and RFI DNA<sup>4</sup> are also cleaved. Stepwise degradation from the 3' end shows that the decamer CAACTTGATA is cleaved by the gene A protein with about equal efficiency to the hexadecamer (Fig. 2, Table 1a). However, elimination of two residues from the 5' end greatly reduces, although it does not completely prohibit, cleavage by the gene A protein (Fig. 2, Table 1b). This suggests that the actual recognition sequence of the gene A protein is shorter than the decamer, possibly the octamer sequence ACTTGATA. This possibility is not inconsistent with the result that the gene A protein does not cleave the synthetic octamer. Similar conclusions were reached from studies on the nuclease activity of the restriction endonucleases *EcoRI*<sup>20,21</sup>, *HpaII* and *MnoI*<sup>22</sup>, using short synthetic DNAs.

It is unlikely that sequences shorter than an octamer sequence can serve as the recognition site of the gene A protein. This conclusion is based on the fact that all possible sequences which have an uninterrupted stretch of seven nucleotides in common with the decamer CAACTTGATA occur in  $\Phi$ X DNA and M13 DNA. These viral, single-stranded DNAs are not cleaved at these sites<sup>12,23,24</sup> (CAACTTG, nucleotides 1,966–1,972 in  $\Phi$ X DNA<sup>7</sup>; AACTTGA, nucleotides 2,492–2,498 and 5,695–5,701 in M13 DNA<sup>25</sup>; ACTTGAT, nucleotides 2,493–2,499 and 5,696–5,702 in M13 DNA<sup>25</sup>; CTTGATA, nucleotides 68–74 in  $\Phi$ X DNA<sup>7</sup>).

In contrast to the gene A protein, the A\* protein cleaves the octamer ACTTGATA. This indicates that the octamer sequence represents the maximum recognition sequence of the A\* protein. The actual recognition sequence is probably less than eight, because the A\* protein has been shown to cleave single-stranded  $\Phi$ X DNA at about 30 different sites<sup>12</sup>.

The possibility that gene A protein is considered to be a nuclease which acts specifically on single-stranded DNA has already been suggested by the finding that the gene A protein nicks supercoiled  $\Phi$ X RFI DNA but not relaxed  $\Phi$ X RF DNA<sup>6,23,26</sup>. Supercoiled DNA has been shown to contain regions of local unwinding, particularly at A+T-rich regions<sup>27</sup>. Interestingly, in the RFI DNAs that are nicked by the gene A protein, the cleavage site is always located in an A+T-rich area (Fig. 5). It is thought that the gene A protein can nick these RFI DNAs, because the recognition sequence is present in a (partially) single-stranded form. However, supercoiled  $\Phi$ X RFI DNA is not nicked by the A\* protein<sup>12,14,23</sup>, indicating that its





**Fig. 5** The nucleotide sequence of the DNA of ΦX174, G4, St-1 and polyoma virus in the region of the gene A protein recognition sequence. The fractions indicate the relative amounts of G and C residues in the different DNA stretches. The ΦX DNA sequence is from Sanger *et al.*<sup>7</sup>, the G4 DNA sequence from Godson *et al.*<sup>36</sup>, the St-1 DNA sequence from Heidekamp *et al.*<sup>10</sup> and the polyoma DNA sequence is from Deininger *et al.*<sup>34</sup>.

recognition sequence is not sufficiently exposed in a single-stranded form. Thus the longer recognition sequence of the gene A protein may be expected to show even less single strandedness in supercoiled ΦX RFI DNA. Nevertheless, supercoiled ΦX RFI DNA is efficiently nicked by the gene A protein. These considerations lead to the conclusion that the gene A protein, in contrast to the A\* protein, can cause unwinding of the DNA double helix at the recognition sequence, which can then be nicked. The unwinding could be driven by the release of (part of) the free energy of the superhelix formation which could take place during the binding of the gene A protein to the ΦX RFI DNA. This unwinding property of the gene A protein is also suggested from the observation that the protein is required for the movement of the replication fork during ΦX DNA replication *in vitro*<sup>5,6</sup>. It seems likely that the DNA unwinding properties of the gene A protein are located in the N-terminal part of the protein chain which is not present in the A\* protein.

The decamer sequence CAACTTGATA is unique in ΦX DNA<sup>7</sup>. It does not occur in M13 DNA<sup>25</sup>, fd DNA<sup>28</sup>, SV40 DNA<sup>29,30</sup>, BKV DNA<sup>31</sup> or pBR322 DNA<sup>32</sup>. However, in polyomavirus DNA, the sequence CAACTTGATA occurs (nucleotides 1,719–1,710 (ref. 33) or 1,737–1,728 (ref. 34)) in the strand with the same polarity as the late mRNAs<sup>33</sup>. The supercoiled polyoma virus component I DNA is not nicked by the gene A protein whereas St-1 RFI DNA in the same reaction mixture is nicked efficiently (F. Heidekamp, personal communication). Comparison of the DNA sequence surrounding CAACTTGATA in polyoma DNA with that of the DNAs of the isometric phages ΦX, G4 and St-1 (Fig. 5) indicates that a characteristic A + T-rich region which is present in the isometric phage DNAs is absent in polyoma DNA. This may explain the

observation that supercoiled polyoma DNA is not nicked by the gene A protein. In single-stranded DNA the gene A protein does not require the A + T-rich region as shown by the present work and the fact that the single-stranded polyomavirus DNA restriction fragment *Hae*III 8, which contains the sequence CAACTTGATA, is cleaved by the gene A protein next to the G residue in this sequence (A.D.M.v.M., unpublished results).

In summary, the successful reaction of ΦX RFI DNA and its initiator protein of DNA replication has been shown to depend on a subtle interplay of the two components of the reaction. The substrate requirements involve (part of) the decamer sequence CAACTTGATA and an adjacent A + T-rich region, which must be present in supercoiled DNA. In supercoiled ΦX RFI DNA this region is sufficiently unwound to bind the gene A protein. This binding causes local unwinding of the DNA double helix which exposes the recognition sequence in a single-stranded form. Subsequently, the gene A protein cleaves one strand, the strand containing the sequence CAACTTGATA. Cleavage occurs at the 3' side of the G residue, and creates a primer for DNA polymerase III holoenzyme to start the rolling circle DNA replication<sup>5</sup>.

We thank Miss H. A. A. M. van Teeffelen for technical assistance, Dr J. H. van de Pol for computer analysis of the ΦX and G4 DNA sequence, P. J. G. F. van Wezenbeek for computer analysis of the M13 DNA sequence, Dr A. J. van der Eb and Dr J. R. Arrand for gifts of polyoma virus DNA, and F. Heidekamp for communicating his unpublished results. The investigation was supported in part by the Netherlands Foundation for Chemical Research (SON), with financial aid from the Netherlands Organisation for the Advancement of Pure Research (ZWO).

Received 2 July; accepted 9 October 1980.

- Sinsheimer, R. L., Starman, B., Nagler, C. & Guthrie, S. J. *molec. Biol.* **4**, 142–160 (1962).
- Francke, B. & Ray, D. S. *J. molec. Biol.* **61**, 565–586 (1971).
- Baas, P. D., Jansz, H. S. & Sinsheimer, R. L. *J. molec. Biol.* **102**, 633–656 (1976).
- Langeveld, S. A. *et al. Nature* **271**, 417–420 (1978).
- Eisenberg, S., Griffith, J. & Kornberg, A. *Proc. natn. Acad. Sci. U.S.A.* **74**, 3198–3203 (1977).
- Ikeda, J. E., Yudelevich, A. & Hurwitz, J. *Proc. natn. Acad. Sci. U.S.A.* **73**, 2669–2673 (1976).
- Sanger, F. *et al. J. molec. Biol.* **125**, 225–246 (1978).
- Eisenberg, S. & Kornberg, A. *J. biol. Chem.* **254**, 5328–5332 (1979).
- van Mansfeld, A. D. M. *et al. Cold Spring Harb. Symp. quant. Biol.* **43**, 331–334 (1979).
- Heidekamp, F., Langeveld, S. A., Baas, P. D. & Jansz, H. S. *Nucleic Acids Res.* **9**, 2009–2021 (1980).
- Dugué, M., Yarranton, G. & Gefter, M. *Cold Spring Harb. Symp. quant. Biol.* **43**, 335–343 (1979).
- Langeveld, S. A., van Mansfeld, A. D. M., de Winter, J. M. & Weisbeek, P. J. *Nucleic Acids Res.* **8**, 2177–2188 (1979).
- Linney, E. A. & Hayashi, M. N. *Nature new Biol.* **245**, 8–9 (1973).
- Langeveld, S. A., van Arkel, G. A. & Weisbeek, P. J. *FEBS Lett.* **114**, 269–272 (1980).
- Arentzen, R., van Boeckel, C. A. A., van der Marel, G. & van Boom, J. H. *Synthesis* **137**–139 (1979).
- de Rooij, J. F. M., Wille-Hazeleger, G., van Deursen, P. H., Serdijn, J. & van Boom, J. H. *Recl. Trav. Chim. Pays-Pas* **98**, 537–548 (1979).
- Brownlee, G. G. & Sanger, F. *Eur. J. Biochem.* **21**, 395–399 (1969).
- Maxam, A. M. & Gilbert, W. *Proc. natn. Acad. Sci. U.S.A.* **74**, 560–564 (1977).
- Maxam, A. M. & Gilbert, W. *Meth. Enzym.* **65**, 499–559 (1980).
- Greene, P. J. *et al. J. molec. Biol.* **99**, 237–261 (1975).
- Goppelt, M., Pingoud, A., Maass, G., Köster, H. & Frank, R. *Eur. J. Biochem.* **104**, 101–107 (1980).
- Baumstark, B. G., Roberts, R. J. & Raj Bhandary, U. L. *J. biol. Chem.* **254**, 8943–8950 (1979).
- Ikeda, J. E., Yudelevich, A., Shimamoto, N. & Hurwitz, J. *J. biol. Chem.* **254**, 9416–9428 (1979).
- Henry, T. J. & Knippers, R. *Proc. natn. Acad. Sci. U.S.A.* **71**, 1549–1553 (1974).
- van Wezenbeek, P. M. G. F., Hulsebos, T. J. M. & Schoenmakers, J. G. G. *Gene* **11**, 129–148 (1980).
- Marians, K., Ikeda, J. E., Schlagman, S. & Hurwitz, J. *Proc. natn. Acad. Sci. U.S.A.* **74**, 1965–1968 (1977).
- Jacob, R. J., Lebowitz, J. & Kleinschmidt, A. K. *J. Virol.* **13**, 1176–1185 (1974).
- Beck, E. *et al. Nucleic Acids Res.* **5**, 4495–4503 (1978).
- Reddy, V. B. *et al. Science* **200**, 494–502 (1978).
- Fiers, W. *et al. Nature* **273**, 113–120 (1978).
- Yang, R. C. A. & Wu, R. *Science* **206**, 456–462 (1979).
- Sutcliffe, J. G. *Cold Spring Harb. Symp. quant. Biol.* **43**, 77–90 (1979).
- Soeda, E., Arrand, J. L., Smolar, N., Walsh, J. E. & Griffin, B. E. *Nature* **283**, 445–453 (1980).
- Deininger, P. L., Esty, A., LaPorte, P., Hsu, H. & Friedmann, T. *Nucleic Acids Res.* **8**, 855–860 (1980).
- van Mansfeld, A. D. M., Vereijken, J. M. & Jansz, H. S. *Nucleic Acids Res.* **3**, 2827–2844 (1976).
- Godson, G. N., Barrell, B. G., Staden, R. & Fiddes, J. C. *Nature* **276**, 236–247 (1978).

## LETTERS

## Transition to oscillatory motion in the Taylor experiment

T. Mullin & T. Brooke Benjamin

Mathematical Institute, 24–29 St Giles, Oxford OX1 3LB, UK

Debates about hydrodynamic stability and the origins of turbulence are often based on the phenomena observable in Taylor's experiment<sup>1</sup> on the flow between concentric circular cylinders, the inner of which rotates while the outer is stationary. To reappraise a central aspect of this subject, we report here the effects of annulus length on the limit of stability for various steady cellular flows. For comparatively small values of the aspect ratio  $\Gamma$ , unforeseen behaviour has been observed indicating enormous sensitivity to end effects. In particular, plots of critical Reynolds number  $R_w$  against  $\Gamma$  are sharply peaked, and the form of oscillations arising at the stability limit changes in successive ranges of  $\Gamma$ . The new phenomena are beyond the reach of any present theory, and they highlight the need for caution when transition observations are interpreted.

The variety of phenomena observable in the Taylor experiment can be classified in terms of a Reynolds number  $R$  whose value fixes dynamical similarity for given proportions of the annular space filled by the fluid: say,  $R = \Omega r_1 d / \nu$ , where  $\Omega$  is the angular velocity of the inner cylinder,  $r_1$  its radius,  $d = r_2 - r_1$  the gap width and  $\nu$  the kinematic viscosity of the fluid. At small  $R$  the flow has no detectable longitudinal or radial component. However, when  $R$  is raised into a narrow, quasi-critical range, typically  $< 100$ , the flow develops a cellular structure, remaining steady and axisymmetric but being such that in adjacent cells the fluid particles move in counter-rotating spiral paths. When  $R$  is raised above a higher threshold value, the flow becomes unsteady with its cellular structure perturbed by circumferential travelling waves. As  $R$  increases further, the temporal variations become progressively more complex, exhibiting several incommensurate frequencies, and eventually a turbulent but perhaps still regularly pulsating state of motion is observed. Recent experimental advances<sup>2,3</sup> have renewed interest in these later stages of the transition to turbulence. In particular, the Taylor experiment should be a test of new theoretical concepts<sup>4</sup> concerning the incipience of turbulence.

Most theoretical studies of the Taylor experiment have been simplified by assuming the annulus to be infinitely long. These have given good estimates for the value of  $R$  at which cells first appear but little insight into the process whereby the number of cells is related to the annulus length. Earlier experiments<sup>5</sup> have, however, shown that the steady cellular flows realizable in the second stage of the Taylor experiment are not unique, and that the length-dependent selection process is complex and quite beyond simulation by the idealized model. Moreover, the multiplicity of steady flows possible at sufficiently high  $R$  values includes various 'anomalous' modes which cannot, for any annulus length, be produced by gradually increasing  $R$  from small values<sup>6</sup>. Although these phenomena have all been qualitatively explained by abstract methods of analysis<sup>7,8</sup>, they have not yet been covered by numerical or other constructive calculations. Non-uniqueness complicates the third, travelling-wave stage of the Taylor experiment<sup>9</sup>, and clearly the complicated solution set in this and the second stage will have to be elucidated further before the final transition to turbulence can be properly understood.

We have modified previous apparatus<sup>5</sup> to give finer control of temperature in the fluid and of rotor speed. The end conditions are virtually symmetric, the bottom of the fluid-filled annular space being a fixed wall and the top being the surface of a PTFE collar whose distance  $l$  from the bottom is continuously adjust-

able from 0 to 126 mm. (Previous, otherwise comparable experiments have used a free upper boundary<sup>10,11</sup>.) The radii of the cylindrical boundaries are  $r_1 = 36.9$  mm and  $r_2 = 60.0$  mm, so that the aspect ratio  $\Gamma = l/d$  is variable from 0 to 5.45.

The working fluid for these experiments was an aqueous solution of glycerol, 50:50 by volume, to which a small quantity of a pearly substance was added for flow visualization. Illuminated laterally, the Taylor cells were seen through the transparent outer cylinder as spiralling myriads of light specks, separated by thin dark bands. The extremely sensitive method of visualization revealed both the finest details of a steady flow and the onset of travelling waves when  $R$  was gradually raised to its critical value. A periodic rise and fall of the cell boundaries could then be seen. When established, however, the time-dependent motions were too complex for their spatial forms to be readily appreciated by the unaided observer. For later measurements of wave speeds, a greater amount of the visualizing additive was used, although not enough to affect the mechanical properties of the liquid but still able to produce vivid images of the kind that has often been recorded<sup>2,9</sup>. As a guide to the identification of angular wavenumbers among the different oscillations observed, photographs and a cine-film were used.

The production of various steady cellular flows in this apparatus, including the anomalous modes, has been described previously<sup>5</sup>. The stability of four such flows is now considered: (1) the two-cell mode in which the fluid spirals in the normal way, radially inwards near the end walls; (2) the normal four-cell mode; (3) the three-cell mode which is alternatively realizable with an abnormally spiralling cell at one end or the other; and (4) the abnormal four-cell mode in which each cell spirals oppositely to its counterpart in (2). The main observations involved establishing a particular mode in a steady state for a measured annulus length  $l$ , and then raising the rotor speed in very small steps until travelling waves appeared. In this way the critical value  $R_w$  of  $R$  marking the limit of stability was found as a function of  $\Gamma$ . After each increment of speed, the system was allowed to settle into its respective steady state, and for consistent results in approaching critical speeds the settling times needed to be prolonged far beyond those suggested by Snyder's<sup>10</sup> empirical estimate.

Having established travelling waves at constant amplitude, the rotor speed was then very gradually reduced, with the same precautions about adequate settling times, until the wavy motion ceased. A definite hysteresis, spanned by the interval from  $R_w$  down to a second critical value  $R'_w < R_w$ , was thus observable in most cases. This was manifested by the sudden cessation of previously vigorous oscillations, the hysteresis limit  $R = R'_w$  could be confidently estimated by our visual method. The frequency of the waves,  $f = \omega/2\pi$  Hz, was measured by timing a predetermined large number of periods with a stopwatch.

Figure 1 shows the results for  $R_w$  and  $R'_w$  plotted against  $\Gamma$ , where the most outstanding feature is the set of high peaks in the stability curves for the four different modes of steady axisymmetric flow. For each mode there is an optimal length of the annulus for which the stable range of rotor speeds is most prolonged, and the maximal values of  $R_w$  are surprisingly great. For the two normal modes, these values are in fact  $\sim 18$  times the critical value of  $R$  for the first appearance of cells according to the idealized theory, and  $\sim 15$  times the estimate of  $R_w$  on a similar basis ignoring end effects<sup>12</sup>. Cole<sup>11</sup> has also observed rapid increases in  $R_w$ , to more than double the estimated value, on reductions of aspect ratio  $\Gamma$  below  $\sim 10$ . (His results, however, do not make it clear whether the same cellular mode had been maintained as  $\Gamma$  was varied.) On the other hand, the well defined optimal length for each mode is quite unexpected, and its distinctness suggests that it should not be exclusive to the modes with comparatively few cells.



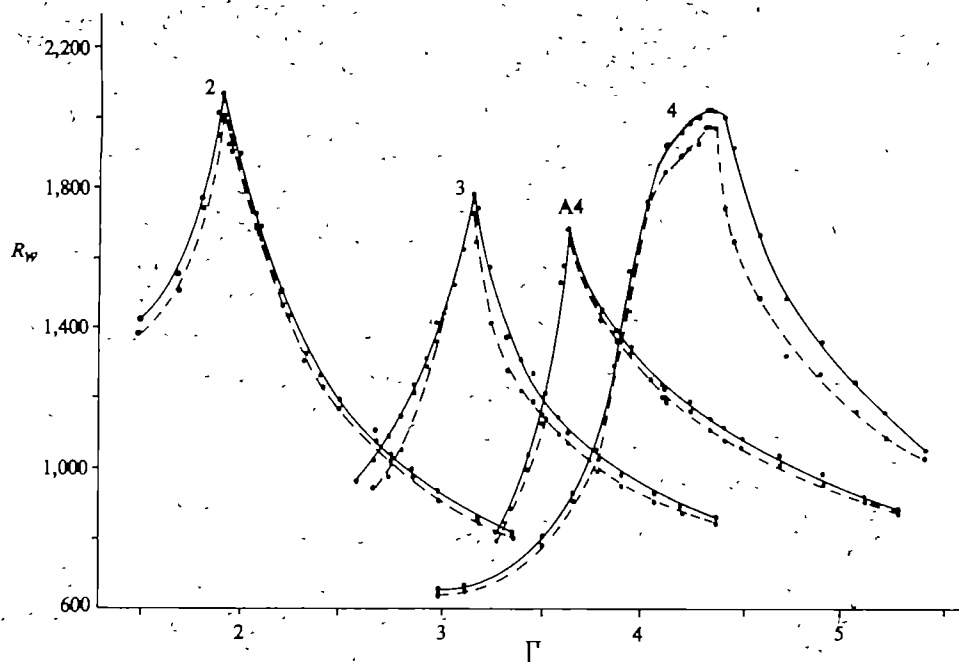


Fig. 1 Stability limit  $R_w$  and hysteresis limit  $R'_w$  as a function of aspect ratio  $\Gamma$ , for four cellular modes.

The curious ridge broadening the peak in the plot of  $R_w$  against  $\Gamma$  for the normal four-cell mode is associated with occurrence of travelling waves that have azimuthal wave number  $n = 1$  (that is, period  $2\pi$  in the cylindrical polar angle). This 'weak wavy mode', so called by Markho *et al.*<sup>13</sup>, was observed only in this region of Fig. 1. For settings  $\Gamma < 4.10$ , to the left of the ridge, the instability of the normal four-cell mode was manifested as waves with  $n = 2$ , giving rise to periodic oscillations of the upper and lower intercellular boundaries but leaving the central boundary steady. With  $\Gamma$  raised into the range 4.10–4.34, however, the unusual wave-form having  $n = 1$  arose; then oscillations appeared on the central interface but none on the other two. After a further increase of  $\Gamma$  into the range 4.34–4.72 which includes the optimal value, the onset of unsteadiness took the more complicated form of a quasi-periodic motion exciting all four cells, which was comprised from waves with  $n = 1$  and those with  $n = 5$  whose frequency was much higher. This form of motion was visibly quite distinct from the singly periodic motions observed elsewhere. For  $\Gamma > 4.72$ , a singly periodic motion was again encountered, but in this case with  $n = 5$ .

The two-cell mode was observed to follow a simpler pattern of behaviour at its stability locus as shown in Fig. 1. It had access there only to periodic waves with either  $n = 3$  or  $n = 5$ , depending on  $\Gamma$ .

The peaks of  $R_w$  for the two anomalous modes are  $\sim 12\%$  and  $22\%$  lower than those for the normal modes, and this deficiency seems consistent with the comparatively high lower limits also set on their ranges of stability<sup>6</sup>. Over a range of  $\Gamma$  upwards from just below the respective optimal value, each of these modes developed singly periodic travelling waves with  $n = 5$  when  $R$  had been raised gradually to  $R_w$ . In common with the normal

modes, however, they could be switched to wave regimes with other values of  $n$  by means of sudden changes in the rotor speed. Over this range each anomalous mode had the striking property that, after the onset of travelling waves, the normally spiralling cells executed distinct oscillations whereas none was observable in the abnormal cells (at one end for the three-cell mode, and at both ends for the anomalous four-cell mode). In fact, for the four-cell mode, increases in speed beyond the threshold value produced a multiply-periodic wave system disturbing the central interface but still causing no observable oscillations in the end cells.

Over a range to the left of the respective peak in Fig. 1, on the other hand, each anomalous mode exhibited another category of time-dependent motion when  $R$  had been raised to  $R_w$ . The motions were seen to be irregular, featuring slow pulsations of large amplitude but without any well defined low frequency. Because there were some moderately energetic components at higher frequencies, the observed motions might perhaps qualify as a primitive form of turbulence. However, their lack of resemblance to any familiar example of turbulence, including flows in our apparatus at much higher  $R$ , makes us wary of such a description.

For conditions at the left-hand end of Fig. 1, the irregular motions grew large enough to cause coalescence of the central and abnormal end cells, whereupon the three-cell mode collapsed into the two-cell mode which duly became steady. A similar situation, where the onset of waves resulted in the eventual collapse of the flow structure, was found for the abnormal four-cell mode in a range of  $\Gamma$ , 3.52–4.07, to the left of the peak in the experimental graph A4. This collapse was into the three-cell mode, which became steady or mildly wavy depending on  $\Gamma$ . Spontaneous mode-jumping in this manner has been described by Coles<sup>9</sup>, referring to arrays of many Taylor cells, but none of his observations exemplified the present case of collapse from an oscillating mode into a steady one.

Most of the observed transitions to time-dependent states of flow evinced appreciable hysteresis, as shown by the experimental plots of  $R'_w$  against  $\Gamma$  (dashed curves in Fig. 1). An interesting feature of the graphs is that the amount of hysteresis,  $R_w - R'_w$ , varies quite abruptly with  $\Gamma$  in certain places, which correspond to the changes that were observed among the types of wavy motion arising at  $R = R_w$ . This feature is particularly prominent near the peak of the graphs for the normal four-cell mode. It had seemed plausible that the irregular, multi-component oscillations of the anomalous modes at annulus lengths less than the optimal would have a large hysteresis, and

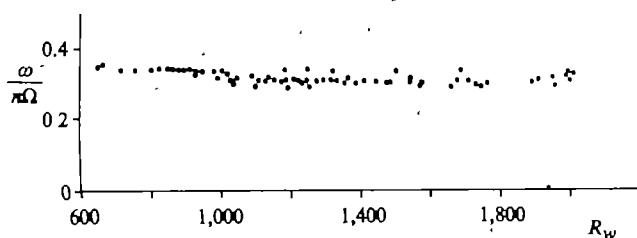


Fig. 2 Dimensionless angular speed of travelling waves that appear at stability limit  $R_w$ .

that as  $R$  was reduced they might first relax into periodic oscillations before the unsteady motion ceased at  $R = R'_w$ ; but no such behaviour was detected experimentally.

The transition has great sensitivity to end effects; but in contrast another, more easily recorded property was found to be surprisingly insensitive to them. Expressed as a multiple of  $\Omega$ , the angular speed  $\omega/n$  of the observed travelling waves turned out to be nearly independent of  $R$ , as shown in Fig. 2 which includes values of  $\omega/n\Omega$  from all our measurements of frequency. The mean value is about 0.32, which is unexpectedly close to corresponding values found previously by others from observations in apparatus with  $\Gamma$  an order of magnitude larger, for example the value 0.34 found by Coles<sup>9</sup>. Considered alone, this property might thus be deceptive as regards the overall importance of end effects.

We thank the SRC for support, and the Department of Engineering Science at Oxford for laboratory facilities.

Received 16 July; accepted 24 October 1980.

1. Taylor, G. I. *Phil. Trans. R. Soc. A* **223**, 289–343 (1923).
2. Fenstermacher, P. R., Swinney, H. L. & Gollub, J. P. *J. Fluid Mech.* **94**, 103 (1979).
3. Walden, R. W. & Donnelly, R. J. *Phys. Rev. Lett.* **42**, 301–304 (1979).
4. Ruelle, D. & Takens, F. *Commun. Math. Phys.* **20**, 167–192 (1971).
5. Benjamin, T. B. *Proc. R. Soc. A* **359**, 27–43 (1978).
6. Benjamin, T. B. & Mullin, T. *Phil. Trans. R. Soc. A* (submitted).
7. Benjamin, T. B. *Proc. R. Soc. A* **359**, 1–26 (1978).
8. Schaeffer, D. G. *Math. Proc. Camb. Phil. Soc.* **87**, 307–337 (1980).
9. Coles, D. *J. Fluid Mech.* **21**, 385–425 (1965).
10. Snyder, H. A. *J. Fluid Mech.* **35**, 273–298 (1969).
11. Cole, J. A. *J. Fluid Mech.* **75**, 1–15 (1976).
12. Eagles, P. M. *J. Fluid Mech.* **49**, 529–550 (1971).
13. Markho, P. H., Jones, C. D. & Mobbs, F. R. *J. Mech. Engng Sci.* **19**, 76–80 (1977).

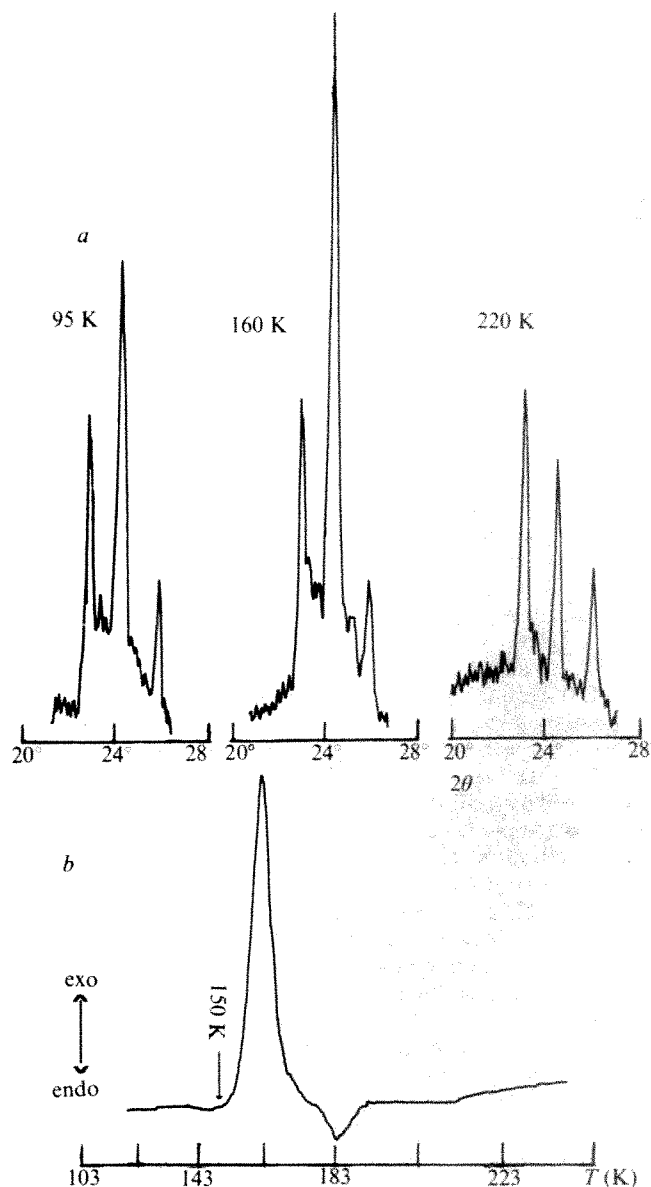
## Complete vitrification in pure liquid water and dilute aqueous solutions

Peter Brüggeller & Erwin Mayer

Institut für Anorganische und Analytische Chemie, Universität Innsbruck, A 6020 Innsbruck, Austria

Pure water can only be vitrified by the very slow condensation of vapour on a metal surface maintained at very low temperatures<sup>1,2</sup>. Attempts to form vitreous ice by rapid cooling of liquid water invariably lead to formation of ice  $I_h$  (ref. 3). (Pryde and Jones<sup>4</sup> did report a heat capacity change of rapidly cooled water at 126 K which they attributed to a glass transition, but could not reproduce this result in subsequent experiments.) Dilute aqueous solutions in contrast to concentrated aqueous solutions<sup>5</sup> behave similarly to water and separate during freezing, even with the highest cooling rates available, into pure ice and concentrated solute<sup>6</sup>. We report here that macroscopic parts of samples of pure liquid water and of dilute aqueous solutions can be vitrified completely by jet-freezing of micrometre-sized aqueous droplets distributed in *n*-heptane as an emulsion—the resulting supercooling effect of  $\sim 40$  K being essential for vitrification<sup>7</sup>.

The formation of vitrified ice from pure liquid water is demonstrated by the differential thermal analysis (DTA) warm-up curve of a jet-frozen emulsion of pure water (Fig. 1b). The exothermic peak at 150 K occurs at the temperature reported for the devitrification of amorphous ice prepared from water vapour<sup>8</sup>. The endothermic peak at 183 K is due to an *n*-heptane impurity. Jet-frozen 0.10 M  $\text{CuCl}_2$  solutions (chosen for ESR requirements) gave similar warm-up curves with the exothermic peak also occurring at 150 K. We have not observed clearly a glass transition. Only a faint endothermic inclination at  $\sim 138$  K in warm-up curves of jet-frozen water and of 0.10 M  $\text{CuCl}_2$  solutions might come from the glass transition of the vitreous phase which compares well with the glass transition temperature of vapour deposited amorphous ice<sup>8</sup>. The glass transition will be unmistakable only in vitreous samples with little or no crystalline impurity, and investigations of vitreous ice formed from water vapour seem to confirm this<sup>8</sup>.



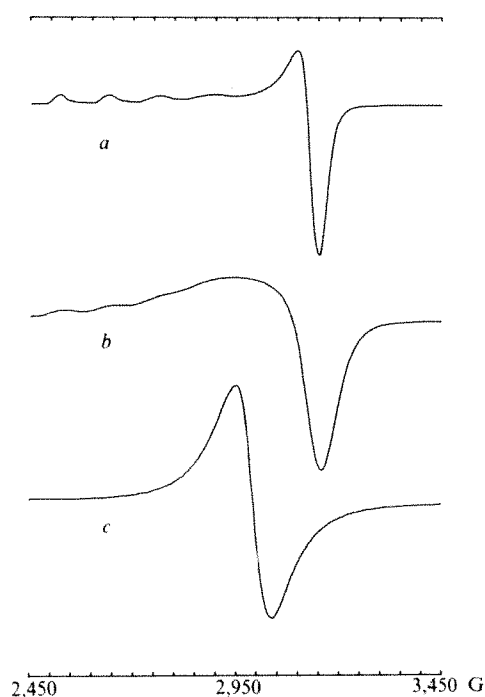
**Fig. 1** *a*, X-ray diffraction pattern ( $\text{Cu K}\alpha$ ) of a jet-frozen emulsified 0.10 M  $\text{CuCl}_2$  solution, heated consecutively from 95 K to 160 and to 220 K. *b*, DTA warm-up curve of jet-frozen emulsified pure liquid water. Heating rate  $6^\circ \text{min}^{-1}$ . The low-temperature DTA apparatus was similar to that used by Rasmussen<sup>9</sup>. The NiCr–Konstantan combination was used as thermocouple and the bottom parts of thin-walled 10-mm diameter NMR tubes were used for sample and reference, and for temperature measurement. About 100 mg of sample were diluted with 300 mg  $\text{CaCO}_3$  and transferred quickly into the precooled DTA apparatus.  $\text{CaCO}_3$  was used as inert reference and in the tube for temperature measurement. Samples were prepared as follows: the emulsion was prepared by dissolving 0.030 g Span 65 (sorbitan tristearate) in 9 ml *n*-heptane, adding 1 ml pure liquid water (*b*) respectively 1 ml 0.10 M aqueous  $\text{CuCl}_2$  solution (*a*) and sonifying the mixture. Droplet size depends strongly on sonifier energy and was adjusted to 1–5  $\mu\text{m}$  (larger droplets supercool insignificantly<sup>7</sup> and the ESR spectra indicated strong aggregation). 5 ml emulsion were jetted through a thick-walled glass tube with a 50  $\mu\text{m}$  aperture, using 100 atm working pressure, into 120 ml of vigorously stirred liquid ethane cooled to  $\sim 90$  K. We preferred ethane to propane as cryomedium because ethane can be pumped off quantitatively at 120 K. For DTA and X-ray experiments *n*-heptane was removed nearly completely by washing the frozen droplets several times with liquid ethane at 110 K. After pumping off the remaining ethane at 120 K the frozen droplets were transferred quickly with a liquid-nitrogen cooled spoon into the precooled apparatus. During the whole procedure the droplets were warmed at most to 130 K. At liquid-nitrogen temperatures special care has to be taken to prevent accumulation of liquid oxygen in the cryomedium.



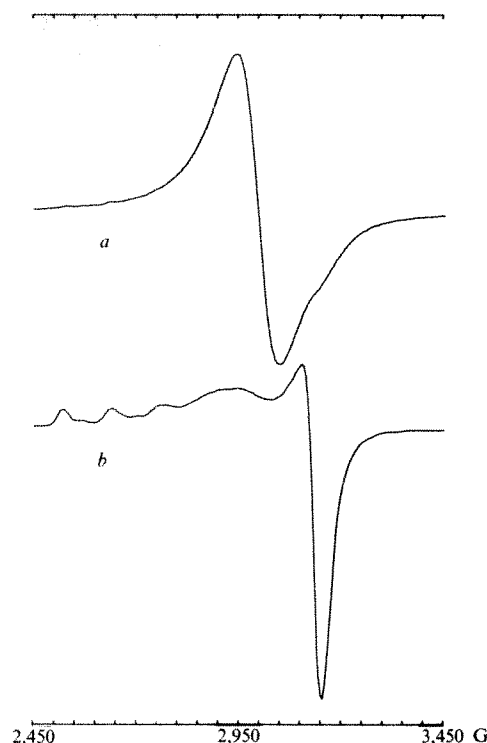
The amount of the vitrified material was determined by calibration with a 50% w/v vitrified glycerol solution. Devitrification of a 50% w/v glycerol solution produces according to Rasmussen and Luyet<sup>9,10</sup> a 73% w/v glycerol solution. We obtain an estimate by comparing the peak areas. To reduce errors both standard and sample were diluted equally with  $\text{CaCO}_3$  and an amount of vitrified glycerol was chosen with a similar signal intensity to our vitrified samples. We found that jet-frozen water/heptane emulsions contain 13% vitrified ice. For jet-frozen emulsified 0.10 M  $\text{CuCl}_2$  solutions a slightly higher value of 16% devitrified ice was obtained after several determinations. This only slightly higher value indicates that the freezing behaviour of a 0.10 M solution is comparable with the freezing behaviour of pure water, the small amount of additional devitrification coming from more concentrated vitrified parts of the solution.

We also investigated the vitrification of aqueous emulsions by X-ray diffraction and ESR spectroscopy. The X-ray diffraction pattern of ice allows us to differentiate between the phases  $I_h$  and  $I_c$  and mixtures of these, by the relative intensities of the three strong reflexes of ice  $I_h$  (for Cu  $K\alpha$ :  $2\theta = 22.8^\circ$ ,  $24.3^\circ$  and  $25.9^\circ$ ) and the strong reflex of ice  $I_c$  ( $2\theta = 24.3^\circ$ )<sup>11,12</sup>. The presence of vitreous components in a partially crystalline sample can be followed by the formation of ice  $I_c$  at the devitrification temperature and the relative increase of the reflex of ice  $I_c$  at  $2\theta = 24.3^\circ$ . Figure 1a shows the characteristic part of the X-ray diffraction pattern of a jet-frozen 0.10 M  $\text{CuCl}_2$  emulsion. The diffraction pattern at 95 K indicates a mixture of ice  $I_h$  and  $I_c$ . At 160 K a drastic increase of the reflex at  $2\theta = 24.3^\circ$  indicates the formation of ice  $I_c$  by devitrification of an amorphous phase. At still higher temperatures, ice  $I_c$  transforms to ice  $I_h$  and at 220 K only the reflexes of  $I_h$  are visible. Our experimental conditions inevitably lead to contamination of the original jet-frozen sample by ice  $I_h$  due to condensation of water vapour during the preparation and transfer of the sample to the X-ray camera, therefore, the resulting X-ray diffraction pattern at 95 K will contain an unknown amount of ice  $I_h$ .

The freezing behaviour of the solute in a dilute solution was studied by ESR spectroscopy. Whereas most other spectroscopic techniques are only sensitive to short-range order (that is,



**Fig. 2** Low temperature (113 K) ESR spectra of: *a*, 0.10 M  $\text{CuCl}_2$  solution, containing 50% (v/v) glycerol for vitrification; *b*, 1.5 M  $\text{CuCl}_2$  solution vitrified as above; *c*, 0.10 M  $\text{CuCl}_2$  slowly frozen by immersion in liquid nitrogen.



**Fig. 3** Low temperature (113 K) ESR spectra of: *a*, 0.10 M  $\text{CuCl}_2$  solution spray-frozen into liquid propane cooled to  $\sim 80$  K. The reported technique<sup>15</sup> was slightly modified: the solution was sprayed into 50 ml of stirred propane and the suspension filtered at 90 K. *b*, A jet-frozen 0.10 M  $\text{CuCl}_2$  emulsion using optimized conditions as described in Fig. 1.

the first hydration sphere), ESR is sensitive to comparatively long range order effects due to the  $1/r^3$  dependence of dipolar interaction<sup>13</sup>. With our system we can differentiate clearly between a 0.10 and a 1.5 M vitrified solution (Fig. 2*a,b*). We used ESR spectroscopy to maximize the various parameters such as cooling conditions and droplet size and found the spectra invaluable for assessing qualitatively the relative amounts of phase separated crystalline and of vitrified material. We used a 0.10 M aqueous  $\text{CuCl}_2$  solution as our ESR test system because: (1) the spectra representing the two extremes—perfect vitrification and complete phase separation—are shown in Fig. 2*a* and *c* and are separated sufficiently for evaluation. (2) At a concentration of 0.10 M the ESR spectrum was the most sensitive to the segregation of ice during the freezing process. At higher concentrations the ESR signal begins to broaden due to dipole-dipole interactions as shown in Fig. 2*b*. At lower concentrations the spectra of glycerol vitrified solutions are nearly identical to the ESR spectrum in Fig. 2*a*. Therefore even drastic segregation of ice from a very dilute solution such as  $10^{-3}$  M, resulting in a dramatic increase of the solute concentration, will not show up in the ESR spectrum. Figure 3*b* shows the ESR spectrum of a jet-frozen emulsion in the 'best' conditions for vitrification. These conditions were identical with the freezing conditions of the pure liquid water sample in Fig. 1*b*. The ESR spectrum is very similar to the spectrum of the perfectly vitrified solution in Fig. 2*a*. Some aggregation of  $\text{CuCl}_2$  is indicated by a broad hump at 2,940 G.

The ESR spectra of jet-frozen 0.10 M  $\text{CuCl}_2$  emulsions display drastic spectral changes with increasing temperature which are irreversible. In Fig. 4 the ESR spectra of a sample warmed for 30 min consecutively to 153 K (*b*), 173 K (*c*) and 193 K (*d*) have to be compared with the spectrum of the original sample at 113 K (*a*). At 153 K the ESR signal starts to broaden approaching within 30 min the width of a 1.5 M vitrified solution (compare with Fig. 2*b*). The increase of the signal at 2,940 G indicates the formation of a highly concentrated  $\text{CuCl}_2$  phase.

At higher temperatures the amount of concentrated  $\text{CuCl}_2$  increases. Evidence from DTA warm-up curves and from the X-ray diffraction patterns of Fig. 1a clearly indicates the process causing the irreversible change of the ESR spectra with temperature. The start at 153 K correlates well with the devitrification temperature determined by DTA. At this temperature ice  $I_c$  (shown by the X-ray diffraction pattern) starts to separate from the vitrified solution, the remaining  $\text{CuCl}_2$  becoming more and more concentrated.

From the theory<sup>3</sup> of the homogeneous nucleation of freezing, the cooling rate necessary for vitrifying a  $\mu\text{m}$ -sized droplet of water was estimated to be  $>10^{10} \text{ K s}^{-1}$  and was considered to be unattainable in practice. To compare our technique with others and to obtain some idea of the relative effects of emulsification and of jet-freezing we investigated the freezing methods usually applied in freeze etching. These methods were too slow to give observable DTA devitrification peaks, and we therefore used ESR spectroscopy. Dropping of  $1 \mu\text{l}$  droplets into liquid Freon at 120 K (the "standard freezing method"<sup>14</sup>—cooling rates up to  $10^3 \text{ K s}^{-1}$ ), yields complete aggregation and the ESR spectrum of a frozen  $0.10 \text{ M CuCl}_2$  solution is identical with the spectrum in Fig. 2c. Even the much faster cooling methods developed by Bachmann and Schmitt<sup>15</sup> (spray-freezing and jet-freezing into liquid propane at 77 K, estimated cooling rates of  $10^5 \text{ K s}^{-1}$ ) do not prevent segregation of the solute from the solvent. The ESR spectrum of a spray-frozen  $0.10 \text{ M CuCl}_2$  solution in Fig. 3a shows mainly aggregated  $\text{CuCl}_2$  and only a minor amount of less concentrated  $\text{CuCl}_2$  is indicated by the shoulder at 3,150 G. Jet-freezing of a  $0.10 \text{ M CuCl}_2$  solution through a  $20 \mu\text{m}$  aperture with 10 atm working pressure into liquid propane gives similar results to spray-freezing. We also tried to obtain a comparison with the cooling methods applied in splat-cooling of liquid metals and alloys<sup>16</sup> by jetting a  $0.10 \text{ M CuCl}_2$  solution through a  $10 \mu\text{m}$  aperture with 100 atm working pressure onto a copper plate cooled to 77 K. The jet was moved as quickly as possible over the surface of the cooled copper plate and its speed was calculated to be  $\sim 100 \text{ m s}^{-1}$  from the diameter of the aperture and consumption of liquid. Although this experiment was not performed using strict splat-quenching conditions we

believe it to be comparable with the 'gun-technique'<sup>16</sup> because of the high speed and small diameter of the jet. The ESR spectrum of the resulting frozen solid indicated complete aggregation. Apparently splat-cooling techniques give very low cooling rates for water and dilute aqueous solutions due to the low conductivities of water and ice.

We estimated our cooling rate by jet-freezing a non-emulsified  $0.10 \text{ M CuCl}_2$  solution, using otherwise identical conditions (glass capillary with  $50 \mu\text{m}$  aperture, 100 atm working pressure into liquid propane at 77 K). The ESR spectrum shows a clear improvement over the ESR spectrum of a spray-frozen sample in Fig. 3a, the signals at 3,050 and 3,150 G being of equal size. We therefore assume the cooling rate to be between  $10^5$  and  $10^6 \text{ K s}^{-1}$ . The further improvement with emulsified solutions in Fig. 3b demonstrates clearly the importance of emulsification and of the resulting supercooling effect for the vitrification of water and dilute aqueous solutions.

We thank Dr L. Bachmann for directing our attention towards this research and for helpful discussions.

Received 21 July, accepted 7 October 1980.

1. Burton, E. F. & Olver, W. F. *Proc. R. Soc. A* **153**, 166 (1935)
2. Venkatesh, C. G. & Rice, S. A. *Science* **186**, 927–928 (1974)
3. Fletcher, N. H. *Rep. Progr. Phys.* **34**, 913–994 (1971)
4. Pryde, J. A. & Jones, G. O. *Nature* **178**, 685–688 (1952)
5. Angell, C. A. & Sato, E. J. *J. chem. Phys.* **49**, 4713–4714 (1968), **52**, 1058–1068 (1970)
6. Volstenholme, G. E. W. & O'Connor, M. *The Frozen Cell* (Churchill, London 1970)
7. Rasmussen, D. H. & MacKenzie, A. P. *J. chem. Phys.* **59**, 5003–5013 (1973)
8. McMillan, J. A. & Lee, S. C. *Nature* **206**, 806–807 (1965)
9. Rasmussen, D. & Luyet, B. *Biodynamics* **10**, 319–331 (1969)
10. Luyet, B. & Rasmussen, D. *Biodynamics* **18**, 167–191 (1968)
11. Dowell, L. G. & Rindert, A. P. *Nature* **188**, 1144–1148 (1960)
12. Olander, D. S. & Rice, S. A. *Proc. natn. Acad. Sci. U.S.A.* **69**, 98–100 (1972)
13. Abragam, A. *The Principles of Nuclear Magnetism*, 126 (Clarendon, Oxford, 1973)
14. Moor, H. & Mithlethaler, J. *J. Cell Biol.* **17**, 609–628 (1963)
15. Bachmann, L. & Schmitt, W. W., *Proc. natn. Acad. Sci. U.S.A.* **68**, 2149–2152 (1971), in *Freeze Etching*, (eds Beaudette, E. L. & Paved, P.) 73–79 (Soc. Franc. Microsc. Electron, Paris 1973)
16. Jones, H. *Rep. Progr. Phys.* **36**, 1425–1497 (1973)

## Lu–Hf total-rock isochron for the eucrite meteorites

P. J. Patchett\*† & M. Tatsumoto\*

\* US Geological Survey, Denver Federal Center, Denver, Colorado 80225

† Colorado School of Mines, Golden, Colorado 80401

The isotope  $^{176}\text{Lu}$  (2.6% of natural lutetium) decays by  $\beta^-$  to  $^{176}\text{Hf}$ , with a long half life. We present here the first Lu–Hf isochron. The eucrite meteorites, a suite of planetary igneous rocks of known age, 4,550 Myr, define a 10-point total-rock isochron with a slope of  $0.0934 \pm 40$ , leading to a value of  $3.53 \pm 0.14 \times 10^{10}$  yr for the  $\beta^-$ -decay half life of  $^{176}\text{Lu}$ . The isochron intercept of  $0.27973 \pm 12$  gives the initial  $^{176}\text{Hf}/^{177}\text{Hf}$  for the inner Solar System at the time of accretion.

Previous geochronological use of the  $^{176}\text{Lu}$ – $^{176}\text{Hf}$  decay scheme involved REE-rich minerals<sup>1,2</sup> in attempts to determine the half life. Faure<sup>3</sup> summarized all physical determinations and suggested a best estimate of  $3.5 \pm 0.2 \times 10^{10}$  yr. However, because  $^{176}\text{Lu}$  is an odd Z-odd N nuclide, then a branching decay is theoretically possible. Dixon *et al.*<sup>4</sup> set an approximate upper limit of 3% on the electron capture to  $^{176}\text{Yb}$ , but to date this possible decay has been neither clearly substantiated nor disproved. It has also not been clearly shown that the Lu–Hf method can be used in isotope chronology and geochemistry.

Using a wide variety of petrological and geochemical criteria, the eucrites constitute a coherent group of cumulate and noncumulate igneous rocks (brecciated to varying degrees), which may have come from a single-parent asteroid<sup>5–7</sup>. In isotope geochemistry, the eucrites are important because they seem to have been produced during a major planetary differentiation 4,550 Myr ago, and to have been isotopically mainly

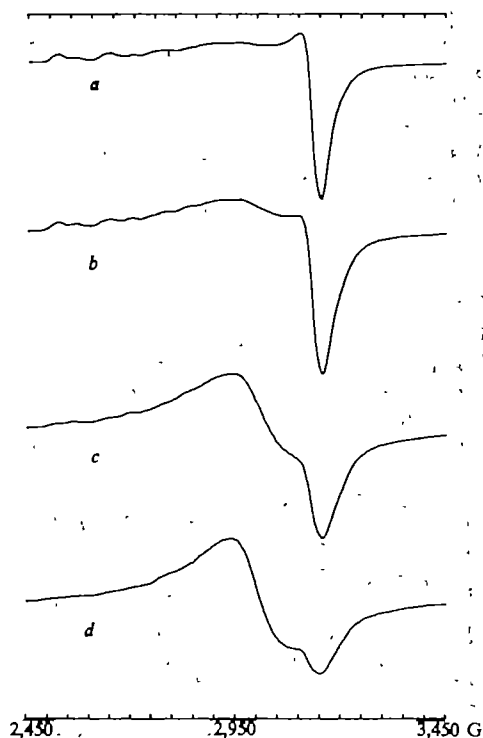


Fig. 4 Low temperature (113 K) ESR spectra of a jet-frozen  $0.10 \text{ M}$  aqueous  $\text{CuCl}_2$ /n-heptane emulsion: a, warmed at most to 113 K; b, c and d warmed consecutively for 30 min to 153 K, 173 K and 193 K respectively.



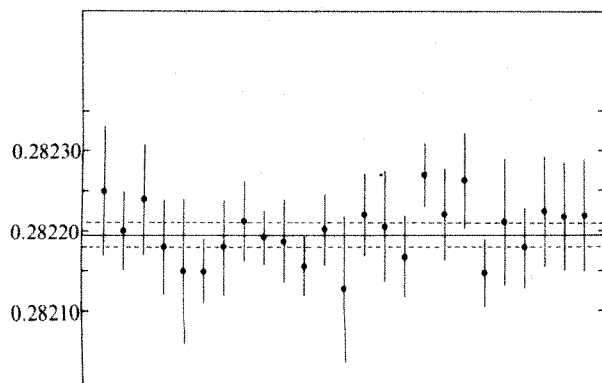
undisturbed since then. Extensive Rb–Sr (refs 8, 9), U–Pb (ref. 10), and Sm–Nd (refs 10–14) studies confirm this, and also that the samples had essentially the same  $^{87}\text{Sr}/^{86}\text{Sr}$  and  $^{143}\text{Nd}/^{144}\text{Nd}$  ratios 4,550 Myr ago. Thus although the eucrites may well have been derived from a single-parent body, this is not a necessary assumption for the present Lu–Hf total-rock isochron exercise, because they have already been shown to be isotopically concordant for the Rb–Sr and Sm–Nd systems, both in age and initial ratio.

Of the 10 samples studied, Stannern, ALHA 77302, Béréba, Nuevo Laredo, Pasamonte, Sioux County and Juvinas are non-cumulate eucrites, consisting of variously brecciated fine- to medium-grained basaltic material. Serra de Magé, Moore County and Moama are cumulate rocks<sup>6</sup>, consisting mainly of coarse-grained unbrecciated pyroxene and plagioclase.

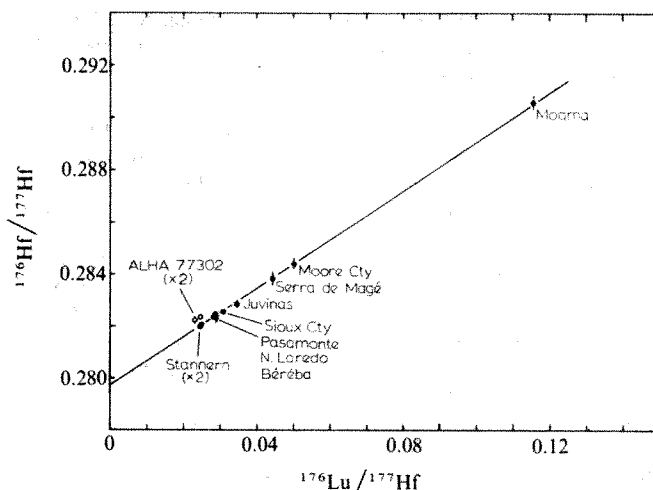
The analytical method is described fully elsewhere<sup>15</sup>. Bomb dissolutions on the disaggregated meteorites were used. The samples were then separated into two aliquots, and mixed  $^{176}\text{Lu}$ – $^{180}\text{Hf}$  spike added to one fraction. Chemical separation for Hf involved three ion-exchange columns and the overall chemical yield was 90%. Lu was not well separated from Yb, but the latter is more volatile and can be easily burned off the sample in the mass spectrometer. Overall blanks were  $<0.1$  ng for Lu and Hf; even for the most Lu, Hf-poor sample, Moama, the sample/blank ratio is  $>600$  for both elements, and hence no corrections for blanks were made. At most, this could result in a 0.15% bias in isochron slope; this is 30 times less than the  $2\sigma$  slope uncertainty, and is clearly insignificant.

Lu was measured on Ta side filaments using a Re centre filament. Hf was measured using a triple Re filament assembly.  $^{179}\text{Hf}/^{177}\text{Hf} = 0.7325$  was used for normalization. The mean value for 25 runs on the Johnson Matthey Hf standard JMC 475 is  $0.282195 \pm 15$  ( $2\sigma$ ) (see Fig. 1). We suggest JMC 475 as an international mass spectrometric Hf standard, and aliquots prepared from a single batch are available on request from Denver. From 1  $\mu\text{g}$  of Hf, a total signal of  $0.5 \times 10^{-11}$  A can be maintained for over 3 h, leading to precision of 0.01–0.03% on  $^{176}\text{Hf}/^{177}\text{Hf}$ .

The low Hf contents of the cumulate eucrites Serra de Magé, Moore County and Moama necessitated use of ion counting for Hf composition runs on these samples. Our two-stage mass spectrometer is equipped with a multiplier as collector, and a pulse-height discriminator to detect pulses. JMC 475 was run using ion counting on the two-stage mass spectrometer immediately before each Hf run on the cumulate eucrites, because of possible bias introduced by using a different machine and by variations in multiplier peak shape. Adjusting the higher values measured for JMC 475 by counting to 0.282195 resulted in corrections of  $-0.00012$  being applied to the Hf compositions of Moore County and Moama, and  $-0.00028$  to Serra de Magé. Corrections for Yb interference in Hf runs were never necessary, and in normal samples, Lu was also absent for all but the first 10–30 ratios of a run. For the samples measured by count-



**Fig. 1**  $^{176}\text{Hf}/^{177}\text{Hf}$  ratios for the Johnson Matthey standard JMC 475 during the eucrite study. The overall mean is  $0.282195 \pm 15$  normalized to  $^{179}\text{Hf}/^{177}\text{Hf} = 0.7325$ .



**Fig. 2** Lu–Hf isochron for the eucrite meteorites. ALHA 77302 is excluded from the regression treatment. Slope,  $0.0934 \pm 0.0040$ ; intercept,  $0.27973 \pm 0.00012$ ; MSWD, 2.50.

ing, corrections for Lu were applied, amounting to absolute downward adjustments in  $^{176}\text{Hf}/^{177}\text{Hf}$  of 0.00002–0.00008.

Lu–Hf isotopic results are listed in Table 1. The Lu/Hf ratio decreases with increasing Lu and Hf concentrations, so that the cumulate eucrites, depleted in trace elements, have Lu/Hf much higher than the noncumulate eucrites. However, over the Hf concentration range 2.4 p.p.m. (Stannern) to 0.8 p.p.m. (Juvinas), the Lu/Hf ratio changes only from 0.18 to 0.25, and there is thus strong coherence between the two elements. In the cumulates, where the residual liquid from crystallization of the pyroxene and plagioclase has been at least partly excluded, this coherence disappears. The cumulate samples (Moama, Lu/Hf = 0.82) presumably became more depleted in Hf than they did in Lu because Hf was more strongly concentrated in the residual liquid. This marked relative depletion of Hf in rocks which do not contain their lowest-melting components, such as cumulates, or residues of partial melting, seems to be an important characteristic of Lu–Hf geochemistry.

We have measured the isotopic composition of Lu in three samples, and find it to be within error of the terrestrial JMC 320 standard ( $37.701 \pm 0.028$ ), particularly taking into account the fact that fractionation cannot be normalized for this two-isotope element. Using large  $\text{Lu}^+$  ion beams from triple filaments, and a Faraday cup collector, we consistently measure  $\sim 37.70$  for JMC320, and 37.55–37.74 for natural samples, depending on fractionation conditions. We cannot reproduce the low values of McCulloch *et al.*<sup>19</sup>, obtained using an electron multiplier, and because we can see no way to correct our measurements objectively for mass fractionation, we have internally standardized all our calculations by using the measured value of  $37.701 \pm 0.028$  for natural  $^{175}\text{Lu}/^{176}\text{Lu}$ . If this ratio is used in any future Lu–Hf geochronology, then all errors will mutually cancel, because the decay constant determined here is based on an isochron whose slope is calculated using the same Lu isotopic composition.  $^{180}\text{Hf}/^{177}\text{Hf} = 1.88651$  (normalized to  $^{179}\text{Hf}/^{177}\text{Hf} = 0.7325$ ) was used for all natural Hf.

Except for the Antarctic eucrite ALHA 77302, the analyses define an isochron (Fig. 2). To increase precision on the initial  $^{176}\text{Hf}/^{177}\text{Hf}$  value, both Stannern results have been included in the regression<sup>16</sup>. The MSWD value of 2.50 suggests a small degree of scatter beyond analytical uncertainties (see Fig. 3), and the  $2\sigma$  errors in slope and intercept (Fig. 2) were obtained by multiplication of the *a priori* uncertainties with  $\sqrt{\text{MSWD}}$  (ref. 16).

ALHA 77302 was analysed twice, and lies clearly above the isochron (Figs 2, 3). The sample was never homogenized, so that the two results are slightly different, with correlated Lu/Hf and  $^{176}\text{Hf}/^{177}\text{Hf}$ . ALHA 77302 has Lu and Hf concentrations very similar to Pasamonte, Nuevo Laredo and Béréba, and distinctly

Table 1 Lu-Hf isotopic data

|               | Lu (p.p.m.) | Hf (p.p.m.) | $^{175}\text{Lu}/^{176}\text{Lu}^*$ | $^{176}\text{Lu}/^{177}\text{Hf}^\dagger$ | $^{176}\text{Hf}/^{177}\text{Hf}^*$ |
|---------------|-------------|-------------|-------------------------------------|---|-------------------------------------|
| Stannern      | 0.4112      | 2.3437      | $37.67 \pm 9$                       | $0.024869 \pm 59$                         | $0.282052 \pm 43$                   |
| Stannern      | 0.4145      | 2.3969      | —                                   | $0.024510 \pm 59$                         | $0.281953 \pm 78$                   |
| ALHA 77302    | 0.2732      | 1.5438      | —                                   | $0.025083 \pm 60$                         | $0.282418 \pm 58$                   |
| ALHA 77302    | 0.2599      | 1.5387      | —                                   | $0.023937 \pm 57$                         | $0.282316 \pm 144$                  |
| Nuevo Laredo  | 0.3599      | 1.8125      | —                                   | $0.028142 \pm 67$                         | $0.282372 \pm 66$                   |
| Béréba        | 0.2649      | 1.2968      | —                                   | $0.028957 \pm 69$                         | $0.282322 \pm 170$                  |
| Pasamonte     | 0.2984      | 1.4792      | $37.74 \pm 3$                       | $0.028593 \pm 67$                         | $0.282490 \pm 63$                   |
| Sioux County  | 0.2439      | 1.1165      | —                                   | $0.030965 \pm 92$                         | $0.282543 \pm 94$                   |
| Juvinas       | 0.1946      | 0.7991      | —                                   | $0.034530 \pm 81$                         | $0.282848 \pm 109$                  |
| Serra de Magé | 0.04297     | 0.1374      | —                                   | $0.044342 \pm 135$                        | $0.283800 \pm 209^\ddagger$         |
| Moore County  | 0.1823      | 0.5159      | $37.62 \pm 15$                      | $0.050105 \pm 152$                        | $0.284384 \pm 202^\ddagger$         |
| Moama         | 0.06631     | 0.08136     | —                                   | $0.11571 \pm 33$                          | $0.290587 \pm 253^\ddagger$         |

\* In-run errors are  $2\sigma_m$ .

† Error includes in-run uncertainties from spiked Lu and Hf runs, an estimated 0.04% uncertainty on run-to-run Lu mass fractionation, and uncertainties on Lu and Hf spike concentration.

‡ Hf composition measured using ion counting on a different mass spectrometer. As a result of standards measured at the same time, Serra de Magé Hf composition has been corrected by  $-0.00028$ , and Moore County and Moama by  $-0.00012$  to correspond to the other results.

lower than Stannern (Table 1). The regular decrease of Lu and Hf upwards along the isochron suggests that the Hf isotopic composition of ALHA 77302 is correct and original (that is similar to Pasamonte, Nuevo Laredo and Béréba), but that the Lu/Hf ratio has been disturbed in post-crystallization time. It seems possible that ALHA 77302 has lost Lu in the recent past, perhaps while embedded for a long time period in the Antarctic ice. The only alternative explanation, that the Hf isotopic composition has been contaminated, is unlikely because any Hf available in quantity on the Earth is probably no more radiogenic than  $^{176}\text{Hf}/^{177}\text{Hf} = 0.284$  (unpublished data), so that a large proportion of such Hf would be needed to raise ALHA 77302 above the isochron. However, we have not conducted leaching experiments on this eucrite.

The intercept of the isochron,  $0.27973 \pm 12$ , gives the  $^{176}\text{Hf}/^{177}\text{Hf}$  of the eucrites at 4,550 Myr, assuming that the age established by other methods can be used for Lu-Hf. As in the case of Nd, it is reasonable, in the absence of evidence to the contrary, to use this value as the primordial Hf isotopic composition for the planets of at least the inner Solar System. At present, however, the chondritic and bulk Earth Lu/Hf ratios are very poorly known, so that isotopic evolution lines cannot be drawn accurately until more data become available. This lack of knowledge is the result of Lu having been analysed with other REE, and Hf usually separately in studies of Zr-Hf fractionation. Our duplicated Hf concentration for Stannern (2.36 p.p.m.) disagrees not only with the neutron activation data of Ehmann *et al.*<sup>17</sup> (1.26 p.p.m.), but also with the isotope

dilution results of Shima<sup>18</sup> (1.23 p.p.m.). This discrepancy can probably only be accounted for by sample heterogeneity, but if our Hf contents of Pasamonte and Stannern are combined with the Zr data of Ehmann *et al.*<sup>17</sup>, then normal Zr/Hf ratios of 35 and 40 are obtained, in contrast to the anomalous 52 and 75 which these authors find using their own Hf contents.

The slope of the isochron,  $0.0934 \pm 0.0040$ , can be used to calculate the  $\beta^-$ -decay constant of  $^{176}\text{Lu}$ , assuming that the total-rock eucrites have been isotopically undisturbed since 4,550 Myr (refs 7-13). The following values are obtained:

$$\lambda^{176}\text{Lu}(\beta^-) = 1.962 \pm 0.081 \times 10^{-11} \text{ yr}^{-1}$$

$$t_{1/2}^{176}\text{Lu}(\beta^-) = 3.53 \pm 0.14 \times 10^{10} \text{ yr}$$

These  $2\sigma$  errors include the scatter component on the isochron; if only the *a priori* uncertainty<sup>16</sup> is used, then the uncertainties on  $\lambda$  and  $t_{1/2}$  are reduced to 0.051 and 0.081 respectively.

The weighted mean of five physical half life determinations made since 1960 (summarized in ref. 3) is  $3.54 \pm 0.11 \times 10^{10} \text{ yr}$ ; this is unchanged if the earlier geological determination<sup>2</sup> of  $3.3 \pm 0.5 \times 10^{10} \text{ yr}$  is included. The agreement between the mean of the physical determinations and the present value based on a Lu-Hf isochron is impressive, and suggests that the value  $3.53 \times 10^{10} \text{ yr}$  for the half life (corresponding to  $\lambda = 1.96 \times 10^{-11} \text{ yr}^{-1}$ ) can now be adopted.

We have ignored the possibility of a minor electron-capture decay of  $^{176}\text{Lu}$  to  $^{176}\text{Yb}$ , so that our half life may be slightly too long. Even if the electron capture does occur, any errors in the age determination will be cancelled out if the half life based on the eucrite isochron is used in future work. This is because the percentage effect on age of an unaccounted-for minor branching decay is essentially linear with time when the decay is slow, as for  $^{176}\text{Lu}$ . If the electron-capture decay can be confirmed and its proportion fixed, then ages calculated using the half life determined here will not need adjustment.

We have established here the usefulness of the  $^{176}\text{Lu}$ - $^{176}\text{Hf}$  decay scheme in isotope chronology, and shown that the igneous eucrite meteorites define an isochron, the slope of which allows the  $\beta^-$ -decay constant of  $^{176}\text{Lu}$  to be determined. The initial  $^{176}\text{Hf}/^{177}\text{Hf}$  ratio of the eucrites at 4,550 Myr probably applies to the Solar System generally, and will be of great importance in calculations of the isotopic evolution of planetary bodies and meteorites.

We thank R. S. Clarke, P. Pellas, C. J. Allègre, C. B. Moore and J. F. Lovering for meteorites, and especially K. Yanai for ALHA 77302. We thank Dan Unruh and Noboru Nakamura for helpful comments. This work was funded by NASA inter-agency transfer order T-783H.

Received 5 September; accepted 2 October 1980

- Herr, W., Marx, E., Eberhardt, P. & Signor, P. Z. *Naturf.* **13a**, 268-273 (1958)
- Boudin, A. & Deutsch, S. *Science* **168**, 1219-1220 (1970).
- Picot, G. *Principles of Isotope Geology* (Wiley, New York, 1977)

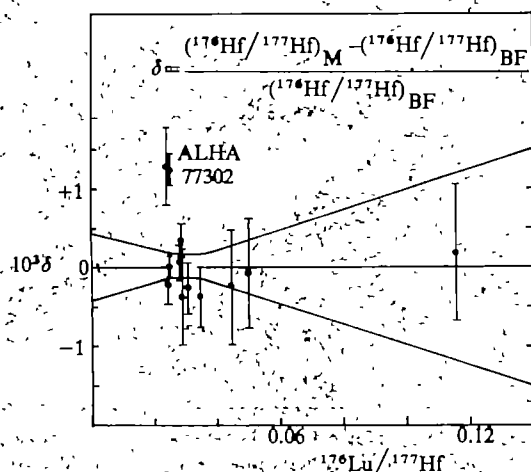


Fig. 3 Deviations in measured  $^{176}\text{Hf}/^{177}\text{Hf}$  (M) of the analyses from those predicted by the best fit line (BF). Isochron error envelope and error bars are  $2\sigma$ . As in the isochron diagram, ALHA 77302 lies clearly above the line.



4. Dixon, D., McNair, A. & Curran, S. C. *Phil. Mag.* **45**, 683–684 (1954).
5. Duke, M. B. & Silver, L. T. *Geochim. cosmochim. Acta* **31**, 1637–1665 (1967).
6. Stolper, E. *Geochim. cosmochim. Acta* **41**, 587–611 (1977).
7. Consolmagno, G. J. & Drake, M. J. *Geochim. cosmochim. Acta* **41**, 1271–1282 (1977).
8. Papanastassiou, D. A. & Wasserburg, G. J. *Earth planet. Sci. Lett.* **5**, 361–376 (1969).
9. Bircik, J. L. & Allègre, C. J. *Earth planet. Sci. Lett.* **39**, 37–51 (1978).
10. Unruh, D. M., Nakamura, N. & Tatsumoto, M. *Earth planet. Sci. Lett.* **37**, 1–12 (1977).
11. Lugmair, G. W. *Meteoritics* **9**, 369 (1974).
12. Nakamura, N., Unruh, D. M., Gensho, R. & Tatsumoto, M. *Lunar Sci. VIII Abstr.* 712–713 (1977).
13. Lugmair, G. W., Scheinin, N. B. & Carlson, R. W. *Meteoritics* **12**, 300–301 (1977).
14. Hamet, J., Nakamura, N., Unruh, D. M. & Tatsumoto, M. *Proc. 9th Lunar Sci. Conf.* 1115–1136 (1978).
15. Patchett, P. J. & Tatsumoto, M. *Contr. Miner. Petrol.* (in the press).
16. York, D. *Earth planet. Sci. Lett.* **5**, 320–324 (1969).
17. Ehmann, W. D., Chyi, L. L., Garg, A. N. & Ali, M. Z. in *Origin and Distribution of the Elements* Vol. II (ed. Ahrens, L. H.) 247–259 (Pergamon, Oxford, 1977).
18. Shima, M. *Geochim. cosmochim. Acta* **43**, 353–362 (1979).
19. McCulloch, M. T., DeLaeter, J. R. & Rosman, K. J. R. *Earth planet. Sci. Lett.* **28**, 308–322 (1976).

## Is the Hercynian belt of Brittany a major shear zone?

Denis Gapais & Claude Le Corre

Centre Armoricain d'Etude Structurale des Socles (CNRS),  
Université de Rennes, avenue du Général-Leclerc, 35042 Rennes  
Cédex, France

**In the Hercynian belt of Brittany (France), large localized shear zones indicate dextral transcurrent shearing. In this letter regional Hercynian structures and their relationships with shearing are considered and information obtained by quartz fabric analysis in the central part of the belt, outside the major shear zones, is presented. Fabric patterns show that a dextral shear component is associated with Hercynian penetrative deformation. Existing geological data are reconsidered in the light of these results, and the extent to which the Hercynian belt of Brittany can be regarded as a 'major shear zone' is discussed.**

The Hercynian belt of Brittany comprises different structural domains which are separated by major crustal discontinuities<sup>1</sup> expressed as transcurrent shear zones (Fig. 1). Within this segment of the west-European Hercynides, Central Brittany is an essentially Hercynian domain<sup>2,3</sup> characterized by structures which follow a roughly east-west trend (Fig. 1). In Central Brittany tectonic structures show the effects of (1) a roughly north-south shortening, (2) diapiric ascent of Hercynian granites, and (3) a dextral transcurrent shearing. Two basic geodynamic models, which involve mainly large-scale transcurrent shearing<sup>4</sup> or north-south compression<sup>1</sup>, have been proposed to account for Hercynian deformation in Central Brittany. In fact, the problem of the bulk deformation regime (coaxial or non-coaxial) is not at all clear. Recent studies have shown that, when developed during shearing, crystallographic fabrics of quartz are generally asymmetric and can be used to deduce the sense of shearing (see ref. 5). Perhaps the first clear field indication of a close relationship between dextral shearing and Hercynian deformation in Central Brittany was that reported by Bouchez and Blaise<sup>6</sup> and Bouchez<sup>7</sup>, on the basis of quartz fabric data. Their results, however, are of very local applicability. Furthermore, clear microtectonic evidence of shearing is lacking within large parts of the belt<sup>8–10</sup>. This has led to a modified geodynamic model<sup>9</sup> in which effects of shearing are mainly restricted to the mapped shear zones (Fig. 1), and remain relatively minor compared with a north-south compression.

Central Brittany is bounded to the north by a rigid continental block, which has been stable since the end of the Proterozoic (see, for example, Mancelian granites) and only slightly affected by the Hercynian orogeny. To the south lies a crystalline block affected mainly by Siluro-Devonian tectono-metamorphic events<sup>1</sup>. Both the northern and the southern limits of Central Brittany are defined by major ductile fault zones, the North and South Armoricain shear zones<sup>1,12–16</sup>. These shear zones, which have a long and complex structural history<sup>1,15,16</sup>, have acted as dextral strike-slip fault zones up to late Hercynian

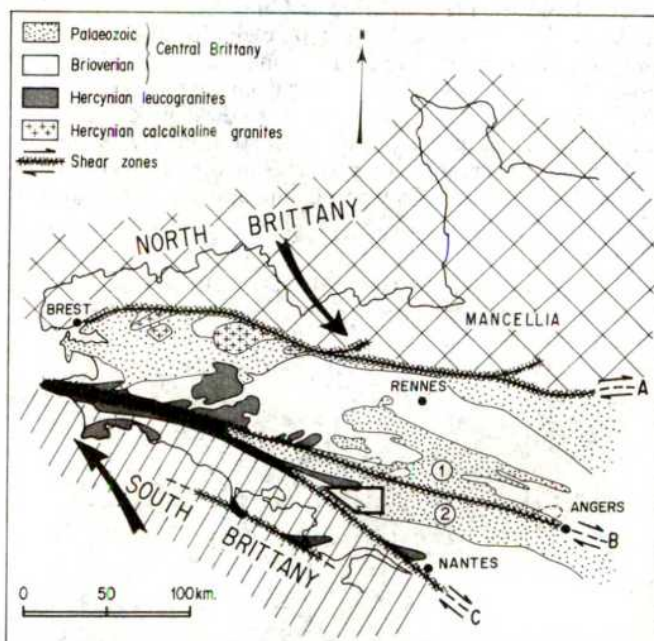
times<sup>14,15,17,18</sup>. Hercynian plutonism<sup>19,20</sup> is concentrated along these shear zones (Fig. 1).

Within Central Brittany, deformation of the sedimentary rock (Proterozoic and Palaeozoic) is mainly expressed as a regional cleavage, generally subvertical, and associated with large-scale folding. Folds are generally upright with low amplitudes<sup>9,10,21</sup>. Fold axes are always subhorizontal or gently plunging. The cleavage is parallel to the principal plane (xy) of the finite strain ellipsoid, and generally exhibits a mineral elongation lineation parallel to the x axis of the finite strain ellipsoid<sup>8,22</sup>. This principal extension direction is parallel, or nearly so, to the regional fold axes. The regional trend of folds and cleavage trajectories varies from west-southwest to east-southeast when moving eastwards through the belt<sup>3</sup>. Local data relating to finite strain (refs 7–9, 11, 22, and S. K. Hanmer, personal communication) indicate a large range of possible shapes of the finite strain ellipsoid. However, when present, stretching on the intermediate axis (y) remains generally weak or moderate. Plane strain ellipsoids are common and even constrictive finite strain is observed.

The axial region of Central Brittany appears as a zone of relatively weak deformation. Zones of more intense deformation are found on moving north or south, towards the North and South Armoricain shear zones. Thus, across the area between Rennes and the southern branch of the South Armoricain shear zone (Fig. 1), we have shown that strain intensity increases towards the south, as a result of Hercynian deformation<sup>8,9,11</sup>. We have also shown<sup>8,9,11,23</sup> that this regional strain gradient is associated with an increase of metamorphism towards the south<sup>3</sup>.

The Hercynian granites were demonstrably intruded during penetrative deformation<sup>2,3,11</sup>. Regional patterns of strain and metamorphism change in the vicinity of plutons (see Fig. 2). Local perturbations can also be observed around pre-Hercynian bodies (for example, Mancelian granites), as a result of their rigid behaviour relative to the country-rocks during the Hercynian orogeny.

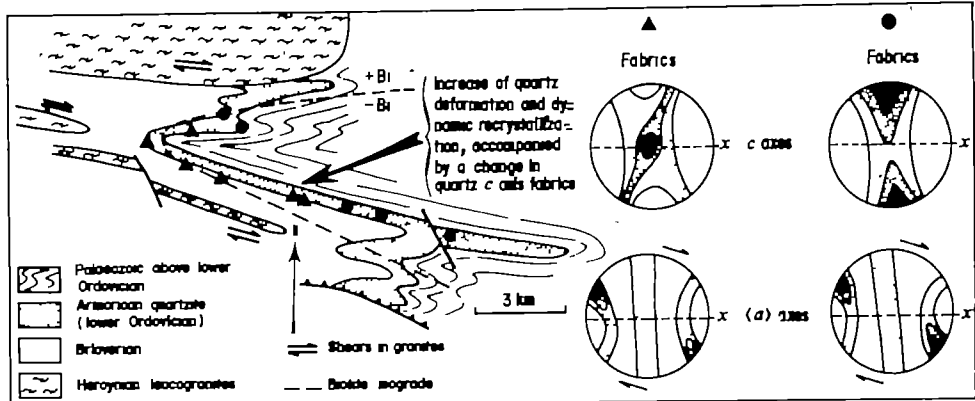
Fabrics and optical microstructures of quartz have been studied in detail within a quartzitic series (Armorican quartzite) of lower Ordovician age. Results given in full elsewhere<sup>15</sup>



**Fig. 1** Simplified geological map of Brittany. The large-scale movements are not precisely determined and arrows indicate only a regional dextral shear component. ①, St Georges-sur-Loire Synclinorium (the inset corresponds to the area of Fig. 2); ②, Sud de Rennes Synclines; A, North Armoricain shear zone; B + C, South Armoricain shear zone (B, northern branch; C, southern branch).



Fig. 2 Geological map of the western part of the St Georges-sur-Loire Synclinorium and variations of fabrics and optical microstructures of quartz within the Armorican quartzite. The dotted line indicates the approximate biotite isograd. The schematic fabric diagrams represent the characteristic  $c$  axes and  $\langle a \rangle$  axes patterns, as inferred from detailed texture goniometry study<sup>10,11</sup>. These patterns indicate a dextral shear component. In the field, the cleavage (dotted line on pole figures, foliation in quartzites) is subvertical, trends roughly N 110°, axial-plane of regional folds. The shear component is acting within a subvertical plane, along a subhorizontal direction.



were obtained from the western part of the St-Georges-sur-Loire Synclinorium (Figs 1 and 2). This Hercynian structure is bounded to the west by Hercynian leucogranites. Associated thermal anomalies are revealed by biotite isograds (Fig. 2). Moving westwards along the southern limb of the synclinorium, an increase of intracrystalline deformation and dynamic recrystallization is observed, leading to a fine-grained quartz mylonite. This is accompanied by a change in quartz  $c$ -axis fabric from a broad girdle with a maximum near the axis of principal shortening to a crossed-girdle pattern with a maximum near the  $y$  axis of the finite strain ellipsoid (Fig. 2). This deformation gradient is attributed to the thermal softening induced by the granites<sup>11</sup>. Quartz fabrics are typically monoclinic. They show a strong maximum of  $\langle a \rangle$  axes oblique with respect to the principal stretching direction  $x$ , and also unequally populated girdles of  $c$ -axes. Such fabrics indicate a dextral shear component<sup>5,10,24</sup> within a subvertical plane, irrespective of the microstructures exhibited by the quartzites (Fig. 2). In some of the quartzites, the occurrence of shear bands and of sigmoidal shadow-zones around rigid objects give further evidence of dextral shearing<sup>10</sup>. Our observations infer that regional shortening and emplacement of granites took place during shear deformation. The leucogranites are themselves penetratively sheared and stretched along the regional extension direction (Figs 1 and 2). Further south from the St-George-sur-Loire Synclinorium, the South Armorican shear zone (Fig. 1) is evidence for more intense shear. On the other hand, on moving north, within moderately deformed zones (such as the Sud de Rennes syndines, Fig. 1), the influence of a shear component becomes less apparent. Over large areas, we have not found any clear evidence for shearing during the main deformation, either from microtectonic criteria or fabric data<sup>8-10</sup>. Indeed, within this domain, the only clear evidences of shearing that has ever been reported is along the northern branch of the South Armorican shear zone<sup>6,17,18</sup> and also along discrete strike-slip microfaults in slates of the country-rocks<sup>9</sup>.

The overall geometry of the structures in Central Brittany (general trends of fold axes, cleavage trajectories and mapped shear zones; principal extension direction subhorizontal and parallel to fold axes) suggests the existence of large-scale dextral transcurrent shearing<sup>4,6</sup>. As shown above, regional strain gradients seem to be closely related to variations in intensity of shearing. Other evidence indicates that the ductile fault zones have acted as dextral strike-slip fault zones, not only in late Hercynian times, but also during the main Hercynian deformation, with associated local strain and metamorphism gradients<sup>6,14</sup>.

Fabric analysis and microtectonic analysis have not given any unequivocal evidence of non-coaxial deformation in weakly deformed zones. This kind of approach, though quite useful in sufficiently deformed rocks, seems to be less satisfactory for rocks exhibiting low strain intensities, where a stable fabric is not attained. Such investigations, if restricted to moderately deformed zones, can therefore lead to incorrect assumptions about the bulk deformation history. Thus, in the area under consideration, it gives only further evidence for regional short-

ening. Also, finite strain assessments which are locally significant cannot be directly extrapolated to provide a quantitative estimate of the geometry of the bulk strain (see ref. 25). In Central Brittany, perturbations induced by granitic bodies introduce further complications. Nevertheless, the overall low amplification of regional folds, bearing in mind that significant ductility contrasts exist between folded series<sup>9,10,21</sup>, is consistent with the observed principal extension subhorizontal and parallel to fold axes and with no evidence for important vertical finite extension. This pattern can be compared with results of bulk plane strain folding experiments<sup>26</sup>. In this way, deformation by shearing is thought to be the main factor limiting the vertical finite extension in Central Brittany.

An oblique convergence of a northern and a southern continental block might account for the observations and would be consistent with structural correlation that can be made between South and Central Brittany<sup>27</sup>. However, it remains difficult to estimate to what extent the bulk process may have differed from a regional simple shearing model. This might be overcome by extending detailed finite strain analysis throughout the whole region to complete the information about strain gradients and be able to calculate the effects of removing strains<sup>28,29</sup>. It has been suggested that the granites along the major shear zones could be the result of localized crustal melting by shear heating<sup>6,30</sup>. However, it has been thought that shear heating cannot in general be sufficient for this purpose<sup>31</sup>. Furthermore, the pattern of regional metamorphism is associated with a regional thermal anomaly which can account for the Hercynian plutonism<sup>3</sup>. The relation between major shear zones and granites can be explained by a thermally initiated strain softening in these zones<sup>32</sup>. Before the shear zones get sufficiently soft to allow most of the deformation to occur in these zones, it is reasonable to expect the entire region to deform as a whole. Regional Hercynian structures could, at least in part, be interpreted in this way. Then, dextral movements could continue along the main shear zones, up to late Hercynian times.

We thank J. P. Brun, P. Choukroune, P. Cobbold, B. Pivette, E. Rutter and S. White for discussions and criticisms.

Received 18 July; accepted 14 October 1980.

- 1 Cogué, J. in *Colloq. int. CNRS, Géologie de l'Himalaya*, 168, 111-129 (1977).
- 2 Le Corre, C. *Bull. B.R.G.M.* 3, 219-254 (1977).
- 3 Haxner, S. K., Le Corre, C. & Berthé, D. *J. Geol. Soc. London* (in the press).
- 4 Matta, Ph. & Ribeiro, A. *C. R. heb. Séanc. Acad. Sci., Paris D280*, 2825-2828 (1975).
- 5 Bouchaz, J. L. *Tectonophysics* 49, T25-T30 (1978).
- 6 Bouchaz, J. L. & Blaise, J. *Bull. Soc. géol. Fr.* 1, 145-157 (1976).
- 7 Bouchaz, J. L. *Tectonophysics* 39, 25-50 (1977).
- 8 Le Corre, C. & Le Théoll, B. *Bull. Soc. géol. Fr.* 6, 1435-1442 (1976).
- 9 Le Corre, C. thesis, Univ. Rennes (1978).
- 10 Gopau, D. thesis, Univ. Rennes (1979).
- 11 Gopau, D. *Bull. Minér.* 102, 249-264 (1979).
- 12 Chaurin, L. *C. R. heb. Séanc. Acad. Sci., Paris D268*, 2859-2861 (1969).
- 13 Perra, F. & Jégouzo, P. *Ann. Rén. Ann. Sci. Terre*, Paris (1975).
- 14 Hirbec, Y. thesis, Univ. Rennes (1979).
- 15 Watts, M. J. & Williams, G. D. *J. struct. Geol.* 1, 323-332 (1979).
- 16 Jégouzo, P. *J. struct. Geol.* 2, 39-47 (1980).
- 17 Berthé, D., Choukroune, P. & Jégouzo, P. *J. struct. Geol.* 1, 31-42 (1979).
- 18 Berthé, D., Choukroune, P. & Gopau, D. *Bull. Minér.* 102, 265-272 (1979).
- 19 Vidal, Ph. *Bull. Soc. géol. Fr.* 15, 232-245 (1973).
- 20 Ponceat, J. J., Charlot, R., Mifidal, A., Chamtraine, J. & Autran, A. *Stress Rén. Ann. Sci. Terre*, Masson (1980).
- 21 Pivette, B. thesis, Univ. Rennes (1978).
- 22 Claffin, M. *Bull. Soc. géol. Fr.* 3, 757-762 (1976).



23. Le Corre, Cl. *Bull. Soc. géol. Fr.* **4**, 547–553 (1975).
24. Lister, G. S. & Williams, P. F. *J. struct. Geol.* **1**, 283–297 (1979).
25. Cobbold, P. *Can. J. Earth Sci.* **8**, 1721–1731 (1977).
26. Watkinson, A. J. *Tectonophysics* **28**, T7–T11 (1975).
27. Vigneress, J. L. *Soc. Géol. minér. Bretagne* (in the press).
28. Cobbold, P. *J. struct. Geol.* **1**, 67–72 (1979).
29. Percevault, M. N. & Cobbold, P. *8ème Réun. Ann. Sci. Terre, Marseille* (1980).
30. Nicolas, A., Bouchez, J. L., Blaise, J. & Poirier, J. P. *Tectonophysics* **42**, 55–73 (1977).
31. Brun, J. P. & Cobbold, P. *J. struct. Geol.* **2**, 149–158 (1980).
32. Poirier, J. P., Bouchez, J. L. & Jonas, J. J. *Earth planet. Sci. Lett.* **43**, 441–453 (1979).

## Clays from New Zealand support the inactive particle theory of soil sensitivity

I. J. Smalley, Craig W. Ross & J. S. Whitton

Soil Bureau, Department of Scientific and Industrial Research, Lower Hutt, New Zealand

**As part of a long-term study of factors contributing to soil sensitivity, investigations have been carried out on some volcanic ash soils from the North Island of New Zealand. We report here that some soils have sensitivities of up to 140 and clay mineral contents of >80%. They apparently owe their high sensitivity to the fact that the clay is halloysite of the spherical variety, and that interparticle interactions with this particular soil mineral are remarkably slight. Although the clay soil has a high liquid limit (~65–80), it has a low plasticity index (~15–30) and its behaviour supports the inactive particle theory of soil sensitivity. When plotted on the Casagrande Plasticity Chart all samples plotted well below the 'A' line.**

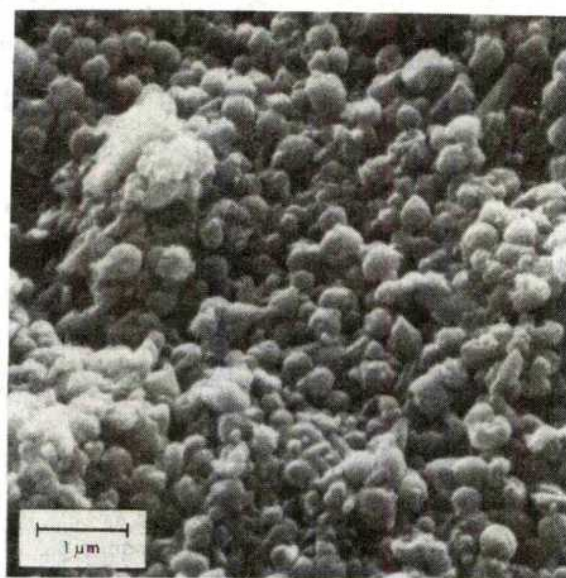
Sensitivity is a measure of the loss in strength which occurs when a soil is disturbed or remoulded. In extreme cases the undisturbed soil strength can be several hundred times as great as the remoulded strength<sup>2</sup>. The ratio of undisturbed to remoulded strength indicates the sensitivity ( $S_t$ ). Soils of extremely high sensitivity (sometimes called quickclays:  $S_t > 50$ ) exist in eastern Canada and in Scandinavia and cause problems by landsliding and retrogressive flowslide behaviour. Various theories have been advanced to explain their properties: the role of interparticle cementation<sup>3</sup>, the leaching theory which has now evolved into a generalized electrochemical approach<sup>4</sup> and the inactive-particle, short-range-bond theory<sup>15</sup> are all being discussed. But choosing between the various approaches has been difficult because of the limited number of high sensitivity soils available. This situation has been helped by the discovery of soils with sensitivities reaching 140 in New Zealand. Initial investigations suggest that the cementation and Rosenqvist factors may not apply.

In August 1979 a damaging landslide occurred at Tauranga, on the northeastern fringe of the central volcanic plateau in the North Island of New Zealand. This landslide had many of the characteristics of a flowslide which occurs in highly sensitive soils and sensitivities of up to 140 were measured, although many much lower values were also recorded (C. Gulliver, personal communication). Mineralogical analyses by differential thermal analysis and X-ray diffraction (XRD) showed that the soil was largely composed (80%+) of hydrated halloysite (10 Å spacing on XRD); minor amounts of quartz and cristobalite were observed. At first sight this apparently contradicts the major requirement of the inactive particle theory, that the clay mineral content be small to negligible; however, the nature of the Tauranga halloysite is such that the observations and the requirements of theory can be reconciled. The inactive particle theory explains very high sensitivities by requiring that there be very little long-range attraction between the soil particles. In the Northern Hemisphere, this requirement is met by specifying that there should be very little active clay mineral content in the soil, and a recent programme of analyses on Canadian soils has shown that they do have low clay mineral contents<sup>6–8</sup>. But in New Zealand it is possible to find soils with a very high clay

mineral content which do not have the 'clayey' or high plasticity indices of soils of similar clay proportion encountered in Northern Hemisphere engineering soil investigations.

Scanning electron microscope studies (by G. Walker; see Fig. 1) show that the soil at Tauranga is composed essentially of spherical halloysite particles. The analytical results from scanning electron microscopy/electron diffraction by X-ray analysis (SEM/EDAX) show a  $\text{SiO}_2/\text{Al}_2\text{O}_3$  ratio of 1:1, which supports halloysite. Some small concretions were completely localized concentrations of iron and manganese (in roughly equal proportions); no sign of cementation was detected. These spherical clay particles (which are single crystalline units and not aggregations) form a very inactive clay with very small interaction with both positive and negative soil water ions; the phosphate uptake for a similar soil is the lowest measured in New Zealand<sup>9</sup>. Thus, although clay mineral particles predominate in the Tauranga material, long-range interparticle forces are essentially absent and the sensitivity is relatively high. The inactive particle theory will need to be generalized to require an absence of long range forces in the soil system rather than a lack of clay mineral materials, although investigations on a sensitive Norwegian soil<sup>11</sup> show that the minimum clay mineral requirement may still operate in the Northern Hemisphere.

Some structural collapse must be involved in the classic quickclay failure and yet the spherical particles might be expected to form a fairly compact structure. SEM reveals some variation in density with 'pores' distributed throughout the soil, and these seem to cause fairly low bulk densities, usually in the range 1.5–1.6 tonnes  $\text{m}^{-3}$ . Natural water contents of the sensitive ash soils were exceptionally high (60–100%) and were often above the liquid limits. The abundant water supports the separated particle once failure has occurred<sup>5</sup> but the initial brittle failure, leading to structural collapse, occurs because of a lack of long-range bonds in the system. Handy<sup>11</sup> has shown that structural collapse in the loess soils of Iowa is promoted by an absence of clay minerals and this observation could indirectly support the inactive particle sensitivity theory. Fedá<sup>12</sup> and Denisov<sup>13</sup> regard loess as a sensitive soil and relate its structural collapse on wetting to the total structural collapse exhibited by a quickclay when it is remoulded. In Iowan loess the primary mineral particles which form the basis of the soil structure are usually quartz with diameters of 20–60  $\mu\text{m}$ , in a Canadian quickclay the particles are quartz and feldspar and the diameters are around 2–5  $\mu\text{m}$  and in the New Zealand volcanic soil the



**Fig. 1** Spherical halloysite particles comprising the sensitive volcanic ash soil at Tauranga; each particle has a diameter of ~0.2  $\mu\text{m}$ . The particles are single crystalline units and not aggregates of smaller particles. (Photo: G. D. Walker, DSIR New Zealand.)



major soil particles are halloysite spheroids with diameters of  $\sim 0.2 \mu\text{m}$ ; they all seem to have a propensity for structural failure, and they all lack long-range forces. (But we have a few reservations about considering loess a truly sensitive soil.)

The existence of the Tauranga soil, with a sensitivity that puts it in the quickclay class (using the Swedish definition) and a remarkable mineralogy, offers the chance of taking another small step towards a general theory of sensitivity. It also supports the approach suggested in the inactive-particle, long-range-bond theory, and it might offer some common ground on which to reconcile the revised approach with the generalized Rosenqvist theory.

We thank Chris Gulliver for drawing our attention to the Tauranga slide and for supplying samples and engineering data.

Received 2 June; accepted 15 October 1980.

1. Smalley, I. J. *Nature* **231**, 310 (1971).
2. Penner, E. *Nature* **197**, 347–348 (1963).
3. Yong, R. N., Sethi, A. J., Booy, E. & Dascal, O. *Engng Geol.* **14**, 83–107 (1979).
4. Rosenqvist, I. Th. *Geol. Appl. Idrogeol.* **10**, 21–32 (1975).
5. Cabrera, J. G. & Smalley, I. J. *Engng Geol.* **7**, 115–133 (1973).
6. Smalley, I. J., Bentley, S. P. & Moon, C. F. *Can. Miner.* **13**, 364–369 (1975).
7. Bentley, S. P. & Smalley, I. J. *Can. Miner.* **16**, 103–112 (1978).
8. Bentley, S. P. & Smalley, I. J. *Engng Geol.* **14**, 209–217 (1979).
9. Theng, B. K. G., Russell, M., Churchman, G. J. & Parfitt, R. L. *Clays Clay Miner.* (in press).
10. Bentley, S. P., Clarke, N. J. & Smalley, I. J. *Can. Miner.* (in the press).
11. Handy, R. L. *Proc. Soil Sci. Soc. Am.* **37**, 281–284 (1973).
12. Fedai, J. *Engng Geol.* **1**, 201–219 (1966).
13. Denisov, N. Ya. *Osnov. Fundam. Mekh. Grunt.* **5**, 5–8 (1963).

## Formation of $\text{C}_4$ – $\text{C}_7$ hydrocarbons from bacterial degradation of naturally occurring terpenoids

John M. Hunt, Robert J. Miller & Jean K. Whelan

Woods Hole Oceanographic Institution, Woods Hole, Massachusetts 02543

**We have recently found many light hydrocarbons, both alkanes and alkenes, in trace amounts (ng compound per g sediment) in Recent marine sediments<sup>1–4</sup>. These hydrocarbons are believed to originate from both biological and low-temperature reactions in the sediments. Understanding their mechanism of formation may allow use of these compounds to decipher the past biological and thermal history of the sediments<sup>4</sup>. To investigate biological origins, we have cultivated mixed populations of bacteria on natural terpenoids and found, as degradation products, both alkanes and alkenes in the  $\text{C}_1$ – $\text{C}_7$  range; this is the first report of  $\text{C}_4$ – $\text{C}_7$  hydrocarbons being formed from microbial activities. Aerobic followed by anaerobic degradation yielded mainly small amounts of straight-chain alkenes. No such products resulted from blanks or controls. The results are consistent with products observed in natural environments.**

The analytical procedure was carried out in 125-ml glass bottles (Hungate method)<sup>5</sup> and 455-ml cans. Both types of vessels were equipped with silicone rubber septa<sup>2</sup> and shown to be gas tight by injecting a positive pressure of helium and testing with an electronic helium leak detector (Gow Mac).

All gases were passed through an alumina trap immersed in dry ice and an Oxisorb trap (Analabs) to remove traces of hydrocarbon or oxygen. All distilled water used in making solutions and media was sparged with helium for 5 min to remove any traces of volatile hydrocarbons. All anaerobic operations and transfers were carried out in a glove bag (12 R) which was alternately evacuated and filled three times with a mixture of 80%  $\text{N}_2$ –20%  $\text{CO}_2$  (the  $\text{CO}_2$  was Matheson, Anaerobe purity). Vessels were kept in the glove bag maintained with a slight positive pressure of 80%  $\text{N}_2$ –20%  $\text{CO}_2$  during bacterial growth to guard against accidental small leaks.

Media was artificial seawater<sup>6</sup> and other nutrients including Pfennig's<sup>7</sup> trace metal stock solution (1 ml per litre). About 30 ml of this media (sterilized and sparged with 20%  $\text{CO}_2$ –80%  $\text{N}_2$ ) containing 0.5–1.5 mg terpene in suspension (farnesol or  $\beta$ -

carotene) per ml medium were added to the sterilized cans and the cans sealed.

A mixed culture of anaerobic bacteria was collected from the sediments in a brackish water pond (Salt Pond) near our laboratory in a collection tube, which was evacuated and filled with an atmosphere of 80%  $\text{N}_2$ –20%  $\text{CO}_2$ . The sample was brought back to the laboratory and further operations were carried out in the glove bag described above. The material was filtered through a 1.2- $\mu\text{m}$  Millipore filter to exclude particulate matter and organisms larger than the desired bacteria. Portions of the filtrate (1 ml) were inoculated into sample cans containing media and farnesol or  $\beta$ -carotene as described above and blank cans which contained everything but the terpene (farnesol or  $\beta$ -carotene). Additional blank cans which had media and terpene substrates but no bacteria were also run with the other blanks. The cans were stored at room temperature and analysed as described below at the end of 144 h.

In the second method, the media was prepared in a device similar to that of Willingham<sup>7</sup>. The media (35 ml) (artificial seawater/Pfennig's solution as described previously plus 0.5 g per litre cysteine-HCl and a few drops of reazurin indicator solution dispensed into the serum bottles after  $\text{CO}_2$  was bubbled through the dispensing device so that the indicator turned from blue to red) was dispensed into the bottles which were subsequently sealed. Substrates and bacteria were added in the same concentrations as used in the cans. The bottles were kept at room temperature and analysed after 196 h. During this time, the reazurin indicator turned from pink to colourless indicating anoxic conditions. Several blanks were run, some using substrates and all carbon sources but no bacteria, others using bacteria and media as described above, but no terpene.

We also wanted to know whether aerobic bacterial metabolism could modify functional groups and make them more susceptible to anaerobic attack. About 4 g of a Noble bacto-agar (VWR) was dissolved by heating in 1 l of a mineral salts medium, autoclaved, cooled and divided into portions. Carbon sources (1.5 g yeast extract and 1.5 g tryptose per litre of medium) were added and several plates were filled with 20 ml of medium. The terpenoids (farnesol and  $\beta$ -carotene) were added initially in low concentrations (10% terpenoid carbon source, 90% yeast/tryptose) and concentrations were gradually increased to prevent inhibition of bacterial growth from too much terpenoid. The final carbon source was 90% terpenoid and 10% yeast extract/tryptose. High bacterial populations were observed by direct microscopic examination for 7 days at these concentrations. Culturing was terminated by dissolving the agar from each plate with concentrated (12 M) HCl (15 ml) and neutralizing with NaOH to pH 7. This solution was placed in the glove bag, sparged with 80%  $\text{N}_2$ –20%  $\text{CO}_2$ , and 30 ml added to the 125-ml Hungate bottles along with 20 ml of the reduced media described above. The bottles were sealed and anaerobic sediment inoculum were introduced into the samples as described previously. Blanks were run with everything but the bacteria and with everything but the terpenoids. Samples were maintained at room temperature and analysed after 210 h. Cultures were terminated by injecting 5 ml of 0.1 M  $\text{HgCl}_2$  into each bottle.

To drive all volatile compounds into the gas phase, the containers were heated at the end of the experiment in a hot water bath at 90°C for 15 min. An aliquot of the gas was withdrawn and analysed on a 200 ft  $\times$  0.01 inch i.d. stainless-steel hexadecane-hexadecene Kel F capillary (WCOT) column<sup>2</sup>. This column will separate most alkanes and alkenes in the  $\text{C}_4$ – $\text{C}_7$  hydrocarbon range as well as compounds with functional groups such as thio-ethers. Compounds were identified by retention time, by co-injection of standards and by gas chromatography-mass spectrometry. All of the compounds found in these experiments had previously been found in Recent sediments<sup>1–4</sup>. Limits of detection by this method are 0.003  $\mu\text{g}$  hydrocarbon per litre of medium.

The hydrocarbons formed in these experiments are listed in Table 1. None of these hydrocarbons was recovered in the blank runs including those with bacteria but no substrate and those



**Table 1** Yield of  $C_4$ – $C_7$  hydrocarbons from microbial degradation of terpenoids

| Mixed culture      | Substrate*         | Products           | Yield†<br>( $\mu$ g per<br>litre<br>medium) |
|--------------------|--------------------|--------------------|---|
| Metal cans         |                    |                    |   |
| Anaerobes          | Farnesol           | Isopentane         | 3   |
|                    |                    | 3-Methylpentane    | $1.5 \pm 0.3$ ‡                             |
| Anaerobes          | $\beta$ -Carotene  | 2-Methylpentane    | 19  |
|                    |                    | 3-Methylpentane    | $16 \pm 2.5$ ‡                              |
|                    |                    | Toluene            | 35  |
| Serum bottles      |                    |                    |   |
| Anaerobes          | Farnesol           | 1-Butene           | 12  |
|                    |                    | 3-Methylpentene    | 11  |
| Anaerobes          | $\beta$ -Carotene  | Methylbutene       | 14  |
| Anaerobes          | $\alpha$ -2-Pinene | Methylbutene       | 15  |
| Aerobes (7 days)   | Farnesol           | 1-Butene           | 141   |
| Anaerobes (8 days) |                    | 2-Hexene           | 9   |
| Aerobes (7 days)   | $\beta$ -Carotene  | 1-Hexene           | 30  |
| Anaerobes (8 days) |                    |                    |   |
| Aerobes (7 days)   | $\alpha$ -2-Pinene | Methylpentene      | 17  |
| Anaerobes (8 days) |                    | 2,2-Dimethylbutane | 21  |

\* About 0.5–1.5 mg of substrate per ml of medium.

† Detection limit 0.003  $\mu$ g per litre medium.

‡ Standard deviation from duplicate cultures.

with substrate but no bacteria. Small amounts of methane, ethane, propane and butane were found in some of the samples, but these were also in blanks that did not contain the terpenoids, so their presence was not considered a result of terpenoid degradation. Also, the samples run in the serum bottles with anaerobic bacteria, but no terpenoids, yielded 50  $\mu$ g per litre of dimethylsulphide and 25  $\mu$ g per litre of  $CS_2$  (detected by gas chromatography). When farnesol was added, these yields increased up to 60  $\mu$ g and 200  $\mu$ g per litre, respectively.

The most significant conclusion is that the anaerobic degradation process formed only a few specific hydrocarbons from each terpenoid. Only alkanes and toluene were formed in the metal cans, whereas alkenes were the main products in the glass serum bottles. The kinetics of alkene formation by the anaerobes is possibly faster than that of alkane formation, but is inhibited by the metal in the can. The formation of branched pentanes from either farnesol or  $\beta$ -carotene is conceivable through the breaking of a carbon-carbon bond in the beta position to the double bonds. It is more difficult to understand the formation of the toluene although methylcyclohexene might be a reasonable precursor<sup>4</sup>.  $\beta$ -Carotene will aromatize to form toluene when heated for 2 weeks at 119 °C (ref. 8). However, when heated at 90 °C for 15 min in the conditions of our experiments, no toluene was found within our detection limit (0.003  $\mu$ g per litre medium). The high yield of toluene in Table 1 only resulted when anaerobes were present in the can. The reason for formation of toluene in the cans but not in the bottles is unclear, but may be due to some effect of the metal in the can. Controls showing no toluene production were: (1) blanks having all substrates including carotene but no bacteria; and (2) bacteria with all carbon sources except carotene. Thus, toluene production due to a metal-catalysed chemical reaction has been ruled out. We did not do aerobic experiments with the metal cans so we cannot conclude that toluene forms exclusively in anaerobic environments.

The anaerobic culturing in the serum bottles yielded mainly branched alkenes. The experiments with aerobes followed by anaerobes yielded mainly straight-chain alkenes and one gem-dimethyl alkane, 2,2-dimethylbutane. The formation of this compound from  $\alpha$ -2-pinene could result from breaking off the 4-carbon ring with the quaternary carbon atom in  $\alpha$ -pinene.

The results of these preliminary microbial degradation experiments fit surprisingly well with our studies of hydrocarbon distributions in marine sediments. In the strongly reducing environment of Walvis Bay, we found that toluene constituted

70% of the  $C_4$ – $C_7$  hydrocarbons in the surface sediments<sup>4</sup>. The present laboratory experiments support the concept that toluene can be an anaerobic degradation product, and show that the gem-dimethyl alkanes, such as neopentane and 2,2-dimethylbutane dominate in sediments where the overlying waters (and topmost sediments) are oxidizing with deeper sediments reducing (Arabian Sea)<sup>3</sup>. These same environments also produced a diverse assemblage of alkenes, including straight-chain pentenes and hexenes. Such compounds seemed to arise from a combination of both aerobic and anaerobic microbial degradation of organic substrates, possibly together with low-temperature chemical reactions. Whelan *et al.*<sup>5</sup> have discussed in detail possible chemical reactions leading to the  $C_4$ – $C_7$  hydrocarbons, such as alcohol dehydration and allylic free radical cleavage. It has also been pointed out that bacterial reworking of algae forms an amorphous biomass high in bacterial bodies that is more readily converted to hydrocarbons in the  $C_{15}$  range<sup>9</sup>. However, we found no references to  $C_4$ – $C_7$  hydrocarbon formation by bacterial reworking.

We are not arguing that these products represent major metabolic paths in the organism. The trace amounts of substrate transformed suggest that these paths probably represent reactions which are incidental to the bacteria. However, the small (p.p.m.–p.p.b.) levels of compounds found in these experiments and in our Recent sediment analyses are comparable so that these microbial processes may explain one source of the compounds in Recent sediments. This is a valuable finding because the presence of a particular set of these molecules in more deeply buried cold sediments may provide information about the nature of the sediment-water interface (oxic or anoxic) when the sediment was buried in past geological time.

This work was supported by the Oceanography Section of the NSF grant OCE 79-19861. We thank Craig Taylor for critical evaluation, and Elizabeth McKenna and Marcia Pratt for culturing aerobes and analysing headspace gases. WHOI No. 4571.

Received 14 July, accepted 14 October 1980

- Hunt, J. M. *Nature* **248**, 411 (1975)
- Whelan, J. K. *Int. Rev. DSDP* **47a**, 531 (1979)
- Hunt, J. M. & Whelan, J. K. *Org. Geochem.* **1**, 219 (1979)
- Whelan, J. K., Hunt, J. M. & Borman, J. *Geochim. cosmochim. Acta* (in the press)
- Ferry, J. G. & Wolfe, R. S. *Microbiology* **107**, 33 (1976)
- Lymap, J. & Fleming, R. H. *J. Mar. Res.* **3**, 134 (1940)
- Willingham, C. A. & Oppenheimer, C. H. *J. Biol. Chem.* **241**, 541 (1964)
- Day, W. C. & Erdman, J. G. *Science* **141**, 808 (1963)
- Lymbach, G. M. *Proc. 9th World Petroleum Congr.* **2**, 357–369 (1975)

## The principal eyes of a jumping spider have a telephoto component

David S. Williams &amp; Peter McIntyre

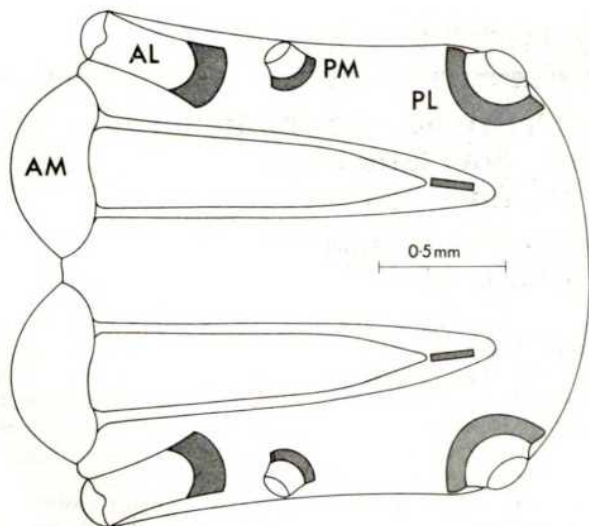
Department of Neurobiology, Research School of Biological Sciences, Australian National University, Canberra, Australia

Jumping spiders are a cosmopolitan family (Salticidae) of predators that can make visual discrimination between prey and mates<sup>1,2</sup>. This task is mediated through the anterior median eyes, described by Land<sup>3</sup> as consisting of a corneal lens and a mottle retina that comprises four layers of receptors embedded in a matrix. The retinal matrix contains a pit distal to the receptors and symmetrically centred on-axis. We have now found that in *Portia fimbriata* (Dolleschall) and some other species, this pit has a refracting interface that increases the focal length of the eye beyond its axial length, thereby magnifying the retinal image and increasing visual resolving power above that possible with only a corneal lens. The most effective part of the conical pit is its rounded apex, which augments the corneal lens to provide a telephoto system that increases the overall focal length by about 1½ times. This mechanism is of particular value to small spiders like *P. fimbriata*, for the possible axial length of their eyes is constrained by the small size of their prosomae (Fig. 1).

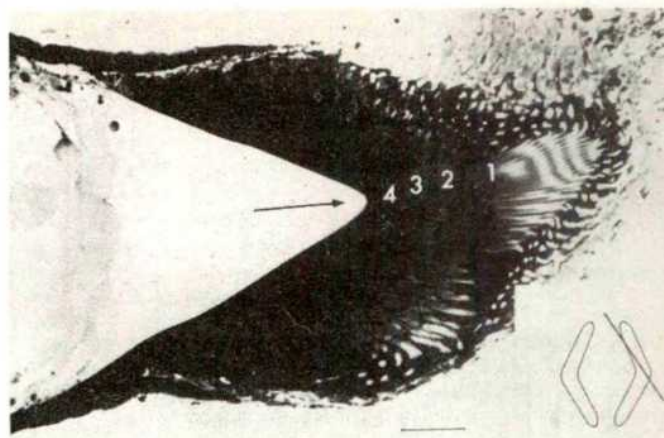


The inside of the pit of the anterior median eye of *P. fimbriata* is structureless and must have a refractive index ( $n$ ) close to that of saline, about 1.336 (Fig. 2). In glutaraldehyde-fixed material, cut while frozen, the matrix behind the pit was found by interferometry to have a uniform  $n$ , a value of  $\sim 1.40$  being obtained from unfixed material. The rounded apex of the pit is about  $20\text{ }\mu\text{m}$  in diameter; the most central region is approximately spherical, with radius of curvature  $\sim 5\text{ }\mu\text{m}$ , and thus acts as the diverging lens of the telephoto system (Fig. 3), with power  $(1.40-1.336)/(-5 \times 10^{-6}) = -12,800$  dioptres. In longitudinal profile, the rounded region is less curved beyond about  $4\text{ }\mu\text{m}$  from the axis and merges into straight sides (Fig. 2). Such an aspherical surface may well give a better image over a wider aperture than a spherical one. The curvature of the pit varies greatly among the different species of salticids and in some cases is so slight that the pit will have negligible power.

From a corneal lens (diameter  $810\text{ }\mu\text{m}$ ) of *P. fimbriata*, dissected out and hung from a drop of saline ( $n = 1.336$ ) to simulate *in situ* conditions<sup>4,5</sup>, a front focal length of  $-1,273\text{ }\mu\text{m}$ , that is, a power of  $+786$  dioptres, was measured (in green light, as was used for the measurements of  $n$ ). The second principal plane of the corneal lens was found nearly to coincide with the front surface of the lens, indicating that the air/cornea interface provides most of the refracting power. The remaining parameter necessary for determination of the optical properties of the telephoto system is the distance,  $d$ , between the corneal lens (more precisely, its second principal plane) and the pit.  $d$  was deduced from ophthalmoscopy, using an apparatus similar to that devised by Land<sup>3,6</sup>. By finding the position in space of the image of a recognizable part of the retina (in this case the virtual image of parts of the receptor cells in the characteristically organized fourth receptor layer, which on-axis lies  $25\text{ }\mu\text{m}$  behind the pit),  $d$  can be calculated from standard thick-lens formulae<sup>7</sup>. (Ideally the properties of the complete dioptric system could be determined directly from the magnification of the ophthalmoscopic image, but this was prevented by uncertainty about exactly which parts of the receptor cells in layer 4 provide the image.) The value determined for  $d$  ( $=1,664\text{ }\mu\text{m}$ ) is to be compared with the focal length in image space of the corneal lens ( $1,273 \times 1.336 = 1,701\text{ }\mu\text{m}$ ). To achieve a reasonable magnification without unduly increasing image distance, the pit must be a short distance inside the focal point of the corneal lens. This condition seems to be satisfied.



**Fig. 1** Diagrammatic horizontal section of the dorsal anterior part of the prosoma of *P. fimbriata*, showing the positions of the anterior (A) and posterior (P) median (M) and lateral (L) eyes. This eye-bearing portion of the prosoma projects dorsally. In the dorso-ventral plane, the posterior eyes lie just above the anterior median retinae.



**Fig. 2** Longitudinal section of an anterior median retina in *P. fimbriata* including part of one arm of its 'boomerang' structure. The material was fixed in glutaraldehyde and  $\text{OsO}_4$ , embedded in Araldite and stained with toluidine blue. Scale bar,  $50\text{ }\mu\text{m}$ . The interior of the pit (arrow) is structureless (the glass cells visible on the left side of the figure do not extend into the pit), but the surrounding retinal matrix has stained densely and homogeneously. Receptor layers are numbered. Horizontally, across the narrow centre of the retina, the distal ends of the layer 1 receptors are arranged as a staircase, such that on the lateral side of the retina they are  $25\text{ }\mu\text{m}$  more distal than on the medial. The overall radius of curvature of the retina in a dorso-ventral plane is far smaller than would be expected if the receptors were organized around the corneal lens. This indicates further that the retina is organized according to the combined properties of the corneal lens and the pit. Inset: Diagram outlining the two anterior median retinae in transverse section at the level of layer 1. The line indicates the plane of the longitudinal section.

Using the above parameters, the position of focus,  $F'$ , of the telephoto system for an object at infinity is  $59\text{ }\mu\text{m}$  behind the pit, corresponding to the distal on-axis region of the second receptor layer, and the magnification achieved by the pit lens is 1.54 (see Fig. 3). The following supports this finding. Comparative ultrastructural studies of salticid principal retinae<sup>8</sup> show that (1) layer 1 receptors in the central region form a high-resolution mosaic whose rhabdom organization implies that the individual rhabdoms are light guides; (2) layer 2 receptors form a coarse central mosaic with probable optical coupling between receptors. In *Plexippus*, recordings from dye-injected cells have identified both layers 1 and 2 as green receptors with peak responses at  $\sim 520\text{ nm}$  (ref. 9). Cells peaking in the green have also been found previously<sup>10</sup>; discrepancies between these results and other published data<sup>11</sup> will be discussed elsewhere<sup>9</sup>. Some salticids, including *P. fimbriata*, seem to discriminate between conspecifics and prey at distances of  $15\text{--}20\text{ cm}$  (refs 12, 13); *Trite planiceps* Simon, a salticid that we find has a significant pit, but lower overall image magnification than *P. fimbriata*, is known to make discriminations at distances of  $20\text{ cm}$  (ref. 12). Thus, a 'best solution' for the dioptric system must provide focused images of objects,  $\sim 20\text{ cm}$  in front of the spider, at the tips of the rhabdoms of layer 1, when  $\lambda = 520\text{ nm}$ . For  $F'$  near the distal ends of the layer 2 receptors, the distal ends of those of layer 1 (Fig. 2) receive best images from objects  $15\text{--}29\text{ cm}$  in front of the spider and have a total depth of field of  $9\text{ cm}$  to  $\infty$ . The depth of field is estimated by compounding the horizontal 'staircase' tiering of the distal ends of layer 1 receptors (which gives the  $15\text{--}29\text{-cm}$  range) with the depth of focus due to diffraction at the aperture of the eye<sup>7</sup> (see below).

The retina of an anterior median eye is boomerang-shaped (Fig. 2), measuring only  $250\text{ }\mu\text{m}$  dorso-ventrally and  $25\text{ }\mu\text{m}$  wide—a size reduction necessary to accommodate the eye's long axis<sup>3</sup> (Fig. 1). At the level of layer 1, the receptors in the centre of



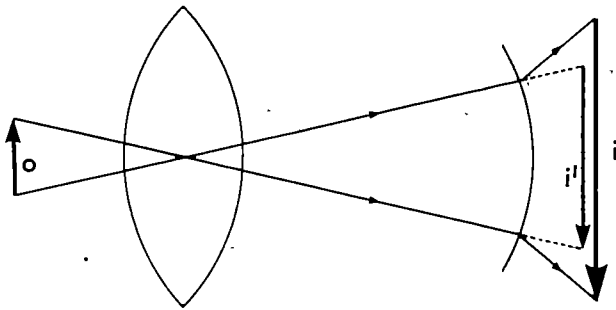


Fig. 3 General schematic illustration of the enlargement of an image by the diverging back element of a telephoto system. o, object; i, image; i', image in absence of diverging surface. The magnification,  $m$ , effected by the pit lens in *P. fimbriata* is given by<sup>7</sup>

$$m = \frac{\text{size of } i}{\text{size of } i'} = P_L/P_T = \left[1 + \frac{P_P(1 - \bar{d}P_L)}{P_L}\right]^{-1}$$

where  $P_T$  is the power of the telephoto lens system, and  $P_L$ ,  $P_P$  the powers of its components, the converging corneal lens and the diverging pit lens respectively  $\bar{d} = d/1.336$ , with  $d$  as defined in the text. This magnification requires an increase in the axial length of the eye of only 22  $\mu\text{m}$

the retina have oval transverse profiles (minimum size 0.8  $\mu\text{m} \times 1.5 \mu\text{m}$ ) and form an hexagonal array with a minimum receptor-row spacing of 1.4  $\mu\text{m}$  (ref. 8), corresponding to a visual angle of 2.4 arc min. (This corresponds to a distance of 0.12 mm at 20 cm in front of the spider.) The resolving ability of a receptor mosaic depends on the angular subtense between neighbouring receptors, that is, on the receptor spacing and focal length of the eye. The receptor spacing at the centre of layer 1 is near the limit imposed by the wave nature of light, because optical crosstalk<sup>14</sup> between the 80–100- $\mu\text{m}$  long rhabdoms would probably be excessive were they much closer together. Therefore, the only way to enhance the anatomical resolving power of the eye is to increase its focal length. Image magnification by the pit achieves this, albeit at the cost of narrowing the field of view of the central retina. About 100 receptors in the centre of layer 1 lie behind the curved region of the pit in a circle of diameter 21  $\mu\text{m}$ —most of the width of the central part of layer 1. In total they have a field of view of 0.6°.

Vertically, the field of view of the eye is extended by the dorsal and ventral extremities of the retina. Light reaching these regions must pass through the sides of the pit which, in longitudinal section, are straight beyond 10  $\mu\text{m}$  from the optic axis and inclined at 30° to it. They produce a range of magnifications of 1.1–1.25, depending on the angle at which rays are incident. Magnification by the whole pit is therefore greatest on-axis, owing to the lens component, and decreases to a negligible amount for very off-axis light. Because off-axis magnification is different for different angles of incidence on the sides of the pit, off-axis focus will be blurred. This poorer image quality is reflected by the receptor mosaic off-axis in layers 1 and 2 where the rhabdoms are larger (~10  $\mu\text{m}$  in diameter) and practically contiguous.

A jumping spider's field of view is extended horizontally by its lateral eyes which, in conjunction with the vertical extremities of the anterior median retinae, allow peripheral detection. Peripheral detection of an object initiates body and anterior median retinal movements that bring images of the object to lie in the centres of the retinae and maintain them there during fixation<sup>6</sup>.

Land<sup>3</sup> suggested that the resolution of the anterior median eyes of two salticid species is probably limited by spherical aberration of their corneal lenses. Our re-examination of the lenses of *P. fimbriata* and several other salticids in a hanging drop and by interference microscopy shows that this defect is corrected by a graded refractive-index distribution in the lens, as in some nocturnal spiders<sup>5,15,16</sup>. Probably, then, the anterior median corneal lenses in salticids are diffraction limited. If this is true of the telephoto system of *P. fimbriata* as a whole, the

maximum or cut-off spatial frequency passed by it is 760  $\text{rad}^{-1}$  (refs 17–19). (The limiting aperture is a ring of pigment, 350  $\mu\text{m}$  in diameter and 315  $\mu\text{m}$  behind the corneal surface. The position of focus is taken as the distal ends of the receptors in layer 1.  $\lambda = 520 \mu\text{m}$ .) The highest spatial frequency that can be reconstructed by layer 1 with minimum receptor-row spacing 1.4  $\mu\text{m}$  and distance 1,980  $\mu\text{m}$  from the posterior nodal point of the telephoto system is  $1,980/2.8 = 710 \text{ rad}^{-1}$ . Therefore, the receptor spacing in the centre of layer 1 seems to be well matched to the telephoto system. In the absence of the pit, the highest frequency reconstructable by the retina would be only 420  $\text{rad}^{-1}$ , which is well below the cut-off frequency for the lens of 850  $\text{rad}^{-1}$ .

A parallel to the pit of *P. fimbriata* is the deep convexiculate fovea found in some vertebrates, notably falconiform birds<sup>20</sup>. It has been proposed that this fovea magnifies the retinal image<sup>20,21</sup> and acts as a focus indicator<sup>22</sup>. The latter is an implausible function for the pit in *P. fimbriata*, for as in other salticids<sup>3</sup>, ophthalmoscopy shows that the eye does not accommodate. Aerodynamic constraints require the heads of birds to be small. Both a group of vertebrates and an invertebrate have therefore adopted the same strategy to improve visual acuity despite a restricted cephalic space.

We thank Robert Jackson for collecting *P. fimbriata* from Queensland, Fred Wanless (British Museum) for identifying them, and David Blest for his critical comments, for providing much anatomical information and for obtaining *Trite planiceps* in New Zealand with the help of Simon Pollard and Robert Jackson. Part of this report has been published elsewhere<sup>23</sup>.

Received 28 July, accepted 20 October 1980

- Crane, J. *Zoologica* 34, 159–214 (1949)
- Drees, O. *Z. Tierpsychol.* 9, 169–209 (1952).
- Land, M. F. *J. exp. Biol.* 51, 443–470 (1969)
- Hornemann, H. *Z. vergl. Physiol.* 7, 201–268 (1928)
- Blest, A. D. & Land, M. F. *Proc. R. Soc. B196*, 197–222 (1977)
- Land, M. F. *J. exp. Biol.* 51, 471–493 (1969)
- Longhurst, R. S. *Geometrical and Physical Optics* (Longman, London, 1973)
- Blest, A. D., McIntyre, P. & Williams, D. S. (in preparation)
- Blest, A. D., Hardie, R. C., McIntyre, P. & Williams, D. S. (in preparation)
- De Voe, R. D. *J. gen. Physiol.* 66, 193–207 (1975)
- Yamashita, S. & Tateda, H. *J. comp. Physiol.* 185, 29–41 (1976)
- Forster, L. M. *N. Z. J. Zool.* 6, 79–93 (1979)
- Jackson, R. R. & Blest, A. D. (in preparation)
- Snyder, A. W. *J. opt. Soc. Am.* 62, 1267–1277 (1972)
- Williams, D. S. *Z. Naturforsch.* 34e, 463–469 (1979)
- Blest, A. D., Williams, D. S. & Kao, L. *Cell Tissue Res.* 211, 391–403 (1980)
- Hopkins, H. H. *Proc. R. Soc. A231*, 91–103 (1955)
- Born, M. & Wolf, E. *Principles of Optics*, 5th edn (Pergamon, Oxford, 1975)
- Snyder, A. W. *J. comp. Physiol.* 116, 161–182 (1977)
- Walls, G. L. *The Vertebrate Eye* (Cranbrook Institute of Science, Bloomfield Hills, Michigan, 1942)
- Snyder, A. W. & Miller, W. H. *Nature* 275, 127–129 (1978)
- Hartmann, L. & Bonnet-Clark, H. C. *Nature* 272, 814–816 (1978)
- Williams, D. S. & McIntyre, P. *Proc. Aust. physiol. pharmac. Soc.* 182P (1980)

## Correlative genetic variation in natural populations of cats, mice and men

Stephen J. O'Brien,\* Mitchell H. Gall† & David L. Levin†

\*Laboratory of Viral Carcinogenesis, National Cancer Institute, National Institute of Health—Frederick Cancer Research Center, Frederick, Maryland 21701

†Biometry Branch, National Cancer Institute, National Institutes of Health, Bethesda, Maryland 20205

The study of the extent and basis of gene-enzyme variation has long been a principal concern of population genetics. Numerous surveys have indicated considerable amounts of genetic variation detectable in natural populations, with few exceptions<sup>1–14</sup>. The variances of average heterozygosities ( $H$ ) between species and among populations within species are large, prompting Lewontin to emphasize the importance of large gene sample sizes<sup>7</sup> and Selander to encourage analysis of variation of

homologous gene-enzyme systems when making species comparisons<sup>8</sup>. We present here a comparative genetic analysis of electrophoretic variation at 57 homologous biochemical loci of cats, mice and men. The distribution of polymorphism among the sampled loci in the three species was nonrandom. A large group of sampled loci (60%) were monomorphic in all three species, whereas a second group (30%) of the loci were polymorphic in two or more species. This conservation of the tolerance of genetic polymorphism is apparently more a characteristic of a particular locus than of the vertebrate species or of the genome. The current hypotheses for classifying polymorphic and monomorphic loci in terms of physiological and physical enzyme characteristics have been re-examined.

Table 1 shows a list of per locus heterozygosities ( $h = 1 - \sum x_i^2$ , where  $x_i$  is the frequency of the  $i$ th allele at a locus) of 57 gene-enzyme systems of one feline, two murine and two human populations. The loci encode homologous enzymes of the species, based on enzymatic, histological and molecular enzyme characteristics<sup>6,15-17</sup> as defined elsewhere<sup>15</sup>. The nomenclature of the human and feline loci conforms to the recommendations given in ref. 18; similarly the mouse nomenclature conforms to recommendations of ref. 19. The 57 loci are those which have been studied in either the cat population<sup>6</sup> or the two mouse populations<sup>10</sup>, and also in human populations<sup>2,20</sup> and for which enzymatic homology has been tentatively established. The feline population is a feral farm cat population studied at 55 loci<sup>6</sup>. The human data are from Harris<sup>20</sup> in almost all cases and represent cumulative estimates summarized by Harris and Hopkinson<sup>2,15</sup>. These estimates of human loci agree well with those presented by Nei and Roychoudhury<sup>21</sup>. In a few cases (*GALA* and *ALB*) the latter estimates are used because these loci are not included by Harris and Hopkinson<sup>2,15,20</sup>.

The LC and BC mouse populations are feral mouse populations collected in Southern California in 1977 and have been described in detail elsewhere<sup>10,22</sup>. To demonstrate that these are representative mouse populations, they were compared with previous surveys, that is, those of the island east of Jutland, Denmark population<sup>5</sup>; the Hallowell Farm, California population<sup>4</sup>; the British mainland population<sup>23</sup>, and the outbred Swiss mouse colony at the Eppeley Institute, Omaha, Nebraska<sup>24</sup>. The 12 polymorphic mouse loci in LC and/or BC listed in Table 1 were all polymorphic in previous mouse surveys. Four of the murine loci *Es-10*, *Glo-1*, *Mod-2*, and *Gpd-1* that are monomorphic in LC and BC, but fall in the polymorphic cluster (1-22 in Table 1), are also polymorphic in other mouse surveys<sup>4,5,23-25</sup>.

The 57 loci in Table 1 are listed according to the extent of polymorphism seen in the three species. The first 22 loci are polymorphic in at least 1 of the 3 species, and, of these, 14 (25% of the total) are polymorphic in 2 species. The estimate rises to 30% if *Glo-1*, *Mod-2*, *Es-10* and *Gpd-1* (which are monomorphic in LC and BC mice but vary between inbred strains and in Swiss, Hallowell Farm and Jutland Island mice) are included. If the distribution of allozyme polymorphism in two species were independent, the frequency of systems which are polymorphic in any two species would be equal to the product of their individual polymorphism frequencies. For example, in our cat sample<sup>6</sup> (Table 1), the proportion of loci tested which were polymorphic ( $P_{cat}$ ) was 0.22 (12/55 loci). The value for the California mice ( $P_{mouse}$ ) sampled was 0.20. Thus, the expected frequency of loci which are polymorphic in both species, if the estimates were independent, equals  $P_{cat} \times P_{mouse} = 0.04$ . The observed frequency of systems which vary in both cat and mouse was 0.14 (5 of 35 loci), nearly 4 times greater than expected.

Table 1 Comparison of biochemical allelic variation of homologous loci of cat, mouse and man

| Human/feline gene | Homologous mouse gene | Subunit number | Subunit molecular weight ( $\times 10^{-3}$ ) | Enzyme class | h = heterozygosity                   |                     |         |                               |      |
|-------------------|-----------------------|----------------|---|--------------|--------------------------------------|---------------------|---------|-------------------------------|------|
|                   |                       |                |   |              | <i>Felis catus</i> (Mid Atlantic US) | <i>Homo sapiens</i> |         | <i>M. musculus domesticus</i> |      |
|                   |                       |                |   |              |                                      | (Caucasian)         | (Negro) | (LC)                          | (BC) |
| 1. PGD            | <i>Pgd</i>            | 2              | 52  | N            | 0.47                                 | 0.04                | 0.09    | 0.24                          | 0.30 |
| 2. HBB            | <i>Hbb</i>            | 4*             | 16  | —            | 0.30                                 | 0.0                 | 0.15    | 0.32                          | 0.44 |
| 3. ESD/ES5        | <i>Es-10</i>          | 2              | 28  | V            | 0.34                                 | 0.18                | 0.18    | 0.0                           | 0.0  |
| 4. PGM3           | —                     | 1              | 53  | R            | 0.38                                 | 0.38                | 0.45    | —                             | —    |
| 5. FUCA           | —                     | 1              | 50  | —            | 0.20                                 | 0.38                | 0.13    | —                             | —    |
| 6. GDH2           | <i>Gpd-1</i>          | 2              | —   | —            | 0.49                                 | —                   | —       | —                             | —    |
| 7. PEPA           | <i>Pep-1</i>          | 2              | 46  | V            | 0.48                                 | 0.38                | 0.31    | 0.0                           | 0.0  |
| 8. ADA            | <i>Ada</i>            | 1              | 34  | R            | 0.53                                 | 0.10                | 0.04    | 0.0                           | 0.0  |
| 9. —/ES1          | <i>Es-2</i>           | 1              | 55  | V            | 0.35                                 | —                   | —       | 0.32                          | 0.50 |
| 10. GPI           | <i>Gpi-1</i>          | 2              | 62  | R            | 0.10                                 | 0.0                 | 0.0     | 0.0                           | 0.05 |
| 11. ME1           | <i>Mod-1</i>          | 4              | 60  | R            | 0.11                                 | 0.0                 | 0.0     | 0.30                          | 0.42 |
| 12. GSR           | <i>Gr-1</i>           | 2              | 50  | —            | 0.0                                  | 0.50                | 0.48    | 0.50                          | 0.50 |
| 13. GPT           | <i>Gpt-1</i>          | 2              | 50  | R            | 0.0                                  | 0.50                | 0.26    | 0.40                          | 0.06 |
| 14. PGM1          | <i>Pgm-2</i>          | 1              | 51  | R            | 0.0                                  | 0.38                | 0.32    | 0.0                           | 0.48 |
| 15. GOT 2         | <i>Got-2</i>          | 2              | 46  | N            | 0.0                                  | 0.04                | 0.15    | 0.47                          | 0.42 |
| 16. ME 2          | <i>Mod-2</i>          | 4              | 60  | R            | 0.0                                  | 0.18                | 0.0     | 0.0                           | 0.0  |
| 17. GLO1          | <i>Glo-1</i>          | —              | —   | —            | 0.0                                  | 0.49                | 0.40    | 0.0                           | 0.0  |
| 18. PFK           | —                     | 4              | 100   | R            | 0.25                                 | 0.0                 | 0.0     | —                             | —    |
| 19. G6PD          | <i>G6PD</i>           | 2              | 53  | R            | 0.0                                  | 0.0                 | 0.46    | 0.0                           | 0.0  |
| 20. ACP1          | <i>Acp-1</i>          | 1              | 15  | V            | 0.0                                  | 0.48                | 0.45    | 0.0                           | 0.0  |
| 21. GOT1          | <i>Got-1</i>          | 2*             | 46  | N            | 0.0                                  | 0.0                 | 0.0     | 0.38                          | 0.0  |
| 22. ID1           | <i>Id-1</i>           | 2              | 48  | N            | 0.0                                  | 0.0                 | 0.0     | 0.51                          | 0.0  |
| 23. APRT          | <i>Aprt</i>           | 2              | 16  | —            | 0.0                                  | 0.0                 | 0.0     | 0.0                           | 0.0  |
| 24. AK1           | <i>Ak-1</i>           | 1              | 22  | R            | 0.0                                  | 0.04                | 0.02    | 0.0                           | 0.0  |
| 25. AK2           | <i>Ak-2</i>           | 1              | 40  | R            | —                                    | 0.0                 | 0.0     | 0.0                           | 0.0  |
| 26. ALDA          | —                     | 4*             | 39  | N            | 0.0                                  | 0.0                 | 0.0     | —                             | —    |
| 27. ADH1          | <i>Adh-2</i>          | 2*             | 40  | R            | —                                    | 0.0                 | 0.0     | 0.0                           | 0.0  |
| 28. CPKB          | —                     | 2*             | 41  | —            | 0.0                                  | 0.0                 | 0.0     | —                             | —    |
| 29. DIA1          | —                     | 1              | 30  | —            | 0.0                                  | 0.0                 | 0.0     | —                             | —    |
| 30. ESA/ES7       | <i>Es-s</i>           | —              | —   | V            | 0.0                                  | 0.0                 | 0.0     | 0.0                           | 0.0  |
| 31. GALA          | —                     | 2              | —   | —            | 0.0                                  | 0.0                 | 0.0     | —                             | —    |
| 32. GALB          | <i>Bgs</i>            | 1              | 72  | —            | 0.0                                  | 0.0                 | 0.0     | —                             | —    |
| 33. GDH1          | —                     | 2              | 111   | —            | 0.0                                  | 0.0                 | —       | —                             | —    |
| 34. GAPD          | <i>Gapdh</i>          | 4              | 36  | R            | —                                    | —                   | 0.0     | 0.0                           | 0.0  |
| 35. GUSB          | <i>Gus</i>            | —              | —   | —            | 0.0                                  | 0.0                 | 0.0     | 0.0                           | 0.0  |

(Table 1 continued overleaf)



Table 1 continued

| Human/feline gene | Homologous mouse gene | Subunit number | Subunit molecular weight ( $\times 10^{-3}$ ) | Enzyme class | h = heterozygosity                   |   |      |   |     |
|-------------------|-----------------------|----------------|---|--------------|--------------------------------------|---|------|---|-----|
|                   |                       |                |   |              | <i>Felis catus</i> (Mid Atlantic US) | <i>Homo sapiens</i> (Caucasian) (Negro) |      | <i>M. musculus domesticus</i> (LC) (BC) |     |
| 36. <i>HEXA</i>   | —                     | —              | —   | —            | 0.0                                  | 0.0                                     | —    | —                                       | —   |
| 37. <i>HEXB</i>   | —                     | —              | —   | —            | 0.0                                  | 0.0                                     | —    | —                                       | —   |
| 38. <i>HK1</i>    | <i>Hk-1</i>           | 1              | 107   | R            | 0.0                                  | 0.0                                     | —    | —                                       | —   |
| 39. <i>HPRT</i>   | <i>Hprt</i>           | 3              | 26  | —            | —                                    | 0.0                                     | 0.0  | 0.0                                     | 0.0 |
| 40. <i>IDH2</i>   | <i>Idh-2</i>          | —              | —   | R            | 0.0                                  | 0.0                                     | 0.0  | 0.0                                     | 0.0 |
| 41. <i>LHDA</i>   | <i>Ldh-1</i>          | 4*             | 35  | N            | 0.0                                  | 0.0                                     | 0.0  | 0.0                                     | 0.0 |
| 42. <i>LDHB</i>   | <i>Ldh-2</i>          | 4*             | 35  | N            | 0.0                                  | 0.0                                     | 0.0  | 0.0                                     | 0.0 |
| 43. <i>MDH1</i>   | <i>Mor-2</i>          | 2*             | 35  | N            | 0.0                                  | 0.0                                     | 0.0  | 0.0                                     | 0.0 |
| 44. <i>MDH2</i>   | <i>Mor-1</i>          | 2              | 35  | N            | 0.0                                  | 0.0                                     | 0.0  | 0.0                                     | 0.0 |
| 45. <i>MPI</i>    | <i>Mpi-1</i>          | 1              | 43  | —            | 0.0                                  | 0.02                                    | —    | 0.0                                     | 0.0 |
| 46. <i>NP</i>     | <i>Np-1</i>           | 3              | 28  | —            | 0.0                                  | 0.0                                     | 0.0  | 0.0                                     | 0.0 |
| 47. <i>PEPB</i>   | <i>Pep-2</i>          | 1              | 55  | V            | 0.0                                  | 0.0                                     | 0.0  | 0.0                                     | 0.0 |
| 48. <i>PEPC</i>   | <i>Dip-1</i>          | 1              | 64  | V            | 0.0                                  | 0.02                                    | 0.01 | 0.0                                     | 0.0 |
| 49. <i>PEPD</i>   | <i>Pep-4</i>          | 2              | 50  | V            | 0.0                                  | 0.0                                     | 0.04 | 0.0                                     | 0.0 |
| 50. <i>PEPS</i>   | <i>Pep-7</i>          | —              | —   | V            | —                                    | 0.0                                     | 0.0  | 0.0                                     | 0.0 |
| 51. <i>PGM2</i>   | <i>Pgm-1</i>          | 1              | 61  | R            | —                                    | 0.0                                     | 0.02 | 0.0                                     | 0.0 |
| 52. <i>PP</i>     | <i>Pyp</i>            | 2              | 23  | —            | 0.0                                  | 0.0                                     | 0.0  | 0.0                                     | 0.0 |
| 53. <i>SOD1</i>   | <i>Sod-1</i>          | 2*             | 16  | V            | —                                    | 0.0                                     | 0.0  | 0.0                                     | 0.0 |
| 54. <i>SOD2</i>   | <i>Sod-2</i>          | 4              | 18  | V            | 0.0                                  | 0.0                                     | 0.0  | 0.0                                     | 0.0 |
| 55. <i>SORD</i>   | —                     | 4              | 38  | N            | 0.0                                  | 0.0                                     | 0.0  | —                                       | —   |
| 56. <i>TPI</i>    | —                     | 2              | 26  | N            | 0.0                                  | 0.0                                     | 0.0  | —                                       | —   |
| 57. <i>ALB</i>    | <i>Alb-1</i>          | —              | 12  | —            | 0.0                                  | 0.0                                     | 0.0  | —                                       | —   |

Enzyme homology (first 2 columns) is based on the following characteristics: (1) substrate specificity; (2) tissue distribution; (3) subcellular organelle association; (4) formation of heteropolymer in somatic cell hybrids; (5) cofactor affinity, and (6) relative electrophoretic mobility. The specific characteristics of each system are described elsewhere<sup>6,15-17</sup>. Subunit number and molecular weight estimates were obtained from refs 39 and 40. Enzyme class after the definitions of Johnson<sup>32</sup>. V, variable substrate class; R, regulatory enzyme class; N, non-regulatory enzyme class. Heterozygosity ( $h$ ) at each locus (assuming Hardy-Weinberg equilibrium) =  $1 - \sum x_i^2$  where  $x_i$  is the frequency of the  $i$ th allele in the population at the locus. A locus is considered to be polymorphic if  $h \geq 0.05$ . If two  $h$  measurements are available, as for LC and BC mice, the species is said to be polymorphic at that locus if either  $h$  value equals or exceeds 0.05. The data are derived from published surveys of feline<sup>6</sup>, human<sup>2,20</sup>, and murine<sup>10</sup> populations. To test for nonrandom distribution of polymorphic loci in the three species sampled, consider only those ( $T = 34$ ) loci for which complete data are available. If  $P_c$ ,  $P_h$ , and  $P_m$  are the numbers of polymorphic loci in the cat, human and murine samples, and  $M_c$ ,  $M_h$  and  $M_m$  are the corresponding numbers of monomorphic loci, then, under independence, the expected number of loci polymorphic in all species ( $PPP$ ) is  $(P_c/T)(P_h/T)(P_m/T)T = 0.7872$  and the expected number of loci monomorphic in all three species ( $MMM$ ) is  $(M_c/T)(M_h/T)(M_m/T)T = 11.7716$ . The expected number of concordant loci ( $PPP + MMM$ ) is 12.5588. The observed value is  $2 + 17 = 19$  concordant loci. The values  $P_c = 7$ ,  $P_h = 13$ ,  $P_m = 10$ ,  $M_c = 27$ ,  $M_h = 21$  and  $M_m = 24$  were obtained from Table 1 using the definition of monomorphic  $h < 0.05$  given above. To determine whether the observed number of concordant  $PPP$  matches ( $Y_1$ ) and concordant  $MMM$  matches ( $Y_2$ ) were significantly greater than expectation, the joint distribution of  $Y_1$  and  $Y_2$  was computed. The number  $X$  of  $PP$  matches for cat and mouse has the hypergeometric mass function  $P(X) = C(P_c, X)C(M_c, P_m - X)/C(T, P_m)$  where  $T = P_c + M_c$  and  $C(n, x) = n!/(x!(n-x)!)$ . Possible values of  $X$  are determined from the  $2 \times 2$  table with margins  $P_c$ ,  $M_c$  and  $P_m$ ,  $M_m$ . Given  $X$ , the conditional joint distribution of  $Y_1$  and  $Y_2$  is given by  $P(Y_1, Y_2|X) = C(X, Y_1)C(b, Y_2)/C(d, P_h - Y_1 + Y_2 - b)/C(T, P_h)$  where  $b = T + X - P_c - P_m$  and  $d = P_c + P_m - 2X$ . Possible values of  $Y_1$  and  $Y_2$  are determined, given  $X$ , from the  $2 \times 3$  table with margins  $X$ ,  $b$ ,  $d$  and  $P_h$ ,  $M_h$ . The joint probability mass function  $P(Y_1, Y_2)$  is obtained for each  $Y_1$  and  $Y_2$  as the sum over all possible  $X$  of terms  $P(X)P(Y_1, Y_2|X)$ . From this distribution it follows that  $P(Y_1 \geq 2) = 0.17410$ ,  $P(Y_2 \geq 17) = 0.00106$  and  $P(Y_1 + Y_2 \geq 19) = 0.00396$ . Thus the number ( $Y_1$ ) of concordant  $PPP$  is not significantly in excess of expectation, but the numbers of  $MMM$  ( $Y_2$ ) and total ( $Y_1 + Y_2$ ) concordances are significantly greater than predicted by chance. To check these calculations, exact means, variances, and covariances of  $Y_1$  and  $Y_2$  were computed using indicator functions and found to agree with those moments of the distribution  $P(Y_1, Y_2)$ . These moment calculations extend the two-dimensional analysis of Everitt<sup>41</sup> to three or more dimensions. In addition, simulation studies confirmed the calculations of  $P(Y_1 \geq 2)$ ,  $P(Y_2 \geq 17)$  and  $P(Y_1 + Y_2 \geq 19)$  above. If the definition of monomorphic is changed from the widely used value  $h < 0.05$  to the very stringent value  $h < 0.01$ , the number of  $MMM$  concordances is reduced to  $Y_2 = 13$  whereas  $Y_1$  is unchanged. Using the corresponding parameters  $P_c = 7$ ,  $M_c = 27$ ,  $P_h = 17$ ,  $M_h = 17$ ,  $P_m = 10$ ,  $M_m = 24$ , we find  $P(Y_1 \geq 2) = 0.2716$ ,  $P(Y_2 \geq 13) = 0.02627$  and  $P(Y_1 + Y_2 \geq 15) = 0.03586$ . Thus, even with this unusually stringent definition of monomorphic, the excess in  $Y_2$  and  $Y_1 + Y_2$  is statistically significant.

\* Indicates those enzyme systems which are inter-locus heteropolymers.

A similar comparison of cat and human<sup>2,6,20</sup> gave an expected overlap frequency of  $P_{cat} \times P_{human} = 0.22 \times 0.28 = 0.06$ ; the observed frequency (Table 1) was  $7/46 = 0.15$ . The mouse-human expectation was 0.06, and the observed match frequency 0.15. The expected frequency of systems polymorphic in all three species assuming random distribution was  $P_c \times P_h \times P_m = 0.01$ . The actual frequency of triple matches was 2 in 36 (0.06). The frequency of polymorphic triplets may actually be higher than indicated because four mouse loci, whose homologues are polymorphic in cat and man, are likely to be polymorphic in mouse, but were not considered as such in our analysis. *Es-10* and *Gpd-1* vary between inbred strains, presumably reflecting allelic variation in their founders<sup>25</sup>. Human and feline *PGM3* have no murine counterpart, although *PGM3* is polymorphic in man, cats and dogs<sup>2,6,26</sup>. *FUCA* is polymorphic in cat and man, but has not yet been typed in any murine population. A three-dimensional statistical analysis of the distribution of polymorphic against monomorphic loci in Table 1 revealed a

significant ( $P = 0.004$ ) excess of monomorphic triplets (that is, loci monomorphic in each species) and polymorphic triplets (loci polymorphic in all three species) over expectation. The statistical methods are shown in Table 1 legend.

The interspecies correlation of the loci which are polymorphic and those which are monomorphic emphasizes the notion that genic polymorphism is a characteristic of certain homologous loci, but not of others in these different species, which have been isolated in evolutionary time for 80 Myr. Certain loci, then, seem to have an adaptive tolerance to accommodate genetic variation whereas others do not, presumably due to selective constraints which physiologically or functionally restrict significant introduction of gene-enzyme variants into a population. An extension of this situation would be the possibility of selective advantage in polymorphism *per se* at the variant loci themselves, in a situation similar to the major histocompatibility complex (MHC) of all vertebrates thus far studied<sup>27,28</sup>. The MHC loci are characteristically polymorphic in natural popu-

lations, often with dozens of segregating alleles rendering virtually 100% heterozygosity within the population.

The molecular and physiological basis of the tendency of specific loci to be polymorphic (or not) is not immediately apparent. A number of adaptive and metabolic models have been proposed to be operative in this decision in *Drosophila* and human populations<sup>29-34</sup>. Enzyme characteristics which have been suggested in this determination include: (1) whether an enzyme has broad substrate specificity and uses exogenous environmental substrates compared with enzymes with narrow substrate specificities and which are members of intermediary enzyme pathways<sup>29-31</sup>; (2) whether or not an enzyme in a pathway exerts a regulatory role<sup>32,33</sup>; (3) the structural gene size as estimated by subunit molecular weight<sup>34,35</sup>; and (4) selective neutrality of the sub-genic portions of polymorphic genes which vary by random mutational substitution<sup>36</sup>. We have estimated the amount of variation in *h* values which can be explained by the first three selective hypotheses using a one-way analysis of variance (data not shown). Although there are tendencies in each case to conform to the models, in no case can more than 10% of the variation be explained by any one model. Whether selective or non-selective factors contribute inordinately to allozyme variation of these systems is not clear.

Finally, the evolutionary conservation of genetic organization and selective factors has also been observed between these three classes of organisms in comparative genetic mapping<sup>16,37,38</sup>. Apparently, blocks of genes have been conserved as linkage groups in a number of cases between cats, mouse and man<sup>16,17,37,38</sup>. The comparative linkage associations and the comparative population structures of these distantly related mammalian genera provide hope for the further understanding of adaptive processes of chromosomal and molecular evolution.

We thank Drs Bruce Grant, Harry Harris, George Johnson and Ross MacIntyre for their discussions during these studies.

Received 5 May, accepted 27 October 1980

- Powell, J. in *Evolutionary Biology* Vol. 8 (eds Dobzhansky, T., Hecht, M. K. & Steere, W. C.) 79-119 (Plenum, New York, 1976)
- Harris, H. & Hopkinson, D. A. *Ann. hum. Genet.* **36**, 9-20 (1972)
- Lewontin, R. C. & Hubby, J. L. *Genetics* **84**, 595-609 (1966)
- Selander, R. K. & Yang, S. Y. *Genetics* **63**, 653-667 (1969)
- Selander, R. K., Hunt, W. G. & Yang, S. Y. *Evolution* **23**, 379-390 (1969)
- O'Brien, S. J. *J. Hered.* **71**, 2-8 (1980)
- Lewontin, R. C. *The Genetic Basis of Evolutionary Change* (Columbia University Press, New York, 1974)
- Selander, R. K. in *Molecular Evolution* (ed. Ayala, F.) 21-45 (Sinauer, Massachusetts, 1976)
- Johnson, G. B. in *Molecular Evolution* (ed. Ayala, F.) (Sinauer, Massachusetts, 1976)
- Race, M. C., Gardner, M. B. & O'Brien, S. J. *Biochem. Genet.* **8**, 915-928 (1980)
- Race, M. C. & Langley, C. H. *Nature* **283**, 855 (1980)
- Boonell, M. L. & Selander, R. K. *Science* **184**, 908-910 (1974)
- Cameron, D. G. & Vyas, E. R. *Biochem. Genet.* **16**, 651-657 (1978)
- Mazlova, M. N., Baccus, R., Pelton, M. R., Smith, M. H. & Gruber, D. in *Proc. 4th Int. Conf. Bear Research and Management* (ed. Martinka, C. J.) (Wildlife Management Inst., in the press)
- Harris, H. & Hopkinson, D. A. *Handbook of Enzyme Electrophoresis in Human Genetics* (North Holland, Amsterdam, 1976)
- Pearson, P. L. *et al. Cytogenet. Cell Genet.* **28**, 82-95 (1979)
- O'Brien, S. J. & Nash, W. G. (submitted)
- Shaw, T. *et al. Cytogenet. Cell Genet.* **28**, 96-116 (1979)
- Committee on Standardization of Genetic Nomenclature for *Mice*. *J. Hered.* **63**, 69-72 (1972)
- Harris, H. *Isosyme Bull.* **18**, 22-25 (1977)
- Nai, M. & Roychoudhury, A. K. *Am. J. hum. Genet.* **26**, 421-443 (1974)
- Gardner, M. B. *Curr. Topics Microbiol. Immun.* **79**, 215-259 (1978)
- Berry, R. J. & Peters, J. *Proc. R. Soc. B197*, 485-503 (1977)
- Race, M. C. & O'Brien, S. J. *Nature* **283**, 157-161 (1980)
- Statits, J. *Cancer Res.* **36**, 4333-4377 (1976)
- Mosier Khan, P., Lou, W. R. T., van der Doos, J. A. & Epstein, R. B. *Transplantation* **18**, 624-628 (1973)
- Klein, J. *Biology of the Mouse Histocompatibility-2 Complex* (Springer, New York, 1975)
- Osozo, D. (ed.) *The Major Histocompatibility System in Man and Animals* (Springer, New York, 1977)
- Gillespie, J. H. & Kojima, K. *Proc. natn. Acad. Sci. U.S.A.* **61**, 582-585 (1968)
- Kojima, K., Gillespie, J. H. & Tobari, Y. N. *Biochem. Genet.* **4**, 627-637 (1970)
- Gillespie, J. H. & Langley, C. H. *Genetics* **76**, 837-848 (1974)
- Johnson, G. B. *Science* **184**, 28-37 (1974)
- Zoccos, E. *Nature* **254**, 446-448 (1975)
- Koehn, R. K. & Eanes, W. F. *Environ. Biol.* **11**, 39-100 (1978)
- Harris, H., Hopkinson, D. A. & Edwards, Y. H. *Proc. natn. Acad. Sci. U.S.A.* **74**, 698-701 (1977)
- Kimura, M. & Ohta, T. *Nature* **229**, 467-499 (1971)
- Lalloy, P. A., Minna, J. D. & Franke, U. *Nature* **274**, 160-163 (1978)
- Lalloy, P. A., Franke, U. & Minna, J. D. *Proc. natn. Acad. Sci. U.S.A.* **75**, 2382-2386 (1978)
- Hopkinson, D. A., Edwards, Y. H. & Harris, H. *Ann. hum. Genet.* **39**, 383-411 (1976)
- Sober, H. A. *Handbook of Biochemistry, Selected Data for Molecular Biology* (CRC, Cleveland, 1970)
- Everitt, B. S. *Br. J. math. stat. Psychol.* **21**, 97-103 (1968)

## Delayed formation of proteoglycan aggregate structures in human articular cartilage disease states

T. R. Oegema Jr

Departments of Orthopaedic Surgery and Biochemistry, University of Minnesota, Minneapolis, Minnesota 55455

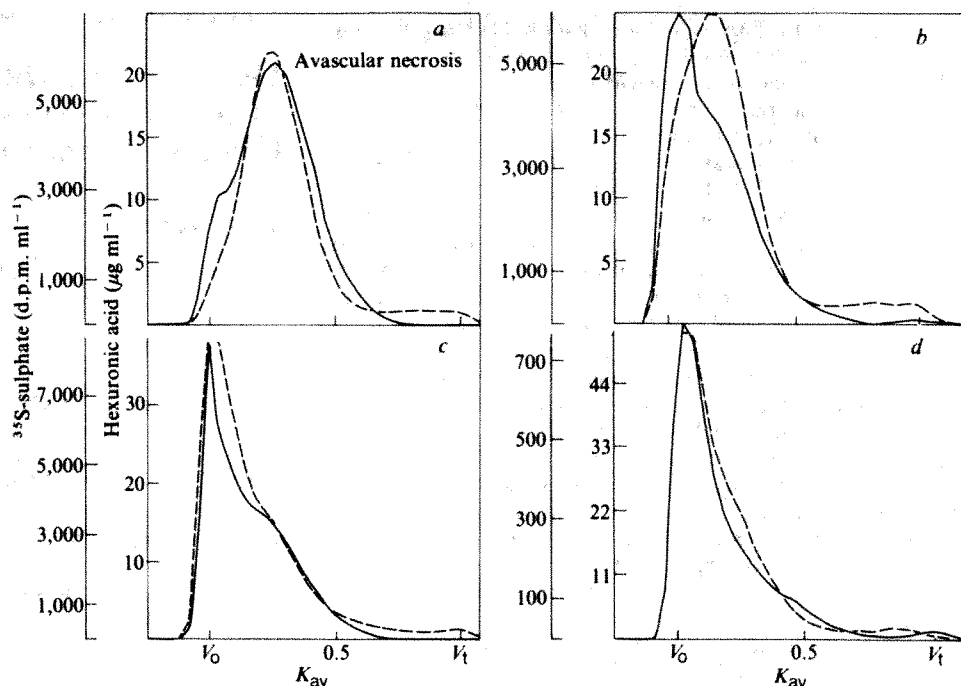
Proteoglycans are major components of many extracellular matrices. In cartilage, they provide reversible resistance to compression and exist as molecules with molecular weights (MWs) of  $1-3 \times 10^6$ . There is a central protein core of MWs approximately  $2 \times 10^5$  (refs 1, 2) with specialized subregions, one containing mainly the chondroitin sulphate chains<sup>3</sup>, another most of the keratan sulphate chains<sup>4</sup>, and a third is a largely globular structure interacting specifically with both hyaluronic acid<sup>5</sup> and a link protein<sup>6</sup> to form stable aggregate structures such as those identified in human articular cartilage<sup>7</sup>. In embryonic<sup>8</sup> and tissue culture systems<sup>9</sup>, proteoglycans are isolated as aggregate structures in as little as 5-10 min after synthesis (sulphation) with no nonaggregating precursor detected. However, Heinegård and Hascall have characterized the small proportion of nonaggregating proteoglycan present in bovine nasal septum cartilage and found that it contained more peptide than the aggregating proteoglycan<sup>10</sup>. Work by Upholt *et al.*<sup>11</sup> has suggested that the MW of unprocessed protein core, synthesized by a wheat-germ translating system from chick sternal cartilage mRNA, is ~340,000, leaving open the possibility of intermediates. I report here the presence, in some human cartilages, of a proteoglycan population that initially will not aggregate with the hyaluronic acid but subsequently can be chased into aggregate.

Human articular cartilage samples were obtained as described previously<sup>12</sup> from normal femoral heads and osteoarthritic joints in the areas immediately adjacent to the osteoarthritic lesion and from kidney-transplant patients undergoing total hip arthroplasty for steroid-induced avascular necrosis. Samples were labelled *in vitro* in RPMI 1640 media as described previously (<sup>35</sup>S-sulphate concentration of 100  $\mu$ Ci ml<sup>-1</sup>) for 4 h (ref. 13) and then part of the sample was extracted with 4 M guanidine hydrochloride in the presence of protease inhibitors<sup>2</sup>. The remainder of the sample was transferred to nonradioactive media containing 0.5 mM sulphate, chased for 18 h, and subsequently extracted as the 4-h samples. The proteoglycan monomer was purified from the extract by a dissociative caesium chloride density-gradient procedure<sup>2</sup>. The proteoglycans were isolated in the bottom two-fifths or D1 fraction and were subsequently examined for incorporated isotope and the ability to interact with hyaluronic acid<sup>2</sup>. The extracted residue was examined for nonextracted, incorporated isotope as described previously<sup>13</sup>.

Results indicated that both 4-h pulse and 18-h chase samples had the same total incorporation, so there was no incorporation of isotope during the chase period. Ninety-five per cent of the incorporated isotope was found in the bottom D1 or proteoglycan monomer fraction. The per cent extractable which varied from cartilage to cartilage (between 38 and 65%) was not different for the paired 4- and 18-h samples, indicating no significant change in the extractable pool size. There were three classes of response: <sup>35</sup>S-sulphate-labelled proteoglycan from normal cartilage ( $n = 2$ ) interacted with hyaluronic acid to the same extent at both 4 and 18 h (60-70%). Proteoglycans from patients with avascular necrosis ( $n = 3$ ) consistently would not interact with hyaluronic acid at 4 h but would interact at 18 h (Fig. 1b, c) with two additional samples having partial response at 4 h. The osteoarthritic cartilage ( $n = 5$ ) gave intermediate



**Fig. 1** The elution profiles for rat chondrosarcoma carrier proteoglycan hexuronic acid (—) and  $^{35}\text{S}$ -sulphate (---) from sepharose CL-2B for  $^{35}\text{S}$ -sulphate-labelled proteoglycans isolated from avascular necrotic human articular cartilage. *a*, 4-h incubation sample with no added hyaluronic acid. *b*, 4-h incubation sample plus 4% (w/w) added hyaluronic acid. *c*, 18-h chase sample plus 4% added hyaluronic acid. *d*, Proteoglycan reisolated after tumour treatment plus 4% hyaluronic acid. For the 4-h sample, the D1-2 fraction contained  $2.37 \times 10^6$  d.p.m. and represented 89% of the extracted d.p.m. and 46.7% of the total incorporated  $^{35}\text{S}$ -sulphate. The 18-h chase D1-2 fraction contained  $2.2 \times 10^6$  d.p.m. and represented 90% of the extracted d.p.m. and 50.8% of the total incorporated  $^{35}\text{S}$ -sulphate. Of the tumour-treated D1-2 fraction, 97% of the incorporated  $^{35}\text{S}$ -sulphate was in the D1-2 or bottom gradient fraction after the treatment, and 90% of the initially added isotope was recovered. The 18-h and tumour-treated controls with no added hyaluronic acid were identical to the 4-h control with no added hyaluronic acid. Carrier (2 mg) was added for each chromatographic run. The proteoglycan extracted from the tissue represented less than 5% of this value. The incubation with the chondrosarcoma included 0.5 g of freely isolated tumour that was finely minced and briefly washed with RPMI 1640 medium. The tumour was incubated for 4 h at 37 °C in 95% air–5%  $\text{CO}_2$  with the labelled proteoglycan that had been dialysed into (3 ml) RPMI 1640. In controls, similarly treated labelled proteoglycans from the chondrosarcoma were recovered unchanged in these incubation conditions. The presence of 10% heat-inactivated fetal calf serum did not alter the results.

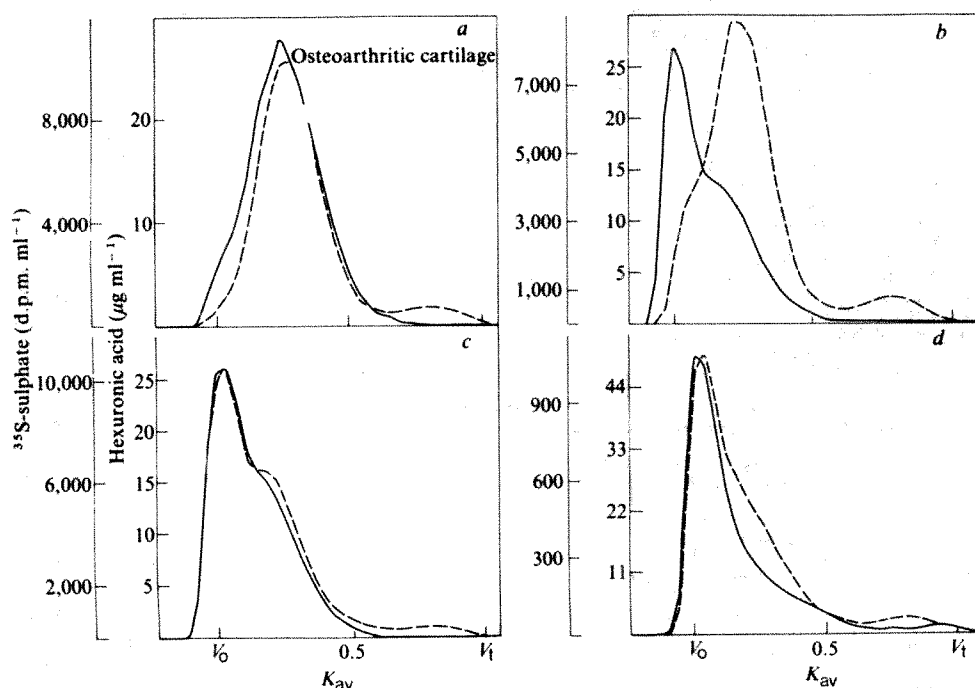


responses with some of the tissues, being unreactive at 4 h (Fig. 2*b*) and 70–80% reactive at 18 h (Fig. 2*c*). In some tissues, the proteoglycans were reactive to the extent of 20–30% at 4 h and were completely (60–70%) reactive at 18 h. When isolated  $^{35}\text{S}$ -sulphate-labelled proteoglycan samples that were non-interactive at 4 h, were treated in the presence of a mince of rat chondrosarcoma<sup>2</sup> for 4 h, reisolated into a dissociative gradient and re-treated with hyaluronic acid, the samples then formed 60–70% aggregate (Figs 1*d*, 2*d*). Controls, in which the tumour was boiled before incubation, showed no conversion to a

hyaluronic interactive form, suggesting a required heat-labile component for conversion.

I therefore suggest that there is a delayed conversion from a hyaluronate-noninteractive precursor to a form that can interact with hyaluronic acid in some osteoarthritic and avascular human cartilages. At present, there is no evidence that this is a classical conversion of a proform to an interactive form or whether there may be a subtle alteration in the structure, such as the slow formation of the correct disulphide bonds in these disease-affected human cartilages. Furthermore, these results may be of

**Fig. 2** The elution profiles for rat chondrosarcoma carrier hexuronic acid (—) and  $^{35}\text{S}$ -sulphate (---) from Sepharose CL-2B for samples of proteoglycans isolated from osteoarthritic cartilage. *a*, 4-h incubation sample with no added hyaluronic acid. *b*, 4-h incubation sample plus 4% (w/w) added hyaluronic acid. *c*, 18-h chase sample plus 4% hyaluronic acid. *d*, Proteoglycan reisolated after treatment with chondrosarcoma plus 4% hyaluronic acid. For the 4-h sample, the D1-2 fraction contained  $1.79 \times 10^6$  d.p.m. and represented 87% of the extracted d.p.m. and 53% of the total incorporated isotope. The 18-h chase D1-2 fraction contained  $1.89 \times 10^6$  d.p.m. and represented 90% of the extracted d.p.m. and 69% of the total incorporated isotope. Of the tumour-treated D1-2 fraction, 97% of the  $^{35}\text{S}$ -sulphate incorporation was in the D1-2 or bottom gradient fraction after the treatment and over 90% of the initially added isotope was recovered. The 18-h and tumour-treated controls with no added hyaluronic acid were identical to the 4-h control with no added hyaluronic acid.



more general application, as the hyaluronic acid-dependent proteoglycan aggregate has recently been reported in other systems<sup>13,14</sup>.

I thank Barbara J. Carpenter for technical assistance. This work was supported by grant CA22558 from the National Institute of Cancer, DHEW and the Orthopaedic Research and Education Foundation.

Received 21 July; accepted 7 October 1980

- 1 Hasegawa, V. C. & Rios, R. L. *J. Biol. Chem.* **247**, 4529–4538 (1972)
- 2 Ogozawa, T. R. Jr, Brown, M. & Dzwonkowski, D. D. *J. Biol. Chem.* **252**, 6470–6477 (1977)
- 3 Hasegawa, D. *J. Biol. Chem.* **252**, 1980–1989 (1977)
- 4 Hasegawa, D. & Axelsson, I. *J. Biol. Chem.* **252**, 1971–1979 (1977)
- 5 Hasegawa, V. C. *J. Supramol. Struct.* **7**, 101–120 (1977)
- 6 Baker, J. R. & Catorson, B. *J. Biol. Chem.* **254**, 2387–2393 (1979)
- 7 Bayliss, M. T. & Ali, S. Y. *Biochem. J.* **176**, 683–693 (1978)
- 8 DeLoe, S., Caplan, A. I. & Hasegawa, V. C. *J. Biol. Chem.* **253**, 4713–4720 (1978)
- 9 Kimura, H. H., Hardingham, T. E., Hasegawa, V. C. & Solursh, M. *J. Biol. Chem.* **254**, 2600–2609 (1979)
- 10 Hasegawa, D. & Hasegawa, V. C. *J. Biol. Chem.* **254**, 927–934 (1979)
- 11 Upbolt, W. B., Vertal, B. M. & Dorfman, A. *Proc. natn. Acad. Sci. USA* **79**, 4847–4851 (1979)
- 12 Thompson, R. C. Jr & Ogozawa, T. R. Jr *Brass. J. Surg.* **61**, 407–416 (1979)
- 13 Ogozawa, T. R. Jr, Bradford, D. S. & Cooper, K. C. *J. Biol. Chem.* **254**, 10579–10581 (1979)
- 14 Ogozawa, T. R. Jr, Hasegawa, V. C. & Eisenstein, R. J. *J. Biol. Chem.* **254**, 1312–1318 (1979)

## Use of aequorin to study excitation-contraction coupling in mammalian smooth muscle

Ian R. Neering\* & Kathleen G. Morgan

Departments of Pharmacology and Physiology and Biophysics, Mayo Foundation, Rochester, Minnesota 55901

Considerable information is available for intact skeletal and cardiac muscle cells on the role of changes in intracellular  $\text{Ca}^{2+}$  ( $[\text{Ca}_i^{2+}]$ ) levels during excitation-contraction coupling<sup>1–3</sup>.  $\text{Ca}_i^{2+}$  levels seem to be similarly important in smooth muscle<sup>4,5</sup>. However, only two published reports describe the use of indicators to directly measure  $[\text{Ca}_i^{2+}]$  in intact smooth muscle cells. One described the use of murexide in molluscan smooth muscle<sup>6</sup>, the other the use of aequorin in single amphibian cells<sup>7</sup>. Their results differed: very long calcium transients were described for the molluscan muscle, compared with very brief ones for the amphibian cells. We present here the first description of the relationship between calcium transients and contraction of whole, mammalian smooth muscle injected with aequorin. The  $\text{Ca}^{2+}$  transient we observed has a slow rise, a long duration, and there was no delay between the peak of the  $\text{Ca}^{2+}$  transient and the onset of force. This contrasts with the amphibian findings but resembles the molluscan data. We observed a delay between the onset of the increase in  $[\text{Ca}_i^{2+}]$  and the onset of the rise in tension which might be explained, at least in part, by the presence of a threshold  $[\text{Ca}_i^{2+}]$  for concentration.

Strips of dog antral circular smooth muscle were prepared as described previously<sup>8</sup>. In each preparation aequorin<sup>9,10</sup>, dissolved in 150 mM KCl, 5 mM HEPES, pH 8.0, was pressure-injected through glass micropipettes into 20–60 cells over an approximately 1-mm<sup>2</sup> area. Light from the aequorin-injected area was detected with an EM1 9635A photomultiplier tube<sup>1</sup>. Figure 1a shows simultaneously recorded light and tension signals in the preparation which gave the largest light response. Both light and tension transients were reproducibly recorded in excess of 128 responses occurring over more than 2 h. This indicates that significant consumption of aequorin was not occurring over this time period. Figure 1b, c shows averaged signals giving a clearer indication of the relationship between light and tension. The onset of the stimulus was coincident with an immediate rapid increase of luminescence (Fig. 1c,

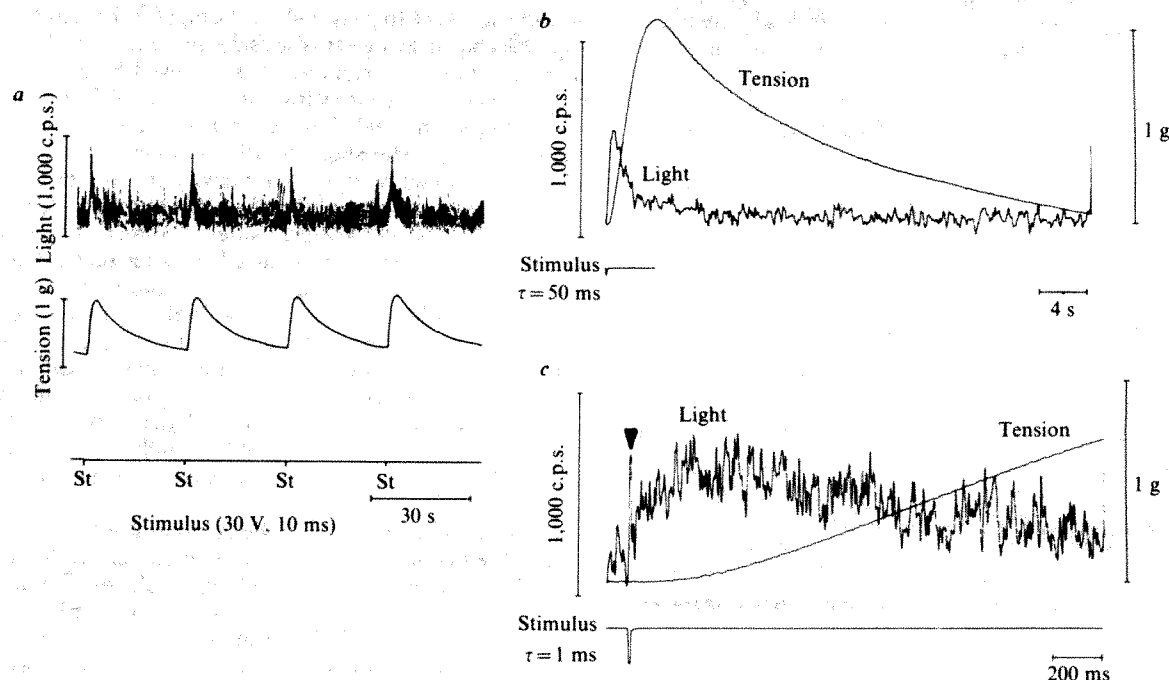
arrowhead) (time to peak 3–4 ms) lasting for the duration of the stimulus and decaying with the same time course as the rise. The short-duration light response was followed by a much slower increase in luminescence with a time to peak of 200 ms (range in five preparations 200–800 ms) and a half decay time of 2 s (range 2–2.5 s). The short-duration response was particularly sensitive to stimulus intensity. At low intensities it was virtually absent, whereas at high intensities light saturated the recording system. At the same, low intensities, the longer-duration light signal and the contraction persisted and an actual potential was still triggered. We think that the short-duration light signal is probably associated with an abnormal membrane response, which has been postulated to explain similar transients in amphibian smooth muscle<sup>7</sup>. Action potentials in canine gastric smooth muscle are often 10 s in duration and seem to involve a  $\text{Ca}^{2+}$  current<sup>8</sup>. Thus, a component of the slower light ( $\text{Ca}^{2+}$ ) transient may occur as a result of  $\text{Ca}^{2+}$  influx during the action potential; however, intracellular release of calcium may also be involved.

It is interesting to compare the responses obtained here with those obtained in other muscles. In amphibian skeletal muscle the delay between onset of the light signal and onset of tension is 5–10 ms at 10 °C (ref. 1); in mammalian Purkinje fibres it is 18–20 ms at 35 °C (ref. 2); in amphibian smooth muscle the delay is greater than 200 ms at 25 °C (ref. 7), whereas for the slow response in our mammalian smooth muscle preparation at 35 °C the delay is 100–160 ms. The value of this latency was not reported for molluscan smooth muscle<sup>6</sup>. Thus, in this respect, mammalian smooth muscle seems to resemble amphibian smooth muscle more closely than the other muscle types. However, the time to peak amplitude of the light responses in mammalian smooth muscle is much greater than in amphibian muscle. Amphibian smooth muscle has a time to peak of only 3 or 4 ms and the light transient is virtually over well before tension development. In contrast, this mammalian smooth muscle has a time to peak of 200–800 ms and a peak light emission coincident with the development of tension. The time to peak for molluscan smooth muscle is similarly long, reaching 1 s or more and corresponding with the development of tension. For comparison, skeletal and cardiac muscles have times to peak of 4 and 8–20 ms, respectively, and the peak light emission occurs during the phase of tension development.

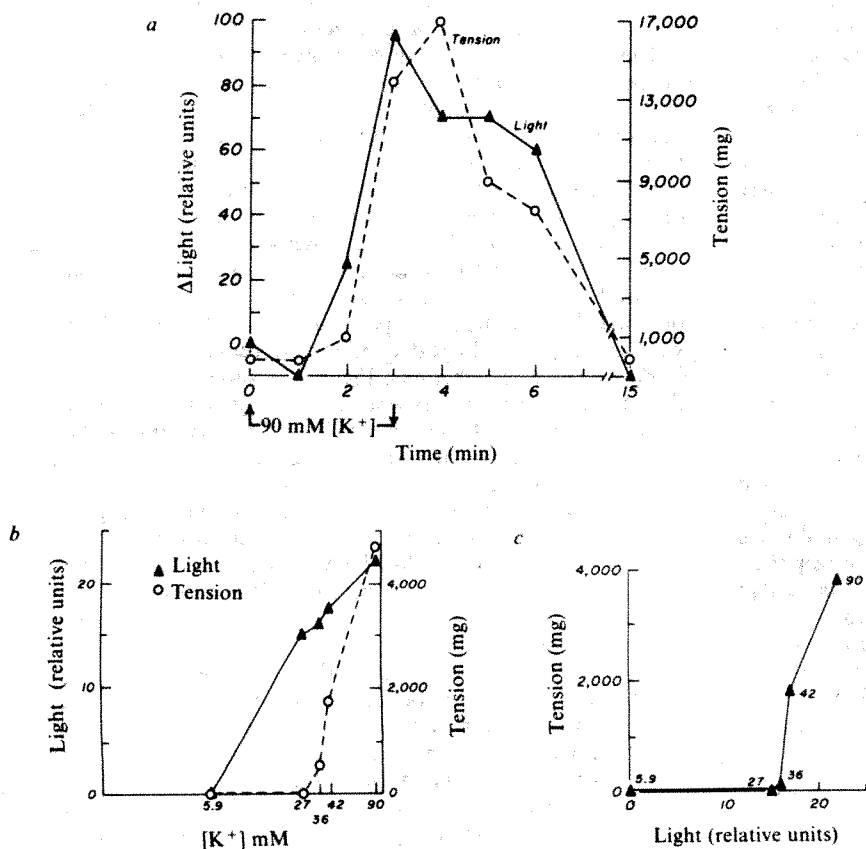
The observation that light emission and hence  $[\text{Ca}_i^{2+}]$  of mammalian smooth muscle rises for a period of more than 100 ms before there is any detectable increase in tension may be interpreted in several ways; either there are relatively slow steps between the elevation of  $\text{Ca}_i^{2+}$  and tension development, or  $[\text{Ca}_i^{2+}]$  is below a threshold concentration necessary for the development of force and some time would be taken in reaching this level, or both of these alternatives occur. The second possibility is supported by the report that this tissue has a voltage threshold for contraction some 30 mV positive to its resting potential<sup>11,12</sup>. To test this possibility and also to determine whether  $[\text{Ca}_i^{2+}]$  is voltage dependent, we recorded calcium levels in depolarized preparations. Figure 2a shows the changes in light and tension with time when an antral strip was depolarized with a solution containing 90 mM  $\text{K}^+$ . This preparation had a 'resting glow' detectable signal averaging. In 5 of 13 preparations demonstrating such a resting glow, there was a decrease in light intensity during the first minute of exposure, however, no regular pattern in this occurrence was noticed. Concentrations of  $\text{K}^+$  of 18–27 mM depolarized the membrane by approximately 15–30 mV (refs 11, 12) and caused increases in light but no increase in tension. Higher levels of  $\text{K}^+$  caused concentration-related increases in light and tension. Figure 2b shows typical plots of both light and tension as a function of  $[\text{K}^+]$  while in Fig. 2c these data are presented as a function of light against tension. Clearly light increased as the  $[\text{K}^+]$  was raised to 27 mM but there was negligible increase of tension up to this level. Microscopic examination of the tissue in these low  $[\text{K}^+]$  solutions failed to reveal any evidence of internal shortening. Thus,  $[\text{Ca}_i^{2+}]$  was increasing at values of membrane potential

\* Present address: Department of Physiology and Pharmacology, University of New South Wales, Box 1, PO Kensington, Sydney, Australia





**Fig. 1** *a*, Simultaneous recordings of light (upper trace) and force of isometric contraction. Light is measured in counts per s from a photon-counting system and force is measured in grammes from a Satham force transducer with a natural frequency of 250 Hz. Individual light and tension responses elicited by 10-ms, 50-V stimuli are shown. The preparation was stimulated through a pair of Pt wires 15 mm apart and parallel to the axis of the circular fibres. Stimulus voltage was chosen to be supramaximal for contraction. Electrical stimuli of these parameters triggered action potentials in this tissue. About 40 cells in this preparation were injected with aequorin. The injection of aequorin had no detectable effect on membrane potential or action potential generation in this spontaneously active tissue. *b*, 32 simultaneous light and tension signals have been averaged to obtain this record. The light signal has been filtered with a 50-ms time constant. *c*, Expanded time scale of the data shown in *b*; recorded with a 1-ms time constant. Arrowhead denotes the brief response associated with stimulus.



**Fig. 2** *a*, Effect of 90 mM K<sup>+</sup> on light emission and isometric tension development. The high [K<sup>+</sup>] solution was substituted for normal Krebs solution at 0 time. ○, Tension; △, light; each data point represents the average of 60, 1-s segments of both light and tension recordings before, during and after exposure to K<sup>+</sup>. High [K<sup>+</sup>] was washed out in this experiment before steady state was established. *b*, Relationship between [K<sup>+</sup>] and light and tension. All data points are from the same preparation, and taken for steady-state responses to each solution. 5.9 mM is the concentration of K<sup>+</sup> in the normal Krebs. *c*, Relationship between light and tension induced by different levels of [K<sup>+</sup>]. This graph shows the same data as *b*. The number beside each symbol represents the [K<sup>+</sup>]. Solutions of high [K<sup>+</sup>] were prepared by equimolar substitution of K<sup>+</sup> for Na<sup>+</sup>. Temperature in all experiments was 32–35 °C (constant in any one experiment).

subthreshold for contraction. This observation supports the contention that resting calcium levels in this tissue are somewhat below a calcium threshold. As this tissue does not normally demonstrate active tone, it may be that such tissues are distinguished from tissues with tonic activity by the level of resting intracellular free calcium concentration.

Whether this 'calcium threshold' is the threshold level of  $\text{Ca}^{2+}$  which activates the myofilaments or that which causes sufficient activation to take up the compliance of the tissue was not determined. Note, however, that with smooth muscle from the fundal region of the stomach<sup>11</sup>, and using the same apparatus for recording contractile tension, significant tension development is detected with as low a  $[\text{K}^+]$  as 12 mM.

Recently, it has been suggested that the action of  $\text{Ca}^{2+}$  on the contractile system of smooth muscle is not direct but, rather, that the  $\text{Ca}^{2+}$  activates a protein kinase which phosphorylates the

myosin and stimulates myosin's interaction with actin<sup>13-15</sup>. This possibility has been used to explain the long delay between the calcium transient and contraction in amphibian smooth muscle<sup>7</sup>. As we do not observe any similar delay in our mammalian smooth muscle preparation, we conclude that such phosphorylation either is not required in mammalian smooth muscle at 35 °C or that it is considerably more rapid than in amphibian smooth muscle at 24 °C. We favour the latter interpretation because the long time course of dephosphorylation<sup>16</sup> could explain the lag between the return of  $[\text{Ca}^{2+}]$  to basal levels and the relaxation of the muscle.

We thank J. R. Blinks and J. H. Szurszewski for many valuable contributions. We also acknowledge use of the facilities of the Friday Harbor Laboratories, University of Washington, for the collection of aequorin. Financial support was provided by the Minnesota Heart Association and USPHS grants AM 17238, HL 12186, HL 07111.

Received 20 August; accepted 1 October 1980.

1. Blinks, J. R., Rüdel, R. & Taylor, S. R. *J. Physiol., Lond.* **277**, 291-323 (1978).
2. Wier, W. G. *Science* **207**, 1085-1087 (1980).
3. Allen, D. G. & Blinks, J. R. *Nature* **273**, 509-513 (1978).
4. Hartshorne, D. J. in *Handbook of Physiology, The Cardiovascular System* Vol. II, 93-120 (Am. Physiol. Soc., Bethesda, Maryland, 1980).
5. Endo, M., Kitazawa, T., Yagi, S., Iino, M. & Kakuta, Y. in *Excitation-Contraction Coupling in Smooth Muscle* (eds Casteels, R. et al.) 199-210 (Elsevier, Amsterdam, 1977).
6. Kometani, K. & Sugi, H. *Experientia* **34**, 1469-1470 (1978).
7. Fay, F. S., Shlevin, H. H., Granger, W. C. & Taylor, S. R. *Nature* **280**, 506-508 (1979).
8. El-Sharkawy, T. Y., Morgan, K. G. & Szurszewski, J. H. *J. Physiol., Lond.* **279**, 291-307 (1978).

9. Blinks, J. R., Prendergast, F. G. & Allen, D. G. *Pharmac. Rev.* **28**, 1-93 (1976).
10. Blinks, J. R. et al. *Meth. Enzym.* **57**, 292-328 (1978).
11. Morgan, K. G., Muir, T. C. & Szurszewski, J. H. *J. Physiol., Lond.* (in the press).
12. Morgan, K. G. & Szurszewski, J. H. *J. Physiol., Lond.* **301**, 229-242 (1980).
13. Chacko, S., Conti, M. A. & Adelstein, R. S. *Proc. natn. Acad. Sci. U.S.A.* **74**, 129-133 (1977).
14. Bremel, R. D., Sobieszek, A. & Small, J. V. in *The Biochemistry of Smooth Muscle* (ed. Stephens, N. L.) 533-549 (University Park Press, Baltimore, 1977).
15. Aksoy, M. O., Williams, D., Sharkey, E. M. & Hartshorne, D. J. *Biochem. biophys. Res. Commun.* **69**, 35-41 (1976).
16. Aksoy, M. O., Dillon, P. F. & Murphy, P. *Fedn Proc.* **39**, 2042-2044 (1980).

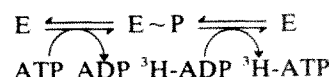
## External Na dependence of ouabain-sensitive ATP:ADP exchange initiated by photolysis of intracellular caged-ATP in human red cell ghosts

Jack H. Kaplan & Richard J. Hollis

Department of Physiology and Biophysics, University of Iowa, Iowa City, Iowa 52242

Coupled active transport of  $\text{Na}^+$  and  $\text{K}^+$  across cellular plasma membranes is mediated by  $(\text{Na}^+ + \text{K}^+)$ -stimulated  $\text{Mg}^{2+}$ -dependent ATPase. Active cation transport by this Na pump involves a cyclic Na-dependent phosphorylation of the enzyme by intracellular ATP and hydrolytic dephosphorylation of the phosphoenzyme, stimulated by  $\text{K}^+$  (ref. 1). In human red blood cells<sup>2</sup>, skeletal muscle<sup>23</sup> and squid axons<sup>3,4</sup>, replacement of extracellular K by Na results in a ouabain-sensitive efflux of Na coupled to an influx of extracellular Na. There is apparently no net Na movement<sup>5</sup> nor net hydrolysis of ATP<sup>6</sup>. The rate of Na:Na exchange is stimulated by increased levels of ADP<sup>7</sup> and exchange transport is not observed in cells totally depleted of intracellular ATP<sup>8</sup>. These characteristics suggest that the biochemical mechanism underlying the Na exchange mode of the Na pump involves phosphorylation of the enzyme by ATP (which requires intracellular Na) followed by its dephosphorylation by ADP. Such a reaction has been observed in partially purified  $(\text{Na}^+ + \text{K}^+)$ ATPase from a variety of sources<sup>9-11</sup> and its dependence on Na concentration has been described<sup>12,13</sup> (although not previously for the red cell enzyme). In the present work, intracellular ATP:ADP exchange reaction was initiated by photoreleased ATP following brief irradiation at 350 nm of ghosts containing caged-ATP<sup>14</sup>. The ouabain-sensitive component of the ensuing ATP:ADP exchange reaction shows a biphasic response to extracellular Na. External Na in the range 0-10 mM has an inhibitory effect whilst increasing concentrations beyond this range stimulate the rate of exchange in a roughly linear fashion up to 100 mM Na. These results represent the first direct demonstration of the sidedness of the effects of Na on this partial sequence in the overall enzyme cycle and bear a qualitative resemblance to the Na effects on the Na-ATPase which occur in the absence of intracellular ADP in human red blood cells<sup>15</sup>.

The biochemical reaction of interest in the present context may be represented as,



and can be measured as the ouabain-sensitive rate of production of  $^3\text{H}$ -ATP from  $^3\text{H}$ -ADP. Although the availability of resealed erythrocyte ghosts has made possible the independent manipulation of intracellular and extracellular cation concentrations, in order to measure the ATP:ADP exchange reaction, three major experimental difficulties had to be overcome: (1) high cytoplasmic adenylate kinase activities (approximately 5 mol per litre of cells per hour); (2) high cytoplasmic nucleoside diphosphokinase (NPDK) activities; (3) endogenous ATPase activities. Furthermore, the preparation of resealed ghosts requires a lengthy incubation procedure for resealing. Since the reaction of interest involves isotopic exchange in the intracellular compartment a recycling system is not appropriate and to measure initial rates of the unidirectional reaction it is necessary that the reaction be initiated after ghost preparation is completed.

Following the lead of Cavieres and Glynn<sup>8</sup> we prepared resealed ghosts with a large dilution of cellular contents and incorporated inside the ghosts the competitive inhibitor of adenylate kinase, diadenosine pentaphosphate ( $\text{Ap}_5\text{A}$ ) (ref. 16). Using a gel filtration column for cell lysis and cytoplasmic dilution<sup>17</sup> and incorporating 50  $\mu\text{M}$   $\text{Ap}_5\text{A}$  into the ghosts we have been able to prepare ghosts containing up to 250  $\mu\text{M}$   $^3\text{H}$ -ADP which after incubation at 37 °C for 2 h contained  $^3\text{H}$ -AMP at levels that were no higher than originally present in the  $^3\text{H}$ -ADP as a contaminant (about 4%). The presence of high cytoplasmic NPDK activities in human erythrocytes is well documented<sup>18</sup> (approximately 5 mol per litre cells per h) and we find that sufficient activity is present even in 300-fold diluted hemolysates to generate micromolar levels of ATP from micromolar ADP and millimolar UTP within several minutes. The enzyme performs the same reaction as the one of interest mediated by the Na pump, that is, the production of  $^3\text{H}$ -ATP from  $^3\text{H}$ -ADP via the dephosphorylation of a phosphoenzyme intermediate. The brain NPDK enzyme is inhibited by Cibacron blue F3GA (J. B. Robinson and E. C. Stellwagen, personal



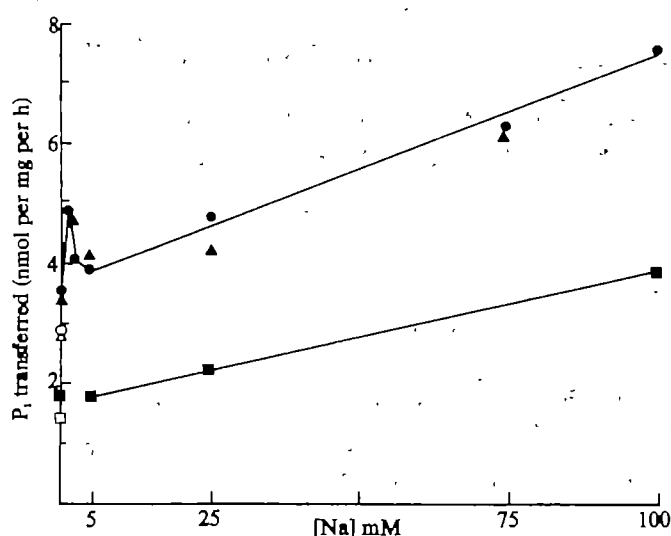
communication). Unfortunately, although this dye is also a very potent inhibitor of the cytoplasmic red cell enzyme, it partitions predominantly into cell membranes. The inhibition of cytoplasmic NADK activity in red cell haemolysates containing Cibacron blue is removed on the addition of red cell membranes (J.H.K. and R.J.H., unpublished data). Amongst the class of dyes which inhibit nucleotide-requiring enzymes<sup>19</sup>, Trypan blue (CI 23850) was found to inhibit cytoplasmic NADK activities in the absence and presence of red cell membranes and in resealed red cell ghosts, without affecting  $(\text{Na}^+ + \text{K}^+)\text{ATPase}$  activities.

To avoid the problems associated with endogenous ATPase activity during ghost incubations at 37 °C (which are required to reseal the ghosts) and also in order to initiate the exchange reaction, we have incorporated caged-ATP into the ghosts. Caged-ATP,  $\text{P}^3\text{-1-(2-nitro)phenylethyl-ATP}$ , is an ATP analogue in which the terminal phosphate of ATP is esterified by a 2-nitrobenzyl moiety. Caged-ATP is resistant to ATPase

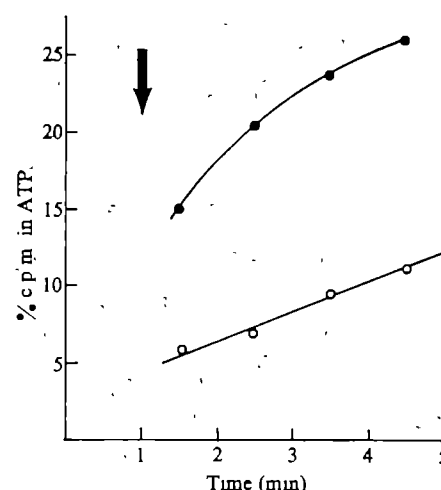
activity because of the esterification of the terminal phosphate residue and is unable to perform ATP-dependent reactions which require phosphorylation. The 2-nitrobenzyl residue is cleaved from the rest of the molecule by irradiation at 350 nm, releasing ATP<sup>14</sup>. We have used caged-ATP as a stable source of ATP that will not undergo reaction during ghost preparation but which subsequently can be 'activated' by the photorelease procedure.

Figure 1 illustrates the Na dependence of ATP:ADP exchange rates in porous red cell membranes. The curve is very similar to that seen using partially purified enzyme from pig kidney outer medulla<sup>10</sup> or dog kidney outer medulla (J.H.K. and M. D. Mone, unpublished), although the specific activity in red cell membranes is some 2–3 orders of magnitude lower than the kidney preparations.

In order to decide which of the Na effects are mediated at extracellular sites, resealed red cell ghosts were prepared containing,  $\text{MgSO}_4$ , NaCl, choline Cl, the kinase inhibitors,



**Fig. 1** The Na dependence of ATP:ADP exchange in porous red cell membranes. Haemoglobin-free membranes were prepared essentially according to the method of Fairbanks *et al.*<sup>21</sup> by lysis of cells at 0 °C in 20 vol of 5 mM sodium phosphate pH 8. Before lysis the cells were washed in 150 mM  $\text{NaHCO}_3$  pH 8.2 to facilitate haemoglobin release<sup>22</sup>. Until use, the white membranes were stored at -20 °C. Thawed membranes were suspended in 5 mM EDTA, 10 mM HEPES pH 7.5 (at 0 °C), incubated at room temperature for 10 min and pelleted (35,000 g, 15 min). The pellet was then resuspended in 150 mM choline chloride, 10 mM HEPES pH 7.6 in 50  $\mu\text{l}$  aliquots at a protein concentration of approximately 3 mg  $\text{ml}^{-1}$ . The reactions were then carried out at 23 °C following the addition of an equal volume of buffered solution containing (final concentration) NaCl + choline chloride to 150 mM, 10 mM  $\text{MgCl}_2$ , 25  $\mu\text{M}$   $^3\text{H}$ -ADP, 25  $\mu\text{M}$  ATP, 100  $\mu\text{M}$   $\text{Ap}_3\text{A}$  and 10 mM HEPES pH 7.6. The reaction was started by the addition of the nucleotides and sampled by quenching in ice-cold 10% trichloroacetic acid at 0.25, 5.25 and 10.25 min. The samples were then frozen before processing. The thawed samples were centrifuged for 2 min at 10,000 g in a Eppendorf microfuge, to pellet the denatured membranes, and samples of the supernatant applied to polyethyleneimine thin layer chromatography plates. The plates were dried and samples of a solution containing 4 mM each of ATP, ADP and AMP applied on top of the experimental samples. The plates were then developed in 0.4 M K phosphate, pH 3.5 and the regions containing ATP, ADP and AMP, visualized using an UV lamp, cut out and placed in scintillation vials. Following the addition of HCl (1 M, 0.5 ml) the vials were placed in an oven at 120 °C for 30 min. After cooling, scintillation fluid was added and then radioactivity co-migrating with each nucleotide counted. Recovery of radioactivity using this procedure was always between 97% and 103% of the amount applied to the chromatography plate. The rates were linear over the time period of the reaction and the initial rate calculated. The curves shown depict the dependence of the exchange rate on Na concentration in experiments using three different preparations of membranes. The open symbols are rates obtained in the absence of Na with  $10^{-4}$  M ouabain in the medium. In the lowest curve Na concentrations between 0 and 5 mM were not used. Although the dependence of rate upon Na concentration was the same in different membrane preparations, the absolute rates did show some variation in different preparations.



**Fig. 2** Photolytic initiation of the ATP:ADP exchange reaction in resealed red cell ghosts. Freshly drawn blood was collected in heparinized tubes and the red cells washed three times in 150 mM choline chloride, 10 mM HEPES pH 7.6 by centrifugation (14,000 g, 5 min), removal of supernatant and resuspension. After the second resuspension the cells were incubated at room temperature for 10 min to ensure completion of pH equilibration. A 10% (by vol) suspension of the cells in the choline buffer was cooled to 0 °C. The suspension was then introduced into the top of a jacketed column of Biorad A50m gel (35 cm  $\times$  5.0 cm) maintained at -1 °C. The column had previously been prepared so that the lower half was equilibrated with 15 mM PIPES, 0.1 mM EDTA pH 6.0, the middle four-tenths of column volume with 20 mM HEPES, pH 7.5 and the upper one-tenth with 150 mM choline Cl, 10 mM HEPES pH 7.6. After introducing the cells into the column they were eluted with buffered choline Cl. The eluate was collected in ice-cold tubes as soon as turbidity was observed in the eluate leaving the column. At this stage the red band of haemoglobin was approximately half-way down the column. The fractions containing membranes were bulked and collected by centrifugation at 0 °C, 31,000 g for 15 min. The supernatant was removed and ice-cold reversal solution containing choline Cl + NaCl (150 mM), 50  $\mu\text{M}$  Trypan blue, 100  $\mu\text{M}$   $\text{Ap}_3\text{A}$ , 10  $\mu\text{M}$   $\text{MgSO}_4$ , 50  $\mu\text{M}$  caged-ATP, 25  $\mu\text{M}$   $^3\text{H}$ -ADP, 10 mM HEPES pH 7.6 was added to the pale pink pellet. After resuspension and incubation in ice for 5 min, the membranes were transferred to a water bath at 37 °C for a further 45 min. The resealed ghosts were then washed three times in 150 mM choline Cl, 10 mM HEPES pH 7.6 by centrifugation (31,000 g, 5 min) and resuspension. The ghosts were packed after the final wash (31,000 g, 15 min) and resuspended in 10% suspension (by vol) in 100 mM NaCl, 50 mM choline Cl, 10 mM HEPES pH 7.6. Aliquots (200  $\mu\text{l}$ ) of the suspension were photolysed in 1 mm path length cuvettes as previously described<sup>14</sup> and at suitable time intervals samples (20  $\mu\text{l}$ ) were added to ice-cold 10% trichloroacetic acid (20  $\mu\text{l}$ ) and rapidly mixed. Duplicate samples were added to distilled water (200  $\mu\text{l}$ ) and placed in a boiling water bath for 1 min. The boiled samples were then cooled and assayed for ATP, ADP and AMP contents using a modification of the procedure of Kimmich *et al.*<sup>20</sup> The samples in trichloroacetic acid were treated as described in the legend to Fig. 1. The filled symbols indicate the rate of appearance of radioactivity in intracellular ATP, the open symbols the rate in the presence of  $10^{-4}$  M ouabain in the external medium. During the time of reaction ATP hydrolysis was less than 5%. The reaction was initiated by photolysis at zero time, the vertical arrow indicates when photolysis was stopped. In unphotolysed ghosts less than 0.04% of the total radioactivity migrated with ATP.

$^3\text{H}$ -ADP and caged-ATP and photolysed to initiate the exchange reaction. A representative time course of the appearance of  $^3\text{H}$ -ATP in such an experiment is shown in Fig. 2. It is clear that a major component of the total exchange reaction is ouabain-sensitive, that is, mediated by the Na pump. Figure 3 shows the data from experiments in which external Na has been systematically varied. In each experiment the rate of ATP:ADP exchange was measured in aliquots of the ghosts suspended at various external Na concentrations. The curves depict the variation of the ATP:ADP exchange rate as a function of the external Na concentration at constant internal Na.

Thus Na pump-mediated ATP:ADP exchange in resealed human red cell ghosts shows a biphasic dependence on extracellular Na concentration. These observations enable us to identify unambiguously each of the three limbs of the Na activation curve in Fig. 1 with intracellular or extracellular sites for Na. At least three classes of sites are observed on the porous membranes (Fig. 1) and of these, the two of lower affinity can now be localized to the extracellular surface of the cell membrane. The higher-affinity extracellular site inhibits the ATP:ADP exchange reaction in the range 0–10 mM Na, the lower affinity site stimulates the reaction in an approximately linear fashion up to 100 mM Na, and thus saturates well beyond the physiological range. The highest affinity Na sites are intracellular and presumably support enzyme phosphorylation. It has been suggested that the stimulation of ATP:ADP exchange reaction rate seen at high Na levels with porous enzyme preparations is due to an increase in the steady-state level of ADP-sensitive phosphoenzyme<sup>13</sup>. Our data extend the earlier observations to include red cell membranes and further specify that the Na sites which are involved in this stimulation are sites for external Na.

The effects of external Na on ATP:ADP exchange described here parallel the dependence of Na:Na exchange in red blood cells on external Na concentration<sup>5</sup>. The question of the relative rates of these reactions has not been directly addressed in the present studies. It would be interesting to know how many Na ions are transported across the membrane each time the phosphorylated pump protein is dephosphorylated by ADP. Although Na entry may require the dephosphorylation step<sup>7</sup> the converse is apparently not true. When external Na is zero and Na entry cannot take place ATP:ADP exchange does occur (Fig. 3). Under these conditions it is not known whether a Na efflux occurs, whether internally bound Na is discharged into the cytosol or whether internal Na remains bound to the enzyme.

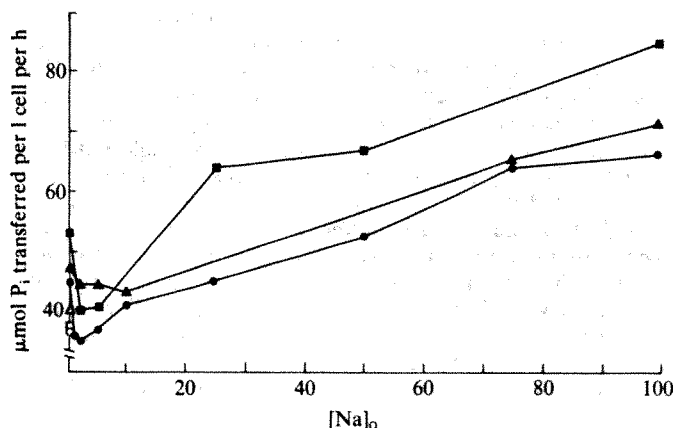


Fig. 3 Dependence of the rate of ATP:ADP exchange on extracellular Na. The procedures used to prepare the ghosts and determine the rate of ATP:ADP exchange were as described in the legends to Figs 1 and 2. The ghosts were suspended in media containing varying Na concentrations before photolysis, maintaining the sum NaCl + choline Cl at 150 mM. The three curves illustrate data from three different batches of resealed ghosts. The open symbols show the rate of ATP:ADP exchange in the absence of extracellular Na and in the presence of  $10^{-4}$  M ouabain. Intracellular Na was determined by flame photometry and was between 11 mM and 16 mM in these experiments.

The determination of the relationship between the rates of isotopic Na movements and ATP:ADP exchange awaits their measurement under varied identical conditions in the same preparation.

We thank Linda J. Kenney for technical assistance, Dr P. G. Wood for advice on gel filtration in the preparation of Haemoglobin-free ghosts and Dr K. G. Beam for comments on the manuscript. This work was supported by NIH grant HL24309 to J.H.K. and by a starter grant from the PMA Foundation.

Received 1 July; accepted 25 September 1980.

- Glynn, I. M. & Karlsh, S. J. D. A. *Rev. Physiol.* **37**, 13–55 (1975).
- Garrahan, P. J. & Glynn, I. M. *J. Physiol., Lond.* **192**, 189–216 (1967).
- Kennedy, B. G. & DeWeer, P. *J. gen. Physiol.* **68**, 405–420 (1976).
- DeWeer, P. *Nature* **219**, 730–731 (1968); **226**, 1251–1252 (1970).
- Garrahan, P. J. & Glynn, I. M. *J. Physiol., Lond.* **192**, 159–174 (1967).
- Garrahan, P. J. & Glynn, I. M. *J. Physiol., Lond.* **192**, 217–235 (1967).
- Glynn, I. M. & Hoffman, J. F. *J. Physiol., Lond.* **218**, 239–256 (1971).
- Cavieses, J. D. & Glynn, I. M. *J. Physiol., Lond.* **297**, 637–645 (1979).
- Fahn, S., Koval, G. J. & Albers, R. W. *J. biol. Chem.* **241**, 1882–1889 (1966).
- Stahl, W. L. *J. Neurochem.* **15**, 499–509; 511–518 (1968).
- Banerjee, S. P. & Wong, S. M. E. *J. biol. Chem.* **247**, 5409–5413 (1972).
- Wildes, R. A., Evans, H. J. & Chiu, J. *Biochim. biophys. Acta* **307**, 162–168 (1973).
- Beauge, L. A. & Glynn, I. M. *J. Physiol., Lond.* **289**, 17–31 (1979).
- Kaplan, J. H., Forbush III, B. & Hoffman, J. F. *Biochemistry* **17**, 1929–1935 (1978).
- Glynn, I. M. & Karlsh, S. J. D. *J. Physiol., Lond.* **256**, 465–496 (1976).
- Lienhard, G. E. & Secemski, I. I. *J. biol. Chem.* **248**, 1121–1123 (1973).
- Wood, P. G. *Fedn. Proc.* **34**, 249 (1975).
- Parks, R. E. Jr. & Agarwal, R. P. *Enzymes* **8**, 307–333 (1973).
- Stellwagen, E. C. *Acc. Chem. Res.* **10**, 92–98 (1977).
- Kimich, G. A., Randies, J. & Brand, J. S. *Analyt. Biochem.* **69**, 187–209 (1975).
- Fairbanks, G., Steck, T. L. & Wallach, D. F. H. *Biochemistry* **10**, 2606–2616 (1971).
- Jennings, M. L. & Passow, H. *Biochim. biophys. Acta* **554**, 498–519 (1979).
- Caldwell, P. C., Hodgkin, A. L., Keynes, R. D. & Shaw, T. I. *J. Physiol., Lond.* **152**, 561–690 (1960).

## Potent carcinogenicity of nitrosodiethanolamine in rats

W. Lijinsky, M. D. Reuber & W. B. Manning

Chemical Carcinogenesis Program, NCI Frederick Cancer Research Center, Frederick, Maryland 21701

Nitrosodiethanolamine is found in synthetic cutting oils and in many cosmetic preparations and is probably the *N*-nitroso compound to which human exposure is greatest<sup>1–3</sup>. It is formed by reaction of the commonly used amines diethanolamine and triethanolamine<sup>4</sup> with nitrosating agents. An assessment of the possible risk in human exposure to nitrosodiethanolamine must be based on sound chronic toxicity data. A previously published chronic test of this compound in rats has shown it to induce liver tumours after very high oral doses<sup>5</sup>, and tumours of the nasal cavity after administration of high repeated doses to Syrian hamsters by subcutaneous injection<sup>6</sup>. To improve our understanding of the carcinogenic potency of nitrosodiethanolamine, we undertook a more extensive study, in which the compound was administered at concentrations ranging from 3,900 to 31,250 parts per million (p.p.m.) in drinking water, to groups of rats for about 6 months. We report here that when the animals were killed, all bore hepatocellular carcinomas, many of which metastasized at the higher doses, indicating that nitrosodiethanolamine is a carcinogen of considerable potency in the rat. However, it is inactive or very weakly active in short-term tests, such as the *Salmonella* mutagenesis test developed by Ames<sup>7</sup>.

Sixty male and sixty female Fischer 344 rats of the colony of the Frederick Cancer Research Center, bred and raised in SPF conditions, were housed in plastic cages with wire-mesh bottoms (five rats per cage). The animals were 6–7 weeks old at the beginning of the experiment, and were randomized into (for



Table 1 Treatment of F 344 rats with solutions of nitrosodiethanolamine (NDELA) in drinking water

| Group | NDELA concentration (p.p.m.) | No. of animals treated |    | No. of animals with liver tumours |    |                     |   |                                |   |
|-------|------------------------------|------------------------|----|-----------------------------------|----|---------------------|---|--------------------------------|---|
|       |                              |                        |    | Hepatocellular carcinomas         |    | Cholangiocarcinomas |   | No. of animals with metastases |   |
|       |                              | ♂                      | ♀  | ♂                                 | ♀  | ♂                   | ♀ |                                |   |
| 1     | 0 (control)                  | 10                     | 10 | 0                                 | 0  | 0                   | 0 | 0                              | 0 |
| 2     | 3,900                        | 10                     | 10 | 10                                | 10 | 1                   | 3 | 0                              | 0 |
| 3     | 7,800                        | 10                     | 10 | 10                                | 10 | 6                   | 5 | 0                              | 0 |
| 4     | 15,600                       | 10                     | 10 | 10                                | 10 | 8                   | 8 | 9                              | 3 |
| 5     | 31,250                       | 10                     | 10 | 10                                | 10 | 10                  | 7 | 10                             | 8 |
| 6     | 62,500                       | 10                     | 10 | —                                 | —  | —                   | — | —                              | — |

*N*-nitrosodiethanolamine was prepared on a large scale as follows. To a 6,000-ml Erlenmeyer flask cooled in an ice bath were added 1 kg diethanolamine (Aldrich), 1.24 kg sodium nitrite (Mallinckrodt) and 1.3 l water. After preliminary agitation to disperse the undissolved solid, the mixture was stirred magnetically overnight. To the homogeneous solution cooled to 0–5 °C in an ice bath was added 1.7 l 12 M HCl dropwise over a period of 4–5 h. Large volumes of brown nitrogen dioxide were evolved. On completion of the acid addition, stirring was continued for 1 h, after which 1,000 ml of methanol was slowly added to the still cold solution. Evolution of methyl nitrite ensued and dictated the rate of methanol addition. The flask was left overnight to complete transesterification. Salts present were removed by filtration using a fritted glass funnel. The filtrate was treated with small portions of a saturated sodium carbonate solution until a pH of 8 was attained. The colour of the solution changed from pale green to golden yellow. This solution was reduced to a viscous suspension by removing a large amount of water on a rotary evaporator. Anhydrous acetone was added to the suspension to decrease the viscosity and the salts in the suspension were removed by vacuum filtration. The filtrate was again reduced to a viscous suspension by removing acetone and residual water. To this suspension was added an equivalent volume of anhydrous acetone and the resulting mixture was filtered to remove the precipitated salts. Acetone was removed from the filtrate to give a golden yellow liquid of high viscosity. Analysis of this material by NMR spectrometry, IR spectrometry and UV spectrometry gave results consistent with the structure of nitrosodiethanolamine and indicated high purity. When 100 g was extracted four times with 100 ml of methylene chloride, the extract concentrated and the residue analysed by gas-liquid chromatography, no identifiable volatile nitrosamines were found at a detection level of 0.03 p.p.m.

each sex) 6 groups of 10. One of the groups served as untreated controls and the remainder were given solutions of nitrosodiethanolamine in neutral (pH 7) tap water that had been filtered through a deionizer. The concentrations of nitrosodiethanolamine and the numbers of animals treated are shown in Table 1.

Treatment consisted of giving the nitrosodiethanolamine solutions at 20 ml per rat each day on 5 days of each week; on the remaining 2 days the animals were given tap water without the nitrosamine. In these conditions almost all the nitrosamine solution was consumed, with little spillage (the tap water was given to replenish any water deficit suffered by the animals). Due to an error in communication, for the first 12 weeks of the experiment the nitrosamine solutions were supplied *ad libitum* for 7 days of each week; this hampered calculation of the exact doses received by each cage of animals, as the animals given the higher concentrations tended to drink more of the drug-containing solution (perhaps it has an appetizing taste). An exception was the 62,500 p.p.m. solution, of which little was drunk and which proved quite toxic, leading to the death of several animals within 2 weeks; treatment with this concentration of nitrosodiethanolamine was discontinued and the animals were discarded.

After 12 weeks the designated treatment regimen was restored and treatment was continued until 34 weeks after the beginning of the experiment. A few animals at the 31,250 and 15,600 p.p.m. concentrations died before the 34th week. All surviving animals were killed at week 34. The dead animals were completely necropsied and all lesions, with most normal tissues, were fixed for histological evaluation.

All the animals in the four long-term treated groups developed hepatocellular carcinomas of the liver. At the higher doses most rats also had cholangiocellular carcinomas. Histologically the hepatocellular carcinomas varied from well differentiated to poorly differentiated to undifferentiated, whereas the cholangiocarcinomas were well differentiated; each liver contained multiple large, invasive carcinomas. None of the untreated control animals had lesions of the liver. At the 31,250 and 15,600 p.p.m. doses, many of the liver carcinomas metastasized to the lungs and peritoneal cavity (Table 1).

Nitrosodiethanolamine is therefore a more potent carcinogen for the liver of Fischer 344 rats than was previously suspected. As liver carcinomas were induced after administration of a

solution containing 3,900 p.p.m. for only 34 weeks, it is likely that considerably lower concentrations will be effective. During most of the experiment the dose of nitrosodiethanolamine received by the animals was kept at 100 ml of solution per week, corresponding to 390 mg of nitrosodiethanolamine per week. This amounted to ~13 g per rat over the course of the treatment or 30 g per kg body weight for the males and 50 g per body weight for the females. This contrasts with the experiment of Druckrey *et al.*<sup>5</sup>, in which a total dose of 150–300 g of nitrosodiethanolamine per kg body weight gave rise to liver tumours in BD rats with a median induction time of 42 weeks.

Concentrations of nitrosodiethanolamine in some cutting oils reaches 3% or 30,000 p.p.m. (ref. 1) and in some cosmetics 48 p.p.m. (ref. 3). Therefore, the data presented here imply that the doses of this compound to which much of the human population is exposed can no longer be dismissed on the grounds that it is a weak carcinogen. Notably nitrosodiethanolamine has been found to penetrate rat skin quite readily<sup>6</sup>, so that skin contact with materials containing nitrosodiethanolamine is likely to present a carcinogenic risk to humans.

A similar study to that in rats was conducted with B6C3F<sub>1</sub> mice, groups of 10 female and 10 male mice being given nitrosodiethanolamine solutions in concentrations of 62,500–3,900 p.p.m. in water. In this case each mouse was allotted 5 ml of solution per day, 5 days a week for 32 weeks. Unlike the rats, mice tolerated the 62,500 p.p.m. concentration quite well. At the end of the study cholangiofibrosis and cirrhosis, as well as some hyperplastic nodules, were found in the livers of many mice receiving the higher doses of nitrosodiethanolamine, but no tumours were observed. This suggests that B6C3F<sub>1</sub> mice are less susceptible to the carcinogenic action of nitrosodiethanolamine than are F 344 rats.

This work was supported by NCI contract NO1-CO-75380.

Received 21 July, accepted 29 October 1980

1. Fan, T. Y. *et al.* *Science* **196**, 70 (1977).
2. Zingmark, P. A. & Rappe, C. *Ames* **6**, 237 (1977).
3. Fan, T. Y. *et al.* *Fd Cosmet Toxicol* **15**, 423 (1977).
4. Lipinsky, W., Kofer, L., Courad, E. & Van de Bogert, R. J. *natn. Cancer Inst.* **49**, 1239 (1972).
5. Druckrey, H., Preussmann, R., Iversen, S. & Schmahl, D. *Z. Krebsforsch.* **69**, 103 (1967).
6. Hilgert, J., Schmitz, I. & Hoffmann, D. *Cancer Lett.* **4**, 55 (1978).
7. Rao, T. K., Young, J. A., Lipinsky, W. & Epler, J. L. *Mutat. Res.* **66**, 1 (1979).
8. Lipinsky, W., Loskoff, A. M. & Sanscoe, E. B. *J. natn. Cancer Inst.* (in the press).

# Thyroid hormone modulation of X ray-induced *in vitro* neoplastic transformation

Duane L. Guernsey

Department of Biochemistry, College of Physicians and Surgeons, Columbia University, New York, New York 10032

Augustinus Ong & Carmia Borek

Radiological Research Laboratory, Department of Radiology and Department of Pathology, College of Physicians and Surgeons, Columbia University, New York, New York 10032

**The direct oncogenic potential of X rays has been demonstrated by the *in vitro* neoplastic transformation of mammalian cells in culture<sup>1</sup>, a technique which permits the study of oncogenesis in the absence of host-specific effects. Although several agents are known to modulate *in vitro* neoplastic transformation by X rays<sup>2</sup>, little is known of the effects of hormones. We now describe experiments which show that the presence of thyroid hormone is necessary for *in vitro* neoplastic transformation by X rays in cells of an established mouse fibroblast culture (C3H/10T1/2) and in early-passage diploid hamster embryo cells.**

Animal studies have shown that altered thyroid status modifies the growth and metastatic potential of implanted tumours<sup>3</sup> as well as the survival rate of animals bearing tumours<sup>6</sup>. We therefore set out to investigate whether this modulation is a direct effect of the hormone on neoplastic transformation. *In vitro* transformation by X rays has been especially well investigated in early-passage primary hamster embryo cells in culture<sup>7,8</sup> and C3H/10T1/2 mouse embryo fibroblasts<sup>9-11</sup>, and qualitatively demonstrated in human diploid cells<sup>12</sup>. Accordingly we have used in this study (1) short-term cultures of diploid hamster embryo cells (HE) obtained as previously described<sup>1,2,7,8</sup>, and (2) the C3H/10T1/2 clone 8 mouse embryo heterodiploid cell line developed by Reznikoff *et al.*<sup>13</sup>.

We have measured the efficacy of X rays in inducing neoplastic transformations in cell cultures of both types when thyroid hormone has been removed from the culture medium and find

that transformation is inhibited. We have also shown that the efficacy of X rays in causing neoplastic transformation is restored when thyroid hormone (triiodothyronine, T<sub>3</sub>) is added to the hormone-depleted medium.

Both cell types are fibroblast-like cells. Cell transformation was detected morphologically and scored as described elsewhere for the hamster embryo cells<sup>1,2,7,8</sup> and for the C3H/10T1/2 mouse cells<sup>9-11,14</sup>. In these earlier studies, the morphological changes associated with the transformed state have been correlated with the oncogenic potential of the cells. The procedures used are described in detail in Table 1 legend. Thyroid hormones (T<sub>3</sub> and thyroxine, T<sub>4</sub>) were removed from heat-inactivated fetal bovine serum as described by Samuels *et al.*<sup>15</sup> using AG1-X10 resin (Biorad). In each experiment, six different experimental culture conditions were used: (1) resin-treated serum (-T<sub>3</sub>), unirradiated; (2) resin-treated serum (-T<sub>3</sub>), irradiated; (3) resin-treated serum, T<sub>3</sub> (Sigma) added (+T<sub>3</sub>), unirradiated; (4) resin-treated serum, T<sub>3</sub> added (+T<sub>3</sub>), irradiated; (5) untreated serum, unirradiated; and (6) untreated serum, irradiated. Table 1 shows that when cells are maintained in media depleted of thyroid hormones (-T<sub>3</sub>), X-ray irradiation-induced transformation is dramatically inhibited in both cell types tested. To support further the role of thyroid hormone in transformation, only T<sub>3</sub> was re-added to resin-treated, serum-supplemented media; the observed transformation frequency on re-addition was similar to control, irradiated cells maintained in untreated-serum-supplemented media.

A dose-response curve for cell survival was carried out, as described elsewhere<sup>7,8</sup>, on each cell type to determine if the elimination of thyroid hormone would differentially affect the survival of the cells after X-ray irradiation. We found that the removal of thyroid hormones from the serum, or the resin treatment, had very little effect on the survival of either cell type (data not shown). Further, it was determined in both cell types that the growth characteristics of cells grown in the absence of T<sub>3</sub> were identical to the growth in the presence of T<sub>3</sub> in resin-treated, serum-supplemented media.

These data indicate that X-ray irradiation-induced *in vitro* transformation of mammalian cells is dramatically inhibited when cells are maintained in the absence of thyroid hormone. This seems to be a direct effect of the hormone as the expected frequency of transformation is restored when T<sub>3</sub> is reintroduced in the culture medium. These results cannot be ascribed to differences in survival or growth characteristics of the cells maintained in the presence or absence of thyroid hormone.

**Table 1** The effect of thyroid hormone on X ray irradiation-induced cell transformation *in vitro* of C3H/10T1/2 mouse cells and hamster embryo cells in culture

| Cells      | Serum treatment/(T <sub>3</sub> condition)             | X rays (Gy) | Total surviving colonies | No. of colonies transformed | Transformation frequency |
|------------|--|-------------|--------------------------|-----------------------------|--------------------------|
| C3H/10T1/2 | Untreated FBS  | 0           | 23,313                   | 0                           | 0                        |
|            | Untreated FBS  | 3           | 27,737                   | 24                          | 8.65 × 10 <sup>-4</sup>  |
|            | Resin-treated FBS/(-T <sub>3</sub> -T <sub>4</sub> )   | 0           | 23,154                   | 0                           | 0                        |
|            | Resin-treated FBS/(-T <sub>3</sub> -T <sub>4</sub> )   | 3           | 33,747                   | 0                           | 0                        |
|            | Resin-treated FBS + T <sub>3</sub> /(+T <sub>3</sub> ) | 0           | 15,884                   | 0                           | 0                        |
|            | Resin-treated FBS + T <sub>3</sub> /(+T <sub>3</sub> ) | 3           | 21,040                   | 16                          | 7.60 × 10 <sup>-4</sup>  |
| HE         | Untreated FBS  | 0           | 2,800                    | 0                           | 0                        |
|            | Untreated FBS  | 2.2         | 4,800                    | 16                          | 3.33 × 10 <sup>-3</sup>  |
|            | Resin-treated FBS/(-T <sub>3</sub> -T <sub>4</sub> )   | 0           | 2,400                    | 0                           | 0                        |
|            | Resin-treated FBS/(-T <sub>3</sub> -T <sub>4</sub> )   | 2.2         | 1,500                    | 0                           | 0                        |
|            | Resin-treated FBS + T <sub>3</sub> /(+T <sub>3</sub> ) | 0           | 2,600                    | 0                           | 0                        |
|            | Resin-treated FBS + T <sub>3</sub> /(+T <sub>3</sub> ) | 2.2         | 3,600                    | 15                          | 4.17 × 10 <sup>-3</sup>  |

Values given are totals of three separate experiments with C3H/10T1/2 cells and two separate experiments with hamster embryo cells. Stock 10<sup>-3</sup> M T<sub>3</sub> in 50% *n*-propanol was diluted in media with 10% resin-treated fetal bovine serum (FBS) to give a final concentration of 10<sup>-7</sup> M T<sub>3</sub> (designated +T<sub>3</sub>). Media without thyroid hormone was prepared with 10% resin-treated FBS and an amount of diluent equal to that added in the +T<sub>3</sub> media. Stock cultures of C3H/10T1/2 cells were maintained in Eagle's basal medium +10% heat-inactivated FBS; hamster embryo cells in Dulbecco's modified Eagle's medium +10% FBS. Both cultures contained penicillin (50 U ml<sup>-1</sup>) and streptomycin (50 µg ml<sup>-1</sup>). All cells were maintained at 37 °C with 5% CO<sub>2</sub> in air throughout the experiment. One week before seeding, stock cultures were placed in the experimental culture media, with and without T<sub>3</sub> (as described in the text) and maintained in these conditions for the duration of the experiment. Twenty-four hours after seeding, the cells were irradiated with X rays at room temperature (2.2 Gy for HE and 3 Gy for C3H/10T1/2 cells), at a dose rate of 0.322 Gy min<sup>-1</sup>, thereafter receiving weekly media changes. After an appropriate incubation period (6 weeks for C3H/10T1/2 and 2 weeks for HE), the cells were fixed and stained with Giemsa and scored for transformation. Both type II and III foci were scored in C3H/10T1/2 experiments.



Experiments, to be published in more detail elsewhere, indicate that when cells are exposed to concentrations of  $T_3$  ranging from  $10^{-11}$  M to  $10^{-7}$  M, X-ray-induced transformation is dose dependent. Additionally, these studies demonstrate that the critical period of exposure to the hormone is a 12-h period before irradiation. This suggests that, in these experimental conditions, thyroid hormone is necessary for the induction and/or potentiation of X-ray irradiation-induced transformation *in vitro*. Thyroid hormone may also have a significant, perhaps even decisive, role in the occurrence of neoplastic transformation *in vivo*. Studies are in progress to define possible mechanisms of action and the involvement of thyroid hormone in neoplastic transformation *in vitro* by chemicals and viruses.

D.L.G. was the recipient of National Research Service Award AM-05948 from the NIH. This investigation was supported by NIH grants CA-22376 and AM-07328, by grant CA-12536 to the Radiological Research Laboratory/Department of Radiology, and grant CA-13696 to the Cancer Center/Institute of Cancer Research awarded by the NCI, DHEW and by contract DE-AC02-78EV04773 from the Department of Energy. We thank Dr I. S. Edelman for providing facilities and support for part of this research. Dr C. Heidelberger provided the C3H/10T1/2 clone 8 mouse embryo heterodiploid cell line.

Received 25 July; accepted 20 October 1980.

1. Borek, C. & Sachs, L. *Nature* **210**, 276-278 (1966); *Proc. natn. Acad. Sci. U.S.A.* **57**, 1522-1527 (1967).
2. Borek, C. *Radiat. Res.* **79**, 209-232 (1979).
3. Dubnik, C. S., Morris, H. P. & Dalton, A. J. *J. natn. Cancer Inst.* **10**, 815-839 (1949).
4. Jabara, A. G. & Maritz, J. S. *Br. J. Cancer* **28**, 161-172 (1973).
5. Kumar, M. S., Chiang, T. & Deodhar, S. D. *Cancer Res.* **39**, 3515-3518 (1979).
6. Mishkin, S., Morris, H. P., Yalovsky, M. & Narisimha Murthy, P. V. *Cancer Res.* **39**, 2371-2375 (1979).
7. Borek, C. & Hall, E. J. *Nature* **243**, 450-453 (1973); *Nature* **252**, 499-501 (1974).
8. Borek, C., Hall, E. J. & Rossi, H. H. *Cancer Res.* **38**, 2997-3005 (1978).
9. Terzaghi, M. & Little, J. B. *Cancer Res.* **36**, 1367-1374 (1976).
10. Han, A. & Elkind, M. M. *Cancer Res.* **39**, 123-130 (1979).
11. Borek, C., Miller, P., Pain, C. & Troll, W. *Proc. natn. Acad. Sci. U.S.A.* **76**, 1800-1803 (1979).
12. Borek, C. *Nature* **283**, 776-778 (1980).
13. Reznikoff, C. A., Bronkow, D. W. & Heidelberger, C. *Cancer Res.* **33**, 3231-3238 (1973).
14. Reznikoff, C. A., Bertram, J. S., Brankow, D. W. & Heidelberger, C. *Cancer Res.* **33**, 3239-3249 (1973).
15. Samuels, H. H., Stanley, F. & Casanova, J. *Endocrinology* **105**, 80-85 (1979).

## Friend leukaemia virus-transformed cells, unlike normal stem cells, form spleen colonies in *Sl/Sl<sup>d</sup>* mice

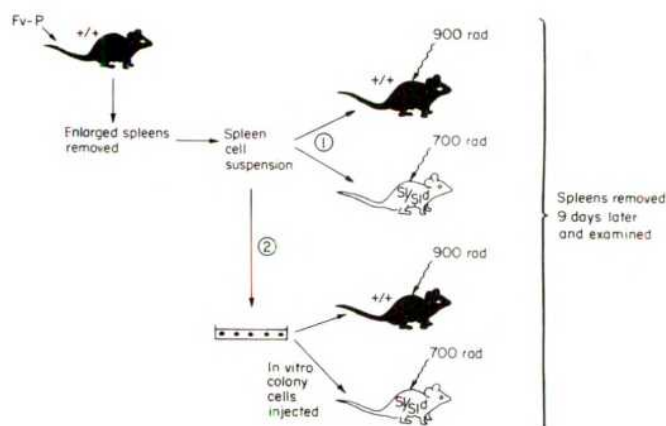
Dixie Mager, Tak W. Mak & Alan Bernstein

The Ontario Cancer Institute and Department of Medical Biophysics, University of Toronto, Toronto, Ontario, Canada M4X 1K9

Neoplastic cells are characterized by partial or total autonomy from the interactions that regulate the behaviour of normal cells in the intact animal. Despite the role of the host cellular environment in governing the proliferation and differentiation of both normal and malignant cells, little is actually known about these host factors. The characterization of host genes that influence both normal cellular processes, as well as susceptibility to tumour induction, is one approach to identifying such factors. Mice carrying two recessive mutations at the *steel* (*Sl*) locus have an environmental defect that affects both normal haematopoietic stem cell function<sup>1,2</sup> as well as susceptibility to Friend leukaemia virus<sup>3-5</sup>. In this study, we have used *Sl/Sl<sup>d</sup>* mice to examine whether malignant transformation by this RNA tumour virus results in a population of cells capable of proliferating even in the defective cellular microenvironment of *Sl/Sl<sup>d</sup>* mice. We report here that late after infection, the leukaemic spleens of Friend virus-infected mice contain cells which, unlike normal haematopoietic stem cells, are able to form macroscopic spleen colonies in irradiated mice of genotype *Sl/Sl<sup>d</sup>*. This observation forms the basis for the first *in vivo* colony assay for leukaemic cells transformed by Friend virus.

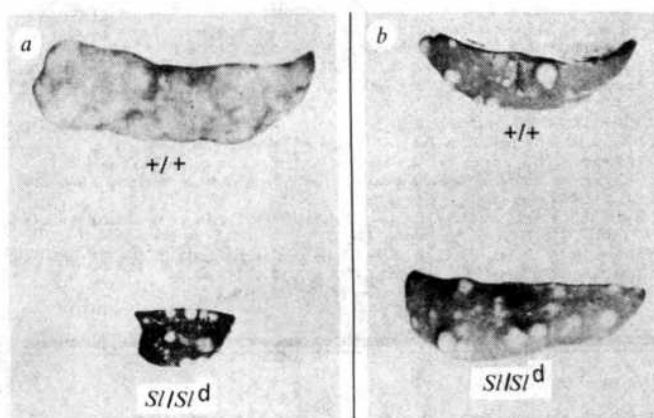
Mice carrying two mutant alleles at the *steel* locus (*Sl/Sl<sup>d</sup>*) exhibit pleiotropic defects, including macrocytic anaemia, sterility and defective pigmentation<sup>6</sup>. Transplantation studies have suggested that the haematopoietic defect in these mice is in the cellular microenvironment in which normal haematopoietic stem cells, and more committed erythroid progenitors, proliferate and differentiate. Haematopoietic cell populations from *Sl/Sl<sup>d</sup>* mice contain normal numbers of stem cells, as measured by their ability to form spleen colonies (colony-forming unit-spleen, CFU-S<sup>7</sup>) in irradiated *+/+* littermates. Thus, the *Sl* locus seems to specify a function, presumably involving short-range cell-cell contacts<sup>8,9</sup>, that regulates the ability of pluripotent stem cells to undergo normal erythropoietic differentiation.

Genetically anaemic *Sl/Sl<sup>d</sup>* mice are also highly resistant to spleen focus induction by the polycythaemia- and anaemia-inducing isolates of Friend spleen focus-forming virus<sup>3-5</sup>. The basis for this resistance is unknown. We presented evidence previously that the spleens from *+/+* mice, infected up to 2 weeks previously with Friend virus, did not contain cells capable of spleen colony formation in irradiated *Sl/Sl<sup>d</sup>* mice<sup>4</sup>. Friend leukaemia seems to be a multi-stage disease in which truly malignant cells capable of extensive proliferation do not appear until late in the disease<sup>10,11</sup>. Thus, the failure to observe spleen colonies in secondary *Sl/Sl<sup>d</sup>* recipients early after infection of *+/+* mice could be attributed to either the absence of any leukaemic stem cells in the *+/+* donor spleens or the inability of Friend virus-transformed cells to proliferate in the *steel* environment.



**Fig. 1** Experimental protocols used to study spleen colony forming ability of Friend virus-infected *+/+* spleen cells. Normal WCB F<sub>1</sub> mice of *+/+* genotype (obtained from crossing mice of strains WC/Re-S1/+ and C57BL/6J-+/+*Sl<sup>d</sup>*) were injected intravenously (i.v.) with  $10^3$  focus-forming units (FFU) of SFFV<sub>P</sub> (spleen focus-forming virus contained in preparations of FV-P). SFFV<sub>P</sub> titres were determined in DBA/2J mice by the spleen-focus assay method<sup>22</sup>. At various times after infection, spleens were removed and single-cell suspensions made in Iscove's Modified Dulbecco's Medium (IMDM) and 5% heat-inactivated fetal calf serum. In the first procedure, the spleen cells were injected i.v. into lethally irradiated *+/+* or *Sl/Sl<sup>d</sup>* recipients. (Mice were irradiated immediately before injection using a <sup>137</sup>Cs biological irradiator.) Nine days later the spleens of recipient mice were fixed in Bouin's solution and examined for spleen colonies. In the second procedure, the spleen cells were plated in methylcellulose using a procedure described elsewhere<sup>15</sup>. In brief,  $10^6$  viable nucleated cells per ml were plated in 2.0% methylcellulose in IMDM (containing  $2 \times 10^{-5}$  M 2-mercaptoethanol) plus 30% heat-inactivated fetal calf serum. Large spherical colonies (containing  $2 \times 10^4$ – $1 \times 10^5$  cells) were picked 14 days later. Colonies were pooled and equal numbers of viable nucleated cells were injected i.v. into irradiated *+/+* or *Sl/Sl<sup>d</sup>* mice. Spleens were examined 9 days later.





**Fig. 2** Appearance of spleen colonies formed by Friend leukaemia virus-transformed  $+/+$  spleen cells obtained from *a*, primary leukaemic spleens or *b*, colonies in methyl cellulose derived from a leukaemic spleen. *a*, Viable nucleated spleen cells ( $5 \times 10^6$ ) from a  $+/+$  mouse infected 10 weeks previously with FV-P were injected into irradiated  $+/+$  or  $Sl/Sl^d$  recipients. Spleens were fixed in Bouin's solution 9 days later. The upper spleen, from a  $+/+$  recipient, is confluent with CFU-S colonies. The lower spleen (approximately half of total) is from an  $Sl/Sl^d$  recipient. Sixteen spleen colonies were counted on this spleen section. *b*, Viable nucleated cells ( $2.5 \times 10^5$ ) from the pooled *in vitro* colonies, described in Fig. 1 legend, derived from a  $+/+$  mouse infected 9 weeks previously with FV-P, were injected into irradiated  $+/+$  or  $Sl/Sl^d$  recipients. Spleen colonies were counted 9 days later. 25 colonies were counted on the  $+/+$  recipient spleen and 31 colonies were found on the  $Sl/Sl^d$  recipient spleen.

To examine the influence of the *steel* environment on both the early and late stages of Friend leukaemia, the ability of  $+/+$  spleen cells from Friend virus-infected mice to proliferate and form macroscopic spleen colonies in irradiated  $Sl/Sl^d$  was measured. Two experimental approaches, outlined in Fig. 1, were followed. In the first procedure, spleen cells, derived from the enlarged spleens of  $+/+$  mice infected at various times previously with a clonal isolate<sup>12</sup> of the polycythaemia-inducing strain of Friend leukaemia virus (FV-P), were injected into either irradiated  $+/+$  or  $Sl/Sl^d$  secondary recipients. As shown in Table 1, spleen cells from either normal  $+/+$  mice or  $+/+$  mice infected up to 5 weeks earlier with FV-P did not contain cells capable of spleen colony formation in irradiated  $Sl/Sl^d$  mice, whereas these same cell populations did contain CFU-S capable of forming spleen colonies in irradiated  $+/+$  littermates. These observations agree with previous findings that CFU-S cannot form spleen colonies in  $Sl/Sl^d$  mice<sup>1</sup>, and extend previous observations from this laboratory that, early after infection with FV-P, the spleens of  $+/+$  mice do not contain cells capable of forming spleen colonies in  $Sl/Sl^d$  mice<sup>4</sup>.

**Table 1** Spleen colony formation by Friend leukaemia virus-transformed spleen cells

| Time after infection | No. of spleen cells injected per mouse | No. of spleen colonies $+/+$ recipients | No. of spleen colonies $Sl/Sl^d$ recipients |
|----------------------|--|---|---|
| Uninfected           | $2 \times 10^6$                        | TMTC* (3)                               | 0 (3)                                       |
| 10 days              | $2 \times 10^6$                        | TMTC (3)                                | 0 (12)                                      |
| 5 weeks              | $5 \times 10^6$                        | TMTC (3)                                | 0 (3)                                       |
| 10 weeks             | $5 \times 10^6$                        | TMTC (3)                                | $24 \pm 8$ (3)                              |

Viable nucleated cells from spleens of uninfected  $+/+$  mice or mice infected with FV-P for various times were injected intravenously into lethally irradiated  $+/+$  or  $Sl/Sl^d$  recipients. Spleens were removed 9 days later. The number of recipient spleens examined in each group is enclosed in parentheses. In every case, the spleens of  $+/+$  recipients were confluent with CFU-S colonies.

\* Too many to count.

However, at a later time after infection (10 weeks), the  $+/+$  leukaemic spleens did contain cells that were now able to form macroscopic spleen colonies in irradiated  $Sl/Sl^d$  hosts (Fig. 2*a* and Table 1). Macroscopically, the nodules or colonies formed by  $+/+$  leukaemic spleen cells in irradiated  $Sl/Sl^d$  mice were less diffuse than, and could be easily distinguished from, both smaller FV-P induced spleen foci, and larger CFU-S derived colonies (Fig. 2*a*). In addition, as shown here and previously<sup>1,4</sup>, CFU-S does not form spleen colonies in  $Sl/Sl^d$  hosts, nor can FV-P-infected cells act as infectious centres in an irradiated host. Thus, the colonies observed in the irradiated  $Sl/Sl^d$  mice are derived from a new cell type that only appears very late after infection with FV-P. One such colony, when placed in cell culture, gave rise directly to a permanent cell line. The properties of this cell line are very similar to cell lines derived from leukaemic spleens after subcutaneous injections into syngeneic secondary recipients<sup>13,14</sup>—the cells grow in suspension, resemble immature erythroid cells, and can be induced to synthesize haemoglobin after treatment with dimethyl sulfoxide (data not shown). Thus, spleen colony formation in irradiated  $Sl/Sl^d$  mice by  $+/+$  leukaemic spleens provides an *in vivo* assay system, free of both an infectious centre and CFU-S background, for the enumeration of a new colony-forming cell that results from transformation by Friend leukaemia virus.

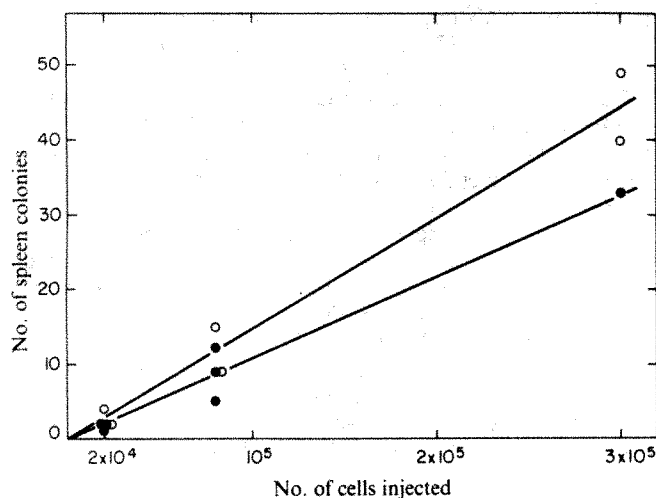
These experiments clearly indicate that, late after infection, Friend virus-infected leukaemic spleens contain cells that can proliferate in the defective  $Sl/Sl^d$  environment. However, the relative colony-forming efficiency of these cells in  $+/+$  and  $Sl/Sl^d$  mice is unknown, because of the CFU-S background when  $+/+$  mice are used as hosts (Table 1). Therefore, the second experimental protocol outlined in Fig. 1 legend was followed. In this procedure, spleen cells from  $+/+$  mice infected 9 weeks previously with FV-P were first cloned in a semi-solid methylcellulose medium in the absence of any exogenous conditioning factors. This *in vitro* assay, which is described more fully elsewhere<sup>15</sup>, seems to detect a population of colony-forming cells similar to that detected by the *in vivo*  $Sl/Sl^d$  assay described above. In brief, these *in vitro* colony-forming cells can only be detected in the advanced stages of Friend disease (greater than 3 weeks) and not in uninfected spleens or in spleens early after infection with Friend virus. The cells in the *in vitro* colonies form spleen colonies in irradiated syngeneic hosts, are tumorigenic and a significant proportion can give rise directly to permanent erythroid cell lines<sup>15</sup>. These cell lines can also be chemically induced to synthesize haemoglobin.

As outlined in Fig. 1 legend, *in vitro* colonies derived from the leukaemic spleens of FV-P-infected  $+/+$  mice were pooled and equal numbers of cells injected into either irradiated  $+/+$  or  $Sl/Sl^d$  hosts. As shown in Fig. 2*b*, approximately equal numbers of macroscopic spleen colonies were observed 9 days later in both normal and genetically anaemic littermates. Furthermore, both the size and macroscopic appearance of the spleen colonies were identical in both sets of mice.

To obtain more quantitative data on the relative colony-forming ability of these FV-P-transformed  $+/+$  cells in  $+/+$  and  $Sl/Sl^d$  hosts, varying numbers of cells, from a cell line that had been established in suspension culture for 6 weeks from a primary colony in methylcellulose, were injected into lethally irradiated  $+/+$  or  $Sl/Sl^d$  recipients. As shown in Fig. 3, the spleen colony-forming ability in either host was a linear function of the number of cells injected, with similar slopes in  $+/+$  and  $Sl/Sl^d$  recipients.

The apparent multi-stage nature of the erythroleukaemia induced by Friend virus has been reported<sup>10,11</sup>. The early stage of Friend disease is characterized by a rapid increase in the number of erythroid colony-forming cells<sup>16,17</sup> with limited proliferative capacity, whereas the late stage is associated with the appearance of spleen cells capable of forming solid tumours in secondary recipients or permanent cell lines in culture<sup>11,13,18,19</sup>. Investigation of the cellular relationship between these stages has been difficult due to the lack of a clonal and quantitative assay for these Friend virus-transformed tumour cells. The





**Fig. 3** Spleen colony formation by a Friend leukaemia virus-transformed cell line in irradiated  $+/+$  and  $SI/SI^d$  recipients. The cell line was derived 6 weeks previously from an *in vitro* colony obtained by plating spleen cells from a  $+/+$  mouse infected 10 weeks previously with FV-P. Various numbers of cells were injected i.v. into irradiated  $+/+$  (●) or  $SI/SI^d$  (○) recipients. Nine days later, spleens were fixed in Bouin's solution and spleen colonies counted.

results presented here indicate that irradiated  $SI/SI^d$  mice are suitable hosts for the definitive enumeration of a class of cells with extensive proliferative capacity that only appear quite late after infection with FV-P. The use of  $SI/SI^d$  secondary recipients eliminates any background colonies contributed by CFU-S in the donor spleens. In addition, although virus is released from the  $+/+$  donor spleen cells, use of irradiated secondary recipients eliminates the background of virus-infected spleen foci of host origin<sup>4</sup> which can arise in unirradiated recipients, even those restrictive for viral replication<sup>20,21</sup>. Thus, this quantitative colony assay should facilitate analysis of the relationship between the early and late stages of Friend leukaemia.

That Friend virus-transformed  $+/+$  cells can form spleen colonies with equal efficiency in both  $+/+$  and  $SI/SI^d$  hosts suggests that these erythroleukaemic cells, unlike normal erythroid progenitor cells, are autonomous of the environmental defect in  $SI/SI^d$  mice. However, mutant  $SI/SI^d$  mice are highly resistant to spleen focus and polycythaemia induction by FV-P, indicating that mutation at the *steel* locus can affect at least the early stages of Friend disease. Thus, the observation that Friend virus-transformed  $+/+$  spleen cells can proliferate to form spleen colonies in  $SI/SI^d$  mice raises the intriguing possibility that progression from the early to late stages of Friend leukaemia is accompanied by the appearance of cells with not only extensive proliferative capacity but also autonomy from a genetically defined cellular regulatory factor.

We thank G. Cheong for technical assistance. Dixie Mager is the recipient of a studentship from the MRC of Canada. This work was supported by grants from the NCI and the MRC of Canada.

Received 1 August; accepted 16 October 1980.

- McCulloch, E. A., Siminovich, L., Till, J. E., Russell, E. S. & Bernstein, S. E. *Blood* **26**, 399-410 (1965).
- Russell, E. S. *Adv. Genet.* **20**, 357-459 (1979).
- Bennett, M., Steeves, R. A., Cudkowicz, G., Mirand, E. A. & Russell, L. B. *Science* **162**, 564-565 (1968).
- McCool, D., Mak, T. W. & Bernstein, A. *J. exp. Med.* **149**, 837-846 (1979).
- MacDonald, M. E. et al. *J. exp. Med.* **151**, 1477-1492 (1980).
- Russell, E. S. & Bernstein, S. E. in *The Biology of the Laboratory Mouse* (ed. Green, E. L.) 351-372 (McGraw-Hill, New York, 1966).
- Till, J. E. & McCulloch, E. A. *Radiat. Res.* **14**, 213-222 (1961).
- Bernstein, S. E. *Am. J. Surg.* **119**, 448-451 (1970).
- Trentin, J. J. et al. in *Morphological and Functional Aspects of Immunity* (eds Landahl-Kiessling, K. et al.) 289-298 (Plenum, New York, 1971).
- Tambourin, P. E., Wendling, F., Jasmin, C. & Smadja-Joffe, F. *Leukemia Res.* **3**, 117-129 (1979).

- Levy, S. B., Blankstein, L. A., Vinton, E. C. & Chambers, T. J. in *Oncogenic Viruses and Host Cell Genes* (eds Ikawa, Y. & Odaka, T.) 409-428 (Academic, New York, 1979).
- Bernstein, A., Mak, T. W. & Stephenson, J. R. *Cell* **12**, 287-294 (1977).
- Friend, C. & Haddad, J. R. *J. natn. Cancer Inst.* **25**, 1279-1289 (1960).
- Friend, C., Scher, W., Holland, J. C. & Sato, T. *Proc. natn. Acad. Sci. U.S.A.* **68**, 378-382 (1971).
- Mager, D., Mak, T. W. & Bernstein, A. *Proc. natn. Acad. Sci. U.S.A.* (in the press).
- Liao, S. K. & Axelrad, A. A. *Int. J. Cancer* **15**, 467-482 (1975).
- Horoszewicz, J. S., Leong, S. S. & Carter, W. A. *J. natn. Cancer Inst.* **54**, 265-267 (1975).
- Ostertag, W., Melderis, H., Steinheider, G., Kluge, N. & Dube, S. *Nature new Biol.* **239**, 231-234 (1972).
- Tambourin, P. et al. in *In vivo and in vitro Erythropoiesis: The Friend System* (ed. Rossi, G. B.) 127-138 (Elsevier, Amsterdam, 1980).
- Steeves, R. A., Bubbers, J. E., Plata, F. & Lilly, G. *Cancer Res.* **38**, 2729-2733 (1978).
- Wendling, F. & Tambourin, P. E. *Int. J. Cancer* **22**, 479-486 (1978).
- Axelrad, A. A. & Steeves, R. A. *Virology* **24**, 513-518 (1964).

## Interferon suppresses antigen- and mitogen-induced leukocyte migration inhibition

R. Szigeti, Maria G. Masucci, G. Masucci, Eva Klein & G. Klein

Department of Tumor Biology, Karolinska Institute, S-104 01 Stockholm 60, Sweden

W. Berthold

Department of Biological Research, D-7950 Biberach/Riss, FRG

Although first recognized by its effect on virus-cell interactions, interferon (IFN)<sup>1</sup> has a variety of other effects<sup>2</sup>. It can affect cell proliferation<sup>3,4</sup>, modify the immune response at several levels<sup>5</sup>, enhance the cytotoxic action of lymphocytes<sup>6-9</sup>, suppress antibody formation<sup>10</sup> and inhibit the development of delayed-type hypersensitivity (DTH) reactions<sup>11,12</sup>. Therefore we have now tested the effect of interferon on leukocyte migration inhibition (LMI), regarded as the counterpart *in vitro* of DTH in humans<sup>13</sup>. We have found that IFN suppresses both mitogen- and antigen-induced LMI, acting directly on the granulocytes but also affecting the lymphokine production of the lymphocytes.

The agarose microdroplet technique<sup>14</sup> was used in two systems: migration inhibition induced by phytohaemagglutinin (PHA) and LMI of leukocytes from Epstein-Barr virus (EBV)-seropositive donors after exposure to EBV antigens. Washed buffy coat cells ( $20 \times 10^6$ ) were mixed with  $135 \mu\text{l}$  nutrient agarose medium containing an equal volume of  $2 \times \text{RPMI}$  1640 medium, supplemented with 20% FCS or NCS and 0.4% agarose. Droplets ( $2 \mu\text{l}$ ) were placed in migration chambers (Sterilin) and after they had solidified, the chambers were filled with medium, with or without mitogen/antigen and incubated in a  $37^\circ\text{C}$  humidified  $\text{CO}_2$  atmosphere for 18-24 h. After incubation the migration areas were measured and the % migration inhibition (MI) calculated according to the formula

$$\% \text{ MI} = \left[ 1 - \frac{\text{mean migration area with antigen}}{\text{mean migration area without antigen}} \right] \times 100$$

Positive MI was recorded when the % inhibition exceeded 20 in the antigen-induced system and 50 with PHA. Purified PHA (Wellcome),  $1 \mu\text{g ml}^{-1}$ , is known to induce LMI of cells from healthy donors<sup>15,16</sup>. We have previously shown that crude extracts of EBV genome-carrying cells ( $50 \mu\text{g per ml}$  protein) or partially purified EBV-determined nuclear antigen (EBNA),  $10 \mu\text{g ml}^{-1}$ , inhibits the leukocyte migration in EBV-seropositive healthy individuals<sup>17,18</sup>. In this study we used a crude extract of the EBV-producer P3HR-1 line and a partially purified<sup>19</sup> EBNA preparation. Human leukocyte interferon (Hu-IFN- $\alpha^1$ , further IFN) was derived from Namalwa cells induced by Sendai virus<sup>20</sup>. The preparation contained  $2.2 \times$

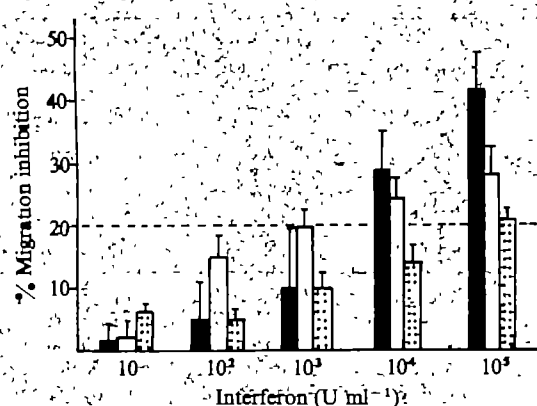


Fig. 1 Effect of IFN on the migration of buffy coat cells (■, 16 experiments) and separated granulocytes (□, 5 experiments). The results are expressed as mean  $\pm$  s.e.m. migration inhibition; 20% inhibition (horizontal dotted line) can be regarded as significant. (□) represents the mean percentage ( $\pm$  s.e.m.) of dead cells among Ficoll-separated lymphocytes after 24 h cultivation in the presence of various concentrations of IFN.

10<sup>5</sup> U per mg protein. The same batch of IFN was also effective in natural killer cell (NK) boosting experiments<sup>21</sup>.

Figure 1 shows that IFN inhibits leukocyte migration when used in high concentrations (10<sup>4</sup>–10<sup>5</sup> U ml<sup>-1</sup>), probably due to its cytotoxic effect on the lymphocytes, as detected by trypan blue exclusion tests in six experiments. At 100 U ml<sup>-1</sup>, IFN had no significant effect on LMI or detectable cytotoxic effect—the viability of the lymphocytes was 95.8  $\pm$  2.1% after 24 h cultivation.

PHA- and antigen-induced LMI was reduced in the presence of 100 U per ml IFN (Table 1). In the PHA system the mean % MI decreased to 32% compared with 61% in the absence of

IFN. Migration of leukocytes from EBV-seronegative persons was not influenced by EBV-antigen preparations nor by addition of 100 U per ml IFN. The leukocyte migration of EBV-seropositive individuals was inhibited by the two antigen preparations (47% and 44% LMI was induced by the crude P3HR-1 cell extract and by the partially purified EBNA preparation, respectively). Migration inhibition was almost completely abolished in the presence of IFN—this effect was also observed when Hu-IFN- $\alpha$  polypeptide<sup>22</sup>, derived from *Escherichia coli*, was tested in the LMI system<sup>23</sup>.

The direct LMI system is complex: the buffy coat contains both the leukocyte migration inhibitory factor (LIF), producer lymphocytes and the indicator (migrating) granulocytes. To determine whether IFN acted on the lymphocyte and/or granulocyte component, we tested the effect of IFN on the migration of separated granulocytes. IFN at the standard dose used in the mitogen and antigen assays (100 U ml<sup>-1</sup>) was slightly inhibitory (Fig. 1). This result suggests that the IFN-mediated decrease of LMI was not due to stimulation of granulocyte movement. In this system, as in other experiments<sup>16</sup>, 1  $\mu$ g per ml PHA had no direct effect on the granulocyte migration. However, addition of lymphokine-containing supernatant of PHA-stimulated lymphocyte cultures inhibited the migration of separated granulocytes (indirect LMI assay) (Fig. 2).

The supernatant-induced migration inhibition was abolished by adding 100 U per ml IFN during the migration period (mean % MI decreased to 18.3% compared with 42.5% in the absence of IFN) (Table 2). Furthermore, 30 min incubation with IFN before addition of the PHA supernatant had the same blocking effect. In the reversed situation (incubation with IFN 30 min after the addition of PHA supernatant) the supernatant-induced migration inhibition was not abolished. These data indicate that IFN blocks the effect of previously released LIF on the granulocytes. This can be due to competition between LIF and IFN for receptor structures present on the granulocyte membranes. Competition of this type was found to occur between IFN and PHA or other substances (such as cholera and tetanus toxin and certain hormones) when measuring the binding of IFN to cell membrane gangliosides (for review see ref. 24).

The indirect LMI assay (granulocyte migration in the presence of lymphokine-containing supernatants, produced by mitogen-stimulated lymphocytes) was also used to detect the effect of IFN on the lymphocyte component. Untreated and mitomycin-C treated lymphocytes were stimulated with PHA, in the presence and absence of 100 U per ml IFN. The IFN specificity of the effect was tested by adding anti-IFN serum

Table 1. PHA- and EBV-antigen-induced LMI in the presence of 100 U per ml IFN.

| PHA<br>(1 $\mu$ g ml <sup>-1</sup> ) |            | P3HR-1 crude extract<br>(50 $\mu$ g ml <sup>-1</sup> ) |            | Partially purified<br>EBNA (10 $\mu$ g ml <sup>-1</sup> ) |            |
|--------------------------------------|------------|--|------------|---|------------|
| -IFN                                 | +IFN       | -IFN   | +IFN       | -IFN  | +IFN       |
| 50                                   | 32         | Seronegative healthy persons                           |            |   |            |
| 61                                   | 45         | 9  | 17         | 16  | 20         |
| 58                                   | 35         | 10   | 16         | 29  | 25         |
| 71                                   | 50         | 14   | 7*         | 14  | 10         |
| 52                                   | 12         | 17   | 12         | 21  | 23         |
| 59                                   | 40         |  |            |   |            |
| 66                                   | 48         | 12.5 $\pm$   | 9.5 $\pm$  | 20.0 $\pm$  | 19.5 $\pm$ |
| 55                                   | 37         | 2.13†  | 2.59       | 3.81  | 3.89       |
| 60                                   | 6          |  |            |   |            |
| 69                                   | 41         | Seropositive healthy persons                           |            |   |            |
| 52                                   | 2*         | 72   | 15         | 28  | 1          |
| 66                                   | 52         | 50   | 18         | 58  | 25         |
| 73                                   | 32         | 45   | 14         | 49  | 9          |
| 50                                   | 11         | 39   | 3          | 35  | 5          |
| 66                                   | 42         | 48   | 10         | 33  | 20         |
|                                      |            | 46   | 10         | 39  | 13         |
| 60 $\pm$                             | 32.0 $\pm$ | 43   | 13         | 50  | 10         |
| 2.05                                 | 4.78       | 48   | 6          | 45  | 2          |
|                                      |            | 40   | 7          | 59  | 7          |
|                                      |            | 40   | 27         | ND  | ND         |
|                                      |            | 42   | 21         | 42  | 8          |
|                                      |            | 49   | 7          | 46  | 23         |
|                                      |            | 46.8 $\pm$   | 7.75 $\pm$ | 44.0 $\pm$  | 8 $\pm$    |
|                                      |            | 2.62   | 2.08       | 2.96  | 1.26       |

Values are % inhibition of migration. ND, not detected.

\* Inhibition = stimulation of migration.

† Mean  $\pm$  s.e.m.

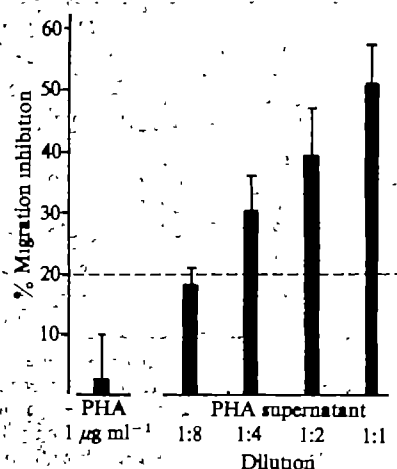


Fig. 2 Inhibitory effect of PHA and PHA supernatant on the migration of separated granulocytes (eight experiments). The results are expressed as mean  $\pm$  s.e.m. % migration inhibition. 20% inhibition (horizontal dotted line) can be regarded as significant.



(provided by K. Cantell). Table 3 shows the results of five experiments. They show that non-proliferating lymphocytes can produce LIF, in analogy with the production of macrophage migration inhibitory factor (MIF)<sup>25</sup>. This precludes the possibility that the IFN-mediated suppression of LMI could be due to its growth-inhibitory effect on the LIF-secreting lymphocytes. In addition, LIF production by both untreated and mitomycin-treated lymphocytes was suppressed by 100 U per ml IFN: 37.6% against 9.2% in the untreated and 31.6% against 8.6% LMI in mitomycin-treated lymphocytes (Table 3). The IFN-induced suppression of LIF production by untreated lymphocytes was completely prevented by the simultaneous addition of anti-IFN serum (37.6% against 9.2%), confirming that IFN itself was responsible for the suppression of LIF production.

**Table 2** Effect of IFN on the granulocyte migration inhibition induced by lymphokine-containing PHA supernatant

| Donor | -IFN       | +IFN*      | +30 min IFN pretreatment† | +IFN 30 min post-treatment‡ |
|-------|------------|------------|---------------------------|-----------------------------|
| 1     | 47         | 24         | ND                        | ND                          |
| 2     | 52         | 5          | ND                        | ND                          |
| 3     | 39         | 6          | 18                        | 35                          |
| 4     | 35         | 13         | 13                        | 28                          |
| 5     | 43         | 26         | 19                        | 39                          |
| 6     | 37         | 9          | 19                        | 42                          |
| 7     | 43         | 29         | 23                        | 41                          |
| 8     | 49         | 21         | 25                        | 52                          |
| 9     | 36         | 21         | 20                        | 38                          |
| 10    | 44         | 17         | 24                        | 38                          |
|       | 42.5 ± 1.9 | 18.3 ± 2.7 | 20.1 ± 1.5                | 39.1 ± 2.6                  |

Values are % inhibition of migration, those at the base of the columns are mean ± s.e.m.

\* Lymphokine production was induced in blood lymphocytes by PHA stimulation.  $2 \times 10^6$  lymphocytes were resuspended in RPMI 1640 supplemented with 10% FCS. PHA ( $1 \mu\text{g ml}^{-1}$ ) was added to the culture. The LIF-containing supernatant was collected after 36–48 h and tested for its ability to induce LMI on purified granulocytes as previously described. 100 U per ml of IFN were added during the migration period together with the PHA supernatant (column 2), 30 min before or after PHA supernatant addition (columns 3 and 4, respectively).

† Lymphocytes were preincubated with IFN for 30 min.

‡ IFN was added 30 min after start of culture.

**Table 3** Effect of IFN and anti-IFN serum on LIF production by untreated and mitomycin-treated lymphocytes

| Donor | Untreated cells |            |                     | Mitomycin-treated* cells |            |
|-------|-----------------|------------|---------------------|--------------------------|------------|
|       | PHA             | PHA+ IFN†  | PHA+ IFN+ anti-IFN‡ | PHA                      | PHA+ IFN   |
| 1     | 39              | 10         | 32                  | 34                       | 12         |
| 2     | 38              | 13         | 45                  | 29                       | 0          |
| 3     | 27              | 0          | 38                  | 18                       | 7          |
| 4     | 39              | 12         | 33                  | 36                       | 11         |
| 5     | 45              | 11         | 40                  | 41                       | 13         |
|       | 37.6 ± 3.2      | 9.2 ± 2.63 | 37.6 ± 2.66         | 31.6 ± 4.37              | 8.6 ± 2.66 |

Values are % migration inhibition induced on separated granulocytes by lymphocyte culture supernatants, produced in various culture conditions. Values at the base of the columns are mean ± s.e.m.

\* Lymphocytes were incubated with  $25 \mu\text{g ml}^{-1}$  mitomycin-C (Sigma) for 30 min, then the cells were washed thoroughly with medium three times and cultivated for LIF production as described in Table 2.

† 100 U  $\text{ml}^{-1}$  IFN was added during the secretion period.

‡ Anti-(100 U  $\text{ml}^{-1}$ ) IFN antiserum was added simultaneously. Addition of the same amount of antiserum to the migrating granulocytes had no toxic effect (MI was 10.5%, not significantly different from the control). The sheep anti-IFN serum has a titre of  $4.5 \times 10^5$  antiviral units per ml.

**Table 4** Effect of preincubation with IFN or IFN + anti-IFN serum on LIF production of lymphocytes after PHA stimulation

| Donor | -IFN      | +IFN         | +IFN + anti-IFN |
|-------|-----------|--------------|-----------------|
| 1     | 52        | 24           | ND              |
| 2     | 41        | 15           | 44              |
| 3     | 41        | 10           | 36              |
| 4     | 42        | 18           | 32              |
|       | 44 ± 3.09 | 16.75 ± 5.85 | 37.3 ± 4.3      |

The cells were incubated for 30 min with 100 U  $\text{ml}^{-1}$  IFN, with or without simultaneous addition of anti-(100 U  $\text{ml}^{-1}$ ) IFN serum, then washed thoroughly with medium three times and cultivated with  $1 \mu\text{g ml}^{-1}$  PHA-P (see Table 2 for culture conditions). Values are % migration inhibition induced on separated granulocytes, by lymphocyte culture supernatants produced in various culture conditions. Values at the base of the columns are mean ± s.e.m. ND, not detected.

In these experiments IFN was present during the migration period, thus a direct effect on the migrating granulocytes cannot be ruled out. Therefore, in the final experiments lymphocytes were preincubated for 30 min with IFN (with or without anti-IFN serum) and subsequently washed before the PHA-stimulation. The results (Table 4) show that preincubation with 100 U per ml IFN was sufficient to reduce significantly LIF production of PHA-activated lymphocytes (44% MI in the untreated and 16.7% in the IFN-pretreated lymphocytes). The suppression of LMI was prevented by the simultaneous addition of anti-IFN serum (37.3% against 16.7%).

These data suggest that IFN has a direct effect on the granulocytes in the LMI system and that it also blocks LIF production by the activated lymphocytes. This could be due to a direct inhibition of the cellular protein synthesis<sup>26</sup> or due to the activation of suppressor cells<sup>27</sup>. We suggest that the latter mechanism could operate *in vivo*, for example in relation to the immunodepression observed during the acute phase of infectious mononucleosis<sup>16,28</sup>. An IFN-like factor in the serum of acute mononucleosis patients was actually found to block LMI<sup>29</sup>.

This work was supported by contract no. NO1 CP 33316 from the Division of Cancer Cause and Prevention, National Cancer Institute and by grants from the Swedish Cancer Society. R.S. is the recipient of a fellowship from the Swedish Institute, Stockholm. M.M. is the recipient of a fellowship from the foundation Blanceflor Boncompagni-Ludovisi, född Bildt, Stockholm. We thank Professor K. Cantell for the anti-IFN serum.

Received 10 September; accepted 23 October 1980.

- Interferon Nomenclature *Nature* **286**, 110 (1980).
- Gresser, I. *Cell Immun.* **34**, 406–411 (1977).
- Gresser, I., Brouty-Boye, D., Thomas, M. T. & Macieira-Coelho, A. *Proc. natn. Acad. Sci. U.S.A.* **66**, 1052–1058 (1970).
- Adams, A., Strander, H. & Cantell, K. *J. gen. Virol.* **28**, 207–217 (1975).
- Epstein, L. in *Interferons and their Actions* (ed. Stewart, W. E.) 91–132 (CRB Press, Ohio, 1977).
- Trinchieri, G. & Santoli, D. *J. exp. Med.* **147**, 1314–1333 (1978).
- Einhorn, S., Blomgren, H. & Strander, H. *Int. J. Cancer* **22**, 405–412 (1978).
- Gidlund, M., Örn, A., Wigzell, H., Senik, A. & Gresser, I. *Nature* **273**, 759–761 (1978).
- Herberman, R. R., Ortaldo, J. R. & Bonnard, G. *Nature* **277**, 221–223 (1979).
- Johnson, H. M., Smith, B. G. & Baron, S. *J. Immun.* **114**, 403–409 (1975).
- Hirsch, M. S., Ellis, D. A. & Black, P. H. *Transplantation* **17**, 234–236 (1974).
- De Maeyer, E., De Maeyer-Guignard, J. & Vandeputte, M. *Proc. natn. Acad. Sci. U.S.A.* **72**, 1753–1757 (1975).
- Søborg, M. & Bendixen, G. *Acta med. scand.* **181**, 247–256 (1967).
- McCoy, J. L., Dean, J. H. & Herberman, R. R. *J. Immun. Meth.* **15**, 355–371 (1977).
- Morison, W. L. *J. clin. Path.* **27**, 113–117 (1974).
- Szigeti, R., Bokay, J., Revesz, T. & Schuler, D. *Allergy* (in the press).
- Szigeti, R., Timar, L. & Revesz, T. *Allergy* **35**, 97–103 (1980).
- Szigeti, R., Luka, J. & Klein, G. *Cell Immun.* (in the press).
- Luka, J., Lindahl, T. & Klein, G. *J. Virol.* **27**, 604–611 (1978).
- Bodo, G. in *Acad. Sci. Acts. Proc. Symp. Preparation, Standardization and Clinical Use of Interferon*, Zagreb (ed. Ikic, D.) 49–57 (1977).
- Masucci, M. G., Masucci, G., Klein, E. & Berthold, W. *Proc. natn. Acad. Sci. U.S.A.* **77**, 3620–3624 (1980).
- Nagata, S. *et al. Nature* **284**, 316–320 (1980).
- Masucci, M. G. *et al. Science* **209**, 1431–1435 (1980).
- Besancon, F. & Ankel, H. *Tex. Rep. Biol. Med.* **35**, 282–289 (1977).
- Rocklin, R. E. *J. Immun.* **110**, 674–678 (1973).
- Fuse, A. & Kuwata, T. *J. gen. Virol.* **33**, 17–24 (1976).
- Kadish, A. S., Tansey, F. A., Yu, G. S. M., Doyle, A. T. & Bloom, B. R. *J. exp. Med.* **151**, 637–650 (1980).
- Mangi, R. J. *et al. New Engl. J. Med.* **291**, 1149–1153 (1974).
- Lai, P. K., Alpers, M. P. & Mackay-Scollay, E. M. *Int. J. Cancer* **20**, 21–29 (1977).

## Prostaglandin modulation of development of cell-mediated immunity in culture

Kam H. Leung & Enrico Mihich

Department of Experimental Therapeutics, Grace Cancer Drug Center, Roswell Park Memorial Institute, New York State Department of Health, Buffalo, New York 14263

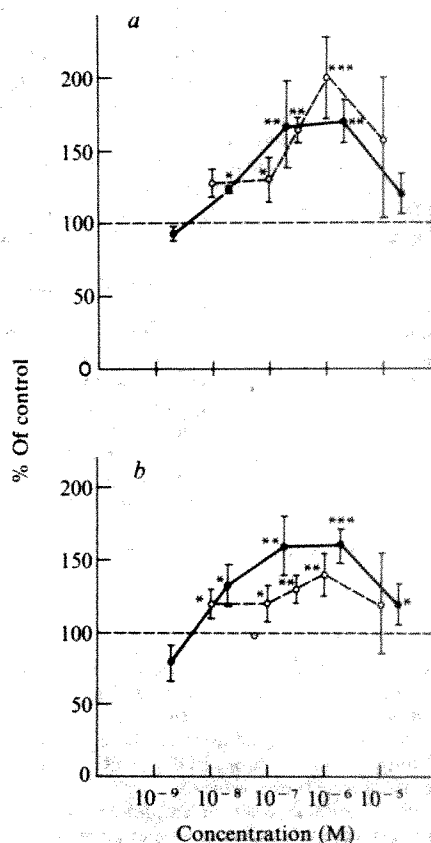
Prostaglandins (PGs) have been implicated as possible modulators of the immune response and various inflammatory processes<sup>1-4</sup>. Various cell components of the immune system are sources of PGs, and mitogen or antigen stimulation of human or murine lymphocytes leads to their enhanced release<sup>5-8</sup>. They are also released from various human and animal tumours<sup>9,10</sup>. Thus, as cells of the immune system are both sensitive to and sources of PGs, these factors may be important as physiological immune regulators. For example, PGs of the E series are capable of inhibiting many effector functions<sup>9-15</sup>. They have also been shown to inhibit the development of the humoral response<sup>16,17</sup>. Although they inhibit the proliferative response to mitogens<sup>18,19</sup>, little is known about their effects on the development of the cell-mediated immune response to antigens. The data summarized here implicate PGs, thromboxane A<sub>2</sub> (TXA<sub>2</sub>) and prostacyclin (PGI<sub>2</sub>) in the regulation of cellular immune responses at the inductive phase. Some of these data have been reported in abstract form<sup>20</sup>.

A dose-response relationship was observed when various numbers of X-ray irradiated P815 mastocytoma cells were cultured with a constant number ( $5 \times 10^6$ ) of allogeneic C57BL/6 spleen cells. The cell-mediated immunity (CMI) was monitored by <sup>3</sup>H-thymidine incorporation and anti-target cell lytic activity (% of specific <sup>51</sup>Cr release) on day 4 in culture. The <sup>3</sup>H-thymidine incorporation into unstimulated lymphocytes was  $1,664 \pm 801$  c.p.m. and increasing the number of stimulator cells from  $1 \times 10^5$  to  $5 \times 10^5$  led to an increase in both <sup>3</sup>H-thymidine incorporation ( $8,576 \pm 3,928$  to  $61,998 \pm 14,079$  c.p.m.) and cytotoxic activity (% specific <sup>51</sup>Cr release  $22.7 \pm 7.7$  to  $52.5 \pm 6.8$ , effector: target cell (E:T) = 50:1). A further increase of stimulator cells to  $1 \times 10^6$  decreased the levels of both these parameters to those of the unstimulated culture. The <sup>3</sup>H-thymidine uptake into the cells was only a measure of the proliferation of the lymphocytes after antigenic stimulation. The ultimate proof of immunological significance of the stimulation is the production of cytolytic effector cells.

Table 1a shows that addition of PGE<sub>1</sub> or PGE<sub>2</sub> on day 0 of culture had an inhibitory effect on <sup>3</sup>H-thymidine incorporation on day 4 of culture. At this time the response was maximal. The <sup>3</sup>H-thymidine incorporation into the lymphocytes was 24% and 38% of the control in the presence of 30 nM PGE<sub>1</sub> and 30 nM PGE<sub>2</sub>, respectively. The agents at these concentrations had no effect on the unstimulated lymphocytes or on the <sup>3</sup>H-thymidine incorporation when added at the time of assay. As indicated by the <sup>51</sup>Cr release assay (Table 1b), 30 nM of PGE<sub>1</sub> or PGE<sub>2</sub> inhibited the development of the CMI by 50%. PGE at the concentrations tested had no effect on the lytic activity of effector cells generated *in vitro* when added at the time of the <sup>51</sup>Cr release assay. This lack of activity on *in vitro*-generated effector cells compared with the effect on *in vivo*-generated effector cells has recently been reported<sup>15</sup>. The concentration of PGE found in inflammatory fluid<sup>7</sup> and in mitogen- or antigen-stimulated cultures<sup>5,6</sup> is in the range of 3–300 nM. Thus, the finding that 30 nM PGE<sub>1</sub> or PGE<sub>2</sub> could inhibit sensitization of lymphocytes is consistent with the hypothesis that, at physiological levels, these agents act as negative-feedback regulators.

Kinetic experiments indicated that PGE<sub>1</sub> affects only the magnitude of the CMI and does not cause a shift in the responses. When PGE<sub>1</sub> was added at various intervals after culture initiation, it was found to act during the inductive phase of the immune response. PGE<sub>1</sub> was active when added to spleen cells as long as 20 h before and up to 24 h after the addition of stimulator cells, but when added 48 h after culture initiation, it was not effective. It has recently been reported that if human peripheral blood lymphocytes are cultured for 24 h before being stimulated by phytohaemagglutinin, their proliferation is no longer inhibited by PGs<sup>21</sup>. However, this study shows that the antigenic stimulation of murine spleen lymphocytes which had been preincubated for 20 h, can still be modulated by PGE<sub>1</sub>. In separate experiments, when PGE<sub>1</sub> was in spleen cell culture for 20 h and was removed by washing before the addition of stimulator cells, little inhibition was observed (data not shown). Thus, these data indicate the reversibility of the effect and the fact that PGE<sub>1</sub> seems to have a relatively long half life in spleen cell cultures. The effect of PGE<sub>1</sub> was also negated if the agent was removed by washing the cells within 8 h after initiation of the culture. By 48 h the effect of PGE<sub>1</sub> was irreversible. In summary, the effects of PGE on the CMI response affect the early period of the induction phase of the response.

The results shown in Fig. 1 indicate that indomethacin, an irreversible inhibitor of cyclooxygenase, the enzyme that catalyses the conversion of arachidonic acid to the endoperoxides PGG<sub>2</sub> and PGH<sub>2</sub> (which are common intermediates for TXA<sub>2</sub>, PGE<sub>2</sub>, PGF<sub>2 $\alpha$</sub> , PGI<sub>2</sub> and other PGs)<sup>22</sup>, augmented



**Fig. 1** Effect of indomethacin and Ro 20-5720 on the development of the CMI. *a*, Thymidine incorporation; *b*, cytotoxicity. The results were expressed in terms of the non-drug-treated control normalized to 100. The control values for the thymidine incorporation for indomethacin and Ro-5720 were  $7,372 \pm 1,370$  and  $15,341 \pm 3,115$  c.p.m., respectively. The control values for <sup>51</sup>Cr release were  $24.3 \pm 3.2$  and  $23.4 \pm 2.6$  c.p.m., respectively. Each value represents the mean % of control  $\pm$  s.d. ( $n=4$ ). \*  $P < 0.005$ , \*\*  $P < 0.001$  and \*\*\*  $P < 0.001$ .



**Table 1** Effects of prostaglandins  $E_1$  and  $E_2$  on  $^3H$ -thymidine incorporation into spleen lymphocytes\* (a) and the cytolytic activity of effector cells (b)

|                                  |                           |  |                        |  |                                       |                         |                        |
|----------------------------------|---------------------------|--|------------------------|--|---------------------------------------|-------------------------|------------------------|
| a                                |                           | Nonstimulated cultures<br>(c.p.m. $\pm$ s.d.) <sup>†</sup>               |                        | Stimulated cultures ( $5 \times 10^5$ P815x)<br>(c.p.m. $\pm$ s.d.) <sup>†</sup> |                                       |                         |                        |
|                                  | PGE concentration<br>(nM) | PGE <sub>1</sub>   | PGE <sub>2</sub>       | PGE <sub>1</sub>   | PGE <sub>2</sub>                      |                         |                        |
| (1) Inductive phase <sup>‡</sup> |                           |  |                        |  |                                       |                         |                        |
|                                  | 0                         | 1,073 $\pm$ 171  |                        | 46,398 $\pm$ 2,874   |                                       |                         |                        |
|                                  | 0.3                       | 1,280 $\pm$ 91 (120) <sup>§</sup>  | 1,628 $\pm$ 360 (181)  | 46,992 $\pm$ 5,912 (101)   | 38,832 $\pm$ 1,987 (84) <sup>  </sup> |                         |                        |
|                                  | 3                         | 1,299 $\pm$ 166 (120)  | 1,530 $\pm$ 220 (142)  | 30,585 $\pm$ 2,440 (66) <sup>§</sup>   | 34,048 $\pm$ 1,766 (73) <sup>§</sup>  |                         |                        |
|                                  | 30                        | 1,110 $\pm$ 363 (102)  | 1,220 $\pm$ 110 (114)  | 11,090 $\pm$ 536 (24) <sup>*</sup>   | 17,512 $\pm$ 1,761 (38) <sup>*</sup>  |                         |                        |
|                                  | 3,000                     | 712 $\pm$ 88 (66) <sup>§</sup>   | 790 $\pm$ 145 (74)     | 5,668 $\pm$ 364 (12) <sup>*</sup>  | 8,224 $\pm$ 1,096 (18) <sup>*</sup>   |                         |                        |
| (2) Effector phase <sup>††</sup> |                           |  |                        |  |                                       |                         |                        |
|                                  | 3                         | ND   | ND                     | 44,439 $\pm$ 3,441 (96)  | 43,285 $\pm$ 2,849 (93)               |                         |                        |
|                                  | 30                        | ND   | ND                     | 45,057 $\pm$ 3,034 (96)  | 44,800 $\pm$ 2,717 (97)               |                         |                        |
|                                  | 3,000                     | 1,348 $\pm$ 325 (126)  | 1,281 $\pm$ 265 (119)  | 49,252 $\pm$ 5,796 (106)   | 46,173 $\pm$ 4,259 (100)              |                         |                        |
| b                                |                           | % Specific <sup>51</sup> Cr release $\pm$ s.d. <sup>†</sup> (E:T ratios) |                        |  |                                       |                         |                        |
|                                  | PGE concentration<br>(nM) | PGE <sub>1</sub>   |                        |  | PGE <sub>2</sub>                      |                         |                        |
|                                  |                           | 50:1   | 25:1                   | 12.5:1   | 50:1                                  | 25:1                    | 12.5:1                 |
| (1) Inductive phase <sup>‡</sup> |                           |  |                        |  |                                       |                         |                        |
|                                  | 0                         | 53.0 $\pm$ 0.7   | 37.7 $\pm$ 2.4         | 23.0 $\pm$ 1.4   | 53.0 $\pm$ 0.7                        | 37.7 $\pm$ 2.4          | 23.0 $\pm$ 1.4         |
|                                  | 0.3                       | 50.9 $\pm$ 3.7<br>(96) <sup>§</sup>                                      | 36.2 $\pm$ 5.1<br>(96) | 19.5 $\pm$ 0.9<br>(85)   | 49.4 $\pm$ 1.4<br>(93)                | 37.9 $\pm$ 1.6<br>(100) | 21.3 $\pm$ 1.6<br>(93) |
|                                  | 3                         | 45.6 $\pm$ 2.0<br>(86) <sup>  </sup>                                     | 31.6 $\pm$ 2.7<br>(84) | 18.0 $\pm$ 1.4<br>(78)   | 47.5 $\pm$ 3.6<br>(90)                | 33.9 $\pm$ 3.2<br>(90)  | 19.8 $\pm$ 1.5<br>(86) |
|                                  | 30                        | 24.3 $\pm$ 0.7<br>(46) <sup>*</sup>                                      | 14.9 $\pm$ 1.4<br>(40) | 6.9 $\pm$ 2.3<br>(30)  | 32.6 $\pm$ 2.0<br>(62) <sup>§</sup>   | 19.7 $\pm$ 1.0<br>(52)  | 12.3 $\pm$ 0.7<br>(53) |
|                                  | 3,000                     | 10.0 $\pm$ 1.1<br>(19) <sup>*</sup>                                      | 5.0 $\pm$ 1.0<br>(10)  | 1.3 $\pm$ 0.8<br>(6)   | 16.4 $\pm$ 2.4<br>(31) <sup>*</sup>   | 10.0 $\pm$ 1.9<br>(27)  | 4.4 $\pm$ 1.2<br>(19)  |
| (2) Effector phase               |                           |  |                        |  |                                       |                         |                        |
|                                  | 3,000                     | 49.1 $\pm$ 2.7<br>(93)   | 33.8 $\pm$ 1.5<br>(90) | ND   | 50.3 $\pm$ 1.1<br>(95)                | 33.5 $\pm$ 1.9<br>(89)  | ND                     |
|                                  | 30,000                    | 47.2 $\pm$ 0.6<br>(89)   | 32.7 $\pm$ 1.0<br>(87) | ND   | 46.8 $\pm$ 1.4<br>(88)                | 32.3 $\pm$ 0.6<br>(86)  | ND                     |

Primary immunization cultures with C57BL/6 mouse spleen cells as responder cells and P815 tumour cells as stimulator cells were established according to published procedures<sup>30</sup>. Briefly, cultures were maintained in RPMI 1640 medium supplemented with 2 mM L-glutamine, 25 mM HEPES (pH 7.45),  $3 \times 10^{-5}$  M mercaptoethanol, 10% heat-inactivated fetal calf serum (FCS, Gibco), 100  $\mu$ g ml<sup>-1</sup> streptomycin, 100 U ml<sup>-1</sup> penicillin and 100  $\mu$ g ml<sup>-1</sup> gentamycin. A suspension of  $5 \times 10^6$  cells in 1.9 ml of supplemented medium was added to 35-mm tissue culture dishes and the cells were incubated at 37 °C in a 5% CO<sub>2</sub> atmosphere. Stimulator cells were X-ray irradiated (4,000R, P815x cells) and test agents were added in 0.1 ml medium to the spleen cell suspension. In some cases, 95% ethyl alcohol (EtOH) was used as initial solvent, but the final concentration did not exceed 0.01% which was shown not to affect the assays. The same volume of medium was added to control cultures. In these conditions, the cytotoxicity of effector cells (E) that developed was proportional to the number of stimulating cells which were varied from  $5 \times 10^5$  to  $2.5 \times 10^6$ . To measure thymidine incorporation, microcultures were incubated in flat-bottom Microtest plates (Linbro) at 37 °C and 5% CO<sub>2</sub> in air. The microcultures consisted of 0.1 ml cell suspension from day 4 culture and 0.1 ml of RPMI medium and 50  $\mu$ l (1  $\mu$ Ci) of [ $Me$ - $^3H$ ]thymidine (specific activity 6.7 Ci mmol<sup>-1</sup>). After 4 h the cultures were collected on glass filter strips with an automatic cell collector. The filters were washed with saline. They were dried and counted in scintillation fluid in a Beckman scintillation counter. *In vitro* effector cells were collected after day 4 and unless otherwise stated, were centrifuged, washed and resuspended in 0.5 ml of medium supplemented with 5% FCS. Cell viability was determined by trypan blue exclusion and was unaffected by the drug treatments. The density of viable effector cells was adjusted to  $1 \times 10^7$  cells ml<sup>-1</sup>.  $^{51}Cr$ -labelled P815 target cells (T) were prepared according to published procedures<sup>31</sup>, and their cell density adjusted to  $2 \times 10^5$  cells ml<sup>-1</sup>. Labelled target cells ( $2 \times 10^4$ ) in 0.1 ml were added to 0.1 ml of effector cells in duplicate 12  $\times$  75-mm plastic tubes (Falcon). The number of effector cells was adjusted to give different E:T ratios—50:1, 25:1 and 12.5:1. The preparations were incubated for 4 h at 37 °C in a humidified CO<sub>2</sub> incubator and the reaction was stopped by adding 2 ml of cold RPMI 1640 medium. The percentage release of radioactive chromium was calculated as follows:

$$\% ^{51}Cr \text{ release} = \frac{\text{c.p.m. in supernatant}}{\text{c.p.m. in supernatant} + \text{c.p.m. in pellet}} \times 100$$

The per cent specific  $^{51}Cr$  release is obtained by subtracting the %  $^{51}Cr$  released from labelled targets in the presence of nonensitized spleen cells from the value obtained in the presence of sensitized spleen cells. All experiments have been reproduced at least twice.

\* Spleen lymphocytes ( $5 \times 10^6$ ) were cultured with  $5 \times 10^5$  P815x cells for 4 days.

<sup>†</sup> These values represent the mean  $\pm$  s.d. where  $n = 3$ .

<sup>‡</sup> The final concentration of either PGE<sub>1</sub> or PGE<sub>2</sub> added at the time of initiation of the culture.

<sup>§</sup> The numbers in parentheses represent per cent of control without PG.

<sup>||</sup> The statistical significance which was determined by the Student's two-tailed *t*-test is indicated by: <sup>§</sup>,  $P < 0.05$ ; <sup>†</sup>,  $P < 0.01$ ; and <sup>\*</sup>,  $P < 0.001$ .

<sup>††</sup> Prostaglandins were added at the time of assay on day 4. ND, not done.

$^3H$ -thymidine incorporation and lytic activity in a concentration-dependent manner. The optimal concentration was  $3 \times 10^{-7}$  M (0.1  $\mu$ g ml<sup>-1</sup>). Ro 20-5720 (*d*,1-6-chloro- $\alpha$ -methyl-carbazole-2-acetic acid), a reversible inhibitor of cyclooxygenase<sup>17</sup>, also augmented the CMI (optimal concentration  $10^{-8}$  M). Inhibitors of PG biosynthesis have been extensively studied (for a recent review, see ref. 23). Inhibitors of cyclooxygenase have been shown previously to inhibit tumour

growth<sup>16</sup>, enhance humoral responses<sup>17</sup> and augment mitogen- or antigen-induced blastogenesis<sup>18,19</sup>.

In addition to the PGs, PGI<sub>2</sub> and TXA<sub>2</sub> are also released by macrophages and lymphocytes<sup>2,23-25</sup>. PGI<sub>2</sub> ( $3 \times 10^{-4}$  M) inhibited the cytolytic activity of effector cells from immunized mice by 20% ( $P < 0.02$ ), whereas at concentrations from  $3 \times 10^{-10}$  M to  $3 \times 10^{-6}$  M it showed no effect on the development of the CMI in culture. This lack of activity may be due to the short

**Table 2** Effects of exogenous PGE<sub>2</sub> on the CMI in the presence or absence of inhibitors of prostaglandin synthesis

| Inhibitors   | Thymidine incorporation |                      |                     | Per cent of control*  |                      |                      | Cytotoxicity |   |    |
|--|-------------------------|----------------------|---------------------|-----------------------|----------------------|----------------------|--------------|---|----|
|  |                         |                      |                     | PGE <sub>2</sub> (nM) |                      |                      |              |   |    |
|  | 0                       | 3                    | 30                  | 0                     | 3                    | 30                   | 0            | 3 | 30 |
| 0  | 100                     | 69 ± 6 <sup>§</sup>  | 30 ± 3 <sup>§</sup> | 100                   | 80 ± 12 <sup>†</sup> | 48 ± 13 <sup>§</sup> |              |   |    |
| Indomethacin (0.1 µg ml <sup>-1</sup> )            | 141 ± 13 <sup>§</sup>   | 76 ± 8 <sup>‡</sup>  | 30 ± 8 <sup>§</sup> | 125 ± 9 <sup>†</sup>  | 94 ± 23              | 37 ± 7 <sup>§</sup>  |              |   |    |
| Imidazole (IDZ) (200 µg ml <sup>-1</sup> )         | 55 ± 11 <sup>§</sup>    | 39 ± 10 <sup>§</sup> | 16 ± 2 <sup>§</sup> | 49 ± 16 <sup>‡</sup>  | 38 ± 11 <sup>§</sup> | 12 ± 8 <sup>§</sup>  |              |   |    |
| Tranylcypromine (Tranyl) (25 µg ml <sup>-1</sup> ) | 144 ± 23 <sup>‡</sup>   | 87 ± 10              | 32 ± 7 <sup>§</sup> | 133 ± 4 <sup>§</sup>  | 127 ± 8 <sup>‡</sup> | 75 ± 16              |              |   |    |
| IDZ/Tranyl (200 µg 25 µg ml <sup>-1</sup> )        | 59 ± 8 <sup>§</sup>     | 35 ± 3 <sup>§</sup>  | 13 ± 1 <sup>§</sup> | 87 ± 21               | 58 ± 25 <sup>‡</sup> | 18 ± 20 <sup>§</sup> |              |   |    |

Spleen cell cultures were exposed to  $3.5 \times 10^5$  P815x cells and indomethacin, imidazole, tranylcypromine or PGE<sub>2</sub> alone or in the indicated combinations.

\* The results were expressed as per cent of non-drug-treated control culture response. The control values for thymidine incorporation and % specific <sup>51</sup>Cr release were  $40,197 \pm 14,977$  and  $49.5 \pm 5.7$  (E:T ratio 50:1), respectively. Each value represents the mean % of control of four experiments  $\pm$  s.d.

<sup>†</sup>  $P < 0.05$ , <sup>‡</sup>  $P < 0.01$ , <sup>§</sup>  $P < 0.001$ .

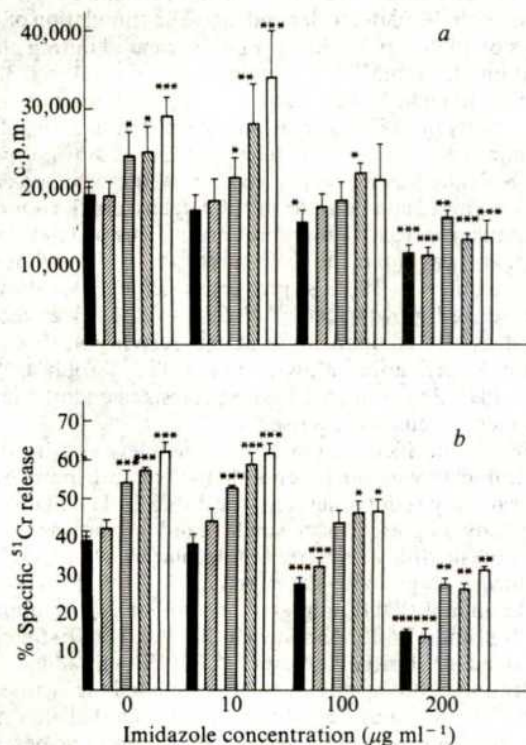
half life of PGI<sub>2</sub> ( $t_{1/2} = 3-5$  min) in culture conditions<sup>26</sup>. The half life of TXA<sub>2</sub> is also extremely short ( $t_{1/2} = 30$  s)<sup>27</sup>. Knowing these facts, tranylcypromine, an inhibitor of PGI<sub>2</sub> synthetase (ID<sub>50</sub> concentration  $160 \mu\text{g ml}^{-1}$ )<sup>26</sup> and imidazole, an inhibitor of thromboxane synthetase (ID<sub>50</sub> concentration  $8 \text{ mM}$ )<sup>27,28</sup>, were tested to assess their effect on the CMI. Note that the effects of these two agents are specific for the respective enzymes and that at the concentrations tested here they do not affect other enzymes of arachidonic acid metabolism. That they may affect other enzyme systems cannot be ruled out. In fact, imidazole is known to stimulate phosphodiesterase<sup>28</sup> and such stimulation reduces cyclic AMP pools and results in either no effect or augmented CMI development (K.H.L., unpublished

results). The data (Fig. 2) show that imidazole (ID<sub>50</sub>  $3 \text{ mM}$  or  $200 \mu\text{g ml}^{-1}$ ) inhibited the development of the CMI whereas tranylcypromine ( $0.2 \text{ mM}$  or  $25 \mu\text{g ml}^{-1}$ ) augmented it in a concentration-dependent manner. When used in combination, imidazole and tranylcypromine were antagonistic in their effect on the CMI. There is, however, an apparent constant minimal per cent reduction of the CMI caused by imidazole regardless of the concentration of tranylcypromine used, and similarly, the augmentation with tranylcypromine in the presence of different concentrations of imidazole remains constant at a certain minimal level. This may reflect the fact that a blockage of TXA<sub>2</sub> synthesis by imidazole leads to a lower TXA<sub>2</sub> pool, but also a consequence of this blockage could be increased synthesis of PGI<sub>2</sub> and PGE<sub>2</sub>. In the presence of imidazole, the effect of tranylcypromine is less effective and vice versa. This may suggest that, apart from inhibition of PGI<sub>2</sub> synthesis by tranylcypromine, some of the action may be due to the possible increased production of TXA<sub>2</sub>.

Table 2 summarizes the effects of exogenous PGE<sub>2</sub> on the CMI in the presence or absence of inhibitors of PG synthesis. The effect of indomethacin was reversible by PGE<sub>2</sub>, indicating that PGE<sub>2</sub> is a negative mediator of the CMI development. The effects of imidazole and PGE<sub>2</sub> were additive. However,  $3 \text{ nM}$  of PGE<sub>2</sub> did not effectively reverse the augmented CMI resulting from the addition of tranylcypromine. More interestingly, the effect of tranylcypromine on the <sup>3</sup>H-thymidine incorporation was abrogated by  $30 \text{ nM}$  of PGE<sub>2</sub>, but its effect on the cytotoxic activity was not completely reversed ( $P < 0.01$ ). This may suggest that PGE<sub>2</sub> is less effective in reversing the action of TXA<sub>2</sub> in the presence of a lower level of PGI<sub>2</sub> and TXA<sub>2</sub>; PGE<sub>2</sub> or PGI<sub>2</sub> may be affecting different subsets of lymphocytes. In the presence of imidazole and tranylcypromine, the effect of PGE<sub>2</sub> was, as in the presence of indomethacin, due to the lower PGI<sub>2</sub> and TXA<sub>2</sub> pools. This seems to indicate that PGI<sub>2</sub> and TXA<sub>2</sub> are more potent than PGE<sub>2</sub> in modulating the development of CMI.

Three implications may be derived from these results: (1) PGI<sub>2</sub> may be a negative (inhibitory) regulator and TXA<sub>2</sub> a positive (augmentative) regulator of the CMI development. (2) Augmentation of the CMI by tranylcypromine may be a consequence of the removal of PGI<sub>2</sub> or of a channelling of PGH<sub>2</sub> into TXA<sub>2</sub> and other PGs. The converse of this argument may be applied to explain the lower CMI response following inhibition of TXA<sub>2</sub> synthesis by imidazole. (3) The relative concentrations of PGI<sub>2</sub>, TXA<sub>2</sub> and PGs may determine the magnitude of the immune response.

We thank Mrs M. J. Ehrke for helpful discussions, Dr J. E. Pike (Upjohn) for PGI<sub>2</sub>, Dr W. E. Scott (Hoffman-LaRoche) for Ro 20-5720, and Ms P. Dickens and K. M. Schrader for preparation of the manuscript. This work fulfilled part of the requirement for the PhD degree of K.H.L.



**Fig. 2** Effect of imidazole or tranylcypromine alone or in combination on the development of the CMI. *a*, Thymidine incorporation; *b*, cytotoxicity. The results were expressed as mean  $\pm$  s.d. ( $n = 4$ ). \*,  $P < 0.005$ , \*\*,  $P < 0.01$  and \*\*\*,  $P < 0.001$ . The concentrations of tranylcypromine were: ■,  $0 \mu\text{g ml}^{-1}$ ; □,  $1 \mu\text{g ml}^{-1}$ ; ▨,  $5 \mu\text{g ml}^{-1}$ ; ▩,  $10 \mu\text{g ml}^{-1}$ ; and ▤,  $25 \mu\text{g ml}^{-1}$ .



Received 23 July; accepted 17 October 1980.

1. Bourne, H. R. *et al. Science* **184**, 19–28 (1974).
2. Pelus, L. M. & Strasser, H. R. *Life Sci.* **20**, 903–914 (1977).
3. Lewis, G. P. *J. reticuloendothel. Soc.* **22**, 389–402 (1977).
4. Goodwin, J. S. & Webb, D. R. *Clin. Immun. Immunopath.* **15**, 106–122 (1980).
5. Ferraris, V. A. & DeRubertis, F. R. *J. clin. Invest.* **54**, 378–386 (1974).
6. Webb, D. R. & Osheroff, P. L. *Proc. natn. Acad. Sci. U.S.A.* **73**, 1300–1304 (1976).
7. Youtten, L. J. F. & McCall, E. in *Prostaglandins in Hematology* (eds Silver, M. J., Smith, J. B. & Kocsis, J. J.) 87–90 (Spectrum, New York, 1977).
8. Humes, J. L. *et al. Nature* **269**, 149–151 (1977).
9. Jaffe, B. M. *Prostaglandins* **6**, 453–461 (1974).
10. Easty, G. C. & Easty, D. M. *Cancer Treat. Rev.* **3**, 217–225 (1976).
11. Henney, C. S., Bourne, H. R. & Lichtenstein, L. M. *J. Immun.* **108**, 1526–1534 (1972).
12. Strom, T. B. *et al. J. exp. Med.* **138**, 381–383 (1973).
13. Gorden, D., Bray, M. A. & Morley, J. *Nature* **262**, 401–402 (1976).
14. Schultz, R. M., Pavlidis, N. A., Stylos, W. A. & Chirigos, M. A. *Science* **202**, 320–321 (1978).
15. Plaut, M. J. *Immun.* **123**, 692–701 (1979).
16. Plescia, O. J., Smith, A. H. & Grinwich, K. *Proc. natn. Acad. Sci. U.S.A.* **72**, 1848–1851 (1975).
17. Webb, D. R. & Nowowiejski, I. *Cell Immun.* **33**, 1–10 (1977).
18. Goodwin, J. S., Bankhurst, A. D. & Messner, R. P. *J. exp. Med.* **146**, 1719–1734 (1977).
19. Webb, D. R. & Nowowiejski, I. *Cell Immun.* **41**, 72–85 (1978).
20. Leung, K. H. & Mihich, E. *63rd A. Meet. Fedn Am. Soc. exp. Biol.*, Dallas, Texas (1–10 April, 1979); 1st Int. Conf. Immunopharmac., Brighton (29 July–1 August, 1980).
21. Goodwin, J. S., Messner, R. P. & Peake, G. T. *J. clin. Invest.* **62**, 753–760 (1978).
22. Samuelsson, B. *et al. A. Rev. Biochem.* **47**, 997–1029 (1978).
23. Vane, J. R. *Adv. Prostaglandin Thromboxane Res.* **4**, 27–44 (1978).
24. Brune, K., Glatt, M., Kalin, H. & Peskar, B. A. *Nature* **274**, 261–263 (1978).
25. Morley, M. A., Bray, M. A., Jones, R. W., Nuteven, D. H. & Van Doryn, D. A. *Prostaglandins* **17**, 730–746 (1979).
26. Gryglewski, R. J., Bunting, S., Moncada, S., Flower, R. J. & Vane, J. R. *Prostaglandins* **12**, 685–713 (1976).
27. Moncada, S. *et al. Prostaglandins* **13**, 611–618 (1977).
28. Parker, C. W., Stevenson, W. F., Huler, M. G. & Kelly, J. P. *J. Immun.* **122**, 1572 (1979).
29. Needleman, P. *et al. Prostaglandins* **14**, 897–907 (1977).
30. Cerottini, J.-C., Engers, H. D., MacDonald, H. R. & Brunner, K. T. *J. exp. Med.* **140**, 703–717 (1974).
31. Mawas, C., Carey, T. & Mihich, E. *Cell Immun.* **6**, 243–260 (1973).

## Platelet-dependent stimulation of prostacyclin synthesis by platelet-derived growth factor

Shaun R. Coughlin\*, Michael A. Moskowitz\*†, Bruce R. Zetter‡, Harry N. Antoniades§ & Lawrence Levine||

\* Laboratory of Neural and Endocrine Regulation, Department of Nutrition and Food Science, Massachusetts Institute of Technology, Cambridge, Massachusetts 02139

† Section of Neurology, Department of Medicine, Peter Bent Brigham Hospital, Harvard Medical School, Boston, Massachusetts 02115

‡ Department of Surgery, Children's Hospital Medical Center, Harvard Medical School, Boston, Massachusetts 02115

§ Center for Blood Research, Department of Nutrition, Harvard School of Public Health, Boston, Massachusetts 02115

|| Department of Biochemistry, Brandeis University, Waltham, Massachusetts 02154

**Prostacyclin (PGI<sub>2</sub>), an unstable metabolite of arachidonic acid synthesized by vascular endothelial and smooth muscle cells, is a potent vasodilator and endogenous inhibitor of platelet aggregation<sup>1–10</sup>. Regulation of PGI<sub>2</sub> synthesis by the vessel wall is not well understood<sup>11–16</sup>. We have investigated the possibility that a product released from platelet granules during degranulation might modify vessel wall PGI<sub>2</sub> biosynthesis. We report here that a non-dialysable, platelet-dependent factor in serum dramatically stimulates PGI<sub>2</sub> synthesis by cultured bovine aortic endothelium, aortic smooth muscle, and adrenal capillary endothelium. Platelet-derived growth factor (PDGF), a releasable peptide contained within platelet alpha granules<sup>17–20</sup>, stimulates PGI<sub>2</sub> synthesis by the above cell types as much as 100-fold. The concentrations of PDGF required to produce these effects are below the level reported in normal human serum<sup>18</sup>. We postulate that *in vivo* released PDGF may increase vessel wall PGI<sub>2</sub> production as part of a negative feedback mechanism controlling platelet aggregation.**

† To whom correspondence should be addressed.

Endothelial cells were cultured from bovine aorta by a modification of previously published techniques (see legend to Table 1)<sup>21–23</sup>. These cells formed confluent monolayers and exhibited light-microscopic and ultrastructural characteristics consistent with endothelium<sup>24–26</sup>. They also contained the endothelial cell marker factor VIII antigen<sup>24</sup>: immunofluorescent studies revealed specific granular staining concentrated in the perinuclear region (anti-bovine factor VIII provided by J. Brown, University of California, San Diego). Bovine aortic smooth muscle cells were cultured as described elsewhere<sup>27</sup>. These appeared spindle-shaped, grew in multilayers with the characteristic 'hill and valley' pattern, and contained prominent myofilamentous bundles characteristic of smooth muscle. Culture and characterization of bovine adrenal capillary endothelium has been reported elsewhere<sup>28</sup>. The capillary endothelial cells used in this study were cloned from single cells and used between passages eight and twelve. Bovine aortic endothelial and smooth muscle cell cultures between passages one and five were used.

Cells in culture were incubated with vehicle or treatment as described in Table 1. Of the total cyclo-oxygenase products made in culture, aortic endothelium made 95% 6-keto prostaglandin F<sub>1α</sub> (6 KF<sub>1α</sub>), capillary endothelium 80%, and aortic smooth muscle 73% 6 KF<sub>1α</sub>. In descending order, lesser amounts of PGF<sub>2α</sub>, PGE<sub>2</sub>, PGD<sub>2</sub> and thromboxane B<sub>2</sub> (TXB<sub>2</sub>) were also made. For comparison, aortic strips *in vitro* made about 96% 6KF<sub>1α</sub> and brain microvessels made 80% (ref. 29).

Serum has been reported to stimulate prostaglandin synthesis by MC5-5 fibroblasts in culture<sup>30</sup>. In preliminary experiments we demonstrated that human or bovine serum also potently stimulated prostaglandin and prostacyclin synthesis in cells of vascular origin, bovine aortic endothelium and smooth muscle. To assess the platelet's contribution to this activity, platelet-rich plasma-derived serum (PRS) and platelet-poor plasma-derived serum (PDS) were prepared (see Table 1) and tested for their ability to stimulate PGI<sub>2</sub> synthesis in culture. The data shown in Table 1 indicate that at least 80% of the stimulatory activity of serum seems to be platelet-dependent. (The stimulation of PGI<sub>2</sub> synthesis by PDS may be due to PDGF released during plasma preparation, thrombin<sup>31</sup>, bradykinin, angiotensin II (ref. 32), or other as yet unidentified compounds.) Preparations with higher specific activity than PRS have been obtained by heating (100 °C for 2.5 min) and extracting platelets into 1.0 M NaCl. (Specific activity is defined as ng 6KF<sub>1α</sub> accumulated per mg of added protein<sup>33</sup>.) These data point to the platelet as a major source of PGI<sub>2</sub>-stimulating activity found in serum. This platelet-dependent activity was nondialysable, stable at 56 °C, and at least partially stable at 100 °C—properties similar to those of platelet-derived growth factor<sup>17</sup>. Because PDGF was recently proposed as the component in serum responsible for phospholipase A<sub>2</sub> activation in Swiss mouse 3T3 fibroblasts<sup>34</sup>, the ability of PDGF to stimulate PGI<sub>2</sub> synthesis in endothelial and smooth muscle cells was assessed.

PDGF was purified<sup>17</sup> from human platelets and incubated with cultured bovine aortic endothelial, smooth muscle, and adrenal capillary endothelial cells (see Table 2). The PDGF used in this study migrated as a single band on polyacrylamide electrophoresis with an apparent molecular weight of 35,000 in non-reducing conditions—after reduction with 5% (v/v) 2-mercaptoethanol PDGF migrated as two bands with apparent MW 13,000 and 17,000. As shown in Table 2, PDGF stimulated dose-dependent biosynthesis of PGI<sub>2</sub>. When added at a concentration of 8.0 ng ml<sup>-1</sup>, PDGF stimulated the synthesis of PGI<sub>2</sub> by 74-, 84- and 15-fold in aortic endothelial, smooth muscle, and capillary endothelial cell cultures, respectively. Followed over a 24-h period, 6KF<sub>1α</sub> accumulated in an essentially linear manner in these cultures. To evaluate the reversibility of PDGF action, cultures were washed five times with 2.5 ml M199 after incubation for 6 h with PDGF (8 ng ml<sup>-1</sup>) and the medium replaced with M199 plus vehicle only. After washing, the rate of 6KF<sub>1α</sub> accumulation returned to that of the unstimulated cultures. Thus, PDGF-induced stimulation

required the continued presence of PDGF in the medium. Similar results were obtained with PRS. In addition to stimulating PGI<sub>2</sub> synthesis, PDGF stimulated PGF<sub>2α</sub> synthesis by the above cell types, with a similar dose response. This suggests that PDGF increases prostaglandin production either by stimulating the cyclo-oxygenase, or, more likely, by increasing arachidonate availability to the cyclo-oxygenase through increasing phospholipid deacylation. In fact, PDGF activation of phospholipase A<sub>2</sub> has recently been reported<sup>34</sup>. Serum stimulates prostaglandin synthesis in a similar manner in these and other cells<sup>30,34</sup>.

Table 1 Platelet-dependent stimulation of PGI<sub>2</sub> synthesis

|  | Control                  | PRS                      | PDS                       |
|--|--------------------------|--------------------------|---------------------------|
| Aortic endothelium<br>6KF <sub>1α</sub> (ng ml <sup>-1</sup> )   | 4.1 ± 0.44 <sup>1</sup>  | 496 ± 87 <sup>2</sup>    | 123 ± 17 <sup>3</sup>     |
| Cells per plate<br>(×10 <sup>-5</sup> )                          | 16.1 ± 0.59 <sup>1</sup> | 20.1 ± 1.1 <sup>2</sup>  | 19.3 ± 0.47 <sup>2</sup>  |
| Aortic smooth muscle<br>6KF <sub>1α</sub> (ng ml <sup>-1</sup> ) | <0.007 <sup>1</sup>      | 9.84 ± 0.24 <sup>2</sup> | 0.85 ± 0.041 <sup>3</sup> |
| Cells per plate<br>(×10 <sup>-5</sup> )                          | 3.60 ± 0.10 <sup>1</sup> | 5.15 ± 0.21 <sup>2</sup> | 4.18 ± 0.44               |

Platelet-rich plasma derived serum (PRS) and platelet-poor plasma-derived serum (PDS) were incubated with vascular cells in culture as described below. Bovine aortic endothelial cells were cultured by a modification of existing techniques<sup>21-23</sup>. Briefly, descending thoracic aortas were excised aseptically from week-old calves within 15 min of death and transported in calcium-magnesium-free Dulbecco's phosphate-buffered saline (PBS) with antibiotics (ABX) (penicillin 50 µg ml<sup>-1</sup>, streptomycin 50 µg ml<sup>-1</sup>, neomycin 100 µg ml<sup>-1</sup> and tylocine 60 µg ml<sup>-1</sup>). The adventitia was removed, the lumen washed with 500 ml of PBS, the intercostals and distal end clamped and the lumen filled with 1 mg ml<sup>-1</sup> collagenase (Worthington Biochemical, 135 U per mg) in Hank's balanced salt solution (Gibco). With the proximal and distal ends occluded, the vessel was incubated by immersion in PBS at 37 °C for 20 min. The collagenase solution was collected, the lumen washed gently four times with culture medium and the washes and collagenase solution were pooled and spun at 100g for 5 min. The pellet was resuspended in culture medium and plated on tissue culture dishes pretreated with gelatin<sup>24</sup> and fibronectin (Collaborative Research) at 1 µg per cm<sup>2</sup>. Culture medium consisted of 1:1 mixture of alpha MEM and Dulbecco's modified Eagle's medium (Gibco) with 20% calf serum (Microbiological Associates), 2 mM added L-glutamine, 25 µg ml<sup>-1</sup> endothelial cell growth supplement (Collaborative Research) and ABX. Bovine aortic smooth muscle and adrenal capillary endothelial<sup>27,28</sup> cells were plated 48 h before the start of an experiment at 1–4 × 10<sup>5</sup> cells per 35 mm tissue culture dish in the appropriate growth conditions for each cell type. At the start of each experiment, the plates were washed twice with 2.5 ml of M199 (Medium 199 (Gibco) with 2 mM added L-glutamine), 2.5 ml of M199 plus vehicle or treatment and the plates returned to the incubator (5% CO<sub>2</sub>/95% air, 37 °C) for the time required. After incubation, the medium was removed and transferred to tubes containing indomethacin (final concentration 4 µM) and frozen until required for assay. Cell numbers were determined using a Coulter Counter (Coulter Electronics) after washing with PBS, briefly treated with trypsin-EDTA solution (Gibco), and suspended in 2% formaldehyde in PBS. PGI<sub>2</sub> and TXA<sub>2</sub> synthesis was assessed by measuring the accumulated levels of their respective stable products<sup>15</sup>, 6KF<sub>1α</sub> and TXB<sub>2</sub>. PGF<sub>2α</sub>, PGE<sub>2</sub>, PGD<sub>2</sub>, TXB<sub>2</sub> and 6KF<sub>1α</sub> concentrations were determined by radioimmunoassay of the incubation medium using techniques described elsewhere<sup>15</sup>. The specificity of this assay system is such that results obtained by direct radioimmunoassay (RIA) of the incubation media are similar to those obtained by first separating the prostaglandins in the media by high performance liquid chromatography and then measuring each fraction by RIA<sup>29,37</sup>. PRS and PDS were prepared by a modification of published techniques<sup>20</sup>. Blood was drawn by venipuncture from normal volunteers into 1/10 volume 3.82% sodium citrate. The anticoagulated whole blood was spun at 100g for 20 min, the platelet-rich plasma (PRP) collected and divided into two portions. One half was clotted by the addition of 1 M CaCl<sub>2</sub> (1 ml per 50 ml PRP) followed by incubation for 3 h at 37 °C. The rest was spun at 2,000g for 15 min, the supernatant collected and the platelet pellet resuspended in 1 M NaCl for future extraction. The supernatant was further spun at 20,000g for 30 min to remove any residual platelets, then clotted with CaCl<sub>2</sub> as above. The resulting PRS and PDS were allowed to stand at 4 °C overnight, centrifuged at 20,000g for 30 min, dialysed (MW cutoff 3,000) against 500 volumes of 145 mM NaCl, 4 mM KCl, 3 mM CaCl<sub>2</sub>, and 1.5 mM MgCl<sub>2</sub>, measured out and frozen for later use. Serotonin was measured in pre-dialysed samples of PRS and PDS by liquid chromatography with electrochemical detection<sup>28</sup> as an index of platelet degranulation. Serotonin levels in the PRS and PDS used in this study were >700 nM and <1 nM, respectively. 500 µl of PRS or PDS were added directly to culture dishes containing 2.0 ml of M199. Twenty-four hour incubations were carried out and culture fluids assayed. 6KF<sub>1α</sub> was not detectable in the dialysed PRS or PDS. Indomethacin (4 µM) inhibited 6KF<sub>1α</sub> synthesis in all cultures by over 99%. Data were analysed by one-way analysis of variance, multiple comparisons were made by the significant difference method<sup>39</sup>. Values shown are mean ± s.e.m. (n = 5). Both PRS and PDS stimulated PGI<sub>2</sub> biosynthesis by bovine aortic endothelial and smooth muscle cells, but PDS was at least five times less active in this capacity. Full recovery of PGI<sub>2</sub> stimulating activity was achieved by recombining platelets and platelet-poor plasma before clotting. Means with different superscripts were significantly different (P < 0.01).

Table 2 PDGF stimulates PGI<sub>2</sub> synthesis

| Cell type                | PDGF<br>(ng ml <sup>-1</sup> ) | 6KF <sub>1α</sub><br>(ng ml <sup>-1</sup> ) | Cell number per plate<br>(×10 <sup>-5</sup> ) |
|--------------------------|--------------------------------|---|---|
| Aortic<br>endothelium    | Vehicle                        | 0.337 ± 0.007 <sup>1</sup>                  | 12.8 ± 0.81                                   |
|                          | 0.08                           | 0.518 ± 0.072 <sup>2</sup>                  | 15.9 ± 0.86                                   |
|                          | 0.80                           | 2.370 ± 0.133 <sup>3</sup>                  | 11.3 ± 0.50                                   |
|                          | 8.00                           | 25.000 ± 5.000 <sup>4</sup>                 | 13.8 ± 1.20                                   |
| Aortic<br>smooth muscle  | Vehicle                        | <0.007 <sup>1</sup>                         | 3.71 ± 0.14 <sup>1</sup>                      |
|                          | 0.08                           | 0.013 ± 0.007 <sup>2</sup>                  | 4.58 ± 0.20 <sup>1</sup>                      |
|                          | 0.80                           | 0.079 ± 0.015 <sup>3</sup>                  | 5.76 ± 0.07 <sup>1</sup>                      |
|                          | 8.00                           | 0.593 ± 0.077 <sup>4</sup>                  | 8.51 ± 0.68 <sup>2</sup>                      |
| Capillary<br>endothelium | Vehicle                        | 0.056 ± 0.015 <sup>1</sup>                  | 5.52 ± 0.54                                   |
|                          | 0.08                           | 0.035 ± 0.003 <sup>1</sup>                  | 5.19 ± 0.25                                   |
|                          | 0.25                           | 0.045 ± 0.001 <sup>1</sup>                  | 4.60 ± 0.32                                   |
|                          | 0.80                           | 0.059 ± 0.010 <sup>1</sup>                  | 4.81 ± 0.29                                   |
|                          | 2.53                           | 0.213 ± 0.018 <sup>2</sup>                  | 4.30 ± 0.51                                   |
|                          | 8.00                           | 0.813 ± 0.059 <sup>3</sup>                  | 5.30 ± 0.78                                   |

Platelet PDGF was purified<sup>17</sup>, added to 1 M NaCl in polypropylene tubes and frozen for later use. PDGF was thawed immediately before use, diluted, if necessary, in 1 M NaCl, and added to 35 mm culture vessels containing 2.5 ml M199. Controls received 25 µM NaCl per plate, the maximum amount of NaCl added to any PDGF-treated culture. This amount of NaCl did not affect prostaglandin production. Twenty-four hour incubations were carried out and culture fluids assayed as described in the text. Prostaglandins were not detected in culture fluid from plates incubated with PDGF (8.0 ng ml<sup>-1</sup>) without cells. Indomethacin inhibited PDGF-stimulated PGI<sub>2</sub> synthesis by 99.8%. Data were analysed as described in the legend to Table 1. Means with different superscripts were significantly different (P < 0.01). Values shown are mean ± s.e.m. (n = 4).

As shown in Table 2, the well known mitogenic effects of PDGF were observed with smooth muscle cells but not with aortic or capillary endothelium. The prostacyclin-stimulating activity of PDGF, however, was seen with all three cell types. Thus the effects of PDGF on arachidonic acid metabolism were not always associated with its effects on cell division.

Thus both a platelet-dependent factor in serum and PDGF stimulate PGI<sub>2</sub> synthesis by vascular cells in culture. Both factors (1) appear to be platelet-derived; (2) are non-dialysable and at least partially heat stable (100 °C for 2.5 min); (3) stimulate cultures with a similar time course (linear 6KF<sub>1α</sub> accumulation over 24 h); (4) act reversibly, and (5) stimulate PGI<sub>2</sub> synthesis most likely by increasing arachidonate availability for cyclo-oxygenase. We therefore suggest that PDGF may be the factor responsible for the platelet-dependent stimulation of PGI<sub>2</sub> synthesis by PRS. The level of PDGF reported in whole human serum is approximately 50 ng ml<sup>-1</sup> (ref. 18), well above the concentrations needed to stimulate PGI<sub>2</sub> synthesis *in vitro* in the present study. Thus PDGF may act locally to increase vascular PGI<sub>2</sub> production after its release *in vivo* at a site of platelet degranulation, as part of a negative feedback mechanism controlling platelet aggregation.

This work was supported by NIH grants NS 15201 and HL 25368. B.Z. was supported by CA-28540. S.C. was supported by the Insurance Medical Scientist Scholarship Fund. M.M. is an Established Investigator of the American Heart Association. L.L. is an American Cancer Society Research Professor of Biochemistry (award PRP-21). H.A. was supported by the Council for Tobacco Research.

Received 24 July, accepted 16 October 1980

- Moncada, S., Gryglewski, R., Bunting, S. & Vane, J. R. *Nature* **263**, 663–665 (1976)
- Bunting, S., Gryglewski, R., Moncada, S. & Vane, J. R. *Prostaglandins* **12**, 897–913 (1976)
- Gryglewski, R., Bunting, S., Moncada, S., Flower, R. & Vane, J. R. *Prostaglandins* **12**, 685–713 (1976)
- Johnson, R. A. *et al.* *Prostaglandins* **12**, 915–928 (1976)
- Baenziger, N. C., Dillendor, M. J. & Majerus, P. W. *Biochem biophys Res Commun* **78**, 294–301 (1977)
- Weksler, B. B., Marcus, A. J. & Jaffe, E. A. *Proc natn Acad Sci U S A* **74**, 3922–3926 (1977)
- Marcus, A. J., Weksler, B. B. & Jaffe, E. A. *J Biol Chem* **253**, 7138–7141 (1978)
- Ryan, J. W., Ryan, U. S., Habibston, D. & Martin, L. *Trans Am Phys Soc* **91**, 343–350 (1978)
- MacIntyre, D. E., Pearson, J. D. & Gordon, J. L. *Nature* **271**, 549–551 (1978)
- Moncada, S. & Vane, J. R. *Fed Proc* **38**, 66–71 (1979)
- Moncada, S. & Vane, J. R. *Br med Bull* **34**, 129–135 (1978)
- Marcus, A. J., Weksler, B. B. & Jaffe, E. A. *J Biol Chem* **253**, 7138–7141 (1978)
- Marcus, A. J. *Prog Hemat* **11**, 147–173 (1979)
- Noodin, P. *et al.* *J Clin Invest* **61**, 839–849 (1978)
- Baenziger, N. L., Baenziger, P. R. & Majerus, P. W. *Cell* **16**, 967–974 (1979)



16. Smith, J. B. *et al.* *Circulation* **58**, 126 (1978).
17. Antoniadis, H. N., Scher, C. D. & Stiles, C. O. *Proc. natn. Acad. Sci. U.S.A.* **76**, 1809–1813 (1979).
18. Antoniadis, H. N. & Scher, C. D. *Proc. natn. Acad. Sci. U.S.A.* **74**, 1973–1977 (1977).
19. Kaplan, D. R., Chao, F. C., Stiles, C. D., Antoniadis, H. N. & Scher, C. D. *Blood* **53**, 1043–1052 (1979).
20. Ross, R., Glomset, J., Kariya, B. & Harker, L. *Proc. natn. Acad. Sci. U.S.A.* **71**, 1207 (1974).
21. Gimbrone, M. A. *Prog. Hemostasis & Thromb.* **3**, 1–28 (1976).
22. Jaffe, E. A., Hayer, L. W. & Wachman, R. L. *J. clin. Invest.* **52**, 2757–2764 (1973).
23. Booyse, F. M., Sedlak, B. J. & Rafelson, M. E. Jr *Thromb. Diath. haemorrh.* **34**, 825–839 (1975).
24. Jaffe, E. A., Nachman, R. C., Becker, C. G. & Minsk, C. R. *J. clin. Invest.* **52**, 2745–2756 (1973).
25. Gimbrone, M. A., Cotran, R. S. & Folkman, J. *J. Cell Biol.* **60**, 673–684 (1974).
26. Schwartz, S. M. *In Vitro* **14**, 966–980 (1978).
27. Ross, R. *J. Cell Biol.* **50**, 172–186 (1971).
28. Folkman, J., Haudenschild, C. & Zetter, B. *Proc. natn. Acad. Sci. U.S.A.* **76**, 5217–5221 (1979).
29. Maurer, P., Moskowitz, M., Levine, L. & Melamed, E. *Prostaglandins Med.* **4**, 153–161 (1980).
30. Hong, S. & Levine, L. *J. biol. Chem.* **251**, 5814–5816 (1976).
31. Weksler, B. B., Ley, C. & Jaffe, E. J. *J. clin. Invest.* **62**, 923–930 (1978).
32. Gryglewski, R., Korb, R. & Splawinski, J. *Haemostasis* **8**, 294–299 (1979).
33. Lowry, O. H., Roseborough, N. J., Farr, A. L. & Randall, R. J. *J. biol. Chem.* **193**, 265–275 (1951).
34. Shier, W. T. *Proc. natn. Acad. Sci. U.S.A.* **77**, 137–141 (1980).
35. Levine, L. & Moskowitz, M. A. *Proc. natn. Acad. Sci. U.S.A.* **76**, 6632–6636 (1979).
36. Levine, L. & Alam, I. *Prostaglandins Med.* **3**, 295–304 (1979).
37. Alam, I., Ohuchi, K. & Levine, L. *Analyt. Biochem.* **93**, 339–345 (1979).
38. Reinhard, J. F., Moskowitz, M. A., Sved, A. F. & Fernstrom, J. D. *Life Sci.* (in the press).
39. Tukey, J. W. *Biometrics* **5**, 99–114 (1949).

## Targeting to cells of fluorescent liposomes covalently coupled with monoclonal antibody or protein A

Lee D. Leserman, Jacques Barbet  
& François Kourilsky

Centre d'Immunologie INSERM-CNRS de Marseille-Luminy,  
Case 906, 13288 Marseille Cedex 2, France

John N. Weinstein

Laboratory of Theoretical Biology, National Cancer Institute,  
National Institutes of Health, Bethesda, Maryland 20205

Many applications envisioned for liposomes in cell biology and chemotherapy require their direction to specific cellular targets<sup>1–3</sup>. The ability to use antibody as a means of conferring specificity to liposomes would markedly increase their usefulness. We report here a method for covalently coupling soluble proteins, including monoclonal antibody and *Staphylococcus aureus* protein A (ref. 4), to small sonicated liposomes, by using the heterobifunctional cross-linking reagent *N*-hydroxysuccinimidyl 3-(2-pyridyldithio)propionate (SPDP, Pharmacia). Liposomes bearing covalently coupled mouse monoclonal antibody against human  $\beta_2$ -microglobulin [antibody B1.1G6 (IgG2a,  $\kappa$ ) (B. Malissen *et al.*, in preparation)] bound specifically to human, but not to mouse cells. Liposomes bearing protein A became bound to human cells previously incubated with the B1.1G6 antibody, but not to cells incubated without antibody. The coupling method results in efficient binding of protein to the liposomes without aggregation and without denaturation of the coupled ligand; at least 60% of liposomes bound functional protein. Further, liposomes did not leak encapsulated carboxyfluorescein (CF) as a consequence of the reaction.

Reaction of SPDP with molecules containing primary amino groups results in the introduction of dithiopyridyl groups through the formation of amide bonds and release of *N*-hydroxysuccinimide<sup>5</sup>. Protein-bound dithiopyridine (DTP) can be readily activated as the thiol derivative by reduction with

**Table 1** Precipitation of protein-bearing liposomes by *S. aureus* strain Cowan I (SaCI)

| Determination                     | <sup>125</sup> I-labelled protein on liposomes:<br>B1.1G6 | Protein A |
|-----------------------------------|---|-----------|
| <sup>125</sup> I-labelled protein | 66%   | 3%        |
| CF in liposomes                   | 62%   | ~10%      |

<sup>125</sup>I-labelled protein-bearing liposomes (20  $\mu$ l, from fraction 8 of the Sepharose 4B column chromatography) were mixed with 1% bovine serum albumin in buffered saline in duplicate 900- $\mu$ l volumes. To some tubes 100  $\mu$ l of 10% SaCI was added; to control tubes only medium was added. After 30 min at 4 °C, tubes were spun 15 min at 2,300g to precipitate the SaCI and bound liposomes. Values represent the % liposomes bound to SaCI, as measured by <sup>125</sup>I counts in the bacterial pellet, and by release of fluorophore by addition of Triton.

dithiothreitol in mild conditions (acidic pH). These thiolated proteins can be reacted with other DTP-substituted molecules to produce covalently coupled products in conditions where homopolymerization and intramolecular cross-linking are kept to a minimum. For coupling of proteins to liposomes we have reacted SPDP with phosphatidylethanolamine (PE) in organic solvent, to form the stable derivative PE-DTP. This compound can be mixed with phosphatidylcholine and cholesterol, and liposomes formed by sonication. Protein containing activated thiol groups can then be coupled.

Figure 1 shows fractions eluted from a small Sepharose 4B column following coupling reactions between liposomes containing 4% PE-DTP and thiolated B1.1G6 (Fig. 1a, b), or thiolated protein A (Fig. 1c, d). Counts of <sup>125</sup>I-labelled protein are seen in the void volume for both proteins (Fig. 1a, c) only when liposomes were present. Figure 1 also shows control incubations of <sup>125</sup>I-labelled proteins incubated alone. In reactions carried out with <sup>14</sup>C-labelled lipid and unlabelled protein (Fig. 1b, d) it can be seen that the liposome peak corresponds to the position of elution of protein in the void volume. This peak is also shown by fluorescence. Due to the high initial concentration of CF (40 mM), the encapsulated CF is strongly quenched<sup>6–8</sup>, but the quenching can be relieved by the addition of detergent. The marked increase of fluorescence seen in fractions 7–9 (Fig. 1b, d) after addition of Triton X-100 confirms the position of the liposome peak. The same panels indicate that there has been only a slight leakage of liposome contents—that is, the fluorescence not increased by detergent (fractions 15–17)—during the

**Table 2** Binding of fluoresceinated proteins or CF-containing protein-bearing liposomes to  $5 \times 10^6$  human peripheral blood leukocytes

| Fluorescent reagent           | pmol protein incubated | pmol CF or fluorescein |           |           |
|-------------------------------|------------------------|------------------------|-----------|-----------|
|                               |                        | Incubated              | +Antibody | –Antibody |
| FTTC-protein A (FPA)          | 30                     | 120                    | 12        | 1.4       |
| Protein A liposomes           | 3.2                    | 118                    | 19        | 1.0       |
| FTTC-goat F(ab') <sub>2</sub> |                        |                        |           |           |
| anti-mouse Ig (F-GaM)         | 110                    | 165                    | 7.7       | 0.2       |
| B1.1G6 liposomes              | 1.3                    | 103                    | ND        | 23*       |

Human peripheral blood leukocytes obtained by standard techniques were incubated in tissue culture medium containing 5% fetal calf serum, in the presence of 25  $\mu$ g ml<sup>–1</sup> B1.1G6 or without antibody. After washing, the cells were mixed with the indicated quantities of protein-bearing liposomes (from fraction 8 of Sepharose 4B column chromatography, Fig. 1), with FPA (Pharmacia) or with F-GaM (Cappel). All incubations were at 4 °C in the presence of 0.02% Na<sub>2</sub>S<sub>2</sub>O<sub>3</sub>. After washing, the cell pellets were lysed with 0.5% Triton and the supernatant measured for fluorescence. The fluorescence of fluoresceinated proteins is corrected for quenching, which is not relieved by Triton. The degree of quenching was determined by the difference between the fluorescence observed and that expected (excitation, 488 nm; emission, 520 nm) for the fluoresceinated proteins for the quantity of fluorescein found to be present by absorption ( $A_{488}$ ), with respect to an unquenched standard. Fluorescein in FPA is 78% quenched and in F-GaM is 44% quenched. The CF in liposomes could be measured directly by fluorescence after relief of quenching by addition of Triton; it was 84–86% quenched in intact liposomes. The quantities of fluorescein or CF incubated and bound were determined by comparison with a known concentration of CF, which has the same fluorescence quantum efficiency as fluorescein. ND, not determined.

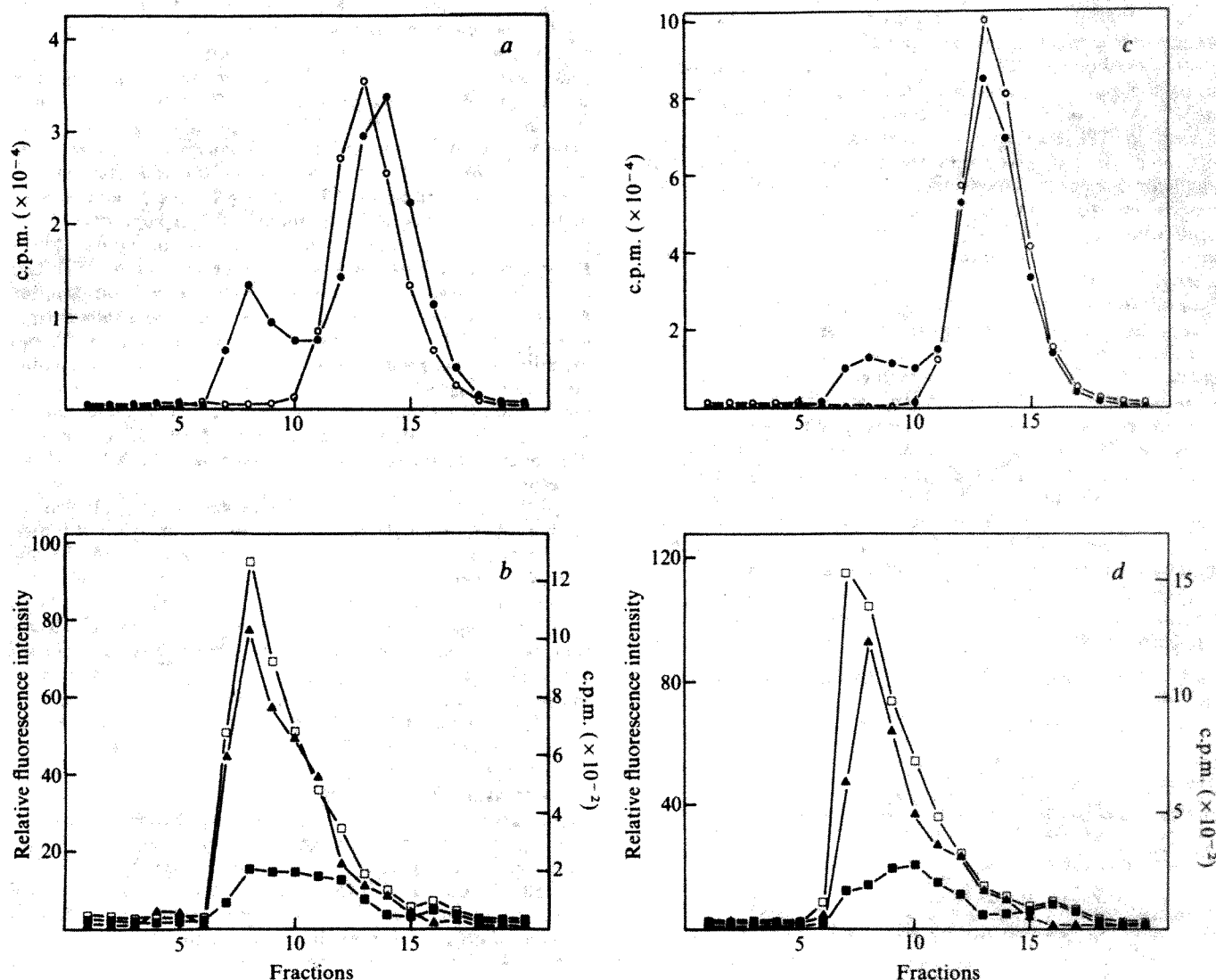
\* Liposomes incubated with  $5 \times 10^6$  mouse spleen cells bound 2.8 pmol CF.

reaction. We have not observed  $^{125}\text{I}$ -labelled protein in the void volume when we chromatographed liposomes and proteins containing DTP groups but not activated by reduction (our unpublished data).

Table 1 shows the results of a representative experiment demonstrating that the protein excluded in the void volume is, in fact, coupled to the surface of the liposomes. This experiment takes advantage of the fact that cells of *S. aureus*, strain Cowan I (SaCI), which express protein A on their surface, will bind to and precipitate certain classes of antibody<sup>9</sup>, including the B1.1G6 class. The result demonstrates that the binding of B1.1G6 antibody to liposomes does not impair recognition of the Fc region of the antibody by the SaCI. Liposomes bearing the covalently bound soluble homologous protein A were not precipitated by the SaCI. The co-precipitation of CF with  $^{125}\text{I}$ -

labelled B1.1G6 indicated that at least 60% of liposomes bear on their surface antibody molecules whose affinity for SaCI is unimpaired.

Liposomal B1.1G6 is also functional with respect to its antibody-combining site (Table 2). B1.1G6-bearing liposomes became bound to human cells, but not to mouse cells. Human cells preincubated with the B1.1G6 antibody and then washed, bound protein A-bearing liposomes; few liposomes were bound if cells were not incubated with the antibody. In experiments not presented here mouse cells preincubated with the monoclonal anti-I-A<sup>k</sup> antibody 10-2-16 (ref. 10) also bound protein A liposomes. The use of protein A on liposomes would thus permit aliquots of a single liposome preparation to be directed at multiple targets, limited only by the availability of antibodies of the appropriate specificity and class.



**Fig. 1** Column chromatography and preparation of protein-bearing liposomes. Protein bound to liposomes or proteins alone were fractionated as follows. The liposome-protein reaction mixture (400  $\mu\text{l}$ ) or 200  $\mu\text{l}$  of  $^{125}\text{I}$ -labelled reduced proteins were applied to a  $1.5 \times 5$  cm column of Sepharose 4B run at  $7.2 \text{ ml h}^{-1}$ ; fractions are 0.6 ml. Aliquots were measured for  $^{125}\text{I}$ ,  $^{14}\text{C}$  and also for CF fluorescence. Fluorescence measurements were made with a Farrand Mark I spectrofluorometer (excitation 488 nm; emission 520 nm) before and after releasing entrapped CF with 0.5% Triton X-100. An unquenched fluorescence standard (66 nM CF) was set at unity for the scale. *a, b*, B1.1G6 and liposomes; *c, d*, protein A and liposomes. The liposome-protein coupling reaction was performed as follows. Dipalmitoyl phosphatidylethanolamine (DPPE, Calbiochem), 10  $\mu\text{mol}$ , was mixed in chloroform/methanol 9:1 (C:M) with  $^{14}\text{C}$ -PE (NEN) to a final specific activity of  $0.15 \mu\text{Ci } \mu\text{mol}^{-1}$ . To 10  $\mu\text{mol}$  was added 12  $\mu\text{mol}$  SPDP and 20  $\mu\text{mol}$  triethylamine. After 2 h at  $25^\circ\text{C}$  the organic phase was extracted with water, dried and the product redissolved in C:M to a final concentration of  $5 \mu\text{mol ml}^{-1}$ . TLC on silical gel revealed a single spot with  $R_f$  0.47 (50  $\mu\text{g}$  sample in  $\text{CHCl}_3/\text{MeOH}/\text{H}_2\text{O}$  65:25:4). The yield (DPPE-DTP) was 90%, based on  $^{14}\text{C}$ . For the formation of liposomes: to 10  $\mu\text{mol}$  dipalmitoyl phosphatidylcholine (DPPC, Sigma) was added 5  $\mu\text{mol}$  cholesterol (Applied Science Labs) and 0.6  $\mu\text{mol}$   $^{14}\text{C}$ -DPPE-DTP, all in C:M. Solvent was evaporated and liposomes formed by sonication under  $\text{N}_2$  for 40 min at  $45^\circ\text{C}$  in the presence of 3 ml 40 mM CF in 0.01 M HEPES-buffered saline, pH 7.45. Unencapsulated CF was removed by gel filtration.  $^{125}\text{I}$ -labelled or unlabelled proteins,  $2.4 \text{ mg ml}^{-1}$ , were incubated with 0.08 mM (for B1.1G6) or 0.5 mM (for protein A) SPDP at pH 7.45 for 30 min at  $25^\circ\text{C}$ . Unreacted SPDP was removed by gel filtration and protein-bound DTP was reduced with 50 mM dithiothreitol in 0.1 M acetate-buffered saline, pH 4.5, for 20 min. Liposomes (500  $\mu\text{l}$ ), at a concentration of 2 mM (in DPPC), were incubated overnight at  $25^\circ\text{C}$  with an equal volume of  $^{125}\text{I}$ -labelled or unlabelled reduced protein,  $1 \text{ mg ml}^{-1}$ , pH 7.45. Samples for  $^{14}\text{C}$  counting were incubated with unlabelled protein.  $\bullet$ ,  $^{125}\text{I}$ -labelled protein incubated with liposomes (*a, c*);  $\circ$ ,  $^{125}\text{I}$ -labelled protein alone (*a, c*);  $\blacktriangle$ ,  $^{14}\text{C}$ -PE in liposomes (*b, d*);  $\blacksquare$ , CF fluorescence before, and  $\square$ , after, addition of Triton (*b, d*).



Table 2 indicates another feature of liposome encapsulation, namely, the large quantity of material that can be carried. The fluorescein/protein (F/P) ratio of directly fluoresceinated antibody (using fluorescein isothiocyanate (FITC)) is limited by denaturation of the antibody to usually not more than 3 or 4 (ref. 11). (Protein A can have a somewhat higher F/P ratio without denaturation.) In this experiment, the F/P ratio for antibody-bearing liposomes is 50 times greater than that of the directly fluoresceinated antibody, and need only be limited by the solubility of the encapsulated material, which for CF is at least sixfold higher than that used here.

Because the coupling conditions minimize homopolymerization of proteins or liposomes, this technique avoids the aggregation and denaturation of IgG observed in techniques associating antibody and liposomes noncovalently, by sonication<sup>12,13</sup>. We have introduced approximately two DTP groups per antibody molecule. In these conditions the titre of the protein is only minimally reduced in a sensitive radioimmunoassay (manuscript in preparation).

We have been unable to associate protein A with liposomes using the glutaraldehyde technique described by Torchilin *et al.*<sup>14,15</sup>. Also, a technique has recently been reported<sup>16</sup> for the formation of PE-derivatives of proteins by reacting them with an activated PE-derivative, following exposure of their intrinsic sulphhydryl residues. The protein-PE complex is then used for passive sensitization of liposomes. This method could not be used with protein A, as it lacks cysteine<sup>17</sup>. In addition, by analogy with 'active' against 'passive' incorporation of dinitrophenyl-PE into liposomes<sup>18</sup>, the inclusion of a prosthetic group into liposomes at the time they are formed, as in the present case, is likely to be a more efficient process.

In experiments to be presented elsewhere, we have encapsulated methotrexate in liposomes to which we have covalently coupled antibody and protein A. In this context we are extending our studies on immunological targeting of methotrexate in liposomes<sup>19,20</sup>. We have also used SPDP to couple albumin, avidin and affinity-purified rabbit antibody to liposomes, and the technique can, in principle, be applied to any compound containing an available amino group. Thus, encapsulation and specific targeting of numerous water-soluble compounds of biological and chemotherapeutic interest is quite feasible.

Pierre Henkart suggested the use of SaCl to precipitate antibody-bearing liposomes. This research was supported by funds from INSERM, CNRS and DRGST (ACC FK, 1980).

**Note added in proof:** A detergent dialysis technique for the association of monoclonal antibodies with liposomes has recently been reported<sup>21</sup>.

Received 14 July; accepted 17 October 1980.

- Gregoriadis, G. (ed.) *Drug Carriers in Biology and Medicine* (Academic, London, 1979).
- Gregoriadis, G. & Allison, A. C. (eds) *Liposomes in Biological Systems* (Wiley, New York, 1980).
- Tom, B. H. & Six, H. R. (eds) *Liposomes and Immunobiology* (Elsevier, Amsterdam, in the press).
- Goding, J. W. *J. Immun. Meth.* **20**, 241-253 (1978).
- Carlsson, J., Drevén, H. & Axén, R. *Biochem. J.* **173**, 723-737 (1978).
- Weinstein, J. N., Yoshikami, S., Henkart, P., Blumenthal, R. & Hagins, W. A. *Science* **195**, 489-492 (1977).
- Weinstein, J. N., Blumenthal, R., Sharrow, S. O. & Henkart, P. *Biochim. biophys. Acta* **509**, 289-299 (1978).
- Leserman, L. D., Weinstein, J. N., Blumenthal, R., Sharrow, S. O. & Terry, W. D. *J. Immun.* **122**, 585-591 (1979).
- Cullen, S. E. & Schwartz, B. D. *J. Immun.* **117**, 136-142 (1976).
- Oi, V. T., Jones, P. P., Goding, J. W., Herzenberg, L. A. & Herzenberg, L. A. *Curr. Topics Microbiol. Immun.* **81**, 115-129 (1978).
- Forni, L. in *Immunological Methods* (eds Lefkowitz, I. & Pernis, B.) 151-166 (Academic, London, 1979).
- Gregoriadis, G. & Neerunjun, D. E. *Biochem. biophys. Res. Commun.* **65**, 537-544 (1975).
- Huang, L. & Kennel, S. J. *Biochemistry* **18**, 1702-1707 (1979).
- Torchilin, V. P., Goldmacher, V. S. & Smirnov, V. N. *Biochem. biophys. Res. Commun.* **85**, 983-985 (1978).
- Torchilin, V. P., Khaw, B. A., Smirnov, V. N. & Haber, E. *Biochem. biophys. Res. Commun.* **89**, 1114-1119 (1979).
- Sinha, D. & Karush, F. *Biochem. biophys. Res. Commun.* **90**, 554-560 (1979).
- Sjodahl, J. *Eur. J. Biochem.* **78**, 471-490 (1977).
- Uemura, K. & Kinsky, S. C. *Biochemistry* **11**, 4085-4094 (1972).
- Leserman, L. D., Weinstein, J. N., Moore, J. J. & Terry, W. D. *Cancer Res.* (in the press).
- Leserman, L. D., Weinstein, J. N., Blumenthal, R. & Terry, W. D. *Proc. natn. Acad. Sci. U.S.A.* **77**, 4089-4093 (1980).
- Huang, A., Huang, L. & Kenne, S. J. *J. biol. Chem.* **255**, 8015-8018 (1980).

## Cell cycle kinetics in human lymphocyte cultures

Kanehisa Morimoto\* & Sheldon Wolff

Laboratory of Radiobiology and Department of Anatomy, University of California, San Francisco, San Francisco, California 94143

Short-term cultures of phytohaemagglutinin (PHA)-stimulated human lymphocytes are widely used to detect chromosome-damaging agents<sup>1,2</sup>, possible human exposure to mutagenic carcinogens<sup>1,2</sup> and the immune response of blood<sup>3</sup>. Because the results are affected by the number of cell divisions before sampling<sup>1,2,4,5</sup>, an accurate knowledge of lymphocyte proliferation in culture is essential for these studies. Unfortunately, the information available on the lymphocyte proliferative characteristics is quite conflicting. For instance, although after stimulation of blood lymphocytes with PHA the cultures soon contain cells that have divided different numbers of times<sup>6,7</sup>; this heterogeneity has been explained variously as a difference in cell-cycle times<sup>8,9</sup> or in the times when the cells start blastogenesis by responding to PHA<sup>10-12</sup>. Prolonged treatment with high concentrations of <sup>3</sup>H-thymidine (TdR) have often been used to investigate lymphocyte proliferation<sup>8,10,13,14</sup>. Incorporated <sup>3</sup>H-TdR can, however, affect cell kinetics<sup>15-19</sup>. The differential staining of sister chromatids<sup>20</sup> in cells dividing for different numbers of times in the presence of bromodeoxyuridine (BUdR) can be used to study cell kinetics<sup>7,8,12</sup>. In experiments combining sister chromatid differential staining and autoradiography, we show here that <sup>3</sup>H-TdR labelling at more than 0.1  $\mu\text{Ci ml}^{-1}$  slows lymphocyte cycling, and that the heterogeneity of different generations of cells is caused by a difference in the times when they start their first DNA synthesis in response to PHA.

PHA-stimulated human lymphocytes were cultured in medium containing BUdR so that cells dividing for the first, second and third time after initiation of culture could be distinguished by the differential staining pattern of sister chromatids in slides stained with fluorescence-plus-Giemsa (FPG)<sup>20</sup>. When metaphase cells from cultures were examined at various times after initiation, it was found that the relative numbers of 1st, 2nd and 3rd or subsequent generation cells shift with increasing culture times (data not shown, see ref. 7). We have already shown that cell division delay induced by chemical treatments is clearly manifested as shifts in the relative proportion of these metaphases<sup>7</sup>.

To measure the effect of <sup>3</sup>H-TdR on cell proliferation, a simple combination method of sister chromatid differential staining and autoradiography was developed (Fig. 1). Cultures were established with 20  $\mu\text{M}$  BUdR and exposed from the 32nd to the 40th hour to <sup>3</sup>H-TdR (specific activity, 52 Ci mmol<sup>-1</sup>) at concentrations of 0.05-5  $\mu\text{Ci ml}^{-1}$ . Consequently, at the highest concentration used the medium contained only 0.1  $\mu\text{M}$  thymidine. An 8-h treatment was selected, because treatments for 4-24 h are commonly used for labelling human lymphocytes in culture. The cultures were then fixed at 64 h and the numbers of cells dividing for the first, second or third time determined in FPG-stained slides<sup>7,12</sup>.

At concentrations above 0.2  $\mu\text{Ci ml}^{-1}$ , <sup>3</sup>H-TdR affects the distribution of each generation metaphase cells in a clear dose-dependent manner (Fig. 2a). In 64-h cultures exposed to  $\leq 0.2 \mu\text{Ci ml}^{-1}$  <sup>3</sup>H-TdR, approximately 10% of the metaphases were in their first division, 40% in their second division and 50% in their third. In cultures exposed to more than 0.2  $\mu\text{Ci ml}^{-1}$  <sup>3</sup>H-TdR, the proportion of 1st-generation metaphases increased, whereas that of 3rd-generation metaphases

\* Permanent address: Department of Public Health, Faculty of Medicine, University of Tokyo, Tokyo 113, Japan.

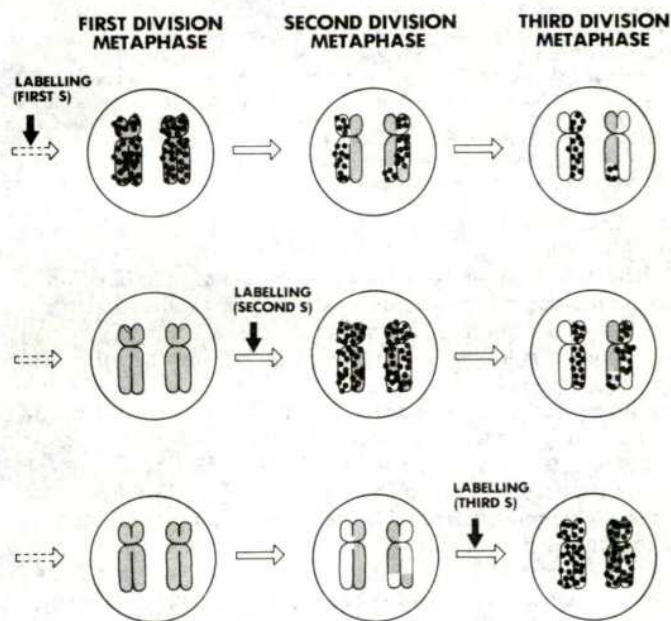


**Table 1** Incidence of labelled metaphases in 64-h cultures pulse-treated with  $^3\text{H}$ -TdR

| Labelling period<br>(h after initiation) | Donor | % Labelled<br>metaphases | % Labelled (or heavily labelled) metaphases among: |        |       |        |       |             |
|--|-------|--------------------------|--|--------|-------|--------|-------|-------------|
|  |       |                          | $X_1$  |        | $X_2$ |        | $X_3$ |             |
|  |       |                          | I  |        | I     |        | I     |             |
| 24-32                                    | A     | 53.0                     | 0  | (0)    | 2.9   | (0)    | 96.3  | (63.0)      |
|  | B     | 43.0                     | 0  | (0)    | 10.6  | (2.1)  | 97.4  | (72.0)      |
| 32-40                                    | A     | 49.0                     | 0  | (0)    | 89.2  | (37.8) | 29.2  | (6.3)       |
|  | B     | 53.0                     | 0  | (0)    | 90.6  | (52.6) | 35.6  | (5.1)       |
| 40-48                                    | A     | 85.0                     | 25.0   | (11.8) | 85.3  | (41.2) | 0     | (0)         |
|  | B     | 65.0                     | 31.6   | (15.8) | 59.2  | (32.7) | 0     | (0)         |
|  |       |                          |  |        |       |        |       | II          |
|  |       |                          |  |        |       |        |       | 0 (0)       |
|  |       |                          |  |        |       |        |       | 0 (0)       |
|  |       |                          |  |        |       |        |       | 4.2 (0)     |
|  |       |                          |  |        |       |        |       | 7.0 (1.8)   |
|  |       |                          |  |        |       |        |       | 98.1 (79.6) |
|  |       |                          |  |        |       |        |       | 93.8 (78.1) |

Labelling was with  $0.1 \mu\text{Ci ml}^{-1}$   $^3\text{H}$ -TdR. I or II represents the metaphases whose labelling pattern indicates the  $^3\text{H}$ -TdR incorporation in the first or second cell cycle, respectively (for details see Fig. 1 legend). The criteria for labelling and the abbreviations used were the same as those in Fig. 2. For metaphases whose labelling pattern indicated  $^3\text{H}$ -TdR incorporation in the second S phase (Fig. 1), if more than one-third (or two-thirds) of the chromosomes were labelled on both chromatids (for 2nd-generation metaphases) or on lightly stained chromatids (for 3rd-generation metaphases), they were designated as labelled (or heavily labelled).

decreased. The percentage of 2nd-generation metaphases exhibited a small peak at  $0.5 \mu\text{Ci ml}^{-1}$  and then at higher concentrations decreased more markedly than did the 3rd-generation metaphases, apparently indicating that the induced mitotic delay in 2nd-generation cells might be longer than that in 3rd-generation cells.



**Fig. 1** Schematic presentation of the simple combination method of  $^3\text{H}$ -TdR labelling and sister chromatid differential staining. When cells are incubated continuously with BUdR and pulse-labelled with  $^3\text{H}$ -TdR at different times after initiation of culture, metaphase cells from resultant cultures have various combinations of the differential staining pattern of sister chromatids and the distribution of autoradiographic silver grains over the chromosomes. The differential staining pattern of sister chromatids yields information on how many times a cell has divided in culture, and the distribution of autoradiographic grains over the chromosomes indicates when the cell synthesized DNA. 1st-Division cells contain chromosomes with both sister chromatids stained uniformly darkly. 2nd-Division cells contain only harlequin chromosomes with one chromatid darkly stained and its sister chromatid lightly stained, whereas 3rd-division cells contain some harlequin chromosomes and other chromosomes with both sister chromatids stained uniformly lightly. For cells which have incorporated  $^3\text{H}$ -TdR in their first S phase, a 1st-division cell has labelling on both chromatids of a chromosome whereas a 2nd-division cell is labelled only on lightly stained chromatids. A 3rd-division cell has labelling on lightly stained chromatids only where both chromatids of a chromosome are lightly stained. For cells which have incorporated  $^3\text{H}$ -TdR in their second S phase, a 1st-division cell has no labelling at all, a 2nd-division cell has labelling on both chromatids and a 3rd-division cell is labelled on lightly stained chromatids where both chromatids of a chromosome are lightly stained as well as where one is lightly stained and one is darkly stained. Such combination patterns of labelling and sister chromatid differential staining are the same in whichever division cycle sister chromatid exchanges take place, although here only those which occurred in the 2nd cell cycle are shown for clarity.

Autoradiograms of the same slides showed that the shift in the relative proportions was more pronounced among labelled metaphases (Fig. 2b), being much more marked in heavily labelled metaphases (Fig. 2c). 'Unlabelled' metaphases, categorized as those other than the labelled cells, showed a small shift in the relative proportions when exposed to more than  $1 \mu\text{Ci ml}^{-1}$   $^3\text{H}$ -TdR (data not shown). The data also indicated that, with exposure to  $^3\text{H}$ -TdR between 32 and 40 h of culture, many more 2nd- than 3rd-generation cells had been labelled in their first S phase (Fig. 2b, c) and that the apparently longer mitotic delay in 2nd-generation metaphase cells (Fig. 2a) was only a reflection of such differential labelling. Labelled 1st-generation metaphases were found only in the cultures exposed to more than  $0.1 \mu\text{Ci ml}^{-1}$   $^3\text{H}$ -TdR. Corresponding decreases in both the mitotic indices and the percentage of transformed cells (Fig. 2d) also occurred. These data indicate that  $^3\text{H}$ -TdR labelling with concentrations above  $0.1 \mu\text{Ci ml}^{-1}$  slows lymphocyte proliferation in culture.

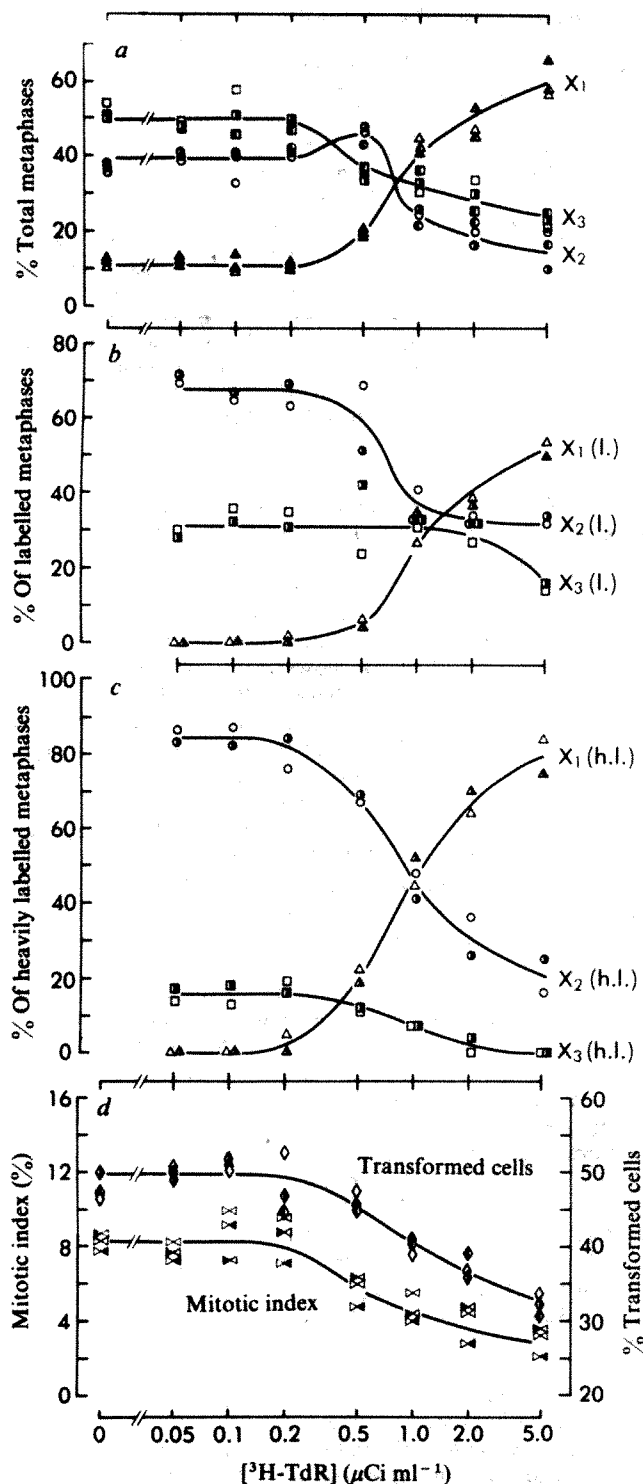
In preliminary experiments we have noted that cell division kinetics are not perturbed by washing the cells and replacing the medium, by treatment with as high as  $10 \mu\text{M}$  cold thymidine, or by the use of BUdR at concentrations up to  $40 \mu\text{M}$  (data not shown). We thus believe that the observed mitotic delay is due to incorporated  $^3\text{H}$ -TdR.

Autoradiograms of FPG-stained cells labelled with  $0.1 \mu\text{Ci ml}^{-1}$   $^3\text{H}$ -TdR at different times after initiation of culture have also shown (Table 1) that the majority of 2nd-generation metaphases seen in a 64-h culture started DNA synthesis at 32-40 h after initiation, and that none of the 1st-generation metaphases started DNA synthesis before 40 h, a quarter of them entering their first S phase at 40-48 h. Most of the 3rd-generation metaphases entered their first S phase at 24-32 h and their second S phase at 40-48 h. These data thus indicate that in cultures, the older-generation cells begin their first DNA synthesis at earlier times after the start of incubation. As shown in Fig. 2, treatment with higher concentrations of  $^3\text{H}$ -TdR perturbs cell division kinetics such that cells with more incorporated  $^3\text{H}$ -TdR have longer cell-cycle times.

Crossen and Morgan<sup>8</sup> have recently found that the small proportion of 1st-division metaphases seen in 72-h cultures treated with  $2 \mu\text{Ci ml}^{-1}$   $^3\text{H}$ -TdR entered S phase before the 34th hour of incubation. We think that this observation of extraordinarily long cell-cycle times is the result of prolonged  $G_2$  phases caused by the radiation from incorporated  $^3\text{H}$ -TdR.

Pollack *et al.*<sup>19</sup> also showed by flow cytometric (FCM) analysis that an 18-h treatment with  $0.5 \mu\text{Ci ml}^{-1}$   $^3\text{H}$ -TdR increased the relative proportion of lymphocytes in the  $G_2$  plus M phase, suggesting an inhibition of cell proliferation. Such a  $G_2$  block, measured by FCM analysis, was also reported in several mammalian cell lines treated with low concentrations of  $^3\text{H}$ -TdR<sup>17,18</sup>. However, the elevation in the  $G_2$ +M peak does not always indicate an actual delay in cell proliferation because the FCM analysis provides only a static representation of the distribution of cells about the cell-cycle phases<sup>17-19</sup> and because a transient





**Fig. 2**  $^3\text{H}$ -TdR-induced changes in the relative proportion of metaphase cells in the 1st (X<sub>1</sub>, triangles), 2nd (X<sub>2</sub>, circles) or 3rd (X<sub>3</sub>, squares) division in 64-h cultures. Changes in the proportion among (a) total, (b) labelled (l.), or (c) heavily labelled (h.l.) metaphases are shown, as are (d) changes in the mitotic indices and the percentage of transformed cells. Two healthy human males aged 30 yr (open symbols) and 33 yr (half-closed symbols) were used as blood donors. Cells were treated with  $^3\text{H}$ -TdR at the appropriate concentration from the 32nd to the 40th hour after initiation of cultures. The treatment with  $^3\text{H}$ -TdR was terminated by washing the cells three times and resuspending them in prewarmed complete medium. A 64-h incubation time was selected because preliminary experiments indicated that the cultures would contain relative proportions of 1st-, 2nd- and 3rd-division metaphases appropriate for the observation of induced perturbations in cell division kinetics. In FPG-stained preparations, cells dividing for the first, second or third time in culture were determined by the differential staining pattern of sister chromatids (Fig. 1). This experiment was repeated with blood from the same donor (left-half-closed symbols). For autoradiography of FPG-stained cells, slides were dipped in a 1% Formvar solution<sup>23</sup> to prevent the formation of chemical grains by direct contact between the autoradiographic nuclear emulsion and the Giemsa stain. The slides were then dipped in Ilford L-4 emulsion and developed after 1–90 days exposure at 4°C. The exposure time was inversely proportional to the  $^3\text{H}$ -TdR concentrations. The degree of labelling was determined by the number of chromosomes labelled in a cell. A 1st-division metaphase was designated as labelled if more than one-third of the chromosomes were labelled on both chromatids; if more than two-thirds of the chromosomes were so labelled the cell was considered to be heavily labelled. Similarly, a second division cell was considered labelled (or heavily labelled) if more than one-third (or two-thirds) of the chromosomes were labelled on the light chromatid. 3rd-Division cells were considered labelled (or heavily labelled) if labelling occurred in the lightly stained chromatids of more than one-sixth (or one-third) of those chromosomes with both chromatids lightly stained in the centromeric regions. These criteria were applied for labelled metaphase cells that incorporated  $^3\text{H}$ -TdR in their first S phase after initiation. Metaphase cells whose labelling pattern indicated  $^3\text{H}$ -TdR incorporation in the second S appeared more frequently in cultures treated at the higher concentrations of  $^3\text{H}$ -TdR. These cells can also be used to indicate cell division delay (data not shown). From each culture 200 metaphases were scored for the distribution of 1st-, 2nd- and 3rd-division cells, and 100 metaphases from each culture were analysed for the distribution of labelled metaphases. Mitotic indices and the percentage of transformed cells were based on 2,000 cells.

a dose-dependent change in the distribution of 1st-, 2nd- and 3rd-division cells in  $^3\text{H}$ -TdR-treated and control cultures<sup>7</sup>.

The present study has thus shown the simple combination of autoradiography and differential staining of sister chromatids to be a sensitive method for detecting mitotic delay in human lymphocyte cultures. It can be easily applied to other cell cultures to check the effect of  $^3\text{H}$ -TdR labelling on cell proliferation. Our data suggest that some information available on human lymphocyte proliferation might be misleading because they were often obtained with lengthy  $^3\text{H}$ -TdR labelling at high concentrations, which induce mitotic delay. We have also presented direct evidence that the heterogeneity with respect to different generation metaphases seen in a culture is a reflection of a difference in the times the cells enter their first DNA-synthesis period, and that the cells have about the same generation times thereafter.

This work was performed under the auspices of the US Department of Energy. K.M. is a Fellow of the Japan Society for the Promotion of Science.

Received 16 June; accepted 25 September 1980.

- Evans, H. J. & Lloyd, D. C. *Mutagen-Induced Chromosome Damage in Man* (Yale University Press, New Haven, 1978).
- Evans, H. J., Court Brown, W. M. & McLean, A. S. *Human Radiation Cytogenetics* (North-Holland, Amsterdam, 1967).
- Oppenheim, J. J. & Rosenstreich, D. L. *Prog. Allergy* **20**, 65–194 (1976).
- Bender, M. A. & Brewen, J. G. *Mutat. Res.* **8**, 383–399 (1969).
- Savage, J. R. K. *Nature* **278**, 687 (1979).
- Tice, R., Schneider, E. L. & Rary, J. M. *Expl Cell Res.* **102**, 232–236 (1976).
- Morimoto, K. & Wolff, S. *Cancer Res.* **40**, 1189–1193 (1980).
- Crossen, P. E. & Morgan, W. F. *Expl Cell Res.* **118**, 423–427 (1979).
- Craig-Holmes, A. P. & Shaw, M. W. *Expl Cell Res.* **99**, 79–87 (1976).
- Soren, L. *Expl Cell Res.* **78**, 201–208 (1973).
- Younkin, L. H. *Expl Cell Res.* **90**, 374–380 (1975).
- Tice, R., Thorne, P. & Schneider, E. L. *Cell Tissue Kinet.* **12**, 1–9 (1979).
- Sasaki, M. S. & Norman, A. *Nature* **210**, 913–914 (1966).
- Beek, B. & Obe, G. *Hum. Genet.* **35**, 57–70 (1976).
- Drew, R. M. & Painter, R. B. *Radiat. Res.* **11**, 535–544 (1959).
- Cleaver, J. E. *Thymidine Metabolism and Cell Kinetics* (North-Holland, Amsterdam, 1967).
- Ehmann, U. K. *Nature* **258**, 633–636 (1975).
- Marz, R. *et al. J. cell. Physiol.* **90**, 1–8 (1977).
- Pollack, A., Bagwell, C. B. & Irvin, G. L. *Science* **203**, 1025–1027 (1979).
- Perry, P. & Wolff, S. *Nature* **251**, 156–158 (1974).
- Purrott, R. J., Vulpis, N. & Lloyd, D. C. *Mutat. Res.* **69**, 275–282 (1980).
- Cleaver, J. E., Thomas, G. H. & Burki, H. J. *Science* **177**, 996–998 (1972).
- Rutledge, M. H. *Chromosoma* **70**, 259–262 (1979).

increase of cells in the G<sub>2</sub> + M can be observed with an unaltered population doubling time of cultured cells<sup>17,18</sup>. Here we have shown directly that an 8-h treatment with as low as 0.2  $\mu\text{Ci ml}^{-1}$   $^3\text{H}$ -TdR delays lymphocyte proliferation in culture.

Purrott *et al.*<sup>21</sup> showed by FPG-differential staining of PHA-stimulated lymphocytes that X-ray irradiation of G<sub>0</sub> cells induces a mitotic delay of 1 h Gy<sup>-1</sup>. In the present experiments accurate estimations of the dose from incorporated  $^3\text{H}$ -TdR and of the amount of delay are not possible because of the complications of both the uptake of  $^3\text{H}$ -TdR and the rate of cell division. Assuming a dose of approximately 5 mGy per disintegration<sup>22</sup>, however, the dose rate received by labelled cells in the first cell cycle after a treatment of 0.5  $\mu\text{Ci ml}^{-1}$   $^3\text{H}$ -TdR can be estimated to be roughly 30 mGy h<sup>-1</sup>. The mitotic delay observed with this treatment is 4–6 h, which was estimated from

## Effects of an Earth-strength magnetic field on electrical activity of pineal cells

P. Semm, T. Schnelder & L. Vollrath

University of Mainz, Department of Anatomy, Neurophysiology Laboratory, 6500 Mainz, Saarstr. 19/21, FRG

Although magnetic fields can influence biological systems, including those of man and other vertebrates<sup>1-4</sup>, no central nervous structure has been identified that might be involved in their detection. From a theoretical point of view, the pineal organ might be such a structure for the following reasons: (1) It is involved in the regulation of circadian rhythms<sup>5</sup> and is thus essential for migratory restlessness ('Zugunruhe')<sup>7</sup>. Orientation at that time can be altered by an artificial magnetic field (MF) with a direction differing by 90° from that of the Earth. Circadian rhythms can be inhibited from phase shifting by compensation of the Earth's MF and can be influenced by an artificial MF<sup>6</sup>. (2) The pineal organ is strongly dependent on its sympathetic innervation<sup>8</sup> and the sympatho-adrenergic system as a whole is sensitive to magnetic stimuli<sup>9</sup>. (3) The pineal organ is a light-sensitive time-keeping organ<sup>10,11</sup> and could form part of a combined compass-solar-clock system, which has been postulated for maintaining orientation in birds<sup>12</sup>. We have therefore investigated the effect of a MF on electrophysiological activity of the guinea pig pineal organ, which is a useful system for such studies on individual cells<sup>11,13</sup>. We report here that activity was depressed by an induced MF and restored when the MF was inverted.

We abandoned attempts to use a small permanent magnet, as the MF produced was neither homogeneous nor accurately measurable in the area of the pineal organ. We used 16 male guinea pigs (300–900 g), anaesthetized with urethane. In each experiment a tracheotomy was performed, and the animal artificially respired and mounted in a stereotaxic frame. Body temperature was maintained using a heating pad and the electrocardiogram continuously monitored. The dorsal surface of the brain was exposed, and a single micropipette inserted into the posterior part of the pineal organ, just under the confluence of the sagittal and transverse sinus. Extracellular activity was

recorded through the micropipette, filled with 4 M NaCl solution saturated with fast green for verifying recording sites histologically. The MF was generated by two Helmholtz coils (radius 3.6 cm), one under the jaw and the other on top of the head, with 3.6 cm distance between them. The strength of the MF in the middle of the two coils was

$$B_H = \left(\frac{4}{5}\right)^{\frac{1}{2}} \cdot \frac{\mu_0 \cdot n \cdot I}{R}$$

where  $B_H$  is the magnetic field strength,  $\mu_0$  the permeability of free space,  $R$  the radius (3.6 cm),  $n$  the winding number (150) and  $I$  the intensity of current (for example:  $I_1$  for 0.3 Oe = 8.0073 mA and  $I_2$  for 0.8 Oe = 21.3528 mA). The MF thus calculated was measured by a Hall-sound and was shown to be relatively homogeneous around the animal's head. The direction of the current and thereby the polarity of the MF could be altered. The artificial MF was added to the vertical component of the Earth's MF when the top coil was made the south pole. It compensated, or inverted, the vertical component when the top coil was made the north pole. The activity maintained by the cells under study was averaged by an averager system with a time base of 1 s per bin (total bin number = 256; a bin is the period of time during which the incoming electrical potentials are summed). The spike number of each averager histogram was determined by an electric counter. The histograms were read and plotted on a recorder every 4 min 16 s.

Before the MF stimulus was applied, we checked that short-term optic and acoustic stimuli had no effect on the pineal cells and that the maintained activity of a given cell was relatively constant (measured for about 16 min, Fig. 1b, c). Then the first MF stimulus of 0.5 Oe was applied for 17 min 4 s and, after 8 min, a second stimulus of the same strength for 8 min. Of a total of 71 cells tested in 16 male guinea pigs, 56 did not respond (Fig. 1a). A cell was classified as sensitive to stimulation only when spontaneous electrical activity was depressed by more than 30%. Fifteen cells (from 11 animals) showed a marked response to MF stimulation; as Fig. 1b and c show, maintained activity was diminished by more than 50%, well out of the range of spontaneous oscillations of pineal electrical activity. The first clear effect could be measured after a latency period of about 2 min, not visible in the figure due to averaging at 4 min 16 s intervals. When the MF was switched off, all cells retained a diminished activity, lasting as long as recording could be continued (up to 30 min in some cases). A second round of the same stimulus had no effect (Fig. 1b, c) even when the strength of the stimulus was varied (not shown).

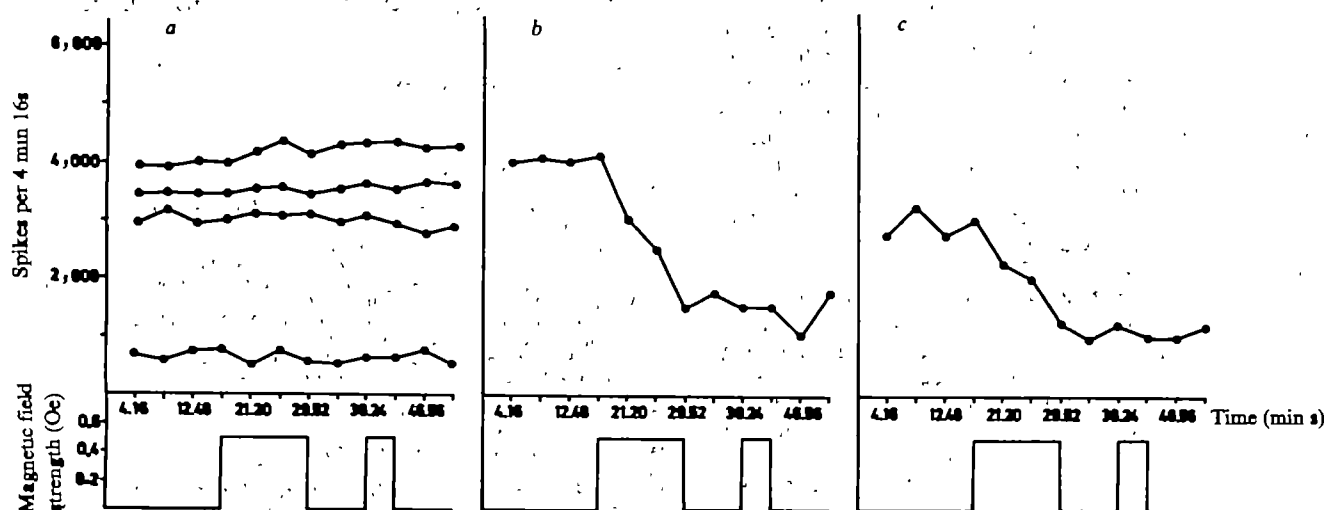
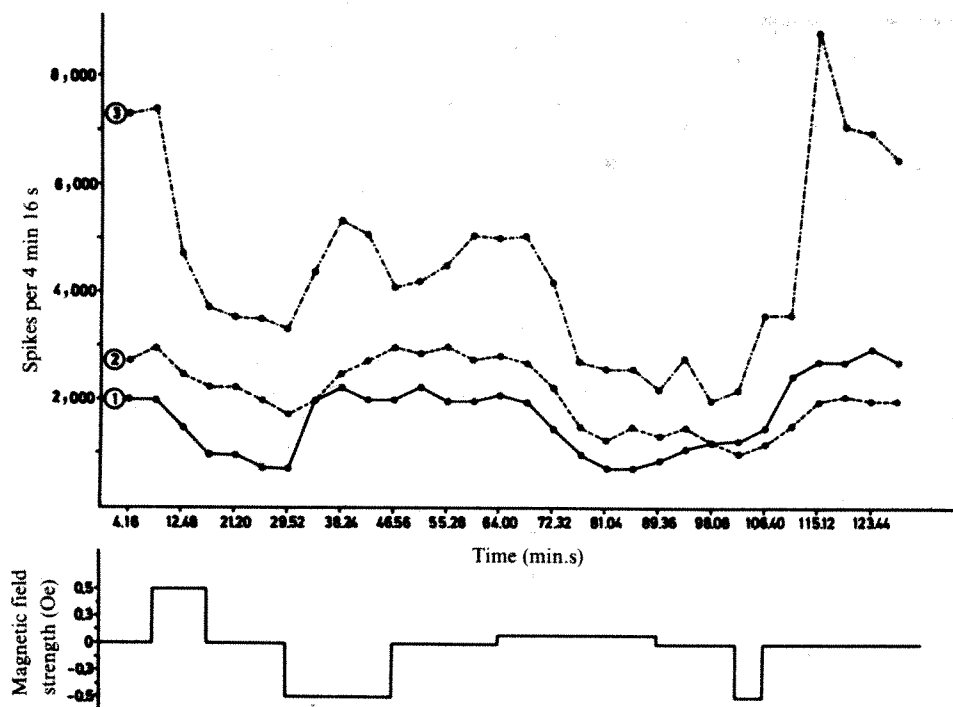


Fig. 1 a, The number of spikes from four single pineal cells (counted every 4 min 16 s, averaging time) which could not be influenced by a magnetic stimulus of 0.5 Oe. b, Reaction of a pineal cell to a MF of 0.5 Oe. c, Another pineal cell, the maintained activity of which is diminished by a MF of 0.5 Oe. A second stimulus had no effect in either cell.





**Fig. 2** The spike number of three single pineal cells. Cell no. 1 shows a clear depression of activity after a magnetic stimulus of 0.5 Oe and remains depressed after cessation of the stimulus. After an inverted stimulus of 0.5 Oe, cell activity returns to output level and is depressed again by a stimulus of 0.10 Oe, south pole up. After a period of depression, activity increases again after a short stimulus of 0.5 Oe with inverted polarity of MF. Cell no. 2 shows a similar reaction, whereas cell no. 3 does not reach its output level after the first application of the inverted MF. After the second inverted magnetic stimulus, cell activity reached output level again.

When the polarity of the MF was changed in 3 of the 15 responsive cells, their activity immediately returned to the initial level (Fig. 2). With the exception of cell no. 3, they all reached this level after 8–12 min. The latency of the renewed activation was also in the range of 2 min (not shown). When the inverted MF was switched off the cells retained their normal activity, which could be depressed again by a low MF stimulus of 0.10 Oe, pointing to a relatively high sensitivity of the cells. After a further inversion of polarity, the cells were again activated. In one case maintained activity could be directly stimulated by an inverted MF (north pole up).

In other brain structures (inferior and superior colliculi, corpus callosum and epithalamus) in identical experimental conditions, no reactions to magnetic stimuli could be measured. Thus, the cellular response of cells to magnetic stimuli is not universal and the reactions measured were not due to magnetic or electrical interference with the recording system.

The role of the pineal organ has been clarified in only a few species. In photoperiodic mammals it influences the hypothalamo-pituitary-gonadal axis and controls the atrophy of the gonads during winter by an increased output of the hormone melatonin<sup>14</sup>. In birds the pineal is involved in the regulation of locomotor activity<sup>15</sup>. In various species the pineal organ is readily influenced by external (light, noise, ambient temperature, olfactory stimuli) and internal (sex steroids, noradrenaline) factors<sup>6</sup>. The heterogeneity of the pineal cells has been demonstrated in the guinea pig although individual functions remain to be elucidated. This may help to explain why not all cells we recorded clearly responded to MF stimuli.

As this is apparently the first report that the pineal responds to changes in an artificial MF, we can offer no corroborative evidence for our findings. Indirect evidence is that migratory restlessness and locomotor activity, which have been clearly shown to be affected by the pineal, can be influenced by artificial or natural MFs. We also feel it is significant that for orientation, in addition to sensing the Earth's MF, time-keeping ability is required<sup>12</sup>. As the pineal organ is a sort of time-keeping device<sup>10</sup>, it might be an ideal site for integration, particularly as birds do not simply switch between magnetic and Sun compasses<sup>12</sup>.

Whether or not the pineal organ itself senses changes of MF is not known. The organ is heavily innervated by sympathetic

fibres<sup>16</sup> and the sympathetic nervous system can be affected by magnetic stimuli, so that the effect may well be indirect. The lack of appreciable amounts of iron in the pineal organ<sup>17,18</sup> makes it unlikely that the magnetite (magnetic iron oxide) required for transducing magnetic stimuli in bacteria<sup>19</sup> is present.

Interestingly, it has been proposed<sup>20</sup> for migratory birds and homing pigeons that the MF is detected in the lateral eyes, although phylogenetically the pineal organ corresponds to the median eye of lower vertebrates<sup>6</sup>. The pineal organ of higher vertebrates is derived from the photoreceptive pineal organ of lower vertebrates<sup>21</sup> and is connected to the lateral eyes by the nucleus suprachiasmaticus and the sympathetic nervous system<sup>22</sup>.

We thank the Volkswagenwerk-Stiftung for financial support.

**Note added in proof:** Recent experiments carried out in our laboratory indicate that pineal cells of homing pigeons, which according to other authors use the natural magnetic field for orientation, also respond clearly to artificial magnetic fields.

Received 30 June; accepted 17 October 1980.

1. Barnothy, M. F. (Plenum, New York, 1964).
2. Barnothy, M. F. Vol. 2 (Plenum, New York, 1969).
3. Markl, H. in *Biophysik* (eds Hoppe, W., Lohman, W., Markl, H. & Ziegler, H.) (Springer, Berlin, 1977).
4. Martin, H. & Lindauer, M. *Fortschr. Zool.* **21**, 211–228 (1973).
5. Martin, H. & Lindauer, M. *J. comp. Physiol.* **122**, 145–187 (1977).
6. Wurtman, R. J., Axelrod, J. & Kelly, D. E. *The Pineal* (Academic, New York, 1968).
7. McMillan, J. P. *J. comp. Physiol.* **79**, 105–112 (1972).
8. Brown, F. A. & Sciow, K. M. *J. interdisciplinary Cycle Res.* **9**, 137–145 (1978).
9. Sakharova, S. A. *Biol. Nauki* **19**, 40–44 (1976).
10. Binkley, S. A., Riebelman, J. B. & Reilly, K. B. *Science* **202**, 1198–1201 (1978).
11. Semm, P. & Vollrath, L. *J. neural Transmission* **47**, 181–190 (1980).
12. Walcott, C. *J. exp. Biol.* **70**, 105–123 (1977).
13. Semm, P. & Vollrath, L. *Neurosci. Lett.* **12**, 93–96 (1979).
14. Reiter, R. *J. Rev. Physiol.* **35**, 305–328 (1973).
15. Turek, F. W. *Science* **194**, 1441–1443 (1976).
16. Kappers, J. A. Z. *Zellforsch. mikrosk. Anat.* **52**, 163–215 (1960).
17. Demmel, U., Höck, A., Kasperek, K. & Feinendegen, L. E. in *Nuclear Activation Techniques in the Life Sciences*, 193–203 (International Atomic Energy Agency, Vienna, 1979).
18. Krstić, R. *Cell Tissue Res.* **174**, 129–137 (1976).
19. Frankel, R. B., Blakemore, R. P. & Wolfe, R. S. *Science* **203**, 1355–1356 (1979).
20. Leask, M. J. M. *Nature* **267**, 144–145 (1977).
21. Collin, J. P. *Ciba Fdn Symp.* **79**–120 (1971).
22. Moore, R. Y., Heller, A., Wurtman, R. J. & Axelrod, J. *Science* **155**, 220–223 (1967).

## $\beta$ -Carboline-3-carboxylic acid ethyl ester antagonizes diazepam activity

S. S. Tenen & James D. Hirsch

Department of Biological Research, G. D. Searle & Company,  
PO Box 5110, Chicago, Illinois 60680

Analogous to the progression of events in the opiate receptor-enkephalin area, the first reports<sup>1-3</sup> that benzodiazepines have selective and specific high-affinity binding sites in brain have stimulated a search for the endogenous 'ligand' or substance that might normally act at these sites<sup>4-9</sup>. Braestrup and co-workers have extracted from human urine a  $\gamma$ -fraction (ref. 10) which they have recently<sup>11</sup> identified as  $\beta$ -carboline-3-carboxylic acid ethyl ester ( $\beta$ CEE). They reported that this substance is extremely potent in displacing <sup>3</sup>H-diazepam from brain binding sites and proposed that a  $\beta$ -carboline-3-carboxylic acid derivative might, in part, be the endogenous ligand for the brain benzodiazepine receptor. We have examined several synthetically derived  $\beta$ -carboline-3-carboxylic acid analogues and now present data obtained from testing only the  $\beta$ CEE described by Braestrup *et al.* In addition to confirming these workers' observation that this compound is a potent displacer of <sup>3</sup>H-diazepam from brain tissue, our pharmacological data indicate that  $\beta$ CEE has activity that is opposite to, rather than similar to, that of diazepam.

The *in vitro* <sup>3</sup>H-diazepam binding assay was carried out in triplicate according to the method of Mackerer *et al.*<sup>12</sup>, using whole rat brain membranes. <sup>3</sup>H-diazepam was present at 4.0 nM and nonspecific binding was determined in the presence of 4  $\mu$ M unlabelled diazepam. Our assay yielded an IC<sub>50</sub> for  $\beta$ CEE of 1.9  $\pm$  0.1 nM (mean  $\pm$  s.e., eight experiments) which closely corresponds to the reported results<sup>11</sup> and is in the range of the most potent benzodiazepines.

Diazepam has anticonvulsant activity and is especially potent in blocking pentylenetetrazole (PTZ)-induced clonic seizures in mice. We determined the PD<sub>50</sub> (50% protective dose) of diaze-

Table 2 The effect of either normal saline or  $\beta$ CEE on the CD<sub>50</sub> of PTZ

| Pretreatments<br>(mg per kg, i.v.) | PTZ<br>dose range<br>(mg per kg, i.v.) | No.<br>of mice | CD <sub>50</sub> of PTZ<br>(mg per kg) |
|------------------------------------|--|----------------|--|
| Normal saline                      | 20-35                                  | 48             | 26.0 (23.8-28.5)                       |
| $\beta$ CEE (3.2)                  | 5-20                                   | 48             | 14.3 (12.3-16.8)                       |
| $\beta$ CEE (10)                   | 5-20                                   | 48             | 12.3 (10.3-14.8)                       |
| $\beta$ CEE (32)                   | 1-15                                   | 48             | 8.3 (6.5-10.6)                         |

The subjects were male HAM/ICR CD-1 mice weighing 20-27 g at the time of the experiments. The CD<sub>50</sub> (convulsive dose for clonic seizures) of PTZ for each of the four experimental conditions was estimated from four dose levels using 12 mice per dose. The CD<sub>50</sub>s (and 95% confidence limits) were calculated by a Searle computer program based on the method of Litchfield and Wilcoxon<sup>13</sup>. The lowest and highest doses of PTZ administered to mice in each pretreatment group are also presented. In all four pretreatment groups none of the mice convulsed at the lowest dose of PTZ and 12 out of 12 mice convulsed at the highest dose.

pam against PTZ-induced clonic seizures in mice pretreated with either normal saline or  $\beta$ CEE at 3.2, 10 or 32 mg per kg. The experimental design was as follows: normal saline or  $\beta$ CEE was given intravenously (i.v.); 5 min later DZM was administered intraperitoneally (i.p.), followed after 20 min by i.v. administration of 35 mg per kg PTZ. Pretreatment with  $\beta$ CEE produced a clear and pronounced dose-responsive increase in the PD<sub>50</sub> of diazepam against PTZ-induced clonic convulsions (Table 1). This antagonism of the anticonvulsant effect of diazepam is best illustrated by examining the effects of  $\beta$ CEE on a single diazepam dose. For example, diazepam at 1 mg per kg (in the control group) blocked PTZ-induced convulsions in all 10 mice tested. However, when pretreated with only 3.2 mg per kg  $\beta$ CEE there was a complete reversal in that all 10 mice convulsed at this same dose of diazepam.

On the basis of these data, it is tempting to speculate that, analogous to the naloxone-opiate relationship, the  $\beta$ CEE antagonism of diazepam is primarily due to competitive receptor occupancy. However, it seems that a more complex relationship exists. We examined the direct effects of  $\beta$ CEE on the dose (CD<sub>50</sub>) of PTZ required to induce clonic convulsions. Mice received i.v. administrations of either normal saline or  $\beta$ CEE, 3.2, 10 or 32 mg per kg, and 25 min later various doses of PTZ were given i.v. As compared with controls,  $\beta$ CEE produced a dose-responsive decrease in the amount of PTZ required to induce clonic convulsions (Table 2). However,  $\beta$ CEE is not in itself a convulsant within the dose range we studied; i.v. doses of up to 75 mg per kg have failed to produce any overt signs of convulsions or tremors.

Thus,  $\beta$ CEE has an unusual pharmacological profile. It potentially displaces <sup>3</sup>H-diazepam from brain membranes, antagonizes the diazepam blockade of PTZ-induced convulsions, lowers the CD<sub>50</sub> of PTZ and has no convulsant activity of its own. This compound might constitute a new and unique class of pharmacological activity. In any case, it should be useful in learning more about the functions of the benzodiazepine receptor and its proposed endogenous ligand. It would be premature to infer that benzodiazepines are 'antagonists' rather than 'agonists' of the naturally occurring ligand, despite the pharmacology of  $\beta$ CEE, until the full identification of the endogenous ligand has been made. Even if the endogenous ligand should involve a  $\beta$ -carboline-3-carboxylic acid derivative we would therefore have tested only what might be a portion or analogue of this ligand. Again, borrowing from the opiate literature, we know that slight modifications of the structure of an agonist can result in markedly different pharmacological activity.

We acknowledge the technical assistance of A. Miller for the pharmacological studies, P. Sumner for the binding studies and P. Yonan for synthesizing  $\beta$ CEE.

Table 1 The effect of pretreatment with either normal saline or  $\beta$ CEE on the PD<sub>50</sub> of diazepam against PTZ-induced clonic convulsions

| Pretreatments<br>(mg per kg, i.v.) | Diazepam<br>dose range<br>(mg per kg, i.p.) | No.<br>of mice | PD <sub>50</sub> of diazepam<br>(mg per kg) |
|------------------------------------|---|----------------|---|
| Normal saline                      | 0.1-1.0                                     | 50             | 0.32 (0.23-0.43)                            |
| $\beta$ CEE (3.2)                  | 0.56-5.6                                    | 50             | 2.7 (2.1-3.5)                               |
| $\beta$ CEE (10)                   | 1.0-10                                      | 50             | 3.8 (2.8-5.2)                               |
| $\beta$ CEE (32)                   | 3.2-32                                      | 50             | 12.6 (9.7-16.3)                             |

The subjects were male HAM/ICR CD-1 mice (obtained from Charles River Breeders), weighing 20-27 g at the time of the experiments. The ED<sub>50</sub> of diazepam that blocked PTZ-induced clonic convulsions is here referred to as the PD<sub>50</sub> of diazepam. The diazepam PD<sub>50</sub> for each of the four pretreatment conditions was derived from five doses of diazepam (covering 1 log dose range in quarter-log steps) with 10 mice per dose. The PD<sub>50</sub>s (and 95% confidence limits) were calculated by a Searle computer program which is based on the method of Litchfield and Wilcoxon<sup>13</sup>. The lowest and highest doses of diazepam administered to the mice in each pretreatment group are also presented. In all four pretreatment groups 10 out of 10 mice convulsed at the lowest diazepam dose and none convulsed at the highest dose. Note that  $\beta$ CEE cannot be dissolved in water; therefore, this compound was administered as a 'suspension' in normal saline with a few drops of PG/Tween-80. All drug concentrations were adjusted so that the mice received 10 ml of this preparation per kg of body weight. Control animals received equal volumes of the saline PG/Tween-80 vehicle. The dorsal tail veins of the mouse were used for all i.v. administrations. Early pilot studies indicated that even the high dose of 32 mg per kg  $\beta$ CEE when administered i.p. failed to show the pharmacological effects reported here.



Received 12 August; accepted 21 October 1980.

1. Squires, R. F. & Braestrup, C. *Nature* **266**, 732-734 (1977).
2. Mohler, H. & Okada, T. *Life Sci.* **20**, 2101-2110 (1977).
3. Braestrup, C., Albrechtsen, R. & Squires, R. F. *Nature* **269**, 702-704 (1977).
4. Colello, G. D., Hockenbery, D. M., Bosmann, H. B., Fuchs, S. & Folkers, K. *Proc. natn. Acad. Sci. U.S.A.* **75**, 6319-6323 (1978).
5. Skolnick, P., Marangos, P. J., Goodwin, F. K., Edwards, M. & Paul, S. *Life Sci.* **23**, 1473-1480 (1978).
6. Ally, A. I. *et al. Neurosci. Lett.* **7**, 31-34 (1978).
7. Asano, T. & Spector, S. *Proc. natn. Acad. Sci. U.S.A.* **76**, 977-981 (1979).
8. Mohler, H., Polc, P., Cumin, R., Pieri, L. & Kettler, R. *Nature* **278**, 563-565 (1979).
9. Davis, L. G. & Cohen, R. K. *Biochem. biophys. Res. Commun.* **92**, 141-148 (1980).
10. Nielsen, M., Gredal, O. & Braestrup, C. *Life Sci.* **25**, 679-686 (1979).
11. Braestrup, C., Nielsen, M. & Olsen, C. E. *Proc. natn. Acad. Sci. U.S.A.* **77**, 2288-2292 (1980).
12. Mackerer, C., Kochman, R. L., Bierschen, B. A. & Bremner, S. S. *J. Pharmac. exp. Ther.* **206**, 405-413 (1978).
13. Litchfield, J. T. Jr & Wilcoxon, F. *J. Pharmac. exp. Ther.* **96**, 99-113 (1949).

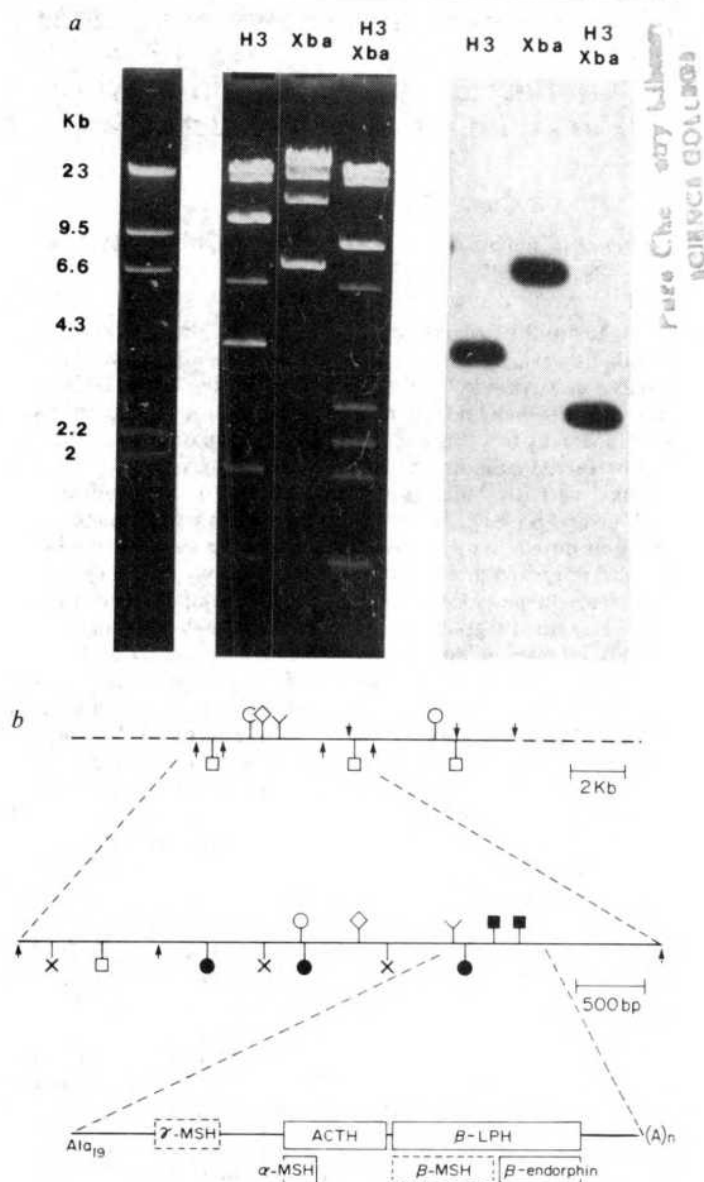
## Most of the coding region of rat ACTH $\beta$ -LPH precursor gene lacks intervening sequences

Jacques Drouin & Howard M. Goodman

Howard Hughes Medical Institute Laboratory, Department of Biochemistry and Biophysics, University of California, San Francisco, California 94143

The peptide hormones ACTH,  $\beta$ -endorphin,  $\alpha$ - and  $\beta$ -melanotropin (MSH) and possibly  $\gamma$ -MSH are synthesized in the pituitary gland by the processing of a 32,000-molecular weight (MW) polypeptide called proopiomelanocortin (POMC)<sup>1-5</sup>. The existence of a further precursor (pre form) to POMC containing an additional N-terminal 'leader' peptide has been suggested by analysis of the *in vitro* translation products of poly(A)-containing RNA from AtT-20 cells, a mouse ACTH-producing cell line of pituitary origin<sup>6</sup>. Nakanishi *et al.*<sup>7</sup> cloned and sequenced a cDNA copy of the bovine prePOMC mRNA. This sequence confirmed the known structure of the carboxyl half of POMC and revealed the presence of a new MSH-like moiety,  $\gamma$ -MSH, within the 16,000-MW amino half of the precursor (16K fragment). Recent experiments have suggested that this peptide may act in synergy with ACTH to increase corticosterone and aldosterone production *in vivo* and *in vitro*<sup>8,9</sup>. We have now isolated from a rat genomic DNA library<sup>10</sup> a segment of a DNA encoding most of POMC, using as probe a mouse 144-base pair cloned cDNA fragment encoding  $\beta$ -MSH and  $\beta$ -endorphin<sup>11</sup>. The cloned rat gene is one of two (or more) closely related POMC genes. The DNA sequence obtained shows that the cloned POMC gene is not interrupted by any intervening sequence (IVS) between the codon for amino acid 19 and the presumptive poly(A) addition site. This region of POMC encodes all the biologically active peptides mentioned above. The DNA sequence encoding the putative  $\gamma$ -MSH and the coding sequence that precedes it are highly conserved between rat and cow. This may indicate an as yet unrecognized biological function(s) for the NH<sub>2</sub>-terminal portion of the 16K fragment.

Polyadenylated RNA from the ACTH-secreting mouse cell line AtT-20 was previously used in this laboratory to clone a 144-base pair cDNA fragment encoding most of the  $\beta$ -MSH and  $\beta$ -endorphin sequences<sup>11</sup>. This mouse cDNA fragment has now been used as a probe to screen<sup>12</sup> a rat genomic DNA library<sup>10</sup> and isolate a fragment of rat DNA encoding POMC. A restriction enzyme cleavage map of the cloned rat DNA fragment was deduced by analysis of the products of double restriction endonuclease digestion and by hybridization of the DNA digests to the cloned mouse cDNA fragment or to single-stranded cDNA synthesized from poly(A)-containing AtT-20 RNA (Fig. 1). A *Xho*I + *Hind*III fragment (1.6 kilobases) contains all the



**Fig. 1** Restriction enzyme cleavage map of the cloned rat POMC gene. A rat genomic DNA library was constructed by cloning, in the bacteriophage  $\lambda$  vector Charon 4A (ref. 35), fragments of rat (Long-Evans) DNA produced by partial digestion with the restriction enzymes *Hae*III and *Alu*I<sup>10</sup>. This library was screened by filter hybridization<sup>12</sup> with the nick-translated<sup>13</sup> 144-base pair mouse cDNA fragment<sup>11</sup> and two clones showing positive hybridization were obtained. Restriction mapping analysis showed that the two clones are similar (not shown) and one of them, containing a 12-kilobase insert, was chosen for further work. *a*, The restriction enzyme cleavage map was deduced by analysis of the products of double restriction endonuclease digestion and by hybridization of the digests to the cloned mouse cDNA fragment. This 144-base pair fragment encodes the  $\beta$ -MSH and  $\beta$ -endorphin sequences. DNA (0.5  $\mu$ g) was digested with the indicated restriction enzymes and separated by electrophoresis on an 0.8% agarose gel. The gel was stained with ethidium bromide and photographed under short-wave UV light (left panel). The DNA was transferred to nitrocellulose paper<sup>13</sup> and hybridization was performed as described previously<sup>14</sup> except that 5  $\times$  SSC (1  $\times$  SSC is 0.15 M sodium chloride, 15 mM trisodium citrate) was used in the hybridization solution and 1  $\times$  SSC in the washes (right panel). A probe was prepared by nick translation<sup>15</sup> of the 144-base pair mouse AtT-20 cloned cDNA fragment. DNA size markers<sup>36</sup> are provided by a *Hind*III (*H3*) digest of wild type  $\lambda$  DNA (left lane). The probe hybridizes only to 3.8-kilobase *Hind*III (*H3*) and 6.7-kilobase *Xba*I (*Xba*) fragments and to a 2.6-kilobase fragment produced by double digestion with *Hind*III + *Xba*I (*H3/Xba*). This 2.6 kilobase fragment was later used for sequencing. *b*, Schematic representation of the restriction endonuclease cleavage map obtained for the cloned rat POMC gene. The solid lines represent the restriction map obtained for the cloned rat DNA and the dotted line the Charon 4A vector DNA. The following symbols are used to indicate the sites of restriction endonuclease cleavage: *Hind*III ( $\uparrow$ ), *Eco*RI ( $\downarrow$ ), *Xba*I ( $\diamond$ ), *Xho*I (*Y*), *Hpa*I (*Hinc*II) ( $\odot$ ), *Bam*HI ( $\square$ ), *Pst*I ( $\bullet$ ), *Acl*I ( $\times$ ) and *Hae*III ( $\blacksquare$ ). All the POMC coding sequences contained in this cloned segment of rat DNA are within the single *Xho*I site (*Y*) and the *Hind*III site ( $\uparrow$ ) at the far right of the middle line of the figure.

cloned rat sequences that are complementary to the mouse cDNA fragment but a larger (2.6 kilobase) *Xba*I + *Hind*III fragment was later used for sequencing.

The restriction map of the cloned rat POMC gene can be compared with POMC sequences present in rat genomic DNA by the filter hybridization method of Southern<sup>13</sup>. Rat HTC cell DNA was digested with various restriction enzymes, transferred to nitrocellulose filters<sup>13</sup> and hybridized<sup>14</sup> to the nick-translated<sup>15</sup> mouse cDNA fragment. Most digests show hybridization of unequal intensity to two bands (Fig. 2); however, a consistent restriction map can be independently derived for the strong and weak hybridizing bands. The sizes of the weakly hybridizing fragments correspond exactly to fragments present in the cloned gene. The cloned gene (Fig. 1) will be referred to as POMC I and the other set of fragments as POMC II. The intensity of the bands corresponding to the two POMC genes in the genomic blot (Fig. 2) suggest that POMC II is present in more copies than POMC I. However, in similar experiments with rat liver DNA, bands corresponding to genes I and II were detected and both were of the same intensity (not shown). The difference in intensity found with DNA from HTC cells could well be due to the heteroploidy of these cells<sup>16</sup>. We conclude from these results that there are at least two POMC genes in the rat, as is the case for rat insulin<sup>17,18</sup>.

The rat POMC I DNA sequence was determined (Fig. 3) and it has the same overall organization as the bovine cDNA sequence<sup>7</sup>. The sequence (Fig. 3) is unambiguously oriented with respect to the restriction map (Fig. 1) by the relative position of the *Xho*I and *Pst*I (at amino acids 23–25) sites. The 5' end of the gene is not present in the sequence and is probably not included in the cloned genomic DNA segment. By comparing the rat sequence with the bovine<sup>7</sup>, human<sup>19</sup> and partial rat amino acid sequences<sup>6</sup>, we can deduce that it encodes part of POMC and starts at the 19th codon (alanine) of the precursor (Fig. 3). An IVS interrupts the coding sequence between amino acids 18 and 19 and the junction between this IVS and the coding region is consistent with the consensus sequence proposed for such boundaries<sup>20</sup>. The agreement between the DNA and the partial amino acid<sup>6,21</sup> sequences (underlined in Fig. 3), together with the very high homology between the rat and bovine DNA sequences in regions of known biological function, support the idea that the sequenced POMC I gene could be expressed; stronger evidence will be provided when cDNA copies of rat POMC are sequenced. Furthermore, recent work on pulse-labelled rat pars intermedia POMC suggests that two forms of the precursor differing in their amino acid sequence are expressed<sup>22</sup>.

Comparison of the rat genomic DNA and bovine cDNA sequences reveals that three regions are highly conserved between them: the  $\gamma$ -MSH region (amino acids 19–74), ACTH (amino acids 98–136) and the  $\beta$ -MSH/ $\beta$ -endorphin region (amino acids 160–209). Not only is the postulated<sup>7</sup>  $\gamma$ -MSH sequence (position 51–62) highly conserved between rat, beef<sup>7</sup> and human<sup>19</sup>, but so is the sequence preceding it (position 19–48). Furthermore, one pair of basic amino acids that delimits  $\gamma$ -MSH in the bovine sequence<sup>7</sup> (position 63, 64) is not conserved in the predicted rat sequence, suggesting that if a  $\gamma$ -MSH peptide was made by processing from this precursor it would be 24 amino acids long rather than 12. This is in agreement with the observation that a synthetic 27-amino acid bovine peptide ( $\gamma$ -MSH) shows similar biological activity to tryptic digests of the 16K fragment<sup>8,9</sup>. These results suggest that the peptide(s) encoded in the  $\gamma$ -MSH region of POMC exert some as yet unrecognized biological function(s).

The predicted rat ACTH sequence is closely homologous to the bovine<sup>7</sup> and other known ACTH<sup>23</sup> sequence. Worthy of mention is the asparagine at position 126 (position 29 of ACTH) within the sequence Asn-Glu-Ser: this residue is likely to be the site of glycosylation in rat and mouse ACTH<sup>3,4</sup>.

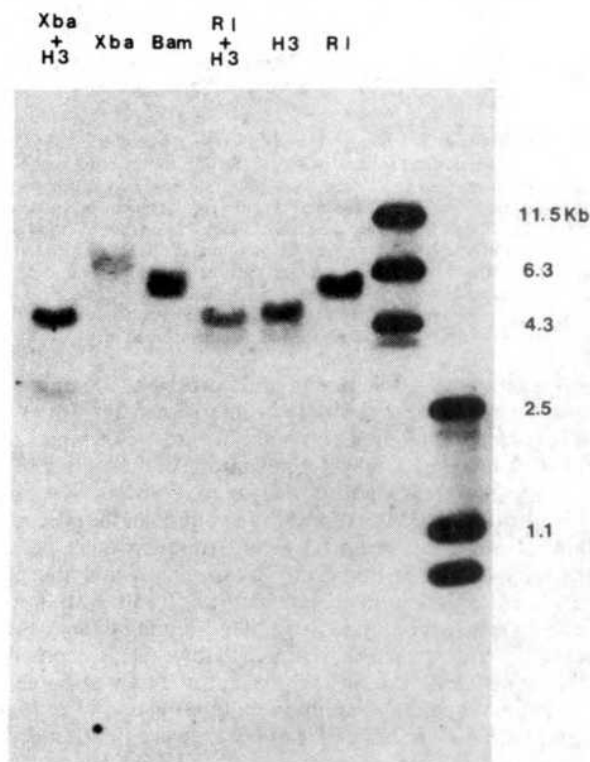
The predicted rat  $\beta$ -MSH sequence is similar to bovine  $\beta$ -MSH but it does not have the pair of basic amino acids that precedes the bovine sequence. Unless a different type of

processing is involved, this would mean that the only peptides carrying the  $\beta$ -MSH sequence that could be produced from this rat POMC would be the NH<sub>2</sub>-terminal fragment of 38 amino acids ( $\gamma$ -LPH) and  $\beta$ -LPH. Human  $\gamma$ - and  $\beta$ -LPH are the only circulating forms of ' $\beta$ -MSH' immunoreactivity that have been detected<sup>24</sup>. A similar situation might exist in the rat.

Two regions of POMC have diverged considerably between the rat and bovine sequences: those preceding (that is, within the 16K fragment) and following (the amino end of  $\beta$ -LPH) ACTH. In the first region, the rat sequence encodes 8 amino acids less than the bovine sequence and rat  $\gamma$ -LPH would be 22 amino acids shorter than its bovine<sup>7</sup> homologue, as suggested by Mains<sup>25</sup>.

The rat 3'-untranslated region is 60 base pairs shorter than the bovine sequence and only the last 54 base pairs are relatively conserved. This conserved segment contains the sequence AATAAA thought to be involved in poly(A) addition<sup>26</sup> and the sequence ACTTCACAGC related to a sequence often observed just before the poly(A) addition site<sup>27</sup>. A 22-base pair sequence and its almost exact reverse complement (18/22 base pairs) are found at a similar distance from the presumptive poly(A) addition site in the rat and bovine 3'-untranslated regions (indicated by arrows in Fig. 3).

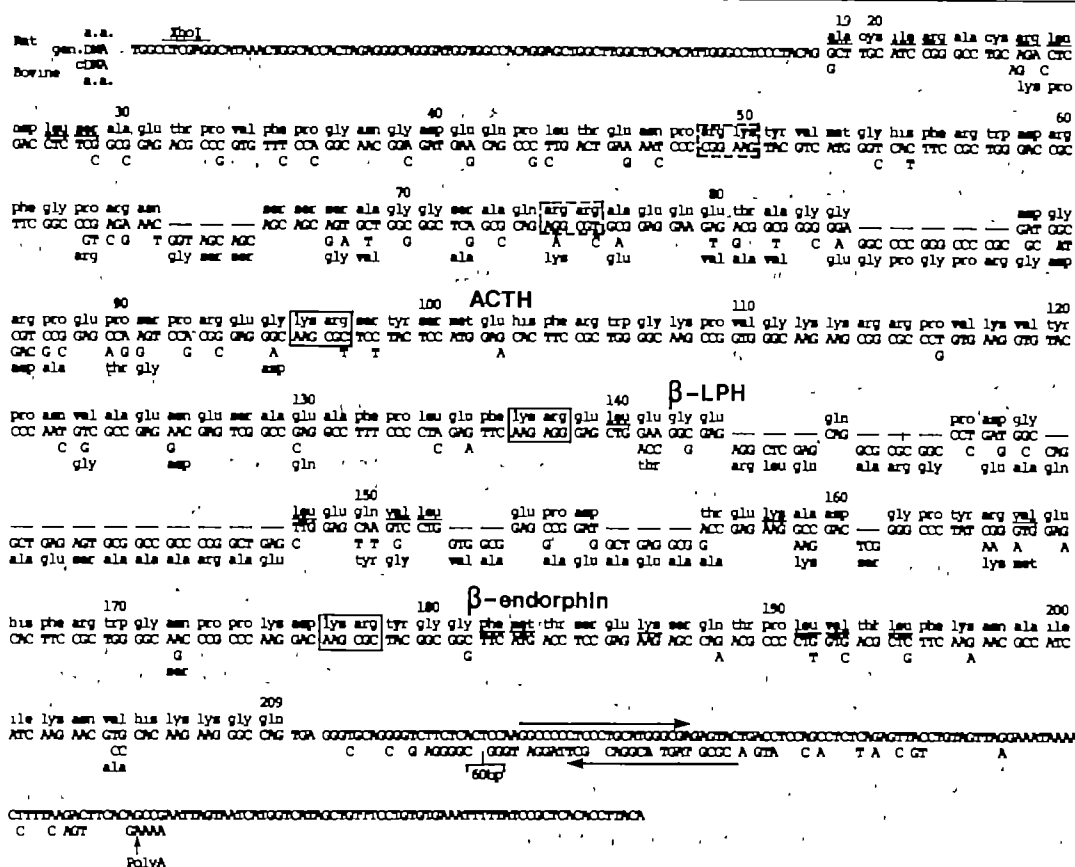
The observation that the bulk of the coding sequence for POMC is uninterrupted by an intervening sequence in the cloned genomic DNA fragment is of interest. The genomic



**Fig. 2** Genomic DNA hybridization. Rat DNA isolated from HTC cells was digested with restriction enzymes and electrophoresed on a 0.8% agarose gel. The transfer to nitrocellulose and the hybridization were done as described in Fig. 1 legend. The two right lanes contain DNA size markers run on the same gel. They are: *Eco*RI-digested pWB91 (11.5 kilobases)<sup>27</sup>, *Eco*RI-digested ColE1 (6.3 kilobases), *Eco*RI-digested pBR322 (4.3 kilobases) and the products of pBR322 digestion with *Ava*I and *Hind*III (2,483, 1,104 and 722 base pairs, respectively)<sup>28</sup>. The 144-base pair mouse cDNA fragment cloned in pBR322 was nick translated<sup>15</sup> and used as probe. *Eco*RI (RI) DNA fragments of 13 and 5.5 kilobases, and two *Hind*III (H3) fragments of 4.4 and 3.8 kilobases, hybridize to the probe. The 3.8-kilobase *Hind*III fragment is not digested by *Eco*RI and corresponds in size and restriction map to the one present in the cloned gene. Both *Bam*HI (Bam) and *Xba*I (Xba) produce broad bands (probably doublets) at about 5.4–5.8 and 6.3–6.7 kilobases, respectively. Another weakly hybridizing *Xba*I fragment of about 2.8 kilobases does not correspond to any fragment found in the cloned gene. Finally, the double digest of *Hind*III + *Xba*I generates a 2.6-kilobase fragment as in the cloned gene and a more intensely hybridizing band at about 4.4 kilobases (Kb).



**Fig. 3** DNA sequence of the rat POMC gene. The DNA nucleotide sequence of the cloned rat POMC gene was determined by the dideoxy chain termination method<sup>29</sup> using single-stranded viral DNA from M13mp2 (refs 40, 41) subclones as templates and the synthetic dodecanucleotide d(TCAGCAGCTTGT) complementary to the phage sequence as a primer. The 2.6-kilobase *Xba*I+*Hind*III fragment that hybridizes to the cloned mouse cDNA probe (Fig. 1) was digested with one of four restriction enzymes (*Hae*III, *A*luI, *Hpa*II or *Rsa*I) for subcloning in M13mp2. These restriction fragments were blunt-end ligated into the 'filled-in' *Eco*RI site of the M13mp2 vector, introduced into the appropriate *Escherichia coli* strain by transformation, and clones containing fragments of the POMC gene identified by plaque hybridization<sup>12</sup> with a probe made from the 2.6-kilobase *Xba*I+*Hind*III fragment. Single-stranded DNA was prepared from 1-ml cultures of each positive candidate<sup>42</sup> and one dideoxy sequencing reaction (ddTTP) was carried out on each to identify similar clones. A representative of each type of recombinant phage obtained was fully sequenced. The complete sequence was deduced by computer-assisted sequence overlap of different clones. More than 95% of the sequence presented was read from both strands and confirmed using different clones, except for the sequence following the *Hae*III site in the 3'-untranslated region, which was read by priming only from the *Hpa*II site at the position of amino acids 154–155. This part of the sequence is therefore less reliable than the rest. The detailed sequencing data are available to investigators on request. The DNA nucleotide sequence and its predicted translation product are shown in comparison with the published bovine cDNA sequence<sup>7</sup>. The amino acid sequence is not numbered from the NH<sub>2</sub> terminus of ACTH as in ref. 7 but from the NH<sub>2</sub> terminus of POMC, which has been determined recently by partial amino acid sequencing of the human<sup>18</sup> and rat<sup>6</sup> polypeptides. The only difference between the predicted amino acid sequence and that determined by Gianoulakis *et al.*<sup>21</sup> is at position 144 (position 6 of  $\beta$ -LPH): they found a phenylalanine whereas the DNA sequence predicts a glutamine. As this residue is the only one where the two sequences do not agree it may be due to a strain difference; one set of data is from Sprague-Dawley and the other (presented here) from Long-Evans rats. The boxed pairs of basic amino acids represent known (solid line) or possible (dashed line) sites of precursor processing.



DNA encoding the functional and structural domains of immunoglobins has been shown to be interrupted by IVSs at the junction between these domains and it was suggested that such gene organization could reflect the evolution of these genes<sup>28–30</sup>; a similar argument was made for the globin genes<sup>31,32</sup>. The three MSH sequences in POMC suggest the evolution of the precursor by duplications of an ancestral gene. Although there are no evolutionary data it is tantalizing to speculate that the precursor's function as a hormone is responsible for its evolution by duplication rather than by IVS-mediated joining of sequences encoding different structural domains. However, it is possible that the cloned gene lost an IVS present in an ancestral gene. The structural constraints imposed by the function of proteins like the immunoglobulins and globins are very different from those exerted on a hormone precursor like POMC. The addition of a new structural domain to the latter would be very unlikely to result in new hormonal activity because this would require the near concomitant appearance of a new receptor molecule on a target cell. On the other hand, evolution of the hormone precursor by duplication would allow the maintenance of the duplicated segment and its slow drifting to another hormonal activity.

Since submission of this manuscript, A. C. Y. Chang *et al.*<sup>33</sup> have published a genomic DNA sequence encoding the same portion of human POMC. The human gene is interrupted by an IVS at about the same position in the coding region and the human sequence diverges from the bovine in the same regions as the rat DNA sequence. Also, Nakanishi *et al.*<sup>34</sup> have published the protein-coding sequence of the bovine ACTH- $\beta$ -lipotropin precursor gene, and find that it is split near the signal peptide region by an intervening sequence of about 2.2 kilobase pairs.

We thank James L. Roberts and Beth Schachter for gifts of AtT-20 poly(A)-containing RNA and HTC DNA, respectively, our colleagues John Fiddes, David Moore, Robert Hallowell and Chi Nguyen-Huu for helpful discussions and critical reading of this manuscript, and Brett McCabe for typing the manuscript. The amino acid sequencing data were made available to us before publication by Dr Michel Chretien. J. D. is supported by a Centennial Fellowship of the MRC of Canada. H.M.G. is an investigator of the Howard Hughes Medical Institute. This work was supported by NIH grant CA 14026.

Received 14 July, accepted 23 October 1980

- 1 Roberts, J. L. & Herbert, E. *Proc. natn. Acad. Sci. U.S.A.* **74**, 4826–4830 (1977)
- 2 Matsu, R. E., Eipper, B. A. & Ling, N. *Proc. natn. Acad. Sci. U.S.A.* **74**, 3014–3018 (1977)
- 3 Eipper, B. A. & Matsu, R. E. *J. supramolec. Struct.* **2**, 247–262 (1978)
- 4 Roberts, J. L., Phillips, M., Rosen, P. A. & Herbert, E. *Biochemistry* **17**, 3609–3618 (1978)
- 5 Crane, P. *et al. Proc. natn. Acad. Sci. U.S.A.* **75**, 4719–4723 (1978)
- 6 Gossard, F., Soudah, N. G., Crane, P., Routhier, R. & Chretien, M. *Biochem. biophys. Res. Commun.* **92**, 1042–1051 (1980)
- 7 Nakanishi, S. *et al. Nature* **278**, 423–427 (1979)
- 8 Podarson, R. C. & Browne, A. C. *Proc. natn. Acad. Sci. U.S.A.* **77**, 2239–2245 (1980)
- 9 Podarson, R. C., Browne, A. C. & Ling, N. *Science* **208**, 1044–1045 (1980)
- 10 Matsu, R. *et al. Cell* **18**, 687–701 (1978)
- 11 Roberts, J. L. *et al. Proc. natn. Acad. Sci. U.S.A.* **76**, 2153–2157 (1979)
- 12 Grunstein, M. & Hogness, D. S. *Proc. natn. Acad. Sci. U.S.A.* **72**, 3961–3965 (1975)
- 13 Southern, E. M. *J. molec. Biol.* **98**, 503–517 (1975)
- 14 Jeffreys, A. J. & Flavell, R. A. *Cell* **12**, 429–439 (1977)
- 15 Rigby, P. W. J., Dieckmann, M., Rhodes, C. & Berg, P. *J. molec. Biol.* **113**, 237–251 (1977)
- 16 Thompson, E. B., Tomkins, G. M. & Curran, J. F. *Proc. natn. Acad. Sci. U.S.A.* **56**, 296–303 (1966)
- 17 Cordell, B. *et al. Cell* **18**, 533–543 (1979)
- 18 Lomedico, P. *et al. Cell* **18**, 545–558 (1979)
- 19 Soudah, N. G. *et al. Biochem. biophys. Res. Commun.* **95**, 1417–1424 (1980)
- 20 Sedl, I., Khoury, G. & Dhar, R. *Nucleic Acids Res.* **6**, 3387 (1979)
- 21 Gianoulakis, C., Soudah, N. G., Routhier, R. & Chretien, M. *Int. J. Peptide Protein Res.* (in the press)
- 22 Crane, P. *et al. Biochemistry* (in the press)

- 23 Dayhoff M. O. *Atlas of Protein Sequence and Structure* Vol. 5, D194-D197 (Natl. Biomed. Res. Pbn, Washington, DC, 1972).
- 24 Bloomfield, G. A., Scott, A. P., Lowry, P. J., Oikar, J. J. H. & Rose, L. H. *Nature* **252**, 492-495 (1974).
- 25 Mame, R. E. & Elipper, B. A. in *Endorphins* (eds Graff, L., Palkovits, M. & Rosen, A. Z.) 79-126 (Akademiai Kiado, Budapest, 1978).
- 26 Proudfoot, N. J. & Brownlee, G. G. *Nature* **263**, 211-214 (1976).
- 27 Benoit, C., O'Hare, K., Brantnach, R. & Chambon, P. *Nucleic Acids Res.* **8**, 127-142 (1980).
- 28 Gilbert, W. *Nature* **271**, 501 (1978).
- 29 Darnell, J. *Science* **202**, 1257-1260 (1978).
- 30 Doolittle, W. *Nature* **272**, 581-582 (1978).
- 31 Eaton, W. A. *Nature* **284**, 183-185 (1980).
- 32 Crank, C. S., Buchanan, S. R. & Boychok, S. *Proc. natn. Acad. Sci. U.S.A.* **77**, 1384-1388 (1980).
- 33 Chang, A. C. Y., Cochot, M. & Cohen, S. N. *Proc. natn. Acad. Sci. U.S.A.* **77**, 4890-4894 (1980).
- 34 Nakanishi, S. *et al.* *Nature* **287**, 752-755 (1980).
- 35 Blattner, F. R. *et al.* *Science* **196**, 161-169 (1977).
- 36 Damsle, D. L., de Wet, J. R. & Blattner, F. F. *J. Virol.* **33**, 390-400 (1980).
- 37 Barnes, W. M. *Science* **196**, 393-394 (1977).
- 38 Sechiff, J. G. *Nucleic Acids Res.* **6**, 2721-2728 (1978).
- 39 Sanger, F., Nicklen, S. & Coulson, A. R. *Proc. natn. Acad. Sci. U.S.A.* **74**, 5463-5467 (1977).
- 40 Messing, J., Groosborn, B., Müller-Hill, B. & Hofschneider, P. H. *Proc. natn. Acad. Sci. U.S.A.* **71**, 3612-3616 (1977).
- 41 Groosborn, B. & Messing, J. *Nature* **272**, 375-377 (1978).
- 42 Winter, G. & Fields, S. *Nucleic Acids Res.* **8**, 1965-1974 (1980).

## Selective processing of $\beta$ -endorphin in regions of porcine pituitary

D. G. Smyth & S. Zakarian

National Institute for Medical Research, The Ridgeway, Mill Hill, London NW7 1AA, UK

The prohormone of  $\beta$ -endorphin is unusual in that it is the precursor of more than one biologically active peptide<sup>1-3</sup> (Fig. 1). The activation of this prohormone, to produce corticotropin (ACTH),  $\alpha$ -melanotropin ( $\alpha$ -MSH) and  $\beta$ -endorphin, would seem to be relatively complex as its processing pattern is known to differ between tissues. Thus ACTH is produced in the anterior pituitary whereas  $\alpha$ -MSH is formed in the pars intermedia<sup>4,5</sup>; similarly, lipotropin and  $\beta$ -endorphin seem to predominate in the anterior pituitary whereas  $\beta$ -endorphin alone has been thought to be the principal component in the pars intermedia. We report here a study of the distribution of  $\beta$ -endorphin-related peptides in various regions of porcine pituitary. The main products in the anterior pituitary were lipotropin and the potent analgesic form of  $\beta$ -endorphin, whereas the main products in the pars intermedia were the inactive lipotropin C'-fragment and its N-acetyl derivative. Thus the processing of the C-terminal region of the  $\beta$ -endorphin prohormone differs markedly between the two regions of porcine pituitary.

We concentrated on the processing of the C-terminal region of the prohormone by studying the distribution of four peptides related to  $\beta$ -endorphin: the C'-fragment of the prohormone

( $\beta$ -endorphin, lipotropin residues 61-91), the C'-fragment (lipotropin residues 61-87), the  $\alpha$ , N-acetyl derivative of the C'-fragment, and the  $\alpha$ , N-acetyl derivative of the C'-fragment<sup>6-8</sup>. These peptides have a similar molecular size and are generally identified and measured together as a single immunoreactive component<sup>9,10</sup>. Their biological activities, however, differ strikingly:  $\beta$ -endorphin has potent analgesic properties<sup>11,12</sup> whereas the C'-fragment is 500 times less potent<sup>13</sup> and the acetyl peptides are inactive<sup>8,14</sup>. The processing of the  $\beta$ -endorphin prohormone to produce active or inactive endorphins may therefore have physiological significance and because the processing could vary between tissues it is clearly important that the individual peptides should be differentiated.

We studied the distribution of  $\beta$ -endorphin-related peptides in the anterior pituitary and pars intermedia plus posterior pituitary by extracting the peptides from dissected regions of porcine pituitary glands. The products were resolved by gel filtration, ion exchange chromatography and high pressure liquid chromatography (HPLC). To locate the eluted peptides (and to allow estimation of peptide recovery) the four known  $\beta$ -endorphin-related peptides, obtained by isolation from porcine pituitary<sup>7,8</sup>, were radioiodinated and trace amounts added to the solvent used to extract the tissues. The peptides resolved by column chromatography were detected and measured by radioimmunoassay (RIA) using an antiserum raised against porcine  $\beta$ -endorphin<sup>15</sup>, and further evidence for the identity and concentrations of the peptides was obtained by comparison of elution positions and peak heights on HPLC with those produced by reference peptides. This extensive chromatographic procedure was necessary because of the complexity of the mixture of pituitary peptides, and because each of the four  $\beta$ -endorphin-related peptides reacted with the  $\beta$ -endorphin antiserum<sup>15</sup>, which prevented their differential estimation by immunoassay of the tissue extracts without previous fractionation.

Gel filtration of the peptides extracted from the anterior pituitary revealed two fractions which differed in molecular size (Fig. 2a); the first emerged in the position of porcine lipotropin and the second contained peptides that eluted in the position of porcine  $\beta$ -endorphin. Resolution of the  $\beta$ -endorphin fraction by ion exchange chromatography showed that the main immunoreactive component co-chromatographed with <sup>125</sup>I-labelled porcine  $\beta$ -endorphin (Fig. 3) and its identity was confirmed by comparison with authentic porcine  $\beta$ -endorphin during HPLC. There was, in addition, a small amount (<4% of the  $\beta$ -endorphin) of other immunoreactive peptides which were chromatographically identical to peptides present in high concentration in the pars intermedia. Thus, apart from these minor components, the principal C-terminal fragments of the  $\beta$ -endorphin prohormone in porcine anterior pituitary are lipotropin and  $\beta$ -endorphin, with  $\beta$ -endorphin accounting for nearly 50% of the total immunoreactive material.

Gel filtration of the peptides extracted from the pars intermedia and posterior pituitary showed a negligible amount of

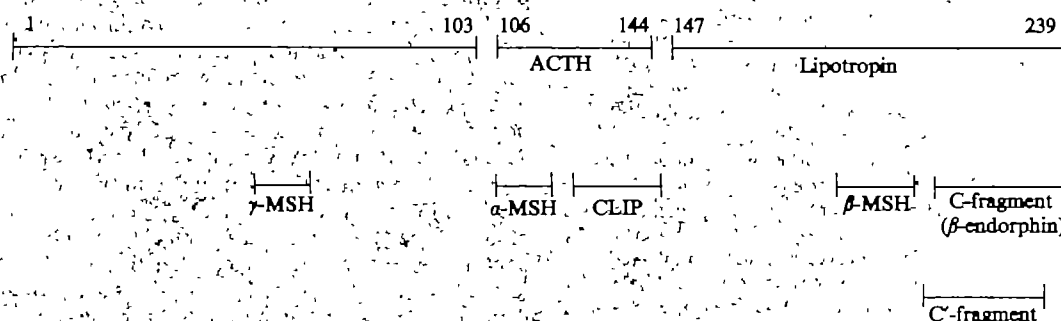
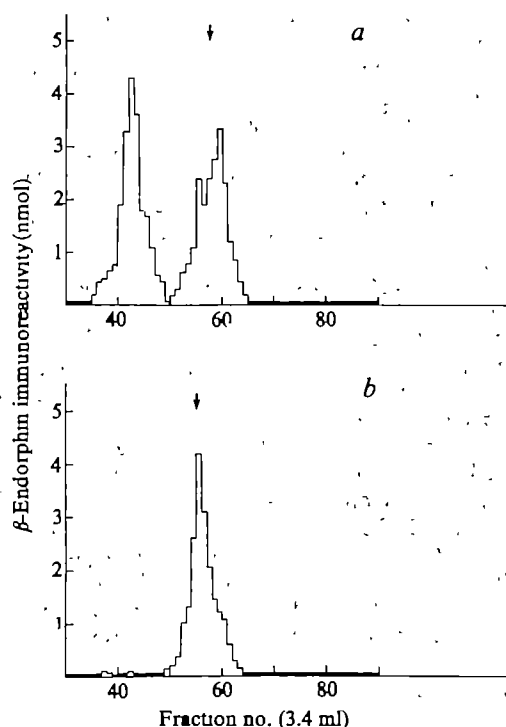


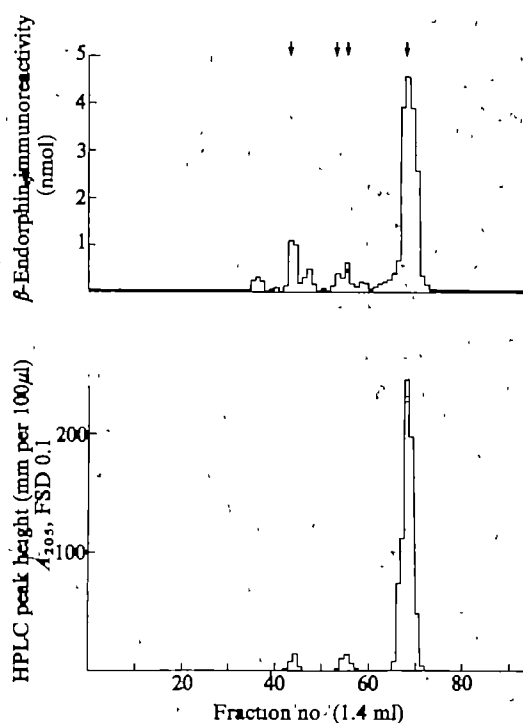
Fig. 1 Schematic representation of the biologically active sections of the 31K prohormone of  $\beta$ -endorphin (according to Nakanishi *et al.*<sup>3</sup>). The numbers represent residue positions in the sequence of the bovine molecule. Each of the peptides indicated is flanked by pairs of basic residues in the prohormone sequence. Several of the prohormone fragments exist both in acetylated and unacetylated forms<sup>8</sup>.



lipotropin or 31K prohormone, but there was a substantial quantity of immunoreactive peptide with the approximate molecular size of  $\beta$ -endorphin (Fig. 2b). The  $\beta$ -endorphin-containing fraction was resolved into at least six components by chromatography on SP-Sephadex C25 (Fig. 4)—note that the biologically active form of  $\beta$ -endorphin (Peak VI) was only a minor component, representing less than 7% of the immunoreactive peptides. Four of the six peptides (Peaks II, IV, V and VI) co-chromatographed with the corresponding radiolabelled markers and their chromatographic behaviour on HPLC was indistinguishable from the corresponding reference peptides ( $\alpha$ ,  $N$ -acetyl C'-fragment, C'-fragment,  $\alpha$ ,  $N$ -acetyl  $\beta$ -endorphin and  $\beta$ -endorphin). Two of the remaining peptides (Peaks I and III), which were not accompanied by radioactive markers, were found to co-chromatograph on SP-Sephadex C25 and on HPLC with peptides formed by mild reaction of C'-fragment or  $\alpha$ ,  $N$ -acetyl C'-fragment with acetic anhydride *in vitro* and did not correspond to products generated by acetylation of  $\beta$ -endorphin. On this basis the two peptides seem to be an  $\epsilon$ ,  $N$ -acetyl derivative of the C'-fragment (Peak III) and an  $\epsilon$ ,  $N$ -acetyl derivative of  $\alpha$ ,  $N$ -acetyl C'-fragment (Peak I).



**Fig. 2** Gel filtration of peptides related to  $\beta$ -endorphin extracted from *a*, porcine anterior pituitary and *b*, porcine pars intermedia plus posterior pituitary. Acid-acetone extraction (acetone/H<sub>2</sub>O/hydrochloric acid, 40/6/1) was carried out at 4 °C on four anterior pituitary lobes or pars intermedia plus posterior pituitary lobes, dissected 20 min *post mortem*. Radiolabelled marker peptides were added before extraction ( $\alpha$ ,  $N$ -acetyl C'-fragment, C'-fragment,  $\alpha$ ,  $N$ -acetyl  $\beta$ -endorphin and  $\beta$ -endorphin were labelled by treatment of 1  $\mu$ g of peptide with 100  $\mu$ Ci of <sup>125</sup>I and  $\sim 6 \times 10^4$  c.p.m. of each peptide was used). The extract was centrifuged at 15,000 r.p.m. for 60 min, acetone was removed by concentration *in vacuo* at 20 °C, and the residual solution diluted in 50% acetic acid in preparation for gel filtration on a Sephadex G75 column (70  $\times$  2.5 cm) in 50% acetic acid. The elution position of the <sup>125</sup>I-labelled  $\beta$ -endorphin related marker peptides is indicated by an arrow. Aliquots (0.25  $\mu$ l) from the anterior pituitary fractions and (0.5  $\mu$ l) from the pars intermedia fractions were immunoassayed using an antiserum to  $\beta$ -endorphin: the antiserum did not cross-react with  $\gamma$ -endorphin or methionine enkephalin but reacted with the  $\alpha$ ,  $N$ -acetyl derivative of  $\beta$ -endorphin and the  $\alpha$ ,  $N$ -acetyl derivative of the C'-fragment, with affinity equal to that of the respective unacetylated parent peptides<sup>15</sup>.



**Fig. 3** Ion exchange chromatography of peptides with the molecular size of  $\beta$ -endorphin, obtained by gel filtration of porcine anterior pituitary extracts. After removal of the acetic acid *in vacuo* at 20 °C from the fractions obtained by gel filtration, chromatography of the peptides was performed on a column (60  $\times$  0.6 cm) of SP-Sephadex C25 in 50% acetic acid with a linear gradient from 0 to 0.6 M sodium chloride, mixer volume 100 ml. The elution positions of the radiolabelled reference peptides ( $\alpha$ ,  $N$ -acetyl C'-fragment, C'-fragment,  $\alpha$ ,  $N$ -acetyl  $\beta$ -endorphin and  $\beta$ -endorphin) are indicated respectively from left to right by the arrows. Aliquots (0.5  $\mu$ l) of the column fractions were dried *in vacuo* and immunoassayed with a  $\beta$ -endorphin antiserum<sup>15</sup>; the amounts of the peptides determined by RIA shown have not been corrected for their immunoreactivities. A second series of aliquots (20–400  $\mu$ l), taken from fractions shown to contain  $\beta$ -endorphin related peptides by RIA, were monitored by HPLC (Waters Associates, Inc.) using a C<sub>18</sub> Bondapak column (30  $\times$  0.4 cm) eluted in 0.01 M hydrochloric acid with a linear gradient (15 min) from 25–40% acetonitrile. The amounts of the peptides shown were determined from the optical density at 205 nm given by the peptide peak occurring at the position of the appropriate unlabelled reference peptide, compared with the peak heights given by known amounts of the marker peptide.

These results show that in the anterior pituitary lipotropin is accompanied by the potent analgesic form of  $\beta$ -endorphin whereas in the pars intermedia the inactive peptides, lipotropin C'-fragment and its  $N$ -acetyl derivative, are the major products. Thus the processing of the C-terminal region of the  $\beta$ -endorphin prohormone differs markedly in the two regions.

The relative amounts of  $\beta$ -endorphin and the C'-fragment, together with their acetylated derivatives, may reflect the activity of proteolytic enzymes with specificity for the respective cleavage sites in lipotropin, the Lys-Arg-Tyr residues at positions 59, 60 and 61 and the Lys-Lys-Gly residues at positions 88, 89 and 90. It may be concluded that the specificity of the processing enzymes in the anterior pituitary differs from that in the pars intermedia. Furthermore, the acetylation of  $\beta$ -endorphin and the C'-fragment takes place almost exclusively in the pars intermedia<sup>16,17</sup>. It is likely that the acetyl endorphins are formed concomitantly with  $\alpha$ -MSH because these acetylated peptides occur in the same region of pituitary (ref. 5 and this communication) and originate as fragments of the same prohormone. Note that the acetyl group is important for the melanotropic activity of  $\alpha$ -MSH<sup>18</sup> but it renders  $\beta$ -endorphin inactive as an opiate. It seems therefore that activation of one

section of the ACTH-endorphin prohormone can be accompanied by inactivation of another.

In an earlier report<sup>15</sup>, we had concluded that the same inactive peptide fragments were present in both the anterior lobe and the pars intermedia of rat pituitary. However, it is now clear that this result was due to slight contamination of the anterior region by cells from the pars intermedia and that the processing patterns are very similar in the corresponding regions of pig and rat pituitary<sup>16</sup>. Thus the differential processing mechanisms are conserved across species.

The two regions of porcine pituitary contain approximately equal amounts of the group of  $\beta$ -endorphin-related peptides whereas in the rat the concentration of the peptides in the pars intermedia is nearly two orders of magnitude greater than that in the anterior pituitary. Studies on the significance of these peptides in different species may therefore be useful in obtaining an understanding of the changing physiological role of the pars intermedia during evolution.

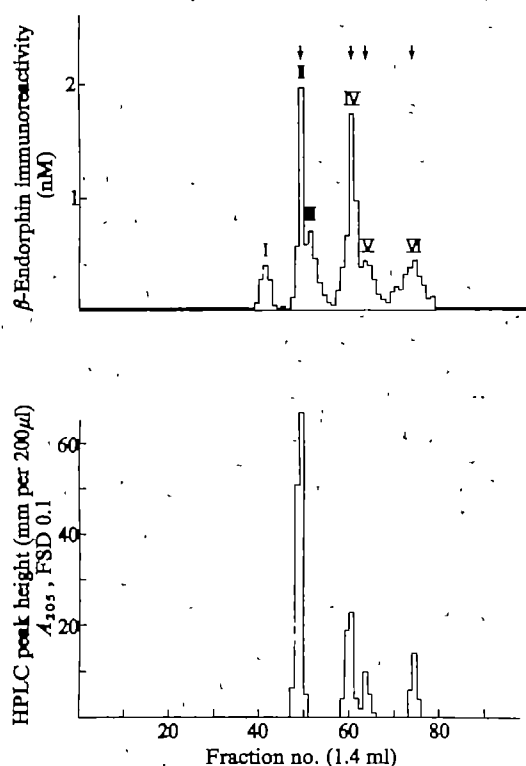
The results of this study demonstrate that specific mechanisms lead to the production of  $\beta$ -endorphin in its opiate active form in porcine anterior pituitary. It is known that ACTH is elaborated in the anterior pituitary and is formed from the same prohormone as  $\beta$ -endorphin; thus two biologically active peptides (ACTH and  $\beta$ -endorphin) are generated together with a potential for synergistic action. However, in the pars intermedia,  $\alpha$ -MSH is accompanied principally by forms of  $\beta$ -endorphin that have been inactivated by proteolysis or acetylation. It

therefore seems that different processing mechanisms acting on the multifunctional prohormone are available to select the appropriate biological activity required in different regions of the pituitary.

We thank Derek Massey and Kamela Maruthainar for technical assistance.

Received 11 August, accepted 4 November 1980

1. Mains, R. E., Eipper, B. A. & Ling, N. *Proc natn Acad Sci USA* **74**, 3014-3018 (1977)
2. Roberts, J. L., Phillips, M., Ross, P. A. & Herbert, E. *Proc natn Acad Sci USA* **75**, 3609-3618 (1978)
3. Nakamatsu, S. *et al. Nature* **278**, 423-426 (1979)
4. Lowry, P. J. & Scott, A. F. *Gen Comp Endocrinol* **26**, 16-23 (1975)
5. Jackson, S. & Lowry, P. J. *J Endocr* **86**, 205-219 (1980)
6. Bradbury, A. F., Smyth, D. G. & Snell, C. R. in *Peptides: Structure and Biological Activity* (eds Walter, R. & Messelböcker, J.) 609-615 (Ann Arbor Sci, Michigan, 1975)
7. Smyth, D. G., Snell, C. R. & Massey, D. E. *Biochem J* **175**, 261-270 (1978)
8. Smyth, D. G., Massey, D. E., Zakarian, S. & Prange, M. D. A. *Nature* **279**, 252-254 (1979)
9. Rosmar, J. *et al. Proc natn Acad Sci USA* **74**, 5162-5165 (1977)
10. Lott, A. S., Soda, T. & Knogor, D. T. *Proc natn Acad Sci USA* **75**, 2950-2954 (1978)
11. Loh, H. H., Tseng, L. F., Wei, E. & Li, C. H. *Proc natn Acad Sci USA* **73**, 2895-2898 (1976)
12. Feldborg, W. S. & Smyth, D. G. *Br J Pharmac* **60**, 445-454 (1977)
13. Gensow, M. J., Doakim, J. F. W., Dostrovsky, J. O. & Smyth, D. G. *Nature* **269**, 167-168 (1977)
14. Doakim, J. F. W., Dostrovsky, J. O. & Smyth, D. G. *Biochem J* **189**, 501-506 (1980)
15. Zakarian, S. & Smyth, D. G. *Proc natn Acad Sci USA* **76**, 5972-5976 (1979)
16. Smyth, D. G., Zakarian, S., Doakim, J. F. W. & Massey, D. E. in *Peptides of the Pars Intermedia* (eds Evered, D. & Lawrence, G.) (Pitman Medical, in the press)
17. Mains, R. E. & Eipper, B. A. in *Peptides of the Pars Intermedia* (eds Evered, D. & Lawrence, G.) (Pitman Medical, in the press)
18. Schweitzer, R. *Ann NY Acad Sci* **297**, 3 (1977)



**Fig. 4** Ion exchange chromatography of peptides with the molecular size of  $\beta$ -endorphin present in porcine pars intermedia plus posterior pituitary. After gel filtration of the tissue extract on Sephadex G75 in 50% acetic acid, the  $\beta$ -endorphin fraction, localized by RIA and by measuring the radioactivity of the marker peptides, was concentrated *in vacuo* at 20°C and added to a column (60×0.6 cm) of SP-Sephadex C25 in 50% acetic acid. Chromatography was performed as in Fig. 3 legend and the elution positions of the four radiolabelled reference peptides ( $\alpha$ , N-acetyl C-fragment, C'-fragment,  $\alpha$ , N-acetyl  $\beta$ -endorphin and  $\beta$ -endorphin) are shown from left to right by arrows. Aliquots (0.5  $\mu$ l) of the eluted fractions were dried *in vacuo* and RIA was carried out using the  $\beta$ -endorphin antiserum. A second series of aliquots (20–400  $\mu$ l) taken from the fractions that contained  $\beta$ -endorphin immunoreactive peptides, were monitored by HPLC (see Fig. 3 legend) and compared with appropriate reference peptides.

## Expression of H-2, laminin and SV40 T and TASA on differentiation of transformed murine teratocarcinoma cells

B. B. Knowles, S. Pan, D. Solter, A. Linnenbach, C. Croce & K. Huebner

The Wistar Institute, 36th Street at Spruce, Philadelphia, Pennsylvania 19104

Murine embryonal carcinoma cells (ECCs) do not express antigens of the major histocompatibility complex (H-2)<sup>1,2</sup>, but do express cell-surface molecules shared with early embryos<sup>3</sup>. ECCs are also characterized by their insusceptibility to infection by various oncogenic viruses<sup>4,7</sup>, and their ability to differentiate into a variety of adult cell types<sup>8</sup>. Differentiation of ECCs *in vitro* can occur spontaneously or can be induced<sup>9–12</sup>. On exposure to retinoic acid the ECC line F9 (ref. 13) differentiates into cells which have the characteristics of parietal endoderm<sup>10,14</sup>. When ECCs are exposed to simian virus 40 (SV40), the SV40 tumour (T) antigen is not expressed<sup>4</sup>, although the virus genome reaches the nucleus<sup>15</sup>, and a primary transcript of the SV40 A gene is made<sup>16</sup>. However, following exposure to retinoic acid, the differentiated cells, like most mouse somatic cells, are susceptible to SV40 abortive infection and synthesize large T and small t antigens<sup>17</sup>. To monitor the molecular events associated with the expression of the SV40 A gene on differentiation, we have constructed an ECC line (F9 12-1) containing a single integrated copy of the SV40 genome<sup>18</sup>. This was accomplished by introducing a recombinant plasmid consisting of pBR322 linked to the herpes simplex type 1 thymidine kinase gene and SV40 genome<sup>19</sup> into a thymidine kinase-deficient F9 cell line<sup>19</sup>. We report here that in F9 12-1 cells exposed to retinoic acid, synthesis of the SV40 A gene product(s), T and tumour-associated specific antigens (TASA), parallels the appearance of the normal hallmarks of differentiation in this cell line, H-2 antigens and the basement membrane protein laminin<sup>20</sup>.

F9 12-1 cells are morphologically identical to murine ECCs. In our experiments (Table 1), we were unable to find any unequivocally SV40 T antigen-positive nuclei; however, because it is difficult to estimate nuclear fluorescence in ECCs due to their characteristic growth in clumps of rounded cells, we



**Table 1** Immunofluorescent assay for detection of antigenic determinants specific to stem cells (SSEA-1), differentiated cells (H-2D<sup>b</sup>) and SV40 T antigen

| Cell line                        | Days following exposure to RA | % Positive cells |                   |                 |
|----------------------------------|-------------------------------|------------------|-------------------|-----------------|
|                                  |                               | SSEA-1           | H-2D <sup>b</sup> | SV40 T antigen* |
| F9 12-1                          | 0                             | 80               | 3                 | 0               |
|                                  | 2                             | 90               | 23                | 2               |
|                                  | 4                             | 25               | 48                | 11              |
|                                  | 7                             | 10               | 58                | 50              |
|                                  | 9                             | 3                | 66                | 65              |
|                                  | 11                            | 4                | 90                | 70              |
|                                  | 15                            | 2                | 95                | 80              |
|                                  | 16                            | 5                | 94                | 90              |
| F9 12-1 clone a (differentiated) |                               | 0                | 100               | 98              |
| K4RSV                            |                               | 0                | 100               | 95              |
| K5RSV                            |                               | 0                | 0                 | 97              |

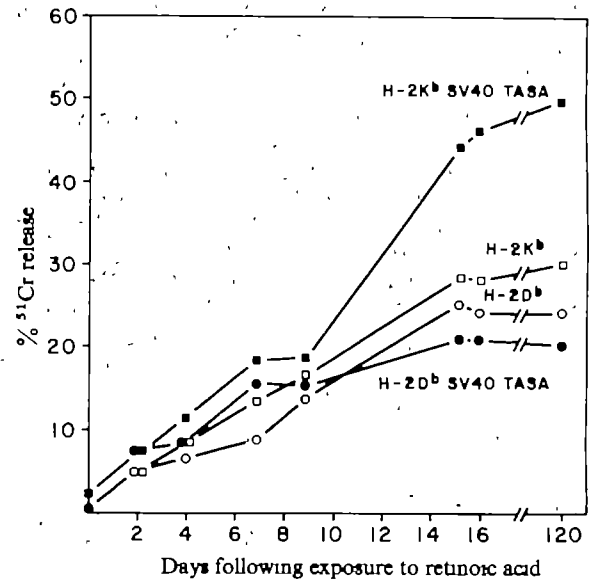
A single-cell suspension of F9 12-1 was placed in 60-mm plastic Petri dishes (Falcon) containing a glass coverlip and cultured in RPMI 1640 with 10% fetal bovine serum (FBS) and  $5 \times 10^{-7}$  M retinoic acid (RA) (*all trans*; Eastman)<sup>10,14</sup>. The medium was replaced with the same medium without retinoic acid 16 h before assay. F9 12-1 and F9 12-1 clone a were cultured in RPMI with 10% FBS. Cells were resuspended by exposure to 0.25% trypsin in phosphate-buffered saline (PBS) containing 0.1 M EDTA. SSEA-1 expression was determined by indirect immunofluorescent assay using monoclonal antibody to SSEA-1 diluted 1:200 (100  $\mu$ l per  $2 \times 10^5$  cells) as described<sup>21</sup> elsewhere. Rabbit IgG, anti-mouse IgG (heavy and light chain specific) (RAMIG) tagged with fluorescein isothiocyanate (FITC) (Cappel) served as the developing reagent; cells were mounted in equal parts of Dulbecco's modified PBS and glycerol on glass slides, with coverlips, and viewed using a Leitz Ortholux microscope with epifluorescence and appropriate filters. Cell suspensions were exposed to a 1:100 dilution of monoclonal antibody B22-249R which detects the H-2D<sup>b</sup> private-specificity 2 (ref. 22). Following exposure to RAMIG-FITC and mounting, cells were scored for fluorescence (see above).

\* Coverlips were washed three times with Dulbecco's modified PBS and fixed by 5 min exposure to  $-20^\circ\text{C}$  acetone and dried. The coverlips were then overlaid with monoclonal antibody to SV40 T antigen, washed and exposed to RAMIG-FITC. Coverlips were mounted in Uvinert aqueous mounting medium (Gurr) and scored for the presence of nuclear fluorescence. In all cases an equivalent amount of IgG from the P3 X63 Ag8 (ref. 23) cell line was used as a control.

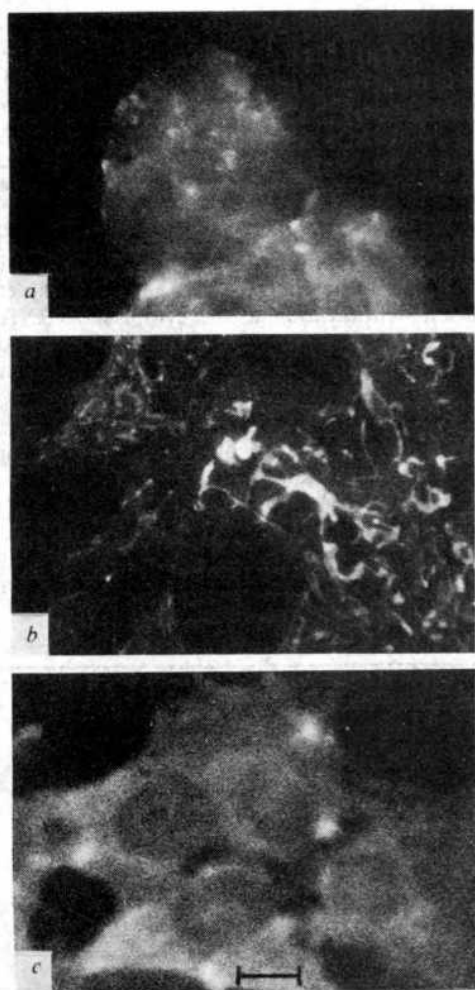
cannot exclude the presence of an occasional SV40 T antigen-positive cell. Like all murine ECCs, the F9 12-1 cell does not express H-2D<sup>b</sup> (Table 1). Although a very low percentage of the cells are weakly fluorescent following reaction with monoclonal antibody to an H-2D<sup>b</sup> antigenic determinant (Table 1), a similar number of fluorescent cells are found when the F9 12-1 cells are incubated with immunoglobulin from the P3X63 Ag8 myeloma cell line. We were also unable to detect those determinants of the H-2K<sup>b</sup> or D<sup>b</sup> molecules recognized by murine cytotoxic T lymphocytes (CTLs) sensitized by allogeneic immunization (Fig. 1). In addition, no SV40 TASA associated with H-2K<sup>b</sup> or H-2D<sup>b</sup> and recognized by SV40-sensitized H-2<sup>b</sup>-restricted CTLs, are expressed. Murine ECCs are characterized by the expression of a stage-specific embryonic antigenic determinant (SSEA-1) which is also found on murine preimplantation embryos beginning at the 8-cell stage and on cells of the inner cell mass<sup>25</sup>. SSEA-1 is secreted into the medium of ECCs and can be detected on 80–100% of all murine ECCs tested. F9 12-1 reacts with the monoclonal antibody that defines the SSEA-1 antigenic determinant (Table 1). A small amount of basement membrane protein is synthesized by F9 cell lines<sup>26</sup>. Antibody to basement membrane protein reacts with a small proportion of cells on the periphery of some of the clumps of the F9 12-1 culture (Fig. 2a). Thus on the basis of morphology, surface-antigen expression and SV40 A gene expression, the F9 12-1 cell seem to behave as other ECCs.

Within 2 days of exposure to retinoic acid some of the F9 12-1 cells assume a flattened, epitheloid morphology. A small percentage of cells express H-2 antigens and the SV40 A gene product(s) T and TASA, are detectable (Table 1, Fig. 1). Most of the cells in these cultures retain the stem cell characteristics. As the cultures are maintained in retinoic acid, differentiation proceeds and after 1 week approximately half the cells morphologically resemble parietal endodermal cells, are synthesizing laminin (Fig. 2b), and express H-2 and SV40 T and TASA.

After 14 days, most of the cells are differentiated, with only a small per cent SSEA-1-positive and over 90% SV40 T- and TASA-positive. These cells also synthesize both laminin and H-2, an indication that cells with the characteristics of parietal



**Fig. 1** Detection of H-2K, H-2D and SV40 TASA in association with H-2K<sup>b</sup> and H-2D<sup>b</sup> in F9 12-1 cells following exposure to retinoic acid. Cells were seeded into 60-mm Petri dishes in RPMI 1640 with 10% FBS and retinoic acid ( $5 \times 10^{-7}$  M) (ref. 10). F9 12-1 clone a cells, exposed 120 d previously to retinoic acid, were grown in RPMI 1640 with 10% FBS. Sixteen hours before assay the cells were re-fed with RPMI 1640 and 10% FBS containing  $^{51}\text{Cr}$ -labelled sodium chromate (NEZ030; 150 Ci per 5 ml). Control target cells (not shown) were SV40-transformed cell lines derived from C57B 10/ScSn congenic mice; K4RSV (H-2K<sup>b</sup>D<sup>b</sup>), K5RSV (H-2K<sup>b</sup>D<sup>b</sup>), LB10SV (H-2K<sup>b</sup>D<sup>b</sup>) and KD2SV (H-2K<sup>b</sup>D<sup>b</sup>) (ref. 24). The  $^{51}\text{Cr}$ -labelled cells were washed, resuspended and incubated for 7 h at a concentration of  $2 \times 10^4$  cells per 0.2 ml, with lymphocytes. Percentage  $^{51}\text{Cr}$ -release was calculated after  $\gamma$  counting of the supernatant fluid and the cells as described elsewhere<sup>24</sup>. Cytotoxic effector cells specific for SV40 TASA associated with H-2K<sup>b</sup> and H-2D<sup>b</sup> were obtained by immunization of B10.A(5R) and B10.A(4R) mice, respectively, with  $10^7$  infectious units of SV40 in each of the hind footpads. One week after immunization, the popliteal lymph nodes were excised, single-cell suspensions prepared and placed in Dulbecco's modified Eagle's minimal essential medium (supplemented with 10% FBS), 2-mercaptoethanol ( $2 \times 10^{-5}$  M), sodium pyruvate (1 mM), Eagle's non-essential amino acids, penicillin and streptomycin) at a concentration of  $10^7$  cells per 10 ml in 25-cm<sup>2</sup> plastic tissue culture flasks (Falcon), and incubated at  $37^\circ\text{C}$ , 5%  $\text{CO}_2$  in humidified air for 3 d before assay<sup>24</sup>. Effector cells specific for H-2K<sup>b</sup> and H-2D<sup>b</sup> were obtained by *in vitro* stimulation of BALB/c AnICR (H-2K<sup>b</sup>D<sup>b</sup>) splenic lymphocytes with irradiated (7,000R) splenic lymphocytes from B10.D2 (R107) (H-2K<sup>b</sup>D<sup>b</sup>) and B10.HTG (H-2K<sup>b</sup>D<sup>b</sup>), respectively. BALB/c cells ( $5 \times 10^6$ ) were incubated with stimulator cells ( $2 \times 10^5$ ) in 2 ml medium per well of a 24-well Linbro plate. After incubation for 6 d at  $37^\circ\text{C}$  in a 5%  $\text{CO}_2$  humidified atmosphere, the cells were either re-stimulated *in vitro* (by the addition of  $2 \times 10^6$  irradiated stimulator cells to  $5 \times 10^6$  viable cells 2 ml medium) and collected after 5 d or used as effectors immediately. Effector to target cell ratio 10:1 for anti-SV40 TASA effectors and 100:1 for anti-H-2 effectors.



**Fig. 2** Immunofluorescent assay for the presence of laminin. Coverslips were fixed (as described in Table 1 legend) and exposed to rabbit anti-mouse basement membrane protein (anti-peak 1) serum<sup>27</sup> (provided by Dr Barry Pierce) and absorbed before use with mouse 3T3 cells (1:12 dilution). FITC-tagged goat IgG anti-rabbit IgG served as the developing reagent. *a*, F9 12-1 before exposure to retinoic acid (RA); *b*, 10 d following exposure to RA; *c*, F9 12-1 clone a.

endoderm express antigens of the major histocompatibility complex.

A differentiated cell line, F9 12-1 clone a, which was cloned from retinoic acid-treated F9 12-1 4 months earlier, was included in these experiments. All cells of this clone express H-2, are SSEA-1-negative, T antigen-positive and express SV40 TASA in association with both H-2K<sup>b</sup> and H-2D<sup>b</sup>. In contrast to the cells monitored for 16 days following retinoic acid treatment, laminin was not detectable in F9 12-1 clone a (Fig. 2c) and the cells appeared fibroblastic. We have previously isolated a differentiated clone (F9 AC clone 9) from retinoic acid-treated F9 cells which has retained its parietal endoderm phenotype for 2 yr in culture. It is possible that, following exposure to retinoic acid, a minor population of fibroblastic cells is always induced and that a representative of these cells gives rise to F9 12-1 clone a. Alternatively, parietal endoderm-like cells may be the only differentiated cells resulting from retinoic acid treatment of F9 cells. However, due to the presence of the SV40 genome, the parietal endoderm phenotype may be transitory with all stable, transformed cells appearing fibroblastic. Experiments are being done to investigate these possibilities.

Recognition of SV40 TASA by virus-specific cytotoxic effector T cells is contingent on expression of the H-2K and D gene products. In contrast to the ECC line PCC3A/1, which does not express H-2 when induced to differentiate by exposure to hexamethylene bisacetamide<sup>11</sup>, each F9 cell which differen-

tiated cells can independently express the H-2K and H-2D gene observed that somatic cell hybrids between F9 and differentiated cells can independently express the H-2K and H-2D gene products<sup>19</sup>, although the mechanism by which this regulatory event occurs remains undefined. Differentiation of the F9 12-1 cell, however, is accompanied by simultaneous expression of both H-2K and H-2D gene products (Fig. 1). This conclusion is based on results with cytotoxic effector cells specific for H-2K<sup>b</sup> and H-2D<sup>b</sup>. In addition, because recognition of SV40 TASA in mice of the H-2<sup>b</sup> haplotype occurs in association with both H-2K<sup>b</sup> and H-2D<sup>b</sup> (ref. 24), the results with cytotoxic effector cells specific for H-2K<sup>b</sup>-SV40 TASA and H-2D<sup>b</sup>-SV40 TASA indicate simultaneous expression of the H-2K<sup>b</sup> and H-2D<sup>b</sup> gene products. Because expression of the H-2 determinants is necessary for CTL recognition of foreign antigens on the cell surface<sup>28</sup>, it is impossible from inspection of the data in Fig. 1 to determine if the SV40 TASA and H-2 antigens appear simultaneously or sequentially. From the data obtained at 2 and 4 days after retinoic acid induction (Table 1), it can be surmised that the H-2D<sup>b</sup> gene product is expressed (and SSEA-1 suppressed) at an earlier time than the SV40 A gene products. However, SV40 T antigen is synthesized in cytoplasm but can only be detected by immunofluorescent techniques following accumulation in the nucleus<sup>29</sup>. Furthermore, cell-surface antigens are more readily detectable by the methods used, so we feel this difference in time of appearance is artefactual. We therefore propose that, following induction of differentiation, there is simultaneous activation of a series of genes, perhaps through the pleiotropic action of a single gene product (for example RNA splicing enzymes<sup>16,17</sup>). Alternatively, a single regulatory event could lead to the synthesis of factors necessary for expression of each of the gene products investigated. The organization of the SV40 genome in relation to the cellular genome in the F9 12-1 cell, the F9 12-1 retinoic acid-treated cells and the F9 12-1 clone a cell is identical (A.L. and K.H., unpublished).

Finally Lehman and Friedrich<sup>30</sup> report that when ECCs are infected with SV40 and then induced to differentiate, SV40 A gene products are not expressed. Free unintegrated SV40 viral DNA was found in these ECCs, and in the differentiated cells derived from them, that was capable of infecting permissive monkey kidney cells, although integrated viral DNA was not detected. The F9 12-1 cells contain integrated SV40 genomes<sup>18</sup> and when they differentiate the SV40 A gene products are expressed. A comparison of these results suggests that integration of the SV40 genome is a prerequisite for the expression of SV40 gene products.

We thank Adrienne Mihalek for technical assistance. This work was supported by grants from the USPHS-NIH, the ACS and the NFM of D.

Received 12 June; accepted 9 October 1980.

- Artzt, K. & Jacob, F. *Transplantation* **17**, 632-634 (1974).
- Forman, J. & Vitteta, E. S. *Proc. natn. Acad. Sci. U.S.A.* **72**, 3661-3665 (1975).
- Solter, D. & Knowles, B. B. *Curr. Topics dev. Biol.* **13**, 139-165 (1979).
- Swartzendruber, D. E. & Lehman, J. M. *J. cell. Physiol.* **85**, 179-188 (1975).
- Boccaro, M. & Kelly, F. *Annls Microbiol. Inst. Pasteur, Paris* **129a**, 227-238 (1978).
- Peries, J., Alves-Cardoso, E., Canivet, M., Debons-Guillemin, M. C. & Lasneret, J. *J. natn. Cancer Inst.* **59**, 463-465 (1977).
- Teich, N. M., Weiss, R. A., Martin, G. R. & Lowy, D. R. *Cell* **12**, 973-982 (1977).
- Martin, G. R. *Cell* **5**, 229-243 (1975).
- Speers, W. C. & Lehman, J. M. *J. cell. Physiol.* **88**, 297-306 (1976).
- Strickland, S. & Mahdavi, V. *Cell* **15**, 393-403 (1978).
- Jakob, H., Dubois, P., Eisen, H. & Jacob, F. *C. r. hebdom. Séanc. Sci., Paris* **286D**, 109-111 (1978).
- Jetten, A. M., Jetten, M. E. R. & Sherman, M. I. *Expl. Cell Res.* **124**, 381-391 (1980).
- Bernstine, E. G., Hooper, M. L., Granchamp, S. & Ephrussi, B. *Proc. natn. Acad. Sci. U.S.A.* **70**, 3899-3903 (1973).
- Solter, D., Shevinsky, L., Knowles, B. B. & Strickland, S. *Dev. Biol.* **70**, 515-521 (1979).
- Swartzendruber, D. E., Friedrich, T. D. & Lehman, J. M. *J. cell. Physiol.* **93**, 25-30 (1977).
- Segal, S., Levine, A. J. & Khoury, G. *Nature* **280**, 335-339 (1979).
- Segal, S. & Khoury, G. *Proc. natn. Acad. Sci. U.S.A.* **76**, 5611-5615 (1979).
- Linnenbach, A., Huebner, K. & Croce, C. M. *Proc. natn. Acad. Sci. U.S.A.* **77**, 4875-4879 (1980).
- Gmur, R., Solter, D. & Knowles, B. B. *J. exp. Med.* **151**, 1349-1359 (1980).
- Howe, C. C. & Solter, D. *Dev. Biol.* **77**, 480-487 (1980).
- Campbell, G. L., Goldstein, L. & Knowles, B. B. *J. Cell Biol.* **64**, 719-724 (1975).
- Lemke, H. G., Hammerling, G. J. & Hammerling, U. *Immun. Rev.* **47**, 175-206 (1979).
- Galfre, G., Howe, S. C., Milstein, C., Butcher, G. W. & Howard, J. C. *Nature* **266**, 550-582 (1977).



- 24 Knowles, B. B., Kocur, M., Pfizmayer, K., Solter, D. & Trinchesi, G. *J. Immunol.* **122**, 1798–1820 (1979)  
 25 Solter, D. & Knowles, B. B. *Proc. natn. Acad. Sci. USA* **75**, 5565–5569 (1978)  
 26 Howe, C. C. & Solter, D. *Dev. Biol.* (in the press)  
 27 Johnson, L. D. & Starcher, B. C. *Biochem. Biophys. Acta* **290**, 158–167 (1972)  
 28 Doherty, P. C., Solter, D. & Knowles, B. B. *Nature* **266**, 361–362 (1977)  
 29 Stepielinski, Z., Knowles, B. B. & Koprowski, H. *Proc. natn. Acad. Sci. USA* **89**, 769–776 (1968)  
 30 Lohman, J. M. & Friedrich, T. D. *J. Supramolec. Struct. Suppl.* **4**, 126 (1980)

## Post-transcriptional regulation of gene expression in guinea pig tissues

Roger K. Craig\*, Ian C. Bathurst†  
 & David G. Herries†

\*Courtauld Institute of Biochemistry, The Middlesex Hospital Medical School, London W1P 7PN, UK

†Department of Biochemistry, University of Leeds, 9 Hyde Terrace, Leeds LS2 9LS, UK

The formation of individual functional mRNA sequences in higher organisms requires many steps in addition to transcription. These include RNA splicing, polyadenylation, base modification, transport from nucleus to cytoplasm and assembly into polyribosomes. Various control mechanisms must also operate. These will function on a quantitative basis to account for the differing frequency of the various classes of cytoplasmic mRNAs, and also on a qualitative basis, because in higher organisms not all the nuclear poly(A)-containing RNA molecules are found in a cytoplasmic poly(A)-containing RNA population from the same tissue<sup>1–10</sup>. During our studies on the mechanisms controlling the accumulation of the poly(A)-containing RNA sequences which occur with high and moderately high frequency in the cytoplasm of the lactating guinea pig mammary gland, it became apparent that >75% of the 20,000 or so poly(A)-containing nuclear RNA sequences were not found in the cytoplasmic poly(A)-containing RNA fraction<sup>4</sup>. Here we demonstrate that many of the poly(A)-containing RNA sequences retained in the nucleus of the lactating guinea pig mammary gland are also present in the nucleus and cytoplasm of the liver of the male guinea pig. These observations provide new evidence for a predominant role of post-transcriptional mechanisms in the regulation of structural gene expression in guinea pig tissue.

Comparison of the base complexity of nuclear and cytoplasmic poly(A)-containing RNA sequences isolated from the lactating guinea pig mammary gland and the male guinea pig liver, demonstrate that the number of different sequences expressed in the nuclear population was similar, but that nearly three times as many poly(A)-containing RNA sequences were present in the cytoplasm of the liver as in the cytoplasm of the mammary gland (Table 1, Fig. 1a). Cross-hybridization studies between the two nuclear poly(A)-containing RNA populations revealed that although each contained similar sequences, there were striking quantitative differences (Fig. 1a). Subsequent hybridization studies using mammary gland nuclear cDNA fractionated into hybridization probes for high- and low-frequency poly(A)-containing RNA sequences showed that sequences present at high frequency in the lactating mammary gland (a group of up to 30 different sequences including the milk proteins<sup>4,5</sup>) were present at very low frequency in the liver (Fig. 1b). In contrast, the most complex population, consisting of sequences which occurred at low frequency in the lactating mammary gland, were present in the liver in comparable amounts (Fig. 1b).

Cross-hybridization studies using mammary gland<sup>4</sup> and liver RNA populations<sup>6</sup> demonstrate that the cytoplasmic poly(A)-containing RNA sequences are all represented within the nuclear poly(A)-containing RNA populations from the same

tissues. This observation, together with the fact that the base complexity of the liver cytoplasmic population is considerably greater than the equivalent lactating mammary gland population suggested that some of those sequences retained in the nucleus of the mammary gland might represent sequences expressed as cytoplasmic poly(A)-containing sequences in liver.

To test this, a cDNA probe representative of those mammary gland poly(A)-containing RNA sequences retained in the nucleus, was hybridized to liver nuclear and cytoplasmic poly(A)-containing RNA. This resulted in maximum hybridization of the probe to nuclear RNA with the expected kinetics, but also significant hybridization to the cytoplasmic RNA population (Fig. 2). We estimate that 3,000–4,000 of those sequences retained in the nucleus of the lactating mammary gland were present in the cytoplasm of the liver. This hybridization cannot be an artefact due to contaminating nuclear sequences within the liver cytoplasmic population because this proportion of the hybridization probe hybridized faster to the liver cytoplasmic poly(A)-containing RNA population than to the liver nuclear poly(A)-containing RNA population. This indicates an enrichment of these sequences within the cytoplasm. Moreover, no significant protection was afforded by a lactating mammary

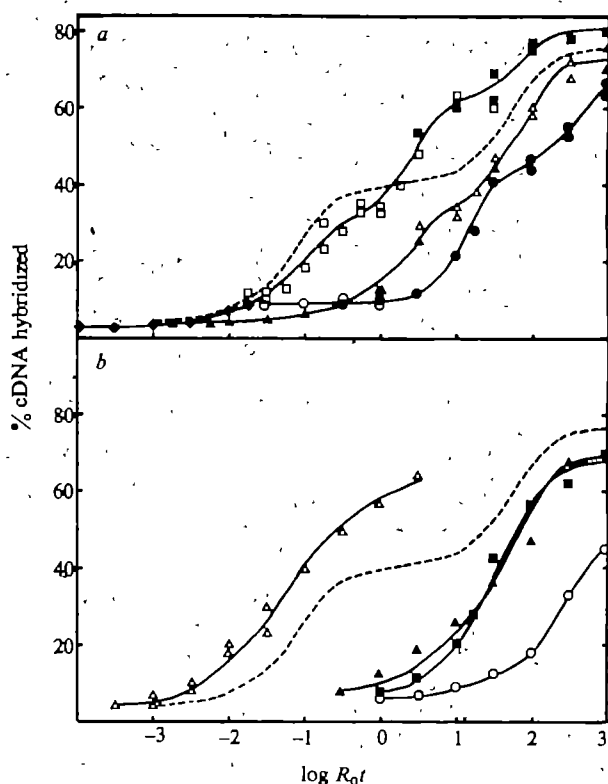


Fig. 1 a, The comparative hybridization kinetics of (1) liver cytoplasmic poly(A)-containing RNA against its homologous cDNA preparation at RNA concentrations of 20  $\mu\text{g ml}^{-1}$  ( $\bullet$ ), 200  $\mu\text{g ml}^{-1}$  ( $\square$ ) and 1  $\text{mg ml}^{-1}$  ( $\blacksquare$ ), (2) liver nuclear poly(A)-containing RNA against its homologous cDNA preparation at RNA concentrations of 100  $\mu\text{g ml}^{-1}$  ( $\triangle$ ) and 1  $\text{mg ml}^{-1}$  ( $\blacktriangle$ ), and (3) the heterologous hybridization of cDNA prepared from mammary gland nuclear poly(A)-containing RNA against liver nuclear poly(A)-containing RNA at RNA concentrations of 200  $\mu\text{g ml}^{-1}$  ( $\circ$ ) and 1  $\text{mg ml}^{-1}$  ( $\bullet$ ). The dashed line represents the hybridization of mammary gland nuclear poly(A)-containing RNA against its homologous cDNA. b, cDNA synthesized from mammary gland nuclear poly(A)-containing RNA was fractionated into high- and low-frequency probes by limited hybridization to a  $R_0t$  value of 1.0 mol nucleotide per 1 s followed by separation of double- and single-stranded sequences on hydroxyapatite<sup>4</sup>. The high-frequency cDNA population was then hybridized to either the mammary gland nuclear poly(A)-containing RNA population at an RNA concentration of 100  $\mu\text{g ml}^{-1}$  ( $\triangle$ ), or the equivalent liver population at an RNA concentration of 1  $\text{mg ml}^{-1}$  ( $\circ$ ). Low-frequency cDNA probes were hybridized to mammary gland ( $\blacktriangle$ ) or liver nuclear poly(A)-containing RNA ( $\blacksquare$ ), both at an RNA concentration of 1  $\text{mg ml}^{-1}$ . The dashed line represents the hybridization of mammary gland nuclear poly(A)-containing RNA against its homologous RNA<sup>4</sup>.

†Present address: Department of Biochemistry, University of Otago, Dunedin, New Zealand

**Table 1** Comparison of the base complexity of nuclear and cytoplasmic poly(A)-containing RNA sequences isolated from lactating guinea pig mammary gland and male guinea pig liver

| Source of RNA         | Transition | Correct $R_{0.1/2}$                           | Complexity                              | No. of species                             | Relative proportion of total population |
|-----------------------|------------|---|---|--|---|
| Liver                 | 1          | $1.16 \times 10^{-2} \pm 4.43 \times 10^{-3}$ | $1.86 \times 10^6 \pm 7.07 \times 10^5$ | $13.3 \pm 5.0$<br>[1.55 $\pm$ 0.3]         | 28<br>[55]                              |
| Post-nuclear fraction | 2          | $6.47 \times 10^{-1} \pm 1.69 \times 10^{-1}$ | $1.03 \times 10^6 \pm 2.70 \times 10^5$ | $741 \pm 194$<br>[31.8 $\pm$ 23.3]         | 45<br>[18]                              |
|                       | 3          | $11.64 \pm 4.70$                              | $1.85 \times 10^7 \pm 7.50 \times 10^6$ | $13,309 \pm 5,395$<br>[3,242 $\pm$ 1,771]  | 27<br>[27]                              |
| Liver                 | 1          | $3.78 \times 10^{-1} \pm 1.00 \times 10^{-1}$ | $6.04 \times 10^5 \pm 1.61 \times 10^5$ | $387 \pm 103$<br>[27.5 $\pm$ 3.7]          | 38<br>[49]                              |
| Nuclear fraction      | 2          | $23.42 \pm 3.29$                              | $3.73 \times 10^7 \pm 5.25 \times 10^6$ | $23,910 \pm 3,365$<br>[18,516 $\pm$ 2,425] | 62<br>[51]                              |

Poly(A)-containing RNA was isolated from total nuclear or cytoplasmic RNA, and  $^3\text{H}$ -labelled cDNA synthesized from each population (specific activity  $1.45 \times 10^7$  c.p.m. per  $\mu\text{g}$ ) using avian myeloblastosis virus reverse transcriptase. Hybridizations were performed in RNA excess and the degree of hybridization determined using  $S_1$  nuclease digestion. Estimations of RNA complexity were based on the comparative hybridization kinetics of a rabbit globin mRNA standard after best line fit by computer and the appropriate adjustment of the observed  $R_{0.1/2}$  values (mol nucleotide per l s). Estimation of the number of sequences in each transition for the liver RNA populations was based on a number average molecular size of 1,590 and 1,390 nucleotides for the nuclear and post-nuclear populations, respectively, as determined by sucrose gradient centrifugation in the presence of formamide. Values in square brackets represent numbers previously calculated for the lactating mammary gland<sup>4</sup>. All procedures were as described previously<sup>4,5,7</sup>. Subsequent best line fits using fractionated cDNA probes in homologous or heterologous hybridizations have been assessed by eye (see Figs 1, 2).

gland cytoplasmic poly(A)-containing RNA population, thereby demonstrating the specificity of the cDNA probe.

The results reveal a remarkable degree of sequence homology within the nuclear poly(A)-containing RNA sequences isolated from two different tissues, one from a male and one from a female animal of the same species. Quantitative differences were also evident, but were restricted to the high-frequency poly(A)-containing RNA sequences. Thus, in common with studies on the distribution of globin<sup>11-15</sup> and ovalbumin<sup>16</sup> mRNA sequences, the RNA sequences found at high frequency in mammary gland tissue<sup>4,5,7</sup> were present at very low frequency in a nuclear poly(A)-containing RNA population and could not be detected in a cytoplasmic poly(A)-containing RNA population isolated from a different tissue within the same species<sup>6</sup>. The accumulation of these sequences seems to be regulated in a different manner from the complex low-frequency poly(A)-containing RNA sequences.

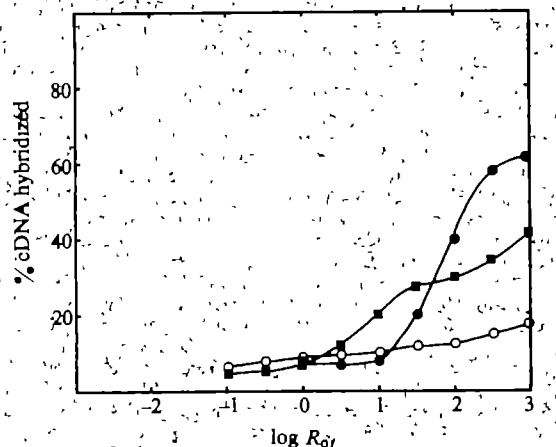
Our observations have a parallel. In sea urchins, post-transcriptional mechanisms seem to predominate, because transcribed single-copy nuclear sequences are common to embryo and adult tissues<sup>8</sup>, but cytoplasmic mRNA populations differ considerably<sup>9,17</sup>. We have investigated two tissues, one of which, the liver, contains a relatively heterogeneous cell population<sup>18</sup> compared with the mammary gland, which is predominantly epithelial<sup>19</sup>. This disparity in cell type presumably accounts for

the increased complexity of the liver cytoplasmic poly(A)-containing RNA population, thereby reflecting different functional requirements of different cell types even within the low-frequency populations. About 75% of the mammary gland low-frequency cytoplasmic poly(A)-containing RNA sequences are also present in the equivalent liver subcellular fraction (I.C.B. and R.K.C., unpublished). Some of these will direct the synthesis of the 'house-keeping' proteins, those proteins required by all cells<sup>9,20,21</sup>, others will represent cell-specific RNA sequences from cell types common to both tissues. The remainder, those not found in the liver, must represent a class of low-frequency poly(A)-containing RNA sequences peculiar to the mammary gland.

Overall, our studies support the concept that post-transcriptional mechanisms determine the accumulation of the low-frequency class of poly(A)-containing RNA sequences within the cytoplasm of guinea pig tissues. Thus although this population of sequences when located in the nucleus of two different tissues is very similar, examination of the relative distribution of these sequences within the cytoplasm reveals considerable tissue-specific differences. The precise nature of these post-transcriptional mechanisms has not been established, but probably involves correct processing of the primary RNA transcripts<sup>22-24</sup>, resulting ultimately in tissue- or cell-specific expression in the cytoplasm.

We thank Professor P. N. Campbell, Dr L. Hall and Dr M. S. Davies for helpful discussions, and the Wellcome Trust for supporting this work. Avian myeloblastosis reverse transcriptase was the gift of Drs J. Beard and J. Gruber.

Received 21 July, accepted 3 October 1980



**Fig. 2** A mammary gland cDNA probe representative of those sequences confined to the nucleus was prepared by hybridizing the cDNA preparation synthesized from nuclear poly(A)-containing RNA with a post-nuclear poly(A)-containing RNA population to a  $R_{0.1/2}$  value of 100 mol nucleotide per l s. Single-stranded cDNA (65% of starting material) was recovered by hydroxylapatite column chromatography<sup>4</sup>, then used as a source of mammary gland nucleus-specific cDNA. This was hybridized to poly(A)-containing RNA from the mammary gland cytoplasmic fraction (○), the liver nuclear (●) and liver cytoplasmic fraction (■), all at an RNA concentration of  $1 \text{ mg ml}^{-1}$ .

- Davidson, E. H. & Britton, R. J. *Science* **204**, 1052-1059 (1979)
- Lowenbaupt, K. & Lingrel, J. B. *Cell* **14**, 337-344 (1978)
- Guyette, W. A., Matsumi, R. J. & Rosen, J. M. *Cell* **17**, 1013-1023 (1979)
- Bathurst, I. C., Craig, R. K., Hornes, D. G. & Campbell, P. N. *Eur. J. Biochem.* **109**, 183-191 (1980)
- Bathurst, I. C., Craig, R. K., Hornes, D. G. & Campbell, P. N. *Biochem. J.* **192**, 489-498 (1980)
- Bathurst, I. C. thesis, Univ. London (1980)
- Craig, R. K., Boulton, A. P., Harrison, O. S., Parker, D. & Campbell, P. N. *Biochem. J.* **181**, 737-759 (1979)
- Kjelson, K. C. & Humphreys, T. *Cell* **12**, 143-155 (1977)
- Galan, G. A. *et al.* *Cell* **7**, 487-505 (1976)
- Bahnen, A., Murty, A. J. & Barnes, G. D. *Nucleic Acids Res.* **8**, 1643-1660 (1980)
- Gilmour, R. S., Harrison, P. A., Winkless, J. D., Affara, N. A. & Paul, J. *Cell Differentiation* **3**, 9-22 (1974)
- Groudine, M. & Weintraub, H. *Proc. natn. Acad. Sci. U.S.A.* **72**, 4464-4468 (1975)
- Humphreys, S., Winkless, J. & Williamson, R. *Cell* **7**, 267-277 (1976)
- Gottschalk, J. M. & Partington, G. H. *Cell* **12**, 953-962 (1977)
- Portman, S. M., Ford, P. J. & Roebash, M. M. *Proc. natn. Acad. Sci. U.S.A.* **74**, 3835-3839 (1977)
- Tsu, S. Y., Tsui, M. J., Lin, C.-T. & O'Malley, B. W. *Biochemistry* **18**, 5726-5731 (1979)
- Lév, Z. *et al.* *Dev. Biol.* **76**, 322-340 (1980)
- Van Bortel, T. J. C. *Trends biochem. Sci.* **4**, 202-205 (1979)
- Pitelka, D. R. in *Lockstein Vol. 4* (ed. Larson, B. L.) 41-66 (1978)
- Axel, R., Fogelson, P. & Schütz, G. *Cell* **7**, 247-254 (1976)
- Hastie, N. D. & Bishop, J. O. *Cell* **9**, 761-774 (1976)
- Wickens, M. P., Woo, S., O'Malley, B. W. & Gordon, J. B. *Nature* **286**, 628-634 (1980)
- Hamer, D. H. & Leder, P. *Cell* **18**, 1299-1302 (1979)
- Early, R. *et al.* *Cell* **20**, 313-319 (1980)



## The higher order structure of chicken erythrocyte chromosomes *in vivo*

J. P. Langmore\* & C. Schutt

MRC Laboratory of Molecular Biology, Hills Road, Cambridge CB2 2QH, UK

Recently eukaryotic chromosomes have been shown to consist of a repeating subunit, called the nucleosome<sup>1</sup>. Although electron microscopy, neutron scattering and X-ray diffraction have been used to determine the low resolution structure of the nucleosome, these techniques have yielded little information about the disposition of nucleosomes within chromosomes. Electron microscopy has produced many models for chromosome structure based on uniform fibres of 150–500 Å diameter or on globular 'superbeads'<sup>2–6</sup>. Unfortunately the models are based on microscope images that fail to reveal the strong structural periodicities shown by X-ray scattering to be characteristic of isolated chromatin in solution. Moreover it has not been demonstrated that the chromosomes of living cells are composed of such fibres. We have used low-angle X-ray scattering to investigate the organization of chromosomes *in vivo* and to account for the previously observed inconsistencies in many X-ray and electron microscope observations. We report here that chicken erythrocytes have a 400 Å periodicity due to a nuclear structure that is directly related to the 300 Å side-by-side packing of chromosome fibres revealed by electron microscopy of embedded cells, and that this periodicity can be preserved in isolated nuclei provided that the proper buffers are used.

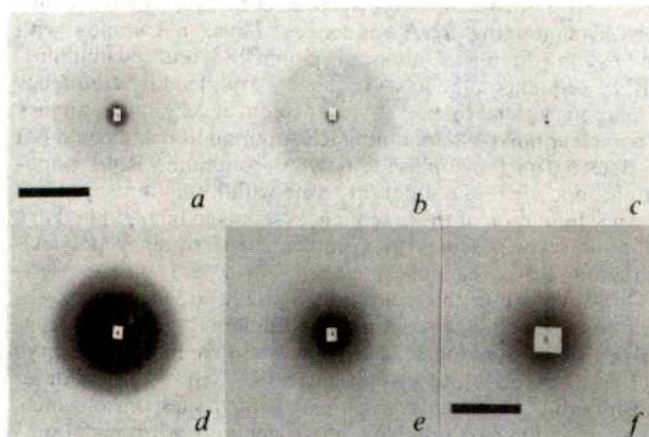
Studies of concentrated isolated chromatin by X-ray and neutron scattering have shown dominant structural periodicities at about 110, 55, 38, 27 and 22 Å<sup>7–14</sup>. The intensities and exact positions of these bands depend on ionic composition of the solution and chromatin concentration. Significantly these low-angle studies have not revealed the 150–500 Å packing bands predicted by all the existing models for chromatin. However, the 110 Å band has been used as indirect evidence that helical 300 Å thick fibres exist<sup>13,14</sup>. Studies of dilute isolated chromatin have shown variable 400–460 Å, weak 200 Å, and weak variable 140 Å periodicities in one case<sup>15</sup>, and absent 400 Å, absent 200 Å, strong 110 Å, absent 55 Å, and strong 33 Å in another case<sup>14</sup>. Unfortunately, solution studies cannot be definitive because partial nuclease digestion and sub-physiological ionic strength are required for chromatin solubility. In fact, as the ionic strength is raised, increasingly compact higher order structures are formed<sup>16–18</sup>.

A typical diffraction pattern from living chicken erythrocytes is shown in Fig. 1a. A shoulder in the intensity is apparent at a spacing of ~400 Å. Patterns from rabbit enucleated erythrocytes do not give rise to this shoulder and possess only low-angle scattering from the concentrated intracellular haemoglobin (Fig. 1b). Buffer alone produced only uniform scattering of low intensity (Fig. 1c). By subtracting the measured intensities of nucleated from enucleated erythrocytes, we produced a difference curve (Fig. 2a) representing the structural differences (presumably nuclear) between these cells. A strong 400 Å peak is present in this curve.

The nuclear origin of the 400 Å peak is demonstrated by diffraction from chicken erythrocyte nuclei isolated by lysis of the cells with MLB buffer (see legend to Fig. 1) of near-

physiological ionic strength and containing magnesium (Figs 1f, 2b). The isolated nuclei also scatter at 200, 106, 60, 38 and 30 Å (Figs 1d, e, 2b, 3a). The nuclear spacings smaller than 400 Å were not obvious in the patterns from whole erythrocytes, due to the reduced contrast and increased background from the high internal concentration of haemoglobin. Diffraction patterns from live chicken and mouse lymphocytes, MOPC-21 and HeLa tissue culture cells, sea urchin, scallop and frog sperm cells, and from nuclei of all these cells clearly show the 106, 60, 38, 30 and 22 Å bands to be common to whole cells as well as their nuclei. Further discussion of these results will be published elsewhere.

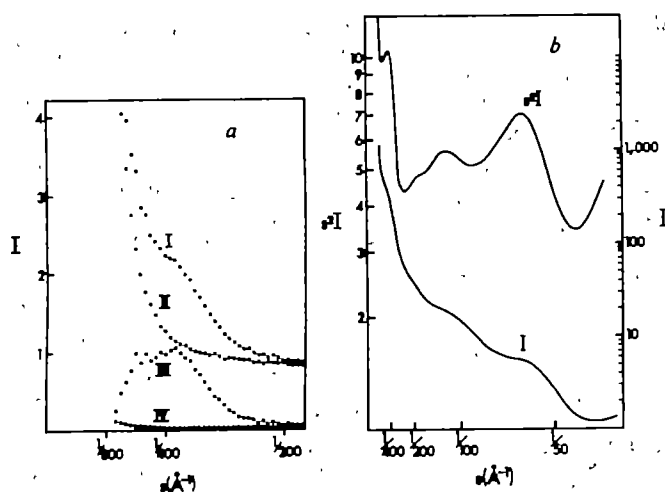
We are confident that the 400 Å band is of chromosomal origin because it is eliminated by nuclease treatment (Fig. 3a). Also thin sections of embedded erythrocytes reveal periodicities of comparable spacings only in the chromocentres (condensed regions of chromatin) and a lack of extraneous cytoplasmic and nuclear structures such as ribosomes, microtubules, mitochondria and nucleoli, which might in other cell types give rise to non-chromosomal low-angle bands. However, electron microscopy of chicken erythrocytes<sup>4</sup> and of isolated nuclei (unpublished results) indicate that the chromocentres have a granular internal structure with a periodicity of only 300 Å, apparently composed of square-packed thick fibres of ~300 Å diameter.



**Fig. 1** Low-angle X-ray diffraction patterns recorded on a Franks<sup>22</sup> camera with two 20-cm bent-glass mirrors and a 33.3-m specimen-to-film distance, mounted on a GX-13 rotating anode X-ray generator (Marconi-Elliott Avionics) producing 1.54 CuK $\alpha$  nickel-filtered radiation. The specimens were cooled to 5 °C and continuously translated over 2–3 cm during the X-ray exposure. The patterns were recorded on Ilford G film and uniformly developed. Aliquots of blood (1 ml, freshly collected with 10 unit ml<sup>-1</sup> heparin) were washed three times by centrifugation at 100g for 5 min in 10 ml of wash buffer (consisting of 130 mM NaCl, 5 mM KCl, 2 mM MgCl<sub>2</sub> and 10 mM HEPES, pH 7.3) and centrifuged into capillaries at 100g. X-ray exposure caused no noticeable haemolysis or uptake of trypan blue. Nuclei were prepared by lysis and resuspension of the pelleted cells three times for 3 min in 10 ml of MLB (consisting of 60 mM KCl, 15 mM NaCl, 15 mM HEPES, pH 7.3, 2 mM MgCl<sub>2</sub>, 0.1% Nonidet P-40 and 1  $\mu$ M fresh phenylmethylsulphonyl fluoride (PMSF)) and centrifuged into capillaries at 1,000g. SDS-polyacrylamide gel electrophoresis of nuclei after X-ray exposure showed no evidence of histone proteolysis. *a*, 4.2 h exposure from living chicken erythrocytes. *b*, 4.5 h exposure from living rabbit erythrocytes. *c*, 16.5 h exposure from wash buffer in capillary. *d*, Pattern from isolated chicken erythrocyte nuclei reproduced to illustrate the 60 Å and 38 Å bands. *e*, Pattern from isolated chicken erythrocytes reproduced to illustrate the 106 Å band. *f*, Pattern from isolated chicken erythrocytes (recorded at 44 cm specimen-to-film distance using Kodak Industrex AA film) reproduced to illustrate the 400 Å band. Length of the bar in *a* represents 1/50 Å<sup>-1</sup> in *a–e*. Bar in *f* represents 1/200 Å<sup>-1</sup> in *f*. *a–c* have been identically reproduced. The 400 Å shoulder is almost as visible by eye as the 106 and 60 Å features. The 200 Å shoulder is very weak and very difficult to visualize in photographic prints. The entire series of reflections from nuclei was consistently observed in more than 20 preparations using various conditions, including pH in the range 6–8, in the presence of 15 mM 2-mercaptoethanol, and in the presence of 1 mM CaCl<sub>2</sub>. Very small amounts of proteolysis eliminate the 400 Å shoulder.

\* Present address: Division of Biological Sciences and Biophysics Research Division, The University of Michigan, Ann Arbor, Michigan 48109.





**Fig. 2** Quantitative analysis of erythrocyte diffraction patterns. *a*, Measured chicken erythrocyte intensities (from the pattern shown in Fig. 1a); curve I, measured rabbit erythrocyte intensities (from the pattern shown in Fig. 1b); curve II, the difference between chicken and rabbit erythrocyte intensities; curve III, measured camera and solvent background (from the pattern shown in Fig. 1c) normalized to 4.3 h exposure time; curve IV, the mode of the difference curve is at  $\sim 380$  Å, and the mean is at  $\sim 410$  Å. *b*, The measured intensities from chicken erythrocyte nuclei in MLB showing a diffraction pattern on a steep background. I, average scattered intensity and  $s$ ,  $2 \sin(\theta/2)/\lambda$  where  $\theta$  is the scattering angle and  $\lambda$  the wavelength. By multiplying the recorded intensities by  $s^2$  we can correct for the random orientation of the fibres with respect to the X-ray beam, and for the high specimen background that seems to decrease as  $1/s^2$ , thereby calculating the true relative strengths (power) of the structural periodicities in the specimen. The chicken intensities are normalized to the rabbit intensities at  $0.005$ – $0.006$  Å $^{-1}$  using a multiplicative factor of 1.3 to correct for the slightly different cell concentrations in the two samples. In this angular range less than 10% of the scattering originates from the nuclei, as estimated by measurements of the steeply falling scattering from isolated nuclei. Two-dimensional densitometry was carried out using a 'Photoscan' (Optronics) controlled by an interactive computer program. A 50- $\mu$ m step size (equivalent to steps of  $s = 0.000098$  Å $^{-1}$ ) was used. Specular optical densities in the range 0–2 were measured and related to X-ray intensities using data applicable to Ilford G film<sup>22</sup>. The intensities at the centre of each pattern were displayed to allow the operator to determine the centre of scattering and to exclude unwanted areas of film from analysis. The scattering centre was established by briefly exposing the film to the direct X-ray beam, by moving the beam stop to one side after recording the diffraction pattern. The accuracy of this centre was checked by comparing the distribution of intensity with radius from above and below, and from left and right, of the centre. The centre was refined until the centre of analysis was to within one half raster unit (25  $\mu$ m) of the scattering centre. To exclude unnecessary camera background and the beam stop shadow on each pattern, a rectangular area covering these unwanted areas was excluded from analysis. Non-excluded data points in the two horizontal quadrants were averaged within annuli of different radii to give the average intensity distribution as a function of radius. The existence of the 400 Å band was also confirmed by the visual appearance of a 400 Å shoulder on all three films in the film pack and by the presence of the 400 Å shoulder in one-dimensional densitometer measurements.

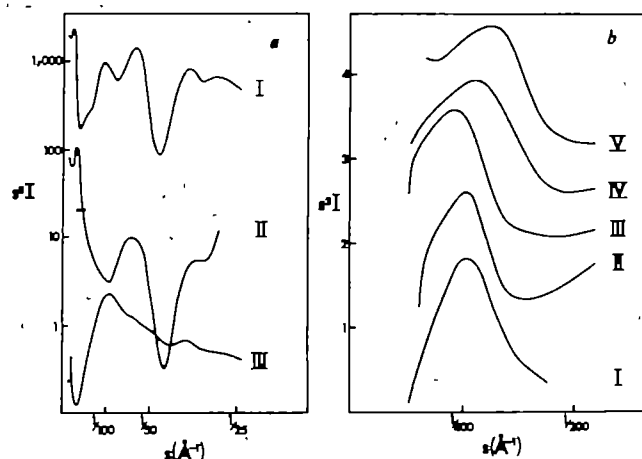
To establish the relevance of the X-ray spacing *in vivo* and *in vitro* to the microscopical structures, we recorded diffraction patterns during the different preparative steps for microscopy. Although fixation and uranyl acetate staining caused a slight expansion of the structure, ethanol dehydration and embedding in epoxy caused broadening and progressive shrinking of the spacing to 310 Å (Fig. 3b). This indicates that the apparent side-by-side partially ordered packing of 300 Å fibres observed by Davies<sup>4</sup> and us in thin sections is probably directly correlated to the more orderly packing of 400 Å fibres *in vivo*. In addition, dehydration distorts the internal structure of the fibres as shown by loss of the 106 and 60 Å bands and appearance of a broad 70 Å band (Fig. 3a), consistent with earlier studies of dehydration<sup>10,12</sup>.

When chromocentres are dispersed by replacing the MgCl<sub>2</sub> (2 mM) of MLB with 2 mM EDTA a homogeneous distribution of thick fibres within the nuclei is seen by electron microscopy and the 400 Å band disappears—all the other reflections are preserved (manuscript in preparation). This substantiates our hypothesis that the 400 Å spacing is from the packing of

nucleofibres and that the 200, 106, 60, 38, 30 and 22 Å periodicities reflect the internal structure of the fibres.

Do our results resolve any long-standing problems in the interpretation of chromatin X-ray patterns? Our consistent observation of a 106 Å band in each cell type and nucleus examined establishes this periodicity as characteristic of intact chromosomes. Previous investigators have been uncertain that this was an invariant feature of chromatin, especially in nuclei<sup>7,8,10,19,20</sup>. We have consistently found the 400 Å band present in chicken erythrocytes and erythrocyte nuclei and absent when the fibres are dispersed, which shows that this band is due only to fibre packing and not to periodicities within the fibres themselves. This contradicts Bram and collaborators who conclude that there is a concentration-independent 300–450 Å periodicity in isolated chromatin fibres<sup>15,20</sup>. Furthermore these investigators were unable to find the characteristic 106 Å band in isolated chromatin or nuclei, perhaps due to their use of very low ionic strength buffers.

The reflections seen in whole cells and isolated nuclei have been difficult to visualize due to their diffuse nature and steep background scattering. The lack of sharpness of the bands was not a preparation artefact, but was due to apparent disorder in chromosome structure. The width of the 400 Å band is probably due to heterogeneity or disorder in the packing of the nucleofibres or because the fibres are organized in small domains. Certainly chromosome fibres do not pack with the high degree of long-range crystalline order found in skeletal muscle or collagen. However, even after embedding in plastic, which causes considerable broadening of the packing band, nucleofibres show a degree of packing order easily recognized in electron micrographs. The diffuse nature of the 200, 106, 60, 38, 30 and 22 Å peaks is not inconsistent with a highly regular nucleofibre internal structure, because in the absence of excellent packing order there are several factors that result in broad bands, including inherent diffuseness of the molecular Fourier transform as in the case of the Bessel functions that describe diffraction from helical fibres, and also random fibre orientation, which leads to overlap of bands at similar angles. In fact, diffraction from the nucleofibre internal structure is no more diffuse than diffraction from randomly oriented double-stranded DNA in solution or in chromatin<sup>4,21</sup>. The presence of a



**Fig. 3** Effects of dehydration and nuclease digestion on X-ray scattering. *a*, Chicken erythrocyte nuclei in MLB (curve I), after embedding in Araldite (curve II), and after nuclease digestion (curve III). For embedding, nuclei were fixed in 1% glutaraldehyde for 10 min at 0 °C, washed in H<sub>2</sub>O, stained in 1% UO<sub>2</sub> for 10 min, dehydrated with increasing concentrations of ethanol, propylene oxide and then Araldite, followed by polymerization at 60 °C for 2 d. Nuclei at a concentration of about 100 A<sub>260</sub> per ml were digested at 37 °C for 15 min with 5,000 units of micrococcal nuclease and 300 units of DNase I. *b*, Diffraction patterns from chicken erythrocyte nuclei: Curve I, *in vivo* from Fig. 2a; curve II, isolated nuclei in MLB; curve III, isolated nuclei in water after fixation and staining as above; curve IV, fixed and stained nuclei in ethanol; curve V, fixed and stained nuclei embedded in Araldite. All curves are arbitrarily positioned on the ordinate in order to minimize overlap, and are therefore not meant to portray the relative intensities but to show the positions of the maximum and minimum in the  $s^2I$  function.



large amount of background scattering in the patterns from living cells and nuclei is not surprising because the fibres are not homogeneously distributed in the sample, but are concentrated in small chromocentres that strongly scatter X rays much as they do visible light. Centrifugation of the nuclei into a transparent pellet eliminates most of this background.

Although the local packing of nucleosomes within chromosomes is conserved among chicken erythrocytes, mouse lymphocytes, HeLa and MOPC-21 cells and several chromatin-containing sperm (as revealed by constancy of the 106, 60, 38, 30 and 22 Å spacings) higher order structure seems to be cell

dependent. For example, lymphocytes have a 330 Å rather than 400 Å periodicity, whereas sperm seem to lack a higher order spacing in the 300–500 Å range (unpublished data). These results suggest that variations in chromosome folding may involve only subtle changes in the local packing of nucleosomes.

J.P.L. was a postdoctoral fellow of the Jane Coffin Childs Fund for Medical Research and also NIGMS (GM06423-01). C.S. is a postdoctoral fellow of the Helen Hay Whitney Foundation. The work was completed under GM27937. We thank A. Klug for useful discussions and R. Staden and T. Wollard for technical assistance.

Received 11 September; accepted 16 October 1980.

1. Felsenfeld, G. *Nature* **271**, 115–122 (1977).
2. Ris, H. & Kubai, D. F. *A. Rev. Genet.* **4**, 263–294 (1970).
3. Davies, H. G. *J. Cell Sci.* **3**, 129–150 (1968).
4. Walmsley, M. E. & Davies, H. G. *J. Cell Sci.* **17**, 113–139 (1975).
5. Finch, J. T. & Klug, A. *Proc. natn. Acad. Sci. U.S.A.* **73**, 1897–1901 (1976).
6. Renz, M., Nehls, P. & Hozier, J. *Proc. natn. Acad. Sci. U.S.A.* **74**, 1879–1882 (1977).
7. Luzzati, V. & Nicolaieff, A. *J. molec. Biol.* **1**, 127–133 (1959).
8. Wilkins, M. H. F., Zubay, G. & Wilson, H. R. *J. molec. Biol.* **1**, 179–185 (1959).
9. Luzzati, V. & Nicolaieff, A. *J. molec. Biol.* **7**, 142–163 (1963).
10. Nicolaieff, A. in *Small Angle X-Ray Scattering* (ed. Brumberger, H.) 221 (Gordon and Breach, New York, 1967).
11. Garrett, R. A. *Biochim. biophys. Acta* **246**, 553–560 (1971).

12. Pooley, A. S., Pardon, J. F. & Richards, B. M. *J. molec. Biol.* **85**, 533–549 (1974).
13. Sperling, L. & Klug, A. *J. molec. Biol.* **112**, 253–263 (1977).
14. Carpenter, B. G., Baldwin, J. P., Bradbury, E. M. & Ibel, K. *Nucleic Acids Res.* **3**, 1739–1746 (1976).
15. Bram, S., Butler-Browne, G., Baudy, P. & Ibel, K. *Proc. natn. Acad. Sci. U.S.A.* **72**, 1043–1045 (1975).
16. Suau, P., Bradbury, E. M. & Baldwin, J. P. *Eur. J. Biochem.* **97**, 593–602 (1979).
17. Campbell, A. M., Cotter, R. I. & Pardon, J. F. *Nucleic Acids Res.* **5**, 1571–1580 (1978).
18. Thoma, F., Koller, Th. & Klug, A. *J. Cell Biol.* **83**, 403–427 (1979).
19. Olins, D. E. & Olins, A. L. *J. Cell Biol.* **53**, 715–736 (1972).
20. Baudy, P. & Bram, S. *Nucleic Acids Res.* **6**, 1721–1727 (1979).
21. Bram, S. & Beeman, W. W. *J. molec. Biol.* **55**, 311–324 (1971).
22. Franks, A. *Proc. phys. Soc.* **B68**, 1054–1064 (1955).
23. Morimoto, H. & Uyeda, R. *Acta crystallogr.* **16**, 1107–1119 (1963).

## Solid-like behaviour of unsheared sickle haemoglobin gels and the effects of shear

Robin W. Briehl

Departments of Physiology and Biochemistry, Albert Einstein College of Medicine, Bronx, New York 10461

**Pathogenesis in sickle cell disease depends on the polymerization of deoxyhaemoglobin S into long fibres followed by 'gel' formation. The 'gelation' renders the affected erythrocytes less deformable than normal so that they obstruct the microvasculature and the 'gelation' process has been one of the targets for the development of therapeutic treatments of sickle cell disease. 'Gelation', however, acts through the rheological properties it induces and rheological abnormalities are therefore the immediate bases of pathogenesis. Although there has been very little study of the rheology of haemoglobin S haemolysates, the 'gels' are generally considered to be highly viscous and thixotropic on the basis of gross observation. Limited and generally qualitative observations show that high viscosity depends on deoxygenation<sup>1,2</sup> and exhibits hysteresis in gelling/ungelling cycles<sup>3</sup>; also that shearing accelerates gelation<sup>3,4</sup> and can induce formation of fibre aggregates and crystals in suspension which, in contrast to the 'gel', are fluid<sup>5</sup>. Using transient and steady state methods it is shown here that unsheared sickle deoxyhaemoglobin preparations are solid-like, consistent with a gel-like nature, whereas shearing converts them to thixotropic viscous systems. These results underline the marked variation and thixotropy the system can undergo and may be relevant to the pathogenesis, clinical course and therapy of sickle cell disease.**

Haemoglobin S solutions were prepared from homozygous haemolysates by chromatography on Whatman DE 52 (ref. 6), dialysis into 0.1 M potassium phosphate, pH 7.0, and deoxygenation at 0°C under nitrogen only. These were transferred cold into a thermostatted Wells-Brookfield RVT Rheolog cone-plate microviscometer in a glove box kept free of oxygen by recirculation of 3% hydrogen in nitrogen over a palladium catalyst. The absence of oxygen was confirmed by (1) a methylene blue indicator, (2) polarographic analysis with a Clark electrode and (3) spectral examination of aliquots of haemoglobin removed from the viscometer. The viscometer cone angle ( $\alpha$ ) was 1.565° so that the speed range from 0.5 to 100 r.p.m. corresponded to shear rates from 1.92 to 384 per s. At 10 r.p.m. the relation between viscosity in centipoise,  $\eta_{cP}$ , and stress ( $\sigma$ ) in dyn cm<sup>-2</sup> is  $\eta_{cP} = 2.61\sigma$ . The cone radius ( $R$ ) was 2.4 cm. The

spring constant ( $k$ ) for the coupling between the synchronous motor and the cone was 1,760 dyn cm. Shearing stress was observed on a digital readout and a continuous record of it and temperature, measured with a thermistor attached to the viscometer cup, was obtained with a Hewlett-Packard 7754A oscillographic recorder. Full scale stress was 245 dyn cm<sup>-2</sup>, occurring at an angular lag of the cone behind the motor of 231°.

After the haemoglobin was introduced into the viscometer, shearing was begun at 10 r.p.m. and gelation was induced by a step increase in temperature. The half time of the step was about 2 s and, the last stages of warming being slower, final temperature was attained within 0.2°C in about 2 min. (Confirmation that sample temperature increased at the same rate as that of the cup was obtained by observing the viscosity of a mixture of glycerol, 75% by weight in water, during a step increase in temperature.) Deoxyhaemoglobin S viscosity remained constant during the delay period incubation<sup>7,8</sup>, after which it began to increase. For preparation of unsheared gels, the viscometer was turned off when viscosity reached 13 cP, about 4 times the solution value, and annealing under neither stress nor shear was then permitted for 30 min.

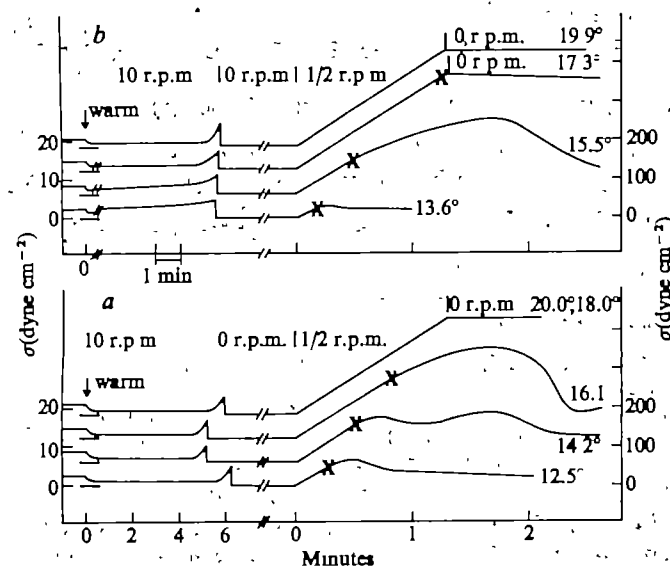
After each experimental procedure, the gel was melted by cooling to 1–2°C for 1 h, the first 10 min in the absence of shear, followed by 40 min at 100 r.p.m. and then 10 min at 10 r.p.m. before the next induction of gelation by warming. Supportive evidence that this melting procedure fully reversed the gelation is provided by (1) the return of viscosity to the previous cold level, (2) constancy of viscosity towards the end of the 40 min period, (3) the reproducibility of the delay time and viscosity progress curve in the next induction of gelation and (4), the lack of change in observed properties of the gel when an experiment was repeated.

In Fig. 1a a gel incubated and annealed at 20°C was subject to slowly increasing stress when the viscometer motor was turned on at 0.5 r.p.m. After the linear increase in stress, upon attaining full scale, the motor was stopped. Stress did not decay. In experiments of up to 10 days, no decay was seen (to within one part in 250). Employing the equation for viscous decay of stress in a cone-plate geometry  $\sigma = \sigma_0 \exp(-3kat/2\pi R^3\eta)$  where  $t$  is time and  $\eta$  is viscosity (in poise), viscosity must be higher than  $3 \times 10^{10}$  cP. This very large value justifies designating the gel as solid-like rather than viscous. When, in some experiments, stress was relieved by rewinding the motor manually, re-application of stress produced identical results, confirming that the solid-like nature of the gel was not damaged.

During application of stress, the rate of increase was, within the limits of measurement (~1%), the same as that obtained (the

maximum rate) when similar stressing was carried out with the cone held fixed by water frozen in the viscometer. Therefore, the cone remained essentially immobile and the gel suffered little or no deformation; that is, because the rate of stress increase reflects deformation of the coupling spring, the rate of rotation of the cone, here essentially zero, can be calculated. A deviation of 1% in the rate of increase of stress from the maximum rate would correspond to an elastic shear modulus of  $165 \text{ dyn cm}^{-2}$ , hence the modulus for the gel was equal to or greater than this.

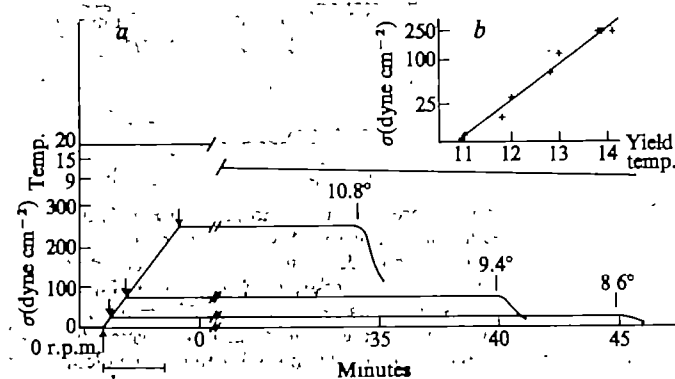
At the three lower temperatures in Fig. 1a the gels showed yield values and peak stresses, both decreasing with decreasing temperature. Figure 1b shows a similar series of experiments, differing only in the time at which temperature was adjusted to the final level; the essential results are the same. Therefore, solid-like strength of gels, manifested in a yield stress, depends



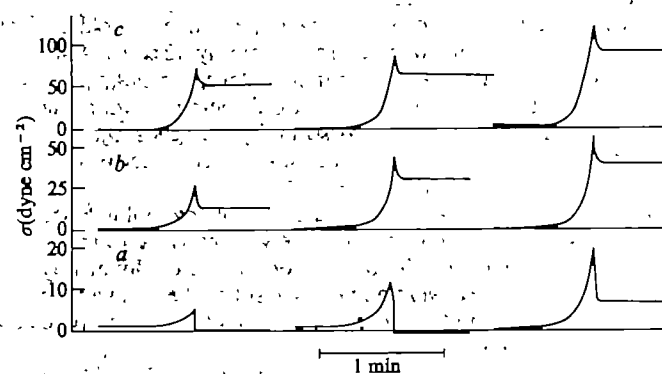
**Fig. 1** *a*, Unsheared gels hold stress up to a yield stress, which depends on temperature. Five experiments were done sequentially on a sample 13.5 mM in haem at different temperatures. The ordinates represent shearing stress ( $\sigma$ ) with a scale factor difference of 10 between left and right hand ordinates; the changes occur at the diagonal lines, at which time there is also a break in the time scale. The zero point on the ordinate scale applies to the experiment at  $12.5^\circ\text{C}$ ; the other curves are displaced upwards for clarity, with each baseline indicated. In each experiment a temperature jump (at the arrow) from  $1^\circ\text{C}$  to  $20^\circ\text{C}$  under shear at 10 r.p.m. resulted in a fall in viscosity (associated with warming). At the end of the delay period, stress and viscosity ( $\eta_{sp}/c = 2.61\sigma$ ) rose until shearing was stopped. The temperature was then decreased in a few minutes from  $20^\circ\text{C}$  to that of the subsequent stressing experiment and the gel was annealed for 30 min under no stress or shear. Stress was then applied by running the synchronous motor at 0.5 r.p.m., stopping it only if stress reached full scale (as in the experiments at  $20.0^\circ\text{C}$  and  $18.0^\circ\text{C}$ ). At  $20.0^\circ\text{C}$  and  $18.0^\circ\text{C}$  the curves were superimposable and both gels held stress at full scale with no decay. At the three lower temperatures the stresses at which the gels broke (as defined by a deviation of  $5 \text{ dyne cm}^{-2}$  from the line of maximal rate of stress increase) are indicated (X); these curves also showed maxima in stress as shearing at 0.5 r.p.m. was continued. *b*, In these experiments (on a different sample) gelation was induced by a temperature jump to a level which then remained unchanged through incubation, annealing and stressing. The delay times associated with the serially decreasing temperatures were 5.7, 11.0, 18.0 and 34.6 min. The viscosity progress curves differed and were more rapid at higher temperatures. The time scale is broken during incubation to make the starts of the 30 min annealing periods coincident. At  $19.9^\circ$  rotating the motor at 0.5 r.p.m. induced stress increase at the maximal rate. After the motor was stopped there was a very slow decay of stress. At  $17.3^\circ\text{C}$  a yield stress was attained just before full scale stress was attained; decay at 0 r.p.m. thereafter was more marked. At the two lower temperatures, successively smaller yield stresses and peak stresses occurred.

on temperature in the manner which would be expected from the endothermic nature of gelation<sup>1,9</sup>. The energy of activation calculated from the delay times in Fig. 1b is  $50 \text{ kcal mol}^{-1}$ , neglecting any temperature-dependent effect of shearing.

Figure 2 defines a yield temperature and, reciprocal to the temperature dependence of yield stress in Fig. 1, shows that it depends on stress.

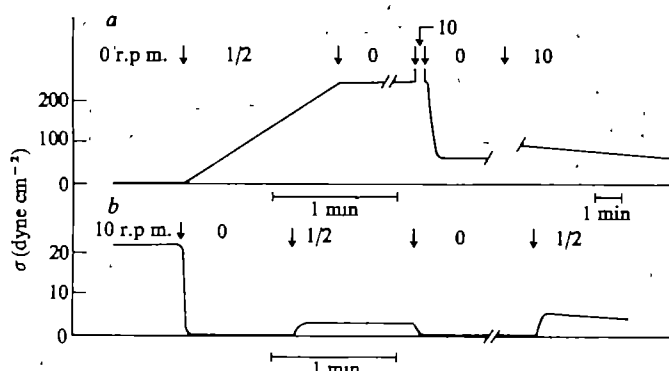


**Fig. 2** Stress dependence of yield temperature. *a*, in separate experiments on a 14.0 mM sample, gels were formed and then annealed at  $20^\circ$  for 30 min as in Fig. 1a. Each gel was then stressed ( $\uparrow$ ) by rotation of the motor at 0.5 r.p.m. until the desired stress was reached ( $\downarrow$ ). At this stress, which did not decay, the gel was cooled slowly, beginning at time 0, until a rapid relaxation occurred, indicative of breaking of the gel. The yield temperatures thus defined, shown on each curve, decrease with decreasing applied stress. The time scale is broken at the diagonal lines. The temperature decrease shown is a superposition of the experiments and, because there were small variations in the rate of cooling, the times of breaking shown are approximate (within 1 min). The yield temperatures at the two higher stresses are each the average of two experiments, differing by  $0.2^\circ\text{C}$  or less. *b*, The dependence of yield temperature on stress (plotted logarithmically) is shown over a large, 40-fold, range of stress in a series of experiments on another sample, 13.7 mM in haem.



**Fig. 3** Solid-like behaviour of gels during the growth stage of gelation. Nine experiments on a 13.4 mM sample at  $26^\circ\text{C}$  are shown. The delay times (defined here as the time required for viscosity to reach 13 cP) were all between 3.62 and 3.82 min. Shearing was carried out at 10 r.p.m. until a desired viscosity, from 13 cP in the first experiment in *a* to 320 cP in the last in *c*, was attained. In *a* full and rapid relaxation to zero stress occurred in the first experiment. In the second, spindle inertia induced a transient oscillation (off scale, below 0) in stress with a final constant value of  $-1.5 \text{ dyn cm}^{-2}$ . In the third experiment the motor was stopped when viscosity was 56 cP. Full relaxation did not occur, as was also the case in all experiments in *b* and *c*. These gels held stresses without long term decay and were therefore solid-like rather than viscous. The rapid partial relaxation occurring immediately after peak viscosity is in whole or part an artefact associated with inertial properties of the cone spindle; it continued to rotate briefly after the motor had stopped and thus the transient rapid decay reflects this as well as (or instead of) any inability of the gel to hold the maximum stress attained. Thus, the final asymptotic stress is a lower limit on the stress the gel might hold.





**Fig. 4** Well sheared gels are viscous. *a* shows, as in Fig. 1, the stressing after annealing of a gel of 13.5 mM deoxyhaemoglobin S at 20°C; full scale stress was held. Then the gel was sheared at 10 r.p.m. for 10 s (during which stress was off scale), resulting in partial relaxation to an asymptotic stress of 64 dyn cm<sup>-2</sup>, indicating viscoplastic behaviour. Fifteen minutes later (during 8 of which the gel was sheared at 10 r.p.m.) the gel showed a time-dependent thixotropic decay in viscosity under continuing shear at 10 r.p.m. After prolonged shear for 120 min at 10 r.p.m., the viscosity reached a final constant value, shown at the start of *b*. Stopping the viscometer then resulted in rapid relaxation to zero stress. Under stressing at 0.5 r.p.m. the gel failed to hold any significant stress, a constant level reflecting viscosity only being attained. On stopping the motor, relaxation was again complete. After 30 min of annealing under no shear, the final part of *b* shows that rotation of the motor at 0.5 r.p.m. resulted in a peak in stress higher than that in the previous stressing, followed by a fall to a level dictated by viscosity, also higher than previously, indicating that some reannealing occurred.

In Fig. 3 shearing was continued after the delay period into the stage of fibre growth<sup>4</sup> to different levels of viscosity. When shearing was stopped after viscosity had reached about 50 cP or more little or no relaxation occurred and the gels held large stresses, showing that the rheological behaviour was essentially solid-like rather than viscous.

By contrast, Fig. 4 shows that well sheared gels held no measurable stresses and were therefore purely viscous. Also, (apparent) viscosity decreased with time under shear and, after a period of no shear, reannealing occurred, demonstrating the presence of viscous thixotropy. Also in Fig. 4, gels subject to brief shear were viscoplastic, manifesting viscous decay to a non-zero asymptotic stress.

These results show that unsheared gels of haemoglobin S are solid-like, well sheared gels are purely viscous, and intermediate, viscoplastic conditions also occur. Also, thixotropy exists in the sense of conversion between solid-like and viscous behaviour as well as in the more usual sense of shear and time dependence of viscosity.

This observation of solid-like behaviour with a plastic yield stress provides justification for the designation 'gel', applied previously even though the system was generally described as 'highly viscous'.

The existence of solid-like properties may have a bearing on pathogenesis in sickle cell disease. An erythrocyte containing a purely viscous interior would deform to an extent dependent on the time integral of stress and thus might eventually pass the microvasculature. On the other hand, a solid-like erythrocyte could not deform unless a critical yield stress were attained. Because shearing history governs the solid-like or viscous nature of the gel, it may also govern the pathogenic potential of each erythrocyte. Whether shear is a favourable or unfavourable factor, however, depends on its effect on gel rheology and also on the fact that it accelerates the delay stage of gelation<sup>3,4</sup>.

Generally, these observations show that gel rheology is highly modifiable even in the absence of alteration of the thermodynamics and kinetics of gelation, and thus that pathogenesis in this highly variable disease may be influenced by the highly variable rheology of gels.

This work was supported in part by United States Public Health Service research grant HL 07451 from the National Heart, Lung and Blood Institute and in part by a grant-in-aid from the New York Heart Association. I thank Nina Louie, Audrey Walker and Jay Zuckerman for technical assistance.

Received 28 July, accepted 7 October 1980

1. Allison, A. C. *Biochem J* **65**, 212-219 (1957)
2. Choon, S., Usami, S., Jan, K.-m., Smith, J. A. & Bertles, J. F. in *Proc. Symp. on Molecular and Cellular Aspects of Sickle Cell Disease* (eds Hercules, J. I., Cottam, G. L., Waterson, M. R. & Schoedter, A. N.) 277-300 (DHEW Publication No. (NIH) 76-1007, 1976)
3. Harris, J. W. & Beuteman, H. B. *J. Lab. clin. Med.* **86**, 564-575 (1975)
4. Briehl, R. W. in *Symp. on the Molecular Basis of Haemoglobin Dysfunction* (ed. Segler, P. B.) (Elsevier, Amsterdam, in the press)
5. Humphrey, J. F. & Steinhardt, J. *Biochem. biophys. Res. Commun.* **69**, 99-105 (1976); *J. molec. Biol.* **112**, 359-375 (1977)
6. Briehl, R. W. & Ewert, S. *J. molec. Biol.* **88**, 445-458 (1973); **89**, 759-766 (1974)
7. Malha, R. & Steinhardt, J. *Biochem. biophys. Res. Commun.* **69**, 887-893 (1974)
8. Hofrichter, J., Ross, P. D. & Eaton, W. A. *Proc. natn. Acad. Sci. U.S.A.* **71**, 4864-4868 (1974)
9. Murayama, M. *Febs Lett.* **15**, 318 (1956)

## A variant surface glycoprotein of *Trypanosoma brucei* synthesized with a C-terminal hydrophobic 'tail' absent from purified glycoprotein

J. C. Boothroyd\*, G. A. M. Cross\*, J. H. J. Hoelmakers† & P. Borst†

\* Wellcome Research Laboratories, Langley Court, Beckenham, Kent BR3 3BS, UK

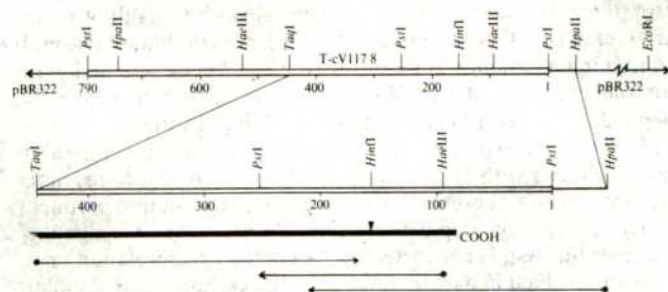
† Universiteit van Amsterdam, Afdeling Medische Enzymologie, Laboratorium voor Biochemie, Jan Swammerdam Instituut, PO Box 60.000, 1005 GA, Amsterdam, The Netherlands

Sequential expression of variant surface glycoproteins (VSGs) enables the parasitic protozoan *Trypanosoma brucei* to evade the immune response of its mammalian hosts<sup>1,2</sup>. Studies of several VSGs, which have been isolated as soluble molecules following disruption of cells in the absence of detergent, have indicated extensive amino acid diversity<sup>3-5</sup> and the absence of a hydrophobic segment which might serve to anchor the carboxy terminus to the membrane<sup>6</sup>. The carboxy-terminal tryptic peptides of six VSGs have recently been characterized and shown to be glycosylated<sup>6</sup>. Three of these VSGs terminated with a glycosylated aspartate or asparagine residue (Asx), suggesting that the VSG was cleaved following synthesis and glycosylation and before characterization. We present here nucleotide sequence data which suggest that the primary translation product of one VSG gene contains a hydrophobic tail at the carboxy terminus which is not found on the isolated, mature glycoprotein<sup>6</sup>. The data also predict that the glycosylated residue is aspartic acid rather than the anticipated asparagine.

We have recently reported the synthesis and molecular cloning into the plasmid pBR322 of complementary DNA (cDNA) molecules corresponding to the VSGs of four variants of a single clone of *T. brucei*<sup>7</sup>. As extensive amino acid sequence data on one of these VSGs (VSG 117) already existed (G. Allen, personal communication), we have selected the corresponding recombinants (T-cV117·1-8) for further study. As purified VSG 117 terminates with a glycosylated Asx<sup>6</sup>, suggesting post-glycosylation proteolytic cleavage of a VSG precursor, we decided first to determine the nucleotide sequence corresponding to the 3' end of the mRNA, coding for the carboxy terminus of the protein.

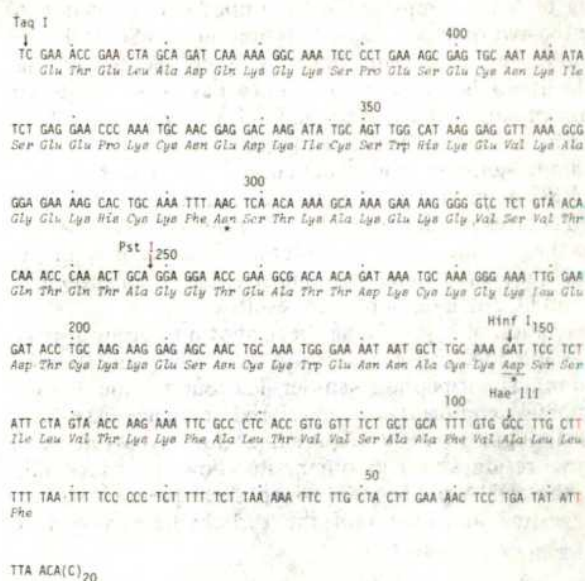
A physical map of the cDNA insert which extended furthest in the 3' direction (T-cV117·8) and the protein region it covers is given in Fig. 1. Also shown are the regions where useful nucleotide sequence information was obtained. Figure 2 presents a representative sequencing gel corresponding to the carboxy-terminal portion of the protein. The complete nucleotide sequence of this region and the implied amino acid sequence are



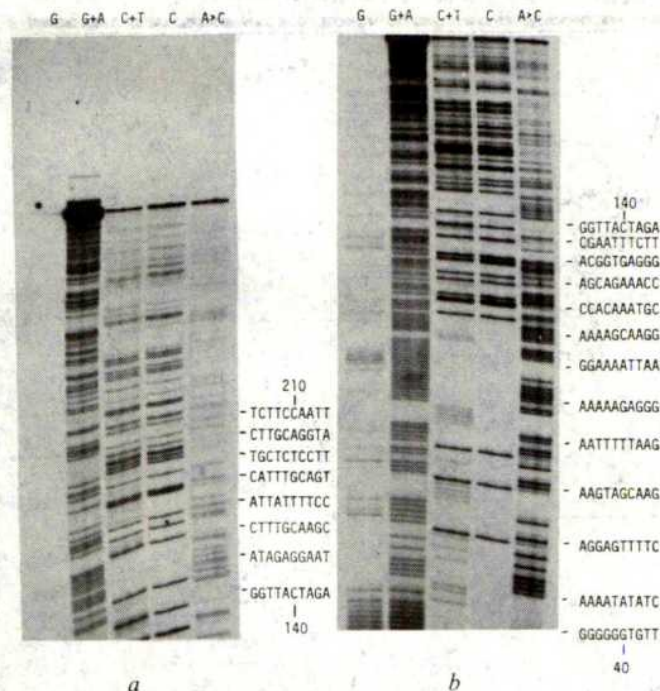


**Fig. 1** Physical map of T-cV117.8 showing restriction endonuclease cutting sites. Distances are in base pairs from the end of the insert nearest the *EcoRI* site of pBR322. These data were obtained by standard mapping procedures and subsequently confirmed by the DNA sequence. Beneath the map are shown the region of the insert which codes for the putative primary translation product and the carboxy terminus of the mature VSG (V). Below this are shown the sites which were [ $5'$ - $^{32}$ P]-end-labelled (●) and the regions where useful sequence information was obtained (→).

given in Fig. 3. The fact that there is neither a poly(A) stretch before the dC tail in Fig. 3 nor the sequence (AATAAA) usually found about 25 nucleotides upstream of the site of poly(A) addition<sup>8</sup> suggests that T-cV117.8 does not extend to the 3' end of the VSG 117 mRNA. This may be an artefact of the process by which these recombinants were constructed or selected<sup>7</sup>. The inferred amino acid sequence shown in Fig. 3 is in complete



**Fig. 3** Summary of nucleotide and protein sequence data. The nucleotide sequence of the coding strand between positions 445 and 1 (see Fig. 1) is given together with the implied amino acid sequence. Only one reading frame is open. The carboxy-terminal residue of the mature, isolated glycoprotein is underlined (see text). Glycosylated residues are marked with asterisks. (C)<sub>20</sub> indicates the dC-tail used to anneal the cDNA insert to the dG-tailed plasmid.



**Fig. 2** Autoradiograph of a representative sequencing gel corresponding to the carboxy terminus of VSG 117. A *HpaII* fragment of DNA from T-cV117.8 was [ $5'$ - $^{32}$ P]-end-labelled with polynucleotide kinase, recut with *TaqI* and purified on a 7% polyacrylamide gel essentially as described<sup>14</sup> except that the eluted fragment was further purified by binding to a 1-ml column of diethylaminoethyl-cellulose followed by elution in 0.5 M NaCl. Base-specific modifications and cleavage were as described<sup>14</sup>, with minor alterations as recently recommended by the authors (A. Maxam and W. Gilbert, personal communication). Analysis was on a thin (0.4-mm) 8% polyacrylamide gel in 7 M urea run at high voltage (1.6–2.0 kV) to reduce secondary structure effects<sup>15</sup>. Aliquots of each sample were loaded on to different tracks of the same gel at 0 (a) and 120 min (b), the gel being run for a total of 270 min. After cooling, the gel was fixed by immersing in 10% (v/v) acetic acid for 20 min, dried under vacuum with heat and autoradiographed at  $-70^{\circ}\text{C}$  in a Kodak cassette containing a Dupont Cronex Xtra-life intensifying screen. The nucleotide sequence corresponding to the C-terminal region of the protein is given to one side. This sequence is of the noncoding strand, the nucleotides being numbered as in Fig. 1.

agreement with independently derived data from the purified glycoprotein (ref. 6 and G. Allen, personal communication) except that protein sequencing indicated the carboxy terminus to be exclusively glycosylated Asx at position 154, whereas the nucleotide sequence shows 23 sense codons beyond this position before a stop codon is reached. It seems, therefore, that at some time after translation of the polypeptide and before characterization of the VSG, a highly specific proteolytic cleavage has occurred 23 amino acids in from the carboxy terminus.

Although we have not directly examined the carboxy-terminal sequence of the primary mRNA translation product, it is a reasonable assumption that it contains the extension predicted by the DNA sequence. This would be consistent with our previous observation<sup>7</sup> that 117 VSG mRNA translated *in vitro* yields a polypeptide which seems to be slightly larger on SDS-polyacrylamide gels than mature VSG isolated from trypanosomes, despite glycosylation of the latter which should increase its apparent molecular weight. The amino acid sequence towards the end of the predicted extension is extremely hydrophobic. We have been unable to define the role of the hydrophobic extension and the time at which it is cleaved. The fact that all six VSGs studied terminate with a glycosylated amino acid<sup>6</sup> suggests cleavage may be a specific event common to VSG processing in *T. brucei*.

Hydrophobic carboxy termini have been reported in surface proteins of influenza virus<sup>9</sup> and *Bacillus stearothermophilus*<sup>10</sup> and may generally serve to anchor membrane-bound cell-surface proteins<sup>11</sup>. Observations that carboxy-terminal glycopeptides of trypanosome VSGs carry an immunologically cross-reacting group<sup>6</sup>, which on living cells is not accessible to antibody<sup>12</sup>, are consistent with the carboxy terminus being in close proximity to the surface membrane. If present in the VSG molecules forming the surface coat of living trypanosomes, the hydrophobic extension could serve a membrane-binding function. However, no precedent exists for the rapid and specific cleavage which would be required to explain the observation that mature VSG is released on cell disruption, even when several inhibitors of proteolysis are present (G.A.M.C., unpublished observations). The existence of such a mechanism for specific cleavage and release of VSG from the cell surface suggests a role in antigenic variation, possibly in allowing



shedding of VSG complexed with antibody. Clarification of whether the hydrophobic extension is present on VSG at the cell surface must await the results of further experiments. Alternatively, the hydrophobic extension could act as a signal sequence during processing and secretion of VSG and could have been removed before arrival at the cell surface (in a manner analogous to amino-terminal leader sequences<sup>11</sup>). Comparison of the mature VSG amino terminus with the sequence inferred from the cDNA corresponding to the 5' end of the mRNA, however, indicates the presence of an amino-terminal extension similar to the signal sequences found on almost all secreted proteins<sup>11</sup> (J.C.B. and G. Allen, unpublished results).

Glycosylation of VSG 117 has been shown to occur at positions 304 and 154 (Fig. 3; ref. 6 and G. Allen, personal communication). The tripeptide Asn-Ser-Thr found at the first site (position 304) conforms to the general sequence Asn-Xxx-Ser/Thr thought to be a requirement for glycosylation at asparagine residues<sup>13</sup>. The other site, however, does not. Instead, the cDNA predicts the tripeptide sequence Asp-Ser-Ser, suggesting attachment of the carbohydrate moiety to

aspartate. To dismiss the possibility that this result was an artefact of the cDNA cloning procedure, a recombinant plasmid containing a genomic copy of the VSG 117 gene was analysed for the presence of the *Hinf*I cleavage site which is strictly dependent on the critical Asp codon (*GATTC*, positions 155–151, Fig. 3). The site was indeed present as defined by single and double digests with *Hinf*I and *Pst*I (J.C.B., unpublished results). It seems certain, therefore, that the primary translation product, at least, has Asp at position 154. We are now investigating whether the Asp is converted to Asn before glycosylation or is instead involved in a novel linkage to the carbohydrate. Similar analyses of cDNAs for other VSGs (now underway) should indicate whether the hydrophobic extension and glycosylated aspartic acid are universal features of the surface glycoproteins of *T. brucei*.

We thank C. A. Paynter for technical assistance, K. M. O'Hare and A. J. Newman for helpful advice and suggestions, G. Allen and A. A. Holder for communicating results before publication and critical reading of the manuscript, and A. C. C. Frasch, A. Bernards, C. Weissmann and M. Winther for supplying recombinant clones of VSG 117.

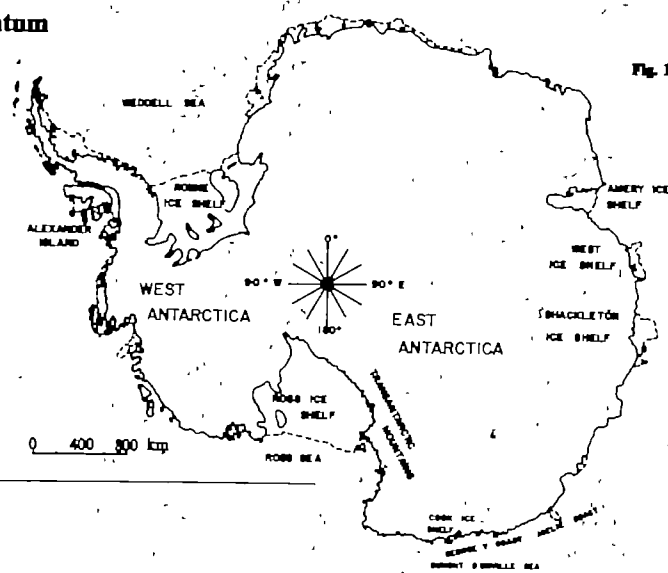
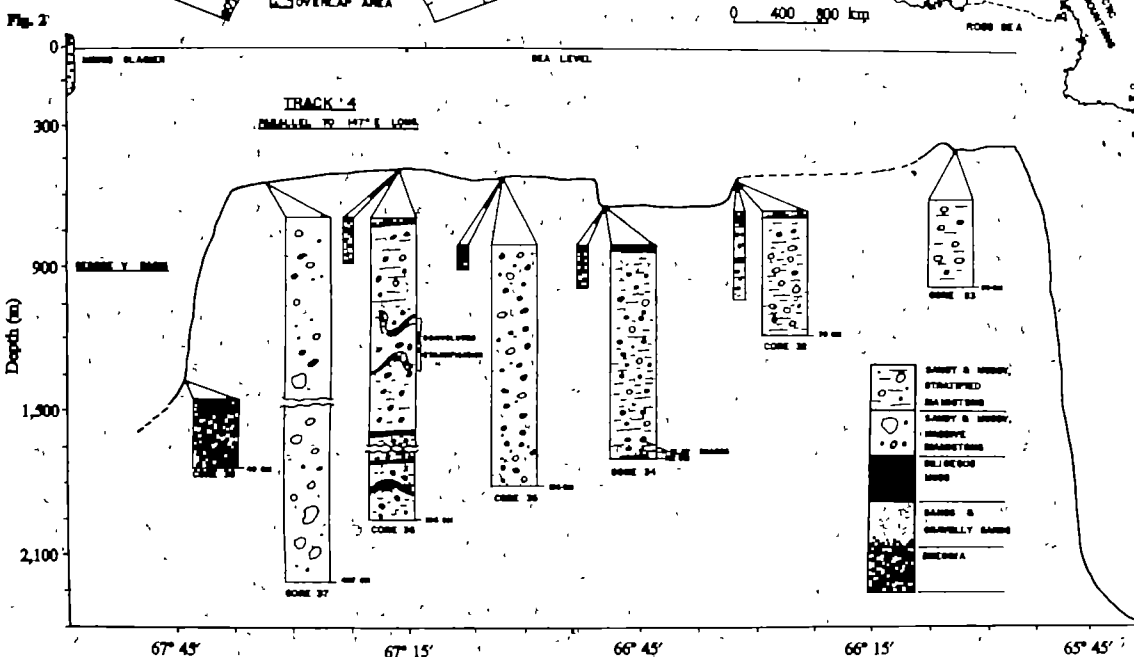
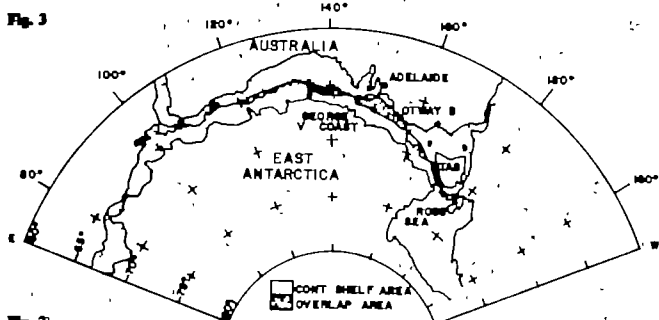
Received 7 June; accepted 1 October 1980

1. Vickerman, K. *Nature* **273**, 613 (1978)
2. Cross, G. A. M. *Proc R Soc B202*, 55 (1978)
3. Cross, G. A. M. *Parasitology* **71**, 393 (1975)
4. Bridgen, P. J., Cross, G. A. M. & Bridgen, J. *Nature* **263**, 613 (1976)
5. Johnson, J. G. & Cross, G. A. M. *Biochem J* **178**, 689 (1979)
6. Holder, A. A. & Cross, G. A. M. *Molec Biochem Parasit* (in the press)
7. Hoernschemper, J. H. J., Borst, P., Van den Burg, J., Weissmann, C. & Cross, G. A. M. *Gene* **8**, 391 (1980).

8. Proudfoot, N. J. & Brownlee, G. G. *Nature* **263**, 211 (1976)
9. Porter, A. G. *et al* *Nature* **282**, 471 (1979)
10. Waxman, D. J. & Strominger, J. L. *J Biol Chem* **254**, 4863 (1979)
11. Davis, B. D. & Tai, P.-C. *Nature* **283**, 433 (1980)
12. Barbet, A. F. & McGuire, T. C. *Proc natn Acad Sci U S A* **76**, 1989 (1980)
13. Marshall, R. D. *Biochem Soc Symp* **40**, 17 (1974)
14. Maxam, A. M. & Gilbert, W. *Proc natn Acad Sci U S A* **74**, 560 (1977)
15. Sanger, F. & Coulson, A. R. *FEBS Lett* **87**, 107 (1978)

### Erratum

Figures 1, 2 and 3 were omitted from the letter 'Lower Cretaceous sediment from the East Antarctic continental shelf' by E. W. Domack *et al.* *Nature* **287**, 625–626.



**Fig. 1** Map of the Antarctic continent showing the locations of regions mentioned in the text.  
**Fig. 2** Profile of the continental shelf off the George V coast showing the relationship of core 38 to other sediments of the shelf (after ref. 7, Fig. 24).  
**Fig. 3** Morphological reconstruction of Australia and East Antarctica showing the positions of localities mentioned in the text (after ref. 9, Fig. 3).

## BOOK REVIEWS

# Science East and West: reflections of Peter Kapitza

Nevill Mott

PETER Leonidovich Kapitza was born on July 9, 1894, and began his scientific work in the Polytechnic Institute of St Petersburg, from which he graduated in 1918. In 1921 he was sent by the Soviet authorities to work under Lord Rutherford in Cambridge, where he stayed until 1934, the Royal Society Mond Laboratory being built especially for his work on the development and effects of high magnetic fields and low temperatures. During this time he retained his Soviet citizenship, returning to Russia from time to time and telling his friends that he thought he was the only man of his country with a passport endorsed for unlimited journeys. However, in 1934, while attending a conference in Leningrad to celebrate the one-hundredth anniversary of the birth of Mendeleev, he was told that he could not return to Britain, and would have to continue his work in the Soviet Union. I was at the same conference, and remember the impression that Kapitza's Rover car, driven from Bergen round the gulf of Finland, made among the few official cars in the streets of Leningrad. In Russia he continued work in low-temperature physics, for which he was awarded a Nobel prize in 1978; after the War he was accused of giving wrong advice about oxygen production and was excluded from his laboratory for several years; rehabilitated, he turned to plasma physics (not nuclear energy as is sometimes thought), and in the past few years has been able to travel abroad.

This book, translated from the Russian, contains a collection of articles and addresses delivered by Kapitza during the past 50 years. Many have appeared elsewhere, for instance "Recollections of Lord Rutherford" and a biographical memoir of L.D. Landau published by the Royal Society, of which Kapitza is a Fellow. His reverence for and gratitude to Rutherford are well known; he writes:

... in the year that Rutherford died there disappeared forever the happy days of free scientific work which gave us such delight in our youth. Science has lost her freedom. Science has become a productive force. ... rich but enslaved, part of her veiled in secrecy.

Sir Nevill Mott is Emeritus Professor of Physics at Cambridge University; he knew Kapitza well between 1930 and 1934.

*Experiment, Theory, Practice: Articles and Addresses of P.L. Kapitza.* Boston Studies in the Philosophy of Science, Vol.46. Pp.429. (Reidel: 1980.) Hardback Dfl.90, \$47.35; paperback Dfl.28, \$14.75.



Peter Kapitza, July 1973

He writes, too, a moving appreciation of Paul Langevin, and of other figures from the past. From the past few years, when he could travel, come addresses to international bodies, such as one on the impact of modern scientific ideas on society to the Unesco symposium on the centenary of Albert Einstein. A few sentences will reflect his views about the way society is going in the developed countries of East and West alike.

The state compels a person to abide by its laws, and society compels him to live in accordance with his traditions. After a certain degree of well-being has been reached people begin to lose their liberty as their prosperity increases, and already the freedom of the individual in the developed countries is extremely limited. Modern society strives to organise people's lives in such a way that they will have an impression of freedom despite their lack of it. This is achieved by means of propa-

ganda and by turning people's interest towards sport, sex and entertainment so as to distract them from reality. Such were the principles on which society was organised in Aldous Huxley's *Brave New World*.

Kapitza seems to feel that it is not so very different in East and West. And in view of this, perhaps the most interesting parts of the book for the Western reader are his addresses to the Presidium of the Academy of Sciences of the USSR, for instance one in 1964, "The Effectiveness of Scientific Work". Here perhaps East and West do not appear so equal. He writes, in criticizing the situation in his own country:

An important factor in morale is to take part in scientific life abroad — at conferences and similar gatherings. As yet we take little part in them. Our delegates are still only one quarter or one fifth as many as those of the USA or other countries [are they now as many?] and often the delegates are selected by bureaucratic methods. . .

And in the same article, he writes that now nearly all those who should be leaders of science spend their time on committees, how every rouble must be accounted for even though money for research is not lacking. A director

cannot dismiss anyone, nor can he provide any incentive. The fettering of the Director, his restricted role in this important matter, is one of the reasons for the low efficiency of our institutes.

The book reveals Peter Kapitza's qualities that all his friends know well — his enormous courage, irrepressible vitality and humour. On humour, writing about theory and experiment, he quotes from the novel, *Gentlemen Prefer Blondes*, "that classical American work. . . 'Love is a good thing but a golden bracelet is forever'." His memory plays him wrong (or does he, as seems hardly credible, quote from a Russian translation?). What Anita Loos wrote in 1925 was "kissing your hand may make you feel very, very good but . . .". However, the point that Kapitza makes is that "theory is a good thing but a good experiment lasts for ever". Rutherford would have agreed, with the last part at any rate.



# Models and mergers in mathematical ecology

Oscar Kempthorne

*Theory of Population Genetics and Evolutionary Ecology: An Introduction.* By J. Roughgarden. Pp.576. (Collier-Macmillan: 1980.) \$24.95, £15.95.

THIS large book is an attempt to present the basic ideation behind two fields of biology — population genetics and ecology — and to initiate the merger between the two which has long been overdue. Population genetics had a pre-Mendelian start with Galton, but, of course, it was the discovery of the Mendelian processes that led to the useful application of concepts of mathematical probability to the subject. Over the same period that Fisher, Wright and Haldane were formulating mathematical theories of the genetics of populations, workers such as Kostitzin, Lotka, Volterra and Gause were developing ideas about the dynamics of populations. In writing this book, Roughgarden is following the tradition of Haldane, Fisher and Norton who took the initial steps in combining the two streams of thought.

Roughgarden's purpose is to formulate mathematical models that incorporate aspects of birth, ageing and death, and to establish the consequences of such models. The mathematics involved in doing this become rather complex, but there is no doubt that this is one of the necessary approaches to a greater understanding of many biological processes. The result of this is that it is now common — indeed necessary — for departments of biology to include members of staff who have had a rigorous training in both biology and mathematics. Roughgarden is obviously an exemplar; he has made a fine effort to give an overall picture of a complicated field.

His book consists of five parts. The first is concerned with the basis of the subject, and in it he develops the elementary theory of a simple infinite Mendelian population with a two-stage life. Individuals contribute according to genotype (but not sex) to male and female genetic pools, newborns arising by the random union of gametes. This leads into what Roughgarden calls "Wright's adaptive topography" (an unfortunate term), with the correct (but misleading) result that such a population will move towards maximum mean fitness. The rest of the opening part of the book is taken up with considerations of the fundamental theorem of natural selection for asexual populations — which has no genetic content at all — genetic drift (for a diallelic locus) and the neutrality controversy. This last chapter provides a good introduction to a somewhat obscure area.

I had anticipated that Part 2 would include detailed discussion of complex genetic systems. In fact, Roughgarden considers only models based on variation at

a multi-allelic single locus and two biallelic loci. Yet, even in this relatively simple case, what is really going on is far from clear (see Fig. 8.8, for example). This is followed by a rather curious chapter on natural selection and quantitative inheritance; the first half is purely biometrical and not Mendelian, the second does incorporate elements of simple Mendelism. Part 2 concludes with a consideration of Fisher's fundamental theorem — which is not at all as fundamental as Fisher thought — and a chapter on non-random mating, a reasonable introduction to inbreeding and assortative mating.

The next section of the book was, to me at least, the most disappointing. It deals with evolution in general, and in spatially varying and temporally varying environments, and with the development of altruism; few results having general implications have come from recent work in these areas.

Once again, in the first five chapters of Part 4, one soon gets involved in difficult integral equations. Here, Roughgarden considers the dynamics of an asexual population in what is a neat, but perhaps oversimplified, presentation. Finally, in this part of the book, stochastic environments are treated; here, it is a great surprise to find the use of Ito and Stratonovich stochastic calculus.

The final section of the book deals with

interacting populations. It starts with a consideration of competition between asexually reproducing populations and leads on to predator-prey models — a useful exposition. Then we are given chapters on coevolution (incorporating a single Mendelian locus and based mostly on Roughgarden's own recent work) and on niche theory and island biogeography.

My overall impression of the book is that it provides a useful but on occasions oversimplified picture of research in the field between 1910 and 1950. Its real value lies in that large portion which deals with more recent work, that undertaken over the past decade, and in this it will undoubtedly be of great value to specialists in mathematical ecology. A deep lacuna in the whole effort is the absence of real quantitative data and then the testing of models by reference to such data. Part of this is due to the immense difficulty of obtaining "hard" data on the dynamics of real ecological systems.

Theoretical ecology incorporating genetics is a young yet complicated area of biological enquiry. We must be grateful to Roughgarden for giving us a base from which to proceed. □

*Oscar Kempthorne is Professor of Statistics and Distinguished Professor in Sciences and Humanities at Iowa State University, Ames, Iowa.*

## Thermodynamics and macromolecules

S. P. Spragg

*An Introduction to Physical Properties of Large Molecules in Solution.* By E. G. Richards. Pp.298. (Cambridge University Press: 1980.) Hardback £18, \$29.50; paperback £5.95, \$9.95.

TO MANY teachers of biophysical chemistry it seems strange to note that over the past two decades instruction on the subject of macromolecules has progressed to a position of marked contrasts. On the one hand, structural descriptions of macromolecules are based on accurate methods of X-ray crystallography, so students persevere in understanding details of this technique. On the other, emphasis in the teaching of the properties of macromolecular solutions has moved slowly away from exact thermodynamic interpretations and so student interest in the fundamental understanding of thermodynamics has waned. It is a pity that some recipe cannot be found which convinces students that the three laws of thermodynamics provide a thread for connecting

many phenomena associated with macromolecular solutions.

The present book contains little philosophical discussion along these lines but it is particularly good at referring proofs back to the fundamental laws of thermodynamics without stating the laws as a starting point. The contents range over configurational statistics of polymers, helix-coil transitions and hydrodynamic properties of macromolecules, as well as providing sound introductions to molecular interactions of neutral molecules and polyampholytes. The lack of experimental results which direct the students' attention to the phenomena under discussion means that the book must be supplemented through lectures; for example, experimental results from the melting curves of nucleic acids would have formed a useful start to the discussion on helix-coil transitions. Further examples will come to the mind of other readers, but this criticism is minor and only serves to show that this book is mainly concerned

with theoretical treatments of problems.

It was particularly pleasing to find a chapter devoted to scattering of electromagnetic radiation (written by S. D. Dover), since some understanding of this phenomenon at a fundamental level is becoming more important as laser technology expands the possibilities of measuring molecular properties on very short time scales.

The book will provide a useful reference text for undergraduates requiring guidance in the application of chemical thermo-

dynamics to describing macromolecular properties. Further, like Professor C. Tanford's well known text on a similar topic (*The Physical Chemistry of Macromolecules*; Wiley, 1961), the content is such that it will also be of value to postgraduates with an interest in the subject.

*S. P. Spragg is Senior Lecturer in Physical Chemistry at the University of Birmingham, UK, with research interests in the solution properties of biological macromolecules.*

## New membranes for old

Harvey Lodish

*Cell Membranes and Viral Envelopes.* Edited by H. A. Blough and J. Tiffany. 2 volumes, pp.848. (Academic: 1980.) Both volumes £40, \$92.

MOST lipid-containing animal viruses bud from either the plasma membrane or internal membranes of infected cells. Much of our knowledge of the structure and assembly of membrane components has come from the use of defined virus model systems. These two volumes represent a noble and needed attempt to bring together reviews on the structure and function of both viral and cellular membranes and their constituents. There are chapters, written by recognized experts, on the basic physical and microscopic techniques used in membrane research, and on the biochemistry of viral and cellular membrane lipids, proteins and carbohydrates. In addition there are contributions on the structure and assembly of particular groups of viruses — influenza virus, retroviruses, Herpes virus and rhabdoviruses — though, oddly, none on the paramyxoviruses or arboviruses.

Most of the contributions to these volumes were written in 1974 and 1975. The end result is that the coverage of publications during the past five years is very erratic. Incredibly, the two chapters written by the editors contain references to very few articles published after 1976. What is worse, the editors apparently exercised little direction over the content of individual chapters, nor did they attempt to rewrite, up-date, or interrelate them. The predictable result is extensive redundancy of data and confusion between chapters.

As one example, the partial sequence of glycophorin used in the chapter on the structure and function of membrane proteins is taken from the 1971 preliminary report; there is no reference to the complete sequence published in 1975 or to the 1978 revised sequence. Oddly, the complete sequence is contained in the following chapter, "Carbohydrates in the Cell

Membrane". Further, in no contribution is there mention of the techniques of fluorescence photobleach recovery, now probably the most widely used method for the determination of the extent and rate of lateral diffusion of cell surface components.

The chapter on carbohydrates of viral envelopes was written in 1974, and is very dated, but some of the more recent structural work is contained in the following chapter, "Glycosylation of Viral Envelope Components". None of the contributions discusses recent work on the importance of proteolytic cleavages in the maturation of viral glycoproteins, such as the influenza haemagglutinin HA or the paramyxovirus fusion protein F. The contribution "Synthesis of Viral Proteins" was also written in 1974-1975, before the site of synthesis of viral glycoproteins in the rough endoplasmic reticulum was known; this chapter, unfortunately, is now largely of historical interest only. Like several others, it contains a one-page addendum which mentions some published work up to the beginning of 1977, but there still remains an inexcusable three-year delay before even this was published.

Some of the individual reviews dealing with more recent developments are of high quality. Many others would have been quite useful had they been published within a year or so of writing, surely a more reasonable lag time. These include those on virus receptors; on influenza virus; on structure and on synthesis of membrane and viral lipids; and on membrane changes in virally transformed cells. The fields covered by this book are expanding very rapidly; as a consequence, these reviews will not be of much value to the contemporary student or researcher. It is indeed unfortunate that the considerable effort expended in writing this book has been largely wasted, as current reviews of these topics would be valuable.

*Harvey Lodish is Professor of Biology at the Massachusetts Institute of Technology, Cambridge, Massachusetts.*

## Geothermal maps

Philip England

*Atlas of Subsurface Temperatures in the European Community.* Compiled by R. Haenel with co-authors. Large format, pp.36+43 maps. Commission of the European Communities/Th. Schäfer: Hannover, 1980.) DM 120.

THE production of subsurface temperature maps for an area the size of the European Economic Community is an undertaking that requires a degree of faith. If it can be assumed that the available, sparsely distributed, temperature and thermal conductivity data adequately characterize the near-surface heat flow of the region (and that this is not perturbed by fluid motion), then it requires only a knowledge of the subsurface geology, and of the thermal conductivity and heat generation of the major lithologies, to extrapolate measured temperatures outward and downwards to make the kind of map this book contains.

These maps are each about 40 cm × 50 cm in size. Seven are 1:5,000,000 maps of subsurface temperature distributions beneath Europe at depths between 500 m and 5 km; six show subsurface temperatures at 1 km for the countries of the EEC; and some 20, with scales of between

### Bring Your Library Up-to-Date With This ANS Edition ... Nuclear Energy in Germany

Winnacker/Wirtz  
6 x 9 hardbound edition  
**\$37.00**

American Nuclear Society  
555 North Kensington Avenue  
La Grange Park, IL 60525 USA

Please take my order for \_\_\_\_\_ books.

- ☐ Payment in full enclosed.  
☐ Bill me and I accept postage and handling charges.

Name \_\_\_\_\_

Org. \_\_\_\_\_

Street \_\_\_\_\_

City \_\_\_\_\_

State \_\_\_\_\_ Zip \_\_\_\_\_

Circle No. 01 on Reader Enquiry Card.





Leo Szilard: *His Version of the Facts*, edited by Spencer R. Weart and Gertrud Weiss Szilard (for review see *Nature* 278, 285; 1979) has been re-issued in paperback by the MIT Press, price \$7.50, £4.95.

1:500,000 and 1:75,000, indicate subsurface temperatures in areas of geothermal interest where the density of subsurface temperature measurements is highest.

Compiling these maps has clearly involved assembling vast amounts of subsurface temperature data (otherwise not readily accessible), and where the density of these observations is high — in the upper kilometre or so of regions of known geothermal potential — the maps may be regarded as reasonably accurate summaries of the available information. Their use is limited, though, when the density of observation is low and when extrapolation over depths of several kilometres is required.

Anyone contemplating buying this book should look first at Plate 2, which shows the density of the available heat flow information in the EEC, and at Plate 39 which indicates the amount of information provided by boreholes. Next they should read, in any one of six languages, the four-page introductory text which gives a brief exposition of how the maps were compiled and of the pitfalls involved in making the kind of extrapolation outlined above. (One point not dealt with adequately is the error involved in assigning values of conductivity and heat production when extrapolating temperatures downwards; the compiler's assumption that the likely uncertainty in these parameters is 10–15% is a wildly optimistic one, and leads him to place misleadingly small error bars on the temperature estimates that he makes.)

Having taken these steps one should be convinced of the difficulties involved in predicting subsurface temperatures from the information available at present, and hence that this book is of little use as a predictor of geothermal resources. The book's remaining attribute, on which it should be judged, lies in the compilation of information that it represents. It is a shame, therefore, that the introduction is so cursory, that so little indication is given of the reliability of the data, and that it was thought necessary to present the information in this elaborate guise.

Philip England is a Research Fellow in the Department of Earth Sciences, Bullard Laboratories, University of Cambridge.

## Herbal facsimiles

Sandra Raphael

*Herbarium Apulei Platonici* (Vol.I) and *Herbolario Volgare* (Vol.II). Facsimile reprints. Introductions by Erminio Caprotti and William T. Stearn. Pp.CXXII + 566. (Edizioni Polifilo: Milan, 1979.) Both volumes L.85,000.

A NEW pair of facsimiles reprints the first Latin and the first vernacular herbals published in Italy, the former in 1481, the latter in 1522. The 1481 book, probably the earliest illustrated herbal printed, is the *Herbarium* of Pseudo-Apuleius, a Graeco-Roman compilation with mediaeval trimmings, surviving in a multitude of manuscripts that indicate its status as a standard source of information on medicinal plants. The crude, diagrammatic woodcuts can have given little help in the identification of the plants described.

The 1522 *Herbolario Volgare* took both

its text and its illustrations from the *Latin Herbarius* printed by Peter Schöffer, Gutenberg's successor, in 1484. The text is another miscellany from an unknown hand, but its pictures are a decorative improvement on those of the Apuleius. The Iringo (sea-holly) is shown here, a plant whose candied roots were regarded as an aphrodisiac as late as the seventeenth century.

Professor Stearn's introductory essay appears in both Italian and English, and the books are fine examples of the exquisite printing of Mardersteig's Stamperia Valdona.

Sandra Raphael is a Senior Editor in the Dictionary Department of Oxford University Press. Her book on illustrated herbals, title?, written in collaboration with Wilfrid Blunt, was published late in 1979.



**CDello Iringo.**

**Cap.LXXVI.**

**L**O iringo sic caldo & humido nel primo grado: Et la sua humidita e maggiore della sua calidita: & quelli che usano la radice condita cō melle moltiplica il sperma: & fa al coito: & allo drizare della uerga: & fa bon nutrimento: Dice serapione & Auicena: Et le radice de iringo cō uno pocho de specie aromatiche si māgiano: ouero con melle o zucararo & cinamomo si acōciano: Lo iringo sic una sorte de spina le foglie delloquale si agionge

18/25 December 1980

# Britain, France and nuclear weapons

Between now and 20 January, when Mr Ronald Reagan will be inaugurated as president of the United States, much important business elsewhere will be conducted in a vacuum. So much is clear from last week's meeting of the NATO Council in Brussels. Many of those present seem to have been as interested to know whether their old colleague, General Douglas Haig, will finish up as United States Secretary of State as in the prospect that threats of economic sanctions against the Soviet Union would deter an invasion of Poland. Yet vacua have their benefits. As boxers tend to free-associate in the nervous minutes before the beginning of a fight, so politicians and others in the West have been talking openly about some of the issues on which American influence will again be dominant in January — defence, arms control and the like. In Britain, this unaccustomed free speech has been mixed with the wild talk inseparable from the accession of Mr Michael Foot as leader of the British Labour Party, for Mr Foot used to be a staunch supporter of unilateral nuclear disarmament for Britain, and has not yet renounced his former views. The Campaign for Nuclear Disarmament can boast of more recruits in the past few months than in the past several years.

Economic issues apart, the most obvious uncertainty is Mr Reagan's position on arms control, and on his plan to renegotiate the Salt II agreement. During the election campaign, his position shifted steadily, from outright repudiation to renegotiation. Soon after 20 January, it should be possible to tell where he now stands, but the signs are encouraging. The Soviet Union has not slammed the door on further talks about the agreement that President Carter shrank from fighting through the US Senate. His successor must by now know the strength of opinion in Europe, especially in Germany, about the need for agreement on short-range as well as strategic nuclear weapons. Anxiety about Poland has only sharpened suspicions that the stability engendered by mutual nuclear deterrence has its drawbacks. With nothing worth mentioning happening at the Madrid conference on the Helsinki accords, Mr Reagan is likely to have calculated that arms control is not, as he once supposed, the wishy-washy plaything of liberals but a considerable political opportunity. That, at least, must be the hope.

Will governments elsewhere be capable of similar (and still unproven) flexibility? The need is most urgent in Britain, as the defence debate in the House of Lords on 3 December showed. Since the invention of nuclear weapons, there have been two British positions on nuclear defence — the belief (shared by all governments in office) that an independent nuclear deterrent is a necessary part of British policy. This is the belief which led the Callaghan government to fit the Polaris submarine missiles with new warheads (at a cost estimated at £1,000 million) and the present government to order a fleet of six Trident nuclear submarines (at a cost of £5,000 million spread over the next ten years). At the other extreme is the view that British bombs are not a strength but a weakness, and should be dismantled. The unilateral position is not homogenous — some ask merely for the abandonment of British nuclear weapons, others would refuse to provide bases for US nuclear weapons or even withdraw from NATO. Nor are the unilateralists entirely wrong-headed in their views. Unilateral nuclear disarmament would bring certain benefits. The snag, which hitherto has far outweighed the advantages, is that there would be a profound change in the character of British political relationships across the Atlantic and across the Channel — and no assurance of British immunity from the consequences of foreign wars.

The novel development is that, in Britain, there is a growing body of opinion sandwiched between the two conventional extremes. In the House of Lords debate, people such as Lord Zuckerman (once Chief Scientist at the Ministry of Defence) and Lord Chalfont (Mr Harold Wilson's Minister for Disarmament) poured cold water on the decision to replace the Polaris submarines with Trident. "If we can afford it, so be it", said Lord Zuckerman, who knows as well as the next British taxpayer that the government's survival will soon depend on its success in cutting public expenditure. The case against the Trident replacement unites an impressive range of interests. The military (represented, for example, by Lord Carver, a distinguished field marshal) would prefer to see the Trident money spent on conventional forces. Strategists (like Chalfont) argue that weapons other than Trident missile submarines would be cheaper and no less effective. None of this implies support for unilateral disarmament — the denial of British bases to US nuclear warheads (in aircraft now, in cruise missiles sometime after 1983), for example. What has happened is merely that entirely sensible opinion has begun to question the most conspicuous cornerstone of British defence policy in the period since 1945.

The British government has been slow to see the way the wind is blowing, or to recognize the advantages of following Mr Reagan's apparent willingness to make the best out of accommodations with his critics. The most immediate embarrassment of the Trident programme is its cost, probably grossly underestimated at £5,000 million. Can it make sense that a government whose chief failure since its election eighteen months ago has been its failure to cut public expenditure should now take on a capital commitment on such a scale, more than half the cost of the US Apollo programme? The decision might be more easily justified if (as some Apollo-builders held in the 1960s) building the Trident submarines would bring uncovenanted technical innovations, but the objective is largely to replicate the nuclear submarines already being built in the United States. It is no wonder that there has been a revival, in the past few weeks, of the old dream of an Anglo-French cruise missile system. That would be cheaper and politically powerful.

These are narrow arguments. The broader question of whether countries such as Britain — France is the only other example — should hang on to independent nuclear forces is more divisive. The conventional British statement of the case is that nuclear weapons are a contribution to collective defence and an assurance of influence in international negotiations, about disarmament as well as making war. The French view, more iconoclastic, is that French security depends in the last resort on French arms. Both arguments are stiffened by chauvinism. With time, each is weakened. Each of them is less convincing as strategic technology becomes more sophisticated. Yet in Western Europe there is a crying need that the European Community should soon acquire what it should always have had — a foreign policy and a defence policy to go with it. Is that where Britain and France may pool their nuclear ambitions after 20 January?

## Nature publication date

As in previous years, this issue of *Nature* (dated 18/25 December) is the last to be published in 1980. Because there are 53 Thursdays in 1981, the next issue, published on 8 January, will be dated 1/8 January 1981.



# US research budget now in better shape

## Dying Congress restores earlier cut-backs

*Washington*

It may not last, but in contrast with previous years, when President Carter's requests for additional funding for science were trimmed back by Congress, the final 1981 research budget looks in even better shape than when it was presented in January 1980.

The Administration revised its initial request in March, reducing a proposed growth in spending on research and development from 11 to 8 per cent. But while Congress has agreed to cuts in other areas of social spending, research and development has been relatively protected.

Last week, for example, when Congress finally agreed to an appropriations bill covering the budgets for 23 assorted federal agencies, only three — the National Aeronautics and Space Administration (NASA), the National Science Foundation (NSF), and the American Battle Monuments Division — received more money than they had asked for.

As in previous years, legislators have been kind to the budget of the National Institutes of Health (NIH). Although the final figure is yet to be agreed, the House has approved an NIH budget of \$3,616 million, and last week the Senate gave its approval to a \$3,686 million budget. Whichever figure is finally decided upon, it will be higher than the \$3,581 million initially requested, and will result in a 5.5 to 7.5 per cent increase in NIH's budget over last year.

In the Department of Energy, threats to the basic research budget — which includes funding for high-energy physics and nuclear physics — were successfully fought off during the summer. The final sum for items under the responsibility of the department's Office of Energy Research will be \$1,145 million, only slightly less than the \$1,203 million requested, with the major reduction being the postponement of improvements to facilities at the national research laboratories.

Only in the case of the Department of Defense, for which the Administration had originally requested a hefty 17 per cent increase in spending on basic research, is the final figure likely to be substantially lower. Congress has approved an appropriations bill which will cut this increase to 12.5 per cent, reducing the planned real increase from 8 to 3.5 per cent. The final figure may be even less, since Congress has also asked the Pentagon to impose further unspecified cuts totalling 4

per cent across the whole of its research and development budget. In the case of NASA and NSF as well, the final figures may be reduced by a requirement that the Office of Management and Budget distributes a further 2 per cent cut across all the agencies covered in the appropriations bill.

Congress has also forced several significant changes in the content of the Administrations proposals for federally-sponsored research programmes.

At NSF, for example, sustained pressure from Senator Edward Kennedy has led to the agreement to introduce a new programme to boost women and minority scientists. Mr Kennedy had added his own "Women in Science" bill to the Senate version of the NSF appropriations bill; and the House finally agreed to a \$30 million programme which will include more than 100 grants for women scientists extra to those which would be otherwise awarded. The NIH budget, on which a final total has yet to be settled, includes an extra \$35 million for training grants which the Administration had suggested be cut back to enable the number of new and

competing research grant awards to be kept constant.

A large part of the increase in NASA's budget will go to cover the additional costs of the much-delayed space shuttle. However, Congress is also becoming increasingly concerned about cost and schedule over-runs in virtually all of the space science programmes.

As a result, Congress has directed NASA to ensure that it receives approval from the National Academy of Sciences before making any substantial programme changes. This move, opposed by several NASA administrators, is supported by Congress as a way of ensuring an adequate response to any future technical difficulties.

Despite the set-backs being experienced by the various space science programmes, almost all have escaped the congressional budget process relatively unscathed, including the proposed new gamma-ray observatory. However, there were warnings that some projects could still be halted through budget rescissions early next year when the new administration takes over.

## Oil, shale or mirage in West Siberia?

The strange story of the supposed Bazhenov oil field in western Siberia, with its reserves of over 600,000 million tonnes of oil, reached the world's newspapers two weeks ago at a particularly sensitive moment. The threat to world oil supplies posed by the Gulf War, and Western contingency plans for a further technological embargo on the Soviet Union should Soviet troops be ordered into Poland, and the impending OPEC meeting in Bali made the announcement of the new field, with reserves surpassing world proved oil reserves, a major consideration for politicians and oil magnates alike.

The report on the Bazhenov field came from Petrostudies, a two-man Swedish team which monitors all open Soviet publications on the oil industry. The consensus of expert opinion, ranging from the CIA to the Soviet oil industry, is that its report is an exaggeration. One French expert went as far as saying that it would amount to a "geological miracle". Petrostudies, however, remains adamant about the size of the find, but is now prepared to concede that a considerable proportion of the oil may not be recoverable.

Challenged with a Soviet statement that the deposit was not oil but shale, Petrostudies director Manlyo Jermol replied that the Bazhenov shale was scientifically important because it contained liquid crude. Until now, he said, it had been believed that such oil was to be found only in porous rocks. He cited the Soviet

geologist, Ivan Nesterov, director of the West Siberian Research Centre for Oil Prospecting who, in 1978, had announced that Soviet research had refuted the old text-book assertion that shales cannot accumulate free oil.

A few days before the Petrostudies announcement, Nesterov was interviewed on Moscow radio in connection with the publication of the guidelines for the new Five Year Plan. On this occasion he was vague about the West Siberian potential. The fields now in production yield more than 300 million tonnes of oil and gas condensate per year, he said — amounting to about half the total Soviet output. But since two thirds of all the fields discovered in the area have not yet been touched, and only one fifth of the oil-bearing region of West Siberia has been explored it is difficult to make reliable estimates of the reserves. Extraction costs, he pointed out, are soaring, the costs of erecting a rig have risen 30 per cent in the last five years, and it has proved impossible to sustain the original growth rate. While maintaining that Western talk about Soviet oil running out in the near future is "highly premature", Nesterov's talk was couched in cautious terms. During the next five years, he said, the Soviet Union will be able to meet its own requirements and its commitments to its trading partners. For the longer term, he gave no hint of any bonanza — shale or otherwise, of the type suggested by Petrostudies.

**Vera Rich**

The one potential casualty, the National Oceanic Satellite System (NOSS) — the proposed successor to the SEASAT satellite — will receive an extra \$6.4 million through the research budget of the Department of Commerce's National Oceanic and Atmospheric Administration (NOAA). NOAA has also received an additional \$1 million for manned undersea facilities, but had \$2 million for acid rain research cut from its budget.

In biomedical research, Congress has rejected proposals from both the House and the Senate for greater supervision of NIH. A bill continuing authorization for the National Cancer Institute and the National Heart, Lung and Blood Institute was passed on 5 December without either the provision for a Presidential Commission on biomedical research priorities, proposed by Senator Edward Kennedy, or controversial new authorizing legislation for the remaining nine research institutes which had been proposed by Representative Henry Waxman.

Cuts in the Defense Department's proposed research programme could set back the growth of ties between the military and universities that have been developing over the past four years, according to Pentagon officials, who warned that in particular proposed new programmes for the Department of the Army may have to be cut back.

Nor will the Defense Department be receiving the hoped-for funds to construct a new production facility for binary chemical weapons. This was deleted by members of the Senate from next year's appropriations bill, on the grounds that if the United States is to resume chemical weapons production, this should be a presidential not a congressional decision.

David Dickson

## Nuclear safety

### European hazards

Brussels

European nuclear power stations are not as vulnerable to operational errors as the one involved in the accident at Three Mile Island, but there is plenty of room for improvement in safety measures in nuclear power stations in the European Economic Community. This conclusion comes from a report submitted to the European Commission's Interdepartmental Coordinating Committee on Nuclear Safety (CCNS). Many of the report's proposals are disputed by the committee in an accompanying reply.

The report comes from a four-man group set up by the European Commission after the Three Mile Island incident. The members of the group were H. Dunster, Deputy Director General of the UK Health and Safety Executive, Professor Latzko of the Technische Hogeschool Delft, Professor Smidt of the Institut für Reaktor Technik der Universität Karlsruhe, and Mr

S. Villani, Director General of the community's Joint Research Centre.

Conditions similar to those which led to the Three Mile Island accident have occurred on several occasions in Europe — the report criticizes the fact that these went almost unnoticed, and calls for a data bank recording all abnormal events in European nuclear power stations.

The siting of nuclear power stations is becoming increasingly politically sensitive in Europe. The report stresses that siting has only a limited part to play in protecting the population, but that there should be a consistent approach among member states to siting nuclear plants, especially in areas close to national borders.

The group also considers that more should be done to minimize the effects of any accidents that may occur: the Commission should study the emergency procedures operating in the various member states, there should be a review of the emergency plans made by the power station operating organizations before they are licenced to operate, and more attention should be given to ways of keeping the public informed in the event of an accident.

The European Commission is criticized for not responding rapidly enough to changing nuclear research needs, for setting up cumbersome committees, and for providing those committees with inadequate technical and administrative services.

According to the Interdepartmental Coordinating Committee, many of the recommendations in the report actually tie in with actions already taken by the Commission, or actions already under consideration. But the rather half-hearted attitude towards nuclear power expressed in the report is not welcomed by the committee. The report says: "no amount of care will totally eliminate the risks of this (nuclear), or any other sort of energy . . . (but) . . . we are finally led to the belief that nuclear sources should continue to play a significant part in the supply of Europe's energy."

Jasper Becker

## Fast reactors

### Low morale

Staff morale may be as much a threat to the British fast reactor programme as the prospect of a public inquiry on the project. The latest sign of this is the resignation of Mr Jack Moore, coordinator of the fast reactor programme at the UK Atomic Energy Authority (UKAEA), at the end of the year. Mr Moore, who is 57, is leaving to take up a post with Motor Columbus engineering consultants in Switzerland. He said earlier this week that at UKAEA he was unlikely to see his work of the past seven years come to fruition before his retirement.

Mr Moore's resignation highlights two potential problems for the staffing policy of the fast reactor team. Although no other

senior staff are reported to be leaving, further delay in a commitment to build a fast reactor may prompt others to go. The second problem is that of the age structure of the design team. Although the UKAEA has been expanding the team by bringing in young people, previous recruitment policies have left a noticeable dearth of people in their forties. When the senior staff retire or leave, their posts will have to be filled by much younger people.

A government statement on the commercial demonstration fast reactor has been expected since the summer. Sir John Hill, chairman of the authority until the end of the year, submitted a proposal to the government a year ago. Mr Moore expects that the government will respond shortly but that it will not make a final decision at this stage. One complication is that the government has not yet responded to the French proposal that Britain should by into commercial exploitation of Super-Phénix.

Meanwhile, the Nuclear Power Company is nearing the completion of a detailed design study, which Mr Moore claims will be superior to current French and Russian designs. The UKAEA would like to submit it to the Central Electricity Generating Board and potential reactor manufacturers so that a site could be chosen and a total project proposal put to the government.

Judy Redfearn

## Satellite communications

### Free for all ahead?

Washington

While the future of US remote-sensing satellites remains entangled in controversy (see *Nature* 14 August), the use of telecommunications satellites is poised for a dramatic expansion.

The Federal Communications Commission (FCC) in Washington has given permission for the launching of 20 new domestic communications satellites, which are likely to increase the capacity of the present system by a factor of four by the mid-1980s.

At least one newspaper company is discussing plans for a nationwide system of locally-produced newspapers linked by satellite, while the Communications Satellite Corporation (Comsat), which owns three of the nine communications satellites at present in orbit, has proposed starting a four-satellite system beaming television programmes directly to private homes within the next few years.

FCC approval for the authorization of the new satellite launches was given unanimously, part of what commission chairman Charles Ferris described as an "open-entry policy" to provide satellite capacity to all who want it.

A separate report prepared by commission staff, for example, has recommended that direct-broadcast satellite television services should be subject to the minimum of regulation, in



the light of competitive pressures from conventional television stations and cable television networks.

The commission is also expected to publish for comment a proposal for squeezing more domestic satellites into geosynchronous orbits, perhaps by reducing the separation of higher-frequency satellites from four to three degrees of longitude.

Such a change, says FCC, would allow the launch of an additional six satellites which had been promised to the commission, but which could not be authorized because of the shortage of available slots.

The launch of the 20 new satellites is likely to result in an increase from 160 to 612 in the number of satellite communications channels available by 1985. Each channel can transmit 1,000 telephone channels or a single television channel.

The new satellites will also create the first major challenge to the giant American Telephone and Telegraph Company (AT&T) in the field of long-distance communication. Two competing companies — General Telephone and Electronics Corporation and the Continental Telephone Corporation — are building their own satellites. AT&T, General Telephone, Southern Pacific Communications Corporation and Hughes Communications will each be constructing their systems for the first time, each having been given permission to build three satellites and launch two.

Local newspaper production could be revolutionized by plans that the Gannett Company is said to be developing for a national newspaper produced in Washington, but beamed to the presses of some of Gannett's 82 local newspapers.

Satellite transmission is already used by the *Wall Street Journal* to print seven editions simultaneously throughout the country. Although no official confirmation has been given of Gannett's plans, it is reported that the initial investment would be about \$100 million; some commentators have pointed out that setting up a single newspaper distributed throughout the country would provide Gannett with the opportunity to become a major voice in national affairs.

Comsat's plans for a satellite-based television network are included in a set of comments which the company has submitted to FCC as part of its preparations for the Region 2 Administrative Radio Conference of the International Telecommunications Union, due to be held in the summer of 1983.

Four satellites would be used to cover the United States, each covering a different time zone, with the most westerly satellite also broadcasting to Hawaii and Alaska. The service would be operated by Satellite Television Corporation, a newly-created subsidiary of Comsat. The market for direct-broadcast satellites is expected to be tested with the modification of two existing spacecraft designs.

David Dickson

## Ariane development

### More trouble

Ground tests of the principal rocket motors of Ariane, putative launch vehicle of the European Space Agency (ESA), have shown brand-new oscillations in the burn — and set the test programme back by a second three months.

Ariane's first test launch in late 1979 reached the planned trajectory, but the second — in May 1980 — ended moments after lift-off with a high frequency oscillation and loss of pressure in one of the first stage engines. A look back at the data for the first launch showed the same oscillation, but at low amplitude; and a re-run of the data accumulated during ground tests showed the same fault.

In October this year, ESA announced that the oscillations (at 2,300 Hz) could be cured by improving tolerances in the manufacture of the injectors, devices like a watering-can rose that mix the fuel and oxidant. This hypothesis will be tested at the end of this month, when new high precision injectors are tried for the first time. Meanwhile a new oscillation has appeared — at 2,700 Hz — and this sets in even with injectors that previously showed no sign of the vibration. While the 2,300 Hz problem "can be regarded as rectified" says ESA hopefully, the 2,700 Hz oscillation "is the subject of thorough investigation and action which still needs some time to complete".

Burn oscillations (called "buzz" or "screaming") are the *bête noire* of liquid fuel engine design and can destroy the engine if they reach high amplitude. One solution is completely to redesign the injector; another is to set Helmholtz resonators, tuned to the critical frequency, into the side of the combustion chamber in such a way as to absorb the oscillation energy.

Solutions such as this, however, verge on complete redesign of the engine — but this may be necessary in the end. The engines were originally designed for the French sounding rocket Diamant (in which similar instabilities were met and solved), but they

were stretched to the limit to meet Ariane's specification of 61 tonnes-weight thrust. The next series of engines, for a bigger Ariane, is based on a different design.

So it is seriously being questioned whether Ariane can meet its first commercial commitments: to launch the French MARECS B and SERIO 2 marine communications and meteorological satellites (which would go up together) and Intelsat V F6. These satellites, and the ESA X-ray astronomy satellite EXOSAT, were originally due for launch in 1981.

For the moment, ESA hopes to have the third test launch in June 1981, and the fourth in the autumn, beginning the commercial series later in the year. If, however, as some fear, the Ariane engines are inherently "marginal", redesign and retesting could take at least a year, and lucrative launch contracts might be lost to American competition. The lead that Ariane appeared to be establishing over the space shuttle — beset by its own problems but now believed to be running smoothly — is narrowing fast.

Robert Walgate

## Halley missions

### NASA to go?

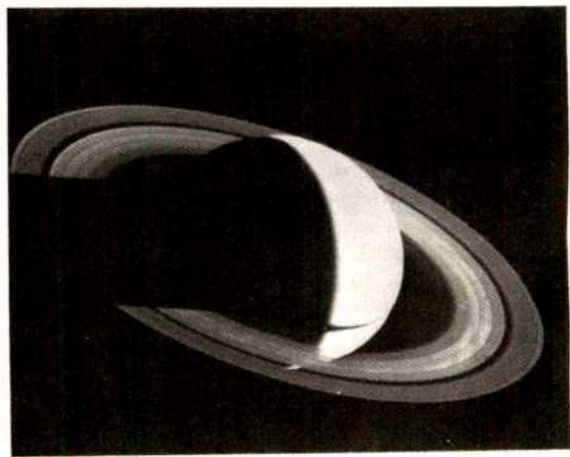
#### Washington

Can the new US Administration be embarrassed into mounting a mission to Halley's comet when it passes through the Solar System in 1986? The proposal has already been passed to president-elect Ronald Reagan from scientists in his home state of California. They point out that the European Space Agency, the Soviet Union and Japan all have plans for separate Halley missions — and that for the United States not also to go would be a major blow to national prestige.

Revised plans for a Halley fly-by were developed earlier this year at the Jet Propulsion Laboratory (JPL) in Pasadena, run for the National Aeronautics and Space Administration (NASA) by the California Institute of Technology (Caltech). Following last year's rejection by the White House of a request for funds to develop an ion-drive — for which money

## Beyond Saturn

Saturn, as seen by Voyager 1 on 16 November, four days after the encounter. Some of the dark spoke-like ring features (*Nature* 4 December) are seen as bright patches due to scattering of sunlight from particles within them. Voyager 1 will be monitored to as great a distance as possible in an attempt to detect the boundary between interplanetary and interstellar space, where the "solar wind" becomes undetectable. Voyager 2 will reach Saturn on 25 August 1981, Uranus in 1986 and Neptune in 1989.





has since been allocated by Congress, but too little and too late — the revised mission would rely on a ballistic launch, limiting its ability to manoeuvre near the comet.

Many JPL scientists still think the mission would be worthwhile, a conclusion backed up by the mission's science committee, headed by Professor John Ververka of Cornell University. And the proposal has already been put to Mr Reagan by Caltech trustee Earle M. Jorgensen, a Los Angeles businessman and close friend of the president-elect.

Scientists at JPL are stressing the question of national pride, one aspect of the space programme that they feel has received relatively little support from the Carter White House. But other members of the space science community are worried that political support for a fly-by mission could prejudice funding for NASA's own favourite scientific project, the Venus Orbiting Imaging Radar (VOIR).

In an unusual move (considered by many a pre-election gambit to win Californian votes), the White House announced in October that it was planned to request funds from Congress for VOIR when the 1982 budget proposals are submitted in January — implying a rejection of the revised Halley plans.

From the scientific point of view, VOIR is reckoned to be more fruitful than the Halley intercept. Members of NASA's space science advisory committee have already stated that they find the possibility of losing VOIR and getting the Halley mission instead to be "extremely distressing".

In addition, however, to the financial attraction — the present Halley plans would make substantial use of instruments developed for the Voyager missions, and its total cost of \$250 million would therefore be only about half that of the proposed VOIR — JPL scientists point out that the chance to observe the comet is a "once in a lifetime opportunity".

Officials from the European Space Agency (ESA) are watching the new developments with some concern, since they feel that a NASA project might well overshadow the more modest goals of ESA's own Halley mission, Giotto, particularly since the latter may not be able to produce photographs of the comet comparable to NASA's.

A substantial NASA involvement in the European effort is now unlikely. Two weeks ago, ESA's space science committee decided to keep the launch a European affair, using the French Ariane rocket, and were therefore not interested in the US offer of using a Delta launcher in exchange for payload space.

US scientists will not be entirely excluded from the European mission. A number are listed as co-investigators in experiments submitted for inclusion in the spacecraft. And ESA is still negotiating terms for Giotto to make use of NASA's deep space tracking network.

NASA, however, is uncomfortable about accepting the unusual role of second fiddle, and supporters of a US mission are emphasizing this possibility in efforts to generate support. Adding the Halley mission to the 1982 budget for NASA would affirm to the world in a "spectacular and dramatic way" that US leadership in high technology stands unsurpassed at the frontiers of knowledge, according to a statement published in the *Congressional Record* by conservative Republican Senator Strom Thurmond. Another supporter is ex-astronaut Senator John Glenn.

If the mission is given the go-ahead, its planners will have a delicate balance to weigh up. Scientifically, more data will be obtained from intercepting the comet after it passes through its perihelion, since solar heating will stimulate the discharge of gas and dust particles. But politically an earlier intercept might be more attractive, as this would pre-empt both the European and the Soviet post-perihelion encounters.

Top NASA administrators are also said to be concerned about the risks of the mission — if the spacecraft is hit by a dust particle there might be no scientific return at all. Scientific and political priorities are therefore likely to meet head-on; nobody is predicting the outcome.

David Dickson

## Polish universities

### Union snag

The drafting commission for the new Bill on Higher Education in Poland met for the first time two weeks ago, under the chairmanship of Professor Zbigniew Redich. The commission was set up by the Minister of Science, Higher Education and Technology, Dr Janusz Gorski. A few days previously, Warsaw University students had staged a sit-in in one of the main buildings of the university to express their lack of confidence in the minister.

The two events are not unconnected; the new bill will give Polish universities considerably more autonomy and a more democratic form of self-government which will include student participation. The two hundred students who occupied a hall in the university's Kazimierzowski Palace were protesting, first and foremost, against the difficulties they are encountering in registering the new Independent Students' Union (NZS). Since students are not "employees", they cannot register as an independent trade union under the Gdansk accords. The first draft of the ministry's "instruction" permitting registration of NZS proved unacceptable to the Warsaw students, although it had been worked out with the participation of NZS delegates. When the ministry negotiator suspended talks with NZS, on the grounds that he must first consult the (now greatly depleted) Socialist Students' Union, NZS considered that the ministry had broken

off negotiations unilaterally and began their sit-in.

After occupying the hall for two days, the students won what they described as a partial concession only — a new ministry instruction on registration to come into force on 20 December. This should allay at least one fear — that without legal status, NZS would be unable to participate in the new "self-government" system of the university. Demands for a national NZS delegate meeting on student problems and for the publication of their grievances in the press were not met.

Neither the concessions by the minister nor the conciliation efforts of the university rector, Dr Henryk Samsonowicz could persuade the students to end their sit-in. Ironically, in view of the fact that NZS cannot legally be a trade union, it ended its protest only in response to a call for restraint issued by the Independent Trade Union Confederation Solidarity.

Vera Rich

## Fissile material

### Counting wrong

Are eleven kilogrammes of highly enriched uranium missing from Dounreay, the UK Atomic Energy Authority's (UKAEA) fast reactor research establishment in North Scotland? The authority cannot say. The amount appears in this year's tally of "materials unaccounted for" (MUF), and is something of an embarrassment. According to the UKAEA, the quantity is within measurement errors on a large throughput, but the throughput cannot be revealed for security reasons and the errors have not been calculated. So it is difficult to give significance to the figure.

All MUF figures announced last week lack error estimates because, an official said on Monday, "errors would have to be combined from many completely different processes and sources".

Nevertheless the 11 kg "loss" at Dounreay was near enough to a critical mass to give the authority pause. In the first three years for which MUF figures were announced, the MUFs at Dounreay for highly enriched uranium were +2.8 kg, +3.7 kg, and +0.3 kg, all indicating paper gains of the material. However, Dounreay was not reprocessing fuel for much of that period, and the present figures relate to the first year (since MUF accounting began) when fuel from the now closed Dounreay fast reactor was being reprocessed.

The figure amounts to a difference between the quantity of  $^{235}\text{U}$  estimated to be on the site at the beginning of the year and the quantity estimated at the end, taking into account traffic on and off site. But much of the  $^{235}\text{U}$  at the beginning was in the form of irradiated fuel rods, and so inaccessible to measurement. The amount in the rods was estimated using knowledge of their position and operating time in the



Dounreay fast reactor, and of the original composition of the rods. At the end of the year, some of these rods had been through reprocessing: here  $^{235}\text{U}$  can be measured easily only at the end of the flow, and by neutron activation analysis in the cans (which are stripped off at the beginning of the process).

When the 11 kg accounting loss was discovered, great efforts were made to recalculate the quantity and check measurements. The new figure was different (the authority will not release it) but it was agreed to keep to the original accounting value. However, the difference was great enough to indicate that the uncertainties in the original estimate were of the same order as its value — about 10 kg. For example, the recalculated figure for  $^{235}\text{U}$  in the original rods was 2 kg different from the first estimate.

However, still no calculation was made of the uncertainty, or "error", on the quantity. And this despite a statement a year ago by Dr A. G. Hamlin, director of the UKAEA Nuclear Materials Accounting Control Team, that "in order to determine whether MUF is really indicative of diversion of material, the safeguards authorities need to know, among other things, the expected level of errors. . .".

Robert Walgate

## US research planning

### NIH reprieved

Washington

The National Institutes of Health (NIH) have avoided the threat of new legislation which would have placed much closer congressional surveillance and control on their research programmes, proposed earlier this year by the House of Representatives health and environment subcommittee (see *Nature*, 22 May).

After intense opposition from medical schools and research institutes — and despite the support of the Secretary of Health and Human Services, Mrs Patricia Harris — proposals put forward by Subcommittee chairman Henry Waxman were mostly dropped when the bill was agreed in final form by the House and the Senate.

Also dropped were equally controversial proposals put forward by Senator Edward Kennedy on the Senate side for a Presidential Commission on biomedical research priorities. Senator Kennedy had wanted to attach this to legislation which re-authorizes the operations of the National Cancer Institute and the National Institute for Heart, Lung and Blood, the only two of NIH's eleven institutes at present requiring such legislation.

NIH themselves opposed both innovations, but were told by Mrs Harris to sit on their hands. Opposition was subsequently led by groups such as the American Association of Medical Colleges, which argued that NIH should be given the greatest possible freedom to

decide on their research strategies.

NIH did not, however, escape completely unscathed. Included in the authorization bill are requirements for additional administrative arrangements covering diabetes research — a pet subject of retiring health subcommittee member Senator Richard Schweiker, expected to become Mr Reagan's Health Secretary — and for research on digestive diseases. NIH officials feel that one disadvantage of the changes proposed by Congressman Waxman is that regular re-authorization of NIH research funds makes it easier for such provisions to be attacked by individual congressmen.

David Dickson

## European environment

### Small gains

Brussels

Agreement has still not been reached by the Environmental Council of the EEC on two pieces of legislation: one concerning the prevention of industrial accidents and the other on the level of mercury discharge. However, new controls on whale imports, the recycling of waste paper, and wildlife habitation have been accepted.

At the meeting in Brussels on 12 December, the so-called "Séveso Directive" again foundered on the French intransigence over transfrontier notification procedures. It had been proposed that information on potentially hazardous plants near frontiers should be made available on a Community basis. The French would prefer notification of neighbouring states bilateral — an idea swiftly rejected by Belgium and Luxembourg. This disagreement is bound to step up the campaign against French nuclear reactors near the Belgium and Luxembourg borders.

The directive on mercury is also meeting resistance from France and Britain. The UK delegation insists that environmental quality objectives be used instead of standard emission limits to measure pollution. In the draft directive — the first to be based on the controversial directive on the control of discharges of dangerous substances into the aquatic environment — it was suggested that the United Kingdom stick to its use of quality controls while the other EEC states use the limit value approach. The French, however, object to this, feeling that pollution abatement costs should be the same throughout the Community. Both this and the industrial accident proposals will now go back to the Committee of Nine's Permanent Representatives for further discussion.

On the bonus side, from 1 January 1982 imports of commercial whale products will be banned. Would-be importers will have to apply for a licence not only for primary products but also for any goods (such as leather) which have been treated with a whale product. Denmark's insistence that

Greenland be excepted from this rule was accepted.

A recommendation obliging the nine member states to take steps to recycle waste paper and pulp was also adopted. Inks or glues which adversely affect the recycling process may fall victim should the legislation be seriously applied.

It was also agreed to finalize the Community's adherence both to the Strasbourg Convention (the Berne Convention) on the protection of European wildlife and their natural habitats and to the Geneva Convention on trans-frontier air pollution.

Jasper Becker

## High-energy physics

### New man, new style

The next director of DESY, the West German particle physics laboratory at Hamburg, will be 49-year-old Dr Volker Soergel, at present a member of the directorate of CERN, the European centre for particle physics in Geneva. Departing DESY director Professor Herwig Schopper announced the appointment during his leaving party at DESY last week.

Schopper moves to CERN in January as director-general; and Soergel will step into his shoes at DESY, even to the point of taking over his predecessor's professorship at the University of Hamburg. But from there on the similarities between the two individuals stop. Schopper had proved himself an extremely able politician in his period at DESY, but is less well known as a physicist; Soergel is a recognized expert on the weak decays of elementary particles, but has yet to learn the ways of Bonn.

However, he is by all accounts an extremely able administrator. According to one ex-CERN physicist, he could complete in ten minutes meetings that should have taken an hour — by resolving conflicts of interest beforehand. In this sense his style is ordered and Germanic. But at the same time, it is said, he can wax enthusiastic "and talk for hours about some harebrained scheme".

At DESY there are plenty of schemes, harebrained or not. A 30-beam synchrotron radiation laboratory opens in January; PETRA, the big electron-positron ring, is being pushed up to 22 GeV per beam in an attempt to find the elusive t-quark; superconducting magnets are being developed; and there are long-term plans for HERA, an 800-GeV proton on 35-GeV electron collider. But first, Soergel must find cash for DESY to pay its electricity bills (see *Nature* 4 December).

Being interested in the weak interaction, he will be keen to run PETRA at the energy where it can take data fastest on weak-electromagnetic interference, and check — in a hitherto impossible way — the Nobel-prize winning Weinberg-Salam unified theory of the weak and electromagnetic interactions. DESY physicists now



estimate that this requires experiments at 16 GeV per beam — not DESY's top energy, but enough to break the present budget if pursued for more than half 1981 running time. Given the cash, they say, they could have a result by May or June. It will be interesting to see if Professor Soergel can get it.

Robert Walgate

## Brazilian agriculture

### Soya beanfeast

Brasilia, November

In the scramble to develop its unexploited resources, officials say that Brazil is turning away from the Amazon Basin to an area of savannah, known locally as the Cerrados, covering about 180 million hectares mainly in the centre of the country. Attempts to open up the Cerrados, including the building of Brasilia, have so far produced only moderate results. But scientists have now convinced the government that the region offers great potential for agriculture.

The problem with savannah regions is that the very old soils have been leached of plant nutrients so only rough scrub supporting inefficient cattle grazing will grow. Aluminium concentrations in the Cerrados are also up to three times more than will be tolerated by most crops. Yet the soil structure and climate are good.



The problems of cultivation in the area are largely the responsibility of a government research institute, in the middle of the region, about 20 miles outside Brasilia. According to Dr Elmar Wagner, its scientific director, the aluminium and acidity problem can be solved by adding limestone, in quantities of roughly 2 tonnes per hectare depending on the crop to be grown. Fertility can be finally restored by adding approximately 150–180 kg of phosphate per hectare, and then maintained by the addition of nitrogen, phosphate, potassium, a trace of zinc and good soil and crop management.

Although Dr Wagner claims that agriculture can be maintained with less fertilizer than is commonly used in industrialized countries, fertilizing such a vast area would be a costly undertaking for Brazil, which has to import most of the raw materials for its fertilizer. So the search is

on for suitable nitrogen fixing crops.

Brazil has already experienced considerable success in breeding soya beans, now its main export crop, which fix all their nitrogen requirement. But attempts in 1979 to introduce nitrogen-fixing soya beans into the Cerrados from the southern coastal states were unsuccessful. Now a team at the Rural University of Rio de Janeiro claims to have discovered why.

According to Joanna Dobereiner, leader of the team, the sudden cultivation of newly-reclaimed tropical soils seems to increase *Streptomyces* fungi which produce antibiotics that kill off nitrogen fixing *Rhizobium* bacteria on the plants' roots. By isolating those strains of *Rhizobium* which survive and inoculating them into soya bean roots, she obtained good soya bean yields in a recent field trial in the Cerrados. She claims that by careful rotation of crops and by use of streptomycin-resistant *Rhizobium*, it may be possible to eliminate most of the need for artificial nitrogen fertilizer which accounts for 70 to 80 per cent of all fertilizer investment.

Most of the growth in farming in the Cerrados since 1975 has been in rough pasture for cattle raising. But Dr Wagner thinks that greater efficiency could be achieved by concentrating on grain crops and forestry. By cultivating most of the area available with improved methods he estimates that the total annual yield of grain crops could rise from 7.5 million tonnes now to 125 million tonnes and that of forestry from 15 million tonnes to 600 million tonnes. Meat production, he says, could be increased from 2.2 million tonnes annually now to 8.0 million tonnes even with pasture area reduced from 144 million to 80 million hectares.

With ambitious plans to cut oil imports further by using alcohol substitutes for petrol and vegetable oil substitutes for diesel, Brazil's need to open up more land to cultivation is becoming crucial. The problem was highlighted this year when Brazil was forced to import black beans from Mexico because some black bean land in the south had been turned over to alcohol production. The question now is whether the Cerrados could be used to grow food, leaving the traditional agricultural lands of the south free for sugar cane for alcohol, or whether the Cerrados itself could be turned over to sugar cane production.

Whatever the decision, the government will be faced with the problem of encouraging the growth of the Cerrados. It has been criticized in the past for encouraging the exploitation of land by wealthy southerners who seek quick profits and who have little interest in long-term development. A major challenge now will be transferring the results of research to the farmer and helping Brazil's underprivileged farming community in the north-east region to take part in the developments.

Judy Redfearn

## Schmitt stars again

Washington

Eight years ago he was collecting rock samples on the Moon. This summer he was a key fund-raiser for presidential candidate Ronald Reagan. And next year he will be the central figure for science in the US Senate, with responsibilities ranging from the programme of the National Aeronautics and Space Administration (NASA) to the budget of the National Institutes of Health (NIH).

A graduate from the California Institute of Technology with a PhD in geology from Harvard, Harrison (Jack) Schmitt won a surprise election victory as Senator for New Mexico in 1976.



Astronaut (right) and Senator (left) Schmitt

Last week he was appointed to head the Senate Commerce Committee's subcommittee on science technology and space. The committee is responsible for overseeing the programmes of both NASA and — if Senator Schmitt has his way — the National Science Foundation.

Not surprisingly, Senator Schmitt has been a keen supporter of the space research programme. With Senator Adlai Stevenson, the subcommittee's present chairman, he has been strongly critical of the Carter Administration's "unimaginative" approach to space policy — and his appointment has been welcomed in the space science community.

More controversial is his selection as chairman of the Senate's labour, health and human services subcommittee — responsible, among other things, for the biomedical research budget of NIH. This post was expected to go to Senator Charles Mathias, a liberal Republican and an enthusiast for biomedical research. But Senator Mathias has now shifted his attention to the Judiciary Committee, where he will counterbalance that committee's new chairman, conservative Senator Strom Thurmond.

Senator Schmitt's attitude towards this area of research is little known. Although a member of the present subcommittee, he has played little part in its deliberations on the NIH budget. As a geologist, he is expected to favour support for basic science; as an astronaut, NIH officials fear he may be drawn towards the high technology aspects of medical care, rather than its social and environmental dimensions.

David Dickson



## CORRESPONDENCE

## Nuclear cheap?

SIR—May I comment belatedly on Professor Jeffery's letter on nuclear costs (*Nature* 23 October, p.674). It is pointless trying to recalculate electricity generation costs on the basis of arbitrary rules. If, as Professor Jeffery believes, capital costs are inadequately reflected, does he propose to recalculate the current costs of coal and its transport in terms of capital expended in the nineteenth century? How does he propose to take account of the fact that if there had been no nuclear contribution the additional fossil fuel supplies would have had to come from expanded output at the marginal and most expensive sources? The costs published by the Central Electricity Generating Board (CEGB) for generation from Magnox nuclear stations and coal and oil fired power stations of similar age and load history, show that on a perfectly proper accountancy basis, including allowance for costs yet to be incurred, the price we would be paying for electricity would be higher now had fossil stations been preferred in the past.

The industry has stressed, however, that this alone is not a guide to future investment, any more than it would be if Magnox fuel costs increased more rapidly than coal and reversed the current cost position. Incidentally Professor Jeffery's projection of fossil fuel prices in terms of the sum of coal and oil prices compounds changes in fuel mix and offsets rising coal prices with the decline in real oil prices following the major price excursion in 1973. It conceals the 60 per cent real increase in coal prices which occurred between 1970 and 1979.

Fuel cycle costs for advanced gas-cooled reactors or pressurized water reactors are different from Magnox in that they refer to oxide fuels with higher burn up for reprocessing in THORP. Estimated future fuel costs are based in part on the expected cost of this plant. Electricity costs for stations yet to be constructed are calculated in constant money terms on a levelized cost basis by summing expected future discounted expenditures and dividing by expected discounted output. Our calculations, which may differ in detail from those of CEGB, suggest that even if coal costs were held steady and uranium prices allowed to rise (both contrary to present trends) nuclear should retain a small cost advantage.

P.M.S. JONES

UK Atomic Energy Authority,  
London SW1, UK

## Biospheric works

SIR—I have just read your article concerning Unesco in the 6 November issue of *Nature*. While I shall refrain from commenting upon the overall content of the article—although for instance we do not know here of any "new technological order" which would have been approved by the recent Belgrade session of our General Conference—there is one point in your text which particularly puzzles me. You state that our programme on Man and the Biosphere (MAB)—in which many scientists and institutions actively participate all over the world—is a source of "largely empty generalizations" and that "people and member governments increasingly ask whether it can be worth its cost".

A few years ago I outlined this programme to your readers in a lead article which appeared in *Nature* of 17th July 1975. The programme was still only emerging from its preparatory phase. It is now fully operational, with close to a thousand very concrete research projects under way in some 75 countries. Around 200 biosphere reserves have been established under the programme in 50 countries. Networks of integrated pilot research, training and demonstration projects have been set up in the humid tropics and in the arid grazing lands. Cities like Rome, Frankfurt or Mexico are being studied as urban systems under MAB. The annual cost of the programme to Unesco is approximately \$2 million only. This catalytic amount has attracted—mainly from industrialized countries—some \$50 millions of extra-budgetary support. In the aggregate it is estimated that national commitments to MAB run at about \$200 millions per year. It would indeed be strange that research organizations would spend such amounts for applied ecological studies leading only to empty generalizations. And everyone present at Belgrade can testify that the programme received enthusiastic support from all governments represented, whether developed or developing.

As a final point, let me indicate that MAB will be 10 years old this year and that we are organizing next October jointly with the International Council of Scientific Unions a conference-exhibit to review the progress of MAB, to evaluate its achievements and shortcomings and to make recommendations for its future. Any constructive criticism which *Nature* and its readers would wish to make would be most appreciated. But sweeping unsubstantiated statements are of no use in this context.

M. BATISSE

Unesco, Paris, France

## More on museums

SIR—May someone who is not by profession a scientist join in your controversy about "Museum pieces"? For like so many other non-scientists I do have a strong interest here, and that an interest of the kind which surely ought, in the present case, to be overriding. That is to say, I am a devoted museum goer myself, with children who also need the help of museums in their education. What we consumers of museum services are entitled to expect from our national institutions is a clear, vivid, fair and balanced presentation of all available materials. When there is fundamental disagreement on any issue of substance between the best qualified professional experts, then we are entitled to be told that such disagreement exists and what the main points at issue are.

Dr L.B. Halstead has made a very serious charge (*Nature* 20 November, p.208) that in the Natural History Museum the exhibits of dinosaurs and of fossil man are now presented in terms of a new theory which none of his critics has yet even suggested represents the consensus of the experts. Nor, it would appear, have those responsible for making up these exhibits and compiling the accompanying booklets done anything to explain and to stress that theirs is only one

view, and that probably a minority view, among those who are best qualified to judge. I would emphasize again that I make no pretensions whatsoever to any such special expertise. But it requires no expertise at all to recognize that Dr Halstead's charges are very serious indeed, and that none of the critics whose letters you have so far published has made any attempt to show that the situation is not in fact as scandalous as Dr Halstead's original letter suggested that it is.

ANTONY FLEW

Department of Philosophy,  
University of Reading, UK

SIR—In response to correspondence from L. B. Halstead (*Nature* 20 November, p. 208), I feel obligated to point out that while science is generally regarded as the outgrowth of processes of the cerebral cortex, Halstead's criticisms of cladistics seem to emanate more from the anterior pituitary.

First, although phylogenetic systematics (cladism) and the punctuated equilibria mode of evolution are largely complementary in their theoretical structure, at least one articulate spokesman for punctuated equilibrium is not a cladist, and therefore it is incorrect to lump the two schools together.

Next, although I am as firmly convinced of gradualism and evolutionary systematics as anyone, it is academic vigilantism to deny the cladists and punctuationalists their day in court. Those views are propounded by extremely competent scholars, whom I perceive to be fundamentally committed to the advancement of our understanding of the history and dynamic processes of life on Earth. This is a different goal (in fact, a directly opposite goal) from that of the creationists, and it is highly inappropriate for Halstead to analogize between their motives.

As for Halstead's innuendo that punctuational evolution is a Communist plot, I confess that I am never quite sure when British people are kidding, but I hope that Halstead was. Gould and Eldredge did spend one page of a thirty-five-page paper (*Paleobiology* 3, 115; 1977) relating their punctuational model of evolutionary change to the more general views of change espoused by Marx. Halstead's criticisms, however, do not address either the issues or the data; they instead take the form: (1) Marxism is wrong; (2) therefore, everything a Marxist says is wrong. This is obscurantism of a most pernicious sort, and side-steps the critical question of whether or not cladism or a punctuational mode of evolution has anything important to contribute to our understanding of the world.

When I see the maxillary and mandibular remains of the Miocene and Pliocene hominoids, I see (along with Halstead, I suspect) anagenesis, migration, allopatric speciation and gradual genetic divergence—without necessary recourse to a punctuational scheme. I do not see, however, how the vituperative essay of Halstead's sheds any new light on any relevant issues. Science should proceed through the critical analysis of ideas and explanations by recourse to the facts at hand: processes of logic and reason. Let us keep our hormones out of it.

JON MARKS

Department of Anthropology,  
University of Arizona, Tucson

## NEWS AND VIEWS

# Climate and variability in the solar constant

from Douglas Gough

AT one time or another almost every fluctuation in the Earth's climate has been attributed by someone to a variation in the solar constant. In many cases alternative, more convincing explanations have been found. For others there is mounting evidence that Milankovich's idea is correct: that variation in terrestrial insolation arising from changes in the elements of the Earth's motion is an important controlling factor. But there remain components of the climatic variation that are otherwise unexplained, and so it has recently become fashionable to study the implications of changes in the solar constant that arise from intrinsic variations in the solar energy flux. This has occurred partly because observational techniques now make it feasible to measure the small fluctuations that many meteorologists and climatologists believe to be sufficient to produce deviations in our weather.

At a recent workshop\* issues concerning the intrinsic variability of the Sun were discussed. The principal aim was to consider observations of the solar luminosity and radius, and to determine to what extent solar phenomena are correlated with changes in terrestrial climate.

The meeting began with a review by G. North (Goddard Space Flight Center) of climate modelling. This very difficult subject is still in a primitive state and any conclusions drawn from it must be viewed with caution. In 1973 the response of a rather sophisticated climate model (that devised by Tzvi Gal-Chen and S. Schneider at the National Center for Atmospheric Research) was investigated to see if a reduction in the solar constant of a few per cent would be sufficient to cause an ice age. The decrease was found not only to bring about an ice age but also produced a result that had not been anticipated: when the solar constant was restored to its original value, or even to a value somewhat higher, the ice would not melt. Astrophysicists believe firmly that the solar luminosity has evolved gradually during the past  $4.7 \times 10^9$  years from about 70 per cent of its present value, and thus the implication of that climatological experiment appeared to be that the Earth must always have been covered with ice. This is evidently not the

case. Therefore it seems inevitable that the climate model must be inadequate. Presumably the Earth has some stabilizing mechanism which operates only on a long time scale and which has not been taken into account. The Earth must be stable to the gradual evolutionary variation of the solar constant, but perhaps not to fluctuations on shorter time scales.

According to North, the situation has not changed since that experiment was performed. There have been various attempts to accommodate the evolutionary rise in the solar luminosity, by supposing the composition of the Earth's atmosphere to have changed such that the resultant variation in the atmospheric greenhouse effect cancelled the effect of the changing solar constant. But this variation has not been coupled either to the flux of incoming radiation, or to the state of the climate, so it appears to be quite accidental that the Sun and the Earth have kept in step. If one accepts that this is unlikely, one is left with what has recently been called the faint Sun paradox: either the astronomers are wrong or the climatologists are wrong; and if the latter is the case, either a long-term climatic stabilizing mechanism must exist or the climate is not really sensitive to changes in insolation on any time scale.

The evolutionary rise in the solar luminosity seems difficult to question, as A. Endal (Louisiana State University) emphasized. It is an apparently straightforward consequence of basic atomic and nuclear physics, gas kinetics and Newtonian gravitation. Therefore the astrophysical conclusion is robust. The sole caveat one might envisage is that perhaps the constant of gravitation ( $G$ ) is decreasing with time, as some cosmologists have suggested. The rate by which  $G$  must decrease to prevent a substantial variation in the solar constant is  $-G/G = 1 \times 10^{-11} \text{ y}^{-1}$ , which is below the present level of detectability. However, in the foreseeable future planetary ranging will no doubt enable measurements to be made.

On the other hand, the climatic balance appears to be rather delicate. A satisfactory self-contained theory does not exist, and the toy models, as North called them, rely on parameters which are determined from present-day empirical evidence and which are assumed to remain constant for all time. Evidently if the dependence of those parameters on the state of the climate were known and could be incorporated into the toy models, a drastic change in the stability

characteristics of those models could result.

To determine whether climate responds to small changes in the solar output, attempts have been made to correlate its variation with the solar cycle. This is a difficult task, since the response is only a small component of total climatic variation. Extensive work has been carried out by J.M. Mitchell, C.W. Stockton and D.M. Meko (in *Solar-terrestrial influences on weather and climate* p.125, eds McCormac, B.M. & Seliga, T.A., Reidel, Dordrecht, 1979), who have obtained an index of the average drought in the US since 1700 from tree-ring analysis. They have found a strong though imperfect correlation with the 22-year cycle, which agrees better with the actual sunspot record than with a regular oscillator with the same mean period. P.R. Bell (IEA) pointed out that an even better correlation exists between the drought record and a combination of the solar cycle and the lunar tides. The agreement is impressive, though its significance was challenged by Mitchell (NOAA, Silver Spring). According to M. Stuiver (University of Washington, Seattle) there is evidence for solar cycle variations in the  $^{14}\text{C}$  record, but there do not seem to be global climatic changes associated with the Maunder and Spörer minima (see *Nature* 286, 868; 1980).

Analyses of this kind have a bearing not only on climatology but also on the physics of solar variability. If an unambiguous relation between climate indices and certain aspects of solar variation could be established, it would be possible to attempt heliochronology from proxy records. Then one might be in a position to establish whether the solar cycle is regulated by an oscillation in which the entire Sun participates, or whether it is a phenomenon that is confined to the convection zone and its immediate environs.

A key to this problem may be the relative changes in the luminosity  $L$  and radius  $R$ , measured by the parameter  $W = \Delta \ln R / \Delta \ln L$ , where  $\Delta$  represents the small change associated with the cycle. It was agreed at the workshop that if the cycle were a purely superficial phenomenon, then  $W \approx 0$ . If, on the other hand, it is deep-seated, the magnitude of  $W$  is of

\*The workshop on solar constant variations was held at the Goddard Institute for Space Studies in Greenbelt, Maryland from 5 to 7 November, 1980. An extensive review of the meeting will be published by S. Sofia in due course.

Douglas Gough is in the Institute of Astronomy and the Department of Applied Mathematics and Theoretical Physics, University of Cambridge.



order (though rather less than) unity. Moreover, it appears that  $W > 0$  if surface variations result from perturbations throughout or at the base of the convection zone, as E.A. Spiegel and N.O. Weiss (*Nature* 287, 616; 1980), for example, have argued, and  $W < 0$  if the perturbing process is confined to the core, as R.H. Dicke (*New Scientist* 83, 12; 1979) upholds. Measurement of  $W$  is thus of great interest.

A whole day of the workshop was devoted to measurements of the solar constant. Rocket and balloon flights have not been frequent enough to gather much reliable information about trends, and ground-based observations have been plagued by interference from the Earth's atmosphere. In a critique of the day's proceedings, C. Fröhlich (Physikalisch-Meteorologisches Observatorium, Davos) concluded that the data were consistent with no variation, but that a secular decrease in  $L$  from 1966 at the rate of 0.1 per cent per decade is not ruled out. It must be appreciated that this apparent trend is merely the result of linear regression through data with large gaps. Recent measurements of visible and ultraviolet sunlight from the Nimbus and SMM satellites suggest a decrease in  $L$  at the rate of about 0.1 per cent per year since 1976, the year of the last sunspot minimum. If all the data are taken into consideration and the possibility of some observational inaccuracy is accepted, one might also see with an eye of faith the hint of a variation associated with the sunspot cycle, with amplitude a few tenths per cent and such that luminosity maxima occur at sunspot minima.

There is another interesting luminosity variation which has a lesser bearing on the main issues confronted at the workshop, and which was agreed by all concerned with the measurements to have occurred. This is an occasional decrease of order 0.1 per cent which persists for about 10 days. On the two occasions on which it has been observed there was a very large sunspot group on the solar disk. Thus it appears that sunspots can reduce the total heat flux through the photosphere for intervals comparable with the turnover time of the larger eddies in the convection zone. This indicates that the sunspot phenomenon is deep-seated, and not confined merely to the supergranular layers as some workers have maintained.

To complete the measurement of  $W$  one must obtain  $R$ . This might be inferred from the effective temperature via the black body radiation law, once the luminosity is known. Spiegel and Weiss (loc. cit) have used estimates of temperature variations made by W.C. Livingston (*Nature* 272, 340; 1978) from the CI 5380 spectrum line. However, Livingston (Kitt Peak Observatory) reported at the workshop that subsequent analyses of other lines, formed higher in the solar atmosphere, do not agree with the earlier conclusion. It appears that the atmospheric temperature

gradient has decreased between 1976 and 1980, but how this relates to the photospheric radius is unclear.

Direct measurements of the solar radius were discussed at some length. Most of this concerned trends on a time scale of centuries, which one might imagine to have been a relaxation from the Maunder minimum. There is a good deal of scatter in the data, and this no doubt has arisen in part from observational error. Eddy (High Altitude Observatory) reported a re-analysis of the Greenwich meridian circle data, and stands by his earlier conclusion (Eddy, J.A. & Boornazian, A.A. *Bull. Am. astr. Soc.* 11, 437; 1979) that the Sun appears to be shrinking, though the rate has been revised downwards. The estimate is now about 0.1 per cent per century, in rough agreement with the values reported by D. Dunham (Computer Science Corporation, Silver Spring) from eclipse analysis, and by B.J. LaBonte and R. Howard (Mount Wilson Observatory) from Mount Wilson photographs. It was noted that this disagrees with I. Shapiro's null result (*Science* 208, 51; 1980) obtained from Mercury transit measurements. Ancient transit measurements, like the Greenwich data, were dependent on observers' judgement, Eddy said, and it is hard to assess the accuracy of the results.

With this remark in mind it is perhaps not surprising that Parkinson *et al.* (*Nature* 288, 548; 1980) have concluded that Eddy and Boornazian's result is not a property of the Sun, but is simply a measure of the variation in not only the observers' opinions but also the seeing conditions and instrumentation. Parkinson *et al.* rediscuss the meridian circle measurements in this light, and also consider Mercury transit and solar eclipse data. They find no convincing evidence for a long term trend, though they do see the hint of a variation on a time scale of about 80 years. It has long been known that this is a time scale

associated with the sunspot cycle (Wolf, R. *Astron. Mitt. Zurich* 14, 1; 1862). It characterizes an irregular amplitude modulation of a kind common to a large class of nonlinear oscillators. It is not unlikely, therefore, that the seat of the modulation is intimately connected with the mechanism of the 22-year oscillation itself. Therefore the phase of the modulation relative to the radius variations is not without interest. Comparing figure 3 of Parkinson *et al.* with the sunspot data (for example, Waldmeier, M. *The sunspot-activity in the years 1610-1960* Schulthess, Zürich, 1961) suggests that maximum radius occurs at about the time when the amplitude of the sunspot cycle is at a minimum.

On a shorter time scale, LaBonte and Howard have deduced from Mount Wilson photoelectric measurements that a decrease in radius of about 0.01 per cent has occurred since 1974. During most of that time sunspot activity was increasing. T. Duvall (Goddard Space Flight Center) has made measurements of  $R$  using the vacuum tower at Kitt Peak National Observatory and H.A. Hill's (University of Arizona) finite Fourier transform definition of the solar limb. At the workshop he reported a decrease of  $0.02 \pm 0.02$  per cent since last December. Hill plans to improve the measurement, and hopes to achieve an accuracy of one part in  $10^7$ .

In summary, we cannot really be sure how either  $L$  or  $R$  is varying on time scales of decades or centuries. Measurements of radius variations over centuries are subject to a good deal of uncertainty, and direct luminosity measurements do not exist. But if one accepts the hints from the most recent observations, one may be tempted to infer that perhaps there are variations in  $L$  and  $R$  over the sunspot cycle, with maxima in both  $L$  and  $R$  occurring at sunspot minima. If that is indeed the case, then  $W > 0$ . □

## Development of spinal sensory systems

from T.M. Jessell and M. Yamamoto

CLASSICAL studies on the development of the spinal cord have focused on the motor neurone and its peripheral target, and the part played by synapse elimination and cell death in the modelling of connections<sup>1</sup>. Yet motor neurone death represents only the first in a series of changes which involve the elimination or reorganization of sensory and spinal neurones and which are

T. M. Jessell and M. Yamamoto are in the Department of Pharmacology, St. George's Hospital Medical School, University of London.

probably not completed until well after birth. Staining techniques that make it possible to trace individual afferent nerves have shown that sensory fibres that can be distinguished on the basis of their peripheral receptive properties also have unique and characteristic terminal arbors in the central nervous system. But how such specificity is generated is only just beginning to be understood.

In the developing rhesus monkey, for example, sensory fibres enter the dorsal horn of the spinal cord during the first

quarter of the gestational period and form well defined synaptic connections with cells occupying the most superficial border of the dorsal horn<sup>2</sup>. Three weeks later, however, these superficial neurones have degenerated, to be replaced by migrating cells that represent the future laminae I and II neurones. This loss of central targets may contribute to the degeneration of sensory neurones that is known to occur during normal development. But not all the sensory axons deprived of their post synaptic targets necessarily degenerate; others may survive to establish new and more stable synapses with superficial dorsal horn neurones<sup>2</sup>.

Moreover, remodelling is not only a question of the elimination and re-establishment of afferent and efferent connections; the spinal inter-neurones themselves undergo extensive morphological changes as they mature. In new-born mammals the neurones in the marginal zone and substantia gelatinosa have stubby, radial dendrites that lack any defined orientation. During the first two weeks after birth they shed some dendrites and elongate others to arrive at their final characteristic morphology<sup>3</sup>. The cues for neuronal elimination and dendritic reorganization in the dorsal horn are unknown and the contribution, if any, of afferent input may be difficult to determine. In the cerebellar cortex where similar problems have been examined in greater detail, the development of Purkinje cell dendrites appears to be partially dependent on intact climbing fibre or granule cell inputs<sup>4,5</sup> although even in the absence of presynaptic elements, a relatively elaborate dendritic arbor can still be generated.

These data raise interesting questions about the mechanisms by which the morphology of individual neurones is changed. At present, the only evidence bearing on this issue is ultrastructural. The additional membrane necessary for elongation of dendrites in the spinal cord, for example, seems to be generated by the fusion of vesicles with existing dendritic plasma membrane<sup>6</sup>; and degenerating spinal dendrites first become apparent as beaded processes containing numerous vesicles that eventually fuse to form cavities. Extraneous synapses on motor-neurones, on the other hand, seem to be removed by a rather more involved procedure. During the early post-natal period the number and distribution of synaptic terminals on motorneurones decreases by about 50 per cent<sup>7</sup>. In a series of beautiful ultrastructural studies, Ronnevi<sup>8</sup> has demonstrated that the phagocytosis of some synaptic terminals on motorneurones may be undertaken by the motorneurone itself. Motorneurone cell bodies can be seen to contain spherical presynaptic inclusions that have double-walled membranes and are packed with synaptic vesicles. The motorneurone is highly selective in the class of synaptic

terminal it engulfs, and other terminals are removed only by glial cells. Very similar double-walled vesicular structures have been noticed in embryonic mouse spinal cord<sup>9</sup> and in the immature cerebellar cortex<sup>10</sup> suggesting that this form of membrane remodelling may in fact be quite common in early development.

While investigations on the specific morphology and connectivity of sensory neurones have only relatively recently been attempted, it has not been until the past year that serious investigations on their specific chemical differentiation have become possible. The difficulty was that no sensory neurotransmitter had been identified, and the breakthrough has come with the discovery of substance P, somatostatin, cholecystokinin (or one of its shorter fragments) and vasoactive-intestinal polypeptide within small dorsal root ganglion neurones<sup>11</sup>. While it is still unclear what part these peptides may play in synaptic transmission or modulation, they have provided several new markers with which to examine the differentiation of sensory neurones. Kessler and Black<sup>12</sup> have shown that the substance P content of rat sensory neurones is markedly increased after post-natal administration of nerve growth factor (NGF), which is already known to be essential for the early development of dorsal root ganglion cells. Conversely, neonatal administration of anti-NGF antibodies depletes substance P from the cell bodies and terminals of immature sensory neurones<sup>13</sup>. Using rhodamine-conjugated NGF<sup>14</sup> it has been possible to show that NGF binds to receptors clustered at the tips of growing axons and is internalized and transported back towards the cell body of the neurone. Whether the internalized receptor complexes play any part in the actions of NGF on sensory neurones is, however, not yet known. Nor is it clear in these circumstances whether NGF is enhancing the survival of neurones already committed to the synthesis of substance P, or inducing substance P synthesis in neurones which would otherwise not have synthesized it. Two recent developments may make it

possible to answer this kind of question. First, there is evidence from experiments *in vitro* for two subpopulations of dorsal root ganglion neurones, only one of which depends for survival on NGF: the other will die in the presence of even a high concentration of NGF, but can be rescued by a factor derived from cultured glioma cells<sup>15,16</sup>. The generation of purified subpopulations of sensory neurones in culture on the basis of their growth-factor sensitivity may thus soon be feasible, and should help to resolve the question of whether the effects of NGF on peptide synthesis are due to selection or induction of cells.

The second important development is the discovery that 'factors' derived from non-neuronal cells can influence peptide synthesis by cultured sensory ganglion cells. Cultures of chick sensory neurones grown in the absence of other kinds of cells contain eight times as much substance P as somatostatin<sup>17</sup>. In the presence of ganglionic non-neuronal cells, the same number of neurones make six times as much somatostatin as substance P. This dramatic switch (analogous to the adrenergic-cholinergic switch reported for autonomic neurones *in vitro*<sup>18</sup>) can be reproduced by adding medium conditioned by non-neuronal cells to 'neurone-alone' cultures, but is independent of NGF-like material. This suggests that early in development a given sensory neurone may have the capacity to synthesize and store more than one peptide. Final determination of peptide expression is probably induced, by factors other than NGF, at a later stage, since somatostatin and substance P are present in separate populations of small dorsal root ganglion neurones in adult animals<sup>19</sup>. Cholecystokinin and vasoactive-intestinal polypeptide are also found in some sensory neurones so the choice open to a single neurone may be greater still.

In adult animals, peptides in sensory neurones have been assumed to function in synaptic transmission. They may however also have a trophic role during development, as has been suggested for the conventional neurotransmitters noradrenaline and 5-hydroxytryptamine. Destruction of noradrenergic neurones in the locus coeruleus of neonatal rats modifies the postnatal arborization of pyramidal cell dendrites in the neocortex<sup>20</sup> while inhibition of 5-hydroxytryptamine synthesis in embryonic rats delays the development of neurones in regions normally receiving a 5-hydroxytryptamine input<sup>21</sup>. Peptides released from immature sensory neurones as they grow into the spinal cord could then regulate the differentiation of surrounding neurones. The use of anti-NGF antibodies or capsaicin to deplete sensory neurones of substance P would provide one method of analysing the role of substance P and possible other peptides in the development of spinal neurones.

1. Purves, D. *Nature* **287**, 585 (1980).
2. Knyihar, E. *et al. Science* **202**, 1206 (1978).
3. Gobel, S. J. *Comp. Neurol.* **180**, 375 (1975).
4. Bradley, P. & Berry, M. *Brain Res.* **142**, 135 (1978).
5. Sotelo, C. *et al. Brain Res.* **98**, 574 (1975).
6. Falls, W. & Gobel, S. F. *Comp. Neurol.* **187**, (1979).
7. Conradi, S. & Ronnevi, L. O. *J. Neurocytol.* **6**, 195 (1977).
8. Ronnevi, L. O. *Brain Res.* **162**, 189 (1979).
9. Vaughn, J. E. & Sims, T. J. *J. Neurocytol.* **7**, 337 (1978).
10. Eckenhoff, M. F. & Pysh, J. J. *J. Neurocytol.* **8**, 623 (1979).
11. Hokfelt, T. *et al. Nature* **284**, 515 (1980).
12. Kessler, J. A. & Black, I. B. *Proc. natn. Acad. Sci. U.S.A.* **77**, 649 (1980).
13. Otten, U. *et al. Nature* **287**, 158 (1980).
14. Levi, A. *et al. Proc. natn. Acad. Sci. U.S.A.* **77**, 3469 (1980).
15. Barde, Y. A. *et al. Proc. natn. Acad. Sci. U.S.A.* **77**, 1199 (1980).
16. Barde, Y. A. *et al. Nature* **274**, 818 (1978).
17. Mudge, A. *Soc. Neurosci. Abstr.* **5**, 584 (1979).
18. Patterson, P. H. A. *Rev. Neurosci.* **1**, 1 (1978).
19. Hokfelt, T. *et al. Neuroscience* **1**, 131 (1976).
20. Maeda, T. M. *et al. Brain Res.* **70**, 515 (1974).
21. Lander, J. M. & Krebs, H. *Dev. Neurosci.* **1**, 15 (1978).



# Successes and failures in human *in vitro* fertilization

from Alexander Lopata

THREE infertile women have given birth to normal infants following *in vitro* fertilization (IVF) and embryo transfer (ET). In each of these women a single embryo had been implanted into the uterus during the early luteal phase of a natural menstrual cycle on one or several occasions<sup>1,2</sup>. Three other women conceived following ET but spontaneously aborted the fetus. One miscarried a 69XXX triploid fetus at 7 weeks gestation, a second miscarried an anatomically normal male fetus whose karyotype showed pleomorphism at 15D and a large Y chromosome at 21 weeks<sup>3</sup>, while the third miscarried a completely normal male fetus at 20 weeks following chorioamnionitis caused by an anaerobic Gram-negative bacillus.

The four pregnancies reported by Edwards and Steptoe<sup>1</sup> resulted from 32 embryo transfers and the two pregnancies reported by Lopata *et al.*<sup>2</sup> were obtained after 14 embryo transfers in 1979. After a number of changes were introduced in their laboratory the latter group carried out 10 additional embryo transfers by mid 1980 but have not obtained further pregnancies. Table 1 was compiled from the combined data and shows that at present the average efficiency of human embryo transfer is approximately 11 per cent whereas the probability of having a child following embryo transfer is three per cent. In contrast to this, live births have not yet occurred following transfer of one or more cultured embryos into the uterus of women whose ovaries had been stimulated with gonadotrophins or with Clomiphene citrate and hCG. Moreover, the efficiency of embryo transfer appears to be very low in these subjects since only three abortive pregnancies resulted from more than 77 embryos transferred by Edwards *et al.*<sup>1</sup> and biochemical evidence of early pregnancy was obtained in only three subjects

following 48 embryos implanted by the Melbourne group.

It should be noted that the computed success rate shown in Table 1 would be much lower if it were calculated on the basis of the total number of subjects monitored (treatment cycles) rather than on the basis of the number of embryo transfers carried out. Edwards and Steptoe monitored 78 menstrual cycles to obtain the 32 embryo transfers, whereas the Melbourne group monitored 69 subjects in 1979 and 63 in 1980. Thus, out of 210 women participating in the IVF and ET programmes, six became pregnant and of these, three delivered normal infants. The large wastage ensues from one of the following: failure to detect the distinct surge of luteinising hormone (LH) which is used for timing oocyte collection; ovulation occurring shortly before the ripe follicle is aspirated; the ovary containing the dominant follicle being inaccessible at laparoscopy; failure to recover an egg when the preovulatory follicle is aspirated; failure of fertilization or normal cleavage of the egg; failure of the embryo to establish pregnancy after it is transferred into the uterus.

Timing the collection of a preovulatory egg on the basis of 3-hourly urinary LH assays to detect the beginning of the gonadotrophin surge, which Edwards and Steptoe and the Melbourne group have used, is complicated by the following considerations. An oscillation in LH excretion is frequently detected before a distinct surge begins. The slope of the gonadotrophin surge and the peak value obtained may vary considerably between patients and often between menstrual cycles in the same patient. As these variations are inherent to the 3-hourly urinary LH assays, the criteria used to judge the start of the surge must be clearly defined to allow comparison of the time intervals (from start of surge to oocyte collection) selected by different groups of investigators.

Timing may begin from the baseline after the LH surge is detected, or from the mid-point of the first 3-hour interval when a sequential increase in LH begins, or from when the level of urinary LH excretion has increased by more than one, or two, standard deviations above the average baseline value. When timing began from the mid-point of the first 3-hour interval at which a sustained increase in urinary LH was detected, it was found that eggs recovered at 24 hours either failed to fertilize *in vitro* or underwent abnormal fertilization, whereas eggs recovered after 26, 28 and 30 hours yielded morphologically normal embryos. The two pregnancies reported by our group resulted from eggs collected 28 hours after the onset of the urinary LH surge. Steptoe *et al.*<sup>3</sup> have reported that their first two pregnancies resulted from eggs collected at 26 hours after the LH surge and the second two pregnancies from eggs aspirated after 24 hours. However, the criteria used for starting the timing of the interval for oocyte collection have not been defined by this latter group.

The time sequence of intrafollicular maturation of preovulatory eggs in women ovulating spontaneously needs to be further investigated. Using ultrasonic scanning of the preovulatory follicle, commencing at 27 hours after the onset of the LH surge and rescanning several times per hour until ovulation occurred, de Crespigny *et al.*<sup>4</sup> found that the interval from the start of the urinary LH surge to ovulation varied from less than 27 hours to 35 hours in nine women. Although this established that the time for follicular rupture varied by up to 8 hours between subjects it is now important to determine whether intrafollicular oocyte maturation requires a more constant time interval and is therefore independent of the actual time of ovulation. If, for example, preovulatory oocytes mature 24 hours after the LH rise, the follicle should be aspirated 25 to 26 hours after the onset of the surge to avoid spontaneous ovulation which occurs in about 20 per cent of subjects by 28 hours. On the other hand if meiotic maturity is incomplete, maturation of the egg in culture for several hours before insemination may improve results. Conversely, even brief periods of culture may be detrimental to mature human eggs, particularly if they resemble mature rabbit eggs which after 2 to 3 hours of ageing in culture remain fertilizable, but yield significantly fewer viable embryos<sup>5</sup>.

*In vitro* fertilization of human eggs has been reported to occur in modified Tyrode's solution formulated by Bavister<sup>6</sup>

**Table 1** The current human embryo transfer efficiency and the probability of having a child by *in vitro* fertilization and embryo transfer

|                               |   |             |  |
|-------------------------------|---|-------------|--|
| <b>Oldham/Cambridge group</b> |   |             |  |
| Embryo transfers              | 32  |             |  |
| Pregnancies                   | 4   |             |  |
| <b>Melbourne group</b>        |   |             |  |
|                               | <b>1979</b>   | <b>1980</b> |  |
| Embryo transfers              | 14  | 10          |  |
| Pregnancies                   | 2   | 0           |  |
| Combined Transfer Efficiency  | $= \frac{\text{Total pregnancies}}{\text{Total embryos transferred}} = \frac{6}{56} = 10.7\%$ |             |  |
| Probability of having a child | $= \frac{\text{Live births}}{\text{Embryos transferred}} = \frac{3}{56} = 5.4\%$              |             |  |

Alexander Lopata is in the Department of Obstetrics and Gynaecology, University of Melbourne, and the Reproductive Biology Unit, Royal Women's Hospital, Carlton, Victoria, Australia.

and adapted by various investigators<sup>7,8,9</sup>, in media described by Biggers, Whitten and Whittingham<sup>10</sup>, and by Hoppe and Pitts<sup>11</sup> as well as in modified Ham's F10 medium<sup>2</sup>. Features common to these media include: a bicarbonate content which has been adjusted to maintain a pH between 7.4 and 7.6 in an atmosphere of 5 per cent CO<sub>2</sub>; an osmolality adjusted to between 280 and 285 mOsmol/kg; supplementation with either crystalline albumin (bovine or human), or with inactivated human serum, both of which are believed to favour *in vitro* capacitation and fertilization. Approximately 10<sup>6</sup> motile spermatozoa per ml of medium are frequently used for inseminating human eggs although concentrations ranging from 0.5 to 2.0 × 10<sup>6</sup> per ml have been employed. The duration of insemination, using washed spermatozoa, resulting in proven fertilization has ranged from 3 to 24 hours<sup>9,12</sup>. It is not known whether the conditions and media currently being used are optimal for human *in vitro* fertilization as adequately controlled experiments and statistical evaluations have not yet been reported.

Ham's F10 medium has been used most successfully for completing syngamy and initiating cleavage in fertilized human eggs, and for supporting development of the embryo up to the blastocyst stage<sup>13,14</sup>. This medium has been reported to be favourable for human preimplantation embryo growth at osmolalities ranging from 280 to 300 mOsmol per kg, and at pH levels from 7.2 to 7.4 in an atmosphere of 5% CO<sub>2</sub> + 5% O<sub>2</sub> + 90% N<sub>2</sub> at 37°C. As a general rule the medium is supplemented with either inactivated human serum, fetal calf serum or human cord serum, at levels ranging from 15 to 30 per cent. Other additions including antibiotics, glutamine, calcium, lactate, pyruvate and crystalline albumin may have been used yet these modifications are not reported in publications. Investigators tend to introduce changes in the culture media and in the procedures they use. The exact culture media used, the supplements added and their final concentration, the final pH and osmolality of the insemination and culture medium, and the duration of

incubation before fresh medium (if any) was introduced into the culture system, have not yet been sufficiently detailed by Edwards *et al.*<sup>1</sup> to enable others working in this area to duplicate the laboratory procedures which have resulted in the four pregnancies following IVF and ET.

Human embryos developed *in vitro* and transferred into the uterus through the cervix have a very low chance of establishing a pregnancy that will continue. The high wastage of transferred embryos may be due to defects in the embryo, endometrium, corpus luteum or the transfer procedure. A cleaving embryo placed in the uterus may fail to develop into a normal blastocyst or it may carry a chromosomal abnormality which causes its

early death. The luteal endometrium may become asynchronous with the stage of development of the embryo, or non-receptive as a result of the absence of humoral or hormonal factors released by the cultured embryo. An inadequately functioning corpus luteum may result from damage sustained by the follicle during oocyte aspiration, or its function may not be sustained due to the absence of an embryonic signal. Poor transfer technique may lead to damage of the embryo, or endometrium, or to failed retention of the embryo in the uterus. It is proposed that a systematic evaluation of all these factors is required before the next significant advance in human IVF and ET will be achieved.

## How heavy is a cold photon?

from N. Dombey

A welcome sign of the healthy state of theoretical physics today is the breakdown of the barriers which are insisted upon by grant-giving bodies and by most physics departments. Our research students in Britain, for example, must be strictly divided into astrophysicists (responsible to the SRC Astronomy, Space and Radio Board), nuclear or particle physicists (Nuclear Physics Board) and 'rest of physics' physicists (Science Board). But however useful (or useless) these divisions may be for experimentalists, they have been increasingly ignored by theorists over the last ten years or so.

The initial serious breakdown of these divisions came in the early 1970s as a result of Wilson's success with the application of renormalizable field theory to the classical problem of phase transitions; for the first time a sensible answer was provided to the question of why many critical indices are universal and independent of the substance undergoing the phase transition.

Many-body physics problems have for long been described in terms of thermodynamic, temperature-dependent Gibbs averages<sup>1</sup> rather than the zero-temperature vacuum expectation values of quantum field theory. It was also widely realised that a continuum limit of a crystal lattice system is applicable when the range of the excitations of interest is large compared with the lattice spacing as it is at a phase transition. But a systematic reduction of the different interactions of solid-state physics to the appropriate field theory came only with Wilson's work (see reference 2). Thus a Heisenberg ferromagnet can be reduced to the theory of an isovector scalar field  $\phi$  with an interaction  $|\phi|^2$  as for pions in particle physics. The critical exponents of the phase transitions can be calculated from the functions defined by the renormalization group equations of the field theory (for a

review see Kogut and Wilson<sup>3</sup>).

A phase transition represents a transition from one type of ordering or symmetry to another: in a ferromagnet, for example, all directions are equivalent above its transition temperature  $T_c$  (in the absence of an external magnetic field) so the system as a whole is rotationally invariant, but below  $T_c$  a ferromagnet will have a direction of magnetization which breaks this rotational symmetry. The interaction Hamiltonian which describes the behaviour of a ferromagnet for  $T < T_c$  as well as  $T > T_c$  is rotationally invariant — but the theory shows that the ground state of the system for  $T < T_c$  is one with the spins preferentially pointing in the same direction and thus does not satisfy rotational invariance. This is an example of 'spontaneous symmetry breaking' and it is characterized by the ground state not possessing the full symmetry of the interaction describing the system. Such theories have been studied now for many years both in solid-state theory (condensed-state theory is a better term to include superconductivity and superfluidity) and in particle theory where the Higgs mechanism of spontaneous symmetry breaking is used in analogy with the theory of superconductivity to generate mass. The best known case of this is the spontaneously broken unified gauge theory  $SU(2) \times U(1)$  of weak and electromagnetic interactions (*Nature* 282, 131; 1979) where the mass of the gauge particles  $W^\pm$ ,  $Z^0$  is generated in this way although in the underlying unbroken gauge theory they would have zero mass.

Thus a class of field theories with similar properties has been studied during the past ten years in both particle theory and condensed-state theory. The linkage with astrophysics and cosmology has more recently paralleled these studies, motivated in particular by the asymmetry of baryons (protons and neutrons) in the universe. According to the generally accepted big-bang theory the universe has been

1. Edwards, R.G., Steptoe, P.C. and Purdy, J.M. *Br. J. Obstet. Gyn.* 87, 737 (1980).
2. Lopata, A., Johnston, I.W., Hoult, I.J. and Speris, A.L. *Fertil. Steril.* 33, 117 (1980).
3. Steptoe, P.C., Edwards, R.G. and Purdy, J.M. *Br. J. Obstet. Gyn.* 87, 757 (1980).
4. de Crespigny, L.Ch., O'Herrilhy, C. and Robinson, H.P. (in preparation).
5. Fraser, L.R. and Dandekar, P.V. *J. exp. Zool.* 184, 303 (1973).
6. Bavister, B.D. *J. Reprod. Fertil.* 13, 544 (1969).
7. Edwards, R.G., Bavister, B.D. and Steptoe, P.C. *Nature* 221, 632 (1969).
8. Soupart, P. and Strong, P.A. *Fertil. Steril.* 25, 11 (1974).
9. Lopata, A., Brown, J.B., Leeton, J.F., Talbot, J.M. and Wood, C. *Fertil. Steril.* 30, 27 (1978).
10. McMaster, R., Yanagimachi, R. and Lopata, A. *Biol. Reprod.* 19, 212 (1978).
11. Hoppe, P.C. and Pitts, S. *Biol. Reprod.* 8, 420 (1973).
12. Lopata, A., McMaster, R., McBain, J.C. and Johnston, W.I.H. *J. Reprod. Fertil.* 52, 339 (1978).
13. Steptoe, P.C., Edwards, R.G. and Purdy, J.M. *Nature* 229, 432 (1971).
14. Lopata, A. and Kohlman, D. *Abstracts of Australian Obstetrical and Gynaecological Research Society*, Armidale (1980).

N. Dombey is in the Department of Physics, University of Sussex.



expanding, and thereby cooling, from a state with infinite temperature and density, and the matter in the universe was created in the early stages of this process. Yet in spite of the law of baryon conservation, the universe contains large numbers of protons and neutrons, not anti-protons and anti-neutrons. Sakharov<sup>3</sup>, in a pioneering and far-sighted paper in 1967, tried to understand how this was possible. He assumed that baryon conservation was not absolute; so anti-protons could decay into electrons or negative muons (but then protons could also decay into  $e^+$  or  $\mu^+$ ). As it was known, however, that CP was violated by a small amount (C is charge conjugation which turns a particle into its anti-particle; P is parity inversion), the rates for proton and anti-proton decay could differ and hence a proton and electron predominance could be built up.

This was viewed as a wild speculation for many years. With the apparent successes of the unified  $SU(2) \times U(1)$  gauge theory of weak and electromagnetic interactions and of quantum chromodynamics (QCD — the  $SU(3)_c$  gauge theory of strong interactions *Nature* 279, 479; 1979), however, many theorists have in recent years considered grand unified gauge theories of which the simplest is the  $SU(5)$  theory of Georgi and Glashow<sup>4</sup> (see also this issue of *Nature* p. 649). This is a theory unifying strong, electromagnetic and weak interactions which is broken by the Higgs mechanism first into the unbroken  $SU(3)_c$  of strong interactions and the  $SU(2) \times U(1)$  of unified weak/electromagnetic interactions, which itself is then broken by the Higgs mechanism in the usual way. A common feature of the grand unified theories is that they contain gauge particles which couple baryons to leptons so that baryon conservation is no longer an exact law.

In order to estimate the size of baryon non-conservation, which would be reflected in a finite rather than infinite proton lifetime, it is necessary to calculate the masses of the gauge particles which mediate these processes. This can be done in the same way as for  $W^\pm$  and  $Z^0$  in  $SU(2) \times U(1)$ : the characteristic mass here is about 100 GeV which is the energy where weak interactions and electromagnetic interactions would have the same strength. Similarly the energy at which electromagnetic interactions become strong is about  $10^{15}$  GeV which therefore is the mass scale of these new particles. Thus the prediction of these theories is that baryons can decay into leptons but, as they would do so only by exchanging a superheavy gauge particle, this happens very rarely.

So there is a hierarchy of gauge theories

$$SU(5) \xrightarrow[100 \text{ GeV}]{10^{15} \text{ GeV}} SU(3)_c \times SU(2) \times U(1) \xrightarrow{\phantom{10^{15} \text{ GeV}}} SU(3)_c \times U(1)$$

where the fully symmetric  $SU(5)$  theory is only realised at energies large compared with  $10^{15}$  GeV so that the mass of all the gauge particles can be neglected; at

energies smaller than  $10^{15}$  GeV but much larger than 100 GeV the mass of  $W^\pm$  and  $Z^0$  can be neglected so that weak and electromagnetic interactions are fully unified; and in our normal low-energy region of laboratory experiments ( $< 100$  GeV) only QCD ( $SU(3)_c$ ) and QED ( $U(1)$ ) remain unbroken symmetries.

This is the present understanding of particle physicists who are eagerly waiting for an example of proton decay. Nevertheless, this hierarchy of gauge theories has immediate cosmological implications for the reasons advanced by Sakharov. We can consider the particles of these gauge theories as interacting with a background heat bath of temperature  $T$ . The appropriate theory would then be applicable to a very hot, very dense gas of particles interacting with the couplings of the gauge theory, provided that this gas had time to come to thermal equilibrium. So now Sakharov's speculation can be given flesh: at temperatures  $T > 10^{28}$  K corresponding to energies above  $10^{15}$  GeV this gas of radiation and particles will interact through a grand unified theory such as  $SU(5)$  with its 24 zero mass gauge particles, and baryons will be created which can then decay into leptons. As the temperature decreases, there is now the possibility of a phase transition of the gas into a new phase with lower symmetry: this has been studied and can indeed happen (see Linde<sup>5</sup> for a general review of the field). In particular, the present baryon-asymmetric state of the universe could be reached in this way, for a baryon asymmetry may have been produced in the early universe which was then 'frozen' in ever since<sup>6</sup>. So the hierarchy above can now be viewed schematically as

$$SU(5) \xrightarrow[10^{15} \text{ K}]{10^{28} \text{ K}} \begin{matrix} SU(3)_c \times SU(2) \times U(1) \\ SU(3)_c \times U(1) \end{matrix}$$

where the dense gas at temperatures above  $10^{28}$  K has the highest symmetry and various phase transitions occur to states of lower symmetry until we reach the present universe with its characteristic cosmic microwave temperature of 2.7 K at which only  $SU(3)_c$  and  $U(1)$  are good symmetries and of the original 24 gauge particles, only the 8 gluons of QCD and the photon of QED remain massless.

This brings us to the letter of Primack and Sher (p. 680, this issue of *Nature*): why they ask, should this hierarchy of broken gauge theories stop at  $SU(3)_c \times U(1)$  and  $T = 10^{15}$  K? Suppose at low enough

temperatures there is a further phase transition into a state of lower symmetry. This could imply "that the  $SU(3)$  gauge symmetry of the strong interactions, quantum chromodynamics, is broken at low temperature. Is it possible that the reason Fairbank and collaborators have been the only group to detect fractionally charged particles — quarks? — is that theirs is the only low temperature search?" This suggestion is due to Deshpande.

Alternatively, or additionally, there is an even more intriguing possibility. Perhaps the  $U(1)$  symmetry of QED is spontaneously broken. This would imply that its gauge particle, the photon, would become massive at a low enough temperature, or more exactly, that a photon gas in equilibrium with a heat bath would undergo a phase transition at  $T = T_c$  so that at temperatures below  $T_c$  each photon in the gas would have a non-zero mass  $\mu(T)$ . There would be various manifestations of a photon mass  $\mu$ . Following the review by Goldhaber and Nieto<sup>7</sup>, one can list four different effects and types of experiment:

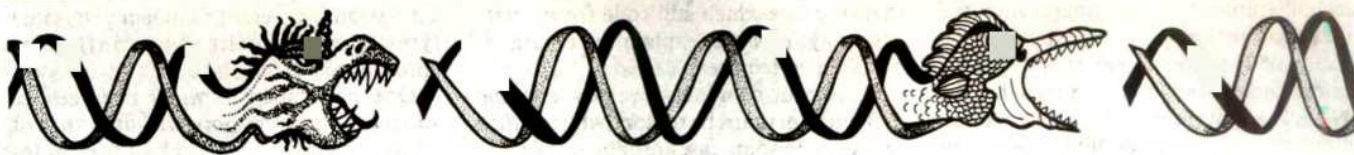
- (i) the velocity of light would vary with its energy (that is, frequency)
- (ii) the electrostatic field would arise from a potential of Yukawa form ( $e^{-\mu r}$ ) rather than the  $1/r$  Coulomb potential. Here  $\hbar = c = 1$ .
- (iii) Ampère's law is violated and the corresponding Maxwell equation becomes  $\nabla \times H = J - \mu^2 A$  where  $A$  is the vector potential; this also leads to an exponential fall-off proportional to  $e^{-\mu r}$  of  $H$  for a magnetic dipole such as the earth, and
- (iv) the dispersion relation between frequency and wave-vector  $k$  becomes  $\omega^2 = k^2 + \mu^2$  in place of  $\omega^2 = k^2$ . This will give a change in arrival time of radio signals from a pulsar dependent on frequency. This can be accurately measured.

Each of these effects gives a bound on  $\mu$  with the best (precise measurements of the Earth's magnetic field) giving  $\mu \leq 3 \times 10^{-15}$  eV, and the others giving upper limits between  $10^{-10}$  and  $10^{-14}$  eV.

Primack and Sher note that all these experiments are performed either at normal temperatures ( $\sim 10^2$  K), or in the case of astronomical measurements, at 2.7 K. Thus they suggest that the photon mass be measured at temperatures much below 2.7 K. One such experiment is shortly to be performed at Sussex University by Clark and his collaborators. It will consist of looking for a frequency shift of a resonant mode in a superconducting cavity as the temperature is reduced in steps from an initial temperature of 4 K, where the photon is certainly massless, to a temperature of 0.05 K. It should be possible to measure the frequency shift (from (iv) above) arising from a phase transition giving the photon mass  $\mu$  to one part in  $10^8$ ; this should give a mass limit at these temperatures of about  $10^{-9}$  eV.  $\square$

1. Abrikosov, A.A., Gorkov, L.P. & Dzyaloshinski, L.E. *Methods of Quantum Field Theory in Statistical Physics* (1963) (translated and edited by R. Silverman, Dover, 1975).
2. Kogut, J. & Wilson, K. *Phys. Rep.* 12C, 75 (1974).
3. Sakharov, A.D. *Pis'ma Zh. Eksp. Teor. Fiz.* 5, 32 (1967).
4. Georgi, H. & Glashow, S.L. *Phys. Rev. Lett.* 32, 438 (1974).
5. Linde, A.D. *Rep. Prog. Phys.* 42, 389 (1979).
6. Yoshimura, S. & Susskind, L. *Phys. Rev. D* 18, 4500 (1978); Toussaint, D., Treiman, S., Wilczek, F. & Zee, A. *Phys. Rev. D* 19, 1036 (1979); Weinberg, S. *Phys. Rev. Lett.* 42, 850 (1979); Ellis, J., Guillard, M. & Nanopoulos, D. *Phys. Lett.* 80B, 360 (1978).
7. Goldhaber, A.S. & Nieto, M.M. *Rev. Mod. Phys.* 43, 277 (1971).





## Selfish DNA

In two review articles in the 17 April issue Doolittle and Sapienza (p. 601) and Orgel and Crick (p. 604) separately suggested that much of the DNA in the genome of higher organisms could be described as 'selfish'. They argued that such DNA has no appreciable phenotypic effect and functions only to ensure its own self-preservation within the genome. This view point stimulated a great deal of comment, some of which was published in the issue of 26 June (p. 617). Now the original authors have joined up with one of their critics and reassessed their ideas in the two articles below. A further comment is added by H. K. Jain.

from L.E. Orgel, F.H.C. Crick and C. Sapienza

DIFFICULTIES have been caused by the words 'selfish', 'junk', 'specific' and 'phenotype' that were used in the two reviews of selfish DNA<sup>1,2</sup>.

Many people dislike the term 'selfish DNA' and a more acceptable alternative might be 'parasitic DNA'. The word 'parasitic' does not imply that the DNA can move between individuals, though certain viral DNAs might do this. It does imply that such DNA can usually move between different chromosomes in the same cell.

The word 'junk' also seems to arouse strong feelings. The idea behind it can be clarified by considering what is meant by 'specific'. We consider a sequence highly specific if the change of any one of its bases almost always has a considerable effect on the organism. An example would be the recognition site for a physiologically relevant restriction enzyme. At the other extreme are sequences whose deletion or extensive alteration would produce a negligible effect. Such sequences could reasonably be called junk. However, there is probably a continuum between these two extremes, including fairly specific sequences, where the alteration of most bases will produce some effect (many sequences coding for protein, and the different signals for starting and stopping transcription are likely to be of this type) and sequences whose deletion or extensive alteration will usually produce a small effect, such as a change in the local rate of recombination. In some cases close similarity of two sequences may be important, while the base sequences themselves may matter hardly at all — for example, within the introns of two neighbouring versions of a gene. The word 'junk' is perhaps too broad to cover all those cases for which the effect of sequence on the phenotype of an organism is small or zero. We hope a more precise terminology will evolve as the facts become better known.

The word 'phenotype' has also caused difficulties in spite of Doolittle and Sapienza's careful use of 'organismal

phenotype' to make their meaning clear. We obviously need two words: one to refer to the phenotype of the organism and the other to apply solely to the 'phenotype' of the parasitic DNA, a distinction we would certainly make in the case of a true parasite. For the former we would suggest 'organismal phenotype' and for the latter, following Cavalier-Smith<sup>3</sup>, 'intra-genomic phenotype', but we would allow the word 'phenotype' alone to be used when the context makes the meaning clear.

In our original definition we said that selfish DNA had two distinct properties: (1) It arises when a DNA sequence spreads by forming additional copies of itself within the genome. (2) It makes no specific contribution to the phenotype. By 'phenotype' we meant organismal phenotype. We intended 'specific' to be understood as 'highly specific' or 'fairly specific' in the discussion above. However it has been pointed out to us by R. Pritchard<sup>4</sup> that 'no... contribution' is unnecessarily strict. It would have been more useful to include also DNA which made a small contribution to the organismal phenotype, either positive or negative. An example of the latter might be a viral DNA which became part of the genome.

There is obviously a continuum of possible selective advantages (positive or negative) to the organism. We had excluded from our definition of selfish DNA those cases where the selective advantage is very high. To decide whether a repeated sequence is parasitic or not, one must determine whether the presence of the repeated sequence in the population is mainly due to the efficiency with which the sequence spreads intragenomically or mainly due to the reproductive success of those individuals in the population who possess repeated copies of the sequence. Only in the former case do we consider it useful to use the term selfish or parasitic DNA, as opposed to useful or symbiotic DNA — the borderline between the two may not be sharp.

In considering the spread of parasitic DNA one should not underestimate the power of natural selection. For example, if a particular transposon was inserted at

random, it would run the risk of inactivating many genes and thus be selected against. A transposon which usually inserted at sites between genes would be at a selective advantage. Sites very near essential genes (as pointed out by Bruce Grant<sup>5</sup>) may be harder to delete than those in the middle of long stretches of junk and so parasitic DNA in the former positions is likely to survive longer. Effects of this type would lead to the selection of selfish DNA sequences that inserted preferentially at special sites in the genome.

Competing theories differ in their analysis of the factors determining the amount of non-specific DNA and of the way in which it comes into existence. Although we cannot at present decide on the quantitative contribution of the different types of non-specific DNA to the genome, it is still helpful to classify the various theories.

We proposed<sup>2</sup> that the amount of non-specific DNA present in a given genome is often determined by the balance between the intragenomic spreading of selfish sequences and phenotypic selection against excess DNA — the weaker the phenotypic selection against non-specific DNA the larger the DNA content of the genome. In another group of theories it is proposed that there is an optimal DNA content for each organism, which may be substantially greater than the amount of specific DNA that is needed to define the phenotype. The amount of non-specific DNA is then principally determined by the difference between the optimal DNA content and the essential content of specific DNA. The theories are not mutually exclusive, but differ substantially in emphasis in their explanation of C-values.

Cavalier-Smith's proposal<sup>3,6</sup> is an interesting example of an 'optimal DNA content' theory. One of his ideas, which we misinterpreted in our previous paper<sup>2</sup>, is that in large cells, particularly in oocytes, the transport of messenger RNA across the nuclear membrane may become a limiting factor and that the only way to increase the

The "selfish DNA" design at the top of the page was created by Linda Angeloff-Sapienza of Halifax, Canada and originally appeared on the cover of the issue of 17 April, 1980.

L.E. Orgel and F.H.C. Crick are at The Salk Institute, San Diego, California and C. Sapienza is in the Department of Biochemistry, Dalhousie University, Halifax, Canada.



rate of transport is by increasing the number of nuclear pores by extending the surface of the membrane. If the area of nuclear membrane is determined by the DNA content of the nucleus, it follows that selection for a larger cell must lead to an increase in the DNA content of the genome. Thus, rather surprisingly, extra non-specific DNA is selected for because it allows such a cell to grow *faster*. While we do not question the logic of the argument, given the various assumptions, we do not find all the assumptions particularly plausible. It may be that there is sometimes selection for increased cell volume and increased nuclear volume. In cells so selected, non-specific DNA can accumulate. Whether it does so because large cells with large nuclei require such accumulation, or because they simply permit it remains to be seen. We feel that more experimental work is needed to unravel the complexities of the situation. In particular, we should like to know in which stages and in which organisms the surface of the nuclear membrane is saturated with nuclear pores.

Cavalier-Smith<sup>3</sup> also cites the widely different DNA contents of germ cells and somatic cells in some invertebrates as evidence against the selfish DNA hypothesis. However these observations can also be explained in terms of the selfish DNA theory. Such DNA 'needs' only to remain in the germ line to function parasitically. On the other hand, organismal selection might sometimes be stronger against surplus DNA in the soma than in the germ line. Thus representation in the germ line but not in the soma may sometimes be an optimal strategy for parasitic DNA. As for B chromosomes, in many cases the evidence appears to us to give some support to the idea (originally proposed by Östergren<sup>7</sup> in 1945) that they are largely parasitic, but there is certainly evidence that they sometimes have phenotypic effects which may possibly be useful<sup>8,9</sup>.

Smith<sup>10</sup> has pointed out that the DNA of vertebrates usually has about 42 per cent GC whereas the GC content of invertebrate and prokaryotic DNA varies over a much wider range. The theory of parasitic DNA has rather little to say on this point. There are many factors which might affect the GC content of an organism's DNA. If much of the parasitic DNA has descended rather recently from insertion elements which themselves originally coded for proteins, then it would not be surprising if their present GC content were similar to

that of genes which still code for protein. This may, perhaps, explain the constancy of GC in vertebrates.

As for our own ideas, we now feel that there may perhaps be reasons why too *little* DNA can in some cases produce a selective disadvantage. For example, Zuckerkandl<sup>11</sup> has suggested that there may be a minimum size for a 'domain' necessary for stability of the chromatin in the folded state. Thus a domain containing only a few genes might benefit from having some non-specific DNA as 'padding'. This would mean that there is indeed an optimal amount for total DNA.

In our original paper<sup>2</sup> we feel that we did not put enough emphasis on the distinction between sequences which are repeated, exactly or nearly exactly, in many tandem repetitions and sequences which are more widely dispersed over the chromosomes and which occur in only one or a few copies in any one place. It seems plausible that these two types of sequence evolved different mechanisms. It is possible that the mechanisms generating the tandemly repeated type are usually more 'ignorant' (in Dover's sense<sup>12</sup>) than the more dispersed type. If the latter have any specific function it is likely to be that of the control, at one level or another, of gene

expression, whereas the tandemly repeated type seem more likely to influence chromosome mechanics.

One possibility to which we feel we should have given more weight is that of 'dead genes', also called 'pseudo-genes'<sup>13,14</sup>; that is, sequences which can no longer code for a protein (or a structural RNA) but which appear to have descended from a sequence that did. Whether these conform to our definition of parasitic DNA remains to be seen, but we suspect this is unlikely, since they usually exist in only a single copy, or as multiple tandem copies in only one place.

In our recent experience most people will agree, after discussion, that ignorant DNA, parasitic DNA, symbiotic DNA (that is, parasitic DNA which has become useful to the organism) and 'dead' DNA of one sort or another are all likely to be present in the chromosomes of higher organisms. Where people differ is in their estimates of the relative amounts. We feel that this can only be decided by experiment. We expect that due to the recent advances in genetic engineering and related techniques much sequence information will accrue in the near future. This should help to decide between the different alternatives. □

## Modes of genome evolution

from Gabriel Dover and W. Ford Doolittle

OUR original articles<sup>1,3</sup> presented antagonistic positions and perhaps obscured many areas of agreement. In essence, we are approaching similar phenomena from different perspectives and it might be useful to clarify where our views agree and differ and to indicate the sorts of evidence which would allow one to decide whether the origin of non-coding DNA in eukaryotic cells is more precisely viewed as 'ignorant'<sup>3</sup> or 'selfish'<sup>1,2</sup>.

The eukaryotic genome is constantly in flux, and this plasticity results from a variety of known and as yet mysterious mechanisms which amplify and disperse segments of DNA throughout a set of chromosomes<sup>4-7</sup>. Replication and recombination are complex processes requiring many enzymes that have evolved by natural selection. What we both wish to stress is that, in establishing these processes, evolution has inadvertently endowed the genome with built-in mechanisms for irregular and recurrent random sequence rearrangements and

created an environment in which elements capable (to varying extents) of promoting their own amplification and dispersion will inevitably arise<sup>1,2,7</sup>. We acknowledge that there is evidence which suggests that some proportion of genome rearrangements may have effects on the biology of an organism (for instance on chromosome behaviour, on nuclear RNA processing, on cell-cycle times, on recombination frequencies and on gene expression; see refs 1-3, 8). Where this is the case, the change in frequency of a sequence rearrangement and the behaviour of elements which promote their own amplification and dispersion will of course depend on the effects they have on fitness. Hence, the net accumulation of these particular families of sequences reflects a balance between the intrinsic rate of accumulation (intra-genomically) and the effect of natural selection on phenotypic differences.

We agree that the amplification and dispersion of segments may occur either at random (sequence-independent or 'ignorant') or with preference for certain sequences (sequence-dependent or 'selfish'). Although both 'ignorant' and 'selfish' are unfortunate terms, they should be understood in the spirit in which they are

- 1 Doolittle, W. F. & Sapienza, C. *Nature* **284**, 601 (1980)
- 2 Orgel, L. E. & Crick, F. H. C. *Nature* **284**, 604 (1980)
- 3 Cavalier-Smith, T. *Nature* **285**, 617 (1980)
- 4 Pritchard, R. (personal communication)
- 5 Grant, B. (personal communication)
- 6 Cavalier-Smith, T. *J. Cell. Sci.* **34**, 247 (1978)
- 7 Östergren, G. *Biol. Notiser* **2**, 157 (1945)
- 8 Jones, R. N. *Int. Rev. Cytol.* **40**, 1 (1975)
- 9 Ames, A. & Dover, G. *Chromosomes* (in the press)
- 10 Smith, T. F. *Nature* **285**, 620 (1980)
- 11 Zuckerkandl, E. (personal communication)
- 12 Dover, G. *Nature* **285**, 618 (1980)
- 13 Loomis, W. *Dev. Biol.* **30**, F3-F4 (1973)
- 14 See, for example, Proudfoot, N. *Nature* **286**, 840 (1980)

Gabriel Dover is in the Department of Genetics, University of Cambridge, UK, and W. Ford Doolittle is in the Department of Biochemistry, Dalhousie University, Canada.

used and defined: sequence-independent and sequence-dependent processes of amplification and dispersion respectively.

The 'selfish process' produces DNAs which are preferentially chosen either by virtue of their nucleotide sequence or by virtue of the fact that they may code for gene products for their own amplification and dispersion. Mobile elements such as bacterial insertion sequences and transposons, the 'Ty-1-like' elements of yeast, the 'copia-like' elements of *Drosophila*, and vertebrate retroviruses, which show surprising similarities in structure and (perhaps) dispersal mechanisms<sup>8</sup> are almost certainly the self-perpetuating products of this sort of process. An alternative term 'self-selection' might usefully describe the process of accumulation of these sequences. Interestingly, there may be an element of self-selection in the process of accumulation and dispersion of some sequence-independent segments. Extensive sharing of similar sequence patterns of repetitive DNAs between chromosomes (see refs 9 and 10), and occasionally between species<sup>11,12</sup>, suggests that an arbitrarily accumulated sequence arrangement preferentially enjoys further rounds of amplification and dispersion<sup>10</sup>. Simulation of unequal recombination by computer appears to show a degree of self-perpetuation of sequences initially chosen at random<sup>13</sup> and also that amplification and dispersion can be part and parcel of the same recombinational irregularity<sup>14</sup>.

A process of recurrent amplification can explain the frequent observation of a greater within-species than between-species sequence homogeneity of shared families<sup>6,9,12</sup>. Similarly, polymorphisms and variations in sequence patterns of ribosomal genes<sup>15</sup>, histone genes<sup>16</sup> and some non-coding families<sup>17-19</sup> in several diverse organisms can be interpreted as the most recent, and hence localized, amplifications of these sequences.

We wish to emphasize, however, that 'ignorant' and 'selfish' self-perpetuation

are terms that uniquely apply to these particular DNA processes and cannot be used, meaningfully, to describe changes in frequencies of other elements that are totally dependent on the natural selection of phenotypes. 'Selfish genes'<sup>20</sup> and 'replicator selection'<sup>21</sup> are not synonymous terms and the evolutionary processes to which they allude are unknown. A very limited accumulation of supernumerary B chromosomes is the only other process that can be described as self-accumulation, often the result of meiotic and mitotic non-disjunction. We doubt if this term can be used to describe the mis-named 'meiotic drive' mechanisms of regular A chromosomes in the rare instances where this occurs. For example, in the case of segregation distortion (SD) in *Drosophila melanogaster*, the preferential recovery of the SD chromosome is not so much due to its accumulation *per se* but is the outcome of dysgenesis of cells carrying the non-SD homologue<sup>22</sup>. This, and other cases, are analogous to the relative changes in frequency of alleles at a gene locus that are the outcome of natural selection; and 'selfish' and 'replicator selection' are misleading descriptions of this process of differential accumulation of alleles and chromosomes.

We do not agree upon the relative contributions of randomly accumulated and preferentially accumulated DNAs to the evolution of eukaryote genomes. It is clear that much of the non-coding DNA of yeast could be of the sort one could call 'selfish'<sup>4,8</sup> whilst non-coding elements of the *D. melanogaster* genome are made up of varying proportions of essentially 'ignorant' repetitive DNA (for example the satellite DNAs<sup>23</sup>) and 'selfish' transposable DNAs (for example the 'copia-like' elements<sup>5</sup>). The scrambled arrangements of repetitive elements in *D. melanogaster* observed by Wensink and co-workers<sup>24</sup>

could reflect either sequence-independent shuffling processes or sequence-dependent insertion of transposable elements, similar to *copia*, at adjacent sites. The available data on repetitive DNA families of species of sea urchins, Gramineae, rodents, primates and insects (see ref.3) do not permit a clear assessment of the mechanisms that gave rise to them, for no direct sequence data are available. The multiple-copy 'Alu I' family of mammalian genomes may have a cellular function<sup>25,26</sup>, but it is not impossible that these are the descendants of a family of transposable elements<sup>27</sup>.

Finally, we suggest that the accumulation of sequences might be affected by constraints on the mechanisms themselves. For example, sequence-dependent amplification and dispersion will favour sequences that accurately contain the required sequence for transposition and that have not drifted too far into unacceptable divergent sequences. Similarly, sequence-independent mechanisms may be constrained to particular lengths of sequences<sup>10</sup>. Such constraints impose a type of selection on sequences, not necessarily as a result of their phenotypic effects but more as a consequence of the molecular mechanisms of replication and recombination.

We do not know what proportions of the repetitive DNAs of 'higher' organisms are amplified and dispersed by either sequence-dependent or sequence-independent mechanisms. Similarly, we do not know to what extent each of these mechanisms is constrained nor do we know the extent to which the frequencies of sequence patterns are an outcome of their possible effects on individual fitness. It is clear, however, that there are several modes of sequence rearrangement within rapidly evolving genomes. The problem now, as with most scientific debates, is one of quantification.

## Incidental DNA

from H.K. Jain

THERE can be two ways of looking at the extraordinarily large amounts of DNA in the eukaryotic genome. One is to keep looking for functions (mostly of a non-conventional nature, for example, determining nucleotypic effects<sup>1</sup>), and the other is to realise that lack of function is precisely what one would expect from a large part of the excess DNA. After all, the most important attributes one would expect of any kind of genetic material in the context of its fundamental role in evolution would be (a) mutability and recombination to create variation and (b)

mechanisms which would help to conserve a large part of this variation in spite of continuous selection, which leads to rejection of a great deal of newly-produced variability. Mechanisms of this kind are already known to exist. Heterozygote advantage is perhaps the most important of them. Ford<sup>2</sup> has argued on the basis of Fisher's<sup>3</sup> theory that heterozygote advantage has evolved because natural selection favours it as a major instrument for the preservation of variability and for keeping the population polymorphic.

Based on similar considerations, one would expect that the property of DNA to show mutability not only in the sense of classical gene mutations and chromosomal

1. Doolittle, W.F. & Sapienza, C. *Nature* **284**, 601 (1980).
2. Orgel, L.E. & Crick, F.H.C. *Nature* **284**, 604 (1980).
3. Dover, G.A. *Nature* **285**, 618 (1980).
4. Cameron, J.R. *et al.* *Cell* **16**, 739 (1979).
5. Potter, S.S. *et al.* *Cell* **17**, 424 (1979).
6. Flavell, R.B. *et al.* in *Genome Organization and Expression in Plants* (Plenum, 1980).
7. Dover, G.A. *Chromosomes Today* **6**, 105 (1977).
8. *Cold Spring Harb. Symp. quant. Biol.* **45** (1980).
9. Dover, G.A. *Nature* **272**, 123 (1978).
10. Brown, S.D.M. & Dover, G.A. *Nucleic Acids Res.* **8**, 781 (1979).
11. Brown, S.D.M. & Dover, G.A. *Nature* **285**, 47 (1980).
12. Donehower, L. & Gillespie, D. *J. molec. Biol.* **134**, 805 (1979).
13. Smith, G.P. *Science* **191**, 528 (1976).
14. Smith, T., Brown, S.D.M. & Dover, G.A. (unpublished results).
15. Wellauer, P.K. *et al.* *J. molec. Biol.* **105**, 487 (1976).
16. Cohn, R.H. & Kedes, L.J. *Cell* **18**, 855 (1979).
17. Cooke, H.J. & Hindley, J. *Nucleic Acids Res.* **6**, 3177 (1979).
18. Christie, N.T. & Skinner, D.M. *Proc. natn. Acad. Sci. U.S.A.* **77**, 2786 (1980).
19. Donehower, L. *et al.* *Proc. natn. Acad. Sci. U.S.A.* **77**, 2129 (1980).
20. Dawkins, R. *The Selfish Gene* (Oxford Univ. Press, 1976).
21. Dawkins, R.A. *Tierpsychology* **47**, 61 (1978).
22. Crow, J.F. *Scientific American* **104**, 1 February (1979).
23. Brullag, E.E. *et al.* *Cold Spring Harb. Symp. quant. Biol.* **42**, 1137 (1977).
24. Wensink, P.C. *et al.* *Cell* **18**, 1231 (1977).
25. Jelinek, W.R. *et al.* *Proc. natn. Acad. Sci. U.S.A.* **77**, 1398 (1980).
26. Rubin, C.M. *et al.* *Nature* **284**, 372 (1980).
27. Bell, G.I. *et al.* *Nucleic Acids Res.* **8**, 4091 (1980).

H.K. Jain is in the Indian Agricultural Research Institute, New Delhi.



rearrangements (for example, of the *Oenothera* kind) but also out-of-step fast replication (or amplification) of some parts of it is one which natural selection would help to evolve and fix in a population. Such a property may not be ascribed to quirks of DNA replication as suggested by Dover<sup>4</sup> but to selection favouring it. Natural selection is concerned not only with the existing variability but even more so with mechanisms which ensure its continued availability. If there is intragenomic selection leading to rapid build-up of some of the DNA sequences (the selfish DNA of Doolittle and Sapienza<sup>5</sup> and Orgel and Crick<sup>6</sup>) we must treat this part of DNA as *incidental* to the fundamental process of mutability so vital for ensuring continued supply of raw material for the production of new genes. It does not follow that all of the DNA produced in this manner will, in fact, acquire a function. A large part of it (or even all of it) may not do so and may be eliminated only on an evolutionary time scale. Meanwhile, new DNA of the same and similar kind may continue to be produced so that at a given point of time there will always be large amounts of non-specific DNA. This fraction is best described as 'incidental' rather than 'selfish' DNA. We may call it incidental because it is a byproduct of the inherent property of mutability of the genome, a characteristic to which natural selection attaches great importance even if it leads to the production of repeated sequences and a wasteful deployment of energy. Viewed in

this light, non-functional DNA is very much a product of natural selection — a selection operating for mutability *per se*. Its relative abundance is probably a function of its nonfunctional nature for any other DNA which carries information of one kind or another would create genetic imbalance and would be quickly rejected.

It is important to recognise that economy has not been a major consideration in the process of evolution. Overproduction and rejection (both quick and prolonged) are not uncommon features of evolution; the excessive amount of DNA should be considered in the same context. Nature places considerable premium on playing safe so that it will not run short of raw material even if this means indiscriminate production leading to sequences which are destined to remain functionless. With our present understanding of the origin of life (far from complete) and its evolution through

several billion years, we must be prepared by now to accept some degree of confusion. After all, the evolutionary process is without any kind of central management, planning and coordination. It is totally dependent on variability arising through errors in the replication of DNA and its subsequent multiplication through recombination, which at times may involve genome fusion<sup>7</sup>. Whatever control mechanisms do exist are themselves a product of these errors which have been seized upon by natural selection to bring about some amount of order. A large number of mutant genes are now known which affect the meiotic process in various ways including chromosome pairing<sup>8,9</sup>, chromosome condensation<sup>10</sup>, preferential segregation<sup>11</sup>, amount of recombination<sup>12,13</sup> and there are also, of course, the mutator genes<sup>14,15</sup>, some of which could possibly be involved in the production of non-specific DNA.

The use of the term 'selfish' may be quite harmless if one does not try to see too much meaning in it. With our recollection of the reactions to Darwin's theory, it is too much to expect that attempts of this kind will not be made. We do not have to be squeamish when science demolishes some of our cherished beliefs. The truth pointed out by Darwin has, in the end, given a more meaningful direction to our social and cultural evolution. By the same token, we do not have to create unnecessary despair if the interesting concept of selfish DNA is misunderstood, as is likely to happen.

1. Cavalier-Smith, T. *Nature* **285**, 617 (1980).
2. Ford, E.B. *Ecological Genetics* (Chapman and Hall, London, 1975).
3. Fisher, R.A. *The Genetical Theory of Natural Selection* (Oxford, 1930).
4. Dover, G. *Nature* **285**, 618 (1980).
5. Doolittle, W.F. & Sapienza, C. *Nature* **284**, 601 (1980).
6. Orgel, L.E. & Crick, F.H.C. *Nature* **284**, 604 (1980).
7. Schwesinger, M.D. *Bact. Rev.* **41**, 872 (1977).
8. Beadle, G.W. *Cytologia* **20**, 269 (1933).
9. Riley, R. *Heredity* **15**, 407 (1960).
10. Rhoades, M.M. & Dempsey, E. *Genetics* **54**, 505 (1966).
11. Rhoades, M.M. & Dempsey, E. *Genetics* **53**, 989 (1966).
12. Baker, B.S. et al. *A. Rev. Genet.* **10**, 53 (1976).
13. Rees, H. *Bot. Rev.* **27**, 288 (1961).
14. Cox, E.C. *A. Rev. Genet.* **10**, 135 (1976).
15. Yanofsky, C. et al. *Proc. natn. Acad. Sci. U.S.A.* **55**, 274 (1966).



## 100 years ago

### NEW GUINEA

from L.M. D'Alberty

"The most perfect harmony seems to reign in families of the Papuan Mahoris, and rare indeed are cases of quarrel among members of one household. They live in communities, sometimes of more than a thousand inhabitants, in well-built villages, worthy to be called small towns, both for their order and cleanliness. They are under the rule of the chiefs or landowners. The chief is looked upon as father of the family. He is called Pacao, and his servant or subject is called Irine. From all I could learn, slavery does not exist, and the sale of human beings is unknown." After describing their daily avocations, amusements, dress, implements, and ornaments (a group of which are figured), he goes on: "Their natural disposition is gentle and placid. They like to spend their time in talking and games, in which men and women take an equal share. Playful and free of speech,



*Durabi, a native of Kiwai Island, at the mouth of the Fly River*

they nevertheless do not transgress the bounds of modesty, either in word or deed. Women and children are included in every conversation, and often take part in public discussions, which are usually held in the evening. Women are always respected, and in some villages they enjoy a certain supremacy, although the government of the house belongs to the husband. Labour may

be said to be fairly divided between the two sexes, and they are accustomed to work from their earliest childhood. . . . Will they be the happier for civilization? This is a difficult problem, and one which cannot be solved until the experiment has been made. For my part I do not doubt that these, more readily than any other savages whom I know, would answer to the call of a civilised nation which, stretching out a paternal hand, would lead them towards our civilisation! To insure success, however, they should be treated as friends, not as slaves; they should be cherished, not destroyed."

Unfortunately our attempts at civilising savages have as yet in every case failed. Are we still, notwithstanding all our wretched failures, to go on in the old way, and allow these interesting and now happy people to be first ruined morally by the teaching of the dregs of our Australian and Pacific traders, and then physically deteriorated by the forced introduction of a form of civilisation utterly unsuited to them? Cannot either philanthropy, or religion, or Government protect these people from all such external influences as have been proved to be unsuited to their condition and stage of development, while aiding them to work out for themselves an indigenous civilisation? Here is perhaps the last chance we have to preserve one remnant of the better class of savages from being crushed under the juggernaut car of our high-pressure civilisation and mad struggle for wealth.

From *Nature* **23**, 23 December, 175, 1880.



## REVIEW ARTICLE

## Why unify?

Howard Georgi

Lyman Laboratory of Physics, Harvard University, Cambridge, Massachusetts 02138

*Unified gauge theories (such as  $SU(5)$ ) of particle interactions are built on the colour  $SU(3)$  and  $SU(2) \times U(1)$  gauge theories which apparently describe strong and weak and electromagnetic interactions at distances as small as  $10^{-16}$  cm. In this article the classical reasons for going beyond  $SU(3) \times SU(2) \times U(1)$  to a fully unified theory such as  $SU(5)$  are reviewed, and a new reason formulated. A class of imaginary worlds similar to our own is considered and it is shown that unification is possible only in ours. This suggests that the low-energy interactions are unique in that they are constructed to make unification possible.*

AS we enter the 1980s, elementary particle theorists have an unusual problem: we know (or think we know) too much. We confidently expect the standard  $SU(3) \times SU(2) \times U(1)$  gauge theory of the strong, weak and electromagnetic interactions to describe particle physics accurately down to distances as small as  $10^{-16}$  cm (ref. 1). The current status of particle physics has been reviewed by Mulvey<sup>2</sup>. This article also briefly discusses the symmetry groups such as  $SU(3)$ , used to describe elementary particles in terms of quark multiplets.

The  $SU(3)$  component of  $SU(3) \times SU(2) \times U(1)$  is the colour  $SU(3)$  theory of strong interactions or quantum chromodynamics (QCD) (the experimental and theoretical background which led to the development of QCD is reviewed in ref. 3). The eight  $SU(3)$  gauge particles are the gluons. They couple to the three colours of the quarks through the eight traceless, hermitian  $3 \times 3$  matrices. The effect of the colour  $SU(3)$  interactions is to confine the coloured quarks into colourless hadrons (for which all the  $SU(3)$  charges vanish).

The  $SU(2) \times U(1)$  component is the Glashow–Weinberg–Salam theory of the weak and electromagnetic interactions. The four  $SU(2) \times U(1)$  gauge particles are the  $W^\pm$  and  $Z^0$  (heavy because the  $SU(2) \times U(1)$  symmetry is spontaneously broken) and the photon.

There are still important questions in the 'low-energy' (<100 GeV) domain of contemporary particle experiments. For example, given the colour  $SU(3)$  theory, how, in detail, do quarks get confined? But the really fundamental questions seem to involve smaller distances and higher energies.

In 1973, it was suggested that the next step beyond  $SU(3) \times SU(2) \times U(1)$  must be the unification of these three gauge groups as subgroups of  $SU(5)$ , so that all of the low-energy particle forces are components of a single, basic force<sup>4</sup>. For a large class of models, including  $SU(5)$ , it was shown that unification must take place at very short distances of the order of  $10^{-29}$  cm (ref. 5).

But why should we go beyond the standard model at all? Here I review the obvious arguments for unification and suggest a new one.

### Experimental evidence

It is appropriate to begin with a few words about the quality of experimental support for the standard  $SU(3) \times SU(2) \times U(1)$  model. The evidence comes from many sources. There is much qualitative support for colour  $SU(3)$  in hadron spectroscopy and for  $SU(2) \times U(1)$  in the structure of weak decays. At a more quantitative level are lepton–lepton scattering and deep inelastic lepton–hadron scattering experiments. Summarizing this: although there is no single convincing datum (like  $g-2$  of the electron for QED), there are many strong indications all pointing in the same direction. Taken together, the evidence for  $SU(3) \times SU(2) \times U(1)$  is rather impressive.

Note that most of the quantitative support for  $SU(3) \times SU(2) \times U(1)$  was obtained after the  $SU(5)$  unification was proposed. Indeed, this is one of the main reasons that unification is taken more seriously now than when it was first suggested.

### Family structure

Intertwined with all the evidence for  $SU(3) \times SU(2) \times U(1)$  is the suggestive and mysterious family structure. Historically, the muon, its neutrino and the strange and charmed quarks were crucial in unravelling the structure of  $SU(3) \times SU(2) \times U(1)$ . But from a modern vantage point, they seem completely extraneous (and the  $\tau$  lepton and  $b$  quark even more so). We would be happy with a world in which only the electron, its neutrino and the up and down quarks exist. In fact, in discussing unification, I will consider only the electron family,  $e^-$ ,  $\nu_e$ , and  $u$  and  $d$ .

### $SU(5)$ unification

The left-handed (LH) fields transform as follows under  $SU(3) \times SU(2) \times U(1)$

$$\begin{aligned} (\nu_e, e^-)_L &: (1, 2)_{-1/2} \\ e_L^+ &: (1, 1)_1 \\ (u, d)_L &: (3, 2)_{1/6} \\ u_L^c &: (\bar{3}, 1)_{-2/3} \\ d_L^c &: (\bar{3}, 1)_{1/3} \end{aligned} \quad (1)$$

where  $c$  indicates charge conjugate; the two numbers in parentheses indicate the  $SU(3)$  and  $SU(2)$  representations (in that order) while the subscript is the  $U(1)$  quantum number (which is just the average electromagnetic charge of the multiplet); colour indices are suppressed.

In  $SU(5)$ , the  $(\nu_e, e^-)_L$  and  $d_L^c$  are combined into a five-dimensional representation of  $SU(5)$  which is conventionally called the  $\bar{5}$ . The corresponding right-handed (RH) fields,  $(e^+, \nu_e^c)_R$  and  $d_R$  thus transform like a  $5$ , the defining representation. The other LH fields transform like an irreducible 10-dimensional representation, the  $10$ .

In this simple structure, the total electromagnetic charge in each multiplet is zero as it must be. Furthermore, any  $SU(5)$  representation except a singlet must transform nontrivially under both the  $SU(2)$  and  $SU(3)$  subgroups, and these do. Finally, this system satisfies a nontrivial constraint, the absence of triangle anomalies, which must be satisfied for the theory to make sense<sup>6,7</sup>. This constraint can be described as follows: write the gauge group generators as matrices acting on the left-handed fermion fields. Then the symmetrized trace of any product of three generators must vanish. In particular, for any three diagonal generators, the product of the eigenvalues summed



over all the LH fermion states must be zero. This constraint is satisfied for the generators of the  $SU(3) \times SU(2) \times U(1)$  subgroup<sup>6-8</sup> and also for the rest of the  $SU(5)$  generators<sup>4</sup>.

## Charge quantization

$SU(5)$  provides a very simple explanation for the experimental fact of charge quantization. The fundamental 5 describes leptons with charges 1 and 0 and quarks with charge  $-1/3$ . Because all  $SU(5)$  representation can be built out of multiples of the 5, all charges are just sums of the fundamental charges and thus multiples of  $1/3$ . More than that there is a relation between colour  $SU(3)$  and charge because the fractional charge  $-1/3$  is carried only by the quarks in the 5. Thus triality zero states (and in particular colour singlet states) have integral charge. Triality one (two) states have charges  $n - 1/3$  ( $n + 1/3$ ) for integral  $n$ .

Given the specific charges in the 5, charge quantization is trivial because by inspection, all the charges in the 5 are commensurate. Actually the charge quantization theorem is deeper and it has a topological aspect. Whenever the unifying gauge group is compact, the charges have to come out commensurate<sup>4</sup>. This is also related to the fact that gauge theories based on simple groups have magnetic monopoles<sup>9</sup> which in turn are related to charge quantization.

## Coupling constant relations

The  $SU(5)$  scheme predicts a relation between the gauge couplings of the three subgroups, so that for example, it predicts  $\sin^2 \theta_w$  in terms of  $\alpha$  and  $\alpha_s$  (ref. 5). The quantitative prediction  $\sin^2 \theta_w \approx 0.205$  is in reasonable agreement with experiment. But, the picture of coupling constant renormalization in which all are equal at very small distances and evolve differently at larger distances gives a satisfying qualitative explanation of the hierarchy of particle interactions. It explains why the strong interactions are strong.

## Baryon number violations

The desire to explain charge quantization and to relate the different coupling constants motivated the search for unified theories from the beginning. Baryon number-violating interactions on the other hand were not sought after. Proton decay appeared unbidden in the  $SU(5)$  scheme and elsewhere<sup>10,11</sup>. But baryon number violation is now seen as an attractive artefact of unification. It yields the most plausible explanation yet proposed for the baryon number of the Universe<sup>12</sup>. Furthermore, current experiments should see proton decay directly and give us an entirely new view on the particle physics world<sup>13</sup>. Pati and Salam<sup>10</sup> have discussed baryon number violation in a partially unified theory. They have also considered<sup>11</sup> an alternative version of unification different from  $SU(5)$  and derived independently and at about the same time. They assume that the colour symmetry is spontaneously broken and the quarks are 'liberated' with integral charge. The baryon-number violation proceeds by a completely different mechanism (depending on colour breakdown) from that in the  $SU(5)$  model. In particular, it predicts baryon decay into final states with lepton number 3 rather than  $-1$ .

## Discussion

Besides these well known successes and predictions, the virtue of the  $SU(5)$  unification is its extreme economy and simplicity. However, this simplicity sometimes makes people suspicious. Can unification really be as simple as ' $2+3=5$ '? I believe that this simplicity is deceptive. The theory is not so much simple as unique. I shall now try to prove the uniqueness of  $SU(5)$  by discussing a class of imaginary worlds which cannot be unified.

First, I will argue that ' $2+2 \neq 4$ '. Consider a world like our own but with two colours instead of three. That is, the gauge group is  $SU(2) \times SU(2) \times U(1)$  and the LH fields are as follows:

$$\begin{aligned} (\nu_e, e^-)_L &: (1, 2)_{-1/2} \\ e_L^+ &: (1, 1)_1 \end{aligned} \quad (2a)$$

as in equation (1); the quarks have charges  $3/4$  and  $-1/4$ ,

$$\begin{aligned} (u, d)_L &: (2, 2)_{1/4} \\ u_L^c &: (2, 1)_{-3/4} \\ d_L^c &: (2, 1)_{1/4} \end{aligned} \quad (2b)$$

The charges of the quarks are determined by the constraint of anomaly cancellation for the  $SU(2) \times SU(2) \times U(1)$  theory.

Of course, this theory does not describe our world. We know that there are three colours and the quark charges are  $2/3$  and  $-1/3$ . But as far as we know, equation (2) describes a possible alternative world. Thus why is our world described by equation (1) rather than equation (2)? The only important difference is that the two-colour theory cannot be unified. This can be seen easily. The 11 fields of equation (2) cannot be divided into two subsets, each of which has total charge zero and is nontrivial with respect to  $SU(2) \times SU(2) \times U(1)$ . Thus any unification must treat all 11 fields as a single irreducible representation. But then the group must be  $SU(11)$  and the resulting theory does not satisfy the anomaly constraint.

Mathematically, we can describe the process of unification as follows: given a representation of a nonsimple group (such as  $SU(3) \times SU(2) \times U(1)$ ) which satisfies the anomaly constraint, find an anomaly-free simple extension (such as  $SU(5)$ ). As the example of  $SU(2) \times SU(2) \times U(1)$  shows, this is not always possible—in fact, it is usually not possible.

It is straightforward to show that in the same sense it is impossible to unify a theory of standard leptons and quarks with more than three colours. That is, we can consider an infinite class of imaginary worlds with gauge group  $SU(n) \times SU(2) \times U(1)$ ,  $n > 3$ , and LH fermions in a representation  $R$  (the quarks have charges  $(1 \pm n)/2n$ ):

$$\begin{aligned} (\nu_e, e^-)_L &: (1, 2)_{-1/2} \\ e_L^+ &: (1, 1)_1 \\ (u, d)_L &: (n, 2)_{1/2n} \\ u_L^c &: (\bar{n}, 1)_{-(n+1)/2n} \\ d_L^c &: (\bar{n}, 1)_{(n-1)/2n} \end{aligned} \quad (3)$$

Again, the charge is chosen to cancel the  $SU(n) \times SU(2) \times U(1)$  anomalies. Here, however, there is an argument against unification which does not involve the charge.

Assume that the unifying group is  $SU(N)$ ,  $N \geq n+2$ . This must be so because of the form of  $R$ . Only  $SU(N)$ ,  $0(4N+2)$  and  $E(6)$  have complex representations and the representations of  $0(4N+2)$  and  $E(6)$  contain other fields besides the leptons and 'quarks' of equation (3). Now consider some conventionally normalized colour generator  $T_c$ . In the representation  $R$  of equation (3),

$$\text{tr}(T_c^2)_R = 2 \quad (4)$$

by explicit calculation. But in the  $N$ -dimensional representation, this same trace satisfies the inequality

$$\text{tr}(T_c^2)_N \geq 1/2 \quad (5)$$

because the  $N$  must contain at least one  $n$  of the  $SU(n)$  subgroup. Now suppose that  $R \neq N$  (and  $R \neq \bar{N}$ ). We can derive a contradiction because the trace in any other representation is too large. It is easy to show that:

$$\frac{\text{tr}(T_c^2)_{R \neq N \text{ or } \bar{N}}}{\text{tr}(T_c^2)_N} \geq (N-2) \geq 4 \quad (6)$$

The first inequality is pure group theory. It is clear from the form of  $R$  that it cannot be a direct sum of more than one  $N$ . The next smallest representation is the  $N(N-1)/2$  which saturates the first inequality. The second inequality follows because  $N \geq$

$n + 2 \geq 6$  in the theories we are discussing. Comparing equations (4), (5) and (6) shows that  $R \neq N$  (or  $\bar{N}$ ) is impossible. Thus  $R$  must be the defining representation of  $SU(N)$ . This too is impossible because the theory has anomalies. The theory described by equation (3) for  $n > 3$  has no anomaly-free simple extension.

Of course, there are anomaly-free simple theories which contain  $SU(n) \times SU(2) \times U(1)$  for  $n \neq 3$ , but they must contain fermions beyond the usual quarks and leptons.  $SU(3) \times SU(2) \times$

$U(1)$  is unique in that it permits unification of quarks and leptons.

This article is based on a talk given at the 1980 Cosener's House conference on Grand Unification. I thank the Rutherford Labs and in particular Chris Maxwell, Gordon Ringland and Mike Teper, and the staff of the Cosener's House for their hospitality and encouragement. I thank Tony Zee for a correction to this work. This work was partly supported by NSF grant PH77-22864.

1. De Rújula, A. *et al.* *Phys. Rev. D* **12**, 147 (1975).

2. Mulvey, J. *Nature* **278**, 403-409 (1979).

3. Marciano, W. & Pagels, H. *Nature* **79**, 479-483 (1979).

4. Georgi, H. & Glashow, S. L. *Phys. Rev. Lett.* **32**, 236 (1974).

5. Georgi, H., Quinn, H. R. & Weinberg, S. *Phys. Rev. Lett.* **33**, 451 (1974).

6. Bouchiat, C., Iliopoulos, J. & Meyer, Ph. *Phys. Lett.* **38B**, 519 (1972).

7. Gross, D. & Jackiw, *Phys. Rev. D* **6**, 477 (1972).

8. Pati, J. C. & Salam, A. *Phys. Rev. D* **8**, 1240 (1973).

9. Coleman, S. in *New Phenomena in Subnuclear Physics* (ed. Zichichi, A.) 297 (Plenum, New York, 1977).

10. Pati, J. C. & Salam, A. *Phys. Rev. Lett.* **31**, 661 (1973).

11. Pati, J. C. & Salam, A. *Phys. Rev. D* **10**, 275 (1974).

12. Nanopoulos, D. V. & Weinberg, S. *Phys. Rev. D* **20**, 2484 (1979).

13. Marshak, M., Winn, D., Steinberg, R. & Sulak, L. *First Workshop on Grand Unification*, (eds Frampton, P. H., Glashow, S. L. & Yildiz, A.) (Math Science Press, Brookline, 1980).

## ARTICLES

# Siderophile-enriched sediments from the Cretaceous-Tertiary boundary

Frank T. Kyte, Zhiming Zhou & John T. Wasson

Institute of Geophysics and Planetary Physics, University of California, Los Angeles, California 90024

*Siderophilic element concentrations are high in sediments from the Cretaceous-Tertiary boundary. An extraterrestrial source is indicated. Concentrations are too high to be understood in terms of the impact of a chondritic asteroid. Either the projectile was a metal-sulphide core or the infalling material (probably weak cometary matter) was slowed down during atmospheric passage.*

REPORTS by Alvarez *et al.*<sup>1,2</sup> of anomalously high Ir concentrations in Cretaceous-Tertiary (CT) boundary sediments led us to analyse samples from its most enriched boundary, the fish clay from Stevns Klint, Denmark, and a Pacific deep-sea drill core which crossed the CT boundary. Alvarez *et al.* interpret the high Ir content as characteristic of an asteroid having a radius of  $10 \pm 4$  km; they attribute the massive extinctions that marked the end of the Cretaceous to stratospheric opacity produced by impact-generated dust.

Because Ir is highly depleted in the Earth's crust relative to solar abundances, or the similar values in chondritic or iron meteorites, it is an ideal tracer for extraterrestrial sources. Other siderophiles (elements concentrated in an Fe-Ni phase if one is present) should also show high concentrations in the high Ir samples. Our procedure allows the rapid determination of several of these elements (Pd, Re, Os, Ir, Pt, Au) to compare their relative abundances in the CT boundary samples with those found in different groups of meteorites. Since starting this study there have been a similar but less comprehensive study of the Stevns Klint clay<sup>3</sup>, and data have been obtained on Ir, Os and several other elements in a boundary clay from Caravaca, Spain<sup>4</sup>.

## Samples

Analyses were performed on 23 samples of the Stevns Klint fish clay and three samples from Deep Sea Drilling Project (DSDP) Leg 62, hole 465A. The Danish specimens 1 and 2 had thicknesses of 3.5 and 2.5 cm respectively, and were sliced parallel to the pronounced bedding to measure variations in composition with stratigraphic position; these yielded 9 and 6 samples, respectively. Unfortunately, we may not have sampled the actual base because siderophiles and sulphide-associated

elements are highest in our lowest samples, whereas Christensen *et al.*<sup>5</sup> report a sharp decrease in concentrations of these elements in the basal, gray, layered marl. Eight specimens (numbers 4-11) which were dark coloured and clay-rich were also analysed; we infer that most of these originated in the lower portion of the section. Some have higher Ir concentrations than those determined in specimens 1 or 2.

Specimens 1 and 2 seem to contain three of the beds described by Christensen *et al.*<sup>5</sup>. In both specimens, sample 1 is the upper portion of a dark brown to grey marl, which must be either bed II or III. Both pairs of samples 2A and 2B are portions of a streaked grey marl corresponding to either bed III or IV. In sample 1, 3 this grades into the overlying lighter coloured marl which is certainly bed V. Here, the remaining samples are interbedded tan marls and fossiliferous chalk layers. The uncertainty in assigning the first two beds was due to: (1) the report<sup>5</sup> that bed IV is intermittent, and found only in the deepest portions of the depositional basins; and (2) that Christensen *et al.*'s bed IV is thicker (3-5 cm) than our second unit (6 mm)<sup>5</sup>.

DSDP hole 465A is located in the Central Pacific at  $33^\circ 49.23'N$  and  $178^\circ 55.14'E$ . Samples were taken from sections 3 and 4 in core 3. These sections primarily consist of a calcareous nannofossil-foraminifera ooze with the consistency of a thick paste; the Cretaceous-Tertiary boundary occurs within this ooze. The upper Cretaceous ooze is white and the lower Tertiary ooze is light tan. Unfortunately, drilling deformed the core and the boundary is smeared over at least 20 cm. Within this interval are several blebs of material containing pyrite (confirmed by our X-ray diffraction studies); these blebs may be fragments of a single 3-mm layer. We describe here the analysis of two samples containing pyrite (465A-1, 2), and one of the white ooze from below the boundary (465A-3).



## Experimental

All samples were dried at 150 °C for 24 h, then ground to a fine powder. Aliquots of 200–400 mg were irradiated with flux monitors at UCLA in a neutron flux of  $2 \times 10^{12} \text{ cm}^{-2} \text{ s}^{-1}$  for instrumental neutron activation analysis (INAA). Aliquots of 40–90 mg were leached with 1M HCl to determine  $\text{CaCO}_3$ .

Separate aliquots of ~1 g of six Stevns Klint samples were similarly irradiated for radiochemical neutron activation analysis (RNAA) of the elements Ir, Os, Pt, Re, Au, Pd, and Ge. After dissolution samples were fused in  $\text{Na}_2\text{O}_2$ , dissolved in HCl, and the noble siderophiles separated as a group on Sraffion resin<sup>6</sup>. Carrier recovery was determined by reactivation. Germanium was separated from the eluate by solvent extraction into  $\text{CCl}_4$  and purified by distillation as  $\text{GeCl}_4$ . The samples have high Br contents, and our determinations were seriously affected by neutron activated Br that was not easily eluted from the resin. The irradiated powders were therefore leached with  $\text{H}_2\text{O}$  before dissolution, reducing Br levels by a factor  $\geq 10$ . We doubt that this procedure removed a significant portion of the noble metals but confirmatory tests are in progress. Aliquots of Smithsonian standard Allende CV chondrite (split 3, pos. 18) were included in the RNAA runs as internal standards.

## Results

Table 1 shows INAA data for 25 elements and two  $\text{CaCO}_3$  determinations (the first based on loss on leaching with 1M HCl, the second based on the assumption that all Ca is present as  $\text{CaCO}_3$ ). The good agreement (67% within 6%) by these independent methods suggest that the latter assumption is correct, and that negligible amounts of other carbonates are present; and also that only a minor fraction of the Ca is in the clay. Table 2 lists the RNAA data for seven elements in six samples of the Danish fish clay. These data confirm the high concentrations of Ir and other siderophiles in the lowest strata. Correction for  $\text{CaCO}_3$  reduces the spread.

Our data on the Stevns Klint fish clay show good general agreement with those of Ganapathy; after allowing for anticipated sampling variations the only significant discrepancies seem to be our 3 times lower Re, 1.9 times higher Pt and 1.6 times lower Au values. Many of our data agree with those of Alvarez *et al.*<sup>1</sup> to within ~20%; we have compared their Stevns Klint samples with our basal samples 1, 1 and 2, 1 which have

similar Ir contents. The chief discrepancies are for a series of elements in which our values are lower by the listed factors: Co, 2.7; Ni, 2.1; Zn, 1.6; As, 2.4; Sb, 2.0. These elements are probably enhanced in strata with high pyrite content, thus the discrepancy can probably be attributed to sampling variations. Curiously, Se concentrations agree even though Se should also be enhanced in sulphide-rich samples.

Our data on DSDP hole 465A add another world location to CT boundaries having Ir concentrations far higher than typical values for pelagic clays<sup>7</sup>. Our Ir concentration of 16 ng per g is lower than those in the Stevns Klint and Caravaca boundary clays, but higher than that at Gubbio.

## Elements in the Stevns Klint fish clay

Relative INAA concentrations of 10 elements are plotted in Fig. 1 as a function of height within Stevns Klint fish clay section 1; all concentrations have been recalculated on a  $\text{CaCO}_3$ -free basis. Bulk  $\text{CaCO}_3$  concentrations are also shown for reference. Only elements whose corrected concentrations either decrease or are constant within 10% are plotted (most lithophiles are not plotted).

The fish clay is finely layered and the variations observed in the section are probably associated with changes in the mineralogy. Thus the very high contents of As, Se and Sb in the lowest sample (Fig. 1) probably reflect higher concentrations of sulphides. But whereas Se levels remain about 6–10 times lower in all higher samples, As and Sb pass through a minimum 4 times lower than the basal sample then rise to final concentrations higher than that in the basal sample. If these high As and Sb concentrations in the higher levels also reflect a high content of sulphides, these were either of a sort that did not enhance Se, or the Se source had decreased greatly before their formation.

More relevant to the present discussion is the behaviour of Ir, which is initially high, decreases by a factor of 2.6 at a height of 15 mm, then gradually rises again to 0.6–0.8 times the basal value. Similar patterns are shown by Fe, Co, and Ni. The trends of Zn and Cr differ from those of Ni and Co chiefly in that the basal values are not appreciably elevated relative to the higher samples. Bromine concentrations are very high in the three lowest samples, then fall rapidly to a plateau 2–3 times lower. As we can leach 90% of this Br with  $\text{H}_2\text{O}$ , it is only weakly bound.

**Table 1** Concentrations\* of 25 elements in the Stevns Klint fish clay and in samples from sections 3 and 4, core 3 of DSDP hole 465A, Leg 62 from the Central Pacific

| Height† |    | Na     | K   | Ca  | Sc  | Cr  | Mn  | Fe   | Co   | Ni  | Zn  | As   | Se    | Br   | Sb   | La | Ce | Nd | Sm  | Eu   | Tb   | Dy  | Yb  | Lu   | Ir   | Th  | CaCO <sub>3</sub> | CaCO <sub>3</sub> |
|---------|----|--------|-----|-----|-----|-----|-----|------|------|-----|-----|------|-------|------|------|----|----|----|-----|------|------|-----|-----|------|------|-----|-------------------|-------------------|
| 1, 1    | 5  | 890    | 2.8 | 234 | 6.7 | 112 | 55  | 14.3 | 23.3 | 239 | 260 | 15.3 | 22.7  | 58.0 | 2.85 | 33 | 28 | 32 | 6.7 | 1.44 | 0.99 | 6.0 | 2.2 | 0.31 | 31.0 | —   | 642               | 584               |
| 1, 2A   | 8  | 870    | 3.3 | 243 | 6.7 | 118 | 62  | 7.4  | 15.7 | 144 | 207 | 6.2  | 2.59  | 59.0 | 1.24 | 30 | 27 | 36 | 6.0 | 1.35 | 0.90 | 5.3 | 2.0 | 0.32 | 17.7 | —   | 659               | 607               |
| 1, 2B   | 11 | 780    | 3.4 | 265 | 6.6 | 106 | 80  | 7.9  | 14.6 | 133 | 206 | 5.4  | 1.93  | 44.0 | 0.94 | 29 | 27 | 32 | 5.8 | 1.36 | 0.88 | 5.4 | 2.1 | 0.30 | 13.8 | —   | 708               | 662               |
| 1, 3    | 15 | 890    | 3.4 | 309 | 5.1 | 56  | 105 | 5.6  | 10.4 | 82  | 144 | 3.2  | 1.50  | 15.0 | 0.55 | 27 | 22 | 26 | 5.4 | 1.25 | 0.84 | 4.8 | 1.9 | 0.27 | 7.0  | —   | 720               | 772               |
| 1, 4    | 20 | 900    | 3.3 | 327 | 5.0 | 38  | 131 | 4.7  | 7.9  | 66  | 126 | 2.7  | 1.47  | 8.2  | 0.50 | 28 | 22 | 26 | 5.7 | 1.30 | 0.87 | 5.1 | 2.0 | 0.27 | 4.6  | —   | 846               | 817               |
| 1, 5A   | 25 | 970    | 3.8 | 310 | 5.9 | 70  | 113 | 8.2  | 11.6 | 111 | 180 | 2.4  | 1.67  | 15.0 | 0.85 | 38 | 34 | 35 | 7.3 | 1.75 | 1.16 | 7.2 | 2.8 | 0.41 | 7.4  | —   | 768               | 768               |
| 1, 5B   | 30 | 880    | 3.1 | 328 | 5.0 | 59  | 142 | 7.8  | 9.9  | 80  | 160 | 7.1  | 1.25  | 13.0 | 0.95 | 31 | 27 | 29 | 5.8 | 1.34 | 0.90 | 5.5 | 2.3 | 0.32 | 5.6  | —   | 808               | 819               |
| 1, 6    | 34 | 1,450  | 1.7 | 370 | 4.2 | 38  | 160 | 5.5  | 6.4  | 60  | 109 | 5.6  | 1.36  | 9.1  | 0.88 | 45 | 39 | 40 | 8.8 | 2.00 | 1.34 | 8.6 | 3.2 | 0.41 | 5.8  | —   | 889               | 924               |
| 1, 7    | 37 | 780    | 2.0 | 346 | 4.1 | 46  | 102 | 6.8  | 8.2  | 94  | 115 | 7.6  | 1.61  | 9.3  | 0.77 | 25 | 22 | 23 | 4.9 | 1.13 | 0.76 | 2.6 | 1.9 | 0.28 | 5.6  | —   | 847               | 964               |
| 2, 1    | 5  | 680    | 2.7 | 224 | 7.6 | 140 | 42  | 17.0 | 31.0 | 298 | 297 | 21.6 | 16.70 | 69.0 | 3.47 | 32 | 30 | 35 | 6.4 | 1.40 | 0.94 | 5.7 | 2.0 | 0.30 | 36.0 | —   | 594               | 559               |
| 2, 2A   | 10 | 710    | 3.5 | 242 | 6.9 | 131 | 62  | 9.1  | 17.8 | 176 | 220 | 9.1  | 2.71  | 57.0 | 1.61 | 27 | 25 | 29 | 5.4 | 1.23 | 0.83 | 4.8 | 1.8 | 0.28 | 19.6 | —   | 667               | 604               |
| 2, 2B   | 16 | 780    | 3.9 | 287 | 6.1 | 85  | 92  | 7.0  | 11.8 | 109 | 177 | 4.2  | 1.96  | 32.0 | 0.71 | 30 | 26 | 29 | 5.9 | 1.37 | 0.94 | 5.4 | 2.2 | 0.30 | 10.8 | —   | 741               | 717               |
| 2, 3    | 22 | 710    | 4.6 | 292 | 6.0 | 87  | 102 | 9.6  | 14.4 | 128 | 202 | 4.2  | 1.47  | 19.0 | 0.66 | 26 | 24 | 23 | 5.1 | 1.20 | 0.80 | 4.7 | 1.8 | 0.28 | 8.0  | —   | 724               | 729               |
| 2, 4    | 26 | 820    | 3.1 | 351 | 5.2 | 41  | 140 | 5.5  | 12.4 | 69  | 135 | 4.0  | 1.28  | 7.7  | 0.67 | 28 | 22 | 26 | 5.6 | 1.29 | 0.90 | 5.0 | 2.2 | 0.28 | 4.5  | —   | 838               | 877               |
| 2, 5    | 30 | 720    | 3.1 | 316 | 5.0 | 68  | 145 | 7.6  | 10.2 | 97  | 158 | 6.3  | 1.30  | 14.0 | 0.77 | 27 | 24 | 24 | 5.2 | 1.22 | 0.80 | 4.7 | 2.0 | 0.30 | 6.5  | —   | 791               | 789               |
| 4       | —  | 790    | 3.2 | 207 | 7.7 | 153 | —   | 19.7 | 38.0 | 392 | 343 | 24.1 | 58.00 | 64.0 | 3.40 | 34 | 33 | —  | 6.2 | 1.54 | 0.96 | —   | 2.0 | —    | 46.0 | 2.8 | 572               | 517               |
| 5       | —  | 780    | 3.2 | 193 | 8.2 | 199 | —   | 20.8 | 33.0 | 281 | 288 | 20.8 | 28.90 | 58.0 | 2.12 | 30 | 28 | —  | 5.6 | 1.37 | 0.84 | —   | 1.8 | —    | 54.0 | 3.3 | 545               | 482               |
| 6       | —  | 840    | 3.6 | 291 | 6.3 | 96  | —   | 6.6  | 12.2 | 118 | 187 | 4.5  | 2.00  | 37.0 | 0.87 | 28 | 27 | —  | 5.5 | 1.28 | 0.90 | —   | 1.9 | —    | 11.9 | 2.9 | 722               | 727               |
| 7       | —  | 910    | 2.8 | 243 | 8.0 | 170 | —   | 13.1 | 26.9 | 239 | 301 | 11.8 | 22.10 | 68.0 | 1.74 | 38 | 38 | —  | 7.5 | 1.77 | 1.11 | —   | 2.3 | —    | 44.0 | 2.8 | 600               | 607               |
| 8       | —  | 810    | 3.4 | 307 | 6.8 | 113 | —   | 9.2  | 16.8 | 162 | 218 | 7.6  | 3.20  | 46.0 | 1.19 | 27 | 30 | —  | 5.3 | 1.25 | 0.83 | —   | 1.7 | —    | 17.8 | 2.7 | 680               | 767               |
| 9       | —  | 890    | 2.9 | 252 | 7.6 | 161 | —   | 19.4 | 38.0 | 309 | 370 | 20.5 | 31.00 | 63.0 | 3.00 | 31 | 29 | —  | 5.8 | 1.32 | 0.88 | —   | 1.9 | —    | 52.0 | 2.7 | 570               | 629               |
| 10      | —  | 880    | 2.7 | 242 | 8.0 | 145 | —   | 8.6  | 19.6 | 235 | 235 | 6.3  | 18.80 | 70.0 | 1.08 | 36 | 35 | —  | 7.0 | 1.65 | 1.12 | —   | 2.3 | —    | 27.2 | 2.6 | 625               | 604               |
| 11      | —  | 720    | 3.4 | 280 | 6.8 | 126 | —   | 6.7  | 14.7 | 160 | 207 | 4.5  | 3.20  | 55.0 | 0.82 | 25 | 27 | —  | 5.1 | 1.18 | 0.78 | —   | 1.6 | —    | 15.8 | 2.6 | 699               | 699               |
| 465A-1  | —  | 13,400 | 3.5 | 264 | 7.4 | 146 | —   | 29.7 | 77.0 | 461 | 318 | 33.8 | 2.10  | 57.0 | 7.30 | 15 | 5  | —  | 2.5 | 0.66 | 0.42 | —   | 1.4 | —    | 15.6 | 2.9 | 685               | 659               |
| 465A-2  | —  | 11,100 | 4.7 | 356 | 4.0 | 49  | —   | 6.2  | 6.3  | 84  | 82  | 6.3  | 0.55  | 54.0 | 5.00 | 19 | 5  | —  | 3.2 | 0.83 | 0.57 | —   | 1.9 | —    | 12.9 | 1.3 | 856               | 889               |
| 465A-3  | —  | 5,600  | —   | 416 | 0.9 | 4   | —   | 0.2  | 1.5  | 14  | 9   | 0.8  | —     | 34.0 | —    | 12 | 2  | —  | 1.8 | 0.47 | 0.35 | —   | 1.4 | —    | <0.7 | 0.1 | 979               | 1,040             |

\*Concentrations in  $\mu\text{g per g}$  except Fe, K, Ca and  $\text{CaCO}_3$ , mg per g, and Ir, ng per g.

†Midpoint heights are relative to the value assigned the lowest sample—see text.

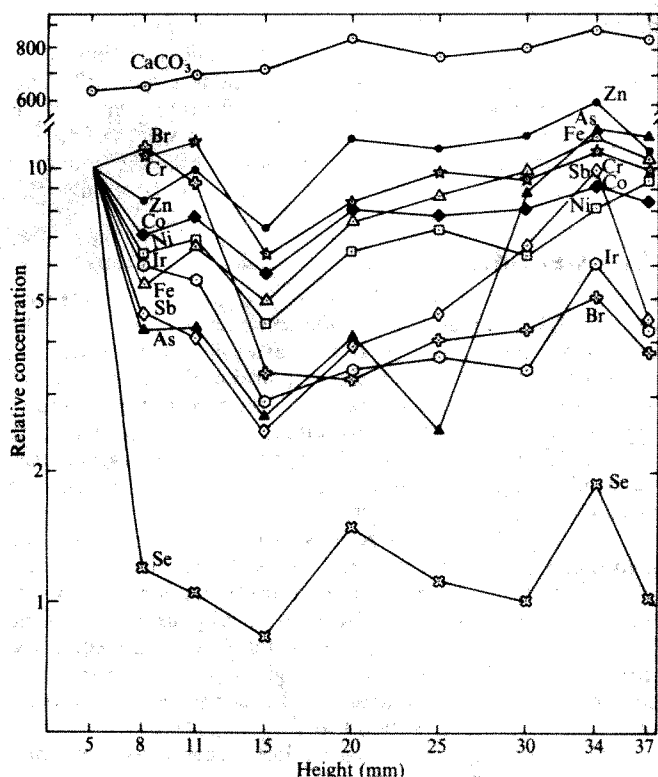


Fig. 1 Abundance profiles for 10 elements in sample 1 from the Stevns Klint fish clay. Data are on a carbonate-free basis and normalized to give sample 1, 1 a value of 10. Only Se is severely depleted up the section and only Ir, As, Sb, and Br also are depleted significantly in most samples. In general, there is little difference between the base and top of the section.

Siderophile concentrations are high in all levels of the fish clay relative to those in normal pelagic clays. The fine lamination of the clay indicates an absence of bioturbation and that there must have been a rather continuous source of siderophile-rich material. The depositional environment here into shallow basins between mounds of Maastrichtian chalk<sup>5</sup>, might have favoured concentration of relatively dense mineral phases. Thus, if Ir is concentrated in such phases these depressions might have become traps for siderophile-rich materials whereas clay minerals were preferentially swept towards lower regions on the continental shelf.

### An extraterrestrial source of the siderophiles?

It has been suggested<sup>1,3,4</sup> that the worldwide enhancement in siderophiles in the CT boundary sediments resulted from the accretion of extraterrestrial material. Alvarez *et al.*<sup>1</sup> inferred an extraterrestrial origin of the Ir anomaly mainly because it is worldwide, coincides with the time of the Cretaceous extinctions, and because asteroidal impacts of the required magnitude should occur about every 100 Myr. They argued against reduction of Ir from the oceanic reservoir, or a worldwide reduction in pelagic sedimentation rates. Smit and Hertogen<sup>4</sup> accepted an extraterrestrial origin primarily because terrestrial sources appeared inadequate to account for the high Ir and Os at the boundary. Ganapathy<sup>3</sup> opted for an extraterrestrial source because common terrestrial rocks have very low siderophile concentrations, and relative abundance patterns in terrestrial rocks and ores are grossly different from the roughly chondritic pattern found in the Stevns Klint clay.

An important observation is that pyrite, FeS<sub>2</sub>, is a ubiquitous component of the CT boundary layers<sup>8</sup>. The formation of pyrite in marine sediments requires reducing conditions and high H<sub>2</sub>S concentrations<sup>9</sup>. In basins like the Norwegian-Danian Trough where the Stevns Klint fish clay formed, these conditions generally reflect the presence of stagnant water in closed basins.

How the required conditions are generated in the deep ocean, for example, at DSDP site 465, is not clear. As a trial hypothesis, we suggest that the reducing conditions are directly associated with the extinction of Cretaceous phytoplankton, and perhaps even resulted from the excess of dead organisms; reducing conditions may have been present in the oceans simultaneously throughout the world.

In fact, such reducing conditions may be necessary to avoid severe fractionation of extraterrestrial siderophiles before deposition. The oceanic residence time of an element is defined as the amount present divided by the steady-state injection or deposition rate. In present-day steady-state conditions, siderophile residence times vary by factors of at least 10<sup>3</sup>. For example, published<sup>10</sup> residence times are 0.20 kyr for Fe, 30 kyr for Co, 90 kyr for Ni and 120 kyr for Au. If these residence times are largely established by kinetic processes<sup>11</sup> such as ingestion by organisms, injection of large amounts of material having a solar Au/Fe ratio into the ocean would result in the first material to fall out having a Au/Fe ratio 600 times smaller than the solar ratio, whereas that in the sediments depositing a few kyr later would be much higher than the solar value.

Long residence times would have to be shortened to values comparable with the depositional periods of the CT sediments and reducing, high sulphide conditions offer plausible circumstances for this to occur. But if the residence times of siderophiles are reduced by a large factor, the deposition rate of oceanic siderophiles of terrestrial origin will be increased by a similar factor. Therefore, any deposition of relatively unfractionated extraterrestrial siderophiles is likely to be accompanied by an enhanced deposition of terrestrial siderophiles, the enhancement factor being roughly proportional to the steady-state oceanic residence time. This exacerbates the problem of separating the terrestrial and extraterrestrial signals.

Figure 2 shows our siderophile data for the six Stevns Klint samples studied by RNAA, and the INAA data available for the DSDP core 465A. In the upper portion element/Ni ratios are normalized to those in CI carbonaceous chondrites, in the lower portion to mean abundances in group IIAB iron meteorites. The following, very approximate, background concentrations based on intercepts on element-Ir diagrams were subtracted from the Stevns Klint samples: 10 mg per g Fe, 20 µg per g Co and 110 µg per g Ni. We had no basis for estimating background levels for the DSDP core. Elements are arranged in order of decreasing nebular condensation temperature<sup>12,13</sup>.

Table 2 Concentrations\* determined by RNAA of seven elements in the Stevns Klint fish clay

|         | Ir  | Os  | Re   | Pt    | Pd  | Au    | Ge    |
|---------|-----|-----|------|-------|-----|-------|-------|
| 4       | 42  | 32  | 9.7  | 60    | 44  | 5.9   | —     |
| 9       | 45  | 60  | 11.7 | 45    | 41  | 5.6   | 1.00  |
| 10      | 29  | 30  | 5.7  | 43    | 30  | 3.4   | 0.98  |
| Allende | 730 | 828 | 71.0 | 1,820 | 705 | 145.0 | 22.00 |
| 5       | 46  | 60  | 11.3 | 69    | 37  | 6.6   | 0.90  |
| 7       | 34  | 53  | 4.3  | 39    | 39  | 5.2   | 0.77  |
| 8       | 18  | 28  | 2.4  | 23    | 21  | 3.7   | 0.81  |
| Allende | 730 | 828 | 70.0 | 1,530 | 705 | 145.0 | 19.00 |

\*Concentrations in ng per g except Ge, µg per g. Each neutron activation run consisted of three clay samples and the Allende CV chondrite.

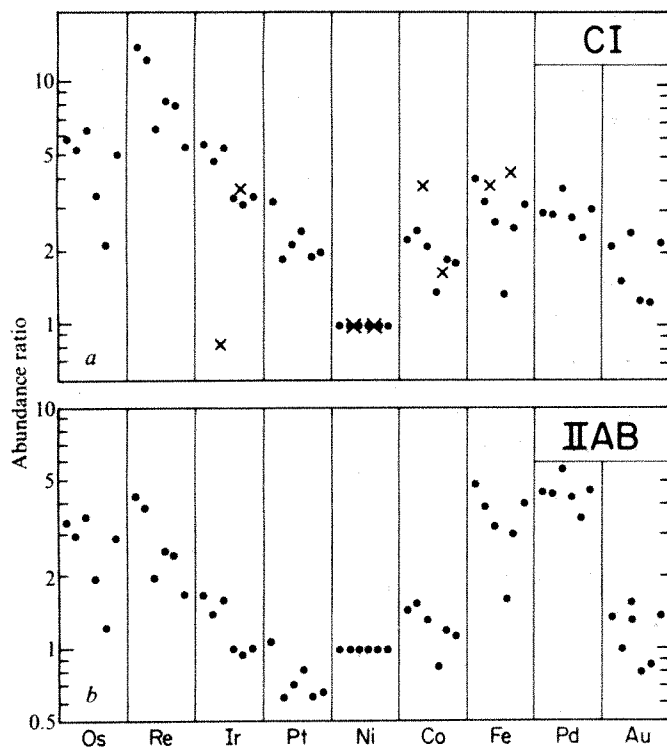
The Stevns Klint samples show significant fractionations relative to any known meteorites. Nickel-normalized abundances of Os and Ir are about 5 times higher than CI values; they are ~3 times higher than the highest chondritic abundances, those in CV chondrites. Although our Re/Ni ratios are about a third of those of Ganapathy<sup>3</sup>, our Re abundance ratios are still about double those for Os and Ir.

If Ni, our normalizing element, were 2.5–3 times higher, the pattern would be generally similar to that of CV chondrites. Although our inferred background Ni value of 110 µg per g may be too high, subtracting no background at all would only increase the average Ni concentration by a factor of ~1.6, much



less than required. Moreover, there are no unique background values that would generate constant ratios of other siderophiles to Ir. If a CI pattern were initially present, then some terrestrial fractionation has surely occurred.

The estimated mean composition of group IIAB iron meteorites shows an enrichment of refractory siderophile (Os, Ir) abundances by about 3 times relative to those in CI chondrites. As shown in Fig. 2b, normalizing to IIAB leads to mean abundance ratios closer to unity than does the CI normalization in Fig. 2a. This conflicts with Ganapathy's<sup>3</sup> inference that the impacting body was not an iron meteorite because 'most iron meteorites (with the exception of group I) show highly variable and noncosmic elemental ratios'. Ganapathy is right that individual, *m*-sized irons often show extreme fractionations associated with fractional crystallization. However, mean siderophile abundance patterns inferred by Willis<sup>14</sup> for entire cores are generally similar to those characteristic of chondrites.



**Fig. 2** Ni-normalized abundance ratios for nine siderophile elements plotted relative to a, CI and b IIAB. The six fish clay samples (●) from left to right are 5, 9, 7, 10, 4 and 8. Plot a shows the INAA data for Pacific core 465A-1 (left side) and 465A-2 (right side). Note that the fractionated patterns can be fit with both meteorite classes. The siderophiles Ge and Sb were not plotted because of the large amount of scatter introduced by correction for terrestrial materials.

A different fractionation pattern is observed in the Central Pacific sample 465A-1 (Fig. 2a). The abundance ratio of Ir is now 0.8, about 5 times lower than in the Stevns Klint clay; the Fe and especially the Co abundance ratios are even higher than in the Danish samples. Sample 465A-2 contained much less pyrite and siderophile abundances similar to the Stevns Klint sample. Perhaps the key message is that relative fractionation of siderophiles has occurred, and that the resulting patterns differ from location to location.

We can now consider whether the CT boundary siderophiles are of extraterrestrial origin. Significant fractions of some siderophiles are surely terrestrial, especially those that have relatively high oceanic residence times. The elements showing the highest abundance ratios in the Stevns Klint fish clay are Os and Ir. Alvarez *et al.*<sup>1</sup> report a concentration of Ir of  $< 4 \times 10^{-13}$  g per g in seawater that together with a mean ocean

depth of 3,700 m and a typical pelagic deposition rates of  $\sim 10^{-13}$  g Ir  $\text{cm}^{-2} \text{yr}^{-1}$  (ref. 7) suggest a residence time of  $\leq 10^6$  yr. It is important to establish this residence time or at least to lower the upper limit. If as seems likely the Ir residence time is comparable with or lower than the  $\sim 100$  kyr values of Ni and Au, the enhanced Ir/Au and Ir/Ni ratios in the CT boundary sediments require that most of the Ir be of extraterrestrial origin.

### An asteroidal impact?

Alvarez *et al.*<sup>1</sup>, Smit and Hertogen<sup>4</sup> and Ganapathy<sup>3</sup> interpret the high CT boundary siderophile contents as being caused by the impact of a large ( $\sim 10$  km) asteroid. Hsü<sup>15</sup> favours a cometary impact, based on the assumption that cometary ices will include chemicals toxic to phytoplankton. Comets apparently consist of roughly equal parts of ice and stony material<sup>16</sup>, thus the mass of impacting cometary material required to supply the observed accumulation of Ir would be twice that for a chondritic asteroid.

These hypotheses have serious problems in explaining the high Ir concentrations in the sediments. Table 3 lists maximum Ir concentrations observed in the four CT boundary sediments for which data are available. Because a negligible portion of the Ir is likely in the  $\text{CaCO}_3$ , the relevant data are those corrected for  $\text{CaCO}_3$ . The final column gives the extraterrestrial component (ETC), the ratio of Ir in the carbonate-free sediment to that in water-free CI chondrites<sup>17</sup>.

Alvarez *et al.*<sup>1</sup> quote the mass of impact ejecta as  $\sim 60$  times the mass of the projectile (R.A.F. Grieve unpublished). In fact, the ratio depends on the impact velocity (Grieve's estimate seems reasonable for  $\sim 20$  km  $\text{s}^{-1}$ ), and the size fraction of the ejecta and projectile material. In the fine fraction of ejecta taken near the rims of fresh lunar craters the ratio is far higher; 4.2 ng per g Ir (ref. 18) in the  $< 4$ - $\mu\text{m}$  fraction of immature soil 61220 (Table 3), implies a ratio of lunar to chondritic material of  $> 100$ . The two other lunar soils<sup>19</sup> listed in Table 3 are mature, that is, their siderophile contents have been enhanced by the continued accretion of projectiles that did not penetrate the regolithic debris layers on the lunar surface. However, we doubt that, following the hypothetical CT event, the ratio in the  $\leq 1$ - $\mu\text{m}$  size fraction having an appreciable stratospheric residence was much less than that in the fine fraction of soil 61220, although we cannot rule out this extreme fractionation.

Examination of the extraterrestrial components (ETC) listed in Table 3 shows that the Danish, Spanish and Central Pacific values are much higher than expected if the projectile had a chondritic composition and the ejecta/projectile ratio were 60. Further, the terrestrial component of the CT boundary sediments is unlikely to consist entirely of ejecta; if half consisted of non-ejecta detrital material, the anticipated ETC would be only  $\sim 0.8\%$ .

Our rare-earth data (Table 1) can be used to examine whether the CT boundary sediment had the same composition worldwide, as would be expected were it composed entirely of ejecta. In fact both the concentrations and the patterns are significantly different: relative to Stevns Klint, DSDP core 465A has half the La concentration, La/Ce ratios are  $\sim 3$  times higher, and La/Yb  $\sim 1.5$  times lower. The Danish sample resembles the average ocean sediment<sup>20</sup> as well as various continental volcanic rocks; the Ce depletion in the Pacific sediment is similar to but less pronounced than the depletion in ocean water. Alteration by interaction with the ocean water during sedimentation is unlikely, because the amount of La in 3 mm of our Pacific sediment exceeds by a factor of 13 that in the overlying 2.5 km of water. We conclude that a substantial non-ejecta contribution is present in one or both sediments.

We have shown that the siderophile pattern is consistent with the projectile being an iron meteorite. The siderophile content of a metal-sulphide core of an asteroid formed from relatively reduced chondritic materials such as H-group chondrites is about 3–4 times greater, that from more oxidized chondritic materials such as L chondrites  $\sim 6$ –7 times greater than those in

a chondritic projectile (a large fraction of all siderophiles except Fe enter the cores in both cases). If we neglect the high ETC of the Stevns Klint sample on the assumption that it reflects selective enrichment of ore minerals, and assume that the non-ejecta component of the other boundary sediments is  $\leq 0.5$ , a metallic core of an oxidized parent body might just account for Spanish and Pacific ETC values. About 20% of the fireballs observed by the Prairie Network enter the Earth's atmosphere at velocities  $\leq 15 \text{ km s}^{-1}$  (ref. 21); if the hypothetical CT object had such a low impact velocity the ejecta/projectile ratio might be  $\sim 30$ , half Grieves's value, and more in keeping with the high ETC values. Impact by interstellar comets or asteroids<sup>22</sup> would tend to result in impact velocities  $> 20 \text{ km s}^{-1}$ .

It is very unlikely that the siderophile enrichment in the CT boundary sediments resulted from the impact with the Earth's surface of a comet or of an asteroid having a chondritic composition. The data seem consistent with the impact of a metallic core, but only if the asteroid were relatively oxidized, the impact velocity were  $\leq 20 \text{ km s}^{-1}$  and if the non-ejecta fraction in the carbonate-free sediment were  $\leq 50\%$ .

### Extraterrestrial materials not impacting the Earth's surface

If the material accreted at the end of the Cretaceous were finely divided, it would be slowed to low velocities in the Earth's atmosphere. Because no ejecta would be produced, the high ETC values would not present a problem.

The most plausible source of finely divided material is an interstellar cloud. It is estimated that the Solar System encounters such clouds each time it passes through an arm of the Galaxy, roughly once each 100 Myr (refs 22–25). The amount of Ir that could be accreted depends on the cloud's density and size.

**Table 3** Maximum Ir concentrations\* observed in samples from the CT boundary at four worldwide locations and the finest fractions of three lunar soils<sup>14,15</sup>

| Location                  | Whole rock | Whole rock<br>-CaCO <sub>3</sub> | Extraterrestrial<br>components†<br>(%) |
|---------------------------|------------|----------------------------------|--|
| Denmark                   | 54         | 120                              | 21                                     |
| Italy                     | 5.5        | 9.1                              | 1.6                                    |
| Spain                     | 27         | 50                               | 9                                      |
| Central pacific           | 13         | 40                               | 7                                      |
| 15100 (<7 $\mu\text{m}$ ) | 19         | 19                               | 3                                      |
| 61200 (<4 $\mu\text{m}$ ) | 4.2        | 4.2                              | 0.7                                    |
| 66080 (<7 $\mu\text{m}$ ) | 22         | 22                               | 4                                      |

\*In ng per g.

†Extraterrestrial components (ETC) were obtained by dividing these concentrations by those in water-free CI chondrites (Ir = 580 ng per g).

A second-order effect is the dependence of the accretion rate on its vectorial velocity, the enhancement factor being approximately  $[1 + (V_{\text{esc}}^2/V_{\text{rel}}^2)]$  where  $V_{\text{rel}}$  is the relative velocity and  $V_{\text{esc}}$  is  $11.2 \text{ km s}^{-1}$ , the escape velocity from the Earth. The relative velocity is commonly estimated to be  $\sim 20 \text{ km s}^{-1}$ . If the velocity is in the range 20–40  $\text{km s}^{-1}$  and the vector is near the orbital plane of the earth, a significant enhancement could occur during some of the Earth's orbit, but the mean enhancement integrated around the orbit is not likely to be as large as a factor of 2. Gravitational focusing by the Sun would significantly enhance the solar accretion rate, but the enhancement of the terrestrial accretion rate would be much less. We will assume no enhancement.

Relative to Si =  $10^6$  atoms, the solar abundance of H is  $2.2 \times 10^{10}$  (ref. 26); our data on CI chondrites indicate an Ir abundance of 0.64. We will assume that these values are appropriate to interstellar clouds in our portion of the Galaxy. If the relative amount of terrestrial Ir was small at all locations, published data<sup>1,3,4</sup> indicate a mean worldwide accumulation

within the range  $8\text{--}80 \times 10^{-9} \text{ g cm}^{-2}$ . An accumulation of  $2 \times 10^{-8} \text{ g cm}^{-2}$  Ir could result from the passage of the Earth through a cloud having a mean density of  $10^5 \text{ H atoms cm}^{-3}$  and a diameter of  $8.6 \times 10^{19} \text{ cm}$  ( $= 5.7 \times 10^6 \text{ AU} = 28 \text{ pc}$ ), an order of magnitude greater than that estimated for the Orion 1 cloud<sup>27</sup>, one of the larger and denser interstellar clouds in our neighbourhood. Thus the probability of passage through such a dense region is probably considerably less than once each 100 Myr. Further, to account for the narrow Ir depth profiles in sediments such as that at Caravaca<sup>4</sup>, the bulk of the interstellar material needs to have been accreted from regions of exceptionally high density ( $\geq 10^6 \text{ H atoms cm}^{-3}$ ), or sedimentation rates must have been  $\leq 10^{-7} \text{ m yr}^{-1}$ , the lowest values observed in abyssal clays today.

Additional arguments against accretion of extrasolar material are a low <sup>244</sup>Pu content (<sup>244</sup>Pu/Ir ratio  $\leq 10^{-4}$ , see ref. 1) and the absence of measurable variations in <sup>191</sup>Ir/<sup>193</sup>Ir and <sup>184</sup>Os/<sup>190</sup>Os ratio<sup>1,3,4</sup>. However, studies of the Allende chondrite showed no variations in <sup>184</sup>Os/<sup>190</sup>Os either in the refractory inclusions having anomalous O isotope compositions or in chromite separates having isotopically anomalous Xe (ref. 28). The absence 4.5 Gyr ago of such variations in materials of diverse isotopic composition suggests that isotopic variations of Os and perhaps Ir as well may also have shown little variation in our part of the Galaxy 65 Myr ago. If the <sup>238</sup>U/Ir atom ratio in the interstellar cloud was equal to the solar value of about 0.03 present at the time the Solar System formed, the <sup>244</sup>Pu/<sup>238</sup>U ratio in the cloud was  $\leq 3 \times 10^{-3}$ , about 5 times lower than that initially present in the oldest meteorites<sup>29</sup>. The mean <sup>244</sup>Pu/<sup>238</sup>U surely varies by factors greater than 5 from cloud to cloud and possibly even within clouds, thus this discrepancy is not severe enough to require rejection of the interstellar cloud accretion model.

As an alternative to interstellar matter, material could enter the Earth's atmosphere as relatively large bodies but disintegrate because of low inherent strength, as thought to have occurred during the Tunguska event. De Laubenfels<sup>39</sup> first suggested that a Tunguska-like event could have triggered the Cretaceous extinctions. The Tunguska projectile was relatively small<sup>31</sup> depositing an energy of  $4 \pm 2 \times 10^{23} \text{ erg}$ , corresponding to  $2 \times 10^{11} \text{ g}$  if the velocity of  $20 \text{ km s}^{-1}$  is assumed. This is  $\sim 10^5$  times smaller than the amount of material inferred from Ir in the European or Pacific CT boundary sediments. The key question is whether in the  $\sim 5 \text{ s}$  atmospheric transit time a  $10^{17}\text{--}10^{18} \text{ g}$  object would break up completely. We doubt that it would and suggest that an object in a non-intersecting orbit broke up into a large number of smaller objects as it passed inside the Roche limit, with a portion of the debris entering new orbits that intersected the Earth's surface.

The Tunguska object has been interpreted as a cometary remnant. In fact, Kresak<sup>32</sup> associated it with Comet Encke. Many comets are structurally weak, as indicated by the fact that at least 10 have broken up without any apparent cause<sup>33,34</sup>. It seems plausible that such weak comets would undergo breakup inside the Roche limit.

About half the meteoritic material entering the Earth's atmosphere seems to be cometary<sup>21</sup>, suggesting that a super Tunguska event of the sort we describe is about as likely as the impact of an asteroid composed of tough materials, perhaps amounting to one event each 100 Myr. In contrast, passage through an interstellar cloud having the required column density would seem to be a far rarer event. We favour the super-Tunguska mechanism.

### Extinction mechanisms

Although infall of a comet may have marked the end of the Cretaceous, we are skeptical about Hsü's<sup>15</sup> marine extinction mechanism, poisoning by toxic cometary substances. Although HCN, CH<sub>3</sub>CN, and CO are certainly toxic for many organisms, the bulk of these would have been oxidized in the fireball that accompanied the cometary accretion. Further, such poisons



would not be selective among different planktonic species and would certainly have also had a deleterious effect on the benthic realm.

We suggest that cometary infall-related marine extinctions resulted either from thermal stress<sup>35,36</sup> or from the opacity of the stratosphere that would accompany the infall of  $10^6$ – $10^7$  times the mass of Tunguska<sup>1</sup>. Total darkness for a few days or a week would lead to the death of most phytoplankton, and a domino effect on the many organisms higher in the food chain.

We are also skeptical about the suggestion<sup>1</sup> that stratospheric opacity lasting for several years was responsible for the death of the dinosaurs and other large land animals. The estimate<sup>1</sup> of  $5 \times 10^{18}$  g of ejecta injected into the stratosphere corresponds to the total mass of the atmosphere above ~48 km, 10% of the atmosphere above ~31 km, and 1% above ~16 km. To keep such large amounts of material suspended, it would have to behave as elastically as gas molecules. In fact, it would probably stick on impact, the coagulation following second-order kinetics. For 2–3 years following the eruption of Krakatoa in 1883 its stratospheric dust produced a reddish-brown solar corona that could be seen in favourable conditions<sup>37</sup>. If favourable conditions were required to see the Krakatoa dust and if second-order kinetics controlled its fallout, clearly no matter how much dust you inject into the stratosphere, within a few months or less the level will drop to a value no more than a few times greater than that present immediately following the Krakatoa explosion. Stratospheric opacity could appreciably reduce photosynthesis by land plants for no more than one season, and probably a much shorter period.

It seems more likely that a major input of energy, whether by asteroidal impact or a super Tunguska, would lead to extensive destruction of forests by the blast wave and accompanying forest fires, as occurred within about a 100 km<sup>2</sup> area about the Tunguska epicentre<sup>38</sup>. Clearly no land animal larger than 25 kg (ref. 39) could have continued to survive in the scorched area near Tunguska.

Another extinction mechanism is required if the siderophiles were accreted from an interstellar cloud. In this case accretion to the solar surface would result in the conversion of gravitational energy to heat, with an increase in the luminosity, and extinctions due to thermal stress<sup>35,40</sup>. A cloud density of  $10^5$  H cm<sup>-3</sup> and a relative velocity of 20 km s<sup>-1</sup>, as used in our estimate, would increase the solar luminosity by 1% (ref. 41). Further, the increase depends on  $V_{rel}^3$ , thus a relative velocity about 25% lower would double the effect. One can easily imagine that as a result of the scatter in velocities and densities within a large interstellar cloud, there is a high probability that during short periods (say 100 yr) the solar luminosity would be increased by 20% or more, resulting in a mean increase in temperature of  $\geq 15$  K. Additional climatic effects are associated with solar

flares and distortions of the solar and terrestrial magnetic fields while the Solar System is immersed in an interstellar cloud<sup>24,25</sup>.

One interesting effect is the reduction of atmospheric O<sub>2</sub> as a result of the accretion of interstellar H<sub>2</sub> to the Earth (see also ref. 42). The estimated accumulation of Ir,  $2 \times 10^{-8}$  cm<sup>-2</sup> corresponds to 3.5 g cm<sup>-2</sup> of H, 14% of the amount required to fully convert atmospheric O<sub>2</sub> to H<sub>2</sub>O. In contrast to CO<sub>2</sub>, there is weak buffering on the atmospheric O<sub>2</sub> content; the level at any time represents a dynamic balance between photosynthetic production and various sinks; adjustment to shifts in the equilibrium abundance requires a few Myr (ref. 43). Baur and Friedl<sup>44</sup> recently suggested that early Mesozoic O<sub>2</sub> levels were only ~60% of present day levels. If levels in the Cretaceous 100 Myr later were also low, the impact of accretion of interstellar H could be still greater than the above estimates.

Undoubtedly many other effects deleterious to one or the other families of organisms would result from immersion of the Solar System in an interstellar cloud.

## Conclusions

A pyrite-bearing CT boundary clay from DSDP hole 465A in the Central Pacific has high concentrations of Ir and other siderophiles, confirming that the high siderophile contents found in shallower sediments are also found in those deposited at depths >2 km. Concentrations of 25 elements as a function of height in the finely layered CT boundary clay from Stevns Klint, Denmark show that although the highest concentrations are found in basal samples, carbonate-free concentrations of siderophiles are relatively high at all heights. The ubiquitous presence of pyrite in CT boundary sediments indicates extensive reducing conditions—these probably led to a reduction in the oceanic residence times and thus enhanced deposition for some terrestrial siderophiles. Nevertheless, we tentatively conclude that most of the Ir in the CT sediments is of extraterrestrial origin. Concentrations of Ir are higher than expected from the surficial impact of a comet or an asteroid of chondritic composition; a metal-sulphide asteroidal core is marginally possible, but it seems more likely that the siderophile-rich material reached terminal velocity in the atmosphere. There is a small possibility that this was dust from an interstellar cloud, but it is more probable that the near-Earth breakup of weak cometary materials produced a series of Tunguska-like events all around the globe.

We thank H. Tappan and A. R. Loeblich for discussions and for the Stevns Klint samples. The collection of the DSDP samples was supported by the NSF and L. Garifal and W. R. Riedel provided these samples. We thank F. Asaro, L. W. Alvarez, P. R. Weissman and J. Hertogen for helpful comments and J. Pai and A. Young for technical assistance.

Received 8 October; accepted 11 November 1980.

- Alvarez, L. W., Alvarez, W., Asaro, F. & Michel, H. V. *Science* **208**, 1095–1108 (1980).
- Alvarez, W., Alvarez, L. W., Asaro, F. & Michel, H. V. *Geol. Soc. Am. Abstr. Prog.* **11**, 378 (1979).
- Ganapathy, R. *Science* **209**, 921–923 (1980).
- Smit, J. & Hertogen, J. *Nature* **285**, 198–200 (1980).
- Christensen, L., Fregerslev, S., Simonsen, A. & Thiede, J. *Bull. geol. Soc. Denmark* **22**, 193–212 (1973).
- Nadkarni, R. A. & Morrison, G. H. *Analyt. Chem.* **46**, 232–236 (1974).
- Crockett, J. G. & Kuo, H. Y. *Geochim. cosmochim. Acta* **43**, 831–842 (1979).
- Percival, S. F. & Fischer, A. G. *Evolut. Theory* **2**, 1–35 (1977).
- Berner, R. A. *Principles of Chemical Sedimentology* (McGraw-Hill, New York 1971).
- Brewer, P. G. in *Chemical Oceanography* (Riley, J. P. & Skirrow, G.) 415–495 (Wiley, New York, 1975).
- Broecker, W. S. *Quat. Res.* **1**, 188–207 (1971).
- Wai, C. M. & Wasson, J. T. *Nature* **282**, 790–793 (1979).
- Palme, H. & Wlotzka, F. *Earth planet. Sci. Lett.* **33**, 45–60 (1976).
- Willis, J. thesis, Univ. California, Los Angeles (1980).
- Hsü, K. J. *Nature* **285**, 201–203 (1980).
- Delsemme, A. H. *Comets, Asteroids, Meteorites* (ed. A. H. Delsemme) 3–12 (University Toledo, 1977).
- Wasson, J. T., Boynton, W. V., Chou, C.-L. & Baedeker, P. A. *The Moon* **13**, 121–141 (1975).
- Boynton, W. V., Chou, C.-L., Bild, R. W., Baedeker, P. A. & Wasson, J. T. *Earth planet. Sci. Lett.* **29**, 21–33 (1976).
- Boynton, W. V. & Wasson, J. T. *Geochim. cosmochim. Acta* **41**, 1073–1082 (1977).
- Haskin, L. A. & Paster, T. P. *Handbook on the Physics and Chemistry of Rare Earths* (eds Gschneidner, K. A. Jr & Eyring, L.) 1–80 (North Holland, Amsterdam 1979).
- Wetherill, G. W. *A. Rev. Earth Planet. Sci.* **2**, 303–331 (1974).
- Napier, W. M. & Clube, S. V. M. *Nature* **282**, 455–459 (1979).
- McCrea, W. H. *Nature* **225**, 607–609 (1975).
- Talbot, R. J., Butler, D. M. & Newman, M. J. *Nature* **262**, 561–563 (1976).
- Begelman, M. C. & Rees, M. J. *Nature* **261**, 298–299 (1976).
- Ross, J. E. & Aller, L. H. *Science* **191**, 1223–1229 (1976).
- Werner, M., Becklin, E. & Neugebauer, G. *Science* **197**, 723–732 (1977).
- Takahashi, H., Higuchi, H., Gros, J., Morgan, J. W. & Anders, D. *Proc. natn. Acad. Sci. U.S.A.* **73**, 4253–4256 (1976).
- Podosek, F. A. *A. Rev. Astr. Astrophys.* **16**, 293–334 (1978).
- De Laubenfels, M. W. *J. Paleontol.* **30**, 207–218 (1956).
- Hunt, J. N., Palmer, R., Penney, W. *Phil. Trans. R. Soc. A* **252**, 275–315 (1960).
- Kresak, L. *Bull. astr. Instr. Czech.* **29**, 129–134 (1978).
- Stefanik, R. P. *Mem. Soc. R. Sci. Liège, Ser. 5* **12**, 29–32 (1966).
- Sekanina, Z. *Icarus* **30**, 574–594 (1977).
- Opik, E. J. *Ir. astr. J.* **5**, 34 (1958).
- Emiliani, C. *EOS* **61**, 505–506 (1980).
- Humphreys, W. J. *Physics of the Air* (McGraw-Hill, New York, 1940).
- Krinov, E. L. *Giant Meteorites* (Pergamon, Oxford, 1966).
- Russell, D. A. *A. Rev. Earth planet. Sci.* **7**, 163–182 (1979).
- McLean, D. M. *Science* **201**, 401–406 (1978).
- Hoyle, F. & Lyttleton, R. A. *Proc. Camb. Phil. Soc. Math. Phys. Sci.* **35**, 405–415 (1939).
- Alvarez, L. W., Alvarez, W., Asaro, R. & Michel, H. V. *Univ. Calif. Rep. LBL-9666* (Lawrence Berkeley Laboratory, 1979).
- Walker, J. C. G. *Am. J. Sci.* **274**, 193–214 (1974).
- Baur, M. E. & Friedl, R. R. *Am. Ass. Adv. Sci. Selected Symp.* **28**, 254–286 (1980).



# Basement heat flow and metalliferous mineralization in England and Wales

**G. C. Brown\*, J. Cassidy\*, E. R. Oxburgh†, J. Plant‡, P. A. Sabine§ & J. V. Watson||**

\* Department of Earth Sciences, The Open University Milton Keynes MK7 6AA, UK

† Department of Mineralogy and Petrology, Downing Place, Cambridge CB2 3EQ, UK

‡ Institute of Geological Sciences (NERC), 154 Clerkenwell Road, London EC1R 5DU, UK

§ Institute of Geological Sciences (NERC), Exhibition Road, London SW7 2DE, UK

|| Department of Geology, Imperial College of Science, South Kensington, London SW7 2BP, UK

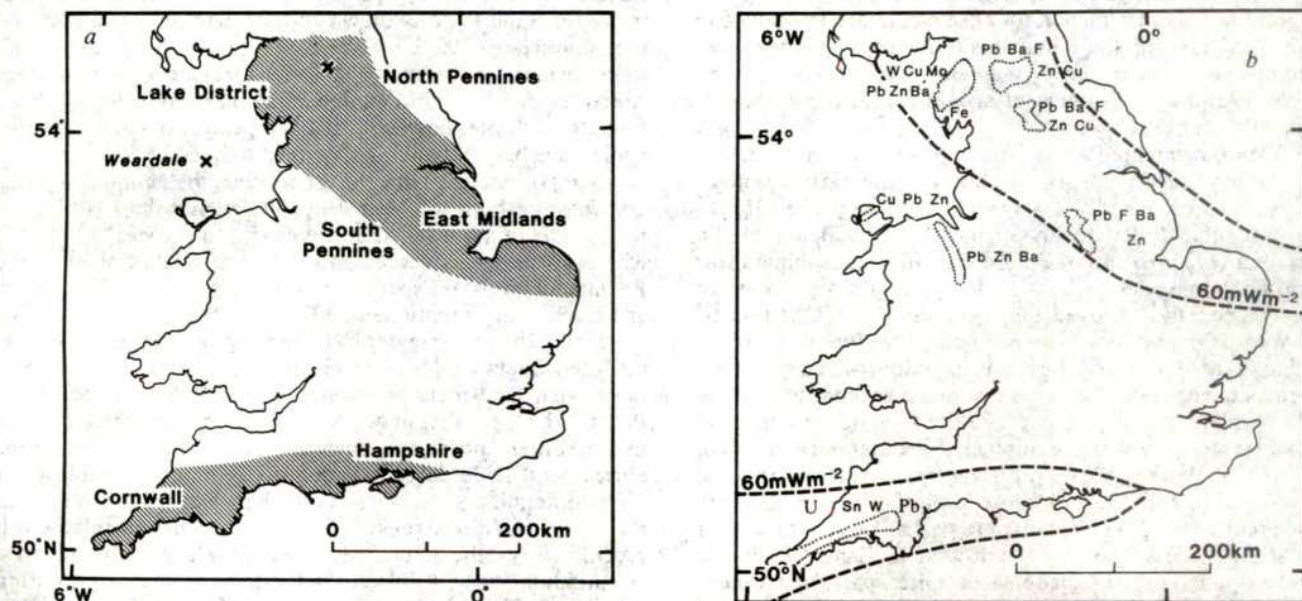
Many examples of epigenetic metalliferous mineralization in central and northern England occur within a province now recognized to be characterized by high heat flow. Our analysis of this correlation leads us to conclude that Caledonian intrusive bodies, with high heat production and thermal conductivity, focused the development of hydrothermal systems responsible both for some types of post-Carboniferous mineralization and for present-day high heat flow.

TWO recent developments in the exploration for geothermal energy and metalliferous mineralization in Britain have highlighted a possible connection between the present-day heat production of rocks (due mainly to the long-lived isotopes  $^{238}\text{U}$ ,  $^{235}\text{U}$ ,  $^{232}\text{Th}$  and  $^{40}\text{K}$ ) and the distribution of epigenetic metalliferous mineralization dating from Hercynian and post-Hercynian times.

First, two high heat flow provinces characterized by surface heat flow  $> 60 \text{ mW m}^{-2}$  have been identified in Britain (Fig. 1a)<sup>1,2</sup>. The northern England high heat flow province (hereafter called the Province) extends as a southeasterly trending zone at least 100-km wide from southern Scotland across the Pennines through Yorkshire to the East Midlands; the south-west England province extends eastwards from Cornwall to Hampshire. Surface heat flow in these provinces is linearly correlated with heat production in crystalline rocks and low-grade metamorphic rocks of the pre-Variscan or Variscan basement, and the provinces show a strong spatial association with the known ore fields of the Lake District, the north and south Pennines (including Derbyshire) and Cornubia (Fig. 1b). Although the mineralized zone in the South Pennines lies on the western margin of the Province, various authors (see refs 3, 4) have indicated that the source of the mineralizing fluids lies to the east. Many occurrences of epigenetic mineralization may, therefore, be related to present-day zones of high heat flow and, where data are available, to above-average basement heat production<sup>5</sup>.

Second, it has become evident that the British granites which are associated with vein mineralization contain unusually high levels of heat-producing elements<sup>6</sup>. These granites seem to have influenced the circulation of hydrothermal fluids not only at the time of emplacement but also, by virtue of their high heat production and relatively high thermal conductivity, long after the period of their consolidation. For example, in south-west England, the Hercynian granites are associated with U-Sn-Pb mineralization, followed by Pb-Zn mineralization at lower temperatures, both dating roughly from the time of emplacement<sup>7</sup>; in addition, U mineralization seems to have continued into Tertiary times<sup>8</sup>. In northern England, where no granites younger than Caledonian are known, mineralization is often located in Carboniferous or post-Carboniferous rocks which post-date the initial cooling of the intrusions, but is known to be spatially related to intrusions under the Alston and Askrigg Blocks and in the Lake District. The model proposed here for the Province whereby hydrothermal convection is maintained by high heat production in granitic rocks has recently been proved quantitatively viable for the origin of uranium deposits in New Hampshire<sup>9</sup>.

Here we examine possible implications of these relationships which provide the basis for current geophysical and geochemical research being sponsored by NERC as part of the coordinated UK Deep Geology programme. Consideration is given to the processes of mineralization in the Province and to the possibility that concealed mineralization may be detectable.



**Fig. 1** *a*, Provinces of high heat flow in central and southern Britain; heat flow in the shaded areas exceeds  $60 \text{ mW m}^{-2}$  indicated by dashed lines in *b*, which also records the spatial occurrence of some important centres of hydrothermal mineralization in England and Wales (heat flow data from refs 2, 16, 22, 23, 31).



## Heat sources and mineralization

Regional geology suggests that the Province cannot be directly related to the distribution of any single stratigraphical unit in the pre-Permian basement (see ref. 2). Devonian and Carboniferous rocks, though present in some areas, are often thin or absent in the northwestern part of the Province. The sub-parallel alignment, on a regional scale, of the Province and the smooth linear anomalies of deep source shown on the 1:625,000 Aeromagnetic map<sup>10</sup> suggests a possible connection with pre-Carboniferous basement structure. Over much of its extent the Province is known to coincide with a Lower Palaeozoic basement-age province<sup>11</sup>; this correlation alone does not account for high heat flow which, instead, may be related to above-average heat production in granitic rocks and greenschist facies shale belts within the basement, both of which contain relatively high levels of radioelements.<sup>2,5,6</sup> The significance of these relationships is discussed below with reference to three principal areas.

(1) In the Lake District, there is a clear spatial relationship between Caledonian granites and later mineralization<sup>12-14</sup>. Average heat productivities in the Shap, Skiddaw and Eskdale granites ( $4.37 \mu\text{W m}^{-3}$ ,  $2.65 \mu\text{W m}^{-3}$ ,  $2.0 \mu\text{W m}^{-3}$ , respectively) are high compared with, for example, an average value of  $1.5 \mu\text{W m}^{-3}$  for Borrowdale volcanics<sup>15</sup> and a range of  $0.6$ – $2.0 \mu\text{W m}^{-3}$  for low-grade metasedimentary and metavolcanic rocks beneath England and Wales<sup>16</sup>. Recent studies<sup>17,18</sup> have shown that these intrusions are characterized by large negative Bouguer anomalies, indicating that large volumes of similar igneous rocks are present at a depth below the present erosion level. In geochemical and geophysical characteristics, these and other late Caledonian intrusions are comparable with the Hercynian plutons of the south-west England high heat flow province<sup>1,6,19</sup>. The relatively unfractionated heat-productivity profile of the Cornubian batholith in particular (requiring that the measured heat productivities are preserved to depths approaching 15 km (ref. 16)) might also apply in the Caledonian plutons. This suggestion is consistent with mineralogical studies<sup>20</sup> indicating that, away from areas of mineralization, uranium in both the Cornubian and late Caledonian granites is held in primary mineral phases. By virtue of their high heat production and thermal conductivity, Caledonian granites beneath the Province would not only have added heat to fuel convective systems involving formation waters in Lower Carboniferous and older sediments beneath thick sedimentary cover<sup>21</sup>, but they might also have continued to act as significant conductive heat-transfer agents during later periods. A mean thermal conductivity of  $3.3 \text{ W m}^{-1} \text{ K}^{-1}$  for comparable Cornubian granites<sup>22</sup> is much higher, for example, than a typical value of  $1.5 \text{ W m}^{-1} \text{ K}^{-1}$  for shale horizons<sup>23</sup>. In some circumstances where upward deformation of sediments has occurred around granites, heat may have been refracted towards those granites (for details, see ref. 5).

(2) Well documented areas<sup>24,25</sup> of epigenetic mineralization above buried Caledonian granites occur in the north Pennines (Fig. 1) at Weardale and Wensleydale. For example, the Rookhope borehole, drilled to investigate the coincidence of the centre of a zonal pattern of Pb–Zn–fluorite–barite mineralization in Carboniferous rocks<sup>26,27</sup> and areas of strong negative Bouguer anomaly<sup>28</sup>, proved the presence of the Caledonian-aged Weardale granite<sup>24</sup>. Whether mineralization in the north Pennine orefield occurred during a single short-lived episode<sup>29</sup> or in repeated episodes<sup>30</sup>, it certainly took place long after these ~400-Myr-old granites had crystallized: a possible link to radioactive heat production is implied. A geothermal gradient of  $31^\circ\text{C km}^{-1}$  at Weardale<sup>31</sup> supports comparisons of the thermal properties of this granite with those of the Cornubian batholith where gradients of  $27$ – $35^\circ\text{C km}^{-1}$  are typical<sup>22</sup>. If the model for mineralization developed for south-west England (ref. 6 and above) is applied to late Caledonian granites, particularly those which are covered by sediments, it follows that concealed mineralization may exist elsewhere in buried sediments which are younger than the granites and with which there would be a close spatial relationship.

(3) The south Pennine–East Midlands section of the Province (Fig. 1) contains the vein and stratiform Pb–Zn–fluorite mineralization of Derbyshire which occupies a tract with NNW elongation. Ford<sup>4</sup> postulated a migration of brines from the North Sea basin to account for the availability of mineralizing fluids in the area. This interpretation, however, (see ref. 32) involves the proposals that the fluids travelled some 150 km up-dip in Carboniferous strata without significant heat loss and that they crossed the Askern structural high<sup>33</sup>. Such difficulties focus attention on the possible influence of local heat sources and, by comparison with the north Pennines, Evans and Maroof<sup>34</sup> suggested that there may be Caledonian intrusive rocks beneath the East Midlands and that these might have exerted an important control. Unfortunately, present geophysical data are equivocal in respect of the presence or absence of buried granite bodies in the south Pennine–East Midlands region. The available deep boreholes penetrate pre-Carboniferous shales with moderate heat production (our unpublished data) and do not reach crystalline basement. Although there is no clear explanation for above-average heat flow in the south-west quadrant of the Province we postulate, by analogy with the Lake District–North Pennine areas, that high basement heat flow related to granites may be responsible: the geophysical implications of this suggestion are receiving further attention. However, we note that water circulating through and rising from deep aquifers beneath horizons of low thermal conductivity provides a more attractive explanation for high heat flow in some parts of the Province, such as east Lincolnshire and Yorkshire, which are underlain by deep sedimentary basins.

## Prerequisites for Pennine mineralization

Epigenetic Pb–Zn vein-type and strata-bound ores of the Mississippi Valley type are characteristically of low-temperature hydrothermal origin<sup>35,36</sup> and, as such, their formation requires slightly elevated thermal gradients, trapped halogen-rich aqueous fluids in permeable rocks and preferably a structural anomaly, such as a fault zone or fractured anticline, to promote fluid circulation. Fluid circulation is also favoured by sources of magmatic or tectonic heat, but these are not essential prerequisites. In the case of Pennine mineralization, it is generally agreed that Lower Carboniferous limestones and sandstones contained the trapped connate water but that the source of base metals was either within Lower Carboniferous shales or within earlier Palaeozoic metasediments<sup>4,30,32,34</sup>. The metals were leached by hydrothermal brines which, from fluid-inclusion studies<sup>32</sup>, are known to have had high salinities and temperatures (~200°C). Some  $^{34}\text{S}/^{32}\text{S}$  ratios for galena<sup>37</sup> and, in particular, the quantity and the rare-earth element geochemistry of fluorite in Pennine mineralization have both been taken to indicate, however, that the genesis of these deposits could have been related to magmatic sources<sup>38</sup>.

An important point of contrast between the Pennine deposits and those of both the Mississippi Valley and the Irish Pb–Zn deposits within Lower Carboniferous host rocks<sup>40,41</sup> is that whereas the latter occurrences are fault-controlled<sup>39</sup>, the Pennine deposits are spatially related to domes. In view of the age discrepancy mentioned earlier, this may be taken as evidence that the role of older Caledonian granites was not only to act as channelways for mineralizing fluids<sup>30</sup>, but that they may have been heat-focusing agents. Flow of fluorine-rich fluids through these granites may have remobilized base metals during hydrothermal processes and may have led to continued enrichment. Differences between the sulphide assemblages of the two Pennine areas suggest a higher temperature regime in the northern (Alston) region<sup>42,43</sup>, a feature which correlates with recent data<sup>5</sup> on the differences in heat flow from the two blocks. In addition to possible contributions from heat-focusing granites, the flow of mineralizing fluids was controlled by faults<sup>44</sup> formed during differential uplift at the end of the Carboniferous, resulting in the deposition of ores at intersections with favourable sedimentary horizons.

## Implications for mineral exploration

The present model is that metalliferous minerals were concentrated magmatically during a Caledonian phase and may have been redeposited in mineral veins near the contemporaneous land surface or on or just beneath a shallow sea floor if later phases of mineralization took place. The process could have continued as long as hydrothermal systems were able to circulate against the hydrostatic gradient, possibly into Tertiary times. The search for minerals should, therefore, be concentrated at and below ancient land or sea-bottom surfaces. Several lines of evidence, including studies of metamorphic facies<sup>16</sup> and levels of granite intrusions<sup>43</sup>, suggest that the present land surface of the northern end of the Province is close to that present at the end of the Devonian. If hydrothermal circulation is able to reach near-surface conditions<sup>6,7</sup>, it follows that most epigenetic mineralization associated with areas that have been positive blocks during post-Devonian time must crop out at, or near, the surface and may be found by established methods of geochemical and geophysical exploration<sup>46,47</sup>. Sedimentary basins containing Carboniferous and later strata, such as those which occupy the central and southeastern part of the Province, may contain deposits at greater depths.

Comparisons with the known history of mineralization in the south-west England high heat flow province (particularly Cornwall, Fig. 1) suggests that the possible existence of two other types of deeply buried deposit in the northern Province is worth consideration. First, in Cornwall, where there is evidence of several post-Hercynian episodes of U remobilization analogous to those discussed above, Sn-W mineralization seems to

have been related only to a high-temperature event closely linked with magmatism. Metals which were not remobilized by low-temperature hydrothermal processes may remain in similarly close association with buried Caledonian granites. Second, stratiform metalliferous deposits in Carboniferous and Permian strata may exist beneath the cratonic cover of Jurassic or younger sediments, more particularly in the southeastern part of the northern Province.

The continuation of mineralizing processes in areas containing radioelement-enriched buried granites, long after the emplacement of those intrusions (see refs 9, 24, 48) is not always widely appreciated. An interesting example of extensive hydrothermal circulation has been recognized in the vicinity of a Tertiary granitic stock near Marysville, Montana<sup>49</sup>, where fluids which circulated in a diffuse fracture system are thought to have set up high thermal gradients near the stock. The igneous rocks themselves are too old for magmatic heat to be responsible for the present-day hydrothermal systems. Other examples of modern hydrothermal systems associated with Palaeozoic radiogenic intrusive bodies from the Eastern Appalachians have been described by Costain and others<sup>50</sup>. Processes of mineralization associated with such hydrothermal systems are likely to be most active in provinces of high heat flow, a consideration which focuses attention on the northern England high heat flow province.

We thank G. M. Brown, F. W. Dunning and D. A. Gray for reviews. This paper is published with the permission of the director of the Institute of Geological Sciences.

Received 2 June, accepted 31 October 1980

1. Tammenang, H. Y. & Whieldon, J. *Geophys. J. R. astr. Soc.* **38**, 83–94 (1974)
2. Richardson, S. W. & Oxburgh, E. R. *Nature* **282**, 565–567 (1979)
3. Bullard, E. C. & Niblett, E. R. *Mem. Nor. R. astr. Soc. Geophys. Suppl.* **6**, 222–238 (1951)
4. Ford, T. D. in *Handbook of Strata-bound and Stratiform Ore Deposits* Vol. 5 (ed Wolf, K. H.) 161–195 (Elsevier, Amsterdam, 1976)
5. England, P. C., Oxburgh, E. R. & Richardson, S. W. *Geophys. J. R. astr. Soc.* **62**, 439–455 (1980)
6. Simpson, P. R., Brown, G. C., Plant, J. & Oettle, D. *Phil. Trans. R. Soc. A* **291**, 385–412 (1979)
7. Sheppard, S. M. F. *J. geol. Soc. Lond.* **133**, 573–591 (1977)
8. Darajoy, A. G., English, T. H., Sprake, O., Proce, E. R. & Avery, D. *Miner. Mag.* **34**, 159–176 (1965)
9. Faka, U., Cathles, L. M. & Holland, H. D. *Econ. Geol.* **73**, 1556–1566 (1978)
10. *1:625,000 Aeromagnetic Maps of Great Britain* (IGS, London, 1965)
11. Wills, L. J. *Mem. geol. Soc. Lond.* **8** (1978)
12. Ineson, P. R. in *Handbook of Strata-bound and Stratiform Ore Deposits* Vol. 5 (ed Wolf, K. H.) 196–230 (Elsevier, Amsterdam, 1976)
13. Fritman, R. J. in *The Geology of the Lake District* (ed Moseley, F.) 226–241 (Yorkshire Geological Society Occasional Publ. 3, 1979)
14. Ineson, P. R. & Mitchell, J. G. *Geol. Mag.* **111**, 521–537 (1974)
15. Cassidy, J. thesis, Liverpool Univ. (1979)
16. Richardson, S. W. & Oxburgh, E. R. *J. geol. Soc. Lond.* **138**, 323–337 (1978)
17. Bott, M. H. P. *J. geol. Soc. Lond.* **130**, 309–331 (1974)
18. Locke, C. A. & Brown, G. C. *Nature* **272**, 526–528 (1978)
19. Brown, G. C., Plant, J. & Lee, M. K. *Nature* **280**, 129–131 (1979)
20. Simpson, P. R., Plant, J. & Cope, M. J. in *Geology, Mining and Extractive Processing of Uranium* (ed Jones, M. J.) 126–139 (Instn Mining and Metallurgy, London, 1976)
21. Russell, M. J. *Trans. Instn Min. Metall.* (Sect. B) **87**, B168–B171 (1978)
22. Whieldon, J., Francis, M. F. & Thomas Betts, A. *Seminar on Geothermal Energy* Vol. 1 175–188 (Commission of the European Communities, Brussels, 1977)
23. Oxburgh, E. R., Richardson, S. W., Bloomer, J. R., Martin, A. & Wright, S. *Seminar on Geothermal Energy* Vol. 1, 155–173 (Commission of the European Communities, Brussels, 1977)
24. Dunham, K. C., Dunham, A. C., Hodge, B. L. & Johnson, G. A. L. *Q. J. geol. Soc. Lond.* **121**, 383–417 (1965)
25. Bott, M. H. P. *Proc. Yorks. geol. Soc.* **36**, 139–168 (1967)
26. Dunham, K. C. *Q. J. geol. Soc. Lond.* **90**, 689–720 (1934)
27. Small, A. T. *Trans. Instn Min. Metall.* (Sect. B) **87**, B10–B13 (1978)
28. Bott, M. H. P. & Mason-Smith, D. Q. *J. geol. Soc. Lond.* **113**, 93–117 (1957)
29. Smith, F. W. & Phillips, R. *Fortschr. Miner.* **82**, 491–494 (1975)
30. Dunham, K. C. in *The Geology and Mineral Resources of Yorkshire* (eds Rayner, D. H. & Hammingway, J. E.) 293–308 (Yorkshire Geological Society Occasional Publ. 2, 1974)
31. Bott, M. H. P., Johnson, G. A. L., Mansfield, J. & Whieldon, J. *Geophys. J. R. astr. Soc.* **27**, 277–288 (1972)
32. Rogers, P. J. *Trans. Instn Min. Metall.* (Sect. B) **86**, B128–B132 (1977)
33. Kent, P. E. *Proc. Yorks. geol. Soc.* **36**, 127–133 (1967)
34. Evans, A. M. & Marroft, S. I. *Min. Mag. Lond.* **134**, 401–411 (1976)
35. Doxy, J. J. *Trans. Instn Min. Metall.* (Sect. B) **79**, B163–B170 (1970)
36. Mitchell, A. H. G. & Garson, M. S. *Miner. Sci. Engng.* **8**, 129–169 (1976)
37. Robinson, B. W. & Ineson, P. R. in *25th Int. geol. Congr. Australia 1976* Abstr. 1, sect. 4A, 183 (1976)
38. Russell, M. J. & Smith, F. W. *Trans. Instn Min. Metall.* (Sect. B) **88**, B30 (1979)
39. Carpenter, A. B., Trout, M. L. & Pickett, E. E. *Econ. Geol.* **69**, 1191–1206 (1974)
40. Morrison, C. J., Davis, G. R. & Sheel, G. M. *Trans. Instn Min. Metall.* (Sect. B) **79**, B174–B185 (1971)
41. Russell, M. J. *Trans. Instn Min. Metall.* (Sect. B) **83**, B128–B133 (1975)
42. Rogers, P. J. *Trans. Instn Min. Metall.* (Sect. B) **87**, B125–B131 (1978)
43. Vaughan, D. J. & Ixer, R. A. *Trans. Instn Min. Metall.* (Sect. B) **89**, B99–B109 (1980)
44. Carter, J. S. & Moore, J. Mc. *Trans. Instn Min. Metall.* (Sect. B) **87**, B90–B93 (1978)
45. Lonke, B. E. in *Geol. J. Spec. Iss.* **10**, 221–248 (1978)
46. Hawkes, H. E. & Webb, J. S. *Geochemistry in Mineral Exploration* (Harper and Row, New York, 1962)
47. Bowles, S. H. U. *Proc. R. Soc.* **339**, 299–311 (1974)
48. Rich, R. A., Peterson, U. & Holland, H. D. *Hydrothermal Uranium Deposits* Vol. 6 (Elsevier, Amsterdam, 1977)
49. *Energy Research and Development (Advances in Res. No. 1 of Hot Dry Rock Assessment Panel)* (ERDA 77–74, Springfield, 1977)
50. Costain, J. K., Glover, L. III & Smith, A. K. *EOS* **61**, 1–3 (1980).

# Pacifica and New Zealand: proposed eastern elements in Gondwanaland's history

P. J. J. Kamp

Earth Sciences and Antarctic Research Unit, University of Waikato, Hamilton, New Zealand

*The origin of the sediments of the Canterbury Suite to the east of the Alpine Fault in New Zealand, cannot have derived from Marie Byrd Land before or during the breaking up of Gondwanaland. It is argued that the sediments may have derived from the lost continent of Pacifica, which is supposed to have separated from Gondwanaland in the late Palaeozoic. Such a mechanism can also account for the recurrence of similar quartzo-feldspathic sediments in California and thus of the Mesozoic dolerites and basalts in southern Africa, Antarctica and Tasmania.*



THE source of voluminous continent-derived sandstones<sup>1</sup> deposited on the Pacific margin of Gondwanaland, but oceanwards of an active arc-trench environment<sup>2</sup>, is a critical problem in the late Palaeozoic-Mesozoic geology of New Zealand and one which has wider implications for Pacific geology. Eastern Gondwanaland (Australia-Antarctica) is precluded as the chief source of the quartzo-feldspathic detritus, known as the Canterbury Suite<sup>1</sup>, for several reasons: (1) the sedimentology of the suite indicates derivation of the sediment from a source in the east (Palaeo Pacific Ocean); (2) the bulk petrography is inconsistent with transportation through the then active volcanic arc bordering eastern Gondwanaland; and (3) alternative explanations, especially of post-depositional juxtapositioning of the Canterbury and Wakatipu<sup>2</sup> Suites by strike-slip faulting subparallel to Antarctica, are excluded by the Mesozoic position with respect to Gondwanaland of the Lord Howe Rise and Campbell Plateau. I propose that this sediment was derived mainly from Pacifica<sup>3</sup>, a continent contiguous with eastern Gondwanaland until its separation from the supercontinent during the late Palaeozoic, its fragmentation in the Triassic and inclusion within the circum-Pacific Cordillera in the early Cenozoic. Pacifica may also be the hitherto unknown source of other anomalous occurrences of quartzo-feldspathic detritus around the Pacific such as the Franciscan assemblage in California<sup>4</sup>. Furthermore, the origin of the extensive Jurassic basalts and dolerites of southern Africa<sup>5</sup>, Antarctica<sup>6</sup> and Tasmania<sup>7</sup> may be related to the separation of Pacifica.

The source of the Canterbury Suite has been debated for many years, and this problem is considered here in three ways. (1) The nature of the Canterbury Suite and the evidence for derivation from an eastern continent is outlined. (2) A new Mesozoic reconstruction of New Zealand relative to Gondwanaland is presented; it is important to consider New Zealand's position as close as possible to the time of Canterbury Suite deposition because the position of accumulation is a constraint on potential source areas. (3) Other problems in

Pacific geology are considered to show that the Canterbury Suite is not an isolated anomaly, and that Pacifica is a general as distinct from a merely local explanation of the source problem.

The fundamental difference between previous hypotheses of the source of the Canterbury Suite and the hypothesis advanced here is one of invoking present continents (Australia-Antarctica) as opposed to a lost continent—Pacifica. In addition to providing a source, the Pacifica model provides a mechanism, through continental fragmentation, for the periodic and rapid derivation of huge volumes of quartzo-feldspathic sediment. Further, the separation and fragmentation of Pacifica are consistent with a generally accepted plate tectonic interpretation<sup>2</sup> of the arc-trench system that formed the adjacent Wakatipu Suite.

### Late Palaeozoic-Mesozoic New Zealand

The late Palaeozoic-Mesozoic geology of New Zealand is dominated by the juxtaposition of two contrasting detrital mineral suites, one the western volcanoclastic Wakatipu Suite of andesitic composition deposited next to the foreland, and the other the quartzo-feldspathic Canterbury Suite deposited in the Pacific Ocean further to the east<sup>1</sup> (Fig. 1). These coeval suites are considered to have formed in contrasting tectonic environments and to have been rafted together in the Mesozoic which culminated in a collision—the Rangitata Orogeny—with intense deformation, metamorphism, uplift and erosion<sup>2</sup>.

The Canterbury Suite comprises two-thirds of the Rangitata Sequence<sup>8</sup> and has an estimated<sup>9</sup> thickness of 30,000 m which is not a true stratigraphical thickness but caused by tectonic stacking or a shifting dopocentre. Derivation from a terrain of granodiorite and minor schistose and metamorphic rock is indicated by the composition of the dominant minerals and rock fragments. In particular Triassic sandstones comprise quartz (40–50%), potash feldspar (10–15%), sodic plagioclase (20%) and minor amounts of muscovite, volcanic rock fragments and chert<sup>1</sup>. These sandstones typically average SiO<sub>2</sub> contents of



**Fig. 1** A map of the New Zealand sub-continent, defined by the 2,000-m isobath, showing the on-land distribution of Palaeozoic foreland rocks<sup>52</sup> and the late Palaeozoic-Mesozoic basement rocks of the Rangitata Sequence<sup>43</sup>. The Canterbury Suite-Wakatipu Suite boundary in southern South Island lies within the Haast Schist belt<sup>1</sup>, and has not been mapped; the boundary shown here is estimated. In North Island the boundary is placed between the Torlesse and Waipapa terrains<sup>16</sup>. Distribution of the ophiolite belt is taken from ref. 53.



67.5% (ref. 10). Tuffs are exceptionally rare. Consistent lithological homogeneity for over 500 km from eastern North Island to Otago (Fig. 1) and in time from Permian to Jurassic indicates the persistence of a continental source capable of supplying a quartzo-feldspathic assemblage for some 100 Myr. Although fossils are generally sparse, those that occur range from late Carboniferous to early Cretaceous<sup>11,12</sup> and biostratigraphic zonation indicates a westward and northward younging of the sediments<sup>2,13</sup>.

Based mainly on the distribution of fossil ages<sup>1</sup> deposition of the Canterbury Suite was remarkably episodic with a small pulse in the late Permian (early Tatarian), a very large pulse in the late early to late Triassic (Ladinian–Norian) and a further large pulse in the late Jurassic (early Kimmeridgian to early Tithonian). The extensive occurrence of a thick Jurassic *mélange* belt which includes reworked Triassic Canterbury Suite sediments<sup>14</sup>, suggests that much of the Jurassic sedimentation pulse was more related to erosion of the earlier Triassic sediments, as a consequence of uplift associated with the first phase of the Rangitata Orogeny<sup>8</sup>, than to tectonic events in the continental source area.

The distribution of depositional facies, detrital conglomerate, plant fossils and the records of directional sedimentary structures all indicate that sediment transport was in all directions and chiefly to the west and north, with non-marine, marginal marine and shallow marine environments in the east and an ocean basin environment in the west<sup>1,15</sup>. The Canterbury Suite thus seems to have been a huge clastic wedge<sup>8</sup> which prograded westward towards a trench, northward to eastern North Island<sup>16</sup>, and southward to a peripheral euxenic deep-marine environment at Chatham Island<sup>17</sup>.

The stratigraphical and sedimentological evidence points towards an eastern source for the Canterbury Suite. Based on the persistence of a similar composition for ~100 Myr, the quantity of sediment and the rate of sediment supply, a primary cratonic region rather than a late Precambrian or Palaeozoic orogenic belt is indicated. Furthermore, the sandstone composition together with the rate of sediment supply in the Triassic, implies rapid uplift in the source area with vigorous physical erosion and with rapid transport to the sea. In short, there seems to have been an orogeny in the source area which climaxed in the Triassic. Hence, there are mechanistic requirements for the source area in addition to constraints on its composition.

In contrast, the Wakatipu Suite (Fig. 1), derived from a calc-alkaline terrain, shows a pronounced lithostratigraphic change from early and middle Permian volcanics, volcanogenic sediments and intrusives, to late Permian, Triassic and Jurassic highly volcanogenic, mostly marine and locally richly fossiliferous sediments, with common tuffs, but no flows. The complex stratigraphy of the Wakatipu Suite is interpreted<sup>2,15</sup> as representing the development in the early Permian of a volcanic arc–trench environment followed later by formation of a subduction zone accretionary wedge and mid-slope basin deposits, and finally a regressive frontal arc wedge of upper slope and slope basin, shelf and non-marine sediments.

### Jurassic reconstruction of modern Gondwanaland

A central problem in reconstructing the Jurassic configuration is the age of the recurved arc through New Zealand, delineated by the Ophiolite belt (Fig. 1). One idea<sup>18,19</sup> is that the curve is Cenozoic in age and formed by 500 km of dextral strain associated with movement on the Alpine Fault. Such models show New Zealand as a linear feature in the late Mesozoic<sup>18,20</sup>, or incorporate 1,000 km of Cenozoic dextral displacement, 500 km of which is attributed to distributed dextral strain<sup>21–23</sup>. Although some Cenozoic crustal strain cannot be excluded<sup>24–26</sup>, 500 km of Cenozoic strain requires excessive distortion of the present outline of New Zealand and this has not been substantiated. An alternative idea is that the bending originated mainly in the Rangitata Orogeny (early Jurassic to mid-

Cretaceous)<sup>8,27,28</sup>. Palaeomagnetic data from South Island<sup>29</sup> and Chatham Island<sup>30</sup> (Fig. 1) seem to preclude significant post-late Cretaceous bending between these localities and may support bending during the Rangitata Orogeny. Furthermore, deformation studies<sup>31</sup> have established the existence of a late Jurassic bend after removing 200 km of Cenozoic dextral strain, an amount which did not excessively distort elements of the land. In the reconstruction to be discussed 200 km of Cenozoic distributed dextral strain is considered to have occurred.

There are two assumptions used in the reconstruction presented as Fig. 2: (1) There has been no major relative movements between Marie Byrd Land and East Antarctica since the late Palaeozoic. (2) There was no relative movement between Marie Byrd Land and the Campbell Plateau in the interval from the late Palaeozoic to the late Cretaceous.

The first assumption is considered to be valid because of the close correspondence in lithologies, ages and structural trends of the Palaeozoic to late Cretaceous geology of North Victoria Land, Marie Byrd Land, New Zealand and Tasmania<sup>32,33</sup>. Each region was affected by a pre-Silurian–late Ordovician metamorphic event and a widespread phase of late Devonian–Early Carboniferous (350–390 Myr BP) plutonism<sup>33</sup>. In Antarctica the trend of the Borchgrevink Orogen extends uninterrupted from the Ford Mountains in western Marie Byrd Land north-northwest through the Ross Sea basement to north-east Victoria Land<sup>34</sup>. Moreover, two Albion to Neocomian (90–142 Myr BP) calc-alkaline magmatic arcs extended from Queensland through New Zealand to Marie Byrd Land before the late Cretaceous break-up<sup>32</sup>. In addition, there is no palaeomagnetic evidence to support large displacements (~10<sup>3</sup> km) between Marie Byrd Land and East Antarctica after the late Cretaceous–early Cenozoic<sup>22</sup>, nor is there evidence during this time for the closing of an ocean basin<sup>34</sup>.

Concerning the second assumption, there are few independent lines of evidence to test the good morphological fit<sup>35</sup> of Campbell Plateau and Marie Byrd Land. In pre-Late Cretaceous times Campbell Basin was a continuation of a sediment-filled trough underlying the eastern Ross Sea shelf<sup>36</sup>. Such a structure would presumably preclude significant late Palaeozoic to late Cretaceous relative movement between Marie Byrd Land and Campbell Plateau.

Because greater New Zealand did not become a landmass until the Rangitata Orogeny (late Triassic to mid-Cretaceous<sup>8</sup>) it is difficult to establish the relative positions of the Canterbury and Wakatipu Suites before the Jurassic, and hence a later Jurassic reconstruction is presented here (Fig. 2). Although some strike-slip faulting may have occurred between the suites in the time between the late early-to late Triassic pulse of sedimentation (Canterbury Suite) and the later Jurassic, it was probably of a small scale (several hundred kilometres), and of dextral character, based on the nature of Cenozoic strike-slip faulting in the New Zealand region.

### Source of the Canterbury Suite

The present non-occurrence of a continent east of New Zealand has led to several proposals invoking a source in the west (North Victoria Land–Tasmania–Victoria (Australia)) or in the south-east (Marie Byrd Land). To enable deposition from the west without contamination by volcanoclastic detritus, bypassing mechanisms have been invoked<sup>13</sup>. However, this idea has been largely discredited on the basis of facies properties and sedimentary environments in the Canterbury Suite<sup>1,37</sup>. Transport between basins of Wakatipu Suite deposition has also been proposed as a working hypothesis for sedimentation and tectonics in the New Zealand geosyncline<sup>16</sup>. However, the extent and continuity of the Stokes Magnetic Anomaly System<sup>19</sup> precludes the occurrence of a break in the arc of sufficient size through which the whole of the Canterbury Suite could have been transported without any contamination by volcanoclastic detritus. A development of the western source is the idea that the sediments were derived from an erosional episode in the Carboniferous before the arc–trench environment formed<sup>31</sup>, but





**Fig. 2** A later Jurassic palaeogeographic map of eastern Gondwanaland with Antarctica in its present-day position. The New Zealand subcontinent is reconstructed against Norton and Sclater's fit<sup>54</sup> of Australia and Antarctica. Q, Queensland; NC, New Caledonia; T, Tasmania; NVL, North Victoria Land; LHR, Lord Howe Rise; NR, Norfolk Ridge; STR, South Tasman Rise; F, Fiordland; NN, Northwest Nelson; NI, North Island; SI, South Island; RS, Ross Sea; CP, Campbell Plateau; CI, Chatham Island. The continental outlines of New Zealand<sup>55</sup>, Australia<sup>56</sup> and Antarctica<sup>57</sup> are taken as the 2,000-m isobath. The line of 'E's' indicates the eastern limit of the pre-late Palaeozoic foreland and the line C-C' relates to the cross-section in Fig. 3. This reconstruction was made by initially establishing the extent, shape and position of the foreland, and then attaching to the foreland margin the 'post-orogenic' form<sup>31</sup> of the Rangitata Sequence. The southwestern extent of the pre-late Palaeozoic Lord Howe Rise<sup>58</sup> was taken from borehole data<sup>59</sup>. The margin of the foreland in Campbell Plateau, which has not been mapped, was placed 130 km south of the ophiolite belt<sup>53</sup>; an equivalent position to the corresponding distance immediately on-land in southeastern South Island (Fig. 1). This position of the margin in Campbell Plateau is consistent with the geology of Campbell Island<sup>60</sup> (Fig. 1), and is similar to an earlier estimate of the margin<sup>52</sup>. 480 km of Cenozoic<sup>61,62</sup> dextral transcurrent displacement on the Alpine Fault was reversed. The Waipounami Fault<sup>63</sup> is considered to be the boundary off eastern South Island where foreland rocks and the Rangitata sequence of Campbell Plateau have been brought into juxtaposition by Cenozoic drifting<sup>22</sup> of the New Zealand sub-continent. The late Cretaceous<sup>64,65</sup> Bounty Trough and Cenozoic<sup>66</sup> Waiau Basin-Solander Trough are closed. The fit of Lord Howe Rise against Australia is the conjectural pre-drift position of the Australian margin based on extrapolation of the Australian margin at the time anomaly 33 formed<sup>67</sup> (82 Myr BP). The reconstruction of Campbell Plateau and Antarctica is a morphological fit<sup>55</sup>. New Caledonia and Norfolk Ridge are placed against Lord Howe Rise. About 100 km of dextral transcurrent displacement is involved to bring the southern part of Norfolk Ridge into the best visually determined morphological fit with Lord Howe Rise. In this reconstruction North Island occurs in a position slightly further south and oceanward of its present position relative to Lord Howe Rise.

such a theory requires an elaborate mechanism to explain the subsequent wholesale reworking westwards back towards the trench.

An eastern source area is now more acceptable although the location has not been specified<sup>1,2,15,38</sup>. In attempts to improve the definition of the eastern source it has been proposed<sup>37</sup> that the Canterbury Suite was formed from sediment derived from Marie Byrd Land and transported northwestwards. However, the Jurassic reconstruction of New Zealand relative to Gondwanaland presented here (Fig. 2) precludes Marie Byrd Land as the source because it lies on the back-arc side of the Canterbury Suite. Moreover, the shape of the clastic wedge comprising the Canterbury Suite is opposite to that expected if Marie Byrd Land were the source; Chatham Island sediments were deposited in a euxenic deep-marine environment yet in a pre-late Cretaceous position (Fig. 2) occur nearer to Marie Byrd Land than the non-marine and shallow marine deposits more distant in South Island.

An alternative idea also involving Marie Byrd Land as the source, but invoking strike-slip faulting of the Canterbury Suite subparallel to the Palaeo Pacific margin of Antarctica has been proposed<sup>39,40</sup>, but not applied to a rigorous Mesozoic reconstruction of eastern Gondwanaland and New Zealand. In taking the later Triassic reconstruction presented here (Fig. 3), and noting particularly the extent of the volcanic arc, to avoid transportation through the arc-trench system some 2,000 km of sinistral strike-slip movement would be required to derive the Canterbury Suite from more eastern parts of Marie Byrd Land. Moreover, the bulk of this movement would need to have occurred between the late early and late Triassic pulse of sedimentation and the first phase of the Rangitata Orogeny (late Triassic-early Jurassic<sup>8</sup>). No mechanism has been proposed and substantiated to account for such rapid movement, and it is in an

opposite sense to Cenozoic strike-slip movement in New Zealand. A model invoking strike-slip faulting would be acceptable only if a lesser amount of fault movement were necessary. This could apparently only be achieved by arbitrarily twisting the Campbell Plateau and Lord Howe Rise into different positions during the Mesozoic, such that until the mid-Jurassic the Canterbury Suite was more proximal to source, yet, by the mid-Cretaceous the Campbell Plateau and Lord Howe Rise were in the pre-breakup late Cretaceous positions. There is no evidence to suggest that before the mid-Cretaceous the Campbell Plateau and Lord Howe Rise had different positions relative to Antarctica and Australia, and hence there is not a substantiated case for Marie Byrd Land as the source of the Canterbury Suite.

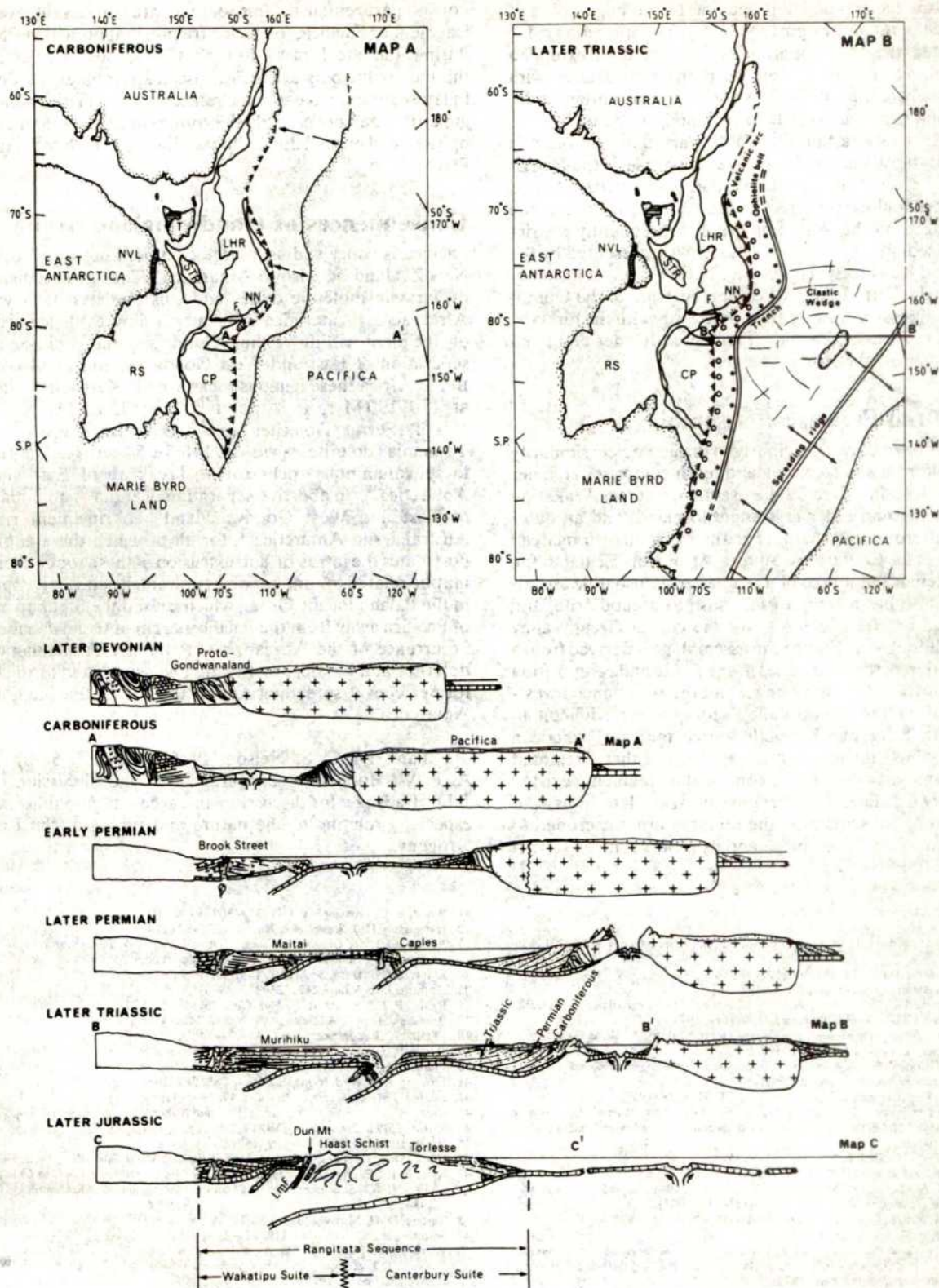
### Pacifica and development of New Zealand

Pacifica was a continent hypothesized from geological evidence<sup>3</sup> to have lain off eastern Gondwanaland until the Triassic. It then fragmented and now occurs as exotic blocks of continental crust within the circum-Pacific Cordillera. The recent demonstration<sup>41</sup> that large parts of western North America are allochthonous adds credibility to Pacifica's fragmenting and subsequently contributing to formation of the Pacific Cordillera.

In discussing Lost Pacifica, Nur and Ben Avraham<sup>3</sup> did not use stratigraphical evidence from New Zealand to support their argument. Pacifica may well be the source of the Canterbury Suite<sup>42</sup>. Not only was Pacifica in the correct position at the right time, but its fragmentation also provides the mechanism for deriving huge volumes of Permian and Triassic sandstone.

I largely agree with the plate tectonic interpretations<sup>2,4,31</sup> for the Wakatipu Suite and the subsequent collision of the two suites, but seek to extend these models eastwards by including Pacifica (Fig. 3).





**Fig. 3** Palaeogeographic maps and schematic cross-sections illustrating a model of the late Palaeozoic-Mesozoic geological development of New Zealand. These show a relationship of the plate tectonic development of the Wakatipu Suite<sup>2,31</sup> and derivation of the Canterbury Suite, to the drift and fragmentation of Pacifica. The later Jurassic cross-section relates to the section line in Fig. 2. The details of map construction and abbreviations are given in Fig. 2, and the terrain names on the cross-sections (for example, Brook Street) are defined elsewhere<sup>2</sup>.

The Rangitata sedimentary-orogenic cycle<sup>43</sup> is postulated to have begun in the late Devonian to early Carboniferous with rifting within the Tuhua Orogen (Fig. 3); fragmentation of supercontinents is believed commonly to occur along old orogenic belts<sup>44</sup>. The spreading centre probably propagated southwards. A reconstruction of New Zealand for the Carboniferous (Fig. 3, map A) shows that the foreland was curved and

the corresponding embayment in Pacifica might have promoted delta formation of the Canterbury Suite. By the Early Permian the Wakatipu arc-trench environment had formed and by the mid-Permian an incipient fracture had developed within Pacifica. The fragmenting of Pacifica (Fig. 3) ensured extensive uplift of the continent during the late Permian and Triassic and derivation, by physical erosion, of detritus which preserved a



quartzo-feldspathic composition because of the huge volumes involved and the rapid transport to the sea. The spreading ridge which initiated the fragmentation of Pacifica then extended south to Antarctica (Fig. 3, map B), perhaps associated with anticlockwise rotation of Gondwanaland concomitant with transformation from Panagea B to A<sup>45</sup>, and by the end of the Triassic was actively rafting the Canterbury Suite on oceanic crust towards the Wakatipu Suite. The first phase of the Rangitata Orogeny ensued in the late Triassic-early Jurassic<sup>8</sup>, and although most folding occurred in the Canterbury Suite, the wedge impinged on the Wakatipu Suite, consequently restricting Jurassic sedimentation to the areas now represented by the Southland and Kawhia Synclines (Fig. 1). The point collision of the clastic wedge (Fig. 3, map B) caused eversion of the Ophiolite and its progressive convergence westwards with the foreland (Fig. 2). In the Jurassic, Pacifica fragmented further and parts were drifting across the Pacific Ocean.

## Source of the Franciscan assemblage

Attention has been drawn previously to the geological similarity between California and New Zealand: each comprises an inner volcanogenic terrain (Great Valley sequence versus Wakatipu Suite) adjacent to an older crystalline foreland, and an outer rarely fossiliferous quartzo-feldspathic terrain (Franciscan assemblage versus Canterbury Suite)<sup>4</sup>. As in New Zealand, the critical problem is the source of the quartzo-feldspathic assemblage which also has a composition close to granodiorite, and was deposited on the Pacific side of the coeval Great Valley sequence. Although the Franciscan assemblage is derived from a continental source, the differences in grain-size and composition between the two sedimentary belts, and the pronounced westward thinning of the Great Valley sequence, are difficult to reconcile with a Sierran-Klamath source for the Franciscan assemblage<sup>4</sup>. This difficulty led to the proposal that a remnant volcanoplutonic arc, possibly a continental fragment, existed between the two sedimentary terrains during the late Jurassic to early Tertiary<sup>46</sup>. Subsequently, the remnant arc was eroded to derive the Franciscan assemblage and its roots subducted so that

now no part remains<sup>4</sup>. This remnant arc could well have been a fragment of Pacifica, for such a fragment approached California during the late Jurassic to early Cretaceous<sup>3</sup>. Consistent with this model, the bulk of the Franciscan assemblage was deposited in latest Jurassic to earliest Cretaceous time (Tithonian-Valanginian)<sup>4</sup>, when presumably the continental fragment was rapidly uplifted and eroded due to interaction with the North American Plate.

## Consequences of Gondwanaland rifting

Pacifica is conceived as a large continent not only adjacent to New Zealand but also to Antarctica<sup>3</sup>. The age and distribution of Jurassic tholeiitic dykes and sills and basaltic lavas from Africa across Antarctica to Tasmania show evidence of a period of incipient rifting within Gondwanaland well before the separation of East and West Gondwanaland at 140–160 Myr BP. In Africa these igneous rocks are the Karroo Basalts dated<sup>3</sup> at 150–190 Myr, in Antarctica the 175±5 Myr old Dufek Massif, Ferrar Dolerites and Kirkpatrick Basalts<sup>47</sup>, and in Tasmania, dolerites aged<sup>7</sup> at 170.5±5 Myr. Rather than link these voluminous rocks to the break-up of East and West Antarctica<sup>48</sup>, an abortive separation of India<sup>49</sup>, an initial rifting of East and West Gondwanaland<sup>50</sup>, or incipient rifting of Australia and Antarctica<sup>51</sup>, for all of which the age of rifting post-dates the intrusion and extrusion of these rocks, their origin may be related to contemporary volcanicity and active spreading in the Palaeo Pacific Ocean which caused the breakup and drift of Pacifica away from the Pacific margin of Gondwanaland. The occurrence of the African, Antarctic and Tasmanian Jurassic dolerites and basalts has already been suggested as related to a former coeval spreading axis in the Palaeo Pacific Ocean off Antarctica<sup>44</sup>.

I thank Dr C. S. Nelson, Professor M. J. Selby and Dr A. P. W. Hodder for encouragement and discussion, and Dr J. D. Bradshaw for discussion and access to unpublished work, especially relating to the nature and timing of the Rangitata Orogeny.

Received 5 August, accepted 22 October 1980

- Andrews, P. B., Spoden, I. G. & Bradshaw, J. D. *N.Z. J. Geol. Geophys.* **19**, 791–819 (1976)
- Coombs, D. S. *et al.* *Am. J. Sci.* **276**, 561–603 (1976).
- Nur, A. & Ben Avraham, Z. *Nature* **270**, 41–43 (1977)
- Blake, M. C., Jones, D. L. & Landa, C. A. in *The Geology of Continental Margins* (eds Burk, C. A. & Drake, C. L.) 853–872 (Springer, New York, 1974)
- Cox, K. G. in *African Magmatism and Tectonics* (eds Clifford, T. N. & Gess, I. G.) 211–236 (Oliver and Boyd, Edinburgh, 1970)
- Barrett, P. J., Grindley, G. W. & Webb, P. N. in *Antarctic Geology and Geophysics* (ed. Adie, R. J.) 319–332 (Oslo University Press, 1972)
- Schmidt, P. W. & McDougall, I. *J. geol. Soc. Aust.* **28**, 321–328 (1977)
- Bradshaw, J. D., Andrews, P. B. & Adams, C. J. *5th Gondwana Symp. Victoria University of Wellington Abstr.* (IUGS Subcommittee on Gondwana Stratigraphy and Paleontology, Wellington, 1980)
- Mitch, A. R. *Trans. R. Soc. N.Z.* **84**, 499–511 (1957)
- Rood, J. J. *Bull. geol. Surv. N.Z.* **87**, 1–60 (1957)
- Campbell, J. D. & Warren, G. *Trans. R. Soc. N.Z.*, *Geol.* **3**, 99–137 (1965)
- Jeonks, T. B. H. & Jeonks, D. G. *Nature* **233**, 117–118 (1971)
- Landa, C. A. & Bishop, D. G. *Bull. geol. Soc. Am.* **83**, 2267–2284 (1972)
- Bradshaw, J. D. *R. Soc. N.Z. J.* **3**, 161–167 (1973)
- Carter, R. M., Hicks, M. D., Norris, R. J. & Turnbull, I. M. in *Sedimentation in Submarine Canyons, Fjords and Trenches* (eds Stanley, D. J. & Kelling, G.) 340–361 (Dowden, Hutchinson and Ross, Stroudsburg, 1978)
- Spoerli, K. B. *Bull. geol. Soc. Am.* **89**, 415–425 (1978)
- Adams, C. J. D. & Robinson, P. *N.Z. J. Geol. Geophys.* **20**, 287–301 (1977)
- Wellman, H. W. *Bull. Aust. Soc. Engng Geophys.* **6**, 55–56 (1975)
- Hunt, T. *N.Z. J. Geol. Geophys.* **21**, 596–606 (1978)
- Cooper, R. A. *Geol. Soc. N.Z. Newsletter* **42**, 31–34 (1976)
- Molnar, P., Atwater, T., Mammernick, J. & Smith, S. M. *Geophys. J. R. astr. Soc.* **40**, 383–420 (1975)
- Wessel, J. K., Hayes, D. E. & Herron, E. M. *Mar. Geol.* **25**, 231–277 (1977)
- Crook, K. A. W. & Bolam, L. *J. geol. Soc. Aust.* **25**, 23–40 (1978)
- Looney, G. J. *Bull. geol. Soc. Am.* **79**, 545–56 (1968)
- Walcott, R. I. *Geophys. J. R. astr. Soc.* **52**, 137–64 (1978)
- Norris, R. J. in *The Origin of the Southern Alps*, *Bull.* **18** (eds Walcott, R. I. & Crosswell, M. M.) (The Royal Society of New Zealand, Wellington, 1979)
- Fleming, C. A. *Q. J. geol. Soc. Lond.* **125**, 125–170 (1970)
- Waterhouse, J. B. *Pacif. Geol.* **9**, 35–73 (1975)
- Oliver, P. J., Munnua, T. C., Grindley, G. W. & Vella, P. *N.Z. J. Geol. Geophys.* **22**, 119–212 (1979)
- Grindley, G. W., Adams, C. J. D., Lumb, J. T. & Wattson, W. A. *N.Z. J. Geol. Geophys.* **20**, 425–467 (1977)
- Wood, B. L. *Tectonophysics* **47**, 339–368 (1978)
- Harrington, H. J. *J. geol. Soc. Aust.* **26**, 276–277 (1979)
- Adams, C. J. *5th Gondwana Symp. Victoria Univ. of Wellington Abstr.* (IUGS Subcommittee on Gondwana Stratigraphy and Paleontology, Wellington, 1980)
- Elliot, D. H. *Am. J. Sci.* **275A**, 45–106 (1975)
- Griffiths, J. R. *Nature* **249**, 336–338 (1974)
- Devey, F. J. & Houtz, R. E. *Mar. Geol.* **25**, 61–72 (1977)
- Bradshaw, J. D. & Andrews, P. B. *Nature* **241**, 14–16 (1973)
- Retallack, G. J. *R. Soc. N.Z. J.* **9**, 397–414 (1979)
- Norris, R. J., Landa, C. A. & Ward, C. M. *Geol. Soc. N.Z. Queenstown Conf. Abstr.* (1977)
- Ward, C. M. & Spoerli, K. B. *J. Geol.* **87**, 187–193 (1979)
- Monger, J. W. H. & Irving, E. *Nature* **238**, 289–294 (1980)
- Pirajno, F. *Geol. Soc. N.Z. Newsletter* **49**, 19–21 (1980)
- Carter, R. M., Landa, C. A., Norris, R. J. & Bishop, D. G. *R. Soc. N.Z. J.* **4**, 5–18 (1974)
- Stutton, J. *Phil. Trans. R. Soc. B279*, 197–205 (1977)
- Irving, E. *Nature* **270**, 304–309 (1977)
- Blake, M. C. & Jones, D. L. *Soc. Econ. Paleontol. Mineral Spec. Publ.* **19**, 255–263 (1974)
- Kyle, P. R., Elliot, D. H. & Ford, A. B. *5th Gondwana Symp. Victoria Univ. of Wellington Abstr.* (IUGS Subcommittee on Gondwana Stratigraphy and Paleontology, Wellington, 1980)
- Tiering, D. H. *Nature* **238**, 92–93 (1972)
- Scrutton, R. A. *Geol. Mag.* **110**, 227–234 (1973)
- Barron, E. J., Harrison, C. G. A. & Hay, W. W. *EOS* **59**, 436–449 (1978)
- Voovers, J. J. & Evans, P. R. in *Gondwana Geology* (ed. Campbell, K. S. W.) 579–607 (ANU Canberra, 1975)
- Cooper, R. A. *R. Soc. N.Z. J.* **9**, 29–84 (1979)
- Devey, F. D. & Christoffel, D. A. *Earth planet. Sci. Lett.* **41**, 14–20 (1978)
- Norton, I. D. & Slater, J. G. *J. geophys. Res.* **84**, 6803–6830 (1979)
- N.Z. Oceanographic Institute *Tectonic Map of the South West Pacific* (DSIR, Wellington, 1970)
- Circum Pacific Council for Energy and Mineral Resources, *Geographic Map of the Circum-Pacific Region* (American Association of Petroleum Geologists, Tulsa, 1978)
- National Mapping Office, Dept. of the Interior, US Antarctic (Map, 2nd edn) (Antarctic Division, Dept. of External Affairs, US, 1956)
- McDougall, I. & van der Lugem, G. *J. Earth planet. Sci. Lett.* **21**, 117–126 (1974)
- Wodzicka, A. *N.Z. J. Geol. Geophys.* **17**, 747–757 (1974)
- Fleming, C. A. *Tectonics* **10**, 52–108 (1962)
- Carter, R. M. & Norris, R. J. *Earth planet. Sci. Lett.* **31**, 85–94 (1976)
- Catton, H. N. C. *N.Z. J. Geol. Geophys.* **22**, 535–553 (1979)
- Caillon, D. *J. N.Z. J. mar. Freshw. Res.* **1**, 16–25 (1967)
- Houtz, R. E., Ewing, J., Ewing, M. & Leonard, A. G. *J. geophys. Res.* **72**, 4713–4739 (1967)
- Kennett, J. P. & Casey, R. E. *N.Z. J. mar. Freshw. Res.* **3**, 20–28 (1969)
- Norris, R. J., Carter, R. M. & Turnbull, I. M. *J. Geol. Soc. Lond.* **135**, 119–205 (1978)
- Wessel, J. K. & Hayes, D. E. *Earth planet. Sci. Lett.* **36**, 77–84 (1977)

# Moloney murine sarcoma proviral DNA is a transcriptional unit

Edmund W. Benz Jr\*, Robert M. Wydro†, Bernardo Nadal-Ginard† & Dino Dina‡

\* Department of Developmental Biology and Cancer, Albert Einstein College of Medicine, Bronx, New York 10461

† Department of Cell Biology, Albert Einstein College of Medicine, Bronx, New York 10461

‡ Department of Genetics and Department of Microbiology and Immunology, Albert Einstein College of Medicine, Bronx, New York 10461

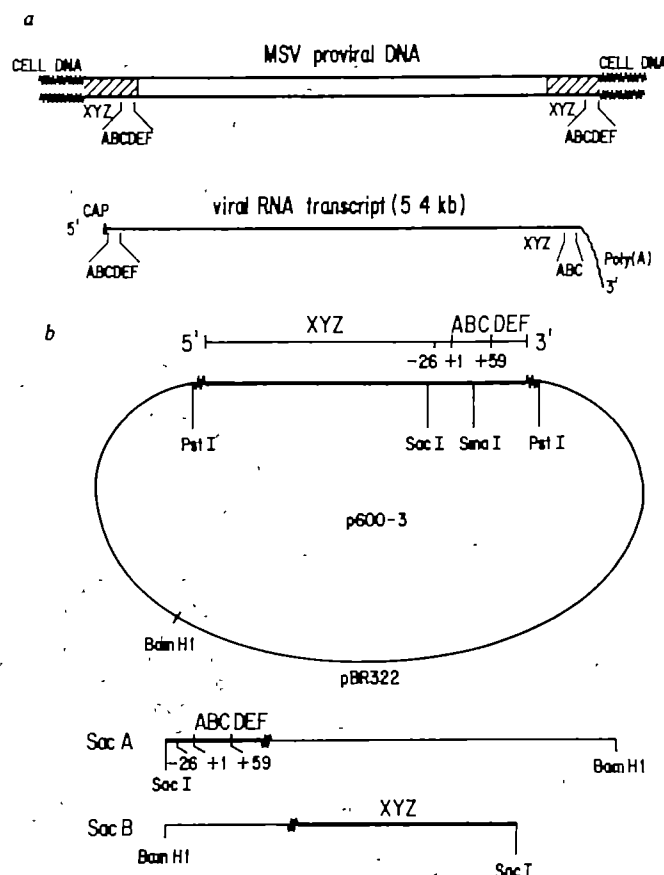
*A portion of Moloney murine sarcoma virus DNA which is repeated at both ends of the provirus has been sequenced. The nucleotide sequence, together with hybridization data obtained with in vitro pulse-labelled nascent viral RNA, indicate that initiation and termination of RNA synthesis occur within that region of the proviral DNA. A model for transcriptional readthrough of termination signals during RNA synthesis in this system is suggested.*

A CRUCIAL STEP in the life cycle of retroviruses is their integration as double-stranded DNA molecules into the DNA of the cell they infect (for a review see ref. 1). The mechanism(s) which regulates transcription of integrated DNA into viral RNA and viral mRNAs has been actively investigated. However, although it is known that cellular RNA polymerase II mediates transcription of the viral genome<sup>2-5</sup>, little is known about the actual sites for initiation and termination of transcription; for example, whether these sites reside on host cell DNA or viral DNA. The size of nuclear virus-specific primary transcripts has not been established; data supporting the presence of both genome-length and longer than genome-length nuclear precursors<sup>6-9</sup> have recently been reported. The discovery that integrated and unintegrated viral DNAs contain a direct repeat at both ends of the DNA and thus are longer than the viral RNA template<sup>10-15</sup> has raised some interesting questions about the potential of the proviral DNA to function as a transcriptional unit. In the case of Moloney murine sarcoma virus (MSV), the

viral DNA carries a 600, base-pair long terminal direct repeat (LTR, which contains the sequences termed XYZABCDE in Fig. 1a)<sup>11</sup>. The mature viral RNA starts and terminates within the LTR with the specific sequence termed 'ABC' (Fig. 1a). This sequence is 59 nucleotides long and is present at both ends of the viral RNA. Its role in reverse transcription has recently been elucidated<sup>16,17</sup>. The genome structure shown in Fig. 1a implies that if MSV functions as a transcriptional unit, the LTR must contain sequences that code for the initiation and termination of RNA synthesis. Alternatively, if transcription starts and terminates outside the proviral DNA, the LTR must carry the information necessary for RNA processing.

We report here DNA sequence data obtained from the LTR DNA cloned into a bacterial plasmid, pBR322. The nucleotide sequence upstream from the region of DNA which codes for the 5' end of the viral RNA (capping site) contains the sequence CAATAAAA, a variation of the typical 'Hogness box', which has been associated with promotion or initiation of transcription

**Fig. 1 a**, Relationship between genomic MSV RNA and integrated DNA. The structure of MSV DNA has been drawn according to results obtained with unintegrated and integrated MSV double-stranded DNA<sup>11,43,46</sup>. The 600-base pair direct repeats (LTRs) are represented by hatched areas. The sequence ABC corresponds to the 59-nucleotide repeat present at either end of viral RNA (ref. 32 and Fig. 3); transcription is from left to right. kb, Kilobases. **b**, Schematic representation of recombinant plasmid p-600-3 from which SacA and SacB DNA fragments were derived. The 600-base pair DNA (LTR) was prepared *in vitro* and purified on agarose gels as described previously<sup>17</sup>. Briefly, S<sub>1</sub> nuclease-treated LTR DNA was tailed with oligo(dC) and plasmid pBR322, cleaved at the PstI site and tailed with oligo(dG). After annealing, the recombinant molecules were selected and amplified in *E. coli*  $\chi$ 1776. Screening was performed with 'strong-stop' MSV cDNA<sup>17,47</sup>. The map of pBR322 is drawn in an anticlockwise orientation. The insert represents the majority of the LTR DNA present on full-length genomic DNA. Its length is 572 nucleotides, of which 518 are viral and the rest G-C tails. Fifty nucleotides are missing from the right end of the sequence and ~15 nucleotides have been deleted at the left end. The numbers +1, +59 and -26 indicate the coordinates of RNA transcription (see Fig. 2) which proceeds from left to right. The SacA and SacB fragments were obtained by digestions with the restriction endonucleases SacI and BamHI. DNA fragments were separated on 5% polyacrylamide gels and electroeluted into dialysis bags. After ethanol precipitation, 1  $\mu$ g of purified DNA was loaded on to Millipore filters. The filters were processed for hybridization and stored under vacuum.





in many of the eukaryotic genes which have been sequenced. The Hogness box is followed by a AATAAA poly(A)-addition signal 70 nucleotides downstream. Hybridization data obtained with *in vitro* pulse-labelled nuclear RNAs indicate that initiation of transcription occurs close to or at sequences corresponding to the viral RNA capping site. The relative position of initiation and polyadenylation sites suggests that a readthrough mechanism may be used in synthesis of mature viral RNA. The potential secondary structure of the RNA transcribed from this portion of the viral genome suggests that in MSV, chain termination may occur by a mechanism similar to attenuation in bacteria<sup>18,19</sup>. A model for such a regulatory mechanism is suggested here.

## DNA sequence data

The long terminal repeat (LTR) present on the unintegrated and integrated viral DNA participates in several crucial steps of the virus life cycle, including DNA synthesis, integration and transcription. To establish whether any specific structural features contained within the LTR might clarify its role in transcription, we have determined the nucleotide sequence of a recombinant plasmid (p-600-3) carrying an insert which represents 518 base pairs of the LTR DNA (Fig. 1b).

Figure 2 shows the nucleotide sequence of the last 177 base pairs (3' end) of the LTR DNA. A Hogness box, which has been found in the majority of eukaryotic genes transcribed by RNA polymerase II (refs 20-23 and ref. 24 for a review), is found 26 nucleotides upstream from the capping site. Although this sequence has been previously considered the structural equivalent of a bacterial 'Pribnow box' (ref. 20), and therefore a promoter, recent evidence suggests that it confers homogeneity

```

      -30      -20      -10      +1      +10
      AGCTCAA TAAAGAGGCC CACAACCCCT CACTCGGCCG GCCAGTCTTC
      TCGAGTT ATTTCTCGG GTGTTGGGA GTGAGCCGCG CGGTGAGAAG

      +20      +30      +40      +50      +60
      CGATAGACTG CGTCGCCCGG GTACCCGTAT TCCCAATAAA GCCTCTTGCT
      GCTATCTGAC GCAGCGGGCC CATGGGCATA AGGGTTATTT CGGAGAACGA

      +70      +80      +90      +100     +110
      GTTTCATCC GAATCGTGGT CTCGTGTTTC CTGGGAGGG TCTCCTCTGA
      CAAACGTAGG CTTAGCACCA GAGCGACAAG GAACCTCC CAGAGGAGACT

      +120     +130     +140
      GTGATTGACT ACCCAGCAGC GGGTCTTTC A
      CACTAAGTGA TGGGTGCTGC CCCCAGAAAG T
  
```

**Fig. 2** Sequence of the right end of the LTR DNA. For sequencing, the 572-base pair insert was released from the plasmid by digestion with *Pst*I and purified on a 5% polyacrylamide gel (acrylamide/bis = 30:1, 20 cm × 20 cm × 1.0 cm). This fragment was digested with *Pvu*II, *Ava*I, *Hha*I, *Sma*I or *Sac*I and end labelled with T4 polynucleotide kinase and [ $\gamma$ -<sup>32</sup>P]ATP (3,000 Ci mmol<sup>-1</sup>, Amersham) or terminal transferase and 3'-[ $\alpha$ -<sup>32</sup>P]dATP (1,000 Ci mmol<sup>-1</sup>, NEN). For strand separation the labelled DNA fragments were dissolved in 30  $\mu$ l of 0.3 M NaOH, 10% glycerol (v/v), 1 mM EDTA and 0.05% bromophenol blue and xylene cyanol, heated at 90°C for 2 min, chilled on ice and immediately fractionated on a 5% polyacrylamide (acrylamide/bis, 60:1) strand-separation gel at 300 V at room temperature in 50 mM Tris-borate, pH 8.3, 1 mM EDTA buffer. These singly end-labelled fragments were sequenced by the chemical cleavage method of Maxam and Gilbert<sup>48</sup>. The nucleotide sequence of both DNA strands was determined except for the last 50 nucleotides. This portion of the sequence has been obtained from strong-stop MSV cDNA synthesized *in vitro*<sup>17</sup>. +1 Indicates the first nucleotide on the viral RNA map, +59 the last one. The Hogness box and the polyadenylation signals are underlined.

to the starting nucleotide or capping site of the transcripts<sup>23</sup>. In its absence, heterogeneous 5' ends are found, but initiation of RNA synthesis is maintained<sup>22,23</sup>. The presence of such a structural element on MSV DNA argues in favour of the possibility that synthesis of mature viral RNA may actually start at this site and that the nucleotide sequence surrounding the capping site and including the Hogness box may serve as a promoter *in vivo*.

A second specific structure, reported for many of the genes transcribed by RNA polymerase II, is the polyadenylation signal AATAAA. This sequence, found at position +45, is followed by another sequence, TTGC or TTTGC<sup>24,25</sup>, at position +63 to +67, immediately downstream from the presumed terminal tetranucleotide TTGC. Comparative data for several other mRNAs<sup>24</sup> and viral RNAs<sup>25,26</sup> indicate that this region is associated with termination of RNA transcription. If transcriptional processes *in vivo* actually use the structural regions described above as regulatory signals, it follows that the LTRs of integrated proviral DNA have a promoter region immediately adjacent to terminator signals.

## Does transcription of MSV RNA start at a cellular or viral promoter?

The presence of sequences in the LTR DNA which correspond to the putative promoter sites of several eukaryotic genes<sup>24</sup> transcribed by RNA polymerase II raises the specific question of whether or not virion RNA is the primary product of nuclear transcription in infected cells. We have therefore isolated nascent, pulse-labelled nuclear RNA synthesized *in vitro* and analysed it by hybridization to different portions of the p-600-3 plasmid DNA (Fig. 2). If transcription started at a cellular site upstream from the viral 'promoter site' (marked -26 in Fig. 1b), LTR sequences (XYZ) upstream from the *Sac*I site would be transcribed and covalently linked to downstream sequences (ABCDEF). If instead transcription started at the putative viral promoter site (Fig. 1b), the 5' ends of virus-specific nuclear RNAs would correspond only to sequences downstream from the *Sac*I site (ABCDEF). By hybridizing *in vitro* pulse-labelled nuclear RNA to LTR sequences downstream from the promoter (*Sac*A fragment, Fig. 1b) or LTR sequences upstream from the promoter (*Sac*B fragment, Fig. 1b), the relative amounts transcribed from these two regions of the LTR DNA have been quantified. This analysis must, however, take into account the fact that mature virion RNA ends with the sequence XYZABC, which can hybridize to both the *Sac*A and *Sac*B fragments. (Table 1 summarizes the distribution of virus-specific nucleotides on the *Sac*A and *Sac*B fragments.) Therefore, before hybridization, we removed polyadenylated mature viral RNA from the nuclear RNA sample by chromatography on oligo(dT)-cellulose (see Table 2 legend). Mature virion RNA was fragmented by alkaline treatment<sup>27</sup> and fractionated by oligo(dT) chromatography. Viral poly(A)<sup>+</sup> and poly(A)<sup>-</sup> RNA fragments were used as controls in the hybridization to DNA-nitrocellulose filters. DNA-nitrocellulose filters carrying specific DNA fragments were prepared as described in Fig. 2 legend.

**Table 1** Distribution of virus-specific sequences on *Sac*A and *Sac*B fragments

| Fragment     | Total virus-specific nucleotides | %   | Nucleotides complementary to 5' viral RNA |    | Nucleotides complementary to 3' viral RNA |    |
|--------------|----------------------------------|-----|---|----|---|----|
|              |                                  |     |   | %  |   | %  |
| p-600-3      | 518                              | 100 | 91  | 17 | 486                                       | 94 |
| <i>Sac</i> A | 128                              | 25  | 91  | 17 | 96  | 18 |
| <i>Sac</i> B | 390                              | 75  | 0   | 0  | 390                                       | 75 |

The number of nucleotides on each fragment was derived from the sequencing data presented in Fig. 2 and unpublished results. The number of hybridizable virus-specific nucleotides from either end of the viral RNA was calculated by taking into account the presence of the 59-nucleotide ABC repeat at the end of the viral RNA. The *Sac*A fragment contains 'promoter-downstream' sequences (ABCDEF) and the *Sac*B fragment carries 'promoter-upstream' sequences (XYZ) (Fig. 1b).

**Table 2** Hybridization of pulse-labelled nuclear RNA from MSV-infected cells to p-600 DNA fragments

| RNA sample                   | Input<br>c.p.m.        | c.p.m.<br>hybridized to<br>SacB (%) | c.p.m.<br>hybridized to<br>SacA (%) |
|------------------------------|------------------------|-------------------------------------|-------------------------------------|
| Nuclear poly(A) <sup>+</sup> | 1.8 × 10 <sup>6</sup>  | 373 (75)                            | 123 (25)                            |
| Viral poly(A) <sup>+</sup>   | 3.2 × 10 <sup>4</sup>  | 1,116 (72)                          | 446 (28)                            |
| Nuclear poly(A) <sup>-</sup> | 1.2 × 10 <sup>7</sup>  | 910 (40)                            | 1,365 (60)                          |
| Viral poly(A) <sup>-</sup>   | 1.12 × 10 <sup>5</sup> | 2,507 (30)                          | 5,988 (70)                          |

Approximately  $2 \times 10^7$  cells were directly lysed on the plate by addition of lysis buffer (25 mM Tris-HCl, pH 7.4, 25 mM NaCl, 5 mM MgCl<sub>2</sub>, 140 mM sucrose, 0.5% Triton X-100). After 10 min in the cold, cells were scraped off the plates with a Teflon-coated razor blade. Complete lysis was achieved by subjecting the cells to 10 strokes with a B pestle in a Dounce homogenizer. Nuclei were pelleted through a sucrose cushion (0.25 M sucrose, 5 mM MgCl<sub>2</sub>, 25 mM Tris pH 7.4) at 4 °C with a table-top centrifuge. The nuclear pellet was resuspended in 1.5 ml of buffer (0.25 M sucrose, 5 mM MgCl<sub>2</sub>, 25 mM Tris pH 7.4) and pelleted again. Final recovery was  $1.1 \times 10^7$  nuclei. The crude nuclei were gently suspended in 150 µl of a solution containing 125 mM Tris pH 7.9, 2 mM MgCl<sub>2</sub>, 5 mM NaF, 1 mg ml<sup>-1</sup> bovine serum albumin, 1 mM ATP, GTP and CTP, 5.8 µM [ $\alpha$ -<sup>32</sup>P]UTP, 50 mM (NH<sub>4</sub>)<sub>2</sub>SO<sub>4</sub> and 1 mM dithiothreitol. The reaction was incubated at 37 °C for 5 min and terminated by the addition of 500 µl of 50 mM Na-acetate pH 5, 6 mM EDTA and 1% SDS. Total incorporation measured by trichloroacetic acid precipitation was  $\sim 3 \times 10^7$  c.p.m. Nuclear RNA was extracted several times with phenol saturated with 0.1 M Na-acetate pH 5.0. After ethanol precipitation, the poly(A)-containing nuclear RNA was fractionated by chromatography on oligo(dT)-cellulose. An aliquot of each RNA fraction was then hybridized to specific p-600 DNA fragments bound to nitrocellulose filters in 1 ml of HEPES hybridization buffer (100 mM HEPES, pH 7, 1 mM EDTA, 0.2% SDS, 0.5 M NaCl and 50% formamide, 48 h at 40 °C). The filters were washed extensively in 2 × SSC at 65 °C and treated with RNase (20 µg ml<sup>-1</sup>, 2 × SSC at room temperature for 1 h). Hybridization experiments were performed in triplicate. In these experiments nonspecific background values (10 c.p.m. per 10<sup>6</sup> c.p.m.) were subtracted from the results presented above.

The nuclear RNA samples labelled with [ $\alpha$ -<sup>32</sup>P]UTP and mature virion RNAs uniformly labelled with <sup>32</sup>P-orthophosphoric acid were hybridized to DNA filters stacked in a scintillation vial (Table 2). If the oligo(dT)-cellulose chromatography step removed all the RNA chains containing the XYZABC portion of the LTR located at the 3' end RNA, the viral poly(A)<sup>-</sup> RNA fragments should hybridize exclusively to the SacA DNA-containing filter. Although the majority of poly(A)<sup>-</sup> RNA counts hybridized to SacA DNA (Table 2), a substantial background (30%) of viral poly(A)<sup>-</sup> RNA hybridized to SacB DNA, implying that oligo(dT)-cellulose chromatography could not completely remove all 3'-terminal fragments of viral RNA molecules. This was not surprising as 10–30% of full-length virion RNA lacks a poly(A) tail (ref. 28 and D.D., unpublished observation). Similarly, we observed that 60% of virus-specific, poly(A)<sup>-</sup>, pulse-labelled nuclear RNA counts hybridized to SacA DNA whereas 40% hybridized to SacB DNA (Table 2). This result implied that pulse-labelled, virus-specific nuclear RNA was very similar to mature virion RNA and that newly synthesized nuclear RNA started primarily at a site on the SacA fragment.

To eliminate the ambiguity due to the background hybridization of 3' sequences in the experiment described above, another experiment was devised. The pulse labelling was performed in the presence of ribonucleoside triphosphate analogue which contained a sulphur atom substituted for oxygen in the  $\gamma$  phosphate position ( $\gamma$ -S NTPs) (see Table 3 legend). Newly initiated chains have the structure  $\gamma$ -S pppN <sup>32</sup>pUp. The incorporation of a  $\gamma$ -S nucleotide at the 5' end of a chain prevents capping of that chain (Furichi and R. N. Wydro, unpublished results), thus allowing its purification by mercury-agarose affinity chromatography<sup>29</sup>. Therefore, RNAs retained by the column terminate with 5'  $\gamma$ -S triphosphate, indicating that these RNAs result from initiation during the pulse label and not from elongation. Because most RNA chains in eukaryotic nuclei start with G or A, only those two substrates were actually used.

After fractionation of the RNA on mercury-agarose columns (see Table 3), a fraction containing the bulk of the nuclear RNA (unbound RNA) and a fraction containing  $\gamma$ -S pppA- and  $\gamma$ -S pppG-initiated chains were obtained (Table 3). The percentage of RNA chains initiated with a substituted nucleotide was

approximately 3% of the total [ $\alpha$ -<sup>32</sup>P]UTP-labelled chains, in agreement with previously obtained results<sup>30,31</sup>. The 'bound' and 'unbound' fractions were hybridized to nitrocellulose filters carrying the SacA and SacB fragments as described above. The hybridization pattern of the unbound fractions of the RNA made in the presence of  $\gamma$ -S ATP and  $\gamma$ -S GTP were quantitatively similar, being proportional to the number of virus-specific nucleotides present on the SacA and SacB fragments (Table 1). This result showed that the substituted nucleotides did not interfere significantly with the elongation of virus-specific RNA chains and that transcription of the whole viral genome occurred.  $\gamma$ -S pppG-initiated chains hybridized preferentially to the SacA fragment. When normalized to the number of virus-specific nucleotides of the SacA and SacB fragments (Table 1), the ratio of the counts hybridized to SacA compared with SacB DNA was greater than 20:1. From these data we concluded that most of the virus-specific RNA chains were initiated within the SacA fragment. The counts which hybridized to the SacB fragment could be due either to the presence of contaminating total RNA in the bound fraction or to a small number of chains initiated at a cellular promoter. The small number of hybridized counts obtained with  $\gamma$ -S pppA-initiated chains supports the conclusion that sulphur groups were not transferred to internal residues of elongating chains.

### A model for chain termination

The evidence presented here strongly suggests that initiation of viral RNA synthesis occurs at a site on proviral DNA contained within the last 177 nucleotides of the 600-base pair repeat. Because the 5' and 3' ends of the primary transcripts of many RNA polymerase II-dependent transcriptional units are conserved during processing of precursor nuclear RNA into mature mRNA (for a summary see refs 24, 25), it is reasonable to assume that virus-specific nuclear RNA chains have the same 3' end as mature virion RNA. As shown in Fig. 3, we have tentatively placed the nucleotide which precedes the poly(A) at position +59 on the basis of oligonucleotide sequence data (ref. 32 and unpublished observations). The DNA sequence between the capping site (+1) and the region immediately following the end of the viral RNA (+59) thus contains signals for poly(A) addition and possibly chain termination. These signals must be ignored by RNA polymerase II during transcription of the LTR at the left end of the proviral DNA (see Fig. 1a); however, the enzyme would have to recognize such signals at the end of transcription, 5,400 nucleotides downstream, as it transcribes the LTR at the right end of the genome.

**Table 3** Hybridization of RNA from MSV-infected cell nuclei pulse-labelled in the presence of  $\gamma$ -S GTP and  $\gamma$ -S ATP to p-600-3 DNA fragments

| RNA sample      | Input<br>c.p.m.    | c.p.m. hybridized<br>to SacB | c.p.m. hybridized<br>to SacA |
|-----------------|--------------------|------------------------------|------------------------------|
| $\gamma$ -S ATP |                    |                              |                              |
| Unbound         | $7.92 \times 10^6$ | 2,225                        | 430                          |
| Bound           | $2.7 \times 10^5$  | 62                           | 22                           |
| $\gamma$ -S GTP |                    |                              |                              |
| Unbound         | $3.82 \times 10^7$ | 8,732                        | 2,652                        |
| Bound           | $9.67 \times 10^5$ | 108                          | 656                          |

RNA was synthesized in the *in vitro* nuclear transcriptional system described in Table 2 legend with the exception that either  $\gamma$ -S ATP or  $\gamma$ -S GTP was added in place of the respective unsubstituted nucleotide triphosphate. The RNA was extracted with phenol as described and ethanol precipitated three times. The RNA was then dissolved in the buffer (10 mM Tris-HCl, pH 7.9, 100 mM NaCl, 10 mM Na<sub>2</sub>EDTA, 0.1% SDS) and applied to a low cross-linked mercury-agarose column as described elsewhere<sup>31</sup>. The bound material was eluted with TNE buffer containing 10 mM dithiothreitol<sup>30</sup>. Eluted fractions (0.5 ml) were monitored for radioactivity by removing aliquots (3 µl for  $\gamma$ -S GTP RNA and 12 µl for  $\gamma$ -S ATP RNA) and measuring Cerenkov radiation in 1.5-ml Eppendorf tubes. Peak fractions were pooled, made 50 µg ml<sup>-1</sup> with tRNA and precipitated overnight with two volumes of ethanol at 20 °C. The RNA synthesized with  $\gamma$ -SGTP was the result of four identical *in vitro* reactions pooled before the extraction of RNA. Hybridizations were performed to filters stacked in scintillation vials as described in Table 2 legend. Experiments were performed with triplicate samples for  $\gamma$ -S GTP. The largest variation between homologous filters in each hybridization was less than 20%. Backgrounds were reproducibly 10 c.p.m. per 10<sup>6</sup> c.p.m. input and have been subtracted from the values presented above.





containing cellular sequences. Note also that our model is not incompatible with the possibility that mature viral RNA is processed from a larger precursor. In this case the large stem and loop structure at the 3' terminus would serve as a recognition site for processing. This model can be tested experimentally. Transfection of cells with plasmids containing the LTR DNA, singly and in tandem repeats, as well as subclones containing specific deletions, should offer a useful approach for studying these phenomena.

We thank J. Pyati for technical assistance, J. Hurwitz for his support and advice, and A. Maxam, D. Schwartz and J. Sims for

Received 28 April; accepted 29 October 1980.

1. Bishop, J. M. & Varmus, H. E. in *Cancer, A Comprehensive Treatise* Vol. 2 (ed. Becker, F. F.) (Plenum, New York, 1975).
2. Monroy, G., Jacquet, M., Groner, V. & Hurwitz, J. *Cold Spring Harb. Symp. quant. Biol.* **39**, 1033-1041 (1974).
3. Jacquet, M., Groner, V. & Hurwitz, J. *Proc. natn. Acad. Sci. U.S.A.* **71**, 2045-2049 (1974).
4. Rymo, L., Parsons, J. T., Coffin, J. M. & Weissmann, C. *Proc. natn. Acad. Sci. U.S.A.* **71**, 2782-2786 (1974).
5. Dinowitz, M. *Virology* **66**, 1-9 (1975).
6. Bishop, J. M. et al. in *Animal Virology* (eds Baltimore, D., Huang, A. & Fox, C. F.) 1-20 (Academic, New York, 1976).
7. Brugge, J. S., Purchio, A. F. & Erikson, R. L. *Virology* **83**, 27-33 (1977).
8. Fan, H. *Cell* **11**, 297-305 (1977).
9. Hsu, T. W., Sabran, J. L., Mark, G. E., Guntaka, R. V. & Taylor, J. M. *J. Virol.* **28**, 810-818 (1978).
10. Hughes, S. H. et al. *Cell* **15**, 1397-1410 (1978).
11. Benz, E. W. Jr & Dina, D. *Proc. natn. Acad. Sci. U.S.A.* **76**, 3294-3298 (1979).
12. Sabram, J. L. et al. *J. Virol.* **29**, 170-178 (1979).
13. Gilboa, E. et al. *Cell* **16**, 863-874 (1979).
14. Yoshimura, F. & Weinberg, R. A. *Cell* **16**, 323-332 (1979).
15. Shank, P. R. et al. *Cell* **15**, 1383-1395 (1978).
16. Haseltine, W. A., Coffin, J. M. & Hageman, T. G. *J. Virol.* **30**, 375-383 (1979).
17. Dina, D. & Benz, E. W. Jr *J. Virol.* **33**, 377-389 (1980).
18. Oxender, D. L., Zurawsky, G. & Yanofsky, C. *Proc. natn. Acad. Sci. U.S.A.* **76**, 5524-5528 (1979).
19. Sanger, F. et al. *Nature* **265**, 687 (1977).
20. Gannon, F. et al. *Nature* **278**, 428-434 (1979).
21. Konkelt, D., Tilghman, S. & Leder, P. *Cell* **15**, 1125-1132 (1978).
22. Baker, C. C., Herisse, J., Courtois, G., Galibert, F. & Ziff, E. *Cell* **18**, 569-580 (1979).

advice and for communicating results before publication. This work was supported by NIH grants CA 24223, CA 26860, CA 13330 and GM 13344. D.D. is a recipient of a Junior Research Faculty Award from ACS; B.N.G. is an Irma T. Hirsch scholar and recipient of a Research Faculty Award from ACS; R.M.W. is a recipient of a NIH postdoctoral fellowship.

Since this manuscript was submitted, the nucleotide sequences of the LTRs of several retroviruses have been reported: by Dhar et al.<sup>41</sup>, Sutcliffe et al.<sup>42</sup>, Czernilofsky et al.<sup>43</sup> and Shimotohno et al.<sup>44</sup>.

23. Grosschedl, R. & Birnstiel, M. L. *Proc. natn. Acad. Sci. U.S.A.* **77**, 1432-1436 (1980).
24. Benoist, C., O'Hare, K., Breathnach, R. & Chambon, P. *Nucleic Acids Res.* **8**, 127-142 (1980).
25. Lovinger, G. G. & Schochetman, G. *Cell* (in the press).
26. Lovinger, G. G. & Schochetman, G. *J. Virol.* **32**, 803-811 (1979).
27. Dina, D. & Beemon, K. *J. Virol.* **23**, 524-532 (1977).
28. Wang, L. H. & Duesberg, P. H. *J. Virol.* **14**, 1515-1529 (1974).
29. Smith, M. M., Reeve, A. E. & Huang, R. C. C. *Biochemistry* **17**, 493-500 (1978).
30. Smith, M. M., Reeve, A. E. & Huang, R. C. C. *Cell* **15**, 615-626 (1978).
31. Wydro, R. M., Brot, N. & Weissbach, H. *Archs Biochem. Biophys.* **201**, 73-80 (1980).
32. Coffin, J. M., Hageman, T. C., Maxam, A. M. & Haseltine, W. A. *Cell* **13**, 761-773 (1978).
33. Keller, E. B. & Calvo, J. M. *Proc. natn. Acad. Sci. U.S.A.* **76**, 6186-6190 (1979).
34. Johnston, H., Barnes, W., Chumley, F., Bossi, L. & Roth, J. *Proc. natn. Acad. Sci. U.S.A.* **77**, 508-512 (1980).
35. Tinoco, I. Jr et al. *Nature new Biol.* **246**, 40 (1973).
36. Sures, I., Lowry, J. & Kedes, L. H. *Cell* **15**, 1033-1044 (1978).
37. Busslinger, M., Portmann, R., Irminger, I. C. & Birnstiel, M. L. *Nucleic Acids Res.* (in the press).
38. Fiers, W. et al. *Nature* **273**, 113-120 (1978).
39. Reddy, V. B. et al. *Science* **200**, 494-502 (1978).
40. Seif, I., Ghoury, G. & Dhar, R. *Cell* **18**, 963-978 (1979).
41. Dhar, R., McClements, W. L., Enquist, L. W. & Vande Woude, G. F. *Proc. natn. Acad. Sci. U.S.A.* **77**, 3937-3941 (1980).
42. Sutcliffe, J. G., Shinnick, T. M., Verma, I. M. & Lerner, R. A. *Proc. natn. Acad. Sci. U.S.A.* **77**, 3302-3306 (1980).
43. Czernilofsky, A. P. et al. *Nucleic Acids Res.* **8**, 2967-2984 (1980).
44. Shimotohno, K., Mizutani, S. & Temin, H. M. *Nature* **285**, 550-554 (1980).
45. Vande Woude, G. F. et al. *Proc. natn. Acad. Sci. U.S.A.* **76**, 1677-1681 (1979).
46. Canaan, E. & Aaronson, S. A. *Proc. natn. Acad. Sci. U.S.A.* **76**, 1677-1681 (1979).
47. Grunstein, M. & Hogness, D. S. *Proc. natn. Acad. Sci. U.S.A.* **72**, 3961-3965 (1975).
48. Maxam, A. M. & Gilbert, W. *Proc. natn. Acad. Sci. U.S.A.* **74**, 560-564 (1977).

## Crystal structure of yeast tRNA<sup>Asp</sup>

D. Moras, M. B. Comarmond, J. Fischer, R. Weiss & J. C. Thierry

Laboratoire de Cristalochimie (ERA 08), Institut Le Bel, Université Louis Pasteur, 4 rue Blaise Pascal, 67070 Strasbourg Cedex, France

J. P. Ebel & R. Giegé

Laboratoire de Biochimie, Institut de Biologie Moléculaire et Cellulaire du CNRS, 15 rue Descartes, 67084 Strasbourg Cedex, France

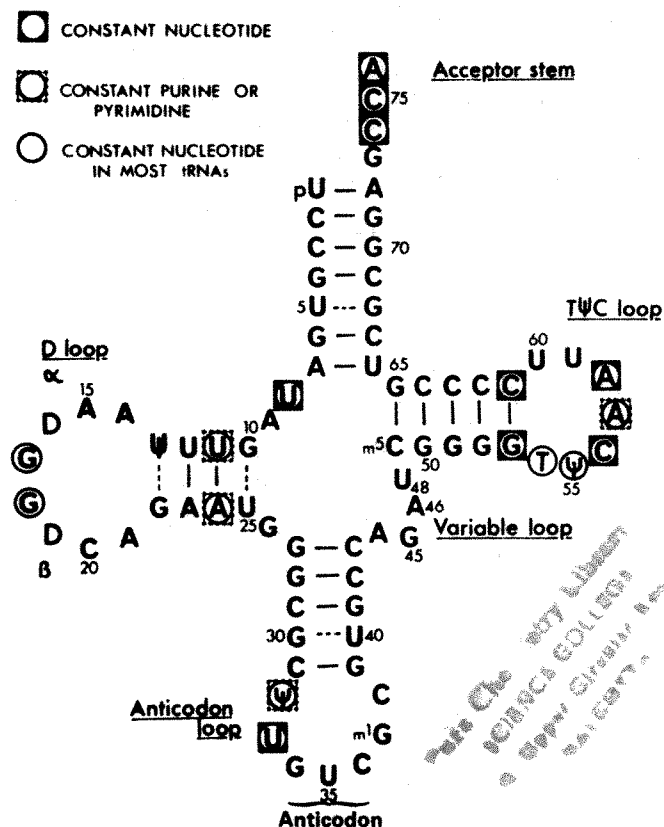
*Two independent, three-dimensional structures of yeast tRNA<sup>Asp</sup>, mainly differing by the conformation of the D loop, have been obtained from a multiple isomorphous replacement (MIR) X-ray analysis at 3.5-Å resolution. The folding of the ribose-phosphate backbone is similar to that found for tRNA<sup>Phe</sup>; major differences concern the relative positioning of the acceptor and anticodon stems, and the conformation of the loops in the two molecules. Crystal packing involves self-complementary GUC anticodon interactions.*

TRANSFER RIBONUCLEIC ACIDS are versatile macromolecules which interact with many components of the protein-synthesizing machinery. Some of the functions of these molecules, like the interaction with the ribosomes, are common to all tRNAs<sup>1,2</sup>; others, like the specific attachment to the aminoacyl-tRNA synthetases, are specific to each particular tRNA<sup>1</sup>. It is therefore expected that all these molecules possess structural similarities at the three-dimensional level, but also differences responsible for their specific functions. To understand the molecular basis of the multifunctional character of tRNA, knowledge of the structure of different tRNAs is necessary.

The first molecular structure of a tRNA obtained from electron-density maps at atomic resolution<sup>3-6</sup>, that of yeast tRNA<sup>Phe</sup>, made possible the elucidation of the folding of the polynucleotide backbone which accommodates the clover-leaf domains in a stable L-shaped structure, the structural justification for most of the invariant residues, and the evidence of tertiary interactions necessary to the stability of the structure.

These features, which might be found in all tRNAs, probably account for the general tRNA functions. The fact that similar information was obtained from two independent structures of tRNA<sup>Phe</sup>, in two different crystal forms, ruled out the possibility of distortions induced by packing forces and gave more confidence for the generality of the L-shaped structure. However, the structural data obtained on yeast tRNA<sup>Phe</sup> did not allow definitive conclusions about the features responsible for the specific functions of the tRNAs. Furthermore, the nature of conformational changes in tRNA, observed by various methods, is still uncertain<sup>7,8</sup>. These facts prompted study of the crystallization of tRNAs presenting structural and functional differences compared with tRNA<sup>Phe</sup>. Emphasis was given to obtaining good crystals of the initiator tRNAs and of tRNAs with short or long extra-loops, or of tRNAs possessing three base pairs in the D stem. In 1977, we succeeded in growing crystals of yeast tRNA<sup>Asp</sup>, which is a tRNA with a short extra-loop, diffracting better than 3.5 Å of resolution<sup>9</sup>.





**Fig. 1** The nucleotide sequence of yeast tRNA<sup>Asp</sup> (ref. 13). For convenience the numbering system of the nucleotides is that of yeast tRNA<sup>Phe</sup>; in the 75-nucleotide long tRNA<sup>Asp</sup>, position 47 in the variable loop has been omitted. Non-classical Watson-Crick base pairs are indicated by broken lines. The invariant and semi-invariant positions (except for initiator tRNAs) and the constant nucleotides in most tRNAs are indicated. Sequence data are taken from the review of Dirheimer *et al.*<sup>26</sup>. The  $\alpha$  and  $\beta$  regions correspond to the parts of the D loop located respectively at the 5' and 3' side of the constant GG sequence.

It was not until 1979 that new structural information on different tRNAs appeared. In yeast tRNA<sup>Met</sup>, which was crystallized in high-salt conditions, only a difference in the position of the anticodon stem with respect to tRNA<sup>Phe</sup> was apparent, but the resolution of the map does not allow a firm conclusion<sup>10</sup>. For the structure of *Escherichia coli* tRNA<sup>Met</sup>, solved using the molecular replacement method, changes from the tRNA<sup>Phe</sup> model were observed which may be of functional importance<sup>11</sup>. Yeast tRNA<sup>Gly</sup> is an exception with an unfolded structure<sup>12</sup>, but this tRNA was crystallized at high temperature in the presence of high amounts of organic solvent.

We report here the first structural results on another elongator tRNA, yeast tRNA<sup>Asp</sup>, based on two independent maps obtained by the MIR method from two interconvertible crystal forms diffracting at high resolution.

### Primary structure

The nucleotide sequence of yeast tRNA<sup>Asp</sup> (ref. 13, Fig. 1) presents some distinctive features compared with yeast tRNA<sup>Phe</sup> and other tRNAs studied by crystallographic methods. An exceedingly high number (nine out of 10) of GC base pairs in the TΨC and anticodon stems confers an important stability to these regions, as confirmed by solution studies<sup>14,15</sup>. Conversely, the D stem does not contain any GC base pair and is therefore particularly unstable. Due to this, the number of base pairs in the D stem of tRNA<sup>Asp</sup> is not well defined and it has long been considered as belonging to class II according to Levitt's tRNA classification<sup>16</sup>. Yeast tRNA<sup>Asp</sup> is also one of the tRNAs containing the fewest number of modified nucleotides: besides the classical D, Ψ and T residues, it only possesses one m<sup>1</sup>G and

one m<sup>5</sup>C. Concerning the general organization of the tRNA<sup>Asp</sup> clover-leaf, the  $\alpha$  and  $\beta$  regions in the D loop (three bases each) differ from those in tRNA<sup>Phe</sup> (four and two bases for the  $\alpha$  and  $\beta$  regions respectively) and the length of the variable loop (four bases) is shorter than in tRNA<sup>Phe</sup> (five bases). Another difference between the two tRNAs is the replacement at position 73 of A in tRNA<sup>Phe</sup> by G in tRNA<sup>Asp</sup>. This position has been proposed as a discriminator site for tRNA aminoacylation<sup>17</sup>. Finally, tRNA<sup>Asp</sup> possesses a self-complementary GUC anticodon<sup>18</sup> which renders it a tempting model system for studying tRNA-mRNA interactions.

### Crystal analysis

We used 150 mg of pure tRNA<sup>Asp</sup>, purified from brewer's yeast tRNAs by countercurrent distribution followed by benzoylated DEAE-cellulose chromatography. For crystallization, tRNA<sup>Asp</sup> was used as a sodium salt, prepared by dialysis against 40 mM sodium cacodylate buffer containing 2 mM MgCl<sub>2</sub>. Crystals were obtained in 62% ammonium sulphate using vapour diffusion techniques<sup>9</sup>. The temperature was a decisive parameter in crystal growth. Crystals suitable for diffractometer measurements were obtained, although in an exceedingly poor yield, by careful monitoring of the concentration of ammonium sulphate against temperature. Before being exposed to X rays, all crystals were stabilized against 70% ammonium sulphate solutions. The space group is C222<sub>1</sub>, with one molecule of tRNA in the asymmetric unit. The solvent content of the crystals, ~75%, is comparable with that of the orthorhombic crystals of yeast tRNA<sup>Phe</sup>. At 20°C, the temperature at which the best crystals are grown, two crystal forms, nonisomorphous and interconvertible, are obtained.

$$\begin{array}{ll}
 a = 61.5 \text{ \AA} & a = 60.3 \text{ \AA} \\
 (A) \quad b = 67.5 \text{ \AA} & \rightleftharpoons (B) \quad b = 68.0 \text{ \AA} \\
 c = 149.5 \text{ \AA} & c = 149.5 \text{ \AA}
 \end{array}$$

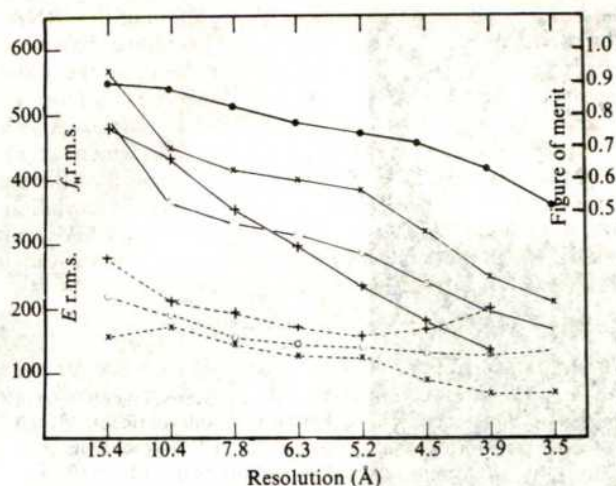
The mean difference in the native  $F$  between the two crystal forms ( $\Sigma|\Delta F|/\Sigma|F|$ ) is of 15% throughout the  $\sin \theta/\lambda$  range. As it was not possible to produce selectively and identify one form or the other, two independent structure determinations had to be carried out by the MIR method. The search for the heavy-atom derivatives was hampered by the interconvertibility of the two crystal forms. For example, it was difficult to obtain a gold derivative of form A, as addition of gold salt drives crystals to an intermediate form close to that of crystals B. Experimental details are given in Fig. 2 legend.

### Electron density map

The shape and limits of the tRNA<sup>Asp</sup> molecule in the crystallographic cell could be drawn from an earlier 5-Å resolution electron-density map phased with two heavy-atom derivatives (Gd and Au, f.o.m. = 0.72). This map revealed an L-shaped structure roughly comparable with that found for tRNA<sup>Phe</sup>. Some characteristic features of the tRNA structure, like the helical stems and the anticodon loop, were clearly recognizable. The region situated near the D and TΨC stems lies close to a 2-fold axis parallel to the crystallographic direction  $a$ , which brings two molecules in close contact in that part of the cell. In this case, the problem of the boundary could be solved by topological considerations and continuity of the helices. At that resolution, however, the precise frontier between the TΨC loop and the CCA end of another molecule could not be unambiguously resolved due to the packing conditions (see below).

The 3.5-Å resolution data confirmed this first analysis and enabled us to trace the complete ribose-phosphate backbone. A few sections of the resulting electron-density map are presented in Fig. 3. Figure 3a shows a portion of the anticodon loop viewed along the direction of the  $a$  axis. Figure 3b represents part of the TΨC stem viewed down the helical stem which runs parallel with the  $a$  axis. In both, the locations of the phosphate groups are indicated by dots and correspond to bulbs of quasi-spherical electron density. A striking feature of this map is the high





**Fig. 2** Refinement statistics of form A. The diffracted intensities were collected on a four-circle Philips PW1100 diffractometer modified for protein work. Great care was taken concerning the decay of intensities in X-ray exposure, this effect being related to the Bragg angle. In standard conditions, a native crystal loses 1% of intensity per h above 3.5-Å resolution. For each crystal, data were collected in successive shells of decreasing resolution, the starting value being determined by the angle to which significant diffraction was observed. For example, for the native data of form B, six crystals were used, scaled together and merged; 5,262 independent significant reflections to 3-Å resolution were then kept, out of 17,440 observed intensities ( $F > 2\sigma F$ ), the agreement factor of intensities being equal to 5.5%. Details concerning the measurement and treatment of the data will be published elsewhere. The best heavy-atom derivative was obtained with gadolinium. The observed unicity of the binding site, when varying the Gd concentration, can be partly explained by the crystallization conditions. Lutetium and lanthane lead to similar results. Gold has two binding sites. The root mean square (r.m.s.) calculated heavy-atom structure amplitudes ( $f_H$ , continuous line) and the r.m.s. lack of closure ( $E$ , broken line) are plotted against resolution for the different isomorphous derivatives used in the refinement:  $\times$ ,  $Gd_2(SO_4)_3$ ;  $+$ ,  $Au(en)_2Cl_3$ ; and  $O$ , the mixed derivative. The distribution of the figure of merit is also indicated ( $\bullet$ ), the overall value being 0.62 for 3,477 phased reflections.

contrast between the electron density of the molecule and the solvent regions. This is even true, but to a lesser extent, for most of the loop regions which are fortunately stabilized by appropriate intermolecular contacts. Except for part of the D loop, the phosphate groups can be identified as the peaks of highest density roughly 6-Å apart. The high content of ammonium sulphate in the crystals with the resulting high ionic strength does not affect the observed signal-to-noise ratio. The background barely reaches the first countour level except in the groove formed by the T $\Psi$ C loop where a higher density can be observed which is not yet related to any molecular feature. The

electron density is also perturbed near the heavy-atom sites where ripples of negative density exist.

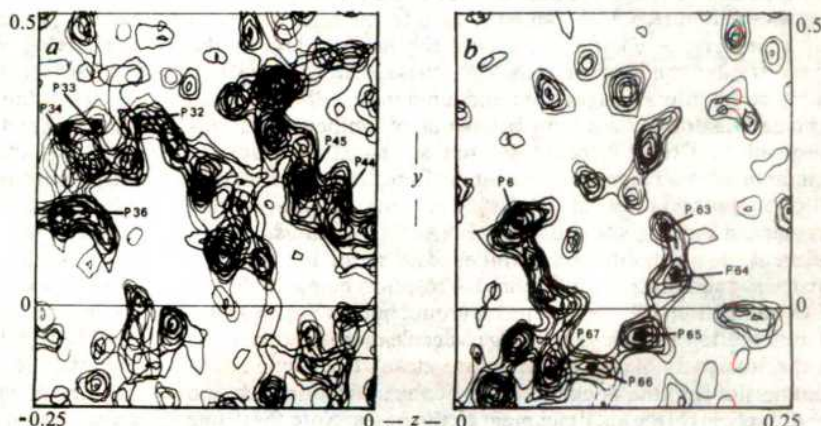
The very high proportion of GC base pairs in tRNA<sup>Asp</sup> probably has an important effect on the stability of the double-helical stems. This in turn is reflected in the experimental electron density. In most places the phosphate groups can be distinguished from the riboses, which appear as flat, connecting densities between the phosphate bulbs. The electron density corresponding to the paired bases can clearly be seen in the double-helical regions; this is also true for many bases of the loop regions which are probably involved in tertiary interactions, either intra- or intermolecular. This is obviously the case for the electron density associated with the T $\Psi$ C and anticodon loop regions, especially the latter which is stabilized by intermolecular contacts across a 2-fold axis. The interactions with the GUC anticodon of another molecule restrain the motion of the atoms. The resulting electron density is thus remarkably strong. At the other extremity of the map, the single-stranded CCA end is clearly visible, due to stabilizing interactions with the T $\Psi$ C loop of the neighbouring molecule. The situation is different in the region of the map corresponding to the D loop which seems weaker in both A and B forms. This was also noticed by Robertus *et al.* in the 3-Å resolution map of the monoclinic form of yeast tRNA<sup>Phe</sup> (ref. 5).

## Model

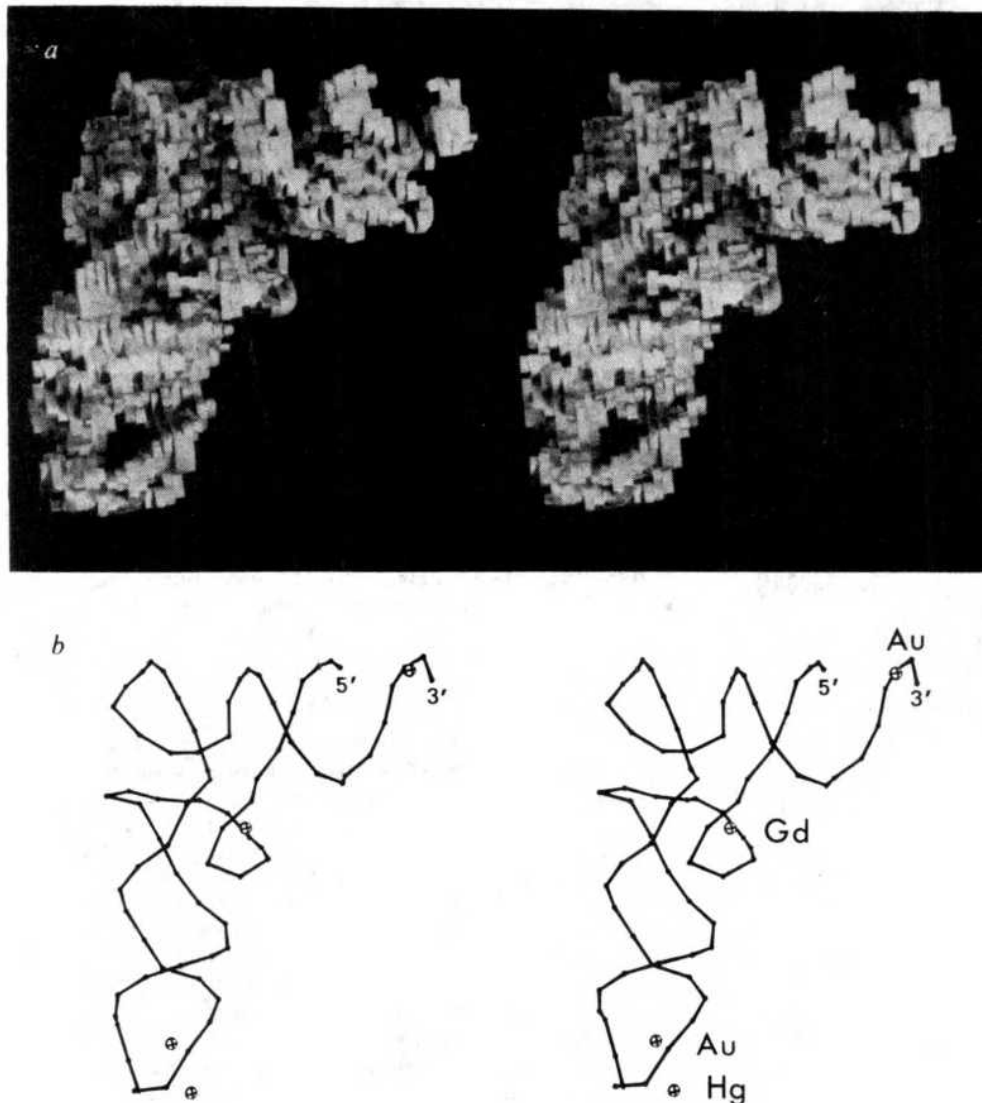
A stereo picture of a balsawood model built out of the 3.5-Å resolution electron-density map of form A is shown in Fig. 4a. This picture corresponds to a view down the crystallographic  $b$  axis. The two major structural units giving the molecule its L shape can be recognized: vertically, from the bottom, the anticodon stem followed by the D stem; horizontally, from the corner of the molecule, the T $\Psi$ C with the amino acid-accepting stem stacked on it. The molecule is approximately 20-Å thick in the viewer's direction. This model can be compared with both balsawood and space-filling models of yeast tRNA<sup>Phe</sup> (refs 19, 20). It clearly shows the more open conformation of the L in tRNA<sup>Asp</sup>, which resembles a boomerang. Two major grooves, sharply cut and without any significant electron density, can be seen in the two limbs of the molecule. These are characteristic of a RNA-type double helix.

The entire ribose-phosphate backbone of tRNA<sup>Asp</sup> deduced from the 3.5-Å resolution maps is presented in Fig. 4b in the same perspective as the balsawood model (ORTEP drawing<sup>21</sup>). The crude position of the peaks of highest density, approximately 6-Å apart from each other, was used as coordinates for the phosphate groups. The overall folding agrees with that observed for tRNA<sup>Phe</sup>. This extends the validity of the tRNA<sup>Phe</sup> model to the short-loop tRNA family and provides direct evidence that the overall folding of a tRNA remains unchanged in high (tRNA<sup>Asp</sup>) or low (tRNA<sup>Phe</sup>) salt concentrations. Even the D stem is clearly visible despite the weakness of its base pairing (two AU and two GU base pairs). This apparently contradicts

**Fig. 3** Two composites of the 3.5-Å MIR map of yeast tRNA<sup>Asp</sup>, form A. *a* Shows the electron density corresponding to part of the anticodon loop and stem (four sections between  $x = -7.7$  and  $-3.7$  Å). This region is characterized by the absence of any significant density in the major groove of the anticodon stem, and by the high electron density of the anticodon loop when compared with that of the nearby helical stem. *b* Shows densities in the amino acid acceptor- and T $\Psi$ C-stem regions (two sections between  $x = 19.4$  and  $20.7$  Å). The electron density corresponding to a Watson-Crick base pair (G6 C67) is seen between P6 and P67.







**Fig. 4** *a*, Stereo picture of a balsawood model of tRNA<sup>Asp</sup> built out of the 3.5-Å resolution electron-density map of form A. The view is down a direction roughly parallel to the crystallographic *b* axis. In that direction the thickness of the molecule is approximately 20 Å. *b*, Stereo view (ORTEP drawing) of the ribose-phosphate backbone presented in the same perspective as the balsawood model. The positions of the heavy-atom binding sites are indicated.

former NMR studies where these interactions, essentially the two AU base pairs, could not be seen in normal ionic conditions; but this is most likely related to the particular distribution of GC and AU base pairs in tRNA<sup>Asp</sup> (ref. 15).

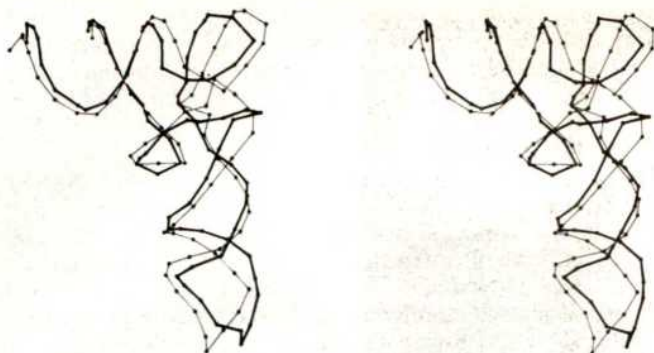
The positions of the heavy-atom binding sites on tRNA<sup>Asp</sup> are also shown in Fig. 4*b*. The lanthanide site is situated near the position of phosphates U8 and A9. It is similar to one of the two strong samarium binding sites in yeast tRNA<sup>Phe</sup> (ref. 22). The distance between the gadolinium site and the phosphates 8 and 9 is ~4 Å; although this is not a refined value, it strongly suggests a direct interaction between the lanthanide and these phosphate groups, as observed in tRNA<sup>Phe</sup>. The fact that this is the unique marked site in tRNA<sup>Asp</sup>, whereas three other binding positions are observed in tRNA<sup>Phe</sup>, can be related to the high structural selectivity of the complexing cavity for lanthanides. In the crystallization medium of tRNA<sup>Asp</sup>, these cations have two strong competitors: magnesium and ammonium. Two possible explanations for the different behaviour of lanthanide cations observed in tRNA<sup>Asp</sup> could be the strong competition of ammonium for weak magnesium binding sites and/or a different D-loop conformation in tRNA<sup>Asp</sup> for the second, strong magnesium binding site found in tRNA<sup>Phe</sup>. Gold binds in two different sites with different affinities. The major site lies near the CCA end (phosphates C75 and A76), thus being indicative of an interaction with the phosphate group, but binding to a base of the TΨC loop of a neighbouring molecule cannot be excluded as the two parts of the molecule are close. The second gold binding site is in the pocket formed by the anticodon loop and most likely involves an attachment to the bases. Note that none

of these gold binding sites is observed in yeast tRNA<sup>Phe</sup> (ref. 23). For a mercury derivative, not used in the phasing, the heavy atom is situated on the 2-fold axis relating the anticodons of two equivalent molecules. It is a good candidate for binding to U35.

### Structural comparison with yeast tRNA<sup>Phe</sup>

Earlier attempts to solve the crystallographic structure of yeast tRNA<sup>Asp</sup> by the molecular-replacement method failed using the structure of yeast tRNA<sup>Phe</sup> as a model. Although the major peak of the rotation function was close to the best possible compromise, no reasonable solution could be obtained from the various translation functions tested. It was only after obtaining an independent chain tracing of tRNA<sup>Asp</sup> from the MIR map and having realized the close similarity of folding with that of tRNA<sup>Phe</sup> that it was possible to position roughly the tRNA<sup>Phe</sup> model in the tRNA<sup>Asp</sup> cell. A 6-Å resolution set of observed structure factors ( $F_o$ ) was then used to obtain the best fit of the two molecules by comparison with the calculated values ( $F_c$ ) derived from the tRNA<sup>Phe</sup> model. An optimization of the six parameters necessary to position the tRNA<sup>Phe</sup> model (the three eulerian rotation angles and the coordinates of the centre of mass of the molecular electron density) was carried out by minimization of  $(F_o - F_c)^2$  quantities by a least-square procedure. Convergence was slow; the reliability factor  $R = \sum \|F_o\| - \|F_c\| / \sum \|F_o\|$  decreased from 0.55 to 0.50 in 19 cycles. The high final  $R$  value for 6-Å resolution data is indicative of poor agreement between the model and the observed data. Details on these procedures will be published elsewhere.





**Fig. 5** Comparison of the ribose-phosphate backbones of yeast tRNA<sup>Asp</sup> in form A (heavy lines) with that of yeast tRNA<sup>Phe</sup> (light lines).

The resulting parameters were used to trace a superposition of the two tRNA backbones shown in Fig. 5. We recall that the tRNA<sup>Asp</sup> is an independent, unrefined model resulting from a crude positioning of phosphate groups. The first overwhelming impression concerns the similarity of the overall folding of both tRNAs. Careful inspection, however, clearly uncovers differences, but at the present level of accuracy only the major ones can be underlined. Figure 5 confirms the more open L conformation of tRNA<sup>Asp</sup>, although the superposition method tends to minimize the differences. The angle formed by the two limbs of the L is increased by more than 10° (Fig. 6). This results in different positioning of the anticodon and of the TΨC stems and loops with respect to fixed acceptor and D stems which superpose well to the corresponding parts of tRNA<sup>Phe</sup>; as a result, the D and anticodon stems are more coaxial. It is tempting to propose that conformational changes in tRNAs could result from concerted movements of the clover-leaf domains different from that suggested by the L-shaped model (see Fig. 6). A concerted behaviour of the D and acceptor stems was also suggested by thermodynamic studies<sup>14</sup> which showed that the simultaneous melting of the tertiary structure and of these two regions is the first step of denaturation of tRNA<sup>Asp</sup>.

A tilt of the anticodon stem is also observed in the initiator tRNA from yeast, but in this tRNA the angle between the acceptor and anticodon stems decreases by ~6° when compared with tRNA<sup>Phe</sup> (J. Sussmann, personal communication). A possible regulatory effect of spermine on the tilt of the anticodon stem was suggested by Quigley *et al.*<sup>24</sup> after discovery of a spermine molecule bound at the hinge region. High salt conditions might have a competitive effect which would induce a structural change at that level. However, the fact that those ionic conditions with similar spermine concentration lead to opposite changes in two different tRNAs greatly weakens such an explanation. In the variable region the deletion of one nucleotide in yeast tRNA<sup>Asp</sup> does not cause an important change. From the superposition diagram, the missing nucleotide is probably U47, which in tRNA<sup>Phe</sup> points towards the exterior of the molecule, the rest of the chain just being stretched toward C49. The resulting shift might, of course, trigger the observed tilt of the anticodon stem, thus making it a characteristic of the tRNAs with four bases in the variable region.

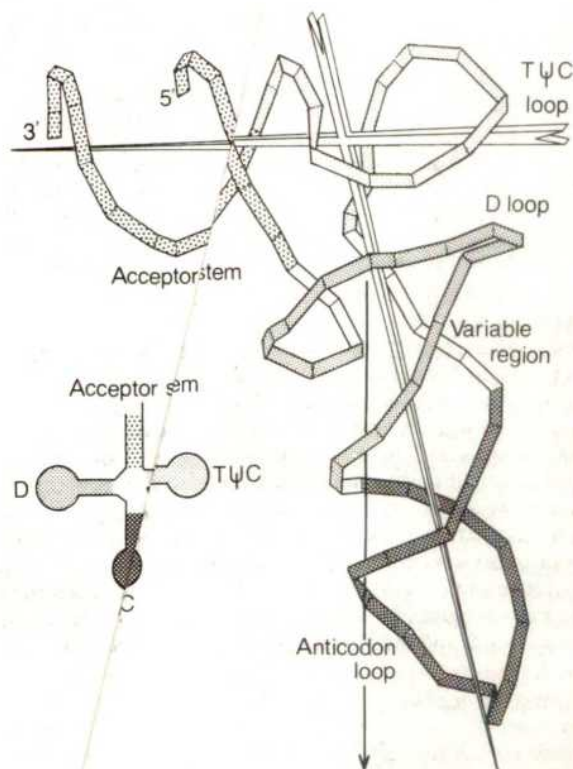
The relative position of the TΨC and D loops is different from that observed in tRNA<sup>Phe</sup>. The precise interactions in this part of the map are not known and further refinements are required. Nevertheless, the interaction scheme between the loops present in tRNA<sup>Phe</sup> is clearly not valid here. For example, the fact that in tRNA<sup>Asp</sup> the two conserved guanines G17 and G18 are moved in the sequence with respect to tRNA<sup>Phe</sup> makes base pairing between G18 and C56 impossible, unless the loop is shifted.

Differences exist even between the two structures of tRNA<sup>Asp</sup> corresponding to the two crystal forms by comparison of the two maps. An averaged map of the density of the two crystal forms shows a much higher contrast everywhere, except in the D-loop

region which is smeared out between nucleotides 16 and 19. This part of the molecule can be otherwise followed on each individual map. The transition between the two forms occurring around 20 °C agrees with the observed differences and stresses the mobility of the D loop. The previously mentioned thermodynamic studies imply that the observed movements of the D loop are not related to a set of especially weak interactions which loosen the structure in that region, as the acceptor stem and the D-stem helix melt simultaneously with a collapse of the tertiary structure.

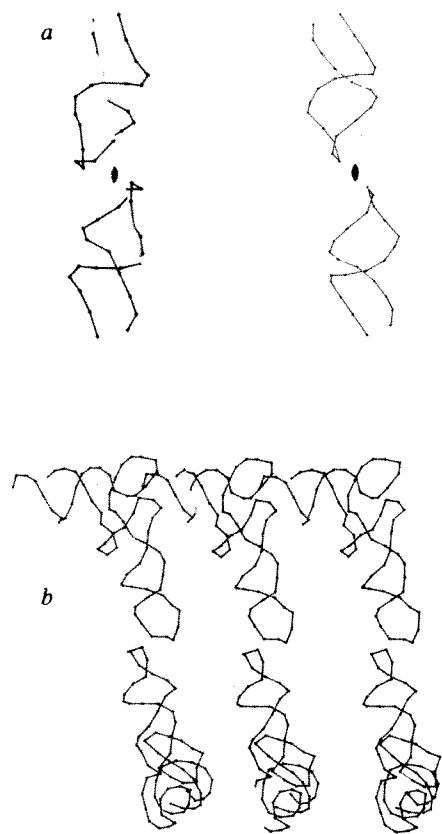
## Intermolecular contacts

Three major intermolecular contacts are involved in the stabilization of the crystal packing of tRNA<sup>Asp</sup>. One contact already mentioned involves interactions between the anticodons of two molecules related by a 2-fold symmetry axis parallel to the crystallographic *b* direction. It assures the crystalline cohesion in the direction of the crystallographic *c* axis. This contact is particularly important because of the self-complementarity of the anticodon GUC of tRNA<sup>Asp</sup>. Grosjean *et al.*<sup>18</sup> have already shown that this association exists in solution. This is reflected, as shown in Fig. 3b, by a high value of the corresponding electron density which compares with that of helical regions. The comparison in that region of the tRNA<sup>Asp</sup> backbone with that of tRNA<sup>Phe</sup> in the orthorhombic form, where one anticodon is stacked on top of the other, is shown in Fig. 7a. Similar stacking interactions in tRNA<sup>Asp</sup> can be excluded by the distances between the related phosphate groups which suggest a base pairing, although the precise nature of these interactions needs a



**Fig. 6** Diagrammatic representation of the ribose-phosphate backbone and of the cloverleaf domains of tRNA<sup>Asp</sup> (indicated by different shadings). The two pointers show the more open conformation of tRNA<sup>Asp</sup> with respect to tRNA<sup>Phe</sup>. Assuming an exact superposition of the acceptor stem in the two molecules, the shift which gives the tRNA<sup>Asp</sup> molecule its boomerang shape results mainly from a different positioning of the AC and TΨC parts of the cloverleaf, the acceptor and D stems being positioned as in tRNA<sup>Phe</sup>. The arrow represents the direction of the helical axis of the anticodon stem in tRNA<sup>Phe</sup>.





**Fig. 7** Packing diagrams. *a*, Anticodon-anticodon interactions. The 2-fold axis-related backbones of the anticodon stem and loop are shown for yeast tRNA<sup>Asp</sup> (left) and for the orthorhombic form of yeast tRNA<sup>Phe</sup> (right). *b*, Partial packing diagram of yeast tRNA<sup>Asp</sup>. For clarity only four out of eight equivalent positions of the space group are traced for one and a half unit cells. The drawing shows the anticodon-anticodon contacts and the interactions between the CCA end and the TΨC loop of adjacent molecules; in the crystals this results in a network of two classes of infinite pseudo-helices, 90° apart. The crystallographic 2-fold axis relating the two anticodons is at 45° from the figure plane.

refined model. The two anticodon loops from the two strands of a double-helical structure which might represent a model of interaction between tRNA and mRNA.

Another strong intermolecular contact, introduced by the C-mode translation, involves the TΨC loop and the acceptor stem of a neighbouring molecule. This results in two infinite, kinked helices related by a dyad and 90° part. Figure 7*b* represents a partial-packing diagram, which underlines the two types of intermolecular contacts described above. A third and quantitatively important intermolecular contact is a consequence of the crystallographic 2-fold axis parallel to *c*. It brings the anticodon stem and the D stem of one molecule in close contact

with the TΨC stem of another one. In this arrangement a cage is formed by the 5' parts of the D stems of the two symmetrically related molecules. The two symmetric gadolinium atoms, 6-Å apart, enter in this cage during isomorphous substitution.

### Biological implications

The three-dimensional structure of tRNA<sup>Asp</sup> confirms the folding originally found in tRNA<sup>Phe</sup>. This result fits with an unitary structural scheme and is probably a consequence of the existence of tertiary interactions brought by the invariant and semi-invariant residues. This scheme brings together both elongator and initiator tRNAs and integrates many properties of these molecules (that is, interactions on the ribosome<sup>1,2</sup>, similar types of interaction in various tRNA-synthetase systems<sup>1</sup>, mischarging of numerous tRNAs by the same synthetase<sup>25</sup>). The tRNA<sup>Asp</sup> structure also presents differences from the canonical tRNA<sup>Phe</sup> model. With the present information, only large differences can be stressed with confidence. The most important deviations concern the respective position of the acceptor and anticodon arms of the boomerang-shaped molecule and the conformation of the loop regions. It may be asked whether the different conformation of tRNA<sup>Asp</sup> is indicative (1) of an archetype of another tRNA class or (2) of another conformation of a standard tRNA structure.

Hypothesis (1) would emphasize the structural role of the clover-leaf organization. In that case, the existing differences between the structure of tRNA<sup>Phe</sup> and the initiator tRNAs on the one hand, and the structure of tRNA<sup>Asp</sup> on the other, should result from differences in the variable loop and/or in the β region. A similar relationship between these tRNAs came out of incorrect aminoacylation studies<sup>25</sup>.

Hypothesis (2) would reflect the conformational flexibility of the tRNA molecules. Would then the conformational changes be induced by the interactions between the self-complementary anticodons, mimicking the ribosomal situation, or is it just a consequence of crystallization conditions, namely high salt concentration? The latter possibility seems to be ruled out by the results obtained with the initiator yeast tRNA<sup>Met</sup>, where similar ionic conditions lead to different structural variations. Probably the induced conformational changes and sequence-bound differences act together to give the observed structural variations. A more accurate model, as well as a detailed comparison of the two electron-density maps available, will increase our knowledge of tRNAs and help answer some of the open questions.

This work was supported by grants from the CNRS (Action Thématique Programmée: Structure Tridimensionnelle des Protéines) and DGRST. We thank M. Delfau for assistance with the purification and crystallization of tRNA<sup>Asp</sup>, M. Schlegel for help with countercurrent distribution of crude tRNA, and A. Cassou, S. Wechsler and J. Born for technical help. We also thank M. G. Rossmann for supplying the Purdue crystallographic programs from which most of the programs used in this study are adapted, A. Lifschitz for the least-square superposition, G. Quigley, N. Woo and A. Rich for discussions and programs, and D. Blow, G. Dirheimer, B. Jacrot and A. Klug for encouragement and helpful discussions.

Received 30 June; accepted 7 October 1980.

- Schimmel, P. R., Söll, D. & Abelson, J. N. (eds) *Transfer RNA: Structure, Properties and Recognition* (Cold Spring Harbor Monogr. Ser. 9A, New York, 1979).
- Clark, B. F. C. in *Ribosomes: Structure, Function and Genetics*, 413-444 (University Park Press, Baltimore, 1979).
- Kim, S. H. *et al. Science* **185**, 435-440 (1974).
- Sussmann, J. L., Holbrook, S. R., Warrant, R. W., Church, G. M. & Kim, H. *J. molec. Biol.* **123**, 607-630 (1978).
- Robertus, J. D. *et al. Nature* **250**, 546-551 (1974).
- Jack, A., Ladner, J. E. & Klug, A. *J. molec. Biol.* **108**, 619-649 (1976).
- Schwarz, U., Manzel, H. M. & Gassen, H. G. *Biochemistry* **15**, 2484-2490 (1976).
- Ehrlich, R., Lefevre, J. L. & Remy, P. *Eur. J. Biochem.* **103**, 145-153 (1980).
- Giegé, R., Moras, D. & Thierry, J. C. *J. molec. Biol.* **115**, 91-96 (1977).
- Schevitz, R. W. *et al. Nature* **278**, 188-190 (1979).
- Woo, N., Roe, B. & Rich, A. *Nature* **286**, 346-351 (1980).
- Wright, H. T., Manor, P. C., Beurling, K., Karpel, R. L. & Fresco, J. L. in *Transfer RNA: Structure, Properties and Recognition*, 145-160 (Cold Spring Harbor Monogr. Ser. 9A, New York, 1979).

- Gangloff, J., Keith, G., Ebel, J. P. & Dirheimer, G. *Nature new Biol.* **230**, 125-127 (1971).
- Coutts, S. M., Gangloff, J. & Dirheimer, G. *Biochemistry* **13**, 3938-3948 (1974).
- Robillard, C. T. *et al. Biochemistry* **15**, 1883-1888 (1976).
- Levitt, M. *Nature* **224**, 759-763 (1969).
- Crothers, D. M., Seno, T. & Söll, D. G. *Proc. natn. Acad. Sci. U.S.A.* **69**, 3063-3067 (1972).
- Grosjean, H., De Henau, S. & Crothers, D. M. *Proc. natn. Acad. Sci. U.S.A.* **75**, 610-614 (1978).
- Rich, A. in *Ribosomes*, 871-884 (Cold Spring Harbor Monogr. Ser. 4, New York, 1974).
- Holbrook, S. R., Sussmann, J. L., Warrant, R. W. & Kim, S. H. *J. molec. Biol.* **123**, 631-660 (1978).
- Johnson, C. K. *ORTEP. Rep. ORNL-3794* (Oak Ridge National Laboratory, Oak Ridge, Tennessee, 1965).
- Jack, A., Ladner, J. E., Rhodes, D., Brown, R. S. & Klug, A. *J. molec. Biol.* **111**, 315-328 (1977).
- Stout, C. D. *et al. Acta Crystallogr.* **B34**, 1529-1544 (1978).
- Quigley, G. J., Teeter, M. M. & Rich, A. *Proc. natn. Acad. Sci. U.S.A.* **75**, 64-68 (1978).
- Ebel, J. P. *et al. Biochimie* **55**, 547-557 (1973).
- Dirheimer, G., Keith, G., Sibley, A. P. & Martin, R. P. in *Transfer RNA: Structure, Properties and Recognition*, 19-41 (Cold Spring Harbor Monogr. Ser. 9A, New York, 1979).

# The structure of histone H1 and its location in chromatin

J. Allan\*, P. G. Hartman†, C. Crane-Robinson† & F. X. Aviles‡

\* Biophysics Laboratories, King's College, London WC2B 5RL, UK

† Biophysics Laboratories, Portsmouth Polytechnic, Portsmouth PO1 2QQ, UK

‡ Department of Biochemistry, Autonomous University, Barcelona, Spain

*On the basis of their primary structure, the lysine-rich histones are a unified family of proteins. Each has an amino acid chain which falls into three distinct domains. Only the central domain (~80 residues) is in a folded conformation. It is protected from trypsin digestion in chromatin and corresponds to the segment of highest sequence conservation. Without the flanking domains it is able to close two full turns of DNA in the nucleosome and can thus locate the H1 molecule.*

THE lysine-rich histones are a group of chromosomal proteins that show considerable sequence variation when contrasted with the core histones. If calf thymus H1 is taken as the archetypal molecule, then rabbit thymus and chicken erythrocyte H1s have sequences very similar to calf<sup>1</sup>, and the trout testis H1 sequence shows only a few variations<sup>2</sup> (Fig. 1). Avian erythrocyte H5 and sea urchin sperm H1 ( $\Phi$ 1) have been considered as specialized versions of H1 but have sequences clearly related to that of calf thymus H1<sup>3-5</sup>. Recent studies of an H1 subfraction from ox liver, H1<sup>o</sup>, indicate it to be intermediate between calf thymus H1 and avian erythrocyte H5 (ref. 6). A partial sequence of an H1 molecule from somatic tissue of sea urchin<sup>7</sup> is also included in Fig. 1. The sequences of both sea urchin H1 molecules show greater homology with H5s, particularly in the central domain, than with the vertebrate H1s. On the basis of primary structure, it is clear that the lysine-rich histones are a unified family.

Studies of extracted lysine-rich histones in free solution have shown conformational homology within the family. Although fully denatured at pH 3 in the absence of salt, they can be induced to fold by increasing the pH and ionic strength, but the folded domain encompasses only a limited portion of the polypeptide chain<sup>8</sup>. For calf thymus H1 the folding domain has been defined as residues 36–121 (ref. 9). Trypsin digestion of histone H5 similarly defines residues 22–100 of that histone as containing all the secondary and tertiary structure<sup>10</sup>. Sea urchin sperm H1 also shows a trypsin-resistant peptide of approximately 80 residues<sup>11</sup>, representing the sequence 36 to about 116 (P. Sautière and P. Puigdomenech, personal communication). The finding that only a limited portion of the chain is folded and trypsin resistant could, however, be a consequence of partial denaturation on extraction and for this reason we have looked to see whether the same domain is protected from digestion in nuclei.

## Trypsin digestion of nuclei

Figure 2 shows a time course of digestion of calf thymus nuclei in isotonic conditions. The H1 subfractions are seen to be gradually degraded to a limiting peptide which runs very close to the peptide (36–121) prepared by trypsin digestion of H1 in free solution<sup>9</sup>. The two peptides have very similar amino acid analyses, and high-resolution proton-resonance spectroscopy shows that the tertiary folding of intact calf thymus H1 and both peptides are the same. We conclude that essentially the same peptide is protected from digestion in nuclei as in free solution.

Digestion experiments with proteases to probe conformation frequently show that protected and folded domains are linked by relatively short bridges of susceptible amino acid residues (hinge regions, for example, *lac* repressor). Does the H1 molecule have

only one, short, protected domain while the remainder is fully accessible to trypsin? Figure 2 shows that at early digestion times many peptides have lengths intermediate between intact H1 and the resistant peptide. The two flanking domains are clearly very accessible in chromatin and therefore probably not in a compact, folded conformation.

## Correlation of primary structure and trypsin-defined conformation

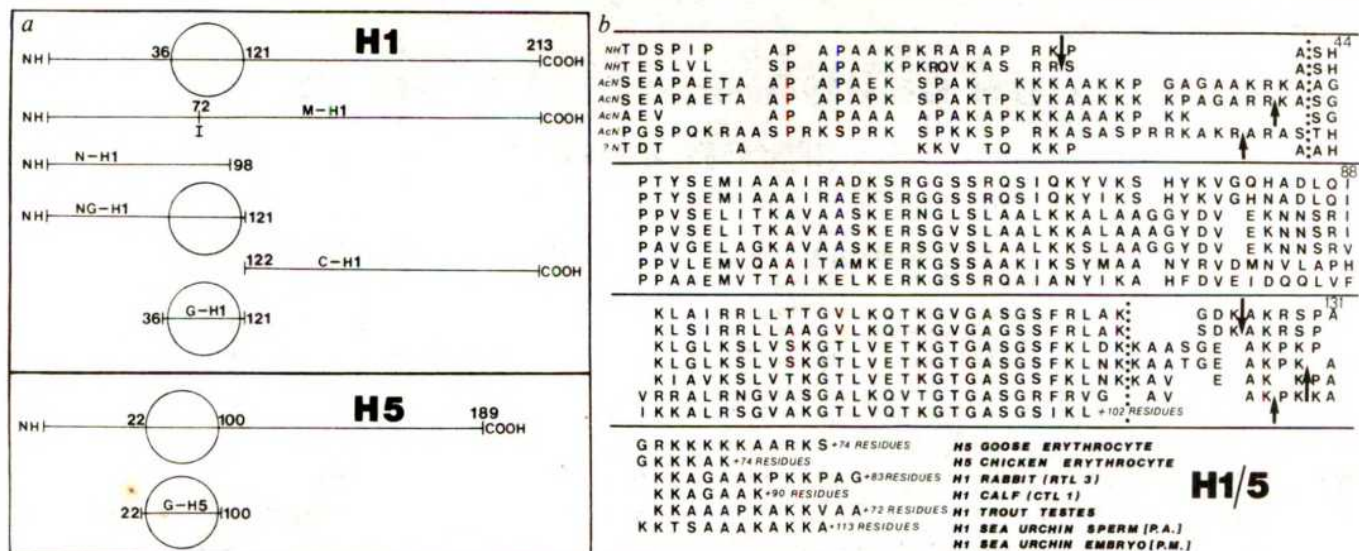
Comparison of the observed trypsin-resistant regions of three rather distant members of the H1 family with the sequence homology (Fig. 1) indicates that the protected domain coincides with the strongly conserved and more hydrophobic region of the sequence in all three cases. Although the conservation of this central domain is less than that of any of the core histones<sup>1,5,12</sup>, it is very much greater than that of the flanking domains. The N-terminal domain shows only low sequence homology throughout the family and varies greatly in length from 40 residues in sea urchin sperm to 13 residues in sea urchin embryos. Homology in the C-terminal domain is less clear-cut as in calf thymus H1, alanine + lysine + proline make up 80% of the residues. As there is considerable replacement of lysine by arginine and of alanine by serine in avian H5, some major restructuring is clearly possible in the C-terminal domain. It is clear, however, that the central, conserved sequences correspond closely with the protected peptides of calf H1, chicken H5 and sea urchin sperm H1, and homologous peptides of ~80 residues are obtained from all three proteins.

Three structural domains of H1 are therefore defined and this view of the molecule is shown in idealized form in Fig. 1. What, then, is the function and spacial arrangement of these three domains of H1 in the structure of chromatin?

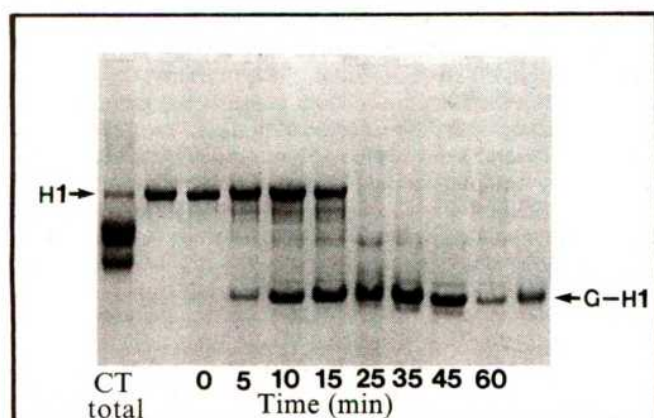
## Experimental approaches to the location and function of H1

H1 has been implicated in chromatin condensation<sup>13-17</sup>. We have tested this function by preparing oligonucleosomes depleted of lysine-rich histone<sup>18</sup>. To this were reassociated peptides of H1 and the sedimentation coefficient of the reconstituted material compared with a control reconstituted with intact H1. Both reassociation and sedimentation were at 80 mM NaCl, conditions in which the extended nucleofilament is almost fully compacted into the higher-order structure<sup>17</sup>. Previous results have shown<sup>19</sup> that a ratio,  $r$ , of 2 moles of intact H1 per nucleosome is required to restore the S-value of the native chromatin and above this value extensive precipitation is





**Fig. 1** *a*, Sequences of several lysine-rich histones aligned for maximum homology. The C-terminal part, consisting largely of proline, alanine and lysine (arginine in H5s), is not fully shown. Vertical dotted lines represent the proposed limits of the strongly conserved globular domain. Bold arrows indicate tryptic cutting points in free-solution digestion of histones at high ionic strength (refs 9–11 and P. Sautière and P. Puigdomenech, personal communication). Sequences are taken from the following: goose H5, chicken H5, rabbit H1 and calf H1, trout testis H1 and sea urchin sperm H1 (*Parechinus angulosus*) (refs 3, 4, 1, 2 and 5 respectively). The sea urchin embryo H1 (*Psammechinus miliaris*) sequence is from a cloned DNA fragment<sup>7</sup>. *b*, Peptides and modified protein from calf thymus histone H1 and chicken erythrocyte H5. Calf thymus H1 was extracted with 5% perchloric acid and purified on Amberlite CG-50. It was iodinated at Tyr 72 by the addition of iodine/potassium iodide at a 1:1 molar ratio of iodine to protein in 15 mM bicarbonate buffer pH 9. The degree of iodination was determined from the NMR spectrum of tyrosine in the disordered protein and found to be 0.95 (ref. 27). NMR was also used to show that the sample of modified H1 (M-H1) does not fold<sup>27</sup>. The introduction of a very bulky atom into a buried residue<sup>35</sup> of a relatively small domain is presumed to prevent folding. The peptide N-H1 was prepared by thrombin digestion of H1 (ref. 36) and purified on CM-cellulose. Identification of the fragment was by amino acid analysis (showing the absence of phenylalanine and the presence of tyrosine), by sizing on the gel (slightly smaller than histone H4 of 102 residues) and by observing the presence of the N-terminal acetyl group in the NMR spectrum. The precise C-terminal point is not established but is  $\pm 5$  residues. The NMR spectrum of the peptide at high ionic strength indicated that it did not form a folded structure<sup>36</sup>. The peptide NG-H1 was also prepared by thrombin digestion<sup>36</sup>. The observation of perturbed peaks in the NMR spectrum of NG-H1 demonstrated that the sample used here folds to form tertiary structure. This peptide is very similar to an abundant natural degradation product of H1, previously labelled 'HMG 8' (ref. 37). We have shown by NMR spectroscopy that HMG 8 contains the folding domain of H1 and is N terminal. Peptide C-H1 was likewise prepared by thrombin digestion of H1. It does not fold<sup>36</sup>. Peptide G-H1 was made by trypsin digestion of H1 in free solution<sup>9</sup> and G-H5 likewise from chicken erythrocyte H5 (ref. 10). Both samples were checked by NMR for the ability to fold. Gel electrophoresis was used to check the purity of the peptides and proteins used.



**Fig. 2** Time course of trypsin digestion of nuclei. Triton X-100-washed calf thymus nuclei were suspended at 20 °C in 0.15 M NaCl, 10 mM Tris, pH 8, at a concentration of  $\sim 2 \text{ mg ml}^{-1}$  DNA. Trypsin was added to a molar ratio of 1:500 with respect to the content of total histone. Soybean trypsin inhibitor was added to aliquots at different times and extraction was with 5% perchloric acid. After precipitation with acetone, the proteins were analysed on 15% polyacrylamide-acid/urea gels<sup>38</sup> and compared with a sample of G-H1, the globular peptide obtained from free-solution digestion of H1 (ref. 9).

observed. Peptides were therefore reconstituted at values of  $r$  up to 2 as a test for their ability to condense the stripped chromatin. As reconstitution of H1 and its peptides results in a monotonic increase in S-value to a maximum of only 1.7 times that of the stripped chromatin, it is assumed that no interparticle cross-linking occurs.

The ability of peptides to compact the nucleofilament has also been tested by observing the rate at which micrococcal nuclease digests the linker DNA between core particles. It is known that removal of H1, with consequent breakdown of the higher-order structure, leads to an 8–10-fold increase in this rate<sup>16</sup> and H1 peptides have therefore been tested for their ability to restore the protection of linker DNA against digestion.

The location of H1 has been tested by nuclease digestion to the level of the core particle monomer. It has been proposed that the primary H1 binding site lies between 140 and 160 base pairs (the best current estimates are 146 and 165 base pairs<sup>20–22</sup>) as there is a pause in nuclease digestion at 165 base pairs and most of the H1 is lost only on subsequent trimming to 146 base pairs<sup>16,23</sup>. The best 'assay' at present for the correct location of H1 is thus the protection of 165 base pairs of DNA in the so-called chromatosome<sup>22,24,25</sup>. Although digestion of native chromatin with staphylococcal nuclease does not give 100% yields of the chromatosome before 146-base pair core particles are produced, nevertheless, if H1 is absent, no protection of 165 base pairs is observed and digestion to 146 base pairs is very much quicker<sup>16</sup>. Several peptides from H1 and H5 have therefore been reconstituted onto chromatin stripped of lysine-rich histones, and micrococcal nuclease digestion used to see whether protection of 165 base pairs is observed at a level comparable to that found in native chromatin.



## Sedimentation studies

Figure 1 shows the positions of the peptides used in the intact chains of H1 and H5. Figure 3 gives sedimentation coefficients of the reconstituted chromatin relative to the stripped chromatin used for each experiment. The results can be summarized as follows: peptide N-H1 (1-98) has no influence on the sedimentation coefficient. The peptide does however bind to the stripped chromatin as it is all found in the pellet after rapid centrifugation and NMR studies have shown that the peptide H1 (1-106) binds to DNA, albeit not strongly<sup>26</sup>. Thus, an N-terminal domain that lacks the folded central domain cannot condense the nucleofilament. Both the globular fragments G-H1 (36-121) and G-H5 (22-100) produce a small increase in S-value, but much below that of intact H1 or H5. If the N-terminal and globular domains are present together, as in the peptide NG-H1 (1-121), the increase in S-value is greater than for the globular domain alone but still only about half of that found for intact H1. When the other half of the molecule is reconstituted, that is, peptide C-H1 (122-213), the increase in S-value is only about one-third of that for intact H1, whereas if both peptides NG-H1 and C-H1 (representing the whole molecule) are reconstituted together the sedimentation increase is similar to that of either peptide alone. It is concluded that no single domain is capable of fulfilling the compacting role of H1, nor is a combination of the N-terminal and globular domains.

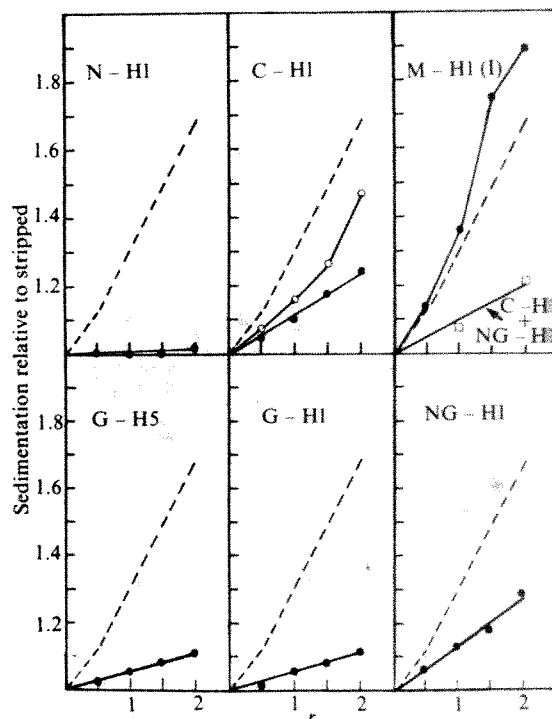
The C-terminal peptide, C-H1, when reconstituted for only 45 min, gives rise to an asymmetric sedimentation zone indicating a structurally heterogeneous sample, whereas after a 20-h incubation a symmetric zone was observed. The short incubation presumably results in irregular location of this peptide, although with time at 80 mM NaCl the peptide may find its correct location. Similar observations were made when the modified H1 (M-H1) was reconstituted, in that an increasingly asymmetric zone was observed as  $r$  was raised. Although at  $r = 2$  the native S-value was restored, with M-H1 the asymmetric peak was of reduced area due to loss of rapidly sedimenting material. Increased incubation time, moreover, did not yield a symmetric sedimentation peak. It is concluded that nonspecific interaction occurs between M-H1 and the stripped chromatin that involves some cross-linking between nucleofilaments and also between incorrect sites on a single nucleofilament.

## Digestion of linker DNA

Native chicken erythrocyte chromatin, or stripped chromatin reconstituted with intact calf thymus H1 or with H5 at  $r = 2$ , is about 10 times more resistant to cleavage within linker DNA than is the stripped chromatin<sup>16,18</sup> (see Fig. 4a, c). Reconstitution with iodinated H1 (M-H1) resulted in linker DNA cleavage at about the same rate as in intact chromatin (Fig. 4b). In contrast, reconstituates made from each of the peptides shown in Fig. 1 had a rate of linker digestion indistinguishable from that of stripped chromatin. It seems, therefore, that only the intact molecule can compact the nucleofilament to the degree necessary for providing linker protection.

## Monomer length fragments

Figure 5a shows that when depleted chromatin is digested with 10 times the amount of nuclease used for linker digestion, the monomer particle is trimmed essentially to a uniform length of ~146 base pairs whereas if intact H1 is reconstituted an additional product of ~168 base pairs appears as with native chromatin<sup>18</sup>. If the N-terminal fragment N-H1 (1-98) is reconstituted, only a 146-base pair band is observed, whereas if NG-H1 (1-121) is used there is considerable protection of ~168 base pairs, as in the reconstitute with intact H1. This suggests that the globular domain is essential for the protection of 168 base pairs. This was confirmed by reconstitution with the globular domain alone, G-H1 (36-121); Fig. 5b shows that, at intermediate digestion times of 2-5 min, the bands corresponding to 168 and 146 base pairs are of comparable intensity, as



**Fig. 3** Sedimentation velocity measurements of reconstituted chromatin. Chicken erythrocyte nuclei were lightly digested with micrococcal nuclease to yield chromatin of 30-50 nucleosome length. This was depleted of H1 and H5 by passage over a DNA-cellulose column at 80 mM NaCl<sup>18</sup>. Proteins and peptides were reconstituted at several values of  $r$  (mol peptide per nucleosome) by direct addition at 80 mM NaCl. The S-values of reconstituates were measured in 5-20% linear sucrose gradients together with native chromatin and H1/H5-stripped chromatin in separate buckets of the same rotor (about 99S and 58S respectively). S-values of reconstituates are expressed relative to that of stripped chromatin. The broken line in each panel represents reconstitution with intact H1 (the S-value of native chromatin is reached at about  $r = 2$  (ref. 19)). Reconstituates were annealed for 45 min except for that with C-H1 which required 20 h for a reproducible result. In the experiment involving two peptides, NG-H1 was added and annealed first and the C-H1 was added subsequently.

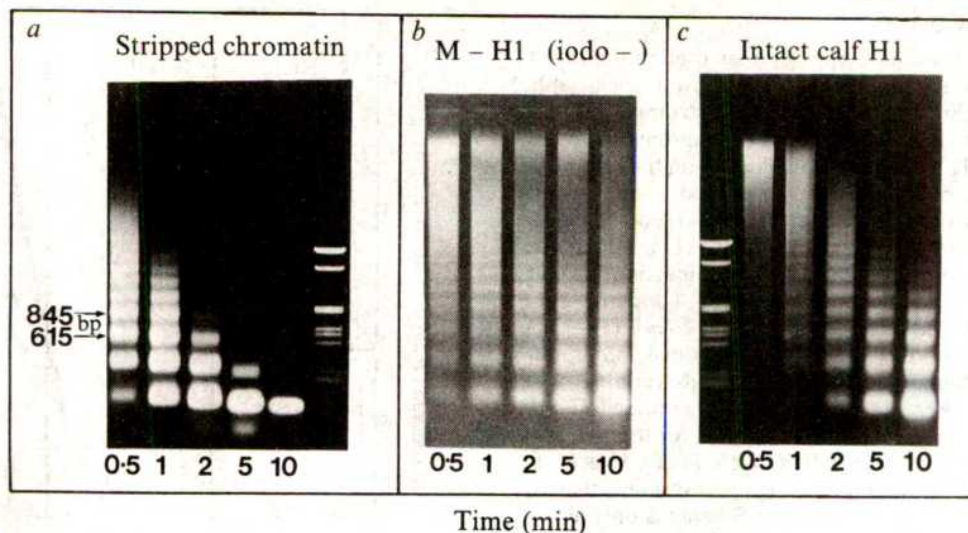
found in reconstituates with intact H1. The C-terminal half of H1 is unable to protect 168 base pairs, as shown by reconstituting with C-H1 (122-213); Fig. 5b shows no evidence of any band around 168 base pairs with this peptide. Thus, only peptides containing the central globular domain of H1 protect the 168-base pair fragment. To test that this domain must not only be present but must also be folded, a reconstitute was made with H1 iodinated at tyrosine residue 72. NMR spectroscopy has already shown that this modification is enough to prevent the molecule from folding<sup>27</sup> as the tyrosine is a buried residue. Figure 5b shows that very little protection of the 168-base pair fragment is afforded by M-H1—although there is some indication of a 10-base pair ladder at earlier digestion times (due probably to considerable compaction of the chromatin by this peptide), by 5 min there is no trace of DNA at the 168-base pair position.

The structural homology between H1 and H5 discussed above implies that the globular domain of H5 should also protect 168 base pairs. This was confirmed by reconstitution with this peptide, G-H5 (22-100). Figure 5b shows a strong and persistent band at ~168 base pairs throughout the digestion.

## Discussion

The above data indicate that: (1) a globular domain of the lysine-rich histones (~80 residues) is protected against trypsin digestion in nuclei, and (2) this domain alone can protect the



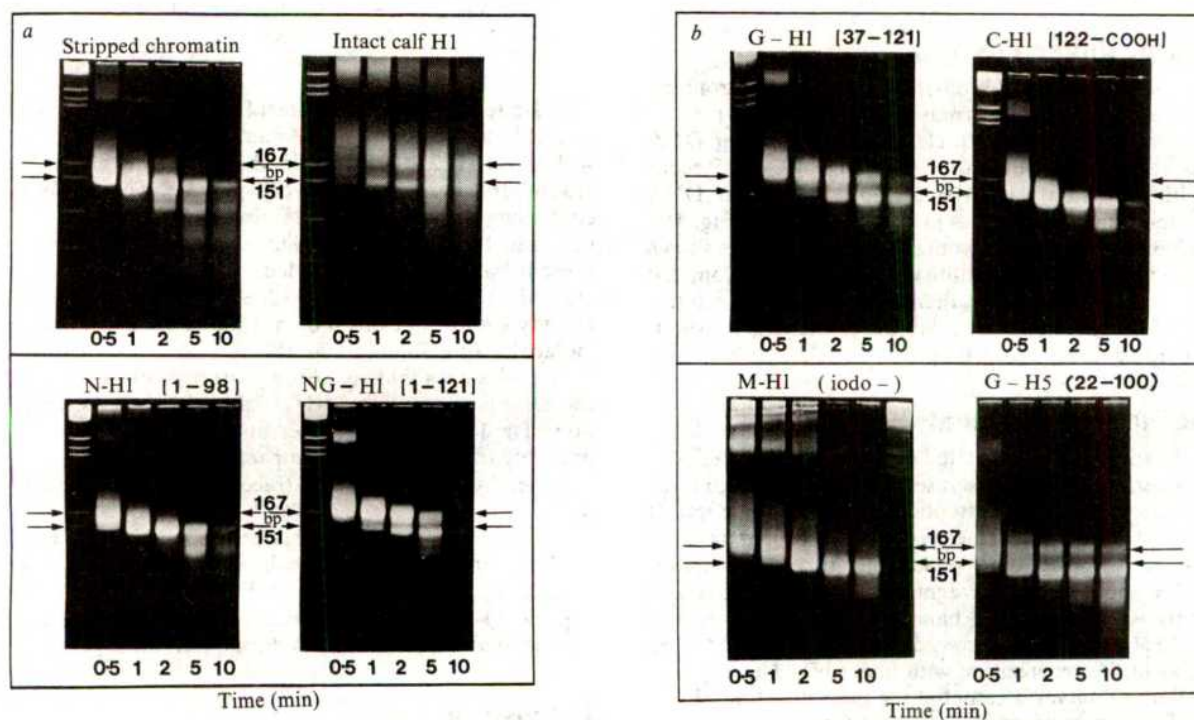


**Fig. 4** Micrococcal nuclease digestion of H1/H5-stripped chromatin and reconstitutes to show preservation of the native nucleosomal repeat and changes in the rate of digestion of linker DNA. Calibration of double-stranded DNA fragments was on 1% agarose stained with ethidium bromide using a *Hae*III digest of PM2 DNA, itself calibrated with a *Taq*I digest of  $\Phi$ X174 RF viral DNA. The DNA repeat length after stripping was  $\sim 210$  base pairs (bp). Both reconstitutes were made at 80 mM NaCl and  $r = 2$ , and the same enzyme/DNA ratio was used in all three experiments.

extra  $\sim 20$  base pairs of DNA present in the chromatosome above that in the core particle. (3) Full compaction of chromatin by H1 may require the intact molecule.

If 146 base pairs represent  $1\frac{1}{2}$  superhelical turns of DNA<sup>28</sup>, then 168 base pairs is approximately two full turns. The globular domain thus seems able to close the second integral turn of DNA. 5'-end-labelling experiments have shown that the DNA extension from core particle to chromatosome is symmetrical,  $\sim 10$  base pairs on both ends (ref. 25 and L. Lutter, personal communication), and this implies a 'symmetrical' placement of the globular domain on the 2-fold axis of the particle. Figure 6 shows a scale model of this type. Crystallographic studies of the

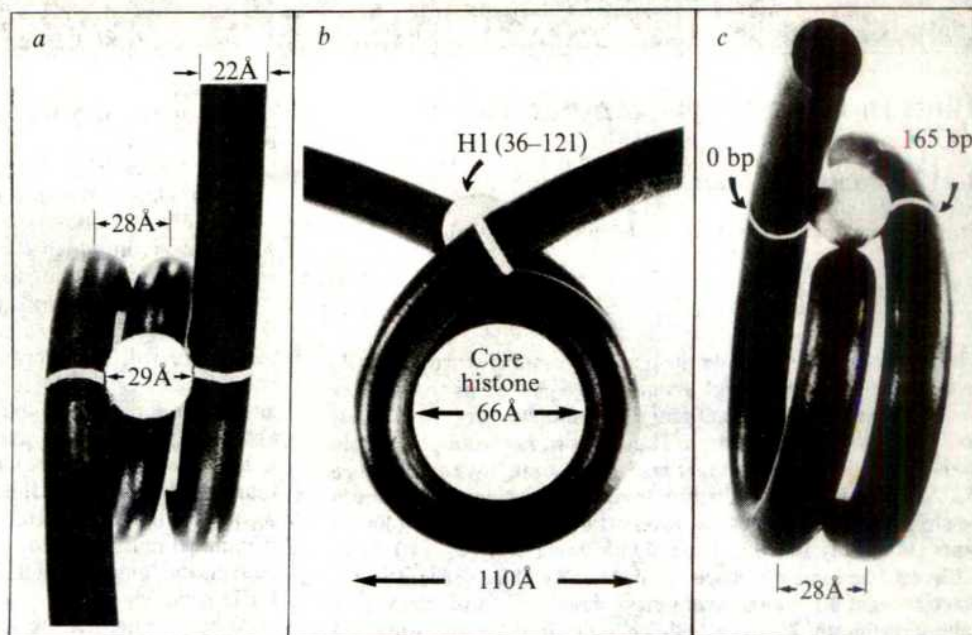
core particle have indicated that the pitch of the DNA is  $\sim 28$  Å (ref. 28) and this is therefore approximately the gap that would be left between the strands of DNA exiting from the particle. We have previously shown by neutron scattering<sup>10</sup> that the diameter of the globular domain of H5 (G-H5, residues 22–100) is 29 Å. (This is very close to the value of 27 Å calculated for a sphere of 79 residues with  $\bar{v} = 0.735$  ml g<sup>-1</sup>.) Recent low-angle neutron-scattering measurements on G-H1 also indicate an essentially spherical particle (J. P. Baldwin and H. W. E. Rattle, personal communication). The diameter of the globular domain is therefore very close to the pitch of the DNA and is thus consistent with the model shown in Fig. 6, in which a 'cage' of



**Fig. 5** Micrococcal nuclease digestion of stripped and reconstituted chromatins to study monomer-particle DNA lengths. Ten times the amount of enzyme was used as compared to Fig. 4. In all eight experiments the same enzyme to DNA ratio was used. Monomer DNA lengths were analysed on 6% polyacrylamide gels, stained with ethidium bromide. A *Hae*III digest of PM2 DNA was used as calibration. bp, Base pairs.



**Fig. 6** Proposed model for the location of the globular domain of the lysine-rich H1-type histones at the exit point of the 165-base pair chromatosome. bp, Base pairs.



three DNA strands is presented for binding of the globular domain.

This model is compatible with a number of reported observations. Singer and Singer have shown that H1 has a preference for super-helical DNA and have implicated the central region in this preference<sup>29</sup>. H1 may thus bind at a point of cross-over between DNA strands. Electron microscopy has shown<sup>17</sup> that only in the presence of H1 do the two DNA strands leave the core particle at the same point, that is, H1 is responsible for bringing the two strands together at exit point. In chromatosomes there is particularly strong cross-linking between H1 and both ends of the duplex DNA, and this contact between H1 and the DNA is on the opposite side of the DNA to that at which the core histones bind; that is, H1 is bound on the outside of the particle<sup>30</sup>. These data can therefore also be assimilated in the model proposed here.

The model in Fig. 6 is the most symmetrical that could be proposed and remembering the necessity for an asymmetric location of H1 (ref. 31) (and H1 is itself asymmetric), some comment is required. An asymmetric model in which 1 mole of H1 protects the extension of just 10 base pairs on one end of the core must be considered as this implies a second (equivalent) binding site giving protection of another 10 base pairs on the other end of the DNA. The existence of a second H1 binding site in the nucleosome has been proposed<sup>19,22</sup> and the precise stoichiometry of lysine-rich histone in chromatin is not yet

certain<sup>23,31-34</sup>. With such a model one would, however, expect that, at  $r=1$ , protection of predominantly a 156-base pair length would be observed, rather than ~168 base pairs, but this has not been found.

The data given above suggest that the primary function of the globular domain is to locate H1 in chromatin by closing the core particle into the chromatosome. This would be expected to involve some increase in sedimentation coefficient (Fig. 3) but does not represent full condensation of the nucleofilament. Which of the other two domains is responsible for this function? As peptide NG-H1 (1-121), which contains both the locating and the N-terminal domains, does not result in the full condensation observed with intact H1, it is concluded that the N-terminal domain is not the main agent. A fundamental structural role for the N-terminal domain is also inconsistent with the considerable sequence and length variability of this domain (Fig. 1), which rather suggests that it provides a functional distinction between different H1 species. The C-terminal domain therefore remains the most likely region for the condensation of the nucleofilament and the very basic and hydrophilic sequence of this domain fit it well for extended ionic interactions with the DNA. The present data suggest, however, that on its own it cannot achieve condensation and must be correctly located in the nucleofilament by the globular domain.

This work was supported in part by a Wellcome Senior Research Fellowship to J.A.

Received 17 July; accepted 8 October 1980.

1. Cole, R. D. in *The Molecular Biology of the Mammalian Genetic Apparatus* (ed. Ts'o, P.) 93 (Elsevier, Amsterdam, 1977).
2. Macleod, A. R., Wong, N. C. & Dixon, G. H. *Eur. J. Biochem.* **78**, 281-291 (1977).
3. Yaguchi, M., Roy, C. & Seligy, V. L. *Biochem. biophys. Res. Commun.* **90**, 1400-1406 (1979).
4. Briand, G. et al. *FEBS Lett.* **112**, 147-151 (1980).
5. Strickland, W. N. et al. *Eur. J. Biochem.* **104**, 567-578 (1980).
6. Smith, B. J., Walker, J. M. & Johns, E. W. *FEBS Lett.* **112**, 42-44 (1980).
7. Schaffner, W. et al. *Cell* **12**, 655-671 (1978).
8. Bradbury, E. M. et al. *Eur. J. Biochem.* **52**, 605-613 (1975).
9. Hartman, P. G., Chapman, G. E., Moss, T. & Bradbury, E. M. *Eur. J. Biochem.* **77**, 45-51 (1977).
10. Aviles, F. J., Chapman, G. E., Kneale, G. G., Crane-Robinson, C. & Bradbury, E. M. *Eur. J. Biochem.* **88**, 363-371 (1978).
11. Puigdomenech, P., Palau, J. & Crane-Robinson, C. *Eur. J. Biochem.* **104**, 263-270 (1980).
12. Yaguchi, M., Roy, C., Dove, M. & Seligy, V. *Biochem. biophys. Res. Commun.* **76**, 100-106 (1977).
13. Littau, V. C., Burdick, C. J., Allfrey, V. G. & Mirsky, A. E. *Proc. natn. Acad. Sci. U.S.A.* **54**, 1204-1212 (1965).
14. Bradbury, E. M., Carpenter, B. G. & Rattle, H. W. E. *Nature* **241**, 123-126 (1973).
15. Billett, M. A. & Barry, J. M. *Eur. J. Biochem.* **49**, 477-484 (1974).
16. Noll, M. & Kornberg, R. D. *J. molec. Biol.* **109**, 393-404 (1977).
17. Thoma, F., Koller, Th. & Klug, A. *J. Cell Biol.* **83**, 403-426 (1979).
18. Allan, J., Staynov, D. Z. & Gould, H. *Proc. natn. Acad. Sci. U.S.A.* **77**, 885-889 (1980).

19. Allan, J. et al. (in preparation).
20. Lutter, L. C. *Nucleic Acids Res.* **6**, 41-56 (1979).
21. Tatchell, K. & Van Holde, K. E. *Proc. natn. Acad. Sci. U.S.A.* **75**, 3583-3587 (1978).
22. Todd, R. D. & Garrard, W. T. *J. biol. Chem.* **254**, 3074-3083 (1979).
23. Varshavsky, A. J., Bakayev, V. V. & Georgiev, G. P. *Nucleic Acids Res.* **3**, 477-492 (1976).
24. Nelson, P. P., Albright, S. C., Wiseman, J. M. & Garrard, W. T. *J. biol. Chem.* **254**, 11751-11760 (1979).
25. Simpson, R. T. *Biochemistry* **17**, 5524-5531 (1978).
26. Bradbury, E. M., Chapman, G. E., Danby, S. E., Hartman, P. G. & Riches, P. L. *Eur. J. Biochem.* **57**, 521-528 (1975).
27. Chapman, G. E., Hartman, P. G., Cary, P. D., Bradbury, E. M. & Lee, D. R. *Eur. J. Biochem.* **86**, 35-44 (1978).
28. Finch, J. T. et al. *Nature* **269**, 29-36 (1977).
29. Singer, D. S. & Singer, M. *Nucleic Acids Res.* **3**, 2531-2547 (1976).
30. Belyavsky, A. V., Bavykin, S. G., Gogvadze, E. G. & Mirzabekov, A. D. *J. molec. Biol.* **139**, 519-536 (1980).
31. Hayashi, K., Hofstaetter, T. & Yakuwa, N. *Biochemistry* **17**, 1880-1883 (1978).
32. Olins, A. L., Carlson, R. D., Wright, E. B. & Olins, D. E. *Nucleic Acids Res.* **3**, 3271-3291 (1976).
33. Weintraub, H. *Nucleic Acids Res.* **5**, 1179-1188 (1978).
34. Goodwin, G. H., Nicholas, R. H. & Johns, E. W. *Biochem. J.* **167**, 485-488 (1977).
35. Giancotti, V., Quadrioglio, F., Cowgill, R. W. & Crane-Robinson, C. *Biochim. biophys. Acta* **624**, 60-65 (1980).
36. Chapman, G. E., Hartman, P. G. & Bradbury, E. M. *Eur. J. Biochem.* **61**, 69-75 (1976).
37. Goodwin, G. H., Walker, J. M. & Johns, E. W. *Biochim. biophys. Acta* **519**, 233-242 (1978).
38. Panyim, S. & Chalkley, R. *Archs Biochem. Biophys.* **130**, 337-346 (1969).



## LETTERS

## Photon mass at low temperature?

Joel R. Primack &amp; Marc A. Sher

Physics Department, University of California, Santa Cruz, California 95064

The theoretical observation that gauge symmetries are generally restored at sufficiently high temperature has led us to consider here the conjecture that gauge symmetries are broken at sufficiently low temperature. The photon, for example, would then acquire a non-zero mass  $m_\gamma$  below some low temperature  $T_0$ . Above this phase-transition temperature, the photon would be strictly massless. Present observational limits on the photon mass show only that  $m_\gamma$  is negligible for  $T > 2.7 \text{ K} \sim 10^{-4} \text{ eV}$ . Although we have not discovered any plausible mechanism for electromagnetic gauge-symmetry breaking and therefore cannot estimate  $T_0$  or  $m_\gamma$ , there is a considerable range of experimentally accessible low temperatures for which there are no stringent constraints on  $m_\gamma$ . Non-zero gluon or graviton masses at low temperatures could also have observable consequences.

The effects of finite temperatures in gauge theories have been studied in some detail<sup>1-3</sup>. It has been shown that, in most models<sup>2,4</sup>, the gauge symmetry is restored at high temperatures, in analogy with superconductivity. In particular, in the context of grand unified theories which unify the strong, weak and electromagnetic interactions, it is now generally agreed that as we go backwards in time to the earliest moments of the big bang, as the temperature  $T$  increases, first the electro-weak  $SU(2) \times U(1)$  gauge symmetry is restored for  $T > T_1 \approx 10^2 \text{ GeV}$  and then the grand unified symmetry is restored for  $T > T_2 \approx 10^{15} \text{ GeV}$  (refs 5, 6). Above  $T_1(T_2)$ , the weak vector bosons (grand unified leptok quark bosons) are strictly massless.

The most dramatic consequence of the conjecture that all gauge symmetries are broken at sufficiently low temperatures is the breakdown of the  $U(1)$  symmetry of quantum electrodynamics (QED) at some low temperature  $T_0$ . In a detailed analysis of both terrestrial and astrophysical observations, Goldhaber and Nieto<sup>7,8</sup> deduced a very small upper limit on the photon mass,  $\sim 10^{-15} \text{ eV}$ . However, all of the observations to which they refer were performed in a heat bath of at least  $2.7 \text{ K}$  ( $\sim 10^{-4} \text{ eV}$ ), the temperature of the cosmic microwave radiation; in fact, many were done at  $\sim 300 \text{ K}$ , room temperature. If the electromagnetic gauge symmetry were broken at a temperature  $T_0$ , then any experiment done at a higher temperature would be done in a  $U(1)$ -symmetric vacuum, and the photon would be exactly massless. Thus, all of the observations considered in ref. 7 only show that  $U(1)$  is an unbroken symmetry above  $2.7 \text{ K}$ —that is  $T_0 \leq 10^{-4} \text{ eV}$ .

We know of no physical mechanism through which the electromagnetic gauge invariance could break down and the photon thereby acquire a mass. Only two mechanisms for breaking a gauge symmetry in a renormalizable way have been discovered: spontaneous and dynamical symmetry breaking. In spontaneous symmetry breaking, exemplified in solid-state physics by the Landau-Ginsburg theory of superconductivity, the photon would acquire a mass through coupling to a charged Higgs scalar field  $\phi^*$  which develops a non-zero vacuum expectation value. However, as shown in ref. 3, because the Higgs field self-coupling  $\lambda$  must be  $\leq 1$  for perturbation theory to be valid, this implies that  $m_\phi \leq 10^{-1} \text{ eV}$  for  $T \sim 300 \text{ K}$ . This is certainly inconsistent with observation, because light charged particles would be pair-produced copiously. Although heavy Higgs particles with very strong self-interactions could conceivably give rise to a phase transition in QED at low temperature, this is

not amenable to perturbative analysis nor, we believe, is it plausible.

The photon cannot acquire a mass through dynamical symmetry breaking. Dynamical symmetry breaking is exemplified in non-relativistic solid-state physics by the BCS theory of superconductivity, in which the photon acquires a mass (Meissner effect) through coupling to Cooper pairs. In relativistic dynamical symmetry breaking<sup>9</sup>, the gauge particle acquires a mass through its coupling to a bound state of a fermion-antifermion pair. This will not work for the photon because of charge conjugation ( $C$ ). A Higgs-type scalar bound state of a fermion-antifermion pair must have even  $C$  and thus could not be absorbed by the odd- $C$  photon to give the photon mass—unless  $C$  is broken in the phase transition. Stern<sup>10</sup> has also pointed out that in a massless field theory in which the coupling constant is within the domain of attraction of an IR-stable origin, there is no dynamical mass generation. Although this condition is met by conventional massless QED, its extension to finite temperature QED is not clear.

Although neither spontaneous nor dynamical symmetry breaking can give rise to a photon mass at low temperature, we regard the conjecture that gauge symmetries are broken at low temperature as sufficiently interesting to warrant experimental test, especially in view of the relative ease of such tests. The main drawback of the lack of an explicit mechanism is that we cannot estimate  $T_0$  or the photon mass,  $m_\gamma$ . The only insight we can offer on  $T_0$  is the observation that  $T \sim 1 \text{ K} \sim 10^{-4} \text{ eV}$  is about as far below the electro-weak phase transition ( $T_1 \sim 10^{11} \text{ eV}$ ) as the grand unified phase transition ( $T_2 \sim 10^{24} \text{ eV}$ ) is above it—in the logarithmic sense, relevant for the renormalization group analyses which determine  $T_1$  and  $T_2$ . Both symmetry-breaking models and physical plausibility suggest that  $m_\gamma \sim T_0$  ( $T_0$  is the only mass scale available). Lacking a specific model, we can offer no insight into the order of the phase transition; in a first (second)-order transition, the photon mass will change discontinuously (continuously) from zero as the system is cooled.

There would be many observable consequences if  $U(1)_{\text{em}}$  were broken below  $T_0$  and the photon acquired a mass  $m_\gamma$ ; we will mention two. The Poisson equation for the electrostatic potential  $V$  acquires an extra mass term

$$(\nabla^2 + m_\gamma^2)V(\mathbf{r}) = -\rho(\mathbf{r}).$$

Then the potential difference between a charged conducting sphere and an inner conducting sphere insulated from the outer one will be<sup>7</sup>

$$\frac{\Delta V}{V} = \frac{1}{2} m_\gamma^2 (a^2 - b^2) + O(m_\gamma^4 a^4)$$

where  $a$  and  $b$  are the radii of the outer and inner spheres. (Generally<sup>7</sup> the effect of  $m_\gamma$  on a system of size  $a$  is  $O(m_\gamma a^2)$ .) This effect could be detected by connecting the inner and outer spheres briefly to allow charge to flow while the system is at low temperature, and later measuring the charge on the inner sphere. A very accurate measurement of  $\Delta V$  would set stringent limits on  $m_\gamma$ , but would not be necessary to detect  $m_\gamma \sim T_0$ . A second way of detecting  $m_\gamma$  would be to measure the resonant frequencies of a superconducting cavity as a function of temperature.

Another consequence of our conjecture is that the  $SU(3)$  gauge symmetry of the strong interactions, quantum chromodynamics (QCD), is broken at low temperature. Is it possible that Fairbank *et al.*<sup>11</sup> have been the only group to detect fractionally charged particles—quarks?—because theirs has been the only low-temperature search (N. Deshpande, personal communication)?

De Rujula *et al.*<sup>12</sup> have devised an MIT-bag model of broken QCD in which the eight  $SU(3)$  gluons get equal mass  $\mu$ , and individual free quarks would have a mass  $M \sim (2\pi\alpha'\mu)^{-1}$  where

$\alpha' = 0.88 \text{ GeV}^{-2}$  is the Regge slope. Their model involves three triplets of coloured Higgs scalars, and  $\mu$  is a function of the parameters of the Higgs self-coupling potential, including the effects of gluon loops<sup>12,13</sup>. In view of the experimental lower limit on  $M$  of several GeV, they must consider  $\mu < 10 \text{ MeV}$ . (They do not discuss the behaviour of their theory as a function of temperature, although the phase transition restoring the colour gauge symmetry would be at temperatures that might be reached in extreme stellar states.)

In the model of De Rújula *et al.* there seems to be no reason why  $\mu$  could not be very small, say  $\sim 10^{-4} \text{ eV}$ . This would exemplify our conjecture: the SU(3) colour gauge symmetry would then be broken at low temperature but restored at high temperature. However, the physical consequences would at first sight seem to be negligible: although free quarks could exist, they would have large mass because of the large size  $V \sim \mu^{-1}$  of their associated colour-confining bags. The only way that light, fractionally charged particles could exist in this model would be apparently for quarks to form colourless bound states with the colour-triplet Higgs scalars. But then we do not know why this would not also happen in the unbroken phase. In any case, this is only a model—perhaps colour symmetry is broken dynamically rather than spontaneously at low temperature. As with QED, in the absence of definitive theoretical analysis we regard the low-temperature behaviour of QCD as uncertain and subject to experimental test. Other possible effects to look for at low temperature besides free quarks are slight shifts in nuclear energy levels. Unlike QED, the effects of QCD symmetry breaking at low temperature might be extremely subtle or even essentially undetectable.

Does our conjecture apply to gravitation? Although the graviton is in a limited sense a gauge particle, with the Lorentz group as the gauge group, it does not (except in non-einsteinian formulations<sup>14,15</sup>) have Yang–Mills dynamics. While several authors<sup>16,17</sup> have recently considered spontaneous symmetry breaking in the context of gravitation, their objective has been to obtain the gravitational coupling constant  $G$  through a scalar field with a nonvanishing vacuum expectation value, rather than to give the graviton a mass at low temperature. The possibility of the graviton having a non-zero rest mass at 2.7 K has been ruled out<sup>18</sup>. It would be possible in principle to observe a graviton mass experimentally, for example, by measuring the force at low temperature on a mass suspended between two unequal masses at a distance such that the force would vanish if the force law were exactly  $r^{-2}$ . If the graviton acquired a mass below some temperature which the universe eventually reaches as it expands, the cosmological consequences would obviously be profound.

One major difficulty with detecting a QCD or gravitational phase transition at low temperature should be emphasized. For a QCD phase transition to occur, it would be necessary for the coloured particles to come to thermal equilibrium with the heat bath. It is not clear that this could happen on a reasonable time scale. Because the gravitational coupling is so weak, it is even more doubtful that equilibrium could be established even on a cosmological time scale. In the case of QED, however, the presence of, for example, a charged Higgs field would lead to rapid equilibration with a photon heat bath.

We note that the simplest test of our conjecture is the measurement of the photon mass at low temperature. A positive result in such an experiment would have important consequences. One could study gauge theory symmetry breaking and phase transitions in the laboratory, the transfer of energy from the gauge boson rest mass to a cosmological constant and vice versa (that is, the apparent creation of energy discussed in ref. 3), a region of space with a different cosmological constant than in our Universe, and so on. We can offer no explanation for  $U(1)_{\text{em}}$  breaking at a low temperature, and there is also no clue as to the value of  $T_0$ . Nonetheless, we have proposed simple experiments which would at least lower the upper limit on the  $U(1)_{\text{em}}$ -breaking phase-transition temperature by a few orders of magnitude.

We thank N. Deshpande, D. Dorfan, T. Goldman, A. Guth, P. Langacker, K. T. Mahanthappa, B. Rosenblum, D. Toussaint and D. Unger, for useful discussions. This work was supported in part by the NSF.

Received 4 September; accepted 28 October 1980.

1. Dolan, L. & Jackiw, R. *Phys. Rev. D* **9**, 3320–3341 (1974).
2. Weinberg, S. *Phys. Rev. D* **9**, 3357–3378 (1974).
3. Linde, A. D. *Phys. Rep.* **42**, 389–435 (1979).
4. Mohapatra, R. N. & Senjanovic, G. *Phys. Rev. Lett.* **42**, 1651–1654 (1979).
5. Georgi, H. & Glashow, S. *Phys. Rev. Lett.* **32**, 438–440 (1974).
6. Langacker, P. *SLAC Preprint (SLAC-PUB-2544, 1980)*.
7. Goldhaber, A. S. & Nieto, M. N. *Rev. Mod. Phys.* **43**, 277–296 (1971).
8. Davis, L., Goldhaber, A. S. & Nieto, M. N. *Phys. Rev. Lett.* **35**, 1402–1405 (1975).
9. Pagels, H. *Phys. Rev. D* **21**, 2336–2347 (1980).
10. Stern, R. *Phys. Rev. D* **14**, 2081–2089 (1976).
11. LaRue, G. S., Fairbank, W. M. & Phillips, J. D. *Phys. Rev. Lett.* **42**, 142–145 (1979).
12. De Rújula, A., Giles, R. C. & Jaffe, R. L. *Phys. Rev. D* **17**, 285–301 (1978); *D* **22**, 227–228 (1980).
13. Georgi, H. *Phys. Rev. D* **22**, 225–226 (1980).
14. Yang, C. N. *Phys. Rev. Lett.* **33**, 445–447 (1974).
15. Fairchild, E. *Phys. Rev. D* **16**, 2438–2447 (1977).
16. Zee, A. *Phys. Rev. Lett.* **42**, 417–421 (1979); **44**, 703–706 (1980).
17. Smolin, L. *Nucl. Phys. B* **160**, 253–268 (1979).
18. Ford, L. H. & Van Dam, H. *Nucl. Phys. B* **169**, 126–136 (1980).

## A study of PSR1237 + 25 at 430 MHz

T. H. Hankins

National Astronomy and Ionosphere Center, Arecibo Observatory, Arecibo, Puerto Rico 00612

G. A. E. Wright

Sonderforschungsbereich: Radioastronomie, Astronomische Institute der Universität Bonn, Auf dem Hügel 71, FRG

PSR1237 + 25, one of the first pulsars to be discovered<sup>1,2</sup>, is characterized by a striking five-peaked integrated intensity profile. Like many other pulsars, PSR1237 + 25 also exhibits the puzzling phenomena of drifting subpulses, 'nulling' and 'mode-switching'. The period of pulsation is 1.38 s, but the radio-emission occurs within an 80 ms interval. We have analysed single-pulse data from this pulsar at 430 MHz to throw light on the still obscure mechanism of pulsar emission. We conclude that the behaviour of PSR1237 + 25 can be explained on the polar-cap model if regular short (S) bursts spiralling in towards the magnetic pole are occasionally interrupted by long (L) bursts along the magnetic axis.

PSR1237 + 25 is nearby (at an estimated distance of 300 pc) and also bright (with a peak flux of 100 Jy at 430 MHz). Despite the complexity of the intensity profile, the position angle remains virtually constant during each pulse. Assuming that the radiation's plane of polarization maintains a fixed angle to the magnetic field lines, this observation is consistent with a model whereby a set of open dipolar field lines surrounding a magnetic pole is being swept perpendicularly across our line-of-sight<sup>3</sup>. Within the framework of this model the instant at which the magnetic pole is pointing directly towards us is given by the longitude at which the linear polarization disappears. We shall adopt this longitude, shown on Fig. 1 as the 'centre' of the profile.

The four principal intensity peaks (1, 2, 4, 5) of the profile can then be ordered in terms of their decreasing displacement,  $r$ , from the central longitude. The sequence obtained is  $r_1, r_5, r_2, r_4$ . The intensities  $I_1, I_5, I_2, I_4$  of the peaks follow the same sequence. Although not apparent in the time resolution of our observations (1.5 ms), component 3 may consist<sup>4</sup> of two closely-separated intensity peaks 3a and 3b.

The fluctuation spectrum of PSR1237 + 25 reveals two distinct features<sup>5</sup>. The first of these is a well-defined periodicity present in the first and fifth components and is  $\sim 2.8$  times the pulsar rotation period,  $P$  (it has been shown<sup>6</sup> that the spectra of different blocks of data show this feature to split into 2 or 3 slightly separated components). The second spectral feature is confined to the third component and is less well-defined, suggesting that it is not indicative of a strict periodicity, but



rather of a more generalized modulation time scale. This time scale is  $\sim 40P$ , or  $\sim 15$  times longer than the first feature. Component 2 may have a weak  $2.8P$ -feature, but component 4 shows no evidence of periodicity.

To see how the individual pulses give rise to these features, we have examined  $>2,000$  consecutive pulses, a typical section of which are shown in Fig. 2. The pulses have been normalized to their peak intensity with the absolute value of the peak given in flux units adjacent to each pulse; this emphasizes the changing morphology of the pulses. The periodicity of approximately three rotation periods is apparent in the first and fifth components, but in general the activity in these components is out of phase, with a peak in 1 preceding that in 5 by one period<sup>6</sup>. There is also evidence<sup>6</sup> of a lesser tendency that activity in component 2 is weak when component 1 is strong, and similarly 4 tends to be weak when 5 is strong. The result of these fluctuations is typically a cycle of approximately three periods. On average, the intensity of the first component exceeds that of the fifth component in the subsequent pulse, while in the third pulse the intensity is considerably reduced and confined to the central components. The cycle then recommences in the first component. The burst-like nature of this sequence will be referred to as an S-burst. A burst begins in the first component and subsequently subsides through the components 1-5-2-4 with the third component either quiescent or closing the burst weakly. Because the bursts last slightly less than three periods (in fact  $2.8P$ ), we gradually see them at different phases.

The simplest interpretation of these observations is that with every rotation of the neutron star the observer's beam diametrically intersects the trajectory of the S-burst in the magnetosphere, and that this trajectory is a spiral (Fig. 3). Although our choice for its sense is arbitrary, clearly the burst must begin in such a way that it first intersects the path of the observer's beam at the longitude of the first component. It then proceeds to describe a spiral with diminishing intensity through the components 5, 2, 4 and, possibly, 3a and 3b. It is also clear from inspection of the individual pulses (see Fig. 2) that in any given pulse emission is often simultaneously present in several components, suggesting that as it moves towards the centre the burst becomes linearly extended along its trajectory.

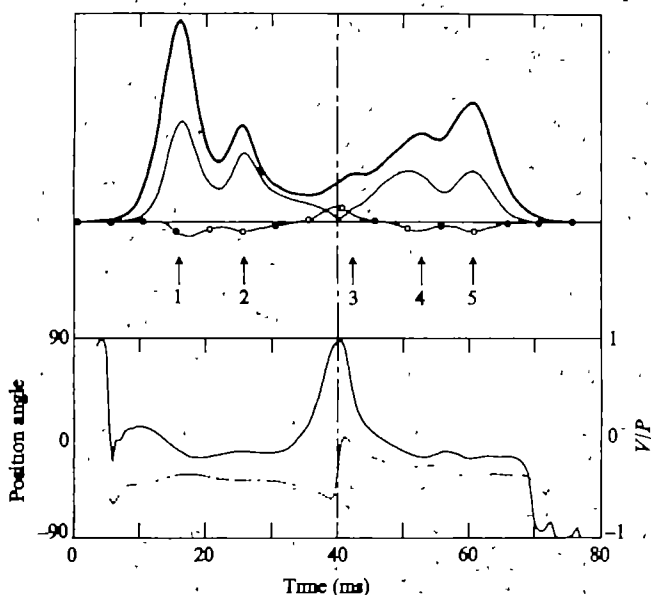


Fig. 1 Integrated polarization profile of 1,593 pulses at 430 MHz, showing the five labelled pulse components. Linear and circular polarization are shown by a light line and a line with small circles, respectively. The linear polarization angle is depicted by the dotted line and the ratio  $V/P$  where  $P = (Q^2 + U^2 + V^2)^{1/2}$  is shown by the lower light line. The 'central' longitude is chosen as the point where linear polarization is a minimum, circular is a maximum, and the position angle is discontinuous.

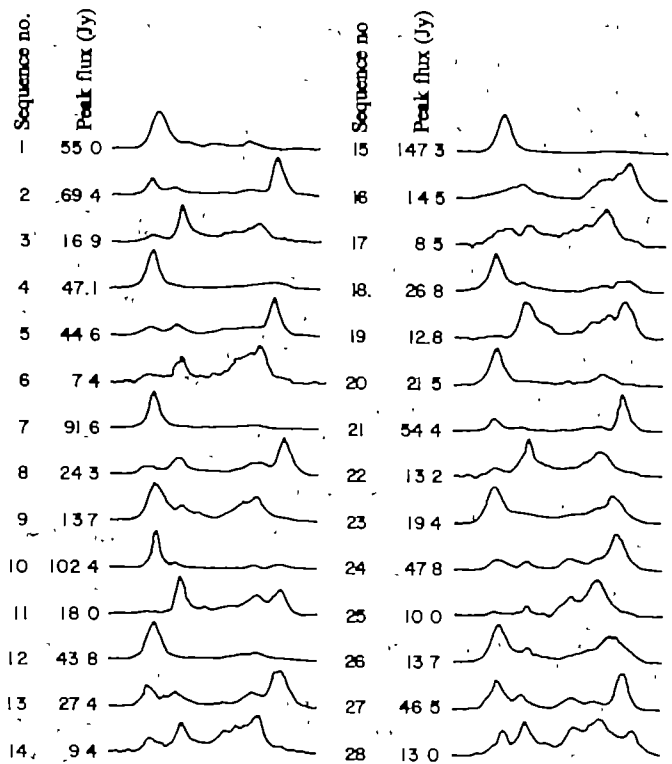


Fig. 2 28 consecutive pulses showing 10 complete S-bursts

Frequently, the burst recommences in component 1 before the previous burst has completely faded from the central components.

Interpreting the succession of the four principal components (1, 5, 2, 4) as successive increases in angular units of  $\pi$  ( $0, \pi, 2\pi, 3\pi$ ), we have plotted in Fig. 4 the natural logarithm of the components' displacements from the central longitude against this angle ( $r$  being normalized by  $r_1$ ). The result is approximately a straight line. This suggests that the burst moves along a logarithmic (or equiangular) spiral whose radius decreases exponentially with angle. Such spirals are described by the equation  $r = r_1 \exp(-\theta \cot \alpha)$ .

Two of the geometric properties of this spiral are of interest: first, its tangent (and hence the trajectory of the burst) makes a constant angle  $\alpha$  with the radius vector. Second, the intersections of any radius vector with successive turns of the spiral form a geometric progression whose common ratio  $k$  is related to the angle  $\alpha$  by  $k = \exp(2\pi \cot \alpha)$ . The straight line in Fig. 4, to which the peaks of the profile closely conform, implies a spiral with  $k \approx 1.62$  and a corresponding angle  $\alpha = 85.5^\circ$ . It may only be coincidence that equiangular spirals are also formed by the shells of *Nautilus Pompilius*<sup>7,8</sup> and other gastropods,  $85^\circ$  being a typical value for their determining angle.

The S-bursts do not, however, repeat indefinitely. At irregular intervals of  $\sim 40$  pulses (or 15 S-bursts) independent activity begins close to the central longitude of the profile (in the third component). This is sometimes, though not always, accompanied by 'nulling', whereby no emission is detected above the noise level ( $0.5$  Jy) for several successive pulses. Among the 2,100 pulses we have inspected there are 22 stretches of sustained nulls (that is, no emission was detected in two or more consecutive pulses, implying that the intrinsic lifetime of the nulls was at least a full rotation period). In every case, the pulses following the nulls showed activity in the third component and in 40% of the cases the nulls were also preceded by such activity (a third component-null association was also noted in the early work of Backer<sup>1</sup>). These 'eruptions' in the third component will be referred to as L-bursts.

Is the  $2.8P$  periodicity 'remembered' during an L-burst so that the S-bursts restart in phase? The splitting of the  $2.8P$  line in the fluctuation spectrum, referred to earlier<sup>2</sup>, is what would be expected of the phase were 'forgotten'. The phase may be lost

during every L-burst or, less frequently, during a null sequence. The amount of splitting would, therefore, depend on the number of L-bursts or nulls included in the data blocks. It may be possible to examine this hypothesis by eliminating nulls and/or L-bursts from the data and re-determining the fluctuation spectrum. This might bring the S-bursts back into phase and make the 2.8P feature free of splitting and broadening. This effect has already been found<sup>11</sup> in PSR0809+74, a pulsar of similar age and period, where nulls occasionally interrupt a highly regular subpulse drift: the nulls sever the drift-bands so that only by removing them from the data is the continuity of the drift restored.

In common with PSR0329+54 and possibly other pulsars, PSR1237+25 switches occasionally into an 'abnormal' mode<sup>2,12-14</sup>, whereby the emission pattern is radically changed. Only one example of this mode occurred in our data, lasting 74 pulses, but unfortunately at a time when interstellar scintillation weakened the definition of the pulses. There is considerable similarity between abnormal mode activity and that observed during the L-bursts. The mode is characterized by sustained activity in the third component and by changes in the longitude of the outer components. No S-burst periodicity can be seen, and we can again only suggest that their repetition has either become irregular or now has a time scale comparable to the rotation period. At our observing frequency (430 MHz) the components in the left hand of the profile are considerably stronger than those on the right: a feature which may be the result of longitudinally-dependent propagation effects.

The polar cap model<sup>15-18</sup> is still the only model which offers a physical explanation for the drift behaviour of sub-pulses. It postulates the existence of a 100-m diameter cap surrounding the magnetic pole on the neutron star's surface, whose outer limits are determined by the last magnetic field lines to close within the light-cylinder. Above the cap a gap of height 100 m forms, in which strong electric fields are maintained both parallel and perpendicular to the magnetic field. Within this volume  $\gamma$  rays with sufficient photon momentum perpendicular to the magnetic field (originating either from the hot surface or

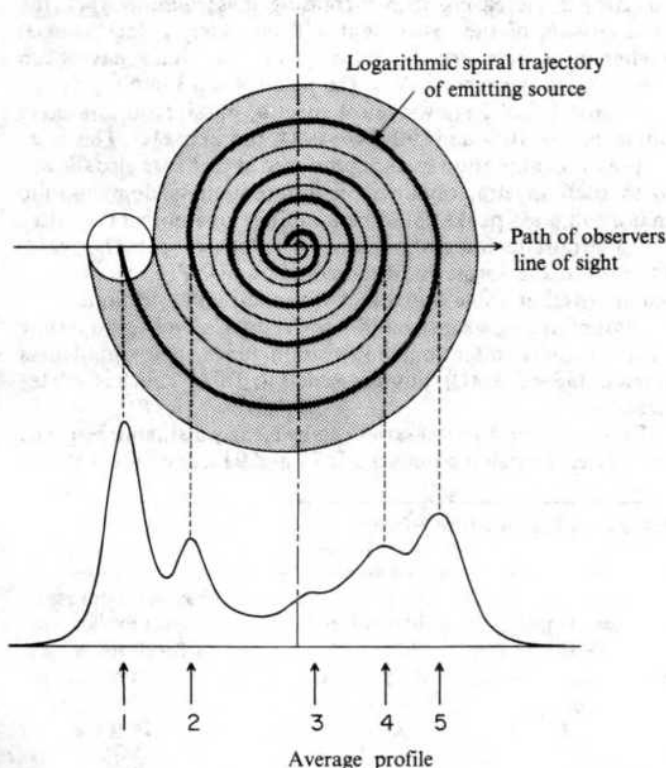


Fig. 3 The proposed spiral path of the S-burst around the magnetic pole and its relation to the observed intensity peaks. The path of the observer's line of sight is shown passing directly over the magnetic pole.

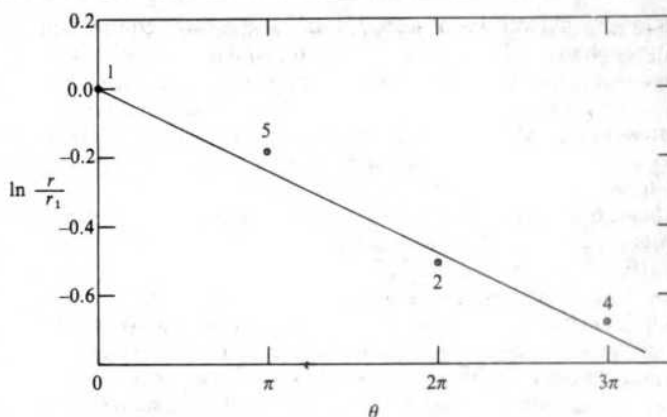


Fig. 4 Plot of  $\ln(r/r_1)$  against  $\theta$ . The straight line corresponds to a logarithmic spiral with a common ratio of  $k = 1.62$ .

from strongly-accelerated particles) generate cascades of electron-positron pairs. These particles are accelerated outwards and, following further pair-creation, excite two-stream instabilities which generate the observed coherent radiation in the upper magnetosphere ( $10^7$ – $10^8$  cm above the cap in the most recent version<sup>17</sup> of the model).

Ruderman and Sutherland<sup>16</sup> have suggested that the drift of sparks around the magnetic pole is the consequence of deviation in the local electric field from its 'force-free' value. The sparks are likely to arise near the edges of the cap where the field-line curvature is largest (and, therefore, where the probability of pair-creation is greatest<sup>19</sup>). Assuming the trajectories to be circles, they arrive at the expression  $5.6B_{12}/P^2$  for the circulation period of the single spark region in units of  $P$  ( $B_{12}$  being the magnetic field strength in  $10^{12}$  G). Inserting the appropriate parameters for PSR1237+25 we obtain a value of  $2.9P$  for the drift period, in close agreement with the observed periodicity of  $2.8P$  for the S-bursts. Ruderman and Sutherland do not discuss the possibility of non-circular drifting, but for an  $85.5^\circ$  spiral the inward radial velocity will only be a fraction  $\cot 85.5^\circ = 0.08$  of the tangential velocity and so in a sense only a second-order effect. No obvious explanation is available for the radial drift: possibly the sparking region, having circumscribed the pole is then for some reason inhibited from repeating its trajectory and moves to an inner radius. Note that a spark following the spiral of Fig. 3 would exploit the entire surface of the cap. Alternatively, we might argue that the presence of the spark will itself distort the electric potential from its axisymmetric form (as pointed out by Jones<sup>18</sup>). There is then no reason to expect the drift trajectory to be perpendicular to the radius. It is also difficult to explain why the inner radius of the sparking region does not move to the pole within milliseconds if the cascade mechanism described by Sturrock<sup>15</sup> is operating. Radial confinement of the spark may be more easily achieved if pair-creation is being sustained by the 'photon splash'<sup>17,18</sup> of  $\gamma$  rays from the surface of the cap.

The simultaneous appearance of the S-bursts in several components suggests that the burst becomes linearly extended along its path. This would occur, for example, if a spark of finite angular size were to drift along a spiral with an angular velocity which increased towards its centre. Constant lateral drift velocity is one, but not the only, possibility. The angular velocity would then increase proportionately with each turn.

The behaviour of the L-bursts cannot be explained on any current theory. Their association with nulling and their modulating effect on the S-bursts suggest that an understanding of their role is crucial. Possibly the S-bursts represent charging and L-bursts discharging of the neutron star. The third component of PSR1237+25 may require a separate physical explanation<sup>10,14</sup>. Perhaps this is a hint as to why in most pulsars nulls interrupt the pulse trains in such an apparently random way<sup>20</sup>: if PSR1237+25 were viewed from any angle other than that which contains the magnetic axis, then the subpulse drift and the



nulling would still be observed, but not the third component. Although a null involves the entire polar cap, its causal mechanism may be confined to the centre and, therefore, seldom seen. Interestingly, in several pulsars Backer<sup>5</sup> has found modulations of typically 100 periods in addition to the short-term drift periodicities. Their possible connection with nulls does not seem to have been investigated.

Multiply-peaked integrated profiles are not uncommon among pulsars<sup>10</sup>, often with asymmetrically distributed peaks. PSR0329+54 and PSR2045-16 are perhaps the best and brightest examples. Intriguingly the binary pulsar<sup>21</sup>, whose individual pulses are too faint to detect, has also an asymmetric triple peak profile. It would, however, be rash to extend the present model to other pulsars without further investigation. The pulsars still have much to teach us, and have hidden their secrets well.

We thank N. Bartel, W. Fawley, L. Fowler, D. Morris and W. Sieber for helpful discussions, and J. M. Rankin for development of the polarization measurement and reduction system at Arecibo. G.A.E.W. thanks the Sonderforschungsbereich: Radioastronomie for support. Much of this work was done while T.H.H. was visiting Max-Planck Institute for Radioastronomy supported by a fellowship from the Alexander von Humboldt Stiftung.

Received 21 July; accepted 20 October 1980.

1. Backer, D. C. *Nature* **228**, 752 (1970).
2. Backer, D. C. *Nature* **228**, 1295 (1970).
3. Radhakrishnan, V. & Cooke, D. J. *Astrophys. Lett.* **3**, 225 (1969).
4. Backer, D. C. thesis, Cornell Univ. (1972).
5. Backer, D. C. *Astrophys. J.* **182**, 245 (1973).
6. Taylor, J. H., Manchester, R. N. & Huguenin, G. R. *Astrophys. J.* **195**, 513 (1975).
7. Lockwood, E. H. *A Book of Curves* (Cambridge University Press, 1961).
8. Thompson, D. W. *On Growth and Form* (Cambridge University Press, 1971).
9. Kahn, P. G. K. & Pompea, S. M. *Nature* **275**, 606 (1978).
10. Backer, D. C. *Astrophys. J.* **209**, 895 (1976).
11. Unwin, S. C., Readhead, A. C. S., Wilkinson, P. N. & Ewing, M. S. *Mon. Not. R. astr. Soc.* **182**, 711 (1978).
12. Lyne, A. G. *Mon. Not. R. astr. Soc.* **153**, 27P (1971).
13. Morris, D., Sieber, N., Ferguson, D. C. & Bartel, N. *Astr. Astrophys.* (in the press).
14. Oster, L. & Sieber, W. *Astr. Astrophys.* **58**, 303 (1977).
15. Sturrock, P. A. *Astrophys. J.* **164**, 529 (1971).
16. Ruderman, M. A. & Sutherland, P. *Astrophys. J.* **196**, 51 (1975).
17. Cheng, A. F. & Ruderman, M. A. *Astrophys. J.* **235**, 576 (1980).
18. Jones, P. B. *Mon. Not. R. astr. Soc.* **184**, 807 (1978).
19. Erber, T. *Rev. Mod. Phys.* **38**, 626 (1966).
20. Richtings, R. T. *Mon. Not. R. astr. Soc.* **176**, 249 (1976).
21. Taylor, J. H., Fowler, L. A. & McCulloch, P. M. *Nature* **277**, 437 (1979).

## Unambiguous mass determination of major stratospheric positive ions

E. Arijs, D. Nevejans & J. Ingels

Belgian Institute for Space Aeronomy, Ringlaan 3, B-1180 Brussels, Belgium

There has been recent considerable interest in the stratospheric ion composition and ion chemistry, especially in view of its possible impact on aerosol formation<sup>1,2</sup> and the possibility of detection of minor constituents with very low concentrations<sup>3,4</sup>. The first composition measurements of positive ions in the stratosphere conducted by a rocket-borne instrument<sup>5</sup>, revealed the existence of the theoretically predicted proton hydrates (PH)<sup>6</sup> and also of some unexpected non-proton hydrates (NPH). (Proton hydrates are primarily ions of the form  $H^+(H_2O)_n$ ). Because low altitude rocket data may be biased by shock wave effects, such as ion fragmentation, the need for balloon flights was strongly felt. In 1978, data obtained with balloon-borne instruments<sup>7-9</sup> partly confirmed and extended the rocket data. There have been several explanations<sup>1,5,7,8,10</sup> of the presence of the observed NPH, but the lack of resolution of the data means an ambiguity still exists about the exact masses of these ions. We report here the first high resolution mass spectra of positive ions in the stratosphere, at 34-km altitude, where the major mass peaks can be identified unambiguously.

The data were obtained with a balloon-borne mass spectrometer, flown on 16 June 1980 with a 100,000 m<sup>3</sup> stratospheric balloon at mid-latitude (CNES launching base at Gap-Tallard, France, 44°33'N). The instrument was launched at 20.38 UT and reached float altitude (34 km) at 22.50 UT, time at which the measurements were started. The flight lasted 8 h and thus mass spectra were obtained in both night-time and day-time conditions. Both positive and negative ions were observed. All measurements were performed at float altitude.

We concentrate here on the masses of the most abundant positive ions during night-time. The data on negative ions will be reported elsewhere.

The instrument primarily consists of a high speed cryopump, described in detail elsewhere<sup>11</sup>, in which a quadrupole mass filter is built and of the associated electronics. The stratospheric ions are sampled through a small orifice (0.2 mm diameter), drilled into a thin stainless steel flange, which can be biased with respect to the gondola (draw-in potential). They are focused into the quadrupole by an electrostatic lens. After mass filtering they reach a high gain electron multiplier, the signals of which are treated by pulse counting techniques. Between the inlet aperture and the mass filter an electron impact ion source is incorporated into the lens system. It can be put on and off by remote control and enables us to analyse the residual gas in the cryopump. Simultaneously a gas mixture of argon, krypton and xenon is injected into the mass spectrometer and an in-flight mass scale calibration is performed, using the well known mass numbers of the different Ar-Kr-Xe isotopes.

The mass spectrometer covers the mass range 0-330 AMU (at high resolution) and is microprocessor controlled. This produces a very flexible system. Several modes of operation can be called on, such as positive ion sampling, negative ion sampling and the neutral or calibration mode. The mass spectra are scanned either with a constant resolution or with a constant peak width. Most of the data for positive ions were obtained with a constant peak width ( $\Delta m$ ) of 0.9 AMU at FWHM. A higher resolution setting implies a lower transmission of the quadrupole mass filter<sup>12</sup>. Because in the constant peak width mode the resolution ( $m/\Delta m$ ) is increasing with increasing mass number ( $m$ ), the transmission of the instrument will be strongly decreased at higher mass numbers. Therefore very few counts have been observed above mass 119 in the positive ion sampling mode.

Figures 1 and 2 show typical spectra, obtained in the mass domains 50-106 and 90-146 AMU respectively. The corresponding calibration spectra produced in flight are also shown. With such spectra, obtained in different mass domains, the major ion mass peaks could be identified unambiguously after the appropriate integration time. The observed mass peaks, fitting into the formerly observed PH and NPH schemes are summarized in Table 1 together with their identification.

Mass 60 is a minor peak and is not shown in Fig. 1. It has only been observed after long integration times in a small mass domain (53-63 AMU), but it is added to Table 1 for completeness.

From Table 1, two ion series can be clearly distinguished. The first series, containing masses 55, 73 and 91 can be identified as

**Table 1** Major observed positive ion mass peaks during night-time at 34 km

| Mass number (AMU) | Identification<br>X = 41 AMU | Observed count rate<br>(mean value<br>counts per s) |
|-------------------|------------------------------|---|
| 55                | $H_3O^+(H_2O)_2$             | 3.7   |
| 60                | $HX^+(H_2O)$                 |   |
| 73                | $H_3O^+(H_2O)_3$             | 20.0  |
| 78                | $HX^+(H_2O)_2$               | 5.7   |
| 91                | $H_3O^+(H_2O)_4$             | 1.9   |
| 96                | $HX^+(H_2O)_3$               | 30.0  |
| 101               | $HX^+X(H_2O)$                | 2.4   |
| 114               | $HX^+(H_2O)_4$               | 0.6   |
| 119               | $HX^+X(H_2O)_2$              | 3.3   |

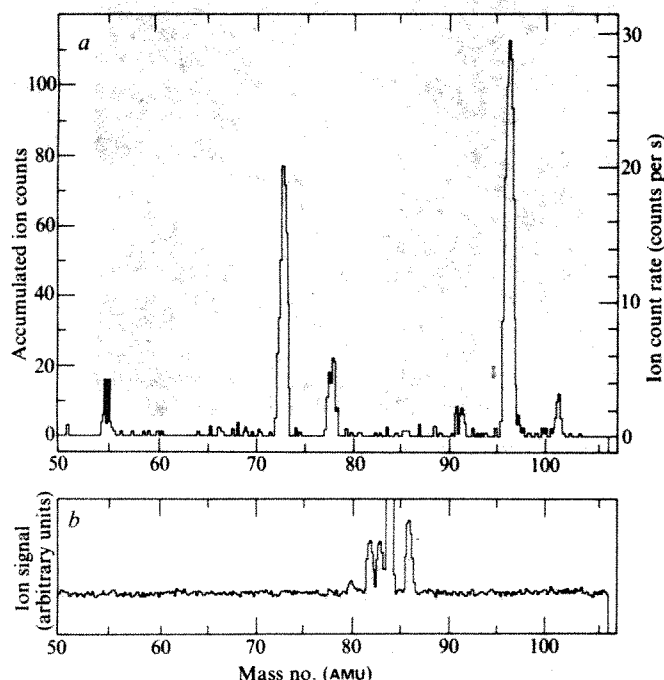
PH with the general formula  $\text{H}_3\text{O}^+ \cdot n\text{H}_2\text{O}$ . As can be expected from the thermochemical data on water ion clustering<sup>13,14</sup> mass 73 is the most abundant peak among the PH. The existence of major masses, fitting the formula  $\text{NH}_4^+ \cdot n\text{NH}_3 \cdot m\text{H}_2\text{O}$  can now be excluded from the present high resolution spectra. This confirms the conclusions about  $\text{NH}_3$  playing no significant part in the stratospheric ion chemistry at 34 km altitude<sup>8</sup>.

A second distinct ion sequence is the one containing masses 60, 78, 96, 114 and 119 AMU. It is generally accepted that these ions are the result of a reaction of the PH with an unknown trace gas X. As was suggested by the Heidelberg group<sup>8</sup> the formula of these NPH has the general form  $\text{XH}^+ \cdot n\text{X} \cdot m\text{H}_2\text{O}$ . Up to now, however, there has been ambiguity about the exact mass number of X and the best information available so far was  $41 \pm 1$  AMU.

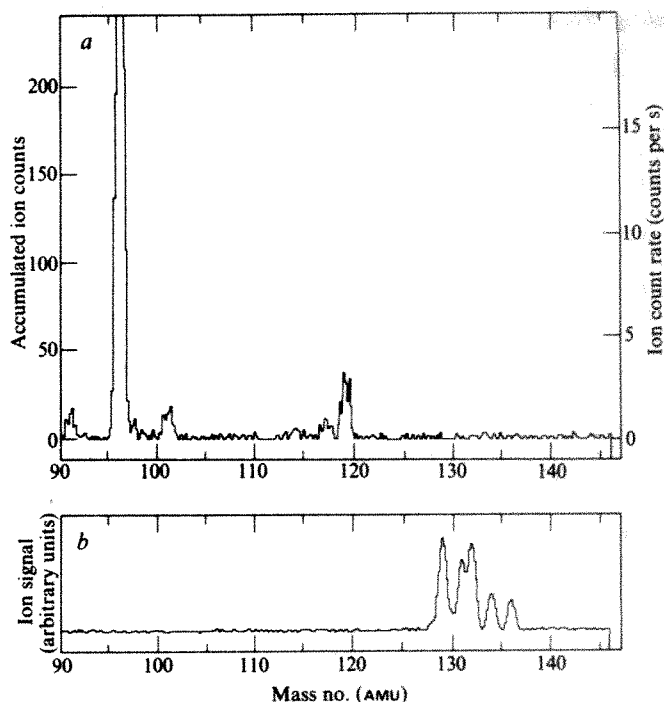
Although Arnold *et al.*<sup>5</sup> at first proposed that formaldehyde was responsible for the presence of NPH in the stratosphere, this theory was rejected after laboratory measurements<sup>15</sup>. More recently, these authors<sup>8</sup> concluded from the measured relative abundances of the PH and NPH that X must have a number density of the order of  $10^5 \text{ cm}^{-3}$  at 36 km and a proton affinity larger than  $175 \text{ kcal mol}^{-1}$ . Consequently they suggested  $\text{CH}_3\text{CN}$  (acetonitrile) as a possible candidate for X.

The fact that no formation mechanism for  $\text{CH}_3\text{CN}$  in the stratosphere was known led Ferguson to the NaOH proposal<sup>1</sup>. The existence of the sodium layer in the atmosphere<sup>16</sup> made this hypothesis quite plausible. The proposal even received support from model calculations<sup>17</sup> and laboratory work<sup>18</sup>. Recently, however, attention has been drawn to some loss mechanisms for NaOH in the stratosphere<sup>10</sup> and MgOH was suggested as a new candidate for X. However, the exact mass, as well as the identity of X has remained an open question.

The most important conclusion, which can be drawn immediately from our data, is that the mass number of the so far unknown molecule X is 41 AMU. Although mass 42 ( $\text{HX}^+$ ) has not been observed, the presence of mass 101 and 119 can only be explained by putting the mass of  $\text{X} = 41$  AMU. The conclusion rules out the hypothesis of X being NaOH (at least during night-time). The other suggestion that X might be solely MgOH is very unlikely. Actually if this were the case, one should



**Fig. 1** *a*, Typical pre-sunrise spectrum obtained in the mass region 50–106 AMU after 14 scans. Each mass unit is divided into six channels. Dwell time per channel, 0.25 s. Duration of one scan, 84 s;  $\Delta m = 0.9$  AMU FWHM. *b*, In-flight calibration obtained in the same mass domain with krypton isotopes. Only one scan is performed here.



**Fig. 2** *a*, Night-time spectrum in the mass region 90–146 AMU. Number of scans is 42. Programmed  $\Delta m = 0.9$  AMU. Real  $\Delta m$  is larger in this domain. *b*, Mass scale calibration performed in flight in the same mass domain with xenon isotopes. Result of one scan.

measure a count rate at masses 97 and 98 of  $\sim 13\%$  of that observed at mass 96, due to the isotopic abundances of  $^{25}\text{Mg}$  and  $^{26}\text{Mg}$ . This is, as Fig. 1 shows, not the case. Nevertheless, the possibility of a small contribution of MgOH to the NPH peaks cannot be ruled out completely; this will have to await high resolution data with large accumulated ion count numbers.

Most of the NPH peaks originate from a molecule with mass 41, different from MgOH. So far the most likely candidate for this molecule seems to be acetonitrile ( $\text{CH}_3\text{CN}$ ), which has a higher proton affinity than water (187.4 kcal compared with 168.9 kcal for  $\text{H}_2\text{O}$ ) (ref. 19) as well as a higher dipole moment (3.92 db compared with 1.85 db for  $\text{H}_2\text{O}$ ) (ref. 20). Although no production mechanism is known for  $\text{CH}_3\text{CN}$  in the stratosphere only a very low concentration ( $10^5 \text{ cm}^{-3}$ ) is required to explain the conversion from PH to NPH. In this framework a critical investigation of some neutral reactions, such as those of active nitrogen (especially in excited states), which can be produced by cosmic rays<sup>21</sup>, with  $\text{CH}_4$ , as well as ion molecule reactions of  $\text{N}^+$  and  $\text{N}_3^+$  with  $\text{CH}_4$  (ref. 22) might be useful to look for a possible source of  $\text{CH}_3\text{CN}$  in the stratosphere. Furthermore the possibility that  $\text{CH}_3\text{CN}$  (which has been observed in interstellar clouds)<sup>23</sup> originates from cosmic dust cannot be overlooked.

Note that no reaction rate coefficients for the ion molecule reaction of PH with  $\text{CH}_3\text{CN}$  have been published. Although they are exothermal and are, therefore, expected to have a large rate coefficient, the study of such reactions at the appropriate temperature is strongly recommended. Up to now, however, the only certain fact about X is its mass number and even the identification of X as acetonitrile remains speculative.

Apart from the masses listed in Table 1, a peak is observed in Fig. 2, which corresponds to 117 AMU. Although this mass can be explained by the ion  $\text{NaOH}_2^+ \cdot \text{NaOH} \cdot 2\text{H}_2\text{O}$ , it is very unlikely that it originates from NaOH because at night the other peaks of the series  $\text{NaOH}_2^+ \cdot n\text{NaOH} \cdot m\text{H}_2\text{O}$  are not observed. It is, therefore, more probable that this peak belongs to a third series  $\text{YH}^+ \cdot n\text{Y} \cdot m\text{H}_2\text{O}$ . The analysis of the minor peaks indicates the existence of other members of this family. However, a more detailed analysis of the present data, as well as high resolution mass spectra with long integration times are needed to identify this series.



Finally, note that the present data are only representative of the night-time ion chemistry at 34-km altitude and that more *in situ* measurements are needed to generalize the conclusions.

We thank the technical staff of the Belgian Institute for Aeronomy and the CNES for the enthusiastic cooperation during the realization of the instrument and the balloon flight. We are also indebted to the NFWO (Belgian National Science Foundation) for partly financing this project.

Received 26 August; accepted 27 October 1980.

1. Ferguson, E. E. *Geophys. Res. Lett.* **5**, 1035-1038 (1978).
2. Arnold, F. *Nature* **284**, 610-611 (1980).
3. Arnold, F. & Fabian, R. *Nature* **283**, 55-57 (1980).
4. Arnold, F., Fabian, R., Henschen, G. & Joos, W. *Planet. Space Sci.* **28**, 681-685 (1980).
5. Arnold, F., Krankowsky, D. & Marien, K. H. *Nature* **267**, 30-32 (1977).
6. Ferguson, E. E. in *The Natural Stratosphere of 1974* (CIAP Monogr. **1**, 5.42-5.54, 1974).
7. Arijis, E., Ingels, J. & Nevejans, D. *Nature* **271**, 642-644 (1978).
8. Arnold, F., Bohringer, H. & Henschen, G. *Geophys. Res. Lett.* **5**, 654-656 (1978).
9. Olsen, J. R. *et al. Rev. Sci. Instrum.* **49**, 643-649 (1978).
10. Murad, E. & Swider, W. *Geophys. Res. Lett.* **6**, 929-932 (1979).
11. Ingels, J., Arijis, E., Nevejans, D., Forth, H. J. & Schaefer, G. *Rev. Sci. Instrum.* **49**, 782-784 (1978).
12. Dawson, P. H. *Quadrupole Mass Spectrometry and its Applications*, 142 (Elsevier, Amsterdam, 1976).
13. Kebarle, P., Searles, S. K., Zolla, A., Scarborough, J. & Arshadi, M. *J. Am. chem. Soc.* **89**, 6393-6399 (1967).
14. Mohnen, V. A. *Pure appl. Geophys.* **84**, 141-153 (1971).
15. Fehsenfeld, F. C., Dotan, I., Albritton, D. L., Howard, C. J. & Ferguson, E. E. *J. geophys. Res.* **83**, 1333-1336 (1978).
16. Megie, C., Bos, F., Blamont, J. E. & Chanin, M. L. *Planet. Space Sci.* **26**, 27-35 (1978).
17. Liu, S. C. & Reid, G. C. *Geophys. Res. Lett.* **6**, 283-286 (1979).
18. Arnold, F. in *Proc. 6th ESA-PAC Symp. on European Rocket and Balloon Programmes*, Bournemouth, 479-496 (1980).
19. Yamdagni, R. & Kebarle, P. *J. Am. chem. Soc.* **98**, 1320-1324 (1976).
20. Nelson, R. D., Lide, D. R. & Maryott, A. A. in *Handbook of Chemistry and Physics*, E-51 and E-52 (Chemical Rubber, 1972).
21. Nicolet, M. *Planet. Space Sci.* **23**, 637-647 (1975).
22. Smith, D., Adams, N. G. & Miller, T. M. *J. chem. Phys.* **69**, 308-317 (1978).
23. Solomon, P. M., Jefferts, K. B., Penzias, A. A. & Wilson, J. W. *Astrophys. J. Lett.* **168**, L107-110 (1971).

## Carbon deposition on metallic surfaces studied by r.f. plasma discharge

J. A. Cairns, J. P. Coad, E. W. T. Richards  
& I. A. Stenhouse

AERE Harwell, Didcot, Oxfordshire OX11 0RA, UK

The accumulation of carbonaceous deposits on surfaces exposed to gases containing hydrocarbons or carbon monoxide is an undesirable phenomenon which can cause contamination of, for example, steel containment vessels and catalyst surfaces. It has been found<sup>1</sup> to occur also in certain conditions on the steel fuel pins of the Advanced Gas Cooled Reactor (AGR). Although in this instance it can be prevented by controlling the coolant composition, there is a strong motivation to understand the basic mechanisms involved. We show here, principally by means of a radio-frequency (r.f.) plasma-discharge system incorporating spectrographic analysis, that the deposits are formed largely as a result of the catalytic activities of the exposed surfaces (even here in the presence of highly ionized gases) and that deposition can be prevented by suitable coatings. These findings have now been confirmed by in-reactor experiments.

Whenever hydrocarbon molecules come into contact with metal surfaces, they exhibit a finite tendency to deposit carbonaceous material. This tendency depends on the chemical nature of the hydrocarbon. (For example, unsaturated molecules are particularly prone to such behaviour.) One example of this effect is the tendency for carbonaceous material to deposit on to the surfaces of the stainless steel fuel pins in an AGR. These fuel pins, which are manufactured from 20%Cr/25%Ni/Nb stabilized steel (20/25/Nb steel) are designed to operate within a temperature range 350-750°C and be subjected to a coolant

which consists mainly of CO<sub>2</sub>, but also contains significant concentrations of CO (a few per cent) and CH<sub>4</sub> (a few hundred p.p.m. by volume). The latter component was specified to suppress any tendency for the CO<sub>2</sub> to oxidize the graphite moderator<sup>2</sup>. Although carbonaceous deposition can be prevented in practice by choosing specific levels of CO and CH<sub>4</sub> additions, it remains important to understand the basic reasons for its formation. The environment within which these events take place, namely the core of a nuclear reactor, renders direct observation very difficult, and subsequent examination of steel specimens exposed to the reactor flux is complicated by their induced radioactivity.

We have subjected specimens of the steel to an r.f. plasma discharge of a CO<sub>2</sub>/CH<sub>4</sub> gas, thereby providing an irradiation environment free from the problems of induced radioactivity. It then becomes possible to compare in laboratory conditions the amounts of carbonaceous material deposited on the steel to that deposited on other surfaces, particularly copper, which has been observed<sup>3</sup> to remain clean in reactor conditions.

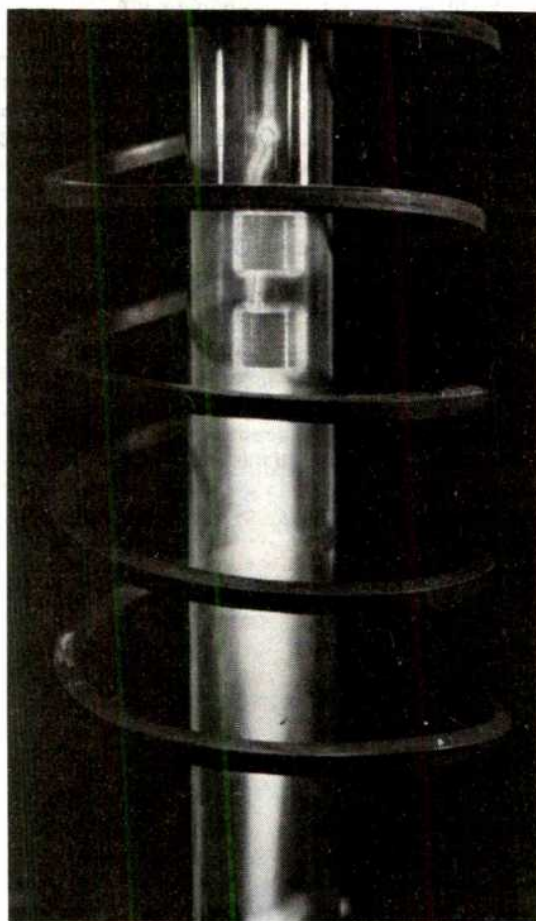


Fig. 1 Experimental arrangement showing specimens suspended in a CH<sub>4</sub>/CO<sub>2</sub> r.f. plasma discharge.

Figure 1 shows the r.f. equipment in operation. Sections of AGR 20/25/Nb steel tubing (15-mm diameter) were mounted in the middle of a silica tube, surrounded by flowing gas at a pressure of 4.7 mbar and subjected to a r.f. plasma discharge (2kV; 2.5 MHz). The gas used was an equivolume CO<sub>2</sub>/CH<sub>4</sub> mixture. This methane level is, of course, much higher than that present in an AGR but it was necessary here to counteract the enhanced oxidative capacity of the CO<sub>2</sub> induced by the intense field. In spite of this, the main effects observed previously in AGR were reproduced. Thus the steel acquired a significant deposit of carbon (0.2-0.5 mg cm<sup>-2</sup>) after 4 h, whereas speci-



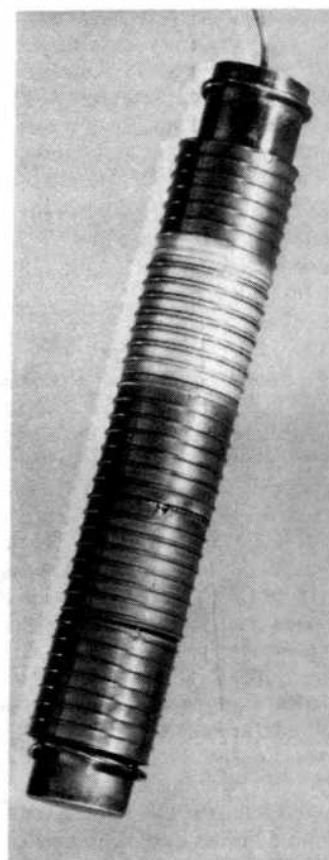
mens of copper mounted alongside the steel remained essentially clean. Incidentally the carbon was measured by combustion in a Leco CS 144 carbon/sulphur analyser and determined as  $\text{CO}_2$  using IR detection.

The above measurements on copper and steel indicate a clear influence of the surface chemistry of the steel in promoting deposition. To nullify this surface activity and thereby suppress the deposition, the steel was coated with a silica layer (1–2- $\mu\text{m}$  thick). A convenient method is to contact the steel with a silica sol, which on heating (to 850 °C for 15 min) densifies to form a dense, protective silica coating<sup>4</sup>. The result was dramatic: the silica-coated steel remained clean throughout its exposure to the  $\text{CO}_2/\text{CH}_4$  discharge, as may be confirmed from Fig. 2 which shows also that nearby uncoated steel specimens acquired carbonaceous deposits. These visual observations were supplemented by carbon analysis, which confirmed that the silica-coated specimen had acquired a negligible amount of deposit. We now consider why the silica-coated specimen remained uncontaminated: was it due to carbonaceous material being removed dynamically with enhanced efficiency throughout the exposure, or was it due to the fact that the silica surface was unable to induce deposition from its surrounding gas, even in the presence of the ionizing environment? The answer can be found by a spectroscopic examination of the light emitted from the plasma, particularly in the vicinity of the specimens.

Light emitted from a 5-cm long section of the discharge was imaged on to the slit of a Hilger medium quartz spectrograph. It was thereby possible to compare the relative emission intensities of individual spectral lines to the region from which they arose in the plasma. Identification of spectral lines and variations in these, as compared with a standard  $\text{CO}_2$  discharge, was done using a Hilger projection comparator. A comparison between some of the species present in the vicinity of a 20/25/Nb steel surface and a corresponding silica-coated specimen, during exposure to an equivolume  $\text{CO}_2/\text{CH}_4$  discharge, is shown in Table 1.

When the gas remote from the sample was examined for these species, it was found to contain principally  $\text{CH}$ ,  $\text{H}$  and  $\text{CO}^+$ , although the signal strengths were lower than in the highly ionized region near the specimens. Of particular interest are the strong signals in the vicinity of the uncoated steel of  $\text{CO}^+$  and  $\text{O}_2^+$ . Both of these were very weak or not detected in the bulk of the plasma or, as seen from Table 1, in the vicinity of the coated steel. Therefore it may be deduced that methane tends to suppress  $\text{O}_2^+$  by gas-phase interaction. It seems reasonable to suggest further that methane is removed dynamically in the vicinity of the uncoated steel (hence the reappearance of  $\text{O}_2^+$ ), being converted under the catalytic influence of the steel's surface to a carbonaceous deposit. This in turn is subject to attack by the oxidizing species, thereby accounting, at least partly, for the appearance there of the strong  $\text{CO}^+$  signal. The lack of carbonaceous deposition on to the silica-coated steel specimen can be understood also: the silica surface, being free from sites which catalyse deposition, remains essentially clean and so there is little  $\text{CO}^+$  production. The  $\text{O}_2^+$  signal is low because the local concentration of methane is retained.

Therefore, the results suggest that carbonaceous deposition on to the steel surface is induced largely by the catalytic activity



**Fig. 2** The reduction in carbonaceous deposition exhibited by a silica-coated steel tube section as compared with nearby, uncoated specimens.

of the surface itself. Surfaces such as silica remain clean because they do not intervene to alter the gas composition in their immediate environment.

The r.f. plasma-discharge system used here has not only highlighted the importance of coatings to prevent carbonaceous deposition, but may be used also to screen suitable coatings for in-reactor assessment. The best coatings identified by this screening have been confirmed to perform well in nuclear reactor conditions.

Finally, there is much scientific literature on the nature of species formed as a result of ionization of  $\text{CO}_2$  and of  $\text{CO}_2/\text{CH}_4$  (ref. 5). However, the main difference between those studies and the present one is that here we emphasize the influence of surfaces, and particularly the 20/25/Nb steel surface in promoting carbonaceous deposition. We cannot be certain that the species identified here at low pressure will exist in that form at AGR pressures and, of course, the composition of the plasma gas examined here differs substantially from that of a genuine AGR coolant. We can conclude, however, that the success in reproducing some of the more significant gas–solid interactions indicates a general validity to the conclusions which have been reached so far.

We thank J. B. Sayers, R. H. Flowers, J. Wright, R. A. Dugdale, J. S. Hislop, C. J. Wood, D. Norfolk, P. Campion, S. J. Thomson and D. Clark for useful discussions, and P. S. Drew and C. F. Ayres for technical assistance.

Received 11 July; accepted 30 October 1980.

1. Wood, C. J. *Nucl. Engng* **22**, 29 (1977).
2. Wright, J., Dominey, D. A., Jacquiss, M. T., Linacre, J. K. & Lind, R. *Proc. 4th Int. Conf. on Peaceful Uses of Atomic Energy* **10**, 415 (1971).
3. Bennett, M. J. *et al.* in *Gas Chemistry in Nuclear Reactors and Large Industrial Plant* (ed. Dyer, A.) 81 (Heyden, London, 1980).
4. Cairns, J. A., Nelson, R. L. & Woodhead, J. L. U.K. Patent Publ. No. 2023453 A (1980).
5. Whickham, A. J., Best, J. V. & Wood, C. J. *Radiat. Phys. Chem.* **10**, 107 (1977).

**Table 1** Comparison of species in the vicinity of 20/25/Nb steel with a silica-coated specimen

| Species         | Wavelength (nm) | 20/25/Nb steel | Silica-coated 20/25/Nb steel |
|-----------------|-----------------|----------------|------------------------------|
| $\text{CO}^+$   | 219–270         | Strong         | Very weak                    |
| $\text{O}_2^+$  | 283.3           | Strong         | Not detected                 |
| $\text{CO}_2^+$ | 288.3–289.6     | Very strong    | Strong                       |
| $\text{CH}$     | 387.2–431.5     | Very strong    | Very strong                  |
| $\text{C}_2$    | 400–440         | Weak           | Weak                         |
| $\text{H}$      | 434–486         | Strong         | Weak                         |



## Generation of light hydrocarbons in sedimentary rocks

J. M. Hunt\*, A. Y. Huc† & J. K. Whelan\*

\* Woods Hole Oceanographic Institution, Woods Hole, Massachusetts 02543

† Laboratoire de Géologie Appliquée, CNRS-ERA 601, Université d'Orléans, 45046 Orléans Cedex, France

Most petroleum arises from the thermal alteration of organic matter in fine-grained sedimentary rocks. The time-temperature conditions of petroleum formation have been defined by numerous laboratory and field studies<sup>1</sup>, but little is known of the conditions in which individual hydrocarbons form in nature. The light hydrocarbons are of particular interest because they are present only in traces in surface sediments, yet they constitute about 30% of a typical petroleum. We have found that the distribution of individual  $C_6$ – $C_8$  hydrocarbons in shale samples from a Gulf of Mexico well indicates that different types of structures are being generated preferentially at different depths. Hydrocarbons with a tertiary carbon atom apparently formed earlier than those with a quaternary carbon because of the greater stability of the intermediate tertiary carbonium ion or free radical.

The samples analysed were well cuttings from a Coastal Offshore Stratigraphic Test (COST) well drilled by a consortium of oil companies about 50 miles east of South Padre Island, off south Texas in the Gulf of Mexico. The cuttings were washed, canned at the well site and kept refrigerated. At the laboratory the drilling mud was washed from the cuttings before analysis.

The  $C_6$ – $C_8$  hydrocarbons were analysed by a headspace method involving the grinding of the cuttings in a closed container and release of the entrained gases in a helium headspace<sup>2</sup>. The gases were analysed by capillary gas chroma-

tography on a column which gives complete resolution of all the  $C_6$ – $C_7$  and part of the  $C_8$  hydrocarbons<sup>3</sup>. Individual hydrocarbons were identified from known retention times and by gas chromatography-mass spectrometry.

The samples analysed in the 4,000–13,000 feet depth interval are Upper Miocene in age whereas the samples extending down to 16,000 feet are Lower Miocene. There are a few silts and sands in the shallow part of the well, but most of the lithology is fine-grained gray shale with organic carbon contents in the range 0.75–1.3%. An over-pressured section extends from about 10,000 feet to total depth.

Figure 1 shows the distribution of total  $C_6$  and  $C_7$  saturated hydrocarbons, alkanes and cycloalkanes in ng per g of sediment. The generation curve for these hydrocarbons shows a threshold of intense generation around 10,000 feet and a peak around 13,500 feet. However, the distribution of individual hydrocarbons shows a different pattern. Figure 2 shows the distributions of two dimethylbutanes and two dimethylpentanes. The differences in these structures is that the 2,2-isomers contain a single quaternary carbon atom and no tertiary carbon atoms, whereas the 2,3-isomers contain two tertiary carbon atoms. The latter structure for both the substituted butane and pentane shows a strong increase in concentration around 10,000 feet. At this depth the subsurface temperature is ~115°C. In contrast, the structures with a quaternary carbon atom show slight increase at 12,000 feet with the major increase around 13,500 feet equal to a subsurface temperature of about 150°C.

Figure 3 shows the hydrocarbon distributions for a  $C_7$  branched alkane and a cycloalkane both containing a tertiary carbon atom. They are compared with a  $C_8$  branched alkane containing a quaternary carbon atom. Again, the latter compound shows no significant increase in concentration before reaching the 13,500-foot depth range. The compounds with the tertiary carbon atoms show this increase at 10,000 feet.

Figure 4 shows two dimethylcyclopentanes in which the only difference is the position of the methyl groups on the ring. In the 1,1-isomer there is a quaternary carbon atom whereas in the 1,2-isomer there are two tertiary carbon atoms. The latter shows increased concentrations at 9,500 feet, the former at ~11,500 feet.

The distribution patterns of the  $C_6$ – $C_8$  hydrocarbons in this well show that there is a significant difference in the time-temperature requirements for the formation of hydrocarbons of different structure. These differences occur over the depth interval from ~10,000 to ~13,500 feet. Deposition rates for the Miocene in this well were ~1,000 feet per Myr, indicating a time differential of ~3.5 Myr and, as previously indicated, a temperature difference of 35°C for the initiation of intense generation of these different hydrocarbons.

There are several possible causes of the observed distributions: (1) a change in organic source material with depth; (2) differential migration; and (3) a change in the generation mechanism as a function of increasing depth (temperature). A change of organic source material with depth can be ruled out by the similarity of capillary gas chromatography analyses carried out on pyrolysis products generated from the organic material<sup>4</sup>. Moreover, migration cannot be the explanation. Light hydrocarbons in this range diffuse from their point of origin towards the surface<sup>5</sup> in such a way as to cause a change in hydrocarbon concentration with molecular size because of differences in diffusion coefficients—for example, between *n*-propane and *n*-hexane. However, for structural isomers such as those in Fig. 2, the quaternary isomers diffuse more rapidly than the tertiary. Neopentane diffuses more rapidly than isopentane, for example<sup>6</sup>. Thus diffusion would lead to the opposite of the observed distributions and cannot be the cause. Similarly, other possible migration mechanisms do not explain the distributions. Separation of isomers due to partial adsorption during migration, or differences in boiling point, would both cause the quaternary structures to occur at shallower depths—to migrate ahead as on a laboratory chromatographic column. Bulk transport in the gas phase might result in some density separation, but again, the

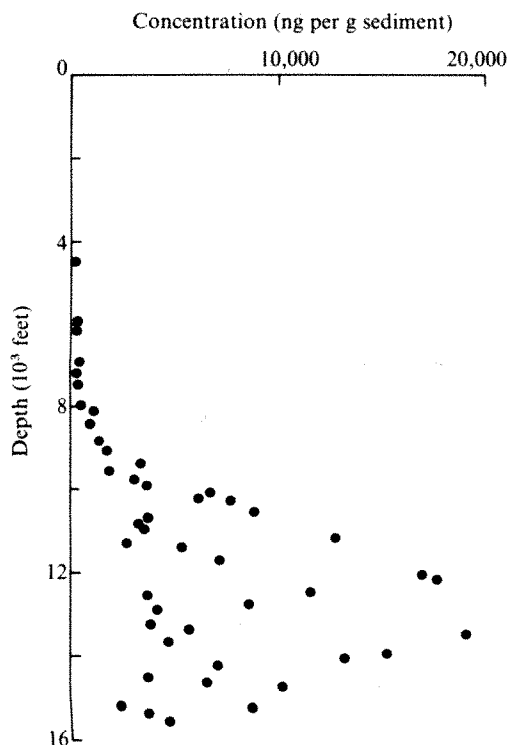
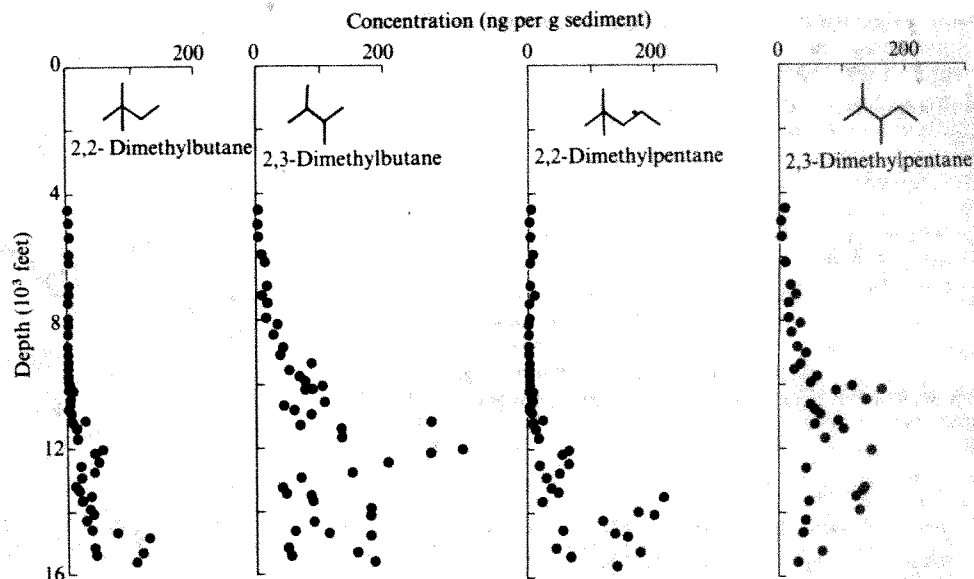


Fig. 1 Concentration plotted against depth of total  $C_6$  plus  $C_7$  saturated hydrocarbons in ng per g of dry sediment in the COST no. 1 well, Gulf of Mexico.

**Fig. 2** Concentration plotted against depth of two C<sub>6</sub> and two C<sub>7</sub> branched alkane isomers in the COST no. 1 well.



quaternary structures are the least dense and would be found shallower instead of deeper.

These arguments suggest that the generation mechanism itself must be the explanation for the profiles observed. It seems unreasonable at these low temperatures (<150 °C) to propose thermodynamic equilibrium between isomeric saturated hydrocarbons, so that we assume that the products preferentially formed at any particular depth result from whichever intermediate (carbonium ion or free-radical) forms most rapidly (kinetic control).

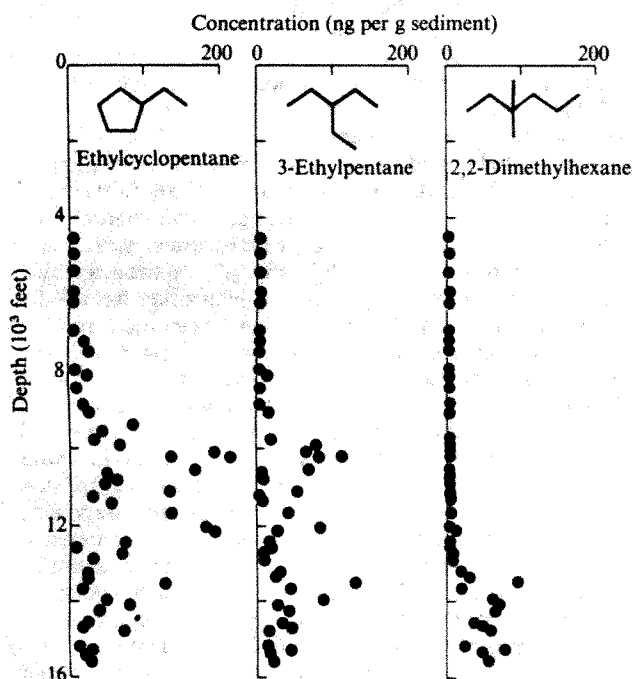
There are two major generation pathways to the observed products from kerogen. Carbonium-ion cracking dominates at lower temperatures (shallower depths) and free-radical cracking dominates at higher temperatures (ref. 1, pp. 122–130). Carbonium ions rearrange whereas free radicals do not<sup>7</sup>. Also, tertiary carbonium ions are more stable than the primary or secondary ions and the latter easily rearrange to the former<sup>7</sup>. Consequently, the increased yield of tertiary structures at 10,000 feet may be the result of intensified carbonium-ion

cracking and isomerization. Carbonium ions with quaternary structures would rapidly rearrange to tertiary products, so that no increase in quaternary hydrocarbons would be observed at this depth.

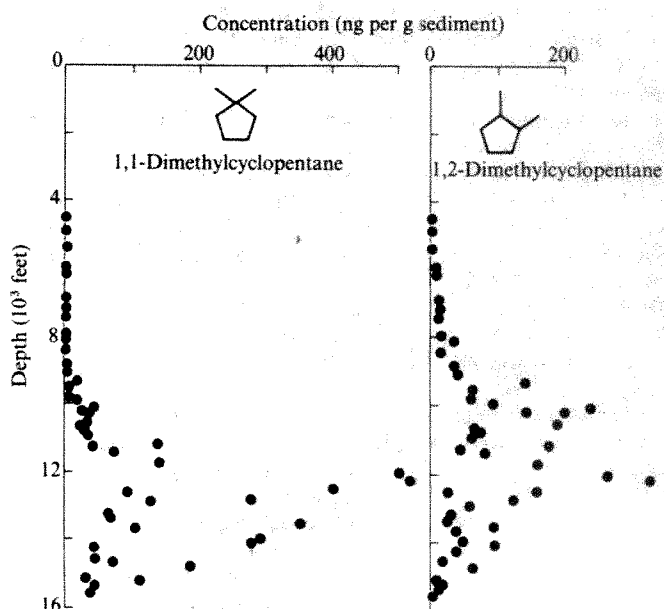
Eventually, as the sediments are buried deeper to higher temperatures, free-radical cracking takes over. This causes an increase in the yield of quaternary structures at 13,500 feet because these free radicals cannot rearrange.

The fact that the yield of tertiary structures is still high at that depth suggests either that tertiary free radicals also are cracking off or that some carbonium-ion cracking is still occurring.

Whether these structures are breaking off as free radicals in the configurations shown or are isomerization products of some carbonium-ion precursors, it is significant that the hydrocarbon content of these shale source-beds is varying substantially with depth. The composition of the C<sub>6</sub>–C<sub>8</sub> hydrocarbon mixture at 10,000 feet is quite different from that at 13,500 feet. This means that attempts to correlate crude oil composition with the hydrocarbons in a presumed source rock or to derive correlations between source rocks will need to account for the formation of different hydrocarbon structures in different time-temperature conditions.



**Fig. 3** Concentration plotted against depth of a C<sub>7</sub> cycloalkane and a C<sub>7</sub> and C<sub>8</sub> branched alkane in the COST no. 1 well.



**Fig. 4** Concentration plotted against depth of two dimethylcyclopentanes in the COST no. 1 well.



Individual hydrocarbons in the gasoline range ( $C_6$ – $C_8$ ) show a significant increase in concentration at varying depths in sedimentary rocks. Hydrocarbon structures with a tertiary carbon atom increased markedly at a subsurface depth equivalent to a time and temperature of 10 Myr and 115 °C. In contrast, structures with a quaternary carbon atom did not show a substantial increase until reaching a depth equivalent to 13.5 Myr and 150 °C. The difference in depth distribution is believed to be due to the formation of carbonium ions from the kerogen at lower temperatures than free radicals. The early-forming carbonium ions then rearrange to the stable tertiary structure. Greater energy (higher temperature) is required to crack the quaternary free-radical structures which do not rearrange.

This work was supported by the Division of Basic Energy Sciences of the US Department of Energy, contract no. EG-77-S-02-4392.

Received 9 July; accepted 21 October 1980.

1. Hunt, J. M. *Petroleum Geochemistry and Geology* 131–143 (Freeman, San Francisco, 1979).
2. Whelan, J. K., Hunt, J. M. & Berman, J. *Geochim. cosmochim. Acta* (in the press).
3. Whelan, J. K. *Init. Rep. DSDP*, 47, 531–539 (1979).
4. Huc, A. Y. & Hunt, J. M. *Geochim. cosmochim. Acta* 44, 1081–1089 (1980).
5. Leythaeuser, D., Schaefer, R. G. & Yukler, A. *Nature* 284, 522–525 (1980).
6. Sahores, J. M. & Witherspoon, P. A. *Adv. Org. Geochem.* 219–230 (1966).
7. March, J. M. *Advances in Organic Chemistry* Ch. 5 (McGraw-Hill, New York, 1968).

## Holocene phosphorite on the East Australian continental margin

G. W. O'Brien & H. H. Veeh

The Flinders University of South Australia, Bedford Park, South Australia 5042, Australia

**Carbonate-fluorapatite, the major component of marine phosphorite, forms within organic-rich diatomaceous sediments in present day conditions along the continental margin of Peru-Chile and South-West Africa (Namibia)<sup>1–4</sup>. Both of these areas are 'West-Coast' phosphogenic provinces<sup>5,6</sup>, characterized by an eastern boundary current, with strong coastal upwelling and associated high organic productivity. We report here the first radiometric evidence supporting Holocene apatite formation in an 'East-Coast' phosphogenic province, the East Australian continental margin, an area of only moderate seasonal upwelling<sup>7,8</sup>.**

The phosphorites of the present study were recovered from the outer continental shelf and upper slope between 29 and 32° S (Fig. 1). In this region, the shelf is fairly narrow (25–40 km) and the slope is unusually steep, with the major shelf break occurring at depths<sup>9,10</sup> between 210 and 450 m. A prominent feature of the oceanography of this area is the East Australian Current, considered a complex series of anti-cyclonic eddies which move generally southwards along the coast<sup>11,12</sup>. Limited upwelling occurs off Evans Head and Laurieton<sup>7,8</sup> (31° 39' S), causing small but significant nutrient enrichments in surface waters.

Phosphorites on the East Australian continental margin were first described by von der Borch<sup>13</sup>, who suggested a mid-Miocene age for them on the basis of palaeontological evidence. Preliminary uranium-series disequilibrium studies<sup>14</sup> confirmed the relict nature of well consolidated, ferruginous phosphorite nodules from the Coffs Harbour region, but also indicated a much younger age ( $5.5 \times 10^4$  yr) for less well consolidated nodules from an area just south of Evans Head. We have examined phosphorites from different locations in an attempt to establish their distribution in space and time, and thus relate their formation to known environmental parameters in this area.

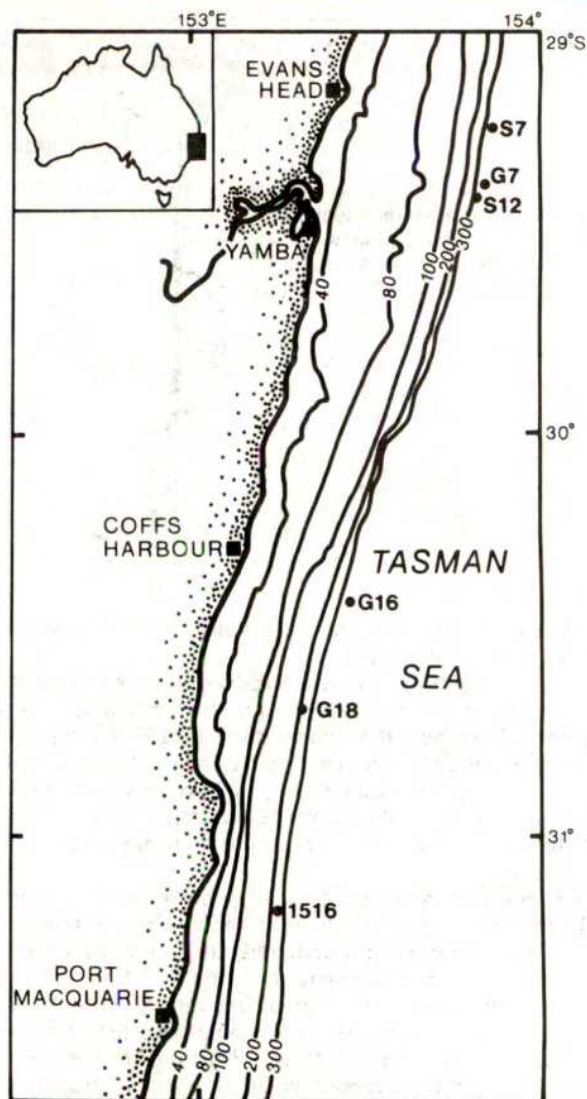


Fig. 1 Location map of phosphatic nodules on the East Australian continental margin. Bathymetric contours (in metres) redrawn from ref. 10.

The nodules fall into two easily distinguishable types—Types I and II. Type I nodules occur within a depth interval 360–420 m on the upper slope, predominantly in the Evans Head–Yamba Head area. These nodules lie within sediments rich in glauconite, biogenic carbonate and quartz and are fairly small (<4 cm diameter), earthy, friable and range in colour from near white to yellow-brown to dark grey. Microscopically, they are seen to be composed of an admixture of silt-sized angular quartz, green to green-brown rounded glauconite as well as calcareous skeletal material which has been cemented by light brownish-tinged cryptocrystalline apatite (collophane). Scanning electron microscopy (SEM, Fig. 2) shows that some phosphate is present as crystallites on the internal surfaces of foraminiferal tests, though no direct evidence for replacement of calcium carbonate by apatite has been observed in these nodules. X-ray diffraction analysis (XRD) of Type I nodules shows quartz, high and low-magnesium calcite, aragonite, glauconite and carbonate fluorapatite as major components. Location G16 differs in that the phosphorite there is present as a poorly consolidated material infilling the interstices between the septa of solitary corals. Type II nodules, which occur off Coffs Harbour in depths of <300 m, are typically fairly large (>5 cm), highly indurated, heavily ferruginized and usually have a 'glazed' appearance. XRD indicates quartz, glauconite, goethite and carbonate fluorapatite as major constituents. Calcite and aragonite are much less abundant in Type II nodules.



**Table 1** Bulk chemical composition, average collophane microprobe analyses and elemental ratios of phosphatic nodules from East Australian continental margin

| Sample no.<br>Type                | Bulk chemical composition* |           |            |              | Average collophane microprobe analyses |       |
|-----------------------------------|----------------------------|-----------|------------|--------------|--|-------|
|                                   | G7-8<br>I                  | G7-9<br>I | G7-10<br>I | 1516-A<br>II | I†                                     | II‡   |
| Fe <sub>2</sub> O <sub>3</sub>    | 4.37                       | 5.83      | 5.42       | 27.48        | 2.42                                   | 8.60  |
| MnO                               | 0.03                       | 0.04      | 0.04       | 0.11         | —                                      | —     |
| TiO <sub>2</sub>                  | 0.37                       | 0.30      | 0.28       | 0.36         | —                                      | —     |
| CaO                               | 29.6                       | 32.2      | 35.3       | 14.3         | 54.59                                  | 51.06 |
| K <sub>2</sub> O                  | 1.05                       | 0.97      | 0.93       | 1.31         | 0.17                                   | 0.11  |
| SiO <sub>2</sub>                  | 28.3                       | 23.5      | 19.4       | 28.1         | 3.48                                   | 1.71  |
| Al <sub>2</sub> O <sub>3</sub>    | 4.30                       | 3.24      | 2.74       | 4.81         | 1.51                                   | 0.99  |
| P <sub>2</sub> O <sub>5</sub>     | 7.5                        | 12.2      | 15.3       | 7.2          | 26.62                                  | 27.38 |
| MgO                               | 1.38                       | 1.35      | 1.24       | 2.51         | 1.27                                   | 1.21  |
| Na <sub>2</sub> O                 | 1.3                        | 1.2       | 0.9        | 0.4          | 0.47                                   | 0.77  |
| SO <sub>3</sub>                   | 0.69                       | 0.74      | 0.85       | 0.41         | 1.12                                   | 1.45  |
| F                                 | 1.9                        | 1.8       | 1.9        | 1.3          | —                                      | —     |
| LOI                               | 19.5                       | 17.6      | 17.1       | 11.7         | —                                      | —     |
| Total                             | 100.29                     | 100.97    | 101.40     | 99.99        | —                                      | —     |
| Less O                            | 0.80                       | 0.76      | 0.80       | 0.55         | —                                      | —     |
| Total                             | 99.49                      | 100.21    | 100.60     | 99.44        | —                                      | —     |
| CaO/P <sub>2</sub> O <sub>5</sub> | 3.95                       | 2.64      | 2.31       | 1.99         | 2.05                                   | 1.86  |
| F/P <sub>2</sub> O <sub>5</sub>   | 0.25                       | 0.15      | 0.12       | 0.18         | —                                      | —     |

\* Determined by X-ray fluorescence spectrography.

† Average of 10 microprobe analyses; ‡ average of 14 microprobe analyses.

Table 1, which summarizes bulk analytical and average collophane microprobe analyses for several nodules, supports the above mentioned differences, with Type I nodules having much lower Fe<sub>2</sub>O<sub>3</sub> contents than do Type II. Whole rock P<sub>2</sub>O<sub>5</sub> contents are low, with a maximum of 15.3% in G7-10, which is slightly below the minimum 18% P<sub>2</sub>O<sub>5</sub> content (50% apatite) that is often taken to define a 'phosphorite'<sup>15</sup>. Strictly speaking, these are really phosphatic nodules.

Uranium-series age determinations were carried out on several Type I and Type II nodules and one solitary coral (Table 2) by methods previously discussed<sup>1-4, 16, 17</sup>. Briefly, the basic assumptions of the U-series method relevant to marine phosphorites are: (1) the uranium entered the apatite phase at the time of its formation, and the time of formation was short compared with the age to be measured; (2) the uranium was derived from seawater; (3) the apatite has remained a closed system with respect to the parent and daughter isotopes; and (4) the apatite was initially free of <sup>230</sup>Th. If these constraints are all satisfied, then the <sup>230</sup>Th/<sup>234</sup>U ratio provides a reliable estimate

of the time of apatite formation. Previous work<sup>4, 18</sup> basically validates assumptions (1)–(3), while the small amount of 'initial' <sup>230</sup>Th usually found in marine phosphorites can be corrected for<sup>4</sup>. The results show that all but one of the Type I nodules show finite ages, and three of these are Holocene. If a correction for non-radiogenic <sup>230</sup>Th is made, based on an assumed <sup>230</sup>Th/<sup>232</sup>Th ratio of 4.0 in common thorium<sup>4</sup>, the Holocene nodules would all be <5,000-yr old. Sample G16-3A represents the phosphatic infilling of a solitary coral. The solid base of the coral itself (100% aragonite) was also dated (G16-3B) and we believe this to be the first time that uranium-series dating of coexisting marine phosphorite and corals has been carried out. The results, which are consistent with the depositional sequence as observed under the microscope, coupled with the generally acknowledged reliability of uranium-series dating of corals, considerably strengthens the arguments presented here. Type II nodules are in radioactive equilibrium and thus beyond the limits of the dating method. Sample 1516-A has in fact suffered some leakage of <sup>234</sup>U similar to many nodules from other areas for which a Miocene age has been independently established<sup>17</sup>.

There are thus two distinctly different types of phosphorite occurring on the East Australian continental margin. Type II nodules, occurring in depths of <300 m, are relict and are probably of mid-Miocene age, as previously suggested<sup>13</sup>. The Type I nodules, on the other hand, are restricted to a narrow depth interval from 360 to 420 m and seem to have formed by cementation of upper-slope sediments with collophane. The spread of ages displayed by Type I nodules suggests that apatite formation has been a continuous process operating in this area for the last several hundred thousand years, rather than being restricted to high stands of sea level during the late Pleistocene<sup>4</sup>. In fact, one of the nodules (G7-12) has an age of 17,500 yr which is very close to the time of the maximum lowering of sea level associated with the last glaciation. The very young ages obtained for several of the samples indicate that apatite formation within East Australian upper slope sediments has only recently ceased, or is even continuing at present.

We have demonstrated that the East Australian continental margin is an area of Holocene phosphate deposition. The general geological and oceanographical characteristics of the region suggest that this deposit may be a modern analogue of McKelvey's<sup>5, 6</sup> East Coast phosphorite deposits. Previously, it has proved difficult to explain many East Coast phosphorite deposits in terms of intense coastal upwelling, and other models, such as an estuarine origin have been proposed<sup>19</sup>. However, a sizeable phosphate deposit, such as the East Australian continental margin deposit, can be produced, even in an area of only moderate seasonal upwelling. Perhaps the East Australian current, predominantly a shelf feature, has resulted in very low sedimentation rates on the upper slope, thus minimizing 'dilution' of the authigenically formed phosphate.

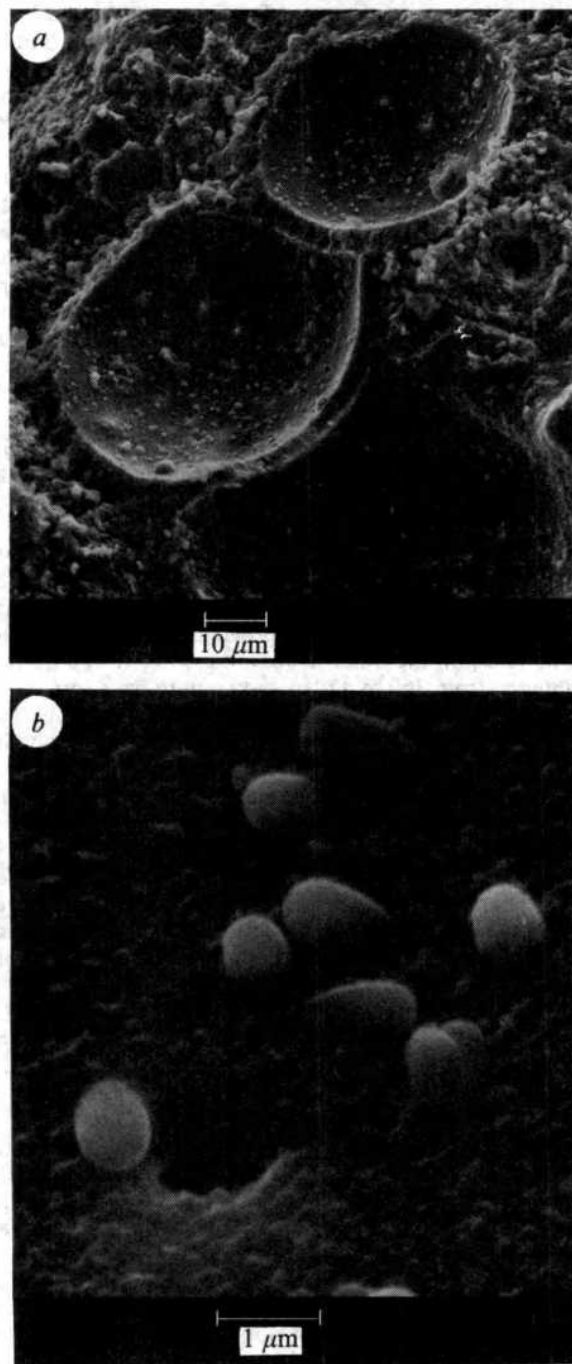
**Table 2** Uranium-series data for phosphatic nodules occurring on the East Australian continental margin

| Sample | Type  | Depth (m) | U (p.p.m.) | Th (p.p.m.) | <sup>234</sup> U/ <sup>238</sup> U | <sup>230</sup> Th/ <sup>234</sup> U | Age (×10 <sup>3</sup> yr) | Age* <sub>c</sub> | <sup>234</sup> U/ <sup>238</sup> U(IV) | U(IV)/U  |
|--------|-------|-----------|------------|-------------|------------------------------------|-------------------------------------|---------------------------|-------------------|--|----------|
| S12-1  | I     | 376       | 229        | 7.3         | 1.14±0.03                          | 0.075±0.007                         | ≤8.5                      | 5±1               | —                                      | —        |
| S7-3   | I     | 412       | 153        | 4.2         | 1.11±0.01                          | 0.45±0.01                           | ≤64                       | 60±2              | 1.06±0.02                              | 109 0.71 |
| G7-8   | I     | 385       | 116        | 3.7         | 1.12±0.01                          | 0.21±0.01                           | ≤25                       | 21±1              | 1.09±0.01                              | 96 0.83  |
| G7-9   | I     | 385       | 90         | 2.7         | 1.10±0.01                          | 0.33±0.02                           | ≤43                       | 40±3              | 1.07±0.01                              | 66 0.73  |
| G7-10  | I     | 385       | 132        | 2.2         | 1.08±0.01                          | 0.79±0.05                           | ≤162                      | 162±23            | 0.94±0.01                              | 108 0.82 |
| G7-12  | I     | 385       | 156        | 3.8         | 1.10±0.01                          | 0.18±0.01                           | ≤21                       | 17.5±1            | 1.06±0.03                              | 101 0.65 |
| G7-17  | I     | 385       | 120        | 4.6         | 1.02±0.01                          | 0.98±0.04                           | >200                      | >200              | 0.81±0.01                              | 94 0.78  |
| G7-29  | I     | 385       | 87         | 2.8         | 1.10±0.01                          | 0.49±0.02                           | ≤71                       | 68±2              | 1.05±0.01                              | 64 0.74  |
| G16-2  | I     | 365       | 99         | 9.2         | 1.17±0.03                          | 0.062±0.006                         | ≤7                        | 0                 | —                                      | —        |
| G16-3A | I     | 365       | 75         | 4.7         | 1.19±0.04                          | 0.079±0.006                         | ≤9                        | 2±0.5             | —                                      | —        |
| G16-3B | Coral | 365       | 4.87       | <0.06       | 1.14±0.02                          | 0.15±0.007                          | 18                        | 18±0.5            | —                                      | —        |
| G18-5  | II    | 210       | 149        | 3.9         | 0.99±0.01                          | 0.94±0.028                          | >200                      | >200              | 0.72±0.01                              | 117 0.79 |
| 1516-A | II    | 241       | 87         | 4.9         | 0.93±0.01                          | 0.95±0.036                          | >200                      | >200              | —                                      | —        |

Errors quoted based on counting statistics (±1σ).

\* Age corrected for common thorium using:  $^{230}\text{Th}_c = ^{230}\text{Th}_m - (4 \times ^{232}\text{Th} \exp(-\lambda_{230}t))$ , where  $^{230}\text{Th}_m$  = measured activity of  $^{230}\text{Th}$ .





**Fig. 2** *a*, Scanning electron micrograph of apatite crystallites on the internal surface of foraminiferal test contained in a phosphatic nodule. (Crystallites confirmed as phosphate-rich by energy dispersive X-ray analysis.) *b*, High magnification of *a* showing relationship of apatite crystals to foraminiferal calcite.

Samples from Locations G7, G16, and G18 were provided by Professor C. C. von der Borch and 1516 by J. Marshall. Others were collected during a CSIRO cruise of RV Sprightly in 1979. Microprobe analyses were performed at Broken Hill Proprietary, Melbourne Research Laboratories and X-ray fluorescence analyses were done by Dr A. R. Milnes. Financial support was provided by the Australian Research Grants Committee. *Note added in proof:* It has been pointed out to us by R. Foster, CSIRO Division of Soils, that the (apatite) crystallites (Fig. 2) could be mineralized bacteria because of the remarkable morphological similarity. If confirmed, this would imply that bacterial activity plays an important role in phosphorite genesis.

Received 24 July; accepted 14 October 1980.

1. Baturin, G. N., Merkulova, K. I. & Chalov, P. I. *Mar. Geol.* **13**, M37-M41 (1972).
2. Veeh, H. H., Burnett, W. C. & Soutar, A. *Science* **181**, 844-845 (1973).

3. Veeh, H. H., Calvert, S. E. & Price, N. B. *Mar. Chem.* **2**, 189-202 (1974).
4. Burnett, W. C. & Veeh, H. H. *Geochim. cosmochim. Acta* **41**, 755-764 (1977).
5. McKelvey, V. E. *U.S. geol. Surv. Bull.* 1252-D, 1-21 (1967).
6. McKelvey, V. E. & Wang, F. H. *U.S. geol. Surv. Misc. Geol. Inv. Map.* 1-632 (1969).
7. Rochford, D. J. *Div. Fish. Oceanogr. Tech. Pap. No. 33* (CSIRO, 1972).
8. Rochford, D. J. *Aust. J. mar. Freshwat. Res.* **26**, 233-243 (1975).
9. Jones, H. A., Davies, P. J. & Marshall, J. F. *J. geol. Soc. Aust.* **22**, 71-78 (1975).
10. Marshall, J. F. *BMR J. Aust. Geol. Geophys.* **4**, 281-288 (1979).
11. Boland, F. M. & Hamon, B. V. *Deep Sea Res.* **17**, 777-794 (1970).
12. Godfrey, J. S., Cresswell, G. R., Golding, T. J., Pearce, A. F. & Boyd, R. *J. phys. Oceanogr.* **10**, 430-440 (1980).
13. Von der Borch, C. C. *J. geol. Soc. Aust.* **16**, 755-759 (1970).
14. Kress, A. G. & Veeh, H. H. *Mar. Geol.* **36**, 143-157 (1980).
15. Bushinsky, G. I. *Isr. Progr. Sci. Trans. Jerus.* (1969).
16. Clarke, R. S. & Altschuler, A. S. *Geochim. cosmochim. Acta* **13**, 127-142 (1958).
17. Kolodny, Y. & Kaplan, I. R. *Geochim. cosmochim. Acta* **34**, 324 (1970).
18. Burnett, W. C., Veeh, H. H. & Soutar, A. *SEPM Spec. Publ.* (in the press).
19. Pevear, D. R. *Econ. Geol.* **61**, 251-256 (1966).

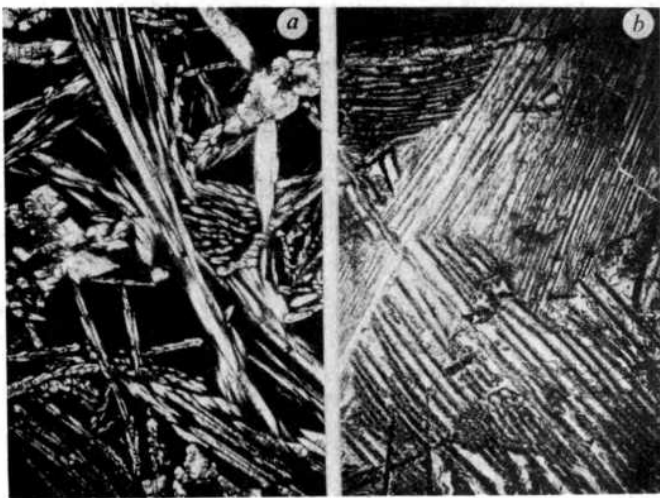
## Boninite at a continental margin

C. P. Wood

New Zealand Geological Survey, PO Box 30368, Lower Hutt, New Zealand

A lava interbedded with Cretaceous sediments deposited on the continental margin of New Zealand has phenocrystic chromite, olivine, low-Ca and high-Ca pyroxenes with quench morphology, normative quartz, and relatively high MgO, Cr and Ni, but very low Ti and Zr; it is shown here to conform to the term boninite as defined by Cameron *et al.*<sup>1</sup>. Such rocks are usually found in geologically oceanic situations, as in the Bonin, and Mariana arc-trench systems of the Western Pacific, or in ophiolites that represent uplifted, oceanic crust formed close to oceanic plate margins, particularly spreading centres, though not necessarily at mid-ocean ridges<sup>2-6</sup>. The New Zealand boninite closely resembles certain ophiolitic lavas, yet its association is not ophiolitic, and this part of New Zealand never was, nor ever became, an oceanic spreading centre<sup>7</sup>. Coeval basalts are alkalic, not tholeiitic as is usual and the occurrence warns against the use of basalt petrochemistry as an indicator of tectonic environment in the absence of supporting geological evidence.

Albian sediments of the Mangapokia Formation in eastern Wairarapa, in the North Island of New Zealand, accumulated as submarine fan or fan-delta deposits, probably at shelf depths in a fault-controlled basin<sup>8</sup>. They comprise at least 1,500 m of flysch-like sediments, with sporadic lavas and sills, most of which are spilitic, alkalic basalts, some with camptonitic affinities. However, near Nagahape almost 10 m of boninitic lava and



**Fig. 1** Textures of Kopi boninite. *a*, Acicular crystals and skeletal chains of augite, and a few lozenges of pigeonite jacketed by augite. Field width, 1.3 mm. *b*, Spinifex texture; oriented blades of chloritized pigeonite rimmed by augite, and a few, dark, cross-cutting olivine dendrites. Matrix is devitrified glass. Field width, 1.3 mm.

**Table 1** Electron probe analyses of representative phenocrysts and average groundmass, and average of six whole-rock analyses (XRF) of Kōpi boninite

|                                | 1     | 2     | 3      | 4a    | 4b    | 5     | 6      | 7a           | 7b            |
|--------------------------------|-------|-------|--------|-------|-------|-------|--------|--------------|---------------|
| SiO <sub>2</sub>               | 0.12  | 55.58 | 55.89  | 51.44 | 51.47 | 50.20 | 55.98  | 52.26 (0.13) | P 900 (100)   |
| TiO <sub>2</sub>               | 0.08  | 0.04  | 0.02   | 0.18  | 0.08  | 0.24  | 0.16   | 0.18 (0.01)  | Cr 1133 (207) |
| Al <sub>2</sub> O <sub>3</sub> | 13.37 | 1.74  | 1.59   | 5.51  | 4.67  | 7.10  | 18.80  | 12.84 (0.24) | Ni 224 (21)   |
| Fe <sub>2</sub> O <sub>3</sub> | 3.85  | —     | —      | —     | —     | —     | —      | 2.96 (1.08)  | Rb 4.8 (1.6)  |
| FeO                            | 18.01 | 7.11  | 8.30   | 7.43  | 6.73  | 8.21  | 7.78   | 6.11 (0.89)  | Sr 39 (4)     |
| MnO                            | —     | 0.19  | 0.18   | 0.22  | 0.12  | 0.16  | 0.12   | 0.17 (0.01)  | Y 7.7 (1.6)   |
| MgO                            | 10.25 | 32.29 | 30.80  | 18.72 | 16.83 | 17.08 | 4.13   | 10.97 (0.46) | Zr 9 (2)      |
| CaO                            | 0.04  | 1.79  | 2.87   | 15.55 | 10.22 | 16.68 | 9.75   | 10.43 (0.30) | Nb <2         |
| Na <sub>2</sub> O              | —     | 0.04  | 0.04   | 0.08  | 0.10  | 0.14  | 3.03   | 1.43 (0.28)  | Ba 63 (30)    |
| K <sub>2</sub> O               | —     | —     | —      | —     | 0.01  | —     | 0.25   | 0.12 (0.04)  |               |
| NiO                            | 0.07  | 0.11  | 0.09   | 0.04  | 0.01  | 0.01  | —      | —            |               |
| Cr <sub>2</sub> O <sub>3</sub> | 53.97 | 0.87  | 0.53   | 0.16  | 0.36  | 0.08  | —      | —            |               |
| Total                          | 99.76 | 99.76 | 100.31 | 99.33 | 99.60 | 99.90 | 100.00 | 97.47        |               |

## Column

- 1 Magnesiochromite, Fe<sub>2</sub>O<sub>3</sub> calculated assuming stoichiometry.
- 2 Bronzite (En<sub>86.0</sub>Fs<sub>10.6</sub>Wo<sub>3.4</sub>).
- 3 Magnesian pigeonite in phenocryst core (En<sub>62.1</sub>Fs<sub>12.4</sub>Wo<sub>5.5</sub>).
- 4 Augites in phenocryst rims; a, low-Ca end of range (En<sub>55.0</sub>Fs<sub>12.2</sub>Wo<sub>32.8</sub>); b, high-Ca end of range (En<sub>48.9</sub>Fs<sub>11.0</sub>Wo<sub>40.1</sub>).
- 5 Augite rim of spinifex-textured pyroxene.
- 6 Average composition of fine-grained groundmass (nine positions; defocused beam) recalculated to 100%.
- 7 Average boninite analysis, standard deviations in parentheses; a, major elements in wt %, 1.92 (0.61) % H<sub>2</sub>O also present; b, trace elements in p.p.m.

hyaloclastite (known as Kōpi boninite) occur within a sequence of coarse quartzofeldspathic sediments derived from a continental hinterland. A water depth of 200–700 m at emplacement is suggested by the bulk sulphur content of 940 p.p.m., and average maximum vesicle diameter of 1.5–2 mm (refs 9, 10). Quartz, chlorite, calcite and laumontite in brecciated boninite indicate zeolite facies alteration, though dense rock is little affected.

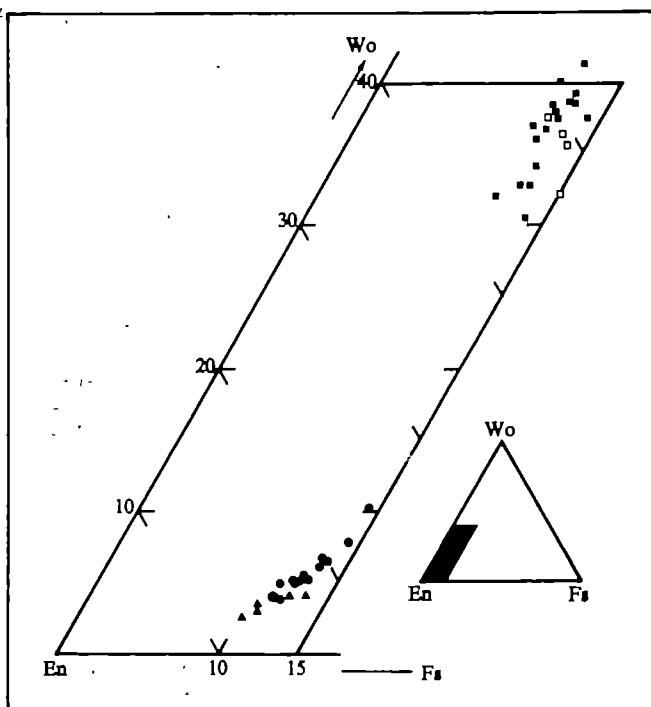
Pillow lava with conspicuous, random needles of pyroxene predominates, though spinifex-textured rock is also present (Fig. 1). Magnesiochromite crystallized first, and is ubiquitous in trace amounts; with average ratios of Cr/(Cr+Al) = 0.71, and Mg/(Mg+Fe<sup>2+</sup>) = 0.51 it falls at the low-Cr, low-Mg margin of the compositional range of boninite and basaltic komatiite chromites<sup>1</sup>. Minor olivine (0.3–1.1 modal %) followed spinel, forming mainly subhedral crystals (<0.5 mm), but with some lantern-and-chain dendrites, particularly in the spinifex rock. Olivine has been replaced completely by quartz, calcite and iron oxides.

There are three types of phenocryst pyroxene, the earliest being rare, unzoned calcic bronzite in the range Mg/(Mg+Fe) = 0.86–0.89 (analysis 2, Table 1). Composite clinopyroxene crystals are the dominant phenocrysts (25.5–38.4 modal %), and in both habit and chemistry they closely resemble the pyroxenes in some rapidly cooled komatiites<sup>11</sup>. They form hollow needles up to 70 × 1 mm which show simple zoning, with a multiply twinned core of pigeonite rimmed by optically continuous augite. Core compositions are continuous with those of bronzite (Fig. 2), straddling the boundary between calcic clinobronzite (En<sub>85</sub>Fs<sub>11</sub>Wo<sub>4</sub>) and highly magnesian pigeonite (En<sub>76</sub>Fs<sub>14</sub>Wo<sub>10</sub>). The crystal forms suggest rapid crystallization from a supercooled liquid to produce these metastable clinopyroxenes, which plot in the miscibility gap between stable high-Ca and low-Ca pyroxenes.

Augite jackets the subcalcic clinopyroxene and sometimes mantles the hollow core; it also occurs as single-phase microphenocrysts and in skeletal chains. In the spinifex rock, oriented blades comprise augite rims on a chloritized core (Fig. 1). Compositions range from En<sub>55.9</sub>Fs<sub>13.4</sub>Wo<sub>30.7</sub> to En<sub>46.9</sub>Fs<sub>11.9</sub>Wo<sub>41.2</sub>, and as the skeletal and spinifex pyroxenes fall within the range of rim compositions (Fig. 2), it seems the composite crystals represent quench overgrowth of calcic clinopyroxene on an earlier, subcalcic core.

Groundmasses comprise fan-spherulitic integrowths mostly too fine to differentiate, but occasionally coarse enough to identify plagioclase (An<sub>67–79</sub>), clinopyroxene and magnetite

(TiO<sub>2</sub> ≈ 7.0%). Interstitial matrix in the spinifex rock varies from devitrified glass, through axiolitic spherulites to well developed, pin-wheel pyroxene spherulites. The average, bulk-matrix analysis (analysis 6, Table 1) resembles aluminous basaltic andesite. The whole-rock analysis (analysis 7a, Table 1) is less siliceous than boninite from the Bonin Islands, but resembles the basaltic lavas found in some ophiolite complexes such as Troodos<sup>2</sup>, and Betts Cove<sup>3</sup>. Cameron *et al.*<sup>1</sup> class all these as boninite, the name adopted here, but other terms such as basaltic komatiite<sup>3</sup>, low-Ti basalt<sup>4</sup>, and magnesian quartz tholeiite<sup>6</sup> have been used for the same rocks. Whatever the name, the combination of relatively high MgO, Cr and Ni, and extremely low TiO<sub>2</sub> and Zr in a quartz-normative



**Fig. 2** Compositions of pyroxenes in Kōpi boninite plotted in part of the system MgSiO<sub>3</sub>–FeSiO<sub>3</sub>–CaSiO<sub>3</sub>. ▲, Bronzite phenocrysts; ●, cores of composite phenocrysts; ■, rims of composite phenocrysts; □, skeletal and spinifex rim pyroxenes.



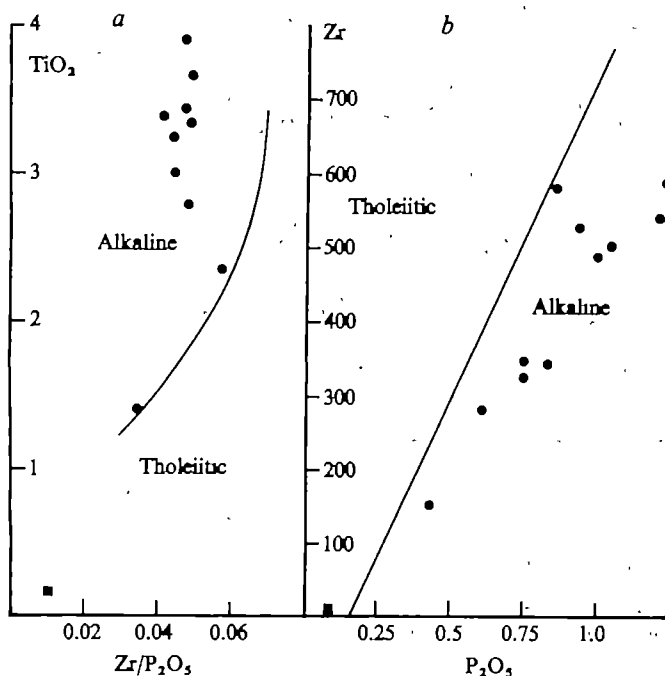


Fig. 3 Kopi boninite (■) and coeval alkaline basaltic rocks (●) plotted using immobile elements to discriminate between alkaline and tholeiitic fields (after ref. 14). a,  $\text{TiO}_2$  (wt%) against the ratio  $\text{Zr}/\text{P}_2\text{O}_5$  (p.p.m.). b, Zr (p.p.m.) against  $\text{P}_2\text{O}_5$  (%).

( $Q = 6.0\%$ ), basic composition places the lava clearly within a spectrum of basaltic to andesitic rocks that are otherwise known only from modern oceanic areas, or ancient ophiolites that were segments of oceanic lithosphere.

The early Cretaceous sediments of eastern Wairarapa are thought to overlie or to represent the youngest part of a sequence of several kilometres of marine sediment of continental provenance, deposited more or less continuously throughout the Mesozoic. An Albian tectonic event deformed the soft sediments and initiated open-shelf deposition<sup>8</sup> which continued till late Tertiary time, when the present uplift and deformation began. Minor intraformational slumping may have occurred during deposition of Mangapokia sediments, but there is no evidence to suggest allochthonous emplacement of the lavas. Thus there is no indication that the area was anything other than a faulted, continent margin at the time the lava was erupted.

In the discussion of genesis of low-Ti magmas, there is general agreement that multistage melting is necessary to give extreme depletion of incompatible elements<sup>1,4-6</sup>. Olivine tholeiite and derivatives, produced by voluminous first-stage melting, are the habitual associates of most low-Ti lavas. However, lavas coeval with the Kopi boninite are alkalic basalts and derivatives, with marked enrichment in P, Ti, Y, Zr and Nb (Fig. 3), presumably generated by deep, low-volume, first-stage melting of upper mantle. Eruption of one or more such magma batches would have efficiently depleted a portion of mantle which then could have risen as a small diapir to melt at shallower depths and produce boninite.

If such a process did occur it is perhaps unusual that the association of boninite with alkalic basalt is so rare. The closest comparison seems to be in the Othris Mountains of Greece, where Cameron *et al.*<sup>1</sup> reported boninite in the Agrilia Formation. There, the associated volcanics are mildly undersaturated, alkaline types<sup>12</sup> erupted at a continental margin during a period of slow splitting, possibly caused either by continental rifting, or the initiation of a marginal ocean basin and nearby subduction zone<sup>13</sup>. It is probable that the eastern margin of the early Cretaceous, New Zealand continent was deeply fractured enough to allow boninite magma to erupt, but even if continental splitting had started it clearly failed to develop. It is certain that a spreading centre never formed at the site of deposition,

and though there is a modern subduction zone to the east of northern New Zealand, the existence of one in early Cretaceous times is a moot point.

I thank P. R. Moore, I. G. Speden, and A. J. Tulloch for discussions and advice, and T. R. Grammer and N. Orr for technical help. Most analytical work was carried out in the Geology Department of Victoria University of Wellington.

Received 15 August, accepted 28 October 1980

- 1 Cameron, W. E., Nisbet, B. G. & Dietrich, V. J. *Nature* **288**, 550-553 (1979)
- 2 Scofield, J. D., Simonson, K. O. & Gass, I. G. *Contrib. Mineral. Petrol.* **51**, 49-64 (1975)
- 3 Simonson, K. O. & Gass, I. G. *Bull. Am. geol. Soc.* **89**, 1220-1230 (1978)
- 4 Ben, S.-S. & Nesbitt, R. W. *Geology* **6**, 689-693 (1978)
- 5 Coash, R. A. & Church, W. R. *Contrib. Mineral. Petrol.* **70**, 29-39 (1979)
- 6 Duncan, R. A. & Gass, I. G. *Geology* **8**, 22-26 (1980)
- 7 Stevens, G. R. & Soggin, R. P. In *The Geology of New Zealand*, 727-745 (Government Printer, Wellington, 1978)
- 8 Moore, P. R. & Speden, I. G. *NZ J. Geol. Geophys.* **22**, 417-433 (1979)
- 9 Moore, J. G. & Schilling, J.-G. *Contrib. Mineral. Petrol.* **41**, 105-118 (1973)
- 10 Jones, J. G. *Am. J. Sci.* **267**, 181-195 (1969)
- 11 Arndt, N. T. *Am. Mineral.* **64**, 856-864 (1979)
- 12 Hyndes, A. *Can. J. Earth Sci.* **11**, 842-853 (1974)
- 13 Smith, A. G. *et al. Econ. geol. Mon.* **68**, 463-481 (1975)
- 14 Winchester, J. A. & Floyd, P. A. *Earth planet. Sci. Lett.* **28**, 459-469 (1976)

## Coefficients of relatedness in sociobiology

Richard E. Michod

Department of Ecology and Evolutionary Biology, University of Arizona, Tucson, Arizona 85721

W. D. Hamilton

Museum of Zoology, University of Michigan, Ann Arbor, Michigan 48109

A much-discussed, quantitative criterion for the spread of an altruistic gene is Hamilton's rule<sup>1,2</sup>

$$\frac{c}{b} < R \quad (1)$$

where  $c$  and  $b$  are additive decrement and increment to fitness of altruist and recipient, respectively, and  $R$  is a measure of genetic relatedness between the two individuals. When rearranged as  $-c.1 + b.R > 0$ , the rule can be interpreted as requiring that the gene-caused action increase the 'inclusive fitness' of the actor. Since its introduction, Hamilton's rule and the attendant concept of inclusive fitness have gained increasing acceptance and use among biologists and have become integral in the field now named sociobiology. However, the essentially heuristic reasoning used in deriving these concepts, along with the lack of a complete specification even in the original outbred model<sup>2</sup>, have led to many investigations into the population genetical underpinnings of Hamilton's rule<sup>3-18</sup>. On the basis of these considerations, several reports<sup>3,10,12,13,18</sup> have proposed new formulae for  $R$ . These formulae have no obvious relation to each other or to the coefficients originally suggested by Hamilton. This proliferation of coefficients is undoubtedly confusing to many and the net effect may be to generate distrust both of the rule and of the notion of inclusive fitness. Our purpose here is to show that these various formulae for  $R$  (refs 3, 10, 12, 13, 18), although independently derived, are actually the same.

What is  $R$  in equation (1)? On the basis of a particular outbred model, Hamilton<sup>1,2</sup> claimed that Wright's<sup>19</sup> 'coefficient of relationship' was the required  $R$ . However, later, giving a heuristic development but no further model, Hamilton<sup>20,21</sup> modified his identification of  $R$  with Wright's coefficient by claiming that equation (1) requires, in principle, a regression coefficient of

genotype of recipient on genotype of altruist, whereas Wright's coefficient is the corresponding correlation coefficient. Such a correlation coefficient will often be the same as the regression coefficient but differs when the interactants are inbred to different extents<sup>18</sup>. These discussions<sup>1,2,20,21</sup> implied that  $R$  was independent of gene frequency and selection, and that equation (1) held for inbred populations (with the regression coefficient as  $R$ ).

However, in recent models<sup>3-17</sup>,  $R$  is taken to be the threshold value of  $c/b$ , below which the cost-benefit ratio must be for the gene to increase. The  $R$  formulated in this operational way need not necessarily correspond to any simple measure of genetic relationship. Some of these models<sup>3-11,14,15,17</sup> specify the whole mating process with respect to interactions within families. Other models<sup>12,13,16</sup> maintain the generality of Hamilton's<sup>2</sup> original approach, and apply to interactants of arbitrary relationship, but fail to specify the population and mating system processes which give rise to  $R$ . If Hamilton's rule is to be useful, it must turn out that  $R$ , as formulated by these various approaches, must not vary widely as gene frequency or the parameters of selection change, except as implied by the simple proportionality to  $c/b$ . In many cases of interest,  $R$  is constant<sup>4,7-9,15</sup>, but in others<sup>3,4,7,10-13,16</sup> dependencies on gene frequency and dominance enter into calculations of  $R$ .

Our analysis here will not consist of any derivations of the coefficients from the gene frequency dynamics, as that is done from different points of view in the various works to be considered<sup>3,10,12,13</sup>. Instead, we will simply convert these various coefficients into a common symbolism and show that they are, in fact, identical. However, before doing so, we should acknowledge an important aspect of the derivations: either selection

must be weak so that standard identity coefficients can be used as measures of genetic relationship, or rather special conditions must be imposed on the models so that there is no selection at internal points of the pedigree patterns studied.

The genetic relationship between two diploid individuals,  $X$  and  $Y$ , at a single locus can be summarized by the following nine 'condensed' identity coefficients  $\Delta_1, \Delta_2, \dots, \Delta_9$ , where  $\Delta_i$  is the probability of genetic identity event  $i$  obtaining (Fig. 1 upper left-hand corner)<sup>22</sup>. These coefficients consider identity states among all four alleles present in  $X$  and  $Y$ . The traditional two-allele coefficients, interpreted as probabilities, are

$$f_X = \Delta_1 + \Delta_2 + \Delta_3 + \Delta_4 \quad f_Y = \Delta_1 + \Delta_2 + \Delta_5 + \Delta_6 \quad (2a)$$

$$f_{XY} = \Delta_1 + \frac{1}{2}(\Delta_3 + \Delta_5 + \Delta_7) + \frac{1}{4}\Delta_8 \quad (2b)$$

where  $f_X$  and  $f_Y$  are the inbreeding coefficients of  $X$  and  $Y$ , respectively, and  $f_{XY}$  is the 'coefficient of consanguinity' between  $X$  and  $Y$ , or the probability that a random allele from  $X$  is identical by descent with a random allele from  $Y$  at the locus of interest. Letting  $X$  denote the altruist and  $Y$  the recipient, the coefficient which we will use to relate the others may now be defined as

$$R = \frac{f_{XY}\alpha + (\Delta_1 + \frac{1}{2}\Delta_3)(1-\alpha)}{\frac{1}{2}\alpha + f_X(1-\frac{1}{2}\alpha)} \quad (3)$$

where  $\alpha = 2q + 2h - 4qh$ ,  $p$  is the frequency of the non-altruist allele  $A$  with  $q = (1-p)$  the frequency of the altruistic allele  $a$ , and  $h$  is the probability that a heterozygote performs an altruistic act. If we express the phenotypes as the probabilities of behaving altruistically (0,  $h$ , 1 corresponding to  $AA$ ,  $Aa$ ,  $aa$ ),

**Fig. 1** Joint and marginal distribution of genetic identity states with genotypes. The nine 'condensed' identity states are given in the upper left-hand corner with probabilities  $\Delta_i$  ( $i = 1, 2, \dots, 9$ ),  $\sum_i \Delta_i = 1$ . The alleles of  $X$  are on top and the alleles of  $Y$  on the bottom. A line connecting alleles indicates identity by descent. Given the occurrence of each identity state, the distribution of the genotypes of  $X$  and  $Y$  are given within the large side and top three boxes, respectively. For example, if identity state 5 obtains, then  $X$  is  $AA$ ,  $Aa$ ,  $aa$  with probabilities  $p^2$ ,  $2pq$ ,  $q^2$ , respectively; the like probabilities for  $Y$  are  $p$ ,  $0$ ,  $q$ , respectively. Given the distribution of identity states, the marginal distribution of genotypes is given in the top left corner of each of these six large boxes. The joint distribution of genotypes are given in the nine large boxes towards the bottom right of the figure. For example, if identity state 3 obtains, then

$$\begin{aligned} P_{00} &= p^2, & P_{01} &= pq, \\ P_{03} &= P_{10} = P_{11} = P_{12} = P_{20} = 0, \\ P_{21} &= pq & \text{and} & P_{22} = q^2. \end{aligned}$$

Y's genotype

AA

Aa

aa

X alleles →   
Y alleles →

$\Delta_1$

$\Delta_2$   $\Delta_3$   $\Delta_4$   $\Delta_5$

$\Delta_6$   $\Delta_7$   $\Delta_8$   $\Delta_9$

$$P_{Y0} = p^2 + f_Y pq$$

|   |                |                |                |
|---|----------------|----------------|----------------|
|   |                |                | p              |
| p | p <sup>2</sup> | p <sup>2</sup> | p              |
| p | p <sup>2</sup> | p <sup>2</sup> | p <sup>2</sup> |

$$P_{Y1} = 2pq(1 - f_Y)$$

|   |     |     |     |
|---|-----|-----|-----|
|   |     |     | -   |
| - | 2pq | 2pq | -   |
| - | 2pq | 2pq | 2pq |

$$P_{Y2} = q^2 + f_Y pq$$

|   |                |                |                |
|---|----------------|----------------|----------------|
|   |                |                | q              |
| q | q <sup>2</sup> | q <sup>2</sup> | q              |
| q | q <sup>2</sup> | q <sup>2</sup> | q <sup>2</sup> |

AA

$$P_{X0} = p^2 + f_X pq$$

|                |                |                |                |
|----------------|----------------|----------------|----------------|
|                |                |                | p              |
| p              | p              | p              | p <sup>2</sup> |
| p <sup>2</sup> | p <sup>2</sup> | p <sup>2</sup> | p <sup>2</sup> |

$$P_{00}$$

|                |                |                |                |
|----------------|----------------|----------------|----------------|
|                |                |                | p              |
| p <sup>2</sup> | p <sup>2</sup> | p <sup>3</sup> | p <sup>2</sup> |
| p <sup>3</sup> | p <sup>2</sup> | p <sup>3</sup> | p <sup>4</sup> |

$$P_{01}$$

|   |    |                   |                   |
|---|----|-------------------|-------------------|
|   |    |                   | -                 |
| - | pq | 2p <sup>2</sup> q | -                 |
| - | -  | p <sup>2</sup> q  | 2p <sup>3</sup> q |

$$P_{02}$$

|                  |   |                 |                               |
|------------------|---|-----------------|-------------------------------|
|                  |   |                 | -                             |
| pq               | - | pq <sup>2</sup> | -                             |
| p <sup>2</sup> q | - | -               | p <sup>2</sup> q <sup>2</sup> |

X's genotype

Aa

$$P_{X1} = 2pq(1 - f_X)$$

|     |     |     |     |
|-----|-----|-----|-----|
|     |     |     | -   |
| -   | -   | -   | 2pq |
| 2pq | 2pq | 2pq | 2pq |

$$P_{10}$$

|                   |   |                  |                   |
|-------------------|---|------------------|-------------------|
|                   |   |                  | -                 |
| -                 | - | -                | pq                |
| 2p <sup>2</sup> q | - | p <sup>2</sup> q | 2p <sup>3</sup> q |

$$P_{11}$$

|   |     |    |                   |
|---|-----|----|-------------------|
|   |     |    | -                 |
| - | -   | -  | -                 |
| - | 2pq | pq | 4p <sup>2</sup> q |

$$P_{12}$$

|                  |   |                 |                  |
|------------------|---|-----------------|------------------|
|                  |   |                 | -                |
| -                | - | -               | pq               |
| 2pq <sup>2</sup> | - | pq <sup>2</sup> | 2pq <sup>3</sup> |

aa

$$P_{X2} = q^2 + f_X pq$$

|                |                |                |                |
|----------------|----------------|----------------|----------------|
|                |                |                | q              |
| q              | q              | q              | q <sup>2</sup> |
| q <sup>2</sup> | q <sup>2</sup> | q <sup>2</sup> | q <sup>2</sup> |

$$P_{20}$$

|                 |   |                  |                               |
|-----------------|---|------------------|-------------------------------|
|                 |   |                  | -                             |
| pq              | - | p <sup>2</sup> q | -                             |
| pq <sup>2</sup> | - | -                | p <sup>2</sup> q <sup>2</sup> |

$$P_{21}$$

|   |    |                  |                  |
|---|----|------------------|------------------|
|   |    |                  | -                |
| - | pq | 2pq <sup>2</sup> | -                |
| - | -  | pq <sup>2</sup>  | 2pq <sup>3</sup> |

$$P_{22}$$

|                |                |                |                |
|----------------|----------------|----------------|----------------|
|                |                |                | q              |
| q <sup>2</sup> | q <sup>2</sup> | q <sup>3</sup> | q <sup>2</sup> |
| q <sup>3</sup> | q <sup>2</sup> | q <sup>3</sup> | q <sup>4</sup> |



Table 1 Joint and marginal distributions of  $X_i$  and  $Y_i$  and  $X_j$  and  $Y_j$ 

|               |       | Y     |                         |                         |                         |
|---------------|-------|-------|-------------------------|-------------------------|-------------------------|
|               |       | $Y_i$ | 0                       | $\frac{1}{2}$           | 1                       |
|               |       | $Y_j$ | 0                       | $h$                     | 1                       |
| $X_i$         | $X_j$ |       |                         |                         |                         |
| 0             | 0     |       | $P_{00}$                | $P_{01}$                | $P_{02}$                |
| $\frac{1}{2}$ | $h$   |       | $P_{10}$                | $P_{11}$                | $P_{12}$                |
| 1             | 1     |       | $P_{20}$                | $P_{21}$                | $P_{22}$                |
|               |       |       | $P_{Y0} = p^2 + f_Y pq$ | $P_{Y1} = 2pq(1 - f_Y)$ | $P_{Y2} = q^2 + f_Y pq$ |
|               |       |       |                         |                         | 1                       |

$P_{ij}$  is the joint distribution of genotypes  $i$  and  $j$  and  $P_{X_i}$ ,  $P_{Y_i}$  are the marginal distributions of the genotypes of  $X$  and  $Y$ , respectively ( $i, j = 0, 1, 2$ ). From the table, the following expressions can be calculated for use in calculations concerning equations (5):  $E(X_i) = hP_{X1} + P_{X2}$ ,  $E(Y_i) = hP_{Y1} + P_{Y2}$ ,  $E(Y_j) = \frac{1}{2}P_{Y1} + P_{Y2} = q$ ,  $E(X_j) = \frac{1}{2}P_{X1} + P_{X2} = q$ ,  $E(Y_i X_j) = \frac{1}{2}hP_{11} + hP_{12} + \frac{1}{2}P_{21} + P_{22}$ ,  $E(X_i X_j) = \frac{1}{2}hP_{X1} + P_{X2}$ ,  $E(X_i Y_j) = \frac{1}{2}hP_{11} + \frac{1}{2}P_{12} + \frac{1}{2}P_{21} + P_{22}$ ,  $E(X_j^2) = \frac{1}{2}P_{X1} + P_{X2}$ .

and the genotypes as the fractions of altruistic alleles (0,  $\frac{1}{2}$ , 1 corresponding to AA, Aa, aa), then  $\alpha$  is simply the regression of phenotype on genotype in a randomly mating population. This convention regarding the genotypes and phenotypes will be used throughout. With a change in notation,  $R$  as given by equation (3) is identical to the coefficient derived by Fleiss and Holtzman<sup>13</sup> (equation (10), where  $P(H) = \Delta_1 + \frac{1}{2}\Delta_3$  and their  $h = \frac{1}{2}\alpha$ ). It is important to note that if the gene effects are additive, if there is no inbreeding or if  $p = q = 0.5$ , then equation (3) reduces to the coefficient proposed by Hamilton<sup>20,21</sup>:

$$R = \frac{2f_{XY}}{1 + f_X} \quad (4)$$

Consequently, the regression coefficient (equation (4)) will be a good estimate of  $R$  in many cases of interest. We now show that the coefficients derived elsewhere in the literature<sup>3,10,12,18</sup> are identical to equation (3).

Below, we index genotypes with a single subscript  $i$ , with  $i = 0, 1, 2$  corresponding to genotypes AA, Aa, aa, respectively. Let  $P_{ij}$  be the joint distribution of genotypes  $i$  and  $j$  in the population with  $i$  being the genotype of  $X$  and  $j$  the genotype of  $Y$  (Fig. 1, Table 1). Let  $X_i$ ,  $X_j$  and  $Y_i$ ,  $Y_j$  denote the genotype and phenotype of  $X$  and  $Y$ , respectively.

Orlove<sup>3</sup> and Orlove and Wood<sup>10</sup> derive  $R = \text{Cov}(X_i, Y_j) / \text{Cov}(X_i, X_j)$  in an outbred model of kin selection in haplodiploid families. Their coefficient<sup>3,10</sup> equals

$$R = \frac{\text{Cov}(Y_i, X_j)}{\text{Cov}(X_i, X_j)} \quad (5)$$

if there is no inbreeding. However, as we now show, equation (5) is more generally correct, as well as being the most concise and intuitive representation of equations (3) or (17).

To relate equation (5) to equation (3), we must first calculate the required covariances. The information needed to do so is given in Table 1, in which the genotypes and phenotypes of  $X$  and  $Y$  are given along with the joint and marginal probabilities. Using this information to evaluate the covariances in equation (5), we obtain directly

$$\frac{\text{Cov}(Y_i, X_j)}{\text{Cov}(X_i, X_j)} = \frac{\frac{1}{2}P_{11}h + hP_{12} + \frac{1}{2}P_{21} + P_{22} - (\frac{1}{2}P_{Y1} + P_{Y2})(hP_{X1} + P_{X2})}{\frac{1}{2}hP_{X1} + P_{X2} - (hP_{X1} + P_{X2})(\frac{1}{2}P_{X1} + P_{X2})} \quad (6)$$

From Table 1, we can also obtain for future use

$$\text{Cov}(Y_i, X_j) = \frac{1}{2}P_{11} + \frac{1}{2}P_{12} + \frac{1}{2}P_{21} + P_{22} - (\frac{1}{2}P_{X1} + P_{X2})(\frac{1}{2}P_{Y1} + P_{Y2}) \quad (7)$$

$$\text{Var}(Y_i) = \frac{1}{4}qp(1 + f_Y) \quad (8a)$$

and

$$\text{Var}(X_i) = \frac{1}{4}qp(1 + f_X) \quad (8b)$$

Substituting equation (7) into the numerator of equation (6)

$$\text{Cov}(Y_i, X_j) = \text{Cov}(Y_i, X_j) + (h - \frac{1}{2})(\frac{1}{2}P_{11} + P_{12} - qP_{X1}) \quad (9)$$

The denominator of equation (6) can be simplified directly to

$$\text{Cov}(X_i, X_j) = pq[\frac{1}{2}\alpha + f_X(1 - \frac{1}{2}\alpha)] \quad (10)$$

As shown in Fig. 1 (see also refs 12, 22, 23), it is possible to express the joint probabilities of the interactions,  $P_{ij}$ , in terms of the condensed identity coefficients and the gene frequency. In particular,

$$\begin{aligned} P_{11} &= 2pq(\Delta_7 + \frac{1}{2}\Delta_8 + 2pq\Delta_9) \\ P_{12} &= pq(\Delta_5 + 2q\Delta_6 + q\Delta_8 + 2q^2\Delta_9) \end{aligned} \quad (11)$$

These formulae (equation (11) and Fig. 1) are only strictly correct for neutral genes; however, it is hoped that they are approximately correct if selection is weak. Substituting equation (11) into equation (9) and recalling

$$P_{X1} = (1 - f_X)2pq$$

we obtain after some algebra

$$\text{Cov}(Y_i, X_j) = \text{Cov}(Y_i, X_j) + \frac{1}{2}pq(\alpha - 1)[\Delta_5 + \Delta_7 + \frac{1}{2}\Delta_8] \quad (12)$$

Letting  $r_{XY}$  be the correlation between the genotypes of  $X$  and  $Y$ , we have

$$\text{Cov}(Y_i, X_j) = r_{XY}[\text{Var}(X_i) \text{Var}(Y_i)]^{1/2} \quad (13)$$

However<sup>19</sup>,

$$r_{XY} = \frac{2f_{XY}}{[(1 + f_X)(1 + f_Y)]^{1/2}} \quad (14)$$

On substituting equations (8) and (14) into equation (13), we obtain

$$\text{Cov}(Y_i, X_j) = f_{XY}pq$$

and so equation (12) becomes

$$\text{Cov}(Y_i, X_j) = f_{XY}pq + \frac{1}{2}pq(\alpha - 1)(\Delta_5 + \Delta_7 + \frac{1}{2}\Delta_8) \quad (15)$$

After rearranging equation (15) and using equation (2b)

$$\text{Cov}(Y_i, X_j) = pq[f_{XY}\alpha + (1 - \alpha)(\Delta_1 + \frac{1}{2}\Delta_3)] \quad (16)$$

On substituting equations (16) and (10) into equation (5), we obtain equation (3) as was to be shown.

Michod<sup>12</sup> (equation (3)) derived the following coefficient for use in Hamilton's rule

$$R = \frac{2xpp' + (1 - x)(1 - 2q)\rho'}{1 + x - 2q} \quad (17)$$

$$\rho' = \frac{(\Delta_1 + \frac{1}{2}\Delta_3)}{q + pf_X} + \frac{q(\Delta_5 + \Delta_7 + \frac{1}{2}\Delta_8)}{q + pf_X} \quad (18a)$$

and

$$\rho' = \frac{\Delta_5 + \Delta_7 + \frac{1}{2}\Delta_8}{1 - f_X} \quad (18b)$$

which are Jacquard's conditional genic structures<sup>12,22,23</sup>. These conditional coefficients in equation (18) give the probability with which  $X$  can predict, on the basis of pedigree ties, the allelic distribution in gametes of  $Y$ . This probability depends on

whether  $X$  is homozygous (equation (18a)) or heterozygous (equation (18b)). In addition, the variable  $x$  appearing in equation (17) is the frequency of altruistic homozygotes among the total class of altruists and is

$$x = \frac{q^2(1-f_x) + f_x q}{q^2(1-f_x) + q f_x + (1-f_x)2pqh} \quad (19)$$

Equation (19) corrects a mistake in Table 1 of Michod<sup>12</sup> where it was thought that the average inbreeding coefficient (averaged over the frequencies of  $X$  and  $Y$  in the population) should be used in equation (19). This is incorrect due to the conditional nature of the altruism. As the gene is only expressed in  $X$ , when  $X$  is in a certain relationship to  $Y$  (the relationship being summarized by the  $\Delta$  values), it is only the frequency of homozygous altruists among all  $X$  individuals which matter in equation (19). This fact alone accounts for the incorrect impression, given in Fig. 2b of that paper<sup>12</sup>, that dominant genes could never increase in frequency. (Fig. 2a of ref. 12 is unaffected by these considerations.) After substituting equations (19) and (18) into equation (17) and collecting the  $\Delta$  values in terms of  $f_{XY}$ , equation (3) is obtained after some rearrangement.

In conclusion, the various coefficients derived in the literature<sup>3,10,12,13,18</sup> for use as  $R$  in Hamilton's rule are equivalent. These coefficients were originally derived from very different points of view. Given the results here, these various approaches support each other and suggest that the one pleomorphic coefficient [equations (3), (5) or (17)] is, indeed, correct.

This work was supported in part by NSF grant DEB 79-10191 to R.E.M. We thank Bob Abugov for discussion and comment.

Received 14 April; accepted 16 October 1980.

1. Hamilton, W. D. *Am. Nat.* **97**, 354-356 (1963).
2. Hamilton, W. D. *J. theor. Biol.* **7**, 1-51 (1964).
3. Orlove, M. J. *J. theor. Biol.* **49**, 289-310 (1975).
4. Levitt, P. R. *Proc. natn. Acad. Sci. U.S.A.* **72**, 4531-4535 (1975).
5. Scudo, F. M. & Ghiselin, M. T. *J. Genet.* **62**, 1-31 (1975).
6. Charnov, E. L. *J. theor. Biol.* **66**, 541-550 (1977).
7. Cavalli-Sforza, L. L. & Feldman, M. W. *Theor. Population Biol.* **14**, 268-281 (1978).
8. Charlesworth, B. *J. theor. Biol.* **72**, 297-319 (1978).
9. Wade, M. J. *Proc. natn. Acad. Sci. U.S.A.* **75**, 6154-6158 (1978); *Am. Nat.* **113**, 399-417 (1979).
10. Orlove, M. J. & Wood, C. L. *J. theor. Biol.* **73**, 679-686 (1978).
11. Craig, R. *Evolution* **33**, 319-334 (1979).
12. Michod, R. E. *J. theor. Biol.* **81**, 223-233 (1979).
13. Flesness, N. R. & Holtzman, R. C. *Am. Nat.* (in the press).
14. Michod, R. E. *Genetics* (in the press).
15. Michod, R. E. & Abugov, R. *Science* **210**, 667-669 (1980).
16. Charlesworth, B. in *Dahlem Workshop on Social Behaviour: Hypothesis and Empirical Tests* (ed. Markl, H.) 11-26 (Verlag Chemie, Weinheim, 1980).
17. Abugov, R. & Michod, R. E. *J. theor. Biol.* (in the press).
18. Michod, R. E. & Anderson, W. W. *Am. Nat.* **114**, 637-647 (1979).
19. Wright, S. *Am. Nat.* **56**, 330-338 (1922).
20. Hamilton, W. D. in *Man and Beast: Comparative Social Behaviour* (eds Eisenberg & Dillon) 57-91 (Smithsonian Institution Press, Washington, DC, 1971).
21. Hamilton, W. D. *A. Rev. Ecol. Syst.* **3**, 193-232 (1972).
22. Jacquard, A. *The Genetic Structure of Populations* (Springer, New York, 1974).
23. Elston, R. C. & Lange, K. *Ann. Hum. Genet.* **39**, 493-496 (1976).

## Proline and valine—cues which stimulate grasshopper herbivory during drought stress?

Brent M. Haglund

Montana Department of Natural Resources and Conservation,  
Biology Department, Montana State University, Bozeman,  
Montana 59717

**Insect herbivores, including members of Orthoptera and Lepidoptera, benefit from increased nitrogen in their food, particularly if it is in the form of easily digested amino acids<sup>1,2</sup>. I report here experimental evidence that grasshoppers detect and preferentially feed on grasses treated with the amino acids proline and valine, which commonly increase in plants under drought stress<sup>3</sup>. This ability may lead to insect concentrations on drought-stressed and nitrogen-enriched plants and thus exacerbate acridid population outbreaks through enhanced growth and survival.**

Ecological studies of grasshoppers and locusts have often considered weather factors to be important determinants of population size or growth rate<sup>4-9</sup>. Dry soil conditions in particular seem to favour population increases of many economically important Orthopteran species<sup>10</sup>. It has been hypothesized that grasshopper growth rates, and consequent survival, increase sharply in drier conditions when perennial grasses have elevated nitrogen (N) levels in parts above ground<sup>1</sup>. Insect herbivores are generally likely to benefit from increased dietary N (ref. 2).

Such elevated nitrogen levels may be the result of increased concentrations of proline<sup>3</sup>. A highly soluble amino acid, proline does not hamper the activities of many photosynthetic enzymes and is able to provide osmotic adjustment in conditions of drought stress or salt accumulation<sup>11-17</sup>. Glycine and valine may function similarly<sup>18</sup>. Leaf laminae accumulate the largest quantities of the newly synthesized proline although it is also found in most other above-ground parts<sup>19</sup>. Genetic varieties of plants which accumulate larger concentrations of free proline tend to survive water stress better and grow faster after stress is relieved<sup>20</sup>.

Mobile herbivores which can detect and concentrate their feeding on N-enriched plants will be favoured relative to conspecifics lacking these abilities. These abilities will be particularly important in environments with food patches of varying N quality. For example, in the northern Great Plains of North America, soil moisture is usually limiting to plant growth in summer. Here forage quality—normally influenced by rainfall—is patchy because thundershowers are local and infrequent.

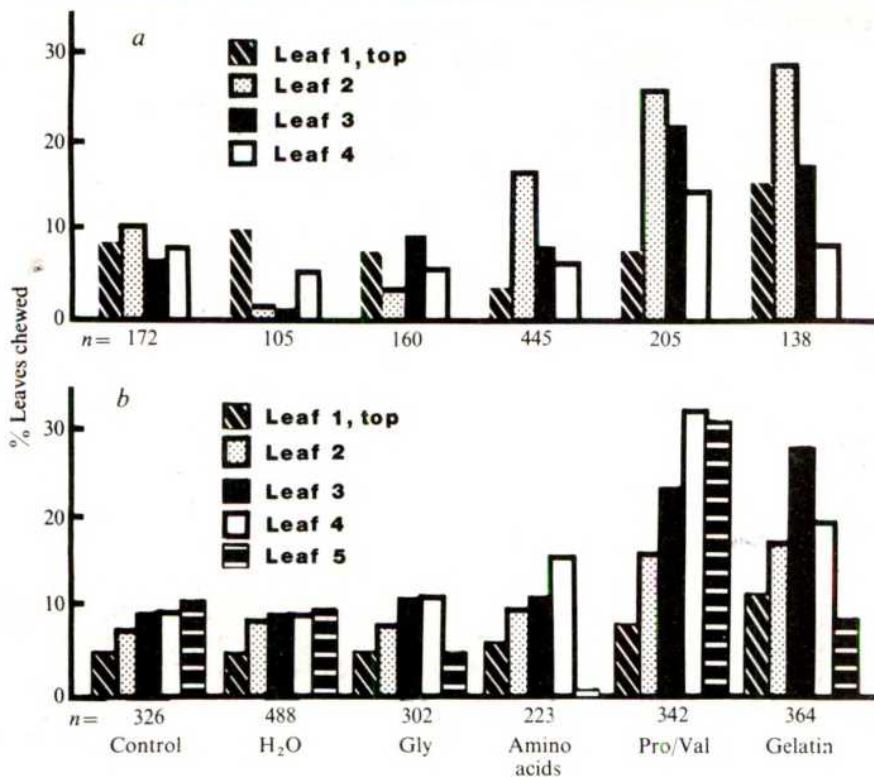
I conducted a field experiment in a native Montana grassland to test the hypothesis that chewing insects can detect plants with elevated amino acid nitrogen levels within the range of levels that occur naturally. A completely randomized two-factor design was replicated three times. Plots of 2 m<sup>2</sup> separated by 4 m buffers were treated. Treatment levels by factor were Factor A (irrigation): none and 25 mm soil surface irrigation; Factor B (foliar sprays): none, 1.6 litre distilled H<sub>2</sub>O, Pro + Val in equal amounts, mixed amino acids in equal amounts (Ala, Arg, Gly, His, Lys, Met, Phe), Gly and gelatin. For the last four treatment levels, amino acids or protein were dissolved in 1.6 litre distilled H<sub>2</sub>O with a concentration equal to 0.7534 g N (except Gly which equalled 7.534 g N). The treatment level was chosen to lie within the range of plant water stress responses and raise the estimated N standing crop by 10%, based on 84 g m<sup>-2</sup> standing crop plant biomass at an estimated 2% total N.

The irrigation treatments were carried out on 9 July 1979 between 0700 and 1000 h; foliar spraying was done by hand on 10 July 1979 from 1230 to 1700 h. Except for the Gly treatment, which was 10 times more concentrated, the maximum possible individual amino acid concentration was 0.93% of plant dry matter compared with measured proline levels of 1% or greater for barley<sup>14</sup>, Bermuda grass<sup>15</sup>, tobacco<sup>16</sup>, clover<sup>21</sup> and several halophyte species<sup>11,17</sup> under water stress. Proline can accumulate to as much as 10-20% of shoot dry weight in *Triglochin maritima*<sup>17</sup>. I estimated that less than one quarter of the spray from any of the treatments contacted the leaves due to low plant density at the site.

The dependent variable measured was percentage of leaves chewed on stems of *Agropyron smithii* with four intact leaves, a C<sub>3</sub> grass, and *Bouteloua gracilis* with five intact leaves, a C<sub>4</sub> grass, stratified by leaf position enumerated from youngest to oldest. Virtually complete collections of stems of these two species were gathered by hand on 6 September 1979. The total number of stems sampled for each of the foliar spray treatments is shown in Fig. 1. Only chewed leaves were counted—broken leaf tips were not recorded.

Chewing was affected by two amino acid treatments but was unaffected by irrigation or the remaining amino acid sprays ( $\chi^2$  test,  $P < 0.001$ ). Because irrigation treatments showed no influence on chewing ( $P > 0.3$ ) data were pooled across water levels in the subsequent analysis. Paired *t*-test analysis of percentage of leaves chewed by leaf position indicated





**Fig. 1** Percentage of leaves chewed by grasshoppers in response to amino acid foliar spray treatments on two grass species: *Agropyron smithii* (a) and *Bouteloua gracilis* (b). Each bar represents the percentage of leaves at each position that were chewed. Leaf position is assigned from the top to the bottom of the stem. Sample size ( $n$ ) is the total number of stems assayed within each treatment.

significant differences ( $P < 0.01$ ) on the second and third leaves of *A. smithii* and on the third, fourth and fifth leaves of *B. gracilis* with Pro and Val. With the gelatin treatment, only the second leaf of *A. smithii* and the third and fourth leaves of *B. gracilis* showed greater numbers of chews. At the time of spraying the first leaf of both species had not emerged; the fourth leaf of *A. smithii* was already brown and probably dead.

Grasshoppers were not responding to an improvement in plant condition due to N enrichment. Forty randomly selected plants from each foliar treatment were measured for stem length, leaf length (numbers two and three) and colour (completely brown or some green remaining). With analysis of variance no difference in these variables could be detected among the treatments ( $P > 0.2$ ).

I conclude that grasshoppers (over 95% of the chewing insects on the plots in July and August and dominated by *Opeia obsura*, *Trachyrachis kiowa* and *Melanoplus sanguinipes*) can detect either proline or valine on plant tissue. They selected grass treated with proline and valine and also grass treated with gelatin containing proline (15%) and valine (3%) residues. Although glycine is an important component (45%) of gelatin, glycine alone had no effect on insect chewing. The possibility that grasshoppers are capable of chemodetection is supported by the documentation<sup>22</sup> of the presence of amino acid receptors in other chewing insects, the Lepidoptera. Aphids are also known to detect amino acids<sup>23</sup>. Furthermore, proline is reported to be a feeding attractant to the snail *Biomphalaria glabrata*<sup>24</sup>.

Proline is used by animals in various ways including intermediate energy metabolism, enzyme synthesis and, in large amounts, for connective tissue. It can also be used for osmoregulation. Insects able to find and consume proline in above average quantities are likely to grow faster. I suggest that proline accumulations will affect chewing insects much less in wet years or in conditions of augmented soil moisture through weather modification or irrigation.

Management implications of this plant-herbivore interaction include the possibility of lowered insect herbivory to the extent that weather modification or irrigation could relieve plant

drought stress. Plants intimately coevolved with their insect herbivores may find partial relief from drought stress by herbivory because it reduces leaf area, allowing water to become more concentrated in remaining leaf tissue<sup>25,26</sup>. However, crop plants genetically engineered for greater proline production in the hopes of raising their drought tolerance and thereby increasing their yield may be at increased risk to insect pests<sup>27</sup>.

I thank T. W. Weaver III for ideas. This research was funded by the High Plains Cooperative Program, Montana Department of National Resources and Conservation grant no. 14-06-D-7577, Water and Power Resources Service, US Department of Interior. Land was made available by the Livestock and Range Research Station, Agricultural Research Service, US Department of Agriculture.

Received 17 April; accepted 15 October 1980.

- White, T. R. C. *Oecologia* **22**, 119-134 (1976).
- Slansky, F. Jr & Feeny, P. *Ecol. Monogr.* **47**, 209-228 (1977).
- Hsiao, T. C. A. *Rev. Pl. Physiol.* **24**, 519-570 (1973).
- Andrewartha, H. G. & Birch, L. C. *The Distribution and Abundance of Animals* (University of Chicago Press, 1954).
- Betts, E. *Anti-Locust Mem.* **6**, 1-25 (1961).
- Dempster, J. P. *Biol. Rev.* **38**, 490-529 (1963).
- Edwards, R. L. *Can. Ent.* **92**, 619-624 (1960).
- Rodell, C. F. *Ecology* **58**, 227-245 (1977).
- Uvarov, B. P. *Trans. ent. Soc. Lond.* **79**, 1-247 (1931).
- Gage, S. H. & Mukerji, M. K. *Envir. Ent.* **6**, 469-479 (1977).
- Cavallieri, A. J. & Huang, A. H. C. *Am. J. Bot.* **66**, 307-312 (1979).
- Hanson, A. D. & Tully, R. E. *Planta* **145**, 45-52 (1979).
- Singh, T. N. *et al. Aust. J. biol. Sci.* **26**, 45-56 (1973a).
- Singh, T. N. *et al. Nature new Biol.* **236**, 188-190 (1972).
- Barnett, N. M. & Naylor, A. W. *Pl. Physiol.* **41**, 1222-1230 (1966).
- Mizusaki, S. *et al. Archs Biochem. Biophys.* **105**, 599 (1964).
- Stewart, G. R. & Lee, J. A. *Planta* **120**, 279-289 (1974).
- Naylor, A. W. in *Water Deficits and Plant Growth* (ed. Kozlowski, T. T.) 241-254 (Academic, New York, 1972).
- Singh, T. N. *et al. Aust. J. biol. Sci.* **26**, 57-63 (1973b).
- Singh, T. N. *et al. Aust. J. biol. Sci.* **26**, 64-72 (1973c).
- Routley, D. G. *Crop Sci.* **6**, 358-361 (1966).
- Schoonhoven, L. M. *Nature* **221**, 1268 (1969).
- Van Emden, H. F. *Insect/Plant Relationships* (Symp. R. ent. Soc., London, 1972).
- Uhazy, L. S. *et al. Science* **201**, 924-926 (1978).
- McNaughton, S. J. *Am. Nat.* **113**, 691-703 (1979).
- Wisnol, K. J. *Range Mgmt* **32**, 194-195 (1979).
- Marx, J. L. *Science* **206**, 1168-1169 (1979).

## Insect populations respond to fluctuating environments

David A. Jillson

Department of Zoology, University of Vermont, Burlington, Vermont 05405

Models of populations inhabiting regularly fluctuating environments suggest that the nature of the population fluctuation is determined by the relative sizes of the characteristic response time of the population,  $T_R$ , and the period of the environmental variation. For example, May's<sup>1</sup> model of a density-regulated population inhabiting a sinusoidally varying environment showed that when the characteristic response time was long relative to the period of environmental fluctuation,  $Y$ , the population averaged out environmental fluctuations, whereas for  $T_R$  short relative to  $Y$ , the population tended to track environmental variations. Characteristic response time is a measure of how quickly a system returns to equilibrium following a disturbance, and for the logistic model and its immediate relatives,  $T_R$  equals the inverse of population growth rate,  $r$ . The present study investigated the responses of populations of the flour beetle, *Tribolium castaneum*, cultured in a series of regularly fluctuating environments. Responses to environmental fluctuations were striking at all periods of environmental fluctuations, but population density declined as environmental period lengthened.

Environmental fluctuations were created by altering the amount of culture medium (95% unbleached wheat flour, 5% brewer's yeast by weight) between 32 and 8 g at regular intervals. This experimental regime represents fluctuations in carrying capacity, for *Tribolium* population size is known to be positively correlated with the amount of culture medium<sup>2</sup>. *T. castaneum* populations were cultured in each of five experimental regimes—a constant 20-g environment, and fluctuating environments with 4-, 8-, 12- and 16-week periods. The periods were chosen to represent intervals ranging from the equivalent of, to much longer than an estimate of *T. castaneum* characteristic response time. *Tribolium* characteristic response time was calculated by taking the inverse of population growth rate. This procedure is accurate if the logistic model is an adequate representation of *Tribolium* population dynamics and was used as simple approximation to  $T_R$ . Estimates of *T. castaneum* population growth rates derived from age-specific survivorship and fecundity schedules range from 0.7 to 1.3 per week<sup>3-6</sup>, corresponding to  $T_R$  of approximately 1 week. Estimates of  $r$  taken from exponential growth phases of *T. castaneum* population growth data<sup>6-8</sup> yield longer response times of 2-6 weeks, and may be more indicative of attainable rates of growth.

Thirty cultures of the corn oil-sensitive strain of *T. castaneum*<sup>9-16</sup> were initiated with 30 adults in a 1:1 sex ratio and 75 unsexed small larvae. Populations were censused at 2-week intervals: larvae, pupae and adults were counted and returned to fresh medium of the appropriate amount. All populations were cultured in 20-g medium for the initial 18 weeks of the experiment to allow the populations to approach demographic and numerical equilibrium. At week 18, six populations were randomly assigned to each of the five treatments, and the series of environmental fluctuations began, continuing until week 64.

Regular though small fluctuations were characteristic of the mean population size over time in the constant 20-g environment (Fig. 1). These intrinsic fluctuations were partly caused by cannibalistic interactions<sup>15-18</sup>. A significant linear regression of mean population size with time showed that populations increased modestly at a rate of only four animals per week.

In contrast, populations in the 4-week treatment increased in density substantially. During weeks 18 to 54, populations increased on average by 21 animals per week. Fluctuations were also seen in this treatment—local increases in population size occurred during periods of 32-g medium, and, except for the decline from week 54 to 56, every decrease occurred in 8-g medium. Bursts of recruitment occurred in the relatively abundant 32-g medium, enhancing the number of small larvae successfully recruited. After two weeks of 8-g medium, 32 g were

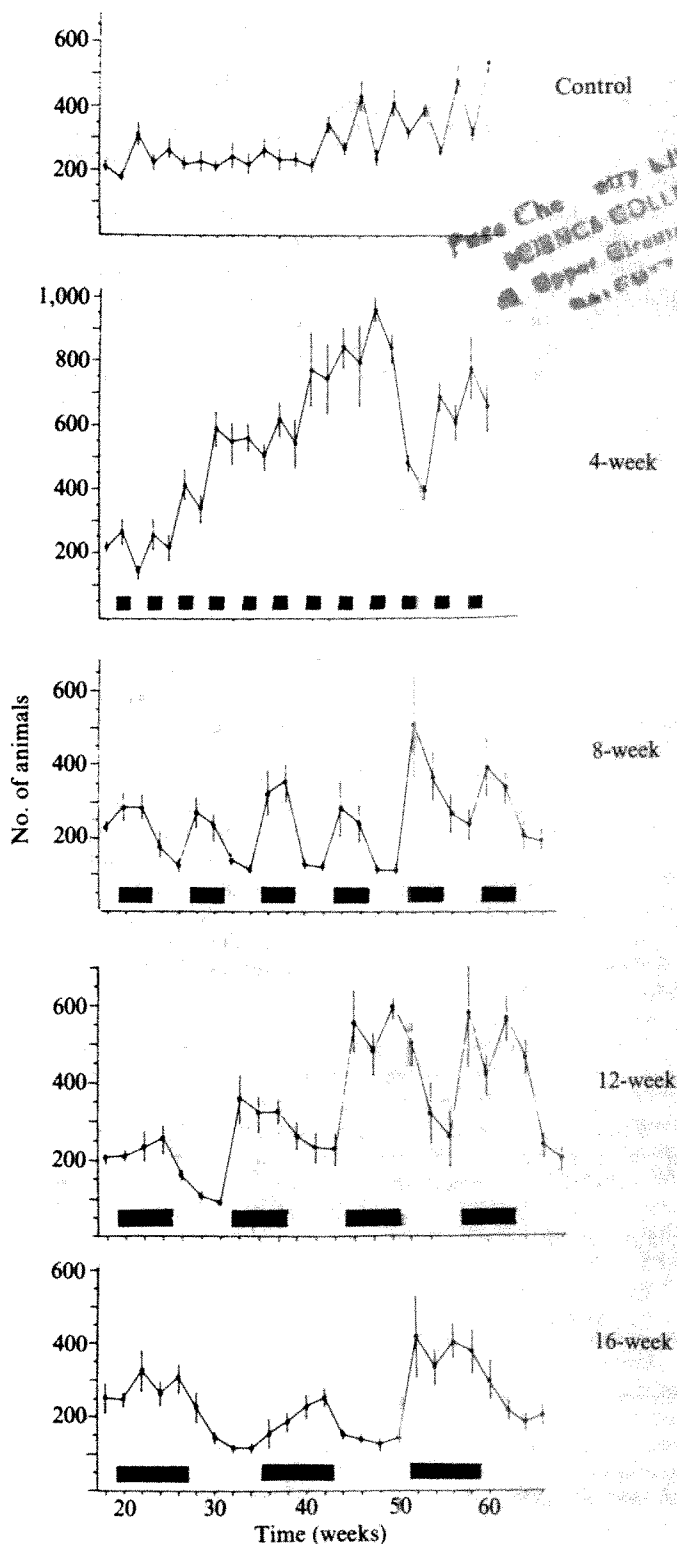


Fig. 1 Mean number ( $\pm$ s.e.) of animals in constant and fluctuating environments. Shaded bars in fluctuating treatments represent periods of 32-g medium, intervening periods had 8-g medium.



available again, the small larval cohort had become large larvae and were able to pupate in abundant medium where cannibalism was reduced. It is most interesting that the 4-week period of environmental fluctuation was ideally suited to the 4-week *T. castaneum* developmental period by maximizing the recruitment of small larvae and minimizing cannibalism on the vulnerable pupae. This treatment attained the highest population densities of the experiment, approximately twice that of the other treatments. This does not agree with predictions that fluctuations in carrying capacity reduce the long-term average population number below that attained in a constant environment<sup>1,19,20</sup>. Wool and Sverdlov<sup>21</sup> reported a similar discrepancy—*Tribolium* productivity tended to be higher in temporally variable than in constant environments. Predictions of a reduction in mean population size were premised on the logistic model, which fails to incorporate the effects of cannibalism, an important factor in *Tribolium* population dynamics<sup>17,18</sup>.

Populations inhabiting the 8-week treatment responded to environmental fluctuations differently from those in the 4-week cycle. Periods of abundant resources supported high densities and vice versa. In contrast to the 4-week treatment, these populations increased only moderately with time. Although bursts of recruitment occurred in 32-g conditions, each cohort of small larvae suffered high losses due to cannibalism when pupation occurred in crowded 8-g conditions.

In the 12-week treatment, mean population size again responded to environmental fluctuations, with population abundance directly proportional to the amount of culture medium. Population peaks tended to contain local dips, reflecting intrinsic patterns of cannibalism on eggs by a cohort of large larvae. Populations in the 16-week treatment also clearly mimicked the physical regime. The three complete cycles of culture medium resulted in three population cycles. Populations in the 12- and 16-week treatments were able to recruit young and undergo pupation in a sequence of 32-g medium, but the next cycle of recruitment was delayed by 6 and 8 weeks respectively by the intervening 8-g period, effectively reducing mean population size.

The proportion of adults in the control and 4-week cycle was relatively constant, and did not display any strong correlation with environmental variability. In contrast, the age distribution in the 8-, 12- and 16-week treatments followed environmental fluctuations, with 80–90% adults found during periods of sparse culture medium, alternating with 20–30% adults in periods of 32-g medium. These demographic oscillations were predominantly caused by recruitment of substantial numbers of immatures in 32-g medium whereas adult numbers remained relatively constant over time.

*Tribolium* populations clearly exhibited changes in density and age distribution in concert with temporal changes in resource availability. In addition, the large mean population size attained in the 4-week treatment was caused by a particular temporal pattern of environmental variation which suited this animal ideally. Although the mean amount of culture medium with time was the same in all treatments, 20 g, differing sequences of resource distribution yielded large differences in population size.

This work was supported by a University of Vermont Institutional Award.

12. Costantino, R. F., Mumma, R. O. & Bruszewski, T. E. *Heredity* **25**, 411–418 (1970).
13. Costantino, R. F. & Rowe, P. M. *Heredity* **29**, 247–252 (1972).
14. Scully, A. M. M. & Costantino, R. F. *Can. J. Genet. Cytol.* **17**, 585–590 (1975).
15. Moffa, A. M. & Costantino, R. F. *Genetics* **87**, 785–805 (1977).
16. Jilison, D. A. & Costantino, R. F. *Am. Nat.* **116**, 206–219 (1980).
17. Lloyd, M. *Ecology* **49**, 245–259 (1968).
18. Desharnais, R. A. & Costantino, R. F. *Can. J. Genet. Cytol.* (in the press).
19. Nisbet, R. M. & Gurney, W. S. C. *J. theor. Biol.* **56**, 459–475 (1976).
20. May, R. M. *Stability and Complexity in Model Ecosystems* (Princeton University Press, New Jersey, 1973).
21. Wool, D. & Sverdlov, E. *Evolution* **30**, 119–129 (1976).

## Multiple extraocular photoreceptive areas on genitalia of butterfly *Papilio xuthus*

Kentaro Arikawa, Eisuke Eguchi\*, Akihiro Yoshida & Kiyoshi Aoki

Life Science Institute, Sophia University, 7-1 Kioicho, Chiyoda-ku, Tokyo, Japan

\* Department of Biology, Yokohama City University, Kanazawa-ku, Yokohama, Japan

Extraocular photoreception has been reported in several orders of insects, and direct photoreception by the central nervous system (CNS) has been shown to be related to the circadian clock in many cases<sup>1</sup>. For example, CNS photoreceptors have been found in the brain and the last abdominal ganglion of the cockroach, *Periplaneta americana*, and in the brain of the silkworm, *Hyalophora cecropia*<sup>2</sup>. In other cases dermal light sensitivity has been deduced from behavioural responses. For instance, the larvae of *Tenebrio molitor* avoid light even after decapitation<sup>3</sup>. The antennae of *Aphis fabae* seem to be the site of light sensitivity responsible for the animal's photokinetic activity<sup>4</sup>. Dermal light sensitivity is demonstrable in all the tergites of the larvae of *Acilius japonicus* and *Dytiscus marginalis*, particularly well developed in the region of terminal abdominal spiracles<sup>5</sup>. We report here, however, the electrophysiological response and morphological characteristics of presumptive photoreceptive sites on the genitalia of the Chinese yellow swallowtail butterfly, *Papilio xuthus* L.

Electrophysiological recordings were made on summer forms of *P. xuthus* collected from a wild population in June 1980. For anatomical studies we used spring forms reared on a semi-artificial diet in the laboratory at 20 °C and with a 8L:16D light regime.

We found that two (N5, N6) of the six pairs (N1–N6, numbered from the most anterior pair) of nerve roots belonging to the last abdominal ganglion contained afferent photosensitive axons. Recordings could be made easily from cut proximal ends of these nerves by means of suction electrodes (Fig. 1a): responses consisted of sustained trains of spikes.

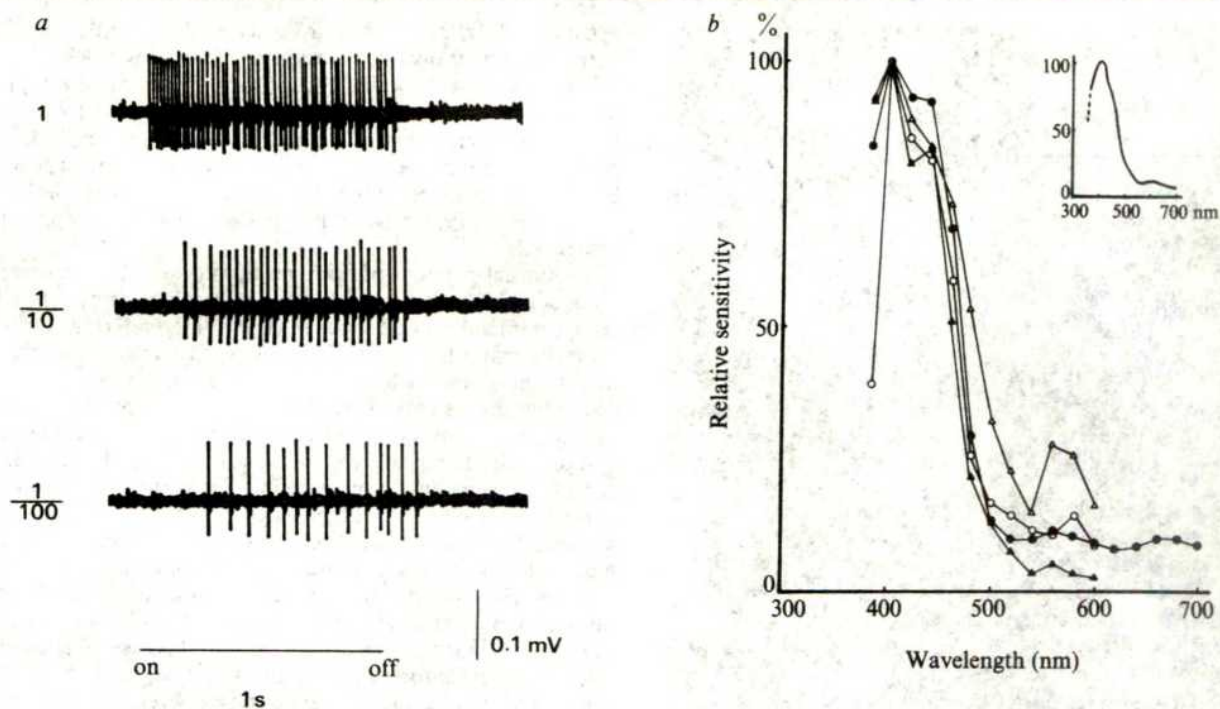
In white light, impulse frequency is related to log *I* (light intensity) by an S-shaped curve. The latent period varies inversely with *I* (Fig. 1a). Spectral sensitivity was determined for the photosensitive units by using 17 monochromatic light bands of 380–700 nm; it peaked at about 400 nm (Fig. 1b). Only one class of units has been recognized.

However, exploration with a 1-mm spot of light demonstrated two distinct photoreceptive areas on each side of the genital region, one (P1) sending afferents to root N6, and the other (P2) connecting with the CNS through N5. P1 and P2 are located in different areas specific to males and females. By anatomical isolation (for P1) and cutting of other nerves (for P2) the photoreceptor sites can be localized as follows.

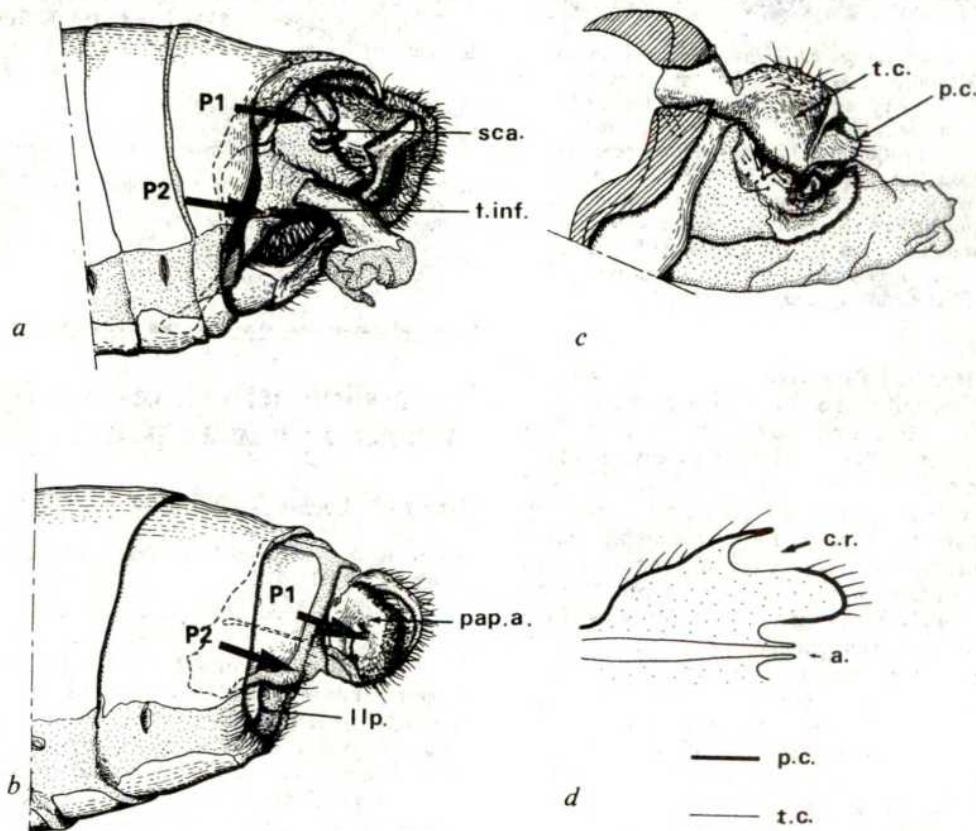
In males ♂ P1 lies in the scaphium whereas ♂ P2 is on the fultura inferior (Fig. 2a). The scaphium is a sclerotized plate-like structure on the dorsal surface of the tuba analis, and the fultura inferior is a ventral part of the terminal diaphragm of

Received 9 July; accepted 13 October 1980.

1. May, R. M. in *Theoretical Ecology* (ed. May, R. M.) 4–25 (Saunders, Philadelphia, 1976).
2. Chapman, R. N. *Ecology* **9**, 111–122 (1928).
3. Leslie, P. H. & Park, T. *Ecology* **30**, 469–477 (1949).
4. Mertz, D. M. *Ecol. Monogr.* **39**, 1–31 (1969).
5. Young, A. M. *Ecology* **51**, 602–619 (1970).
6. Jilison, D. A. thesis, Univ. Rhode Island (1977).
7. Park, T., Leslie, P. H. & Mertz, D. B. *Physiol. Zool.* **37**, 97–162 (1964).
8. Park, T. *Physiol. Zool.* **27**, 177–238 (1954).
9. Costantino, R. F., Bell, A. E. & Rogler, J. C. *Nature* **210**, 221–222 (1966).
10. Costantino, R. F., Bell, A. E. & Rogler, J. C. *Heredity* **22**, 529–539 (1967).
11. Costantino, R. F., Rogler, J. C. & Bell, A. E. *Heredity* **23**, 477–483 (1968).

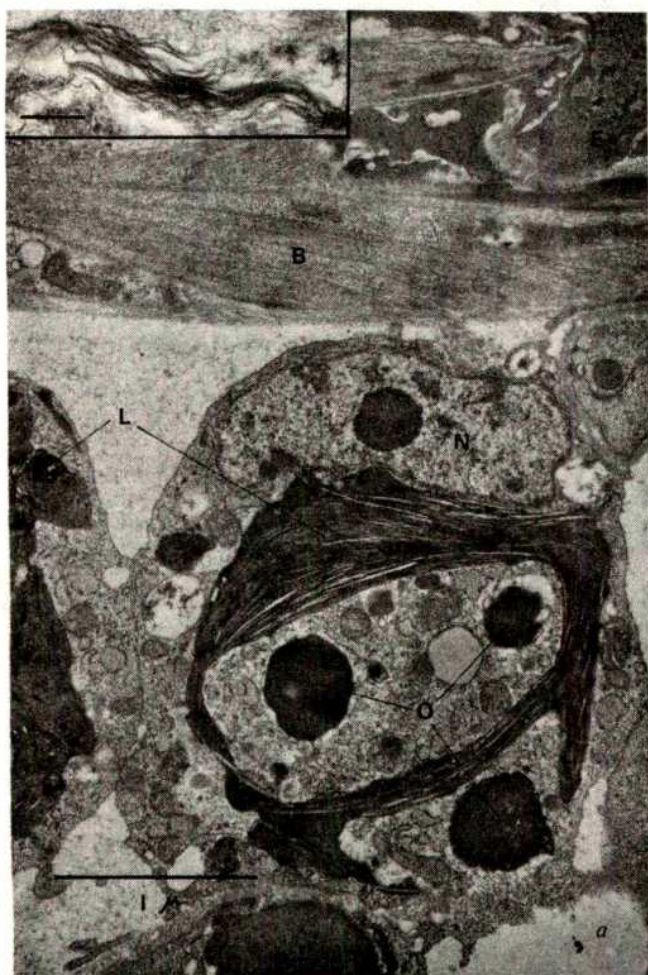


**Fig. 1** Electrophysiological responses. *a*, Typical spike train evoked by a 1-s flash of white light. Numbers at the left are the relative light intensities ( $I \sim 5,000$  lx). Recording from N5 of the last abdominal ganglion of a male *P. xuthus*. This nerve receives afferents from the fultura inferior (P2). Similar responses were obtained from N5 as well as N6 in both sexes. *b*, Spectral sensitivity of four individuals:  $\circ$  and  $\bullet$ , males recorded from N6;  $\Delta$ , female recorded from N6;  $\triangle$ , female recorded from N5. Spike numbers at  $\lambda_{\max} = 400$  nm were taken as 100%. Inset, averaged curve.



**Fig. 2** Location (four arrows in *a* and *c*) and external features of *P. xuthus* photoreceptive sites identified by response to stimulation by a 1-mm spot of light. *a*, Tip of male abdomen seen laterally from the left side with left valva removed; *b*, tip of female abdomen seen laterally from the left side; *c*, detail of male scaphium; *d*, schematic horizontal section of the concave light sensitive area of the papilla analis. sca., Scaphium; f.inf., fultura inferior; pap.a., papilla analis; llp., lamella postvaginalis; p.c., pigmented cuticle; t.c., transparent cuticle; c.r., concave region; a., anus.





**Fig. 3** Presumed photoreceptive cell in the male scaphium. *a*, Overall view (scale = 1  $\mu$ m); *b*, detail of lamellated structure in the cytoplasm of the cell (scale = 0.1  $\mu$ m). Specimens were prefixed for 4–5 h with 2.0% glutaraldehyde and 2.0% paraformaldehyde in 0.1 M cacodylate buffer solution at pH 7.4 at room temperature. After washing, the tissue was post-fixed for 2–3 h in 2.0%  $\text{OsO}_4$  in the same buffer, dehydrated in an acetone series and embedded in Epon. Cut with a diamond knife, sections were stained with uranyl acetate and lead citrate and observed with a JEM 100B electron microscope. N, nucleus; B, basement membrane; L, lamellated body; E, epidermal cell; O, oil droplet.

male butterflies. In females  $\text{P1}$  lies on the papilla analis and  $\text{P2}$  lies laterally on the membrane between the papilla analis and the lamella postvaginalis (Fig. 2*b*). The papillae anales covered with chitinous hairs are strongly sclerotized lobes between which the anus and ostium oviductus open to the exterior.

Externally these various photoreceptor sites are marked by small areas of transparent cuticle, which elsewhere is pigmented and opaque. Thus the scaphium is pale brown over most of its surface but has a transparent area on its inner margin. Also the papilla analis is strongly pigmented except for a concave posterior region which is transparent and free of hairs (Fig. 2*d*).

When the transparent  $\text{P1}$  genital areas are covered with opaque material the afferent responses in  $\text{N6}$  are blocked completely. When this opaque material is removed, light-induced spikes reappear as in the normal preparation (Fig. 1). This shows that the photoreceptive elements of  $\text{P1}$  are illuminated through its local clear cuticular area. Similar transparent spots as described above, characterize the  $\text{P2}$  area but the effect of screening them has not been tested yet.

To localize further the receptor elements involved in  $\text{P1}$  and  $\text{P2}$  we examined these areas by transmission electron microscopy. That revealed, directly under the basement membrane of the epidermis, cells containing well-developed lamellated

organelles (Fig. 3*a*). These are essentially the same under the corresponding transparent cuticle of both  $\text{P1}$  and  $\text{P2}$ .

These lamellated bodies occupy a large volume of cytoplasm and may be associated with the photosensitivity. Lamellated bodies resembling those identified in the butterfly scaphium and papilla analis have been observed in the eyes of other invertebrates—for example, in the distal photoreceptor cells of the eye of the scallop *Pecten*<sup>6</sup> and the proximal region of cephalopod visual cells<sup>7</sup>.

The visual pigment of both vertebrates and invertebrates is embedded in elaborate disk-like or microvillus arrays of photoreceptor membrane. However, the epidermal cells of these butterfly photoreceptors show no such surface cytoplasmic membrane system, suggesting that they are not the light sensitive units in this case. However, there are other cells directly beneath the transparent cuticle and epidermis, with extensive cytoplasmic membrane systems, and they may be the photoreceptive organelles. A more convincing demonstration of such a function would depend on both proof of the appropriate axonal or synaptic connection to supply the observed spikes in  $\text{N6}$ , and a more detailed study of the lamellated membrane systems. Fine structural changes due to light and dark adaptation, as well as evidence for localization of visual pigment molecules might also prove diagnostic in this case. Whether and how these receptors are functional in copulation or other reproductive behaviour remain to be discovered.

We also obtained responses to white light stimulation of the genitalia with 6 other species of Papilionidae and 10 species from 6 of the 7 other butterfly families found in Japan (Libytheidae have not been tested yet). However, no such responses could be detected electrophysiologically in either nocturnal (two species tested) or diurnal (four species tested) moths.

We thank Mr Jun Emoto, Nanzan University, for critical comments and Dr Talbot H. Waterman, Yale University, and Dr Jean M. Michalec, Sophia University, for reviewing the manuscript. This work was supported in part by a Grant-in-Aid for Scientific Research 411201 and 510906 from the Ministry of Education, Science and Culture of Japan.

Received 7 August; accepted 30 October 1980.

1. Bennett, M. F. in *Handbook of Sensory Physiology* Vol. 7, 6A (ed. Autrum, H.) 641–664 (Springer, New York, 1979).
2. Saunders, D. S. *Insect Clocks* (Pergamon, Oxford, 1976).
3. Tucelesco, J. *Bull. Biol.* no. 4, 1–35 (1933).
4. Booth, C. O. *Nature* **197**, 265–266 (1963).
5. Schöne, H. Z. *vergl. Physiol.* **33**, 63–98 (1951).
6. Barber, V. C. et al. *Z. Zellforsch.* **76**, 295–359 (1967).
7. Yamamoto, T. et al. *J. Cell Biol.* **25**, 345–359 (1965).

## Reversible activation–inactivation of renin in human plasma

Brenda J. Leckie & Norah K. McGhee

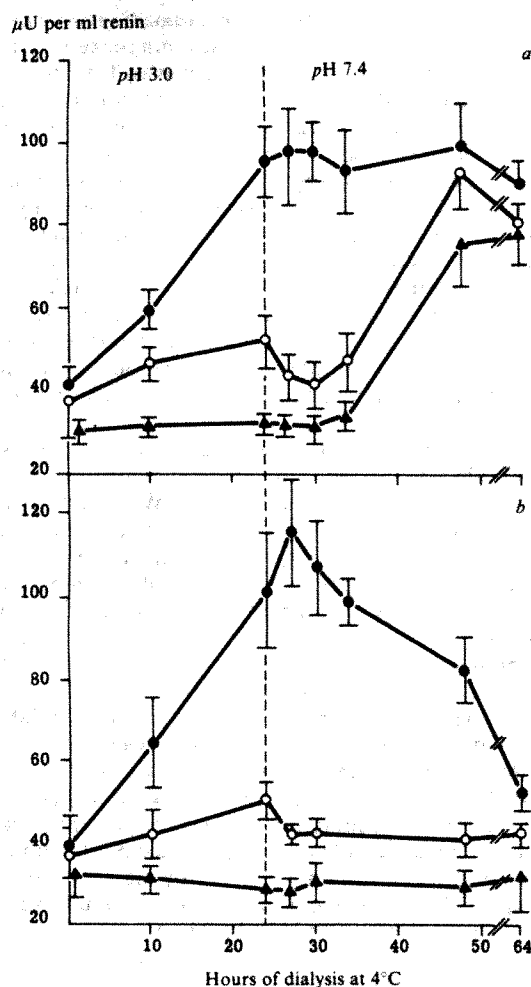
Medical Research Council Blood Pressure Unit, Western Infirmary, Glasgow G11 6NT, UK

Renin, an aspartate protease, cleaves the  $\alpha$ -globulin angiotensinogen to produce the decapeptide angiotensin I, which is then converted to the vasoactive hormone angiotensin II by the action of a peptidase 'converting enzyme'. An inactive form of renin<sup>1–3</sup> sometimes termed prorenin<sup>4</sup> is present in normal human plasma. Its enzymatic activity is increased by exposure to a pH of 3.0 or 3.3 followed by dialysis towards neutral pH. Only a small proportion of the inactive renin is activated during the acid stage of dialysis, most of the activation apparently taking place during the subsequent dialysis to pH 5.7 (ref. 4) or 7.5 (ref. 5). Furthermore, if inhibitors of serine proteases are added to the plasma, the amount of inactive renin activated by this

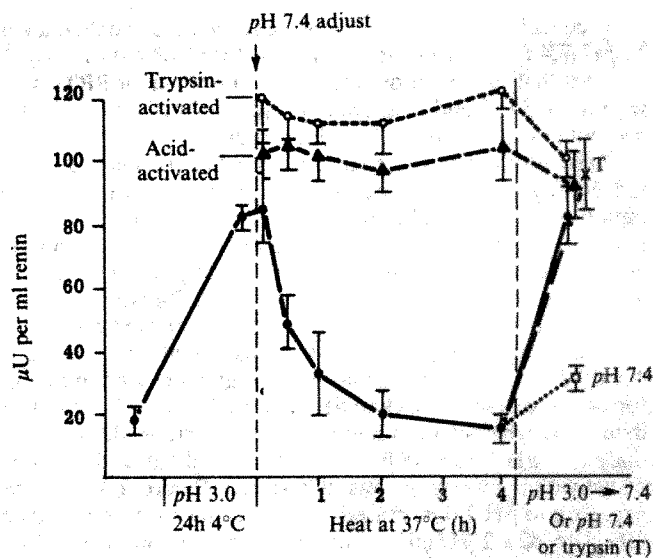


dialysis procedure is reduced<sup>4,6</sup>. These results suggest that acid-activation is mediated by serine proteases. The role of enzymes such as plasma kallikrein, plasmin and renal kallikrein as physiological activators of inactive renin has recently been discussed<sup>5,9</sup>. In our study of the activation of plasma inactive renin we have now found that, contrary to previous reports<sup>4,5</sup>, complete activation of inactive renin takes place during the acid stage of dialysis. This activation can be reversed if plasma is rapidly adjusted to pH 7.4 and warmed. The next step in the acid-activation procedure, that is, dialysis to neutral pH, renders the initial acid-activation irreversible. These results were completely unexpected, and we offer an explanation that reassesses the nature of inactive renin and the activation process.

In the first series of experiments we studied the change in the renin concentration of normal male plasma during acid-activation in the presence and absence of soya bean trypsin inhibitor (Fig. 1). Samples of plasma (0.5 ml) were dialysed to pH 3.0 for 24 h at 4°C (ref. 1) and then taken to pH 7.4 at 4°C. At intervals, plasma was removed from the dialysis bags and transferred to 50 µl soya bean trypsin inhibitor (SBTI) solution<sup>6</sup> to



**Fig. 1** The renin concentration (ordinate) in normal human plasma during dialysis at 4°C to pH 3.0 followed by dialysis to pH 7.4. *a*, 0.5-ml samples of plasma were dialysed against 15 ml of pH 3.0 glycine/HCl buffer<sup>1</sup> at 4°C. At 0, 10 and 24 h, samples were removed from the dialysis bags and added to 50 µl of a 5 mg ml<sup>-1</sup> solution of SBTI to give a final concentration of 19 µmol per 1 SBTI. 50 µl of 3 M Tris-HCl buffer was added and the renin concentration assayed immediately by measuring the rate of angiotensin I generation from ox angiotensinogen<sup>10</sup>. ●, Immediate assay; ○, assay after 1 h at 37°C; ▲, assay after 5 h at 37°C. *b*, As for *a* except that 19 µmol per 1 SBTI was added to the plasma before the start of dialysis. Mean  $\pm$  s.e.m. of four experiments.



**Fig. 2** ●, Plasma was dialysed to pH 3.0 for 24 h at 4°C then 1/10 volume of 3 M Tris-HCl buffer added and the plasma warmed at 37°C. After 4 h the remaining plasma was dialysed to pH 3.0 and dialysed back to pH 7.4 at 4°C. Controls were dialysed to pH 7.4 for 48 h at 4°C (□). ▲, Plasma was dialysed to pH 3.0 for 24 h at 4°C and dialysed back to pH 7.4 at 4°C before the addition of 3 M Tris-HCl buffer and warming. ○, Plasma was trypsin-activated before being treated as described above. Mean  $\pm$  s.e.m. of three experiments.

give a final concentration of 19 µmol l<sup>-1</sup> SBTI. The inhibitor was used to prevent any activation of inactive renin by plasma proteases after removal of the sample from the dialysis bag<sup>6</sup>. The pH of the plasma was adjusted to between 7.4 and 7.5 at 4°C with the addition of 50 µl 3 M Tris-HCl buffer, pH 7.6, and the samples were immediately assayed for renin<sup>10</sup>. The renin was re-assayed after the samples had been incubated for 1 h at 37°C and again after 5 h. In a parallel series of experiments, 19 µmol l<sup>-1</sup> SBTI was added to the plasma before the start of the dialysis. Samples were dialysed as before, except that no further SBTI was added before adjustment of the pH and the samples were assayed for renin. Figure 1*a* shows the results of experiments in which plasma was dialysed without SBTI and assayed for renin immediately after adjustment to pH 7.4. During dialysis at pH 3.0 the renin concentration increased from 41  $\pm$  4 µU ml<sup>-1</sup> to 95  $\pm$  8 µU ml<sup>-1</sup> (mean  $\pm$  s.e.m.,  $P < 0.01$ ). During the subsequent dialysis to pH 7.4, the renin concentration did not change: 98  $\pm$  9 µU ml<sup>-1</sup> at 24 h (that is, 48 h from the start of the experiment) and 89  $\pm$  6 µU ml<sup>-1</sup> after 40 h (64 h from the start). Thus dialysis to pH 3.0 completely activated the inactive renin in this plasma. We confirmed that activation was complete by treating a separate portion of the plasma with trypsin<sup>10</sup>, which gave a renin concentration of 100  $\pm$  12 µU ml<sup>-1</sup> similar to that of 95  $\pm$  8 µU ml<sup>-1</sup> obtained with acid alone.

A different pattern was obtained if the samples were allowed to stand at 37°C for 1 h before being assayed. In this case, the renin concentration apparently increased to only 52  $\pm$  6 µU ml<sup>-1</sup> after the pH 3.0 stage of dialysis, but to 91  $\pm$  7 µU ml<sup>-1</sup> after dialysis to pH 7.4. If the plasma was assayed after 5 h at 37°C there was an apparent lack of activation during the pH 3.0 stage of dialysis. This pattern of activation is similar to that obtained elsewhere<sup>4,5</sup>.

Figure 1*b* shows the results of the experiments in which SBTI was added to the plasma before the start of dialysis. The activation obtained during the pH 3.0 stage of dialysis was similar to that for renin in plasma dialysed without SBTI. However, during the dialysis to pH 7.4 in the presence of SBTI the renin concentration in the plasma fell slowly over 40 h so that the final value of 58  $\pm$  5 µU ml<sup>-1</sup> was lower than that after the dialysis to pH 3.0 alone ( $P < 0.05$ ) and also lower than the



renin concentration in plasma dialysed at pH 3.0 and then taken to pH 7.4 for 40 h in the absence of SBTI ( $P < 0.01$ ). When samples that had been dialysed in the presence of SBTI were warmed at 37 °C and re-assayed, no apparent activation of renin was noted throughout both periods of dialysis.

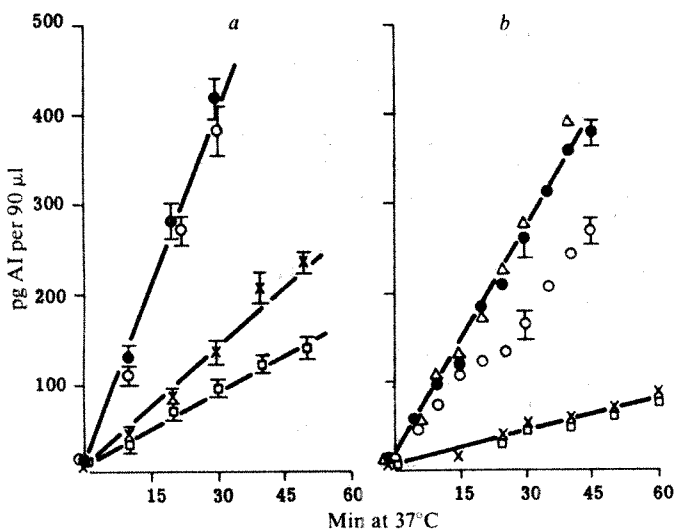
These results showed that the activation of inactive renin induced by acid dialysis could be reversed if the plasma was rapidly neutralized and warmed. We investigated the reversal in a second series of experiments using another sample of pooled normal plasma. The plasma was dialysed to pH 3.0 for 24 h at 4 °C, assayed for renin then adjusted to pH 7.4 with 3 M Tris-HCl buffer at 4 °C and re-assayed. The plasma was warmed at 37 °C and the renin concentration measured at intervals. After 4 h at 37 °C the remaining plasma was again dialysed to pH 3.0 for 24 h and dialysed back to pH 7.4 for a further 24 h at 4 °C to determine whether the renin could be re-activated. A control dialysis to pH 7.4 for 48 h at 4 °C was carried out, and the effect of activation by trypsin was also tested. Figure 2 shows that exposure to pH 3.0 increased plasma renin concentration from  $19 \pm 3$  to  $82 \pm 2 \mu\text{U ml}^{-1}$ . During the incubation at 37 °C the renin concentration fell to the level in untreated plasma. If this incubated plasma was either acid-activated or trypsin-activated the renin concentration was restored to  $81 \pm 4 \mu\text{U ml}^{-1}$ , or  $97 \pm 11 \mu\text{U ml}^{-1}$  respectively. Therefore, the loss of renin on warming at 37 °C is not an irreversible denaturation similar to that of active renin exposed to pH 11.4 for 2 h (ref. 11). Incubated plasma dialysed to pH 7.4 showed a renin concentration of only  $36 \pm 6 \mu\text{U ml}^{-1}$ . This was higher than the renin levels in untreated plasma but it is possible that cryoactivation<sup>4</sup> had occurred during the 48 h at 4 °C.

Experiments were also carried out with plasma that had been dialysed to pH 3.0 and dialysed back to pH 7.4 for 48 h at 4 °C

before addition of 3 M Tris-HCl buffer and incubation at 37 °C. This plasma showed no reversal of the high renin concentration when warmed, nor did trypsin-treated plasma (Fig. 2).

The reversible activation-inactivation of renin in plasma was not due to an assay artefact. Falsely high renin concentrations can be obtained if proteolytic enzymes present in the radioimmunoassay mixture destroy the iodinated angiotensin I (results in preparation). False high results could also be obtained if a substance that cross-reacted with our angiotensin I antibody was generated during the dialysis of plasma to pH 3.0. A falsely low result could be obtained if the angiotensin I produced during the renin assay was destroyed by peptidases. However, none of the plasma samples contained detectable amounts of angiotensin I-like material before the start of the incubation with ox angiotensinogen. Thus the high renin concentrations obtained after dialysis of the plasma to pH 3.0 were not due to high 'blank' concentrations of angiotensin I (Fig. 3). The rate of production of angiotensin I was proportional to the time of incubation with ox angiotensinogen (Fig. 3), for all samples of treated plasma, except three out of six samples that had been dialysed to pH 3.0 without subsequent dialysis to pH 7.4. In these, the rate of angiotensin I generation decreased with increasing time of incubation in the renin assay. This cannot be due to an artefact such as substrate exhaustion which should equally affect other samples of the same renin concentration, but might be expected if the 'activated' renin in acid-treated plasma was being inactivated during the renin assay. We measured the recovery of angiotensin I incubated with plasma in the presence of angiotensin I antibody<sup>10</sup>. Recovery was >96% during the period of the renin assay, after correction for any generation of angiotensin I in the plasma. Therefore the antibody could protect angiotensin I against peptidases in the treated plasma samples. We considered the possibility of artefacts due to the presence of a protease such as cathepsin D which could generate angiotensin I from ox angiotensinogen. However, cathepsin D is not likely to cleave ox angiotensinogen at our assay pH of 6.9–7.0 (ref. 12). We conclude therefore that our results reflect a genuine change in the enzymatic activity of plasma inactive renin.

Since this study we have heard that another group using a different renin assay method also finds that plasma inactive renin is activated by exposure to acid alone (W. Hsueh, personal communication). Hsueh *et al.*<sup>13</sup> suggest that acidification alters the structure of the inactive renin molecule in such a way as to render it more susceptible to the action of proteases such as renal kallikrein<sup>9</sup>. We suggest an alternative explanation. Human plasma contains many protease inhibitors. There are high molecular weight forms of renin in mouse plasma that may consist of active renin bound to a plasma protein<sup>14</sup>. Furthermore, inactive forms of renin in extracts of pig<sup>15</sup>, rabbit<sup>16</sup> and dog<sup>17</sup> kidney consist of active renin bound to a renin 'inhibitor'. The inactive renin in human plasma may be a similar material. Exposure to acid may result in a conformational change in either renin or inhibitor leading to dissociation of the complex. Restoration of alkaline pH and incubation at 37 °C could result in re-association. By contrast, dialysis of the acidified plasma towards pH 7.4 at 4 °C could result in loss of the binding capacity of the inhibitor if plasma serine proteases either destroy the inhibitor by proteolysis or bind to it in competition with renin.



**Fig. 3** Rate of production of angiotensin I from ox angiotensinogen by renin in two samples of normal plasma, using an antibody-trapping method<sup>10</sup>. Plasma was treated as follows: ●, dialysed to pH 3.0 at 4 °C and dialysed back to pH 7.4 at 4 °C; ○, dialysed to pH 3.0 at 4 °C, rapidly adjusted to pH 7.4 at 4 °C and assayed; □, as for ○ but the plasma was incubated for 5 h at 37 °C before assay; ×, untreated plasma; Δ, trypsin-activated plasma (sample b only). The pg angiotensin I per 90 µl incubation mixture (ordinate) is plotted against time of incubation (abscissa). The range of the radioimmunoassay is 30–500 pg angiotensin I per 90 µl. Note that all samples of plasma including (○) and (□) show undetectable amounts of angiotensin at the start of the assay and that rate of production of angiotensin I is linear with time except for plasma b treated as for (○) (see text). In plasma a, heating at 37 °C for 5 h reduced the renin concentration below that of untreated plasma although for four separate experiments this was not significant ( $P > 0.05$ ). Bars show s.e. for triplicate assays.

Received 1 September; accepted 27 October 1980.

1. Leckie, B. J. *et al.* *Circulation Res.* **40**, 46–51 (1977).
2. Derkx, F. H. M. *et al.* *Lancet* **ii**, 496–498 (1978).
3. Bord, G. W. *Lancet* **i**, 215–218 (1977).
4. Atlas, S. A., Sealey, J. E. & Laragh, J. H. *Circulation Res.* **43**, Suppl. 1, 128–135 (1978).
5. Derkx, F. H. M., Bouma, B. N., Schalekamp, M. P. A. & Schalekamp, M. A. D. H. *Nature* **280**, 315–316 (1979).
6. Leckie, B. J. *Clin. Sci. molec. Med.* **55**, 133s–134s (1978).
7. Sealey, J. E., Atlas, S. A., Laragh, J. H., Silverberg, M. & Kaplan, A. P. *Proc. natn. Acad. Sci. U.S.A.* **76**, 5914–5918 (1979).
8. Rumpf, K. W. *et al.* *Nature* **283**, 482 (1980).
9. Sealey, J. E., Atlas, S. A., Laragh, J. H., Oza, N. B. & Ryan, J. W. *Nature* **275**, 144–145 (1978).
10. Millar, J. A., Leckie, B. J., Morton, J. J., Jordan, J. & Tree, M. *Clinica chim. Acta* **101**, 5–15 (1980).

11. Arakawa, K., Ikeda, M., Fukuyama, J. & Sakai, T. *J. clin. Endocr. Metab.* **42**, 599–602 (1976).
12. Hackenthal, E., Hackenthal, R. & Hilgenfeldt, U. *Biochim. biophys. Acta* **522**, 574–588 (1978).
13. Hsueh, W. A., Carlson, E. J., O'Connor, D. & Warren, S. *Clin. Res.* **28**, 331 (1980).
14. Poulsen, K. *et al. Clin. Sci. molec. Med.* **55**, 125s–128s (1978).
15. Boyd, G. W. *Circulation Res.* **35**, 426–438 (1974).
16. Leckie, B. J. & McConnell, A. *Circulation Res.* **36**, 513–519 (1975).
17. Kawamura, M., Ikemoto, F., Funakawa, S. & Yamamoto, K. *Clin. Sci. molec. Med.* **57**, 345–350 (1979).

## Ability of kallikrein to generate angiotensin II-like pressor substance and a proposed 'kinin-tensin enzyme system'

Kikuo Arakawa & Haruo Maruta

Department of Internal Medicine, Fukuoka University School of Medicine, Fukuoka, Japan 814

Pig pancreatic kallikrein liberates kallidin from kininogen<sup>1</sup>, whereas trypsin releases bradykinin<sup>2</sup>. Recently, both kallikrein and trypsin have been reported to convert inactive plasma renin to active renin<sup>3,4</sup>. However, we found that at pH 6.0, trypsin generated an angiotensin II-like pressor substance from human plasma protein in the absence of converting enzyme<sup>5</sup>. This has been isolated and found to have the same amino acid composition as angiotensin II<sup>6</sup>. Thus, *in vitro* trypsin can directly liberate both the depressor, bradykinin, in weak alkaline conditions, and the pressor, angiotensin II, at weakly acidic pH, from the appropriate substrates. We have now investigated whether kallikrein—a serine protease like trypsin—also generates a pressor substance at weakly acidic pH. Our results demonstrate that it does. We therefore suggest that kallikrein may be involved in a direct link between the pressor and depressor systems and we propose the term 'kinin-tensin system' for this sort of one-enzyme system capable of generating both depressor and pressor substances.

Human plasma protein Cohn's fraction IV-4 was used as substrate because it is rich in angiotensinogen<sup>7</sup>, as well as kallidinogen<sup>8</sup>. However, it was not a pure preparation, and was shown to contain renin which can be inactivated by alkali treatment<sup>9</sup>. Possible contamination with prorenin, cathepsin D and angiotensin I-converting enzyme was excluded or eliminated as follows: first, to activate any prorenin present, fraction IV-4 was treated by acid according to Yokosawa *et al.*<sup>3</sup>, and second, inactivation of the activated renin was achieved by treatment with alkali according to Arakawa *et al.*<sup>9</sup>. Trypsin- or kallikrein-activatable prorenin<sup>3,4</sup> was similarly treated. As shown in Table 1, the absence of angiotensin I formation indicated that these treatments were effective in removing any activatable prorenin and renin. Acid protease, or cathepsin D activity was not detected using denatured bovine haemoglobin as the substrate<sup>10</sup>. Angiotensin I-converting enzyme activity was also not detected when assayed by the method of Cushman and Cheung<sup>11</sup>. Thus, the alkali-treated substrate was shown to be free from any interfering components.

For pure pig pancreatic kallikrein two components, kallikrein A and B, were revealed by cellulose acetate electrophoresis at pH 8.6 (150 V, 1.5 h). Trypsin and chymotrypsin migrate different and could not be detected. The preparation did not hydrolyse benzoyl-L-tyrosine ethyl ester<sup>12</sup>, which indicated that there was no contamination by chymotrypsin, and it was also shown to be free from cathepsin D and angiotensin I-converting enzyme, by the same methods used for the above substrate.

The pretreated human plasma protein fraction IV-4 and the pure kallikrein preparation were incubated at pH 3.0–10.0, and after incubation vasoactive substances (Table 2) were analysed using the rat blood pressure bioassay. The bioassay showed formation of a pressor substance at pH 4.0–6.0, and depressor

**Table 1** Proof of non-contamination by trypsin- or kallikrein-activatable prorenin in substrate, human plasma protein fraction IV-4

| Total amount of the pressor substance formed from 10 mg of substrate    |                             |            |  |                             |            |             |
|---|-----------------------------|------------|--|-----------------------------|------------|-------------|
| Incubation of trypsin-activated fraction IV-4 with renin-free substrate |                             |            | Incubation of kallikrein-activated fraction IV-4 with renin-free substrate |                             |            |             |
| Incubation (min)  | Bioassay (equiv. to AII ng) | AI-RI (ng) | AII-RI (ng)  | Bioassay (equiv. to AII ng) | AI-RI (ng) | AII-RI (ng) |
| 0   | 0                           | 0          | 0.04   | 13.6                        | 0          | 12.5        |
| 15  | 0                           | 0          | 0.04   | 15.2                        | 0          | 17.5        |
| 30  | 0                           | 0          | 0.03   | 13.8                        | 0          | 16.0        |
| 60  | 0                           | 0          | 0.03   | 8.9                         | 0          | 15.7        |
| 120   | 0                           | 0          | 0.03   | 8.0                         | 0          | 14.0        |

Before incubation, to activate acid-activatable prorenin which might be contained in fraction IV-4, it was treated by dialysis against 0.05 M glycine-HCl buffer containing 0.1 M NaCl, pH 3.3, for 20 h, followed by a second dialysis against 0.1 M Tris-HCl buffer containing 0.1 M NaCl, pH 7.5, for 2 h. To inactivate the resultant activated renin, it was treated at pH 11.3 with 1.0 M NaOH for 2 h. pH was adjusted to 7.0 with 1.0 M HCl and it was dialysed against distilled water, and lyophilised. All these experiments were done at 4 °C. To activate trypsin- or kallikrein-activatable prorenin, 10 mg of the above-treated fraction IV-4 of 920 ng angiotensin I equivalent were dissolved in 1 ml of 0.1 M Tris-HCl buffer, pH 7.5, and added with 0.4 mg of trypsin (Miles, specific activity 3,000 NF units) or 0.5 mg of hog pancreatic kallikrein (Sanwa Chemicals, specific activity 768 µg equivalents bradykinin per min per mg, pH 8.0). Incubation was at 25 °C for 10 min in the case of trypsin and 1 h for kallikrein. The reaction was stopped by the addition of 5 mg aprotinin (Bayer, 5,000 KIU per mg protein). Finally, 100 µl of the above trypsin- or kallikrein-treated mixture were incubated with 10 mg of the renin-free substrate, or alkali-treated fraction IV-4<sup>3</sup>. The incubation was done in 2 ml of 0.1 M sodium phosphate buffer, pH 6.0, containing 200 µl of 0.1 M Na<sub>2</sub>EDTA, 20 µl of 0.45 M 8-hydroxyquinoline sulphate and 5 µl of 10% 2,3-dimercapto-1-propanol as angiotensinase inhibitors, at 37 °C for 0, 15, 30, 60 and 120 min. Reaction was stopped by boiling for 10 min. Products were bioassayed in rat blood pressure, and radioimmunoassayed for angiotensin I (AI-RI) and angiotensin II (AII-RI). Control experiments using 10 mg of acid- and alkali-treated fraction IV-4 without treatment by trypsin or kallikrein showed no formation of pressor substance. Trypsin- or kallikrein-treated fraction IV-4 produced a small amount of angiotensin II, but not angiotensin I.

substance(s) at the other pHs. Pepstatin, a renin inhibitor<sup>13</sup>, did not inhibit the pressor formation (Table 2), indicating that a renin-like enzyme was not involved. In control experiments without kallikrein, the alkali-treated fraction IV-4 did not generate any pressor substance in identical conditions, as reported elsewhere<sup>5,9</sup>. Kallikrein alone without substrate also did not generate pressor. These data are therefore consistent with the liberation of a vasoconstrictor by kallikrein and parallel previous results with trypsin<sup>5,6</sup>.

The pressor effect was not only similar in pattern to that of angiotensin II, but was also inhibited by the angiotensin II-antagonist, [1-Sar,8-Ile]-angiotensin II (Fig. 1), but not by SQ 14225, the converting-enzyme inhibitor (Fig. 2). Bioassay value of the pressor activity coincided with the radioimmunoassay value for angiotensin II, but not for angiotensin I, as shown in Table 2. It therefore seems likely that the pressor effect is due to the release of angiotensin II, in contrast to angiotensin I formed from the non-alkali-treated substrate in the absence of kallikrein<sup>9</sup>. Unless unknown mechanisms are involved, it is probably derived from angiotensinogen by a single cleavage. The methods used in the purification of the kallikrein and substrate indicate that the activation of prorenin<sup>3,4</sup> is not involved. Involvement of tonin is also unlikely because tonin has never been found in any animal organ other than rat submaxillary gland and pure pig pancreatic kallikrein is unlikely to contain it.

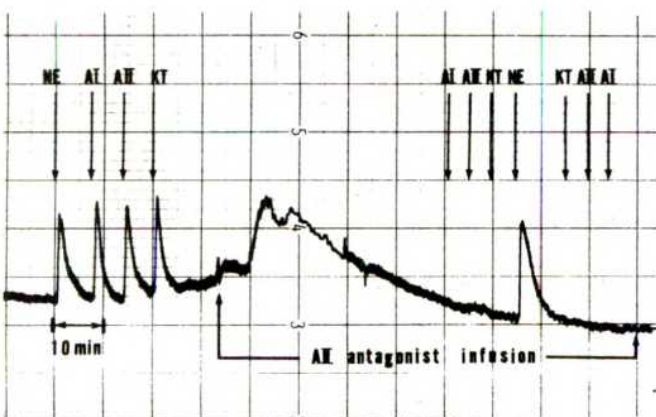
Thus both trypsin and kallikrein have been shown to be involved in the direct release of both pressor and depressor



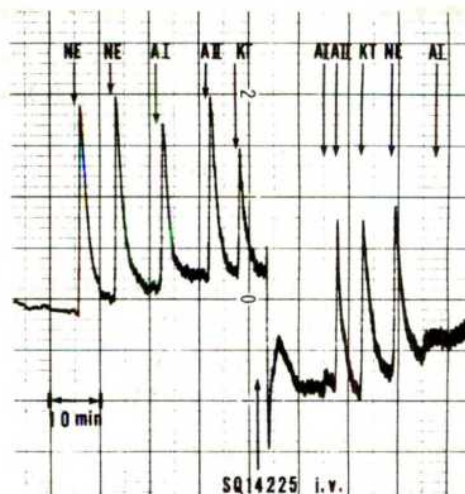
**Table 2** Comparison of values of the pressor substance formed at pH values 3–10 by kallikrein assayed by different methods

| pH | Total amount of pressor substance formed after 18 h incubation |            |             |                             |            |             |
|----|--|------------|-------------|-----------------------------|------------|-------------|
|    | Without pepstatin  |            |             | With pepstatin              |            |             |
|    | Bioassay (equiv. to AII ng)                                    | AI-RI (ng) | AII-RI (ng) | Bioassay (equiv. to AII ng) | AI-RI (ng) | AII-RI (ng) |
| 3  | 145.0  | 21         | 251.0       | 0                           | 0          | 16.8        |
| 4  | 1,760.0  | 10         | 1,770.0     | 1,636.0                     | 0          | 1,664.0     |
| 5  | 1,520.0  | 8          | 1,892.0     | 1,912.0                     | 0          | 2,580.8     |
| 6  | 370.0  | 28         | 340.0       | 87.2                        | 0          | 70.0        |
| 7  | 5.5  | 13         | 15.7        | 0                           | 0          | 14.8        |
| 8  | 75.0   | 0          | 15.4        | 0                           | 0          | 4.9         |
| 9  | 54.0   | 0          | 6.6         | 0                           | 0          | 2.7         |
| 10 | 69.0   | 0          | 7.1         | 0                           | 0          | 3.0         |

10 mg of acid- and alkali-treated fraction IV-4 and 0.5 mg of pig pancreatic kallikrein were incubated in 2 ml of Britton-Robinson's universal buffer. The buffer was prepared from acid mixture (0.04 M phosphoric acid, 0.04 M acetic acid, and 0.04 M boric acid) adjusted to each desired pH value (3.0–10.0) using 0.2 M NaOH in the presence of angiotensinase inhibitors and  $4 \times 10^{-7}$  M SQ 14225, with or without  $5.4 \times 10^{-5}$  M pepstatin at 37 °C for 18 h. The vasoactive substances were extracted from the reaction mixture with hot ethanol and the extract evaporated to dryness under reduced pressure at 45 °C. Bioassays and radioimmunoassays for angiotensin I (AI-RI) and angiotensin II (AII-RI) in the products revealed that kallikrein generated pressor substance from acid- and alkali-treated fraction IV-4 at weakly acidic pH (4.0–6.0). Bioassay values of the pressor substance corresponded well with angiotensin II radioimmunoassay values. Pepstatin showed no inhibitory effect.



**Fig. 1** Mode of pressor activity of kallikrein-generated pressor substance and effects of angiotensin II antagonist. Kallikrein-generated pressor substance was assayed by blood pressure in a female Wistar rat anaesthetized with intraperitoneal sodium amobarbital (100 mg per kg body weight) and ganglion-blocked with subcutaneous pentolinium tartrate (4 mg per kg body weight)<sup>14</sup>. Blood pressure was determined using a catheter inserted into the carotid artery by Hewlett-Packard pressure amplifier (Model 8805 C) and Yokogawa flat-recorder (Type 3051) connected to a Statham p23Db transducer. The samples were injected into a femoral vein, with [1-Sar,8-Ile]-angiotensin II injected into another femoral vein. By continuous infusion of [1-Sar,8-Ile]-angiotensin II at a rate of 50 ng per 0.05 ml per min, pressor activities of [5-Ile]-angiotensin I, [5-Ile]-angiotensin II, and kallikrein-generated pressor substance were inhibited, but that of noradrenaline was not. NE, 20 ng noradrenaline. AI, 6 ng angiotensin I. AII, 2 ng angiotensin II. KT, kallikrein-generated pressor substance.



**Fig. 2** Mode of pressor activity of kallikrein-generated pressor substance and effects of converting-enzyme inhibitor, SQ 14225. SQ 14225 was given by a bolus intravenous injection at a dose of 0.8 mg per kg body weight. It almost completely inhibited pressor action of [5-Ile]-angiotensin I, but not that of [5-Ile]-angiotensin II, kallikrein-generated pressor substance and noradrenaline. Symbols are the same as those in Fig. 1.

substances. Two opposing activities—depressor and pressor—are built into a one-enzyme system and the direction of the reaction may be determined by only a slight pH shift between 5.0 and 8.0. It is suggested that the term 'kinin(s)' be restricted to vasodepressor(s) and the term 'tensin(s)' to vasopressor(s). Based on this nomenclature, 'kinin-tensin enzyme system' may be coined for this type of one-enzyme system with bidirectional circulatory activities, such as the trypsin-(bradykinin and/or angiotensin II) system<sup>6</sup>, and the kallikrein-(kinin and/or angiotensin II) system.

We are attempting to purify and identify the pressor substance released by kallikrein *in vitro*, and examining the possibility that a comparable reaction occurs for the regulation of tissue perfusion *in vivo*. The fact that there must have been cleavage of the Phe-His bond by trypsin and kallikrein suggests that a more fundamental enzymological study with regard to their substrate specificity would be of interest.

This study was supported in part by grants-in-aid from the Japanese Ministry of Education (B-148195 and B-548200), the Fukuoka University Research Institute, and the Rinsho-yakuri-Kenkyushinko Foundation. We thank Miss M. Yanagiuchi and Y. Taniguchi for technical assistance.

Received 9 May; accepted 16 October 1980.

- Habermann, E. & Blennemann, G. *Naunyn-Schmiedeberg's Arch. exp. Path. Pharmacol.* **249**, 357–373 (1964).
- Elliot, D. F., Horton, E. W. & Lewis, G. P. *Biochem. J.* **78**, 60–65 (1961).
- Sealey, J. E., Atlas, S. A., Laragh, J. H., Oza, N. B. & Ryan, J. W. *Nature* **275**, 144–145 (1978).
- Yokosawa, N., Takahashi, N., Inagami, T. & Page, D. L. *Biochim. biophys. Acta* **569**, 211–219 (1976).
- Arakawa, K., Ikeda, M., Fukuyama, J. & Sakai, T. *J. clin. Endocr. Metab.* **42**, 599–602 (1976).
- Arakawa, K., Yuki, M. & Ikeda, M. *Biochem. J.* **187**, 647–653 (1980).
- Arakawa, K., Minohara, A., Yamada, J., Uemura, N. & Nakamura, M. *Clinica chim. Acta* **22**, 309–315 (1968).
- Habermann, E. *Handb. exp. Pharmacol.* **25**, 250–288 (1970).
- Arakawa, K., Minohara, A., Uemura, N., Sakai, T. & Ikeda, M. *Endocr. jap.* **22**, 472–432 (1975).
- Barret, A. J. *Biochem. J.* **104**, 601–608 (1967).
- Cushman, D. W. & Cheung, H. S. *Biochem. Pharmacol.* **20**, 1637–1648 (1971).
- Hummel, B. C. W. *Can. J. Biochem. Physiol.* **37**, 1393–1399 (1959).
- Aoyagi, T. *et al. J. Antibiotics* **25**, 689–694 (1972).
- Arakawa, K., Nakatani, M., Minohara, A. & Nakamura, M. *Biochem. J.* **104**, 900–906 (1967).



## Are opioid peptides co-transmitters in noradrenergic vesicles of sympathetic nerves?

Steven P. Wilson\*, Richard L. Klein†, Kwen-Jen Chang‡, Milton S. Gasparis†, O. Humberto Viveros\* & Wen-Hsun Yang†

\*Department of Medicinal Biochemistry, Wellcome Research Laboratories, Triangle Research Park, North Carolina 27709

†Department of Pharmacology and Toxicology, University of Mississippi Medical Center, Jackson, Mississippi 39216

‡Department of Molecular Biology, Wellcome Research Laboratories, Research Triangle Park, North Carolina 27709

Biogenic amines and peptide hormones co-exist in paraneurons<sup>1</sup> or amine precursor uptake and decarboxylation (APUD) cells<sup>2</sup>. Opioid peptide immunohistochemistry occurs in the gland cells and nerve endings of the adrenal medulla<sup>3</sup>, and both dopamine  $\beta$ -hydroxylase (EC 1.14.17.1) and enkephalin-like immunohistochemistry occurs in some small intensely fluorescent and sympathetic ganglion cells<sup>4</sup>. Direct biochemical assays demonstrate opiate-like peptides (OLPs) including Met- and Leu-enkephalin in the adrenal medulla, and the highest specific activity is attained in the purified adrenomedullary chromaffin granule fraction<sup>5</sup>. Chromaffin cells also synthesize enkephalins *de novo*<sup>6</sup>. Adrenal medullae from larger species, including ox and man, contain much more OLP material than those from smaller species such as rodents<sup>5,7</sup>; fortunately so, because only from ox is it practical to purify both chromaffin granules and splenic nerve vesicles at particle purity and yield suitable for chemical composition studies. In ox and man the large dense-cored vesicles (LDVs) comprise 30–50% of the vesicle population in terminals of blood vessels, spleen and vas deferens, equivalent to 80–90% of the total terminal vesicle capacity. For these reasons, we chose bovine splenic nerve in which to investigate the localization of OLPs in the peripheral sympathetic system. Our results, reported here and based on direct biochemical analyses, indicate that OLPs, putative transmitters and noradrenaline probably co-exist in sympathetic C-fibres, which constitute 98% of the bovine splenic nerve. Further, the OLPs and noradrenaline can probably co-exist in the large dense-cored noradrenergic vesicles of this nerve. We believe the obtained 1:60 molar ratio of opioid peptides:noradrenaline to be the highest yet demonstrated for enkephalins in any neurotransmitter organelle or tissue.

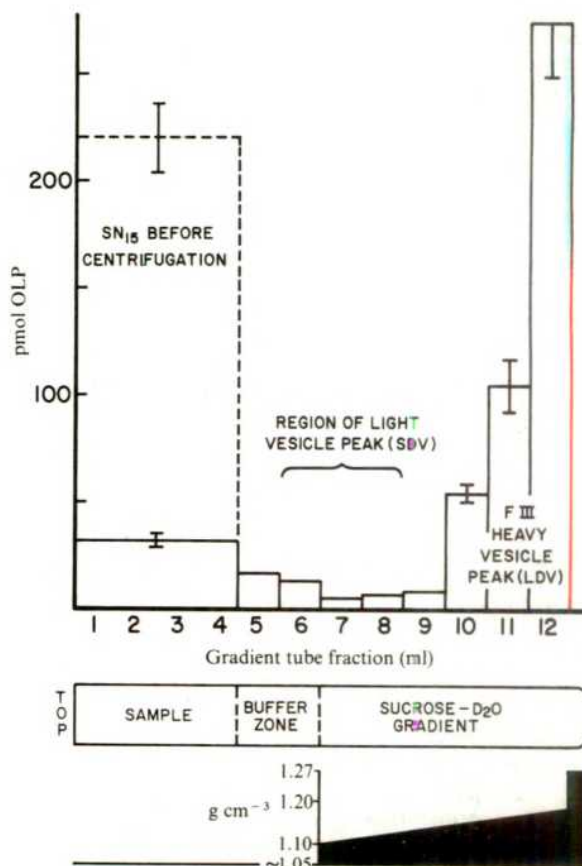
The distribution of OLPs in the sucrose-D<sub>2</sub>O density gradient used to purify noradrenergic LDVs is shown in Fig. 1. Of the original peptide activity layered onto the density gradient (SN<sub>15</sub>), 14.6% is soluble and remains above the buffer zone. About 90% of the recoverable, sedimentable OLP material (Table 1) occurs in the heavy vesicle fractions (FIII, fractions 11 and 12) where LDVs equilibrate<sup>8</sup>. Negligible OLPs distribute in the less dense regions of the gradient, including the zone (fractions 6–8) where small dense-cored vesicles typically equilibrate.

The pattern of OLP distribution in the density gradient is almost identical to that of noradrenaline in sedimentable particles<sup>9</sup>, except that about one-third of the noradrenaline readily leaks from the vesicles during tissue homogenization. Dopamine  $\beta$ -hydroxylase also occurs at the highest specific activity in the heavy vesicle peak (Table 1), but about one-third is scattered throughout the gradient at lower buoyant densities<sup>9</sup>. This is explained by the occurrence of 'immature' LDVs from the

proximal end of the nerve, with full enzyme content but low noradrenaline content, and by depletion of matrix material resulting from vesicle rupture during isolation or from previous exocytosis.

Specific activities and recoveries of OLPs at various steps in the purification of LDVs are presented in Table 1 and compared with the analogous data for noradrenaline and dopamine  $\beta$ -hydroxylase. The molar ratio of noradrenaline:OLPs remains ~100:1 and the units of dopamine  $\beta$ -hydroxylase:nmol OLPs at ~1:1 throughout the purification process. The higher purification of OLPs over dopamine  $\beta$ -hydroxylase or noradrenaline (50-fold and 35-fold, respectively) is in keeping with its more restricted localization to LDVs and selective retention.

The stepwise recoveries of OLPs, dopamine  $\beta$ -hydroxylase and noradrenaline vary for particular reasons. Due to their molecular weight of ~500, OLPs should be released from the LDVs only by physical lysis or by exocytosis from nerve terminals, and therefore, relatively little should occur in the soluble phase of the nerve homogenate. However, the peptides are also readily degraded by ubiquitous peptidases<sup>10</sup> and this could be partly responsible for the 25–35% loss reflected in recoverable peptide (Table 1 legend).



**Fig. 1** Opiate-like peptide distribution following density gradient centrifugation. Purified LDVs were prepared from bovine splenic nerve<sup>8,12,13</sup> obtained 10–15 min post mortem using a modified sucrose-D<sub>2</sub>O density gradient sampling procedure<sup>9</sup>. OLPs were preserved in extracts containing 1.0 M acetic acid and measured by displacement of [<sup>125</sup>I]-[D-Ala<sup>2</sup>, D-Leu<sup>5</sup>]enkephalin (0.25 mM; specific activity 2 Ci  $\mu$ mol<sup>-1</sup>) from rat brain membrane receptors<sup>19</sup>. SN<sub>15</sub> is the supernatant obtained from the desheathed splenic nerve homogenate after centrifugation at 10,500g for 15 min. FIII is the purified heavy vesicle fraction containing LDVs and includes fractions (ml) 11 and 12 of the sucrose-D<sub>2</sub>O density gradient based on their similar noradrenaline content per mg protein.



**Table 1** Opiate-like peptide (OLP), noradrenaline (NA) and dopamine  $\beta$ -hydroxylase (D $\beta$ H) content and recovery in purified vesicles from bovine splenic nerve

| Fraction   | NA<br>(nmol per<br>mg*† protein) | %<br>Recovery<br>per step | D $\beta$ H*‡<br>(units per mg<br>protein)§ | %<br>Recovery<br>per step | OLPs<br>(nmol per mg<br>protein) | %<br>Recovery<br>per step | Protein<br>(mg per<br>gradient)¶ |
|--|----------------------------------|---------------------------|---|---------------------------|----------------------------------|---------------------------|----------------------------------|
| Whole nerve homogenate                             | 1.0                              |                           | 0.011                                       |                           | 0.10 ± 0.0008<br>(n = 12)        |                           | 82–110                           |
| SN <sub>15</sub> (sedimentable<br>(total)¶)        | 7.1                              | 67.8                      | 0.024                                       | 57.6                      | 0.020 ± 0.006<br>(n = 5)         | 51–63                     | 27–31<br>62–73                   |
| FIII (fractions 11 and 12 of density<br>gradient)  | 32.0                             | 66.6                      | 0.388                                       | 52.0                      | 0.524 ± 0.043<br>(n = 11)        | 89–93*                    | 0.7–1.09                         |
| Purification**                                     | 32x                              |                           | 35x   |                           | 52x                              |                           |                                  |
| Overall recovery in gradient from SN <sub>15</sub> |                                  | ~95                       |   | ~100                      |                                  | 69<br>(64–75)             |                                  |

\* Ref. 9.

† Ref. 13.

‡ M.S.G., W.-H.Y. and R.L.K., unpublished.

§ Unit of D $\beta$ H activity equals 1  $\mu$ mol octopamine synthesized per min at 37 °C in a medium containing 20 mM tryamine as substrate.

¶ Protein distribution is based on the modified density gradient with 2.0 ml buffer zone.

¶ Percentage soluble OLPs in SN<sub>15</sub> (total) averaged 14.6% ± 1.0 (n = 12).\* Recovery is corrected for 25.3–36.4% loss of OLPs which was due to degradation or other factors and is based on the actual overall recovery in the gradient from 4.0 ml SN<sub>15</sub>.\*\* Protein content per gradient and purification are uncorrected for nonspecifically adsorbed albumin content. OLP data are  $\pm$ s.e.m.**Table 2** Distribution of opiate-like peptides in vesicles purified from sequential segments of bovine splenic nerve

| Content                    | Proximal segment | Middle segment | Distal segment              | % Increase |
|----------------------------|------------------|----------------|-----------------------------|------------|
| Per g nerve segment weight |                  |                |                             |            |
| mg LDV protein             | 0.13 ± 0.02      | 0.16 ± 0.03    | 0.23 ± 0.01<br>(P < 0.01)   | 68%        |
| nmol OLP                   | 0.65 ± 0.06      | 0.80 ± 0.07    | 1.08 ± 0.12<br>(P < 0.02)   | 65%        |
| units D $\beta$ H*         | 0.047 ± 0.01     | 0.059 ± 0.01   | 0.083 ± 0.01<br>(P < 0.005) | 77%        |
| nmol ATP†                  | 0.76 ± 0.02      | —              | 1.32 ± 0.07<br>(P < 0.005)  | 74%        |
| nmol NA‡                   | 3.08 ± 0.20      | 5.13 ± 0.28    | 8.40 ± 0.17<br>(P < 0.001)  | 273%       |
| Per mg LDV protein         |                  |                |                             |            |
| nmol OLP                   | 0.74 ± 0.10      | 0.62 ± 0.16    | 0.64 ± 0.10                 | No change  |
| units D $\beta$ H*         | 0.62 ± 0.07      | 0.66 ± 0.08    | 0.64 ± 0.08                 | No change  |
| nmol ATP†                  | 10.0 ± 0.3       | —              | 10.1 ± 0.5                  | No change  |
| nmol NA‡                   | 44.0 ± 2.6       | 57.0 ± 3.2     | 70.0 ± 4.0<br>(P < 0.005)   | 59%        |

Date are  $\pm$ s.e.m., n = 4 paired experiments with duplicate OLP determinations in which vesicles were prepared identically and simultaneously from equal weights of desheathed splenic nerve segments: proximal and middle segments (extraspinal) were ~5–6 cm long and the distal segment (intrasplenic) was 15–30 cm long. See Table 1 legend for a definition of a unit of D $\beta$ H activity.

\* Ref. 9.

† Ref. 17.

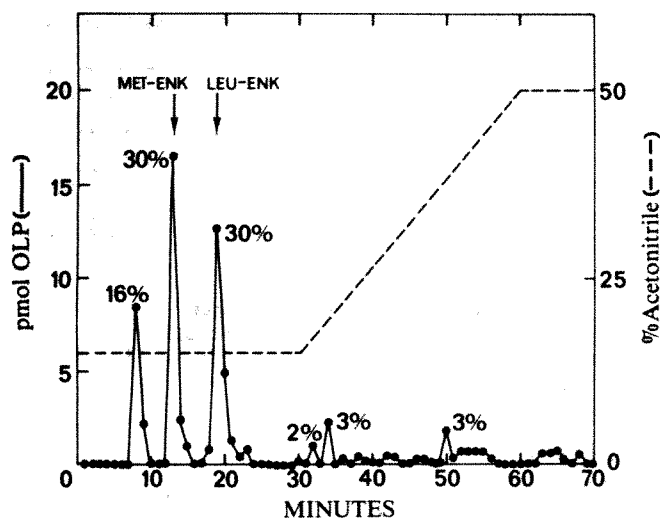
‡ Refs 14, 18.

In the purified LDV fraction of the density gradient, FIII, the OLP content averages 0.5–0.6 nmol per mg protein. An additional twofold purification is to be expected for the LDVs by differential centrifugation of fraction FIII<sup>9,12,13</sup>. This should result in OLP levels of ~1.0 nmol per mg protein, uncorrected for nonspecifically adsorbed bovine serum albumin, which amounts to at least one-third of the total protein in the vesicle fraction.

Analysis of purified LDV pellet extracts by HPLC reveals three major and several minor peaks with opioid activity (Fig. 2). Two of the major peaks, each representing 30% of the recovered opioid, have retention times identical to those of Met- and Leu-enkephalin standards. The <sup>3</sup>H-Leu-enkephalin internal standard also eluted with a retention time of 19 min. The major opioid component with a retention time of 8 min probably corresponds to oxidized Met-enkephalin<sup>6</sup>. Recovery of opioid activity on the Amberlite column is 48%, compared with 80% for <sup>3</sup>H-Leu-enkephalin internal standard, which is similar to recoveries in acetic acid extracts of adrenomedullary chromaffin

cells<sup>6</sup>. This probably represents the loss of opioid peptides of a larger molecular size than enkephalins<sup>11</sup>. Recovery of OLPs eluted from the Amberlite column and subsequently subjected to HPLC is 70%, similar to the 60% recovery of <sup>3</sup>H-Leu-enkephalin standard. Using the recovery of <sup>3</sup>H-Leu-enkephalin to correct for losses of Met- and Leu-enkephalin during the chromatographic separations, these two peptides comprise 40–50% of the total opioid activity in LDV material.

Table 2 shows data from experiments designed to measure the levels of OLPs in the nerve vesicles as they are transported distally from the nerve cell bodies in the coeliac ganglion to the varicosities in the spleen. The amount of OLPs per gramme fresh nerve weight increases 60–70% in the distal direction and is equal to the increase in protein of the purified vesicle fraction, the latter being a measure of relative vesicle numbers per segment. Similar increases occur in dopamine  $\beta$ -hydroxylase activity and the ATP content, based on nerve segment fresh weight. Thus, OLPs, like dopamine  $\beta$ -hydroxylase and ATP, do not change significantly when expressed on the basis of total



**Fig. 2** High performance liquid chromatographic separation of opiate like peptides from bovine splenic nerve large dense-cored vesicles. An acid extract (2.6 ml) of LDV pellets was applied to a column of Amberlite XAD-2 (2 ml bed volume). The eluate was reappplied to the resin and the resin washed four times with 5 ml of 0.2 M acetic acid. Enkephalins were eluted from the column with 5 ml of 0.2 M acetic acid in methanol. The eluate was evaporated to dryness under  $N_2$  and resuspended in water for application to the HPLC column. HPLC was carried out on a Partisil PXS-10, 10/25 ODS column. After sample application the column was eluted ( $1 \text{ ml min}^{-1}$ ) with 15% acetonitrile/10 mM ammonium acetate, pH 4.2, for 30 min followed by a gradient of 15–50% acetonitrile for 30 min. OLPs, opiate-like peptides; ENK, enkephalin.

protein in the purified LDV fraction from sequential nerve segments. In contrast, noradrenaline content per gram nerve fresh weight increases 273% in the sequential nerve segments. Thus, noradrenaline is synthesized and accumulated by the vesicles during axoplasmic transport, the content increasing ~60% per mg LDV protein<sup>14</sup>. This increase occurs exclusively in the fast release pool of 'newly synthesized' transmitter<sup>15</sup>.

This research was supported in part by grants NSF BNS-79-12951 and NIMH 1R03-MH35481 to R.L.K. and the AHA-Miss. Affil. and BRSG S07-RR05386 from the NIH to W.H.Y. Parts of this research have been reported elsewhere<sup>16</sup>.

Received 24 July; accepted 15 October 1980.

- Fujita, T. & Kobayashi, S. *Trends neurol. Sci.* 27–30 (1979).
- Pearse, A. G. E. *J. Histochem. Cytochem.* 17, 303–313 (1969).
- Schultzberg, M. *et al. Neuroscience* 3, 1169–1186 (1978).
- Schultzberg, M. *et al. Neuroscience* 4, 249–270 (1979).
- Viveros, O. H., Diliberto, E. J., Hazum, E. & Chang, K.-J. *Molec. Pharmacol.* 16, 1101–1107 (1979).
- Wilson, S. P., Chang, K.-J. & Viveros, O. H. *Proc. natn. Acad. Sci. U.S.A.* 77, 4364–4368 (1980).
- Viveros, O. H., Diliberto, E. J., Hazum, E. & Chang, K.-J. *Adv. biochem. Psychopharmacol.* 22, 191–204 (1980).
- Thureson-Klein, A., Klein, R. L. & Lagercrantz, H. *J. Neurocytol.* 2, 13–27 (1973).
- Klein, R. L. *et al. J. Neurobiol.* 10, 291–307 (1979).
- Snyder, S. H. *Science* 209, 976–982 (1980).
- Lewis, R. V. *et al. Science* 208, 1459–1461 (1980).
- Lagercrantz, H., Klein, R. L. & Stjärne, L. *Life Sci.* 9, 639–650 (1970).
- Yen, S. S., Klein, R. L. & Chen-Yen, S. H. *J. Neurocytol.* 2, 1–12 (1973).
- Klein, R. L. in *Frontiers in Catecholamine Research* (eds Usdin, E. & Snyder, S.) 423–425 (Pergamon, Oxford, 1973).
- Klein, R. L. & Harden, T. K. *Life Sci.* 16, 315–322 (1975).
- Klein, R., Gasparis, M., Yang, W., Viveros, O. & Wilson, S. *Trans. Am. Soc. neurochem.* 11, 230 (1980).
- Yen, S. S., Klein, R. L., Chen-Yen, S. H. & Thureson-Klein, A. *J. Neurobiol.* 7, 11–22 (1976).
- Chen-Yen, S. H. thesis, Univ. Mississippi (1975).
- Miller, R. J., Chang, K.-J., Cooper, B. & Cuatrecasas, P. *J. biol. Chem.* 253, 531–538 (1978).

## Differential regulation of the $\alpha_2$ -adrenergic receptor by $Na^+$ and guanine nucleotides

Thomas Michel, Brian B. Hoffman & Robert J. Lefkowitz

Howard Hughes Medical Institute Laboratory, Departments of Medicine (Cardiology) and Biochemistry, Duke University Medical Center, Durham, North Carolina 27710

Many hormones interact with receptors which stimulate the enzyme adenylate cyclase. Less well characterized are those receptors which mediate an inhibition of adenylate cyclase activity<sup>1</sup>. However, guanine nucleotides are clearly important in the regulation of both stimulatory and inhibitory receptors<sup>2</sup>. Monovalent cations, notably  $Na^+$ , regulate many inhibitory receptor systems but apparently not stimulatory receptors<sup>1</sup>. We investigate here the effects of  $Na^+$  and guanine nucleotides on the adenylate cyclase-coupled inhibitory  $\alpha_2$ -adrenergic receptor of the rabbit platelet<sup>3</sup>. Computer modelling of adrenaline competition curves with <sup>3</sup>H-dihydroergocryptine (<sup>3</sup>H-DHE) indicates that adrenaline induces two distinct affinity states of the  $\alpha_2$  receptor—one of higher ( $\alpha_{2H}$ ) and the other of lower ( $\alpha_{2L}$ ) affinity. Guanylyl-5'-yl-imidodiphosphate (Gpp(NH)p) seems to reduce adrenaline affinity by converting the high-affinity state into the low-affinity form of the receptor. In contrast,  $Na^+$  reduces adrenaline affinity at both the high- and low-affinity states of the  $\alpha_2$  receptor while preserving receptor heterogeneity. Thus, guanine nucleotides and  $Na^+$  differ in the manner by which each reduces agonist affinity for the  $\alpha_2$ -adrenergic receptor.

The rabbit platelet's  $\alpha$  receptors were found to be exclusively of the  $\alpha_2$  subtype by the computer modelling of competition curves of the antagonists prazosin and yohimbine with <sup>3</sup>H-DHE<sup>4</sup> which were best described by a model of one class of binding sites with yohimbine much more potent than prazosin (data not shown). This is similar to the situation in human platelets<sup>5</sup>.

Agonist interactions with the rabbit platelet's  $\alpha_2$ -adrenergic receptor are shown in Fig. 1 and Table 1. Without added  $Na^+$  or guanine nucleotides, the adrenaline competition curve with <sup>3</sup>H-DHE yielded a shallow binding isotherm with a slope factor ('pseudo' Hill coefficient) of 0.67 suggesting the presence of heterogeneous binding states. Computer modelling indicated the presence of two classes of binding states with high ( $\alpha_{2H}$ )- and low ( $\alpha_{2L}$ )-affinity states for adrenaline of  $K_d$   $6.3 \times 10^{-9}$  M and  $1.5 \times 10^{-7}$  M, respectively. The addition of Gpp(NH)p (0.1 mM) caused the adrenaline competition curve to shift to lower affinity and to become steep with a slope factor of 1.0. These curves were best fitted by a model with one class of binding states of lower affinity ( $K_d = 1.3 \times 10^{-7}$  M), with this affinity not significantly different from the lower affinity binding state ( $K_d \alpha_{2L} = 1.5 \times 10^{-7}$  M) found in the absence of added Gpp(NH)p. These effects of Gpp(NH)p are very similar to those previously reported for the  $\beta$ -adrenergic receptor in frog erythrocytes<sup>6</sup> and for  $\alpha_2$ -adrenergic receptors in human platelets<sup>5</sup>. In the absence of Gpp(NH)p, 57% of the  $\alpha_2$  receptors are in the  $\alpha_{2H}$  state, the remainder are in the  $\alpha_{2L}$  state, and the ratio  $K_d \alpha_{2L}/K_d \alpha_{2H}$  is 24 (see Table 1). When 0.1 mM Gpp(NH)p is added, all of the  $\alpha_2$  receptors are present in the lower-affinity state ( $\alpha_{2L}$ ); there is no change in the total number of receptors present.

We have previously shown that 100 mM NaCl causes a maximal decrease in agonist affinity at these receptors<sup>7</sup>. In the presence of 100 mM NaCl, competition curves of (–)-adrenaline and <sup>3</sup>H-DHE are shifted to lower overall affinity and increased steepness relative to control curves (Fig. 1, Table 1). The observed slope factor, 0.8, is still, however, significantly less



**Table 1** Parameters derived from computer modelling of competition curves of (–)adrenaline with <sup>3</sup>H-DHE in rabbit platelet membranes in the presence and absence of NaCl and Gpp(NH)p

| Additions                            | n | EC <sub>50</sub> (M)     | K <sub>dα<sub>2H</sub></sub> (M) | K <sub>dα<sub>2L</sub></sub> (M) | $\frac{K_{d\alpha_{2L}}}{K_{d\alpha_{2H}}}$ | % R <sub>H</sub> | % R <sub>L</sub> | Slope factor |
|--------------------------------------|---|--------------------------|----------------------------------|----------------------------------|---|------------------|------------------|--------------|
| None*                                | 3 | 7.2±2.0×10 <sup>-8</sup> | 6.3±1.0×10 <sup>-9</sup>         | 1.5±0.3×10 <sup>-7</sup>         | 24  | 57±8             | 43±7             | 0.67±0.07    |
| 0.1 mM Gpp(NH)p†                     | 3 | 2.6±0.8×10 <sup>-7</sup> | —                                | 1.3±0.3×10 <sup>-7</sup> ‡       | —   | 0                | 100              | 1.0±0.10¶    |
| 100 mM NaCl*                         | 5 | 2.5±0.3×10 <sup>-6</sup> | 4.2±0.5×10 <sup>-7</sup>         | 3.2±0.5×10 <sup>-6</sup>         | 8   | 51±20            | 49±18            | 0.78±0.09    |
| 0.1 mM Gpp(NH)p<br>plus 100 mM NaCl† | 4 | 4.2±0.5×10 <sup>-6</sup> | —                                | 2.1±0.5×10 <sup>-6</sup> §       | —   | 0                | 100              | 1.1±0.15¶    |

Binding assays were performed as described in the text. The parameters are derived from the computer modelling of the competition curves shown graphically in Fig. 1. The competition curves are the means of *n* experiments, each done in duplicate. EC<sub>50</sub> refers to the competitor concentration yielding half-maximal inhibition of <sup>3</sup>H-DHE binding. K<sub>dα<sub>2H</sub></sub> and K<sub>dα<sub>2L</sub></sub> refer to the dissociation constants of the high- and low-affinity states, respectively. The fraction of α receptors in these states is shown as %R<sub>H</sub> and %R<sub>L</sub>, respectively. See text for details.

- \* Two-state fit significantly better than one-state fit (*P* < 0.01).
- † Two-state fit not significantly better than one-state fit (*P* > 0.05).
- ‡ Value not significantly different from K<sub>dα<sub>2L</sub></sub> in absence of NaCl and Gpp(NH)p (*P* > 0.05).
- § Value not significantly different from K<sub>dα<sub>2L</sub></sub> in presence of NaCl without added Gpp(NH)p (*P* > 0.05).
- || Slope factor significantly different from 1.0 (*P* < 0.05).
- ¶ Slope factor not significantly different from 1.0 (*P* > 0.05).

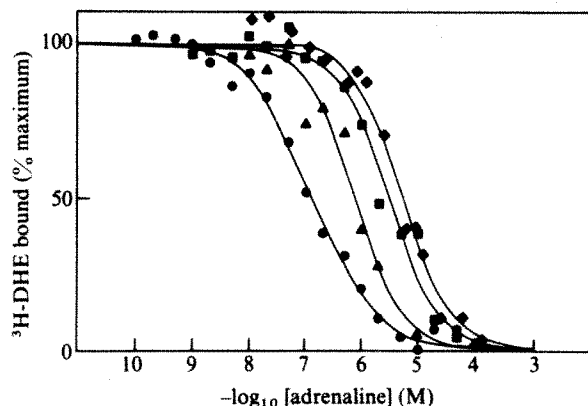
than 1.0 (*P* < 0.05). The competition curve is significantly better fitted by a model with two classes of binding states for adrenaline. The proportion of the α<sub>2</sub>-receptor population in the high (R<sub>H</sub>)- and low (R<sub>L</sub>)-affinity states is not significantly changed from the control curve, with %R<sub>H</sub> = 51 and %R<sub>L</sub> = 49. However, adrenaline affinity is reduced at both the high- and low-affinity states. There is a greater relative reduction in affinity at the high-affinity state, as shown by the ratio of K<sub>dα<sub>2L</sub></sub>/K<sub>dα<sub>2H</sub></sub> being 8 in the presence of 100 mM Na<sup>+</sup> compared with a ratio of 24 in the absence of added Na<sup>+</sup>. These results indicate that both Na<sup>+</sup> and Gpp(NH)p reduce agonist affinity, but that Gpp(NH)p abolishes the heterogeneity of agonist binding whereas receptor heterogeneity is maintained in the presence of Na<sup>+</sup>.

Addition of 0.1 mM Gpp(NH)p to adrenaline competition curves in the presence of 100 mM Na<sup>+</sup> causes a further decrease in agonist affinity and an increase in the slope factor to 1.1 (Table 1; Fig. 1). The competition curves in the presence of Gpp(NH)p and Na<sup>+</sup> are best described by a model with a homogeneous class of binding states. The affinity of this state for adrenaline (K<sub>d</sub> = 2.1×10<sup>-6</sup> M) is not significantly different from the K<sub>dα<sub>2L</sub></sub> of 3.2×10<sup>-6</sup> M determined in the presence of Na<sup>+</sup> alone without added Gpp(NH)p. Thus, the effect of Gpp(NH)p in the presence

of Na<sup>+</sup> is apparently to convert receptors in the α<sub>2H</sub> state into the α<sub>2L</sub> state, entirely analogous to the effect of this nucleotide on adrenaline competition curves in the absence of added Na<sup>+</sup>.

In rabbit platelet membranes, prostaglandin E<sub>1</sub> (PGE<sub>1</sub>) causes a 10–12-fold increase in adenylate cyclase activity<sup>3,7</sup>. In the absence of added NaCl, (–)adrenaline (0.1 mM) causes a small but significant decrease (11±6%, data from five experiments) in PGE<sub>1</sub>-stimulated (0.01 mM PGE<sub>1</sub>) adenylate cyclase activity, from 169±20 pmol cyclic AMP per min per mg protein to 150±17 pmol cyclic AMP per min per mg protein. In the presence of 100 mM NaCl, there is a threefold greater maximal inhibition (31±4%) of PGE<sub>1</sub>-stimulated adenylate cyclase activity by adrenaline, from 207±21 down to 143±18 pmol cyclic AMP per min per mg protein (five experiments, significantly greater inhibition than in the absence of Na<sup>+</sup>, *P* < 0.005). The potentiation of adrenaline-mediated inhibition of PGE<sub>1</sub>-stimulated adenylate cyclase by Na<sup>+</sup> is dose dependent, with a half-maximal effect at a Na<sup>+</sup> concentration of 30 mM (data not shown). In the conditions used in this assay, addition of GTP over a wide concentration range (10<sup>-7</sup>–10<sup>-4</sup> M) had no apparent effect on the inhibition of adenylate cyclase by adrenaline in either the presence or absence of Na<sup>+</sup>.

**Fig. 1** Competition curves of <sup>3</sup>H-DHE with (–)adrenaline in the presence and absence of Na<sup>+</sup> and Gpp(NH)p. Isolation of rabbit platelet plasma membranes was as previously described<sup>10</sup> with the exception that the lysate pellet was washed once in resuspension buffer containing 50 mM Tris-HCl and 10 mM MgCl<sub>2</sub>·6H<sub>2</sub>O, pH 7.5. The final resuspension was in this buffer to a protein concentration of 1–3 mg ml<sup>-1</sup>. Radioligand binding assays were in a total volume of 0.2 ml which consisted of 0.025 ml of <sup>3</sup>H-DHE (33 Ci mmol<sup>-1</sup>, NEN) and 0.075 ml of drug in resuspension buffer with NaCl added to yield indicated final concentrations. Incubations (25 °C for 30 min) were started by addition of 0.1 ml of membranes. The assay was terminated by rapid vacuum filtration with a 20-ml wash with resuspension buffer at 25 °C. The concentration of <sup>3</sup>H-DHE in these assays was 4 nM; specific radioligand binding to α receptors was 60–70% of total binding. The affinity of <sup>3</sup>H-DHE binding was 3×10<sup>-9</sup> M in all conditions used in these assays. Computer modelling of competition curves was done as described previously<sup>5,19–23</sup>. For each treatment, competition curves were constructed with each point determined in duplicate. <sup>3</sup>H-DHE binding, as a fraction of binding in the absence of competitor, was computed at each concentration of competitor. Then the results of the individual experiments were meaned and subjected to computer analysis. This analysis provided parameter estimates and standard errors which represent the confidence limits of the computer estimates. The computer program for the data analysis, which is based on the law of mass action, involves nonlinear least squares curve fitting<sup>20</sup> using a generalized model for complex ligand–receptor systems<sup>19</sup>. The computer technique provides an objective evaluation of whether the data are best fitted by a one- or two-receptor-state model. A fit of the data to two states of binding was accepted only if the fit was significantly improved (*P* < 0.05) over that for a one-state fit. The modelling provides values for the affinity constants of the competing ligand for the different states of the receptor and the proportion of the states present when a two-state fit is involved. Slope factors ('pseudo' Hill coefficients) and half-maximal inhibitory concentrations (EC<sub>50</sub>s) in the various experimental conditions were determined using a four-parameter logistic equation, as previously described<sup>22</sup>. Adenylate cyclase assays were performed as described previously<sup>7</sup> with slight modifications. The incubation mixture, in a final volume of 50 μl, consisted of 0.1 mM ATP, 1–2×10<sup>6</sup> c.p.m. of [α-<sup>32</sup>P]ATP and an ATP-regenerating system (in which none of the reagents is Na<sup>+</sup> salts), 50 mM Tris-HCl pH 7.5, 10 mM MgCl<sub>2</sub>, indicated concentrations of NaCl and 1–2 mg ml<sup>-1</sup> membrane protein. PGE<sub>1</sub> at 10<sup>-5</sup> M caused an 8–12-fold stimulation of adenylate cyclase, with half-maximal stimulation by 10<sup>-7</sup> M in either the presence or absence of NaCl. Protein was determined by the method of Lowry<sup>24</sup> using bovine serum albumin as standard. ●, No additions; ▲, +0.1 mM GppNHp; ■, +100 mM NaCl; ◆, +0.1 mM GppNHp + 100 mM NaCl.



The individual and additive reduction in agonist affinity promoted by  $\text{Na}^+$  and guanine nucleotides is characteristic of diverse receptor systems which inhibit adenylate cyclase<sup>1,2,7-12</sup>. Several studies have shown that the presence of one or both of these agents is required for the effective coupling of hormone binding to enzyme inhibition<sup>1,2,13-16</sup>. The present experiments have demonstrated that  $\alpha$ -adrenergic receptor-mediated inhibition of adenylate cyclase is potentiated by  $\text{Na}^+$ . Note that the concentration of  $\text{Na}^+$  yielding half-maximal reduction in agonist affinity ( $40 \text{ mM Na}^+$ )<sup>7</sup> is similar to the  $\text{Na}^+$  concentration yielding half-maximal potentiation of adrenaline-mediated adenylate cyclase inhibition reported here. Our study did not demonstrate a GTP requirement for  $\alpha$ -receptor-mediated adenylate cyclase inhibition. Presumably this reflects the presence of sufficient GTP in the adenylate cyclase assay used in this study to permit adenylate cyclase regulation in the absence of added guanine nucleotides.

These investigations have demonstrated heterogeneity of agonist binding to the  $\alpha_{2L}$  and  $\alpha_{2H}$  states of the  $\alpha_2$ -adrenergic receptor, with the  $\alpha_{2H}$  state seemingly converted into the low-affinity form by guanine nucleotides. These observations resemble the situation described for the  $\beta$ -adrenergic receptor<sup>6</sup>, which promotes the GTP-dependent activation of adenylate cyclase. Applying both biochemical<sup>17</sup> and computer-modelling techniques<sup>6-18</sup> to the  $\beta$ -adrenergic receptor system, it has been proposed that heterogeneity of agonist binding and its regulation by guanine nucleotides are the result of the interaction of the receptor with a GTP-binding nucleotide regulatory protein in the membrane. It seems plausible that the  $\alpha_2$ -adrenergic receptor interacts with an analogous membrane-bound nucleotide regulatory protein<sup>13</sup>, and that this interaction is important in the guanine nucleotide-mediated modulation of agonist affinity states. We have shown that  $\text{Na}^+$  does not abolish heterogeneity of agonist binding, and thus presumably the interaction of  $\alpha$  receptor and nucleotide regulatory protein is maintained even in the presence of  $\text{Na}^+$  as the addition of guanine nucleotides further reduces agonist affinity. In contrast to guanine nucleotides,  $\text{Na}^+$  reduces affinity of both the high- and low-affinity states, and this effect of  $\text{Na}^+$  may be independent of the nucleotide regulatory protein. Perhaps the action of  $\text{Na}^+$  is mediated via the receptor itself or through an interaction with another membrane component distinct from the nucleotide regulatory protein.

In conclusion, these studies have indicated distinctly different roles for guanine nucleotides and  $\text{Na}^+$  in the regulation of the adenylate cyclase-coupled inhibitory  $\alpha_2$ -adrenergic receptor. Although further studies are needed to establish the molecular basis of this differential regulation, the present data suggest that  $\text{Na}^+$  effects may be mediated through independent mechanisms. Understanding the basis of the effects of  $\text{Na}^+$  on either the receptor or other membrane components is relevant to the mechanism of hormone and drug inhibition of adenylate cyclase.

This work was supported by NIH grants HL16037 and HL20339. T.M. is a student in the Medical Scientist Training Program (NIH grant GM07171). B.B.H. is a Fellow of the MRC of Canada. R.J.L. is an Investigator of the Howard Hughes Medical Institute.

Received 28 May; accepted 11 August 1980.

- Jakobs, K. H. *Molec. cell. Endocr.* **16**, 147-156 (1979).
- Rodbard, M. *Nature* **284**, 17-22 (1980).
- Harwood, J. P., Moskowitz, J. & Krishna, G. *Biochem. biophys. Acta* **261**, 444-456 (1972).
- Hoffman, B. B., De Lean, A., Wood, C. L., Schocken, D. D. & Lefkowitz, R. J. *Life Sci.* **24**, 1739-1746 (1979).
- Hoffman, B. B., Mullikin-Kilpatrick, D. & Lefkowitz, R. J. *J. biol. Chem.* **255**, 4645-4652 (1980).
- Kent, R. S., De Lean, A. & Lefkowitz, R. J. *Molec. Pharmacol.* **17**, 14-23 (1980).
- Tsai, B. S. & Lefkowitz, R. J. *Molec. Pharmacol.* **14**, 540-548 (1978).
- Blume, A. J. *Proc. natn. Acad. Sci. U.S.A.* **75**, 1713-1717 (1978).
- Rosenberger, L. B., Yamamura, H. I. & Roeske, W. R. *J. biol. Chem.* **255**, 820-823 (1980).
- Tsai, B. S. & Lefkowitz, R. J. *Molec. Pharmacol.* **16**, 61-68 (1979).
- Glossman, H. & Presek, P. *Naunyn-Schmiedeberg's Archs Pharmacol.* **306**, 67-73 (1979).
- Greenberg, D. A., U'Prichard, D. C., Sheehan, P. & Snyder, S. H. *Brain Res.* **140**, 378-384 (1978).
- Steer, M. L. & Wood, A. J. *J. biol. Chem.* **254**, 10791-10797 (1979).
- Blume, A. J., Lichtenstein, D. & Boone, G. *Proc. natn. Acad. Sci. U.S.A.* **76**, 5626-5630 (1979).

- Lichtenstein, D., Boone, G. & Blume, A. J. *Cyclic Nucleotide Res.* **5**, 367-375 (1979).
- Aktories, K., Schultz, G. & Jakobs, K. H. *FEBS Lett.* **107**, 100-104 (1979).
- Limbird, L. E., Gill, D. M. & Lefkowitz, R. J. *Proc. natn. Acad. Sci. U.S.A.* **77**, 775-779 (1980).
- Stadel, J. M., De Lean, A. & Lefkowitz, R. J. *J. biol. Chem.* **255**, 1436-1441 (1980).
- Feldman, H. A. *Analyt. Biochem.* **48**, 317-338 (1972).
- Fletcher, J. E. & Schrager, R. I. *A User's Guide to Least Squares Curve Fitting Tech. Rep.* No. 1 (U.S. Dep. of Health, Education and Welfare, 1973).
- Rodbard, D. & Frazier, G. R. *Meth. Enzym.* **37B**, 3-22 (1975).
- De Lean, A., Munson, P. J. & Rodbard, D. *Am. J. Physiol.* **235**, E97-E102 (1978).
- Hancock, A. A., De Lean, A. & Lefkowitz, R. J. *Molec. Pharmacol.* **16**, 1-9 (1979).
- Lowry, O. H., Rosebrough, N. J., Fain, A. L. & Randall, R. J. *J. biol. Chem.* **193**, 265-275 (1951).

## No junctional communication between epithelial cells in hydra

S. W. de Laat\*, L. G. J. Tertoolen\* & C. J. P. Grimmlikhuijzen†‡

\* Hubrecht Laboratory, International Embryological Institute, Uppsalalaan 8, 3584 CT Utrecht, The Netherlands

† Max-Planck-Institut für medizinische Forschung, Abteilung Biophysik, Jahnstrasse 29, 6900 Heidelberg, FRG

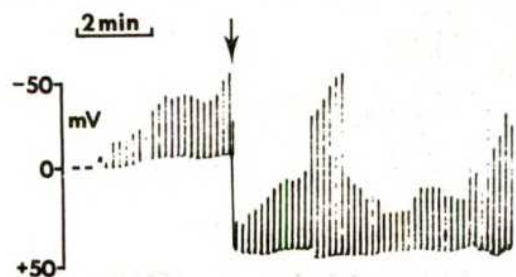
Diffusion gradients of morphogens have been inferred as a basis for the control of morphogenesis in hydra<sup>1,2</sup>, and morphogenetic substances have been found which, on the basis of their molecular weight (MW), should be able to pass gap junctions<sup>3-7</sup>. There have been several reports of the presence of gap junctions between epithelial cells of hydra<sup>8-13</sup>. However, until now, there has been no report published on whether these junctions enable the epithelial cells to exchange molecules of small molecular weight, as has been described in other organisms<sup>14-20</sup>. Therefore we decided to investigate the communicative properties of the junctional membranes by electrophysiological methods and by intracellular-dye iontophoresis. We report here that no electrotonic coupling is detectable between epithelial cells of *Hydra attenuata* in: (1) intact animals, (2) head-regenerating animals, (3) cell re-aggregates, and (4) hydra that have become nerve-free. Furthermore we show that epithelial cells are unable to exchange low-molecular weight fluorescent dyes.

Electrotonic coupling between epithelial cells was measured by conventional intracellular glass microelectrodes<sup>21</sup>. Current pulses were passed and voltages recorded through a single microelectrode. In the intact animal measurements were performed in the head, mid-gastric and foot regions with the two electrodes positioned at short distances (<100  $\mu\text{m}$ ) along the longitudinal or latitudinal axis of the body column. The chances of impalement of epithelial cells were high as this cell type covers most of the surface of the animal<sup>11</sup>. In addition to normal animals, we tested for electrotonic coupling in animals in which we could expect special morphogenetic regulation. In head-regenerating animals electrotonic coupling was monitored at regular intervals in the new head region, starting 30 min after head removal and continuing until new tentacles had appeared (2 days). In another experiment we dissociated hydra into its separate component cells and allowed these to reaggregate, sort, and form new animals<sup>22</sup>. We made measurements all over the aggregates from 2 h after the onset of aggregation until new heads appeared (3 days). Phenotypic variants of hydra that consisted almost totally of epithelial cells were also measured. These so-called nerve-free hydra have similar gap junctions to normal animals<sup>13</sup> and are useful in microelectrode studies as they do not contract spontaneously and offer better chances for impaling epithelial cells only.

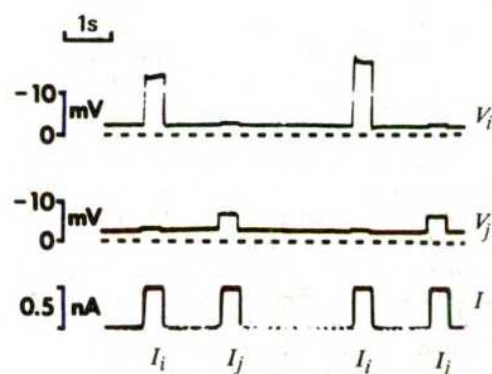
By careful impalement with the microelectrodes it was possible to distinguish in intact animals between the ectodermal and the endodermal cells. Figure 1 shows an example of a recording in which the measurement was initially taken from an ectodermal cell, and further penetration resulted in the impalement of an underlying endodermal cell. Ectodermal cells have

‡ To whom correspondence should be addressed.





**Fig. 1** Example of an intracellular recording of the membrane potential and input resistance from epithelial cells of intact normal hydra. Initially an ectodermal cell was impaled, but on further penetration (arrow) the microelectrode moved into an underlying endodermal cell. The recording demonstrates the occurrence of spontaneous fluctuations in membrane potential and input resistance, and the difference in membrane potential between ectodermal and endodermal cells. The input resistance was determined as the ratio between the deflection of the membrane potential and the amplitude of the current pulse. Intracellular voltages were measured and current pulses ( $5 \times 10^{-10}$  A, 500 ms) were passed through a single 3 M KCl-filled glass microelectrode by the use of a bridge circuit to compensate for the electrode impedance. Hydra was kept in a medium composed of 1 mM  $\text{CaCl}_2$ , 0.1 mM  $\text{MgCl}_2$ , 0.1 mM KCl, 0.5 mM  $\text{Na}_2\text{HPO}_4$ , adjusted to pH 7.6 with phosphoric acid. Microelectrode tip potentials ( $<10$  mV) and resistances (20–40 M $\Omega$ ) were determined and compensated in this medium. The electrode properties depend on the ionic strength of the medium. In a control experiment we measured a decrease in tip potential  $<+5$  mV and electrode resistance  $<15$  M $\Omega$  upon changing to a 305 mosm salt solution (about equivalent to the cytoplasm). For this reason membrane potentials and input resistances are expected to be 5 mV more negative and 15 M $\Omega$  greater, respectively, than measured. The mobility of the intact and the head-regenerating animals was reduced during the measurements by adding 2% of the polymer Tylose (Hoechst) to the medium. This allowed continuous recordings of up to 15 min. With nerve-free animals and cell aggregates no Tylose was used.



**Fig. 2** Lack of electrotonic coupling between visibly adjacent ectodermal cells in nerve-free hydra. The figure gives an example of the maximum deflection in membrane potential that could be observed on passing current into an adjacent cell—in nearly all measurements no visible deflection could be observed. In all experiments described in the text the coupling ratio  $V_i/V_j$  was  $<0.04$ , where  $V_i$  and  $V_j$  are the deflection in the membrane potential of cell  $i$  and cell  $j$ , respectively, when a current pulse is passed from cell  $j$  to the grounded medium. Nerve-free hydra were obtained as described<sup>13</sup> and consisted of more than 95% epithelial cells. Conditions as in Fig. 1.

membrane potentials ranging between +5 and -15 mV, whereas endodermal cells have membrane potentials of +25 to +50 mV. This was confirmed by histological examination of fixed animals after marking the impaled cells with Lucifer Yellow CH. The difference in membrane potential between both types of epithelial cells agrees with earlier observations by Kass-Simon and Diesl on isolated epithelial cells<sup>23</sup>. In both types of cell we found spontaneous fluctuations in membrane potential and input resistance (Fig. 1). As no significant differences in membrane potentials and input resistances were found between intact, nerve-free and head-regenerating animals, these data were pooled (Table 1). In early re-aggregates we could not distinguish between ectodermal and endodermal cells. Here the membrane potentials ranged between -15 and +25 mV, with mean value  $+9.1 \pm 5.3$  mV (s.e.m.),  $N = 7$ . The input resistance ranged between 35 and 100 M $\Omega$ , with a mean value of  $68.6 \pm 7.6$  M $\Omega$ ,  $N = 7$  (see also Fig. 1).

Over 100 measurements failed to show electrotonic coupling among ectodermal cells, among endodermal cells, or between ectodermal and endodermal cells in all the experimental conditions, including those in which special morphogenetic regulation



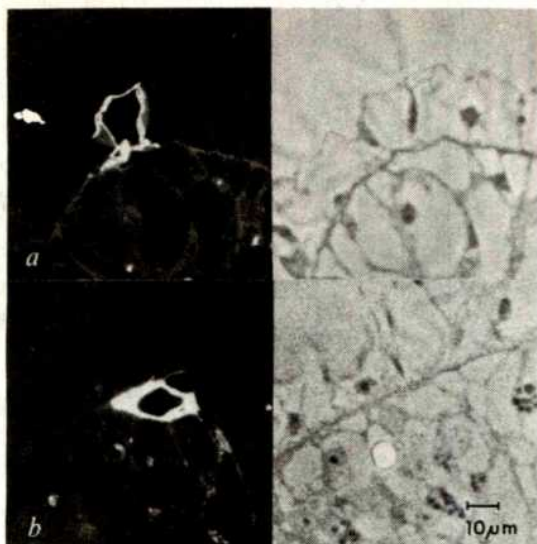
**Fig. 3** Example of a micrograph taken 30 min after iontophoresis of Lucifer Yellow CH into an epithelial cell in nerve-free hydra. No transfer of dye to other cells was observed in any of the experimental conditions applied. Similar results were obtained with fluorescein. The tip of a regular microelectrode was filled with a 3% aqueous solution of Lucifer Yellow CH, whereas the remainder of the electrode system was filled with 3 M LiCl. The dye was introduced iontophoretically into the cell by applying repetitive hyperpolarizing current pulses of  $2 \times 10^{-9}$  A and 1.5 s duration at 0.5 s intervals for 1 min. Fluorescence was observed and photomicrographs were taken as described<sup>27</sup>.

might be expected. Taking into account the resolution limit of our registration system, the coupling ratio  $V_i/V_j$  (see Fig. 2 legend) was always smaller than 0.04. An example of a measurement in nerve-free hydra is shown in Fig. 2.

It might be argued that possible leakage of calcium from the medium into the cells during the impalement might have caused a closure of the gap junctions<sup>20</sup>. To check this, we repeated the measurements in calcium-free medium. We also determined the possible effect of the trans-epithelial potential which normally exists between the gastric cavity and the external medium<sup>24,25</sup>. By insertion of a capillary into the mouth this potential was abolished. In all these circumstances we found normal membrane potentials, input resistances and absence of electrotonic coupling.

In addition to our electrophysiological experiments we studied the exchange of Lucifer Yellow CH (MW, 457) and fluorescein (MW, 330) between epithelial cells. Lucifer Yellow CH<sup>26,27</sup> particularly, was extremely effective for tracing dye coupling due to its excellent spectral properties, its rapid spread through an injected cell, and good retention by the cell during histological processing. In over 75 experiments fluorescent dye was introduced iontophoretically from a glass microelectrode into epithelial cells at different positions along the body column of intact and nerve-free animals. The localization of the dye was





**Fig. 4** Micrographs of 1- $\mu$ m histological sections of normal hydra fixed after iontophoresis of Lucifer Yellow into an ectodermal cell (a) and endodermal cell (b); left: fluorescence, right: phase contrast (unstained). Conditions as in Fig. 3. The animals were fixed in 4% formaldehyde for 24 h at 4°C, dehydrated in dimethoxypropanal (DMP) for 1 h, embedded in Spurr low-viscosity embedding medium by placing in Spurr/DMP (1:1) for 5 h, Spurr/DMP (3:1) for 12 h and Spurr only for 8 h. Polymerization was at 60°C for 12 h.

monitored by fluorescence microscopy up to 1 h after application. Throughout this time the fluorescence remained definitively located within a single cell, without detectable transfer to neighbouring cells (Fig. 3). Some of the animals were fixed after introduction of Lucifer Yellow CH into a number of epithelial cells and examined after histological processing (Fig. 4). From observation of serial 1- $\mu$ m sections we made the following conclusions: (1) there was no transfer of the dye between epithelial cells, (2) the absence of electrotonic and dye coupling was not due to positioning of the micro-electrode in the large vacuoles—iontophoretically applied Lucifer Yellow CH was definitively located within the cytoplasm, (3) the impalement did not cause apparent cell damage, (4) ectodermal and endodermal cells have different membrane potentials (see above).

Our observations show that the epithelial cells in hydra are not able to exchange ions and fluorescent dyes of low molecular weight. We conclude that: (1) gap junctions between epithelial cells of hydra, observed by electron microscopy, do not function as communicative intercellular junctions—they might be of a primitive type, involved in the formation of connective junctions, (2) morphogenetic substances probably diffuse via the extracellular space, (3) nerve-free hydra which are still able to contract on electrical or mechanical stimulation<sup>28</sup> cannot conduct the contraction pulse along electrotonically coupled epithelial cells—they may use paracrine communication.

We thank Dr W. W. Stewart for his gift of Lucifer Yellow CH, Dr H. C. Schaller for her interest, and the Deutsche Forschungsgemeinschaft (Scha 253/6) for financial support.

**Table 1** Membrane potential and input resistance in hydra epithelial cells

|          | Membrane potential (mV)  | Input resistance (M $\Omega$ ) |
|----------|--------------------------|--------------------------------|
| Ectoderm | $-2.5 \pm 1.2$ (N = 16)  | $38.8 \pm 4.7$ (N = 16)        |
| Endoderm | $+36.0 \pm 1.3$ (N = 40) | $45.5 \pm 2.9$ (N = 40)        |

Mean number of cells  $\pm$  s.e.m. are given. The spontaneous fluctuations in each cell (see Fig. 1) were averaged by taking values of the membrane potential and the input resistance at 1-min intervals.

Received 23 July; accepted 16 October 1980.

- Gierer, A. & Meinhardt, H. *Kybernetik* **12**, 30–39 (1972).
- Wolpert, L., Clarke, M. R. B. & Hornbrugh, A. *Nature new Biol.* **239**, 101–105 (1972).
- Schaller, H. C. *J. Embryol. exp. Morph.* **29**, 27–38 (1973).
- Berking, S. *Wilhelm Roux's Arch. dev. Biol.* **181**, 215–225 (1977).
- Grimmelikhuijzen, C. J. P. *Cell Differentiation* **8**, 267–273 (1979).
- Grimmelikhuijzen, C. J. P. & Schaller, H. C. *Trends biochem. Sci.* **4**, 265–267 (1979).
- Schmidt, T. & Schaller, H. C. *Wilhelm Roux's Arch. dev. Biol.* **188**, 133–139 (1980).
- Hand, A. R. & Gobel, S. J. *J. Cell Biol.* **52**, 397–408 (1972).
- Filshie, B. K. & Flower, N. E. *J. Cell. Sci.* **23**, 151–172 (1977).
- Wood, R. L. *J. ultrastruct. Res.* **58**, 299–315 (1977).
- West, D. L. *Tissue Cell* **10**, 629–646 (1978).
- Wood, R. L. *Cell Tissue Res.* **199**, 319–338 (1979).
- Lepault, J., McDowall, A. W. & Grimmelikhuijzen, C. J. P. *Cell Tissue Res.* **209**, 217–224 (1980).
- Gilula, N. B., Reeves, O. R. & Steinbach, A. *Nature* **235**, 262–265 (1972).
- Bennett, M. V. L. *Fedn Proc.* **32**, 65–75 (1973).
- Azarnia, R., Larsen, W. J. & Loewenstein, W. R. *Proc. natn. Acad. Sci. U.S.A.* **71**, 880–884 (1974).
- Johnson, R., Hammer, M., Sheridan, J. D. & Revel, J. P. *Proc. natn. Acad. Sci. U.S.A.* **71**, 4536–4540 (1974).
- Pitts, J. D. & Simms, J. W. *Expl Cell Res.* **104**, 153–163 (1977).
- Loewenstein, W. R. in *Differentiation and Development* (eds Ahmed, F., Russell, T. R., Schultz, J. & Werner, J.) 399–409 (Academic, New York, 1978).
- Loewenstein, W. R. *Biochim. biophys. Acta* **560**, 1–65 (1979).
- de Laat, S. W., Barts, P. W. J. A. & Bakker, M. I. *J. Membrane Biol.* **27**, 109–129 (1976).
- Gierer, A. *et al.* *Nature new Biol.* **239**, 98–101 (1972).
- Kass-Simon, G. & Diesl, V. K. *Nature* **265**, 75–77 (1977).
- Josephson, R. K. & Macklin, M. *Science* **156**, 1629–1631 (1967).
- Josephson, R. K. & Macklin, M. *J. gen. Physiol.* **53**, 638–665 (1969).
- Stewart, W. W. *Cell* **14**, 741–759 (1978).
- de Laat, S. W., Tertoolen, L. G. J., Dorresteyn, A. W. C. & van den Biggelaar, J. A. M. *Nature* **287**, 546–548 (1980).
- Campbell, R. D., Josephson, R. K., Swab, W. E. & Rushforth, N. B. *Nature* **262**, 388–390 (1976).

## Receptor binding and internalization of immobilized transcobalamin II by mouse leukaemia cells

Kiyoshi Takahashi\*, Mehdi Tavassoli\* & Donald W. Jacobsen††

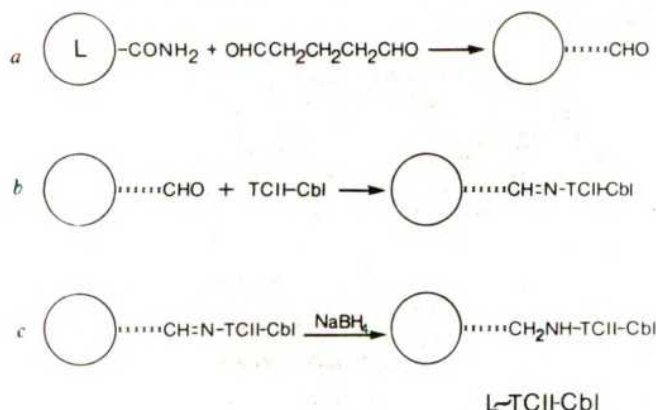
Departments of \*Clinical Research and †Biochemistry, Scripps Clinic and Research Foundation, La Jolla, California 92037

Membrane transport of vitamin B<sub>12</sub> (cyanocobalamin; Cbl) into mammalian cells is mediated by the serum protein transcobalamin II (TCII)<sup>1–3</sup>. In mouse leukaemia L1210 cells, TCII-Cbl binds to membrane receptors in a rapid, temperature-independent step and is internalized by a slow, temperature-dependent process<sup>4</sup>. To delineate the location of receptors on these cells, we have constructed a visual probe by covalently coupling purified TCII-Cbl to submicrometre latex particles<sup>5</sup> (minibeads). We report here that when L1210 cells are incubated with minibeads containing TCII-Cbl at 4°C and examined by scanning electron microscopy (SEM), the particles are found attached predominantly to microvilli. Incubation of the cells at 37°C results in the internalization of the minibeads. As visualized by transmission electron microscopy (TEM), this endocytotic process seems to occur in clathrin-coated pits and vesicles<sup>6,7</sup> at the cell surface.

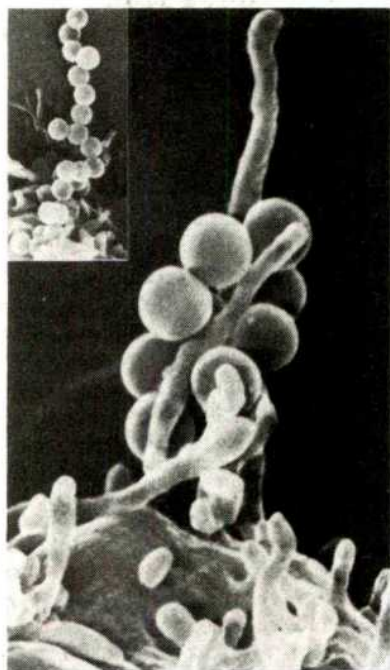
Recent work has demonstrated that cultured L1210 cells attach tightly to large (70  $\mu$ m) Sepharose beads coated with Cbl-TCII<sup>8</sup>. Although the binding of numerous cells (~150 cells per bead) somewhat obscured the contact zone between the bead and the cell, it was apparent that cellular microvilli made intimate and extensive contact with the bead surface. To identify specific receptor areas for TCII-Cbl on L1210 cell surfaces and perhaps confirm the apparent role of microvilli in the transport process, we have repeated these experiments using small (0.35  $\mu$ m) latex particles derivatized with TCII-Cbl. The latter were prepared by a method modified from Weston and

† To whom correspondence should be addressed.

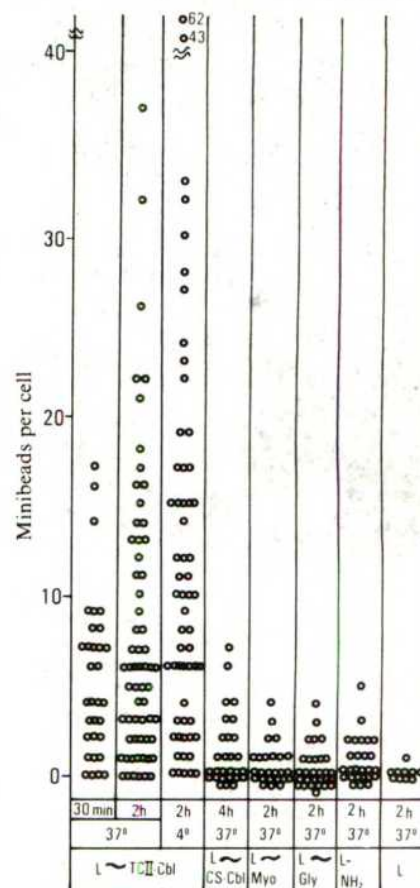




**Fig. 1** Synthesis and structure of the receptor probe L~TCII-Cbl. Amide-modified polystyrene latex particles (0.35  $\mu\text{m}$ ; Dow) were suspended to 5% (w/v) in 0.1 M  $\text{NaHCO}_3$  (pH 8.0) and 8% glutaraldehyde was added to a final concentration of 5% (step a). After 24 h at 37 °C, excess glutaraldehyde was removed by dialysis against 0.1 M  $\text{NaHCO}_3$  (pH 8.8) for 24 h at 4 °C. Rabbit serum TCII-Cbl (100  $\mu\text{g}$ ), purified by the method of D.W.J. *et al.*<sup>10</sup>, was added to 1 ml of a 0.1% suspension of the glutaraldehyde-modified minibeads in 0.1 M  $\text{NaHCO}_3$  (pH 8.8) (step b). After 6 h at room temperature, the preparation was treated with 0.2 M  $\text{NaBH}_4$  for 15 min at 4 °C (step c). The L~TCII-Cbl minibeads were pelleted by centrifugation (40,000g for 20 min) and washed three times with phosphate-buffered saline (pH 7.4).



**Fig. 2** Binding of L~TCII-Cbl to microvilli of L1210 cells. Cultured L1210 cells were suspended for 2 h (4 °C) with 0.04% L~TCII-Cbl in RPMI 1640 medium containing 5% fetal bovine serum, collected by centrifugation (150g for 7 min) and washed twice with serum-free medium. A drop of cell suspension was placed on a round coverslip pretreated with poly-L-lysine (50  $\mu\text{g ml}^{-1}$ ) and fixed in modified Karnovsky's solution containing 0.125 M cacodylate buffer (pH 6.8) for 7 min. The coverslip was then rinsed three times with 0.125 M cacodylate (pH 7.3) and postfixed in similarly buffered 2%  $\text{OsO}_4$  for 15 min at room temperature. After dehydration and displacement in Freon 113, the cells were critical point-dried and sputter coated with platinum-palladium.  $\times 18,000$ , inset  $\times 4,500$ .



**Fig. 3** Binding capacity of L1210 cells for L~TCII-Cbl and control minibeads. Incubation conditions were as described in Fig. 2 legend except that time and temperature varied as indicated. Each circle represents the number of minibeads bound per cell. Scoring was made on SEM prints of cells randomly selected at low magnification ( $\times 500$ ; well below the resolution required to detect minibeads) and then photographed at higher magnification ( $\times 6,000$ ). These data represent two separate preparations of L~TCII-Cbl. Control studies used plain (L) or amide-modified (L~NH<sub>2</sub>) latex, or minibeads on which TCII-Cbl was replaced by glycine (L~Gly), myoglobin (L~Myo) or the non-TCII Cbl-binder from chicken serum (L~CS-Cbl).

Avrameas<sup>9</sup> to form the receptor probe L~TCII-Cbl shown in Fig. 1. The same method was used to prepare control minibeads derivatized with glycine, myoglobin or the non-TCII Cbl-binder from chicken serum.

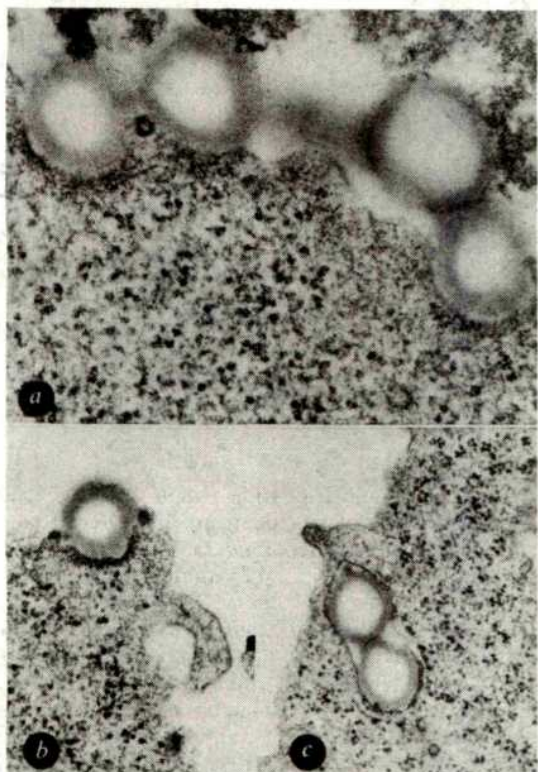
Cultured L1210 cells were incubated with L~TCII-Cbl at 4 or 37 °C for 0.5, 2 or 4 h. The cells were then collected, washed, fixed and processed for SEM and TEM. As shown in Fig. 2, SEM revealed extensive interaction between L~TCII-Cbl and microvilli. In some cases, these minibeads decorated the entire length of the microvillus, suggesting a localized and highly concentrated region of TCII-Cbl receptors. Minibead clusters were occasionally seen closer to the cell surface, but shorter microvilli could have been responsible for this effect. Quantitative data (Fig. 3) obtained from SEM prints indicated that minibeads containing TCII-Cbl bound equally well at 4 or 37 °C, averaging 12 and 10 per cell, respectively. The specificity of the interaction is also shown in Fig. 3. Thus, unmodified minibeads or minibeads derivatized with glycine, myoglobin or the non-TCII Cbl-binder from chicken serum did not bind to L1210 cells.

When cells were incubated with L~TCII-Cbl at 37 °C and then examined in sections using TEM, various stages of internalization were visualized (Fig. 4). Small clusters of minibeads appeared at the cell surface and were embedded in coated pits



and coated vesicles. The latter were morphologically similar to vesicles containing the structural protein clathrin, but were somewhat larger ( $\sim 0.35 \mu\text{m}$ ) than those commonly encountered in adsorptive endocytosis ( $0.05\text{--}0.25 \mu\text{m}$ )<sup>6</sup>.

These studies provide visual evidence for the localization of TCII-Cbl receptors on the microvilli of L1210 cells and suggest that the complex is internalized at the surface of the cell. Although it is not clear how the receptor complex reaches the surface for endocytosis, at least two mechanisms can be invoked: either the microvilli retract and become contiguous with the surface, or the receptor complex laterally diffuses along the



**Fig. 4** Internalization of L-TCII-Cbl by L1210 cells. Incubation conditions were as described in Fig. 2 legend except that the temperature was  $37^\circ\text{C}$ . Cells were prepared, fixed and dehydrated as for SEM, and then embedded in Spurr resin and thin-sectioned. After staining with uranyl acetate and lead citrate, preparations were examined by TEM. *a* Shows several minibeads on the cell surface, two of which seem to be in the process of internalization.  $\times 21,000$ . *b* Shows a minibead within a vesicle which seems to be coated by clathrin.  $\times 15,000$ . *c* Shows two minibeads completely internalized within a common vesicle.  $\times 10,000$ .

microvilli and on to the surface for subsequent endocytosis. In either case, internalization of L-TCII-Cbl seems to occur via clathrin-coated pits and vesicles in a temperature-dependent fashion.

This work was supported by NIH grants AM-25510 (M.T.), AM-25406 (D.W.J.), CA-16600, DOE contract EV00899 (M.T.) and American Cancer Society grant CH-31.

## Growth-modulating plasma tripeptide may function by facilitating copper uptake into cells

Loren Pickart\*, Jonathan H. Freedman†, W. John Loker‡, Jack Peisach†, Christopher M. Perkins‡, Ronald E. Stenkamp§ & Boris Weinstein‡

\* Virginia Mason Research Center, Seattle, Washington 98101

† Department of Molecular Pharmacology, Albert Einstein College of Medicine, Bronx, New York 10461

‡ Department of Chemistry and § Department of Biological Structure, University of Washington, Seattle, Washington 98195

The plasma tripeptide glycyl-L-histidyl-L-lysine (GHL), when added at nanomolar concentrations to a wide group of cultured systems, produces a disparate set of responses ranging from the stimulation of growth and differentiation to outright toxicity<sup>1-3</sup>. Such diverse actions imply that this tripeptide mediates some basic biochemical function common to many types of cells and organisms. During the isolation of GHL we found the compound to co-isolate through a number of steps with approximately equimolar copper and about 1/5 molar iron<sup>4</sup>. Maximal effects on hepatoma cells (HTC<sub>4</sub>) were seen when the peptide was added with copper and iron to the growth medium<sup>1</sup>. Structure-function studies revealed that several tripeptides with a histidyl-lysyl linkage were nearly as active as GHL<sup>1</sup>. The association of GHL with copper and a homology similarity between the tripeptide and the copper transport sites on albumin and  $\alpha$ -fetoprotein, where the cupric atom is bound to a histidyl residue adjacent to a basic residue, suggested that GHL may act as a copper transport factor<sup>4</sup>. We report here that the tripeptide readily forms complexes with copper(II) and enhances the uptake of the metal into cultured hepatoma cells.

GHL was synthesized by coupling *N*<sup>ε</sup>-t-butyloxycarbonyl-*N*<sup>im</sup>-benzyloxycarbonyl-L-histidine to benzyl *N*<sup>ε</sup>-benzyloxycarbonyl-L-lysine using a mixed anhydride procedure involving isobutyl chloroformate and *N*-methyl morpholine to yield benzyl *N*<sup>ε</sup>-t-butyloxycarbonyl-*N*<sup>im</sup>-benzyloxycarbonyl-L-histidyl-*N*<sup>ε</sup>-benzyloxycarbonyl-L-lysinate. The protected dipeptide was dissolved in methanol saturated with HCl to cleave the t-butyloxycarbonyl protecting group and to precipitate benzyl *N*<sup>im</sup>-benzyloxycarbonyl-L-histidyl-*N*<sup>ε</sup>-benzyloxycarbonyl-L-lysinate hydrochloride. Neutralization of this salt with triethyl amine gave the free dipeptide amine, which on joining to *N*<sup>ε</sup>-benzyloxycarbonylglycine by a mixed anhydride method, formed benzyl *N*<sup>ε</sup>-benzyloxycarbonylglycyl-*N*<sup>im</sup>-benzyloxycarbonyl-L-histidyl-*N*<sup>ε</sup>-benzyloxycarbonyl-L-lysinate. Hydrogenolysis of this fully protected compound produced the free peptide and chromatography on silica gel yielded crystalline GHL that had satisfactory microanalytical and amino acid analyses, as well as spectral data (IR and NMR).

When GHL was added to hepatoma (HTC<sub>4</sub>) cells, which had been cultured in low serum (0.75%) fetal calf serum, it was observed that the tripeptide elevated copper uptake in a dose-dependent manner from 10 to 200 ng ml<sup>-1</sup>. Higher concentrations of the compound were less effective and very high concentrations of the tripeptide (10  $\mu\text{g ml}^{-1}$ ) were inhibitory to copper uptake into the cells. When the compound was added at 200 ng ml<sup>-1</sup>, copper uptake increased approximately 2.4-fold after 4 h incubation (Fig. 1). The tripeptide's effect was rapid and the rise in the intake of copper at 30 min was 50% of the 4-h value. Addition of the constituent amino acids of GHL at a molar ratio 300-fold greater than that found in the parent compound at 200 ng ml<sup>-1</sup> did not alter the rate of copper transfer (Fig. 1). By contrast, the tripeptide had no significant effect on the transport of ferrous (<sup>59</sup>Fe) iron into the cells. These

Received 22 July; accepted 16 October 1980.

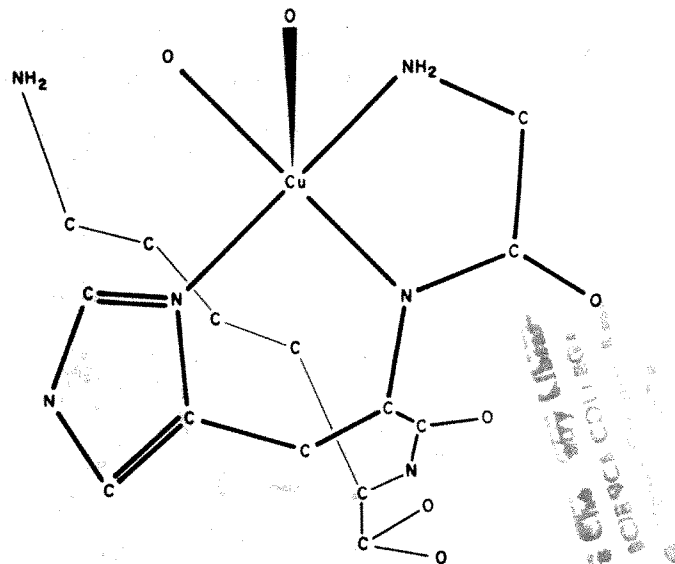
- Cooper, B. A. & Paranchych, W. *Nature* **191**, 393-395 (1961).
- Mahoney, M. J. & Rosenberg, L. E. in *Cobalamin* (ed. Babor, B. M.) 369-402 (Wiley-Interscience, New York, 1975).
- Youngdahl-Turner, P., Mellman, I. S., Allen, R. H. & Rosenberg, L. E. *Exp Cell Res.* **118**, 127-134 (1979).
- DiGirolamo, P. M. & Huennekens, F. M. *Archs Biochem. Biophys.* **168**, 386-393 (1975).
- Molday, R. S., Dreyer, W. J., Rembaum, A. & Yen, S. P. S. *J. Cell Biol.* **64**, 75-88 (1975).
- Pearse, B. *Trends biochem. Sci.* **5**, 131-134 (1980).
- Goldstein, J. L., Anderson, R. G. W. & Brown, M. S. *Nature* **279**, 679-685 (1979).
- Jacobsen, D. W., Montejano, Y. D., Vitols, K. S. & Huennekens, F. M. *Blood* **55**, 160-163 (1980).
- Weston, P. D. & Avrameas, S. *Biochem. biophys. Res. Commun.* **45**, 1574-1580 (1971).
- Jacobsen, D. W. & Montejano, Y. D. in *Vitamin B12* (eds Zagalak, B. & Friedrich, W.) 947-954 (de Gruyter, Berlin, 1979).



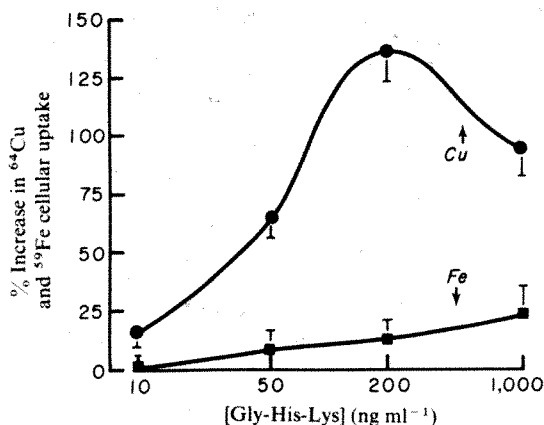
results suggest that GHL transports copper, and perhaps other related metals, into cells in culture.

This possibility is further supported by evidence that the tripeptide readily forms chelates with cupric ions. A single crystal X-ray diffraction study of a GHL-Cu complex showed the existence of a tridentate bonding structure involving the N-terminal group of glycine, the nitrogen atom of the first amide bond, and the imine nitrogen atom of the imidazole ring of histidine. The  $\epsilon$ -terminal amine group on the lysine side chain remains free and is not bound to the copper atom (Fig. 2). The electron paramagnetic resonance spectrum (EPR) of the peptide was determined on a frozen, aqueous solution (0.55 mM) in the presence of Cu(II) (0.50 mM) at 77 K and 9.073 GHz. The magnetic parameters obtained from the axial spectrum were  $A_{\parallel}$  210 G,  $g_{\parallel}$  2.335, and  $g_{\perp}$  2.057. These data indicate that the  $d_{x^2-y^2}$  orbital is the highest d-orbital, a result consistent with strong interactions between a copper ion and four ligands in a near-equatorial arrangement. The super-hyperfine structure present in the EPR spectrum supported the involvement of the copper with at least one nitrogen donor atom in a near-planar coordination. Electron spin echo studies confirmed the coordination of imidazole to copper and there was no indication from the EPR spectrum for dipolar interactions between two adjacent copper atoms<sup>5</sup>. The combined X-ray and EPR results are consistent with the idea of a GHL-Cu complex in solution that is monomeric in nature.

These experiments at low-serum conditions of cell culture suggest an increase in copper transport serves as a mechanism for the action of GHL and may explain the range of responses to



**Fig. 2** Structure of GHL-Cu crystals. X-ray analysis indicates that the N-terminal group of glycine, the adjacent nitrogen in the first amide linkage of the peptide chain and the unprotonated nitrogen of the imidazole ring of histidine form bonds to copper. EPR measurements suggest that the GHL-Cu complex exists as a monomeric species in dilute solution. The detailed interpretation of the X-ray and EPR data will be published elsewhere.



**Fig. 1** Effect of glycyl-L-histidyl-L-lysine (GHL) on the uptake of <sup>64</sup>Cu and <sup>59</sup>Fe into hepatoma cells in culture. Hepatoma (HTC<sub>4</sub>) cells were cultured for 3 days in 90% Eagle's basal medium plus 10% Swim's S-77 medium and 0.7% fetal calf serum in plastic T-flasks (25 cm<sup>2</sup>, 10<sup>6</sup> cells per flask) by methods previously detailed<sup>1</sup>. GHL was then added to the cultures at the indicated dosages. <sup>64</sup>Cu (1  $\mu$ Ci, 4.9 Ci per g) was added and glycine, histidine and lysine were present in 300-fold molar excess over GHL at 200 ng ml<sup>-1</sup>. The cells were incubated for 4 h at 37 °C, the media removed, and the cells washed four times with phosphate buffer saline, pH 7.4 (Gibco), at 0 °C, incubated in 0.01% trypsin for 15 min, and then cells were removed from the flask. The hepatoma cells were centrifuged at 2,000g for 30 min at 0 °C then homogenized in distilled water. The cellular debris was removed by centrifugation at 10,000g for 10 min and aliquots of the supernatant, representing copper from the cellular cytosol, counted by normal scintillation counting methods<sup>21</sup>. The cellular uptake of radiolabelled Cu at the various dosages of GHL ( $\pm$ s.d.) for six experiments is given in Fig. 1. In the complete absence of serum, GHL was only one-quarter as active in stimulating Cu uptake. The control Cu uptakes at 0.5, 1 and 2 h were, respectively, 51%, 72% and 84% of the 4-h value. The uptake of radiolabelled Fe (1  $\mu$ Ci per flask, 6.2 Ci per g) was determined in the same way as for Cu.

the compound. Synthetic tripeptide, when added to culture media at concentrations of 10–200 ng ml<sup>-1</sup>, has been found to: (1) enhance the growth of hepatoma cells<sup>3</sup>, thyroid follicular cells<sup>6</sup> and T-strain mycoplasma<sup>7</sup>; (2) stimulate the growth and differentiation of *Ascaris* larvae<sup>8</sup>, lymphocytes<sup>9</sup> and neurones<sup>10,11</sup>; (3) assist the establishment in culture of 19 cancer cell lines from human tumours<sup>12</sup>; (4) raise the viability of eosinophils<sup>13</sup>, endometrial cells<sup>14</sup>, fibroblasts<sup>15</sup>, kidney cells<sup>16</sup>, liver cell and organ cultures<sup>3,17</sup>, macrophages<sup>18</sup>, mast cells<sup>19,20</sup> and placental organ cultures<sup>21</sup>; (5) inhibit the growth of glial<sup>10</sup> and L929 cells<sup>22</sup>; and (6) increase antibody cytotoxicity towards parasitic worms (*Schistosoma mansoni*)<sup>23</sup>. Different patterns of cellular response to an increased copper(II) intake would rationalize the range of biological effects observed by various workers.

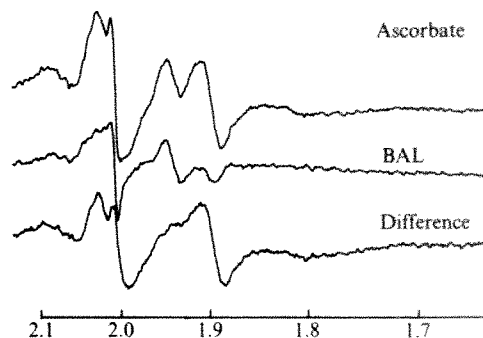
Furthermore, these results clearly delineate a structural model for a molecule that delivers transition metals to cellular receptors. The first two residues of the GHL molecule are involved in the bonding of the copper, whereas the side chain of lysine may be involved in the recognition of receptors that function in the uptake of the copper into cells. This possibility is further strengthened by the obvious analogies to the copper transport sites on plasma albumin or, in the fetus, on  $\alpha$ -fetoprotein, in which the histidyl residue that binds the copper is immediately adjacent to either a lysyl or an arginyl residue.<sup>4</sup> These considerations imply that the combination of a histidyl unit next to a basic residue constitutes a biologically active structure critical for the uptake of copper into cells.

We thank Drs Lyle H. Jensen and Norman J. Rose for their help and advice, and Madams Barbara Charles and Ruth Rehbein for the typing. The work was supported by USPHS grants AM 17702, CA 28858, GM 10828, HL 13399 and RR 00558.

Received 30 July; accepted 16 October 1980.

- Pickart, L. & Thaler, M. *Nature new Biol.* **243**, 85–87 (1973); *J. Chromat.* **175**, 65–73 (1979); *FEBS Lett.* **104**, 119–122 (1979); *J. cell Physiol.* **102**, 129–139 (1980).
- Schlesinger, D. H., Pickart, L. & Thaler, M. *Experientia* **33**, 324–325 (1977).
- Pickart, L., Thayer, L. & Thaler, M. *Biochem. biophys. Res. Commun.* **54**, 562–566 (1973).
- Aoyagi, T., Ikenaka, T. & Ichida, F. *Cancer Res.* **38**, 3483–3486 (1978).
- Peisach, J. in *Mechanisms of Oxidizing Enzymes* (eds Singer, T. P. & Ondarza, R. N.) 385–406 (Elsevier, Amsterdam, 1978).
- Ambesi-Impombato, F. S., Parks, L. A. M. & Coon, H. G. *Proc. natn. Acad. Sci. U.S.A.* **77**, 3455–3459 (1980).

7. Robertson, J. A. *J. clin. Microbiol.* **7**, 127–132 (1978).
8. Stromberg, B. E., Khoury, P. B. & Soulsby, E. J. L. *Int. J. Parasit.* **7**, 149–151 (1977).
9. Dessaint, J. P., Camus, D., Fischer, E. & Capron, A. *Eur. J. Immun.* **7**, 624–629 (1977).
10. Sensenbrenner, M., Jaros, G. G., Moonen, G. & Mandel, P. *Neurobiology* **5**, 207–213 (1975).
11. Lindner, G., Grosse, G. & Henklein, P. *Z. mikrosk.-anat. Forsch.* **93**, 820–828 (1979).
12. Simon, W. E. & Holzel, F. *J. Cancer Res. clin. Oncol.* **94**, 307–323 (1979).
13. Capron, M., Capron, A., Torpier, G., Bazin, H., Bout, D. & Joseph, M. *Eur. J. Immun.* **8**, 127–133 (1978).
14. Svanberg, L. & Astedt, B. *Experientia* **35**, 818–819 (1979).
15. Leung, M. K., Fessler, L. J., Greenberg, D. B. & Fessler, J. H. *J. biol. Chem.* **254**, 224–232 (1979).
16. Astedt, B., Barlow, G. & Holmberg, L. *Thromb. Res.* **11**, 149–153 (1977).
17. Eriksson, S., Alm, R. & Astedt, B. *Biochim. biophys. Acta* **542**, 496–505 (1978).
18. Joseph, M., Dessaint, J. P. & Capron, A. *Cell Immun.* **34**, 247–258 (1977).
19. Capron, M., Rousseaux, J., Mazingue, C., Bazin, H. & Capron, A. *J. Immun.* **121**, 2518–2526 (1978).
20. Mazingue, C., Dessaint, J. P. & Capron, A. *J. immun. Meth.* **21**, 65–77 (1978).
21. Holmberg, L., Lecander, I., Persson, B. & Astedt, B. *Biochim. biophys. Acta* **544**, 128–137 (1978).
22. Slotta, K. H., Golub, A. L. & Lopez, V. *Hoppe-Seyler's Z. physiol. Chem.* **356**, 367–376 (1975).
23. Torpier, G., Quaissi, M. A. & Capron, A. *J. ultrastruct. Res.* **67**, 276–287 (1979).



**Fig. 1** EPR spectrum of sub-mitochondrial particles ( $70 \text{ mg ml}^{-1}$  in  $0.25 \text{ M}$  sucrose,  $50 \text{ mM}$  morpholinopropane sulphonic acid buffer,  $\text{pH } 7.0$ ) reduced for  $3 \text{ min}$  at  $20^\circ\text{C}$  with  $5 \text{ mM}$  ascorbate in the presence of  $10 \mu\text{M}$   $N,N,N',N'$ -tetramethyl- $p$ -phenylenediamine,  $20 \mu\text{M}$  cytochrome  $c$  and  $4 \text{ mM}$  KCN. The EPR spectra were measured at  $36 \text{ K}$ ,  $5 \text{ mW}$  microwave power,  $9.33 \text{ GHz}$  frequency and  $6.3 \text{ G}$  modulation amplitude. The spectra plotted were 20–25 times scan averaged and corrected for differences in tube diameter and protein concentration. The top spectrum is that of untreated particles and the middle one after incubation with  $10 \text{ mM}$  BAL (2,3-dimercaptopropanol) and shaking in air for  $30 \text{ min}$  at  $36^\circ\text{C}$  (ref. 11). The bottom spectrum is the difference: control minus BAL-treated.

## Identification of the BAL-labile factor

E. C. Slater & S. de Vries

Laboratory of Biochemistry, BCP Jansen Institute, University of Amsterdam, Plantage Muidergracht 12, 1018 TV Amsterdam, The Netherlands

One of us has previously reported<sup>1</sup> that treatment of the Keilin and Hartree heart-muscle preparation<sup>2</sup> with 2,3-dimercaptopropanol (BAL), in the presence of air, leads to the complete inactivation of the succinate oxidase system with little if any effect on the activities of succinate dehydrogenase (until more than half the BAL was oxidized) or cytochrome  $c$  oxidase. The inactivation of the complete succinate oxidase system requires the oxidation of BAL by air in the presence of the enzyme. It is not caused by  $\text{H}_2\text{O}_2$  or BAL disulphides produced during the oxidation of BAL. Spectroscopic studies identified the block as lying between cytochromes  $b$  and  $c$ . It was suggested that a BAL-labile factor is present which transfers electrons from cytochrome  $b$  to cytochrome  $c$  and which is destroyed by coupled oxidation with BAL. The factor is also required for NADH oxidation<sup>3</sup>. Subsequent work showed that it is not identical with cytochrome  $c_1$  (ref. 4), myoglobin present in the preparation<sup>5</sup> or the antimycin-binding site<sup>6</sup>. We report here that this factor is identical to the iron-sulphur protein in the central portion of the respiratory chain first identified by Rieske<sup>6</sup>.

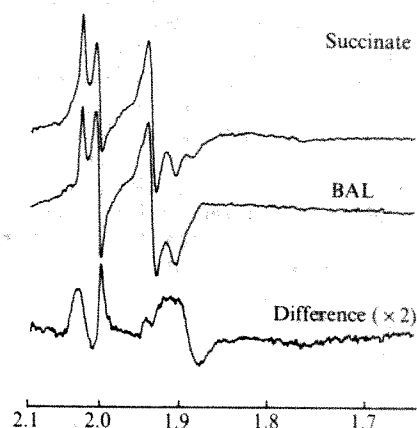
The following clues led us to this identification: (1) Deul and Thorn's observation<sup>5</sup> that, whereas after either BAL treatment or addition of antimycin electron flow between cytochromes  $b$  and  $c$  is blocked, the addition of antimycin to BAL-treated preparations causes a block in the reduction of cytochrome  $b$ . (2) Trumpower's observation<sup>7</sup> that in preparations of succinate/cytochrome  $c$  oxidoreductase from which Racker's 'oxidation factor'<sup>8</sup> has been extracted electron transfer between cytochromes  $b$  and  $c_1$  is impaired, but that in the presence of antimycin the reduction of cytochrome  $b$  is blocked. (3) The recent identification by Trumpower<sup>9</sup> of the active principle in Racker's preparations of oxidation factor as Rieske's iron-sulphur protein.

Direct evidence that BAL specifically destroys the Rieske iron-sulphur protein has now been obtained by electron paramagnetic resonance (EPR) spectrometry.

The EPR spectrum of sub-mitochondrial particles reduced with ascorbate in the presence of tetramethyl- $p$ -phenylenediamine, cytochrome  $c$  and cyanide (Fig. 1) shows lines characteristic of the Rieske iron-sulphur protein:  $g_z = 2.03$ ,  $g_y = 1.89$  and  $g_x = 1.80$ . There is an additional line at about  $1.94$  derived from partial reduction of one of the iron-sulphur clusters associated with succinate dehydrogenase, and a free radical

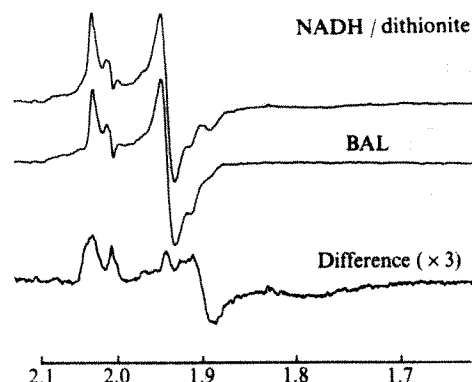
at about  $g = 2.0$  derived from the semiquinone of ubiquinone and from ascorbate. (The broad line at about  $2.1$  is probably due to contaminating copper.) After BAL treatment, the signals of the Rieske iron-sulphur protein completely disappeared. The residual signals are due to the free radical and the  $g_y$  and  $g_z$  lines of the iron-sulphur cluster of succinate dehydrogenase. The difference spectrum shows the three lines characteristic of the Rieske iron-sulphur protein.

Figures 2 and 3 show similar spectra obtained after reduction with succinate and  $\text{NADH} + \text{Na}_2\text{S}_2\text{O}_4$ , respectively. Although the  $g_z$  and  $g_y$  lines are now overshadowed by signals from other iron-sulphur clusters reduced at the lower potentials, the difference spectra (control minus BAL-treated) are in both cases dominated by the signals of the Rieske cluster. The complete elimination of the broad  $g_x$  line at  $1.80$ , which is characteristic of the Rieske iron-sulphur protein, is particularly clear. Lines at  $g = 1.92$  and  $2.01$  in the difference spectrum in Fig. 3 are



**Fig. 2** EPR spectrum of sub-mitochondrial particles reduced for  $10 \text{ min}$  at  $30^\circ\text{C}$  with  $20 \text{ mM}$  succinate in the presence of  $20 \mu\text{M}$  cytochrome  $c$  and  $4 \text{ mM}$  KCN. Conditions were as in Fig. 1 legend, except that the gain used for the direct spectra was  $1/1.6$  times that in Fig. 1, and that in the difference spectrum was twice that in the direct spectrum.





**Fig. 3** EPR spectrum of sub-mitochondrial particles reduced for 10 min at 20 °C with 2 mM NADH (pH 7.2) and dithionite in the presence of 20  $\mu$ M cytochrome *c* and 4 mM KCN. Conditions were as in Fig. 1 legend, except that the gain used for the direct spectra was 1/3.2 times that in Fig. 1, and that in the difference spectrum was three times that in the direct spectrum.

probably due to destruction by BAL treatment of an iron-sulphur protein in the outer membrane of the mitochondrion, fragments of which are present in sub-mitochondrial particles<sup>10</sup>.

Figure 3 shows that, although the mitochondrial inner membrane contains about 10 different iron-sulphur clusters, only that belonging to the Rieske protein is destroyed by BAL

treatment of sub-mitochondrial particles, thus confirming the specificity of BAL treatment<sup>11</sup>.

The nature of the chemical reaction between BAL, oxygen and the iron-sulphur protein is not established. It is possible that a disulphide bridge is formed between BAL and one of the cysteine molecules or the inorganic sulphur that is bound to the iron atom in the iron-sulphur cluster. The specificity of the BAL action may be due to the relative accessibility of this strongly hydrophilic compound to the Rieske iron-sulphur cluster.

We conclude that the BAL-labile factor is identical to the Rieske iron-sulphur protein; the oxidation factor has also been identified with this protein<sup>9</sup>. BAL treatment is therefore a useful technique for specifically eliminating the Rieske iron-sulphur cluster from the respiratory chain of sub-mitochondrial particles.

This work was supported in part by a grant from the Netherlands Organization for the Advancement of Pure Research (ZWO) under the auspices of the Netherlands Foundation for Chemical Research (SON).

Received 21 August; accepted 4 November 1980.

1. Slater, E. C. *Nature* **161**, 405–407 (1948).
2. Keilin, D. & Hartree, E. F. *Proc. R. Soc. B* **129**, 277–306 (1940).
3. Slater, E. C. *Nature* **165**, 674–676 (1950).
4. Slater, E. C. *Nature* **163**, 532 (1949).
5. Deul, D. H. & Thorn, M. B. *Biochim. biophys. Acta* **59**, 426–436 (1962).
6. Rieske, J. S., Hansen, R. E. & Zaugg, W. S. *J. biol. Chem.* **239**, 3017–3022 (1964).
7. Trumpower, B. L. *Biochem. biophys. Res. Commun.* **70**, 73–80 (1976).
8. Nishibayashi-Yamashita, H., Cunningham, C. & Racker, E. *J. biol. Chem.* **247**, 698–704 (1972).
9. Trumpower, B. L. & Edwards, C. A. *J. biol. Chem.* **254**, 8697–8706 (1979).
10. Heidrich, H.-G., Albracht, S. P. J. & Bäckström, D. *FEBS Lett.* **95**, 314–318 (1978).
11. Slater, E. C. *Biochem. J.* **45**, 14–30 (1949).

## 1,25-Dihydroxycholecalciferol stimulation of a mitochondrial protein in chick intestinal cells

Adrian N. Hobden\*, Marilyn Harding & D. Eric M. Lawson

Dunn Nutritional Laboratory, University of Cambridge and Medical Research Council, Milton Road, Cambridge CB4 1XJ, UK

The steroid hormone 1,25-dihydroxycholecalciferol (1,25-(OH)<sub>2</sub>D<sub>3</sub>) stimulates the absorption of dietary calcium by the small intestine of animals although the exact mechanism by which this is achieved remains unclear. However, it has long been known that a soluble, calcium-binding protein (CaBP), is produced in large amounts in the cytoplasm of the intestinal cells of animals after *in vivo* administration of vitamin D<sub>3</sub> or 1,25-(OH)<sub>2</sub>D<sub>3</sub> (refs 1, 2). We report here that 1,25-(OH)<sub>2</sub>D<sub>3</sub> administered *in vivo* to rachitic chickens also stimulates production of another protein with molecular weight (MW) 39,000–42,000 which is insoluble in the absence of detergent, is found in the outer mitochondrial membrane and is produced in advance of maximum calcium transport.

Synthesis of CaBP is not optimal until after maximum stimulation of calcium transport by 1,25-(OH)<sub>2</sub>D<sub>3</sub> (ref. 3)—there is significant stimulation of calcium transport before any CaBP can be detected in the intestinal cell. Thus CaBP cannot have a direct effect on calcium transport and other factors which are responsive to *in vivo* administration of 1,25-(OH)<sub>2</sub>D<sub>3</sub> have been sought. Two such factors, proteins of MW 45,000 and 84,000, have been identified in the intestinal brush borders of chickens<sup>4,5</sup>. However, only small quantities of these proteins

were produced after administration of 1,25-(OH)<sub>2</sub>D<sub>3</sub> possibly indicating additional rather than *de novo* synthesis. The function of these proteins is unknown although any role for them in calcium uptake would possibly be at the level of absorption of calcium from the intestinal lumen into the cytoplasm. Once calcium has crossed the intestinal brush border membrane, it has to be transported across the cell to the basal membranes and then into the capillaries. We therefore looked for any changes in protein composition of intestinal mitochondria following *in vivo* administration of 1,25-(OH)<sub>2</sub>D<sub>3</sub> to rachitic chickens.

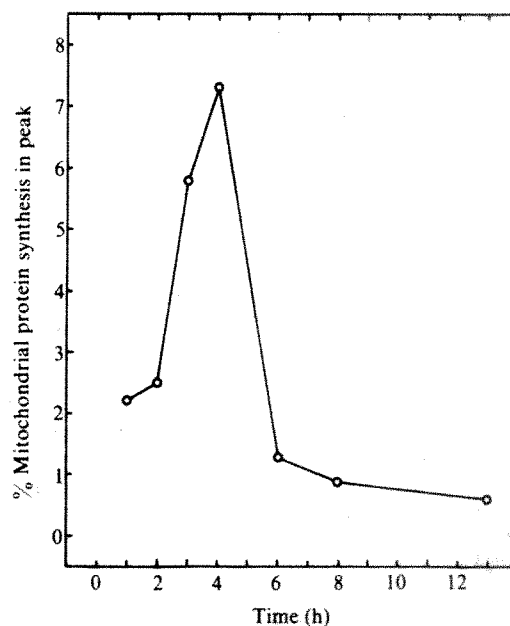
At various times following administration of 125 ng of 1,25-(OH)<sub>2</sub>D<sub>3</sub>, the rachitic chickens were killed and slices of their everted jejunum incubated in medium containing [<sup>14</sup>C]leucine. Mitochondria were isolated from the slices and their proteins electrophoresed through SDS gels together with proteins (labelled with [4,5-<sup>3</sup>H]leucine) from the intestinal mitochondria of 1,25-(OH)<sub>2</sub>D<sub>3</sub>-deficient chickens. The gels were sliced and the radioactivity in each slice determined. Examination of the ratio of <sup>14</sup>C:<sup>3</sup>H in each slice revealed that an extra protein (or additional amounts of a protein) was being produced in the birds subjected to 1,25-(OH)<sub>2</sub>D<sub>3</sub> administration (Fig. 1). The level of synthesis of this protein was quantified from the double-label plot<sup>6</sup> (Fig. 1) and a time course of synthesis determined (Fig. 2). This additional mitochondrial protein maximally accounted for over 7% of total mitochondrial protein synthesis (Fig. 2). Comparison with the time courses for other events which follow *in vivo* administration of 1,25-(OH)<sub>2</sub>D<sub>3</sub> (refs 3, 4) reveals that maximum production of this mitochondrial protein (at 4 h) occurred before maximum calcium transport (at 8 h) and well before maximum synthesis of CaBP (Fig. 3). Although the MW and the time course of appearance (Fig. 3) were similar to those of a protein previously observed in intestinal brush borders<sup>4,5</sup> the mitochondrial protein was produced in greater amounts (P. Wilson, personal communication), had a consistently smaller MW (39,000–42,000) and did not behave like actin (putatively identified as the brush border protein<sup>5</sup>) on gel electrophoresis in 8 M urea. We suggest therefore that the mitochondrial protein is a novel product of the

\* To whom correspondence should be addressed.

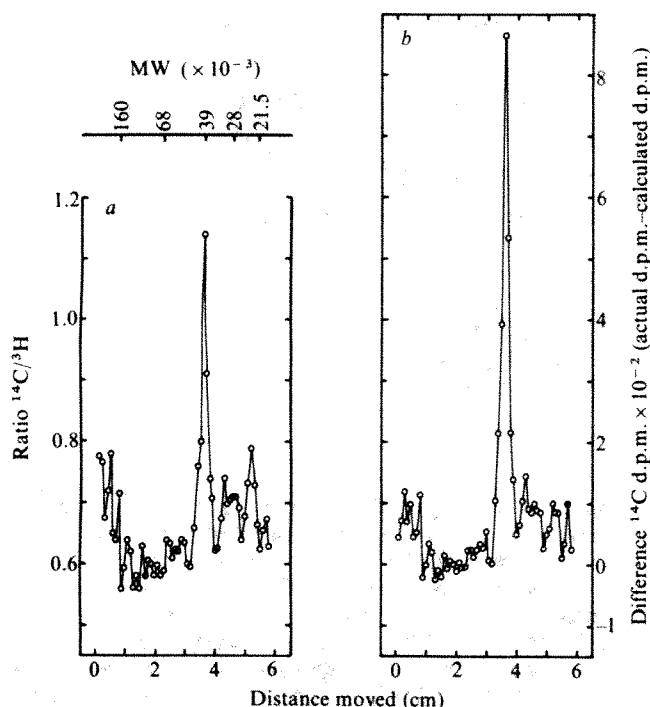
intestinal cells which is produced following *in vivo* administration of  $1,25\text{-(OH)}_2\text{D}_3$ .

Partial fractionation of the intestinal mitochondria into inner membrane, outer membrane and soluble protein fractions was achieved by sonication and sucrose density-gradient centrifugation<sup>7</sup>. In this way we showed that the novel mitochondrial protein had a distribution between the fractions similar to the enzyme rotenone-insensitive NADH-cytochrome *c* reductase (Fig. 4), a marker for the outer mitochondrial membrane<sup>7</sup>. Thus it seems that this protein is a constituent of the outer mitochondrial membrane. Little or no protein was found in the soluble fraction and it could not be solubilized unless a detergent (0.1% v/v Triton X-100) was present in the buffer.

Mitochondria from a wide variety of tissues can accumulate large amounts of calcium<sup>8-10</sup> and they have long been thought to be involved in calcium transport across intestinal cells<sup>11,12</sup>. However, the influence of vitamin  $\text{D}_3$  and  $1,25\text{-(OH)}_2\text{D}_3$  on the

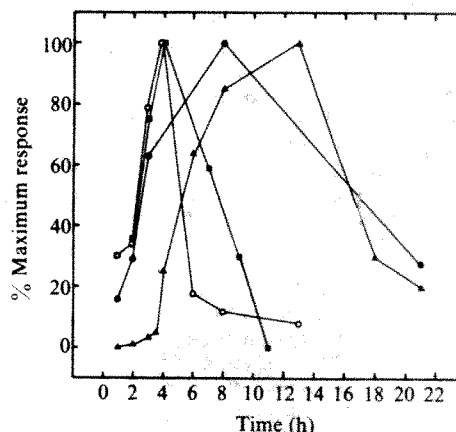


**Fig. 2** Time course of synthesis of mitochondrial protein. Slices of everted chick jejunum from vitamin D-deficient chicks or those dosed at various times before death with 125 ng of  $1,25\text{-(OH)}_2\text{D}_3$  were incubated with radioactive leucine and their mitochondria prepared as described in Fig. 1 legend. Mitochondrial proteins from chicks dosed with  $1,25\text{-(OH)}_2\text{D}_3$  at a certain time before death were mixed with those from vitamin D-deficient chicks electrophoresed and counted as described previously (Fig. 1 legend). The level of  $^{14}\text{C}$  radioactivity observed in the peak at MW 39,000–42,000 in a difference plot<sup>6</sup> (see Fig. 1b) was estimated and expressed as percentage of total  $^{14}\text{C}$  on the gel.



**Fig. 1** Mitochondrial proteins synthesized in intestinal slices from  $1,25\text{-(OH)}_2\text{D}_3$ -dosed or deficient chickens. Flasks containing 0.5 g of everted chick jejunal slices (about 2 mm thick) were incubated in 10 ml of Krebs Improved Ringer 1 medium<sup>18</sup> for 2 h with shaking in  $\text{O}_2/\text{CO}_2$  (19:1) atmosphere at  $37^\circ\text{C}$ . Slices from vitamin D-deficient chicks or those dosed 4 h before death with 125 ng of  $1,25\text{-(OH)}_2\text{D}_3$  were incubated with  $[4,5\text{-}^3\text{H}]\text{leucine}$  (125  $\mu\text{Ci}$ ) and  $[U\text{-}^{14}\text{C}]\text{leucine}$  (25  $\mu\text{Ci}$ ), respectively. After incubation the slices were washed several times with 0.9% w/v NaCl and their mitochondria isolated<sup>19</sup>. Mitochondria from dosed and deficient chicks were mixed (50,000–100,000 d.p.m. of  $^3\text{H}$ , 25,000–50,000 d.p.m. of  $^{14}\text{C}$  and  $\sim 0.5$  mg protein) and dissociated before electrophoresis by heating at  $70^\circ\text{C}$  for 30 min in a solution containing dithiothreitol (15  $\text{mg ml}^{-1}$ ), SDS (10  $\text{mg ml}^{-1}$ ), Tris (12  $\text{mg ml}^{-1}$ ) and glycerol (0.1 ml). After electrophoresis in SDS-polyacrylamide<sup>5</sup> the gel was washed for several hours in acetic acid/propan-2-ol/water (2:5:13) by volume and cut into 1-mm sections. Each slice was treated with 0.5 ml 90% (v/v) NCS tissue solubilizer (Amersham/Searle) at  $60^\circ\text{C}$  for 2 h in closed vials. After cooling, 0.5 ml of NCS tissue solubilizer and 10 ml of scintillator containing 0.01% 1,4-bis-(5-phenyloxazol-2-yl) benzene and 0.4% 2,5-diphenyloxazole in toluene was added to the digested gel and radioactivity estimated in a Packard Tri-Carb scintillation spectrometer model 2650. Quenching corrections were made by means of automatic external standard and correlation curves for combined  $^{14}\text{C}$  and  $^3\text{H}$ . a, Ratio of  $^{14}\text{C}/^3\text{H}$  in each slice of gel; b, difference between observed  $^{14}\text{C}$  radioactivity in each slice and that expected if each slice had the average ratio of  $^{14}\text{C}/^3\text{H}$  (ref. 6).

mitochondria of intestinal cells has received little attention. Vitamin  $\text{D}_3$  administered *in vitro* and *in vivo* seems to alter the ability of kidney mitochondria to retain calcium *in vitro*<sup>13,14</sup> and some authors report that CaBP can influence the release of calcium from intestinal mitochondria<sup>11</sup>. In addition, a small yet direct effect of  $1,25\text{-(OH)}_2\text{D}_3$  on calcium uptake by intestinal mitochondria *in vitro* has been demonstrated<sup>15</sup>. In this experiment it was suggested that the direct effect might be of only secondary importance—the steroid caused a much greater increase in calcium uptake merely by increasing cytoplasmic concentrations of calcium. Such an effect would account for the

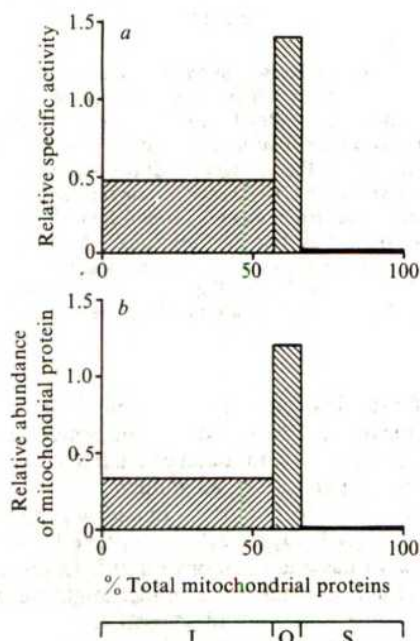


**Fig. 3** Time course of events occurring in the rachitic chick intestine after a single intracardial injection of  $1,25\text{-(OH)}_2\text{D}_3$  (125 ng).  $\circ$ , Synthesis of mitochondrial protein;  $\blacksquare$ , synthesis of brush border protein<sup>4</sup>;  $\bullet$ , calcium transport *in vitro*<sup>3</sup>;  $\blacktriangle$ , synthesis of CaBP (ref. 3).



transient accumulation of calcium by intestinal mitochondria *in vivo* after administration of vitamin D<sub>3</sub> (ref. 16).

We have been unable to find any role for this novel mitochondrial protein in calcium transport. Although the protein may be required to regulate some aspect of mitochondrial calcium transport, most studies have suggested that these processes are controlled both by the electrochemical gradient which is established across the inner mitochondrial membrane and by a calcium carrier, associated with the inner membrane, which catalyses a continuous efflux of calcium (for a review see ref. 17). The outer mitochondrial membrane is considered to be of little importance in calcium transport. However, the evidence for CaBP stimulation of calcium release from mitochondria<sup>11</sup> suggests an intermediary role for the mitochondrial protein in this process. Alternatively it may act independently of CaBP and sequester calcium from the mitochondrial intramembrane space thus facilitating calcium efflux and calcium transport across the intestinal cell. We do not know whether the protein is produced *de novo* or merely at a greater rate after *in vivo* administration of 1,25-(OH)<sub>2</sub>D<sub>3</sub>. Further experiments are required to answer these questions.



**Fig. 4** Distribution of newly synthesized protein between sub-mitochondrial fractions. Mitochondria from the jejuna of vitamin D-deficient chicks ([4,5-<sup>3</sup>H]leucine-labelled) or from such chicks dosed 4 h before death with 125 ng 1,25-(OH)<sub>2</sub>D<sub>3</sub> ([U-<sup>14</sup>C]leucine-labelled) as described in Fig. 1 legend were mixed 2:1 dosed: deficient (by weight) and sub-mitochondrial particles were prepared essentially by the method of Sottocasa *et al.*<sup>7</sup>. The mixture of mitochondria (20 mg protein ml<sup>-1</sup>) was resuspended in 7.5 ml 10 mM Tris-phosphate pH 7.4 at 20 °C, left on ice for 10 min and mixed with 2.5 ml 1.8 M sucrose, 2 mM (Na)<sub>2</sub>ATP, 2 mM MgSO<sub>4</sub> followed by a further 10 min on ice. Aliquots (3.5 ml) of this final mixture were sonicated on ice for three 15-s periods, with 30-s rests between each sonication, using a 9.5-mm diameter probe at an amplitude of 4 μm in a MSE ultrasonic disintegrator Mk 2. The sonicated mitochondria were then pooled and layered onto 8.5 ml 0.76 M sucrose, 5 mM Tris-phosphate pH 7.4, which was itself layered on 14 ml 1.32 M sucrose, 5 mM Tris-phosphate pH 7.4 in a Beckman SW 27 tube. After centrifugation for 3 h at 24,000 r.p.m. and 4 °C in a Beckman SW 27 rotor three fractions were collected—the pellet, designated the inner mitochondrial membrane fraction (I); material at the interface of the 0.76M and 1.32M sucrose, designated outer mitochondrial membrane fraction (O); and the top layer, designated soluble proteins (S). Portions of each fraction were assayed for: *a*, the presence of rotenone-insensitive NADH-cytochrome *c* reductase<sup>7</sup> or *b*, the percentage of total <sup>14</sup>C-labelled protein synthesis present in the peak at MW 39,000–42,000 following SDS-gel electrophoresis and a difference plot (see Figs 1, 2).

Received 21 August; accepted 27 October 1980.

1. Wasserman, R. H., Corradino, R. A. & Taylor, A. N. *J. biol. Chem.* **243**, 3978–3986 (1968).
2. Wasserman, R. H., Taylor, A. N. & Fullmer, C. S. *Biochem. Soc. spec. Publ.* **3**, 55–74 (1974).
3. Spencer, R., Charman, M., Wilson, P. & Lawson, E. *Nature* **263**, 161–163 (1976).
4. Wilson, P. W. & Lawson, D. E. M. *Biochim. biophys. Acta* **497**, 805–811 (1977).
5. Wilson, P. W. & Lawson, D. E. M. *Biochem. J.* **173**, 627–631 (1978).
6. Mayol, R. F. *Molec. cell. Endocr.* **2**, 133–146 (1975).
7. Sottocasa, G. L., Kuylenstierna, B., Ernster, L. & Bergstrand, A. *J. Cell Biol.* **32**, 415–438 (1967).
8. Lehninger, A. L., Carafoli, E. & Rossi, C. S. *Adv. Enzym.* **29**, 259–321 (1967).
9. Lehninger, A. L. *Biochem. J.* **119**, 129–138 (1970).
10. Bygrave, F. L. *Biol. Rev.* **53**, 43–79 (1978).
11. Hamilton, J. W. & Holdsworth, E. S. *Biochem. biophys. Res. Commun.* **40**, 1324–1330 (1970).
12. Omdahl, J. L. & De Luca, H. F. *Physiol. Rev.* **53**, 327–372 (1973).
13. Engstrom, G. W. & De Luca, H. F. *J. biol. Chem.* **237**, 974–975 (1962).
14. Engstrom, G. W. & De Luca, H. F. *Biochemistry* **3**, 203–209 (1964).
15. Bikle, D. D., Askew, E. W., Zolock, D. J., Morrissey, R. L. & Herman, R. H. *Biochim. biophys. Acta* **598**, 561–574 (1980).
16. Sampson, H. W., Matthews, J. L., Martin, J. H. & Kunin, A. S. *Calcified Tissue Res.* **5**, 305–316 (1970).
17. Nicholls, D. G. & Crompton, M. *FEBS Lett.* **111**, 261–268 (1980).
18. Dawson, R. M. C. in *Data for Biochemical Research* 2nd edn (eds Dawson, R. M. C., Elliot, C. D., Elliot, W. H. & Jones, K. M.) 476–508 (Clarendon, Oxford, 1969).
19. Freeman, K. B. *Biochem. J.* **94**, 494–501 (1965).

## Role of *src* gene in growth regulation of Rous sarcoma virus-infected chicken embryo fibroblasts

Gordon Parry, James C. Bartholomew & Mina J. Bissell\*

Laboratory of Chemical Biodynamics, Lawrence Berkeley Laboratory, University of California, Berkeley, California 94720

We report here a study of the mechanisms leading to loss of growth control in chicken embryo fibroblasts transformed by Rous sarcoma virus (RSV). We have been particularly concerned with the role of the *src* gene in this process, and have used RSV mutants temperature sensitive (*ts*) for transformation to investigate the nature of the growth regulatory lesion. The two principal findings were (1) the stationary phase of the cell cycle (*G*<sub>1</sub>) in chick embryo fibroblasts seems to have two distinct regulatory compartments (using the terminology of Brooks *et al.*<sup>1</sup> we refer to these as 'Q' and 'A' states). When rendered stationary at 41.5 °C by serum deprivation, normal cells enter a Q state, but cells infected with the *ts*-mutant occupy an A state. (2) Whereas normal cells can occupy either state depending on culture conditions, the *ts*-infected cells, at 41.5 °C, do not seem to enter Q even though a known *src* gene product, a kinase, is reported to be inactive at this temperature<sup>2,3</sup>. We discuss the possibility that viral factors other than the active *src* protein kinase influence growth control in infected cultures.

The experiments involved plating cultures at high density and low serum content in 35-mm plates in medium containing 0.5% chicken serum (see Fig. 1 legend), and maintaining them at either 41.5 or 35 °C for 36–48 h before starting an experiment. DNA synthesis was followed by staining cells with propidium iodide and analysing cellular fluorescence by flow cytometry. After 48 h in 0.5% serum, cells infected with the *ts* mutants LA24, LA29 or NY68 mainly occupied the *G*<sub>1</sub> compartment if cultured at 41.5 °C. However, a significant proportion was found in S if cultures were maintained at 35 °C (Table 1). Cultures maintained at 41.5 °C and then shifted to 35 °C were found to enter S approximately 8 h after shift (Fig. 1). These data confirm the early work of Bell *et al.*<sup>4</sup>. The lag period before entry into S was distinctly longer when normal cells seeded at high density

\* To whom reprint requests should be addressed.



**Table 1** Growth regulation in ts-mutants LA29 and LA24 (Prague A) and NY68 (Schmidt Rupp A)

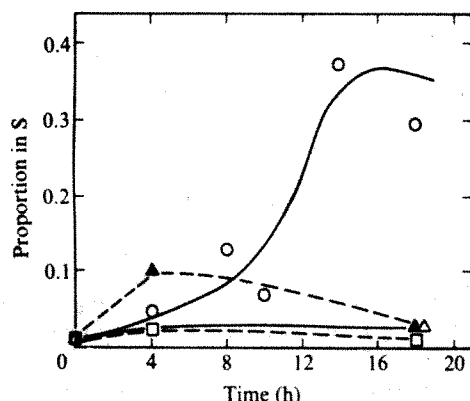
|              | Fraction of the population in cell cycle phase |       |                     |
|--------------|--|-------|---------------------|
|              | G <sub>1</sub>                                 | S     | G <sub>2</sub> + M* |
| 41.5 °C      |  |       |                     |
| Normal cells | 0.694  | 0.027 | 0.279               |
| NY 68        | 0.688  | 0.028 | 0.304               |
| LA 29        | 0.688  | 0.042 | 0.271               |
| LA 24        | 0.688  | 0.028 | 0.304               |
| 35 °C        |  |       |                     |
| Normal cells | 0.703  | 0.012 | 0.286               |
| NY 68        | 0.423  | 0.324 | 0.253               |
| LA 29        | 0.407  | 0.478 | 0.114               |
| LA 24        | 0.498  | 0.424 | 0.078               |

Chicken embryo fibroblasts were cultured as described in Fig. 1 legend except that 4 h after plating, some cultures were shifted to 35 °C whereas others were maintained at 41.5 °C. Cultures were kept at these temperatures for 48 h and the distribution of cells throughout the cycle analysed after this time period, using the procedures described in Fig. 1 legend. The cells in the G<sub>2</sub> + M category include some G<sub>1</sub> doublets which were not dissociated in our experimental conditions and thus the values in this category do not reflect true G<sub>2</sub> + M estimations.

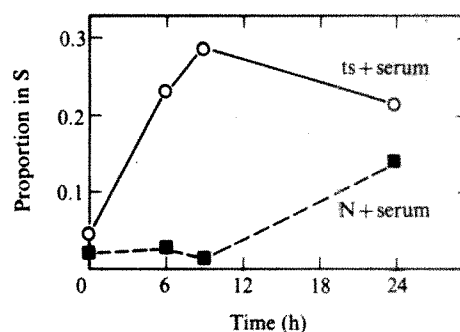
\* Doublet population significant.

and maintained in low serum were stimulated to initiate DNA synthesis by serum addition at 41.5 °C. In six separate experiments, normal cells at 41.5 °C were found to enter S phase 12–14 h after stimulation, but surprisingly, LA24-infected cells entered S phase only 6–8 h after stimulation (Fig. 2). These results implied that in the stationary state normal and LA24-infected cultures were at different stages of the G<sub>1</sub> phase.

If normal cells were initially plated at a lower density or serum stimulated 24 h after plating instead of 48 h, then their lag period before entry into S approached that of LA24-infected cultures (Fig. 3). This clearly demonstrated that there are two



**Fig. 1** Kinetics of entry of chicken embryo fibroblasts into S phase after shift from 41.5 to 35 °C. Tertiary cells were plated in medium 199 supplemented with 2% tryptose broth, 0.5% chicken serum and 0.1% glucose, at a density of  $2 \times 10^6$  per 35-mm plate. They were kept at 41.5 °C for 36–38 h and either maintained at this temperature for a further 18 h or shifted to 35 °C. At given times, plates were removed and the cells collected and stained with propidium iodide as described elsewhere<sup>11</sup>. The stained cells were subsequently analysed in a flow cytometer and histograms of the distribution of cells throughout the cell cycle obtained. The proportion of cells in S was determined using a fitting procedure, and data analysed using a program described elsewhere<sup>12</sup>. ○, LA24-infected cells cultured at 41.5 °C and shifted to 35 °C; △, normal cells cultured at 41.5 °C and shifted to 35 °C; □, LA24-infected cells cultured at 41.5 °C and held at that temperature, and ▲, normal cells cultured at 41.5 °C and held at that temperature.



**Fig. 2** Serum stimulation of DNA synthesis in normal and LA24-infected cells maintained at 41.5 °C. Cells were seeded at  $2.0$ – $2.5 \times 10^6$  per 35-mm dish, cultures as in Fig. 1 and maintained at 41.5 °C for 48 h. DNA synthesis was initiated by the addition of 200 µl of calf serum to the cultures (no medium change: 2 ml medium per plate) and the proportion of cells in S at times after addition was determined as described in Fig. 1 legend. ○, LA24-infected cells; ■, normal cells (N).

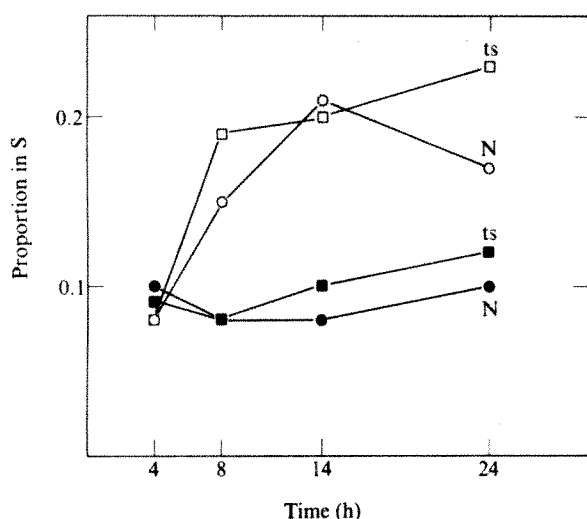
compartments in the stationary phase of the chick embryo fibroblast cell cycle and that, by manipulating culture conditions, normal cells can be made to occupy either compartment. In contrast, it was not possible to force the LA24-infected cells into the compartment with a 12–14 h lag even by plating the cells at much higher densities than the normal cells or by growing them strictly at 42 °C. Thus, viral factors in the stationary ts-infected cells prevent these cells from entering the state which would necessitate the longer lag period. Experiments with cells infected with transformation-defective virus showed that their lag period from serum stimulation to entry into S was similar to that of normal cells (data not shown).

That chicken embryo fibroblasts apparently have two distinct stationary states within the G<sub>1</sub> phase is consistent with the recent work of Brooks *et al.*<sup>1</sup>, who discuss the evidence for two stationary states (Q and A) in mammalian cell-cycle models. Our data suggest that this is also true for the avian cell cycle, the Q state being a long-lag compartment and the A state the short-lag compartment.

Our data also indicate that virally coded factor(s) active at the non-permissive temperature must be responsible for maintaining the infected cells in the short-lag stationary stage in G<sub>1</sub> or preventing the cells from moving into the long-lag compartment. At present, the only known activity coded for by the *src* gene is a protein kinase, pp60<sup>src</sup>, which has been shown to be temperature sensitive in ts-mutants<sup>3</sup>. It is possible to argue that a low level of kinase is expressed at 41.5 °C and that this is sufficient to advance the cells further along the cycle. Such levels, however, would have to be very small in LA24-infected cells because the *in vivo* (cellular) activity of the kinase has been shown to be similar to that in uninfected controls even at 41 °C. Furthermore, in experiments carried out with cells cultured at strictly 42 °C, when such 'leakiness' would be minimized, the same differences in cycle position were observed. Also, note that in earlier studies which examined the expression of many transformation parameters at permissive and non-permissive temperatures using LA24, we failed to detect leakiness of other usual transformation parameters at the non-permissive temperature<sup>6,7</sup>.

A more feasible alternative is that an activity other than the kinase is responsible for these observations—this could be another activity associated with pp60<sup>src</sup> at the non-permissive temperature or a different protein coded for by a different reading frame of the *src* gene. Support for this suggestion comes from the observation in neuroretinal cells that the growth-regulating activity of *src* and its other transformation-related





**Fig. 3** Stimulation of DNA synthesis in normal and LA24-infected cells maintained at lower density at 41.5 °C. Cells were seeded at  $1.2 \times 10^6$  per 35-mm plate in the conditions described in Fig. 1 legend. They were kept at 41.5 °C for 18–24 h. DNA synthesis was initiated by changing the medium with fresh medium containing 2–5% chick or calf serum. Proportion of cells in S was determined as described in Fig. 1 legend. Closed symbols, control cultures; open symbols, serum-stimulated cultures.

functions may be dissociable<sup>8</sup>. Calothy *et al.*<sup>8</sup> have isolated an RSV mutant, PA-101, which is defective for 'transformation', but causes proliferation of neuroretinal cells. The 60,000 molecular weight (60K) *src* protein produced by these cells is inactive as a kinase in the immune complex assay (J. M. Bishop, personal communication).

Other observations on cells infected with temperature-sensitive RSV mutants are interesting in terms of these results. Poste and Flood<sup>9</sup> found that infected cells formed tumours at both 41 and 35 °C when grown on chicken chorioallantoic membranes. Harley and Goldfine<sup>10</sup> found that in contrast to several types of normal cells, infected cells need not synthesize lipids before initiating DNA synthesis when shifted from 41 to 35 °C. Finally, it was found that infected cells cultured at 41 °C were more sensitive to tumour promoters than were normal cells<sup>7</sup>. Data reported here, together with these observations, are consistent with the idea that cells infected with temperature-sensitive RSV mutants are in an initiated or committed state at the non-permissive temperature, and provide strong evidence for the multi-stage model of viral oncogenesis which has been discussed in detail elsewhere<sup>7</sup>.

We thank Jill Hatie and Deborah Farson for help with cell culture, Krishnakali Das for data analysis, and J. Michael Bishop for allowing us to cite unpublished data. This work was supported by the Division of Biomedical and Environmental Research, United States Department of Energy, under contract W-740-ENG-48, and an SRC (UK) fellowship to G.P.

Received 18 July; accepted 27 October 1980.

- Brooks, R. F., Bennett, D. C. & Smith, J. A. *Cell* **19**, 493–504 (1980).
- Collet, M. S. & Erikson, R. L. *Proc. natn. Acad. Sci. U.S.A.* **75**, 2021–2014 (1978).
- Rübsamen, H., Friis, R. R. & Bauer, H. *Proc. natn. Acad. Sci. U.S.A.* **76**, 967–971 (1979).
- Bell, J. G., Wyke, J. A. & Macpherson, I. A. *J. gen. Virol.* **27**, 127–134 (1975).
- Sefton, B. M., Hunter, T., Beemon, K. & Eckhart, W. *Cell* (in the press).
- Parry, G. & Hawkes, S. P. *Proc. natn. Acad. Sci. U.S.A.* **75**, 3703–3707 (1978).
- Bissell, M. J., Hatie, C. & Calvin, M. *Proc. natn. Acad. Sci. U.S.A.* **76**, 348–352 (1979).
- Calothy, G., Doirier, F., Dambrine, G. & Pessac, B. *Virology* **89**, 75–84 (1978).
- Poste, G. & Flood, M. K. *Cell* **17**, 789–800 (1979).
- Harley, J. B. & Goldfine, H. *Expl Cell Res.* **118**, 47–54 (1979).
- Teng, M., Bartholomew, J. C. & Bissell, M. J. *Nature* **268**, 739–741 (1977).
- Bartholomew, J. C., Pearlman, A. L., Landolph, J. R. & Straub, K. *Cancer Res.* **39**, 2538–2543 (1979).

## An embryo protein induced by SV40 virus transformation of mouse cells

Peter T. Mora, K. Chandrasekaran  
& Vivian W. McFarland

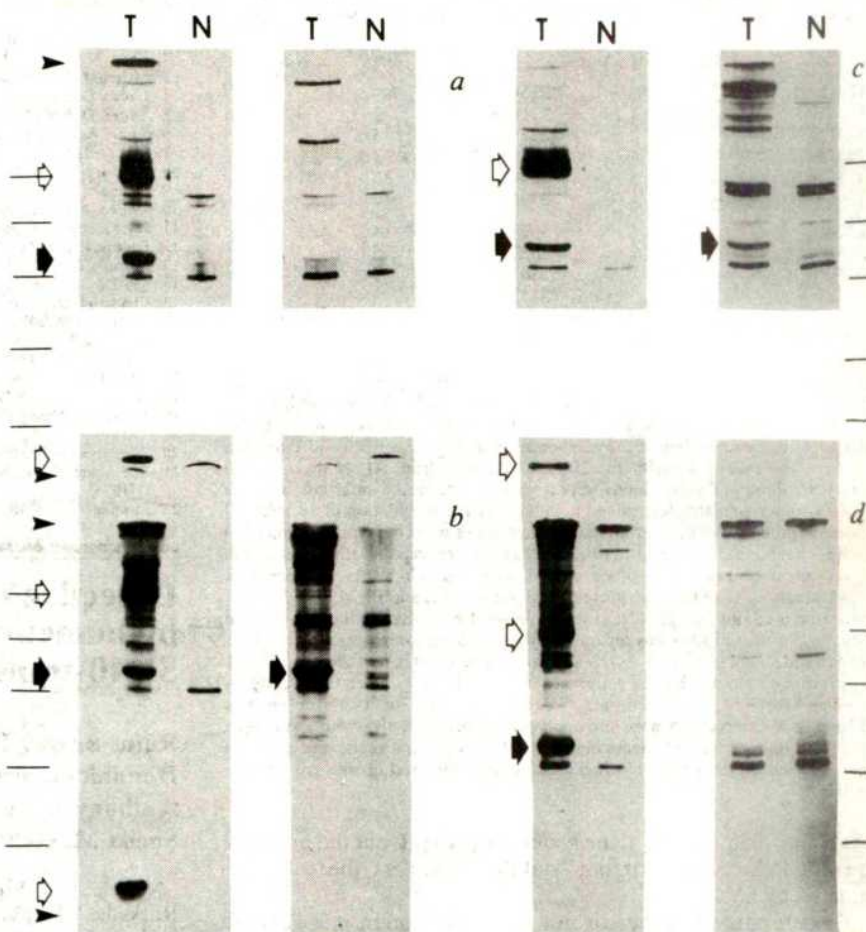
National Institutes of Health, National Cancer Institute, Bethesda, Maryland 20205

A specific protein of molecular weight (MW) ~55,000 (55K) was found recently by immunoprecipitation in all SV40 virus-transformed mammalian cells<sup>1–8</sup>, in addition to the SV40 large T antigen (~94K) and small t antigen (~17K), which are the only proteins coded by the 'early half' of the SV40 genome. The 55K protein is encoded by cellular DNA; its peptide pattern is different from that of the SV40 antigens and it is species specific in mouse, rat, hamster, monkey and human SV40-transformed (or infected) cells<sup>6–9</sup>. A 55K protein with a similar peptide pattern was found in mouse embryonal carcinoma cells not exposed to SV40<sup>4,5</sup>. Similar proteins were reported in mouse sarcomas and leukaemias induced by a great variety of aetiological agents and also in a spontaneously transformed mouse fibroblast cell line<sup>10</sup>, and it has been suggested that the protein may be a general correlate of cellular tumorigenicity<sup>11–13</sup>. We now report that the ~55K protein is present in primary cell cultures from 12–14-day old mouse embryos, but not in 16-day old mouse embryos. The embryo protein has a peptide pattern virtually indistinguishable from that of the SV40-induced protein. We also show by comparing closely related cell families that spontaneously transformed highly tumorigenic mouse cells do not possess the 55K protein.

The large T antigen, the ~55K cellular protein and the small t antigen were the major labelled proteins specifically immunoprecipitated from an SV40-transformed cloned mouse fibroblast cell \*215CSC with the SV40 tumour (T) serum<sup>1–9</sup>, as shown in the left half of the panels of Fig. 1. In the right half of Fig. 1a, the 'parent' clone 210C, not transformed by SV40, does not show these specifically immunoprecipitable proteins, and thus also lacks the 55K protein<sup>1</sup>. The T serum used is able to precipitate the cellular 55K protein independently of the presence of SV40 large T antigen, as shown on the embryonal carcinoma cell line F9 (right half of Fig. 1b)<sup>4,5,14</sup>.

Mouse embryos at various post-implantation stages were investigated and compared. Primary cultures from 12-day old mouse embryos showed the presence of specifically immunoprecipitable ~55K protein (see dark arrow in the right half of Fig. 1c). Similarly, 10–14-day mouse embryo primary cultures also possessed the 55K protein (data not shown). Equally or more highly radioactive immunoprecipitates from primary cultures from 16-day old mouse embryos exhibited no specific immunoprecipitable protein in the 55K region (right half of Fig. 1d). Apparently, beyond a certain embryonic developmental stage, significant amounts of the protein are no longer synthesized in primary cultures. When the primary embryo cultures from 12-, 14- or 17-day embryos were replated and labelled, none of the secondary or subsequent passages tested showed detectable significant amounts of 55K protein (data not shown; see also data on 210C and other established mouse and other embryo cell lines<sup>1–8</sup>). Thus, the cells which synthesize detectable 55K cellular protein in primary culture either are no longer present in further cultures in sufficient amounts or do not synthesize the 55K protein in significant amounts. In preliminary experiments with M. Dziadek we have now detected the 55K protein in 13-day mouse embryo organ cultures of liver, brain and carcass, but not in similar 16-day old embryo organ cultures, indicating that the protein indeed correlates with stages

**Fig. 1** Detection of the 55K protein in various cells. Preconfluent, exponentially growing cells in tissue culture<sup>21</sup> were labelled for 3 h with L-[<sup>35</sup>S]methionine, extracted, immunoprecipitated with either serum from hamster bearing SV40-induced tumour (T serum) or with normal (N) preimmune hamster serum, and subjected to SDS-polyacrylamide gel electrophoresis and fluorography, as described elsewhere<sup>1</sup>. Left to right, pairwise: panel a, the SV40-transformed clonal mouse embryo cell line \*215CSC and the parent clone 210C; panel b, \*215CSC and F9 teratocarcinoma cells; panel c, \*215CSC and 12-day old AL/N mouse embryo primary culture; panel d, \*215CSC and 16-day old embryo primary (see Table 1 legend for the abbreviations used for the cells). Dark wide arrows indicate the ~55K cellular protein, the open arrows the position of the SV40 large T and small t antigens, and the narrow arrows the top and bottom of the separating gels. Lines on the side of the panels show the positions of the MW marker proteins: Phosphorylase a, 94K; bovine serum albumin, 66.5K; ovalbumin, 45K; DNase I, 31K; trypsinogen, 24K; lactoglobulin, 18K. Embryo cells were obtained as follows. A virgin 8-week old AL/N female was placed in a cage with one 8-week old AL/N male mouse; 16 h later the female was checked for vaginal plug and removed from the cage. This day was designated day 0. After various (10–17) days of pregnancy, the females were killed, the uterus excised and individual embryos (average seven or eight per mouse) removed in sterile conditions. Embryos were dissected free of extraembryonic membranes, combined, minced, washed with phosphate-buffered saline pH 7.4, gently trypsinized and plated for primary cultures, as described elsewhere<sup>21</sup>. In a procedure similar to that used for all the other cells after one change of growth medium, preconfluent exponentially growing cells of the primary cultures were labelled as above. Equal volumes of the cell extract supernatants were immunoprecipitated with T or N serum, as described previously<sup>1</sup>. The input radioactivities of the T serum precipitates were 30–40% higher than the N serum precipitates, resulting in the more intense protein bands in the former. Overexposed fluorograms (7 days) are presented to facilitate detection of any (possible) 55K proteins in the N serum precipitates.

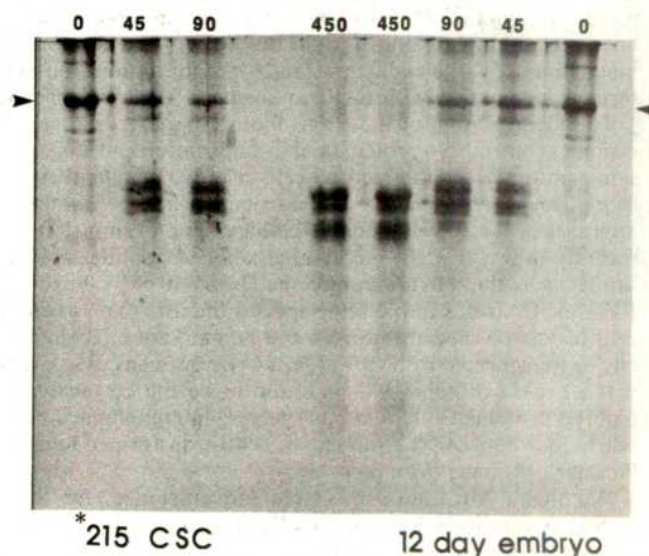


of embryogenesis and that its synthesis in the appropriate primary cultures is not a result of culture artefacts (for example, cell 'stimulation' or selection).

To obtain enough labelled 55K embryo protein for a proteolytic peptide comparison, it was necessary to have at least three synchronously pregnant AL/N mice and combine 12-day old embryos for primary culture. The 55K band, separated on an SDS-polyacrylamide gel as in Fig. 1, was cut out and eluted from the gel. A similar amount of labelled SV40-induced protein was obtained from \*215CSC cells. The two labelled proteins were subjected separately to limited proteolysis with increasing amounts of *Staphylococcus aureus* V8 protease and re-electrophoresed<sup>15</sup>. Figure 2 shows seven to nine methionine-labelled peptides with identical mobilities, appearing symmetrically with increased enzyme concentrations, from the

SV40-transformed \*215CSC cells (left half) and the 12-day old embryo primary cells (right half of fluorogram). Thus, the 55K protein in 12-day old embryos is very similar (or identical) to the SV40-induced (or stabilized) 55K cellular protein. Preliminary findings with D. Simmons also show very similar (or identical) two-dimensional electrophoresis and chromatography patterns<sup>8</sup> for the methionine-labelled tryptic peptides of the two proteins. Comparison of the proteins from SV40-transformed cells from different species suggests that the protein is an evolutionarily conserved protein<sup>8</sup>, and might thus have an essential cellular function. The results indicate that the host gene(s) for such protein(s) is functioning constitutively in the embryo during a certain phase of embryogenesis. In established embryo cells

**Fig. 2** Comparison of peptides obtained by partial proteolysis of the isolated 55K proteins from 12-day old embryo primary cells and from the SV40-transformed \*215CSC cells. Twenty 12-day old AL/N embryos were used for primary cultures and labelled as in Fig. 1. The \*215CSC cells were also labelled similarly. Immunoprecipitates with T serum were separated as in Fig. 1. The 55K protein bands were located, cut out, homogenized in a buffer containing 10 mM NaHCO<sub>3</sub>, 0.1% SDS, 0.1%  $\beta$ -mercaptoethanol and 20% sucrose<sup>15</sup>, and extracted at 37 °C overnight. The extraction mixture was centrifuged and the supernatant sampled for counting. The total radioactivities recovered were 35,889 c.p.m. from the embryo cells and 23,940 c.p.m. from the \*215CSC cells. Four aliquots (20  $\mu$ l) each of the two supernatants, containing 8,545 c.p.m. (embryo) and 5,700 c.p.m. (\*215CSC), were placed in wells in the 3% spacing gel. Homogenizing buffer<sup>1</sup> (10  $\mu$ l) containing 0, 45, 90 and 450 ng of *Staphylococcus aureus* V8 protease (Miles) was placed in the wells as shown on the top of the figure. The wells were filled with a sample electrophoresis buffer<sup>22</sup>, subjected to electrophoresis (30 V, 3 h) until the marker dye had penetrated 1 inch of the stacking gel. Electrophoresis continued at 140 V for 2 h, until the dye reached the bottom of the gel. The gel was stained, destained and fluorographed as before<sup>1</sup>. Exposure was for 20 days. The solid arrow points to the undigested 55K protein present in largest amount in the gel columns from the buffer controls.





**Table 1** Absence of correlation between tumorigenicity and the 55K protein

| Cell     | TD <sub>50</sub> | 55K protein | Cell     | TD <sub>50</sub> | 55K protein |
|----------|------------------|-------------|----------|------------------|-------------|
| 104C     | 2                | —           | *215CSC  | 6.4              | +           |
| *106CSC  | 4                | +           | *221CSCT | 2                | +           |
| 124CSCT  | 2                | —           | *222CSCT | <3               | +           |
| 127CSCT  | <2               | —           | 223CSCT  | 3                | —           |
| 128CSCT  | <2               | —           | *224CSCT | 2                | +           |
| 134CSCTC | >4               | —           | 219CT    | <2               | —           |
| 210C     | 6.4              | —           | 301T     | 4                | —           |
| 213CSC   | 5.5              | —           | *303TCS  | >5               | +           |
| *214CSC  | >6               | +           | *314TSCT | >5               | +           |
|          |                  |             | *315TSCT | 5                | +           |

Properties of mouse embryo cell lines from three cell 'families'. The relation and generation of the cells are indicated with the postfix letters in sequence: C denotes a clone (obtained by a single-cell technique<sup>20</sup>); S, SV40 transformed; C, recloned; T, tumour cell line obtained from the clone immediately above (by injecting 10<sup>5</sup>–10<sup>7</sup> cells into a syngeneic mouse and re-establishing a cell line from the tumour<sup>19</sup>). An asterisk before the number denotes that the cell is SV40 T-antigen positive. The cells in the 100 and 200 families were from AL/N strain mouse embryo<sup>19</sup>; those in the 300 family were from BALB/c mouse embryo. The TD<sub>50</sub> denotes tumorigenicity, determined by intramuscular inoculation of 10-fold cell dilutions (minimum of three each) into batches of 6–8-week old syngeneic mice (10 mice per batch): TD<sub>50</sub> = log<sub>10</sub>[number of cells producing rapidly lethal sarcomas in 50% of the mice inoculated]; observed and calculated as in ref. 19. The presence (+) or absence (—) of the 55K protein was determined as in Fig. 1. The SV40 T antiserum used (lot 78 × 222, NCI) was capable of precipitating the 55K protein alone, when such protein was separated by gel electrophoresis from the SV40 T antigen and eluted separately (as in Fig. 2) and reprecipitated (not shown) (see also the precipitation of the F9 and embryo cells in Fig. 1). Also, when the T-antigen-negative labelled cell extracts were mixed with excess of T-antigen-positive unlabelled cell extracts no more immunoprecipitable radioactive counts were seen in the 55K region than without mixing (data not shown). Some of the cells had been characterized previously for biochemical, tissue culture and *in vivo* growth properties<sup>19,20</sup>.

(including many clones<sup>1</sup>), the genes are present, but the proteins are not induced and/or not 'stabilized', unless the cells are infected by SV40.

To determine whether or not the 55K protein is a general correlate of cellular tumorigenicity, the presence of the 55K protein in three families of established mouse fibroblast cells were compared with tumorigenicity in the syngeneic mouse. There was no correlation at all in the mouse embryo fibroblast cells tested (Table 1). The highly malignant sarcomagenic cells in all three families from two strains (AL/N and BALB/c) of mice, which became tumorigenic by spontaneous transformation (cells 104C, 124CSCT, 127CSCT, 128CSCT, 219CT and 301T), did not possess detectable amounts of 55K protein when tested with the SV40 T antiserum, whereas the correlation was found without exception in all three families with the cells expressing SV40 T antigen and the 55K protein<sup>1</sup>. Tumour cell lines 124, 127 and 128CSCT and the 134CSCTC clone carry late SV40 DNA, but are revertant in the sense that they do not possess the SV40 early gene<sup>16</sup>. This shows that the continued presence of at least one copy<sup>16</sup> of the SV40 early gene (as in \*106CSC) and its protein product (T antigen) is sufficient and, in established cell lines, necessary not only for the initiation<sup>5</sup> but also for the maintenance of the induction (and/or stabilization—possibly through interaction with the T antigen<sup>17</sup>) of the 55K protein.

The identification of the SV40-induced mouse cellular 55K protein as an embryo protein (and by implication and analogy to similar proteins synthesized by cells of other mammals transformed by other means<sup>6–11,13</sup>) has opened up new molecular approaches for developmental biology. For example, it was recently shown that the methionine-labelled peptides are very similar when the cells are transformed by SV40 or by the related BK and JC viruses in the same species (hamster), or when the cells of related species (monkey and human) are infected lytically or transformed by SV40<sup>9</sup>. Our work now leads us to expect that all these proteins will be found to be the corresponding embryo proteins in the various species. Immunological cross-reactivities between the surface of SV40-transformed and fetal hamster cells have been reported<sup>18</sup>.

We thank Mr Lorenzo Waters for assistance, Dr S. W. Luborsky for discussion, and Drs D. Simmons and M. Dziadek for allowing us to quote results.

Received 18 June; accepted 6 November 1980.

- Chang, C., Simmons, D. T., Martin, M. A. & Mora, P. T. *J. Virol.* **31**, 463–471 (1979).
- Kress, M., May, E., Cassingena, R. & May, P. J. *J. Virol.* **31**, 472–483 (1979).
- Meleiro, J. A., Stitt, D. T., Mangel, W. F. & Carroll, R. B. *Virology* **93**, 466–480 (1979).
- Linzer, D. I. H. & Levine, A. J. *Cell* **17**, 43–52 (1979).
- Linzer, D. I. H., Maltzman, W. & Levine, A. J. *Virology* **98**, 308–318 (1979).
- Smith, A. E., Smith R. & Paucha, E. *Cell* **18**, 335–346 (1979).
- Meleiro, J. A., Tur, S. & Carroll, R. B. *Proc. natn. Acad. Sci. U.S.A.* **77**, 97–101 (1980).
- Simmons, D. T., Martin, M. A., Mora, P. T. & Chang, C. J. *J. Virol.* **44**, 650–657 (1980).
- Simmons, D. J. *J. Virol.* **36**, 519–525 (1980).
- DeLeo, A. J. *et al. Proc. natn. Acad. Sci. U.S.A.* **76**, 2420–2424 (1979).
- Jay, G. *et al. Cold Spring Harb. Symp. quant. Biol.* **44**, 469–664 (1980).
- Pollack, R. *et al. Cold Spring Harb. Symp. quant. Biol.* **44**, 681–688 (1980).
- Luka, J., Jörnval, H. & Klein, G. *J. Virol.* **35**, 592–602 (1980).
- Segal, S., Levine, A. J. & Khoury, G. *Nature* **280**, 335–338 (1979).
- Cleveland, D. W., Fischer, S. G., Kirschner, M. W. & Laemmli, U. K. *J. biol. Chem.* **252**, 1102–1106 (1977).
- Küster, J. M., Mora, P. T., Brown, M. & Khoury, G. *Proc. natn. Acad. Sci. U.S.A.* **74**, 4796–4800 (1977).
- Lane, D. P. & Crawford, L. V. *Nature* **278**, 261–263 (1979).
- Weppner, W. A. & Coggin, J. H. Jr *Cancer Res.* **40**, 1380–1387 (1980).
- Mora, P. T., Chang, C., Couvillion, L., Küster, J. M. & McFarland, V. W. *Nature* **269**, 36–40 (1977).
- Winterbourne, D. J. & Mora, P. T. *J. biol. Chem.* **253**, 5109–5120 (1978).
- McFarland, V. W., Mora, P. T., Schultz, A. & Pancake, S. J. *cell. Physiol.* **85**, 101–111 (1975).
- Laemmli, U. K. *Nature* **227**, 680–685 (1970).

## Defective repair of alkylated DNA by human tumour and SV40-transformed human cell strains

Rufus S. Day III\*, Chuck H. J. Ziolkowski\*, Dominic A. Scudiero†, Sharon A. Meyer†, Anthony S. Lubiniecki‡, Anthony J. Girardi§, Sheila M. Galloway|| & Gaither D. Bynum¶

\* Nucleic Acids Section, LMC, CIP, DCCP, NCI, NIH, 9000 Rockville Pike, Bethesda, Maryland 20205

† Chemical Carcinogenesis Program, Frederick Cancer Research Center, Frederick, Maryland 21701

‡ Flow Laboratories, 7655 Old Spring House Road, McLean, Virginia 22101

§ Institute for Medical Research, Copewood and Davis Streets, Camden, New Jersey 08103

|| Litton Bionetics, 5516 Nicholson Lane, Kensington, Maryland 20795

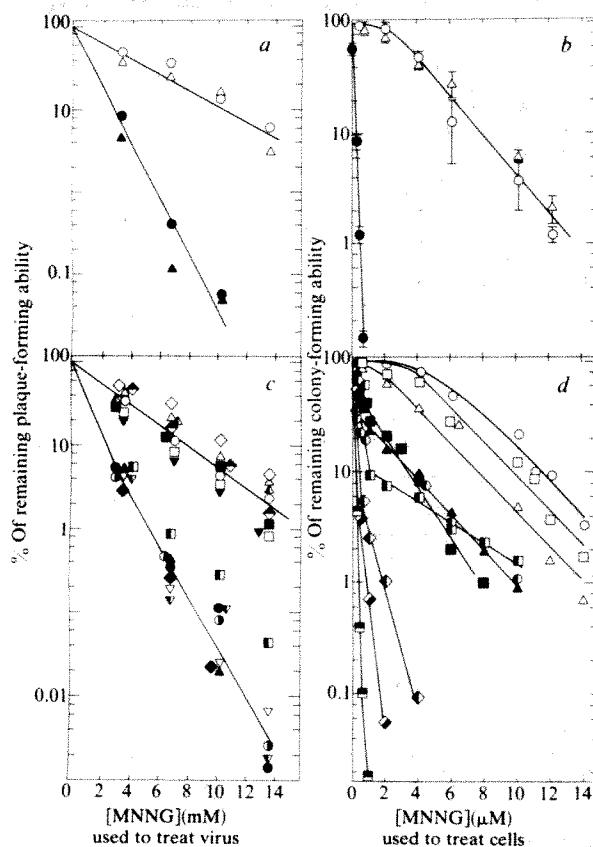
¶ Section on Cellular Aging, Laboratory of Comparative Cellular Physiology, Gerontology Research Center, NIA, Baltimore, Maryland 21224

We have identified a group of 8 (among 39) human tumour cell strains deficient in the ability to support the growth of adenovirus 5 preparations treated with *N*-methyl-*N*'-nitro-*N*-nitrosoguanidine (MNNG), but able to support the growth of non-treated adenovirus normally<sup>1,2</sup>. This deficient behaviour defines the Mer<sup>−</sup> phenotype<sup>3</sup>. Strains having the Mer<sup>−</sup> phenotype were found to arise from tumours originating in four different organs. Relative to Mer<sup>+</sup> strains, Mer<sup>−</sup> tumour strains showed greater sensitivity to MNNG-produced killing, greater MNNG-stimulated 'DNA repair' synthesis and a more rapid MNNG-produced decrease in semi-conservative DNA synthesis<sup>2</sup>. Here we report that (1) Mer<sup>−</sup> strains are deficient in removing O<sup>6</sup>-methylguanine (O<sup>6</sup>-MeG) from their DNA after [*Me*-<sup>14</sup>C]MNNG treatment (Table 1); (2) Mer<sup>−</sup> tumour strains originate from tumours arising in patients having Mer<sup>+</sup> normal fibroblasts (Fig. 1a, b); (3) SV40 transformation of (Mer<sup>+</sup>) human fibroblasts often converts them to Mer<sup>−</sup> strains (Fig. 1c, d); (4) MNNG produces more sister chromatid exchanges (SCEs) in Mer<sup>−</sup> than in Mer<sup>+</sup> cell strains (Fig. 2).

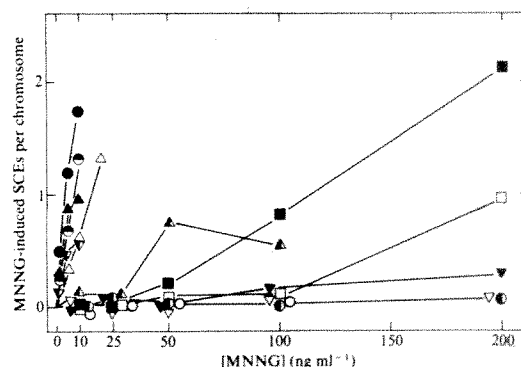
Mer<sup>+</sup> and Mer<sup>−</sup> strains were treated with <sup>14</sup>C-MNNG and analysed directly following and 20-h after treatment for DNA-bound O<sup>6</sup>-MeG and *N*<sup>7</sup>-MeG (*N*<sup>7</sup>-methylguanine; see Table 1). O<sup>6</sup>-MeG is not removed appreciably from the DNA of Mer<sup>−</sup> strains over the 20-h incubation period. However, the amount of O<sup>6</sup>-MeG (relative to *N*<sup>7</sup>-MeG) found in the DNA of MNNG-treated Mer<sup>+</sup> strains shortly after MNNG treatment is about

threefold less than that found in Mer<sup>-</sup> strains, presumably reflecting active removal by Mer<sup>+</sup> strains of O<sup>6</sup>-MeG during the 1-h MNNG treatment (ref. 3 and B. Strauss, personal communication). During the 20-h incubation after MNNG treatment, the Mer<sup>+</sup> strains continued to remove O<sup>6</sup>-MeG from their DNA. By contrast, in the Mer<sup>-</sup> strains, the O<sup>6</sup>-MeG/N<sup>7</sup>-MeG ratio increased, presumably reflecting the slow loss of N<sup>7</sup>-MeG from the DNA expected at 37°C (refs 3-6). (Our data are consistent with a half life for DNA-bound N<sup>7</sup>-MeG of ~46 h, which is in the range of those published<sup>5,6</sup>.)

We questioned whether the tumours that gave rise to the Mer<sup>-</sup> tumour strains arose in persons who were entirely composed of Mer<sup>-</sup> cells (indicating possible genetic inheritance of the condition) or whether the non-tumour cells of such patients would be Mer<sup>+</sup> (indicating that the Mer<sup>-</sup> condition may be a property of only tumour cells). To investigate this question experimentally, we obtained strains of normal fibroblasts prepared from two patients whose tumours had given rise to the Mer<sup>-</sup> A427N and Hs750T strains. The normally appearing fibroblast strains, A427F and Hs750M, were both found to be Mer<sup>+</sup> (Fig. 1a). Studies of post-MNNG colony-forming ability (Fig. 1b) established that the fibroblast lines A427F and Hs750M had sensitivities to MNNG similar to those of human fibroblasts (see refs 2, 7, and Fig. 1d). The A427N tumour line, however, showed the increased sensitivity to MNNG-produced



**Fig. 1** a, b, MNNG-produced inactivation of adenovirus 5 (a) and of colony-forming ability (b) using normal or tumour cell strains from the same patient. Patient 1: ○, A427F (normal fibroblast strain) and ●, A427N (lung tumour strain). Patient 2: △, Hs750M (normal fibroblast strain) and ▲, Hs750T (stomach tumour strain). For a, adenovirus 5 was inactivated with MNNG and subsequently assayed for plaque-forming ability using monolayers of the above strains as described<sup>19</sup>. For colony-forming ability (b), cells were seeded at low density, treated with MNNG and grown to colonies as described elsewhere<sup>7</sup>. No colony data are presented for Hs750T because it did not form colonies. Virus plaquing efficiencies and cellular colony-forming efficiencies were in the ranges of those reported previously and were not correlated with the sensitivities observed. c, d, MNNG-produced inactivation of adenovirus 5 (c) and of colony-forming ability (d) using normal human fibroblasts, SV40-transformed fibroblasts and Mer<sup>-</sup> tumour strains. The cell strains used were: ○, AT5BIVA2; △, WI38; ▲, WI38VA13; ◆, GM54; ■, GM638; ○, IMR90; ● and ●, IMR90-830; ●, IMR90-890; □, WI26; ■, WI26VA4; ▲, GM637; ▼, XP12; ▼, W98VA1; ◆, SV80; ▼, WI8VA2; ■, A172; ◆, A875; ◆, BE.



**Fig. 2** Number of MNNG-induced SCEs as a function of MNNG concentration used to treat cells of five Mer<sup>-</sup> and seven Mer<sup>+</sup> strains. Confluent cells were split into 75-cm<sup>2</sup> flasks containing DMEM or McCoy's 5A plus 10% fetal calf serum. The next morning, stocks of MNNG were diluted into the medium to obtain the desired concentrations. Bromodeoxyuridine was added to 10 μg ml<sup>-1</sup>. After 57-80 h of incubation, colcemid (10 μg ml<sup>-1</sup>, Gibco) was added to 0.1-0.2 μg ml<sup>-1</sup>. After 4 h further incubation, the cells were collected, centrifuged and resuspended in 5 ml 0.04-0.075 M KCl, centrifuged and fixed in 5 ml methanol/glacial acetic acid, 3:1, and dried on to slides. For differential staining, slides were either immersed in 4'-6-diamidino-2-phenylindole at 10 μg ml<sup>-1</sup> of distilled water for at least 3 min, removed and treated with three drops 0.2 M NaPO<sub>4</sub> buffer, pH 11.5, or stained by a modified Hoechst 33258-Giemsa technique<sup>20,21</sup>. The chromosomes of at least 15 metaphase cells were counted to determine each point. Standard deviations were typically 0.2-0.3 of the average. The cell strains used, followed by the zero dose level of SCEs per chromosome, were: Mer<sup>-</sup>: ●, A1336 (0.34); ●, A2095 (0.14); ▼, A1235 (0.18); ▲, WI38VA13 (0.38); △, A253 (0.26); Mer<sup>+</sup>: □, A388 (0.35); ○, IMR90 (0.16); ■, A549 (0.15); ●, A673 (0.14); ▲, A704 (0.20); ▼, HuTu80 (0.16); and ▼, W98VA1 (0.64).

killing characteristic of Mer<sup>-</sup> tumour strains (ref. 2 and Fig. 1d); tumour strain Hs750T did not form colonies. Therefore, the respective patients were not entirely composed of Mer<sup>-</sup> cells, showing that generalized inheritance of the Mer<sup>-</sup> condition did not occur.

SV40-transformed human fibroblast strains were tested for their Mer phenotype to determine whether the Mer<sup>-</sup> phenotype was characteristic only of certain strains derived from human tumours, or if human strains transformed by other means were also Mer<sup>-</sup>. Of 11 SV40-transformed strains, 7 were found to be Mer<sup>-</sup> and 4 Mer<sup>+</sup> (Fig. 1c Table 1). The available non-transformed human fibroblast 'parents' of these transformed strains (Table 2) were all Mer<sup>+</sup>, including three strains (IMR90, WI38 and GM54) that gave rise to Mer<sup>-</sup> transformed strains (Table 2). The result indicates that SV40 transformation often converts Mer<sup>+</sup> strains to Mer<sup>-</sup> strains, or selects Mer<sup>-</sup> variants as targets for transformation.

The SV40-produced Mer<sup>-</sup> strains were not as sensitive as Mer<sup>-</sup> tumour strains to the killing effects of MNNG (Fig. 1d), suggesting that either the Mer<sup>-</sup> tumour strains are defective in the ability to remove an additional MNNG-produced lesion, or that the cellular response of the two groups of Mer<sup>-</sup> strains to O<sup>6</sup>-MeG differs. Further, although the SV40-produced Mer<sup>-</sup> cells were more MNNG sensitive than their parent fibroblasts, they were not more sensitive to MNNG-produced killing than were Mer<sup>+</sup> SV40-transformed cells, and, therefore, were not killed by O<sup>6</sup>-MeG, which they are deficient in excising. (To be certain that the Mer<sup>-</sup> phenotype of the tumour strains was not caused by adventitious SV40 infection, we found, using our assay<sup>8</sup>, that SV40 T-antigen was not detectable in any of the eight Mer<sup>-</sup> tumour strains described above. By contrast, and as a control, more than 95% of the nuclei of the SV80 strain contained T-antigen.)

Sister chromatid exchanges<sup>9,10</sup> reflect cellular DNA damage due to various mutagenic and carcinogenic agents<sup>10,11</sup> and are increased in damaged cells lacking certain DNA repair processes<sup>12,13</sup>. Figure 2 shows that Mer<sup>-</sup> strains, including one (WI38VA13) derived from normal fibroblasts (WI38), gave rise to detectable levels of SCEs at much (up to 250-fold) lower concentrations of MNNG than did Mer<sup>+</sup> strains. However, there



| Mer <sup>-</sup> strains | After 1 h MNNG treatment (c.p.m.) |                     |   | After 1 h MNNG treatment +<br>20 h incubation (c.p.m.) |                     |   |
|--------------------------|-----------------------------------|---------------------|---|--|---------------------|---|
|                          | N <sup>7</sup> -MeG               | O <sup>6</sup> -MeG | O <sup>6</sup> -MeG/N <sup>7</sup> -MeG | N <sup>7</sup> -MeG                                    | O <sup>6</sup> -MeG | O <sup>6</sup> -MeG/N <sup>7</sup> -MeG |
| A427N                    | 1,221.5                           | 139.5               | 0.114                                   | 1,164.1  | 169.1               | 0.145                                   |
| A253                     | 1,365.0                           | 132.8               | 0.097                                   | 963.8  | 129.0               | 0.134                                   |
| SV80                     | 419.0                             | 33.1                | 0.079                                   | 319.3  | 36.5                | 0.114                                   |
| A172                     | 643.3                             | 43.9                | 0.068                                   | 398.0  | 57.9                | 0.145                                   |
| HeLa S3                  | 933.8                             | 84.7                | 0.091                                   | 493.4  | 51.2                | 0.104                                   |
| A2095                    | 271.6                             | 30.6                | 0.113                                   | 145.8  | 19.7                | 0.135                                   |
| A875                     | 712.3                             | 65.5                | 0.092                                   | 272.6  | 37.0                | 0.136                                   |
| A1617                    | 734.3                             | 72.1                | 0.098                                   | 440.2  | 51.4                | 0.117                                   |
| BE                       | 762.7                             | 74.1                | 0.097                                   | 400.2  | 62.8                | 0.157                                   |
| GM638                    | 1,182.9                           | 129.1               | 0.109                                   | 845.9  | 126.4               | 0.149                                   |
| IMR90-830                | 1,334.0                           | 156.1               | 0.117                                   | 521.0  | 67.1                | 0.129                                   |
| W18VA2                   | 1,664.2                           | 186.2               | 0.112                                   | 1,199.4  | 163.0               | 0.136                                   |
| W138VA13                 | 1,183.1                           | 105.6               | 0.089                                   | 760.9  | 99.6                | 0.131                                   |
| Average                  |                                   |                     | 0.098                                   |  |                     | 0.133                                   |
| Mer <sup>+</sup> strains |                                   |                     |   |  |                     |   |
| HeLa CCL2                | 926.2                             | 25.2                | 0.027                                   | 529.2  | 10.0                | 0.019                                   |
| A549                     | 1,007.2                           | 39.7                | 0.039                                   | 832.9  | 12.0                | 0.014                                   |
| HT29                     | 1,519.5                           | 26.2                | 0.017                                   | 927.3  | 8.1                 | 0.009                                   |
| H4                       | 1,020.8                           | 35.3                | 0.035                                   | 613.6  | 10.7                | 0.017                                   |
| HuTu80                   | 388.0                             | 6.3                 | 0.017                                   | 170.9  | 2.6                 | 0.015                                   |
| W98VA1                   | 3,183.3                           | 133.7               | 0.042                                   | 2,004.8  | 21.9                | 0.011                                   |
| A388                     | 514.4                             | 27.0                | 0.052                                   | 434.6  | 8.4                 | 0.019                                   |
| A704                     | 328.2                             | 8.7                 | 0.027                                   | 175.2  | 0.9                 | 0.005                                   |
| Average                  |                                   |                     | 0.032                                   |  |                     | 0.014                                   |

**Table 2** Human strains used in the present study

| Tumour strains   |                                       |             | Fibroblast strains |                          |             |
|------------------|---------------------------------------|-------------|--------------------|--------------------------|-------------|
| Mer <sup>-</sup> | Tumour of origin                      | Source      | Mer <sup>+</sup>   | Tumour of origin         | Source      |
| A427N            | Lung carcinoma                        | <i>a</i>    | Hs750M             | Muscle tissue            | <i>a</i>    |
| A253             | Epidermoid carcinoma, neck            | <i>a</i>    | A427F              | Lung                     | <i>b</i>    |
| A172             | Astrocytoma                           | <i>a</i>    | WI26               | Embryonic lung           | <i>e</i>    |
| HeLa S3          | Cervical carcinoma                    | <i>c</i>    | WI38               | Embryonic lung           | <i>e</i>    |
| A2095            | Synovial cell sarcoma                 | <i>b</i>    | IMR90              | Embryonic lung           | <i>f, d</i> |
| A875             | Melanoma                              | <i>b</i>    | GM54               | Human                    | <i>f</i>    |
| A1617            | Adenocarcinoma, colon                 | <i>b</i>    |                    |                          |             |
| BE               | Colon carcinoma                       | <i>d</i>    |                    | SV40-transformed strains |             |
| Hs750T           | Stomach carcinoma, metastatic to lung |             | Mer <sup>-</sup>   | Fibroblast of origin     |             |
|                  |                                       | <i>a</i>    | SV80               | Fetal fibroblast strain  | <i>a</i>    |
| A1336            | Ovarian carcinoma                     | <i>b</i>    | XP12               | XP12RO                   | <i>c</i>    |
| A1235            | Astrocytoma                           | <i>b</i>    | GM638              | GM54                     | <i>f</i>    |
| Mer <sup>+</sup> |                                       |             | IMR90-830          | IMR90                    | <i>g</i>    |
| HeLa CCL2        | Cervical carcinoma                    | <i>c</i>    | IMR90-890          | IMR90                    | <i>g</i>    |
| A549             | Lung carcinoma                        | <i>b</i>    | WI38VA13           | WI38                     | <i>e, g</i> |
| HT29             | Colon carcinoma                       | <i>d</i>    | WI8VA2             | WI8                      | <i>g</i>    |
| H4               | Neuroglioma                           | <i>a</i>    | Mer <sup>+</sup>   |                          |             |
| HuTu80           | Stomach tumour                        | <i>a</i>    | AT5BIVA2           | AT5BI                    | <i>g</i>    |
| A388             | Epidermoid carcinoma                  | <i>a, b</i> | W98VA1             | W98                      | <i>g</i>    |
| A704             | Kidney carcinoma                      | <i>a, b</i> | WI26VA4            | WI26                     | <i>g</i>    |
| A673             | Rhabdomyosarcoma                      | <i>a</i>    | GM637              | GM37                     | <i>c, f</i> |

tibility to MNNG-produced SCEs in addition to the differences noted in our introduction. Further, the demonstration of the Mer<sup>-</sup> behaviour of the HeLa S3 and XP12 strains, known to be more mutable by alkylating agents than either the HeLa CCL2 or the GM637 strain<sup>14,15</sup>, provides a link between the Mer<sup>-</sup> phenotype and increased sensitivity to mutagenesis by alkylating agents.

The two SV40-transformed human strains, identified here as Mer<sup>-</sup> (XP12, derived from a xeroderma pigmentosum (XP) patient) and Mer<sup>+</sup> (GM637, derived from a control person), are divergent both in their susceptibilities to MNNG-produced SCEs (XP12 was the more sensitive<sup>12</sup>) and in their abilities to remove O<sup>6</sup>-alkylguanines from their DNA<sup>4,16</sup> (GM637 showed such excision, XP12 did not). These differences were provisionally hypothesized to be another manifestation of the repair defect in XP fibroblasts that leads to deficient repair of UV ray-damaged DNA. We believe that these differences are more probably due to the SV40-produced molecular changes that lead to the expression of the Mer<sup>-</sup> phenotype.

The identification and characterization of the Mer<sup>-</sup> phenotype in many transformed human cell lines, but not in normal human fibroblasts, leave us unable to decide whether the Mer<sup>-</sup> repair deficiency enhances (or is produced by) transformation, or whether virally produced transformation often leaves a Mer<sup>-</sup> 'footprint'. That 1-chloroethyl-1-nitrosourea (CNU) produces

more DNA cross-links in Mer<sup>-</sup> than in Mer<sup>+</sup> tumour strains (see accompanying manuscript<sup>17</sup>) further suggests that the presence or absence of the Mer repair system may be the molecular reason for the *in vivo* failure or success of chemotherapeutic regimens using agents (1,3-bis-chloroethylnitrosourea (BCNU) or 3-cyclohexyl-1-chloroethyl-1-nitrosourea (CCNU)) having modes of action similar to that of CNU.

We thank Drs Kurt Kohn, R. M. Baker and Len Erickson for helpful discussions. Dr Kohn first suggested investigating the Mer phenotype of WI38VA13 and Dr Baker provided strains HeLa CCL2, HeLa S3, GM637, and XP12 and data before publication. We also thank Dr S. A. Aaronson for the supply of human tumour cell strains, all of which begin with 'A' in this work, Dr Hermann Autrup both for providing us with N<sup>3</sup>-MeA, N<sup>7</sup>-MeG and O<sup>6</sup>-MeG standards and for encouragement, Dr Tsuyoshi Kakefuda for instruction in HPLC techniques and for his patience, and Dr Ken Kraemer for suggestions concerning the manuscript.

Received 29 July; accepted 27 October 1980.

- Day, R. S. III & Ziolkowski, C. H. J. *Nature* **279**, 797-799 (1979).
- Day, R. S. III, Ziolkowski, C. H. J., Scudiero, D. A., Meyer, S. A. & Mattern, M. R. *Carcinogenesis* **1**, 21-32 (1980).
- Montesano, R., Bresil, H. & Margison, G. P. *Cancer Res.* **39**, 1798-1802 (1979).
- Bodell, W. J., Singer, B., Thomas, G. H. & Cleaver, J. E. *Nucleic Acids Res.* **6**, 2819-2829 (1979).
- Altamirano-Dimas, M., Sklar, R. & Strauss, B. *Mutat. Res.* **60**, 197-206 (1979).
- Singer, B. *J. natn. Cancer Inst.* **62**, 1329-1339 (1979).
- Scudiero, D. A. *Cancer Res.* **40**, 984-990 (1980).
- Kaplan, M. M., Giard, D. J., Blattner, W. A., Lubiniecki, A. S. & Fraumeni, J. F. Jr *Proc Soc. exp. Biol. Med.* **148**, 660-664 (1975).
- Latt, S. A. *Proc. natn. Acad. Sci. U.S.A.* **71**, 3162-3166 (1974).
- Perry, P. & Evans, H. J. *Nature* **258**, 121-125 (1975).
- Casano, A. V., Thompson, L. H., Lindl, P. A. & Minkler, J. L. *Nature* **270**, 551-553 (1978).
- Wolff, S. A., Rodin, B. & Cleaver, J. E. *Nature* **265**, 387-389 (1977).
- De Weerd-Kastelein, E. A., Keijzer, W., Rainaldi, G. & Bootsma, D. *Mutat. Res.* **45**, 253-261 (1977).
- Baker, R. M., Van Voorhis, W. C. & Spencer, L. A. *Proc. natn. Acad. Sci. U.S.A.* **76**, 5249-5253 (1979).
- Baker, R. M., Zuerndorfer, G. & Mandel, R. *Environ. Mutagenesis* **2**, 269-270 (1980).
- Goth-Goldstein, R. *Nature* **267**, 81-82 (1977).
- Erickson, L. C., Laurent, G., Sharkey, N. A. & Kohn, K. *Nature* **288**, 727-729 (1980).
- Girardi, A. J., Jensen, F. C. & Koprowski, H. *J. cell. comp. Physiol.* **65**, 69-84 (1965).
- Day, R. S. III *Photochem. Photobiol.* **19**, 9-13 (1974).
- Goto, K., Maeda, S., Kano, Y. & Sugiyama, T. *Chromosoma* **66**, 351-359 (1978).
- Perry, P. & Wolff, S. *Nature* **251**, 156-158 (1974).

## DNA cross-linking and monoadduct repair in nitrosourea-treated human tumour cells

Leonard C. Erickson\*, Guy Laurent, Nancy A. Sharkey & Kurt W. Kohn

Laboratory of Molecular Pharmacology, Developmental Therapeutics Program, Division of Cancer Treatment, National Cancer Institute, National Institutes of Health, Bethesda, Maryland 20205

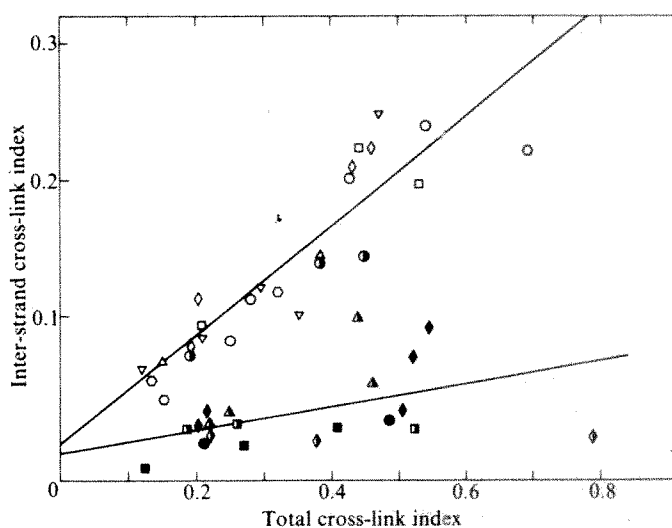
The 1-(2-chloroethyl)-1-nitrosoureas are potent anti-cancer drugs<sup>1,2</sup> which produce DNA inter-strand cross-links in a two-step reaction sequence. The first step was proposed to be an addition of a chloroethyl group to a guanine-O<sup>6</sup> position of DNA<sup>3</sup>; the second step, which occurs over a period of several hours in the absence of free drug<sup>3-6</sup>, could then form an inter-strand cross-link by the slow reaction of the bound chloroethyl group with a nucleophilic site on the opposite DNA strand. The delay between the formation of chloroethyl monoadducts and the formation of inter-strand cross-links allows time for a DNA repair mechanism, capable of removing the monoadducts, to prevent the cross-linking. We recently proposed this mechanism to account for a difference in inter-strand cross-linking between a normal and a transformed human cell strain<sup>6</sup>. Day and his coworkers (see refs 7, 8 and previous paper<sup>9</sup>) found that some human tumour cell strains (designated Mer<sup>-</sup> phenotype) are deficient in the ability to repair O<sup>6</sup>-methylguanine lesions in DNA. We therefore hypothesized that the repair function that removes O<sup>6</sup>-methylguanine residues from DNA would also remove chloroethyl monoadducts and hence prevent chloroethylnitrosourea-induced inter-strand cross-linking. We now present evidence that supports this hypothesis and indicates also that the O<sup>6</sup>-methylguanine repair confers resistance to cell killing by chloroethylnitrosourea.

Thirteen human cell strains, most of them derived from malignant tumours, were studied (Table 1). The phenotype of each strain was classified as Mer<sup>+</sup> or Mer<sup>-</sup> by R. Day, on the

basis of whether or not the cells were proficient in supporting the growth of adenovirus 5 treated with N-methyl-N'-nitro-N-nitrosoguanidine<sup>7-9</sup>.

The cells were treated with 1-(2-chloroethyl)-1-nitrosourea (CNU) for 1 h and then incubated for 6 h to allow inter-strand cross-links to form<sup>5,6</sup>. Inter-strand cross-linking and DNA-protein cross-linking were determined by the alkaline elution method<sup>10-12</sup>, using the same procedures as in our previous study<sup>6</sup>. The elution assay, when performed directly (without proteinase), measures the combined effect of inter-strand and DNA-protein cross-links. The major contribution to this measurement, in the case of chloroethylnitrosoureas, is from DNA-protein cross-links<sup>5,6</sup>. The assay with proteinase greatly reduces or eliminates the DNA-protein cross-links, and is assumed to be a measure of inter-strand cross-linking<sup>11</sup>.

The results show a clear correlation between inter-strand



**Fig. 1** Inter-strand cross-linking (assay with proteinase) plotted against DNA-protein cross-linking, estimated by assay without proteinase in the same experiment. Cross-link index is defined in Table 1 legend. Open symbols, Mer<sup>-</sup> strains; closed and half-closed symbols, Mer<sup>+</sup> strains. The symbols representing individual cell strains are shown in Table 1.

\* To whom correspondence should be addressed at: Building 37, Room 5D17, National Institutes of Health, National Cancer Institute, Bethesda, Maryland 20205.



**Table 1** Alkaline elution assays of DNA inter-strand and DNA-protein cross-linking by 1-(2-chloroethyl)-1-nitrosourea (CNU) (cross-link index  $\times 10^3$ )

| Cell strain | Origin                 | Mer phenotype | Inter-strand cross-linking (proteinase assay) |                            | Total cross-linking (no proteinase) |                 |
|-------------|------------------------|---------------|---|----------------------------|-------------------------------------|-----------------|
|             |                        |               | 50 $\mu$ M CNU                                | 100 $\mu$ M CNU            | 50 $\mu$ M CNU                      | 100 $\mu$ M CNU |
| ■ HT29      | Colon ca.              | +             | 0 (-13-+13) <sup>3</sup>                      | 7 (0-17) <sup>3</sup>      | 126, 135                            | 268, 410        |
| ● IMR90     | Embryonic lung         | +             | 3 (-3-+7) <sup>3</sup>                        | 23 (23-24) <sup>3</sup>    | 210, 216                            | 485             |
| ◆ A2182     | Lung ca.               | +             | 14 (8-20) <sup>3</sup>                        | 31                         | 154, 218                            | 788             |
| ◊ A673      | Rhabdomyosarcoma       | +             | 16 (12-20) <sup>3</sup>                       | 16                         | 186, 261                            | 523             |
| ◆ A549      | Lung ca.               | +             | 33 (20-54) <sup>4</sup>                       | 52 (19-91) <sup>4</sup>    | 203, 216                            | 504, 545        |
| ▲ HT1080    | Fibrosarcoma           | +             | 62 (20-107) <sup>4</sup>                      | 127 (51-230) <sup>3</sup>  | 221, 251                            | 437, 462        |
| ● A431      | Epidermoid ca. (vulva) | +             | 69 (60-76) <sup>3</sup>                       | 143 (142-144) <sup>2</sup> | 190, 190                            | 385, 446        |
| ○ A1336     | Ovarian ca.            | -             | 69 (38-177) <sup>3</sup>                      | 221                        | 135, 152                            | 692             |
| ▽ A427      | Lung ca.               | -             | 72 (61-84) <sup>4</sup>                       | 149 (101-247) <sup>4</sup> | 122, 208                            | 295, 471        |
| □ BE        | Colon ca.              | -             | 81 (71-93) <sup>3</sup>                       | 201 (182-224) <sup>4</sup> | 166, 207                            | 438, 530        |
| ◇ A172      | Astrocytoma (grade IV) | -             | 84 (62-113) <sup>3</sup>                      | 217 (209-225) <sup>2</sup> | 193, 204                            | 432, 457        |
| △ VA13      | SV40-transformed WI-88 | -             | 88 (50-146) <sup>3</sup>                      | 232 (145-320) <sup>2</sup> | 148, 152                            | 384             |
| ○ A875      | Melanoma               | -             | 112 (82-142) <sup>3</sup>                     | 240 (201-281) <sup>3</sup> | 250, 281                            | 540             |

Cells previously labelled with [2-<sup>14</sup>C]thymidine (0.01  $\mu$ Ci ml<sup>-1</sup>, 24 h) were treated with 50 or 100  $\mu$ M CNU for 1 h in culture medium (Dulbecco's modified Eagle's medium, 10% heat-inactivated fetal calf serum, 0.02 M HEPES buffer) and then incubated for 6 h in drug-free medium. Control cells were similarly run without drug treatment. After collection,  $2-5 \times 10^5$  cells were mixed with  $5 \times 10^5$  L1210 mouse leukaemia cells whose DNA had been labelled with <sup>3</sup>H-thymidine (0.1  $\mu$ Ci ml<sup>-1</sup>, 24 h); these cells served as internal standards. The mixed cell suspensions were exposed to 300 R of <sup>137</sup>Cs  $\gamma$ -ray irradiation at 0 °C just before alkaline elution, which was carried out by the same procedures as used in our previous study<sup>6</sup>. Cells were deposited on 2- $\mu$ m-pore size polyvinyl chloride filters and lysed with 2% SDS, 0.02 M EDTA, 0.1 M glycine, pH 10, with or without 0.5 mg ml<sup>-1</sup> proteinase K. Alkaline elution was with tetrapropylammonium hydroxide/0.02 M H<sub>2</sub>EDTA, pH 12.1, pumped at a rate of 2 ml h<sup>-1</sup>. When proteinase K was used, the eluting solution also contained 0.1% SDS. When proteinase K was not used, the lysis solution was washed out with 0.04 M Na-EDTA, pH 10, before elution at pH 12.1. Cross-link index is defined as  $[(1-R_0)/(1-R_1)]^{1/2} - 1$ , where  $R_0$  and  $R_1$  are the 'relative retention' for untreated and CNU-treated cells, respectively<sup>5</sup>. Relative retention is the fraction of the <sup>14</sup>C-DNA remaining on the filter when 30% of the internal standard <sup>3</sup>H-DNA remained on the filter. The range of values obtained in independent experiments are given in parentheses; the superscript indicates the number of experiments. Symbols in the first column on the left are used to represent the cell strains in Figs 1 and 2. ca., carcinoma. Cell strains: IMR90, normal human embryo cells obtained from W. Nichols; VA13, an SV40-transformed derivative of normal human embryo strain WI38; BE, obtained from B. Giovannella; HT29, obtained from E. Jensen. The other strains were obtained from R. Day.

cross-linking (proteinase assay) and methylation repair capacity (Table 1). The six strains deficient in this capacity (Mer<sup>-</sup> phenotype) produced consistently higher inter-strand cross-linking levels than did five of the seven Mer<sup>+</sup> strains studied.

The remaining two Mer<sup>+</sup> strains (A431 and HT1080) gave deviant results. Strain A431 yielded high inter-strand cross-linking values, in the range of the Mer<sup>-</sup> strains. In view of this result, Day (personal communication) restudied the A431 culture, and found that with continued passage the culture had attained a large Mer<sup>-</sup> component. In the case of the HT1080 strain, the first two inter-strand cross-link determinations were low, well within the Mer<sup>+</sup> range, whereas the last two determinations were high, well within the Mer<sup>-</sup> range. This observation raises the question of whether cells in culture can lose the Mer<sup>+</sup> phenotype.

In addition to assays for inter-strand cross-links, most of the experiments included assays for DNA-protein cross-links. The assays for total cross-links (no proteinase), which we take to be essentially measures of DNA-protein cross-linking, showed no significant differences between the Mer<sup>+</sup> and Mer<sup>-</sup> strains (Table 1). Hence, the differences in inter-strand cross-linking cannot be attributed simply to differences in drug uptake or inactivation.

DNA-protein cross-links form without delay<sup>5,6</sup> and probably involve different sites of linking to DNA from inter-strand cross-links. If the differences in inter-strand cross-linking are principally due to differences in a specific DNA repair mechanism, DNA-protein cross-linking, apparently little affected by such repair, could be a measure of the extent of drug entry and intracellular reactivity in particular experiments. The use of DNA-protein cross-linking as a gauge of intracellular drug delivery is plausible also because chloroethylnitrosoureas are lipid soluble, and hence their entry into cells is not likely to be limited by membrane barriers.

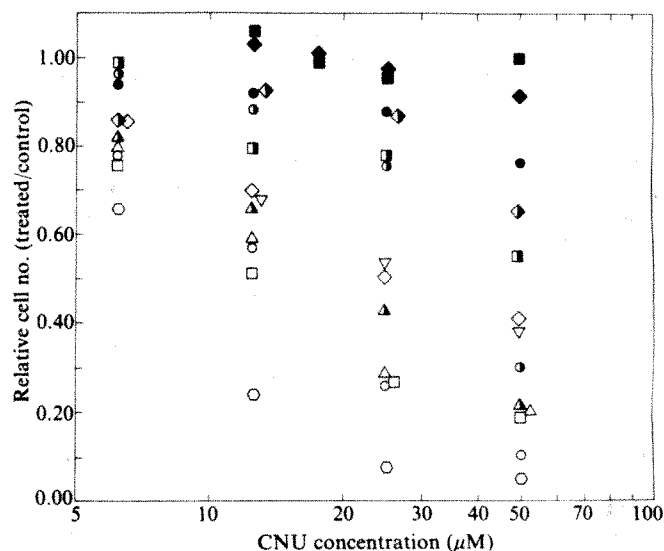
Using this concept, the value for inter-strand cross-linking (proteinase assay) was plotted against the value for DNA-protein cross-linking (no proteinase) obtained in the same experiment (Fig. 1). The cell strains are seen to give a bimodal distribution, the Mer<sup>-</sup> strains (open symbols) being clearly separated from most of the Mer<sup>+</sup> strains (closed and half-closed symbols). The A431 (Mer<sup>+</sup>) strain again falls within the Mer<sup>-</sup> group (half closed circles). The segregation of the cell strains into two distinct groups is analogous to the distinct grouping with respect to methylation repair noted by Day and his

coworkers<sup>7-9</sup>. This lends additional support to the idea that the cells differ with respect to a discrete phenotype.

The cytotoxic sensitivity of the cell strains to CNU was determined in terms of inhibition of cell proliferation (Fig. 2). Results with this assay have been found to be consistent with colony formation assays<sup>6</sup>. The six Mer<sup>-</sup> strains (open symbols) were clearly more sensitive to CNU than were five of the seven Mer<sup>+</sup> strains.

The exceptions again were strains A431 (Fig. 2, half-closed circles) and HT1080 (Fig. 2, half-closed triangles). The A431 strain exhibited low sensitivity at low drug concentrations and high sensitivity at high concentration. It is possible that this strain has a limited capacity for O<sup>6</sup>-alkyl guanine repair, so that at low levels of DNA damage it seems to be Mer<sup>+</sup>, but at high levels seems to be Mer<sup>-</sup>.

Our results, together with those of Day and his colleagues<sup>7-9</sup>, suggest that the loss of a specific DNA repair function could simultaneously make cells susceptible to neoplastic transformation and make the resulting tumours vulnerable to



**Fig. 2** Effect of CNU treatment on proliferation of various cell strains. Cells were treated with CNU for 1 h. After drug removal, the cells were allowed to proliferate in fresh medium for 3 days (three to five doubling times for control cells). Symbols are as in Fig. 1 and Table 1.

chemotherapy with certain DNA damaging agents. The loss of the ability to repair  $O^6$ -alkyl guanine lesions in DNA could make the cells susceptible to the mutagenic effects of methylating agents and related carcinogens. Such cells would have an increased likelihood of malignant transformation, and could give rise to the  $Mer^-$  tumours. Our results suggest that such tumours may be vulnerable to DNA cross-linking by 1-(2-chloroethyl)-1-nitrosoureas.

Recent evidence indicates that repair of  $O^6$ -methylguanine and  $O^6$ -ethylguanine involves destruction rather than excision of these residues from DNA<sup>13-15</sup>. As  $O^6$ -alkylation markedly alters the bond conjugation in the guanine ring, this could be the recognition feature for an enzyme which acts on the ring regardless of the identity of the alkylating group. Thus,  $O^6$ -methylguanine and  $O^6$ -2-chloroethylguanine residues might be destroyed by the same enzyme.

We thank Dr Rufus Day for providing cell strains which he had determined to have the  $Mer^-$  or  $Mer^+$  phenotype, and for many fruitful discussions. G.L. was supported by grants from the Fogarty International Center (NIH) and the Rose and Jean Hoguet Foundation.

Received 15 July; accepted 27 October 1980.

1. Wheeler, G. P. *Handbk exp. Pharmac.* **38**, 65-84 (1975).
2. Carter, S. K. *Cancer Treat. Rep.* **60**, 645-811 (1976).
3. Kohn, K. W. *Cancer Res.* **37**, 1450-1454 (1977).
4. Lown, J. W., McLaughlin, L. W. & Chang, Y.-M. *Bioorgan. Chem.* **7**, 97-110 (1978).
5. Ewig, R. A. G. & Kohn, K. W. *Cancer Res.* **38**, 3197-3203 (1978).
6. Erickson, L. C., Bradley, M. O., Ducore, J. M., Ewig, R. A. G. & Kohn, K. W. *Proc. natn. Acad. Sci. U.S.A.* **77**, 467-471 (1980).
7. Day, R. S. III & Ziolkowski, C. H. *Nature* **279**, 797-799 (1979).
8. Day, R. S. III, Ziolkowski, C. H., Scudiero, D. A., Meyer, S. A. & Mattern, M. R. *Carcinogenesis* **1**, 21 (1980).
9. Day, R. S. III *et al.* *Nature* **288**, 724-729 (1980).
10. Kohn, K. W., Erickson, L. C., Ewig, R. A. G. & Friedman, C. A. *Biochemistry* **15**, 4629-4637 (1976).
11. Kohn, K. W. *Meih. Cancer Res.* **16**, 291-345 (1979).
12. Kohn, K. W., Ewig, R. A. G., Erickson, L. C. & Zwelling, L. A. in *A Laboratory Manual of Research Procedures* (eds Friedberg, E. C. & Hanawalt, P. C.) (Dekker, New York, in the press).
13. Robins, P. & Cairns, J. *Nature* **280**, 74-76 (1979).
14. Karran, P. & Lindahl, T. *Nature* **280**, 76-77 (1979).
15. Renard, A. & Verly, W. G. *FEBS Lett.* **114**, 98-102 (1980).

## Transient haem-globin interactions in photodeligated carboxyhaemoglobin and subunits

L. Lindqvist\*, S. El Mohsni\*†, F. Tfibel\* & B. Alpert†

\* Laboratoire de Photophysique Moléculaire du CNRS, Université de Paris-Sud, 91405 Orsay Cédex, France

† Laboratoire de Biologie Physico-Chimique, UER Biomédicale, 45 rue des Saints-Pères, 75270 Paris Cédex 06, France

Although the fixation of ligand to haemoglobin (Hb) is known to be accompanied by changes in protein conformation<sup>1</sup> regulating the oxygen exchange in blood, the mechanism triggering these changes remains undecided<sup>2-4</sup>. We now report a dynamic approach to this problem using results obtained in a nanosecond laser photolysis study of carboxyhaemoglobin (HbCO) and its isolated subunits. The study is based on our previous observation<sup>5</sup> of a structural evolution of free Hb after photodeligation, manifested through slight variations of the protein spectrum in the microsecond range. It is now found that the isolated subunits also show this behaviour. The duration of the spectral evolution is  $\sim 2\mu s$  for the three proteins and the activation energy of the process  $\sim 9 \text{ kcal mol}^{-1}$ . The spectral evolution is attributed to local conformation changes at the haem region, occurring during the structural relaxation of the freshly deligated protein. The results for the isolated chains show that such changes exist even in the absence of the R-T transition.

Hb and its isolated subunits were prepared from fresh human adult blood using standard procedures<sup>6,7</sup>. Aqueous solutions of the proteins at pH 7.0 (0.1 M potassium phosphate buffer) were degassed by pumping, and potassium dithionite was added to

eliminate the last traces of oxygen. The CO-complexes were obtained by exposure of these solutions to CO; dissolved excess CO was removed by rough pumping, and an atmosphere of argon was applied above the solutions. The experiments were performed at 22 °C except where otherwise stated.

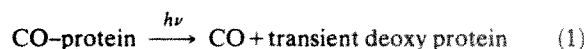
Photolysis light pulses of wavelength 530 nm and pulsewidth 7 ns at half-maximum were obtained from an Nd-glass laser. Maximum energy incident in the samples was 100 mJ. Optical transmission changes in the irradiated solutions (across 1 mm) were measured as a function of time at different wavelengths<sup>5</sup>.

We previously<sup>5</sup> showed that photodeligated Hb initially has an absorption spectrum slightly different from that of stable deoxy Hb (Fig. 1a); however, this difference disappears within a few microseconds. We have established<sup>8</sup> that this behaviour is not a multiphoton effect; such effects can always be suspected in pulsed laser studies<sup>9</sup>. The existence of a microsecond evolution of photodeligated Hb has also recently been confirmed by resonance Raman spectroscopy<sup>10</sup>.

Figure 1b and c show spectra measured after 100% photodeligation of the subunit CO complexes by laser excitation. The Soret band of the  $\alpha$  chain is reduced in intensity compared with that of the stable deoxy protein, although to a smaller extent (7%) than that observed for Hb (18%). The corresponding Soret bands of the  $\beta$  chain seem to be coincident with each other. No distortion of the  $\alpha$  and  $\beta$  subunit spectra was detectable in the 500-600 nm range, in contrast with the 10 nm displacement of the 555 nm band to the red observed for Hb<sup>5</sup>.

The distortion in the spectrum of  $\alpha$  chain disappeared after a few microseconds. (When calculating the amplitude of spectral variation in this time range, correction was made for the partial (30-40%) recovery of the ligated proteins occurring during the first few hundred nanoseconds, due to geminate recombination<sup>5,8</sup>.) A microsecond spectral variation was also observed for the  $\beta$  chain, although of very low amplitude. This variation showed that the Soret band of the photodeligated  $\beta$  chain is initially depressed by  $\sim 1\%$  compared with that of the stable deoxy protein, a difference too small to appear in the transient spectrum shown in Fig. 1c.

The kinetics of the spectral evolution for the three proteins were obtained from measurements at 430 nm. Exponential decays showed that the transient form of the deligated proteins relaxes in a first-order reaction. The reactions occurring on excitation can then be written

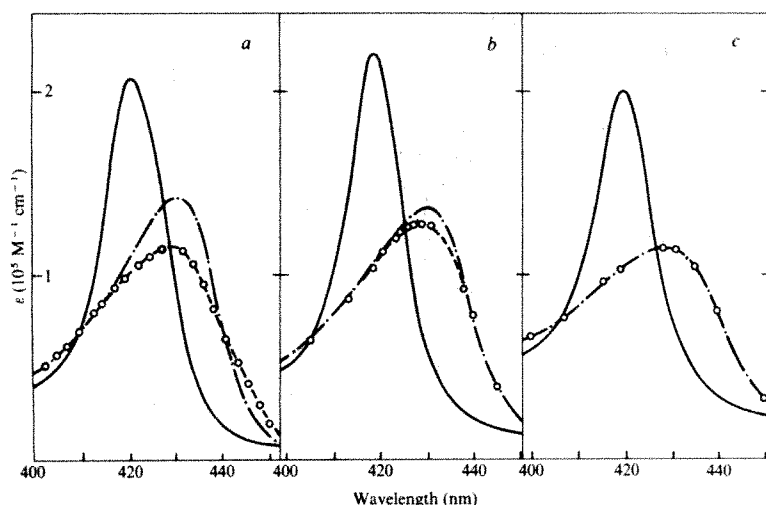


The rate constant  $k$  is  $4.1 \times 10^5 \text{ s}^{-1}$  ( $\pm 10\%$ ) for Hb,  $6.6 \times 10^5 \text{ s}^{-1}$  ( $\pm 10\%$ ) for  $\alpha$  and  $6 \times 10^5 \text{ s}^{-1}$  ( $\pm 30\%$ ) for  $\beta$ . Activation energies ( $E_a$ ) were determined from the temperature dependence of  $k$  (13-35 °C). Figure 2 shows the results in an Arrhenius plot. A value of  $E_a = 9 \pm 1 \text{ kcal mol}^{-1}$  was obtained for Hb and  $\alpha$ . The results for the  $\beta$  chain, although only semi-quantitative, indicate that its  $E_a$  value is at least of the same order of magnitude as that of the other two proteins.

The spectral evolution (process (2)) is most probably due to changes in the haem environment occurring during structural relaxation of the proteins following photodeligation. Such a relaxation must occur in Hb because the reversible binding of ligand to this protein is known to be accompanied by a rearrangement of the four chains with respect to each other<sup>2</sup> (the quaternary change) and by tertiary conformation changes, including small readjustments of the haem-protein contacts<sup>11-13</sup>. Structural studies of the isolated chains are lacking; however, X-ray investigations of myoglobin<sup>14</sup> have shown that readjustments in the haem region occur on ligand binding to this non-cooperative protein and one may expect a similar behaviour for the isolated  $\alpha$  and  $\beta$  chains.

As the non-cooperative isolated subunits show the evolution effect, the relaxation cannot be explained by the occurrence of a



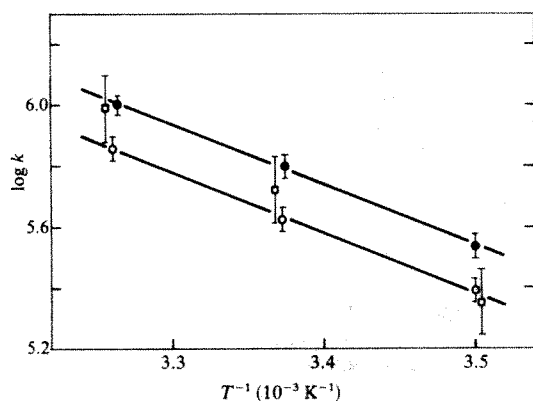


**Fig. 1** Transient absorption spectra (○) of Hb (a), α (b) and β (c) measured after pulsed laser photodissociation of the corresponding CO complexes (end-of-pulse spectra). The absorption spectra of the CO-proteins (—) and the stable deoxy proteins (---) are also shown. Haem concentration ~50 μM.

quaternary structure change. However, it is striking that the spectral variation for Hb is not the mean of those for the isolated chains but is instead appreciably enhanced. This enhancement indicates that the α and β haem regions of this cooperative protein undergo more profound changes, probably because of the quaternary structure relaxation.

Gibson discovered in his early flash-photolytic studies<sup>15</sup> the transient appearance of a spectrally distorted form of deoxy Hb with high reactivity ('quickly reacting form'). More recently, Sawicki and Gibson<sup>16</sup> reported the transient spectrum observed following laser irradiation (of 1 μs duration) of HbCO. They did not detect any similar effect with the isolated chains and therefore stressed the role of the quaternary change in the transient Hb spectrum. Apart from the shape of this latter spectrum, our results differ from those of Sawicki and Gibson. However, differences in experimental conditions (time resolution, pH) preclude a more detailed comparison.

The  $E_a$  value of the spectral evolution observed in the present study is high, considering the weakness of the interactions determining the tertiary conformation. It is, on the other hand, of the same order of magnitude as the energy of the haem-proximal histidine (F8) coordination bond (~10 kcal mol<sup>-1</sup>, as estimated from results for cobaltoporphyrins<sup>17</sup>). Also, the rate constant of process (2) is in the frequency range of the dissociation rate (10<sup>5</sup>–10<sup>6</sup> s<sup>-1</sup>) for a number of five-coordinate complexes of ferroporphyrins with nitrogenous bases<sup>18,19</sup>. It is therefore tempting to suggest that the structural change in deoxy Hb (process (2)) is controlled by the thermally activated opening of the haem-histidine (F8) coordination bond. Removal of the stress in the unrelaxed deoxy Hb may be facilitated by haem and histidine movements during the transient opening of this bond.



**Fig. 2** Temperature variation of the rate constant  $k$  associated with the spectral evolution (process (2)) of photodissociated Hb (○), α (●) and β (□) on an Arrhenius plot. The high uncertainty in the points for the β subunit are due to the extremely small spectral change observed for this protein.

Received 14 July; accepted 4 November 1980.

1. Perutz, M. F., Muirhead, H., Cox, J. M. & Goaman, L. C. *G. Nature* **219**, 131–139 (1968).
2. Perutz, M. F. *Nature* **228**, 726–734 (1970).
3. Eisenberger, P., Shulman, R. G., Kincaid, B. M., Brown, G. S. & Ogawa, S. *Nature* **274**, 30–34 (1978).
4. Little, R. G. & Ibers, J. A. *J. Am. chem. Soc.* **96**, 4452–4463 (1974).
5. Alpert, B., El Mohsni, S., Lindqvist, L. & Tübel, F. *Chem. Phys. Lett.* **64**, 11–16 (1979).
6. Perutz, M. F. *J. Crystal Growth* **2**, 54–56 (1968).
7. Geraci, G., Parkhurst, L. J. & Gibson, Q. H. *J. biol. Chem.* **244**, 4664–4667 (1969).
8. Alpert, B., Lindqvist, L., El Mohsni, S. & Tübel, F. in *Interaction between Iron and Proteins in Oxygen and Electron Transport* (ed. Ho, C.) (Elsevier, Amsterdam, in the press).
9. Greene, B. I., Hochstrasser, R. M., Weisman, R. B. & Eaton, W. A. *Proc. natn. Acad. Sci. U.S.A.* **75**, 5255–5259 (1978).
10. Friedman, J. M. & Lyons, K. B. *Nature* **284**, 570–572 (1980).
11. Anderson, L. J. *J. molec. Biol.* **79**, 495–506 (1973).
12. Makinen, M. W. & Eaton, W. A. *Nature* **247**, 62–64 (1974).
13. Gelin, B. R. & Karplus, M. *Proc. natn. Acad. Sci. U.S.A.* **74**, 801–805 (1977).
14. Phillips, S. E. V. *Nature* **273**, 247–248 (1978).
15. Gibson, Q. H. *Biochem. J.* **71**, 293–303 (1959).
16. Sawicki, C. A. & Gibson, Q. H. *J. biol. chem.* **251**, 1533–1542 (1976).
17. Drago, R. S., Beugelsdijk, T., Breese, J. A. & Cannady, J. P. *J. Am. chem. Soc.* **100**, 5374–5382 (1978).
18. White, D. K., Cannon, J. B. & Traylor, T. G. *J. Am. chem. Soc.* **101**, 2443–2454 (1979).
19. Lavalette, D., Tétreau, C. & Mometeau, M. *J. Am. chem. Soc.* **101**, 5395–5401 (1979).

## Human immunoglobulin variable region genes—DNA sequences of two V<sub>κ</sub> genes and a pseudogene

David L. Bentley & T. H. Rabbitts

MRC Laboratory of Molecular Biology, Hills Road, Cambridge CB2 2QH, UK

The study of immunoglobulin genes at the molecular level can allow us to elucidate the origin of antibody diversity. Investigations of immunoglobulin gene structure in the mouse have shown that light chains are encoded by three gene segments: the C gene encoding the constant region and the V and J genes encoding the variable region. In antibody-producing cells the V and J genes join together to create a complete immunoglobulin gene<sup>1,2</sup>. No data are available on the structure of human light chain variable region genes, but the variable regions of over 150 human κ light chain proteins have been sequenced and they comprise four distinct subgroups<sup>3–5</sup>. Here we report the complete DNA sequences of three human κ variable region (V<sub>κ</sub>) genes isolated from fetal liver DNA. The sequences demonstrate that two non-allelic genes encoding subgroup I proteins have more than 90% nucleotide homology in both coding and non-coding regions. Comparison of these human genes with two complete DNA sequences of mouse V<sub>κ</sub> genes<sup>6,7</sup> shows that V<sub>κ</sub> gene structure is highly conserved between the two species, which suggests that V<sub>κ</sub> genes rearrange during the differentiation of human lymphocytes by a very similar mechanism to that in the mouse<sup>8,9</sup>. The sequence of a defective

$V_{\kappa}$  gene is also described—this gene is unable to code for a functional immunoglobulin due to substitutions, deletions and insertions in its sequence. It is analogous to the pseudogenes<sup>10</sup> of globin<sup>11-13</sup> and *Xenopus* 5S RNA<sup>14</sup>.

To isolate human  $V_{\kappa}$  genes, we used the ability of mouse and human  $V$  gene sequences to cross-hybridize<sup>15</sup>. A mouse  $V_{\kappa}$  plus constant region cDNA clone derived from MPC11 plasmacytoma cells<sup>16</sup> was used as a probe to screen a library of fragments of human fetal liver DNA<sup>17</sup> cloned in the  $\lambda$  phage vector, Charon 4A (ref. 18). About 150,000 clones were screened and one hybridizing clone, HK101, was isolated. Restriction fragments containing the  $V_{\kappa}$  coding region were subcloned in an M13 phage vector<sup>19</sup> and sequenced by the chain-terminator method<sup>20,21</sup>.

The DNA sequence of the HK101  $V_{\kappa}$  gene is shown in Fig. 1. The predicted amino acid sequence was compared with the protein sequences of human  $\kappa$  light chains<sup>3</sup> which allowed this gene to be assigned to the  $V_{\kappa}I$  subgroup. Comparison with two mouse  $V_{\kappa}$  genes that have been completely sequenced<sup>6,7</sup> showed that the gene apparently codes for a hydrophobic signal peptide 22 amino acids long and the first 95 V-region residues of the secreted protein. This analysis also allowed us to identify a 125-base intervening sequence within the region coding for the signal peptide. The absence of a J region sequence shows that this V gene is in the germ-line configuration, that is, it has not undergone V-J joining.

Figure 1 compares the sequences of the human  $V_{\kappa}$  gene HK101 and the mouse  $V_{\kappa}$  gene K2 (ref. 7) and demonstrates

that  $V_{\kappa}$  gene structure is conserved between man and mouse. One conserved feature of the structural gene is the position of the intervening sequence between amino acids -4 and -5 of the signal peptide. The intervening sequence of human<sup>22</sup> and mouse<sup>23</sup> heavy chain V genes is also located at this position. Both human and mouse  $V_{\kappa}$  genes only encode amino acids up to position 95 of the complete light chain. Thus  $\kappa$  light chain genes of both species are interrupted within the third antigen-binding or complementarity-determining region at position 95. This implies that in man, as in the mouse, the carboxy-terminal portion of a  $V_{\kappa}$  region is encoded by a separate  $J_{\kappa}$  gene.

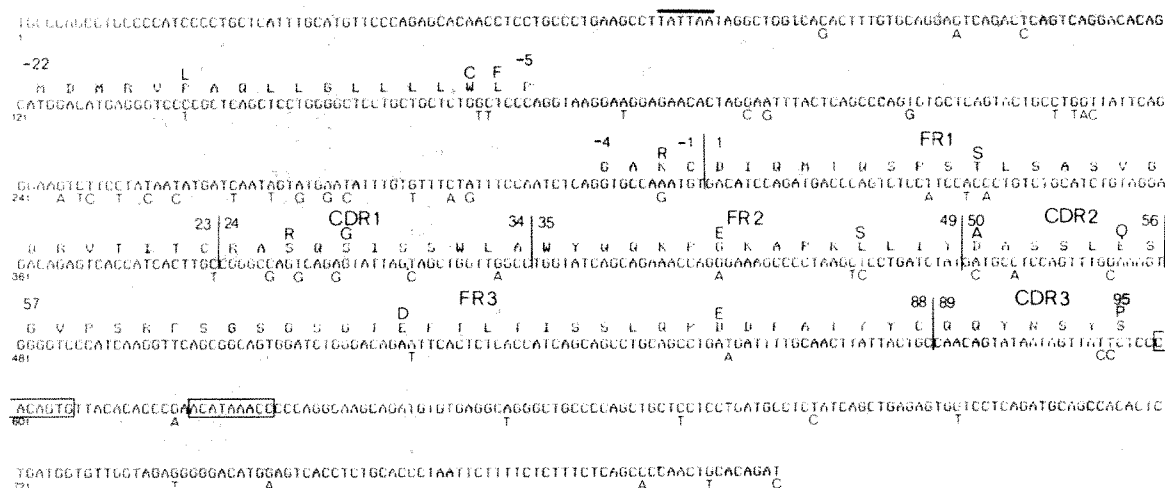
Also conserved between man and mouse are two short lengths of sequence adjacent to the 3' side (downstream) of the  $V_{\kappa}$  genes (see Fig. 1) that are thought to be recognized by the mechanism which joins V and J segments to create a complete immunoglobulin gene<sup>8,9</sup>. These 'V-J joining sequences', 7 and 9 bases long, are identical in the human HK101 gene and the mouse K2 and MOPC 41 genes<sup>6,7</sup>. Closely related sequences have been found adjacent to variable region genes of mouse  $\lambda$  light chains<sup>24</sup> as well as human<sup>22</sup> and mouse heavy chains<sup>23</sup>. These observations imply that very similar gene-rearrangement mechanisms operate on mouse and human light and heavy chain V genes.

The two coding segments of the human HK101 gene are 75% and 76% homologous to the mouse sequences MOPC 41 and K2 whereas the intervening sequences have only 50% and 60% homology. More rapid evolutionary divergence of intervening sequences relative to coding sequences has also been observed for globin<sup>25</sup>, vitellogenin<sup>26</sup> and insulin genes<sup>27</sup>. However, the 5'



**Fig. 1** Sequence comparison of human (HK101) and mouse (K2)<sup>7</sup>  $V_{\kappa}$  genes. The HK101 gene was isolated from a library of human fetal liver DNA fragments cloned in Charon 4A (ref. 17) by plaque-hybridization screening<sup>36</sup> using the nick-translated<sup>37</sup> mouse  $V_{\kappa} + C_{\kappa}$  cDNA clone  $\mu\kappa(11)24$  (ref. 16) as a probe. The HK101 V gene was identified within a 4.8-kilobase fragment of the recombinant  $\lambda$  phage by Southern blot hybridization<sup>29</sup> using  $\mu\kappa(11)24$  as the probe. This fragment was subcloned in the plasmid pBR322 and the *Pst*I sites within the insert were mapped by the method of Smith and Birnstiel<sup>38</sup>. Two *Pst*I fragments (with junctions at codons 79/80) containing the coding region were cloned in the phage vector M13mp2/*Pst*, which was constructed by blunt-end ligation of a *Pst*I linker octanucleotide to the *Eco*RI site of M13mp2 (ref. 19) which had been filled with the Klenow fragment of *Pol*I (ref. 39). The single-stranded DNA of recombinant M13 phage was used as a template for sequencing by the chain-terminator method<sup>20,21</sup> with a 26-base pair primer<sup>40</sup>. Although we have not sequenced over the junction of these two *Pst*I fragments, their alignment was derived from restriction mapping data and from sequencing of a closely related gene, HK102, where we sequenced through the *Pst*I site at this position. In the two sequences shown, broken lines have been inserted to maximize homology between the human and mouse genes using the computer program XMATCH<sup>41</sup>. The derived protein sequence is given in the one letter code. The framework (FR) and complementarity-determining (CDR) regions of the protein are indicated. The two 'V-J joining sequences' are boxed.



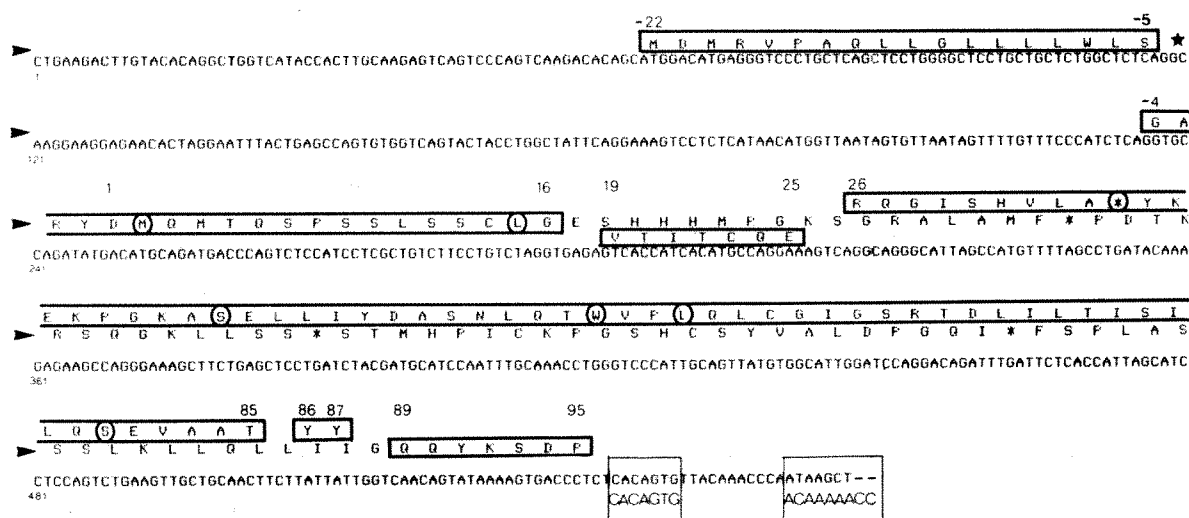


**Fig. 2** Sequence of a second human V $\kappa$  gene, HK102. The HK102 gene was selected from the library of cloned human DNA fragments using as probe the HK101 *Pst*I fragment coding up to amino acid 79 subcloned in the plasmid pBR322. The HK102 V gene was sequenced by a rapid procedure in which recombinant  $\lambda$  phage DNA was digested with a restriction enzyme to yield a mixture of small (<500 base pairs) fragments which was then 'shotgun' cloned into an M13 vector treated with phosphatase to prevent self-ligation<sup>42</sup>. The resulting recombinants containing fragments of the variable region coding sequence were selected by plaque hybridization screening<sup>36</sup> using the HK101 V segment probe. *Sau*3A fragments were cloned in M13mp2/Bam<sup>43</sup> and *Alu*I fragments in M13mp73 (J. Messing, unpublished results). Use of two restriction enzymes made it possible to overlap all junctions between fragments except for the junction between *Alu*I fragments at position -15/-14 of the protein. These two fragments were aligned by analogy with the HK101 sequence. 58% of the sequence was obtained on both strands derived from independent M13 clones. The HK101 V $\kappa$  nucleotide and amino acid sequences are marked at points where they differ from HK102. A sequence related to the TATAAA box important for the initiation of transcription by RNA polymerase II in other genes<sup>44</sup> is overlined. The 'V-J joining sequences' are boxed.

and 3' sequences closely flanking mouse and human V $\kappa$  genes are as homologous as the coding regions. In the 130 bases 5' (upstream) of the first codon, HK101 and K2 are 72% homologous (excluding an insertion of 10 bases in the human sequence) and in the 90 bases 3' of the last codon they are 74% homologous. Further downstream no significant homology could be detected. The conservation of non-coding flanking sequences may suggest that they have functional significance for transcription or gene rearrangement but these predictions require experimental verification. It is apparent from the comparison of mouse and human V $\kappa$  genes that during evolution non-coding sequences diverge from one another in different ways from coding sequences. Divergent coding regions are related primarily by base substitutions, whereas non-coding regions also

contain insertions, deletions and duplications as observed for the mouse  $\beta$ -globin genes<sup>28</sup> and *Xenopus* vitellogenin genes<sup>26</sup>.

As a first step towards a full description of diversity among germ-line V $\kappa$  genes we have isolated and sequenced two other human V $\kappa$  genes. The sequence of one of these, HK102, is shown in Fig. 2. HK101 and HK102 are probably non-allelic V $\kappa$  genes because we have identified restriction fragments corresponding to both of these in the DNA from each of 7 unrelated individuals using the Southern hybridization technique<sup>29</sup> (D.L.B. and T.H.R., in preparation). The HK101 and HK102 V $\kappa$  genes are more than 94% homologous throughout the coding region and the 5' and 3' flanking sequences (Fig. 2), and, as in the mouse-human comparison (Fig. 1), the intervening sequences are considerably less homologous (82%) than the



**Fig. 3** The DNA sequence of a human V $\kappa$  pseudogene. Isolation of the gene, HK100, and the DNA sequencing strategy was as for HK102 (Fig. 2 legend). All junctions between *Alu*I and *Sau*3A fragments were sequenced. 92% of the sequence was obtained in both strands and the region where only one strand was sequenced was confirmed on two independent clones. The in-phase reading frame is indicated with arrows. The reading frames which correspond to normal immunoglobulin protein are in heavy boxes and amino acid positions are marked according to the standard numbering of normal  $\kappa$  light chains<sup>3</sup>. Asterisks mark termination codons and circles mark positions where highly conserved amino acids have been replaced due to apparent base-pair substitutions. The unconventional sequence at the 5' end of the intervening sequence is indicated by a star. Putative 'V-J joining sequences' are in light boxes. The final two blank positions refer to unidentified nucleotides beyond the *Alu*I fragment sequenced.

coding and flanking sequences. Both the HK101 and HK102 genes encode proteins that can be assigned to the  $V_{\alpha}Ib^{30}$  subgroup but neither is identical to any known complete protein sequence. However, the HK102 sequence is closely related to the EU light chain protein<sup>31</sup> from which it differs by 6 amino acids in the first 95. HK101 and HK102 differ at 14 amino acid residues in the signal peptide and in each of the framework and complementarity-determining regions of the protein. It seems likely that the extensive homology between these two human sequences is due to their recent common ancestry or to some gene correction mechanism<sup>32</sup>.

The sequence of a third human  $V_{\alpha}$  gene, HK100 (Fig. 3), is remarkable because it apparently cannot encode a functional immunoglobulin. The reading frame of this gene contains three in-phase termination codons which are a result of four small insertions and deletions in the DNA sequence relative to normal  $V_{\alpha}$  genes such as HK101 or HK102. These apparent mutations are a 2-base deletion at amino acid position 17/18, a 4-base insertion at 25/26, a 3-base insertion at 85/86 and a 1-base insertion in the invariant Cys codon at position 88. In addition, a number of apparent nucleotide substitutions in the coding region of HK100 change highly conserved amino acid residues at positions 2, 15, 44, 57, 60 and 80. A substitution at amino acid 35 replaces an invariant Trp codon, TGG, with a TGA nonsense codon (which is not in phase, however). Overall, the sequence of this abnormal gene and its flanking regions is 78% homologous to the HK101 sequence after maximizing homology<sup>41</sup>. The sequence of the HK100  $V_{\alpha}$  gene suggests that it evolved by a mechanism typical of non-coding sequences, involving insertions and deletions as well as substitutions.

We do not know whether the HK100 V gene is capable of being transcribed but it is unlikely that a transcript could be correctly processed. The 5' end of the intervening sequence begins with a GC dinucleotide, not the highly conserved GT normally found at this position<sup>33</sup>. This GC sequence has never been observed in 36 known functional RNA splicing sites<sup>34</sup>.

Furthermore the HK100  $V_{\alpha}$  gene may not be able to undergo V-J joining. Examination of the two sequence blocks downstream of the gene, thought to be important for V gene rearrangement, shows that the HK100 sequence possesses the first CACAGTG block but lacks a good match with the ACAAAAACC consensus sequence for the second block. In fact it differs from the consensus at four of the first seven positions (see Fig. 1) whereas no other known  $V_{\alpha}$  gene differs from the consensus at more than one position<sup>35</sup>.

Other genes apparently unable to encode functional products have been discovered for 5S rRNA and  $\alpha$  and  $\beta$  globin (see ref. 10 for a review) and these have been termed pseudogenes. The HK100  $V_{\alpha}$  gene is the first example of an immunoglobulin variable region pseudogene.

We thank Dr T. Maniatis for providing the library of cloned human DNA and Drs Perry, Marcu and Schibler for the plasmid p $\alpha$ (11)24 (ref. 16), J. Karn for Sau3A, and B. J. Meyer, J. Sims and S. Fields for critical reading of the manuscript.

Received 16 October, accepted 24 November 1980

- Brack, C. *et al.* *Cell* **15**, 1-14 (1978).
- Sechman, J. G. & Leder, P. *Nature* **276**, 790-795 (1978).
- Kabat, E. A. *et al.* *NJH Publ. No.* 80-2008 (1979).
- Milstein, C. *Nature* **216**, 330-332 (1967).
- Wang, A. C. *et al.* *Nature new Biol.* **243**, 126-127 (1973).
- Sechman, J. G. *et al.* *Nature* **280**, 370-375 (1979).
- Nishioaka, Y. & Leder, P. *J. Biol. Chem.* **255**, 3691-3694 (1980).
- Sakano, H. *et al.* *Nature* **280**, 288-294 (1979).
- Max, E. E. *et al.* *Proc. natn. Acad. Sci. U.S.A.* **76**, 3450-3454 (1979).
- Proudfoot, N. J. *Nature* **280**, 840-841 (1980).
- Jahn, C. L. *et al.* *Cell* **21**, 159-168 (1980).
- Lacy, E. & Maniatis, T. *Cell* **21**, 545-553 (1980).
- Proudfoot, N. J. & Maniatis, T. *Cell* **21**, 537-544 (1980).
- Jacq, C., Miller, J. R. & Brownlee, G. G. *Cell* **12**, 109-120 (1977).
- Rabbitts, T. H., Matthysen, G. & Haxllyn, P. H. *Nature* **284**, 238-243 (1980).
- Schibler, U., Märcu, K. B. & Perry, R. P. *Cell* **18**, 1495-1509 (1978).
- Lawn, R. M. *et al.* *Cell* **15**, 1157-1174 (1978).
- Blattner, F. *et al.* *Science* **196**, 161-169 (1977).
- Grosveld, B. & Meeling, J. *Nature* **272**, 375-377 (1978).
- Sanger, F., Nicklen, S. & Coulson, A. R. *Proc. natn. Acad. Sci. U.S.A.* **74**, 5463-5467 (1977).
- Schreier, P. H. & Cortese, R. *J. molec. Biol.* **129**, 169-172 (1979).
- Matthysen, G. & Rabbitts, T. H. *Proc. natn. Acad. Sci. U.S.A.* (in the press).
- Early, P. *et al.* *Cell* **19**, 981-999 (1980).

- Bernard, O. *et al.* *Cell* **15**, 1133-1144 (1978).
- van den Berg, J. *et al.* *Nature* **276**, 37-44 (1978).
- Wahl, W. *et al.* *Cell* **20**, 107-117 (1980).
- Parier, F. *et al.* *Cell* **20**, 555-566 (1980).
- Konkel, M. *et al.* *Cell* **18**, 865-873 (1979).
- Southern, E. M. *J. molec. Biol.* **98**, 503-517 (1975).
- Milstein, C. P. & Deverson, E. V. *Biochem. J.* **123**, 945-958 (1971).
- Gottlieb, P. D. *et al.* *Biochemistry* **9**, 3155-3161 (1970).
- Tartof, K. D. *Am. Rev. Genet.* **9**, 355-385 (1975).
- Brathnach, R. *et al.* *Proc. natn. Acad. Sci. U.S.A.* **75**, 4853-4857 (1978).
- Lerner, M. R. *et al.* *Nature* **283**, 220-224 (1980).
- Sakano, H. *et al.* *Nature* **286**, 676-683 (1980).
- Benton, W. D. & Davis, R. W. *Science* **196**, 180-182 (1977).
- Makats, T., Jeffrey, A. & Kleid, D. O. *Proc. natn. Acad. Sci. U.S.A.* **72**, 1184-1188 (1975).
- Smith, H. O. & Birnstiel, M. L. *Nucleic Acids Res.* **3**, 2387-2398 (1976).
- Backman, K., Pishano, M. & Gilbert, W. *Proc. natn. Acad. Sci. U.S.A.* **73**, 4174-4178 (1976).
- Anderson, S. *et al.* *Nucleic Acids Res.* **8**, 1731-1745 (1980).
- Staden, R. *Nucleic Acids Res.* **6**, 2601-2610 (1979).
- Ullrich, A. *et al.* *Science* **196**, 1313-1319 (1977).
- Rothstein, R. J. *et al.* *Meth. Enzym.* **68**, 98-109 (1979).
- Cordas, J. *et al.* *Science* **209**, 1406-1414 (1980).

## Dimethyl sulphoxide reduces anti-receptor antibody titres in experimental myasthenia gravis

Alan Pestronk & Daniel B. Drachman

Johns Hopkins University, School of Medicine, Department of Neurology, 1721 E. Madison Street, Baltimore, Maryland 21205

The basic abnormality in myasthenia gravis (MG) is a reduction of acetylcholine receptors (AChRs) at neuromuscular junctions, due to an autoimmune attack directed against the receptors<sup>1</sup>. Several lines of evidence support the idea that humoral immune mechanisms play an important part in this process: anti-AChR antibodies are present in the sera of more than 80% of myasthenic patients<sup>2-4</sup>; the pathogenicity of the antibodies has been demonstrated by passive transfer of IgG from myasthenic patients to mice which reproduces the typical features of MG in the recipient animals<sup>5,6</sup>; finally, procedures that reduce levels of anti-AChR antibody, such as plasmapheresis, produce improvement in the clinical symptoms of MG<sup>7</sup>. Present treatments of MG depend largely on the prolonged use of immunosuppressive drugs, which have significant drawbacks<sup>1,8-10</sup>, for they usually produce only a slow fall in antibody titres, and have toxic side effects. An agent that could produce a rapid and sustained fall of autoantibody titre might have wide application in the treatment of MG and other autoimmune diseases. In the course of testing immunosuppressive drugs for their effect in treating experimental autoimmune MG (EAMG), we discovered that the vehicle used to dissolve some of these agents, dimethyl sulphoxide (DMSO), itself produced a rapid and sustained fall of anti-AChR antibody titre. We now report similar results for a controlled trial of DMSO treatment in rats with EAMG.

EAMG was produced in female Lewis rats (200-225 g) by immunizing them with 50  $\mu$ g of AChR, emulsified in an equal volume of Freund's complete adjuvant, injected intradermally. AChR was extracted from the electric organs of *Torpedo californicus* with Triton X-100 and purified by affinity chromatography, using  $\alpha$ -toxin from the venom of the cobra *Naja naja siamensis* covalently linked to Sepharose 4B beads as the binding ligand<sup>11</sup>.

Measurement of anti-AChR antibodies was carried out by a double precipitation radioimmunoassay like those previously described<sup>2,4</sup>. Antibodies directed against *Torpedo* AChR were measured using as the antigen  $0.5 \times 10^{-12}$  moles of purified *Torpedo* AChR coupled to <sup>125</sup>I- $\alpha$ -bungarotoxin (<sup>125</sup>I- $\alpha$ -BTX). Serial dilutions of sera from the experimental rats were used, and precipitation was produced by the addition of goat anti-rat IgG. The antibody titre, determined from the linear portion of the dilution curve, is expressed as moles  $\times 10^{-9}$  of  $\alpha$ -BTX precipitated per litre. For determinations of antibody against rat AChR, an aliquot of Triton-extracted denervated rat muscle containing  $0.5 \times 10^{-12}$  moles of AChR was used as the antigen,



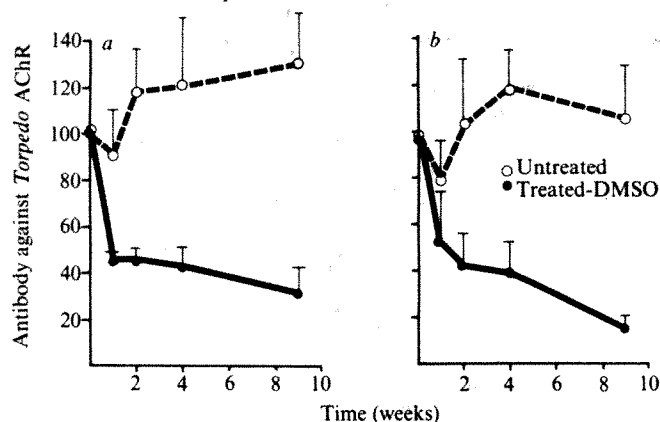
coupled to  $^{125}\text{I}$ - $\alpha$ -BTX as above. These assays were sensitive to antibody concentrations of  $0.5 \times 10^{-9}$  moles per l of serum. Determinations of antibodies against both *Torpedo* AChR (the immunizing antigen) and rat AChR (the 'self' antigen) were made repeatedly up to 2 months after the start of the experiment. Levels of rat IgG were measured in sera from treated and control EAMG animals by a commercial radial immunodiffusion assay (Hyland).

The original purpose of our investigations was to examine whether frentizole, a drug thought to be particularly effective in suppressing humoral immune responses, would reduce the levels of anti-AChR antibody in rats with EAMG. Because frentizole is poorly soluble in water it was administered in DMSO solution; control EAMG animals received DMSO alone. Our results showed that anti-AChR titres fell by 50% within 1 week in both experimental and control animals.

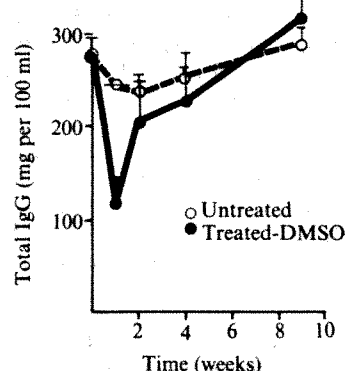
A therapeutic trial of DMSO alone was therefore undertaken to determine whether DMSO was responsible for the fall in the antibody titre. Experimental rats with EAMG were treated with a 2-week course of daily intraperitoneal injections of DMSO (1.0 ml) starting 1 month after immunization with AChR. Control EAMG animals immunized at the same time were given injections of physiological saline.

After 1 week of treatment with DMSO the titre of anti-*Torpedo* AChR antibody decreased to a mean of 46% of pretreatment levels. The titres remained markedly reduced, reaching 32% of pretreatment levels 6 weeks after discontinuation (Fig. 1a). In contrast, antibody titres in control animals remained elevated, eventually rising to a level 30% higher than that at the start of the study (Fig. 1a). There was also a rapid reduction in levels of the autoantibody, against rat AChR. One week after the start of DMSO treatment anti-rat AChR antibody titres had fallen to 48% of pretreatment levels (Fig. 1b). By the end of the study, the mean anti-rat AChR antibody titre was 14% of the pretreatment level, and 12% of the level in untreated controls. In control animals autoantibody titres remained relatively constant, averaging 5% higher at the end of the study. Serum concentrations of IgG were initially reduced by DMSO treatment, being 42% of pretreatment levels after 1 week. However, in contrast to the anti-AChR antibody, IgG rapidly returned to pretreatment levels (Fig. 2). By 2 weeks after the end of the treatment course, the mean IgG level was not significantly different from the levels in pretreatment or control animals.

We carried out additional control experiments which showed that DMSO did not interfere with the assay for anti-AChR antibody. Antibody titres were not significantly affected by levels of DMSO of up to 0.5% in serum. Further, antibody titres



**Fig. 1** a, Antibody titres against *Torpedo* AChR; b, antibody titres against rat AChR. Dashed line indicates titres in untreated EAMG rats, solid line those in DMSO-treated EAMG rats. Treatment was given at time 0 (4 weeks after induction of EAMG). Antibody titres at time 0 were normalized to 100%. The absolute values of antibody at this time were  $640\text{--}2,300 \text{ mol} \times 10^{-9} \text{ l}^{-1}$  against *Torpedo* AChR and  $5\text{--}60 \text{ mol} \times 10^{-9} \text{ l}^{-1}$  against rat AChR. Subsequent values represent the mean of percentages of the initial titre (from eight treated and seven untreated rats)  $\pm$  s.e.



**Fig. 2** Levels of total IgG. Dashed line indicates levels in untreated EAMG rats, solid line those in DMSO-treated EAMG rats. Treatment was given at time 0 (4 weeks after induction of EAMG).

in EAMG animals treated 8 h previously with a single dose of DMSO did not differ from titres in untreated animals.

Our results show that treatment with DMSO reduced antibody titres against both foreign (*Torpedo*) and self (rat) AChR. The fall in titres was rapid and sustained, and titres did not rise even after DMSO was discontinued. The mechanism by which DMSO reduces antibody titres is unknown. The fall in anti-AChR antibody titres is not attributable to a direct effect of DMSO on the antibody, as there was no change in the titre after acute treatment with DMSO. The effect is not due to interference with the antibody assay, because relatively high serum concentrations of DMSO had no effect on antibody measurement. In addition, the half life of DMSO is less than 1 day<sup>12</sup> and anti-AChR antibody titres remained low for at least 6 weeks after the cessation of treatment. A more likely explanation for the fall in titres is that DMSO reduced the production of antibody by lymphoid cells. It remains to be determined whether this effect is due to a direct action of DMSO on antibody-producing cells or to an indirect effect on immune regulatory mechanisms such as suppressor cells. In any case, active immune responses may be especially susceptible to DMSO, for anti-AChR antibody titres remained low, whereas the total IgG concentration returned to normal.

It is encouraging that the fall of anti-AChR antibody titres after DMSO treatment is comparable to that which results from plasmapheresis. This suggests that DMSO might be effective in the treatment of diseases such as MG where antibodies have an important pathogenic role<sup>1</sup> and plasmapheresis provides only temporary improvement<sup>7</sup>. The finding that at the longer times after treatment, autoantibodies against AChR remained depressed whereas the total levels of IgG returned to normal may be relevant to the potential usefulness of DMSO in human disease states.

Thus, we have found that DMSO treatment produces a rapid and sustained fall in anti-AChR antibody in EAMG. It seems likely that DMSO might also be effective in ameliorating other active humoral immune responses. If so, DMSO may provide an effective new treatment for immune diseases mediated by autoantibodies.

This work was supported by grants from the NIH and the Muscular Dystrophy Association of America.

Received 7 August; accepted 24 October 1980.

- Drachman, D. B. *New Engl. J. Med.* **298**, 136–142, 186–193 (1978).
- Lindstrom, J. M., Seybold, M. E., Lennon, V. A. & Whittingham, S. *Neurology* **26**, 1054–1059 (1979).
- Mittag, T., Kornfeld, P., Tormay, A. & Woo, C. *New Engl. J. Med.* **294**, 691–694 (1976).
- Appel, S. H., Almon, R. R. & Levy, N. *New Engl. J. Med.* **293**, 760–761 (1975).
- Toyka, K. V. *et al.* *New Engl. J. Med.* **296**, 125–131 (1977).
- Howard, J. F. & Sanders, D. B. *Neurology* **30**, 760–764 (1980).
- Dau, P. C. (ed.) *Plasmapheresis and Immunobiology of Myasthenia Gravis* (Houghton Mifflin, Boston, 1979).
- Hertel, G., Mertens, H. G., Ruether, P. & Ricker, K. in *Plasmapheresis and the Immunobiology of Myasthenia Gravis* (ed. Dau, P. C.) Ch. 29 (Houghton Mifflin, Boston, 1979).
- Sanders, D. B., Howard, J. F., Johns, T. R. & Campa, J. F. in *Plasmapheresis and the Immunobiology of Myasthenia Gravis* (ed. Dau, P. C.) 289–306 (Houghton Mifflin, Boston, 1979).
- Rowland, L. P. *Trans. Am. neurol. Ass.* **133**, 277–302 (1978).
- Eldefrawi, M. E. & Eldefrawi, A. T. *Archs Biochem. Biophys.* **159**, 362–373 (1973).
- Hucker, H. B., Ahmad, P. M. & Miller, E. A. *J. Pharmac. exp. Ther.* **154**, 176–184 (1966).

# Anomalous region on Mars: implications for near-surface liquid water\*

S. H. Zisk

NEROC Haystack Observatory, Westford, Massachusetts 01886

P. J. Mouginis-Mark

Department of Geological Sciences, Brown University, Providence, Rhode Island 02912

*An anomalous region has been identified on Mars from the 1971 and 1973 Earth-based Goldstone radar data. This region is characterized by coincident very high radar reflectivities, and unusual smoothness. Very few realistic surface morphologies can generate such return-signals. Liquid water within ~50–100 cm of the surface is one possibility, an interpretation strengthened by an apparent seasonal variation in surface reflectivity for the same locality.*

ANALYSIS of radar measurements of the martian surface enables textural-compositional differences of materials to be interpreted on a scale unobtainable from orbital images<sup>1–3</sup>. Estimates of the dielectric constant (from inherent reflectivity) and small-scale slope statistics (see, for example, the C-factor analysis developed by Hagfors<sup>4</sup>) can be used to characterize surface units<sup>5</sup> or to delineate areas with unusual material properties.

An extensive data base was compiled from Earth-based radar measurements of the martian surface by Downs *et al.*<sup>2</sup> in 1971 and 1973 at the Jet Propulsion Laboratory's Goldstone Facility. This combined set of observations gave almost complete coverage between 14 and 22° S. The high dielectric constant of liquid water compared with both ice and dry geological materials<sup>6</sup> means that radar observations should provide excellent evidence for or against the existence of water on Mars. In particular, this radar data set can provide additional evidence regarding the existence of near-equatorial regions of H<sub>2</sub>O outgassing ('oases') proposed by Huguenin *et al.*<sup>7,8</sup>. Liquid water should affect the radar characteristics of the surface, if any overburden is relatively transparent to the radar energy. If the water were allowed to form a free surface, as opposed to an adsorbed layer on a mineral substrate, then the radar-reflecting facets would be expected to be nearly horizontal due to gravitational forces. Hence this type of surface would give a radar return with a very high smoothness as well as high reflectivity. We report here our attempts to search for anomalous areas within the radar data set, where both high reflectivity and C-factor values could be attributed to a layer of liquid water or damp soil.

## Experimental method

The radar determination of surface smoothness and reflectivity is derived from the observed variation of echo strength as a function of local incidence angle<sup>4,6</sup>. The radar echo at any incidence angle is the incoherent sum of reflections from surface facets within the resolution cell which are oriented perpendicular to the radar beam. Strictly speaking, the reflecting surfaces are the Fresnel zones of these elements, so that the cross-section of each surface element depends on its radius of curvature or, where the radius is large, on its area<sup>6</sup>. The size of the radar

resolution cell is much larger than even the planetary-radius Fresnel zone. It is fixed by the resolution of the radar signal in time-delay and Doppler frequency, which respectively determine the resolution along the projected axis of rotation and at right angles to it. For the radar data considered here, the resolution cell measures ~80 km by 10 km, compared with the 0.9-km size of the Fresnel zone for the planet's radius of curvature<sup>2</sup>.

The C-factor parameter used to describe the surface smoothness quantitatively was derived by Hagfors<sup>4</sup>. He postulated a set of models for surface topography (based on observations of the Moon), for each of which he calculated the number distribution of surface-facet slopes, and thence the expected curve of radar strength compared with incidence angle (C-factor template). The radar-observed curve was computer-fitted to these hypothetical curves to determine the best-fit value for the C-factor. For areas with moderate to high smoothness (C-factor > 100), the expression for the r.m.s. surface slope  $a_{rms}$  is

$$a_{rms} = C^{-1/2} \text{ rad}$$

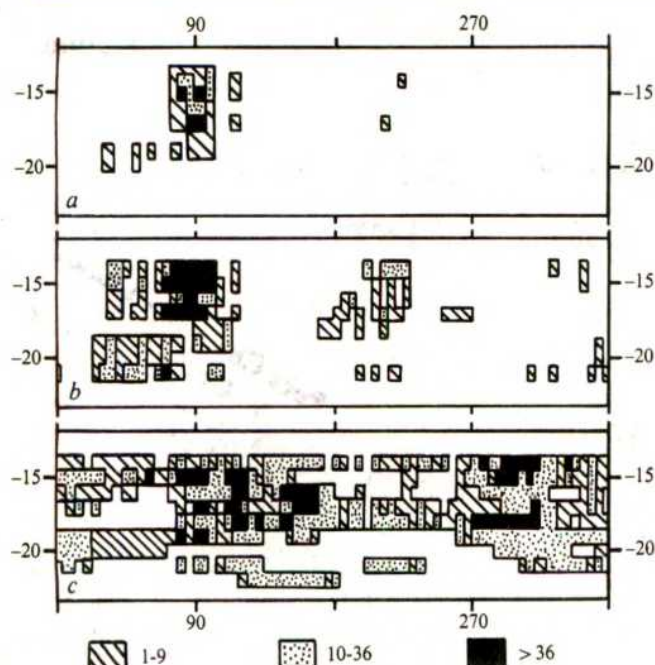
For real surfaces which do not match these models, the measured curve of echo strength compared with the incidence angle will not agree well with any of the templates, and a large standard error will result from the fitting process. Smooth, random surfaces will generally show a good fit to the templates, because there is little dependence on the details of the model. Surfaces with high relief, on the other hand, cannot usually be described well by only one parameter. Also, a non-random surface such as an area of sand-dunes or a cluster of comparable-size craters, cannot be described well by the standard C-factor parameter at any observable amplitude of relief.

The morphology of the surface determines the shape of the curve and hence the value of C-factor. The amplitude of the curve is a function only of the reflectivity of the material of which the surface is composed, and is another independent output from the template-fitting process.

In the present radar measurements, the same surface-resolution element was observed at various incidence angles (by using the Doppler resolution in longitude) to form the curve of echo strength versus incidence angle. There is therefore no implicit

\* **Erratum:** Due to an error in the *Nature* office, the original rather than the subsequently revised version of this article appeared in the issue of 13 November (288, 126–129, 1980). We here reprint the article in its correct form.





**Fig. 1** Number density of radar sample points with given characteristics per  $1^\circ$  latitude,  $5^\circ$  longitude sample bins. *a*, Reflectivity  $>9\%$  and *C*-factor  $>3,200$  coincidentally; *b*, *C*-factor  $>3,200$ ; *c*, reflectivity  $>9\%$ . Note that although data points with high reflectivity or *C*-factor occur over a wide area of Mars, coincident high values in both parameters are found exclusively at the 'oasis' areas proposed by Huguenin *et al.*<sup>7,8</sup> (Solis Lacus, at  $15\text{--}30^\circ$  S,  $80\text{--}90^\circ$  W; and Noachis-Hellespontus, at  $15\text{--}25^\circ$  S,  $305\text{--}315^\circ$  W).

assumption of large-area uniformity of the surface, as was the case for some earlier measurements. Any systematic variation in surface composition as, for example, a low-reflectivity mantled surface interspersed with high-relief, high-reflectivity rock formations, will show up as a poor fit (high standard error) to the *C*-factor templates<sup>5</sup>. A mixture of high- and low-reflectivity materials exhibiting the same morphology will yield a low-error *C*-factor value, with an intermediate reflectivity. Other surface configurations can be hypothesized and their radar-measured parameters calculated. The reverse calculation, however, from the radar data to the surface configuration, cannot be carried out unambiguously for all combinations of reflectivity and *C*-factor. As the surface becomes less smooth, the variety of possible configurations increases and the reliability of the template-fitting becomes much worse, partly because of the reduced strength of the widely-scattered signal and partly because of the above-mentioned variety of possible surface topographies.

## Analysis

The data were scanned for regions with a coincident high reflectivity and smoothness. Limits of  $9\%$  reflectivity and  $3,200$  *C*-factor (r.m.s. slopes  $<1^\circ$ ) were chosen arbitrarily. Variations from  $9$  to  $11\%$  and from  $2,400$  to  $3,200$  respectively had only a slight effect on the shape of the anomalous area and on the number of observation points. For these measurement values, the formal errors (standard deviations) were  $\sim 10\%$  of the data value.

Figure 1*a* illustrates the areocentric position and number densities of these high-reflectivity, high-smoothness measurements. Only two regions on the planet share this combined radar characteristic. The most prominent is a region centred at  $16^\circ$  S  $90^\circ$  W. There is also a pair of smaller areas to the north-west of Hellas. These two regions are remarkably close to the Solis Lacus ( $25^\circ$  S,  $85^\circ$  W) and Noachis-Hellespontus ( $20^\circ$  S,  $310^\circ$  W) proposed by Huguenin *et al.*<sup>7,8</sup>.

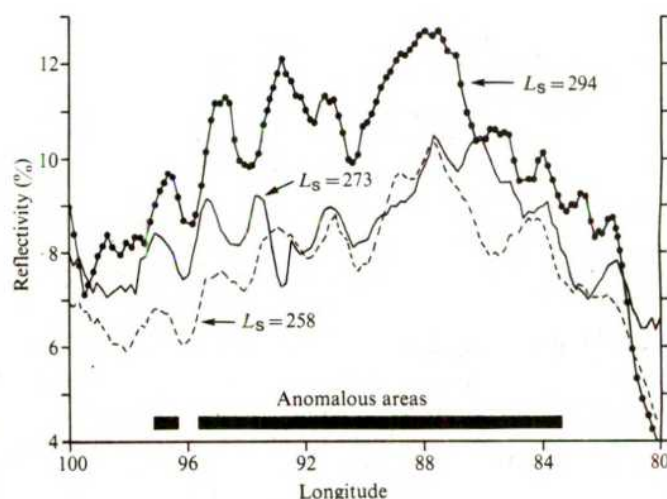
For comparison, Fig. 1*b,c* indicates the areas having only their reflectivity or *C*-factor above the defined limits. Note that there are many areas of high reflectivity, indicating a profusion of well-compacted or rocky soils on the martian surface. Areas of high smoothness are less common, although they are not restricted to the anomalies described here.

As an argument for the reality of the anomalous areas, note that the map of Fig. 1*a* includes radar measurements from both the 1971 and 1973 conjunctions. Almost no anomalous data points occur elsewhere on the planet, despite the near-global coverage of the data set between  $14$  and  $22^\circ$  S. In the  $300 \times 300$  km anomaly itself, on the other hand, there are several hundred points.

## Seasonal variability

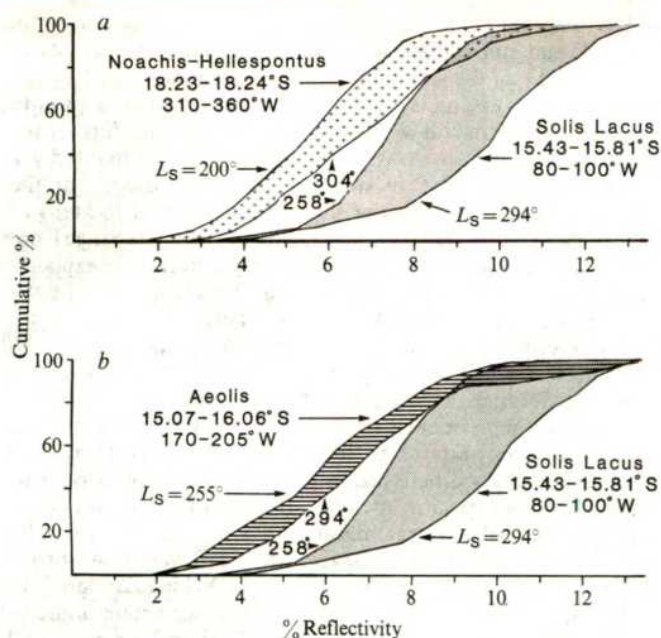
Additional characteristics of Solis Lacus can be determined by comparing radar data derived for nearly coincident ground tracks at different times of the martian year. Note that practical limitations of Earth-based radar systems dictate that radar observations of the sub-Earth region must be made near opposition, and hence near local martian summer. Winter measurements would at best be extremely difficult to make using Earth-based radar.

A combination of data from the 1971 and 1973 oppositions provides an example of overlapping radar swaths: latitudes  $15.45^\circ$  S,  $15.43^\circ$  S, and  $15.81^\circ$  S were sampled between  $80$  and  $100^\circ$  W during the seasonal range from early to middle local martian summer ( $L_s = 258^\circ$ ,  $273^\circ$  and  $294^\circ$  respectively). Note that, as  $L_s$  represents the longitude of the Sun as seen from Mars, the difference between  $L_s = 258^\circ$  and  $294^\circ$  is roughly equivalent to the shift from early June to mid-July on Earth (Northern Hemisphere). Because of the nearly identical locations of these radar profiles (the north-south extent of the radar resolution cell is  $1.3^\circ$ , giving an overlap of at least  $70\%$  between swaths), the reflectivity curves for identical surfaces should be very similar. However, Fig. 2 indicates that there is a discrepancy in the reflectivity between  $L_s = 258^\circ$  and  $273^\circ$ . The  $273^\circ$  profile indicates an increase of  $1.0\text{--}1.5\%$  in the reflectivity compared to the same longitude at  $L_s = 258^\circ$ , while the  $294^\circ$  profile shows a further enhancement of  $2.5\text{--}3.5\%$ . For large parts of the region between  $82$  and  $100^\circ$  W, there is a systematically higher reflectivity with advancing  $L_s$ , that is season. Such a



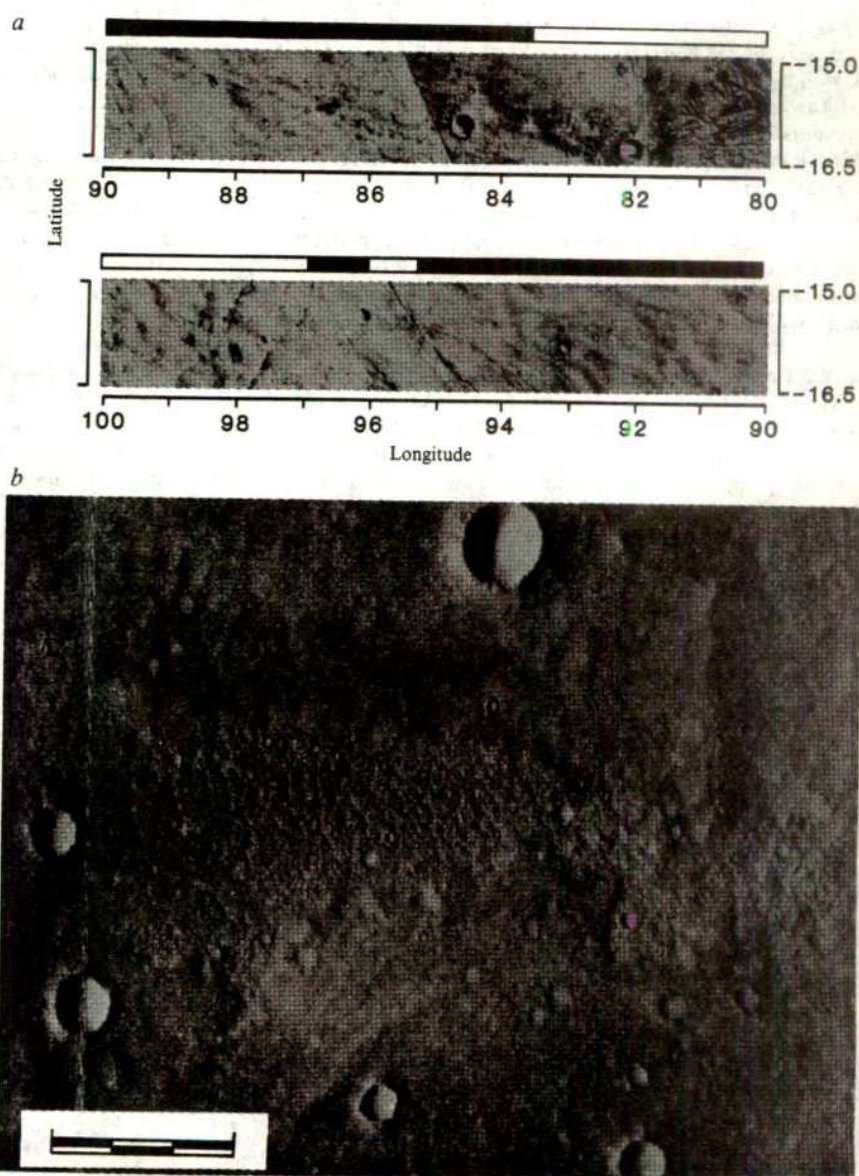
**Fig. 2** Temporal variations in radar reflectivity for an area of Solis Lacus at  $15.43\text{--}15.81^\circ$  S. Curves represent a running 5-point average at  $0.16^\circ$  longitude intervals. Radar data was taken during 1971 ( $L_s = 258^\circ$ ) and 1973 ( $L_s = 273^\circ$  and  $294^\circ$ ) Mars oppositions at latitudes  $15.44$ ,  $15.43$  and  $15.81^\circ$  S respectively. The 'anomalous areas' refer to parts of the ground track at  $L_s = 294^\circ$  where reflectivity is  $>9\%$  and *C*-factor  $>3,200$  (see also Fig. 4*a*).





**Fig. 3** The seasonal variations in radar reflectivity compared here for three regions of Mars. The horizontal axis is reflectivity and the vertical axis is the percentage of data points having less than the indicated reflectivity. *a*, Compares the strongly anomalous Solis Lacus area with the weakly anomalous Noachis-Hellespontus region. *b*, Compares Solis Lacus with an area in Aeolis, which is taken to be representative of Mars as a whole and shows no anomaly. Note that all three areas display an increase in percentage reflectivity with increasing martian season, but that Solis Lacus has a much more pronounced seasonal change, in addition to its higher absolute radar reflectivity.

**Fig. 4** Viking Orbiter Images of the anomalous radar areas. *a*, Ground track shown in Fig. 2; *b*, high resolution for an area in Solis Lacus at 18.7°S. Note that the images do not support a hypothetical smooth, mantle-free surface as an explanation of the radar anomaly. Numerous 10-km craters and lava flow fronts are in evidence (USGS photomosaics I-1183 and I-1190; and Viking frame 773A10). Scale bar, 3 km.





phenomenon seems to be real, since some parts of the data (for example, between 83–84° W and 88–92° W for  $L_s = 258^\circ$  and  $273^\circ$ ) show no difference in reflectivity despite their respective acquisition dates in 1971 and 1973. This is strong evidence for the adequacy of the calibration of the original radar data, and also for the lack of any temporal variation in the data from instrumental causes.

In another test for possible systematic effects, we are searching the radar data at areas other than the observed anomaly for quasi-seasonal variability. Some of the results are depicted in Fig. 3. Figure 3a presents a plot of the range of variability of the reflectivity with  $L_s$  for Noachis-Hellespontus, which contains the only cluster of anomalous points outside the Solis Lacus region. Figure 3b presents Aeolis as an example of a non-anomalous region. Figure 3 shows that there is a 'seasonal' variability in much of the observed area, in the same sense (increased reflectivity with advancing summer); but that Solis Lacus exhibits the greatest range by more than a factor of 2 of those areas so far examined. The general variability may indicate scattered expressions of near-surface water and/or permafrost; or possibly a low-level, systematic and time-dependent flaw in the calibration.

## Discussion

Measurements showing a high radar reflectivity (high dielectric constant) would be expected not only for water surfaces, but also for large areas of smooth rock within 1 m of the surface. In these conditions, anorthositic rock, with a dielectric constant  $K$  of about 5, would have a reflectivity of about 15% (basalt, with  $K = 9$ , is >25%; water, with  $K = 81$ , is >65%) if it covered the entire surface area of the radar cell (~750 km<sup>2</sup>). Figure 4 presents Viking Orbiter images of the same area as Fig. 2. Although few craters larger than ~10 km diameter are within the radar ground track, many moderately well preserved lava flow fronts can be easily identified. Morphologically comparable lava flows elsewhere on Mars either have radar reflectivities of 2–6% or  $C$ -factors <2,000 (refs 5, 9, 10). Unless the small-scale surface texture of the Solis Lacus region is unrelated to its large-scale appearance in Fig. 3, the hypothesis of an extensive rock pediment is untenable as an explanation for the high values of radar reflectivity and  $C$ -factor.

Moreover, to explain a seasonal variability in the reflectivity of a solid rock surface, one must hypothesize, for example, an absorptive overburden which is regularly scoured away as the summer progresses. The thickness of overburden required for the observed changes in dielectric constant have been calculated on the basis of published dielectric constants and absorption lengths for basaltic rock and loosely-compacted rock powder<sup>11</sup>. Although resonant effects of thin highly-planar soil and rock layers might be observed in laboratory conditions, such conditions do not exist on a planetary surface. Consequently, the reflectivity was calculated for a random-thickness soil layer masking a solid rock surface. Assuming dielectric constants of 2.0 for soil and 8.0 for rock, the net reflection coefficient for bare rock is 23%; for a soil layer at least 14 cm (one wavelength) thick, is 11%; and drops to 6% for a soil depth of 1.4 m. For lunar rock chemistry rather than terrestrial rock chemistry, the 6% reflectivity would require more than 10 m of rock-free soil. The problem is complicated by other factors such as variation in

soil porosity with depth, but the conclusion, nevertheless, is that for rock and soil surface to exhibit a measured reflectivity of more than 11%, the soil thickness must be in the range from 10 to 20 cm over the entire area; and that an additional deposit of the order of 1 m of soil would be required to reduce further the dielectric constant to 8%. Although there is undoubtedly a seasonal redistribution of martian dust, photographs at the Viking Lander sites<sup>12</sup> do not show the buildup of the tens of centimetres of dust that would be needed to effect a change from 11 to 8% in the average radar reflectivity. Alternative explanations, such as seasonal changes in the bulk chemistry of the near-surface rocks, seem also to be unlikely.

Conversely, a transition from frozen water (reflectivity >7%) to liquid water (reflectivity >64%) would produce just such a striking difference in the observed radar reflectivity. Considerable supporting evidence exists that permits the presence of liquid water on Mars to be hypothesized. The large martian channel systems are believed to be the products of large-scale release and surface flow of water from confined aquifers<sup>13,14</sup>. Thermal and IR-spectral measurements of the North Polar cap<sup>15</sup> indicate abundant water ice, while 1–3 wt% of adsorbed water was detected in samples taken by the Viking Landers<sup>16</sup>. In addition, on a smaller scale, both spectrophotometer measurements made during the 1973 dust storm<sup>17</sup> and measurements from the Viking water-vapour mapping experiment<sup>18</sup> indicate that a considerable amount of H<sub>2</sub>O outgassing occurs at present within Solis Lacus. Although the surface temperatures at the Viking Lander sites are only in the range 230–250 K (ref. 19), for an assumed analogy with terrestrial geology the water reservoir could be highly saline due to the salts leached from the surrounding rocks<sup>20</sup>. For Mars, saline solutions have been shown to be stable in their liquid phase in current surface conditions at temperatures as low as 210 K (ref. 21).

We conclude, therefore, that only surface materials containing liquid water are consistent with: (1) the coincident very high radar reflectivities and  $C$ -factor values; (2) the photographically observed surface morphology; and (3) the increase in reflectivity values from spring to summer. Some inferences can also be made about the regional extent of the near-surface expression of the liquid water at Solis Lacus. An extensive liquid water surface (such as a lake) would have a much higher reflectivity than the observed maximum value of about 16%. More likely is a reduction in the reflectivity by an overlying layer of soil, as outlined above for the rock-soil combination, or, alternatively (or additionally), the liquid water might be observable only through random patches of the surface because of variations in the thickness or density of the overburden. In the latter case, the observed reflection values would be from a mixture of high and low reflectivity surface elements. In this case, the  $C$ -factor measurements would depend mainly on the highly reflecting regions (the oases) rather than the dry intervening areas. In either case, we are convinced by the radar data that liquid water does indeed exist near the surface of Solis Lacus during Southern Hemisphere summer.

We thank George Downs for radar data, and Richard Simpson and Gordon Pettengill for helpful comments. This research was partly supported by NASA under grants NSG-7179, NSG-7569, and NSG-7570. Haystack Observatory is operated by MIT under NSF grant AST-7920168.

Received 7 April; accepted 13 October 1980.

- Pettengill, G. H., Shapiro, I. I. & Rogers A. E. E. *Icarus* **18**, 22–28 (1973).
- Downs, G. S., Reichley, P. E. & Green, R. R. *Icarus* **26**, 273–312 (1975).
- Simpson, R. A., Tyler, G. L. & Lipa, B. J. *Icarus* **32**, 147–167 (1977).
- Hagfors, T. *J. geophys. Res.* **69**, 3779–3784 (1964).
- Mouginis-Mark, P. J. & Zisk, S. H. *Lunar planet. Sci.* **11**, 771–773 (1980).
- Evans, J. V. & Hagfors, T. *J. Radar Astronomy* (McGraw-Hill, New York, 1968).
- Huguenin, R. L., Clifford, S. M., Sullivan, C. A. & Miller, K. J. *NASA Tech. Mem.* 80339, 208–214 (1979).
- Huguenin, R. L. & Clifford, S. M. *Bull. Am. astr. Soc.* **11**, 580 (1979).
- Mouginis-Mark, P. J. & Zisk, S. H. *Lunar planet. Sci.* **11**, 768–770 (1980).
- Mouginis-Mark, P. J., Cintala, M. J. & Whitford-Stark, J. L. *Lunar planet. Sci.* **11**, 762–764 (1980).
- Campbell, M. J. & Ulrichs, J. *J. geophys. Res.* **74**, 5867–5880 (1969).
- Arvidson, R., Guinness, E. & Lee, S. *Nature* **278**, 533–535 (1979).
- Baker, V. R. *J. geophys. Res.* **84**, 7985–7993 (1979).
- Carr, M. H. *J. geophys. Res.* **84**, 2995–3007 (1979).
- Kieffer, H. H., Chase, S. C., Martin, T. Z., Miner, E. D. & Palluconi, F. D. *Science* **194**, 1341–1344 (1976).
- Anderson, D. M. & Tice, A. R. *J. molec. Evolut.* **14**, 33–38 (1979).
- McCord, T. B., Huguenin, R. L. & Johnson, G. *Icarus* **31**, 293–314 (1977).
- Farmer, C. B., Davies, D. W., Holland, A. L., LaPorte, D. D. & Doms, P. E. *J. geophys. Res.* **82**, 4255 (1977).
- Hess, S. L., Leovy, C. B., Ryan, J. A. & Tillman, J. E. *J. geophys. Res.* **82**, 4559–4574 (1977).
- McGinnis, L. O. *Proc. 2nd Colloq. Plan. Water Hanover*, New Hampshire, 7–10 (1978).
- Brass, G. W. *Icarus* **42**, 20–28 (1980).

## MATTERS ARISING

## Superoxide involvement in negative air ion effects

INTEREST in research on the biological effects of small negative air ions has been due to the variety of claims made for them, ranging from lethal effects on micro-organisms to therapeutic effects on humans<sup>1-3</sup>. In spite of the promising results reported, there has been a lack of understanding of the underlying biochemical basis. This is not surprising because the exact nature of the air ions has not been defined by those concerned. Consequently, there has been no investigation of the interaction between well defined ionized air species and biological systems of different degrees of complexity, which could have provided the basis for understanding the possible biological impact. Recently, however, experiments have been reported by Kellogg *et al.*<sup>4</sup> which "support the concept that the negative air ions responsible for bacterial death consist solely or in part of hydrated superoxide anions". This conclusion was based on the observation that the enzyme superoxide dismutase (SOD) completely protected bacteria against killing by air ionization. This enzyme is known to remove  $O_2^-$  efficiently by catalysing its disproportionation into hydrogen peroxide and molecular oxygen. The negative air ions in that study were produced by a corona discharge-type negative ion generator.

We suggest caution in adopting this conclusion. The negative ion species generated in air by corona discharge have been identified accurately by mass spectrometry<sup>5</sup>. At atmospheric pressure, in static or dynamic conditions,  $CO_3^-$  is the dominant species produced. Such ions were found to be due to small concentrations of  $CO_2$  in air. The  $CO_2$  apparently reacts with  $O^-$  or  $O_3^-$  to form  $CO_3^-$ . It was estimated that only about 40 p.p.m. of  $CO_2$  is needed at atmospheric pressure to convert all oxygen ions to  $CO_3^-$  species. Superoxide anion,  $O_2^-$ , was detected in small amounts only at a gas pressure lower than 200 torr, a maximum of about 15%  $O_2^-$  being produced at 20 torr.

We know of no published report that  $CO_3^-$  can be converted to  $O_2^-$  in water. We have tested<sup>6</sup> the possible generation of  $O_2^-$  from ionized air in aqueous medium by simple and straightforward chemical assay such as reduction of nitroblue tetrazolium (NBT) to the corresponding formazan<sup>7</sup>. A 5-day exposure of an aqueous solution of NBT ( $10^{-5}$  M) to the ion generator (Modulon Corona discharge-type operated at a maximum discharge current of 0.1 mA) provided no indication of conversion to formazan. Also, no evidence could be obtained of the production of hydrogen peroxide, the product of  $O_2^-$  self-disproportionation

( $k = 4 \times 10^5 \text{ M}^{-1} \text{ s}^{-1}$ , ref. 8) in water exposed to the ion generator (1 ml water, 10 cm distance from the needle, 24-h exposure).

Finally, the negative ion flux in the work of Kellogg *et al.*<sup>4</sup> was  $5 \mu\text{A}$ . This corresponds to about  $3 \times 10^{13}$  electron charges per s or  $1.1 \times 10^{17}$  electron charges per h. Even if all the negative charges produced  $O_2^-$ , and neglecting its decay, this is equivalent to  $1.8 \times 10^{-7} \text{ mol } O_2^- \text{ per h}$ . This differs significantly from  $3 \times 10^{-4} \text{ mol } O_2^- \text{ per h}$  as the stated level of  $O_2^-$  in the same work.

We have no ready explanation for the protection by SOD against bacterial killing by negative air ions observed by Kellogg *et al.*<sup>4</sup>. Only by carefully duplicating their experiments and manipulating the variables in their system could one hope to explain the observed data. Whatever the explanation, however, it is very unlikely to be mediated by superoxide radical anion.

Regarding the general mechanism of action of negative ion generators (which are almost exclusively of corona discharge-type), we find it surprising that no attention has been paid to the striking resemblance between them and electrostatic precipitators. These latter devices, well known in the chemical industry, efficiently collect dust, fumes and mists by charging the particles in an electrostatic field created by negative corona discharge electrodes<sup>9</sup>.

We suggest that the same effects attributed to some undefined small negative air ions could be explained by the electrical field produced by the generation of ions. Such a field could cause, for example, the enhanced migration of microbial cells, reminiscent of electrophoresis, which ends in agglutination or adsorption to the walls, resulting in a lower plate count.

The claimed feeling of well-being produced by ion generators<sup>1-3</sup> could be due to an atmosphere free of aerosols and dirt, cleaned by electrostatic precipitation. Would not any other air-filtration device give the same results?

I. ROSENTHAL

Division of Food Technology,  
Agricultural Research Organization,  
The Volcani Center, PO Box 6,  
Bet Dagan, Israel  
and

Department of Chemistry,  
Nuclear Research Center-Negev,  
PO Box 9001, Beer-Sheva, Israel

E. BEN-HUR

Department of Radiobiology,  
Nuclear Research Center-Negev,  
PO Box 9001, Beer-Sheva, Israel

1. Knoll, M., Fichmeier, J. & Schön, R. W. *Adv. Electron. Electron Phys.* **19**, 178-244 (1964).

2. Gualtierotti, R., Kornbluh, I. H. & Sirtori, C. *Bioclimatology and Aeroionotherapy* (Carlo Elba Foundation, Milan, 1968).
3. Kreuger, A. P. & Reed, E. J. *Science* **193**, 1209-1213 (1976).
4. Kellogg, E. W., Yost, M. G., Barthakur, N. & Kreuger, A. P. *Nature* **281**, 400-401 (1979).
5. Shahin, M. M. *Appl. Opt. Suppl.* **3**, 106-110 (1969).
6. Rosenthal, I., Juven, B. J., Gordin, S. & Ben-Hur, E. *J. appl. Bact.* **46**, 451-454 (1979).
7. Beauchamp, C. O. & Fridovich, I. *Analyt. Biochem.* **44**, 276-287 (1971).
8. Bielski, B. H. J. & Allen, A. O. *J. phys. Chem.* **81**, 1048-1050 (1977).
9. Kirk, R. E. & Othmer, D. F. (eds) *Encyclopedia of Chemical Technology* Vol. 5, 646-665 (1954).

KELLOGG, YOST AND KRUEGER  
REPLY—We have several points to make in reply to the comments by Rosenthal and Ben-Hur. First, no one has yet definitely characterized the chemical nature of negative air ions. The work by Shahin<sup>1</sup> on the ionic species produced by corona discharge seems quite interesting, and he does clearly identify the predominant negative ion made in his system (at atmospheric pressure) as  $CO_3^-$ . However, his system differs from ours<sup>2</sup> in several ways, including the maximal current used (1 mA compared with our 0.01 mA) and the corona discharge voltage (12 kV compared with our 5 kV). We cannot determine whether these differences would affect the negative ions produced. However, even if our system did make  $CO_3^-$  as the principal negative ion species, Shahin's work does not preclude the production of  $HO_2$ , which as an uncharged species would go undetected by mass spectroscopic methods, and which would give rise to  $O_2^-$  in solution.

We do know of a number of studies that support the  $O_2^-(H_2O)_n$  negative air ion concept. For example, Mohnen<sup>3</sup> summarized his work as follows: "An attempt has been made to determine theoretically a reaction scheme to explain the formation of negative small ions in the troposphere and lower stratosphere. The terminal ions are found to be hydrated  $O_2^-$  and  $CO_4^-$ . The degree of hydration depends on temperature, and the mean number of water molecules attached to those ions is of the order of 3 or 4. As soon as the water vapor concentration is less than the concentration of carbon dioxide (about 8 km), the terminal ion is found to be hydrated  $CO_4^-$ . The reaction scheme is based on measured and reasonably estimated reaction rate constants determined by using U.S. standard atmosphere for the neutral gas composition." Regardless of the identity of negative ions in air, this does not preclude their transformation to other ions, such as  $O_2^-$  on addition to solution. Our data, which showed strong protection against negative ion bacterial kill by superoxide dismutase (SOD), but not by denatured SOD, strongly indicated  $O_2^-$  involvement in this negative ion effect, which occurred whether one considers negative air ions as  $O_2^-(H_2O)_n$  or not.



The negative air ion system used by Rosenthal *et al.*<sup>4</sup> to test for  $O_2^-$  production, by looking for nitroblue tetrazolium (NBT) reduction, or  $H_2O_2$  accumulation, had several gross inadequacies. They neither grounded, nor even stirred, their target solutions and could not in fact even demonstrate a bactericidal effect of negative air ions, an effect repeatedly confirmed in numerous published reports. Our own work has shown that the effect of negative ions on NBT gives results that seem neither simple nor straightforward. We found that although negative ion treatment did not cause reduction of NBT to the formazan, it did cause the NBT solution to change spectrally, while concomitantly losing its susceptibility to reduction to the formazan by dithionite. Although SOD completely prevented this effect, we also found that denatured SOD, and even bovine serum albumin, gave complete protection. Our results with NBT, although unexplained, offer no evidence either for or against superoxide involvement in negative air ion effects.

Similarly, the failure of Rosenthal *et al.* to find evidence for  $H_2O_2$  production in solutions exposed to negative ions does not in any way argue against  $O_2^-$  involvement. They failed to understand that one cannot simply 'add' negative charges indefinitely to a target solution, and as their system consisted simply of  $H_2O$  exposed to an ion generator without grounding, or even stirring, one would not expect to find sufficient  $H_2O_2$  accumulation for measurement by even the most sensitive methods, let alone less sensitive chemical methods such as the iodometric that they used.

We apologize that we did inadvertently give an incorrect value for the maximal possible flux of  $O_2^-$  in our system— $0.18 \mu M h^{-1}$  gives a correct estimation of this flux. Over a 5-h period, this gives a ratio of  $\approx 1.4 \times 10^{10}$  negative ions per bacterium. Although the mechanism of bacterial kill remains obscure, it does not seem to occur by agglutination due to electrostatic effects, because early in our experimental series we observed no agglutination of samples in direct microscopic examination. Furthermore, previous studies using polonium-210 or tritium as ion sources have also demonstrated bacterial kill, despite having a field substantially lower than that seen in corona discharge generators<sup>5</sup>. Earlier work using corona discharge generators<sup>6</sup> found a reversal of damage to cells on exposure to intense visible light, an effect which should not occur with agglutination. Finally, the time required for cell death was much less than the minimal time for agglutination predicted by the von Smoluchowski equation<sup>7</sup>. Many other studies have shown the varied biological activity of negative air ions<sup>8-13</sup>, so the suggestion by Rosenthal and Ben-Hur that all negative ion effects are derived from an electric field or electrostatic pre-

cipitation effects appears at odds with the experimental facts of the literature.

E. W. KELLOGG III

Membrane Bioenergetics Group,  
Lawrence Berkeley Laboratory  
and

Department of Physiology-Anatomy,  
University of California,  
Berkeley, California 94720

M. G. YOST

A. P. KRUEGER

Department of Biomedical and  
Environmental Health Sciences,  
School of Public Health,  
University of California,  
Berkeley, California 94720

- Shahin, M. M. *Appl. Opt. Suppl.* **3**, 106-110 (1969).
- Kellogg, E. W. III, Yost, M. G., Barthakur, N. & Krueger, A. P. *Nature* **281**, 400-401 (1978).
- Mohnen, V. A. *Geophys. Res.* **75**, 1717-1721 (1970).
- Rosenthal, I., Juven, B. J., Gordin, S. & Ben-Hur, R. J. *appl. Bact.* **46**, 451-454 (1979).
- Krueger, A. P., Smith, R. F. & Go, I. G. *J. gen. Physiol.* **41**, 359-381 (1957).
- Krueger, A. P., Reed, E. J., Brook, K. B. & Day, M. B. *Int. J. Biometeor.* **19**, 65-71 (1975).
- von Smoluchowski, *Phys. Z.* **17**, 557, 583 (1916).
- Krueger, A. P., Strubbe, A. E., Yost, M. G. & Reed, E. J. *Int. J. Biometeor.* **22**, 202-212 (1978).
- Krueger, A. P., Kotaka, S. & Andriese, P. C. *Int. J. Biometeor.* **9**, 201-209 (1965).
- Kotaka, S., Krueger, A. P. & Andriese, P. C. *Int. J. Biometeor.* **12**, 85-92 (1968).
- Krueger, A. P., Andriese, P. C. & Kotaka, S. *Int. J. Biometeor.* **12**, 225-239 (1968).
- Gilbert, G. O. *Int. J. Biometeor.* **17**, 267-275 (1973).
- Frey, A. H. *J. comp. Physiol. Psychol.* **63**, 121-125 (1967).

## Role of $PGE_2$ in anion exchange in gastric mucosa

IT has been suggested by Schiessel *et al.*<sup>1</sup> that a prostaglandin ( $PGE_2$ ) increases  $Cl^-HCO_3^-$  exchange in gastric mucosa, thereby protecting surface cells against excessive back-diffusion of  $H^+$  from the lumen. Their evidence is necessarily indirect, because it is not known whether such exchange occurs at the nutrient membrane of the surface cell (as demanded by their hypothesis) or, indeed, whether exchange diffusion is a characteristic of this cell type. The authors do show an increase in  $Cl^-$  fluxes across the isolated mucosa due to  $PGE_2$ , and because anion exchange is rather nonspecific in this preparation<sup>2</sup>, as in red blood cells<sup>3,4</sup>, it is reasonable to suppose that exchange of  $Cl^-$  for  $HCO_3^-$  is also increased.

The authors, however, are guilty of a logical *non sequitur*: they deduce that  $PGE_2$  increases exchange of cell  $Cl^-$  for nutrient  $HCO_3^-$  from a negative finding, that  $PGE_2$  does not affect the depression in nutrient to secretory  $Cl^-$  flux due to the removal of secretory  $Cl^-$  (trans-concentration effect<sup>5</sup>). Exchange of  $Cl^-$  across the epithelium requires a suitable partner anion, yielding a null electrical current. In the secretory solution, the authors use replacement anions (isethionate, sulphate) which do not exchange for  $Cl^-$ , and this fact cannot be altered by a drug such as  $PGE_2$ .

The criticism here raises a pertinent question: does a modest level of  $HCO_3^-$  in

the secretory solution reduce the trans-concentration effect, and does  $PGE_2$  then further reduce the effect? Evidence on this question would bear more directly on the authors' hypothesis.

RICHARD P. DURBIN

Department of Anatomy, University of  
Umeå, Umeå, Sweden

- Schiessel, R., Matthews, J., Barzilai, A., Merhav, A. & Silen, W. *Nature* **283**, 671-673 (1980).
- Durbin, R. P., Kitahara, S., Stahlmann, K. & Heinz, E. *Am. J. Physiol.* **207**, 1177-1180 (1964).
- Gunn, R. B., Dalmark, M., Tosteson, D. C. & Wieth, J. O. *J. gen. Physiol.* **61**, 185-206 (1973).
- Dalmark, M. *J. gen. Physiol.* **67**, 223-234 (1976).
- Heinz, E. & Durbin, R. P. *J. gen. Physiol.* **41**, 101-117 (1957).

SCHIESEL *ET AL.* REPLY—We acknowledge the validity of the argument that  $PGE_2$  cannot alter the trans-concentration effect because replacement anions which do not exchange for  $Cl^-$ , were used in the secretory solution, and we were aware of that fact. In these experimental conditions, however, failure of  $PGE_2$  to affect  $J_{Cl^-}$  (the flux of  $^{36}Cl^-$  measured from nutrient to secretory solutions) more than about the 50% usually found in control experiments in our laboratory suggests that the  $PGE_2$  does not affect either of the remaining components of  $Cl^-$  flux—the active or diffusional components. An unfortunate phrasing of the sentence describing our findings may have led to the misunderstanding that we believed these experiments rigorously excluded the possibility that  $PGE_2$  affects exchange diffusion of  $Cl^-$ .

We agree that much of the evidence for our hypothesis is necessarily indirect. The finding that  $PGE_2$  did not sustain  $Cl^-$  flux in metiamide-inhibited tissues when  $HCO_3^-$  was absent from the nutrient solution supports this hypothesis, however. It is also possible that  $PGE_2$  causes an increase in  $Cl^-$  permeability without change in exchange diffusion of  $HCO_3^-/Cl^-$  exchange.

The suggested experiments would be interesting, but in our opinion difficult to interpret and not definitive in excluding an effect of  $PGE_2$  on exchange diffusion of  $Cl^-$ . If all three components of the  $Cl^-$  flux are operative when a suitable exchangeable anion (not  $Cl^-$ ) is in the secretory solution, stimulation of  $Cl^-$  flux by  $PGE_2$  would not specifically define the effect of  $PGE_2$  on any of the three components of  $Cl^-$  flux. Conversely, failure of  $PGE_2$  to stimulate  $Cl^-$  flux in these conditions might be interpreted as evidence that either a direct  $Cl^-Cl^-$  exchange at the secretory membrane is required for the  $PGE_2$  effect or that the non- $Cl^-$  anion inhibited the effect of  $PGE_2$ .

WILLIAM SILEN

RUDOLF SCHIESEL

JEFFREY MATTHEWS

AMI BARZILAI

ARYEH MERHAV

Departments of Surgery,  
Harvard Medical School,  
Beth Israel Hospital  
Boston, Massachusetts 02215

## BOOK REVIEWS

## Tertiary sector of the science industry

Edward Shils

THE activities of thinking and observing which are involved in the pursuit of scientific knowledge occur in a setting of many other activities and institutions which are not themselves scientific knowledge but which are indispensable to it. These include the intellectual relationships among individual scientists, within institutions, within and between countries; the traditions of institutions — such as laboratories — in which scientific work is done; the organs and institutions through which scientists communicate the results of their research; and the processes through which problems are selected and knowledge is sifted, rejected, affirmed, extended, elaborated and revised. It is in these actions and places that the “public” character of science is exhibited. They constitute what has come to be known as “the scientific community”, a complex made up of as many scientific sub-communities as there are fields of specialization, and institutions and countries in which scientific work is done.

In addition, there are the institutions and arrangements which bring scientific traditions into the focus of attention of young persons who might become scientists, and those processes by which aspirant scientists are inducted into the intellectual and moral discipline of scientific work. Since scientific work requires apparatus and time free from other obligations, the institutional arrangements whereby scientists are enabled to live and to have what they need to do scientific work are likewise parts of this immediately necessary complement to the advancement of scientific knowledge.

Around all this there have grown up a large number of supplementary activities which are not integral or immediately necessary to the pursuit of scientific knowledge and its incorporation, by application, into technology. Among these are the historiography of science and medicine and of the technology used in economic life and warfare, systematic analysis of the logical and epistemological structure of scientific propositions, reflection on the moral and other merits and demerits of scientific knowledge and of technology in

*A Guide to the Culture of Science, Technology, and Medicine.* Edited by Paul T. Durbin. (Free Press/Collier Macmillan: 1980.) \$45, £30.

their many forms, the sociological study of the structure of scientific communities and of particular scientific institutions, and discussions about whether and how science should be governed by authorities outside itself. Some of this penumbral intellectual effort has been carried on by academics. Some of it has become established in academic institutions as parts of existing disciplines such as history, philosophy and sociology. Some is part of journalism and of amateur scholarship.

Finally, at some distance from immediate involvement with the pursuit of scientific knowledge, there are the ramifications of science into the way of life and outlook of the ordinary members of society — its impact on their moral notions and conduct, their cosmological and religious beliefs, their conceptions of mankind and the world, and their ideas about and knowledge of science itself.

All of this vast complex may be called “the culture of science”. It is an immense subject, deserving of studious attention because it permeates so much of modern civilization.

*A Guide to the Culture of Science, Technology and Medicine* is a collaborative attempt to summarize the state of knowledge regarding the culture of science. It is a thick volume of nine parts, ranging in length from 30 to about 60 pages. The parts deal with the history of science, written by Arnold Thackray; the history of technology, by Carroll Pursell; the history of medicine, by Gert Brieger; the philosophy of science in its “historical, social and value aspects”, by Alex Michalos; the philosophy of medicine, by H. Tristram Engelhardt and Edmund Erde; the sociology of science and technology, by Jerry Gaston; medical sociology and science and technology in medicine, by Linda Aiken and Howard Freeman; and science policy studies by Diane Crane. Each essay is accompanied by a long and excellent bibliography.

As is inevitable with such a work, the outcome is very uneven. Most noticeably, the quality of the contributions is unrelated to their length. Two of the least valuable — those on the history of technology and the

philosophy of science — are respectively the shortest and nearly the longest in the volume. The long essay on the philosophy of science contains less about the culture of science than any of the others; it is a series of mechanically assembled summaries and bibliographical references, some of them patently second-hand. Some, but not all of the defects of this particular essay are attributable to the author; they are also due to the dreary literature which he has to summarize, a literature which is self-contained, having little to do with what scientists do and know.

It is not accidental that the richest contributions are those by Brieger, by Engelhardt and Erde, and by Aiken and Freeman. Each of these essays benefits from the authors’ intimacy with medical practice and biomedical science, and from the long traditions of learning and reflection by physicians and biomedical scientists; in these there is an exceptional awareness of moral issues. Exceptional, because although the contributors to the volume were apparently enjoined by the editorial board to pay particular attention to moral issues and questions of “values”, most of the authors deal with them in a perfunctory way, as if they were acting under orders and did not have their heart in it. It is only in those essays dealing with medicine — and in Mitcham’s essay on the philosophy of technology — that the moral or “value” problems are treated as genuine issues which practitioners and investigators are under compelling obligation to reflect upon, and to take into account in their actions.

How are we to explain this difference between the humdrum and insightful character of some of these essays and the lively realism of others? The answer to this seems to me to lie in the fact that, for some of the authors, the “culture of science, technology and medicine” is something to be written about from the outside, as an academic quasi-discipline with its own self-justifying traditions. They regard it as something to be studied and written about, but not as something in which they participate. This bespeaks a deficiency in their understanding of the concept. They do not really see the literature of their subjects as parts of the “culture” — despite the title of the book to which they have contributed. The centrality of scientific knowledge to the “culture of

Edward Shils is Professor of Sociology and Social Thought at the University of Chicago and editor of *Minerva*. His most recent book is *The Calling of Sociology* (University of Chicago Press, 1980).



science" seems to have escaped some of the contributors to this book, not least the sociologists among them.

Here, a word should be said about the contributions of sociology to the present volume. In the essay which deals with medical sociology and science and technology in medicine, the authors devote less than one-fourth of their space to the former and, although they deal with it appreciatively, they see that it touches only spottily on their topic. They point out that it is guided by the tradition of sociology as an academic discipline. What they are indicating is that medical sociology, with all its merits, has not really become part of the culture of science, technology and medicine. The same must be said about the way in which the sociology of science and technology is presented here.

The editors themselves must bear some of the onus for this faulty understanding of the culture of science. Otherwise how could they have omitted any treatment of the impact of scientific knowledge on the

outlook and conduct of ordinary members of modern societies? There is nothing in the book about that. Nor is there anything about scientific education. And, except for passing comments in the essays on the history of science and medicine, there is no serious consideration of the process of the growth of scientific knowledge. The editors have found the right name for their subject but they have not found the subject to which to apply it.

In the preface it is stated that "more than anything else, the volume should be useful to teachers of interdisciplinary courses in technology and values or science and society". If their expectation is realized, it will help to maintain such courses of study in their present superficiality and in their arbitrary and distorted conception of their subject. This book has considerable value but it is not a guide for those who are too isolated for their own good from science, technology and medicine, and who do not understand their own peculiar place in its culture. □

presented in this review, unfortunately, is based on the authors' own work, with the consequence that the chapter is too short to cover these interesting viruses in sufficient depth.

The final contribution is a review on the prospects in human retrovirus research. It does, however, present a somewhat unusual perspective as it is more cautious than previous reviews on the subject. The chapter is well balanced and covers the appropriate material comprehensively.

Overall, the book is an adequate compilation of many useful reviews. What is missing, however, is a final section that brings together the diverse ideas and information — instead of leaving the chapters as separate entities — and a discussion of the direction that future work in this field should take. It is also rather unfortunate that, at the time of completion of the book (early 1979), information on molecular cloning studies and structures of proviruses was still scanty, for additional material on these subjects would improve the book. This kind of drawback is perhaps inevitable in such multi-author reviews covering fast-moving areas of research. Nevertheless, this book should stand as a good source of references. It should also be of value to biochemists with a special interest in retroviruses and to pre- and postdoctoral fellows entering the field. □

Tak W. Mak is a Senior Staff Scientist at The Ontario Cancer Institute and an Associate Professor of Medical Biophysics at the University of Toronto.

## Retrovirus research

Tak W. Mak

*Molecular Biology of RNA Tumor Viruses.* Edited by John R. Stephenson. Pp. 528. (Academic: 1980.) \$49.50, £34.20.

THE momentum that was given to retrovirus research by the discovery of reverse transcriptase is still strong. Today, ten years after that discovery, the field remains one of the most active areas in biology. The book, a collection of 12 reviews by as many groups, is an attempt to take stock and evaluate the progress in the field. In general, the reviews are informative though a few chapters are somewhat narrow in that they tend to dwell on the authors' own work. A more important criticism, however, is that the choice of topics suffers from lack of an overall balance that would accurately reflect the efforts in different aspects of retrovirus research. For example, the reviews tend to emphasize mammalian retroviruses, with a strong accent on murine type-C viruses, while omitting much of the avian viruses and their genetics.

The book begins with a good account of the historical development of retrovirus research, from the discovery of Rous sarcoma virus to the present. The three chapters which follow all deal with mammalian type-C retrovirus genes and their transmission. The first is a summary of the efforts to delineate further evolutionary relationships among primates and mice through studies of their endogenous retrovirus sequences. The next, on murine endogenous type-C viruses, is a comprehensive account of the

genetics and regulation of murine type-C retroviruses. It contains many helpful tables to aid readers in understanding this complicated field. The third of these opening contributions is on the integration and transmission of exogenous murine type-C virus. It contains some interesting information on germ line integration of exogenous virus. However, it seems rather brief and repetitive after the two preceding, rather ampler, chapters.

The next two contributions are on transforming viruses and retrovirus genomes, respectively. They are both useful reviews. They complement each other well and are presented at an appropriate level for such a volume. That which deals with retrovirus genomes, however, is too short to cover the genome structures of both avian and murine retroviruses. Expansion of this chapter or addition of another article to include more on avian retroviruses and the biochemistry of retroviruses would have been desirable.

The seventh and eighth chapters are on type-C viral proteins and their primary structures. They contain an in-depth look at the proteins of type-C retrovirus and would be useful for investigators interested in the subject. Next come two contributions on reverse transcriptase and heteroduplex mapping — both of which are informative and contain detailed surveys of reverse transcriptase enzymology and heteroduplex mapping of viral genomes. The eleventh chapter is a discussion of type-B and type-D retroviruses. Most of the information

## Evolving theories

Adrian Friday

*Phylogenetic Patterns and the Evolutionary Process. Method and Theory in Comparative Biology.* By Niles Eldredge and Joel Cracraft. Pp. 349. (Columbia University Press: 1980.) \$27.50, £15.50.

ELDRIDGE and Cracraft's central theme is that estimates of the pattern of evolutionary history logically precede the making of hypotheses about the process of evolution.

Estimation of the pattern of evolutionary relationships is inevitably carried out by the comparison of similarities between organisms. To Eldredge and Cracraft, shared similarities do not all have equal status in this enterprise but, following the ideas of the late Willi Hennig, a way of organizing such information is to construct a series of nested sets each characterized by at least one evolutionary innovation (Hennig's "synapomorphy"). That these are innovations emphasizes to the authors the importance in such analysis of interpreting the pathway of change in biological characters. Decisions about the sequence of change can often be difficult



to make, but the stark alternative interpretation of the pattern of differences between organisms as a static, instantaneous phenomenon is clearly not one likely to appeal to evolutionary biologists. To quote Eldredge and Cracraft (p.55): "The concept of nested sets of synapomorphy makes sense only if it is assumed that change has taken place . . .".

The so-called "problem of homology" is presented as not being a problem when phylogenetic homologies are equated with the evolutionary innovations defining sets. Accordingly, evolutionary convergence is interpreted as non-homologous similarity: the sceptical might regard this as more a definition than a solution.

For Eldredge and Cracraft, a diagram summarizing set membership is a "cladogram" and includes no designation of ancestral versus descendant organisms. If such additional conjectures are made, the diagram then becomes a phylogenetic tree. The difference is seen as an important one: the cladogram being the more general statement. However, no mention is made of the valuable work of G.F. Estabrook which defines these concepts more precisely from a rather different viewpoint.

The authors present the structure of a cladogram as subject to rejection and replacement by an alternative hypothesis. In this way hypotheses of set membership can be corroborated. Rejection is achieved by the examination of more characters. Where these contradict the original partitioning, they may do so in concerted fashion and force a re-examination, not only of the old scheme of hierarchies, but also of our biological understanding of the characters used to define them. A statement that: "The criterion of parsimony specifies our acceptance of the least rejected hypothesis" (p.70) may seem unexceptionable to many, but: "In evolutionary terms, therefore, we prefer the cladistic hypothesis which minimizes convergence" (also p.70) appears unfortunate in view of the authors' otherwise clinical view of parsimony as an inevitable component of the hypothetico-deductive method rather than a principle of the evolutionary process.

In the final chapter the separate nature of microevolution, speciation and macroevolution is emphasized (with due acknowledgement to the ideas of Sewall Wright and S. N. Salthe). On this subject the book becomes repetitious and risks losing its momentum in nested reappraisals of previous sections. Certainly, a reading of such recent books as R. C. Lewontin's *The Genetic Basis of Evolutionary Change* (Columbia University Press, 1974), M. J. D. White's *Modes of Speciation* (Freeman, 1978) and S. M. Stanley's *Macroevolution* (Freeman, 1979) reinforces the lack of a unified theory underlying the events of evolution.

Ironically, the conflict between pattern and process can be brought out by con-

sidering the approach of population geneticists to the estimation of kinship relationships using gene frequency data measured in human populations, clearly a "microevolutionary" study (an example is given in E. A. Thompson's *Human Evolutionary Trees*; Cambridge University Press, 1975). This type of estimation is a statistical exercise involving the prior construction of a probabilistic model of change. When we attempt to apply such a methodologically rigorous approach to anatomical characters it is difficult to frame a plausible model for the process.

What Eldredge and Cracraft's book

suggests to me, in defiance of their declared theme, is that our lack of a model for the relevant processes of evolution hampers the convincing reconstruction of the pattern of evolutionary relationships. The majority of readers would probably not agree. In any case, the book is strongly recommended to allies and opponents alike. It solicits underlinings and exclamation marks and is mostly elegantly argued and enjoyable.

Adrian Friday is Assistant Curator of Vertebrates at the University Museum of Zoology, Cambridge, UK.

## Humphry Davy and geological conundrums

G.Y. Craig

*Humphry Davy on Geology: The 1805 Lectures for the General Audience.* Edited by R. Siegfried and R.H. Dott. Pp.169. (University of Wisconsin Press: 1980.) \$17.50, £9.



Sir Humphry Davy

HUMPHRY Davy, chemist and inventor, lectured on a variety of scientific subjects at the Royal Institution in London between 1801 and 1812. From 1805 onwards he gave a course of ten lectures in geology. Happily, full hand-written notes on eight of his lectures have been preserved, and with two further transcripts by a copyist now provide the only complete lecture course known among Davy's surviving papers.

In their introductory chapter the editors outline Davy's career and comment on his geological philosophy. Davy himself explains his stance in the first lecture:

Geology, perhaps more than any other department of natural philosophy, is a science of contemplation. It requires no experience or complicated apparatus, no minute processes upon the unknown properties of matter. It demands only an inquiring mind and senses alive to the facts

almost everywhere presented in nature. As it may be acquired without much difficulty, so it may be improved without much painful exertion.

Almost a century later Sir Archibald Geikie commented in his biography of Murchison that it also required a stout pair of legs!

Davy's style is clear, his writing elegant, his criticisms courteous, and throughout he reveals the caution typical of the chemist. The first four lectures, excluding a general introductory lecture, are largely concerned with a review of earlier theoretical speculations, ranging from Greek philosophers to late-eighteenth century writers. In the following six lectures he describes rocks and outcrops, both from his own observations and from those of the other naturalists. Conundrums are many, resolutions are few. Why should limestone stick more firmly to sandstone than to schist? There is a report of fishes in basalt! Is coal formed by heat from vegetable matter?—yet the strata above and below don't appear to have been subjected to heat. Sensible personal observations blended with second-hand reports, contradictory theories and a belief in a purposeful progression of life inevitably lead to difficulty. Davy does not attempt to develop an independent theory of his own, but with the critical and perhaps slightly superior view of an experimental chemist has as much to be wary about. Since he is not prepared to be a Neptunist, and is unwilling to be a Plutonist, he finds himself on occasions in an impossible position:

All the facts seem to render it probable that the basaltic rocks usually found in alternation with the common secondary rocks cannot be of igneous origin. But the proposition of the impossibility of the formation of this substance by fire must not be advanced.

Davy was not the first lecturer in geology in Britain; he was preceded by Walker at Edinburgh and by Beddoes at Oxford and Bristol. And although there was no



# text books from MACMILLAN PRESS

## FROM DNA TO PROTEIN: The Transfer of Genetic Information MARIA SZEKELY

This is the first textbook which discusses gene structure on the basis of recent discoveries of overlapping and split genes and which genetic information can be encoded into the genetic material and how it can be transferred to other materials.

A perfectly up-to-date account of our present knowledge of the structure and expression of genes in prokaryotic and eukaryotic organisms and the only available text showing the correlation between the structure and function of nucleic acids.

March, £18.00, 0 333 21836 1  
£9.95, 0 333 21828 8

## HUMAN REPRODUCTION AND DEVELOPMENTAL BIOLOGY D. J. BEGLEY, J. A. FIRTH and J. R. S. HOULT

An integrated approach to describe the cellular and physiological processes of human reproduction and embryological development in relation to their underlying mechanisms and to their practical applications in medicine. The book combines anatomy, biochemistry, physiology and pharmacology, making it more suitable for modern preclinical and human biology courses.

February, £20.00, 0 333 23423 5  
£9.95, 0 333 23424 3

## GYNAECOLOGICAL CYTOLOGY

MATHILDE E. BOON and  
METTE LISE TABBERS-  
BOUMEESTER

Dr Boon and Dr Tabbers-Boumeester have, over the past ten years, developed the course in diagnostic cytology which was first given in Leiden in 1969.

In this volume they present their insight into both the study of diagnostic cytology, and into the teaching of this increasingly important subject. To illustrate the modern concepts of cytopathology, examples of more advanced approaches are included: as well as scanning and electron microscopy there are details of DNA measurements, morphometry and immunopathology.

June, £25.00, 0 333 26117 8  
£14.00, 0 333 26118 6

Macmillan Press books are available from leading booksellers  
If you have difficulty obtaining these titles please write to  
Tony Watson, Macmillan Retail Ltd, Houndmills,  
Basingstoke, Hants, enclosing purchase price + 70p (p&p).

**M** MACMILLAN  
PRESS

elementary textbook as we know it at the time, Playfair's *Illustrations of the Huttonian Theory* was certainly available. It would be interesting to know the names of the people who attended Davy's classes and the influence that he had on them. We know for instance from Geikie's biography that R.I. Murchison attended Davy's class in 1812 and that in 1823 Davy encouraged Murchison to go up to London and take some lectures in chemistry, etc. Davy's further irresistible bait was that he would soon get Murchison into the Royal Society (Davy was at that time its President!). Perhaps then Davy's greatest contribution to geology was to persuade Murchison to

abandon fox-hunting and take up geology instead.

Geologists and historians will be grateful to the editors for producing this book and continuing the tradition of academics in the mid-western United States in providing, indeed specializing in, transcripts and facsimile copies of the works of the late-eighteenth and early-nineteenth century philosophers of the Earth. Future historians of the history of science will no doubt one day wish to consider the reason for this phenomenon.

G.Y. Craig is Professor of Geology at the University of Edinburgh.

## Cellular regulatory mechanisms

John Mowbray

*Principles of Metabolic Control in Mammalian Systems.* Edited by R.H. Herman, R.M. Cohn and P.D. McNamara. Pp.670. (Plenum: 1980.) \$35, £22.05.

THE editors of this large book are also the main contributors as authors or co-authors of 11 of the 15 chapters. Their aim, according to the preface, is to discern basic regulatory principles and to embody these in a theoretical approach which can be applied to any set of metabolic reactions. Anyone conversant with the development of metabolic regulation in recent years could be forgiven the thought that such an attempt is premature; close reading of the resulting volume has unfortunately done nothing to dispel my prejudice in this respect. This does not mean that the work should be dismissed out-of-hand, for there is a patent need to collate and review critically the diffuse literature on cellular regulation so that the various arguments may be widely appreciated and tested.

The subject is not one for those without a basic grounding in biochemistry, and yet many of the chapters are padded out with rather large amounts of elementary textbook information. The second chapter, for example, discusses metabolic networks from a non-linear, non-equilibrium, thermodynamic point of view in the first part and defines, as in a primer, hydrophobic, electrostatic, covalent and van der Waals interactions in the second part. In similar vein the special purpose of the book receives little or no contribution from the chapters on enzymes and coenzymes, protein synthesis, DNA replication and the cell cycle, membrane enzymes and membrane structure. All of these topics are better presented (there is a noticeable dearth of diagrams in this volume) in most textbooks for the beginner, and are readily accessible in expert reviews or monographs for the more

advanced reader. On the other hand, a topic not well covered as yet, protein degradation, is presented in a straightforward account with the methodological reservations adequately expounded.

Of the chapters devoted to regulatory mechanisms, the opening chapter in the book develops the hierarchical classification of metabolic processes from which the authors believe important principles can be deduced. The lists and tables are informative, albeit less than comprehensive. In a later contribution, modulation of enzyme activity is discussed without achieving the penetration of specialist monographs like those by Newsholme and Start (Wiley, 1973), or Ferdinand (Wiley, 1976), and it lacks the breadth of some recent reviews. The account of feedback/forward on complex pathways such as glycolysis strikes me as difficult to follow without the aid of diagrams unless one is already familiar with the examples. The chapter "Secretion Mechanisms" is a good, clear account with sufficient references for further reading, and that on the role of compartmentation is well written and nicely balanced with examples taken from key processes. Finally, the chapter dealing with hormone mechanisms has an interesting section on comparative biochemical endocrinology which is perhaps too complex for the novice, and a comprehensive though somewhat uncritical treatment of fast-acting hormones. By contrast the treatment of steroid hormones is cursory in the extreme, spoiling what is otherwise one of the better chapters.

In the end, while there are selected chapters one can recommend to one's students, this is a book for the specialist who can win the grains of very real effort the editors have sown from the chaff of their self-indulgence.

John Mowbray is a Lecturer in Biochemistry at University College London.